ISSN 1007-9327 (print)
ISSN 2219-2840 (online)

World Journal of *Gastroenterology*

World J Gastroenterol 2022 September 7; 28(33): 4744-4928



Published by Baishideng Publishing Group Inc

World Journal of Gastroenterology

Contents

Weekly Volume 28 Number 33 September 7, 2022

REVIEW

4744 Regulation of transforming growth factor-β signaling as a therapeutic approach to treating colorectal cancer

Maslankova J, Vecurkovska I, Rabajdova M, Katuchova J, Kicka M, Gayova M, Katuch V

MINIREVIEWS

4762 Immunological mechanisms of fecal microbiota transplantation in recurrent *Clostridioides difficile* infection

Soveral LF, Korczaguin GG, Schmidt PS, Nunes IS, Fernandes C, Zárate-Bladés CR

4773 Albumin administration in patients with cirrhosis: Current role and novel perspectives

de Mattos ÂZ, Simonetto DA, Terra C, Farias AQ, Bittencourt PL, Pase THS, Toazza MR, de Mattos AA, Alliance of Brazilian Centers for Cirrhosis Care – the ABC Group

ORIGINAL ARTICLE

Basic Study

4787 Novel therapeutic diiminoquinone exhibits anticancer effects on human colorectal cancer cells in two-dimensional and three-dimensional *in vitro* models

Monzer A, Wakimian K, Ballout F, Al Bitar S, Yehya A, Kanso M, Saheb N, Tawil A, Doughan S, Hussein M, Mukherji D, Faraj W, Gali-Muhtasib H, Abou-Kheir W

Case Control Study

4812 Previous hepatitis B viral infection–an underestimated cause of pancreatic cancer

Batskikh S, Morozov S, Dorofeev A, Borunova Z, Kostyushev D, Brezgin S, Kostyusheva A, Chulanov V

Retrospective Cohort Study

4823 Effectiveness, safety, and drug sustainability of biologics in elderly patients with inflammatory bowel disease: A retrospective study

Hahn GD, LeBlanc JF, Golovics PA, Wetwittayakhlang P, Qatomah A, Wang A, Boodaghians L, Liu Chen Kiow J, Al Ali M, Wild G, Afif W, Bitton A, Lakatos PL, Bessissow T

Retrospective Study

4834 Prevalence and factors associated with vitamin C deficiency in inflammatory bowel disease

Gordon BL, Galati JS, Yang S, Longman RS, Lukin D, Scherl EJ, Battat R

4846 Development and validation of a risk prediction score for the severity of acute hypertriglyceridemic pancreatitis in Chinese patients

Liu ZY, Tian L, Sun XY, Liu ZS, Hao LJ, Shen WW, Gao YQ, Zhai HH

World Journal of Gastroenterology

Weekly Volume 28 Number 33 September 7, 2022

Contents

Observational Study

4861 Are bowel symptoms and psychosocial features different in irritable bowel syndrome patients with abdominal discomfort compared to abdominal pain?

Fang XC, Fan WJ, Drossman DD, Han SM, Ke MY

Randomized Clinical Trial

4875 Peroral endoscopic myotomy *vs* laparoscopic myotomy and partial fundoplication for esophageal achalasia: A single-center randomized controlled trial

de Moura ETH, Jukemura J, Ribeiro IB, Farias GFA, de Almeida Delgado AA, Coutinho LMA, de Moura DTH, Aissar Sallum RA, Nasi A, Sánchez-Luna SA, Sakai P, de Moura EGH

SYSTEMATIC REVIEWS

4890 Chinese herbal formula shen-ling-bai-zhu-san to treat chronic gastritis: Clinical evidence and potential mechanisms

Jin W, Zhong J, Song Y, Li MF, Song SY, Li CR, Hou WW, Li QJ

SCIENTOMETRICS

4909 Global research trends in the field of liver cirrhosis from 2011 to 2020: A visualised and bibliometric study

Gan PL, Huang S, Pan X, Xia HF, Zeng XY, Ren WS, Zhou X, Lv MH, Tang XW

CASE REPORT

4920 Ectopic bronchogenic cyst of liver misdiagnosed as gallbladder diverticulum: A case report

Dong CJ, Yang RM, Wang QL, Wu QY, Yang DJ, Kong DC, Zhang P

LETTER TO THE EDITOR

4926 Prediction of moderately severe and severe acute pancreatitis in pregnancy: Several issues

Yang QY, Hu JW

World Journal of Gastroenterology

Weekly Volume 28 Number 33 September 7, 2022

Contents

ABOUT COVER

Editorial Board Member of *World Journal of Gastroenterology*, Osamu Toyoshima, MD, PhD, Director, Department of Gastroenterology, Toyoshima Endoscopy Clinic, Tokyo 157-0066, Japan. t@ichou.com

AIMS AND SCOPE

The primary aim of *World Journal of Gastroenterology* (*WJG*, *World J Gastroenterol*) is to provide scholars and readers from various fields of gastroenterology and hepatology with a platform to publish high-quality basic and clinical research articles and communicate their research findings online. *WJG* mainly publishes articles reporting research results and findings obtained in the field of gastroenterology and hepatology and covering a wide range of topics including gastroenterology, hepatology, gastrointestinal endoscopy, gastrointestinal surgery, gastrointestinal oncology, and pediatric gastroenterology.

INDEXING/ABSTRACTING

The *WJG* is now abstracted and indexed in Science Citation Index Expanded (SCIE, also known as SciSearch®), Current Contents/Clinical Medicine, Journal Citation Reports, Index Medicus, MEDLINE, PubMed, PubMed Central, Scopus, Reference Citation Analysis, China National Knowledge Infrastructure, China Science and Technology Journal Database, and Superstar Journals Database. The 2022 edition of Journal Citation Reports® cites the 2021 impact factor (IF) for *WJG* as 5.374; IF without journal self cites: 5.187; 5-year IF: 5.715; Journal Citation Indicator: 0.84; Ranking: 31 among 93 journals in gastroenterology and hepatology; and Quartile category: Q2. The *WJG*'s CiteScore for 2021 is 8.1 and Scopus CiteScore rank 2021: Gastroenterology is 18/149.

RESPONSIBLE EDITORS FOR THIS ISSUE

Production Editor: *Ying-Yi Yuan*; **Production Department Director:** *Xiang Li*; **Editorial Office Director:** *Jia-Ru Fan*.

NAME OF JOURNAL
World Journal of Gastroenterology

ISSN
ISSN 1007-9327 (print) ISSN 2219-2840 (online)

LAUNCH DATE
October 1, 1995

FREQUENCY
Weekly

EDITORS-IN-CHIEF
Andrzej S Tarnawski

EDITORIAL BOARD MEMBERS
http://www.wjgnet.com/1007-9327/editorialboard.htm

PUBLICATION DATE
September 7, 2022

COPYRIGHT
© 2022 Baishideng Publishing Group Inc

INSTRUCTIONS TO AUTHORS
https://www.wjgnet.com/bpg/gerinfo/204

GUIDELINES FOR ETHICS DOCUMENTS
https://www.wjgnet.com/bpg/GerInfo/287

GUIDELINES FOR NON-NATIVE SPEAKERS OF ENGLISH
https://www.wjgnet.com/bpg/gerinfo/240

PUBLICATION ETHICS
https://www.wjgnet.com/bpg/GerInfo/288

PUBLICATION MISCONDUCT
https://www.wjgnet.com/bpg/gerinfo/208

ARTICLE PROCESSING CHARGE
https://www.wjgnet.com/bpg/gerinfo/242

STEPS FOR SUBMITTING MANUSCRIPTS
https://www.wjgnet.com/bpg/GerInfo/239

ONLINE SUBMISSION
https://www.f6publishing.com

© 2022 Baishideng Publishing Group Inc. All rights reserved. 7041 Koll Center Parkway, Suite 160, Pleasanton, CA 94566, USA

E-mail: bpgoffice@wjgnet.com https://www.wjgnet.com

World Journal of Gastroenterology

Submit a Manuscript: https://www.f6publishing.com

World J Gastroenterol 2022 September 7; 28(33): 4744-4761

DOI: 10.3748/wjg.v28.i33.4744

ISSN 1007-9327 (print) ISSN 2219-2840 (online)

REVIEW

Regulation of transforming growth factor-β signaling as a therapeutic approach to treating colorectal cancer

Jana Maslankova, Ivana Vecurkovska, Miroslava Rabajdova, Jana Katuchova, Milos Kicka, Michala Gayova, Vladimir Katuch

Specialty type: Biochemistry and molecular biology

Provenance and peer review: Unsolicited article; Externally peer reviewed.

Peer-review model: Single blind

Peer-review report's scientific quality classification

Grade A (Excellent): A
Grade B (Very good): B, B
Grade C (Good): C, C, C
Grade D (Fair): D
Grade E (Poor): 0

P-Reviewer: Gao W, China; Ghazy A, Egypt; Kiuchi J, Japan; Liang H, China; Luo ZW, China

Received: May 12, 2022
Peer-review started: May 12, 2022
First decision: June 19, 2022
Revised: July 6, 2022
Accepted: August 16, 2022
Article in press: August 16, 2022
Published online: September 7, 2022

Jana Maslankova, Ivana Vecurkovska, Miroslava Rabajdova, Department of Medical and Clinical Biochemistry, Faculty of Medicine, Pavol Jozef Safarik University in Kosice, Kosice 04011, Slovakia

Jana Katuchova, Milos Kicka, First Department of Surgery, Medical Faculty of Safarik University, Kosice 04011, Kosicky kraj, Slovakia

Michala Gayova, Department of Burns and Reconstructive Surgery, Medical Faculty at Safarik University and University Hospital, Kosice 04011, Slovakia

Vladimir Katuch, Department of Neurosurgery, Medical Faculty at Safarik University and University Hospital, Kosice 04011, Slovakia

Corresponding author: Jana Katuchova, MD, PhD, Doctor, Professor, Surgeon, First Department of Surgery, Medical Faculty of Safarik University, 1 Trieda SNP, Kosice 04011, Kosicky kraj, Slovakia. jana.katuchova@upjs.sk

Abstract

According to data from 2020, Slovakia has long been among the top five countries with the highest incidence rate of colorectal cancer (CRC) worldwide, and the rate is continuing to rise every year. In approximately 80% of CRC cases, allelic loss (loss of heterozygosity, LOH) occurs in the long arm of chromosome 18q. The most important genes that can be silenced by 18q LOH or mutations are small mothers against decapentaplegic homolog (SMAD) 2 and SMAD4, which are intracellular mediators of transforming growth factor (TGF)-β superfamily signals. TGF-β plays an important role in the pro-oncogenic processes, including such properties as invasion, epithelial-mesenchymal transition (commonly known as EMT), promotion of angiogenesis, and immunomodulatory effects. Several recent studies have reported that activation of TGF-β signaling is related to drug resistance in CRC. Because the mechanisms of drug resistance are different between patients in different stages of CRC, personalized treatment is more effective. Therefore, knowledge of the activation and inhibition of factors that affect the TGF-β signaling pathway is very important.

Key Words: Small mothers against decapentaplegic homologs; Transforming growth factor-beta; Colorectal cancer; Marker; Signaling pathway

©The Author(s) 2022. Published by Baishideng Publishing Group Inc. All rights reserved.

Core Tip: A thorough understanding of the complete transforming growth factor (TGF)-β/small mothers against decapentaplegic homolog signaling pathway is important for defining its functions during pathological processes of colorectal cancer. Inhibitors specifically targeting TGF-β pathway mediators that reduce the expression of a particular protein may lead to fewer/milder adverse effects. However, the dual role of the TGF-β pathway in the onset and progression of cancer complicates the physiological/pathological and, thus, clinical situation. In recent years, research has shown that modification of members of this pathway is a promising approach for clinical procedures. Long-term treatment should emphasize personalized and targeted therapy.

Citation: Maslankova J, Vecurkovska I, Rabajdova M, Katuchova J, Kicka M, Gayova M, Katuch V. Regulation of transforming growth factor-β signaling as a therapeutic approach to treating colorectal cancer. *World J Gastroenterol* 2022; 28(33): 4744-4761
URL: https://www.wjgnet.com/1007-9327/full/v28/i33/4744.htm
DOI: https://dx.doi.org/10.3748/wjg.v28.i33.4744

INTRODUCTION

According to data from 2020, Slovakia has long been among the top five countries with the highest incidence rate of colorectal cancer (CRC) worldwide, and this rate continues to rise every year[1]. Although significant progress has been made in the diagnosis, screening, and treatment of patients with advanced CRC, therapeutic options are still limited, requiring the discovery of additional markers to act as prognostic predictors[2].

Up to 60%-65% of colorectal tumors have no family history (sporadic) and are the result of somatic mutations and epigenetic changes due to factors such as a lifestyle with limited physical activity, alcoholism and smoking[3]. CRC can arise as a result of these genetic and epigenetic aberrations (Figure 1): Chromosomal instability (CIN; 65%-85%), methylation of the CpG island (CIMP; 10%-20%), and DNA microsatellite instability (MSI; 12%-15%)[4]. Some authors have noted that patients with a tumor-bearing the CpG island methylator phenotype will have a worse prognosis compared to patients with a CIMP-negative tumor[5-7]. The instability of DNA microsatellite regions is characterized by mutations in the genome that arise due to defects in mismatch repair genes and can affect and inactivate tumor suppressor genes, leading to malignant transformation[8,9]. CIN is caused by the gain or loss of whole or large parts of chromosomes, leading to karyotype variability between cells. CIN results in chromosome imbalance (aneuploidy), subchromosomal genomic amplification, and loss of heterozygosity (LOH)[10].

This type of classification, based on a single molecular marker, is not very informative in the early diagnosis of CRC; thus, a combination of several molecular markers has been proposed as a better classification approach for patients with CRC. Moreover, the joint efforts of the CRC Subtyping Consortium have led to a formal proposal for the stratification of CRC cases into the following four molecular subtypes (referred to as CMS1-4)[11,12] (Figure 2; Table 1).

CMS1 is usually a right-sided (proximal) tumor, commonly diagnosed in older age females, and is associated with worse survival after relapse. This subtype is characterized by hypermethylation of CpG islands, which causes loss of tumor suppressor function and has a low prevalence of somatic copy number alterations (referred to as SCNAs). The hypermethylation of promoter regions of the MMR genes causes MSI[11].

CMS2 is mainly located on the left side (distal part of the colon) and is often diagnosed in men, with a better prognosis and a higher survival rate, even after relapse. This gene expression profile is characterized by low mutation rate. CMS2 also represents over-activation of epidermal growth factor (EGF)-related signaling pathways, with higher expression of the epidermal growth factor receptor (EGFR)[13]. Finally, Guinney *et al*[11] reported that CMS2 has more copy number gains in oncogenes and losses in tumor suppressor genes than the other CMSs.

CMS3 is another right-sided subtype and is the most frequently diagnosed in patients with evident metabolomics disease[13]. Although KRAS mutation is present in every CMS, it occurs more frequently in CMS3[11].

CMS4 tumors exhibit extremely low levels of hypermutation and are defined by an activated transforming growth factor (TGF)-β pathway and by epithelial-mesenchymal transition (EMT), making them generally more chemoresistant[13]. CMS4 tumors tend to be diagnosed at more advanced stages (III and IV); indeed, the poor prognosis of CMS4 (compared to the relatively favorable prognoses of CMS1 and CMS2) in non-metastatic disease have been demonstrated[11].

Table 1 Characteristics of individual colorectal cancer subtypes

CMS1	CMS2	CMS3	CMS4
(MSI immune)	(Canonical)	(Metabolic)	(Mesenchymal)
CIMP high	CIN	CIN, CIMP low	CIN
Hypermethylation			
SCNA-low	SCNA-high	SCNA-intermediate	SCNA-high
BRAF mutant		KRAS mutant	
Activation of immune cells	WNT, MYC activation	Metabolic deregulation	TGF- activation
Worse survival after relapse	Superior survival after relapse		Worse relapse-free and overall survival

SCNA: Somatic copy number alteration; CIN: Chromosomal instability; CIMP: Methylation of the CpG island; TGF: Transforming growth factor.

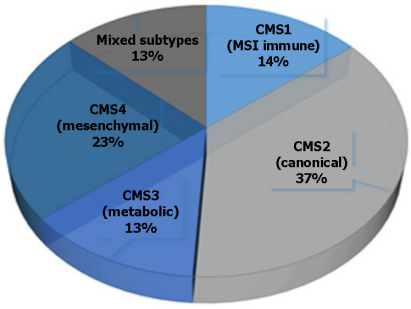


Figure 1 Representation of individual colorectal cancer subtypes.

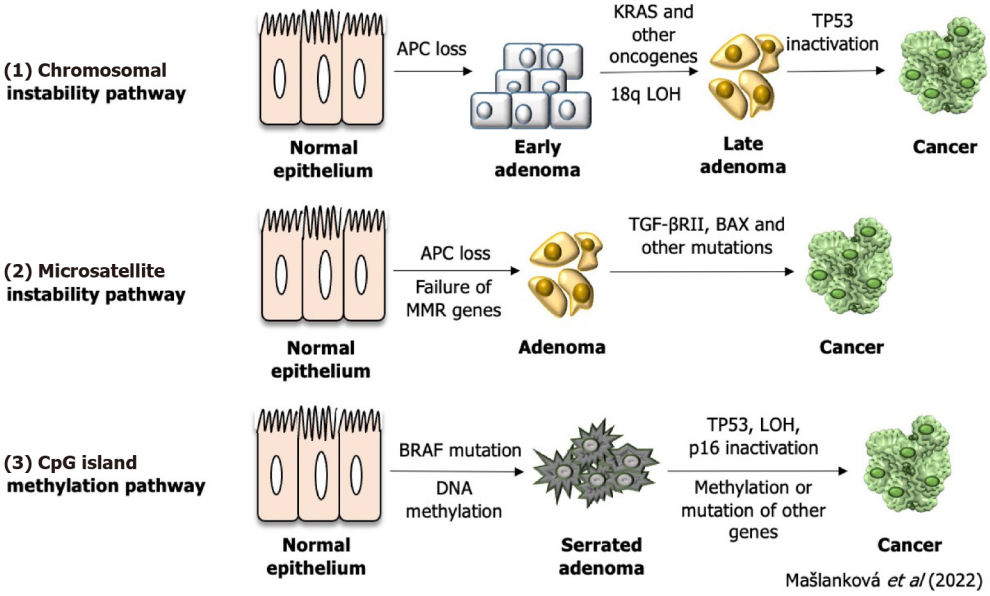


Figure 2 Three genetic and epigenetic aberrations of colorectal cancer formation. LOH: Loss of heterozygosity; TGF: Transforming growth factor.

The basic characteristics of each CRC subtype, CMS1-4, are summarized in Table 1.

Approximately 80% of colorectal tumors have loss of an allele in the long arm of chromosome 18q, followed by LOH on chromosome 17p (75%-80%), 8p (40%), 5q (30%), and finally 22q (20%-30%). Allelic loss in chromosome 18q has been reported in 70% of cases of primary CRC with late-stage adenomas and shows a strong correlation with poor prognosis [14]. Patients with 18q LOH have a particularly poor prognosis in stage II disease, leading to the conclusion that stage II adjuvant therapy is important for these patients[15].

There are many candidate tumor suppressor genes in 18q, including small mothers against decapentaplegic homolog (SMAD) 2, SMAD4, netrin receptor DCC (DCC), and Cdk5 and Abl enzyme substrate 1 *(CABLES1*)[16]. The most important genes that can be silenced by 18q LOH or mutations are SMAD2 and SMAD4, which are intracellular mediators of TGF-β superfamily signaling[17].

TGF-β SUPERFAMILY SIGNALING

TGF-β superfamily signaling is mainly divided into the following two subfamilies: TGF-β-activin-nodal and bone morphogenetic protein (BMP). The TGF-β ligand (comprised of the TGF-β1, -β2, and -β3 isoforms) is a multifunctional member of the cytokine family, playing an important role in such cellular responses as cell proliferation, differentiation, and pathological processes. TGF-β itself plays a key role in the processes of EMT and fibrosis[18].

The canonical (SMAD-dependent) TGF-β signaling pathway (Figure 3) utilizes serine/threonine kinase receptors (TGF-βRI/TGF-βRII) in the plasma membrane and phosphorylates their cytoplasmic effectors SMAD2 and SMAD3. TGF-βRI receptors differ from TGF-βRII by the presence of an N-terminal glycine/serine-rich (GS) domain, which regulates kinase activity and SMAD binding. TGF-βRII receptor phosphorylates serine and threonine residues within the GS domain of TGF-βRI, and activated TGF-βRI receptor phosphorylates the distal C-termini of SMAD2 and SMAD3. An anchor of SMAD receptor activation, a SMAD cofactor that directly interacts with SMAD2/3, is required to anchor SMAD2/3 proteins to the TGF-β receptor. After phosphorylation, SMAD2 and SMAD3 dimers form heteromeric complexes with SMAD4 and then translocate to the nucleus. They act as transcription factors, mediate the expression of various genes, and promote various biological functions in the tumor microenvironment, resulting in tumor suppression[19].

A conserved branch of the TGF-β superfamily involves BMP signaling. BMP canonical signaling is triggered upon the binding of soluble ligands to serine-threonine kinase receptors, BMPRI and BMPRII, in the plasma membrane. Activated BMP receptors stimulate various intracellular signaling pathways. This canonical pathway is characterized by phosphorylation of SMAD1/5/8, which subsequently forms a gene-regulatory complex with SMAD4. Alternative BMP signaling can occur *via* the non-canonical pathway and is due to the presence of multiple intracellular kinases (Figure 3)[20].

While TGF-β-induced extracellular matrix production promotes tumor development, the inhibitory response to TGF suppresses tumor formation. Thus, the level of TGF-β receptor activation can alter the outcome of TGF-β signaling from suppression to oncogenesis. The TGF-β/SMAD signaling pathway has a dual effect; during tumor initiation and early stages, it stops the cell cycle and triggers apoptosis and in later stages, it promotes tumorigenesis and increases tumor progression and invasiveness[21]. TGF-β signaling causes cell cycle arrest and death during tumor initiation, acting as a tumor suppressor. However, it has also been demonstrated to increase tumor cell proliferation, EMT, and stem-like activity during tumor progression, as well as fibrosis, inflammation, and angiogenesis[22-24].

TGF-β AND ITS ROLE IN TUMOR SUPPRESSION

TGF-β signaling regulates cell proliferation mainly by inhibiting cell cycle progression through a mechanism that arrests the cell in the G1 phase. In most epithelial, endothelial, and hematopoietic cells, this arrest occurs through the activation of cyclin-dependent kinase (CDK) inhibitors, such as p21CIP1 and p15INK4b. TGF-β signaling also inhibits c-Myc oncogene transcription as well as DNA-binding protein inhibitors (ID1-3) and nuclear factors, which play key roles in cell differentiation and progression from the G1 to S phase of the cell cycle[25].

The canonical TGF-β signaling pathway can induce apoptosis by modulating the expression of various members of the B-cell lymphoma 2 (Bcl-2) family such as death receptor fibroblast death-associated antigen (FAS), DNA damage-inducible (GADD) 45-β, and kinase associated with by death (DAPK), which depends on the type of cells where the signaling takes place. It can also induce growth arrest and modulate caspases to induce intrinsic and extrinsic apoptosis[18].

TGF-β AND ITS ROLE IN TUMOR PROMOTION

In later stages of cancer, TGF-β may adversely promote tumor progression and metastasis[18]. The TGF-β signaling pathway activates the promoter activity of the translation inhibitory protein 4E-BP1 (regulator of eukaryotic translation initiation factor-4F (eIF4E) through SMAD4, thereby suppressing translation, cell growth and proliferation [26]. TGF-β also promotes the secretion of matrix metalloproteases (MMPs), mainly MMP-2 and MMP-9, and inhibits the activity of their tissue inhibitors (TIMPs) [27].

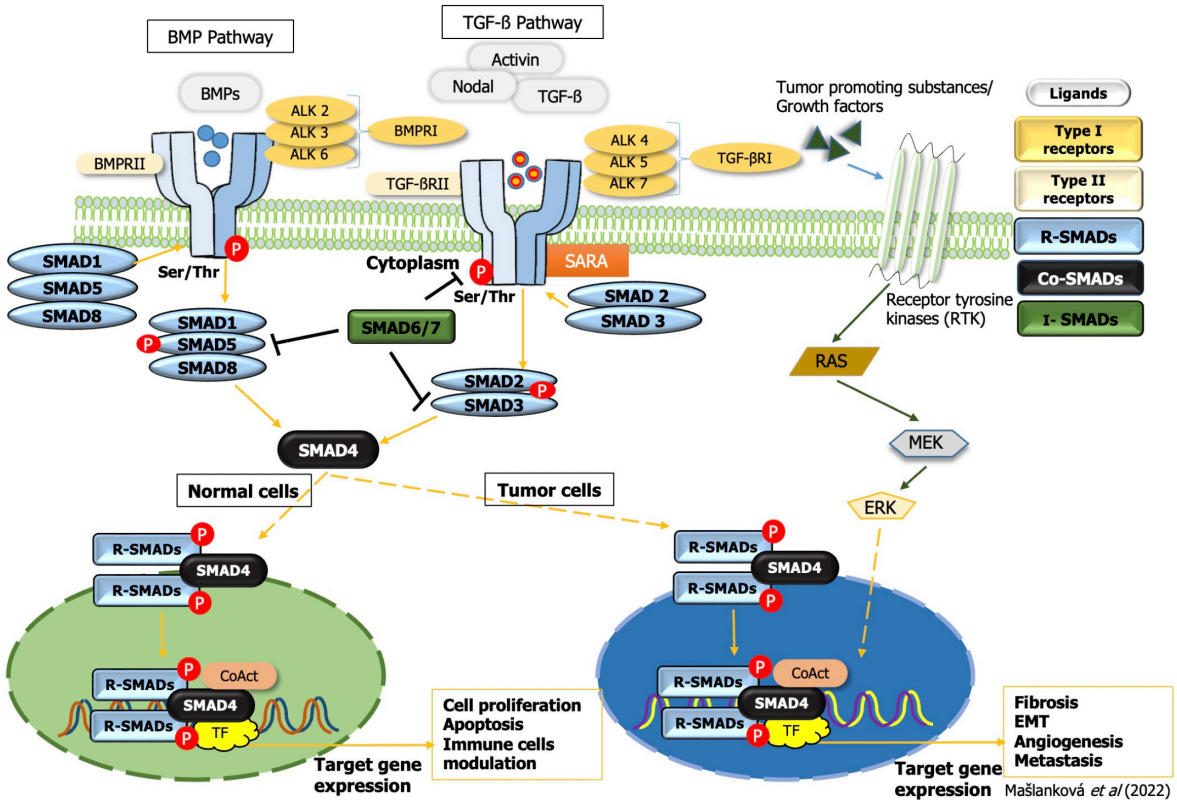


Figure 3 Transforming growth factor-beta superfamily signal transduction. TGF: Transforming growth factor; EMT: Epithelial-mesenchymal transition; ERK: Extracellular signal-regulated kinase; BMP: Bone morphogenetic protein; SMAD: Small mothers against decapentaplegic homolog.

Fibrotic processes are well known to play a key role in promoting malignancy, and TGF-β is one of the most prominent inducers of fibrotic processes. During fibrosis, abundant ECM components accumulate due to activated myofibroblasts. In tumor tissue, solidified stroma stimulates tumor cell proliferation, migration, and survival. Fibrosis plays a vital role in EMT regulation, promotes angiogenesis and hypoxia, and inhibits anti-tumor immunity. Ultimately, the degree of tissue fibrosis is related to tumor aggression and poor patient prognosis[28].

TGF-β collaborates closely with BMP during fibrosis, due to their structural similarity and shared signal transmission modality. Their role is to regulate fibrosis-causing processes, like EMT. The interaction of TGF-β and BMP to form a complex with SMAD4, together with SMAD7 which elicits an inhibitory effect, affects the balance between the activation of SMADs that are members of the TGF-β signaling pathway (SMAD2/3) and SMADs that are part of the BMP signaling pathway (SMAD1/5/8). Therefore, many studies report antagonistic roles of TGF-β and BMP[29,30]; according to them, BMP activity is antifibrotic. Fewer studies support the opposite trend. Specifically, Katsuno *et al*[31] determined that BMP signaling can promote TGF-β signaling through the activation of protein arginine N-methyltransferase (PRMT1), which methylates SMAD6/7. SMAD6/7, in turn, activates SMAD1/3/5, resulting in the promotion of EMT during fibrosis and the maintenance of the tumor cell phenotype in malignancies[29,31].

TGF-β/SMAD RECEPTORS

Each of the isoforms of TGF-β (-1, -2, -3) binds to serine/threonine kinases, which belong to the group of transmembrane receptors and can bind to TGF-βI and TGF-βII. The name of TGF-βRI is also an activin-like receptor kinase (ALK). Seven types of TGF-βRIs have been identified to date (ALK1-7), five types of TGF-βRIIs (TGF-βRII, BMPRII, ACVRII, ACVRIIB, and AMHRII), and two types of TGF-βRIIIs (betaglycan and endoglin). All TGF-βRs consist of a C-terminal cytoplasmatic domain of a serine/threonine kinase, an internal transmembrane region, and an N-terminal domain, which binds ligands [18].

TGF-β receptors, SMAD proteins, and their mutation or inactivation have been described in many publications, along with their role in the progression of malignancies[32,33]. The loss of TGF-β tumor suppressor functions, which play a key role in inhibition in normal epithelial cells as well as in tumor cells, leads to oncogenic processes. Many human cancers, including CRC, are resistant to TGF-β-mediated growth inhibition, however. This resistance may be due to mutation or functional inactivation

of TGF-βRI, decreased expression of TGF-βRI or TGF-βRII, and inactivation mutations of individual members of the TGF-β signaling pathway, such as SMAD2 and SMAD4[25]. Reportedly, approximately 20%-30% of CRCs contain mutations of TGF-βRII, and mostly involve colon cancer cells with MSI. One of the most frequent MSI mutations detected occurs in a coding polyadenine tract in exon 3 of the TGF-β RII gene. Some studies have even suggested that one of the important factors contributing to CRC transformation is the inactivation of TGFβR2, which increases cell proliferation due to prolonged activation of cdk4 expression[34-36].

Not only TGF-βRII but also TGF-βRI may contain a similar hypermutable polyadenine sequence resulting from mismatch repair defects, and the mutant allele (known as TGF-βRI6A) has been described to predispose to colon cancer, with a reported frequency of 100%[37].

SMADs

The mammalian TGF-β receptor family contains five SMAD substrates (SMAD1, SMAD2, SMAD3, SMAD5 and SMAD8); these are commonly referred to as receptor-regulated SMADs or R-SMADs[19]. Bone morphogenetic protein (BMP) and anti-Müeller receptors have high affinity for SMAD 1, 5, and 8 and TGF-β, activin and nodal receptors bind SMAD 2 and 3 proteins. SMAD4 belongs to the co-SMAD group, the second class of the SMAD family, which serves as a common partner for all R-SMADs such as SMAD2, SMAD3, SMAD1, SMAD5, and SMAD8 to form heterotrimeric complexes. These heterotrimeric SMAD complexes are subsequently translocated to nuclei, where they bind to specific promoters to act as DNA-specific transcriptional regulators of target genes[38]. SMAD6 and SMAD7 have inhibitory roles in the TGF-β/SMAD signaling pathway[39,40].

SMAD proteins are composed of approximately 500 amino acids and consist of two globular domains [MAD homology (MH) 1 and MH2] joined by a linker region. The N-terminal domain of MH1 is highly conserved in all R-SMADs and SMAD4, but not in SMADs 6 and 7, and contains a hairpin structure with DNA-binding capability. The MH2 domain contains hydrophobic elements that bind to TGF-βR and BMPR transmembrane receptors. The linker region is quite different between the different subgroups, whereas the C-terminal domain (MH2) is identical in all SMAD proteins[19]. The MH2 domain is involved in SMAD protein homooligomerization and heterooligomerization, cytoplasmic anchoring, and transcription. In normal (healthy) and premalignant cells, the TGF-β tumor signaling pathway has a suppressive role, but this pathway can be inhibited, damaged, or even used by cancer cells to promote oncogenic functions[38]. The known roles of individual SMAD proteins during the onset and progression of CRC are summarized in Table 2.

In 65% of colon adenocarcinomas and 50% of rectal adenocarcinomas, mutations in any of the 43 genes that encode proteins of the TGF-β pathway superfamily have been described[19]. Many proteins interact with the SMADs to modulate their activity. Therefore, by regulating these proteins, we can influence the process of carcinogenesis[41].

Role of SMAD2/3

Many studies describe the significant role of SMAD2/3 in the EMT process, which is activated by the TGF-β signaling pathway. The most important difference between SMAD2 and SMAD3 is that the MH1 region of SMAD2 has two more amino acid fragments than SMAD3. Due to this amino acid difference, SMAD3 can directly bind to DNA and has transcriptional activity, whereas SMAD2 lacks transcriptional activity[42,43].

Although SMAD3 is highly homologous to SMAD2, the roles of SMAD2 and SMAD3 are different in the TGF-β signaling process. SMAD3 plays a very important role as a mediator of EMT, as demonstrated by inhibition or knockdown of SMAD3, which blocked cell migration induced by the TGF-β signaling pathway. Therefore, regulation of SMAD3 protein expression is a very important regulatory step in EMT prevention[44].

The results of Liu *et al*[45] point to other important differences between SMAD2 and SMAD3. SMAD2 is mostly located in the cytoplasm, whereas a large amount of SMAD3 is distributed in the nucleus. Western blot analysis was performed in that study, which provided evidence to support the conclusion that in the absence of TGF-β activation, endogenous SMAD2 is found mainly in the cytoplasm, while large amounts of SMAD3 are found in the nucleus of human embryonic stem cells, kidney cells, and skin fibroblast cells. This otherness in different cell compartments of SMAD2 and SMAD3 proteins may reflect their activity in TGF-beta-induced signal transduction.

Analyses of tissue and experiments with explanted tissue have revealed strongly reduced phosphorylated SMAD3 and increased levels of its inhibitor SMAD7 in Crohn's disease tissue and a moderate reduction in ulcerative colitis (UC) tissue[46]. UC poses a high risk of developing CRC; however, the molecular mechanisms underlying the transition from UC to CRC are unclear[47].

Wang *et al*[48] showed that it was possible to increase the transcriptional activity of SMAD3, phosphorylation of SMAD2, and reduction of SMAD7 expression by knocking out signal transducer and activator of transcription 3 (STAT3), which ultimately led to the suppression of tumor progression in CRC. STAT3 is a member of the STAT protein family and can promote oncogenesis of CRC through

Table 2 Roles of individual small mothers against decapentaplegic homolog proteins in the onset and progression of colorectal cancer

Type of SMAD	Role in colorectal cancer	References
SMAD1	Participates in the modification of cell growth, differentiation, apoptosis and other processes that are essential in the regulation of the body's immune system	[39-42]
	Promotes epithelial-mesenchymal transition process	
	By increasing the expression of ATG5 induces autophagy	
SMAD2	Inhibits the expression of related functional genes, cell proliferation and regulates the transcriptional response that promotes cell apoptosis	[43,44]
	Expression of SMAD2 is correlated with patient survival	
SMAD3	In the formation of a tumor, depending on the stage of the cancer, it plays the double role of an oncogene or a tumor suppressor gene	[45-48]
	Reduces its expression through mir-4429, and inhibits the appearance, development and metastasis of cancer cells	
SMAD4	Plays a very important role in the transduction of the TGF-β signaling pathway	[32,49]
	Maintains the cell cycle in the G1 phase, which leads to abnormal tumor proliferation	
	Is a tumor suppressor gene	
	High mutation rate of SMAD4 in CRC patients was associated with poor prognosis, but not with clinical stage	
SMAD5	Mediates TGF-β superfamily ligand signaling pathway and thus influences cancer progression	[50]
	No relevant studies on the role of SMAD5 in CRC patients have been found in the last 5 years	
SMAD6	Regulates TGF-β signaling pathway, promotes angiogenesis, stimulates extracellular matrix, and inhibits immunity, thus contributing to tumor growth, diffusion, and metastasis	[51]
	No relevant studies on the role of SMAD6 in CRC patients have been found in the last 5 years	
SMAD7	Plays a dual role in different tumor stages, acting as a tumor suppressor gene by inhibiting proliferation and promoting apoptosis in the early stage, and increasing invasion in the late stage, promoting epithelial-mesenchymal transition, which correlates with the degree of malignancy	[52,53]

SMAD: Small mothers against decapentaplegic homolog; ATG5: Autophagy-related gene 5; CRC: Colorectal cancer; TGF: Transforming growth factor.

various pathways.

Liu *et al*[49] reported that treatment with exogenous interleukin 6 (IL-6) stimulated STAT3 activation, increased TGF-β-induced SMAD3 and Snail expression, and inhibited the EMT process, suggesting that the Janus kinase/signal transducer and activator of transcription 3 (JAK/STAT3) pathway is required for TGF-β-induced EMT and cancer cell migration and invasion by upregulating SMAD3 and Snail expression. Moreover, Xu *et al*[50] showed that the expression of SMAD2 is correlated with patient survival. Their results demonstrated that the MIR22 host gene (MIR22HG) has been shown to play a role in suppressing colorectal tumors by binding competitively to SMAD2, thereby preventing the interaction between SMAD2 and SMAD4. These data suggest that the MIR22HG silencing promotes the EMT process and thus tumorigenicity in CRC.

Many papers have been published in recent years that link the action of the TGF-β signaling pathway to other pathways. The mitogen-activated protein kinase (MAPK) pathway may phosphorylate a group of proteins that are responsible for altering cell behavior, or conversely, proteins of this pathway may be activated by extracellular molecules such as cytokines produced by the TGF-β signaling pathway. The extracellular signal-regulated kinase (ERK) pathway inhibits the TGF-β pathway by phosphorylating SMAD2 and SMAD3 without translocating them to the nucleus[51,52].

Despite the important roles of SMAD2 and SMAD3 in the TGF-β signaling process, the prevalence of mutations was estimated up to 6%. Fleming *et al*[53] showed that the percentage of mutations increased with the combined prevalence of SMAD4, SMAD2, and SMAD3 mutations to 14.8% in primary sporadic CRCs.

Lin *et al*[54] described that nitrilase 1 (NIT1) suppresses the proliferation of CRC cells through a positive feedback loop between NIT1 and the TGFβ/SMAD signaling pathway because SMAD3 transcriptionally upregulates at the transcriptional level. NIT1 belongs to the carbon-nitrogen hydrolase superfamily and plays an important role in the suppression of CRC.

Role of SMAD4

A key component of TGF-β signaling is SMAD4, which plays an important role as a so-called switch in deciding whether to stop the cell cycle or progress to the spread of cancer[32]. Impaired TGF-β signaling

due to the deletion of SMAD4 is detected in 16%-25% of CRCs[55]. Sadeghi *et al*[56] found SMAD4 mutations in 33.3% of analyzed tissues collected from patients with CRC.

Most SMAD4 mutations occur in the MH2 domain, although this domain represents only 41.5% of the coding sequence of the entire SMAD4 protein[56-58]. The MH2 domain is essential for homodimerization and heterooligomerization with SMAD2 or SMAD3 proteins. Therefore, mutations in this region can cause blocks to the growth, inhibition, and apoptosis that is otherwise generally induced by TGF-β. Moreover, SMAD4 mutations promote inflammation by TGF-β and thus may expand genetically damaged cells during tumorigenesis[56]. The most frequent mutation of the SMAD4 gene has been described in CRC which leads to the formation of a salt bridge between Arg361 and Asp351 and which affects homodimerization and heterooligomerization with SMAD2 and SMAD3[59,60].

Sadeghi *et al*[56] further described in their publication that the other significant mutations in CRC are at codons 264 and 271 of SMAD4 protein, which are located in the linker domain, a region required for subcellular localization and transcriptional activation.

Analyzes of tissue sections by immunohistochemical methods of carcinomas from various organs, including the gastrointestinal tract have shown a loss of SMAD4 expression in > 50% of colorectal carcinomas, which is associated with lymph node metastases. SMAD4 loss has been seen in 58% of pancreatic adenocarcinomas, 27% of appendiceal adenocarcinomas, 16% of cholangiocarcinomas, 10% of lung adenocarcinomas, and < 5% of esophageal, breast, gastric, and mucinous ovarian adenocarcinomas [61]. Although the LOH on chromosome 18q can be the main cause of SMAD4 loss in CRC, there are other posttranscriptional and posttranslational mechanisms that may contribute to SMAD4 protein loss or dysfunction, such as ubiquitylation, sumoylation, or interference with regulatory microRNA (miRNA)[62].

Regarding the correlation between SMAD proteins and clinicopathological characteristics, Yang *et al* [63] showed that SMAD4 concentrations in CRC patients were significantly higher in the N0 stage compared to patients with NI stage. Regarding patients in advanced stages (TNM III-IV), reduced concentrations of SMAD4 were recorded in them compared to patients in early stages (TNM I-II). In addition, SMAD4 was significantly decreased in patients who were older than 65 years.

Szeglin *et al*[64] determined probes and corresponding genes from analysis of SMAD-binding elements (SBEs) that were correlated with SMAD4 expression. They subsequently confirmed that a SMAD4-modulated gene profile predicted disease-free survival in stage II and III CRC. According to them, this gene profile has prognostic potential in selected CRC patients.

Role of SMAD7

SMAD7 acts as an inhibitor of SMAD in the TGF-β/SMAD pathway and may prevent TGF-β-dependent SMAD2/SMAD4 complex formation and inhibit SMAD2 accumulation in the nucleus (Figure 4). SMAD7 may also promote the dephosphorylation and inactivation of TGF-βRI with cooperation of the E3 ubiquitin ligase SMURF1/2. SMAD7 may also localize to the nucleus and limit the binding of the SMAD2-3/SMAD4 complex to specific SMAD-responsive DNA sequences[65]. So, SMAD7 plays an important role in both the cytoplasm and the nucleus, thereby maintaining the balance in the TGF-β induced signaling pathway. Inactivation of any component in this pathway will result in accelerated cell growth and dysregulation of apoptosis signals, leading to uncontrolled cell growth and differentiation, and the induction of cancer cells[66]. Therefore, overproduction of SMAD7 leads to significantly decreased EMT in response to TGF-β[67].

Several studies have reported the significant role of SMAD7 in sporadic CRC. According to results published by Li *et al*[66], SMAD7 is a target of miR-424, which is implicated in the regulation of SMAD7 expression *via* the circTBL1XR1/miR-424 axis.

Boulay and colleagues, in 264 biopsy samples from CRC patients, showed that the deletion of SMAD7 is less common than deletion of SMAD4 and SMAD2, and patients with such a SMAD7 deletion have a significantly better prognosis than patients without a deletion. Their findings demonstrated that patients with SMAD7 deletions had a low ratio of death risk and relapse, which clearly defined SMAD7 as a negative prognostic marker in CRC patients[68,69].

SMAD7 and SMAD4 genes are deregulated in CRC, whereas there is a markedly higher increase in SMAD7 expression (~ 11.3-fold) than SMAD4 expression (approximately 2-fold) in tumor cells[70]. SMAD7 protein expression is closely related to Dukes' stage, CRC invasion depth, and lymph node metastases, and positively correlates with CRC expression[66].

Less frequently, it has been reported that SMAD7 also has an anti-cancer effect. Gastrointestinal carcinomas, such as CRC, are characterized by frequent genetic alterations in SMAD components. Furthermore, depending on the stage of the tumor, SMAD7 activity can transition from tumor-suppressive to tumor-promoting (*i.e.*, early *vs* advanced). Given the opposing roles of TGF signaling, these seemingly contradicting functions are not surprising[71,72].

REGULATION OF TGF-β SIGNALING PATHWAY BY NON-CODING RNAs

Genes that encode proteins represent less than 2% of the total human genome, while approximately 90%

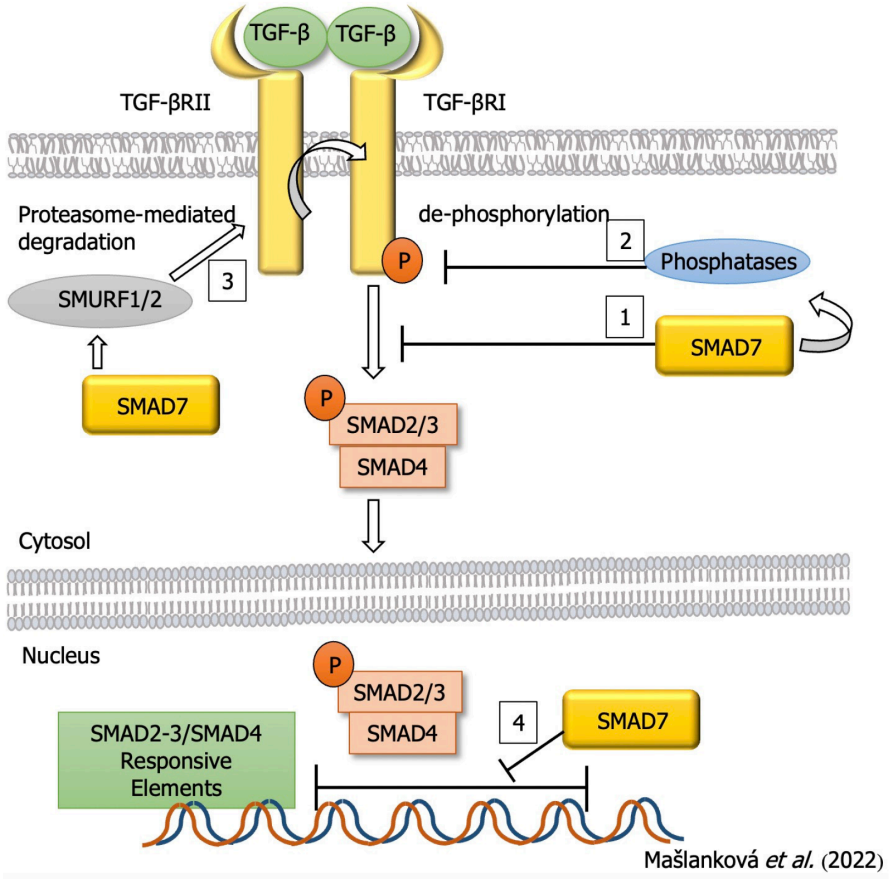


Figure 4 Inhibitory effect of small mothers against decapentaplegic homolog 7 on the process of colorectal cancer development. TGF: Transforming growth factor; SMAD: Small mothers against decapentaplegic homolog.

of the human genome consists of non-coding RNAs (ncRNAs) that do not encode proteins. ncRNAs are divided into two larger groups[73]; in one are the housekeeping ncRNAs, including the very abundant rRNAs and tRNAs, and in the other are the regulatory ncRNAs, including long ncRNAs (lncRNAs), microRNAs (miRNAs), circular RNAs (circRNAs), PIWI-interacting RNAs, small tRNA-derived RNAs (tRFs), small nuclear RNAs (snoRNAs), siRNAs and others. The most studied classes of ncRNAs are lncRNAs, miRNAs, and circRNAs. These types of ncRNAs very significantly regulate or are regulated by the TGF-β signaling pathway[74].

LNCRNAs AS REGULATORS IN CRC

lncRNAs influence gene expression through several mechanisms, such as silencing of the X chromosome, modification of chromatin, imprinting of the genome, activation of transcription, and nuclear transport. Imbalance in regulation of lncRNA transcription has been associated with apoptosis, angiogenesis, proliferation, invasion, metastasis and drug resistance of CRC[74].

The lncRNAs cancer susceptibility candidate 9 (CASC9) and small nucleolar RNA host gene 6 (SNHG6) can positively regulate the TGF-β pathway in CRC. CASC9, in particular, increases the stabilization of TGF-β2 mRNA[75], and a study by Zhang *et al*[76] showed that it targets miRNA-542-3p and could also increase chemoresistance. The lncRNA SNHG6, on the other hand, targets miR-26a-5p and increases the resistance of CRC cells to 5-fluorouracil (5-FU).

The lncRNA nuclear paraspeckle assembly transcript 1 (NEAT1) has been verified to participate in the development and progression of colon cancer[77].

CTBP1-AS2 has an important role in CRC proliferation and metastasis. While CTBP1-AS2 has been shown to significantly promote activation of the TGF-β/SMAD2/3 signaling pathway, miR93-5p (a downstream molecule of CTBP1-AS2) has been shown to target the 3′-untranslated region (UTR) of TGF-β. Furthermore, investigations of the functionally of miR-93-5p showed that its overexpression exerts an anti-cancer effect by inhibiting the TGF-β/SMAD2/3 pathway[78].

miRNAs AS REGULATORS IN CRC

miRNA regulates the transcription of genes encoding proteins at the post-transcriptional level. They perform this task by binding to complementary sequences located in the 3′-UTRs of their target mRNAs [79]. miRNAs are also competitively inhibited by lncRNAs[24].

In TGF-β signaling, miRNAs can play a stimulatory role, as shown in cells treated with anti-metabolites and anti-microtubule medicines; this is similar to what has been reported in cases of chemo-resistance against DNA damaging agents. In particular, miR-423-5p, miR-552, miR-34a, and the miR-17-92 cluster (miR-17, miR-18a, miR-19a, miR-19b, miR-20a, and miR-92a) are examples of miRNAs that regulate TGF-β signaling in CRC. Furthermore, SMAD2, SMAD4, and TGF-βRII genes are markedly associated with miRNA-155 and miR-22, both of which strongly correlate with tumor properties, suggesting clinical utility in immunotherapy[24]. miR-4666-3p and miR-329 act as tumor suppressor genes, affecting TGF-βR1 and thus preventing the activation of the TGF-β1/Smad pathway[80]. Finally, miR-147 overexpression has been shown to inhibit EMT and the TGF-β/SMAD pathway in colon cancer cells[81].

circRNAs AS REGULATORS IN CRC

circRNAs are formed by back-splicing of linear RNA and connections *via* covalent linkage. circRNAs can prevent miRNAs from binding to the 3′-UTR sequence of a particular gene, by attachment to miRNAs, ultimately regulating gene expression by activating mRNA cleavage or subsequent translation [82].

circPTEN1 is significantly downregulated in CRC and its expression is positively correlated with patient prognosis. circPTEN1 binds to the MH2 domain of SMAD4 and prevents the interaction between SMAD4 and SMAD2/3, which leads to suppression of translocation of the SMAD complex into the nucleus, followed by the activation of the transcription of downstream genes that regulate the EMT by the TGF-β signaling pathway[83].

circPACRGL acts as a miR-142-3p/miR-506-3p sponge to promote TGF-β1 expression and, thus, promote the differentiation of N1 to N2 neutrophils[84].

Gaining a more comprehensive understanding of the role of ncRNAs in CRC may lead to new approaches in the treatment of this disease; however, currently, only a limited number of identified and characterized lncRNAs and circRNAs with a confirmed regulatory role in CRC are known. There remains an urgent need to investigate the role of other lncRNAs and circRNAs that may facilitate the prognosis, diagnosis and treatment of CRC.

TREATMENT OF CRC

Over the last 10 years, researchers have developed a new anticancer therapy for patients with advanced or metastatic cancer. Several recent studies have shown that drug resistance in the treatment of various cancers, including CRC, is associated with the activation of TGF-β signaling[24]. 5-FU, an anticancer agent that belongs to the category of antimetabolites, is widely used to regulate metabolic pathways that are essential for cancer cell proliferation and survival. 5-FU is a standard chemotherapeutic used for the treatment of CRC patients, and a large proportion of these patients relapse or metastasize during the course of treatment. In patients with CRC, drug resistance is a key cause of chemotherapy failure and disease progression[85,86]. Recent research suggests that SMAD4 expression levels correlate with the prognosis and response to 5-FU and can help guide therapeutic decisions regarding its administration [87,88]. Reduced concentrations of SMAD3 or loss of SMAD4 suppress the expression of tumor suppressor genes that are induced by the TGF-β signaling pathway, which in turn leads to the expression of anti-apoptotic proteins Bcl-2 and Bcl-Wand increased survival of cancer cells resistance to 5-fluorouracil in CRC[89].

The role of TGF-β/SMAD signaling in tumor radiotherapy is controversial. It has been described in some studies that fibrosis is induced by upregulation of SMAD2/3 after radiation exposure. Reactive oxygen species (ROS) are involved in irradiation (IR)-induced fibrosis through TGF-β signaling. SMAD molecules that are activated by the TGF-β signaling pathway regulate ROS production by upregulating *NADP oxidase* 4[89,90]. Mutations in some genes, such as tumor protein p53, Ras, SMAD4, and EMT, are important in radioresistance or radiosensitization and can be controlled by SMAD-dependent or SMAD-independent TGF-β pathways[91]. Publications in recent years suggest that TGF-β signaling through various mechanisms, especially through miRNA-mediated regulation, plays an important role in the resistance of tumor cells to DNA-damaging agents. In CRC, miR-34a interacts directly with the 3′-untranslated region of SMAD4 and suppresses TGF-β/SMAD4 signaling. In patients with oxaliplatin-resistant CRC, miR-34a is downregulated to increase macroautophagy by activating the TGF-β/SMAD pathway[92,93].

ANTI-TGF-β THERAPIES

The objective of targeting TGF-β signaling as a therapeutic approach to treat cancer is supported by a plethora of findings from genetic and preclinical studies. Several strategies have been tested thus far that aim to block the TGF-β signaling pathway (Figure 5). These include: (1) Preventing TGF-β production or expression of its receptor by antisense oligonucleotides (ASOs; short synthetic single-stranded nucleic acids that bind to RNA to regulate gene expression); (2) preventing TGF-β activation *via* integrin-blocking antibodies, in which the antibodies compete with the TGF-β ligand to bind to its receptor, as well as the ability to block the activation of latent TGF-β (both steps are crucial for TGF-β to elicit its protumorogenic and immunosuppressive responses); (3) inhibiting the interaction between TGF-β and its receptor with neutralizing antibodies to TGF-β, blocking antibodies to TGF-βRII or ligand traps (engineered soluble forms of the receptor that compete with the cell-bound receptor); (4) preventing intracellular TGF-β receptor signal transduction *via* small-molecule *kinase* inhibitors, which bind to the ATP-binding domain of TGF-β kinase and inhibit *ATP kinase* activity, thereby blocking the downstream signaling cascade[94]; (5) immune checkpoint inhibitors (ICIs), which have essential roles in modulating the immune system. This group includes monoclonal antibodies that send inhibitory signals to T cells, enhancing T cells' antitumor immune response and improving antitumor defense. In addition to immunoregulatory cells such as regulatory T cells (Tregs), M2 macrophages, and myeloid-derived suppressor cells (MDSCs), the cytokine TGF-β also has the ability to control and modulate T cell functions. This is facilitated by the release of molecules that are able to activate specific ICIs. In this way, activation of inhibitory immune checkpoints, such as cytotoxic T-lymphocyte-associated protein-4 (CTLA-4), programmed cell death-1/Ligand (PD-1/PD-L1), lymphocyte-activation gene 3 (LAG3), or T-cell immunoglobulin-and mucin domain-3-containing molecule 3 (TIM-3) can disrupt cytotoxic T-lymphocyte (CTL) proliferation in CRC and reduce the immune response against cancer[95]; (6) vaccine-based approaches to modulate TGF-β signaling, which have been applied with the aim of facilitating the immune destruction of cancer cells in many different tumor types. It is important to realize that tumors are able to prevent the activation of the immune system by hiding tumor cell antigens and also suppress the immune system. Thus, cancer vaccines will help to activate and maintain an anti-tumor immune response; and (7) adoptive cell therapy, which is a form of passive immunotherapy that involves transferring immune cells or molecules to the host[96].

Many of these agents have been or are being evaluated in clinical trials to treat CRC (Table 3).

SMALL MOLECULE INHIBITORS OF SMAD EXPRESSION AND PHOSPHORYLATION

Since SMAD molecules have an important role in the TGF-β signaling pathway, great efforts have been made for the search of SMAD activation inhibitors. Indeed, it has been shown that SMAD3 silencing can suppress cancer cell growth and metastasis by increasing the cancer-killing activity of natural killer (NK) cells. Thus, the selective inhibition of the SMAD3 protein with a potent, low toxicity drug could provide a promising anticancer treatment. Some compounds have shown good inhibitory activity against SMAD 2 or SMAD3 through direct or indirect downregulation of their respective expressions and phosphorylations[97].

Peptide aptamers or DNA aptamers are artificial short peptides, respectively single-stranded DNA or RNA nucleotides, which are antibody-like in function. Aptamers can bind specific molecules with high specificity and affinity. SMAD2-and SMAD3-binding aptamers have also been established. Upon binding to SMAD2 or SMAD3, the aptamer prevents their binding and complex formation, thereby arresting TGF-β signaling[98,99]. Aptamers also have the potential to be used more frequently in clinical practice, from disease diagnosis to targeted delivery of therapeutic agents. Their simplicity in manufacturing and lengthy shelf life significantly improve this potential[100].

The specific inhibitor of SMAD3 (SIS3) is a synthetic substance that specifically inhibits the phosphorylation of SMAD3 and thus its binding to SMAD4[101]. Furthermore, targeting the inhibition of SMAD3 is currently considered a promising therapeutic strategy in the treatment of cancer[102].

MEDICATION THERAPEUTIC STRATEGIES THROUGH THE TGF-B /SMAD SIGNALING PATHWAY

The effects of several potential molecules that induce tumor growth or inhibit the proliferation and metastasis of carcinoma cells through regulation of the TGF-β/SMAD signaling pathway have been described[103]. Baicalein is a major flavonoid, originally extracted from the edible medicinal plants of *Scutellaria baicalensis* and *S. lateriflora*. Baicalein reduces the concentrations of phosphorylated SMAD2 and SMAD3, without affecting the total levels of SMAD2 and SMAD3 and thus inhibits the TGF-β /SMAD2/3 signaling pathway in fibroblasts in vitro and in vivo without affecting SMAD 1, 5, and 8 in the BMP signaling pathway[104].

Table 3 Clinical trials of drugs for the treatment of colorectal cancer (United States National Library of Medicine; ClinicalTrials.gov)

Clinical trials (phase)	Drug	Target	Mechanism of action
Antisense oligonucleotides			
NCT00844064 (I)	AP12009 (trabedersen)	TGF-β2	By binding to TGF-βII mrna, its expression is reduced
Antibodies			
NCT04952753 (II)	NIS793	TGF-β	Reduction of active cytokine, reduction of SMAD2/3 phosphorylation, and reduction of TGF-β target gene expression
NCT02947165 (I)	NIS793	TGF-β	Reduction of active cytokine, reduction of SMAD2/3 phosphorylation, and reduction of TGF-β target gene expression
NCT01646203(I)	IMC-TR1	TGF-βRII	Reduction of active cytokine, reduction of SMAD2/3 phosphorylation, and reduction of TGF-β target gene expression
Ligand traps			
NCT03436563 (I/II)	M7824	TGF-βRII	Bifunctional anti-PD-L1/TGF-βRII trap fusion protein
NCT02517398(I)	Bintrafusp alfa	TGF-βRII and PD-L1	First-in-class bifunctional fusion protein composed of a mab against PD-L1 fused to the extracellular domain of the TGF-β receptor II
NCT04856787 (II/III)	SHR-1701	TGF-βRII	Bifunctional anti-PD-L1/TGF-βRII agent
Small molecule receptor kinase inhibitors			
NCT04031872 (I/II)	LY3200882; capecitabine	TGF-βRI	By blocking ATP binding to TGF-βR, receptor kinase activity and signal transduction are reduced
NCT05400122 (I)	Vactosertib	TGF-βRI	Inhibits the activity of TGF-βR1
NCT03724851 (I/II)	Vactosertib + Pembroli-zumab	TGF-βRI	Inhibits the activity of TGF-βR1
NCT03470350 (I/II)	Galunisertib	TGF-βRI	Inhibits the activity of TGF-βR1
Immune checkpoints			
NCT04540159		TGF-β1	Measuring the level Active TGF-β1 by flow-cytometric analysis in the intraabdominal ascites
Adoptive cell therapy			
NCT03431311 (I/II)	ACT	TGF-βII	ACT with Radium-1 TCR + T cells transiently redirected against the TGF-βRII frameshift antigen which is expressed in MSI+ colon cancer.
NCT05040568 (I)	CB-NK-TGF-Î²R2-/NR3C1		Immunotherapy with ex vivo preactivated and expanded CB-NK cells in combination with cetuximab

ACT: Adoptive cell therapy; TGF: Transforming growth factor.

Ginseng is valued as the most important medicinal plant in traditional Chinese medicine. The major constituents of ginseng are ginsenosides. Ginsenoside Rg3 has an inhibitory effect on the TGF-β/SMAD and ERK signaling pathways in keloid fibroblasts and increases mRNA expression levels in SMAD7 [105]. Dai *et al*[106] showed that ginsenoside Rb2 can inhibit the expression of SMAD4 and phosphorylated SMAD2/3 in CRC cells.

Kaempferol is a natural flavanol, a type of flavonoid, found in a variety of plants and plant-derived foods, including kale, beans, tea, spinach, and broccoli. It binds to the TβRI, leading to its inactivation. This results in inhibition of the TGF-β/SMAD signaling pathway due to reduced phosphorylation of SMAD2/3[107].

Loureirin B, a flavonoid extracted from *Dracaena cochinchinensis*, is used in traditional Chinese medicine (TCM). Loureirin B upregulates the expression of MMP-1, MMP-3, MMP-9, and MMP-13 and thus causes degradation of extracellular matrix, inhibits the phosphorylation of SMAD2 and SMAD3 and thus effectively suppresses the TGF-β/SMAD pathway[108].

Galangin is a polyphenolic compound derived primarily from different medicinal herbs, the effect of which is the downregulation of SMAD2 and SMAD3 phosphorylation without altering the expression of total SMAD2, SMAD3, SMAD4, SMAD6, and SMAD7[109].

Celastrol is a pharmacologically active substance extracted from *Tripterygium wilfordii* Hook F, which is used in TCM to treat cancer and other inflammatory diseases[110]. Zhang *et al*[111] showed that celastrol reduces the levels of SMAD4 and phosphorylated SMAD2/3. Together, celastrol may inhibit

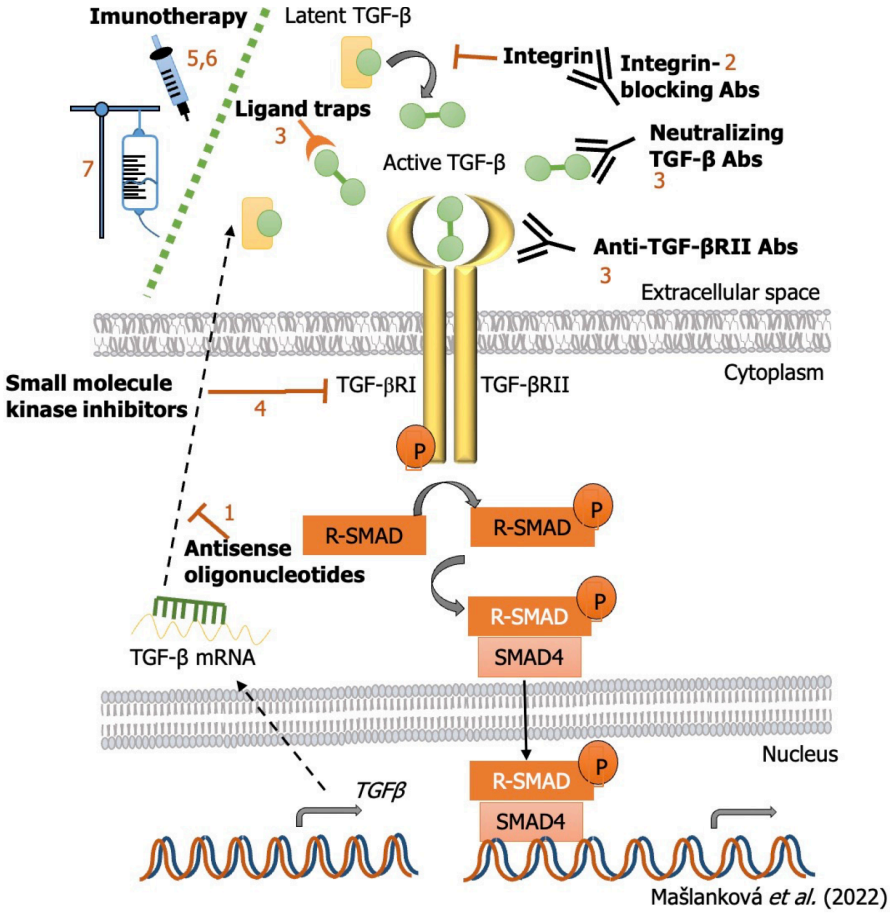


Figure 5 Inhibition strategies of transforming growth factor-β signaling pathway and miRNAs targets for colorectal cancer treatment.
TGF: Transforming growth factor; SMAD: Small mothers against decapentaplegic homolog.

CRC through TGF-β, which is a promising treatment for CRC.

Qingjie Fuzheng granules are TCM comprising a 4-herb mixture, composed of *Hedyotis diffusa* Willd, malt, *Astragalus*, and *S. barbata* D. Don significantly inhibits the expression of several key proteins in the canonical TGF-β/SMAD pathway, including TGF-β, phosphorylated SMAD2/3, and SMAD4. This inhibition leads to a decrease in the ratio of N-cadherin to E-cadherin, indicating that EMT is inhibited [111].

CONCLUSION

Antitumor immunity is mediated by macrophages, NK cells, granulocytes (polymorphonuclear leukocytes, PMNs), T cells, and antibodies. In recent years, the particular role of PMNs in regulation of adaptive immunity, especially in cancer, has emerged. PMNs in cancer are functionally diverse, with some authors describing their antitumor activity, but the number of publications in which the authors confirm their negative regulation of immune responses and their presence in cancer patients associated with poor prognosis and therapeutic outcomes is increasing. These cells suppress the physiological role of T and B lymphocytes and NK cells, and also promote tumor progression and metastasis through non-immune mechanisms. Cytokines produced by tumor cells [vascular endothelial growth factor (VEGF), TGF-β] also play a similar role when they inhibit T cell development and function. TGF-β, as an immunosuppressive factor, significantly affects the proliferation, activation, and differentiation of immune effector cells. Epigenetic changes that may be affected by the TGF-β pathway in CRC should be carefully studied because the mechanisms of drug resistance are different between patients in different stages of cancer and personalized treatment is more effective. Therefore, knowledge of the activation and inhibition of factors that affect the TGF-β signaling pathway is very important.

ACKNOWLEDGEMENTS

This review is a summary work consisting of the results of many authors. We would like to thank all the authors whose work we have included in this review article and apologize to the authors whose relevant work has not been included in this review article.

FOOTNOTES

Author contributions: Maslankova J, Vecurkovska I, Rabajdova M, Katuchova J, Kicka M, Gayova M, and Katuch V contributed equally to the study's conception, design and undertaking, and to manuscript preparation; all authors have read and approve the final manuscript.

Conflict-of-interest statement: The authors declare having no conflict of interests for this article.

Open-Access: This article is an open-access article that was selected by an in-house editor and fully peer-reviewed by external reviewers. It is distributed in accordance with the Creative Commons Attribution NonCommercial (CC BY-NC 4.0) license, which permits others to distribute, remix, adapt, build upon this work non-commercially, and license their derivative works on different terms, provided the original work is properly cited and the use is non-commercial. See: https://creativecommons.org/Licenses/by-nc/4.0/

Country/Territory of origin: Slovakia

ORCID number: Jana Maslankova 0000-0002-2786-0620; Miroslava Rabajdova 0000-0001-9562-5756; Jana Katuchova 0000-0001-5479-6444; Vladimir Katuch 0000-0001-8044-4012.

S-Editor: Chen YL
L-Editor: A
P-Editor: Zhang XD

REFERENCES

1 **Xi Y**, Xu P. Global colorectal cancer burden in 2020 and projections to 2040. *Transl Oncol* 2021; **14**: 101174 [PMID: 34243011 DOI: 10.1016/j.tranon.2021.101174]
2 **Lech G**, Słotwiński R, Słodkowski M, Krasnodębski IW. Colorectal cancer tumour markers and biomarkers: Recent therapeutic advances. *World J Gastroenterol* 2016; **22**: 1745-1755 [PMID: 26855534 DOI: 10.3748/wjg.v22.i5.1745]
3 **Ahmad R**, Singh JK, Wunnava A, Al-Obeed O, Abdulla M, Srivastava SK. Emerging trends in colorectal cancer: Dysregulated signaling pathways (Review). *Int J Mol Med* 2021; **47** [PMID: 33655327 DOI: 10.3892/ijmm.2021.4847]
4 **Wang W**, Kandimalla R, Huang H, Zhu L, Li Y, Gao F, Goel A, Wang X. Molecular subtyping of colorectal cancer: Recent progress, new challenges and emerging opportunities. *Semin Cancer Biol* 2019; **55**: 37-52 [PMID: 29775690 DOI: 10.1016/j.semcancer.2018.05.002]
5 **Wang F**, Xia X, Yang C, Shen J, Mai J, Kim HC, Kirui D, Kang Y, Fleming JB, Koay EJ, Mitra S, Ferrari M, Shen H. *SMAD4* Gene Mutation Renders Pancreatic Cancer Resistance to Radiotherapy through Promotion of Autophagy. *Clin Cancer Res* 2018; **24**: 3176-3185 [PMID: 29602802 DOI: 10.1158/1078-0432.CCR-17-3435]
6 **Reynolds IS**, Furney SJ, Kay EW, McNamara DA, Prehn JHM, Burke JP. Meta-analysis of the molecular associations of mucinous colorectal cancer. *Br J Surg* 2019; **106**: 682-691 [PMID: 30945755 DOI: 10.1002/bjs.11142]
7 **Gallois C**, Laurent-Puig P, Taieb J. Methylator phenotype in colorectal cancer: A prognostic factor or not? *Crit Rev Oncol Hematol* 2016; **99**: 74-80 [PMID: 26702883 DOI: 10.1016/j.critrevonc.2015.11.001]
8 **Andre T**, Amonkar M, Norquist JM, Shiu KK, Kim TW, Jensen BV, Jensen LH, Punt CJA, Smith D, Garcia-Carbonero R, Sevilla I, De La Fouchardiere C, Rivera F, Elez E, Diaz LA Jr, Yoshino T, Van Cutsem E, Yang P, Farooqui M, Le DT. Health-related quality of life in patients with microsatellite instability-high or mismatch repair deficient metastatic colorectal cancer treated with first-line pembrolizumab versus chemotherapy (KEYNOTE-177): an open-label, randomised, phase 3 trial. *Lancet Oncol* 2021; **22**: 665-677 [PMID: 33812497 DOI: 10.1016/S1470-2045(21)00064-4]
9 **De' Angelis GL**, Bottarelli L, Azzoni C, De' Angelis N, Leandro G, Di Mario F, Gaiani F, Negri F. Microsatellite instability in colorectal cancer. *Acta Biomed* 2018; **89**: 97-101 [PMID: 30561401 DOI: 10.23750/abm.v89i9-S.7960]
10 **Pino MS**, Chung DC. The chromosomal instability pathway in colon cancer. *Gastroenterology* 2010; **138**: 2059-2072 [PMID: 20420946 DOI: 10.1053/j.gastro.2009.12.065]
11 **Guinney J**, Dienstmann R, Wang X, de Reyniès A, Schlicker A, Soneson C, Marisa L, Roepman P, Nyamundanda G, Angelino P, Bot BM, Morris JS, Simon IM, Gerster S, Fessler E, De Sousa E Melo F, Missiaglia E, Ramay H, Barras D, Homicsko K, Maru D, Manyam GC, Broom B, Boige V, Perez-Villamil B, Laderas T, Salazar R, Gray JW, Hanahan D, Tabernero J, Bernards R, Friend SH, Laurent-Puig P, Medema JP, Sadanandam A, Wessels L, Delorenzi M, Kopetz S, Vermeulen L, Tejpar S. The consensus molecular subtypes of colorectal cancer. *Nat Med* 2015; **21**: 1350-1356 [PMID: 26457759 DOI: 10.1038/nm.3967]
12 **Fontana E**, Eason K, Cervantes A, Salazar R, Sadanandam A. Context matters-consensus molecular subtypes of colorectal cancer as biomarkers for clinical trials. *Ann Oncol* 2019; **30**: 520-527 [PMID: 30796810 DOI: 10.1093/annonc/mdz052]

13 **Stintzing S**, Wirapati P, Lenz HJ, Neureiter D, Fischer von Weikersthal L, Decker T, Kiani A, Kaiser F, Al-Batran S, Heintges T, Lerchenmüller C, Kahl C, Seipelt G, Kullmann F, Moehler M, Scheithauer W, Held S, Modest DP, Jung A, Kirchner T, Aderka D, Tejpar S, Heinemann V. Consensus molecular subgroups (CMS) of colorectal cancer (CRC) and first-line efficacy of FOLFIRI plus cetuximab or bevacizumab in the FIRE3 (AIO KRK-0306) trial. *Ann Oncol* 2019; **30**: 1796-1803 [PMID: 31868905 DOI: 10.1093/annonc/mdz387]

14 **Nguyen HT**, Duong HQ. The molecular characteristics of colorectal cancer: Implications for diagnosis and therapy. *Oncol Lett* 2018; **16**: 9-18 [PMID: 29928381 DOI: 10.3892/ol.2018.8679]

15 **Wang W**, Wang GQ, Sun XW, Chen G, Li YF, Zhang LY, Qiu HB, Huang CY, Zhan YQ, Zhou ZW. Prognostic values of chromosome 18q microsatellite alterations in stage II colonic carcinoma. *World J Gastroenterol* 2010; **16**: 6026-6034 [PMID: 21157981 DOI: 10.3748/wjg.v16.i47.6026]

16 **Vacante M**, Borzì AM, Basile F, Biondi A. Biomarkers in colorectal cancer: Current clinical utility and future perspectives. *World J Clin Cases* 2018; **6**: 869-881 [PMID: 30568941 DOI: 10.12998/wjcc.v6.i15.869]

17 **Samanta D**, Datta PK. Alterations in the Smad pathway in human cancers. *Front Biosci (Landmark Ed)* 2012; **17**: 1281-1293 [PMID: 22201803 DOI: 10.2741/3986]

18 **Baba AB**, Rah B, Bhat GR, Mushtaq I, Parveen S, Hassan R, Hameed Zargar M, Afroze D. Transforming Growth Factor-Beta (TGF-β) Signaling in Cancer-A Betrayal Within. *Front Pharmacol* 2022; **13**: 791272 [PMID: 35295334 DOI: 10.3389/fphar.2022.791272]

19 **Gough NR**, Xiang X, Mishra L. TGF-β Signaling in Liver, Pancreas, and Gastrointestinal Diseases and Cancer. *Gastroenterology* 2021; **161**: 434-452.e15 [PMID: 33940008 DOI: 10.1053/j.gastro.2021.04.064]

20 **Frey P**, Devisme A, Schrempp M, Andrieux G, Boerries M, Hecht A. Canonical BMP Signaling Executes Epithelial-Mesenchymal Transition Downstream of SNAIL1. *Cancers (Basel)* 2020; **12** [PMID: 32326239 DOI: 10.3390/cancers12041019]

21 **Karathanasi V**, Tosios KI, Nikitakis NG, Piperi E, Koutlas I, Trimis G, Sklavounou A. TGF-β1, Smad-2/-3, Smad-1/-5/-8, and Smad-4 signaling factors are expressed in ameloblastomas, adenomatoid odontogenic tumors, and calcifying cystic odontogenic tumors: an immunohistochemical study. *J Oral Pathol Med* 2013; **42**: 415-423 [PMID: 23157422 DOI: 10.1111/jop.12016]

22 **Gu S**, Feng XH. TGF-β signaling in cancer. *Acta Biochim Biophys Sin (Shanghai)* 2018; **50**: 941-949 [PMID: 30165534 DOI: 10.1093/abbs/gmy092]

23 **Luo J**, Chen XQ, Li P. The Role of TGF-β and Its Receptors in Gastrointestinal Cancers. *Transl Oncol* 2019; **12**: 475-484 [PMID: 30594036 DOI: 10.1016/j.tranon.2018.11.010]

24 **Zhang M**, Zhang YY, Chen Y, Wang J, Wang Q, Lu H. TGF-β Signaling and Resistance to Cancer Therapy. *Front Cell Dev Biol* 2021; **9**: 786728 [PMID: 34917620 DOI: 10.3389/fcell.2021.786728]

25 **Seoane J**, Gomis RR. TGF-β Family Signaling in Tumor Suppression and Cancer Progression. *Cold Spring Harb Perspect Biol* 2017; **9** [PMID: 28246180 DOI: 10.1101/cshperspect.a022277]

26 **Hao Y**, Baker D, Ten Dijke P. TGF-β-Mediated Epithelial-Mesenchymal Transition and Cancer Metastasis. *Int J Mol Sci* 2019; **20** [PMID: 31195692 DOI: 10.3390/ijms20112767]

27 **Muscella A**, Vetrugno C, Cossa LG, Marsigliante S. TGF-β1 activates RSC96 Schwann cells migration and invasion through MMP-2 and MMP-9 activities. *J Neurochem* 2020; **153**: 525-538 [PMID: 31729763 DOI: 10.1111/jnc.14913]

28 **Piersma B**, Hayward MK, Weaver VM. Fibrosis and cancer: A strained relationship. *Biochim Biophys Acta Rev Cancer* 2020; **1873**: 188356 [PMID: 32147542 DOI: 10.1016/j.bbcan.2020.188356]

29 **Dituri F**, Cossu C, Mancarella S, Giannelli G. The Interactivity between TGFβ and BMP Signaling in Organogenesis, Fibrosis, and Cancer. *Cells* 2019; **8** [PMID: 31547567 DOI: 10.3390/cells8101130]

30 **Ning J**, Zhao Y, Ye Y, Yu J. Opposing roles and potential antagonistic mechanism between TGF-β and BMP pathways: Implications for cancer progression. *EBioMedicine* 2019; **41**: 702-710 [PMID: 30808576 DOI: 10.1016/j.ebiom.2019.02.033]

31 **Katsuno Y**, Qin J, Oses-Prieto J, Wang H, Jackson-Weaver O, Zhang T, Lamouille S, Wu J, Burlingame A, Xu J, Derynck R. Arginine methylation of SMAD7 by PRMT1 in TGF-β-induced epithelial-mesenchymal transition and epithelial stem-cell generation. *J Biol Chem* 2018; **293**: 13059-13072 [PMID: 29907569 DOI: 10.1074/jbc.RA118.002027]

32 **Zhao M**, Mishra L, Deng CX. The role of TGF-β/SMAD4 signaling in cancer. *Int J Biol Sci* 2018; **14**: 111-123 [PMID: 29483830 DOI: 10.7150/ijbs.23230]

33 **Zhang T**, Liu W, Meng W, Zhao H, Yang Q, Gu SJ, Xiao CC, Jia CC, Fu BS. Downregulation of miR-542-3p promotes cancer metastasis through activating TGF-β/Smad signaling in hepatocellular carcinoma. *Onco Targets Ther* 2018; **11**: 1929-1939 [PMID: 29670368 DOI: 10.2147/OTT.S154416]

34 **Fricke F**, Mussack V, Buschmann D, Hausser I, Pfaffl MW, Kopitz J, Gebert J. TGFBR2dependent alterations of microRNA profiles in extracellular vesicles and parental colorectal cancer cells. *Int J Oncol* 2019; **55**: 925-937 [PMID: 31432155 DOI: 10.3892/ijo.2019.4859]

35 **Grady WM**. Polymerase Slippage Restoration of Frameshifted TGFBR2 in Colorectal Cancer: A Novel Paradigm. *Gastroenterology* 2015; **148**: 1276-1279 [PMID: 25921376 DOI: 10.1053/j.gastro.2015.04.023]

36 **Jung B**, Staudacher JJ, Beauchamp D. Transforming Growth Factor β Superfamily Signaling in Development of Colorectal Cancer. *Gastroenterology* 2017; **152**: 36-52 [PMID: 27773809 DOI: 10.1053/j.gastro.2016.10.015]

37 **Zhou R**, Huang Y, Cheng B, Wang Y, Xiong B. TGFBR1*6A is a potential modifier of migration and invasion in colorectal cancer cells. *Oncol Lett* 2018; **15**: 3971-3976 [PMID: 29467907 DOI: 10.3892/ol.2018.7725]

38 **Sinha A**, Iyengar PV, Ten Dijke P. E3 Ubiquitin Ligases: Key Regulators of TGFβ Signaling in Cancer Progression. *Int J Mol Sci* 2021; **22** [PMID: 33418880 DOI: 10.3390/ijms22020476]

39 **de Ceuninck van Capelle C**, Spit M, Ten Dijke P. Current perspectives on inhibitory SMAD7 in health and disease. *Crit Rev Biochem Mol Biol* 2020; **55**: 691-715 [PMID: 33081543 DOI: 10.1080/10409238.2020.1828260]

40 **Miyazawa K**, Miyazono K. Regulation of TGF-β Family Signaling by Inhibitory Smads. *Cold Spring Harb Perspect Biol*

2017; **9** [PMID: 27920040 DOI: 10.1101/cshperspect.a022095]
41 **Tecalco-Cruz AC**, Ríos-López DG, Vázquez-Victorio G, Rosales-Alvarez RE, Macías-Silva M. Transcriptional cofactors Ski and SnoN are major regulators of the TGF-β/Smad signaling pathway in health and disease. *Signal Transduct Target Ther* 2018; **3**: 15 [PMID: 29892481 DOI: 10.1038/s41392-018-0015-8]
42 **Chen HY**, Chiang YF, Huang JS, Huang TC, Shih YH, Wang KL, Ali M, Hong YH, Shieh TM, Hsia SM. Isoliquiritigenin Reverses Epithelial-Mesenchymal Transition Through Modulation of the TGF-β/Smad Signaling Pathway in Endometrial Cancer. *Cancers (Basel)* 2021; **13** [PMID: 33799801 DOI: 10.3390/cancers13061236]
43 **Ma X**, Gao Y, Chen Y, Liu J, Yang C, Bao C, Wang Y, Feng Y, Song X, Qiao S. M2-Type Macrophages Induce Tregs Generation by Activating the TGF-β/Smad Signalling Pathway to Promote Colorectal Cancer Development. *Onco Targets Ther* 2021; **14**: 5391-5402 [PMID: 34908844 DOI: 10.2147/OTT.S336548]
44 **Chen N**, Balasenthil S, Reuther J, Frayna A, Wang Y, Chandler DS, Abruzzo LV, Rashid A, Rodriguez J, Lozano G, Cao Y, Lokken E, Chen J, Frazier ML, Sahin AA, Wistuba II, Sen S, Lott ST, Killary AM. DEAR1 is a chromosome 1p35 tumor suppressor and master regulator of TGF-β-driven epithelial-mesenchymal transition. *Cancer Discov* 2013; **3**: 1172-1189 [PMID: 23838884 DOI: 10.1158/2159-8290.CD-12-0499]
45 **Liu L**, Liu X, Ren X, Tian Y, Chen Z, Xu X, Du Y, Jiang C, Fang Y, Liu Z, Fan B, Zhang Q, Jin G, Yang X, Zhang X. Smad2 and Smad3 have differential sensitivity in relaying TGFβ signaling and inversely regulate early lineage specification. *Sci Rep* 2016; **6**: 21602 [PMID: 26905010 DOI: 10.1038/srep21602]
46 **Monteleone G**, Kumberova A, Croft NM, McKenzie C, Steer HW, MacDonald TT. Blocking Smad7 restores TGF-beta1 signaling in chronic inflammatory bowel disease. *J Clin Invest* 2001; **108**: 601-609 [PMID: 11518734 DOI: 10.1172/jci12821]
47 **Romano M**, DE Francesco F, Zarantonello L, Ruffolo C, Ferraro GA, Zanus G, Giordano A, Bassi N, Cillo U. From Inflammation to Cancer in Inflammatory Bowel Disease: Molecular Perspectives. *Anticancer Res* 2016; **36**: 1447-1460 [PMID: 27069120 DOI: 10.1007/s00384-020-03726-4]
48 **Wang G**, Yu Y, Sun C, Liu T, Liang T, Zhan L, Lin X, Feng XH. STAT3 selectively interacts with Smad3 to antagonize TGF-β signalling. *Oncogene* 2016; **35**: 4388-4398 [PMID: 26616859 DOI: 10.1038/onc.2015.446]
49 **Liu RY**, Zeng Y, Lei Z, Wang L, Yang H, Liu Z, Zhao J, Zhang HT. JAK/STAT3 signaling is required for TGF-β-induced epithelial-mesenchymal transition in lung cancer cells. *Int J Oncol* 2014; **44**: 1643-1651 [PMID: 24573038 DOI: 10.3892/ijo.2014.2310]
50 **Xu J**, Shao T, Song M, Xie Y, Zhou J, Yin J, Ding N, Zou H, Li Y, Zhang J. MIR22HG acts as a tumor suppressor *via* TGFβ/SMAD signaling and facilitates immunotherapy in colorectal cancer. *Mol Cancer* 2020; **19**: 51 [PMID: 32127004 DOI: 10.1186/s12943-020-01174-w]
51 **Haque S**, Morris JC. Transforming growth factor-β: A therapeutic target for cancer. *Hum Vaccin Immunother* 2017; **13**: 1741-1750 [PMID: 28575585 DOI: 10.1080/21645515.2017.1327107]
52 **Boye A**. A cytokine in turmoil: Transforming growth factor beta in cancer. *Biomed Pharmacother* 2021; **139**: 111657 [PMID: 34243626 DOI: 10.1016/j.biopha.2021.111657]
53 **Fleming NI**, Jorissen RN, Mouradov D, Christie M, Sakthianandeswaren A, Palmieri M, Day F, Li S, Tsui C, Lipton L, Desai J, Jones IT, McLaughlin S, Ward RL, Hawkins NJ, Ruszkiewicz AR, Moore J, Zhu HJ, Mariadason JM, Burgess AW, Busam D, Zhao Q, Strausberg RL, Gibbs P, Sieber OM. SMAD2, SMAD3 and SMAD4 mutations in colorectal cancer. *Cancer Res* 2013; **73**: 725-735 [PMID: 23139211 DOI: 10.1158/0008-5472.CAN-12-2706]
54 **Lin C**, Zhang J, Lu Y, Li X, Zhang W, Lin W, Zheng L. NIT1 suppresses tumour proliferation by activating the TGFβ1-Smad2/3 signalling pathway in colorectal cancer. *Cell Death Dis* 2018; **9**: 263 [PMID: 29449642 DOI: 10.1038/s41419-018-0333-3]
55 **Razzaque MS**, Atfi A. TGIF1-Twist1 axis in pancreatic ductal adenocarcinoma. *Comput Struct Biotechnol J* 2020; **18**: 2568-2572 [PMID: 33005315 DOI: 10.1016/j.csbj.2020.09.023]
56 **Najjar Sadeghi R**, Saeedi N, Sahba N, Sadeghi A. SMAD4 mutations identified in Iranian patients with colorectal cancer and polyp. *Gastroenterol Hepatol Bed Bench* 2021; **14**: S32-S40 [PMID: 35154600]
57 **McCarthy AJ**, Chetty R. *Smad4/DPC4*. *J Clin Pathol* 2018; **71**: 661-664 [PMID: 29720405 DOI: 10.1136/jclinpath-2018-205095]
58 **Zi Z**. Molecular Engineering of the TGF-β Signaling Pathway. *J Mol Biol* 2019; **431**: 2644-2654 [PMID: 31121181 DOI: 10.1016/j.jmb.2019.05.022]
59 **Liao X**, Hao Y, Zhang X, Ward S, Houldsworth J, Polydorides AD, Harpaz N. Clinicopathological characterization of SMAD4-mutated intestinal adenocarcinomas: A case-control study. *PLoS One* 2019; **14**: e0212142 [PMID: 30730996 DOI: 10.1371/journal.pone.0212142]
60 **Mehrvarz Sarshekeh A**, Advani S, Overman MJ, Manyam G, Kee BK, Fogelman DR, Dasari A, Raghav K, Vilar E, Manuel S, Shureiqi I, Wolff RA, Patel KP, Luthra R, Shaw K, Eng C, Maru DM, Routbort MJ, Meric-Bernstam F, Kopetz S. Association of SMAD4 mutation with patient demographics, tumor characteristics, and clinical outcomes in colorectal cancer. *PLoS One* 2017; **12**: e0173345 [PMID: 28267766 DOI: 10.1371/journal.pone.0173345]
61 **Ritterhouse LL**, Wu EY, Kim WG, Dillon DA, Hirsch MS, Sholl LM, Agoston AT, Setia N, Lauwers GY, Park DY, Srivastava A, Doyle LA. Loss of SMAD4 protein expression in gastrointestinal and extra-gastrointestinal carcinomas. *Histopathology* 2019; **75**: 546-551 [PMID: 31054158 DOI: 10.1111/his.13894]
62 **Silva VR**, Santos LS, Dias RB, Quadros CA, Bezerra DP. Emerging agents that target signaling pathways to eradicate colorectal cancer stem cells. *Cancer Commun (Lond)* 2021; **41**: 1275-1313 [PMID: 34791817 DOI: 10.1002/cac2.12235]
63 **Yang L**, Liu Z, Tan J, Dong H, Zhang X. Multispectral imaging reveals hyper active TGF-β signaling in colorectal cancer. *Cancer Biol Ther* 2018; **19**: 105-112 [PMID: 29219668 DOI: 10.1080/15384047.2017.1395116]
64 **Szeglin BC**, Wu C, Marco MR, Park HS, Zhang Z, Zhang B, Garcia-Aguilar J, Beauchamp RD, Chen XS, Smith JJ. A SMAD4-modulated gene profile predicts disease-free survival in stage II and III colorectal cancer. *Cancer Rep (Hoboken)* 2022; **5**: e1423 [PMID: 34114372 DOI: 10.1002/cnr2.1423]
65 **Troncone E**, Marafini I, Stolfi C, Monteleone G. Involvement of Smad7 in Inflammatory Diseases of the Gut and Colon Cancer. *Int J Mol Sci* 2021; **22** [PMID: 33920230 DOI: 10.3390/ijms22083922]

66 **Li N**. CircTBL1XR1/miR-424 axis regulates Smad7 to promote the proliferation and metastasis of colorectal cancer. *J Gastrointest Oncol* 2020; **11**: 918-931 [PMID: 33209488 DOI: 10.21037/jgo-20-395]

67 **Alidoust M**, Hamzehzadeh L, Khorshid Shamshiri A, Afzaljavan F, Kerachian MA, Fanipakdel A, Aledavood SA, Allahyari A, Bari A, Moosanen Mozaffari H, Goshayeshi L, Pasdar A. Association of SMAD7 genetic markers and haplotypes with colorectal cancer risk. *BMC Med Genomics* 2022; **15**: 8 [PMID: 35016683 DOI: 10.1186/s12920-021-01150-3]

68 **Boulay JL**, Mild G, Lowy A, Reuter J, Lagrange M, Terracciano L, Laffer U, Herrmann R, Rochlitz C. SMAD7 is a prognostic marker in patients with colorectal cancer. *Int J Cancer* 2003; **104**: 446-449 [PMID: 12584741 DOI: 10.1002/ijc.10908]

69 **Stolfi C**, De Simone V, Colantoni A, Franzè E, Ribichini E, Fantini MC, Caruso R, Monteleone I, Sica GS, Sileri P, MacDonald TT, Pallone F, Monteleone G. A functional role for Smad7 in sustaining colon cancer cell growth and survival. *Cell Death Dis* 2014; **5**: e1073 [PMID: 24556688 DOI: 10.1038/cddis.2014.49]

70 **Rosic J**, Dragicevic S, Miladinov M, Despotovic J, Bogdanovic A, Krivokapic Z, Nikolic A. SMAD7 and SMAD4 expression in colorectal cancer progression and therapy response. *Exp Mol Pathol* 2021; **123**: 104714 [PMID: 34717960 DOI: 10.1016/j.yexmp.2021.104714]

71 **Stolfi C**, Marafini I, De Simone V, Pallone F, Monteleone G. The dual role of Smad7 in the control of cancer growth and metastasis. *Int J Mol Sci* 2013; **14**: 23774-23790 [PMID: 24317436 DOI: 10.3390/ijms141223774]

72 **Troncone E**, Monteleone G. Smad7 and Colorectal Carcinogenesis: A Double-Edged Sword. *Cancers (Basel)* 2019; **11** [PMID: 31052449 DOI: 10.3390/cancers11050612]

73 **Diamantopoulos MA**, Tsiakanikas P, Scorilas A. Non-coding RNAs: the riddle of the transcriptome and their perspectives in cancer. *Ann Transl Med* 2018; **6**: 241 [PMID: 30069443 DOI: 10.21037/atm.2018.06.10]

74 **Jia Z**, An J, Liu Z, Zhang F. Non-Coding RNAs in Colorectal Cancer: Their Functions and Mechanisms. *Front Oncol* 2022; **12**: 783079 [PMID: 35186731 DOI: 10.3389/fonc.2022.783079]

75 **Luo K**, Geng J, Zhang Q, Xu Y, Zhou X, Huang Z, Shi KQ, Pan C, Wu J. LncRNA CASC9 interacts with CPSF3 to regulate TGF-β signaling in colorectal cancer. *J Exp Clin Cancer Res* 2019; **38**: 249 [PMID: 31186036 DOI: 10.1186/s13046-019-1263-3]

76 **Zhang H**, Wang J, Yu T, Lu J, Yu Z. Silencing LncRNA CASC9 inhibits proliferation and invasion of colorectal cancer cells by MiR-542-3p/ILK. *PLoS One* 2022; **17**: e0265901 [PMID: 35427373 DOI: 10.1371/journal.pone.0265901]

77 **Azizidoost S**, Ghaedrahmati F, Anbiyaee O, Ahmad Ali R, Cheraghzadeh M, Farzaneh M. Emerging roles for lncRNA-NEAT1 in colorectal cancer. *Cancer Cell Int* 2022; **22**: 209 [PMID: 35676702 DOI: 10.1186/s12935-022-02627-6]

78 **Li Q**, Yue W, Li M, Jiang Z, Hou Z, Liu W, Ma N, Gan W, Li Y, Zhou T, Chen S. Downregulating Long Non-coding RNAs CTBP1-AS2 Inhibits Colorectal Cancer Development by Modulating the miR-93-5p/TGF-β/SMAD2/3 Pathway. *Front Oncol* 2021; **11**: 626620 [PMID: 33937030 DOI: 10.3389/fonc.2021.626620]

79 **Jung G**, Hernández-Illán E, Moreira L, Balaguer F, Goel A. Epigenetics of colorectal cancer: biomarker and therapeutic potential. *Nat Rev Gastroenterol Hepatol* 2020; **17**: 111-130 [PMID: 31900466 DOI: 10.1038/s41575-019-0230-y]

80 **Chao HM**, Wang TW, Chern E, Hsu SH. Regulatory RNAs, microRNA, long-non coding RNA and circular RNA roles in colorectal cancer stem cells. *World J Gastrointest Oncol* 2022; **14**: 748-764 [PMID: 35582099 DOI: 10.4251/wjgo.v14.i4.748]

81 **Ning X**, Wang C, Zhang M, Wang K. Ectopic Expression of miR-147 Inhibits Stem Cell Marker and Epithelial-Mesenchymal Transition (EMT)-Related Protein Expression in Colon Cancer Cells. *Oncol Res* 2019; **27**: 399-406 [PMID: 29426374 DOI: 10.3727/096504018X15179675206495]

82 **Vakhshiteh F**, Hassani S, Momenifar N, Pakdaman F. Exosomal circRNAs: new players in colorectal cancer. *Cancer Cell Int* 2021; **21**: 483 [PMID: 34521402 DOI: 10.1186/s12935-021-02112-6]

83 **Zheng L**, Liang H, Zhang Q, Shen Z, Sun Y, Zhao X, Gong J, Hou Z, Jiang K, Wang Q, Jin Y, Yin Y. circPTEN1, a circular RNA generated from PTEN, suppresses cancer progression through inhibition of TGF-β/Smad signaling. *Mol Cancer* 2022; **21**: 41 [PMID: 35135542 DOI: 10.1186/s12943-022-01495-y]

84 **Shang A**, Gu C, Wang W, Wang X, Sun J, Zeng B, Chen C, Chang W, Ping Y, Ji P, Wu J, Quan W, Yao Y, Zhou Y, Sun Z, Li D. Exosomal circPACRGL promotes progression of colorectal cancer *via* the miR-142-3p/miR-506-3p- TGF-β1 axis. *Mol Cancer* 2020; **19**: 117 [PMID: 32713345 DOI: 10.1186/s12943-020-01235-0]

85 **Che J**, Pan L, Yang X, Liu Z, Huang L, Wen C, Lin A, Liu H. Thymidine phosphorylase expression and prognosis in colorectal cancer treated with 5-fluorouracil-based chemotherapy: A meta-analysis. *Mol Clin Oncol* 2017; **7**: 943-952 [PMID: 29285354 DOI: 10.3892/mco.2017.1436]

86 **Kugimiya N**, Nishimoto A, Hosoyama T, Ueno K, Takemoto Y, Harada E, Enoki T, Hamano K. JAB1-STAT3 activation loop is associated with recurrence following 5-fluorouracil-based adjuvant chemotherapy in human colorectal cancer. *Oncol Lett* 2017; **14**: 6203-6209 [PMID: 29113268 DOI: 10.3892/ol.2017.6994]

87 **Lin Z**, Zhang L, Zhou J, Zheng J. Silencing Smad4 attenuates sensitivity of colorectal cancer cells to cetuximab by promoting epithelialmesenchymal transition. *Mol Med Rep* 2019; **20**: 3735-3745 [PMID: 31485652 DOI: 10.3892/mmr.2019.10597]

88 **Oyanagi H**, Shimada Y, Nagahashi M, Ichikawa H, Tajima Y, Abe K, Nakano M, Kameyama H, Takii Y, Kawasaki T, Homma KI, Ling Y, Okuda S, Takabe K, Wakai T. SMAD4 alteration associates with invasive-front pathological markers and poor prognosis in colorectal cancer. *Histopathology* 2019; **74**: 873-882 [PMID: 30636020 DOI: 10.1111/his.13805]

89 **Vu T**, Yang S, Datta PK. MiR-216b/Smad3/BCL-2 Axis Is Involved in Smoking-Mediated Drug Resistance in Non-Small Cell Lung Cancer. *Cancers (Basel)* 2020; **12** [PMID: 32668597 DOI: 10.3390/cancers12071879]

90 **Dai YH**, Li XQ, Dong DP, Gu HB, Kong CY, Xu Z. P27 Promotes TGF-*β*-Mediated Pulmonary Fibrosis *via* Interacting with MTORC2. *Can Respir J* 2019; **2019**: 7157861 [PMID: 31641391 DOI: 10.1155/2019/7157861]

91 **Cheng Q**, Li C, Yang CF, Zhong YJ, Wu D, Shi L, Chen L, Li YW, Li L. Methyl ferulic acid attenuates liver fibrosis and hepatic stellate cell activation through the TGF-β1/Smad and NOX4/ROS pathways. *Chem Biol Interact* 2019; **299**: 131-139 [PMID: 30543783 DOI: 10.1016/j.cbi.2018.12.006]

92 **Sun C**, Wang FJ, Zhang HG, Xu XZ, Jia RC, Yao L, Qiao PF. miR-34a mediates oxaliplatin resistance of colorectal

cancer cells by inhibiting macroautophagy *via* transforming growth factor-β/Smad4 pathway. *World J Gastroenterol* 2017; **23**: 1816-1827 [PMID: 28348487 DOI: 10.3748/wjg.v23.i10.1816]

93 **Chen L**, Zhu Q, Lu L, Liu Y. MiR-132 inhibits migration and invasion and increases chemosensitivity of cisplatin-resistant oral squamous cell carcinoma cells *via* targeting TGF-β1. *Bioengineered* 2020; **11**: 91-102 [PMID: 31906769 DOI: 10.1080/21655979.2019.1710925]

94 **Teixeira AF**, Ten Dijke P, Zhu HJ. On-Target Anti-TGF-β Therapies Are Not Succeeding in Clinical Cancer Treatments: What Are Remaining Challenges? *Front Cell Dev Biol* 2020; **8**: 605 [PMID: 32733895 DOI: 10.3389/fcell.2020.00605]

95 **Makaremi S**, Asadzadeh Z, Hemmat N, Baghbanzadeh A, Sgambato A, Ghorbaninezhad F, Safarpour H, Argentiero A, Brunetti O, Bernardini R, Silvestris N, Baradaran B. Immune Checkpoint Inhibitors in Colorectal Cancer: Challenges and Future Prospects. *Biomedicines* 2021; **9** [PMID: 34572263 DOI: 10.3390/biomedicines9091075]

96 **Lynch D**, Murphy A. The emerging role of immunotherapy in colorectal cancer. *Ann Transl Med* 2016; **4**: 305 [PMID: 27668225 DOI: 10.21037/atm.2016.08.29]

97 **Wang QM**, Tang PM, Lian GY, Li C, Li J, Huang XR, To KF, Lan HY. Enhanced Cancer Immunotherapy with Smad3-Silenced NK-92 Cells. *Cancer Immunol Res* 2018; **6**: 965-977 [PMID: 29915022 DOI: 10.1158/2326-6066.CIR-17-0491]

98 **Huang J**, Chen X, Fu X, Li Z, Huang Y, Liang C. Advances in Aptamer-Based Biomarker Discovery. *Front Cell Dev Biol* 2021; **9**: 659760 [PMID: 33796540 DOI: 10.3389/fcell.2021.659760]

99 **Lee J**, Ryu M, Bae D, Kim HM, Eyun SI, Bae J, Lee K. Development of DNA aptamers specific for small therapeutic peptides using a modified SELEX method. J Microbiol 2022 [DOI: 10.1007/s12275-022-2235-4]

100 **Alhamhoom Y**, As Sobeai HM, Alsanea S, Alhoshani A. Aptamerbased therapy for targeting key mediators of cancer metastasis (Review). *Int J Oncol* 2022; **60** [PMID: 35425991 DOI: 10.3892/ijo.2022.5355]

101 **Ji X**, Wang H, Wu Z, Zhong X, Zhu M, Zhang Y, Tan R, Liu Y, Li J, Wang L. Specific Inhibitor of Smad3 (SIS3) Attenuates Fibrosis, Apoptosis, and Inflammation in Unilateral Ureteral Obstruction Kidneys by Inhibition of Transforming Growth Factor β (TGF-β)/Smad3 Signaling. *Med Sci Monit* 2018; **24**: 1633-1641 [PMID: 29555895 DOI: 10.12659/msm.909236]

102 **Wu N**, Lian G, Sheng J, Wu D, Yu X, Lan H, Hu W, Yang Z. Discovery of a novel selective water-soluble SMAD3 inhibitor as an antitumor agent. *Bioorg Med Chem Lett* 2020; **30**: 127396 [PMID: 32738967 DOI: 10.1016/j.bmcl.2020.127396]

103 **Zhang T**, Wang XF, Wang ZC, Lou D, Fang QQ, Hu YY, Zhao WY, Zhang LY, Wu LH, Tan WQ. Current potential therapeutic strategies targeting the TGF-β/Smad signaling pathway to attenuate keloid and hypertrophic scar formation. *Biomed Pharmacother* 2020; **129**: 110287 [PMID: 32540643 DOI: 10.1016/j.biopha.2020.110287]

104 **Zhang YF**, Zhou SZ, Cheng XY, Yi B, Shan SZ, Wang J, Li QF. Baicalein attenuates hypertrophic scar formation *via* inhibition of the transforming growth factor-β/Smad2/3 signalling pathway. *Br J Dermatol* 2016; **174**: 120-130 [PMID: 26301336 DOI: 10.1111/bjd.14108]

105 **Tang M**, Bian W, Cheng L, Zhang L, Jin R, Wang W, Zhang Y. Ginsenoside Rg3 inhibits keloid fibroblast proliferation, angiogenesis and collagen synthesis in vitro *via* the TGFβ/Smad and ERK signaling pathways. *Int J Mol Med* 2018; **41**: 1487-1499 [PMID: 29328420 DOI: 10.3892/ijmm.2018.3362]

106 **Dai G**, Sun B, Gong T, Pan Z, Meng Q, Ju W. Ginsenoside Rb2 inhibits epithelial-mesenchymal transition of colorectal cancer cells by suppressing TGF-β/Smad signaling. *Phytomedicine* 2019; **56**: 126-135 [PMID: 30668333 DOI: 10.1016/j.phymed.2018.10.025]

107 **Li H**, Yang L, Zhang Y, Gao Z. Kaempferol inhibits fibroblast collagen synthesis, proliferation and activation in hypertrophic scar *via* targeting TGF-β receptor type I. *Biomed Pharmacother* 2016; **83**: 967-974 [PMID: 27522259 DOI: 10.1016/j.biopha.2016.08.011]

108 **Bai X**, He T, Liu J, Wang Y, Fan L, Tao K, Shi J, Tang C, Su L, Hu D. Loureirin B inhibits fibroblast proliferation and extracellular matrix deposition in hypertrophic scar *via* TGF-β/Smad pathway. *Exp Dermatol* 2015; **24**: 355-360 [PMID: 25683490 DOI: 10.1111/exd.12665]

109 **Zhang Y**, Shan S, Wang J, Cheng X, Yi B, Zhou J, Li Q. Galangin inhibits hypertrophic scar formation *via* ALK5/Smad2/3 signaling pathway. *Mol Cell Biochem* 2016; **413**: 109-118 [PMID: 26728998 DOI: 10.1007/s11010-015-2644-3]

110 **Shi J**, Li J, Xu Z, Chen L, Luo R, Zhang C, Gao F, Zhang J, Fu C. Celastrol: A Review of Useful Strategies Overcoming its Limitation in Anticancer Application. *Front Pharmacol* 2020; **11**: 558741 [PMID: 33364939 DOI: 10.3389/fphar.2020.558741]

111 **Zhang L**, Liu J, Lin S, Tan J, Huang B, Lin J. Qingjie Fuzheng Granule Inhibited the Migration and Invasion of Colorectal Cancer Cells by Regulating the lncRNA ANRIL/let-7a/TGF-*β*1/Smad Axis. *Evid Based Complement Alternat Med* 2020; **2020**: 5264651 [PMID: 32714407 DOI: 10.1155/2020/5264651]

World Journal of Gastroenterology

Submit a Manuscript: https://www.f6publishing.com

World J Gastroenterol 2022 September 7; 28(33): 4762-4772

DOI: 10.3748/wjg.v28.i33.4762

ISSN 1007-9327 (print) ISSN 2219-2840 (online)

MINIREVIEWS

Immunological mechanisms of fecal microbiota transplantation in recurrent *Clostridioides difficile* infection

Lucas F Soveral, Gabriela G Korczaguin, Pedro S Schmidt, Isabel S Nunes, Camilo Fernandes, Carlos R Zárate-Bladés

Specialty type: Gastroenterology and hepatology

Provenance and peer review: Invited article; Externally peer reviewed.

Peer-review model: Single blind

Peer-review report's scientific quality classification

Grade A (Excellent): A
Grade B (Very good): B
Grade C (Good): C
Grade D (Fair): D
Grade E (Poor): 0

P-Reviewer: Chen Q, China; Tieranu CG, Romania; Zhang F, China

Received: March 12, 2022
Peer-review started: March 12, 2022
First decision: April 6, 2022
Revised: May 6, 2022
Accepted: August 16, 2022
Article in press: August 16, 2022
Published online: September 7, 2022

Lucas F Soveral, Gabriela G Korczaguin, Pedro S Schmidt, Isabel S Nunes, Camilo Fernandes, Carlos R Zárate-Bladés, Laboratory of Immunoregulation, Department of Microbiology, Immunology, and Parasitology, Center for Dysbiosis Control, Federal University of Santa Catarina, Florianopolis 88037-000, Brazil

Camilo Fernandes, Division of Infectious Diseases, Hospital Nereu Ramos, Florianopolis 88025-301, Brazil

Corresponding author: Carlos R Zárate-Bladés, MD, MSc, PhD, Assistant Professor, Laboratory of Immunoregulation, Department of Microbiology, Immunology, and Parasitology, Center for Dysbiosis Control, Federal University of Santa Catarina, CCB Novo, 8o andar, Rua da Prefeitura Universitária, Setor Córrego Grande, Campus UFSC, Florianopolis 88037-000, Brazil. zarate.blades@ufsc.br

Abstract

Fecal microbiota transplantation (FMT) is a successful method for treating recurrent *Clostridioides difficile* (*C. difficile*) infection (rCDI) with around 90% efficacy. Due to the relative simplicity of this approach, it is being widely used and currently, thousands of patients have been treated with FMT worldwide. Nonetheless, the mechanisms underlying its effects are just beginning to be understood. Data indicate that FMT effectiveness is due to a combination of microbiological direct mechanisms against *C. difficile*, but also through indirect mechanisms including the production of microbiota-derived metabolites as secondary bile acids and short chain fatty acids. Moreover, the modulation of the strong inflammatory response triggered by *C. difficile* after FMT seems to rely on a pivotal role of regulatory T cells, which would be responsible for the reduction of several cells and soluble inflammatory mediators, ensuing normalization of the intestinal mucosal immune system. In this minireview, we analyze recent advances in these immunological aspects associated with the efficacy of FMT.

Key Words: Fecal microbiota transplantation; Immunity; Mechanism; Dysbiosis; Pseudomembranous colitis; *Clostridioides difficile*

©The Author(s) 2022. Published by Baishideng Publishing Group Inc. All rights reserved.

Core Tip: Fecal microbiota transplantation (FMT) is an excellent treatment option of pseudomembranous colitis due to *Clostridiodes difficile* infection (CDI) because of its remarkable effectiveness. Moreover, FMT is a promising therapy for several other disorders in which dysbiosis is an important pathological factor. The mechanisms of FMT have begun to be dissected and include the restoration of the commensal microbial community structure and the modulation of several components of the immune system. This minireview focus on the FMT immune-related mechanisms for CDI.

Citation: Soveral LF, Korczaguin GG, Schmidt PS, Nunes IS, Fernandes C, Zárate-Bladés CR. Immunological mechanisms of fecal microbiota transplantation in recurrent *Clostridioides difficile* infection. *World J Gastroenterol* 2022; 28(33): 4762-4772
URL: https://www.wjgnet.com/1007-9327/full/v28/i33/4762.htm
DOI: https://dx.doi.org/10.3748/wjg.v28.i33.4762

INTRODUCTION

The human microbiota is a complex community of microorganisms that reside on the skin and mucosal surfaces, with gut microbiota being by far the most studied microbial subcommunity[1]. Firmicutes and Bacteroidetes are the most prevalent phyla in the human gut, followed by Actinobacteria and Proteobacteria[2]. Interestingly, mammals directly or indirectly receive signals from the microbiota for adequate development and functioning throughout life[3]. These signals are important for several systems of the human body. The interaction of the microbiota with the immune system is probably the best example of how important the commensal microbiota is for the host, given that the absence of microbiota results in an immune system with fewer and less varied components, as well as delayed immune responses[3,4]. Moreover, the presence of a normal microbiota restricts the colonization of pathogens by direct and indirect mechanisms. This function of the microbiota is known as colonization resistance[5,6]. Furthermore, the alteration of intestinal microbiota composition is called dysbiosis and commonly results in disease development.

CLOSTRIDIOIDES DIFFICILE INFECTION AND INTESTINAL DYSBIOSIS CORRECTION WITH FMT

Clostridioides difficile (*C. difficile*) is a spore-forming bacillus with the capacity to retain crystal violet staining, denoting that its cell wall is rich in peptidoglycans and, therefore, becomes positive in the staining procedure created by Hans Christian Gram in 1884[7]. Although *C. difficile* could be part of the intestinal commensal microbiota, toxin-producing strains are pathogenic. Nonetheless, the ingestion of toxin-producing *C. difficile* does not necessarily result in disease development because the microbiota is able to avoid colonization and overgrowth of this pathobiont[8]. However, *C. difficile* infection (CDI) is well known to occur due to a combination of two factors: (1) Ingestion of the bacillus spores during hospitalization, where the circulation of strains capable of expressing toxins A, B, and C - which damage the intestinal epithelium - is more common; and (2) Receiving or having recently received broad-spectrum antibiotic therapy, which will cause intestinal dysbiosis[8,9]. Thus, antibiotic exposure followed by acute episodes of diarrhea is the main clinical indicator of CDI. The detection of toxins associated with colonoscopic and/or histopathologic findings will confirm the diagnosis of pseudomembranous colitis[10]. Elderly persons are more affected by the disease; however, CDI is becoming more frequent in younger populations and with no association with previous hospitalizations[8,11]. The emergence of hypervirulent and antibiotic-resistant *C. difficile* strains contributed to the burden of worldwide cases of antibiotic-associated diarrhea and pseudomembranous colitis[8,10]. In fact, CDI may range from mild or self-limiting diarrhea to severe cases and the development of sequelae, including toxic megacolon and fulminant colitis. CDI is commonly treated by antibiotics (Metronidazole, Vancomycin, and Fidaxomicin) with efficacy rates ranging from 76% (Metronidazole) to as high as 97% (Vancomycin and Fidaxomicin)[12,13]. However, as with many other broad-spectrum antibiotics, *C. difficile* can also develop resistance mechanisms to these and other antibiotics[14]. Furthermore, antibiotic therapy, which treats CDI, will enhance dysbiosis and will predispose the patient to CDI relapse[15]. In fact, it is well known that 20%-30% of antibiotic-treated CDI cases subsequently develop recurrent episodes of the infection (rCDI)[16-18].

FMT is primarily indicated for treating pseudomembranous colitis due to rCDI[19,20]. The use of FMT for rCDI is based on several studies reporting the effectiveness of FMT, supporting it as the most effective treatment for this disease. In a systematic review on FMT effectiveness against rCDI that included 45 studies (36 cohort studies and nine randomized clinical trials), it was shown that FMT has

91% effectiveness after eight weeks of repeated treatment - far superior to the use of antibiotics[21]. According to the United States Food and Drug Administration, FMT may be performed after two failed courses of antibiotics[22]. The fecal material for FMT may be obtained from a relative or unrelated donor and administered using a nasogastric or nasoduodenal tube or by colonoscopy[19,20,23,24]. More recently, successful FMT treatments using lyophilized solutions and capsules have been reported[25-27]. Commonly, the administration of one or two courses of FMT results in clinical remission as early as one day after the first FMT[23,24,28]. Its effects are based mainly on the restoration of eubiosis[29]. This implies that FMT effectiveness relies on microbiologic mechanisms, or in other words, the restoration of colonization-resistance-related mechanisms[30-32]. However, indirect mechanisms of colonization resistance include the crosstalk with different components of the immune system, which will be important for both maintaining the integrity of the intestinal mucosa or restoring that integrity if the disease is already present, as is the case of pseudomembranous colitis due to CDI[9,33].

Notably, FMT restores the capacity of the microbial community to convert primary bile acids (BAs) into secondary BAs, such as deoxycholic acid and ursodeoxycholic acid, which can inhibit *C. difficile* germination and epithelial apoptosis[34]. Although not directly shown in FMT, the optimal biotransformation of BAs by microbiota also modulates the repertoire and functions of colonic RORγt+ T regulatory (Treg) cells, contributing to intestinal homeostasis[35]. Moreover, higher levels of primary BAs in the stool, such as taurocholic acid - which can promote the spore germination of *C. difficile* - have been reported in rCDI patients compared to healthy individuals as well as compared to patients experiencing their first episode of CDI[36]. This is compatible with the bile salt hydrolase (*BSH*) gene abundance reduction - which metabolizes BAs - in rCDI patients compared to healthy and first episode CDI individuals[24]. Furthermore, BSH functional activity is rapidly restored in rCDI patients after FMT [23]. Taken together, these data indicate that gut microbial BAs metabolism is one of the molecular mechanisms of FMT to successfully treat rCDI.

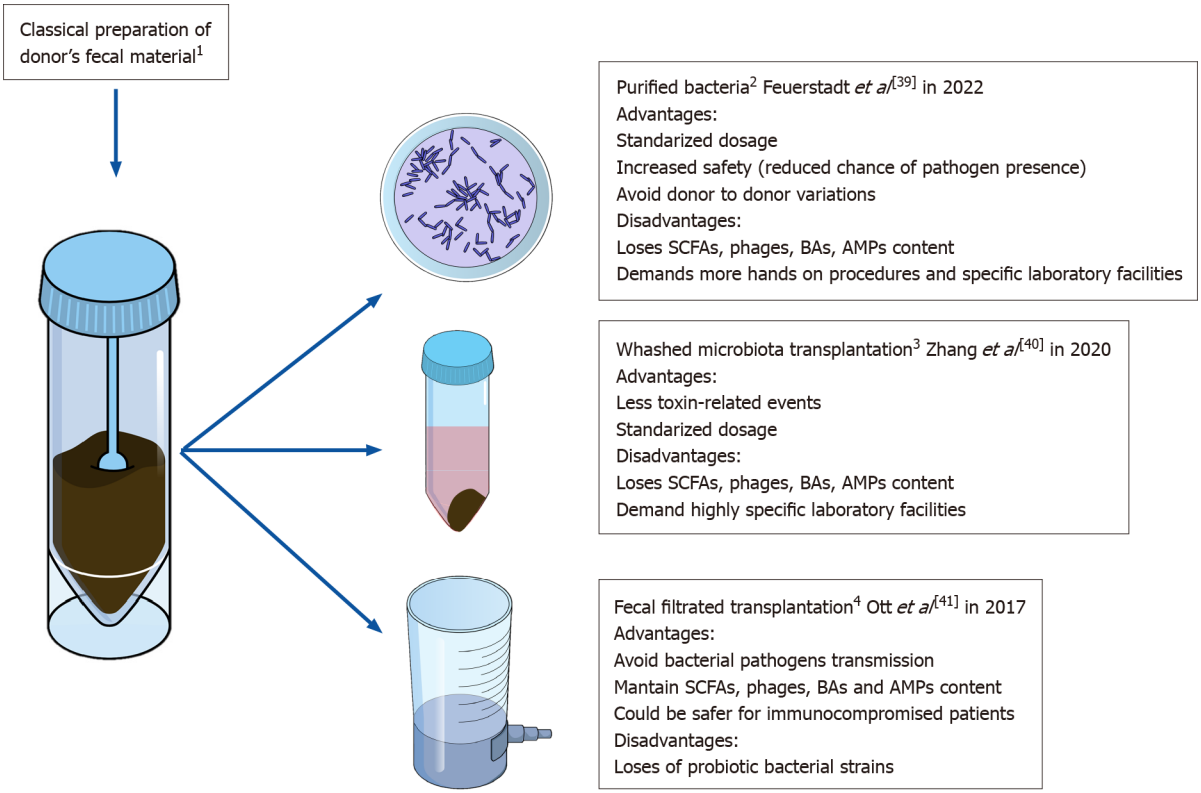
Similarly, the recovery of microbiota functions after FMT is linked to the repopulation of short-chain fatty acids (SCFAs) producer bacteria - mainly members of the Clostridiales clade that include several butyrate producers[37]. SCFAs are known to serve as the main source of energy for colonocytes but also play a role in homeostasis maintenance, inducing the differentiation into effector and Treg cells in the intestinal lamina propria (LP)[38]. BAs and SCFAs are bacterial metabolites with pleiotropic effects on the immune system but, acting together, they may play a crucial role in reducing the inflammation in the intestine after FMT[35].

One important aspect of FMT refers to means of improving it by using simpler preparations that could offer more standardized formulations, being more patient-friendly, and avoiding any type of potential risks by not using an undefined combination of living microorganisms, as is the case with FMT. In this regard, Feuerstadt *et al*[39] have recently reported the use of oral capsules composed of live purified Firmicute bacterial spores in a phase 3 clinical trial of patients with rCDI. Of the 89 patients treated with this formulation and followed for eight weeks, they observed recurrence in 11 patients (12%) compared to 37 patients (40% of recurrence) in the placebo group[39].

On the other hand, Zhang *et al*[40] proposed to submit the fecal material of standard FMT to a combinatorial method of filtration and centrifugation to offer a safer, more precise and quality-controllable microbiome transplant. The authors called this material "washed microbiota transplantation" (WMT) and provided evidence of reduced levels of pro-inflammatory molecules such as leukotriene B4, corticosterone, and prostaglandin G2 in mice which were intraperitoneally injected with WMT. Despite that washed microbiota has been used successfully to treat ulcerative colitis and Crohn's disease since 2014, it has not been evaluated in the context of rCDI[40].

Interestingly, Ott *et al*[41] showed that a single administration of sterile fecal filtrate (FFT), which contains bacterial components, bacteriophages, and bacteriocins but not whole bacterial cells, was able to eliminate symptoms and avoided the recurrence of CDI in 5 patients. This finding could overturn the necessity of living bacteria and successful engraftment of donor microbiota to reach the protective effect of FMT in rCDI patients. A possible explanation for this result could be that bacteria cell wall components and DNA fragments, which remain after filtration, stimulate the host's innate immune responses, with subsequent reprogramming of the mucosal immune mechanisms against the pathogen while promoting the restoration of homeostasis. The authors also proposed an additional explanation in which the massive transfer of bacteriophages from the donor to the host would be able to correct dysbiosis in rCDI patients. Although the study does not assess BAs or SCFAs content in the FFT, it is reasonable to consider that these metabolites could also participate in the effects reached by FFT since they are expected to persist after the filtration process. The absence of potential bacterial pathogens in the transplanted material - as is the case when using FFT - could represent an important advantage for the use of FFT in immunodeficient patients instead of living bacteria. In addition, FFT could also be better standardized. Therefore, FFT needs to be explored in detail in a larger group of patients and compared to FMT. Figure 1 summarizes these FMT variations and their key features.

Taking together all these studies, one may conclude that immune pathways activated during the response to *C. difficile* are important not only to identify the mechanisms that effectively contribute to its elimination but also to determine which immune components are activated or respond to FMT.



DOI: 10.3748/wjg.v28.i33.4762 **Copyright** ©The Author(s) 2022.

Figure 1 Advantages and disadvantages of non-classical preparations methods of donor's fecal material prior to fecal microbiota transplantation. [1]Classical preparation consist in dissolve donor's fecal material by blending with saline water and filter out residual solid feces through gauze or fabric. [2]Isolation of different bacteria strains directly from donor's fecal material. [3]Basically, this method consists in consecutively centrifugation of microbiota from donors to remove the supernadants. [4]Uses filtration systens to retain debris and bacterial load from the donor's fecal material. SCFAs: Short-chain fatty acids; AMPs: Antimicrobial peptides; BAs: Bile acids.

ESSENTIAL CONCEPTS OF THE IMMUNE RESPONSE DURING CDI

As there are recent and excellent reviews on the immune response to *C. difficile*[10,42,43], in this section, we present the main characteristics of this host-pathogen interaction.

The immune response to *C. difficile* is characterized by the development of an inflammatory reaction with Th1 and Th17 components. This response starts with bacterial sensing by epithelial cells and the release of interleukin (IL)-1 and IL-8 with high capacity to attract neutrophils[44,45]. Type-1 innate lymphoid cells (ILC-1) also participate in the response by secreting interferon-γ (IFN-γ)[46]. Antigen-presenting cells (APCs), including macrophages and dendritic cells (DCs), are important to capture and process *C. difficile* antigens, migrate to draining lymph nodes, and activate specific T cells[47]. Under these circumstances, Th1 cells are generated, but the secretion of IL-6 and IL-23 provide sufficient stimuli for the expansion of Th17 cells[48]. While these aspects of the immune response could be pivotal for appropriate enhancement of several bacteria-killing mechanisms by innate cells, it is already known that an exacerbated immune response signifies the development of pseudomembranous colitis, which is the histopathological lesion caused by the inflammatory response taking place in the colon[49]. To avoid the development of an immunopathological response, two important branches of immunity are required. First, the activation of Treg cells with the secretion of immune regulatory cytokines IL-10 and transforming growth factor-β (TGF-β)[50]. The source of these regulatory cytokines may also be enriched from other cell subsets such as intestinal epithelial cells, for example, which have the ability to secrete relevant quantities of TGF-β[50,51]. Secondly, recent studies have indicated the importance of active Th2 components present in patients with CDI who do not develop histopathological lesions but, instead, resolve the infection. These elements include mainly ILC-2 and eosinophils as the main cell populations[52,53], as well as type 2 cytokines, including IL-4, IL-5, IL-13, IL-25, and IL-33[54-56].

While the participation of Th1, Th17, and Treg cells during the response to bacteria with the characteristics of *C. difficile* is easy to understand, the type 2 component - which appears to have remarkable importance for the host to avoid an overreacting inflammatory response - is unexpected. Therefore, the antigenic components responsible for the activation of ILC-2 and eosinophils during CDI are new essential factors to be identified to better understand the effective immune response against *C. difficile*.

Table 1 Main clinical and experimental studies about the immunological mechanisms associated to fecal microbiota transplantation efficacy

Ref.	Model / clinical study	Main findings
Ekmekciu *et al*[57], 2017	Mice treated with antibiotic cocktail followed by FMT	Recovery of INF-γ, IL-17, IL-22 and IL-10 producer CD4+ T cells in intestinal LP. FMT failed to recover CD8+ T and B cells in LP after antibiotic exposure
Burrello *et al* [58], 2018	Mice treated with DSS followed by oral gavage of mucus and feces from healthy mice	Treatment increased Camp, S100A8, Muc1 and Muc4, reduced MHC-II+ cells and normalized populations of ILC-2, ILC-3, F4/80+ macrophages and CD11b+ Ly6G+ neutrophils
	In vitro stimulation of LPMCs stimulated with FMT or DSS-derived microbiota	FMT reduced IL-1β, TNF-α and IFN-γ and increased IL-10
	IL-10 receptor blockade in DSS mice prior of FMT treatment	Blockade of IL-10 resulted in reduction in colon length, increased weight loss and expression of *IL-1β, TNF and IFNγ* genes
Littmann *et al*[59], 2021	Use of different KO mice to evaluate B and T (CD8+, Th1, Th17 and Treg) cells	Treg cells play a pivotal role for FMT to achieve the effects against CDI
Monaghan *et al*[60], 2021	Multiomic analysis of fecal, sera and PBMC samples of patients with severe (n = 3) or fulminant (n = 1) CDI treated with FMT in 6 occasions plus fidaxomicin (severe cases) or vancomycin and metronidazole (fulminant case)	One patient (severe CDI) did not respond to treatment. The fulminant case responded after FMT in 10 occasions plus antibiotics. 78 features were identified differentiating responders to the non-responder. Non responsiveness was associated to higher levels of MMP-2, TWEAK, IL-26, sTNF-R1, sTNF-R2, effector memory CD8 T cells and circulation of senescent T cells; and lower TCR diversity repertoire, B cell and regulatory B cell frequencies

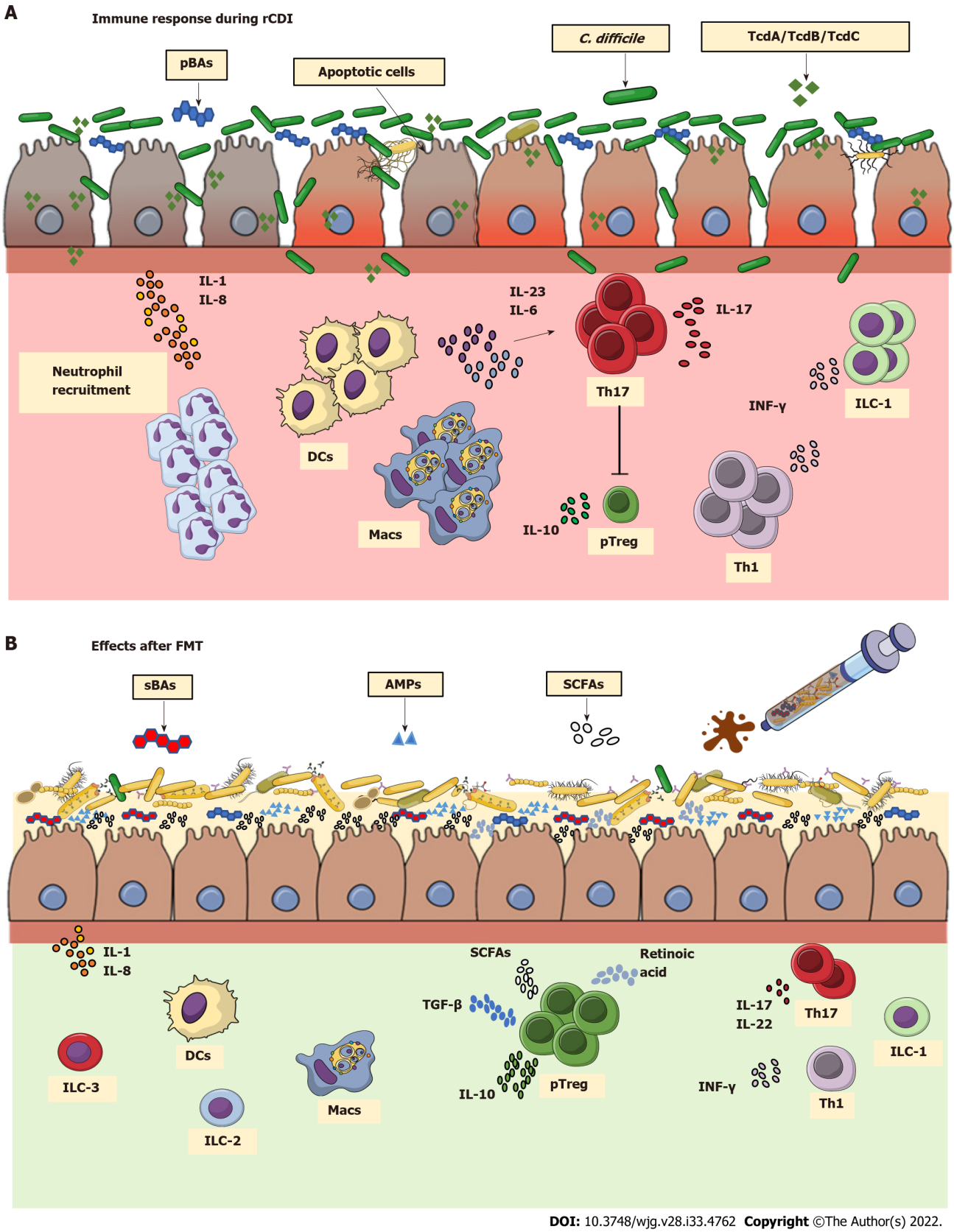
IL: Interleukin; FMT: Fecal microbiota transplantation; INF: Interferon; LP: Lamina propria; DSS: Dextran sodium sulfate; LPMCs: Lamina propria mononuclear cells; Muc: Mucin; TNF: Tumor necrosis factor; Treg: T regulatory; KO: Knockout; CDI: *Clostridioides difficile* infection; PBMC: Peripheral blood mononuclear cell; ILC: Innate lymphoid cells.

IMMUNOLOGICAL EFFECTS ASSOCIATED WITH FMT EFFICACY TO TREAT RCDI

One important attempt to gain knowledge to elucidate the immunological events elicited by FMT to successfully treat rCDI was made by Ekmekciu *et al*[57]. In this article, the investigators evaluated the effects on the immune system of mice treated for eight weeks with a cocktail of five antibiotics followed by FMT to resolve the dysbiosis caused by the antibiotic exposure. After successfully showing the depletion of the intestinal microbiota and reduction of proliferating cells in the intestines, as well as the restoration of both parameters soon after FMT, the authors evaluated different populations of the immune system. The investigators found that CD4+ T lymphocyte frequencies decreased after antibiotic treatment in the gut LP and mesenteric lymph nodes and presented recovery from the seventh day after FMT. Paradoxically, the absolute number of CD4+ T lymphocytes increased in the spleen and did not return to normal levels 28 d after FMT. CD8+ T cells showed the same profile as CD4+ T cells in LP, mesenteric lymph nodes, and the spleen, but not in the colon. The number of colonic CD8+ T cells presented a huge reduction after the antibiotic treatment, and FMT failed to induce the recovery of these cells. In parallel, B cells presented equivalent alterations to those of T cells in the gut (including an important reduction in the colon with no recovery after FMT), mesenteric lymph nodes, and the spleen, yet only in absolute cell numbers and not in cell frequencies[57].

The microbiota depletion due to the antibiotic treatment also resulted in a reduction of T cells with memory/effector phenotype ($CD44^{hi}$), Tregs, and co-stimulatory molecules in DCs, with the restoration of all these parameters after FMT. The authors also found that IFN-γ, IL-17, IL-22, and IL-10-producing T cells decreased with antibiotic treatment but were restored with FMT[57].

Subsequently, using the classical dextran sodium sulfate (DSS) colitis model, Burrello *et al*[58] provided a more profound and dynamic analysis of the effects of FMT in resolving intestinal inflammation. They used the $CXCR6^{egfp}$ reporter mice, in which T cells may be tracked, including the invariant natural killer T cell population. The investigators treated mice with DSS for seven days and, after a two-day recovery period, the mice received FMT on three consecutive days. The mice received a preparation of intestinal mucus on the first day and feces from healthy donor mice on the second and third days. Evaluations were performed one and five days after the last FMT. They found that FMT reduced the production of IL-1β and increased the production of antimicrobial peptides (Camp and S100A8) and mucins (Muc1 and Muc4), all in the colonic epithelium. In parallel, they observed effects on the innate and adaptive immune systems in DSS colitic mice treated with FMT. In the innate immune system, DSS inflammation induced the expansion of ILC-2 and ILC-3, F4/80+ macrophages, and CD11β+ Ly6G+ neutrophils, followed by a reduction of these populations after FMT. Furthermore, FMT strongly reduced MHC-II+ cells, indicating that the bacteriotherapy also affected APCs. These observations were correlated with the evaluation of LP mononuclear cells (LPMCs) stimulated with FMT or DSS-derived microbiota, *in vitro*. They found that innate and adaptive LPMCs stimulated with FMT-derived microbiota produced less IL-1β, tumor necrosis factor-α, and IFN-γ pro-inflammatory cytokines while increasing the production of IL-10. Moreover, the investigators went further, attempting to determine



DOI: 10.3748/wjg.v28.i33.4762 **Copyright** ©The Author(s) 2022.

Figure 2 The immune response during recurrent *Clostridioides difficile* infection and after fecal microbiota transplantation treatment. A: During recurrent *Clostridioides difficile* (*C. difficile*) infection, the depletion of commensal microbiota results in higher levels of primary bile acids (BAs). These molecules are known to trigger the *C. difficile* vegetative state and its expansion, resulting in production of toxin (Tcd) A, TcdB, and TcdC, which cause apoptosis of enterocytes and release of interleukin (IL)-1 and IL-8 in the lamina propria (LP). Consequently, there is extensive recruitment of neutrophils dendritic cells, and macrophages and type 1 innate lymphocytes (ILC-1) in an attempt to cope with the infection. These cells produce pro-inflammatory cytokines including IL-6, IL-23, interferon (IFN)-γ, which induce Th17 and Th1 differentiation. This inflammatory state dominated by IL-17 and IFN-γ promotes tissue damage, which could spread along the intestines, and is accompanied with absence of innate ILC-2 and reduction of peripheral T regulatory (Treg) cells; B: The therapeutic effects of FMT involve

the reestablishment of a wide variety of commensal microorganisms that directly and indirectly antagonize *C. diffcile*. Commensal strains that produce secondary Bas and short chain fatty acids are re-established, as well as the production of antimicrobial peptides by epithelial cells together with the reconstitution of the barrier integrity. These effects allow to reduce the activation of innate immunocytes, the expansion of Treg cells which produce IL-10, and subsequent normalization of Th1 and Th17 cell frequencies in the LP. IL: Interleukin; FMT: Fecal microbiota transplantation; TNF: Tumor necrosis factor; INF: Interferon; SCFAs: Short-chain fatty acids; AMPs: Antimicrobial peptides; TGF: Transforming growth factor; pBAs: Primary bile acids; sBAs: Secondary bile acids; DCs: Dendritic cell; ILC: Innate lymphoid cells; rCDI: Recurrent *Clostridioides difficile* infection; Treg: T regulatory; Macs: Macrophages.

the importance of IL-10 secretion for the beneficial effects of FMT to treat DSS colitis. Using a concomitant administration of IL-10 blockade in DSS mice during the FMT treatment, the authors demonstrated the pivotal importance of this regulatory cytokine for inflammation resolution, including the normalization of the histological score and intestinal weight[58].

More recently, Littmann *et al*[59] were able to confirm the importance of IL-10-producing cells for the host to be able to respond effectively to FMT. Their 2021 report started by considering that if the host immune system is not important for FMT to resolve the intestinal inflammation during CDI, then immune-deficient mice should be equally effective as wild-type animals to respond to FMT. To test their hypothesis, they used *Rag1* double knockout animals (*Rag1*$^{-/-}$), which lack T and B cells, and compared CDI course before and after FMT. They observed that CDI persisted in *Rag1*$^{-/-}$ animals but not in wild-type (WT) littermates nor *Rag1*^{HET} controls. Importantly, they confirmed this observation by excluding the possibility that the microbiota composition of *Rag1*$^{-/-}$, which is known to be different from the microbiota of *Rag1*^{HET} mice, was indeed the reason for the differential responses to FMT. They were able to do so by performing three additional control experiments. First, they analyzed and compared the microbiota composition of *Rag1*$^{-/-}$, *Rag1*^{HET}, and WT mice. Second, they transferred WT or *Rag1*$^{-/-}$ microbiota to antibiotic-treated *Rag1*$^{-/-}$ and *Rag1*^{HET} mice. Third, they employed germ-free C57BL/6 mice, which were cohoused with *Rag1*$^{-/-}$ or *Rag1*^{HET} mice. These mice were treated with antibiotics, infected with *C. difficile*, and then treated with FMT. All these experiments confirmed that the difference in the responses to FMT in *Rag1-/-* or *Rag1*^{HET} depended on an adaptive immune cell population and not on differences in microbiome composition prior to FMT. Next, the investigators focused on determining which adaptive immune cell population is important for FMT efficacy. By using specific knock-out animals, they excluded the importance of B cells, CD8+ T cells, Th17, and Th1 CD4+ cells. In contrast, the transient specific ablation of Treg cells using the diphtheria toxin Foxp3-DTR mice demonstrated that Treg cells are pivotal to observing the effects of FMT against CDI. Moreover, Littman *et al*[59] also showed that FMT engraftment is different depending on the immune activation status of the host, as well as that the microbiota post-FMT is metabolically distinct depending on the functionality of the host immune system.

Finally, Monaghan *et al*[60] performed a systems biology-based study to interrogate the interaction among microbiome-metabolome-immune system in the context of FMT applied to patients with severe or fulminant CDI. They studied four patients unresponsive to antibiotic therapy and treated with sequential FMT. Three patients were responders against one non-responder. The evaluations included microbiome and associated metabolome profile in fecal samples as well as the evaluation of blood samples to access the epigenomic, metabolomic, glycomic, immune proteomic, immunophenotyping, functional immune assays, and the T cell receptor repertoire. Although the small sample size did not allow the authors to draw clear conclusions, they suggest that immunosenescent signals could be associated with non-responsiveness to FMT, since they found strong correlations between peripheral senescent T cells and host factors including butyrate, serum hydroxybutyrate, fecal urso- iso- and hyodeoxycholic acids, serum immunoglobulin G Fc N-glycopeptides, and microbial taxa including *Pseudomonas* at the genus level[60]. The main findings of the studies recently discussed are listed in Table 1.

In summary, the studies described here indicate that FMT effectiveness rely not only on the capacity of donor eubiotic microbiota to be able to expulse *C. difficile*, but also to produce key metabolic products as secondary BAs and SCFAs. These metabolites, together with the displacement of the pathogen which represents less injury and consequently reduction of pathogen-derived antigens for innate and adaptive immunity activation, allow Treg cells to expand and increase the production of IL-10. This regulatory activity becomes pivotal for different types of immune cell populations and their produced cytokines to return to normal levels dampening inflammation, as shown in Figure 2.

CONCLUSION

The findings discussed here provide a new perspective on the therapeutic effects of FMT to restore eubiosis. This ability refers, in our opinion, two key aspects: (1) The material to be transplanted must contain the appropriate elements to displace the pathogen and modulate the immune system of the patient effectively; and (2) The status of the immune system of the patient is decisive at the moment of receiving the transplant, which means that the patient's immune system must be able to respond

adequately to the FMT stimuli.

FMT is an effective option for the resolution of rCDI and is being used around the world increasingly. Moreover, recent studies show its efficacy in treating the first episode of CDI as well as its repeated use can treat severe and fulminant CDI forms[60]. Although the concept of the method is simple, it is a labor-intensive procedure and requires the acceptance of the patient to be treated with this kind of transplant, even if FMT-derived capsules are used. Nonetheless, as FMT is increasingly showing its benefits in a variety of clinical situations (*e.g.*, autism spectrum disorders, type 2 diabetes, and, of course, different types of inflammatory bowel diseases), this should guarantee not only the continuing use of FMT but also the advancement of basic research seeking to identify the molecular microbiological components that are pivotal for FMT efficacy. In addition, the new evidence discussed here shows the importance of disclosing in detail the immunological pathways that must be activated/deactivated during the FMT process. At the same time, it is necessary to consider that several of these observations came from animal studies, and where FMT was used to treat colitis induced by DSS or antibiotic cocktails but not by *C. difficile* infection. Nonetheless, all these efforts should lead to the identification of molecular factors that may become candidates for the development of new and more conventional therapeutic products that could replace FMT in the future or improve its results.

FOOTNOTES

Author contributions: Soveral LF, Korczaguin GG, and Schmidt PS collected the literature and wrote the first draft, conceptualized the table and figures, and contributed equally to this work; Nunes IS and Fernandes C corrected the first draft; Zárate-Bladés CR conceptualized the structure of the text and critically revised the manuscript for important intellectual content; and all authors read and approved the final version of the manuscript.

Supported by the grant "Programa de ciência tecnologia e inovação aos grupos de pesquisa da Universidade Federal de Santa Catarina", FAPESC (2021TR000301); Soveral LF is a graduate student fellow of Fundação de Amparo à Pesquisa e Inovação do Estado de Santa Catarina, FAPESC (3003/2021); Schmidt PS is student fellow of Programa Institucional de Iniciação Cientifica e Tecnológica, PIBIC of the Conselho Nacional de Desenvolvimento Científico e Tecnológico, CNPq (2021/949248); Nunes IS is a graduate student fellow of Coordenação de Aperfeiçoamento de Pessoal de Nível Superior, CAPES (202003075).

Conflict-of-interest statement: All the authors report no relevant conflicts of interest for this article.

Open-Access: This article is an open-access article that was selected by an in-house editor and fully peer-reviewed by external reviewers. It is distributed in accordance with the Creative Commons Attribution NonCommercial (CC BY-NC 4.0) license, which permits others to distribute, remix, adapt, build upon this work non-commercially, and license their derivative works on different terms, provided the original work is properly cited and the use is non-commercial. See: https://creativecommons.org/Licenses/by-nc/4.0/

Country/Territory of origin: Brazil

ORCID number: Lucas F Soveral 0000-0003-4373-9027; Gabriela G Korczaguin 0000-0002-1453-7816; Pedro S Schmidt 0000-0002-4348-3319; Isabel S Nunes 0000-0003-1730-3529; Camilo Fernandes 000-0003-3603-6155; Carlos R Zárate-Bladés 0000-0002-7728-7869.

S-Editor: Wang JJ
L-Editor: A
P-Editor: Wang JJ

REFERENCES

1 **Ursell LK**, Metcalf JL, Parfrey LW, Knight R. Defining the human microbiome. *Nutr Rev* 2012; **70** Suppl 1: S38-S44 [PMID: 22861806 DOI: 10.1111/j.1753-4887.2012.00493.x]
2 **Ruan W**, Engevik MA, Spinler JK, Versalovic J. Healthy Human Gastrointestinal Microbiome: Composition and Function After a Decade of Exploration. *Dig Dis Sci* 2020; **65**: 695-705 [PMID: 32067143 DOI: 10.1007/s10620-020-06118-4]
3 **Thursby E**, Juge N. Introduction to the human gut microbiota. *Biochem J* 2017; **474**: 1823-1836 [PMID: 28512250 DOI: 10.1042/BCJ20160510]
4 **Belkaid Y**, Harrison OJ. Homeostatic Immunity and the Microbiota. *Immunity* 2017; **46**: 562-576 [PMID: 28423337 DOI: 10.1016/j.immuni.2017.04.008]
5 **Bohnhoff M**, Drake BL, Miller CP. Effect of streptomycin on susceptibility of intestinal tract to experimental Salmonella infection. *Proc Soc Exp Biol Med* 1954; **86**: 132-137 [PMID: 13177610 DOI: 10.3181/00379727-86-21030]
6 **van der Waaij D**, Berghuis-de Vries JM, Lekkerkerk Lekkerkerk-v. Colonization resistance of the digestive tract in conventional and antibiotic-treated mice. *J Hyg (Lond)* 1971; **69**: 405-411 [PMID: 4999450 DOI: 10.1017/S0022172400021653]

7 **Breakwell DP**, Moyes RB, Reynolds J. Differential staining of bacteria: capsule stain. *Curr Protoc Microbiol* 2009; **Appendix** 3: Appendix 3I [PMID: 19885936 DOI: 10.1002/9780471729259.mca03is15]

8 **Czepiel J**, Dróżdż M, Pituch H, Kuijper EJ, Perucki W, Mielimonka A, Goldman S, Wultańska D, Garlicki A, Biesiada G. Clostridium difficile infection: review. *Eur J Clin Microbiol Infect Dis* 2019; **38**: 1211-1221 [PMID: 30945014 DOI: 10.1007/s10096-019-03539-6]

9 **Kim S**, Covington A, Pamer EG. The intestinal microbiota: Antibiotics, colonization resistance, and enteric pathogens. *Immunol Rev* 2017; **279**: 90-105 [PMID: 28856737 DOI: 10.1111/imr.12563]

10 **Frisbee AL**, Petri WA Jr. Considering the Immune System during Fecal Microbiota Transplantation for Clostridioides difficile Infection. *Trends Mol Med* 2020; **26**: 496-507 [PMID: 32359480 DOI: 10.1016/j.molmed.2020.01.009]

11 **Ogielska M**, Lanotte P, Le Brun C, Valentin AS, Garot D, Tellier AC, Halimi JM, Colombat P, Guilleminault L, Lioger B, Vegas H, De Toffol B, Constans T, Bernard L. Emergence of community-acquired Clostridium difficile infection: the experience of a French hospital and review of the literature. *Int J Infect Dis* 2015; **37**: 36-41 [PMID: 26092300 DOI: 10.1016/j.ijid.2015.06.007]

12 **Zar FA**, Bakkanagari SR, Moorthi KM, Davis MB. A comparison of vancomycin and metronidazole for the treatment of Clostridium difficile-associated diarrhea, stratified by disease severity. *Clin Infect Dis* 2007; **45**: 302-307 [PMID: 17599306 DOI: 10.1086/519265]

13 **Okumura H**, Fukushima A, Taieb V, Shoji S, English M. Fidaxomicin compared with vancomycin and metronidazole for the treatment of Clostridioides (Clostridium) difficile infection: A network meta-analysis. *J Infect Chemother* 2020; **26**: 43-50 [PMID: 31624029 DOI: 10.1016/j.jiac.2019.07.005]

14 **Spigaglia P**. Recent advances in the understanding of antibiotic resistance in Clostridium difficile infection. *Ther Adv Infect Dis* 2016; **3**: 23-42 [PMID: 26862400 DOI: 10.1177/2049936115622891]

15 **Kachrimanidou M**, Tsintarakis E. Insights into the Role of Human Gut Microbiota in *Clostridioides difficile* Infection. *Microorganisms* 2020; **8** [PMID: 32023967 DOI: 10.3390/microorganisms8020200]

16 **Garey KW**, Sethi S, Yadav Y, DuPont HL. Meta-analysis to assess risk factors for recurrent Clostridium difficile infection. *J Hosp Infect* 2008; **70**: 298-304 [PMID: 18951661 DOI: 10.1016/j.jhin.2008.08.012]

17 **Kelly CP**. Can we identify patients at high risk of recurrent Clostridium difficile infection? *Clin Microbiol Infect* 2012; **18** Suppl 6: 21-27 [PMID: 23121551 DOI: 10.1111/1469-0691.12046]

18 **Maroo S**, Lamont JT. Recurrent clostridium difficile. *Gastroenterology* 2006; **130**: 1311-1316 [PMID: 16618421 DOI: 10.1053/j.gastro.2006.02.044]

19 **Vindigni SM**, Surawicz CM. Fecal Microbiota Transplantation. *Gastroenterol Clin North Am* 2017; **46**: 171-185 [PMID: 28164849 DOI: 10.1016/j.gtc.2016.09.012]

20 **Cammarota G**, Ianiro G, Tilg H, Rajilić-Stojanović M, Kump P, Satokari R, Sokol H, Arkkila P, Pintus C, Hart A, Segal J, Aloi M, Masucci L, Molinaro A, Scaldaferri F, Gasbarrini G, Lopez-Sanroman A, Link A, de Groot P, de Vos WM, Högenauer C, Malfertheiner P, Mattila E, Milosavljević T, Nieuwdorp M, Sanguinetti M, Simren M, Gasbarrini A; European FMT Working Group. European consensus conference on faecal microbiota transplantation in clinical practice. *Gut* 2017; **66**: 569-580 [PMID: 28087657 DOI: 10.1136/gutjnl-2016-313017]

21 **Baunwall SMD**, Lee MM, Eriksen MK, Mullish BH, Marchesi JR, Dahlerup JF, Hvas CL. Faecal microbiota transplantation for recurrent *Clostridioides difficile* infection: An updated systematic review and meta-analysis. *EClinicalMedicine* 2020; **29-30**: 100642 [PMID: 33437951 DOI: 10.1016/j.eclinm.2020.100642]

22 **Bakken JS**, Borody T, Brandt LJ, Brill JV, Demarco DC, Franzos MA, Kelly C, Khoruts A, Louie T, Martinelli LP, Moore TA, Russell G, Surawicz C; Fecal Microbiota Transplantation Workgroup. Treating Clostridium difficile infection with fecal microbiota transplantation. *Clin Gastroenterol Hepatol* 2011; **9**: 1044-1049 [PMID: 21871249 DOI: 10.1016/j.cgh.2011.08.014]

23 **Vanny P**, Machiavelli A, Wippel C, De andrade J, Zamparette C, Tartari D, Sincero T, Pinto A, Zárate-Bládes CR. Therapeutic Use of Commensal Microbes: Fecal/Gut Microbiota Transplantation. In: Atta-ur-Rahman FRS. Frontiers in Clinical Drug Research - Anti-Infectives: Volume 5. Sharjah: Bentham Science Publishers, 2018: 41-110

24 **Rossen NG**, MacDonald JK, de Vries EM, D'Haens GR, de Vos WM, Zoetendal EG, Ponsioen CY. Fecal microbiota transplantation as novel therapy in gastroenterology: A systematic review. *World J Gastroenterol* 2015; **21**: 5359-5371 [PMID: 25954111 DOI: 10.3748/wjg.v21.i17.5359]

25 **Vigvári S**, Sipos D, Solt J, Vincze Á, Kocsis B, Nemes Z, Kappéter Á, Feiszt Z, Kovács B, Péterfi Z. Faecal microbiota transplantation for Clostridium difficile infection using a lyophilized inoculum from non-related donors: A case series involving 19 patients. *Acta Microbiol Immunol Hung* 2019; **66**: 69-78 [PMID: 29239198 DOI: 10.1556/030.64.2017.042]

26 **Youngster I**, Mahabamunuge J, Systrom HK, Sauk J, Khalili H, Levin J, Kaplan JL, Hohmann EL. Oral, frozen fecal microbiota transplant (FMT) capsules for recurrent Clostridium difficile infection. *BMC Med* 2016; **14**: 134 [PMID: 27609178 DOI: 10.1186/s12916-016-0680-9]

27 **Varga A**, Kocsis B, Sipos D, Kása P, Vigvári S, Pál S, Dembrovszky F, Farkas K, Péterfi Z. How to Apply FMT More Effectively, Conveniently and Flexible - A Comparison of FMT Methods. *Front Cell Infect Microbiol* 2021; **11**: 657320 [PMID: 34150673 DOI: 10.3389/fcimb.2021.657320]

28 **Weingarden A**, González A, Vázquez-Baeza Y, Weiss S, Humphry G, Berg-Lyons D, Knights D, Unno T, Bobr A, Kang J, Khoruts A, Knight R, Sadowsky MJ. Dynamic changes in short- and long-term bacterial composition following fecal microbiota transplantation for recurrent Clostridium difficile infection. *Microbiome* 2015; **3**: 10 [PMID: 25825673 DOI: 10.1186/s40168-015-0070-0]

29 **Waldbaum C**, López F, Antelo P, Sorda J. [Faecal microbiota transplantation for Clostridioides difficile infection]. *Medicina (B Aires)* 2020; **80**: 633-639 [PMID: 33254107 DOI: 10.1038/s41575-020-0350-4]

30 **Wilson KH**, Perini F. Role of competition for nutrients in suppression of Clostridium difficile by the colonic microflora. *Infect Immun* 1988; **56**: 2610-2614 [PMID: 3417352 DOI: 10.1128/iai.56.10.2610-2614.1988]

31 **Rea MC**, Sit CS, Clayton E, O'Connor PM, Whittal RM, Zheng J, Vederas JC, Ross RP, Hill C. Thuricin CD, a posttranslationally modified bacteriocin with a narrow spectrum of activity against Clostridium difficile. *Proc Natl Acad Sci U S A* 2010; **107**: 9352-9357 [PMID: 20435915 DOI: 10.1073/pnas.0913554107]

32 **Ng KM**, Ferreyra JA, Higginbottom SK, Lynch JB, Kashyap PC, Gopinath S, Naidu N, Choudhury B, Weimer BC, Monack DM, Sonnenburg JL. Microbiota-liberated host sugars facilitate post-antibiotic expansion of enteric pathogens. *Nature* 2013; **502**: 96-99 [PMID: 23995682 DOI: 10.1038/nature12503]

33 **Khoruts A**, Sadowsky MJ. Understanding the mechanisms of faecal microbiota transplantation. *Nat Rev Gastroenterol Hepatol* 2016; **13**: 508-516 [PMID: 27329806 DOI: 10.1038/nrgastro.2016.98]

34 **Weingarden AR**, Chen C, Bobr A, Yao D, Lu Y, Nelson VM, Sadowsky MJ, Khoruts A. Microbiota transplantation restores normal fecal bile acid composition in recurrent Clostridium difficile infection. *Am J Physiol Gastrointest Liver Physiol* 2014; **306**: G310-G319 [PMID: 24284963 DOI: 10.1152/ajpgi.00282.2013]

35 **Song X**, Sun X, Oh SF, Wu M, Zhang Y, Zheng W, Geva-Zatorsky N, Jupp R, Mathis D, Benoist C, Kasper DL. Microbial bile acid metabolites modulate gut RORγ^{+} regulatory T cell homeostasis. *Nature* 2020; **577**: 410-415 [PMID: 31875848 DOI: 10.1038/s41586-019-1865-0]

36 **Allegretti JR**, Kearney S, Li N, Bogart E, Bullock K, Gerber GK, Bry L, Clish CB, Alm E, Korzenik JR. Recurrent Clostridium difficile infection associates with distinct bile acid and microbiome profiles. *Aliment Pharmacol Ther* 2016; **43**: 1142-1153 [PMID: 27086647 DOI: 10.1111/apt.13616]

37 **Seekatz AM**, Theriot CM, Rao K, Chang YM, Freeman AE, Kao JY, Young VB. Restoration of short chain fatty acid and bile acid metabolism following fecal microbiota transplantation in patients with recurrent Clostridium difficile infection. *Anaerobe* 2018; **53**: 64-73 [PMID: 29654837 DOI: 10.1016/j.anaerobe.2018.04.001]

38 **Park J**, Kim M, Kang SG, Jannasch AH, Cooper B, Patterson J, Kim CH. Short-chain fatty acids induce both effector and regulatory T cells by suppression of histone deacetylases and regulation of the mTOR-S6K pathway. *Mucosal Immunol* 2015; **8**: 80-93 [PMID: 24917457 DOI: 10.1038/mi.2014.44]

39 **Feuerstadt P**, Louie TJ, Lashner B, Wang EEL, Diao L, Bryant JA, Sims M, Kraft CS, Cohen SH, Berenson CS, Korman LY, Ford CB, Litcofsky KD, Lombardo MJ, Wortman JR, Wu H, Auniņš JG, McChalicher CWJ, Winkler JA, McGovern BH, Trucksis M, Henn MR, von Moltke L. SER-109, an Oral Microbiome Therapy for Recurrent *Clostridioides difficile* Infection. *N Engl J Med* 2022; **386**: 220-229 [PMID: 35045228 DOI: 10.1056/NEJMoa2106516]

40 **Zhang T**, Lu G, Zhao Z, Liu Y, Shen Q, Li P, Chen Y, Yin H, Wang H, Marcella C, Cui B, Cheng L, Ji G, Zhang F. Washed microbiota transplantation vs. manual fecal microbiota transplantation: clinical findings, animal studies and *in vitro* screening. *Protein Cell* 2020; **11**: 251-266 [PMID: 31919742 DOI: 10.1007/s13238-019-00684-8]

41 **Ott SJ**, Waetzig GH, Rehman A, Moltzau-Anderson J, Bharti R, Grasis JA, Cassidy L, Tholey A, Fickenscher H, Seegert D, Rosenstiel P, Schreiber S. Efficacy of Sterile Fecal Filtrate Transfer for Treating Patients With Clostridium difficile Infection. *Gastroenterology* 2017; **152**: 799-811.e7 [PMID: 27866880 DOI: 10.1053/j.gastro.2016.11.010]

42 **Sehgal K**, Khanna S. Immune response against *Clostridioides difficile* and translation to therapy. *Therap Adv Gastroenterol* 2021; **14**: 17562848211014817 [PMID: 33995585 DOI: 10.1177/17562848211014817]

43 **Nibbering B**, Gerding DN, Kuijper EJ, Zwittink RD, Smits WK. Host Immune Responses to Clostridioides difficile: Toxins and Beyond. *Front Microbiol* 2021; **12**: 804949 [PMID: 34992590 DOI: 10.3389/fmicb.2021.804949]

44 **Xu H**, Yang J, Gao W, Li L, Li P, Zhang L, Gong YN, Peng X, Xi JJ, Chen S, Wang F, Shao F. Innate immune sensing of bacterial modifications of Rho GTPases by the Pyrin inflammasome. *Nature* 2014; **513**: 237-241 [PMID: 24919149 DOI: 10.1038/nature13449]

45 **Hasegawa M**, Yamazaki T, Kamada N, Tawaratsumida K, Kim YG, Núñez G, Inohara N. Nucleotide-binding oligomerization domain 1 mediates recognition of Clostridium difficile and induces neutrophil recruitment and protection against the pathogen. *J Immunol* 2011; **186**: 4872-4880 [PMID: 21411735 DOI: 10.4049/jimmunol.1003761]

46 **Abt MC**, Lewis BB, Caballero S, Xiong H, Carter RA, Sušac B, Ling L, Leiner I, Pamer EG. Innate Immune Defenses Mediated by Two ILC Subsets Are Critical for Protection against Acute Clostridium difficile Infection. *Cell Host Microbe* 2015; **18**: 27-37 [PMID: 26159718 DOI: 10.1016/j.chom.2015.06.011]

47 **Ishida Y**, Maegawa T, Kondo T, Kimura A, Iwakura Y, Nakamura S, Mukaida N. Essential involvement of IFN-gamma in Clostridium difficile toxin A-induced enteritis. *J Immunol* 2004; **172**: 3018-3025 [PMID: 14978106 DOI: 10.4049/jimmunol.172.5.3018]

48 **McDermott AJ**, Falkowski NR, McDonald RA, Pandit CR, Young VB, Huffnagle GB. Interleukin-23 (IL-23), independent of IL-17 and IL-22, drives neutrophil recruitment and innate inflammation during Clostridium difficile colitis in mice. *Immunology* 2016; **147**: 114-124 [PMID: 26455347 DOI: 10.1111/imm.12545]

49 **Gebhard RL**, Gerding DN, Olson MM, Peterson LR, McClain CJ, Ansel HJ, Shaw MJ, Schwartz ML. Clinical and endoscopic findings in patients early in the course of clostridium difficile-associated pseudomembranous colitis. *Am J Med* 1985; **78**: 45-48 [PMID: 3966488 DOI: 10.1016/0002-9343(85)90460-7]

50 **Atarashi K**, Tanoue T, Shima T, Imaoka A, Kuwahara T, Momose Y, Cheng G, Yamasaki S, Saito T, Ohba Y, Taniguchi T, Takeda K, Hori S, Ivanov II, Umesaki Y, Itoh K, Honda K. Induction of colonic regulatory T cells by indigenous Clostridium species. *Science* 2011; **331**: 337-341 [PMID: 21205640 DOI: 10.1126/science.1198469]

51 **Bauché D**, Marie JC. Transforming growth factor β: a master regulator of the gut microbiota and immune cell interactions. *Clin Transl Immunology* 2017; **6**: e136 [PMID: 28523126 DOI: 10.1038/cti.2017.9]

52 **Frisbee AL**, Saleh MM, Young MK, Leslie JL, Simpson ME, Abhyankar MM, Cowardin CA, Ma JZ, Pramoonjago P, Turner SD, Liou AP, Buonomo EL, Petri WA Jr. IL-33 drives group 2 innate lymphoid cell-mediated protection during Clostridium difficile infection. *Nat Commun* 2019; **10**: 2712 [PMID: 31221971 DOI: 10.1038/s41467-019-10733-9]

53 **Cowardin CA**, Buonomo EL, Saleh MM, Wilson MG, Burgess SL, Kuehne SA, Schwan C, Eichhoff AM, Koch-Nolte F, Lyras D, Aktories K, Minton NP, Petri WA Jr. The binary toxin CDT enhances Clostridium difficile virulence by suppressing protective colonic eosinophilia. *Nat Microbiol* 2016; **1**: 16108 [PMID: 27573114 DOI: 10.1038/nmicrobiol.2016.108]

54 **Kulaylat AS**, Buonomo EL, Scully KW, Hollenbeak CS, Cook H, Petri WA Jr, Stewart DB Sr. Development and Validation of a Prediction Model for Mortality and Adverse Outcomes Among Patients With Peripheral Eosinopenia on Admission for Clostridium difficile Infection. *JAMA Surg* 2018; **153**: 1127-1133 [PMID: 30208386 DOI: 10.1001/jamasurg.2018.3174]

55 **Buonomo EL**, Cowardin CA, Wilson MG, Saleh MM, Pramoonjago P, Petri WA Jr. Microbiota-Regulated IL-25 Increases

Eosinophil Number to Provide Protection during Clostridium difficile Infection. *Cell Rep* 2016; **16**: 432-443 [PMID: 27346351 DOI: 10.1016/j.celrep.2016.06.007]

56 **De Salvo C**, Wang XM, Pastorelli L, Mattioli B, Omenetti S, Buela KA, Chowdhry S, Garg RR, Goodman WA, Rodriguez-Palacios A, Smith DE, Abbott DW, Cominelli F, Bamias G, Xin W, Lee JJ, Vecchi M, Pizarro TT. IL-33 Drives Eosinophil Infiltration and Pathogenic Type 2 Helper T-Cell Immune Responses Leading to Chronic Experimental Ileitis. *Am J Pathol* 2016; **186**: 885-898 [PMID: 26908008 DOI: 10.1016/j.ajpath.2015.11.028]

57 **Ekmekciu I**, von Klitzing E, Fiebiger U, Escher U, Neumann C, Bacher P, Scheffold A, Kühl AA, Bereswill S, Heimesaat MM. Immune Responses to Broad-Spectrum Antibiotic Treatment and Fecal Microbiota Transplantation in Mice. *Front Immunol* 2017; **8**: 397 [PMID: 28469619 DOI: 10.3389/fimmu.2017.00397]

58 **Burrello C**, Garavaglia F, Cribiù FM, Ercoli G, Lopez G, Troisi J, Colucci A, Guglietta S, Carloni S, Guglielmetti S, Taverniti V, Nizzoli G, Bosari S, Caprioli F, Rescigno M, Facciotti F. Therapeutic faecal microbiota transplantation controls intestinal inflammation through IL10 secretion by immune cells. *Nat Commun* 2018; **9**: 5184 [PMID: 30518790 DOI: 10.1038/s41467-018-07359-8]

59 **Littmann ER**, Lee JJ, Denny JE, Alam Z, Maslanka JR, Zarin I, Matsuda R, Carter RA, Susac B, Saffern MS, Fett B, Mattei LM, Bittinger K, Abt MC. Host immunity modulates the efficacy of microbiota transplantation for treatment of Clostridioides difficile infection. *Nat Commun* 2021; **12**: 755 [PMID: 33531483 DOI: 10.1038/s41467-020-20793-x]

60 **Monaghan TM**, Duggal NA, Rosati E, Griffin R, Hughes J, Roach B, Yang DY, Wang C, Wong K, Saxinger L, Pučić-Baković M, Vučković F, Klicek F, Lauc G, Tighe P, Mullish BH, Blanco JM, McDonald JAK, Marchesi JR, Xue N, Dottorini T, Acharjee A, Franke A, Li Y, Wong GK, Polytarchou C, Yau TO, Christodoulou N, Hatziapostolou M, Wang M, Russell LA, Kao DH. A Multi-Factorial Observational Study on Sequential Fecal Microbiota Transplant in Patients with Medically Refractory *Clostridioides difficile* Infection. *Cells* 2021; **10** [PMID: 34831456 DOI: 10.3390/cells10113234]

World Journal of Gastroenterology

Submit a Manuscript: https://www.f6publishing.com

World J Gastroenterol 2022 September 7; 28(33): 4773-4786

DOI: 10.3748/wjg.v28.i33.4773

ISSN 1007-9327 (print) ISSN 2219-2840 (online)

MINIREVIEWS

Albumin administration in patients with cirrhosis: Current role and novel perspectives

Ângelo Zambam de Mattos, Douglas Alano Simonetto, Carlos Terra, Alberto Queiroz Farias, Paulo Lisboa Bittencourt, Tales Henrique Soares Pase, Marlon Rubini Toazza, Angelo Alves de Mattos, Alliance of Brazilian Centers for Cirrhosis Care – the ABC Group

Specialty type: Gastroenterology and hepatology

Provenance and peer review: Invited article; Externally peer reviewed.

Peer-review model: Single blind

Peer-review report's scientific quality classification

Grade A (Excellent): 0
Grade B (Very good): B
Grade C (Good): C
Grade D (Fair): 0
Grade E (Poor): 0

P-Reviewer: Ferrarese A, Italy; Rabago LR, Spain

Received: March 27, 2022
Peer-review started: March 27, 2022
First decision: May 9, 2022
Revised: June 5, 2022
Accepted: July 5, 2022
Article in press: July 5, 2022
Published online: September 7, 2022

Ângelo Zambam de Mattos, Angelo Alves de Mattos, Graduate Program in Medicine: Hepatology, Federal University of Health Sciences of Porto Alegre, Porto Alegre 90050-170, Brazil

Douglas Alano Simonetto, Division of Gastroenterology and Hepatology, Mayo Clinic, Rochester, MN 55902, United States

Carlos Terra, Department of Gastroenterology, State University of Rio de Janeiro, Rio de Janeiro 20550-170, Brazil

Alberto Queiroz Farias, Department of Gastroenterology, University of São Paulo, São Paulo 01246-903, Brazil

Paulo Lisboa Bittencourt, Gastroenterology and Hepatology Unit, Hospital Português, Salvador 40130-030, Brazil

Tales Henrique Soares Pase, Internal Medicine Unit, Irmandade Santa Casa de Misericórdia de Porto Alegre, Porto Alegre 90020-090, Brazil

Marlon Rubini Toazza, Gastroenterology and Hepatology Unit, Irmandade Santa Casa de Miseric órdia de Porto Alegre, Porto Alegre 90020-090, Brazil

Corresponding author: Ângelo Zambam de Mattos, MD, MSc, PhD, Professor, Graduate Program in Medicine: Hepatology, Federal University of Health Sciences of Porto Alegre, 245, Sarmento Leite Street, Porto Alegre 90050-170, Brazil. angmattos@hotmail.com

Abstract

Mortality in cirrhosis is mostly associated with the development of clinical decompensation, characterized by ascites, hepatic encephalopathy, variceal bleeding, or jaundice. Therefore, it is important to prevent and manage such complications. Traditionally, the pathophysiology of decompensated cirrhosis was explained by the peripheral arterial vasodilation hypothesis, but it is currently understood that decompensation might also be driven by a systemic inflammatory state (the systemic inflammation hypothesis). Considering its oncotic and nononcotic properties, albumin has been thoroughly evaluated in the prevention and management of several of these decompensating events. There are formal evidence-based recommendations from international medical societies proposing that albumin be administered in individuals with cirrhosis undergoing

large-volume paracentesis, patients with spontaneous bacterial peritonitis, those with acute kidney injury (even before the etiological diagnosis), and those with hepatorenal syndrome. Moreover, there are a few randomized controlled trials and meta-analyses suggesting a possible role for albumin infusion in patients with cirrhosis and ascites (long-term albumin administration), individuals with hepatic encephalopathy, and those with acute-on-chronic liver failure undergoing modest-volume paracentesis. Further studies are necessary to elucidate whether albumin administration also benefits patients with cirrhosis and other complications, such as individuals with extraperitoneal infections, those hospitalized with decompensated cirrhosis and hypoalbuminemia, and patients with hyponatremia.

Key Words: Cirrhosis; Albumin; Paracentesis; Spontaneous bacterial peritonitis; Acute kidney injury; Hepatorenal syndrome

©The Author(s) 2022. Published by Baishideng Publishing Group Inc. All rights reserved.

Core tip: Mortality in cirrhosis is mostly associated with clinical decompensation. Albumin has oncotic and nononcotic properties, which may contribute to the prevention and management of such complications. This review discusses the current recommendations and the novel perspectives regarding the use of albumin in cirrhosis.

Citation: de Mattos ÂZ, Simonetto DA, Terra C, Farias AQ, Bittencourt PL, Pase THS, Toazza MR, de Mattos AA, Alliance of Brazilian Centers for Cirrhosis Care – the ABC Group. Albumin administration in patients with cirrhosis: Current role and novel perspectives. *World J Gastroenterol* 2022; 28(33): 4773-4786
URL: https://www.wjgnet.com/1007-9327/full/v28/i33/4773.htm
DOI: https://dx.doi.org/10.3748/wjg.v28.i33.4773

INTRODUCTION

Cirrhosis and chronic liver diseases rank as the conditions with the 10th highest mortality rate worldwide[1]. Deaths are mostly related to the development of clinical decompensation of cirrhosis, and 4%–12% of individuals with cirrhosis present with at least one episode of decompensation annually[2]. This is why preventing and treating decompensating events in cirrhosis are constant concerns of gastroenterologists and hepatologists.

Albumin administration has been studied in the prophylaxis and management of different forms of decompensation of cirrhosis for many years. Albumin is exclusively synthesized by hepatocytes, and it is characterized as a water-soluble, negatively charged, 67-kDa protein, with a half-life of approximately 20 d in normal conditions. It is the most abundant protein in serum and in extracellular fluids, and it has multiple roles, including oncotic, antioxidative, detoxifying, anti-inflammatory, endothelium stabilizing, and immunomodulatory functions[3]. Traditionally, most decompensating events of cirrhosis were explained by the peripheral arterial vasodilation hypothesis[4], and albumin was considered potentially useful mainly due to its oncotic property, as it is responsible for 75% of plasma oncotic pressure[3]. However, with the current understanding that decompensation of cirrhosis is at least partly driven by a systemic inflammatory state (the systemic inflammation hypothesis)[5-8], the nononcotic properties of albumin have gained much attention[3].

This article reviews the current role and novel perspectives for albumin administration in cirrhosis. Table 1 shows the main indications for which there are formal recommendations for the use of albumin in cirrhosis as well as other potential situations in which albumin may play a role.

LARGE VOLUME PARACENTESIS

Large volume paracentesis (LVP) is the current standard of care for the management of refractory and tense ascites due to its efficacy and low rate of complications[9-11]. However, the drainage of large volumes of ascitic fluid increases cardiac output and reduces peripheral vascular resistance and effective circulating volume, leading to arterial hypotension, acute kidney injury (AKI), hepatic encephalopathy (HE), worsening of hyponatremia, and decreased survival rates. This severe condition is termed paracentesis-induced circulatory dysfunction (PICD) and is defined by a rise of more than 50% in the basal plasma renin activity a few days after the procedure, indicating the detrimental effect of volume depletion on effective volemia[12-15].

Table 1 Current recommendations and potential indications for albumin administration in cirrhosis

Current recommendations[1]	Potential indications
Large-volume paracentesis	Modest-volume paracentesis
Acute kidney injury	Extraperitoneal infections
Hepatorenal syndrome	Long-term albumin administration in cirrhosis with ascites
Spontaneous bacterial peritonitis	Decompensated cirrhosis with hypoalbuminemia
	Hepatic encephalopathy
	Hyponatremia
	Cirrhotic cardiomyopathy
	Acute-on-chronic liver failure

[1]Recommendations for albumin administration according to the European Association for the Study of the Liver[9] and the American Association for the Study of Liver Diseases[11].

Several randomized controlled trials (RCTs) have shown that PICD can be prevented by intravenous human albumin administration, particularly in cases of paracentesis exceeding 5 L and that albumin is more effective than other plasma expanders[13,16-18]. In the seminal study by Ginès *et al*[13] for instance, 105 patients were randomized to be submitted to paracentesis with or without albumin infusion, and individuals receiving albumin developed less episodes of hyponatremia ($P < 0.01$) and renal impairment ($P < 0.05$).

In 2012, a meta-analysis of 17 RCTs, including 1225 patients with ascites undergoing LVP, showed that in comparison to alternative treatments albumin reduced the incidence of PICD [odds ratio = 0.39, 95% confidence interval (CI): 0.27-0.55], hyponatremia (odds ratio = 0.58, 95%CI: 0.39–0.87), and mortality (odds ratio = 0.64, 95%CI: 0.41–0.98), which appeared to be definitive evidence regarding the role of albumin infusion in LVP[19]. However, in 2019 another meta-analysis, including 25 RCTs, revisited this issue. According to this systematic review, there was no evidence of significant reduction in mortality or renal impairment when any volume expansion was compared to no volume expansion at all, but it should be highlighted that only one and two RCTs using albumin actually contributed to the analyses of these outcomes, respectively. When albumin was compared to other plasma expanders, there were significant benefits of using albumin regarding prevention of PICD [risk ratio (RR) = 1.98, 95%CI: 1.31–2.99] and hyponatremia (RR = 1.49, 95%CI: 1.03–2.14), but there was no evidence of significant differences between treatments regarding renal impairment (RR = 1.17, 95%CI: 0.71–1.91) and mortality (RR = 1.03, 95%CI: 0.82–1.30)[20].

The use of vasoconstrictors, such as vasopressin, midodrine, and noradrenaline, has been proposed as an alternative to albumin in order to overcome the marked arterial vasodilation and arterial hypotension associated with PICD, but evidence on the clinical utility of such drugs is limited in this context. An RCT compared the effect of midodrine and standard albumin doses in preventing PICD in 50 patients with cirrhosis and tense refractory ascites. Midodrine therapy was associated with higher incidence of AKI, worsening of hyponatremia, and higher plasma renin activity and plasma aldosterone concentration, suggesting that this drug is not as effective as intravenous albumin in preventing PICD after LVP[21].

Despite the existence of some doubts concerning the benefits of albumin on hard outcomes (renal impairment and mortality), its clear benefits on important surrogate outcomes (PICD and hyponatremia) allow albumin to be recommended in patients with cirrhosis undergoing paracentesis of more than 5 L. According to the European Association for the Study of the Liver, it should be administered at a dose of 8 g/L ascitic fluid removed[9], while the American Association for the Study of Liver Diseases recommends it is used at doses of 6–8 g/L ascites removed[11].

Modest volume paracentesis (< 5 L) seems to have less serious impacts on hemodynamic and neurohumoral systems, and therefore it might be safe to perform the paracentesis without administering albumin[22]. The exception to this seems to apply to patients with acute-on-chronic liver failure (ACLF) undergoing paracentesis < 5 L because these individuals usually have an intense hemodynamic impairment that theoretically increases the risk of PICD. A recent study randomized 80 subjects with ACLF undergoing paracentesis < 5 L to receive standard doses of albumin or no fluid expansion and demonstrated that PICD was significantly more common in the control group than in the albumin group (70.0% *vs* 30.0%, $P = 0.001$), with significantly higher incidences of HE (50.0% *vs* 27.0%, $P = 0.04$), hyponatremia (67.5% *vs* 22.5%, $P < 0.001$), AKI (62.5% *vs* 30%, $P = 0.001$), and short-term mortality (62.5% *vs* 27.5%, $P = 0.003$)[23].

AKI AND HEPATORENAL SYNDROME

AKI is a common complication of cirrhosis, reported in up to one-third of hospitalized patients with advanced liver disease[24-27]. The diagnostic criteria of AKI in cirrhosis have evolved over the years and are currently based on an acute increase in serum creatinine by ≥ 0.3 mg/dL or ≥ 50% from baseline [28]. The new definition and classification proposed by the International Club of Ascites has allowed for earlier recognition of AKI and implementation of therapeutic strategies, such as intravenous albumin use.

Hypovolemia accounts for about one-half of all cases of AKI in cirrhosis, and it is often driven by excessive use of diuretics and/or fluid losses from lactulose-induced diarrhea. In addition to diuretic withdrawal, intravenous albumin at 1 g/kg/d (maximum 100 g/d) for 2 d has been recommended for volume expansion, especially in patients with AKI stage ≥ 1b[9,11] since mortality appears to significantly increase from this stage on[24,29-32]. Response failure to a 2-d fluid challenge with albumin is suggestive of hepatorenal syndrome (HRS), formerly classified as type 1 and currently as HRS–AKI, once structural kidney injury has been excluded. Recent history of shock, nephrotoxic drugs, proteinuria, microhematuria, and hydronephrosis on renal ultrasound must be ruled out for the diagnosis of HRS–AKI, which is one of exclusion[9,11,28,33].

The benefits of albumin in HRS, a functional kidney injury driven by reduction in renal blood flow, extend beyond just plasma volume expansion. This has been demonstrated in a study comparing albumin with hydroxyethyl starch, a synthetic colloid, in patients with spontaneous bacterial peritonitis (SBP). Administration of albumin resulted in significant improvement on systemic hemodynamics, whereas this effect was not appreciated in the starch group[34]. Furthermore, albumin carries important anti-inflammatory and antioxidant properties, and it has been shown to bind circulating bacterial products, thus preventing their negative consequences on the systemic circulation[35,36]. This has led to the extension of albumin use past the initial fluid challenge at a recommended dose of 20–40 g/d[9,11,28]. Although albumin alone has a limited role in HRS–AKI[37,38], the benefit of added albumin to vasoconstrictor therapy in HRS has been demonstrated in one nonrandomized study comparing terlipressin with terlipressin plus albumin. Despite being a small study, it demonstrated that the combination therapy group had a significantly higher response rate compared to terlipressin monotherapy (77% *vs* 25%, $P = 0.03$)[39].

It is important to note that excessive albumin use in AKI and HRS can be detrimental and contribute to development of pulmonary edema and respiratory failure. This concern has been raised in the recently published CONFIRM study, a large RCT comparing terlipressin with placebo[38]. Concomitant albumin was given in > 80% of patients in both arms at a mean total dose of 200–240 g over 5 d (40–50 g/d). A higher incidence of respiratory failure was observed in the terlipressin group (14% *vs* 5%), presumably secondary to pulmonary edema because of the known cardiovascular effects of terlipressin in combination with excessive albumin use[40]. Thus, volume status should be closely monitored in these patients and judicious albumin use is recommended.

SBP

Bacterial infections occur in 25%–35% of the patients hospitalized with advanced cirrhosis[41], and they are associated with increased morbidity and mortality[42,43], particularly when acquired in the hospital or in healthcare facilities, due to the presence of multidrug resistant organisms[44-48]. SBP is frequently reported as the most common infection in subjects with cirrhosis and ascites[44,45] and one of the main precipitants of ACLF[49]. It is diagnosed in the presence of a polymorphonuclear cell count > 250/mm^3 in the ascitic fluid, and it is usually treated with third-generation cephalosporins in those patients with community-acquired infection[9,11].

However, since the publication of the pivotal RCT by Sort *et al*[50] in 1999, it is clear that this infection should not be treated exclusively with antibiotics. In that study, 126 hospitalized patients with SBP were randomized to receive intravenous cefotaxime *versus* intravenous cefotaxime plus albumin administered at a dose of 1.5 g/kg body weight at baseline, followed by 1 g/kg on day 3. The authors described a threefold reduction in the incidence of renal impairment favoring the albumin group (33% *vs* 10%, $P = 0.002$). More importantly, 3-mo mortality was also significantly lower in the albumin group (41% *vs* 22%, $P = 0.03$), which was attributed to the decrease in the incidence of AKI[50].

The benefit of using albumin in SBP was initially attributed to plasma expansion and/or prevention of circulatory dysfunction[34,50,51], but it actually seems that albumin infusion leads to a reduction of plasma levels of nitric oxide, tumor necrosis factor-α, endotoxin and interleukin-6[52]. These findings favor the concept that albumin is more than a colloid and that it has anti-inflammatory properties in individuals with decompensated cirrhosis[53].

In the study by Sort *et al*[50], renal impairment was negligible in both groups of patients in the presence of baseline bilirubin levels < 4 mg/dL and serum creatinine level < 1 mg/dL, suggesting that albumin administration might be restricted to higher-risk subjects. Nevertheless, subsequent data have disputed those findings[54,55]. In this regard, a meta-analysis including four RCTs[34,50-52] evaluated

the role of albumin in SBP and concluded that albumin was associated with a lower incidence of renal impairment and mortality, not identifying a significant difference in albumin effects according to baseline levels of bilirubin or renal function[56]. Since then, several international guidelines recommend the use of high-dose albumin in patients with SBP, even in patients at lower risk for renal impairment[9,11,57]. However, there still is some controversy regarding albumin dosing and schedule since the use of lower doses of albumin were associated with a reduction in proinflammatory cytokines in an RCT[52], and no major differences in outcomes were observed in a subsequent Brazilian trial comparing standard *versus* lower doses of albumin in SBP[58].

EXTRAPERITONEAL INFECTIONS

Infections (not only SBP) characterize state 6 (end-state) in the clinical course of cirrhosis[59], as they increase the risk for AKI, HRS, organ failure, and ACLF[60]. It has also been recently demonstrated that infections are the most important precipitating factor for acute decompensation of cirrhosis, even in patients without ACLF[61]. On the other hand, in compensated cirrhosis, the role of infections is not completely understood. A recent cohort study has demonstrated that 17% of patients with compensated cirrhosis developed infections, particularly respiratory and urinary tract infections, which led to decompensation of cirrhosis in 26% of cases and to an increased mortality rate[62].

Therefore, considering the importance of infections in the prognosis of cirrhosis, improving the efficacy of therapeutic strategies would be of the utmost importance. In SBP, as previously discussed, the addition of albumin to antibiotic treatment represented an important improvement in the therapeutic strategy[50], and it was natural to study if a similar intervention could reach the same results in extraperitoneal infections. The rationale behind this proposal is that albumin is a multifunctional protein, which also has important nononcotic properties, as previously mentioned[3]. Furthermore, individuals with cirrhosis are not only quantitatively deficient in albumin but also qualitatively, which highlights the concept of the effective albumin concentration[63,64].

Some RCTs have evaluated the subject of albumin administration in infections other than SBP. In the first of them, patients with cirrhosis and extraperitoneal infections were randomized to receive antibiotics plus albumin (same doses as for SBP) or antibiotics alone, and albumin led to improved circulatory and renal functions. In that study, there was no significant difference in 3-mo survival between groups, but albumin use was an independent predictive factor of survival after adjusting for other factors[65].

In the second RCT, despite delaying the onset of renal failure, albumin was not able to significantly reduce its incidence or improve survival. Besides, 8.3% of subjects receiving albumin developed pulmonary edema as a complication[66]. It is noteworthy, however, that the study had important methodological limitations.

In the third RCT, albumin was associated with a higher resolution of ACLF as well as with lower incidence of nosocomial infections. Nevertheless, once again, there was no significant difference between groups regarding mortality[67]. An important limitation of this study is the fact that only 23% of the estimated sample was actually enrolled in the trial[68].

In order to further examine this subject, our group has performed a meta-analysis of RCTs evaluating the role of albumin in extraperitoneal infections. In that meta-analysis, there was no evidence of significant benefit of albumin in reducing renal dysfunction (RR = 0.55, 95%CI: 0.25–1.19, P = 0.13) or mortality in 30 d (RR = 1.62, 95%CI: 0.92–2.84, P = 0.09) and 90 d (RR = 1.27, 95%CI: 0.89–1.83, P = 0.19)[69]. Therefore, at this moment, a general recommendation cannot be made regarding the administration of albumin in patients with cirrhosis and extraperitoneal infections[9]. Still, there might be a role for albumin in a subgroup of extraperitoneal infections, particularly the most severe of them[70].

LONG-TERM ALBUMIN ADMINISTRATION

Ascites is the most common among severe complications of cirrhosis[71], and it marks state 4 in the natural history of this disease[59]. Ascites is associated with a 5-year mortality of 50%, and persistent ascites predicts mortality independently of the Model for End-Stage Liver Disease score[59,72]. Therefore, strategies aiming at the increase in survival of patients with cirrhosis and ascites are constantly pursued.

Long-term albumin administration has been studied in the management of patients with cirrhosis and ascites for many decades. The rationale for its use relies on the hypothesis that albumin could reduce effective arterial hypovolemia through plasma expansion and that the nononcotic properties of albumin could act against the systemic inflammation that is behind decompensation of cirrhosis[3,5]. Once again, the concept of effective albumin concentration should be highlighted in this context[63]. As albumin is quantitatively and qualitatively deficient in cirrhosis, leading to alterations in the transport and metabolism of substances as well as to the impairment of systems associated with the redox balance, inflammation, and coagulation, it is hypothesized that albumin supplementation could prevent

the decompensation of cirrhosis[73-77].

Five RCTs evaluated the role of long-term albumin administration in patients with cirrhosis and ascites. The first study evaluated a small sample of subjects with persistent ascites already under treatment with diuretics. Albumin was used at doses of 25–100 g every 1–2 d according to serum colloid osmotic pressure, and 25–100 g every 1–2 wk thereafter. The osmotic pressure was improved in individuals receiving albumin, but mortality was not different between groups[78].

After that, two Italian RCTs evaluated the matter. Gentilini *et al*[79] enrolled patients with ascites unresponsive to a low-sodium diet, while Romanelli *et al*[80] studied individuals with their first episode of grade 2–3 ascites. Both studies randomized patients to receive albumin at doses of 25 g every week for 12 mo and every other week thereafter[79,80]. In the former study, albumin led to significantly lower cumulative probabilities of recurrence of ascites and hospitalization, but there was no benefit regarding mortality[79]. In the latter, though, patients receiving albumin had a significantly lower probability of recurrence of ascites and a higher cumulative survival rate[80].

Finally, in 2018, two more RCTs on long-term albumin administration were published. Solà *et al*[81] evaluated albumin at doses of 40 g twice a month in combination with midodrine for patients with cirrhosis and ascites in the waiting list for liver transplantation, but there was no significant difference in survival or in complications of cirrhosis between study groups. The high rate of transplantation in that study might have led patients to be treated with albumin for an insufficient period of time (since they were quickly transplanted). The fact that the renin–angiotensin–aldosterone system activity did not completely normalize in subjects receiving albumin also supports the hypothesis that higher doses and longer duration of albumin administration might have been necessary[81].

On the other hand, Caraceni *et al*[82] randomized patients with persistent ascites to receive albumin 40 g twice a week for 2 wk and once a week thereafter or no plasma expansion. Individuals receiving albumin had significantly better results than their counterparts regarding mortality, need for paracentesis, SBP, extraperitoneal infections, HE, renal dysfunction, HRS, hyponatremia, and hyperkalemia [82].

Considering the differences in the results of these studies, we have performed a meta-analysis on this issue. Pooling the data from all five RCTs, it was demonstrated that albumin significantly reduced recurrence of ascites/need for paracentesis (RR = 0.56, 95%CI: 0.48–0.67, $P < 0.001$). There was also a trend towards a lower risk of mortality favoring albumin, but it did not reach statistical significance (RR = 0.88, 95%CI: 0.67–1.14, $P = 0.33$). There was no evidence of significant differences between groups regarding refractory ascites, SBP, HE, gastrointestinal bleeding, or adverse events[83].

We understand the main reason for the study by Caraceni *et al*[82] having reached such outstanding results relates to the doses of albumin used. In a recent study, the effects of different doses of long-term albumin administration were compared. While high-dose albumin (1.5 g/kg/wk) led to normalization of serum levels of albumin, improvement of circulatory and cardiac function, and reduction in plasma levels of cytokines, low-dose albumin (1.0 g/kg every 2 wk) did not[84]. It is noteworthy that the trial by Caraceni *et al*[82] was the one using the highest dose of albumin among the five RCTs on this issue, and, even so, the dose used was only slightly higher than that considered insufficient in the abovementioned study[84]. Moreover, while changes in serum levels of albumin were not different between groups in the trial by Solà *et al*[81], the intervention group had a normalization of serum albumin in the study by Caraceni *et al*[82], which reinforces the idea of insufficient doses of albumin in the former trial.

Furthermore, in a *post hoc* analysis of the study by Caraceni *et al*[82], the authors demonstrated that a serum level of albumin of 4 g/dL at 1 mo should be the target in long-term albumin administration in order for the highest survival rates to be achieved. In that publication, the authors suggested the hypothesis of the albumin gap, associating the amount of albumin required not only to baseline albumin levels but also to the severity of liver disease and highlighting the importance of the concept of effective albumin concentration[63].

Therefore, considering the abovementioned evidence, we believe that long-term albumin administration in patients with cirrhosis and ascites will probably become a formal recommendation in the near future. It must be emphasized, though, that the most recent guidelines still did not include this indication of albumin use in cirrhosis[11,85]. Hopefully, the ongoing PRECIOSA trial (NCT03451292) will provide us with more definitive data on this issue.

OTHER INDICATIONS

Decompensated cirrhosis

A recent RCT (the ATTIRE study), including 777 patients hospitalized for decompensated cirrhosis with baseline serum albumin levels < 3 g/dL, evaluated the effects of increasing these levels by daily intravenous administration of albumin. In that study, albumin administration was not superior to placebo in preventing a composite endpoint of infection, AKI and death[86].

Nevertheless, there are important points to consider. (1) No information on the distribution of patients between groups according to the Child–Pugh classification was provided. This is of great importance due to the recognized heterogeneity of such a group of patients. In fact, this could influence

the response to albumin infusion; (2) Ascites relates to the severity of circulatory dysfunction in patients with advanced cirrhosis. Although ascites was present in 62% of patients in the albumin group and in 71% in the control group, there was no information about its grade, the percentage of individuals with refractory ascites, use of diuretics, and their doses. Furthermore, there were no data on serum sodium concentration, another important marker of circulatory dysfunction; (3) There were no data on the severity or type of infections and their effects on circulatory function. Previous research suggests that giving albumin to patients with cirrhosis may be especially effective in the subset of patients with circulatory and renal dysfunction[50]; and (4) Finally, evidence shows that high doses of albumin are required for individuals with cirrhosis to benefit[84] and that the target level of serum albumin should be 4 g/dL[63]. Patients in the trial by China *et al*[86] reached levels barely over 3 g/dL. Therefore, it is likely that they did not receive enough albumin to benefit from the intervention.

The results of the ATTIRE study should be interpreted with caution, as it seems that rather than trying to make a general recommendation on albumin administration in decompensated cirrhosis, it might be more appropriate to define the best albumin administration strategy and the subgroup of patients with cirrhosis who could benefit most from its effects.

HE

The understanding of the pathophysiology of HE has increased in recent years. Thus, besides the traditional concept that implies cerebral exposure to ammonia as the basic mechanism for HE occurrence, new proposals suggest that the activation of inflammatory mediators, cerebral blood flow alterations due to circulatory dysfunction, and oxidative stress altogether contribute to the astrocytic injury leading to HE[87]. Albumin, a multifunctional protein, as previously mentioned in this review, could therefore play an important role in the treatment of HE.

In 2004, a pilot study evaluated the effects of plasma expansion with albumin in patients with cirrhosis and diuretic-induced HE. Albumin was more effective than a gelatin-based colloid solution in improving HE grade and lowering plasma concentrations of malondialdehyde, an oxidative stress marker[88]. After that pilot study, a multicenter, double-blind RCT found no significant differences between albumin or saline solution in the resolution of HE in patients with cirrhosis hospitalized with this complication. However, the same study demonstrated a significant improvement in 90-d survival in the albumin group (69.2% *vs* 40.0%, P = 0.02)[89]. In yet another RCT that compared lactulose plus albumin (group 1) *versus* lactulose alone (group 2) for the treatment of HE, 75% of patients in group 1 and only 53% of those in group 2 had complete reversal of HE (P = 0.03). Moreover, mortality was significantly lower in group 1 (18.3% *vs* 31.6%, P = 0.04)[90]. In this regard, a recent meta-analysis of RCTs aimed at clarifying the role of albumin in HE. In that study, albumin administration was able to significantly improve HE (RR = 0.60, 95%CI: 0.38–0.95, P = 0.03) and mortality (RR = 0.54, 95%CI: 0.33–0.90, P = 0.02)[91].

In another clinical context, that of the prophylaxis of TIPS-induced HE, Riggio *et al*[92] compared patients receiving albumin to a historical control group and found no significant difference in the incidence of overt HE[92]. However, the important methodological limitations of that study must be kept in mind when appraising its results.

Considering what was presented, despite the absence of a formal recommendation for the administration of albumin in the treatment of HE, it seems that there is initial evidence favoring its use. Further studies should be encouraged in this regard.

Hyponatremia

Hyponatremia is an important marker of prognosis in cirrhosis as it can induce neurological complications, and it is associated with reduced survival. Hyponatremia in cirrhosis results from a reduction in free water excretion due to nonosmotic secretion of antidiuretic hormone caused by splanchnic vasodilation. The use of albumin may decrease antidiuretic hormone secretion by improving relative hypovolemia, and therefore it might be useful in the management of hyponatremia[9].

In a small series, McCormick *et al*[93] observed complete reversal of hyponatremia after albumin infusion to three patients with decompensated cirrhosis. Moreover, an RCT evaluated the role of albumin infusion in hyponatremic subjects with cirrhosis, showing a significant improvement in serum sodium concentration, an increase in free water clearance, and a reduction in vasopressin concentration in the albumin group when compared to the placebo group[94]. Furthermore, in a large cohort of patients with cirrhosis and hyponatremia, albumin use was independently associated with the normalization of serum sodium levels[95]. More recently, in an analysis of the ATTIRE trial database, albumin infusions also led to an improvement in hyponatremia, which did not translate into benefits regarding hard outcomes[86]. Therefore, due to the scarcity of data, other studies are needed before albumin infusion can be recommended as a therapeutic option in patients with cirrhosis and hyponatremia.

Cirrhotic cardiomyopathy

Albumin seems to prevent cardiac output reduction and plasma renin activity increase in patients with cirrhosis more effectively than other plasma expanders[3]. The increase in cardiac output induced by albumin seems to be independent of volume expansion[96], which might be explained by the reversal of

the negative effects of tumor necrosis factor-alpha and oxidative stress on cardiac contractility[97].

ACLF

Considering the exacerbated systemic inflammatory state associated with the pathophysiology of ACLF and the anti-inflammatory properties of albumin, it could be hypothesized that albumin might play a role in the treatment of ACLF. There are limited data on this issue at the moment[98], but an RCT on albumin in extraperitoneal infections has demonstrated that individuals receiving this intervention had higher rates of ACLF resolution than their counterparts. Moreover, subjects receiving albumin had evidence of suppression of the systemic inflammation (decrease in white blood cells, C reactive protein, and interleukin-6), which was not specific for those with ACLF[67].

On the other hand, there remains a concern that administered albumin could be modified and added up to the pool of pathological albumin of such severely ill patients[98]. It is noteworthy that patients with cirrhosis, particularly those with advanced disease, have an impairment of albumin function in all of its domains and, therefore, a reduction in effective albumin concentration[64,76]. In this regard, research on ways of improving the quality of commercially available albumin is of the utmost importance since it could lead to an increase in albumin effectiveness as well as to a reduction in costs [3].

PREDICTION OF RESPONSE TO ALBUMIN ADMINISTRATION

Not all patients receiving albumin will benefit from it, and biomarkers capable of identifying those most likely to benefit from it would be extremely useful[3]. Effective albumin concentration, which reflects the portion of the albumin pool with normal structure and function, is superior to total albumin in stratifying individuals with compensated cirrhosis, acute decompensation, or ACLF as well as in distinguishing patients with or without complications of cirrhosis. Therefore, effective albumin concentration seems to be promising as a predictor of prognosis and treatment response in these patients. However, further studies are required not only regarding effective albumin concentration but also for other biomarkers[64,99].

ADVERSE EVENTS

Albumin infusion is generally safe, but careful evaluation of the patient is necessary in order to avoid complications, particularly volume overload and pulmonary edema[38,86]. Other uncommon complications of albumin might relate to contamination by blood-derived pathogens as well as to its administration to individuals allergic to albumin and to those with severe anemia, severe coagulopathy with pulmonary hemorrhage, or with subcutaneous bleeding[98,100].

ECONOMIC ASPECTS

Albumin administration has traditionally been considered costly. However, its cost has decreased over time. More importantly, albumin administration was proven cost-effective in different settings when evaluated using a decision-tree economic model. In that study, when compared to saline, gelatin, and no fluid expansion, albumin was the dominant treatment (more effective and less costly) for patients undergoing LVP. Regarding individuals with SBP, combining albumin and antibiotics was more cost-effective than using antibiotics alone in all three evaluated countries, and it was the dominant strategy in two of them. Finally, in HRS, combining albumin and a vasoconstrictor was the dominant strategy when compared to using a vasoconstrictor alone. Therefore, the concept of albumin administration being costly should be revisited since it is not only cost-effective but also cost-saving in most settings [101].

CONCLUSION

Due to the pathophysiological mechanisms behind decompensations of cirrhosis, albumin plays an important role in their prevention and management through its oncotic and nononcotic properties. International medical societies have made formal evidence-based recommendations for albumin administration in LVP, AKI, HRS and SBP. Promising evidence suggests that long-term albumin in patients with ascites, albumin in modest-volume paracentesis in individuals with ACLF, and albumin in HE are also probably beneficial. Further studies are needed to elucidate the role of albumin in other clinical scenarios, such as extraperitoneal infections, decompensated cirrhosis with hypoalbuminemia, and hyponatremia.

FOOTNOTES

Author contributions: All authors contributed to this paper with conception of the manuscript, literature review and analysis, drafting and critical revision of the manuscript, and approval of the final version of the paper.

Conflict-of-interest statement: All authors report no relevant conflicts of interest for this article.

Open-Access: This article is an open-access article that was selected by an in-house editor and fully peer-reviewed by external reviewers. It is distributed in accordance with the Creative Commons Attribution NonCommercial (CC BY-NC 4.0) license, which permits others to distribute, remix, adapt, build upon this work non-commercially, and license their derivative works on different terms, provided the original work is properly cited and the use is non-commercial. See: https://creativecommons.org/Licenses/by-nc/4.0/

Country/Territory of origin: Brazil

ORCID number: Ângelo Zambam de Mattos 0000-0002-3063-0199; Douglas Alano Simonetto 0000-0003-4095-8144; Carlos Terra 0000-0003-3069-128X; Alberto Queiroz Farias 0000-0002-5572-663X; Paulo Lisboa Bittencourt 0000-0003-0883-4870; Tales Henrique Soares Pase 0000-0001-7474-2048; Marlon Rubini Toazza 0000-0001-6561-487X; Angelo A de Mattos 0000-0003-2417-9765.

S-Editor: Ma YJ
L-Editor: Kerr C
P-Editor: Ma YJ

REFERENCES

1 **GBD 2019 Diseases and Injuries Collaborators**. Global burden of 369 diseases and injuries in 204 countries and territories, 1990-2019: a systematic analysis for the Global Burden of Disease Study 2019. *Lancet* 2020; **396**: 1204-1222 [PMID: 33069326 DOI: 10.1016/S0140-6736(20)30925-9]
2 **Moon AM**, Singal AG, Tapper EB. Contemporary Epidemiology of Chronic Liver Disease and Cirrhosis. *Clin Gastroenterol Hepatol* 2020; **18**: 2650-2666 [PMID: 31401364 DOI: 10.1016/j.cgh.2019.07.060]
3 **Bernardi M**, Angeli P, Claria J, Moreau R, Gines P, Jalan R, Caraceni P, Fernandez J, Gerbes AL, O'Brien AJ, Trebicka J, Thevenot T, Arroyo V. Albumin in decompensated cirrhosis: new concepts and perspectives. *Gut* 2020; **69**: 1127-1138 [PMID: 32102926 DOI: 10.1136/gutjnl-2019-318843]
4 **Schrier RW**, Arroyo V, Bernardi M, Epstein M, Henriksen JH, Rodés J. Peripheral arterial vasodilation hypothesis: a proposal for the initiation of renal sodium and water retention in cirrhosis. *Hepatology* 1988; **8**: 1151-1157 [PMID: 2971015 DOI: 10.1002/hep.1840080532]
5 **Bernardi M**, Moreau R, Angeli P, Schnabl B, Arroyo V. Mechanisms of decompensation and organ failure in cirrhosis: From peripheral arterial vasodilation to systemic inflammation hypothesis. *J Hepatol* 2015; **63**: 1272-1284 [PMID: 26192220 DOI: 10.1016/j.jhep.2015.07.004]
6 **Moreau R**, Jalan R, Gines P, Pavesi M, Angeli P, Cordoba J, Durand F, Gustot T, Saliba F, Domenicali M, Gerbes A, Wendon J, Alessandria C, Laleman W, Zeuzem S, Trebicka J, Bernardi M, Arroyo V; CANONIC Study Investigators of the EASL–CLIF Consortium. Acute-on-chronic liver failure is a distinct syndrome that develops in patients with acute decompensation of cirrhosis. *Gastroenterology* 2013; **144**: 1426-1437, 1437.e1 [PMID: 23474284 DOI: 10.1053/j.gastro.2013.02.042]
7 **Clària J**, Stauber RE, Coenraad MJ, Moreau R, Jalan R, Pavesi M, Amorós À, Titos E, Alcaraz-Quiles J, Oettl K, Morales-Ruiz M, Angeli P, Domenicali M, Alessandria C, Gerbes A, Wendon J, Nevens F, Trebicka J, Laleman W, Saliba F, Welzel TM, Albillos A, Gustot T, Benten D, Durand F, Ginès P, Bernardi M, Arroyo V; CANONIC Study Investigators of the EASL-CLIF Consortium and the European Foundation for the Study of Chronic Liver Failure (EF-CLIF). Systemic inflammation in decompensated cirrhosis: Characterization and role in acute-on-chronic liver failure. *Hepatology* 2016; **64**: 1249-1264 [PMID: 27483394 DOI: 10.1002/hep.28740]
8 **Trebicka J**, Fernandez J, Papp M, Caraceni P, Laleman W, Gambino C, Giovo I, Uschner FE, Jimenez C, Mookerjee R, Gustot T, Albillos A, Bañares R, Janicko M, Steib C, Reiberger T, Acevedo J, Gatti P, Bernal W, Zeuzem S, Zipprich A, Piano S, Berg T, Bruns T, Bendtsen F, Coenraad M, Merli M, Stauber R, Zoller H, Ramos JP, Solè C, Soriano G, de Gottardi A, Gronbaek H, Saliba F, Trautwein C, Özdogan OC, Francque S, Ryder S, Nahon P, Romero-Gomez M, Van Vlierberghe H, Francoz C, Manns M, Garcia E, Tufoni M, Amoros A, Pavesi M, Sanchez C, Curto A, Pitarch C, Putignano A, Moreno E, Shawcross D, Aguilar F, Clària J, Ponzo P, Jansen C, Vitalis Z, Zaccherini G, Balogh B, Vargas V, Montagnese S, Alessandria C, Bernardi M, Ginès P, Jalan R, Moreau R, Angeli P, Arroyo V; PREDICT STUDY group of the EASL-CLIF Consortium. The PREDICT study uncovers three clinical courses of acutely decompensated cirrhosis that have distinct pathophysiology. *J Hepatol* 2020; **73**: 842-854 [PMID: 32673741 DOI: 10.1016/j.jhep.2020.06.013]
9 **European Association for the Study of the Liver**. EASL Clinical Practice Guidelines for the management of patients with decompensated cirrhosis. *J Hepatol* 2018; **69**: 406-460 [PMID: 29653741 DOI: 10.1016/j.jhep.2018.03.024]
10 **Moore KP**, Wong F, Gines P, Bernardi M, Ochs A, Salerno F, Angeli P, Porayko M, Moreau R, Garcia-Tsao G, Jimenez W, Planas R, Arroyo V. The management of ascites in cirrhosis: report on the consensus conference of the International Ascites Club. *Hepatology* 2003; **38**: 258-266 [PMID: 12830009 DOI: 10.1053/jhep.2003.50315]
11 **Biggins SW**, Angeli P, Garcia-Tsao G, Ginès P, Ling SC, Nadim MK, Wong F, Kim WR. Diagnosis, Evaluation, and

Management of Ascites, Spontaneous Bacterial Peritonitis and Hepatorenal Syndrome: 2021 Practice Guidance by the American Association for the Study of Liver Diseases. *Hepatology* 2021; **74**: 1014-1048 [PMID: 33942342 DOI: 10.1002/hep.31884]

12 **Ruiz-del-Arbol L**, Monescillo A, Jimenéz W, Garcia-Plaza A, Arroyo V, Rodés J. Paracentesis-induced circulatory dysfunction: mechanism and effect on hepatic hemodynamics in cirrhosis. *Gastroenterology* 1997; **113**: 579-586 [PMID: 9247479 DOI: 10.1053/gast.1997.v113.pm9247479]

13 **Ginès P**, Tító L, Arroyo V, Planas R, Panés J, Viver J, Torres M, Humbert P, Rimola A, Llach J. Randomized comparative study of therapeutic paracentesis with and without intravenous albumin in cirrhosis. *Gastroenterology* 1988; **94**: 1493-1502 [PMID: 3360270 DOI: 10.1016/0016-5085(88)90691-9]

14 **Bernardi M**, Ricci CS, Zaccherini G. Role of human albumin in the management of complications of liver cirrhosis. *J Clin Exp Hepatol* 2014; **4**: 302-311 [PMID: 25755577 DOI: 10.1016/j.jceh.2014.08.007]

15 **Zaccherini G**, Tufoni M, Iannone G, Caraceni P. Management of Ascites in Patients with Cirrhosis: An Update. *J Clin Med* 2021; **10** [PMID: 34830508 DOI: 10.3390/jcm10225226]

16 **Ginès A**, Fernández-Esparrach G, Monescillo A, Vila C, Domènech E, Abecasis R, Angeli P, Ruiz-Del-Arbol L, Planas R, Solà R, Ginès P, Terg R, Inglada L, Vaqué P, Salerno F, Vargas V, Clemente G, Quer JC, Jiménez W, Arroyo V, Rodés J. Randomized trial comparing albumin, dextran 70, and polygeline in cirrhotic patients with ascites treated by paracentesis. *Gastroenterology* 1996; **111**: 1002-1010 [PMID: 8831595 DOI: 10.1016/s0016-5085(96)70068-9]

17 **Sola-Vera J**, Miñana J, Ricart E, Planella M, González B, Torras X, Rodríguez J, Such J, Pascual S, Soriano G, Pérez-Mateo M, Guarner C. Randomized trial comparing albumin and saline in the prevention of paracentesis-induced circulatory dysfunction in cirrhotic patients with ascites. *Hepatology* 2003; **37**: 1147-1153 [PMID: 12717396 DOI: 10.1053/jhep.2003.50169]

18 **Moreau R**, Valla DC, Durand-Zaleski I, Bronowicki JP, Durand F, Chaput JC, Dadamessi I, Silvain C, Bonny C, Oberti F, Gournay J, Lebrec D, Grouin JM, Guémas E, Golly D, Padrazzi B, Tellier Z. Comparison of outcome in patients with cirrhosis and ascites following treatment with albumin or a synthetic colloid: a randomised controlled pilot trail. *Liver Int* 2006; **26**: 46-54 [PMID: 16420509 DOI: 10.1111/j.1478-3231.2005.01188.x]

19 **Bernardi M**, Caraceni P, Navickis RJ, Wilkes MM. Albumin infusion in patients undergoing large-volume paracentesis: a meta-analysis of randomized trials. *Hepatology* 2012; **55**: 1172-1181 [PMID: 22095893 DOI: 10.1002/hep.24786]

20 **Simonetti RG**, Perricone G, Nikolova D, Bjelakovic G, Gluud C. Plasma expanders for people with cirrhosis and large ascites treated with abdominal paracentesis. *Cochrane Database Syst Rev* 2019; **6**: CD004039 [PMID: 31251387 DOI: 10.1002/14651858.CD004039.pub2]

21 **Hamdy H**, ElBaz AA, Hassan A, Hassanin O. Comparison of midodrine and albumin in the prevention of paracentesis-induced circulatory dysfunction in cirrhotic patients: a randomized pilot study. *J Clin Gastroenterol* 2014; **48**: 184-188 [PMID: 23842215 DOI: 10.1097/MCG.0b013e31829ae376]

22 **Peltekian KM**, Wong F, Liu PP, Logan AG, Sherman M, Blendis LM. Cardiovascular, renal, and neurohumoral responses to single large-volume paracentesis in patients with cirrhosis and diuretic-resistant ascites. *Am J Gastroenterol* 1997; **92**: 394-399 [PMID: 9068457]

23 **Arora V**, Vijayaraghavan R, Maiwall R, Sahney A, Thomas SS, Ali R, Jain P, Kumar G, Sarin SK. Paracentesis-Induced Circulatory Dysfunction With Modest-Volume Paracentesis Is Partly Ameliorated by Albumin Infusion in Acute-on-Chronic Liver Failure. *Hepatology* 2020; **72**: 1043-1055 [PMID: 31849085 DOI: 10.1002/hep.31071]

24 **Fagundes C**, Barreto R, Guevara M, Garcia E, Solà E, Rodríguez E, Graupera I, Ariza X, Pereira G, Alfaro I, Cárdenas A, Fernández J, Poch E, Ginès P. A modified acute kidney injury classification for diagnosis and risk stratification of impairment of kidney function in cirrhosis. *J Hepatol* 2013; **59**: 474-481 [PMID: 23669284 DOI: 10.1016/j.jhep.2013.04.036]

25 **Wu CC**, Yeung LK, Tsai WS, Tseng CF, Chu P, Huang TY, Lin YF, Lu KC. Incidence and factors predictive of acute renal failure in patients with advanced liver cirrhosis. *Clin Nephrol* 2006; **65**: 28-33 [PMID: 16429839 DOI: 10.5414/cnp65028]

26 **Piano S**, Rosi S, Maresio G, Fasolato S, Cavallin M, Romano A, Morando F, Gola E, Frigo AC, Gatta A, Angeli P. Evaluation of the Acute Kidney Injury Network criteria in hospitalized patients with cirrhosis and ascites. *J Hepatol* 2013; **59**: 482-489 [PMID: 23665185 DOI: 10.1016/j.jhep.2013.03.039]

27 **Sujan R**, Cruz-Lemini M, Altamirano J, Simonetto DA, Maiwall R, Axley P, Richardson T, Desai V, Cabezas J, Vargas V, Kamath PS, Shah VH, Sarin SK, Bataller R, Singal AK. A Validated Score Predicts Acute Kidney Injury and Survival in Patients With Alcoholic Hepatitis. *Liver Transpl* 2018; **24**: 1655-1664 [PMID: 30153377 DOI: 10.1002/lt.25328]

28 **Angeli P**, Ginès P, Wong F, Bernardi M, Boyer TD, Gerbes A, Moreau R, Jalan R, Sarin SK, Piano S, Moore K, Lee SS, Durand F, Salerno F, Caraceni P, Kim WR, Arroyo V, Garcia-Tsao G. Diagnosis and management of acute kidney injury in patients with cirrhosis: revised consensus recommendations of the International Club of Ascites. *J Hepatol* 2015; **62**: 968-974 [PMID: 25638527 DOI: 10.1016/j.jhep.2014.12.029]

29 **Huelin P**, Piano S, Solà E, Stanco M, Solé C, Moreira R, Pose E, Fasolato S, Fabrellas N, de Prada G, Pilutti C, Graupera I, Ariza X, Romano A, Elia C, Cárdenas A, Fernández J, Angeli P, Ginès P. Validation of a Staging System for Acute Kidney Injury in Patients With Cirrhosis and Association With Acute-on-Chronic Liver Failure. *Clin Gastroenterol Hepatol* 2017; **15**: 438-445.e5 [PMID: 27720915 DOI: 10.1016/j.cgh.2016.09.156]

30 **Bansho ETO**, Silva PES, Colombo BS, Wildner LM, Bazzo ML, Dantas-Corrêa EB, Schiavon LL, Narciso-Schiavon JL. Prognostic Significance of The New Criteria for Acute Kidney Injury in Cirrhosis. *Ann Hepatol* 2018; **17**: 461-469 [PMID: 29735786 DOI: 10.5604/01.3001.0011.7390]

31 **Schacher FC**, Mattos AA, Mulazzani CM, Detanico RB, Favero B, Fonseca BB, Felix PH, Pase THS, Kupski C, Machado MB, Coral GP, Wiltgen D, Mattos AZ. IMPACT OF ACUTE KIDNEY INJURY STAGING ON PROGNOSIS OF PATIENTS WITH CIRRHOSIS. *Arq Gastroenterol* 2020; **57**: 244-248 [PMID: 32935742 DOI: 10.1590/S0004-2803.202000000-46]

32 **Leão GS**, de Mattos AA, Picon RV, Schacher FC, John Neto G, Jotz RF, Chiesa T, Bombassaro IZ, Possebon JPP, Coral GP, Tovo CV, de Mattos ÂZ. The prognostic impact of different stages of acute kidney injury in patients with

decompensated cirrhosis: a prospective cohort study. *Eur J Gastroenterol Hepatol* 2021; **33**: e407-e412 [PMID: 33731594 DOI: 10.1097/MEG.0000000000002120]

33 **Angeli P**, Garcia-Tsao G, Nadim MK, Parikh CR. News in pathophysiology, definition and classification of hepatorenal syndrome: A step beyond the International Club of Ascites (ICA) consensus document. *J Hepatol* 2019; **71**: 811-822 [PMID: 31302175 DOI: 10.1016/j.jhep.2019.07.002]

34 **Fernández J**, Monteagudo J, Bargallo X, Jiménez W, Bosch J, Arroyo V, Navasa M. A randomized unblinded pilot study comparing albumin versus hydroxyethyl starch in spontaneous bacterial peritonitis. *Hepatology* 2005; **42**: 627-634 [PMID: 16108036 DOI: 10.1002/hep.20829]

35 **Stocker R**, Glazer AN, Ames BN. Antioxidant activity of albumin-bound bilirubin. *Proc Natl Acad Sci U S A* 1987; **84**: 5918-5922 [PMID: 3475708 DOI: 10.1073/pnas.84.16.5918]

36 **Cantin AM**, Paquette B, Richter M, Larivée P. Albumin-mediated regulation of cellular glutathione and nuclear factor kappa B activation. *Am J Respir Crit Care Med* 2000; **162**: 1539-1546 [PMID: 11029374 DOI: 10.1164/ajrccm.162.4.9910106]

37 **Boyer TD**, Sanyal AJ, Wong F, Frederick RT, Lake JR, O'Leary JG, Ganger D, Jamil K, Pappas SC; REVERSE Study Investigators. Terlipressin Plus Albumin Is More Effective Than Albumin Alone in Improving Renal Function in Patients With Cirrhosis and Hepatorenal Syndrome Type 1. *Gastroenterology* 2016; **150**: 1579-1589.e2 [PMID: 26896734 DOI: 10.1053/j.gastro.2016.02.026]

38 **Wong F**, Pappas SC, Curry MP, Reddy KR, Rubin RA, Porayko MK, Gonzalez SA, Mumtaz K, Lim N, Simonetto DA, Sharma P, Sanyal AJ, Mayo MJ, Frederick RT, Escalante S, Jamil K; CONFIRM Study Investigators. Terlipressin plus Albumin for the Treatment of Type 1 Hepatorenal Syndrome. *N Engl J Med* 2021; **384**: 818-828 [PMID: 33657294 DOI: 10.1056/NEJMoa2008290]

39 **Ortega R**, Ginès P, Uriz J, Cárdenas A, Calahorra B, De Las Heras D, Guevara M, Bataller R, Jiménez W, Arroyo V, Rodés J. Terlipressin therapy with and without albumin for patients with hepatorenal syndrome: results of a prospective, nonrandomized study. *Hepatology* 2002; **36**: 941-948 [PMID: 12297842 DOI: 10.1053/jhep.2002.35819]

40 **Krag A**, Bendtsen F, Mortensen C, Henriksen JH, Møller S. Effects of a single terlipressin administration on cardiac function and perfusion in cirrhosis. *Eur J Gastroenterol Hepatol* 2010; **22**: 1085-1092 [PMID: 20453655 DOI: 10.1097/MEG.0b013e32833a4822]

41 **Mattos AA**, Wiltgen D, Jotz RF, Dornelles CMR, Fernandes MV, Mattos ÂZ. Spontaneous bacterial peritonitis and extraperitoneal infections in patients with cirrhosis. *Ann Hepatol* 2020; **19**: 451-457 [PMID: 32533951 DOI: 10.1016/j.aohep.2020.04.010]

42 **Gustot T**, Felleiter P, Pickkers P, Sakr Y, Rello J, Velissaris D, Pierrakos C, Taccone FS, Sevcik P, Moreno C, Vincent JL; EPIC II Group of Investigators. Impact of infection on the prognosis of critically ill cirrhotic patients: results from a large worldwide study. *Liver Int* 2014; **34**: 1496-1503 [PMID: 24606193 DOI: 10.1111/liv.12520]

43 **Arvaniti V**, D'Amico G, Fede G, Manousou P, Tsochatzis E, Pleguezuelo M, Burroughs AK. Infections in patients with cirrhosis increase mortality four-fold and should be used in determining prognosis. *Gastroenterology* 2010; **139**: 1246-1256, 1256.e1 [PMID: 20558165 DOI: 10.1053/j.gastro.2010.06.019]

44 **D'Oliveira RAC**, Pereira LCD, Codes L, Rocha MS, Bittencourt PL. Analysis of Healthcare Associated and Hospital Acquired Infections in Critically Ill Patients with Cirrhosis. *Arq Gastroenterol* 2022; **59**: 102-109 [PMID: 35442319 DOI: 10.1590/S0004-2803.202200001-18]

45 **Fernández J**, Acevedo J, Castro M, Garcia O, de Lope CR, Roca D, Pavesi M, Sola E, Moreira L, Silva A, Seva-Pereira T, Corradi F, Mensa J, Ginès P, Arroyo V. Prevalence and risk factors of infections by multiresistant bacteria in cirrhosis: a prospective study. *Hepatology* 2012; **55**: 1551-1561 [PMID: 22183941 DOI: 10.1002/hep.25532]

46 **Piano S**, Singh V, Caraceni P, Maiwall R, Alessandria C, Fernandez J, Soares EC, Kim DJ, Kim SE, Marino M, Vorobioff J, Barea RCR, Merli M, Elkrief L, Vargas V, Krag A, Singh SP, Lesmana LA, Toledo C, Marciano S, Verhelst X, Wong F, Intagliata N, Rabinowich L, Colombato L, Kim SG, Gerbes A, Durand F, Roblero JP, Bhamidimarri KR, Boyer TD, Maevskaya M, Fassio E, Kim HS, Hwang JS, Gines P, Gadano A, Sarin SK, Angeli P; International Club of Ascites Global Study Group. Epidemiology and Effects of Bacterial Infections in Patients With Cirrhosis Worldwide. *Gastroenterology* 2019; **156**: 1368-1380.e10 [PMID: 30552895 DOI: 10.1053/j.gastro.2018.12.005]

47 **Fernández J**, Prado V, Trebicka J, Amoros A, Gustot T, Wiest R, Deulofeu C, Garcia E, Acevedo J, Fuhrmann V, Durand F, Sánchez C, Papp M, Caraceni P, Vargas V, Bañares R, Piano S, Janicko M, Albillos A, Alessandria C, Soriano G, Welzel TM, Laleman W, Gerbes A, De Gottardi A, Merli M, Coenraad M, Saliba F, Pavesi M, Jalan R, Ginès P, Angeli P, Arroyo V; European Foundation for the Study of Chronic Liver Failure (EF-Clif). Multidrug-resistant bacterial infections in patients with decompensated cirrhosis and with acute-on-chronic liver failure in Europe. *J Hepatol* 2019; **70**: 398-411 [PMID: 30391380 DOI: 10.1016/j.jhep.2018.10.027]

48 **Costabeber AM**, Mattos AA, Sukiennik TC. Prevalence of bacterial resistance in hospitalized cirrhotic patients in southern brazil: a new challenge. *Rev Inst Med Trop Sao Paulo* 2016; **58**: 36 [PMID: 27253738 DOI: 10.1590/S1678-9946201658036]

49 **Fernández J**, Acevedo J, Wiest R, Gustot T, Amoros A, Deulofeu C, Reverter E, Martínez J, Saliba F, Jalan R, Welzel T, Pavesi M, Hernández-Tejero M, Ginès P, Arroyo V; European Foundation for the Study of Chronic Liver Failure. Bacterial and fungal infections in acute-on-chronic liver failure: prevalence, characteristics and impact on prognosis. *Gut* 2018; **67**: 1870-1880 [PMID: 28847867 DOI: 10.1136/gutjnl-2017-314240]

50 **Sort P**, Navasa M, Arroyo V, Aldeguer X, Planas R, Ruiz-del-Arbol L, Castells L, Vargas V, Soriano G, Guevara M, Ginès P, Rodés J. Effect of intravenous albumin on renal impairment and mortality in patients with cirrhosis and spontaneous bacterial peritonitis. *N Engl J Med* 1999; **341**: 403-409 [PMID: 10432325 DOI: 10.1056/NEJM199908053410603]

51 **Xue H**, Lin B, Mo J, Li J. Effect of albumin infusion on preventing the deterioration of renal function in patients with spontaneous bacterial peritonitis. *Zhonghua Xiaohuabing Zazhi* 2002; **3**: 32-34 [DOI: 10.1046/j.1443-9573.2002.00062.x]

52 **Chen TA**, Tsao YC, Chen A, Lo GH, Lin CK, Yu HC, Cheng LC, Hsu PI, Tsai WL. Effect of intravenous albumin on endotoxin removal, cytokines, and nitric oxide production in patients with cirrhosis and spontaneous bacterial peritonitis.

Scand J Gastroenterol 2009; **44**: 619-625 [PMID: 19191184 DOI: 10.1080/00365520902719273]
53 **Paine CH**, Biggins SW, Pichler RH. Albumin in Cirrhosis: More Than a Colloid. *Curr Treat Options Gastroenterol* 2019; **17**: 231-243 [PMID: 30968341 DOI: 10.1007/s11938-019-00227-4]
54 **Terg R**, Gadano A, Cartier M, Casciato P, Lucero R, Muñoz A, Romero G, Levi D, Terg G, Miguez C, Abecasis R. Serum creatinine and bilirubin predict renal failure and mortality in patients with spontaneous bacterial peritonitis: a retrospective study. *Liver Int* 2009; **29**: 415-419 [PMID: 18803587 DOI: 10.1111/j.1478-3231.2008.01877.x]
55 **Poca M**, Concepción M, Casas M, Alvarez-Urturi C, Gordillo J, Hernández-Gea V, Román E, Guarner-Argente C, Gich I, Soriano G, Guarner C. Role of albumin treatment in patients with spontaneous bacterial peritonitis. *Clin Gastroenterol Hepatol* 2012; **10**: 309-315 [PMID: 22094025 DOI: 10.1016/j.cgh.2011.11.012]
56 **Salerno F**, Navickis RJ, Wilkes MM. Albumin infusion improves outcomes of patients with spontaneous bacterial peritonitis: a meta-analysis of randomized trials. *Clin Gastroenterol Hepatol* 2013; **11**: 123-30.e1 [PMID: 23178229 DOI: 10.1016/j.cgh.2012.11.007]
57 **Aithal GP**, Palaniyappan N, China L, Härmälä S, Macken L, Ryan JM, Wilkes EA, Moore K, Leithead JA, Hayes PC, O'Brien AJ, Verma S. Guidelines on the management of ascites in cirrhosis. *Gut* 2021; **70**: 9-29 [PMID: 33067334 DOI: 10.1136/gutjnl-2020-321790]
58 **de Araujo A**, de Barros Lopes A, Rossi G, da Silva GV, Ananias P, Ness S, Alvares-da-Silva MR. Low-dose albumin in the treatment of spontaneous bacterial peritonitis: should we change the standard treatment? *Gut* 2012; **61**: 1371-1372 [PMID: 22217507 DOI: 10.1136/gutjnl-2011-301739]
59 **D'Amico G**, Morabito A, D'Amico M, Pasta L, Malizia G, Rebora P, Valsecchi MG. Clinical states of cirrhosis and competing risks. *J Hepatol* 2018; **68**: 563-576 [PMID: 29111320 DOI: 10.1016/j.jhep.2017.10.020]
60 **Piano S**, Angeli P. Bacterial Infections in Cirrhosis as a Cause or Consequence of Decompensation? *Clin Liver Dis* 2021; **25**: 357-372 [PMID: 33838855 DOI: 10.1016/j.cld.2021.01.006]
61 **Trebicka J**, Fernandez J, Papp M, Caraceni P, Laleman W, Gambino C, Giovo I, Uschner FE, Jansen C, Jimenez C, Mookerjee R, Gustot T, Albillos A, Bañares R, Jarcuska P, Steib C, Reiberger T, Acevedo J, Gatti P, Shawcross DL, Zeuzem S, Zipprich A, Piano S, Berg T, Bruns T, Danielsen KV, Coenraad M, Merli M, Stauber R, Zoller H, Ramos JP, Solé C, Soriano G, de Gottardi A, Gronbaek H, Saliba F, Trautwein C, Kani HT, Francque S, Ryder S, Nahon P, Romero-Gomez M, Van Vlierberghe H, Francoz C, Manns M, Garcia-Lopez E, Tufoni M, Amoros A, Pavesi M, Sanchez C, Praktiknjo M, Curto A, Pitarch C, Putignano A, Moreno E, Bernal W, Aguilar F, Clària J, Ponzo P, Vitalis Z, Zaccherini G, Balogh B, Gerbes A, Vargas V, Alessandria C, Bernardi M, Ginès P, Moreau R, Angeli P, Jalan R, Arroyo V; PREDICT STUDY group of the EASL-CLIF CONSORTIUM. PREDICT identifies precipitating events associated with the clinical course of acutely decompensated cirrhosis. *J Hepatol* 2021; **74**: 1097-1108 [PMID: 33227350 DOI: 10.1016/j.jhep.2020.11.019]
62 **Villanueva C**, Albillos A, Genescà J, Garcia-Pagan JC, Brujats A, Calleja JL, Aracil C, Bañares R, Morillas RM, Poca M, Peñas B, Augustin S, Abraldes JG, Alvarado E, Torres F, Bosch J; PreDesCI Study Investigators. Bacterial infections adversely influence the risk of decompensation and survival in compensated cirrhosis. *J Hepatol* 2021; **75**: 589-599 [PMID: 33905794 DOI: 10.1016/j.jhep.2021.04.022]
63 **Caraceni P**, Tufoni M, Zaccherini G, Riggio O, Angeli P, Alessandria C, Neri S, Foschi FG, Levantesi F, Airoldi A, Simone L, Svegliati-Baroni G, Fagiuoli S, Laffi G, Cozzolongo R, Di Marco V, Sangiovanni V, Morisco F, Toniutto P, Gasbarrini A, De Marco R, Piano S, Nardelli S, Elia C, Roncadori A, Baldassarre M, Bernardi M; ANSWER Study Investigators. On-treatment serum albumin level can guide long-term treatment in patients with cirrhosis and uncomplicated ascites. *J Hepatol* 2021; **74**: 340-349 [PMID: 32853747 DOI: 10.1016/j.jhep.2020.08.021]
64 **Baldassarre M**, Naldi M, Zaccherini G, Bartoletti M, Antognoli A, Laggetta M, Gagliardi M, Tufoni M, Domenicali M, Waterstradt K, Paterini P, Baldan A, Leoni S, Bartolini M, Viale P, Trevisani F, Bernardi M, Caraceni P. Determination of Effective Albumin in Patients With Decompensated Cirrhosis: Clinical and Prognostic Implications. *Hepatology* 2021; **74**: 2058-2073 [PMID: 33710623 DOI: 10.1002/hep.31798]
65 **Guevara M**, Terra C, Nazar A, Solà E, Fernández J, Pavesi M, Arroyo V, Ginès P. Albumin for bacterial infections other than spontaneous bacterial peritonitis in cirrhosis. A randomized, controlled study. *J Hepatol* 2012; **57**: 759-765 [PMID: 22732511 DOI: 10.1016/j.jhep.2012.06.013]
66 **Thévenot T**, Bureau C, Oberti F, Anty R, Louvet A, Plessier A, Rudler M, Heurgué-Berlot A, Rosa I, Talbodec N, Dao T, Ozenne V, Carbonell N, Causse X, Goria O, Minello A, De Ledinghen V, Amathieu R, Barraud H, Nguyen-Khac E, Becker C, Paupard T, Botta-Fridlung D, Abdelli N, Guillemot F, Monnet E, Di Martino V. Effect of albumin in cirrhotic patients with infection other than spontaneous bacterial peritonitis. A randomized trial. *J Hepatol* 2015; **62**: 822-830 [PMID: 25463545 DOI: 10.1016/j.jhep.2014.11.017]
67 **Fernández J**, Angeli P, Trebicka J, Merli M, Gustot T, Alessandria C, Aagaard NK, de Gottardi A, Welzel TM, Gerbes A, Soriano G, Vargas V, Albillos A, Salerno F, Durand F, Bañares R, Stauber R, Prado V, Arteaga M, Hernández-Tejero M, Aziz F, Morando F, Jansen C, Lattanzi B, Moreno C, Campion D, Gronbaek H, Garcia R, Sánchez C, García E, Amorós A, Pavesi M, Clària J, Moreau R, Arroyo V. Efficacy of Albumin Treatment for Patients with Cirrhosis and Infections Unrelated to Spontaneous Bacterial Peritonitis. *Clin Gastroenterol Hepatol* 2020; **18**: 963-973.e14 [PMID: 31394283 DOI: 10.1016/j.cgh.2019.07.055]
68 **Mattos ÂZ**, Leão GS, Mattos AA. Albumin for Infections Other Than Spontaneous Bacterial Peritonitis: Still Not an Answer. *Clin Gastroenterol Hepatol* 2020; **18**: 1247-1248 [PMID: 31743756 DOI: 10.1016/j.cgh.2019.11.026]
69 **Leão GS**, John Neto G, Jotz RF, Mattos AA, Mattos ÂZ. Albumin for cirrhotic patients with extraperitoneal infections: A meta-analysis. *J Gastroenterol Hepatol* 2019; **34**: 2071-2076 [PMID: 31353630 DOI: 10.1111/jgh.14791]
70 **Fernández J**, Acevedo J, Prado V, Mercado M, Castro M, Pavesi M, Arteaga M, Sastre L, Juanola A, Ginès P, Arroyo V. Clinical course and short-term mortality of cirrhotic patients with infections other than spontaneous bacterial peritonitis. *Liver Int* 2017; **37**: 385-395 [PMID: 27558198 DOI: 10.1111/liv.13239]
71 **John JA**, de Mattos AA, da Silva Miozzo SA, Comerlato PH, Porto M, Contiero P, da Silva RR. Survival and risk factors related to death in outpatients with cirrhosis treated in a clinic in Southern Brazil. *Eur J Gastroenterol Hepatol* 2015; **27**: 1372-1377 [PMID: 26426832 DOI: 10.1097/MEG.0000000000000480]

72 **Heuman DM**, Abou-Assi SG, Habib A, Williams LM, Stravitz RT, Sanyal AJ, Fisher RA, Mihas AA. Persistent ascites and low serum sodium identify patients with cirrhosis and low MELD scores who are at high risk for early death. *Hepatology* 2004; **40**: 802-810 [PMID: 15382176 DOI: 10.1002/hep.20405]

73 **Bernardi M**, Caraceni P. Novel perspectives in the management of decompensated cirrhosis. *Nat Rev Gastroenterol Hepatol* 2018; **15**: 753-764 [PMID: 30026556 DOI: 10.1038/s41575-018-0045-2]

74 **Garcia-Martinez R**, Caraceni P, Bernardi M, Gines P, Arroyo V, Jalan R. Albumin: pathophysiologic basis of its role in the treatment of cirrhosis and its complications. *Hepatology* 2013; **58**: 1836-1846 [PMID: 23423799 DOI: 10.1002/hep.26338]

75 **Jalan R**, Schnurr K, Mookerjee RP, Sen S, Cheshire L, Hodges S, Muravsky V, Williams R, Matthes G, Davies NA. Alterations in the functional capacity of albumin in patients with decompensated cirrhosis is associated with increased mortality. *Hepatology* 2009; **50**: 555-564 [PMID: 19642174 DOI: 10.1002/hep.22913]

76 **Domenicali M**, Baldassarre M, Giannone FA, Naldi M, Mastroroberto M, Biselli M, Laggetta M, Patrono D, Bertucci C, Bernardi M, Caraceni P. Posttranscriptional changes of serum albumin: clinical and prognostic significance in hospitalized patients with cirrhosis. *Hepatology* 2014; **60**: 1851-1860 [PMID: 25048618 DOI: 10.1002/hep.27322]

77 **Bernardi M**, Zaccherini G, Caraceni P. Pro: The Role of Albumin in Pre-Liver Transplant Management. *Liver Transpl* 2019; **25**: 128-134 [PMID: 30346096 DOI: 10.1002/lt.25356]

78 **WILKINSON P**, SHERLOCK S. The effect of repeated albumin infusions in patients with cirrhosis. *Lancet* 1962; **2**: 1125-1129 [PMID: 14000766 DOI: 10.1016/s0140-6736(62)90895-4]

79 **Gentilini P**, Casini-Raggi V, Di Fiore G, Romanelli RG, Buzzelli G, Pinzani M, La Villa G, Laffi G. Albumin improves the response to diuretics in patients with cirrhosis and ascites: results of a randomized, controlled trial. *J Hepatol* 1999; **30**: 639-645 [PMID: 10207805 DOI: 10.1016/s0168-8278(99)80194-9]

80 **Romanelli RG**, La Villa G, Barletta G, Vizzutti F, Lanini F, Arena U, Boddi V, Tarquini R, Pantaleo P, Gentilini P, Laffi G. Long-term albumin infusion improves survival in patients with cirrhosis and ascites: an unblinded randomized trial. *World J Gastroenterol* 2006; **12**: 1403-1407 [PMID: 16552809 DOI: 10.3748/wjg.v12.i9.1403]

81 **Solà E**, Solé C, Simón-Talero M, Martín-Llahí M, Castellote J, Garcia-Martínez R, Moreira R, Torrens M, Márquez F, Fabrellas N, de Prada G, Huelin P, Lopez Benaiges E, Ventura M, Manríquez M, Nazar A, Ariza X, Suñé P, Graupera I, Pose E, Colmenero J, Pavesi M, Guevara M, Navasa M, Xiol X, Córdoba J, Vargas V, Ginès P. Midodrine and albumin for prevention of complications in patients with cirrhosis awaiting liver transplantation. A randomized placebo-controlled trial. *J Hepatol* 2018; **69**: 1250-1259 [PMID: 30138685 DOI: 10.1016/j.jhep.2018.08.006]

82 **Caraceni P**, Riggio O, Angeli P, Alessandria C, Neri S, Foschi FG, Levantesi F, Airoldi A, Boccia S, Svegliati-Baroni G, Fagiuoli S, Romanelli RG, Cozzolongo R, Di Marco V, Sangiovanni V, Morisco F, Toniutto P, Tortora A, De Marco R, Angelico M, Cacciola I, Elia G, Federico A, Massironi S, Guarisco R, Galioto A, Ballardini G, Rendina M, Nardelli S, Piano S, Elia C, Prestianni L, Cappa FM, Cesarini L, Simone L, Pasquale C, Cavallin M, Andrealli A, Fidone F, Ruggeri M, Roncadori A, Baldassarre M, Tufoni M, Zaccherini G, Bernardi M; ANSWER Study Investigators. Long-term albumin administration in decompensated cirrhosis (ANSWER): an open-label randomised trial. *Lancet* 2018; **391**: 2417-2429 [PMID: 29861076 DOI: 10.1016/S0140-6736(18)30840-7]

83 **Sandi BB**, Leão GS, de Mattos AA, de Mattos ÂZ. Long-term albumin administration in patients with cirrhosis and ascites: A meta-analysis of randomized controlled trials. *J Gastroenterol Hepatol* 2021; **36**: 609-617 [PMID: 32914468 DOI: 10.1111/jgh.15253]

84 **Fernández J**, Clària J, Amorós A, Aguilar F, Castro M, Casulleras M, Acevedo J, Duran-Güell M, Nuñez L, Costa M, Torres M, Horrillo R, Ruiz-Del-Árbol L, Villanueva C, Prado V, Arteaga M, Trebicka J, Angeli P, Merli M, Alessandria C, Aagaard NK, Soriano G, Durand F, Gerbes A, Gustot T, Welzel TM, Salerno F, Bañares R, Vargas V, Albillos A, Silva A, Morales-Ruiz M, Carlos García-Pagán J, Pavesi M, Jalan R, Bernardi M, Moreau R, Páez A, Arroyo V. Effects of Albumin Treatment on Systemic and Portal Hemodynamics and Systemic Inflammation in Patients With Decompensated Cirrhosis. *Gastroenterology* 2019; **157**: 149-162 [PMID: 30905652 DOI: 10.1053/j.gastro.2019.03.021]

85 **de Franchis R**, Bosch J, Garcia-Tsao G, Reiberger T, Ripoll C; Baveno VII Faculty. Baveno VII - Renewing consensus in portal hypertension. *J Hepatol* 2022; **76**: 959-974 [PMID: 35120736 DOI: 10.1016/j.jhep.2021.12.022]

86 **China L**, Freemantle N, Forrest E, Kallis Y, Ryder SD, Wright G, Portal AJ, Becares Salles N, Gilroy DW, O'Brien A; ATTIRE Trial Investigators. A Randomized Trial of Albumin Infusions in Hospitalized Patients with Cirrhosis. *N Engl J Med* 2021; **384**: 808-817 [PMID: 33657293 DOI: 10.1056/NEJMoa2022166]

87 **Wright G**, Jalan R. Ammonia and inflammation in the pathogenesis of hepatic encephalopathy: Pandora's box? *Hepatology* 2007; **46**: 291-294 [PMID: 17661413 DOI: 10.1002/hep.21843]

88 **Jalan R**, Kapoor D. Reversal of diuretic-induced hepatic encephalopathy with infusion of albumin but not colloid. *Clin Sci (Lond)* 2004; **106**: 467-474 [PMID: 14678008 DOI: 10.1042/CS20030357]

89 **Simón-Talero M**, García-Martínez R, Torrens M, Augustin S, Gómez S, Pereira G, Guevara M, Ginés P, Soriano G, Román E, Sánchez-Delgado J, Ferrer R, Nieto JC, Sunyé P, Fuentes I, Esteban R, Córdoba J. Effects of intravenous albumin in patients with cirrhosis and episodic hepatic encephalopathy: a randomized double-blind study. *J Hepatol* 2013; **59**: 1184-1192 [PMID: 23872605 DOI: 10.1016/j.jhep.2013.07.020]

90 **Sharma BC**, Singh J, Srivastava S, Sangam A, Mantri AK, Trehanpati N, Sarin SK. Randomized controlled trial comparing lactulose plus albumin versus lactulose alone for treatment of hepatic encephalopathy. *J Gastroenterol Hepatol* 2017; **32**: 1234-1239 [PMID: 27885712 DOI: 10.1111/jgh.13666]

91 **Is B**, Bombassaro IZ, Tovo CV, de Mattos ÂZ, Ahlert M, Chiesa T, de Mattos AA. Albumin in the management of hepatic encephalopathy: A systematic review and meta-analysis. *Ann Hepatol* 2021; **26**: 100541 [PMID: 34600143 DOI: 10.1016/j.aohep.2021.100541]

92 **Riggio O**, Nardelli S, Pasquale C, Pentassuglio I, Gioia S, Onori E, Frieri C, Salvatori FM, Merli M. No effect of albumin infusion on the prevention of hepatic encephalopathy after transjugular intrahepatic portosystemic shunt. *Metab Brain Dis* 2016; **31**: 1275-1281 [PMID: 26290375 DOI: 10.1007/s11011-015-9713-x]

93 **McCormick PA**, Mistry P, Kaye G, Burroughs AK, McIntyre N. Intravenous albumin infusion is an effective therapy for hyponatraemia in cirrhotic patients with ascites. *Gut* 1990; **31**: 204-207 [PMID: 2311979 DOI: 10.1136/gut.31.2.204]

94 **Jalan R**, Mookerjee R, Cheshire L, Williams R, Davies N. Albumin infusion for severe hyponatremia in patients with refractory ascites: a randomized clinical trial. *J Hepatol* 2007; **46** Suppl 1: S95 [DOI: 10.1016/s0168-8278(07)61830-3]

95 **Bajaj JS**, Tandon P, O'Leary JG, Biggins SW, Wong F, Kamath PS, Garcia-Tsao G, Maliakkal B, Lai JC, Fallon M, Thuluvath P, Vargas HE, Subramanian RM, Thacker LR, Reddy RK. The Impact of Albumin Use on Resolution of Hyponatremia in Hospitalized Patients With Cirrhosis. *Am J Gastroenterol* 2018; **113**: 1339 [PMID: 29880972 DOI: 10.1038/s41395-018-0119-3]

96 **Shasthry SM**, Kumar M, Khumuckham JS, Sarin SK. Changes in cardiac output and incidence of volume overload in cirrhotics receiving 20% albumin infusion. *Liver Int* 2017; **37**: 1167-1176 [PMID: 28135785 DOI: 10.1111/liv.13375]

97 **Bortoluzzi A**, Ceolotto G, Gola E, Sticca A, Bova S, Morando F, Piano S, Fasolato S, Rosi S, Gatta A, Angeli P. Positive cardiac inotropic effect of albumin infusion in rodents with cirrhosis and ascites: molecular mechanisms. *Hepatology* 2013; **57**: 266-276 [PMID: 22911662 DOI: 10.1002/hep.26021]

98 **Jagdish RK**, Maras JS, Sarin SK. Albumin in Advanced Liver Diseases: The Good and Bad of a Drug! *Hepatology* 2021; **74**: 2848-2862 [PMID: 33772846 DOI: 10.1002/hep.31836]

99 **Caraceni P**, O'Brien A, Gines P. Long-term albumin treatment in patients with cirrhosis and ascites. *J Hepatol* 2022; **76**: 1306-1317 [PMID: 35589252 DOI: 10.1016/j.jhep.2022.03.005]

100 **Caraceni P**, Domenicali M, Tovoli A, Napoli L, Ricci CS, Tufoni M, Bernardi M. Clinical indications for the albumin use: still a controversial issue. *Eur J Intern Med* 2013; **24**: 721-728 [PMID: 23790570 DOI: 10.1016/j.ejim.2013.05.015]

101 **Runken MC**, Caraceni P, Fernandez J, Zipprich A, Carlton R, Bunke M. The cost-effectiveness of albumin in the treatment of decompensated cirrhosis in Germany, Italy, and Spain. *Health Econ Rev* 2019; **9**: 22 [PMID: 31278624 DOI: 10.1186/s13561-019-0237-7]

World Journal of Gastroenterology

Submit a Manuscript: https://www.f6publishing.com

World J Gastroenterol 2022 September 7; 28(33): 4787-4811

DOI: 10.3748/wjg.v28.i33.4787

ISSN 1007-9327 (print) ISSN 2219-2840 (online)

ORIGINAL ARTICLE

Basic Study

Novel therapeutic diiminoquinone exhibits anticancer effects on human colorectal cancer cells in two-dimensional and three-dimensional *in vitro* models

Alissar Monzer, Kevork Wakimian, Farah Ballout, Samar Al Bitar, Amani Yehya, Mariam Kanso, Nour Saheb, Ayman Tawil, Samer Doughan, Maher Hussein, Deborah Mukherji, Walid Faraj, Hala Gali-Muhtasib, Wassim Abou-Kheir

Specialty type: Medicine, research and experimental

Provenance and peer review: Invited article; Externally peer reviewed.

Peer-review model: Single blind

Peer-review report's scientific quality classification

Grade A (Excellent): 0
Grade B (Very good): B
Grade C (Good): C
Grade D (Fair): 0
Grade E (Poor): 0

P-Reviewer: Capello D, Italy; Fruhling P, Sweden

Received: March 18, 2022
Peer-review started: March 18, 2022
First decision: June 11, 2022
Revised: June 24, 2022
Accepted: August 5, 2022
Article in press: August 5, 2022
Published online: September 7, 2022

Alissar Monzer, Farah Ballout, Samar Al Bitar, Department of Biology, American University of Beirut, Beirut 1107-2020, Lebanon

Kevork Wakimian, Amani Yehya, Wassim Abou-Kheir, Department of Anatomy, Cell Biology and Physiological Sciences, American University of Beirut, Beirut 1107-2020, Lebanon

Mariam Kanso, Samer Doughan, Maher Hussein, Walid Faraj, Department of Surgery, American University of Beirut Medical Center, Beirut 1107-2020, Lebanon

Nour Saheb, Ayman Tawil, Department of Pathology and Laboratory Medicine, American University of Beirut Medical Center, Beirut 1107-2020, Lebanon

Deborah Mukherji, Department of Internal Medicine, American University of Beirut Medical Center, Beirut 1107-2020, Lebanon

Hala Gali-Muhtasib, Department of Biology and Center for Drug Discovery, American University of Beirut, Beirut 1107-2020, Lebanon

Corresponding author: Wassim Abou-Kheir, MSc, PhD, Associate Professor, Department of Anatomy, Cell Biology and Physiological Sciences, American University of Beirut, Bliss street-Hamra, Beirut 1107-2020, Lebanon. wa12@aub.edu.lb

Abstract

BACKGROUND

Colorectal cancer (CRC) is the second leading cause of cancer-related mortality. Cancer stem cells (CSCs) in CRC, which are spared by many chemotherapeutics, have tumorigenic capacity and are believed to be the reason behind cancer relapse. So far, there have been no effective drugs to target colon CSCs. Diiminoquinone (DIQ) has shown promising effects on targeting colon cancer. However, there is limited research on the effects of DIQ on eradicating CSCs in CRC.

AIM

To investigate the anticancer potential of DIQ on colon CSCs in two-dimensional

(2D) and three-dimensional (3D) models using colonospheres and patient-derived organoids.

METHODS

Various 2D methods have been used to assess the effect and the mechanism of DIQ on HCT116 and HT29 cell lines including cell proliferation and viability assays, migration and invasion assays, immunofluorescence staining, and flow cytometry. The potency of DIQ was also assessed in 3D culture using the sphere formation assay and colon cancer patient-derived organoid model.

RESULTS

Our results showed that DIQ significantly inhibited cell proliferation, migration, and invasion in HCT116 and HT29 cell lines. DIQ treatment induced apoptosis along with an accumulation of HCT116 and HT29 cancer cells in the sub-G1 region and an increase in reactive oxygen species in both CRC cell lines. DIQ reduced sphere-forming and self-renewal ability of colon cancer HCT116 and HT29 stem/progenitor cells at sub-toxic doses of 1 μmol/L. Mechanistically, DIQ targets CSCs by downregulating the main components of stem cell-related -catenin, AKT, and ERK oncogenic signaling pathways. Potently, DIQ displayed a highly significant decrease in both the count and the size of the organoids derived from colon cancer patients as compared to control and 5-fluorouracil conditions.

CONCLUSION

This study is the first documentation of the molecular mechanism of the novel anticancer therapeutic DIQ *via* targeting CSC, a promising compound that needs further investigation.

Key Words: Diiminoquinone; Anticancer activity; Colorectal cancer; Cancer stem cells; Patient-derived organoids; Colonospheres

©The Author(s) 2022. Published by Baishideng Publishing Group Inc. All rights reserved.

Core Tip: Diiminoquinone has anticancer activity against colorectal cancer. Diiminoquinone targets chemoresistant cancer stem cells in three-dimensional *in vitro* models by downregulating the main components of stem cell-related -catenin, AKT, and ERK oncogenic signaling pathways. Our findings highlight diiminoquinone's novel therapeutic potential against colorectal cancer.

Citation: Monzer A, Wakimian K, Ballout F, Al Bitar S, Yehya A, Kanso M, Saheb N, Tawil A, Doughan S, Hussein M, Mukherji D, Faraj W, Gali-Muhtasib H, Abou-Kheir W. Novel therapeutic diiminoquinone exhibits anticancer effects on human colorectal cancer cells in two-dimensional and three-dimensional *in vitro* models. *World J Gastroenterol* 2022; 28(33): 4787-4811

URL: https://www.wjgnet.com/1007-9327/full/v28/i33/4787.htm

DOI: https://dx.doi.org/10.3748/wjg.v28.i33.4787

INTRODUCTION

Colorectal cancer (CRC) ranks as the third most common cancer worldwide in 2020 in terms of incidence in men and women, and the second most common cause of cancer deaths in 2020 reaching 935000 deaths according to GLOBOCAN 2020 data[1].

Current medical treatment of CRC includes a wide array of systemic therapies, which include chemotherapeutics [such as 5-fluorouracil (5FU)], targeted therapy (such as epidermal growth factor receptor inhibitors), in addition to immunotherapy, depending on the stages of CRC. High mortality and recurrence rates of CRC are mainly correlated to metastasis, treatment resistance[2,3], and presence of chemoresistant cancer stem cells (CSCs)[4,5]. Although 5FU is the standard chemotherapy for CRC, either alone or in combination with other treatments, it has been ineffective and found to cause drug resistance[6,7]. Around 75% of patients with metastatic CRC receiving chemotherapy develop recurrence within 18 mo[8]. Although the field has witnessed several advances on the quest to control advanced and metastatic colon cancer with some newly developed drugs, there is still a pressing need to fully understand colon cancer biology, develop novel treatment approaches and pre-clinical models, and identify useful therapeutics targeting CSCs and chemoresistant cells and aiming at increasing patient survival.

Recently, we have witnessed the development of different types of *in vitro* three-dimensional (3D) culture systems to recapitulate the *in vivo* cancer growth[9,10]. 3D culture systems mainly include organoid models and multicellular spheroid models[11]. Cancer treatment, particularly using 3D culture

for targeting CSC, is rapidly progressing toward personalized medicine taking into consideration the individual molecular biology and genetic variability of tumors. Introducing *in vitro* patient-derived organoid culture systems to 3D models have revolutionized CRC research[12,13].

CSCs are characterized by their self-renewal, pluripotency, and tumor expansion potential of differentiated cell populations with altered molecular and cellular phenotypes[14]. They are responsible for angiogenic induction and apoptotic resistance. This small subpopulation is associated with tumor invasion and metastasis, therapeutic resistance, cancer relapse, and poor prognosis in patients[15]. CSCs are present within solid tumors, and they are recognized to be resistant to chemotherapies such as 5FU or oxaliplatin[4]. Intriguingly, there are no effective drugs to target CSCs in CRC. Therefore, targeting this population holds hope for treatment response.

Studies have reported that some quinones, which are often secondary metabolites derived from plants, possess anticancer activity[16]. They are present and clinically used in a variety of cancer treatments, such as the anthracyclines daunorubicin, doxorubicin, and mitoxantrone, acting through the redox quinone-hydroquinone system[17]. Anthraquinones are a class of natural compounds that possess anticancer properties against various skin cancer cells and breast cancer cells[18]. Studies have shown that thymoquinone, which has a basic quinone structure, induces apoptosis and halts metastasis in CRC [19,20]. Also, iminoquinone exerts anticancer effects through inhibition of cell survival/proliferation and inhibition of oncogene expression[21].

The novel diiminoquinone (DIQ) compound has recently shown potent anticancer effects against the HCT116 CRC cell line as reported in our previous study[22]. The activity of DIQ is believed to be based on the structural similarities between quinones and diiminoquinones. Here, we investigated the anticancer activities and targeting mechanism(s) of DIQ against human colon CSCs using colonosphere cultures and patient-derived organoids. This study represents the first comprehensive documentation of the activity of DIQ against colon CSCs, findings that will provide the basis for proposing this stable and non-toxic compound for clinical testing and future discovery of new effective treatments for patients with colon cancer.

MATERIALS AND METHODS

Cell culture condition

Human CRC cell lines HCT116 and HT29 and non-tumorigenic fetal human intestinal FH74Int cell line were purchased from ATCC (ATCC, Manassas, VA, United States). HCT116 and HT29 cell lines were cultured and maintained in RPMI 1640 (Sigma-Aldrich, St. Louis, MO, United States) and L-glutamine (Sigma-Aldrich). FH74Int cells were grown in DMEM (Lonza, Verviers, Belgium) supplemented with 10 μg/mL insulin and 1% sodium pyruvate. Cell culture media was supplemented with antibiotics [1% penicillin-streptomycin (100 U/mL)], 10% heat-inactivated fetal bovine serum (FBS) (Sigma-Aldrich), and 5 μg/mL Plasmocin™ Prophylactic (InvivoGen, San Diego, CA, United States). Cells were maintained in an incubator at 37 °C in a humidified atmosphere of 5% CO_2 and 95% air and were routinely checked for mycoplasma contamination. All cells were mycoplasma free.

DIQ preparation and treatment

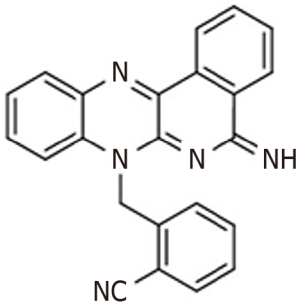
The purified compound DIQ (Figure 1) was synthesized by Professor Makhlouf Haddadin (Department of Chemistry, American University of Beirut)[22]. Stocks of the purified compound DIQ were prepared by dissolving 5 mg in 1 mL 100% dimethyl sulfoxide (Pan Biotech, Aidenbach, Germany). DIQ dilutions were stored at -20 °C. The stock solutions were then dissolved in cell culture medium such that the percentage of dimethyl sulfoxide on cells was less than 0.1%.

MTT cell viability assay

The anti-proliferative effects of DIQ were measured *in vitro* by using MTT [3-(4, 5-dimethylthiazol-2-yl)-2, 5-diphenyltetrazolium bromide] (Sigma-Aldrich) assay according to the manufacturer's instructions. HCT116 WT, HT29, and FHSInt74 cells were seeded in 96-well culture plates at a density of 10000 cells per well and incubated overnight. Then, the subconfluent cells were treated in triplicate with different concentrations of DIQ diluted in 100 μL complete media for 24, 48, and 72 h. For each time point, 10 μL of 5 mg/mL [in 1 × phosphate-buffered saline (PBS)] MTT reagent was added to each well and incubated at 37 °C for 4 h. The reduced MTT dye was solubilized with absolute isopropanol (Sigma-Aldrich) (100 μL/well) after which MTT optical density was measured at 595 nm by an ELISA reader (Multiskan Ex; ThermoFisher Scientific, Waltham, MA, United States). The percent cell proliferation with respect to control was determined for each drug dose.

Trypan blue exclusion assay

HCT116, HT29, and FHSInt74 cell lines were seeded in duplicates in 24-well culture plates at a density of 50000, 80000, and 100000 cells/300 μL complete media per well, respectively. Cells were incubated overnight then treated in duplicate with various concentrations of DIQ (1, 4, and 10 μmol/L) for 24, 48,



DOI: 10.3748/wjg.v28.i33.4787 **Copyright** ©The Author(s) 2022.

Figure 1 Chemical structure of the diiminoquinone compound.

and 72 h. Attached live cells were harvested by trypsin EDTA and added to the supernatant. The cell pellet was resuspended in 300 µL media. Live cells were counted using a hemocytometer. The percentage cell viability was expressed as percentage growth relative to the control condition of each time point and are derived from the mean of triplicates wells. Each experiment was repeated at least three times.

Wound healing assay

For wound healing, or scratch assay, CRC cells were seeded in 24-well plates and incubated until they reached 80%-90% confluence. Cells were then treated with 10 µg/mL mitomycin C (Sigma-Aldrich) to block cellular proliferation. A sterile 200 µL tip was used to scratch wounds of the same width on each monolayer. After washing the plates twice with PBS (Sigma-Aldrich) to remove the detached cells, the remaining cells were cultured in complete media with or without DIQ treatment at the IC_{50} concentration. Images using bright-field microscopy were subsequently taken at 0 h and 72 h to compare the wound width. The wound width was measured and expressed as a percentage of the relative wound width. The experiment was repeated three times with duplicate measurements in each experiment.

Transwell invasion assay

For the transwell invasion assay, 0.3×10^5 HCT116 and 0.5×10^5 HT29 cells were seeded in serum-free medium in the top chamber of 24-well inserts (pore size, 8 µm; Falcon, ThermoFisher Scientific) coated with 1:10 dilution in cold PBS of Matrigel™ (BD Bioscience, Franklin Lakes, NJ, United States). A medium supplemented with 10% FBS was used as a chemoattractant in the lower chamber. Cells with or without DIQ treatment were allowed to migrate through the membrane coated with Matrigel™ at 37 °C in a 5% CO_2 incubator for 72 h. Non-migratory cells in the upper chamber were then gently scraped off with a cotton-tip applicator. Invading cells on the lower surface of the membrane were fixed and stained with hematoxylin and eosin. After staining, the total number of invading cells was counted using an inverted light microscope (10 × objective) from six consecutive fields for each well.

Reactive oxygen species

The level of intracellular reactive oxygen species (ROS) in HCT116 and HT29 was measured using the fluorescent probe dihydroethidium (DHE). For DHE staining, cells were seeded at a density of 50000 cells on coverslips in 24-well cell culture plates and allowed to become 40%-50% confluent. Following 48 h incubation with DIQ treatment at the IC_{50} dose, CRC cells were fixed in 4% formaldehyde for 20 min. After fixation, CRC cells were washed twice with 1 × PBS, then incubated with 20 µmol/L DHE dye (Invitrogen, Carlsbad, CA, United States). After 45 min staining, the DHE stain was removed, and the cells were washed with 1 × PBS. Mounting media with 4',6-diamidino-2-phenylindole dye was added. Fluorescence images were taken immediately under a Zeiss LSM710 Laser confocal microscope (Carl Zeiss, Oberkochen, Germany) equipped with Zen software to process the images.

Cell cycle analysis

Cells were seeded at 5×10^5 cells in 6-well cell culture plates and incubated overnight prior to drug treatment for 24 and 72 h. Cells were then harvested and washed in PBS then fixed in 70% ice-cold ethanol added dropwise to the cell pellet while vortexing for 30 min on ice. To ensure that only DNA was stained, fixed cells were incubated for 30 min at 37 °C with 100 µL of propidium iodide (PI) (Sigma) solution [6 µL RNase, 30 µL PI (1 mg/mL)] in the dark in a flow tube (BD Falcon, ThermoFisher Scientific). A total of 10000 gated events were acquired in order to assess the proportions of cells in different stages of the cell cycle. Cell cycle analysis was performed by flow cytometry using Guava EasyCyte8 Flow Cytometer-Millipore. GuavaSoft™ 2.7 Software.

Annexin V-PI staining

HCT116 and HT29 cells were seeded at a density of 5 × 10^5 cells in 6-well cell culture plates and incubated overnight prior to drug treatment for 72 h. Cells were then harvested and washed in cold PBS. The pellet was resuspended in 100 µL binding buffer and stained with 5 µL annexin V-FITC and 5 µL PI in the dark for 30 min at room temperature. Then, 400 µL binding buffer was added, and apoptotic cells were analyzed with fluorescence-activated cell sorting flow cytometry.

Sphere formation assay

Self-renewal capacity is deemed to be one of the major defining hallmarks of stem/progenitor cells. Thus, to determine whether DIQ was able to target the self-renewing CSC pool, we investigated sphere formation capability over 5 generations. The sphere formation assay was used as previously reported by our laboratory[23,24]. Briefly, 1000 single cells/well in 96-well culture plate were suspended in cold Matrigel™/serum-free medium (1:1) in a total volume of 10 µL. Cells were seeded uniformly in a circular manner around the bottom rim of the well and allowed to solidify in the incubator at 37 °C for 1 h. Subsequently, 100 µL of RPMI with 5% FBS treated with DIQ was added gently in the middle of each well. Each experimental condition was performed in duplicate. Spheres were replenished with warm media as in the original seeding every other day. Spheres were counted in the 96-well plate dishes after 8 to 12 d of sphere culture, and bright field images of the spheres were obtained using Axiovert microscope from Zeiss at × 10 magnification. Images were analyzed by Carl Zeiss Zen 2012 image software to determine sizes. Sphere-formation unit (SFU) was calculated for each generation as follows: SFU = number of spheres formed/number of cells originally plated. Results were represented as percentage of the SFU of each condition.

Sphere propagation assay

To enrich the stem-like population of cells, the media was aspirated from the well. Collected spheres using cold media were incubated in 300 µL of Trypsin/EDTA at 37 °C for 1-3 min and then passed through 27-gauge syringes three times. Single cells resulting from the dissociation of spheres were replated and treated at the same density of 1000 cells/well in 96-well culture plates as previously described. We believe that at least 5 generations of colonospheres were required to enrich the subpopulation of progenitor/stem-like colon cancer cells.

Immunofluorescence imaging of colonospheres

Spheres at generation 1 were collected with cold RPMI media and centrifuged to washout all Matrigel™ debris. After centrifugation, spheres were fixed in situ in 4% paraformaldehyde (PFA) at room temperature for 20 min. The PFA was aspirated gently, and spheres were permeabilized with 0.5% Triton X-100 for 30 min at room temperature. After carefully aspirating the permeabilization solution, spheres were blocked using the sphere blocking buffer [0.1% bovine serum albumin (BSA), 0.2% Triton X-100, 0.05% Tween-20, and 10% normal goat serum in PBS] for 2 h at room temperature. Spheres were washed in PBS then incubated overnight with different primary antibodies for assessment of treatment and characterization including Ki67, CD44, Gamma H2A histone family member X (γH2AX), cytokeratin (CK)19 and CK8 (refer to Table 1 for details on antibodies used). After gentle washing with PBS containing 0.1% Tween-20, spheres were incubated with Alexa-488 and/or 568-conjugated IgG (Invitrogen) for 2 h at room temperature. Spheres were mounted with the antifade Fluorogel II with 4′,6-diamidino-2-phenylindole (Abcam, Cambridge, United Kingdom). Confocal fluorescent images were acquired and analyzed using the Carl Zeiss LSM 710 Laser scanning microscope.

Western blot analysis

For two-dimensional (2D) western blot results, cells were plated in 12-well plates, treated with DIQ, and then collected. For 3D western blot results, HCT116 and HT29 cells were plated in 24-well plates (3 × 10^5 cells/well) with or without treatment to form spheres. At day 8-10, spheres were collected with cold RPMI media then washed with PBS to remove any residual media. Proteins were then extracted with RIPA lysis buffer (sc-24948; Santa Cruz Biotechnology, Dallas, TX, United States). Protein extracts were quantified using the DC Bio-Rad Protein Assay (Bio-Rad Laboratories, Hercules, CA, United States) according to the manufacturer's protocol. Equal amounts of protein lysate were mixed with 5% β-mercaptoethanol and 2X Laemmli Sample Buffer (Bio-Rad Laboratories), electrophoresed in 12% sodium dodecyl sulfate-polyacrylamide gel electrophoresis, and then transferred to 0.45 µm nitrocellulose membrane (Bio-Rad Laboratories) for 2 h. Membranes were blocked for 1 h with 5% skim milk in tris-buffered saline with 0.1% tween 20, then blotted with primary antibodies (antibodies used are listed in Table 2) overnight at 4 °C. The next day, membranes were washed three times with tris-buffered saline with 0.1% tween 20 and blotted with corresponding secondary antibodies for 1 h at room temperature. Hybridization with GAPDH-HRP (6C5) coupled antibody was performed for 1 h at room temperature as the housekeeping gene. Membranes were developed, and target proteins were detected using the enhanced chemiluminescence system (Bio-Rad Laboratories). Images were generated and quantified using ChemiDoc™ Imaging Systems (Bio-Rad Laboratories).

Table 1 List of primary and secondary antibodies used in immunofluorescent staining

Antibody name	Species	Dilution	Catalog number	Company
Primary antibodies				
CK8	Mouse	1:200	904801	Biolegend
CK19	Rabbit	1:200	ab15463	Abcam
CD44	Mouse	1:100	sc-7297	Santa Cruz Biotechnology
Ki67	Mouse	1:50	sc-23900	Santa Cruz Biotechnology
p- HistoneH2AX	Rabbit	1:200	#9718S	Cell Signaling
Secondary antibodies				
Alexa fluoro 488	Goat anti-mouse	1:200	A-28175	Invitrogen
Alexa fluoro 568	Goat anti-rabbit	1:200	A-11011	Invitrogen
Phalloidin		1:200	R415	Invitrogen

Table 2 List of primary and secondary antibodies used in western blot experiments

Antibody name	Species	Dilution	Catalog number	Company
Primary antibodies				
p53	Rabbit	1:50	sc-6243	Santa Cruz Biotechnology
p21	Rabbit	1:1000	sc-2947	Cell Signaling
CD133	Rabbit	1:500	#64326S	Cell Signaling
β-catenin	Mouse	1:200	sc-7963	Santa Cruz Biotechnology
PCNA	Mouse	1:50	sc-25280	Santa Cruz Biotechnology
p-ERK	Mouse	1:300	sc-7383	Santa Cruz Biotechnology
ERK	Rabbit	1:300	sc-93	Santa Cruz Biotechnology
p-AKT	Rabbit	1:1000	#4060	Cell Signaling
AKT	Rabbit	1:1000	#4691	Cell Signaling
GAPDH-HRP (6C5)	Mouse	1:20,000	#MAB5476	Abnova
Secondary antibodies				
Goat anti-mouse	Goat	1:1000	sc-516102	Santa Cruz Biotechnology
Mouse anti-rabbit	Mouse	1:1000	sc-2357	Santa Cruz Biotechnology

Ethical consideration of patient derived-organoid culture

The study with all its experimental protocols was conducted under the Institutional Review Board approvals of the American University of Beirut and American University of Beirut Medical Center to obtain patient information and human colorectal tissue samples from consenting patients. All protocols were performed in accordance with The Code of Ethics of the World Medical Association (Declaration of Helsinki) and in agreement with all ethical considerations of the Institutional Review Board for experiments involving human subjects. Oral consent was obtained from all patients, and confidentiality was maintained. For colectomy specimens, a core biopsy was taken from the area most likely to be involved with cancer according to the surgeon and pathologist recommendations.

Tissue processing and patient-derived organoid culture

Colon tumor tissue from patients was rinsed with PBS and manually minced using sterile scalpels. The majority of minced fragments was employed for organoid culturing; remaining fragments were transferred directly to 4% PFA for histological examination. According to the protocol described by Boehnke *et al*[25], minced fragments for organoid culturing were digested in advanced adDMEM/F12 (Gibco, ThermoFisher Scientific) supplemented with 1 × P/S, collagenase IV (Sigma-Aldrich), and amphotericin B (Sigma-Aldrich) at 37 °C for 1 h. During incubation, the tissue fragments were repeatedly suspended with a 100 µL micropipette. To exclude undigested tissue fragments, the suspension was filtered through a 100 µm cell strainer (Corning, Corning, NY, United States). The

flowthrough was subjected to consecutive filtrations when needed. Isolated cells were seeded in 24-well plates with Matrigel at a cell density of 20000 single cells/well. Then, 20 µL drops were plated into the middle of the well. The plate was placed upside down in the 37 °C incubator for 15 min to allow the Matrigel to solidify. Finally, 300 µL of prewarmed human colon growth medium plus Y-27632 was added into each well. Cells were cultured with adDMEM/F12 additional with various factors added to maintain tumor biological traits and growth activity. Medium was changed every 2-3 d. Cultures were passaged when the aggregates reached 800 µm diameter. Organoids were counted at day 8-12 of each passage under Axiovert inverted microscope at × 10 magnification, and then images of organoids were taken at the same magnification. Images were then analyzed by Carl Zeiss Zen 2012 image software to determine size. The organoid formation count (OFC) was calculated at each generation by counting the number of organoids formed, starting with the same number of input cells in all conditions.

Passaging of the established patient-derived organoids

Organoids were collected when they reached the appropriate size and confluency for passaging (8-12 d after plating). To dissolve Matrigel, ice-cold medium was used, and organoids were collected. Organoids were then centrifuged at 200 g for 5 min at 4 °C. After that, the pellet was resuspended in 1 mL ice-cold adDMEM/F12 to dissolve residual Matrigel. After counting the cells in the pellet, the cells were resuspended in 90% cold Matrigel and seeded as a 5 µL drop in 96-well plate. Cells were cultured with adDMEM/F12 additional with various factors added to maintain the tumor's biological traits and growth activity. Medium was changed every 2-3 d with or without DIQ treatment. Cultures were passaged when the aggregates reached 800 µm diameter. The previous steps were repeated for several generations.

Cell line-derived organoid protocol

Briefly, 5000 HCT116 and HT29 single cells/well in 96-well culture plate were suspended in cold Matrigel™/serum-free medium (9:1) in a total volume of 5 µL as drops in the middle of individual wells of 96-well culture plates. Plated colon cells were allowed to solidify in the incubator at 37 °C for 30 min. Subsequently, 200 µL/well of advanced DMEM/F12 media with several factors, with or without DIQ treatment, was added. Each experimental condition was performed in duplicate. Organoids were replenished with warm media as in the original seeding every other day. Organoids were counted in the 96-well plate dishes after 8 to 12 d of organoid culture, and bright field images of the organoids were obtained using Axiovert microscope from Zeiss at × 10 magnification.

Immunofluorescence and morphological analysis of colonospheres and colorectal organoids

Spheres/organoids were collected with cold RPMI media and centrifuged to wash all Matrigel™ debris. After centrifugation, spheres/organoids were fixed in situ in 4% PFA at room temperature for 20 min. The PFA was aspirated gently, and spheres/organoids were permeabilized with 0.5% Triton X-100 for 30 min at room temperature. After carefully aspirating the permeabilization solution, spheres/organoids were blocked using the blocking buffer (0.1% BSA, 0.2% Triton X-100, 0.05% Tween-20, and 10% normal goat serum in PBS) for 2 h at room temperature. Spheres/organoids were washed in PBS then incubated overnight with different primary antibodies for assessment of treatment and characterization (refer to Table 1 for details on antibodies used). After gentle washing with PBS containing 0.1% Tween-20, spheres/organoids were incubated with Alexa-488 and/or 568-conjugated IgG (Invitrogen) for 2 h at room temperature. Spheres/organoids were mounted with the antifade Fluorogel II with 4',6-diamidino-2-phenylindole (Abcam). Confocal fluorescent images were acquired and analyzed using the Carl Zeiss LSM 710 Laser scanning microscope. Paraffin embedding, microtome sectioning, and standard hematoxylin and eosin staining were all performed by the Histology Laboratory at the Diana Tamari Sabbagh building; all steps were performed at room temperature.

Animal experiments

Animal experiments were performed according to approved protocols by the Institutional Animal Care and Use Committee of the American University of Beirut. Mice were housed under optimum conditions of temperature and light set in specific pathogen-free animal housing. Mice were kept in plastic cages covered with sawdust and had unrestricted access to a commercial mouse diet (24% protein, 4.5% fat, 4% fiber) and water. Animals were sacrificed by cervical dislocation following deep anesthesia with isoflurane. For tumor induction in mice, a group of 6-8-wk old non-obese diabetic severe combined immunodeficiency male mice were inoculated subcutaneously into the flanks with 100 HCT116-derived spheres in a total volume of 50 µL growth media and Matrigel™ (1:1). Upon the detection of a palpable tumor post cell/sphere injection, group 1 injected with 3D spheres was treated with saline (control group), and group 2 injected with 3D spheres was treated with DIQ (20 mg/kg). Mice were treated three times/wk until tumor burden necessitated that we sacrificed the animals. Tumor size was measured every other day using Mitutoyo caliper throughout the study. Mice were monitored daily for signs of morbidity. Body weight recordings were carried out biweekly.

Statistical analysis

All statistical tests were performed using GraphPad Prism 7 (version 7.0; GraphPad Software Inc., La Jolla, CA, United States). Student's *t* test, One-way or two-way analysis of variance tests were used in this study. In all statistical tests, the mean of treated groups was compared to the mean of control groups. Statistical significance was reported at *P* values of < 0.05. $^{a}P < 0.05$; $^{b}P < 0.01$; $^{c}P < 0.001$. Experimental values were means ± standard error of the mean.

RESULTS

DIQ reduced the cell proliferation of human CRC cell lines in 2D in vitro models

To assess the effect of DIQ compound on the proliferation of human CRC cell lines cultured in 2D monolayers, we employed the MTT assay. Two human CRC cell lines, HCT116 and HT29, were treated with different concentrations of DIQ (1, 4, and 10 μmol/L) for 24, 48, and 72 h. The MTT results revealed that DIQ significantly inhibited the proliferation of HCT116 and HT29 human CRC cells at micromolar concentrations in a time- and dose-dependent manner (Figure 2A). Interestingly, a concentration of DIQ as low as 4 μmol/L was able to inhibit cell proliferation by approximately more than 30% at 24 h in HCT116 and HT29 cell lines and more than 50% cell reduction was observed at 48 h and 72 h in both cell lines. The mean IC_{50} values of DIQ was approximately 4 μmol/L in both cell lines (Figure 2A). The effect of DIQ on the viability of the human CRC cell lines was further confirmed by trypan blue exclusion method, and there was consistency between the MTT results and trypan blue exclusion assay (Figure 2B). Interestingly, DIQ treatment had relatively limited toxicity to the human non-tumorigenic intestinal FHS74Int cells when applied at doses up to 5 μmol/L and over a 72-h period (Supplementary Figure 1A).

DIQ inhibited migration and invasion of CRC cells

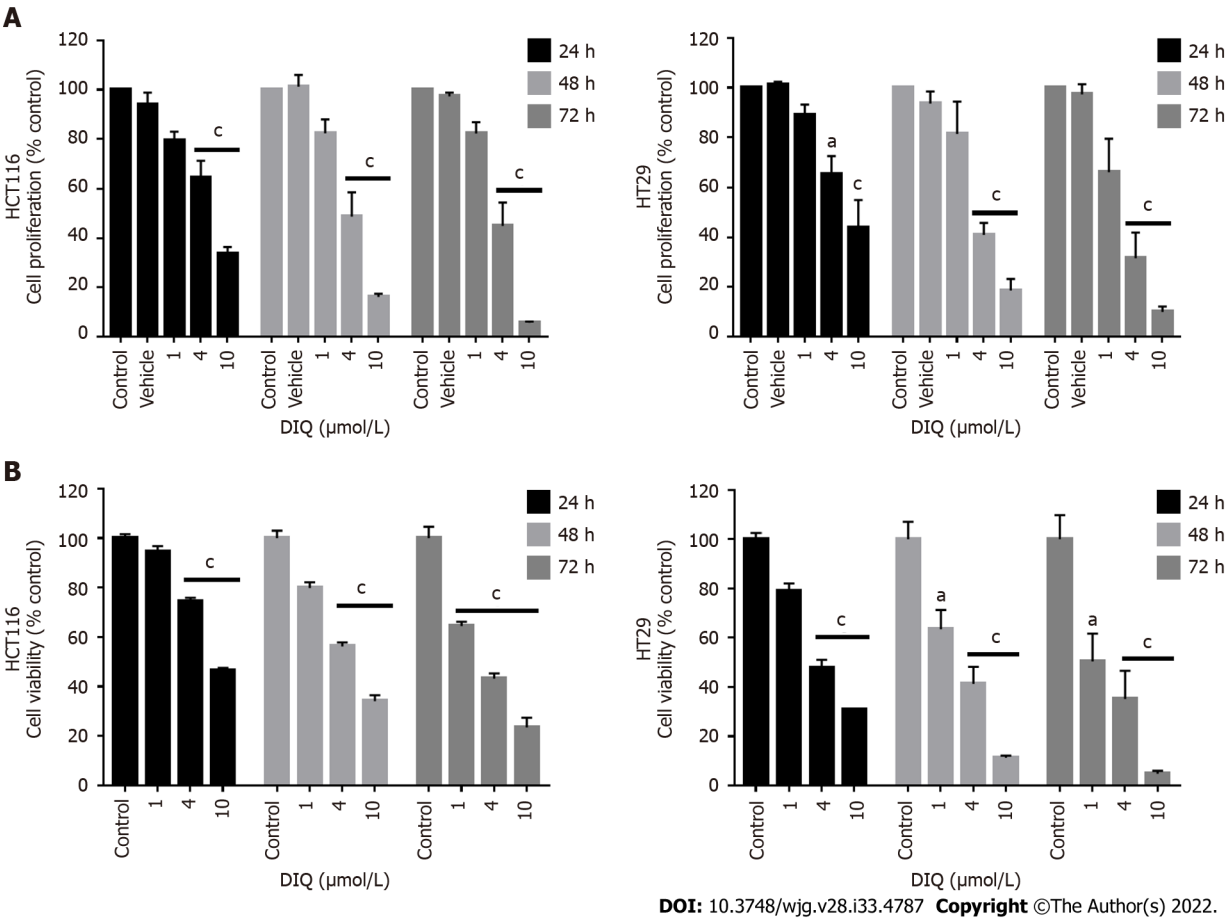
One of the most well-known properties of cancer cells is their ability to break away from their site and invade neighboring tissues[26]. Wound healing and transwell invasion assays were employed to evaluate the effects of DIQ on human CRC cell migration and invasion. DIQ at the corresponding IC_{50} concentration significantly suppressed and slowed down the cell migration ability of both cell lines at 72 h compared to the vehicle-treated control cells as determined by the wound healing assay (Figure 3A). The treatments failed to close the wound by more than 70% in both cell lines compared with control conditions, which were able to almost completely close the wound (Figure 3A). In addition, DIQ showed significant inhibitory potential on CRC cell invasion. The number of HCT116 and HT29 invasive cells were remarkably decreased in response to FBS in treated conditions reaching a value of less than two-fold compared to the control condition at 72 h (Figure 3B).

DIQ induced cell cycle arrest and apoptosis in CRC cells

To evaluate the underlying mechanism of growth inhibition by DIQ in CRC, the cell cycle distribution analysis of HCT116 and HT29 cells treated with the IC_{50} concentration of DIQ for 72 h was performed using flow cytometry. As shown in Figure 4A, DIQ treatment in HCT116 cells caused G1 arrest with concomitant decreases in the S and G2/M fractions mainly after 72 h. No changes in the cell cycle were noticed after treating both cell lines with DIQ for 24 h. DIQ effect on the HCT116 cell cycle was pronounced at 72 h. The proportion of HCT116 cells in G1 phase was increased from 45.6% in control cells to 60.2% in cells treated with DIQ for 72 h, while the proportion of cells in G2/M phase decreased from 35.2% to 21.5% (Figure 4A). However, in HT29 cells, DIQ treatment induced S phase (38.35%) cell cycle arrest after 72 h treatment and depleted cells at G1 and G2/M phases. Interestingly, upon treatment with 4 μmol/L DIQ, the percentage of HCT116 and HT29 cells in the sub-G1 phase significantly increased reaching 3.5- and 5.0-fold at 72 h, respectively, suggesting that the reduction in cell viability in response to DIQ could be due to cell death (Figure 4A). To further confirm whether growth inhibition was related to apoptosis, Annexin V and PI staining was performed. As shown in Figure 4A, after treating CRC cells with DIQ at the indicated concentrations for 72 h, the total apoptotic cell populations were significantly increased in both cell lines reaching 61% in HCT116 and 70% in HT29 cells.

DIQ induced the production of ROS in CRC cells

Recently, targeting cancer *via* ROS-based mechanisms has been reported as a radical therapeutic approach[27]. To investigate the effect of DIQ on cellular stress and the involvement of oxidative stress in their anti-proliferative effect in CRC, ROS production was examined by DHE stain intensity. DHE is a fluorescent dye that can easily permeate cell membranes and has been widely used to quantify cellular $O2^{-}$ and H_2O_2 by producing red fluorescent products. Our results showed that a significant increase of the DHE staining intensity was observed in treated cells at 48 h as compared to the control (Figure 4B). Thus, DIQ treatment induced ROS production in both CRC cell lines.



DOI: 10.3748/wjg.v28.i33.4787 **Copyright** ©The Author(s) 2022.

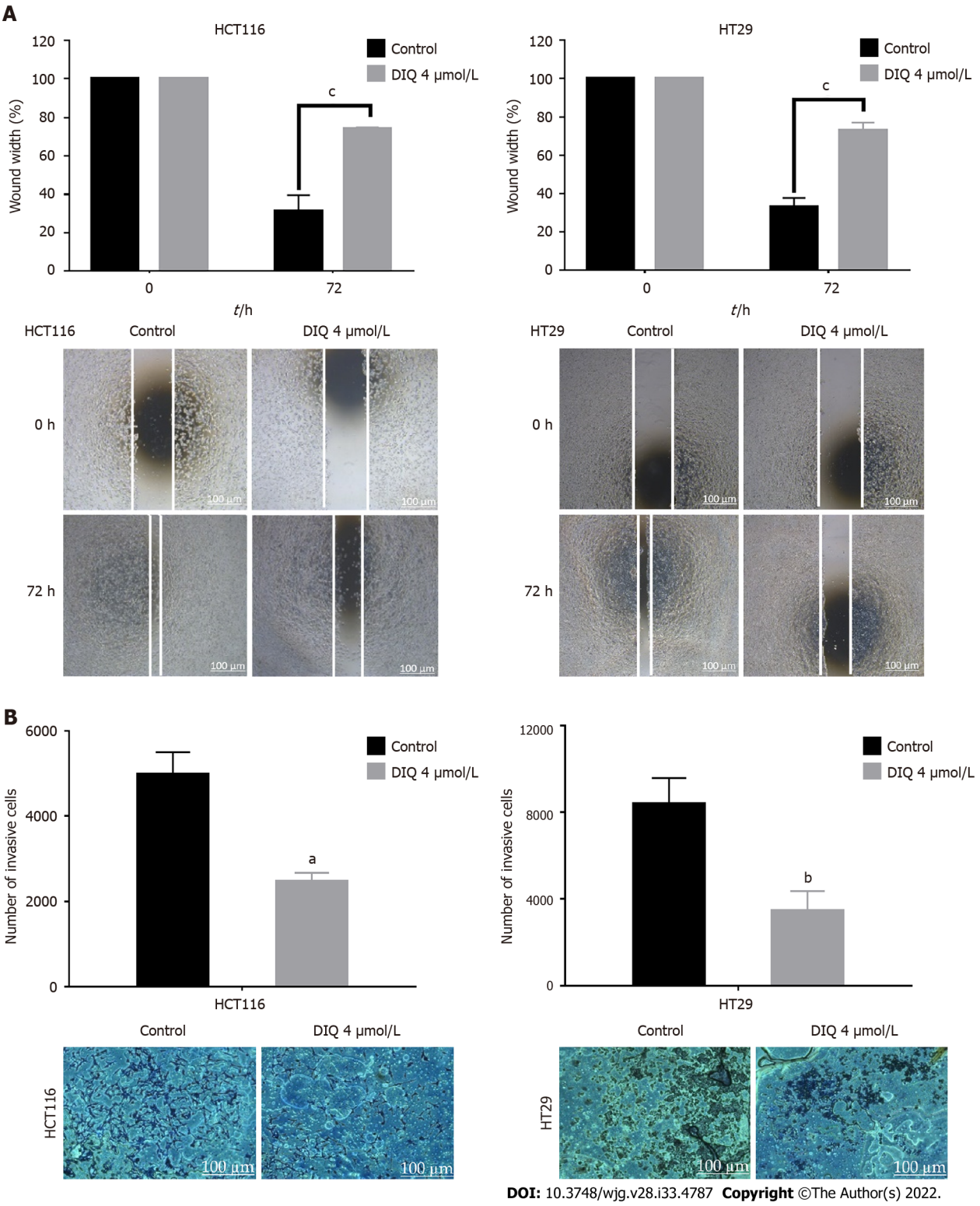
Figure 2 Diiminoquinone reduced the proliferation and the viability of HCT116 and HT29 colorectal cancer cell lines in a time- and dose-dependent manner. A: The anticancer effect of different concentrations of diiminoquinone (DIQ) on the proliferation of HCT116 and HT29 cells using the MTT assay was determined in triplicates at 24, 48, and 72 h. Results were expressed as the percentage of proliferation of the treated group compared to the control at every time point; B: The anticancer effect of different concentrations of DIQ on the viability of HCT116 and HT29 cells using the trypan blue exclusion assay was determined in triplicates at 24, 48, and 72 h. Results were expressed as percentage of viable cells of the treated group compared to the control at every time point. Data represent an average of three independent experiments and is reported as mean ± standard error of the mean ($^aP < 0.05$, $^bP < 0.01$, $^cP < 0.001$).

DIQ altered the expression of the cell cycle and proliferation markers in CRC cells

To determine the association between the observed cell cycle arrest and the increased ROS in HCT116 and HT29, western immunoblot analyses were performed on total cell extracts prepared from 2D-treated cells to detect possible changes in the expression of cell cycle and proliferation markers. As shown in Figure 4C, the expression levels of p53 and p21, which are cell cycle regulators of the G1 phase, were upregulated by 1.28-fold and 1.42-fold, respectively, in HCT116 upon DIQ treatment as compared to control conditions. Whereas, in HT29 treated cells, p53 was downregulated and p21 was significantly upregulated by 1.8-fold, suggesting that the inhibitory mechanism of DIQ is different in HCT116 and HT29 cells. The expression of the proliferation-associated proteins, such as AKT, p-AKT, ERK, p-ERK, and proliferating cell nuclear antigen (PCNA), were markedly decreased by DIQ treatment in both cell lines (Figure 4F). In addition, the expression levels of stem cell markers, CD133 and β-catenin, were also downregulated in both CRC cell lines.

DIQ targeted the enriched population of human CRC stem cells in 3D

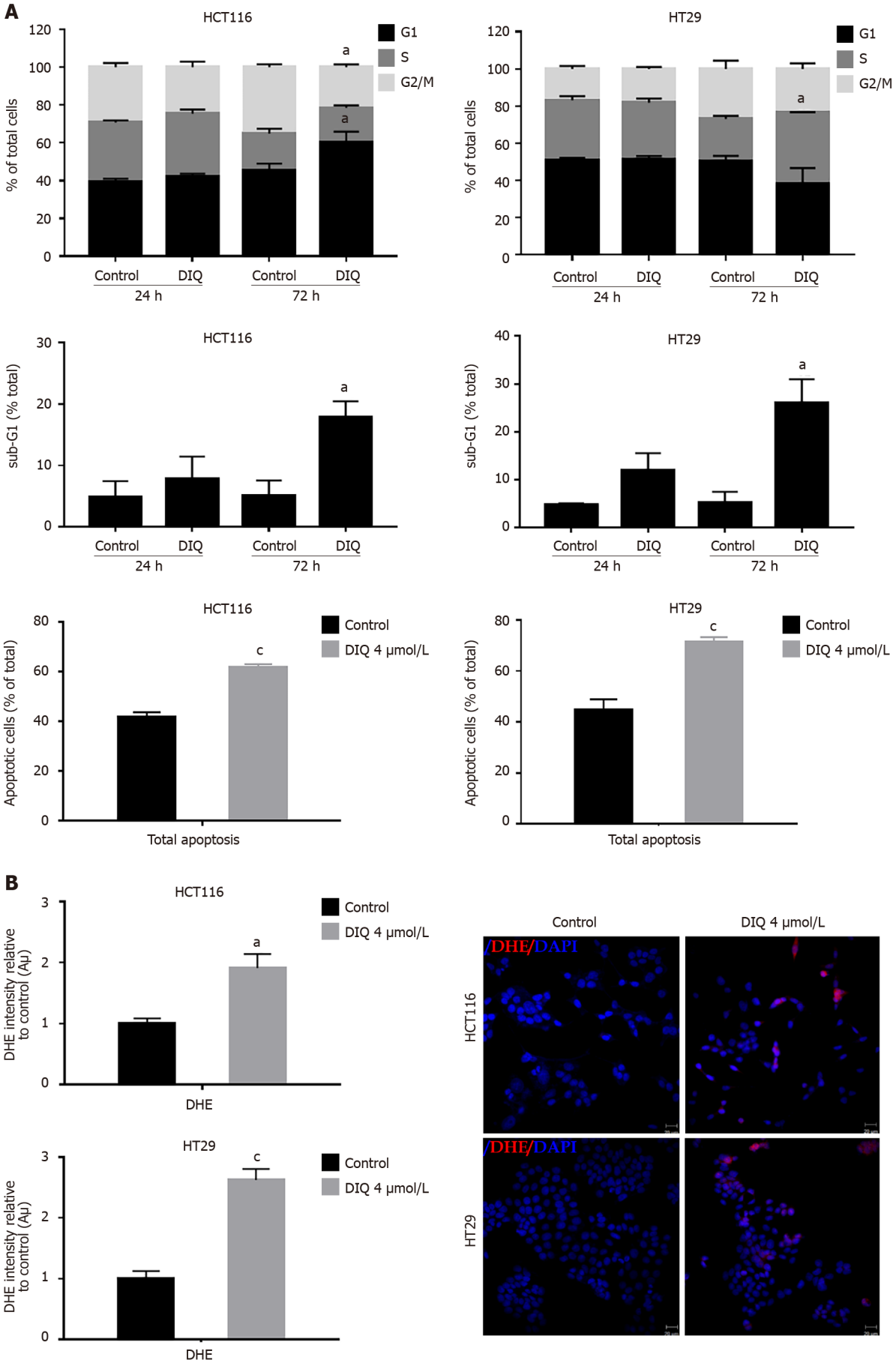
We investigated colonosphere formation of HCT116 and HT29 cells, a salient feature of CSCs. To better visualize their sphere forming capabilities in 3D cultures, HCT116 and HT29 cells were cultured as single cells in Matrigel™ for 8-12 d in the presence of DIQ. The spheres were then visualized under an inverted light microscope, and bright-field images were taken (Figure 5). Cells that were able to form spheres in the first generation were collected and propagated by dissociating spheres into single cells and reseeding the same number of cells (1000 cells/well). The assay was performed until the fifth generation. Our data showed that both HCT116 and HT29 cells formed spheres, suggesting the presence of a unique population with stem cell-like properties. Notably, a clear dose-dependent attenuation of the SFU at generation 1 for both cell lines was observed when treated with different concentrations of DIQ (0.5 and 1 μmol/L). The SFU was always significantly and remarkably lower in drug-treated cells compared to that of the control condition by more than 50% (Figure 5). Consecutive propagations of

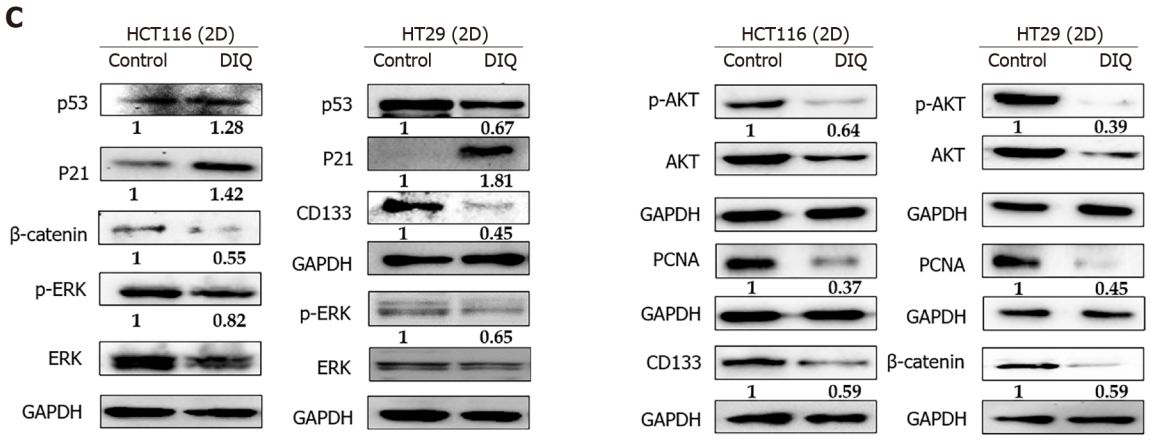


DOI: 10.3748/wjg.v28.i33.4787 **Copyright** ©The Author(s) 2022.

Figure 3 Diiminoquinone reduced the migration and the invasion of HCT116 and HT29 colorectal cancer cells. A: HCT116 and HT29 cells were seeded in 24-well plates. A scratch was made on confluent cells using a 200 μL tip, and images were taken at 0 h and 72 h with or without the indicated treatment. Quantification of the distance of the wound closure was assessed over time. Representative images of wound healing assay at × 5 magnification (scale = 100 μm); B: Colorectal cancer cells were seeded onto the Matrigel-coated membrane in the top chamber of the transwell and were either treated or not with the indicated concentration in the presence of fetal bovine serum in the lower chamber. Cells that invaded to the lower chamber after 72 h were fixed, stained with hematoxylin and eosin, counted, and are represented as the number of invading cells compared to the control. Data represent an average of three independent experiments and is reported as mean ± standard error of the mean ($^{a}P < 0.05$, $^{b}P < 0.01$, $^{c}P < 0.001$). DIQ: Diiminoquinone.

formed spheres at each generation with successive treatment with DIQ were performed up to 5 generations. Interestingly, our results showed additional inhibition of the SFU upon DIQ treatment when the cells were propagated from generation 1 up to generation 5 spheres. We observed that 1 μmol/L of DIQ treatment decreased SFU of HCT116 cells by more than 10 times compared to the


A
HCT116
HT29
G1
S
G2/M
% of total cells
Control
DIQ
24 h
72 h
sub-G1 (% total)
Apoptotic cells (% of total)
DIQ 4 μmol/L
Total apoptosis
B
DHE intensity relative to control (Aμ)
DHE
Control
DIQ 4 μmol/L
/DHE/DAPI



DOI: 10.3748/wjg.v28.i33.4787 **Copyright** ©The Author(s) 2022.

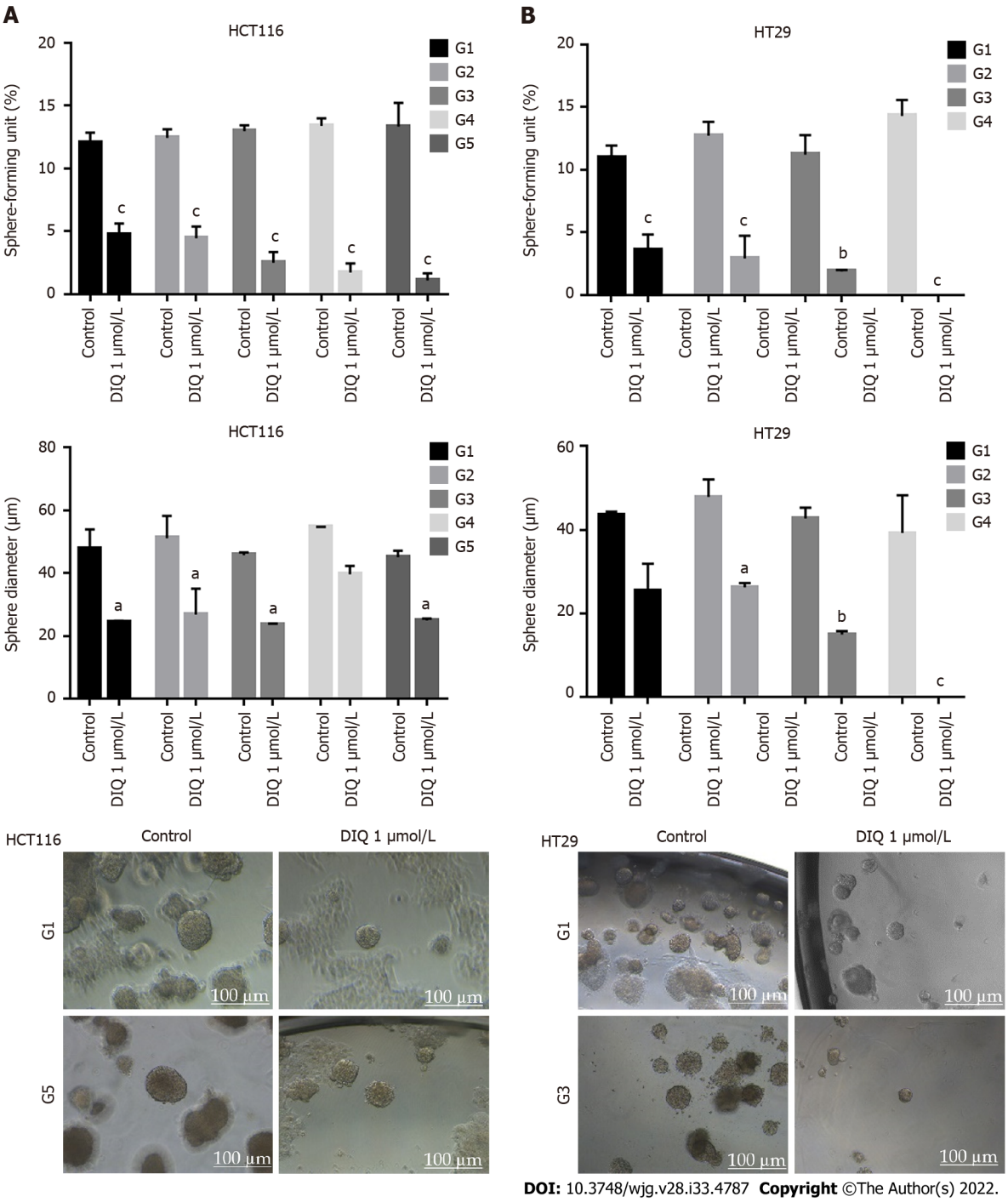
Figure 4 Diiminoquinone induced an accumulation of HCT116 and HT29 cancer cells in the sub-G1 region and apoptosis along with an increase in reactive oxygen species production. A: The distribution of phases of the cell cycle upon diiminoquinone (DIQ) treatment at 24 h and 72 h in HCT116 and HT29 cells using propidium iodide-based flow cytometric analysis of DNA content was shown. Data represent the average of three independent experiments and are reported as mean ± standard error of the mean ($^aP < 0.05$, $^bP < 0.01$, $^cP < 0.001$); B: Reactive oxygen species (ROS) production in HCT116 and HT29 cells was detected by dihydroethidium (DHE) staining. Representative images of colorectal cancer cells exposed to DIQ stained with DHE for ROS content (red color). Cell nuclei were stained with 4',6-diamidino-2-phenylindole (DAPI) (blue). A summary of the quantification of the red fluorescence intensity was represented; C: Lysates of colorectal cancer cells treated with 4 μmol/L DIQ were immunoblotted for p53, p21, β-catenin, p-ERK, ERK, p-AKT, AKT, and proliferating cell nuclear antigen (PCNA). Bands were detected by enhanced chemiluminescence and quantified using ChemiDoc MP Imaging System. Data represent an average of three independent experiments and is reported as mean ± standard error of the mean ($^aP < 0.05$, $^bP < 0.01$, $^cP < 0.001$).

control (13.3%) at generation 5 reaching approximately 1%. Moreover, as shown in Figure 5, HT29 cells were more sensitive to DIQ, and there was an eradication of spheres at generation 4 (SFU = 0%) compared to the control (14.28%). In addition to assessing its effect on self-renewal capacity, DIQ significantly decreased the sizes of the spheres by more than 50% as compared to untreated control conditions. Further decrease in sphere sizes was recognized over the 5 generations in both cell lines depicting pronounced additive effect of the treatments on the formed spheres upon propagation (Figure 5). Thus, DIQ has led to fewer and smaller HCT116 and HT29 spheres. Interestingly, DIQ treatment did not show any significant effect on the size and SFU of FHS74Int-derived spheres over 5 generations (Supplementary Figure 2B). Taken together, these findings suggest that DIQ specifically targeted the colorectal CSC.

DIQ induced apoptosis and inhibited proliferation of human CRC stem cells

Spheres collected at generation 1 were subjected to immunofluorescence analysis of the expression of the proliferation marker Ki67, cytokeratin epithelial markers, CK8 and CK19, and the stem cell marker CD44. Our data revealed that Ki67, CK8, and CK19 expression were significantly reduced in treated spheres derived from HCT116 and HT29 cell lines (Figure 6A-D). The downregulation of the CK19 marker in both HCT116 and HT29 spheres at generation 1 could be an indicator of an inhibition of the epithelial-mesenchymal transition process. Immunofluorescence staining showed high expression of CD44 in control spheres at generation 1 indicating enriched stemness in these cells. Treatment with DIQ showed a significant reduction of CD44 expression in HCT116 and HT29 colonospheres as compared to the control, which is in tune with the downregulation of the CRC stem marker CD133 data (Figure 6C and E). Finally, DIQ effect on DNA damage was studied by assessing the expression of γH2AX. Our results revealed that the expression of γH2AX was markedly increased in treated spheres in both cell types (Figure 6D).

To further assess the effect of DIQ on the enriched CSCs population, we were interested in determining the effect of DIQ on the expression of proliferation markers, stem cell markers, and Wnt signaling molecules of CSCs using western blot. Consistent with the western blot analyses of 2D CRC cells, the expression of the proliferation markers p-AKT and p-ERK were remarkably downregulated by DIQ treatment in both HCT116 and HT29-derived spheres confirming inhibitory effects of DIQ on the proliferation of 3D CSC colonospheres (Figure 6E). Western blot analysis revealed a decrease in the levels of the proliferation marker PCNA post treatment consistent with the data that DIQ decreased the size of HCT116 and HT29-derived spheres (Figure 6E). For the Wnt signaling studies, we investigated treatment effects on β-catenin, which plays an important role in colon cancer stemness properties. Western blot analysis showed a downregulation of β-catenin expression in treated compared to untreated spheres. Analysis of p53 and p21 protein expression in HCT116 spheres upon DIQ treatment showed upregulation of these proteins by 1.32-fold and 1.99-fold, respectively, further confirming apoptosis induction (Figure 6E). Only p21 expression was upregulated in HT29 cells by 1.26-fold as compared to non-treated spheres, whereas the expression of p53 was not affected by DIQ treatment in



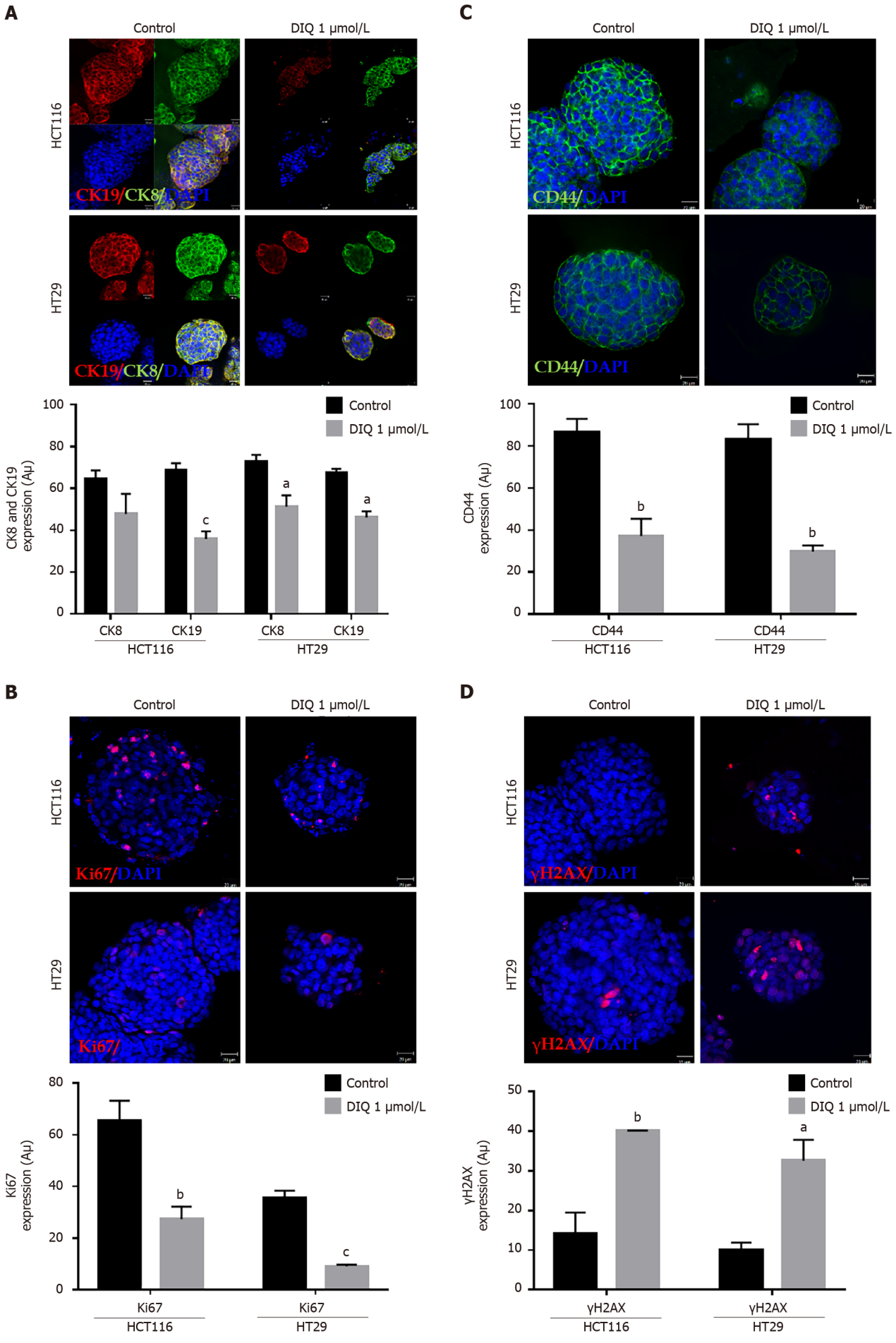
DOI: 10.3748/wjg.v28.i33.4787 **Copyright** ©The Author(s) 2022.

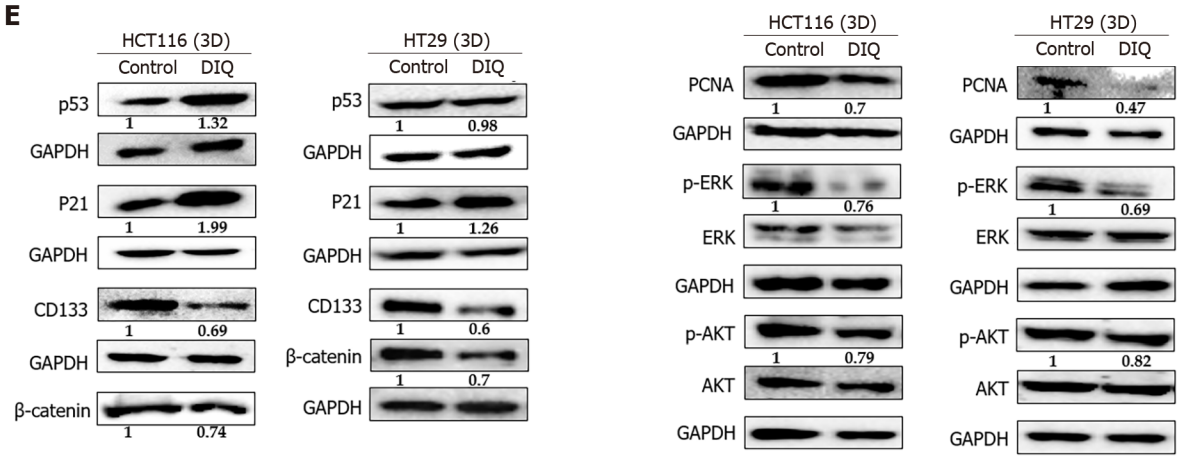
Figure 5 Diiminoquinone reduced the sphere-forming and self-renewal ability of colon cancer stem/progenitor cells. A: HCT116 and B: HT29 cells were seeded at a density of 1000 single cells/well in Matrigel™ for 8 d with and without 1 μmol/L diiminoquinone (DIQ) at generation 1. Spheres were propagated for five generations in duplicates for each condition. Media or treatment was replenished every 2 d. Spheres were counted at day 8-12 of sphere culture. Results are expressed as sphere-formation unit, which was calculated according to the following formula: sphere-formation unit = (number of spheres counted/number of input cells) × 100. Quantification of the average size of generation 1 to generation 5 colon cancer spheres with or without treatment conditions. Spheres sizes were measured by Carl Zeiss Zen 2012 image software. Data represent an average diameter (μm) of 50 measured spheres. Representative bright field images of HCT116 and HT29 colon spheres in Matrigel™ taken by the Axiovert inverted microscope are shown. Data represent an average of three independent experiments and is reported as mean ± standard error of the mean ($^aP < 0.05$, $^bP < 0.01$, $^cP < 0.001$).

HT29 spheres.

DIQ had antitumor potential in non-obese diabetic severe combined immunodeficiency mice injected with HCT116 spheres

To investigate the antitumor effect of DIQ on targeting the CSC population of cells *in vivo*, we subcutaneously injected two groups of non-obese diabetic severe combined immunodeficiency mice with 100 spheres derived from HCT116 cells. Mice developed tumors in 2 wk and were then treated


A
Control
DIQ 1 μmol/L
HCT116
HT29
CK19/CK8/DAPI
CK8 and CK19 expression (Aμ)
Control
DIQ 1 μmol/L
CK8
CK19
HCT116
HT29
C
CD44/DAPI
CD44 expression (Aμ)
B
Ki67/DAPI
Ki67 expression (Aμ)
D
γH2AX/DAPI
γH2AX expression (Aμ)



DOI: 10.3748/wjg.v28.i33.4787 **Copyright** ©The Author(s) 2022.

Figure 6 Diiminoquinone induced apoptosis and inhibited proliferation in colon cancer stem/progenitor cells. Representative immunofluorescence imaging of control and diiminoquinone (DIQ)-treated HCT116 and HT29 spheres collected at generation 1. A-D: Spheres stained for cytokeratin (CK)8 (green) and CK19 (red) (A), KI67 (B), CD44 (C), and gamma H2A histone family member X (γH2AX) (D) were obtained using confocal microscopy. The nuclei were stained with anti-fade reagent Fluorogel II with 4',6-diamidino-2-phenylindole (DAPI). The quantification of the intensity of CK8, CK19, CD44, and Ki67 stain in control and DIQ-treated spheres was performed using Carl Zeiss Zen 2012 image software. Stain intensity was normalized to size. Scale bar 20 μm; E: Analysis of p53, p21, CD133, β-catenin, proliferating cell nuclear antigen (PCNA), p-ERK, ERK, p-AKT, and AKT protein expression in HCT116 and HT29 generation 1 spheres upon treatment is shown. GAPDH served as an internal control. Bands were detected by enhanced chemiluminescence using ChemiDoc MP Imaging System. Fold expression changes normalized to GAPDH and to total ERK and total AKT in the cases of p-ERK and p-AKT expression, respectively, are given. Data represent an average of three independent experiments and is reported as mean ± standard error of the mean ($^aP < 0.05$, $^bP < 0.01$, $^cP < 0.001$).

with 20 mg/kg DIQ three times per week for 21 d. DIQ treatment did not cause any change in the body weight or death of mice, indicating no toxicity.

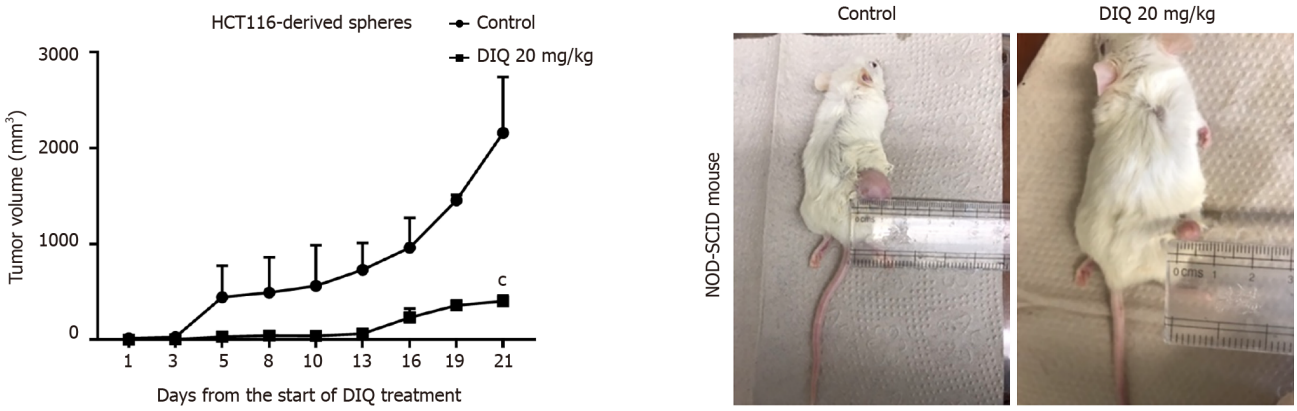
DIQ significantly inhibited tumor growth in the treated group when compared to the control group particularly at day 21 (Figure 7). Interestingly, the average tumor volume was 403.2 mm^3 in DIQ-treated mice at sacrifice, while it was 2158.5 mm^3 in the control group (Figure 7).

Assessment of the effect of DIQ treatment on the established colon cancer patient derived organoids: Organoids as models for DIQ assessment

We established a 3D organoid system from fresh tissue samples obtained from different stages of 5 random colon cancer consenting patients. As described in the methods section, a total of 20000 single cells derived from freshly digested tissues were plated per 20 μL droplets of 90% Matrigel™ in 24-well plates. Cells were plated depending on the total cell count that was successfully derived from the tissue specimens. Despite the expected challenges in modeling colon cancer, we succeeded in establishing colon organoids from patients undergoing colectomy. Organoids formed at generation 1 were dissociated, propagated to generation 2, and the effect of DIQ on the organoids formed was assessed. The growth of organoids was determined by the total number (OFC) and size (diameter) of the organoids formed. The response of colon cancer patient-derived organoids to DIQ was compared to that of 5FU, which is the standard first-line treatment option for CRC. This response was evaluated on 5 random treatment-naïve patients with different clinical data. We succeeded in establishing colon organoids and propagating them. The two different doses of DIQ (0.5 and 1 μmol/L) displayed a highly significant inhibition in the OFC and the size of tumor organoids derived from the 5 studied patients when they were compared to the control group in a dose-dependent manner (Figures 8-10). These results were consistent with the response of HCT116 and HT29 cell line-derived organoids to DIQ treatment. DIQ elicited a statistically significant decrease in both OFC and size of cell line-derived organoids (Supplementary Figure 2).

In Patient 1, organoids were successfully propagated up to generation 6 as shown in Figure 8. Interestingly, an increase in the number of tumor organoids formed was observed with each propagation, thus indicating enrichment of stem cells and enhancement of the establishment of colon organoids. Characterization of the established patient 1-derived organoids was performed by studying the expression of the CRC epithelial lineage markers CK19 and CK8 and the stem cell marker CD44. Using immunofluorescence staining, the tumor organoids showed a positive expression of CK19, CK8, and CD44 confirming the presence of stem-like/progenitor CRC cells within the bulk of our patient-derived organoids.

As shown in Figure 9, a reduction in the OFC and size of the treated organoids was noticed in patient 3 with rectal mucinous adenocarcinoma (pT2 stage). Characterization of patient 3derived organoids and corresponding tissue was assessed by investigating the expression of CK19 and CD44 markers using immunofluorescence staining. These organoids mimicked the heterogeneity of corresponding tumor



DOI: 10.3748/wjg.v28.i33.4787 **Copyright** ©The Author(s) 2022.

Figure 7 Diiminoquinone reduced tumor growth in non-obese diabetic severe combined immunodeficiency mice. Non-obese diabetic severe combined immunodeficiency (NOD-SCID) mice (5 mice/group) were injected with 100 HCT116 generation 1 spheres. Tumor growth was monitored by measuring the tumor volume during 21 d of treatment (3 times per week) with either 20 mg/kg diiminoquinone (DIQ) or physiologic saline. Representative images of control and DIQ-treated mice at day 21. Data represent an average of two independent experiments and is reported as mean ± standard error of the mean ($^{a}P < 0.05$, $^{b}P < 0.01$, $^{c}P < 0.001$).

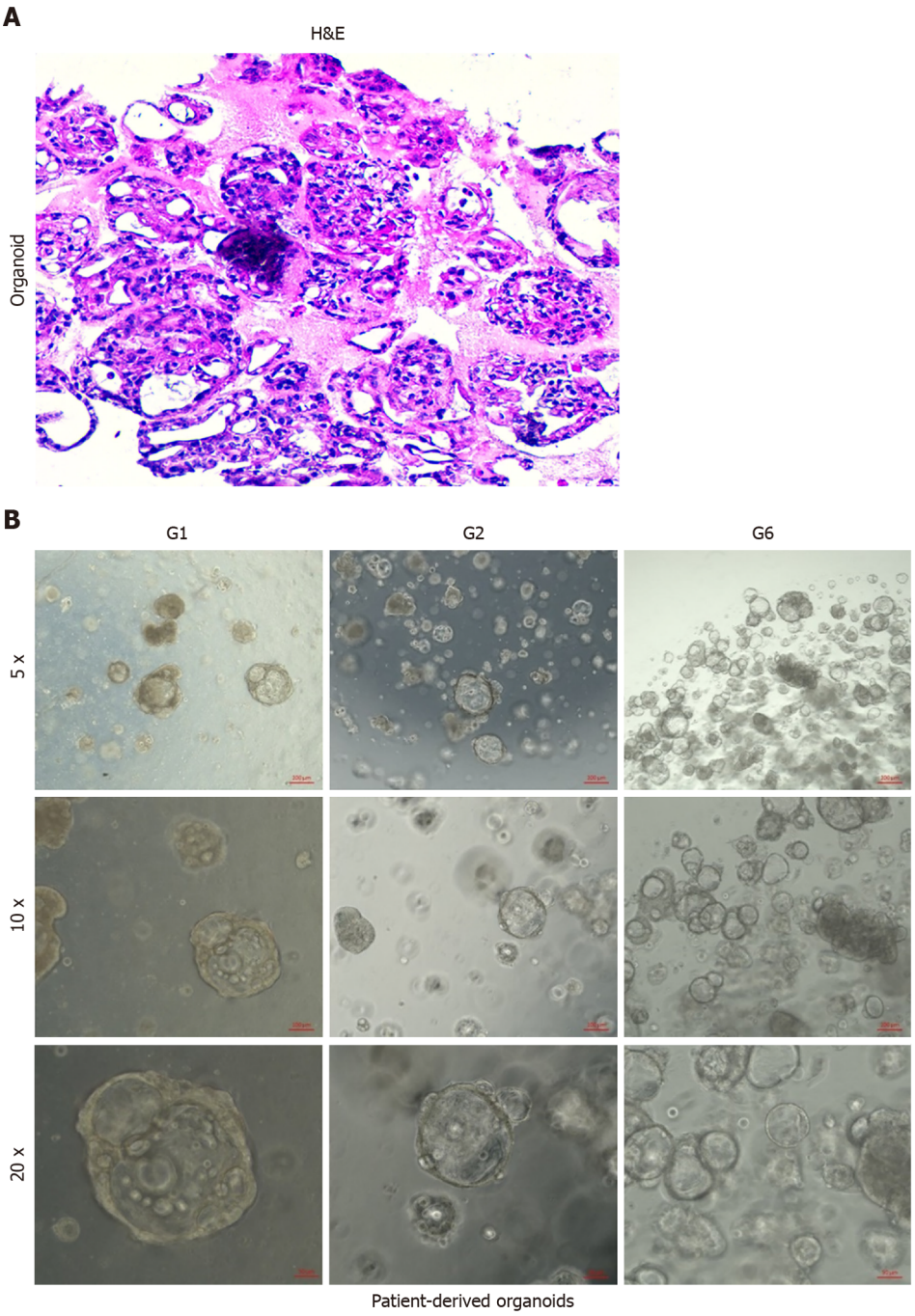
tissue. Strong expression of CK19 and CD44 was noted in organoids consistent with the corresponding tumor tissue (Figure 9). The co-expression of CK19 and CD44 was decreased upon treatment in a dose-dependent manner (Figure 9B). In Patients 2 and 5, both exhibited similar grade (grade 2) moderately differentiated sigmoid colon adenocarcinoma and were of the same stage (pT3). DIQ treatment at concentrations as low as 0.5 μmol/L displayed a decrease in the growth of the organoids in Patient 2 and an eradication of organoids in Patient 5 (Figure 10). Organoid formation was eradicated upon DIQ (0.5 and 1 μmol/L) treatment in Patient 4, who was diagnosed with moderately differentiated (grade 2) pT2 sigmoid colon adenocarcinoma. Interestingly, the effect of DIQ on the OFC and the size of the organoids was more potent than that of 5FU particularly in patients 2, 4, and 5 (Figure 10).

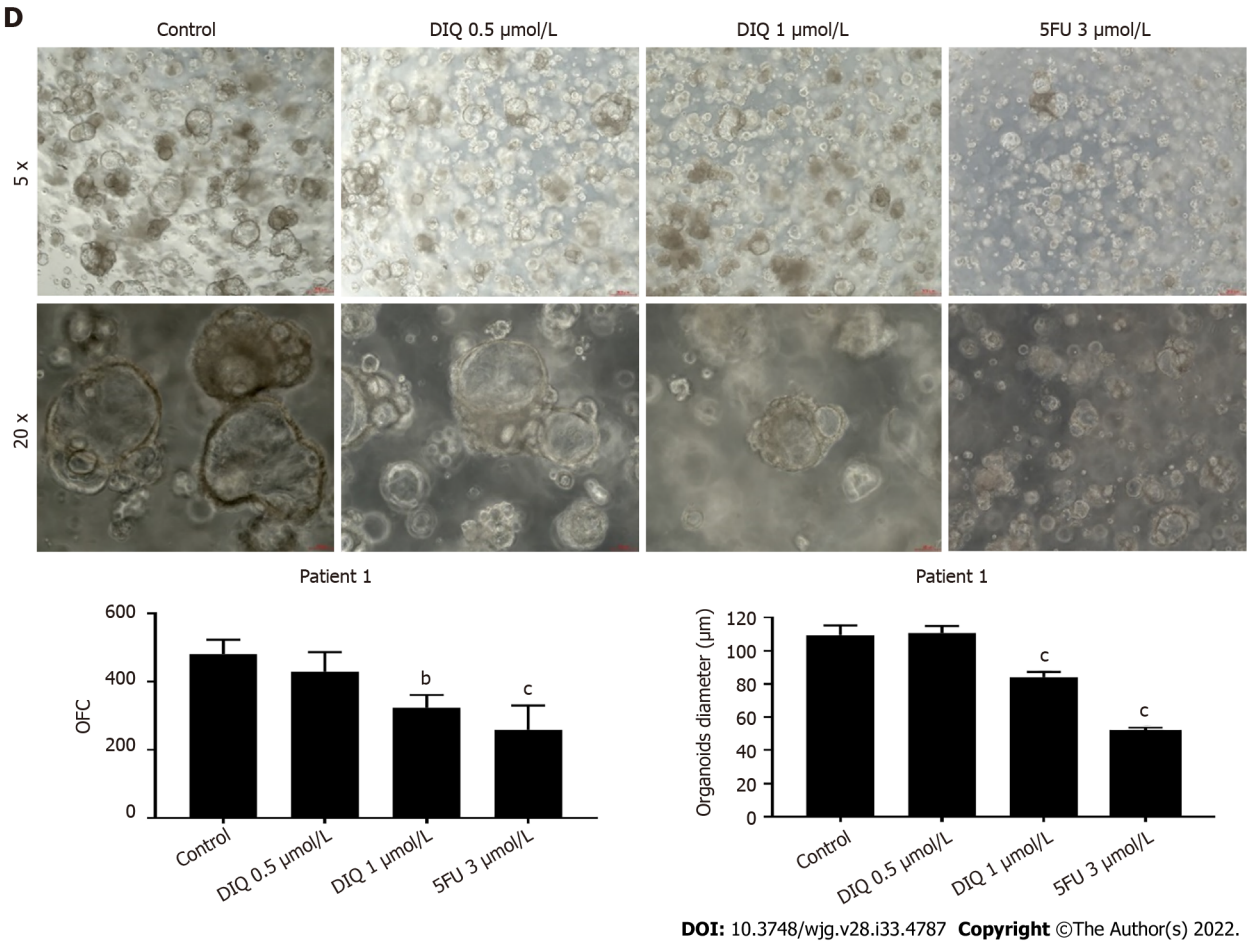
DISCUSSION

In this study, we investigated the anticancer activity of DIQ in 2D and 3D models of human colon cancer. DIQ reduced the sphere forming and self-renewal ability of CRC HCT116 and HT29 stem cells at sub-toxic doses. Mechanistically, DIQ targeted CSCs by reducing the proliferation marker Ki67 and CRC stem cell markers CD44 and CK19 as well as inducing DNA damage through increasing γH2AX expression and downregulating the main components of stem cell-related -catenin, AKT, and ERK oncogenic signaling pathways. DIQ displayed a highly significant decrease in both the count and the size of the organoids derived from colon cancer patients as compared to control and 5FU conditions. Furthermore, in 2D culture, DIQ significantly inhibited cell proliferation, migration, and invasion of HCT116 and HT29 cell lines. DIQ also induced apoptosis and an increase in ROS along with an accumulation of cells in the sub-G1 region. Consistent with the *in vitro* data, DIQ exhibited reduction in the tumor growth and proliferation *in vivo*.

Our major focus in this study was to evaluate the ability of DIQ to target CSCs in HCT116 and HT29 cells using a 3D sphere formation assay. CSCs are a rare subpopulation of stem-like tumor cells that are responsible for tumor relapse[28,29]. The increase of SFU in both CRC cell lines from generation 1 up to generation 5 suggests an enrichment in CSCs upon propagation, thus confirming the advantage of using the 3D sphere formation assay. Treatment of HCT116 and HT29 cells with DIQ at a concentration as low as 1 μmol/L targeted the subpopulation of stem/progenitor cells over five generations as reflected by the drastic decrease in the SFU and the sphere size in both cell lines. HT29 spheres were more sensitive to 1 μmol/L DIQ, and an eradication of HT29 spheres occurred at generation 3. The interesting finding of DIQ not affecting non-tumorigenic FHS74Int cells makes DIQ somewhat selective to cancer cells, which is the most essential aspect sought after in anticancer drugs.

To understand what molecular pathways could be targeted by DIQ, we focused mainly on the pathways implicated in CSCs. Multiple signaling systems are involved in resistance of CSCs to therapy. It is widely accepted that the Wnt/β-catenin pathway is the most relevant signaling pathway for colon cancer development. Wnt signaling contributes to stem cell development, tumorigenicity, and oncogenesis[30,31]. This pathway is mechanistically responsible for drug resistance of colon CSCs. Increasing evidence validates that this pathway can interact with other oncogenic signaling pathways, such as those involving MAPK, PI3K, AKT, and ERK, which are aberrantly activated in many human cancers[32,33]. Indeed, evidence has shown that AKT and ERK are overexpressed in human CRC[32].


A
H&E
Organoid
B
G1
G2
G6
5 x
10 x
20 x
Patient-derived organoids
C
CD44/DAPI
CK19/CK8/DAPI
Organoid
20 μm



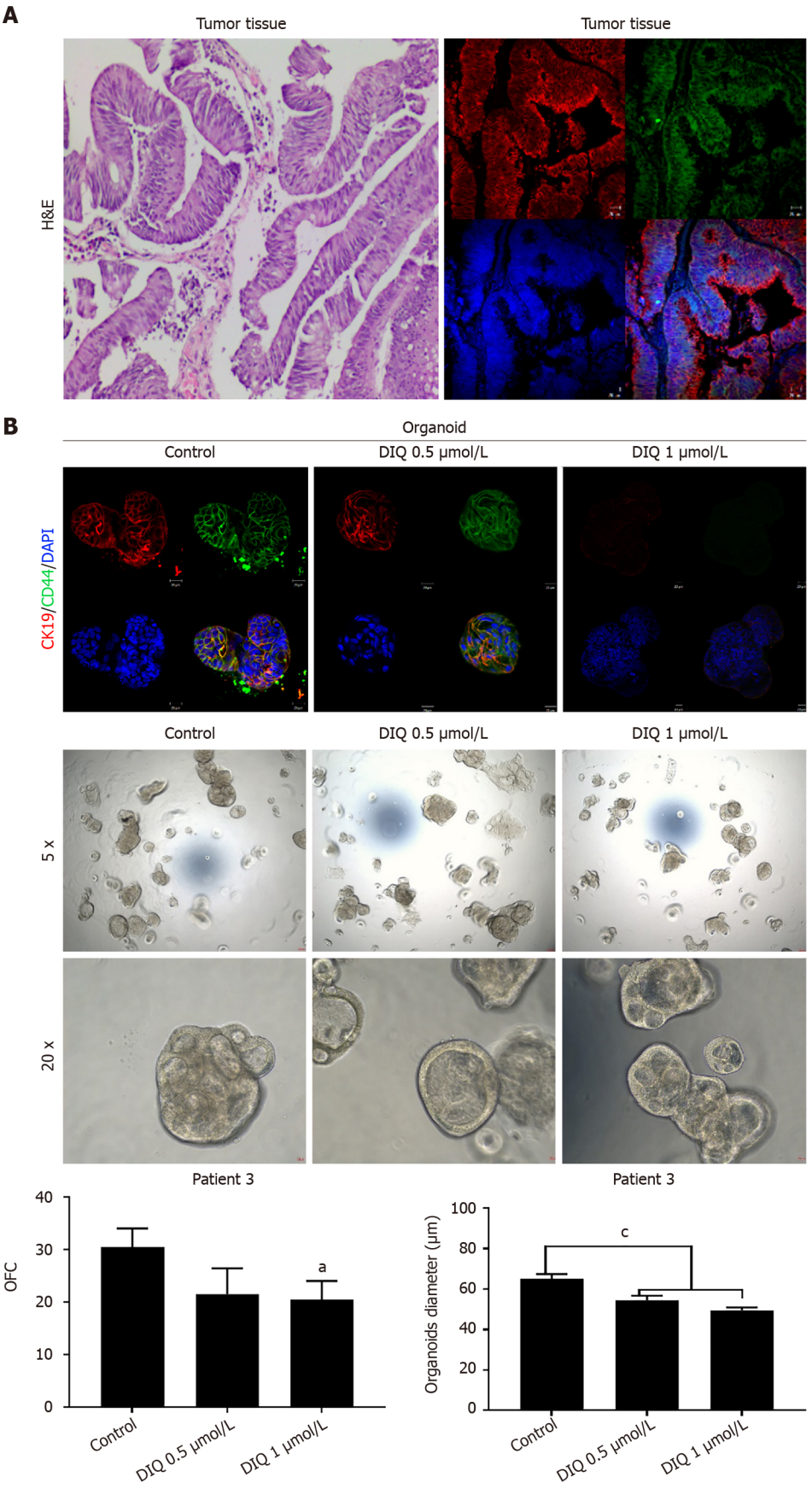
DOI: 10.3748/wjg.v28.i33.4787 **Copyright** ©The Author(s) 2022.

Figure 8 Establishment and characterization of patient-derived organoids from colon cancer patient 1. A: Representative image of organoids derived from patient 1 stained with hematoxylin and eosin (HE); B: Representative bright-field images of organoids at generation (G)1, G2, and G6. Fresh tumor tissues were enzymatically digested, and single cells were plated in 90% growth factor-reduced Matrigel. G1 organoids were successfully propagated up to G6. Images were visualized by Axiovert inverted microscope at × 5, × 10, and × 20 magnification. Scale bar 100 μm; C: Immunofluorescent images of organoids stained with colon lineage epithelial markers cytokeratin (CK)19 and CK8 and stem cell marker CD44. The nuclei were stained with anti-fade Fluorogel II with 4',6-diamidino-2-phenylindole (DAPI). Representative confocal microscopy images were acquired using a Zeiss LSM 710 laser scanning confocal microscope. Scale bar 100 μm; D: Representative bright-field images of G2 organoids treated with diiminoquinone (DIQ) (0.5 and 1 μmol/L) or 5-fluorouracil (5FU) (3 μmol/L). Organoid formation count (OFC) and size were calculated, and mean values were reported as mean ± standard error of the mean ($^{a}P < 0.05$, $^{b}P < 0.01$, $^{c}P < 0.001$). Images were visualized by Axiovert inverted microscope at × 5 and × 20 magnification. Scale bar 100 μm.

Thus, identifying drugs that target these oncogenic pathways could make a solid rationale for the targeted therapy of cancers. The result of western blot analysis showed that the ratio of both phosphorylated AKT to total AKT (p-AKT/AKT) and phosphorylated ERK to total ERK (p-ERK/ERK), which are key players of AKT/ERK pathways, were decreased upon DIQ treatment in CRC spheres. These findings suggest that DIQ suppressed sphere growth and formation *via* dual inhibition of AKT/ERK dependent signaling pathways.

We additionally investigated the protein levels of the key stem cell markers in CRC, CD133, and β-catenin, which are involved in chemotherapy resistance. Interestingly, the expression of CD133 and β-catenin were dramatically downregulated after DIQ treatment. Moreover, upon DIQ treatment, there was a significant decrease in the expression of CD44 and CK19 in both CRC cell lines, which were highly expressed in control spheres, along with a decrease in the expression of Ki67 and PCNA. It is interesting to note that CK19, which is considered a tumor marker in CRC, is specifically and stably expressed in primary and metastatic CRC cells. Altogether, this suggests that DIQ could be considered a novel therapeutic compound for suppressing CSC self-renewal.

DIQ-mediated apoptosis and inhibition of cell cycle progression was dependent on the upregulation of p21, which is a known tumor suppressor[34], promotes ROS accumulation, binds to PCNA, and inhibits cell cycle progression[35]. ROS is one of the major inducer of DNA damage. Induction of ROS generation induces increased stress on cancer cells leading to cancer cell death. Interestingly, DIQ treatment induced ROS production in CRC cell lines suggesting that an increase in ROS might also be involved in the anticancer effects of DIQ.



DOI: 10.3748/wjg.v28.i33.4787 **Copyright** ©The Author(s) 2022.

Figure 9 Effect of diiminoquinone on established patient-derived organoids from colon cancer patient 3. A: Immunohistochemistry images of tissue derived from patient 3 stained with hematoxylin and eosin (HE). Immunofluorescent images of tissue stained with colon lineage epithelial markers cytokeratin (CK)19 and stem cell marker CD44. The nuclei were stained with anti-fade Fluorogel II with 4', 6-diamidino-2-phenylindole (DAPI). Representative confocal

microscopy images were acquired using a Zeiss LSM 710 laser scanning confocal microscope. Scale bar 20 μm; B: Immunofluorescent images of organoids derived from colon cancer patient 3 at generation (G)2 in the presence and absence of diiminoquinone (DIQ) treatment (0.5 and 1 μmol/L) stained with colon lineage epithelial markers CK19 and stem cell marker CD44. The nuclei were stained with anti-fade Fluorogel II with DAPI. Representative confocal microscopy images were acquired using a Zeiss LSM 710 laser scanning confocal microscope. Scale bar 20 μm. Representative bright-field images of organoids derived from colon cancer patient 3 at G2 in the presence and absence of DIQ treatment (0.5 and 1 μmol/L). Organoid formation count and size were calculated, and mean values were reported as mean ± standard error of the mean ($^{a}P < 0.05$, $^{b}P < 0.01$, $^{c}P < 0.001$). Images were visualized by Axiovert inverted microscope at × 5 and × 20 magnification. Organoid formation count (OFC) and size of G were calculated, and mean values were reported as mean ± standard error of the mean ($^{a}P < 0.05$, $^{b}P < 0.01$, $^{c}P < 0.001$). Scale bar 100 μm.

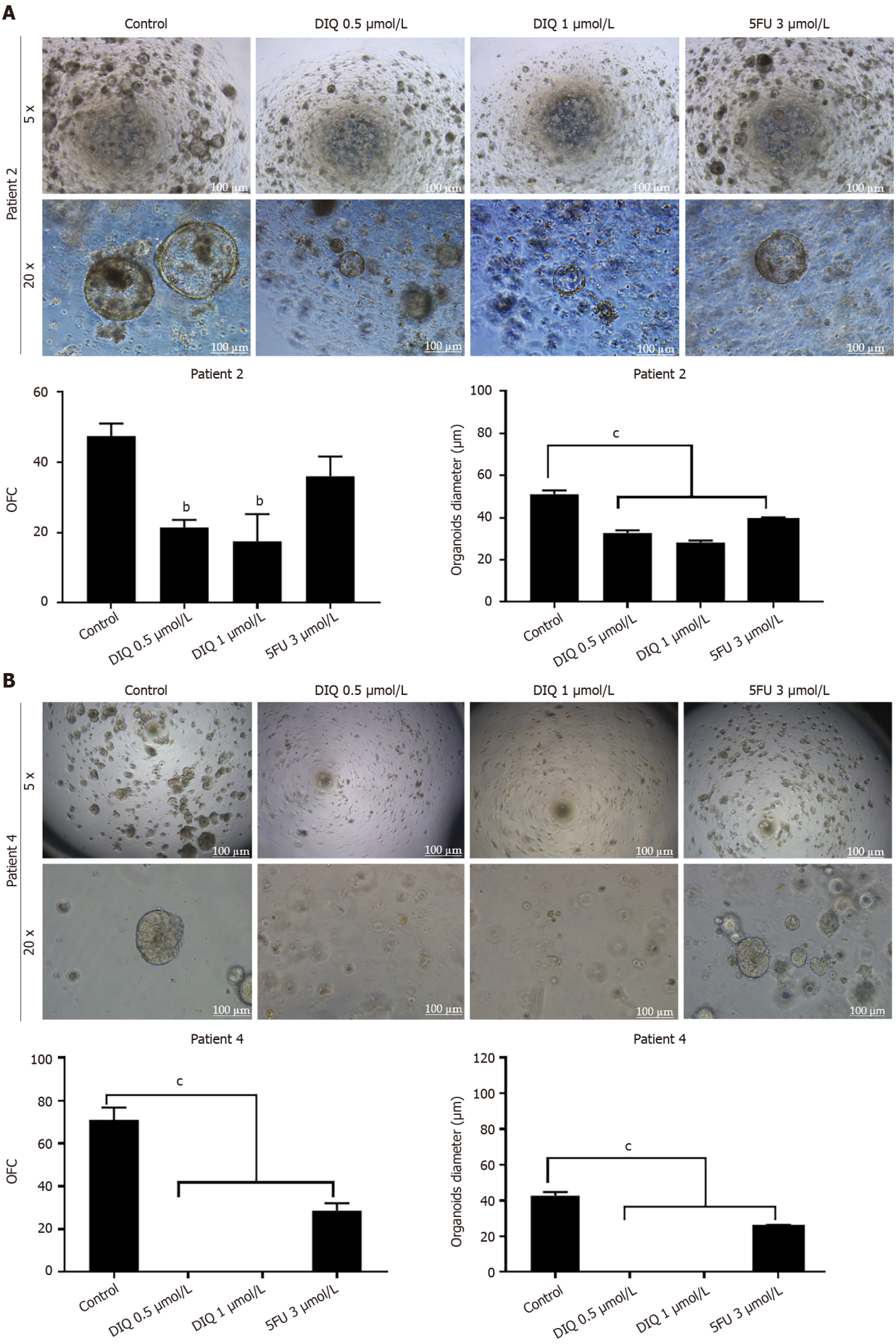
Since DIQ-induced apoptosis in HCT116 colonospheres through an increase in TUNEL positivity as we previously reported[22], we assessed whether DNA damage was activated in the spheres derived from both cell lines. We evaluated the expression of γH2AX, which is a DNA double-strand damage biomarker and could be a classical cancer prognostic factor[36,37]. The loss of DNA damage in CRC is involved in the development of therapeutic resistance[37]. In addition, quinones and oxaliplatin have been shown to induce apoptosis of CRC cells by activating DBS and activating γH2AX expression[7,38]. Interestingly, DIQ increased the expression of γH2AX in both CRC cells; clearly emphasizing that DIQ is a potent inducer of DNA damage.

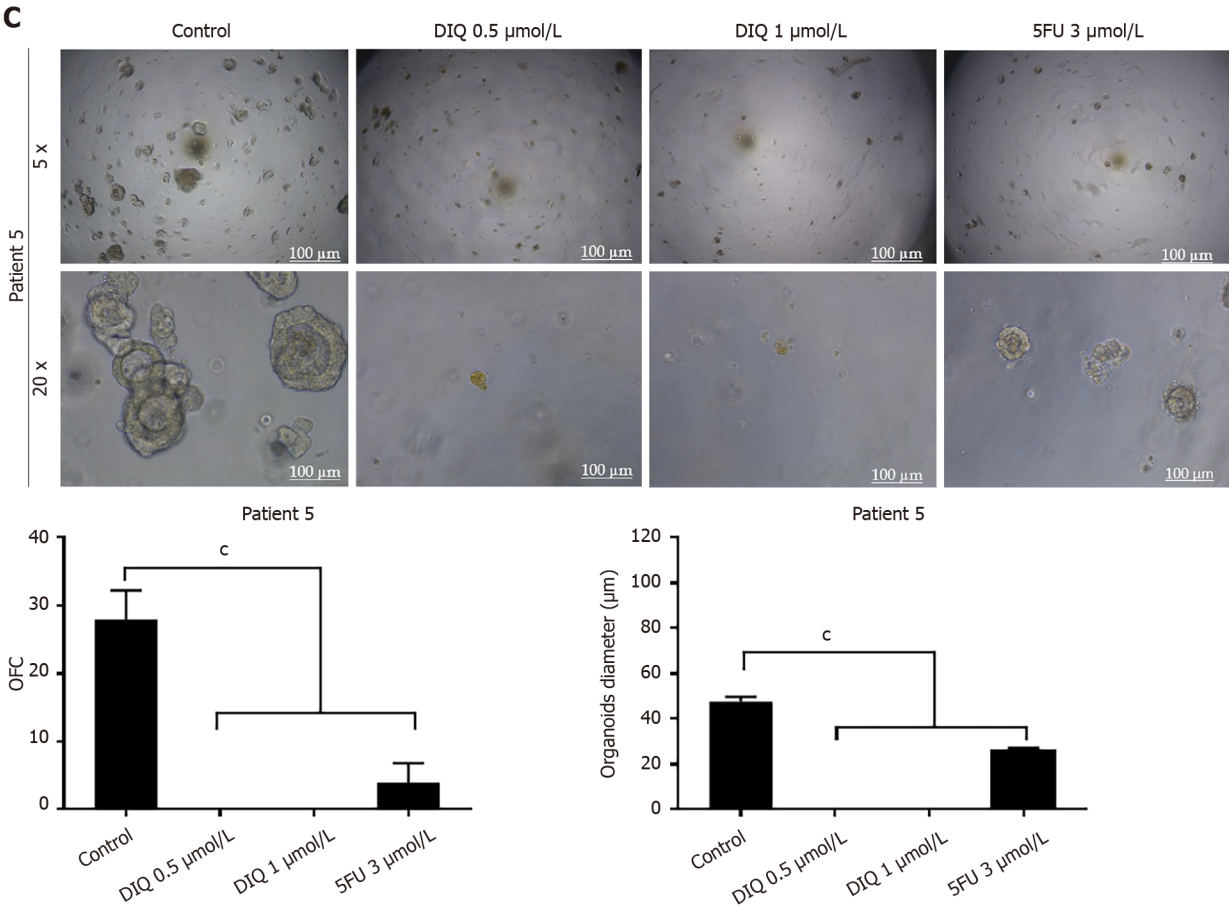
Interestingly, this study has also demonstrated effects of DIQ in patient-derived organoids. This model closely recapitulates tissue architecture and cellular composition and is used to assess the self-renewal and differentiation capacities of the organoid CSC, including growth kinetics and drug sensitivity[12,13]. Testing drug efficacy in colon patient-derived organoids holds great promise for personalized medicine and exhibits a significant potential to predict patient response and connect compound screening and clinical trials[39,40]. Since drug resistance to chemotherapy is a serious challenge in treating solid tumors, drug exposure studies on the patient-derived organoids help in choosing specific chemotherapy regimens for patients with malignant disease. Since chemotherapy response in CRC treatment varies between patients, the current study used patient-derived CRC organoids to evaluate the antineoplastic effect of DIQ in targeting stem cells. The established colon organoids expressed the CRC epithelial marker lineage CK19 and the CSC cell marker CD44. This observed co-expression recapitulates the architecture and the characteristics of colon tissues. Notably, DIQ caused a prominent inhibitory effect on the growth of CRC organoids from various patients at different CRC stages, emphasizing its antitumor potential in CRC patients. This effect was either more than or as potent as that of 5FU, emphasizing its inhibitory effect. The results of response of HCT116 and HT29 cell-derived organoids to DIQ treatments were consistent with that of patient-derived organoids. We, therefore, for the first time revealed that DIQ targeted the CSC in patient-derived colon organoids.

The present study has several limitations. The two major limitations in organoid establishment and subsequent applications were the small size of the patient tissue and the availability of tissues at the time of the study. As a clinical study, the patient sample size was relatively small. Additionally, the percentage success rate of deriving colon patient derived organoids was not more than 42%; only 5 out of 12 specimens were successfully established as colon organoids. This could possibly be due to limitations in tissue quality as well. A larger cohort is still required to further investigate and evaluate the effect of DIQ in translational medicine.

CONCLUSION

In conclusion, we demonstrated for the first time that DIQ reduces self-renewal capacity of colorectal tumors and prevents therapy resistance in patient-derived organoids through interfering with the stem cell Wnt/-catenin and AKT and ERK pathways that are involved in CRC tumorigenesis. Also, the effect of DIQ was involved in the major cell fate responses including apoptosis, cell cycle arrest, and stress response. DIQ inhibits the key processes of CRC tumorigenesis, including cell growth, proliferation, migration, and invasion. Our findings strongly suggest that DIQ could be a promising compound for treatment of CRC patients and could be clinically used as a non-toxic compound for targeting human colon cancer stem/progenitor cells.


A
Control
DIQ 0.5 μmol/L
DIQ 1 μmol/L
5FU 3 μmol/L
Patient 2
5 x
20 x
100 μm
Patient 2
OFC
b
b
Control
DIQ 0.5 μmol/L
DIQ 1 μmol/L
5FU 3 μmol/L
Patient 2
Organoids diameter (μm)
c
B
Control
DIQ 0.5 μmol/L
DIQ 1 μmol/L
5FU 3 μmol/L
Patient 4
5 x
20 x
100 μm
Patient 4
OFC
c
Control
DIQ 0.5 μmol/L
DIQ 1 μmol/L
5FU 3 μmol/L
Patient 4
Organoids diameter (μm)
c



DOI: 10.3748/wjg.v28.i33.4787 **Copyright** ©The Author(s) 2022.

Figure 10 Diiminoquinone reduced the growth of the patient-derived organoids from different colon cancer patients. A: Representative bright field images of generation (G)1 organoids derived from patient 2 (grade 2; stage T3) grown with or without diiminoquinone (DIQ) or 5-fluorouracil (5FU). Organoid formation count (OFC) was calculated in duplicate wells per condition. The quantification of the average diameter was calculated. The data of OFC and size are presented in two separate graphs; B: Representative bright field images of G4 organoids derived from patient 4 (grade 2; stage T2) grown with or without DIQ or 5FU. OFC was calculated in duplicate wells per condition. The quantification of the average diameter size was calculated. The data of OFC and size are presented in two separate graphs; C: Representative bright field images of G2 organoids derived from patient 5 (grade 2; stage T3) grown with or without DIQ or 5FU. OFC was calculated in duplicate wells per condition. The quantification of the average diameter was calculated. The average mean of OFC and size are presented in two separate graphs. All mean values were reported as mean ± standard error of the mean ($^{a}P < 0.05$, $^{b}P < 0.01$, $^{c}P < 0.001$). Scale bar, 100 μm.

ARTICLE HIGHLIGHTS

Research background

Colorectal cancer (CRC) is a multistep genetic disorder caused by sequential mutational events in signal transduction pathways occurring along with progression of the cancer. Quinone containing compounds have been reported as one of the promising novel anticancer therapeutics against CRC. However, the effects of diiminoquinone (DIQ) on CRC stem cells have not been extensively investigated yet.

Research motivation

To explore the promising anticancer effects of a novel quinone, DIQ, on CRC.

Research objectives

To investigate the anticancer potential of novel therapeutic DIQ on CRC using two-dimensional and three-dimensional models.

Research methods

MTT and trypan blue exclusion assays were employed to assess the anti-proliferative effect of DIQ on HCT116 and HT29 cell lines *in vitro*. Propidium iodide DNA and dihydroethidium staining were performed to determine cell cycle distribution and reactive oxygen species production in response to DIQ, respectively. Wound healing and transwell invasion assays were used to determine the invasion and migration ability of DIQ, respectively. Then, a sphere formation model was used to evaluate the potency of DIQ on targeting cancer stem cells in CRC cells for up to five generations. Immunofluor-

escent analysis and western blot were performed to elucidate the mechanism of action of DIQ in CRC. Organoid model was used to assess DIQ response on established organoids from fresh colorectal tissue samples from consenting patients.

Research results

DIQ reduced the self-renewal capacity of CRC cells and targeted the growth of colon cancer patient-derived organoids. DIQ downregulated the expression of key markers involved in the oncogenic stem cell Wnt/-catenin, AKT, and ERK signaling pathways that are involved in CRC tumorigenesis. Also, DIQ decreased proliferation, migration, and invasion and induced apoptosis, cell-cycle arrest, and reactive oxygen species.

Research conclusions

Our findings strongly suggest that DIQ could be a promising novel therapeutic for the treatment of CRC patients. This study represents the first documentation of the molecular mechanism of the novel anticancer therapeutics DIQ *via* targeting cancer stem cells, findings that have potential therapeutic implications for colon cancer patients.

Research perspectives

Further research on the DIQ mechanisms that are involved in CRC tumorigenesis is needed to be performed in the future. A larger cohort is still required to further investigate and evaluate the effects of DIQ in translational medicine.

ACKNOWLEDGEMENTS

We are thankful to all members of the Gali-Muhtasib and Abou-Kheir Laboratory and the staff of the core facilities in the DTS Building at the American University of Beirut for their technical help and support.

FOOTNOTES

Author contributions: Monzer A carried out lab work as part of her PhD thesis, wrote the manuscript, and performed data analysis and interpretation of data (*e.g.*, biostatistics, statistical analysis, and editing); Wakimian K, Ballout F, Al Bitar S, and Yehya A performed initial lab work and participated in data collection; Faraj W, Tawil A, Doughan S, Hussein M, Kanso M, and Saheb N helped in clinical data curation and the consent form for colon cancer patient samples at the American University of Beirut Medical Center; Gali-Muhtasib H and Abou-Kheir W conceived the project, supervised the work, and edited the manuscript draft; All authors have reviewed and approved the final manuscript.

Institutional review board statement: All specimens from the patients were obtained after their informed consent. All experiments involving human subjects were performed in agreement with all ethical considerations of the Institutional Review Board.

Institutional animal care and use committee statement: Prior to any mouse experiment, all mice protocols were reviewed and approved by the Institutional Animal Care and Use Committee (American University of Beirut, Institutional Animal Care and Use Committee).

Conflict-of-interest statement: All the authors report no relevant conflicts of interest for this article.

Data sharing statement: No additional data are available.

ARRIVE guidelines statement: The ARRIVE Guidelines have been adopted. The authors have read the ARRIVE Guidelines, and the manuscript was prepared and revised according to the ARRIVE Guidelines.

Open-Access: This article is an open-access article that was selected by an in-house editor and fully peer-reviewed by external reviewers. It is distributed in accordance with the Creative Commons Attribution NonCommercial (CC BY-NC 4.0) license, which permits others to distribute, remix, adapt, build upon this work non-commercially, and license their derivative works on different terms, provided the original work is properly cited and the use is non-commercial. See: https://creativecommons.org/Licenses/by-nc/4.0/

Country/Territory of origin: Lebanon

ORCID number: Samar Al Bitar 0000-0002-0016-1029; Samer Doughan 0000-0002-6584-6977; Deborah Mukherji 0000-0002-0192-5828; Walid Faraj 0000-0002-0156-7960; Hala Gali-Muhtasib 0000-0001-6840-3015; Wassim Abou-Kheir 0000-0001-9719-9324.

S-Editor: Gong ZM
L-Editor: Filipodia
P-Editor: Li X

REFERENCES

1 **Sung H**, Ferlay J, Siegel RL, Laversanne M, Soerjomataram I, Jemal A, Bray F. Global Cancer Statistics 2020: GLOBOCAN Estimates of Incidence and Mortality Worldwide for 36 Cancers in 185 Countries. *CA Cancer J Clin* 2021; **71**: 209-249 [PMID: 33538338 DOI: 10.3322/caac.21660]
2 **Rawla P**, Sunkara T, Barsouk A. Epidemiology of colorectal cancer: incidence, mortality, survival, and risk factors. *Prz Gastroenterol* 2019; **14**: 89-103 [PMID: 31616522 DOI: 10.5114/pg.2018.81072]
3 **Hsieh MH**, Kung PT, Kuo WY, Ke TW, Tsai WC. Recurrence, death risk, and related factors in patients with stage 0 colorectal cancer: A nationwide population-based study. *Medicine (Baltimore)* 2020; **99**: e21688 [PMID: 32899000 DOI: 10.1097/MD.0000000000021688]
4 **Phi LTH**, Sari IN, Yang YG, Lee SH, Jun N, Kim KS, Lee YK, Kwon HY. Cancer Stem Cells (CSCs) in Drug Resistance and their Therapeutic Implications in Cancer Treatment. *Stem Cells Int* 2018; **2018**: 5416923 [PMID: 29681949 DOI: 10.1155/2018/5416923]
5 **Mitra A**, Mishra L, Li S. EMT, CTCs and CSCs in tumor relapse and drug-resistance. *Oncotarget* 2015; **6**: 10697-10711 [PMID: 25986923 DOI: 10.18632/oncotarget.4037]
6 **Phua LC**, Mal M, Koh PK, Cheah PY, Chan EC, Ho HK. Investigating the role of nucleoside transporters in the resistance of colorectal cancer to 5-fluorouracil therapy. *Cancer Chemother Pharmacol* 2013; **71**: 817-823 [PMID: 23271323 DOI: 10.1007/s00280-012-2054-0]
7 **Ballout F**, Monzer A, Fatfat M, Ouweini HE, Jaffa MA, Abdel-Samad R, Darwiche N, Abou-Kheir W, Gali-Muhtasib H. Thymoquinone induces apoptosis and DNA damage in 5-Fluorouracil-resistant colorectal cancer stem/progenitor cells. *Oncotarget* 2020; **11**: 2959-2972 [PMID: 32821342 DOI: 10.18632/oncotarget.27426]
8 **Brandi G**, De Lorenzo S, Nannini M, Curti S, Ottone M, Dall'Olio FG, Barbera MA, Pantaleo MA, Biasco G. Adjuvant chemotherapy for resected colorectal cancer metastases: Literature review and meta-analysis. *World J Gastroenterol* 2016; **22**: 519-533 [PMID: 26811604 DOI: 10.3748/wjg.v22.i2.519]
9 **Edmondson R**, Broglie JJ, Adcock AF, Yang L. Three-dimensional cell culture systems and their applications in drug discovery and cell-based biosensors. *Assay Drug Dev Technol* 2014; **12**: 207-218 [PMID: 24831787 DOI: 10.1089/adt.2014.573]
10 **Chaicharoenaudomrung N**, Kunhorm P, Noisa P. Three-dimensional cell culture systems as an *in vitro* platform for cancer and stem cell modeling. *World J Stem Cells* 2019; **11**: 1065-1083 [PMID: 31875869 DOI: 10.4252/wjsc.v11.i12.1065]
11 **Fang Y**, Eglen RM. Three-Dimensional Cell Cultures in Drug Discovery and Development. *SLAS Discov* 2017; **22**: 456-472 [PMID: 28520521 DOI: 10.1177/1087057117696795]
12 **Young M**, Reed KR. Organoids as a Model for Colorectal Cancer. *Curr Colorectal Cancer Rep* 2016; **12**: 281-287 [PMID: 27656116 DOI: 10.1007/s11888-016-0335-4]
13 **Huch M**, Knoblich JA, Lutolf MP, Martinez-Arias A. The hope and the hype of organoid research. *Development* 2017; **144**: 938-941 [PMID: 28292837 DOI: 10.1242/dev.150201]
14 **Bao B**, Ahmad A, Azmi AS, Ali S, Sarkar FH. Overview of cancer stem cells (CSCs) and mechanisms of their regulation: implications for cancer therapy. *Curr Protoc Pharmacol* 2013; **Chapter** 14: Unit 14.25 [PMID: 23744710 DOI: 10.1002/0471141755.ph1425s61]
15 **Chang JC**. Cancer stem cells: Role in tumor growth, recurrence, metastasis, and treatment resistance. *Medicine (Baltimore)* 2016; **95**: S20-S25 [PMID: 27611935 DOI: 10.1097/MD.0000000000004766]
16 **Lu JJ**, Bao JL, Wu GS, Xu WS, Huang MQ, Chen XP, Wang YT. Quinones derived from plant secondary metabolites as anti-cancer agents. *Anticancer Agents Med Chem* 2013; **13**: 456-463 [PMID: 22931417]
17 **Pereyra CE**, Dantas RF, Ferreira SB, Gomes LP, Silva-Jr FP. The diverse mechanisms and anticancer potential of naphthoquinones. *Cancer Cell Int* 2019; **19**: 207 [PMID: 31388334 DOI: 10.1186/s12935-019-0925-8]
18 **Huang Q**, Lu G, Shen HM, Chung MC, Ong CN. Anti-cancer properties of anthraquinones from rhubarb. *Med Res Rev* 2007; **27**: 609-630 [PMID: 17022020 DOI: 10.1002/med.20094]
19 **Mehanna MM**, Sarieddine R, Alwattar JK, Chouaib R, Gali-Muhtasib H. Anticancer Activity of Thymoquinone Cubic Phase Nanoparticles Against Human Breast Cancer: Formulation, Cytotoxicity and Subcellular Localization. *Int J Nanomedicine* 2020; **15**: 9557-9570 [PMID: 33293807 DOI: 10.2147/IJN.S263797]
20 **Guler EM**, Sisman BH, Kocyigit A, Hatiboglu MA. Investigation of cellular effects of thymoquinone on glioma cell. *Toxicol Rep* 2021; **8**: 162-170 [PMID: 33489775 DOI: 10.1016/j.toxrep.2020.12.026]
21 **Wang W**, Rayburn ER, Velu SE, Chen D, Nadkarni DH, Murugesan S, Zhang R. A novel synthetic iminoquinone, BA-TPQ, as an anti-breast cancer agent: *in vitro* and *in vivo* activity and mechanisms of action. *Breast Cancer Res Treat* 2010; **123**: 321-331 [PMID: 19936915 DOI: 10.1007/s10549-009-0638-0]
22 **Monzer A**, Jabotian N, Ballout F, Zhu JS, Kurth MJ, Haddadin MJ, Gali-Muhtasib H. Novel 2-(5-Imino-5*H*-isoquinolones[3,4-*b*]quinoxalin-7-ylmethyl)-benzonitrile (DIQ3) and Other Related Derivatives Targeting Colon Cancer Cells: Syntheses and in Vitro Models. *ACS Omega* 2019; **4**: 3205-3212 [PMID: 30842984 DOI: 10.1021/acsomega.8b02698]
23 **Mouhieddine TH**, Nokkari A, Itani MM, Chamaa F, Bahmad H, Monzer A, El-Merahbi R, Daoud G, Eid A, Kobeissy FH, Abou-Kheir W. Metformin and Ara-a Effectively Suppress Brain Cancer by Targeting Cancer Stem/Progenitor Cells. *Front Neurosci* 2015; **9**: 442 [PMID: 26635517 DOI: 10.3389/fnins.2015.00442]

24 **Abou-Kheir W**, Hynes PG, Martin P, Yin JJ, Liu YN, Seng V, Lake R, Spurrier J, Kelly K. Self-renewing Pten-/- TP53-/- protospheres produce metastatic adenocarcinoma cell lines with multipotent progenitor activity. *PLoS One* 2011; **6**: e26112 [PMID: 22022528 DOI: 10.1371/journal.pone.0026112]

25 **Boehnke K**, Iversen PW, Schumacher D, Lallena MJ, Haro R, Amat J, Haybaeck J, Liebs S, Lange M, Schäfer R, Regenbrecht CR, Reinhard C, Velasco JA. Assay Establishment and Validation of a High-Throughput Screening Platform for Three-Dimensional Patient-Derived Colon Cancer Organoid Cultures. *J Biomol Screen* 2016; **21**: 931-941 [PMID: 27233291 DOI: 10.1177/1087057116650965]

26 **Jiang WG**, Sanders AJ, Katoh M, Ungefroren H, Gieseler F, Prince M, Thompson SK, Zollo M, Spano D, Dhawan P, Sliva D, Subbarayan PR, Sarkar M, Honoki K, Fujii H, Georgakilas AG, Amedei A, Niccolai E, Amin A, Ashraf SS, Ye L, Helferich WG, Yang X, Boosani CS, Guha G, Ciriolo MR, Aquilano K, Chen S, Azmi AS, Keith WN, Bilsland A, Bhakta D, Halicka D, Nowsheen S, Pantano F, Santini D. Tissue invasion and metastasis: Molecular, biological and clinical perspectives. *Semin Cancer Biol* 2015; **35** Suppl: S244-S275 [PMID: 25865774 DOI: 10.1016/j.semcancer.2015.03.008]

27 **Shi X**, Zhang Y, Zheng J, Pan J. Reactive oxygen species in cancer stem cells. *Antioxid Redox Signal* 2012; **16**: 1215-1228 [PMID: 22316005 DOI: 10.1089/ars.2012.4529]

28 **Yu Z**, Pestell TG, Lisanti MP, Pestell RG. Cancer stem cells. *Int J Biochem Cell Biol* 2012; **44**: 2144-2151 [PMID: 22981632 DOI: 10.1016/j.biocel.2012.08.022]

29 **Rich JN**. Cancer stem cells: understanding tumor hierarchy and heterogeneity. *Medicine (Baltimore)* 2016; **95**: S2-S7 [PMID: 27611934 DOI: 10.1097/MD.0000000000004764]

30 **Nwabo Kamdje AH**, Takam Kamga P, Tagne Simo R, Vecchio L, Seke Etet PF, Muller JM, Bassi G, Lukong E, Kumar Goel R, Mbo Amvene J, Krampera M. Developmental pathways associated with cancer metastasis: Notch, Wnt, and Hedgehog. *Cancer Biol Med* 2017; **14**: 109-120 [PMID: 28607802 DOI: 10.20892/j.issn.2095-3941.2016.0032]

31 **Ma J**, Cheng J, Gong Y, Tian L, Huang Q. Downregulation of Wnt signaling by sonic hedgehog activation promotes repopulation of human tumor cell lines. *Dis Model Mech* 2015; **8**: 385-391 [PMID: 25713298 DOI: 10.1242/dmm.018887]

32 **Ye Q**, Cai W, Zheng Y, Evers BM, She QB. ERK and AKT signaling cooperate to translationally regulate survivin expression for metastatic progression of colorectal cancer. *Oncogene* 2014; **33**: 1828-1839 [PMID: 23624914 DOI: 10.1038/onc.2013.122]

33 **Braicu C**, Buse M, Busuioc C, Drula R, Gulei D, Raduly L, Rusu A, Irimie A, Atanasov AG, Slaby O, Ionescu C, Berindan-Neagoe I. A Comprehensive Review on MAPK: A Promising Therapeutic Target in Cancer. *Cancers (Basel)* 2019; **11** [PMID: 31652660 DOI: 10.3390/cancers11101618]

34 **Al Bitar S**, Gali-Muhtasib H. The Role of the Cyclin Dependent Kinase Inhibitor p21$^{cip1/waf1}$ in Targeting Cancer: Molecular Mechanisms and Novel Therapeutics. *Cancers (Basel)* 2019; **11** [PMID: 31575057 DOI: 10.3390/cancers11101475]

35 **Waga S**, Hannon GJ, Beach D, Stillman B. The p21 inhibitor of cyclin-dependent kinases controls DNA replication by interaction with PCNA. *Nature* 1994; **369**: 574-578 [PMID: 7911228 DOI: 10.1038/369574a0]

36 **Mah LJ**, El-Osta A, Karagiannis TC. gammaH2AX: a sensitive molecular marker of DNA damage and repair. *Leukemia* 2010; **24**: 679-686 [PMID: 20130602 DOI: 10.1038/leu.2010.6]

37 **Palla VV**, Karaolanis G, Katafigiotis I, Anastasiou I, Patapis P, Dimitroulis D, Perrea D. gamma-H2AX: Can it be established as a classical cancer prognostic factor? *Tumour Biol* 2017; **39**: 1010428317695931 [PMID: 28351323 DOI: 10.1177/1010428317695931]

38 **Chiu SJ**, Lee YJ, Hsu TS, Chen WS. Oxaliplatin-induced gamma-H2AX activation *via* both p53-dependent and -independent pathways but is not associated with cell cycle arrest in human colorectal cancer cells. *Chem Biol Interact* 2009; **182**: 173-182 [PMID: 19735649 DOI: 10.1016/j.cbi.2009.08.019]

39 **Fatehullah A**, Tan SH, Barker N. Organoids as an *in vitro* model of human development and disease. *Nat Cell Biol* 2016; **18**: 246-254 [PMID: 26911908 DOI: 10.1038/ncb3312]

40 **Azar J**, Bahmad HF, Daher D, Moubarak MM, Hadadeh O, Monzer A, Al Bitar S, Jamal M, Al-Sayegh M, Abou-Kheir W. The Use of Stem Cell-Derived Organoids in Disease Modeling: An Update. *Int J Mol Sci* 2021; **22** [PMID: 34299287 DOI: 10.3390/ijms22147667]

World Journal of Gastroenterology

Submit a Manuscript: https://www.f6publishing.com

World J Gastroenterol 2022 September 7; 28(33): 4812-4822

DOI: 10.3748/wjg.v28.i33.4812

ISSN 1007-9327 (print) ISSN 2219-2840 (online)

ORIGINAL ARTICLE

Case Control Study

Previous hepatitis B viral infection–an underestimated cause of pancreatic cancer

Sergey Batskikh, Sergey Morozov, Alexey Dorofeev, Zanna Borunova, Dmitry Kostyushev, Sergey Brezgin, Anastasiya Kostyusheva, Vladimir Chulanov

Specialty type: Gastroenterology and hepatology

Provenance and peer review: Invited article; Externally peer reviewed.

Peer-review model: Single blind

Peer-review report's scientific quality classification
Grade A (Excellent): 0
Grade B (Very good): B, B, B
Grade C (Good): C
Grade D (Fair): 0
Grade E (Poor): 0

P-Reviewer: Pham TTT, Viet Nam; Sultana C, Romania; Tai DI, Taiwan

Received: April 20, 2022
Peer-review started: April 20, 2022
First decision: June 2, 2022
Revised: June 15, 2022
Accepted: August 16, 2022
Article in press: August 16, 2022
Published online: September 7, 2022

Sergey Batskikh, Department of Hepatology, Moscow Clinical Scientific Center N.A. A.S. Loginov, Moscow 111123, Russia

Sergey Morozov, Department of Gastroenterology, Hepatology and Nutrition, Federal Research Center of Nutrition, Biotechnology and Food Safety, Moscow 115446, Russia

Alexey Dorofeev, Zanna Borunova, Department of Scientific and Clinical Laboratory Research, Moscow Clinical Scientific Center N.A. A.S. Loginov, Moscow 111123, Russia

Dmitry Kostyushev, Sergey Brezgin, Anastasiya Kostyusheva, Vladimir Chulanov, Laboratory of Genetic Technologies, Sechenov University, Moscow 119435, Russia

Dmitry Kostyushev, Sergey Brezgin, Vladimir Chulanov, Division of Biotechnology, Scientific Center for Genetics and Life Sciences, Sirius University of Science and Technology, Sochi 354340, Russia

Vladimir Chulanov, Laboratory of Genetic Technologies and Translational Research, National Medical Research Center for Tuberculosis and Infectious Diseases of Ministry of Health of Russia, Moscow 127994, Russia

Corresponding author: Sergey Morozov, MD, PhD, Doctor, Senior Researcher, Department of Gastroenterology, Hepatology and Nutrition, Federal Research Center of Nutrition, Biotechnology and Food Safety, Kashirskoye Shosse 21, Moscow 115446, Russia.
morosoffsv@mail.ru

Abstract

BACKGROUND

The etiology of pancreatic cancer remains unclear. This limits the possibility of prevention and effective treatment. Hepatitis B virus (HBV) is responsible for the development of different types of cancer, but its role in pancreatic cancer is still being discussed.

AIM

To assess the prevalence of previous HBV infection and to identify viral biomarkers in patients with pancreatic ductal adenocarcinoma (PDAC) to support the role of the virus in etiology of this cancer.

METHODS
The data of 130 hepatitis B surface antigen-negative subjects were available for the final analysis, including 60 patients with PDAC confirmed by cytology or histology and 70 sex- and age-matched controls. All the participants were tested for HBV biomarkers in blood [antibody to hepatitis B core antigen (anti-HBc), antibody to hepatitis B surface antigen (anti-HBs) and HBV DNA], and for those with PDAC, biomarkers in resected pancreatic tissues were tested (HBV DNA, HBV pregenomic RNA and covalently closed circular DNA). We performed immunohistochemistry staining of pancreatic tissues for hepatitis B virus X antigen and Ki-67 protein. Non-parametric statistics were used for the analysis.

RESULTS
Anti-HBc was detected in 18/60 (30%) patients with PDAC and in 9/70 (13%) participants in the control group (P = 0.029). Accordingly, the odds of PDAC in anti-HBc-positive subjects were higher compared to those with no previous HBV infection (odds ratio: 2.905, 95% confidence interval: 1.191-7.084, standard error 0.455). HBV DNA was detected in 8 cases of PDAC and in 6 of them in the pancreatic tumor tissue samples only (all patients were anti-HBc positive). Blood HBV DNA was negative in all subjects of the control group with positive results of the serum anti-HBc test. Among 9 patients with PDAC, 5 revealed signs of replicative competence of the virus (covalently closed circular DNA with or without pregenomic RNA) in the pancreatic tumor tissue samples. Hepatitis B virus X antigen expression and active cell proliferation was revealed by immunohistochemistry in 4 patients with PDAC in the pancreatic tumor tissue samples.

CONCLUSION
We found significantly higher risks of PDAC in anti-HBc-positive patients. Detection of viral replication and hepatitis B virus X protein expression in the tumor tissue prove involvement of HBV infection in pancreatic cancer development.

Key Words: Hepatitis B virus; Previous hepatitis B; Occult hepatitis B virus infection; Pancreatic cancer; Pancreatic ductal adenocarcinoma

©The Author(s) 2022. Published by Baishideng Publishing Group Inc. All rights reserved.

Core Tip: Hepatitis B viral (HBV) infection is responsible for different types of cancer. Its role in pancreatic ductal adenocarcinoma (PDAC) remains unclear. This study assessed the prevalence of previous HBV infection and to identify viral biomarkers in patients with PDAC to support the role of the virus in the etiology of this cancer. Anti-HBc-positive subjects had an almost 3-fold greater chance of PDAC compared to the controls. Detection of viral replication and hepatitis B virus X protein expression in the tumor tissue show a possible involvement of HBV infection in pancreatic cancer development. Previous HBV infection is currently an underestimated cause of PDAC.

Citation: Batskikh S, Morozov S, Dorofeev A, Borunova Z, Kostyushev D, Brezgin S, Kostyusheva A, Chulanov V. Previous hepatitis B viral infection–an underestimated cause of pancreatic cancer. *World J Gastroenterol* 2022; 28(33): 4812-4822
URL: https://www.wjgnet.com/1007-9327/full/v28/i33/4812.htm
DOI: https://dx.doi.org/10.3748/wjg.v28.i33.4812

INTRODUCTION

Pancreatic cancer (PC) is an aggressive gastrointestinal malignancy with a low rate of early detection, poor survival and a limited number of therapeutic options. It causes more than 430000 deaths yearly worldwide[1]. This makes PC the third leading cause of cancer-related deaths in the United States and the fourth in the European Union[2,3]. The incidence rate of PC is growing, while the improvement in the survival rates is negligible[4]. Pancreatic ductal adenocarcinoma (PDAC) is the most prevalent type of PC and is found in 85% of cases[5]. The etiology of PC remains unclear, which limits the possibility for prevention and effective treatment. Early detection of PC remains a challenge. Therefore, it is still relevant to explore etiological factors of PDAC further and to identify subjects at risk of the disease. Numerous risk factors for the disease have been identified (smoking, excessive alcohol intake, history of chronic pancreatitis, obesity and diabetes, *etc*)[6]. Some viruses, including hepatitis B virus (HBV), are responsible for the development of different types of cancer, but their role in PC is still being discussed

[7].

In endemic regions, like Southeast Asia, the blood markers of current HBV infection are commonly found in subjects with PC[8]. Some authors from endemic regions report that HBV infection is not associated with the risk of developing PC after adjusting for age, sex, diabetes and smoking[9].

Cohort studies from Northern Europe (Denmark, Sweden), where HBV infection is not widespread, showed conflicting results and made an association between PC and HBV infection questionable[10-12]. In most of these studies, association of PC with previous HBV infection (PBI) was not considered. However, it may be important as the risk of liver cancer development perseveres even after hepatitis B surface antigen (HBsAg) loss[13-15].

Cancerogenic mechanisms of HBV infection may be explained by the integration of viral DNA fragments into the genome of host cells or persistence of the viral genome as a covalently closed circular DNA (cccDNA), which plays the role of viral reservoir and template for life-long synthesis of new virions. Both are responsible for preserved expression of viral proteins (especially HBx), which can lead to potentially oncogenic mutations[16-18].

Thus, not only active hepatitis B, but also previous HBV infection may contribute to PC development. Detection of HBV DNA and viral antigens in the pancreatic tumor tissues may provide direct evidence of the involvement of the virus in the etiology of this cancer. However, only a few studies demonstrated the presence of HBV DNA (cccDNA) and/or viral antigens in pancreatic tumor tissue. Therefore, the aim of our study was to assess the prevalence of PBI and to identify viral biomarkers in patients with PDAC to support the role of the virus in the etiology of this cancer.

MATERIALS AND METHODS

Study population

The study was based on the data of complex examination of patients that applied for PC treatment to Moscow Clinical Scientific Center named after A.S. Loginov from January 2019 to November 2020. Subjects of the control group were also recruited. The study (registered AAAA-A18-118021590196-1, AAAA-A20-120051990006-1 at www.rosrid.ru) was approved by the Local Ethics Committee and was conducted in accordance with the Declaration of Helsinki (1968) and its consequent revisions. All subjects signed a written informed consent form before the enrollment.

Inclusion criteria

Patients of both sexes, older than 18 years, willing to participate in the study were eligible.

In the group of PC, we enrolled patients with histologically or cytologically confirmed PDAC. In the control group we enrolled generally healthy subjects who applied for routine check-ups or treatment of other non-malignant gastrointestinal conditions and whose data of abdominal ultrasound and/or computed tomography revealed no signs of focal lesions in the pancreas.

Exclusion criteria

Other/indeterminate types of PC or non-malignant lesions beside PDAC (for the main group); positive blood test for HBsAg, hepatitis C virus or HIV antibodies; past surgery for PC; current or previous treatment with interferons, nucleos(t)ide analogues for HBV infection or other reasons; clinically significant diseases or health disorders, making it impossible to perform procedures required by the study protocol.

Confirmation of the conditions of interest

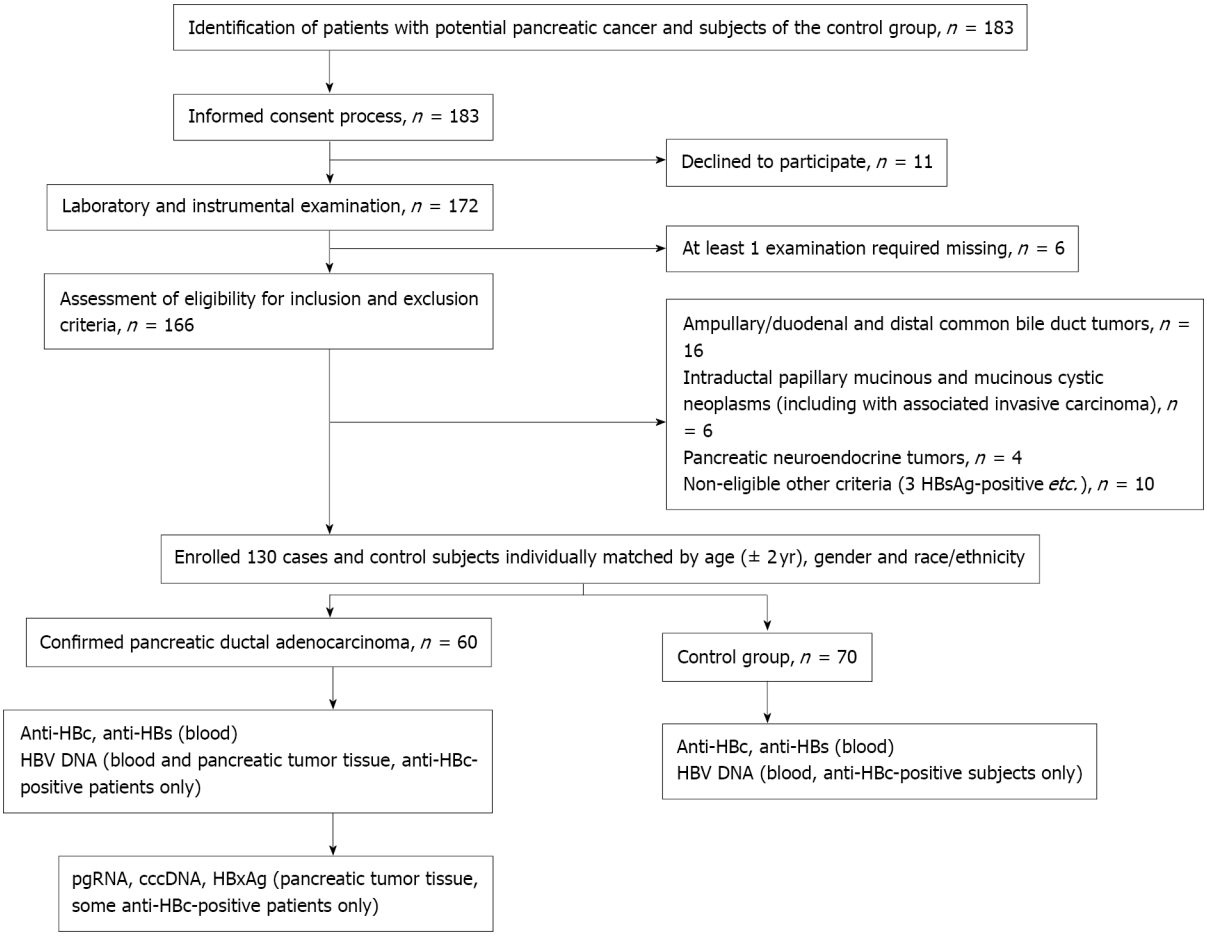
PBI was defined as the presence of antibody to hepatitis B core antigen (anti-HBc) with or without antibody to hepatitis B surface antigen (anti-HBs) or HBV DNA in serum[19]. Control subjects were matched for age (within 2 years), sex and race/ethnicity with the PDAC patients. Study design is shown in Figure 1.

Study procedures

To exclude health conditions able to affect results of the study, all patients underwent routine diagnostic procedures (including but not limited to blood tests, electrocardiogram, abdominal ultrasound and chest X-ray) within standards of care.

All the participants were tested for HBV biomarkers in blood (HBsAg, anti-HBc, anti-HBs). Those HBsAg-negative with positive anti-HBc result were tested for HBV DNA in blood. Anti-HBc-positive patients with PDAC were examined for HBV DNA in the pancreatic tumor tissue.

Tumor tissues of anti-HBc-positive patients with PDAC underwent examination for HBV biomarkers (HBV pregenomic RNA and cccDNA) and immunohistochemistry staining for hepatitis B virus X antigen (HBxAg) and Ki-67 protein in cases of the signed informed consent for these tests and sufficient quantity and good quality of the samples.



DOI: 10.3748/wjg.v28.i33.4812 **Copyright** ©The Author(s) 2022.

Figure 1 Study design and patient allocation chart. cccDNA: Covalently closed circular DNA; HBV: Hepatitis B virus; HBsAg: Hepatitis B surface antigen; anti-HBc: Antibody to hepatitis B core antigen; anti-HBs: Antibody to hepatitis B surface antigen; pgRNA: Pregenomic RNA.

All anti-HBc-positive participants were tested for the presence of HBV DNA in the blood. In addition, all 18 anti-HBc-positive patients with PDAC were tested for the presence of HBV DNA in pancreatic tumor tissue. In 8 of them, the quality and quantity of samples were suitable for additional testing for HBV pregenomic RNA and cccDNA. Five patients had eligible samples according to these criteria and gave additional consent for immunohistochemical staining for HBxAg and Ki-67 protein.

Collection of samples: Blood samples were taken after overnight fasting, coded and processed immediately at the local laboratory according to the standard instructions.

Pancreatic tumor tissue samples were obtained during surgery or diagnostic biopsy, coded and processed locally. They were stained with hematoxylin-eosin and assessed by a qualified morphologist.

Immunology: Serum samples were tested for HBsAg, anti-HBc IgG, anti-HBs, hepatitis C virus and HIV antibodies. These tests were performed with the use of a Sunrise analyzer (Tecan GmbH, Austria) and specific immunoassays kits (Vector-Best Co., Russia).

Analysis of HBV nucleic acids: Plasma HBV DNA was isolated using commercial AmpliSens Riboprep kit (AmpliSens Biotechnologies, Russia) according to manufacturer's instructions and quantified using the PCR assay AmpliSens HBV-FL (AmpliSens Biotechnologies) kit (lower limit of detection of 10 IU/mL).

To isolate nucleic acids from biopsies, samples were first homogenized in the MagNA Lyser (Roche Diagnostics, Switzerland). HBV DNA was isolated by AmpliSens Riboprep kit (AmpliSens Biotechnologies) and quantified by AmpliSens HBV-FL (AmpliSens Biotechnologies) kit.

To quantify cccDNA, nucleic acids were first treated with T5 exonuclease (New England Biolabs, United Kingdom) at 37 °C for 60 min and inactivation at 70 °C for 20 min[20]. HBV cccDNA was quantified with specific sets of primers and probes and normalized to genomic β-globin.

Specific sets of primers (Table 1) and TaqMan fluorescent probes were used for PCR analysis to detect HBV DNA in pancreatic tissue samples.

Table 1 List of specific sets of primers and probes used for the analysis

Target	Sequence	
cccDNA	Fw	CCGTGTGCACTTCGCTTCA
	Rev	GCACAGCTTGGAGGCTTGA
	Probe	FAM-CATGGAGACCACCGTGAACGCCC-BHQ1
β-globin	-	V31-FEP-CE (AmpliSens)
		HPV HCR-Screen (AmpliSens)

cccDNA: Covalently closed circular DNA; Fw: Forward; Rev: Reverse; HPV: Human papillomavirus; HCR: High carcinogenic risk; AmpliSens: AmpliSens Biotechnologies, Russia.

To analyze pregenomic HBV RNA (pgRNA HBV), nucleic acids were treated with RNase-free DNase I (NEB) for 30 min at 37 °C, purified by using AmpliSens Riboprep kit (AmpliSens Biotechnologies), reverse transcribed by AmpliSens Reverta-FL (AmpliSens Biotechnologies) and quantified by AmpliSens HBV-FL (AmpliSens Biotechnologies) kit. CFX96 Real-Time System (Bio-Rad, United States) PCR machine was used for the analysis of plasma and pancreatic tissue samples.

Immunohistochemistry of pancreatic tissues was performed after deparaffinization. Slides were fixed in 4% paraformaldehyde, washed three times in Tris-HCl (50 mM, pH 8.0) followed by incubation with a blocking buffer (0.02% of Triton X-100, 10% horse serum, and 150 mmol/L NaCl in Tris-HCl, 50 mmol/L, pH 8.0) for 30 min and 1 h staining with primary rabbit anti-HBx (ab39716) (Abcam, United Kingdom). Then, slides were washed three times for 5 min in a washing buffer (0.02% of Triton X-100 and 200 mmol/L NaCl in Tris-HCl, 50 mmol/L, pH 8.0) and incubated for 1 h with secondary Alexa Fluor 594 goat anti-rabbit antibodies (ab150080) (Abcam). After that, the slides were treated with primary tagged Alexa Fluor® 488 rabbit anti-Ki-67 (ab197234) and Hoechst 33342 (ab228551) for 1 h, washed three times for 5 min in washing buffer and finally mounted with a Fluoroshield reagent (Abcam). Images were captured using Thunder imaging systems (Leica Microsystems, Germany) with 10 × objectives. Ki-67 and HBxAg staining was analyzed using LAS X (Leica Microsystems). Ki-67 index was counted as the percentage of Ki-67-positive cells[21].

Statistical analysis

Statistica 12.0 software (StatSoft Inc., United States) was used for analysis of the data. Statistical processing of the obtained data was carried out using nonparametric statistics. Quantitative indicators were preliminarily assessed for compliance with the normal distribution using the Kolmogorov-Smirnov and Lilliefors tests. When quantitative indicators' distributions differed from normal, we used medians and the interquartile ranges (25%-75%) for the description and processed the data using the Mann-Whitney *U* test. Nominal data were compared using Pearson $\chi 2$ test with Yates's correction. *P* values < 0.05 were considered significant. Odds ratio (OR) and 95% confidence interval (95%CI) calculations were performed to assess the association between PDAC and PBI marker detection.

RESULTS

Data of 60 patients with PDAC and 70 participants of the control group were available for the final analysis. Demographic and viral characteristics of the participants are shown in Table 2.

In patients with PDAC, anti-HBc antibodies were found more often than in the control group (P = 0.029). Accordingly, the odds of PDAC in anti-HBc-positive subjects were significantly higher compared to those who had no PBI (OR: 2.905, 95%CI: 1.191-7.084, standard error 0.455).

Overall, HBV DNA was found in 8 anti-HBc-positive patients with PDAC. In 2 subjects it was detected in both the blood and pancreatic tumor samples, whereas in the other 6 participants the testing gave positive results only in the pancreatic tumor tissues. No positive results for HBV DNA were obtained in the control group.

The data from special examination of the blood and pancreatic tissue samples are shown in Table 3. The markers confirming replicative competence of HBV (cccDNA with or without pgRNA) were found in the pancreatic tumor tissue samples in 5 patients with PDAC. In 1 subject with a positive test on HBV DNA in the pancreatic tissue examination on cccDNA and pgRNA was not performed.

In those with detectable HBV DNA, viral load in the pancreatic tissue was 632 (390-851) IU/mL [median (25%-75%)].

HBxAg expression and active cells' proliferation was revealed by immunohistochemistry in 4 participants with PDAC in the pancreatic tumor tissue samples (Table 3 and Figure 2). The number of HBx-expressing cells in them did not exceed 10%.

Table 2 Study population characteristics

	PDAC, *n* = 60	Control, *n* = 70
Age in yr, Me (25%-75%)	64 (59-69)	62 (58-65)
Race/Ethnicity		
White/Caucasian, *n* (%)	56 (93.3)	65 (92.9)
Asian, *n* (%)	4 (6.7)	5 (7.1)
Females, *n* (%)	33 (55.0)	45 (64.3)
Anti-HBc (total), *n* (%)	18 (30.0)[a]	9 (12.9)
Anti-HBc + anti-HBs, *n* (%)	8 (13.3)	5 (7.1)
Anti-HBc (only), *n* (%)	10 (16.7)	4 (5.7)
HBV DNA (blood and/or pancreatic tissue), *n* (%[1])	8 (44.4)[a]	0
HBV DNA (pancreatic tissue only), *n* (%[1])	6 (33.3)[a]	0

[a]$P < 0.05$ pancreatic ductal adenocarcinoma *vs* control (Yates corrected χ^2).
[1]The percentage is according to the number of anti-hepatitis B core antigen-positive cases.
PDAC: Pancreatic ductal adenocarcinoma; Me: Median; HBV: Hepatitis B virus; HBc: Hepatitis B core antigen; HBs: Hepatitis B surface antigen.

Table 3 The results of special examination of subjects with pancreatic ductal adenocarcinoma

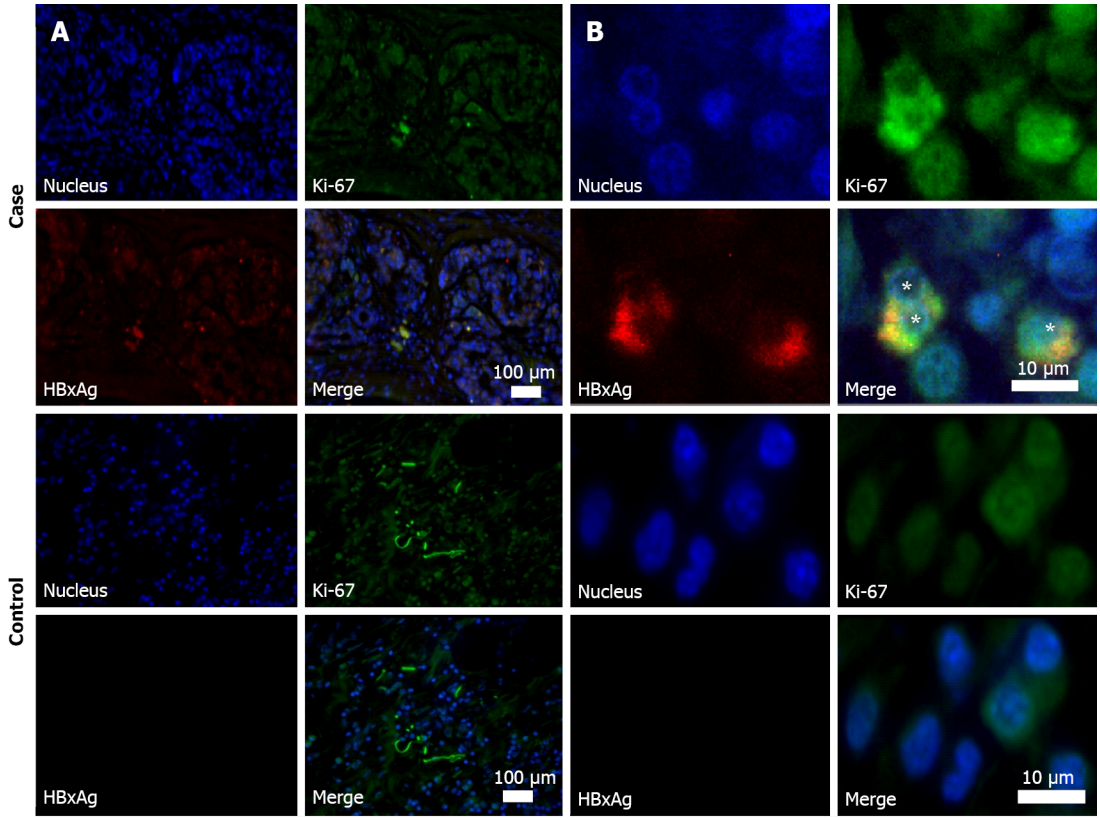
No.	Sex	Age in yr	Blood samples				Pancreatic tissue				
			HBsAg	Anti-HBc	Anti-HBs	HBV DNA, IU/mL	HBV DNA, IU/mL	pgRNA HBV, IU/mL	cccDNA, copies/cell × 10^{-6}	HBxAg	HBx-positive cells[1], %
1	M	50	Neg	Pos	Neg	Tnd	653	Tnd	257	Pos	3.9
2	F	58	Neg	Pos	Pos	Tnd	415	797	1440	Np	Np
3	M	60	Neg	Pos	Pos	Tnd	1183	Tnd	Tnd	Pos	3.7
4	M	61	Neg	Pos	Pos	Tnd	364	520	314	Pos	3.4
5	F	63	Neg	Pos	Pos	Tnd	Tnd	Tnd	Tnd	Neg	0
6	F	66	Neg	Pos	Pos	134	868	Np	Np	Np	Np
7	M	69	Neg	Pos	Pos	Tnd	610	Tnd	Tnd	Np	Np
8	M	69	Neg	Pos	Pos	Tnd	302	1428	1384	Np	Np
9	F	70	Neg	Pos	Pos	126	834	Tnd	1026	Pos	9.9

[1]Data are shown as median values by several fields of vision.
HBsAg: Hepatitis B surface antigen; anti-HBc: Antibody to hepatitis B core antigen; anti-HBs: Antibody to hepatitis B surface antigen; pgRNA: Pregenomic RNA; cccDNA: Covalently closed circular DNA; HBxAg: Hepatitis B virus X antigen; Np: Not performed; Tnd: Target not detected; Neg: Negative; Pos: Positive; HBV: Hepatitis B virus; M: Male; F: Female.

Ki-67 proliferative index in subjects with PDAC in the cohort of special examination was 79.1 (45.2–86.4) [median (25%-75%)]. All HBx-expressing cells were also Ki-67 positive.

DISCUSSION

The results of the present study demonstrate the association of PBI with PDAC and provide direct molecular evidence for the presence of HBV biomarkers in the pancreatic tumor tissue. In 8 of our patients with PDAC, HBV DNA was detected in the pancreatic tumor tissue. In 5 of them, replicative competence of HBV DNA in the pancreas was supported by detection of cccDNA (with or without pgRNA). Identification of cccDNA and pgRNA (transcribed only from cccDNA) additionally suggests that these patients saved a silent replication of the virus in the pancreatic tissue. Detection of the virus nucleic acids in pancreatic tissue only (with no HBV DNA present in blood) in most of subjects excludes



DOI: 10.3748/wjg.v28.i33.4812 **Copyright** ©The Author(s) 2022.

Figure 2 Immunohistochemistry of resected pancreatic tumor tissues (obtained during surgery). Case: Anti-HBc-positive patient with pancreatic ductal adenocarcinoma. Control: Patient with pancreatic ductal adenocarcinoma, who was negative for hepatitis B virus biomarkers. A: Images at magnification × 10; B: Images at magnification × 100. Samples were stained for Ki-67 protein (green fluorescence) and X antigen of hepatitis B virus of (HBxAg) (red fluorescence). Cell nuclei were counterstained by Hoechst33342 dye (blue). Asterisks indicate HBxAg/Ki-67 co-stained cells.

the possibility of artificial contamination of the tumor tissue samples.

Viral infections, including those caused by HBV were recognized among the modifiable risk factors of PC development[22,23]. The data of a meta-analysis of case-control and observational studies (number of subjects with PC: 5883) showed that the odds of PC were significantly higher in chronic or inactive HBsAg carriers [OR: 1.60 (95%CI: 1.26-2.05)] and anti-HBc-positive but anti-HBs-negative individuals [OR: 1.76 (95%CI: 1.05-2.93)] compared to those who were never exposed to HBV infection[7,24]. In our study, the odds of PDAC were even higher, and anti-HBc-positive subjects had an almost 3-fold greater chance of PDAC compared to the controls.

Only a few studies have demonstrated molecular evidence of possible HBV involvement in pancreatic tumor development by identifying HBV DNA (cccDNA) and/or its antigens in pancreatic tumor tissue, and only a limited number of subjects (especially HBsAg-negative but anti-HBc-positive) were involved[25,26]. Although certain pathogenetic mechanisms of PC associated with hepatitis B infection need to be explained in specially planned studies, some assumptions could be made.

HBV is a known carcinogen and is one of the main causes of hepatocellular carcinoma in endemic regions[8]. However, in HBV endemic areas, such as Africa and East Asia, there is a relatively low rate of PC-related deaths. Probably due to high mortality from other causes (including HBV-associated hepatocellular carcinoma), there is not enough time for the development of PC in people with PBI.

HBV integrates into the genome of infected cells, causes genomic aberrations, enhances expression of oncogenes or inhibits tumor suppressors and leads to the cancer development[14]. Similar mechanisms are possible in non-liver carcinogenesis, including the pancreas[25,27]. Pancreatic beta cells and hepatocytes develop from the ventral foregut endoderm during ontogenesis and thus may share characteristics that are favorable for HBV replication and virus-induced tumor development[28]. It seems that malignant transformation in the pancreas is not provoked by direct cellular damage and is caused by the integration of HBV DNA into the genome of pancreatic cells and subsequent disruption of the functions of anti-oncogenes or by stimulation of pro-oncogenes' activity[29]. The replication of HBV in pancreatic tissue may decrease with time. However, DNA fragments of the virus integrated into the genome of host cells continue to express viral proteins (especially regulatory protein X) of HBV responsible for carcinogenesis. The expression capability of HBx from integrated fragments of the viral genome in tumor tissues when replication is absent was confirmed in hepatocellular carcinoma[30-32].

In our study, immunohistochemistry revealed expression of HBx in the pancreatic tumor tissue in 4 out of 5 HBsAg-negative and anti-HBc-positive patients with PDAC. Replicative competence of HBV (detected cccDNA) was found in 3 of them. This may mean that in 1 patient, expression of HBx was caused only by the integration of the virus into the genome of pancreatic cells. These fragments of viral DNA, which preserve the open reading frame and express HBx, may serve as a basis for carcinogenesis in subjects with PDAC. Although this mechanism may play a role in primary cancer development, its role in PC recurrence is not clear, and further studies are necessary. The low-grade replication may also play a role in HBV reactivation, especially in cases when immunodepressants are used. However, this question is insufficiently studied.

It is not clear whether the number of HBxAg expressing cells is important for cancer development. In hepatocellular carcinoma of HBsAg-negative HBV DNA-positive subjects, the relative number of HBxAg-expressing cells is about 30% within the tumor tissue and 20% in the rest of the liver tissue[33]. Similar data for PC are lacking. According to our results, the number of cells producing HBxAg in PDAC is about 4%. It seems that the number of cells producing HBx protein is less important than their presence, at least for PC development. This may be indirectly confirmed by the fact that in all HBxAg-positive subjects in our study proliferative index Ki-67 was significantly higher than 50%, whereas similarly high values of this marker were only found in about 12% of subjects with PDAC[21,34].

Detection of cccDNA in pancreatic tissue in HBsAg-negative subject supports the need for revision of the statements of the Taormina Workshop (2018), which defines occult HBV infection as the presence of replication-competent HBV DNA (*i.e.* cccDNA in the liver and/or HBV DNA in the blood of people who test negative for HBsAg by currently available assays)[16]. As extrahepatic HBV replication may occur in HBsAg-negative subjects (which was confirmed in the course of our study), it is reasonable not to indicate in the statement the specific organ for HBV DNA (cccDNA) detection.

Involvement of PBI in PC development requires revision of the ultimate targets of antiviral treatment. "Sterilizing cure" (undetectable HBsAg in blood in combination with the absence of DNA HBV in any tissues, including cccDNA and integrated viral DNA) was recognized unachievable in the near future [35]. However, "functional cure" (defined as sustained clearance of HBs with or without HBs-seroconversion and non-detectable HBV DNA in blood after the course of treatment) evidently cannot affect the expression of oncogenic proteins of HBV (especially HBx) and thus diminish the chances of cancer development. Although it is impossible to achieve eradication of cccDNA and integrated fragments of the viral genome with currently existing means, this should be stated as the ultimate goal for future therapy options.

The limitation of the study is a relatively small number of patients. Moreover, examination of the tumor tissues on cccDNA, pgRNA and HBxAg was possible for only a few of the 18 anti-HBc-positive subjects with PDAC due to the quality of the obtained specimens. Further randomized multicenter studies are necessary to confirm the obtained results, prove the role of HBV infection in the etiology of PC and clarify carcinogenic mechanisms in them.

CONCLUSION

An almost three-fold risk of PDAC was found in HBsAg-negative but anti-HBc-positive subjects. Detection of silent viral replication and pro-oncogenic HBx protein expression in the tumor tissue suggest involvement of HBV infection in PC development. PBI seems to be an underestimated cause of PDAC at the moment.

ARTICLE HIGHLIGHTS

Research background

The etiology of pancreatic cancer is unclear. This limits possibilities for its prevention and effective treatment. Hepatitis B virus (HBV) is responsible for the development of hepatocellular carcinoma and different types of extrahepatic cancer, but its role in the etiology of pancreatic cancer is still being discussed.

Research motivation

The epidemiological relationship of previous HBV infection (PBI) with pancreatic cancer and identification of viral biomarkers within the tumor tissue may provide support for this. However, there is still a lack of such reports, especially from non-endemic regions for HBV infection.

Research objectives

In our study, we aimed to assess the prevalence of PBI and to identify viral biomarkers in patients with pancreatic ductal adenocarcinoma (PDAC) to support the role of the virus in the etiology of this cancer.

Research methods

The data of 130 hepatitis B surface antigen-negative subjects were included in the final analysis (60 patients with PDAC confirmed by cytology or histology and 70 sex- and age-matched controls). All the participants were tested for HBV biomarkers in blood (antibody to hepatitis B core antigen, antibody to hepatitis B surface antigen and HBV DNA). Those with PDAC were tested for biomarkers in resected pancreatic tissues [HBV DNA, HBV pregenomic RNA and covalently closed circular DNA (cccDNA)]. Additionally, we performed immunohistochemistry staining of pancreatic tissues for hepatitis B virus X antigen and Ki-67 protein. Non-parametric statistics were used for the analysis.

Research results

We have established that 18/60 (30%) patients with PDAC and 9/70 (13%) participants in the control group (P = 0.029) were anti-hepatitis B core antigen-positive. HBV DNA was detected in 8 anti-hepatitis B core antigen-positive patients of PDAC (in 6 of them—in the pancreatic tumor tissue samples only) but in neither subjects of the control group. In 5 patients with PDAC we revealed signs of replicative competence of the virus (cccDNA with or without pregenomic RNA) in the pancreatic tumor tissue samples. Hepatitis B virus X antigen expression and active cells' proliferation was revealed by immunohistochemistry in 4 participants with PDAC in the pancreatic tumor tissue samples.

Research conclusions

PBI seems to be an underestimated cause of PDAC.

Research perspectives

Larger studies are necessary to assess risks of PDAC in subjects with PBI and define HBV-associated mechanisms of carcinogenesis in them.

ACKNOWLEDGEMENTS

The authors acknowledge all study participants.

FOOTNOTES

Author contributions: Batskikh S and Morozov S designed this study; Batskikh S collected and analyzed the data; Borunova Z, Dorofeev A, Kostyushev D, Brezgin S, Kostyusheva A and Chulanov V performed laboratory analyses; Batskikh S, Morozov S and Kostyushev D prepared the figures; Batskikh S performed statistical analysis; Morozov S and Batskikh S drafted the manuscript; All authors critically revised the manuscript and approved its final version.

Supported by Ministry of Science and Higher Education of Russian Federation, No. FGMF-2022-0005; Russian Science Foundation, No. 20-15-00373; and Moscow Healthcare Department, No. AAAA-A18-118021590196-1.

Institutional review board statement: The study was reviewed and approved by the Local Ethics Committee of Moscow Clinical Research Center, No. 9/2016, dated 12DEC2016 and was conducted in accordance with the Declaration of Helsinki (1968) and its consequent revisions.

Informed consent statement: All subjects signed a written informed consent form before the enrollment.

Conflict-of-interest statement: Dr. Batskikh reports grants from Moscow Department of Health during the conduct of the study; personal fees from ABBVIE, personal fees from MSD, personal fees from R-PHARM, outside the submitted work. Dr. Morozov reports grants from Ministry of Science and Higher Education of Russia, during the conduct of the study; personal fees from AstraZeneca, personal fees from Dr. Falk, personal fees from AlfaSigma, grants from Russian Science Foundation, personal fees from Takeda, outside the submitted work. Dr. Chulanov reports grants from Russian Foundation for Basic Research, grants from Russian Foundation for Basic Research, outside the submitted work. Dr. Kostyushev, Dr. Kostyusheva and Dr. Brezgin report grants from Russian Foundation for Basic Research, grants from Russian Foundation for Basic Research, during the conduct of the study. Dr. Dorofeev and Dr. Borunova have nothing to disclose.

Data sharing statement: No additional data are available.

STROBE statement: The authors have read the STROBE Statement—checklist of items, and the manuscript was prepared and revised according to the STROBE Statement—checklist of items.

Open-Access: This article is an open-access article that was selected by an in-house editor and fully peer-reviewed by external reviewers. It is distributed in accordance with the Creative Commons Attribution NonCommercial (CC BY-

NC 4.0) license, which permits others to distribute, remix, adapt, build upon this work non-commercially, and license their derivative works on different terms, provided the original work is properly cited and the use is non-commercial. See: https://creativecommons.org/Licenses/by-nc/4.0/

Country/Territory of origin: Russia

ORCID number: Sergey Batskikh 0000-0002-5917-203X; Sergey Morozov 0000-0001-6816-3058; Alexey Dorofeev 0000-0001-9754-7579; Zanna Borunova 0000-0001-5251-1513; Dmitry Kostyushev 0000-0002-1851-7441; Sergey Brezgin 0000-0003-4792-0739; Anastasiya Kostyusheva 0000-0002-2335-6582; Vladimir Chulanov 0000-0001-6303-9293.

S-Editor: Fan JR
L-Editor: Filipodia
P-Editor: Fan JR

REFERENCES

1 **Bray F**, Ferlay J, Soerjomataram I, Siegel RL, Torre LA, Jemal A. Global cancer statistics 2018: GLOBOCAN estimates of incidence and mortality worldwide for 36 cancers in 185 countries. *CA Cancer J Clin* 2018; **68**: 394-424 [PMID: 30207593 DOI: 10.3322/caac.21492]
2 **NIH**. National Cancer Institute. Cancer Stats Facts: Pancreatic Cancer. [cited 4 January 2022]. Available from: https://seer.cancer.gov/statfacts/html/pancreas.html
3 **European Commission**. European Cancer Information System. [cited 6 January 2022]. Available from: https://ecis.jrc.ec.europa.eu/explorer.php
4 **Maisonneuve P**. Epidemiology and burden of pancreatic cancer. *Presse Med* 2019; **48**: e113-e123 [PMID: 30878335 DOI: 10.1016/j.lpm.2019.02.030]
5 **Mostafa ME**, Erbarut-Seven I, Pehlivanoglu B, Adsay V. Pathologic classification of "pancreatic cancers": current concepts and challenges. *Chin Clin Oncol* 2017; **6**: 59 [PMID: 29307199 DOI: 10.21037/cco.2017.12.01]
6 **Tempero MA**, Malafa MP, Al-Hawary M, Behrman SW, Benson AB, Cardin DB, Chiorean EG, Chung V, Czito B, Del Chiaro M, Dillhoff M, Donahue TR, Dotan E, Ferrone CR, Fountzilas C, Hardacre J, Hawkins WG, Klute K, Ko AH, Kunstman JW, LoConte N, Lowy AM, Moravek C, Nakakura EK, Narang AK, Obando J, Polanco PM, Reddy S, Reyngold M, Scaife C, Shen J, Vollmer C, Wolff RA, Wolpin BM, Lynn B, George GV. Pancreatic Adenocarcinoma, Version 2.2021, NCCN Clinical Practice Guidelines in Oncology. *J Natl Compr Canc Netw* 2021; **19**: 439-457 [PMID: 33845462 DOI: 10.6004/jnccn.2021.0017]
7 **Liu X**, Zhang ZH, Jiang F. Hepatitis B virus infection increases the risk of pancreatic cancer: a meta-analysis. *Scand J Gastroenterol* 2021; **56**: 252-258 [PMID: 33399501 DOI: 10.1080/00365521.2020.1868568]
8 **Arbuthnot P**, Kew M. Hepatitis B virus and hepatocellular carcinoma. *Int J Exp Pathol* 2001; **82**: 77-100 [PMID: 11454100 DOI: 10.1111/j.1365-2613.2001.iep0082-0077-x]
9 **Chang MC**, Chen CH, Liang JD, Tien YW, Hsu C, Wong JM, Chang YT. Hepatitis B and C viruses are not risks for pancreatic adenocarcinoma. *World J Gastroenterol* 2014; **20**: 5060-5065 [PMID: 24803819 DOI: 10.3748/wjg.v20.i17.5060]
10 **Andersen ES**, Omland LH, Jepsen P, Krarup H, Christensen PB, Obel N, Weis N; DANVIR Cohort Study. Risk of all-type cancer, hepatocellular carcinoma, non-Hodgkin lymphoma and pancreatic cancer in patients infected with hepatitis B virus. *J Viral Hepat* 2015; **22**: 828-834 [PMID: 25650146 DOI: 10.1111/jvh.12391]
11 **Huang J**, Magnusson M, Törner A, Ye W, Duberg AS. Risk of pancreatic cancer among individuals with hepatitis C or hepatitis B virus infection: a nationwide study in Sweden. *Br J Cancer* 2013; **109**: 2917-2923 [PMID: 24178755 DOI: 10.1038/bjc.2013.689]
12 **Sundquist K**, Sundquist J, Ji J. Risk of hepatocellular carcinoma and cancers at other sites among patients diagnosed with chronic hepatitis B virus infection in Sweden. *J Med Virol* 2014; **86**: 18-22 [PMID: 24038002 DOI: 10.1002/jmv.23754]
13 **European Association for the Study of the Liver**. EASL 2017 Clinical Practice Guidelines on the management of hepatitis B virus infection. *J Hepatol* 2017; **67**: 370-398 [PMID: 28427875 DOI: 10.1016/j.jhep.2017.03.021]
14 **Brechot C**, Pourcel C, Louise A, Rain B, Tiollais P. Presence of integrated hepatitis B virus DNA sequences in cellular DNA of human hepatocellular carcinoma. *Nature* 1980; **286**: 533-535 [PMID: 6250074 DOI: 10.1038/286533a0]
15 **Zhao LH**, Liu X, Yan HX, Li WY, Zeng X, Yang Y, Zhao J, Liu SP, Zhuang XH, Lin C, Qin CJ, Zhao Y, Pan ZY, Huang G, Liu H, Zhang J, Wang RY, Wen W, Lv GS, Zhang HL, Wu H, Huang S, Wang MD, Tang L, Cao HZ, Wang L, Lee TL, Jiang H, Tan YX, Yuan SX, Hou GJ, Tao QF, Xu QG, Zhang XQ, Wu MC, Xu X, Wang J, Yang HM, Zhou WP, Wang HY. Genomic and oncogenic preference of HBV integration in hepatocellular carcinoma. *Nat Commun* 2016; **7**: 12992 [PMID: 27703150 DOI: 10.1038/ncomms12992]
16 **Raimondo G**, Locarnini S, Pollicino T, Levrero M, Zoulim F, Lok AS; Taormina Workshop on Occult HBV Infection Faculty Members. Update of the statements on biology and clinical impact of occult hepatitis B virus infection. *J Hepatol* 2019; **71**: 397-408 [PMID: 31004683 DOI: 10.1016/j.jhep.2019.03.034]
17 **Fanning GC**, Zoulim F, Hou J, Bertoletti A. Therapeutic strategies for hepatitis B virus infection: towards a cure. *Nat Rev Drug Discov* 2019; **18**: 827-844 [PMID: 31455905 DOI: 10.1038/s41573-019-0037-0]
18 **Fanning GC**, Zoulim F, Hou J, Bertoletti A. Author Correction: Therapeutic strategies for hepatitis B virus infection: towards a cure. *Nat Rev Drug Discov* 2020; **19**: 291 [PMID: 31913354 DOI: 10.1038/s41573-019-0057-9]
19 **Lok AS**, Everhart JE, Di Bisceglie AM, Kim HY, Hussain M, Morgan TR; HALT-C Trial Group. Occult and previous hepatitis B virus infection are not associated with hepatocellular carcinoma in United States patients with chronic hepatitis

C. *Hepatology* 2011; **54**: 434-442 [PMID: 21374690 DOI: 10.1002/hep.24257]

20 **Qu B**, Ni Y, Lempp FA, Vondran FWR, Urban S. T5 Exonuclease Hydrolysis of Hepatitis B Virus Replicative Intermediates Allows Reliable Quantification and Fast Drug Efficacy Testing of Covalently Closed Circular DNA by PCR. *J Virol* 2018; **92** [PMID: 30232183 DOI: 10.1128/JVI.01117-18]

21 **Pergolini I**, Crippa S, Pagnanelli M, Belfiori G, Pucci A, Partelli S, Rubini C, Castelli P, Zamboni G, Falconi M. Prognostic impact of Ki-67 proliferative index in resectable pancreatic ductal adenocarcinoma. *BJS Open* 2019; **3**: 646-655 [PMID: 31592095 DOI: 10.1002/bjs5.50175]

22 **Hassan MM**, Li D, El-Deeb AS, Wolff RA, Bondy ML, Davila M, Abbruzzese JL. Association between hepatitis B virus and pancreatic cancer. *J Clin Oncol* 2008; **26**: 4557-4562 [PMID: 18824707 DOI: 10.1200/JCO.2008.17.3526]

23 **Midha S**, Chawla S, Garg PK. Modifiable and non-modifiable risk factors for pancreatic cancer: A review. *Cancer Lett* 2016; **381**: 269-277 [PMID: 27461582 DOI: 10.1016/j.canlet.2016.07.022]

24 **Wang Y**, Yang S, Song F, Cao S, Yin X, Xie J, Tu X, Xu J, Xu X, Dong X, Lu Z. Hepatitis B virus status and the risk of pancreatic cancer: a meta-analysis. *Eur J Cancer Prev* 2013; **22**: 328-334 [PMID: 23165286 DOI: 10.1097/CEJ.0b013e32835b6a21]

25 **Song C**, Lv J, Liu Y, Chen JG, Ge Z, Zhu J, Dai J, Du LB, Yu C, Guo Y, Bian Z, Yang L, Chen Y, Chen Z, Liu J, Jiang J, Zhu L, Zhai X, Jiang Y, Ma H, Jin G, Shen H, Li L, Hu Z; China Kadoorie Biobank Collaborative Group. Associations Between Hepatitis B Virus Infection and Risk of All Cancer Types. *JAMA Netw Open* 2019; **2**: e195718 [PMID: 31199446 DOI: 10.1001/jamanetworkopen.2019.5718]

26 **Chen Y**, Bai X, Zhang Q, Wen L, Su W, Fu Q, Sun X, Lou Y, Yang J, Zhang J, Chen Q, Wang J, Liang T. The hepatitis B virus X protein promotes pancreatic cancer through modulation of the PI3K/AKT signaling pathway. *Cancer Lett* 2016; **380**: 98-105 [PMID: 27339327 DOI: 10.1016/j.canlet.2016.06.011]

27 **Dejean A**, Lugassy C, Zafrani S, Tiollais P, Brechot C. Detection of hepatitis B virus DNA in pancreas, kidney and skin of two human carriers of the virus. *J Gen Virol* 1984; **65** (Pt 3): 651-655 [PMID: 6699625 DOI: 10.1099/0022-1317-65-3-651]

28 **Wandzioch E**, Zaret KS. Dynamic signaling network for the specification of embryonic pancreas and liver progenitors. *Science* 2009; **324**: 1707-1710 [PMID: 19556507 DOI: 10.1126/science.1174497]

29 **Sherman M**. Pancreatic cancer in chronic hepatitis B. *Liver Int* 2010; **30**: 339-341 [PMID: 20456036 DOI: 10.1111/j.1478-3231.2009.02202.x]

30 **Tu T**, Budzinska MA, Vondran FWR, Shackel NA, Urban S. Hepatitis B Virus DNA Integration Occurs Early in the Viral Life Cycle in an *In Vitro* Infection Model *via* Sodium Taurocholate Cotransporting Polypeptide-Dependent Uptake of Enveloped Virus Particles. *J Virol* 2018; **92** [PMID: 29437961 DOI: 10.1128/JVI.02007-17]

31 **Kew MC**. Hepatitis B virus x protein in the pathogenesis of hepatitis B virus-induced hepatocellular carcinoma. *J Gastroenterol Hepatol* 2011; **26** Suppl 1: 144-152 [PMID: 21199526 DOI: 10.1111/j.1440-1746.2010.06546.x]

32 **Geng M**, Xin X, Bi LQ, Zhou LT, Liu XH. Molecular mechanism of hepatitis B virus X protein function in hepatocarcinogenesis. *World J Gastroenterol* 2015; **21**: 10732-10738 [PMID: 26478665 DOI: 10.3748/wjg.v21.i38.10732]

33 **Poussin K**, Dienes H, Sirma H, Urban S, Beaugrand M, Franco D, Schirmacher P, Bréchot C, Paterlini Bréchot P. Expression of mutated hepatitis B virus X genes in human hepatocellular carcinomas. *Int J Cancer* 1999; **80**: 497-505 [PMID: 9935147 DOI: 10.1002/(sici)1097-0215(19990209)80:4<497::aid-ijc3>3.0.co;2-8]

34 **Kim H**, Park CY, Lee JH, Kim JC, Cho CK, Kim HJ. Ki-67 and p53 expression as a predictive marker for early postoperative recurrence in pancreatic head cancer. *Ann Surg Treat Res* 2015; **88**: 200-207 [PMID: 25844354 DOI: 10.4174/astr.2015.88.4.200]

35 **Cornberg M**, Lok AS, Terrault NA, Zoulim F; 2019 EASL-AASLD HBV Treatment Endpoints Conference Faculty. Guidance for design and endpoints of clinical trials in chronic hepatitis B – Report from the 2019 EASL-AASLD HBV Treatment Endpoints Conference‡. *J Hepatol* 2020; **72**: 539-557 [PMID: 31730789 DOI: 10.1016/j.jhep.2019.11.003]

World Journal of Gastroenterology

Submit a Manuscript: https://www.f6publishing.com

World J Gastroenterol 2022 September 7; 28(33): 4823-4833

DOI: 10.3748/wjg.v28.i33.4823

ISSN 1007-9327 (print) ISSN 2219-2840 (online)

ORIGINAL ARTICLE

Retrospective Cohort Study

Effectiveness, safety, and drug sustainability of biologics in elderly patients with inflammatory bowel disease: A retrospective study

Gustavo Drügg Hahn, Jean-Frédéric LeBlanc, Petra Anna Golovics, Panu Wetwittayakhlang, Abdulrahman Qatomah, Anna Wang, Levon Boodaghians, Jeremy Liu Chen Kiow, Maryam Al Ali, Gary Wild, Waqqas Afif, Alain Bitton, Peter Laszlo Lakatos, Talat Bessissow

Specialty type: Gastroenterology and hepatology

Provenance and peer review: Unsolicited article; Externally peer reviewed.

Peer-review model: Single blind

Peer-review report's scientific quality classification
Grade A (Excellent): 0
Grade B (Very good): B
Grade C (Good): C
Grade D (Fair): 0
Grade E (Poor): 0

P-Reviewer: Rodrigues AT, Brazil; Sitkin S, Russia

Received: January 28, 2022
Peer-review started: January 28, 2022
First decision: March 11, 2022
Revised: March 17, 2022
Accepted: August 14, 2022
Article in press: August 14, 2022
Published online: September 7, 2022

Gustavo Drügg Hahn, Petra Anna Golovics, Panu Wetwittayakhlang, Abdulrahman Qatomah, Anna Wang, Levon Boodaghians, Maryam Al Ali, Gary Wild, Waqqas Afif, Alain Bitton, Peter Laszlo Lakatos, Talat Bessissow, Division of Gastroenterology, IBD Center, McGill University Health Center, Montreal H3G 1A4, Quebec, Canada

Gustavo Drügg Hahn, School of Medicine, Graduate Course Sciences in Gastroenterology and Hepatology, Universidade Federal do Rio Grande do Sul, Porto Alegre 90000-000, Brazil

Jean-Frédéric LeBlanc, Division of Gastroenterology, McGill University Health Centre, Montreal H3G 1A4, Quebec, Canada

Petra Anna Golovics, Department of Gastroenterology, Hungarian Defense Forces, Medical Centre, Budapest 1134, Hungary

Panu Wetwittayakhlang, Unit of Gastroenterology and Hepatology, Division of Internal Medicine, Faculty of Medicine, Prince of Songkla University, Songkhla 90110, Thailand

Jeremy Liu Chen Kiow, Department of Gastroenterology, Centre Hospitalier de l'Université de Montréal, Montreal H2X 3E4, Quebec, Canada

Corresponding author: Peter Laszlo Lakatos, AGAF, DSc, FEBG, MD, PhD, Chief Physician, Professor, Division of Gastroenterology, IBD Center, McGill University Health Center, 1650 Ave. Cedar, D7.211, Montreal H3G 1A4, Quebec, Canada. kislakpet99@gmail.com

Abstract

BACKGROUND

Biologic therapy resulted in a significant positive impact on the management of inflammatory bowel disease (IBD) however data on the efficacy and side effects of these therapies in the elderly is scant.

AIM

To evaluate retrospectively the drug sustainability, effectiveness, and safety of the biologic therapies in the elderly IBD population.

METHODS

Consecutive elderly (≥ 60 years old) IBD patients, treated with biologics [inflixi-

mab (IFX), adalimumab (ADAL), vedolizumab (VDZ), ustekinumab (UST)] followed at the McGill University Inflammatory Bowel Diseases Center were included between January 2000 and 2020. Efficacy was measured by clinical scores at 3, 6-9 and 12-18 mo after initiation of the biologic therapy. Patients completing induction therapy were included. Adverse events (AEs) or serious AE were collected during and within three months of stopping of the biologic therapy.

RESULTS

We identified a total of 147 elderly patients with IBD treated with biologicals during the study period, including 109 with Crohn's disease and 38 with ulcerative colitis. Patients received the following biologicals: IFX (28.5%), ADAL (38.7%), VDZ (15.6%), UST (17%). The mean duration of biologic treatment was 157.5 (SD = 148) wk. Parallel steroid therapy was given in 34% at baseline, 19% at 3 mo, 16.3% at 6-9 mo and 6.5% at 12-18 mo. The remission rates at 3, 6-9 and 12-18 mo were not significantly different among biological therapies. Kaplan-Meyer analysis did not show statistical difference for drug sustainability (P = 0.195), time to adverse event (P = 0.158) or infection rates (P = 0.973) between the four biologics studied. The most common AEs that led to drug discontinuation were loss of response, infusion/injection reaction and infection.

CONCLUSION

Current biologics were not different regarding drug sustainability, effectiveness, and safety in the elderly IBD population. Therefore, we are not able to suggest a preferred sequencing order among biologicals.

Key Words: Inflammatory bowel disease; Biologics; Elderly; Efficacy; Safety; Adverse events

©The Author(s) 2022. Published by Baishideng Publishing Group Inc. All rights reserved.

Core Tip: Data on the efficacy and side effects of biologic therapies in the elderly inflammatory bowel disease (IBD) population is scant. Our single center study evaluates retrospectively the drug sustainability, effectiveness, and safety of approved biologic therapies in this sensitive population. The major finding of our study was that the drug sustainability and safety of the different biologicals were not significantly different in a large real-world, elderly IBD cohort treated in this single tertiary IBD center. As a consequence, we are still not able to suggest a preferred sequencing order among biologicals.

Citation: Hahn GD, LeBlanc JF, Golovics PA, Wetwittayakhlang P, Qatomah A, Wang A, Boodaghians L, Liu Chen Kiow J, Al Ali M, Wild G, Afif W, Bitton A, Lakatos PL, Bessissow T. Effectiveness, safety, and drug sustainability of biologics in elderly patients with inflammatory bowel disease: A retrospective study. *World J Gastroenterol* 2022; 28(33): 4823-4833

URL: https://www.wjgnet.com/1007-9327/full/v28/i33/4823.htm

DOI: https://dx.doi.org/10.3748/wjg.v28.i33.4823

INTRODUCTION

Crohn's disease (CD) and ulcerative colitis (UC) are chronic immune-mediated diseases classified as inflammatory bowel diseases (IBD), which can result in progressive bowel damage and disability. Although more common in young adults, the prevalence and the incidence of IBD are increasing in the elderly[1]. Approximately 10%-15% of new IBD diagnoses occur in individuals over 60 years (elderly-onset IBD), while the majority of older patients with IBD are classified as adult-onset IBD, meaning they were diagnosed with IBD between 18-59 years old[2-4]. There has been a revolution in the medical therapy of IBD with the advent of biological agents in the past two decades leading to improved clinical outcomes. Biological therapies were also associated with adverse events (AEs), including infusion/injection reactions, infections, and malignancies. Elderly IBD patients are in many ways a difficult-to-treat patient population, and may be even more vulnerable to AEs due to advanced age, comorbidities and polypharmacy[5].

The proportion of elderly IBD patients in randomized clinical trials (RCTs) is usually small, therefore there is lack of data concerning effectiveness and safety profiles of biologic therapies in this population. This relative paucity of data together with the higher frequency of comorbidities, polypharmacy, and the perceived toxicity of IBD drug therapies in the elderly patients may likely explain the underuse of biological agents and the reported higher rates of steroid use. As reported by studies from France, Sweden and Hong Kong, only 1%-3% of elderly IBD patients received biologic therapy within five to ten

years of follow-up[6-8].

The expected rate of AE and medication interactions may significantly influence the choice of therapy in the elderly IBD population. In a study from Leuven, advanced age was associated with higher rates of serious AEs (SAEs) on anti-tumor necrosis factor (TNF) therapy, such as infections and malignancy[9]. In contrast, recent data from pooled analyses of RCTs suggest that the advanced age, and not anti-TNF exposure, was associated with increased rates of SAE and hospitalizations[10].

Furthermore, landmark trials evaluating the more recently approved biologic agents, such as vedolizumab (VDZ) or ustekinumab (UST), suggested a more beneficial overall safety profile[11,12]. However, the existing literature is limited regarding effectiveness and safety of these agents in the elderly population. A *post hoc* analysis of the GEMINI trials reported that in IBD patients above 55 years old the efficacy and safety of VDZ was similar to younger IBD patients, while the safety profile was not different from placebo[13]. Relatively few data are available in elderly IBD patients on the efficacy or safety on anti-TNFs and on the new biologicals. One of the first studies in elderly patients was Busquets *et al*[14] which performed a systematic review on efficacy and safety of anti-TNFs in the elderly, however mainly in patients with rheumatic diseases. It concluded that elderly patients on anti-TNF therapy have higher number of AEs, and similar efficacy, when compared with younger patients. The aim of our study was to measure the rates of biologic therapy sustainability in elderly IBD patients, as well as to report their effectiveness and safety profile.

MATERIALS AND METHODS

Study design

Consecutive elderly patients (aged 60 years or over) previously or currently treated with a biologic agent and followed at the McGill University Health Centre Inflammatory Bowel Diseases Center between January 2000 and January 2020 were included retrospectively. The efficacy of treatment with a biologic agent was assessed by clinical score, biochemical and endoscopy. Clinical response and remission using the Harvey-Bradshaw Index (HBI) and Mayo score were measured at baseline, 3 mo, 6-9 mo, and 12-18 mo of follow up. Patients included were patients with IBD, with an age of 60 years or older, whose current or prior treatment included biological agents (anti-TNF, VDZ or UST). Patients with contra-indications to biologic therapy, or patients with less than 3 mo follow-up were excluded. For patients with multiple biological exposure, data for the last biological therapy was collected.

Local electronic medical charts were used to identify elderly IBD patients on infliximab (IFX), adalimumab (ADAL), VDZ or UST. We collected demographic data (age, gender), comorbidities, age at diagnosis, disease duration, disease extent and phenotype (Montreal classification)[15], prior gastrointestinal surgeries, C-reactive protein, fecal calprotectin, radiological or endoscopic reports and clinical symptoms of IBD activity. Additional therapeutic variables measured were treatment duration and dosage, prior or concomitant immunosuppression, parallel steroid therapy. Comorbidity was measured by the Charlson Comorbidity Index (CCI), where a CCI of 0 represents absence of comorbidity[16]. AE, SAE, hospitalizations [duration and reasons (medical, surgical, unrelated) for hospitalization] and mortality were collected. SAE was grouped into four distinct categories: Infection (infection reported during the course of biologic therapy not requiring hospitalization), severe infection (any infection reported during the course of biologic therapy that needed hospitalization), malignancy, IBD-related surgeries (excluding elective surgical management of perianal lesions). If a treatment-related complication did not fit the previously-mentioned criteria for a SAE, then it was considered an AE, including acute infusion reactions (within one hour of dose administration), hypersensitivity reactions, non-allergic skin rash, mild infections and other AE. Patient-related data were collected through the MUHC electronic medical record (Oacis Clinical Information System).

Outcomes

The primary outcome was the drug sustainability and comparative time-dependent safety analysis in elderly patients with IBD (aged 60 years or over) on different biologic therapy. Secondary outcomes included the comparison of rates of clinical, biochemical, and endoscopic remission in elderly IBD patients according to the biologic therapy used. Clinical response was defined as a decrease in the HBI by 3 points or more from baseline for CD or a similar decrease in the partial Mayo Score (pMayo) by 3 or more for UC, while clinical remission was defined as an overall HBI of less than 5 for CD or an overall pMayo of less than 2 for UC[17].

AE or SAE occurring within three months of the last biologic dose were considered to be related to the biologic agent. SAEs were defined as potentially life-threatening or leading to death, hospitalization, or prolongation of hospitalization, or causing significant disruption in normal life functions. Infections and malignancy were separately captured. Reasons for discontinuation of the biologic agent were also evaluated.

Statistical analysis

Statistical analysis was performed using Statistical Package for the Social Sciences (SPSS 20.0; SPSS INC., Chicago, Illinois). Descriptive statistics were used to summarize patient and treatment-related characteristics along with means ± SD, and common themes highlighted using qualitative data analysis. Chi-square test or Fisher exact test was used to compare categorical variables while the Student's unpaired *t*-test was used to compare continuous variables. Kaplan Meier curves were plotted with COX regression analysis to assess differences in drug sustainability, infections or AE stratified by the different biological agents. A $P < 0.05$ was defined as statistically significant.

Ethical considerations

This study was reviewed and approved by the McGill University Health Centre Research Ethics Board under the ethical approval number: 2019-5209. The research protocol conforms to ethical guidelines of the 1975 Declaration of Helsinki (6th revision, 2008) and local regulations. Informed consent was obtained from each patient included in the study.

RESULTS

Demographic and baseline factors

A total of 147 elderly patients with IBD were identified, including 109 patients with CD and 38 patients with UC. The majority of patients (75.5%) were diagnosed before the age of 60, thus adult-onset, elderly IBD patients. Disease location was predominantly ileocolonic (47.7%) in patients with CD and pancolitis for patients with UC (63.2%). Among patients with CD, 21.1% suffered from perianal disease. The CCI was at least 1 in 95.2% of elderly IBD patients, at least 3 in 47.6% and above 4 in 12.9%. Approximately 45.6% (67 patients) of all included patients underwent at least one surgical resection related to IBD. 70 elderly IBD patients (47.6%) had previous exposure to other biologics. Over the study period, 35.4% of patients had received a course of systemic steroids at least once, while 17% were treated with concomitant immunomodulatory therapy. The mean duration of biological therapy was 157.5 (SD = 148) wk. Extraintestinal manifestations had been diagnosed in 10.9% of elderly IBD patients. Table 1 summarizes disease characteristics and history of IBD-related therapy.

Drug sustainability, time to AE or infection

Figure 1A (see appendix section) shows the time to treatment discontinuation stratified by the biological agent by Kaplan-Meier and Cox regression analysis. No significant difference was found among the four biologicals ($P = 0.195$) (Figure 1A). According to Figure 1B, the time to AE was not significantly different in a Kaplan-Meier and Cox regression analysis among the four biologics ($P = 0.158$). Figure 1C shows the time to infections stratified by the biological agent. There was no statistical difference among the biologicals among the respective time to infection curves ($P = 0.973$). SAE was observed in only one patient (0.6%), who presented fever of unknown origin, needing hospitalization.

Efficacy

Figure 2A (see appendix section) shows the rates of clinical response and remission in elderly IBD patients treated with different biologicals according to HBI or Mayo scores at 3 mo. When assessing the clinical response in patients with CD, 71% of the patients on ADAL, 70% on UST, 65.2% on IFX and 60% on VDZ achieved clinical response at 3 mo. Regarding clinical remission in CD at 3 mo, 61.3% of patients on ADAL, followed by 54.2% on UST, 50% on VDZ and 47.8% on IFX achieved clinical remission. When looking at clinical response at 3 mo in patients with UC, 80% of the patients on ADAL, followed by VDZ with 44.4% and IFX with 40% responded. With regards to clinical remission at 3 mo, 40% patients on ADAL achieved clinical remission, 30% on IFX and 20% on VDZ.

The rates of clinical remission in elderly IBD patients treated with different biologicals according to HBI or Mayo scores at 6-9 mo are show in Figure 2B (see appendix section). Regarding clinical response in CD, 71.4% of patients on UST achieved clinical response at 6-9 mo, followed by 60.9 % on IFX, 58.3% on VDZ and 54.1% on ADAL. As for clinical remission in CD, 56.5% of patients on IFX, 50% on UST, 45.9% on ADAL and 41.7% on VDZ achieved clinical remission at 6-9 mo. When evaluating clinical response in UC, 55.6% of patients on IFX, followed by 45.5% on VDZ, 42.9% on ADAL reached clinical response at 6-9 mo. As for clinical remission in UC, 42.9% of patients on ADAL, 36.4% on VDZ and 33.3% on IFX achieved this outcome.

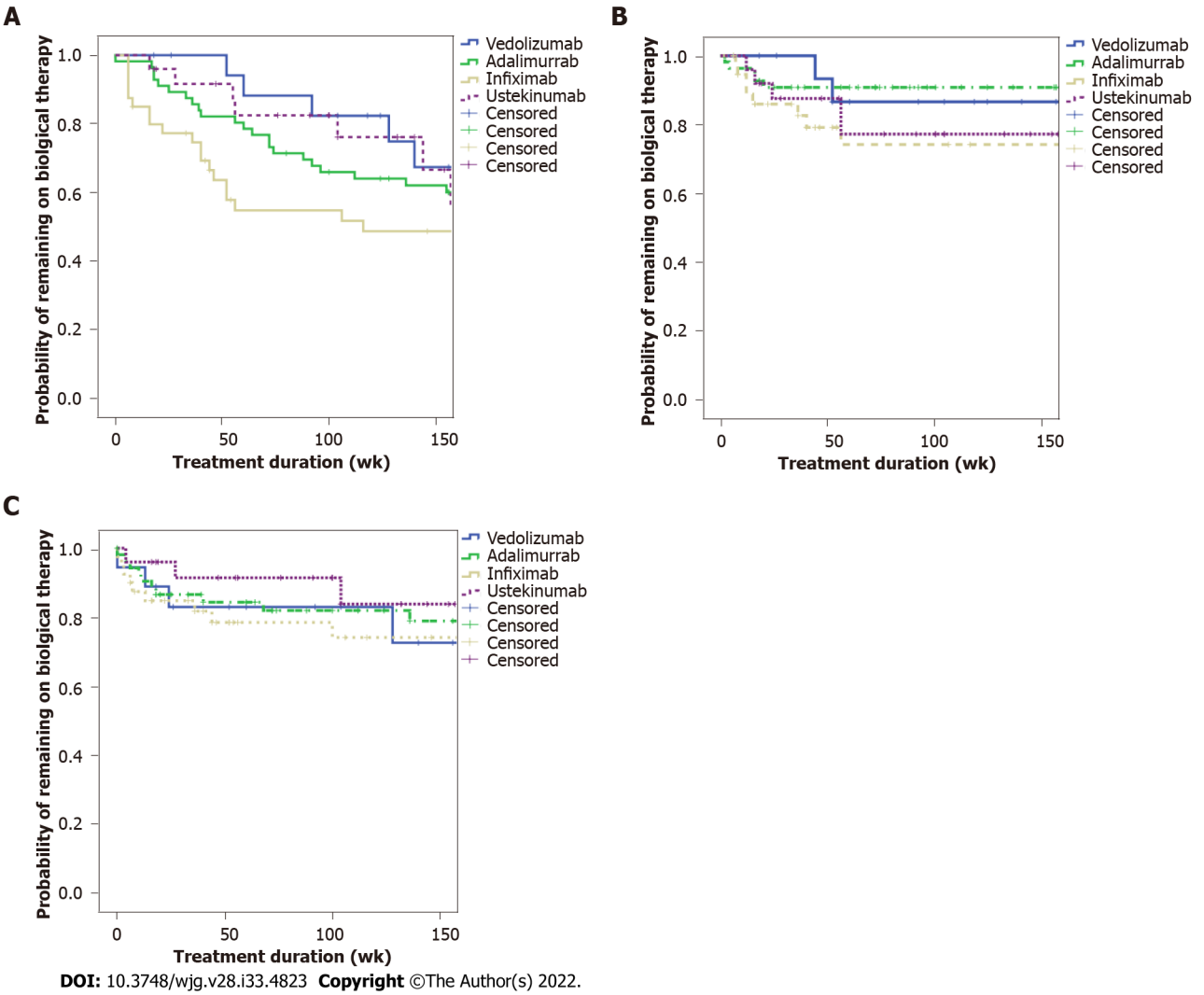
The rates of clinical remission in elderly IBD patients treated with different biologicals according to HBI or Mayo scores after 12-18 mo are presented in Figure 2C (see appendix section). Regarding clinical remission in patients with CD, 55.6% of patients on ADAL, followed by 40% on VDZ, 37.5% on IFX and 30% on UST achieved remission. As for clinical remission in patients with UC, approximately 62.5% of patients on IFX, followed by 50% on ADAL and 45.5% on VDZ achieved remission. Clinical response and remission rates were not significantly different across biologicals in either CD or UC at any time points (P = ns for each assessment), as shown in Figure 2 (see appendix section). Given the retrospective

Table 1 Disease characteristics at baseline and history of inflammatory bowel disease-related therapy

		Biological therapy			
		Vedolizumab % (*n* = 23)	Adalimumab % (*n* = 57)	Infliximab % (*n* = 42)	Ustekinumab % (*n* = 25)
Age at IBD diagnosis (yr)	< 60	69 (16)	81 (46)	71 (30)	76 (19)
	≥ 60	30 (7)	19 (11)	28 12	24 (6)
IBD type	CD	52 (12)	81 (46)	64 (27)	96 (24)
	UC	48 (11)	19 (11)	36 (15)	4 (1)
CD location	Ileal (L1)	17 (4)	24 (14)	9 (4)	12 (3)
	Colonic (L2)	4 (1)	21 (12)	19 (8)	24 (6)
	Ileocolonic (L3)	26 (6)	31 (18)	38 (16)	48 (12)
	Isolated upper GI disease (L4)	4 (1)	3 (2)	2 (1)	4 (1)
	Combined upper GI disease with L1, 2 or 3	4 (1)	2 (1)	2 (1)	12 (3)
Disease behavior	Luminal (B1)	17 (4)	38 (22)	24 (10)	32 (8)
	Stricturing (B2)	26 (6)	28 (16)	28 (12)	44 (11)
	Penetrating (B3)	13 (3)	16 (9)	17 (7)	24 (6)
CD perianal	Presence of perianal disease	9 (2)	12 (7)	24 (10)	16 (4)
UC extension	Proctitis (E1)	0	2 (1)	0	0
	Left-sided (E2)	26 (6)	5 (3)	5 (2)	0
	Pancolitis (E2)	22 (5)	12 (7)	26 (11)	4 (1)
UC severity (Mayo score)	1	13 (3)	9 (5)	5 (2)	0
	2	17 (4)	7 (4)	17 (7)	0
	3	17 (4)	3 (2)	9 (4)	4 (1)
Charlson Comorbidity Index	0	0	9 (5)	5 (2)	0
	1-2	56 (13)	54 (31)	38 (16)	36 (9)
	3-4	26 (6)	28 (16)	48 (20)	36 (9)
	More than 4	17 (4)	9 (5)	7 (3)	28 (7)
History of malignancy	Active within last 5 yr	4 (1)	3 (2)	2 (1)	8 (2)
	Active more than 5 yr prior	4 (1)	2 (1)	5 (2)	0
Prior resective surgery	Surgical resection ≥ 1	43 (10)	44 (25)	33 (14)	72 (18)
Previous exposure to biologics	Bio-naïve	39 (9)	54 (31)	76 (32)	20 (5)
	Previous exposure to anti-TNF	61 (14)	46 (26)	21 (9)	80 (20)
	Previous exposure to VDZ	0	0	7 (3)	4 (1)
	Previous exposure to UST	9 (2)	0	2 (1)	4 (1)
Concomitancy of 5-ASA	Yes	39 (9)	14 (8)	8 (19)	16 (4)
Concomitancy of systemic steroids at baseline	Yes	43 (10)	26 (15)	40 (17)	40 (10)
Concomitancy of immunomodulator at baseline	Yes	9 (2)	17 (10)	26 (11)	8 (2)
History of an extraintestinal manifestation	Musculoskeletal	0	3 (2)	5 (2)	4 (1)
	Ocular	0	3 (2)	5 (2)	8 (2)
	Mucocutaneous	4 (1)	3 (2)	7 (3)	12 (3)
	Primary sclerosing	4 (1)	0	0	4 (1)

	cholangitis

CD: Crohn's disease; UC: Ulcerative colitis; IBD: Inflammatory bowel disease; GI: Gastrointestinal; 5-ASA: 5-aminosalicylic acid; TNF: Tumor necrosis factor; VDZ: Vedolizumab; UST: Ustekinumab.



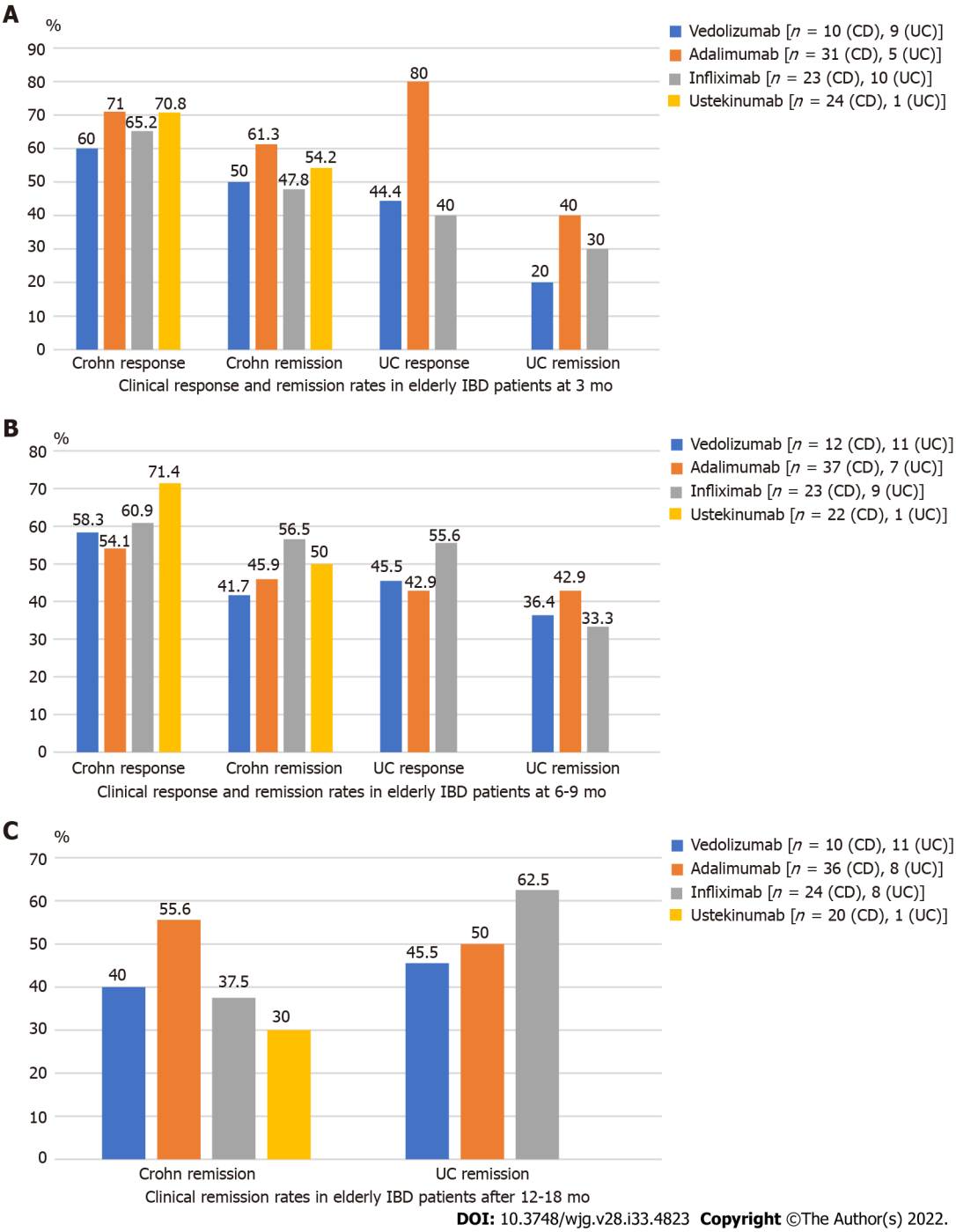
DOI: 10.3748/wjg.v28.i33.4823 **Copyright** ©The Author(s) 2022.

Figure 1 Time based on biologic therapy. A: Treatment discontinuation; B: Adverse event; C: Infection.

nature of the study and the lack of standardization of the collected measurements for endoscopic and biomarkers, the statistical analysis was inconclusive, therefore the data is not presented.

DISCUSSION

The major finding of our study was that the drug sustainability and safety of the different biologicals were not significantly different in a large real-world, elderly IBD cohort treated in this single tertiary IBD center. Peyrin-Biroulet *et al*[18] evaluated the efficacy and safety profile of anti-TNF in IBD patients, showing no difference in the frequency of mortality, malignancies and serious infections between anti-TNF and control group. Similarly, Lichtenstein *et al*[19] reported that the occurrence of death was similar between patients treated with anti-TNF and those who received other treatments only; however, an increased risk of infections was seen in patients treated with IFX. Borren and Ananthakrishnan[20] reported that older age was associated with an increased risk of malignancy compared to younger age. Elderly patients on biologics had a 3-fold increase in risk of infection compared to those who were not using biologics, yet there were no significant differences in odds of malignancy or mortality compared to older patients that were not using biologics.



DOI: 10.3748/wjg.v28.i33.4823 **Copyright** ©The Author(s) 2022.

Figure 2 Clinical response and remission rates in elderly inflammatory bowel disease patients treated with different biologicals according to Harvey-Bradshaw Index or Mayo scores. A: At 3 mo; B: At 6-9 mo; C: After 12-18 mo. CD: Crohn's disease; UC: Ulcerative colitis; IBD: Inflammatory bowel disease.

Regarding efficacy and safety profile of biological therapy in the elderly patients, Asscher *et al*[21]. assessed the safety and effectiveness of anti-TNF therapy in IBD patients over 60 years. Elderly patients on anti-TNF therapy have an increased risk of serious infections compared with elderly IBD patients who are not on anti-TNF therapy, not compared to younger patients who receive anti-TNF, though. However, comorbidity has been shown to be an indicator of SAE in patients exposed to anti-TNF. Effectiveness was similar between elderly and younger patients. Lobatón *et al*[9] also evaluated efficacy and safety of anti-TNF therapy in an elderly IBD population and showed a worse short-term clinical response to anti-TNFs at 10 wk after anti-TNF initiation, meaning that the probability of drug discontinuation during the follow-up (whatever the reason) was higher; but when excluding primary non response, this proportion became similar between the two groups. No differences were found in long-term efficacy among the initial responders (79.5% *vs* 82.8%; $P = 0.64$). As for safety, a higher risk of SAE was found in elderly IBD patients treated with anti-TNFs (risk ratio = 4.7; $P < 0.001$) compared to the

younger subgroup[9]. Along with that, our study also reported statistically similar rates of 3 mo clinical response and 6-12 mo clinical response and remission among the four types of biologics studied (ADAL, IFX, VDZ and UST). Regarding safety, time to AE and to infection were also not statistically different.

The efficacy and safety of the anti-TNFs are extensively studied, less real world or comparative data are available for the new biologicals. In the landmark clinical trials, they appeared to be a safer option compared to the anti-TNFs, although in indirect comparisons. Recently, comparative efficacy and safety data became available in IBD patients. The SEAVUE study compared UST with ADAL for induction and maintenance of biological-naïve patients with moderate to severe CD. With regards to safety, 34.0% of UST-treated and 40.5% of the ADAL-treated patients had infections, 2.6% and 7.2% had SAEs, and 6.3% and 11.3% had AEs leading to therapy discontinuation in non-elderly IBD patients[22]. VARSITY trial compared VDZ with ADAL in patients with moderately to severely active UC, mainly patients without previous exposure to biologics. Numerical differences were observed in the reported AEs. Of note, the exposure-adjusted incidence rate of infection was 23.4 per 100 patients-year in the VDZ group and 34.6 per 100 patients-year in the ADAL group[23].

As for the elderly IBD population on new biologicals, there is still a paucity of data concerning efficacy and safety from real world studies. Cohen *et al*[24] evaluated the efficacy and safety of VDZ in elderly IBD patients compared to non-elderly patients. Equal effectiveness in both groups was reported; however, there was a higher risk of infections among the elderly on VDZ, which could be related to age and due to underlying diseases[24]. Garg *et al*[25] evaluated the safety and efficacy of UST in elderly CD patients. Efficacy and safety were similar in this relatively small cohort in elderly and non-elderly IBD patients; elderly patients were less likely severe, though, and both groups had 95% previous exposure to biologics. Furthermore, the mucosal healing rates observed in the elderly cohort were in check with other real-world studies performed in non-elderly IBD patients. As for safety, UST use in elderly IBD was not associated with higher rates of infusion reaction, infections, or postoperative complications as compared to the non-elderly patients[25]. In line with these studies, ours showed no significant difference in time to AEs and infection among elderly IBD patients treated with anti-TNF, VDZ and UST.

The strength of our study is that represents a single center cohort with harmonized treatment and follow-up strategies across IBD specialists. In addition, a complex analysis of effectiveness and safety was performed in a relatively large elderly IBD cohort. However, the present study has limitations. First, there was a relatively low number of elderly patients on new biological therapies. Second, it consists of a retrospective cohort with intrinsic problems of accuracy and potential biases such as recall bias and reporting bias, specially of AEs and mild infections, which patients may not have announced or may not have been documented. Third, follow-up on biomarkers, fecal calprotectin and endoscopy were not uniform for timing. Fourth and last, rates of previous exposure to biologicals were different for new biologics *vs* anti-TNFs.

CONCLUSION

Current biologic therapies were not different concerning drug sustainability, effectiveness, and safety in the elderly IBD population. Based on these results, a preferred sequencing order among biologicals for this specific population is not possible to be suggested thus, larger studies in elderly IBD population are warranted.

ARTICLE HIGHLIGHTS

Research background

Biologic therapy resulted in a significant positive impact on the treatment of inflammatory bowel disease (IBD) however data on the efficacy and side effects of these therapies in the elderly is scant.

Research motivation

To further evaluate and develop more studies regarding treatment efficacy and safety of biological therapies in a specific and sensitive population, such as the elderly IBD patients, since there is not much evidence about it on medical literature so far.

Research objectives

Retrospectively evaluate the drug sustainability, effectiveness, and safety of the biologic therapies in the elderly IBD population.

Research methods

Consecutive elderly (≥ 60 years old) IBD patients, treated with biologics [infliximab (IFX), adalimumab

(ADAL), vedolizumab (VDZ), ustekinumab (UST)] followed at the McGill University Inflammatory Bowel Diseases Center were included between January 2000 and 2020. Efficacy was measured by clinical scores at 3, 6-9 and 12-18 mo after initiation of the biologic therapy. Patients completing induction therapy were included. Adverse events (AEs) or serious AEs were collected during and within three months of stopping of the biologic therapy.

Research results

A total of 147 elderly patients with IBD were identified and treated with biologicals during the study period, including 109 with Crohn's disease and 38 with ulcerative colitis. Patients received the following biologicals: IFX (28.5%), ADAL (38.7%), VDZ (15.6%), UST (17%). The mean duration of biological therapy was 157.5 (SD = 148) wk. Parallel steroid therapy was given in 34% at baseline, 19% at 3 mo, 16.3% at 6-9 mo and 6.5% at 12-18 mo. The remission rates at 3, 6-9 and 12-18 mo were not significantly different among biological therapies. Kaplan-Meyer analysis did not show statistical difference for drug sustainability ($P = 0.195$), time to adverse event ($P = 0.158$) or infection rates ($P = 0.973$) between the four studied biologicals. The most common AEs that led to drug discontinuation were loss of response, infusion/injection reaction and infection.

Research conclusions

Current biologics were not different regarding drug sustainability, effectiveness, and safety in the elderly IBD population. Therefore, it is not possible to suggest a preferred sequencing order among biologics.

Research perspectives

The authors expect that this article may help other IBD physicians and gastroenterologists in their decision process for treating elderly IBD patients with biological therapy.

FOOTNOTES

Author contributions: Hahn GD and Bessissow T are guarantors of the manuscript; LeBlanc JF and Bessissow T designed the study; LeBlanc JF, Qatomah A, Wang A, Boodaghians L, Liu Chen Kiow J and Al Ali M performed the data collection; Drügg Hahn G, LeBlanc JF, Golovics PA, Wetwittayakhlang P, Lakatos PL and Bessissow T performed the data interpretation; Lakatos PL performed the statistical analysis; Drügg Hahn G wrote the initial draft of the manuscript, and Golovics PA, Wetwittayakhlang P, Wild G, Afif W, Bitton A, Lakatos PL and Bessissow T were involved in the critical revision of the manuscript; and all the authors reviewed and approved the final manuscript.

Institutional review board statement: The study was approved by the Research Ethics Board of McGill University Health care center, Montreal, Quebec, Canada, under protocol No. 2019-5209. Individual patient-level data were de-identified to maintain confidentiality in all steps of study analysis. This study was conducted in compliance with regulations stated in the 1975 Declaration of Helsinki.

Informed consent statement: Informed consent was obtained from each patient included in the study.

Conflict-of-interest statement: Hahn GD, Qatomah A, Wang A, Boodaghians L, Liu Chen Kiow J, Al Ali M, and Wild G declared no conflict of interest; LeBlanc JF has been a speaker or advisory board member for Janssen and Takeda; Golovics PA has been a speaker for AbbVie, Takeda, Fresenius, Ferring; Wetwittayakhlang P has been a speaker and/or advisory board member: Takeda, Pfizer, Janssen, Ferring, A. Menerini, and MSD; Afif W has been a speaker for Janssen, Prometheus, Dynacare, Takeda, AbbVie Theradiag; Bitton A has been a member of Advisory Boards - Abbvie, Pfizer, Takeda, Janssen, Merck; Speaker's bureau - Abbvie, Janssen, Takeda, Pfizer; Lakatos PL has been a speaker and/or advisory board member for AbbVie, Arena, Falk Pharma GmbH, Ferring, Genetech, Janssen, Kyowa Hakko Kirin Pharma, Mitsubishi Tanabe Pharma Corporation, MSD, Pfizer, Roche, Shire, Takeda and Tillots, and has received unrestricted research grants from AbbVie, MSD and Pfizer; Bessissow T has been a speaker or advisory board member for Takeda, Janssen, Abbvie, Merck, Pfizer, Pendopharm, Ferring, Shire, Sandoz, BMS, Roche, Fresenius Kabi, Viatris.

Data sharing statement: The main data are given in this article. The data are available from the corresponding author upon request.

STROBE statement: The authors have read the STROBE Statement-checklist of items, and the manuscript was prepared and revised according to the STROBE Statement-checklist of items.

Open-Access: This article is an open-access article that was selected by an in-house editor and fully peer-reviewed by external reviewers. It is distributed in accordance with the Creative Commons Attribution NonCommercial (CC BY-NC 4.0) license, which permits others to distribute, remix, adapt, build upon this work non-commercially, and license

their derivative works on different terms, provided the original work is properly cited and the use is non-commercial. See: https://creativecommons.org/Licenses/by-nc/4.0/

Country/Territory of origin: Canada

ORCID number: Gustavo Drügg Hahn 0000-0003-1963-7848; Jean-Frédéric LeBlanc 0000-0002-8477-6337; Petra Anna Golovics 0000-0003-3195-183X; Panu Wetwittayakhlang 0000-0002-5962-4112; Abdulrahman Qatomah 0000-0001-9528-6301; Anna Wang 0000-0002-1023-1465; Levon Boodaghians 0000-0003-3107-7396; Jeremy Liu Chen Kiow 0000-0003-2486-3647; Maryam Al Ali 0000-0003-0502-4899; Gary Wild 0000-0002-9625-3437; Waqqas Afif 0000-0001-6869-0982; Alain Bitton 0000-0001-7214-1978; Peter Laszlo Lakatos 0000-0002-3948-6488; Talat Bessissow 0000-0003-2610-1910.

S-Editor: Wang JJ
L-Editor: A
P-Editor: Wang JJ

REFERENCES

1 **Jeuring SF**, van den Heuvel TR, Zeegers MP, Hameeteman WH, Romberg-Camps MJ, Oostenbrug LE, Masclee AA, Jonkers DM, Pierik MJ. Epidemiology and Long-term Outcome of Inflammatory Bowel Disease Diagnosed at Elderly Age-An Increasing Distinct Entity? *Inflamm Bowel Dis* 2016; **22**: 1425-1434 [PMID: 26933752 DOI: 10.1097/MIB.0000000000000738]
2 **Rozich JJ**, Luo J, Dulai PS, Collins AE, Pham L, Boland BS, Sandborn WJ, Singh S. Disease- and Treatment-related Complications in Older Patients With Inflammatory Bowel Diseases: Comparison of Adult-onset *vs* Elderly-onset Disease. *Inflamm Bowel Dis* 2021; **27**: 1215-1223 [PMID: 33252124 DOI: 10.1093/ibd/izaa308]
3 **Ananthakrishnan AN**, Donaldson T, Lasch K, Yajnik V. Management of Inflammatory Bowel Disease in the Elderly Patient: Challenges and Opportunities. *Inflamm Bowel Dis* 2017; **23**: 882-893 [PMID: 28375885 DOI: 10.1097/MIB.0000000000001099]
4 **Gisbert JP**, Chaparro M. Systematic review with meta-analysis: inflammatory bowel disease in the elderly. *Aliment Pharmacol Ther* 2014; **39**: 459-477 [PMID: 24405149 DOI: 10.1111/apt.12616]
5 **Hruz P**, Juillerat P, Kullak-Ublick GA, Schoepfer AM, Mantzaris GJ, Rogler G; on behalf of Swiss IBDnet, an official working group of the Swiss Society of Gastroenterology. Management of the Elderly Inflammatory Bowel Disease Patient. *Digestion* 2020; **101** Suppl 1: 105-119 [PMID: 31935714 DOI: 10.1159/000503099]
6 **Everhov ÅH**, Halfvarson J, Myrelid P, Sachs MC, Nordenvall C, Söderling J, Ekbom A, Neovius M, Ludvigsson JF, Askling J, Olén O. Incidence and Treatment of Patients Diagnosed With Inflammatory Bowel Diseases at 60 Years or Older in Sweden. *Gastroenterology* 2018; **154**: 518-528.e15 [PMID: 29102619 DOI: 10.1053/j.gastro.2017.10.034]
7 **Mak JWY**, Lok Tung Ho C, Wong K, Cheng TY, Yip TCF, Leung WK, Li M, Lo FH, Ng KM, Sze SF, Leung CM, Tsang SWC, Shan EHS, Chan KH, Lam BCY, Hui AJ, Chow WH, Ng SC. Epidemiology and Natural History of Elderly-onset Inflammatory Bowel Disease: Results From a Territory-wide Hong Kong IBD Registry. *J Crohns Colitis* 2021; **15**: 401-408 [PMID: 32914171 DOI: 10.1093/ecco-jcc/jjaa181]
8 **Charpentier C**, Salleron J, Savoye G, Fumery M, Merle V, Laberenne JE, Vasseur F, Dupas JL, Cortot A, Dauchet L, Peyrin-Biroulet L, Lerebours E, Colombel JF, Gower-Rousseau C. Natural history of elderly-onset inflammatory bowel disease: a population-based cohort study. *Gut* 2014; **63**: 423-432 [PMID: 23408350 DOI: 10.1136/gutjnl-2012-303864]
9 **Lobatón T**, Ferrante M, Rutgeerts P, Ballet V, Van Assche G, Vermeire S. Efficacy and safety of anti-TNF therapy in elderly patients with inflammatory bowel disease. *Aliment Pharmacol Ther* 2015; **42**: 441-451 [PMID: 26104047 DOI: 10.1111/apt.13294]
10 **Cheng D**, Cushing KC, Cai T, Ananthakrishnan AN. Safety and Efficacy of Tumor Necrosis Factor Antagonists in Older Patients With Ulcerative Colitis: Patient-Level Pooled Analysis of Data From Randomized Trials. *Clin Gastroenterol Hepatol* 2021; **19**: 939-946.e4 [PMID: 32371165 DOI: 10.1016/j.cgh.2020.04.070]
11 **Feagan BG**, Rutgeerts P, Sands BE, Hanauer S, Colombel JF, Sandborn WJ, Van Assche G, Axler J, Kim HJ, Danese S, Fox I, Milch C, Sankoh S, Wyant T, Xu J, Parikh A; GEMINI 1 Study Group. Vedolizumab as induction and maintenance therapy for ulcerative colitis. *N Engl J Med* 2013; **369**: 699-710 [PMID: 23964932 DOI: 10.1056/NEJMoa1215734]
12 **Feagan BG**, Sandborn WJ, Gasink C, Jacobstein D, Lang Y, Friedman JR, Blank MA, Johanns J, Gao LL, Miao Y, Adedokun OJ, Sands BE, Hanauer SB, Vermeire S, Targan S, Ghosh S, de Villiers WJ, Colombel JF, Tulassay Z, Seidler U, Salzberg BA, Desreumaux P, Lee SD, Loftus EV Jr, Dieleman LA, Katz S, Rutgeerts P; UNITI–IM-UNITI Study Group. Ustekinumab as Induction and Maintenance Therapy for Crohn's Disease. *N Engl J Med* 2016; **375**: 1946-1960 [PMID: 27959607 DOI: 10.1056/NEJMoa1602773]
13 **Yajnik V**, Khan N, Dubinsky M, Axler J, James A, Abhyankar B, Lasch K. Efficacy and Safety of Vedolizumab in Ulcerative Colitis and Crohn's Disease Patients Stratified by Age. *Adv Ther* 2017; **34**: 542-559 [PMID: 28070861 DOI: 10.1007/s12325-016-0467-6]
14 **Busquets N**, Carmona L, Surís X. [Systematic review: safety and efficacy of anti-TNF in elderly patients]. *Reumatol Clin* 2011; **7**: 104-112 [PMID: 21794793 DOI: 10.1016/j.reuma.2010.02.001]
15 **Satsangi J**, Silverberg MS, Vermeire S, Colombel JF. The Montreal classification of inflammatory bowel disease: controversies, consensus, and implications. *Gut* 2006; **55**: 749-753 [PMID: 16698746 DOI: 10.1136/gut.2005.082909]
16 **Charlson ME**, Pompei P, Ales KL, MacKenzie CR. A new method of classifying prognostic comorbidity in longitudinal studies: development and validation. *J Chronic Dis* 1987; **40**: 373-383 [PMID: 3558716 DOI: 10.1016/0021-9681(87)90171-8]

17 **Vermeire S**, Schreiber S, Sandborn WJ, Dubois C, Rutgeerts P. Correlation between the Crohn's disease activity and Harvey-Bradshaw indices in assessing Crohn's disease severity. *Clin Gastroenterol Hepatol* 2010; **8**: 357-363 [PMID: 20096379 DOI: 10.1016/j.cgh.2010.01.001]

18 **Peyrin-Biroulet L**, Deltenre P, de Suray N, Branche J, Sandborn WJ, Colombel JF. Efficacy and safety of tumor necrosis factor antagonists in Crohn's disease: meta-analysis of placebo-controlled trials. *Clin Gastroenterol Hepatol* 2008; **6**: 644-653 [PMID: 18550004 DOI: 10.1016/j.cgh.2008.03.014]

19 **Lichtenstein GR**, Feagan BG, Cohen RD, Salzberg BA, Diamond RH, Price S, Langholff W, Londhe A, Sandborn WJ. Serious infection and mortality in patients with Crohn's disease: more than 5 years of follow-up in the TREAT™ registry. *Am J Gastroenterol* 2012; **107**: 1409-1422 [PMID: 22890223 DOI: 10.1038/ajg.2012.218]

20 **Borren NZ**, Ananthakrishnan AN. Safety of Biologic Therapy in Older Patients With Immune-Mediated Diseases: A Systematic Review and Meta-analysis. *Clin Gastroenterol Hepatol* 2019; **17**: 1736-1743.e4 [PMID: 30616024 DOI: 10.1016/j.cgh.2018.12.032]

21 **Asscher VER**, van der Vliet Q, van der Aalst K, van der Aalst A, Brand EC, van der Meulen-de Jong AE, Oldenburg B, Pierik MJ, van Tuyl B, Mahmmod N, Maljaars PWJ, Fidder HH; Dutch ICC. Anti-tumor necrosis factor therapy in patients with inflammatory bowel disease; comorbidity, not patient age, is a predictor of severe adverse events. *Int J Colorectal Dis* 2020; **35**: 2331-2338 [PMID: 32860081 DOI: 10.1007/s00384-020-03716-6]

22 **Irving PM**, Sands BE, Hoops T, Izanec JL, Gao LL, Gasink C, Greenspan A, Allez M, Danese S, Hanauer SB, Jairath V, Kuehbacher T, Lewis JD, Loftus EV, Mihaly JrE, Panaccione R, Scherl E, Shchukina O, Sandborn WJ. OP02 Ustekinumab *vs* adalimumab for induction and maintenance therapy in Moderate-to-Severe Crohn's Disease: The SEAVUE study. *J Crohns Colitis* 2021; **15**: S001-S002 [DOI: 10.1093/ecco-jcc/jjab075.001]

23 **Sands BE**, Peyrin-Biroulet L, Loftus EV Jr, Danese S, Colombel JF, Törüner M, Jonaitis L, Abhyankar B, Chen J, Rogers R, Lirio RA, Bornstein JD, Schreiber S; VARSITY Study Group. Vedolizumab versus Adalimumab for Moderate-to-Severe Ulcerative Colitis. *N Engl J Med* 2019; **381**: 1215-1226 [PMID: 31553834 DOI: 10.1056/NEJMoa1905725]

24 **Cohen NA**, Plevris N, Kopylov U, Grinman A, Ungar B, Yanai H, Leibovitzh H, Isakov NF, Hirsch A, Ritter E, Ron Y, Shitrit AB, Goldin E, Dotan I, Horin SB, Lees CW, Maharshak N. Vedolizumab is effective and safe in elderly inflammatory bowel disease patients: a binational, multicenter, retrospective cohort study. *United European Gastroenterol J* 2020; **8**: 1076-1085 [PMID: 32807038 DOI: 10.1177/2050640620951400]

25 **Garg R**, Aggarwal M, Butler R, Achkar JP, Lashner B, Philpott J, Cohen B, Qazi T, Rieder F, Regueiro M, Click B. Real-World Effectiveness and Safety of Ustekinumab in Elderly Crohn's Disease Patients. *Dig Dis Sci* 2022; **67**: 3138-3147 [PMID: 34160735 DOI: 10.1007/s10620-021-07117-9]

World Journal of Gastroenterology

Submit a Manuscript: https://www.f6publishing.com

World J Gastroenterol 2022 September 7; 28(33): 4834-4845

DOI: 10.3748/wjg.v28.i33.4834

ISSN 1007-9327 (print) ISSN 2219-2840 (online)

ORIGINAL ARTICLE

Retrospective Study

Prevalence and factors associated with vitamin C deficiency in inflammatory bowel disease

Benjamin Langan Gordon, Jonathan S Galati, Stevie Yang, Randy S Longman, Dana Lukin, Ellen J Scherl, Robert Battat

Specialty type: Gastroenterology and hepatology

Provenance and peer review: Unsolicited article; Externally peer reviewed.

Peer-review model: Single blind

Peer-review report's scientific quality classification

Grade A (Excellent): 0
Grade B (Very good): 0
Grade C (Good): C, C
Grade D (Fair): 0
Grade E (Poor): 0

P-Reviewer: Ferreira-Duarte M, Portugal; Rathnaswami A, India

Received: March 14, 2022
Peer-review started: March 14, 2022
First decision: May 9, 2022
Revised: May 23, 2022
Accepted: August 6, 2022
Article in press: August 6, 2022
Published online: September 7, 2022

Benjamin Langan Gordon, Jonathan S Galati, Department of Medicine, New York Presbyterian/Weill Cornell Medical Center, New York, NY 10065, United States

Stevie Yang, Randy S Longman, Dana Lukin, Ellen J Scherl, Robert Battat, Department of Gastroenterology and Hepatology, New York Presbyterian/Weill Cornell Medical Center, New York, NY 10021, United States

Corresponding author: Robert Battat, MD, Assistant Professor, Department of Gastroenterology and Hepatology, New York Presbyterian/Weill Cornell Medical Center, 1315 York Avenue, Mezzanine, New York, NY 10021, United States. rbattat20@icloud.com

Abstract

BACKGROUND

Patients with inflammatory bowel disease (IBD) are prone to several nutritional deficiencies. However, data are lacking on vitamin C deficiency in Crohn's disease (CD) and ulcerative colitis (UC) patients, as well as the impact of clinical, biomarker and endoscopic disease severity on the development of vitamin C deficiency.

AIM

To determine proportions and factors associated with vitamin C deficiency in CD and UC patients.

METHODS

In this retrospective study, we obtained clinical, laboratory and endoscopic data from CD and UC patients presenting to the IBD clinic at a single tertiary care center from 2014 to 2019. All patients had an available plasma vitamin C level. Of 353 subjects who met initial search criteria using a cohort discovery tool, 301 ultimately met criteria for inclusion in the study. The primary aim described vitamin C deficiency (≤ 11.4 μmol/L) rates in IBD. Secondary analyses compared proportions with deficiency between active and inactive IBD. Multivariate logistic regression analysis evaluated factors associated with deficiency.

RESULTS

Of 301 IBD patients, 21.6% had deficiency, including 24.4% of CD patients and 16.0% of UC patients. Patients with elevated C-reactive protein (CRP) (39.1% *vs* 16.9%, $P < 0.001$) and fecal calprotectin (50.0% *vs* 20.0%, $P = 0.009$) had signifi-

cantly higher proportions of deficiency compared to those without. Penetrating disease (P = 0.03), obesity (P = 0.02) and current biologic use (P = 0.006) were also associated with deficiency on univariate analysis. On multivariate analysis, the objective inflammatory marker utilized for analysis (elevated CRP) was the only factor associated with deficiency (odds ratio = 3.1, 95% confidence interval: 1.5-6.6, P = 0.003). There was no difference in the presence of clinical symptoms of scurvy in those with vitamin C deficiency and those without.

CONCLUSION

Vitamin C deficiency was common in IBD. Patients with elevated inflammatory markers and penetrating disease had higher rates of vitamin C deficiency.

Key Words: Inflammatory bowel disease; Crohn's disease; Ulcerative colitis; Vitamin C deficiency; Scurvy; Malnutrition

©The Author(s) 2022. Published by Baishideng Publishing Group Inc. All rights reserved.

Core Tip: This study aimed to determine proportions and factors associated with vitamin C deficiency in inflammatory bowel disease (IBD) patients. In 301 patients, 21.6% had vitamin C deficiency, including 24.4% of Crohn's disease and 16.0% of ulcerative colitis patients. Patients with elevated C-reactive protein (39.1% *vs* 16.9%) and fecal calprotectin (50.0% *vs* 20.0%) had higher proportions of deficiency compared to those without, as did patients with penetrating disease (36.2% *vs* 20.8%). This study provides the largest data on vitamin C deficiency in IBD, and demonstrates that deficiency is common in this population, particularly those with markers of active luminal or penetrating disease.

Citation: Gordon BL, Galati JS, Yang S, Longman RS, Lukin D, Scherl EJ, Battat R. Prevalence and factors associated with vitamin C deficiency in inflammatory bowel disease. *World J Gastroenterol* 2022; 28(33): 4834-4845

URL: https://www.wjgnet.com/1007-9327/full/v28/i33/4834.htm

DOI: https://dx.doi.org/10.3748/wjg.v28.i33.4834

INTRODUCTION

Inflammatory bowel diseases (IBD), including Crohn's disease (CD) and ulcerative colitis (UC), are chronic inflammatory disorders of the gastrointestinal tract that affect over 1.5 million people in the United States alone[1,2]. Several nutritional deficiencies are well described in patients with IBD, the most common being iron, vitamin B12, vitamin D, zinc, and calcium[3-7]. However, far less literature exists on vitamin C (ascorbic acid) deficiency in this population. While the prevalence of scurvy - the clinical manifestations of vitamin C deficiency - has largely declined in the 21st century, up to 7% of the United States population still possesses vitamin C deficiency. The risk of deficiency is particularly increased in smokers, obese patients, and patients from low-income backgrounds[8]. Among those also at risk are patients with poor vitamin C intake and malabsorptive processes.

Traditionally, in IBD patients, vitamin C deficiency is thought to originate from insufficient consumption, malabsorption, and altered metabolism of vitamin C. Although not routinely recommended, many IBD patients adhere to low-residue diets to decrease gut motility and bacterial fermentation of fiber. Unfortunately, several regimens exclude fresh fruit and vegetables, the main dietary sources of vitamin C[9]. Inadequate consumption is often compounded by malabsorption of vitamin C in these patients. Ascorbate is primarily absorbed in the jejunum and ileum, which are often affected in CD[10]. In addition, patients with IBD have been shown to have polymorphisms in genes encoding vitamin C transporters necessary for vitamin C uptake[11,12]. Lastly, tumor necrosis factor-alpha (TNF-α), a proinflammatory cytokine often elevated in IBD, also downregulates transcription of transporters necessary for vitamin C uptake[13,14].

Vitamin C deficiency can lead to impaired uptake and utilization of iron, poor wound healing, and bleeding[15,16]. The diagnosis of vitamin C deficiency can be all the more challenging to make in patients with IBD, as many nonspecific symptoms of scurvy - fatigue, arthralgias, and cutaneous manifestations - can confound systemic symptoms of CD and UC. Prior studies of patients with IBD have described inadequate vitamin C intake and suboptimal serum vitamin C levels in 22%-70% and 15%-84%, respectively[9,17-20]. Notably, these studies have been small, excluded patients with UC, and occurred prior to the advent of biologic medications. Importantly, cohorts lacked data on clinical, biomarker and endoscopic measures of disease activity to assess for their impact on vitamin C deficiency.

IBD patients are at risk for malnutrition and vitamin C deficiency is an easily reversible condition. Thus, it is essential to understand the prevalence of and factors associated with vitamin C deficiency in this population to better identify those at risk. For this reason, this study aimed to determine rates of vitamin C deficiency in patients with CD and UC and investigate potential factors associated with the development of vitamin C deficiency in this population.

MATERIALS AND METHODS

Patient population

Data were extracted from chart review of patients presenting to the IBD clinic at a single tertiary institution from 2014 to 2019. Patients were identified using a cohort discovery tool (Informatics for Integrating Biology and the Bedside, National Center for Biomedical Computing, Partners HealthCare System, Boston, Massachusetts) at Weill Cornell Medicine, New York. Search criteria included age 18 years and older, diagnosis of CD or UC, and a plasma vitamin C measurement drawn from 2014 to 2019. International Classification of Diseases 10th edition codes were used to identify patients with CD (K50.x) and UC (K51.x). Exclusion criteria included lack of a CD or UC diagnosis, plasma vitamin C level, or IBD-related visit at the time that plasma vitamin C measurement was performed. Three hundred fifty-three subjects matched initial search criteria. In patients with multiple plasma vitamin C levels, the lowest value and associated visit were utilized. This study was conducted retrospectively from data obtained for clinical purposes. The study was approved by the institutional review board at Weill Cornell Medicine, who confirmed that no ethical approval was required.

Data extraction

We extracted covariates readily available in the electronic medical record. Baseline characteristics were collected, including age, sex, race, body mass index (BMI), smoking history, type of IBD (CD or UC), disease duration and prior IBD-related surgeries (*i.e.*, total proctocolectomy, ileocolonic resection, small bowel resection, *etc.*). Endoscopic scores - within six months of plasma vitamin C level assessment - were collected when available. Disease location and behavior were defined by the Montreal classification for IBD[21]. Patients were evaluated for current and prior IBD medications, including biologic agents such as TNF-α inhibitors (infliximab, adalimumab, golimumab, and certolizumab pegol), vedolizumab, and ustekinumab. Additional laboratory values collected within one week of plasma vitamin C levels were included in the analysis. When available, C-reactive protein (CRP), iron, transferrin saturation, ferritin, vitamin B12, vitamin D, 25-hydroxy, and fecal calprotectin were obtained. Iron deficiency was defined as ferritin < 30 ng/mL and transferrin saturation < 16% in those with quiescent disease and ferritin < 100 ng/mL and transferrin saturation < 16% in those with active disease[22]. Vitamin B12 deficiency was defined as serum vitamin B12 level < 200 pg/mL or < 148 pmol/L[7]. Vitamin D deficiency or insufficiency was defined as serum vitamin D, 25-hydroxy level ≤ 20 ng/mL [23]. From the electronic medical record, we also extracted data on symptoms typically associated with vitamin C deficiency (*i.e.*, scurvy) at the IBD visit when plasma vitamin C level was obtained. These included fatigue, arthritis/arthralgias, skin findings (rash, hyperpigmentation, *etc.*), easy bruising, gingivitis, poor wound healing, perifollicular findings (hemorrhage, folliculitis) and alopecia.

Outcomes and definitions

The primary study outcome was the prevalence of vitamin C deficiency in IBD patients. Vitamin C deficiency was defined as plasma vitamin C level < 11.4 μmol/L[24,25]. Inadequate vitamin C level or marginal deficiency was defined as 11.4-28.0 μmol/L, consistent with prior studies[24,25]. Secondary analyses were performed to assess whether clinical, biomarker or endoscopic disease activity were associated with deficiency. Patients were assessed for clinical disease activity using the Harvey-Bradshaw Index for CD[26] and modified partial Mayo score for UC[27]. Clinically active disease was defined as Harvey-Bradshaw Index > 5 for CD. For UC, clinically active disease was defined as either stool frequency or rectal bleeding > 1 on the modified partial Mayo score. Elevated CRP was defined as > 0.9 mg/dL and elevated fecal calprotectin was defined as > 250 μg/g. Endoscopically severe disease was defined as simple endoscopic score CD > 15 for CD and Mayo endoscopic score ≥ 2 for UC[28-30]. Additional outcomes based on biologic plausibility included the association of vitamin C deficiency with IBD type (CD or UC), obesity (BMI ≥ 30), use of biologic medications, disease location in the small intestine, penetrating disease, IBD-related surgery, elevated CRP, elevated fecal calprotectin, iron deficiency, clinically active disease and endoscopically severe disease.

Statistical analysis

The primary outcome described the prevalence of vitamin C deficiency in patients with IBD. To address this outcome, based on previous data in 137 CD patients showing a 15% prevalence of vitamin C deficiency[17], in our exploratory cohort of 301 patients, we expected that a two-sided 95% confidence interval (CI) for the prevalence could be constructed to be within ± 4.0% of the observed prevalence

proportion. Statistical review was performed by the corresponding author, who has extensive experience performing statistical analyses for clinical research.

For secondary outcomes, variables (listed above) were selected based on biologic plausibility for abnormal vitamin C absorption. To address these secondary outcomes, we performed chi-squared tests or Fisher's exact tests as appropriate to compare the proportions of vitamin C deficiency between groups. A multivariate logistic regression was performed on covariates selected based on biologic plausibility. These included presence of small bowel disease, penetrating disease, history of IBD-related surgery, obesity, current biologic medication use, elevated CRP, and clinically active disease. Variables with $P \leq 0.2$ were selected for inclusion in the final model. CRP was selected as the sole objective inflammatory marker for sample size considerations (*i.e.*, fecal calprotectin and endoscopy data had limited sample size) and to avoid multicollinearity with these other inflammatory assessments. All analyses were performed using Stata Version 16.0 (StataCorp, College Station, TX). Continuous variables were expressed as means ± SD. The multivariate analysis was expressed as odds ratio (OR) with 95%CI.

RESULTS

Baseline demographics

A total of 301 CD or UC patients with available plasma vitamin C levels were included in the study. Baseline characteristics of the entire cohort are described in Table 1. The mean age of the cohort was 47.6 ± 17.4 years. One hundred ninety (63.1%) subjects were female, and 230 (76.4%) were Caucasian. A total of 201 (66.8%) patients had a diagnosis of CD and 100 (33.2%) had a diagnosis of UC. The mean duration of disease was 17.0 ± 13.6 years. A total of 109 (36.2%) patients had a history of IBD-related surgery and 133 patients (44.2%) were undergoing treatment with a biologic agent at the time of plasma vitamin C level collection. Six patients (2.0%) were active smokers and 42/291 (14.4%) had a BMI ≥ 30. Fifty-nine of 252 patients (23.4%) had iron deficiency, 1/264 (0.4%) had vitamin B12 deficiency, and 38/259 (14.7%) had vitamin D deficiency or insufficiency. Of 292 patients with available disease activity scores, 134 (45.9%) had clinically active disease. Of 113 patients with available endoscopies, 20 (17.7%) had endoscopically severe disease.

Proportion of IBD patients with vitamin C deficiency

The mean vitamin C level was 35.7 ± 27.8 μmol/L in the entire IBD cohort. For analysis of the primary outcome, 21.6% of IBD patients (65/301) had vitamin C deficiency (< 11.4 μmol/L). An additional 24.6% of IBD patients (74/301) had inadequate vitamin C levels (11.4-28.0 μmol/L). CD patients had numerically higher prevalence of vitamin C deficiency than those with UC, although this result did not reach statistical significance (24.4% *vs* 16.0%, $P = 0.1$, Figure 1).

Secondary outcomes: Factors associated with vitamin C deficiency in all IBD patients

In all IBD patients, those with elevated CRP had higher proportions of vitamin C deficiency (39.1% *vs* 16.9%, $P < 0.001$, Table 2) compared to those without elevated CRP. Similarly, patients with elevated fecal calprotectin had higher rates of vitamin C deficiency (50.0% *vs* 20.0%, $P = 0.009$) compared to those without fecal calprotectin elevation. In a subgroup with available endoscopic data, those with severe inflammation ($n = 20$) had numerically higher deficiency rates compared to those without severe inflammation (35.0% *vs* 22.6% $P = 0.2$). However, comparable rates of deficiency existed between those with and without clinically active disease (26.1% *vs* 18.4%, $P = 0.1$). Obesity (35.7% *vs* 19.7%, $P = 0.02$) and current biologic medication use (28.6% *vs* 15.6%, $P = 0.006$) were associated with increased rates of vitamin C deficiency on univariate analysis. Among patients on current biologic therapy ($n = 133$), there were higher proportions of vitamin C deficiency in those using TNF-α inhibitors (17/48) compared with those using non-TNF-α (16/85) biologics (35.4% *vs* 18.8%, $P = 0.03$). Iron deficiency (28.8% *vs* 20.2%, $P = 0.2$), vitamin D deficiency/insufficiency (28.9% *vs* 21.3%, $P = 0.3$), surgery (25.7% *vs* 19.3%, $P = 0.2$), and active smoking (50.0% *vs* 21.0%, $P = 0.1$) were not associated with higher deficiency rates. On multivariate analysis, elevated CRP was the only factor significantly associated with vitamin C deficiency (OR = 3.1, 95%CI: 1.5-6.6, $P = 0.003$). Presence of small bowel disease, penetrating disease, history of IBD-related surgery, obesity, use of a biologic agent, and clinically active disease were not.

Secondary outcomes: Factors associated with vitamin C deficiency stratified by disease

Among CD patients, patients with penetrating disease had significantly higher rates of vitamin C deficiency compared to patients without penetrating disease (36.2% *vs* 20.8%, $P = 0.03$, Table 2). In CD patients, both elevated CRP (41.2% *vs* 17.9%, $P = 0.001$) and fecal calprotectin (56.3% *vs* 26.3%, $P = 0.04$) were persistently associated with higher proportions of vitamin C deficiency compared to those without elevated biomarkers. In subgroups of CD patients with endoscopic data available, those with endoscopically severe disease ($n = 12$) had numerically increased prevalence of vitamin C deficiency (41.7% *vs* 27.7%, $P = 0.3$). Similarly, CD patients with clinically active disease had numerically higher rates of deficiency (30.2% *vs* 20.2%, $P = 0.1$). CD patients with small bowel involvement did not have higher

Table 1 Baseline characteristics

	All IBD patients (*n* = 301)
Female sex	190 (63.1%)
Age (yr)	47.6 ± 17.4
Ethnicity	
Caucasian	230 (76.4%)
Hispanic	16 (5.3%)
African-American	5 (1.7%)
Asian	14 (4.7%)
Not specified	36 (12.0%)
BMI	24.8 ± 5.2
Obesity (BMI ≥ 30)[1]	42 (14.4%)
Active smoking	6 (2.0%)
CD	201 (66.8%)
Disease location	
Ileal	57 (28.4%)
Colonic	34 (16.9%)
Ileocolonic	108 (53.7%)
Upper disease	10 (5.0%)
Behavior	
Non-stricturing, non-penetrating	106 (52.7%)
Stricturing	74 (36.8%)
Penetrating	47 (23.4%)
UC	100 (36.8%)
Disease location[1]	
Proctitis	14 (14.7%)
Left-sided colitis	45 (47.4%)
Pancolitis	36 (37.9%)
Disease duration (yr)	17.0 ± 13.6
IBD related surgery	109 (36.2%)
IBD medications	
Current biologic use	133 (44.2%)
Past/ever biologic use	166 (55.1%)
Clinically active disease[1]	134 (45.9%)
CD	96 (49.2%)
UC	38 (39.2%)
Endoscopically severe disease[1]	20 (17.7%)
CD	12 (15.6%)
UC	8 (22.2%)

[1]Ten patients had unknown body mass index. Five ulcerative colitis (UC) patients had unknown disease location. Nine patients did not have disease activity available (6 Crohn's disease, 3 UC). One hundred thirteen inflammatory bowel disease patients had endoscopies available.
Clinically active disease was defined as Harvey-Bradshaw index > 5 for Crohn's disease (CD), and stool frequency or rectal bleeding > 1 on modified partial Mayo score for ulcerative colitis (UC). Endoscopically severe disease was defined as simple endoscopic score CD > 15 in CD and endoscopic Mayo

score ≥ 2 in UC. IBD: Inflammatory bowel disease; CD: Crohn's disease; UC: Ulcerative colitis; BMI: Body mass index.

Table 2 Prevalence of vitamin C deficiency in covariate populations

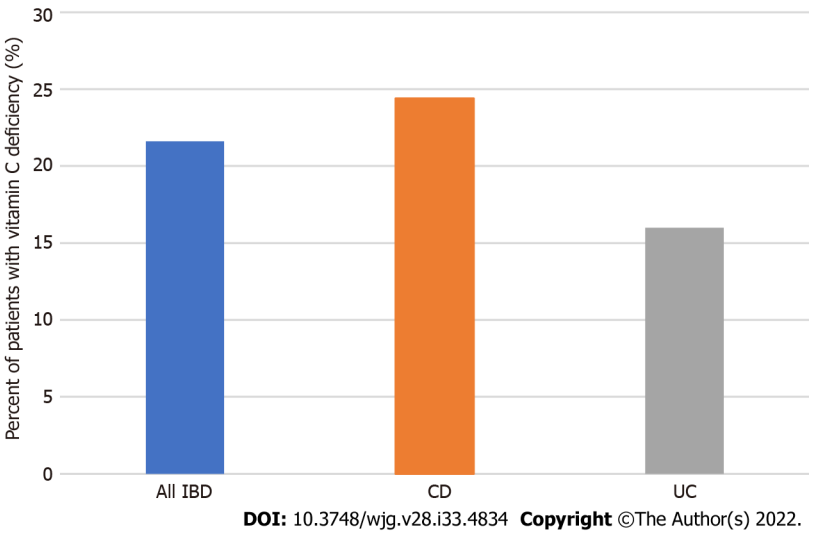
Covariates	Prevalence of vitamin C deficiency in patients with covariate	Prevalence of vitamin C deficiency in patients without covariate	*P* value
IBD type			
CD	49/201 (24.4%)	-	0.1
UC	16/100 (16.0%)	-	0.1
Small bowel disease	38/165 (23.0%)	11/36 (30.6%)	0.3
Penetrating disease	17/47 (36.2%)	32/154 (20.8%)	0.03[1]
IBD related surgery	28/109 (25.7%)	37/192 (19.3%)	0.2
CD	25/96 (26.0%)	24/105 (22.9%)	0.6
UC	3/13 (23.1%)	13/87 (14.9%)	0.4
Obesity (BMI ≥ 30)	15/42 (35.7%)	49/249 (19.7%)	0.02[1]
Active smoking	3/6 (50.0%)	62/295 (21.0%)	0.1
Current biologic use	38/133 (28.6%)	26/167 (15.6%)	0.006[1]
CRP > 0.9 mg/dL	25/64 (39.1%)	36/213 (16.9%)	< 0.001[1]
CD	21/51 (41.2%)	24/134 (17.9%)	0.001[1]
UC	4/13 (30.8%)	12/79 (15.2%)	0.2
Fecal calprotectin > 250 ug/g	10/20 (50.0%)	12/60 (20.0%)	0.009[1]
CD	9/16 (56.3%)	10/38 (26.3%)	0.04[1]
UC	1/4 (25.0%)	2/22 (9.1%)	0.4
Iron deficiency	17/59 (28.8%)	39/193 (20.2%)	0.2
Vitamin D deficiency/insufficiency	11/38 (28.9%)	47/221 (21.3%)	0.3
Clinically active disease	35/134 (26.1%)	29/158 (18.4%)	0.1
CD	29/96 (30.2%)	20/99 (20.2%)	0.1
UC	6/38 (15.8%)	9/59 (15.3%)	0.9
Endoscopically severe disease	7/20 (35.0%)	21/93 (22.6%)	0.2
CD	5/12 (41.7%)	18/65 (27.7%)	0.3
UC	2/8 (25.0%)	3/28 (10.7%)	0.3

[1]Patients with penetrating disease, obesity, biologic use, elevated C-reactive protein and elevated fecal calprotectin had increased frequency of vitamin C deficiency.

Clinically active disease was defined as Harvey-Bradshaw index > 5 for Crohn's disease (CD), and stool frequency or rectal bleeding > 1 on modified partial Mayo score for ulcerative colitis (UC). Endoscopically severe disease was defined as simple endoscopic score CD > 15 in CD and endoscopic Mayo score ≥ 2 in UC. IBD: Inflammatory bowel disease; CD: Crohn's disease; UC: Ulcerative colitis; BMI: Body mass index; CRP: C-reactive protein.

rates of vitamin C deficiency compared to those without small bowel involvement (23.0% *vs* 30.6%, P = 0.3).

In small subgroups of UC patients with available data, numerical differences persisted between those with elevated CRP (n = 13) and those with elevated fecal calprotectin (n = 4) when compared to those without elevated biomarkers (CRP: 30.8% *vs* 15.2%, P = 0.2; fecal calprotectin: 25.0% *vs* 9.1%, P = 0.4). In a small subset of UC patients with available endoscopic data, those with endoscopically severe disease (n = 8) had numerically increased frequency of vitamin C deficiency (25.0% *vs* 10.7%, P = 0.3). However, clinically active disease was not associated with higher rates of vitamin C deficiency when compared to those with quiescent disease (15.8% *vs* 15.3%, P = 0.9).



DOI: 10.3748/wjg.v28.i33.4834 **Copyright** ©The Author(s) 2022.

Figure 1 Prevalence of vitamin C deficiency in inflammatory bowel disease. In total, 21.6% of all inflammatory bowel disease patients had vitamin C deficiency, including 24.4% of Crohn's disease patients and 16.0% of ulcerative colitis patients. IBD: Inflammatory bowel disease; CD: Crohn's disease; UC: Ulcerative colitis.

Symptoms of vitamin C deficiency

When comparing patients with and without vitamin C deficiency, there was no difference in the presence of one or more clinical features of scurvy (66.2% *vs* 58.5%, $P = 0.3$, Table 3). Furthermore, both groups had similar rates of arthritis, cutaneous findings, easy bruising, gingivitis, perifollicular findings and alopecia. Patients with vitamin C deficiency were more likely to report fatigue than those with normal vitamin C levels (43.1% *vs* 27.5%, $P = 0.02$). Moreover, vitamin C deficient patients were more likely to report poor wound healing (4.6% *vs* 0.4%, $P = 0.03$).

DISCUSSION

Though many consider scurvy a historical disease of seafarers, the current study demonstrates that vitamin C deficiency affects a significant minority of IBD patients. In 301 patients, 21.6% of IBD patients had vitamin C deficiency, including 24.4% of CD patients and 16.0% of UC patients. This is approximately three-fold higher than the prevalence of vitamin C deficiency in the overall United States population[8].

Strikingly, in IBD patients with elevated objective markers of inflammation, such as CRP and fecal calprotectin, vitamin C deficiency rates ranged from 39%-50%. Similarly, CD patients with penetrating phenotype had higher deficiency rates. On multivariate analysis, the association between elevated CRP and vitamin C deficiency persisted. To our knowledge, this study uniquely examines the relationship between objectively quantified intestinal inflammation (using endoscopy, $n = 113$, or fecal calprotectin, $n = 80$) and vitamin C deficiency in a large cohort. Subgroup analysis in patients with available endoscopic data was concordant with biomarker data, with numerically higher rates of deficiency in those with significant intestinal inflammation. In UC, biomarkers and endoscopic data were more limited, with few patients in groups with elevated CRP, fecal calprotectin and endoscopic inflammation available. Absolute rates of deficiency were non-significantly lower in UC, but numerical differences between UC patients with and without inflammation were similar to these differences in CD. Notably, even in patients without objective evidence of inflammatory disease - based on CRP, calprotectin, and endoscopic score - rates of deficiency ranged from 17%-23%.

This study is the largest to date to report on the prevalence of vitamin C deficiency in IBD. Additionally, the current study significantly increases available data in both CD and UC by utilizing a well characterized cohort to provide analyses on factors associated with deficiency. Previous smaller studies have shown vitamin C deficiency rates of 15%-84% in CD patients[9,17-20]. The variability of decreased vitamin C levels in these studies largely stems from differences in sample sizes and reference ranges.

While previous studies report inadequate vitamin C intake in UC[31], to our knowledge, there are no prior studies describing proportions with vitamin C deficiency in UC. Vitamin C deficiency would be biologically plausible in CD as CD often affects the primary sites of vitamin C absorption in the small bowel. Interestingly, in UC patients (without small bowel disease), 16% had vitamin C deficiency. While dietary data was not available in this study, avoidance of vitamin C rich foods likely contributed to the development of vitamin C deficiency in patients with UC, as has been reported in previous studies[31]. Moreover, patients with UC often have elevated TNF-α, which has been shown to downregulate

Table 3 Clinical features of vitamin C deficiency

	Vitamin C deficiency (*n* = 65)	Normal vitamin C level (*n* = 236)	*P* value
Presence of ≥ 1 clinical feature(s) of scurvy	43 (66.2%)	138 (58.5%)	0.3
None	22 (33.8%)	98 (41.5%)	-
Fatigue	28 (43.1%)	65 (27.5%)	0.02[1]
Arthritis/arthralgias	27 (41.5%)	96 (40.7%)	0.9
Skin findings (rash, hyperpigmentation)	9 (13.8%)	29 (12.3%)	0.7
Easy bruising	6 (9.2%)	9 (3.8%)	0.1
Gingivitis	3 (4.6%)	6 (2.5%)	0.4
Poor wound healing	3 (4.6%)	1 (0.4%)	0.03[1]
Perifollicular findings (hemorrhage, folliculitis)	2 (3.1%)	1 (0.4%)	0.1
Alopecia	1 (1.5%)	5 (2.1%)	1.0

[1]Patients with vitamin C deficiency were more likely to report fatigue and poor wound healing.
There was no difference in presence of clinical features of scurvy between patients with vitamin C deficiency and those without.

transporters involved in vitamin C uptake[13,14].

The current study found penetrating disease to be associated with vitamin C deficiency. Previously, development of metabolic bone disease has been associated with a penetrating phenotype[32], although few studies have commented on the development of micronutrient deficiency in CD patients with penetrating disease. Penetrating disease often involves the small bowel and also likely reflects more active, refractory CD. Thus, patients with penetrating phenotypes may be at higher risk of both malabsorption - *via* inflamed tissue and enteric fistulas - and poor consumption - *via* dietary avoidance of foods rich in vitamin C that may exacerbate symptoms. These data are consistent with CRP and fecal calprotectin elevations also being associated with deficiency. Interestingly, presence of small bowel disease was not associated with increased risk of vitamin C deficiency in CD, despite the jejunum and ileum being the primary sites of vitamin C absorption. However, historical disease location may have been confounded by patients with inactive small bowel disease. Further studies on patients with active small intestinal disease would be required prior to concluding a lack of association between disease location and deficiency status.

While obesity and biologic medication use have biologic plausibility for deficiency and were associated on univariate analysis[8,13,14,33], the study results in aggregate more strongly support active IBD being associated with vitamin C deficiency. Only CRP was associated with vitamin C deficiency on multivariate analysis. However, it should be noted that in non-IBD populations[8], obesity has been shown to be associated with higher rates of vitamin C deficiency. Prior studies suggest that increased access to low-cost, high-calorie, micronutrient-poor food may explain the association between obesity and multiple vitamin deficiencies[33]. The association of current biologic medication use and vitamin C deficiency is less clear and may be due to this being a marker of a more severe disease course. In a subgroup analysis of patients using biologic therapy, patients on TNF-α inhibitors had higher rates of deficiency compared to those on non-TNF-α agents (*i.e.*, vedolizumab, ustekinumab, *etc.*), which runs counter to our understanding of TNF-α in vitamin C deficiency. TNF-α is known to downregulate transcription of transporters required for vitamin C uptake[13,14], and thus, one might expect that patients using TNF-α inhibitors would have lower, not higher proportions of deficiency. This further supports the use of anti-TNF agents or biologics as a surrogate for disease severity. Future studies may be warranted to better investigate this mechanism.

This study also highlights the difficulty in making a diagnosis of vitamin C deficiency in patients with IBD. In our cohort, there was no difference in the presence of clinical features of scurvy in patients with vitamin C deficiency compared to those with normal vitamin C levels. Many sequelae of vitamin C deficiency are nonspecific and can mimic or coexist with active IBD, including fatigue, arthralgias, oral lesions, bleeding, poor wound healing, anemia, and iron deficiency[15]. Unfortunately, more specific findings in scurvy, such as perifollicular hemorrhage and follicular hyperkeratosis, occur in only a small minority of vitamin C deficient patients, as our study reiterates. Given the challenge of diagnosing scurvy in this population, providers should have a low threshold to test for vitamin C deficiency and counsel on adequate vitamin C intake. Unlike the relapsing and often refractory nature of IBD in many patients, vitamin C supplementation can lead to rapid resolution of symptoms, including some incorrectly ascribed to IBD. Even in IBD patients with unmeasured vitamin C levels, empiric supplementation is not unreasonable, given vitamin C's role as an antioxidant, preventing free radical damage and reducing extracellular oxidants[24]. However, future studies demonstrating that vitamin C supple-

mentation can decrease inflammatory burden or improve clinical symptoms would be necessary prior to recommending empiric supplementation as standard of care for this population.

Study limitations include the use of retrospective chart review. This study did not find an association between clinical disease severity and vitamin C deficiency. However, clinical disease indices, particularly in CD, poorly correlate with mucosal disease[34]. Though this study examined the relationship between endoscopic activity and vitamin C deficiency, analyses on this relationship were limited by the small number of patients with significant endoscopic inflammation (n = 20). Yet, numerical differences based on endoscopic inflammation were consistent with CRP and fecal calprotectin data, suggesting that intestinal inflammation impacts vitamin C deficiency. Multivariate analyses utilized a single objective marker of inflammation to avoid multicollinearity. CRP was selected as few patients had elevated fecal calprotectin (n = 20) or significant endoscopic inflammation (n = 20), whereas 277 patients had CRP data available. Additionally, given the retrospective nature of our study, data are restricted to patients who had plasma vitamin C measurements available; these patients were not necessarily being screened for deficiency. Selection bias may exist as such laboratory values may have restricted the population to those more prone to have vitamin C deficiency. Nonetheless, nearly 40% of our study population had no symptoms of scurvy when their vitamin C level was obtained, indicating a sizable component of our cohort were simply being monitored for standard nutritional deficiencies. An additional limitation of this study was that measurements of all micronutrients were not performed. The retrospective nature of our study also limits our examination of whether inadequate consumption was associated with higher rates of deficiency, or whether fasting status at serum collection impacted vitamin C level, as dietary data was not available. The use of chart review to assess for symptoms of vitamin C deficiency is also a limitation that may have led to under-detection of symptoms related to deficiency. Some providers may not routinely screen for symptoms related to scurvy (*i.e.*, gingivitis, alopecia, *etc.*) and these items may not be reflected in providers' notes. Thus, reporting bias may exist. Despite this, vitamin C deficiency symptoms were infrequently documented. Lastly, this cohort was comprised of patients at an IBD center affiliated with a tertiary care center. Thus, the subjects in this study may have more severe disease, potentially impacting the generalizability of these data.

CONCLUSION

The current study demonstrates that vitamin C deficiency exists in a significant portion of patients with IBD, particularly those with objective markers of active luminal or penetrating disease. Clinical features of scurvy did not differ between patients with and without deficiency, reinforcing the challenge of diagnosing scurvy in this population, as symptoms of vitamin C deficiency and IBD may overlap. In summary, vitamin C deficiency exists in a considerable fraction of IBD patients. Thus, identifying and treating this easily reversible condition in these patients is essential.

ARTICLE HIGHLIGHTS

Research background

Patients with inflammatory bowel disease (IBD) are prone to several nutritional deficiencies, including iron, vitamin B12 and vitamin D. However, there is a lack of data on vitamin C deficiency in this population, as well as the impact of clinical, biomarker and endoscopic disease severity on the development of vitamin C deficiency.

Research motivation

As IBD patients are already at risk of malnutrition and as vitamin C deficiency is an easily reversible condition, it would be valuable to understand the prevalence of and factors associated with vitamin C deficiency in this population.

Research objectives

The primary objective assessed the prevalence of vitamin C deficiency in IBD patients. Secondary objectives evaluated proportions with deficiency between active and inactive IBD - using clinical, laboratory and endoscopic data - to better identify those at risk of deficiency.

Research methods

In this retrospective study, clinical, laboratory and endoscopic data were collected from all Crohn's disease (CD) and ulcerative colitis (UC) patients who had available plasma vitamin C levels presenting to the IBD clinic at a single tertiary care center from 2014 to 2019. Of 353 subjects who met initial search criteria using a cohort discovery tool, 301 ultimately met criteria for inclusion in the study. The primary aim described vitamin C deficiency (≤ 11.4 μmol/L) rates in IBD, with secondary analyses comparing

proportions with deficiency between active and inactive IBD. Multivariate logistic regression analysis evaluated factors associated with deficiency.

Research results

In 301 IBD patients, 21.6% had vitamin C deficiency, including 24.4% of CD and 16.0% of UC patients. Patients with elevated C-reactive protein (CRP) (39.1% *vs* 16.9%, $P < 0.001$) and fecal calprotectin (50.0% *vs* 20.0%, $P = 0.009$) had higher proportions of deficiency compared to those without. Other factors associated with vitamin C deficiency included the presence of penetrating disease ($P = 0.03$), obesity ($P = 0.02$) and current biologic medication use ($P = 0.006$). On multivariable analysis, the objective inflammatory marker utilized for analysis (CRP) was the only factor associated with deficiency (odds ratio = 3.1, 95% confidence interval: 1.5-6.6, $P = 0.003$).

Research conclusions

This study provides the largest data on vitamin C deficiency in patients with IBD, uniquely assesses factors associated with deficiency and provides rigorous assessment of inflammatory status using objective markers. Vitamin C deficiency was common in IBD, particularly those with objective markers of active luminal or penetrating disease. As vitamin C deficiency exists in over one-fifth of IBD patients, it is essential to identify and treat this easily reversible condition in this population.

Research perspectives

Future prospective studies with well characterized cohorts, and data on diet, other micronutrient deficiencies, endoscopic assessment, and vitamin C supplementation, may be warranted to further elucidate factors associated with vitamin C deficiency and the impact of supplementation on clinical course in IBD patients.

FOOTNOTES

Author contributions: Battat R is the guarantor of the article; Gordon BL, Galati JS, Longman RS, Lukin D, Scherl EJ and Battat R contributed to the design of the study; Gordon BL, Galati JS, and Yang S collected the data; Gordon BL and Battat R analyzed the data; Gordon BL, Scherl EJ, Lukin D and Battat R wrote the paper; and all authors read and approved the final version of the manuscript.

Institutional review board statement: This study was reviewed and approved by the institutional review board at Weill Cornell Medicine.

Informed consent statement: This study was conducted retrospectively from data obtained for clinical purposes. The study was approved by the institutional review board at Weill Cornell Medicine, who confirmed that no ethical approval or informed consent was required.

Conflict-of-interest statement: Gordon BL, Galati JS, Yang S have none to report; Longman RS consulted Pfizer, Bristol Myers Squibb; Lukin D consults for Boehringer Ingelheim, Palatin Technologies, Pfizer; research support: AbbVie, Janssen, Kenneth Rainin Foundation, Takeda; Scherl EJ consulted AbbVie, Crohn's and Colitis Foundation of America (CCFA), Entera Health, Evidera, GI Health Foundation, Janssen, Protagonist, Seres, Takeda, Bristol Myers Squibb; research support: AbbVie, AstraZeneca, CCFA, Janssen, Pfizer, National Institute of Health, New York Crohn's Foundation, UCSF-CCFA Clinical Research Alliance, Genentech, Seres, Celgene, UCB, Johns Hopkins University, National Institute of Diabetes and Digestive and Kidney; Shareholder: Gilead; Honoraria: GI Health Foundation, Janssen; Battat R provide research support, fund for the Future Award and Jill Roberts Funds at the Department of Medicine, Weill Cornell Medicine.

Data sharing statement: The datasets used and analyzed in this current study are available from the corresponding author on reasonable request.

Open-Access: This article is an open-access article that was selected by an in-house editor and fully peer-reviewed by external reviewers. It is distributed in accordance with the Creative Commons Attribution NonCommercial (CC BY-NC 4.0) license, which permits others to distribute, remix, adapt, build upon this work non-commercially, and license their derivative works on different terms, provided the original work is properly cited and the use is non-commercial. See: https://creativecommons.org/Licenses/by-nc/4.0/

Country/Territory of origin: United States

ORCID number: Benjamin Langan Gordon 0000-0001-8861-010X; Dana Lukin 0000-0003-4581-2267; Robert Battat 0000-0002-7421-9764.

S-Editor: Wang JJ

L-Editor: A
P-Editor: Wang JJ

REFERENCES

1 **Loftus EV Jr**. Clinical epidemiology of inflammatory bowel disease: Incidence, prevalence, and environmental influences. *Gastroenterology* 2004; **126**: 1504-1517 [PMID: 15168363 DOI: 10.1053/j.gastro.2004.01.063]
2 **Loftus EV Jr**. Update on the Incidence and Prevalence of Inflammatory Bowel Disease in the United States. *Gastroenterol Hepatol (N Y)* 2016; **12**: 704-707 [PMID: 28035199]
3 **Hwang C**, Ross V, Mahadevan U. Micronutrient deficiencies in inflammatory bowel disease: from A to zinc. *Inflamm Bowel Dis* 2012; **18**: 1961-1981 [PMID: 22488830 DOI: 10.1002/ibd.22906]
4 **Vagianos K**, Bector S, McConnell J, Bernstein CN. Nutrition assessment of patients with inflammatory bowel disease. *JPEN J Parenter Enteral Nutr* 2007; **31**: 311-319 [PMID: 17595441 DOI: 10.1177/0148607107031004311]
5 **Jeejeebhoy KN**, Duerksen DR. Malnutrition in Gastrointestinal Disorders: Detection and Nutritional Assessment. *Gastroenterol Clin North Am* 2018; **47**: 1-22 [PMID: 29413007 DOI: 10.1016/j.gtc.2017.09.002]
6 **Battat R**, Kopylov U, Szilagyi A, Saxena A, Rosenblatt DS, Warner M, Bessissow T, Seidman E, Bitton A. Vitamin B12 deficiency in inflammatory bowel disease: prevalence, risk factors, evaluation, and management. *Inflamm Bowel Dis* 2014; **20**: 1120-1128 [PMID: 24739632 DOI: 10.1097/MIB.0000000000000024]
7 **Battat R**, Kopylov U, Byer J, Sewitch MJ, Rahme E, Nedjar H, Zelikovic E, Dionne S, Bessissow T, Afif W, Waters PJ, Seidman E, Bitton A. Vitamin B12 deficiency in inflammatory bowel disease: a prospective observational pilot study. *Eur J Gastroenterol Hepatol* 2017; **29**: 1361-1367 [PMID: 28953003 DOI: 10.1097/MEG.0000000000000970]
8 **Schleicher RL**, Carroll MD, Ford ES, Lacher DA. Serum vitamin C and the prevalence of vitamin C deficiency in the United States: 2003-2004 National Health and Nutrition Examination Survey (NHANES). *Am J Clin Nutr* 2009; **90**: 1252-1263 [PMID: 19675106 DOI: 10.3945/ajcn.2008.27016]
9 **Filippi J**, Al-Jaouni R, Wiroth JB, Hébuterne X, Schneider SM. Nutritional deficiencies in patients with Crohn's disease in remission. *Inflamm Bowel Dis* 2006; **12**: 185-191 [PMID: 16534419 DOI: 10.1097/01.MIB.0000206541.15963.c3]
10 **Said HM**. Intestinal absorption of water-soluble vitamins in health and disease. *Biochem J* 2011; **437**: 357-372 [PMID: 21749321 DOI: 10.1042/BJ20110326]
11 **Shaghaghi MA**, Kloss O, Eck P. Genetic Variation in Human Vitamin C Transporter Genes in Common Complex Diseases. *Adv Nutr* 2016; **7**: 287-298 [PMID: 26980812 DOI: 10.3945/an.115.009225]
12 **Amir Shaghaghi M**, Bernstein CN, Serrano León A, El-Gabalawy H, Eck P. Polymorphisms in the sodium-dependent ascorbate transporter gene SLC23A1 are associated with susceptibility to Crohn disease. *Am J Clin Nutr* 2014; **99**: 378-383 [PMID: 24284447 DOI: 10.3945/ajcn.113.068015]
13 **Sands BE**, Kaplan GG. The role of TNFalpha in ulcerative colitis. *J Clin Pharmacol* 2007; **47**: 930-941 [PMID: 17567930 DOI: 10.1177/0091270007301623]
14 **Subramanian VS**, Sabui S, Subramenium GA, Marchant JS, Said HM. Tumor necrosis factor alpha reduces intestinal vitamin C uptake: a role for NF-κB-mediated signaling. *Am J Physiol Gastrointest Liver Physiol* 2018; **315**: G241-G248 [PMID: 29631379 DOI: 10.1152/ajpgi.00071.2018]
15 **Hirschmann JV**, Raugi GJ. Adult scurvy. *J Am Acad Dermatol* 1999; **41**: 895-906; quiz 907 [PMID: 10570371 DOI: 10.1016/s0190-9622(99)70244-6]
16 **Smith A**, Di Primio G, Humphrey-Murto S. Scurvy in the developed world. *CMAJ* 2011; **183**: E752-E755 [PMID: 21555388 DOI: 10.1503/cmaj.091938]
17 **Imes S**, Dinwoodie A, Walker K, Pinchbeck B, Thomson AB. Vitamin C status in 137 outpatients with Crohn's disease. Effect of diet counseling. *J Clin Gastroenterol* 1986; **8**: 443-446 [PMID: 3760522 DOI: 10.1097/00004836-198608000-00012]
18 **Hodges P**, Gee M, Grace M, Thomson AB. Vitamin and iron intake in patients with Crohn's disease. *J Am Diet Assoc* 1984; **84**: 52-58 [PMID: 6690565]
19 **Hughes RG**, Williams N. Leucocyte ascorbic acid in Crohn's disease. *Digestion* 1978; **17**: 272-274 [PMID: 640276 DOI: 10.1159/000198118]
20 **Linaker BD**. Scurvy and vitamin C deficiency in Crohn's disease. *Postgrad Med J* 1979; **55**: 26-29 [PMID: 432168 DOI: 10.1136/pgmj.55.639.26]
21 **Satsangi J**, Silverberg MS, Vermeire S, Colombel JF. The Montreal classification of inflammatory bowel disease: controversies, consensus, and implications. *Gut* 2006; **55**: 749-753 [PMID: 16698746 DOI: 10.1136/gut.2005.082909]
22 **Gasche C**, Berstad A, Befrits R, Beglinger C, Dignass A, Erichsen K, Gomollon F, Hjortswang H, Koutroubakis I, Kulnigg S, Oldenburg B, Rampton D, Schroeder O, Stein J, Travis S, Van Assche G. Guidelines on the diagnosis and management of iron deficiency and anemia in inflammatory bowel diseases. *Inflamm Bowel Dis* 2007; **13**: 1545-1553 [PMID: 17985376 DOI: 10.1002/ibd.20285]
23 **Giustina A**, Adler RA, Binkley N, Bouillon R, Ebeling PR, Lazaretti-Castro M, Marcocci C, Rizzoli R, Sempos CT, Bilezikian JP. Controversies in Vitamin D: Summary Statement From an International Conference. *J Clin Endocrinol Metab* 2019; **104**: 234-240 [PMID: 30383226 DOI: 10.1210/jc.2018-01414]
24 **Granger M**, Eck P. Dietary Vitamin C in Human Health. *Adv Food Nutr Res* 2018; **83**: 281-310 [PMID: 29477224 DOI: 10.1016/bs.afnr.2017.11.006]
25 **Robitaille L**, Hoffer LJ. A simple method for plasma total vitamin C analysis suitable for routine clinical laboratory use. *Nutr J* 2016; **15**: 40 [PMID: 27102999 DOI: 10.1186/s12937-016-0158-9]
26 **Harvey RF**, Bradshaw JM. A simple index of Crohn's-disease activity. *Lancet* 1980; **1**: 514 [PMID: 6102236 DOI: 10.1016/s0140-6736(80)92767-1]

27 **Lewis JD**, Chuai S, Nessel L, Lichtenstein GR, Aberra FN, Ellenberg JH. Use of the noninvasive components of the Mayo score to assess clinical response in ulcerative colitis. *Inflamm Bowel Dis* 2008; **14**: 1660-1666 [PMID: 18623174 DOI: 10.1002/ibd.20520]

28 **Daperno M**, D'Haens G, Van Assche G, Baert F, Bulois P, Maunoury V, Sostegni R, Rocca R, Pera A, Gevers A, Mary JY, Colombel JF, Rutgeerts P. Development and validation of a new, simplified endoscopic activity score for Crohn's disease: the SES-CD. *Gastrointest Endosc* 2004; **60**: 505-512 [PMID: 15472670 DOI: 10.1016/s0016-5107(04)01878-4]

29 **Schroeder KW**, Tremaine WJ, Ilstrup DM. Coated oral 5-aminosalicylic acid therapy for mildly to moderately active ulcerative colitis. A randomized study. *N Engl J Med* 1987; **317**: 1625-1629 [PMID: 3317057 DOI: 10.1056/NEJM198712243172603]

30 **Danese S**, Sandborn WJ, Colombel JF, Vermeire S, Glover SC, Rimola J, Siegelman J, Jones S, Bornstein JD, Feagan BG. Endoscopic, Radiologic, and Histologic Healing With Vedolizumab in Patients With Active Crohn's Disease. *Gastroenterology* 2019; **157**: 1007-1018.e7 [PMID: 31279871 DOI: 10.1053/j.gastro.2019.06.038]

31 **Urbano AP**, Sassaki LY, Dorna MS, Carvalhaes MA, Martini LA, Ferreira AL. Nutritional intake according to injury extent in ulcerative colitis patients. *J Hum Nutr Diet* 2013; **26**: 445-451 [PMID: 23560822 DOI: 10.1111/jhn.12064]

32 **Cravo M**, Guerreiro CS, dos Santos PM, Brito M, Ferreira P, Fidalgo C, Tavares L, Pereira AD. Risk factors for metabolic bone disease in Crohn's disease patients. *Inflamm Bowel Dis* 2010; **16**: 2117-2124 [PMID: 20848459 DOI: 10.1002/ibd.21297]

33 **Via M**. The malnutrition of obesity: micronutrient deficiencies that promote diabetes. *ISRN Endocrinol* 2012; **2012**: 103472 [PMID: 22462011 DOI: 10.5402/2012/103472]

34 **Falvey JD**, Hoskin T, Meijer B, Ashcroft A, Walmsley R, Day AS, Gearry RB. Disease activity assessment in IBD: clinical indices and biomarkers fail to predict endoscopic remission. *Inflamm Bowel Dis* 2015; **21**: 824-831 [PMID: 25738372 DOI: 10.1097/MIB.0000000000000341]

World Journal of Gastroenterology

Submit a Manuscript: https://www.f6publishing.com

World J Gastroenterol 2022 September 7; 28(33): 4846-4860

DOI: 10.3748/wjg.v28.i33.4846

ISSN 1007-9327 (print) ISSN 2219-2840 (online)

ORIGINAL ARTICLE

Retrospective Study

Development and validation of a risk prediction score for the severity of acute hypertriglyceridemic pancreatitis in Chinese patients

Zi-Yu Liu, Lei Tian, Xiang-Yao Sun, Zong-Shi Liu, Li-Jie Hao, Wen-Wen Shen, Yan-Qiu Gao, Hui-Hong Zhai

Specialty type: Gastroenterology and hepatology

Provenance and peer review: Unsolicited article; Externally peer reviewed.

Peer-review model: Single blind

Peer-review report's scientific quality classification

Grade A (Excellent): A
Grade B (Very good): 0
Grade C (Good): C
Grade D (Fair): 0
Grade E (Poor): 0

P-Reviewer: Hegyi P, Hungary; Tang XB, China

Received: June 12, 2022
Peer-review started: June 12, 2022
First decision: July 12, 2022
Revised: July 25, 2022
Accepted: August 16, 2022
Article in press: August 16, 2022
Published online: September 7, 2022

Zi-Yu Liu, Li-Jie Hao, Wen-Wen Shen, Yan-Qiu Gao, Hui-Hong Zhai, Department of Gastroenterology, Xuanwu Hospital, Capital Medical University, Beijing 100053, China

Lei Tian, Department of Hematology and Hematopoietic Cell Transplantation, City of Hope National Medical Center, Los Angeles, CA 91010, United States

Xiang-Yao Sun, Department of Orthopedics, Xuanwu Hospital, Capital Medical University, Beijing 100053, China

Zong-Shi Liu, Department of Geriatric, Guangzhou First People's Hospital, School of Medicine, South China University of Technology, Guangzhou 510180, Guangdong Province, China

Corresponding author: Hui-Hong Zhai, MD, PhD, Chief Physician, Doctor, Professor, Department of Gastroenterology, Xuanwu Hospital, Capital Medical University, No. 45 Changchun Street, Beijing 100053, China. zhaihuihong@263.net

Abstract

BACKGROUND

The frequency of acute hypertriglyceridemic pancreatitis (AHTGP) is increasing worldwide. AHTGP may be associated with a more severe clinical course and greater mortality than pancreatitis caused by other causes. Early identification of patients with severe inclination is essential for clinical decision-making and improving prognosis. Therefore, we first developed and validated a risk prediction score for the severity of AHTGP in Chinese patients.

AIM

To develop and validate a risk prediction score for the severity of AHTGP in Chinese patients.

METHODS

We performed a retrospective study including 243 patients with AHTGP. Patients were randomly divided into a development cohort (n = 170) and a validation cohort (n = 73). Least absolute shrinkage and selection operator and logistic regression were used to screen 42 potential predictive variables to construct a risk score for the severity of AHTGP. We evaluated the performance of the nomogram and compared it with existing scoring systems. Last, we used the best cutoff value

(88.16) for severe acute pancreatitis (SAP) to determine the risk stratification classification.

RESULTS

Age, the reduction in apolipoprotein A1 and the presence of pleural effusion were independent risk factors for SAP and were used to construct the nomogram (risk prediction score referred to as AAP). The concordance index of the nomogram in the development and validation groups was 0.930 and 0.928, respectively. Calibration plots demonstrate excellent agreement between the predicted and actual probabilities in SAP patients. The area under the curve of the nomogram (0.929) was better than those of the Bedside Index of Severity in AP (BISAP), Ranson, Acute Physiology and Chronic Health Evaluation (APACHE II), modified computed tomography severity index (MCTSI), and early achievable severity index scores (0.852, 0.825, 0.807, 0.831 and 0.807, respectively). In comparison with these scores, the integrated discrimination improvement and decision curve analysis showed improved accuracy in predicting SAP and better net benefits for clinical decisions. Receiver operating characteristic curve analysis was used to determine risk stratification classification for AHTGP by dividing patients into high-risk and low-risk groups according to the best cutoff value (88.16). The high-risk group (> 88.16) was closely related to the appearance of local and systemic complications, Ranson score ≥ 3, BISAP score ≥ 3, MCTSI score ≥ 4, APACHE II score ≥ 8, C-reactive protein level ≥ 190, and length of hospital stay.

CONCLUSION

The nomogram could help identify AHTGP patients who are likely to develop SAP at an early stage, which is of great value in guiding clinical decisions.

Key Words: Nomogram; Severity; Acute pancreatitis; Prediction model

©The Author(s) 2022. Published by Baishideng Publishing Group Inc. All rights reserved.

Core Tip: A risk prediction score (referred to as AAP), including age, the level of apolipoprotein A1 and the presence of pleural effusion, was first built to predict the severity of acute hypertriglyceridemic pancreatitis in Chinese patients. After calibration and verification, this score was shown to have high predictive accuracy and good performance. The risk score could help identify patients who are likely to develop severe acute pancreatitis at an early stage. In comparison with other scores, these scores showed improved accuracy in predicting and better net benefits for clinical decisions. AAP could be of great value in guiding clinical decisions as a convenient and specific tool.

Citation: Liu ZY, Tian L, Sun XY, Liu ZS, Hao LJ, Shen WW, Gao YQ, Zhai HH. Development and validation of a risk prediction score for the severity of acute hypertriglyceridemic pancreatitis in Chinese patients. *World J Gastroenterol* 2022; 28(33): 4846-4860

URL: https://www.wjgnet.com/1007-9327/full/v28/i33/4846.htm

DOI: https://dx.doi.org/10.3748/wjg.v28.i33.4846

INTRODUCTION

Hypertriglyceridemia (HTG) is the third most common cause of acute pancreatitis (AP)[1]. The frequency of acute hypertriglyceridemic pancreatitis (AHTGP) as a type of AP is increasing worldwide[2]. One multicenter study conducted in Beijing found that AHTGP was present in 10.36% of patients with AP[3,4]. Furthermore, some evidence suggests that AHTGP may be associated with a more severe clinical course and greater mortality than pancreatitis caused by other causes[1,5,6]. Patients with severe AP (SAP) characteristically have pancreatic necrosis or distant organ failure with a mortality rate of up to 40%[7]. Early identification of patients with severe inclination is essential for the delivery of specific interventions or intensive care support in a timely manner, as well as for improving prognosis. This indicates the importance of predicting the severity of AHTGP[8].

At present, four commonly used AP scoring systems are available for the early identification of SAP, including the Acute Physiology and Chronic Health Evaluation (APACHE II), Ranson score, the Bedside Index of Severity in AP (BISAP), and the modified computed tomography (CT) severity index (MCTSI). However, they have limitations[9]. APACHE II collects a large number of parameters, making it complicated and inconvenient to use and poor at predicting disease within 24 h of disease onset. The Ranson score consists of 11 indicators, which must be evaluated upon admission and 48 h following admission. Some of these indicators are not routinely collected during early stages of AP, so early

prediction is difficult[10]. BISAP uses five indicators to determine AP severity 24 h after admission. It is easy to use but has low sensitivity for predicting SAP[11]. The MCTSI has outstanding performance in predicting local complications. But it is poor in predicting severity[12]. The AP prediction accuracy could be improved by combining several scoring systems, but it was inconvenient. Without a new scoring system, it was difficult to increase the prediction accuracy[13].

Moreover, many studies have demonstrated that single laboratory indicators can be used to predict the severity of AHTGP, such as the neutrophil-lymphocyte ratio (NLR), white blood cell (WBC) count, red blood cell distribution width (RDW), serum calcium (Ca^{2+}) and C-reactive protein (CRP), which are easy to use in practice but lack high sensitivity or specificity[2,14]. It should be noted that serum triglyceride (TG) levels dose-dependently worsen the outcome of AP[6], but there is still controversy[5]. Recently, several new clinical prediction models have been developed to predict the severity of AP[15,16]. The early achievable severity index (EASY) prediction score as an artificial intelligence model was recently developed based on machine learning for the early and easy prediction of severity in AP[17]. However, almost all of them were developed for all etiologies of pancreatitis and not for HTG-induced pancreatitis separately.

In conclusion, AHTGP may be associated with a more severe clinical course and greater mortality. Early prediction and detection of patients who are likely to develop SAP is of great importance. The purpose of this study is to develop and validate a fast, simple, accurate, and reproducible risk score for predicting severe AHTGP at an early stage.

MATERIALS AND METHODS

Patient selection and data processing

The study involved a retrospective review of 243 patients diagnosed with AHTGP who were admitted to the Intensive Care Unit of a gastroenterology department of Xuanwu Hospital from November 2012 to January 2022. All patients were diagnosed with AHTGP for the first time, and the possibility of other pancreatic diseases (recurrent AP, chronic pancreatitis, or pancreatic cancer) and cases with missing data were excluded. The following data were recorded: Basic demographics, medical history, vital signs, laboratory tests and X-ray of the chest within 24 h. Pancreatic examinations under CT or magnetic resonance imaging within 72 h. All patients received routine management after admission. This study was approved by the Ethics Committee of the Xuanwu Hospital of Capital Medical University; written informed consent was waived considering the retrospective study design.

Diagnosis and scoring systems

The diagnostic criteria for AHTGP were elevated TG level (> 11.30 mmol/L, or 5.65-11.30 mmol/L with lactescent serum) and two or more of the following three symptoms: (1) Abdominal pain consistent with AP; (2) Levels of amylase and/or lipase at least three times above the upper limit of normal; and (3) Abdominal imaging consistent with changes in AP. According to the Atlanta classification revised in 2012, AP severity was divided into three groups based on organ failure status and local and/or systemic complications. The absence of organ failure and local or systemic complications was considered to indicate mild AP (MAP). The presence of transient (within 48 h) organ failure and/or local complications or exacerbation of comorbid disease was regarded as moderately severe AP (MSAP). The presence of persistent (> 48 h) organ failure was considered to indicate SAP. The respiratory, cardiovascular, and renal systems were assessed to identify organ failure, which was defined as a modified Marshall score > 2 for one of these three systems. Acute peripancreatic fluid collection, pancreatic pseudocyst, acute necrotic collection, walled-off necrosis, and infected pancreatic necrosis were defined as local complications[18].

As part of the validation process, five scoring systems were compared to our risk prediction score. Within 24 h of admission, laboratory tests and radiological examinations were conducted to determine APACHE II and BISAP scores. The Ranson score was derived from laboratory tests performed within 48 h of admission. The MCTSI score was determined from CT scans performed within 72 h of admission. The EASY prediction score as an artificial intelligence model was recently developed to predict the severity of AP. It consists of four parts (personal details, anamnestic data, admission data and blood test results) with a total of 23 predictors. We calculated the predicted severity scores for all subjects on a web application (http://easy-app.org/) in the Streamlit Python-based framework.

Potential predictive variables

We selected 42 potential predictive variables based on the literature and previous clinical experience, including demographic variables, medical history, clinical signs, laboratory findings, and imaging results. Demographic variables included continuous and categorical variables: Age, body mass index (BMI), smoking status, and drinking habits. Medical history included categorical variables: Diabetes, hypertension, hyperlipemia, and fatty liver. Clinical signs included continuous variables: Respiratory rate (RR), heart rate (HR), systolic blood pressure, and diastolic blood pressure. Laboratory findings performed within 24 h of admission included WBC, NLR[14], RDW[19], platelet counts (PLT), mean

platelet volume (MPV)[20], platelet distribution width (PDW)[21], total cholesterol (TC)[22], TG[6], high-density lipoprotein cholesterol level to low-density lipoprotein cholesterol level ratio (H/L ratio)[23], apolipoprotein A1 (ApoA1)[24], total bilirubin (TBIL), aspartate transaminase (AST), alanine aminotransferase (ALT), alkaline phosphatase (ALP), albumin (ALB)[25], blood urea nitrogen (BUN)[24], serum creatinine (Cr)[26], free triiodothyronine (fT3)[27], CRP, procalcitonin (PCT), serum sodium (Na), serum potassium (K), serum Ca^{2+}, prothrombin time (PT), activated partial thromboplastin time (APTT), thrombin time (TT), fibrinogen (FIB)[28], and D-dimer levels[29]. Imaging results included the presence of a pleural effusion according to the chest X-ray within 24 h of admission[30].

Outcomes

We defined the severity of AHTGP according to the revised Atlanta classification given the extensive acceptance of this guideline[18]. SAP was defined as persistent organ failure and was used as the clinical outcome measure.

Statistical analysis

Statistical comparisons between the non-SAP (MAP + MSAP) and SAP groups were performed with analysis of variance or the Mann–Whitney U test for continuous variables and the chi-square test or Fisher's exact test for categorical variables. There were 42 variables entered into the selection process, as described here. Least absolute shrinkage and selection operator (LASSO) regression was applied to minimize the potential collinearity of variables measured from the same patient and overfitting of variables. The most predictive covariates were selected by the minimum (λ min). Subsequently, variables identified by LASSO regression analysis and some other important clinical variables were entered into univariable and multivariable logistic regression analyses for further predictor selection. Clinical patient samples were randomly divided (3:1) into development and validation cohorts. We constructed a nomogram and validated the accuracy estimates by using 1000 bootstrap resamples to reduce overfitting. To quantify the discrimination performance of the nomogram for predicting SAP, the concordance index (C-index) was measured in the development set and validation cohort. By plotting the calibration curve, we analyzed the relationship between the observed incidence and predicted probability in the development set and the validation set. Integrated discrimination improvement (IDI) was established to evaluate the improvement of the risk prediction score with other existing scoring systems in the whole set. Decision curve analysis (DCA) was applied to quantify the clinical usefulness of the nomogram in the whole set. All statistical analyses were performed by R software (https://www.r-project.org/, The R Foundation) and Empower-Stats software (http://www.empowerstats.com, X&Y Solutions, Inc., Boston, MA, United States).

Risk group

To determine the risk stratification classification for AHTGP, the best cutoff value for SAP calculated through the ROC curve was used to divide patients into high-risk and low-risk groups. The differences in clinical manifestations and prognoses between the high- and low-risk groups were also compared to evaluate the efficacy of our risk score.

RESULTS

Clinical characteristics

A total of 243 records from patients diagnosed with AHTGP and discharged from the intensive care units (ICUs) during our study period were included for analysis. The baseline characteristics of the study population are summarized in Table 1. The average age of the entire cohort was 40.12 ± 10.12 years, and there were more males (n = 188, 77.37%) than females (n = 55, 22.63%). We divided our AP patients into two groups, non-SAP (MAP + MSAP) and SAP. The total rate of SAP was 25.51%. There was no significant difference in age, sex or BMI between the two groups. Furthermore, there was no significant difference in medical history between the two groups. In terms of vital signs, patients with SAP had a significantly higher heart rate (92.23 ± 16.29 *vs* 107.58 ± 18.65, $P < 0.001$) and respiratory rate (20.47 ± 4.38 *vs* 25.27 ± 6.21, $P < 0.001$) index than patients in the non-SAP group. Patients in the two groups showed no significant differences in laboratory findings, including PLT, MPV, H/L ratio, TBIL, ALT, ALP, fT3, Na, K, and TT. However, there were differences in WBC, NLR, RDW, PDW, TC, TG, ApoA1, AST, ALB, BUN, Cr, CRP, PCT, ESR, Ca^{2+}, PT, APTT, FIB, and D-dimer. For imaging results, pleural effusions were significantly more frequently observed among SAP patients (12.71% *vs* 74.19%, $P < 0.001$).

Predictor selection

Forty-two variables measured at the hospital within 24 h of admission were included in the LASSO regression. After LASSO regression selection (Figure 1), with a lambda of 0.028, 10 variables remained significant predictors of SAP, including age, HR, RR, ApoA1, WBC, Bun, Cr, Ca^{2+}, D-dimer, and the

Table 1 Demographic and clinical characteristics of patients in the non-severe acute pancreatitis and severe acute pancreatitis groups

Patient characteristics	All (*n* = 243)	Non-SAP (*n* = 181)	SAP (*n* = 62)	*P* value
Demographic variables				
Sex, *n* (%)				0.297
Male	188 (77.37)	143 (79.00)	45 (72.60)	
Female	55 (22.63)	38 (21.00)	17 (27.40)	
Age (yr)	40.12 ± 10.12	39.60 ± 10.10	41.60 ± 10.20	0.190
BMI (kg/m^2)	28.27 ± 4.25	28.10 ± 4.00	28.70 ± 4.90	0.367
Medical history				
Diabetes, *n* (%)				0.648
Yes	139 (57.20)	102 (56.40)	37 (59.70)	
No	104 (42.80)	79 (43.65)	25 (40.30)	
Hypertension, *n* (%)				0.164
Yes	59 (24.28)	48 (26.50)	11 (17.70)	
No	184 (75.72)	133 (73.50)	51 (82.30)	
Hyperlipidemia, *n* (%)				0.250
Yes	152 (62.55)	64 (35.40)	27 (43.50)	
No	91 (37.45)	64 (35.40)	27 (43.50)	
Fatty liver, *n* (%)				0.073
Yes	185 (76.13)	143 (79.00)	42 (67.70)	
No	58 (23.87)	38 (21.00)	20 (32.30)	
Drinking, *n* (%)				0.483
Yes	120 (49.38)	87 (48.10)	33 (53.20)	
No	123 (50.62)	94 (51.90)	29 (46.80)	
Smoking, *n* (%)				0.386
Yes	133 (54.73)	102 (56.40)	31 (50.00)	
No	110 (45.27)	79 (43.60)	31 (50.00)	
Clinical signs				
HR (bpm)	96.14 ± 18.17	92.23 ± 16.30	107.58 ± 18.65	< 0.001
R (bpm)	21.66 ± 5.33	20.47 ± 4.38	25.27 ± 6.21	< 0.001
SBP (mmHg)	133.50 ± 17.52	133.51 ± 16.56	133.48 ± 20.21	0.992
DBP (mmHg)	81.13 ± 12.03	80.85 ± 11.28	81.92 ± 14.08	0.548
		Non-SAP (*n* = 181, 74.49%)	**SAP (*n* = 62, 25.51%)**	
Laboratory findings				
WBC (× 10^9/L)	12.53 ± 3.86	11.96 ± 3.63	14.41 ± 3.97	< 0.001
NLR	9.94 ± 7.27	8.82 ± 6.98	13.19 ± 7.15	< 0.001
RDW (fL)	12.87 ± 0.72	12.80 ± 0.69	13.08 ± 0.78	0.009
PLT (× 10^9/L)	218.91 ± 61.98	216.09 ± 57.99	227.15 ± 72.30	0.226
MPV (fL)	10.75 ± 1.05	10.68 ± 1.01	10.95 ± 1.14	0.074
PDW (fL)	12.66 ± 2.22	12.47 ± 2.09	13.23 ± 2.47	0.018
TC (mmol/L)	10.15 ± 4.11	9.54 ± 3.62	11.94 ± 4.92	< 0.001
TG (mmol/L)	21.08 ± 7.50	20.17 ± 7.31	23.75 ± 7.49	0.001
H/L ratio	0.96 ± 1.36	0.96 ± 1.36	0.97 ± 1.36	0.946

ApoA1 (g/L)	1.02 ± 0.35	1.11 ± 0.34	0.75 ± 0.23	< 0.001
TBIL (μmol/L)	14.16 ± 8.29	13.81 ± 7.11	15.16 ± 11.03	0.987
AST (U/L)	29.78 ± 17.41	27.40 ± 13.03	36.76 ± 25.20	< 0.001
ALT (U/L)	31.04 ± 28.70	30.80 ± 29.94	31.73 ± 24.94	0.826
ALP (U/L)	73.91 ± 25.30	73.59 ± 22.70	74.84 ± 31.88	0.737
ALB (g/L)	41.57 ± 5.91	42.22 ± 5.53	39.66 ± 6.58	0.003
BUN mmol/L	4.32 ± 2.03	4.05 ± 1.39	5.10 ± 3.12	< 0.001
Cr (μmol/L)	62.62 ± 42.98	56.64 ± 15.83	80.10 ± 78.56	< 0.001
fT3 (pmol/L)	1.97 ± 0.37	1.99 ± 0.36	1.91 ± 0.41	0.134
CRP (mg/L)	160.20 ± 127.36	133.55 ± 112.64	237.99 ± 136.59	< 0.001
PCT (ng/mL)	0.80 ± 1.93	0.59 ± 1.72	1.42 ± 2.35	0.003
ESR (mm/h)	42.57 ± 24.76	40.71 ± 25.10	47.99 ± 23.06	0.045
Na (mmol/L)	133.97 ± 4.29	134.28 ± 4.09	133.07 ± 4.76	0.054
K (mmol/L)	4.02 ± 0.46	3.97 ± 0.35	4.19 ± 0.67	0.080
Ca^{2+} (mmol/L)	2.13 ± 0.26	2.19 ± 0.18	1.96 ± 0.36	< 0.001
PT (s)	13.26 ± 0.98	13.12 ± 0.84	13.68 ± 1.21	< 0.001
APTT (s)	37.82 ± 5.28	37.35 ± 5.14	39.22 ± 5.45	0.016
TT (s)	15.07 ± 1.10	15.08 ± 1.09	15.05 ± 1.13	0.823
FIB (g/L)	5.70 ± 2.21	5.41 ± 2.10	6.56 ± 2.32	< 0.001
D-dimer (μg/L)	1.34 ± 1.83	0.94 ± 0.98	2.51 ± 2.94	< 0.001
Imaging results				
Pleural effusion, *n* (%)				< 0.001
Yes	69 (28.40)	23 (12.71)	46 (74.19)	
No	174 (71.61)	158 (87.30)	16 (25.81)	

BMI: Body mass index; RR: Respiratory rate; HR: Heart rate; SBP: Systolic blood pressure; DBP: Diastolic blood pressure; SAP: Severe acute pancreatitis; Non-SAP: Mild acute pancreatitis and moderately sever acute pancreatitis; WBC: White blood cell; NLR: Neutrophil to lymphocyte ratio; RDW: Red blood cell distribution width; PLT: Platelet counts; RDW: MPV Mean platelet volume; PDW: Platelet distribution width; TC: Total cholesterol; TG: Triglyceride; HDL-C: High-density lipoprotein cholesterol; LDL-C: Low-density lipoprotein cholesterol; ApoA1: Apolipoprotein A1; TBIL: Total bilirubin; AST: Aspartate transaminase; ALT: Alanine aminotransferase; ALP: Alkaline phosphatase; ALB: Albumin; BUN: Blood urea nitrogen; Cr: Creatinine; fT3: Free triiodothyronine; CRP: C-reactive protein; PCT: Procalcitonin; Na: Sodium; K: Potassium; Ca^{2+}: Calcium; PT: Prothrombin time; APTT: Activated partial thromboplastin time; TT: Thrombin time; FIB: Fibrinogen; SAP: Severe acute pancreatitis; Non-SAP: Mild acute pancreatitis and moderately sever acute pancreatitis.

presence of pleural effusion. According to a previous study, TG levels dose-dependently increase the severity of AP[6]. The presence of metabolic syndrome and its components associated with increasing AP severity were also important factors[31,32]. Therefore, we included TG level, BMI, history of hypertension and diabetes in the regression analysis. Based on the Endocrine Society Clinical Practice Guideline and previously published study, we divided TG levels into three groups as classified by variables (group 1: < 11.3 mmol/L; group 2: 11.3-22.59 mmol/L; group 3: ≥ 22.6 mmol/L) for clinical use [6].

Univariable and multivariable logistic regression

Inclusion of these 14 variables in a logistic regression model resulted in four variables that were independently statistically significant predictors of SAP (Table 2): Age (OR: 1.07; 95%CI: 1.01-1.14; P = 0.033), ApoA1 (OR: 0.02; 95%CI: 0.00-0.12; P < 0.0001), Ca^{2+} (OR: 0.11; 95%CI: 0.01-0.90; P = 0.040) and the presence of pleural effusion (OR: 15.61; 95%CI: 5.05-48.24; P < 0.0001).

Construction and validation of the nomogram

Clinical patient samples were randomly divided (3:1) into development and validation cohorts. Due to the small sample size, we used 1000 bootstrap resamples for development and validation to reduce over-the-fit bias. The multivariable analyses demonstrated that age, the reduction in ApoA1 and Ca^{2+}, and the presence of pleural effusion were independent risk factors for SAP. Considering that the level of

Table 2 Univariable and multivariable logistic regression analyses of predictive factors for severe acute pancreatitis in all subjects

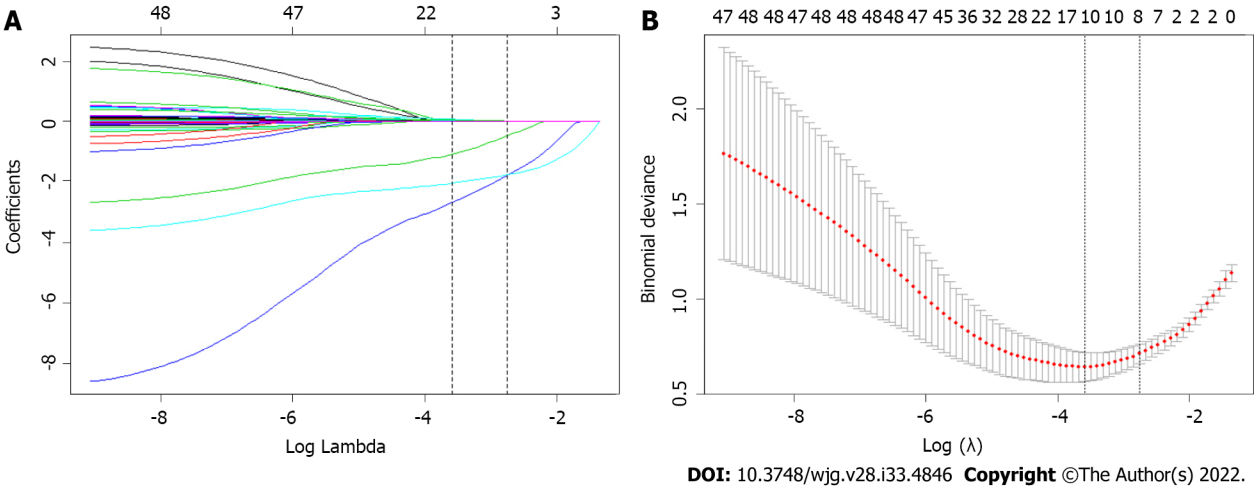
Variables	Univariable regression		Multivariable regression	
	OR (95%CI)	*P* value	OR (95%CI)	*P* value
Age	1.02 (0.99-1.05)	0.190	1.07 (1.01-1.14)	0.033
BMI (kg/m^2)	1.03 (0.96-1.10)	0.366	1.08 (0.94-1.24)	0.278
Hypertension				
No	1.00		1.00	
Yes	0.60 (0.29-1.24)	0.167	1.02 (0.99-1.06)	0.201
Diabetes				
No	1.00		1.00	
Yes	1.15 (0.64-2.06)	0.648	1.27 (0.38-4.24)	0.693
HR (bpm)	1.05 (1.03-1.07)	< 0.0001	1.02 (0.99-1.06)	0.201
RR (bpm)	1.20 (1.12-1.28)	< 0.0001	1.12 (0.99-1.26)	0.068
TG (mmol/L)				
< 11.3	1.00		1.00	
11.3-22.6	2.06 (0.57-7.49)	0.273	4.20 (0.40-44.25)	0.232
≥ 22.6	3.43 (0.96-12.20)	0.057	5.95 (0.56-62.75)	0.138
ApoA1 (g/L)	0.01 (0.00-0.05)	< 0.0001	0.02 (0.00-0.12)	< 0.0001
Cr (μmol/L)	1.02 (1.01-1.03)	0.002	1.01 (0.99-1.02)	0.458
Bun (μmol/L)	1.27 (1.10-1.48)	0.001	1.29 (0.92-1.81)	0.145
WBC (× 10^9/L)	1.18 (1.09-1.28)	< 0.0001	1.08 (0.95-1.24)	0.248
Ca^{2+} (mmol/L)	0.02 (0.01-0.09)	< 0.0001	0.11 (0.01-1.02)	0.040
D-dimer (μg/L)	1.69 (1.35-2.12)	< 0.0001	1.24 (0.94-1.63)	0.122
Pleural effusion	19.75 (9.64-40.48)	< 0.0001	15.62 (5.05-48.24)	< 0.0001

BMI: Body mass index; RR: Respiratory rate; HR: Heart rate; SBP: Systolic blood pressure; WBC: White blood cell; ApoA1: Apolipoprotein A1; BUN: Blood urea nitrogen; Cr: Creatinine; Ca: Calcium; SAP: Severe acute pancreatitis; OR: Odds ratio.

TG, BMI and history of hypertension and diabetes may also be important predictors, we constructed three predictive models based on different combinations of these factors. The logistic regression function was as follows: Model 1 (including age, ApoA1, and pleural effusion): Log (odds of SAP) = -0.15 (constant) + 0.06 × age - 5.49 × ApoA1 + 3.57 × (pleural effusion = 1); Model 2 (including age, ApoA1, Ca^{2+} and pleural effusion): Log (odds of SAP) = 4.86 (constant) + 0.06 × age - 5.32 × ApoA1 - 2.40 × Ca^{2+} + 3.31 × (pleural effusion = 1); Model 3 (including age, diabetes, hypertension, BMI, TG, ApoA1 and pleural effusion): Log (odds of SAP) = -7.30 (constant) + 0.09 × age + 0.15 × BMI - 0.35 × (hypertension = 1) - 1.09 × (diabetes = 1) - 6.72 × ApoA1 + 3.98 × (pleural effusion = 1) +3.39 × (TG = 1) + 3.23 × (TG = 2). ROC curve analysis was applied to evaluate the diagnostic performance of the three predictive models (Supplementary Figure 1). Model 1 had no significant differences in receiver operating characteristic curves (AUCs) and IDI between Model 2 and Model 3 (Supplementary Table 1). For clinical convenience and easy application, we selected Model 1 with the fewest factors as the final risk prediction score and constructed the nomogram (referred to as AAP) (Figure 2). The C-index for the development and validation cohorts after bootstrapping were 0.930 (95%CI: 0.893-0.967) and 0.928 (95%CI: 0.867-0.990), respectively (Figure 3A and B). This suggested a nomogram with good discrimination. The calibration curve of the nomogram is presented in Figure 3C and D. Calibration plots fall on a 45-degree diagonal line, which shows good agreement between the predicted and actual probabilities in SAP patients in the development and validation cohorts.

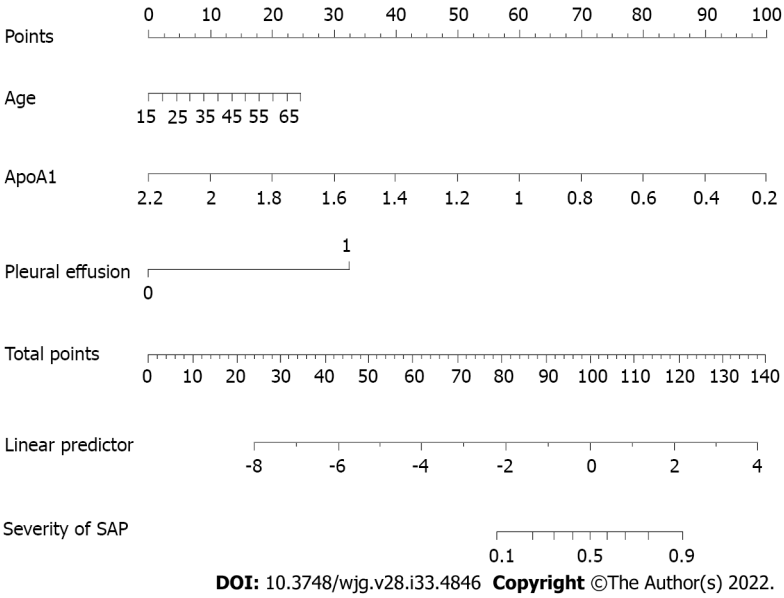
Clinical use

An ROC curve analysis was applied to evaluate the diagnostic efficacy of the new risk prediction score (referred to as AAP) and other clinical scoring systems, including the BISAP, Ranson, APACHE II, MCTSI and EASY. The AUC values of AAP, BISAP, RASON, APACHE II, MCTSI and EASY to predict SAP were 0.929 (95%CI: 0.889-0.958), 0.852 (95%CI: 0.801-0.894), 0.825 (95%CI: 0.771-0.871), 0.807



DOI: 10.3748/wjg.v28.i33.4846 **Copyright** ©The Author(s) 2022.

Figure 1 Feature selection using the least absolute shrinkage and selection operator binary logistic regression model. A: Least absolute shrinkage and selection operator (LASSO) coefficient profiles of the 42 baseline features; B: Tuning parameter (λ) selection in the LASSO model using 10-fold cross-validation *via* minimum criteria.



DOI: 10.3748/wjg.v28.i33.4846 **Copyright** ©The Author(s) 2022.

Figure 2 Nomogram for predicting severe acute pancreatitis for patients in the development cohort. SAP: Severe acute pancreatitis.

(95%CI: 0.752-0.855), 0.831 (95%CI: 0.778-0.876), and 0.807 (95%CI: 0.743-0.871), respectively (Figure 4). AAP achieved the highest AUC in predicting SAP among the scoring systems (Table 3). The improvement in the prediction of SAP was evaluated by calculating the IDI. IDIs were employed to compare the discriminative ability between the new model and the other clinical scoring systems. These results demonstrated that our nomogram has a greater potential for accurately predicting SAP than the other four clinical scoring systems (Table 4).

DCA was used to compare the clinical usability and benefits of the nomogram throughout the whole cohort. DCA plots showed that our nomogram had greater net benefits than other system scores for predicting the severity of AP patients, which demonstrated its utility in clinical decision-making (Figure 5).

Risk stratification based on the Nomogram for SAP

To determine the risk stratification classification for AP, the best cutoff value (88.16) for SAP calculated through the ROC curve was used to divide patients into high-risk and low-risk groups. We further analyzed the relationship between the AAP cutoff value (88.16) and clinical parameters. The high-risk group was closely related to local and system complications: Ranson ≥ 3, BISAP ≥ 3, MCTSI ≥ 4, APACHE-II ≥ 8, CRP ≥ 190, and the length of hospital stay (Table 5).

Table 3 Comparison of diagnostic performance for predicting severe acute pancreatitis between the AAP and other existing clinical scores

Variables	Δ AUC	95%CI	Z statistic	*P* value
AAP-APACHE II	0.122	0.057-0.187	3.661	0.000
AAP-BISAP	0.076	0.007-0.198	3.839	0.000
AAP-MCTSI	0.098	0.027-0.305	3.111	0.002
AAP-Ranson	0.104	0.048-0.159	3.670	0.000
AAP-EASY	0.122	0.056-0.188	3.606	0.000

AAP: Our risk prediction score referred to as AAP; EASY: EASY prediction score; Δ AUC: Difference of areas under curve between AAP and other clinical scores; SE: Standard error; CI: Confidence interval; SAP: Severe acute pancreatitis.

Table 4 Diagnostic performance of the integrated discrimination improvement between the AAP and other clinical scores

Variables	IDI	SE	95%CI	Z statistic	*P* value
AAP-APACHE-II	0.201	0.077	0.050-0.352	2.601	0.009
AAP-BISAP	0.095	0.052	0.037-0.115	1.828	0.068
AAP-MCTSI	0.166	0.071	0.036-0.160	2.339	0.019
AAP-Ranson	0.216	0.063	0.093-0.338	3.444	0.001
AAP-EASY	0.205	0.082	0.045-0.365	2.513	0.012

IDI: Integrated discrimination improvement; SE: Standard error; CI: Confidence interval; AAP: Our risk prediction score referred to as AAP; EASY: EASY prediction score; SAP: Severe acute pancreatitis.

DISCUSSION

AHTGP has grown in incidence and importance. According to the previously published literature, HTG is the third most common cause of AP[6]. Clinically, AHTGP is similar to other forms of AP, but it is associated with significantly higher complication rates, severity, and mortality[5,6]. Thus, recognizing risk factors for severe AHTGP in the early stages is very important for triaging patients appropriately to ICUs and providing specific treatments. In the present study, we developed a convenient and specific nomogram based on three predictors for predicting the severity of patients with AHTGP. The nomogram showed great calibration and discriminatory abilities in both the development and validation groups. In addition, our nomogram has shown improved prognostic reliability, accuracy and the best net benefit when compared to other clinical scoring systems, such as BISAP, Ranson, APACHE II, CTSI and an artificial intelligence model, the EASY prediction score. Moreover, the model could distinguish patients into low-risk and high-risk groups according to the best cutoff point (88.16). Patients with higher scores had a higher probability of developing SAP than those with lower scores. The cutoff point can help doctors in making medical decisions.

As mentioned in the introduction, four commonly used AP scoring systems, including APACHE II, Ranson, BISAP, and MCTSI, have limitations on their abilities to identify SAP early. According to our results, our prediction score AAP has three easily available parameters lower than other scoring systems, which is easy for clinical application. Meanwhile, it has better performance in diagnostic efficacy and clinical decision-making for patients with AHTGP. It is worth mentioning that an artificial intelligence model-EASY prediction score consisting of 23 parameters was developed recently based on a multicenter, multinational, prospective and observational study[17]. We applied this model to our research population. Although it achieved a high AUC in predicting SAP, it was still the lowest among the AAP and four commonly used AP scoring systems. This may suggest that the prediction ability of the EASY model is limited for pancreatitis caused by HTG.

Notably, we introduced a new predictor, ApoA1, into our risk score compared with other clinical scoring systems. Recent studies have shown a negative correlation between ApoA1 and the severity of AP, and decreased serum levels of ApoA1 have been linked to the occurrence of SAP in patients[24,33]. The mechanism can be explained as follows: In SAP patients, excessive inflammatory cytokines inhibit synthesis. Recent studies showed a negative correlation between ApoA1 and the severity of AP, and decreased serum levels of ApoA1 have been linked to the occurrence of SAP in patients and lead to lipoprotein degradation[34]. Our previous study showed that the best cutoff point of ApoA1 for

Table 5 The relationship between risk stratification and clinical parameters

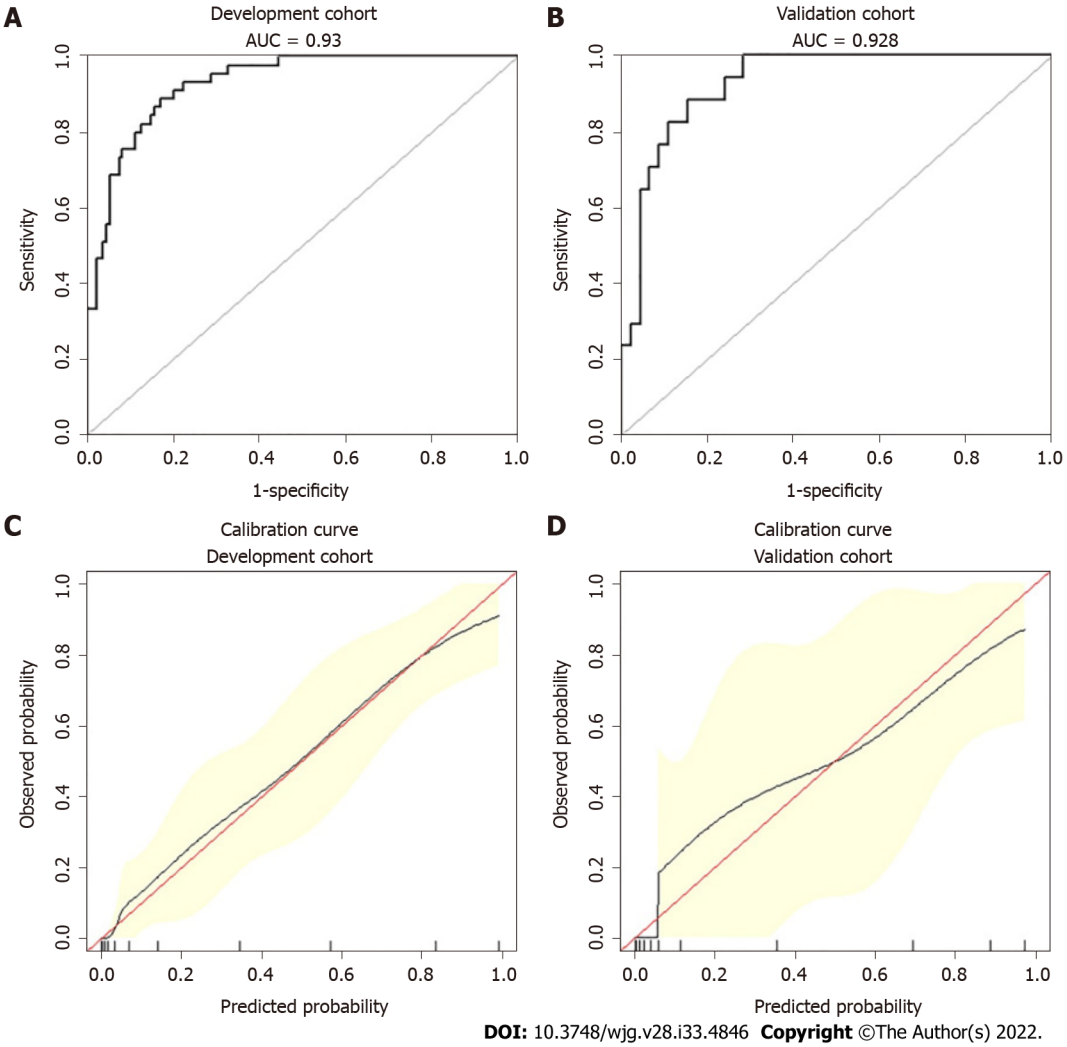
	Low-risk group (*n* = 158)	High-risk group (*n* = 85)	*P* value
Local complications			
APFC	43 (27.22%)	68 (80.00%)	< 0.001
PPC	3 (1.90%)	10 (11.77%)	0.001
ANC	3 (1.90%)	22 (25.88%)	< 0.001
WON	0 (0.00%)	4 (4.71%)	0.014
Systemic complications			
SIRS	92 (58.23%)	72 (84.71%)	< 0.001
Respiratory failure	29 (18.35%)	59 (69.41%)	< 0.001
Renal failure	0 (0.00%)	13 (15.29%)	< 0.001
Cardiovascular failure	2 (1.27%)	5 (5.88%)	0.040
Clinical Scoring Systems			
Ranson ≥ 3	28 (17.72%)	53 (62.35%)	< 0.001
BISAP ≥ 3	0 (0.00%)	4 (4.71%)	0.014
MCTSI ≥ 4	15 (9.49%)	53 (62.35%)	< 0.001
APACHE-II ≥ 8	73 (46.20%)	68 (80.00%)	< 0.001
CRP ≥ 190	42 (26.58%)	44 (51.77%)	< 0.001
Hospital day, days	13.51 ± 5.45	20.04 ± 8.14	< 0.001

APFC: Acute peripancreatic fluid collection; PPC: Pancreatic pseudocyst; ANC: Acute necrotic collection; WON: Walled-off necrosis; IPN: Infected pancreatic necrosis; SIRS: Systemic inflammatory response syndrome.

predicting severe acute hyperlipidemic pancreatitis was 0.8 g/L, whose sensitivity, specificity and Youden index were 0.877, 0.674 and 0.55, respectively[35]. Another study performed by Li *et al*[33] showed that ApoA1 predicts the optimal critical value of SAP to be 0.8 g/L, whose sensitivity, specificity and Youden index were 0.551, 0.757 and 0.693, respectively[33]. Therefore, ApoA1 has been found to be a reliable and validated indicator of SAP. Therefore, ApoA1 included in our model could increase the specificity and sensitivity of the nomogram.

Pleural effusion is one of the most common thoracic complications in AP patients. According to recent studies, the prevalence ranges from 46.0% to 72.3%[36]. The disruption of the pancreatic duct may result in leakage of pancreatic secretions directly into the peritoneal cavity *via* the transdiaphragmatic lymphatic channels[37]. According to the up-to-date revised Atlanta criteria, pleural effusion is a strong individual predictor of SAP. Additionally, pleural effusion is a valuable indicator of BISAP score. Yan *et al*[30] showed that on the basis of PEV, the AUC of 0.816 for predicting severe AP, with a threshold of 69.00 mL, and the sensitivity and specificity were 84.23% and 81.07, respectively. According to this study, pleural effusion volume can serve as a clinical biomarker to predict the severity and outcome of AP[30].

The evidence indicates that patients with HTG present a more severe form of pancreatitis. A previous study confirmed that HTG dose-dependently increases the complications and severity of AP[6]. However, a meta-analysis including 11965 patients from 16 eligible studies found no significant difference in AP severity based on the extent of HTG[5]. This study also explored the association between HTG levels and the severity of AHTGP. Compared to patients with TGs lower than 11.3 mmol/L, we found that patients with TGs above 22.6 mmol/L had a higher OR (OR: 5.95; 95%CI: 0.56-62.75; P = 0.232) than patients with TGs between 11.3 and 22.59 mmol/L (OR: 4.20; 95%CI: 0.40-44.25; P = 0.138). We speculated that there was a trend for HTG to dose-dependently increase the severity of AHTGP. Previous studies showed that the presence of metabolic syndrome and its components, including obesity, diabetes and hypertension, were significantly associated with increasing AP severity [31,32]. Our study showed that there was a trend that the presence of obesity (OR: 1.08; 95%CI: 0.94-1.24; P = 0.278), diabetes (OR: 1.27; 95%CI: 0.38-4.24; P = 0.693) and hypertension (OR: 1.02; 95%CI: 0.99-1.06; P = 0.201) increased the risk of SAP. However, the P values were not significant, probably because of our small sample size. The small sample size of our study makes it difficult to make extensive recommendations. The next step is to conduct a multicenter prospective cohort study with a large sample size to further explore this important issue.



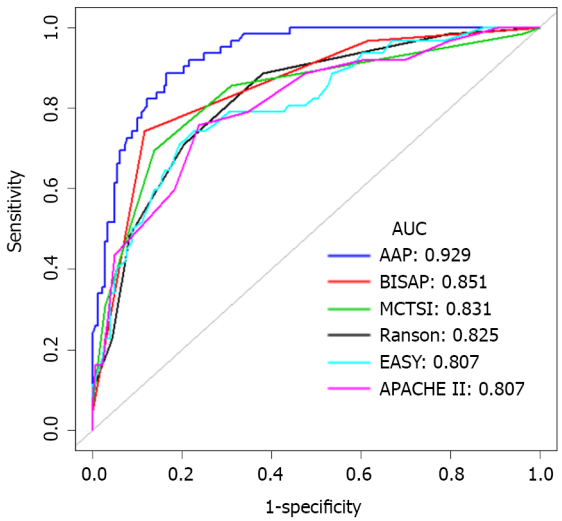
DOI: 10.3748/wjg.v28.i33.4846 **Copyright** ©The Author(s) 2022.

Figure 3 Receiver operating characteristic curves and calibration curves of the nomogram for predicting severe acute pancreatitis. A: Receiver operating characteristic curves (AUCs) in the development group; B: AUC in the validation group; C: Calibrations of the nomogram for predicting severe acute pancreatitis (SAP) in the development group; D: Calibrations of the nomogram for predicting SAP in the validation group.

The novelties and strengths of our study include the following: To the best of our knowledge, this is the first study attempting to develop a risk prediction score for HTG-induced pancreatitis. We also compared the risk prediction score with existing scoring systems in a sample of Chinese patients for predicting the severity of AHTGP. Although the established and validated nomogram in our study may provide a convenient and specific tool to assist physicians in clinical decisions, there are some limitations to be taken into account. First, this study was retrospective, so selection and detection bias could exist. Second, it was a single-center study with a small sample size, which lacked multicenter data verification. There is a need to externally validate the risk score prior to clinical use. Furthermore, the data used to develop and validate the score are all from China, which limits their generalizability to other parts of the world.

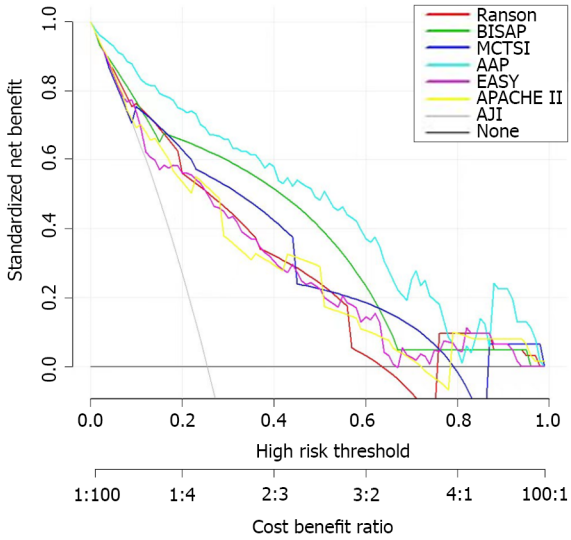
CONCLUSION

In this study, we developed a risk score to estimate the prediction of developing SAP among patients with AHTGP based on three variables commonly measured on admission to the hospital. Estimating the risk score could help identify patients who are likely to develop SAP at an early stage. It could be of great value in guiding clinical decisions as a convenient and specific tool and optimizing the use of medical resources by supporting appropriate treatment.



DOI: 10.3748/wjg.v28.i33.4846 **Copyright** ©The Author(s) 2022.

Figure 4 Receiver operating characteristic curves for the AAP and other existing clinical scoring systems, such as Bedside Index of Severity in acute pancreatitis, Ranson, Acute Physiology and Chronic Health Evaluation II), modified computed tomography severity index and early achievable severity index prediction scores. AAP: Our risk prediction score referred to as AAP; EASY: The EASY prediction score is an artificial intelligence model for predicting the severity of acute pancreatitis.



DOI: 10.3748/wjg.v28.i33.4846 **Copyright** ©The Author(s) 2022.

Figure 5 Decision curve analysis for the nomogram. AAP: Our risk prediction score referred to as AAP; EASY: The EASY prediction score is an artificial intelligence model for predicting the severity of acute pancreatitis.

ARTICLE HIGHLIGHTS

Research background

The frequency of acute hypertriglyceridemic pancreatitis (AHTGP) is in-creasing worldwide. AHTGP may be associated with a more severe clinical course and greater mortality than pancreatitis caused by other causes. Early identification of patients with severe inclination is essential for clinical deci-sion-making and improving prognosis. Hence, constructing a risk prediction score with high predictive accuracy and clinical utility for assessing the severity of AHTGP patients is of great importance.

Research motivation

Early prediction and detection of AHTGP patients who are likely to develop severe acute pancreatitis (SAP) is of great importance. Almost of existing clinical scores were developed for all etiologies of pancreatitis and not for hypertriglyceridemia (HTG)-induced pancreatitis separately. To the best of our knowledge, this is the first study attempting to develop a risk prediction score for HTG-induced pancreatitis. This risk score may help guide clinical decisions for these patients.

Research objectives

The purpose of this study was to establish a risk prediction score with easy use and high performance for predicting the severity of AHTGP patients in China, which will help doctors make rational clinical decisions.

Research methods

We performed a retrospective study of patients with AHTGP. Least absolute shrinkage and selection operator and logistic regression were used to screen predictive variables to construct a nomogram for predicting the severity of AHTGP. The predictive accuracy of the nomogram was estimated using the concordance index. The performance of the nomogram was estimated using a calibration curve. We evaluated the predictive accuracy and net benefit of the risk score and compared it with existing scoring systems *via* receiver operating characteristic curve analysis and decision curve analysis. We used the best cutoff value for SAP to determine the risk stratification classification.

Research results

A risk prediction score consisting of three predictors commonly measured on admission was constructed to predict the severity of SAP. More importantly, our nomogram exhibited high predictive accuracy and good performance. In addition, our nomogram has shown improved prognostic reliability, accuracy and the best net benefit when compared to other clinical scoring systems, such as Bedside Index of Severity in AP, Ranson, Acute Physiology and Chronic Health Evaluation II, modified computed tomography severity index and an artificial intelligence model, the early achievable severity index prediction score. Moreover, the risk prediction score could distinguish patients into low-risk and high-risk groups according to the best cutoff point. The cutoff point can help doctors in making medical decisions.

Research conclusions

This risk prediction score have potential usefulness in predicting the presence of SAP at an early stage. It could be of great value in guiding clinical decisions as a convenient and specific tool and optimizing the use of medical resources by supporting appropriate treatment.

Research perspectives

To the best of our knowledge, this is the first study attempting to develop a risk prediction score for HTG-induced pancreatitis. But, this was a single-center study with a small sample size, which lacked multi-center data verification. The next step is to conduct a multicenter prospective cohort study with a large sample size to construct specific risk score and externally validate the risk score prior to clinical use.

ACKNOWLEDGEMENTS

The authors express special thanks to Gui-Qi Zhu (Department of Liver Surgery, Liver Cancer Institute, Zhongshan Hospital, Fudan University, Shanghai, 200032, China) for his advice on data analysis.

FOOTNOTES

Author contributions: Liu ZY and Zhai HH designed the current study as the principal investigators; Liu ZY and Tian L were involved in the study conception and design; Hao LJ, Shen WW and Gao YQ collected data; Liu ZY, Sun XY and Liu ZS drafted the plans for the data analyses, conducted statistical analyses and interpreted the data; Liu ZY drafted the manuscript; Tian L was responsible for language editing; All authors were involved in interpretation of the results and revision of the manuscript, and all approved the final version of the manuscript, the corresponding author attests that all the listed authors meet the authorship criteria and that no others meeting the criteria have been omitted.

Supported by 2021 National Natural Youth Cultivation Project of Xuanwu Hospital of Capital Medical University, No. QNPY2021018.

Institutional review board statement: This study was reviewed and approved by the Ethics Committee of the Xuanwu Hospital of Capital Medical University, No. 2022102.

Informed consent statement: Written informed consent was waived considering the retrospective study design.

Conflict-of-interest statement: All the authors report no relevant conflicts of interest for this article.

Data sharing statement: The clinical data was available from the corresponding author at zhaihuihong@263.net. And

no additional data are available.

Open-Access: This article is an open-access article that was selected by an in-house editor and fully peer-reviewed by external reviewers. It is distributed in accordance with the Creative Commons Attribution NonCommercial (CC BY-NC 4.0) license, which permits others to distribute, remix, adapt, build upon this work non-commercially, and license their derivative works on different terms, provided the original work is properly cited and the use is non-commercial. See: https://creativecommons.org/Licenses/by-nc/4.0/

Country/Territory of origin: China

ORCID number: Zi-Yu Liu 0000-0002-4095-3346; Lei Tian 0000-0002-5609-0098; Xiang-Yao Sun 0000-0001-9385-2402; Zong-Shi Liu 0000-0003-2431-8374; Li-Jie Hao 0000-0002-9130-9542; Wen-Wen Shen 0000-0002-2495-3530; Yan-Qiu Gao 0000-0001-7670-2381; Hui-Hong Zhai 0000-0002-8452-6311.

S-Editor: Fan JR
L-Editor: A
P-Editor: Fan JR

REFERENCES

1 **Hassanloo J**, Béland-Bonenfant S, Paquette M, Baass A, Bernard S. Prevalence, severity and management of hypertriglyceridemia-associated pancreatitis; A 7-year retrospective cohort study at canadian quaternary care hospitals. *J Clin Lipidol* 2022 [PMID: 35659855 DOI: 10.1016/j.jacl.2022.05.064]
2 **Sun YM**, Gao F, Chen X, Zhang J. The relationship between triglyceride level and the severity of acute hypertriglyceridemic pancreatitis in Chinese patients. *Turk J Gastroenterol* 2020; **31**: 633-639 [PMID: 33090100 DOI: 10.5152/tjg.2020.18335]
3 **Zheng Y**, Zhou Z, Li H, Li J, Li A, Ma B, Zhang T, Liao Q, Ye Y, Zhang Z, Yang Y, Wang Z, Yang J, Li F. A multicenter study on etiology of acute pancreatitis in Beijing during 5 years. *Pancreas* 2015; **44**: 409-414 [PMID: 25438072 DOI: 10.1097/MPA.0000000000000273]
4 **Tai WP**, Lin XC, Liu H, Wang CH, Wu J, Zhang NW, Chen W. A Retrospective Research of the Characteristic of Hypertriglyceridemic Pancreatitis in Beijing, China. *Gastroenterol Res Pract* 2016; **2016**: 6263095 [PMID: 26880892 DOI: 10.1155/2016/6263095]
5 **Kiss L**, Fűr G, Mátrai P, Hegyi P, Ivány E, Cazacu IM, Szabó I, Habon T, Alizadeh H, Gyöngyi Z, Vigh É, Erőss B, Erős A, Ottoffy M, Czakó L, Rakonczay Z Jr. The effect of serum triglyceride concentration on the outcome of acute pancreatitis: systematic review and meta-analysis. *Sci Rep* 2018; **8**: 14096 [PMID: 30237456 DOI: 10.1038/s41598-018-32337-x]
6 **Mosztbacher D**, Hanák L, Farkas N, Szentesi A, Mikó A, Bajor J, Sarlós P, Czimmer J, Vincze Á, Hegyi PJ, Erőss B, Takács T, Czakó L, Németh BC, Izbéki F, Halász A, Gajdán L, Hamvas J, Papp M, Földi I, Fehér KE, Varga M, Csefkó K, Török I, Farkas HP, Mickevicius A, Maldonado ER, Sallinen V, Novák J, Ince AT, Galeev S, Bod B, Sümegi J, Pencik P, Dubravcsik Z, Illés D, Gódi S, Kui B, Márta K, Pécsi D, Varjú P, Szakács Z, Darvasi E, Párniczky A, Hegyi P; Hungarian Pancreatic Study Group. Hypertriglyceridemia-induced acute pancreatitis: A prospective, multicenter, international cohort analysis of 716 acute pancreatitis cases. *Pancreatology* 2020; **20**: 608-616 [PMID: 32402696 DOI: 10.1016/j.pan.2020.03.018]
7 **Harshit Kumar A**, Singh Griwan M. A comparison of APACHE II, BISAP, Ranson's score and modified CTSI in predicting the severity of acute pancreatitis based on the 2012 revised Atlanta Classification. *Gastroenterol Rep (Oxf)* 2018; **6**: 127-131 [PMID: 29780601 DOI: 10.1093/gastro/gox029]
8 **de Pretis N**, Amodio A, Frulloni L. Hypertriglyceridemic pancreatitis: Epidemiology, pathophysiology and clinical management. *United European Gastroenterol J* 2018; **6**: 649-655 [PMID: 30083325 DOI: 10.1177/2050640618755002]
9 **Cho JH**, Kim TN, Chung HH, Kim KH. Comparison of scoring systems in predicting the severity of acute pancreatitis. *World J Gastroenterol* 2015; **21**: 2387-2394 [PMID: 25741146 DOI: 10.3748/wjg.v21.i8.2387]
10 **Wang L**, Zeng YB, Chen JY, Luo Q, Wang R, Zhang R, Zheng D, Dong YH, Zou WB, Xie X, Du YQ, Li ZS. A simple new scoring system for predicting the mortality of severe acute pancreatitis: A retrospective clinical study. *Medicine (Baltimore)* 2020; **99**: e20646 [PMID: 32502051 DOI: 10.1097/MD.0000000000020646]
11 **Yang YX**, Li L. Evaluating the Ability of the Bedside Index for Severity of Acute Pancreatitis Score to Predict Severe Acute Pancreatitis: A Meta-Analysis. *Med Princ Pract* 2016; **25**: 137-142 [PMID: 26613249 DOI: 10.1159/000441003]
12 **Yang L**, Liu J, Xing Y, Du L, Chen J, Liu X, Hao J. Comparison of BISAP, Ranson, MCTSI, and APACHE II in Predicting Severity and Prognoses of Hyperlipidemic Acute Pancreatitis in Chinese Patients. *Gastroenterol Res Pract* 2016; **2016**: 1834256 [PMID: 27882045 DOI: 10.1155/2016/1834256]
13 **Mounzer R**, Langmead CJ, Wu BU, Evans AC, Bishehsari F, Muddana V, Singh VK, Slivka A, Whitcomb DC, Yadav D, Banks PA, Papachristou GI. Comparison of existing clinical scoring systems to predict persistent organ failure in patients with acute pancreatitis. *Gastroenterology* 2012; **142**: 1476-82; quiz e15 [PMID: 22425589 DOI: 10.1053/j.gastro.2012.03.005]
14 **Huang L**, Chen C, Yang L, Wan R, Hu G. Neutrophil-to-lymphocyte ratio can specifically predict the severity of hypertriglyceridemia-induced acute pancreatitis compared with white blood cell. *J Clin Lab Anal* 2019; **33**: e22839 [PMID: 30737845 DOI: 10.1002/jcla.22839]
15 **Hong W**, Lillemoe KD, Pan S, Zimmer V, Kontopantelis E, Stock S, Zippi M, Wang C, Zhou M. Development and

validation of a risk prediction score for severe acute pancreatitis. *J Transl Med* 2019; **17**: 146 [PMID: 31068202 DOI: 10.1186/s12967-019-1903-6]

16 **Qiu Q**, Nian YJ, Guo Y, Tang L, Lu N, Wen LZ, Wang B, Chen DF, Liu KJ. Development and validation of three machine-learning models for predicting multiple organ failure in moderately severe and severe acute pancreatitis. *BMC Gastroenterol* 2019; **19**: 118 [PMID: 31272385 DOI: 10.1186/s12876-019-1016-y]

17 **Kui B**, Pintér J, Molontay R, Nagy M, Farkas N, Gede N, Vincze Á, Bajor J, Gódi S, Czimmer J, Szabó I, Illés A, Sarlós P, Hágendorn R, Pár G, Papp M, Vitális Z, Kovács G, Fehér E, Földi I, Izbéki F, Gajdán L, Fejes R, Németh BC, Török I, Farkas H, Mickevicius A, Sallinen V, Galeev S, Ramírez-Maldonado E, Párniczky A, Erőss B, Hegyi PJ, Márta K, Váncsa S, Sutton R, Szatmary P, Latawiec D, Halloran C, de-Madaria E, Pando E, Alberti P, Gómez-Jurado MJ, Tantau A, Szentesi A, Hegyi P; Hungarian Pancreatic Study Group. EASY-APP: An artificial intelligence model and application for early and easy prediction of severity in acute pancreatitis. *Clin Transl Med* 2022; **12**: e842 [PMID: 35653504 DOI: 10.1002/ctm2.842]

18 **Banks PA**, Bollen TL, Dervenis C, Gooszen HG, Johnson CD, Sarr MG, Tsiotos GG, Vege SS; Acute Pancreatitis Classification Working Group. Classification of acute pancreatitis--2012: revision of the Atlanta classification and definitions by international consensus. *Gut* 2013; **62**: 102-111 [PMID: 23100216 DOI: 10.1136/gutjnl-2012-302779]

19 **Cheng T**, Liu BF, Han TY, Pan P, Liu JZ, Yu H. Efficiency of red cell distribution width in predicting severity and mortality of patients with acute pancreatitis: A protocol for systematic review and meta-analysis. *Medicine (Baltimore)* 2021; **100**: e24658 [PMID: 33578595 DOI: 10.1097/MD.0000000000024658]

20 **Lei JJ**, Zhou L, Liu Q, Xiong C, Xu CF. Can mean platelet volume play a role in evaluating the severity of acute pancreatitis? *World J Gastroenterol* 2017; **23**: 2404-2413 [PMID: 28428720 DOI: 10.3748/wjg.v23.i13.2404]

21 **Wang F**, Meng Z, Li S, Zhang Y, Wu H. Platelet Distribution Width Levels Can Be a Predictor in the Diagnosis of Persistent Organ Failure in Acute Pancreatitis. *Gastroenterol Res Pract* 2017; **2017**: 8374215 [PMID: 29445395 DOI: 10.1155/2017/8374215]

22 **Hong W**, Zimmer V, Basharat Z, Zippi M, Stock S, Geng W, Bao X, Dong J, Pan J, Zhou M. Association of total cholesterol with severe acute pancreatitis: A U-shaped relationship. *Clin Nutr* 2020; **39**: 250-257 [PMID: 30772093 DOI: 10.1016/j.clnu.2019.01.022]

23 **Wu Q**, Zhong X, Fu M, Yang H, Bo H, Liao X, Hu Z, Wang B, Zhang Z, Jin X, Kang Y. High-density lipoprotein cholesterol to low-density lipoprotein cholesterol ratio in early assessment of disease severity and outcome in patients with acute pancreatitis admitted to the ICU. *BMC Gastroenterol* 2020; **20**: 164 [PMID: 32460705 DOI: 10.1186/s12876-020-01315-x]

24 **Zhou CL**, Zhang CH, Zhao XY, Chen SH, Liang HJ, Hu CL, Chen NW. Early prediction of persistent organ failure by serum apolipoprotein A-I and high-density lipoprotein cholesterol in patients with acute pancreatitis. *Clin Chim Acta* 2018; **476**: 139-145 [PMID: 29183667 DOI: 10.1016/j.cca.2017.11.028]

25 **Kaplan M**, Ates I, Akpinar MY, Yuksel M, Kuzu UB, Kacar S, Coskun O, Kayacetin E. Predictive value of C-reactive protein/albumin ratio in acute pancreatitis. *Hepatobiliary Pancreat Dis Int* 2017; **16**: 424-430 [PMID: 28823374 DOI: 10.1016/S1499-3872(17)60007-9]

26 **Wan J**, Shu W, He W, Zhu Y, Zeng H, Liu P, Xia L, Lu N. Serum Creatinine Level and APACHE-II Score within 24 h of Admission Are Effective for Predicting Persistent Organ Failure in Acute Pancreatitis. *Gastroenterol Res Pract* 2019; **2019**: 8201096 [PMID: 30984258 DOI: 10.1155/2019/8201096]

27 **Yang WQ**, Yang Q, Chen WJ, Zhang XB, Xu QQ, Qiao Y, Xu XH, Liu L, Lu XY, Zhu CQ. Low FT3 is a valuable predictor of severe acute pancreatitis in the emergency department. *J Dig Dis* 2018; **19**: 431-438 [PMID: 29802762 DOI: 10.1111/1751-2980.12609]

28 **Thong VD**, Mong Trinh NT, Phat HT. Factors associated with the severity of hypertriglyceridemia induced acute pancreatitis. *Medicine (Baltimore)* 2021; **100**: e25983 [PMID: 34032712 DOI: 10.1097/MD.0000000000025983]

29 **Liu C**, Zhou X, Ling L, Chen S, Zhou J. Prediction of mortality and organ failure based on coagulation and fibrinolysis markers in patients with acute pancreatitis: A retrospective study. *Medicine (Baltimore)* 2019; **98**: e15648 [PMID: 31124944 DOI: 10.1097/MD.0000000000015648]

30 **Yan G**, Li H, Bhetuwal A, McClure MA, Li Y, Yang G, Zhao L, Fan X. Pleural effusion volume in patients with acute pancreatitis: a retrospective study from three acute pancreatitis centers. *Ann Med* 2021; **53**: 2003-2018 [PMID: 34727802 DOI: 10.1080/07853890.2021.1998594]

31 **Niknam R**, Moradi J, Jahanshahi KA, Mahmoudi L, Ejtehadi F. Association Between Metabolic Syndrome and Its Components with Severity of Acute Pancreatitis. *Diabetes Metab Syndr Obes* 2020; **13**: 1289-1296 [PMID: 32425564 DOI: 10.2147/DMSO.S249128]

32 **Szentesi A**, Párniczky A, Vincze Á, Bajor J, Gódi S, Sarlós P, Gede N, Izbéki F, Halász A, Márta K, Dobszai D, Török I, Farkas H, Papp M, Varga M, Hamvas J, Novák J, Mickevicius A, Maldonado ER, Sallinen V, Illés D, Kui B, Erőss B, Czakó L, Takács T, Hegyi P. Multiple Hits in Acute Pancreatitis: Components of Metabolic Syndrome Synergize Each Other's Deteriorating Effects. *Front Physiol* 2019; **10**: 1202 [PMID: 31620021 DOI: 10.3389/fphys.2019.01202]

33 **Li Y**, Zheng R, Gao F, Wang L, Feng S, Li J, Huang Z. Association between high-density lipoprotein cholesterol and apolipoprotein A-I and severe acute pancreatitis: a case-control study. *Eur J Gastroenterol Hepatol* 2021; **33**: 1517-1523 [PMID: 34723873 DOI: 10.1097/MEG.0000000000002095]

34 **Vuilleumier N**, Dayer JM, von Eckardstein A, Roux-Lombard P. Pro- or anti-inflammatory role of apolipoprotein A-1 in high-density lipoproteins? *Swiss Med Wkly* 2013; **143**: w13781 [PMID: 23740387 DOI: 10.4414/smw.2013.13781]

35 **Liu Z**, Liu Z, Zhang M. Correlation of apolipoprotein levels with the severity of hyperlipidemic acute pancreatitis. *Chin J Gen Pract* 2019; 1070-1071

36 **Raghuwanshi S**, Gupta R, Vyas MM, Sharma R. CT Evaluation of Acute Pancreatitis and its Prognostic Correlation with CT Severity Index. *J Clin Diagn Res* 2016; **10**: TC06-TC11 [PMID: 27504376 DOI: 10.7860/JCDR/2016/19849.7934]

37 **Kumar P**, Gupta P, Rana S. Thoracic complications of pancreatitis. *JGH Open* 2019; **3**: 71-79 [PMID: 30834344 DOI: 10.1002/jgh3.12099]

World Journal of Gastroenterology

Submit a Manuscript: https://www.f6publishing.com

World J Gastroenterol 2022 September 7; 28(33): 4861-4874

DOI: 10.3748/wjg.v28.i33.4861

ISSN 1007-9327 (print) ISSN 2219-2840 (online)

ORIGINAL ARTICLE

Observational Study

Are bowel symptoms and psychosocial features different in irritable bowel syndrome patients with abdominal discomfort compared to abdominal pain?

Xiu-Cai Fang, Wen-Juan Fan, Douglas D Drossman, Shao-Mei Han, Mei-Yun Ke

Specialty type: Gastroenterology and hepatology

Provenance and peer review: Unsolicited article; Externally peer reviewed.

Peer-review model: Single blind

Peer-review report's scientific quality classification

Grade A (Excellent): 0
Grade B (Very good): B, B
Grade C (Good): 0
Grade D (Fair): 0
Grade E (Poor): 0

P-Reviewer: Caballero-Mateos AM, Spain; Losurdo G, Italy

Received: January 19, 2022
Peer-review started: January 19, 2022
First decision: April 10, 2022
Revised: April 19, 2022
Accepted: August 6, 2022
Article in press: August 6, 2022
Published online: September 7, 2022

Xiu-Cai Fang, Wen-Juan Fan, Mei-Yun Ke, Department of Gastroenterology, Peking Union Medical College Hospital, Chinese Academy of Medical Sciences and Peking Union Medical College, Beijing 100730, China

Wen-Juan Fan, Department of Gastroenterology, Tongji Hospital, Tongji Medical College, Huazhong University of Science & Technology, Wuhan 430030, Hubei Province, China

Douglas D Drossman, Center of Functional GI and Motility Disorders, University of North Carolina, Chapel Hill, NC 27517, United States

Douglas D Drossman, Center for Education and Practice of Biopsychosocial Care, Drossman Gastroenterology, Durham, NC 27713, United States

Douglas D Drossman, Rome Foundation, Rome Foundation, Raleigh, NC 27614, United States

Shao-Mei Han, Department of Epidemiology and Statistics, Institute of Basic Medical Sciences, Chinese Academy of Medical Sciences & School of Basic Medicine, Peking Union Medical College, Beijing 100005, China

Corresponding author: Xiu-Cai Fang, MD, Professor, Department of Gastroenterology, Peking Union Medical College Hospital, Chinese Academy of Medical Sciences and Peking Union Medical College, No. 1 Shuaifuyuan, Wangfujing, Dongcheng District, Beijing 100730, China. fangxiucai2@aliyun.com

Abstract

BACKGROUND

The Rome IV criteria eliminated abdominal discomfort for irritable bowel syndrome (IBS), which was previously included in Rome III. There are questions as to whether IBS patients with abdominal discomfort (seen in Rome III but not Rome IV) are different from those with abdominal pain (Rome IV).

AIM

To compare bowel symptoms and psychosocial features in IBS patients diagnosed with Rome III criteria with abdominal discomfort, abdominal pain, and pain & discomfort.

METHODS

We studied IBS patients meeting Rome III criteria. We administered the IBS symptom questionnaire, psychological status, and IBS quality of life. Patients were classified according to the predominant abdominal symptom associated with defecation into an only pain group, only discomfort group, and pain & discomfort group. We compared bowel symptoms, extraintestinal symptoms, IBS quality of life, psychological status and healthcare-seeking behaviors, and efficacy among the three groups. Finally, we tested risk factors for symptom reporting in IBS patients.

RESULTS

Of the 367 Rome III IBS patients enrolled, 33.8% (124 cases) failed to meet Rome IV criteria for an IBS diagnosis. There were no meaningful differences between the pain group (n = 233) and the discomfort group (n = 83) for the following: (1) Frequency of defecatory abdominal pain or discomfort; (2) Bowel habits; (3) Coexisting extragastrointestinal pain; (4) Comorbid anxiety and depression; and (5) IBS quality of life scores except more patients in the discomfort group reported mild symptom than the pain group (22.9% *vs* 9.0%). There is a significant tendency for patients to report their defecatory and non-defecatory abdominal symptom as pain alone, or discomfort alone, or pain & discomfort (all $P < 0.001$).

CONCLUSION

IBS patients with abdominal discomfort have similar bowel symptoms and psychosocial features to those with abdominal pain. IBS symptoms manifesting abdominal pain or discomfort may primarily be due to different sensation and reporting experience.

Key Words: Irritable bowel syndrome; Abdominal pain; Abdominal discomfort; Diagnosis; Psychosocial distress; Quality of life

©The Author(s) 2022. Published by Baishideng Publishing Group Inc. All rights reserved.

Core Tip: It is generally accepted that abdominal pain is the most predominant symptom of irritable bowel syndrome (IBS), and Rome IV eliminated abdominal discomfort as diagnostic criteria for IBS. Asian studies showed about one-third of IBS patients diagnosed using Rome III criteria had abdominal discomfort alone. In this study, we compared bowel symptoms, extraintestinal symptoms, IBS-quality of life, psychological status and healthcare-seeking behaviors, and efficacy between the abdominal pain and abdominal discomfort groups expecting to find a difference between the two groups but did not. We also assessed risk factors for symptom reporting for IBS patients.

Citation: Fang XC, Fan WJ, Drossman DD, Han SM, Ke MY. Are bowel symptoms and psychosocial features different in irritable bowel syndrome patients with abdominal discomfort compared to abdominal pain? *World J Gastroenterol* 2022; 28(33): 4861-4874
URL: https://www.wjgnet.com/1007-9327/full/v28/i33/4861.htm
DOI: https://dx.doi.org/10.3748/wjg.v28.i33.4861

INTRODUCTION

Irritable bowel syndrome (IBS) is a common functional bowel disorder with a global prevalence of 4.1% according to the Rome IV criteria and 10.1% with Rome III criteria[1]. Using the Rome III definition, IBS is characterized by recurrent abdominal pain or discomfort associated with altered bowel frequency or stool form[2]. However, the term "discomfort" was deleted from the 2016 Rome IV diagnostic criteria because some languages do not have a word for discomfort or it has different meanings in different languages or cultures[3,4]. Possibly abdominal discomfort has qualitative and quantitative levels of distinction with abdominal pain[5]. The data from a population-based survey of adults in the United States, Canada, and the United Kingdom showed that eliminating "discomfort" from the criteria for IBS affected diagnostic rates only slightly[6], and only 10% of Rome III-IBS patients among the Swedish cohort did not fulfill Rome-IV IBS diagnosis due to reporting only abdominal discomfort and not pain [7]. However, clinical studies from Thailand and central China revealed that about one-third of patients with IBS diagnosed using Rome III criteria had abdominal discomfort alone[8,9]. This rate is as high as 84.2% from another clinical retrospective report from Tianjin, China[10]. Evidence regarding pathophysiological differences between abdominal pain and abdominal discomfort such as whether these symptoms are categorically different or exist on a continuum of severity is lacking[11,12]. It is also unclear whether there are clinical or phenotypical distinctions with IBS presenting with abdominal pain

vs abdominal discomfort as to how this change of criteria impacts the clinical practice.

This study aimed to: (1) Compare the bowel and extraintestinal symptoms of patients with IBS presenting with abdominal discomfort alone to those with pain alone as well as with pain & discomfort; (2) Evaluate the anxiety, depression, quality of life (QOL), and symptom reporting tendency for patients with pain and discomfort; and (3) Validate whether the discomfort is milder than pain on a continuum of severity for Chinese patients. The clinical data were drawn from the IBS database of Peking Union Medical College Hospital.

MATERIALS AND METHODS

Subjects

Consecutive patients with IBS aged 18-65 years from Peking Union Medical College Hospital gastroenterology clinics were enrolled in this study from June 2009 to February 2016. All patients met Rome III diagnostic and subtype criteria[2], including IBS with diarrhea (IBS-D), IBS with constipation (IBS-C), and mixed IBS. Patients with organic gastrointestinal diseases and metabolic diseases were excluded based on the results of routine tests for blood, urine, stool; liver, kidney, and thyroid function, measurements of carcinoembryonic antigen, erythrocyte sedimentation rate, and C-reactive protein, and abdominal ultrasound and colonoscopy/barium enema in the past year. The participating patients provided oral or written consent to participate before study enrollment. This study was approved by the Peking Union Medical College Hospital Ethics Committee (S-234).

IBS symptom questionnaire

The IBS symptom questionnaire was administered by well-trained investigators in face-to-face interviews. The questionnaire was adapted from a previous symptom-related questionnaire for adult functional gastrointestinal disorders in Beijing[13], the Rome III diagnostic questionnaire for adult functional gastrointestinal disorders, and the Rome III psychosocial alarm questionnaire for functional gastrointestinal disorders[2]. Information collected included demographic data, IBS disease course, frequency and severity of IBS symptoms, defecation-related symptoms, extraintestinal symptoms, physical examination and supplementary examination results, and IBS treatments in the whole disease course and the last year.

Patients were evaluated according to abdominal pain, abdominal discomfort, or both abdominal pain & discomfort just before defecation (pre-defecatory), at IBS onset, and between IBS symptom episodes without association to defecation (ordinary). Patients with the presence or worsening of pre-defecatory abdominal pain and without pre-defecatory abdominal discomfort were categorized as the pain group regardless of whether they had abdominal pain or discomfort during the ordinary period. Similarly, patients with pre-defecatory abdominal discomfort and without pre-defecatory abdominal pain were categorized as the discomfort group, and patients with pre-defecatory abdominal pain and discomfort were categorized as the pain & discomfort group.

The main intestinal symptom score for IBS-D was calculated according to the report by Zhu *et al*[14]. Diagnosis of gastroesophageal reflux disease and functional dyspepsia were made according to the Montreal consensus[15] and Rome III diagnostic and subtype criteria[2], respectively. Patients who did not met Rome IV diagnostic criteria for IBS (including patients with pre-defecatory abdominal discomfort alone or symptom frequency < 1 d/wk) were evaluated for possible diagnoses of other functional bowel disorders using Rome IV criteria, including functional diarrhea, functional constipation, functional abdominal bloating/distension, and unspecified functional bowel disorder[3].

QOL evaluation

The simplified Chinese version of the IBS-QOL instrument was used to evaluate patient QOL[16], which was translated from IBS-QOL[17] and well validated. This instrument was completed by patients according to the instructions provided; the total score and eight domain scores were calculated as in a previous publication[14].

Psychological evaluation

The Hamilton Anxiety (HAMA) and Hamilton Depression (HAMD) scales were used to evaluate patient psychological status by specially trained professionals through conversation and observation. A HAMA score ≥ 14 was judged as anxiety and ≥ 21 as moderate-to-severe anxiety. A HAMD score ≥ 17 was judged as depression and ≥ 24 as moderate-to-severe depression[18,19].

Statistical analysis

All analyses were performed using SPSS version 19.0 (IBM Corporation, Somers, NY, United States). Parametric distribution was evaluated by Kolmogorov-Smirnov test. Parametric and categorical data are presented as mean ± SD or rate, respectively. Nonparametric data were presented as median and interquartile range. Comparisons among the three groups were made by one-way analysis of variance

for parametric data, Kruskal-Wallis test for nonparametric data, and χ^2 test for categorical variables. Spearman's test was performed to assess nonparametric correlations between two quantitative variables. Bonferroni test was used to adjust for pairwise comparison among the three groups after analysis of variance. Multiple logistic regression analysis was used to determine the independent factors for abdominal pain or abdominal discomfort. $P < 0.05$ was considered statistically significant.

RESULTS

Demographic data

In total, 367 patients meeting Rome III criteria for IBS were enrolled in this study (205 males and 162 females), with an average age of 43.0 ± 11.4 years.

There were 233 patients (63.5%) in the pain group, 83 patients (22.6%) in the discomfort group, and 51 patients (13.9%) in the pain & discomfort group. There were more males in the discomfort group than in the pain group (67.5% *vs* 50.2%, $P = 0.01$). There were no significant differences in age, body mass index, educational level, physical work, family economic status, marriage status, the average IBS disease course, and IBS subtype distribution among the three groups ($P > 0.05$) (Table 1).

Characteristics of abdominal pain, discomfort, and pain & discomfort

In the three groups, the locations of abdominal pain, discomfort, or pain & discomfort before defecation were mainly in the umbilical region, lower abdomen, and left lower quadrant. There was no significant difference in distribution of symptom location, even though more patients in the discomfort group reported the symptom location as "others" (indicating varied or obscure locations) than in the pain group (21.7% *vs* 10.3%, $P = 0.009$). There was a significant difference in the severity of pain and/or discomfort among the three groups ($P = 0.007$), and more patients in the discomfort group reported mild symptom than those in the pain group. There was no significant difference in frequency among the three groups (Table 2).

There were significant differences in the prevalence of ordinary abdominal pain or/and discomfort among the three groups ($P < 0.001$). More patients in the pain group reported ordinary abdominal pain than those in the discomfort group and pain & discomfort group, while more patients in the discomfort group reported ordinary abdominal discomfort than those in the pain group and pain & discomfort group. In the pain & discomfort group, 54.9% of patients reported having ordinary pain and discomfort, which was significantly higher than the other two groups (Table 2).

In total, there were 52 patients (14.2%) with onset frequency of < 1 d/wk (*i.e.* 3 d/mo), including 37 cases in the pain group, 11 cases in the discomfort group, and 4 cases in the pain & discomfort group. The proportion of less frequency was 15.9%, 13.3%, and 7.8%, respectively, without significant difference ($P = 0.32$). According to Rome IV diagnostic criteria, a total of 124 patients (33.8%) would not meet an IBS diagnosis (Figure 1).

Bowel movements and stool form

In 345 patients with IBS-D, the average bowel movements during symptom non-onset period of the pain group (1.5 ± 0.9/d) were less than the discomfort group (1.8 ± 1.1/d) and the pain & discomfort group (1.9 ± 1.1/d) ($P = 0.004$), but there were no significant differences in average bowel movements during symptom onset period (3.8 ± 1.5 *vs* 3.8 ± 1.4 *vs* 3.6 ± 1.5, $P > 0.05$) (Figure 2A). There were no significant differences in stool form during symptom non-onset and onset periods among the three groups (all $P > 0.05$) (Figure 2B).

Abdominal pain and/or discomfort improvement after defecation

Abdominal pain and/or discomfort improved after defecation except for 1 patient in the pain group. There was no significant difference in the waiting time and degree for improvement among the three groups (Figure 2C and D).

In IBS-D patients, the main intestinal symptom score was 9.3 ± 1.6 in the pain group, 9.4 ± 1.5 in the discomfort group, and 9.6 ± 1.3 in the pain & discomfort group ($P > 0.05$).

Defecation-related symptoms

The prevalence of defecation related symptoms such as abdominal bloating, urgency, sensation of incomplete evacuation, and passing mucus were high overall for all 3 groups. More patients in the discomfort group reported having urgency, sensation of incomplete evacuation, and passing mucus than those in the pain group (all $P < 0.05$). In the pain & discomfort group, the prevalence of abdominal bloating, abdominal distension, and anorectal pain was significantly higher than that in the pain group (all $P < 0.05$) (Table 2).

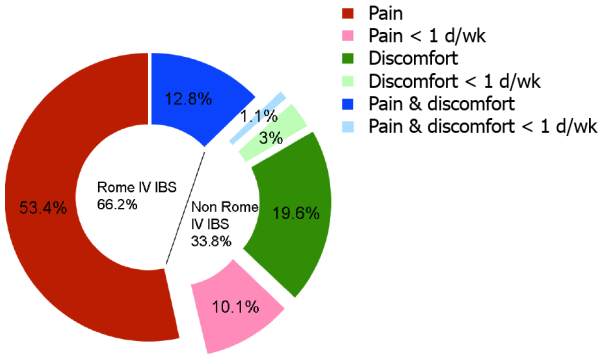
Extraintestinal symptoms

There were no significant differences in the prevalence of gastroesophageal reflux disease or functional

Table 1 Demographic data for irritable bowel syndrome patients with abdominal pain alone, abdominal discomfort alone, and abdominal pain & discomfort

Variable	Pain group (*n* = 233)	Discomfort group (*n* = 83)	Pain & discomfort group (*n* = 51)	*P* value
Male, %	117 (50.2)	56 (67.5)	32 (62.7)	0.01[2]
Age in yr	43.7 ± 11.7	42.3 ± 10.6	40.8 ± 11.0	0.23
BMI in kg/m^2	23.0 ± 4.0	22.8 ± 4.0	22.3 ± 3.8	0.56
Education level, college and above, %	71 (30.5)	29 (34.9)	13 (25.5)	0.51
Physical labor, %	135 (57.9)	42 (50.6)	34 (66.7)	0.18
Family economic status, well-off & above, %	105 (45.1)	44 (53.0)	18 (35.3)	0.13
Marriage status, married, %	201 (86.3)	71 (85.5)	41 (80.4)	0.56
IBS disease course in yr[1]	6.0 (7.5)	5.3 (7.0)	6.0 (7.0)	0.38
IBS type				0.06
IBS-D, %	95.7	96.4	86.3	
IBS-C, %	3.0	2.4	7.8	
IBS-M, %	1.3	1.2	5.9	

[1]Data presented as median (interquartile range), Kruskal-Wallis test. Note: *P* value is the difference among pain group, discomfort group, and pain & discomfort group, superscript letter is significantly different at a $P < 0.05$.
[2]The difference is between the pain group and discomfort group.
Data presented as number (%) or mean ± SD. Analysis of variance and χ^2 tests. IBS-D: Irritable bowel syndrome with diarrhea; BMI: Body mass index; IBS-C: Irritable bowel syndrome with constipation; IBS-M: Mixed irritable bowel syndrome.



DOI: 10.3748/wjg.v28.i33.4861 **Copyright** ©The Author(s) 2022.

Figure 1 Constitution diagram of irritable bowel syndrome patients diagnosed with Rome III and Rome IV criteria. About one-third of irritable bowel syndrome patients (parts dragged out of ring) diagnosed with Rome III criteria failed in irritable bowel syndrome diagnosis with Rome IV criteria because of only having abdominal discomfort before defecation (in green, 22.6%) or frequency of abdominal pain less than 1 d/wk (in light colors, 14.2%), which 3% of patients among them have discomfort alone with less frequency (in light green). IBS: Irritable bowel syndrome.

dyspepsia between the pain group and the discomfort group ($P > 0.05$), but the prevalence of epigastric pain syndrome, mainly epigastric pain was higher in the pain group than the discomfort group (21.0% *vs* 7.2%, 18.5% *vs* 6.0%, $P < 0.05$). More patients in the pain & discomfort group reported early satiation, dyspareunia, and menstrual pain for women than in the pain group (all $P < 0.05$). The prevalence of dyspareunia in the pain & discomfort group was also higher than in the discomfort group ($P < 0.001$) (Table 3).

Comorbid anxiety and depression

There were no significant differences in HAMA score, HAMD score, or the prevalence and severity of anxiety and depression among the three groups (Table 4).

IBS-QOL

The QOL of patients with IBS showed an obvious decrease with an IBS-QOL score of 72.2 ± 17.9 in the

Table 2 Characteristics of bowel symptoms in irritable bowel syndrome patients with abdominal pain alone, abdominal discomfort alone, and abdominal pain & discomfort

Variable	Pain group (*n* = 233)	Discomfort group (*n* = 83)	Pain & discomfort group (*n* = 51)	*P* value
Location[1], %				0.213
Left lower quadrant	67 (28.8)	14 (16.9)	12 (23.5)	
Umbilical	79 (33.9)	27 (32.5)	20 (39.2)	
Lower abdomen	65 (27.9)	23 (27.7)	15 (29.4)	
Epigastric	11 (4.7)	2 (2.4)	2 (3.9)	
Whole abdomen	12 (4.0)	8 (9.6)	5 (9.8)	
Others	24 (10.3)	18 (21.7)	7 (13.7)	
Severity, %				0.007
Mild	21 (9.0)	19 (22.9)	6 (11.7)	
Moderate	160 (68.7)	55 (66.3)	37 (72.6)	
Severe	52 (22.3)	9 (10.8)	8 (15.7)	
Frequency, %				0.290
3 d/mo	37 (15.9)	11 (13.3)	4 (7.84)	
1 d/wk	25 (10.7)	5 (6.0)	2 (3.9)	
>1 d/wk	108 (46.4)	38 (45.8)	27 (52.94)	
Every day	63 (27.0)	29 (34.9)	18 (35.3)	
Ordinary pain/discomfort, %				< 0.001
Pain alone	84 (36.1)	6 (7.2)	6 (11.8)	
Discomfort alone	21 (9.0)	43 (51.8)	3 (5.9)	
Pain & discomfort	7 (3.0)	2 (2.4)	28 (54.9)	
No pain or discomfort	121 (51.9)	32 (38.6)	14 (27.4)	
Defecation-related symptoms, %				
Abdominal bloating	93 (39.9)	43 (51.8)	35 (68.6)	0.001[3]
Abdominal distension	21 (9.0)	13(15.7)	12 (23.5)	0.01[3]
Urgency	197 (84.6)	80 (96.4)	42 (82.4)	0.01[2,4]
Defecation straining	70 (30.0)	25 (30.1)	23 (45.1)	0.10
Sensation of anorectal obstruction	62 (26.6)	30 (36.1)	19 (37.3)	0.13
Anorectal pain	28 (12.0)	15 (18.1)	17 (33.3)	0.001[3]
Sensation of incomplete evacuation	164 (70.4)	74 (89.2)	39 (76.5)	0.003[2]
Passing mucus	141 (60.5)	66 (79.5)	39 (76.5)	0.002[2]

[1]Some patients reported more than one location. χ^2 test, data presented as number (%).
[2]The difference is between pain group and discomfort group.
[3]The difference is between pain group and pain & discomfort group.
[4]The difference is between discomfort group and pain & discomfort group.
P value is the difference among pain group, discomfort group, and pain & discomfort group, and superscript letters are significantly different at a $P < 0.05$.

pain group, 72.0 ± 20.0 in the discomfort group, and 70.4 ± 15.0 in the pain & discomfort group while comparing to the mean overall score in healthy Chinese subjects (95.50 ± 6.73 with the scores on each of the eight domains being ≥ 90.00)[16]. The most meaningful impairment for all 3 groups was food avoidance, following by dysphoria, interference with activity, and health worry. There were no significant differences in the eight domain scores between the pain group and discomfort group (Figure 3), while patients in the pain & discomfort group had lower QOL than patients having discomfort alone ($P = 0.03$).

Table 3 Coexisting extraintestinal symptoms of irritable bowel syndrome patients with abdominal pain alone, abdominal discomfort alone, and abdominal pain & discomfort

Variable	Pain group (*n* = 233)	Discomfort group (*n* = 83)	Pain & discomfort group (*n* = 51)	*P* value
GERD, %	60 (25.8)	14 (16.9)	10 (19.6)	0.20
Heartburn	35 (15.0)	6 (7.2)	6 (11.8)	0.18
Acid reflux	44 (18.9)	10 (12.1)	5 (9.8)	0.15
Food regurgitation	14 (6.0)	4 (4.8)	3 (5.9)	0.92
Retrosternal chest pain	10 (4.3)	3 (3.6)	2 (3.9)	0.96
Functional dyspepsia, %	86 (36.9)	23 (27.7)	18 (35.3)	0.32
Epigastric pain syndrome	49 (21.0)	6 (7.2)	7 (13.7)	0.01[2]
Epigastric pain	43 (18.5)	5 (6.0)	7 (13.7)	0.02[2]
Epigastric burning	12 (5.2)	2 (2.4)	3 (5.9)	0.54
Postprandial distress syndrome	64 (27.5)	22 (26.5)	15 (29.4)	0.94
Postprandial fullness	57 (24.5)	20 (24.1)	9 (17.7)	0.57
Early satiation	14 (6.0)	6 (7.2)	9 (17.7)	0.02[3]
Somatic pain, %				
Headache	17 (45.9)	37 (44.6)	26 (51.0)	0.76
Neck pain	21 (9.0)	7 (8.4)	3 (5.9)	0.77
Backache	41 (17.6)	8 (9.6)	7 (13.7)	0.21
Dyspareunia	12 (5.2)	6 (7.2)	11 (21.6)	< 0.001[3,4]
Menstrual pain[1]	30 (25.9)	10 (37.0)	11 (57.9)	0.016[3]

[1]The number of female patients in the abdominal pain, abdominal discomfort, and pain & discomfort groups was 116, 27, and 19, respectively. χ^2 test. Data presented as number (%).
[2]*P* value is difference between the pain group and the discomfort group.
[3]The difference is between the pain group and the pain & discomfort group.
[4]The difference is between the discomfort group and the pain & discomfort group.
P value is the difference among the pain group, discomfort group, and pain & discomfort group, and superscript letters are significantly different at $P < 0.05$. GERD: Gastroesophageal reflux disease.

Healthcare-seeking behaviors and efficacy

There were no significant differences among the three groups in the average number of consultations and colonoscopies in the whole disease course and the average consultations and intermittent and long-term medication use in the last year (all $P > 0.05$). More patients in discomfort group used antispasmodics (muscarinic cholinergic receptor antagonists and selective intestinal calcium channel blockers), and all patients who used the antispasmodics had a reasonably good response (response rate over 50%). The overall satisfaction rate (including complete satisfaction and satisfaction) with medical care showed no significant difference among the three groups ($P > 0.05$) (Table 5).

Risk factors for IBS patients describing pre-defecatory symptoms as abdominal pain alone, discomfort alone, and pain & discomfort

Twelve variables differing between the pain group and the discomfort group at a *P* value with significant difference in Tables 1-3 were utilized for a multiple logistic regression analysis. We found that male patients [odds ratio (OR) = 1.955, 95% confidence interval (CI): 1.104-3.462, $P = 0.021$] and patients with mild defecatory abdominal pain or discomfort (OR = 4.020, 95%CI: 1.436-11.253, $P = 0.008$) were the predictors for patients to describe their pre-defecatory symptoms as abdominal discomfort alone rather than abdominal pain alone (Table 6). Similar analyses were performed between the pain group and the pain & discomfort group (11 variables) and the discomfort group and the pain & discomfort group (10 variables). We found that abdominal bloating (OR = 2.238, 95%CI: 1.080-4.638, $P = 0.030$) and anorectal pain (OR = 2.979, 95%CI: 1.347-6.585, $P = 0.007$) were the predictors for patients to describe their symptom as pain & discomfort rather than pain alone (Table 6), and no predictors were found for patients to describe their symptom as discomfort alone or pain & discomfort.

Table 4 Comorbid anxiety and depression among irritable bowel syndrome patients with abdominal pain alone, abdominal discomfort alone, and abdominal pain & discomfort

Variable	Pain group (*n* = 233)	Discomfort group (*n* = 83)	Pain & discomfort group (*n* = 51)	*P* value
HAMA score	16.1 ± 7.3	15.5 ± 7.3	17.3 ± 7.4	0.36
Comorbid anxiety, %	141 (60.5)	49 (59.0)	38 (74.5)	0.14
Mild	69 (29.6)	25 (30.1)	21 (41.2)	0.26
Moderate-severe	72 (30.9)	24 (28.9)	17 (33.3)	0.86
HAMD score	13.2 ± 6.2	12.3 ± 6.1	14.3 ± 5.5	0.18
Comorbid depression, %	66 (28.3)	22 (26.5)	18 (35.3)	0.53
Mild	54 (23.2)	20 (24.1)	17 (33.3)	0.31
Moderate-severe	12 (5.2)	2 (2.4)	1 (2.0)	0.40
Comorbid anxiety & depression, %	62 (26.6)	20 (24.1)	18 (35.3)	0.35

Data presented as mean ± SD or number (%). Student's *t* test and $\chi 2$ tests. *P* value is difference among the pain group, discomfort group, and pain & discomfort group. HAMA: Hamilton Anxiety Scale; HAMD: Hamilton Depression Scale.

Table 5 Consultations and medications of irritable bowel syndrome patients with abdominal pain alone, abdominal discomfort alone, and abdominal pain & discomfort

Variable	Pain group (*n* = 233)	Discomfort group (*n* = 83)	Pain & discomfort group (*n* = 51)	*P* value
In the whole disease course				
Consultation times per year[1]	4.6 ± 6.7	5.7 ± 6.2	4.2 ± 4.1	0.54
Colonoscopies[2]	1.9 ± 1.4	1.5 ± 0.8	1.6 ± 0.9	0.22
In the last year				
Consultation times[1]	4.0 ± 5.7	4.5 ± 4.5	4.9 ± 4.7	0.54
Medications, intermittent and long-term use, %	164 (70.4)	56 (67.5)	43 (84.3)	0.09
Antispasmodics use				
Use rate	29 (12.4)	24 (28.9)	12 (23.5)	0.002[3]
Response rate	22 (75.9)	13 (54.2)	10 (83.3)	0.12
Overall satisfaction to medical care, %	125 (53.7)	39 (47.0)	21 (41.2)	0.21

[1]Consultation times were average consultation times of consulters.
[2]Colonoscopies were average colonoscopies of patients who performed colonoscopies.
[3]The difference is between the pain group and the discomfort group.
Data presented as mean ± SD or number (%). Analysis of variance and χ^2 test. *P* value is difference among pain group, discomfort group, and pain & discomfort group, and superscript letter is significantly different at a $P < 0.05$.

Diagnosis of patients with abdominal discomfort alone according to Rome IV criteria

Among 83 patients having pre-defecatory abdominal discomfort alone and not meeting Rome IV criteria for IBS, 48 patients (57.8%) met the diagnosis for functional diarrhea, 28 patients (33.7%) for functional abdominal bloating/distension, 2 patients (2.4%) for functional constipation, and 5 patients (6.0%) were classified as unspecified functional bowel disorder.

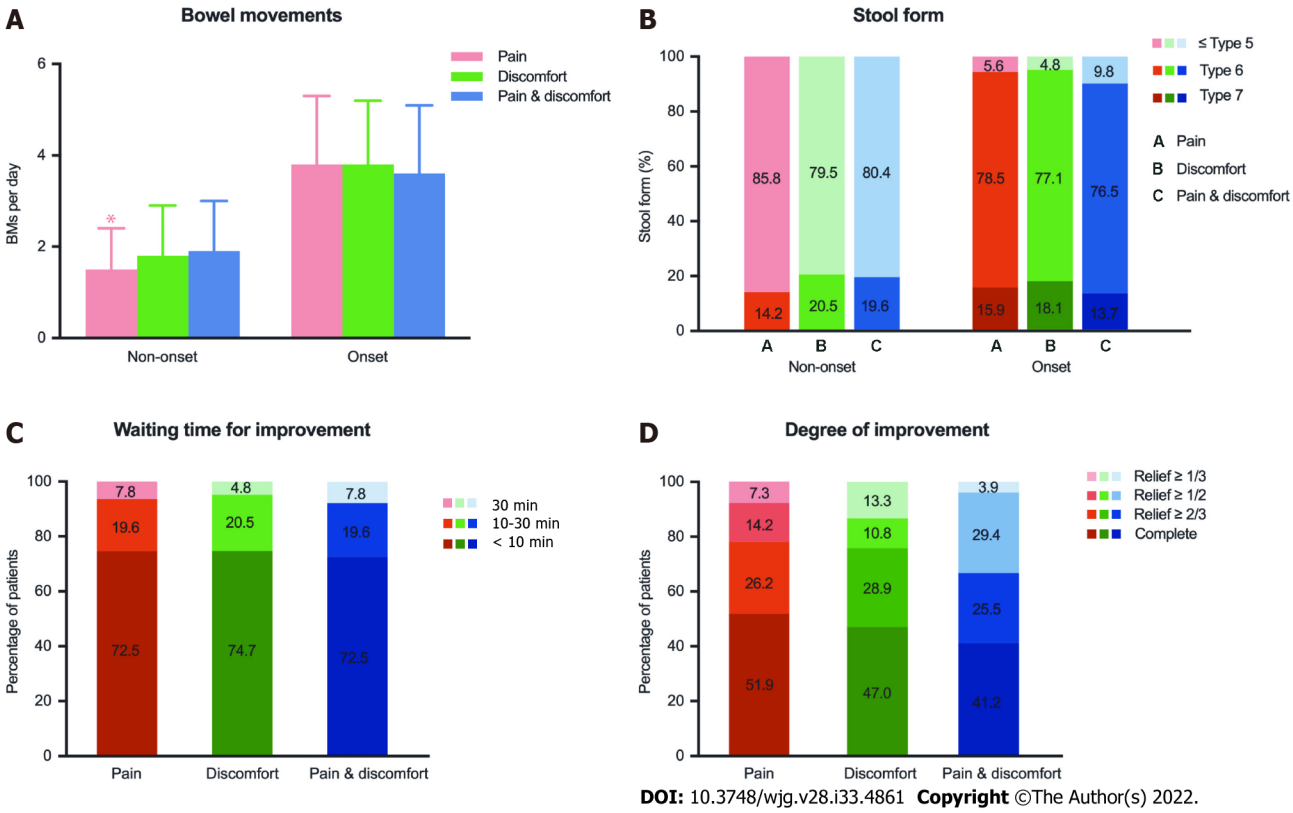
DISCUSSION

The present study comprehensively compared the bowel symptoms and psychosocial features of IBS

Table 6 Risk factors for irritable bowel syndrome patients describing symptoms as abdominal pain alone, abdominal discomfort alone, and abdominal pain & discomfort

	Partial regression coefficient	Standard error	Wald χ^2	95%CI	*P* value
Abdominal discomfort alone *vs* abdominal pain alone					
Male sex	0.671	0.291	5.293	1.955 (1.104-3.462)	0.021[a]
Severity (mild defecatory pain or discomfort)	1.391	0.525	7.018	4.020 (1.436-11.253)	0.008[a]
Abdominal pain alone *vs* abdominal pain & discomfort					
Abdominal bloating	0.805	0.372	4.692	2.238 (1.080-4.638)	0.030[a]
Anorectal pain	1.091	0.405	7.272	2.979 (1.347-6.585)	0.007[a]

[a]$P < 0.05$. Multiple logistic regression analysis. Superscript letter is significantly different at a $P < 0.05$.
CI: Confidence interval.



DOI: 10.3748/wjg.v28.i33.4861 **Copyright** ©The Author(s) 2022.

Figure 2 Comparison of bowel movements and stool forms in irritable bowel syndrome with diarrhea patients and improvement of abdominal pain or discomfort after defecation in irritable bowel syndrome patients among the abdominal pain alone, abdominal discomfort alone, and abdominal pain & discomfort groups. A: Bowel movements during irritable bowel syndrome with diarrhea non-onset and onset status; B: Stool forms based on Bristol Stool Form Scale during irritable bowel syndrome with diarrhea non-onset and onset status; C: Degree of improvement of abdominal pain and discomfort with defecation; D: Waiting time for improvement of abdominal pain and discomfort with defecation in irritable bowel syndrome patients. Numbers in the column are percentages. [b]$P < 0.01$. BM: Bowel movement.

patients with pre-defecatory abdominal pain alone to pre-defecatory abdominal discomfort alone, and abdominal pain & discomfort. We found that patients with abdominal discomfort had similar bowel and extraintestinal symptoms, comorbid anxiety and depression, QOL, and healthcare-seeking behaviors to those with abdominal pain.

It is generally accepted that abdominal pain is the most predominant symptom of IBS[3]; however, a previous clinical study from the United States found only 21% of IBS patients with moderate to severe symptoms reported their predominant symptom in terms of abdominal pain[11]. Another study conducted by Lembo *et al*[12] showed that the proportions of IBS patients who reported pain or gas

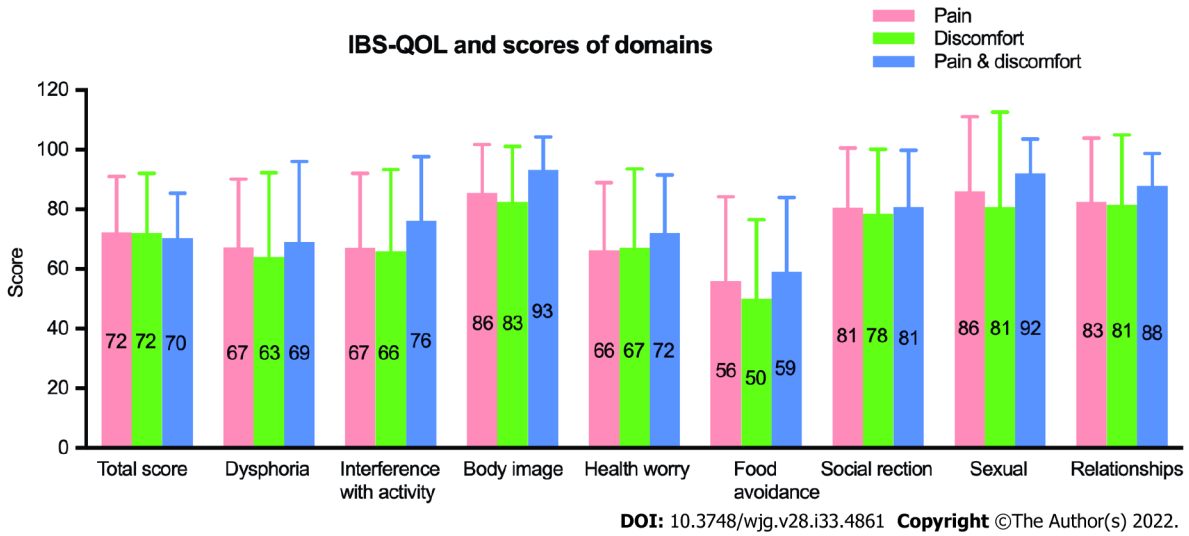


Figure 3 Comparison of irritable bowel syndrome-quality of life. There were no significant differences in the total score and eight domain scores among the three groups. Numbers in the column are percentages. IBS-QOL: Irritable bowel syndrome-quality of life.

(bloating-type discomfort) as one of their viscerosensory symptoms were similar (60% *vs* 66%). Currently, several studies compared the diagnostic rate between Rome III and IV criteria for IBS in the general population and consulting cohorts. The proportions of having abdominal discomfort varied among the western countries (2.4%-9.9%)[6,7,20,21] and the eastern countries (29.8%-84.2%)[8-10]. In this study, IBS patients with abdominal discomfort accounted for 22.6%. The elimination of abdominal discomfort from the diagnostic criteria had little effect on the diagnosis of IBS for the western countries [3], while a significant proportion of IBS patients were no longer IBS in Asian, including in China[8-10].

The significant difference between the western and eastern countries indicates there may be cultural factors that affect the experience and reporting of abdominal symptoms. The definition of abdominal pain is more uniformly accepted, while the definition for abdominal discomfort is ambiguous; "discomfort means an uncomfortable sensation not described as pain" according to the Rome III criteria[2]. Further, there are no comparison studies concerning abdominal discomfort descriptions in cross-cultural cohorts. In this study, Chinese patients with IBS accurately reported abdominal discomfort, including the location and association with defecation (both in pre-defecatory and non-defecatory periods), as well as other defecation related symptoms (*i.e.* urgency and so on). Symptom characteristics were similar with abdominal pain, which indicated that abdominal discomfort was a relatively explicit symptom for Chinese patients, unlike the impression from a cognitive study from American IBS patients [6] in which abdominal discomfort might encompass a wide range of symptoms such as bloating, gas, fullness, flatulence, sensation of incomplete evacuation, and urgency.

Abdominal pain and discomfort are both visceral perceptions of abnormality on the same continuum with pain appearing at the more severe end of the spectrum[11]. In this study, there were no meaningful differences between the pain alone group and discomfort alone group in frequencies as well as the main intestinal symptom score for IBS-D patients except more patients in the discomfort group reported mild symptoms than the pain group. In addition, we found patients with mild defecatory abdominal pain or discomfort were predisposed to describe their pre-defecatory symptoms as abdominal discomfort alone rather than abdominal pain alone, which indicated abdominal discomfort may appear as the milder form of pain. However, it was reported that more IBS patients rank abdominal discomfort as their most bothersome symptom than abdominal pain (60% *vs* 29% in America[12], 15.3% *vs* 4.5% of IBS-C in Japan [22]), and the severity of abdominal discomfort had the strongest independent relationship with QOL impairment[10]. Patients in the three groups had similar healthcare-seeking behavior and satisfaction to medical care in this study. We speculated in terms of the symptom itself, the overall severity of IBS, and occupation of medical resources that abdominal discomfort is as important as abdominal pain.

Nevertheless, more patients in the discomfort group reported accompanying urgency, sensation of incomplete evacuation, and passing mucus than the pain group. Patients with abdominal pain & discomfort had a higher prevalence of abdominal bloating/distension and anorectal pain than patients with abdominal pain alone, and a lower score of QOL than patients with abdominal discomfort alone. In addition, we found that abdominal bloating and anorectal pain were the predictors for patients to describe their symptom as pain & discomfort rather than pain alone, suggesting coexisting symptoms played important roles in the generation of discomfort feeling.

We noticed that the previous studies seldom paid attention to the abdominal symptoms of IBS patients during non-defecatory period. An interesting finding in this study is more patients having pre-defecatory abdominal discomfort alone also reported non-defecatory abdominal discomfort than the other two groups, and a similar report tendency for patients with pain alone and pain & discomfort

during defecatory period and non-defecatory period. In terms of extraintestinal symptoms, more patients in the pain group reported coexisting epigastric pain. The possible explanation for this reporting tendency is individual sensation and reporting experience to the similar stimulations and pathophysiological changes[11].

The relationships between diary stress, psychological distress, and severity of abdominal discomfort symptoms in women with IBS have been noted[23]. In this study, the scores of HAMA and HAMD and comorbid anxiety and depression were comparable between the pain group and the discomfort group. The impact of mental status to the symptom sensation and reporting could be ignored.

To date, studies on the pathophysiology of IBS mainly focused on abdominal pain[12,24-27]. As far as we know, there was no direct evidence focused on mechanism of abdominal discomfort or comparison of the difference of pathogenesis between abdominal pain and discomfort. Abdominal discomfort could simultaneously improve with abdominal pain and/or bloating to antispasmodics tiropramide and octylonium, secretagogue linaclotide, or simethicone and *Bacillus* coagulans for IBS or IBS-C patients[28-31]. It is unclear whether the treatments focused on bloating, diarrhea, or constipation could relieve the abdominal discomfort for those patients having defecatory abdominal discomfort alone while they are diagnosed as other bowel disorders according to Rome IV criteria (as shown in the results). Therefore, we realized that it may be more beneficial to classify patients with bowel-related abdominal discomfort into IBS from a therapeutic consideration.

There are several limitations in this study. We only included the IBS patients with typical changes of bowel habits, *i.e.* IBS-D and IBS-C. Therefore, some mixed IBS and IBS-unclassified patients might be missed[7,31]. We enrolled patients with Rome III criteria and did not concern the abdominal pain and discomfort during or soon after bowel movement. The proportion of Rome III suspected IBS patients with this kind of pain or discomfort was low (2.9% according to Bai *et al*[9]). Moreover, we did not ask patients to describe the difference between abdominal pain and discomfort. The data for response to therapies were retrospective recall, including prescription and over-the-counter. In addition, the prevalence of IBS in the general population for males was lower than females (4.1% *vs* 5.4%)[32], but an equal or higher ratio of male to female consulting patients was reported in clinical studies[9,14]. It is unclear whether male patients have more vigorous healthcare seeking behaviors or priority of medical care than female patients, but more female patients reported frequent consultations and colonoscopies during the whole disease course of IBS than male patients[33]. IBS-D is the predominant subtype, which accounted for 74.1% in the general population of South China[34] and 66.3% in consulting patients[31]. In addition, this was a single-center study.

CONCLUSION

Chinese patients with IBS can differentiate and report abdominal pain or/and abdominal discomfort as their key bowel symptom. The patients with abdominal discomfort had similar bowel symptoms and psychosocial features to those with abdominal pain. There is a tendency for IBS patients to report their defecatory and non-defecatory abdominal symptom as pain alone, discomfort alone, or pain and discomfort. Pre-defecatory abdominal discomfort should be considered as an important symptom for IBS patients. Further studies focused on the pathophysiology and therapeutic response (including the cultural influence) of abdominal pain and discomfort are needed.

ARTICLE HIGHLIGHTS

Research background

The Rome IV criteria eliminated abdominal discomfort for irritable bowel syndrome (IBS), which was previously included in the Rome III criteria. Asian studies showed the rate of IBS patients with abdominal discomfort alone was high.

Research motivation

There are questions as to whether IBS patients with abdominal discomfort (seen in Rome III but not Rome IV) are different from those with abdominal pain (Rome IV).

Research objectives

To compare the bowel and extraintestinal symptoms of patients with IBS presenting with abdominal discomfort alone to those with pain alone as well as with pain & discomfort and to evaluate the anxiety, depression, quality of life, and symptom reporting tendency for patients with pain and discomfort.

Research methods

We enrolled IBS patients and collected their clinical data. Patients were classified to the pain only group,

the discomfort only group, and the pain & discomfort group. We compared bowel symptoms, extraintestinal symptoms, IBS-quality of life, psychological status and healthcare-seeking behaviors, and efficacy among the three groups and tested risk factors for symptom reporting in IBS patients.

Research results

About one-third of patients meeting Rome III criteria failed to meet Rome IV criteria for an IBS diagnosis. There were no meaningful differences between the pain group and discomfort group for frequency of defecatory abdominal pain or discomfort, bowel habits, coexisting extragastrointestinal pain, comorbid anxiety and depression, and IBS-quality of life scores.

Research conclusions

IBS patients with abdominal discomfort have similar bowel symptoms and psychosocial features to those with abdominal pain.

Research perspectives

Further studies focused on the pathophysiology and therapeutic response (including the cultural influence) of abdominal pain and discomfort are needed.

ACKNOWLEDGEMENTS

The authors thank their colleagues in the Department of Gastroenterology, Peking Union Medical College Hospital for their contributions to the enrollment of IBS patients.

FOOTNOTES

Author contributions: Fang XC was responsible for study concept and design, data collection and interpretation, and drafting and revision of the manuscript; Fan WJ participated in data collection, data analysis, and figure drafting; Drossman DD was responsible for critical revision; Han SM participated in data analysis; Ke MY participated in critical revision; all authors approved the final version of the manuscript as submitted.

Supported by the Program of International S & T Cooperation, No. 2014DFA31850; the National Natural Science Foundation of China, No. 81870379 and No. 81370488; and the Project of the National Key Technologies R & D Program in the 11th Five Year Plan period, No. 2007BAI04B01.

Institutional review board statement: This study was reviewed and approved by the Peking Union Medical College Hospital Ethics Committee, No. S-234.

Informed consent statement: All study participants provided oral or written consent to participate before study enrollment.

Conflict-of-interest statement: There are no conflicts of interest to report.

Data sharing statement: No additional data are available.

STROBE statement: The authors have read the STROBE Statement—checklist of items, and the manuscript was prepared and revised according to the STROBE Statement—checklist of items.

Open-Access: This article is an open-access article that was selected by an in-house editor and fully peer-reviewed by external reviewers. It is distributed in accordance with the Creative Commons Attribution NonCommercial (CC BY-NC 4.0) license, which permits others to distribute, remix, adapt, build upon this work non-commercially, and license their derivative works on different terms, provided the original work is properly cited and the use is non-commercial. See: https://creativecommons.org/Licenses/by-nc/4.0/

Country/Territory of origin: China

ORCID number: Xiu-Cai Fang 0000-0002-5600-8779; Wen-Juan Fan 0000-0002-2927-9266; Douglas D Drossman 0000-0002-8178-0453; Shao-Mei Han 0000-0003-2081-7969; Mei-Yun Ke 0000-0001-5793-9500.

S-Editor: Chen YL
L-Editor: Filipodia
P-Editor: Yuan YY

REFERENCES

1 **Sperber AD**, Bangdiwala SI, Drossman DA, Ghoshal UC, Simren M, Tack J, Whitehead WE, Dumitrascu DL, Fang X, Fukudo S, Kellow J, Okeke E, Quigley EMM, Schmulson M, Whorwell P, Archampong T, Adibi P, Andresen V, Benninga MA, Bonaz B, Bor S, Fernandez LB, Choi SC, Corazziari ES, Francisconi C, Hani A, Lazebnik L, Lee YY, Mulak A, Rahman MM, Santos J, Setshedi M, Syam AF, Vanner S, Wong RK, Lopez-Colombo A, Costa V, Dickman R, Kanazawa M, Keshteli AH, Khatun R, Maleki I, Poitras P, Pratap N, Stefanyuk O, Thomson S, Zeevenhooven J, Palsson OS. Worldwide Prevalence and Burden of Functional Gastrointestinal Disorders, Results of Rome Foundation Global Study. *Gastroenterology* 2021; **160**: 99-114.e3 [PMID: 32294476 DOI: 10.1053/j.gastro.2020.04.014]

2 **Drossman DA**, Corazziari E, Delvaux M. Rome III-functional gastrointestinal disorders. 3th ed. BW & A Books, inc: Durham, 2006

3 **Mearin F**, Lacy BE, Chang L, Chey WD, Lembo AJ, Simren M, Spiller R. Bowel Disorders. *Gastroenterology* 2016 [PMID: 27144627 DOI: 10.1053/j.gastro.2016.02.031]

4 **Fang X**, Francisconi CF, Fukudo S, Gerson MJ, Kang JY, Schmulson W MJ, Sperber AD. Multicultural Aspects in Functional Gastrointestinal Disorders (FGIDs). *Gastroenterology* 2016 [PMID: 27144623 DOI: 10.1053/j.gastro.2016.02.013]

5 **Spiegel BM**, Bolus R, Agarwal N, Sayuk G, Harris LA, Lucak S, Esrailian E, Chey WD, Lembo A, Karsan H, Tillisch K, Talley J, Chang L. Measuring symptoms in the irritable bowel syndrome: development of a framework for clinical trials. *Aliment Pharmacol Ther* 2010; **32**: 1275-1291 [PMID: 20955447 DOI: 10.1111/j.1365-2036.2010.04464.x]

6 **Palsson OS**, Whitehead W, Törnblom H, Sperber AD, Simren M. Prevalence of Rome IV Functional Bowel Disorders Among Adults in the United States, Canada, and the United Kingdom. *Gastroenterology* 2020; **158**: 1262-1273.e3 [PMID: 31917991 DOI: 10.1053/j.gastro.2019.12.021]

7 **Aziz I**, Törnblom H, Palsson OS, Whitehead WE, Simrén M. How the Change in IBS Criteria From Rome III to Rome IV Impacts on Clinical Characteristics and Key Pathophysiological Factors. *Am J Gastroenterol* 2018; **113**: 1017-1025 [PMID: 29880963 DOI: 10.1038/s41395-018-0074-z]

8 **Patcharatrakul T**, Thanapirom K, Gonlachanvit S. Application of Rome III vs. Rome IV diagnostic criteria for irritable bowel syndrome (IBS) in clinical practice: is the newer the better? *Gastroenterology* 2017; **152**: S717

9 **Bai T**, Xia J, Jiang Y, Cao H, Zhao Y, Zhang L, Wang H, Song J, Hou X. Comparison of the Rome IV and Rome III criteria for IBS diagnosis: A cross-sectional survey. *J Gastroenterol Hepatol* 2017; **32**: 1018-1025 [PMID: 27862281 DOI: 10.1111/jgh.13642]

10 **Wang B**, Zhao W, Zhao C, Jin H, Zhang L, Chen Q, Wang B. What impact do Rome IV criteria have on patients with IBS in China? *Scand J Gastroenterol* 2019; **54**: 1433-1440 [PMID: 31829752 DOI: 10.1080/00365521.2019.1698650]

11 **Sach J**, Bolus R, Fitzgerald L, Naliboff BD, Chang L, Mayer EA. Is there a difference between abdominal pain and discomfort in moderate to severe IBS patients? *Am J Gastroenterol* 2002; **97**: 3131-3138 [PMID: 12492200 DOI: 10.1111/j.1572-0241.2002.07110.x]

12 **Lembo T**, Naliboff B, Munakata J, Fullerton S, Saba L, Tung S, Schmulson M, Mayer EA. Symptoms and visceral perception in patients with pain-predominant irritable bowel syndrome. *Am J Gastroenterol* 1999; **94**: 1320-1326 [PMID: 10235213 DOI: 10.1111/j.1572-0241.1999.01009.x]

13 **Pan G**, Lu S, Ke M, Han S, Guo H, Fang X. Epidemiologic study of the irritable bowel syndrome in Beijing: stratified randomized study by cluster sampling. *Chin Med J (Engl)* 2000; **113**: 35-39 [PMID: 11775207]

14 **Zhu L**, Huang D, Shi L, Liang L, Xu T, Chang M, Chen W, Wu D, Zhang F, Fang X. Intestinal symptoms and psychological factors jointly affect quality of life of patients with irritable bowel syndrome with diarrhea. *Health Qual Life Outcomes* 2015; **13**: 49 [PMID: 25925746 DOI: 10.1186/s12955-015-0243-3]

15 **Vakil N**, van Zanten SV, Kahrilas P, Dent J, Jones R; Global Consensus Group. The Montreal definition and classification of gastroesophageal reflux disease: a global evidence-based consensus. *Am J Gastroenterol* 2006; **101**: 1900-20; quiz 1943 [PMID: 16928254 DOI: 10.1111/j.1572-0241.2006.00630.x]

16 **Huang WW**, Zhou FS, Bushnell DM, Diakite C, Yang XH. Cultural adaptation and application of the IBS-QOL in China: a disease-specific quality-of-life questionnaire. *Qual Life Res* 2007; **16**: 991-996 [PMID: 17440830 DOI: 10.1007/s11136-006-9141-9]

17 **Patrick DL**, Drossman DA, Frederick IO, DiCesare J, Puder KL. Quality of life in persons with irritable bowel syndrome: development and validation of a new measure. *Dig Dis Sci* 1998; **43**: 400-411 [PMID: 9512138 DOI: 10.1023/a:1018831127942]

18 **Hamilton M**. The assessment of anxiety states by rating. *Br J Med Psychol* 1959; **32**: 50-55 [PMID: 13638508 DOI: 10.1111/j.2044-8341.1959.tb00467.x]

19 **Hamilton M**. A rating scale for depression. *J Neurol Neurosurg Psychiatry* 1960; **23**: 56-62 [PMID: 14399272 DOI: 10.1136/jnnp.23.1.56]

20 **Black CJ**, Yiannakou Y, Houghton LA, Ford AC. Epidemiological, Clinical, and Psychological Characteristics of Individuals with Self-reported Irritable Bowel Syndrome Based on the Rome IV vs Rome III Criteria. *Clin Gastroenterol Hepatol* 2020; **18**: 392-398.e2 [PMID: 31154027 DOI: 10.1016/j.cgh.2019.05.037]

21 **Vork L**, Weerts ZZRM, Mujagic Z, Kruimel JW, Hesselink MAM, Muris JWM, Keszthelyi D, Jonkers DMAE, Masclee AAM. Rome III vs Rome IV criteria for irritable bowel syndrome: A comparison of clinical characteristics in a large cohort study. *Neurogastroenterol Motil* 2018; **30** [PMID: 28804974 DOI: 10.1111/nmo.13189]

22 **Kanazawa M**, Miwa H, Nakagawa A, Kosako M, Akiho H, Fukudo S. Abdominal bloating is the most bothersome symptom in irritable bowel syndrome with constipation (IBS-C): a large population-based Internet survey in Japan. *Biopsychosoc Med* 2016; **10**: 19 [PMID: 27274765 DOI: 10.1186/s13030-016-0070-8]

23 **Hertig VL**, Cain KC, Jarrett ME, Burr RL, Heitkemper MM. Daily stress and gastrointestinal symptoms in women with irritable bowel syndrome. *Nurs Res* 2007; **56**: 399-406 [PMID: 18004186 DOI: 10.1097/01.NNR.0000299855.60053.88]

24 **Ludidi S**, Mujagic Z, Jonkers D, Keszthelyi D, Hesselink M, Kruimel J, Conchillo J, Masclee A. Markers for visceral hypersensitivity in patients with irritable bowel syndrome. *Neurogastroenterol Motil* 2014; **26**: 1104-1111 [PMID:

24920528 DOI: 10.1111/nmo.12365]

25 **Josefsson A**, Rosendahl A, Jerlstad P, Näslin G, Törnblom H, Simrén M. Visceral sensitivity remains stable over time in patients with irritable bowel syndrome, but with individual fluctuations. *Neurogastroenterol Motil* 2019; **31**: e13603 [PMID: 31012215 DOI: 10.1111/nmo.13603]

26 **Wouters MM**, Balemans D, Van Wanrooy S, Dooley J, Cibert-Goton V, Alpizar YA, Valdez-Morales EE, Nasser Y, Van Veldhoven PP, Vanbrabant W, Van der Merwe S, Mols R, Ghesquière B, Cirillo C, Kortekaas I, Carmeliet P, Peetermans WE, Vermeire S, Rutgeerts P, Augustijns P, Hellings PW, Belmans A, Vanner S, Bulmer DC, Talavera K, Vanden Berghe P, Liston A, Boeckxstaens GE. Histamine Receptor H1-Mediated Sensitization of TRPV1 Mediates Visceral Hypersensitivity and Symptoms in Patients With Irritable Bowel Syndrome. *Gastroenterology* 2016; **150**: 875-87.e9 [PMID: 26752109 DOI: 10.1053/j.gastro.2015.12.034]

27 **Larsson MB**, Tillisch K, Craig AD, Engström M, Labus J, Naliboff B, Lundberg P, Ström M, Mayer EA, Walter SA. Brain responses to visceral stimuli reflect visceral sensitivity thresholds in patients with irritable bowel syndrome. *Gastroenterology* 2012; **142**: 463-472.e3 [PMID: 22108191 DOI: 10.1053/j.gastro.2011.11.022]

28 **Lee KN**, Lee OY, Choi MG, Sohn CI, Huh KC, Park KS, Kwon JG, Kim N, Rhee PL, Myung SJ, Lee JS, Lee KJ, Park H, Lee YC, Choi SC, Jung HK, Jee SR, Choi CH, Kim GH, Park MI, Sung IK. Efficacy and Safety of Tiropramide in the Treatment of Patients With Irritable Bowel Syndrome: A Multicenter, Randomized, Double-blind, Non-inferiority Trial, Compared With Octylonium. *J Neurogastroenterol Motil* 2014; **20**: 113-121 [PMID: 24466452 DOI: 10.5056/jnm.2014.20.1.113]

29 **Johnston JM**, Kurtz CB, Macdougall JE, Lavins BJ, Currie MG, Fitch DA, O'Dea C, Baird M, Lembo AJ. Linaclotide improves abdominal pain and bowel habits in a phase IIb study of patients with irritable bowel syndrome with constipation. *Gastroenterology* 2010; **139**: 1877-1886.e2 [PMID: 20801122 DOI: 10.1053/j.gastro.2010.08.041]

30 **Urgesi R**, Casale C, Pistelli R, Rapaccini GL, de Vitis I. A randomized double-blind placebo-controlled clinical trial on efficacy and safety of association of simethicone and Bacillus coagulans (Colinox®) in patients with irritable bowel syndrome. *Eur Rev Med Pharmacol Sci* 2014; **18**: 1344-1353 [PMID: 24867512]

31 **Yao X**, Yang YS, Cui LH, Zhao KB, Zhang ZH, Peng LH, Guo X, Sun G, Shang J, Wang WF, Feng J, Huang Q. Subtypes of irritable bowel syndrome on Rome III criteria: a multicenter study. *J Gastroenterol Hepatol* 2012; **27**: 760-765 [PMID: 21929652 DOI: 10.1111/j.1440-1746.2011.06930.x]

32 **Zhao Y**, Zou D, Wang R, Ma X, Yan X, Man X, Gao L, Fang J, Yan H, Kang X, Yin P, Hao Y, Li Q, Dent J, Sung J, Halling K, Wernersson B, Johansson S, He J. Dyspepsia and irritable bowel syndrome in China: a population-based endoscopy study of prevalence and impact. *Aliment Pharmacol Ther* 2010; **32**: 562-572 [PMID: 20497141 DOI: 10.1111/j.1365-2036.2010.04376.x]

33 **Fan WJ**, Xu D, Chang M, Zhu LM, Fei GJ, Li XQ, Fang XC. Predictors of healthcare-seeking behavior among Chinese patients with irritable bowel syndrome. *World J Gastroenterol* 2017; **23**: 7635-7643 [PMID: 29204063 DOI: 10.3748/wjg.v23.i42.7635]

34 **Xiong LS**, Chen MH, Chen HX, Xu AG, Wang WA, Hu PJ. A population-based epidemiologic study of irritable bowel syndrome in South China: stratified randomized study by cluster sampling. *Aliment Pharmacol Ther* 2004; **19**: 1217-1224 [PMID: 15153175 DOI: 10.1111/j.1365-2036.2004.01939.x]

World Journal of Gastroenterology

Submit a Manuscript: https://www.f6publishing.com

World J Gastroenterol 2022 September 7; 28(33): 4875-4889

DOI: 10.3748/wjg.v28.i33.4875

ISSN 1007-9327 (print) ISSN 2219-2840 (online)

ORIGINAL ARTICLE

Randomized Clinical Trial

Peroral endoscopic myotomy *vs* laparoscopic myotomy and partial fundoplication for esophageal achalasia: A single-center randomized controlled trial

Eduardo Turiani Hourneaux de Moura, José Jukemura, Igor Braga Ribeiro, Galileu Ferreira Ayala Farias, Aureo Augusto de Almeida Delgado, Lara Meireles Azeredo Coutinho, Diogo Turiani Hourneaux de Moura, Rubens Antonio Aissar Sallum, Ary Nasi, Sergio A Sánchez-Luna, Paulo Sakai, Eduardo Guimarães Hourneaux de Moura

Specialty type: Gastroenterology and hepatology

Provenance and peer review: Invited article; Externally peer reviewed.

Peer-review model: Single blind

Peer-review report's scientific quality classification

Grade A (Excellent): 0
Grade B (Very good): B
Grade C (Good): C
Grade D (Fair): 0
Grade E (Poor): 0

P-Reviewer: Bortolotti M, Italy; Sweis R, United Kingdom

Received: May 4, 2022
Peer-review started: May 4, 2022
First decision: June 2, 2022
Revised: July 7, 2022
Accepted: August 6, 2022
Article in press: August 6, 2022
Published online: September 7, 2022

Eduardo Turiani Hourneaux de Moura, Igor Braga Ribeiro, Paulo Sakai, Eduardo Guimarães Hourneaux de Moura, Departamento de Gastroenterologia, Faculdade de Medicina, Universidade de Sao Paulo, Serviço de Endoscopia Gastrointestinal do Hospital das Clínicas HCFMUSP, Sao Paulo 05403-010, Brazil

José Jukemura, Rubens Antonio Aissar Sallum, Ary Nasi, Division of Esophageal Surgery, Hospital das Clínicas, University of São Paulo School of Medicine, Sao Paulo 05403-010, Brazil

Galileu Ferreira Ayala Farias, Aureo Augusto de Almeida Delgado, Lara Meireles Azeredo Coutinho, Diogo Turiani Hourneaux de Moura, Departamento de Gastroenterologia, Faculdade de Medicina, Universidade de Sao Paulo, Hospital das Clínicas, University of São Paulo School of Medicine, Sao Paulo 05403-010, Brazil

Sergio A Sánchez-Luna, Department of Internal Medicine, The University of Alabama at Birmingham Heersink School of Medicine, Basil I. Hirschowitz Endoscopic Center of Excellence, Division of Gastroenterology and Hepatology, Birmingham, AL 35233, United States

Corresponding author: Igor Braga Ribeiro, MD, PhD, Associate Research Scientist, Attending Doctor, Doctor, Research Scientist, Departamento de Gastroenterologia, Faculdade de Medicina, Universidade de Sao Paulo, Serviço de Endoscopia Gastrointestinal do Hospital das Clínicas HCFMUSP, Av. Dr Enéas de Carvalho Aguiar, 225, 6o Andar, Bloco 3, Cerqueira Cesar, Sao Paulo 05403-010, Brazil. igorbraga1@gmail.com

Abstract

BACKGROUND

Achalasia is a rare benign esophageal motor disorder characterized by incomplete relaxation of the lower esophageal sphincter (LES). The treatment of achalasia is not curative, but rather is aimed at reducing LES pressure. In patients who have failed noninvasive therapy, surgery should be considered. Myotomy with partial fundoplication has been considered the first-line treatment for non-advanced achalasia. Recently, peroral endoscopic myotomy (POEM), a technique that

employs the principles of submucosal endoscopy to perform the equivalent of a surgical myotomy, has emerged as a promising minimally invasive technique for the management of this condition.

AIM

To compare POEM and laparoscopic myotomy and partial fundoplication (LM-PF) regarding their efficacy and outcomes for the treatment of achalasia.

METHODS

Forty treatment-naive adult patients who had been diagnosed with achalasia based on clinical and manometric criteria (dysphagia score ≥ II and Eckardt score > 3) were randomized to undergo either LM-PF or POEM. The outcome measures were anesthesia time, procedure time, symptom improvement, reflux esophagitis (as determined with the Gastroesophageal Reflux Disease Questionnaire), barium column height at 1 and 5 min (on a barium esophagogram), pressure at the LES, the occurrence of adverse events (AEs), length of stay (LOS), and quality of life (QoL).

RESULTS

There were no statistically significant differences between the LM-PF and POEM groups regarding symptom improvement at 1, 6, and 12 mo of follow-up (P = 0.192, P = 0.242, and P = 0.242, respectively). However, the rates of reflux esophagitis at 1, 6, and 12 mo of follow-up were significantly higher in the POEM group (P = 0.014, P < 0.001, and P = 0.002, respectively). There were also no statistical differences regarding the manometry values, the occurrence of AEs, or LOS. Anesthesia time and procedure time were significantly shorter in the POEM group than in the LM-PF group (185.00 ± 56.89 and 95.70 ± 30.47 min *vs* 296.75 ± 56.13 and 218.75 ± 50.88 min, respectively; P = 0.001 for both). In the POEM group, there were improvements in all domains of the QoL questionnaire, whereas there were improvements in only three domains in the LM-PF group.

CONCLUSION

POEM and LM-PF appear to be equally effective in controlling the symptoms of achalasia, shortening LOS, and minimizing AEs. Nevertheless, POEM has the advantage of improving all domains of QoL, and shortening anesthesia and procedure times but with a significantly higher rate of gastroesophageal reflux.

Key Words: Esophageal achalasia; Gastroesophageal reflux; Deglutition disorders; Heller myotomy; Fundoplication; Randomized controlled trial

©The Author(s) 2022. Published by Baishideng Publishing Group Inc. All rights reserved.

Core Tip: This randomized controlled trial compared the efficacy and outcomes of laparoscopic myotomy and partial fundoplication (LM-PF) with those of peroral endoscopic myotomy (POEM) for the treatment of patients with achalasia of any etiology. There were no statistically significant differences between the LM-PF and POEM groups regarding symptoms. However, the rates of reflux esophagitis were significantly higher in the POEM group. POEM and LM-PF appear to be equally effective in controlling the symptoms of achalasia, shortening length of hospital stay, and minimizing adverse events. However, POEM has the advantage of shortening anesthesia and procedure times.

Citation: de Moura ETH, Jukemura J, Ribeiro IB, Farias GFA, de Almeida Delgado AA, Coutinho LMA, de Moura DTH, Aissar Sallum RA, Nasi A, Sánchez-Luna SA, Sakai P, de Moura EGH. Peroral endoscopic myotomy *vs* laparoscopic myotomy and partial fundoplication for esophageal achalasia: A single-center randomized controlled trial. *World J Gastroenterol* 2022; 28(33): 4875-4889

URL: https://www.wjgnet.com/1007-9327/full/v28/i33/4875.htm

DOI: https://dx.doi.org/10.3748/wjg.v28.i33.4875

INTRODUCTION

Achalasia is a rare benign esophageal motor disorder characterized by incomplete relaxation of the lower esophageal sphincter (LES)[1-3]. For primary or idiopathic achalasia, the underlying etiology has yet to be clearly defined; secondary achalasia results from any one of several systemic diseases including infectious, autoimmune, and drug-induced disorders[4-6]. In both cases, the most common

symptoms are progressive dysphagia, regurgitation, and weight loss. The symptom intensity and treatment response can be assessed with validated scales such as the Eckardt score[2,7,8]. The diagnosis requires the proper integration between reported symptoms and the interpretation of diagnostic tests such as a barium esophagogram, esophagogastroduodenoscopy (EGD), and manometry—either conventional esophageal manometry (EM) or high-resolution manometry (HRM)[9-12].

The treatment of achalasia is not curative but rather is aimed at reducing LES pressure[13-17]. In patients who have failed noninvasive therapy, surgery should be considered[18]. Myotomy with partial fundoplication has been considered the first-line treatment for non-advanced achalasia[19].

Recently, peroral endoscopic myotomy (POEM), a technique that employs the principles of submucosal endoscopy to perform the equivalent of a surgical myotomy, has emerged as a promising minimally invasive technique for the management of this condition[20]. This technique was first described in 1980 and subsequently modified to create what is now POEM[21,22].

This randomized controlled trial (RCT) compared the efficacy and outcomes of laparoscopic myotomy and partial fundoplication (LM-PF) with those of POEM for the treatment of patients with achalasia of any etiology. We also compared the two procedures in terms of the incidence of reflux esophagitis.

MATERIALS AND METHODS

Study design and participants

This was a single-center RCT in which we evaluated 40 treatment-naive patients with esophageal achalasia. We included patients ≥ 18 years of age who had been diagnosed with achalasia based on clinical and manometric criteria (dysphagia score ≥ II and Eckardt score > 3) and who provided informed consent. Patients who had previously undergone endoscopic or surgical procedures involving the esophagogastric junction (EGJ) were excluded, as were those with liver cirrhosis, esophageal varices, Barrett's esophagus, esophageal strictures, premalignant or malignant EGJ lesions, coagulopathies, pseudoachalasia, esophageal diverticulum, severe cardiopulmonary diseases, or severe systemic diseases, as well as those who were at high surgical risk and those who were pregnant or lactating.

Randomization strategy

An investigator who was unaffiliated with the trial created the randomization list. Specific software (www.randomizer.org) was used, and participants were randomly allocated at a 1:1 ratio to the experimental (POEM) group or the comparison (LM-PF) group.

Sample size calculation

The sample size was calculated to identify statistical significance between LM-PF and POEM regarding reflux esophagitis rates, which were assumed to be 5% and 40% after LM-PF and POEM, respectively [23]. To achieve a power of 80% with an alpha of 0.05, we estimated the minimum sample size to be 38 (19 patients in each group). Taking potential losses into consideration, we chose to include a total of 40 patients.

Techniques

POEM: All POEM procedures were performed by a single operator with extensive experience in the technique. Prophylactic intravenous antibiotics and a proton pump inhibitor (PPI) were administered 30 min before intubation and general anesthesia.

After the gastroscope was introduced, the esophageal lumen and mucosa were thoroughly cleaned. This was followed by submucosal injection of 10 mL of 0.5% indigo carmine. An incision was made into the mucosa of the posterior wall, between 5 and 6 o'clock, at 10 cm above the EGJ. The incision was made with a dual-function submucosal dissection knife (HybridKnife; Erbe, Tübingen, Germany) in Endocut Q mode (effect 2, width 3, and interval 5). Subsequently, spray coagulation (effect 2 at 40 W) was used to create a submucosal tunnel extending 3-4 cm beyond the EGJ into the proximal stomach. In all patients, full-thickness myotomy—including the circular and longitudinal muscle layers—was performed in Endocut Q mode. The myotomy was initiated 2 cm distal from the mucosal entry point and extended 3-4 cm into the proximal stomach. The mucosal incision was closed by using through-the-scope clips (Supplementary Figures 1 and 2).

A barium esophagogram was obtained on postoperative day 1. In the absence of complications, the patient was started on a clear liquid diet and subsequently advanced to a full liquid diet for 14 d.

LM-PF: All LM-PF procedures were performed by members of the foregut surgery group. After pneumoperitoneum had been established, five trocars were positioned, after which the left hepatic lobe was retracted to access the EGJ (Supplementary Figure 3). That was followed by division of the phrenoesophageal ligament, dissection, and isolation of the distal esophagus from adjacent structures; and anterolateral dislocation of the distal esophagus. The anterior gastric adipose tissue and the anterior vagus nerve were dissected and separated from the esophagus and stomach, after which myotomy of

the circular and longitudinal muscle layers was performed, extending from 5-6 cm above the EGJ to 2-3 cm below the EGJ. Partial fundoplication between the esophagus and stomach was then performed by placing sutures in three planes: Posterior—two to three sutures; left lateral—four to five sutures (on the left side); and right anterior—a line of sutures covering the myotomy, thus interposed with the gastric fundus on the right. In the absence of complications, patients were started on a clear liquid diet on the morning following the procedure and maintained on a mechanical soft diet for 14 d after discharge.

Diagnosis and follow-up

Clinical assessments: Although achalasia subtyping is defined based on HRM, in this study, the achalasia subtype was evaluated according to the degree of esophageal dilation on the barium esophagogram and esophageal motor activity on EM or HRM. Given that Chagas disease, which often involves the esophagus, is common in Brazil, all patients were screened for anti-*Trypanosoma cruzi* antibodies by enzyme-linked immunosorbent assay and indirect immunofluorescence. Weight loss, dysphagia, and pain were assessed before the procedure, as well as at 6 and 12 mo after the procedure, by using the Eckardt score. Patients with an Eckardt score ≥ 3 were categorized as symptomatic. The clinical evaluation of gastroesophageal reflux (GER) and the diagnosis of GER disease (GERD) was based on the application of the GER Disease Questionnaire (GerdQ)[24] (Supplementary Figure 4).

EGD: We performed EGD before the procedure, as well as at 6 and 12 mo after. Esophagitis was graded according to the Los Angeles classification system[25]. We performed chromoendoscopy with narrow-band imaging and 2.5% Lugol's solution to screen for esophageal cancer. Suspicious lesions were biopsied.

Barium esophagogram: To assess esophageal emptying before and 12 mo after the procedure, we used a timed barium esophagogram, as previously described[26]. The degree of esophageal emptying is qualitatively estimated by comparing 1- and 5-min images or by measuring the height and width (in centimeters) of the barium column at both times, calculating the approximate area, and determining the percentage change in the area.

EM: Conventional EM was performed before and 12 mo after the procedure. It should be noted that HRM technology was not available in Brazil when the trial began. To perform conventional EM, we used an eight-channel computerized polygraph under pneumohydraulic capillary infusion at a flow rate of 0.6 mL/min/channel. Preparation was required with a 12-h fast and suspension of medications that alter esophageal motility. The technique consists of passing a probe through the nostril and checking the position in the stomach through deep inspiration. With the patient in the supine position, the probe is pulled centimeter by centimeter to measure the mean respiratory pressure and pressure inversion point, and then one of the channels is positioned distal to 3 cm from the upper edge of the LES and the other channels are distant 5 cm apart. Finally, the catheter is pulled up to the upper esophageal sphincter. Through the average of the four distal radial channels of the conventional manometry catheter, the maximum expiratory pressure (MEP) was identified, which best represents the LES pressure itself.

Quality of life: To evaluate the quality of life (QoL), we used the Medical Outcomes Study 36-item Short-Form Health Survey (SF-36)[27,28]. The SF-36 comprises 36 questions covering eight domains: Physical functioning, role-physical, bodily pain, general health, vitality, social functioning, role-emotional, and mental health.

Adverse events: Among the adverse events (AEs) recorded, pneumoperitoneum requiring drainage or puncture was categorized as a minor AE, as was minor mucosal damage requiring endoscopic closure. Major AEs were defined as pneumoperitoneum leading to hemodynamic instability and premature interruption of the procedure; bleeding requiring a blood transfusion and accompanied by hemodynamic instability or requiring an additional intervention; major mucosal damage requiring endoscopic closure or increasing the length of stay (LOS); or fistula/dehiscence of the incision with signs of fever or infection associated with hemodynamic instability. For AEs occurring in the LM-PF group, we used the Clavien-Dindo classification[29].

Outcome measures and data collection

For POEM and LM-PF, the following outcome measures were evaluated: Operative time; length of the myotomy in the esophagus and stomach; myotomy site; complications; and LOS. Patient data were collected on the Research Electronic Data Capture platform.

Follow-up

At 1, 6, and 12 mo after the interventions, the Eckardt score was determined, the SF-36 was applied, EGD was performed, and timed barium esophagograms were obtained. Conventional EM was performed at 6 and 12 mo. Patients received the maximum dose of PPI for the first 30 d postprocedure, and those who presented with erosive esophagitis at follow-up endoscopy were maintained on PPI

treatment for 8 wk. Treatment success was defined as symptom improvement (≤ 3-point reduction in the Eckardt score), an LES pressure < 15 mmHg[30-32], and a > 50% reduction in the height of the barium column at 1 min. Treatment failure was defined as symptom persistence in patients with an Eckardt score ≥ 3.

Statistical analysis

We performed descriptive analyses of all study variables. Quantitative variables were expressed as means with standard deviations or as medians with interquartile ranges. Qualitative variables are expressed as absolute and relative frequencies. For the comparison of means between the two groups, the Student's *t*-test was used. When the assumption of normality was rejected, the nonparametric Mann-Whitney test was used. To test the homogeneity between proportions, the chi-square test or Fisher's exact test was used. Repeated-measures analysis of variance was used to compare the groups over the course of the study. When the assumption of normality was rejected, the nonparametric Mann-Whitney test and Friedman test were used. The data were processed with the SPSS Statistics software package, version 17.0 for Windows (SPSS Inc., Chicago, IL, United States). $P < 0.05$ was considered statistically significant.

RESULTS

Population characteristics

Between March 2017 and February 2018, 40 patients diagnosed with achalasia were enrolled and randomized to undergo LM-PF ($n = 20$) or POEM ($n = 20$), as detailed in Figure 1. Nine (22.5%) of the forty patients (five in the POEM group and four in the LM-PF group) tested positive for anti-*T. cruzi* antibodies, indicating exposure to Chagas disease. At baseline, there was no statistical difference between the two groups in terms of sex, age, etiology, grade, symptom duration, weight, body mass index, or Eckardt score (Table 1). The study was terminated after all patients had been followed for at least 12 mo.

Treatment outcomes

Eckardt scores at 1, 6, and 12 mo were lower than the baseline scores in both groups—1.0, 0.5, and 0.50, respectively, *vs* 8.0, in the POEM group; and 0.0, 0.0, and 0.0, respectively, *vs* 8.5, in the LM-PF group—and the differences were statistically significant ($P < 0.001$; Table 2). There were no statistical differences between the two groups for the Eckardt scores at 1, 6, and 12 mo of follow-up ($P = 0.192$, $P = 0.242$, and $P = 0.242$, respectively).

In the POEM group, treatment success was confirmed at 1 mo in all 20 patients, at 6 mo in 18 of the patients (90%), and at 12 mo in 19 (95%). In the LM-PF group, treatment success was confirmed at 1 mo and was maintained at 6 and 12 mo in all 20 patients. As shown in Table 3, there was no statistical difference between the two groups regarding treatment success at 1, 6, or 12 mo ($P = 0.487$ and $P = 1.000$ for 6 and 12 mo, respectively).

In both groups, there were significant postprocedural improvements in dysphagia, although the differences were not significant at 1, 6, or 12 mo ($P = 0.602$; $P = 0.565$, and $P = 0.547$, respectively). However, statistically significant improvements in weight loss, chest pain, and regurgitation were observed in both groups (Supplementary Tables 1 and 2). The postprocedure rate of GER, as assessed with the GerdQ, was higher in the POEM group than in the LM-PF group (64.6% *vs* 11.1%; $P < 0.02$).

Endoscopic findings

At 1, 6, and 12 mo, only 20, 18, and 18 POEM group patients, respectively, underwent EGD, as did only 17, 16, and 17 LM-PF group patients, respectively. The remaining patients declined to undergo EGD because they were asymptomatic. The rates of esophagitis were significantly higher in the POEM group than in the LM-PF group at 1, 6, and 12 mo of follow-up ($P = 0.014$, $P < 0.001$, and $P = 0.002$, respectively). In the LM-PF group, 1 patient had esophagitis (classified as grade A) at 6 mo and 2 patients had esophagitis (classified as grades B and C, respectively) at 12 mo. In the POEM group, esophagitis was observed at 1 mo in 5 patients (being classified as grade A in one, grade B in three, and grade C in one), at 6 mo in 10 patients (being classified as grade A in three, grade B in two, and grade C in five), and at 12 mo in 11 patients (being classified as grade A in five, grade C in four, and grade D in two). At 1, 6, and 12 mo, the rates of esophagitis were 0.0%, 5.6%, and 11.1%, respectively, in the LM-PF group and 29.4%, 62.5%, and 64.6%, respectively, in the POEM group (Table 4).

Barium esophagogram

Table 5 shows the results of the barium esophagogram. In both groups, the heights of the barium column at 1 and 5 min were significantly lower at 1, 6, and 12 mo than at baseline ($P < 0.001$). There was no statistical difference between the two groups regarding the barium column height values at 1 and 5 min in the follow-up periods (intent-to-treat analysis: $P = 0.429$ and 0.773; per-protocol analysis: $P =$

Table 1 Characteristics of the study population

Variable	Total (*n* = 40)	Group		*P* value
		LM-PF (*n* = 20)	POEM (*n* = 20)	
Male, *n* (%)	26 (65)	14 (70.0)	12 (60.0)	0.507
Age in yr, mean ± SD	44.55 (13.77)	44.20 (13.21)	44.90 (14.64)	0.875
Etiology of achalasia, *n* (%)				1.000
Chagas disease	9 (22.5)	4 (20.0)	5 (25.0)	
Idiopathic	31 (77.5)	16 (80.0)	15 (75.0)	
BMI in kg/m^2, mean ± SD	22.78 (4.49)	22.79 (4.41)	22.77 (4.70)	0.988
Eckardt score, median (IQR)	8.00 (6.25-9.00)	8.50 (7.25-9.75)	8.00 (6.00-9.00)	0.478

BMI: Body mass index; IQR: Interquartile range; LM-PF: Laparoscopic myotomy and partial fundoplication; POEM: Peroral endoscopic myotomy.

Table 2 Eckardt scores

Time point	Total (*n* = 40), median (IQR)	Group		*P* value[1]
		LM-PF (*n* = 20), median (IQR)	POEM (*n* = 20), median (IQR)	
Baseline	8.00 (6.25-9.00)	8.50 (7.25-9.75)	8.00 (6.00-9.00)	0.478
1 mo	0.00 (0.00-1.00)	0.00 (0.00-1.00)	1.00 (0.00-1.00)	0.192
6 mo	0.00 (0.00-1.75)	0.00 (0.00-1.00)	0.50 (0.00-2.00)	0.242
12 mo	0.00 (0.00-1.75)	0.00 (0.00-1.00)	0.50 (0.00-2.00)	0.242

[1]Nonparametric Mann-Whitney test.
IQR: Interquartile range; LM-PF: Laparoscopic myotomy and partial fundoplication; POEM: Peroral endoscopic myotomy.

Table 3 Treatment success

Time point	Total (*n* = 40), *n* (%)	Group		*P* value[1]
		LM-PF (*n* = 20), *n* (%)	POEM (*n* = 20), *n* (%)	
1 mo	40 (100.0)	20 (100.0)	20 (100.0)	-
6 mo	38 (95.0)	20 (100.0)	18 (90.0)	0.487
12 mo	39 (97.50)	20 (100.0)	19 (95.0)	1.000

[1]Fisher's exact test.
LM-PF: Laparoscopic myotomy and partial fundoplication; POEM: Peroral endoscopic myotomy.

0.505 and 0.922).

EM

In both groups, the MEP values were significantly lower at 6 and 12 mo than at baseline (Table 6). There was no statistical difference between the two groups at either of those time points (intention-to-treat analysis: $P = 0.848$).

AEs, LOS, anesthesia time, and procedure time

Table 7 describes the AEs, LOS, anesthesia time, and procedure time, in the sample as a whole and by groups. There was no statistical difference between the two groups regarding the rate of AEs ($P = 0.605$). The relevant complications observed in the immediate postprocedural period included empyema requiring thoracostomy in one (5%) of the LM-PF patients, and inadvertent intraoperative mucosal damage in three (15%) of the POEM patients (treated with endoscopic clipping). The clinical outcomes were favorable in all patients. The mean LOS was 3.95 ± 3.36 d in the LM-PF group, compared with 3.40 ± 0.75 d in the POEM group ($P = 0.483$). The mean anesthesia time and mean procedure time were both

Table 4 Reflux esophagitis

Time point	*n* (%) of Total	Group		*P* value[1]
		LM-PF, *n* (%) of Total	POEM, *n* (%) of Total	
Baseline	1 (2.5) of 40	0 (0.0) of 20	1 (5.0) of 20	1.000
1 mo	5 (13.5) of 37	0 (0.0) of 20	5 (29.4) of 17	0.014
6 mo	11 (32.4) of 34	1 (5.6) of 18	10 (62.5) of 16	< 0.001
12 mo	13 (37.1) of 35	2 (11.1) of 18	11 (64.6) of 17	0.002

[1]Fisher's exact test.
LM-PF: Laparoscopic myotomy and partial fundoplication; POEM: Peroral endoscopic myotomy.

Table 5 Height of the barium column in cm

Variable	Total (*n* = 40)	Group	
		LM-PF (*n* = 20)	POEM (*n* = 20)
Height at 1 min			
Baseline	17.48 (8.11)	16.97 (6.70)	17.99 (9.46)
1 mo	9.90 (5.88)	11.39 (4.18)	8.42 (6.99)
6 mo	8.91 (4.49)	9.61 (3.72)	8.22 (5.15)
12 mo	10.35 (3.38)	10.98 (2.73)	9.73 (3.90)
Height at 5 min			
Baseline	15.31 (8.13)	14.92 (7.06)	15.69 (9.24)
1 mo	5.53 (5.41)	6.30 (4.84)	4.75 (5.95)
6 mo	5.69 (5.14)	5.99 (4.56)	5.39 (5.77)
12 mo	8.31 (4.96)	8.66 (4.92)	7.97 (5.10)

Data are presented as mean ± SD. LM-PF: Laparoscopic myotomy and partial fundoplication; POEM: Peroral endoscopic myotomy.

Table 6 Esophageal manometry results of lower esophageal sphincter pressure in mmHg

Variable	Time point	Total (*n* = 40)	Group	
			LM-PF (*n* = 20)	POEM (*n* = 20)
Maximal expiratory pressure	Baseline	25.98 (10.42)	24.53 (9.90)	27.43 (10.98)
	6 mo	10.44 (5.86)	9.93 (5.45)	10.94 (6.34)
	12 mo	10.11 (5.09)	9.34 (4.19)	10.87 (5.85)

Data are presented as mean ± SD. LM-PF: Laparoscopic myotomy and partial fundoplication; POEM: Peroral endoscopic myotomy.

shorter in the POEM group than in the LM-PF group (185.00 ± 56.89 and 95.70 ± 30.47 min, respectively, *vs* 296.75 ± 56.13 and 218.75 ± 50.88 min, respectively; $P < 0.001$ for both).

QoL

Table 8 shows the results obtained with the SF-36. In the POEM group, there were postprocedural improvements in all SF-36 domains, whereas there were improvements in only three domains (physical functioning, energy/fatigue, and general health) in the LM-PF group.

Table 7 Adverse events, length of hospital stay, anesthesia time, and procedure time

Variable	Total (*n* = 40)	Group		*P* value
		LM-PF (*n* = 20)	POEM (*n* = 20)	
Adverse events, *n* (%)	4 (10.0)	1 (5.0)	3 (15.0)	0.605[a]
Length of hospital stay in d	3.68 (2.42)	3.95 (3.36)	3.40 (0.75)	0.483[b]
Anesthesia time in min	240.88 (79.46)	296.75 (56.13)	185.00 (56.89)	< 0.001[b]
Procedure time in min	157.23 (74.81)	218.75 (50.88)	95.70 (30.47)	< 0.001[b]

[a]Fisher's exact test.
[b]Student's *t*-test.
Data are presented as mean ± SD, unless noted otherwise. LM-PF: Laparoscopic myotomy and partial fundoplication; POEM: Peroral endoscopic myotomy.

Table 8 Quality of life

SF-36 domain	Baseline score		*P* value	Score at 12 mo		*P* value
	LM-PF (*n* = 20), median (IQR)	POEM (*n* = 20), median (IQR)		LM-PF (*n* = 20), median (IQR)	POEM (*n* = 20), median (IQR)	
Physical functioning	95.00 (70.0-100.0)	77.50 (62.25-95.0)	0.165	100.0 (90.0-100.0)	92.50 (66.25-100.0)	0.183
Role-physical	100.0 (56.25-100.0)	25.0 (0.00-68.75)	0.012	100.0 (100.0-100.0)	100.0 (56.25-100.0)	0.445
Role-emotional	100.0 (33.30-100.0)	33.30 (0.00-66.70)	0.021	100.0 (66.70-100.0)	100.0 (41.65-100.0)	0.640
Vitality	67.5 (46.25-88.75)	52.50 (36.25-65.00)	0.052	85.0 (56.25-100.0)	80.0 (56.25-90.0)	0.341
Mental health	74.0 (54.0-95.0)	58.0 (44.0-75.0)	0.030	94.0 (69.0-100.0)	80.0 (57.0-91.0)	0.174
Social functioning	81.25 (62.50-100.0)	56.25 (37.50-71.88)	0.006	100.0 (78.13-100.0)	93.75 (40.63-100.0)	0.174
Bodily pain	73.75 (49.38-97.50)	62.50 (45.0-79.38)	0.201	90.0 (78.13-100.0)	80.0 (55.0-97.50)	0.142
General health	50.0 (31.25-83.75)	55.0 (41.25-65.0)	0.698	82.50 (61.25-100.0)	67.50 (52.50-100.0)	0.445

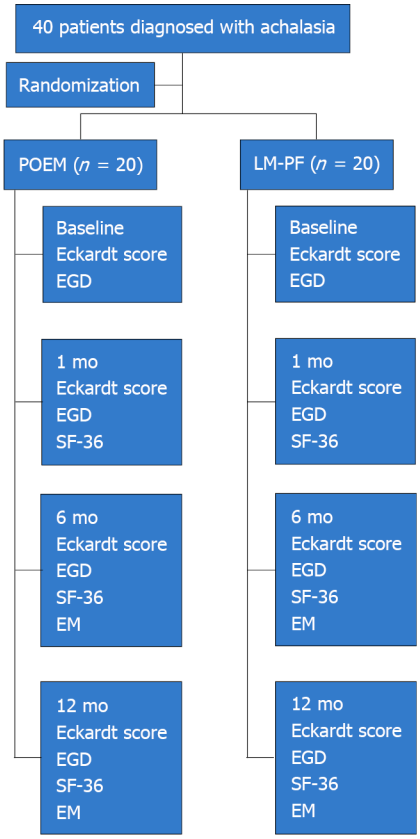
IQR: Interquartile range; LM-PF: Laparoscopic myotomy and partial fundoplication; POEM: Peroral endoscopic myotomy; SF-36: Medical Outcomes Study 36-item Short-Form Health Survey.

DISCUSSION

In this single-center RCT comparing POEM and LM-PF in treatment-naive patients with achalasia, a significant proportion of the patients evaluated had achalasia attributed to Chagas disease. In a study by Farias *et al*[33], no statistical difference was observed between idiopathic and Chagas disease-associated achalasia regarding treatment success and AEs with POEM.

For years, LM-PF has been considered the gold-standard treatment for achalasia[34], because it provides good clinical results, has a low reintervention rate, and has adequate reproducibility. In the first study involving the use of endoscopic myotomy[21], conducted in 1980, all 17 of the patients in the sample showed symptom improvement. Although, technical improvements proposed by Inoue *et al*[22] in 2010 and several cohort studies comparing POEM and LM-PF[35-45] over the last decade have proved its safety and efficacy in the management of achalasia, the POEM technique is still not fully standardized[22].

The first RCT comparing the two techniques in the treatment of idiopathic achalasia[46], including 221 patients, demonstrated clinical success rates at 1 year and 2 years of follow-up of 84.8% and 83.0%, respectively, in the POEM group, comparable to the 83.5% and 81.7%, respectively, observed for the LM-PF group. In our study, the clinical success rate at the end of the 1st year was 95% in the POEM group and 100% in the LM-PF group, with no statistical difference between the two techniques. This discrepancy between our results and those of the earlier trial may be related to the fact that approximately 35% of the patients evaluated in that trial had previously received some type of treatment, which could have increased the degree of technical difficulty in dissection secondary to submucosal fibrosis.



DOI: 10.3748/wjg.v28.i33.4875 **Copyright** ©The Author(s) 2022.

Figure 1 Flow chart of the study timeline. EGD: Esophagogastroduodenoscopy; EM: Esophageal manometry (conventional); LM-PF: Laparoscopic myotomy and partial fundoplication; POEM: Peroral endoscopic myotomy; SF-36: Medical Outcomes Study 36-item Short-Form Health Survey.

We observed no statistical differences between the two techniques concerning Eckardt scores for dysphagia, regurgitation, chest pain, and weight loss, at 1, 6, and 12 mo of follow-up, which demonstrates the noninferiority of POEM to the LM-PF.

Immediate postprocedural complications occurred in 10% of the 40 patients evaluated in the present study. There were no cases of death in our sample, and the rate of AEs did not differ significantly between the two techniques. In our study, all POEM procedures involved a full-thickness myotomy, which made pneumoperitoneum an expected event. Pneumoperitoneum is a common finding after POEM and is not indicative of an unfavorable outcome for the patient. We categorized pneumoperitoneum as an AE only if abdominal decompression was required.

Anesthesia and procedure times were shorter for POEM than for LM-PF. That can be explained by the fact that the POEM involved full-thickness myotomy and did not involve fundoplication. There was no difference between the two procedures in terms of LOS and QoL.

We found that POEM and LM-PF both resulted in significant decreases in the 1- and 5-min barium column heights at 1, 6, and 12 mo after the procedures, demonstrating a clear decrease in resistance to the passage of contrast at the level of the EGJ. Sanagapalli *et al*[47] showed an association of significant improvement in symptoms when there is a mean reduction in the residual barium column height by about 53%. The LES pressure (MEP) on conventional EM was significantly lower throughout the follow-up period than at baseline, and there was no significant difference between the two groups.

In this study, the rates of treatment success were comparable between surgical and endoscopic myotomy, both providing symptom improvement, as well as objective improvement in radiological and manometric parameters, at 1, 6, and 12 mo. A recent systematic review and meta-analysis demonstrated that the incidence of GER is higher after POEM than after laparoscopic Heller myotomy[48]. That is in agreement with our findings. The evaluation of GER in our study was based on the typical clinical manifestations of GERD or the identification of erosive esophagitis by EGD. All patients with symptoms and suggestive endoscopic findings of GER received PPI treatment with suspension or maintenance according to the clinical and endoscopic response. A significant limitation of our study was the absence of pHmetry evaluation, which is the main method for GERD evaluation. Prior to our study, we considered that the pHmetry evaluation would be compromised because patients with esophageal achalasia present retention of food residues in the esophageal mucosa and the fermentation of those residues can decrease the intraluminal pH and thus be a confounding factor in the diagnosis of GERD. However, Smart *et al*[49] showed that such fermentation would affect only pre-procedure pHmetry,

without much influence on the post-procedure pHmetry.

Erosive esophagitis, especially grade C or D, is considered indicative of GER after endoscopy in patients without a history of the condition[50]. We consider that patients undergoing POEM have a wider esophagogastric transition that favors a higher rate of GER compared to LM-PF, despite similar LES pressures between the groups. Werner *et al*[46] also showed more GER in patients undergoing POEM despite no differences in manometry compared to LM-PF.

The POEM technique has undergone numerous changes since its initial description by Inoue *et al*[22]. It has been shown that short- to medium-term efficacy is comparable between myotomy of the circular muscle layer only and full-thickness myotomy, as well as that the latter, despite significantly reducing the duration of POEM, may increase the risk of GERD[51,52]. Likewise, there is uncertainty about whether myotomy should be performed in the anterior or posterior wall, the latter technique being associated with a higher incidence of GER[53,54], although other studies have failed to demonstrate that [55,56]. In the present study, we chose a long posterior full-thickness myotomy, because of the greater technical ease[43,57,58].

The results obtained in our study corroborate those of a previous study demonstrating the noninferiority of POEM to LM-PF for symptom control in patients with achalasia, except for postprocedure GER[46]. That raises the question of which technical changes we should study. Therefore, it is valid to perform in-depth analyses of oblique fiber preservation techniques[59], as well as the use of POEM with fundoplication[60,61]. One study[58] demonstrated that preservation of the oblique muscle, using the two penetrating vessels as an anatomical landmark, can significantly reduce the frequency of post-POEM GER, although that should be interpreted with caution because it was a retrospective cohort study, without strict methodological criteria, and with limited reproducibility. In the present study, we employed the conventional POEM technique as previously described[62], and the preservation of the two penetrating vessels was not standardized. The postprocedural occurrence of GERD symptoms in our sample was > 50%, similar to what has been reported by other authors. Despite not including patients undergoing POEM, a recent study[63] showed that achalasia patients with post-treatment reflux symptoms demonstrate esophageal hypersensitivity to chemical and mechanical stimuli, which may determine symptom generation.

Another strategy proposed to minimize the occurrence of GER after POEM is performing transoral incisionless fundoplication. In one pilot study[60], that procedure was reported to have a 100% success rate in terms of symptom control, acid exposure time, and the need for antisecretory drugs. In another pilot study[61], standard POEM combined with endoscopic fundoplication (POEM-F) was employed, and no complications were observed. A recent retrospective study followed patients for 12 mo after POEM-F[64], and showed that the incidence of postprocedural GER was only 11.1%. Albeit attractive, POEM-F has several potential limitations[65]. First, it is necessary to perform POEM in the anterior wall, contrary to the current trend of using a posterior wall approach. Second, it may not be possible to perform POEM-F in patients who have previously undergone anterior myotomy and experience symptom recurrence due to submucosal fibrosis. Third, the long-term durability of this type of fundoplication is still unknown.

In our opinion, it will take some time for the literature to reveal whether endoscopic or surgical myotomy is the best long-term option for the treatment of achalasia. Two crucial points that weigh unfavorably on the POEM procedure, in terms of the possibility that it will come to be widely indicated for the treatment of achalasia[66,67]. The first is the paucity of high-quality (randomized) technical studies comparing POEM with the well-established techniques of pneumatic dilatation of the cardia and laparoscopic myotomy with fundoplication, which could show, at least, the noninferiority of POEM. The second is the lack of studies with long (> 5 years) follow-up periods, which could demonstrate the true reintervention rate, based on the identification of serious late complications, including GER requiring fundoplication and dysphagia resulting from an inadequate myotomy[68]. Currently, the results at 2-3 years are similar between the endoscopic and surgical myotomy techniques concerning the clinical parameters, except for the greater occurrence of GER after the endoscopic technique, which typically responds well to antisecretory drug treatment. However, those data are accompanied by uncertainties that will only be resolved over time.

CONCLUSION

Our results allow us to conclude that LM-PF and POEM are equally effective in controlling the clinical symptoms of achalasia at 1, 6, and 12 mo. Although the use of the POEM technique results in a significantly higher rate of postprocedure GER, it also shortens anesthesia and procedure times. We found no differences between the two methods regarding LOS, the occurrence of AEs, or QoL. In the POEM group, there was an improvement in all domains of QoL.

ARTICLE HIGHLIGHTS

Research background

Achalasia is a rare benign esophageal motor disorder characterized by incomplete relaxation of the lower esophageal sphincter (LES). The treatment of achalasia is not curative but rather aimed at reducing the LES pressure. Surgical myotomy with partial fundoplication is traditional the gold standard method for the management of these patients. Peroral endoscopic myotomy (POEM) use its increasing due to it satisfactory results.

Research motivation

Since there is still no definition of the best treatment for achalasia, the objective of this study was to compare the techniques used.

Research objectives

This study aimed to compare POEM and laparoscopic myotomy and partial fundoplication (LM-PF) regarding their efficacy and outcomes for the treatment of achalasia.

Research methods

This was a single-center randomized controlled clinical trial.

Research results

There were no significant differences between the LM-PF and POEM groups regarding symptom improvement at 1, 6, and 12 mo of follow-up. Rates of reflux esophagitis were significantly higher in the POEM group. There were also no statistical differences regarding manometry values or the occurrence of adverse events or length of stay. Anesthesia time and procedure time were significantly shorter in the POEM group than in the LM-PF group. In the POEM group, there was an improvement in all domains of quality of life.

Research conclusions

POEM and LM-PF are equally effective in controlling symptoms of achalasia. POEM has the advantage of reducing anesthesia and procedure times, but with a significantly higher rate of gastroesophageal reflux.

Research perspectives

Future research should focus on long-term follow-up and outcomes of different techniques. It is possible that the improvement in the POEM technique may contribute to new perspectives on reflux symptoms.

FOOTNOTES

Author contributions: de Moura ETH contributed to the conception and design of the study; de Moura ETH, Ribeiro IB, de Moura DTH, Aissar Sallum RA, Nasi A, Sánchez-Luna SA, Sakai P, and de Moura EGH analyzed and interpreted the data, drafted the article, revised the article for important intellectual content, and approved the final version; Jukemura J, de Almeida Delgado AA, and Coutinho LMA analyzed and interpreted the data, revised the article for important intellectual content, and approved the final version; Farias GFA analyzed and interpreted the data, and approved the final version.

Institutional review board statement: The study was approved by the Research Ethics Committee of the University of São Paulo School of Medicine, No. CAAE: 23460613000000068.

Clinical trial registration statement: The trial was registered at ClinicalTrials.gov, No. NCT02138643.

Informed consent statement: All subjects agreed to participate in this study after informed consent and ethical permission were obtained.

Conflict-of-interest statement: All the authors report no relevant conflicts of interest for this article.

Data sharing statement: No additional data are available.

CONSORT 2010 statement: The authors have read the CONSORT 2010 Statement, and the manuscript was prepared and revised according to the CONSORT 2010 Statement.

Open-Access: This article is an open-access article that was selected by an in-house editor and fully peer-reviewed by external reviewers. It is distributed in accordance with the Creative Commons Attribution NonCommercial (CC BY-NC 4.0) license, which permits others to distribute, remix, adapt, build upon this work non-commercially, and license

their derivative works on different terms, provided the original work is properly cited and the use is non-commercial. See: https://creativecommons.org/Licenses/by-nc/4.0/

Country/Territory of origin: Brazil

ORCID number: Eduardo Turiani Hourneaux de Moura 0000-0002-5247-318X; José Jukemura 0000-0002-3943-7088; Igor Braga Ribeiro 0000-0003-1844-8973; Galileu Ferreira Ayala Farias 0000-0003-0242-3691; Aureo Augusto de Almeida Delgado 0000-0003-1183-9840; Lara Meireles Azeredo Coutinho 0000-0002-9059-0512; Diogo Turiani Hourneaux de Moura 0000-0002-7446-0355; Rubens Antonio Aissar Sallum 0000-0003-1823-0042; Ary Nasi 0000-0001-6928-4281; Sergio A Sánchez-Luna 0000-0001-6870-2226; Paulo Sakai 0000-0003-3088-9210; Eduardo Guimarães Hourneaux de Moura 0000-0003-1215-5731.

S-Editor: Fan JR
L-Editor: Filipodia
P-Editor: Fan JR

REFERENCES

1 **Gregersen H**, Lo KM. Pathophysiology and treatment of achalasia in a muscle mechanical perspective. *Ann N Y Acad Sci* 2018; **1434**: 173-184 [PMID: 29756656 DOI: 10.1111/nyas.13711]
2 **Mayberry JF**. Epidemiology and demographics of achalasia. *Gastrointest Endosc Clin N Am* 2001; **11**: 235-248, v [PMID: 11319059]
3 **Sadowski DC**, Ackah F, Jiang B, Svenson LW. Achalasia: incidence, prevalence and survival. A population-based study. *Neurogastroenterol Motil* 2010; **22**: e256-e261 [PMID: 20465592 DOI: 10.1111/j.1365-2982.2010.01511.x]
4 **Reynolds JC**, Parkman HP. Achalasia. *Gastroenterol Clin North Am* 1989; **18**: 223-255 [PMID: 2668168]
5 **Yu L**, Li J, Wang T, Zhang Y, Krasna MJ. Functional analysis of long-term outcome after Heller's myotomy for achalasia. *Dis Esophagus* 2010; **23**: 277-283 [PMID: 20002701 DOI: 10.1111/j.1442-2050.2009.01031.x]
6 **Vaezi MF**, Pandolfino JE, Vela MF. ACG clinical guideline: diagnosis and management of achalasia. *Am J Gastroenterol* 2013; **108**: 1238-49; quiz 1250 [PMID: 23877351 DOI: 10.1038/ajg.2013.196]
7 **Eckardt VF**. Clinical presentations and complications of achalasia. *Gastrointest Endosc Clin N Am* 2001; **11**: 281-292, vi [PMID: 11319062]
8 **Winter H**, Shukla R, Elshaer M, Riaz AA. Current management of achalasia – A review. *Br J Med Pract* 2015; **8** [DOI: 10.12968/hmed.2012.73.2.117]
9 **Ellis FH Jr**, Olsen AM. Achalasia of the esophagus. *Major Probl Clin Surg* 1969; **9**: 1-221 [PMID: 4949995]
10 **Gross R**, Johnson LF, Kaminski RJ. Esophageal emptying in achalasia quantitated by a radioisotope technique. *Dig Dis Sci* 1979; **24**: 945-949 [PMID: 510096 DOI: 10.1007/BF01311951]
11 **Ehlers AP**, Oelschlager BK, Pellegrini CA, Wright AS, Saunders MD, Flum DR, He H, Farjah F. Achalasia Treatment, Outcomes, Utilization, and Costs: A Population-Based Study from the United States. *J Am Coll Surg* 2017; **225**: 380-386 [PMID: 28602724 DOI: 10.1016/j.jamcollsurg.2017.05.014]
12 **Cappell MS**, Stavropoulos SN, Friedel D. Updated Systematic Review of Achalasia, with a Focus on POEM Therapy. *Dig Dis Sci* 2020; **65**: 38-65 [PMID: 31451984 DOI: 10.1007/s10620-019-05784-3]
13 **Spiess AE**, Kahrilas PJ. Treating achalasia: from whalebone to laparoscope. *JAMA* 1998; **280**: 638-642 [PMID: 9718057 DOI: 10.1001/jama.280.7.638]
14 **Boeckxstaens GE**, Zaninotto G, Richter JE. Achalasia. *Lancet* 2014; **383**: 83-93 [PMID: 23871090 DOI: 10.1016/S0140-6736(13)60651-0]
15 **Bonifácio P**, de Moura DTH, Bernardo WM, de Moura ETH, Farias GFA, Neto ACM, Lordello M, Korkischko N, Sallum R, de Moura EGH. Pneumatic dilation versus laparoscopic Heller's myotomy in the treatment of achalasia: systematic review and meta-analysis based on randomized controlled trials. *Dis Esophagus* 2019; **32** [PMID: 30380036 DOI: 10.1093/dote/doy105]
16 **Vaezi MF**, Felix VN, Penagini R, Mauro A, de Moura EG, Pu LZ, Martínek J, Rieder E. Achalasia: from diagnosis to management. *Ann N Y Acad Sci* 2016; **1381**: 34-44 [PMID: 27571581 DOI: 10.1111/nyas.13176]
17 **Herbella FA**, Moura EG, Patti MG. Achalasia 2016: Treatment Alternatives. *J Laparoendosc Adv Surg Tech A* 2017; **27**: 6-11 [PMID: 27754816 DOI: 10.1089/lap.2016.0468]
18 **Martins RK**, Ribeiro IB, DE Moura DTH, Hathorn KE, Bernardo WM, DE Moura EGH. PERORAL (POEM) OR SURGICAL MYOTOMY FOR THE TREATMENT OF ACHALASIA: A SYSTEMATIC REVIEW AND META-ANALYSIS. *Arq Gastroenterol* 2020; **57**: 79-86 [PMID: 32294740 DOI: 10.1590/S0004-2803.202000000-14]
19 **Jung HK**, Hong SJ, Lee OY, Pandolfino J, Park H, Miwa H, Ghoshal UC, Mahadeva S, Oshima T, Chen M, Chua ASB, Cho YK, Lee TH, Min YW, Park CH, Kwon JG, Park MI, Jung K, Park JK, Jung KW, Lim HC, Jung DH, Kim DH, Lim CH, Moon HS, Park JH, Choi SC, Suzuki H, Patcharatrakul T, Wu JCY, Lee KJ, Tanaka S, Siah KTH, Park KS, Kim SE; Korean Society of Neurogastroenterology and Motility. 2019 Seoul Consensus on Esophageal Achalasia Guidelines. *J Neurogastroenterol Motil* 2020; **26**: 180-203 [PMID: 32235027 DOI: 10.5056/jnm20014]
20 **Kahaleh M**, Tyberg A, Suresh S, Lambroza A, Gaidhane M, Zamarripa F, Martínez GM, Carames JC, Moura ET, Farias GF, Porfilio MG, Nieto J, Rey M, Rodriguez Casas F, Mondragón Hernández OV, Vargas-Rubio R, Canadas R, Hani A, Munoz G, Castillo B, Lukashok HP, Robles-Medranda C, de Moura EG. How does per-oral endoscopic myotomy compare to Heller myotomy? *Endosc Int Open* 2020; **8**: E1392-E1397 [PMID: 33015342 DOI: 10.1055/a-1223-1521]
21 **Ortega JA**, Madureri V, Perez L. Endoscopic myotomy in the treatment of achalasia. *Gastrointest Endosc* 1980; **26**: 8-10 [PMID: 7358270 DOI: 10.1016/s0016-5107(80)73249-2]

22 **Inoue H**, Minami H, Kobayashi Y, Sato Y, Kaga M, Suzuki M, Satodate H, Odaka N, Itoh H, Kudo S. Peroral endoscopic myotomy (POEM) for esophageal achalasia. *Endoscopy* 2010; **42**: 265-271 [PMID: 20354937 DOI: 10.1055/s-0029-1244080]

23 **de Pascale S**, Repici A, Puccetti F, Carlani E, Rosati R, Fumagalli U. Peroral endoscopic myotomy versus surgical myotomy for primary achalasia: single-center, retrospective analysis of 74 patients. *Dis Esophagus* 2017; **30**: 1-7 [PMID: 28575245 DOI: 10.1093/dote/dox028]

24 **Jones R**, Junghard O, Dent J, Vakil N, Halling K, Wernersson B, Lind T. Development of the GerdQ, a tool for the diagnosis and management of gastro-oesophageal reflux disease in primary care. *Aliment Pharmacol Ther* 2009; **30**: 1030-1038 [PMID: 19737151 DOI: 10.1111/j.1365-2036.2009.04142.x]

25 **Lundell LR**, Dent J, Bennett JR, Blum AL, Armstrong D, Galmiche JP, Johnson F, Hongo M, Richter JE, Spechler SJ, Tytgat GN, Wallin L. Endoscopic assessment of oesophagitis: clinical and functional correlates and further validation of the Los Angeles classification. *Gut* 1999; **45**: 172-180 [PMID: 10403727 DOI: 10.1136/gut.45.2.172]

26 **de Oliveira JM**, Birgisson S, Doinoff C, Einstein D, Herts B, Davros W, Obuchowski N, Koehler RE, Richter J, Baker ME. Timed barium swallow: a simple technique for evaluating esophageal emptying in patients with achalasia. *AJR Am J Roentgenol* 1997; **169**: 473-479 [PMID: 9242756 DOI: 10.2214/ajr.169.2.9242756]

27 **Ware JE Jr**, Sherbourne CD. The MOS 36-item short-form health survey (SF-36). I. Conceptual framework and item selection. *Med Care* 1992; **30**: 473-483 [PMID: 1593914]

28 **Ciconelli RM**, Ferraz MB, Santos W, Meinão I. Tradução para a língua portuguesa e validação do questionário genérico de avaliação de qualidade de vida SF-36 (Brasil SF-36). *Rev Bras Reumatol* 1999; **39**: 143-50. s2 [DOI: 10.1590/s1413-81232011000800010]

29 **Dindo D**, Demartines N, Clavien PA. Classification of surgical complications: a new proposal with evaluation in a cohort of 6336 patients and results of a survey. *Ann Surg* 2004; **240**: 205-213 [PMID: 15273542 DOI: 10.1097/01.sla.0000133083.54934.ae]

30 **Müller M**, Eckardt AJ, Wehrmann T. Endoscopic approach to achalasia. *World J Gastrointest Endosc* 2013; **5**: 379-390 [PMID: 23951393 DOI: 10.4253/wjge.v5.i8.379]

31 **Müller M**, Keck C, Eckardt AJ, Werling S, Wehrmann T, König J, Gockel I. Outcomes of pneumatic dilation in achalasia: Extended follow-up of more than 25 years with a focus on manometric subtypes. *J Gastroenterol Hepatol* 2018; **33**: 1067-1074 [PMID: 29140553 DOI: 10.1111/jgh.14044]

32 **Ghoshal UC**, Rangan M. A review of factors predicting outcome of pneumatic dilation in patients with achalasia cardia. *J Neurogastroenterol Motil* 2011; **17**: 9-13 [PMID: 21369487 DOI: 10.5056/jnm.2011.17.1.9]

33 **Farias GFA**, de Moura DTH, de Moura ETH, de Rezende DT, Hathorn KE, Nasi A, Queiroz NSF, de Moura EGH. Peroral endoscopic myotomy (POEM): a comparative study between Chagasic and idiopathic achalasia. *Endosc Int Open* 2020; **8**: E506-E512 [PMID: 32258372 DOI: 10.1055/a-1035-9288]

34 **Zaninotto G**, Bennett C, Boeckxstaens G, Costantini M, Ferguson MK, Pandolfino JE, Patti MG, Ribeiro U Jr, Richter J, Swanstrom L, Tack J, Triadafilopoulos G, Markar SR, Salvador R, Faccio L, Andreollo NA, Cecconello I, Costamagna G, da Rocha JRM, Hungness ES, Fisichella PM, Fuchs KH, Gockel I, Gurski R, Gyawali CP, Herbella FAM, Holloway RH, Hongo M, Jobe BA, Kahrilas PJ, Katzka DA, Dua KS, Liu D, Moonen A, Nasi A, Pasricha PJ, Penagini R, Perretta S, Sallum RAA, Sarnelli G, Savarino E, Schlottmann F, Sifrim D, Soper N, Tatum RP, Vaezi MF, van Herwaarden-Lindeboom M, Vanuytsel T, Vela MF, Watson DI, Zerbib F, Gittens S, Pontillo C, Vermigli S, Inama D, Low DE. The 2018 ISDE achalasia guidelines. *Dis Esophagus* 2018; **31** [PMID: 30169645 DOI: 10.1093/dote/doy071]

35 **Hungness ES**, Teitelbaum EN, Santos BF, Arafat FO, Pandolfino JE, Kahrilas PJ, Soper NJ. Comparison of perioperative outcomes between peroral esophageal myotomy (POEM) and laparoscopic Heller myotomy. *J Gastrointest Surg* 2013; **17**: 228-235 [PMID: 23054897 DOI: 10.1007/s11605-012-2030-3]

36 **Ujiki MB**, Yetasook AK, Zapf M, Linn JG, Carbray JM, Denham W. Peroral endoscopic myotomy: A short-term comparison with the standard laparoscopic approach. *Surgery* 2013; **154**: 893-7; discussion 897 [PMID: 24074429 DOI: 10.1016/j.surg.2013.04.042]

37 **Bhayani NH**, Kurian AA, Dunst CM, Sharata AM, Rieder E, Swanstrom LL. A comparative study on comprehensive, objective outcomes of laparoscopic Heller myotomy with per-oral endoscopic myotomy (POEM) for achalasia. *Ann Surg* 2014; **259**: 1098-1103 [PMID: 24169175 DOI: 10.1097/SLA.0000000000000268]

38 **Teitelbaum EN**, Rajeswaran S, Zhang R, Sieberg RT, Miller FH, Soper NJ, Hungness ES. Peroral esophageal myotomy (POEM) and laparoscopic Heller myotomy produce a similar short-term anatomic and functional effect. *Surgery* 2013; **154**: 885-91; discussion 891 [PMID: 24074428 DOI: 10.1016/j.surg.2013.04.051]

39 **Leeds SG**, Burdick JS, Ogola GO, Ontiveros E. Comparison of outcomes of laparoscopic Heller myotomy versus per-oral endoscopic myotomy for management of achalasia. *Proc (Bayl Univ Med Cent)* 2017; **30**: 419-423 [PMID: 28966450 DOI: 10.1080/08998280.2017.11930212]

40 **Hanna AN**, Datta J, Ginzberg S, Dasher K, Ginsberg GG, Dempsey DT. Laparoscopic Heller Myotomy vs Per Oral Endoscopic Myotomy: Patient-Reported Outcomes at a Single Institution. *J Am Coll Surg* 2018; **226**: 465-472.e1 [PMID: 29410262 DOI: 10.1016/j.jamcollsurg.2017.12.050]

41 **Chan SM**, Wu JC, Teoh AY, Yip HC, Ng EK, Lau JY, Chiu PW. Comparison of early outcomes and quality of life after laparoscopic Heller's cardiomyotomy to peroral endoscopic myotomy for treatment of achalasia. *Dig Endosc* 2016; **28**: 27-32 [PMID: 26108140 DOI: 10.1111/den.12507]

42 **Kumagai K**, Tsai JA, Thorell A, Lundell L, Håkanson B. Per-oral endoscopic myotomy for achalasia. Are results comparable to laparoscopic Heller myotomy? *Scand J Gastroenterol* 2015; **50**: 505-512 [PMID: 25712228 DOI: 10.3109/00365521.2014.934915]

43 **Kumbhari V**, Khashab MA. Peroral endoscopic myotomy. *World J Gastrointest Endosc* 2015; **7**: 496-509 [PMID: 25992188 DOI: 10.4253/wjge.v7.i5.496]

44 **Ramirez M**, Zubieta C, Ciotola F, Amenabar A, Badaloni A, Nachman F, Nieponice A. Per oral endoscopic myotomy vs. laparoscopic Heller myotomy, does gastric extension length matter? *Surg Endosc* 2018; **32**: 282-288 [PMID: 28660419 DOI: 10.1007/s00464-017-5675-x]

45 **Kahaleh M**, Xu MM, Zamarripa F, Martínez G, Arantes VN, Rodriguez FC, Castillo B, Andalib I, Tyberg A, Lambroza A, Saumoy M, Carames JC, Baptista A, Robles-Medranda C, Lukashok H, Gaidhane M, Valencia JMB, Moura ETHD, Moura EGHD. POEM in Latin America: The Rise of a New Standard. *J Clin Gastroenterol* 2019; **53**: e352-e355 [PMID: 30702485 DOI: 10.1097/MCG.0000000000001161]

46 **Werner YB**, Hakanson B, Martinek J, Repici A, von Rahden BHA, Bredenoord AJ, Bisschops R, Messmann H, Vollberg MC, Noder T, Kersten JF, Mann O, Izbicki J, Pazdro A, Fumagalli U, Rosati R, Germer CT, Schijven MP, Emmermann A, von Renteln D, Fockens P, Boeckxstaens G, Rösch T. Endoscopic or Surgical Myotomy in Patients with Idiopathic Achalasia. *N Engl J Med* 2019; **381**: 2219-2229 [PMID: 31800987 DOI: 10.1056/NEJMoa1905380]

47 **Sanagapalli S**, Plumb A, Maynard J, Leong RW, Sweis R. The timed barium swallow and its relationship to symptoms in achalasia: Analysis of surface area and emptying rate. *Neurogastroenterol Motil* 2020; **32**: e13928 [PMID: 32578341 DOI: 10.1111/nmo.13928]

48 **Schlottmann F**, Luckett DJ, Fine J, Shaheen NJ, Patti MG. Laparoscopic Heller Myotomy Versus Peroral Endoscopic Myotomy (POEM) for Achalasia: A Systematic Review and Meta-analysis. *Ann Surg* 2018; **267**: 451-460 [PMID: 28549006 DOI: 10.1097/SLA.0000000000002311]

49 **Smart HL**, Foster PN, Evans DF, Slevin B, Atkinson M. Twenty four hour oesophageal acidity in achalasia before and after pneumatic dilatation. *Gut* 1987; **28**: 883-887 [PMID: 3653757 DOI: 10.1136/gut.28.7.883]

50 **Mota RCL**, de Moura EGH, de Moura DTH, Bernardo WM, de Moura ETH, Brunaldi VO, Sakai P, Thompson CC. Risk factors for gastroesophageal reflux after POEM for achalasia: a systematic review and meta-analysis. *Surg Endosc* 2021; **35**: 383-397 [PMID: 32206921 DOI: 10.1007/s00464-020-07412-y]

51 **Gu L**, Ouyang Z, Lv L, Liang C, Zhu H, Liu D. Safety and efficacy of peroral endoscopic myotomy with standard myotomy versus short myotomy for treatment-naïve patients with type II achalasia: a prospective randomized trial. *Gastrointest Endosc* 2021; **93**: 1304-1312 [PMID: 33058884 DOI: 10.1016/j.gie.2020.10.006]

52 **Duan T**, Tan Y, Zhou J, Lv L, Liu D. A Retrospective Study of Peroral Endoscopic Full-Thickness Myotomy in Patients with Severe Achalasia. *J Laparoendosc Adv Surg Tech A* 2017; **27**: 770-776 [PMID: 28557560 DOI: 10.1089/lap.2016.0445]

53 **Tan Y**, Lv L, Wang X, Zhu H, Chu Y, Luo M, Li C, Zhou H, Huo J, Liu D. Efficacy of anterior versus posterior per-oral endoscopic myotomy for treating achalasia: a randomized, prospective study. *Gastrointest Endosc* 2018; **88**: 46-54 [PMID: 29571969 DOI: 10.1016/j.gie.2018.03.009]

54 **Ramchandani M**, Nabi Z, Reddy DN, Talele R, Darisetty S, Kotla R, Chavan R, Tandan M. Outcomes of anterior myotomy versus posterior myotomy during POEM: a randomized pilot study. *Endosc Int Open* 2018; **6**: E190-E198 [PMID: 29399617 DOI: 10.1055/s-0043-121877]

55 **Ichkhanian Y**, Abimansour JP, Pioche M, Vosoughi K, Eleftheriadis N, Chiu PWY, Minami H, Ogihara K, Sanaei O, Jovani M, Khashab MA. Outcomes of anterior versus posterior peroral endoscopic myotomy 2 years post-procedure: prospective follow-up results from a randomized clinical trial. *Endoscopy* 2021; **53**: 462-468 [PMID: 32572862 DOI: 10.1055/a-1204-4242]

56 **Rodríguez de Santiago E**, Mohammed N, Manolakis A, Shimamura Y, Onimaru M, Inoue H. Anterior versus posterior myotomy during poem for the treatment of achalasia: systematic review and meta-analysis of randomized clinical trials. *J Gastrointestin Liver Dis* 2019; **28**: 107-115 [PMID: 30851179 DOI: 10.15403/jgld.2014.1121.281.pom]

57 **Swanström LL**, Rieder E, Dunst CM. A stepwise approach and early clinical experience in peroral endoscopic myotomy for the treatment of achalasia and esophageal motility disorders. *J Am Coll Surg* 2011; **213**: 751-756 [PMID: 21996484 DOI: 10.1016/j.jamcollsurg.2011.09.001]

58 **Tanaka S**, Toyonaga T, Kawara F, Watanabe D, Hoshi N, Abe H, Ariyoshi R, Ohara Y, Takao T, Morita Y, Umegaki E, Kodama Y. Novel per-oral endoscopic myotomy method preserving oblique muscle using two penetrating vessels as anatomic landmarks reduces postoperative gastroesophageal reflux. *J Gastroenterol Hepatol* 2019; **34**: 2158-2163 [PMID: 31373050 DOI: 10.1111/jgh.14814]

59 **Tanaka S**, Kawara F, Toyonaga T, Inoue H, Bechara R, Hoshi N, Abe H, Ohara Y, Ishida T, Morita Y, Umegaki E. Two penetrating vessels as a novel indicator of the appropriate distal end of peroral endoscopic myotomy. *Dig Endosc* 2018; **30**: 206-211 [PMID: 28846807 DOI: 10.1111/den.12957]

60 **Tyberg A**, Choi A, Gaidhane M, Kahaleh M. Transoral incisional fundoplication for reflux after peroral endoscopic myotomy: a crucial addition to our arsenal. *Endosc Int Open* 2018; **6**: E549-E552 [PMID: 29756011 DOI: 10.1055/a-0584-6802]

61 **Inoue H**, Ueno A, Shimamura Y, Manolakis A, Sharma A, Kono S, Nishimoto M, Sumi K, Ikeda H, Goda K, Onimaru M, Yamaguchi N, Itoh H. Peroral endoscopic myotomy and fundoplication: a novel NOTES procedure. *Endoscopy* 2019; **51**: 161-164 [PMID: 30654395 DOI: 10.1055/a-0820-2731]

62 **Zhou PH**, Cai MY, Yao LQ, Zhong YS, Ren Z, Xu MD, Qin XY. Peroral Endoscopic Myotomy for Esophageal Achalasia by HybridKnife: A Case Report. *Case Rep Gastrointest Med* 2012; **2012**: 325479 [PMID: 22900214 DOI: 10.1155/2012/325479]

63 **Ponds FA**, Oors JM, Smout AJPM, Bredenoord AJ. Reflux symptoms and oesophageal acidification in treated achalasia patients are often not reflux related. *Gut* 2021; **70**: 30-39 [PMID: 32439713 DOI: 10.1136/gutjnl-2020-320772]

64 **Bapaye A**, Dashatwar P, Dharamsi S, Pujari R, Gadhikar H. Single-session endoscopic fundoplication after peroral endoscopic myotomy (POEM+F) for prevention of post gastroesophageal reflux - 1-year follow-up study. *Endoscopy* 2021; **53**: 1114-1121 [PMID: 33291157 DOI: 10.1055/a-1332-5911]

65 **Reddy ND**. Peroral endoscopic myotomy with fundoplication: are we there yet! *Endoscopy* 2019; **51**: 111-112 [PMID: 30695805 DOI: 10.1055/a-0820-3129]

66 **Patti MG**, Andolfi C, Bowers SP, Soper NJ. POEM vs Laparoscopic Heller Myotomy and Fundoplication: Which Is Now the Gold Standard for Treatment of Achalasia? *J Gastrointest Surg* 2017; **21**: 207-214 [PMID: 27844266 DOI: 10.1007/s11605-016-3310-0]

67 **Liu-Burdowski J**, Duarte-Chavez R, Kahaleh M. Per-oral Endoscopic Myotomy: State of the Art. *J Clin Gastroenterol* 2022; **56**: 16-22 [PMID: 34653065 DOI: 10.1097/MCG.0000000000001620]

68 **McKay SC**, Dunst CM, Sharata AM, Fletcher R, Reavis KM, Bradley DD, DeMeester SR, Müller D, Parker B, Swanström LL. POEM: clinical outcomes beyond 5 years. *Surg Endosc* 2021; **35**: 5709-5716 [PMID: 33398572 DOI: 10.1007/s00464-020-08031-3]

World Journal of Gastroenterology

Submit a Manuscript: https://www.f6publishing.com

World J Gastroenterol 2022 September 7; 28(33): 4890-4908

DOI: 10.3748/wjg.v28.i33.4890

ISSN 1007-9327 (print) ISSN 2219-2840 (online)

SYSTEMATIC REVIEWS

Chinese herbal formula shen-ling-bai-zhu-san to treat chronic gastritis: Clinical evidence and potential mechanisms

Wei Jin, Juan Zhong, Yang Song, Ming-Fei Li, Shi-Yi Song, Chun-Run Li, Wei-Wei Hou, Qing-Jie Li

Specialty type: Gastroenterology and hepatology

Provenance and peer review: Unsolicited article; Externally peer reviewed.

Peer-review model: Single blind

Peer-review report's scientific quality classification

Grade A (Excellent): A, A
Grade B (Very good): 0
Grade C (Good): 0
Grade D (Fair): 0
Grade E (Poor): 0

P-Reviewer: Gadour E, United Kingdom; Nassar M, United States

Received: January 12, 2022
Peer-review started: January 12, 2022
First decision: March 8, 2022
Revised: March 16, 2022
Accepted: August 6, 2022
Article in press: August 6, 2022
Published online: September 7, 2022

Wei Jin, Yang Song, Ming-Fei Li, Wei-Wei Hou, Department of Emergency, Hospital of Chengdu University of Traditional Chinese Medicine, Chengdu 610075, Sichuan Province, China

Juan Zhong, Shi-Yi Song, Chun-Run Li, Chengdu University of Traditional Chinese Medicine, Chengdu 610075, Sichuan Province, China

Qing-Jie Li, Interventional Operation Room, Hospital of Chengdu University of Traditional Chinese Medicine, Chengdu 610075, Sichuan Province, China

Corresponding author: Wei-Wei Hou, MD, PhD, Chief Doctor, Department of Emergency, Hospital of Chengdu University of Traditional Chinese Medicine, No. 39 Shierqiao Road, Chengdu 610075, Sichuan Province, China. houww2018@cdutcm.edu.cn

Abstract

BACKGROUND

Chronic gastritis (CG) is an inflammatory disease of the gastric mucosa. Shen-ling-bai-zhu san (SLBZS), a traditional Chinese medicine formula, is widely used for treating CG. Nevertheless, its effects are currently unclear.

AIM

To determine the clinical evidence and potential mechanisms of SLBZS for the treatment of CG.

METHODS

We systematically searched 3 English (PubMed, Embase, Medline) and 4 Chinese databases (Cochrane Library Central Register of Controlled Trials, China National Knowledge Infrastructure database, Wanfang Data Knowledge Service Platform, and the VIP information resource integration service platform) without language or publication bias restriction. Qualified studies were selected according to pre-set inclusion and exclusion criteria. RevMan 5.3 software was used for meta-analysis and literature quality assessment, Stata 14.0 software was used for sensitivity analysis, GRADE profiler 3.6 was used to evaluate the quality of evidence. And then, network pharmacology analysis was applied to primary research the mechanisms of action of SLBZS on CG.

RESULTS

Fourteen studies were finally included, covering 1335 participants. Meta-analysis indicated that: (1) SLBZS was superior to conventional therapies [risk ratio (RR): 1.29, 95% confidence interval (CI): 1.21 to 1.37, $P < 0.00001$]; (2) SLBZS was better

than conventional therapies [RR: 0.24, 95% confidence interval (95%CI): 0.11 to 0.55, $P = 0.0007$] in terms of recurrence rate and reversal of *Helicobacter pylori* positivity (RR: 1.20, 95%CI: 1.11 to 1.30, $P < 0.00001$); and (3) The safety of SLBZS for CG remains unclear. According to the GRADE method, the quality of evidence was not high. Besides, SNZJS might treat CG by acting on related targets and pathways such as EGFR tyrosine kinase inhibitor resistance, the PI3K-Akt signaling pathway, and others.

CONCLUSION

SLBZS might be useful in treating CG, but long-term effects and specific clinical mechanisms of it maintain unclear. More samples and high-quality clinical experiments should be assessed and verified in the next step.

Key Words: Chronic gastritis; Shen-ling-bai-zhu-san; Chinese herbal formula; Systematic review; Network pharmacology

©The Author(s) 2022. Published by Baishideng Publishing Group Inc. All rights reserved.

Core Tip: A 2012 clinical practice guideline recommended Shenling Baizhu Powder for the Pattern of Spleen and Stomach Deficiency chronic gastritis (CG). The 2020 clinical guideline did not recommended Shen-ling-bai-zhu san (SLBZS), possibly because of inadequate clinical evidence and pharmacological mechanisms. We designed our study to focus on evidence of efficacy and potential mechanisms. Our study showed that SLBZS might be useful in treating CG; however, its long-term effects and mechanisms of action are unclear. Due to the poor quality of the evidence, more samples and high-quality clinical studies should be tested.

Citation: Jin W, Zhong J, Song Y, Li MF, Song SY, Li CR, Hou WW, Li QJ. Chinese herbal formula shen-ling-bai-zhu-san to treat chronic gastritis: Clinical evidence and potential mechanisms. *World J Gastroenterol* 2022; 28(33): 4890-4908

URL: https://www.wjgnet.com/1007-9327/full/v28/i33/4890.htm

DOI: https://dx.doi.org/10.3748/wjg.v28.i33.4890

INTRODUCTION

Chronic gastritis (CG) is a set of inflammatory diseases of the gastric mucosa[1] and is one of the common diseases of the digestive system. The disease often relapses, accompanied by symptoms that severely affect the quality of life. Chronic atrophic gastritis is associated with intestinal metaplasia and intraepithelial neoplasia, increasing gastric cancer risk. Globally, on average, more than 50% of people may have CG at any given moment[2]. A pathological study of 8892 patients in China found that atrophic gastritis, intestinal metaplasia, and dysplasia were prevalent, occurring in 25.8%, 23.6%, and 7.3% of the population, respectively[3].

The treatment of CG with gastric mucosal repair consists of antacids, antacids, and gastric mucosal protective agents[4-7]. Nevertheless, the efficacy of triple or quadruple therapy is not ideal, and there are frequent side effects[8]. For these reasons, complementary and alternative medicine therapies such as acupuncture[9-12], moxibustion[13,14], and Chinese herbal formulas[15,16] are sought as alternative therapies.

The Chinese herb formula Shenling Baizhu Powder, also known as Shen-ling-bai-zhu-san (SLBZS), is a widely used prescription for digestive tract disease in China derived from the classic herb monograph "*Taipinghuiminhejijufang*" written in the Song dynasty[17]. Ten commonly used herbs constitute SLBZS; these include Baizhu (*Atractylodes macrocephala* Koidz), Fuling (*Smilax glabra* Roxb), Yiyiren [*Coix lacryma-jobi var*. ma-yuen (Rom.Caill.) Stapf], Renshen (*Panax ginseng* C.A.Mey), Shanyao (*Dioscorea oppositifolia* L), Baibiandou (*Lablab purpureus subsp*. purpureus), Lianzi (*Nelumbo nucifera Gaertn*), Sharen (*Amomum villosum* Lour), Jiegeng (*Platycodon grandiflorus*) and Gancao (*Glycyrrhiza uralensis* Fisch. ex DC). In China, clinical studies suggested that SLBZS treats CG[18,19] with efficacy. Nevertheless, mechanistic studies based on animal experiments are lacking.

Furthermore, a 2012 Clinical practice guideline[20] recommended Shenling Baizhu Powder for the Pattern of Spleen and Stomach Deficiency CG. The pathogenesis can be summarized as the stomach failing to be nourished because of splenic and gastric qi deficiency and disturbance of qi movement. A 2020 clinical guideline did not recommend SLBZS, possibly because of inadequate clinical evidence and pharmacological mechanisms[21]. Efficacy evidence and potential mechanistic studies are required.

Table 1 Search strategy

Number	Search terms
1	Mesh descriptor (Medicine, Traditional) explode all trees
2	(Medicine, Chinese Traditional*): ti,ab,kw
3	Mesh descriptor(Drugs, Chinese Herbal) explode all trees,
4	((Chinese Drugs, Plant*) or (Chinese Herbal Drugs*) or (Herbal Drugs, Chinese*) or (Plant Extracts, Chinese*) or (Chinese Plant Extracts*) or(Extracts, Chinese Plant*)): ti,ab,kw
5	Mesh descriptor (shen-ling-bai-zhu) explode all trees
6	((shen-ling-bai-zhu powder*) or (shen-ling-bai-zhu formula*) or (shen-ling-bai-zhu decoction*) or (shen-ling-bai-zhu decoction*) or (Shen-ling-bai-zhu powder*) or (Shen-ling-bai-zhu formula*) or (Shen-ling-bai-zhu formula*)): ti,ab,kw
7	Or 1-6
8	Mesh descriptor: (Chronic gastritis) explode all trees
9	((Chronic gastritis*) or (Digestive System Diseases*) or (Gastrointestinal Diseases*) or (Gastroenteritis*) or (Gastritis*) or (Chronic, gastritis*)): ti, ab, kw
10	Or 8-9
11	Mesh descriptor: (randomized controlled trials) explode all trees
12	(random*) or (randomly*) or (allocation*) or (random allocation*) or (placebo*) or (double blind*) or (clinical trials*) or (randomized control trial*) or (RCT*) or (controlled clinical trials*): ti, ab, kw
13	Or: 11-12
14	7 and 10 and 13

MATERIALS AND METHODS

Study registration

We registered this review and meta-analysis at the PROSPERO website (https://www.crd.york.ac.uk/PROSPERO/#recordDetails), an international prospective system review registration website. The registration number was CRD42020212979. We conducted the study based on the details of this protocol.

Database search

Our investigators independently searched PubMed, Embase, Medline, Cochrane Library Central Register of Controlled Trials, China National Knowledge Infrastructure database, Wanfang Data Knowledge Service Platform, and the VIP information resource integration service platform from their inception to November 2021. There were no limitations on language or publication status. They also searched conference articles and clinical registries for possible related trials.

Search terms

We adopted a search strategy that combined medical subject headings and free words. Two authors (YS, MFL) searched and screened all citations independently. The search strategy was as follows (Table 1): The search strategy followed the Preferred Reporting Items for Systematic Reviews and Meta-Analyses statement[22].

Inclusion criteria

Randomized controlled trials (RCTs) or quasi-RCTs that reported the effects of SLBZS on CG were included.

Participants: Studies that evaluated patients with a diagnosis of CG were included. For example, we used diagnostic criteria from the standardized consensus on the diagnosis of CG from the Branch of Spleen and Stomach Diseases of the Chinese Society of Traditional Chinese Medicine, China, that depends on endoscopy and pathological examinations[23]. We excluded studies that included CG patients complicated with hypertension, diabetes, heart disease, or severe allergic diseases. There was no restriction on the setting of interest or other population characteristics.

Interventions: SLBZ powder was the primary prescription, regardless of its dosage form, dosage, or course of treatment. If there were other medications, formulas, or traditional Chinese medicine (TCM) therapies (such as acupuncture, moxibustion, and ear-acupressure) in the treatment group, the control groups must also receive these therapies.

Comparisons: Western medicine, active control, and placebo were acceptable. If SLBZ + western medicine was applied in the experimental group, western medicine in the control group must be consistent.

Outcome measures: We considered efficacy outcomes as primary outcome measures, including effectiveness, recurrence rate, symptom score, *Helicobacter pylori* (*H. pylori*) eradication, and quality-of-life assessment. Secondary outcome measures were adverse events directly related to CG.

Exclusion criteria

The exclusion criteria were as follows: (1) The study was not an RCT, *e.g.*, retrospective study, cross-sectional study, observational study, case study, animal study, or others; (2) for multiple reports or repeated publications from the same study, we retained the one with a more significant number of details; (3) diagnostic criteria were not reported in trials, disease not CG; and (4) studies or trials used SLBZS as a part of complex interventions; for example, SLBZS decoction plus another herbal medicine formula *vs* acupuncture therapies. Western medicine is inconsistent in two groups.

Study selection and data extraction

According to our study registration protocol, two reviewers (WJ, QJL) independently performed trial searches, study selection, and raw data extraction. A third reviewer (JZ) checked the extracted data. We resolved conflicts through consensus.

Risk of bias assessment

According to the Cochrane Handbook details[24], we performed the risk of bias assessment analysis using the Cochrane collaborative bias risk tool in Review Manager 5.3 software. We resolved conflicts by consultation with a third investigator (WWH).

Statistical analysis

We used Review Manager 5.3 and Stata 14.0 software for statistical analysis. We calculated 95% confidence interval (CI) and mean difference for continuous variables and 95%CI and risk ratio (RR) for dichotomous variables. Differences with $P < 0.05$ were statistically significant. We determined the heterogeneity of data using Cochrane χ^2 and I^2 tests. We used a fixed-effect model if there was no significant heterogeneity; otherwise, we used a random-effect model. We conducted subgroup analyses to explore the source of heterogeneity. We determined publication bias by examining funnel plots and Egger's tests for more than ten trials. We used sensitivity analysis to explore the stability of the results. GRADE profiler 3.6 software was applied to evaluate the quality of evidence.

Mechanisms of network pharmacology of SLBZD to treat CG

Collection and screening of pharmacodynamic components in TCM System Pharmacology Database and analysis platform (TCMSP, HTTP://ibts.hkbu.edu.hk/LSP/tcmsp.php) in ginseng, atractylodes, poria cocos, yam, white hyacinth bean, lotus seed, coix seed, amomum fruit, radix platycodi, radix glycyrrhizae as keyword query filter chemical composition. The database contains about 500 drugs listed in the Chinese Pharmacopoeia, providing absorption, distribution, metabolism and excretion, ingredient data, and target and disease information. Oral bioavailability (OB) and drug-like properties (DL) are essential indexes determining whether a compound can be developed into a drug. Based on the relevant literature, OB and DL were set to > 30% and > 0.18, respectively, and the screened compounds were used as candidate ingredients[25,26].

Target prediction of pharmacodynamic components, the simplified molecular Linear Input specification (Simles) number, and Mol structure of each candidate component were retrieved using PubChem. We arranged candidate target genes using PharmMapper online (http://Lilab-ecust.cn/pharmmapper/index.html) and Swiss target prediction (HTTP://www.swisstargetprediction.ch/), and we arranged the standbys in an Excel form.

Prediction of disease Targets Genes associated with CG was identified by searching for "Chronic Gastritis" in GeneCards (http://www.genecards.org/).

Network construction and analysis

SLBZ Powder's candidate components and target genes were screened and imported into Cytoscape 3.7.2 software using Excel to obtain a component-target network diagram. The predicted disease candidate targets were imported into the online protein interaction (String) database, the species organism was set as human (*Homo sapiens*), and the PPI map was obtained. The PPI map was imported into Cytoscape 3.7.2 software. The potential targets of Shenlingbaizhu Powder in chronic gastritis can be obtained by merging the component-target network diagram and disease target PPI diagram using Merge software, which can be imported into the online String database the interaction map of potential targets.

Functional mechanism analysis of potential targets GO enrichment analysis, and Kyoto Encyclopedia of Genes and Genomes (KEGG) pathway enrichment annotation analysis of potential target genes were performed using the R package clusterProfiler.

Table 2 Excluded 11 studies after reading the full text

Reason	Ref. (*n* = 11)
Intervention combined with other decoction (*n* = 3)	**Li GS**. Observation on the curative effect of Shenling Baizhu Powder and Taohong Siwu Decoction in treating chronic gastritis. *Zhongyi Linchuang Zazhi* 2007; **19** (10): 260-261
	Yang Y. Shenlingbaizhu san and zhaqupingwei powder combined with western medicine in the treatment of chronic gastritis randomized paraller controlled study. *Shiyong Zhongyi Neike Zazhi* 2013; **27** (10): 40-41
	Yang SX. Clinical study on the treatment of Chronic functional diarrhea with Shenling Baizhu Powder and Lizhong Decoction. *Yatai Chuantong Yixue* 2017; **30** (13): 145-146
Intervention combined with other decoction, no diagnostic criteria (*n* = 2)	**Jin JZ**. Shenling Baizhu Powder and Zuojin pill to treat chronic gastritis. *Shiyong Zhongyi Neike Zazhi* 2011; **27** (11): 752
	Gao CZ, Yang SM. Observation on curative effect of cefaclor combined with Shenlingbaizhu granule and Muxiang Shunqi pill in treating chronic gastritis. *Zhonghua Yixue Chuangxin Zazhi* 2012; **9** (22): 127-128
No diagnostic criteria (*n* = 1)	**Shi ZR**. Clinical observation on 8 cases of chronic gastritis treated by Shenling Baizhu Powder. *Neimenggu Zhongyi Zazhi* 2014 [DOI: 10.16040/j.cnki.cn15-1101.2014.07.024]
Not CG(*n* = 1)	**Zhang WW**. Clinical observation on 96 cases of spleen deficiency and stomachache treated with Shenling Baizhu Powder. *Zhongguo Minzuyixue Yu Minzuyaoxue* 2013; **9** (12): 80
Intervention combined with acupuncture (*n* = 3)	**Yang FX**. Acupuncture combined with Shenling Baizhu Powder to treat chronic gastritis with spleen deficiency and dampness. *Kouqiang Yixue Dianzi Zazhi* 2015; **6** (13): 140-143
	Wu XR. 30 cases of chronic gastritis with spleen deficiency and dampness treated by acupuncture combined with Shenling Baizhu Powder. *Guangming Zhongyi* 2015; **30** (5): 1018-1020
	Wu CY. Analysis of curative effect of acupuncture combined with Shenling Baizhu Powder on chronic gastritis with spleen deficiency and dampness. *Jixu Yixue Jiaoyu Zazhi* 2019; **33** (10): 161-162
Intervention combined with other decoction, WM are inconsistent in two groups (*n* = 1)	**Yan Z**. Clinical study of cefaclor combined with Shenling Baizhu granule and Muxiang Shunqi pill in treating chronic gastritis. *Yatai Chuantong Yixue* 2015; **11** (18): 106-107

RESULTS

Database search results

We retrieved 335 trials from 6 databases. When duplicate records were deleted, 177 remained. We excluded 152 studies by reading the title and abstract of the papers, including seven repeatedly published studies, ninety-five reports on the SLBZS experience of experienced TCM doctors, four retrospective studies, seventeen observation studies, one case report, and twenty-eight studies of diseases that were not CG. We read the full texts of the remaining 25 records. We deleted 11 records because of exclusion criteria (Table 2).

Finally, we included 14 studies in our review (flowchart of database search and study identification is shown in Figure 1).

Study characteristics

There were 14 Chinese-language RCTs, comprising 1335 participants aged 15-68 years[27-40], published between 2008 and 2020. Interventions in these studies were SLBZS *vs* conventional medicine or SLBZS + conventional medicine *vs* conventional medicine. In conventional medicine therapy, there were four methods, including monotherapy in four trials[27,33,34,37], combined therapy in one study[36], triple therapy in seven studies[28,31,32,35,38-40] and two trials of quadruple therapy[29,30]. There were various treatment durations, including 4, 5, 8, and 12 wk.

Total effectiveness was the primary outcome measure in all trials. All trials reported balanced baseline characteristics. Five trials (36%) recorded adverse events[29,31,34,36,38], and three studies reported recurrence rates[34,38,40]. Two studies reported participant withdrawal information[31,34]. No study reported influence on the quality of life as an outcome measure. Characteristics of included studies are shown in Table 3.

Risk of bias assessment

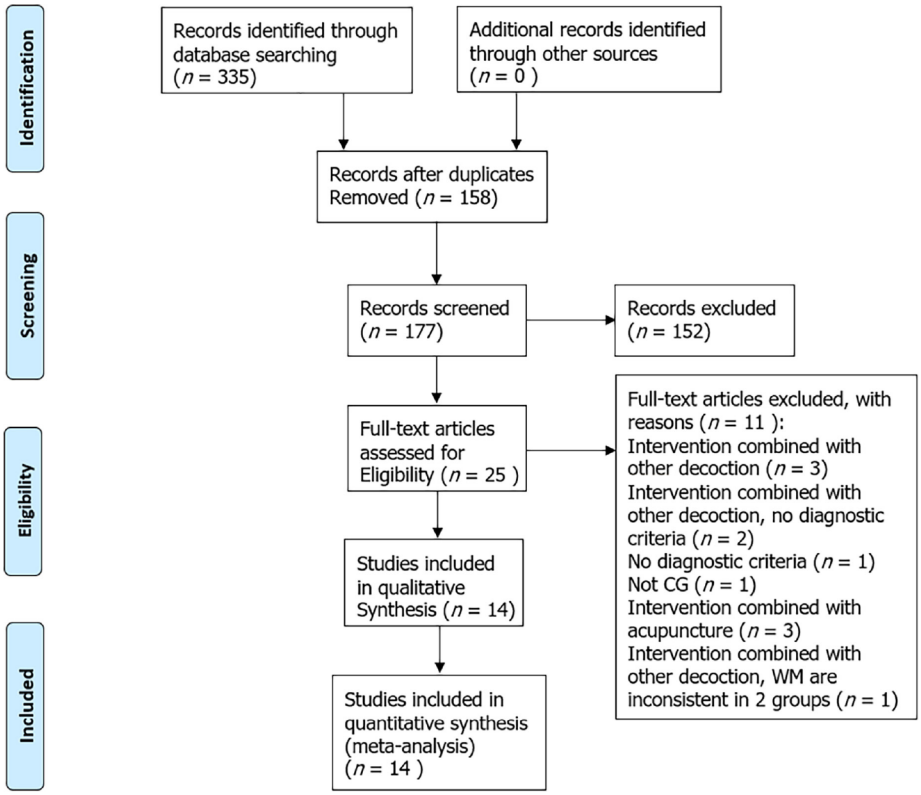
(1) Fourteen trials were consistent at baseline, and all tests referred to RCTs, three studies[28,39,40] mentioned randomization using the "random number table" method; (2) all studies not reported "distribution hidden" method; (3) the "blinding method" was not reported in any study, two studies[31,34] reported "No cases withdrawal and dropped-out," and three studies[34,38,40] reported "recurrence rate"; (4) selective reporting may come out in studies that there were too few indicators were noted; and (5) we considered some support from pharmaceutical companies that the ethics committee would not approve as other bias. If herbs were offered free by pharmaceutical companies, bias might taint the results. Two studies[34,36] reported that an ethics committee approved the study, suggesting a low bias level. For another 12 studies, we could not determine the effects of other potential sources of bias

Table 3 Characteristics of included studies

Ref.	Study design	Sample size (E/C)	Gender (E/C) and age (yr)	Duration	Interventions		Period	Outcome measure	Balance report of baseline
					Control group	Experimental group			
Yun[27], 2014	RCT	48 (24/24)	(13/11) (10/14); (34.96 ± 11. 39)/(34.08 ± 12.82)	Not mentioned	Rabeprazole enteric-coated capsule	Rabeprazole enteric-coated capsule + SLBZD	4 wk	Effective rate	$P > 0.05$
Chen *et al*[28], 2014	RCT	79 (40/39)	(24/16) (23/16); (42.6 ± 13.1)/43.5 ± 13.4	6-17 mo/6-19 mo	Triple therapy (clarithromycin sustained-release tablets + rabeprazole sodium capsule + metronidazole tablets)	Triple therapy + SLBZD	4 wk	Effective rate	$P > 0.05$
Chen *et al*[29], 2018	RCT	60 (30/30)	(14/16) (15/15); (55.45 ± 6.55)/(55.46 ± 6.44)	3-12 mo	Quadruple therapy (rabeprazole sodium capsule + amoxicillin + clarithromycin sustained-release tablets + biskal-citrate)	Quadruple therapy + SLBZD	8 wk	Effective rate; H. Pylori eradication; adverse event	$P > 0.05$
Du[30], 2017	RCT	48 (26/22)	(14/12) (12/10); (40.7 ± 6.1)/(41.2 ± 6.6)	7 mo-9 years/6 mo-8 years	Quadruple therapy (amoxicillin clavulanic potassium chewable tablets + metronidazole + omeprazole + compound bismuth aluminate capsule)	SLBZD	5 wk	Effective rate	$P > 0.05$
Gu[31], 2017	RCT	98 (49/49)	Not mentioned; 19-58	Not mentioned	Triple therapy (omeprazole + clarithromycin + amoxicillin)	Triple therapy + SLBZD	4 wk	Effective rate; H. Pylori eradication rate; adverse event	$P > 0.05$
Li *et al* [32], 2020	RCT	66 (33/33)	(19/14) (18/15); (58.54 ± 4.65)/(58.62 ± 4.57)	4-17 years/4-18 years	Triple therapy (mosapride tablet + polyzyme tablets + lansoprazole tablets)	Triple therapy + SLBZD	12 wk	Effective rate	$P > 0.05$
Tang [33], 2014	RCT	60 (30/30)	(16/14) (17/13); (22-46)/(23-52)	Not mentioned	Omeprazole enteric-coated capsules	Omeprazole Enteric-coated Capsules + SLBZD	8 wk	Effective rate	$P > 0.05$
Xia[34], 2015	RCT	300 (150/150)	Not mentioned; 18-85	Not mentioned	Omeprazole enteric-coated capsules	SLBZD	8 wk	Effective rate; recurrence rate; adverse event	$P > 0.05$
Xu *et al* [35], 2018	RCT	60 (30/30)	(17/13) (16/14); (55.6 ± 16.4)/(56.8 ± 14.9)	4-20 years/4-19 years	Triple therapy (mosapride tablet + polyzyme tablets + lansoprazole tablets)	Triple therapy+SLBZD	12 wk	Effective rate	$P > 0.05$
Zhang *et al*[36], 2020	RCT	68 (34/34)	(15/19) (17/17); (44.8 ± 5.0)/(45.2 ± 5.4)	1-12 years/2-14 years	Combination therapy (omeprazole + compound bismuth aluminate granules)	Combination therapy + SLBZD	8 wk	Effective rate; adverse events	$P > 0.05$
Zhao and Lin [37], 2010	RCT	80 (40/40)	(37/3) (38/2); (46.2 ± 6.7)/(44.2 ± 5.7)	2-7 years/2-8 years	No alcohol, famotidine	No alcohol, famotidine + SLBZD	4 wk	Effective rate;	$P > 0.05$
Zheng [38], 2014	RCT	92 (46/46)	(28/18) (30/16); (34 ± 5.34)/(33 ± 5.76)	5 mo-6 years/7 mo-6 years	Triple therapy (amoxicillin dispersion tablet + omeprazole enteric-coated capsules + clarithromycin tablet)	SLBZD	4 wk	Effective rate; adverse events; recurrence rate	$P > 0.05$
Zhuang *et al*[39], 2019	RCT	106 (53/53)	(65/41); (46.20 ± 8.75)	1-11 years	Triple therapy (omeprazole enteric-coated tablets + clarithromycin dispersible tablets+amoxil capsule)	Triple therapy + SLBZD	4 wk	Effective rate; H. Pylori's negative conversion rate	$P > 0.05$
Zou[40], 2015	RCT	170 (85/85)	(86/84); (40.9 ± 11.1)	Not mentioned	Triple therapy (amoxicillin + clarithromycin + omeprazole)	Triple therapy + SLBZD	8 wk	Effective rate; H. Pylori's negative	$P > 0.05$

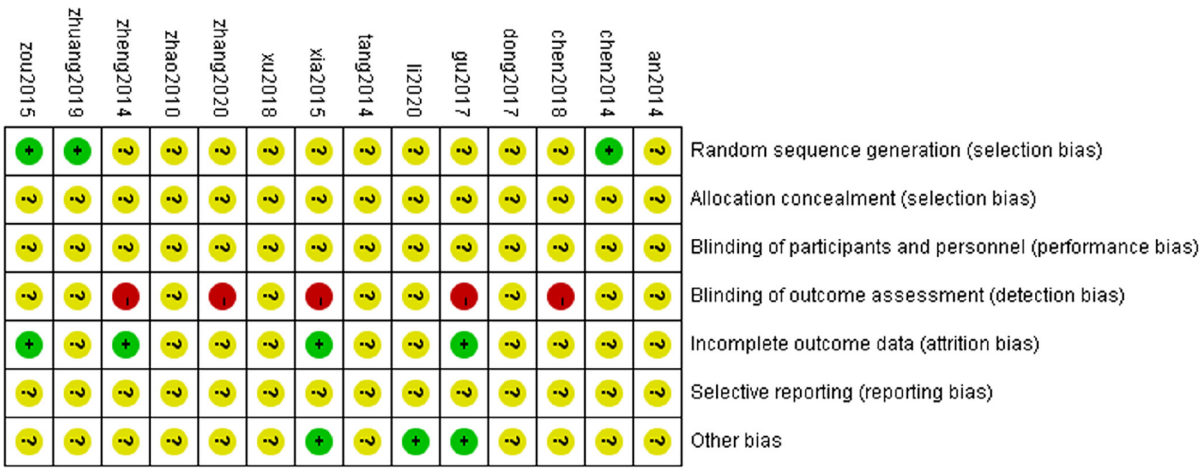
	conversion rate; recurrence rate

RCT: Randomized controlled trial; *H. Pylori*: *Helicobacter pylori*; SLBZS: Shen-ling-bai-zhu san.



DOI: 10.3748/wjg.v28.i33.4890 **Copyright** ©The Author(s) 2022.

Figure 1 Flowchart of database searching and study identification.



DOI: 10.3748/wjg.v28.i33.4890 **Copyright** ©The Author(s) 2022.

Figure 2 Risk of bias summary.

because there were no reports of herbs' sources. Details are displayed in Table 4. The included studies were therefore classified as low quality (Figure 2).

Evaluation of outcome measures

Total effectiveness: Total effectiveness is a composite endpoint composed of improved symptoms and

Table 4 Methodological quality details of all included studies

Ref.	Baseline	Randomization	Allocation concealment	Blind method	Withdrawal or dropped-out	Follow up	Protocol and registration	Ethics committee approved
Yun[27], 2014	Comparability	Random	NR	NR	NR	NR	NR	NR
Chen *et al* [28], 2014	Comparability	Random number table	NR	NR	NR	NR	NR	NR
Chen *et al* [29], 2018	Comparability	Random	NR	NR	NR	NR	NR	NR
Du[30], 2017	Comparability	Random	NR	NR	NR	NR	NR	NR
Gu[31], 2017	Comparability	Random	NR	NR	No cases withdrawal and dropped-out	NR	NR	Approved
Li *et al*[32], 2020	Comparability	Random	NR	NR	NR	NR	NR	Approved
Tang[33], 2014	Comparability	Random	NR	NR	NR	NR	NR	NR
Xia[34], 2015	Comparability	Random	NR	NR	No cases withdrawal and dropped-out	Recurrence rate	NR	Approved
Xu *et al* [35], 2018	Comparability	Random	NR	NR	NR	NR	NR	NR
Zhang *et al* [36], 2020	Comparability	Random	NR	NR	NR	NR	NR	NR
Zhao and Lin[37], 2010	Comparability	Random	NR	NR	NR	NR	NR	NR
Zheng[38], 2014	Comparability	Random	NR	NR	NR	Recurrence rate	NR	NR
Zhuang *et al*[39], 2019	Comparability	Random number table	NR	NR	NR	NR	NR	NR
Zou[40], 2015	Comparability	Random number table	NR	NR	NR	Recurrence rate	NR	NR

NR: Not Reported.

gastroscopy. The results fall into three categories: Obviously effective, effective, and invalid, according to clinical Research on New Chinese Medicines[41]. The details are as follows. Clinical cure: Epigastric pain and symptoms disappeared, gastroscopy returned to normal, *i.e.*, gastric mucosa repair, the disappearance of active inflammation, and mild chronic inflammation; Obviously effective: Epigastric pain and symptoms disappear or diminish. Gastroscopy showed significant improvement; that is, gastric mucosa was nearly normal, active inflammation was gone, and there was less chronic inflammation; Effective: Relief of epigastric pain and other symptoms. Gastroscopy showed reduced gastric mucosal lesions; that is, gastric mucosa was essentially normal, active inflammation was gone, and less chronic inflammation; and Invalid: no improvement or aggravation of clinical symptoms and signs. Gastroscopy showed no change. There were slight differences in this outcome's composition in various studies due to the non-uniform efficacy assessment criteria. All 14 RCTs compared the total effectiveness rate of SLBZS in patients with CG. SLBZS was superior to conventional therapies (RR: 1.29, 95%CI: 1.22 to 1.37, $P < 0.00001$) (Figure 3A). Heterogeneity in the total effectiveness was very small ($P = 0.91$, $I^2 = 0\%$).

We created subgroups based on the duration of treatment (4, 5, 8, or 12 wk) (Supplementary Table 1), comparison type (SLBZS *vs* conventional medicine or SLBZS + conventional medicine *vs* conventional medicine alone) (Supplementary Table 2), and intervention method (monotherapy, combined therapy, triple therapy, or quadruple therapy) (Supplementary Table 3). These subgroup analyses showed that the effectiveness rate of SLBZS did not differ based on the duration of treatment, combination with other medications, or intervention method (all $P > 0.05$) (Table 5).

Table 5 Subgroup analysis of total effectiveness

Subgroup method (total effective rate)	Items	Number of comparisons	Results (risk ratio, 95%CI)	*P* value for overall effect	I^2	*P* value for subgroup difference
Course of treatment	All comparisons	14	1.29 (1.22,1.37)	< 0.00001	0%	
Supplementary Table 1	4 wk	5	1.27 (1.17,1.37)	< 0.00001	0%	
	5 wk	1	1.45 (1.04, 2.03)	0.03	NA	0.58
	8 wk	5	1.28 (1.16, 1.40)	0.02	0%	
	12 wk	2	1.44 (1.19, 1.74)	0.0002	0%	
Comparison type	All comparisons	14	1.23 (1.14, 1.32)	< 0.00001	47%	
Supplementary Table 2	SLBZS *vs* CM	3	1.23 (1.10, 1.38)	0.0003	0%	0.93
	SLBZS + CM *vs* CM	11	1.23 (1.11, 1.35)	< 0.0001	57%	
Intervention method	All comparisons	14	1.29 (1.22, 1.37)	< 0.0001	0%	
Supplementary Table 3	Monotherapy	4	1.25 (1.12, 1.40)	< 0.0001	5%	
	Combined therapy	1	1.41 (1.08, 1.84)	0.01	NA	0.82
	Triple therapy	7	1.30 (1.21,1.40)	< 0.0001	0%	
	Quadruple therapy	2	1.35 (1.11, 1.64)	0.003	0%	

NA: Not available; CM: Conventional medicine; SLBZS: Shen-ling-bai-zhu san.

Table 6 Adverse events

Study	Experiment group	Control group
Zhang, 2020	Diarrhea (2/34)	Dizziness (2/34) and dry mouth (1/34)
Chen, 2018	Headache (1/30), diarrhea (1/30), nausea (1/30)	Headache (2/30), diarrhea (1/30), nausea (2/30), constipation (1/30), rash (1/30)
Zheng, 2014	None	Headache and rash (17.39%)

Recurrence rate: Three studies reported recurrence rate[34,38,40]. Pooled raw data showed that SLBZS was better than conventional therapies (RR: 0.24, 95%CI: 0.11 to 0.55, $P = 0.0007$, Figure 3B).

HP negative conversion rate: Four trials noted the reversal rate for *Helicobacter pylori* (*H. pylori*) positivity[29,31,39,40]. Meta-analysis showed that SLBZS was superior to conventional therapies (RR: 1.20, 95%CI: 1.11 to 1.30, $P < 0.00001$, Figure 3C).

Other results

One trial compared the time required for symptom improvement in patients with CG[38]. The experimental group was superior to the control group regarding effects on epigastric stagnation, abdominal distension, belching, acid regurgitation, and nausea ($P < 0.05$).

There were no reports of significant responses or improvement in the quality-of-life data in these studies. One study reported the Questionnaire for Comprehensive Quality of Life Assessment responses pre- and post-treatment in two groups[36]. After two consecutive months of treatment, scores in all dimensions improved, and the treatment group's score was significantly higher than that of the treatment group ($P < 0.05$).

Publication bias

Funnel plots showed the publication bias of the effectiveness rate (Figure 4A). The funnel plot of the effective rate was symmetric, suggesting no significant publication bias. Egger's test results agreed with the funnel plots ($P = 0.005$ and 0.000, respectively).

Adverse events

Of the 14 studies, nine RCTs did not mention adverse events[27,28,30,32,33,35,36,39,40]. Two studies

Table 7 GRADE evidence for the effect of Shen-ling-bai-zhu san

Quality assessment							Summary of findings					
							No of patients		Effect		Quality	Importance
No of studies	Design	Limitations	Inconsistency	Indirectness	Imprecision	Other considerations	RQLQ	Control	Relative (95%CI)	Absolute		
Effective rate												
14	Randomized trials	Serious[1]	Serious[2]	Serious[3]	No serious imprecision[4]	None	595/670 (88.8%)	459/665 (69%)	RR 1.45 (1.22 to 1.37)	200 more per 1000 (from 152 more to 255 fewer)	Very low	Critical
								0.676		196 more per 1000 (from 149 fewer to 250 more)		
Recurrence rate												
3	Randomized trials	Serious[1]	Serious[2]	Serious[3]	No serious imprecision[4]	None	7/281 (2.5%)	31/281 (11%)	RR 0.24 (0.11 to 0.55)	84 fewer per 1000 (from 50 fewer to 98 fewer)	Very low	Important
								0.177		135 fewer per 1000 (from 58 fewer to 158 fewer)		
HP negative conversion rate												
4	Randomized trials	No serious limitations[1]	Very serious[2]	No serious indirections[3]	No serious imprecision[4]	None	207/217 (95.4%)	170/270 (78.3%)	RR 1.2 (1.11 to 1.3)	157 more per 1000 (from 86 more to 135 more)	Moderate	Important
								0.815		163 more per 1000 (from 90 more to 244 more)		

[1]Randomized controlled trial design method is not reported.
[2]The risk of bias assessment is mostly "unclear risk" because there are not enough details in articles.
[3]Studies come from China.
[4]There is significant heterogeneity between studies.

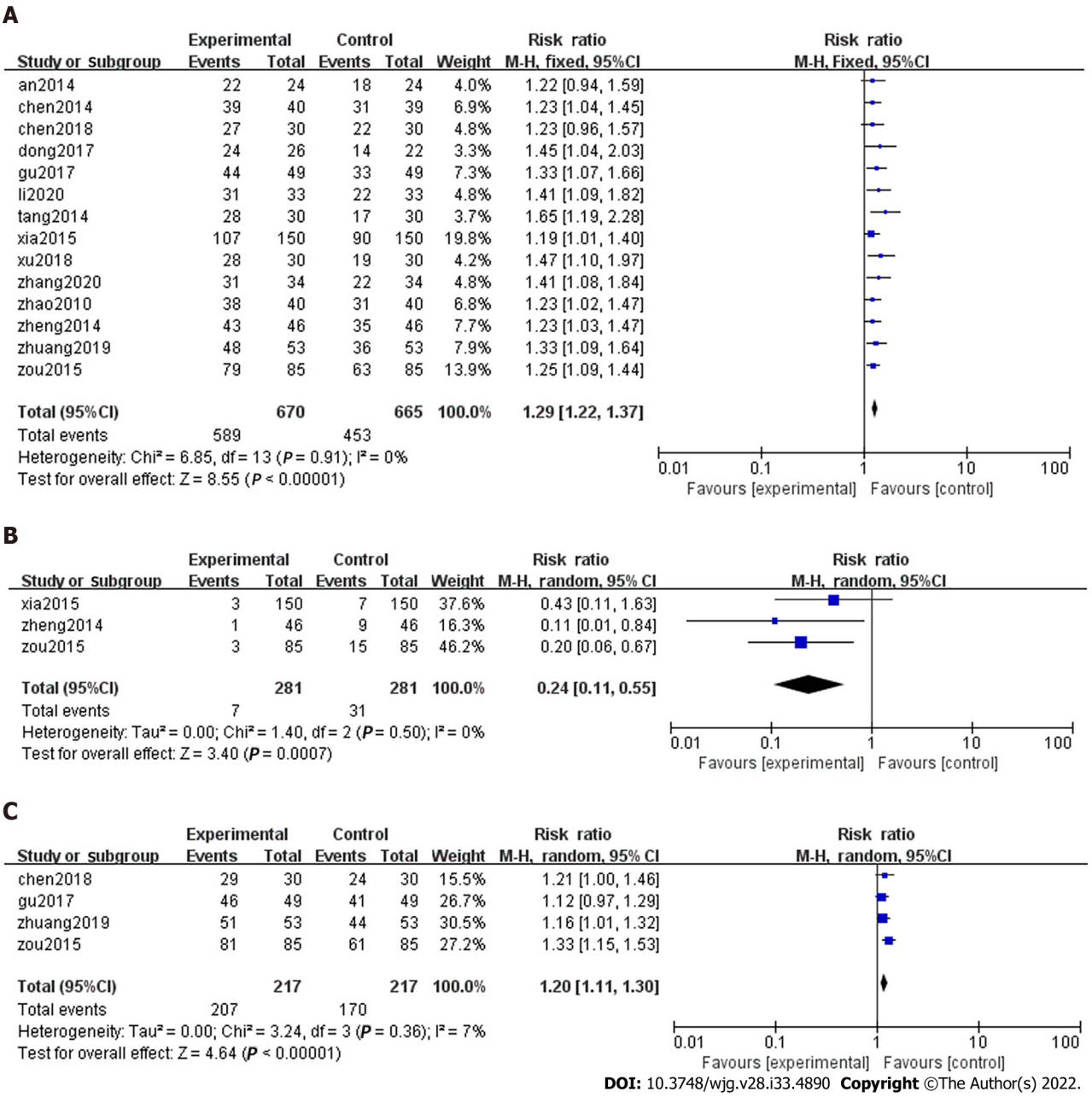
mentioned no prominent adverse events[34,29]. Three trials reported adverse events (Table 6); however, no study commented on methods used to manage these events.

GRADE evidence for the effect of SLBZD

GRADE results of SLBZD is shown in (Table 7). However, the quality of evidence was very low or moderate because of the poor methodological quality.

Network pharmacology results of SLBZS

Composition and targets of SCBZS: According to the OB > 30% and DL > 0.18 standard screening, we screened 189 ingredients, including seven in Baizhu (*Atractylodes macrocephala* Koidz), 15 in Fuling (Smilax glabra Roxb), 9 in Yiyiren [*Coix lacryma-jobi var.* ma-yuen (Rom.Caill.) Stapf], 22 in Renshen (*Panax ginseng* C.A.Mey), 15 in Shanyao (*Dioscorea oppositifolia* L), one in Baibiandou (*Lablab purpureus* subsp. purpureus), 11 in Lianzi (*Nelumbo nucifera* Gaertn.), 92 in Gancao (*Glycyrrhiza uralensis* Fisch. ex



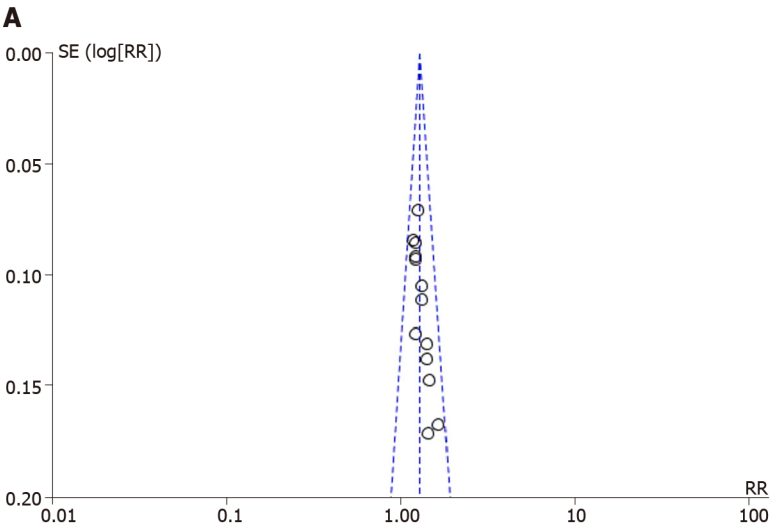
DOI: 10.3748/wjg.v28.i33.4890 **Copyright** ©The Author(s) 2022.

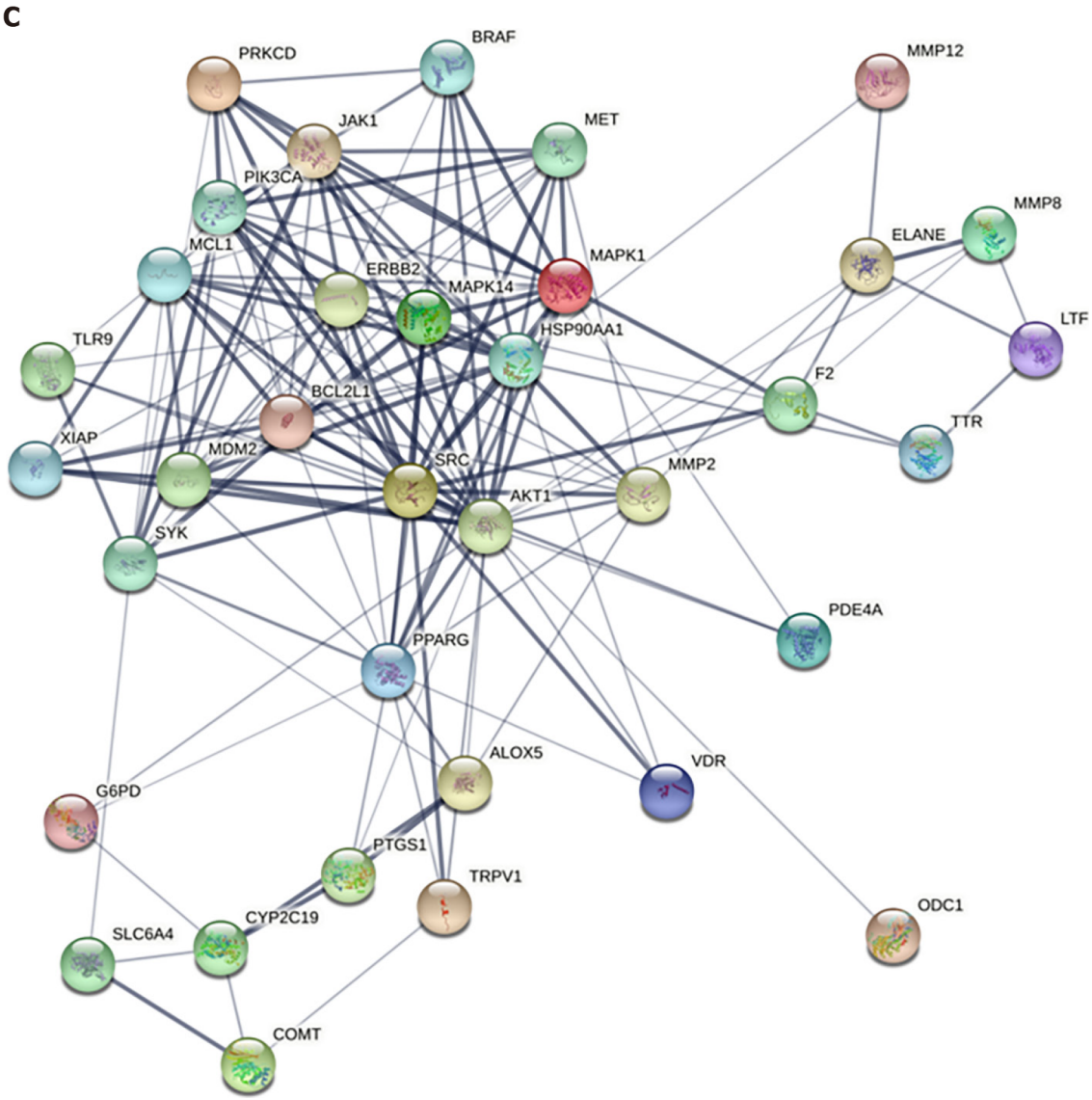
Figure 3 Forest plot. A: Forest plot for total effectiveness; B: Forest plot for recurrence rate; C: Forest plot for the reversal rate of Helicobacter pylori positivity. 95%CI: 95% confidence interval.

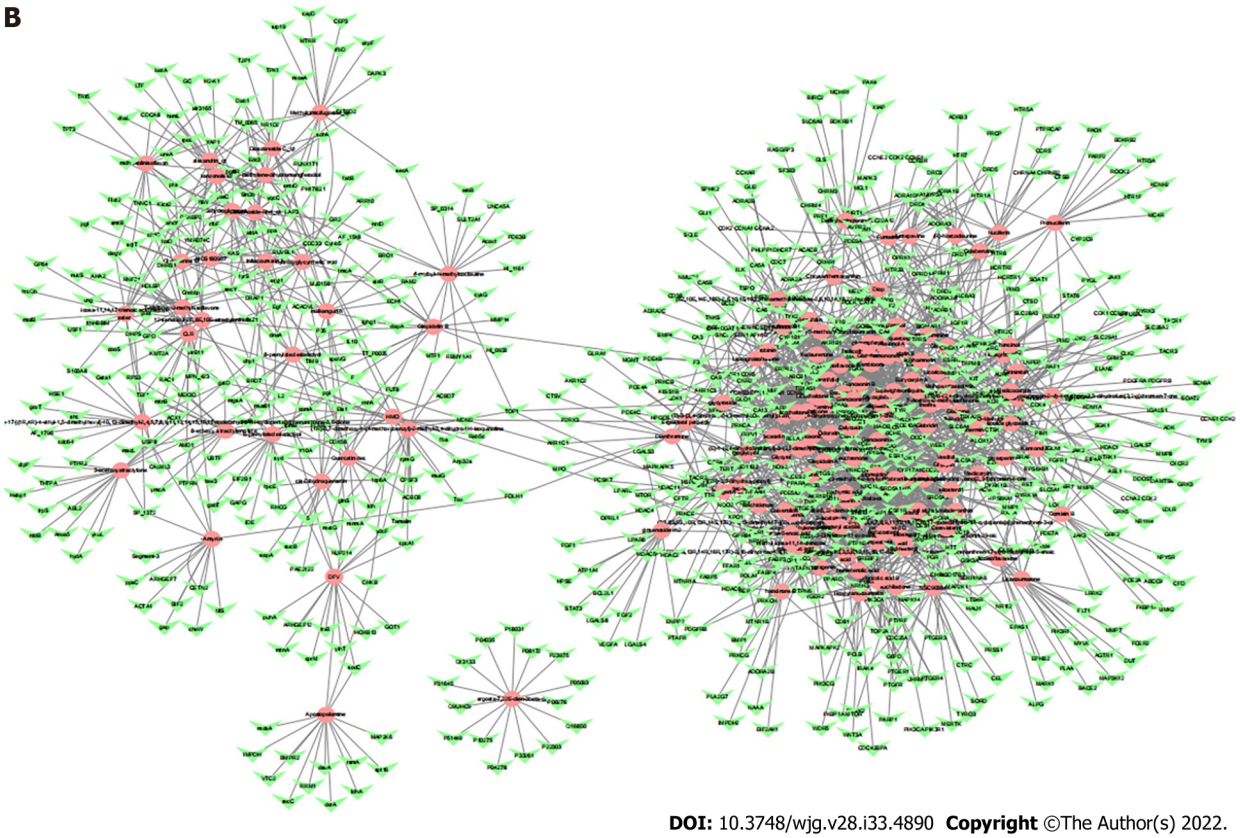
DC), ten in Sharen (*Amomum villosum* Lour.), and seven in Jiegeng (*Platycodon grandiflorus*). The repeated components and components with no target were deleted, leaving 158 candidate components. Each candidate component's top 15 target genes were selected, and duplicated genes were identified, with 693 candidate target genes.

PPI network: The component-target network diagram of Shen-ling-bai-zhu Powder visually shows the interaction between pharmacodynamic components and target genes of Shen-ling-bai-zhu Powder (Figure 4B). The network contains 851 nodes with 2445 sides, among which 158 nodes represent candidate ingredients and 693 nodes represent candidate target genes related to drug candidate ingredients. The average number of neighborhood nodes was 5.561. There were 300 nodes and 3325 edges in the disease target interaction network, and the average number of neighborhood nodes in the network was 34.635. A total of 35 potential targets of SLBZS on chronic gastritis can be obtained by analyzing the component-target and disease target interaction networks. Figure 4C visually shows the interaction relationship between potential targets.

GO enrichment analysis and KEGG pathway enrichment analysis: The results of GO analysis showed that in the BP category, differentially expressed genes were concentrated in the regulation of reactive oxygen species metabolic process, response to oxidative stress, cellular response to chemical stress, and


A
SE (log[RR])
0.00
0.05
0.10
0.15
0.20
0.01
0.1
1.00
10
100
RR


C
PRKCD
BRAF
MMP12
JAK1
MET
PIK3CA
MMP8
ELANE
MCL1
MAPK1
ERBB2
MAPK14
LTF
TLR9
HSP90AA1
F2
BCL2L1
TTR
XIAP
MDM2
SRC
MMP2
AKT1
SYK
PDE4A
PPARG
ALOX5
VDR
G6PD
PTGS1
TRPV1
ODC1
CYP2C19
SLC6A4
COMT



DOI: 10.3748/wjg.v28.i33.4890 **Copyright** ©The Author(s) 2022.

Figure 4 Funnel plot and network. A: Funnel plot of total effectiveness rate; B: Network plot of the active compounds of Shen-ling-bai-zhu san (SLBZS) target and chronic gastritis (CG) target; C: SLBZS-CG target protein interaction network.

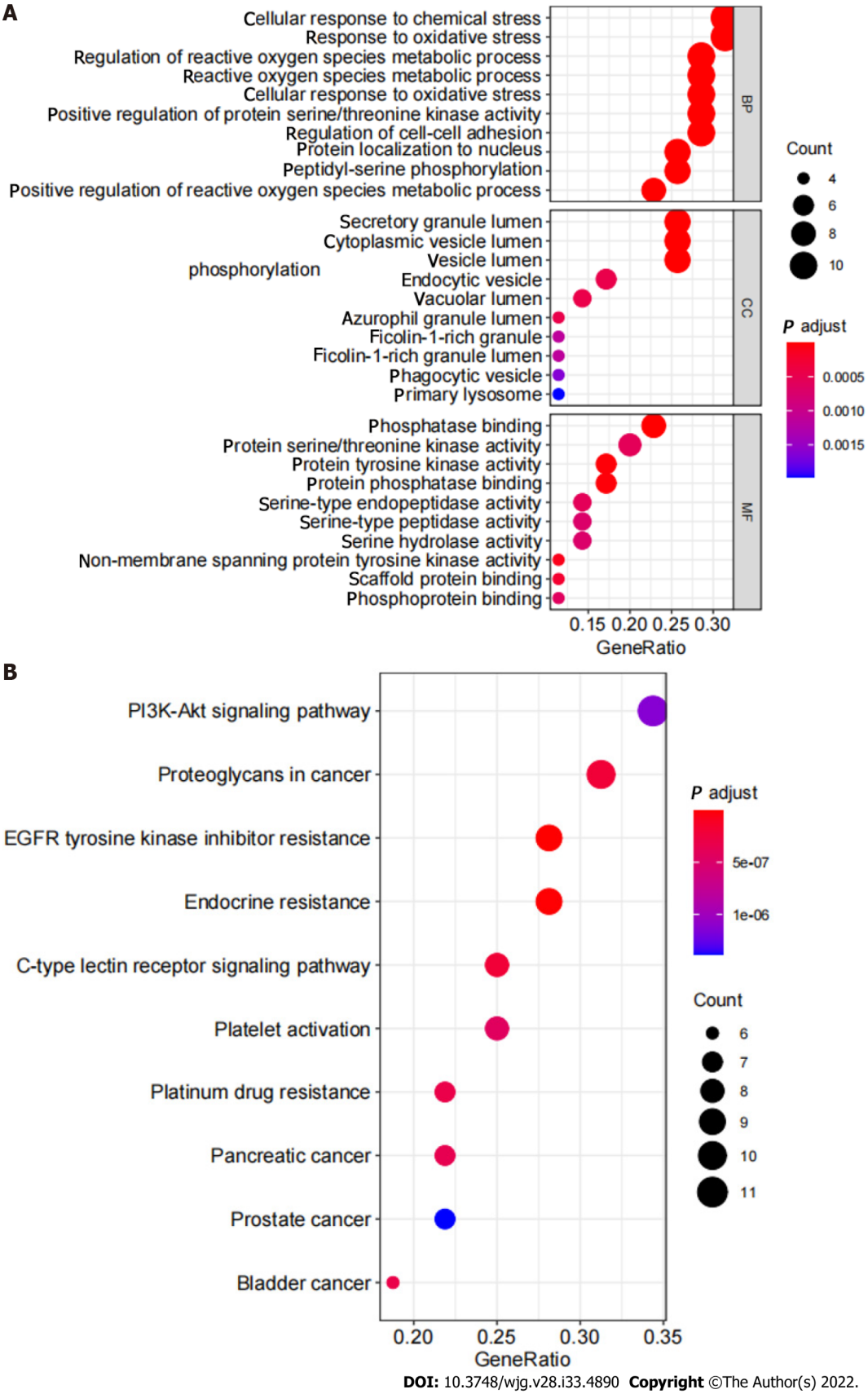
others. Differentially expressed genes are enriched in vesicle lumen, cytoplasmic vesicle lumen, and secretory granule lumen in the CC category. Differentially expressed genes are enriched in tyrosine kinase activity, protein serine/threonine kinase activity, and phosphatase binding (Figure 5A). KEGG pathway analysis results showed that the differentially expressed genes involved EGFR tyrosine kinase inhibitor resistance and the PI3K-Akt signaling pathway (Figure 5B, Figure 6).

DISCUSSION

Effectiveness and safety of a formula used for CG treatment were evaluated by us. We also summarized the possible pharmacological mechanisms based on collecting as many medical records as possible. Before our study, at least two systematic reviews[42,43] focused on the efficacy of Chinese herbal medicine formulas as CG treatments. However, neither of these reviews included SLBZS as an experimental intervention, and there are no animal studies of SLBZS for CG.

Analysis of the 14 RCTs suggested that SLBZS reverses *H. pylori* seropositivity and recurrence rates in patients with CG more so than in western medicine. SLBZS formula treats CG based on the current evidence. There were insignificant heterogeneity and publication bias. The safety is not yet established. The study designs were not rigorous, and the GRADE assessment presented moderate and low quality. Therefore, large numbers of rigorously designed RCTs are required to obtain conclusive evidence for the effect and safety of SLBZS for CG.

CG is a common digestive system disorder characterized by an inflammatory condition of the gastric mucosa. CG also leads to mental and psychological disorders like interpersonal sensitivity and depression[44]. On the one hand, studies demonstrated that the link between gut flora and depression is strong[45-47], and gut peptides are essential regulators of microbiota-gut-brain signaling in health and stress-related psychiatric illnesses[45]. On the other hand, intestinal flora can be transformed by TCM compounds[48]. Chinese medicine can regulate the composition and metabolism of intestinal flora and regulate intestinal flora by affecting the secretion of brain-gut peptide and monoamine neurotransmitters, thus improving depression behavior[47-49]. Hence, the anti-inflammatory effect of regulating gut microbiota could represent a complementary and alternative direction for CG with depression symptoms.



DOI: 10.3748/wjg.v28.i33.4890 **Copyright** ©The Author(s) 2022.

Figure 5 GO analysis and Kyoto Encyclopedia of Genes and Genomes enrichment analysis. A: GO analysis of the critical targets of Shen-ling-bai-zhu san (SLBZS) in treatment for chronic gastritis (CG); B: Kyoto Encyclopedia of Genes and Genomes enrichment analysis of the critical targets of SLBZS in treatment for CG.

Main pharmacological mechanisms

According to a study based on Chinese Medicine theory[50], the mechanism of TCM in treating CG is related to neuroprotective mechanisms, immune protective mechanisms, endocrine protective mechanisms, and other factors. A rat study showed that *Xiangshaliujunzi* decoction improved chronic atrophic gastritis symptoms by activating the TLR2, TLR4/MAPK/NF-κB/iNOS/NO signal pathway [51]. SLBZD reduced intestinal adenoma formation in adenomatous polyposis coli multiple intestinal neoplasia mice by suppressing hypoxia-inducible factor 1α-induced CD4 + CD25 + forkhead box P3 regulatory T cells[19]. Nevertheless, the mechanisms of SLBZS in CG have not been clarified.

In the present study, based on the network pharmacology analysis of drug and disease targets, a collateral relationship revealed the mechanism of SLBZS in the treatment of CG. First, we identified candidate target genes of SLBZS. Then, a protein interaction data network was generated, from which we obtained 36 related protein targets. The most protein targets included SRC, MAPK14, PPARG, and ERBB2. Critical GO entries were included regulation of reactive oxygen species metabolic process, response to oxidative stress, cellular response to chemical stress, protein tyrosine kinase activity, protein serine/threonine kinase activity, phosphatase binding, and others. Key signal pathways were identified in the KEGG enrichment analysis, primarily in EGFR tyrosine kinase inhibitor resistance, the PI3K-Akt signaling pathway, and others.

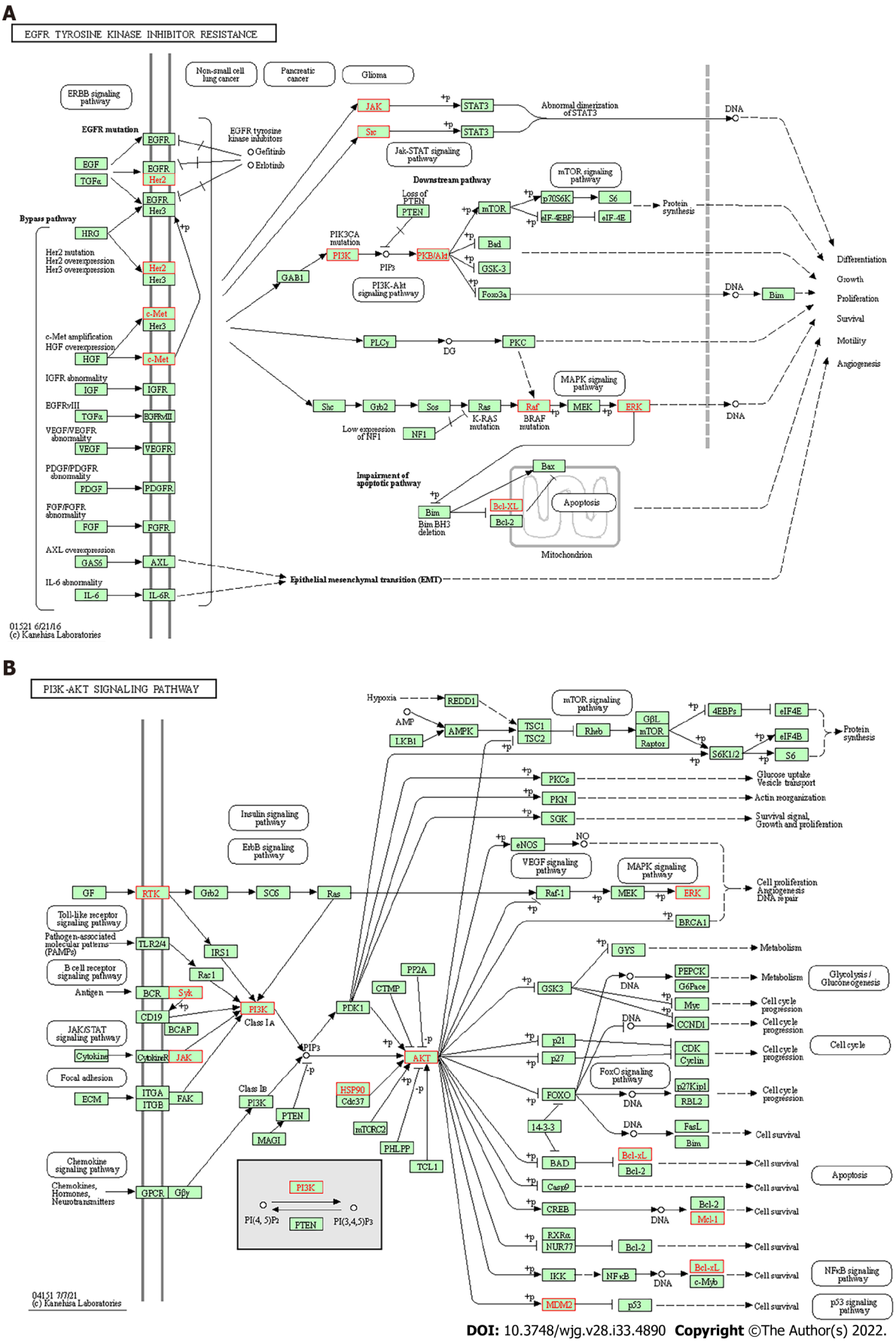
A study found that alterations in gastric cell stress-adaptive mechanisms due to *H. pylori* appear crucial during chronic infection[52]; therefore, response to oxidative stress of SLBZS to improve CG symptoms may determine the mechanism. In a future study, we will combine chemical analysis with network pharmacology to study the pharmacological effects of complex formulations comprehensively. The candidate target proteins and the formula's active ingredients are predicted by analyzing the corresponding networks. The chemical ingredients may be fully identified through experiments to confirm their presence in the formula. Therefore, further animal and clinical experiments are needed for research and exploration.

Limitations

This study had many limitations: (1) Only small sample sizes Chinese-language RCTs were included, and there were some defects in research design that resulted in the low or moderate quality of evidence; (2) most studies had design flaws like it focused only on results without illustrating a specific implementation of the random method, blind method, and follow-up reporting; (3) despite using validated documents supporting effectiveness assessment criteria, our non-uniform efficacy evaluation approach might influence outcomes and results. It might be challenging to employ the same effectiveness assessment criteria for each trial, as these criteria varied with each update; (4) adverse effects and recurrence rates information is rare reported; (5) the dosage of SLBZS has not been standardized and unified, and therefore the reasonable dosage was difficult to determined; (6) the pharmacology mechanism is unclear, especially the specific analysis of active ingredients and side effects; and (7) conflicts of interest of study investigators or funders may influence the risk of bias due to missing results. None of our included studies clearly reported their Chinese herbal sources, particularly whether pharmaceutical companies provided support. It is difficult to determine whether there were conflicts of interest. Presentation of herb sources in future studies could help determine bias.

CONCLUSION

This meta-analysis included 14 RCTs and summarized the clinical efficacy and potential mechanisms of the Chinese herbal formula SLBZS in treating CG. However, the methodological quality of the studies was not high, the risk of relapses and adverse reactions was underreported, and related mechanisms lacked validation; therefore, rigorous RCTs and basic science studies should be designed further to determine a definitive association between SLBZS and CG.



DOI: 10.3748/wjg.v28.i33.4890 **Copyright** ©The Author(s) 2022.

Figure 6 Schematic diagram. A: Schematic diagram of main Kyoto Encyclopedia of Genes and Genomes (KEGG) pathway, EGFR tyrosine kinase inhibitor resistance; B: Schematic diagram of the main KEGG pathways, PI3K-AKT signaling pathway, arrows represent activation effect, T-arrows represent inhibition effect, and segments show activation or inhibition effects.

ARTICLE HIGHLIGHTS

Research background

The effects and safety of Shen-ling-bai-zhu san (SLBZS) are currently unclear.

Research motivation

A 2012 clinical practice guideline recommended SLBZ Powder for the Pattern of Spleen and Stomach Deficiency CG. The 2020 clinical guideline did not recommend SLBZS, possibly because of inadequate clinical evidence and pharmacological mechanisms. We designed our study to focus on evidence of efficacy and potential mechanisms. This controversy needed clarified.

Research objectives

To determine the clinical evidence and potential mechanisms of SLBZS for the treatment of CG.

Research methods

Evidence-based meta-analysis and network pharmacology methods.

Research results

Fourteen articles were eventually included, covering 1335 participants. SLBZS might treat CG by acting on related targets and pathways such as EGFR tyrosine kinase inhibitor resistance, the PI3K-Akt signaling pathway, and others.

Research conclusions

SLBZS might be useful in treating CG, but its long-term effects and specific clinical mechanisms keep unclear.

Research perspectives

More samples and high-quality clinical studies should be tested and verified in the next step.

FOOTNOTES

Author contributions: Jin W and Zhong J designed the protocol; this work was conducted by Jin W, Zhong J, Li QJ, Song Y, and Hou WW; the manuscript was drafted by Zhong J and revised by Li MF, Song SY, and Li CR; Jin W and Zhong J contributed equally to this work and should be regarded as co-first authors; all authors approved the final manuscript before submission.

Conflict-of-interest statement: There are no conflicts of interest to report.

PRISMA 2009 Checklist statement: The authors have read the PRISMA 2009 Checklist, and the manuscript was prepared and revised according to the PRISMA 2009 Checklist.

Open-Access: This article is an open-access article that was selected by an in-house editor and fully peer-reviewed by external reviewers. It is distributed in accordance with the Creative Commons Attribution NonCommercial (CC BY-NC 4.0) license, which permits others to distribute, remix, adapt, build upon this work non-commercially, and license their derivative works on different terms, provided the original work is properly cited and the use is non-commercial. See: https://creativecommons.org/Licenses/by-nc/4.0/

Country/Territory of origin: China

ORCID number: Wei Jin 0000-0002-7849-8203; Juan Zhong 0000-0002-7805-0185; Yang Song 0000-0003-4987-2099; Ming-Fei Li 0000-0001-5476-3335; Shi-Yi Song 0000-0001-6921-876X; Chun-Run Li 0000-0003-4300-5680; Wei-Wei Hou 0000-0002-5921-2724; Qing-Jie Li 0000-0003-1011-7846.

S-Editor: Chen YL
L-Editor: Filipodia
P-Editor: Yu HG

REFERENCES

1 **Bacha D**, Walha M, Ben Slama S, Ben Romdhane H, Bouraoui S, Bellil K, Lahmar A. Chronic gastritis classifications. *Tunis Med* 2018; **96**: 405-410 [PMID: 30430483]
2 **Sipponen P**, Maaroos HI. Chronic gastritis. *Scand J Gastroenterol* 2015; **50**: 657-667 [PMID: 25901896 DOI:

10.3109/00365521.2015.1019918]
3 **Du Y**, Bai Y, Xie P, Fang J, Wang X, Hou X, Tian D, Wang C, Liu Y, Sha W, Wang B, Li Y, Zhang G, Shi R, Xu J, Huang M, Han S, Liu J, Ren X, Wang Z, Cui L, Sheng J, Luo H, Zhao X, Dai N, Nie Y, Zou Y, Xia B, Fan Z, Chen Z, Lin S, Li ZS; Chinese Chronic Gastritis Research group. Chronic gastritis in China: a national multi-center survey. *BMC Gastroenterol* 2014; **14**: 21 [PMID: 24502423 DOI: 10.1186/1471-230X-14-21]
4 **Li XY**, Zhang JY, Wu TN, Li M. Efficacy and safety evaluation of two regimens including Esomeprazole and amoxicillin for eradication of Helicobacter pylori associated chronic gastritis. *Zhongguo Yiyuan Yaoxue Zazhi* 2020; **40**: 427-431
5 **Liu XM**, Deng ZM, Lian YC. Effect of Rebapat combined with triple therapy on gastrointestinal hormone and immune function in patients with chronic atrophic gastritis. *Jilin Yixue* 2020; **41**: 2655-2656
6 **Cheng YX**. Effects of quadruple therapy and traditional triple therapy on gastrointestinal function and symptoms in patients with Hp positive chronic gastritis. *Zhongguo Shiyong Yiyao* 2020; **15**: 121-123
7 **Wu L**, Du ZQ. The effect of Xiaopi and Weifang combined with quadruple therapy on the efficacy, gastric function and serum inflammatory factors in patients with HP-related chronic atrophic gastritis. *Zhongguo Zhongyiyao Zazhi* 2020; **22**: 1-14
8 **Flores-Treviño S**, Mendoza-Olazarán S, Bocanegra-Ibarias P, Maldonado-Garza HJ, Garza-González E. Helicobacter pylori drug resistance: therapy changes and challenges. *Expert Rev Gastroenterol Hepatol* 2018; **12**: 819-827 [PMID: 29976092 DOI: 10.1080/17474124.2018.1496017]
9 **Li Z**, Zhang H, Wang D, Chen X, Li S. [Research progress on mechanism of acupuncture for chronic atrophic gastritis]. *Zhongguo Zhen Jiu* 2016; **36**: 1117-1120 [PMID: 29231537 DOI: 10.13703/j.0255-2930.2016.10.035]
10 **Wang L**, Li G. [Warm acupuncture for chronic atrophic gastritis with spleen-stomach deficiency cold]. *Zhongguo Zhen Jiu* 2017; **37**: 135-138 [PMID: 29231474 DOI: 10.13703/j.0255-2930.2017.02.007]
11 **Zhao J**, Cheng H, Ding Y. [Research progress of fire needling for chronic gastritis]. *Zhongguo Zhen Jiu* 2018; **38**: 223-228 [PMID: 29473371 DOI: 10.13703/j.0255-2930.2018.02.032]
12 **Xu J**, Zheng X, Cheng KK, Chang X, Shen G, Liu M, Wang Y, Shen J, Zhang Y, He Q, Dong J, Yang Z. NMR-based metabolomics Reveals Alterations of Electro-acupuncture Stimulations on Chronic Atrophic Gastritis Rats. *Sci Rep* 2017; **7**: 45580 [PMID: 28358020 DOI: 10.1038/srep45580]
13 **Liu CC**, Chen JL, Chang XR, He QD, Shen JC, Lian LY, Wang YD, Zhang Y, Ma FQ, Huang HY, Yang ZB. Comparative metabolomics study on therapeutic mechanism of electro-acupuncture and moxibustion on rats with chronic atrophic gastritis (CAG). *Sci Rep* 2017; **7**: 14362 [PMID: 29084954 DOI: 10.1038/s41598-017-13195-5]
14 **Liu X**, She C, Zhong H, Liu T, Cao JN, Zhang C, Liu M, Chang XR. [Effect of moxibustion at "Zusanli"(ST36) on metabolites of gastric tissue in rats with chronic atrophic gastritis based on metabonomics]. *Zhen Ci Yan Jiu* 2019; **44**: 113-119 [PMID: 30945487 DOI: 10.13702/j.1000-0607.180149]
15 **Wu XX**, Li X, Dang ZQ, Luo WZ, Zhao CP, Yu K. [Clinical therapy of Zisheng decoction recipe for chronic atrophic gastritis with intestinal metaplasia]. *Zhongguo Zhong Yao Za Zhi* 2017; **42**: 4882-4887 [PMID: 29493162 DOI: 10.19540/j.cnki.cjcmm.20170919.004]
16 **Tian G**, Wu C, Li J, Liang B, Zhang F, Fan X, Li Z, Wang Y, Liu D, Lai-Han Leung E, Chen J. Network pharmacology based investigation into the effect and mechanism of Modified Sijunzi Decoction against the subtypes of chronic atrophic gastritis. *Pharmacol Res* 2019; **144**: 158-166 [PMID: 30991106 DOI: 10.1016/j.phrs.2019.04.012]
17 **Wang Y**, Zhang S, Zhou Q, Meng M, Chen W. Efficacy of Shenlingbaizhu formula on irritable bowel syndrome: a systematic review. *J Tradit Chin Med* 2020; **40**: 897-907 [PMID: 33258340 DOI: 10.19852/j.cnki.jtcm.2020.06.001]
18 **Cui ZG**, Shu MY. Observation on curative effect of cefclone combined with Shenlingbaizhu granules and Muxiang shunqi pills on chronic gastritis. *Zhongguo Yixue Chuangxin* 2012; **9**: 2012
19 **Xu W**, Han Q, Liang S, Li L, Sun X, Shao M, Yao X, Xu W. Modified Shenlingbaizhu decoction reduces intestinal adenoma formation in adenomatous polyposis coli multiple intestinal neoplasia mice by suppression of hypoxia-inducible factor 1α-induced CD4+CD25+forkhead box P3 regulatory T cells. *J Tradit Chin Med* 2018; **38**: 22-32 [PMID: 32185948]
20 **Tang XD**, Lu B, Zhou LY, Zhan SY, Li ZH, Li BS, Gao R, Wang FY, Wang P, Yang JQ, Liu G, Zhang YQ, Che GX, Lin M, Bian LQ, Zhao YP; China Academy of Chinese Medical Sciences, Beijing. Clinical practice guideline of Chinese medicine for chronic gastritis. *Chin J Integr Med* 2012; **18**: 56-71 [PMID: 22231707 DOI: 10.1007/s11655-012-0960-y]
21 **Standardization project group of Clinical Application Guide for Dominant Diseases of Chinese Patent Medicine Treatment**. Clinical Application Guide of Chinese Patent Medicine in treating Chronic Gastritis (2020). *Zhongguo Zhongyixi Jiehe Zazhi* 2021; **2**: 157-163
22 **Yan Z**. Clinical study of cefaclor combined with Shenlingbaizhu granules and Muxiang shunqi pills in treatment of chronic gastritis. *Yatai Chuantong Yixue* 2015; **11**: 106-107
23 **Ai ZZ**, Zai YW. Overview of Shenling Baizhu Powder in the Treatment of Digestive System Diseases. *Liaoning Zhongyiyao Daxue Xuebao* 2008; **10**: 201-202
24 **Cumpston M**, Li T, Page MJ, Chandler J, Welch VA, Higgins JP, Thomas J. Updated guidance for trusted systematic reviews: a new edition of the Cochrane Handbook for Systematic Reviews of Interventions. *Cochrane Database Syst Rev* 2019; **10**: ED000142 [PMID: 31643080 DOI: 10.1002/14651858.ED000142]
25 **Wang N**, Zheng Y, Gu J, Cai Y, Wang S, Zhang F, Chen J, Situ H, Lin Y, Wang Z. Network-pharmacology-based validation of TAMS/CXCL-1 as key mediator of XIAOPI formula preventing breast cancer development and metastasis. *Sci Rep* 2017; **7**: 14513 [PMID: 29109519 DOI: 10.1038/s41598-017-15030-3]
26 **Lee AY**, Park W, Kang TW, Cha MH, Chun JM. Network pharmacology-based prediction of active compounds and molecular targets in Yijin-Tang acting on hyperlipidaemia and atherosclerosis. *J Ethnopharmacol* 2018; **221**: 151-159 [PMID: 29698773 DOI: 10.1016/j.jep.2018.04.027]
27 **Yun A**. 48 cases of chronic gastritis were treated with Jiawei Shenling Baizhu Powder. *Guangming Zhongyi* 2014; **29**: 305-306
28 **Chen XL**, Zhong RG, Zhang JZ, Xu LZ. Clinical observation on the treatment of chronic erosive gastritis by triple therapy combined with Shenling Baizhu Powder. *Xinzhongyi* 2014; **46**: 64-66

29 **Chen XY**, Wang W, Li H. Clinical efficacy and safety of Shenling Baizhu powder as an adjunctive treatment for atrophic gastritis with Helicobacter pylori infection. *Shijie Huaren Xiaohua Zazhi* 2018; **26**: 488-493

30 **Du DG**. Experience of treating chronic erosive gastritis, gastric ulcer and Helicobacter pylori infection with Shenling Baizhu Powder. *Linchuang Yixue Zazhi* 2017; **30**: 13-14

31 **Gu XX**. Chronic Gastritis Randomized Controlled Study Shenling Baizhu Powder Combined Western Medicin Treatment. *Shiyong Zhongyi Neike Zazhi* 2017; **31**: 55-56

32 **Li L**, Zhao L, Feng W, Jiang YL, Yang WX, Wang TG, Xiao GH. Clinical effect of Jiawei Shenling Baizhu Powder on chronic atrophic gastritis with weakness of spleen and stomach. *Neimenggu Zhongyiyao* 2020; **39**: 30-31

33 **Tang YJ**. Effective observation of Shenlingbaizhu Decoction for Chronic Ga. *Quanmin Jiankang Zazhi* 2014; **12**: 36-37

34 **Xia CH**. Randomized Controlled Study of Chronic Gastritis Shenling Baizhu Powder combined Western Medicine. *Shiyong Zhongyi Neike Zazhi* 2015; **29**: 71-72

35 **Xu MF**, Sheng HP, Xu JL. Clinical observation on the treatment of chronic atrophic gastritis with spleen-stomach weakness by Jiawei Shenling Baizhu Powder. *Zhongxiyi Jiehe Xinxueguanbing Dianzi Zazhi* 2018; **30**: 160-161

36 **Zhang L**, Huang PY. Clinical Analysis of Shen ling Bai zhu Powder Combined with Western Medicine in Treatment of Hp-negative Erosive Gastritis. *Shiyong Zhongyi Neike Zazhi* 2020; **34**: 101-103 [DOI: 10.13729/j.issn.1671-7813.Z20190352]

37 **Zhao BQ**, Lin SQ. Clinical Observation on Therapeutic Effect of ShenLin BaiZhu San in Patients with Chronic Alcoholic Gastritis. *Gansu Zhongyiyao Zazhi* 2020; **30**: 23

38 **Zheng YH**. Study of Efficacy of Dialectically Adjusted Dosage of Shenlin Baizhu Powder in Treating Chronic Superficial Gastritis for Patients with Spleen and Stomach Deficiency. *Zhonghua Zhongyiyao Xuekan* 2014; **31**: 2533-2535

39 **Zhuang T**, Zhou Y. Observation on the effect of Treating chronic gastritis caused by Hp infection with Shenling Baizhu Powder. *Dangdai Yiyao Lintan* 2019; **17**: 207-210

40 **Zou ZY**. Clinical study of dialectically adjusted dosage of Shenlingbaizhu Powder in treatment bof Chronic Superficial Gastritis Patients with Spleen and Stomach Deficiency. *Dangdai Yiyao Lintan* 2015; **13**: 18-19

41 **Li J**, Chen J, Tang W. The consensus of integrative diagnosis and treatment of acute pancreatitis-2017. *J Evid Based Med* 2019; **12**: 76-88 [PMID: 30806495 DOI: 10.1111/jebm.12342]

42 **Dai YK**, Zhang YZ, Li DY, Ye JT, Zeng LF, Wang Q, Hu L. The efficacy of Jianpi Yiqi therapy for chronic atrophic gastritis: A systematic review and meta-analysis. *PLoS One* 2017; **12**: e0181906 [PMID: 28738092 DOI: 10.1371/journal.pone.0181906]

43 **Cao Y**, Zheng Y, Niu J, Zhu C, Yang D, Rong F, Liu G. Efficacy of Banxia Xiexin decoction for chronic atrophic gastritis: A systematic review and meta-analysis. *PLoS One* 2020; **15**: e0241202 [PMID: 33108375 DOI: 10.1371/journal.pone.0241202]

44 **Zhao X**, Wu M, Zhang D, Sun Y, Yang Y, Xie H, Su Y, Jia J, Zhang S. The relationship of interpersonal sensitivity and depression among patients with chronic atrophic gastritis: The mediating role of coping styles. *J Clin Nurs* 2018; **27**: e984-e991 [PMID: 29052273 DOI: 10.1111/jocn.14114]

45 **Lach G**, Schellekens H, Dinan TG, Cryan JF. Anxiety, Depression, and the Microbiome: A Role for Gut Peptides. *Neurotherapeutics* 2018; **15**: 36-59 [PMID: 29134359 DOI: 10.1007/s13311-017-0585-0]

46 **Peirce JM**, Alviña K. The role of inflammation and the gut microbiome in depression and anxiety. *J Neurosci Res* 2019; **97**: 1223-1241 [PMID: 31144383 DOI: 10.1002/jnr.24476.]

47 **Hao WZ**, Li XJ, Zhang PW, Chen JX. A review of antibiotics, depression, and the gut microbiome. *Psychiatry Res* 2020; **284**: 112691 [PMID: 31791704 DOI: 10.1016/j.psychres.2019.112691]

48 **Ma Y**, Guo LN, Liu YL. Advances in the study of intestinal flora and depression. *Shiyong Yixue Zazhi* **34**: 324-327 [DOI: 10.3969/j.issn.1006-5725.2018.02.042]

49 **Meng ZQ**, Chen H, Du Y. Research progress of intestinal microflora and Chinese herbal medicine and their combination in the field of depression. *Zhongyaoxue* 2020; **31**: 2918-2923 [DOI: 10.6039/j.issn.1001-0408.2020.23.18]

50 **Yan ZM**, Bao A, Li HN, Liu SW, Hai XH. Research progress on mechanism of TCM in treating chronic gastritis. *Liaoning Zhongyiyao Zazhi* 2019; **46**: 435-438 [DOI: 10.13192/j.issn.1000-1719.2019.02.068]

51 **Lin ZQ**, Wang DX, Hong SS, Fu XY. Effects of Xiangsha Liujunzi decoction on TLR signal pathway in gastric mucosa tissues of rats with Helicobacter pylori-induced chronic atrophic gastritis. *Zhongguo Zhong Yao Za Zhi* 2016; **41**: 3078-3083 [PMID: 28920352 DOI: 10.4268/cjcmm20161623]

52 **Díaz P**, Valenzuela Valderrama M, Bravo J, Quest AFG. *Helicobacter pylori* and Gastric Cancer: Adaptive Cellular Mechanisms Involved in Disease Progression. *Front Microbiol* 2018; **9**: 5 [PMID: 29403459 DOI: 10.3389/fmicb.2018.00005]

World Journal of Gastroenterology

Submit a Manuscript: https://www.f6publishing.com

World J Gastroenterol 2022 September 7; 28(33): 4909-4919

DOI: 10.3748/wjg.v28.i33.4909

ISSN 1007-9327 (print) ISSN 2219-2840 (online)

SCIENTOMETRICS

Global research trends in the field of liver cirrhosis from 2011 to 2020: A visualised and bibliometric study

Pei-Ling Gan, Shu Huang, Xiao Pan, Hui-Fang Xia, Xin-Yi Zeng, Wen-Sen Ren, Xian Zhou, Mu-Han Lv, Xiao-Wei Tang

Specialty type: Gastroenterology and hepatology

Provenance and peer review: Unsolicited article; Externally peer reviewed.

Peer-review model: Single blind

Peer-review report's scientific quality classification

Grade A (Excellent): 0
Grade B (Very good): B, B, B
Grade C (Good): 0
Grade D (Fair): 0
Grade E (Poor): 0

P-Reviewer: El-Shabrawi MH, Egypt; Fernandes SA, Brazil; Silva LD, Brazil

Received: April 14, 2022
Peer-review started: April 14, 2022
First decision: June 10, 2022
Revised: June 17, 2022
Accepted: August 6, 2022
Article in press: August 6, 2022
Published online: September 7, 2022

Pei-Ling Gan, Xiao Pan, Hui-Fang Xia, Xin-Yi Zeng, Wen-Sen Ren, Xian Zhou, Mu-Han Lv, Xiao-Wei Tang, Department of Gastroenterology, The Affiliated Hospital of Southwest Medical University, Luzhou 646099, Sichuan Province, China

Pei-Ling Gan, Xiao Pan, Hui-Fang Xia, Xin-Yi Zeng, Wen-Sen Ren, Xian Zhou, Mu-Han Lv, Xiao-Wei Tang, Department of Gastroenterology, Nuclear Medicine and Molecular Imaging Key Laboratory of Sichuan Province, Luzhou 646000, Sichuan Province, China

Shu Huang, Department of Gastroenterology, The People's Hospital of Lianshui, Huaian 223400, Jiangsu Province, China

Corresponding author: Xiao-Wei Tang, MD, PhD, Doctor, Department of Gastroenterology, The Affiliated Hospital of Southwest Medical University, No. 25 Taiping Street, Jiangyang Region, Luzhou 646099, China. solitude5834@hotmail.com

Abstract

BACKGROUND

Liver cirrhosis is the leading cause of liver-related mortality worldwide. It is currently a global health challenge.

AIM

This research intended to explore and analyse research trends and frontiers in this field during the last 10 years, providing new inspiration for clinical decision-making and scientific research.

METHODS

Publications on hepatic cirrhosis research were retrieved from the Web of Science Core Collection on April 4, 2021. Bibliometric visualisation was conducted through VOSviewer and CiteSpace.

RESULTS

The analytic research was based on original articles and reviews. A total of 7775 records of hepatic cirrhosis published from 2011 to 2020 were retrieved. In the past ten years, the number of related annual publications has increased significantly, especially in the United States and China. All publications were distributed among 109 countries. The United States contributed the most (21.95%) and was consistently the leading driving force, with a solid academic reputation in this area. The University of Barcelona distributed the most related articles (177

articles) and was cited the most frequently. The *Journal of Hepatology* ranked third in the top 10 journals, which has the highest impact factor (impact factor 2019 = 20.582). Jasmohan S. Bajaj was the most productive author (72 articles). Burst keywords (*e.g.*, sofosbuvir, burden, care, sarcopenia, chronic liver failure, human gut microbiome, and nonalcoholic fatty liver disease) and a succession of reference citation bursts have provided clues about research frontiers in recent years.

CONCLUSION

This study identified developing trends in the evolution of liver cirrhosis to provide new inspiration for researchers.

Key Words: Liver cirrhosis; Bibliometric research; Research frontiers; VOSviewer; CiteSpace; Visualization

©The Author(s) 2022. Published by Baishideng Publishing Group Inc. All rights reserved.

Core Tip: This research explored and analyzed research trends and frontiers in this field during the last 10 years, further providing new inspiration for scientific research. We found sarcopenia, human gut microbiome, and nonalcoholic fatty liver disease are of particular interest in studies of cirrhosis. Treatment of diseases that cause cirrhosis, such as hepatitis C, is also a hot topic.

Citation: Gan PL, Huang S, Pan X, Xia HF, Zeng XY, Ren WS, Zhou X, Lv MH, Tang XW. Global research trends in the field of liver cirrhosis from 2011 to 2020: A visualised and bibliometric study. *World J Gastroenterol* 2022; 28(33): 4909-4919

URL: https://www.wjgnet.com/1007-9327/full/v28/i33/4909.htm

DOI: https://dx.doi.org/10.3748/wjg.v28.i33.4909

INTRODUCTION

Liver cirrhosis is a common clinical chronic progressive disease with high mortality caused by one or more factors. It is the fifth leading cause of adult deaths, the top cause of liver-related death worldwide [1], and the eighth of the primary diseases in economic cost[2]. Cirrhosis is a heterogeneous disease classified into two prognosis stages: compensated cirrhosis and decompensated cirrhosis[3]. In the early stage, due to the essential liver compensatory function, there are no visible symptoms. Later, the primary symptoms are liver function impairment and portal hypertension, and multiple systems are affected. Ascites, upper gastrointestinal haemorrhage, secondary infection, hepatic encephalopathy, canceration, and other complications are common in the late stage. Thus, cirrhosis is a high-burden treatment option for patients, health care systems, and the government.

Bibliometric research is a quantitative analytic method that employs mathematics and statistics to determine scientific activity[4]. It can help researchers identify the research focus and trends of a particular subject. In addition, the research results may be beneficial to future research.

Professor Chen (Drexel University) created CiteSpace V, a Java-based information visualisation program for bibliometric analysis. Researchers may assess a discipline's evolution and identify frontier trends intuitively by providing numerous data in the form of knowledge maps[5]. CiteSpace has recently been used for bibliometric analysis in various fields; however, there is yet to be a bibliometric analysis of cirrhosis. In this study, we first used CiteSpace V to analyse articles on liver cirrhosis from 2011 to 2020 utilizing the Web of Science Core Collection (WoSCC) database, providing new inspiration for clinical decision-making and scientific research.

MATERIALS AND METHODS

Data collection and search strategy

Data were retrieved from the WoSCC on a single day, April 4, 2021. WoSCC offers extensive citation index information for over 8000 influential and famous journals globally. It is a comprehensive database, notably in natural science and medicine. The following were included in the search strategy: title = "cirrhosis," database selected = Web of Science Core Collection, time span = 2011–2020. Only original articles and reviews were included. We obtained 7775 records for this study. A flowchart representing the retrieval strategies is shown in Supplementary Figure 1. In addition, high-quality references were retrieved and cited by the Reference Citation Analysis (https://www.referencecitation-analysis.com/) database.

Analysis tool

For bibliometric analysis, Microsoft Excel 2016, VOSviewer, and CiteSpace were chosen. Information on authors, journals, institutions, and countries may be integrated with these computer systems. Parameters such as article count, impact factor (IF), centrality, and occurrence/citation burst were utilized in this article. Productivity was measured by the number of articles published and was used to identify productive individuals or groups. The IF was obtained using Journal Citation Reports (JCR). The IF is a recognized metric for assessing a journal's impact worldwide. The IF in this study was based on JCR (2019). The network visualisation maps were constructed using VOSviewer to examine the cooperative relationships between countries and institutions with highly cocited references. Coauthorship analysis identifies research output. We selected "countries" and "organizations" as the unit of analysis. CiteSpace V adopts a time slicing technique to create a timeline of network models and integrates these individual networks to produce an overview network for the systematic analysis of the relevant publications. In this study, we utilized CiteSpace V to conduct a cocitation analysis of the references and clusters. After that, a timeline view of cocited references was built. As a result, we were able to clarify the origin and period of certain clustering fields[6]. These parameters help identify potential collaborative relationships in the field of liver cirrhosis. Furthermore, an occurrence burst denotes a word that appears often over a specific period, whereas a citation burst denotes a reference that is referenced frequently during a specific period[7]. Keywords and references with the highest citation bursts were selected to demonstrate research hot spots and frontiers because they can identify whether relevant scholars have paid extensive attention to these areas in a specific period[5].

RESULTS

Publication output and temporal trend

A total of 7775 publications satisfied the search criteria. Table 1 lists the top-10 cited articles in descending order based on the number of citations. Figure 1A depicts the global distribution of yearly publications on cirrhosis research from 2011 to 2020. The overall worldwide publishing trend rose from 520 to 955 between 2011 and 2020. However, during the periods of 2015-2017 and 2019-2020, the number of publications showed a modest decrease. The annual publication trends of the top 10 academic output countries are presented in Figure 1B. The number of publications on cirrhosis published by the United States and China has increased remarkably within the last decade.

Distribution by country and institution

All of the publications come from 109 countries and 6902 institutions. The distribution of countries/regions that published no fewer than 100 papers is shown in Supplementary Figure 2. Table 2 contains detailed information on the top 10 countries. The United States had the most publications (1707 publications), followed by China (1672 publications) and Japan (711 publications). Among the top 10 countries, France exhibits high academic quality, and its citation/article ratio (46.67) was far greater than that of other listed countries.

Using VOSviewer, we constructed a network visualisation map for liver cirrhosis research publications to assess international collaborations. Collaborations between countries and institutions are depicted in Supplementary Figure 3. Nodes with higher co-occurrence were classified as the same colour. Nodes with similar colours formed one cluster, indicating that they had closer cooperative relationships. The width of the lines describes the magnitude of the collaboration. As shown, the United States had the highest total link strength, suggesting that it cooperated most with other countries worldwide. The country that collaborated the most with the United States was China. The most productive institutions are listed in Table 3. The University of Barcelona (177 publications) ranked first, followed by Virginia Commonwealth University (120 publications) and University College London (119 publications). The cluster coloured in green was led by the University of Barcelona, collaborating most with Virginia Commonwealth University. Furthermore, three of the top 10 institutions are in the United States, two are in China, and two are in Italy, suggesting that these three countries have many outstanding research groups in this field.

Distribution by journals and authors

Liver cirrhosis research articles were published in 1511 journals. The number of articles in the top 10 journals ranged from 119 to 259, accounting for 22.73% of the total (1767) (Supplementary Table 1). Among these journals, *Liver International* contributed the highest number of publications on cirrhosis research (259 publications, IF 2019 = 5.175), followed by *Hepatology* (242 publications, IF 2019 = 14.679) and *Journal of Hepatology* (212 publications, IF 2019 = 20.582). *Journal of Hepatology* had the highest IF, and its citation/article ratio (68.30) was far more than that of other listed journals. The most frequently cited journal was *Hepatology* (14922 citations). The following most frequently cited journals were *Journal of Hepatology* (14479 citations) and *Liver International* (5721 citations).

Table 1 The top 10 cited articles of Web of Science Core Collection bibliometrics in cirrhosis research field

Rank	First author	Journal	Title	Number of citations (WoSCC)	Type of articles
1	Moreau R	*Gastroenterology* 2013; 144(7): 1426-1437, 1437.e1-9	Acute-on-chronic liver failure is a distinct syndrome that develops in patients with acute decompensation of cirrhosis	1113	Retrospective study
2	Marcellin P	*Lancet* 2013; 381(9865): 468-475	Regression of cirrhosis during treatment with tenofovir disoproxil fumarate for chronic hepatitis B: a 5-year open-label follow-up study	946	Randomized controlled trial
3	Kowdley KV	*N Engl J Med* 2014; 370(20): 1879-1888	Ledipasvir and Sofosbuvir for 8 or 12 weeks for chronic HCV without cirrhosis	872	Prospective study
4	Qin N	*Nature* 2014; 513(7516): 59-64	Alterations of the human gut microbiome in liver cirrhosis	793	Retrospective study
5	Anstee QM	*Nat Rev Gastroenterol Hepatol* 2013; 10(6): 330-344	Progression of NAFLD to diabetes mellitus, cardiovascular disease or cirrhosis	758	Review
6	Tsochatzis EA	*Lancet* 2014; 383(9930): 1749-1761	Liver cirrhosis	686	Review
7	Poordad F	*N Engl J Med* 2014; 370(21): 1973-1982	ABT-450/r-Ombitasvir and Dasabuvir with Ribavirin for hepatitis C with cirrhosis	675	Randomized controlled trial
8	Garcia-Tsao G	*Hepatology* 2017; 65(1): 310-335	Portal hypertensive bleeding in cirrhosis: risk stratification, diagnosis, and management: 2016 Practice Guidance by the American Association for the Study of Liver Diseases	539	Practice guideline
9	Conti F	*J Hepatol* 2016; 65(4): 727-733	Early occurrence and recurrence of hepatocellular carcinoma in HCV-related cirrhosis treated with direct-acting antivirals	495	Prospective study
10	Chen Y	*Hepatology* 2011; 54(2): 562-572	Characterization of fecal microbial communities in patients with liver cirrhosis	450	Randomized controlled trial

WoSCC: Web of Science Core Collection.

Table 2 The top 10 countries that published articles on cirrhosis research

Rank	Country	Number of articles	Number of citations	Citations per article
1	United States	1707	46238	27.09
2	China	1672	19452	11.63
3	Japan	711	11215	15.77
4	Italy	651	22183	34.08
5	Spain	486	19497	40.12
6	Germany	477	12862	26.96
7	England	458	19842	43.32
8	France	391	18247	46.67
9	South Korea	310	5077	16.38
10	India	302	3661	12.12

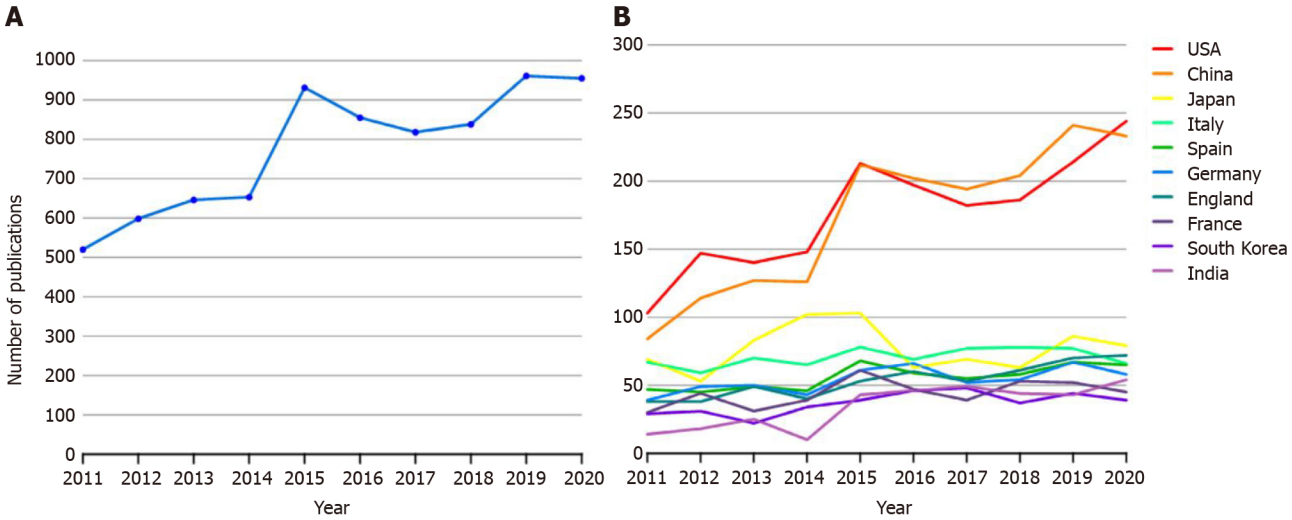
A total of 35653 authors contributed to the overall output. The most productive authors are listed in Supplementary Table 2. Jasmohan S. Bajaj published 72 articles, ranking first in the number of publications, followed by M. Eric Gershwin (70 articles) and Qi Xingshun (61 articles). Pere Gines had the highest citation/article ratio (89.27), followed by Paolo Angeli (74.07) and Guadalupe Garcia-Tsao (69.13).

Analysis of keywords

Figure 2 shows the top 25 keywords with the strongest occurrence burst. The occurrence burst, which demonstrated a sharp rise over a certain period, referred to frontier disciplines and dynamic changes in

Table 3 The top 10 institutions that published articles on cirrhosis research

Rank	Institutions	Number of articles	Number of citations	Country
1	University of Barcelona	177	11087	Spain
2	Virginia Commonwealth University	120	5826	United States
3	University College London	119	5134	England
4	Mayo Clinic	117	4074	USA
5	University of Padua	111	5430	Italy
6	Capital Medical University	109	646	China
7	University of California, Davis	102	4515	USA
8	Zhejiang University	102	2404	China
9	University of Copenhagen	99	1521	Denmark
10	University of Milan	98	5108	Italy



DOI: 10.3748/wjg.v28.i33.4909 **Copyright** ©The Author(s) 2022.

Figure 1 Trends in the number of publications and analysis of countries in the field of cirrhosis. A: The annual worldwide publication output; B: The annual publication output for the top 10 countries.

a particular field. Hot topics were represented by keywords whose occurrence burst lasted until 2020. The most recent burst keywords were "sofosbuvir" (2016–2020), "burden" (2017–2020), "care" (2017–2020), "sarcopenia" (2018–2020), "chronic liver failure" (2018–2019), "human gut microbiome" (2018–2020), "nonalcoholic fatty liver disease (NAFLD)" (2018–2020), "American association" (2018–2020), and "ma" (2018–2020).

Analysis of references

In bibliometric research, reference analysis is an important indication. The pieces of literature with the strongest citation burst are considered to be the knowledge fundamentals of the research frontiers. Clusters along horizontal timelines are depicted in Figure 3, which is a timeline visualisation in CiteSpace. From left to right, each cluster is presented. The publication time legend is displayed at the top. The clusters were arranged vertically and in declining order of size. The largest cluster is presented at the top. Cocitation linkages are shown by the stained curves. Large-sized nodes were especially concerning since they were highly cited. The most cited references in a given year are displayed under each timeline. Clusters were numbered from 0. Cluster #0 was the largest cluster. As shown in the timeline overview, the largest cluster in this study was #0 acute kidney injury, indicating a significant research interest and direction in recent years. This was followed by #1 hepatitis C, #2 clonal selection theory, #3 hepatic encephalopathy, #4 Liver cirrhosis, and #5 variceal bleeding. Some clusters remained active until 2020. Figure 4 depicts cirrhosis-related references with the strongest citation burst during the last 10 years. Citation bursts until the end of 2020 were led by de Franchis *et al* (2015), who had the strongest burst (40.22), followed by Garcia-Tsao *et al* (2017), Tsochatzis *et al* (2014), Vilstrup *et al* (2014),

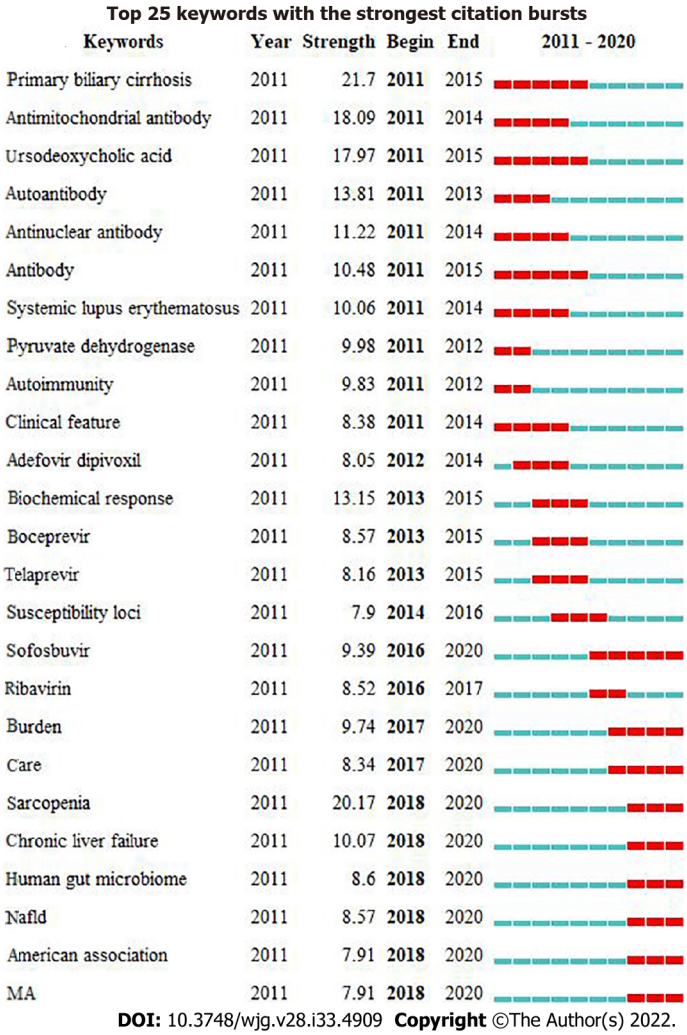


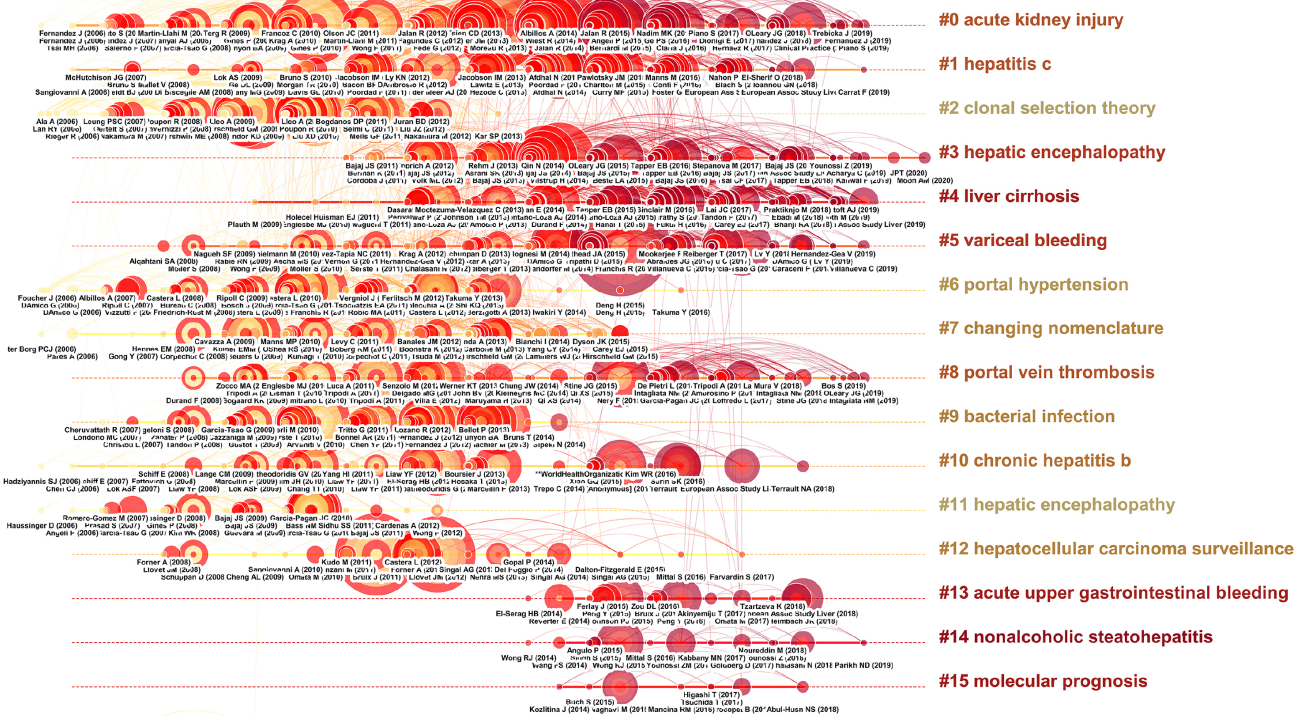
Figure 2 Keywords with the strongest occurrence burst on cirrhosis research.

Mokdad *et al* (2014), Albillos *et al* (2014), Jalan *et al* (2014), and Heimbach *et al* (2018).

DISCUSSION

Liver cirrhosis is a chronic disease with high mortality and is a serious public health problem, afflicting more than 160 million people globally in 2017[8]. The most common cause is chronic viral hepatitis, specifically hepatitis B virus (HBV) and hepatitis C virus (HCV)[3,9]. Previous studies have shown that the prevalence of liver cirrhosis varies by region. East Asia has the most significant prevalence of liver cirrhosis. In contrast, Southern Latin America has the lowest incidence of 12.1%[9]. Furthermore, the worldwide incidence of liver cirrhosis is increasing continuously, and it ranks eighth in terms of economic cost among significant diseases[2], even though various public health measures have been implemented. As a result, to better comprehend the advanced research hotspots in the field of cirrhosis, a study is necessary.

From the retrieved data, we can easily conclude that the general research trend of liver cirrhosis has been growing, especially in China and the United States. Eight of the top 10 countries that most produce related research were developed countries, while 2 were developing countries. The United States had the most publications, followed by China and Japan, and India ranked last. In 2017, among individuals with prevalent liver cirrhosis worldwide, HBV infection accounted for approximately 28.72%. East Asia has the highest prevalence of liver cirrhosis. China had the world's greatest number of patients. Therefore, China and India rank among the top 10 countries in terms of the occurrence of liver cirrhosis and may be relevant for these potential causes. However, in terms of citations per article, although China temporarily ranked in the top position in number of articles, it still has a long way to go to improve the overall quality of articles. China must continue to increase research in this area and strengthen collaborations with other countries. In contrast, although only a few French articles were published, they were of high academic quality.



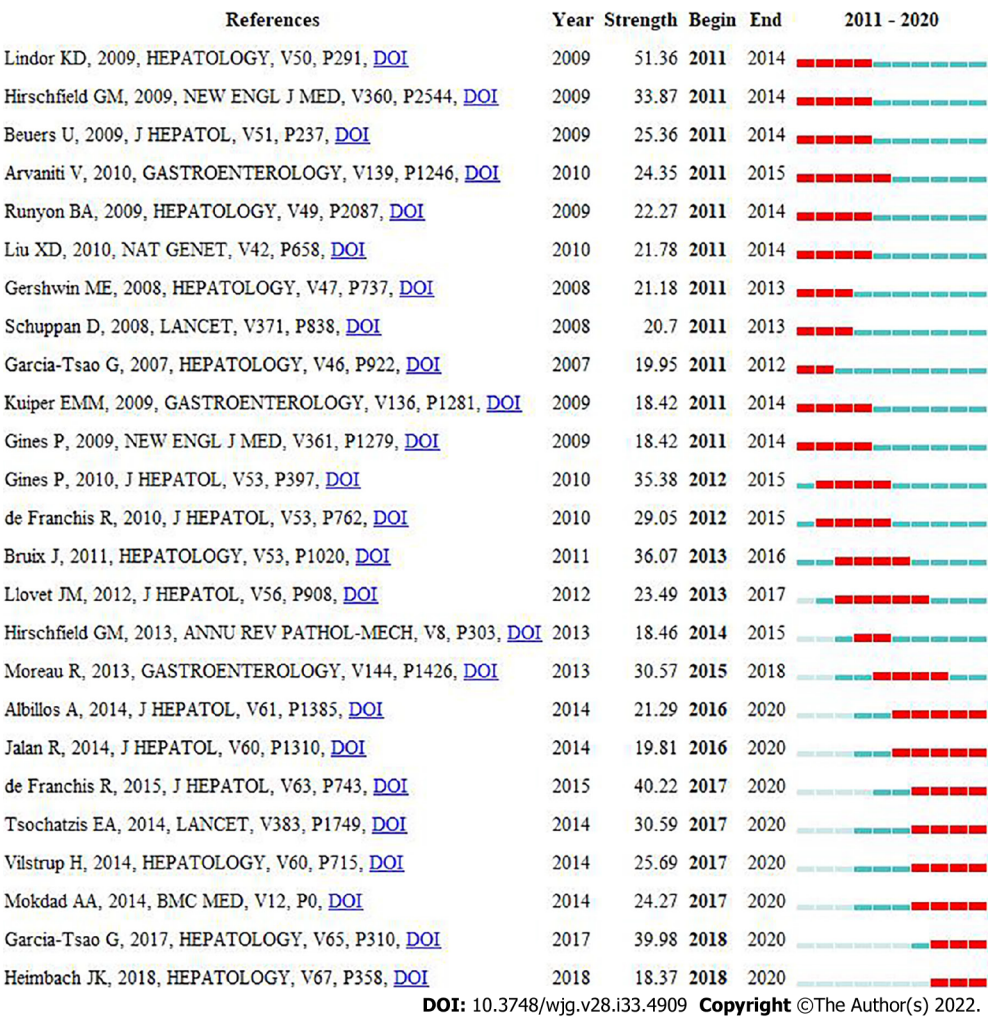
DOI: 10.3748/wjg.v28.i33.4909 **Copyright** ©The Author(s) 2022.

Figure 3 A timeline visualization of the largest clusters.

Nine of the top 10 institutions were universities, suggesting that universities are the most common research groups. Three of the top 10 institutions were from the United States (Virginia Commonwealth University, Mayo Clinic, and University of California, Davis); thus, the United States is the main domain in the field. Two of the top 10 institutions were from China (Capital Medical University and Zhejiang University), and two institutions were from Italy (the University of Padua and University of Milan). According to the findings of this analysis, the three countries have numerous great research groups in this area.

In this study, we found some great research works from some excellent authors. They made significant contributions to this discipline. For example, Guadalupe Garcia-Tsao ranked 7th among the top 10 authors, and her practice guideline of portal hypertensive bleeding in cirrhosis also ranked among the top 10[10]. Her study effort provides academic researchers and clinical professionals with a better and deeper understanding of risk stratification, diagnosis, and management of portal hypertensive bleeding in liver cirrhosis. Moreau *et al*[11] analysed data from patients with cirrhosis and acute decompensation (AD) to establish diagnostic criteria for acute-on-chronic liver failure (ACLF), which he discovered was distinct from AD. In addition, his research demonstrated that ACLF mortality is linked to loss of organ function and high leukocyte counts and that ACLF is particularly severe in individuals with no prior history of AD.

CiteSpace V was used to detect keyword bursts in this study. These statistics are potentially valuable in forecasting research frontiers. The keywords "sofosbuvir," "burden," "care," "sarcopenia," "chronic liver failure," "human gut microbiome," and the "NAFLD" are expected to appear often in the following years, indicating emerging trends. The top five cirrhosis frontiers are as follows: (1) Sarcopenia: The skeletal muscle is the body's largest organ, and atrophy comes from a change in the balance of protein production and degradation towards protein breakdown. Primary sarcopenia is a loss of skeletal muscle strength, mass, or physical function owing to ageing, whereas secondary sarcopenia is recognized as a loss of skeletal muscle strength, mass, or physical function due to underlying disorders. Liver cirrhosis is one of the representational disorders that might be complicated with secondary sarcopenia. In patients with cirrhosis, muscle mass loss worsens as their liver reserve deteriorates. Sarcopenia and frailty have a negative impact on clinical outcomes and prognosis. It has been convincingly demonstrated that patients with cirrhosis, sarcopenia, and frailty have a lower quality of life and survival, more cirrhotic complications and infections, and poorer outcomes following liver transplant surgery[12-14]. As a result, emphasis must be placed on early detection, active diagnosis, and treatment. Consequently, further investigations in the context of assessment criteria for sarcopenia and frailty are warranted to deepen our current knowledge of sarcopenia and frailty in patients with cirrhosis; (2) Chronic liver failure: ACLF, a clinical syndrome in patients with chronic liver disease, is more often discussed clinically. It is associated with multiple organ failure and increased short-term mortality. It is a significant cause of mortality in people with cirrhosis. Although the precise causative mechanism is



DOI: 10.3748/wjg.v28.i33.4909 **Copyright** ©The Author(s) 2022.

Figure 4 References with the strongest citation burst on cirrhosis research.

unknown, systemic inflammation plays a critical role in its pathogenesis, and the strength of this inflammatory response paralleled the severity of ACLF. Aside from organ failure and a very high risk of short-term death, patients with ACLF exhibited other characteristics that separated them from non-ACLF patients. They were, for example, younger, had more alcoholic cirrhosis and less HCV-related cirrhosis, and mainly had a higher frequency of active alcoholism and severe bacterial infections[11]. More research for new findings into the mechanisms underlying ACLF, risk prediction models, therapeutic targets, and liver transplantation for ACLF is needed; (3) Sofosbuvir: An oral nucleotide analogue inhibitor of the HCV-specific NS5B polymerase has been approved to treat chronic HCV infection. A study showed that ledipasvir-sofosbuvir for eight weeks was associated with a high rate of sustained virologic response among previously untreated patients with HCV genotype 1 infection without cirrhosis[15]. A recent article published in *The Lancet Gastroenterology & Hepatology* stated that ravidasvir plus sofosbuvir was effective in patients with chronic HCV infection. Furthermore, by offering a new affordable, simple, and efficacious public health tool for large-scale implementation, this treatment has the potential to eradicate HCV-related morbidity and mortality[16]; (4) Human gut microbiome: The function of gut microbiota in human health and disease has recently received much attention. Several chronic illnesses have been linked to the gut microbiota, such as obesity[17-19], inflammatory bowel disease[20], diabetes mellitus[21], and NAFLD[22]. Through the hepatic portal and bile secretion systems, the liver interacts directly with the gut. Enteric dysbiosis, namely, the translocation of bacteria and their products over the gut epithelial barrier, is involved in the development of liver cirrhosis. However, the phylogenetic and functional composition alterations in the human gut microbiota associated with this progression remain obscure[23]. Furthermore, research suggests that microbiome manipulation to eliminate manganese and reduce GABA levels in the gut might provide a novel therapeutic approach for treating hepatic encephalopathy[24]. In addition, novel probiotics may be helpful in the prevention of the aggravation of liver cirrhosis. More broadly, microbiome manipulation may offer up new pathways for the treatment of liver cirrhosis. A combination of microbial genes distinguishes patients with liver cirrhosis from healthy individuals with high specificity. This might pave the way for a novel method of monitoring and preventing liver cirrhosis; and (5) NAFLD: NAFLD is a

progressive liver disease spectrum encompassing simple steatosis, nonalcoholic steatohepatitis (NASH), fibrosis, and, eventually, cirrhosis. NAFLD is closely associated with characteristics of metabolic syndrome such as abdominal obesity, insulin resistance, glucose intolerance or type 2 diabetes (T2DM), and atherogenic dyslipidaemia[25]. Over the last few decades, people's lifestyles have become more sedentary, and dietary habits have changed, leading to an increase in the prevalence of obesity and insulin resistance[26,27]. In light of this, NAFLD quickly became the most common cause of abnormal liver biochemistry in both developed and developing countries. Several prior epidemiological studies have identified a strong association between NAFLD and an elevated risk of developing T2DM. In addition, patients with NAFLD, whether adults or adolescents, have several risk factors for cardiovascular disease. A notable minority proportion of NAFLD patients proceed to a more severe disease characterized by NASH and fibrosis and cirrhosis or, in some circumstances, progress to hepatocellular carcinoma[28]. The mechanisms linking NAFLD to the diseases mentioned above and the current pharmacological treatments for NAFLD need to be further explored.

The articles with the strongest citation burst are potentially valuable for exploring research frontiers. In this study, #0 acute kidney injury was the largest cluster, and #3 hepatic encephalopathy remained active until the most recent publication year for a cited reference. References with the top three citation bursts were as follows: (1) de Franchis *et al*[29] contributed to the writing of expanding consensus in portal hypertension, further elaborating the stratifying risk and individualizing care for portal hypertension; (2) Garcia-Tsao *et al*[10] coauthored a practice guideline and elaborated the risk stratification, diagnosis, and management of portal hypertensive bleeding in cirrhosis; and (3) Tsochatzis *et al*[30] reviewed the current understanding of cirrhosis as a dynamic process and outlined therapeutic options for preventing and treating complications of cirrhosis based on the subclassification in clinical stages. Meanwhile, we proposed a new concept for managing patients with cirrhosis and the challenge in the 21st century.

Limitations

To the best of our knowledge, this study was the first bibliometric analysis of cirrhosis in the past ten years. This study, however, has certain limitations. First, we considered the WoSCC database a reputable and reliable service for publications and citations; hence, we extracted data only from it. This may restrict the coverage of all available articles and result in a reduced number of documents included in the analysis. Second, the search method may also have been insufficient because we only searched for publications with the phrase "cirrhosis," which may have resulted in a paucity of papers due to other terminology. Finally, we analysed the data selectively. We mainly utilized a quantitative analysis approach, while little emphasis has been paid to the qualitative aspects of this study. As a result, certain critical points and details may have been missed. All of the considerations mentioned above may lead to bias in the results. Hence, the results should be interpreted with caution.

CONCLUSION

This study might aid researchers in identifying new trends in cirrhosis from 2011 to 2020, thus, providing new inspiration for scientific research.

ARTICLE HIGHLIGHTS

Research background

Liver cirrhosis is a common clinical chronic progressive disease with high mortality caused by one or more factors.

Research motivation

Identifying new trends in cirrhosis from 2011 to 2020, thus, providing new inspiration for scientific research.

Research objectives

This research intended to explore and analyse research trends and frontiers in this field of cirrhosis during the last 10 years.

Research methods

Using VOSviewer and CiteSpace, assess a discipline's evolution and identify frontier trends intuitively by knowledge maps.

Research results

The general research trend of liver cirrhosis has been growing, especially in China and the United States. The keywords "sofosbuvir," "burden," "care," "sarcopenia," "chronic liver failure," "human gut microbiome," and the "NAFLD" are expected to appear often in the following years, indicating emerging trends. The top five cirrhosis frontiers are Sarcopenia, Chronic liver failure, Sofosbuvir, Human gut microbiome and Nonalcoholic fatty liver disease.

Research conclusions

This study identified developing trends in the evolution of liver cirrhosis to provide new inspiration for researchers.

Research perspectives

The top five cirrhosis frontiers are sarcopenia, chronic liver failure, sofosbuvir, human gut microbiome and nonalcoholic fatty liver disease.

FOOTNOTES

Author contributions: Gan PL, Huang S and Pan X contributed equally to this work; Gan PL, Zhou X, Lv MH and Tang XW designed the research study; Gan PL, Huang S, Pan X, Xia HF and Zeng XY performed the research; Pan X and Ren WS contributed analytic tools; Gan PL, Huang S and Pan X analyzed the data and wrote the manuscript; All authors have read and approve the final manuscript.

Conflict-of-interest statement: We declared that no conflicts of interest or financial ties to disclose.

PRISMA 2009 Checklist statement: The authors have read the PRISMA 2009 Checklist, and the manuscript was prepared and revised according to the PRISMA 2009 Checklist.

Open-Access: This article is an open-access article that was selected by an in-house editor and fully peer-reviewed by external reviewers. It is distributed in accordance with the Creative Commons Attribution NonCommercial (CC BY-NC 4.0) license, which permits others to distribute, remix, adapt, build upon this work non-commercially, and license their derivative works on different terms, provided the original work is properly cited and the use is non-commercial. See: https://creativecommons.org/Licenses/by-nc/4.0/

Country/Territory of origin: China

ORCID number: Pei-Ling Gan 0000-0003-2487-1321; Shu Huang 0000-0001-7284-469X; Xiao Pan 0000-0003-1232-8487; Hui-Fang Xia 0000-0003-3469-8024; Xin-Yi Zeng 0000-0002-7926-2980; Wen-Sen Ren 0000-0003-4078-5933; Xian Zhou 0000-0001-9200-5412; Mu-Han Lü 0000-0001-8881-5092; Xiao-Wei Tang 0000-0001-6064-0526.

S-Editor: Zhang H
L-Editor: A
P-Editor: Yuan YY

REFERENCES

1 **GBD 2017 Causes of Death Collaborators**. Global, regional, and national age-sex-specific mortality for 282 causes of death in 195 countries and territories, 1980-2017: a systematic analysis for the Global Burden of Disease Study 2017. *Lancet* 2018; **392**: 1736-1788 [PMID: 30496103 DOI: 10.1016/S0140-6736(18)32203-7]
2 **Scaglione S**, Kliethermes S, Cao G, Shoham D, Durazo R, Luke A, Volk ML. The Epidemiology of Cirrhosis in the United States: A Population-based Study. *J Clin Gastroenterol* 2015; **49**: 690-696 [PMID: 25291348 DOI: 10.1097/MCG.0000000000000208]
3 **Westbrook RH**, Dusheiko G. Natural history of hepatitis C. *J Hepatol* 2014; **61**: S58-S68 [PMID: 25443346 DOI: 10.1016/j.jhep.2014.07.012]
4 **Oelrich B**, Peters R, Jung K. A bibliometric evaluation of publications in urological journals among European Union countries between 2000-2005. *Eur Urol* 2007; **52**: 1238-1248 [PMID: 17673361 DOI: 10.1016/j.eururo.2007.06.050]
5 **Chen C**. CiteSpace II: Detecting and visualizing emerging trends and transient patterns in scientific literature. 2006; 57: 359-377 [DOI: 10.1002/asi.20317]
6 **Chen C**, Dubin R, Kim MC. Emerging trends and new developments in regenerative medicine: a scientometric update (2000 - 2014). *Expert Opin Biol Ther* 2014; **14**: 1295-1317 [PMID: 25077605 DOI: 10.1517/14712598.2014.920813]
7 **Chen C**, Hu Z, Liu S, Tseng H. Emerging trends in regenerative medicine: a scientometric analysis in CiteSpace. *Expert Opin Biol Ther* 2012; **12**: 593-608 [PMID: 22443895 DOI: 10.1517/14712598.2012.674507]
8 **Liu Z**, Jiang Y, Yuan H, Fang Q, Cai N, Suo C, Jin L, Zhang T, Chen X. The trends in incidence of primary liver cancer caused by specific etiologies: Results from the Global Burden of Disease Study 2016 and implications for liver cancer prevention. *J Hepatol* 2019; **70**: 674-683 [PMID: 30543829 DOI: 10.1016/j.jhep.2018.12.001]

9 **de Carvalho JR**, Villela-Nogueira CA, Perez RM, Portugal FB, Flor LS, Campos MR, Schramm JMA. Burden of Chronic Viral Hepatitis and Liver Cirrhosis in Brazil - the Brazilian Global Burden of Disease Study. *Ann Hepatol* 2017; **16**: 893-900 [PMID: 29055917 DOI: 10.5604/01.3001.0010.5280]

10 **Garcia-Tsao G**, Abraldes JG, Berzigotti A, Bosch J. Portal hypertensive bleeding in cirrhosis: Risk stratification, diagnosis, and management: 2016 practice guidance by the American Association for the study of liver diseases. *Hepatology* 2017; **65**: 310-335 [PMID: 27786365 DOI: 10.1002/hep.28906]

11 **Moreau R**, Jalan R, Gines P, Pavesi M, Angeli P, Cordoba J, Durand F, Gustot T, Saliba F, Domenicali M, Gerbes A, Wendon J, Alessandria C, Laleman W, Zeuzem S, Trebicka J, Bernardi M, Arroyo V; CANONIC Study Investigators of the EASL–CLIF Consortium. Acute-on-chronic liver failure is a distinct syndrome that develops in patients with acute decompensation of cirrhosis. *Gastroenterology* 2013; **144**: 1426-1437, 1437.e1 [PMID: 23474284 DOI: 10.1053/j.gastro.2013.02.042]

12 **European Association for the Study of the Liver**. EASL Clinical Practice Guidelines on nutrition in chronic liver disease. *J Hepatol* 2019; **70**: 172-193 [PMID: 30144956 DOI: 10.1016/j.jhep.2018.06.024]

13 **Ebadi M**, Montano-Loza AJ. Sarcopenia and Frailty in the Prognosis of Patients on the Liver Transplant Waiting List. *Liver Transpl* 2019; **25**: 7-9 [PMID: 30472786 DOI: 10.1002/lt.25386]

14 **Sinclair M**, Gow PJ, Grossmann M, Angus PW. Review article: sarcopenia in cirrhosis--aetiology, implications and potential therapeutic interventions. *Aliment Pharmacol Ther* 2016; **43**: 765-777 [PMID: 26847265 DOI: 10.1111/apt.13549]

15 **Kowdley KV**, Gordon SC, Reddy KR, Rossaro L, Bernstein DE, Lawitz E, Shiffman ML, Schiff E, Ghalib R, Ryan M, Rustgi V, Chojkier M, Herring R, Di Bisceglie AM, Pockros PJ, Subramanian GM, An D, Svarovskaia E, Hyland RH, Pang PS, Symonds WT, McHutchison JG, Muir AJ, Pound D, Fried MW; ION-3 Investigators. Ledipasvir and sofosbuvir for 8 or 12 weeks for chronic HCV without cirrhosis. *N Engl J Med* 2014; **370**: 1879-1888 [PMID: 24720702 DOI: 10.1056/NEJMoa1402355]

16 **Andrieux-Meyer I**, Tan SS, Thanprasertsuk S, Salvadori N, Menétrey C, Simon F, Cressey TR, Said HRHM, Hassan MRA, Omar H, Tee HP, Chan WK, Kumar S, Thongsawat S, Thetket K, Avihingsanon A, Khemnark S, Yerly S, Ngo-Giang-Huong N, Siva S, Swanson A, Goyal V, Bompart F, Pécoul B, Murad S. Efficacy and safety of ravidasvir plus sofosbuvir in patients with chronic hepatitis C infection without cirrhosis or with compensated cirrhosis (STORM-C-1): interim analysis of a two-stage, open-label, multicentre, single arm, phase 2/3 trial. *Lancet Gastroenterol Hepatol* 2021; **6**: 448-458 [PMID: 33865507 DOI: 10.1016/S2468-1253(21)00031-5]

17 **Ley RE**, Turnbaugh PJ, Klein S, Gordon JI. Microbial ecology: human gut microbes associated with obesity. *Nature* 2006; **444**: 1022-1023 [PMID: 17183309 DOI: 10.1038/4441022a]

18 **Turnbaugh PJ**, Hamady M, Yatsunenko T, Cantarel BL, Duncan A, Ley RE, Sogin ML, Jones WJ, Roe BA, Affourtit JP, Egholm M, Henrissat B, Heath AC, Knight R, Gordon JI. A core gut microbiome in obese and lean twins. *Nature* 2009; **457**: 480-484 [PMID: 19043404 DOI: 10.1038/nature07540]

19 **Turnbaugh PJ**, Ley RE, Mahowald MA, Magrini V, Mardis ER, Gordon JI. An obesity-associated gut microbiome with increased capacity for energy harvest. *Nature* 2006; **444**: 1027-1031 [PMID: 17183312 DOI: 10.1038/nature05414]

20 **Garrett WS**, Gallini CA, Yatsunenko T, Michaud M, DuBois A, Delaney ML, Punit S, Karlsson M, Bry L, Glickman JN, Gordon JI, Onderdonk AB, Glimcher LH. Enterobacteriaceae act in concert with the gut microbiota to induce spontaneous and maternally transmitted colitis. *Cell Host Microbe* 2010; **8**: 292-300 [PMID: 20833380 DOI: 10.1016/j.chom.2010.08.004]

21 **Qin J**, Li Y, Cai Z, Li S, Zhu J, Zhang F, Liang S, Zhang W, Guan Y, Shen D, Peng Y, Zhang D, Jie Z, Wu W, Qin Y, Xue W, Li J, Han L, Lu D, Wu P, Dai Y, Sun X, Li Z, Tang A, Zhong S, Li X, Chen W, Xu R, Wang M, Feng Q, Gong M, Yu J, Zhang Y, Zhang M, Hansen T, Sanchez G, Raes J, Falony G, Okuda S, Almeida M, LeChatelier E, Renault P, Pons N, Batto JM, Zhang Z, Chen H, Yang R, Zheng W, Yang H, Wang J, Ehrlich SD, Nielsen R, Pedersen O, Kristiansen K. A metagenome-wide association study of gut microbiota in type 2 diabetes. *Nature* 2012; **490**: 55-60 [PMID: 23023125 DOI: 10.1038/nature11450]

22 **Yan AW**, Fouts DE, Brandl J, Stärkel P, Torralba M, Schott E, Tsukamoto H, Nelson KE, Brenner DA, Schnabl B. Enteric dysbiosis associated with a mouse model of alcoholic liver disease. *Hepatology* 2011; **53**: 96-105 [PMID: 21254165 DOI: 10.1002/hep.24018]

23 **Gill SR**, Pop M, Deboy RT, Eckburg PB, Turnbaugh PJ, Samuel BS, Gordon JI, Relman DA, Fraser-Liggett CM, Nelson KE. Metagenomic analysis of the human distal gut microbiome. *Science* 2006; **312**: 1355-1359 [PMID: 16741115 DOI: 10.1126/science.1124234]

24 **Qin N**, Yang F, Li A, Prifti E, Chen Y, Shao L, Guo J, Le Chatelier E, Yao J, Wu L, Zhou J, Ni S, Liu L, Pons N, Batto JM, Kennedy SP, Leonard P, Yuan C, Ding W, Hu X, Zheng B, Qian G, Xu W, Ehrlich SD, Zheng S, Li L. Alterations of the human gut microbiome in liver cirrhosis. *Nature* 2014; **513**: 59-64 [PMID: 25079328 DOI: 10.1038/nature13568]

25 **de Alwis NM**, Day CP. Non-alcoholic fatty liver disease: the mist gradually clears. *J Hepatol* 2008; **48** Suppl 1: S104-S112 [PMID: 18304679 DOI: 10.1016/j.jhep.2008.01.009]

26 **Ratziu V**, Bellentani S, Cortez-Pinto H, Day C, Marchesini G. A position statement on NAFLD/NASH based on the EASL 2009 special conference. *J Hepatol* 2010; **53**: 372-384 [PMID: 20494470 DOI: 10.1016/j.jhep.2010.04.008]

27 **Das K**, Das K, Mukherjee PS, Ghosh A, Ghosh S, Mridha AR, Dhibar T, Bhattacharya B, Bhattacharya D, Manna B, Dhali GK, Santra A, Chowdhury A. Nonobese population in a developing country has a high prevalence of nonalcoholic fatty liver and significant liver disease. *Hepatology* 2010; **51**: 1593-1602 [PMID: 20222092 DOI: 10.1002/hep.23567]

28 **Anstee QM**, Targher G, Day CP. Progression of NAFLD to diabetes mellitus, cardiovascular disease or cirrhosis. *Nat Rev Gastroenterol Hepatol* 2013; **10**: 330-344 [PMID: 23507799 DOI: 10.1038/nrgastro.2013.41]

29 **de Franchis R**; Baveno VI Faculty. Expanding consensus in portal hypertension: Report of the Baveno VI Consensus Workshop: Stratifying risk and individualizing care for portal hypertension. *J Hepatol* 2015; **63**: 743-752 [PMID: 26047908 DOI: 10.1016/j.jhep.2015.05.022]

30 **Tsochatzis EA**, Bosch J, Burroughs AK. Liver cirrhosis. *Lancet* 2014; **383**: 1749-1761 [PMID: 24480518 DOI: 10.1016/S0140-6736(14)60121-5]

World Journal of Gastroenterology

Submit a Manuscript: https://www.f6publishing.com

World J Gastroenterol 2022 September 7; 28(33): 4920-4925

DOI: 10.3748/wjg.v28.i33.4920

ISSN 1007-9327 (print) ISSN 2219-2840 (online)

CASE REPORT

Ectopic bronchogenic cyst of liver misdiagnosed as gallbladder diverticulum: A case report

Cheng-Ji Dong, Ru-Ming Yang, Qi-Long Wang, Qing-Yuan Wu, Da-Ji Yang, De-Cai Kong, Ping Zhang

Specialty type: Gastroenterology and hepatology

Provenance and peer review: Unsolicited article; Externally peer reviewed.

Peer-review model: Single blind

Peer-review report's scientific quality classification

Grade A (Excellent): 0
Grade B (Very good): B, B
Grade C (Good): 0
Grade D (Fair): 0
Grade E (Poor): 0

P-Reviewer: Samizadeh B, Iran; Yin F, United States

Received: March 17, 2022
Peer-review started: March 17, 2022
First decision: April 10, 2022
Revised: April 13, 2022
Accepted: August 16, 2022
Article in press: August 16, 2022
Published online: September 7, 2022

Cheng-Ji Dong, Qing-Yuan Wu, Da-Ji Yang, De-Cai Kong, Ping Zhang, Department of Hapatopancreatobiliary Surgery, The First Bethune Hospital of Jilin University, Changchun 130021, Jilin Province, China

Ru-Ming Yang, Department of Breast Surgery, The First Bethune Hospital of Jilin University, Changchun 130021, Jilin Province, China

Qi-Long Wang, Department of Vascular Surgery, The First Bethune Hospital of Jilin University, Changchun 130021, Jilin Province, China

Corresponding author: Ping Zhang, MD, Chief Doctor, Professor, Department of Hapato-pancreatobiliary Surgery, The First Bethune Hospital of Jilin University, No. 71 Xinmin Street, Changchun 130021, Jilin Province, China. z_ping@jlu.edu.cn

Abstract

BACKGROUND

Ectopic bronchogenic cysts are a type of congenital cystic tumor that are extremely difficult to diagnose and can be ectopically located in various organs, with the possibility of malignant transformation. Here we report a case of an ectopic bronchogenic cyst in the liver initially misdiagnosed as a gallbladder diverticulum.

CASE SUMMARY

The patient was a middle-aged woman whose chief complaint was intermittent pain in the upper abdomen. Imaging examination revealed a cystic space in the left inner lobe of the liver. She was admitted to our hospital for treatment. Based on abdominal examination and imaging findings, the initial diagnosis was gallbladder diverticulum with cholestasis combined with chronic cholecystitis. However, following intraoperative observations and postoperative pathologic assessment, the diagnosis was revised to ectopic bronchogenic cyst of the liver.

CONCLUSION

Radiologists, hepatobiliary and pancreatic surgeons, gastrointestinal surgeons, urologists, and even neurosurgeons should be aware and consider a possible diagnosis of ectopic bronchogenic cysts, especially when other types of cyst, cystadenoma, and other diseases are excluded. The disease and its complications should be detected and correctly diagnosed and treated as early as possible in order to avoid adverse outcomes.

Key Words: Ectopic bronchogenic cyst; Misdiagnosis; Gallbladder diverticulum; Benign tumor; Cystadenoma; Case report

©The Author(s) 2022. Published by Baishideng Publishing Group Inc. All rights reserved.

Core Tip: Ectopic bronchogenic cysts are the rarest type of bronchogenic cyst and can be ectopically located in different organs. When various specialists diagnose cysts, cystadenomas, and other diseases, the possibility of ectopic bronchogenic cyst should not be discounted. We report a case of an ectopic bronchogenic cyst in the liver that was misdiagnosed as gallbladder diverticulum. Early surgical intervention is the most effective strategy to prevent disease transformation.

Citation: Dong CJ, Yang RM, Wang QL, Wu QY, Yang DJ, Kong DC, Zhang P. Ectopic bronchogenic cyst of liver misdiagnosed as gallbladder diverticulum: A case report. *World J Gastroenterol* 2022; 28(33): 4920-4925
URL: https://www.wjgnet.com/1007-9327/full/v28/i33/4920.htm
DOI: https://dx.doi.org/10.3748/wjg.v28.i33.4920

INTRODUCTION

A bronchogenic cyst is a rare congenital cystic tumor that can generally be classified as one of three types—namely, intrapulmonary, mediastinal, and heterotopic (the most rare)[1-3]. Bronchogenic cysts often develop ectopically in the neck, retroperitoneum, and stomach wall; very few cases of ectopic cysts in the liver have been reported[4]. Ectopic bronchogenic cysts often have no specific clinical manifestations, imaging characteristics, or changes in laboratory indices, making preoperative diagnosis extremely difficult. The cysts are typically discovered during routine physical examinations or because of complications resulting from the compression of surrounding organs or tissues. Here we report a case of an ectopic bronchogenic cyst in the liver that was preoperatively diagnosed as cholecystic diverticulum with cholestasis.

CASE PRESENTATION

Chief complaints

A 40-year-old woman presented with intermittent upper abdominal pain.

History of present illness

Physical examination at the primary hospital revealed a space-occupying lesion above the gallbladder in the left inner lobe of the liver that was complicated by chronic cholecystitis. The patient was transferred to our hospital for further treatment.

History of past illness

The patient was physically fit.

Personal and family history

Her family history was noncontributory.

Physical examination

A physical examination of the abdomen showed no muscle tension, tenderness, or rebound pain. No abdominal mass was detected; the liver was not touched under the ribs, and the Murphy sign was positive.

Laboratory examinations

Laboratory examinations including routine blood and blood coagulation, liver function, biochemistry, tumor markers, and infection markers revealed no abnormalities.

Imaging examinations

Abdominal color Doppler ultrasound showed a cystic echo beside the gallbladder in the left inner lobe of the liver with a size of 3.2 cm × 1.6 cm. The boundary was clear, the ultrasound transmission was poor, a bile mud echo was observed, there was no blood flow signal, and there appeared to be a

connection with the neck of the gallbladder. Gallbladder diverticulum with cholestasis and chronic cholecystitis was suspected. Hepatobiliary, pancreatic, and splenic multi-slice plain computed tomography (CT) scanning and 3-phase enhanced scans showed an elliptical low-density shadow above the gallbladder in the left inner lobe of the liver, with a CT value of about 55 HU. Intrahepatic bile ducts were not dilated. The gallbladder was not enlarged but the wall was slightly thickened, and there was no abnormal density in the cavity. The cystic space-occupying lesion above the gallbladder in the left inner lobe of the liver strongly suggested gallbladder diverticulum with cholestasis. Magnetic resonance cholangiopancreatography (MRCP) was performed to determine the relationship between the lesion and the gallbladder. There was an oval abnormal signal in the gallbladder fossa area about 2.9 cm × 2.0 cm in size. T1-weighted imaging (T1WI) and T2-weighted imaging (T2WI) and diffusion-weighted imaging showed a high-signal shadow and the apparent diffusion coefficient was consistent with a slightly high-signal shadow; the edges of the shadow were thin, smooth, and clear, and there was no enhancement at the lesion center. The lesion appeared to be connected to the cystic duct given the limited fluid signal shadow in the gallbladder fossa area of the intrahepatic lobe (Figure 1).

FINAL DIAGNOSIS

Based on the patient's symptoms, abdominal examination, and imaging findings, the initial diagnosis was gallbladder diverticulum with cholestasis combined with chronic cholecystitis. However, based on intraoperative findings and postoperative pathologic results, the diagnosis was later confirmed as ectopic bronchogenic cyst in the liver.

TREATMENT

The patient underwent laparoscopic cholecystectomy and cystectomy of the left inner lobe of the liver. During the operation, it was observed that the cyst and gallbladder were connected to a pedicle but not to each other. Dark green bile was drained from the gallbladder, and light yellow turbid fluid was observed inside the cyst (Figure 2).

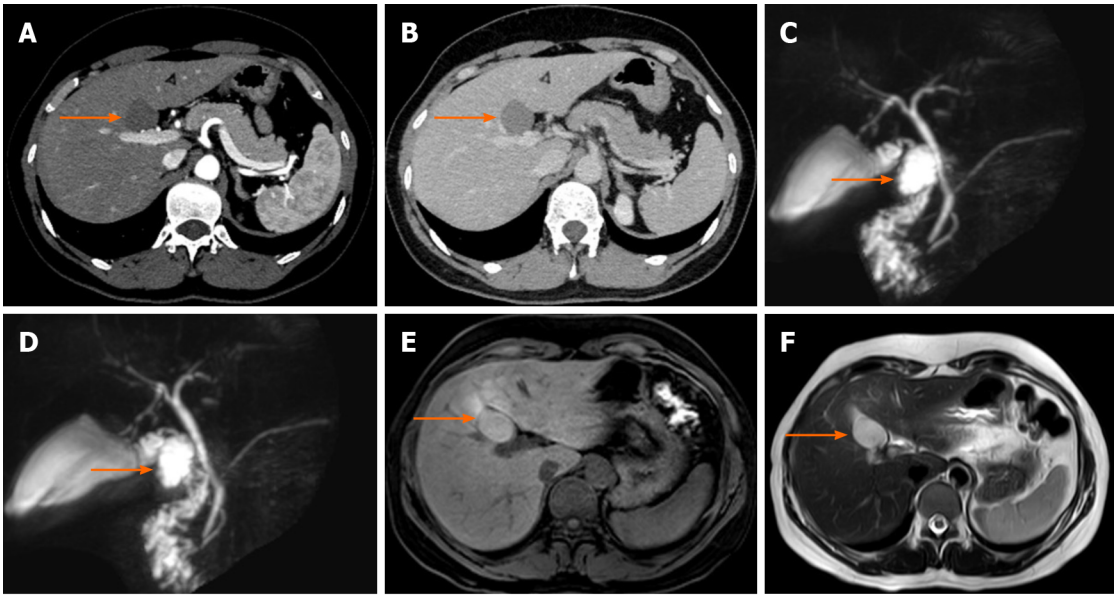
OUTCOME AND FOLLOW-UP

After the operation, we carried out a pathologic examination on the excised specimen. The outer part of the cyst was connected to the gallbladder; the volume was 2 cm × 2 cm × 2 cm, the wall thickness was 0.1-0.2 cm, and the inner wall was smooth and light brown. The cyst wall was fibrous under microscopic examination, with visible muscle tissue. Part of the mucosal epithelium on the inner surface was absent, and the remaining inner surface was partly lined with pseudostratified ciliated columnar epithelium and mucous epithelium. Serous and mucous glands were observed in the lamina propria, consistent with bronchogenic cysts. The intraoperative findings combined with histopathologic examination refuted the preoperative diagnosis of gallbladder diverticulum complicated by cholestasis (Figure 3). No recurrence was found in the color Doppler ultrasonography 6 mo after the operation.

DISCUSSION

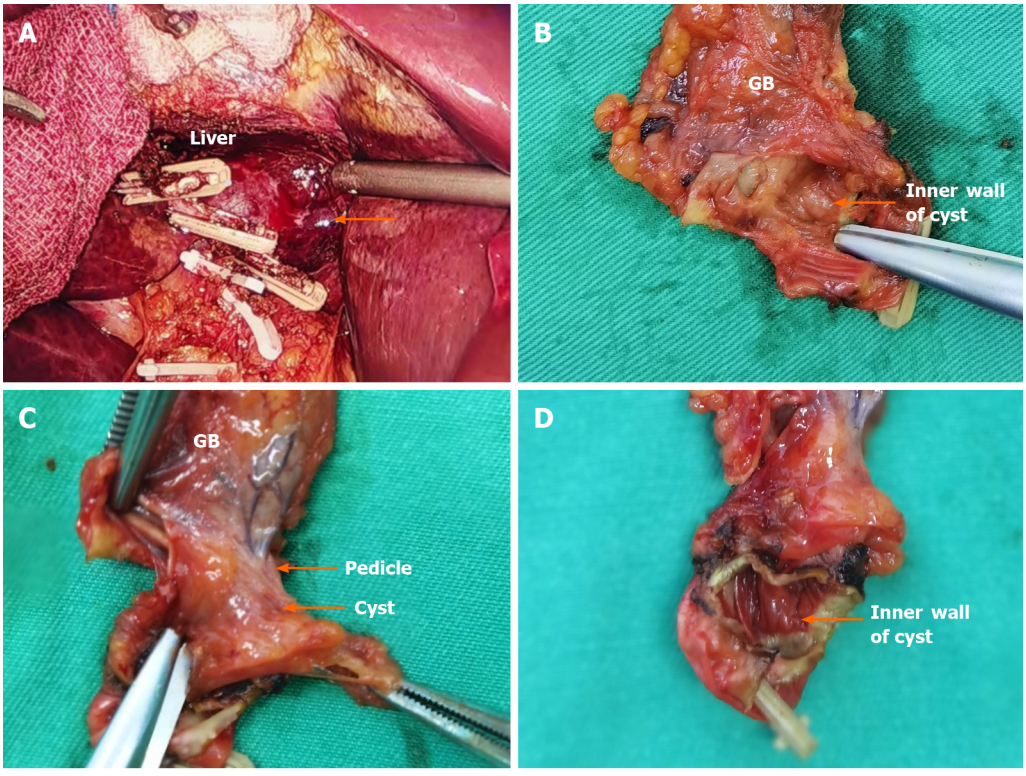
Ectopic bronchogenic cysts can occur at any age, with similar prevalence in men and women. There are few specific manifestations but clinical symptoms can arise when a cyst compresses nearby organs or tissues. For example, a patient developed new abdominal pain and gross hematuria that may have been caused by the aggravation of a lump originating from the left adrenal gland[5]; the pain was intermittent, which may have been related to chronic cholecystitis. Similarly, ectopic bronchogenic cysts have no special imaging findings. Magnetic resonance imaging (MRI) examinations often show isointense shadows on T1WI and high-intensity shadows on T2WI that are not enhanced by the contrast agent. However, in some patients, both T1WI and T2WI show significant enhancement[6]. In our patient, T1WI showed a slightly high-signal shadow and T2WI showed a high-signal shadow; a retrospective analysis of the MRI findings was more suggestive of ectopic bronchogenic cysts, which are associated with elevated levels of the tumor markers carcinoembryonic antigen, carbohydrate antigen (CA)19-9, and CA72-4[7,8].

In countries where bronchogenic cysts are endemic, they are often associated with hydatid disease [9]. The diagnosis and differential diagnosis of ectopic bronchogenic cysts is extremely difficult and they are often confused with other types of cyst and serous or mucinous cystadenoma. The pathogenesis of ectopic bronchogenic cysts in the abdominal cavity is complex and diverse. It has been proposed to



DOI: 10.3748/wjg.v28.i33.4920 **Copyright** ©The Author(s) 2022.

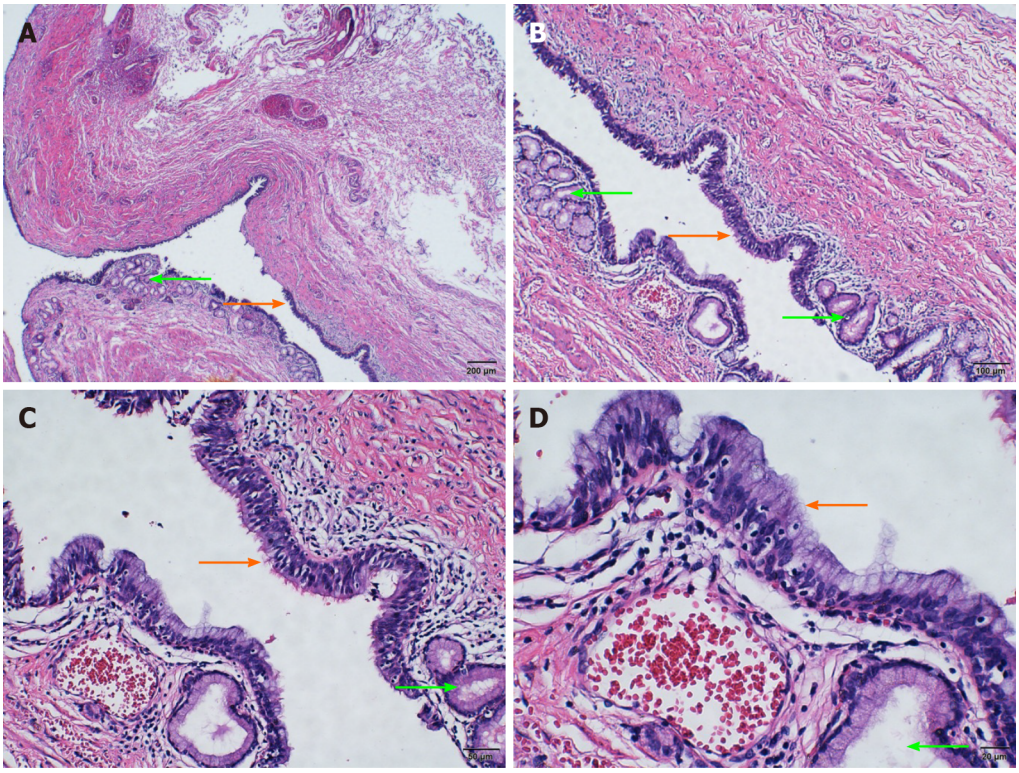
Figure 1 Ectopic bronchogenic cyst in a 40-year-old woman. The location of the cyst is indicated by an orange arrow. Magnetic resonance cholangiopancreatography (MRCP) showed that the cyst was locally connected to the cystic duct. A: Hepatobiliary and pancreatic enhanced computed tomography (CT) arterial phase; B: Hepatobiliary and pancreatic enhanced CT venous phase; C and D: MRCP; E: T1-weighted imaging showed a slightly high signal shadow; F: T2-weighted imaging showed a high signal shadow.



DOI: 10.3748/wjg.v28.i33.4920 **Copyright** ©The Author(s) 2022.

Figure 2 Gross examination of the surgically excised ectopic bronchogenic cyst. A: The gallbladder and cyst were removed under laparoscopy, revealing the smooth wound surface (orange arrow) connecting the cyst and liver; B: The inner wall of the cyst. The cyst contained light yellow turbid liquid; C: The cyst was connected to the gallbladder *via* a pedicle; D: Inner wall of the cyst.

originate in the embryonic foregut, which develops from the primordial malformed trachea and bronchial tree in the early embryo; bacteria shed from this structure migrate to the caudal side of the foregut, which forms the abdominal organ or retroperitoneal bronchus cyst. The thoracic and abdominal cavities are thought to be connected in the early embryonic stage. At 6 wk of gestation, the pleura and



DOI: 10.3748/wjg.v28.i33.4920 **Copyright** ©The Author(s) 2022.

Figure 3 Histopathologic examination by hematoxylin and eosin staining. The cyst wall was fibrous and muscle tissue was visible. The mucosal epithelium of the inner surface of the cyst wall was partially detached, and the remaining inner surface was partly lined with pseudostratified ciliated columnar epithelium (orange arrow) and mucous epithelium. Serous and mucous glands were observed in the lamina propria (green arrow). A: 4 ×; B: 10 ×; C: 20 ×; D: 40 ×.

peritoneum fuse and develop into a mature diaphragm. The body cavity is divided into the mature thoracic cavity and abdominal cavity. The abdominal buds of the tracheobronchial tree are squeezed and migrate into the abdominal cavity at the same time, leading to ectopic bronchogenic cysts in the abdominal cavity[10]. Clarifying the detailed mechanism underlying the development of bronchogenic cysts will facilitate their detection, diagnosis, and treatment.

Most ectopic bronchogenic cysts require surgical removal, and histopathologic examination of surgical specimens must be performed to confirm the diagnosis. Immunopositivity for cytokeratin (CK)7 and thyroid transcription factor 1 and immunonegativity for CK20 and calretinin in the epithelial lining also strongly support a diagnosis of bronchogenic cysts[7,11]. In terms of treatment, as ectopic bronchogenic cysts can be ectopic to different organs, the speed at which they develop and their biological behaviors vary[1,2]. Ectopic bronchogenic cysts are also easily confused with cystic diseases of adjacent organs, patients with bronchogenic cysts or suspected ectopic bronchogenic cysts should be examined by a surgeon, especially when the cyst is small as it may be missed. Thus, immunohistochemistry is useful when bronchial cysts cannot be differentially diagnosed based on histology and microscopic examination alone, and excision by using laparoscopy or robotic surgery and histopathology remain the first choices for treatment and definitive diagnosis[12].

CONCLUSION

Ectopic bronchogenic cysts are a congenital cystic tumor that are extremely difficult to diagnose and can be ectopically located in various organs, and have a risk of malignant transformation. Radiologists, hepatobiliary and pancreatic surgeons, gastrointestinal surgeons, urologists, and even neurosurgeons should be aware of these cysts. During diagnosis and treatment of a suspected cyst or cystadenoma, the possibility of ectopic bronchogenic cysts should be considered. The disease and its complications should be detected and diagnosed and treated as early as possible to avoid adverse consequences.

FOOTNOTES

Author contributions: Zhang P and Dong CJ performed the surgery, reviewed the literature, and contributed to manuscript drafting; Dong CJ, Yang RM, and Wang QL wrote the manuscript; Dong CJ, Wu QY, Yang DJ, and Kong

DC were involved in the clinical management of the patient; all authors gave final approval for the submitted version of the manuscript.

Informed consent statement: Written, informed consent was obtained from the patient for publication of this report.

Conflict-of-interest statement: The authors declare that they have no conflict of interest.

CARE Checklist (2016) statement: The authors have read the CARE Checklist (2016), and the manuscript was prepared and revised according to the CARE Checklist (2016).

Open-Access: This article is an open-access article that was selected by an in-house editor and fully peer-reviewed by external reviewers. It is distributed in accordance with the Creative Commons Attribution NonCommercial (CC BY-NC 4.0) license, which permits others to distribute, remix, adapt, build upon this work non-commercially, and license their derivative works on different terms, provided the original work is properly cited and the use is non-commercial. See: https://creativecommons.org/Licenses/by-nc/4.0/

Country/Territory of origin: China

ORCID number: Cheng-Ji Dong 0000-0001-7359-6501; Ru-Ming Yang 0000-0003-3593-3735; Qi-Long Wang 0000-0002-0475-2037; Qing-Yuan Wu 0000-0001-9692-7166; Da-Ji Yang 0000-0002-2266-1606; De-Cai Kong 0000-0002-2204-6283; Ping Zhang 0000-0003-4944-2937.

S-Editor: Yan JP
L-Editor: A
P-Editor: Yan JP

REFERENCES

1 **Mumtaz A**, Dhanani R, Faisal M, Maqbool H, Iqbal Khan A. Bronchogenic Cyst in the Cervical Region: A Rare Entity - A Case Report and Review of the Literature. *Cureus* 2021; **13**: e14413 [PMID: 33987062 DOI: 10.7759/cureus.14413]
2 **Hu L**, Fan J, Wang T, Tang G. Ectopic Bronchogenic Cyst in Abdomen- A Rare Special Type. *Am J Med Sci* 2021; **361**: e59-e60 [PMID: 33865550 DOI: 10.1016/j.amjms.2020.11.014]
3 **Martinod E**, Pons F, Azorin J, Mouroux J, Dahan M, Faillon JM, Dujon A, Lajos PS, Riquet M, Jancovici R. Thoracoscopic excision of mediastinal bronchogenic cysts: results in 20 cases. *Ann Thorac Surg* 2000; **69**: 1525-1528 [PMID: 10881835 DOI: 10.1016/s0003-4975(99)01438-1]
4 **Kim KH**, Kim JI, Ahn CH, Kim JS, Ku YM, Shin OR, Lee EJ, Lim KW. The first case of intraperitoneal bronchogenic cyst in Korea mimicking a gallbladder tumor. *J Korean Med Sci* 2004; **19**: 470-473 [PMID: 15201519 DOI: 10.3346/jkms.2004.19.3.470]
5 **Anderson MI**, O'Reilly KJ, Costabile RA. Retroperitoneal bronchogenic cyst mimicking a pheochromocytoma. *J Urol* 2001; **166**: 1379-1380 [PMID: 11547079 DOI: 10.1016/S0022-5347(05)65774-6]
6 **Ubukata H**, Satani T, Motohashi G, Konishi S, Goto Y, Watanabe Y, Nakada I, Tabuchi T. Intra-abdominal bronchogenic cyst with gastric attachment: report of a case. *Surg Today* 2011; **41**: 1095-1100 [PMID: 21773899 DOI: 10.1007/s00595-010-4398-6]
7 **Yuan K**, Shu M, Ma Y, Feng W, Ye J, Yuan Y. Ectopic bronchogenic cyst in the retroperitoneal region: a case report and literature review of adult patients. *BMC Surg* 2021; **21**: 347 [PMID: 34544401 DOI: 10.1186/s12893-021-01341-w]
8 **He WT**, Deng JY, Liang H, Xiao JY, Cao FL. Bronchogenic cyst of the stomach: A case report. *World J Clin Cases* 2020; **8**: 1525-1531 [PMID: 32368546 DOI: 10.12998/wjcc.v8.i8.1525]
9 **Limaiem F**, Mlika M. Bronchogenic Cyst. 2021 Jul 20. In: StatPearls [Internet]. Treasure Island (FL): StatPearls Publishing; 2022 Jan- [PMID: 30725658]
10 **Mirilas P**. Embryogenesis of Ectopic Bronchogenic Cysts: Keep It Simple. *J Invest Surg* 2020; **33**: 574-575 [PMID: 30574822 DOI: 10.1080/08941939.2018.1542049]
11 **Nishida N**, Hata Y, Nomoto K. Intramyocardial bronchogenic cyst: histological appearance and a review of the literature. *Cardiovasc Pathol* 2017; **28**: 64-67 [PMID: 28334597 DOI: 10.1016/j.carpath.2017.03.005]
12 **Taira N**, Kawasaki H, Atsumi E, Ichi T, Kawabata T, Saio M, Yoshimi N. Mucoepidermoid Carcinoma of Arising from a Bronchogenic Cyst of the Diaphragm. *Ann Thorac Cardiovasc Surg* 2018; **24**: 247-250 [PMID: 29367500 DOI: 10.5761/atcs.cr.17-00131]

World Journal of Gastroenterology

Submit a Manuscript: https://www.f6publishing.com

World J Gastroenterol 2022 September 7; 28(33): 4926-4928

DOI: 10.3748/wjg.v28.i33.4926

ISSN 1007-9327 (print) ISSN 2219-2840 (online)

LETTER TO THE EDITOR

Prediction of moderately severe and severe acute pancreatitis in pregnancy: Several issues

Qun-Ying Yang, Jian-Wen Hu

Specialty type: Gastroenterology and hepatology

Provenance and peer review: Unsolicited article; Externally peer reviewed.

Peer-review model: Single blind

Peer-review report's scientific quality classification

Grade A (Excellent): 0
Grade B (Very good): B
Grade C (Good): C
Grade D (Fair): 0
Grade E (Poor): 0

P-Reviewer: Juneja D, India; Shalaby MN, Egypt

Received: May 1, 2022
Peer-review started: May 1, 2022
First decision: June 19, 2022
Revised: June 22, 2022
Accepted: August 16, 2022
Article in press: August 16, 2022
Published online: September 7, 2022

Qun-Ying Yang, Jian-Wen Hu, Department of Gastroenterology, Dongyang People's Hospital, Dongyang 322100, Zhejiang Province, China

Corresponding author: Jian-Wen Hu, PhD, Professor, Department of Gastroenterology, Dongyang People's Hospital, No. 60 Wuning West Road, Dongyang 322100, Zhejiang Province, China. 18367908196@163.com

Abstract

We reviewed a study addressing the development and validation of a prediction model for moderately severe and severe acute pancreatitis in pregnancy. We identified some statistical deficiencies in this article. In addition, we believe that the role of cholesterol as a predictor should be described in more detail.

Key Words: Acute pancreatitis; Prediction model; Statistical analyses; Cholesterol

©The Author(s) 2022. Published by Baishideng Publishing Group Inc. All rights reserved.

Core Tip: This is a comment on a study involving the development and validation of a prediction model for moderately severe and severe acute pancreatitis in pregnancy. We believe that the role of cholesterol as a predictor should be more clearly described.

Citation: Yang QY, Hu JW. Prediction of moderately severe and severe acute pancreatitis in pregnancy: Several issues. *World J Gastroenterol* 2022; 28(33): 4926-4928
URL: https://www.wjgnet.com/1007-9327/full/v28/i33/4926.htm
DOI: https://dx.doi.org/10.3748/wjg.v28.i33.4926

TO THE EDITOR

We were pleased to read the high-level article published by Yang *et al*[1]. In this article, the authors developed and validated a nomogram with good accordance for the prediction of moderately severe and severe acute pancreatitis in pregnancy (MSIP). The authors reported a nomogram that incorporated numerous blood indices for albumin, lactate dehydrogenase, triglyceride, and cholesterol levels, thus facilitating the early individualized prediction of the severity of acute pancreatitis in pregnancy

(APIP). This study is of great significance for the clinical management of APIP. However, in our opinion, this article has some problems that need to be discussed further.

First, we found that some data that were not suitable for this article. In the result sections, we noticed that 134 patients were classified as having mild acute pancreatitis in pregnancy (MAIP) and 56 as having MSIP. However, Figure 1 (https://www.wjgnet.com/1007-9327/full/v28/i15/WJG-28-1588-g001.htm) and Table 1 (https://www.wjgnet.com/1007-9327/full/v28/i15/1588-T1.htm) showed that the number of patients with MAIP and MSIP was 136 and 54, respectively. This inconsistency should be addressed.

In addition, there are problems associated with the statistical analyses in that the methods used for statistical analyses should be described in more detail. In Table 1 (https://www.wjgnet.com/1007-9327/full/v28/i15/1588-T1.htm) and Table 2 (https://www.wjgnet.com/1007-9327/full/v28/i15/1588-T2.htm), the authors should provide more accurate statistical values, including Student's *t*-values or χ^2 values, instead of just providing *P* values. Most of the variables mentioned by the authors in Table 1 (https://www.wjgnet.com/1007-9327/full/v28/i15/1588-T1.htm) and Table 2 (https://www.wjgnet.com/1007-9327/full/v28/i15/1588-T2.htm), such as cholesterol and platelets, are not labeled with units of measurement. Moreover, *P*-values were not listed in the statistical results for "trimester of pregnancy on admission".

In the Discussion section, the authors mentioned that hypercholesterolemia is a known risk factor for cardiovascular diseases. In fact, high-density lipoprotein (HDL) and non-HDL cholesterol have opposite associations with cardiovascular diseases[2], and plasma HDL cholesterol concentrations correlate negatively with the risk of cardiovascular diseases[3]. The authors mentioned that cholesterol is a predictive factor for MSIP, and the cholesterol levels of patients with MAIP and MSIP were 7.34 ± 5.63 and 12.80 ± 6.64, respectively, in Table 1 (https://www.wjgnet.com/1007-9327/full/v28/i15/1588-T1.htm). The authors mentioned some previous studies in their Discussion section. We took a close look at these studies and found that only one recent study[4] showed that low levels of total cholesterol (TC) and high TC within 24 h of admission were independently associated with an increased risk of severe acute pancreatitis. Other studies[5-7] have suggested that serum levels of HDL cholesterol are inversely correlated with disease severity in patients with predicted severe acute pancreatitis. However, this study showed that cholesterol is a predictive factor for MSIP but not HDL. This is a confusing statement. We believe that the present study is inconsistent with previous studies and that the role of cholesterol as a predictor should be more clearly described.

FOOTNOTES

Author contributions: Yang QY reviewed the literature and contributed to manuscript drafting; Hu JW was responsible for the revision of the manuscript for important intellectual content; all authors issued final approval for the version to be submitted.

Conflict-of-interest statement: All the authors report no relevant conflicts of interest for this article.

Open-Access: This article is an open-access article that was selected by an in-house editor and fully peer-reviewed by external reviewers. It is distributed in accordance with the Creative Commons Attribution NonCommercial (CC BY-NC 4.0) license, which permits others to distribute, remix, adapt, build upon this work non-commercially, and license their derivative works on different terms, provided the original work is properly cited and the use is non-commercial. See: https://creativecommons.org/Licenses/by-nc/4.0/

Country/Territory of origin: China

ORCID number: Qun-Ying Yang 0000-0002-4196-440X; Jian-Wen Hu 0000-0002-6452-8790.

S-Editor: Fan JR
L-Editor: Wang TQ
P-Editor: Fan JR

REFERENCES

1 **Yang DJ**, Lu HM, Liu Y, Li M, Hu WM, Zhou ZG. Development and validation of a prediction model for moderately severe and severe acute pancreatitis in pregnancy. *World J Gastroenterol* 2022; **28**: 1588-1600 [PMID: 35582133 DOI: 10.3748/wjg.v28.i15.1588]

2 **NCD Risk Factor Collaboration (NCD-RisC)**. National trends in total cholesterol obscure heterogeneous changes in HDL and non-HDL cholesterol and total-to-HDL cholesterol ratio: a pooled analysis of 458 population-based studies in Asian and Western countries. *Int J Epidemiol* 2020; **49**: 173-192 [PMID: 31321439 DOI: 10.1093/ije/dyz099]

3 **Pownall HJ**, Rosales C, Gillard BK, Gotto AM Jr. High-density lipoproteins, reverse cholesterol transport and atherogenesis. *Nat Rev Cardiol* 2021; **18**: 712-723 [PMID: 33833449 DOI: 10.1038/s41569-021-00538-z]

4 **Hong W**, Zimmer V, Basharat Z, Zippi M, Stock S, Geng W, Bao X, Dong J, Pan J, Zhou M. Association of total cholesterol with severe acute pancreatitis: A U-shaped relationship. *Clin Nutr* 2020; **39**: 250-257 [PMID: 30772093 DOI: 10.1016/j.clnu.2019.01.022]
5 **Peng YS**, Chen YC, Tian YC, Yang CW, Lien JM, Fang JT, Wu CS, Hung CF, Hwang TL, Tsai YH, Lee MS, Tsai MH. Serum levels of apolipoprotein A-I and high-density lipoprotein can predict organ failure in acute pancreatitis. *Crit Care* 2015; **19**: 88 [PMID: 25851781 DOI: 10.1186/s13054-015-0832-x]
6 **Khan J**, Nordback I, Sand J. Serum lipid levels are associated with the severity of acute pancreatitis. *Digestion* 2013; **87**: 223-228 [PMID: 23751273 DOI: 10.1159/000348438]
7 **Hong W**, Lin S, Zippi M, Geng W, Stock S, Zimmer V, Xu C, Zhou M. High-Density Lipoprotein Cholesterol, Blood Urea Nitrogen, and Serum Creatinine Can Predict Severe Acute Pancreatitis. *Biomed Res Int* 2017; **2017**: 1648385 [PMID: 28904946 DOI: 10.1155/2017/1648385]



Published by **Baishideng Publishing Group Inc**
7041 Koll Center Parkway, Suite 160, Pleasanton, CA 94566, USA
Telephone: +1-925-3991568
E-mail: bpgoffice@wjgnet.com
Help Desk: https://www.f6publishing.com/helpdesk
https://www.wjgnet.com



© 2022 Baishideng Publishing Group Inc. All rights reserved.

ISSN 1007-9327 (print)
ISSN 2219-2840 (online)

World Journal of *Gastroenterology*

World J Gastroenterol 2022 September 14; 28(34): 4929-5092



Published by Baishideng Publishing Group Inc

World Journal of Gastroenterology

Contents

Weekly Volume 28 Number 34 September 14, 2022

REVIEW

4929 Therapeutic strategies for post-transplant recurrence of hepatocellular carcinoma

Sposito C, Citterio D, Virdis M, Battiston C, Droz Dit Busset M, Flores M, Mazzaferro V

MINIREVIEWS

4943 Diagnosis, treatment, and current concepts in the endoscopic management of gastroenteropancreatic neuroendocrine neoplasms

Iabichino G, Di Leo M, Arena M, Rubis Passoni GG, Morandi E, Turpini F, Viaggi P, Luigiano C, De Luca L

4959 Efficacy of cytapheresis in patients with ulcerative colitis showing insufficient or lost response to biologic therapy

Iizuka M, Etou T, Sagara S

ORIGINAL ARTICLE

Basic Study

4973 Long noncoding RNA ZNFX1-AS1 promotes the invasion and proliferation of gastric cancer cells by regulating LIN28 and CAPR1N1

Zhuo ZL, Xian HP, Sun YJ, Long Y, Liu C, Liang B, Zhao XT

4993 Oxidized low-density lipoprotein stimulates CD206 positive macrophages upregulating CD44 and CD133 expression in colorectal cancer with high-fat diet

Zheng SM, Chen H, Sha WH, Chen XF, Yin JB, Zhu XB, Zheng ZW, Ma J

5007 Ji-Chuan decoction ameliorates slow transit constipation *via* regulation of intestinal glial cell apoptosis

Wang XM, Lv LX, Qin YS, Zhang YZ, Yang N, Wu S, Xia XW, Yang H, Xu H, Liu Y, Ding WJ

Retrospective Cohort Study

5023 Pregnancy and fetal outcomes of chronic hepatitis C mothers with viremia in China

Pan CQ, Zhu BS, Xu JP, Li JX, Sun LJ, Tian HX, Zhang XH, Li SW, Dai EH

Retrospective Study

5036 Trends in hospitalization for alcoholic hepatitis from 2011 to 2017: A USA nationwide study

Wakil A, Mohamed M, Tafesh Z, Niazi M, Olivo R, Xia W, Greenberg P, Pyrsopoulos N

5047 Analysis of invasiveness and tumor-associated macrophages infiltration in solid pseudopapillary tumors of pancreas

Yang J, Tan CL, Long D, Liang Y, Zhou L, Liu XB, Chen YH

World Journal of Gastroenterology

Weekly Volume 28 Number 34 September 14, 2022

Contents

Observational Study

5058 Impact of adalimumab on disease burden in moderate-to-severe ulcerative colitis patients: The one-year, real-world UCanADA study

Bessissow T, Nguyen GC, Tarabain O, Peyrin-Biroulet L, Foucault N, McHugh K, Ruel J

CASE REPORT

5076 Gastrointestinal tumors in transplantation: Two case reports and review of literature

Stammler R, Anglicheau D, Landi B, Meatchi T, Ragot E, Thervet E, Lazareth H

5086 Spontaneous expulsion of a duodenal lipoma after endoscopic biopsy: A case report

Chen ZH, Lv LH, Pan WS, Zhu YM

World Journal of Gastroenterology

Weekly Volume 28 Number 34 September 14, 2022

Contents

ABOUT COVER

Editorial Board Member of *World Journal of Gastroenterology*, Abhinav Vasudevan, BMed, MPH, FRACP, PhD, Staff Physician and Medical Lead in Inflammatory Bowel Diseases, Department of Gastroenterology and Hepatology, Eastern Health, Box Hill 3128, Australia

AIMS AND SCOPE

The primary aim of *World Journal of Gastroenterology* (*WJG*, *World J Gastroenterol*) is to provide scholars and readers from various fields of gastroenterology and hepatology with a platform to publish high-quality basic and clinical research articles and communicate their research findings online. *WJG* mainly publishes articles reporting research results and findings obtained in the field of gastroenterology and hepatology and covering a wide range of topics including gastroenterology, hepatology, gastrointestinal endoscopy, gastrointestinal surgery, gastrointestinal oncology, and pediatric gastroenterology.

INDEXING/ABSTRACTING

The *WJG* is now abstracted and indexed in Science Citation Index Expanded (SCIE, also known as SciSearch®), Current Contents/Clinical Medicine, Journal Citation Reports, Index Medicus, MEDLINE, PubMed, PubMed Central, Scopus, Reference Citation Analysis, China National Knowledge Infrastructure, China Science and Technology Journal Database, and Superstar Journals Database. The 2022 edition of Journal Citation Reports® cites the 2021 impact factor (IF) for *WJG* as 5.374; IF without journal self cites: 5.187; 5-year IF: 5.715; Journal Citation Indicator: 0.84; Ranking: 31 among 93 journals in gastroenterology and hepatology; and Quartile category: Q2. The *WJG*'s CiteScore for 2021 is 8.1 and Scopus CiteScore rank 2021: Gastroenterology is 18/149.

RESPONSIBLE EDITORS FOR THIS ISSUE

Production Editor: *Hua-Ge Yu*; **Production Department Director:** *Xu Guo*; **Editorial Office Director:** *Jia-Ru Fan.*

NAME OF JOURNAL
World Journal of Gastroenterology

ISSN
ISSN 1007-9327 (print) ISSN 2219-2840 (online)

LAUNCH DATE
October 1, 1995

FREQUENCY
Weekly

EDITORS-IN-CHIEF
Andrzej S Tarnawski

EDITORIAL BOARD MEMBERS
http://www.wjgnet.com/1007-9327/editorialboard.htm

PUBLICATION DATE
September 14, 2022

COPYRIGHT
© 2022 Baishideng Publishing Group Inc

INSTRUCTIONS TO AUTHORS
https://www.wjgnet.com/bpg/gerinfo/204

GUIDELINES FOR ETHICS DOCUMENTS
https://www.wjgnet.com/bpg/GerInfo/287

GUIDELINES FOR NON-NATIVE SPEAKERS OF ENGLISH
https://www.wjgnet.com/bpg/gerinfo/240

PUBLICATION ETHICS
https://www.wjgnet.com/bpg/GerInfo/288

PUBLICATION MISCONDUCT
https://www.wjgnet.com/bpg/gerinfo/208

ARTICLE PROCESSING CHARGE
https://www.wjgnet.com/bpg/gerinfo/242

STEPS FOR SUBMITTING MANUSCRIPTS
https://www.wjgnet.com/bpg/GerInfo/239

ONLINE SUBMISSION
https://www.f6publishing.com

© 2022 Baishideng Publishing Group Inc. All rights reserved. 7041 Koll Center Parkway, Suite 160, Pleasanton, CA 94566, USA
E-mail: bpgoffice@wjgnet.com https://www.wjgnet.com

World Journal of Gastroenterology

Submit a Manuscript: https://www.f6publishing.com

World J Gastroenterol 2022 September 14; 28(34): 4929-4942

DOI: 10.3748/wjg.v28.i34.4929

ISSN 1007-9327 (print) ISSN 2219-2840 (online)

REVIEW

Therapeutic strategies for post-transplant recurrence of hepatocellular carcinoma

Carlo Sposito, Davide Citterio, Matteo Virdis, Carlo Battiston, Michele Droz Dit Busset, Maria Flores, Vincenzo Mazzaferro

Specialty type: Gastroenterology and hepatology

Provenance and peer review: Invited article; Externally peer reviewed.

Peer-review model: Single blind

Peer-review report's scientific quality classification

Grade A (Excellent): A, A
Grade B (Very good): 0
Grade C (Good): 0
Grade D (Fair): 0
Grade E (Poor): 0

P-Reviewer: Chang A, Thailand; Kim IH, South Korea

Received: January 27, 2022
Peer-review started: January 27, 2022
First decision: February 24, 2022
Revised: March 5, 2022
Accepted: July 26, 2022
Article in press: July 26, 2022
Published online: September 14, 2022

Carlo Sposito, Davide Citterio, Matteo Virdis, Carlo Battiston, Michele Droz Dit Busset, Maria Flores, Vincenzo Mazzaferro, HPB Surgery, Hepatology and Liver Transplantation, Fondazione IRCCS Istituto Nazionale Tumori di Milano, Milan 20133, Italy

Carlo Sposito, Vincenzo Mazzaferro, Department of Oncology and Hemato-Oncology, University of Milan, Milan 20100, Italy

Corresponding author: Carlo Sposito, MD, Associate Professor, Surgeon, HPB Surgery, Hepatology and Liver Transplantation, Fondazione IRCCS Istituto Nazionale Tumori di Milano, *Via* Venezian 1, Milan 20133, Italy. carlo.sposito@istitutotumori.mi.it

Abstract

Despite stringent selection criteria, hepatocellular carcinoma recurrence after liver transplantation (LT) still occurs in up to 20% of cases, mostly within the first 2–3 years. No adjuvant treatments to prevent such an occurrence have been developed so far. However, a balanced use of immunosuppression with minimal dose of calcineurin inhibitors and possible addition of mammalian target of rapamycin inhibitors is strongly advisable. Moreover, several pre- and post-transplant predictors of recurrence have been identified and may help determine the frequency and duration of post-transplant follow-up. When recurrence occurs, the outcomes are poor with a median survival of 12 mo according to most retrospective studies. The factor that most impacts survival after recurrence is timing (within 1–2 years from LT according to different authors). Several therapeutic options may be chosen in case of recurrence, according to timing and disease presentation. Surgical treatment seems to provide a survival benefit, especially in case of late recurrence, while the benefit of locoregional treatments has been suggested only in small retrospective studies. When systemic treatment is indicated, sorafenib has been proved safe and effective, while only few data are available for lenvatinib and regorafenib in second line. The use of immune checkpoint inhibitors is controversial in this setting, given the safety warnings for the risk of acute rejection.

Key Words: Liver transplantation; Hepatocellular carcinoma; Immunosuppression; Recurrence; Surgical treatment; Locoregional treatment; Systemic treatment

©The Author(s) 2022. Published by Baishideng Publishing Group Inc. All rights reserved.

Core tip: Hepatocellular carcinoma (HCC) is becoming the most common indication for liver transplantation (LT). The problem of tumor recurrence after LT, that occurs in up to 20% of cases, is becoming of increasing interest. We reviewed of the available literature on HCC recurrence after LT. The best preventive measures still rely on pretransplant selection criteria, since no dedicated follow-up guidelines exist and no post-LT adjuvant treatments are available. When recurrence occurs, the prognosis is poor. However, aggressive surgical treatment, particularly in the case of late recurrence, may provide a significant survival benefit.

Citation: Sposito C, Citterio D, Virdis M, Battiston C, Droz Dit Busset M, Flores M, Mazzaferro V. Therapeutic strategies for post-transplant recurrence of hepatocellular carcinoma. *World J Gastroenterol* 2022; 28(34): 4929-4942
URL: https://www.wjgnet.com/1007-9327/full/v28/i34/4929.htm
DOI: https://dx.doi.org/10.3748/wjg.v28.i34.4929

INTRODUCTION

Hepatocellular carcinoma (HCC) is the most common liver cancer and the fourth leading cause of cancer-related mortality[1,2]. From the time of its initial developments in the early 1960s, liver transplantation (LT) appeared as the ideal cure for HCC on liver cirrhosis because of the perspective to cure at the same time both the tumor and the underlying liver disease. However, the first experiences were disappointing with many authors reporting 5-year survival < 40%, mainly because of recurrences of the primary tumor[3-6]. A retrospective review of these discouraging results progressively led to the observation that survival of patients was directly related to the stage of HCC at the time of LT. This was the basis on which a prospective study was conducted in Milan applying *a priori* restrictive criteria for the selection of HCC candidates for LT (namely a single nodule ≤ 5 cm or two or three nodules ≤ 3 cm, each with no macrovascular invasion at pretransplant imaging). The seminal paper published in 1996 demonstrated that LT under such criteria achieved better long-term results than any other therapy, with outcomes similar to LT for nononcological indications[7]. The so called Milan criteria (MC) were subsequently validated by many other groups reporting 5-year survival rates of ≥ 70%, and became the benchmark for selecting patients with HCC for LT. Pooled recurrence rates have been reported to be around 8% for patients within MC *versus* 28% for patients beyond these criteria, according to a recent meta-analysis[8]. Thus, HCC recurs in a proportion of recipients who are within MC, while LT may provide cure for some patients who are beyond these criteria. When recurrence occurs, survival is poor and post-LT HCC recurrence is the factor that most affects long-term outcomes in this setting. Considering that HCC represents the most common indication for LT in the USA, and that since the introduction of direct antiviral agents against hepatitis C virus the proportion of patients undergoing LT for HCC is increasing worldwide[9,10], the problem of tumor recurrence will probably affect a growing number of patients. However, to date, treatment of HCC recurrence following LT is largely understudied and dedicated guidelines are lacking. The aim of this paper is to provide a review of the current evidence on therapeutic strategies for patients with HCC recurrence after LT.

PREVENTION OF POST-LT HCC RECURRENCE

Tumor recurrence may be linked to remaining (previously undetected) extrahepatic HCC at the time of LT, or result from the post-LT engraftment of circulating HCC clones[11]. It is extrahepatic in 50%–60% of cases, with lung, bones and adrenal glands being the most frequently affected sites[12]. Timing of HCC recurrence is variable, but in most cases it occurs within 3 years after LT. Early recurrence (< 1 year after LT) is associated with a significantly worse prognosis, while later recurrence might result in better outcomes and even in cure in selected cases[13].

Prevention of recurrence through selection criteria

Considering that the risk of post-LT recurrence is strictly related to pretransplant HCC stage and treatment, recurrence is firstly prevented by the application of pre-LT selection criteria able to identify patients at higher risk. Proposals for expansion of MC have been initially developed using tumor morphology, namely size and number of nodules. In fact, these factors have been demonstrated as surrogate markers of microvascular invasion (MVI) and/or poor tumor differentiation, which are the principal determinants of biological aggressiveness and therefore of the risk of post-LT recurrence[14]. Expanded criteria increased the acceptable size and number of HCC nodules with respect to MC, but the considerable heterogeneity coupled with differences in accuracy of liver imaging techniques

probably represent the greatest limitation of criteria based only on morphology.

To overcome these limits, criteria incorporating serum markers as surrogates of biological tumor features such as α-fetoprotein (AFP) have been proposed. In particular, by combining the morphological characteristics of the tumor and AFP values it was possible to develop selection criteria for LT definitively exceeding MC, while even decreasing the risk of post-LT recurrence[15,16]. A strategy combining tumor burden with the assessment of response to pre-LT locoregional treatment (LRT) as a marker of favorable tumor biology has gained broader acceptance[17]. For patients beyond MC, a common strategy is to downstage patients by means of LRT or surgical therapy. In fact, patients successfully downstaged within accepted criteria share the same prognosis as patients within the criteria *ab initio* and so far[18], response to therapies appears as one of the best surrogates of favorable tumor biology and thus an optimal selection tool for candidates for LT[17,19,20]. Patients progressing in the pre-LT period despite LRT have significantly worse post-LT outcomes with respect to patients with stable or responding disease. Finally, tumor differentiation, MVI, presence of circulating cancer cells and genomic markers have also been suggested as selection criteria for LT, but these assessments require biopsy, which might induce tumor seeding. Furthermore, it is well known that tumors are heterogeneous and show areas of varying degrees of differentiation and genomic features.

Post-LT surveillance

Considering that post-LT recurrence is mostly asymptomatic, and that early detection of recurrence may have a positive impact on long-term outcomes, post-LT surveillance has an important role in this setting. However, no guidelines from the major Hepato-bilio-pancreatic societies are available and surveillance protocols are mostly center-specific, often with a high heterogeneity between centers as recently reported[21]. Few retrospective studies on post-LT surveillance have been published to date, and several questions regarding frequency, duration, and imaging modality for a cost-effective surveillance remain open.

For imaging modality, cross-sectional imaging of the abdomen [with either multiphase computed tomography (CT) or magnetic resonance imaging] and noncontrast lung CT scan allow detection of the most frequent sites of recurrent HCC[21,22]. Cross-sectional imaging of the brain, bone scintigraphy or positron emission tomography–CT are indicated only in case of clinical suspicion and not on a regular basis, while it seems reasonable to check for AFP levels at each surveillance visit even if no data is available to support this indication.

Given that the majority of recurrences occur within the first 3 years after LT, there is general agreement to indicate surveillance imaging and visits more frequently in this time frame (*i.e.*, every 4–6 mo) and yearly thereafter[22]. Some authors suggest interrupting surveillance after 5 years. However, recurrences (either *de novo* tumors or true recurrences) have been repeatedly reported up to 10–15 years after LT[23]; considering that late HCC relapse is associated with a better prognosis with respect to earlier events and that it is sometimes curable, it seems reasonable to prolong yearly surveillance for at least ten years.

Ideally, frequency and duration of surveillance would be based on the assessed risk of post-LT HCC recurrence. Several proposals have been made in this sense, and the RETREAT score[24] (that includes AFP at LT, presence of MVI and sum of maximum size + number of vital nodules) is the most recent and promising predictor in terms of discriminative power and validation on a large scale registry. However, no prospective validation is available to date, and the cost-effectiveness of a surveillance program based on the risk of recurrence has yet to be demonstrated.

The impact of surveillance programs on post-recurrence survival has been scarcely studied. A recent multicenter study on 232 patients who experienced HCC recurrence found that increasing number of post-LT surveillance scans (with cut-off at three surveillance scans within the first 2 years) was associated with improved survival and possibility of undergoing potentially curative treatments[25].

Role of immunosuppression

Improvements in the management of immunosuppression reduced rejection episodes favoring long-term graft survival; calcineurin inhibitors (CNIs) tacrolimus and cyclosporine played a fundamental role in this improvement. However, several studies demonstrated that CNI exposure is associated with an increased risk of tumor recurrence with a dose-dependent effect[26]. It is likely that the immunosuppression induced by CNIs prevents the immune system from detecting and destroying circulating or dormant HCC cells and therefore, dosage of CNIs should be maintained with the aim of balancing this risk without increasing the risk of rejection episodes.

Mammalian target of rapamycin inhibitors (mTORis) sirolimus and everolimus are another class of immunosuppressants targeting some HCC pathways, which showed antiangiogenic and antiproliferative effects in experimental models[27]. Data from retrospective studies and meta-analyses suggest that, compared to CNIs, the use of mTORis reduces the risk of post-LT HCC recurrence and increases long-term survival. In the most recent meta-analysis including 23 comparative studies [17 observational and 6 randomized controlled trials (RCTs)] with 6495 patients, recurrence-free survival (RFS) was significantly increased with mTORi-based therapy at 1 and 3 years with a nonsignificant increase at 5 years[28]. Overall survival (OS) was also significantly improved, as well as recurrence rate being lower in the mTORi arm without differences based on the type of mTORi. However, only one RCT that

compared post-LT immunosuppression containing mTORi (sirolimus) *versus* not containing mTORi [29]. In this international RCT of 525 patients there appeared to be an advantage in the sirolimus group regarding RFS in the first 3–5 years. However, this benefit was subsequently lost with further follow-up and the trial failed to meet the primary endpoint of demonstrating a significant reduction of recurrences in the mTORi-containing immunosuppression group.

Adjuvant treatments after LT

Several attempts had been performed with chemotherapy as an adjuvant treatment to prevent HCC recurrence after LT[30,31]. HCC is a chemoresistant tumor; therefore, cytotoxic systemic therapies have failed to provide any consistent benefit in this setting and have been abandoned in the last decade[32]. Sorafenib, an oral multikinase inhibitor that shows significant improvement in survival of patients with advanced HCC, has been tested in small studies in the setting of adjuvant treatment for HCC after LT. Despite some initial signs of efficacy, with one phase I study showing a significant reduction in the risk of HCC recurrence with a maximum tolerable dose of sorafenib 200 mg twice daily[33], other single-center case series failed to confirm these data and to date no RCTs are available. Lenvatinib, a more recent targeted therapy for advanced HCC, has not been prospectively tested in the adjuvant setting; a small retrospective case series confirmed an acceptable drug safety and patient tolerance but did not show any significant reduction in terms of HCC recurrence[34]. Immune checkpoints inhibitors (ICIs) have emerged as a treatment option for advanced-stage HCC. No studies are available on ICIs as post-LT adjuvant treatment. A recent systematic review and pooled analysis reviewed 14 patients receiving ICIs for recurrent disease after LT for HCC: 11 of them (78.6%) died, and graft rejection was the cause of death in five cases (45.4%). The high rejection rate raises the question of safety of ICIs in transplanted patients, even in the setting of overt recurrence[35]. Thus, to date, no anticancer treatments can be recommended to prevent HCC recurrence after LT, and it is unlikely that they will become available in the near future.

TREATMENT OF POST-LT HCC RECURRENCE

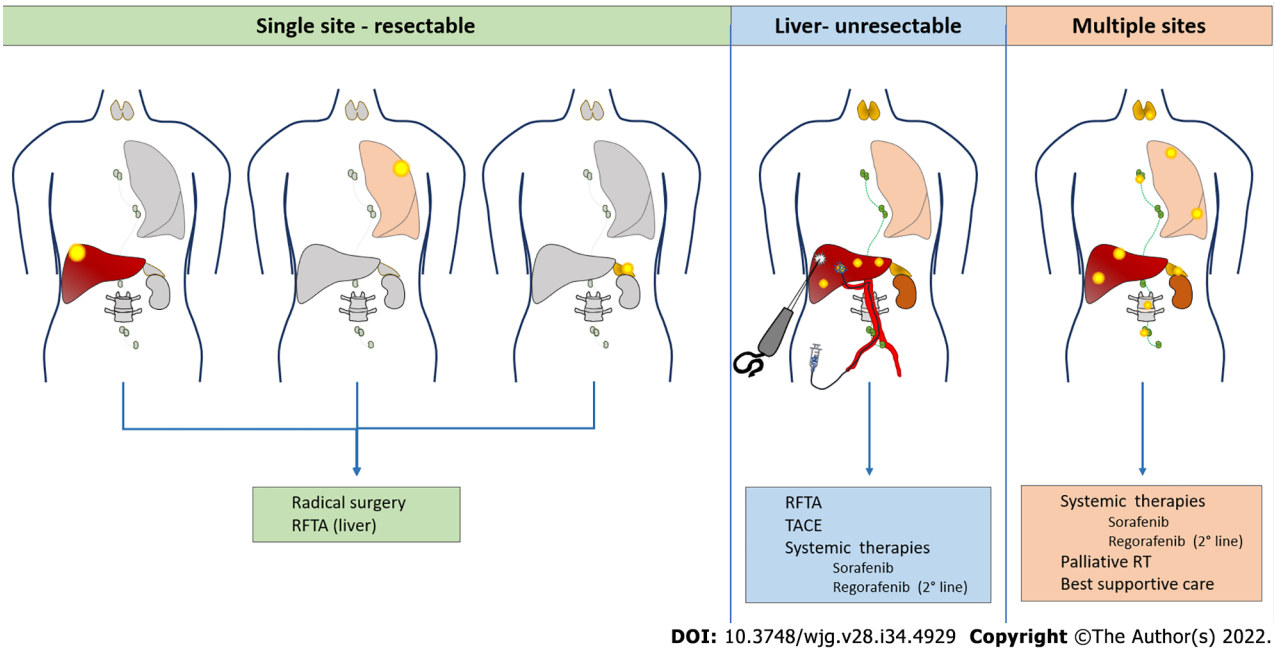
Literature concerning the efficacy of each treatment modality is scarce, with the many limitations related to the small number of patients included, the frequent use of combined treatment and the different patterns of recurrence, all acting as confounding factors. In the majority of cases (50%–60%) recurrence is extrahepatic and affects the following sites: lungs (40%–60%), bones (25%–30%), adrenal glands (10%), lymph nodes (10%) and peritoneum (10%)[12]. Liver-only recurrence occurs in 15%–40% of patients, while combined liver and extrahepatic recurrence accounts for 30%–40% of cases. The therapeutic options clearly depend on location, multifocality and clinical presentation of recurrence (Figure 1).

Surgery

Liver resection is safe and provides a survival benefit in case of intrahepatic oligorecurrence[36,37], with a median survival of 28–65 mo observed for patients receiving surgery, compared to 5–15 mo in those receiving systemic treatment only[38-41]. Surgical treatment is feasible in 25%–50% of cases with higher morbidity rate (60%–80%) with respect to primary liver resections[42-44], mainly because of the risk of infections in the context of immunosuppression.

Sapisochin *et al*[39] retrospectively analyzed 121 patients with HCC recurrence after LT, finding that not being amenable to resection or ablation was an independent predictor of poor prognosis [hazard ratio (HR) = 4.7, 95% confidence interval (CI): 2.7–8.3). An Italian multicenter study analyzed 21 patients with recurrence and reported a significantly better 4-year survival rate in patients treated with surgical resection for intra- and extrahepatic recurrence compared to those with unresectable disease (57% *vs* 14%, P = 0.02)[45]. In another series of 106 patients, treatment for recurrent HCC most commonly included chemotherapy (73.5%), surgical resection (23.3%), external beam radiation (13.6%), and ablation (3.9%), with the majority of patients receiving nonsurgical therapies (59.2%). The highest survival rates at 3 years were observed in patients receiving surgical therapy alone (60%), followed by patients receiving both surgical and nonsurgical therapy (37%), patients receiving only nonsurgical therapy (11%), and patients receiving no treatment (0%)[40]. Time from LT to recurrence is one of the most important prognostic factors, and patients with late recurrence show more favorable 5-year outcomes survival with resection compared to those of patients who recur earlier[46].

Surgery may enhance long-term survival also in patients with pulmonary recurrences amenable to resection, with 5-year survival rates ranging from 34% to 44% in those undergoing metastasectomy[47-52]. A benefit from surgical treatment is also reported for other sites of recurrence in smaller case series, including vertebrae[53], adrenal glands[54,55], lymph nodes[56], peritoneum[57] and pharynx[58]. In patients with multiple recurrences, some benefits have also been gained from repeated resections, probably reflecting less aggressive tumor biology[41].



DOI: 10.3748/wjg.v28.i34.4929 **Copyright** ©The Author(s) 2022.

Figure 1 Hepatocellular carcinoma recurrence after liver transplantation: Treatment possibilities according to disease presentation. RT: Radiotherapy; RFTA: Radiofrequency thermal ablation; TACE: Transarterial chemoembolization.

Locoregional therapies

Radiofrequency ablation (RFA) for liver recurrences may be proposed with a curative intent for small lesions, with the advantages of a percutaneous approach. In a retrospective single-center series, Huang *et al*[44] compared 15 patients with post-LT HCC recurrence treated surgically with 11 patients treated with RFA. This study demonstrated similar 5-year OS (35% for surgery *vs* 28% for RFA) but a tendency to a worse 5-year disease-free survival in the RFA group (16% *vs* 0%). Another study evaluating safety and efficacy of microwave ablation on a series of 11 patients found this technique safe and tolerable, with a 15.8% rate of local tumor progression after treatment and 15.3% survival at 2 years[59].

Multifocal intrahepatic recurrences may be amenable to transarterial chemoembolization (TACE). The largest series collected 28 patients treated by conventional TACE[60]. There were no significant post-treatment complications and the targeted tumor reduced in size by ≥ 25% in 19 patients (67.9%). However, intrahepatic recurrence or extrahepatic metastases occurred in 26 patients (92.9%) within 6 mo. The 3- and 5-year survival rates following TACE were 6% and 0%, respectively, with a mean survival time of 9 mo. A single-center retrospective investigation compared 14 patients treated with TACE with 14 matched controls who did not receive TACE but chemotherapy, radiotherapy or supportive care. Eight of the 14 patients treated with TACE (57%) showed partial tumor response and had a significantly longer survival compared to those who did not[61].

Systemic therapies

The effectiveness of systemic therapies for HCC recurrence following LT is largely unstudied because these patients have been routinely excluded from clinical trials. Sorafenib has been increasingly administered for treatment of post LT recurrences, and some data have been collected in the literature regarding its safety and efficacy in this setting. In a case–control study from Sposito *et al*[62], sorafenib provided improved median survival after HCC recurrence untreatable by surgery or LRT with respect to best supportive care (10.6 *vs* 2.2 mo). A meta-analysis published 2 years later reported a pooled 1-year survival of 36% (range 18%–90%)[63]. The main limitation of sorafenib in transplanted patients is toxicity, often leading to dose reduction, as reported by several studies[62,64]. Close monitoring is warranted for these patients, particularly in case of immunosuppression with mTORis, since this association may lead to severe adverse events[65-70]. Regorafenib may be proposed as a second-line treatment in case of progression under sorafenib[71]. In a recent multicenter study, second line treatment with regorafenib after sorafenib discontinuation provided a median survival of 13.1 mo compared with 5.5 mo with best supportive care in post-LT HCC relapse[72]. Recently approved tyrosine kinase inhibitors (lenvatinib[73] and cabozantinib[74]) and monoclonal antibodies (ramucirumab[75]) will soon be introduced in clinical practice also for the treatment of post-LT recurrence, giving us the opportunity to collect data about their efficacy and toxicity in this setting[76]. Currently, immunotherapy is changing the landscape of systemic therapies for HCC[77-79], but its safety after LT represents a point of concern, since ICIs may cause allograft rejection and other serious adverse events[80-85].

FACTORS IMPACTING SURVIVAL AFTER HCC RECURRENCE

Studies evaluating the outcome of patients with post-LT HCC recurrence mostly consist of small and heterogeneous series burdened by significant biases in terms of transplant criteria, availability of different treatments and patients' selection to curative and palliative options[86]. Survival of post-LT HCC recurrence is dismal and significantly worse than relapse after resection (median OS around 12 mo *vs* nearly 2 years in transplanted and resected patients, respectively), and immunosuppression is a potential driver of such a difference[87,88]. A number of factors have an impact on survival, and there is a small subset of patients with more favorable prognosis in whom curative treatments may be undertaken. Table 1 summarizes the results of studies evaluating the prognostic factors and outcome of treatment for HCC relapse after LT.

Time to recurrence and primary tumor features

Several studies showed that time from LT to recurrence has a primary role on outcomes, with early relapse being associated with poor prognosis either when defined as occurring within 6 mo[89-93], 1 year[39,94,95] or 2 years[96]. Many factors related to the primary tumor biology and aggressiveness affect time to recurrence and/or post-relapse survival: size (with cutoffs > 30 or > 50 mm)[45,97], staging outside MC[45], bilobar spread[97], absence of peritumoral capsule[45], poorly differentiated tumors[91,94,95], total tumor volume[92], presence of micro- or macrovascular invasion and pre-LT lymphocyte to neutrophil ratio[39,40,91,92]. The use of mTORi in the post-LT setting seems to be related to better post-recurrence outcomes, as shown both in eastern and western series[93,95]. Moreover, a history of graft rejection has also been associated with improved outcomes, possibly due to more active anticancer immunity[92].

It has been suggested that the observed difference in outcomes between early and late recurrences lies in different underlying biological mechanisms. However, this does not turn into a difference in the site of recurrence. In fact, occurrence of extrahepatic, combined intra- and extrahepatic or intrahepatic relapses do not seem to be different in early *versus* late recurrences[97]. While early relapses may be due to undetected extrahepatic metastases or circulating HCC clones implanting in a target organ during or soon after LT, late recurrences are possibly related to a second hit leading to late engrafting of HCC cells remaining latent during the initial post-LT period. In the latter, immunosuppression may also play a role[23]. As for intrahepatic late relapses, a further mechanism to be considered is *de novo* occurrence of HCC, usually arising in the context of chronic liver disease or cirrhosis due to recurrence of primary hepatitis, ischemic biliary injury or chronic rejection, several years after LT[98]. In such instances, results are expected to parallel those of nontransplant recipients with localized HCC, in which surgery or LRTs are effective in controlling the disease.

Pattern, features and resectability of recurrence

Aside from primary disease features, other studies have focused on the pattern of recurrence as a relevant prognostic factor for post-recurrence survival. As expected, limited disease spread with localized nodules (oligorecurrence), either hepatic or extrahepatic, has been associated to better outcomes than disseminated multifocal recurrence in several series[36-38,41,45,90]. In addition, a different prognostic impact of hepatic *versus* extrahepatic localization has been repeatedly reported. Hong *et al* showed that liver involvement as the first recurrence site was associated with worse survival, with fewer patients amenable to resection among intrahepatic rather than extrahepatic localizations[93]. A monocentric French series on 70 HCC recurrences also identified intrahepatic location as an unfavorable prognostic factor, which was confirmed in a Latin American series on 105 post-LT recurrences showing a lower probability of treatment in patients with hepatic relapses[41,94]. It may be speculated that this is related to the biological mechanism underlying tumor relapse, with recurrences due to undetected metastases at the time of LT more likely to occur at extrahepatic sites and associated with decreased burden as compared to circulating HCC clones, biologically more aggressive tumors, and being more likely to implant in the new liver. Of note, peritoneal and bone localizations were also reported as a poor prognostic factors[37,91,95]. Nevertheless, evidence deriving from several studies shows that the best outcomes are observed in patients with unifocal, often extrahepatic disease, easily amenable to surgical resection[36-38,41,45]. In the large series by Sapisochin *et al*[39] cited above, not being amenable to curative-intent treatment (resection or ablation) was an independent indicator of poor survival, together with AFP ≥ 100 ng/mL at the time of relapse. In another single-center study from the USA by Bodzin *et al*[40] on 106 recurrences, a prominent prognostic role of recurrence-related factors (AFP at relapse, > 3 nodules, maximum size of recurrence and bone spread) rather than primary disease features was shown. By combining such factors, a risk score model was built, with accurate stratification of recurrent patients into low-risk (median survival of 70.6 mo), medium-risk (12.2 mo) and high-risk (3.4 mo) subgroups.

Due to selection bias of surgical patients towards later recurrences, more favorable localizations, less aggressive disease and better performance status, the independent prognostic role of either recurrence pattern or resectability is questionable. The limited disease spread may make patients more likely to undergo surgical excision on the one hand, or simply reflect a different tumor biology, etiology, and

Table 1 Studies evaluating the prognostic factors and outcome of treatment for hepatocellular carcinoma relapse after liver transplantation

Ref.	No. of patients	Type of study	Site of recurrence	Treatment	mTTR	mOS	Negative outcome predictors
Sapisochin *et al* [39], 2015	121 (15.5%)	Retrospective multicenter	18.4% liver, 47.4% extrahepatic, 34.2% liver + extra	31.4% surgery/ablation, 42.1% palliative, 26.4% BSC	14 mo	12.2 mo (1 yr 54%; 3 yr 19%; 5 yr 14%)	No curative treatment. RFS < 1 yr. AFP > 100 ng/mL
Ho *et al*[96], 2020	349 (16.4%)	National registry	≥ 38.1% liver, ≥ 20.3% extrahepatic/(liver + extra)	4.6% surgery, 6.3% ablation, 32.1% RT, 27.2% TACE, 20.3% Sorafenib, 20.3% BSC	17.8 mo	11.2 mo (1 yr 57%; 3 yr 24.7%; 4 yr 19%)	LT era > 2008 (due to listing of downstaged patients). No curative treatment. Sorafenib/RT
Hong *et al*[93], 2019	92 (17.3%) (LDLT)	Retrospective multicenter	37% liver, 34.8% lung, 28.3% bone, 16.3% lymph nodes	38% surgery, 51.1% TACE, 38% RT, 45.7% Sorafenib	11.3 mo	11.7 mo (1 yr 59.5%; 3 yr 23%; 5 yr 11.9%)	TTR < 6 mo. No curative treatment. Multiorgan involvement. Explant tumor size > 5 cm. mTORi (late)
Toso *et al*[92], 2013	30 (12.8%)	Retrospective multicenter	46.6% liver, 43.3% lung, 23.3% bone, 13.3% other	20% surgery, 10% TACE/RF/PEI, 70% CT/BSC	14.2 mo	33 mo	Graft rejection 0-6 mo. TTR
Bodzin *et al* [40], 2017	106 (12.4%)	Retrospective multicenter	37.8% liver, 55.7% lung, 25.5% bone, 3.8% brain	23.3% surgery, 3.9% RFA, 13.6% RT, 73.5% CT, 17% BSC	15.8 mo	10.6 mo	MELD at LT > 23. TTR. > 3 recurrent nodules. Size of recurrence. Bone recurrence. AFP at recurrence. Donor Na. Pre-LT NLR
Fernandez-Sevilla *et al*[41], 2017	70 (14.2%)	Retrospective single center	2.8% liver, 72.9% extrahepatic, 24.3% liver + extra	31.4% surgery, 8.6% TACE, 28.6% Sorafenib	17 mo	19 mo (1 yr 65%; 3 yr 26%; 5 yr 5%)	AFP > 100 ng/mL. Intrahepatic. Multifocal. No surgical treatment
Maccali *et al* [94], 2021	105 (16.6%)	Retrospective multicenter	23.8% liver, 21% liver + extra, 55.2% extrahepatic	9.5% surgery, 2.9% TACE, 4.8% RT, 44.8% CT/Sorafenib	13 mo	6.2 mo	RFS < 1 yr. No surgical, loco-regional or systemic treatment
Ekpanyapong *et al*[95], 2020	96 (13.5%)	Retrospective single center	21.9% liver, 78.1% extrahepatic/(liver + extra)	27.1% surgery. 5.2% RFA. 1% TACE. 10.4% RT. 39.6% Sorafenib. 16.7% BSC	17.1 mo	10.1 mo (1 yr 48%; 3 yr 16%)	AFP > 1000 ng/mL. Poorly differentiated HCC. Bilirubin ≥ 1.2 mg/dL and albumin < 3.5 mg/dL at recurrence. Peritoneal disease
Regalia *et al* [45], 1998	21 (15.9%)	Retrospective multicenter	19% liver, 19% lung, 14% bone, 38% multiple sites	33.3% surgery, 19% CT, 14.3% RT/CT-RT, 23.8% BSC	7.8 mo	1 yr 62%; 3 yr 29%; 4 yr 23%	Related to early recurrence: Explant tumor size > 3 cm; outside Milan Criteria; absence of capsule
Kornberg *et al* [38], 2010	16 (26.7%)	Retrospective single center	25% liver, 25% bone, 31.2% lung,6.2% brain, 6.2% peritoneum, 6.2% adrenal gland	43.7% surgery, 18.7% RT, 6.2% TACE, 6.2 Sorafenib, 31.2 %BSC	23 mo	10.5 mo	No surgical treatment. Early recurrence (< 24 mo)
Alshahrani *et al* [57], 2018	232 (15.6%)	Retrospective single center	31% liver, 57.8% extrahepatic, 13.4% multiple sites	-	-	1 yr 60.2%; 3 yr 28.3%; 5 yr 20.5%; 10 yr 7%	Early recurrence
Taketomi *et al* [100], 2010	17 (16.8%) (LDLT)	Retrospective single center	-	53% surgery, 47% other	12.9 mo	1 yr 76.5%; 3 yr 51.3%; 5 yr 34.2%	No surgical treatment. Early recurrence
Roh *et al*[90], 2014	63 (13.8%)	Retrospective single center	22% liver, 16% lung, 52% multiple sites, 10% other	6% surgery, 38% local treatment, 16% systemic treatment, 33% combined treatment, 13% BSC	12.9 mo	12.2 mo	Bone involvement. Early recurrence (< 6 mo). Multi-organ
Valdivieso *et al* [36], 2010	23 (12.6%)	Retrospective single center	8.7% liver, 21.7% liver + extra, 69.5% extrahepatic	47.8% surgery, 17.4 systemic treatment, 34.8% BSC	23.4 mo	R0 33.2 mo, other 11.9 mo	R0 surgical treatment
Mehta *et al* [101], 2020	84 (11.6%)	Retrospective multicenter	26.2% liver, 48.8% extrahepatic, 25% multiple sites	-	13 mo	-	-
Sharma *et al*	17 (18%)	Retrospective	35.3% liver, 64.7%	-	25.2	-	-

[102], 2012		single center	multiple sites		mo		
Shin *et al*[91], 2010	28 (20.3%) (LDLT)	Retrospective single center	50% liver, 25% extrahepatic, 25% multiple sites	Liver: TACE. Extrahepatic: Systemic therapy/RT	7.9 mo	11.7 mo (1 yr 52.8%; 3 yr 15.8%)	Major vascular invasion. Poorly differentiated HCC. No surgical treatment. Bone metastases
Schlitt *et al* [103], 1999	39 (56.5%)	Retrospective single center	23.1% liver, 38.5 liver + extra, 38.5% extrahepatic	38.4% surgery, 41% BSC, 12.8% systemic treatment, 2.5% TACE, 5.1% RT	14.5 mo	8 mo (non-surgical treatment)	-
Escartin *et al* [104], 2007	28 (15.2%)	Retrospective single center	14.3% liver, 46.4% extrahepatic, 39.3% multiple sites	-	-	7 mo	-
Cescon *et al* [105], 2010	34 (12%)	Retrospective single center	8.8% liver, 20.6% extrahepatic, 70.6% multiple sites	100% systemic treatment (in combination with: 5.9% surgery, 3% RT, 3% RFA, 3% IA CT)	12 mo	-	-
Roayaie *et al* [37], 2004	57 (18.3%)	Retrospective single center	15.8 % liver, 52.6% extrahepatic, 31.6% multiple sites	31.6% surgery, 5.2% TACE, 26.3% systemic treatment, 7% RT, 29.8% BSC	12.2 mo	8.7 mo	Bone metastases. No surgical treatment. Early recurrence

RFS: Relapse free survival; OS: Overall survival; RT: Radiotherapy; BSC: Best supportive care; IA CT: Intra-arterial chemotherapy. RFA: Radiofrequency ablation; LT: Liver transplant; mTTR: Median time to recurrence; mOS: Median overall survival; TACE: Transarterial chemoembolization; HCC: Hepatocellular carcinoma; PEI: Percutaneous ethanol injection; LDLT: Living donor liver transplantation.

stage of recurrence on the other hand, as compared to more advanced cases of multifocal recurrence. Even when radical resection cannot be undertaken, it is widely accepted that any kind of treatment of recurrence has a positive prognostic impact. In the multicenter Latin American study, propensity score matching was used to evaluate the adjusted treatment effect considering selection bias. Patients treated with both sorafenib and surgery/TACE had better survival compared to the best supportive care regardless of time to recurrence[95]. Although randomized data are unlikely to be available in this context and retrospective comparisons are impaired by intrinsic differences between single site/oligometastatic and disseminated recurrence, surgical treatment remains an independent predictor of improved outcome following post-LT recurrence[37-39,41].

Serum markers

As for primary disease and post-LT outcome, AFP at recurrence as an indicator of disease spread, MVI and biological aggressiveness was frequently reported as a strong predictor of prognosis, with cutoffs varying from 100 to 1000 ng/mL[39-41,95]. The difference in survival for patients with high AFP was evident regardless of curative-intent treatment, confirming its value as a marker of unfavorable biological features, and its ability to guide the clinical management of patients affected by HCC recurrence. Finally, other biochemical markers at recurrence were associated with shorter survival: High bilirubin, possibly as a reflection of graft dysfunction, and low albumin, related to poor nutritional status as a general prognostic factor outlined in several series[96,99].

CONCLUSION

HCC recurrence after LT is still a dreadful event, occurring in up to 20% of cases. It might be prevented by stringent pretransplant selection criteria incorporating biological markers of aggressiveness (such as response to therapy, serum markers, histological factors) in addition to size and number of tumors. Several advances in this sense have been made in the last decade, allowing patients with HCC broader access to LT with more precise prediction of outcomes. In the post-LT period, surveillance should be driven by post-LT risk stratification, and the RETREAT score seems to be the best cost-effective approach. No adjuvant treatments after LT have been validated to prevent HCC recurrence; however, a balanced use of immunosuppression with minimal dose of CNIs and possibly the addition of mTORi is strongly advisable. Median post-recurrence survival is 12 mo: the interplay between time to recurrence (with a negative impact of earlier events) and the possibility of a radical treatment is the strongest determinant of survival.

FOOTNOTES

Author contributions: Sposito C wrote and revised the paper; Citterio D, Virdis M, Battiston C, Droz Dit Busset M and Flores M wrote the paper and the tables; Virdis M drew the figures; Flores M and Battiston C did literature research; Mazzaferro V have reviewed the paper for important intellectual content.

Conflict-of-interest statement: All the authors report no relevant conflicts of interest for this article.

Open-Access: This article is an open-access article that was selected by an in-house editor and fully peer-reviewed by external reviewers. It is distributed in accordance with the Creative Commons Attribution NonCommercial (CC BY-NC 4.0) license, which permits others to distribute, remix, adapt, build upon this work non-commercially, and license their derivative works on different terms, provided the original work is properly cited and the use is non-commercial. See: https://creativecommons.org/Licenses/by-nc/4.0/

Country/Territory of origin: Italy

ORCID number: Carlo Sposito 0000-0002-2276-2669; Davide Citterio 0000-0002-0708-8733; Matteo Virdis 0000-0002-1944-2357; Carlo Battiston 0000-0001-6826-7893; Michele Droz Dit Busset 0000-0002-5967-6828; Maria Flores 0000-0001-7195-6251; Vincenzo Mazzaferro 0000-0002-4013-8085.

S-Editor: Wang JJ
L-Editor: Kerr C
P-Editor: Wang JJ

REFERENCES

1 **Villanueva A**. Hepatocellular Carcinoma. *N Engl J Med* 2019; **380**: 1450-1462 [PMID: 30970190 DOI: 10.1056/NEJMra1713263]
2 **Bray F**, Ferlay J, Soerjomataram I, Siegel RL, Torre LA, Jemal A. Global cancer statistics 2018: GLOBOCAN estimates of incidence and mortality worldwide for 36 cancers in 185 countries. *CA Cancer J Clin* 2018; **68**: 394-424 [PMID: 30207593 DOI: 10.3322/caac.21492]
3 **Iwatsuki S**, Starzl TE, Sheahan DG, Yokoyama I, Demetris AJ, Todo S, Tzakis AG, Van Thiel DH, Carr B, Selby R, Madariaga J. Hepatic resection vs transplantation for hepatocellular carcinoma. *Ann Surg* 1991; **214**: 221-229 [DOI: 10.1097/00000658-199109000-00005]
4 **Yokoyama I**, Carr B, Saitsu H, Iwatsuki S, Starzl TE. Accelerated growth rates of recurrent hepatocellular carcinoma after liver transplantation. *Cancer* 1991; **68**: 2095-2100 [PMID: 1655200 DOI: 10.1002/1097-0142(19911115)68:10<2095::aid-cncr2820681002>3.0.co;2-y]
5 **Bismuth H**, Chiche L, Adam R, Castaing D, Diamond T, Dennison A. Liver resection versus transplantation for hepatocellular carcinoma in cirrhotic patients. *Ann Surg* 1993; **218**: 145-151 [PMID: 8393649 DOI: 10.1097/00000658-199308000-00005]
6 **Ringe B**, Pichlmayr R, Wittekind C, Tusch G. Surgical treatment of hepatocellular carcinoma: experience with liver resection and transplantation in 198 patients. *World J Surg* 1991; **15**: 270-285 [PMID: 1851588 DOI: 10.1007/BF01659064]
7 **Mazzaferro V**, Regalia E, Doci R, Andreola S, Pulvirenti A, Bozzetti F, Montalto F, Ammatuna M, Morabito A, Gennari L. Liver transplantation for the treatment of small hepatocellular carcinomas in patients with cirrhosis. *N Engl J Med* 1996; **334**: 693-699 [PMID: 8594428 DOI: 10.1056/NEJM199603143341104]
8 **Tan DJH**, Wong C, Ng CH, Poh CW, Jain SR, Huang DQ, Muthiah MD. A Meta-Analysis on the Rate of Hepatocellular Carcinoma Recurrence after Liver Transplant and Associations to Etiology, Alpha-Fetoprotein, Income and Ethnicity. *J Clin Med* 2021; **10** [PMID: 33440759 DOI: 10.3390/jcm10020238]
9 **Yang JD**, Larson JJ, Watt KD, Allen AM, Wiesner RH, Gores GJ, Roberts LR, Heimbach JA, Leise MD. Hepatocellular Carcinoma Is the Most Common Indication for Liver Transplantation and Placement on the Waitlist in the United States. *Clin Gastroenterol Hepatol* 2017; **15**: 767-775.e3 [PMID: 28013117 DOI: 10.1016/j.cgh.2016.11.034]
10 **Kwong AJ**, Kim WR, Flemming JA. De Novo Hepatocellular Carcinoma Among Liver Transplant Registrants in the Direct Acting Antiviral Era. *Hepatology* 2018; **68**: 1288-1297 [PMID: 29672886 DOI: 10.1002/hep.30045]
11 **Toso C**, Mentha G, Majno P. Liver transplantation for hepatocellular carcinoma: five steps to prevent recurrence. *Am J Transplant* 2011; **11**: 2031-2035 [PMID: 21831154 DOI: 10.1111/j.1600-6143.2011.03689.x]
12 **Sapisochin G**, Bruix J. Liver transplantation for hepatocellular carcinoma: outcomes and novel surgical approaches. *Nat Rev Gastroenterol Hepatol* 2017; **14**: 203-217 [PMID: 28053342 DOI: 10.1038/nrgastro.2016.193]
13 **Goldaracena N**, Mehta N, Scalera I, Sposito C, Atenafu EG, Yao FY, Muiesan P, Mazzaferro V, Sapisochin G. Multicenter validation of a score to predict prognosis after the development of HCC recurrence following liver transplantation. *HPB (Oxford)* 2019; **21**: 731-738 [PMID: 30391218 DOI: 10.1016/j.hpb.2018.10.005]
14 **Mazzaferro V**, Llovet JM, Miceli R, Bhoori S, Schiavo M, Mariani L, Camerini T, Roayaie S, Schwartz ME, Grazi GL, Adam R, Neuhaus P, Salizzoni M, Bruix J, Forner A, De Carlis L, Cillo U, Burroughs AK, Troisi R, Rossi M, Gerunda GE, Lerut J, Belghiti J, Boin I, Gugenheim J, Rochling F, Van Hoek B, Majno P; Metroticket Investigator Study Group. Predicting survival after liver transplantation in patients with hepatocellular carcinoma beyond the Milan criteria: a retrospective, exploratory analysis. *Lancet Oncol* 2009; **10**: 35-43 [PMID: 19058754 DOI: 10.1016/S1470-2045(08)70284-5]

15 **Duvoux C**, Roudot-Thoraval F, Decaens T, Pessione F, Badran H, Piardi T, Francoz C, Compagnon P, Vanlemmens C, Dumortier J, Dharancy S, Gugenheim J, Bernard PH, Adam R, Radenne S, Muscari F, Conti F, Hardwigsen J, Pageaux GP, Chazouillères O, Salame E, Hilleret MN, Lebray P, Abergel A, Debette-Gratien M, Kluger MD, Mallat A, Azoulay D, Cherqui D; Liver Transplantation French Study Group. Liver transplantation for hepatocellular carcinoma: a model including α-fetoprotein improves the performance of Milan criteria. *Gastroenterology* 2012; **143**: 986-94.e3; quiz e14 [PMID: 22750200 DOI: 10.1053/j.gastro.2012.05.052]

16 **Mazzaferro V**, Sposito C, Zhou J, Pinna AD, De Carlis L, Fan J, Cescon M, Di Sandro S, Yi-Feng H, Lauterio A, Bongini M, Cucchetti A. Metroticket 2.0 Model for Analysis of Competing Risks of Death After Liver Transplantation for Hepatocellular Carcinoma. *Gastroenterology* 2018; **154**: 128-139 [PMID: 28989060 DOI: 10.1053/j.gastro.2017.09.025]

17 **Lai Q**, Avolio AW, Graziadei I, Otto G, Rossi M, Tisone G, Goffette P, Vogel W, Pitton MB, Lerut J; European Hepatocellular Cancer Liver Transplant Study Group. Alpha-fetoprotein and modified response evaluation criteria in solid tumors progression after locoregional therapy as predictors of hepatocellular cancer recurrence and death after transplantation. *Liver Transpl* 2013; **19**: 1108-1118 [PMID: 23873764 DOI: 10.1002/lt.23706]

18 **Yao FY**, Mehta N, Flemming J, Dodge J, Hameed B, Fix O, Hirose R, Fidelman N, Kerlan RK Jr, Roberts JP. Downstaging of hepatocellular cancer before liver transplant: long-term outcome compared to tumors within Milan criteria. *Hepatology* 2015; **61**: 1968-1977 [PMID: 25689978 DOI: 10.1002/hep.27752]

19 **Otto G**, Herber S, Heise M, Lohse AW, Mönch C, Bittinger F, Hoppe-Lotichius M, Schuchmann M, Victor A, Pitton M. Response to transarterial chemoembolization as a biological selection criterion for liver transplantation in hepatocellular carcinoma. *Liver Transpl* 2006; **12**: 1260-1267 [PMID: 16826556 DOI: 10.1002/Lt.20837]

20 **Millonig G**, Graziadei IW, Freund MC, Jaschke W, Stadlmann S, Ladurner R, Margreiter R, Vogel W. Response to preoperative chemoembolization correlates with outcome after liver transplantation in patients with hepatocellular carcinoma. *Liver Transpl* 2007; **13**: 272-279 [PMID: 17256758 DOI: 10.1002/Lt.21033]

21 **Aggarwal A**, Te HS, Verna EC, Desai AP. A National Survey of Hepatocellular Carcinoma Surveillance Practices Following Liver Transplantation. *Transplant Direct* 2021; **7**: e638 [PMID: 33324743 DOI: 10.1097/TXD.0000000000001086]

22 **Berenguer M**, Burra P, Ghobrial M, Hibi T, Metselaar H, Sapisochin G, Bhoori S, Kwan Man N, Mas V, Ohira M, Sangro B, van der Laan LJW. Posttransplant Management of Recipients Undergoing Liver Transplantation for Hepatocellular Carcinoma. Working Group Report From the ILTS Transplant Oncology Consensus Conference. *Transplantation* 2020; **104**: 1143-1149 [PMID: 32217940 DOI: 10.1097/TP.0000000000003196]

23 **Verna EC**, Patel YA, Aggarwal A, Desai AP, Frenette C, Pillai AA, Salgia R, Seetharam A, Sharma P, Sherman C, Tsoulfas G, Yao FY. Liver transplantation for hepatocellular carcinoma: Management after the transplant. *Am J Transplant* 2020; **20**: 333-347 [PMID: 31710773 DOI: 10.1111/ajt.15697]

24 **Mehta N**, Heimbach J, Harnois DM, Sapisochin G, Dodge JL, Lee D, Burns JM, Sanchez W, Greig PD, Grant DR, Roberts JP, Yao FY. Validation of a Risk Estimation of Tumor Recurrence After Transplant (RETREAT) Score for Hepatocellular Carcinoma Recurrence After Liver Transplant. *JAMA Oncol* 2017; **3**: 493-500 [PMID: 27838698 DOI: 10.1001/jamaoncol.2016.5116]

25 **Lee DD**, Sapisochin G, Mehta N, Gorgen A, Musto KR, Hajda H, Yao FY, Hodge DO, Carter RE, Harnois DM. Surveillance for HCC After Liver Transplantation: Increased Monitoring May Yield Aggressive Treatment Options and Improved Postrecurrence Survival. *Transplantation* 2020; **104**: 2105-2112 [PMID: 31972705 DOI: 10.1097/TP.0000000000003117]

26 **Rodríguez-Perálvarez M**, Tsochatzis E, Naveas MC, Pieri G, García-Caparrós C, O'Beirne J, Poyato-González A, Ferrín-Sánchez G, Montero-Álvarez JL, Patch D, Thorburn D, Briceño J, De la Mata M, Burroughs AK. Reduced exposure to calcineurin inhibitors early after liver transplantation prevents recurrence of hepatocellular carcinoma. *J Hepatol* 2013; **59**: 1193-1199 [PMID: 23867318 DOI: 10.1016/j.jhep.2013.07.012]

27 **Semela D**, Piguet AC, Kolev M, Schmitter K, Hlushchuk R, Djonov V, Stoupis C, Dufour JF. Vascular remodeling and antitumoral effects of mTOR inhibition in a rat model of hepatocellular carcinoma. *J Hepatol* 2007; **46**: 840-848 [PMID: 17321636 DOI: 10.1016/j.jhep.2006.11.021]

28 **Grigg SE**, Sarri GL, Gow PJ, Yeomans ND. Systematic review with meta-analysis: sirolimus- or everolimus-based immunosuppression following liver transplantation for hepatocellular carcinoma. *Aliment Pharmacol Ther* 2019; **49**: 1260-1273 [PMID: 30989721 DOI: 10.1111/apt.15253]

29 **Geissler EK**, Schnitzbauer AA, Zülke C, Lamby PE, Proneth A, Duvoux C, Burra P, Jauch KW, Rentsch M, Ganten TM, Schmidt J, Settmacher U, Heise M, Rossi G, Cillo U, Kneteman N, Adam R, van Hoek B, Bachellier P, Wolf P, Rostaing L, Bechstein WO, Rizell M, Powell J, Hidalgo E, Gugenheim J, Wolters H, Brockmann J, Roy A, Mutzbauer I, Schlitt A, Beckebaum S, Graeb C, Nadalin S, Valente U, Turrión VS, Jamieson N, Scholz T, Colledan M, Fändrich F, Becker T, Söderdahl G, Chazouillères O, Mäkisalo H, Pageaux GP, Steininger R, Soliman T, de Jong KP, Pirenne J, Margreiter R, Pratschke J, Pinna AD, Hauss J, Schreiber S, Strasser S, Klempnauer J, Troisi RI, Bhoori S, Lerut J, Bilbao I, Klein CG, Königsrainer A, Mirza DF, Otto G, Mazzaferro V, Neuhaus P, Schlitt HJ. Sirolimus Use in Liver Transplant Recipients With Hepatocellular Carcinoma: A Randomized, Multicenter, Open-Label Phase 3 Trial. *Transplantation* 2016; **100**: 116-125 [PMID: 26555945 DOI: 10.1097/TP.0000000000000965]

30 **Olthoff KM**, Rosove MH, Shackleton CR, Imagawa DK, Farmer DG, Northcross P, Pakrasi AL, Martin P, Goldstein LI, Shaked A. Adjuvant chemotherapy improves survival after liver transplantation for hepatocellular carcinoma. *Ann Surg* 1995; **221**: 734-41; discussion 731 [PMID: 7794077 DOI: 10.1097/00000658-199506000-00012]

31 **Hsieh CB**, Chou SJ, Shih ML, Chu HC, Chu CH, Yu JC, Yao NS. Preliminary experience with gemcitabine and cisplatin adjuvant chemotherapy after liver transplantation for hepatocellular carcinoma. *Eur J Surg Oncol* 2008; **34**: 906-910 [PMID: 18166289 DOI: 10.1016/j.ejso.2007.11.014]

32 **Fujiki M**, Aucejo F, Kim R. Adjuvant treatment of hepatocellular carcinoma after orthotopic liver transplantation: do we really need this? *Clin Transplant* 2013; **27**: 169-177 [PMID: 23216662 DOI: 10.1111/ctr.12042]

33 **Siegel AB**, El-Khoueiry AB, Finn RS, Guthrie KA, Goyal A, Venook AP, Blanke CD, Verna EC, Dove L, Emond J, Kato T, Samstein B, Busuttil R, Remotti H, Coffey A, Brown RS Jr. Phase I trial of sorafenib following liver transplantation in

patients with high-risk hepatocellular carcinoma. *Liver Cancer* 2015; **4**: 115-125 [PMID: 26020033 DOI: 10.1159/000367734]

34 **Han B**, Ding H, Zhao S, Zhang Y, Wang J, Gu J. Potential Role of Adjuvant Lenvatinib in Improving Disease-Free Survival for Patients With High-Risk Hepatitis B Virus-Related Hepatocellular Carcinoma Following Liver Transplantation: A Retrospective, Case Control Study. *Front Oncol* 2020; **10**: 562103 [PMID: 33365268 DOI: 10.3389/fonc.2020.562103]

35 **Ziogas IA**, Evangeliou AP, Giannis D, Hayat MH, Mylonas KS, Tohme S, Geller DA, Elias N, Goyal L, Tsoulfas G. The Role of Immunotherapy in Hepatocellular Carcinoma: A Systematic Review and Pooled Analysis of 2,402 Patients. *Oncologist* 2021; **26**: e1036-e1049 [PMID: 33314549 DOI: 10.1002/onco.13638]

36 **Valdivieso A**, Bustamante J, Gastaca M, Uriarte JG, Ventoso A, Ruiz P, Fernandez JR, Pijoan I, Testillano M, Suarez MJ, Montejo M, Ortiz de Urbina J. Management of hepatocellular carcinoma recurrence after liver transplantation. *Transplant Proc* 2010; **42**: 660-662 [PMID: 20304217 DOI: 10.1016/j.transproceed.2010.02.014]

37 **Roayaie S**, Schwartz JD, Sung MW, Emre SH, Miller CM, Gondolesi GE, Krieger NR, Schwartz ME. Recurrence of hepatocellular carcinoma after liver transplant: patterns and prognosis. *Liver Transpl* 2004; **10**: 534-540 [PMID: 15048797 DOI: 10.1002/Lt.20128]

38 **Kornberg A**, Küpper B, Tannapfel A, Katenkamp K, Thrum K, Habrecht O, Wilberg J. Long-term survival after recurrent hepatocellular carcinoma in liver transplant patients: clinical patterns and outcome variables. *Eur J Surg Oncol* 2010; **36**: 275-280 [PMID: 19857941 DOI: 10.1016/j.ejso.2009.10.001]

39 **Sapisochin G**, Goldaracena N, Astete S, Laurence JM, Davidson D, Rafael E, Castells L, Sandroussi C, Bilbao I, Dopazo C, Grant DR, Lázaro JL, Caralt M, Ghanekar A, McGilvray ID, Lilly L, Cattral MS, Selzner M, Charco R, Greig PD. Benefit of Treating Hepatocellular Carcinoma Recurrence after Liver Transplantation and Analysis of Prognostic Factors for Survival in a Large Euro-American Series. *Ann Surg Oncol* 2015; **22**: 2286-2294 [PMID: 25472651 DOI: 10.1245/s10434-014-4273-6]

40 **Bodzin AS**, Lunsford KE, Markovic D, Harlander-Locke MP, Busuttil RW, Agopian VG. Predicting Mortality in Patients Developing Recurrent Hepatocellular Carcinoma After Liver Transplantation: Impact of Treatment Modality and Recurrence Characteristics. *Ann Surg* 2017; **266**: 118-125 [PMID: 27433914 DOI: 10.1097/SLA.0000000000001894]

41 **Fernandez-Sevilla E**, Allard MA, Selten J, Golse N, Vibert E, Sa Cunha A, Cherqui D, Castaing D, Adam R. Recurrence of hepatocellular carcinoma after liver transplantation: Is there a place for resection? *Liver Transpl* 2017; **23**: 440-447 [PMID: 28187493 DOI: 10.1002/lt.24742]

42 **Sommacale D**, Dondero F, Sauvanet A, Francoz C, Durand F, Farges O, Kianmanesh R, Belghiti J. Liver resection in transplanted patients: a single-center Western experience. *Transplant Proc* 2013; **45**: 2726-2728 [PMID: 24034033 DOI: 10.1016/j.transproceed.2013.07.032]

43 **Chok KSh**. Management of recurrent hepatocellular carcinoma after liver transplant. *World J Hepatol* 2015; **7**: 1142-1148 [PMID: 26052403 DOI: 10.4254/wjh.v7.i8.1142]

44 **Huang J**, Yan L, Wu H, Yang J, Liao M, Zeng Y. Is radiofrequency ablation applicable for recurrent hepatocellular carcinoma after liver transplantation? *J Surg Res* 2016; **200**: 122-130 [PMID: 26277218 DOI: 10.1016/j.jss.2015.07.033]

45 **Regalia E**, Fassati LR, Valente U, Pulvirenti A, Damilano I, Dardano G, Montalto F, Coppa J, Mazzaferro V. Pattern and management of recurrent hepatocellular carcinoma after liver transplantation. *J Hepatobiliary Pancreat Surg* 1998; **5**: 29-34 [PMID: 9683751 DOI: 10.1007/pl00009947]

46 **Chok KS**, Chan SC, Cheung TT, Chan AC, Fan ST, Lo CM. Late recurrence of hepatocellular carcinoma after liver transplantation. *World J Surg* 2011; **35**: 2058-2062 [PMID: 21597889 DOI: 10.1007/s00268-011-1146-z]

47 **Tomimaru Y**, Sasaki Y, Yamada T, Eguchi H, Takami K, Ohigashi H, Higashiyama M, Ishikawa O, Kodama K, Imaoka S. The significance of surgical resection for pulmonary metastasis from hepatocellular carcinoma. *Am J Surg* 2006; **192**: 46-51 [PMID: 16769274 DOI: 10.1016/j.amjsurg.2005.12.006]

48 **Jeong YH**, Hwang S, Lee GD, Choi SH, Kim HR, Kim YH, Park SI, Kim DK. Surgical Outcome of Pulmonary Metastasectomy for Hepatocellular Carcinoma Recurrence in Liver Transplant Patients. *Ann Transplant* 2021; **26**: e930383 [PMID: 33972494 DOI: 10.12659/AOT.930383]

49 **Bates MJ**, Farkas E, Taylor D, McFadden PM. Pulmonary resection of metastatic hepatocellular carcinoma after liver transplantation. *Ann Thorac Surg* 2008; **85**: 412-415 [PMID: 18222234 DOI: 10.1016/j.athoracsur.2007.10.065]

50 **Han KN**, Kim YT, Yoon JH, Suh KS, Song JY, Kang CH, Sung SW, Kim JH. Role of surgical resection for pulmonary metastasis of hepatocellular carcinoma. *Lung Cancer* 2010; **70**: 295-300 [PMID: 20353879 DOI: 10.1016/j.lungcan.2010.02.014]

51 **Finn RS**, Qin S, Ikeda M, Galle PR, Ducreux M, Kim TY, Kudo M, Breder V, Merle P, Kaseb AO, Li D, Verret W, Xu DZ, Hernandez S, Liu J, Huang C, Mulla S, Wang Y, Lim HY, Zhu AX, Cheng AL; IMbrave150 Investigators. Atezolizumab plus Bevacizumab in Unresectable Hepatocellular Carcinoma. *N Engl J Med* 2020; **382**: 1894-1905 [PMID: 32402160 DOI: 10.1056/NEJMoa1915745]

52 **Hwang S**, Kim YH, Kim DK, Ahn CS, Moon DB, Kim KH, Ha TY, Song GW, Jung DH, Kim HR, Park GC, Namgoong JM, Yoon SY, Jung SW, Park SI, Lee SG. Resection of pulmonary metastases from hepatocellular carcinoma following liver transplantation. *World J Surg* 2012; **36**: 1592-1602 [PMID: 22411088 DOI: 10.1007/s00268-012-1533-0]

53 **Hu JG**, Lu Y, Lin XJ. En Bloc lumpectomy of T12 vertebra for progressive hepatocellular carcinoma metastases following liver transplantation: A case report. *Medicine (Baltimore)* 2020; **99**: e18756 [PMID: 31914098 DOI: 10.1097/MD.0000000000018756]

54 **Abdel Wahab M**, Shehta A, Ibrahim EM, Eldesoky RT, Sultan AA, Zalata KR, Fathy O, Elshoubary M, Salah T, Yassen AM, Elmorshedi M, Monier A, Farouk A, Shiha U. Adrenalectomy for solitary recurrent hepatocellular carcinoma five years after living donor liver transplantation: A case report. *Int J Surg Case Rep* 2019; **54**: 23-27 [PMID: 30513494 DOI: 10.1016/j.ijscr.2018.11.062]

55 **Jalbani IK**, Nazim SM, Tariq MU, Abbas F. Adrenalectomy for solitary metastasis of Hepatocellular carcinoma post liver transplantation: Case report and literature review. *Pak J Med Sci* 2016; **32**: 1044-1046 [PMID: 27648064 DOI: 10.12669/pjms.324.10339]

56 **Ikegami T**, Yoshizumi T, Kawasaki J, Nagatsu A, Uchiyama H, Harada N, Harimoto N, Itoh S, Motomura T, Soejima Y, Maehara Y. Surgical Resection for Lymph Node Metastasis After Liver Transplantation for Hepatocellular Carcinoma. *Anticancer Res* 2017; **37**: 891-895 [PMID: 28179348 DOI: 10.21873/anticanres.11395]

57 **Alshahrani AA**, Ha SM, Hwang S, Ahn CS, Kim KH, Moon DB, Ha TY, Song GW, Jung DH, Park GC, Cho HD, Kwon JH, Kang SH, Lee SG. Clinical Features and Surveillance of Very Late Hepatocellular Carcinoma Recurrence After Liver Transplantation. *Ann Transplant* 2018; **23**: 659-665 [PMID: 30237389 DOI: 10.12659/AOT.910598]

58 **Tohyama T**, Sakamoto K, Tamura K, Nakamura T, Watanabe J, Wakisaka H, Takada Y. Pharyngeal metastasis following living-donor liver transplantation for hepatocellular carcinoma: a case report and literature review. *World J Surg Oncol* 2020; **18**: 109 [PMID: 32466780 DOI: 10.1186/s12957-020-01873-0]

59 **Zhai H**, Liang P, Yu XL, Cheng Z, Han ZY, Liu F, Yu J. Microwave ablation in treating intrahepatic recurrence of hepatocellular carcinoma after liver transplantation: An analysis of 11 cases. *Int J Hyperthermia* 2015; **31**: 863-868 [PMID: 26608701 DOI: 10.3109/02656736.2015.1091953]

60 **Ko HK**, Ko GY, Yoon HK, Sung KB. Tumor response to transcatheter arterial chemoembolization in recurrent hepatocellular carcinoma after living donor liver transplantation. *Korean J Radiol* 2007; **8**: 320-327 [PMID: 17673843 DOI: 10.3348/kjr.2007.8.4.320]

61 **Zhou B**, Shan H, Zhu KS, Jiang ZB, Guan SH, Meng XC, Zeng XC. Chemoembolization with lobaplatin mixed with iodized oil for unresectable recurrent hepatocellular carcinoma after orthotopic liver transplantation. *J Vasc Interv Radiol* 2010; **21**: 333-338 [PMID: 20116286 DOI: 10.1016/j.jvir.2009.11.006]

62 **Sposito C**, Mariani L, Germini A, Flores Reyes M, Bongini M, Grossi G, Bhoori S, Mazzaferro V. Comparative efficacy of sorafenib versus best supportive care in recurrent hepatocellular carcinoma after liver transplantation: a case-control study. *J Hepatol* 2013; **59**: 59-66 [PMID: 23500153 DOI: 10.1016/j.jhep.2013.02.026]

63 **Mancuso A**, Mazzola A, Cabibbo G, Perricone G, Enea M, Galvano A, Zavaglia C, Belli L, Cammà C. Survival of patients treated with sorafenib for hepatocellular carcinoma recurrence after liver transplantation: a systematic review and meta-analysis. *Dig Liver Dis* 2015; **47**: 324-330 [PMID: 25641331 DOI: 10.1016/j.dld.2015.01.001]

64 **Toso C**, Mentha G, Majno P. Integrating sorafenib into an algorithm for the management of post-transplant hepatocellular carcinoma recurrence. *J Hepatol* 2013; **59**: 3-5 [PMID: 23567081 DOI: 10.1016/j.jhep.2013.03.029]

65 **Invernizzi F**, Iavarone M, Zavaglia C, Mazza S, Maggi U, Cesarini L, Antonelli B, Airoldi A, Manini MA, Sangiovanni A, Rossi G, Donato MF, Saverio Belli L, Lampertico P. Experience With Early Sorafenib Treatment With mTOR Inhibitors in Hepatocellular Carcinoma Recurring After Liver Transplantation. *Transplantation* 2020; **104**: 568-574 [PMID: 31517781 DOI: 10.1097/TP.0000000000002955]

66 **Piguet AC**, Saar B, Hlushchuk R, St-Pierre MV, McSheehy PM, Radojevic V, Afthinos M, Terracciano L, Djonov V, Dufour JF. Everolimus augments the effects of sorafenib in a syngeneic orthotopic model of hepatocellular carcinoma. *Mol Cancer Ther* 2011; **10**: 1007-1017 [PMID: 21487053 DOI: 10.1158/1535-7163.MCT-10-0666]

67 **Herden U**, Fischer L, Schäfer H, Nashan B, von Baehr V, Sterneck M. Sorafenib-induced severe acute hepatitis in a stable liver transplant recipient. *Transplantation* 2010; **90**: 98-99 [PMID: 20606568 DOI: 10.1097/TP.0b013e3181daac69]

68 **Waidmann O**, Hofmann WP, Zeuzem S, Trojan J. mTOR inhibitors and sorafenib for recurrent heptocellular carcinoma after orthotopic liver transplantation. *J Hepatol* 2011; **54**: 396-398 [PMID: 21111506 DOI: 10.1016/j.jhep.2010.08.038]

69 **De Simone P**, Crocetti L, Pezzati D, Bargellini I, Ghinolfi D, Carrai P, Leonardi G, Della Pina C, Cioni D, Pollina L, Campani D, Bartolozzi C, Lencioni R, Filipponi F. Efficacy and safety of combination therapy with everolimus and sorafenib for recurrence of hepatocellular carcinoma after liver transplantation. *Transplant Proc* 2014; **46**: 241-244 [PMID: 24507059 DOI: 10.1016/j.transproceed.2013.10.035]

70 **Bhoori S**, Toffanin S, Sposito C, Germini A, Pellegrinelli A, Lampis A, Mazzaferro V. Personalized molecular targeted therapy in advanced, recurrent hepatocellular carcinoma after liver transplantation: a proof of principle. *J Hepatol* 2010; **52**: 771-775 [PMID: 20347502 DOI: 10.1016/j.jhep.2010.01.025]

71 **Iavarone M**, Invernizzi F, Czauderna C, Sanduzzi-Zamparelli M, Bhoori S, Amaddeo G, Manini MA, López MF, Anders M, Pinter M, Rodríguez MJB, Cristóbal MR, Soteras GA, Piñero F, Villadsen GE, Weinmann A, Crespo G, Mazzaferro V, Regnault H, Giorgio M, González-Diéguez ML, Donato MF, Varela M, Wörns MA, Bruix J, Lampertico P, Reig M. Preliminary experience on safety of regorafenib after sorafenib failure in recurrent hepatocellular carcinoma after liver transplantation. *Am J Transplant* 2019; **19**: 3176-3184 [PMID: 31365177 DOI: 10.1111/ajt.15551]

72 **Iavarone M**, Invernizzi F, Ivanics T, Mazza S, Zavaglia C, Sanduzzi-Zamparelli M, Fraile-López M, Czauderna C, Di Costanzo G, Bhoori S, Pinter M, Manini MA, Amaddeo G, Yunquera AF, Piñero F, Blanco Rodríguez MJ, Anders M, Aballay Soteras G, Villadsen GE, Yoon PD, Cesarini L, Díaz-González Á, González-Diéguez ML, Tortora R, Weinmann A, Mazzaferro V, Romero Cristóbal M, Crespo G, Regnault H, De Giorgio M, Varela M, Prince R, Scudeller L, Donato MF, Wörns MA, Bruix J, Sapisochin G, Lampertico P, Reig M. Regorafenib Efficacy After Sorafenib in Patients With Recurrent Hepatocellular Carcinoma After Liver Transplantation: A Retrospective Study. *Liver Transpl* 2021; **27**: 1767-1778 [PMID: 34388851 DOI: 10.1002/lt.26264]

73 **Kudo M**, Finn RS, Qin S, Han KH, Ikeda K, Piscaglia F, Baron A, Park JW, Han G, Jassem J, Blanc JF, Vogel A, Komov D, Evans TRJ, Lopez C, Dutcus C, Guo M, Saito K, Kraljevic S, Tamai T, Ren M, Cheng AL. Lenvatinib versus sorafenib in first-line treatment of patients with unresectable hepatocellular carcinoma: a randomised phase 3 non-inferiority trial. *Lancet* 2018; **391**: 1163-1173 [PMID: 29433850 DOI: 10.1016/S0140-6736(18)30207-1]

74 **Abou-Alfa GK**, Meyer T, Cheng AL, El-Khoueiry AB, Rimassa L, Ryoo BY, Cicin I, Merle P, Chen Y, Park JW, Blanc JF, Bolondi L, Klümpen HJ, Chan SL, Zagonel V, Pressiani T, Ryu MH, Venook AP, Hessel C, Borgman-Hagey AE, Schwab G, Kelley RK. Cabozantinib in Patients with Advanced and Progressing Hepatocellular Carcinoma. *N Engl J Med* 2018; **379**: 54-63 [PMID: 29972759 DOI: 10.1056/NEJMoa1717002]

75 **Zhu AX**, Kang YK, Yen CJ, Finn RS, Galle PR, Llovet JM, Assenat E, Brandi G, Pracht M, Lim HY, Rau KM, Motomura K, Ohno I, Merle P, Daniele B, Shin DB, Gerken G, Borg C, Hiriart JB, Okusaka T, Morimoto M, Hsu Y, Abada PB, Kudo M; REACH-2 study investigators. Ramucirumab after sorafenib in patients with advanced hepatocellular carcinoma and increased α-fetoprotein concentrations (REACH-2): a randomised, double-blind, placebo-controlled, phase

3 trial. *Lancet Oncol* 2019; **20**: 282-296 [PMID: 30665869 DOI: 10.1016/S1470-2045(18)30937-9]

76 **Rimassa L**, Personeni N, Czauderna C, Foerster F, Galle P. Systemic treatment of HCC in special populations. *J Hepatol* 2021; **74**: 931-943 [PMID: 33248171 DOI: 10.1016/j.jhep.2020.11.026]

77 **El-Khoueiry AB**, Sangro B, Yau T, Crocenzi TS, Kudo M, Hsu C, Kim TY, Choo SP, Trojan J, Welling TH Rd, Meyer T, Kang YK, Yeo W, Chopra A, Anderson J, Dela Cruz C, Lang L, Neely J, Tang H, Dastani HB, Melero I. Nivolumab in patients with advanced hepatocellular carcinoma (CheckMate 040): an open-label, non-comparative, phase 1/2 dose escalation and expansion trial. *Lancet* 2017; **389**: 2492-2502 [PMID: 28434648 DOI: 10.1016/S0140-6736(17)31046-2]

78 **Finn RS**, Ryoo BY, Merle P, Kudo M, Bouattour M, Lim HY, Breder V, Edeline J, Chao Y, Ogasawara S, Yau T, Garrido M, Chan SL, Knox J, Daniele B, Ebbinghaus SW, Chen E, Siegel AB, Zhu AX, Cheng AL; KEYNOTE-240 investigators. Pembrolizumab As Second-Line Therapy in Patients With Advanced Hepatocellular Carcinoma in KEYNOTE-240: A Randomized, Double-Blind, Phase III Trial. *J Clin Oncol* 2020; **38**: 193-202 [PMID: 31790344 DOI: 10.1200/JCO.19.01307]

79 **Zhu AX**, Finn RS, Edeline J, Cattan S, Ogasawara S, Palmer D, Verslype C, Zagonel V, Fartoux L, Vogel A, Sarker D, Verset G, Chan SL, Knox J, Daniele B, Webber AL, Ebbinghaus SW, Ma J, Siegel AB, Cheng AL, Kudo M; KEYNOTE-224 investigators. Pembrolizumab in patients with advanced hepatocellular carcinoma previously treated with sorafenib (KEYNOTE-224): a non-randomised, open-label phase 2 trial. *Lancet Oncol* 2018; **19**: 940-952 [PMID: 29875066 DOI: 10.1016/S1470-2045(18)30351-6]

80 **Kittai AS**, Oldham H, Cetnar J, Taylor M. Immune Checkpoint Inhibitors in Organ Transplant Patients. *J Immunother* 2017; **40**: 277-281 [PMID: 28719552 DOI: 10.1097/CJI.0000000000000180]

81 **Friend BD**, Venick RS, McDiarmid SV, Zhou X, Naini B, Wang H, Farmer DG, Busuttil RW, Federman N. Fatal orthotopic liver transplant organ rejection induced by a checkpoint inhibitor in two patients with refractory, metastatic hepatocellular carcinoma. *Pediatr Blood Cancer* 2017; **64** [PMID: 28643391 DOI: 10.1002/pbc.26682]

82 **Biondani P**, De Martin E, Samuel D. Safety of an anti-PD-1 immune checkpoint inhibitor in a liver transplant recipient. *Ann Oncol* 2018; **29**: 286-287 [PMID: 29293878 DOI: 10.1093/annonc/mdx548]

83 **DeLeon TT**, Salomao MA, Aqel BA, Sonbol MB, Yokoda RT, Ali AH, Moss AA, Mathur AK, Chascsa DM, Rakela J, Bryce AH, Borad MJ. Pilot evaluation of PD-1 inhibition in metastatic cancer patients with a history of liver transplantation: the Mayo Clinic experience. *J Gastrointest Oncol* 2018; **9**: 1054-1062 [PMID: 30603124 DOI: 10.21037/jgo.2018.07.05]

84 **Gassmann D**, Weiler S, Mertens JC, Reiner CS, Vrugt B, Nägeli M, Mangana J, Müllhaupt B, Jenni F, Misselwitz B. Liver Allograft Failure After Nivolumab Treatment-A Case Report With Systematic Literature Research. *Transplant Direct* 2018; **4**: e376 [PMID: 30255136 DOI: 10.1097/TXD.0000000000000814]

85 **Lipson EJ**, Bodell MA, Kraus ES, Sharfman WH. Successful administration of ipilimumab to two kidney transplantation patients with metastatic melanoma. *J Clin Oncol* 2014; **32**: e69-e71 [PMID: 24493726 DOI: 10.1200/JCO.2013.49.2314]

86 **de'Angelis N**, Landi F, Carra MC, Azoulay D. Managements of recurrent hepatocellular carcinoma after liver transplantation: A systematic review. *World J Gastroenterol* 2015; **21**: 11185-11198 [PMID: 26494973 DOI: 10.3748/wjg.v21.i39.11185]

87 **Pelizzaro F**, Gambato M, Gringeri E, Vitale A, Cillo U, Farinati F, Burra P, Russo FP. Management of Hepatocellular Carcinoma Recurrence after Liver Transplantation. *Cancers (Basel)* 2021; **13** [PMID: 34638365 DOI: 10.3390/cancers13194882]

88 **Shalaby S**, Burra P. De novo and recurrent malignancy. *Best Pract Res Clin Gastroenterol* 2020; **46-47**: 101680 [PMID: 33158464 DOI: 10.1016/j.bpg.2020.101680]

89 **Jeyarajah DR**, Doyle MBM, Espat NJ, Hansen PD, Iannitti DA, Kim J, Thambi-Pillai T, Visser BC. Role of yttrium-90 selective internal radiation therapy in the treatment of liver-dominant metastatic colorectal cancer: an evidence-based expert consensus algorithm. *J Gastrointest Oncol* 2020; **11**: 443-460 [PMID: 32399284 DOI: 10.21037/jgo.2020.01.09]

90 **Roh YN**, David Kwon CH, Song S, Shin M, Man Kim J, Kim S, Joh JW, Lee SK. The prognosis and treatment outcomes of patients with recurrent hepatocellular carcinoma after liver transplantation. *Clin Transplant* 2014; **28**: 141-148 [PMID: 24372624 DOI: 10.1111/ctr.12286]

91 **Shin WY**, Suh KS, Lee HW, Kim J, Kim T, Yi NJ, Lee KU. Prognostic factors affecting survival after recurrence in adult living donor liver transplantation for hepatocellular carcinoma. *Liver Transpl* 2010; **16**: 678-684 [PMID: 20440777 DOI: 10.1002/lt.22047]

92 **Toso C**, Cader S, Mentha-Dugerdil A, Meeberg G, Majno P, Morard I, Giostra E, Berney T, Morel P, Mentha G, Kneteman NM. Factors predicting survival after post-transplant hepatocellular carcinoma recurrence. *J Hepatobiliary Pancreat Sci* 2013; **20**: 342-347 [PMID: 22710887 DOI: 10.1007/s00534-012-0528-4]

93 **Hong SK**, Lee KW, Yoon KC, Kim HS, Ahn SW, Kim H, Lee JM, Cho JH, Yi NJ, Suh KS. Different prognostic factors and strategies for early and late recurrence after adult living donor liver transplantation for hepatocellular carcinoma. *Clin Transplant* 2019; **33**: e13703 [PMID: 31464006 DOI: 10.1111/ctr.13703]

94 **Maccali C**, Chagas AL, Boin I, Quiñonez E, Marciano S, Vilatobá M, Varón A, Anders M, Hoyos Duque S, Lima AS, Menendez J, Padilla-Machaca M, Poniachik J, Zapata R, Maraschio M, Chong Menéndez R, Muñoz L, Arufe D, Figueroa R, Soza A, Fauda M, Perales SR, Vergara Sandoval R, Bermudez C, Beltran O, Arenas Hoyos I, McCormack L, Mattera FJ, Gadano A, Parente García JH, Tani CM, Augusto Carneiro D'Albuquerque L, Carrilho FJ, Silva M, Piñero F. Recurrence of hepatocellular carcinoma after liver transplantation: Prognostic and predictive factors of survival in a Latin American cohort. *Liver Int* 2021; **41**: 851-862 [PMID: 33217193 DOI: 10.1111/liv.14736]

95 **Ekpanyapong S**, Philips N, Loza BL, Abt P, Furth EE, Tondon R, Khungar V, Olthoff K, Shaked A, Hoteit MA, Reddy KR. Predictors, Presentation, and Treatment Outcomes of Recurrent Hepatocellular Carcinoma After Liver Transplantation: A Large Single Center Experience. *J Clin Exp Hepatol* 2020; **10**: 304-315 [PMID: 32655233 DOI: 10.1016/j.jceh.2019.11.003]

96 **Ho CM**, Lee CH, Lee MC, Zhang JF, Chen CH, Wang JY, Hu RH, Lee PH. Survival After Treatable Hepatocellular Carcinoma Recurrence in Liver Recipients: A Nationwide Cohort Analysis. *Front Oncol* 2020; **10**: 616094 [PMID: 33598433 DOI: 10.3389/fonc.2020.616094]

97 **El-Domiaty N**, Saliba F, Vibert E, Karam V, Sobesky R, Ibrahim W, Pittau G, Ciacio O, Salloum C, Amer K, Saeed MA, Shawky JA, Sa Cunha A, Rosmorduc O, Cherqui D, Adam R, Samuel D. Early Versus Late Hepatocellular Carcinoma Recurrence After Transplantation: Predictive Factors, Patterns, and Long-term Outcome. *Transplantation* 2021; **105**: 1778-1790 [PMID: 32890134 DOI: 10.1097/TP.0000000000003434]

98 **Au KP**, Chok KSH. Multidisciplinary approach for post-liver transplant recurrence of hepatocellular carcinoma: A proposed management algorithm. *World J Gastroenterol* 2018; **24**: 5081-5094 [PMID: 30568386 DOI: 10.3748/wjg.v24.i45.5081]

99 **Nagai S**, Mangus RS, Kubal CA, Ekser B, Fridell JA, Klingler KR, Maluccio MA, Tector AJ. Prognosis after recurrence of hepatocellular carcinoma in liver transplantation: predictors for successful treatment and survival. *Clin Transplant* 2015; **29**: 1156-1163 [PMID: 26458066 DOI: 10.1111/ctr.12644]

100 **Taketomi A**, Fukuhara T, Morita K, Kayashima H, Ninomiya M, Yamashita Y, Ikegami T, Uchiyama H, Yoshizumi T, Soejima Y, Shirabe K, Maehara Y. Improved results of a surgical resection for the recurrence of hepatocellular carcinoma after living donor liver transplantation. *Ann Surg Oncol* 2010; **17**: 2283-2289 [PMID: 20204531 DOI: 10.1245/s10434-010-0999-y]

101 **Mehta N**, Bhangui P, Yao FY, Mazzaferro V, Toso C, Akamatsu N, Durand F, Ijzermans J, Polak W, Zheng S, Roberts JP, Sapisochin G, Hibi T, Kwan NM, Ghobrial M, Soin A. Liver Transplantation for Hepatocellular Carcinoma. Working Group Report from the ILTS Transplant Oncology Consensus Conference. *Transplantation* 2020; **104**: 1136-1142 [PMID: 32217938 DOI: 10.1097/TP.0000000000003174]

102 **Sharma P**, Welch K, Hussain H, Pelletier SJ, Fontana RJ, Marrero J, Merion RM. Incidence and risk factors of hepatocellular carcinoma recurrence after liver transplantation in the MELD era. *Dig Dis Sci* 2012; **57**: 806-812 [PMID: 21953139 DOI: 10.1007/s10620-011-1910-9]

103 **Schlitt HJ**, Neipp M, Weimann A, Oldhafer KJ, Schmoll E, Boeker K, Nashan B, Kubicka S, Maschek H, Tusch G, Raab R, Ringe B, Manns MP, Pichlmayr R. Recurrence patterns of hepatocellular and fibrolamellar carcinoma after liver transplantation. *J Clin Oncol* 1999; **17**: 324-331 [PMID: 10458250 DOI: 10.1200/JCO.1999.17.1.324]

104 **Escartin A**, Sapisochin G, Bilbao I, Vilallonga R, Bueno J, Castells L, Dopazo C, Castro E, Caralt M, Balsells J. Recurrence of hepatocellular carcinoma after liver transplantation. *Transplant Proc* 2007; **39**: 2308-2310 [PMID: 17889173 DOI: 10.1016/j.transproceed.2007.06.042]

105 **Cescon M**, Ravaioli M, Grazi GL, Ercolani G, Cucchetti A, Bertuzzo V, Vetrone G, Del Gaudio M, Vivarelli M, D'Errico-Grigioni A, Dazzi A, Di Gioia P, Lauro A, Pinna AD. Prognostic factors for tumor recurrence after a 12-year, single-center experience of liver transplantations in patients with hepatocellular carcinoma. *J Transplant* 2010; **2010** [PMID: 20862199 DOI: 10.1155/2010/904152]

World Journal of Gastroenterology

Submit a Manuscript: https://www.f6publishing.com

World J Gastroenterol 2022 September 14; 28(34): 4943-4958

DOI: 10.3748/wjg.v28.i34.4943

ISSN 1007-9327 (print) ISSN 2219-2840 (online)

MINIREVIEWS

Diagnosis, treatment, and current concepts in the endoscopic management of gastroenteropancreatic neuroendocrine neoplasms

Giuseppe Iabichino, Milena Di Leo, Monica Arena, Giovanni Giuseppe Rubis Passoni, Elisabetta Morandi, Francesca Turpini, Paolo Viaggi, Carmelo Luigiano, Luca De Luca

Specialty type: Gastroenterology and hepatology

Provenance and peer review: Invited article; Externally peer reviewed.

Peer-review model: Single blind

Peer-review report's scientific quality classification

Grade A (Excellent): 0
Grade B (Very good): B, B, B
Grade C (Good): C, C
Grade D (Fair): 0
Grade E (Poor): 0

P-Reviewer: Alali AA, Kuwait; Hu HG, China; Shah OJ, India; Wang WQ, China

Received: April 11, 2022
Peer-review started: April 11, 2022
First decision: May 12, 2022
Revised: June 29, 2022
Accepted: August 22, 2022
Article in press: August 22, 2022
Published online: September 14, 2022

Giuseppe Iabichino, Milena Di Leo, Monica Arena, Giovanni Giuseppe Rubis Passoni, Elisabetta Morandi, Francesca Turpini, Paolo Viaggi, Luca De Luca, Digestive Endoscopy Unit, ASST Santi Paolo e Carlo, Milano 20144, Italy

Carmelo Luigiano, Gastroenterology Section, Grande Ospedale Metropolitano "Bianchi-Melacrino-Morelli", Reggio Calabria 89124, Italy

Corresponding author: Luca De Luca, MD, Director, Doctor, Digestive Endoscopy Unit, ASST Santi Paolo e Carlo, Via Antonio di Rudinì 8, Milano 20144, Italy. lucadeluca1210@gmail.com

Abstract

Gastroenteropancreatic neuroendocrine neoplasms (GEP-NENs) are rare tumors derived from the neuroendocrine cell system, which that have increased in incidence and prevalence in recent years. Despite improvements in radiological and metabolic imaging, endoscopy still plays a pivotal role in the number of GEP-NENs. Tumor detection, characterization, and staging are essential in management and treatment planning. Upper and lower gastrointestinal (GI) endoscopy is essential for correct localization of the primary tumor site of GI NENs. Endoscopic ultrasonography (EUS) has an important role in the imaging and tissue acquisition of pancreatic NENs and locoregional staging of GI neuroendocrine tumors. Correct staging and histological diagnosis have important prognostic implications. Endoscopic operating techniques allow the removal of small GI NENs in the early stage of mucosal or submucosal invasion of the intestinal wall. Preoperative EUS-guided techniques may help the surgeon locate small and deep tumors, thus avoiding formal pancreatic resections in favor of parenchymal-sparing surgery. Finally, locoregional ablative treatments have been proposed in recent studies with promising results in selected patients.

Key Words: Neuroendocrine neoplasms; Gastrointestinal endoscopy; Endoscopic resection; Endoscopic ultrasound; Ablative technique; Tissue acquisition

©The Author(s) 2022. Published by Baishideng Publishing Group Inc. All rights reserved.

Core Tip: Gastroenteropancreatic neuroendocrine neoplasms (GEP-NENs) are complex neoplasms that present many clinical challenges. This review reports endoscopic management of patients with GEP-NENs. Endoscopic procedures allow diagnosis, local staging, and tissue acquisition. Early NENs of the stomach, duodenum, or rectum are generally removed by endoscopic operating techniques. New endoscopic ultrasonography-guided operative techniques may help the surgeon locate small and deep tumors or treat small pancreatic NENs.

Citation: Iabichino G, Di Leo M, Arena M, Rubis Passoni GG, Morandi E, Turpini F, Viaggi P, Luigiano C, De Luca L. Diagnosis, treatment, and current concepts in the endoscopic management of gastroenteropancreatic neuroendocrine neoplasms. *World J Gastroenterol* 2022; 28(34): 4943-4958
URL: https://www.wjgnet.com/1007-9327/full/v28/i34/4943.htm
DOI: https://dx.doi.org/10.3748/wjg.v28.i34.4943

INTRODUCTION

Gastroenteropancreatic neuroendocrine neoplasms (GEP-NENs) are rare neoplasms arising from neuroendocrine cells distributed in the GEP tract. Most commonly, the primary lesion is located in the gastric mucosa, small and large intestine, rectum, and pancreas[1].

The incidence of GEP-NENs has substantially increased over the last decades. Data from the Surveillance, Epidemiology, and End Results registry show that the incidence of GEP-NENs has increased 6.4 fold since the program's inception in 1973. This phenomenon may be related to the increasing number of radiological imaging and endoscopic examinations performed[1,2].

Approximately 15%-30% of GEP-NENs are functioning tumors with hormone-related symptoms; the remaining 70%-85% are nonfunctioning and detected incidentally or because the patient has symptoms of mass effects or distant metastases[3]. The management of GEP-NENs requires a multidisciplinary approach. Since GEP-NENs are less frequent than other malignancies, endoscopic management of these tumors may not be fully understood.

This review focuses on the endoscopic diagnosis and treatment of GEP-NENs.

Site

The GEP tract represents the most common localization of NENs. Gastrointestinal NENs (GI-NENs) develop from the stomach (23%), appendix (21%), small bowel (15%), and rectum (14%). Esophageal and colonic NENs are rare tumors that account for a small percentage of GI-NENs. Pancreatic NENs (Pan-NENs) represent about 1% of all pancreatic neoplasms but their prevalence is around 10%[1].

Grade

The World Health Organization subclassifies GEP-NENs based on the mitotic count and Ki-67 index (Table 1). This classification defines both well-differentiated neuroendocrine tumors (NETs) and poorly differentiated neuroendocrine carcinomas (NECs). NETs are divided into grade 1 (Ki-67 index < 3, mitotic rate < 2), grade 2 (Ki-67 index 3-20, mitotic rate 2-20), and grade 3 (Ki-67 index > 20, mitotic rate > 20). NECs exhibit poorly differentiated morphology with significant atypia and frequently have geographic necrosis. Tumors involving both neuroendocrine and non-neuroendocrine cells are classified as mixed NENs and non-NENs[4].

Staging

There are two major classifications in current clinical use: the European Neuroendocrine Tumor Society (ENETS) tumor, node and metastasis (TNM) system and the American Joint Committee on Cancer TNM system[5,6].

Functional status

Clinically, GEP-NENs can be classified into nonfunctioning and functioning tumors. The functioning tumors secrete substances that cause appreciable clinical symptoms, whereas the nonfunctioning neoplasms do not secrete any substance or the substance produced is inactive. The hormones produced and clinical symptoms vary by site of the primary GEP-NENs. Clinical symptoms include hypoglycemic syndrome, carcinoid syndrome, Zollinger-Ellison syndrome, watery diarrhea-hypokalemia-achlorhydria syndrome, and glucagonoma (Table 2)[7].

Biomarker levels

Chromogranin A is currently the most commonly used biomarker for GEP-NENs. It has a 10%-35% specificity, and its sensitivity ranges from 32% to 92%. Serotonin and its metabolite 5-hydroxyindole

Table 1 2019 World Health Organization classification of neuroendocrine neoplasms of the gastrointestinal tract and hepatopancreatobiliary organs

NENs	Differentiation	Grade	Mitotic rate	Ki-67 index %
NET, G1	Well differentiated	Low	< 2	< 3
NET, G2	Well differentiated	Intermediate	2-20	3-20
NET, G3	Well differentiated	High	> 20	> 20
NEC, small cell type	Poorly differentiated	High	> 20	> 20
NEC, large cell type	Poorly differentiated	High	> 20	> 20
MiNEN	Well or poorly differentiated	Variable	Variable	Variable

NEN: Neuroendocrine neoplasm; NET: Neuroendocrine tumor; NEC: Neuroendocrine carcinoma; MiNEN: Mixed neuroendocrine-non-neuroendocrine neoplasm.

Table 2 The hormones produced by the primary gastroenteropancreatic neuroendocrine neoplasms

Tissue	Hormones	Symptoms/Syndrome
Gastric	Histamine, CGA	Atypical flush, wheeze, angioedema
Duodenal	CGA, somatostatin, gastrin	Cholelithiasis, steatorrhea, diabetes, ZE syndrome (gastrinoma)
Jejuno-ileal, appendiceal, cecal	Serotonin, CGA, pancreastatin	Carcinoid syndrome
Colorectal	Pancreatic polypeptide	No hormonal symptoms
Pancreatic	Insulin	Recurrent hypoglycemia
	Glucagon	Diarrhea, glossitis, necrolytic migratory erythema, weight loss, hyperglycemia, blood clots
	VIP	Diarrhea, hypokalemia, achlorhydria
	ACTH	Cushingoid facies, weight gain, diabetes, hypertension
	GHRH	Acromegalic features, diabetes
	PTHRP	Hypercalcemia
	Gastrin	Pain, diarrhea (ZE syndrome)
	Somatostatin	Diabetes, cholelithiasis, steatorrhea, weight loss
	Serotonin	Flushing, diarrhea (carcinoid syndrome)

5HIAA: 5-hydroxyindoleacetic acid; ACTH: Adrenocorticotrophic hormone; CGA: Chromogranin A; F-PNET: Functional pancreatic neuroendocrine tumor; GHRH: Growth hormone releasing hormone; MEN1: Multiple endocrine neoplasia type 1; NF1: Neurofibromatosis type 1; PTHRP: Parathyroid hormone-related peptide; VIP: Vasoactive intestinal polypeptide; ZE: Zollinger Ellison.

acetic acid have been measured in blood and urine samples, respectively, as markers of carcinoid syndrome. However, the sensitivity of this biomarker is as low as 35% in the absence of carcinoid syndrome[8].

Several other potential biomarkers include neuron-specific enolase, human chorionic gonadotropin, alpha-fetoprotein, and pancreatic polypeptide. These circulating biomarkers are useful to aid diagnosis, but are of insufficient value to accurately identify the primary tumor site, correlate with tumor grade, and differentiate low-level malignancy from high-grade disease[9].

In recent years, new biomarkers have been evaluated that may correlate with clinical outcomes and be useful as better prognostic indicators. These include microRNAs, long noncoding RNAs, circulating tumor cells, and DNA methylation patterns[10].

Any associated syndromes

Most GEP-NENs are sporadic, but they also can arise as part of inherited familial syndromes. About 5% of patients with GEP-NENs harbor genomic mutations with well-characterized familial syndromes such as multiple endocrine neoplasia type 1 (MEN1), von Hippel-Lindau (VHL) disease, tuberous sclerosis (TSC), and neurofibromatosis type 1 (NF1)[11].

MEN1 is an autosomal-dominant syndrome, characterized by NENs of the anterior pituitary, parathyroid glands, and pancreas. VHL syndrome is an autosomal-dominant syndrome characterized by a variety of benign and malignant neoplasms including clear renal cell carcinomas, pheochromocytomas, hemangioblastomas, retinal angiomas, paragangliomas, and pNENs. TSC is an autosomal-dominant syndrome characterized by widespread, low-grade tumors, and hamartomas in multiple organs including the brain, heart, skin, eyes, kidney, lung, and liver. pNENs are described in only 1% to 5% of cases. NF1 is an autosomal-dominant syndrome characterized by ubiquitous neurofibromas; multiple cafe-au-lait skin spots; and susceptibility to gliomas, myeloid leukemia, pheochromocytomas, and occasionally pNENs[12].

DIAGNOSIS

Gastric NENs

Gastric NENs (G-NENs) are neoplasms derived from the enterochromaffin-like cells of the gastric mucosa. They are classified into types I, II and III according to their clinical and pathophysiological characteristics (Table 3)[13].

Type I G-NENs correspond to the majority of G-NENs found in the stomach (70%-80%) and are associated with autoimmune chronic atrophic gastritis and hypergastrinemia, type II G-NENs lesions are caused by gastrinomas and commonly found in patients with Zollinger-Ellison syndrome (ZES) and MEN1, and type III G-NENs lesions consist of a sporadic lesion and are unrelated to gastrin hypersecretion.

Patients with G-NENs typically present with nonspecific symptoms and the diagnosis is made by upper gastrointestinal (GI) endoscopy for symptoms such as abdominal pain, nausea, bleeding, and anemia. Despite the low incidence of G-NET, recent data have demonstrated an increase due to an expanding use of upper endoscopy, improvement of endoscopes, and more attention to identification and characterization of gastric lesion[14]. Type I G-NENs occur in the corpus and/or fundus and are multiple small reddish polyps, usually subcentimetrics. They are associated with a chronic atrophic gastritis with an excellent prognosis. Tumor extension is limited to the mucosa or submucosa.

Type II G-NENs are similar to type I lesions but the adjacent gastric folds have a hypertrophic gastric mucosa and occasionally have multiple areas of ulceration of gastric and duodenal mucosa. Type II G-NENs are involved in MEN1 and ZES and have a good prognosis, similar to type I. Type III G-NENs are single, large (> 2 cm), sometimes ulcerated, more aggressive and associated with local and distant spread, and involve the muscular layer (Figure 1)[15]. The prognosis of this subgroup is poor.

At the time of diagnosis, biopsy samples should be taken from the lesions and multiple gastric biopsies (antrum, body, and fundus) should be performed for etiologic orientation.

Endoscopic ultrasonography (EUS) should be performed if the lesion is greater than 1 cm in order to assess the layer of origin, tumor size, echogenicity, margins, wall invasion, and regional lymph nodes. At EUS, G-NENs present as rounded isoechoic or hypoechoic tumors, localized in the second (deeper mucosal) or third (submucosal) echo layers. EUS diagnostic accuracy for evaluation of subepithelial lesion including G-NET is suboptimal (43%-67%)[16]. EUS is a very accurate technique for assessing tumor size and muscularis propria integrity, factors that seem to condition the potential for distant metastasis[17].

In type I and II G-NENs, staging EUS is frequently performed to evaluate indication to endoscopic treatment. For patients suspected of having type II G-NENs, EUS evaluation must be performed for the assessment of any duodenal or Pan-NENs. In Type III G-NENs, EUS is indicated to stage the disease by assessing the presence of regional lymph node involvement[18].

Duodenal NENs

Duodenal NENs (D-NENs) are solitary, small lesions generally discovered incidentally on imaging studies or endoscopy. They are generally classified into five different tumor types: duodenal gastrinomas, somatostatinomas, nonfunctional D-NENs, duodenal gangliocytic paragangliomas, and high-grade poorly differentiated NEC[19].

Most D-NENs are localized predominantly in the first and second duodenal portion and are nonfunctioning with a low risk of local or distant metastases. Functioning D-NENs are typically associated with higher metastatic power. The presence of multiple D-NENs should raise suspicion of MEN1-ZES[19].

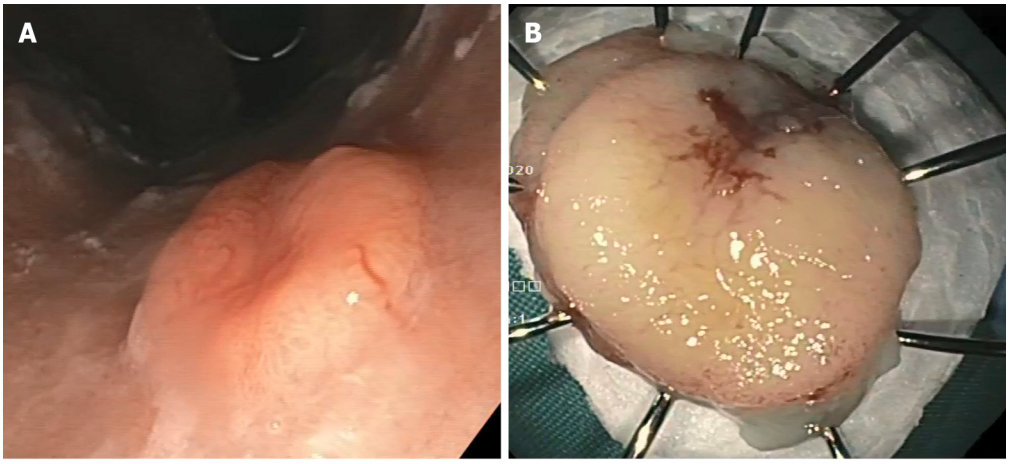
D-NENs located in the ampullary/periampullary region have more aggressive behavior and poorer overall survival than D-NENs located elsewhere in the duodenum[20,21].

On upper GI endoscopy, D-NENs have the appearance of submucosal tumors with a surface color often identical to the surrounding mucosa (Figure 2). As the tumor enlarges, a depression may form in the center, which is eventually replaced by an ulcer crater[22].

EUS evaluation is useful for duodenal subepithelial lesions characterization; the accuracy of combined endoscopic/EUS imaging for all duodenal lesions is 84.9%[23].

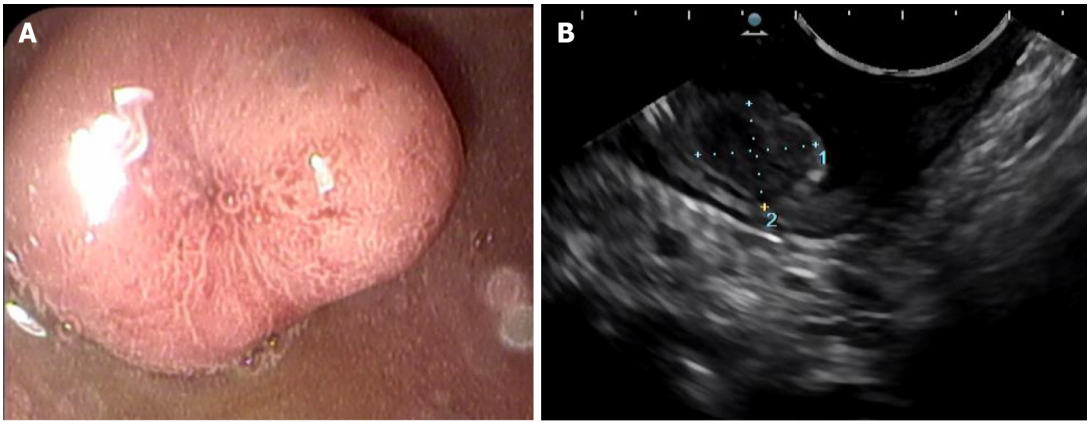
Table 3 Characteristics of the subtypes of neuroendocrine neoplasms of the stomach

Characteristics	Type I	Type II	Type III
Prevalence	70%-80%	5%-10%	10%-20%
Background	Autoimmune chronic atrophic gastritis	Gastrinomas (Zollinger-Ellison syndrome)	Normal mucosa
Number of lesions	Multiple	Multiple	Single
Size of tumors	1-2 cm	1 cm	> 2 cm
Site of tumor	Corpus and/or fundus	Corpus and/or fundus	Anywhere
Serum gastrin levels	Elevated	Elevated	Normal
Gastric pH	High	Low	Normal
Invasion	Rare	More common	Common
Prognosis (5-yr survival)	Excellent (90%-95%)	Good (70%-90%)	Worse (less than 35%)



DOI: 10.3748/wjg.v28.i34.4943 **Copyright** ©The Author(s) 2022.

Figure 1 Gastric neuroendocrine neoplasm. A: Endoscopic image demonstrates a flat lesion in the stomach fundus with depressed center; B: Endoscopic en bloc resection was achieved.



DOI: 10.3748/wjg.v28.i34.4943 **Copyright** ©The Author(s) 2022.

Figure 2 Duodenal neuroendocrine neoplasm. A: Endoscopic image demonstrates a sessile polyp with central depression; B: Endoscopic ultrasound demonstrates a hypoechoic intramural structure in the submucosal layer of the duodenal wall.

EUS is also useful to exclude locoregional lymph node metastases and thus the indication for endoscopic mucosal resection in case of lesions > 1 cm. At EUS evaluation, D-NENs are usually located in the submucosal layer and are rounded, hypoechoic, well-demarcated small lesions. Fine needle aspiration (FNA) should also be performed in cases of nondiagnostic histopathology[18]. Duoden-

oscopy and EUS are indicated to identify the primary tumor in the case of ZES and in patients with MEN1[24].

Small bowel NENs

Small bowel NENs (SB-NENs) are the most common NENs developing distant metastases; however, their prognosis remains favorable[25]. They tend to present in later stages because clinical symptoms are often insidious and the diagnosis often occurs in the course of an intervention for intestinal obstruction or bleeding[26].

Accurate localization and staging of SB-NENs often involve a combination of several imaging modalities. Endoscopic examinations such as capsule endoscopy and double-balloon enteroscopy are useful in identifying occult SB-NENs when no primary tumor was found on conventional imaging. Macroscopically, most SB-NENs are sessile nodules or ulcerated lesions usually measuring between 1 and 2 cm or as multiple tumors[27,28].

Appendix NENs

Appendiceal NENs (A-NENs) are usually discovered incidentally at final pathological examination after an appendectomy is performed for acute appendicitis. Colonoscopic examination of the entire large bowel is mandatory given the frequency of synchronous colorectal neoplasia[27]. A-NENs usually have a good prognosis. In most cases, appendicectomy alone is considered curative; however, in selected cases with high malignant potential, the right hemicolectomy could be considered[29].

Colorectal NENs

Colonic NENs (C-NENs) and rectal NENs (R-NENs) are two different clinical entities. C-NENs have more aggressive features and much worse prognosis than R-NENs[30]. Nearly 70% of C-NENs are located in the ascending colon, particularly in the cecum with a mean size of 5 cm at presentation. The patients generally experience late symptoms such as abdominal pain, GI bleeding, and weight loss, and most of them have local or distant metastasis[15].

Most R-NENs are diagnosed through screening sigmoidoscopy and/or colonoscopy while only a small fraction have symptoms such as diarrhea, abdominal pain, or rectal bleeding.

The majority of R-NENs are small size lesions less than 1 cm and only 5% present are larger than 2 cm [31].

Endoscopically, R-NENs appear as sessile or semipedunculated polypoid lesions with normal or a yellow-discolored mucosa, frequently located in the midrectum. Larger lesions can have different endoscopic characteristics such as ulcerations, depressions or hyperemic color, which can be suggestive of aggressive disease[30].

At EUS, R-NENs have the aspect of nodular, hypoechoic, or isoechoic submucosal tumor clearly demarcated from the surrounding tissue[18].

EUS-FNA can be helpful to make a differential diagnosis with other subephitelial lesion[32] with a diagnostic accuracy of 85.1%[33].

According to the current ENETS consensus, an EUS should also be performed in order to assess the depth of rectal wall invasion and regional lymphadenopathy prior to endoscopic resection[34].

A complete colonoscopy is indicated after a diagnosis of a R-NENs to exclude concomitant colon cancer and other NENs[35].

Pan-NENs

Pan-NENs comprise 1% to 2% of pancreatic neoplasms[36]. Pan-NENs are classified as functioning or nonfunctioning depending on whether they cause hormonal overproduction syndrome. Functioning Pan-NENs include insulinoma, gastrinoma, VIPoma, and glucagonoma. Nonfunctioning Pan-NENs comprise the largest group of Pan-NENs and do not produce syndromes of hormonal excess. Nonfunctioning Pan-NENs often manifest later in the course of the disease or are discovered incidentally during abdominal imaging examinations performed for other diseases[37].

EUS is a very useful tool in the management of Pan-NENs and has been considered the imaging study of choice to be performed after other negative noninvasive imaging studies are negative[38].

Puli *et al*[39] assessed the diagnostic accuracy of EUS for detection of Pan-NENs. This meta-analysis demonstrated an excellent accuracy of EUS in this setting with a sensitivity of 87.2% and a specificity of 98.0%.

A meta-analysis of 2015 assessed incremental benefit of preoperative EUS for the detection of suspected Pan-NENs after other investigative modalities have been attempted. EUS increased the overall Pan-NENs detection by over 25% and was particularly useful in functioning Pan-NENs, typically smaller in size (*i.e.* insulinomas or gastrinoma)[40].

EUS is also very useful in assessing the presence of multiple lesions, size lesion and especially the distance between the lesion and the main pancreatic duct, a factor that can drive the decision on which surgical approach (*i.e.* enucleation *vs* resection)[18]. Pancreatic enucleation is commonly performed for Pan-NENs with a low risk of malignant progression but post-operative pancreatic fistula risk is higher for neoplasms located close to the duct[41].

EUS is of course useful for differential diagnosis of Pan-NENs with other solid pancreatic lesions. Pan-NENs are solid lesions and on EUS examination, appear as well-demarcated, hypoechoic lesions with a homogeneous pattern. However, because Pan-NENs grow expansively, they may also appear as cystic or indistinguishable from pancreatic adenocarcinomas.

In Pan-NENs EUS guided tissue acquisition is considered the procedure of choice to reach cytologic diagnosis, but also ascertainment of tumor grade by determining the Ki-67 proliferation index and mitotic count (Figure 3).

EUS-FNA provides a cytological specimen with a sensitivity ranging between 80% and 90%, specificity at 96%[18]. The adequacy and concordance of Ki-67 evaluation of EUS-FNA compared with histology remains unclear especially for tumor > 20 mm[42,43]. To overcome these limitations of cytological Ki-67 determination, sampling with needles for EUS-guided fine-needle biopsy (EUS-FNB) have been introduced with good results[44,45]. In a recent retrospective study EUS-FNB outperformed EUS-FNA for Ki-67 proliferation index determination[46].

EUS elastography (EUS-E) is a newer tool of diagnostic EUS for differential diagnosis of solid pancreatic lesions. It is a technique that analyzes pancreatic stiffness being a useful tool for the differential diagnosis of pancreatic masses with a qualitative or quantitative elastographic assessment. A meta-analysis by Zhang *et al*[47] showed a sensitivity and specificity of quantitative EUS-E for the differentiation of benign and malignant pancreatic masses of 0.95 and 0.61, respectively. Iglesias-García *et al*[48] evaluated the accuracy of quantitative EUS-E for the differential diagnosis of solid pancreatic masses. EUS-E was helpful in differentiating pancreatic cancer from Pan-NENs with a sensitivity of 100% and a specificity of 88%. In another study, elastographic analysis was accurate in discriminating between benign and malignant pancreatic lesions, without difference between NENs and other nonmalignant lesions[49].

Recently, shear wave elastography (SWE) has been introduced as a quantitative absolute measurement of tissue hardness. Ohno *et al*[50] compared the diagnostic performances of EUS-SWE and conventional strain elastography for solid pancreatic lesions without significant differences.

To date EUS-E does not provide sufficient diagnostic accuracy to replace tissue diagnosis but it plays a significant role in those cases of suspected pancreatic cancer where biopsy sampling was inconclusive and can help to select the area of the pancreatic lesion to be sampled[51].

Contrast-enhanced EUS (CE-EUS) consists of an intravenous injection of contrast media during the EUS examination so parenchymal perfusion and the microvasculature of the pancreas can be visualized. Pancreatic cancer is observed as a hypoenhanced heterogeneous lesion whereas Pan-NENs are observed as well-demarcated lesions with hyperenhancement in the arterial phase.

CE-EUS increased the accuracy of EUS for both the detection and characterization of solid pancreatic lesions[52].

Kitano *et al*[53] prospectively evaluated how accurately CE-EUS characterizes pancreatic lesions and hyperenhanced lesions were diagnosed as Pan-NENs with a sensitivity of 79% and specificity of 99%. Several studies have examined CE-EUS in the differentiation between malignant and benign Pan-NENs [39,40]. Heterogeneous enhancement at an early arterial phase with fewer vessels and more fibrosis is associated with an aggressive tumor[54]. Palazzo *et al*[55] reported a sensitivity of 86% and a specificity of 96% in prediction tumor aggressiveness in Pan-NENs with the use of CE-EUS.

NET could be found also in the bile ducts[56]; however, the incidence is very low. In the literature, only 100 cases of biliary tree NETs were described and they have an excellent prognosis[57]. In these cases, complete surgical excision offers optimal treatment with no evidence of chemotherapy or radiotherapy's role in the management.

ENDOSCOPIC THERAPY

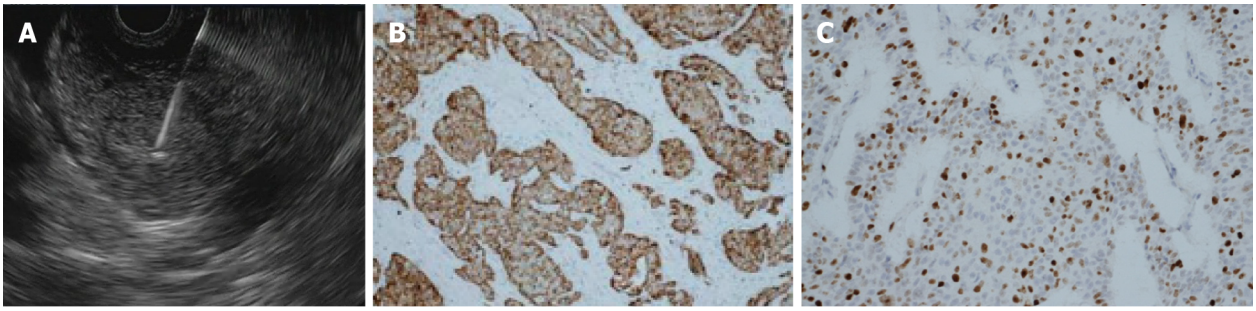
In the last 10 years, the approach of GEP-NENs progressively included endoscopic resection technique. The choice of the treatment modality needs of a careful assessment and depends by multiple factors. The indication of endoscopic respective therapy does not include NET of appendix, colon and biliary tree while for pancreatic NET the suitable endoscopic approaches are ablative techniques.

G-NENs

Most type I G-NENs are limited to the mucosa or submucosa and they rarely invade the muscularis propria or metastasize to local lymph nodes if < 10 mm. Current guidelines suggested removing all tumors ≥ 10 mm[16]. EUS is recommended to identify possible involvement of regional lymph nodes and invasion beyond the submucosa prior to resection. Endoscopic resection (ER) either by endoscopic mucosal resection (EMR) or endoscopic submucosal dissection (ESD) is the treatment of choice when EUS demonstrates the lesion to be localized to the mucosa or submucosa[58].

Surgical treatment is the option for lesions which are predicted to be T2 (lesion larger than 20 mm or grading G3) or lesions with positive margins[58].

Sato *et al*[59] showed in a low number of cases that about 66% of type I G-NENs resected by EMR had a positive vertical margin, whereas no case with ESD had positive vertical or horizontal margins. Kim *et*



DOI: 10.3748/wjg.v28.i34.4943 **Copyright** ©The Author(s) 2022.

Figure 3 Pancreatic neuroendocrine neoplasm. A: Endoscopic ultrasound revealed a 15 mm hypoechoic lesion of the pancreas; B: Stained immunohistochemically for chromogranin showing diffuse and strong positivity (original magnification 400 ×), consistent with a poorly differentiated neuroendocrine tumor infiltrating the entire thickness of the muscle tissue to the head of the pancreas; C: The proliferation index (Ki-67) < 20%.

al[60] evaluated the clinical usefulness of ESD with that of EMR for resection of type I G-NENs with an estimated size of ≤ 10 mm. ESD yielded a significantly higher histologic complete resection rate than EMR, particularly in the vertical resection margin.

Noh *et al*[61] evaluated outcomes of endoscopic treatment for type 1 G-NENs below 20 mm in diameter. The complete resection rate was significantly higher in the ESD group than in the EMR group with similar procedure-related adverse events. For type II G-NENs local or limited excision can be recommended and indication for treatment type is similar to type 1 G-NENs[24,62]. Type III G-NENs are more associated with deeper invasion of the gastric wall, higher risk of nodal metastasis than type I and II G-NENs and surgery is considered the initial therapeutic approach[58]. ER has been proposed for small lesions. Kwon *et al*[63] investigated the clinical outcomes of type 3 G-NENs (mean tumor size of 10.2 ± 6.3 mm) after endoscopic treatment with a median follow-up of 46 mo. Of the 45 included in the follow-up, no evidence of tumor recurrence was found. Authors concluded that endoscopic treatment could be applied for type 3 G-NENs smaller than 2 cm, confined in the submucosal layer and without lymphovascular invasion. In Figure 4, we summarize the current recommendations for G-NENs.

D-NENs

Most D-NENs are located in the first or second part of the duodenum, with 20% of them occurring in the periampullary region[21]. Current guidelines indicate ER for small (≤ 10 mm) nonperiampullary D-NENs confined to the submucosal layer, without lymph node or distant metastasis. Either endoscopic or surgical resection is allowed, for nonperiampullary D-NENs measuring 10-20 mm without metastatic risk (G1, no muscolaris invasion, no lymph-vascular invasion and no lymph-node metastasis)[24,58].

There are different ER techniques, such as cap technique, EMR, EMR with ligation device and ESD [58].

Gincul *et al*[64] evaluated the feasibility and outcome of endoscopic treatment of D-NENs (including 7 ampullary G1/G2 NETs with ≤ 20 mm) with EMR. The resection rate was R0 only in 51.6% (16/31) of patients. During a median follow-up period of 56 mo, 2 patients (8.3%) presented a tumor recurrence. Morbidity was 38 % (11/29) and mortality was 3% (one severe bleeding).

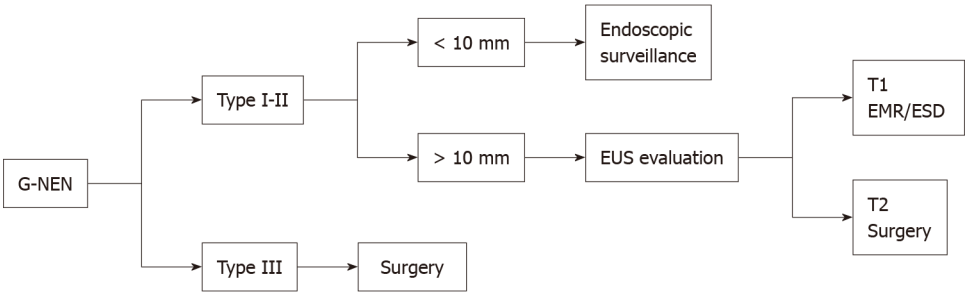
Nishio *et al*[65] assessed the efficacy, safety and the long-term outcomes of ESD for nonperiampullary D-NENs ≤ 10 mm in diameter. En bloc, R0 and curative resection were achieved in 100% (8/8), 88% (7/8), and 88% (7/8) of tumors, respectively. During a median follow-up of 34.0 mo none of the patients showed evidence of local recurrence or distant metastasis. Perforation occurred in 2 patients (16%) without need for surgery.

In a recent review, Brito *et al*[66] evaluated the effectiveness and complications of ER techniques in patients with D-NETs ≤ 20 mm. Polypectomy was associated with a high occurrence of incomplete resections. Among the mucosectomies, EMR with cap or EMR with injection was associated with lower frequencies of compromised margin and recurrent surgery. Endoscopic submucosal dissection was not associated with recurrence but it was associated with a higher occurrence of bleeding and perforation.

ER of D-NENs is complex and associated with significant morbidity. EMR is associated with a lower R0 resection rate than ESD. ESD is associated with better pathologically confirmed resection but with a higher morbidity rate and should be restricted to expert centers[67]. ESGE guidelines suggests choosing between EMR, ESD, and endoscopic full thickness resection (EFTR) to resect nonampullary, nonfunctional duodenal NENs of < 15 mm, depending on size, location, depth of invasion, and local expertise [16].

Ampullary D-NENs have a less favorable prognosis than nonampullary D-NENs and pancreaticoduodenectomy is recommended regardless of size[24].

Local resection might be sufficient for small highly differentiated ampullary D-NENs without node metastases especially in patients with comorbidities[24].



DOI: 10.3748/wjg.v28.i34.4943 **Copyright** ©The Author(s) 2022.

Figure 4 Algorithm for gastric neuroendocrine neoplasm management. EMR: Endoscopic mucosal resection; ESD: Endoscopic submucosal dissection; EUS: Endoscopic ultrasonography; G-NEN: Gastric neuroendocrine neoplasm.

In one of the largest studies of EMR of D-NENs above reported, Gincul *et al*[64] included 7 ampullary G1/G2 D-NENs with ≤ 20 mm. In this subgroup of patients, R0 resection was achieved in 5 patients (71%) without recurrence with a median follow-up period of 56 mo.

Shimai *et al*[68] reported 3 patients with an ampullary D-NENS, who underwent endoscopic papillectomy without tumor recurrence or metastasis after a follow-up of 2 years. In Figure 5, we summarize the current recommendations for D-NENs.

R-NENs

The current guidelines recommend ER for R-NENs < 10 mm in size with no risk factors for metastasis. R-NENs larger than 20 mm are candidates for surgical resection. There is controversy over R-NENs of intermediate size 10-19 mm (Figure 6). R-NENs with these sizes have a poorer prognosis compared with those < 10 mm[34]. The main factors associated with the risk of lymph-node metastases are atypical endoscopic aspect (presence of mucosal depression or ulceration), suspicious pararectal lymph node at EUS, invasion of the muscularis propria, G2, and lymphovascular invasion. Rectal NET with any risk factor for metastasis should be considered for surgical resection with lymphadenoctomy. For lesions measuring 10-19 mm without factors associated with metastatic risk the most appropriate resection techniques may be ESD or transanal endoscopic microsurgery (TEM)[24-34].

The appropriate endoscopic technique resection should allow for en bloc oncological excision. Optimal endoscopic treatment modality for R-NENs has not yet been achieved.

Conventional polypectomy is associated with a low rate of complete resection as most of the R-NENs are submucosal. Son *et al*[69] reported a complete resection rate by conventional polypectomy of 30.9%.

EMR is simple and has low complication rates but can sometimes cause incomplete resection and difficulty in pathologic evaluation because even small R-NENs can invade the submucosa. Several studies, assessing efficacy of EMR, have reported complete resection rates ranging from 30%-70%[70-74].

Therefore, several m-EMR methods have been reported and included cap-assisted EMR (EMR-C), EMR with a ligating device (EMR-L), and EMR after circumferential precutting (EMR-P).

EMR-L is performed suctioning the lesion into the ligating device and cutting by using a round snare after placing bands around the base of tissue suctioned. EMR-C is performed with a transparent cap fitted to the scope, followed by snare cautery resection. These techniques allow the cutting of the submucosal layer from the muscularis propria[75].

Lee *et al*[75] performed a retrospective study comparing EMR-L and EMR-C, concluding that EMR-L may achieve both a higher endoscopic rate and a histologic complete resection rate. An analysis of 17 studies reported that the complete resection rate of R-NENs using EMR-L was 94.8% compared with 72.4% for EMR-C[76].

EMR-P is performed by lifting the mucosa with a saline injection, making a circumferential incision using the tip of the snare or special endoknives and resecting the tumor with a snare. This technique has the advantages, unlike the other m-EMR procedures, of not being affected by lesion size. Several studies have investigated the usefulness of EMR-P for resection of R-NENs showing a complete resection rate from 81.2% to 96.7% with a short procedure time, and an acceptable safety profile[77-79].

Recently Park *et al*[80] evaluated the safety and efficacy of underwater endoscopic mucosal resection in the treatment of small R-NENs (< 10 mm) with high R0 resection rates similar to ESD.

ESD is an advanced endoscopic technique employing a submucosal injection to lift the lesion away from the muscularis propria layer. Dedicated devices are then used to dissect around the entire lesion in the submucosal plane. This technique results in a high en bloc resection rate although more complicated, time consuming and with higher risk of complications than EMR and m-EMR[81].

Zhou *et al*[82] performed a meta-analysis comparing ESD with EMR and m-EMR in the treatment of R-NENs smaller than 15 mm in diameter. Complete resection rate was significantly higher in the ESD group than in the EMR group and comparable between the ESD group and the m-EMR group. A recent meta-analysis compared efficacy of ESD and EMR in curing R-NENs. This study showed that ESD is

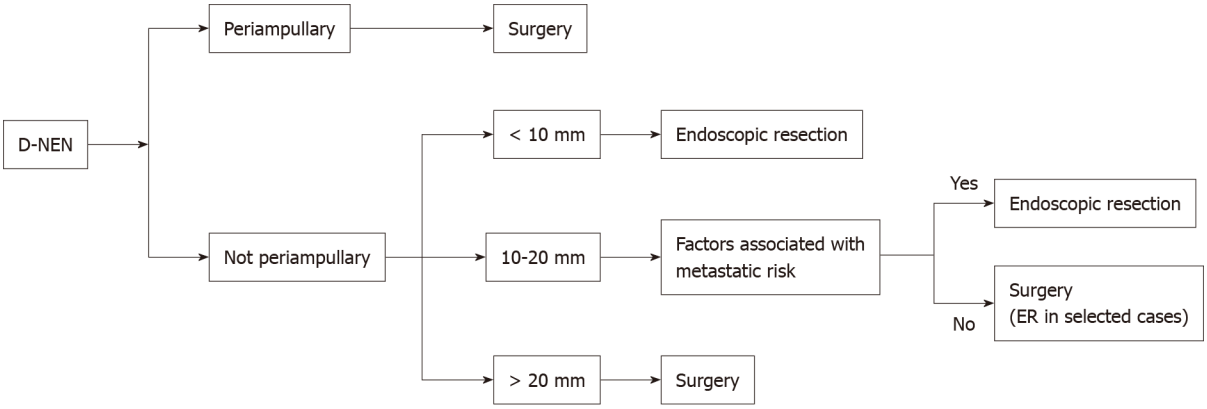


Figure 5 Algorithm for duodenal neuroendocrine neoplasms management. D-NEN: Duodenal neuroendocrine neoplasm; ER: Endoscopic resection.

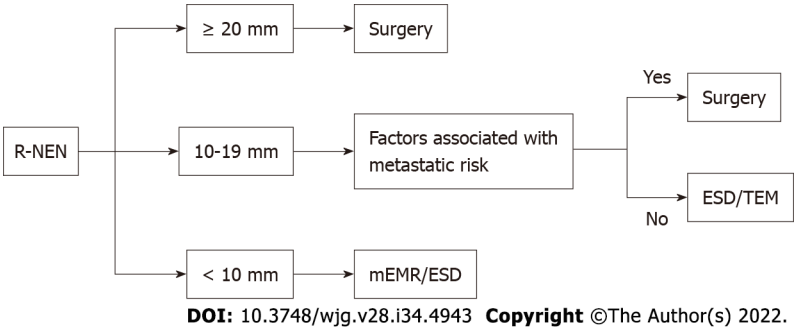


Figure 6 Algorithm for rectal neuroendocrine neoplasms management. ESD: Endoscopic submucosal dissection; mEMR: Modified endoscopic mucosal resection; R-NEN: Rectal neuroendocrine neoplasm; TEM: Transanal endoscopic microsurgery.

more effective in curing R-NENs of 10-20 mm in size than EMR without significant differences for R-NENs smaller than 10 mm[83].

In patients with an incomplete resection from EMR techniques, ESD may be indicated as salvage therapy[24,84].

A recent new endoscopic technique is EFTR, which is performed using a full thickness resection device (FTRD). The FTRD uses a transparent cap with a modified over-the-scope clip (OTSC) mounted over a standard colonoscope. The lesion is pulled into the cap and the pseudopolyp created by the OTSC closure is then resected with the snare preloaded in the tip of the cap. Meier *et al*[85] conducted a study evaluating EFTR in 40 cases of R-NENs showing effectiveness of this method (R0 resection rate in 95%) in addition to feasibility (median time, 18.5 min) and safety.

Pan-NENs

Patients with small Pan-NENs are candidates for pancreatic-sparing procedures such as central pancreatectomy or enucleation. Small Pan-NENs can be difficult to detect intra-operatively by palpation only. EUS-guided techniques to facilitate small Pan-NENs localization especially during laparoscopy surgery are tattooing or fiducial markers implantation. These techniques allow a precise localization of lesions ensuring adequate margins of resection and preserving normal pancreatic parenchyma[86].

Endoscopic ultrasound-guided fine needle tattooing (EUS-FNT) is a safe, easy to perform and useful new method to mark preoperatively small Pan-NENs. Generally, a 22-gauge standard needle allows easy injection of the tattooing solution. The needle is inserted inside the target lesion or immediately near the lesion borders into the normal parenchyma. The most frequently solution utilized is a sterile carbon-based ink which is nondegradable and remains in the tissues indefinitely[87].

Recently Rosa *et al*[88] evaluated EUS-FNT in facilitating intra-operative detection of Pan-NENs (8 insulinoma and 8 nonfunctional Pan-NENs.) The tattoo mark was detected in all but one patient. Only a small hematoma secondary to the EUS-FNT was observed.

The placement of fiducial markers implantation under EUS guidance is another technique to facilitate Pan-NENs localization during surgery. Fiducials are implantable radiographic markers that have been used for many years to mark soft tissue in radiology. The fiducial is easily visible during an intraoperative ultrasound[86].

Law *et al*[89] reported on two consecutive patients with small Pan-NENs who underwent fiducial placement. In both of the reported cases, the fiducials were visualized by intraoperative ultrasound, and the surgical resection was successful without procedure-related complications.

In recent years endoscopic ultrasound-guided ablation therapy has emerged as a new therapeutic option for solid pancreatic tumors, especially for Pan-NENs in elderly patients and candidates unfit for surgery. There are two main techniques used, EUS-guided radiofrequency ablation (EUS-RFA) and EUS-guided ethanol ablation (EUS-EA)[90]. Functioning and multiple Pan-NENs seem to be the ideal target for endoscopic ultrasound -guided ablation therapy resolving symptomatic hormonal syndromes. In case of nonfunctioning Pan-NENs, these techniques could be a therapeutic option in the case of patients unfit to surgery[91].

EUS-EA can be safe and useful for the control of symptoms in patients with small insulinomas[91-93].

Jürgensen *et al*[92] reported the first case of EUS–EA of a 13 mm pancreatic insulinoma in a 78-year-old woman. The patient exhibited no further hypoglycemic episodes with no recurrence of the tumor on follow-up.

Levy *et al*[93] reported a small series of 5 patients for EUS-EA of insulinomas; they observed that symptomatic relief was relieved almost immediately after the procedure and maintained during the follow-up.

Qin *et al*[94] reported a series of 4 patients for EUS-EA of insulinomas with no recurrence of hypoglycemia and complications during follow-up.

Choi *et al*[95] reported the largest cohort of 32 patients with nonfunctioning Pan-NENs treated with EUS–EA. In 24 out of 40 tumors (60%) complete ablation was achieved.

The other less invasive locoregional therapy for Pan-NENs is EUS-RFA. Multiple case reports of EUS-RFA of insulinomas showed complete regression of the clinical syndrome[96-98].

Regarding nonfunctioning Pan-NENs, Barthet *et al*[99] conducted a prospective multicenter study including 12 patients with 14 Pan-NENs (mean size 13.1 mm) treated with EUS-RFA. Among the 14 Pan-NENs, at 1-year follow-up, 12 had completely disappeared (86% tumor resolution). Two adverse events occurred (one pancreatitis, one pancreatic ductal stenosis). Another case series included 11 patients with nonfunctioning Pan-NENs. A complete radiological response was achieved in 8 of 11 patients treated with EUS-RFA. Two cases of mild pancreatitis occurred[100].

CONCLUSION

GEP-NENs are on the rise. The reasons for this phenomenon are a better awareness of an increased and more widespread use of GI endoscopy and advanced radiological imaging[1]. The overall survival rate for patients with GEP-NENs has improved in the last years[2]. This achievement is due to both early detection and better therapeutic strategies of GEP-NENs.

Endoscopy is the only method of choice to detect asymptomatic GI-NENs at an early stage. Most patients with early, GI-NENs can be treated with ER or surveillance.

Pan-NENs are relatively rare tumors but their number is increasing, mainly because of the advances in various diagnostic imaging modalities as EUS. Newer advancement in the field of EUS such as the evolution of needles, EUS-E and CE-EUS can provide useful information with an improvement in the management of Pan-NENs. EUS-guided tumor ablation therapies can be a therapeutic option in selected patients unfit for surgery.

The literature evidence on this field is growing every day. For the nature of our study (mini-review) and the very wide issue, we collected and summarized the most important evidence regarding the endoscopic treatment underlying current guideline. We believe that a systematic review the literature with meta-analysis (when applicable) for every specific GI-NENs is needed to prove and confirm the role of endoscopy in diagnosis and therapy of many types of GI-NENs.

FOOTNOTES

Author contributions: All authors made substantial contributions to the conception of the study and literature search, drafted the manuscript or revised it critically for important intellectual content, and approved the final version of the manuscript to be published.

Conflict-of-interest statement: The authors have no conflicts of interest to declare.

Open-Access: This article is an open-access article that was selected by an in-house editor and fully peer-reviewed by external reviewers. It is distributed in accordance with the Creative Commons Attribution NonCommercial (CC BY-NC 4.0) license, which permits others to distribute, remix, adapt, build upon this work non-commercially, and license their derivative works on different terms, provided the original work is properly cited and the use is non-commercial. See: https://creativecommons.org/Licenses/by-nc/4.0/

Country/Territory of origin: Italy

ORCID number: Giuseppe Iabichino 0000-0003-3786-7292; Milena Di Leo 0000-0002-5933-8474; Monica Arena 0000-0002-2958-3655; Giovanni Giuseppe Rubis Passoni 0000-0001-9934-8311; Elisabetta Morandi 0000-0002-5568-5831; Francesca Turpini 0000-0002-4408-0810; Paolo Viaggi 0000-0002-3467-7031; Carmelo Luigiano 0000-0001-5719-3948; Luca De Luca 0000-0002-3290-3103.

S-Editor: Zhang H
L-Editor: Filipodia
P-Editor: Zhang H

REFERENCES

1 **Niederle MB**, Hackl M, Kaserer K, Niederle B. Gastroenteropancreatic neuroendocrine tumours: the current incidence and staging based on the WHO and European Neuroendocrine Tumour Society classification: an analysis based on prospectively collected parameters. *Endocr Relat Cancer* 2010; **17**: 909-918 [PMID: 20702725 DOI: 10.1677/ERC-10-0152]
2 **Dasari A**, Shen C, Halperin D, Zhao B, Zhou S, Xu Y, Shih T, Yao JC. Trends in the Incidence, Prevalence, and Survival Outcomes in Patients With Neuroendocrine Tumors in the United States. *JAMA Oncol* 2017; **3**: 1335-1342 [PMID: 28448665 DOI: 10.1001/jamaoncol.2017.0589]
3 **Milan SA**, Yeo CJ. Neuroendocrine tumors of the pancreas. *Curr Opin Oncol* 2012; **24**: 46-55 [PMID: 22080942 DOI: 10.1097/CCO.0b013e32834c554d]
4 **Nagtegaal ID**, Odze RD, Klimstra D, Paradis V, Rugge M, Schirmacher P, Washington KM, Carneiro F, Cree IA; WHO Classification of Tumours Editorial Board. The 2019 WHO classification of tumours of the digestive system. *Histopathology* 2020; **76**: 182-188 [PMID: 31433515 DOI: 10.1111/his.13975]
5 **Luo G**, Javed A, Strosberg JR, Jin K, Zhang Y, Liu C, Xu J, Soares K, Weiss MJ, Zheng L, Wolfgang CL, Cives M, Wong J, Wang W, Sun J, Shao C, Tan H, Li J, Ni Q, Shen L, Chen M, He J, Chen J, Yu X. Modified Staging Classification for Pancreatic Neuroendocrine Tumors on the Basis of the American Joint Committee on Cancer and European Neuroendocrine Tumor Society Systems. *J Clin Oncol* 2017; **35**: 274-280 [PMID: 27646952 DOI: 10.1200/JCO.2016.67.8193]
6 **Amin MB**, Greene FL, Edge SB, Compton CC, Gershenwald JE, Brookland RK, Meyer L, Gress DM, Byrd DR, Winchester DP. The Eighth Edition AJCC Cancer Staging Manual: Continuing to build a bridge from a population-based to a more "personalized" approach to cancer staging. *CA Cancer J Clin* 2017; **67**: 93-99 [PMID: 28094848 DOI: 10.3322/caac.21388]
7 **Dillon JS**. Workup of Gastroenteropancreatic Neuroendocrine Tumors. *Surg Oncol Clin N Am* 2020; **29**: 165-183 [PMID: 32151354 DOI: 10.1016/j.soc.2019.10.002]
8 **Fang JM**, Li J, Shi J. An update on the diagnosis of gastroenteropancreatic neuroendocrine neoplasms. *World J Gastroenterol* 2022; **28**: 1009-1023 [PMID: 35431496 DOI: 10.3748/wjg.v28.i10.1009]
9 **Oberg K**, Modlin IM, De Herder W, Pavel M, Klimstra D, Frilling A, Metz DC, Heaney A, Kwekkeboom D, Strosberg J, Meyer T, Moss SF, Washington K, Wolin E, Liu E, Goldenring J. Consensus on biomarkers for neuroendocrine tumour disease. *Lancet Oncol* 2015; **16**: e435-e446 [PMID: 26370353 DOI: 10.1016/S1470-2045(15)00186-2]
10 **Sansone A**, Lauretta R, Vottari S, Chiefari A, Barnabei A, Romanelli F, Appetecchia M. Specific and Non-Specific Biomarkers in Neuroendocrine Gastroenteropancreatic Tumors. *Cancers (Basel)* 2019; **11** [PMID: 31382663 DOI: 10.3390/cancers11081113]
11 **Fernandez CJ**, Agarwal M, Pottakkat B, Haroon NN, George AS, Pappachan JM. Gastroenteropancreatic neuroendocrine neoplasms: A clinical snapshot. *World J Gastrointest Surg* 2021; **13**: 231-255 [PMID: 33796213 DOI: 10.4240/wjgs.v13.i3.231]
12 **Cives M**, Strosberg JR. Gastroenteropancreatic Neuroendocrine Tumors. *CA Cancer J Clin* 2018; **68**: 471-487 [PMID: 30295930 DOI: 10.3322/caac.21493]
13 **Rindi G**, Luinetti O, Cornaggia M, Capella C, Solcia E. Three subtypes of gastric argyrophil carcinoid and the gastric neuroendocrine carcinoma: a clinicopathologic study. *Gastroenterology* 1993; **104**: 994-1006 [PMID: 7681798 DOI: 10.1016/0016-5085(93)90266-f]
14 **Basuroy R**, Srirajaskanthan R, Prachalias A, Quaglia A, Ramage JK. Review article: the investigation and management of gastric neuroendocrine tumours. *Aliment Pharmacol Ther* 2014; **39**: 1071-1084 [PMID: 24628514 DOI: 10.1111/apt.12698]
15 **Ahmed M**. Gastrointestinal neuroendocrine tumors in 2020. *World J Gastrointest Oncol* 2020; **12**: 791-807 [PMID: 32879660 DOI: 10.4251/wjgo.v12.i8.791]
16 **Deprez PH**, Moons LMG, O'Toole D, Gincul R, Seicean A, Pimentel-Nunes P, Fernández-Esparrach G, Polkowski M, Vieth M, Borbath I, Moreels TG, Nieveen van Dijkum E, Blay JY, van Hooft JE. Endoscopic management of subepithelial lesions including neuroendocrine neoplasms: European Society of Gastrointestinal Endoscopy (ESGE) Guideline. *Endoscopy* 2022; **54**: 412-429 [PMID: 35180797 DOI: 10.1055/a-1751-5742]
17 **Varas MJ**, Gornals JB, Pons C, Espinós JC, Abad R, Lorente FJ, Bargalló D. Usefulness of endoscopic ultrasonography (EUS) for selecting carcinoid tumors as candidates to endoscopic resection. *Rev Esp Enferm Dig* 2010; **102**: 577-582 [PMID: 21039065 DOI: 10.4321/s1130-01082010001000002]
18 **Zilli A**, Arcidiacono PG, Conte D, Massironi S. Clinical impact of endoscopic ultrasonography on the management of neuroendocrine tumors: lights and shadows. *Dig Liver Dis* 2018; **50**: 6-14 [PMID: 29102525 DOI:

10.1016/j.dld.2017.10.007]
19 **Hoffmann KM**, Furukawa M, Jensen RT. Duodenal neuroendocrine tumors: Classification, functional syndromes, diagnosis and medical treatment. *Best Pract Res Clin Gastroenterol* 2005; **19**: 675-697 [PMID: 16253893 DOI: 10.1016/j.bpg.2005.05.009]
20 **Yao JC**, Hassan M, Phan A, Dagohoy C, Leary C, Mares JE, Abdalla EK, Fleming JB, Vauthey JN, Rashid A, Evans DB. One hundred years after "carcinoid": epidemiology of and prognostic factors for neuroendocrine tumors in 35,825 cases in the United States. *J Clin Oncol* 2008; **26**: 3063-3072 [PMID: 18565894 DOI: 10.1200/JCO.2007.15.4377]
21 **Randle RW**, Ahmed S, Newman NA, Clark CJ. Clinical outcomes for neuroendocrine tumors of the duodenum and ampulla of Vater: a population-based study. *J Gastrointest Surg* 2014; **18**: 354-362 [PMID: 24114680 DOI: 10.1007/s11605-013-2365-4]
22 **Sato Y**, Hashimoto S, Mizuno K, Takeuchi M, Terai S. Management of gastric and duodenal neuroendocrine tumors. *World J Gastroenterol* 2016; **22**: 6817-6828 [PMID: 27570419 DOI: 10.3748/wjg.v22.i30.6817]
23 **Pavlovic Markovic A**, Rösch T, Alempijevic T, Krstic M, Tomic D, Dugalic P, Sokic Milutinovic A, Bulajic M. Endoscopic ultrasound for differential diagnosis of duodenal lesions. *Ultraschall Med* 2012; **33**: E210-E217 [PMID: 23129520 DOI: 10.1055/s-0032-1313135]
24 **de Mestier L**, Lepage C, Baudin E, Coriat R, Courbon F, Couvelard A, Do Cao C, Frampas E, Gaujoux S, Gincul R, Goudet P, Lombard-Bohas C, Poncet G, Smith D, Ruszniewski P, Lecomte T, Bouché O, Walter T, Cadiot G; Thésaurus National de Cancérologie Digestive (TNCD). Digestive Neuroendocrine Neoplasms (NEN): French Intergroup clinical practice guidelines for diagnosis, treatment and follow-up (SNFGE, GTE, RENATEN, TENPATH, FFCD, GERCOR, UNICANCER, SFCD, SFED, SFRO, SFR). *Dig Liver Dis* 2020; **52**: 473-492 [PMID: 32234416 DOI: 10.1016/j.dld.2020.02.011]
25 **Scott AT**, Howe JR. Management of Small Bowel Neuroendocrine Tumors. *Surg Oncol Clin N Am* 2020; **29**: 223-241 [PMID: 32151357 DOI: 10.1016/j.soc.2019.11.006]
26 **Scott AT**, Howe JR. Management of Small Bowel Neuroendocrine Tumors. *J Oncol Pract* 2018; **14**: 471-482 [PMID: 30096273 DOI: 10.1200/JOP.18.00135]
27 **Hirabayashi K**, Zamboni G, Nishi T, Tanaka A, Kajiwara H, Nakamura N. Histopathology of gastrointestinal neuroendocrine neoplasms. *Front Oncol* 2013; **3**: 2 [PMID: 23346552 DOI: 10.3389/fonc.2013.00002]
28 **Sivero L**, Telesca DA, Ruggiero S, Russo T, Amato M, Bianco T, Amato B, Formisano C, Avellino M, Napolitano V. Endoscopic diagnosis and treatment of neuroendocrine tumors of the digestive system. *Open Med (Wars)* 2016; **11**: 369-373 [PMID: 28352822 DOI: 10.1515/med-2016-0067]
29 **Toumpanakis C**, Fazio N, Tiensuu Janson E, Hörsch D, Pascher A, Reed N, O Apos Toole D, Nieveen van Dijkum E, Partelli S, Rinke A, Kos-Kudla B, Costa F, Pape UF, Grozinsky-Glasberg S, Scoazec JY; The ENETS 2016 Munich Advisory Board Participants; ENETS 2016 Munich Advisory Board Participants. Unmet Needs in Appendiceal Neuroendocrine Neoplasms. *Neuroendocrinology* 2019; **108**: 37-44 [PMID: 30235454 DOI: 10.1159/000493894]
30 **Broecker JS**, Ethun CG, Postlewait LM, Le N, McInnis M, Russell MC, Sullivan P, Kooby DA, Staley CA, Maithel SK, Cardona K. Colon and Rectal Neuroendocrine Tumors: Are They Really One Disease? *Am Surg* 2018; **84**: 717-726 [PMID: 29966574 DOI: 10.1177/000313481808400525]
31 **McDermott FD**, Heeney A, Courtney D, Mohan H, Winter D. Rectal carcinoids: a systematic review. *Surg Endosc* 2014; **28**: 2020-2026 [PMID: 24584484 DOI: 10.1007/s00464-014-3430-0]
32 **Cazacu IM**, Singh BS, Luzuriaga Chavez AA, Koduru P, Ejaz S, Weston BR, Ross WA, Lee JH, Roy-Chowdhuri S, Bhutani MS. EUS and EUS-guided FNA/core biopsies in the evaluation of subepithelial lesions of the lower gastrointestinal tract: 10-year experience. *Endosc Ultrasound* 2020; **9**: 329-336 [PMID: 32913150 DOI: 10.4103/eus.eus_51_20]
33 **Chen HT**, Xu GQ, Teng XD, Chen YP, Chen LH, Li YM. Diagnostic accuracy of endoscopic ultrasonography for rectal neuroendocrine neoplasms. *World J Gastroenterol* 2014; **20**: 10470-10477 [PMID: 25132764 DOI: 10.3748/wjg.v20.i30.10470]
34 **Caplin M**, Sundin A, Nillson O, Baum RP, Klose KJ, Kelestimur F, Plöckinger U, Papotti M, Salazar R, Pascher A; Barcelona Consensus Conference participants. ENETS Consensus Guidelines for the management of patients with digestive neuroendocrine neoplasms: colorectal neuroendocrine neoplasms. *Neuroendocrinology* 2012; **95**: 88-97 [PMID: 22261972 DOI: 10.1159/000335594]
35 **Kamp K**, Damhuis RA, Feelders RA, de Herder WW. Occurrence of second primary malignancies in patients with neuroendocrine tumors of the digestive tract and pancreas. *Endocr Relat Cancer* 2012; **19**: 95-99 [PMID: 22194442 DOI: 10.1530/ERC-11-0315]
36 **Ito T**, Sasano H, Tanaka M, Osamura RY, Sasaki I, Kimura W, Takano K, Obara T, Ishibashi M, Nakao K, Doi R, Shimatsu A, Nishida T, Komoto I, Hirata Y, Nakamura K, Igarashi H, Jensen RT, Wiedenmann B, Imamura M. Epidemiological study of gastroenteropancreatic neuroendocrine tumors in Japan. *J Gastroenterol* 2010; **45**: 234-243 [PMID: 20058030 DOI: 10.1007/s00535-009-0194-8]
37 **Massironi S**, Sciola V, Peracchi M, Ciafardini C, Spampatti MP, Conte D. Neuroendocrine tumors of the gastro-entero-pancreatic system. *World J Gastroenterol* 2008; **14**: 5377-5384 [PMID: 18803349 DOI: 10.3748/wjg.14.5377]
38 **Falconi M**, Eriksson B, Kaltsas G, Bartsch DK, Capdevila J, Caplin M, Kos-Kudla B, Kwekkeboom D, Rindi G, Klöppel G, Reed N, Kianmanesh R, Jensen RT; Vienna Consensus Conference participants. ENETS Consensus Guidelines Update for the Management of Patients with Functional Pancreatic Neuroendocrine Tumors and Non-Functional Pancreatic Neuroendocrine Tumors. *Neuroendocrinology* 2016; **103**: 153-171 [PMID: 26742109 DOI: 10.1159/000443171]
39 **Puli SR**, Kalva N, Bechtold ML, Pamulaparthy SR, Cashman MD, Estes NC, Pearl RH, Volmar FH, Dillon S, Shekleton MF, Forcione D. Diagnostic accuracy of endoscopic ultrasound in pancreatic neuroendocrine tumors: a systematic review and meta analysis. *World J Gastroenterol* 2013; **19**: 3678-3684 [PMID: 23801872 DOI: 10.3748/wjg.v19.i23.3678]
40 **James PD**, Tsolakis AV, Zhang M, Belletrutti PJ, Mohamed R, Roberts DJ, Heitman SJ. Incremental benefit of preoperative EUS for the detection of pancreatic neuroendocrine tumors: a meta-analysis. *Gastrointest Endosc* 2015; **81**: 848-56.e1 [PMID: 25805462 DOI: 10.1016/j.gie.2014.12.031]

41 **Giuliani T**, Marchegiani G, Girgis MD, Crinò SF, Muthusamy VR, Bernardoni L, Pea A, Ramera M, Paiella S, Landoni L, Gabbrielli A, Salvia R, Donahue TR, Bassi C. Endoscopic placement of pancreatic stent for "Deep" pancreatic enucleations operative technique and preliminary experience at two high-volume centers. *Surg Endosc* 2020; **34**: 2796-2802 [PMID: 32180000 DOI: 10.1007/s00464-020-07501-y]

42 **Paiella S**, Landoni L, Rota R, Valenti M, Elio G, Crinò SF, Manfrin E, Parisi A, Cingarlini S, D'Onofrio M, Scarpa A, Lawlor RT, Bernardoni L, Capelli P, Nessi C, Miotto M, Gabbrielli A, Bassi C, Salvia R. Endoscopic ultrasound-guided fine-needle aspiration for the diagnosis and grading of pancreatic neuroendocrine tumors: a retrospective analysis of 110 cases. *Endoscopy* 2020; **52**: 988-994 [PMID: 32498099 DOI: 10.1055/a-1180-8614]

43 **Boutsen L**, Jouret-Mourin A, Borbath I, van Maanen A, Weynand B. Accuracy of Pancreatic Neuroendocrine Tumour Grading by Endoscopic Ultrasound-Guided Fine Needle Aspiration: Analysis of a Large Cohort and Perspectives for Improvement. *Neuroendocrinology* 2018; **106**: 158-166 [PMID: 28494461 DOI: 10.1159/000477213]

44 **Leeds JS**, Nayar MK, Bekkali NLH, Wilson CH, Johnson SJ, Haugk B, Darne A, Oppong KW. Endoscopic ultrasound-guided fine-needle biopsy is superior to fine-needle aspiration in assessing pancreatic neuroendocrine tumors. *Endosc Int Open* 2019; **7**: E1281-E1287 [PMID: 31579710 DOI: 10.1055/a-0990-9611]

45 **Kamata K**, Ashida R, Yasukawa S, Chiba Y, Fukutake N, Nebiki H, Kurita A, Takaoka M, Ogura T, Shiomi H, Asada M, Yasuda H, Shigekawa M, Yanagisawa A, Kudo M, Kitano M. Histological diagnosis and grading of pancreatic neuroendocrine tumor by endoscopic ultrasound-guided fine needle biopsy using a 25-gauge needle with a core trap: A multicenter prospective trial. *Pancreatology* 2020; **20**: 1428-1433 [PMID: 32952043 DOI: 10.1016/j.pan.2020.08.023]

46 **Crinò SF**, Ammendola S, Meneghetti A, Bernardoni L, Conti Bellocchi MC, Gabbrielli A, Landoni L, Paiella S, Pin F, Parisi A, Mastrosimini MG, Amodio A, Frulloni L, Facciorusso A, Larghi A, Manfrin E. Comparison between EUS-guided fine-needle aspiration cytology and EUS-guided fine-needle biopsy histology for the evaluation of pancreatic neuroendocrine tumors. *Pancreatology* 2021; **21**: 443-450 [PMID: 33390343 DOI: 10.1016/j.pan.2020.12.015]

47 **Zhang B**, Zhu F, Li P, Yu S, Zhao Y, Li M. Endoscopic ultrasound elastography in the diagnosis of pancreatic masses: A meta-analysis. *Pancreatology* 2018; **18**: 833-840 [PMID: 30093353 DOI: 10.1016/j.pan.2018.07.008]

48 **Iglesias-Garcia J**, Larino-Noia J, Abdulkader I, Forteza J, Dominguez-Munoz JE. Quantitative endoscopic ultrasound elastography: an accurate method for the differentiation of solid pancreatic masses. *Gastroenterology* 2010; **139**: 1172-1180 [PMID: 20600020 DOI: 10.1053/j.gastro.2010.06.059]

49 **Carrara S**, Di Leo M, Grizzi F, Correale L, Rahal D, Anderloni A, Auriemma F, Fugazza A, Preatoni P, Maselli R, Hassan C, Finati E, Mangiavillano B, Repici A. EUS elastography (strain ratio) and fractal-based quantitative analysis for the diagnosis of solid pancreatic lesions. *Gastrointest Endosc* 2018; **87**: 1464-1473 [PMID: 29329992 DOI: 10.1016/j.gie.2017.12.031]

50 **Ohno E**, Kawashima H, Ishikawa T, Iida T, Suzuki H, Uetsuki K, Yashika J, Yamada K, Yoshikawa M, Gibo N, Aoki T, Kataoka K, Mori H, Yamamura T, Furukawa K, Nakamura M, Hirooka Y, Fujishiro M. Diagnostic performance of endoscopic ultrasonography-guided elastography for solid pancreatic lesions: Shear-wave measurements versus strain elastography with histogram analysis. *Dig Endosc* 2021; **33**: 629-638 [PMID: 32662150 DOI: 10.1111/den.13791]

51 **Cosgrove D**, Piscaglia F, Bamber J, Bojunga J, Correas JM, Gilja OH, Klauser AS, Sporea I, Calliada F, Cantisani V, D'Onofrio M, Drakonaki EE, Fink M, Friedrich-Rust M, Fromageau J, Havre RF, Jenssen C, Ohlinger R, Săftoiu A, Schaefer F, Dietrich CF; EFSUMB. EFSUMB guidelines and recommendations on the clinical use of ultrasound elastography. Part 2: Clinical applications. *Ultraschall Med* 2013; **34**: 238-253 [PMID: 23605169 DOI: 10.1055/s-0033-1335375]

52 **He XK**, Ding Y, Sun LM. Contrast-enhanced endoscopic ultrasound for differential diagnosis of pancreatic cancer: an updated meta-analysis. *Oncotarget* 2017; **8**: 66392-66401 [PMID: 29029521 DOI: 10.18632/oncotarget.18915]

53 **Kitano M**, Kudo M, Yamao K, Takagi T, Sakamoto H, Komaki T, Kamata K, Imai H, Chiba Y, Okada M, Murakami T, Takeyama Y. Characterization of small solid tumors in the pancreas: the value of contrast-enhanced harmonic endoscopic ultrasonography. *Am J Gastroenterol* 2012; **107**: 303-310 [PMID: 22008892 DOI: 10.1038/ajg.2011.354]

54 **Takada S**, Kato H, Saragai Y, Muro S, Uchida D, Tomoda T, Matsumoto K, Horiguchi S, Tanaka N, Okada H. Contrast-enhanced harmonic endoscopic ultrasound using time-intensity curve analysis predicts pathological grade of pancreatic neuroendocrine neoplasm. *J Med Ultrason (2001)* 2019; **46**: 449-458 [PMID: 31377939 DOI: 10.1007/s10396-019-00967-x]

55 **Palazzo M**, Napoléon B, Gincul R, Pioche M, Pujol B, Lefort C, Fumex F, Hautefeuille V, Fabre M, Cros J, Felce M, Couvelard A, Sauvanet A, Lévy P, Ruszniewski P, Palazzo L. Contrast harmonic EUS for the prediction of pancreatic neuroendocrine tumor aggressiveness (with videos). *Gastrointest Endosc* 2018; **87**: 1481-1488 [PMID: 29325706 DOI: 10.1016/j.gie.2017.12.033]

56 **De Luca L**, Tommasoni S, de Leone A, Bianchi ML, de Nictolis M, Baroncini D. Neuroendocrine tumor of the extrahepatic bile duct: a tumor in an unusual site visualized by cholangioscopy. *Endoscopy* 2013; **45** Suppl 2: E338-E339 [PMID: 24150737 DOI: 10.1055/s-0032-1326453]

57 **Altiti M**, Al-Sa'afin AJ, Al-Tawarah T, Suleihat A, Abulhaj S, Mahseeri M. Biliary tree neuroendocrine tumor, an incidental finding. *Int J Surg Case Rep* 2021; **82**: 105940 [PMID: 33964717 DOI: 10.1016/j.ijscr.2021.105940]

58 **Delle Fave G**, O'Toole D, Sundin A, Taal B, Ferolla P, Ramage JK, Ferone D, Ito T, Weber W, Zheng-Pei Z, De Herder WW, Pascher A, Ruszniewski P; Vienna Consensus Conference participants. ENETS Consensus Guidelines Update for Gastroduodenal Neuroendocrine Neoplasms. *Neuroendocrinology* 2016; **103**: 119-124 [PMID: 26784901 DOI: 10.1159/000443168]

59 **Sato Y**, Takeuchi M, Hashimoto S, Mizuno K, Kobayashi M, Iwafuchi M, Narisawa R, Aoyagi Y. Usefulness of endoscopic submucosal dissection for type I gastric carcinoid tumors compared with endoscopic mucosal resection. *Hepatogastroenterology* 2013; **60**: 1524-1529 [PMID: 23933946 DOI: 10.5754/hge121185]

60 **Kim HH**, Kim GH, Kim JH, Choi MG, Song GA, Kim SE. The efficacy of endoscopic submucosal dissection of type I gastric carcinoid tumors compared with conventional endoscopic mucosal resection. *Gastroenterol Res Pract* 2014; **2014**: 253860 [PMID: 24693280 DOI: 10.1155/2014/253860]

61 **Noh JH**, Kim DH, Yoon H, Hsing LC, Na HK, Ahn JY, Lee JH, Jung KW, Choi KD, Song HJ, Lee GH, Jung HY.

Clinical Outcomes of Endoscopic Treatment for Type 1 Gastric Neuroendocrine Tumor. *J Gastrointest Surg* 2021; **25**: 2495-2502 [PMID: 33825119 DOI: 10.1007/s11605-021-04997-0]

62 **De Luca L**, Di Berardino M, Mangiavillano B, Repici A. Gastric endoscopic submucosal dissection in Western countries: Indications, applications, efficacy and training perspective. *World J Gastrointest Surg* 2021; **13**: 1180-1189 [PMID: 34754386 DOI: 10.4240/wjgs.v13.i10.1180]

63 **Kwon YH**, Jeon SW, Kim GH, Kim JI, Chung IK, Jee SR, Kim HU, Seo GS, Baik GH, Choi KD, Moon JS. Long-term follow up of endoscopic resection for type 3 gastric NET. *World J Gastroenterol* 2013; **19**: 8703-8708 [PMID: 24379589 DOI: 10.3748/wjg.v19.i46.8703]

64 **Gincul R**, Ponchon T, Napoleon B, Scoazec JY, Guillaud O, Saurin JC, Ciocirlan M, Lepilliez V, Pioche M, Lefort C, Adham M, Pialat J, Chayvialle JA, Walter T. Endoscopic treatment of sporadic small duodenal and ampullary neuroendocrine tumors. *Endoscopy* 2016; **48**: 979-986 [PMID: 27494453 DOI: 10.1055/s-0042-112570]

65 **Nishio M**, Hirasawa K, Ozeki Y, Sawada A, Ikeda R, Fukuchi T, Kobayashi R, Makazu M, Sato C, Maeda S. Short- and long-term outcomes of endoscopic submucosal dissection for non-ampullary duodenal neuroendocrine tumors. *Ann Gastroenterol* 2020; **33**: 265-271 [PMID: 32382229 DOI: 10.20524/aog.2020.0477]

66 **Brito HP**, Torres IT, Turke KC, Parada AA, Waisberg J, Botelho RV. Comparison of endoscopic resection techniques for duodenal neuroendocrine tumors: systematic review. *Endosc Int Open* 2021; **9**: E1214-E1221 [PMID: 34447867 DOI: 10.1055/a-1487-5594]

67 **Amoyel M**, Belle A, Dhooge M, Ali EA, Hallit R, Prat F, Dohan A, Terris B, Chaussade S, Coriat R, Barret M. Endoscopic management of non-ampullary duodenal adenomas. *Endosc Int Open* 2022; **10**: E96-E108 [PMID: 35047339 DOI: 10.1055/a-1723-2847]

68 **Shimai S**, Yamamoto K, Sofuni A, Tsuchiya T, Ishii K, Tanaka R, Tonozuka R, Honjo M, Mukai S, Fujita M, Nagai K, Asai Y, Matsunami Y, Kurosawa T, Kojima H, Honma H, Minami H, Yamaguchi H, Itoi T. Three Cases of Ampullary Neuroendocrine Tumor Treated by Endoscopic Papillectomy: A Case Report and Literature Review. *Intern Med* 2020; **59**: 2369-2374 [PMID: 32611953 DOI: 10.2169/internalmedicine.4568-20]

69 **Son HJ**, Sohn DK, Hong CW, Han KS, Kim BC, Park JW, Choi HS, Chang HJ, Oh JH. Factors associated with complete local excision of small rectal carcinoid tumor. *Int J Colorectal Dis* 2013; **28**: 57-61 [PMID: 22821140 DOI: 10.1007/s00384-012-1538-z]

70 **Kim KM**, Eo SJ, Shim SG, Choi JH, Min BH, Lee JH, Chang DK, Kim YH, Rhee PL, Kim JJ, Rhee JC, Kim JY. Treatment outcomes according to endoscopic treatment modalities for rectal carcinoid tumors. *Clin Res Hepatol Gastroenterol* 2013; **37**: 275-282 [PMID: 22959100 DOI: 10.1016/j.clinre.2012.07.007]

71 **Yang DH**, Park Y, Park SH, Kim KJ, Ye BD, Byeon JS, Myung SJ, Yang SK. Cap-assisted EMR for rectal neuroendocrine tumors: comparisons with conventional EMR and endoscopic submucosal dissection (with videos). *Gastrointest Endosc* 2016; **83**: 1015-22; quiz 1023 [PMID: 26460225 DOI: 10.1016/j.gie.2015.09.046]

72 **Nakamura K**, Osada M, Goto A, Iwasa T, Takahashi S, Takizawa N, Akahoshi K, Ochiai T, Nakamura N, Akiho H, Itaba S, Harada N, Iju M, Tanaka M, Kubo H, Somada S, Ihara E, Oda Y, Ito T, Takayanagi R. Short- and long-term outcomes of endoscopic resection of rectal neuroendocrine tumours: analyses according to the WHO 2010 classification. *Scand J Gastroenterol* 2016; **51**: 448-455 [PMID: 26540372 DOI: 10.3109/00365521.2015.1107752]

73 **Jeon JH**, Cheung DY, Lee SJ, Kim HJ, Kim HK, Cho HJ, Lee IK, Kim JI, Park SH, Kim JK. Endoscopic resection yields reliable outcomes for small rectal neuroendocrine tumors. *Dig Endosc* 2014; **26**: 556-563 [PMID: 24447261 DOI: 10.1111/den.12232]

74 **Kim HH**, Park SJ, Lee SH, Park HU, Song CS, Park MI, Moon W. Efficacy of endoscopic submucosal resection with a ligation device for removing small rectal carcinoid tumor compared with endoscopic mucosal resection: analysis of 100 cases. *Dig Endosc* 2012; **24**: 159-163 [PMID: 22507089 DOI: 10.1111/j.1443-1661.2011.01190.x]

75 **Lee J**, Park YE, Choi JH, Heo NY, Park J, Park SH, Moon YS, Nam KH, Kim TO. Comparison between cap-assisted and ligation-assisted endoscopic mucosal resection for rectal neuroendocrine tumors. *Ann Gastroenterol* 2020; **33**: 385-390 [PMID: 32624659 DOI: 10.20524/aog.2020.0485]

76 **de Mestier L**, Brixi H, Gincul R, Ponchon T, Cadiot G. Updating the management of patients with rectal neuroendocrine tumors. *Endoscopy* 2013; **45**: 1039-1046 [PMID: 24163193 DOI: 10.1055/s-0033-1344794]

77 **Cheung DY**, Choi SK, Kim HK, Kim SS, Chae HS, Seo KJ, Cho YS. Circumferential submucosal incision prior to endoscopic mucosal resection provides comparable clinical outcomes to submucosal dissection for well-differentiated neuroendocrine tumors of the rectum. *Surg Endosc* 2015; **29**: 1500-1505 [PMID: 25277474 DOI: 10.1007/s00464-014-3831-0]

78 **So H**, Yoo SH, Han S, Kim GU, Seo M, Hwang SW, Yang DH, Byeon JS. Efficacy of Precut Endoscopic Mucosal Resection for Treatment of Rectal Neuroendocrine Tumors. *Clin Endosc* 2017; **50**: 585-591 [PMID: 29020763 DOI: 10.5946/ce.2017.039]

79 **Huang J**, Lu ZS, Yang YS, Yuan J, Wang XD, Meng JY, Du H, Wang HB. Endoscopic mucosal resection with circumferential incision for treatment of rectal carcinoid tumours. *World J Surg Oncol* 2014; **12**: 23 [PMID: 24472342 DOI: 10.1186/1477-7819-12-23]

80 **Park SS**, Han KS, Kim B, Chang Kim B, Hong CW, Sohn DK, Chang HJ. Comparison of underwater endoscopic mucosal resection and endoscopic submucosal dissection of rectal neuroendocrine tumors (with videos). *Gastrointest Endosc* 2020; **91**: 1164-1171.e2 [PMID: 31904380 DOI: 10.1016/j.gie.2019.12.039]

81 **Maione F**, Chini A, Milone M, Gennarelli N, Manigrasso M, Maione R, Cassese G, Pagano G, Tropeano FP, Luglio G, De Palma GD. Diagnosis and Management of Rectal Neuroendocrine Tumors (NETs). *Diagnostics (Basel)* 2021; **11** [PMID: 33923121 DOI: 10.3390/diagnostics11050771]

82 **Zhou X**, Xie H, Xie L, Li J, Cao W, Fu W. Endoscopic resection therapies for rectal neuroendocrine tumors: a systematic review and meta-analysis. *J Gastroenterol Hepatol* 2014; **29**: 259-268 [PMID: 24118068 DOI: 10.1111/jgh.12395]

83 **Yong JN**, Lim XC, Nistala KRY, Lim LKE, Lim GEH, Quek J, Tham HY, Wong NW, Tan KK, Chong CS. Endoscopic submucosal dissection versus endoscopic mucosal resection for rectal carcinoid tumor. A meta-analysis and meta-regression with single-arm analysis. *J Dig Dis* 2021; **22**: 562-571 [PMID: 34472210 DOI: 10.1111/1751-2980.13048]

84 **Ramage JK**, De Herder WW, Delle Fave G, Ferolla P, Ferone D, Ito T, Ruszniewski P, Sundin A, Weber W, Zheng-Pei Z, Taal B, Pascher A; Vienna Consensus Conference participants. ENETS Consensus Guidelines Update for Colorectal Neuroendocrine Neoplasms. *Neuroendocrinology* 2016; **103**: 139-143 [PMID: 26730835 DOI: 10.1159/000443166]

85 **Meier B**, Albrecht H, Wiedbrauck T, Schmidt A, Caca K. Full-thickness resection of neuroendocrine tumors in the rectum. *Endoscopy* 2020; **52**: 68-72 [PMID: 31614372 DOI: 10.1055/a-1008-9077]

86 **Melita G**, Pallio S, Tortora A, Crinò SF, Macrì A, Dionigi G. Diagnostic and Interventional Role of Endoscopic Ultrasonography for the Management of Pancreatic Neuroendocrine Neoplasms. *J Clin Med* 2021; **10** [PMID: 34203922 DOI: 10.3390/jcm10122638]

87 **Rimbas M**, Larghi A, Fusaroli P, Dong Y, Hollerbach S, Jenssen C, Săftoiu A, Sahai AV, Napoleon B, Arcidiacono PG, Braden B, Burmeister S, Carrara S, Cui XW, Hocke M, Iglesias-Garcia J, Kitano M, Oppong KW, Sun S, Di Leo M, Petrone MC, B Teoh AY, Dietrich CF. How to perform EUS-guided tattooing? *Endosc Ultrasound* 2020; **9**: 291-297 [PMID: 32883923 DOI: 10.4103/eus.eus_44_20]

88 **Rosa F**, Rimbaș M, Rizzatti G, Quero G, Fiorillo C, Impagnatiello M, D'Aversa F, Costamagna G, Alfieri S, Larghi A. EUS-guided fine needle tattooing (EUS-FNT) for preoperative localization of small pancreatic neuroendocrine tumors (p-NETs): a single-center experience. *Surg Endosc* 2021; **35**: 486-492 [PMID: 32959183 DOI: 10.1007/s00464-020-07996-5]

89 **Law JK**, Singh VK, Khashab MA, Hruban RH, Canto MI, Shin EJ, Saxena P, Weiss MJ, Pawlik TM, Wolfgang CL, Lennon AM. Endoscopic ultrasound (EUS)-guided fiducial placement allows localization of small neuroendocrine tumors during parenchymal-sparing pancreatic surgery. *Surg Endosc* 2013; **27**: 3921-3926 [PMID: 23636530 DOI: 10.1007/s00464-013-2975-7]

90 **Zhang L**, Tan S, Huang S, Zhong C, Lü M, Peng Y, Tang X. The safety and efficacy of endoscopic ultrasound-guided ablation therapy for solid pancreatic tumors: a systematic review. *Scand J Gastroenterol* 2020; **55**: 1121-1131 [PMID: 32730715 DOI: 10.1080/00365521.2020.1797870]

91 **Testoni SGG**, Healey AJ, Dietrich CF, Arcidiacono PG. Systematic review of endoscopy ultrasound-guided thermal ablation treatment for pancreatic cancer. *Endosc Ultrasound* 2020; **9**: 83-100 [PMID: 32295966 DOI: 10.4103/eus.eus_74_19]

92 **Jürgensen C**, Schuppan D, Neser F, Ernstberger J, Junghans U, Stölzel U. EUS-guided alcohol ablation of an insulinoma. *Gastrointest Endosc* 2006; **63**: 1059-1062 [PMID: 16733126 DOI: 10.1016/j.gie.2005.10.034]

93 **Levy MJ**, Thompson GB, Topazian MD, Callstrom MR, Grant CS, Vella A. US-guided ethanol ablation of insulinomas: a new treatment option. *Gastrointest Endosc* 2012; **75**: 200-206 [PMID: 22078104 DOI: 10.1016/j.gie.2011.09.019]

94 **Qin SY**, Lu XP, Jiang HX. EUS-guided ethanol ablation of insulinomas: case series and literature review. *Medicine (Baltimore)* 2014; **93**: e85 [PMID: 25255024 DOI: 10.1097/MD.0000000000000085]

95 **Choi JH**, Park DH, Kim MH, Hwang HS, Hong SM, Song TJ, Lee SS, Seo DW, Lee SK. Outcomes after endoscopic ultrasound-guided ethanol-lipiodol ablation of small pancreatic neuroendocrine tumors. *Dig Endosc* 2018; **30**: 652-658 [PMID: 29575213 DOI: 10.1111/den.13058]

96 **Lakhtakia S**, Ramchandani M, Galasso D, Gupta R, Venugopal S, Kalpala R, Reddy DN. EUS-guided radiofrequency ablation for management of pancreatic insulinoma by using a novel needle electrode (with videos). *Gastrointest Endosc* 2016; **83**: 234-239 [PMID: 26394384 DOI: 10.1016/j.gie.2015.08.085]

97 **Limmer S**, Huppert PE, Juette V, Lenhart A, Welte M, Wietholtz H. Radiofrequency ablation of solitary pancreatic insulinoma in a patient with episodes of severe hypoglycemia. *Eur J Gastroenterol Hepatol* 2009; **21**: 1097-1101 [PMID: 19685572 DOI: 10.1097/meg.0b013e328323d70e]

98 **Rossi S**, Viera FT, Ghittoni G, Cobianchi L, Rosa LL, Siciliani L, Bortolotto C, Veronese L, Vercelli A, Gallotti A, Ravetta V. Radiofrequency ablation of pancreatic neuroendocrine tumors: a pilot study of feasibility, efficacy, and safety. *Pancreas* 2014; **43**: 938-945 [PMID: 24717825 DOI: 10.1097/MPA.0000000000000133]

99 **Barthet M**, Giovannini M, Lesavre N, Boustiere C, Napoleon B, Koch S, Gasmi M, Vanbiervliet G, Gonzalez JM. Endoscopic ultrasound-guided radiofrequency ablation for pancreatic neuroendocrine tumors and pancreatic cystic neoplasms: a prospective multicenter study. *Endoscopy* 2019; **51**: 836-842 [PMID: 30669161 DOI: 10.1055/a-0824-7067]

100 **Oleinikov K**, Dancour A, Epshtein J, Benson A, Mazeh H, Tal I, Matalon S, Benbassat CA, Livovsky DM, Goldin E, Gross DJ, Jacob H, Grozinsky-Glasberg S. Endoscopic Ultrasound-Guided Radiofrequency Ablation: A New Therapeutic Approach for Pancreatic Neuroendocrine Tumors. *J Clin Endocrinol Metab* 2019; **104**: 2637-2647 [PMID: 31102458 DOI: 10.1210/jc.2019-00282]

World Journal of Gastroenterology

Submit a Manuscript: https://www.f6publishing.com

World J Gastroenterol 2022 September 14; 28(34): 4959-4972

DOI: 10.3748/wjg.v28.i34.4959

ISSN 1007-9327 (print) ISSN 2219-2840 (online)

MINIREVIEWS

Efficacy of cytapheresis in patients with ulcerative colitis showing insufficient or lost response to biologic therapy

Masahiro Iizuka, Takeshi Etou, Shiho Sagara

Specialty type: Gastroenterology and hepatology

Provenance and peer review: Invited article; Externally peer reviewed.

Peer-review model: Single blind

Peer-review report's scientific quality classification

Grade A (Excellent): 0
Grade B (Very good): B
Grade C (Good): C, C, C
Grade D (Fair): 0
Grade E (Poor): 0

P-Reviewer: Ali SNH, Jordan; Li HY, China; Sitkin S, Russia; Wen XL, China

Received: May 30, 2022
Peer-review started: May 30, 2022
First decision: June 18, 2022
Revised: July 16, 2022
Accepted: August 16, 2022
Article in press: August 16, 2022
Published online: September 14, 2022

Masahiro Iizuka, Shiho Sagara, Akita Health Care Center, Akita Red Cross Hospital, Akita 010-0001, Japan

Masahiro Iizuka, Takeshi Etou, Department of Gastroenterology, Akita Red Cross Hospital, Akita 010-1495, Japan

Corresponding author: Masahiro Iizuka, MD, PhD, Director, Doctor, Akita Health Care Center, Akita Red Cross Hospital, 3-4-23 Nakadori, Akita 010-0001, Japan.
maiizuka@woody.ocn.ne.jp

Abstract

For the optimal management of refractory ulcerative colitis (UC), secondary loss of response (LOR) and primary non-response to biologics is a critical issue. This article aimed to summarize the current literature on the use of cytapheresis (CAP) in patients with UC showing a poor response or LOR to biologics and discuss its advantages and limitations. Further, we summarized the efficacy of CAP in patients with UC showing insufficient response to thiopurines or immunomodulators (IM). Eight studies evaluated the efficacy of CAP in patients with UC with inadequate responses to thiopurines or IM. There were no significant differences in the rate of remission and steroid-free remission between patients exposed or not exposed to thiopurines or IM. Three studies evaluated the efficacy of CAP in patients with UC showing an insufficient response to biologic therapies. Mean remission rates of biologics exposed or unexposed patients were 29.4 % and 44.2%, respectively. Fourteen studies evaluated the efficacy of CAP in combination with biologics in patients with inflammatory bowel disease showing a poor response or LOR to biologics. The rates of remission/response and steroid-free remission in patients with UC ranged 32%-69% (mean: 48.0%, median: 42.9%) and 9%-75% (mean: 40.7%, median: 38%), respectively. CAP had the same effectiveness for remission induction with or without prior failure on thiopurines or IM but showed little benefit in patients with UC refractory to biologics. Although heterogeneity existed in the efficacy of the combination therapy with CAP and biologics, these combination therapies induced clinical remission/response and steroid-free remission in more than 40% of patients with UC refractory to biologics on average. Given the excellent safety profile of CAP, this combination therapy can be an alternative therapeutic strategy for UC refractory to biologics. Extensive prospective studies are needed to understand the efficacy of combination therapy with CAP and biologics.

Key Words: Ulcerative colitis; Inflammatory bowel disease; Cytapheresis; Granulocyte and monocyte adsorptive apheresis; Anti-tumor necrosis factor-α antibody; Combination therapy

©The Author(s) 2022. Published by Baishideng Publishing Group Inc. All rights reserved.

Core Tip: Management of refractory ulcerative colitis (UC) experiencing primary non-response or loss of response to biologics is a critical issue. We first summarized the efficacy of cytapheresis (CAP) for such patients. Although CAP tended to have lower effects for induction of remission in patients with UC who were refractory to biologics, combination therapies with CAP and biologics induced clinical remission or response in more than 40% of such patients with UC on average. Given the excellent safety profile of CAP, we believe that this combination therapy can be an alternative therapeutic strategy for such refractory UC patients.

Citation: Iizuka M, Etou T, Sagara S. Efficacy of cytapheresis in patients with ulcerative colitis showing insufficient or lost response to biologic therapy. *World J Gastroenterol* 2022; 28(34): 4959-4972
URL: https://www.wjgnet.com/1007-9327/full/v28/i34/4959.htm
DOI: https://dx.doi.org/10.3748/wjg.v28.i34.4959

INTRODUCTION

Ulcerative colitis (UC) is a chronic inflammatory bowel disease (IBD) of the colon characterized by a relapsing and remittent course[1,2]. Multiple factors, such as genetic background, environmental and luminal factors, and mucosal immune dysregulation, have been suggested to contribute to UC pathogenesis[1]. Several treatments for UC are available to induce and maintain the clinical remission of the disease. For patients with mild to moderate UC, 5-aminosalicylic acid (5-ASA) is generally used, and more than 90% of patients receive 5-ASA within 1 year of diagnosis[3]. Corticosteroids (CSs) are the first-line treatment to induce remission in moderate to severe UC[2]. It was reported that immediate outcomes from CSs were complete remission in 54%, partial remission in 30%, and no response in 16% of patients[4]. Despite the effectiveness of CSs in patients with UC, it has been reported that the rate of steroid dependence was 17%-22% at 1 year following treatment with the initial CS therapy and increased to 38% mostly within 2 years[4-8].

Thiopurines have been conventionally used for the treatment of steroid-dependent UC[9-14]. The rates of the induction of CS-free remission with thiopurines in steroid-dependent patients with UC were reported to be 44% and 53%, respectively[13,14]. However, it has also been reported that thiopurine therapy has failed in approximately 25% of IBD patients within 3 mo after treatment initiation, mostly due to drug intolerance or toxicity[11].

Along with the recent advancements in the treatment for UC, effective treatments, including biologics [anti- tumor necrosis factor-α (TNF-α) antibodies[15-25], anti-integrin monoclonal antibody[26]], Janus kinase (JAK) inhibitor[27] and tacrolimus[28,29], have been developed for refractory UC. A meta-analysis showed that anti-TNF-α antibodies had more clinical benefits than placebo as evidenced by the former's increased frequency of clinical, steroid-free, and endoscopic remission and decreased frequency of colectomy[30]. It has been reported that the rates of induction of steroid-free remission in refractory patients with UC with anti-TNF-α antibodies ranged from 40.0%-76.5%[2,16,18,21,22,24]. Vedolizumab (VDZ) is an anti-integrin monoclonal antibody. Studies on VDZ showed that clinical response and remission were achieved in 51% and 30% of patients with UC by week 14, respectively [31]. However, despite the significant efficacy of biologics for UC, secondary loss of response (LOR) is a common clinical problem. It was reported that the rate of LOR to anti-TNF-α antibodies in UC ranged from 23%-46% at 12 mo after anti-TNF-α initiation[32]. It was also reported that the incidence rates of LOR to adalimumab (ADA) and infliximab (IFX) were 58.3% and 59.1% during maintenance therapy, respectively (mean follow-up: 139 and 158.8 wk, respectively)[33]. Recent data from a systematic review showed that the pooled incidence rates of LOR to VDZ were 47.9 and 39.8 per 100 person-years of follow-up among patients with Crohn's disease (CD) and UC, respectively[34]. Considering these results, secondary LOR as well as primary non-response to biologics, are a critical issue for the optimal management of refractory UC. In this context, recent studies have shown the efficacy of use of cytapheresis (CAP) in such patients with UC[35-51].

CAP is a non-pharmacological extracorporeal therapy and has been developed as a treatment for UC [52-58]. CAP is performed using two methods, namely, granulocyte and monocyte adsorptive apheresis (GMA), which uses cellulose acetate beads (Adacolumn, JIMRO Co., Ltd., Takasaki, Japan), and leukocytapheresis (LCAP), which uses polyethylene phthalate fibers (Cellsorba., Asahi Kasei Medical Co., Ltd., Tokyo, Japan)[42,52]. GMA selectively depletes elevated levels of granulocytes and monocytes

from the patients' circulation, but spares most of the lymphocytes[52]. LCAP exerts its anti-inflammatory effects by removing activated leukocytes or platelets from the peripheral blood through extracorporeal circulation[42]. It has been reported that CAP is an effective therapeutic strategy for active refractory UC with fewer adverse effects[52-59]. In addition, it is notable that there have been no reports showing LOR to CAP during the treatment.

As described above, recent studies have shown the efficacy of the use of CAP in patients with UC showing a poor response or LOR to biologics, but the results of these studies have not been summarized to date. The purpose of this article is to summarize the current literature on the use of CAP as an alternative therapeutic strategy for patients with UC showing insufficient response or LOR to biologics and discuss the advantages and limitations of this strategy. We also summarized the efficacy of CAP for patients with UC showing insufficient response to thiopurines or immunomodulators (IM)[36,37,42,58-62].

LITERATURE SEARCH STRATEGY

Electric search for studies published before December 2021 was performed in the PubMed databases. The search terms used were as follows; ulcerative colitis, inflammatory bowel disease, cytapheresis, GMA, biologics, loss of response, anti-TNF-α antibody, infliximab, adalimumab, golimumab, vedolizumab, ustekinumab, combination therapy, thiopurine, and immunomodulator. Reference lists of all relevant articles were searched for further studies. The search was restricted to articles in the English language and included prospective studies, retrospective studies, case series, case reports, and randomized control studies. Subsequently, we generated a state-of-the-art comprehensive review by summarizing the data on the efficacy of CAP in patients with UC (or IBD) showing insufficient or lost response to biologic therapy, and efficacy of CAP in patients with UC showing insufficient response to thiopurines or IM.

EFFICACY OF CAP IN PATIENTS WITH UC SHOWING INSUFFICIENT RESPONSE TO THIOPURINES OR IM

There were eight studies that evaluated the efficacy of CAP in patients having UC with insufficient response to thiopurines (Table 1)[36,37,42,58-62]. These studies include three prospective studies, two retrospective studies, one historical cohort study, one single-arm, open-label, multicentre trial, and one multicenter cohort study. Among them, four studies showed remission rates, and four studies showed steroid-free remission rates in CAP therapy in patients with UC concomitantly treated with thiopurines or IM. Although the background of the patients in these studies were different, the remission rates in CAP therapy ranged from 40.3%-73% (mean ± SD: 56.25 ± 16.03%, median: 55.85%, interquartile range: 41.475%-71.425%) and the steroid-free remission rates in CAP therapy ranged from 36%-56.3% (mean ± SD: 47.25 ± 9.99%, median: 48.35%, interquartile range: 37.425%-55.975%) (Figure 1). Among these studies, four[37,42,58,59] compared the rates of clinical remission between the patients exposed to thiopurines or IM and the patients unexposed to them. In all four studies significant differences were not observed in the rates of remission between patients exposed to thiopurines or IM and control. In three of the four studies, the remission rates in patients with UC concomitantly exposed to thiopurines or IM ranged from 45%-73% (mean ± SD: 61.57 ± 14.69%, median: 66.7%), and those in patients unexposed to thiopurines or IM ranged from 48%-71% (mean ± SD: 62.7 ± 12.8%, median: 69.1%) (Figure 2A).

Specifically, Yokoyama *et al*[42] used LCAP in their study and demonstrated that the clinical remission rate of the patients concomitantly using thiopurines was 73% and that of the patients without using thiopurines was 71%. They showed that in univariate analysis, concomitant use of thiopurine did not show statistically significant differences between the remission and nonremission groups (P = 0.623). Yamamoto *et al*[37] used GMA in their study and showed that the clinical remission rate of patients exposed to immunosuppressants was 45%, and that of the patients unexposed to immunosuppressants was 48%. They showed that in the univariate analysis, exposure to immunosuppressants did not affect the likelihood of clinical remission in the treatment of GMA (P = 0.61).

Regarding the rate of steroid-free remission, two studies[59,62] compared the rates of steroid-free remission between the patients concomitantly treated with thiopurines or IM and the patients treated without them. These studies showed that significant differences were not observed between the patients concomitantly treated with thiopurines or IM and patients treated without them. The steroid-free remission rates in patients with UC concomitantly treated with thiopurines or IM were 41.7% and 56.3% (mean: 49%) and the rates of steroid-free remission in patients with UC treated without thiopurines or IM were 45.5% and 53.5% (mean: 49.5%), respectively (Figure 2B). Specifically, Ishiguro *et al*[62] showed that in the univariate analysis, IM therapy was not associated with remission induction rate by GMA (P = 1.00). However, they also showed that in the multivariate analysis, only IM therapy was associated with an increased risk of relapse (OR: 37.6877, 95%CI: 2.4178-587.4632; P = 0.0013).

Table 1 Efficacy of cytapheresis in patients with ulcerative colitis showing insufficient response to thiopurine or immunomodulators

Ref.	Study type	Total number of patients included in the study	Number of patients insufficient response to thiopurine or IM	Regimen of CAP	Rate of remission	Rate of steroid- free remission
Cabriada *et al*[60], 2010	Prospective study	18 (SD)	18	GMA or LCAP (5-10 sessions, 1 session/wk)		55%
Takayama *et al*[58], 2013	Historical cohort study	90	14	GMA or LCAP (5-10 sessions, 1-2/wk)	49% (total Pts), pre-use of IM had little effects on the response to therapy	
Yokoyama *et al*[42], 2014	Prospective Observation Study	623 (for efficacy assessment)	196	LCAP (5-10 sessions, mean 8.4), intensive LCAP was performed in > 70% of Pts	73% (Pts concomitantly treated with thiopurine), 71% (Pts treated without thiopurine), $P = 0.623$	
Imperiali *et al*[61], 2017	Prospective multicenter study	33 (SD)	33	GMA (5 sessions, 1 session/wk)		36%
Yamamoto *et al*[37], 2018	Retrospective study	593	159	GMA (5 sessions, 1 to 5 sessions/wk), 5 or 6 GMA were added in Pts who did not achieve clinical remission	45% (Pts exposed to IM), 48% (Pts unexposed to IM), $P = 0.61$	
Dignass *et al* [36], 2016	Single-arm, open-label, multicentre trial	86 (SD)	83	GMA (5-10 sessions, 1 session/wk)	40.3%	
Ishiguro *et al*[62], 2020	Multicenter cohort study	102, SD or SR UC Pts were not included	16	GMA (mean number of GMA 9.9 sessions, 1-3 sessions/wk)		56.3% (Pts concomitantly treated with IM), 53.5% (Pts treated without IM), $P = 1.00$
Iizuka *et al* [59], 2021	Retrospective study	55 (SD: 33, SR: 21)	12	GMA or LCAP [5-20 sessions (mean 8.8), 1-2 sessions/wk (in principle)]	66.7% (Pts concomitantly treated with thiopurine), 69.1% (all Pts), no significant differences	41.7% (Pts concomitantly treated with thiopurine), 45.5% (all Pts), no significant differences

CAP: Cytapheresis; GMA: Granulocyte and monocyte adsorptive apheresis; LCAP: Leukocytapheresis; IM: Immunomodulators (or immunosuppressants); Pts: Patients; SD: Steroid dependent patients; SR: Steroid refractory patients; Intensive LCAP: Defined as performing ≥ 4 leukocytapheresis treatment within the first 2 wk.

In summary, it was suggested that CAP has the same effectiveness for induction of remission in patients with UC with and without prior failure to thiopurines or IM.

EFFICACY OF CAP IN PATIENTS WITH UC SHOWING PREVIOUS BIOLOGICS FAILURE

Three studies have evaluated the efficacy of CAP in patients with UC showing an insufficient response to anti-TNF-α therapy or exposure to biologics compared with biologic naïve patients with UC[35-37] (Table 2). These studies include two retrospective studies and one single-arm open-label multicentre trial. Among these studies, Yamamoto *et al*[37] showed that the clinical remission rate of the patients exposed to biologics was 31%, and that of the patients unexposed to biologics was 48% ($P = 0.01$). They showed that in the univariate analysis, biologic naïve patients responded well to GMA ($P = 0.01$). In multivariate analysis, exposure to biologics was an independent significant factor affecting the clinical efficacy of GMA ($P = 0.01$). Dignass *et al*[36] conducted a study on a large cohort of steroid-dependent patients with UC refractory to immunosuppressant and /or biologic treatment to provide additional clinical data regarding the safety and efficacy of Adacalumn (GMA). They showed that remission was achieved at week 12 in 31/77 [40.3% (95%CI: 29.2, 52.1)] of patients who failed on immunosuppressants, 10/36 [27.8% (95%CI: 14.2, 45.2)] of patients who failed on anti-TNF-α treatment, and 9/30 [30.0% (95%CI: 14.7, 49.4)] of patients who failed on both immunosuppressants and anti-TNF-αtreatment. Their results suggested that the remission rate using Adacalumn tended to be lower in patients who failed on anti-TNF-α treatment or on both immunosuppressants and anti-TNF-α treatment compared to that of the patients who failed on immunosuppressants. The remission rates in patients with UC exposed to anti-TNF-α treatment in the two studies were 27.8% and 31% (mean: 29.4%), and the remission rates in

Table 2 Efficacy of cytapheresis in patients with ulcerative colitis showing previous biologics failure

Ref.	Study type	Biologics exposure	Number of patients (total number of patients in the study)	Regimen of CAP	Rate of remission	Rate of steroid-free remission
Cabriada *et al*[35], 2012	Retrospective study (results of nationwide Spanish registry)	IFX	33 (total: 142 SD)	GMA (95% of the Pts), 1-10 sessions (median 5 sessions)		37% (all Pts), no differences in clinical remission were found among those Pts with previous thiopurine or IFX failure
Dignass *et al* [36], 2016	Single-arm, open-label, multicentre trial	TNF-α	37 (total: 86 SD)	GMA (5-10 sessions, 1 session/wk)	27.8% (Pts who failed on TNF-α), 40.3% (Pts who failed on immunosup-pressants	
Yamamoto *et al*[37], 2018	Retrospective study	(1) IFX; and (2) ADA	(1) 31; and (2) 36 (total: 593)	GMA (5 sessions, 1 to 5 sessions/wk), 5 or 6 GMA were added in Pts who did not achieve clinical remission	31% (Pts exposed to biologics), 48% (Pts unexposed to biologics), P = 0.01	

CAP: Cytapheresis; SD: Steroid dependent patients; GMA: Granulocyte and monocyte adsorptive apheresis; Pts: Patients; IFX: Infliximab; TNF-α: Tumor necrosis factor-α; ADA: Adalimumab.

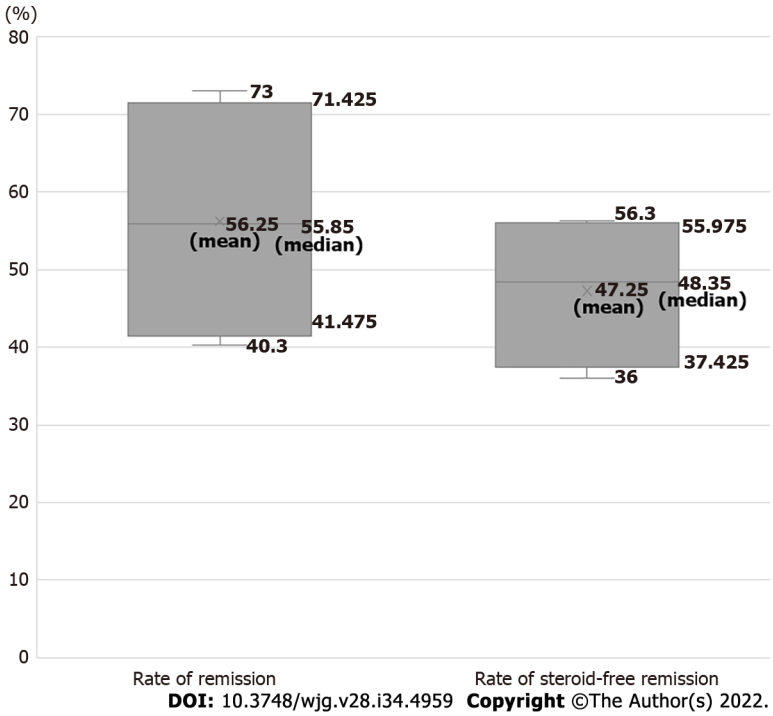
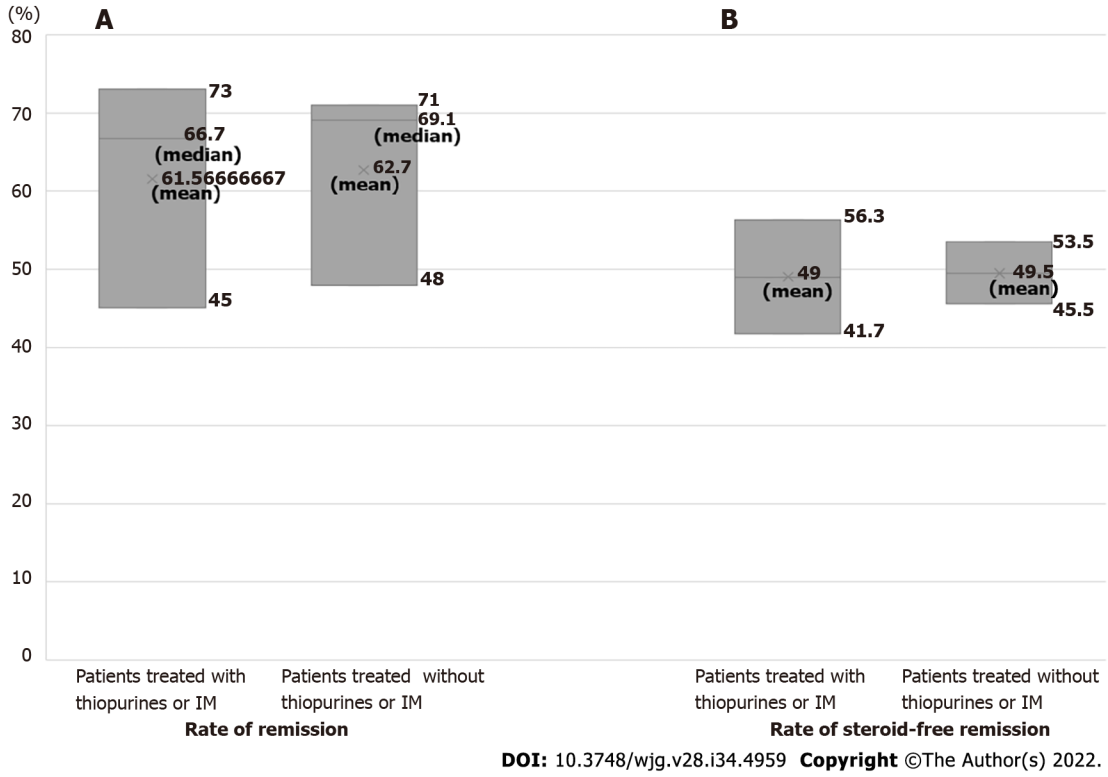


Figure 1 Remission and steroid-free remission rates in cytapheresis therapy in patients with ulcerative colitis concomitantly treated with thiopurines or immunomodulators. Box plot shows that, in cytapheresis therapy, the remission rates range from 40.3%-73% (mean: 56.25%, median: 55.85%, interquartile range: 41.475%-71.425%) and the rates of steroid-free remission range from 36%-56.3% (mean: 47.25%, median: 48.35%, interquartile range: 37.425%-55.975%).

patients with UC unexposed to anti-TNF-α treatment were 40.3% and 48% (mean: 44.15%), respectively (Figure 3).

Cabriada *et al*[35] conducted a clinical study including 142 steroid-dependent patients with UC [previous thiopurines failure 98 (69%), previous IFX failure 33 (23%)] to evaluate the short and long-term effectiveness and safety of leukocytapheresis therapy by means of a nationwide registry of clinical practice. Although the rate of remission in patients who were refractory to thiopurines or IFX was not described in the paper, no differences in clinical remission were found among those with previous thiopurine or IFX failure.



DOI: 10.3748/wjg.v28.i34.4959 **Copyright** ©The Author(s) 2022.

Figure 2 Remission and steroid-free remission rates in cytapheresis therapy in patients with ulcerative colitis concomitantly treated with thiopurines or immunomodulators and in those treated without thiopurines or immunomodulators. A: Box plot shows that the rates of remission in patients concomitantly treated with thiopurines or immunomodulators (IM) and in those treated without thiopurines or IM range from 45%-73% (mean: 61.57%, median: 66.7%) and 48%-71% (mean: 62.7%, median: 69.1%), respectively; B: The rates of steroid-free remission in patients with ulcerative colitis (UC) concomitantly treated with thiopurines or IM are 41.7% and 56.3% (mean: 49%), and those in patients with UC treated without thiopurines or IM are 45.5% and 53.5% (mean: 49.5%), respectively.

In summary, it is controversial whether CAP has a similar clinical effect in patients with UC who failed biologics treatment and in biologic naïve patients with UC due to limited studies. However, based on these studies, it is suggested that CAP tended to have less efficacy for induction of clinical remission in patients with UC who failed on anti-TNF-α treatment compared to biologic naïve patients with UC.

EFFICACY OF COMBINATION THERAPY WITH CAP AND BIOLOGICS IN IBD PATIENTS SHOWING INSUFFICIENT RESPONSE OR LOSS OF RESPONSE TO BIOLOGICS

Efficacy of the combination therapy with CAP and biologics

There have been 14 studies that evaluated the efficacy of the combination therapy of CAP and biologics in IBD patients that were refractory to biologics[38-51] (Table 3). These studies include two prospective studies, four retrospective studies, one preliminary study, and seven case reports. These studies include eight studies evaluating combination therapy with GMA or LCAP and anti-TNF-α (IFX: 6 studies; ADA: 1 study; IFX, ADA, golimumab: 1 study), four studies with GMA and VDZ, one study with GMA and ustekinumab, and one exceptional study with GMA and a pan-JAK inhibitor tofacitinib. Among these 14 studies, seven studies[42,44,45,47-50] examined the efficacy of combination therapies in patients with UC, five studies[38-41,46] examined its efficacy for CD patients, and two studies[43,51] examined its efficacy for both UC and CD patients.

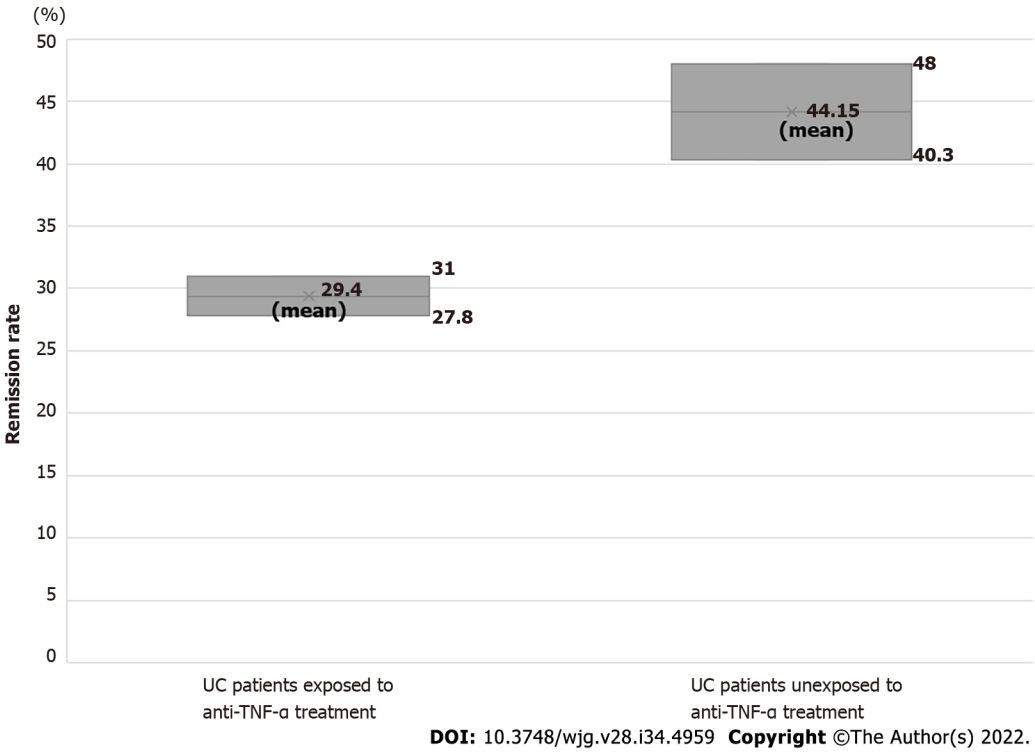
As shown in Table 3, there were differences in the background of the patients and methods of combination therapies among the studies, and heterogeneity existed in the efficacy of the combination therapies with CAP and biologics among the studies. The rates of remission or response to combination therapies in IBD (UC and CD) patients in these studies excluding seven case reports ranged from 32%-100% (mean ± SD: 62.72 ± 26.65%, median: 57.85%, interquartile range: 40.175%-89.275%) and the rates of steroid-free remission ranged from 9%-75% (mean ± SD: 43 ± 27.4%, median: 44%, interquartile range: 16.25%-68.75%), respectively (Figure 4). Regarding the efficacy of the combination therapies in patients with UC, three studies showed the rates of remission or response, and three studies showed steroid-free remission in the combination therapies of CAP and biologics in patients with UC refractory to biologics. The rates of remission or response ranged from 32%-69% (mean ± SD: 47.97 ± 19.0%, median: 42.9%),

Table 3 Efficacy of combination therapy with cytapheresis and biologics in inflammatory bowel disease patients showing insufficient response or loss of response to biologics

Ref.	Study type	Biologics to which insufficient response or LOR was shown	Number of patients	Methods of combination therapy	Regimen of CAP	Rate of remission	Rate of response	Rate of steroid-free remission	Rate of AE (%)
González Carro *et al* [38], 2006	Case report	IFX (LOR)	CD 1	IFX + GMA	GMA 1 session/8 wk, 12 mo	100%			
Fukunaga *et al*[39], 2010	Case report	IFX (LOR)	CD 1	IFX + GMA	GMA 1 sessions/wk, 3 consecutive weeks × 3 courses and maintenance therapy	100%			0/1 (0%)
Sono *et al* [40], 2012	Prospective study	IFX (LOR)	CD 15	IFX + GMA	GMA 1 session/wk, 5 consecutive wk		46.7%; a fall in CDAI by more than 15%		
Ozeki *et al* [41], 2012	Case report	(1) IFX (failure); (2) ADA (failure); (3) Steroid refractory and *etc.*	(1) CD 1; (2) CD 1; and (3) CD 3	ADA + GMA	GMA 2 sessions/wk, 5 consecutive wk	100%			0/5 (0%)
Yokoyama *et al*[42], 2014	Prospective observational study	IFX	UC 42	IFX + LCAP	LCAP 5-10 sessions (mean 8.4), intensive LCAP was performed in > 70% of Pts	69.0% (Pts concomitantly treated with IFX)			
Yokoyama *et al*[43], 2018	Case report	IFX (LOR)	UC 2; CD 1	IFX + GMA	GMA 1 session/wk, 3 consecutive wk or more	UC 100%, CD 100%			
Scrivo *et al* [44], 2018	Case report	VDZ (primary nonresponse to VDZ; Previous LOR to IFX; Primary non-response to ADA)	UC 1	VDZ + GMA	GMA 1 session/wk,5 wk			100%	0/1 (0%)
Sáez-González *et al* [45], 2018	Case report	VDZ (primary nonresponse to VDZ; Primary nonresponse to ADA and IFX)	UC 1	VDZ + GMA	GMA 2 sessions/wk, 5 wk + 14 monthly maintenance sessions			100%	
Tanida *et al* [46], 2018	Retrospective study	(1) IFX (LOR); (2) ADA (LOR); (3) Steroid refractory	(1) CD 1; (2) CD 1; and (3) CD 1	UST + GMA	GMA: 2 sessions/wk, for 5 consecutive wk	100%		50%	0/3 (0%)
Rodríguez-Lago *et al* [47], 2019	Retrospective multicenter study	Anti-TNF therapy (IFX 23, ADA 18, GLM 6); Primary nonresponse 49%, LOR 51%	UC 47	Anti-TNF therapy + GMA	GMA 1 sessions/wk 45%, 2 sessions/wk 55%; 5-10 sessions 51%, > 10 sessions 19% (median of 10 sessions)		32%	9%	2/47 (4%)
Rodríguez-Lago *et al* [48], 2019	Retrospective multicentre pilot study	VDZ (primary nonresponse 25%, secondary LOR 75%); All Pts had previously received anti-TNF agents (IFX 88%, ADA 50%, GLM 38%)	UC 8	VDZ + GMA	GMA: 5-38 sessions (median 15), biweekly 75%, weekly 25%; maintenance GMA 75%, monthly 38%, every 2 wk 25%		Partial Mayo score decreased ($P = 0.01$)	38%	0/8 (0%)
Nakamura *et al*[49], 2020	Case report	VDZ (primary nonresponse to VDZ; Serious	UC 1	VDZ + GMA	semiweekly GMA, 4 wk	100%			

		allergy to IFX)						
Tanida *et al* [50], 2020	Retrospective study	(1) IFX(LOR); (2) ADA (LOR); (3) Steroid refractory or dependent	(1) UC 2; (2) UC 2; and (3) UC 3	TOF + GMA	GMA: 2 sessions/wk, total 10 sessions		75%	3/7 (43%)
Yokoyama *et al*[51], 2020	Preliminary study	IFX (LOR)	UC 7; CD 7	IFX + GMA	1 or 2 sessions/wk, for 5 consecutive wk, Pts who did not achieved remission by week 8 underwent another GMA (1 session/wk, 5 consecutive wk)	All IBD 64.3%, UC 42.9%, CD 85.7%		0/14 (0%)

LOR: Loss of response; CAP: Cytapheresis; CD: Crohn's disease; GMA: Granulocyte and monocyte adsorptive apheresis; UC: Ulcerative colitis; LCAP: Leukocytapheresis; AE: Adverse events; IFX: Infliximab; ADA: Adalimumab; Pts: Patients; VED: Vedolizumab; UST: Ustekinumab; TNF-α: Tumor necrosis factor-α; GLM: Golimumab; TOF: Tofacitinib; Intensive LCAP: Defined as performing ≥ 4 leukocytapheresis within the first 2 wk.

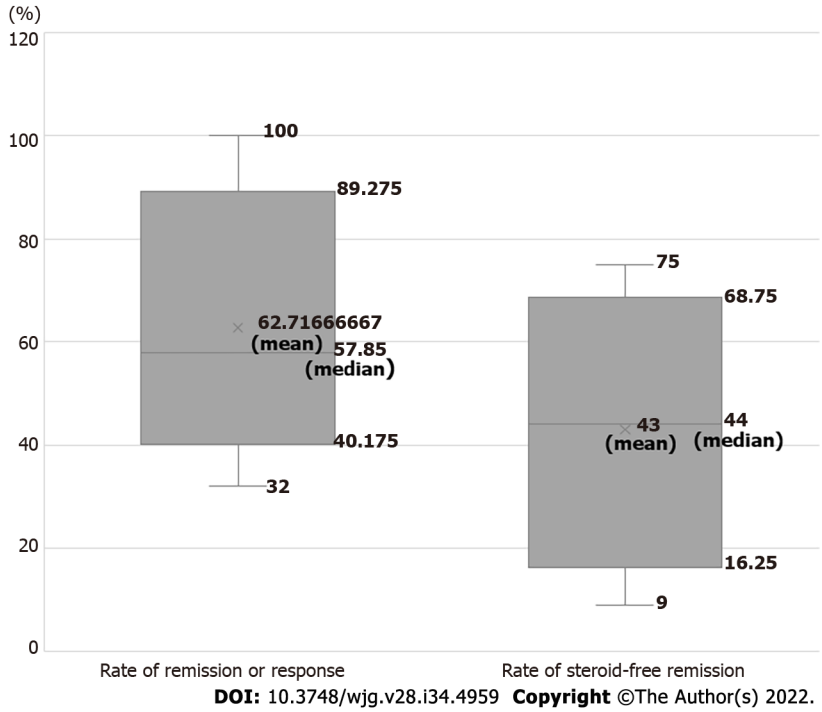


DOI: 10.3748/wjg.v28.i34.4959 Copyright ©The Author(s) 2022.

Figure 3 Remission rates in cytapheresis therapy in patients with ulcerative colitis exposed to anti-tumor necrosis factor-α treatment and in those unexposed to anti-tumor necrosis factor-α treatment. The remission rates in patients with ulcerative colitis (UC) exposed to anti-tumor necrosis factor-α (TNF-α) treatment are 27.8% and 31% (mean: 29.4%), and those in patients with UC unexposed to anti-TNF-α treatment are 40.3% and 48% (mean: 44.15%), respectively.

and the rates of steroid-free remission in patients with UC ranged from 9%-75% (mean ± SD: 40.7 ± 33.1%, median: 38%), respectively (Figure 5). On the other hand, the rates of remission or response in CD patients ranged from 46.7%-100% (mean ± SD: 77.5 ± 27.6%, median 85.7%), and the rate of steroid-free remission in CD patients was 50%.

Regarding the efficacy of the combination therapy, Rodríguez-Lago *et al*[47] found no differences in the efficacy depending on the type of anti-TNF received during the combination therapy. They also reported that the response to the combination therapy was inversely proportional to the number of previous anti-TNF agents, but it was not influenced by the presence of primary non-response or secondary LOR. Another important aspect being considered is the regimen of CAP prescribed because an intensified regimen with longer and biweekly sessions has demonstrated rapid and higher efficacy rates without increasing the number of adverse events (AEs)[47,57]. In Table 3, it seems that the studies using a higher frequency of biweekly CAP or intensive CAP tended to demonstrate good clinical efficacy.



DOI: 10.3748/wjg.v28.i34.4959 Copyright ©The Author(s) 2022.

Figure 4 Rates of remission or response and steroid-free remission in the combination therapies of cytapheresis and biologics in inflammatory bowel disease patients showing insufficient response or loss of response to biologics. Box plot shows that the remission rates in the combination therapies of cytapheresis and biologics range from 32%-100% (mean: 62.72%, median: 57.85%, interquartile range: 40.175%-89.275%), and the rates of steroid-free remission in the combination therapies range from 9%-75% (mean: 43%, median: 44%, interquartile range: 16.25%-68.75%).

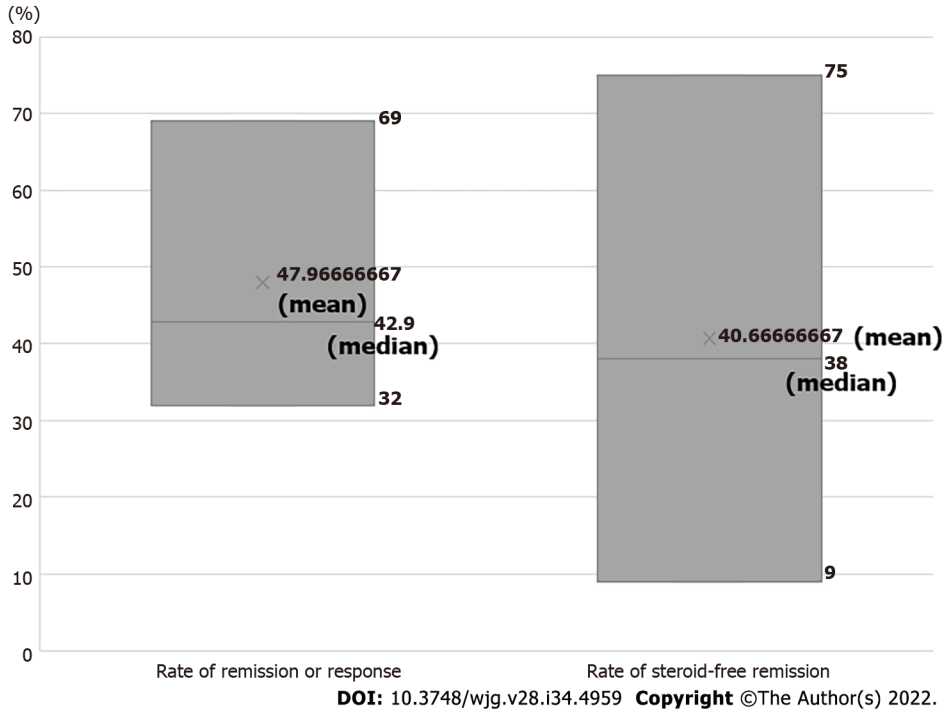
Safety of the combination therapy

One of the strengths of CAP is its safety profile[63]. Of note, several studies have reported the excellent safety of CAP[36,42,52,56,63]. Among these studies, Hibi *et al*[56] evaluated the safety of Adacolumn in 697 patients with UC in 53 medical institutions. They reported that no serious AEs were observed, and only mild to moderate adverse events were observed in 7.7% of patients. In addition, Motoya *et al*[52] showed that the incidence of AEs among elderly patients was similar in all patients. Regarding the safety of the combination therapy with CAP and biologics, eight out of 14 studies listed in Table 3 reported the rate of AEs[39,41,44,46-48,50,51]. Six of the eight studies reported no adverse events. On the other hand, Rodríguez-Lago *et al*[47] reported 4% (2/47) AEs related to the technique (anxiety and headache), and Tanida *et al*[50] reported 43% (3/7) AEs (one had orolabial herpes, one had a transient increase in creatinine phosphokinase due to intense physical exercise, and one had triglyceride increase). However, Tanida *et al*[50] described that AEs observed in their study were consistent with the AEs reported in the oral clinical trials for tofacitinib in ulcerative colitis induction 1 and 2 trials, suggesting that AEs observed in their study were due to AEs from tofacitinib. In summary, AEs were observed in five out of 86 patients (5.8%) in the eight studies.

Based on these results, combination therapy with CAP and biologics is safe and well- tolerated.

Possible mechanisms of the efficacy of the combination therapy with CAP and biologics

Regarding the mechanism of the efficacy of the combination therapy of CAP and biologics, Rodriguez-Largo *et al*[47] suggested that the benefit may be related to multiple mechanisms of action. They suggested that GMA could reduce the circulating inflammatory burden in addition to direct improvement in disease activity, thus allowing the anti-TNF to restore its response. They also suggested an alternative hypothesis that states that the benefits come from the possible interaction between both treatments. This interaction could be an improvement in blood trough levels of the drug, a reduction of anti-drug antibodies, or both. In this context, several studies supported their hypothesis. Soluble TNF receptors are known to neutralize TNF without invoking a TNF-like response. Saniabadi *et al*[64] reported that blood levels of soluble TNF-α receptors I and II increased in IBD patients who underwent Adacolumn therapy. Hanai *et al*[65] also showed that soluble TNF-α receptor I/II, which are believed to have potent anti-inflammatory actions, were significantly increased in the peripheral blood at the end of the GMA session. Sono *et al*[40] showed an increase in plasma IL-10 and a decrease in circulating immune complexes and anti-nuclear antibodies during GMA therapy in GMA-responder CD patients with LOR to IFX. Furthermore, Yokoyama *et al*[43] showed that upon GMA therapy, the average plasma trough IFX increased from 0.91 μg/mL to 1.46 μg/mL, with concomitant decreases in C-reactive protein, IL-6, and IL-17A in IBD patients experiencing LOR to IFX. In their recent study, Yokoyama *et al*[51]



DOI: 10.3748/wjg.v28.i34.4959 **Copyright** ©The Author(s) 2022.

Figure 5 Rates of remission or response and steroid-free remission in the combination therapies of cytapheresis and biologics in patients with ulcerative colitis showing insufficient response or loss of response to biologics. Box plot shows that the remission rates in the combination therapies of cytapheresis and biologics range from 32%-69% (mean: 47.97%, median: 42.9%), and the rates of steroid-free remission in the combination therapies range from 9%-75% (mean: 40.7%, median: 38%).

showed that the levels of antibodies to IFX in patients with LOR to IFX were significantly elevated compared with those indicating a sustained clinical remission. They also showed that in patients who received IFX + GMA combination therapy, the IBD symptoms significantly improved together with a decrease in antibodies to IFX. These studies suggest the possibility that GMA therapy can decrease IFX antibodies and increase plasma trough IFX in patients with LOR to IFX.

Regarding combination therapy with GMA and VDZ, it was hypothesized that this strategy might target the migration of leukocytes into the inflamed tissue by combining their mechanism of action. The peripheral inflammatory cells affected by VDZ may be removed by the ability of GMA to adsorb multiple immune cells[48]. Nakamura *et al*[49] also suggested that VDZ and GMA were able to strengthen the suppression of the migration of leukocytes into the inflamed tissue by combining their mechanisms of action. Since the migration of peripheral inflammatory cells from the blood vessels is blocked by VDZ, multiple immune cells-including the congested ones in the peripheral blood- can be removed by GMA. Thus, considering the mechanism of action of GMA and VDZ, it is suggested that this combination therapy can synergically strengthen the therapeutic effects of each therapy.

Summary of the combination therapies with CAP and biologics

In summary, combination therapies of CAP and biologics can safely induce clinical remission or response and steroid-free remission in 32%-100% (mean: 62.72%, median: 57.85%) and 9%-75% (mean: 43%, median: 44%) of the IBD patients and in 32%-69% (mean: 47.97%, median: 42.9%) and 9%-75% (mean: 40.7%, median: 38%) of patients with UC refractory to biologics, respectively. In addition, it is a strong point of CAP that there have been no reports showing LOR to CAP during treatment. Given the excellent safety profile of CAP, these results suggest that this combination therapy can be an effective and alternative therapeutic strategy for patients with UC that experienced primary non-response or LOR to biologics. The economic burden of GMA may also be considered in decision-making[63]. A recent study showed that the availability of biosimilars had reduced the costs of anti-TNF agents, but GMA still has a cost slightly below the new biologicals (*i.e.*, ustekinumab and vedolizumab) with an even better safety profile[63]. In this context, Tominaga *et al*[66] evaluated the efficacy, safety, and treatment cost of prednisolone (PSL) and GMA in 41 patients with active UC who had achieved remission with GMA or with orally administered PSL. They showed that adverse events were reported in 12.5% of the GMA group and 35.3% of the PSL group. The average medical cost was 12739.4€/patient in the GMA group and 8751.3€ in the PSL group ($P < 0.05$). From these results, they concluded that the higher cost of GMA is offset by its good safety profile.

CONCLUSION

Summarizing the results of previous studies, it is suggested that CAP has the same effectiveness for induction of remission in patients having UC with or without prior failure of thiopurines or IM. It is controversial whether CAP has a similar clinical effect in patients with UC that failed on previous biologics therapy and in biologic naïve patients. However, it seems that CAP tended to be less effective for induction of clinical remission in patients with UC that were refractory to biologics therapy. Although there was heterogeneity in the efficacy of the combination therapy with CAP and biologics in patients with IBD refractory to biologics, it is notable that combination therapies with CAP and biologics induced clinical remission or response and steroid-free remission in more than 40% of patients with UC that failed on previous biologics therapy on average. Given the excellent safety profile of CAP, it is suggested that this combination therapy can be an alternative therapeutic strategy for patients with UC that were refractory to biologics. However, the number of studies examining this combination therapy has been small and limited to date. Larger prospective studies are needed to better understand the efficacy of the combination therapy of CAP and biologics for refractory patients with UC.

FOOTNOTES

Author contributions: Iizuka M was responsible for the conception and design of the study, literature review and analysis, drafting and critical revision and editing, and final approval of the final version; Etou T and Sagara S was responsible for the critical revision and final approval of the final version.

Conflict-of-interest statement: There is no conflicts of interest associated with any of the senior author or other coauthors contributed their efforts in this manuscript.

Open-Access: This article is an open-access article that was selected by an in-house editor and fully peer-reviewed by external reviewers. It is distributed in accordance with the Creative Commons Attribution NonCommercial (CC BY-NC 4.0) license, which permits others to distribute, remix, adapt, build upon this work non-commercially, and license their derivative works on different terms, provided the original work is properly cited and the use is non-commercial. See: https://creativecommons.org/Licenses/by-nc/4.0/

Country/Territory of origin: Japan

ORCID number: Masahiro Iizuka 0000-0002-4920-2805; Takeshi Etou 0000-0001-8402-7689; Shiho Sagara 0000-0002-1900-7937.

S-Editor: Zhang H
L-Editor: A
P-Editor: Zhang H

REFERENCES

1 **Kobayashi T**, Siegmund B, Le Berre C, Wei SC, Ferrante M, Shen B, Bernstein CN, Danese S, Peyrin-Biroulet L, Hibi T. Ulcerative colitis. *Nat Rev Dis Primers* 2020; **6**: 74 [PMID: 32913180 DOI: 10.1038/s41572-020-0205-x]
2 **Khan HM**, Mehmood F, Khan N. Optimal management of steroid-dependent ulcerative colitis. *Clin Exp Gastroenterol* 2015; **8**: 293-302 [PMID: 26648749 DOI: 10.2147/CEG.S57248]
3 **Nguyen NH**, Fumery M, Dulai PS, Prokop LJ, Sandborn WJ, Murad MH, Singh S. Comparative efficacy and tolerability of pharmacological agents for management of mild to moderate ulcerative colitis: a systematic review and network meta-analyses. Lancet Gastroenterol Hepatol 2018;3:742-753 [DOI: 10.1016/S2468-1253(18)30231-0]
4 **Faubion WA Jr**, Loftus EV Jr, Harmsen WS, Zinsmeister AR, Sandborn WJ. The natural history of corticosteroid therapy for inflammatory bowel disease: a population-based study. *Gastroenterology* 2001; **121**: 255-260 [PMID: 11487534]
5 **Ho GT**, Chiam P, Drummond H, Loane J, Arnott ID, Satsangi J. The efficacy of corticosteroid therapy in inflammatory bowel disease: analysis of a 5-year UK inception cohort. *Aliment Pharmacol Ther* 2006; **24**: 319-330 [PMID: 16842459]
6 **Edwards FC**, Truelove SC. The course and prognosis of ulcerative colitis. *Gut* 1963; **4**: 299-315 [PMID: 14084741]
7 **Farmer RG**, Easley KA, Rankin GB. Clinical patterns, natural history, and progression of ulcerative colitis. A long-term follow-up of 1116 patients. *Dig Dis Sci* 1993; **38**: 1137-1146 [PMID: 8508710]
8 **Khan N**, Abbas A, Williamson A, Balart L. Prevalence of corticosteroids use and disease course after initial steroid exposure in ulcerative colitis. *Dig Dis Sci* 2013; **58**: 2963-2969 [PMID: 23812861 DOI: 10.1007/s10620-013-2748-0]
9 **Park SK**, Yang SK, Ye BD, Kim KJ, Yang DH, Jung KW, Park SH, Kim JW, Byeon JS, Myung SJ, Kim JH. The long-term efficacy of azathioprine in steroid-dependent ulcerative colitis. *Scand J Gastroenterol* 2013; **48**: 1386-1393 [PMID: 24164382 DOI: 10.3109/00365521.2013.845908]
10 **Bär F**, Sina C, Fellermann K. Thiopurines in inflammatory bowel disease revisited. *World J Gastroenterol* 2013; **19**: 1699-1706 [PMID: 23555158 DOI: 10.3748/wjg.v19.i11.1699]
11 **Jharap B**, Seinen ML, de Boer NK, van Ginkel JR, Linskens RK, Kneppelhout JC, Mulder CJ, van Bodegraven AA.

Thiopurine therapy in inflammatory bowel disease patients: analyses of two 8-year intercept cohorts. *Inflamm Bowel Dis* 2010; **16**: 1541-1549 [PMID: 20155846 DOI: 10.1002/ibd.21221]

12 **van Gennep S**, de Boer NK, D'Haens GR, Löwenberg M. Thiopurine Treatment in Ulcerative Colitis: A Critical Review of the Evidence for Current Clinical Practice. *Inflamm Bowel Dis* 2017; **24**: 67-77 [PMID: 29272488 DOI: 10.1093/ibd/izx025]

13 **Ardizzone S**, Maconi G, Russo A, Imbesi V, Colombo E, Bianchi Porro G. Randomised controlled trial of azathioprine and 5-aminosalicylic acid for treatment of steroid dependent ulcerative colitis. *Gut* 2006; **55**: 47-53 [PMID: 15972298]

14 **Rosenberg JL**, Wall AJ, Levin B, Binder HJ, Kirsner JB. A controlled trial of azathioprine in the management of chronic ulcerative colitis. *Gastroenterology* 1975; **69**: 96-99 [PMID: 1097295]

15 **Rutgeerts P**, Sandborn WJ, Feagan BG, Reinisch W, Olson A, Johanns J, Travers S, Rachmilewitz D, Hanauer SB, Lichtenstein GR, de Villiers WJ, Present D, Sands BE, Colombel JF. Infliximab for induction and maintenance therapy for ulcerative colitis. *N Engl J Med* 2005; **353**: 2462-2476 [PMID: 16339095 DOI: 10.1056/NEJMoa050516]

16 **Armuzzi A**, Pugliese D, Danese S, Rizzo G, Felice C, Marzo M, Andrisani G, Fiorino G, Sociale O, Papa A, De Vitis I, Rapaccini GL, Guidi L. Infliximab in steroid-dependent ulcerative colitis: effectiveness and predictors of clinical and endoscopic remission. *Inflamm Bowel Dis* 2013; **19**: 1065-1072 [PMID: 23448790 DOI: 10.1097/MIB.0b013e3182802909]

17 **Sjöberg M**, Magnuson A, Björk J, Benoni C, Almer S, Friis-Liby I, Hertervig E, Olsson M, Karlén P, Eriksson A, Midhagen G, Carlson M, Lapidus A, Halfvarson J, Tysk C; Swedish Organization for the Study of Inflammatory Bowel Disease (SOIBD). Infliximab as rescue therapy in hospitalised patients with steroid-refractory acute ulcerative colitis: a long-term follow-up of 211 Swedish patients. *Aliment Pharmacol Ther* 2013; **38**: 377-387 [PMID: 23799948 DOI: 10.1111/apt.12387]

18 **Barreiro-de Acosta M**, Lorenzo A, Mera J, Dominguez-Muñoz JE. Mucosal healing and steroid-sparing associated with infliximab for steroid-dependent ulcerative colitis. *J Crohns Colitis* 2009; **3**: 271-276 [PMID: 21172286 DOI: 10.j.crohns]

19 **Mocciaro F**, Orlando A, Scimeca D, Cottone M. [Infliximab in moderate to severe steroid-dependent or steroid-refractory ulcerative colitis]. *Recenti Prog Med* 2007; **98**: 560-564 [PMID: 18044405]

20 **Gavalas E**, Kountouras J, Stergiopoulos C, Zavos C, Gisakis D, Nikolaidis N, Giouleme O, Chatzopoulos D, Kapetanakis N. Efficacy and safety of infliximab in steroid-dependent ulcerative colitis patients. *Hepatogastroenterology* 2007; **54**: 1074-1079 [PMID: 17629042]

21 **Sandborn WJ**, van Assche G, Reinisch W, Colombel JF, D'Haens G, Wolf DC, Kron M, Tighe MB, Lazar A, Thakkar RB. Adalimumab induces and maintains clinical remission in patients with moderate-to-severe ulcerative colitis. *Gastroenterology* 2012; **142**: 257-65.e1 [PMID: 22062358 DOI: 10.1053/j.gastro.2011.10.032]

22 **Italian Group for the Study of Inflammatory Bowel Disease**, Armuzzi A, Biancone L, Daperno M, Coli A, Pugliese D, Annese V, Aratari A, Ardizzone S, Balestrieri P, Bossa F, Cappello M, Castiglione F, Cicala M, Danese S, D'Incà R, Dulbecco P, Feliciangeli G, Fries W, Genise S, Gionchetti P, Gozzi S, Kohn A, Lorenzetti R, Milla M, Onali S, Orlando A, Papparella LG, Renna S, Ricci C, Rizzello F, Sostegni R, Guidi L, Papi C. Adalimumab in active ulcerative colitis: a "real-life" observational study. *Dig Liver Dis* 2013; **45**: 738-743 [PMID: 23683530 DOI: 10.1016/j.dld.2013.03.018]

23 **Sandborn WJ**, Feagan BG, Marano C, Zhang H, Strauss R, Johanns J, Adedokun OJ, Guzzo C, Colombel JF, Reinisch W, Gibson PR, Collins J, Järnerot G, Hibi T, Rutgeerts P; PURSUIT-SC Study Group. Subcutaneous golimumab induces clinical response and remission in patients with moderate-to-severe ulcerative colitis. *Gastroenterology* 2014; **146**: 85-95; quiz e14 [PMID: 23735746 DOI: 10.1053/j.gastro.2013.05.048]

24 **Bosca-Watts MM**, Cortes X, Iborra M, Huguet JM, Sempere L, Garcia G, Gil R, Garcia M, Muñoz M, Almela P, Maroto N, Paredes JM. Short-term effectiveness of golimumab for ulcerative colitis: Observational multicenter study. *World J Gastroenterol* 2016; **22**: 10432-10439 [PMID: 28058024 DOI: 10.3748/wjg.v22.i47.10432]

25 **Tursi A**, Allegretta L, Buccianti N, Della Valle N, Elisei W, Forti G, Faggiani R, Gallina S, Hadad Y, Larussa T, Lauria A, Luzza F, Lorenzetti R, Mocci G, Penna A, Polimeni N, Pranzo G, Ricciardelli C, Zampaletta C, Picchio M. Effectiveness and Safety of Golimumab in Treating Outpatient Ulcerative Colitis: A Real-Life Prospective, Multicentre, Observational Study in Primary Inflammatory Bowel Diseases Centers. *J Gastrointestin Liver Dis* 2017; **26**: 239-244 [PMID: 28922435 DOI: 10.15403/jgld.2014.1121.263.trs]

26 **Feagan BG**, Rutgeerts P, Sands BE, Hanauer S, Colombel JF, Sandborn WJ, Van Assche G, Axler J, Kim HJ, Danese S, Fox I, Milch C, Sankoh S, Wyant T, Xu J, Parikh A; GEMINI 1 Study Group. Vedolizumab as induction and maintenance therapy for ulcerative colitis. *N Engl J Med* 2013; **369**: 699-710 [PMID: 23964932 DOI: 10.1056/NEJMoa1215734]

27 **Sandborn WJ**, Su C, Sands BE, D'Haens GR, Vermeire S, Schreiber S, Danese S, Feagan BG, Reinisch W, Niezychowski W, Friedman G, Lawendy N, Yu D, Woodworth D, Mukherjee A, Zhang H, Healey P, Panés J; OCTAVE Induction 1, OCTAVE Induction 2, and OCTAVE Sustain Investigators. Tofacitinib as Induction and Maintenance Therapy for Ulcerative Colitis. *N Engl J Med* 2017; **376**: 1723-1736 [PMID: 28467869 DOI: 10.1056/NEJMoa1606910]

28 **Ogata H**, Matsui T, Nakamura M, Iida M, Takazoe M, Suzuki Y, Hibi T. A randomised dose finding study of oral tacrolimus (FK506) therapy in refractory ulcerative colitis. *Gut* 2006; **55**: 1255-1262 [PMID: 16484504 DOI: 10.1136/gut.2005.081794]

29 **Baumgart DC**, Pintoffl JP, Sturm A, Wiedenmann B, Dignass AU. Tacrolimus is safe and effective in patients with severe steroid-refractory or steroid-dependent inflammatory bowel disease--a long-term follow-up. *Am J Gastroenterol* 2006; **101**: 1048-1056 [PMID: 16573777]

30 **Lv R**, Qiao W, Wu Z, Wang Y, Dai S, Liu Q, Zheng X. Tumor necrosis factor alpha blocking agents as treatment for ulcerative colitis intolerant or refractory to conventional medical therapy: a meta-analysis. *PLoS One* 2014; **9**: e86692 [PMID: 24475168 DOI: 10.1371/journal.pone.0086692]

31 **Engel T**, Ungar B, Yung DE, Ben-Horin S, Eliakim R, Kopylov U. Vedolizumab in IBD-Lessons From Real-world Experience; A Systematic Review and Pooled Analysis. *J Crohns Colitis* 2018; **12**: 245-257 [PMID: 29077833 DOI: 10.1093/ecco-jcc/jjx143]

32 **Ben-Horin S**, Kopylov U, Chowers Y. Optimizing anti-TNF treatments in inflammatory bowel disease. *Autoimmun Rev* 2014; **13**: 24-30 [PMID: 23792214]

33 **Ma C**, Huang V, Fedorak DK, Kroeker KI, Dieleman LA, Halloran BP, Fedorak RN. Outpatient Ulcerative Colitis Primary

Anti-TNF Responders Receiving Adalimumab or Infliximab Maintenance Therapy Have Similar Rates of Secondary Loss of Response. *J Clin Gastroenterol* 2015; **49**: 675-682 [PMID: 25389599 DOI: 10.1097/MCG.0000000000000265]

34 **Peyrin-Biroulet L**, Danese S, Argollo M, Pouillon L, Peppas S, Gonzalez-Lorenzo M, Lytras T, Bonovas S. Loss of Response to Vedolizumab and Ability of Dose Intensification to Restore Response in Patients With Crohn's Disease or Ulcerative Colitis: A Systematic Review and Meta-analysis. *Clin Gastroenterol Hepatol* 2019; **17**: 838-846.e2 [PMID: 29935327 DOI: 10.1016/j.cgh.2018.06.026]

35 **Cabriada JL**, Domènech E, Ibargoyen N, Hernández V, Clofent J, Ginard D, Gutiérrez-Ibarluzea I, Hinojosa J. Leukocytapheresis for steroid-dependent ulcerative colitis in clinical practice: results of a nationwide Spanish registry. *J Gastroenterol* 2012; **47**: 359-365 [PMID: 22105230 DOI: 10.1007/s00535-011-0499-2]

36 **Dignass A**, Akbar A, Hart A, Subramanian S, Bommelaer G, Baumgart DC, Grimaud JC, Cadiot G, Makins R, Hoque S, Bouguen G, Bonaz B. Safety and Efficacy of Granulocyte/Monocyte Apheresis in Steroid-Dependent Active Ulcerative Colitis with Insufficient Response or Intolerance to Immunosuppressants and/or Biologics [the ART Trial]: 12-week Interim Results. *J Crohns Colitis* 2016; **10**: 812-820 [PMID: 26818659 DOI: 10.1093/ecco-jcc/jjw032]

37 **Yamamoto T**, Iida T, Ikeya K, Kato M, Matsuura A, Tamura S, Takano R, Tani S, Osawa S, Sugimoto K, Shimoyama T, Hanai H. A multicenter retrospective study aiming to identify patients who respond well to adsorptive granulomonocytapheresis in moderately to severely active ulcerative colitis. *Clin Transl Gastroenterol* 2018; **9**: 170 [PMID: 29977035 DOI: 10.1038/s41424-018-0037-0]

38 **González Carro P**, Pérez Roldán F, Roncero García Escribano O, Lafuente R, Legaz Huidobro ML, Amigo Echenagusía A. Case report: combination therapy with granulocyte apheresis and infliximab for refractory Crohn's disease. *J Clin Apher* 2006; **21**: 249-251 [PMID: 16607627 DOI: 10.1002/jca.20093]

39 **Fukunaga K**, Yokoyama Y, Kamikozuru K, Yoshida K, Kikuyama R, Nagase K, Nakamura S, Takei Y, Miwa H, Matsumoto T. Selective depletion of peripheral granulocyte/monocyte enhances the efficacy of scheduled maintenance infliximab in Crohn's disease. *J Clin Apher* 2010; **25**: 226-228 [PMID: 20544712 DOI: 10.1002/jca.20242]

40 **Sono K**, Yamada A, Yoshimatsu Y, Takada N, Suzuki Y. Factors associated with the loss of response to infliximab in patients with Crohn's disease. *Cytokine* 2012; **59**: 410-416 [PMID: 22633084 DOI: 10.1016/j.cyto.2012.04.026]

41 **Ozeki K**, Tanida S, Mizoshita T, Tsukamoto H, Ebi M, Mori Y, Kataoka H, Kamiya T, Joh T. Combination Therapy with Intensive Granulocyte and Monocyte Adsorptive Apheresis plus Adalimumab: Therapeutic Outcomes in 5 Cases with Refractory Crohn's Disease. *Case Rep Gastroenterol* 2012; **6**: 765-771 [PMID: 23341799 DOI: 10.1159/000346312]

42 **Yokoyama Y**, Matsuoka K, Kobayashi T, Sawada K, Fujiyoshi T, Ando T, Ohnishi Y, Ishida T, Oka M, Yamada M, Nakamura T, Ino T, Numata T, Aoki H, Sakou J, Kusada M, Maekawa T, Hibi T. A large-scale, prospective, observational study of leukocytapheresis for ulcerative colitis: treatment outcomes of 847 patients in clinical practice. *J Crohns Colitis* 2014; **8**: 981-991 [PMID: 24556083 DOI: 10.1016/j.crohns.2014.01.027]

43 **Yokoyama Y**, Kamikozuru K, Watanabe K, Nakamura S. Inflammatory bowel disease patients experiencing a loss of response to infliximab regain long-term response after undergoing granulocyte/monocyte apheresis: A case series. *Cytokine* 2018; **103**: 25-28 [PMID: 29291447 DOI: 10.1016/j.cyto.2017.12.030]

44 **Scrivo B**, Vitello A, Cappello M. Response to "The combination therapy with cytapheresis plus vedolizumab in a corticosteroid-dependent patient with ulcerative colitis and previous Anti-TNF alfa failure". *Dig Liver Dis* 2018; **50**: 1103-1104 [PMID: 29871799 DOI: 10.1016/j.dld.2018.05.001]

45 **Sáez-González E**, Aguas M, Huguet JM, Nos P, Beltrán B. Combination therapy with cytapheresis plus vedolizumab in a corticosteroid-dependent patient with ulcerative colitis and previous ANTI-TNF-α drug failure. *Dig Liver Dis* 2018; **50**: 415-417 [PMID: 29397323 DOI: 10.1016/j.dld.2018.01.124]

46 **Tanida S**, Mizoshita T, Ozeki K, Katano T, Tanaka M, Nishie H, Shimura T, Okamoto Y, Kubota E, Kataoka H, Joh T. Combination Therapy With Intensive Granulocyte and Monocyte Adsorptive Apheresis Plus Ustekinumab in Patients With Refractory Crohn's Disease. *Ther Apher Dial* 2018; **22**: 295-300 [PMID: 29790276 DOI: 10.1111/1744-9987.12697]

47 **Rodríguez-Lago I**, Sempere L, Gutiérrez A, Núñez A, Leo Carnerero E, Hinojosa E, Mora M, Cañete F, Mañosa M, Herrera C, Beltrán B, Forés A, Arjona D, Barreiro-de Acosta M, Khorrami S, Aguirre U, Ginard D, Cabriada JL. Granulocyte-monocyte apheresis: an alternative combination therapy after loss of response to anti-TNF agents in ulcerative colitis. *Scand J Gastroenterol* 2019; **54**: 459-464 [PMID: 30982369 DOI: 10.1080/00365521.2019.1600715]

48 **Rodríguez-Lago I**, Benítez JM, Sempere L, Sáez-González E, Barreiro-de Acosta M, de Zárate JO, Cabriada JL. The combination of granulocyte-monocyte apheresis and vedolizumab: A new treatment option for ulcerative colitis? *J Clin Apher* 2019; **34**: 680-685 [PMID: 31518013 DOI: 10.1002/jca.21746]

49 **Nakamura M**, Yamamura T, Maeda K, Sawada T, Mizutani Y, Ishikawa E, Ohashi A, Kajikawa G, Furukawa K, Ohno E, Honda T, Kawashima H, Ishigami M, Fujishiro M. Refractory Ulcerative Colitis Improved by Scheduled Combination Therapy of Vedolizumab and Granulocyte and Monocyte Adsorptive Apheresis. *Intern Med* 2020; **59**: 3009-3014 [PMID: 32727993 DOI: 10.2169/internalmedicine.5302-20]

50 **Tanida S**, Ozeki K, Mizoshita T, Kitagawa M, Ozeki T, Tanaka M, Nishie H, Shimura T, Kubota E, Kataoka H. Combination Therapy With Tofacitinib Plus Intensive Granulocyte and Monocyte Adsorptive Apheresis as Induction Therapy for Refractory Ulcerative Colitis. *J Clin Med Res* 2020; **12**: 36-40 [PMID: 32010420 DOI: 10.14740/jocmr4037]

51 **Yokoyama Y**, Sawada K, Aoyama N, Yoshimura N, Sako M, Hirai F, Kashiwagi N, Suzuki Y. Efficacy of Granulocyte and Monocyte Adsorptive Apheresis in Patients With Inflammatory Bowel Disease Showing Lost Response to Infliximab. *J Crohns Colitis* 2020; **14**: 1264-1273 [PMID: 32166331 DOI: 10.1093/ecco-jcc/jjaa051]

52 **Motoya S**, Tanaka H, Shibuya T, Osada T, Yamamoto T, Hongo H, Mizuno C, Saito D, Aoyama N, Kobayashi T, Ito H, Tanida S, Nojima M, Kokuma S, Hosoi E. Safety and effectiveness of granulocyte and monocyte adsorptive apheresis in patients with inflammatory bowel disease in special situations: a multicentre cohort study. *BMC Gastroenterol* 2019; **19**: 196 [PMID: 31752695 DOI: 10.1186/s12876-019-1110-1]

53 **Yamamoto T**, Umegae S, Matsumoto K. Mucosal healing in patients with ulcerative colitis during a course of selective leukocytapheresis therapy: a prospective cohort study. *Inflamm Bowel Dis* 2010; **16**: 1905-1911 [PMID: 20310015 DOI: 10.1002/ibd.21260]

54 **Lindberg A**, Eberhardson M, Karlsson M, Karlén P. Long-term follow-up with Granulocyte and Monocyte Apheresis re-treatment in patients with chronically active inflammatory bowel disease. *BMC Gastroenterol* 2010; **10**: 73 [PMID: 20604939 DOI: 10.1186/1471-230X-10-73]

55 **Sandborn WJ**. Preliminary data on the use of apheresis in inflammatory bowel disease. *Inflamm Bowel Dis* 2006; **12** Suppl 1: S15-S21 [PMID: 16378006]

56 **Hibi T**, Sameshima Y, Sekiguchi Y, Hisatome Y, Maruyama F, Moriwaki K, Shima C, Saniabadi AR, Matsumoto T. Treating ulcerative colitis by Adacolumn therapeutic leucocytapheresis: clinical efficacy and safety based on surveillance of 656 patients in 53 centres in Japan. *Dig Liver Dis* 2009; **41**: 570-577 [PMID: 19211314 DOI: 10.1016/j.dld]

57 **Sakuraba A**, Motoya S, Watanabe K, Nishishita M, Kanke K, Matsui T, Suzuki Y, Oshima T, Kunisaki R, Matsumoto T, Hanai H, Fukunaga K, Yoshimura N, Chiba T, Funakoshi S, Aoyama N, Andoh A, Nakase H, Mizuta Y, Suzuki R, Akamatsu T, Iizuka M, Ashida T, Hibi T. An open-label prospective randomized multicenter study shows very rapid remission of ulcerative colitis by intensive granulocyte and monocyte adsorptive apheresis as compared with routine weekly treatment. *Am J Gastroenterol* 2009; **104**: 2990-2995 [PMID: 19724269 DOI: 10.1038/ajg.2009.453]

58 **Takayama T**, Kanai T, Matsuoka K, Okamoto S, Sujino T, Mikami Y, Hisamatsu T, Yajima T, Iwao Y, Ogata H, Hibi T. Long-term prognosis of patients with ulcerative colitis treated with cytapheresis therapy. *J Crohns Colitis* 2013; **7**: e49-e54 [PMID: 22633997 DOI: 10.1016/j.crohns.2012.05.005]

59 **Iizuka M**, Etou T, Shimodaira Y, Hatakeyama T, Sagara S. Cytapheresis re-induces high-rate steroid-free remission in patients with steroid-dependent and steroid-refractory ulcerative colitis. *World J Gastroenterol* 2021; **27**: 1194-1212 [PMID: 33828394 DOI: 10.3748/wjg.v27.i12.1194]

60 **Cabriada JL**, Ibargoyen N, Hernández A, Bernal A, Castiella A. Sustained remission after steroids and leukocytapheresis induced response in steroid-dependent ulcerative colitis: results at 1 year. *Dig Liver Dis* 2010; **42**: 432-435 [PMID: 19833566 DOI: 10.1016/j.dld.2009.09.001]

61 **Imperiali G**, Amato A, Terpin MM, Beverina I, Bortoli A, Devani M, Viganò C; Study Group on IBD (GSMII). Granulocyte-Monocyte Apheresis in Steroid-Dependent, Azathioprine-Intolerant/Resistant Moderate Ulcerative Colitis: A Prospective Multicenter Study. *Gastroenterol Res Pract* 2017; **2017**: 9728324 [PMID: 29403531 DOI: 10.1155/2017/9728324]

62 **Ishiguro Y**, Ohmori T, Umemura K, Iizuka M. Factors associated with the outcomes in ulcerative colitis patients undergoing granulocyte and monocyte adsorptive apheresis as remission induction therapy: A multicenter cohort study. *Ther Apher Dial* 2021; **25**: 502-512 [PMID: 33029920 DOI: 10.1111/1744-9987.13594]

63 **Domènech E**, Grífols JR, Akbar A, Dignass AU. Use of granulocyte/monocytapheresis in ulcerative colitis: A practical review from a European perspective. *World J Gastroenterol* 2021; **27**: 908-918 [PMID: 33776362 DOI: 10.3748/wjg.v27.i10.908]

64 **Saniabadi AR**, Hanai H, Suzuki Y, Ohmori T, Sawada K, Yoshimura N, Saito Y, Takeda Y, Umemura K, Kondo K, Ikeda Y, Fukunaga K, Nakashima M, Beretta A, Bjarnason I, Lofberg R. Adacolumn for selective leukocytapheresis as a non-pharmacological treatment for patients with disorders of the immune system: an adjunct or an alternative to drug therapy? *J Clin Apher* 2005; **20**: 171-184 [PMID: 15892107 DOI: 10.1002/jca.20046]

65 **Hanai H**, Watanabe F, Yamada M, Sato Y, Takeuchi K, Iida T, Tozawa K, Tanaka T, Maruyama Y, Matsushita I, Iwaoka Y, Saniabadi A. Correlation of serum soluble TNF-alpha receptors I and II levels with disease activity in patients with ulcerative colitis. *Am J Gastroenterol* 2004; **99**: 1532-1538 [PMID: 15307873 DOI: 10.1111/j.1572-0241.2004.30432.x]

66 **Tominaga K**, Nakano M, Hoshino M, Kanke K, Hiraishi H. Efficacy, safety and cost analyses in ulcerative colitis patients undergoing granulocyte and monocyte adsorption or receiving prednisolone. *BMC Gastroenterol* 2013; **13**: 41 [PMID: 23452668 DOI: 10.1186/1471-230X-13-41]

World Journal of Gastroenterology

Submit a Manuscript: https://www.f6publishing.com

World J Gastroenterol 2022 September 14; 28(34): 4973-4992

DOI: 10.3748/wjg.v28.i34.4973

ISSN 1007-9327 (print) ISSN 2219-2840 (online)

ORIGINAL ARTICLE

Basic Study

Long noncoding RNA ZNFX1-AS1 promotes the invasion and proliferation of gastric cancer cells by regulating LIN28 and CAPR1N1

Zhong-Ling Zhuo, Hai-Peng Xian, Yu-Jing Sun, Yan Long, Chang Liu, Bin Liang, Xiao-Tao Zhao

Specialty type: Gastroenterology and hepatology

Provenance and peer review: Unsolicited article; Externally peer reviewed.

Peer-review model: Single blind

Peer-review report's scientific quality classification

Grade A (Excellent): 0
Grade B (Very good): B
Grade C (Good): 0
Grade D (Fair): 0
Grade E (Poor): 0

P-Reviewer: Kotelevets SM, Russia

Received: August 2, 2021
Peer-review started: August 2, 2021
First decision: October 2, 2021
Revised: October 29, 2021
Accepted: August 23, 2022
Article in press: August 23, 2022
Published online: September 14, 2022

Zhong-Ling Zhuo, Hai-Peng Xian, Yan Long, Chang Liu, Xiao-Tao Zhao, Department of Clinical Laboratory, Peking University People's Hospital, Beijing 100044, China

Zhong-Ling Zhuo, The Key Laboratory of Geriatrics, Peking University Fifth School of Clinical Medicine, Beijing 100730, China

Yu-Jing Sun, Department of Clinical Laboratory, Peking University International Hospital, Beijing 100044, China

Bin Liang, Department of Gastrointestinal Surgery, Peking University People's Hospital, Beijing 100044, China

Corresponding author: Xiao-Tao Zhao, MD, Director, Department of Clinical Laboratory, Peking University People's Hospital, No. 11 Xizhimen South Street, Beijing 100044, China. zhaoxt@bjmu.edu.cn

Abstract

BACKGROUND

Long noncoding RNA (lncRNA) ZNFX1-AS1 (ZFAS1) is a newly discovered lncRNA, but its diagnostic value in gastric cancer is unclear.

AIM

To investigate the potential role of ZFAS1 in gastric cancer and to evaluate the clinical significance of ZFAS1 as a biomarker for gastric cancer screening.

METHODS

Quantitative real-time polymerase chain reaction (qRT-PCR) was used to screen for gastric cancer-associated lncRNAs in gastric cancer patients, gastric stromal tumor patients, gastritis or gastric ulcer patients, and healthy controls. Correlations between ZFAS1 expression and clinicopathological features were analyzed. The biological effects of ZFAS1 on the proliferation, migration, and invasion of gastric cancer cells were studied by MTT, colony formation, and transwell migration assays. The potential mechanism of ZFAS1 was demonstrated using enzyme-linked immunosorbent assay and qRT-PCR. The relationship between ZFAS1 and tumorigenesis was demonstrated using *in vivo* tumor formation assays.

RESULTS
The plasma level of lncRNA ZFAS1 was significantly higher in preoperative patients with gastric cancer than in individuals in the other 4 groups. Increased expression of ZFAS1 was significantly associated with lymph node metastasis, advanced TNM stage, and poor prognosis. ZFAS1 regulated the proliferation, migration, and invasion of gastric cancer cells and regulated the growth of gastric cancer cells *in vivo*. LIN28 and CAPRIN1 were identified as key downstream mediators of ZFAS1 in gastric cancer cells.

CONCLUSION
LncRNA ZFAS1 promoted the invasion and proliferation of gastric cancer cells by modulating LIN28 and CAPRIN1 expression, suggesting that ZFAS1 can be used as a potential diagnostic and prognostic biomarker in gastric cancer.

Key Words: Long noncoding RNA; ZNFX1-AS1; Gastric cancer; Biomarker; Invasion; Proliferation

©The Author(s) 2022. Published by Baishideng Publishing Group Inc. All rights reserved.

Core Tip: Long noncoding RNA (lncRNA) ZNFX1-AS1 (ZFAS1) is a newly discovered lncRNA, but its diagnostic value in gastric cancer is unclear. This study aimed to investigate the potential role of ZFAS1 in gastric cancer and to evaluate the clinical significance of ZFAS1 as a biomarker for gastric cancer screening. LncRNA ZFAS1 promoted invasion and proliferation of gastric cancer cells by modulating LIN28 and CAPRIN1, suggesting that ZFAS1 can be used as a potential biomarker for the diagnosis and prognosis of gastric cancer.

Citation: Zhuo ZL, Xian HP, Sun YJ, Long Y, Liu C, Liang B, Zhao XT. Long noncoding RNA ZNFX1-AS1 promotes the invasion and proliferation of gastric cancer cells by regulating LIN28 and CAPR1N1. *World J Gastroenterol* 2022; 28(34): 4973-4992
URL: https://www.wjgnet.com/1007-9327/full/v28/i34/4973.htm
DOI: https://dx.doi.org/10.3748/wjg.v28.i34.4973

INTRODUCTION

Gastric carcinoma is the 2nd primary cause of death due to carcinoma and the 6th most common cancer worldwide. Approximately 1000000 new cases of gastric cancer are diagnosed each year, and approximately 800000 patients die from the disease, accounting for approximately 8.2% of global cancer-related mortality[1]. The progression-free survival (PFS) rate and prognosis of gastric carcinoma highly depend on the TNM stage of the disease. The high mortality is associated with the faultiness of standard screening protocols and lack of overt early symptoms[1]. Therefore, early detection and optimal treatment are necessary to improve the prognosis of gastric carcinoma. However, current biologic markers, such as carbohydrate antigen 199 (CA-199) and carcinoembryonic antigen (CEA), have low sensitivity and specificity[2]. Therefore, there is an urgent need to find novel biomarkers for early diagnosis of gastric cancer.

Long noncoding RNAs (lncRNAs) are a class of non-protein-coding RNA molecules > 200 nucleotides in length[3]. Recently, some studies have reported that lncRNAs are involved in protein modification and gene expression and that their dysregulation leads to a variety of genetic diseases[4-6]. Published articles have also shown that lncRNAs exhibit significant regulatory effects on transcription patterns in malignant tumors, some of which involve tumor cell invasion and metastasis, with a poor prognosis[6, 7]. For example, H19 and SUMO1 pseudogene 3 (SUMO1P3) are upregulated in gastric cancer, while gastric cancer-associated transcript 1 is downregulated[7-11]. Additionally, HOTAIR overexpression may be associated with tumor escape mechanisms[12]. These studies strongly suggest that lncRNAs underlie the molecular etiology of gastric carcinoma. It is worth noting that the detection of circulating lncRNAs provides a new gastric biomarker for gastric cancer that is expected to be useful for monitoring and screening patients with gastric cancer[13].

Here, we selected 15 candidate cancer-associated lncRNAs. Among these lncRNAs, lncRNA ZNFX1-AS1 (ZFAS1) was found to be upregulated in the plasma of preoperative gastric cancer patients compared with healthy controls, and expression of ZFAS1 was significantly associated with lymphatic invasion, advanced TNM stage, and poor prognosis. We then investigated the biological effects of ZFAS1 on the survival, proliferation, and migration of gastric cancer cells. The underlying mechanism of ZFAS1 and the relationship between ZFAS1 and tumorigenesis were identified. These results showed that lncRNA ZFAS1 is a potential biomarker for gastric cancer.

MATERIALS AND METHODS

Sample collection and ethics statement

All samples were obtained from Peking University People's Hospital between July 2015 and June 2016. Seventy-five matched (pre- and postoperative) whole blood and serum samples were collected from patients who underwent gastrointestinal surgery for gastric resection. In addition, intraperitoneal free cancer cell (IFCC) samples were collected from 60 of these patients. Other whole blood and serum specimens were collected from 60 gastric stromal tumor patients (before surgery), 60 gastritis or ulcer patients (before treatment), and 75 healthy controls. All specimens were collected with the corresponding patient information, such as age, sex, and collection time. In addition, the tumor size, tumor location (evaluated according to the National Comprehensive Cancer Network Clinical Practice Guidelines in Oncology, Version II[14]), pathological type, degree of differentiation (based on the World Health Organization Classification of Tumors of the Digestive System, 4th edition[15]), TNM stage and lymphatic invasion status (based on the American Joint Committee on Cancer Staging Manual, 7th edition[16]) of the corresponding patients were collected.

Plasma and serum samples were collected in BD vacutainer ethylenediamine tetraacetic acid tubes and BD vacutainer somatostatin tubes (BD Biosciences, NJ, United States), respectively. Preoperative samples of patients with gastric cancer were obtained at least 2 mo before surgery or after radiotherapy or chemotherapy. Postoperative samples from these patients were collected 7-10 d after surgery. Samples from patients with gastric stromal tumor or gastritis/peptic ulcer were collected before any treatment was administered. The healthy control samples were randomly collected from normal subjects. For plasma samples, a special centrifugation protocol (2348 × g for 30 min at 4 °C; 4696 × g for 5 min at 4 °C; 10733 × g for 5 min at 4 °C) was performed to prevent contamination with cellular nucleic acids. Plasma and IFCC samples were stored at -80 °C in 3 volumes of TRIzol® reagent (Qiagen, CA, United States) for further analysis. Serum samples were analyzed directly[17]. This study was approved by the Research Ethics Committee of Peking University People's Hospital. Patient data and samples were treated according to the ethical and legal criteria adopted in the 2013 Declaration of Helsinki. Written informed consent for ethical approval and patient consent was obtained from all participants.

RNA extraction and quantitative real-time polymerase chain reaction

This method is the same as that described in our previously published article[17]. LncRNA was extracted from plasma using a Direct-zol™ RNA MiniPrep R2050i Kit (Zymo Research, CA, United States) according to the manufacturer's protocol. The concentration and purity of total RNA were measured using a NanoDrop 2000c spectrophotometer (Thermo Fisher Scientific, MA, United States). Total RNA was then solubilized using RNase-free water, and reverse transcription was immediately performed using PrimeScript RT Master Mix (Takara Bio, Kyushu, Japan) according to the manufacturer's instructions. After reverse transcription, quantitative polymerase chain reaction (qPCR) was performed in a LightCycler 480 Instrument II (Roche Diagnostics, Basel, Switzerland) using TransStart Green qPCR SuperMix (TransGen, Beijing, China) according to the supplier's instructions. The primers used for qPCR were designed with Primer Premier V 5.0 (Premier Biosoft International, CA, United States) and were synthesized by Beijing Sunbiotech Co., Ltd. (Beijing, China). The sequences of all primers, including those specific for GAPDH, are listed in Table 1. PCR was carried out with initial denaturation at 95 °C for 3 min followed by 40 cycles of 1 min at 95 °C and 1 min at 60 °C with subsequent detection. Due to the stability of GAPDH in plasma, it was chosen as the internal control for data standardization. For the calculations, the equation $\Delta C_q = C_{q\ \text{selected lncRNA}} - C_{q\ \text{GAPDH lncRNA}}$ was used, where ΔC_q was defined as the difference in the quantification cycle (C_q) values. Every specimen was analyzed in triplicate, and the experiment was repeated 3 times.

Cell culture

The human gastric cancer cell lines BGC-823 and SGC-7901 were a gift from Peking University People's Hospital Gastrointestinal Surgery Laboratory and were maintained in RPMI 1640 medium (Invitrogen, CA, United States) supplemented with 10% fetal bovine serum (FBS) (Gibco, CA, United States). The flask was incubated in a humidified incubator at 37 °C under 5% CO_2 in air.

LncRNA silencing and overexpression

ZFAS1-siRNA against ZFAS1 was synthesized by GenePharma (Shanghai, China). BGC-823 and SGC7901 cells were grown in 6-well plates (2 × 10^5cells/well) and transfected for 36 h using Lipofectamine RNAiMAX Transfection Reagent (Invitrogen, CA, United States). The ZFAS1 siRNA sequences were as follows: ZFAS1 siRNA1, 5′-AGACGCGAAAGAACGAAUGTT-3′; ZFAS1 siRNA2, 5′-UUACAAGGCAGACUGAAUCTT-3′; and ZFAS1 siRNA3, 5′-UAUGCAGGUAGGCAGUUAGTT-3′. The GAPDH siRNA and negative control siRNA sequences were as follows: GAPDH siRNA, 5'-ACGUGACACGUUCGGAGAATT-3' and negative control siRNA, 5'-ACGUGCAC AGUACUAGGAATT-3'.

Table 1 List of all primers used to screen gastric cancer-associated long noncoding RNAs

Name	Forward-primer	Reverse-primer
GAPDH	ACCCACTCCTCCACCTTTGAC	TGTTGCTGTAGCCAAATTCGTT
H19	TACAACCACTGCACTACCTG	TGGAATGCTTGAAGGCTGCT
CCAT1	CATTGGGAAAGGTGCCGAGA	ACGCTTAGCCATACAGAGCC
HOTAIR	GGTAGAAAAAGCAACCACGAAGC	ACATAAACCTCTGTCTGTGAGTGCC
LINC00152	CTCCAGCACCTCTACCTGTTG	GGACAAGGGATTAAGACACACA
ZNFX1-AS1	CCAGTTCCACAAGGTTAC	GCAGGTAGGCAGTTAGAA
PVT1	CTTGAGAACTGTCCTTACG	CAGATGAACCAGGTGAAC
GAS5	CACAGGCATTAGACAGAA	AGGAGCAGAACCATTAAG
SNHG12	GACTTCCGGGGTAATGACAG	GCCTTCTGCTTCCCATAGAG
TUG1	TAGCAGTTCCCCAATCCTTG	CACAAATTCCCATCATTCCC
CHET1	CCCCACAAATGAAGACACT	TTCCCAACACCCTATAAGAT
SUMP1P3	ACTGGGAATGGAGGAAGA	TGAGAAAGGATTGAGGGAAAAG
GACAT3	GGGGGCTTGTTTCTTTGTGTAG	CATTCGGCTCTGACCTCTCAC
ABHD11-AS1	GAACGGGATGAAGCCATTG	GCTGATTCTGGACCTGCTG
GACAT2	TGGATGCTTACAAAGGACTGG	CTGCAATTACGGAAAGAGCTG
uc001lsz	GACGGCACCTACTACACCTT	GCTGACCACCTTGTTGTTGAA

The ZFAS1 overexpression short hairpin RNA (ZFAS1-shRNA1), sh-ZFAS1 directed against ZFAS1 short hairpin RNA (ZFAS1-shRNA2), and NC-shRNA short hairpin RNA constructs were synthesized by GenePharma (Shanghai, China). The sequences of ZFAS1-shRNA1, ZFAS1-shRNA2, and NC-shRNA are shown in Table 2. BGC-823 and SGC7901 cells were grown in 6-well plates (2×10^5 cells/well) and transduced for 36 h using Polybrene (GenePharma, REVG0001) and Enhanced Infection Solution (GenePharma, REVG0002).

MTT assay

After transduction with NC-shRNA, ZFAS1-shRNA1, and ZFAS1-shRNA2, BGC823 and SGC7901 cells were trypsinized, and six replicates of 12×10^3 cells per well were seeded in 96-well plates, with wells without cells used as blank wells. Proliferation was measured by an MTT (Sigma Aldrich, St. Louis, MO, United States) transformation assay. Briefly, 20 mL of MTT solution (5 mg/mL) was added to each well, and cells were grown for 4 h at 37 °C. After adding 100 mL of the dissolved solution (10% SDS in 0.01 M HCl solution), cells were further cultured at 37 °C for 3 h. The specific optical density of all wells was then measured at 490 nm.

Transwell migration assay

BGC823 and SGC7901 cells were suspended in serum-free medium after transduction with NC-shRNA, ZFAS1-shRNA1, and ZFAS1-shRNA2 and inoculated into transwell chambers with inserts of 8 μm pore size. Medium containing 10% FBS was placed in the bottom chamber. After 36 h of incubation, cells that migrated through the membrane to the lower surface were fixed with paraformaldehyde, stained with crystal violet, counted, and photographed. The results are shown as the average of three independent experiments.

Colony formation assay

BGC823 and SGC7901 cells transduced with NC-shRNA, ZFAS1-shRNA1, and ZFAS1-shRNA2 were seeded into 6-well plates (1000 cells per well) and cultured in a humidified incubator at 37 °C in 5% CO_2 for 10 d. The medium was changed every 3 d. At the end of the incubation period, the cultured cells were fixed with 4% paraformaldehyde and stained with crystal violet to assess the number of colonies. The results are shown as the average of three independent experiments.

Prediction and expression of ZFAS1 binding proteins

Binding proteins of lncRNA ZFAS1 were predicted based on the starBase V2.0 database (http://starbase.sysu.edu.cn). The primers specific for the mRNA sequences of the genes encoding the binding proteins were designed according to the nucleic acid sequence information for the corresponding proteins in GenBank (https://www.ncbi.nlm.nih.gov/genbank/) with a primer design tool (

Table 2 The sequences of ZNFX1-AS1-shRNA1, ZNFX1-AS1-shRNA2 and NC-shRNA

	Sequence
ZFAS1-shRNA1	ACCGGTCGGGGGCCCAGGGTGGAGAGCACGAGGGCCTGGCCCAGGCACGGCCGGCGCCTCCGCCCTCGA GGAGGGCGTCACCTCAGCTCCCCCCGGCGGCGGAGCCGGCGGGCTCAGGCGGGCGCGGCTGAGGGGAGCGGAC CGCGGGGGGCGGGAGATGACTGCGCCCAAGGCCTTTGCGGGCCTCAGCCGGCCCCAGAGGAAGGGGAACCCGT CGAGCGGTTTGGTGCGTGTGAAGCGCGACATGGCGAGGAAGCGGACAAGCCCGGGTGGCCCGGCGTGTAGAGG GAAGGGGGCGGGGCTAGACGCGGCCTGGACAACTACTAGAGCGCCTCGGGCTGTGCTGCTCGAGACTACATTT CCCAGAGCGACGCGCGCGGAGCGGGCGGGAAAGAGAGCGTTTCGGGTCCAGTGCGCAGGTGCGAAAGCCATCT TTGGTTATATAAGGGAGGTTCAGGAAGCCATTCGTTCTTTCGCGTCTGCGGTGCCCGGAGTGTGGTACTTCTC CTAGTTGCAGTCAGGCTTCATACGCTATTGTCCTGCCCGTTAGAGCAGCCAGCGGGTACAGAATGGATTTTGG AAGAGGGAGTCACCACTGGACCTCCAAGGAAGCCACGTGCAGACATCTACAACCTTCGATCTCCTGACGAGTT TATTGTTGGCCAAAACCAGGCTTTGATTGAACCAGGATGAATGCGGGTGTTGGAAGTAGAATATATATATACA TATAAAATTGGTTGGGAGCCACGTGTACCAGTGTGTGTTGATCTTGGCTTGATTCAGTCTGCCTTGTAACAGA AACTGGCGATGGAATATGAGAGGAGCCCTCTGGAAAGAAAAGGACAGACCCTGTGCTTTCATGAAAGTGAAGA TCTGGCTGAACCAGTTCCACAAGGTTACTGTATACATAGCCTGAGTTTAAAAGGCTGTGCCCACTTCAAGAAT GTCATTGTTAGACTTTGAAATTTCTAACTGCCTACCTGCATAAAGAAAATAAAATCTTTTAAATCAAAAGCTAGC
ZFAS1-shRNA2	TTACAAGGCAGACTGAATCTT
NC-shRNA	TTCTCCGAACGTGTCACGT

ZFAS1: ZNFX1-AS1.

http://www.ncbi.nlm.nih.gov/tools/primer-Blast). The sequences of all primers, including those specific for GAPDH, are listed in Table 3.

NC-shRNA, ZFAS1-shRNA1, and ZFAS1-shRNA2 were transduced into BGC823 and SGC7901 cells, and mRNA was then reverse transcribed. The mRNA expression levels of the genes encoding the candidate lncRNA ZFAS 1 binding proteins were determined by quantitative real-time-PCR (qRT-PCR) using the primers listed in Table 3. The experimental method was the same as that described previously.

Protein extraction and enzyme-linked immunosorbent assay

Stably transfected cells, as well as tumor/lymph node tissue from BALB/c nude mice, were lysed with NP40 cell lysis buffer (Invitrogen, CA, United States) supplemented with SigmaFAST™ protease inhibitor tablets (Sigma Aldrich, St. Louis, MO, United States). LIN28, CAPRIN1, CEA, and CK20 were detected by enzyme-linked immunosorbent assay (ELISA) using a Mouse Protein lin-28 homolog A (Lin28a) ELISA Kit (ELISAGenie, Dublin, Ireland), a Human Caprin 1 (CAPRIN1) ELISA Kit (Abbexa, Cambridge, United Kingdom), a CEA ELISA Kit (Bioss, United Kingdom) and CK20 ELISA kits (FKBIO, Chengdu, China), respectively.

In vivo tumor formation assay

Four-week-old female athymic BALB/c nude mice were maintained under specific pathogen-free conditions and operated on according to the protocol approved by the Beijing Medical Laboratory Animal Management Committee. NC-shRNA-, ZFAS1-shRNA1-, and ZFAS1-shRNA2-transduced BGC823 cells were harvested. For tumor formation assays, 10^7 cells were injected subcutaneously into one side of each mouse. Tumor growth was examined every week, and the tumor volume was calculated using the equation V = 0.5 × D × d2 (V, volume; D, longitudinal diameter; d, latitudinal diameter). The expression of lncRNA ZFAS1 in BALB/c mouse blood was detected by qRT-PCR every week, and the primer sequences are listed in Table 1. The expression of LIN28 and CAPRIN1 proteins in BALB/c nude mouse tumors and the expression of CEA and CK20 in BALB/c nude mouse lymph nodes were detected by ELISA after four weeks. This study was conducted in strict accordance with the National Institutes of Health Guidelines for the Care and Use of Laboratory Animals. The program was approved by the Animal Experiment Ethics Committee of Peking University People's Hospital.

Statistical analysis

The formula $2^{-\Delta\Delta Ct}$ were used to calculate the levels of relative lncRNA expression in plasma[18]. Based on this formula, all relative lncRNA expression levels in plasma were evaluated. Continuous variables were described by the mean ± SD (normal distribution), or the median and interquartile range M (P25, P75) (non-normal distribution). The *t*-test or Mann-Whitney *U* test was used according to the data distribution to identify statistically significant differences. For categorical variables, the percentages of patients in each category were calculated using the χ^2 test or Fisher's exact test. In addition, receiver operating characteristic (ROC) curve analysis was performed to assess the diagnostic value of circulating lncRNA and traditional tumor markers in distinguishing between gastric carcinoma patients and healthy subjects. Statistical analysis was performed using SPSS software version 19.0 (IBM Corp., Armonk, NY, United States). *P* values less than 0.05 were considered significant.

Table 3 List of primers used to detect mRNA expression of long noncoding RNA binding proteins

Name	Forward-primer (5' to 3')	Reverse-primer (5'to 3')
GAPDH	ACCCACTCCTCCACCTTTGAC	TGTTGCTGTAGCCAAATTCGTT
UPF1	GGTCCCTGATAATTATGGCGATG	ACGGCATAAACCTGGGAGTG
eIF4AIII	GGCATCTACGCTTACGGTTT	CAGCCAACTCTCTTGTGGGA
IGF2BP1	AGCTCCTTTATGCAGGCTCC	GAGCCTTGAATTGGGCCTCT
FMRP	CTCAAGGCTTGGCAGGGTATG	CCGTGCCCCCTATTTCTGTA
LIN28	AGATCAAAAGGAGACAGGTGCT	AATAGCCCCCACCCATTGTG
IGF2BP2	ACCCTCTCGGGTAAAGTGGA	GTTGACAACGGCGGTTTCTG
FUS	GCAAGATGGATTCCAGGGGTG	TCCAGGAAAGTGAAAAGGGGG
ZC3H7B	TGTGCAAAGGAGGAGATCGAC	ACAGACGGAGAGTCCTTGGT
IGF2BP3	CCTGGTGAAGACTGGCTACG	CCAGCACCTCCCACTGTAAAT
CAPRIN1	CTGCTGGCTGGCTAAGTCC	GGCCGAGGGCATCGTG

RESULTS

Relative expression of a selected subgroup of lncRNAs (plasma) from 15 gastric cancer patients and 15 healthy control subjects

Fifteen matched samples from preoperative and postoperative gastric cancer patients and samples from 15 healthy control subjects were used as the sample cohort. The general characteristics and clinicopathological features of all subjects are provided in Table 4. The relative expression of the 15 lncRNAs, namely, uc001 Lsz/HOTAIR/CCAT1/H19/GACAT2/ABHD11-AS1/GACAT3 /SUMO1P3/CHET1/TUG1/SNHG12/GAS5/PVT1/LINC00152, and ZFAS1, was evaluated in the plasma of all subjects. As mentioned in Figure 1, the levels of lncRNA ZFAS1 in preoperative patient plasma were significantly higher than those in postoperative patient and healthy control subject plasma ($P < 0.01$).

Relative levels of the lncRNA ZFAS1 in the plasma of healthy control subjects, gastritis/peptic ulcer patients, GIST patients, and preoperative and postoperative gastric cancer patients

The general characteristics and clinicopathological features of 60 healthy control subjects, 60 gastritis/peptic ulcer patients, 60 GIST patients, and 60 patients with matched preoperative and postoperative data are summarized in Table 5. The relative levels of ZFAS1 in the plasma of all subjects were assessed by qRT-PCR. As shown in Figure 2A, the levels of lncRNA ZFAS1 in preoperative patient plasma were significantly higher than those in plasma from the individuals in the other four groups ($P < 0.01$).

Relative levels of lncRNA ZFAS1 (plasma) in preoperative gastric carcinoma patients (different TNM stages)

We used the ΔΔCt formula to calculate the relative levels of lncRNA ZFAS1 in the samples (plasma) of patients with different TNM stages, including 20 patients with stage I and II disease and 40 patients with stage III and IV disease. As mentioned in Figure 2B, the median relative levels of lncRNA ZFAS1 in healthy controls, patients with stage I and II disease, and patients with stage III and IV disease were 0.81, 1.61, and 2.52, respectively. The relative levels in early- and advanced-stage patients were significantly higher than that in healthy controls ($P < 0.01$).

Relative levels of lncRNA ZFAS1 in 60 matched plasma samples from pre-operative and post-operative gastric carcinoma patients

Sixty matched pre-operative and post-operative samples (plasma) were included in our research. We found that the median relative levels of ZFAS1 before and after surgery were 2.22 and 1.01, respectively. The level decreased in 55 of the 60 gastric cancer patients (92%) approximately 10 d after surgery ($P < 0.01$; Figure 2C).

Correlation between the relative level of lncRNA ZFAS1 in IFCC and plasma samples

Sixty matched preoperative patient plasma and IFCC samples were collected. We used the ΔΔCt method to evaluate the relative levels of ZFAS1 in plasma and IFCC. As shown in Figure 2D, the relative levels of ZFAS1 in plasma and IFCC were strongly positively correlated ($R^2 = 0.76$, $P < 0.01$).

Table 4 General characteristics and clinicopathological factors of gastric cancer patients and healthy control subjects

Variables	Gastric cancer (*n* = 15)	Healthy control (*n* = 15)
Gender		
Male	12	12
Female	3	3
Age (yr)		
Mean	61	62
Range	48-70	47-80
Tumor site[1]		
Upper third	3	-
Middle third	4	-
Lower third	8	-
Tumor size		
≥ 5 cm	6	-
< 5 cm	9	-
Pathological differentiation[2]		
Undifferentiated or poorly differentiated	12	-
Others	3	-
TNM classification[3]		
I + II	4	-
III + IV	11	-
Lymphatic invasion[3]		
Positive	11	-
Negative	4	-

[1]According to National Comprehensive Cancer Network Clinical Practice Guidelines in Oncology: Version I, 2016.
[2]According to World Health Organization Classification of Tumors of the Digestive System: 4th edition.
[3]According to the American Joint Committee on Cancer Staging Manual: 7th edition.

Diagnostic accuracy of plasma ZFAS1 and traditional serum biomarkers

ROC analysis revealed that the area under the curve (AUC) value of plasma ZFAS1 for discriminating gastric cancer patients from healthy control subjects was 0.85 (Figure 2E). The highest AUC value of any traditional serum biomarker was 0.63, while the AUC value of the other traditional biomarkers was lower than that of CEA. The highest accuracy of plasma ZFAS1 was obtained at a cutoff level of 1.00, where its sensitivity and specificity for identifying gastric carcinoma patients were 0.82 and 0.72, respectively.

ZFAS1 amplification is correlated with poor prognosis in gastric cancer

To explore the correlations between the relative ZFAS1 level and gastric cancer clinicopathological characteristics, we divided the patients into groups by sex, age, tumor site/size/lymphatic invasion/pathological differentiation status and TNM classification (Table 6). Data analysis indicated that the relative ZFAS1 expression level was strongly associated with tumor size (P = 0.01), TNM classification (P = 0.02), and lymphatic invasion (P = 0.03). We then divided patients into two groups by the median relative ZFAS1 level. Kaplan-Meier survival analysis was used to assess the potential correlation between the relative ZFAS1 expression level and patient prognosis. As shown in Figures 2F and G, patients with a high ZFAS1 level had shorter overall survival (OS) and PFS times than those with a low ZFAS1 level. This result suggests that ZFAS1 is a potential prognostic biomarker in gastric cancer patients.

ZFAS1 knockdown inhibited the viability, migration, and proliferation of gastric cancer cells

The expression level of ZFAS1 was positively correlated with lymph node metastasis, suggesting that ZFAS1 may be involved in tumor metastasis. Therefore, we studied the effect of ZFAS1 knockdown on

Table 5 General characteristics and clinicopathological factors of gastric cancer patients and healthy control subjects

Variables	Healthy control (*n* = 60)	Gastritis/peptic ulcer (*n* = 60)	GIST (*n* = 60)	Gastric cancer (*n* = 60)
Gender				
Male	46	37	35	46
Female	14	23	25	14
Age (yr)				
Mean	61	60	60	61
Range	37-91	37-89	30-85	37-91
Tumor site[1]				
Upper third	-	-	-	13
Middle third	-	-	-	14
Lower third	-	-	-	33
Tumor size				
≥ 5 cm	-	-	-	29
< 5 cm	-	-	-	31
Pathological differentiation[2]				
Undifferentiated or poorly differentiated	-	-	-	45
Others	-	-	-	15
TNM classification[3]				
I + II	-	-	-	20
III + IV	-	-	-	40
Lymphatic invasion[3]				
Positive	-	-	-	43
Negative	-	-	-	17

[1]According to National Comprehensive Cancer Network Clinical Practice Guidelines in Oncology: Version I, 2016.
[2]According to World Health Organization Classification of Tumors of the Digestive System: 4th edition.
[3]According to the American Joint Committee on Cancer Staging Manual: 7th edition.
GIST: Gastric stromal tumor.

gastric cancer cells. To verify the efficiency of ZFAS1 knockdown and prevent off-target effects, we first transfected three targeted siRNAs, ZFAS1-siRNA1, ZFAS1-siRNA2, and ZFAS1-siRNA3, into BGC823 and SGC7901 cells. Fluorescence microscopy was used to test the transfection efficiency. As shown in Figure 3, all three siRNAs significantly reduced the expression level of ZFAS1 in transfected BGC823 and SGC7901 cells. Next, we constructed ZFAS1-shRNA2 (with a sequence based on that of ZFAS1-siRNA2) and transduced it into BGC823 and SGC7901 cells. The MTT and colony formation assay results showed that compared to control cells transduced with NC-shRNA, BGC823 and SGC7901 cells with ZFAS1 knockdown showed significant decreases in viability and proliferation (Figures 4 and 5). The transwell migration assay showed that ZFAS1 knockdown in BGC823 and SGC7901 cells significantly inhibited cell migration (Figure 6). In summary, our data suggest that knockdown of ZFAS1 reduces the viability, proliferation, and migration of gastric cancer cells.

ZFAS1 overexpression enhanced the viability, migration, and proliferation of gastric cancer cells

To further investigate the function of ZFAS1 in gastric cancer, we transduced ZFAS1-shRNA1 into BGC823 and SGC7901 cells to overexpress ZFAS1 and evaluated the transduction efficiency by fluorescence microscopy. As shown in Figure 7, the expression level of ZFAS1 was significantly increased in transduced BGC823 and SGC7901 cells. The MTT and colony formation assay results showed that compared to control cells transfected with NC-shRNA, BGC823 and SGC7901 cells overexpressing ZFAS1 showed significant increases in viability and proliferation (Figures 4 and 5). The transwell migration assay showed that ZFAS1 overexpression in BGC823 and SGC7901 cells significantly promoted cell migration (Figure 6). In summary, our data indicate that overexpression of ZFAS1 enhances the viability, proliferation, and migration of gastric cancer cells.

Table 6 Correlation between the relative expression of long noncoding RNA HULC or ZNFX1-AS1 and clinicopathologic factors

Variables	Number of cases	*P* value
Gender		
Male	46	0.99
Female	14	
Age (yr)		
≤ 61	28	0.26
> 61	32	
Tumor site[1]		
Upper third	13	0.12
Middle third	14	
Lower third	33	
Tumor size		
≥ 5 cm	29	0.01
< 5 cm	31	
Pathological differentiation[2]		
Undifferentiated or poorly differentiated	45	0.55
Others	15	
TNM classification[3]		
I + II	20	0.02
III + IV	40	
Distant metastasis[3]		
Positive	5	0.97
Negative	55	
Lymphatic invasion[3]		
Positive	43	0.03
Negative	17	

[1]According to National Comprehensive Cancer Network Clinical Practice Guidelines in Oncology: Version I, 2016.
[2]According to World Health Organization Classification of Tumors of the Digestive System: 4th edition.
[3]According to the American Joint Committee on Cancer Staging Manual: 7th edition.

LIN28 and CAPRIN1 are the key downstream mediators of ZFAS1 in gastric cancer cells

To further investigate the mechanism by which lncRNA ZFAS1 affects the aggressiveness of gastric cancer, we used the starBase V2.0 database to analyze binding proteins of lncRNA ZFAS1[19]. The results showed that a total of 10 proteins had more than three binding sites for lncRNA ZFAS1. These proteins were UPF1, eIF4AIII, IGF2BP1, FMRP, LIN28, IGF2BP2, FUS, ZC3H7B, IGF2BP3, and CAPRIN1. We then analyzed the mRNA expression levels of these proteins in BGC823 and SGC7901 cells transduced with ZFAS1-shRNA1 and ZFAS1-shRNA2. Our goal was to determine which proteins exhibited changes in expression consistent with the change in ZFAS1 expression. The qRT-PCR results showed that ZFAS1 overexpression significantly increased the expression of LIN28 and CAPRIN1 ($P < 0.05$) and that ZFAS1 knockdown significantly decreased the expression of LIN28 and CAPRIN1 ($P < 0.05$) (Figure 8). ELISA showed the same results (Figure 9).

Association of ZFAS1 with the tumorigenesis of gastric cancer cells in vivo

To further investigate whether ZFAS1 overexpression or knockdown affects tumor growth *in vivo*, BGC823 cells stably transduced with NC-shRNA, ZFAS1-shRNA1 and ZFAS1-shRNA2 were inoculated into 4-wk female athymic BALB/c nude mice. The expression of lncRNA ZFAS1 in nude mice was detected weekly by qRT-PCR. The results showed that the expression of lncRNA ZFAS1 in the three groups of nude mice increased over time. The expression level in the ZFAS1-shRNA1 group was higher

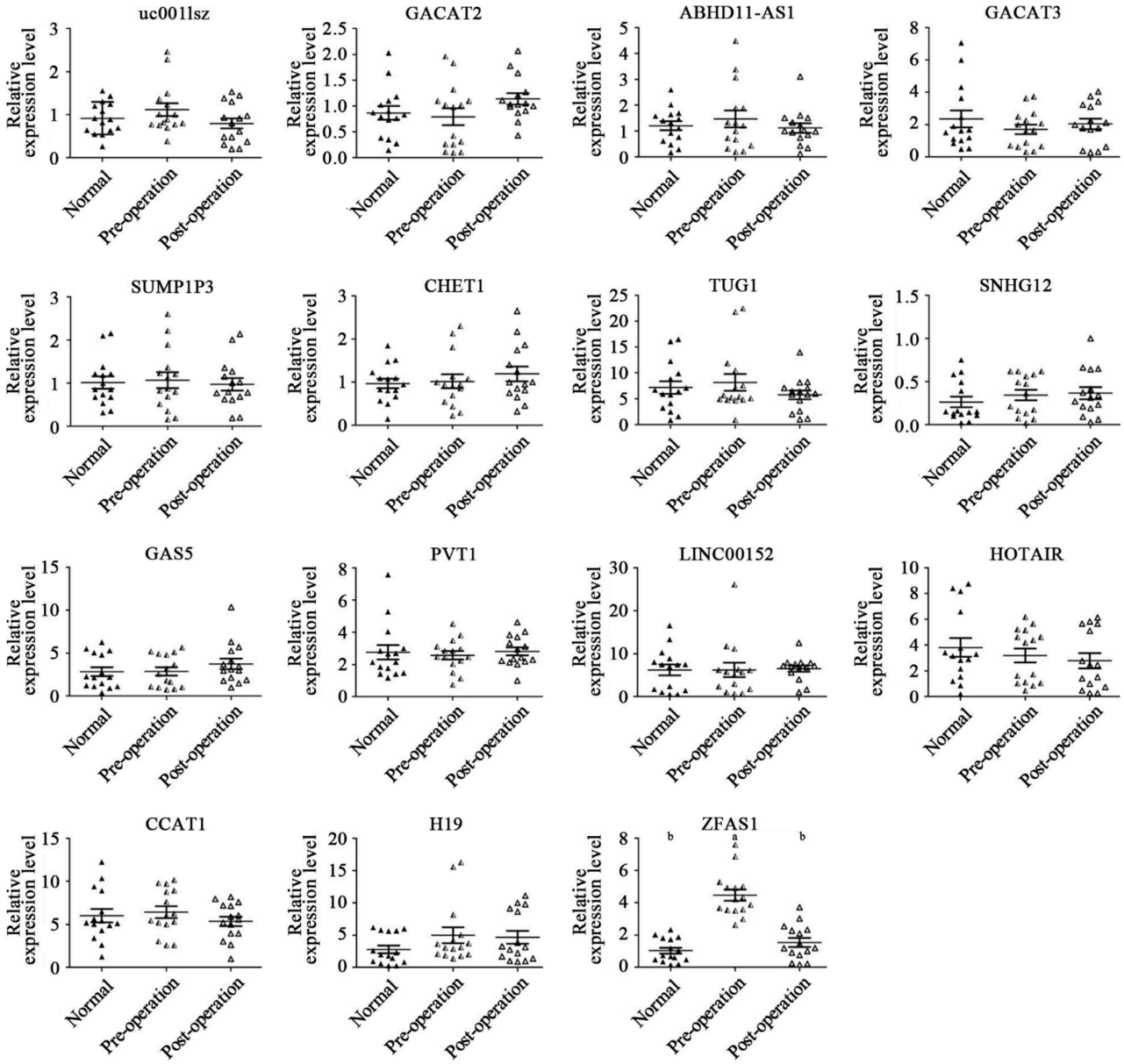


Figure 1 Relative expression levels of a selected subset of plasma long noncoding RNAs in 15 matched preoperative and postoperative gastric cancer patients and 15 healthy control subjects. Scatter plot of long noncoding RNA relative expression levels in the plasma of preoperative patients (preoperative; *n* = 15), postoperative patients (postoperative; *n* = 15), and healthy control subjects (normal; *n* = 15), as assessed by quantitative polymerase chain reaction. The upper and lower bars indicate the ± SD values, and the middle bar indicates the median value. *P* values ($^{a}P < 0.05$; $^{b}P < 0.01$) were determined using the *t*-test.

than that in the control group, and the expression level in the ZFAS1-shRNA2 group was lower than that in the control group (Figure 10A). Images of tumors from nude mice are shown in Figures 10B and C. Tumor size and weight were measured weekly; compared with tumors in the control group, tumors in the ZFAS1-shRNA1 group were significantly larger and heavier, and tumors in the ZFAS1-shRNA2 group were significantly smaller and lighter (Figures 10D and E). Next, in tumor tissue, ELISA confirmed that the expression of LIN28 and CAPRIN1 was significantly increased in tumors in the ZFAS1-shRNA1 group compared with those in the control group ($P < 0.05$), while the expression of LIN28 and CAPRIN1 was significantly decreased in tumors in the ZFAS1-shRNA2 group ($P < 0.05$) (Figure 10F). In addition, ELISA showed significant increases in CEA and CK20 expression in lymph nodes in the ZFAS1-shRNA1 group compared with the control group ($P < 0.05$) and significant decreases in CEA and CK20 expression in lymph nodes in the ZFAS1-shRNA2 group ($P < 0.05$) (Figure 10G), confirming the relationship between lncRNA ZFAS1 expression and lymph node metastasis in gastric cancer cells. In conclusion, our results indicate that ZFAS1 overexpression promotes the growth of gastric cancer cells *in vivo* and that ZFAS1 knockdown inhibits the growth of gastric cancer cells *in vivo*.

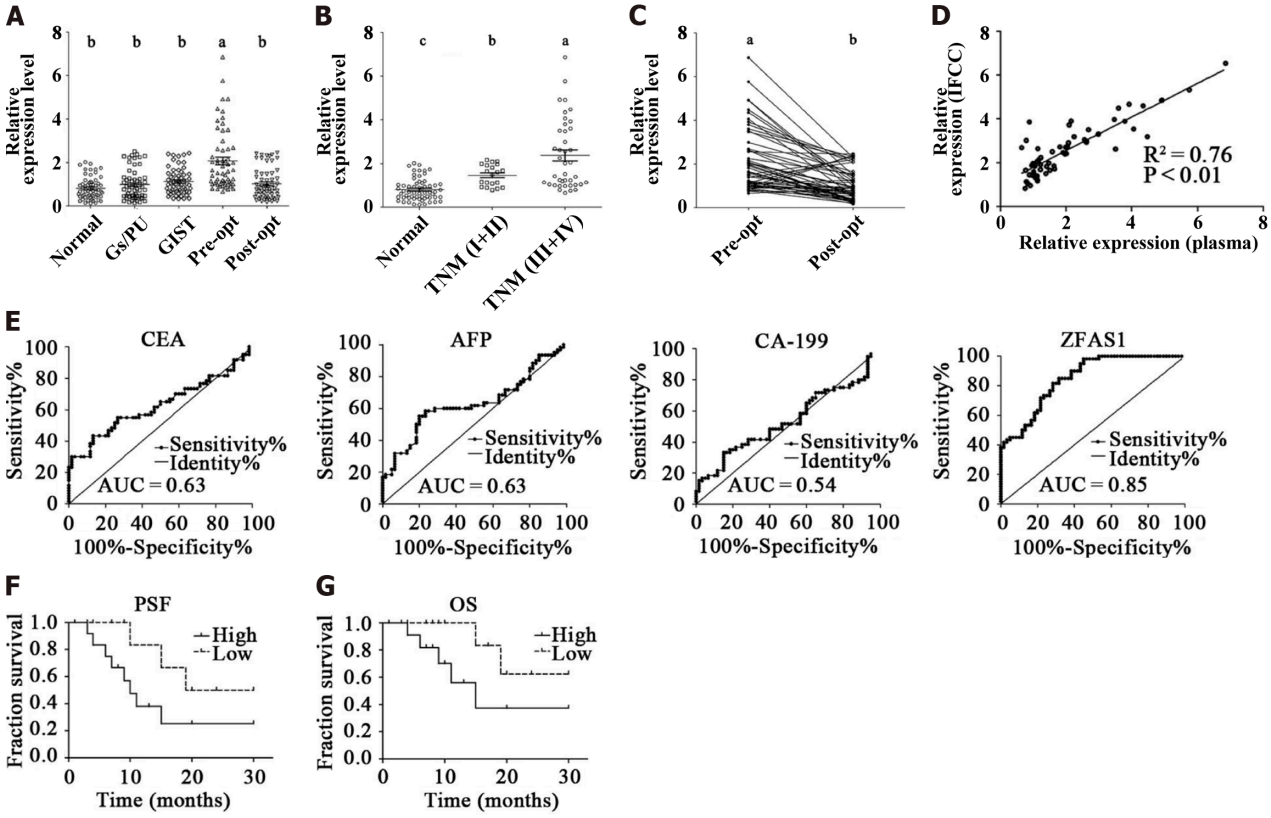


Figure 2 ZNFX1-AS1 is a potential diagnostic and prognostic biomarker. A: Scatter plot of long noncoding RNA (lncRNA) relative expression levels in the plasma of healthy control subjects (normal; *n* = 60), gastritis/peptic ulcer patients (Gs/PU patients; *n* = 60), gastric stromal tumor patients (GIST; *n* = 60), preoperative patients (pre-opt; *n* = 60), and postoperative patients (post-opt; *n* = 60), as assessed by real-time polymerase chain reaction (PCR); B: Scatter plot of lncRNA relative expression levels in the plasma of healthy control subjects (normal; *n* = 60), early-stage patients (TNM I + II; *n* = 20), and advanced-stage patients (TNM III + IV; *n* = 40), as assessed by real-time PCR; C: The endpoints indicate the relative expression levels of lncRNA ZNFX1-AS1 (ZFAS1) in preoperative (pre-opt) and postoperative (post-opt) patient plasma, while the lines connecting the pairs of endpoints indicate the trends in the relative expression levels in the matched preoperative and postoperative patient plasma; D: The linear correlations between the relative expression of lncRNAs in plasma and infrequent clonal complexes were analyzed. *P* values ($^{a}P < 0.05$; $^{b}P < 0.01$; $^{c}P < 0.001$) were determined using the *t*-test; E: Receiver operating characteristic curves showing the area under the curve values of plasma ZFAS1 and traditional serum biomarkers; F: Progression-free survival times indicating the potential prognostic value of ZFAS1 in gastric cancer patients; G: Overall survival times indicating the potential prognostic value of ZFAS1 in gastric cancer patients. Gs/PU: Gastritis/peptic ulcer patients; GIST: Gastric stromal tumor; AUC: Area under the curve; CEA: Carcinoembryonic antigen; AFP: Alpha fetoprotein; CA-199: Carbohydrate antigen 199; OS: Overall survival; PFS: Progression-free survival.

DISCUSSION

Gastric cancer is a common malignancy that is particularly difficult to diagnose early[20]. However, traditional biomarkers have low specificity and low sensitivity. As lncRNA research has intensified, many lncRNAs have been determined to be involved in the development, progression, and prognosis of gastric cancer[21], but their diagnostic value as gastric cancer markers needs further study. By reviewing the literature, we selected 15 candidate lncRNAs that have high expression in gastric tumor tissues. Next, the relative levels of these 15 candidate lncRNAs were evaluated in the plasma of 15 normal subjects and 15 matched samples from preoperative and postoperative patients with gastric cancer. The results showed that the plasma level of only ZFAS1 was significantly higher in preoperative gastric cancer patients than in normal subjects and postoperative gastric cancer patients (Figure 1). Therefore, we selected ZFAS1 as a follow-up research object. Moreover, we confirmed that lncRNAs can exist stably in peripheral blood, consistent with the findings of Li *et al*[22]. Therefore, lncRNA ZFAS1 may be a potential plasma biomarker for gastric cancer.

We recollected plasma from 60 healthy control subjects, 60 gastritis/peptic ulcer patients, 60 GIST patients, and 60 matched preoperative and postoperative patients to further validate the aforementioned results. Our data indicated that the expression of ZFAS1 in the peripheral blood of patients with gastric cancer was significantly higher than that of healthy controls and patients with benign gastrointestinal disease (Figure 2A), consistent with previous reports. Our data also showed that ZFAS1 is significantly associated with advanced TNM stage and lymphatic invasion (Figure 2B). There was a sharp decrease in the relative level of ZFAS1 in peripheral blood after surgery (Figure 2C). We also evaluated traditional serological markers such as CEA, CA-199, and alpha fetoprotein in the 60 preoperative patients. Compared with traditional biomarkers, plasma lncRNA ZFAS1 had higher

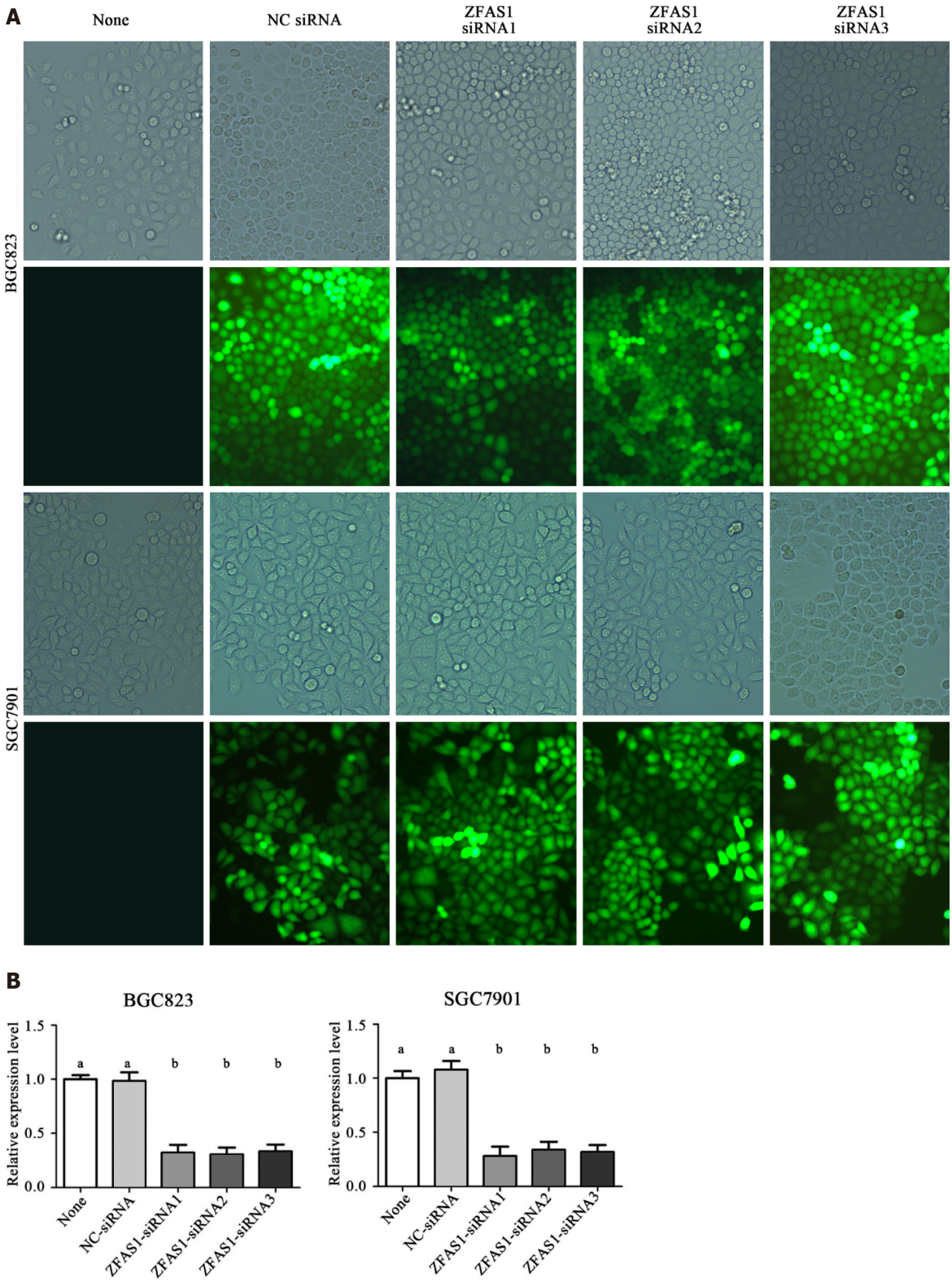


Figure 3 Fluorescence microscopy was used to verify the transfection efficiency of ZNFX1-AS1-siRNA1, ZNFX1-AS1-siRNA2 and ZNFX1-AS1-siRNA3. A: The same position of BGC823 cells and SGC7901 cells under a normal microscope and fluorescence microscope, respectively; B: The relative expression of long noncoding RNA ZNFX1-AS1 (ZFAS1) in five groups of cells (None, NC-siRNA, ZFAS1-siRNA1, ZFAS1-siRNA2, ZFAS1-siRNA3) was evaluated by quantitative reverse transcription polymerase chain reaction. ZFAS1: ZNFX1-AS1. $^{a}P < 0.05$; $^{b}P < 0.01$.

sensitivity and specificity (Figure 2E). In addition, the relative level of ZFAS1 in plasma was significantly correlated with that in IFCCs (Figure 2D). This indicates that lncRNA ZFAS1 is released into the peripheral blood by gastric tumors. This suggests that ZFAS1 may promote the progression of gastric cancer. Both the PFS and OS analysis results showed (Figures 2F and G) that a high level of lncRNAs in peripheral blood was not favorable for patients. Thus, lncRNAs may be used not only for early diagnosis but also for postoperative evaluation of patients.

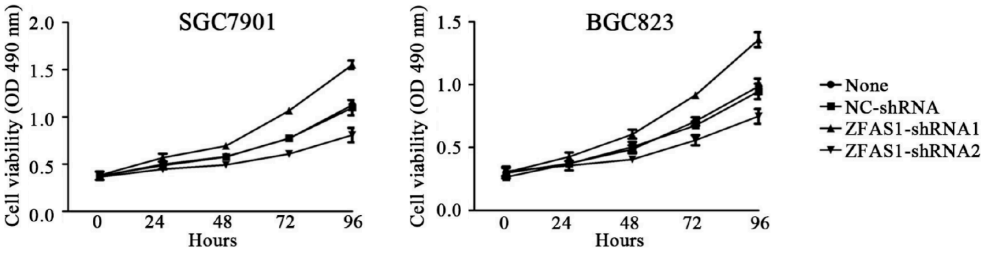


Figure 4 MTT assays were performed to determine the viability of ZGCS1-shRNA1- and ZNFX1-AS1-shRNA2-transduced BGC823 and SGC7901 cells. OD: Optical density.

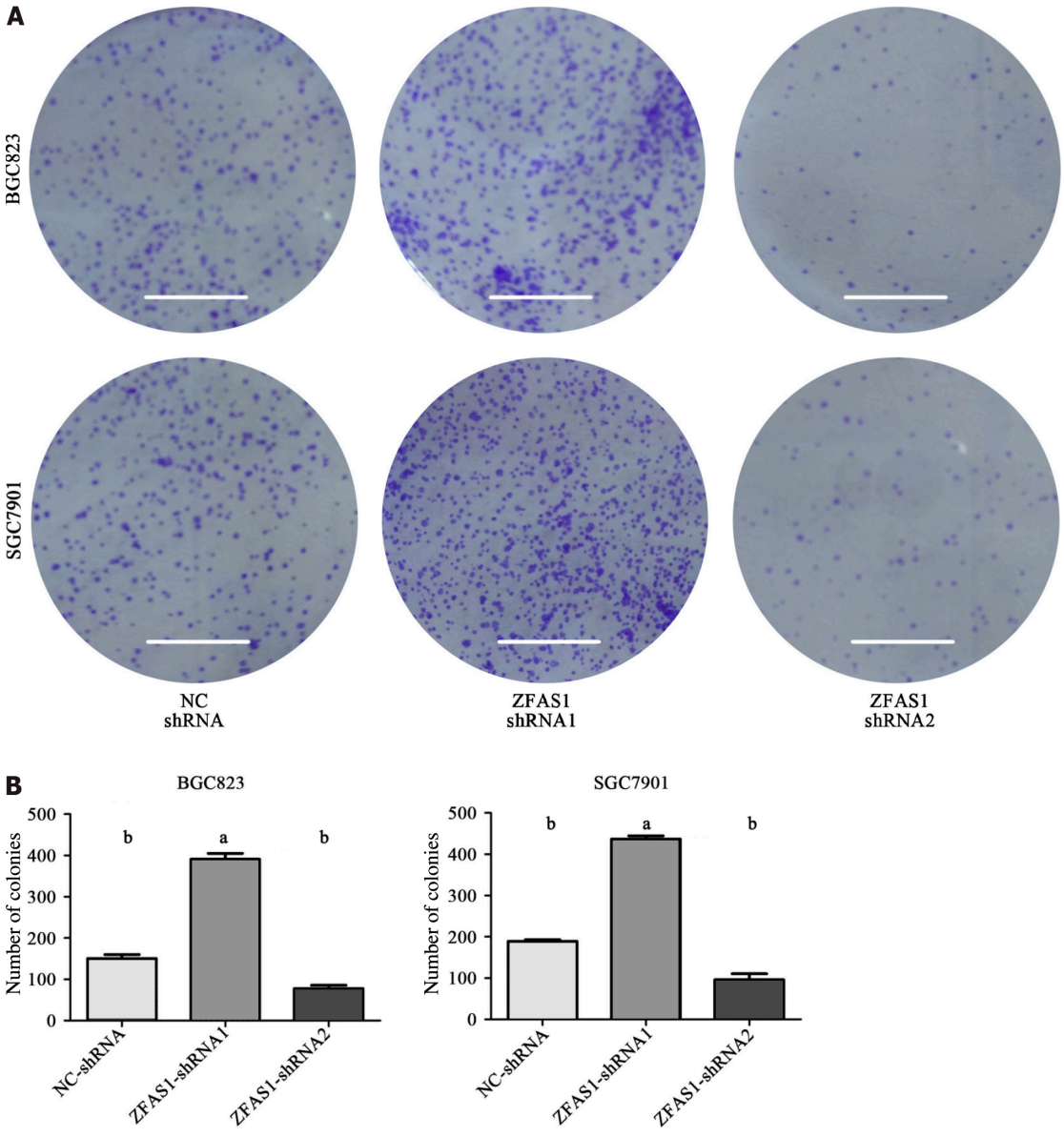


Figure 5 Colony formation assays were performed to determine the proliferation of BGC823 and SGC7901 cells transduced with ZNFX1-AS1-shRNA1 and ZNFX1-AS1-shRNA2. A: BGC823 cells and SGC7901 cells were subjected to colony formation assay after transduction, and the number of spots was analyzed; B: The number of spots for the three groups [NC-shRNA, ZNFX1-AS1 (ZFAS1)-shRNA1, ZFAS1-shRNA2] in the colony formation assays were compared. ZFAS1: ZNFX1-AS1. $^{a}P < 0.05$; $^{b}P < 0.01$.

In addition, ZFAS1 is reported to be involved in metabolism, prognosis, and cell proliferation in liver cancer[23,24]. It has been reported that the expression of ZFAS1 in gastric cancer tissues is significantly higher than that in adjacent tissues and that ZFAS1 expression is related to the prognosis of gastric cancer patients[25,26]. siRNA transfection techniques were used to determine the appropriate lncRNA ZFAS1 interference sequence. We used three types of siRNAs (ZFAS1 siRNA1, ZFAS1 siRNA2, and

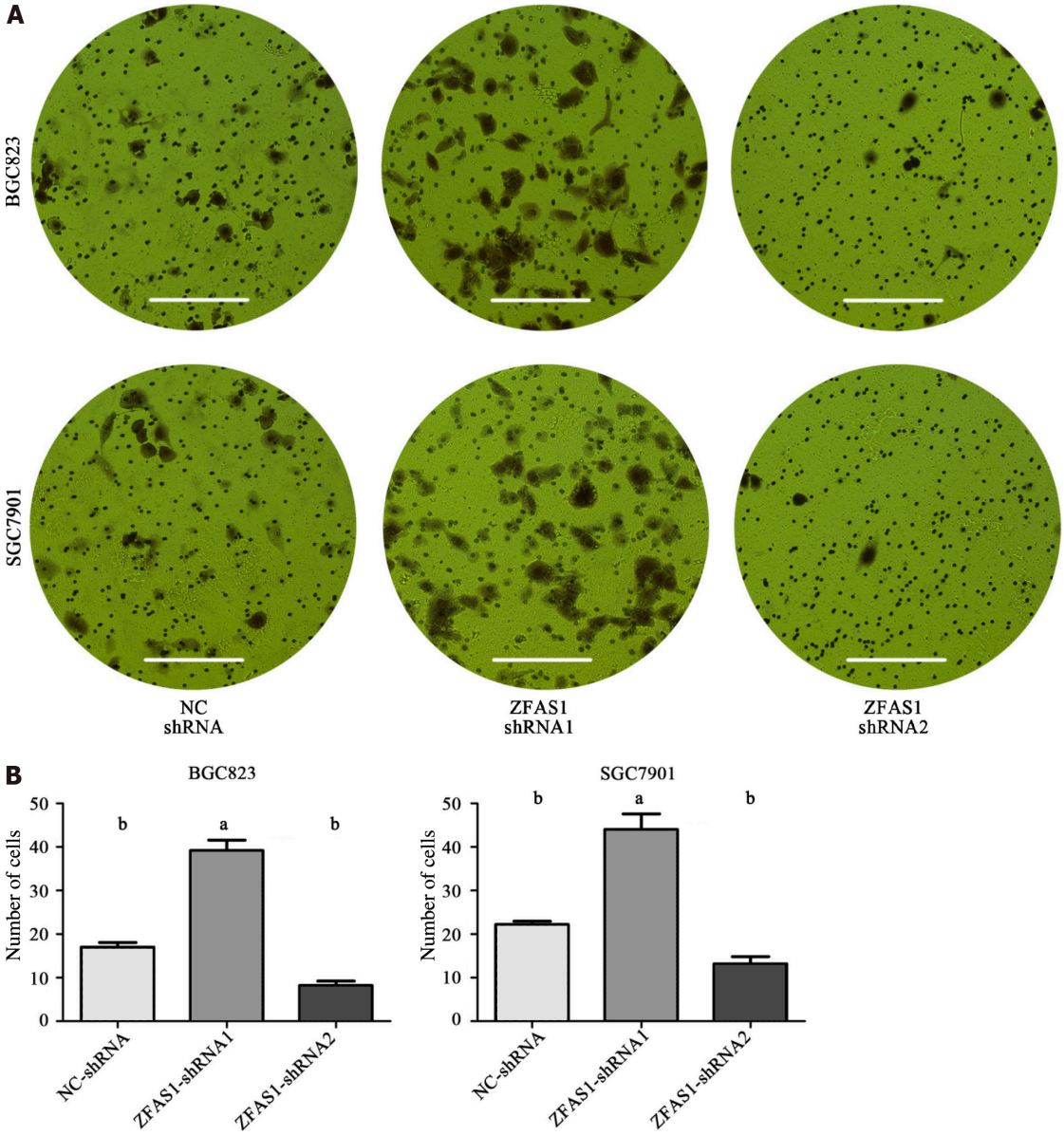


Figure 6 Transwell migration assays were performed to determine the migration ability of ZNFX1-AS1-shRNA1- and ZNFX1-AS1-shRNA2-transduced BGC823 and SGC7901 cells. A: BGC823 cells and SGC7901 cells were subjected to transwell migration assay after transduction, and the number of cell was calculated; B: The number of cells for the three groups [NC-shRNA, ZNFX1-AS1 (ZFAS1)-shRNA1, ZFAS1-shRNA2] in the transwell migration assays were compared. $^{a}P < 0.05$; $^{b}P < 0.01$. ZFAS1: ZNFX1-AS1.

ZFAS1 siRNA3) to interfere with the expression of ZFAS1 in cell lines to prevent off-target effects. All these siRNAs significantly reduced the expression of lncRNA ZFAS1 in BGC823 cells and SGC7901 cells (Figure 3). We finally selected the ZFAS1 siRNA2 sequence to construct ZFAS1-shRNA2 and successfully generated BGC823 cells and SGC7901 cells with low expression of lncRNA ZFAS1. BGC823 cells and SGC7901 cells with stable knockdown of lncRNA ZFAS1 were also successfully cultured. We further employed loss-of-function and gain-of-function studies to assess the role of ZFAS1 in gastric cancer cell proliferation and migration by MTT, transwell, and colony formation assays (Figures 4, 5 and 6). We observed that ZFAS1 knockdown inhibited gastric cancer cell proliferation and migration, whereas ZFAS1 overexpression had the opposite effects.

We then studied the mechanism by which ZFAS1 affects the proliferation and invasion of gastric cancer cells. The starBase V2.0 database was used to analyze the lncRNA ZFAS1 binding proteins[19]. Only 10 proteins had more than three binding sites for lncRNA ZFAS1. We found that the changes in the mRNA expression of LIN28 and CAPRIN1 were consistent with the change in ZFAS1 expression in gastric cancer cells (Figure 8). The LIN28 protein is thought to play an important role in gastrointestinal tumors[27,28]. In colorectal cancer, LIN28 has been shown to enhance tumor cell invasion *via* the Wnt pathway, whereas overexpression of LIN28 also recruits the microRNA let-7 to enhance tumor cell metastasis[28]. In gastric cancer, LIN28 affects the human epidermal growth factor receptor 2 level through posttranscriptional regulation, which in turn affects the invasive ability of gastric cancer cells.

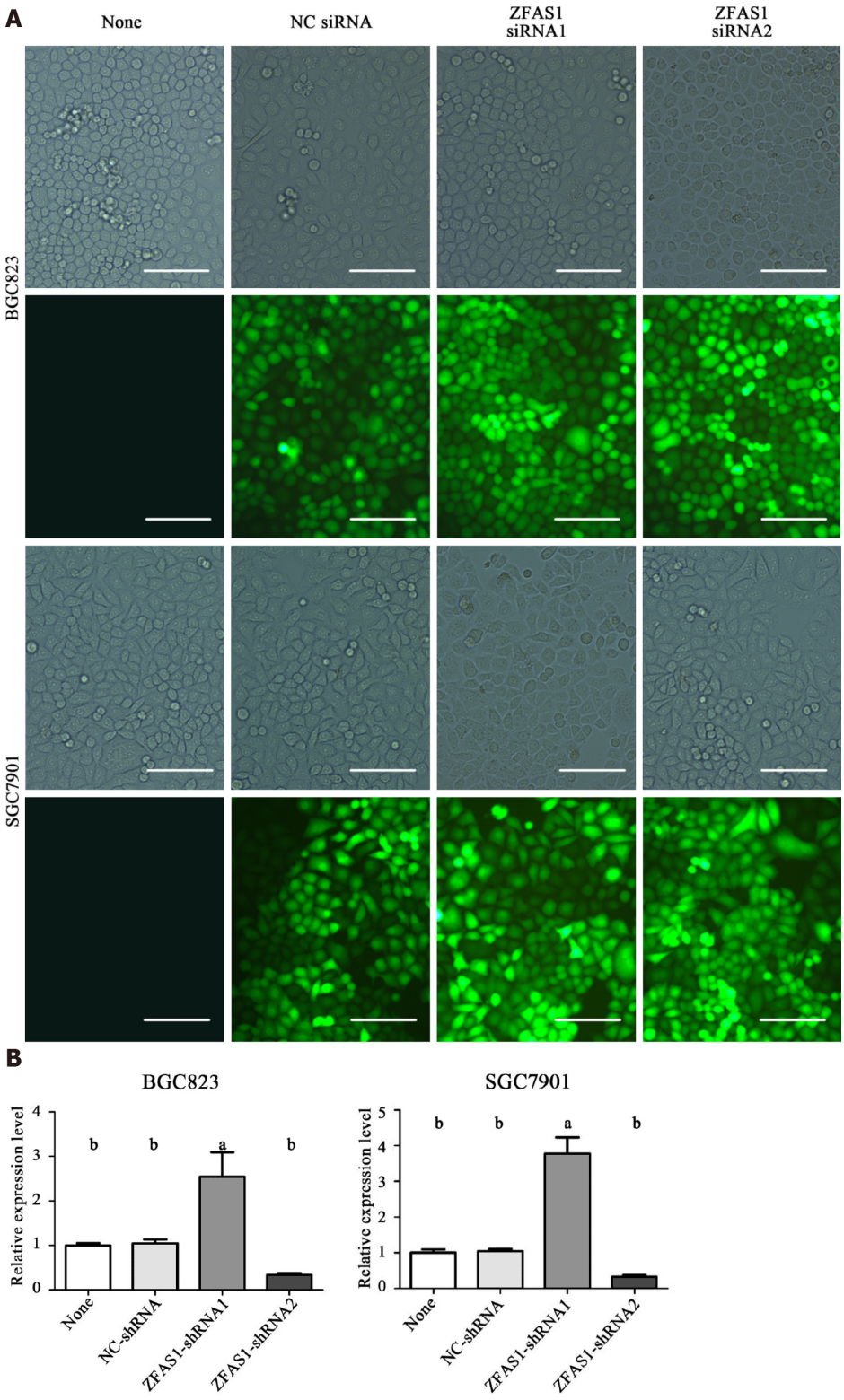


Figure 7 Fluorescence microscopy was used to test the transduction efficiency of ZNFX1-AS1-shRNA1 and ZNFX1-AS1-shRNA2. A: The same position of BGC823 cells and SGC7901 cells under a normal microscope and fluorescence microscope, respectively; B: The relative expression of long noncoding RNA ZNFX1-AS1 (ZFAS1) in four groups of cells (None, NC-shRNA, ZFAS1-shRNA1, ZFAS1-shRNA2) was evaluated by quantitative reverse transcription polymerase chain reaction. ZFAS1: ZNFX1-AS1. $^{a}P < 0.05$; $^{b}P < 0.01$.

In addition, LIN28 is an independent risk factor for the prognosis of gastric cancer. This result suggests that LIN28 may be a key protein downstream of lncRNA ZFAS1 and that lncRNA ZFAS1 may enhance the proliferation and invasion of gastric cancer cells by regulating LIN28. CAPRIN1 is thought to be involved in cell invasion in a variety of tumors[29-31]. In osteosarcoma, CAPRIN1 has been shown to cause cisplatin resistance and abnormal apoptosis of tumor cells *via* the Akt pathway and the ERK1/2 pathway[31], and it can also be used as an independent risk predictor for breast cancer. The changes in

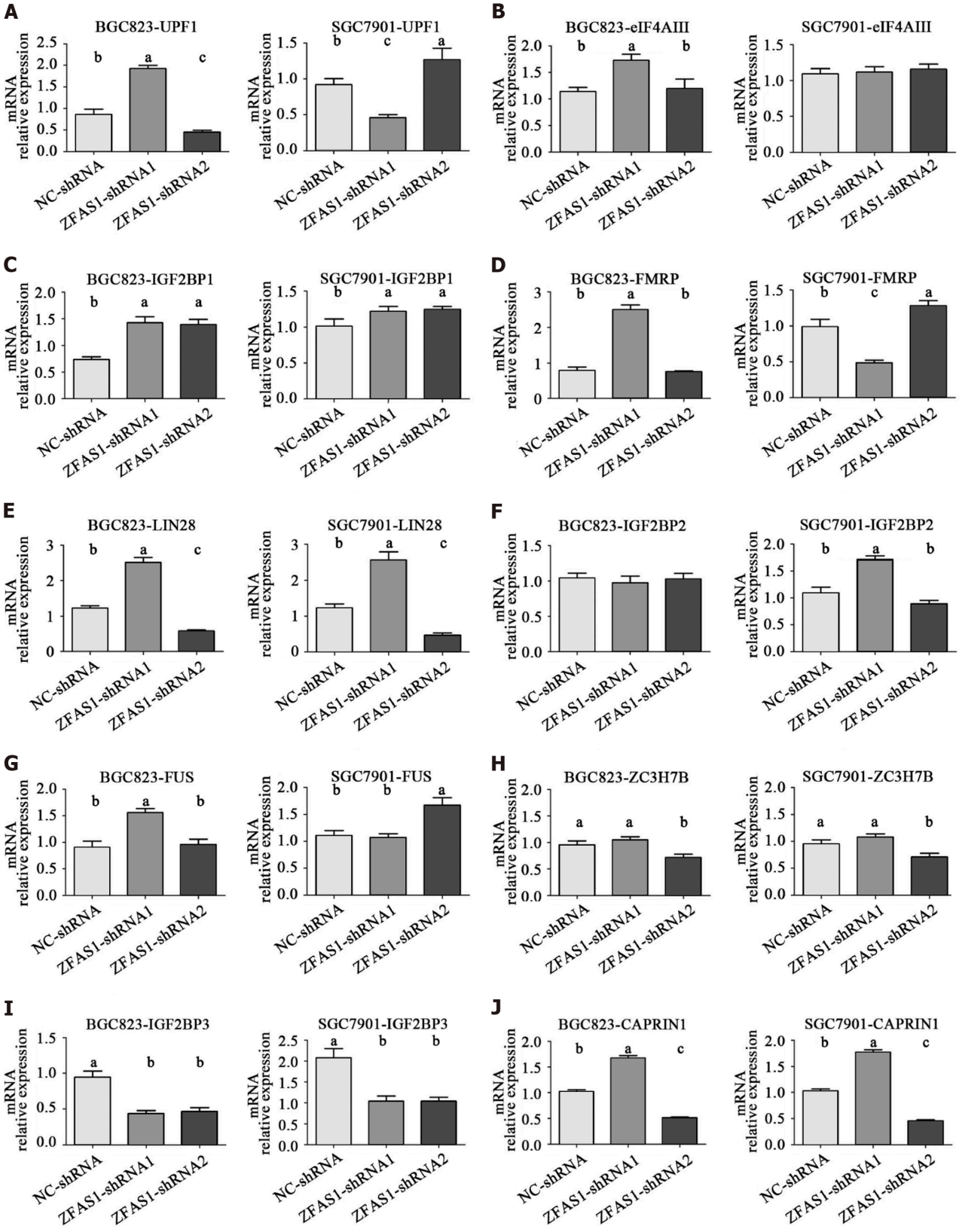


Figure 8 The relative mRNA levels of genes encoding ZNFX1-AS1 binding proteins in transduced BGC823 and SGC7901 cells were determined by quantitative reverse transcription polymerase chain reaction. A: UFP1; B: eIF4AIII; C: IGF2BP1; D: FMRP; E: LIN28; F: IGF2BP2; G: FUS; H: ZC3H7B; I: IGF2BP3; J: CAPRIN1. AFAS1: ZNFX1-AS1. $^{a}P < 0.05$; $^{b}P < 0.01$.

the mRNA expression of LIN28 and CAPRIN1 were consistent with knockdown and overexpression of ZFAS1, whereas LIN28 and CAPRIN1 were significantly associated with tumor invasion, which explains the mechanism connecting ZFAS1 with lymphatic invasion in tumor patients. ZFAS1 has been shown to silence the expression of Kruppel-like factor 2 and naked cuticle homolog 2 by binding to

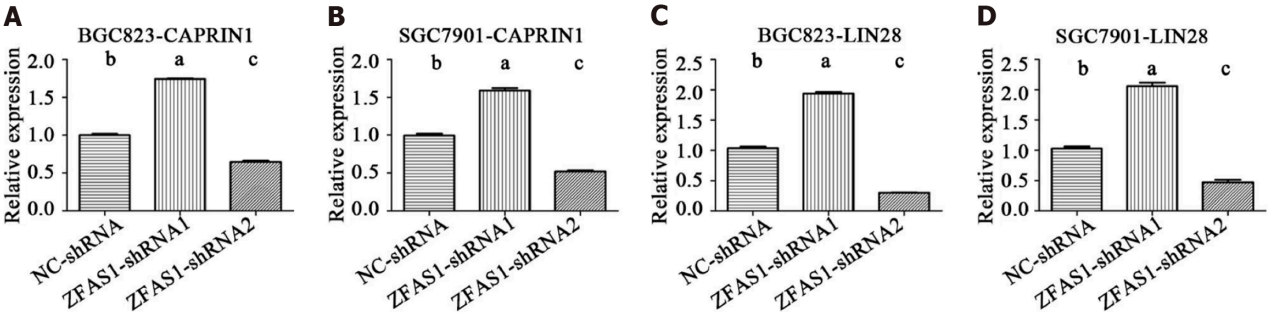


Figure 9 The relative protein levels of LIN28 and CAPRIN1 in transduced BGC823 and SGC7901 cells were determined by enzyme-linked immunosorbent assay. A: The levels of CAPRIN1 in transduced BGC823 cells; B: The levels of CAPRIN1 in transduced SGC7901 cells; C: The levels of LIN28 in transduced BGC823 cells; D: The levels of LIN28 in transduced SGC7901 cells. $^{a}P < 0.05$; $^{b}P < 0.01$.

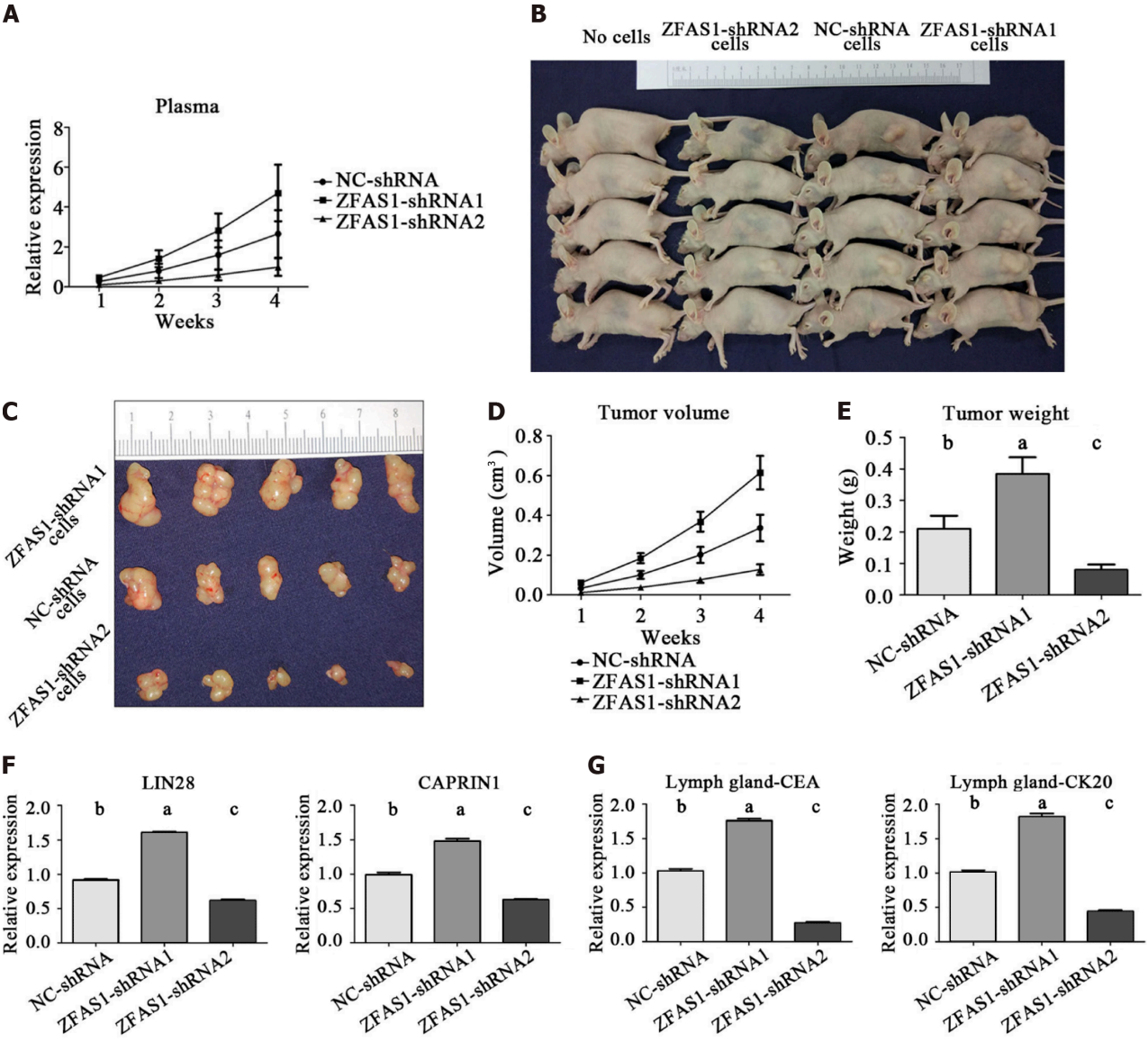


Figure 10 Effect of ZNFX1-AS1 on gastric cancer cell tumorigenesis *in vivo*. A: The expression of long noncoding RNA ZNFX1-AS1 in BALB/c nude mice was detected weekly by quantitative reverse transcription polymerase chain reaction; B and C: Images of tumors from BALB/c nude mice; D and E: Tumor size and weight were measured weekly; F: Expression of LIN28 and CAPRIN1 in tumors of BALB/c nude mice; G: Expression of carcinoembryonic antigen and CK20 in lymph nodes of BALB/c nude mice. CEA: Carcinoembryonic antigen; ZFAS1: ZNFX1-AS1. $^{a}P < 0.05$; $^{b}P < 0.01$; $^{c}P < 0.001$.

polycomb repressive complex 2 and lysine-specific demethylase 1, leading to the development of gastric cancer[25]. In addition, it promotes the development of liver cancer tumor cells[23]. CAPRIN1 may play a key role in the regulation of tumor cell proliferation and invasion *via* lncRNA ZFAS1.

In this study, we validated the above hypothesis by establishing tumor-bearing mice. The expression level of lncRNA ZFAS1 in the plasma of mice injected with tumor cells with high expression of lncRNA ZFAS1 was significantly higher than that in mice in the other two groups (Figure 10A). The *in vivo* experiments also indicated that ZFAS1 overexpression promoted gastric cancer cell proliferation and migration, whereas ZFAS1 knockdown had the opposite effect (Figures 10B-E). The data also demonstrated that LIN28 and CAPRIN1 are still regulated by lncRNA ZFAS1 in mice (Figure 10F). CK20 and CEA are classical biomarkers of gastric cancer cells in tissues. The CEA and CK20 levels in the lymph nodes of nude mice injected with tumor cells with high expression of lncRNA ZFAS1 were significantly higher than those in mice in the other two groups (Figure 10G). This further demonstrated that high expression of lncRNA ZFAS1 may enhance the invasion of gastric cancer cells.

CONCLUSION

In conclusion, we demonstrated in this study that the lncRNA ZFAS1 level is increased in the plasma of gastric cancer patients. LncRNA ZFAS1 promotes the invasion and proliferation of gastric cancer cells by modulating LIN28 and CAPRIN1 expression. These findings indicate that ZFAS1 plays an oncogenic role in gastric cancer and can be used as a potential diagnostic biomarker and a new therapeutic target for gastric cancer.

ARTICLE HIGHLIGHTS

Research background

Long noncoding RNA (lncRNA) ZNFX1-AS1 (ZFAS1) is a newly discovered lncRNA, but its diagnostic value in gastric cancer is unclear.

Research motivation

We investigated the biological effects of ZFAS1 on the survival, proliferation, and migration of gastric cancer cells.

Research objectives

This study aimed to investigate the potential role of ZFAS1 in gastric cancer and to evaluate the clinical significance of ZFAS1 as a biomarker for gastric cancer screening.

Research methods

RNA extraction, quantitative realtime polymerase chain reaction, lncRNA silencing and overexpression, MTT assay, transwell migration assay, Colony formation assay, protein extraction, immunosorbent assay, and *in vivo* tumor formation assay were performed in this study.

Research results

ZFAS1 amplification was correlated with poor prognosis in gastric cancer. ZFAS1 knockdown inhibited the viability, migration, and proliferation of gastric cancer cells. ZFAS1 overexpression enhanced the viability, migration, and proliferation of gastric cancer cells. LIN28 and CAPRIN1 were the key downstream mediators of ZFAS1 in gastric cancer cells. ZFAS1 was associated with the tumorigenesis of gastric cancer cells *in vivo*.

Research conclusions

LncRNA ZFAS1 is a potential biomarker for gastric cancer.

Research perspectives

ZFAS1 plays an oncogenic role in gastric cancer and can be used as a potential diagnostic biomarker and a new therapeutic target for gastric cancer.

ACKNOWLEDGEMENTS

The authors would like to thank Peking University People's Hospital Gastrointestinal Surgery Laboratory for providing the cell lines.

FOOTNOTES

Author contributions: Zhuo ZL analyzed the experimental data and completed the draft of the manuscript; Xian HP completed all of the experiments; Sun YJ, Long Y, and Liu C collected all of the clinical data; Liang B and Zhao XT are responsible for designing the work and for final approval of the version to be published.

Supported by Beijing Natural Science Foundation, No. 7172225.

Institutional review board statement: This study was approved by the Research Ethics Committee of Peking University People's Hospital. Patient data and samples were treated according to the ethical and legal criteria adopted in the 2013 Declaration of Helsinki. Written informed consent for ethical approval and patient consent was obtained from all participants.

Institutional animal care and use committee statement: This study was approved by the Peking University People's Hospital Animal Use Protocol & Ethic Review.

Conflict-of-interest statement: All the authors report no relevant conflicts of interest for this article.

Data sharing statement: The datasets used and/or analyzed during the current study are available from the corresponding author on reasonable request.

ARRIVE guidelines statement: The authors have read the ARRIVE guidelines, and the manuscript was prepared and revised according to the ARRIVE guidelines.

Open-Access: This article is an open-access article that was selected by an in-house editor and fully peer-reviewed by external reviewers. It is distributed in accordance with the Creative Commons Attribution NonCommercial (CC BY-NC 4.0) license, which permits others to distribute, remix, adapt, build upon this work non-commercially, and license their derivative works on different terms, provided the original work is properly cited and the use is non-commercial. See: https://creativecommons.org/Licenses/by-nc/4.0/

Country/Territory of origin: China

ORCID number: Zhong-Ling Zhuo 0000-0001-9284-4785; Xiao-Tao Zhao 0000-0001-6104-8989.

S-Editor: Wang JJ
L-Editor: Webster JR
P-Editor: Chen YX

REFERENCES

1 **Bray F**, Ferlay J, Soerjomataram I, Siegel RL, Torre LA, Jemal A. Global cancer statistics 2018: GLOBOCAN estimates of incidence and mortality worldwide for 36 cancers in 185 countries. *CA Cancer J Clin* 2018; **68**: 394-424 [PMID: 30207593 DOI: 10.3322/caac.21492]
2 **Riquelme I**, Ili C, Roa JC, Brebi P. Long non-coding RNAs in gastric cancer: mechanisms and potential applications. *Oncotarget* 2016 [DOI: 10.18632/oncotarget.9396]
3 **Sun J**, Song Y, Chen X, Zhao J, Gao P, Huang X, Xu H, Wang Z. Novel long non-coding RNA RP11-119F7.4 as a potential biomarker for the development and progression of gastric cancer. *Oncol Lett* 2015; **10**: 115-120 [PMID: 26170986 DOI: 10.3892/ol.2015.3186]
4 **Vance KW**, Sansom SN, Lee S, Chalei V, Kong L, Cooper SE, Oliver PL, Ponting CP. The long non-coding RNA Paupar regulates the expression of both local and distal genes. *EMBO J* 2014; **33**: 296-311 [PMID: 24488179 DOI: 10.1002/embj.201386225]
5 **Wapinski O**, Chang HY. Long noncoding RNAs and human disease. *Trends Cell Biol* 2011; **21**: 354-361 [DOI: 10.1016/j.tcb.2011.04.001]
6 **Qi P**, Xu MD, Ni SJ, Huang D, Wei P, Tan C, Zhou XY, Du X. Low expression of LOC285194 is associated with poor prognosis in colorectal cancer. *J Transl Med* 2013; **11**: 122 [PMID: 23680400 DOI: 10.1186/1479-5876-11-122]
7 **Mei D**, Song H, Wang K, Lou Y, Sun W, Liu Z, Ding X, Guo J. Up-regulation of SUMO1 pseudogene 3 (SUMO1P3) in gastric cancer and its clinical association. *Med Oncol* 2013; **30**: 709 [PMID: 23996296 DOI: 10.1007/s12032-013-0709-2]
8 **Yang F**, Bi J, Xue X, Zheng L, Zhi K, Hua J, Fang G. Up-regulated long non-coding RNA H19 contributes to proliferation of gastric cancer cells. *FEBS J* 2012; **279**: 3159-3165 [PMID: 22776265 DOI: 10.1111/j.1742-4658.2012.08694.x]
9 **Sun W**, Wu Y, Yu X, Liu Y, Song H, Xia T, Xiao B, Guo J. Decreased expression of long noncoding RNA AC096655.1-002 in gastric cancer and its clinical significance. *Tumour Biol* 2013; **34**: 2697-2701 [PMID: 23645148 DOI: 10.1007/s13277-013-0821-0]
10 **Xiao B**, Guo J. Long noncoding RNA AC096655.1-002 has been officially named as gastric cancer-associated transcript 1, GACAT1. *Tumour Biol* 2013; **34**: 3271 [PMID: 23754450 DOI: 10.1007/s13277-013-0916-7]
11 **Song H**, Sun W, Ye G, Ding X, Liu Z, Zhang S, Xia T, Xiao B, Xi Y, Guo J. Long non-coding RNA expression profile in human gastric cancer and its clinical significances. *J Transl Med* 2013; **11**: 225 [PMID: 24063685 DOI:

10.1186/1479-5876-11-225]
12 **Song B**, Guan Z, Liu F, Sun D, Wang K, Qu H. Long non-coding RNA HOTAIR promotes HLA-G expression *via* inhibiting miR-152 in gastric cancer cells. *Biochem Biophys Res Commun* 2015; **464**: 807-813 [PMID: 26187665 DOI: 10.1016/j.bbrc.2015.07.040]
13 **Arita T**, Ichikawa D, Konishi H, Komatsu S, Shiozaki A, Shoda K, Kawaguchi T, Hirajima S, Nagata H, Kubota T, Fujiwara H, Okamoto K, Otsuji E. Circulating long non-coding RNAs in plasma of patients with gastric cancer. *Anticancer Res* 2013; **33**: 3185-3193 [PMID: 23898077]
14 **Levy MH**, Back A, Benedetti C, Billings JA, Block S, Boston B, Bruera E, Dy S, Eberle C, Foley KM, Karver SB, Knight SJ, Misra S, Ritchie CS, Spiegel D, Sutton L, Urba S, Von Roenn JH, Weinstein SM. NCCN clinical practice guidelines in oncology: palliative care. *J Natl Compr Canc Netw* 2009; **7**: 436-473 [PMID: 19406043 DOI: 10.6004/jnccn.2009.0031]
15 **Nagtegaal ID**, Odze RD, Klimstra D, Paradis V, Rugge M, Schirmacher P, Washington KM, Carneiro F, Cree IA; WHO Classification of Tumours Editorial Board. The 2019 WHO classification of tumours of the digestive system. *Histopathology* 2020; **76**: 182-188 [PMID: 31433515 DOI: 10.1111/his.13975]
16 **Edge SB**, Compton CC. The American Joint Committee on Cancer: the 7th edition of the AJCC cancer staging manual and the future of TNM. *Ann Surg Oncol* 2010; **17**: 1471-1474 [PMID: 20180029 DOI: 10.1245/s10434-010-0985-4]
17 **Xian HP**, Zhuo ZL, Sun YJ, Liang B, Zhao XT. Circulating long non-coding RNAs HULC and ZNFX1-AS1 are potential biomarkers in patients with gastric cancer. *Oncol Lett* 2018; **16**: 4689-4698 [PMID: 30197680 DOI: 10.3892/ol.2018.9199]
18 **Livak KJ**, Schmittgen TD. Analysis of relative gene expression data using real-time quantitative PCR and the 2(-Delta Delta C(T)) Method. *Methods* 2001; **25**: 402-408 [PMID: 11846609 DOI: 10.1006/meth.2001.1262]
19 **Li JH**, Liu S, Zhou H, Qu LH, Yang JH. starBase v2.0: decoding miRNA-ceRNA, miRNA-ncRNA and protein-RNA interaction networks from large-scale CLIP-Seq data. *Nucleic Acids Res* 2014; **42**: D92-D97 [PMID: 24297251 DOI: 10.1093/nar/gkt1248]
20 **Ferlay J**, Soerjomataram I, Dikshit R, Eser S, Mathers C, Rebelo M, Parkin DM, Forman D, Bray F. Cancer incidence and mortality worldwide: sources, methods and major patterns in GLOBOCAN 2012. *Int J Cancer* 2015; **136**: E359-E386 [PMID: 25220842 DOI: 10.1002/ijc.29210]
21 **Shao Y**, Ye M, Jiang X, Sun W, Ding X, Liu Z, Ye G, Zhang X, Xiao B, Guo J. Gastric juice long noncoding RNA used as a tumor marker for screening gastric cancer. *Cancer* 2014; **120**: 3320-3328 [PMID: 24986041 DOI: 10.1002/cncr.28882]
22 **Li Q**, Shao Y, Zhang X, Zheng T, Miao M, Qin L, Wang B, Ye G, Xiao B, Guo J. Plasma long noncoding RNA protected by exosomes as a potential stable biomarker for gastric cancer. *Tumour Biol* 2015; **36**: 2007-2012 [PMID: 25391424 DOI: 10.1007/s13277-014-2807-y]
23 **Li T**, Xie J, Shen C, Cheng D, Shi Y, Wu Z, Deng X, Chen H, Shen B, Peng C, Li H, Zhan Q, Zhu Z. Amplification of Long Noncoding RNA ZFAS1 Promotes Metastasis in Hepatocellular Carcinoma. *Cancer Res* 2015; **75**: 3181-3191 [PMID: 26069248 DOI: 10.1158/0008-5472.CAN-14-3721]
24 **Askarian-Amiri ME**, Crawford J, French JD, Smart CE, Smith MA, Clark MB, Ru K, Mercer TR, Thompson ER, Lakhani SR, Vargas AC, Campbell IG, Brown MA, Dinger ME, Mattick JS. SNORD-host RNA Zfas1 is a regulator of mammary development and a potential marker for breast cancer. *RNA* 2011; **17**: 878-891 [PMID: 21460236 DOI: 10.1261/rna.2528811]
25 **Nie F**, Yu X, Huang M, Wang Y, Xie M, Ma H, Wang Z, De W, Sun M. Long noncoding RNA ZFAS1 promotes gastric cancer cells proliferation by epigenetically repressing KLF2 and NKD2 expression. *Oncotarget* 2017; **8**: 38227-38238 [PMID: 27246976 DOI: 10.18632/oncotarget.9611]
26 **Pan L**, Liang W, Fu M, Huang ZH, Li X, Zhang W, Zhang P, Qian H, Jiang PC, Xu WR, Zhang X. Exosomes-mediated transfer of long noncoding RNA ZFAS1 promotes gastric cancer progression. *J Cancer Res Clin Oncol* 2017; **143**: 991-1004 [PMID: 28285404 DOI: 10.1007/s00432-017-2361-2]
27 **Wang Q**, Zhou J, Guo J, Teng R, Shen J, Huang Y, Xie S, Wei Q, Zhao W, Chen W, Yuan X, Chen Y, Wang L. Lin28 promotes Her2 expression and Lin28/Her2 predicts poorer survival in gastric cancer. *Tumour Biol* 2014; **35**: 11513-11521 [PMID: 25128063 DOI: 10.1007/s13277-014-2481-0]
28 **Tu HC**, Schwitalla S, Qian Z, LaPier GS, Yermalovich A, Ku YC, Chen SC, Viswanathan SR, Zhu H, Nishihara R, Inamura K, Kim SA, Morikawa T, Mima K, Sukawa Y, Yang J, Meredith G, Fuchs CS, Ogino S, Daley GQ. LIN28 cooperates with WNT signaling to drive invasive intestinal and colorectal adenocarcinoma in mice and humans. *Genes Dev* 2015; **29**: 1074-1086 [PMID: 25956904 DOI: 10.1101/gad.256693.114]
29 **Bidet K**, Dadlani D, Garcia-Blanco MA. G3BP1, G3BP2 and CAPRIN1 are required for translation of interferon stimulated mRNAs and are targeted by a dengue virus non-coding RNA. *PLoS Pathog* 2014; **10**: e1004242 [PMID: 24992036 DOI: 10.1371/journal.ppat.1004242]
30 **Gong B**, Hu H, Chen J, Cao S, Yu J, Xue J, Chen F, Cai Y, He H, Zhang L. Caprin-1 is a novel microRNA-223 target for regulating the proliferation and invasion of human breast cancer cells. *Biomed Pharmacother* 2013; **67**: 629-636 [PMID: 23953883 DOI: 10.1016/j.biopha.2013.06.006]
31 **Sabile AA**, Arlt MJ, Muff R, Husmann K, Hess D, Bertz J, Langsam B, Aemisegger C, Ziegler U, Born W, Fuchs B. Caprin-1, a novel Cyr61-interacting protein, promotes osteosarcoma tumor growth and lung metastasis in mice. *Biochim Biophys Acta* 2013; **1832**: 1173-1182 [PMID: 23528710 DOI: 10.1016/j.bbadis.2013.03.014]

World Journal of Gastroenterology

Submit a Manuscript: https://www.f6publishing.com

World J Gastroenterol 2022 September 14; 28(34): 4993-5006

DOI: 10.3748/wjg.v28.i34.4993

ISSN 1007-9327 (print) ISSN 2219-2840 (online)

ORIGINAL ARTICLE

Basic Study

Oxidized low-density lipoprotein stimulates CD206 positive macrophages upregulating CD44 and CD133 expression in colorectal cancer with high-fat diet

Shi-Min Zheng, Hao Chen, Wei-Hong Sha, Xiao-Fen Chen, Jian-Bin Yin, Xiao-Bo Zhu, Zhong-Wen Zheng, Juan Ma

Specialty type: Gastroenterology and hepatology

Provenance and peer review: Unsolicited article; Externally peer reviewed.

Peer-review model: Single blind

Peer-review report's scientific quality classification

Grade A (Excellent): A
Grade B (Very good): B
Grade C (Good): C, C
Grade D (Fair): 0
Grade E (Poor): 0

P-Reviewer: Chen XX, China; Elchaninov AV, Russia; Ortiz-Masia D, Spain

Received: March 14, 2022
Peer-review started: March 14, 2022
First decision: April 11, 2022
Revised: May 15, 2022
Accepted: August 22, 2022
Article in press: August 22, 2022
Published online: September 14, 2022

Shi-Min Zheng, Hao Chen, Wei-Hong Sha, Xiao-Fen Chen, Xiao-Bo Zhu, Zhong-Wen Zheng, Juan Ma, Department of Gastroenterology and Hepatology, Guangdong Provincial People's Hospital, Guangdong Academy of Medical Sciences, Guangzhou 510080, Guangdong Province, China

Shi-Min Zheng, Wei-Hong Sha, Xiao-Fen Chen, Juan Ma, Medical College, Shantou University, Shantou 515041, Guangdong Province, China

Wei-Hong Sha, Jian-Bin Yin, Juan Ma, Medical College, Southern Medical University, Guangzhou 510515, Guangdong Province, China

Jian-Bin Yin, Center for Orthopaedic Surgery, The Third Affiliated Hospital of Southern Medical University, Guangzhou 510630, Guangdong Province, China

Corresponding author: Juan Ma, PhD, Doctor, Department of Gastroenterology and Hepatology, Guangdong Provincial People's Hospital, Guangdong Academy of Medical Sciences, No. 106, Zhongshan 2nd Road, Guangzhou 510080, Guangdong Province, China.
mjlqh@163.com

Abstract

BACKGROUND

Oxidized low-density lipoprotein (ox-LDL), which is abnormally increased in the serum of colorectal cancer (CRC) patients consuming a high-fat diet (HFD), may be one of the risk factors for the development of CRC. Ox-LDL exerts a regulatory effect on macrophages and may influence CRC through the tumor microenvironment. The role of ox-LDL in CRC remains unclear.

AIM

To investigate the role of ox-LDL through macrophages in HFD associated CRC.

METHODS

The expression of ox-LDL and CD206 was detected in colorectal tissues of CRC patients with hyperlipidemia and HFD-fed mice by immunofluorescence. We stimulated the macrophages with 20 μg/mL ox-LDL and assessed the expression levels of CD206 and the cytokines by cell fluorescence and quantitative polymerase chain reaction. We further knocked down LOX-1, the surface receptor of

ox-LDL, to confirm the function of ox-LDL in macrophages. Then, LoVo cells were co-cultured with the stimulated macrophages to analyze the CD44 and CD133 expression by western blot.

RESULTS

The expression of ox-LDL and the CD206 was significantly increased in the stroma of colorectal tissues of CRC patients with hyperlipidemia, and also upregulated in the HFD-fed mice. Moreover, an increased level of CD206 and decreased level of inducible nitric oxide synthase were observed in macrophages after ox-LDL continuous stimulation. Such effects were inhibited when the surface receptor LOX-1 was knocked down in macrophages. Ox-LDL could induce CD206+ macrophages, which resulted in high expression of CD44 and CD133 in co-cultured LoVo cells.

CONCLUSION

Ox-LDL stimulates CD206+ macrophages to upregulate CD44 and CD133 expression in HFD related CRC.

Key Words: Oxidized low-density lipoprotein; CD206 positive macrophages; CD44; CD133

©The Author(s) 2022. Published by Baishideng Publishing Group Inc. All rights reserved.

Core Tip: Obesity increases the risk of colorectal cancer (CRC), but the mechanism remains unknown. CD206+ macrophages promote CRC. It has been established that the prevalence of CRC was higher in people consuming a high-fat diet (HFD) and HFD fed mice with up-regulated CD206+ macrophages levels in colorectal tissue. Oxidized low-density lipoprotein (ox-LDL) is a lipid peroxide which has been found to be increased in serum of CRC patients. Importantly, ox-LDL exerts a regulatory effect on macrophages and may regulate CRC through the tumor microenvironment. Our study showed that ox-LDL stimulates CD206+ macrophages to up-regulate CD44 and CD133 expression in HFD associated CRC.

Citation: Zheng SM, Chen H, Sha WH, Chen XF, Yin JB, Zhu XB, Zheng ZW, Ma J. Oxidized low-density lipoprotein stimulates CD206 positive macrophages upregulating CD44 and CD133 expression in colorectal cancer with high-fat diet. *World J Gastroenterol* 2022; 28(34): 4993-5006
URL: https://www.wjgnet.com/1007-9327/full/v28/i34/4993.htm
DOI: https://dx.doi.org/10.3748/wjg.v28.i34.4993

INTRODUCTION

Obesity is a widespread health condition. There is ample evidence to suggest that obesity increases the risk of colorectal cancer (CRC)[1]. A prospective cohort study of 85256 women found that obese individuals had a 1.93 times higher risk of CRC by age 50 than normal-weight individuals[2]. Excessive intake of dietary fat, *e.g.*, a high-fat diet (HFD), is the main cause of obesity and one of the important reasons for the increased incidence of CRC[3]. However, the specific mechanism of CRC remains unknown. It is currently believed that HFD promotes intestinal cancer by increasing the number and malignant potential of intestinal stem cells[4,5].

Interestingly, it has been shown that HFD could activate systemic inflammation and increase the malignant potential of intestinal tumors by upregulating the expression of macrophages[6,7]. It has been established that macrophages exhibit multiple phenotypes, like those positive for CD206, CD163, or inducible nitric oxide synthase (iNOS)[8]. Importantly, some types of macrophages promote cell repair and proliferation, like CD206+ macrophages[9]. An increasing body of evidence suggests that CD206+ macrophages in the tumor microenvironment promote CRC development, and a positive correlation has been documented between the level of CD206+ macrophages and the degree of tumor malignancy[10]. Moreover, metastasis can be promoted through the interactions of CD206+ macrophages with CRC cells [11]. Liu *et al*[7] found that the prevalence of CRC was higher in people on a HFD with upregulated CD206+ macrophage levels in colon tissue. Moreover, when mice with intestinal microflora disorder were fed an HFD, it was found that CD206+ macrophages in colon tissues correlated with the number of colon tumors and the degree of malignancy, suggesting that the increased CD206+ macrophage level induced by an HFD could exert a significant promoting effect on CRC.

HFD can cause low-grade inflammation and oxidative stress in the whole body, leading to increased lipid levels such as cholesterol and low-density lipoprotein[6]. Oxidized low-density lipoprotein (ox-LDL) is a lipid peroxide produced under oxidative stress that can be used to assess oxidative stress and lipid metabolism in the body. Several studies on obese people have found that the serum ox-LDL level in CRC patients was higher than that in the control group with a healthy intestinal tract[12-14].

Importantly, ox-LDL exerts a regulatory effect on macrophages and may regulate CRC through the tumor microenvironment[15]. However, the mechanisms underlying macrophage regulation in CRC by ox-LDL remain unclear. In addition, the regulatory role of macrophages on tumors may be related to tumor stem cells. In this regard, Yang *et al*[16] found that CD44 levels were gradually increased in lung cancer tissue with an increase in the level of CD206+ macrophages. Lv *et al*[17] also found that CD133 levels were upregulated in thyroid cancer with the increasing CD206+ macrophages. CD206+ macrophages share a similar relationship with CD44 and CD133 in CRC. In this study, the expression and corresponding effects of ox-LDL in colorectal tissue from hyperlipidemia patients were studied to explore the regulatory effects of ox-LDL on macrophages and the tumor stem cell markers CD44 and CD133 in the colorectal stroma. Our findings will provide a new mechanism of increased CRC susceptibility with HFD.

MATERIALS AND METHODS

Patient samples

Colonoscopy was performed on hyperlipidemia patients with CRC, with no prior radiotherapy, chemotherapy, or surgery. Healthy colorectal tissues were collected from volunteers who underwent colonoscopy in the physical examination. CRC (cancer, n = 16, male:female = 10:6) and normal colorectal tissues (normal, n = 20, male:female = 11:9) were collected. The average age of all patients was 57 ± 6 years old. All tissue samples were examined by experienced pathologists. All the CRC tissues that we collected were adenocarcinoma. After sampling, tissue samples were fixed in 4% paraformaldehyde. All patients were treated at the Guangdong Provincial People's Hospital, and the tissue samples were collected by the same endoscopist. The human study was approved by the Ethics Committee of Guangdong Provincial People's Hospital. Informed consent was obtained from all patients before the beginning of the study.

Animal model

Six C57/BL6 mice aged 4 wk assigned to an HFD group were fed an HFD (#H10141, China) for a total of 12 wk. Another six C57/BL6 mice aged 4 wk were assigned to a control group and fed a normal diet (normal grade, #02, China) for the same duration. After 12 wk, the mice were sacrificed for colorectal tissue harvesting. All tissues were immediately transferred to 4% paraformaldehyde. Animal experiments were also approved by the Ethics Committee of Guangdong Provincial People's Hospital.

Specimen processing

After the above clinical and animal specimens were fixed at room temperature for 24 h, tissue sections were prepared as follows. The tissues were first dehydrated and then embedded with paraffin. The paraffin-embedded tissues were cut into 3 μm-thick sections and cross-sections of the intestinal tissue were observed.

Animal histological analysis

Three- micron-thick mice tissue slices were cut and dried in a 65 °C oven for 120 min. The slices were stained with hematoxylin and eosin, dehydrated, and cleared. Finally, the slices were dried and sealed with neutral gum. All samples were examined by experienced pathologists.

Immunofluorescence staining

The specimens were dried in a 65 °C oven for 2 h for dewaxing and dehydration, and then soaked in deionized water for 5 min. The tissue specimens were soaked in sodium citrate solution overnight in a 60 °C water bath to expose the antigen. The sections were immersed in phosphate buffer solution (PBS) and then incubated with 10% goat serum at 37 °C for 1 h for antigen blocking. The slices were incubated at 4 °C for 12 h with the corresponding primary antibody, rewarmed at room temperature, and washed with PBS. The cells were incubated with 100 μL/well working solution containing Alexa Fluor 594-conjugated goat anti-rabbit secondary antibody at room temperature for 1 h in the dark. 4,6-diamino-2-phenylindole (DAPI; Thermo Fisher Science, United States) was used for nuclear counterstaining. The stained slides were imaged using an inverted fluorescence microscope (magnification, × 400; Olympus Corporation).

For calculation of the rate of ox-LDL positive cells in immunofluorescence (IF) staining, three fields were randomly selected from each section to observe the stroma of colorectal tissue under a 400 × microscope. For iNOS-F4/80 or CD206-F4/80 double staining, the number of iNOS, CD206, and F4/80 positive cells and total cells was counted, and the rate of iNOS and F/480, or CD206 and F4/80 positive cells was calculated. For ox-LDL-CD206 or LOX-1-CD206 double staining, the number of positive cells and total cells was counted, and their rate was calculated. The mean value of the rates from three fields was the positive cell rate of each section. All the analyses were double-blind and graded by two or more observers.

Cell experiments

Cell lines and culture: The human colorectal adenocarcinoma cell line (LoVo) and mouse monocyte-macrophage leukemia cell line (RAW 264.7) were purchased from the American Center for Typical Culture Preservation (ATCC, United States). The human monocytic leukemia cell line was purchased from Wuhan Penoside Company (THP-1, #CL-0233, China). The maintenance medium for cell culture was Dulbecco modified Eagle medium (DMEM, Gibco) containing glucose (4.5 g/L), 10% fetal bovine serum, 100 U/mL penicillin, and 100 mg/mL streptomycin. All cells were cultured under standard cell culture conditions of 37 °C, 5% CO_2, and 95% humidity.

Lipoprotein induction and RNA extraction: THP-1 cells were inoculated in 6-well plates, and 50 μg/mL ox-LDL was added 24 h and 72 h after sample collection. The confluence of cells in both groups was maintained at 60%-70% at the beginning of treatment, while the control group did not receive any treatment. The samples were centrifuged (800 rpm, 3 min) and washed with sterile PBS, and re-centrifuged (800 rpm, 3 min). Then, total RNA was extracted from tissues or cells using TRIzol reagent, according to the manufacturer's instructions. The RNA samples were stored at -80 °C.

Cell fluorescence: RAW264.7 cells were inoculated in 12-well plates and treated with 50 μg/mL ox-LDL for 72 h when the cell confluence reached 60%-70%, while the control group did not receive any treatment. After 72 h, the culture medium was discarded, and the cells were treated with 4% paraformaldehyde for 15 min. The cells were washed with PBS, blocked with 10% sheep serum at 37 °C for 1 h, and incubated with PBS solution dissolved in 1% BSA and 0.1% TritonX-100 followed by primary antibody [rabbit anti-CD206 antibody (1:100, #18704-1-AP, United States)] at 4 °C for 12 h. The cells were then washed with PBS, and incubated with the AlexaFluor594 conjugated secondary antibody (1:500) at room temperature in the dark for 1 h. The cells were washed with PBS, one drop of DAPI was added to each well, and images were obtained under the corresponding fluorescence channel using an inverted fluorescence microscope. The method used to calculate the IF-positive cell rate was the same as above.

Co-culture and protein extraction: LoVo cells and THP-1 cells were inoculated in the lower and upper chambers of 12-well transwell plates, respectively. The cell density was 60%-70%, and cells were incubated with ox-LDL (#S24879, China) for 72 h. There were no THP-1 cells in the upper compartment of the culture plate in the control group, and the other conditions were the same as those for the treatment group. The culture medium was discarded 72 h later, and cells were gently moistened with PBS. Total protein of LoVo cells in each group was extracted with RIPA lysis buffer on ice. Protein concentration was detected by the BCA method, and protein samples were stored at -80 °C.

Quantitative polymerase chain reaction

RNA concentration was determined first, and the samples were diluted to ensure that the concentrations were consistent. The RNA was reverse-transcribed to cDNA in a 20 μL system, and the total RNA content was kept below 1000 ng. Then, the cDNA was used as the template for quantitative polymerase chain reaction (qPCR) amplification. ABI 7300 real-time PCR software was used to analyze the PCR results and detect the Ct value of the sample. *GAPDH* was used as the internal reference gene, and the relative quantitative analysis was carried out by the $2^{-\Delta\Delta Ct}$ method. The primer sequences used are shown in Table 1.

LOX-1 small interfering RNA transfection

Small interfering RNA (siRNA) was used to inhibit the expression of LOX-1 in macrophages. LOX-1 siRNA or siRNA negative control (GenePharma, GenePharma, Suzhou, China) was introduced into THP-1 cells *via* Liposome 3000 (3 μL/mL) for 24 h. The sequence of LOX-1 siRNA used is shown in Table 2.

Western blot analysis

Protein samples (10 μg) were separated by 10% sodium dodecyl sulfate-polyacrylamide gel electrophoresis and transferred to a PVDF membrane. The membrane was then blocked with 5% skim milk. One hour later, anti-CD44 antibody (1:5000, # AB189524, United Kingdom) and anti-GAPDH antibody (1:10000, # AB9458, United Kingdom) were added. After incubating with the primary antibody, the membrane was washed with TBST. The samples were then incubated with horseradish peroxidase-labeled secondary antibody (1:3000) for 1 h at room temperature. After washing with TBST, immune reactive bands were analyzed after protein band visualization with enhanced chemiluminescence reagents.

Statistical analysis

Microsoft Excel 2019 worksheet was used to summarize the experimental results and generate tables. Adobe Photoshop 2020 software was used to process the images, and GraphPad Prism 8.0.2 software was used for statistical analyses. The Chi-square test or unpaired *t*-test was performed to compare the difference between two groups. One-way ANOVA test was performed to compare the difference among

Table 1 Forward and reverse primer sequences of *GAPDH*, inducible nitric oxide synthase, *CD206*, and *LOX-1*

Gene	Forward primer (5'-3')	Reverse primer (5'-3')
GAPDH	CTGTTCGACAGTCAGCCGCATC	GCGCCCAATACGACCAAATCCG
INOS	TTCAGTATCACAACCTCAGCAAG	TGGACCTGCAAGTTAAAATCCC
CD206	TGGAGAGGGAAGAGAGTGAACA	GCCCATAAGTGTGCTCTGAA
LOX-1	GTGGCATGGAGAAAACTGTTAC	CATCCAAAGACAAGCACTTCTC

iNOS: Inducible nitric oxide synthase.

Table 2 Sequence of LOX-1 small interfering RNA

si-LOX-1	Forward sequence (5'-3')	Reverse sequence (5'-3')
1	UUUGCUACUCUCUUCAGUGTT	CACUGAAGAGAGUAGCAAATT
2	UUGCUUGCUGGAUGAAGUCTT	GACUUCAUCCAGCAAGCAATT
3	UUUCUGACUCCUGUGAAGCTT	GCUUCACAGGAGUCAGAAATT

more than two groups, and the Dunnett *post-hoc* test was used for multiple comparisons. The data were assessed for normality before conducting the unpaired *t*-test and one-way ANOVA test. A P value < 0.05 was considered statistically significant. All tests were carried out more than three times.

RESULTS

Ox-LDL expression is increased in the stroma of CRC tissue

To explore the distribution and expression of ox-LDL in CRC, we collected tissue samples from CRC patients with hyperlipidemia (n = 16) and normal subjects (n = 20) and performed IF staining for ox-LDL. The results showed that compared with normal colorectal tissues, the expression of ox-LDL was significantly increased in the stroma of CRC tissues (Figures 1A and 1E). It has been reported that LOX-1 is the surface receptor of ox-LDL in macrophages[12]. LOX-1-positive cells were also abundantly detected in CRC tissues (Figures 1C and 1G).

CD206+ macrophages are increased in the stroma of CRC tissue

Double IF for CD206-F4/80 or iNOS-F4/80 showed that the number of CD206+ macrophages increased significantly in the stroma of CRC tissue (Figures 1I-L). Besides, double IF also showed the number of CD206+/ox-LDL+ cells and CD206+/LOX-1+ cells increased abundantly in CRC tissue (Figures 1B, 1D, 1F, and 1H).

Establishment of HFD mouse model

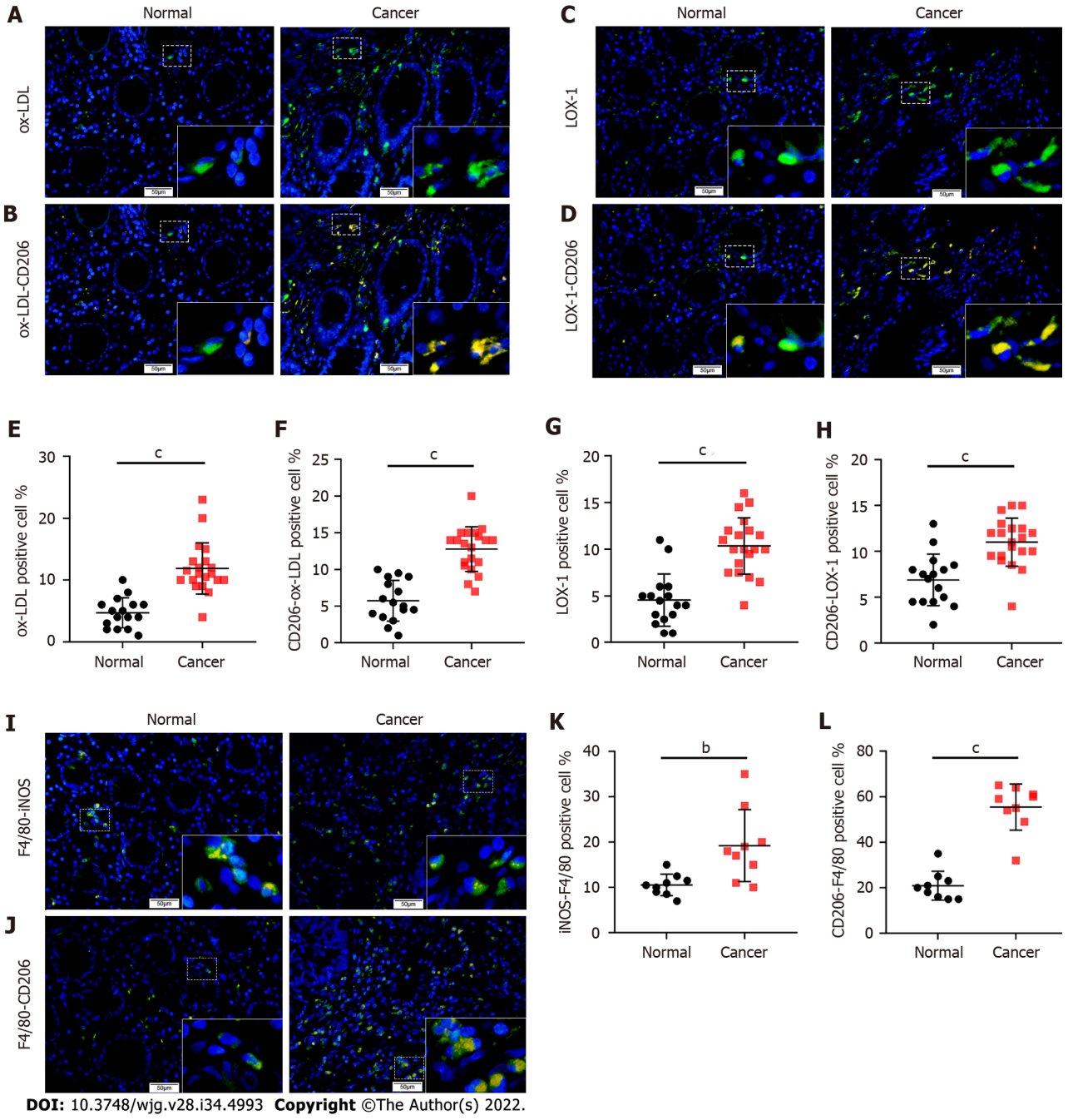
Four-week-old C57 mice were fed an HFD, and mice of the same age were fed a normal diet as controls. After 20 wk, the mice were sacrificed, and colorectal tissue specimens were harvested (n = 6). The colorectal length of control mice and HFD-fed mice was measured, respectively. We found that the colorectal length of HFD mice was shorter (Figures 2A and 2B). Subsequently, the tissue samples were sectioned and stained with hematoxylin and eosin. The staining results showed that glandular nuclei and interstitial cells in the colorectal tissues of HFD mice were slightly enlarged but to a milder degree than those usually observed with intraepithelial neoplasia (Figure 2C).

HFD increases ox-LDL expression and CD206 positive macrophages in the colorectal stroma of mice

After establishing the HFD-fed mouse model, we performed double IF staining for CD206-F4/80 or iNOS-F4/80 in the colorectal tissue sections of the control and HFD-fed mice. We found that the number of CD206 positive macrophages was significantly increased in the colorectal stroma of HDF-fed mice (Figures 3A, 3B, 3E, and 3F). The number of CD206+/ox-LDL+ cells and CD206+/LOX-1+ cells also increased significantly in the colorectal stroma of HDF-fed mice (Figures 3C, 3D, 3G, and 3H).

Continuous ox-LDL stimulation promotes CD206+ macrophages

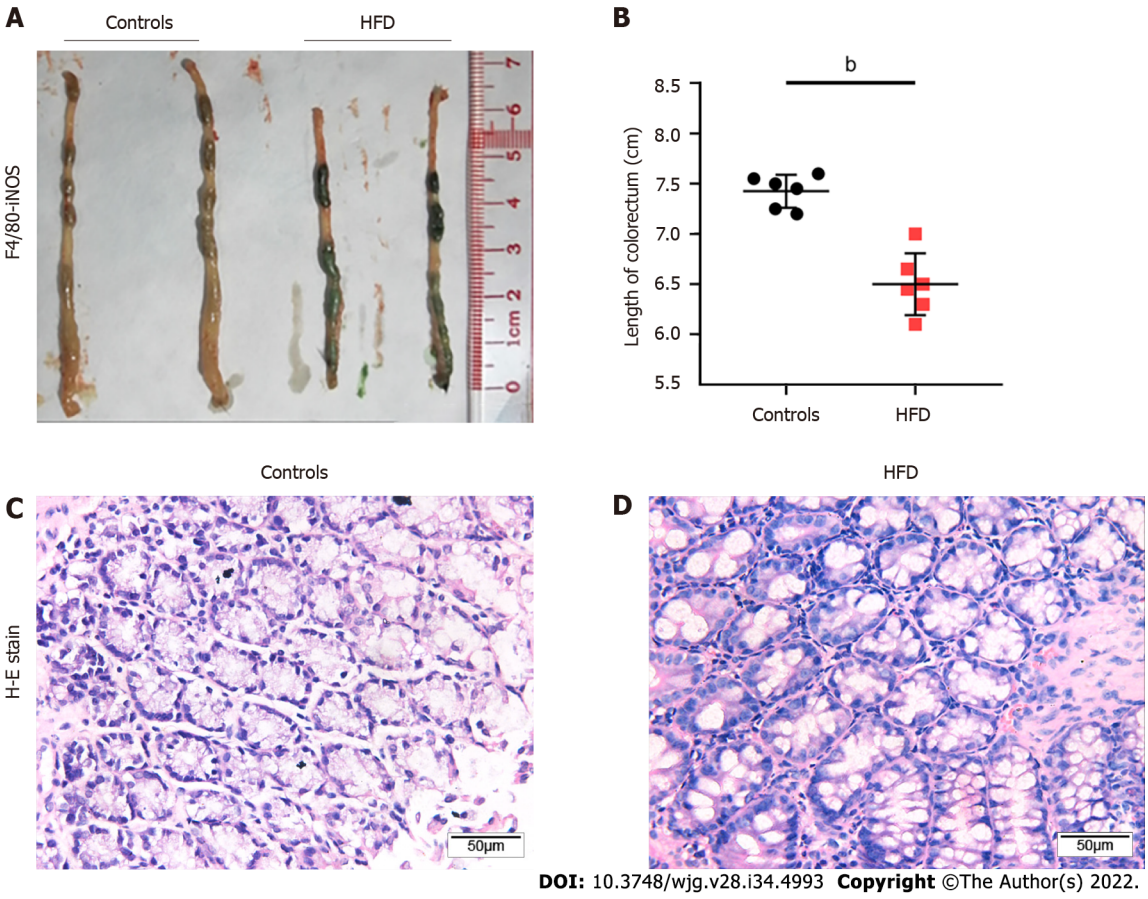
To explore whether ox-LDL is related to macrophage polarization, we stimulated human monocytic leukemia cells (THP-1) with ox-LDL for 24 h and 72 h *in vitro*. qPCR results showed that the expression level of *CD206* gradually increased with increased stimulation time. However, the expression level of



DOI: 10.3748/wjg.v28.i34.4993 **Copyright** ©The Author(s) 2022.

Figure 1 Increased expression of oxidized low-density lipoprotein and CD206 in the stroma of colorectal cancer tissue. A: Immunofluorescence (IF) images of oxidized low-density lipoprotein (ox-LDL) expression in colorectal tissues (scale bars represent 50 μm); B: Double IF images of CD206-ox-LDL expression in colorectal tissues (scale bars represent 50 μm); C: IF images of LOX-1 expression in colorectal tissues (scale bars represent 50 μm); D: Double IF images of CD206-LOX-1 expression in colorectal tissues (scale bars represent 50 μm); E: Histogram of ox-LDL expression in colorectal tissues based on IF results in Figure 1A; F: Quantification of CD206 and ox-LDL positive cells in colorectal tissues based on IF results in Figure 1B; G: Histogram of LOX-1 expression in colorectal tissues based on IF results in Figure 1C; H: Quantification of CD206 and LOX-1 positive cells in colorectal tissues based on IF results in Figure 1D; I: Double IF images of inducible nitric oxide synthase (iNOS)-F4/80 expression in colorectal tissues (scale bars represent 50 μm); J: Double IF images of CD206-F4/80 expression in colorectal tissues (scale bars represent 50 μm); K: Quantification of iNOS positive macrophages in colorectal tissues based on IF results in Figure 1I; L: Quantification of CD206 positive macrophages in colorectal tissues based on IF results in Figure 1J. Data are shown as the mean ± SD. Statistical analyses were conducted using an unpaired *t*-test. The boxed area is enlarged in the bottom right corner. $^{b}P < 0.01$, $^{c}P < 0.001$. ox-LDL: Oxidized low-density lipoprotein; iNOS: Inducible nitric oxide synthase.

iNOS increased in a short period and then decreased significantly below the initial level (Figure 4A). In addition, ox-LDL was used to stimulate mouse leukemic monocyte/macrophage cell line (RAW 264.7) for 72 h, and IF detection for CD206 was conducted. The results showed that CD206+ macrophages significantly increased in RAW 264.7 cells 3 d after ox-LDL stimulation (Figures 4B and 4C). Overall, we found that CD206+ macrophages gradually increased with continuous stimulation with ox-LDL, while iNOS+ macrophages initially increased then decreased in the later stages.



DOI: 10.3748/wjg.v28.i34.4993 **Copyright** ©The Author(s) 2022.

Figure 2 Establishment of a high-fat diet mouse model. A: Length of colorectal segment of controls and high-fat diet (HFD) mice; B: Quantification of the length of colorectal segment of controls and HFD mice; C: Histopathological colorectal tissue sections of controls and HFD mice (scale bars represent 50 μm). Data are shown as the mean ± SD. Statistical analyses were conducted using an unpaired *t*-test. $^{b}P < 0.01$. HFD: High-fat diet; H-E stain: Hematoxylin-eosin staining; iNOS: Inducible nitric oxide synthase.

In order to confirm the relationship between ox-LDL and CD206+ cells, we transfected LOX-1 siRNA into THP-1 cells to inhibit the expression of LOX-1, the specific receptor of ox-LDL (Figure 4D). After 72 h of ox-LDL stimulation, the inhibition of iNOS expression and the promotion of CD206 expression were significantly weakened in THP-1 cells transfected with LOX-1 siRNA (Figure 4E). Further examination of the function of CD206+ macrophages showed that after 72 h of ox-LDL stimulation, the levels of the CD206+ macrophage-related cytokines interleukin IL-4, IL-10, and tumor necrosis factor TNF-β increased significantly in THP-1 cells except IL-13 (Figure 4F).

Macrophages promote the expression of tumor stem cell markers CD44 and CD133 in an ox-LDL-stimulated high-fat microenvironment

To investigate whether the occurrence of CRC is related to macrophages in the colorectal stroma and a high-fat microenvironment, we simultaneously inoculated human colorectal adenocarcinoma cells (LoVo) and THP-1 cells into transwell culture plates supplemented with 20 μg/mL ox-LDL for 72 h (Figure 5A). Thus, a high-lipid microenvironment was established to stimulate macrophages *in vitro* (n = 5). Western blot analysis showed that CD44 and CD133 expression was significantly increased in LoVo cells co-cultured with THP-1+ ox-LDL compared with ox-LDL alone (Figures 5C and 5D). We further transfected LOX-1 siRNA or siRNA negative control into THP-1 cells, and provided ox-LDL stimulation and co-cultured with LoVo cells again (Figure 5B). After ox-LDL stimulation, the levels of CD44 and CD133 in LoVo cells were inhibited when we knocked down LOX-1 in THP-1 cells (Figures 5E and 5F).

DISCUSSION

An increasing body of evidence suggests that HFD increases the risk of CRC. Importantly, studies have demonstrated the relationship between HFD and cancer by establishing animal models. HFD is often associated with abnormal oxidative stress and elevated lipid levels. Ox-LDL is a metabolite that reflects oxidative stress and lipid metabolism and is associated with various tumors. Ma *et al*[18] hypothesized

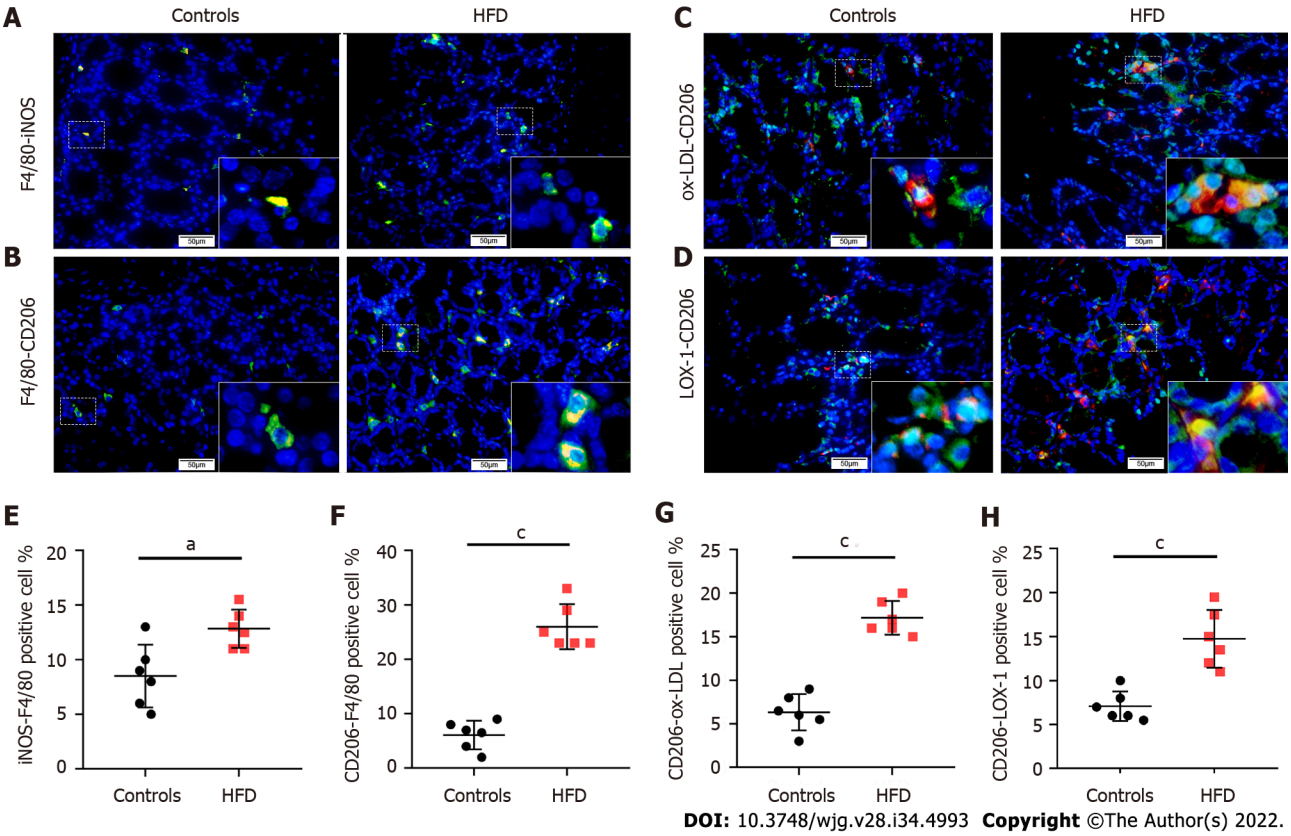


Figure 3 High-fat diet leads to increased expression of oxidized low-density lipoprotein and an increase of CD206 positive macrophages in mouse colorectal stroma. A: Double immunofluorescence (IF) images of inducible nitric oxide synthase (iNOS)-F4/80 expression in colorectal tissues of controls and high-fat diet (HFD)-fed mice (scale bars represent 50 μm); B: Double IF images of inducible nitric oxide synthase CD206-F4/80 expression in colorectal tissues of controls and HFD-fed mice (scale bars represent 50 μm); C: Double IF images of CD206-oxidized low-density lipoprotein (ox-LDL) expression in colorectal tissues of controls and HFD-fed mice (scale bars represent 50 μm); D: Double IF images of CD206-LOX-1 expression in colorectal tissues of controls and HFD-fed mice (scale bars represent 50 μm); E: Quantification of iNOS positive macrophages in colorectal tissues based on IF results in Figure 3A; F: Quantification of CD206 positive macrophages in colorectal tissues based on IF results in Figure 3B; G: Quantification of CD206 and ox-LDL positive cells in colorectal tissues based on IF results in Figure 3C; H: Quantification of CD206 and LOX-1 positive cells in colorectal tissues based on IF results in Figure 3D. Data are shown as the mean ± SD. Statistical analyses were conducted using an unpaired *t* test. The boxed area is enlarged in the bottom right corner. $^{a}P < 0.05$, $^{c}P < 0.001$. ox-LDL: Oxidized low-density lipoprotein; HFD: High-fat diet; iNOS: Inducible nitric oxide synthase.

that ox-LDL could promote gastric cancer metastasis and demonstrated that ox-LDL could promote vascular proliferation and lymphatic metastasis in gastric cancer by activating the nuclear factor-kappa B signaling pathway in animal and cell experiments. Ox-LDL may play a potential role in promoting HFD associated CRC. It has been reported that ox-LDL is correlated with CRC in patients with dyslipidemia, and the serum ox-LDL level of CRC patients is higher than that in subjects without tumors[19]. A study from Egypt found that the serum ox-LDL level of obese colon cancer patients was higher than that in obese patients with a healthy intestine; a positive correlation was found between the serum ox-LDL level and the degree of tumor malignancy[13]. Furthermore, it was found that the serum ox-LDL level of patients after surgery was significantly lower than that before surgery[14]. These findings suggest that ox-LDL is a potential predictor and prognostic biomarker of CRC. However, the above experiments were conducted using blood serum tests of CRC patients. To the best of our knowledge, no study has documented ox-LDL expression in colorectal tissue. Herein, we provided compelling evidence that ox-LDL was abnormally expressed in CRC patients with hyperlipidemia at the tissue level. In this regard, the ox-LDL level was upregulated in the cancer tissue of CRC patients, especially in the stroma. Besides, we demonstrated that LOX-1, the surface receptor of ox-LDL, was also upregulated in CRC tissues. Consistently, increased ox-LDL and LOX-1 levels were documented in the colorectal tissues of HFD-fed mice, suggesting the regulatory role of ox-LDL in the tumor microenvironment in CRC.

Macrophages, the most important immune cells in the tumor microenvironment, exhibit multiple phenotypes and exert various function[8]. It has been shown that iNOS+ macrophages inhibit tumor progression mainly by playing a pro-inflammatory role[20], while CD206+ macrophages promote cell repair and cell proliferation and growth, thus promoting tumor progression[9]. Different macrophages exhibit dynamic changes in the tumor microenvironment, and CD206+ macrophages are closely related to CRC development[21]. Existing clinical studies have reported that the CD206+ macrophage level is

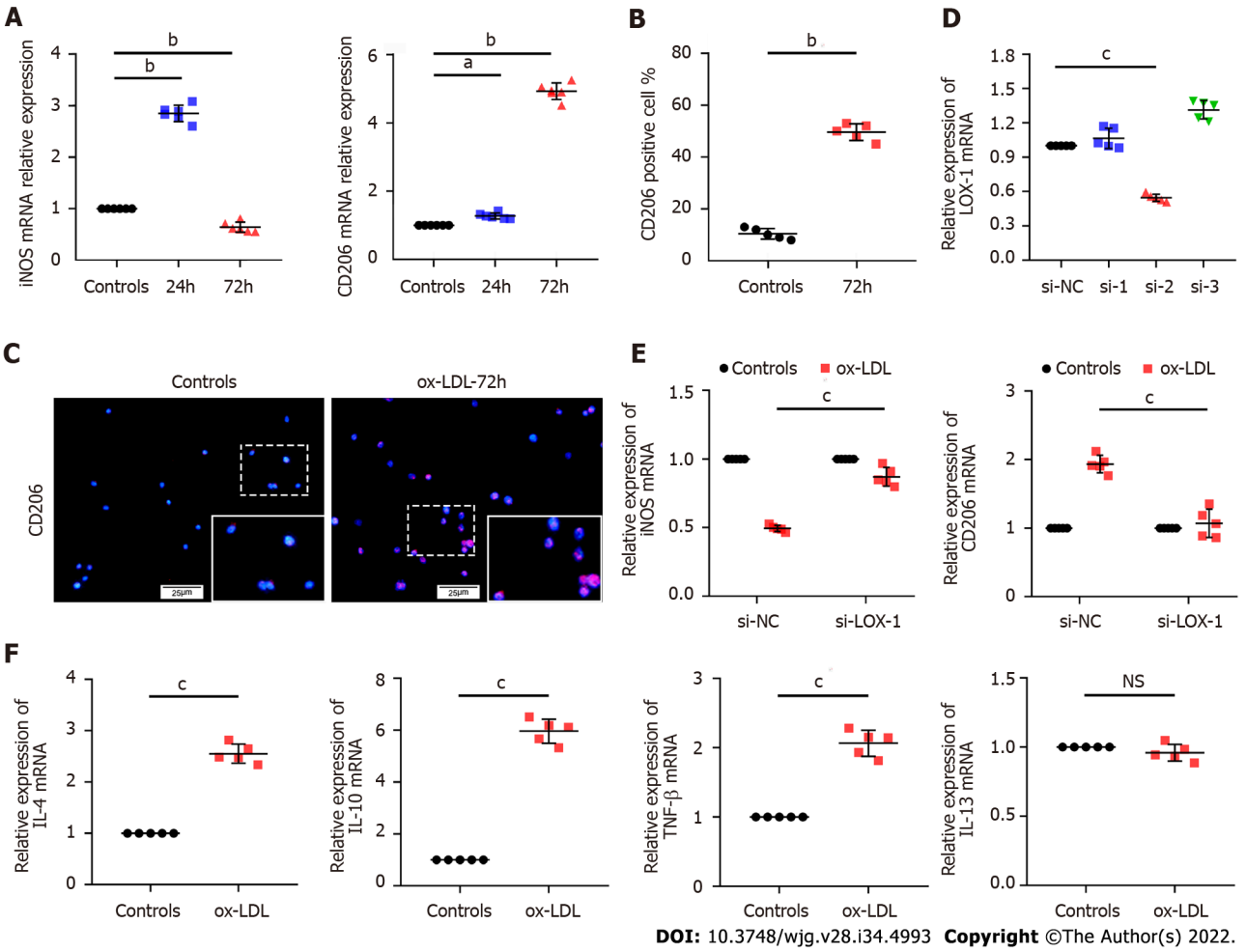
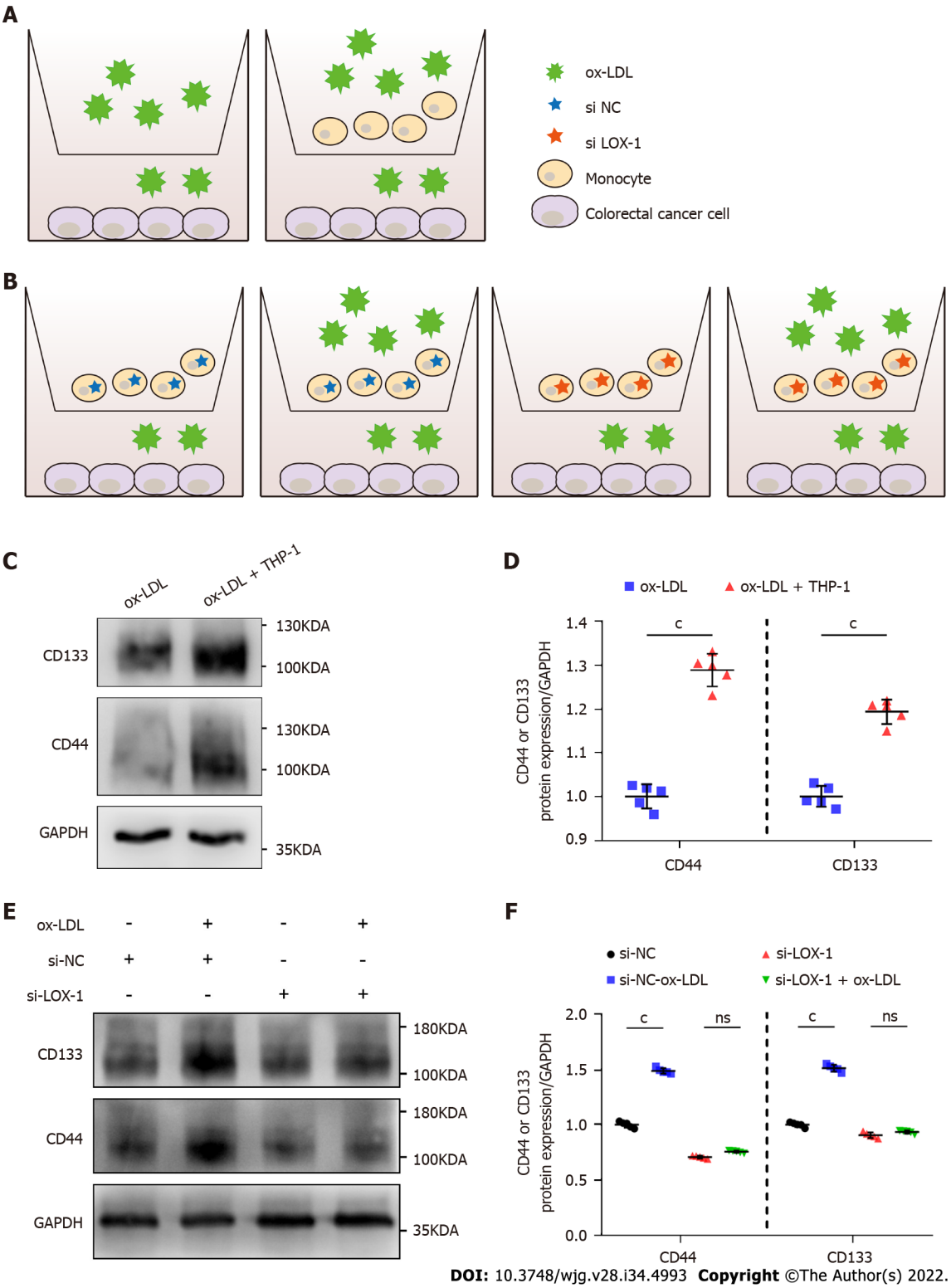


Figure 4 Continuous stimulation with oxidized low-density lipoprotein promotes CD206+ macrophages. A: Quantitative polymerase chain reaction (qPCR) detection of mRNA expression of *CD206* and inducible nitric oxide synthase (*iNOS*) in THP-1 cells after oxidized low-density lipoprotein (ox-LDL) stimulation; B: Quantification of CD206-positive cells in RAW 264.7 cells based on IF results in Figure 4C; C: Cell fluorescence images of CD206 expression in RAW 264.7 cells after ox-LDL stimulation (scale bars represent 25 μm); D: qPCR detection of the expression of *LOX-1* mRNA in THP-1 cells after transfection with *LOX-1* small interfering RNA of different sequences; E: qPCR detection of the expression of *iNOS* and *CD206* mRNA in THP-1 cells with low expression of *LOX-1* stimulated with ox-LDL; F: qPCR detection of the expression of interleukin *IL-4, IL-10, IL-13*, and tumor necrosis factor-β mRNA in THP-1 cells after 72 h of ox-LDL stimulation. Data are shown as the mean ± SD. Statistical analyses were conducted using an unpaired *t* test (Figure 4A, 4D, 4E, and 4F) or one-way analysis of variance followed by Dunnett's multiple comparison test (Figure 4B). The boxed area is enlarged in the bottom right corner. $^{a}P < 0.05$, $^{b}P < 0.01$, $^{c}P < 0.001$. ox-LDL: Oxidized low-density lipoprotein; iNOS: Inducible nitric oxide synthase; IL: Interleukin; TNF: Tumor necrosis factor; si-NC: Small interfering RNA negative control.

positively correlated with the TNM stage, the number of metastasized lymph nodes, and the degree of vascular invasion[22], and high CD206+ macrophage expression suggests a poor prognosis. Han *et al* [11] found that CD206+ macrophages in the tumor microenvironment could promote CRC metastasis through interaction with CRC cells. CD206+ macrophages have been reported to be elevated in colorectal tissues in patients with hyperlipidemia. A higher prevalence of CRC was detected in subjects with an HFD in a retrospective cohort study conducted by Liu *et al*[7]. In the present study, CD206+ macrophages were upregulated in colorectal tissues in patients with hyperlipidemia. In addition, animal experiments also confirmed that an increase in the number of intestinal tumors in HFD-fed mice was accompanied by a higher level of CD206+ macrophages, which correlated with the degree of malignancy of the tumor[7]. Our study demonstrated that CD206+ macrophages were highly expressed in the stroma of CRC tissues compared with normal tissues. These results suggest that the elevated level of CD206+ macrophages induced by HFD exerted a stimulatory effect on CRC. We also found that CD206+/ox-LDL+ cells and CD206+/LOX-1+ cells were highly expressed in the colorectal stroma of HDF-fed mice and CRC patients. In addition, studies confirmed that ox-LDL exert a regulatory effect on macrophages, and iNOS+ macrophages increased 24 h after ox-LDL induction *in vitro*[15]. Our study further found that CD206+ macrophages occurred in THP-1 cells under continuous ox-LDL stimulation. A high level of CD206+ macrophages was observed in RAW264.7 cells after ox-LDL stimulation for 72 h. Further examination of the function of CD206+ macrophages showed that after ox-LDL stimulation for 72 h, the levels of CD206+ macrophage-related cytokines IL-4, IL-10, and TNF-β increased significantly in THP-1 cells. Our study demonstrated that following the knockdown of LOX-1, the number of CD206+ macrophages mediated by ox-LDL was significantly depressed. Based on our results, we hypothesized



DOI: 10.3748/wjg.v28.i34.4993 **Copyright** ©The Author(s) 2022.

Figure 5 Macrophages promote the expression of CD44 in LoVo cells in an oxidized low-density lipoprotein-stimulated hyperlipidemic microenvironment. A: Flow diagram of the experimental result in Figure 5C; B: Flow diagram of the experimental result in Figure 5E; C: Protein expression of CD44 and CD133 in LoVo cells after oxidized low-density lipoprotein (ox-LDL) or THP-1 + ox-LDL stimulation detected by western blot; D: Quantification of CD44 and CD133 expression in LoVo cells based on western blot results in Figure 5C; E: Protein expression of CD44 and CD133 in LoVo cells after THP-1 + ox-LDL stimulation detected by western blot. The THP-1 cells were transfected with si-LOX-1 or small interfering RNA negative control; F: Quantification of CD44 and CD133 expression in LoVo cells based on western blot results in Figure 5E. Data are shown as the mean ± SD. Statistical analyses were conducted using an unpaired *t* test. $^{a}P < 0.05$, $^{b}P < 0.01$, $^{c}P < 0.001$. ox-LDL: Oxidized low-density lipoprotein; si-NC: Small interfering RNA negative control.

that ox-LDL could promote the progression of CRC by continuous stimulation of macrophages to induce CD206+ macrophages.

In addition, ox-LDL is also associated with tumor stem cells. Yang *et al*[23] found that ox-LDL could increase the malignancy of tumor stem cells in bladder cancer, thus promoting the development of bladder cancer. Active cell proliferation has been documented in gastrointestinal tissue from HFD-fed mice, with increased malignancy of tumor stem cells, which has been attributed to the inflammatory environment in colorectal tissue[4,5,24]. The high level of CD206+ macrophages in HFD-fed mice may play a certain role in this process. After THP-1 cells were stimulated with ox-LDL for 72 h and co-cultured with LoVo cells, the levels of the tumor stem cell markers CD44 and CD133 significantly increased in LoVo cells. Further, when we knocked down LOX-1 in macrophages, the increase in the levels of CD44 and CD133 was not that obvious in CRC cells, confirming that ox-LDL mediated the CD206+ macrophages to upregulate CD44 and CD133 expression in colon cancer cells.

CONCLUSION

In this study, we hypothesized that HFD could induce ox-LDL and its surface receptor LOX-1 accumulation in CRC tissue, suggesting the regulatory role of ox-LDL in the microenvironment of CRC. Furthermore, continuous stimulation of ox-LDL on macrophages induced CD206+ macrophages, which could further promote the increase of CD44 and CD133 levels in CRC cells. However, there are many limitations to our study. First of all, this study was a single-center study, and the sample size of included clinical specimens was relatively small. Larger sample size and multi-center prospective studies are needed to confirm our findings. Moreover, the mechanism underlying the effects of ox-LDL and the relevant signaling pathways were not explored, warranting further studies. In conclusion, we demonstrated that HFD causes ox-LDL accumulation in the colorectal tissue and upregulates CD44 and CD133 expression in colorectal cells by inducing CD206+ macrophages. These findings provide evidence for a new mechanism of increased CRC susceptibility with HFD.

ARTICLE HIGHLIGHTS

Research background

Oxidized low-density lipoprotein (ox-LDL), abnormally increased in the serum of patients with colorectal cancer (CRC) associated with a high-fat diet (HFD), may be one of the risk factors for CRC. Ox-LDL exerts a regulatory effect on macrophages, is associated with cancer stem cells, and may regulate CRC through the tumor microenvironment. The role of ox-LDL in CRC remains unclear. It is essential to explore the function of ox-LDL to explore the pathogenesis of HFD associated CRC.

Research motivation

The expression of ox-LDL in human colorectal cancerous tissues and colorectal tissues of hyperlipidemic mice was detected, and the function of ox-LDL in the macrophages in the tumor microenvironment was explored. Our key point is that ox-LDL up-regulates CD44 and CD133 in HFD associated CRC, which is mediated by macrophages. Our study will provide a new idea for the mechanism of HFD associated CRC.

Research objectives

The study aimed to investigate the role of ox-LDL through macrophage in HFD associated CRC.

Research methods

The expression of ox-LDL and CD206 was detected in colorectal tissues of CRC patients with hyperlipidemia and HFD-fed mice by immunofluorescence. We stimulated macrophages with 20 ug/mL ox-LDL and assessed the expression levels of CD206 and cytokines by cell fluorescence and quantitative polymerase chain reaction. We further knocked down LOX-1, the surface receptor of ox-LDL, to confirm the function of ox-LDL in macrophages. Then, LoVo cells were co-cultured with the stimulated macrophages to analyze the CD44 and CD133 expression by western blot.

Research results

The expression of ox-LDL and CD206 was significantly increased in the stroma of colorectal tissues of CRC patients with hyperlipidemia, and also upregulated in the HFD-fed mice. Moreover, an increased level of CD206 and decreased level of inducible nitric oxide synthase were observed in macrophages after the continuous stimulation of ox-LDL. Such effects were inhibited when the surface receptor LOX-1 was knocked down in macrophages. Ox-LDL could induce CD206+ macrophages, which resulted in high expression of CD44 and CD133 in co-cultured LoVo cells.

Research conclusions

Our study found that HFD could induce ox-LDL accumulation in CRC tissue, suggesting the regulatory role of ox-LDL in the microenvironment of CRC. Continuous stimulation of macrophages with ox-LDL induced CD206+ macrophages, which could further promote the increase of CD44 and CD133 levels in CRC cells.

Research perspectives

Our future study will collect more samples. We look forward to make a convincing analysis to identify the correlation between ox-LDL and progression and survival of the enrolled patients in the near future. We will explore the potential signal pathways related to ox-LDL promoting M2-type macrophages by using the technology of single cell sequencing and/or RNA-Seq assay. We are confident that it will provide exciting data in the near future.

ACKNOWLEDGEMENTS

We thank Ms. Lin-Lin Huang (Department of Gastroenterology, Guangdong Provincial People's Hospital, Guangdong Academy of Medical Sciences, Guangzhou, China) for kindly providing LoVo cells. We really appreciate Mr. Ren-Gui Lin and Ms. Yu-Liang Huang (The Third School of Clinical Medicine, Southern Medical University, Guangzhou, China) for kindly assisting in the completion of the experiments.

FOOTNOTES

Author contributions: Zheng SM, Sha WH, Chen H, and Ma J designed and coordinated the study; Zheng SM, Chen XF, Yin JB, Zhu XB, and Zheng ZW performed the experiments; Zheng SM and Yin JB acquired and analyzed the data; Chen XF, Zhu XB, and Zheng ZW interpreted the data; Zheng SM, Sha WH, and Chen H wrote the manuscript; and all authors approved the final version of the article.

Supported by Science and Technology Program of Guangzhou, No. 202102080007.

Institutional review board statement: The institutional review board of the Guangdong General Hospital approved the study protocol. All procedures performed in studies involving human participants were in accordance with the ethical standards of the institutional and national research committee and with the 1964 Helsinki declaration and its later amendments or comparable ethical standards.

Institutional animal care and use committee statement: The animal protocol was designed to minimize pain or discomfort to the animals. The animals were acclimatized to laboratory conditions (23 °C, 12 h/12 h light/dark, 50% humidity, ad libitum access to food and water) for 2 wk prior to experimentation.

Conflict-of-interest statement: All the authors report no relevant conflicts of interest for this article.

Data sharing statement: Technical appendix, statistical code, and dataset available from the corresponding author at email: mjlqh@163.com. Participants gave informed consent for data sharing.

ARRIVE guidelines statement: The authors have read the ARRIVE guidelines, and the manuscript was prepared and revised according to the ARRIVE guidelines.

Open-Access: This article is an open-access article that was selected by an in-house editor and fully peer-reviewed by external reviewers. It is distributed in accordance with the Creative Commons Attribution NonCommercial (CC BY-NC 4.0) license, which permits others to distribute, remix, adapt, build upon this work non-commercially, and license their derivative works on different terms, provided the original work is properly cited and the use is non-commercial. See: https://creativecommons.org/Licenses/by-nc/4.0/

Country/Territory of origin: China

ORCID number: Shi-Min Zheng 0000-0003-1104-9005; Hao Chen 0000-0003-4339-3441; Wei-Hong Sha 0000-0001-7610-3813; Juan Ma 0000-0003-1256-4914.

S-Editor: Wang JJ
L-Editor: Wang TQ
P-Editor: Wu RR

REFERENCES

1 **Sung H**, Ferlay J, Siegel RL, Laversanne M, Soerjomataram I, Jemal A, Bray F. Global Cancer Statistics 2020: GLOBOCAN Estimates of Incidence and Mortality Worldwide for 36 Cancers in 185 Countries. *CA Cancer J Clin* 2021; **71**: 209-249 [PMID: 33538338 DOI: 10.3322/caac.21660]

2 **Liu PH**, Wu K, Ng K, Zauber AG, Nguyen LH, Song M, He X, Fuchs CS, Ogino S, Willett WC, Chan AT, Giovannucci EL, Cao Y. Association of Obesity With Risk of Early-Onset Colorectal Cancer Among Women. *JAMA Oncol* 2019; **5**: 37-44 [PMID: 30326010 DOI: 10.1001/jamaoncol.2018.4280]

3 **Keum N**, Giovannucci E. Global burden of colorectal cancer: emerging trends, risk factors and prevention strategies. *Nat Rev Gastroenterol Hepatol* 2019; **16**: 713-732 [PMID: 31455888 DOI: 10.1038/s41575-019-0189-8]

4 **Mana MD**, Hussey AM, Tzouanas CN, Imada S, Barrera Millan Y, Bahceci D, Saiz DR, Webb AT, Lewis CA, Carmeliet P, Mihaylova MM, Shalek AK, Yilmaz ÖH. High-fat diet-activated fatty acid oxidation mediates intestinal stemness and tumorigenicity. *Cell Rep* 2021; **35**: 109212 [PMID: 34107251 DOI: 10.1016/j.celrep.2021.109212]

5 **van Driel MS**, van Neerven SM, Vermeulen L. High-Fat Diet Impacts on Tumor Development in the Gut. *Trends Cancer* 2021; **7**: 664-665 [PMID: 34219052 DOI: 10.1016/j.trecan.2021.06.005]

6 **Lin HY**, Weng SW, Shen FC, Chang YH, Lian WS, Hsieh CH, Chuang JH, Lin TK, Liou CW, Chang CS, Lin CY, Su YJ, Wang PW. Abrogation of Toll-Like Receptor 4 Mitigates Obesity-Induced Oxidative Stress, Proinflammation, and Insulin Resistance Through Metabolic Reprogramming of Mitochondria in Adipose Tissue. *Antioxid Redox Signal* 2020; **33**: 66-86 [PMID: 31950846 DOI: 10.1089/ars.2019.7737]

7 **Liu T**, Guo Z, Song X, Liu L, Dong W, Wang S, Xu M, Yang C, Wang B, Cao H. High-fat diet-induced dysbiosis mediates MCP-1/CCR2 axis-dependent M2 macrophage polarization and promotes intestinal adenoma-adenocarcinoma sequence. *J Cell Mol Med* 2020; **24**: 2648-2662 [PMID: 31957197 DOI: 10.1111/jcmm.14984]

8 **Murray PJ**, Allen JE, Biswas SK, Fisher EA, Gilroy DW, Goerdt S, Gordon S, Hamilton JA, Ivashkiv LB, Lawrence T, Locati M, Mantovani A, Martinez FO, Mege JL, Mosser DM, Natoli G, Saeij JP, Schultze JL, Shirey KA, Sica A, Suttles J, Udalova I, van Ginderachter JA, Vogel SN, Wynn TA. Macrophage activation and polarization: nomenclature and experimental guidelines. *Immunity* 2014; **41**: 14-20 [PMID: 25035950 DOI: 10.1016/j.immuni.2014.06.008]

9 **Li R**, Zhou R, Wang H, Li W, Pan M, Yao X, Zhan W, Yang S, Xu L, Ding Y, Zhao L. Gut microbiota-stimulated cathepsin K secretion mediates TLR4-dependent M2 macrophage polarization and promotes tumor metastasis in colorectal cancer. *Cell Death Differ* 2019; **26**: 2447-2463 [PMID: 30850734 DOI: 10.1038/s41418-019-0312-y]

10 **Noy R**, Pollard JW. Tumor-associated macrophages: from mechanisms to therapy. *Immunity* 2014; **41**: 49-61 [PMID: 25035953 DOI: 10.1016/j.immuni.2014.06.010]

11 **Han L**, Wang S, Wei C, Fang Y, Huang S, Yin T, Xiong B, Yang C. Tumour microenvironment: a non-negligible driver for epithelial-mesenchymal transition in colorectal cancer. *Expert Rev Mol Med* 2021; **23**: e16 [PMID: 34758892 DOI: 10.1017/erm.2021.13]

12 **Khaidakov M**, Mehta JL. Do atherosclerosis and obesity-associated susceptibility to cancer share causative link to oxLDL and LOX-1? *Cardiovasc Drugs Ther* 2011; **25**: 477-487 [PMID: 21881851 DOI: 10.1007/s10557-011-6330-8]

13 **Keshk WA**, Zineldeen DH, Wasfy RE, El-Khadrawy OH. Fatty acid synthase/oxidized low-density lipoprotein as metabolic oncogenes linking obesity to colon cancer *via* NF-kappa B in Egyptians. *Med Oncol* 2014; **31**: 192 [PMID: 25173531 DOI: 10.1007/s12032-014-0192-4]

14 **Salehi SS**, Mirmiranpour H, Rabizadeh S, Esteghamati A, Tomasello G, Alibakhshi A, Najafi N, Rajab A, Nakhjavani M. Improvement in Redox Homeostasis after Cytoreductive Surgery in Colorectal Adenocarcinoma. *Oxid Med Cell Longev* 2021; **2021**: 8864905 [PMID: 34381561 DOI: 10.1155/2021/8864905]

15 **Pei C**, Zhang Y, Wang P, Zhang B, Fang L, Liu B, Meng S. Berberine alleviates oxidized low-density lipoprotein-induced macrophage activation by downregulating galectin-3 *via* the NF-κB and AMPK signaling pathways. *Phytother Res* 2019; **33**: 294-308 [PMID: 30402951 DOI: 10.1002/ptr.6217]

16 **Yang P**, Rhea PR, Conway T, Nookala S, Hegde V, Gagea M, Ajami NJ, Harribance SL, Ochoa J, Sastry JK, Cohen L. Human Biofield Therapy Modulates Tumor Microenvironment and Cancer Stemness in Mouse Lung Carcinoma. *Integr Cancer Ther* 2020; **19**: 1534735420940398 [PMID: 32975128 DOI: 10.1177/1534735420940398]

17 **Lv J**, Liu C, Chen FK, Feng ZP, Jia L, Liu PJ, Yang ZX, Hou F, Deng ZY. M2like tumourassociated macrophagesecreted IGF promotes thyroid cancer stemness and metastasis by activating the PI3K/AKT/mTOR pathway. *Mol Med Rep* 2021; **24** [PMID: 34184083 DOI: 10.3892/mmr.2021.12249]

18 **Ma C**, Xie J, Luo C, Yin H, Li R, Wang X, Xiong W, Zhang T, Jiang P, Qi W, Zhou T, Yang Z, Wang W, Ma J, Gao G, Yang X. OxLDL promotes lymphangiogenesis and lymphatic metastasis in gastric cancer by upregulating VEGFC expression and secretion. *Int J Oncol* 2019; **54**: 572-584 [PMID: 30483757 DOI: 10.3892/ijo.2018.4648]

19 **Suzuki K**, Ito Y, Wakai K, Kawado M, Hashimoto S, Toyoshima H, Kojima M, Tokudome S, Hayakawa N, Watanabe Y, Tamakoshi K, Suzuki S, Ozasa K, Tamakoshi A; Japan Collaborative Cohort Study Group. Serum oxidized low-density lipoprotein levels and risk of colorectal cancer: a case-control study nested in the Japan Collaborative Cohort Study. *Cancer Epidemiol Biomarkers Prev* 2004; **13**: 1781-1787 [PMID: 15533907]

20 **Lee JW**, Lee SM, Chun J, Im JP, Seo SK, Ha N, Il Choi Y, Kim JS. Novel Histone Deacetylase 6 Inhibitor CKD-506 Inhibits NF-κB Signaling in Intestinal Epithelial Cells and Macrophages and Ameliorates Acute and Chronic Murine Colitis. *Inflamm Bowel Dis* 2020; **26**: 852-862 [PMID: 31895948 DOI: 10.1093/ibd/izz317]

21 **Inagaki K**, Kunisho S, Takigawa H, Yuge R, Oka S, Tanaka S, Shimamoto F, Chayama K, Kitadai Y. Role of tumor-associated macrophages at the invasive front in human colorectal cancer progression. *Cancer Sci* 2021; **112**: 2692-2704 [PMID: 33964093 DOI: 10.1111/cas.14940]

22 **Ma X**, Gao Y, Chen Y, Liu J, Yang C, Bao C, Wang Y, Feng Y, Song X, Qiao S. M2-Type Macrophages Induce Tregs Generation by Activating the TGF-β/Smad Signalling Pathway to Promote Colorectal Cancer Development. *Onco Targets Ther* 2021; **14**: 5391-5402 [PMID: 34908844 DOI: 10.2147/OTT.S336548]

23 **Yang L**, Sun J, Li M, Long Y, Zhang D, Guo H, Huang R, Yan J. Oxidized Low-Density Lipoprotein Links

Hypercholesterolemia and Bladder Cancer Aggressiveness by Promoting Cancer Stemness. *Cancer Res* 2021; **81**: 5720-5732 [PMID: 34479964 DOI: 10.1158/0008-5472.CAN-21-0646]

24 **Beyaz S**, Mana MD, Roper J, Kedrin D, Saadatpour A, Hong SJ, Bauer-Rowe KE, Xifaras ME, Akkad A, Arias E, Pinello L, Katz Y, Shinagare S, Abu-Remaileh M, Mihaylova MM, Lamming DW, Dogum R, Guo G, Bell GW, Selig M, Nielsen GP, Gupta N, Ferrone CR, Deshpande V, Yuan GC, Orkin SH, Sabatini DM, Yilmaz ÖH. High-fat diet enhances stemness and tumorigenicity of intestinal progenitors. *Nature* 2016; **531**: 53-58 [PMID: 26935695 DOI: 10.1038/nature17173]

World Journal of Gastroenterology

Submit a Manuscript: https://www.f6publishing.com

World J Gastroenterol 2022 September 14; 28(34): 5007-5022

DOI: 10.3748/wjg.v28.i34.5007

ISSN 1007-9327 (print) ISSN 2219-2840 (online)

ORIGINAL ARTICLE

Basic Study

Ji-Chuan decoction ameliorates slow transit constipation *via* regulation of intestinal glial cell apoptosis

Xiu-Min Wang, Li-Xia Lv, Yue-Si Qin, Yu-Zhu Zhang, Ni Yang, Shu Wu, Xiu-Wen Xia, Hong Yang, Hong Xu, Ying Liu, Wei-Jun Ding

Specialty type: Gastroenterology and hepatology

Provenance and peer review: Unsolicited article; Externally peer reviewed.

Peer-review model: Single blind

Peer-review report's scientific quality classification
Grade A (Excellent): 0
Grade B (Very good): 0
Grade C (Good): C, C
Grade D (Fair): 0
Grade E (Poor): 0

P-Reviewer: Khayyat YM, Saudi Arabia; Kumar A, India

Received: May 20, 2022
Peer-review started: May 20, 2022
First decision: July 13, 2022
Revised: July 19, 2022
Accepted: August 21, 2022
Article in press: August 21, 2022
Published online: September 14, 2022

Xiu-Min Wang, Yu-Zhu Zhang, Ni Yang, Shu Wu, Xiu-Wen Xia, Hong Yang, Wei-Jun Ding, Department of Fundamental Medicine, Chengdu University of Traditional Chinese Medicine, Chengdu 610072, Sichuan Province, China

Xiu-Min Wang, Hong Xu, Department of Proctology, Chengdu First People's Hospital, Chengdu 610041, Sichuan Province, China

Li-Xia Lv, Department of Endocrinology and Metabolism, Chengdu First People's Hospital, Chengdu 610041, Sichuan Province, China

Yue-Si Qin, Department of Dermatology, Chengdu First People's Hospital, Chengdu 610041, Sichuan Province, China

Ying Liu, Department of Preventive Medicine, Shantou University Medical College, Shantou 515063, Guangdong Province, China

Corresponding author: Wei-Jun Ding, PhD, Full Professor, Department of Fundamental Medicine, Chengdu University of Traditional Chinese Medicine, No. 1166 Liutai Avenue, Wenjiang District, Chengdu 610072, Sichuan Province, China. dingweijun@cdutcm.edu.cn

Abstract

BACKGROUND

Slow transit constipation (STC) is a common intestinal disease with increasing incidence. STC results from various factors, such as the enteric nervous system and metabolic changes. As a classical formula of traditional Chinese medicine, Ji-Chuan decoction (JCD) has been extensively and effectively used in STC treatment, yet its pharmacological mechanism remains unclear.

AIM

To explore the integrated regulatory pattern of JCD against STC through hyphenated techniques from metabolism, network pharmacology and molecular methods.

METHODS

STC model mice were generated by intragastric administration of compound diphenoxylate (10 mg/kg/d) for 14 d. The STC mice in the low dose of JCD (3.04 g/kg), middle dose of JCD (6.08 g/kg) and high dose of JCD (12.16 g/kg) groups

were orally administered JCD solution once a day for 2 wk. The acetylcholine (ACH) level was examined by enzyme-linked immunosorbent assay. The pathological features of colon tissue were observed by hematoxylin and eosin staining. The differentially expressed metabolites and metabolic pathways were tested by nontargeted metabolomics. The main targets and core ingredients of JCD were identified by network pharmacology, and the expression of AKT was confirmed by immunohistochemistry. Finally, the pathways involved in JCD treatment were predicted using a combination of differentially expressed metabolites and targets, and intestinal glial cell apoptosis was demonstrated by immunofluorescence.

RESULTS

JCD significantly promoted intestinal motility, increased the levels of the excitatory neurotransmitter ACH and reduced intestinal inflammation in STC mice. Untargeted metabolomics results showed that JCD significantly restored metabolic dysfunction and significantly affected taurine and hypotaurine metabolism. Network pharmacology and molecular experiments showed that JCD regulates AKT protein expression, and the core component is quercetin. Combined analysis demonstrated that apoptosis may be an important mechanism by which JCD relieves constipation. Further experiments showed that JCD reduced enteric glial cell (EGC) apoptosis.

CONCLUSION

This work demonstrated that reducing EGC apoptosis may be the critical mechanism by which JCD treats STC. These findings call for further molecular research to facilitate the clinical application of JCD.

Key Words: Slow-transit constipation; Ji-Chuan decoction; Taurine and hypotaurine metabolism; AKT; Enteric glial cell; Apoptosis

©The Author(s) 2022. Published by Baishideng Publishing Group Inc. All rights reserved.

Core Tip: Slow transit constipation (STC) model mice, which were established with compound diphenoxylate, were effectively treated with Ji-Chuan decoction (JCD). The results show that JCD can promote intestinal motility, increase acetylcholine content, reduce enteric inflammation, improve metabolic dysfunction, and reduce enteric glial cell apoptosis. This work demonstrated that reducing enteric glial cell apoptosis may be the critical mechanism by which JCD treats STC. These findings call for further molecular research to facilitate the clinical application of JCD.

Citation: Wang XM, Lv LX, Qin YS, Zhang YZ, Yang N, Wu S, Xia XW, Yang H, Xu H, Liu Y, Ding WJ. Ji-Chuan decoction ameliorates slow transit constipation *via* regulation of intestinal glial cell apoptosis. *World J Gastroenterol* 2022; 28(34): 5007-5022
URL: https://www.wjgnet.com/1007-9327/full/v28/i34/5007.htm
DOI: https://dx.doi.org/10.3748/wjg.v28.i34.5007

INTRODUCTION

Chronic constipation is a common complaint and can generally be divided into defecatory disorder, mixed constipation, normal transit constipation and slow transit constipation (STC). STC is the major type of chronic constipation characterized by a substantial increase in bowel transit time. STC has become an epidemic that particularly impacts the quality of life of elderly patients[1]. Despite high morbidity worldwide, the etiology of STC is poorly understood. An accumulation of publications indicates that multiple factors have been documented in the pathogenesis of STC[2-4]. Consequently, an interdisciplinary approach is necessary for exploring its pathological characteristics and developing therapies based on multiple components and multiple targets, such as traditional Chinese medicine (TCM)[5,6]. The active components of Ma-Zi-Ren-Wan could safely and effectively relieve the severity of functional constipation. Based on network pharmacology[7], the anti-STC mechanism of Gui-ren-Run-chang granules, another TCM formula, is associated with repairing the SCF/c-kit pathway and reducing aquaporin-4 expression in the colon[8].

Ji-Chuan decoction (JCD) is a representative TCM formula that originated from Jing-Yue-Zhang in the Ming Dynasty. It has been extensively used for STC and other gastroenteric disorders for hundreds of years[9]. JCD, as a typical TCM prescription, is composed of six herbs and includes multiple bioactive ingredients and complex targets. Studies have shown that JCD can effectively shorten colonic transit

time, improve anorectal dynamics, regulate gastrointestinal neurotransmitters, alleviate constipation symptoms in STC patients, and improve the quality of life of STC patients[9,10]. After 1 mo of continuous use, only a few patients experienced adverse reactions such as dizziness (1.7%) and dry mouth (1.7%)[10]. Our clinical practice confirmed that JCD was a useful formula for STC therapy. *Cistanche deserticola* (*C. deserticola*) is the monarch drug for JCD, and the combination of geniposide and Lactobacillus plantarum KSFY06 has been shown to have anti-montmorillonite-induced constipation effects in Kunming mice[11,12]. However, direct experimental study of the effects of JCD against STC remains to be performed. In this work, we attempt to assess the laxative effect of JCD against STC through a multiomics approach, including metabolomics and TCM network pharmacology, to explore the integrated therapeutic mechanism of JCD.

MATERIALS AND METHODS

Reagents and JCD preparation

Rabbit anti-AKT monoclonal antibody (No: bs-0115R) was provided by Bioss. The biotin secondary antibody anti-rabbit working solution (Goat, SP-9001) was provided by Beijing Zhongshan Jinqiao Biological Technology Co., Ltd. Glial fibrillary acidic protein (GFAP) (mouse, code: ab4648) and Caspase3 (rabbit, code: ab4051) were purchased from Abcam. CY3-labeled goat anti-mouse immunoglobulin G (IgG) (code: 202110) and fluorescein isothiocyanate-labeled goat anti-rabbit IgG (code: GB22303) were purchased from Servicebio.

The JCD solution was prepared according to the protocol described by Cui *et al*[13]. A clinical packet of JCD is composed of six Chinese herbs, *i.e.*, *Angelica sinensis* (15 g), *C. deserticola* (9 g), *Achyranthes bidentata* (*A. bidentata*) (6 g), *Fructus aurantii* (*F. aurantii*) (4.5 g), *Alisma orientalis* (3 g) and *Cimicifuga heracleifuga* (3 g). Six packets of JCD were purchased from Chengdu Hospital of Integrated TCM and Western Medicine and identified by Dr. Wan Lin from Chengdu University of TCM. These herbs were then soaked in 2430 mL ddH_2O (w/v 1:10) for 30 min and decocted for 20 min. Combined solutions following three decoctions were filtered by a 0.22-μm filter, concentrated to 0.81 g of crude herb per milliliter by a vapor evaporator, and stored at -20 °C for further use. In the past, scholars have studied the hyphenated to liquid chromatography characteristic fingerprints of JCD substances[14].

STC model-made, JCD treatment and sample collection

This experiment was approved by the Animal Ethics Committee, Chengdu University of TCM (license 2016-16). Thirty C57BL/6J male mice, aged 7 wk and weight 20.21 ± 2.10 g, were purchased from Chongqing Evansville Laboratory Animal Co., Ltd. (Chongqing, China). The animals were adaptively fed for 7 d in an environment with relative humidity of 45%-55%, a 12-h light/dark cycle and temperature of 22 ± 2 °C. The mice were then randomly divided into six groups, with five animals in each group: Healthy control (HC), STC model (STC), positive drug treatment (mosapride, MSP), low dose of JCD (JCDL), middle dose of JCD (JCDM) and high dose of JCD (JCDH). Mice in the HC group were orally administered normal saline (0.1 mL/10 g/d) as a negative control. The other mice were induced as the STC models by oral administration of compound diphenoxylate (10 mg/kg/d) for 14 d. After model identification, mice in the MSP group were orally administered with MSP (2.5 mg/kg); mice in the JCDL (3.04 g/kg), JCDM (6.08 g/kg) and JCDH (12.16 g/kg) groups were orally administered with JCD; and normal saline (0.1 mL/10 g/d) was gavaged in the HC and STC groups. Each mouse was administered treatments once a day for 14 d. Body weight, food intake and water intake were monitored every week. At the end of experiment, the feces of each mouse were collected under sterile procedures, frozen in liquid nitrogen and stored at -80 °C for further use.

The number of defecation particles within 6 h was counted, and the wet weight of the stool samples was evaluated. Then, the dry weight of the stool was weighed after drying at 60 °C for 12 h in a desiccator, and the moisture content of the stool was calculated. The colonic samples were harvested after euthanasia[15]. The acetylcholine (ACH) concentrations were detected by enzyme-linked immunosorbent assay.

Evaluation of the intestinal propulsive rate

The intestinal propulsive rate was measured after the last administration as follows[16]: All mice were fasted for 12 h and allowed free access to water. Then, mice were fed charcoal powder in 10% acacia gum. After 30 min, the abdomen was opened and the intestines were removed. The length from the pylorus to the ileocecal junction, as well as the charcoal transport distance were measured. The intestinal propulsive rate was calculated by the following formula[17]: Charcoal transit ratio (%) = distance of charcoal transport (cm)/length from pylorus to ileocecal junction (cm) × 100%.

Hematoxylin and eosin and immunofluorescence staining

The collected tissue samples were fixed with 10% formalin, dehydrated with alcohol, and embedded in paraffin wax. The embedded tissues were then sliced into 5-μm slices using a microtome (Leica, Buffalo

Grove, United States) and stained with hematoxylin and eosin (HE). The pathological features were imaged by a digital microscope (Xiamen, China), and the optical densities were quantified using Image-Pro Plus 6.0.

Ultrahigh-pressure liquid chromatography coupled with tandem mass spectrometry analysis

Metabolomics was performed with a Vanquish UHPLC (Thermo, Germany) coupled with a Q Exactive™ HF (Thermo, Germany) platform (Novogene, Beijing, China) as previously described. Fecal samples (100 mg) were ground in liquid nitrogen, incubated on ice for 5 min, and centrifuged at 15000 × g for 20 min at 4 °C. The supernatant was diluted with liquid chromatography-mass spectrometry grade water to a final concentration of 53% methanol. After another centrifugation step, the supernatant was injected into the liquid chromatography-tandem mass spectrometry system for analysis. Samples were injected into a Hypesil Gold column (C18) using a 17-min linear gradient at a flow rate of 0.2 mL/min. The eluents in positive polarity mode were Eluent A (0.1% FA in water) and Eluent B (methanol). The eluents for negative polarity mode were Eluent A (5 mmol/L ammonium acetate, pH 9.0) and Eluent B (methanol). The solvent gradient was set as follows: 2% B, 1.5 min; 2%-100% B, 12.0 min; 100% B, 14.0 min; 100%-2% B, 14.1 min; and 2% B, 17 min. The Q Exactive™ HF mass spectrometer was operated in positive/negative mode with a spray voltage of 3.2 kV, a capillary temperature of 320 °C, a sheath gas flow of 40 arb, and an auxiliary gas flow of 10 arb. Then, the data were matched to the mzCloud, mzVault, and MassList databases for accurate qualitative and relative quantitative results. The threshold for differential metabolites was set as variable importance in the projection (VIP) > 1.0, fold change (FC) > 1.5 or < 0.667 and P value < 0.05. The metabolic functions and relevant metabolic pathways were enriched by MetaboAnalyst 5.0 (https://www.metaboanalyst.ca/).

Network pharmacology analysis and immunohistochemical validation

TCMSP (https://tcmsp-e.com/) was applied to find the chemical components and corresponding targets of JCD, with OB ≥ 30% and DL ≥ 0.18. The UniProt database (https://www.UniProt.org/) was used to correct potential targets. The chemical composition and corresponding targets of JCD were checked by BAT-MAN (http://bionet.ncpsb.org.cn/batman-tcm/index.php), with a score cutoff over 500. Then, the targets obtained from TCMSP and BAT-MAN were combined and deduplicated. Taking "slow transfer constipation" as the keyword, the target points with a score greater than 5.0 were collected from the GeneCard database (https://www.genecards.org/), and all the targets collected from OMIM (https://omim.org/) were included in the follow-up study. The common genes of drug targets and disease genes were put into the STRING11.0 (https://string-db.org/) database to construct a protein-protein interaction (PPI) network. The relevant data were imported into Cytoscape (3.7.1) software in tsv format, and the cytoHubba plug-in was used to display the top 30 nodes in the betweenness algorithm as Hub nodes and to display them in Excel. The distribution pattern and expression levels of AKT, which is one of the most important hub nodes in colonic tissues, were analyzed by immunohistochemistry. Rabbit anti-AKT antibody (Bioss; 1:100) was applied overnight at 4 °C, followed by horseradish peroxidase-conjugated goat anti-rabbit IgG incubation at room temperature for 30 min, and diaminobenzidine was used for staining. The graphic processing software Image-Pro plus 6.0 was used to quantify the expression of AKT. Five fields of each slide were randomly observed, and the optical density values were determined. The components acting on AKT are considered core components of JCD.

Integrated analysis of differentially expressed metabolites and target genes

The HGNC database (https://www.genenames.org/) was applied to transform the obtained JCD target genes into mouse genes. The Joint-Pathway analysis of MetaboAnalyst 5.0 was used to enrich differentially expressed metabolites (DEMs) and target genes associated with JCD. Except for those nominated by other diseases, the top 25 pathways were selected for integrated analysis. The degree of apoptosis of enteric glial cells (EGCs) in colon tissue was analyzed by immunofluorescence. Rabbit anti-caspase3 antibody (Abcam; 1:100) was applied overnight at 4 °C, and mouse anti-GFAP antibody (Abcam; 1:100) was stained at 37 °C for 30 min followed by 4',6-diamidino-2-phenylindole for 10 min at room temperature. ImageJ graphics processing software was used to calculate the apoptosis of EGCs. Five fields of each slide were randomly observed, and densitometric values were estimated.

Statistical analysis

Data processing and statistical analyses were performed by Graph Pad Prism 7 (GraphPad, La Jolla, CA, United States). Data are expressed as the mean ± SD. One-way analysis of variance was used to compare the data of six groups. Student's t test was used for the pairwise comparison of data. The results were considered significant when P < 0.05.

RESULTS

JCD promoted intestinal motility, increased excitatory neurotransmitters and reduced intestinal inflammation in STC mice

General restoration of STC symptoms was observed after JCD treatment. The food intake, water intake and body weight in the JCDH and JCDM groups were similar to those in the HC group (Supplementary Table 1). Compared with HC mice, the average number of stool particles collected from STC mice was markedly reduced. After JCD administration, the average number of stool particles collected from the JCDL, JCDM and JCDH groups was significantly increased and was similar to the level of the positive control drug MSP (Figure 1A). Compared with the HC group, the dry weight, wet weight, and water content of the feces in the STC group were significantly decreased, and the dry weight, wet weight, and water content of the feces in the MSP, JCDM, and JCDH groups were significantly increased (Table 1). Compared with the HC group, the intestinal propulsion rate was significantly decreased in the STC mice, whereas the intestinal propulsion rate was significantly increased in the JCDM, JCDH, and MSP groups (Figure 1B). Finally, the concentrations of excitatory neurotransmitters (colon ACH) in STC mice were significantly reduced, while those in the three JCD groups were significantly increased (Figure 1C).

In addition, pathological observations demonstrated that JCD significantly reduced constipation-associated intestinal inflammation. Pathological observation demonstrated typical pathology of intestinal inflammation in STC mice, with inflammatory infiltration and necrosis in the distal colon. JCD repaired the colonic injuries in a dose-dependent manner (Figure 2). Briefly, the results showed that JCD exerts its effects by enhancing intestinal motility, promoting excitatory neurotransmitters and inhibiting intestinal inflammation in STC mice. Therefore, it is considered that the modeling was successful.

JCD beneficially regulated taurine and hypotaurine metabolism

Forty-two DEMs (Supplementary Table 2) (negative ion mode) between the HC and STC groups and 86 DEMs (Supplementary Table 3) between the STC and JCDH groups were identified (the sample chromatogram in negative ion mode is shown in Supplementary Figure 1). Among the DEMs, eighteen were altered by the modeling process but recovered after JCDH treatment (Supplementary Table 4). As shown in Figure 3A, the closely focused cluster of quality control (QC) samples indicated the reproducibility of the experiments. Figures 3B and C display the fecal DEMs observed after modeling and JCDH treatment. Compared with the STC group, the R2 (evaluation of the modeling ability) and Q2 (description of the predictive ability) of the HC and JCDH groups indicated that the orthogonal partial least squares-discrimination analysis model had high predictability and reliability. Compared with the STC group, the R2 intercepts of the HC and JCDH groups were 0.94 and 0.92, respectively, and the Q2 intercepts were 0.72 and 0.88, respectively (Figures 3D and E). Figures 3F and G show the DEMs by volcano maps. Furthermore, taurine and hypotaurine metabolism were the main pathways impacted by JCDH treatment (Figure 3H).

The core target of JCD is AKT, and the core component is quercetin

To further determine the therapeutic mechanism of JCD in STC, we performed a network pharmacology analysis. After data screening, 45 active pharmaceutical ingredients (Supplementary Table 2), 280 related targets, and 1372 disease targets were obtained. Comparing the goals related to JCD and STC, 89 common goals were identified and registered in the STRING database. Cytoscape 3.7.2 software was used to construct a PPI network, including 132 nodes and 2492 interactive edges (Figure 4A). According to the betweenness centrality value, the top 30 hub nodes were identified (Figures 4B and C), and AKT was considered one of the important targets. Immunohistochemistry confirmed that colonic AKT expression was significantly suppressed in STC mice compared with the HC group, whereas JCD significantly reversed this effect (Figures 4D and E). The chemical that acts on AKT is considered to be the core component of JCD, *i.e.,* the quercetin from *A. bidentata* and *C. deserticola,* baicalein, kaempferol and wogonin from *A. bidentata*, and naringenin from *F. aurantii* (Table 2).

JCD inhibited EGC apoptosis

To comprehensively probe the pharmacological mechanism of JCD, a joint-pathway analysis was performed based on DEMs and common genes from network pharmacology. Twenty-five remarkable pathways are presented in Figure 5A. Apoptosis may be an important signaling pathway in the treatment of STC by JCD. GFAP is an EGC marker. Immunofluorescence double-labeling of GFAP and caspase3 showed that compared with the HC group, the apoptotic rate of EGCs in the STC group was significantly increased, while those in the JCDH and JCDM groups were significantly decreased (Figures 5B and C), confirming the predicted results.

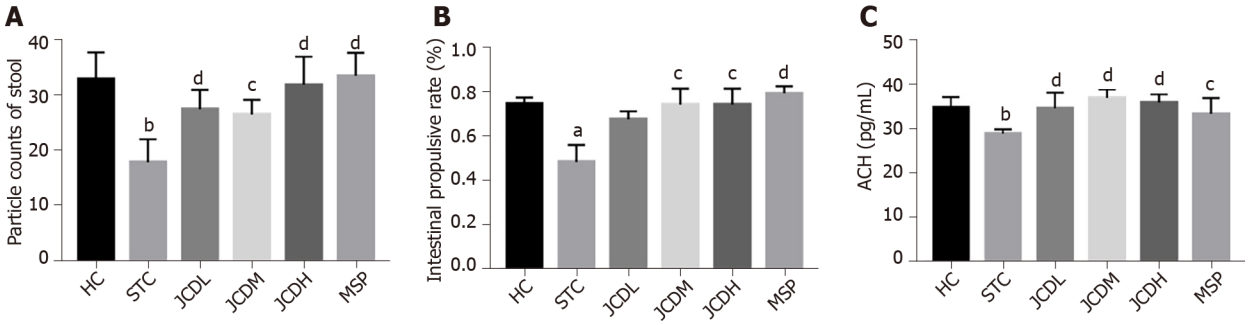
Table 1 Dry weight, wet weight and moisture content of feces of mice in each group

Grouping/feces index	Wet weight (g/mou)	Dry weight (g/mou)	Moisture content (%/mou)
HC	0.26 ± 0.02	0.18 ± 0.01	0.30 ± 0.04
STC	0.12 ± 0.01[a]	0.10 ± 0.01[c]	0.18 ± 0.01[c]
JCDL	0.25 ± 0.01	0.18 ± 0.01	0.29 ± 0.02
JCDM	0.26 ± 0.02[a]	0.18 ± 0.02[c]	0.30 ± 0.02[c]
JCDH	0.26 ± 0.02[a]	0.18 ± 0.01[c]	0.31 ± 0.02[c]
MSP	0.27 ± 0.03[b]	0.19 ± 0.02[c]	0.30 ± 0.01[c]

[a]$P < 0.05$: Compared with the healthy control group.
[b]$P < 0.01$: Compared with the healthy control group.
[c]$P < 0.05$: Compared with the slow transit constipation group.
Data are expressed as the mean ± SD. HC: Healthy control; STC: Slow transit constipation; JCD: Ji-Chuan decoction; JCDL: Low-dose Ji-Chuan decoction treatment; JCDM: Middle-dose Ji-Chuan decoction treatment; JCDH: High-dose Ji-Chuan decoction treatment; MSP: Mosapride treatment.

Table 2 The core ingredients of Ji-Chuan decoction

Molecular name	Oral bioavailability (%)	Drug like
Baicalein	33.52	0.21
Kaempferol	41.88	0.24
Naringenin	59.29	0.21
Quercetin	46.43	0.28
Wogonin	30.68	0.23

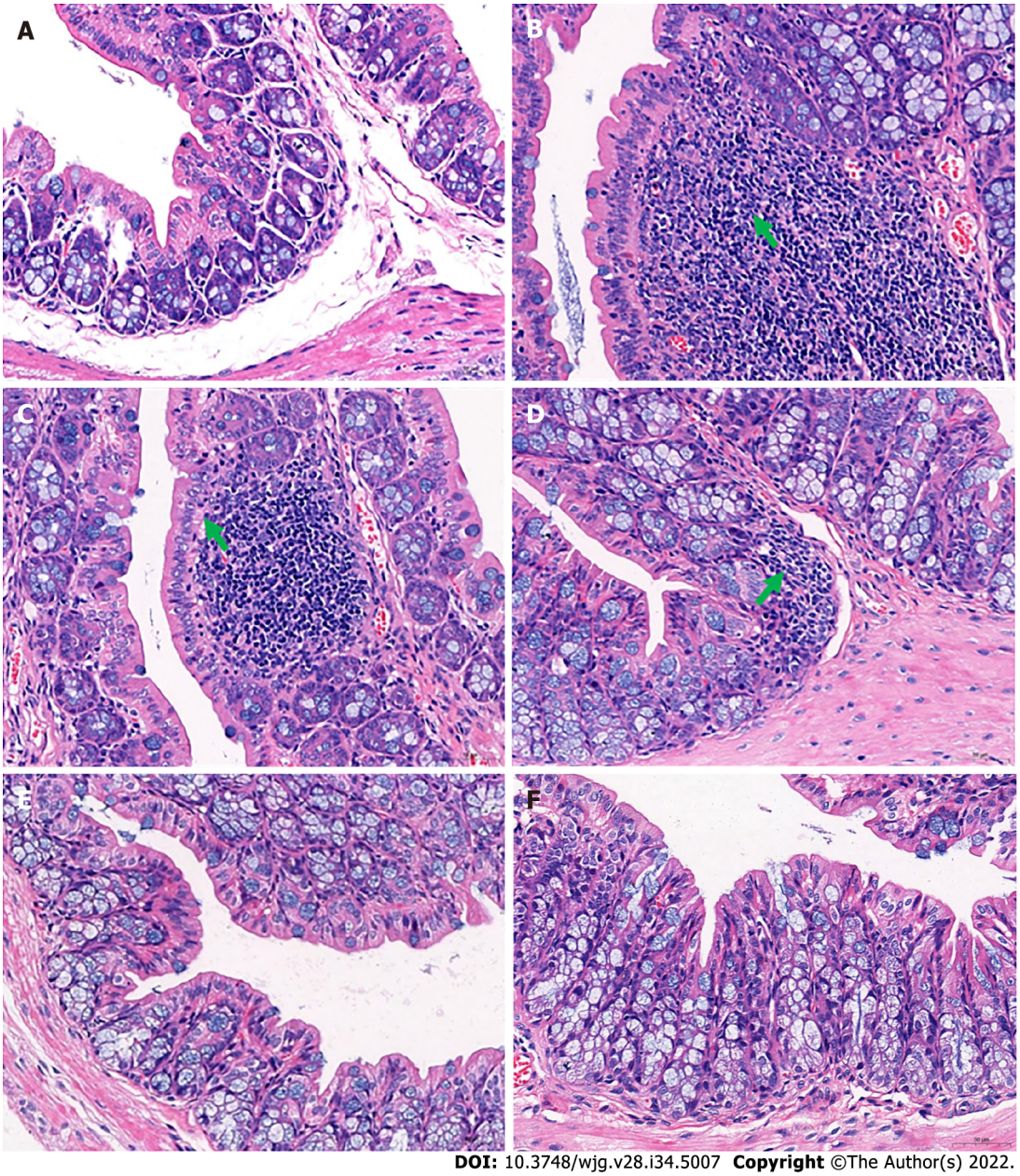


DOI: 10.3748/wjg.v28.i34.5007 **Copyright** ©The Author(s) 2022.

Figure 1 Results of the constipation-related index. A: Particle counts of stool; B: Intestinal propulsive rate; C: The expression levels of colonic acetylcholine. ACH: Acetylcholine; HC: Healthy control; STC: Slow transit constipation; JCD: Ji-Chuan decoction; JCDL: Low-dose Ji-Chuan decoction treatment; JCDM: Middle-dose Ji-Chuan decoction treatment; JCDH: High-dose Ji-Chuan decoction treatment; MSP: Mosapride treatment. Compared with the healthy control group: [a]$P < 0.05$, [b]$P < 0.01$. Compared with the slow transit constipation group: [c]$P < 0.05$, [d]$P < 0.01$.

DISCUSSION

JCD is an established TCM formula that is a particularly effective therapy for STC differentiated by TCM as Spleen and Kidney Yang deficiency syndrome[9], yet its pharmaceutical mechanism remains unclear. We explored the therapeutic mechanism of JCD in a dose-dependent manner and observed that the best effect was achieved by JCDH. The compound diphenoxylate is widely used to induce STC in animal models and can inhibit the peristaltic reflex of intestinal mucosa. It is easier to induce constipation than the commonly used loperamide and is more available than morphine[17]. It is easier to induce constipation than other loperamides and easier to obtain than morphine[17]. The holistic view is shared between systems biology and TCM[18]; therefore, we used key disciplines of systems biology, such as metabolomics and network pharmacology, to effectively reveal the integrated mechanism of JCD for STC.

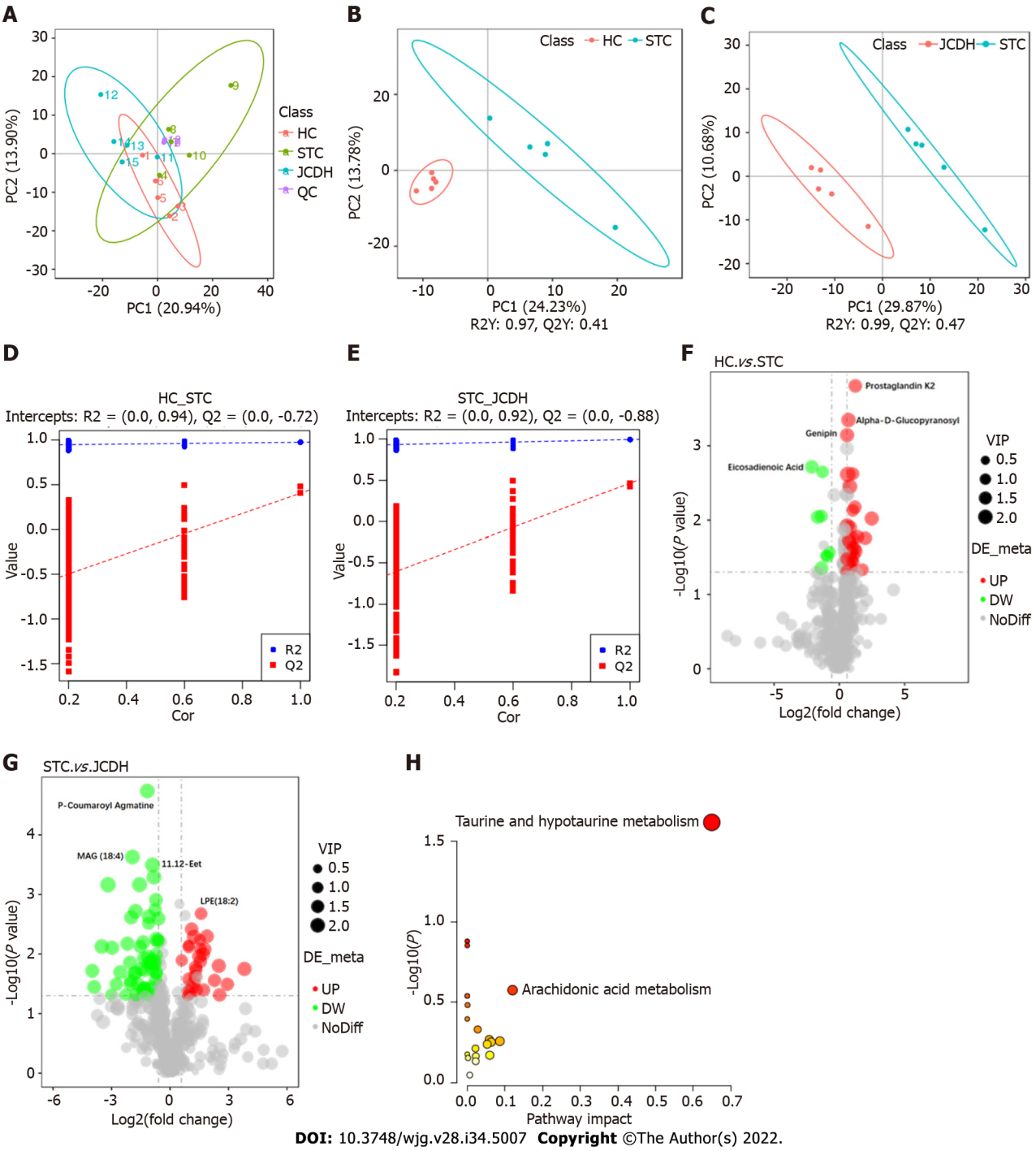


DOI: 10.3748/wjg.v28.i34.5007 **Copyright** ©The Author(s) 2022.

Figure 2 Histological changes in the distal colon. A: Distal colon of the healthy control group; B: In the distal colons of mice in the slow transit constipation group, more severe inflammatory infiltration was observed; C: In the distal colons of mice in the low-dose Ji-Chuan decoction (JCD) treatment group, more severe inflammatory infiltration was observed; D: In the distal colon of mice in the middle-dose JCD group, there was reduced inflammation; E: High-dose JCD treatment restored the normal tissue morphology of the distal colon of constipated mice; F: Mosapride treatment restored the normal tissue morphology of the distal colon of constipated mice. Sections were observed at 400 × using a light microscope.

JCD substantially improved the manifestation of STC in mice

Constipation refers to laborious defecation, dry and hard stools and low stool volume. Effective drugs will increase key indices of constipation, such as the quantity and water content of the feces and the intestinal propulsive rate[19,20]. In this study, we observed that JCD substantially improved almost all indices tested in this work (Figures 1A and B, Table 1). The intestinal propulsive rates, extensively used to evaluate the pathological degree and curative effect of constipation, were significantly decreased after diphenoxylate treatment. Similar anti-constipation effects were obtained among the JCDM, JCDH and the positive reagent MSP groups (Figure 1B). In addition, the three JCD doses could statistically increase the concentration of excitatory neurotransmitter (ACH) (Figure 1C), suggesting that the increase in excitatory neurotransmitter is a critical approach for anti-constipation by JCD[3]. Our colonic pathological observation showed that JCD significantly reduced inflammatory infiltration and repaired pathological damage caused by the compound diphenoxylate in a dose-dependent manner (Figure 2), confirming previous studies[21]. Therefore, our work indicates an integrated effect of JCD on STC by promoting excitatory neurotransmitters, inhibiting gastroenteric inflammation and accelerating intestinal motility.

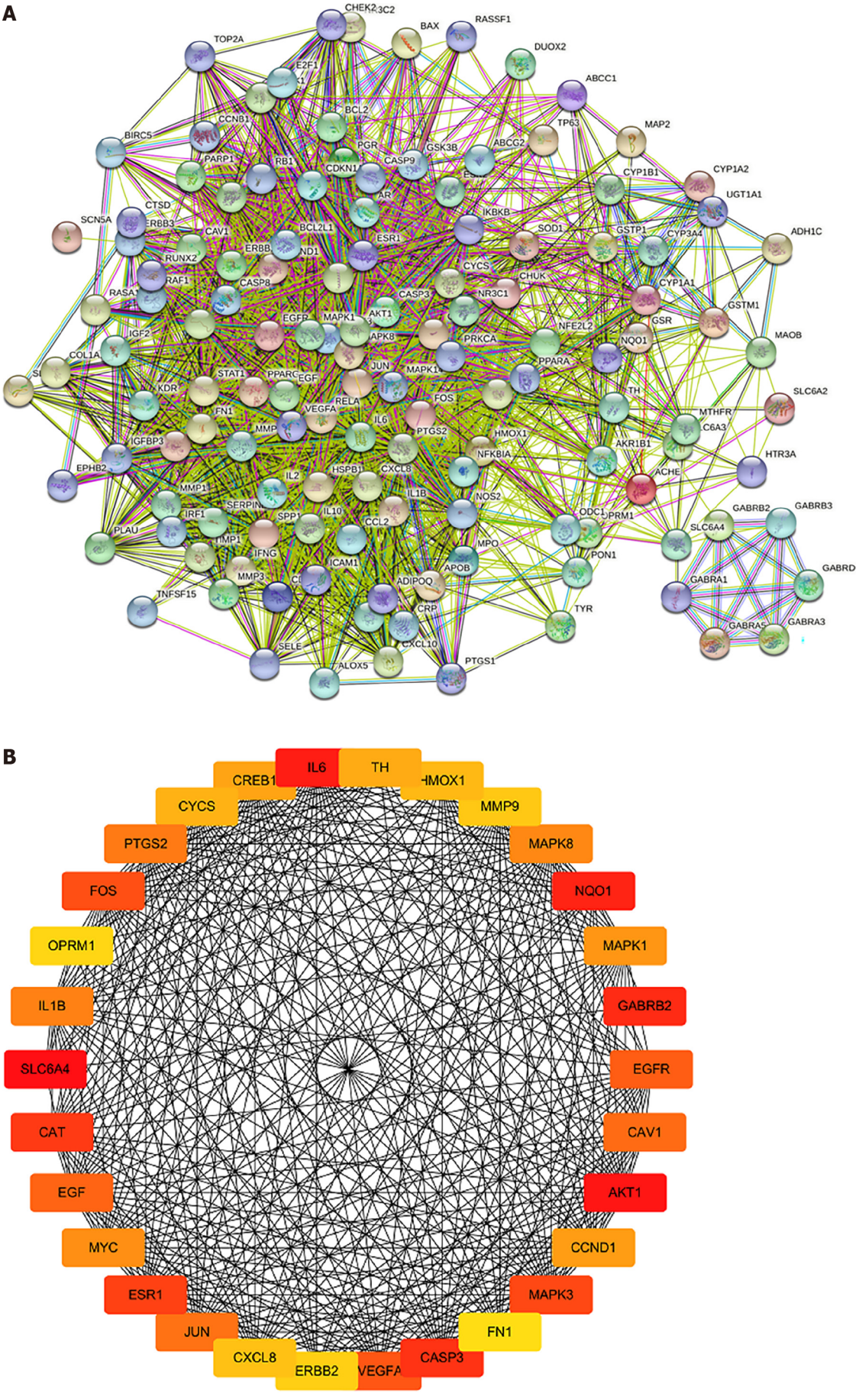


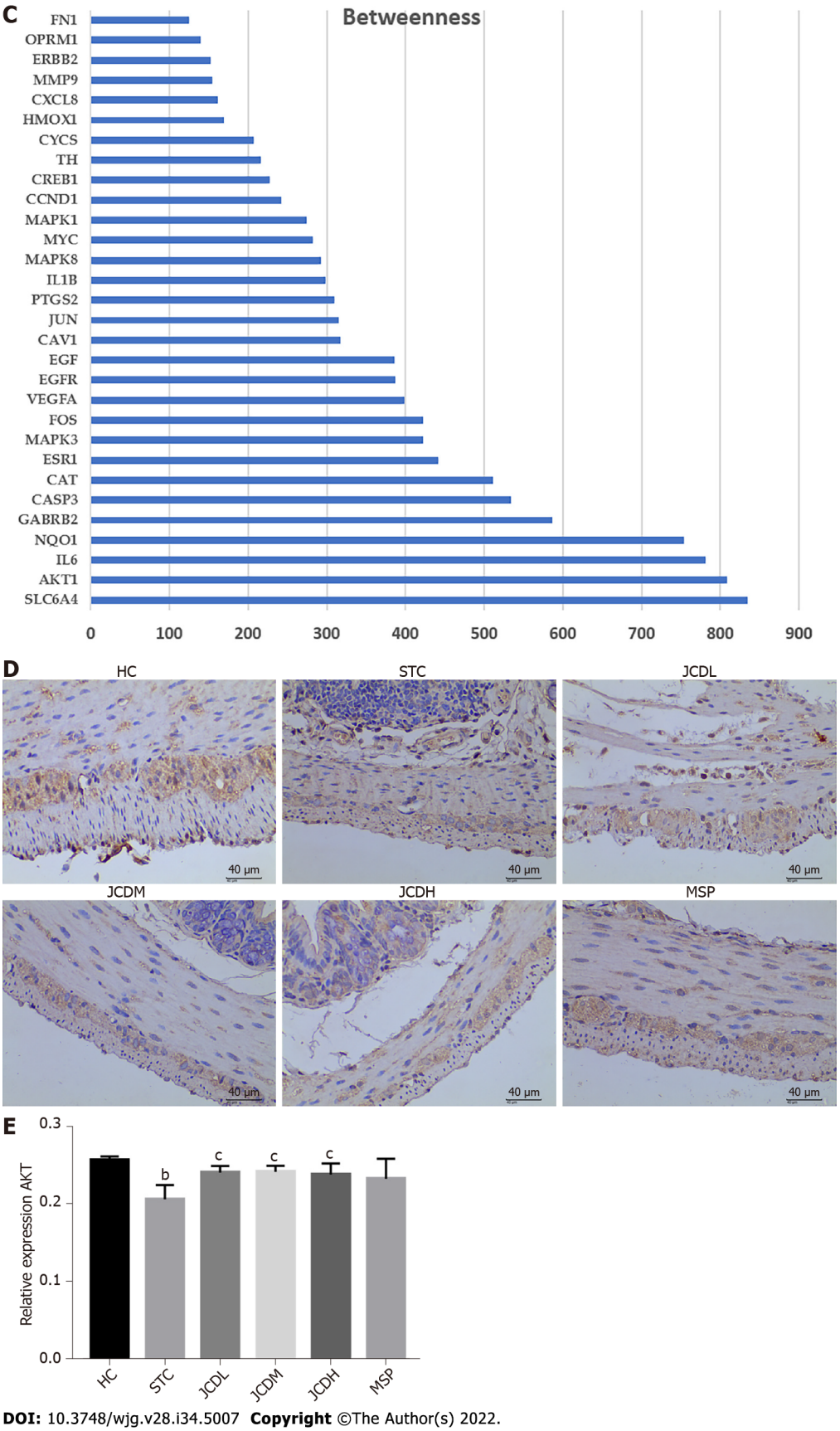
DOI: 10.3748/wjg.v28.i34.5007 **Copyright** ©The Author(s) 2022.

Figure 3 Different intestinal metabolites detected by ultrahigh-pressure liquid chromatography coupled with tandem mass spectrometry.
A: Principal component analysis; B: Orthogonal partial least squares discrimination analysis score plots of intestinal metabolic profiling in the healthy control (HC) *vs* slow transit constipation (STC) groups; C: STC *vs* high-dose Ji-Chuan decoction (JCDH) treatment groups under negative ion mode; D: Permutation test in negative ion mode of the HC *vs* STC groups; E: Permutation test in negative ion modes of the STC *vs* JCDH groups; F: Volcano plot of the different metabolites between the STC and HC groups; G: Volcano plot of the different metabolites between the JCDH and STC groups; H: Critical metabolic pathways of the STC *vs* JCDH groups. HC: Healthy control; STC: Slow transit constipation; JCD: Ji-Chuan decoction; JCDL: Low-dose Ji-Chuan decoction treatment; JCDM: Middle-dose Ji-Chuan decoction treatment; JCDH: High-dose Ji-Chuan decoction treatment; MSP: Mosapride treatment; MAG: 1-(6Z,9Z,12Z,15Z-Octadecatetraenoyl)-sn-glycerol; 11.12-EET: (5Z,8Z,14Z)-11,12-Epoxyeicosa-5,8,14-trienoic acid; LPE: 2-(9Z,12Z-octadecadienoyl)-sn-glycero-3-phosphoethanolamine; QC: Quality control.

JCD altered critical enteric metabolites, especially taurine and hypotaurine

The metabolome results showed that the pathways involving taurine and hypotaurine metabolism were important for the anti-constipation effect of JCD. Taurine is a sulfur-containing α-amino acid with anti-inflammatory properties that can be sequentially converted into homocysteine, cystathionine, cysteine and/or hypotaurine[22,23]. The concentration of taurine was significantly reduced in loperamide-induced constipation rats, and red liriope ameliorated constipation and increased the level of taurine[24, 25]. Our work also showed that the contents of taurine and its metabolite hypotaurine were negatively


A
CHEK2
BAX
RASSF1
TOP2A
DUOX2
ABCC1
BCL2
BIRC5
TP63
MAP2
PARP1
RB1
CDKN1
GSK3B
ABCG2
CYP1B1
CYP1A2
UGT1A1
CTSD
ERBB3
SCN5A
CAV1
BCL2L1
ESR1
SOD1
GSTP1
CYP3A4
ADH1C
RUNX2
ERBB
ND1
CYCS
CHUK
RAF1
CASP8
CYP1A1
RASA1
CASP3
NR3C1
GSTM1
EGFR
MAPK1
AKT1
GSR
IGF2
APK8
NFE2L2
MAOB
PRKCA
NQO1
COL1A1
PPARA
JUN
MAPK14
STAT1
PPARG
EGF
KDR
TH
SLC6A2
FOS
RELA
FN1
VEGFA
MTHFR
IL6
C6A3
MMP
PTGS2
HMOX1
IGFBP3
AKR1B1
NFKBIA
HTR3A
EPHB2
HSPB1
CXCL8
ACHE
IL2
MMP1
IL1B
NOS2
SERPINE1
IRF1
SPP1
IL10
ODC1
PRM1
GABRB2
GABRB3
PLAU
CCL2
SLC6A4
MMP7
MPO
IFNG
PON1
ICAM1
APOB
GABRD
MMP3
ADIPOQ
GABRA1
TNFSF15
CRP
TYR
GABRA5
GABRA3
SELE
CXCL10
ALOX5
PTGS1
B
IL6
TH
CREB1
HMOX1
CYCS
MMP9
PTGS2
MAPK8
FOS
NQO1
OPRM1
MAPK1
IL1B
GABRB2
SLC6A4
EGFR
CAT
CAV1
EGF
AKT1
MYC
CCND1
ESR1
MAPK3
JUN
FN1
CXCL8
CASP3
ERBB2
VEGFA



DOI: 10.3748/wjg.v28.i34.5007 **Copyright** ©The Author(s) 2022.

Figure 4 Network construction, screening and validation of the core targets for Ji-Chuan decoction treatment of slow transit constipation. A: Protein-protein interaction (PPI) network; B: Top 30 protein targets with the largest betweenness in the PPI network; C: Betweenness analysis of the top 30 protein targets; D and E: The relative expression of AKT as assessed by immunofluorescent staining. AKT: Serine/threonine-protein kinase; HC: Healthy control; STC: Slow transit constipation; JCD: Ji-Chuan decoction; JCDL: Low-dose Ji-Chuan decoction treatment; JCDM: Middle-dose Ji-Chuan decoction treatment; JCDH: High-dose Ji-Chuan decoction treatment; MSP: Mosapride treatment; SLC6A4: Sodium-dependent serotonin transporter; AKT1: RAC-alpha serine/threonine-protein

kinase; IL: Interleukin; NQO1: NAD(P)H dehydrogenase (quinone)1; GABRB2: Gammaaminobutyric acid receptor subunit beta-2; CASP3: Caspase-3; CAT: Catalase; ESR1: Estrogen receptor; MAPK3: Mitogen-activated protein kinase 3; FOS: Proto-oncogene c-Fos; VEGFA: Vascular endothelial growth factor A; EGFR: Epidermal growth factor receptor; EGF: Pro-epidermal growth factor; CAV1: Caveolin-1; JUN: Transcription factor AP-1; PTGS2: Prostaglandin G/H synthase 2; MAPK8: Mitogen-activated protein kinase 8; MYC: Myc proto-oncogene protein; MAPK1: Mitogen-activated protein kinase 1; CCND1: G1/S-specific cyclin-D1; CREB1: Cyclic AMP-responsive element-binding protein 1; TH: Thyroid hormone; CYCS: Cytochrome c; HMOX1: Heme oxygenase 1; MMP9: Matrix metalloproteinase-9; ERBB2: Receptor tyrosine-protein kinase erbB-2; FN1: Fibronectin. Data are expressed as the mean ± SD. Compared with the healthy control group: $^{b}P < 0.01$. Compared with the slow transit constipation group: $^{c}P < 0.05$, $^{d}P < 0.01$.

associated with the manifestation of STC and positively associated with intestinal transit rates[26]. However, the molecular mechanism of taurine on gastrointestinal motility and the regulatory mechanisms of JCD remain to be further explored.

JCD restored the levels of AKT, a key protein involved in apoptosis regulation

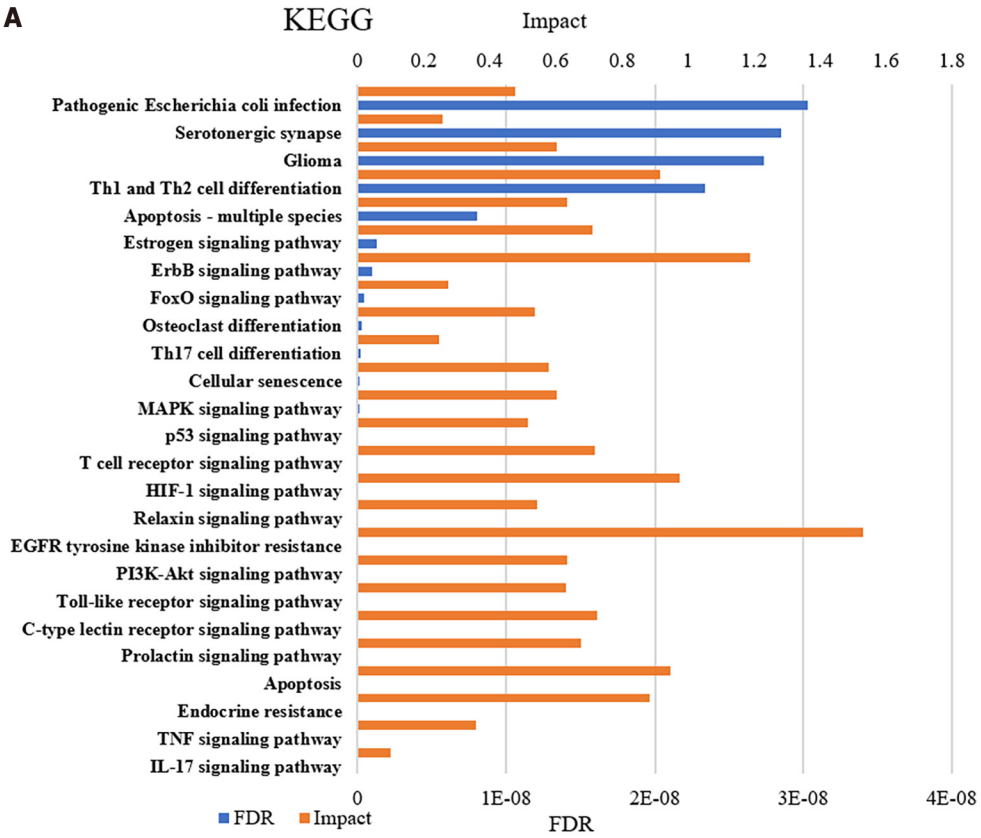
PPI network prediction showed that AKT is the core target of JCD for STC therapy. In our experiments, STC mice showed downregulated expression of AKT, while all three doses of JCD treatment reversed the abnormally reduced expression levels. AKT plays an important role in cell survival and apoptosis. Previous studies have shown that high glucose levels can induce EGC apoptosis through the AKT pathway, which is closely related to intestinal motility[27]. Another study showed that EGCs could protect the nervous system from hyperglycemia-induced damage by activating the Akt/GSK-3β pathway[28]. Therefore, we speculate that the treatment of STC with JCD may be related to EGC apoptosis.

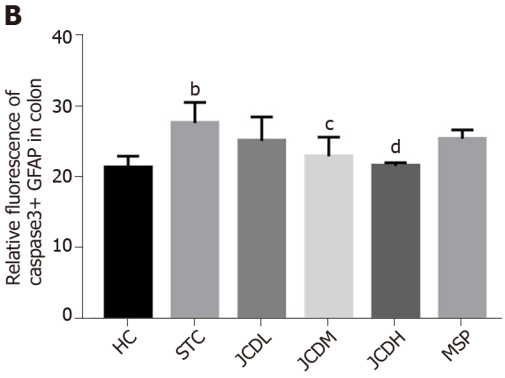
JCD rescued excessive EGC apoptosis

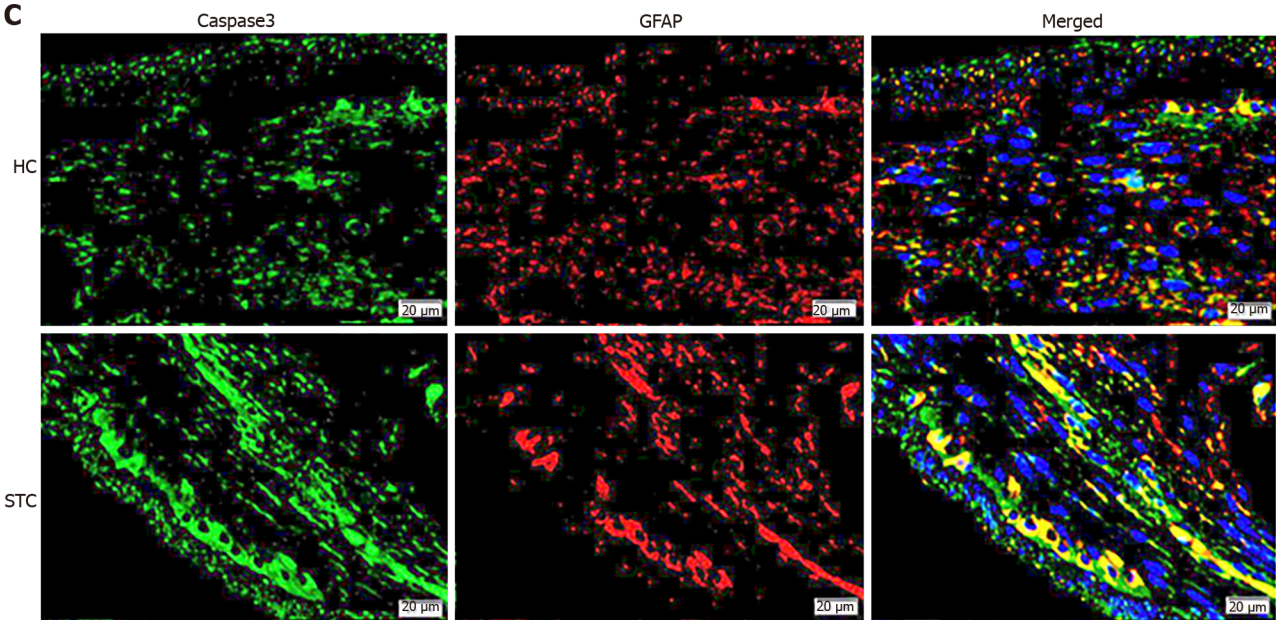
Experimental evidence in humans and animals suggests that EGCs play a key role in regulating gastrointestinal motility and transit[29-32]. A cohort study of twenty-six STC patients showed reduced EGCs compared with ten healthy volunteers[33]. EGC can increase the expression of Akt and ZO-1 by releasing glial cell-derived neurotrophic factor, indirectly regulating the integrity of the intestinal epithelial barrier, reducing intestinal inflammation and improving delayed colonic transit[34,35]. Another study showed that enteric glial LPAR1 signaling regulates gastrointestinal motility through EGCs and may contribute to chronic intestinal pseudo-obstruction in humans[36]. Activation of opioid receptors in EGCs may be associated with morphine-induced constipation[37]. Previous studies have shown that the key components of JCD are associated with neural apoptosis, and many of them also involve changes in AKT protein. For example, wogonin, a key component of JCD identified in this paper, can prevent hippocampal injury after brain trauma through antioxidation and anti-apoptosis, which has been shown to occur through the PI3K/Akt/nuclear factor E2-related factor 2 (Nrf2)/HO-1 pathway[38]. Baicalein reduces sevoflurane-induced neurodegeneration, improves learning and memory retention in rats, and modulates the PI3/Akt/GSK-3β and JNK/ERK signaling pathways[39]. Kaempferol prevents cerebral ischemia-reperfusion injury by interfering with oxidative and inflammatory stress-induced apoptosis[40]. Quercetin is involved in neuroprotection by regulating Nrf2, paraoxonase 2, JNK, tumour necrosis factor alpha, PGC-1α, MAPKs, CREB and PI3K/Akt[41]. Naringenin can effectively inhibit Aβ25-35-induced neuronal injury in PC12 cells by regulating the ER and PI3K/Akt pathways[42]. To our knowledge, the current work is the first to demonstrate that JCD can improve constipation by reducing EGC apoptosis. Our work applied a multiomics strategy to explore the therapeutic mechanism of JCD in the treatment of STC and found some interesting evidence that remains to be elucidated in more detail in the future. The JCDH group of mice exhibited a better effect, suggesting that a suitable dose needs to be further evaluated.

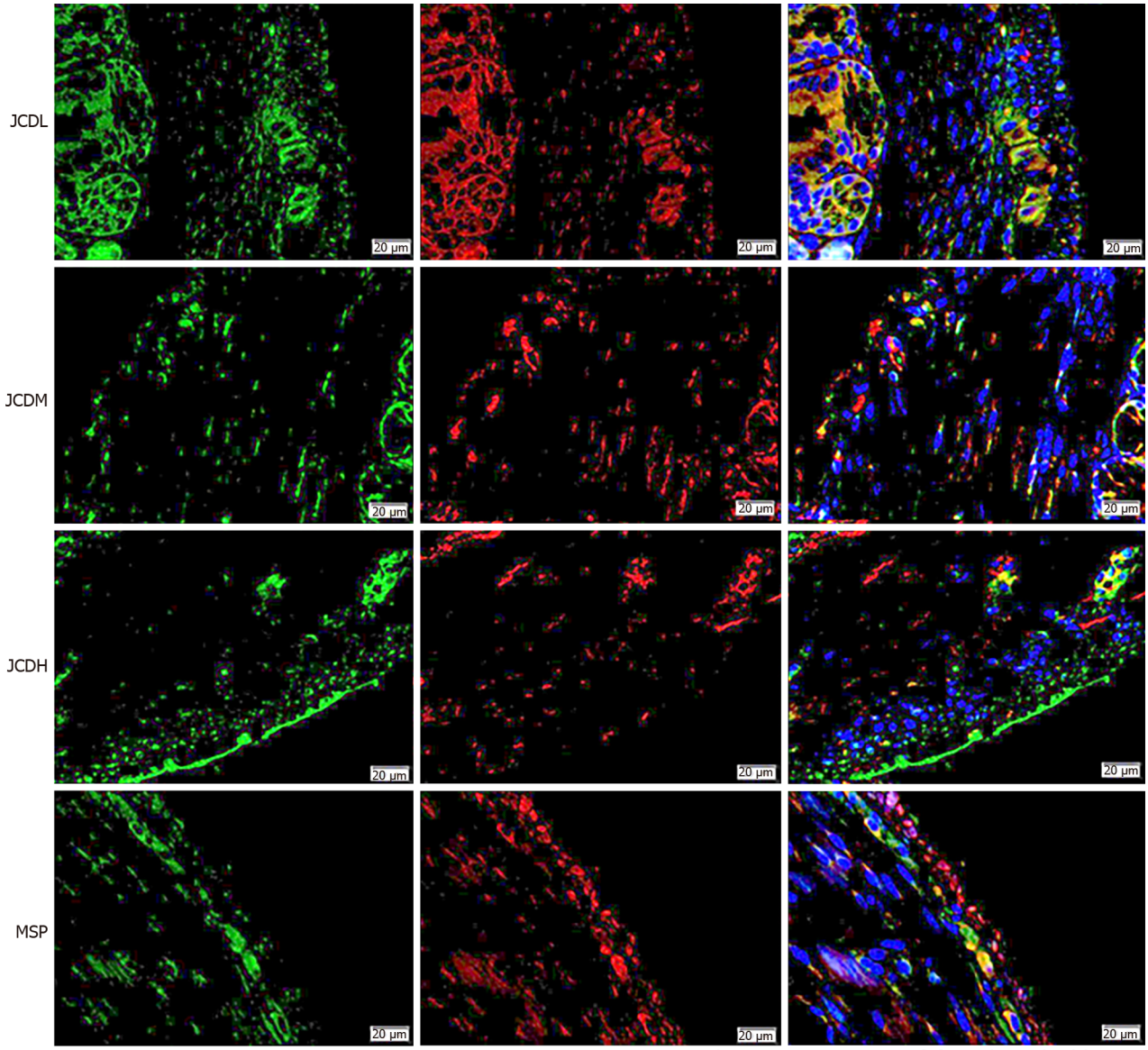
CONCLUSION

This work demonstrated that reduced enteric EGC apoptosis may be the critical mechanism of JCD in STC therapy. These findings call for further molecular research to facilitate the clinical application of JCD.


A
KEGG
Impact
0
0.2
0.4
0.6
0.8
1
1.2
1.4
1.6
1.8
Pathogenic Escherichia coli infection
Serotonergic synapse
Glioma
Th1 and Th2 cell differentiation
Apoptosis - multiple species
Estrogen signaling pathway
ErbB signaling pathway
FoxO signaling pathway
Osteoclast differentiation
Th17 cell differentiation
Cellular senescence
MAPK signaling pathway
p53 signaling pathway
T cell receptor signaling pathway
HIF-1 signaling pathway
Relaxin signaling pathway
EGFR tyrosine kinase inhibitor resistance
PI3K-Akt signaling pathway
Toll-like receptor signaling pathway
C-type lectin receptor signaling pathway
Prolactin signaling pathway
Apoptosis
Endocrine resistance
TNF signaling pathway
IL-17 signaling pathway
0
1E-08
2E-08
3E-08
4E-08
FDR
FDR
Impact


B
Relative fluorescence of caspase3+ GFAP in colon
40
30
20
10
0
b
c
d
HC
STC
JCDL
JCDM
JCDH
MSP


C
Caspase3
GFAP
Merged
HC
STC
20 μm



DOI: 10.3748/wjg.v28.i34.5007 **Copyright** ©The Author(s) 2022.

Figure 5 Integrative analysis and experimental validation of improved network pharmacology and metabolites. A: Integration analysis between the modified network pharmacology and metabolites. The ordinate stands for pathways, the primary abscissa stands for minus false discovery rates, and the secondary abscissa stands for impact; B and C: The relative expression of Caspase3+ Glial fibrillary acidic protein was assessed by immunofluorescent staining. GFAP: Glial fibrillary acidic protein; HC: Healthy control; STC: Slow transit constipation; JCD: Ji-Chuan decoction; JCDL: Low-dose Ji-Chuan decoction treatment; JCDM: Middle-dose Ji-Chuan decoction treatment; JCDH: High-dose Ji-Chuan decoction treatment; MSP: Mosapride treatment; FDR: False discovery rates; KEGG: Kyoto Encyclopedia of Genes and Genomes; Th: Thyroid hormone; EGFR: Epidermal growth factor receptor; MAPK: Mitogen-activated protein kinase; IL: Interleukin; TNF: Tumor necrosis factor; HIF: Hypoxia-inducible factor. Data are expressed as the mean ± SD. Compared with the healthy control group: $^{a}P < 0.05$, $^{b}P < 0.01$. Compared with the slow transit constipation group: $^{c}P < 0.05$, $^{d}P < 0.01$.

ARTICLE HIGHLIGHTS

Research background

Slow transit constipation (STC) is a common intestinal disorder without an effective therapeutic regimen. Ji-Chuan Decoction (JCD) is an established formula for STC. However, its pharmacological mechanism is still unclear.

Research motivation

To determine the ingredients and mechanism of JCD for STC treatment.

Research objectives

To explore the integrated regulatory pattern of JCD against STC through hyphenated techniques from metabolism, network pharmacology and molecular methods.

Research methods

STC model mice were generated by gavage of diphenoxylate for 14 d. STC mice in the low- (3.04 g/kg), medium- (6.08 g/kg) and high-dosage (12.16 g/kg) JCD groups were orally administered. The acetylcholine (ACH) level was detected by enzyme-linked immunosorbent assay. AKT expression and enteric glial cell (EGC) apoptosis were demonstrated by immunofluorescence. The differentially expressed metabolites were tested by nontargeted metabolomics. The targets and core ingredients were identified by network pharmacology.

Research results

JCD significantly promotes intestinal motility, increases colonic ACH content and reduces inflammation in STC mice. It markedly restores the misaligned metabolites, including taurine/hypotaurine, and rescues AKT expression with quercetin. Inhibition of EGC apoptosis is a potential mechanism by which JCD relieves constipation.

Research conclusions

Regulating gut metabolites and reducing EGC apoptosis in STC mice may be the key mechanism of JCD for STC treatment.

Research perspectives

Further investigation into the molecular interactions among the JCD ingredients and metabolites, intestinal microbiota and host response in STC mice is necessary.

ACKNOWLEDGEMENTS

The authors would like to acknowledge Yao Zheng-Hong (Novogene, Beijing, Master of Agriculture), for skillful technical assistance.

FOOTNOTES

Author contributions: Wang XM, Xu H, and Ding WJ designed and coordinated the study; Wang XM, Lv LX, Qin YS, Zhang YZ, Yang N, Wu S, Xia XW, and Yang H performed the experiments and acquired and analyzed the data; Liu Y interpreted the data; Ding WJ contributed to critical revision of the manuscript; and all authors read and approved the final manuscript.

Supported by the National Natural Science Foundation of China, No. 82074151; and the Experimental Formulary Sichuan Youth Science and Technology Innovation Research Team, No. 2020JDTD0022.

Institutional animal care and use committee statement: This experiment was approved by the Animal Ethics Committee, Chengdu University of TCM (license 2016-16).

Conflict-of-interest statement: All the authors report no relevant conflicts of interest for this article.

Data sharing statement: No additional data are available.

ARRIVE guidelines statement: The authors have read the ARRIVE guidelines, and the manuscript was prepared and revised according to the ARRIVE guidelines.

Open-Access: This article is an open-access article that was selected by an in-house editor and fully peer-reviewed by external reviewers. It is distributed in accordance with the Creative Commons Attribution NonCommercial (CC BY-NC 4.0) license, which permits others to distribute, remix, adapt, build upon this work non-commercially, and license their derivative works on different terms, provided the original work is properly cited and the use is non-commercial. See: https://creativecommons.org/Licenses/by-nc/4.0/

Country/Territory of origin: China

ORCID number: Xiu-Min Wang 0000-0002-3088-8579; Li-Xia Lv 0000-0001-5216-1605; Yue-Si Qin 0000-0002-5327-9554; Yu-Zhu Zhang 0000-0001-6779-0711; Ni Yang 0000-0002-5613-6041; Shu Wu 0000-0002-8729-8801; Xiu-Wen Xia 0000-0003-1962-1221; Hong Yang 0000-0002-5145-4243; Hong Xu 0000-0002-3905-7835; Ying Liu 0000-0002-3318-3486; Wei-Jun Ding 0000-0002-4933-7347.

S-Editor: Wang JJ
L-Editor: A
P-Editor: Wang JJ

REFERENCES

1 **Nelson AD**, Camilleri M, Chirapongsathorn S, Vijayvargiya P, Valentin N, Shin A, Erwin PJ, Wang Z, Murad MH. Comparison of efficacy of pharmacological treatments for chronic idiopathic constipation: a systematic review and network meta-analysis. *Gut* 2017; **66**: 1611-1622 [PMID: 27287486 DOI: 10.1136/gutjnl-2016-311835]

2 **Yeh KM**, Johansson O, Le H, Rao K, Markus I, Perera DS, Lubowski DZ, King DW, Zhang L, Chen H, Liu L. Cystic fibrosis transmembrane conductance regulator modulates enteric cholinergic activities and is abnormally expressed in the enteric ganglia of patients with slow transit constipation. *J Gastroenterol* 2019; **54**: 994-1006 [PMID: 31392489 DOI: 10.1007/s00535-019-01610-9]

3 **Russell JP**, Mohammadi E, Ligon C, Latorre R, Johnson AC, Hoang B, Krull D, Ho MW, Eidam HS, DeMartino MP, Cheung M, Oliff AI, Kumar S, Greenwood-Van Meerveld B. Enteric RET inhibition attenuates gastrointestinal secretion and motility *via* cholinergic signaling in rat colonic mucosal preparations. *Neurogastroenterol Motil* 2019; **31**: e13479 [PMID: 30311722 DOI: 10.1111/nmo.13479]

4 **Kim JE**, Park JW, Kang MJ, Choi HJ, Bae SJ, Choi Y, Lee YJ, Seo S, Hong JT, Hwang DY. Laxative Effect of Spicatoside A by Cholinergic Regulation of Enteric Nerve in Loperamide-Induced Constipation: ICR Mice Model. *Molecules* 2019; **24** [PMID: 30836659 DOI: 10.3390/molecules24050896]

5 **Zhong LLD**, Zheng G, Da Ge L, Lin CY, Huang T, Zhao L, Lu C, Lu AP, Bian ZX. Chinese herbal medicine for constipation: zheng-based associations among herbs, formulae, proprietary medicines, and herb-drug interactions. *Chin Med* 2016; **11**: 28 [PMID: 27347002 DOI: 10.1186/s13020-016-0099-4]

6 **Whiting RL**, Ford AC. Efficacy of traditional chinese medicine in functional constipation. *Am J Gastroenterol* 2011; **106**: 1003; author reply 1003-1003; author reply 1004 [PMID: 21540906 DOI: 10.1038/ajg.2011.14]

7 **Huang T**, Ning Z, Hu D, Zhang M, Zhao L, Lin C, Zhong LLD, Yang Z, Xu H, Bian Z. Uncovering the Mechanisms of Chinese Herbal Medicine (MaZiRenWan) for Functional Constipation by Focused Network Pharmacology Approach. *Front Pharmacol* 2018; **9**: 270 [PMID: 29632490 DOI: 10.3389/fphar.2018.00270]

8 **Ali MZ**, Mehmood MH, Haneef M, Saleem M, Ishrat G, Siddiqi HS, Gilani AU, Ahmed M. A flavonoid driven phyto-pharmacological effects of Capparis decidua Edgew. in rodents. *Pak J Pharm Sci* 2020; **33**: 333-342 [PMID: 32122866]

9 **Dai L**, Zhong LL, Ji G. Irritable bowel syndrome and functional constipation management with integrative medicine: A systematic review. *World J Clin Cases* 2019; **7**: 3486-3504 [PMID: 31750331 DOI: 10.12998/wjcc.v7.i21.3486]

10 **Zhang SX**, Zhang XA, An YK. Effect of Jichuanjian on Gastrointestinal Function□Serum Intestinal Neurotransmitters andIntestinal Flora in Elderly with Chronic Functional Constipation. *Chin J ETMF* 2018; **24**: 169-174 [DOI: 10.13422/j.cnki.syfjx.20182131]

11 **Gan Y**, Liang J, Diao W, Zhou X, Mu J, Pang L, Tan F, Zhao X. *Lactobacillus plantarum* KSFY06 and geniposide counteract montmorillonite-induced constipation in Kunming mice. *Food Sci Nutr* 2020; **8**: 5128-5137 [PMID: 32994973 DOI: 10.1002/fsn3.1814]

12 **Zhang Y**, Wang Y, Yang S, Xiao Y, Guan H, Yue X, Wang X, Li X. The Difference of Chemical Components and Biological Activities of the Raw Products slices and the Wine Steam-Processed Product from Cistanche deserticola. *Evid Based Complement Alternat Med* 2019; **2019**: 2167947 [PMID: 31007699 DOI: 10.1155/2019/2167947]

13 **Cui H**, Li Y, Wang Y, Jin L, Yang L, Wang L, Liao J, Wang H, Peng Y, Zhang Z, Liu X. Da-Chai-Hu Decoction Ameliorates High Fat Diet-Induced Nonalcoholic Fatty Liver Disease Through Remodeling the Gut Microbiota and Modulating the Serum Metabolism. *Front Pharmacol* 2020; **11**: 584090 [PMID: 33328987 DOI: 10.3389/fphar.2020.584090]

14 **Shi C**, Li X, Feng J, Huang Y, Wang Y, Chen J, Li S. Study on HPLC characteristic fingerprint of substance benchmark of classical famou sprescription of Jichuan Decoction. *Zhong Cao Yao* 2020; **51**: 3930-3936

15 **Lee HY**, Kim JH, Jeung HW, Lee CU, Kim DS, Li B, Lee GH, Sung MS, Ha KC, Back HI, Kim SY, Park SH, Oh MR, Kim MG, Jeon JY, Im YJ, Hwang MH, So BO, Shin SJ, Yoo WH, Kim HR, Chae HJ, Chae SW. Effects of Ficus carica paste on loperamide-induced constipation in rats. *Food Chem Toxicol* 2012; **50**: 895-902 [PMID: 22178225 DOI: 10.1016/j.fct.2011.12.001]

16 **Nagakura Y**, Naitoh Y, Kamato T, Yamano M, Miyata K. Compounds possessing 5-HT3 receptor antagonistic activity inhibit intestinal propulsion in mice. *Eur J Pharmacol* 1996; **311**: 67-72 [PMID: 8884238 DOI: 10.1016/0014-2999(96)00403-7]

17 **Yang A**, Yan Y, He H, Gao Y, He K, Shi H, Liu M. Comparative study on four models for preparing functional constipation in mice. *China Med Eng* 2019; **27**: 1-4 [DOI: 10.19338/j.issn.1672-2019.2019.03.001]

18 **Meng X**, Ma J, Kang AN, Kang SY, Jung HW, Park YK. A Novel Approach Based on Metabolomics Coupled With Intestinal Flora Analysis and Network Pharmacology to Explain the Mechanisms of Action of Bekhogainsam Decoction in the Improvement of Symptoms of Streptozotocin-Induced Diabetic Nephropathy in Mice. *Front Pharmacol* 2020; **11**: 633 [PMID: 32508632 DOI: 10.3389/fphar.2020.00633]

19 **Qian Y**, Zhao X, Kan J. Preventive effect of resistant starch on activated carbon-induced constipation in mice. *Exp Ther Med* 2013; **6**: 228-232 [PMID: 23935751 DOI: 10.3892/etm.2013.1096]

20 **Gibson GR**, Probert HM, Loo JV, Rastall RA, Roberfroid MB. Dietary modulation of the human colonic microbiota: updating the concept of prebiotics. *Nutr Res Rev* 2004; **17**: 259-275 [PMID: 19079930 DOI: 10.1079/NRR200479]

21 **Ren X**, Liu L, Gamallat Y, Zhang B, Xin Y. Enteromorpha and polysaccharides from enteromorpha ameliorate loperamide-induced constipation in mice. *Biomed Pharmacother* 2017; **96**: 1075-1081 [PMID: 29198923 DOI: 10.1016/j.biopha.2017.11.119]

22 **Obeid OA**, Johnston K, Emery PW. Plasma taurine and cysteine levels following an oral methionine load: relationship with coronary heart disease. *Eur J Clin Nutr* 2004; **58**: 105-109 [PMID: 14679374 DOI: 10.1038/sj.ejcn.1601755]

23 **Wójcik OP**, Koenig KL, Zeleniuch-Jacquotte A, Costa M, Chen Y. The potential protective effects of taurine on coronary heart disease. *Atherosclerosis* 2010; **208**: 19-25 [PMID: 19592001 DOI: 10.1016/j.atherosclerosis.2009.06.002]

24 **Kim JE**, Lee YJ, Kwak MH, Jun G, Koh EK, Song SH, Seong JE, Kim JW, Kim KB, Kim S, Hwang DY. Metabolomics approach to serum biomarker for loperamide-induced constipation in SD rats. *Lab Anim Res* 2014; **30**: 35-43 [PMID:

24707303 DOI: 10.5625/lar.2014.30.1.35]
25 **Kim JE**, Lee YJ, Ryu SH, Park JW, Kang MJ, Choi HJ, Bae SJ, Choi Y, Kang HG, Kim KB, Kim S, Lim Y, Hwang DY. Metabolomics approach to serum biomarker for laxative effects of red *Liriope platyphylla* in loperamide-induced constipation of SD rats. *Lab Anim Res* 2019; **35**: 9 [PMID: 32257897 DOI: 10.1186/s42826-019-0009-x]
26 **Lee DS**, Jo HG, Kim MJ, Lee H, Cheong SH. Laxative Effects of Taurine on Loperamide-Induced Constipation in Rats. *Adv Exp Med Biol* 2019; **1155**: 261-271 [PMID: 31468405 DOI: 10.1007/978-981-13-8023-5_25]
27 **Chen Y**, Liu G, He F, Zhang L, Yang K, Yu H, Zhou J, Gan H. MicroRNA 375 modulates hyperglycemia-induced enteric glial cell apoptosis and Diabetes-induced gastrointestinal dysfunction by targeting Pdk1 and repressing PI3K/Akt pathway. *Sci Rep* 2018; **8**: 12681 [PMID: 30140011 DOI: 10.1038/s41598-018-30714-0]
28 **Luo P**, He WX, Li C, Chang MJ. Enteric glial cells exert neuroprotection from hyperglycemia-induced damage *via* Akt/GSK3β pathway. *Neuroreport* 2021; **32**: 875-881 [PMID: 34029286 DOI: 10.1097/WNR.0000000000001670]
29 **Neunlist M**, Rolli-Derkinderen M, Latorre R, Van Landeghem L, Coron E, Derkinderen P, De Giorgio R. Enteric glial cells: recent developments and future directions. *Gastroenterology* 2014; **147**: 1230-1237 [PMID: 25305504 DOI: 10.1053/j.gastro.2014.09.040]
30 **Ochoa-Cortes F**, Turco F, Linan-Rico A, Soghomonyan S, Whitaker E, Wehner S, Cuomo R, Christofi FL. Enteric Glial Cells: A New Frontier in Neurogastroenterology and Clinical Target for Inflammatory Bowel Diseases. *Inflamm Bowel Dis* 2016; **22**: 433-449 [PMID: 26689598 DOI: 10.1097/MIB.0000000000000667]
31 **Rao M**, Rastelli D, Dong L, Chiu S, Setlik W, Gershon MD, Corfas G. Enteric Glia Regulate Gastrointestinal Motility but Are Not Required for Maintenance of the Epithelium in Mice. *Gastroenterology* 2017; **153**: 1068-1081.e7 [PMID: 28711628 DOI: 10.1053/j.gastro.2017.07.002]
32 **Grubišić V**, Gulbransen BD. Enteric glia: the most alimentary of all glia. *J Physiol* 2017; **595**: 557-570 [PMID: 27106597 DOI: 10.1113/JP271021]
33 **Bassotti G**, Villanacci V, Maurer CA, Fisogni S, Di Fabio F, Cadei M, Morelli A, Panagiotis T, Cathomas G, Salerni B. The role of glial cells and apoptosis of enteric neurones in the neuropathology of intractable slow transit constipation. *Gut* 2006; **55**: 41-46 [PMID: 16041063 DOI: 10.1136/gut.2005.073197]
34 **Zhang DK**, He FQ, Li TK, Pang XH, Cui DJ, Xie Q, Huang XL, Gan HT. Glial-derived neurotrophic factor regulates intestinal epithelial barrier function and inflammation and is therapeutic for murine colitis. *J Pathol* 2010; **222**: 213-222 [PMID: 20632386 DOI: 10.1002/path.2749]
35 **Liu GX**, Yang YX, Yan J, Zhang T, Zou YP, Huang XL, Gan HT. Glial-derived neurotrophic factor reduces inflammation and improves delayed colonic transit in rat models of dextran sulfate sodium-induced colitis. *Int Immunopharmacol* 2014; **19**: 145-152 [PMID: 24462388 DOI: 10.1016/j.intimp.2014.01.008]
36 **Ahmadzai MM**, McClain JL, Dharshika C, Seguella L, Giancola F, De Giorgio R, Gulbransen BD. LPAR1 regulates enteric nervous system function through glial signaling and contributes to chronic intestinal pseudo-obstruction. *J Clin Invest* 2022; **132** [PMID: 35166239 DOI: 10.1172/JCI149464]
37 **Gao H**, Zhang Y, Li Y, Chang H, Cheng B, Li N, Yuan W, Li S, Wang Q. μ-Opioid Receptor-Mediated Enteric Glial Activation Is Involved in Morphine-Induced Constipation. *Mol Neurobiol* 2021; **58**: 3061-3070 [PMID: 33624141 DOI: 10.1007/s12035-021-02286-0]
38 **Feng Y**, Ju Y, Yan Z, Ji M, Yang M, Wu Q, Wang L, Sun G. Protective role of wogonin following traumatic brain injury by reducing oxidative stress and apoptosis *via* the PI3K/Nrf2/HO1 pathway. *Int J Mol Med* 2022; **49** [PMID: 35179214 DOI: 10.3892/ijmm.2022.5109]
39 **Wang S**, Zhou Y. Baicalein Inhibits Neuroapoptosis Via Pathways in Sevoflurane Induced Rats. *Transl Neurosci* 2018; **9**: 88-98 [PMID: 30042862 DOI: 10.1515/tnsci-2018-0015]
40 **Wang J**, Mao J, Wang R, Li S, Wu B, Yuan Y. Kaempferol Protects Against Cerebral Ischemia Reperfusion Injury Through Intervening Oxidative and Inflammatory Stress Induced Apoptosis. *Front Pharmacol* 2020; **11**: 424 [PMID: 32351385 DOI: 10.3389/fphar.2020.00424]
41 **Grewal AK**, Singh TG, Sharma D, Sharma V, Singh M, Rahman MH, Najda A, Walasek-Janusz M, Kamel M, Albadrani GM, Akhtar MF, Saleem A, Abdel-Daim MM. Mechanistic insights and perspectives involved in neuroprotective action of quercetin. *Biomed Pharmacother* 2021; **140**: 111729 [PMID: 34044274 DOI: 10.1016/j.biopha.2021.111729]
42 **Zhang N**, Hu Z, Zhang Z, Liu G, Wang Y, Ren Y, Wu X, Geng F. Protective Role Of Naringenin Against $A\beta_{25-35}$-Caused Damage *via* ER and PI3K/Akt-Mediated Pathways. *Cell Mol Neurobiol* 2018; **38**: 549-557 [PMID: 28699113 DOI: 10.1007/s10571-017-0519-8]

World Journal of Gastroenterology

Submit a Manuscript: https://www.f6publishing.com

World J Gastroenterol 2022 September 14; 28(34): 5023-5035

DOI: 10.3748/wjg.v28.i34.5023

ISSN 1007-9327 (print) ISSN 2219-2840 (online)

ORIGINAL ARTICLE

Retrospective Cohort Study

Pregnancy and fetal outcomes of chronic hepatitis C mothers with viremia in China

Calvin Q Pan, Bao-Shen Zhu, Jian-Ping Xu, Jian-Xia Li, Li-Juan Sun, Hong-Xia Tian, Xi-Hong Zhang, Su-Wen Li, Er-Hei Dai

Specialty type: Gastroenterology and hepatology

Provenance and peer review: Unsolicited article; Externally peer reviewed.

Peer-review model: Single blind

Peer-review report's scientific quality classification
Grade A (Excellent): 0
Grade B (Very good): B, B
Grade C (Good): C
Grade D (Fair): 0
Grade E (Poor): 0

P-Reviewer: Han GR, China; Lewis-Ximenez L, Brazil; Tamori A, Japan

Received: May 24, 2022
Peer-review started: May 24, 2022
First decision: June 27, 2022
Revised: July 9, 2022
Accepted: August 25, 2022
Article in press: August 25, 2022
Published online: September 14, 2022

Calvin Q Pan, Center for Liver Diseases, Beijing Ditan Hospital, Capital Medical University, Beijing 100015, China

Calvin Q Pan, Division of Gastroenterology and Hepatology, Department of Medicine, NYU Langone Health, NYU School of Medicine, Flushing, NY 11355, United States

Bao-Shen Zhu, Jian-Ping Xu, Jian-Xia Li, Li-Juan Sun, Hong-Xia Tian, Su-Wen Li, Department of Obstetrics and Gynecology, The Fifth Hospital of Shijiazhuang, Hebei Medical University, Shijiazhuang 050021, Hebei Province, China

Xi-Hong Zhang, School of Public Health, North China University of Science and Technology, Tangshan 063210, Hebei Province, China

Xi-Hong Zhang, Er-Hei Dai, Division of Liver Disease, Department of Medicine, The Fifth Hospital of Shijiazhuang, Hebei Medical University, Shijiazhuang 050021, Hebei Province, China

Corresponding author: Er-Hei Dai, MD, Professor, Division of Liver Disease, Department of Medicine, The Fifth Hospital of Shijiazhuang, Hebei Medical University, No. 42 Ta'nan Road, Yuhua Distinct, Shijiazhuang 050021, Hebei Province, China. daieh2008@126.com

Abstract

BACKGROUND

Data that assess maternal and infant outcomes in hepatitis C virus (HCV)-infected mothers are limited.

AIM

To investigate the frequency of complications and the associated risk factors.

METHODS

We performed a cohort study to compare pregnancy and fetal outcomes of HCV-viremic mothers with those of healthy mothers. Risk factors were analyzed with logistic regression.

RESULTS

Among 112 consecutive HCV antibody-positive mothers screened, we enrolled 79 viremic mothers. We randomly selected 115 healthy mothers from the birth

registry as the control. Compared to healthy mothers, HCV mothers had a significantly higher frequency of anemia [2.6% (3/115) *vs* 19.0% (15/79), $P < 0.001$] during pregnancy, medical conditions that required caesarian section [27.8% (32/115) *vs* 48.1% (38/79), $P = 0.004$], and nuchal cords [9.6% (11/115) *vs* 34.2% (27/79), $P < 0.001$]. In addition, the mean neonatal weight in the HCV group was significantly lower (3278.3 ± 462.0 *vs* 3105.1 ± 459.4 gms; $P = 0.006$), and the mean head circumference was smaller (33.3 ± 0.6 *vs* 33.1 ± 0.7 cm; $P = 0.03$). In a multivariate model, HCV-infected mothers were more likely to suffer anemia [adjusted odds ratio (OR): 18.1, 95% confidence interval (CI): 4.3-76.6], require caesarian sections (adjusted OR: 2.6, 95%CI: 1.4-4.9), and have nuchal cords (adjusted OR: 5.6, 95%CI: 2.4-13.0). Their neonates were also more likely to have smaller head circumferences (adjusted OR: 2.1, 95%CI: 1.1-4.3) and lower birth weights than the average (≤ 3250 gms) with an adjusted OR of 2.2 (95%CI: 1.2-4.0). The vertical transmission rate was 1% in HCV-infected mothers.

CONCLUSION

Maternal HCV infections may associate with pregnancy and obstetric complications. We demonstrated a previously unreported association between maternal HCV viremia and a smaller neonatal head circumference, suggesting fetal growth restriction.

Key Words: Hepatitis C virus viremia; Mother-to-child transmission; Pregnancy complications; Maternal health; Infant hepatitis C virus infection

©The Author(s) 2022. Published by Baishideng Publishing Group Inc. All rights reserved.

Core Tip: Although hepatitis C virus (HCV) affects a significant number of pregnant women, there is limited data regarding the impact of HCV active infection on pregnancy and infant outcomes. The current cohort study compared maternal complications and fetal development of HCV mothers with detectable levels of HCV RNA with those of healthy mothers. The study demonstrates a previously unreported association between maternal HCV viremia and a smaller neonate head circumference. In addition, HCV viremia was an independent predictor for negative maternal outcomes including anemia during pregnancy, medical conditions that required caesarian section, and nuchal cords. These findings increase the need for close antenatal surveillance in HCV mothers with viremia for maternal complications and delayed fetal development.

Citation: Pan CQ, Zhu BS, Xu JP, Li JX, Sun LJ, Tian HX, Zhang XH, Li SW, Dai EH. Pregnancy and fetal outcomes of chronic hepatitis C mothers with viremia in China. *World J Gastroenterol* 2022; 28(34): 5023-5035
URL: https://www.wjgnet.com/1007-9327/full/v28/i34/5023.htm
DOI: https://dx.doi.org/10.3748/wjg.v28.i34.5023

INTRODUCTION

Hepatitis C virus (HCV) infection is a common infectious disease that affects the liver and remains a significant global health burden[1]. Although spontaneous viral clearance may occur in approximately 15% of patients who have acute HCV infection, the majority develop a chronic HCV infection. Among patients who have chronic hepatitis C, approximately 10%-15% will progress to cirrhosis within the first 20 years of infection, which eventually becomes decompensated without appropriate therapy and places them at high risk of developing liver cancer[2]. The prevalence of antibodies to HCV (HCV-Ab) in pregnant women is 0.1% to 2.4%, although it is much higher in some endemic areas[3]. The proportion of pregnant women with HCV-Ab positivity and active infection with viremia is approximately 60% to 70%[3].

Globally, up to 8% of pregnant women are infected with HCV in highly endemic areas[4]. In the United States, surveillance published in 2017 revealed a nationwide increase in HCV infection among pregnant women, which is an increasing but potentially modifiable threat to maternal and child health [5]. The proportion of infants born to HCV-infected women is also increasing in the United States[6]. It has been reported that vertical transmission is the most common mechanism of HCV infection in children, occurring in approximately 6% of infants born to women with HCV infection[7]. The risk of HCV vertical transmission increases if the maternal serum HCV viral load is above 10^5 copies/mL[8,9]. In addition, published studies have suggested that vertical transmission encompasses several potential transmission routes from an infected woman to her newborn, including intrauterine, intrapartum, and postnatal routes[10-13]. According to the American Association for the Study of Liver Diseases

guidelines, all pregnant women should be tested for HCV infections, ideally at the time of initiation of prenatal care[14].

Although HCV affects a significant number of pregnant women, there are limited data regarding the impact of HCV active infection on pregnancy and infant outcomes. Prior studies of HCV and pregnancy have focused on the vertical transmission rates of HCV infection using limited assessments of the effects of chronic HCV infections on maternal health, complications during delivery, and fetal complications [15]. Therefore, there are data gaps in supporting strategies for the clinical management of mothers with HCV infections during pregnancy. Additionally, the identification of adverse consequences could improve current perinatal care and monitoring recommendations. With that in mind, we conducted a retrospective cohort study to compare the frequency and severity of adverse maternal outcomes during pregnancy, as well as fetal and infant outcomes, between mothers with HCV viremia and healthy mothers.

MATERIALS AND METHODS

Study design, setting, and patient selection

This is a single-center retrospective observational cohort study conducted at a tertiary referral university hospital located in Shijiazhuang city of Hebei province in China, which receives referrals from different levels of community medical clinics and health facilities in the city. The study site mainly included mothers with infectious diseases, including hepatitis B, hepatitis C, and human immunodeficiency virus (HIV). The Institutional Review Board approved the study, and the need for informed consent was waived. Local standards of care for prenatal care include regular clinic visits approximately every 4 to 6 wk during pregnancy for mothers who are infected with chronic viral hepatitis. Mothers received a symptom-directed physical exam, blood tests, and ultrasonography exams from the early second trimester to delivery. Viral hepatitis and HIV screening were performed at the first prenatal visit (often during the first or early second trimester), and hospital delivery was mandated in the entire province except in an emergency event.

In the current study, patients who attended the services in the prenatal care clinic from November 1, 2011 to May 31, 2020 were screened for eligibility. Adult patients (age > 18 years old) who had a diagnosis of HCV-Ab positivity for at least six months and detectable levels of HCV RNA (> 15 IU/mL) during prenatal screening were eligible for enrollment. Major exclusion criteria were the following: Coinfection with hepatitis B virus, hepatitis D virus, or HIV; current or history of intravenous drug use or sexually transmitted diseases; liver cancer; autoimmune liver disease; primary biliary cirrhosis; and alcohol-related liver diseases (consumption of more than 20 g/day of alcohol for > 5 years). Patients with other liver diseases, including inherited liver diseases and drug-induced liver injury, were also excluded. For each patient included in the HCV group, a healthy mother was identified and selected from the Delivery Suite Registry at random. The selection was based on their infants' date of birth (± 30 d) matched to those of the HCV mothers with similar baseline values (matched for gestational days and parity). Based on the ratio of approximately 1:1 to match the number of subjects enrolled in the HCV group, a similar number of subjects was included in the healthy mother group. All patients included in the study were not smoking, drinking alcohol, or using any recreational drugs since these variables may affect the infants' outcomes.

Laboratory measurements for subjects in the study were all performed by the central laboratory in the medical center. HCV-Ab was tested by a chemiluminescent microparticle immunoassay (Autobio, Zhengzhou, China). Serum HCV RNA levels were measured with the real-time quantitative polymerase chain reaction method by using the Cobas TaqMan polymerase chain reaction assay according to the laboratory manuals (Roche Diagnostics, United States). An undetectable level was defined as below the lowest level of quantitation = 15 IU/mL. The comprehensive chemistry panel was tested using a HITACHI 7600 fully automatic biochemical analyzer, with the ULN of alanine aminotransferase (ALT) set at 40 U/L (Wako Pure Chemical Industries, Ltd. Japan).

Patient data collection and outcome assessment

Using an electronic medical record system and paper charts, we collected the following maternal data: Patients' demographic information and pertinent clinical data, including a history of liver disease or hepatocellular carcinoma, pregnancy or obstetric complications; medication lists; positive physical findings, including pelvimetry, labor outcomes, and modes of delivery; laboratory results of completed blood count, coagulation tests, chemistry panels with ALT, and virological tests; and imaging results if available. Pertinent data were assessed at all visits starting from gestational week 12 with a four-week interval before delivery, at delivery, and at postpartum weeks 12, 24, and 36. Perinatal information for fetal development, including birth weight, height, Apgar scores, gestational age, and perinatal complications such as birth trauma and neonatal jaundice, was extracted from the neonatal records. Infant outcomes, such as intrauterine growth restriction, birth defects, macrosomia, low birth weight, and meconium staining stool, were collected.

The primary assessment was to analyze the frequency of maternal complications (both pregnancy and obstetrics complications) and negative fetal outcomes in HCV-infected mothers with viremia *vs* those in healthy mothers. In addition, vertical transmission rates were analyzed among mothers with HCV infection. Secondary assessments were the association between demographic or clinical features and negative maternal or fetal outcomes in a multivariable logistic regression analysis. The current study used the following criteria to define the vertical transmission of HCV and considered the transmission confirmed if any of the following occurred: (1) Detection of HCV RNA in an infant who is 3 to 6 months old; (2) Detection of HCV RNA in the infant on at least 2 occasions; (3) Finding elevated serum aminotransferase levels in an HCV-Ab positive child (ULN = 40 U/mL); or (4) Confirming an identical viral genotype between mother and child[3].

Statistical analysis

Data analyses were performed using the Statistical Package for Social Science for Windows, Version 25.0 (SPSS Inc., IBM, New York, United States). Frequencies and percentages were used to summarize the categorical variables. Fisher's exact tests or chi-squared tests were used when comparing data between and within groups. Depending on the underlying distribution of the data, descriptive values are expressed as the means ± SD or medians and interquartile ranges. The student's t-test was used to assess continuous variables between groups. The maternal outcomes or infant outcomes were calculated *per* pregnant mother and/or *per* infant when appropriate. The baseline demographic or characteristic variables were analyzed as independent variables, whereas the negative maternal or infant outcomes were considered dependent variables. Risk factors identified from the univariate analysis (P value < 0.05) were further analyzed in the multivariate logistic regression model. The aforementioned risk factors associated with negative outcomes are presented with crude and adjusted odds ratios (ORs) with 95% confidence intervals (CIs). All tests were two-tailed with a 95%CI, and a P value < 0.05 was considered significant.

RESULTS

Patient characteristics

Among the 122 consecutive HCV antibody-positive pregnant women screened, 30 were not eligible due to undetectable levels of HCV RNA throughout the pregnancy. In addition, 13 patients were excluded because they were coinfected with HIV (n = 6) or hepatitis B virus (n = 7). As a result, seventy-nine patients who had HCV viremia during pregnancy were eligible for the HCV group. In addition, 115 healthy mothers were identified and selected from the Delivery Suite Registry at random (delivery date ± 30 d matched to those cases in the HCV-infected group with similar baseline variables). As a result, our cohort consisted of 194 pregnant women with 79 and 115 mothers in the HCV group and a healthy mother (noninfected) group, respectively. The patient selection process is shown in Figure 1. All patients in the HCV group had no clinical indicator for liver decompensation. The clinical characteristics of the study patients are presented in Table 1. The demographic characteristics were well matched between the two groups in the majority of variables, including pre-pregnancy mean BMI, the number of parities or pluralities, mean gestational days, and mean ALT at delivery. However, mothers in the healthy group had a significantly older mean age (29.4 ± 4.9 *vs* 25.8 ± 4.7 years, P < 0.001), a low frequency of intertuberous diameter < 8.5 cm (29.6% *vs* 48.1%, P = 0.009) and were taller (160.9 ± 4.0 *vs* 159.6 ± 3.8 cm, P < 0.001) than those in the HCV group.

Maternal outcomes

Data from gestational week 12 to delivery about pregnancy or obstetric complications and maternal laboratory abnormalities were analyzed. The following pregnancy and obstetric complications were identified in both groups (Table 2): Preterm labor, preeclampsia, eclampsia, gestational hypertension, anemia, abnormal renal or thyroid function, oligohydramnios, gestational diabetes, nuchal cord, umbilical cord prolapses, postpartum hemorrhage, premature rupture of membranes, and cesarean section due to medical needs. When comparing the aforementioned outcomes or laboratory abnormalities between the HCV-infected and healthy individuals, a significantly higher frequency of anemia during pregnancy was observed in the HCV group [19.0% (15/79) *vs* 2.6% (3/115), P < 0.001]. In addition, a significantly higher frequency of nuchal cords [34.2% (27/79) *vs* 9.6% (11/115); P < 0.001] and cesarean sections due to medical needs [48.1% (38/79) *vs* 27.8% (32/115); P = 0.004] was reported in the HCV group. The frequencies of other pregnancy or obstetric complications did not differ between the two groups (Table 2).

Fetal and infant outcomes

When comparing the fetal and infant outcomes between the HCV-infected and healthy mother groups (Table 3), we observed a significantly lower mean ± SD body weight in neonates who were born to HCV-infected mothers (3105.1 ± 459.4 *vs* 3278.3 ± 462.0 gms; P = 0.006). However, the frequency of low

Table 1 The demographic and clinical characteristics of mothers and infants

Variables presented with *n* (%), mean ± SD, or specified	HCV mothers with viremia (*n* = 79)[1]	Healthy mothers (*n* = 115)[1]	*P* value
Maternal characteristics			
Age (yr)	25.8 ± 4.7	29.4 ± 4.9	< 0.001
< 20	2/79 (2.5)	0/115 (0.0)	0.003
20-34	73/79 (92.4)	94/115 (81.7)	
≥ 35	4/79 (5.1)	21/115 (18.3)	
Height, cm	159.6 ± 3.8	160.9 ± 4.0	0.02
Pre-pregnancy BMI	27.4 ± 3.4	27.5 ± 3.1	0.80
< 23	4/79 (5.1)	3/115 (2.6)	0.44
23-29	53/79 (67.1)	86/115 (74.8)	
≥ 29	22/79 (27.8)	26/115 (22.6)	
History of miscarriage	1/79 (1.3)	1/115 (0.9)	> 0.99
History of stillbirth	2/79 (2.5)	2/115 (1.7)	> 0.99
Previous uterine surgery	28/79 (35.4)	35/115 (30.4)	0.46
Parity			
0-1	47/79 (59.5)	62/115 (53.9)	0.44
≥ 2	32/79 (40.5)	53/115 (46.1)	
Plurality			
0-1	47/79 (59.5)	62/115 (53.9)	0.44
> 2	32/79 (40.5)	53/115 (46.1)	
Gestational (days)	273.8 ± 9.5	276.0 ± 9.1	0.11
Interspinous distance, median (IRQ), cm	25.0 (24.0, 25.0)	25.0 (24.0, 25.0)	0.23
Intercristal distance, median (IRQ), cm	27.0 (27.0, 28.0)	27.0 (27.0, 28.0)	0.40
External conjugate, median (IRQ), cm	20.0 (20.0, 21.0)	20.0 (20.0, 21.0)	0.33
Intertuberous diameter, median (IRQ), cm	8.5 (8.0, 8.5)	8.5 (8.0, 8.5)	0.006
< 8.5	38/79 (48.1)	34/115 (29.6)	0.009
≥ 8.5	41/79 (51.9)	81/115 (70.4)	
Hemoglobin, median (IRQ), g/L	111.0 (100.0, 119.0)	110.0 (100.0, 119.0)	0.88
< 110	37/79 (46.8)	51/115 (44.3)	0.73
≥ 110	42/79 (53.2)	64/115 (55.7)	
Platelet, median (IRQ), × 109/L	207.0 (166.0, 242.0)	201.0 (167.0, 242.0)	0.95
Prothrombin time, median (IRQ), seconds	10.6 (10.1, 11.1)	10.5 (10.0, 11.1)	0.40
ALT at delivery, U/L	26.3 ± 20.1	16.6 ± 56.7	0.15
HCV RNA at delivery, IU/mL	19, 217, 509 ± 35, 745, 723	-	-

[1]All mothers in the study had a singleton pregnancy.

HCV: Hepatitis C virus; ALT: Alanine aminotransferase; IRQ: Interquartile range; BMI: Body mass index.

birth weight (< 2500 g) did not differ between the two groups [8.9% (7/79) *vs* 3.5% (4/115); $P = 0.20$]. The other variables did not differ between the two groups. In addition, neonates in the HCV group had a significantly smaller mean head circumference (33.1 ± 0.7 *vs* 33.3 ± 0.6 cm; $P = 0.03$). The other measurements did not differ between the two groups, which included gestational weeks, the percentage of neonates that reached full-term or small for gestational age at delivery, and the mean height at birth. There were no miscarriages, stillbirths, birth defects, or Apgar scores < 7 at 5 min after birth in the entire cohort.

Table 2 Maternal outcomes in the hepatitis C virus viremic group *vs* the control group

Variables, *n* (%)	HCV-infected group (*n* = 79), %	Healthy mother group (*n* = 115), %	*P* value
Pregnancy complications			
Preterm (< 37 wk)	1/79 (1.3)	0/115 (0.0)	> 0.99
Preeclampsia	3/79 (3.8)	0/115 (0.0)	0.07
Eclampsia	0/79 (0.0)	2/115 (2.5)	0.17
Gestational hypertension	0/79 (0.0)	4/115 (3.5)	0.15
Abnormal thyroid function	4/79 (5.1)	1/115 (0.9)	0.16
Gestational diabetes	4/79 (5.1)	4/115 (3.5)	0.72
Oligohydramnios	6/79 (7.6)	3/115 (2.6)	0.16
Abnormal renal function	49/79 (62.0)	64/115 (55.7)	0.38
Anemia during pregnancy	15/79 (19.0)	3/115 (2.6)	< 0.001
Obstetric complications			
Rates of cesarean section[1]	38/79 (48.1)	32/115 (27.8)	0.004
Nuchal cord	27/79 (34.2)	11/115 (9.6)	< 0.001
Umbilical cord prolapses	1/79 (1.3)	0/115 (0.0)	0.41
Postpartum hemorrhage	1/79 (1.3)	0/115 (0.0)	0.41
Premature rupture of membranes	3/79 (3.8)	4/115 (3.5)	> 0.99

[1]The rates of cesarean section were calculated based on the number of cases performed due to medical needs. Patients who requested a cesarean section without medical indications were not included.

Among infants who were born to HCV-infected mothers, all were tested HCV-Ab positive at birth, and one had a detectable level of HCV RNA (2165 IU/mL). All infants in the study cohort were breastfed. Their HCV-Ab became negative beyond six months, except for the one who had HCV viremia at birth. This infant continued to have HCV antibodies and detectable levels of HCV RNA measured at the ages of three months and nine months, meeting the criteria of chronic hepatitis C infection. The HCV transmission rate in our study was 1.3% (n = 1/79). In the review of maternal characteristics, the mother was 25 years old with a maternal HCV RNA level of 2.58 × 5 Log_{10} IU/mL at delivery. She had a history of blood transfusion and was diagnosed with chronic HCV infection during prenatal screening. Her pregnancy was uneventful, with normal levels of ALT throughout the entire pregnancy. She delivered a girl with normal physical development at gestational week 39 plus 5 d.

Risk factors associated with negative outcomes

When comparing the pregnancy and obstetric complications between the two groups, we found that a significantly higher frequency of anemia, nuchal cord, and cesarean section due to medical needs occurred among HCV-infected mothers. The crude and adjusted ORs with 95%CIs of each risk factor are presented in Table 4. The analyses indicated that HCV infection was the only factor associated with anemia (adjusted OR: 18.1, 95%CI: 4.3-76.6), increased numbers of C sections due to medical needs (adjusted OR: 2.6, 95%CI: 1.4-4.9), and nuchal cords during pregnancies (adjusted OR: 5.6, 95%CI: 2.4-13.0). Since a significantly smaller head circumference and lower mean birth weight were the only two negative fetal outcomes identified in infants from HCV-infected mothers, we analyzed the maternal risk factors (Table 5) and found that maternal HCV infection was associated with these negative outcomes. The adjusted ORs of maternal HCV infection associated with a smaller head circumference and birth weight ≤ 3250 gms were 2.1 (95%CI: 1.1-4.3) and 2.2 (95%CI: 1.2-4.0), respectively.

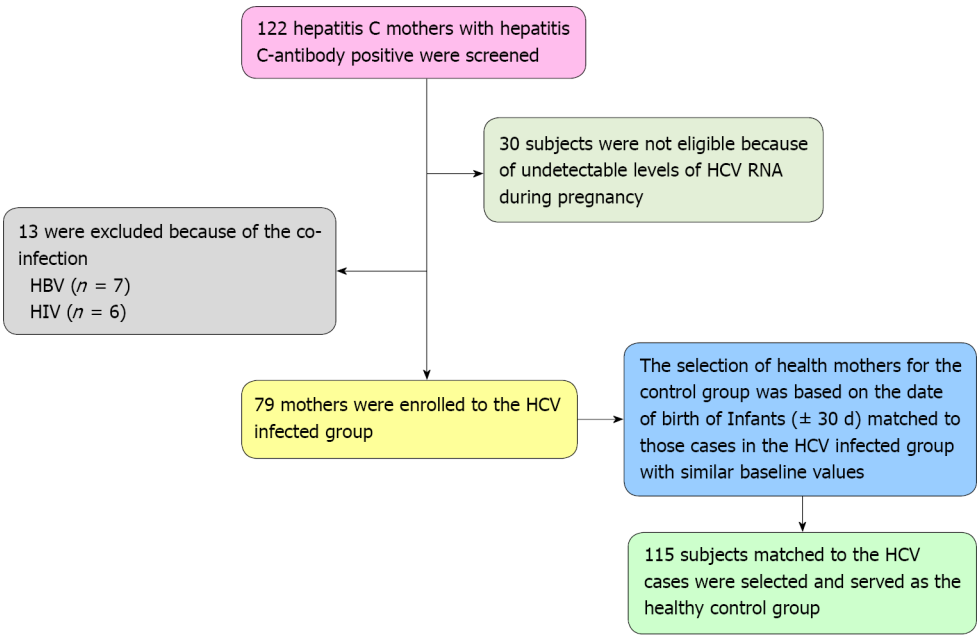
DISCUSSION

Although HCV vertical transmission can occur in up to 5.8% of mother-infant pairs[16], many children can clear HCV infection spontaneously[17]. The disease can also be cured with oral antiviral therapy starting at the age of 3[17]. Therefore, the clinical landscape of managing HCV-infected mothers has recently shifted from addressing HCV vertical transmission to the assessment and management of negative pregnancy or neonatal outcomes. Published studies have linked several negative pregnancy outcomes to maternal HCV infection, including intrahepatic cholestasis[18-20], gestational diabetes[21-

Table 3 The fetal and infant outcomes in the two study groups

Infant characteristics at birth[1] variables presented with *n* (%) or mean ± SD	Infants from HCV-infected mothers (*n* = 79)	Infants from healthy mothers (*n* = 115)	*P* value
Gestational weeks	39.1 ± 1.4	39.4 ± 1.3	0.11
Full-term birth	74/79 (93.7)	107/115 (93.0)	0.86
Meconium staining positive	8/79 (10.1)	11/115 (9.6)	> 0.99
Height at birth, cm	49.0 ± 1.6	49.4 ± 1.0	0.05
Head circumference, cm	33.1 ± 0.7	33.3 ± 0.6	0.03
Weight at birth, gms	3105.1 ± 459.4	3278.3 ± 462.0	0.006
≤ 3250 gms	49/79 (62.0)	52/115 (45.2)	0.02
< 2500 gms	7/79 (8.9)	4/115 (3.5)	0.20
Small for gestational age[2]	1/79 (1.3)	1/115 (0.9)	> 0.99
Birth defects	0/79 (0.0)	0/115 (0.0)	> 0.99
Apgar score < 7 at 5 min	0/79 (0.0)	0/115 (0.0)	> 0.99
HCV-Ab (+) at birth, *n* (%)	79/79 (100)	-	-
Detectable HCV RNA, *n* (%)	1/79 (1.27)	-	-

[1]All cases in the study were singleton.
[2]Small for gestational age; defined as a birth weight below the 10th percentile for each gestational age using sex-specific criteria.
HCV: Hepatitis C virus.



DOI: 10.3748/wjg.v28.i34.5023 **Copyright** ©The Author(s) 2022.

Figure 1 Flow Chart for patients enrolled in the study. Data analyses included 194 patients. Among the 122 patients with hepatitis C antibody positive evaluated, 79 were eligible and enrolled. A control group with healthy uninfected patients (*n* = 115) was selected to match the infected patients. Patients were divided into two groups: a hepatitis C patient group and a healthy control group comparison. HCV: Hepatitis C virus; HBV: Hepatitis B virus; HIV: Human immunodeficiency virus.

23], the premature rupture of the membranes[24,25], the requirement for cesarean delivery[24,25], preterm delivery[23], small for gestational age[26], and low birth weight[26]. However, its effect on restriction or disturbance of intrauterine fetal growth remains inconclusive[21,23,26-28].

Our study assessed both maternal and fetal outcomes in viremic mothers with HCV infections. To our knowledge, this is the first study from China to assess pregnancy outcomes in HCV viremic mothers. We found that HCV might be associated with a higher frequency of nuchal cords and a smaller neonatal

Table 4 Risk factors associated with obstetric complications

Clinical variables	Case/exposed[1]	Crude OR (95%CI); *P* value	Adjusted OR (95%CI); *P* value
C-section[2]			
Age, *n* (%)			
< 35	59/194 (30.4)	1	1
≥ 35	11/194 (5.7)	1.5 (0.6-3.4); *P* = 0.38	1.5 (0.6-3.9); *P* = 0.42
Nulliparity, *n* (%)			
No	37/194 (19.1)	1	1
Yes	33/194 (17.0)	0.6 (0.3-1.0); *P* = 0.06	0.6 (0.3-1.1); *P* = 0.08
BMI, *n* (%)			
< 30	57/194 (29.4)	1	1
≥ 30	13/194 (6.7)	1.3 (0.6-2.7); *P* = 0.56	1.2 (0.5-2.7); *P* = 0.65
HCV infection, *n* (%)			
No	32/194 (16.5)	1	1
Yes	38/194 (19.6)	2.4 (1.3-4.4); *P* = 0.004	2.6 (1.4-4.9); *P* = 0.003
Intertuberous diameter, *n* (%)			
≥ 8.5	41/194 (21.1)	1	1
< 8.5	29/194 (14.9)	1.3 (0.7-2.2); *P* = 0.41	2.6 (1.4-4.9); *P* = 0.65
Nuchal cord			
Age, *n* (%)			
< 35	33/194 (17.0)	1	1
≥ 35	5/194 (2.6)	1.0 (0.4-2.9); *P* = 0.96	2.8 (0.8-10.3); *P* = 0.11
Nulliparity, *n* (%)			
No	13/194 (6.7)	1	1
Yes	25/194 (12.9)	1.6 (0.8-3.5); *P* = 0.19	2.0 (0.9-4.8); *P* = 0.11
BMI, *n* (%)			
< 30	32/194 (16.5)	1	1
≥ 30	6/194 (3.1)	0.9 (0.4-2.5); *P* = 0.90	0.7 (0.2-1.9); *P* = 0.44
HCV infection, *n* (%)			
No	11/194 (5.7)	1	1
Yes	27/194 (13.9)	4.9 (2.3-10.7); *P* < 0.001	5.6 (2.4-13.0); *P* < 0.001
Intertuberous diameter, *n* (%)			
≥ 8.5	20/194 (10.3)	1	1
< 8.5	18/194 (9.3)	1.3 (0.7-2.4); *P* = 0.35	1.3 (0.6-2.8); *P* = 0.51
Maternal anemia during pregnancy			
Age, *n* (%)			
< 35	19/194 (9.8)	1	1
≥ 35	3/194 (1.5)	1.1 (0.3-3.9); *P* = 0.91	2.5 (0.5-13.3); *P* = 0.28
Nulliparity, *n* (%)			
No	13/194 (6.7)	1	1
Yes	9/194 (4.6)	0.5 (0.2-1.2); *P* = 0.13	0.5 (0.2-1.4); *P* = 0.18
BMI, *n* (%)			
< 30	20/194 (10.3)	1	1

≥ 30	2/194 (1.0)	0.5 (0.1-2.1); $P = 0.33$	0.4 (0.1-1.8); $P = 0.21$
HCV infection, *n* (%)			
No	3/194 (1.5)	1	1
Yes	19/194 (9.8)	11.8 (3.4-41.6); $P < 0.001$	18.1 (4.3-76.6); $P < 0.001$
Intertuberous diameter, *n* (%)			
≥ 8.5	13/194 (6.7)	1	1
< 8.5	9/194 (4.6)	1.2 (0.5-3.0); $P = 0.35$	0.8 (0.3-2.3); $P = 0.72$

[1]Case/exposed: The case refers to the number of patients who presented with the specified variable and the Exposed refers to the total number of patients in the entire study cohort.
[2]The rates of cesarean section were calculated based on the number of cases performed due to medical needs. Patients who requested a cesarean section without medical indications were not included.
BMI: Body mass index; OR: Odds ratio; HCV: Hepatitis C virus.

head circumference, which has not been reported in the literature before. We also found that HCV viremia was linked to pregnancy anemia, cesarean sections due to medical needs, and low gestational weight in neonates. In addition, we observed that lower birth weight was associated with maternal infection, which was consistent with published data from the United States and Europe[23,26]. In the context of all infants in our study being breastfed, the HCV vertical transmission rate was 1.27%, which was within the range (0.2%-6%) of the already published studies[16,29].

Early studies by Jaffery *et al*[30] and Bohman *et al*[31] found that fetal outcomes did not differ between HCV-positive mothers and healthy controls[30,31]. However, in a study by Salemi *et al*[29], the risk of an adverse neurological outcome was higher in infants born to HCV mothers, including feeding difficulties (OR: 1.32, 95%CI: 1.06-1.64) and neonatal seizures (OR: 1.74, 95%CI: 0.98-3.10)[29]. The aforementioned studies have limitations of lacking a well-defined study population because the diagnosis of HCV was based on the HCV antibody, and HCV RNA was not always tested. Paternoster *et al*[24] observed that intrahepatic cholestasis was more common in HCV-RNA-positive mothers than in HCV-RNA-negative mothers, suggesting that HCV viremia may lead to different outcomes[19]. In addition, cofounders such as intravenous drug use or sexually transmitted diseases may not be adjusted in studies based on pregnancy registries[26,32]. These factors could contribute to the discrepancies among the study findings. In the context of the paucity of data and infrequency of fetal negative events, Huang *et al*[33] performed a meta-analysis and found that low birth weight was linked to maternal HCV infection (OR: 1.97, 95%CI: 1.43-2.71)[33].

In our study, birth weight ≤ 3250 gms was associated with HCV exposure. There was also a trend of HCV-exposed neonates with a birth weight of < 2500 gms. More importantly, our cohort demonstrates a previously unreported association between maternal HCV viremia and a smaller neonatal head circumference. Our findings provide new evidence supporting the intrauterine restriction of fetal growth in a well-defined HCV population, which enrolled only HCV-infected mothers with detectable levels of HCV RNA who had no history of intravenous drug use or sexually transmitted diseases.

Although the mechanism of fetal growth restriction is not fully understood, several studies have suggested that HCV-induced inflammation in the placenta may cause fetal development restriction. In an *in vitro* study, HCV infected a human cytotrophoblast and changed its ultrastructure dramatically upon infection[33]. In addition, Hurtado *et al*[34] observed that the cytotoxicity of natural killer cells and natural killer T cells was enhanced in the placenta, and placental natural killer T-cell cytotoxicity was further increased by HCV infections[34]. Several population-based retrospective cohort studies reported higher rates of gestational diabetes in HCV-infected mothers than in noninfected mothers[35,36], but the association was limited to women with excessive weight gain during pregnancy. Our study did not show such complications, which is likely because our patients are Asians with a much lower body mass index than those in other studies[21,24,26].

In this cohort study, some limitations should be addressed. Being a single-center retrospective design, this study has a limited capacity when adjusting or balancing all covariates between the HCV-exposed and HCV nonexposed groups. Additionally, we did not have HCV genotype data. However, published studies in China indicated that the majority of Chinese patients with HCV had genotype 1[36]. Second, cohort data about HCV antibody-positive but nonviremic mothers are limited: These mothers were not enrolled in our study due to the small number of patients in our center ($n = 30$, Figure 1). Further studies in this subgroup will add to the understanding of pregnancy outcomes. Third, the liver fibrosis stages for patients with HCV infection were not assessed in this study, although all patients had no clinical indications of liver decompensation. Therefore, future studies might be needed to investigate whether HCV-infected patients with advanced fibrosis have negative maternal and fetal outcomes. Last, the frequency of negative events in HCV-infected mothers could be underestimated due to the maternal mean age being younger than that of healthy mothers.

Table 5 Risk factors associated with fetal negative outcomes

Clinical variables	Case/exposed[1]	Crude OR (95%CI)	Adjusted OR (95%CI)
Head circumference ≤ 33 cm at birth			
Maternal age, *n* (%)			
< 35	118 /194 (60.8)	1	1
≥ 35	18 /194 (9.3)	1.1 (0.4-2.8); *P* = 0.82	2.0 (0.7-5.7); *P* = 0.19
Nulliparity, *n* (%)			
No	53/194 (27.3)	1	1
Yes	83 /194 (42.8)	1.9 (1.0-3.6); *P* = 0.04	2.4 (1.2-4.9); *P* = 0.01
BMI, *n* (%)			
< 30	120/194 (61.9)	1	1
≥ 30	16/194 (8.2)	0.4 (0.2-0.8); *P* = 0.008	0.3 (0.1-0.7); *P* = 0.003
HCV infection, *n* (%)			
No	75/194 (38.7)	1	1
Yes	61/194 (31.4)	1.8 (0.9-3.5); *P* = 0.08	2.1 (1.1-4.3); *P* = 0.03
Intertuberous diameter, *n* (%)			
≥ 8.5	85/194 (43.8)	1	1
< 8.5	51/194 (26.3)	1.1 (0.6-2.0); *P* = 0.86	1.0 (0.5-2.0); *P* = 0.75
Weight at birth ≤ 3250 gms			
Age, *n* (%)			
< 35	88/194 (45.4)	1	1
≥ 35	13/194 (6.7)	1.0 (0.4-2.3); *P* > 0.99	1.7 (0.6-4.3); *P* = 0.29
Nulliparity, *n* (%)			
No	39/194 (20.1)	1	1
Yes	62/194 (32.0)	1.6 (0.9-2.8); *P* = 0.13	1.8 (0.9-3.4); *P* = 0.07
BMI, *n* (%)			
< 30	88/194 (45.4)	1	1
≥ 30	13 /194 (6.7)	0.6 (0.3-1.2); *P* = 0.16	0.5 (0.2-1.1); *P* = 0.09
HCV infection HCV, *n* (%)			
No	52/194 (26.8)	1	1
Yes	49/194 (25.3)	2.0 (1.1-3.5); *P* = 0.02	2.2 (1.2-4.0); *P* = 0.01
Intertuberous diameter, *n* (%)			
≥ 8.5	61/194 (31.4)	1	1
< 8.5	40/194 (20.6)	1.2 (0.7-2.2); *P* = 0.46	1.1 (0.6-2.1); *P* = 0.66

[1]Case/exposed: The case refers to the number of patients who presented with the specified variable and the Exposed refers to the total number of patients in the entire study cohort.
BMI: Body mass index; OR: Odds ratio.

CONCLUSION

In conclusion, our study demonstrates a previously unreported association between maternal HCV viremia and a smaller neonatal head circumference. Given our new findings on the intrauterine restriction of fetal growth from HCV exposure, screening all mothers during pregnancy for HCV should be a mandatory practice. More importantly, our findings indicate a need for close antenatal surveillance for maternal complications and delayed fetal development in HCV mothers with viremia. Last, our data support that preconception health management should include HCV screening, so HCV infection can be treated before pregnancy to improve the health of both the mothers and infants.

ARTICLE HIGHLIGHTS

Research background

Hepatitis C virus (HCV) infection remains a significant global health burden, and there is a high proportion of women with antibodies to HCV positive whose active infection with viremia. In addition, HCV infection among pregnant women is an increasing but potentially modifiable threat to maternal and child health.

Research motivation

Although HCV affects a significant number of pregnant women, there is limited data regarding the impact of HCV active infection on pregnancy and infant outcomes. Therefore, there are data gaps in supporting strategies for clinical management of mothers with HCV infections during pregnancy.

Research objectives

We conducted a retrospective cohort study to compare the frequency and severity of adverse maternal outcomes during pregnancy, as well as fetal and infant outcomes between mothers with HCV viremia and healthy mothers.

Research methods

A retrospective observational cohort study was conducted to compare pregnancy and fetal outcomes of HCV-viremic mothers with those of healthy mothers. After HCV mothers with viremia and healthy mothers were enrolled, we collected their demographic information and pertinent clinical data using an electronic medical record system and paper charts. Perinatal information for fetal development and infant outcomes were extracted from the neonatal records. Data analyses were performed using the Statistical Package for Social Science for Windows, Version 25.0 (SPSS Inc., IBM, New York, United States).

Research results

Our study enrolled 79 viremic mothers and 115 healthy mothers. Compared to healthy mothers, HCV mothers had a significantly higher frequency of anemia, caesarian section, and nuchal cords during pregnancy. In addition, the mean neonatal weight and head circumference in the HCV group was significantly lower. In a multivariate model, similar results were found.

Research conclusions

Our study demonstrates the association between maternal HCV viremia and a smaller neonate head circumference. We also confirmed the high frequency of pregnancy and obstetric complications in HCV viremic mothers.

Research perspectives

Multi-center and large sample studies are needed to verify these results in the future and to investigate if HCV-infected patients with advanced fibrosis have negative maternal and fetal outcomes.

ACKNOWLEDGEMENTS

We thank the medical staff in the Department of Obstetrics and Gynecology, The Fifth Hospital of Shijiazhuang, for their support and assistance during our study. We also like to thank Mr. Andrew Park (Northern Valley Regional High School at Old Tappan, United States) for proofreading the manuscript.

FOOTNOTES

Author contributions: Pan CQ provided the concept and designed the study, wrote the manuscript, communicated with the journal, and addressed comments from reviewers; Dai EH and Zhu BS obtained the funding and supervised the study; Pan CQ, Zhang XH, and Dai EH performed data analyses; All other authors contributed to the data collection.

Supported by The Ministry of Science and Technology of China for the National Five-Year Key Projects in Infectious Diseases, No. 2015ZX10004801.

Institutional review board statement: The study was reviewed and approved by the Institutional Review Board of the Fifth Hospital of Shijiazhuang in China.

Informed consent statement: The informed consent was waived.

Conflict-of-interest statement: Dr. Pan received grants from Gilead. He also serves as a speaker for Gilead and Abbvie. Other authors have nothing to be disclosed.

Data sharing statement: The authors agree to share anonymized Individual Patient Data (IPD) upon request or as required by law and/or regulation with qualified external researchers. Approval of such requests is at the authors' discretion and is dependent on the nature of the request, the merit of the research proposed, the availability of the data, and the intended use of the data. Data requests should be sent to Erhei Dai MD at email: daieh2008@126.com

STROBE statement: The authors have read the STROBE Statement—checklist of items, and the manuscript was prepared and revised according to the STROBE Statement—checklist of items.

Open-Access: This article is an open-access article that was selected by an in-house editor and fully peer-reviewed by external reviewers. It is distributed in accordance with the Creative Commons Attribution NonCommercial (CC BY-NC 4.0) license, which permits others to distribute, remix, adapt, build upon this work non-commercially, and license their derivative works on different terms, provided the original work is properly cited and the use is non-commercial. See: https://creativecommons.org/Licenses/by-nc/4.0/

Country/Territory of origin: China

ORCID number: Calvin Q Pan 0000-0002-3723-6688; Er-Hei Dai 0000-0001-8835-6199.

S-Editor: Fan JR
L-Editor: A
P-Editor: Fan JR

REFERENCES

1 National Institutes of Health Consensus Development Conference Statement: Management of hepatitis C 2002 (June 10-12, 2002). *Gastroenterology* 2002; **123**: 2082-2099 [PMID: 12454863 DOI: 10.1053/gast.2002.1232082]
2 **Chen SL**, Morgan TR. The natural history of hepatitis C virus (HCV) infection. *Int J Med Sci* 2006; **3**: 47-52 [PMID: 16614742 DOI: 10.7150/ijms.3.47]
3 **Roberts EA**, Yeung L. Maternal-infant transmission of hepatitis C virus infection. *Hepatology* 2002; **36**: S106-S113 [PMID: 12407583 DOI: 10.1053/jhep.2002.36792]
4 **Spera AM**, Eldin TK, Tosone G, Orlando R. Antiviral therapy for hepatitis C: Has anything changed for pregnant/Lactating women? *World J Hepatol* 2016; **8**: 557-565 [PMID: 27134703 DOI: 10.4254/wjh.v8.i12.557]
5 **Patrick SW**, Bauer AM, Warren MD, Jones TF, Wester C. Hepatitis C Virus Infection Among Women Giving Birth - Tennessee and United States, 2009-2014. *MMWR Morb Mortal Wkly Rep* 2017; **66**: 470-473 [PMID: 28493860 DOI: 10.15585/mmwr.mm6618a3]
6 **Koneru A**, Nelson N, Hariri S, Canary L, Sanders KJ, Maxwell JF, Huang X, Leake JA, Ward JW, Vellozzi C. Increased Hepatitis C Virus (HCV) Detection in Women of Childbearing Age and Potential Risk for Vertical Transmission - United States and Kentucky, 2011-2014. *MMWR Morb Mortal Wkly Rep* 2016; **65**: 705-710 [PMID: 27442053 DOI: 10.15585/mmwr.mm6528a2]
7 **Benova L**, Mohamoud YA, Calvert C, Abu-Raddad LJ. Vertical transmission of hepatitis C virus: systematic review and meta-analysis. *Clin Infect Dis* 2014; **59**: 765-773 [PMID: 24928290 DOI: 10.1093/cid/ciu447]
8 **Ceci O**, Margiotta M, Marello F, Francavilla R, Loizzi P, Francavilla A, Mautone A, Impedovo L, Ierardi E, Mastroianni M, Bettocchi S, Selvaggi L. Vertical transmission of hepatitis C virus in a cohort of 2,447 HIV-seronegative pregnant women: a 24-month prospective study. *J Pediatr Gastroenterol Nutr* 2001; **33**: 570-575 [PMID: 11740231 DOI: 10.1097/00005176-200111000-00011]
9 **Hayashida A**, Inaba N, Oshima K, Nishikawa M, Shoda A, Hayashida S, Negishi M, Inaba F, Inaba M, Fukasawa I, Watanabe H, Takamizawa H. Re-evaluation of the true rate of hepatitis C virus mother-to-child transmission and its novel risk factors based on our two prospective studies. *J Obstet Gynaecol Res* 2007; **33**: 417-422 [PMID: 17688606 DOI: 10.1111/j.1447-0756.2007.00582.x]
10 **Resti M**, Azzari C, Mannelli F, Moriondo M, Novembre E, de Martino M, Vierucci A. Mother to child transmission of hepatitis C virus: prospective study of risk factors and timing of infection in children born to women seronegative for HIV-1. Tuscany Study Group on Hepatitis C Virus Infection. *BMJ* 1998; **317**: 437-441 [PMID: 9703524 DOI: 10.1136/bmj.317.7156.437]
11 **Mok J**, Pembrey L, Tovo PA, Newell ML; European Paediatric Hepatitis C Virus Network. When does mother to child transmission of hepatitis C virus occur? *Arch Dis Child Fetal Neonatal Ed* 2005; **90**: F156-F160 [PMID: 15724041 DOI: 10.1136/adc.2004.059436]
12 **Arshad M**, El-Kamary SS, Jhaveri R. Hepatitis C virus infection during pregnancy and the newborn period--are they opportunities for treatment? *J Viral Hepat* 2011; **18**: 229-236 [PMID: 21392169 DOI: 10.1111/j.1365-2893.2010.01413.x]
13 **Pembrey L**, Newell ML, Tovo PA; EPHN Collaborators. The management of HCV infected pregnant women and their children European paediatric HCV network. *J Hepatol* 2005; **43**: 515-525 [PMID: 16144064 DOI: 10.1016/j.jhep.2005.06.002]
14 **AASLD**. HCV Guidance: Recommendations for Testing, Managing, and Treating Hepatitis C. [cited 10 February 2022].

Available from: https://wwwhcvguidelinesorg/evaluate/testing-and-linkage

15 **Society for Maternal-Fetal Medicine (SMFM)**; Hughes BL, Page CM, Kuller JA. Hepatitis C in pregnancy: screening, treatment, and management. *Am J Obstet Gynecol* 2017; **217**: B2-B12 [PMID: 28782502 DOI: 10.1016/j.ajog.2017.07.039]

16 **Duan Z**, Jia JD, Hou J, Lou L, Tobias H, Xu XY, Wei L, Zhuang H, Pan CQ. Current challenges and the management of chronic hepatitis C in mainland China. *J Clin Gastroenterol* 2014; **48**: 679-686 [PMID: 24921215 DOI: 10.1097/MCG.0000000000000109]

17 **Reddick KL**, Jhaveri R, Gandhi M, James AH, Swamy GK. Pregnancy outcomes associated with viral hepatitis. *J Viral Hepat* 2011; **18**: e394-e398 [PMID: 21692952 DOI: 10.1111/j.1365-2893.2011.01436.x]

18 **Connell LE**, Salihu HM, Salemi JL, August EM, Weldeselasse H, Mbah AK. Maternal hepatitis B and hepatitis C carrier status and perinatal outcomes. *Liver Int* 2011; **31**: 1163-1170 [PMID: 21745298 DOI: 10.1111/j.1478-3231.2011.02556.x]

19 **Pergam SA**, Wang CC, Gardella CM, Sandison TG, Phipps WT, Hawes SE. Pregnancy complications associated with hepatitis C: data from a 2003-2005 Washington state birth cohort. *Am J Obstet Gynecol* 2008; **199**: 38.e1-38.e9 [PMID: 18486089 DOI: 10.1016/j.ajog.2008.03.052]

20 **Money D**, Boucoiran I, Wagner E, Dobson S, Kennedy A, Lohn Z, Krajden M, Yoshida EM. Obstetrical and neonatal outcomes among women infected with hepatitis C and their infants. *J Obstet Gynaecol Can* 2014; **36**: 785-794 [PMID: 25222357 DOI: 10.1016/S1701-2163(15)30480-1]

21 **Dibba P**, Cholankeril R, Li AA, Patel M, Fayek M, Dibble C, Okpara N, Hines A, Ahmed A. Hepatitis C in Pregnancy. *Diseases* 2018; **6** [PMID: 29702563 DOI: 10.3390/diseases6020031]

22 **Epstein RL**, Espinosa C. Hepatitis C Virus in Neonates and Infants. *Clin Perinatol* 2021; **48**: 343-357 [PMID: 34030818 DOI: 10.1016/j.clp.2021.03.007]

23 **Geenes V**, Williamson C. Intrahepatic cholestasis of pregnancy. *World J Gastroenterol* 2009; **15**: 2049-2066 [PMID: 19418576 DOI: 10.3748/wjg.15.2049]

24 **Paternoster DM**, Fabris F, Palù G, Santarossa C, Bracciante R, Snijders D, Floreani A. Intra-hepatic cholestasis of pregnancy in hepatitis C virus infection. *Acta Obstet Gynecol Scand* 2002; **81**: 99-103 [PMID: 11942897]

25 **Locatelli A**, Roncaglia N, Arreghini A, Bellini P, Vergani P, Ghidini A. Hepatitis C virus infection is associated with a higher incidence of cholestasis of pregnancy. *Br J Obstet Gynaecol* 1999; **106**: 498-500 [PMID: 10430202 DOI: 10.1111/j.1471-0528.1999.tb08305.x]

26 **Rac MW**, Sheffield JS. Prevention and management of viral hepatitis in pregnancy. *Obstet Gynecol Clin North Am* 2014; **41**: 573-592 [PMID: 25454991 DOI: 10.1016/j.ogc.2014.08.004]

27 **Prasad MR**, Honegger JR. Hepatitis C virus in pregnancy. *Am J Perinatol* 2013; **30**: 149-159 [PMID: 23389935 DOI: 10.1055/s-0033-1334459]

28 **Floreani A**. Hepatitis C and pregnancy. *World J Gastroenterol* 2013; **19**: 6714-6720 [PMID: 24187446 DOI: 10.3748/wjg.v19.i40.6714]

29 **Salemi JL**, Whiteman VE, August EM, Chandler K, Mbah AK, Salihu HM. Maternal hepatitis B and hepatitis C infection and neonatal neurological outcomes. *J Viral Hepat* 2014; **21**: e144-e153 [PMID: 24666386 DOI: 10.1111/jvh.12250]

30 **Jaffery T**, Tariq N, Ayub R, Yawar A. Frequency of hepatitis C in pregnancy and pregnancy outcome. *J Coll Physicians Surg Pak* 2005; **15**: 716-719 [PMID: 16300710]

31 **Bohman VR**, Stettler RW, Little BB, Wendel GD, Sutor LJ, Cunningham FG. Seroprevalence and risk factors for hepatitis C virus antibody in pregnant women. *Obstet Gynecol* 1992; **80**: 609-613 [PMID: 1407881]

32 **Berkley EM**, Leslie KK, Arora S, Qualls C, Dunkelberg JC. Chronic hepatitis C in pregnancy. *Obstet Gynecol* 2008; **112**: 304-310 [PMID: 18669727 DOI: 10.1097/AOG.0b013e318180a4f3]

33 **Huang QT**, Hang LL, Zhong M, Gao YF, Luo ML, Yu YH. Maternal HCV infection is associated with intrauterine fetal growth disturbance: A meta-analysis of observational studies. *Medicine (Baltimore)* 2016; **95**: e4777 [PMID: 27583932 DOI: 10.1097/MD.0000000000004777]

34 **Nie QH**, Gao LH, Cheng YQ, Huang XF, Zhang YF, Luo XD, Wang JQ, Wang YY. Hepatitis C virus infection of human cytotrophoblasts cultured in vitro. *J Med Virol* 2012; **84**: 1586-1592 [PMID: 22930506 DOI: 10.1002/jmv.23380]

35 **Hurtado CW**, Golden-Mason L, Brocato M, Krull M, Narkewicz MR, Rosen HR. Innate immune function in placenta and cord blood of hepatitis C--seropositive mother-infant dyads. *PLoS One* 2010; **5**: e12232 [PMID: 20814429 DOI: 10.1371/journal.pone.0012232]

36 **Trevisanuto D**, Peruzzetto C, Cavallin F, Vedovato S, Cosmi E, Visentin S, Chiarelli S, Zanardo V. Fetal placental inflammation is associated with poor neonatal growth of preterm infants: a case-control study. *J Matern Fetal Neonatal Med* 2013; **26**: 1484-1490 [PMID: 23560517 DOI: 10.3109/14767058.2013.789849]

World Journal of Gastroenterology

Submit a Manuscript: https://www.f6publishing.com

World J Gastroenterol 2022 September 14; 28(34): 5036-5046

DOI: 10.3748/wjg.v28.i34.5036

ISSN 1007-9327 (print) ISSN 2219-2840 (online)

ORIGINAL ARTICLE

Retrospective Study

Trends in hospitalization for alcoholic hepatitis from 2011 to 2017: A USA nationwide study

Ali Wakil, Mujtaba Mohamed, Zaid Tafesh, Mumtaz Niazi, Raquel Olivo, Weiyi Xia, Patricia Greenberg, Nikolaos Pyrsopoulos

Specialty type: Gastroenterology and hepatology

Provenance and peer review: Unsolicited article; Externally peer reviewed.

Peer-review model: Single blind

Peer-review report's scientific quality classification
Grade A (Excellent): 0
Grade B (Very good): B
Grade C (Good): C, C, C
Grade D (Fair): 0
Grade E (Poor): 0

P-Reviewer: Lu XL, China; Radford-Smith DE, United Kingdom; Xu CF, China

Received: February 7, 2022
Peer-review started: February 7, 2022
First decision: April 10, 2022
Revised: May 1, 2022
Accepted: July 25, 2022
Article in press: July 25, 2022
Published online: September 14, 2022

Ali Wakil, Zaid Tafesh, Mumtaz Niazi, Raquel Olivo, Nikolaos Pyrsopoulos, Department of Gastroenterology and Hepatology, Rutgers New Jersey Medical School, Newark, NJ 07103, USA

Mujtaba Mohamed, Department of Gastroenterology and Hepatology, Marshall University Hospital, Huntington, WV 25701, USA

Weiyi Xia, Patricia Greenberg, Department of Biostatistics & Epidemiology, Rutgers School of Public Health, Piscataway, NJ 08854, USA

Corresponding author: Nikolaos Pyrsopoulos, FAASLD, AGAF, FRCP, MD, PhD, Chief Doctor, Professor, Department of Gastroenterology and Hepatology, Rutgers New Jersey Medical School, 185 S. Orange Avenue MSB H Rm - 536, Newark, NJ 07103, United States. pyrsopni@njms.rutgers.edu

Abstract

BACKGROUND

Severe alcoholic hepatitis (AH) is one of the most lethal manifestations of alcohol-associated liver disease. In light of the increase in alcohol consumption worldwide, the incidence of AH is on the rise, and data examining the trends of AH admission is needed.

AIM

To examine inpatient admission trends secondary to AH, along with their clinical outcomes and epidemiological characteristics.

METHODS

The National Inpatient Sample (NIS) database was utilized, and data from 2011 to 2017 were reviewed. We included individuals aged ≥ 21 years who were admitted with a primary or secondary diagnosis of AH using the International Classification of Diseases (ICD)-9 and its correspondent ICD-10 codes. Hepatitis not related to alcohol was excluded. The national estimates of inpatient admissions were obtained using sample weights provided by the NIS.

RESULTS

AH-related hospitalization demonstrated a significant increase in the USA from 281506 (0.7% of the total admission in 2011) to 324050 (0.9% of the total admi-ssion

in 2017). The median age was 54 years. The most common age group was 45–65 years (range 57.8%–60.7%). The most common race was white (63.2%–66.4%), and patients were predominantly male (69.7%–71.2%). The primary healthcare payers were Medicare (29.4%–30.7%) and Medicaid (21.5%–32.5%). The most common geographical location was the Southern USA (33.6%–34.4%). Most patients were admitted to a tertiary care center (50.2%–62.3%) located in urban areas. Mortality of AH in this inpatient sample was 5.3% in 2011 and 5.5% in 2017. The most common mortality-associated risk factors were acute renal failure (59.6%–72.1%) and gastrointestinal hemorrhage (17.2%–20.3%). The total charges were noted to range between $25242.62 and $34874.50.

CONCLUSION

The number of AH inpatient hospitalizations significantly increased from 2011 to 2017. This could have a substantial financial impact with increasing healthcare costs and utilization. AH-mortality remained the same.

Key Words: Alcoholic hepatitis; Cirrhosis; Fatty liver disease; Alcohol abuse

©The Author(s) 2022. Published by Baishideng Publishing Group Inc. All rights reserved.

Core tip: This study demonstrated a significant increase in the number of hospitalizations due to alcoholic-associated hepatitis (AH) throughout the USA, with an overall increase in the cost and financial burden of the disease. These trends were in line with the increase in the incidence of alcohol misuse across the years. This study provides potential data for future prospective research to help trigger more aggressive screening and prevention methods for alcohol abuse to prevent AH. Additionally, there is a need for the development of novel therapeutic agents targeting the disease since AH treatment is limited.

Citation: Wakil A, Mohamed M, Tafesh Z, Niazi M, Olivo R, Xia W, Greenberg P, Pyrsopoulos N. Trends in hospitalization for alcoholic hepatitis from 2011 to 2017: A USA nationwide study. *World J Gastroenterol* 2022; 28(34): 5036-5046

URL: https://www.wjgnet.com/1007-9327/full/v28/i34/5036.htm

DOI: https://dx.doi.org/10.3748/wjg.v28.i34.5036

INTRODUCTION

Alcohol-associated liver disease (ALD) comprises a spectrum of liver diseases ranging from reversible fatty liver to severe alcohol-associated hepatitis (AH) and cirrhosis, to acute-on-chronic liver failure[1]. All manifestations of ALD may overlap and can develop after heavy alcohol consumption for at least 6 mo[2]. AH is a clinical syndrome with acute onset jaundice in the presence of heavy alcohol misuse[2]. Mild AH patients with alcohol abstinence can have a good outcome. However, those with severe disease defined by Maddrey's discriminant function ≥ 32, or model for end-stage liver disease score ≥ 20, have a high 30-d mortality rate[1]. ALD is one of the leading causes of cirrhosis and it is the second leading indication for liver transplantation in the USA according to the Scientific Registry of Transplant Recipients data[3]. Alcohol consumption continues to be on the rise, with global data extrapolated from the World Health Organization showing the average annual per capita alcohol consumption has risen from 5.5 L in 2005 to 6.4 L in 2018[4]. Consequently, global alcohol-attributable mortality in 2016 has increased to 38.8 per 100000 people and 1759 disability-adjusted life-years per 100000 people[4]. According to a study from Denmark, during the study period (1999–2008), the annual incidence rate of AH was reported to increase for both men and women from 37 to 46 per 100000 and from 24 to 34 per 100 000, respectively[5]. The 5-year overall mortality in this study was found to be 56% and was significantly higher in patients with cirrhosis compared to patients without cirrhosis (69% *vs* 47%, respectively)[5]. In the USA, a study evaluating the United States National Inpatient Sample (NIS) database showed that out of 325 000 hospital admissions in 2010, 0.8% were AH-related[6]. With the availability of highly effective direct-acting antivirals therapy for chronic hepatitis C, the burden of chronic liver disease (CLD) is shifting towards ALD and non-ALD[7,8]. Studies have demonstrated that there is an increasing trend in consuming alcohol in the USA[9-12], with the initiation of alcohol at younger ages[13-15], and binging representing the most frequent pattern of alcohol consumption[16]. As a consequence of this upward trend in alcohol use disorder, it is anticipated that the correlating rise in ALD will have significant health, social and economic burdens accredited to the increase in hospitalization rate, as well as the elevated support required for these patients in an outpatient setting[8].

According to the 2007 NIS database, a significant healthcare cost and use of resources were reported [17]. Another study using the NIS database from 2012 to 2016, reported a higher admissions rate for CLD with a 26.2% increase in hospitalization costs and an $18.8 billion economic burden in 2016[18]. Despite the advances in medicine, the currently available therapeutics for severe AH are scarce and only limited to corticosteroids, which contributes to the high mortality of this disease[1].

Given the increased prevalence of alcohol misuse in the USA, this study aimed to provide a relatively recent descriptive analysis of trends in AH hospitalization within the USA. Data were obtained using the NIS database from 2011 to 2017.

MATERIALS AND METHODS

Data source

The Healthcare Cost and Utilization Project (HCUP) is a collection of databases and contains the NIS database[19]. The NIS is the largest publicly available inpatient database that encompasses a range of different data encoded by International Classification of Diseases (ICD) codes from more than 1000 hospitals, constituting a 20% sample data of all US hospitals. The database enables data extraction on a broad range of health conditions and specific populations, including cost and quality of health services, medical practice patterns, and outcomes of treatments on a national level.

Study design and study population

This was a retrospective analysis. All subjects in the database ≥ 21 years old who were hospitalized with a discharge diagnosis of AH from 2011 to 2017 were included. To minimize ascertainment bias, we classified hospitalization as AH-related if it was associated with a primary admission diagnosis of AH or a primary discharge diagnosis. A secondary AH-related hospitalization was classified as having the AH diagnosis anywhere in the admission diagnosis (25 diagnoses) or anywhere in the discharge diagnoses. We excluded all non-alcohol-related hepatitis diagnoses using ICD-9 and ICD-10. This included autoimmune hepatitis, acute and chronic viral hepatitis A–E, and nonalcoholic steatohepatitis. All data were weighted using discharge level values, to produce an accurate estimate of the patient population nationwide. AH-related hospitalization was identified by ICD-9 and ICD-10 discharge diagnosis codes. The ICD codes included were alcohol-associated hepatitis, alcoholic fatty liver disease, and alcohol-associated cirrhosis (Table 1). Previous validation studies have shown that the discharge diagnosis captures the cause of hospitalization accurately, such as in primary biliary cholangitis[20], coronary artery disease[21], and hepatitis B and C[11]. Other outcomes examined were inpatient mortality. We identified known risk factors related to mortality in patients with the following: acute renal failure (ARF), gastrointestinal bleeding, and sepsis (Table 2). Patient age, sex, household income, race, and geographic region (Northeast, Midwest, South and West) were obtained. The primary payer for the hospitalization was categorized as Medicare, Medicaid, private insurance, self-pay, or others. The types of hospitals were categorized into teaching, non-teaching community, and rural hospitals. Hospitalization characteristics were presented separately where the primary reason for hospitalization was AH *versus* AH presenting as a secondary condition. These characteristics included in-hospital mortality, length of stay, and discharge disposition.

Statistical analysis

Patients were first screened and selected based on the presence of an AH diagnosis. The temporal trend of the AH-related hospitalization was tested by Cochran–Armitage test. The patient demographics, additional clinical characteristics, and clinical outcome measures were then summarized using the median with interquartile range for continuous variables, or frequencies with percentages for categorical variables. To compare these variables among different years, Kruskal–Wallis and χ^2 tests were used. These demographics and variables were tested against the year. Overall and between-categorical group P values were reported for categorical variables. Prevalence of AH-related diagnosis among HCUP dataset and mortality-related risk factors among AH patients who died during hospitalization in 2011–2017 were tested using the χ^2 test. A multivariable logistic model was fitted and resulting odds ratios (OR) with 95% confidence intervals were used to test for association between the risk factors and the primary outcome of in-hospital mortality, further adjusting for demographics and additional clinical characteristics. Due to the desire to have population-level interpretations, survey weights were applied to all patient-level observations as provided in the NIS database. All reported P values were two-sided, and the significance cut-off was set at 0.05. The Bonferroni adjustment was used to adjust for multiple testing in between-categorical χ^2 test and logistic regression. Data analyses were completed in SAS version 9.4 (SAS Institute Inc., Cary, NC, USA) and R studio (R version 3.6.0, R Foundation for Statistical Computing, Vienna, Austria).

Table 1 Diagnosis to be included International Classification of Diseases-9 and its correspondent International Classification of Diseases-10

ICD-9	Correspondent ICD-10
571.0 alcoholic fatty liver	K.70 alcoholic fatty liver
571.1 acute alcoholic hepatitis	K.70.11 alcoholic hepatitis with ascites
	K.70.10 alcoholic hepatitis without ascites
571.2 alcoholic cirrhosis of liver	Correspondent ICD-10 found
571.3 alcoholic liver damage, unspecified	K70.40 alcoholic hepatic failure without coma
	K70.41 alcoholic hepatic failure with coma
	K70.9 alcoholic liver disease, unspecified

ICD: International Classification of Diseases.

Table 2 Trend of alcoholic hepatitis-related hospitalization 2011 to 2017

	2011	2012	2013	2014	2015	2016	2017	*P*
Total admission, *n*	38590733	36484846	35597792	35358818	35769942	35675421	35798453	
AH-related admission, *n* (%)	281506 (0.7)	274365 (0.8)	278580 (0.8)	291435 (0.8)	308765 (0.9)	313235 (0.9)	324050 (0.9)	< 0.001
Admission when primary admission diagnosis is AH, *n* (%)	47140 (0.1)	45710 (0.1)	46715 (0.1)	48395 (0.1)	54955 (0.2)	66170 (0.2)	71290 (0.2)	< 0.001

AH: Alcoholic hepatitis.

RESULTS

AH-related hospitalization showed an increase from 281506 (0.7% of the total in 2011) to 324050 (0.9% of the total in 2017; $P < 0.01$) (Figure 1). This included all AH-related admissions when AH was not the primary or secondary diagnosis. There was also an increase in the number of admissions when the primary admission diagnosis was AH (47140 in 2011 to 71290 in 2017) ($P < 0.01$; Table 2).

Results from demographic observations showed that the median age of patients hospitalized with AH was 54 years. The most common age group was 45–65 years (58.4%–60.7%; $P < 0.01$); the most common race was white (63.2%–66.4%; $P < 0.01$); patients were predominantly male (69.7%–71.2%; $P < 0.01$); and the primary healthcare payers were Medicare (29.4%–30.7%; $P < 0.01$) and Medicaid (21.5%–32.5%; $P < 0.01$). The most common geographical location was the southern region of the USA (33.6%–34.4%; $P = 0.017$). Most patients were admitted to tertiary hospitals (50.2%–62.3%; $P < 0.01$) in urban areas. The most common presenting diagnosis was AH (63.5%–69%; $P < 0.01$). The most common outcome was routine discharge (60%–63.3%; $P < 0.01$). The median length of stay was 5.98 d (SD = 7.11) in 2011 which increased to 6.14 d (SD = 7.43) in 2017 ($P < 0.01$). Total charge for hospitalized patients with AH ranged between $46507.47 (SD = 87193.29) and $63574.52 (SD = 108850.63; $P < 0.01$) (Table 3).

The mortality of AH-related hospitalizations was 5.3% in 2011 and 5.5% in 2017 ($P < 0.01$). Risk factors that could be associated with AH mortality were sepsis (increased from 7.4% in 2011 to 48.3% in 2017; $P < 0.01$), renal failure (59.6% in 2011 to 72.1% in 2018; $P < 0.01$), and gastrointestinal (GI) hemorrhage (17.2% in 2011 to 20.3% in 2017; $P = 0.048$) (Table 4). Multivariable regression analysis on death during hospitalization was performed and demonstrated higher odds of mortality in the following group: age > 65 years (OR 3.55; $P < 0.0001$), female (OR 1.13; $P < 0.0001$), large academic hospital (OR 1.3; $P < 0.0001$), sepsis (OR 3.33; $P < 0.0001$), GI hemorrhage (OR 2.31; $P < 0.0001$), and ARF (OR 7.19; $P < 0.0001$) (Table 5).

DISCUSSION

ALD is a spectrum of diseases ranging from hepatic steatosis to fibrosis and eventually cirrhosis, with continued alcohol use[22]. Alcohol consumption has been on the rise in the USA. Previously, a large survey conducted by the National Epidemiologic Survey showed a prevalence of alcohol use over any 12-mo period to rise from 65% to 72%, with an overall increase in alcohol consumption between 2001

Table 3 Summary statistics of demographic of hospitalized alcoholic hepatitis patients, 2011 to 2017

Characteristic	AH-related admission							*P*[1]	
	2011	2012	2013	2014	2015	2016	2017	Overall	Between-group
n	281506	274365	278580	291435	308765	313235	324050		
Age in years at admission [median (Q1, Q3)]	54.0 (46.0, 61.0)	54.0 (46.0, 61.0)	54.0 (46.0, 62.0)	54.0 (46.0, 62.0)	54.0 (46.0, 62.0)	54.0 (46.0, 62.0)	55.0 (46.0, 62.0)	< 0.001	
Age group (yr)								< 0.001	
< 25, *n* (%)	1545 (0.5)	1215 (0.4)	1135 (0.4)	1295 (0.4)	1320 (0.4)	1635 (0.5)	1535 (0.5)		0.011
25-44, *n* (%)	57738 (20.5)	57040 (20.8)	58155 (20.9)	61335 (21.0)	66670 (21.6)	69165 (22.1)	70935 (21.9)		< 0.001
45-64, *n* (%)	170876 (60.7)	166030 (60.5)	167810 (60.2)	174765 (60.0)	181845 (58.9)	182905 (58.4)	187350 (57.8)		< 0.001
≥65, *n* (%)	51348 (18.2)	50080 (18.3)	51480 (18.5)	54040 (18.5)	58930 (19.1)	59530 (19.0)	64230 (19.8)		< 0.001
Gender								< 0.001	
Male, *n* (%)	198491 (70.5)	195350 (71.2)	196820 (70.7)	203735 (69.9)	216650 (70.2)	218295 (69.7)	227080 (70.1)		< 0.001
Female, *n* (%)	83016 (29.5)	79000 (28.8)	81725 (29.3)	87615 (30.1)	92075 (29.8)	94810 (30.3)	96965 (29.9)		< 0.001
Missing, *n* (%)	0 (0.0)	15 (0.0)	35 (0.0)	85 (0.0)	40 (0.0)	130 (0.0)	5 (0.0)		
Race								< 0.001	
White, *n* (%)	178031 (63.2)	180550 (65.8)	183125 (65.7)	193560 (66.4)	202205 (65.5)	207155 (66.1)	214760 (66.3)		< 0.001
Black, *n* (%)	27402.8 (9.7)	27045 (9.9)	26625 (9.6)	27630 (9.5)	29145 (9.4)	28025 (8.9)	29290 (9.0)		< 0.001
Hispanic, *n* (%)	37280 (13.2)	36670 (13.4)	38575 (13.8)	38905 (13.3)	43390 (14.1)	45870 (14.6)	49135 (15.2)		< 0.001
Asian or Pacific Islander, *n* (%)	2235 (0.8)	2370 (0.9)	2680 (1.0)	2855 (1.0)	3565 (1.2)	3520 (1.1)	3840 (1.2)		< 0.001
Native American, *n* (%)	5056 (1.8)	5985 (2.2)	5720 (2.1)	5910 (2.0)	6725 (2.2)	7140 (2.3)	7565 (2.3)		< 0.001
Other, *n* (%)	7134 (2.5)	7760 (2.8)	6940 (2.5)	7785 (2.7)	7780 (2.5)	8305 (2.7)	9085 (2.8)		0.030
Missing, *n* (%)	24368.5 (8.7)	13985 (5.1)	14915 (5.4)	14790 (5.1)	15955 (5.2)	13220 (4.2)	10375 (3.2)		
Median household income national quartile for patient ZIP code								< 0.001	
$1-$38999, *n* (%)	79993 (28.4)	83510 (30.4)	80530 (28.9)	85525 (29.3)	95660 (31.0)	94940 (30.3)	95785 (29.6)		< 0.001
$39000-$47999, *n* (%)	69137 (24.6)	66095 (24.1)	71125 (25.5)	76895 (26.4)	72860 (23.6)	77800 (24.8)	83130 (25.7)		< 0.001
$48000-$62999, *n* (%)	68313 (24.3)	62360 (22.7)	65010 (23.3)	65695 (22.5)	72025 (23.3)	73690 (23.5)	75805 (23.4)		< 0.001
$63000 or more, *n* (%)	56576 (20.1)	53795 (19.6)	53035 (19.0)	54360 (18.7)	59515 (19.3)	58905 (18.8)	60560 (18.7)		< 0.001
Missing, *n* (%)	7487.7 (2.7)	8605 (3.1)	8880 (3.2)	8960 (3.1)	8705 (2.8)	7900 (2.5)	8770 (2.7)		
Primary expected payer								< 0.001	
Medicare, *n* (%)	82774 (29.4)	81905 (29.9)	85335 (30.6)	88860 (30.5)	93460 (30.3)	94160 (30.1)	99510 (30.7)		< 0.001
Medicaid, *n* (%)	60601 (21.5)	61975 (22.6)	62490 (22.4)	86040 (29.5)	96230 (31.2)	100255 (32.0)	105305 (32.5)		< 0.001
Private including HMO, *n* (%)	71261 (25.3)	65885 (24.0)	65405 (23.5)	70445 (24.2)	76095 (24.6)	75795 (24.2)	76200 (23.5)		< 0.001
Self-pay, *n* (%)	45272 (16.1)	43865	42785 (15.4)	31705	28095 (9.1)	27930 (8.9)	28890 (8.9)		< 0.001

		(16.0)		(10.9)				
No charge, *n* (%)	4980.6 (1.8)	3455 (1.3)	5330 (1.9)	3235 (1.1)	3195 (1.0)	2995 (1.0)	2610 (0.8)	< 0.001
Other, *n* (%)	15296.9 (5.4)	16515 (6.0)	16670 (6.0)	10555 (3.6)	11150 (3.6)	11625 (3.7)	10805 (3.3)	< 0.001
Missing, *n* (%)	1320 (0.5)	765 (0.3)	565 (0.2)	595 (0.2)	540 (0.2)	475 (0.2)	730 (0.2)	
Bed size of hospital								< 0.001
Small, *n* (%)	32567 (11.6)	36820 (13.4)	37640 (13.5)	54105 (18.6)	54870 (17.8)	57875 (18.5)	64035 (19.8)	< 0.001
Medium, *n* (%)	73628 (26.2)	77055 (28.1)	76680 (27.5)	86355 (29.6)	94260 (30.5)	91795 (29.3)	97445 (30.1)	< 0.001
Large, *n* (%)	175312 (62.3)	160490 (58.5)	164260 (59.0)	150975 (51.8)	159635 (51.7)	163565 (52.2)	162570 (50.2)	< 0.001
Region of hospital								0.001
Northeast, *n* (%)	53252 (18.9)	51120 (18.6)	51855 (18.6)	53795 (18.5)	56100 (18.2)	57590 (18.4)	59600 (18.4)	0.16
Midwest, *n* (%)	61095 (21.7)	59575 (21.7)	60330 (21.7)	64160 (22.0)	67170 (21.8)	68655 (21.9)	72150 (22.3)	0.42
South, *n* (%)	95441 (33.9)	94365 (34.4)	95705 (34.4)	98035 (33.6)	105260 (34.1)	105730 (33.8)	108555 (33.5)	0.017
West, *n* (%)	71718 (25.5)	69305 (25.3)	70690 (25.4)	75445 (25.9)	80235 (26.0)	81260 (25.9)	83745 (25.8)	0.046
Location teaching status of hospital								< 0.001
Rural, *n* (%)	28721 (10.2)	27135 (9.9)	26909.9 (9.7)	23195 (8.0)	23990 (7.8)	24250 (7.7)	25035 (7.7)	< 0.001
Urban non-teaching, *n* (%)	127976 (45.5)	113625 (41.4)	112610 (40.4)	84150 (28.9)	88965 (28.8)	87650 (28.0)	77930 (24.0)	< 0.001
Urban teaching, *n* (%)	124809 (44.3)	133605 (48.7)	139060 (49.9)	184090 (63.2)	195810 (63.4)	201335 (64.3)	221085 (68.2)	< 0.001

[1]Missing data is excluded from the *P* value calculation.
AH: Alcoholic hepatitis; HMO: Health Maintenance Organization.

Table 4 Mortality-related risk factors in alcoholic hepatitis patients who expired while hospitalized, 2011 to 2017

	2011	2012	2013	2014	2015	2016	2017	*P*
n	15002	14845	15310	15885	16385	17435	17785	
Sepsis, *n* (%)	1111 (7.4)	950 (6.4)	980 (6.4)	1170 (7.4)	2850 (17.4)	8145 (46.7)	8595 (48.3)	< 0.001
GI hemorrhage, *n* (%)	2582 (17.2)	2755 (18.6)	2715 (17.7)	3230 (20.3)	3025 (18.5)	3355 (19.2)	3395 (19.1)	0.042
Acute renal failure, *n* (%)	8941 (59.6)	9450 (63.7)	9780 (63.9)	10485 (66.0)	11265 (68.8)	12325 (70.7)	12825 (72.1)	< 0.001

GI: Gastrointestinal.

and 2012[23].

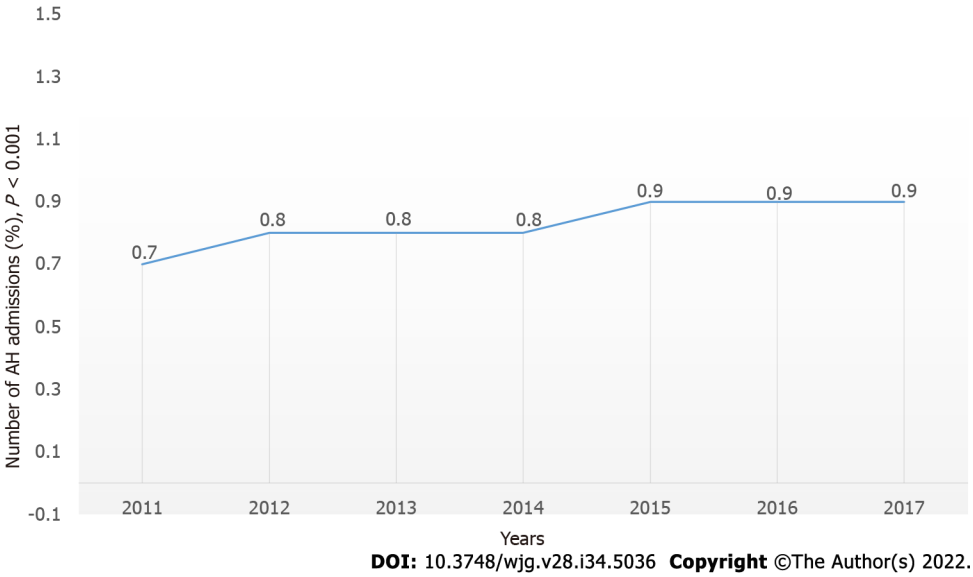
Our study included all AH-related admissions from 2011 to 2017 in the NIS database. Out of the 38.5 million admissions in 2011, about 281 506 (0.7%) were due to AH. This number increased to 324050 (0.9%) out of 35.7 million admissions in 2017 ($P < 0.001$; Figure 1). Moreover, the number of admissions due to a primary diagnosis of AH increased by almost 1.5 times between 2011 and 2017 from 47140 (0.1%) to 71290 (0.2%) ($P < 0.001$). These are alarming figures, and they match the results of increased alcohol consumption and binge drinking in the USA[8,12]. This has major consequences as AH continues to cause significant morbidity and mortality. Additionally, we found that each AH-related admission costs on average $46000 to $63000 with an average in-hospital length of stay of 4 d per admission. About 60% of those patients had Medicare or Medicaid insurance as the primary expected payer. These increasing admissions, as reported previously, escalates the burden on the healthcare system and the public payer funded by tax dollars[24].

Table 5 Multivariable logistic regression on death during hospitalization among alcoholic hepatitis-related admission[1] from 2011 to 2017

Variables	Levels	Odds ratio		
		Estimate	95% confidence interval	*P* after Bonferroni correction[2]
Age groups (yr)	< 25	1.0		Reference
	25-44	1.89	1.28-2.79	0.039
	45-64	2.85	1.93-4.21	< 0.0001
	65/65+	3.55	2.4-5.25	< 0.0001
Sex	Male	Reference		
	Female	1.13	1.09-1.17	< 0.0001
Race	White	1.0		Reference
	Black	0.82	0.77-0.86	< 0.0001
	Hispanic	0.94	0.9-0.98	0.20
	Asian or Pacific Islander	0.92	0.8-1.07	1.00
	Native American	1.04	0.94-1.15	1.00
	Other	1.12	1.02-1.22	0.36
Primary expected payer	Medicare	1.0		Reference
	Medicaid	1.12	1.07-1.18	0.00020
	Private including HMO	1.11	1.06-1.17	0.00025
	Self-pay	1.37	1.29-1.45	< 0.0001
	No charge	0.92	0.78-1.09	1.00
	Other	1.45	1.34-1.57	< 0.0001
Median household income national quartile for patient ZIP code	$1-$38999	1.0		Reference
	$39000-$47999	0.98	0.94-1.02	1.00
	$48000-$62999	0.95	0.92-1	0.84
	$63000 or more	0.9	0.86-0.94	0.00021
Bed size of hospital	Small	1.0		Reference
	Medium	1.2	1.14-1.26	< 0.0001
	Large	1.3	1.25-1.37	< 0.0001
Region of hospital	Northeast	1.0		Reference
	Midwest	0.91	0.87-0.96	0.0062
	South	1	0.96-1.05	1.00
	West	1.08	1.03-1.14	0.023
Location/teaching status of hospital	Rural	1.0		Reference
	Urban non-teaching	1.03	0.97-1.1	1.00
	Urban teaching	1.08	1.02-1.15	0.28
Sepsis	Yes	3.33	3.2-3.47	< 0.0001
GI hemorrhage	Yes	2.31	2.22-2.4	< 0.0001
Acute renal failure	Yes	7.19	6.96-7.42	< 0.0001

[1]Outcome is death during hospitalization (n = 1901436).
[2]P value adjusted by Bonferroni correction to account for multiple testing.

GI: Gastrointestinal; HMO: Health Maintenance Organization.



DOI: 10.3748/wjg.v28.i34.5036 **Copyright** ©The Author(s) 2022.

Figure 1 Trends in alcoholic hepatitis-related admissions from 2011 to 2017.

The increase in AH burden has a huge impact on trends of liver transplantation and consequently, organ allocation. Recent data showed that in select patients with severe AH, early liver transplantation resulted in high survival rates in the early transplant of AH at 6 mo *vs* no transplant (77% *vs* 23%)[25, 26]. Based on these results, many liver transplant centers around the USA are performing liver transplants for select severe AH patients. Consequently, this has resulted in ALD surpassing chronic hepatitis C virus infection as the leading indication for liver transplantation[27].

Our study showed that the majority of AH hospitalized individuals were middle-aged white men. This is not surprising, as more men consume alcohol above the recommended safety levels compared to women[24]; although women are more susceptible to developing AH within a shorter period and less exposure to alcohol compared to men[28].

We observed that the mortality of hospitalized patients with AH was about 5%, which has remained similar from 2011 to 2017. We also examined some of the major mortality-related risk factors among AH patients who expired during hospitalization. ARF was the most common finding in these patients and increased from 59.6% in 2011 to 72% in 2017. A possible explanation of these results may include the lack of therapy for severe AH with ARF since the benefit of steroids is unknown in this patient population as the steroids or pentoxifylline for AH trial excluded patients with ARF defined as creatinine > 5.7 mg/dL[29]. In addition, hepatorenal syndrome is associated with high mortality, which could be as high as 80% at 2 wk[30]. Sepsis and GI bleeding were also noted as mortality-risk factors in almost 48% and 19%, respectively, in patients who died from AH in 2017. Sepsis had a significant increase from 7.4% in 2014 to 46.7% in 2016 and 48.3% in 2017. This likely resulted from implementing the conversion of ICD-9 to ICD-10 on October 1, 2015. Sepsis is coded for by one code in ICD-9 (995.91), in contrast, there are 26 codes for different types of sepsis in ICD-10, which could potentially explain the sharp rise in sepsis rate. Additionally, AH patients usually present with fever and leukocytosis meeting Systemic Inflammatory Response Syndrome, criteria leading clinicians to code for sepsis even without an active infection present.

A regression analysis was performed that showed that advanced age, female gender, ARF, sepsis and GI bleeding were the most prominent risk factors. These mortality risk factors do not establish causality, since there is no etiology of death in the NIS database. Moreover, there is no information as to whether these risk factors were resolved or not during hospitalization since it was captured by the ICD codes used.

One limitation of this study was the accuracy of the NIS database in capturing ICD-9 and ICD-10 codes. For instance, some AH-related admissions could have been reported as jaundice or hepatic failure, which would exclude those patients from our analysis. There was also no information regarding the outcomes of AH patients once they were discharged. This has resulted in a lower in-hospital mortality rate (about 5%) compared to the established high 30-d mortality of AH patients (30%–50%) [31]. The mortality rate in our study is the percentage of patients who died while hospitalized only.

CONCLUSION

We observed that AH-related hospitalization continued to increase during the study period. This could have a substantial impact on increasing healthcare costs and utilization among patients hospitalized for AH. Mortality remained the same throughout the study period. These findings are alarming and should trigger more aggressive screening and prevention of alcohol abuse to prevent the increasing cases of AH and its consequences.

ARTICLE HIGHLIGHTS

Research background

Alcoholic hepatitis (AH) is a significant healthcare issue with rising alcohol use in the USA. Alcohol-associated liver disease is the second leading indication for liver transplantation after surpassing chronic hepatitis C infection.

Research motivation

With increasing alcohol consumption there is a need to measure the magnitude of AH effects.

Research objectives

The study aimed to examine the trends in hospitalization of AH patients across the USA. The second aim was to look at the mortality of hospitalized patients, along with the risk factors associated with death while hospitalized.

Research methods

Data were extracted from National Inpatient Sample database using discharge diagnosis codes of International Classification of Diseases (ICD)-9 and their corresponding ICD-10. We included hospitalization for the years from 2011 to 2017.

Research results

AH inpatient hospitalization increased from 0.7% of total admissions to 0.9% of total admissions. Mortality for admitted patients remained the same.

Research conclusions

There has been an increase in AH hospitalization that could affect the healthcare system. Acute renal failure, sepsis and gastrointestinal hemorrhage are highly associated with increased mortality in AH patients.

Research perspectives

New studies should focus on finding new therapeutic targets of AH. New studies should look for improved strategies to limit alcohol misuse.

FOOTNOTES

Author contributions: Wakil A contributed to the manuscript writing, methodology, editing, project administration; Mohamed M contributed to the manuscript writing and editing; Tafesh, Z, Olivo R and Niazi M contributed to the reviewing and editing; Greenberg P and Xia W contributed to the statistical analysis, data extraction; Pyrsopoulos N contributed to the supervision, reviewing and editing; all authors have read and approved the final manuscript.

Institutional review board statement: This study was done using the NIS database which does not require approval from the IRB, thus no IRB approval was needed for this study.

Informed consent statement: Patients were not required to give informed consent to the study because the analysis used anonymous clinical data using NIS database which contains no identifying patient information and does not require informed consent to use the data.

Conflict-of-interest statement: All authors have no relevant conflict of interest.

Data sharing statement: No additional data are available.

Open-Access: This article is an open-access article that was selected by an in-house editor and fully peer-reviewed by external reviewers. It is distributed in accordance with the Creative Commons Attribution NonCommercial (CC BY-NC 4.0) license, which permits others to distribute, remix, adapt, build upon this work non-commercially, and license

their derivative works on different terms, provided the original work is properly cited and the use is non-commercial. See: https://creativecommons.org/Licenses/by-nc/4.0/

Country/Territory of origin: United States

ORCID number: Ali Wakil 0000-0002-9377-4691; Mujtaba Mohamed 0000-0003-2067-817X; Zaid Tafesh 0000-0002-3927-9569; Mumtaz Niazi 0000-0002-4740-5131; Raquel Olivo 0000-0003-3845-5900; Weiyi Xia 0000-0002-1435-266X; Patricia Greenberg 0000-0001-6652-5019; Nikolaos Pyrsopoulos 0000-0002-6950-8174.

Corresponding Author's Membership in Professional Societies: American Association for the Study of Liver Diseases, No. 218688; American College of Gastroenterology.

S-Editor: Yan JP
L-Editor: Kerr C
P-Editor: Yan JP

REFERENCES

1 **Gao B**, Bataller R. Alcoholic liver disease: pathogenesis and new therapeutic targets. *Gastroenterology* 2011; **141**: 1572-1585 [PMID: 21920463 DOI: 10.1053/j.gastro.2011.09.002]
2 **Singal AK**, Kamath PS, Gores GJ, Shah VH. Alcoholic hepatitis: current challenges and future directions. *Clin Gastroenterol Hepatol* 2014; **12**: 555-64; quiz e31 [PMID: 23811249 DOI: 10.1016/j.cgh.2013.06.013]
3 **Kwong AJ**, Kim WR, Lake JR, Smith JM, Schladt DP, Skeans MA, Noreen SM, Foutz J, Booker SE, Cafarella M, Snyder JJ, Israni AK, Kasiske BL. OPTN/SRTR 2019 Annual Data Report: Liver. *Am J Transplant* 2021; **21** Suppl 2: 208-315 [PMID: 33595192 DOI: 10.1111/ajt.16494]
4 **World Health Organization**. Global Status Report on Alcohol and Health 2018. Poznyak V, Rekve D, editor. Geneva: World Health Organization, 2018
5 **Sandahl TD**, Jepsen P, Thomsen KL, Vilstrup H. Incidence and mortality of alcoholic hepatitis in Denmark 1999-2008: a nationwide population based cohort study. *J Hepatol* 2011; **54**: 760-764 [PMID: 21126790 DOI: 10.1016/j.jhep.2010.07.016]
6 **Singal AK**, Kuo YF, Anand BS. Hepatitis C virus infection in alcoholic hepatitis: prevalence patterns and impact on in-hospital mortality. *Eur J Gastroenterol Hepatol* 2012; **24**: 1178-1184 [PMID: 22735607 DOI: 10.1097/MEG.0b013e328355cce0]
7 **Williams R**. The pervading influence of alcoholic liver disease in hepatology. *Alcohol Alcohol* 2008; **43**: 393-397 [PMID: 18385413 DOI: 10.1093/alcalc/agn013]
8 **Neff GW**, Duncan CW, Schiff ER. The current economic burden of cirrhosis. *Gastroenterol Hepatol (N Y)* 2011; **7**: 661-671 [PMID: 22298959]
9 **Yörük BK**. Legalization of Sunday alcohol sales and alcohol consumption in the United States. *Addiction* 2014; **109**: 55-61 [PMID: 24103041 DOI: 10.1111/add.12358]
10 **Xuan Z**, Nelson TF, Heeren T, Blanchette J, Nelson DE, Gruenewald P, Naimi TS. Tax policy, adult binge drinking, and youth alcohol consumption in the United States. *Alcohol Clin Exp Res* 2013; **37**: 1713-1719 [PMID: 23711219 DOI: 10.1111/acer.12152]
11 **Niu B**, Forde KA, Goldberg DS. Coding algorithms for identifying patients with cirrhosis and hepatitis B or C virus using administrative data. *Pharmacoepidemiol Drug Saf* 2015; **24**: 107-111 [PMID: 25335773 DOI: 10.1002/pds.3721]
12 **Shirazi F**, Singal AK, Wong RJ. Alcohol-associated Cirrhosis and Alcoholic Hepatitis Hospitalization Trends in the United States. *J Clin Gastroenterol* 2021; **55**: 174-179 [PMID: 32520887 DOI: 10.1097/MCG.0000000000001378]
13 **Siegel M**, DeJong W, Naimi TS, Heeren T, Rosenbloom DL, Ross C, Ostroff J, Jernigan DH. Alcohol brand preferences of underage youth: results from a pilot survey among a national sample. *Subst Abus* 2011; **32**: 191-201 [PMID: 22014249 DOI: 10.1080/08897077.2011.601250]
14 **Miller TR**, Levy DT, Spicer RS, Taylor DM. Societal costs of underage drinking. *J Stud Alcohol* 2006; **67**: 519-528 [PMID: 16736071 DOI: 10.15288/jsa.2006.67.519]
15 **Siegel MB**, Naimi TS, Cremeens JL, Nelson DE. Alcoholic beverage preferences and associated drinking patterns and risk behaviors among high school youth. *Am J Prev Med* 2011; **40**: 419-426 [PMID: 21406275 DOI: 10.1016/j.amepre.2010.12.011]
16 **Bor J**, Basu S, Coutts A, McKee M, Stuckler D. Alcohol use during the great recession of 2008-2009. *Alcohol Alcohol* 2013; **48**: 343-348 [PMID: 23360873 DOI: 10.1093/alcalc/agt002]
17 **Jinjuvadia R**, Liangpunsakul S; Translational Research and Evolving Alcoholic Hepatitis Treatment Consortium. Trends in Alcoholic Hepatitis-related Hospitalizations, Financial Burden, and Mortality in the United States. *J Clin Gastroenterol* 2015; **49**: 506-511 [PMID: 25198164 DOI: 10.1097/MCG.0000000000000161]
18 **Hirode G**, Saab S, Wong RJ. Trends in the Burden of Chronic Liver Disease Among Hospitalized US Adults. *JAMA Netw Open* 2020; **3**: e201997 [PMID: 32239220 DOI: 10.1001/jamanetworkopen.2020.1997]
19 **Myers RP**, Shaheen AA, Fong A, Wan AF, Swain MG, Hilsden RJ, Sutherland L, Quan H. Validation of coding algorithms for the identification of patients with primary biliary cirrhosis using administrative data. *Can J Gastroenterol* 2010; **24**: 175-182 [PMID: 20352146 DOI: 10.1155/2010/237860]
20 **Rawson NS**, Malcolm E. Validity of the recording of ischaemic heart disease and chronic obstructive pulmonary disease in the Saskatchewan health care datafiles. *Stat Med* 1995; **14**: 2627-2643 [PMID: 8619104 DOI: 10.1002/sim.4780142404]

21 **Agency for Healthcare Research and Quality**. Overview of the National (Nationwide) Inpatient Sample (NIS). Sep 13, 2021. [cited Feb 6, 2022]. Available from: http://www.hcup-us.ahrq.gov/nisoverview.jsp

22 **O'Shea RS**, Dasarathy S, McCullough AJ; Practice Guideline Committee of the American Association for the Study of Liver Diseases; Practice Parameters Committee of the American College of Gastroenterology. Alcoholic liver disease. *Hepatology* 2010; **51**: 307-328 [PMID: 20034030 DOI: 10.1002/hep.23258]

23 **Grant BF**, Chou SP, Saha TD, Pickering RP, Kerridge BT, Ruan WJ, Huang B, Jung J, Zhang H, Fan A, Hasin DS. Prevalence of 12-Month Alcohol Use, High-Risk Drinking, and DSM-IV Alcohol Use Disorder in the United States, 2001-2002 to 2012-2013: Results From the National Epidemiologic Survey on Alcohol and Related Conditions. *JAMA Psychiatry* 2017; **74**: 911-923 [PMID: 28793133 DOI: 10.1001/jamapsychiatry.2017.2161]

24 **Mathurin P**, Moreno C, Samuel D, Dumortier J, Salleron J, Durand F, Castel H, Duhamel A, Pageaux GP, Leroy V, Dharancy S, Louvet A, Boleslawski E, Lucidi V, Gustot T, Francoz C, Letoublon C, Castaing D, Belghiti J, Donckier V, Pruvot FR, Duclos-Vallée JC. Early liver transplantation for severe alcoholic hepatitis. *N Engl J Med* 2011; **365**: 1790-1800 [PMID: 22070476 DOI: 10.1056/NEJMoa1105703]

25 **Crabb DW**, Im GY, Szabo G, Mellinger JL, Lucey MR. Diagnosis and Treatment of Alcohol-Associated Liver Diseases: 2019 Practice Guidance From the American Association for the Study of Liver Diseases. *Hepatology* 2020; **71**: 306-333 [PMID: 31314133 DOI: 10.1002/hep.30866]

26 **Goldberg D**, Ditah IC, Saeian K, Lalehzari M, Aronsohn A, Gorospe EC, Charlton M. Changes in the Prevalence of Hepatitis C Virus Infection, Nonalcoholic Steatohepatitis, and Alcoholic Liver Disease Among Patients With Cirrhosis or Liver Failure on the Waitlist for Liver Transplantation. *Gastroenterology* 2017; **152**: 1090-1099.e1 [PMID: 28088461 DOI: 10.1053/j.gastro.2017.01.003]

27 **Liangpunsakul S**. Clinical characteristics and mortality of hospitalized alcoholic hepatitis patients in the United States. *J Clin Gastroenterol* 2011; **45**: 714-719 [PMID: 21085006 DOI: 10.1097/MCG.0b013e3181fdef1d]

28 **Roerecke M**, Vafaei A, Hasan OSM, Chrystoja BR, Cruz M, Lee R, Neuman MG, Rehm J. Alcohol Consumption and Risk of Liver Cirrhosis: A Systematic Review and Meta-Analysis. *Am J Gastroenterol* 2019; **114**: 1574-1586 [PMID: 31464740 DOI: 10.14309/ajg.0000000000000340]

29 **Thursz MR**, Richardson P, Allison M, Austin A, Bowers M, Day CP, Downs N, Gleeson D, MacGilchrist A, Grant A, Hood S, Masson S, McCune A, Mellor J, O'Grady J, Patch D, Ratcliffe I, Roderick P, Stanton L, Vergis N, Wright M, Ryder S, Forrest EH; STOPAH Trial. Prednisolone or pentoxifylline for alcoholic hepatitis. *N Engl J Med* 2015; **372**: 1619-1628 [PMID: 25901427 DOI: 10.1056/NEJMoa1412278]

30 **Ginès A**, Escorsell A, Ginès P, Saló J, Jiménez W, Inglada L, Navasa M, Clària J, Rimola A, Arroyo V. Incidence, predictive factors, and prognosis of the hepatorenal syndrome in cirrhosis with ascites. *Gastroenterology* 1993; **105**: 229-236 [PMID: 8514039 DOI: 10.1016/0016-5085(93)90031-7]

31 **Lucey MR**, Mathurin P, Morgan TR. Alcoholic hepatitis. *N Engl J Med* 2009; **360**: 2758-2769 [PMID: 19553649 DOI: 10.1056/NEJMra0805786]

World Journal of Gastroenterology

Submit a Manuscript: https://www.f6publishing.com

World J Gastroenterol 2022 September 14; 28(34): 5047-5057

DOI: 10.3748/wjg.v28.i34.5047

ISSN 1007-9327 (print) ISSN 2219-2840 (online)

ORIGINAL ARTICLE

Retrospective Study

Analysis of invasiveness and tumor-associated macrophages infiltration in solid pseudopapillary tumors of pancreas

Jie Yang, Chun-Lu Tan, Dan Long, Yan Liang, Li Zhou, Xu-Bao Liu, Yong-Hua Chen

Specialty type: Gastroenterology and hepatology

Provenance and peer review: Unsolicited article; Externally peer reviewed.

Peer-review model: Single blind

Peer-review report's scientific quality classification

Grade A (Excellent): A
Grade B (Very good): 0
Grade C (Good): C
Grade D (Fair): 0
Grade E (Poor): 0

P-Reviewer: Kitamura K, Japan; Rahmati M, Iran

Received: May 17, 2022
Peer-review started: May 17, 2022
First decision: August 1, 2022
Revised: August 5, 2022
Accepted: August 25, 2022
Article in press: August 25, 2022
Published online: September 14, 2022

Jie Yang, Chun-Lu Tan, Xu-Bao Liu, Yong-Hua Chen, Department of Pancreatic Surgery, West China Hospital, Sichuan University, Chengdu 610041, Sichuan Province, China

Dan Long, Key Laboratory of Transplant Engineering and Immunology of the Ministry of Health, West China Hospital, Sichuan University, Chengdu 610041, Sichuan Province, China

Yan Liang, Li Zhou, Core Facilities, West China Hospital, Sichuan University, Chengdu 610041, Sichuan Province, China

Corresponding author: Yong-Hua Chen, MD, Professor, Department of Pancreatic Surgery, West China Hospital, Sichuan University, No. 37 Guoxue Alley, Wuhou District, Chengdu 610041, Sichuan Province, China. chenyonghua2007@163.com

Abstract

BACKGROUND

Solid pseudopapillary tumor (SPT) is a rare pancreatic tumor. Considering its malignant behaviors, SPT has been classified as a low-grade malignant tumor. Indeed, only 9.2% of all SPT patients are initially diagnosed as malignant with invasion or metastasis. Thus, one of the challenges in managing SPT patients is predicting malignant behavior.

AIM

To investigate the malignant behavior and tumor-associated macrophage (TAM) infiltration between different histopathologic features of SPT patients.

METHODS

Twenty-five formalin-fixed paraffin-embedded tissue samples from 22 patients pathologically diagnosed with an SPT between 2009 and 2019 at West China Hospital were included in this retrospective study. Integrity of the capsule and growth pattern of the tumor cells was assessed microscopically in hematoxylin-eosin (HE)-stained sections. Based on the histopathological features, the SPT patients were divided into two groups: capsule or invasion. Clinical features, malignant behavior, and TAM infiltration were compared between the two groups.

RESULTS

Among the 22 SPT patients, 11 were identified for each group, having either a capsule or invasion histopathologic feature. Malignant behavior was more frequent in the invasion group, including 2 patients who had peripheral organ

invasion, 3 with liver metastasis, and 1 with both lymph node and spleen metastases (P= 0.045). Ki-67 index of more than 3% was also more frequent in the invasion group (P = 0.045). Immunohistochemical analysis showed that the invasion group had a significant increase of CD68-positive TAMs in intratumor and peritumor sites in comparison with the capsule group (all P < 0.0001). Similarly, CD163-positive M2-like macrophages were also markedly increased in the intratumor and peritumor sites in the invasion group (all P < 0.0001). At the liver metastasis site, both intratumor and peritumor tissues showed relatively high-level CD68-positive TAMs and CD163-positive M2-like macrophages infiltration. However, the differences between the intratumor, peritumor and normal hepatic tissues did not reach statistical significance (all P > 0.05).

CONCLUSION

SPT patients with invasion evident under microscope were more likely to exhibit malignant behavior and TAM infiltration, especially M2-like macrophages. This finding can help in future investigations of the underlying mechanism of TAM-mediated SPT malignant behavior.

Key Words: Pancreatic neoplasms; Solid pseudopapillary tumors; Malignancy; Tumor-associated macrophages; Histological labeling; Immunohistochemistry

©The Author(s) 2022. Published by Baishideng Publishing Group Inc. All rights reserved.

Core Tip: In the present study, we reviewed 22 solid pseudopapillary tumor (SPT) patients to investigate the malignant behavior and tumor-associated macrophage (TAM) infiltration between different histopathologic features. The results showed that invasion detected under microscope was associated with the malignant behavior and TAM infiltration. The phenomenon of increased infiltration of TAMs, especially M2-like macrophages in the invasion feature, might help us to investigate the underlying mechanism of TAM-mediated SPT malignant behavior, as well as to potentially treat recurrent and metastatic SPT by targeting TAMs.

Citation: Yang J, Tan CL, Long D, Liang Y, Zhou L, Liu XB, Chen YH. Analysis of invasiveness and tumor-associated macrophages infiltration in solid pseudopapillary tumors of pancreas. *World J Gastroenterol* 2022; 28(34): 5047-5057

URL: https://www.wjgnet.com/1007-9327/full/v28/i34/5047.htm

DOI: https://dx.doi.org/10.3748/wjg.v28.i34.5047

INTRODUCTION

Solid pseudopapillary tumor (SPT) is a rare pancreatic tumor, first reported by Frantz in 1959[1]. Considering its malignant behaviors, including the invasion of peripheral organs and metastasis at diagnosis or recurrence after surgical resection, the World Health Organization (WHO) has classified SPT as a low-grade malignant tumor[2,3]. The overall prognosis of SPT patients is good, with 5-year and 10-year survival rates up to 89.5% and 86.3%, respectively[4]. Reportedly, among all SPT patients, only 9.2% are initially diagnosed as malignant with invasion or metastasis[3]. Thus, one of the challenges in managing SPT patients lies in predicting malignant behavior.

Currently, clinical features are being studied to predict the malignant behaviors of SPT. For instance, patients over 40 years of age have been found to be more likely to develop malignant SPT[5,6]. The computed tomography (CT) imaging features of multiple and geographic uptake type and progressive enhancement during the delayed phase have shown potential predictive power[6,7]. One of the most frequently mentioned predictive factors is capsule or incomplete capsule of SPT, with the latter being significantly correlated with malignancy[1,5,8-10]. However, the capsule or incomplete capsule state is primarily assessed on CT imaging. Assessment of the integrity of a capsule and growth pattern of tumor cells, especially on SPT margins under the microscope, might reflect the real biological behavior of SPT.

Macrophages that infiltrate or surround the tumor microenvironment are termed as tumor-associated macrophages (TAMs)[11]. TAMs, especially those of the M2-like macrophage subtype, could enhance tumor invasion and metastasis[12]. However, only limited studies are available regarding the role of TAMs in the SPT microenvironment and their relationship with malignant behavior of SPT. Herein, we classified SPT patients in either a capsule group or invasion group based on the integrity of capsule and growth pattern of tumor cells determined microscopically, and compared the clinical features and malignant behaviors between the two groups. Furthermore, we used immunohistochemical (IHC) staining to analyze the infiltration of TAMs, especially the M2-like macrophages, in primary SPT and

liver metastasis sites.

MATERIALS AND METHODS

Patients and tissues

Twenty-five formalin-fixed paraffin-embedded tissue samples (including 22 tumors and peritumor tissues, and 3 metastatic sites) from 22 patients pathologically diagnosed with an SPT according to WHO 2010 criteria between 2009 and 2019 at West China Hospital were included in this retrospective study. All the samples were obtained by surgery and reviewed by two expert pathologists blinded to the original data. This study was approved by the biomedical ethics committee from our hospital with written informed consent from all subjects (2014 Trial No. 37).

Data collection and definition

Based on the integrity of the capsule and growth pattern of tumor cells, especially on tumor margins, evident in hematoxylin-eosin (HE)-stained sections under a microscope, SPT patients were divided into two groups: the capsule or invasion group. The invasion feature was defined as a tumor with an incomplete fibrous capsule with tumor cells invasively present in normal pancreatic tissue, as determined microscopically. On the other hand, a capsule feature is considered when the tumor has an intact fibrous envelope (Figure 1).

The malignant behaviors of SPT at diagnosis, including deep infiltration into the surrounding tissue and lymph node or distant organ metastasis, were recorded. The Ki-67 index was measured based on a manual visual counting method[13], and 3% was chosen as the cut-off value, according to findings from a recent study[14].

Clinical data was collected, including sex, age, serum tumor marker CA19-9, CA125, carcinoembryonic antigen, and neuron-specific enolase (NSE). Tumor size (largest diameter of the tumor), tumor location (head and neck or body and tail), component of the tumor (solid and cystic or solid), capsule or incomplete capsule, and calcification were also measured based on the CT imaging data and surgical specimens.

IHC analysis

IHC staining was used to evaluate the intratumoral and peritumoral presence of TAMs (CD68-positive) and M2-like macrophages (CD163-positive), a subtype of TAM, in primary and metastasis site tissues. Five micrometer-thick sequential tissue sections were obtained from paraffin-embedded tissue samples and used for the IHC analysis as described in previous studies[15,16]. The primary antibodies used in IHC staining were antibodies against CD68 (rabbit anti-human, D4B9C, dilution 1:400; Cell Signaling Technology, Danvers, MA, United States) and CD163 (rabbit anti-human, D6U1J, dilution 1:500; Cell Signaling Technology). Anti-rabbit IgG, horseradish peroxidase-linked antibody was used as the secondary antibody. For the assessment of expression of CD68- and CD163-positive cells, the tissue sections were screened using each immunohistochemistry slide at the low power fields (× 4), and the hot spots were selected. Immune cell staining was scored by counting the number of stained immune cells in three high power fields (× 400) in the hot spots. IHC sections were independently assessed by three authors (Yang J, Chen YH, and Zhou L).

Statistical methods

All statistical analyses were carried out using Statistical Package for Social Sciences (SPSS) Version 24 (IBM Corp., Armonk, NY, United States). Categorical variables are expressed as percentages (%), and continuous variables are expressed as medians. Normality and homogeneity of the data were assessed by Shapiro–Wilk's and Levene's tests, respectively. Fisher's exact test and Mann–Whitney test were used to detect di□erences in categorical and continuous variables between groups of patients. A P value < 0.05 was considered statistically significant.

RESULTS

Patient characteristics

Among the 22 SPT patients, 11 were identified for each group based on the capsule or invasion histopathologic feature, respectively. The clinical and pathological characteristics between the capsule and invasion groups are shown in Table 1. The patients included 4 males and 18 females, ranging in age from 12 years to 65 years (median age of 35 years) and showed no difference between the two groups (P = 0.586 and P= 0.146, respectively). Only 3 patients showed CA19-9 or CA125 elevation in the invasion group. Interestingly, 2 patients in the capsule group and 5 in the invasion group showed positivity for NSE, although the difference did not reach statistical significance (P = 0.361). All 22 patients received surgical treatment, which included 4 pancreaticoduodenectomies, 10 distal pancreatectomies, 7 central

Table 1 Clinical and pathological characteristics between capsule and invasion solid pseudopapillary tumor patients

	Capsule group, *n* = 11	Invasion group, *n* = 11	*P* value
Age, yr (Median, range)	26 (12, 46)	36 (15, 65)	0.146
Sex (Female)	10	8	0.586
Positive serum tumor marker			
CA19-9	0	1	1.000
CA125	0	2	0.476
CEA	0	0	-
NSE	2	5	0.361
Surgical procedure			-
Pancreaticoduodenectomy	1	3	
Distal pancreatectomy	5	5	
Total pancreatectomy	1	0	
Central pancreatectomy	4	3	
Combined segmental hepatectomy	0	3	
Tumor size (Median, range)	4.8 (2.0-8.1)	4.0 (1.3-8.8)	0.834
Tumor location			1.000
Head and neck	6	5	
Body and tail	5	6	
Component of the tumor			0.387
Solid	3	6	
Solid and cystic	8	5	
Calcification	3	2	1.000
Capsule assessed by CT imaging	9	2	0.004
Peripheral organ invasion	0	2	0.476
Metastasis	0	4[a]	0.045
Lymph node	0	1	
Liver	0	3	
Spleen	0	1	
Ki-67 Index > 3%	0	4	0.045

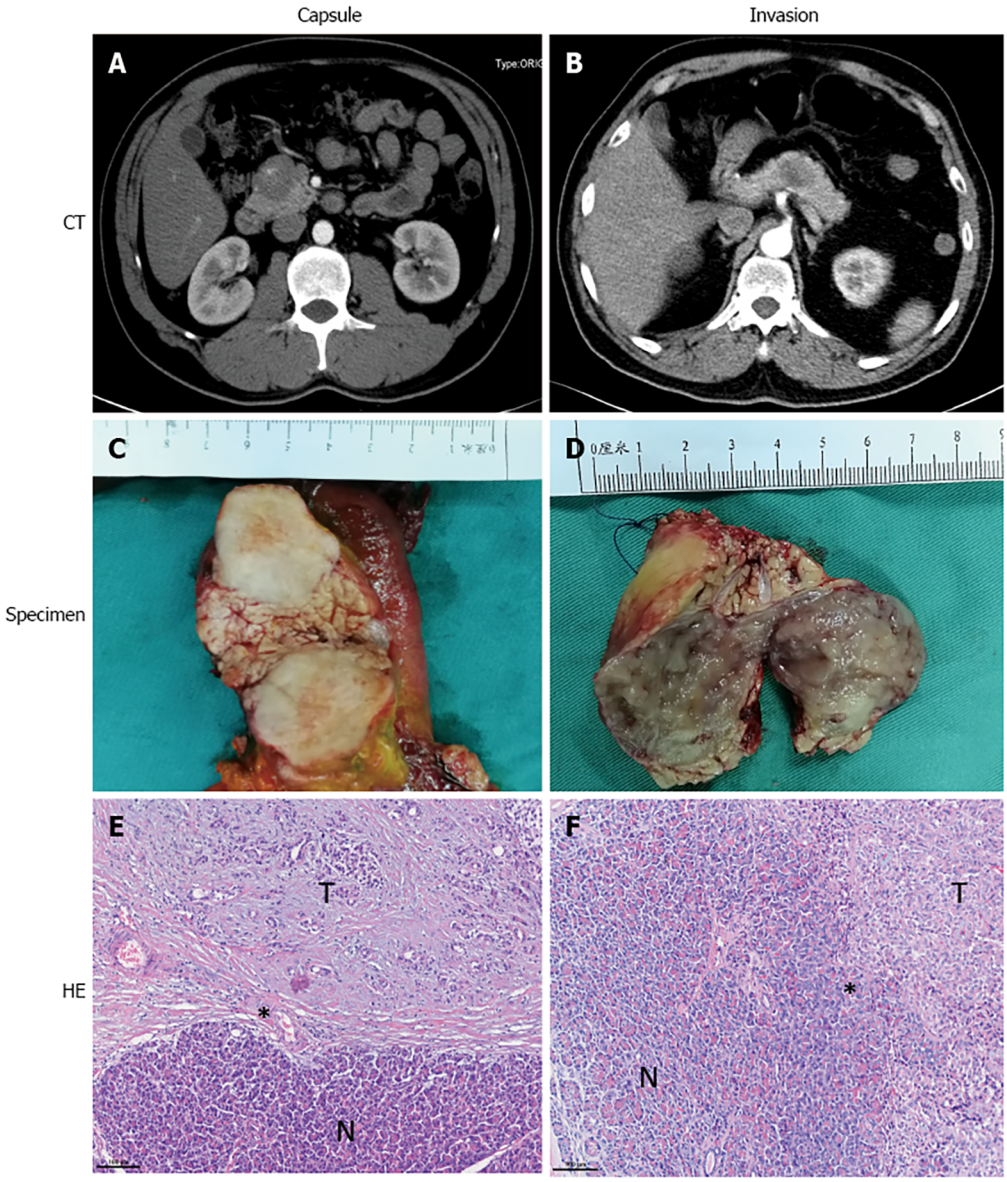
[a]1 patient had both spleen and lymph node metastasis.
CEA: Carcino-embryonic antigen; CT: Computed tomography; NSE: Neuron-specific enolase.

pancreatectomies, and 1 total pancreatectomy. All 3 patients with liver metastasis received combined segmental hepatectomy.

No difference was evident in tumor size, location, component, nor calcification between the two groups. However, compared with the capsule group, malignant behavior of SPTs was more frequent in the invasion group, including in 2 patients with peripheral organ invasion, 3 with liver metastasis, and 1 with lymph node and spleen metastases (P = 0.045). Furthermore, Ki-67 index more than 3% was also more frequent in the invasion group (P = 0.045).

TAM infiltration in primary tumor site

Since the invasion group had increased malignant behavior compared with the capsule group, we compared the infiltration of TAMs in the SPT microenvironment between the two groups. All primary tumor samples of the 22 patients showed positivity for macrophage and M2-like macrophage infiltration in IHC analysis. Although the intratumoral macrophage infiltration was increased in both groups compared with normal pancreatic tissue, the invasion group had a significant increase of intratumoral macrophage infiltration compared with the capsule group (all P < 0.0001; Figure 2A-C). A similar trend



DOI: 10.3748/wjg.v28.i34.5047 **Copyright** ©The Author(s) 2022.

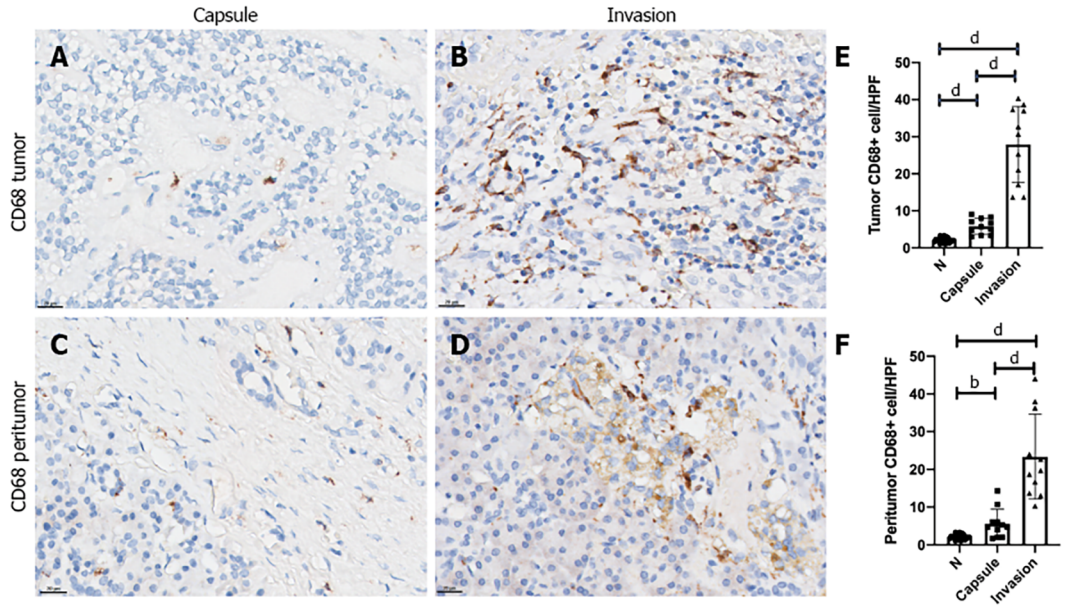
Figure 1 Computed tomography imaging, specimen and histopathologic features of capsulized and invasive solid pseudopapillary tumors. A, C and E: For the capsulized solid pseudopapillary tumors (SPTs), computed tomography (CT) imaging (A) and specimen (C) showed a clear distinction from surrounding pancreatic tissue, and an intact fibrous envelope on the tumor margin on hematoxylin and eosin (HE)-stained section (E); B, D and F: Invasive SPT was indistinguishable from surrounding normal pancreatic tissue on CT imaging (B) and in the specimen (D), and tumor cells showed infiltrative growth into normal pancreatic tissue on HE-stained section (F). N: Normal pancreas tissue; T: Tumor. *Tumor margin.

was observed for infiltrated peritumor macrophages. The TAM infiltration in peritumoral tissue, especially in the tumor margin, was markedly increased in the invasion group compared with capsule group ($P < 0.0001$; Figure 2D-F).

As a subtype of TAMs, the expression of CD163-positive M2-like macrophages was relatively low compared with CD68-positive TAMs. Elevation in both intratumor and peritumor sites in both the invasion group and capsule group compared with the normal pancreas tissue was evident by IHC (all $P < 0.0001$; Figure 3). Similarly, the expression of CD163-positive M2-like macrophages was also markedly increased in the intratumor and peritumor sites in the invasion group in comparison to the capsule group (all $P < 0.0001$; Figure 3).

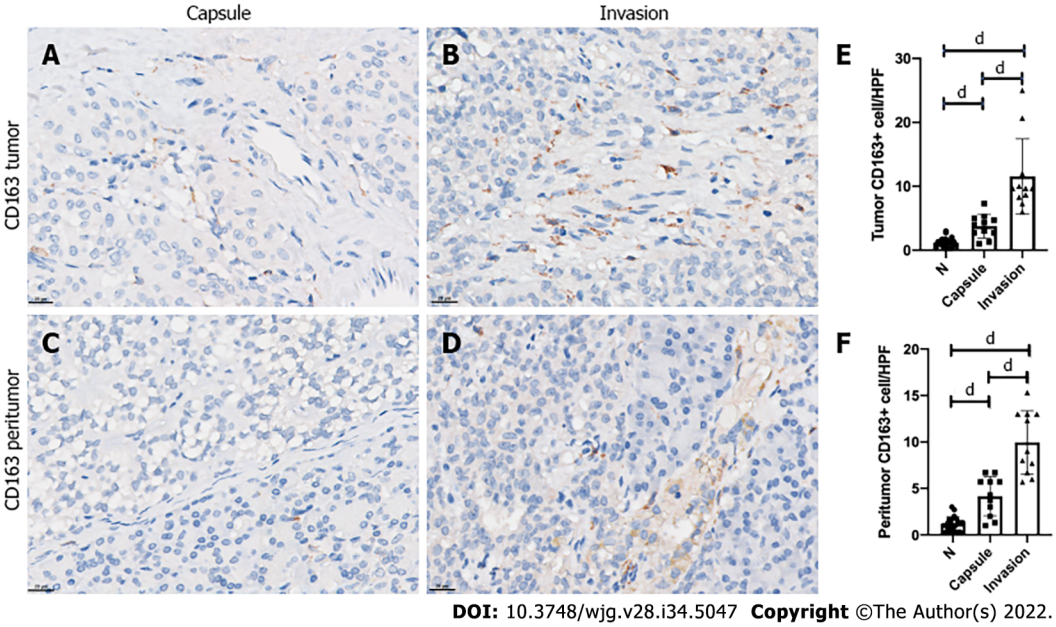
TAM infiltration in liver metastasis site

Tumors in the liver metastasis sites also showed invasion features. Tumor cells were observed as invasively grown into normal hepatic cells, and no complete fibrous capsule was found on HE-stained sections (Figure 4A and B). Liver metastasis of 3 SPT patients showed positivity for macrophage and M2-like macrophage infiltration. Like the primary tumor site of the invasion group, both intratumor and peritumor areas of the metastasis site had relatively high-level CD68-positive TAM infiltration.



DOI: 10.3748/wjg.v28.i34.5047 **Copyright** ©The Author(s) 2022.

Figure 2 Invasion group showed increased tumor-associated CD68-positive macrophage infiltration compared with capsule group by immunohistochemical analysis. A-F: Immunohistochemical-stained imaging and analysis of tumor (A-C) and peritumor (D-F) infiltrated with CD68-positive macrophages in representative patients from the capsule (A, D) and invasion (B, E) groups. N: Normal pancreas tissue. $^{b}P < 0.01$; $^{d}P < 0.0001$.



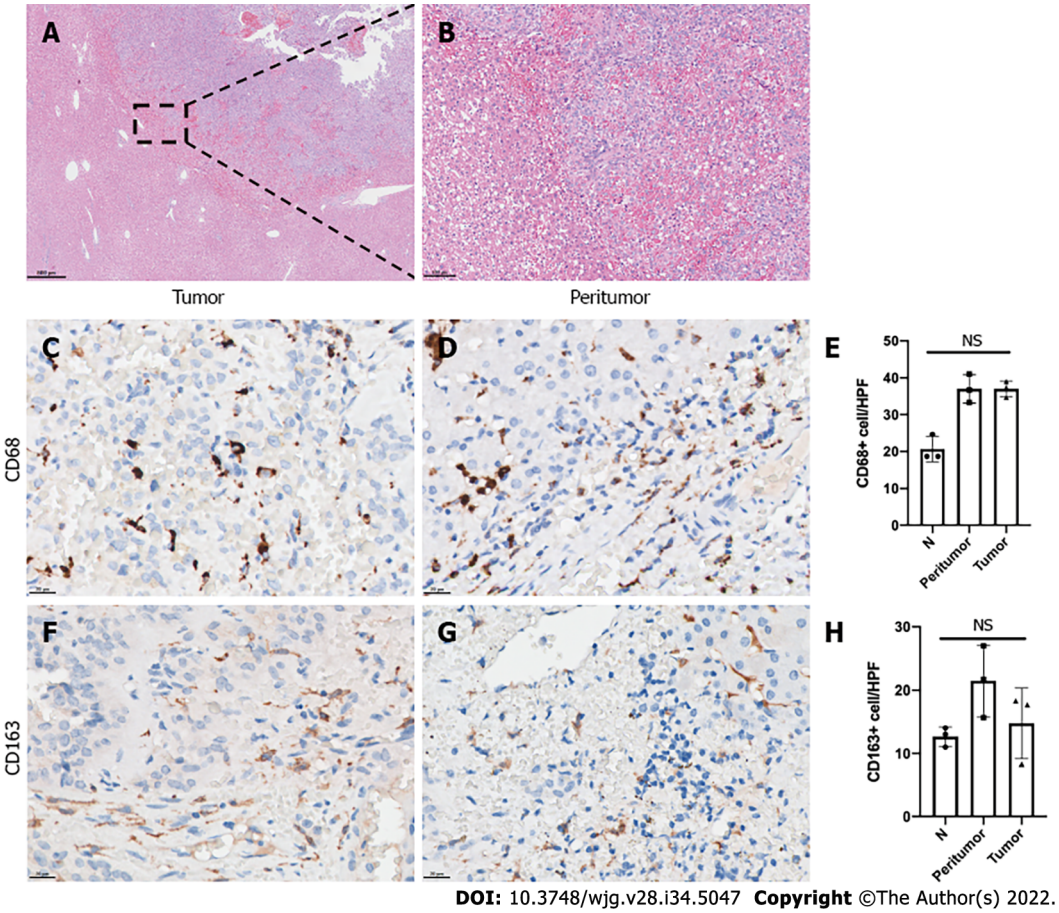
DOI: 10.3748/wjg.v28.i34.5047 **Copyright** ©The Author(s) 2022.

Figure 3 Invasion group showed increased tumor-associated CD163-positive M2-like macrophage infiltration compared with capsule group by immunohistochemical analysis. A-F: Immunohistochemical-stained images and analysis of tumor (A-C) and peritumor (D-F) tissues infiltrated with CD163-positive M2-like macrophages in representative patients from the capsule (A, D) and invasion (B, E) groups. N: Normal pancreas tissue. $^{d}P < 0.0001$.

However, there was no difference between the intratumor, peritumor and normal hepatic tissues. The CD163-positive M2-like macrophages had relatively high expression in both the intratumor and peritumor metastasis sites. No statistically significant difference was found upon comparison of the CD163-positive M2-like macrophage infiltration of intratumor, peritumor and normal hepatic tissues.

DISCUSSION

In the present study, we found that the invasion feature evident under a microscope was associated



DOI: 10.3748/wjg.v28.i34.5047 **Copyright** ©The Author(s) 2022.

Figure 4 Tumor-associated macrophage infiltration in liver metastasis sites of solid pseudopapillary tumor patients. A and B: Hematoxylin-eosin staining of the liver metastasis site of representative solid pseudopapillary tumor (SPT) patients; C-H: Immunohistochemical-stained imaging and analysis of intratumor and peritumor CD68 (C-E) and CD163 (F-H) expression in the liver metastasis site of representative SPT patients. N: Normal hepatic tissue; NS: No significance.

with malignant behavior of SPT. Additionally, we elaborated the spatial distribution of TAMs in the SPT tumor microenvironment and showed distinct expression of TAMs and M2-like macrophages between tissues with invasion and capsule features. Furthermore, we also described the intratumor and peritumor distribution of TAMs and M2-like macrophages in the liver metastases site. Considering the malignant behavior of SPTs, this study may provide a histopathological basis for identification of malignant SPTs. The phenomenon of increased infiltration of TAMs, especially M2-like macrophages, in the invasion feature might help in subsequent investigations of the underlying mechanism of TAM-mediated SPT malignant behavior, as well as to potentially treat recurrent and metastatic SPT by targeting TAMs.

The incomplete capsule feature assessed by CT imaging has been widely used and is considered able to predict malignant behavior of SPT[4]. Ye *et al*[1] showed this incomplete capsule group had a larger tumor size, an exogenous growth pattern, a malignant tendency during intraoperative frozen biopsy, and more likely to have invasion into the vasculature or organs. Indeed, in our study, the capsule or incomplete capsule measured by CT imaging was consistent with the capsule or invasion feature detected upon evaluation under a microscope. However, 2 patients in each group had distinct results. Considering the increased malignant behaviors of these SPT patients, we are concerned that assessment by CT imaging might miss patients with invasion features that could be detected with a microscope.

Other tumor types, such as small renal cell carcinoma, colorectal cancer and urinary bladder carcinoma, also have histopathological features of capsule or invasion as growth patterns, and the invasive growth feature has been shown as associated with worse prognosis of patients[17-19].

The intact fibrous envelope in extracellular matrix (ECM) might serve as a barrier for tumor cell invasion[20]. In our study, none of the 11 SPT patients with a capsule feature showed malignant behavior, such as invasion to surrounding tissues and distant metastasis. TAMs can secrete several proteolytic enzymes, including matrix metalloproteinases (MMPs, such as MMP7, MMP2, and MMP9), which can mediate the ECM degradation[21]. Particularly, M2-like macrophages could produce chitinase 3-like protein 1 to upregulate MMP expression and promote the invasiveness of gastric and breast cancer cells[22]. The expression of TAMs and M2-like macrophages in peritumor tissues of patients in the invasion group were significantly higher than those in the capsule group, which may be

related to the pathological characteristics of incomplete fibrous capsule and tumor cells' invasive growth pattern, and thus the malignant behaviors. Furthermore, the epithelial-mesenchymal transition hotpot, another mechanism associated with tumor cell invasiveness that mainly occurred at the peritumor site, was also accompanied by TAM infiltration in abundance in hepatocellular carcinoma patients[23]. Of interest, a recent study found that lipid-loaded TAMs could also sustain invasiveness in prostate cancer[24].

Metastasis to the liver through the portal venous system is a common route for the metastasis of pancreatic tumors. Indeed, 3 SPT patients in our study had liver metastasis. TAMs were involved in vascularization in a tumor environment and intravasation of tumor cells, two major mechanisms for tumor metastasis[11,25]. Vascular endothelial growth factor-A (VEGFA) is one of the primary factors driving expansion of the tumor vascular vascularization[26]. Infiltration of TAMs was associated with increased VEGFA expression and vascular density in tumor microenvironment[27,28]. This is probably because the TAMs could promote the expression of VEGFA in vascular endothelial cells by producing WNT7B[29]. Indeed, elevated expressions of fibroblast growth factor, placental growth factor, and anti-inflammatory cytokines, such as transforming growth factor-beta (TGF-β) and IL-10 in M2-like macrophages, could potentially enhance the vascularization[30,31]. Furthermore, tumor-associated M2-like macrophages could directly facilitate tumor metastasis by binding tumor cells and mediating their intravasation[32]. Therefore, when an SPT has an invasion feature, the increase of TAMs, especially M2-like macrophages, might facilitate metastasis compared with an SPT that has a capsule feature.

In addition to the vascularization and intravasation in primary tumor sites, the metastasis process includes the formation of a pre-metastatic niche followed by the growth phase[33]. TAMs in the pre-metastatic niche show an immunosuppressive phenotype characterized by elevated programmed death ligand-1 and nitric oxide synthase expression[34]. Macrophages are recruited during expansion of the metastatic site in the liver, through the CCL2–CCR2 signaling pathway[35]. Blocking the CCL2–CCR2 signaling axis was shown to reduce macrophage infiltration and metastatic expansion[36]. Few studies have reported the polarization of macrophages within or around liver metastasis sites[37]. In our study, we observed relatively more infiltration of TAMs, especially M2-like macrophages, in both intratumor and peritumor sites after the formation of SPT liver metastases. More importantly, to understand the role of TAMs in the formation of liver metastases, dynamic observation of the temporal and spatial changes of TAMs from a pre-metastatic niche to a pro-metastasis site is required.

Recently, Yang *et al*[14] classified SPT patients by the Ki-67 index based on their similar biological behavior in the 2017 WHO's pancreatic neuroendocrine tumor grade. In that study, the Ki-67 index was significantly associated with recurrence of SPT[14]. Regarding the Ki-67 index in the malignant behavior of SPT, in our research, a Ki-67 index more than 3% was observed in 4 patients in the invasion group, including 1 patient with peripheral organ invasion, 1 with both lymph node and spleen metastases, and 2 with liver metastasis. However, the Ki-67 index was only 1% in the remaining patient with peripheral organ invasion and liver metastasis. Indeed, previous meta-analyses that evaluated the Ki-67 index to predict malignant behavior of SPTs demonstrated distinct results, which might be due to the limited number of patients included and differences in the methods used to assess the Ki-67 index[38,39]. A multicenter study is needed to reveal the role of Ki-67 index in SPT patients. TAMs might be involved in the regulation of tumor cell Ki-67 expression. Lindsten *et al*[40] showed that increased infiltration of macrophages was associated with decreased progesterone receptor (commonly known as PR) expression and increased Ki-67 expression in breast tumor cells. Considering the regular expression of PR in SPT[41], the potential influence of TAMs on Ki-67 index in SPT needs further investigation.

Limitations of the present study should be noted. One of the limitations of this study was that the retrospective design and the paucity of the number of patients did not allow us to investigate causal associations between the TAMs and the invasiveness of SPT. In addition, a single immunohistochemical marker to identify target cells might not reflect the real proportion of M2-like macrophages in TAMs, so we did not compare this proportion between invasion and capsule groups in our study. The dichotomy of M1 and M2 classification of human TAM polarizations was not as obvious as in mouse, so we used M2-like macrophages instead. Further analysis of the specific distribution and function of TAMs in SPT patients using flow cytometry and a single-cell sequencing method might be used.

CONCLUSION

SPT patients with the invasion feature were more likely to demonstrate malignant behavior. These patients also showed increased infiltration of TAMs, especially M2-like macrophages, in both intratumor and peritumor sites compared with patients with the capsule feature.

ARTICLE HIGHLIGHTS

Research background

Solid pseudopapillary tumor (SPT) has been classified as a low-grade malignant tumor, and indeed only 9.2% patients of all SPT patients are initially diagnosed as malignant with invasion or metastasis. Thus, one of the challenges in managing SPT patients is predicting malignant behavior. One of the most frequently mentioned predictive factors is whether the tumor had a capsule or incomplete capsule as assessed by computed tomography imaging. However, assessing the integrity of the capsule and growth pattern of tumor cells, especially on SPT margins, using a microscope might reflect the real biological behavior of SPT. Tumor-associated macrophages (TAMs), especially the M2-like macrophages subtype, could enhance tumor invasion and metastasis; however, only limited studies are available regarding the role of the TAMs in the SPT microenvironment and their relationship with malignant behaviors of SPT.

Research motivation

The present study suggests that an invasiveness feature, as determined using a microscope is a good predictive factor for the malignant behavior of an SPT and illustrates the macrophage infiltration in the tumor microenvironment of an SPT.

Research objectives

Instead of assessing the integrity of the capsule on computed tomographic imaging, we divided SPT patients into two groups, either with invasion or capsule, based on the integrity of capsule and growth pattern of the tumor cells, especially on the tumor margins, under the microscope; we then investigated differences in the malignant behavior and TAM infiltration between these two groups.

Research methods

Hematoxylin-eosin-stained sections of SPT patients were used to assess the integrity of the capsule and growth pattern of tumor cells, especially on tumor margins. Immunohistochemical staining was used to evaluate the intratumoral and peritumoral presence of TAMs (CD68-positive) and M2-like macrophages (CD163-positive).

Research results

Malignant behavior was present more frequently in the invasion group, including in 2 patients with peripheral organ invasion, 3 with liver metastasis, and 1 with both lymph node and spleen metastases. Immunohistochemical analysis found that the invasion group had a significant increase of CD68-positive TAMs and CD163-positive M2-like macrophages in intratumoral and peritumoral sites in comparison with the capsule group.

Research conclusions

SPT patients with invasion detected using a microscope were more likely to have a tumor that demonstrated malignant behavior and TAM infiltration, especially of M2-like macrophages.

Research perspectives

This study may provide a histopathological basis for identification of malignant SPT. The phenomenon of increased infiltration of TAMs, especially M2-like macrophages in the invasion feature, might help us to investigate the underlying mechanism of TAM-mediated SPT malignant behavior, as well as to potentially treat recurrent and metastatic SPT by targeting TAMs.

FOOTNOTES

Author contributions: Yang J, Tan CL, Long D, Liang Y, Zhou Li, Liu XB, and Chen YH designed the research study; Yang J, Tan CL, Liu XB, and Chen YH performed the research; Yang J, Long D, Liang Y, Zhou Li, and Chen YH analyzed the data and wrote the manuscript; all authors have read and approved the final manuscript.

Supported by Natural Science Foundation of China, No. 82071746; Key Research and Development Projects in Sichuan Province, No. 2019YFS0043; and 1 3 5 Project for Disciplines of Excellence–Clinical Research Incubation Project, West China Hospital, Sichuan University, No. ZY2017302.

Institutional review board statement: The study was reviewed and approved by the Medical Ethics Committee of West China Hospital at Sichuan University (2014 Trial No. 37).

Informed consent statement: All study participants or their legal guardians provided informed written consent about personal and medical data collection prior to study enrollment.

Conflict-of-interest statement: All authors report no relevant conflict of interest for this article.

Data sharing statement: No additional data are available.

Open-Access: This article is an open-access article that was selected by an in-house editor and fully peer-reviewed by external reviewers. It is distributed in accordance with the Creative Commons Attribution NonCommercial (CC BY-NC 4.0) license, which permits others to distribute, remix, adapt, build upon this work non-commercially, and license their derivative works on different terms, provided the original work is properly cited and the use is non-commercial. See: https://creativecommons.org/Licenses/by-nc/4.0/

Country/Territory of origin: China

ORCID number: Jie Yang 0000-0001-9352-162X; Chun-Lu Tan 0000-0002-7315-1964; Yong-Hua Chen 0000-0001-8485-0755.

S-Editor: Wu YXJ
L-Editor: A
P-Editor: Wu YXJ

REFERENCES

1 **Ye J**, Ma M, Cheng D, Yuan F, Deng X, Zhan Q, Shen B, Peng C. Solid-pseudopapillary tumor of the pancreas: clinical features, pathological characteristics, and origin. *J Surg Oncol* 2012; **106**: 728-735 [PMID: 22688864 DOI: 10.1002/jso.23195]
2 **Papavramidis T**, Papavramidis S. Solid pseudopapillary tumors of the pancreas: review of 718 patients reported in English literature. *J Am Coll Surg* 2005; **200**: 965-972 [PMID: 15922212 DOI: 10.1016/j.jamcollsurg.2005.02.011]
3 **Yu PF**, Hu ZH, Wang XB, Guo JM, Cheng XD, Zhang YL, Xu Q. Solid pseudopapillary tumor of the pancreas: a review of 553 cases in Chinese literature. *World J Gastroenterol* 2010; **16**: 1209-1214 [PMID: 20222163 DOI: 10.3748/wjg.v16.i10.1209]
4 **You L**, Yang F, Fu DL. Prediction of malignancy and adverse outcome of solid pseudopapillary tumor of the pancreas. *World J Gastrointest Oncol* 2018; **10**: 184-193 [PMID: 30079144 DOI: 10.4251/wjgo.v10.i7.184]
5 **Wang J**, Chen X, Wang C, Cui W, Ren S, Wang Z, Li H. Differentiation of aggressive from non-aggressive pancreatic solid pseudopapillary neoplasms using computed tomography. *Abdom Radiol (NY)* 2019; **44**: 2448-2458 [PMID: 30850890 DOI: 10.1007/s00261-019-01969-6]
6 **Kim JS**, Hao EI, Rho SY, Hwang HK, Lee WJ, Yoon DS, Kang CM. Clinical Pattern of Preoperative Positron Emission Tomography/Computed Tomography (PET/CT) Can Predict the Aggressive Behavior of Resected Solid Pseudopapillary Neoplasm of the Pancreas. *Cancers (Basel)* 2021; **13** [PMID: 33925678 DOI: 10.3390/cancers13092119]
7 **Rastogi A**, Assing M, Taggart M, Rao B, Sun J, Elsayes K, Tamm E, Bhosale P. Does Computed Tomography Have the Ability to Differentiate Aggressive From Nonaggressive Solid Pseudopapillary Neoplasm? *J Comput Assist Tomogr* 2018; **42**: 405-411 [PMID: 29287021 DOI: 10.1097/RCT.0000000000000698]
8 **Park JK**, Cho EJ, Ryu JK, Kim YT, Yoon YB. Natural history and malignant risk factors of solid pseudopapillary tumors of the pancreas. *Postgrad Med* 2013; **125**: 92-99 [PMID: 23816775 DOI: 10.3810/pgm.2013.03.2634]
9 **Song H**, Dong M, Zhou J, Sheng W, Zhong B, Gao W. Solid Pseudopapillary Neoplasm of the Pancreas: Clinicopathologic Feature, Risk Factors of Malignancy, and Survival Analysis of 53 Cases from a Single Center. *Biomed Res Int* 2017; **2017**: 5465261 [PMID: 29094047 DOI: 10.1155/2017/5465261]
10 **Song H**, Dong M. The Prognostic Factors of Preoperative Prognostic Nutritional Index and Radiological Findings of Solid Pseudopapillary Tumors of Pancreas: A Single-Center Experience of 14 Years. *Cancer Manag Res* 2020; **12**: 5689-5699 [PMID: 32765072 DOI: 10.2147/CMAR.S256650]
11 **Lin Y**, Xu J, Lan H. Tumor-associated macrophages in tumor metastasis: biological roles and clinical therapeutic applications. *J Hematol Oncol* 2019; **12**: 76 [PMID: 31300030 DOI: 10.1186/s13045-019-0760-3]
12 **Qian BZ**, Pollard JW. Macrophage diversity enhances tumor progression and metastasis. *Cell* 2010; **141**: 39-51 [PMID: 20371344 DOI: 10.1016/j.cell.2010.03.014]
13 **Reid MD**, Bagci P, Ohike N, Saka B, Erbarut Seven I, Dursun N, Balci S, Gucer H, Jang KT, Tajiri T, Basturk O, Kong SY, Goodman M, Akkas G, Adsay V. Calculation of the Ki67 index in pancreatic neuroendocrine tumors: a comparative analysis of four counting methodologies. *Mod Pathol* 2015; **28**: 686-694 [PMID: 25412850 DOI: 10.1038/modpathol.2014.156]
14 **Yang F**, Wu W, Wang X, Zhang Q, Bao Y, Zhou Z, Jin C, Ji Y, Windsor JA, Lou W, Fu D. Grading Solid Pseudopapillary Tumors of the Pancreas: the Fudan Prognostic Index. *Ann Surg Oncol* 2021; **28**: 550-559 [PMID: 32424583 DOI: 10.1245/s10434-020-08626-z]
15 **Rahmati M**, Rashno A. Automated image segmentation method to analyse skeletal muscle cross section in exercise-induced regenerating myofibers. *Sci Rep* 2021; **11**: 21327 [PMID: 34716401 DOI: 10.1038/s41598-021-00886-3]
16 **Rahmati M**, Taherabadi SJ. The effects of exercise training on Kinesin and GAP-43 expression in skeletal muscle fibers of STZ-induced diabetic rats. *Sci Rep* 2021; **11**: 9535 [PMID: 33953268 DOI: 10.1038/s41598-021-89106-6]
17 **Krüger S**, Noack F, Böhle A, Feller AC. Histologic tumor growth pattern is significantly associated with disease-related survival in muscle-invasive transitional cell carcinoma of the urinary bladder. *Oncol Rep* 2004; **12**: 609-613 [PMID: 15289845]

18 **Morikawa T**, Kuchiba A, Qian ZR, Mino-Kenudson M, Hornick JL, Yamauchi M, Imamura Y, Liao X, Nishihara R, Meyerhardt JA, Fuchs CS, Ogino S. Prognostic significance and molecular associations of tumor growth pattern in colorectal cancer. *Ann Surg Oncol* 2012; **19**: 1944-1953 [PMID: 22189472 DOI: 10.1245/s10434-011-2174-5]

19 **Li G**, Xiao T, Wang K, Zhang R, Wang A, Yan C, Wang C. Histopathological validation of safe margin for nephron-sparing surgery based on individual tumor growth pattern. *World J Surg Oncol* 2021; **19**: 255 [PMID: 34454535 DOI: 10.1186/s12957-021-02375-3]

20 **Mierke CT**. The matrix environmental and cell mechanical properties regulate cell migration and contribute to the invasive phenotype of cancer cells. *Rep Prog Phys* 2019; **82**: 064602 [PMID: 30947151 DOI: 10.1088/1361-6633/ab1628]

21 **Kessenbrock K**, Plaks V, Werb Z. Matrix metalloproteinases: regulators of the tumor microenvironment. *Cell* 2010; **141**: 52-67 [PMID: 20371345 DOI: 10.1016/j.cell.2010.03.015]

22 **Chen Y**, Zhang S, Wang Q, Zhang X. Tumor-recruited M2 macrophages promote gastric and breast cancer metastasis *via* M2 macrophage-secreted CHI3L1 protein. *J Hematol Oncol* 2017; **10**: 36 [PMID: 28143526 DOI: 10.1186/s13045-017-0408-0]

23 **Fu XT**, Dai Z, Song K, Zhang ZJ, Zhou ZJ, Zhou SL, Zhao YM, Xiao YS, Sun QM, Ding ZB, Fan J. Macrophage-secreted IL-8 induces epithelial-mesenchymal transition in hepatocellular carcinoma cells by activating the JAK2/STAT3/Snail pathway. *Int J Oncol* 2015; **46**: 587-596 [PMID: 25405790 DOI: 10.3892/ijo.2014.2761]

24 **Masetti M**, Carriero R, Portale F, Marelli G, Morina N, Pandini M, Iovino M, Partini B, Erreni M, Ponzetta A, Magrini E, Colombo P, Elefante G, Colombo FS, den Haan JMM, Peano C, Cibella J, Termanini A, Kunderfranco P, Brummelman J, Chung MWH, Lazzeri M, Hurle R, Casale P, Lugli E, DePinho RA, Mukhopadhyay S, Gordon S, Di Mitri D. Lipid-loaded tumor-associated macrophages sustain tumor growth and invasiveness in prostate cancer. *J Exp Med* 2022; **219** [PMID: 34919143 DOI: 10.1084/jem.20210564]

25 **Fu LQ**, Du WL, Cai MH, Yao JY, Zhao YY, Mou XZ. The roles of tumor-associated macrophages in tumor angiogenesis and metastasis. *Cell Immunol* 2020; **353**: 104119 [PMID: 32446032 DOI: 10.1016/j.cellimm.2020.104119]

26 **Claesson-Welsh L**, Welsh M. VEGFA and tumour angiogenesis. *J Intern Med* 2013; **273**: 114-127 [PMID: 23216836 DOI: 10.1111/joim.12019]

27 **Valković T**, Dobrila F, Melato M, Sasso F, Rizzardi C, Jonjić N. Correlation between vascular endothelial growth factor, angiogenesis, and tumor-associated macrophages in invasive ductal breast carcinoma. *Virchows Arch* 2002; **440**: 583-588 [PMID: 12070596 DOI: 10.1007/s004280100458]

28 **Laoui D**, Van Overmeire E, Di Conza G, Aldeni C, Keirsse J, Morias Y, Movahedi K, Houbracken I, Schouppe E, Elkrim Y, Karroum O, Jordan B, Carmeliet P, Gysemans C, De Baetselier P, Mazzone M, Van Ginderachter JA. Tumor hypoxia does not drive differentiation of tumor-associated macrophages but rather fine-tunes the M2-like macrophage population. *Cancer Res* 2014; **74**: 24-30 [PMID: 24220244 DOI: 10.1158/0008-5472.CAN-13-1196]

29 **Yeo EJ**, Cassetta L, Qian BZ, Lewkowich I, Li JF, Stefater JA 3rd, Smith AN, Wiechmann LS, Wang Y, Pollard JW, Lang RA. Myeloid WNT7b mediates the angiogenic switch and metastasis in breast cancer. *Cancer Res* 2014; **74**: 2962-2973 [PMID: 24638982 DOI: 10.1158/0008-5472.CAN-13-2421]

30 **Jetten N**, Verbruggen S, Gijbels MJ, Post MJ, De Winther MP, Donners MM. Anti-inflammatory M2, but not pro-inflammatory M1 macrophages promote angiogenesis in vivo. *Angiogenesis* 2014; **17**: 109-118 [PMID: 24013945 DOI: 10.1007/s10456-013-9381-6]

31 **Cui X**, Morales RT, Qian W, Wang H, Gagner JP, Dolgalev I, Placantonakis D, Zagzag D, Cimmino L, Snuderl M, Lam RHW, Chen W. Hacking macrophage-associated immunosuppression for regulating glioblastoma angiogenesis. *Biomaterials* 2018; **161**: 164-178 [PMID: 29421553 DOI: 10.1016/j.biomaterials.2018.01.053]

32 **Wang J**, Cao Z, Zhang XM, Nakamura M, Sun M, Hartman J, Harris RA, Sun Y, Cao Y. Novel mechanism of macrophage-mediated metastasis revealed in a zebrafish model of tumor development. *Cancer Res* 2015; **75**: 306-315 [PMID: 25492861 DOI: 10.1158/0008-5472.CAN-14-2819]

33 **Tsilimigras DI**, Brodt P, Clavien PA, Muschel RJ, D'Angelica MI, Endo I, Parks RW, Doyle M, de Santibañes E, Pawlik TM. Liver metastases. *Nat Rev Dis Primers* 2021; **7**: 27 [PMID: 33859205 DOI: 10.1038/s41572-021-00261-6]

34 **Morrissey SM**, Zhang F, Ding C, Montoya-Durango DE, Hu X, Yang C, Wang Z, Yuan F, Fox M, Zhang HG, Guo H, Tieri D, Kong M, Watson CT, Mitchell RA, Zhang X, McMasters KM, Huang J, Yan J. Tumor-derived exosomes drive immunosuppressive macrophages in a pre-metastatic niche through glycolytic dominant metabolic reprogramming. *Cell Metab* 2021; **33**: 2040-2058.e10 [PMID: 34559989 DOI: 10.1016/j.cmet.2021.09.002]

35 **Grossman JG**, Nywening TM, Belt BA, Panni RZ, Krasnick BA, DeNardo DG, Hawkins WG, Goedegebuure SP, Linehan DC, Fields RC. Recruitment of CCR2^{+} tumor associated macrophage to sites of liver metastasis confers a poor prognosis in human colorectal cancer. *Oncoimmunology* 2018; **7**: e1470729 [PMID: 30228938 DOI: 10.1080/2162402X.2018.1470729]

36 **Zhao L**, Lim SY, Gordon-Weeks AN, Tapmeier TT, Im JH, Cao Y, Beech J, Allen D, Smart S, Muschel RJ. Recruitment of a myeloid cell subset (CD11b/Gr1 mid) *via* CCL2/CCR2 promotes the development of colorectal cancer liver metastasis. *Hepatology* 2013; **57**: 829-839 [PMID: 23081697 DOI: 10.1002/hep.26094]

37 **Brodt P**. Role of the Microenvironment in Liver Metastasis: From Pre- to Prometastatic Niches. *Clin Cancer Res* 2016; **22**: 5971-5982 [PMID: 27797969 DOI: 10.1158/1078-0432.Ccr-16-0460]

38 **Zou C**, Yang F, Wu W, Fu D. Ki-67 and malignancy in solid pseudopapillary tumor of the pancreas: A systematic review and meta-analysis. *Pancreatology* 2020; **20**: 683-685 [PMID: 32247627 DOI: 10.1016/j.pan.2020.03.015]

39 **Yepuri N**, Naous R, Meier AH, Cooney RN, Kittur D, Are C, Jain A, Dhir M. A systematic review and meta-analysis of predictors of recurrence in patients with Solid Pseudopapillary Tumors of the Pancreas. *HPB (Oxford)* 2020; **22**: 12-19 [PMID: 31350105 DOI: 10.1016/j.hpb.2019.06.005]

40 **Lindsten T**, Hedbrant A, Ramberg A, Wijkander J, Solterbeck A, Eriksson M, Delbro D, Erlandsson A. Effect of macrophages on breast cancer cell proliferation, and on expression of hormone receptors, uPAR and HER-2. *Int J Oncol* 2017; **51**: 104-114 [PMID: 28498427 DOI: 10.3892/ijo.2017.3996]

41 **Zalatnai A**, Kis-Orha V. Solid-pseudopapillary Neoplasms of the Pancreas is still an Enigma: a Clinicopathological Review. *Pathol Oncol Res* 2020; **26**: 641-649 [PMID: 31209654 DOI: 10.1007/s12253-019-00671-8]

World Journal of Gastroenterology

Submit a Manuscript: https://www.f6publishing.com

World J Gastroenterol 2022 September 14; 28(34): 5058-5075

DOI: 10.3748/wjg.v28.i34.5058

ISSN 1007-9327 (print) ISSN 2219-2840 (online)

ORIGINAL ARTICLE

Observational Study

Impact of adalimumab on disease burden in moderate-to-severe ulcerative colitis patients: The one-year, real-world UCanADA study

Talat Bessissow, Geoffrey C Nguyen, Osman Tarabain, Laurent Peyrin-Biroulet, Nathalie Foucault, Kevin McHugh, Joannie Ruel

Specialty type: Gastroenterology and hepatology

Provenance and peer review: Unsolicited article; Externally peer reviewed.

Peer-review model: Single blind

Peer-review report's scientific quality classification

Grade A (Excellent): 0
Grade B (Very good): B, B, B
Grade C (Good): 0
Grade D (Fair): 0
Grade E (Poor): 0

P-Reviewer: Innocenti T, Italy; Kaewput W, Thailand

Received: March 30, 2022
Peer-review started: March 30, 2022
First decision: June 10, 2022
Revised: July 27, 2022
Accepted: August 17, 2022
Article in press: August 17, 2022
Published online: September 14, 2022

Talat Bessissow, Department of Medicine, McGill University Health Center, Montreal H3G 1A4, Quebec, Canada

Geoffrey C Nguyen, Mount Sinai Hospital Inflammatory Bowel Disease Centre, Toronto M5T 3L9, Ontario, Canada

Osman Tarabain, Dr. O. Tarabain Clinic, Windsor N8W 1E6, Ontario, Canada

Laurent Peyrin-Biroulet, Department of Gastroenterology, University of Lorraine, CHRU-Nancy, Nancy F-54000, France

Nathalie Foucault, Kevin McHugh, AbbVie Corporation, Saint-Laurent H4S 1Z1, Quebec, Canada

Joannie Ruel, Department of Medicine, Sherbrooke University Hospital Center, Sherbrooke J1H 5N4, Quebec, Canada

Corresponding author: Talat Bessissow, FRCP (C), MD, MSc, Associate Professor, Department of Medicine, McGill University Health Center, 1650 Avenue Cedar, Montreal H3G 1A4, Quebec, Canada. talat.bessissow@mcgill.ca

Abstract

BACKGROUND

A gap remains in documenting the impact of anti-tumor necrosis factor therapy on disease burden in ulcerative colitis (UC) patients treated in a real-world setting. The use of patient-reported outcomes (PROs) has been discussed as a primary endpoint in the context of the FDA PRO Guidance, for labelling purposes. Specifically, the efficacy and safety of adalimumab have been demonstrated in pivotal trials; however, data are needed to understand how clinical results translate into improvements in key aspects of the daily lives of UC patients, such as symptoms, health-related quality of life (HRQoL), and disability.

AIM

To assess real-world effectiveness of adalimumab on PRO measures in patients with moderate-to-severe UC.

METHODS

UCanADA was a single arm, prospective, 1-year multicenter Canadian post-marketing observational study in which multiple PRO questionnaires were completed—with psychologic distress/depression symptoms as the primary endpoint—by patients with moderate-to-severe UC. Assessments were performed during patients' routine care visit schedule, which was at the initiation of adalimumab (baseline), after induction (approximately 8 wk), and 52 wk after baseline. Additional optional assessments between weeks 8 and 52 were collected at least once but no more than two times during this period. Serious safety events and per-protocol adverse events were collected.

RESULTS

From 23 Canadian centres, 100 patients were enrolled and 48 completed the study. Measured with the Patient Health Questionnaire–9 items at week 52, 61.5% (40/65) [95% confidence interval (CI): 49.7%-73.4%] of the patients improved in psychologic distress/depression symptoms, which was slightly higher in completers [65.9% (29/44); 95%CI: 51.9%-79.9%)]. At week 52, clinical response and clinical remission were achieved respectively by 65.7% (44/73) and 47.8% (32/73) of the patients. The odds of improving depressive symptoms for those achieving a clinical remission at week 52 was 7.94 higher compared with those not achieving a clinical remission (CI: 1.42, 44.41; P = 0.018). Significant changes from baseline to weeks 8 and 52 were observed in disability, HRQoL, and fatigue. Meaningful improvement was reported in work impairment.

CONCLUSION

At week 52, over 60% of the UCanADA patients had depressive symptoms significantly reduced, as well as HRQoL, fatigue symptoms, and work impairment improved. No new safety signals were detected.

Key Words: Disease burden; Patient-reported outcome; Depressive symptoms; Ulcerative colitis; Adalimumab; Real-world data

©The Author(s) 2022. Published by Baishideng Publishing Group Inc. All rights reserved.

Core Tip: In real-world at week 52, over 60% of patients with moderate-to-severe ulcerative colitis treated with adalimumab had their depressive symptoms improved, as well as their quality of life, fatigue symptoms, and work impairment. No new safety signals were detected.

Citation: Bessissow T, Nguyen GC, Tarabain O, Peyrin-Biroulet L, Foucault N, McHugh K, Ruel J. Impact of adalimumab on disease burden in moderate-to-severe ulcerative colitis patients: The one-year, real-world UCanADA study. *World J Gastroenterol* 2022; 28(34): 5058-5075
URL: https://www.wjgnet.com/1007-9327/full/v28/i34/5058.htm
DOI: https://dx.doi.org/10.3748/wjg.v28.i34.5058

INTRODUCTION

Ulcerative colitis (UC)—an intermittent, idiopathic, and chronic disease of the colon—has a worldwide incidence of 1 to 20 *per* 100000 individuals and a prevalence of 5 to 500 *per* 100000 individuals[1,2]. As of 2018 in Canada, it is estimated that 120000 individuals live with this disease.

The burden of UC has been recognized to extend beyond its clinical signs and physical symptoms such as bloody diarrhea and abdominal pain, including the development of anxiety/depression, a decreased health-related quality of life (HRQoL), an impact on work productivity and social interactions, and impairments in sexual function[3-6]. As such, having access to multidisciplinary, collaborative, chronic disease models of care improves patients' HRQoL[7].

Around 30% of patients with inflammatory bowel disease (IBD) experience psychiatric disorders, and depression/anxiety in these patients have been shown to be three times greater than in the general population[8]. In UC patients, the prevalence of depression symptoms and disorders have been estimated as 16.7% [95% confidence interval (CI): 12.0%-21.4%][9]. Assessing the severity of depression in over 158000 IBD patients, a Patient Health Questionnaire–9 items (PHQ-9) pooled mean score of 7.6 (95%CI: 6.3-8.8, on a 0-27 scale) has been reported, which can be interpreted as a mild depression[9,10].

Among physical symptoms, fatigue, which is not relieved by rest and implies limitations of daily activities[11], has been reported by 42% to 47% of UC patients at diagnosis[12]. Fatigue has been shown to impact IBD patients' QoL and is experienced by those of all ages, with some studies suggesting a

greater burden in women[13-17]. In a recent review on IBD, Nocerino *et al*[18] documented strong associations between fatigue and sleep disturbance and inadequate sleep, highlighting a proportion of more than 50% of both active and inactive IBD patients reporting sleep deficiency.

Consistent with the increasing inclusion of patient's voice in all aspects of health care as in UC therapies[19] and aiming to align with the FDA guidance[20], the use of patient-reported outcome (PRO) questionnaires are more and more used as clinical endpoints in IBD studies[21]. The use of PRO instruments helps understand patients' preferences, which in turn has been shown to be associated with treatment acceptance and adherence[22-25].

In IBD populations, depression/anxiety has been measured with a wide range of tools, including the PHQ-9[9,26-29]. The Inflammatory Bowel Disease Questionnaire (IBDQ) and its short version (SIBDQ) as well as the EuroQol 5-Dimentions, 5 Levels (EQ-5D-5L) questionnaire have been used to assess HRQoL[30-34], fatigue has been assessed by the Functional Assessment Chronic Illness Therapy–Fatigue (FACIT-F) questionnaire[18,35-37], and work productivity with the Work Productivity and Activity Impairment (WPAI) questionnaire[26,30,38-40].

Developed and validated in 2012 in a population-based cohort, the inflammatory bowel disease disability index (IBD-DI) is specific to assess disability in IBD patients[41-43]. On a 0-100 scale, the mean (interquartile range) value of the IBD-DI was 35.3 (Q1 = 19.6; Q3 = 51.8). Higher IBD-DI values were associated with female gender ($P < 0.001$), clinical disease activity ($P < 0.0001$), and disease duration ($P = 0.02$)[42].

To provide real-world data on improvements in daily lives of UC patients, the overall goal of the UCanADA study was to gather evidence on effectiveness, quality of life, disability, and work productivity during an adalimumab treatment. The primary objective was to evaluate psychological distress/depression symptoms using change from baseline in the PHQ-9 after 1 year of a real-world adalimumab treatment in moderate-to-severe UC patients.

MATERIALS AND METHODS

Study design and patients

In this prospective, single arm, 1-year multicenter Canadian post-marketing observational study, adults (≥ 18 years) with a confirmed diagnosis of UC and a moderate-to-severe disease activity–evidenced by either a Mayo endoscopic subscore (MES) of 2 or 3 from endoscopic investigation in the previous 3-mo closest to the baseline visit, or a Mayo rectal bleeding subscore ≥ 2 and a calprotectin value greater than 250 mg/g–were enrolled if they were prescribed adalimumab as part of their treatment by their treating physician. If a patient was previously treated with vedolizumab or any anti-tumor necrosis factor (TNF) agent (except adalimumab), an appropriate washout period took place *per* routine practice, which period varied usually from 2 to 3 mo.

Excluded from the study were patients who either previously received adalimumab, used infliximab or any anti-TNF agent and did not clinically respond at any time unless they experienced a treatment limiting reaction; had a history of subtotal colectomy with ileorectostomy or colectomy with ileoanal pouch, Kock pouch, or ileostomy for UC or planned bowel surgery; had a current diagnosis of indeterminate colitis, ulcerative proctitis only, or with a current diagnosis and/or have a history of Crohn's disease; had other TNF immune-modulated disease; OR had a significant history of renal, neurologic, psychiatric, endocrinologic, metabolic, immunologic, cardiovascular, or hepatic disease that in the opinion of the investigator would adversely affect his/her participating in this study. Also, we excluded from the study pregnant or breast-feeding female patients and patients currently participating in another prospective study including controlled clinical trials.

Eligible patients were approached to participate in the study after a decision to change the patient's therapy for adalimumab was already made by the treating physician. To participate in the study and to disclose personal health information, all patients were required to sign a patient authorization form (or written informed consent), which was approved by an Independent Ethics Committee/Institutional Review Board (ClinicalTrials.gov Identifier: NCT02506179). The study was conducted between July 2015 and December 2019 in 23 Canadian sites, with approximately half of the sites being community based and the other half academic based.

Assessments

Patients were followed for 52 wk post initiation of adalimumab treatment (baseline). The assessments were performed during patients' routine care visits schedule, coinciding approximately to 8 and 52 wk after baseline, in accordance with the Canadian approved label (product monograph) and as *per* regional requirements. The completers population was defined as patients who received at least one dose of treatment, and at least one follow-up appointment and did not terminate the study early or discontinue.

During these visits, the patients' medical history and changes in medical conditions, previous and concomitant medications, and disease severity and activity [clinical response defined as simple clinical colitis activity index (SCCAI)[44] decrease from baseline of ≥ 2, clinical remission defined as SCCAI

score ≤ 2, endoscopic evaluation (MES), assessment of rectal bleeding (Mayo Rectal bleeding Subscore), and the physician's global assessment (PGA)] were assessed.

Also, patients were required to fill, on paper at the physician's office, eight PRO questionnaires for evaluating: The presence and severity of depression (PHQ-9 using a 0-27 scale)[10], the entire spectrum of limitations in functioning in patients (IBD-DI questionnaire evaluating 4 domains of body functions, activity and participation, body structures, and environmental factors)[41], HRQoL (EQ-5D-5L questionnaire comprising mobility, self-care, usual activities, pain/discomfort, and anxiety/depression using a 0-1 scale)[45], SIBDQ questionnaire assessing the social, emotional, bowel, and systemic domains on a 1-7 scale[46], fatigue (FACIT-F questionnaire having a fatigue subscale score with a range from 0 to 52)[47], sleep related outcomes [Medical Outcomes Study Sleep scale (MOS Sleep) 12-item questionnaire including sleep disturbance, sleep awakening short of breath or with headache, sleep adequacy, somnolence, and quantity of sleep/optimal sleep][48], work related outcomes [WPAI: UC V2.0[49] presenting percentages of absenteeism (work time missed), presenteeism (impairment while working), an overall work impairment (overall productivity loss, accounting for both absenteeism and presenteeism), and activity impairment (impairment in activities outside work)], and Valuation of Lost Productivity (VOLP) questionnaire[50], assessing the impact of health conditions on lost productivity in monetary units. The order by which the PRO questionnaires were filled was varied to limit the potential of missing data that would systemically be found for a particular instrument.

Safety assessments included serious adverse events (AEs), any non-serious event of malignancy in patients 30 years of age and younger[51], unusual failure in efficacy, and AEs leading to discontinuation. These were coded using Medical Dictionary for Regulatory Activities version 17.1.

Study size and statistical methods

The sample size was calculated assuming a proportion of 15% of patients would improve their PHQ-9 score compared with baseline and change severity category. Using an alpha of 0.05 with a lower CI of 6%, a sample size of 72 patients would be needed. To account for a potential 25% attrition over the course of one year, the sample size was increased to 100 patients. It was anticipated that up to 30% of the 100 moderate-to-severe UC patients newly treated with adalimumab would have prior experience with biologics.

The primary effectiveness endpoint—the proportion of patients with a change in depressive symptoms using the PHQ-9 score from baseline following initiation of adalimumab and after 1 year of treatment—was calculated, and the 95%CIs were estimated. Changes in PHQ-9 scores from baseline were tested by paired sample *t*-test. Least-square mean (LS mean) of the changes were also estimated by the mixed effect repeated measures models where baseline values were included as a covariate. Changes in severity categories were tested by Bowker's test (*kxk* table where $k > 2$) or McNemar's test (2 × 2 table).

To understand the independent effect of clinical effectiveness on the probability of improving in PHQ-9 at week 52, a logistic regression analysis was conducted to examine the effect of clinical response and clinical remission adjusting for the baseline PHQ-9 score and other potential prognostic factors. A similar analysis was conducted to assess the association between clinical effectiveness on changes of PHQ-9 scores from baseline. LS mean of the changes associated with clinical response and clinical remission was estimated by the mixed effect repeated measures models using all follow-up visits.

For secondary outcomes, the IBD-DI, EQ-5D-5L, SIBDQ, FACIT-F, and MOS Sleep, scores at baseline, week 8, and week 52 were summarized, and changes in scores from baseline were tested by paired sample *t*-tests. LS mean of the changes were also estimated by the mixed effect repeated measures models where the baseline value was included as a covariate. Productivity outcomes (WPAI and VOLP) at baseline, week 52, and changes in outcome from baseline were summarized. The 95%CIs for the changes were estimated by bootstrapped percentile CIs based on samples of 10000.

The sensitivity to change for the IBD-DI was evaluated using the effective size (ES) and the standardized response mean (SRM). For both statistics, values of 0.020, 0.50, and 0.80 or greater were used to represent small, moderate, and large, respectively. The association between the change in PROs (EQ-5D-5L, SIBDQ, FACIT-F, and MOS Sleep) and clinical response/remission (effectiveness) were assessed using a mixed model for repeated measures using observations from all follow-up visits with the baseline value included in the model as a covariate. All models with repeated measures included a random intercept with the effectiveness variable (fixed, forced-in), visit (fixed, forced-in), baseline value of the PRO measure (fixed, forced-in) and other covariates. Cross-sectional regression models included an intercept with the effectiveness variable (forced-in), baseline value of the PRO measure (fixed) and other covariates. Least squares means, *P* value and 2-sided 95%CI of the difference between the two groups defined by the clinical effectiveness were determined. Additional details on the statistical analysis used to determine the correlation between effectiveness (clinical response and remission) rates and PRO measures are provided in the Supplementary material section.

Missing data were imputed only for the sensitivity analysis of the primary outcome. For missing responses on PRO questionnaire items, missing data were handled *per* the imputation solutions provided in the coding of the PRO instruments. To assess the impact of missing data on the primary endpoint estimate, the sensitivity analysis was performed using two imputation methods: Non-responder imputation (NRI), defined as patients who did not provide week 52 effectiveness data or

dropped out of the study prior to week 52 were considered as no improvement; and last observation carried forward (LOCF) defined as the last effectiveness assessment prior to week 52 was used for those missing week 52 assessment.

All calculations and analyses were performed using SAS version 9.4 (Cary, NC: SAS Institute Inc.) under the Windows 10 Enterprise operating system at the Centre for Health Evaluation and Outcome Sciences, in Vancouver, Canada.

RESULTS

Patients

One hundred patients from 23 Canadian sites were included in the study (Figure 1). Respectively, 94, 48, and 98 patients were included in the effectiveness population [intent-to-treat (ITT) population], the completers population, and the safety population. Patients in the ITT population had a mean age (SD) of 42.5 (15.3) years and a mean body mass index of 25.4 (4.5) kg/m^2 (Table 1). The majority was White (93.6%) and male (59.6%). The mean age at UC diagnosis was 34.5 (15.3) years, and the mean duration of disease was 7.9 (8.0) years. Forty-eight (48%) patients completed the study.

Impact on psychological distress/depression symptoms

Following routine care treatment with adalimumab, the proportion of patients who improved in psychological distress/depressive symptoms using the PHQ-9 total score at week 52—defined as a change in PHQ-9 total score from baseline, the study primary endpoint—was 61.5% (40/65) (95%CI: 49.7%-73.4%) for the ITT population and 65.9% (29/44) (95%CI: 51.9%-79.9%) for the completers population (Figure 2A). To assess the impact of missing data, the sensitivity analyses conducted on the primary endpoint showed that the proportions of patients who improved in psychological distress/depressive symptoms, using the NRI and LOCF imputation methods, were similar to the proportion obtained using the original non-imputed data analysis, with the ITT population (Supplementary Table 1).

Overall, changes from baseline in the PHQ-9 total score were significant at weeks 8 and 52 (P = 0.010), with changes slightly higher for the completers population [-2.5 (6.1) and -3.4 (6.8) at weeks 8 and 52] than in the ITT population [-2.2 (6.1) -2.4 (7.1)] on a 0-27 scale (Table 2). The proportion of patients with a PHQ-9 total score 10 (yellow flag category, *i.e.*, moderate or more severe depression) was 25.6% (21/82) at week 8, which slightly increased to 29.2% (19/65) at week 52 for the ITT population. These proportions were lower and stable over time (18%-19%) for the completers population. For patients with severe depressive symptoms (red flag category), the proportions improved from 19.1% (18/94) and 16.7% (8/48) at baseline to 12.3% (8/65) and 2.3% (1/44) at week 52 for the ITT population and completers population, respectively.

The PHQ-9 questionnaire items that showed the highest improvement from baseline were 'Poor appetite or overeating' (response 'Not at all' increased by 23.3% from baseline to week 52, and response 'Nearly every day' decreased by 20.3% from baseline to week 52), 'Little interest or pleasure in doing things' (response 'Not at all' increased by 15.3% from baseline to week 52, and response 'Nearly every day' decreased by 12.1% from baseline to week 52), and 'Feeling tired or having little energy' (response 'Not at all' increased by 8.2% from baseline to week 52, and response 'Nearly every day' decreased by 20.3% from baseline to week 52) (Supplementary Table 2).

Clinical endpoints

The proportions of patients who achieved a clinical response (decrease from baseline ≥ 2 in SCCAI score) remained similar throughout the study [64.2% (52/81) at week 8 and 65.7% (44/67) at week 52], and the proportion who achieved clinical remission (SCCAI score ≤ 2) slightly increased [41.5% (34/82) at week 8 and 47.8% (32/67) at week 52] in the ITT population (Figure 2B). For the completers population, these proportions increased during the study for both the clinical response and clinical remission, reaching 85.4% (35/41) and 73.2% (30/41), respectively, at week 52 (Supplementary Table 3).

Similarly, the proportions of patients who achieved endoscopic healing remained constant between weeks 8 and 52 [42.9% (6/14) had a Mayo endoscopic score of 0 or 1 and 11.5% (3/26), had a fecal calprotectin concentration < 50 μg/g] in the ITT population (Figure 2C), whereas in the completers population, the proportions increased over time [71.4% (5/7) and 80.0% (8/10), measured with the Mayo endoscopic score and 7.7% (1/13) and 11.8% (2/17) measured with the fecal calprotectin concentration, at weeks 8 and 52, respectively] (Supplementary Table 3).

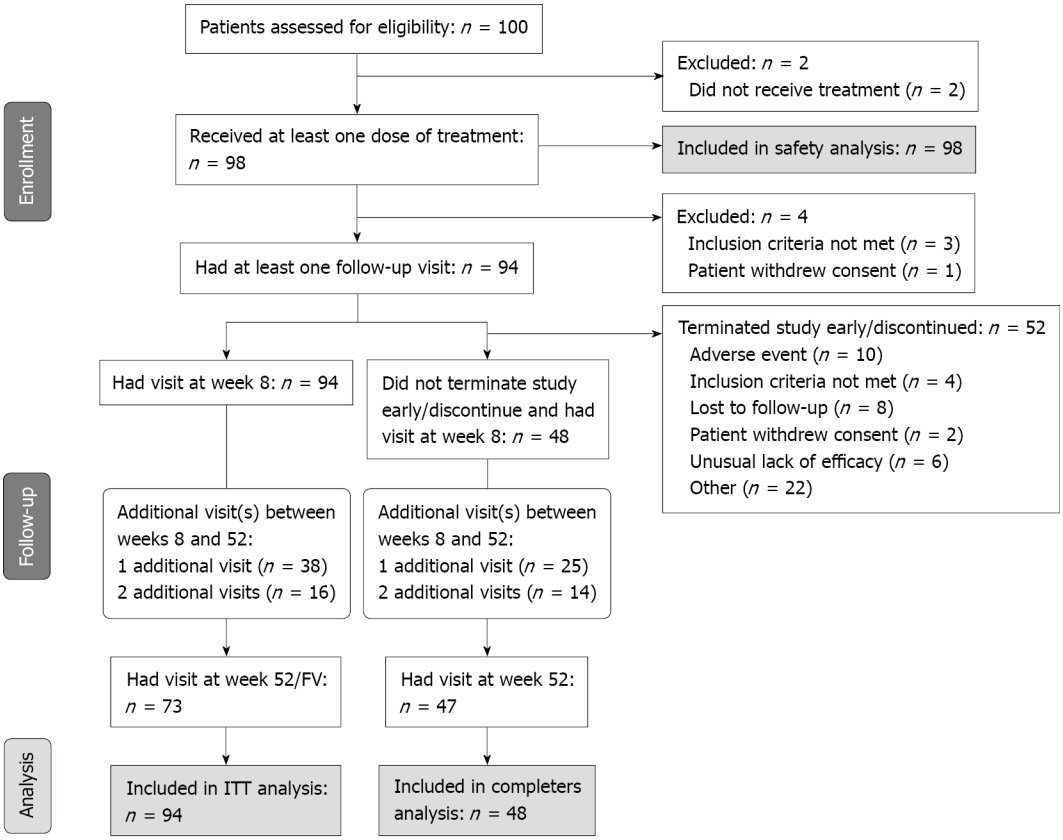
No major changes were observed over time in the extracolonic feature, with the majority of patients not having arthritis at both baseline and follow-up visit [81.5% (66/81) at week 8 and 82.1% (55/67) at week 52] (Figure 2D). The proportion of patients who had arthritis at baseline and none at follow-up was 8.6% (7/81) at week 8 and 9.0% (6/67) at week 52. Similar proportions were observed in the completers population (Supplementary Table 3).

Table 1 Baseline patient and disease characteristics

Characteristics		*N*	*n* (%) or mean ± SD
Age		94	42.5 (15.3)
Gender	Male	94	56 (59.6)
BMI (kg/m^2)		91	25.4 (4.5)
Race	American Indian/Alaska Native	94	1 (1.1)
	Asian		5 (5.3)
	White		88 (93.6)
Employment status	Disability		2 (2.1)
	Employed (fulltime, part time < 35 h/week)		63 (67.0)
	Homemaker		3 (3.2)
	Retired		12 (12.8)
	Student		6 (6.4)
	Temporary leave of absence		1 (1.1)
	Unemployed		6 (6.4)
	Unknown		1 (1.1)
Tobacco use	Current smoker	94	2 (2.1)
	Former smoker		34 (36.2)
	Never smoked		55 (58.5)
	Unknown		3 (3.2)
Alcohol use	Non-drinker	94	20 (21.3)
	Ex-drinker		5 (5.3)
	Light (less than 2 drinks *per* day)		61 (64.9)
	Moderate (2-4 drinks *per* day)		5 (5.3)
	Unknown		3 (3.2)
Age at UC diagnosis (yr)		98	34.5 (15.3)
Disease duration (yr)		98	7.9 (8.0)
Family history of UC	No	98	59 (60.2)
	Yes		20 (20.4)
	Unknown		19 (19.4)
Montreal classification of extent of UC	E2	97	55 (56.7)
(prior 3 mo)	E3		42 (43.3)
Mayo Endoscopic Subscore	1	90	1 (1.1)
(prior 3 mo)	2		66 (73.3)
	3		23 (25.6)
Endoscopy (prior 6 mo)	Yes	98	91 (92.9)
UC-related ED visit (prior 6 mo)	Yes	98	13 (13.3)
UC-related hospitalization (prior 6 mo)	Yes	98	12 (12.2)
Previous biologic use	Yes	44	5 (11.4)
Medication use:	Corticosteroids	98	63 (64.3)
Since UC diagnosis to prior 6 mo	Imuran (azathioprine)		37 (37.8)
	6-MP		8 (8.2)
	5-ASA		83 (84.7)

	Methotrexate		5 (5.1)
	Cyclosporine		1 (1.0)
Medication use:	Corticosteroids	98	61 (62.2)
Since prior 6 mo to current	Imuran (azathioprine)		39 (39.8)
	6-MP		5 (5.1)
	5-ASA		67 (68.4)
	Methotrexate		8 (8.2)
	Cyclosporine		0 (0.0)

Montreal classification of extent of UC: E2 = left sided (distal) ulcerative colitis, E3 = extensive (pancolitis) ulcerative colitis; Mayo endoscopic subscore: 0 = normal or inactive disease, 1 = mild disease, 2 = moderate disease, 3 = severe disease; 5-ASA: 5-aminosalicylic acid; 6-MP: Mercaptopurine; BMI: Body mass index; ED: Emergency department; UC: Ulcerative colitis.



DOI: 10.3748/wjg.v28.i34.5058 **Copyright** ©The Author(s) 2022.

Figure 1 UCanADA study flow diagram. The intent-to-treat population was defined as patients who received at least one dose of treatment and had at least one follow-up appointment. The completers population was defined as patients who received at least one dose of treatment, and at least one follow-up appointment and did not terminate the study early or discontinue. The safety population was defined as patients who received at least one dose of treatment. FV: Final visit; ITT: Intent-to-treat.

The proportion of patients who were PGA responders, defined as a decrease from baseline of ≥ 1 point, varied from 66.7% (50/75) to 61.5% (40/65) for the ITT population (Figure 2E) and from 73.2% (30/41) to 83.7% (36/43) for the completers population, from week 8 to week 52, respectively (Supplementary Table 3). While at baseline the majority of patients had moderate disease [73.9% (68/92)], at week 8 the highest proportion of patients had mild disease [35.5% (27/76)], and at week 52, 50.0% (33/66) of patients were assessed as normal (Figure 2E). The proportion of patients assessed with severe disease remained comparable between week 8 [5.3% (4/76)] and week 52 [6.1% (4/66)]. Similar results were reported for the completers population (Supplementary Table 3).

A proportion of 5.5% (4/73) of patients reported complications including hospitalization and surgery at week 52 in the ITT population (Supplementary Table 4), and none were reported among the completers population (Supplementary Table 3). The proportion of patients with current steroid use

Table 2 Patient Health Questionnaire–9 items at week 8 and week 52/final visit

Outcome	ITT			Completers		
	Baseline (*n* = 94)	Week 8 (*n* = 94)	Week 52/final visit (*n* = 73)	Baseline (*n* = 48)	Week 8 (*n* = 48)	Week 52/final visit (*n* = 47)
PHQ-9 total score						
n	94	82	65	48	43	44
mean ± SD	8.8 (6.3)	6.8 (5.3)	6.5 (5.6)	8.2 (6.7)	5.8 (5.6)	4.6 (4.3)
Median	8.0	6.0	5.0	5.0	5.0	3.0
Min, Max	0.0, 26.0	0.0, 26.0	0.0, 22.0	1.0, 26.0	0.0, 26.0	0.0, 15.0
Change from baseline						
n		82	65		43	44
mean ± SD		-2.2 (6.1)	-2.4 (7.1)		-2.5 (6.1)	-3.4 (6.8)
P value		0.002	0.008		0.010	0.002
PHQ-9 category, *n* (%)						
Minimal	35 (37.2)	31 (37.8)	28 (43.1)	23 (47.9)	21 (48.8)	25 (56.8)
Mild	23 (24.5)	30 (36.6)	18 (27.7)	8 (16.7)	14 (32.6)	11 (25.0)
Moderate	18 (19.1)	14 (17.1)	11 (16.9)	9 (18.8)	4 (9.3)	7 (15.9)
Moderately severe	11 (11.7)	4 (4.9)	7 (10.8)	4 (8.3)	2 (4.7)	1 (2.3)
Severe	7 (7.4)	3 (3.7)	1 (1.5)	4 (8.3)	2 (4.7)	0 (0.0)
P value		0.280	0.681		0.610	0.542
PHQ-9: Yellow flag category, *n* (%)						
	36 (38.3)	21 (25.6)	19 (29.2)	17 (35.4)	8 (18.6)	8 (18.2)
P value		0.028	0.083		0.021	0.059
PHQ-9: Red flag category, *n* (%)						
Yes	18 (19.1)	7 (8.5)	8 (12.3)	8 (16.7)	4 (9.3)	1 (2.3)
P value		0.013	0.134		0.180	0.034

The yellow flag category was defined as the proportion of patients with a Patient Health Questionnaire–9 total score ≥ 10, and the red flag category was defined as patients with severe depressive symptoms. ITT: Intent-to-treat; Max: Maximum; Min: Minimum; PHQ-9: Patient Health Questionnaire–9 items.

decreased between week 8 and week 52 from 29.4% (25/85) to 19.2% (14/73) in the ITT population and from 22.2% (10/45) to 12.8% (6/47) in the completers population.

Improvement in IBD-DI

The mean change from baseline in IBD-DI increased from -10.7 (17.21) at week 8 to -13.8 (22.24) at week 52 ($P < 0.001$), with proportions of patients who improved disability increasing from 72.6% (53/73) to 74.1% (40/54) over time in the ITT population (Figure 2F). Results from the completers population were slightly higher [mean change from baseline = -14.69 (17.99) and -20.09 (17.74) and improved disability = 81.4% (35/43) and 88.9% (32/36) at weeks 8 and 52, respectively] (Supplementary Table 5).

The IBD-DI was moderately sensitive to change for the ITT population, varying from -0.61 to -0.77 for ES and had a SRM of -0.62 (Supplementary Table 6). For the completers population, the IBD-DI was greatly sensitive to change. The ES varied from -0.75 to 1.08 and the SRM varied from -0.82 to -1.13

Correlations between PHQ-9 and clinical outcomes

A correlation analysis showed that at week 52 an improvement in PHQ-9 total score was associated with the baseline PHQ-9 score, with a higher baseline score predicting a greater improvement on the PHQ-9 (Table 3). No associations were detected between an improvement in PHQ-9 and clinical response; however, an association was measured with clinical remission in the ITT analysis (OR: 7.94; 95%CI: 1.42-44.41; $P = 0.018$), though this was not statistically significant in the completer analysis.

Table 3 Association between clinical response/remission and improvement in Patient Health Questionnaire–9 items total score at week 52/final visit–intent-to-treat and completers populations

Analysis population	Parameter	Model coefficient (SE)	Est. odds ratio (95%CI)	*P* value
Clinical response				
ITT	Baseline PHQ-9 total score	0.17 (0.06)	1.19 (1.05-1.34)	0.005
	Clinical response at week 52: Yes versus No	0.30 (0.65)	1.35 (0.38-4.84)	0.648
	UC duration (years)	0.11 (0.05)	1.11 (1.00-1.24)	0.051
Completers	Baseline PHQ-9 total score	0.20 (0.10)	1.22 (1.00-1.48)	0.049
	Clinical response at week 52: Yes versus No	-1.29 (1.29)	0.28 (0.02-3.43)	0.317
	UC duration (years)	0.14 (0.08)	1.15 (0.98-1.35)	0.079
Clinical remission				
ITT	Baseline PHQ-9 total score	0.28 (0.09)	1.33 (1.11-1.59)	0.002
	Clinical remission at week 52: Yes versus No	2.07 (0.88)	7.94 (1.42-44.41)	0.018
	UC duration (years)	0.11 (0.06)	1.11 (1.00-1.24)	0.054
Completers	Baseline PHQ-9 total score	0.22 (0.11)	1.24 (1.00-1.53)	0.045
	Clinical remission at week 52: Yes versus No	1.39 (1.07)	4.00 (0.50-32.37)	0.193
	UC duration (years)	0.14 (0.08)	1.15 (0.98-1.36)	0.095

Clinical response based on simple clinical colitis activity index (SCCAI): decrease from baseline of ≥ 2; Clinical remission: SCCAI ≤ 2; CI: Confidence interval; ITT: Intent-to-treat; PHQ-9: Patient Health Questionnaire–9 Items; SE: Standard error.

A regression analysis between the PHQ-9 total score and clinical response/remission at week 52 showed an association at week 52 using the ITT population ($P < 0.001$), but not in the completer population ($P \geq 0.098$) (Supplementary Table 7).

Impact on other PROs and correlation with clinical outcomes

For the other PRO tools used to assess the impact of the adalimumab treatment, changes from baseline at weeks 8 and 52 were significant for the EQ-5D-5L utility score, SIBDQ total score, FACIT-F total score, MOS Sleep Problems Index I and Sleep Problems Index II ($P = 0.049$) measured in the ITT population (Table 4) and the completers population (Supplementary Tables 8 and 9). A regression analysis showed that changes in the PRO measures between baseline and week 52 were all significantly associated with clinical outcomes ($P < 0.001$), except for the MOS Sleep measures ($P \geq 0.064$) (Supplementary Table 10).

The SIBDQ items of social function and bowel symptoms improved the most from baseline [mean change at week 52, 1.09 (2.11) and 0.93 (1.66), respectively on a 1-7 scale] ($P < 0.001$) (Table 4). Observing the FACIT-F measures, patients reported gaining more over time from the physical fatigue [3.86 (7.11)] than from the functional fatigue [2.58 (6.36)], emotional fatigue [2.06 (5.26)], and social impact of fatigue [1.32 (4.60)], at week 52 ($P = 0.024$). For the MOS Sleep subscales, only the sleep adequacy subscale significantly improved over time, with a mean change from baseline of 11.69 (5.26) at week 52 ($P < 0.001$).

All the WPAI scores improved from baseline, and the ones that improved the most were activity impairment [-16.9% (29.8) at week 8 and -16.7% (33.6) at week 52], *i.e.*, activities performed outside of work, and overall work impairment [-16.2% (30.2) at week 8 and -14.5% (34.4) at week 52], which combines absenteeism and presenteeism at work (Table 4). Similar results were reported for the completers (Supplementary Table 11).

For the VOLP, the most important changes were reported at week 52 and were related to paid work [paid work productivity loss in the past x months = -42.2 (115.7) hours and any paid work productivity loss in the past x months = -17% (-16.7%)] and lost productivity [any costs of lost productivity in the past x month = -15% (11.6%) hours and total costs of lost productivity in the past x months ($) = -1998 (-7299.7) $]. Study completers reported slightly higher results (Supplementary Table 11).

Safety

The safety profile was consistent with the known safety profile of adalimumab. During the study, 18 (18.4%) patients experienced at least one AE (Table 5). The AEs reported by more than 1% of patients

Table 4 Change from baseline in other patient-reported outcomes at weeks 8 and 52–intent-to-treat population

PRO measure	Baseline	Change from baseline				
	n (%) or mean ± SD	*N*	Week 8, *n* (%) or mean ± SD	*P* value	*N*	Week 52, *n* (%) or mean ± SD	*P* value
EQ-5D-5L	0.78 (0.17)	83	0.05 (0.17)	0.021	65	0.06 (0.24)	0.049
SIBDQ							
Total score	4.26 (1.08)	83	0.60 (1.08)	< 0.001	65	0.71 (1.24)	< 0.001
Social function	4.40 (1.91)	82	0.93 (1.78)	< 0.001	64	1.09 (2.11)	< 0.001
Emotional function	4.32 (0.78)	83	0.23 (0.82)	0.013	65	0.20 (0.93)	0.093
Bowel symptoms	4.25 (1.33)	83	0.69 (1.50)	< 0.001	65	0.93 (1.66)	< 0.001
Systemic symptoms	4.11 (1.63)	83	0.63 (1.33)	< 0.001	65	0.68 (1.56)	< 0.001
FACIT-F							
Fatigue subscale	30.10 (13.76)	83	3.78 (12.29)	0.006	65	5.41 (13.87)	0.003
Physical fatigue	17.67 (6.59)	83	2.44 (6.27)	< 0.001	65	3.86 (7.11)	< 0.001
Social impact of fatigue	20.69 (5.02)	82	0.52 (3.97)	0.234	65	1.32 (4.60)	0.024
Emotional fatigue	15.37 (4.71)	83	1.10 (4.24)	0.021	65	2.06 (5.26)	0.002
Functional fatigue	15.65 (5.54)	83	2.07 (5.43)	< 0.001	65	2.58 (6.36)	0.002
Trial outcome index	63.42 (24.02)	83	8.29 (21.79)	< 0.001	65	11.85 (24.85)	< 0.001
FACT-G total score	69.38 (16.99)	82	6.16 (15.58)	< 0.001	65	9.82 (18.58)	< 0.001
FACIT-F total score	99.48 (29.04)	82	9.99 (26.34)	< 0.001	65	15.23 (30.64)	< 0.001
MOS Sleep							
Sleep problems index I	40.46 (19.16)	83	-4.14 (15.89)	0.020	65	-6.56 (16.21)	0.002
Sleep problems index II	42.30 (19.69)	83	-3.47 (15.66)	0.047	65	-4.92 (16.75)	0.021
Sleep disturbance scale	41.52 (25.58)	83	-3.67 (20.82	0.112	65	-4.22 (22.30)	0.132
Snoring scale	30.22 (33.08)	81	0.00 (24.49)	1.000	63	2.54 (25.78)	0.437
Short of breath scale	11.06 (19.37)	83	2.41 (21.50)	0.310	65	3.08 (19.12)	0.199
Sleep adequacy	42.13 (26.96)	83	8.07 (26.01)	0.006	65	11.69 (26.31)	< 0.001
Somnolence scale	43.12 (27.35)	83	-1.37 (22.42)	0.581	65	-4.00 (25.24)	0.206
Sleep quantity	6.73 (1.41)	82	0.13 (1.29)	0.371	63	0.34 (1.31)	0.042
WPAI[1]							
Work time missed (%)	18.9 (31.1)	48	-6.7 (30.9)		37	-9.4 (35.0)	
Work impairment while working (%)	39.5 (28.5)	46	-14.8 (33.1)		38	-14.5 (35.8)	
Overall work impairment (%)	44.2 (30.1)	42	-16.2 (30.2)		35	-14.5 (34.4)	
Activity impairment (%)	46.0 (31.9)	83	-16.9 (29.8)		64	-16.7 (33.6)	
VOLP							
Any paid work productivity loss in the past x months (%)	45 (76.3)	58	-5 (-4.6)		47	-17 (-16.7)	
Paid work productivity loss in the past x months (hours)	98.5 (122.7)	51	13.5 (127.8)		42	-42.2 (115.7)	
Any unpaid work productivity loss in the past 7 d (%)	20 (29.0)	61	-8 (-9.3)		48	-7 (-1.9)	
Unpaid work productivity loss in the past 7 d (hours)	3.9 (11.6)	61	-3.4 (12.4)		48	-1.9 (14.8)	
Any costs of lost productivity in the past x month (%)	47 (79.7)	58	-5 (-7.3)		47	-15 (-11.6)	

Total costs of lost productivity in the past x months ($)	6075.8 (8890.9)	51	-1328 (5594.9)	42	-1998 (7299.7)

[1]Due to health.

EQ-5D-5L: EuroQol 5-Dimensions, 5 Levels; CI: Confidence interval; FACIT-F: Functional Assessment Chronic Illness Therapy-Fatigue; MOS: Medical Outcomes Study; PRO: Patient-reported outcome; SIBDQ: Short Quality of Life in Inflammatory Bowel Disease Questionnaire.

Table 5 Overview of adverse events–safety population

	Events (*n* = 55)	Patients (*n* = 98)
All AEs	55	18 (18.4%)
Severe AEs	10 (18.2%)	5 (5.1%)
AEs related to study drug	17 (30.9%)	12 (12.2%)
Mild	5 (29.4%)	4 (4.1%)
Moderate	6 (35.3%)	6 (6.1%)
Severe	4 (23.5%)	2 (2.0%)
Not provided	2 (11.8%)	2 (2.0%)
Serious AEs	27 (49.1%)	7 (7.1%)
Number of patients with AEs		
Resulting in hospitalization		6 (6.1%)
Resulting in study drug discontinuation		15 (15.3%)
Malignancy in patients ≤ 30 yr	0	0
Death	0	0

Percentages of patients were calculated based on the total number of patients. Percentages of events were based on the total number of events.
AE: Adverse event.

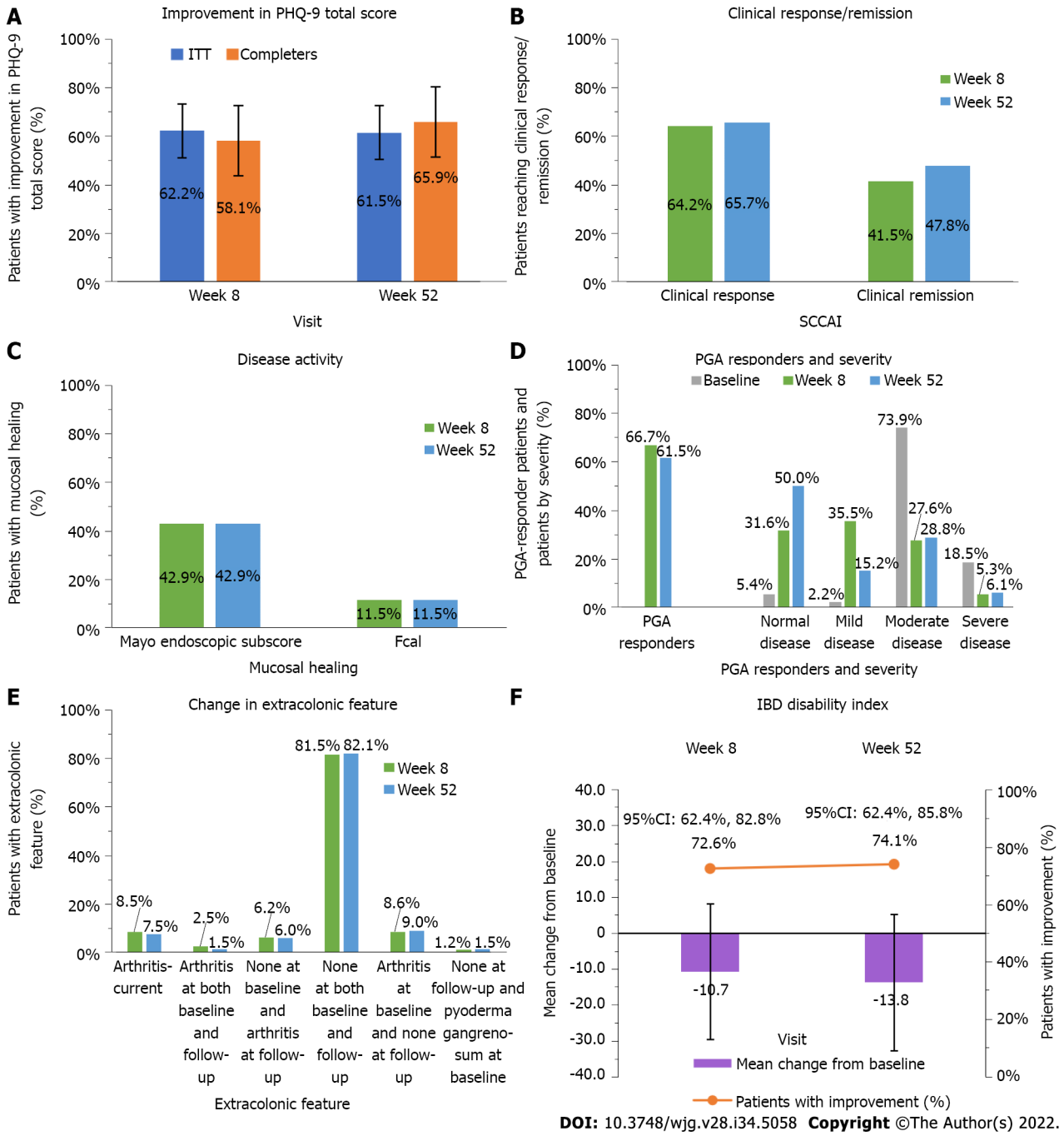
were: Colitis ulcerative [6 (6.1%) patients], drug ineffective [6 (6.1%) patients], haematochezia [2 (2.0%) patients], and arthralgia [2 (2.0%) patients]. Each of the severe AEs was experienced by only one (1.0%) patient, which included one event each of anal fissure, colitis, dysphagia, and mouth ulceration. One patient experienced two events of severe oesophagitis.

Two (2.0%) patients experienced serious treatment-related AEs that were assessed by the investigator to be reasonably possibly related to adalimumab: 1 (1.0%) patient experienced two events of severe oesophagitis that led to hospitalization and prolongation of hospitalization, and one event of severe aggravated colitis that led to hospitalization; 1 (1.0%) patient experienced severe injection site pain. There was one report of cutaneous basal cell cancer in a 63-year-old male. Monitored as *per* protocol safety variable, there were no reports of malignancy in patients 30 years of age and younger. No death was reported during the study, and no new signal or unexpected trend was identified for the patient population.

DISCUSSION

To fill an information gap on Canadian real-world data on the effectiveness of adalimumab on PRO measures in moderate-to-severe UC patients, and consistent with the FDA guidelines on the use of PRO measures to support labelling claims[20], the UCanADA study enrolled 100 patients from 23 centres using as a primary endpoint the change from baseline in depressive symptoms at week 52, measured by the PHQ-9 questionnaire.

The PHQ-9 measures in study UCanADA showed that over 60% of the study population improved in psychological distress/depression symptoms during the real-world adalimumab treatment, with most gains observed at week 52 in the completers population (65.9%). Significant changes from baseline were observed at week 8, which were maintained at week 52 and were slightly higher for the completers population (P = 0.010). Despite this improvement, these scores may be interpreted as a remaining mild depression in patients[10] and not necessarily a clinically meaningful change[52-54], which indicates a potential relevance to offer psychological support to this population[7,55]. In the present observational



DOI: 10.3748/wjg.v28.i34.5058 **Copyright** ©The Author(s) 2022.

Figure 2 Effect of a real-world adalimumab treatment on effectiveness and patient-reported outcomes in moderate-to-severe ulcerative colitis patients. A: Proportion of patients who improved in Patient Health Questionnaire–9 items total score at week 52 in the intent-to-treat and completers populations (%), improvement defined as change from baseline, bars show 95% confidence intervals; B: Proportion of patients achieving clinical response/remission at weeks 8 and 52 (%), measured by the simple clinical colitis activity index (SCCAI) ≤ 2; C: Proportion of patients with endoscopic healing at weeks 8 and 52 (%), healing measured as a Mayo endoscopic subscore of 0 or 1 or a fecal calprotectin concentration < 50 μg/g; D: Proportion of patients with extracolonic feature at weeks 8 and 52 (%), measured by the SCCAI; E: Proportion of physician's global assessment responders and severity at weeks 8 and 52 (%), responders defined as with a decrease from baseline of ≥ 1 point; F: inflammatory bowel disease index mean change from baseline and proportion of patients who improved (%). Bars represent standard deviations. PRO: Patient-reported outcome; UC: Ulcerative colitis; PHQ-9: Patient Health Questionnaire–9; IBD: Inflammatory bowel disease; SCCAI: Simple clinical colitis activity index; ITT: Intent-to-treat; PGA: Physician's global assessment.

study, while patients who had a preliminary failure to biologics were excluded, patients with secondary failures were included, which may have led to the inclusion of patients with greater psychological burden than biologic-naïve patients.

Our results show a significant change from baseline in PHQ-9 score earlier during treatment than those of a recently reported cohort of 1804 UC outpatients, who were included regardless of treatment assignment or disease activity[26]. However, a similar decrease in PHQ-9 score was measured in UC patients at least 30 d after being initiated on an anti-TNF therapy (including infliximab, adalimumab, or

certolizumab) and/or immunomodulator therapy (methotrexate or azathioprine)[29].

At week 52, clinical response and clinical remission were achieved respectively by 65.7% and 47.8% of the ITT population, and 85.4% and 73.2% of the completers population. These results are comparable to those from the InspirADA study at week 8, in which 463 moderate-to-severe UC patients from 92 international sites were treated with adalimumab following usual clinical practice[40].

To our knowledge, UCanADA is the first study reporting associations between PHQ-9 scores and clinical response/remission in UC patients in a real-world setting. A regression analysis showed that in the ITT population, the odds of improving depressive symptoms for those achieving a clinical remission at week 52 was 7.94 higher compared to those not achieving a clinical remission (OR: 7.94; 95%CI: 1.42-44.41; $P = 0.018$).

These results–as well as the significant associations measured between the PHQ-9 total score and clinical response/remission at week 52 ($P < 0.001$) and between clinical response/remission and IBD-DI, EQ-5D-5L, SIBDQ total score, and FACIT-F fatigue subscale ($P = 0.002$)–are consistent with the other findings showing a relationship between disease activity and HRQoL[34,35,56]. In a 6-mo study including 199 UC patients, a consistent and almost linear relationship was demonstrated between SCCAI values and the EQ-5D-5L index values (correlation: ρ: -0.53; $P < 0.001$)[34].

Other studies conducted in UC patients reported correlations between disease activity indexes and HRQoL measures. Aniwan *et al*[35] reported a good correlation between the SIBDQ and the combination of self-rated rectal bleeding and stool frequency using the 6-point partial Mayo score (ClinPRO2) and MES, from a study on 90 UC patients ($r = -0.70$; $P < 0.01$). Assessed on 110 UC patients, a significant correlation has been reported between SIBDQ and SCCAI and MES alone ($r = −0.79$ and $r = −0.58$, respectively)[56]. Consistent with our findings, these support an association between clinical remission and improved HRQoL.

To the PHQ-9 item 'Feeling tired or having little energy' between baseline and week 52, the proportion of patients feeling it 'Nearly every day' decreased by 20%, and those feeling it 'Not at all' increased by 8%. These results are in line with the significant decrease in fatigue shown in the FACIT-F total score and fatigue subscale ($P = 0.006$).

As fatigue has been reported to be strongly associated with sleep disturbances in IBD patients[18], not surprisingly our scores from the MOS sleep problems indexes I and II also significantly improved during the study, as well as sleep adequacy and sleep quantity subscores ($P = 0.042$ at week 52). Using the NIH PROMIS questionnaire in 160 patients with IBD using either and anti-TNF or vedolizumab, Stevens *et al*[57] reported significant and meaningful improvement in sleep quality by week 6 ($P = 0.009$), which was paralleled by a significant reduction in depression ($P < 0.05$), as measured in the UCanADA study population. These results reinforce the need to assess sleep disorders a part of an algorithmic approach for the systemic workup of fatigue[18].

Also related to fatigue, in a study including 1185 IBD patients (462 with UC), Williet *et al*[58] reported a strong correlation between FACIT-F score and IBD-DI measure ($r = -0.78$) as well as overall work impairment ($r = -0.70$). Similar trends were observed in UCanADA, *i.e.*, a significant improvement in fatigue (FACIT-F total score; $P < 0.001$) mirrored by a significant improvement in IBD-DI measures ($P < 0.001$) as well as a meaningful improvement in overall work impairment during the study. Our IBD-DI measures are similar to those reported from other UC populations[43]. In a meta-analysis including 3167 IBD patients, Lo *et al*[43] reported a significant lower disease disability rates in patients on biological treatment than those on corticosteroids ($P < 0.01$).

At week 8 and week 52, there was a gain between 15% and 17% in work impairment, overall work impairment, and activity impairment in the UCanADA study population. These represent less gains than those reported from the InspirADA population at week 26; however, they were twice as high as the minimal clinically important difference of 7% in WPAI outcome[59].

Limitations of the research methods used in this study are related to, but may not have been limited to, the observational nature of the study with regards to missing data, which has been alleviated with the use of sensitivity analyses for the primary endpoint. This study consisted of a small cohort of patients, and only 48 (48%) patients completed the study. However, the results between the ITT population and completers population were fairly consistent. The PRO questionnaires being self-administered provide subjective data as opposed to objective data. The collection of secondary PROs data may be subject to a recall bias.

CONCLUSION

At week 52 in a real-world setting, adalimumab was effective in reducing depressive symptoms in patients with UC, with more than 60% of the patients achieving an improvement the PHQ-9 with a mean improvement of 2.4 points. A broad range of PROs including HRQoL and work productivity also significantly improved during the study. The safety profile was consistent with the known safety profile of adalimumab, and no new signal or unexpected trend was identified for the patient population.

ARTICLE HIGHLIGHTS

Research background

The efficacy and safety of adalimumab have been demonstrated in pivotal trials, but there remained a need to assess more holistically how the clinical results translate into concrete improvements in key aspects of the daily lives of ulcerative colitis (UC) patients, such as symptoms, health-related quality of life (HRQoL), and disability.

Research motivation

Although some patient-reported outcomes (PROs) from existing studies may have items capturing some of these aspects, limited data was available for adalimumab in UC, specifically on psychological distress/depression, disability, fatigue, and pain or sleep quality in real-life setting.

Research objectives

The overarching goal for the UCanADA study was to assess the real-life effectiveness of adalimumab on PRO measures, while taking the opportunity to use the inflammatory bowel disease disability index to assess the impact of adalimumab on key components of patients' functioning when affected with moderate-to-severe UC.

Research methods

UCanADA was a single arm, prospective, 1-year multicenter Canadian post-marketing observational study in which multiple PRO questionnaires were completed—with psychologic distress/depression symptoms as the primary endpoint—by patients with moderate-to-severe UC. Assessments were performed during patients' routine care visit schedule, which was at the initiation of adalimumab (baseline), after induction (approximately 8 wk), and 52 wk after baseline. Additional optional assessments between weeks 8 and 52 were collected at least once but no more than two times during this period. Serious safety events and per-protocol adverse events were collected.

Research results

One hundred patients were included in this final analysis, with 94 (94%) patients included in the efficacy population (identified as the intent-to-treat (ITT) population), 48 (48%) patients included in the completers' population, and 98 (98%) patients included in the safety population. The primary endpoint–the proportion of patients who achieved a change from baseline, defined as an improvement in total severity score relative to baseline, in the Patient Health Questionnaire–9 items (PHQ-9) measure at week 52–was 61.5% [40/65 patients; 95% confidence interval (CI): 49.7%-73.4%] for the ITT population and 65.9% (29/44 patients; 95%CI: 51.9%-79.9%) for completers. The safety profile was consistent with the known safety profile of adalimumab, and no new signal or unexpected trend was identified for the patient population.

Research conclusions

At week 52, adalimumab, used in a real-life study, was effective in reducing depressive symptoms in patients with UC, with more than 60% of the patients achieving an improvement the PHQ-9 with a mean improvement of 2.4 points. Thus, the treatment with adalimumab contributed to reducing the depressive symptoms frequently experienced in patients with UC as well as improving a broad range of PROs such as HRQoL and work productivity, as assessed with PRO instruments. The safety profile was consistent with the known safety profile of adalimumab, and no new signal or unexpected trend was identified for the patient population.

Research perspectives

Improvements in PHQ-9 were associated with clinical remission. Beyond the PHQ-9, significant improvements in several PROs were observed suggesting an improvement in HRQoL and work productivity as well. The population in the study, as well as the inclusion and exclusion criteria, was representative of the target population. In addition, coinciding the study visits with the patient's routine care visit schedule helped increase generalizability of the PRO instruments by decreasing the impact on real life.

ACKNOWLEDGEMENTS

AbbVie and the authors thank all study investigators (Dr. Kenneth Atkinson, Columbia Gastroenterology Management Ltd.; Dr. Guy Aumais, CHUM-Hôpital Maisonneuve-Rosemont; Dr. Rahman Bacchus, Dr. Rahman Bacchus Medicine Corporation; Dr. Andrew Bellini, Bellini Medicine Professional Corporation; Dr. Edmond-Jean Bernard, Le Centre des Maladies Inflammatoires et Intestinales de

Montréal (CMIIM); Dr. Ian Bookman, Kensington Cancer Screening Clinic; Dr. Raymond Bourdages, CHAU - Hôpital Hotel-Dieu de Levis; Dr. Brian Bressler, Gastrointestinal Research Institute (GIRI); Dr. Sharyle Fowler, Royal University Hospital; Dr. Alexandre Gougeon, Centre Hospitalier de l'Université Laval (CHUL); Dr. Daniel Green, Oshawa Clinic; Dr. Vivian Huang, Zeidler Ledcor Centre; Dr. Mark MacMillan, Dr. Everett Chalmers Regional Hospital; Dr. Remo Panaccione, University of Calgary Gastrointestinal Research Group; Dr. Denis Petrunia, Discovery Clinical Services; Dr. Ranjit Singh, PerCuro Clinical Research Ltd.; Dr. Richmond Sy, Ottawa Hospital - General Campus; Dr. Audrey Weber, CHUM – Hôpital St-Luc; and Dr. Chadwick Williams, Dr. Chadwick Ian Williams Professional) for their contribution and the patients for their participation in this study. Thank you also to Daphne Guh, MSc., from the Centre for Health Evaluation and Outcome Sciences, and Nick Bansback, Ph.D. from University of British Columbia, for the statistical analyses. Medical writing support was provided by Judy Chiu, MPH, from the Centre for Health Evaluation and Outcome Sciences, and Nathalie Ross, PhD, MWC, from McDougall Scientific Ltd. All of these contributors were funded by AbbVie, Inc. AbbVie sponsored the study and medical writing support for this manuscript; contributed to the design; participated in the collection, analysis, and interpretation of data as well as in writing, reviewing, and approving the final version of this manuscript. No honoraria or payments were made for authorship.

FOOTNOTES

Author contributions: Bessissow T was involved in study design, coordinating the data collection, interpretation of the results, and review and revision of the manuscript; Ruel J, Nguyen GC, and Tarabain O were involved in coordinating the data collection, interpretation of the results, and review and revision of the manuscript; Foucault N and McHugh K were involved in study design, interpretation of the results, and review and revision of the manuscript.

Institutional review board statement: All sites had the study reviewed and approved by an ethics committee. While CEC Advarra IRB Services (Aurora, Ontario, Canada) reviewed and approved for some sites, other sites were approved through local/multi centres ethics committees (Dr. Everett Chalmers Regional Hospital, MUHC-Royal Victoria Hospital, CHUM-Hôpital Maisonneuve-Rosemont, CHAU-Hôpital Hôtel-Dieu de Levis, Royal University Hospital, Centre Hospitalier de l'Université de Sherbrooke, CHUM-Hôpital St-Luc, Zeidler Ledcor Centre, Ottawa Hospital-General Campus, Mount Sinai Hospital, London Health Sciences Centre, Centre Hospitalier de l'Université Laval (CHUL), University of Calgary Gastrointestinal Research Group).

Informed consent statement: All patients were required to sign a patient authorization form (or written informed consent) to participate in the study, and to disclose personal health information.

Conflict-of-interest statement: The authors have either received research support from, served as consultant, speakers bureau, scientific officer, participants of steering committees and advisory boards, and/or received honoraria from the following sponsors: T.B.: AbbVie, Janssen, Takeda, Merck, Pfizer, Roche, Bristol Myers Squibb, Gilead, Sandoz, Ferring, Alimentiv Inc. (formerly Robarts Clinical Trials); J.R.: AbbVie, Janssen, Takeda, Pfizer, Sandoz, Ferring, Alimentiv Inc. (formerly Robarts Clinical Trials); G.N.: AbbVie and Takeda; O.T.: AbbVie; N.F. and K.M.: are employees of AbbVie and may own AbbVie stock; L.P.B.: Dr. Peyrin-Biroulet reports personal fees from Galapagos, AbbVie, Janssen, Genentech, Ferring, Tillots, Celltrion, Takeda, Pfizer, Index Pharmaceuticals, Sandoz, Celgene, Biogen, Samsung Bioepis, Inotrem, Allergan, MSD, Roche, Arena, Gilead, Amgen, BMS, Vifor, Norgine, Mylan, Lilly, Fresenius Kabi, OSE Immunotherapeutics, Enthera, Theravance, Pandion Therapeutics, Gossamer Bio, Viatris, Thermo Fisher. Grants from AbbVie, MSD, Takeda, Fresenius Kabi. Stock options: CTMA.

Data sharing statement: AbbVie is committed to responsible data sharing regarding the clinical trials we sponsor. This includes access to anonymized, individual and trial-level data (analysis data sets), as well as other information (*e.g.*, protocols and Clinical Study Reports), as long as the trials are not part of an ongoing or planned regulatory submission. This includes requests for clinical trial data for unlicensed products and indications. This clinical trial data can be requested by any qualified researchers who engage in rigorous, independent scientific research, and will be provided following review and approval of a research proposal and Statistical Analysis Plan (SAP) and execution of a Data Sharing Agreement (DSA). Data requests can be submitted at any time and the data will be accessible for 12 mo, with possible extensions considered. For more information on the process, or to submit a request, visit the following link: https://www.abbvie.com/our-science/clinical-trials/clinical-trials-data-and-information-sharing/data-and-information-sharing-with-qualified-researchers.html.

STROBE statement: The authors have read the STROBE Statement—checklist of items, and the manuscript was prepared and revised according to the STROBE Statement—checklist of items.

Open-Access: This article is an open-access article that was selected by an in-house editor and fully peer-reviewed by external reviewers. It is distributed in accordance with the Creative Commons Attribution NonCommercial (CC BY-NC 4.0) license, which permits others to distribute, remix, adapt, build upon this work non-commercially, and license

their derivative works on different terms, provided the original work is properly cited and the use is non-commercial. See: https://creativecommons.org/Licenses/by-nc/4.0/

Country/Territory of origin: Canada

ORCID number: Talat Bessissow 0000-0003-2610-1910; Geoffrey C Nguyen 0000-0001-7083-7429; Laurent Peyrin-Biroulet 0000-0003-2536-6618; Kevin McHugh 0000-0001-9331-1614; Joannie Ruel 0000-0001-6996-0120.

S-Editor: Fan JR
L-Editor: A
P-Editor: Fan JR

REFERENCES

1 **Ford AC**, Moayyedi P, Hanauer SB. Ulcerative colitis. *BMJ* 2013; **346**: f432 [PMID: 23386404 DOI: 10.1136/bmj.f432]
2 **Danese S**, Fiocchi C. Ulcerative colitis. *N Engl J Med* 2011; **365**: 1713-1725 [PMID: 22047562 DOI: 10.1056/NEJMra1102942]
3 **McCormick JB**, Hammer RR, Farrell RM, Geller G, James KM, Loftus EV Jr, Mercer MB, Tilburt JC, Sharp RR. Experiences of patients with chronic gastrointestinal conditions: in their own words. *Health Qual Life Outcomes* 2012; **10**: 25 [PMID: 22401607 DOI: 10.1186/1477-7525-10-25]
4 **Mikocka-Walus A**, Knowles SR, Keefer L, Graff L. Controversies Revisited: A Systematic Review of the Comorbidity of Depression and Anxiety with Inflammatory Bowel Diseases. *Inflamm Bowel Dis* 2016; **22**: 752-762 [PMID: 26841224 DOI: 10.1097/MIB.0000000000000620]
5 **Regueiro M**, Greer JB, Szigethy E. Etiology and Treatment of Pain and Psychosocial Issues in Patients With Inflammatory Bowel Diseases. *Gastroenterology* 2017; **152**: 430-439.e4 [PMID: 27816599 DOI: 10.1053/j.gastro.2016.10.036]
6 **Yarlas A**, Rubin DT, Panés J, Lindsay JO, Vermeire S, Bayliss M, Cappelleri JC, Maher S, Bushmakin AG, Chen LA, DiBonaventura M. Burden of Ulcerative Colitis on Functioning and Well-being: A Systematic Literature Review of the SF-36® Health Survey. *J Crohns Colitis* 2018; **12**: 600-609 [PMID: 29718244 DOI: 10.1093/ecco-jcc/jjy024]
7 **Jones JL**, Nguyen GC, Benchimol EI, Bernstein CN, Bitton A, Kaplan GG, Murthy SK, Lee K, Cooke-Lauder J, Otley AR. The Impact of Inflammatory Bowel Disease in Canada 2018: Quality of Life. *J Can Assoc Gastroenterol* 2019; **2**: S42-S48 [PMID: 31294384 DOI: 10.1093/jcag/gwy048]
8 **Zhang CK**, Hewett J, Hemming J, Grant T, Zhao H, Abraham C, Oikonomou I, Kanakia M, Cho JH, Proctor DD. The influence of depression on quality of life in patients with inflammatory bowel disease. *Inflamm Bowel Dis* 2013; **19**: 1732-1739 [PMID: 23669400 DOI: 10.1097/MIB.0b013e318281f395]
9 **Neuendorf R**, Harding A, Stello N, Hanes D, Wahbeh H. Depression and anxiety in patients with Inflammatory Bowel Disease: A systematic review. *J Psychosom Res* 2016; **87**: 70-80 [PMID: 27411754 DOI: 10.1016/j.jpsychores.2016.06.001]
10 **Kroenke K**, Spitzer RL, Williams JB. The PHQ-9: validity of a brief depression severity measure. *J Gen Intern Med* 2001; **16**: 606-613 [PMID: 11556941 DOI: 10.1046/j.1525-1497.2001.016009606.x]
11 **Barsevick AM**, Cleeland CS, Manning DC, O'Mara AM, Reeve BB, Scott JA, Sloan JA; ASCPRO (Assessing Symptoms of Cancer Using Patient-Reported Outcomes). ASCPRO recommendations for the assessment of fatigue as an outcome in clinical trials. *J Pain Symptom Manage* 2010; **39**: 1086-1099 [PMID: 20538190 DOI: 10.1016/j.jpainsymman.2010.02.006]
12 **Grimstad T**, Norheim KB, Isaksen K, Leitao K, Hetta AK, Carlsen A, Karlsen LN, Skoie IM, Gøransson L, Harboe E, Aabakken L, Omdal R. Fatigue in Newly Diagnosed Inflammatory Bowel Disease. *J Crohns Colitis* 2015; **9**: 725-730 [PMID: 25994356 DOI: 10.1093/ecco-jcc/jjv091]
13 **Jelsness-Jørgensen LP**, Bernklev T, Henriksen M, Torp R, Moum BA. Chronic fatigue is associated with impaired health-related quality of life in inflammatory bowel disease. *Aliment Pharmacol Ther* 2011; **33**: 106-114 [PMID: 21083587 DOI: 10.1111/j.1365-2036.2010.04498.x]
14 **Romberg-Camps MJ**, Bol Y, Dagnelie PC, Hesselink-van de Kruijs MA, Kester AD, Engels LG, van Deursen C, Hameeteman WH, Pierik M, Wolters F, Russel MG, Stockbrügger RW. Fatigue and health-related quality of life in inflammatory bowel disease: results from a population-based study in the Netherlands: the IBD-South Limburg cohort. *Inflamm Bowel Dis* 2010; **16**: 2137-2147 [PMID: 20848468 DOI: 10.1002/ibd.21285]
15 **Cohen BL**, Zoëga H, Shah SA, Leleiko N, Lidofsky S, Bright R, Flowers N, Law M, Moniz H, Merrick M, Sands BE. Fatigue is highly associated with poor health-related quality of life, disability and depression in newly-diagnosed patients with inflammatory bowel disease, independent of disease activity. *Aliment Pharmacol Ther* 2014; **39**: 811-822 [PMID: 24612278 DOI: 10.1111/apt.12659]
16 **Graff LA**, Vincent N, Walker JR, Clara I, Carr R, Ediger J, Miller N, Rogala L, Rawsthorne P, Lix L, Bernstein CN. A population-based study of fatigue and sleep difficulties in inflammatory bowel disease. *Inflamm Bowel Dis* 2011; **17**: 1882-1889 [PMID: 21830266 DOI: 10.1002/ibd.21580]
17 **Jonefjäll B**, Simrén M, Lasson A, Öhman L, Strid H. Psychological distress, iron deficiency, active disease and female gender are independent risk factors for fatigue in patients with ulcerative colitis. *United European Gastroenterol J* 2018; **6**: 148-158 [PMID: 29435325 DOI: 10.1177/2050640617703868]
18 **Nocerino A**, Nguyen A, Agrawal M, Mone A, Lakhani K, Swaminath A. Fatigue in Inflammatory Bowel Diseases: Etiologies and Management. *Adv Ther* 2020; **37**: 97-112 [PMID: 31760611 DOI: 10.1007/s12325-019-01151-w]
19 **Daperno M**, Armuzzi A, Danese S, Fries W, Liguori G, Orlando A, Papi C, Principi M, Rizzello F, Viscido A, Gionchetti P. Unmet Medical Needs in the Management of Ulcerative Colitis: Results of an Italian Delphi Consensus. *Gastroenterol*

Res Pract 2019; **2019**: 3108025 [PMID: 31565051 DOI: 10.1155/2019/3108025]
20 **Food and Drug Administration**. Guidance for industry patient-reported outcome measures: Use in medical product development to support labeling claims. In: Services USDoHaH, editor, 2009: 39
21 **Bojic D**, Bodger K, Travis S. Patient Reported Outcome Measures (PROMs) in Inflammatory Bowel Disease: New Data. *J Crohns Colitis* 2017; **11**: S576-S585 [PMID: 27797917 DOI: 10.1093/ecco-jcc/jjw187]
22 **Bastemeijer CM**, Voogt L, van Ewijk JP, Hazelzet JA. What do patient values and preferences mean? *Patient Educ Couns* 2017; **100**: 871-881 [PMID: 28043713 DOI: 10.1016/j.pec.2016.12.019]
23 **Zhang Y**, Coello PA, Brożek J, Wiercioch W, Etxeandia-Ikobaltzeta I, Akl EA, Meerpohl JJ, Alhazzani W, Carrasco-Labra A, Morgan RL, Mustafa RA, Riva JJ, Moore A, Yepes-Nuñez JJ, Cuello-Garcia C, AlRayees Z, Manja V, Falavigna M, Neumann I, Brignardello-Petersen R, Santesso N, Rochwerg B, Darzi A, Rojas MX, Adi Y, Bollig C, Waziry R, Schünemann HJ. Using patient values and preferences to inform the importance of health outcomes in practice guideline development following the GRADE approach. *Health Qual Life Outcomes* 2017; **15**: 52 [PMID: 28460638 DOI: 10.1186/s12955-017-0621-0]
24 **Postmus D**, Mavris M, Hillege HL, Salmonson T, Ryll B, Plate A, Moulon I, Eichler HG, Bere N, Pignatti F. Incorporating patient preferences into drug development and regulatory decision making: Results from a quantitative pilot study with cancer patients, carers, and regulators. *Clin Pharmacol Ther* 2016; **99**: 548-554 [PMID: 26715217 DOI: 10.1002/cpt.332]
25 **Ho M**, Saha A, McCleary KK, Levitan B, Christopher S, Zandlo K, Braithwaite RS, Hauber AB; Medical Device Innovation Consortium's Patient Centered Benefit-Risk Steering Committee. A Framework for Incorporating Patient Preferences Regarding Benefits and Risks into Regulatory Assessment of Medical Technologies. *Value Health* 2016; **19**: 746-750 [PMID: 27712701 DOI: 10.1016/j.jval.2016.02.019]
26 **Ghosh S**, Sensky T, Casellas F, Rioux LC, Ahmad T, Márquez JR, Vanasek T, Gubonina I, Sezgin O, Ardizzone S, Kligys K, Petersson J, Suzuki Y, Peyrin-Biroulet L. A Global, Prospective, Observational Study Measuring Disease Burden and Suffering in Patients with Ulcerative Colitis Using the Pictorial Representation of Illness and Self-Measure Tool. *J Crohns Colitis* 2020 [PMID: 32722760 DOI: 10.1093/ecco-jcc/jjaa159]
27 **Moon JR**, Lee CK, Hong SN, Im JP, Ye BD, Cha JM, Jung SA, Lee KM, Park DI, Jeen YT, Park YS, Cheon JH, Kim H, Seo B, Kim Y, Kim HJ; MOSAIK study group of the Korean Association for Study of Intestinal Diseases. Unmet Psychosocial Needs of Patients with Newly Diagnosed Ulcerative Colitis: Results from the Nationwide Prospective Cohort Study in Korea. *Gut Liver* 2020; **14**: 459-467 [PMID: 31533398 DOI: 10.5009/gnl19107]
28 **Geiss T**, Schaefert RM, Berens S, Hoffmann P, Gauss A. Risk of depression in patients with inflammatory bowel disease. *J Dig Dis* 2018; **19**: 456-467 [PMID: 29989345 DOI: 10.1111/1751-2980.12644]
29 **Horst S**, Chao A, Rosen M, Nohl A, Duley C, Wagnon JH, Beaulieu DB, Taylor W, Gaines L, Schwartz DA. Treatment with immunosuppressive therapy may improve depressive symptoms in patients with inflammatory bowel disease. *Dig Dis Sci* 2015; **60**: 465-470 [PMID: 25274158 DOI: 10.1007/s10620-014-3375-0]
30 **Armuzzi A**, Tarallo M, Lucas J, Bluff D, Hoskin B, Bargo D, Cappelleri JC, Salese L, daCosta DiBonaventura M. The association between disease activity and patient-reported outcomes in patients with moderate-to-severe ulcerative colitis in the United States and Europe. *BMC Gastroenterol* 2020; **20**: 18 [PMID: 31964359 DOI: 10.1186/s12876-020-1164-0]
31 **Walter E**, Hausberger SC, Groß E, Siebert U. Health-related quality of life, work productivity and costs related to patients with inflammatory bowel disease in Austria. *J Med Econ* 2020; **23**: 1061-1071 [PMID: 32713223 DOI: 10.1080/13696998.2020.1801187]
32 **Teich N**, Grümmer H, Jörgensen E, Liceni T, Holtkamp-Endemann F, Fischer T, Hohenberger S. Golimumab in real-world practice in patients with ulcerative colitis: Twelve-month results. *World J Gastroenterol* 2020; **26**: 2852-2863 [PMID: 32550760 DOI: 10.3748/wjg.v26.i21.2852]
33 **Paschos P**, Katsoula A, Salanti G, Giouleme O, Athanasiadou E, Tsapas A. Systematic review with network meta-analysis: the impact of medical interventions for moderate-to-severe ulcerative colitis on health-related quality of life. *Aliment Pharmacol Ther* 2018; **48**: 1174-1185 [PMID: 30378141 DOI: 10.1111/apt.15005]
34 **Panés J**, Domènech E, Aguas Peris M, Nos P, Riestra S, Juliá de Páramo B, Cea-Calvo L, Romero C, Marín-Jiménez I. Association between disease activity and quality of life in ulcerative colitis: Results from the CRONICA-UC study. *J Gastroenterol Hepatol* 2017; **32**: 1818-1824 [PMID: 28370253 DOI: 10.1111/jgh.13795]
35 **Aniwan S**, Bruining DH, Park SH, Al-Bawardy B, Kane SV, Coelho Prabhu N, Kisiel JB, Raffals LE, Papadakis KA, Pardi DS, Tremaine WJ, Loftus EV Jr. The Combination of Patient-Reported Clinical Symptoms and an Endoscopic Score Correlates Well with Health-Related Quality of Life in Patients with Ulcerative Colitis. *J Clin Med* 2019; **8** [PMID: 31387259 DOI: 10.3390/jcm8081171]
36 **Saraiva S**, Cortez-Pinto J, Barosa R, Castela J, Moleiro J, Rosa I, da Siva JP, Dias Pereira A. Evaluation of fatigue in inflammatory bowel disease - a useful tool in daily practice. *Scand J Gastroenterol* 2019; **54**: 465-470 [PMID: 31012338 DOI: 10.1080/00365521.2019.1602669]
37 **Villoria A**, García V, Dosal A, Moreno L, Montserrat A, Figuerola A, Horta D, Calvet X, Ramírez-Lázaro MJ. Fatigue in out-patients with inflammatory bowel disease: Prevalence and predictive factors. *PLoS One* 2017; **12**: e0181435 [PMID: 28749985 DOI: 10.1371/journal.pone.0181435]
38 **Christiansen LK**, Lo B, Bendtsen F, Vind I, Vester-Andersen MK, Burisch J. Health-related quality of life in inflammatory bowel disease in a Danish population-based inception cohort. *United European Gastroenterol J* 2019; **7**: 942-954 [PMID: 31428419 DOI: 10.1177/2050640619852532]
39 **Yarlas A**, Maher SM, Bayliss MS, Lovley A, Cappelleri JC, DiBonaventura MD. Psychometric validation of the work productivity and activity impairment questionnaire in ulcerative colitis: results from a systematic literature review. *J Patient Rep Outcomes* 2018; **2**: 62 [PMID: 30547275 DOI: 10.1186/s41687-018-0088-8]
40 **Travis S**, Feagan BG, Peyrin-Biroulet L, Panaccione R, Danese S, Lazar A, Robinson AM, Petersson J, Pappalardo BL, Bereswill M, Chen N, Wang S, Skup M, Thakkar RB, Chao J. Effect of Adalimumab on Clinical Outcomes and Health-related Quality of Life Among Patients With Ulcerative Colitis in a Clinical Practice Setting: Results From InspirADA. *J Crohns Colitis* 2017; **11**: 1317-1325 [PMID: 28981846 DOI: 10.1093/ecco-jcc/jjx093]
41 **Peyrin-Biroulet L**, Cieza A, Sandborn WJ, Coenen M, Chowers Y, Hibi T, Kostanjsek N, Stucki G, Colombel JF;

International Programme to Develop New Indexes for Crohn's Disease (IPNIC) group. Development of the first disability index for inflammatory bowel disease based on the international classification of functioning, disability and health. *Gut* 2012; **61**: 241-247 [PMID: 21646246 DOI: 10.1136/gutjnl-2011-300049]

42 **Gower-Rousseau C**, Sarter H, Savoye G, Tavernier N, Fumery M, Sandborn WJ, Feagan BG, Duhamel A, Guillon-Dellac N, Colombel JF, Peyrin-Biroulet L; International Programme to Develop New Indexes for Crohn's Disease (IPNIC) group; International Programme to Develop New Indexes for Crohn's Disease (IPNIC) group. Validation of the Inflammatory Bowel Disease Disability Index in a population-based cohort. *Gut* 2017; **66**: 588-596 [PMID: 26646934 DOI: 10.1136/gutjnl-2015-310151]

43 **Lo B**, Prosberg MV, Gluud LL, Chan W, Leong RW, van der List E, van der Have M, Sarter H, Gower-Rousseau C, Peyrin-Biroulet L, Vind I, Burisch J. Systematic review and meta-analysis: assessment of factors affecting disability in inflammatory bowel disease and the reliability of the inflammatory bowel disease disability index. *Aliment Pharmacol Ther* 2018; **47**: 6-15 [PMID: 28994131 DOI: 10.1111/apt.14373]

44 **Walmsley RS**, Ayres RC, Pounder RE, Allan RN. A simple clinical colitis activity index. *Gut* 1998; **43**: 29-32 [PMID: 9771402 DOI: 10.1136/gut.43.1.29]

45 **Kind P**. The EuroQol instrument - an index of health-related quality of life. In: Spilker B, editor Quality of Life and Pharmacoeconomics in Clinical Trials 2nd ed. Philadelphia, PA: Lippincott-Raven Publishers, 1996

46 **Irvine EJ**, Zhou Q, Thompson AK. The Short Inflammatory Bowel Disease Questionnaire: a quality of life instrument for community physicians managing inflammatory bowel disease. CCRPT Investigators. Canadian Crohn's Relapse Prevention Trial. *Am J Gastroenterol* 1996; **91**: 1571-1578 [PMID: 8759664]

47 **Tinsley A**, Macklin EA, Korzenik JR, Sands BE. Validation of the functional assessment of chronic illness therapy-fatigue (FACIT-F) in patients with inflammatory bowel disease. *Aliment Pharmacol Ther* 2011; **34**: 1328-1336 [PMID: 21999576 DOI: 10.1111/j.1365-2036.2011.04871.x]

48 **Hays R**, Stewart A. Sleep Measures. In: Stewart A, Ware J, editors. Measuring functioning and well-being; the medical outcomes study approach Duke edition: Duke University Press; 1992: 235–259

49 **Zhang W**, Bansback N, Boonen A, Young A, Singh A, Anis AH. Validity of the work productivity and activity impairment questionnaire--general health version in patients with rheumatoid arthritis. *Arthritis Res Ther* 2010; **12**: R177 [PMID: 20860837 DOI: 10.1186/ar3141]

50 **Zhang W**, Bansback N, Kopec J, Anis AH. Measuring time input loss among patients with rheumatoid arthritis: validity and reliability of the Valuation of Lost Productivity questionnaire. *J Occup Environ Med* 2011; **53**: 530-536 [PMID: 21508868 DOI: 10.1097/JOM.0b013e318218abf1]

51 **U.S. Food and Drug Administration**. FDA Drug Safety Communication: UPDATE on Tumor Necrosis Factor (TNF) blockers and risk for pediatric malignancy. 2018. [cited 10 January 2022]. Available from: https://www.fda.gov/drugs/drug-safety-and-availability/fda-drug-safety-communication-update-tumor-necrosis-factor-tnf-blockers-and-risk-pediatric

52 **Round JM**, Lee C, Hanlon JG, Hyshka E, Dyck JRB, Eurich DT. Changes in patient health questionnaire (PHQ-9) scores in adults with medical authorization for cannabis. *BMC Public Health* 2020; **20**: 987 [PMID: 32576158 DOI: 10.1186/s12889-020-09089-3]

53 **Hudgens S**, Floden L, Blackowicz M, Jamieson C, Popova V, Fedgchin M, Drevets WC, Cooper K, Lane R, Singh J. Meaningful Change in Depression Symptoms Assessed with the Patient Health Questionnaire (PHQ-9) and Montgomery-Åsberg Depression Rating Scale (MADRS) Among Patients with Treatment Resistant Depression in Two, Randomized, Double-blind, Active-controlled Trials of Esketamine Nasal Spray Combined With a New Oral Antidepressant. *J Affect Disord* 2021; **281**: 767-775 [PMID: 33261932 DOI: 10.1016/j.jad.2020.11.066]

54 **Turkoz I**, Alphs L, Singh J, Jamieson C, Daly E, Shawi M, Sheehan JJ, Trivedi MH, Rush AJ. Clinically meaningful changes on depressive symptom measures and patient-reported outcomes in patients with treatment-resistant depression. *Acta Psychiatr Scand* 2021; **143**: 253-263 [PMID: 33249552 DOI: 10.1111/acps.13260]

55 **Moayyedi P**, Andrews CN, MacQueen G, Korownyk C, Marsiglio M, Graff L, Kvern B, Lazarescu A, Liu L, Paterson WG, Sidani S, Vanner S. Canadian Association of Gastroenterology Clinical Practice Guideline for the Management of Irritable Bowel Syndrome (IBS). *J Can Assoc Gastroenterol* 2019; **2**: 6-29 [PMID: 31294724 DOI: 10.1093/jcag/gwy071]

56 **Theede K**, Kiszka-Kanowitz M, Nordgaard-Lassen I, Mertz Nielsen A. The Impact of Endoscopic Inflammation and Mucosal Healing on Health-related Quality of Life in Ulcerative Colitis Patients. *J Crohns Colitis* 2015; **9**: 625-632 [PMID: 25956537 DOI: 10.1093/ecco-jcc/jjv081]

57 **Stevens BW**, Borren NZ, Velonias G, Conway G, Cleland T, Andrews E, Khalili H, Garber JG, Xavier RJ, Yajnik V, Ananthakrishnan AN. Vedolizumab Therapy Is Associated with an Improvement in Sleep Quality and Mood in Inflammatory Bowel Diseases. *Dig Dis Sci* 2017; **62**: 197-206 [PMID: 27796768 DOI: 10.1007/s10620-016-4356-2]

58 **Williet N**, Sarter H, Gower-Rousseau C, Adrianjafy C, Olympie A, Buisson A, Beaugerie L, Peyrin-Biroulet L. Patient-reported Outcomes in a French Nationwide Survey of Inflammatory Bowel Disease Patients. *J Crohns Colitis* 2017; **11**: 165-174 [PMID: 27516406 DOI: 10.1093/ecco-jcc/jjw145]

59 **Binion DG**, Louis E, Oldenburg B, Mulani P, Bensimon AG, Yang M, Chao J. Effect of adalimumab on work productivity and indirect costs in moderate to severe Crohn's disease: a meta-analysis. *Can J Gastroenterol* 2011; **25**: 492-496 [PMID: 21912760 DOI: 10.1155/2011/938194]

World Journal of Gastroenterology

Submit a Manuscript: https://www.f6publishing.com

World J Gastroenterol 2022 September 14; 28(34): 5076-5085

DOI: 10.3748/wjg.v28.i34.5076

ISSN 1007-9327 (print) ISSN 2219-2840 (online)

CASE REPORT

Gastrointestinal tumors in transplantation: Two case reports and review of literature

Romain Stammler, Dany Anglicheau, Bruno Landi, Tchao Meatchi, Emilia Ragot, Eric Thervet, Hélène Lazareth

Specialty type: Gastroenterology and hepatology

Provenance and peer review: Unsolicited article; Externally peer reviewed.

Peer-review model: Single blind

Peer-review report's scientific quality classification

Grade A (Excellent): A
Grade B (Very good): B, B
Grade C (Good): 0
Grade D (Fair): 0
Grade E (Poor): 0

P-Reviewer: Harouachi A, Morocco; Karki S, Nepal; Shuang WB, China

Received: March 7, 2022
Peer-review started: March 7, 2022
First decision: April 5, 2022
Revised: April 19, 2022
Accepted: August 6, 2022
Article in press: August 6, 2022
Published online: September 14, 2022

Romain Stammler, Eric Thervet, Hélène Lazareth, Department of Nephrology, Georges Pompidou European Hospital, Paris 75015, France

Dany Anglicheau, Department of Renal Transplantation, Necker-Enfants Malades Institute, French National Institutes of Health and Medical Research U1151, Paris 75015, France

Dany Anglicheau, Bruno Landi, Eric Thervet, Hélène Lazareth, Université Paris Cité, Assistance Publique des Hôpitaux de Paris, Paris 75001, France

Bruno Landi, Department of Gastroenterology and Digestive Oncology, Georges Pompidou European Hospital, Paris 75015, France

Tchao Meatchi, Department of Pathology, Georges Pompidou European Hospital, Paris 75015, France

Emilia Ragot, Department of Digestive Surgery, Georges Pompidou European Hospital, Paris 75015, France

Corresponding author: Hélène Lazareth, MD, PhD, Doctor, Department of Nephrology, Georges Pompidou European Hospital, 20, rue Leblanc, Paris 75015, France.
helene.lazareth@gmail.com

Abstract

BACKGROUND

Gastrointestinal stromal tumors (GISTs) are the most common mesenchymal tumors of the gastrointestinal tract. As most of them harbor a *KIT* mutation (75%), selective kinase inhibitors are the therapeutic option and show a sustained objective response among patients with metastatic or unresectable GISTs. A well-known higher risk of neoplasm has been described among renal transplant recipients (RTRs). Nevertheless, only few cases of GIST onset among transplant patients have been reported in the literature.

CASE SUMMARY

Here, we describe 2 cases of gastric GIST occurring during the follow-up of RTRs. We also review the existing literature concerning GIST occurrence in transplant patients. In total and in association with our 2 cases, 16 patients have been reported. The median age was 59.5 years and 69% were male. With a median tumor size of 45 mm, no patient displayed metastatic dissemination at diagnosis.

Time from transplantation to diagnosis was highly variable between 5 mo and 21 years. Histopathological data mostly revealed high risk of progression (43%). Death increased to 29% during follow-up. Surgical treatment was systematically performed when the tumor was operable (94%). The use of adjuvant therapy was uncommon (19%).

CONCLUSION
GISTs represent rare but potentially severe malignant complication among transplant patients.

Key Words: Gastrointestinal stromal tumors; Imatinib mesylate; Transplantation; Kidney transplantation; Proto-oncogene protein c-KIT; Case report

©The Author(s) 2022. Published by Baishideng Publishing Group Inc. All rights reserved.

Core Tip: Although a well-known higher risk of neoplasm has been described among renal transplant recipients (RTRs), few cases of gastrointestinal stromal tumors (GISTs) have been reported. We describe 2 cases of gastric GIST among RTRs and provide a review of the literature. We report 16 patients with a median age of 59.5 years, and 69% were male. No patient displayed metastasis at diagnosis. Time from transplantation to diagnosis varied between 5 mo and 21 years. Histopathology revealed high risk of progression (43%). Death increased to 29%. Surgical treatment was commonly performed (94%). The use of adjuvant therapy was uncommon (19%).

Citation: Stammler R, Anglicheau D, Landi B, Meatchi T, Ragot E, Thervet E, Lazareth H. Gastrointestinal tumors in transplantation: Two case reports and review of literature. *World J Gastroenterol* 2022; 28(34): 5076-5085
URL: https://www.wjgnet.com/1007-9327/full/v28/i34/5076.htm
DOI: https://dx.doi.org/10.3748/wjg.v28.i34.5076

INTRODUCTION

Gastrointestinal stromal tumors (GISTs) are the most common mesenchymal tumors of the gastrointestinal (GI) tract[1]. GISTs arise from interstitial cells of Cajal (ICC), which are specialized mesenchymal cells located within the muscle of the GI tract. ICC play a critical role in regulating smooth muscle function and GI tract motility[2]. GISTs are mainly located in the stomach (55%) or the small bowel (30%). About 10% to 47% of patients have metastatic disease at diagnosis[3-5]. About 95% of GISTs display positive staining for the receptor tyrosine kinase KIT (or CD117), 75% of these tumors harbor a *KIT* gene mutation and 10% a platelet-derived growth factor receptor A (*PDGFRA*) gene mutation[6]. Among KIT-negative GISTs, immunohistochemical expression of discovered on GIST-1 (DOG-1) was found in 76% of the cases[7]. Consequently, selective tyrosine kinase inhibitors targeting KIT receptor have been used. The first one, imatinib mesylate (Gleevec®; Novartis, Basel, Switzerland), has shown a sustained objective response in a phase III trial among patients with metastatic or unresectable GISTs in immunocompetent patients[8].

In renal transplant recipients (RTRs), an increased risk of cancer has been reported especially for non-melanoma skin cancer, virus-associated cancer and lymphoproliferative disorders[9]. Currently, malignancy represents a major cause of mortality among RTRs[10]. Nonetheless, only few cases of GIST have been reported among transplant patients. Overall, 8 cases of GIST[11-17] and 2 cases of extra GIST (EGIST)[14,18] have previously been reported in RTRs and respectively 3 cases[19-21] and 1 case[22] in liver transplant recipients.

We report 2 cases of GIST occurring in RTRs and provide a review of the existing literature concerning GIST occurrence in transplant patients.

CASE PRESENTATION

Chief complaints

Case 1: A 60-year-old Caucasian man without any symptoms.

Case 2: A 56-year-old Caucasian man presented with upper GI hemorrhage.

History of present illness

Case 1: Hepatic magnetic resonance imaging (MRI) was performed to explore abnormal hepatic tests.

MRI revealed a 32 mm spherical tumor of the lesser curvature of the stomach.

Case 2: The upper GI hemorrhage led to gastric endoscopy, which revealed a spherical gastric tumor in the fundus.

History of past illness

Case 1: He had end-stage renal disease with a kidney biopsy compatible with nephronophthisis despite negative screening for mutation in hepatocyte nuclear factor 1 beta (*HNF1B*) gene. Hemodialysis was initiated in 2016. In October 2019, he received a kidney transplant from a deceased donor. The initial immunosuppressive therapy combined basiliximab, steroids, tacrolimus, and everolimus. Renal function at hospital discharge was 94 μmol/L, (normal range 53 μmol/L to 97 μmol/L). Initial maintenance immunosuppressive therapy associated steroids, tacrolimus, and everolimus. Due to relapsing lymphocele, everolimus was switched to mycophenolate mofetil (MMF). Moreover, a pre-existing mild cytolysis and cholestasis worsened after transplantation leading to the discontinuation of cotrimoxazole and MMF, which were replaced by atovaquone and belatacept (NULOJIX®; Bristol-Myers Squibb, New York, NY, United States), respectively.

Case 2: The patient developed end-stage renal disease of unknown origin. He received a kidney transplantation from a deceased donor. Due to preformed donor specific antibodies (anti-Cw15, mean fluorescence intensity of 6130) on the day of transplantation, induction immunosuppressive therapy combined basiliximab, steroids, MMF, cyclosporine, and intravenous immunoglobulins. At 10 d after surgery, a kidney biopsy was performed due to delayed graft function. It revealed acute tubular necrosis associated with possible acute humoral rejection (g1 cpt0 v0 i0 t0 according to Banff's classification[23,24], C4d immunostaining was negative). A treatment with high dose steroids, five plasma exchanges and rituximab[25] was initiated allowing improvement of renal function with a nadir in serum creatinine level of 170 μmol/L. Maintenance immunosuppressive therapy included steroids, cyclosporine, and MMF.

Personal and family history

Case 1: His other past medical history consisted in nonalcoholic steatohepatitis, Hashimoto's thyroiditis, and hypertension.

Case 2: The patient had no significant personal or family history.

Physical examination

Case 1: On admission, physical examination was unremarkable.

Case 2: Physical examination was unremarkable except for hematemesis.

Laboratory examinations

Case 1: The patient had mild cytolysis and cholestasis without any other biological abnormality.

Case 2: No abnormal blood test was noticed on admission.

Imaging examinations

Case 1: Body computed tomography (CT) scan confirmed the absence of metastatic dissemination.

Case 2: Body CT scan was consistent with local tumor without metastatic localizations.

Initial diagnosis

Case 1: Upper GI endoscopy found a 3 cm submucosal tumor of the lesser curvature of the stomach. Tumor biopsies were performed using endoscopic ultrasound guidance. Cytological examination revealed spindle-shaped cells that showed positive staining for c-KIT and DOG-1 in immunohistochemistry, confirming the diagnosis of GIST (Figure 1).

Case 2: The gastric endoscopy revealed a spherical gastric tumor in the fundus with a typical macroscopic aspect of GIST.

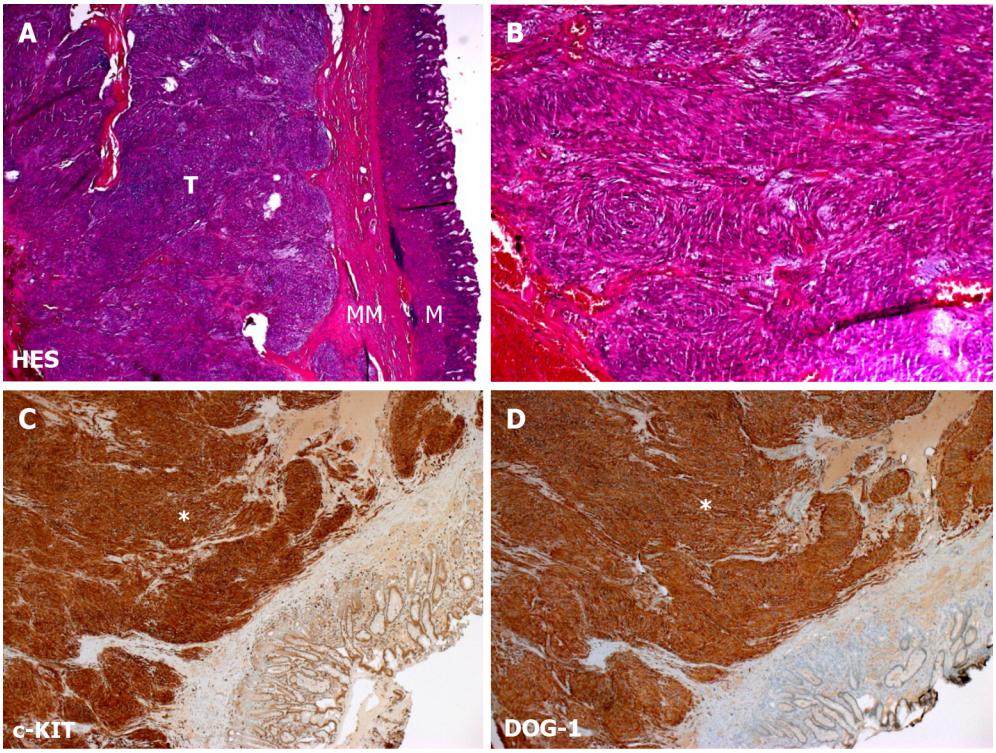
Initial treatment

Case 1: Partial gastrectomy was performed without complication.

Case 2: Partial gastrectomy was performed.

Course of illness in the hospital

Case 1: No complication associated with the GIST of its treatment was noticed.



DOI: 10.3748/wjg.v28.i34.5076 **Copyright** ©The Author(s) 2022.

Figure 1 Histopathological features of case 1 gastrointestinal stromal tumor. A: Hematoxylin and eosin staining showing exophytic development of a tumor from the mucosa musculus (magnification, 2.5 ×); B: Hematoxylin and eosin staining showing spindle cell morphology composed of relatively uniform cells arranged in short fascicles (magnification, 20 ×); C: Immunohistochemistry showing strong positive staining for the protooncogene c-KIT (white asterisk; magnification, 5 ×); D: Immunohistochemistry showing strong positive staining for discovered on gastrointestinal stromal tumor protein 1 (white asterisk; magnification, 5 ×). M: Mucosa; MM: Mucosa musculus; T: Tumor.

Case 2: The patient was rapidly discharged after partial gastrectomy without complication.

FINAL DIAGNOSIS

Case 1

Histopathology revealed a 27 mm stromal tumor strongly positive for KIT and moderately positive for DOG-1 with a mitotic count of 2 mitosis for 5 mm^2. The tumor harbored an exon 11 (p. Val559Ala c.1676T>C) *KIT* mutation[23].

Case 2

Histopathology report described a 51 mm GIST strongly positive for KIT harboring a mitotic count of 10 mitosis for 5 mm^2. Of note, an exon 18 D842V *PDGFRA* mutation was identified.

TREATMENT

Case 1

Regarding the very low risk of progression, no adjuvant therapy was initiated.

Case 2

No adjuvant treatment was initiated at the time of diagnosis.

Table 1 Characteristics of 16 transplanted patients with gastrointestinal stromal tumors

	Overall number	
Male sex, *n* (%)	16	11 (69)
Age (yr), median (min; max)	16	59.5 (23; 74)
Type of organ transplantation, *n* (%)	16	
Kidney		12 (75)
Liver		4 (25)
Location of primitive tumor, *n* (%)	16	
Stomach		9 (56)
Small bowel		3 (19)
Colon		1 (6)
Other: pelvis, perineum, mesentery		3 (19)
Time from transplantation to diagnosis (mo), median (min; max)	16	32 (5; 252)
Metastatic dissemination at diagnosis, *n* (%)	16	0 (0)
Tumor size (mm), median (min; max)	15	45 (10; 230)
Risk of progression according to Joensuu's criteria, *n* (%)	14	
Very low		2 (14)
Low		4 (29)
Intermediate		2 (14)
High		6 (43)
Surgical treatment, *n* (%)	16	15 (94)
Adjuvant treatment, *n* (%)	16	3 (19)
Modification of immunosuppression, *n* (%)	11	9 (82)
Death during follow-up, *n* (%)	14	4 (29)

OUTCOME AND FOLLOW-UP

Case 1

The patient remains in remission at the 1-year follow-up.

Case 2

Two years later, a follow-up MRI revealed hepatic vascular nodules compatible with metastatic lesions. Treatment with imatinib mesylate was initiated. In the absence of a tumor response, imatinib was discontinued 4 mo later and sunitinib (SUTENT©; Bayer, Germany), an anti-angiogenic multikinase inhibitor (anti vascular endothelial growth factor-1, -2, -3, PDGFR-α,-β, c-KIT, fms-like tyrosine kinase 3, and RET) was introduced. Five months later, the onset of thrombopenia, neutropenia, and hepatic cytolysis led to replacement of sunitinib with regorafenib (STIVARGA©; Bayer Pharma AG, Germany), another multikinase inhibitor. Due to side effects and tumor progression, regorafenib was discontinued and dasatinib (SPRYCEL©; Bristol-Myers Squibb, New York, NY, United States) was introduced. Disease progression finally led to stopping all therapies in April 2019. Selective transarterial embolization was performed complicated with artery dissection of the kidney transplant requiring stent implantation. The patient was finally admitted with a clinical presentation of hydrops concomitant with acute renal injury and peritoneal carcinosis. The patient eventually died due to disease progression.

DISCUSSION

GISTs represent an uncommon malignant complication of immunosuppression state in solid organ transplantation. We describe 2 cases of typical GIST occurring early in the course of kidney transplantation. The first patient developed an isolated gastric GIST 5 mo after transplantation and the second 4 years after. Both were nonmetastatic at diagnosis although the second patient developed

Table 2 Clinical features and immunosuppression regimen of 16 transplant patients with gastrointestinal stromal tumor

Ref.	Age (yr)/sex	Transplanted organ	Time from transplantation to diagnosis	Location of primitive GIST	Metastasis at diagnosis	Evolution/delay	Immunosuppression before diagnosis	Immunosuppression after diagnosis
Agaimy and Wünsch [11]	59/F	Kidney	40 mo	Stomach	No	Relapse 68 mo	Not described	Not described
Agaimy and Wünsch [11]	58/F	Kidney	96 mo	Small bowel	No	Not described	Not described	Not described
Saidi *et al* [19]	54/M	Liver	11 mo	Colon	No	Not described	Tac, Aza	Not described
Camargo *et al*[22]	64/M	Liver	7 mo	Perineum	No	Not described	Tac, mycophenolate sodium	Not described
Tu *et al* [18]	57/F	Kidney	6 mo	Pelvis	No	Not described	Steroids, CsA, MMF	CsA and MMF at half dosage; rapamycin-containing regimens-teroids withdrawn
Mulder *et al*[12]	72/M	Kidney	21 yr	Stomach	No	Peritoneal metastasis/24 mo	Steroids, CsA	Steroids, CsA (60% reduction in dosage)
Mrzljak *et al*[20]	53/M	Liver	12 mo	Jejunum	No	No	Tac, MMF	Same
Cimen *et al*[13]	46/F	Kidney	18 yr	Stomach	No	Not described	Steroids, CsA, Aza	Same with reduced dosage of CsA
Cheung *et al*[14]	64/M	Kidney	2 yr	Stomach	No	Yes/2 yr	Steroids, Tac, MMF	Steroids, Tac (reduced dosage), everolimus
Cheung *et al*[14]	48/M	Kidney	1 yr	Mesentery	Multiple tumors	No	CsA, MMF	CsA withdrawal, sirolimus introduction
Patiño *et al*[15]	23/F	Kidney	13 yr	Stomach	No	Local relapse/3 yr	Steroids, Tac, MMF	Not described
Xie *et al* [21]	60/M	Liver	11 mo	Stomach	No	No	Tac, sirolimus, MMF	Same
Elkabets *et al*[17]	74/M	Kidney	7 yr	Stomach	No	No	Steroids, CsA, MMF	Switch CsA to mTOR inhibitor
Takahashi *et al*[16]	64/M	Kidney	72 mo	Small bowel	No	No	Steroids, CsA, MMF	Stop CsA
Stammler *et al*	60/M	Kidney	5 mo	Stomach	No	No	Steroids, Tac, MMF	Switch MMF to belatacept
Stammler *et al*	64/M	Kidney	51 mo	Stomach	No	Yes/23 mo	Steroids, CsA, MMF	Switch CsA to Tac

Aza: Azathioprine; CsA: Cyclosporine; F: Female; GIST: Gastrointestinal stromal tumor; M: Male; MMF: Mycophenolate mofetil; mTOR: Mammalian target of rapamycin; Tac: Tacrolimus.

multiple hepatic metastasis 2 years after complete tumor resection. Of note, the mutation of *PDGFRA* D842V in the second case was associated with resistance to imatinib mesylate.

We looked for previously reported cases of GIST in the literature during the course of transplantation. We searched PubMed and Web of Science databases using the following Medical Subject Headings words: "Gastrointestinal stromal tumors" AND "Kidney transplantation" or "Gastrointestinal stromal tumors" AND "Transplantation." Using these terms, we found 8 and 31 articles, respectively. Only 12 articles were analyzed. From 2007 to 2020, 14 cases of GIST have been reported in transplant recipients [11-22]. We excluded reports of GIST occurring among nontransplant or bone marrow transplant patients. We also excluded article types different than case reports or case series.

Table 1 summarizes the main features of these patients including the 2 cases described in the present manuscript. Tables 2 and 3 give details on the 14 cases reported. In our literature review, the typical patient profile was a male patient with a median age of 59.5-years-old, who developed large nonmetastatic gastric tumors (median size, 45 mm). The delay between transplantation and diagnosis was highly

Table 3 Histopathological features, treatments, and outcome of 16 transplant patients with gastrointestinal stromal tumor

Ref.	Size (mm)	Mitotic count	Fletcher's criteria	Joensuu's criteria	Mutation identified	Resection	Initial adjuvant treatment	Second line treatment	Outcome
Agaimy and Wünsch[11]	35	< 5/50	Low	Low	Not described	Yes	No	Not described	Alive and relapse free at 68 mo
Agaimy and Wünsch[11]	230	14/50	High	High	Not described	Yes	No	Not described	Not described
Saidi *et al* [19]	25	1/50	Low	High	Not described	Yes	No	Not described	Alive and relapse free at 18 mo
Camargo *et al*[22]	50	5/50	Intermediate	High	Not described	Yes	No	Not described	Alive and relapse free at 20 mo
Tu *et al*[18]	45	2-3/50	Low	Low	*PDGFRA* exon 18 V824V	Yes	No	Not described	Alive and relapse free 24 mo
Mulder *et al* [12]	50	> 10/50	High	High	Not described	Yes	No	Imatinib 400 mg/d then 200 mg/d	Died 44 mo
Mrzljak *et al* [20]	10	1/50	Very low	Very low	Not described	Yes	No	No	Died 3 yr after from acute leukemia
Cimen *et al* [13]	150	14/50	High	High	*KIT* T574del	Yes	Imatinib 400 mg/d	Not described	Alive and relapse free at 12 mo
Cheung *et al* [14]	30	9/50	Intermediate	Intermediate	Not described	Yes	No	No	Died from pneumonia at 2 yr
Cheung *et al* [14]	Not described	Not described	Not described	Not described	Not described	No	Imatinib 400 mg/d for 1 yr	Switch CsA to sirolimus	Alive and relapse free at 10 yr
Patiño *et al* [15]	58	Not described	Intermediate or high	Intermediate of high	Not described	Yes	No	Imatinib 400 mg/d	Alive and relapse free/5 yr after imatinib initiation
Xie *et al*[21]	10	< 5/50	Very low	Very low	*KIT* exon 11	Yes	No	No	Not described
Elkabets *et al*[17]	31	Not described	Not described	Not described	Not described	Yes	No	No	Alive and relapse free at 40 mo
Takahashi *et al*[16]	110	20/50	High	High	*KIT* exon 11	Yes	Imatinib 400 mg/d reduced to 3000 mg/d	No	Alive and relapse free at 18 mo
Stammler *et al*	27	2/5	Low	Low	*KIT* exon 11	Yes	No	No	Alive and relapse free at 2 mo
Stammler *et al*	51	10/50	High	High	*PDGFRA* exon 18	Yes	No	Sunitinib then regorafenib then dasatinib	Died 56 mo later

CsA: Cyclosporine.

variable, ranging between 5 mo and 21 years. Histopathological data mostly revealed high risk of progression (42.8%) and death occurred in 29% of the cases during follow-up. Surgical treatment was systematically performed if the tumor features were suitable (94%). The use of adjuvant therapy was uncommon (19%).

Several prognostic classifications have been used to evaluate the risk of recurrence of GIST after surgery. In 2002, Fletcher *et al*[26] claimed size of the tumor and mitotic count, Miettinen and Lasota[27] in 2006 added tumor location and Joensuu *et al*[28] in 2012 adjoined rupture of the tumoral capsule and male gender. Heinrich *et al*[29] demonstrated that *PDGFRA* and *c-KIT* were mutually exclusive proto-oncogenic mutations with similar biologicals consequences, even if associated with different prognostics. Molecular predictors of response to imatinib have been widely studied. Underlying *KIT* or *PDGFRA* mutations are the strongest predictors of imatinib sensitivity[30]. Mutations directly located in the *PDGFRA* binding site of imatinib or inducing variations in tridimensional conformation of the tyrosine kinase receptor and subsequently hiding the binding site, may explain inefficacy of therapy. For instance, *KIT* exon 9 mutation is less sensitive to imatinib and *PDFGRA* exon 18 D842V mutations is associated with imatinib resistance. Nevertheless, these mutations have been correlated with opposite

courses of the disease, indolent for *PDFGRA* exon 18 D842V mutation but aggressive for *KIT* exon 9 mutation[31]. These data should highlight the importance of molecular biomarkers to evaluate prognosis of GIST or EGIST at diagnosis.

Guidelines for the diagnosis, treatment, and follow-up of GIST have recently been published[32]. Management of local or locoregional disease should always aim for complete resection whenever possible. Otherwise, neoadjuvant treatment with imatinib for 6 to 12 mo should be used in case of sensitive mutation with an overall response rate of 50%[30]. Moreover, high-risk patients, as previously described, should receive adjuvant imatinib for a duration of 3 years[33]. Imatinib remains the first-line therapy for metastatic GIST. Several other targeted therapies such as sunitinib or regorafenib have emerged as second- or third-line treatment, and more recently avapritinib and ripretinib. Several biomarkers, such as *KIT* or *PDGFRA* mutations, are used as predictive factors for tumoral response to refine therapeutic strategies[32]. Data are missing concerning the level of tyrosine kinase inhibitors' efficacy in transplanted patients.

Data about the management of immunosuppressive therapy after the diagnosis of GIST are scarce. As both imatinib mesylate and cyclosporin are extensively metabolized by cytochrome P450 3A4, interaction occurrence has been documented[12]. Reduction in the dosage of cyclosporin should be performed if this treatment is maintained. Mammalian target of rapamycin inhibitors (mTORis) have shown antiproliferative properties among transplant patients. Schöffski *et al*[34] highlighted the potential efficacy of association of everolimus and imatinib in imatinib-resistant GIST in a phase II trial. Cheung *et al*[14] reported a case of complete tumoral response with sirolimus in a transplant patient with imatinib-resistant GIST. Among the patients described in Tables 1 and 2, mTORis have been initiated or switched in 4 of them. Three of them were alive and relapse-free at last follow-up and the last patient died from pneumonia 2 years after GIST diagnosis.

This study had several limitations. First, the retrospective analysis of GIST cases impairs the reliability of the data. Very few cases of GIST occurring after solid organ transplantation have been described in the last 15 years reducing the significance of this literature review. Moreover, it was unclear if GIST was a *de novo* feature in our first patient because of the short delay (5 mo) between transplantation and tumor discovery. Unfortunately, the latest available CT scan was performed 7 years before the transplantation. However, some previous cases reported GIST onset within the 1st year following transplantation[14,18-22].

CONCLUSION

To conclude, GISTs represent rare but potentially severe malignant complication among transplant patients. Further analysis of prognosis value of new biomarkers should improve therapeutic strategies.

FOOTNOTES

Author contributions: Stammler R and Lazareth H designed the study; Stammler R, Lazareth H, Anglicheau D, Meatchi T, Ragot E, and Thervet E investigated the patients and collected the data; Stammler R, Lazareth H, and Landi B interpreted the data and wrote the manuscript; all authors revised the manuscript and approved the final version.

Informed consent statement: Written informed consent was obtained from the patient for publication of this case report and any accompanying images.

Conflict-of-interest statement: The authors have no conflicts of interest to report.

CARE Checklist (2016) statement: The authors have read the CARE Checklist (2016), and the manuscript was prepared and revised according to the CARE Checklist (2016).

Open-Access: This article is an open-access article that was selected by an in-house editor and fully peer-reviewed by external reviewers. It is distributed in accordance with the Creative Commons Attribution NonCommercial (CC BY-NC 4.0) license, which permits others to distribute, remix, adapt, build upon this work non-commercially, and license their derivative works on different terms, provided the original work is properly cited and the use is non-commercial. See: https://creativecommons.org/Licenses/by-nc/4.0/

Country/Territory of origin: France

ORCID number: Romain Stammler 0000-0002-0533-5964; Bruno Landi 0000-0002-4841-7919; Hélène Lazareth 0000-0002-1500-3736.

S-Editor: Yan JP
L-Editor: Filipodia

P-Editor: Yan JP

REFERENCES

1 **Rubin BP**, Heinrich MC, Corless CL. Gastrointestinal stromal tumour. *Lancet* 2007; **369**: 1731-1741 [PMID: 17512858 DOI: 10.1016/S0140-6736(07)60780-6]

2 **Sanders KM**, Kito Y, Hwang SJ, Ward SM. Regulation of Gastrointestinal Smooth Muscle Function by Interstitial Cells. *Physiology (Bethesda)* 2016; **31**: 316-326 [PMID: 27488743 DOI: 10.1152/physiol.00006.2016]

3 **Søreide K**, Sandvik OM, Søreide JA, Giljaca V, Jureckova A, Bulusu VR. Global epidemiology of gastrointestinal stromal tumours (GIST): A systematic review of population-based cohort studies. *Cancer Epidemiol* 2016; **40**: 39-46 [PMID: 26618334 DOI: 10.1016/j.canep.2015.10.031]

4 **DeMatteo RP**, Lewis JJ, Leung D, Mudan SS, Woodruff JM, Brennan MF. Two hundred gastrointestinal stromal tumors: recurrence patterns and prognostic factors for survival. *Ann Surg* 2000; **231**: 51-58 [PMID: 10636102 DOI: 10.1097/00000658-200001000-00008]

5 **Emile JF**, Brahimi S, Coindre JM, Bringuier PP, Monges G, Samb P, Doucet L, Hostein I, Landi B, Buisine MP, Neuville A, Bouché O, Cervera P, Pretet JL, Tisserand J, Gauthier A, Le Cesne A, Sabourin JC, Scoazec JY, Bonvalot S, Corless CL, Heinrich MC, Blay JY, Aegerter P. Frequencies of KIT and PDGFRA mutations in the MolecGIST prospective population-based study differ from those of advanced GISTs. *Med Oncol* 2012; **29**: 1765-1772 [PMID: 21953054 DOI: 10.1007/s12032-011-0074-y]

6 **Corless CL**, Barnett CM, Heinrich MC. Gastrointestinal stromal tumours: origin and molecular oncology. *Nat Rev Cancer* 2011; **11**: 865-878 [PMID: 22089421 DOI: 10.1038/nrc3143]

7 **Lopes LF**, West RB, Bacchi LM, van de Rijn M, Bacchi CE. DOG1 for the diagnosis of gastrointestinal stromal tumor (GIST): Comparison between 2 different antibodies. *Appl Immunohistochem Mol Morphol* 2010; **18**: 333-337 [PMID: 20571340 DOI: 10.1097/PAI.0b013e3181d27ec8]

8 **Demetri GD**, von Mehren M, Blanke CD, Van den Abbeele AD, Eisenberg B, Roberts PJ, Heinrich MC, Tuveson DA, Singer S, Janicek M, Fletcher JA, Silverman SG, Silberman SL, Capdeville R, Kiese B, Peng B, Dimitrijevic S, Druker BJ, Corless C, Fletcher CD, Joensuu H. Efficacy and safety of imatinib mesylate in advanced gastrointestinal stromal tumors. *N Engl J Med* 2002; **347**: 472-480 [PMID: 12181401 DOI: 10.1056/NEJMoa020461]

9 **Vajdic CM**, McDonald SP, McCredie MR, van Leeuwen MT, Stewart JH, Law M, Chapman JR, Webster AC, Kaldor JM, Grulich AE. Cancer incidence before and after kidney transplantation. *JAMA* 2006; **296**: 2823-2831 [PMID: 17179459 DOI: 10.1001/jama.296.23.2823]

10 **Awan AA**, Niu J, Pan JS, Erickson KF, Mandayam S, Winkelmayer WC, Navaneethan SD, Ramanathan V. Trends in the Causes of Death among Kidney Transplant Recipients in the United States (1996-2014). *Am J Nephrol* 2018; **48**: 472-481 [PMID: 30472701 DOI: 10.1159/000495081]

11 **Agaimy A**, Wünsch PH. Gastrointestinal stromal tumours (GIST) in kidney transplant recipients--a report of two cases. *Nephrol Dial Transplant* 2007; **22**: 1489-1490 [PMID: 17277341 DOI: 10.1093/ndt/gfl807]

12 **Mulder KE**, Egorin MJ, Sawyer MB. Renal dysfunction in a renal transplant patient treated concurrently with cyclosporine and imatinib. *Invest New Drugs* 2012; **30**: 2400-2402 [PMID: 22116657 DOI: 10.1007/s10637-011-9769-3]

13 **Cimen S**, Guler S, Panek R, Alwayn I. Gastrointestinal stromal tumour in a recipient with kidney transplantation. *BMJ Case Rep* 2015; **2015** [PMID: 26032701 DOI: 10.1136/bcr-2014-207178]

14 **Cheung CY**, Lo SH, Chan CK, Li FK, Cheng IK, Chau KF. Gastrointestinal stromal tumors in kidney transplant recipients: Report of two cases and literature review. *Asia Pac J Clin Oncol* 2017; **13**: 104-106 [PMID: 27461055 DOI: 10.1111/ajco.12506]

15 **Seculini Patiño CE**, Tabares AH, Laborie MV, Diller A. [Gastrointestinal stromal tumor and renal transplant]. *Medicina (B Aires)* 2017; **77**: 334-336 [PMID: 28825581 DOI: 10.21037/gist.2018.11.01]

16 **Takahashi R**, Shinoda K, Ishida T, Hamamoto Y, Morita S, Akita H, Kitaoka S, Tamaki S, Asanuma H, Yoshida T, Jinzaki M, Kameyama K, Oya M. Small intestinal perforation due to a huge gastrointestinal stromal tumor in a kidney transplant recipient: a case report and literature review. *BMC Nephrol* 2019; **20**: 120 [PMID: 30943904 DOI: 10.1186/s12882-019-1310-5]

17 Erratum for the Research Article: "mTORC1 Inhibition Is Required for Sensitivity to PI3K p110α Inhibitors in *PIK3CA*-Mutant Breast Cancer" by M. Elkabets, S. Vora, D. Juric, N. Morse, M. Mino-Kenudson, T. Muranen, J. Tao, A. B. Campos, J. Rodon, Y. H. Ibrahim, V. Serra, V. Rodrik-Outmezguine, S. Hazra, S. Singh, P. Kim, C. Quadt, M. Liu, A. Huang, N. Rosen, J. A. Engelman, M. Scaltriti, J. Baselga. *Sci Transl Med* 2018; **10** [PMID: 30429358 DOI: 10.1126/scitranslmed.aav9425]

18 **Tu H**, Li Q, Cai J, Chen Z, Yang H, Jiang H, Mao Y, Shou Z, Chen J. Extragastrointestinal stromal tumor in a kidney transplant recipient. *Clin Exp Nephrol* 2012; **16**: 350-353 [PMID: 22009637 DOI: 10.1007/s10157-011-0550-x]

19 **Saidi RF**, Sepehr A, Cosimi AB, Hertl M. Gastrointestinal stromal tumor in a liver transplant recipient. *Transplantation* 2008; **85**: 1363 [PMID: 18475199 DOI: 10.1097/TP.0b013e31816c7e2f]

20 **Mrzljak A**, Košuta I, Škrtić A, Kardum-Skelin I, Vrhovac R. Metachronous gastrointestinal stromal tumor and acute leukemia after liver transplantation for cholangiocellular carcinoma: is there a link? *Case Rep Oncol* 2013; **6**: 163-168 [PMID: 23626555 DOI: 10.1159/000348817]

21 **Xie M**, Rao W, Zhang P, Zhao Q, Tian Z. Endoscopic full-thickness resection for a gastrointestinal stromal tumor in a liver transplant recipient: A case report. *Medicine (Baltimore)* 2019; **98**: e16669 [PMID: 31374043 DOI: 10.1097/MD.0000000000016669]

22 **Camargo MA**, Boin I, Mainnardi JP, de Lourdes M, Ayrizono S, Coy CS, Leonardi MI, Meirelles L, Leonardi LS, Escanhoela CA. Extragastrointestinal stromal tumor and liver transplantation: case report and review. *Transplant Proc*

2008; **40**: 3781-3783 [PMID: 19100489 DOI: 10.1016/j.transproceed.2008.04.017]

23 **Pai T**, Bal M, Shetty O, Gurav M, Ostwal V, Ramaswamy A, Ramadwar M, Desai S. Unraveling the spectrum of *KIT* mutations in gastrointestinal stromal tumors: An Indian Tertiary Cancer Center Experience. *South Asian J Cancer* 2017; **6**: 113-117 [PMID: 28975118 DOI: 10.4103/sajc.sajc_275_16]

24 **Roufosse C**, Simmonds N, Clahsen-van Groningen M, Haas M, Henriksen KJ, Horsfield C, Loupy A, Mengel M, Perkowska-Ptasińska A, Rabant M, Racusen LC, Solez K, Becker JU. A 2018 Reference Guide to the Banff Classification of Renal Allograft Pathology. *Transplantation* 2018; **102**: 1795-1814 [PMID: 30028786 DOI: 10.1097/TP.0000000000002366]

25 **Roberts DM**, Jiang SH, Chadban SJ. The treatment of acute antibody-mediated rejection in kidney transplant recipients-a systematic review. *Transplantation* 2012; **94**: 775-783 [PMID: 23032865 DOI: 10.1097/TP.0b013e31825d1587]

26 **Fletcher CD**, Berman JJ, Corless C, Gorstein F, Lasota J, Longley BJ, Miettinen M, O'Leary TJ, Remotti H, Rubin BP, Shmookler B, Sobin LH, Weiss SW. Diagnosis of gastrointestinal stromal tumors: A consensus approach. *Hum Pathol* 2002; **33**: 459-465 [PMID: 12094370 DOI: 10.1053/hupa.2002.123545]

27 **Miettinen M**, Lasota J. Gastrointestinal stromal tumors: pathology and prognosis at different sites. *Semin Diagn Pathol* 2006; **23**: 70-83 [PMID: 17193820 DOI: 10.1053/j.semdp.2006.09.001]

28 **Joensuu H**, Vehtari A, Riihimäki J, Nishida T, Steigen SE, Brabec P, Plank L, Nilsson B, Cirilli C, Braconi C, Bordoni A, Magnusson MK, Linke Z, Sufliarsky J, Federico M, Jonasson JG, Dei Tos AP, Rutkowski P. Risk of recurrence of gastrointestinal stromal tumour after surgery: an analysis of pooled population-based cohorts. *Lancet Oncol* 2012; **13**: 265-274 [PMID: 22153892 DOI: 10.1016/S1470-2045(11)70299-6]

29 **Heinrich MC**, Corless CL, Duensing A, McGreevey L, Chen CJ, Joseph N, Singer S, Griffith DJ, Haley A, Town A, Demetri GD, Fletcher CD, Fletcher JA. PDGFRA activating mutations in gastrointestinal stromal tumors. *Science* 2003; **299**: 708-710 [PMID: 12522257 DOI: 10.1126/science.1079666]

30 **Kee D**, Zalcberg JR. Current and emerging strategies for the management of imatinib-refractory advanced gastrointestinal stromal tumors. *Ther Adv Med Oncol* 2012; **4**: 255-270 [PMID: 22942908 DOI: 10.1177/1758834012450935]

31 **Palomba G**, Paliogiannis P, Sini MC, Colombino M, Casula M, Manca A, Pisano M, Sotgiu G, Doneddu V, Palmieri G, Cossu A. KIT and PDGFRa mutational patterns in Sardinian patients with gastrointestinal stromal tumors. *Eur J Cancer Prev* 2021; **30**: 53-58 [PMID: 32091431 DOI: 10.1097/CEJ.0000000000000581]

32 **Casali PG**, Abecassis N, Aro HT, Bauer S, Biagini R, Bielack S, Bonvalot S, Boukovinas I, Bovee JVMG, Brodowicz T, Broto JM, Buonadonna A, De Álava E, Dei Tos AP, Del Muro XG, Dileo P, Eriksson M, Fedenko A, Ferraresi V, Ferrari A, Ferrari S, Frezza AM, Gasperoni S, Gelderblom H, Gil T, Grignani G, Gronchi A, Haas RL, Hassan B, Hohenberger P, Issels R, Joensuu H, Jones RL, Judson I, Jutte P, Kaal S, Kasper B, Kopeckova K, Krákorová DA, Le Cesne A, Lugowska I, Merimsky O, Montemurro M, Pantaleo MA, Piana R, Picci P, Piperno-Neumann S, Pousa AL, Reichardt P, Robinson MH, Rutkowski P, Safwat AA, Schöffski P, Sleijfer S, Stacchiotti S, Sundby Hall K, Unk M, Van Coevorden F, van der Graaf WTA, Whelan J, Wardelmann E, Zaikova O, Blay JY; ESMO Guidelines Committee and EURACAN. Gastrointestinal stromal tumours: ESMO-EURACAN Clinical Practice Guidelines for diagnosis, treatment and follow-up. *Ann Oncol* 2018; **29**: iv68-iv78 [PMID: 29846513 DOI: 10.1093/annonc/mdy095]

33 **Joensuu H**, Eriksson M, Sundby Hall K, Reichardt A, Hartmann JT, Pink D, Ramadori G, Hohenberger P, Al-Batran SE, Schlemmer M, Bauer S, Wardelmann E, Nilsson B, Sihto H, Bono P, Kallio R, Junnila J, Alvegård T, Reichardt P. Adjuvant Imatinib for High-Risk GI Stromal Tumor: Analysis of a Randomized Trial. *J Clin Oncol* 2016; **34**: 244-250 [PMID: 26527782 DOI: 10.1200/JCO.2015.62.9170]

34 **Schöffski P**, Reichardt P, Blay JY, Dumez H, Morgan JA, Ray-Coquard I, Hollaender N, Jappe A, Demetri GD. A phase I-II study of everolimus (RAD001) in combination with imatinib in patients with imatinib-resistant gastrointestinal stromal tumors. *Ann Oncol* 2010; **21**: 1990-1998 [PMID: 20507881 DOI: 10.1093/annonc/mdq076]

World Journal of Gastroenterology

Submit a Manuscript: https://www.f6publishing.com

World J Gastroenterol 2022 September 14; 28(34): 5086-5092

DOI: 10.3748/wjg.v28.i34.5086

ISSN 1007-9327 (print) ISSN 2219-2840 (online)

CASE REPORT

Spontaneous expulsion of a duodenal lipoma after endoscopic biopsy: A case report

Zhi-Hao Chen, Li-Hong Lv, Wen-Sheng Pan, Yi-Miao Zhu

Specialty type: Gastroenterology and hepatology

Provenance and peer review: Unsolicited article; Externally peer reviewed.

Peer-review model: Single blind

Peer-review report's scientific quality classification
Grade A (Excellent): 0
Grade B (Very good): B
Grade C (Good): C, C
Grade D (Fair): 0
Grade E (Poor): 0

P-Reviewer: Morozov S, Russia; Skok K, Austria

Received: March 3, 2022
Peer-review started: March 3, 2022
First decision: June 11, 2022
Revised: July 24, 2022
Accepted: August 21, 2022
Article in press: August 21, 2022
Published online: September 14, 2022

Zhi-Hao Chen, Wen-Sheng Pan, Yi-Miao Zhu, Department of Gastroenterology, Zhejiang Provincial People's Hospital, Hangzhou 310014, Zhejiang Province, China

Zhi-Hao Chen, Wen-Sheng Pan, Yi-Miao Zhu, Affiliated Hospital, People's Hospital of Hangzhou Medical College, Hangzhou 310014, Zhejiang Province, China

Li-Hong Lv, Department of Gastroenterology, Xianju County People's Hospital, Taizhou 317300, Zhejiang Province, China

Corresponding author: Yi-Miao Zhu, MM, Doctor, Department of Gastroenterology, Zhejiang Provincial People's Hospital, No. 158 Shangtang Road, Gongshu District, Hangzhou 310014, Zhejiang Province, China. zhuyimiao01@163.com

Abstract

BACKGROUND

Gastrointestinal (GI) lipomas are benign submucosal tumors of mature adipocytes that arise mainly in the colon and stomach, sometimes in the ileum and jejunum, and rarely in the duodenum. Patients with symptomatic lipomas require endoscopic or surgical treatment. Spontaneous expulsion of lipomas after biopsy is a rare condition that has limited case reports.

CASE SUMMARY

A 56-year-old man presented to our hospital with intermittent postprandial epigastric fullness. Esophagogastroduodenoscopy (EGD) revealed a 10-mm soft yellowish submucosal lesion with the "pillow sign," located in the second portion of duodenum. Endoscopic ultrasonography (EUS) using a 12-MHz catheter probe showed a hyperechoic, homogenous, and round solid lesion (OLYMPUS EUS EU-ME2, UM-DP12-25R, 12-MHz radial miniprobe, Olympus Corporation, Tokyo, Japan). Deep biopsy was performed using the bite-on-bite technique with forceps. Histological examination was compatible with submucosal lipoma. The lesion spontaneously expelled 12 d after the biopsy. Follow-up EUS performed after 2 mo confirmed this condition.

CONCLUSION

Deep biopsy could lead to spontaneous GI lipoma expulsion. This might be the first step in lipoma diagnosis and treatment.

Key Words: Lipoma; Duodenal neoplasms; Spontaneous expulsion; Endoscopic biopsy;

Adipose tissue; Case report

©The Author(s) 2022. Published by Baishideng Publishing Group Inc. All rights reserved.

Core Tip: Gastrointestinal lipomas are benign tumors consisting of mature adipocytes. Symptomatic patients may require endoscopic or surgical treatment. Here, we report a case of duodenal papillary lipoma, which was spontaneously expelled 12 d after a bite-on-bite deep biopsy with forceps. The spontaneous expulsion of the lipoma shows the possibility of performing a deep biopsy as a fenestration in the first step as a diagnostic and therapeutic procedure.

Citation: Chen ZH, Lv LH, Pan WS, Zhu YM. Spontaneous expulsion of a duodenal lipoma after endoscopic biopsy: A case report. *World J Gastroenterol* 2022; 28(34): 5086-5092
URL: https://www.wjgnet.com/1007-9327/full/v28/i34/5086.htm
DOI: https://dx.doi.org/10.3748/wjg.v28.i34.5086

INTRODUCTION

Gastrointestinal (GI) lipomas are benign submucosal tumors of mature adipocytes that are commonly found incidentally on endoscopy and imaging. They arise throughout the GI tract, mainly in the colon (65%-75%), followed by the ileum and jejunum (25%)[1]. The duodenum is a rare site of GI lipomas, with only 4% of lipomas affected, mostly in the second portion of the duodenum[1]. Lipomas are rarely symptomatic and have no malignant potential. However, they occasionally result in hemorrhage, abdominal pain, intestinal intussusception, or obstructive jaundice, which are related to the characteristics of the lipoma, such as its size and location[1,2]. Symptomatic duodenal lipomas require treatment. They can be excised endoscopically or surgically. This report presents a case of duodenal lipoma diagnosed by endoscopic ultrasonography (EUS) that was spontaneously expelled 12 d after a bite-on-bite deep biopsy with forceps.

CASE PRESENTATION

Chief complaints

A 56-year-old Chinese man presented to our gastroenterology department with intermittent postprandial epigastric fullness for half a year.

History of present illness

The patient had early satiety and mild reflux, especially after greasy meals, without abdominal pain, melena, fever, or jaundice. The symptoms were moderate and paroxysmal, which affected his appetite. No weight loss was reported during the past half a year. There was no history of abdominal surgery.

History of past illness

The patient's past medical history was non-contributory.

Personal and family history

The patient has none family history.

Physical examination

On physical examination, the patient's vital signs were stable with a 37.2 °C body temperature on admission. The subject's height was 170 cm and weight was 80 kg, with body mass index of 27.68 kg/m^2. No obvious abnormalities were observed upon pulmonary and cardiac examination. There was no tenderness, mass, unusual bowel sounds, or Murphy's sign upon abdominal examination. No jaundice or superficial lymphadenopathy was observed.

Laboratory examinations

The analyses of complete blood count, blood biochemistry, and serum tumor marker levels were within the normal range.

Imaging examinations

Esophagogastroduodenoscopy (EGD) revealed a 10-mm soft yellowish submucosal lesion with the "pillow sign," located in the second portion of the duodenum, directly upon the duodenal papilla (Figures 1A and B). Contrast-enhanced computed tomography (CT) revealed a suspicious low-density lesion in the periampullary region without enhancement (Figure 1C). Further EUS (OLYMPUS EUS EU-ME2, UM-DP12-25R, 12-MHz radial miniprobe, Olympus Corporation, Tokyo, Japan) revealed a hyperechoic, homogenous, round solid lesion arising from the submucosal layer, accompanied by echo attenuation (Figure 1D).

FINAL DIAGNOSIS

Deep biopsy was performed *via* the bite-on-bite technique using forceps (Micro-Tech Co. Ltd., Nanjing, China) (Figure 1E). Microscopic examination showed a small amount of roundish adipocytes in the submucosa layer, expressing S-100. Tiny lipid droplets were observed in cell cytoplasm. The glands of epithelium were neatly arranged on top. The small fragments of biopsy compatible with a submucosal lipoma. (Figures 1F-H). Based on the classic endoscopic signs, EUS characteristics and histology of the lesion, a diagnosis of duodenal lipoma was made. No bleeding, perforation, or any other complications were observed the patient.

TREATMENT

During endoscopy, the patient underwent neither resection nor hemostatic procedures after the biopsy. Prokinetics and proton pump inhibitor were prescribed to relieve the symptoms. Considering the size and location of the lipoma, we suggested that the patient remain under observation. However, the patient was extremely anxious about the lesion and insisted on its removal; thus, endoscopic resection and prophylactic pancreatic duct stenting were attempted.

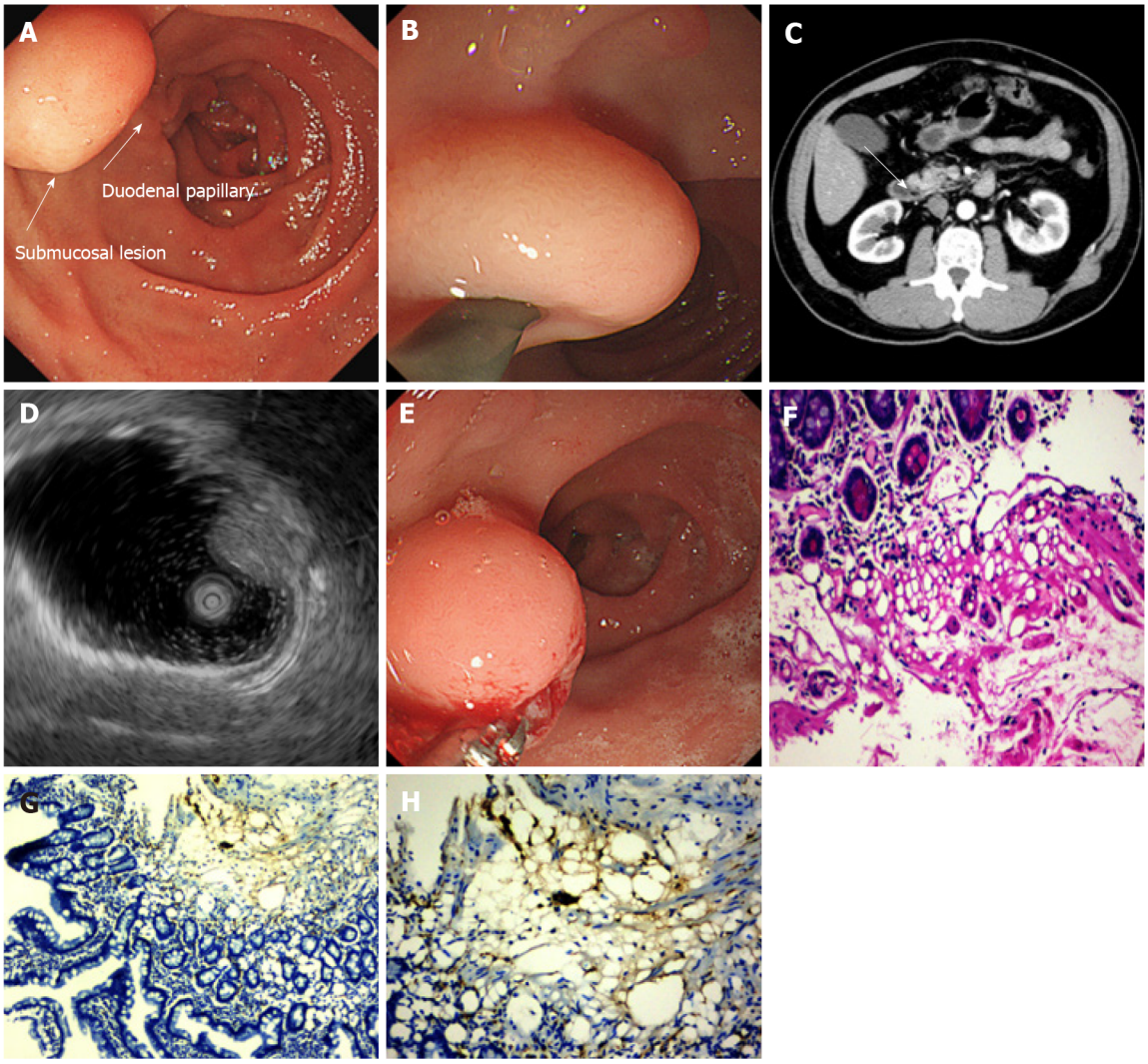
OUTCOME AND FOLLOW-UP

The patient reported milder symptoms and fewer episodes after prescription. However, he insisted on resection. On endoscopic resection, which was 12 d after the biopsy, the lipoma had disappeared, with only a red scar and inflammatory mucosa residue in situ of the lesion (Figures 2A and B). Two months after the first EUS, a follow-up EUS was performed, showing that macroscopically the site displayed signs of inflammation and scarring. And the former lesion no longer existed in the surrounding duodenal wall in EUS (Figures 2C-E). After endoscopy, mild symptoms occasionally occurred during the follow-up period, without medications.

DISCUSSION

Duodenal lipoma is a rare benign tumor of the GI tract accounting for 4% of GI lipomas, most of which occur in the second portion of the duodenum[1,2]. Duodenal lipoma can be symptomatic or asymptomatic, depending on the size and location. Moreover, 80% of symptomatic duodenal lipomas have a diameter of > 2 cm, mainly manifesting as intestinal obstruction, hemorrhage, and jaundice[2,3]. The tumor in our case was a submucosal lipoma, which accounts for > 90% of intestinal lipomas, with the others arising from the intermuscular tissue and subserosa[4]. Imaging of lipomas is well recognized. CT shows well-defined border tumors in a uniform low density with fat attenuation of -120 HU to -60 HU, while magnetic resonance imaging shows high-intensity lesion with on T1-weighted, iso-signal intensity on T2-weighted, and low intensity on fat-suppressed T2-weighted imaging[5,6]. The classic endoscopic signs as "pillow sign," "tenting sign," and "naked fat sign" indicate the possibility of lipomas. The typical EUS finding for submucosal lipomas is a homogeneous hyperechoic mass originating from the submucosal layer, with echo attenuation behind and/or inside the rear area[7]. In our case, the duodenal lipoma was present in the second portion of the duodenum, immediately upon the duodenal papilla, with classic imaging on EGD, CT, and EUS, with pathologically confirmation.

Symptomatic lipomas require treatment, including removal *via* endoscopy or surgical excision. There are four techniques for endoscopic excision: Dissection-based resection, endoscopic mucosal resection (EMR), loop-assisted resection, and unroofing[8] (Figure 3). Dissection-based resection defines as endoscopic procedure mainly using dissection-based techniques, such as ESD. Loop-assisted resection is the procedure performed with loop for haemostatic or removal reasons. Because of the poor conduction of electric current in the adipose tissue, endoscopists must apply a higher electrical output during

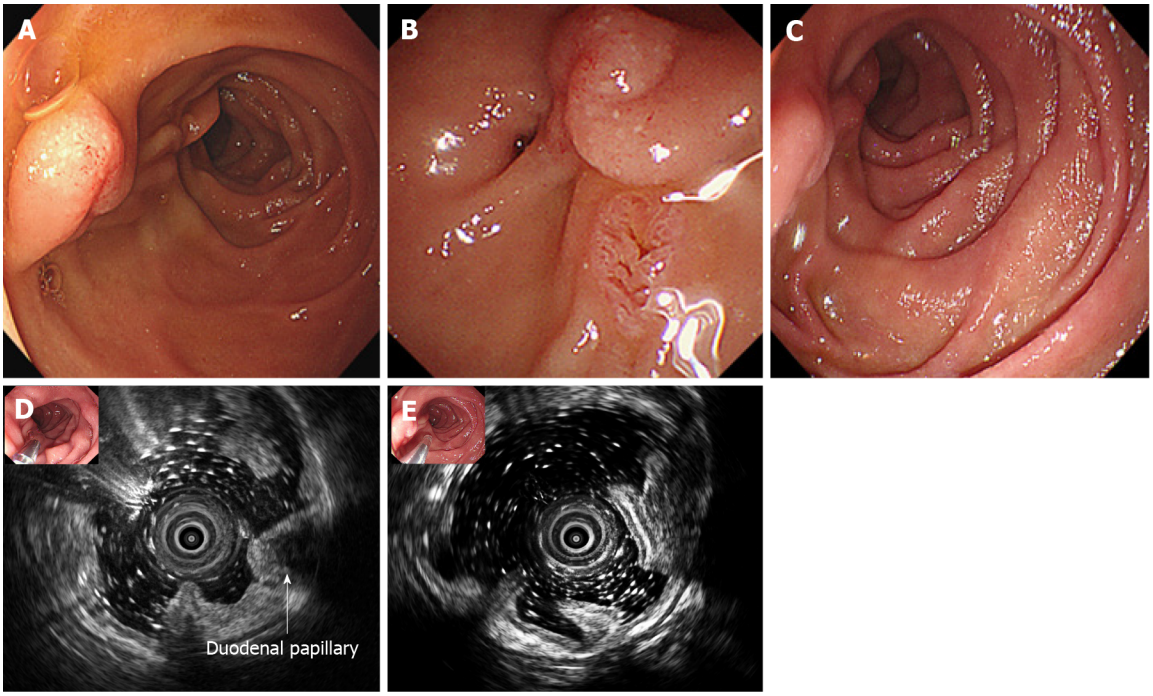


DOI: 10.3748/wjg.v28.i34.5086 **Copyright** ©The Author(s) 2022.

Figure 1 Imaging findings at the time of diagnosis. A and B: Esophagogastroduodenoscopy revealed a 10-mm soft yellowish submucosal lesion with the "pillow sign," located in the second portion of duodenum, immediately upon the duodenal papillary; C: Abdominal contrast-enhanced computed tomography shows a suspicious low-density lesion in the periampullary region without enhancement (white arrow); D: Endoscopic ultrasonography with a 12-MHz catheter probe showed a hyperechoic, homogenous, and round solid lesion with echo attenuation, arising from the submucosal layer; E: Deep biopsy *via* bite-on-bite technique with forceps was performed; F-H: Microscopic examination showed a small amount of roundish adipocyte in the submucosa layer, expressing S-100. Tiny lipid droplets were observed in cell cytoplasm. The glands of epithelium were neatly arranged on top (F: Hematoxylin and eosin staining, × 200; G: Immunohistochemical S-100 stain, × 100; H: IHC S-100 stain, × 200).

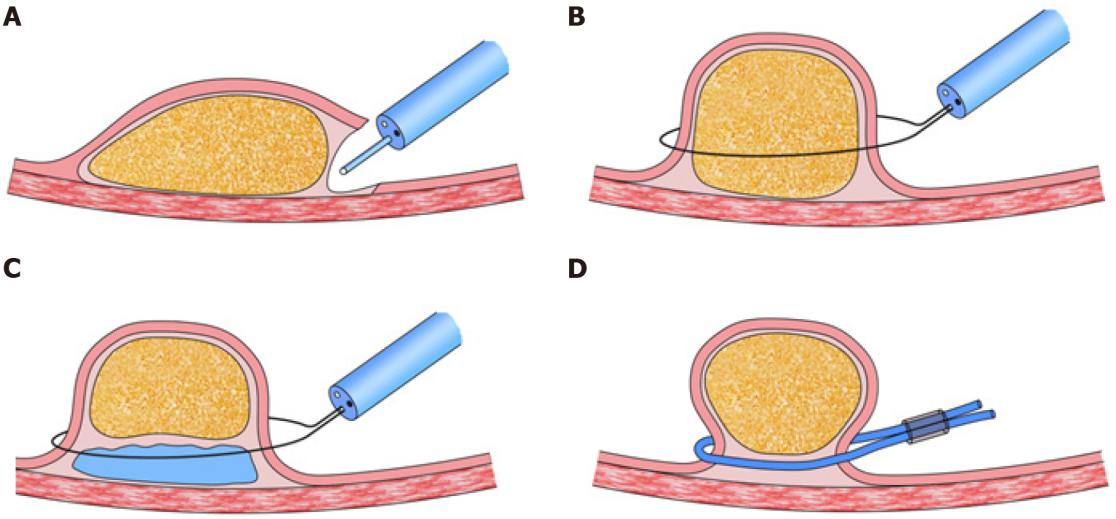
resection, which increases the possibility of complications, such as hemorrhage and perforation, especially for giant lipomas. The unroofing technique, which cuts off the upper half of the lesion, with the remaining adipose tissue extruded from the open surface, was first applied by Mimura *et al*[9]. Its efficacy and safety have been approved by several authors in case reports[10-14]. Bronswijk *et al*[8] collected 24 studies (77 lesions included) of endoscopic treatment for colon lipomas, and a systematic review indicated that endoscopic resolution rates were 60%, 100%, 93.6%, and 93.1% for unroofing, dissection-based resection, EMR, and loop-assisted resection, respectively. The former two techniques reported no adverse events, whereas the latter two showed complication rates of 12.9%-13.8%. Yamamoto *et al*[15] proposed a two-step hybrid technique that combined endoscopic unroofing with EMR for giant lipomas.

Spontaneous disappearance or expulsion of lipomas is an extremely rare manifestation that had limited case reports. There have been some cases of spontaneous expulsion per rectum of submucosal lipomas without any intervention. With a certain volume, these submucosal lipomas cause intussusception, which might lead to ischemia, necrosis, and breakage, and the lipomas were spontaneously expelled[4,16-20]. In our case, the lipoma was spontaneously expelled after deep biopsy *via* the bite-on-bite technique with forceps, which we suspected was the result of fat extravasation from the biopsy site as fenestration over time. There were a few cases of spontaneous expulsion after biopsy of GI lipoma[21-24]. Kurahara *et al*[21] first reported a gastric lipoma that was expelled after biopsy. Ishiyama *et al*[22] reported the expulsion of a colonic lipoma after biopsy. We speculated that, in these cases, three



DOI: 10.3748/wjg.v28.i34.5086 **Copyright** ©The Author(s) 2022.

Figure 2 Follow-up endoscopic view of the lesion. A and B: 12 d after the biopsy, the lipoma was spontaneously expelled, with red scar and inflammatory mucosa residue in situ of the lesion; C-E: Follow-up endoscopic ultrasonography after 2 mo revealed that the *in situ* mucosa was smooth, and the former lesion no longer existed in the surrounding duodenal wall or periduodenal papilla region.



DOI: 10.3748/wjg.v28.i34.5086 **Copyright** ©The Author(s) 2022.

Figure 3 Techniques for endoscopic excision of gastrointestinal lipomas[14]. A: Dissection-based resection technique; B: Unroofing technique; C: Endoscopic mucosal resection; D: Loop-assisted resection technique.

conditions need to be met for the lipoma to disappear: (1) The overlying mucosa and tumor capsule must be damaged by either acquired opening, such as unroofing and deep biopsy, or spontaneous opening, such as ischemia and ulceration; (2) The lipoma should arise from the submucosal layer; and (3) The extravasation rate, which depends on the tumor volume and size of the fenestration, should be faster than the mucosal healing rate. In this case, the special anatomical position might have facilitated pancreatic lipase and bile digestion of the lipoma to speed up the discharge process.

The treatment techniques and cases of spontaneous expulsion lipomas indicate that we might conduct a deep biopsy based on bite-on-bite techniques or more intense "tunneled biopsy" as fenestration routinely when a lipoma is diagnosed with typical EUS and EGD. Such biopsies could aid in further diagnosis in pathology and reduce the size or even remove the lesion as a treatment, particularly in cases where the lesion is relatively large or located in the small intestine[25]. A simple deep biopsy

during diagnosis might decrease the complications caused by the lesion itself or by the next step of endoscopic or surgical resection. Larger studies are necessary to make conclusion on the efficacy of fenestration on lipoma and algorithm of treatment.

CONCLUSION

In this case, we present the spontaneous expulsion of a duodenal lipoma 12 d after a bite-on-bite deep biopsy. Treatments for benign and slow-growing tumors include endoscopic dissection-based resection, EMR, loop-assisted resection, endoscopic unroofing, and surgical resection. The expulsion of lipoma after biopsy enlightens us the possibility of taking a deep biopsy as a fenestration in the first step as the diagnostic and therapeutic procedure.

ACKNOWLEDGEMENTS

Yi-Miao Zhu would extend her sincere gratitude to Yuan Chen for his careful review of the pathology, valuable suggestions, and inspiring advice of the case. Special thanks should go to her beloved husband for his continuous support and encouragement.

FOOTNOTES

Author contributions: Chen ZH, Lv LH, and Zhu YM assembled, analyzed, and interpreted the patient's data and case presentation; Zhu YM and Pan WS reviewed the literature; Chen ZH and Zhu YM prepared the original manuscript; Zhu YM edited and critically revised the manuscript; all authors contributed to writing the manuscript; and all authors read and approved the final manuscript.

Supported by the Medical Technology and Education of Zhejiang Province of China, No. Y202146136.

Informed consent statement: Written informed consent was obtained from the patient's guardian for the publication of this case report and any accompanying images.

Conflict-of-interest statement: All the authors report no relevant conflicts of interest for this article.

CARE Checklist (2016) statement: The authors read the CARE Checklist (2016), and the manuscript was prepared and revised according to the CARE checklist (2016).

Open-Access: This article is an open-access article that was selected by an in-house editor and fully peer-reviewed by external reviewers. It is distributed in accordance with the Creative Commons Attribution NonCommercial (CC BY-NC 4.0) license, which permits others to distribute, remix, adapt, build upon this work non-commercially, and license their derivative works on different terms, provided the original work is properly cited and the use is non-commercial. See: https://creativecommons.org/Licenses/by-nc/4.0/

Country/Territory of origin: China

ORCID number: Wen-Sheng Pan 0000-0002-2347-1695; Yi-Miao Zhu 0000-0002-1745-4063.

S-Editor: Wang JJ
L-Editor: A
P-Editor: Wang JJ

REFERENCES

1 **O'Riordan BG**, Vilor M, Herrera L. Small bowel tumors: an overview. *Dig Dis* 1996; **14**: 245-257 [PMID: 8843980 DOI: 10.1159/000171556]
2 **Pei MW**, Hu MR, Chen WB, Qin C. Diagnosis and Treatment of Duodenal Lipoma: A Systematic Review and a Case Report. *J Clin Diagn Res* 2017; **11**: PE01-PE05 [PMID: 28892976 DOI: 10.7860/JCDR/2017/27748.10322]
3 **Wilson JM**, Melvin DB, Gray G, Thorbjarnarson B. Benign small bowel tumor. *Ann Surg* 1975; **181**: 247-250 [PMID: 1078626]
4 **Kang B**, Zhang Q, Shang D, Ni Q, Muhammad F, Hou L, Cui W. Resolution of intussusception after spontaneous expulsion of an ileal lipoma per rectum: a case report and literature review. *World J Surg Oncol* 2014; **12**: 143 [PMID: 24884620 DOI: 10.1186/1477-7819-12-143]
5 **Genchellac H**, Demir MK, Ozdemir H, Unlu E, Temizoz O. Computed tomographic and magnetic resonance imaging

findings of asymptomatic intra-abdominal gastrointestinal system lipomas. *J Comput Assist Tomogr* 2008; **32**: 841-847 [PMID: 19204441 DOI: 10.1097/RCT.0b013e318159a4b5]

6 **Kovač JD**, Dunjić MK, Bjelović M, Banko B, Lilić G, Milenković R, Micev M, Maksimović R. Magnetic resonance imaging features of multiple duodenal lipomas: a rare cause of intestinal obstruction. *Jpn J Radiol* 2012; **30**: 676-679 [PMID: 22752443 DOI: 10.1007/s11604-012-0098-z]

7 **Chen HT**, Xu GQ, Wang LJ, Chen YP, Li YM. Sonographic features of duodenal lipomas in eight clinicopathologically diagnosed patients. *World J Gastroenterol* 2011; **17**: 2855-2859 [PMID: 21734794 DOI: 10.3748/wjg.v17.i23.2855]

8 **Bronswijk M**, Vandenbroucke AM, Bossuyt P. Endoscopic treatment of large symptomatic colon lipomas: A systematic review of efficacy and safety. *United European Gastroenterol J* 2020; **8**: 1147-1154 [PMID: 32746773 DOI: 10.1177/2050640620948661]

9 **Mimura T**, Kuramoto S, Hashimoto M, Yamasaki K, Kobayashi K, Kobayashi M, Oohara T. Unroofing for lymphangioma of the large intestine: a new approach to endoscopic treatment. *Gastrointest Endosc* 1997; **46**: 259-263 [PMID: 9378215 DOI: 10.1016/s0016-5107(97)70097-x]

10 **Kim GW**, Kwon CI, Song SH, Jin SM, Kim KH, Moon JH, Hong SP, Park PW. Endoscopic resection of giant colonic lipoma: case series with partial resection. *Clin Endosc* 2013; **46**: 586-590 [PMID: 24143327 DOI: 10.5946/ce.2013.46.5.586]

11 **Lee KJ**, Kim GH, Park DY, Shin NR, Lee BE, Ryu DY, Kim DU, Song GA. Endoscopic resection of gastrointestinal lipomas: a single-center experience. *Surg Endosc* 2014; **28**: 185-192 [PMID: 23996333 DOI: 10.1007/s00464-013-3151-9]

12 **Shin EK**, Kim KJ, Seo JA, Paek JH, Choi IS, Moon W, Park MI, Park SJ. [A case of giant colonic lipoma showing spontaneous resolution after endoscopic partial resection]. *Korean J Gastroenterol* 2007; **50**: 199-202 [PMID: 17885287]

13 **Soares JB**, Gonçalves R, Rolanda C. Endoscopic resection of a large colonic lipoma by unroofing technique. *Endoscopy* 2011; **43** Suppl 2 UCTN: E407 [PMID: 22275025 DOI: 10.1055/s-0030-1256938]

14 **Sugimoto K**, Sato K, Maekawa H, Sakurada M, Orita H, Ito T, Saita M, Ikota M, Yoshida Y, Yamano M. Unroofing technique for endoscopic resection of a large colonic lipoma. *Case Rep Gastroenterol* 2012; **6**: 557-562 [PMID: 22949897 DOI: 10.1159/000342350]

15 **Yamamoto K**, Ikeya T, Shiratori Y. Endoscopic unroofing and mucosal resection for a large colonic lipoma with intussusception: an effective hybrid technique. *VideoGIE* 2021; **6**: 190-192 [PMID: 33898900 DOI: 10.1016/j.vgie.2020.11.018]

16 **Misra SP**, Singh SK, Thorat VK, Gulati P, Malhotra V, Anand BS. Spontaneous expulsion per rectum of an ileal lipoma. *Postgrad Med J* 1988; **64**: 718-719 [PMID: 3251232 DOI: 10.1136/pgmj.64.755.718]

17 **Hamila F**, Elghali MA, Bouriga R, Haj Khlifa MH, Fadhl H, Jarrar MS, Letaief R. Partial spontaneous anal expulsion of the right colon lipoma: An exceptional diagnostic circumstance. *Int J Surg Case Rep* 2017; **41**: 414-416 [PMID: 29546005 DOI: 10.1016/j.ijscr.2017.10.059]

18 **Robertson DA**, Saweirs W, Low-Beer TS. Spontaneous expulsion of a large colonic tumour. *Br Med J (Clin Res Ed)* 1982; **285**: 1084 [PMID: 6812756 DOI: 10.1136/bmj.285.6348.1084]

19 **Zamboni WA**, Fleisher H, Zander JD, Folse JR. Spontaneous expulsion of lipoma per rectum occurring with colonic intussusception. *Surgery* 1987; **101**: 104-107 [PMID: 3492056]

20 **Stebbings WS**, Staunton MD. Spontaneous expulsion of a large submucosal colonic lipoma. *J R Soc Med* 1989; **82**: 624-625 [PMID: 2810300 DOI: 10.1177/014107688908201021]

21 **Kurahara K**, Aoyagi K, Hizawa K, Yao T, Iida M, Fujishima M. Spontaneous disappearance of a gastric lipoma after endoscopic biopsy: report of an unusual case. *Endoscopy* 1999; **31**: S31 [PMID: 10376473]

22 **Ishiyama S**, Tashiro Y, Nagayasu K, Niwa K, Ono S, Sugimoto K, Hata M, Kamiyama H, Komiyama H, Takahashi M, Yaginuma Y, Kojima Y, Goto M, Tanaka M, Sengoku H, Okuzawa A, Tomiki Y, Sakamoto K. Spontaneous disappearance of a giant colonic lipoma after endoscopic biopsy. *Endoscopy* 2011; **43** Suppl 2 UCTN: E16 [PMID: 21271519 DOI: 10.1055/s-0030-1255826]

23 **João M**, Cunha I, Gravito-Soares E, Gravito-Soares M, Amaro P, Figueiredo P. An Atypical Presentation of a Colonic Lipoma: Avoiding Surgery with a Deeper Endoscopic Look. *GE Port J Gastroenterol* 2022; **29**: 45-50 [PMID: 35111963 DOI: 10.1159/000513967]

24 **Sidani SM**, Tawil AN, Sidani MS. Extraction of a large self-amputated colonic lipoma: A case report. *Int J Surg* 2008; **6**: 409-411 [PMID: 18947813 DOI: 10.1016/j.ijsu.2006.05.003]

25 **Koutsoumpas A**, Perera R, Melton A, Kuker J, Ghosh T, Braden B. Tunneled biopsy is an underutilised, simple, safe and efficient method for tissue acquisition from subepithelial tumours. *World J Clin Cases* 2021; **9**: 5822-5829 [PMID: 34368301 DOI: 10.12998/wjcc.v9.i21.5822]



Published by **Baishideng Publishing Group Inc**
7041 Koll Center Parkway, Suite 160, Pleasanton, CA 94566, USA
Telephone: +1-925-3991568
E-mail: bpgoffice@wjgnet.com
Help Desk: https://www.f6publishing.com/helpdesk
https://www.wjgnet.com



© 2022 Baishideng Publishing Group Inc. All rights reserved.

ISSN 1007-9327 (print)
ISSN 2219-2840 (online)

World Journal of *Gastroenterology*

World J Gastroenterol 2022 September 21; 28(35): 5093-5239



Published by Baishideng Publishing Group Inc

World Journal of Gastroenterology

Contents

Weekly Volume 28 Number 35 September 21, 2022

REVIEW

5093 Robotic, self-propelled, self-steerable, and disposable colonoscopes: Reality or pipe dream? A state of the art review

Winters C, Subramanian V, Valdastri P

5111 Noncoding RNAs as additional mediators of epigenetic regulation in nonalcoholic fatty liver disease

Zaiou M

MINIREVIEWS

5129 Combination strategies for pharmacologic treatment of non-alcoholic steatohepatitis

Suri J, Borja S, Lim JK

ORIGINAL ARTICLE

Basic Study

5141 Long noncoding RNA negative regulator of antiviral response contributes to pancreatic ductal adenocarcinoma progression *via* targeting miR-299-3p

Wang HQ, Qian CH, Guo ZY, Li PM, Qiu ZJ

5154 Alcohol promotes epithelial mesenchymal transformation-mediated premetastatic niche formation of colorectal cancer by activating interaction between laminin-γ2 and integrin-β1

Nong FF, Liang YQ, Xing SP, Xiao YF, Chen HH, Wen B

Retrospective Cohort Study

5175 Natural history and outcomes of patients with liver cirrhosis complicated by hepatic hydrothorax

Romero S, Lim AK, Singh G, Kodikara C, Shingaki-Wells R, Chen L, Hui S, Robertson M

Observational Study

5188 Gut microbiota of hepatitis B virus-infected patients in the immune-tolerant and immune-active phases and their implications in metabolite changes

Li YN, Kang NL, Jiang JJ, Zhu YY, Liu YR, Zeng DW, Wang F

5203 Dynamic blood presepsin levels are associated with severity and outcome of acute pancreatitis: A prospective cohort study

Xiao HL, Wang GX, Wang Y, Tan ZM, Zhou J, Yu H, Xie MR, Li CS

Prospective Study

5217 High prevalence of chronic viral hepatitis B and C in Minnesota Somalis contributes to rising hepatocellular carcinoma incidence

Mohamed EA, Giama NH, Abdalla AO, Shaleh HM, Oseini AM, Ali HA, Ahmed F, Taha W, Ahmed Mohammed H, Cvinar J, Waaeys IA, Ali H, Allotey LK, Ali AO, Mohamed SA, Harmsen WS, Ahmmad EM, Bajwa NA, Afgarshe MD, Shire AM, Balls-Berry JE, Roberts LR

LETTER TO THE EDITOR

5230 Urotensin II level is elevated in inflammatory bowel disease patients

Zhang Y, Chen GX

5233 Hepatitis B viral infection and role of alcohol

Muro M, Collados-Ros A, Legaz I

CORRECTION

5237 Correction to "Inhibiting heme oxygenase-1 attenuates rat liver fibrosis by removing iron accumulation"

Wang QM, Du JL, Duan ZJ, Guo SB, Sun XY, Liu Z

ABOUT COVER

Editorial Board of *World Journal of Gastroenterology*, Yoichi Matsuo, MD, PhD, Professor, Department of Gastroenterological Surgery, Nagoya City University Graduate School of Medical Sciences, Kawasumi 1, Mizuho-cho, Mizuho-ku, Nagoya 4678601, Japan. matsuo@med.nagoya-cu.ac.jp

AIMS AND SCOPE

The primary aim of *World Journal of Gastroenterology* (*WJG*, *World J Gastroenterol*) is to provide scholars and readers from various fields of gastroenterology and hepatology with a platform to publish high-quality basic and clinical research articles and communicate their research findings online. *WJG* mainly publishes articles reporting research results and findings obtained in the field of gastroenterology and hepatology and covering a wide range of topics including gastroenterology, hepatology, gastrointestinal endoscopy, gastrointestinal surgery, gastrointestinal oncology, and pediatric gastroenterology.

INDEXING/ABSTRACTING

The *WJG* is now abstracted and indexed in Science Citation Index Expanded (SCIE, also known as SciSearch®), Current Contents/Clinical Medicine, Journal Citation Reports, Index Medicus, MEDLINE, PubMed, PubMed Central, Scopus, Reference Citation Analysis, China National Knowledge Infrastructure, China Science and Technology Journal Database, and Superstar Journals Database. The 2022 edition of Journal Citation Reports® cites the 2021 impact factor (IF) for *WJG* as 5.374; IF without journal self cites: 5.187; 5-year IF: 5.715; Journal Citation Indicator: 0.84; Ranking: 31 among 93 journals in gastroenterology and hepatology; and Quartile category: Q2. The *WJG*'s CiteScore for 2021 is 8.1 and Scopus CiteScore rank 2021: Gastroenterology is 18/149.

RESPONSIBLE EDITORS FOR THIS ISSUE

Production Editor: *Yi-Xuan Cai*; **Production Department Director:** *Xiang Li*; **Editorial Office Director:** *Jia-Ru Fan.*

NAME OF JOURNAL
World Journal of Gastroenterology

ISSN
ISSN 1007-9327 (print) ISSN 2219-2840 (online)

LAUNCH DATE
October 1, 1995

FREQUENCY
Weekly

EDITORS-IN-CHIEF
Andrzej S Tarnawski

EDITORIAL BOARD MEMBERS
http://www.wjgnet.com/1007-9327/editorialboard.htm

PUBLICATION DATE
September 21, 2022

COPYRIGHT
© 2022 Baishideng Publishing Group Inc

INSTRUCTIONS TO AUTHORS
https://www.wjgnet.com/bpg/gerinfo/204

GUIDELINES FOR ETHICS DOCUMENTS
https://www.wjgnet.com/bpg/GerInfo/287

GUIDELINES FOR NON-NATIVE SPEAKERS OF ENGLISH
https://www.wjgnet.com/bpg/gerinfo/240

PUBLICATION ETHICS
https://www.wjgnet.com/bpg/GerInfo/288

PUBLICATION MISCONDUCT
https://www.wjgnet.com/bpg/gerinfo/208

ARTICLE PROCESSING CHARGE
https://www.wjgnet.com/bpg/gerinfo/242

STEPS FOR SUBMITTING MANUSCRIPTS
https://www.wjgnet.com/bpg/GerInfo/239

ONLINE SUBMISSION
https://www.f6publishing.com

© 2022 Baishideng Publishing Group Inc. All rights reserved. 7041 Koll Center Parkway, Suite 160, Pleasanton, CA 94566, USA
E-mail: bpgoffice@wjgnet.com https://www.wjgnet.com

World Journal of Gastroenterology

Submit a Manuscript: https://www.f6publishing.com

World J Gastroenterol 2022 September 21; 28(35): 5093-5110

DOI: 10.3748/wjg.v28.i35.5093

ISSN 1007-9327 (print) ISSN 2219-2840 (online)

REVIEW

Robotic, self-propelled, self-steerable, and disposable colonoscopes: Reality or pipe dream? A state of the art review

Conchubhair Winters, Venkataraman Subramanian, Pietro Valdastri

Specialty type: Gastroenterology and hepatology

Provenance and peer review: Invited article; Externally peer reviewed.

Peer-review model: Single blind

Peer-review report's scientific quality classification

Grade A (Excellent): 0
Grade B (Very good): 0
Grade C (Good): C, C
Grade D (Fair): 0
Grade E (Poor): 0

P-Reviewer: Cheng KC, China; Pattarajierapan S, Thailand

Received: May 6, 2022
Peer-review started: May 6, 2022
First decision: June 8, 2022
Revised: June 21, 2022
Accepted: September 1, 2022
Article in press: September 1, 2022
Published online: September 21, 2022

Conchubhair Winters, Venkataraman Subramanian, Leeds Institute of Medical Research, University of Leeds, St. James's University Hospital, Leeds LS9 7TF, United Kingdom

Pietro Valdastri, School of Electronic and Electrical Engineering, University of Leeds, Leeds LS2 9JT, United Kingdom

Corresponding author: Conchubhair Winters, MBChB, Doctor, Research Fellow, Leeds Institute of Medical Research, University of Leeds, St. James's University Hospital, Beckett Street, Leeds LS9 7TF, United Kingdom. c.r.winters@leeds.ac.uk

Abstract

Robotic colonoscopes could potentially provide a comfortable, less painful and safer alternative to standard colonoscopy. Recent exciting developments in this field are pushing the boundaries to what is possible in the future. This article provides a comprehensive review of the current work in robotic colonoscopes including self-propelled, steerable and disposable endoscopes that could be alternatives to standard colonoscopy. We discuss the advantages and disadvantages of these systems currently in development and highlight the technical readiness of each system to help the reader understand where and when such systems may be available for routine clinical use and get an idea of where and in which situation they can best be deployed.

Key Words: Robot-enhanced procedures; Colonoscopy; Endoscopy; Capsule endoscopy; Colorectal cancer; Colonic polyp

©The Author(s) 2022. Published by Baishideng Publishing Group Inc. All rights reserved.

Core Tip: Colorectal cancer is a common cause of cancer related mortality. Detection and removal of precancerous polyps reduces the risk of colorectal cancer. Colonoscopy is the gold standard investigation for colorectal polyps and cancer but can be uncomfortable due to the mechanics of the procedure. Robotics has the potential to reduce the discomfort and improve the procedure for patients, while improving key performance indicators. Robotics can offer a more intuitive endoscopic appearance, using various methods to negotiate the colon to reduce discomfort. Robotics could lead to a more effective, better tolerated, safer, autonomous colonoscopy with minimal operator interaction.

Citation: Winters C, Subramanian V, Valdastri P. Robotic, self-propelled, self-steerable, and disposable colonoscopes: Reality or pipe dream? A state of the art review. *World J Gastroenterol* 2022; 28(35): 5093-5110
URL: https://www.wjgnet.com/1007-9327/full/v28/i35/5093.htm
DOI: https://dx.doi.org/10.3748/wjg.v28.i35.5093

INTRODUCTION

Colorectal cancer incidence

Colorectal cancer (CRC) is the third most diagnosed cancer and the second most common cause of cancer related mortality worldwide[1]. Many countries, particularly those with a high human development index (HDI), continue to see an increasing incidence[2]. Rapid increases in the incidence of CRC can be seen in countries transitioning from medium to high HDI[2]. Although CRC aetiology is heterogeneous, the majority are sporadic, and the increasing incidence has been attributed to the western lifestyle and increasing levels of obesity[3].

The majority of CRCs have a detectable precursor lesion, a colonic polyp, which can be present for many years before cancer develops[4]. Endoscopic resection of colonic polyps has been shown to reduce cancer related mortality by up to 53%[5]. More and more countries are utilising screening programmes to control the increasing incidence of CRC. Screening programmes vary in nature and often utilise faecal testing such as faecal immunochemical testing (FIT). However, colonoscopy remains the gold standard for diagnosing and removing colonic polyps. Colonoscopy is also utilised in many polyp, colitis, and hereditary CRC surveillance programmes[6-9].

Despite the recommendations for colonoscopy as a diagnostic, screening, or surveillance tool, it is often underutilised. Delays in colonoscopy following a positive FIT has been shown to increase the likelihood of finding advanced adenomas, CRC, and advanced CRC[10]. A meta-analysis looking at second evaluation after a positive faecal occult blood test found that only 72.5% underwent a second evaluation in the form of any lower gastrointestinal investigation[11]. Additionally, a recent international survey of FIT screening programmes found that only 79% of those with a positive FIT underwent a colonoscopy[12]. Studies from Lee *et al*[13] and Zorzi *et al*[14] suggest the risk of CRC related mortality is double in those with a positive FIT who refuse colonoscopy than those who undergo a colonoscopy [13,14].

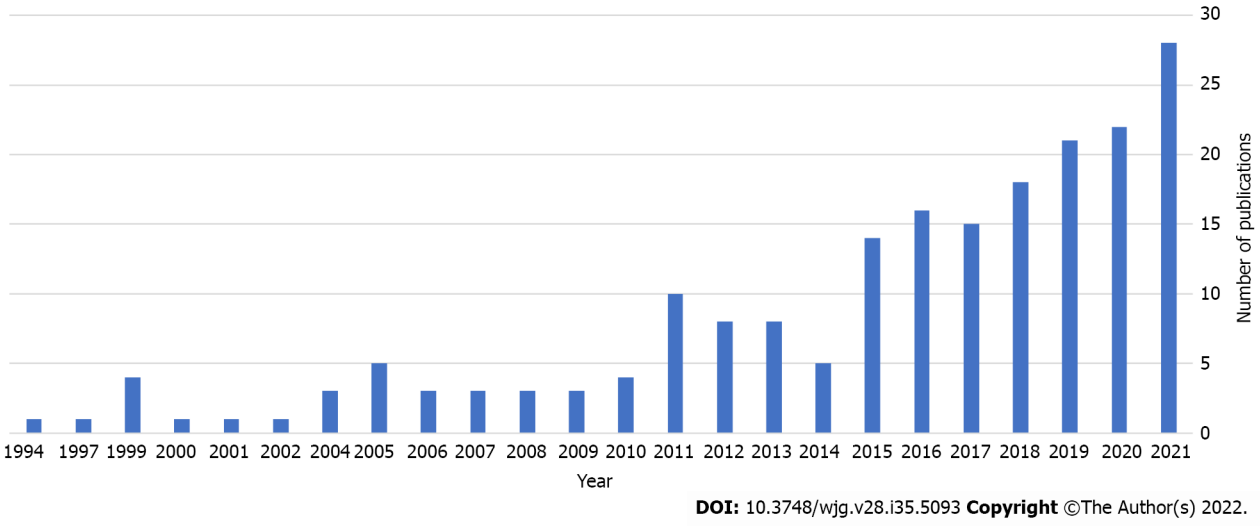
The reason for a lack of follow-up investigation may be the decision of a healthcare worker, for example due to co-morbidity. However, approximately 10% of those with a positive faecal blood test that are not followed up are due to patient refusal to have a colonoscopy[15]. Alternative tests such as computed tomography colonography (CTC) and colon capsule are available, and their merits will be discussed in future sections. Several qualitative studies have been done exploring the barriers and facilitators to colonoscopy. Although the barriers are numerous, complex, and interrelated, previous bad experiences of colonoscopy and fear of pain or discomfort are commonly cited[15-17].

History of colonoscopy

The first descriptions of an endoscope came from Bozzini in 1805 which he called the Lichtleiter (light conductor)[18,19]. Several rigid endoscopes were subsequently invented, but it was over a century before Wolfe and Schindler developed the semi-rigid gastroscope which paved the way for our endoscopes of today[20]. The evolution of the modern endoscope gained speed in the 1950s when Hirschowitz and Curtiss developed the fibreoptic endoscope[21]. A flexible endoscope was developed in Japan to assess of the lower GI tract, the first colonoscope, and by the late 1960s Shinya introduced therapeutics by performing the first polypectomy[21,22]. The charged couple device (CCD) was developed and in the 1980s the videoendoscope was born. Since then, the optics have been the mainstay of research focus and endoscope advancements. We have ever evolving improvements in the optics such as high definition, magnification, and an increasing range of image enhancement virtual chromoendoscopy options. And although the technique by which we perform colonoscopy has been refined, reducing risk and discomfort, we still push and torque a semirigid tube from the distal end to advance around the colon. The introduction of electromagnetic guidance, such as ScopeGuide (ScopeGuide Endoscope Insertion Tube System, Olympus America, Inc., Allentown, PA), allowed further refinement of the technique. However, it was not until the 1990s, with advances in robotics, that the potential for a new way to perform colonoscopy was explored.

Robots in endoscopy

Following Food and Drug Administration (FDA) approval in 2000 of robotic surgical master-slave platforms such as da Vinci and Zeus, there has been an upsurge in interest in robotic endoscopic devices. Figure 1 shows the increasing number of robotic colonoscopy articles on PubMed[23]. Robotic colonoscopy has potential benefits over conventional colonoscopy (CC) for the patient as well as the endoscopist and service provider. Robotics in colonoscopy is not only limited to diagnostic procedures,



DOI: 10.3748/wjg.v28.i35.5093 **Copyright** ©The Author(s) 2022.

Figure 1 PubMed search for "robotic colonoscopy" showing the increasing number of papers over the last 3 decades[23].

the additional dexterity and triangulation offered by many robotic platforms has great potential in therapeutic procedures such as endoscopic submucosal dissection (ESD).

Recent advances in robotics and miniaturisation, as well as the evolving nature of artificial intelligence (AI) in endoscopy, make this the perfect time to explore robotic colonoscopy. The expanding use of surgical robotic platforms should make patients and endoscopists more accepting of these new technologies in endoscopy. The potential for teleoperated endoscopes to facilitate "medical distancing" is also a concept of increasing interest given the current severe acute respiratory syndrome coronavirus 2 global pandemic.

For robotics to be accepted in endoscopy they must not only offer the same role as CC, but more. The ideal robotic colonoscope should fulfil several criteria as listed in Table 1.

POTENTIAL BENEFITS OF ROBOTIC COLONOSCOPY OVER CC

Patients

Much work in robotic colonoscopy is aimed at delivering a less painful and lower risk endoscopic procedure by reducing the forces on the colonic mucosa and tethering structures. The principal method of reducing this discomfort is through altering the actuation method. Many devices have taken inspiration from nature through biomimicry, for example inchworm or snake like movements. Others use external actuation, such as magnets to pull the device through the colon. A lower discomfort procedure also offers the potential for less anaesthetic/sedative use, further lowering the risk of colonoscopy[24]. Miniaturisation, and particularly capsule endoscopy, have the potential to offer a less invasive, less embarrassing, and more convenient option for patients. Some devices may even be provided in a community setting, negating the need to travel to hospital. Although incomplete colonoscopy rates have improved over the last few decades, there remain a number of patients who require a second procedure. Robotics has the potential to reduce the number of failed procedures by improving caecal intubation rates (CIRs).

Endoscopists

Training in both the diagnostic and therapeutic aspects of colonoscopy take considerable time[25,26]. Robotics has the potential to make colonoscopy training easier through more intuitive controls, autonomous features and the increased dexterity offered by many platforms. Less loop formation and lower discomfort rates could translate into improved completion rates. The improvement in manoeuvrability could reduce polyp miss rates and potential post-colonoscopy CRCs. Robotics has the potential to 'democratise' colonoscopy, reducing the variability in polyp detection rates by improving the detection rates of less well performing endoscopists. Many platforms are aiming to improve the ergonomics of colonoscopy in an attempt to reduce fatigue and endoscopy related musculoskeletal injuries[27,28].

Service providers

Our forebearers in surgical robotics have yet to provide any clear answers as to the cost effectiveness of robotic procedures. The initial purchase costs are often high, but the cost benefit thereafter is unclear

Table 1 The features of the ideal robotic colonoscope

No.	Ideal robotic colonoscope features
1	Affordable
2	Acceptable to patients and endoscopists
3	More comfortable than conventional colonoscopy
4	Lower risk than conventional colonoscopy
5	Improved caecal intubation rate compared to conventional colonoscopy
6	Offer at least comparable mucosal visibility with the option of image enhancement (virtual chromoendoscopy)
7	Capable of taking biopsies and therapeutics such as polypectomy
8	Offer integration with artificial intelligence for polyp detection and characterisation
9	Ideally have autonomous features, such as self-navigation
10	Reduce the training time to achieve competence compared to conventional colonoscopy
11	Procedure times should be less than, but must not be significantly longer than, conventional colonoscopy
12	Have sustainability in mind in the manufacturing, reprocessing or disposal of the device

and variable between procedures[29-32]. The Endotics robotic colonoscope, discussed in detail later, claims to offer a cost neutral alternative to standard colonoscopy[33]. Although few robotic colonoscopes are at a technology readiness level (TRL) to perform health economics studies, we will aim to discuss several potential benefits to service providers.

Unsedated procedures offer cost and efficiency saving benefits through utilisation of less anaesthetic and recovery staff, as well as a quicker turnaround within the department. There is an increasing demand on endoscopy services caused by an aging population, increasing environmental and behavioural risk factors, and ever increasing screening and surveillance populations[34]. The addition of the recent pandemic associated service provision issues and enhanced infection control and prevention measures are stretching endoscopy departments to their limit[35]. The ideal robotic colonoscope to ease these pressures would require less staff and be quicker, pain-free, teleoperated, mobile and have therapeutic capabilities. A single use device would negate the cost associated with reprocessing, as well as potentially reducing cross contamination[36]. Improvements in sustainability may also be achieved using single use devices which reduce the need for carbon- and water-heavy reprocessing facilities.

AVAILABLE ALTERNATIVES TO COLONOSCOPY

Alternative procedures to assess the colon are required if a patient refuses or is unfit for a colonoscopy, or in the event of an incomplete colonoscopy. There are a number of alternatives to CC, most commonly CTC and colon capsule endoscopy (CCE). The advantages and limitations of these commonly used alternatives are shown in Table 2.

CTC, until the recent adoption of CCE, was the most commonly used alternative to colonoscopy. CTC has a similar sensitivity to colonoscopy for the detection of large (> 10 mm) polyps and CRC[37,38]. CTC is better tolerated than CC and over half of patients have an additional pathology detected on the scan [37,39]. However, approximately 30% of CTC patients require further investigation, often in the form of a colonoscopy to remove polyps[38]. CTC is significantly less sensitive than colonoscopy for detection of small polyps and flat lesions such as sessile serrated lesions[40].

CCE is better tolerated than CC[41]. A recent meta-analysis showed that when compared with CC, CCE had a sensitivity and specificity of 87% and 88% respectively, for detection of polyps ≥ 6 mm[42]. However, a large retrospective study by Benech *et al*[43], showed that 19% of CCEs had a missed advanced adenoma when they underwent a further procedure[43]. When comparing CTC to CCE, Spada *et al*[44] compared 100 patients with an incomplete colonoscopy and found a relative sensitivity of 2.0 in favour of CCE for identifying polyps ≥ 6 mm[44]. The recently published TOPAZ study also suggested CCE was superior to CTC for the detection of polyps ≥ 6 mm and non-inferior for polyps ≥ 10 mm[45]. However, some inherent biases and flaws in methodology of the TOPAZ study have been pointed out by Burr *et al*[46] which cast some doubt on the validity of these results[46]. A meta-analysis of CTC *vs* CCE in incomplete colonoscopies showed that CCE had superior diagnostic yields for all polyp sizes (37% *vs* 10%), but poorer completion rates (76% *vs* 98%)[47].

Magnetic resonance imaging techniques, magnetic resonance colonography (MRC), have also been evaluated as an alternative to CC. MRC has the benefits of being non-invasive and not carry the radiation risks associated with CTC. However, magnetic resonance imaging scanners can be claustro-

Table 2 Advantages and limitations of conventional colonoscopy alternatives

Procedure	Advantages	Limitations
Conventional colonoscopy	Extensive knowledge base and expertise already available, diagnostic and therapeutic capabilities. Gold standard	Bowel cleansing required, painful for some (sedative and analgesics often required), prolonged training period required, risk of perforation due to forces required
CT colonography [39,41,101]	Lower intensity bowel cleansing, shorter procedure, less discomfort (no sedation or analgesia needed), other intraabdominal pathology can be detected, lower risk of perforation, better patient tolerance	Low dose radiation used, lower sensitivity for small and flat polyps, no therapeutic capability, no direct mucosal visualisation, limited evidence of a benefit in CRC incidence or mortality
Wireless capsule colonoscopy	Minimally invasive, painless, better patient tolerability, low perforation risk	Aggressive bowel cleansing required, lower sensitivity than CC for polyps, no control of the capsule, no therapeutic capability, risk of capsule retention, limited battery life can cut out before complete colon visualisation

CRC: Colorectal cancer; CC: Conventional colonoscopy; CT: Computed tomography.

phobic for some and are very time consuming procedures. A meta-analysis in 2009 found the sensitivity of MRC for the detection of CRC was 100%, but was only 84% for polyps ≥ 10 mm[48]. A study in 30 lynch syndrome patients who underwent tandem MRC then colonoscopy, found that MRC was unable to detect any lesions under 10 mm, including one missed cancer[49]. Another study of MRC in asymptomatic individuals found MRC and colonoscopy had sensitivities of 78.4% and 97.3%, respectively, for polyps ≥ 6 mm[50]. Although some meta-analysis suggest MRC has a good sensitivity for the detection of CRC, other meta-analysis suggest the sensitivity for detection of all lesions could be as low as 75%[51].

CHALLENGES FOR ROBOTIC COLONOSCOPY

As technologies advance, many of the technical challenges to robotic colonoscopy are being resolved. The deformable, slick surface of the colon and it's many and varying orientations and bends make for a challenging environment and a multitude of solutions have been proposed by various research teams.

Locomotion

The first challenge for any robotic device is locomotion. Passive locomotion is adopted by most capsule endoscopes, in which the device passes through the gastrointestinal tract by natural peristalsis. However, the lack of control has the consequence of potentially missing lesions and rules out any therapeutic application.

Actively controlled robotic colonoscopes can be divided into internally and externally actuated devices. Internally actuated devices control propulsion by interacting directly with the surrounding environment by means of wheels, propellers, belts or bio-mimicked animal-like movements. Much inspiration for the locomotion of these devices has been taken from nature with many attempting to copy the movements of animals such as snakes, earthworms, or caterpillars, and some even mimicking the movement of micro cilia. These actuation principles are achieved using electromechanical or pneumatic mechanisms, or a combination of both. External actuation involved controlling the internal device by means of an external mechanism such as magnetic fields and field gradients. With external magnetic actuation comes the challenge of localisation of the endoscope within its environment.

Localisation

Localisation refers to the position and orientation (*i.e.*, pose) of the device. Localisation can be relative or absolute. Relative localisation is a well-developed technology and is implemented in a number of wireless capsule endoscopes (WCE) giving an estimated position with respect to the anatomy. Absolute localisation gives an accurate position and orientation. Several proposed solutions have been investigated in endoscopes including magnetic, ultrasound, radiofrequency and computer-vision technology. Many WCEs use radiofrequency localisation, current capsules have an error in position on average 38 mm and up to 100 mm[52]. Magnetic localisation is gaining increasing academic interest, and can be combined with magnetic actuation. Magnetic localisation can perform a 6 degrees of freedom (DOF) localisation with an average error in position and orientation under 5 mm and 6 mm, respectively[53].

Miniaturisation

Miniaturisation is a challenge for all robotic colonoscopes, but is of particular importance in capsule endoscopy. A capsule endoscope contains several components: External case, optical window, light emitting diode (LED), lens, image sensor, radio frequency transmitter, antenna, and a power source.

Powering a capsule endoscope to allow for the variable colonic transit times requires a battery sufficiently large and often means adjusting the frames *per* seconds, and ultimately sensitivity, to preserve battery life. All this must then fit within a safe size for transit through the GI tract. Most capsule endoscopes are 11 mm in diameter and up to 32 mm in length with a battery life now exceeding 10 h and often containing two cameras[34]. One proposed method to overcome the miniaturisation challenge is external actuation *via* magnetic coupling, reducing the size of the battery in capsules and the need for intricate mechanisms of locomotion. One such commercially available capsule endoscope which already takes advantage of magnetic coupling is the NaviCam (Ankon Technologies, Wuhan, Shanghai, China) for inspection of the upper gastrointestinal tract[54].

Patient tolerance

The goal for most robotic colonoscopes is to improve the patient experience. For most devices this takes the form of reducing discomfort and risk. Capsule endoscopes achieve this by causing no distortion to the GI tract during their passive transit. Actively controlled devices aim to traverse the colon retrograde while reducing distortion and pressure exerted, resulting in less pain. Potentially also reducing the risk of perforation associated with the forces often required to torque and push around the colon in CC. Various actuation methods aim to tackle this problem by rolling, walking, inching, slithering, or pulling with magnets along the colon.

Cost

Not many robotic colonoscopy devices have health economic studies assessing their financial impact. Even the colon capsule, which is now available as an alternative to CC in some health services such as the National Health Service in the United Kingdom, has yet to show any cost effectiveness benefit over CC[55].

Sustainability

Reprocessing presents a massive challenge in robotic colonoscopy due to the intricacy of some devices. Many researchers are pursuing the potential of single use devices. With over 18 million endoscopic procedure *per* year in the United States, endoscopy is the third highest generator of waste in healthcare. Endoscope reprocessing uses up to 100 L of water as well as the electricity, heat, disinfectants and detergents[56]. Single use endoscopes have the potential to avoid this carbon heavy process. Provided the disposal of the device does not incur a higher carbon footprint, single use robotic devices have the potential to present a greener option for colonoscopy.

Autonomy

Perhaps the most notable evidence of robotic autonomy in day-to-day life is in automotive vehicles which can park and even navigate with minimal external input. However, medical robotics is also seeing an evolution in autonomy. Standard colonoscopy is completely under the control of the endoscopist with no autonomy. The introduction of AI for polyp detection has moved endoscopy into the first level of autonomy by visually assisting the endoscopist. Robotic colonoscopes have the potential to push the levels of autonomy much further. Devices capable of autonomously navigating the colon are being researched. However, with such levels of autonomy come challenges such as ethical and legal considerations.

TRL

TRL assessment was introduced by NASA in the 1980 to replace the traditional research and development categories: Basic research, feasibility, development, and demonstration[57]. TRL provides an objective 9 stage assessment of how advanced a technology is towards adoption[58]. When discussing each device, we will attempt to give our objective assessment of the TRL of each device. The score assigned will range from 1 (basic principles of the technology observed and report) to 9 (proof of real-world successful use of the technology) as described in Table 3, and a score will be assigned to each device described alongside the device characteristics in Table 4.

ROBOTIC COLONOSCOPES

For the purpose of this review article a selection of the most advanced platforms will be discussed, dividing them into active flexible platforms, passive devices, robot assisted platforms and robotic platforms with therapeutic applications. A table offering additional detail on the devices, as well as several more devices, is available in Supplementary Table 1.

Table 3 Technology readiness levels as applicable to robotic colonoscopy[57,102,103]

TRL	Definition	Supporting information relevant to robotic colonoscopy
1	Basic principles observed and reported	Published research on the core principals of the technology
2	Technology concept and/or application formulated	Moving from principals to applied research with potential applications speculated
3	Analytical and experimental proof of concept	Active research and development proving the concept within a laboratory setting. Benchtop testing
4	Component validation in laboratory environment	Proof of concept and safety in an *ex-vivo* animal colon
5	Component/system validation in a relevant environment	*In-vivo* animal testing with an aim at providing relevant evidence for human testing or FDA approval
6	High fidelity alpha protype demonstration in a relevant environment	Clinical trials assessing feasibility and safety in small number of humans
7	Beta prototype demonstrated in a relevant environment	Clinical safety and effectiveness trials. Determination of risks and adverse events. Final design validation
8	Completed system and qualified to relevant requirement/standards through testing and demonstration	FDA or equivalent approval
9	Actual system proven through successful operation	Device being marked with post-market studies proving real world operational capability

Adopted from United States Department of Defense Technology Readiness Assessment (TRA) Guidance document, and the supporting evidence required from the United States Department of Defense Technology Readiness Assessment (TRA) Desk book. TRL: Technology readiness level; FDA: Food and Drug Administration.

Table 4 Active flexible colonoscopy platforms with technology readiness level

Device name (manufacturer)	Latest study	Outcomes	TRL
Aer-O-Scope-*GI View Ltd., Ramat Gan, Israel*[21,59-61,63,64]	2016: Human tandem study, 58 CRC screening patients. CIR: 98.2%. CIT: 11 min. 87.5% of polyps detected. No PREMs	CE marked and FDA approved. Balloon propulsion model no longer manufactured	8
ColonoSight-*Stryker GI Ltd., Haifa, Israel*[65,66]	2008: Human study on 178 participants. CIR 90%. CIT: 11.2 min. No PREMs	FDA approved. No longer manufactured	8
Consis medical-*Beer'Sheva, Israel*[21,67]	None available	No regulatory approvals	3
Endoculus-*Department of Mechanical Engineering & Division of Gastroenterology, University of Colorado, United States*[20]	2020: *In-vivo* and *ex-vivo* porcine colon in one. Unable to traverse an *in-vivo* colon, but capable of negotiating an *ex-vivo* porcine colon	No regulatory approvals	4
ENDOO robotic colonoscope-*Endoo Project, Pisa, Italy*[87-89]	2020: *Ex-vivo* porcine colon human simulator study	No regulatory approvals	4
Endotics-*ERA Endoscopy SRL, Peccioli, Italy*[69-74]	2020**:** Learning curve study of 57 participants. CIR and CIT improved to 100% and 22 min following a learning block. PREMs: Mild or no discomfort in most	CE marked and FDA approved. Commercially available in Europe and Japan	8
Invendoscope-*Invendo Medical GmbH, Weinheim, Germany (acquired by Ambu A/S, Copenhagen, Denmark in 2017)*[21,77-79]	2018: Human study on 40 participants using the SC210 model. CIR 95%. CIT 14.2 min. No PREMs on this study, but previous studies reported lower pain scores than CC	CE marked and FDA approved. No longer manufactured	8
Magnetic Flexible Endoscope-*STORM lab, Leeds, United Kingdom & Nashville, TN, United States*[4,53,85,86,104]	2020: *In-vivo* porcine study. Clinical trial due 2022	No regulatory approvals	5

TRL: Technology readiness level; CIR: Caecal intubation rate; CIT: Caecal intubation time; FDA: Food and Drug Administration; CRC: Colorectal cancer; CC: Conventional colonoscopy; CE: Capsule endoscopy.

Active flexible colonoscopy platforms

Aer-O-Scope: The Aer-O-Scope (GI View Ltd., Ramat Gan, Israel) is a single use flexible colonoscope that uses a CO_2 propulsion system to self-advance through the colon. With a 200° field of view offered by two cameras it aims to offer better visibility behind folds while reducing discomfort. The device works by inflating two polyurethane balloons (Figure 2), the first balloon is inflated at the rectum to create a seal, a second balloon which pulsates and has a hydrophilic coating to reduce friction is inflated proximal to the first. Using the seal between the balloons, CO_2 is inflated, and the pneumatic force



Figure 2 Aer-O-Scope (GI View Ltd., Ramat Gan, Israel). A: Single use colonoscope scanner; B: Workstation. Citation: Images supplied directly by the manufacturer with email detailing permission to use attached as a text file.

propels the proximal balloon forward. To protect the colon, the system controls the pressure so it does not exceed 60 mbar[59]. The most recent version of the device is equipped with two working channels to allow therapeutics[21]. Tip control is achieved using a hand-held controller. Once in the caecum, the pressures are reversed to propel the proximal balloon back towards the rectum while maintaining colonic distension for visibility.

Safety of this novel propulsion method was first demonstrated in 20 pigs in 2006 were only minor petechiae and no adverse events were noted[60]. That study was quickly followed by a clinical trial in the same year on 12 healthy young adults[61]. In this study 10 out of 12 procedures were completed to the caecum with the other two stopping at the hepatic flexure. In both these cases CC was also unable to progress beyond the hepatic flexure due to redundant colon in one and pain in the other. Caecal intubation occurred in an average of 14 min for the 10 completed. Two subjects requested analgesia, while the other 10 had a non-sedated procedure. Mild localised submucosal petechial lesions, thought to be related to balloon friction, were noted on 4 of the follow-up conventional colonoscopies. No other clinically significant adverse events were reported.

A further prospective, non-randomised clinic trial was published in 2016 on 58 CRC screening patients who underwent tandem colonoscopies with the Aer-O-Scope followed by CC[59]. Caecal intubation was achieved in 98.2% (94.4% in the training cohort and 100% in the study cohort). The Aer-O-Scope detected 87.5% of the polyps found by CC, and 100% of those ≥ 5 mm. Caecal intubation was achieved in a mean of 11 min. No mucosal damage or adverse events were reported. Patients were sedated and no patient related experience measures have been reported on.

A prospective clinical trial using the Aer-O-Scope completed recruitment on clinicaltrial.gov in November 2021 but the results have not yet been published at the time of writing and are likely to be for a newer model of the colonoscope[62]. The Aer-O-Scope is CE marked and received FDA approval in 2016[63]. GI View Ltd no longer produce the self-propelled version of the Aer-O-Scope, instead opting to use the technology on a new version which is a single use robotic colonoscope without the balloon self-propulsion[64].

Following correspondence with GI View Ltd, they felt the advances in colonoscopy technique, with improved CIRs and within shorter times, limited the need for a self-propelled device. Instead, they are choosing to concentrate on a single use colonoscope with a larger lens aimed at improved polyp detection, while maintaining similar controls to reduce the need for new training.

ColonoSight: ColonoSight (Stryker GI Ltd., Haifa, Israel) is a self-advancing system composed of a reusable colonoscope (EndoSight) covered by a single use plastic sleeve (ColonoSleeve). The Colono-Sleeve is a multi-lumen sheath that is inflated with air and progressively unfolds to propel the device through the colonic lumen. The IntraPull force that insufflates the air for propulsion is controlled using a foot pedal. The other controls resemble those of a standard colonoscope using a wheel and pully angulation control system. Push, pull and torque can also be used, similar to standard colonoscopy. On

reaching the caecum, air insufflation is directed toward the tip, insufflating and reversing the pressure. A CCD camera with an LED is used to capture image, eliminating the need for fibre optics. The device contains a working channel for therapeutic tools. The outer surface, tip and channels of the endoscope are single use, therefore negating the need for reprocessing of the reusable EndoSight component[65].

Shike *et al*[65] describe that the operation and safety of the instrument was first tested on animals (12 pigs and 7 sheep) with a mean progression into the colon of 80 cm. *In-vitro* dye and culture studies as well as *in-vivo* culture testing confirmed the integrity of the disposable sleeve to protect against bacterial transfer. A clinical trial published in 2008 included 178 participants achieved a 90% CIR in a mean caecal intubation time (CIT) of 11.2 min. The CIR in the final 50 participants was 94%, suggesting a possible learning curve effect. 40 participants underwent polypectomy, with biopsies and argon plasma coagulation was also performed. No immediate complications were noted, and no complications were reported at a two week follow-up telephone call. Participants received intravenous sedation and no patient experience measures are reported on. Physicians reported the IntraPull helped progress the device[65]. The ColonoSight Model 510B received FDA approval in 2004[66]. Stryker GI Ltd acquired Sightline Technologies Ltd, the original manufacturer, in 2006 and the device is no longer manufactured. The reason for discontinuation is not clear, but Stryker GI Ltd have focused on laparoscopic endoscopic equipment rather than colonoscopes, so they may not have had the infrastructure to market a new colonoscope or they may have chosen to integrate the technology into laparoscopic equipment.

Consis medical: Consis medical (Beer'Sheva, Israel) have developed a semi-disposable, single use colonoscope that self-propels along the colon by means of an inverted sleeve pressurised with water. The head of the device can be removed and sterilised at the end of the procedure, with the sleeve cartridge being disposable[67]. The reusable head contains a camera, light source, steering system and water/air nozzle. Human colon simulation and animal tests were due to take place in 2018 but no published results are yet available[21].

Endoculus: Endoculus (University of Colorado, United States) is a multi-DOF fixed tether single use robotic capsule endoscope. Locomotion is *via* two independently controlled motor drives with micro-pillared treads, offering 2-DOF skid steering. *Via* a fixed tether the Endoculus contains channels for insufflation and irrigation, and a working channel for introduction of endoscopic instruments. The tip of the capsule contains a complementary metal-oxide-semiconductor (CMOS) camera and an adjustable LED. The fixed tether is narrow in diameter and very flexible, however the motorised tip is larger than a standard colonoscope at 6.0 cm × 3.0 cm × 2.3 cm. The research team feel the device could be made smaller with advanced manufacturing techniques[68].

In-vivo testing was carried out in a porcine colon. The device was inserted manually to 10 cm but was then unable to negotiate the sigmoid colon. The research team postulated that this was due to friction from the narrow sigmoid colon in a pig on the non-tread sides of the device. *Ex-vivo* testing on a porcine colon was subsequently conducted on a 40 cm mid colon section. The Endoculus was capable of negotiating the *ex-vivo* colon at speeds up to 40 mm/s both in an insufflated 6 cm diameter colon and also in a collapsed lumen[68].

Endotics: Endotics (ERA Endoscopy SRL, Peccioli, Italy) is an FDA and CE marked biomimicking colonoscope on sale in Europe and Japan[69]. The electropneumatic system uses proximal and distal clamps to attach to the colon wall and in a semi-autonomous process of extension and retraction of the shaft between the clamps it progresses along the colon in an inchworm fashion. Image is captured *via* an integrated CMOS camera lit by an LED light source. The device has a 3 mm working channel, insufflation and suction, and is single use. A 180° steerable head is controlled using a handheld control unit[70].

In-vitro studies reported in 2009 showed the Endotics E-worm system reduced the pressure on sensors around a pig colon by 90% compared to CC. An *in-vivo* animal study showed no complication of the clamping system at follow-up colonoscopy 7 d later[71]. In a pilot tandem study of 40 patients in 2009 the Endotics system only managed to achieve a CIR of 27.5% with mean CIT of 57 minutes, compared to a CIR of 82.5% for CC. The patient experience for the Endotics system was reported to be much better with average pain and discomfort scores of 0.9 and 1.1 out of 10, compared to 6.9 and 6.8 for CC[71].

A second tandem human study on 71 participants was published by Tumino *et al*[72] in 2010 aimed at assessing the Endotics ability to detect polyps. The CIR was 81.6% for the Endotics system and 94.3% for CC, with mean CIT 45.1 (± 18.5) min compared to 23.7 (± 7.2) min, respectively. None of the participants required sedation for the Endotics procedure, with 14/71 asking for sedation during the subsequent CC procedure. The Endotics system showed a sensitivity of 93.3% for the detection of polyps, detecting 14/15 polyps seen on CC. 6/71 (8.4%) of participants reported mild adverse events (nausea, headache, abdominal pain and discomfort) which the authors say, due to the tandem nature of the study, couldn't be distinguished from bowel cleansing or CC related adverse events[72].

A retrospective analysis of 5 years of Endotics examination in a single centre in Italy reported on 102 procedures performed due to incomplete CC. The Endotics system was able to complete a colonoscopy

in 95/102 (93.1%) of these patients. Mean CIT was 51 (± 22.5) min[73]. A learning curve study from Trecca *et al*[74] in 2020 presents two blocks of 27 and 28 participants. The CIR improved from 92.7% to 100% and the CIT from 55 to 22 min between the first and second block. The polyp detection rate and adenoma detection rate was 40% and 26.7%, respectively. The procedure was reported as mild or no distress in most cases with 92.7% willing to have a repeat Endotics procedure[74].

Endotics have performed a health economics study comparing Endotic robotic colonoscopy to standard colonoscopy in the Italian healthcare system and found the robotic colonoscopy to be comparable in price to standard colonoscopy, €441.25 *vs* €426.25, respectively[33].

Invendoscope

The Invendoscope (Invendo Medical GmbH, Weinheim, Germany) has a number of models with several CE and FDA approvals[75,76]. The single use computer-assisted device is propelled through the colon by an inverted sleeve driven by 8 wheels (Figure 3). The wheels grip the inside of the inverted sleeve to move forward and backwards. Control is *via* a handheld joystick. The tip of the colonoscope is robotically assisted and can be defected up to 180°, is equipped with three LEDs and a CMOS vision chip with an 114° field of view. Standard colonoscope functions such as insufflation, suction and irrigation are available, as well as a 3.2 mm working channel.

Animal testing using the SC20 model on the *in-vivo* small bowel of 5 pigs showed the device could be inserted through 3 small bowel loops and there was no mucosal damage found on microscopic pathological examination[77]. In a clinical trial of the SC40 model published in 2008, using two varying length prototypes in 34 participants, CIRs of 79% and 90% were achieved. CITs were 26 min and 20 min. The shorter of the two prototypes had a lower CIR, longer procedure time and more pain and bloating. Five cases had to be excluded due to instrument defects. Two of the failures to achieve caecal intubation were due to pain. Overall, the participants gave a mean acceptance rating of 1.96 (range 1-6). No immediate or delayed complications were reported[77].

A clinical trial on the Invendo SC20 model published by Groth *et al*[78] in 2011 found a CIR of 98.4% in 61 volunteers. Median CIT was 15 min and only 3/61 (4.9%) requested sedation. There were 32 polypectomies and no device-related complications reported. Water instillation was used in half of the cases to aid progression. Endoscope malfunctions were experienced in 2 cases. Post-procedure pain and discomfort scores were 1.6 and 2.3 out of 6, respectively[78].

Invendo Medical GmbH was acquired by Ambu in 2017 and the SC40 inverted sleeve wheel driven prototype has been replaced by the SC200 and then the SC210 which are manually inserted single use devices utilising robotic tip controls[21].

Only a conference abstract could be found on the Invendo SC210 model. In this clinical trial 40 participants underwent colonoscopy with the SC210, CIR was 95% with a median CIT of 14.2 min. Most patients (35/40) received propofol sedation. Twelve patients had polypectomies performed. There were 3 complaints of abdominal pain post-procedure and one self-limiting haemorrhage from the sigmoid colon, but no major complications[79].

The SC210 model no longer has any robotic locomotion, with the only robotics left being tip deflection, making it predominantly a single use colonoscope. Since the acquisition by Ambu, the Invendoscope is no longer on the market. Following correspondence with Ambu, the long scope length (220 cm) required for the self-propelled version made it difficult to control looping. Physicians also reportedly found it difficult to transition to the robotic tip control of the SC210 so Ambu have decided to focus on conventional control mechanisms.

Robotic capsule colonoscope

A European FP6 project called "Versatile Endoscopic Capsule for GI TumOr Recognition and therapy" (VECTOR project) was tasked to explore magnetic capsule endoscopy from 2006 to 2011. One of the outputs of the project was a magnetically controlled capsule for colonoscopy. A 13.5 mm × 29.5 mm endoscopic capsule containing 6 LEDs and a CCD camera capable of 550 × 582 pixel resolution and a 120° field of view was designed. The capsule also contained 3 permanent magnets and a triaxial magnetic sensor to monitor the magnetic link. Power and transmission to and from the capsule was achieved *via* a 2 mm cable. The capsule was controlled using an external permanent magnet fixed to a robotic arm end effector which was found to offer more precision than manual control[80]. The robotic arm has 6 DOF and an additional 7th DOF was added at the end effector-magnet connection. The capsule trajectory is controlled by means of controlling the robotic arm and the magnetic attraction between the external and internal magnets pulls the capsule along the colon. The initial version of the device was not able to insufflate the colon, so a Foley catheter had to be passed rectally to insufflate[81].

A benchtop study of the magnetic capsule colonoscope was undertaken, including 11 endoscopist and 11 trainees, who performed the robotic capsule colonoscopy and CC on an *ex-vivo* porcine colon used to simulate a human colon. All 22 participants were able to complete the procedure using both the robotic capsule and conventional colonoscope. Pins inserted in the phantom colon were found with a mean accuracy of 80.9% (± 11.0%) in the robotic capsule procedures and 85.8% (± 9.9%) in the CC procedures[81].

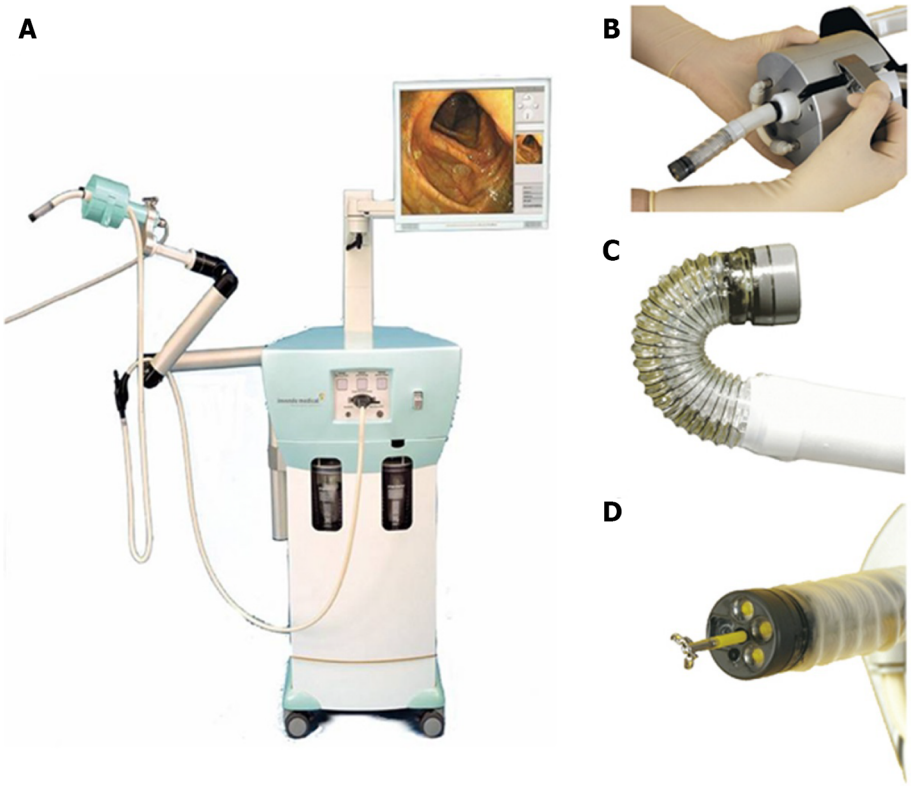


Figure 3 Invendoscope SC20 (Invendo Medical GmbH, Weinheim, Germany). A: Workstation; B: Drive unit; C: Deflectable tip; D: Working channel. Citation: Groth S, Rex DK, Rösch T, Hoepffner N. High cecal intubation rates with a new computer-assisted colonoscope: a feasibility study. *Am J Gastroenterol* 2011; 106: 1075-1080. Copyright© The Authors 2020. Published by Creative Commons Attribution-NonCommercial-No Derivative Works 3.0 License.

The next prototype from the same team of researchers, named the Magnetic Air Capsule, included a soft multi-lumen tether to allow insufflation, washing, suctioning, lens cleaning and a working channel for passing therapeutic tools. *Ex-vivo* testing on a porcine colon within a human phantom model was undertaken using 12 participants and all participants were able to complete an 85 cm phantom colonoscopy, with 85% (± 11%) of the beads found. *In-vivo* porcine testing proved the device was capable of traversing an average distance of 800 (± 40) mm in an average of 900 (± 195) seconds[82].

The VECTOR project team were also able to explore several other aspects of robotic colonoscope design. Experiments exploring the human robot interface were conducted and teleoperated (remote control) was found to be more reliable than a human/robot cooperative haptic control using a torque/force sensor[83].

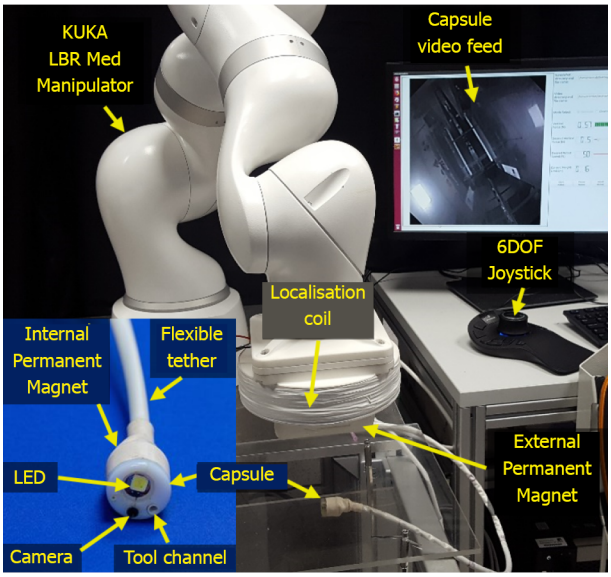
Following on from the VECTOR project, some of the research team have gone on to develop the technologies further in the ENDOO magnetic colonoscope and the magnetic flexible endoscope (MFE).

MFE

The MFE research team (STORM lab, Leeds, United Kingdom and Nashville, TN, United States) has developed the soft tether capsule colonoscope technology further (Figure 4). Advancements in the localisation and real time pose estimation allow closed loop control of the endoscope. Closed loop control allows the user to steer the endoscope based on what they see from the video feed rather than controlling movement of the robotic arm and attempting to translate that into the movement desired of the endoscope tip[53,84]. Further developments have allowed the capsule to levitate in the colon lumen rather than skimming along the mucosal surface. Autonomous navigation and autonomous retroflexion have been demonstrated in porcine studies[4,85]. Laboratory based learning curve studies and task load assessments suggest a quicker learning curve than with CC and a lower perceived workload[86]. *In-vivo* porcine studies have not demonstrated any safety concerns and even novice user were able to navigate the device 85 cm into a pig colon[84]. The platform is currently undergoing final pre-clinical steps in preparation for first-in-human trials.

ENDOO

The ENDOO project (Pisa, Italy) was a European H2020 project between 2015 and 2019 that also designed a magnetically actuated soft tether robot. A permanent magnet in the capsular tip of the endoscope is pulled through the colon using closed loop interaction with an external permanent magnet on an industrial anthropomorphic robotic arm[87,88]. The capsular tip has two 1080p CMOS cameras to allow stereoscopic, 3-dimensional, views. Four LEDs offer white light illumination, and 4 ultraviolet



DOI: 10.3748/wjg.v28.i35.5093 **Copyright** ©The Author(s) 2022.

Figure 4 Magnetic flexible endoscope (STORM lab, Leeds, United Kingdom and Nashville, TN, United States).

LEDs allow narrow band imaging. The 160 cm soft tether carries 4 channels, including a 3.7 mm working channel, providing suction, irrigation, lens cleaning and insufflation. The soft tether also integrates nylon cables to allow variable stiffness of the shaft.

Ex-vivo testing using a porcine colon in a human abdomen simulator compared key functionalities, forces generated, simulated polyp detection and usability when compared to CC in 10 expert endoscopists and 5 trainees. The forces generated by the robotic colonoscope were significantly less than those generated by CC, with cumulative interaction forces of 16.5N for CC and 1.67N for the robotic colonoscope. The robotic colonoscope was able to complete the procedure 67% of the time with a comparable polyp detection rate to CC[89].

PASSIVE COLONOSCOPY

Passive colonoscopes are capsule devices designed to assess the colon with movement through the gastrointestinal tract passively *via* natural peristalsis. There is now a commercially available colon capsule endoscope, the Pillcam™ COLON2 (Given Imaging, Yokneam Illit, Israel). Researchers have also been exploring the addition of further robotics within capsular devices in an attempt to overcome some of their disadvantages. Advances in miniaturisation, image capture and batteries have allowed researchers the space within the small confines of a safe capsule size to add further robotics. A full review of these devices is beyond the scope of this review but have been done in detail by Manfredi[90] and Slawinski *et al*[91].

ROBOT ASSISTED FLEXIBLE ENDOSCOPY PLATFORMS

The previously described robotic platforms aim to provide an alternative to CC. However, some researchers have been developing platforms to assist with some of the challenges of performing CC by adapting the current colonoscope. Adding robotic controls to existing endoscopes could improve the ergonomics and assist with the difficult learning curve associated with colonoscopy.

The Endodrive (ECE Medical Products, Erlangen, Germany) is a platform using a rotating engine and foot pedal to control shaft insertion. Rotation and tip control is still required[92]. Rozeboom *et al*[93] present a robotic-assisted flexible colonoscope that uses an add-on to the handle of the colonoscope that convert the wheel control mechanism into a robotic joystick control. CIR using Rozeboom's device was 68%[93]. Robotic steering and automated lumen centralisation (RS-ALC, Enschede, Netherlands) is another platform which uses joystick control of an add-on to the endoscope handle with the addition of lumen centralisation software. A study of novices and experts on a colon simulation model found that novices had a faster CIT and polyp detection rate with the RS-ALC than CC. The opposite was found of experts, who found CC better[94]. The master–slave endoscopic operation robot (EOR; Kyushu Institute of Technology, Kitakyushu, Japan) which is in its third iteration, added on therapeutic tools. The EOR version 3 uses a rotary motor, rotating handle, torque sensor and mini joystick which allows haptic

feedback and 4 axis movement. An *ex-vivo* colon phantom study using 8 endoscopists performed 48 colonoscopies with a CIR of 100% and CIT of 118.5 (± 89.4) seconds[69].

ROBOTIC FLEXIBLE ENDOSCOPES WITH THERAPEUTIC APPLICATIONS

Advances in the therapeutic capabilities of gastrointestinal endoscopy and the evolution of natural orifice transluminal endoscopy (NOTES) have led researchers to look to robotics to enhance the dexterity offered by our endoscopes. A number of systems have been developed that claim to offer greater triangulation, dexterity and DOF to improve our ability to perform procedures such as ESD, third space endoscopy and NOTES. Examples include Endoluminal Assistant for Surgical Endoscopy (EASE; KARL STORZ/IRCAD, Strasbourg, France) (Figure 5), K-FLEX (EasyEndo Surgical, Daejeon, Korea) and the MASTER (EndoMASTER Pte, Singapore)[95-97]. A detailed review of these devices is beyond the scope of this review article but has been done by Lim[98].

CONCLUSION

Endoscopy is an expanding speciality with colonoscopy demand rising by at least 5% *per* year[99,100]. Yet a significant number of people decline to undergo colonoscopy due to several factors including pain and previous bad experiences[16,17]. Robotics has the potential to provide an alternative to CC. However, the ideal robotic platform must be affordable; versatile and capable of performing precise movements while maintaining patient comfort. The potential for robotics to improve the dexterity of an endoscope in the ever-expanding field of therapeutic endoscopy is also worth consideration and likely to be something we will see in the future. Researchers developing new medical devices must keep sustainability in mind. And with a global pandemic in the forefronts of everyone's minds, the potential for robotics to provide a 'medically distanced' procedure will be appealing to many.

AI has not been covered in this review article but is likely to be integrated in robotic colonoscopes. AI in endoscopy has many facets, including image assistance for lesion detection or characterisation, but also integrates closely with robotics in the form of autonomous movement/navigation. Although for many this seems like science fiction and not yet requiring discussion, the technology is available. The MFE device can autonomously navigate a pig colon.

However, advances in AI and increasingly autonomous tasks introduce a number a challenges. Regulatory, ethical and legal uncertainty is likely to take time to overcome, hindering commercialisation. Integration is therefore likely to be slow, with a gradual increase in the autonomy of devices despite the technology being available for further autonomy.

The technology to allow a completely autonomous colonoscopy, including diagnostics, with an endoscopist only required on a supervisory capacity is not so far away. Autonomous robotic colonoscopy has the potential to increased capacity with fewer operators required to perform more procedures. Endoscopists could potentially be trained much quicker. Robotics has the potential to raise the standard of procedures, democratising colonoscopy, thus reducing post-colonoscopy CRCs, reducing complications and improving the colonoscopy experience for patients.

Some of the devices discussed have reached TRLs of 8 and gained FDA or CE marking, however few have yet been adopted enough to perform post-marketing studies or health economics studies. Although, the Endotics health economics study has shown promising result, health economics studies in other areas of robotic healthcare, such as surgery, have been fraught with conflicting results.

Several of the discussed robotic colonoscopes have been modified, removing some of the robotics and opting to pursue the single use colonoscope market. It is probable that the improvements in endoscopy technique have put off commercialisation for the purpose of improved caecal intubation. However, much of the need for these devices is to improve patient experience, which now seems to be the focus of many research teams. What may seem like more intuitive controls will still be different to the standard endoscope controls experienced endoscopists have grown used to. Resistance to change is going to be a challenge for all new devices.

These technologies are often expensive initially, but the cost should not be confused with the potential cost effectiveness of a test which is more acceptable, with the subsequent reduction in morbidity and mortality. Technological advances are happening at an exponential rate and although none of the device to date have challenged the dominance of CC, it is probable that one will in the very near future.

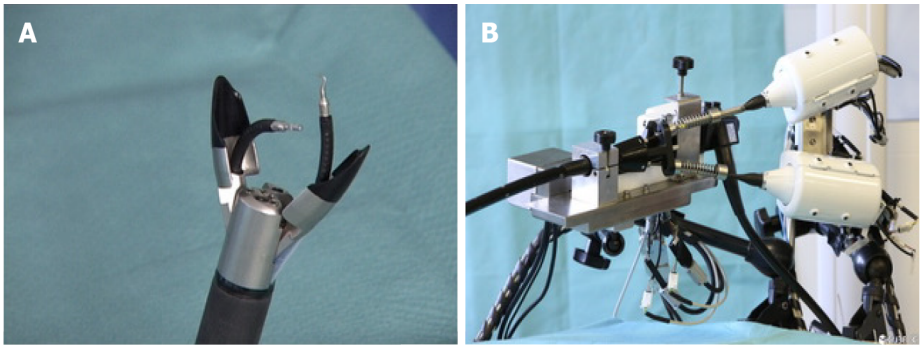


Figure 5 Endoluminal assistant for surgical endoscopy (EASE; KARL STORZ/IRCAD, Strasbourg, France). A: Flexible tip with antagonistic tendons with tools attached; B: Slave unit. Citation: Permission for use and images provided directly by the lab who developed the device. Email confirmation attached as a text file.

FOOTNOTES

Author contributions: Winters C wrote the article; Valdastri P and Subramanian V made substantial contributions to the content, offered critical revisions and approved the final version of the article.

Supported by Cancer Research UK (CRUK) Early Detection and Diagnosis Research Committee, No. 27744.

Conflict-of-interest statement: Winters C, Subramanian V and Valdastri P report a grant from Cancer Research UK, during the conduct of the article. Any opinions, findings and conclusions, or recommendations expressed in this article are those of the authors and do not necessarily reflect the views of CRUK.

Open-Access: This article is an open-access article that was selected by an in-house editor and fully peer-reviewed by external reviewers. It is distributed in accordance with the Creative Commons Attribution NonCommercial (CC BY-NC 4.0) license, which permits others to distribute, remix, adapt, build upon this work non-commercially, and license their derivative works on different terms, provided the original work is properly cited and the use is non-commercial. See: https://creativecommons.org/Licenses/by-nc/4.0/

Country/Territory of origin: United Kingdom

ORCID number: Conchubhair Winters 0000-0001-5773-2876; Venkataraman Subramanian 0000-0003-3603-0861.

Corresponding Author's Membership in Professional Societies: British Society of Gastroenterology.

S-Editor: Fan JR
L-Editor: A
P-Editor: Fan JR

REFERENCES

1 **Sung H**, Ferlay J, Siegel RL, Laversanne M, Soerjomataram I, Jemal A, Bray F. Global Cancer Statistics 2020: GLOBOCAN Estimates of Incidence and Mortality Worldwide for 36 Cancers in 185 Countries. *CA Cancer J Clin* 2021; **71**: 209-249 [PMID: 33538338 DOI: 10.3322/caac.21660]
2 **Arnold M**, Sierra MS, Laversanne M, Soerjomataram I, Jemal A, Bray F. Global patterns and trends in colorectal cancer incidence and mortality. *Gut* 2017; **66**: 683-691 [PMID: 26818619 DOI: 10.1136/gutjnl-2015-310912]
3 **Keum N**, Giovannucci E. Global burden of colorectal cancer: emerging trends, risk factors and prevention strategies. *Nat Rev Gastroenterol Hepatol* 2019; **16**: 713-732 [PMID: 31455888 DOI: 10.1038/s41575-019-0189-8]
4 **Slawinski PR**, Taddese AZ, Musto KB, Sarker S, Valdastri P, Obstein KL. Autonomously Controlled Magnetic Flexible Endoscope for Colon Exploration. *Gastroenterology* 2018; **154**: 1577-1579.e1 [PMID: 29530377 DOI: 10.1053/j.gastro.2018.02.037]
5 **Medical Technologies Innovation and Knowledge Centre**. The Medical Technologies Innovation and Knowledge Centre. [cited 10 April 2022]. Available from: https://medical-technologies.co.uk/
6 **Lamb CA**, Kennedy NA, Raine T, Hendy PA, Smith PJ, Limdi JK, Hayee B, Lomer MCE, Parkes GC, Selinger C, Barrett KJ, Davies RJ, Bennett C, Gittens S, Dunlop MG, Faiz O, Fraser A, Garrick V, Johnston PD, Parkes M, Sanderson J, Terry H; IBD guidelines eDelphi consensus group, Gaya DR, Iqbal TH, Taylor SA, Smith M, Brookes M, Hansen R, Hawthorne AB. British Society of Gastroenterology consensus guidelines on the management of inflammatory bowel disease in adults. *Gut* 2019; **68**: s1-s106 [PMID: 31562236 DOI: 10.1136/gutjnl-2019-318484]
7 **Monahan KJ**, Bradshaw N, Dolwani S, Desouza B, Dunlop MG, East JE, Ilyas M, Kaur A, Lalloo F, Latchford A, Rutter

MD, Tomlinson I, Thomas HJW, Hill J; Hereditary CRC guidelines eDelphi consensus group. Guidelines for the management of hereditary colorectal cancer from the British Society of Gastroenterology (BSG)/Association of Coloproctology of Great Britain and Ireland (ACPGBI)/United Kingdom Cancer Genetics Group (UKCGG). *Gut* 2020; **69**: 411-444 [PMID: 31780574 DOI: 10.1136/gutjnl-2019-319915]

8 **Rutter MD**, East J, Rees CJ, Cripps N, Docherty J, Dolwani S, Kaye PV, Monahan KJ, Novelli MR, Plumb A, Saunders BP, Thomas-Gibson S, Tolan DJM, Whyte S, Bonnington S, Scope A, Wong R, Hibbert B, Marsh J, Moores B, Cross A, Sharp L. British Society of Gastroenterology/Association of Coloproctology of Great Britain and Ireland/Public Health England post-polypectomy and post-colorectal cancer resection surveillance guidelines. *Gut* 2020; **69**: 201-223 [PMID: 31776230 DOI: 10.1136/gutjnl-2019-319858]

9 **Hassan C**, Antonelli G, Dumonceau JM, Regula J, Bretthauer M, Chaussade S, Dekker E, Ferlitsch M, Gimeno-Garcia A, Jover R, Kalager M, Pellisé M, Pox C, Ricciardiello L, Rutter M, Helsingen LM, Bleijenberg A, Senore C, van Hooft JE, Dinis-Ribeiro M, Quintero E. Post-polypectomy colonoscopy surveillance: European Society of Gastrointestinal Endoscopy (ESGE) Guideline - Update 2020. *Endoscopy* 2020; **52**: 687-700 [PMID: 32572858 DOI: 10.1055/a-1185-3109]

10 **Mutneja HR**, Bhurwal A, Arora S, Vohra I, Attar BM. A delay in colonoscopy after positive fecal tests leads to higher incidence of colorectal cancer: A systematic review and meta-analysis. *J Gastroenterol Hepatol* 2021; **36**: 1479-1486 [PMID: 33351959 DOI: 10.1111/jgh.15381]

11 **Gingold-Belfer R**, Leibovitzh H, Boltin D, Issa N, Tsadok Perets T, Dickman R, Niv Y. The compliance rate for the second diagnostic evaluation after a positive fecal occult blood test: A systematic review and meta-analysis. *United European Gastroenterol J* 2019; **7**: 424-448 [PMID: 31019712 DOI: 10.1177/2050640619828185]

12 **Selby K**, Senore C, Wong M, May FP, Gupta S, Liang PS. Interventions to ensure follow-up of positive fecal immunochemical tests: An international survey of screening programs. *J Med Screen* 2021; **28**: 51-53 [PMID: 32054392 DOI: 10.1177/0969141320904977]

13 **Lee YC**, Li-Sheng Chen S, Ming-Fang Yen A, Yueh-Hsia Chiu S, Ching-Yuan Fann J, Chuang SL, Chiang TH, Chou CK, Chiu HM, Wu MS, Wu CY, Chia SL, Chiou ST, Chen HH. Association Between Colorectal Cancer Mortality and Gradient Fecal Hemoglobin Concentration in Colonoscopy Noncompliers. *J Natl Cancer Inst* 2017; **109** [PMID: 28376228 DOI: 10.1093/jnci/djw269]

14 **Zorzi M**, Battagello J, Selby K, Capodaglio G, Baracco S, Rizzato S, Chinellato E, Guzzinati S, Rugge M. Non-compliance with colonoscopy after a positive faecal immunochemical test doubles the risk of dying from colorectal cancer. *Gut* 2022; **71**: 561-567 [PMID: 33789965 DOI: 10.1136/gutjnl-2020-322192]

15 **Dalton ARH**. Incomplete diagnostic follow-up after a positive colorectal cancer screening test: a systematic review. *J Public Health (Oxf)* 2018; **40**: e46-e58 [PMID: 28069989 DOI: 10.1093/pubmed/fdw147]

16 **Kerrison RS**, Sheik-Mohamud D, McBride E, Whitaker KL, Rees C, Duffy S, von Wagner C. Patient barriers and facilitators of colonoscopy use: A rapid systematic review and thematic synthesis of the qualitative literature. *Prev Med* 2021; **145**: 106413 [PMID: 33412167 DOI: 10.1016/j.ypmed.2020.106413]

17 **Kerrison RS**, Travis E, Dobson C, Whitaker KL, Rees CJ, Duffy SW, von Wagner C. Barriers and facilitators to colonoscopy following fecal immunochemical test screening for colorectal cancer: A key informant interview study. *Patient Educ Couns* 2022; **105**: 1652-1662 [PMID: 34607734 DOI: 10.1016/j.pec.2021.09.022]

18 **Meester RG**, Doubeni CA, Zauber AG, Goede SL, Levin TR, Corley DA, Jemal A, Lansdorp-Vogelaar I. Public health impact of achieving 80% colorectal cancer screening rates in the United States by 2018. *Cancer* 2015; **121**: 2281-2285 [PMID: 25763558 DOI: 10.1002/cncr.29336]

19 **Ramai D**, Zakhia K, Etienne D, Reddy M. Philipp Bozzini (1773-1809): The earliest description of endoscopy. *J Med Biogr* 2018; **26**: 137-141 [PMID: 29405817 DOI: 10.1177/0967772018755587]

20 **Visconti TAC**, Otoch JP, Artifon ELA. Robotic endoscopy. A review of the literature. *Acta Cir Bras* 2020; **35**: e202000206 [PMID: 32348403 DOI: 10.1590/s0102-865020200020000006]

21 **Ciuti G**, Skonieczna-Żydecka K, Marlicz W, Iacovacci V, Liu H, Stoyanov D, Arezzo A, Chiurazzi M, Toth E, Thorlacius H, Dario P, Koulaouzidis A. Frontiers of Robotic Colonoscopy: A Comprehensive Review of Robotic Colonoscopes and Technologies. *J Clin Med* 2020; **9** [PMID: 32486374 DOI: 10.3390/jcm9061648]

22 **Holme Ø**, Løberg M, Kalager M, Bretthauer M, Hernán MA, Aas E, Eide TJ, Skovlund E, Lekven J, Schneede J, Tveit KM, Vatn M, Ursin G, Hoff G; NORCCAP Study Group†. Long-Term Effectiveness of Sigmoidoscopy Screening on Colorectal Cancer Incidence and Mortality in Women and Men: A Randomized Trial. *Ann Intern Med* 2018; **168**: 775-782 [PMID: 29710125 DOI: 10.7326/M17-1441]

23 **PubMed**. PubMed search "Robotic Colonoscopy". National Library of Medicine; 2021. [cited 10 January 2022]. Available from: https://pubmed.ncbi.nlm.nih.gov/

24 **Wernli KJ**, Brenner AT, Rutter CM, Inadomi JM. Risks Associated With Anesthesia Services During Colonoscopy. *Gastroenterology* 2016; **150**: 888-94; quiz e18 [PMID: 26709032 DOI: 10.1053/j.gastro.2015.12.018]

25 **Maida M**, Alrubaiy L, Bokun T, Bruns T, Castro V, China L, Conroy G, Trabulo D, Van Steenkiste C, Voermans RP, Burisch J, Ianiro G. Current challenges and future needs of clinical and endoscopic training in gastroenterology: a European survey. *Endosc Int Open* 2020; **8**: E525-E533 [PMID: 32258375 DOI: 10.1055/a-1093-0877]

26 **Siau K**, Anderson JT, Valori R, Feeney M, Hawkes ND, Johnson G, McKaig BC, Pullan RD, Hodson J, Wells C, Thomas-Gibson S, Haycock AV, Beales ILP, Broughton R, Dunckley P; Joint Advisory Group on Gastrointestinal Endoscopy (JAG). Certification of UK gastrointestinal endoscopists and variations between trainee specialties: results from the JETS e-portfolio. *Endosc Int Open* 2019; **7**: E551-E560 [PMID: 30957005 DOI: 10.1055/a-0839-4476]

27 **Shergill AK**, Harris Adamson C. Failure of an engineered system: The gastrointestinal endoscope. *Tech Gastrointest Endosc* 2019; **21**: 116-123 [DOI: 10.1016/j.tgie.2019.02.001]

28 **Yung DE**, Banfi T, Ciuti G, Arezzo A, Dario P, Koulaouzidis A. Musculoskeletal injuries in gastrointestinal endoscopists: a systematic review. *Expert Rev Gastroenterol Hepatol* 2017; **11**: 939-947 [PMID: 28705042 DOI: 10.1080/17474124.2017.1356225]

29 **Merola G**, Sciuto A, Pirozzi F, Andreuccetti J, Pignata G, Corcione F, Milone M, De Palma GD, Castaldo R, Pecchia L,

Ceccarelli G, Bracale U. Is robotic right colectomy economically sustainable? *Surg Endosc* 2020; **34**: 4041-4047 [PMID: 31617088 DOI: 10.1007/s00464-019-07193-z]

30 **Gomolin A**, Gotlieb W, Lau S, Salvador S, Racovitan F, Abitbol J. Mandate to evaluate robotic surgery implementation: a 12-year retrospective analysis of impact and future implications. *J Robot Surg* 2022; **16**: 783-788 [PMID: 34741713 DOI: 10.1007/s11701-021-01327-z]

31 **Partelli S**, Ricci C, Cinelli L, Montorsi RM, Ingaldi C, Andreasi V, Crippa S, Alberici L, Casadei R, Falconi M. Evaluation of cost-effectiveness among open, laparoscopic and robotic distal pancreatectomy: A systematic review and meta-analysis. *Am J Surg* 2021; **222**: 513-520 [PMID: 33853724 DOI: 10.1016/j.amjsurg.2021.03.066]

32 **Lundin ES**, Carlsson P, Wodlin NB, Nilsson L, Kjölhede P. Cost-effectiveness of robotic hysterectomy *vs* abdominal hysterectomy in early endometrial cancer. *Int J Gynecol Cancer* 2020; **30**: 1719-1725 [PMID: 32863275 DOI: 10.1136/ijgc-2020-001611]

33 **Sicuro R**, Tumino E, Lambiase C, Mamone D. Robotic Colonoscopy: Comparative Analysis of Costs Compared to Painless Conventional Colonoscopy. 2020 Preprint. Available from: Research Square [DOI: 10.21203/rs.3.rs-104356/v1]

34 **Shenbagaraj L**, Thomas-Gibson S, Stebbing J, Broughton R, Dron M, Johnston D, Shaw T, Haboubi HN, Green JT. Endoscopy in 2017: a national survey of practice in the UK. *Frontline Gastroenterol* 2019; **10**: 7-15 [PMID: 30651952 DOI: 10.1136/flgastro-2018-100970]

35 **Calderwood AH**, Calderwood MS, Williams JL, Dominitz JA. Impact of the COVID-19 Pandemic on Utilization of EGD and Colonoscopy in the United States: An Analysis of the GIQuIC Registry. *Tech Innov Gastrointest Endosc* 2021; **23**: 313-321 [PMID: 34345871 DOI: 10.1016/j.tige.2021.07.003]

36 **Larsen S**, Kalloo A, Hutfless S. The hidden cost of colonoscopy including cost of reprocessing and infection rate: the implications for disposable colonoscopes. *Gut* 2020; **69**: 197-200 [PMID: 31413166 DOI: 10.1136/gutjnl-2019-319108]

37 **Halligan S**, Dadswell E, Wooldrage K, Wardle J, von Wagner C, Lilford R, Yao GL, Zhu S, Atkin W. Computed tomographic colonography compared with colonoscopy or barium enema for diagnosis of colorectal cancer in older symptomatic patients: two multicentre randomised trials with economic evaluation (the SIGGAR trials). *Health Technol Assess* 2015; **19**: 1-134 [PMID: 26198205 DOI: 10.3310/hta19540]

38 **Atkin W**, Dadswell E, Wooldrage K, Kralj-Hans I, von Wagner C, Edwards R, Yao G, Kay C, Burling D, Faiz O, Teare J, Lilford RJ, Morton D, Wardle J, Halligan S; SIGGAR investigators. Computed tomographic colonography versus colonoscopy for investigation of patients with symptoms suggestive of colorectal cancer (SIGGAR): a multicentre randomised trial. *Lancet* 2013; **381**: 1194-1202 [PMID: 23414650 DOI: 10.1016/S0140-6736(12)62186-2]

39 **Halligan S**, Wooldrage K, Dadswell E, Shah U, Kralj-Hans I, von Wagner C, Faiz O, Teare J, Edwards R, Kay C, Yao G, Lilford RJ, Morton D, Wardle J, Atkin W; SIGGAR Investigators. Identification of Extracolonic Pathologies by Computed Tomographic Colonography in Colorectal Cancer Symptomatic Patients. *Gastroenterology* 2015; **149**: 89-101.e5 [PMID: 25796362 DOI: 10.1053/j.gastro.2015.03.011]

40 **IJspeert JE**, Tutein Nolthenius CJ, Kuipers EJ, van Leerdam ME, Nio CY, Thomeer MG, Biermann K, van de Vijver MJ, Dekker E, Stoker J. CT-Colonography vs. Colonoscopy for Detection of High-Risk Sessile Serrated Polyps. *Am J Gastroenterol* 2016; **111**: 516-522 [PMID: 27021193 DOI: 10.1038/ajg.2016.58]

41 **Ghanouni A**, Halligan S, Plumb A, Boone D, Wardle J, von Wagner C. Non- or full-laxative CT colonography vs. endoscopic tests for colorectal cancer screening: a randomised survey comparing public perceptions and intentions to undergo testing. *Eur Radiol* 2014; **24**: 1477-1486 [PMID: 24817084 DOI: 10.1007/s00330-014-3187-9]

42 **Kjølhede T**, Ølholm AM, Kaalby L, Kidholm K, Qvist N, Baatrup G. Diagnostic accuracy of capsule endoscopy compared with colonoscopy for polyp detection: systematic review and meta-analyses. *Endoscopy* 2021; **53**: 713-721 [PMID: 32858753 DOI: 10.1055/a-1249-3938]

43 **Benech N**, Vinet O, Gaudin JL, Benamouzig R, Dray X, Ponchon T, Galmiche JP, Sacher-Huvelin S, Samaha E, Saurin JC; ONECC Study Group. Colon capsule endoscopy in clinical practice: lessons from a national 5-year observational prospective cohort. *Endosc Int Open* 2021; **9**: E1542-E1548 [PMID: 34540548 DOI: 10.1055/a-1526-0923]

44 **Spada C**, Hassan C, Barbaro B, Iafrate F, Cesaro P, Petruzziello L, Minelli Grazioli L, Senore C, Brizi G, Costamagna I, Alvaro G, Iannitti M, Salsano M, Ciolina M, Laghi A, Bonomo L, Costamagna G. Colon capsule *vs* CT colonography in patients with incomplete colonoscopy: a prospective, comparative trial. *Gut* 2015; **64**: 272-281 [PMID: 24964317 DOI: 10.1136/gutjnl-2013-306550]

45 **Cash BD**, Fleisher MR, Fern S, Rajan E, Haithcock R, Kastenberg DM, Pound D, Papageorgiou NP, Fernández-Urién I, Schmelkin IJ, Rex DK. Multicentre, prospective, randomised study comparing the diagnostic yield of colon capsule endoscopy *vs* CT colonography in a screening population (the TOPAZ study). *Gut* 2021; **70**: 2115-2122 [PMID: 33443017 DOI: 10.1136/gutjnl-2020-322578]

46 **Burr NE**, Plumb A, Sood R, Rembacken B, Tolan DJM. CT colonography remains an important test for colorectal cancer. *Gut* 2022; **71**: 217-218 [PMID: 33753420 DOI: 10.1136/gutjnl-2021-324399]

47 **Deding U**, Kaalby L, Bøggild H, Plantener E, Wollesen MK, Kobaek-Larsen M, Hansen SJ, Baatrup G. Colon Capsule Endoscopy vs. CT Colonography Following Incomplete Colonoscopy: A Systematic Review with Meta-Analysis. *Cancers (Basel)* 2020; **12** [PMID: 33202936 DOI: 10.3390/cancers12113367]

48 **Zijta FM**, Bipat S, Stoker J. Magnetic resonance (MR) colonography in the detection of colorectal lesions: a systematic review of prospective studies. *Eur Radiol* 2010; **20**: 1031-1046 [PMID: 19936754 DOI: 10.1007/s00330-009-1663-4]

49 **Lim EJ**, Leung C, Pitman A, Stella DL, Brown G, Slattery M, Marion K, Macrae F. Magnetic resonance colonography for colorectal cancer screening in patients with Lynch syndrome gene mutation. *Fam Cancer* 2010; **9**: 555-561 [PMID: 20495877 DOI: 10.1007/s10689-010-9350-9]

50 **Graser A**, Melzer A, Lindner E, Nagel D, Herrmann K, Stieber P, Schirra J, Mansmann U, Reiser MF, Göke B, Kolligs FT. Magnetic resonance colonography for the detection of colorectal neoplasia in asymptomatic adults. *Gastroenterology* 2013; **144**: 743-750.e2 [PMID: 23415805 DOI: 10.1053/j.gastro.2012.12.041]

51 **Gao Y**, Wang J, Lv H, Xue Y, Jia R, Liu G, Bai W, Wu Y, Zhang L, Yang J. Diagnostic value of magnetic resonance and computed tomography colonography for the diagnosis of colorectal cancer: A systematic review and meta-analysis. *Medicine (Baltimore)* 2019; **98**: e17187 [PMID: 31574825 DOI: 10.1097/MD.0000000000017187]

52 **Bianchi F**, Masaracchia A, Shojaei Barjuei E, Menciassi A, Arezzo A, Koulaouzidis A, Stoyanov D, Dario P, Ciuti G. Localization strategies for robotic endoscopic capsules: a review. *Expert Rev Med Devices* 2019; **16**: 381-403 [PMID: 31056968 DOI: 10.1080/17434440.2019.1608182]

53 **Taddese AZ**, Slawinski PR, Pirotta M, De Momi E, Obstein KL, Valdastri P. Enhanced Real-Time Pose Estimation for Closed-Loop Robotic Manipulation of Magnetically Actuated Capsule Endoscopes. *Int J Rob Res* 2018; **37**: 890-911 [PMID: 30150847 DOI: 10.1177/0278364918779132]

54 **Dupont PE**, Nelson BJ, Goldfarb M, Hannaford B, Menciassi A, O'Malley MK, Simaan N, Valdastri P, Yang GZ. A decade retrospective of medical robotics research from 2010 to 2020. *Sci Robot* 2021; **6**: eabi8017 [PMID: 34757801 DOI: 10.1126/scirobotics.abi8017]

55 **England PH**. Bowel Cancer Screening: Programme Overview. 2019. [cited 10 April 2022]. Available from: https://www.gov.uk/guidance/bowel-cancer-screening-programme-overview

56 **Siau K**, Hayee BH, Gayam S. Endoscopy's Current Carbon Footprint. *Tech Innov Gastrointest Endosc* 2021; **23**: 344-352 [DOI: 10.1016/j.tige.2021.06.005]

57 **Tapia-Siles SC**, Coleman S, Cuschieri A. Current state of micro-robots/devices as substitutes for screening colonoscopy: assessment based on technology readiness levels. *Surg Endosc* 2016; **30**: 404-413 [PMID: 26092000 DOI: 10.1007/s00464-015-4263-1]

58 **Taherdoost H**. A review of technology acceptance and adoption models and theories. *Procedia Manuf* 2018; **22**: 960-967

59 **Gluck N**, Melhem A, Halpern Z, Mergener K, Santo E. A novel self-propelled disposable colonoscope is effective for colonoscopy in humans (with video). *Gastrointest Endosc* 2016; **83**: 998-1004.e1 [PMID: 26391735 DOI: 10.1016/j.gie.2015.08.083]

60 **Pfeffer J**, Grinshpon R, Rex D, Levin B, Rösch T, Arber N, Halpern Z. The Aer-O-Scope: proof of the concept of a pneumatic, skill-independent, self-propelling, self-navigating colonoscope in a pig model. *Endoscopy* 2006; **38**: 144-148 [PMID: 16479421 DOI: 10.1055/s-2006-925089]

61 **Vucelic B**, Rex D, Pulanic R, Pfefer J, Hrstic I, Levin B, Halpern Z, Arber N. The aer-o-scope: proof of concept of a pneumatic, skill-independent, self-propelling, self-navigating colonoscope. *Gastroenterology* 2006; **130**: 672-677 [PMID: 16530508 DOI: 10.1053/j.gastro.2005.12.018]

62 **View G**. Validation of Aer-O-Scope Colonoscope System Cecal Intubation. ClinicalTrials.gov: U.S. National Library of Medicine; 2019. [cited 8 April 2022]. Available from: https://clinicaltrials.gov/ct2/show/NCT03949777?cond=aer-o-scope&draw=2&rank=1

63 **Federal Drug Administration**. Aer-O-Scope FDA approval. Department of Health & Human Services 30th June 2016. [cited 8 April 2022]. Available from: https://www.gao.gov/products/gao-16-729r

64 **View G**. Aer-O-Scope. GI View. [cited 8 April 2022]. Available from: https://www.giview.com/

65 **Shike M**, Fireman Z, Eliakim R, Segol O, Sloyer A, Cohen LB, Goldfarb-Albak S, Repici A. Sightline ColonoSight system for a disposable, power-assisted, non-fiber-optic colonoscopy (with video). *Gastrointest Endosc* 2008; **68**: 701-710 [PMID: 18501356 DOI: 10.1016/j.gie.2007.12.062]

66 **Federal Drug Administration**. Colonosight FDA approval. Department of Health & Human Services 24th November 2003. [cited 8 April 2022]. Available from: https://www.fda.gov/

67 **Medical C**. Consis Medical. Consis-medical; 2018 [updated 2018]. [cited 8 April 2022]. Available from: http://consis-medical.com/

68 **Formosa GA**, Prendergast JM, Edmundowicz SA, Rentschler ME. Novel Optimization-Based Design and Surgical Evaluation of a Treaded Robotic Capsule Colonoscope. *IEEE Transact Robot* 2020; **36**: 545-552 [DOI: 10.1109/tro.2019.2949466]

69 **Kume K**, Sakai N, Goto T. Development of a novel endoscopic manipulation system: the Endoscopic Operation Robot ver.3. *Endoscopy* 2015; **47**: 815-819 [PMID: 25910062 DOI: 10.1055/s-0034-1391973]

70 **Boškoski I**, Orlandini B, Papparella LG, Matteo MV, De Siena M, Pontecorvi V, Costamagna G. Robotics and Artificial Intelligence in Gastrointestinal Endoscopy: Updated Review of the Literature and State of the Art. *Curr Robot Rep* 2021; **2**: 43-54 [DOI: 10.1007/s43154-020-00040-3]

71 **Cosentino F**, Tumino E, Passoni GR, Morandi E, Capria A. Functional evaluation of the endotics system, a new disposable self-propelled robotic colonoscope: *in vitro* tests and clinical trial. *Int J Artif Organs* 2009; **32**: 517-527 [PMID: 19844894 DOI: 10.1177/039139880903200806]

72 **Tumino E**, Sacco R, Bertini M, Bertoni M, Parisi G, Capria A. Endotics system *vs* colonoscopy for the detection of polyps. *World J Gastroenterol* 2010; **16**: 5452-5456 [PMID: 21086563 DOI: 10.3748/wjg.v16.i43.5452]

73 **Tumino E**, Parisi G, Bertoni M, Bertini M, Metrangolo S, Ierardi E, Cervelli R, Bresci G, Sacco R. Use of robotic colonoscopy in patients with previous incomplete colonoscopy. *Eur Rev Med Pharmacol Sci* 2017; **21**: 819-826 [PMID: 28272700]

74 **Trecca A**, Catalano F, Bella A, Borghini R. Robotic colonoscopy: efficacy, tolerability and safety. Preliminary clinical results from a pilot study. *Surg Endosc* 2020; **34**: 1442-1450 [PMID: 31932942 DOI: 10.1007/s00464-019-07332-6]

75 **Federal Drug Administration**. Invendoscope E210 FDA approval. Public Health Service 27 September 2017. [cited 8 April 2022]. Available from: https://www.fda.gov/

76 **Federal Drug Administration**. Invendoscope E200 FDA approval. Public Health Service: Department of Health & Human Services 15 July 2016. [cited 8 April 2022]. Available from: https://www.docin.com/p-1892232862.html

77 **Rösch T**, Adler A, Pohl H, Wettschureck E, Koch M, Wiedenmann B, Hoepffner N. A motor-driven single-use colonoscope controlled with a hand-held device: a feasibility study in volunteers. *Gastrointest Endosc* 2008; **67**: 1139-1146 [PMID: 18355823 DOI: 10.1016/j.gie.2007.10.065]

78 **Groth S**, Rex DK, Rösch T, Hoepffner N. High cecal intubation rates with a new computer-assisted colonoscope: a feasibility study. *Am J Gastroenterol* 2011; **106**: 1075-1080 [PMID: 21386833 DOI: 10.1038/ajg.2011.52]

79 **Straulino F**, Genthner A, Kiesslich R, Eickhoff A. Sa1938 Colonoscopy with the sterile single use endoscope INVENDOSCOPE SC210. *Gastrointest Endosc* 2018; **87** [DOI: 10.1016/j.gie.2018.04.459]

80 **Ciuti G**, Donlin R, Valdastri P, Arezzo A, Menciassi A, Morino M, Dario P. Robotic *vs* manual control in magnetic

steering of an endoscopic capsule. *Endoscopy* 2010; **42**: 148-152 [PMID: 20017088 DOI: 10.1055/s-0029-1243808]
81 **Arezzo A**, Menciassi A, Valdastri P, Ciuti G, Lucarini G, Salerno M, Di Natali C, Verra M, Dario P, Morino M. Experimental assessment of a novel robotically-driven endoscopic capsule compared to traditional colonoscopy. *Dig Liver Dis* 2013; **45**: 657-662 [PMID: 23453360 DOI: 10.1016/j.dld.2013.01.025]
82 **Valdastri P**, Ciuti G, Verbeni A, Menciassi A, Dario P, Arezzo A, Morino M. Magnetic air capsule robotic system: proof of concept of a novel approach for painless colonoscopy. *Surg Endosc* 2012; **26**: 1238-1246 [PMID: 22179445 DOI: 10.1007/s00464-011-2054-x]
83 **Salerno GCM**, Lucarini G, Valdastri P, Arezzo A, Menciassi A, Morino M, Dario P. A Comparative Evaluation of Control Interfaces for a Robotic-Aided Endoscopic Capsule Platform. *IEEE Trans Robot* 2012; **28**: 534-538 [DOI: 10.1109/TRO.2011.2177173]
84 **Martin JW**, Scaglioni B, Norton JC, Subramanian V, Arezzo A, Obstein KL, Valdastri P. Enabling the future of colonoscopy with intelligent and autonomous magnetic manipulation. *Nat Mach Intell* 2020; **2**: 595-606 [PMID: 33089071 DOI: 10.1038/s42256-020-00231-9]
85 **Pittiglio G**, Barducci L, Martin JW, Norton JC, Avizzano CA, Obstein KL, Valdastri P. Magnetic Levitation for Soft-Tethered Capsule Colonoscopy Actuated With a Single Permanent Magnet: A Dynamic Control Approach. *IEEE Robot Autom Lett* 2019; **4**: 1224-1231 [PMID: 31304240 DOI: 10.1109/LRA.2019.2894907]
86 **Mamunes AP**, Campisano F, Martin J, Scaglioni B, Mazomenos E, Valdastri P, Obstein KL. Magnetic flexible endoscope for colonoscopy: an initial learning curve analysis. *Endosc Int Open* 2021; **9**: E171-E180 [PMID: 33532555 DOI: 10.1055/a-1314-9860]
87 **Bianchi F**, Ciuti G, Koulaouzidis A, Arezzo A, Stoyanov D, Schostek S, Oddo CM, Menciassi A, Dario P. An innovative robotic platform for magnetically-driven painless colonoscopy. *Ann Transl Med* 2017; **5**: 421 [PMID: 29201873 DOI: 10.21037/atm.2017.09.15]
88 **Endoo Project**. Endoo EU Project; 2020. [cited 8 April 2022]. Available from: http://www.endoo-project.eu/
89 **Verra M**, Firrincieli A, Chiurazzi M, Mariani A, Lo Secco G, Forcignanò E, Koulaouzidis A, Menciassi A, Dario P, Ciuti G, Arezzo A. Robotic-Assisted Colonoscopy Platform with a Magnetically-Actuated Soft-Tethered Capsule. *Cancers (Basel)* 2020; **12** [PMID: 32887238 DOI: 10.3390/cancers12092485]
90 **Manfredi L**. Endorobots for Colonoscopy: Design Challenges and Available Technologies. *Front Robot AI* 2021; **8**: 705454 [PMID: 34336938 DOI: 10.3389/frobt.2021.705454]
91 **Slawinski PR**, Obstein KL, Valdastri P. Capsule endoscopy of the future: What's on the horizon? *World J Gastroenterol* 2015; **21**: 10528-10541 [PMID: 26457013 DOI: 10.3748/wjg.v21.i37.10528]
92 **Endoskopie EC**. Endodrive systems workstation. www.ece-medical-systems.com: Ece medical systems. [cited 8 April 2022]. Available from: http://www.endodrive.de/
93 **Rozeboom ED**, Bastiaansen BA, de Vries ES, Dekker E, Fockens PA, Broeders IA. Robotic-assisted flexible colonoscopy: preliminary safety and efficiency in humans. *Gastrointest Endosc* 2016; **83**: 1267-1271 [PMID: 26551732 DOI: 10.1016/j.gie.2015.10.046]
94 **Pullens HJ**, van der Stap N, Rozeboom ED, Schwartz MP, van der Heijden F, van Oijen MG, Siersema PD, Broeders IA. Colonoscopy with robotic steering and automated lumen centralization: a feasibility study in a colon model. *Endoscopy* 2016; **48**: 286-290 [PMID: 26126158 DOI: 10.1055/s-0034-1392550]
95 **Mascagni P**, Lim SG, Fiorillo C, Zanne P, Nageotte F, Zorn L, Perretta S, de Mathelin M, Marescaux J, Dallemagne B. Democratizing Endoscopic Submucosal Dissection: Single-Operator Fully Robotic Colorectal Endoscopic Submucosal Dissection in a Pig Model. *Gastroenterology* 2019; **156**: 1569-1571.e2 [PMID: 30768985 DOI: 10.1053/j.gastro.2018.12.046]
96 **Hwang M**, Kwon DS. K-FLEX: A flexible robotic platform for scar-free endoscopic surgery. *Int J Med Robot* 2020; **16**: e2078 [PMID: 31945797 DOI: 10.1002/rcs.2078]
97 **Lomanto D**, Wijerathne S, Ho LK, Phee LS. Flexible endoscopic robot. *Minim Invasive Ther Allied Technol* 2015; **24**: 37-44 [PMID: 25627436 DOI: 10.3109/13645706.2014.996163]
98 **Lim SG**. The development of robotic flexible endoscopic platforms. *Inter J Gastrointest Interven* 2020; **9**: 9-12 [DOI: 10.18528/ijgii190022]
99 **Comas M**, Mendivil J, Andreu M, Hernández C, Castells X. Long-Term Prediction of the Demand of Colonoscopies Generated by a Population-Based Colorectal Cancer Screening Program. *PLoS One* 2016; **11**: e0164666 [PMID: 27732635 DOI: 10.1371/journal.pone.0164666]
100 **Ravindran S**, Bassett P, Shaw T, Dron M, Broughton R, Johnston D, Healey CJ, Green J, Ashrafian H, Darzi A, Coleman M, Thomas-Gibson S. National census of UK endoscopy services in 2019. *Frontline Gastroenterol* 2021; **12**: 451-460 [PMID: 34712462 DOI: 10.1136/flgastro-2020-101538]
101 **Lauby-Secretan B**, Vilahur N, Bianchini F, Guha N, Straif K; International Agency for Research on Cancer Handbook Working Group. The IARC Perspective on Colorectal Cancer Screening. *N Engl J Med* 2018; **378**: 1734-1740 [PMID: 29580179 DOI: 10.1056/NEJMsr1714643]
102 **Director RD**. Technology Readiness Assessment (TRA) Deskbook. US Department of Defense, 2009
103 **Engineering ASoDfRa**. Technology Readiness Assessment (TRA) Guidance. US Department of Defense, 2011
104 **Slawinski PR**, Taddese AZ, Musto KB, Obstein KL, Valdastri P. Autonomous Retroflexion of a Magnetic Flexible Endoscope. *IEEE Robot Autom Lett* 2017; **2**: 1352-1359 [PMID: 28289703 DOI: 10.1109/LRA.2017.2668459]

World Journal of Gastroenterology

Submit a Manuscript: https://www.f6publishing.com

World J Gastroenterol 2022 September 21; 28(35): 5111-5128

DOI: 10.3748/wjg.v28.i35.5111

ISSN 1007-9327 (print) ISSN 2219-2840 (online)

REVIEW

Noncoding RNAs as additional mediators of epigenetic regulation in nonalcoholic fatty liver disease

Mohamed Zaiou

Specialty type: Medicine, research and experimental

Provenance and peer review: Invited article; Externally peer reviewed.

Peer-review model: Single blind

Peer-review report's scientific quality classification

Grade A (Excellent): 0
Grade B (Very good): B
Grade C (Good): C, C
Grade D (Fair): 0
Grade E (Poor): 0

P-Reviewer: Tarantino G, Italy; Trifan A, Romania; Ulasoglu C, Turkey

Received: July 15, 2022
Peer-review started: July 15, 2022
First decision: July 25, 2022
Revised: July 28, 2022
Accepted: August 25, 2022
Article in press: August 25, 2022
Published online: September 21, 2022

Mohamed Zaiou, Institut Jean Lamour, UMR CNRS 7198, CNRS, University of Lorraine, Nancy 54011, France

Corresponding author: Mohamed Zaiou, PhD, Professor, Institut Jean Lamour, UMR CNRS 7198, CNRS, University of Lorraine, 2 allée André Guinier, BP 50840, Nancy 54011, France. mohamed.zaiou@univ-lorraine.fr

Abstract

Nonalcoholic fatty liver disease (NAFLD) has emerged as the most common cause of chronic liver disorder worldwide. It represents a spectrum that includes a continuum of different clinical entities ranging from simple steatosis to non-alcoholic steatohepatitis, which can evolve to cirrhosis and in some cases to hepatocellular carcinoma, ultimately leading to liver failure. The pathogenesis of NAFLD and the mechanisms underlying its progression to more pathological stages are not completely understood. Besides genetic factors, evidence indicates that epigenetic mechanisms occurring in response to environmental stimuli also contribute to the disease risk. Noncoding RNAs (ncRNAs), including microRNAs, long noncoding RNAs, and circular RNAs, are one of the epigenetic factors that play key regulatory roles in the development of NAFLD. As the field of ncRNAs is rapidly evolving, the present review aims to explore the current state of knowledge on the roles of these RNA species in the pathogenesis of NAFLD, highlight relevant mechanisms by which some ncRNAs can modulate regulatory networks implicated in NAFLD, and discuss key challenges and future directions facing current research in the hopes of developing ncRNAs as next-generation non-invasive diagnostics and therapies in NAFLD and subsequent progression to hepatocellular carcinoma.

Key Words: MicroRNAs; Nonalcoholic fatty liver disease; Steatohepatitis; Noncoding RNAs; Circular RNAs; Biomarker

©The Author(s) 2022. Published by Baishideng Publishing Group Inc. All rights reserved.

Core Tip: Nonalcoholic fatty liver disease (NAFLD) covers a spectrum of hepatic pathologies, ranging from simple steatosis to nonalcoholic steatohepatitis, all of which can evolve to cirrhosis and in some cases to hepatocellular carcinoma. There are now indications that noncoding RNAs (ncRNAs), a component of epigenetic mechanisms, contribute to the pathogenesis of NAFLD and may serve as potential prognostic and diagnostic biomarkers. However, little is known about the role of these RNA species in NAFLD and its progressive forms. This paper discusses the current state of research on the role of most clinically relevant ncRNAs in the pathogenesis of NAFLD.

Citation: Zaiou M. Noncoding RNAs as additional mediators of epigenetic regulation in nonalcoholic fatty liver disease. *World J Gastroenterol* 2022; 28(35): 5111-5128
URL: https://www.wjgnet.com/1007-9327/full/v28/i35/5111.htm
DOI: https://dx.doi.org/10.3748/wjg.v28.i35.5111

INTRODUCTION

Nonalcoholic fatty liver disease (NAFLD) has emerged as a liver disorder with an increasing prevalence but unclear etiology. The disease covers a wide spectrum of histologic lesions, ranging from simple steatosis to its subtype, nonalcoholic steatohepatitis (NASH), which is characterized by inflammation and hepatocyte injury. Over several years, NASH can progress to more serious disease stages, such as cirrhosis and hepatocellular carcinoma (HCC)[1]. Based on the close association between hepatic steatosis and metabolic dysregulation, international consensus guidelines recommended the renaming of NAFLD to metabolic-associated fatty liver disease[2,3]. The prevalence of NAFLD depends on race and ethnicity. In the United Sates, the estimated prevalence of NAFLD was reported to be about 32%[4]. However, estimates are likely higher in other populations that are currently witnessing the rapid rise in the incidence of type 2 diabetes mellitus (T2DM), obesity, metabolic and insulin resistance syndrome, and dyslipidemia rates[5,6].

NAFLD is sometimes called the "silent killer", because most patients with the condition are typically asymptomatic in the early stages until the liver is severely damaged. The unsuspected disease condition is often found incidentally when liver enzyme levels, such as alanine aminotransferase, are elevated in routine laboratory work-up or hepatic steatosis appears on imaging for reasons other than liver symptoms or signs. Currently, liver biopsy remains the gold standard method for NAFLD diagnosis and degree of liver injury evaluation[7]. Computed tomography scans and ultrasound can also be performed as part of the standard evaluation of NAFLD. However, these methods have a number of limitations, including invasiveness, low sensitivity, sampling variability, and inaccurate diagnosis[8,9]. The American Association for the Study of Liver Diseases has identified uncertainties about these diagnostic tools, which represent a barrier to the effective treatment of patients with NAFLD[10]. Thus, there is increased recognition of the need to develop non-invasive biomarkers that have the ability to identify simple steatosis from NASH patients who are at high risk of progression to cirrhosis and HCC conditions.

Many concepts important to understanding the pathogenesis of NAFLD have arisen. The traditional view of this complex disease suggests that an interplay between genetic and triggering and/or modifying environmental events is the fundamental basis for disease initiation and development[11,12]. Over the last several years, a growing body of functional evidence has pointed towards a central role of epigenetic factors in fatty liver diseases, including NAFLD. Epigenetics was redefined multiple times and Cavalli and Heard described it as "the study of molecules and mechanisms that can perpetuate alternative gene activity states in the context of the same DNA sequence"[13]. Epigenetic machinery could be another layer that orchestrates gene expression and provides a molecular link between genetic and environment effects on NAFLD. Thus, the integration of epigenetic information may represent another opportunity to tackle the complexity of NAFLD and identify new predictive biomarkers and potential therapeutic targets of this disease. Indeed, recent advancements in the emerging field of epigenetics have revealed that epigenetic mechanisms and associated systems may regulate many aspects of the pathogenesis of NAFLD[3,14]. Unlike genetic alterations, epigenetic alterations can be mostly heritable and reversible. Thus, further discoveries in the field could enable the development of epigenetic tools that can be used not only to complement current strategies for early disease diagnosis and optimal individualized patient risk stratification but also to improve therapy.

To date, the most studied epigenetic mechanisms include DNA methylation, histone modifications, and noncoding RNA (ncRNA)-based regulation. While certain epigenetic mechanisms underlying DNA and chromatin modifications in NAFLD were addressed elsewhere[15,16], only relevant studies shedding light on the roles played by ncRNAs' machinery will be reviewed next.

EMERGING ROLE OF NCRNAS IN THE PATHOGENESIS OF NAFLD

For decades, only the portion of the genome that is transcribed into mRNA (approximately 2%) was the central focus of basic science and medical research. The remaining 98% was simply believed non-functional and referred to as "junk DNA" or "dark matter"[17]. Due to advances in high-throughput sequencing technologies enabling more in-depth genomic and transcriptomic analyses, the Encyclopedia of DNA Elements project revealed that up to 80% of the human genome is transcribed, generating a multitude of functional transcripts commonly referred to as ncRNAs[18,19]. The biological significance of these nonprotein coding transcripts is now becoming evident, with many ncRNAs found to have epigenetic activity and substantial roles in regulating diverse cellular processes. Indeed, they can affect gene expression by interacting with the transcriptional apparatus, and regulating chromatin structure and RNA processing mechanisms[20]. There is also proof that interaction and crosstalk between different species of ncRNA groups can create complicated and intertwined networks that can affect gene expression[21]. Regulatory ncRNAs mainly consist of microRNAs (miRNAs) (< 30 nucleotides), long noncoding RNAs (lncRNAs) (≥ 200 nucleotides)[19], and circular RNAs (circRNAs). Due to their stability and easy detection in biological fluids, ncRNAs are continuously investigated as promising diagnostic and therapeutic tools in metabolic diseases. A growing body of literature indicates that ncRNAs are abundantly expressed in the liver and their altered expression patterns are associated with various types of liver diseases including NAFLD[22,23]. Moreover, ncRNAs reveal significant differences in expression according to the severity of NAFLD and histological features[24]. In the next sections, the role of miRNAs, lncRNAs, and circRNAs will be discussed, to better improve our understanding of their appealing potential as biomarkers for early NAFLD/NASH staging and therapeutic targets.

miRNAs in NAFLD

miRNAs are small, highly conserved short single-stranded ncRNAs (approximately 18-22 nucleotides in length) with epigenetic functions able to transcriptionally regulate gene expression of other RNAs notably mRNAs[25]. They are transcribed in the cell nucleus and transported to the cytoplasm, where they are processed into mature miRNAs[26]. With respect to their function, miRNAs primarily regulate gene expression by promoting mRNA degradation or repressing their translation. They serve as master regulators that control the expression of thousands of coding and noncoding genes. Prior research suggests that more than 60% of human coding genes are potential targets of miRNAs[27]. Mounting evidence reveals that dysregulation in miRNAs' expression is associated with molecular processes of various forms of metabolic and liver diseases, including NAFLD conditions[3,28-30]. Indeed, several differentially expressed miRNAs play key roles in the development of NAFLD in animal models and humans[30-33], essentially through the regulation of several pathogenic processes including altered lipid and glucose metabolism, insulin resistance, and inflammation pathways[34,35]. Because miRNAs are stably detected in biofluids and can circulate within microvesicles, exosomes, or apoptotic bodies, or bound to RNA-binding proteins, interest in studying these molecules has increased tremendously. Additionally, considerable research has demonstrated that these RNA species may offer new insights into disease biology, and their easy profiling in the serum has raised enthusiasm about their potential use in clinical practice as biomarkers for early diagnosis and clinical monitoring of NAFLD progression [36,37]. While a plethora of miRNAs are associated with fatty liver diseases, only those shown to be repeatedly involved in different stages of NAFLD will be discussed next.

miR-21

There is evidence that miR-21-mediated regulation may play an important role in the pathogenesis of several types of liver diseases[38]. Dysregulated miR-21 expression has been reported in animal models of steatohepatitis and human NASH. Specifically, the levels of circulating miR-21 and its expression in the liver are heavily elevated in both NAFLD patients and mouse models[39-41]. Likewise, circulating miR-21 Levels are significantly increased in patients suffering from NASH compared to NAFL and healthy controls[42]. Other studies have shown that inhibiting miR-21 can alleviate steatosis by activating peroxisome proliferator-activated receptor alpha (PPARα)[40,43]. In support of these findings, another report indicated that hepatocyte-specific knockout (KO) of miR-21 in mice improved high-fat diet (HFD)-induced steatosis through upregulation of multiple miR-21-targeted pathways governing lipid metabolism[44]. Similarly, miR-21 abrogation along with obeticholic acid treatment significantly reduced NASH in mice[45].

Moreover, miR-21 plays a key role in hepatic lipid metabolism by promoting hepatic lipid accumulation *via* its interaction with several proteins including sterol regulatory element binding protein (SREBP1)[46] and 3-hydroxy-3-methylglutaryl-co-enzyme A reductase (HMGCR)[47]. Additionally, miR-21 can target phosphatase and tensin homolog, which prevents hepatic steatosis[48], and PPARα expression, which induces inflammation and fibrosis progression and activates lipid oxidation in NAFLD[40]. Other investigations have revealed that miR-21 can inactivate the Wnt/β-catenin signaling pathway by targeting low-density lipoprotein (LDL) receptor-related protein 6, thereby aggravating lipid accumulation and inflammation[49]. Mechanistic studies have also demonstrated that miR-21

promotes hepatic insulin resistance and steatosis in diet-induced obese mice through the regulation of several key transcription factors, such as forkhead box protein O1, insulin-induced gene 2, signal transducer and activator of transcription 3, and hepatocyte nuclear factor 4-alpha (HNF4-α)[44]. Together, these studies clearly show that miR-21 plays an essential role in key transitions of NAFLD pathogenesis. Such findings hold the potential to develop miR-21 as a reliable serum biomarker to identify patients "at risk" for NASH.

miR-29a

The miR-29 family of miRNAs consists of miR-29a, miR-29b, and miR-29c members[50], and are mainly expressed in hepatocytes and hepatic stellate cells (HSCs)[51,52]. A body of evidence suggests that miR-29a is significantly associated with diagnostic relevance of NAFLD[31,53], NASH[54] and liver fibrosis [54,55], as well as aggressiveness and prognosis of HCC[31]. López-Riera *et al*[56] identified circulating miR-29a as one of the potential biomarkers that could predict drug-induced NAFLD in humans. Yang *et al*[57] found that serum miR-29a levels were significantly lower in NAFLD patients compared to controls. Furthermore, another study revealed that miR-29a disrupts DNA methyltransferase 3β (DNMT3β) to improve diet-induced NASH in mice. Mattis *et al*[58] used a mouse model to demonstrate that miR-29a protects hepatocytes from steatosis by repressing lipoprotein lipase in hepatocytes. Moreover, miR-29a inhibits glycogen synthase kinase 3 beta to repress sirtuin 1 (SIRT1)-mediated mitochondrial biogenesis and improve methionine–choline-deficient diet-induced NASH in mice[59]. Roderburg *et al*[52] reported that miR-29 family members are downregulated in mouse models of liver fibrosis and in human fibrotic livers. A recent study indicated that miR-29a plays a regulatory role in NAFLD by improving HFD-induced steatohepatitis and liver fibrosis through the suppression of cluster of differentiation 36 (CD36)[31]. Together, these findings highlight the potential of miR-29a-targeted therapy for the treatment of NAFLD and its advanced stages.

miR-33a/miR33b

In humans, the miR-33 family comprises two members, miR-33a and miR-33b (miR-33a/b), which are co-transcribed with the sterol regulatory element-binding protein 2 (SREBP2) and 1 respectively, and their main targets are SREBP and SREBP2 and ATP-binding cassette subfamily A member 1 (ABCA1). miR-33a/b is implicated in fatty liver disease and plays key roles in lipid metabolism and transport by targeting a number of genes involved in cholesterol homeostasis and insulin signaling pathways[60,61]. In mice, there is only one miR-33 isoform, which is an ortholog form of human miR-33a[60].

In addition, expression levels of miR-33 are increased in the liver tissues of patients with NAFLD[62]. Circulating miR-33a is associated with steatosis and inflammation in patients with NAFLD after liver transplantation and can serve as an independent predictor of these pathological conditions[63]. The expression of hepatic miR-33a/miR-144 is increased in NASH patients with morbid obesity[64]. A further study in mice also demonstrated that miR-33 can regulate hepatic lipogenesis signaling and may serve as a potential circulating biomarker of NAFLD[65].

From a therapeutic perspective, several studies have demonstrated that treatment with anti-miR-33 therapeutic agents can significantly reduce plaque burden in mouse models of atherosclerosis and offer promise for treating cardiovascular disease[66-68]. However, a previously published clinical trial indicated that increased expression of miR-33a in the liver is associated with steatohepatitis in morbidly obese humans and metabolic dysfunction[64]. In line with this, long-term therapeutic silencing of miR-33 in mice leads to the development of adverse outcomes, including hypertriglyceridemia and hepatic steatosis[69,70]. miR-33 KO mice exposed to HFD developed marked worsening of obesity and liver steatosis *via* targeting SREBP1[71]. Recently, Price *et al*[61] provided additional evidence that genetic loss of miR-33 results in an increase in food intake and promotes obesity and insulin resistance. Thus, further research is needed to fully understand the role of miR-33a/b in NAFLD, which may provide new insights into the physiopathology of various forms of this disease.

miR-34a

The miR-34 family comprises three members: miR-34a, miR-34b, and miR-34c. miR-34a expression levels are increased both in the liver and serum of patients with NAFLD and NASH compared to healthy controls and are positively correlated with total cholesterol (TC) and triglyceride (TG) levels[72, 73]. miR-34 regulates many transcription factors, such as HNF4-α, SIRT1, and p53, which are involved in lipid metabolism, cholesterol synthesis, and fatty acid b-oxidation[72,74]. In addition, Xu *et al*[73] demonstrated that miR-34a inhibits hepatic very LDL secretion by promoting steatosis through interaction with HNF4-α in patients with NASH and mice fed HFD. miR-34a regulates steatosis by directly targeting PPARα expression in NAFLD[75]. Recently, another study demonstrated that the miR-34a/SIRT1/AMPK pathway is involved in mitochondrial dysfunction in a mouse NASH model[76]. Higher circulating levels of miR-34a have been seen in patients with NAFLD and NASH and mice fed HFD[73,77]. An association of miR-34a and miR-122 with dyslipidemia among patients with NAFLD has also been reported[78], and both miRNAs could be useful biomarkers in children with obesity and NAFLD[79]. Finally, in a meta-analysis study, miR-34a, miR-122, and miR-192 were identified as potential diagnostic markers to segregate NAFL from NASH[32]. Here, miR-34 showed the best

diagnostic accuracy for discriminating NASH *vs* NAFLD.

miR-122

miR-122 is the most abundant and extensively studied hepatic miRNA representing about 70% of the total miRNA in the liver[80]. Current evidence indicates that miR-122 plays an essential role in different aspects of liver function as well as in the epigenetic modulation of several genes linked to chronic hepatic pathology[72,80,81]. miR-122 is involved in the regulation of lipid and cholesterol metabolism. Animal experiments have revealed that inhibition of miR-122 results in a decrease of hepatic fatty acid and cholesterol synthesis rate, reduction in plasma cholesterol levels, enhanced liver fatty acid oxidation, and protection of HFD-fed mice from hepatic steatosis[82,83]. Further investigations have reported that miR-122 targets specific genes of cholesterol biosynthesis, such as *HMGCR*, microsomal TG transfer protein, 3-hydroxy-3-methylglutaryl-coenzyme A (CoA) synthase 1, fatty acid synthase, and acetyl-CoA carboxylase[33,82,83], suggesting a role in the pathogenesis of NAFLD.

Excessive accumulation of TG in the cytoplasm of hepatocytes is a hallmark of NAFLD. Genetic deletion of miR-122 Locus in mice results in TG accumulation in the liver and hepatic steatosis that progresses to NASH, fibrosis, and HCC[81,84], whereas restoration of miR-122a expression reduces disease symptoms and tumorigenesis[84]. Consistent with the results from animal investigations, reduced expression of miR-122 is observed in hepatic tissues of NASH patients compared to that in simple steatosis and healthy controls[72,80]. Interestingly, changes in miRNA expression profiles were observed at various stages of NAFLD, including simple fatty liver, NASH, and liver fibrosis to HCC. In this respect, a study reported that in NAFLD patients, the hepatic miR-122 Levels were lower in patients with mild steatosis compared to those with severe steatosis, while hepatic and serum miR-122 Levels were significantly higher in patients with mild fibrosis than in those with severe fibrosis[74].

Conversely, elevated serum levels of miR-122 have been found in patients with NAFLD patients compared to controls, and these levels are positively correlated with disease severity[85,86]. These data are in line with reports demonstrating that circulating levels of miR-122 are positively associated with fatty liver disease, T2DM, obesity, and atherosclerosis[80,87,88]. Additionally, NASH patients exhibit increased levels of miR-122 in the serum[80] and decreased hepatic expression of this RNA[72]. Although studies have consistently demonstrated that miR-122 expression differs between hepatocytes and blood, mechanisms underlying such an inverse correlation are certainly complex and need further attention. Attempts have been made to explain the observed difference in expression between the two tissues. The elevated levels of circulating miR-122 could be attributed to its secretion *via* liver exosomes. In agreement with this, Gallo *et al*[89] reported that miR-122 is localized in abundance to secreted liver exosomes. However, it must be acknowledged that the dynamic of miRNAs expression, secretion, and transport is complex and the contribution of other tissues such as adipose tissue to the pool of miR-122 Levels must not be ruled out.

miR-155

miR-155 is a multifunctional miRNA known to regulate numerous fundamental processes such as immunity, inflammation, lipid metabolism, and cancer[90,91]. Several studies have reported that miR-155 is one of the biologically most relevant miRNAs in several liver diseases including NAFLD[92,93]. In this respect, a study by Wang *et al*[94] demonstrated that the level of miR-155 is decreased in liver tissue and peripheral blood of NAFLD patients compared with healthy controls. Other studies indicated that miR-155 activity was also decreased in patients with NAFLD, which could be attributed to the adipogenic transcription factors CCAAT/enhancer binding protein (C/EBP)-α, C/EBP-β, PPAR-γ and LXRα[94,95]. On the other hand, miR-155-deficient mice fed a HFD developed increased hepatic steatosis compared to controls[94], while conditionally liver-specific overexpression of miR-155 reduced serum and hepatic levels of TC, TG, and high-density lipoprotein, and alleviated NAFLD[93]. These results suggest that miR-155 has a protective role in NAFLD and its pathological conditions. However, conflicting study results have somewhat dimmed the promise of using this miRNA to prevent NAFLD. For instance, miR-155 KO mice fed a methionine-choline-deficient diet showed a decrease in steatosis along with a reduction in the expression of genes involved in fatty acid metabolism and fibrosis, but not liver injury or inflammation[95]. Upon ingestion of a diet high in fat, high in cholesterol, and high in sucrose, miR-155 KO mice displayed less liver injury, decreased steatosis, and attenuation in fibrosis compared to control mice[96]. The ambiguous miR-155 roles suggest that this transcript may exert pleiotropic functions depending on the etiology and disease context. Another scenario is that miR-155-containing exosomes or miR-155-containing microvesicles released from cells into the surrounding tissue could contribute to the observed differences in results. As an example, adipose tissue-derived miR-155 upregulated by HFD was shown to induce hepatic insulin resistance in murine models[97]. Thus, further studies are warranted to clarify the contradictory results and determine the role of miR-155 in intracellular lipid accumulation and NAFLD development and progression.

miR-192

miR-192 is highly expressed in quiescent HSCs. Overexpression of miR-192 significantly suppresses the activity of these cells by reducing the proliferation and migratory potential of primary mouse HSCs[98].

A previous study found that circulating miR-192 is differentially expressed in NAFLD patients and even identified a miRNA panel (hsa-miR-122-5p, hsa-miR-1290, hsa-miR-27b-3p, and hsa-miR-192-5p) with high diagnostic accuracy for this disease[99]. Another study indicated that serum levels of miR-192-5p were significantly elevated in NAFLD patients and positively associated with hepatic inflammatory activity score and disease progression[100]. Recently, Wang *et al*[101] observed that miR-34a, miR-122, and miR-192 represent suitable biomarkers to distinguish NAFLD and NASH severity. Another study found that in NASH patients levels of miR-192 were elevated in serum, while decreased in the liver[80]. Similar to miR-122, miR-192 was increased in NASH serum compared with steatosis and downregulated in NASH liver, both in human and animal models, suggesting that these miRNAs are released from hepatocytes during pathophysiological states associated with cell membrane impairment[42,100]. A recent meta-analysis identified several miRNAs as potential biomarkers of NAFLD and NASH, including miR-34a, miR-122, and miR-192[32]. Together, these findings suggest that circulating miRNA-192 Levels may represent a potential noninvasive diagnostic biomarker and therapeutic target for the different stages of NAFLD.

miR-375

miR-375 is highly expressed in pancreatic islets and considered to be an essential regulator of glucose homeostasis and insulin secretion[102]. miR-122, miR-192, and miR-375 are significantly upregulated in NAFLD patients compared to controls[80]. miR-375 is involved in the pathogenesis of NAFLD and its inhibition suppresses the production of inflammatory cytokines tumor necrosis factor-alpha as well as interluekin-6, increased the expression of adiponectin, and suppressed lipid accumulation in palmitate (PA)-induced HepG2 cells[103]. These preliminary data suggest that miR-375 as well as the above discussed miRNAs (Table 1) could be promising targets for the prevention and progression of NAFLD.

LncRNAs in NAFLD pathogenesis

LncRNAs are relatively long RNA transcripts (> 200 nucleotides) that lack coding potential[104]. They are regulatory molecules transcribed from intergenic, exonic, or the distal protein-coding regions by RNA polymerase II and capped at the 5′-end and polyadenylated at the 3′-end[104]. Regarding their functions, there are subsets of lncRNAs that act as guides by binding to proteins and directing their localization, providing dynamic scaffolds providing a central platform for the transient assembly of multiple proteins and RNAs[105] and decoys that bind targeted proteins or miRNAs to limit their availability and function by acting as a molecular sink[106]. However, other functions related to these RNA species may arise as research in the field rapidly progresses. Over the last decade, dysregulation of lncRNAs has been linked to the pathophysiology of various human diseases, such as cancer, diabetes, and cardiovascular diseases[107]. In the context of NAFLD, some reports have noted that lncRNA expression patterns are dysregulated, suggesting that these molecules may represent potential drivers of NAFLD biology and have utility as clinical biomarkers. However, the role of lncRNAs in the development and progression of NAFLD still remains relatively unexplored. Herein, we provide a scientific update on lncRNAs relevant to NAFLD and its stages.

H19 LncRNA

The lncRNA H19 (H19) is a transcription product of the *H19* gene and represents one of the first discovered lncRNAs. H19 predominantly acts to affect miRNAs stability in different physiological and pathological conditions[108]. In recent years, H19 has attracted great attention in the research of liver diseases due to its aberrant expression and extensive involvement in several hepatic metabolic processes [109]. In this respect, existing evidence has shown that overexpression of H19 results in hepatic metabolic reprogramming and exacerbates diet-induced fatty liver[110]. In agreement with this, Liu *et al* [111] reported that expression of H19 induces hepatic steatosis by activating both the lipogenic transcription factor MLX interacting protein-like and the mammalian target of rapamycin complex 1 signaling pathways. In animal models, knockdown of H19 inhibited steatosis and alleviated hepatic lipogenesis by directly regulating the miR-130a/PPARγ axis in NAFLD[112]. However, further studies would be useful for determining the precise contribution of H19 to the pathogenesis of NAFLD.

Blnc1

Brown fat lncRNA 1 (Blnc1) is implicated in the regulation of adipocyte differentiation and function [113] and may serve as a regulator of triacylglycerol biosynthesis. Recently, Zhao *et al*[114] reported that hepatic Blnc1 expression was strongly linked to activation of lipogenesis in mouse models of obesity and NAFLD, whereas its liver-specific inactivation abrogated HFD-induced hepatic steatosis and insulin resistance, and protected mice from diet-induced NASH pathogenesis. Conversely, overexpression of Blnc1 in epididymal white fat tissue improved whole body insulin sensitivity, partially attenuated systemic dyslipidemia and glucose metabolism, and markedly protected against diet-induced obesity hepatic steatosis, probably *via* enhancement of mitochondrial biogenesis and function in white fat[115]. Overall, these results suggest that Blnc1 has different regulatory mechanisms and distinct functions in the liver and white adipose tissue.

Table 1 Selected microRNAs shown to be highly involved in the pathogenesis of nonalcoholic fatty liver disease

miRNA	Circulation level	Tissue expression	Main functional and pathophysiological impacts	Ref.
miR-21	↑	↑	Promotes lipogenesis Involved in NASH, fibrosis, and HCC Targets several metabolic and inflammatory signaling pathways related to the pathogenesis of NAFLD	[38-40,42,44]
miR-29a	↑	↓	Highly connected with the diagnostic relevance of NAFLD, NASH, and HCC Modulates oxidative stress and inflammation in the context of NAFLD	[31,53,52,58]
miR-33a/b	↑	↑	Involved in lipid metabolism, glucose homeostasis and hepatic lipogenesis Associated with steatosis and inflammation in patients with NAFLD/NASH	[61-63,65]
miR-34a	↑	↑	Regulates lipoprotein metabolism and promotes liver steatosis Involved in NAFLD/NASH Correlates with the severity of hepatic inflammatory activity Can serve as a biomarker to distinguish NAFLD from NASH patients	[72,73,75]
miR-122	↑	↓	Modulates several genes linked to chronic hepatic pathology and lipid metabolism Promotes hepatic steatosis Serum miR-122 correlates positively with markers of NAFLD severity as well as with NASH	[74,82-84]
miR-155	↑	↑	Regulates key cellular events in NAFLD/NASH Promotes insulin resistance	[96,97]
miR-192	↑	↓	Significantly elevated in NAFLD patients and positively associated with hepatic inflammatory activity score and disease progression Increased in serum from NASH patients compared with steatosis Could be a potential biomarker of NAFLD and NASH	[32,80,100]
miR-375	↑	↑	Involved in the pathogenesis of NAFLD/NASH/fibrosis Key regulator of glucose homeostasis and insulin secretion	[80,102]

HCC: Hepatocellular carcinoma; miRNAs: MicroRNAs; NAFLD: Nonalcoholic fatty liver disease; NASH: Nonalcoholic steatohepatitis.

lncHR1

The lncRNA HCV regulated 1 (lncHR1) was recently identified as a novel human-specific lncRNA that has an effect on lipid metabolism. A study by Li *et al*[116] reported that in an HFD mouse model, overexpression of lncHR1 inhibited fatty acid synthase and lowered oleic acid-induced hepatic cell TG and lipid droplets' accumulation by inhibiting *SREBP1c* gene expression. These findings are relevant to NAFLD since dyslipidemia in patients with NAFLD is atherogenic in nature and it is characterized by increased levels of serum TG. Furthermore, elevated TG levels in the circulation are associated with metabolic syndrome and cardiovascular disease[117].

Metastasis-associated lung adenocarcinoma transcript 1

Metastasis-associated lung adenocarcinoma transcript 1 (MALAT1) is one of the highly conserved lncRNAs shown to play a significant role in many diseases, including cancer, diabetes, and insulin resistance. A previous study showed that excess PA increases MALAT1 expression, activated SREBP1c and induced intracellular lipid accumulation in hepatocytes, whereas inhibition of MALAT1 expression decreased nuclear SREBP1c level and lipid accumulation both *in vitro* and *in vivo*[118]. Further analysis by these authors revealed that the reduction of MALAT1 in the liver improved insulin sensitivity in ob/ob mice. They concluded that MALAT1 may promote hepatic steatosis and insulin resistance by increasing nuclear SREBP1c protein stability in hepatocytes[118]. Furthermore, results from lncRNA profiling in the liver biopsies of NAFLD patients demonstrated the potential of MALAT1 as a regulator of liver inflammation and fibrosis and insulin resistance by targeting the C-X-C motif chemokine ligand 5[119]. Consistent with these observations, another study found that MALAT1 expression was significantly increased in NASH patients compared to NAFLD individuals with simple steatosis and controls[120]. Previous studies have reported that MALAT is overexpressed in both HCC cell lines and clinical tissue samples[121,122], providing additional evidence that this lncRNA could be used as a

biomarker of liver damage and HCC development.

Nuclear enriched abundant transcript 1

Nuclear enriched abundant transcript 1 (NEAT1) is a nuclear lncRNA involved in various liver diseases [123]. It is involved in adipogenesis processes, including lipolysis, lipid uptake, and LDL oxidation. A recent study indicated that the NEAT1 and mTOR signaling pathway proteins were increased in NAFLD *in vitro* and *in vivo* while downregulation of NEAT1 alleviated NAFLD *via* the mTOR/S6K1 signaling pathway in rat model[124]. Additionally, NEAT1 plays an important role in the activation of estrogen receptor alpha to regulate water-glycerol transporter (AQP7)-mediated hepatic steatosis[125]. Chen *et al*[126] found that NEAT1 promotes steatosis by sponging miR-146a-5p, subsequently increasing the expression of Rho-kinase1 (ROCK1) and significantly inducing the AMPK/SREBP pathway. Silencing of NEAT1 alleviated fibrosis and inflammatory responses by regulating the miR-506/GLI3 axis in an NAFLD cellular model[127]. A recent study indicated that NEAT1 and paternally expressed gene 3 were highly expressed in the liver and HSCs from NASH mice and silencing of NEAT1 effectively reduced the fibrotic characteristics of HSCs in the setting of NASH[128]. These results corroborate previous findings by Leti *et al*[119] indicating that NEAT1 is upregulated in the fibrosis of NASH patients compared to controls. Together, these studies highlight the potential value of NEAT1 for aiding in the prognosis and diagnosis of NASH.

Ultra-conserved element

Ultra-conserved element (UC372) is a lncRNA associated with impaired homeostasis of lipid metabolism and may play a role in the pathogenesis of NAFLD. UC372 is upregulated in a murine model of T2DM (db/db mice), HFD-fed mice, and NAFLD patients, indicating a role in liver steatosis and fatty liver[129]. Mechanistically, UC372 may drive hepatic steatosis through binding to pri-miR-195/pri-miR-4668, thus preventing miR-195/miR-4668 from regulating the expression of target genes associated with lipid synthesis and uptake, including acetyl-CoA carboxylase, fatty acid synthase, stearoyl-CoA desaturase 1, and lipid uptake-related genes such as CD36[129]. These preliminary results suggest that UC372 may be a promising target for therapies combating hepatic steatosis.

Maternally expressed gene 3

Maternally expressed gene 3 (MEG3), also known as gene trap locus 2, is another lncRNA that plays a regulatory role in the carcinogenesis and progression of several types of cancer. MEG3 is also suspected to be involved in the pathogenesis of NAFLD. In this respect, an early study reported that expression of hepatic MEG3 was consistently decreased in the chemokine (C-C motif) ligand 4 (CCl4)-induced mouse progressive liver fibrosis model compared to normal tissues, and HSCs may be one of the main sources of the MEG3 Levels present in CCl4-treated livers[130]. The same study revealed that MEG3 was also downregulated in human liver fibrotic tissues compared with control liver tissues. In line with this these studies, Huang *et al*[131] showed that the downregulation of MEG3 in *in vitro* and *in vivo* models of NAFLD is negatively correlated with lipogenesis-related genes, and that overexpression of MEG3 alleviates lipid overaccumulation in HepG2 cells. The downregulation of MEG3 in two models of NAFLD (free fatty acid-challenged primary hepatocytes and HFD-induced mouse) was also indicated in a more recent study by Zou *et al*[132].

In contradiction with these results, hepatic MEG3 Levels are significantly increased in liver fibrosis and NASH cirrhosis in human patients[133]. Similarly, MEG3 was shown to be one of the most differentially expressed lncRNAs in the vascular endothelium in diet-induced obese mice, and its expression was elevated in human nonalcoholic fatty livers and NASH livers, whereas its knockdown potentiated obesity-induced insulin resistance and impaired glucose homeostasis[134]. These conflicting results underline the complexity of MEG regulation, and further studies are required to clarify the biological significance of MEG3 and its potential role MEG3 either as a biomarker or a therapeutic target for NAFLD.

Highly upregulated in liver cancer

The lncRNA highly upregulated in liver cancer (HULC) was the first identified lncRNA specifically overexpressed in HCC. HULC, a functionally important lncRNA, promotes HCC growth, metastasis and drug resistance[135]. HULC expression was found to be increased in the liver tissue of NAFLD rats [136]. Inhibition of this lncRNA improves hepatic fibrosis and lipid deposition and decreases hepatocyte apoptosis in rats with NAFLD *via* inhibition of the mitogen-activated protein kinase signaling pathway in liver tissue[136]. Interestingly, the antidiabetic drug metformin was also reported to decrease HULC by inhibiting the expression of specificity protein 1 transcription factor in liver cancer cells[137]. Indeed, metformin was shown to improve insulin resistance and hyperinsulinemia and increase insulin sensitivity. This drug is now recommended and has proven to be effective for the treatment of NAFLD [138]. Collectively, these findings suggest that HULC could be a promising target for NAFLD diagnosis, staging, and therapy.

Homeobox transcript antisense intergenic RNA

Homeobox (HOX) transcript antisense intergenic RNA (HOTAIR) is a lncRNA that resides on a boundary of the HOXC locus on chromosome 12q13.13. HOTAIR is increased in different forms of cancers and involved in diverse cellular functions. In NAFLD, free fatty acid treatment promotes TG accumulation in HepG2 cells, significantly induces HOTAIR expression and inhibits phosphatase and tensin homolog expression[139]. A recent study reported that HOTAIR was activated in NAFLD, and HOTAIR knockdown significantly inhibited the development of NAFLD *via* mediation of miR-130b-3p/ROCK1/AMPK axis, further suggesting a target for NAFLD[140]. HOTAIR shows several oncogenic functions in HCC and its expression levels are increased in liver fibrosis, which causes acceleration of carcinogenesis in hepatitis B virus-infected patients[141]. Other investigations have reported that HOTAIR can serve as a competing endogenous RNA to sponge miR-29b and then repress DNMT3b, which contributes to hepatic fibrosis[141].

Fatty liver-related lncRNA 2

The lncRNA fatty liver-related lncRNA 2 (FLRL2) is located in the intronic region of the aryl hydrocarbon receptor nuclear translocator-like (*Arntl*) gene, and *Arntl* is predicted as a cis target of FLRL2. FLRL2 was identified as a potential key molecule in the pathogenesis of NAFLD. This nuclear-localized lncRNA is downregulated in the NAFLD mouse model, suggesting a role in the pathogenesis of this disease[142]. Further mechanistic studies have demonstrated that overexpression of FLRL2 alleviates NAFLD through activation of the Arntl-SIRTA pathway, inhibits lipogenesis, and reduces hepatic steatosis in HFD mice[143]. These results render FLRL2 another promising therapeutic candidate for the treatment of NAFLD and its complications. Finally, the above-discussed lncRNAs with their potential functions in NAFLD are also summarized in Table 2.

circRNAs in NAFLD

As their name implies, circRNAs are single-stranded covalently closed RNA species formed through back-splicing. Distinct characteristics of circRNAs, such as high stability, evolutionary conservation among species, exonuclease resistance, and existence in body fluids endow this class of RNAs with numerous potential functions ranging from miRNA and protein sponges to gene transcriptional regulators and protein/peptide translators. Moreover, circRNAs are dysregulated in numerous pathological conditions and may potentially serve as novel diagnostic biomarkers and therapeutic targets.

Although there is increasing evidence linking circRNAs to the pathogenesis of metabolic diseases, studies centered on the investigation of circRNAs in NAFLD were only recently conducted[144-146]. Data from recent literature suggest that circRNAs are involved in several fundamental processes governing the onset and progression of NAFLD and display aberrant expression[147]. For instance, a circRNA_0046367 was decreased in HFD-induced hepatic steatosis[148]. Subsequently, the authors of this study demonstrated that normalization of circRNA_0046367 Levels prevents lipid peroxidation and mitochondrial dysfunction in steatosis through miR-34a sponging and PPARα downregulation. In a further analysis, the same research laboratory identified an additional circRNA: circRNA_0046366, whose expression was also diminished during free fatty acid-induced hepatocellular steatosis in high fat-treated HepG2 cells[149]. In HepG2 cells with hepatic steatosis induced by high-fat stimulation, circRNA_021412 was associated with hepatic steatosis *via* the circRNA_021412/miR-1972/LPIN1axis [150]. circRNA microarrays analysis in an HFD mouse model revealed that circScd1 expression was significantly decreased in NAFLD tissues compared to that in controls. Consistent with this, knockdown of circScd1 promoted hepatosteatosis through the regulation of the Janus kinase 2 and signal transducer and activator of transcription 5 signaling pathway[151]. In an *in vitro* model of NAFLD, Hsa_circ_0048179 was shown to attenuate free fatty acid-induced steatosis *via* Hsa_circ_0048179/miR-188-3p/glutathione peroxidase 4 signaling[152]. circRNA profiling in a NASH mouse model identified circRNA_29981 as the circRNA most significantly differentially expressed in this setting[153].

More recently, Jin *et al*[147] indicated that the circRNA_002581-miR-122-CPEB1 axis aggravates NASH partially through autophagy suppression, while silencing of circRNA_002581 significantly attenuated lipid droplet accumulation, eliminated liver damage in both mouse and cellular models of NASH. Chen *et al*[154] indicated that silencing of circ_0071410 alleviates hepatic stellate activation, a key step of liver cirrhosis. HSCs are the primary cell type responsible for liver fibrosis. In the CCl4-induced mouse model of liver fibrosis, mmu_circ_34116 was able to inhibit HSCs activation[155]. In a mouse model of NAFLD, Chen *et al*[156] found that circ_0057558 can promote NAFLD by regulating ROCK1/AMPK signaling through targeting miR-206. Interestingly, a novel mitochondrial genome-encoded circRNA termed mitochondrial steatohepatitis-associated circRNA ATP5B regulator (SCAR) was identified recently[157]. The latter study found SCAR to be significantly downregulated in liver fibroblasts from patients with NASH. Additionally, the overexpression of SCAR inhibited mitochondrial reactive oxygen species output and fibroblast activation *via* shutting down mitochondrial permeability transition pore. More importantly, *in vivo* targeting of SCAR alleviated HFD-induced cirrhosis and insulin resistance implying that circRNA SCAR may serve as a therapeutic target for NASH[157].

Table 2 Relevant dysregulated long noncoding RNAs associated with alterations in liver metabolism and nonalcoholic fatty liver disease

lncRNA	Expression	Main functional and pathophysiological effects	Ref.
MALAT1	↑	Promotes cell proliferation, migration, and invasion in several different human cancers including HCC Promotes hepatic steatosis and insulin resistance Hepatic MALAT1 levels are higher in NASH patients with fibrosis Promotes NAFLD progression and increase with the severity of the disease	[119-122]
NEAT1	↑	Promotes adipogenesis, lipogenesis, and lipid absorption Modulates fibrosis and inflammatory responses Silencing NEAT1 alleviated fibrosis and inflammatory in a NAFLD cellular model	[124,126,127]
MEG3	↓	Involved in lipid metabolism and glucose homeostasis Correlates with steatosis and inflammation (NASH) in patients with NAFLD	[131-134]
HULC	↑	Promotes HCC growth and metastasis Promotes NAFLD development Metformin decreases HULC expression	[135,136]
HOTAIR	↑	Activates lipid accumulation in hepatocytes and promotes hepatic steatosis development Expression profile is significantly increased in oleic acid-induced steatosis and during the development of HFD-induced NAFLD Accelerates liver fibrosis and carcinogenesis	[139-141]
FLRL2	↓	Decreases endoplasmic reticulum stress and liver inflammation Alleviates NAFLD and steatosis in mouse model	[143]

FLR2: Fatty liver-related lncRNA 2; H19: H19 imprinted maternally expressed transcript; HCC: Hepatocellular carcinoma; HFD: High-fat diet; HOTAIR: HOX transcript antisense RNA; MALAT1: Metastasis-associated lung adenocarcinoma transcript 1; lncRNAs: Long noncoding RNAs; MEG3: Maternally expressed 3; NAFLD: Nonalcoholic fatty liver disease; NASH: Nonalcoholic steatohepatitis; NEAT1: Nuclear paraspeckle assembly transcript 1; HULC: Hepatocellular carcinoma upregulated long noncoding RNA.

Together, these findings suggest that certain circRNAs, including those summarized in Table 3, are likely to contribute to NAFLD phenotype, which makes them attractive targets for the development of diagnostic and interventional pharmacology. However, circRNA data are still lacking functional evidence and their underlying mechanisms are still awaiting elucidation. Nevertheless, further carefully designed prospective studies to emphasize and validate the potential use of circRNAs as NAFLD biomarkers are expected to yield new insights into the pathogenesis of this disease state.

CONCLUSION

The findings from the above research clearly indicate that alterations in miRNA, circRNA and lncRNA expression play critical roles in cellular physiology and many diseases, including NAFLD and cancer. Thus, these ncRNA subsets are promising non-invasive biomarkers for the diagnosis and stratification of patients with NAFLD and could inform future personalized treatments designed for this condition. Even though the concept is promising and optimism is high, there is a consensus that research in the field still has limitations and technical challenges. (1) Sustained research efforts in the ncRNAs field have aimed to develop biomarkers to support the diagnostic process in patients with NAFLD. Unfortunately, most of the studies were carried out in subjects who already display patterns of worsening symptoms and are seeking medical care. To overcome this challenge, an alternative option would be to investigate the status of ncRNAs in the general population, which may assess the risk and capture early stages of disease initiation and evolution. This strategy could help achieve early diagnosis in individuals at risk for NAFLD but yet asymptomatic, and determine whether the overserved aberration in ncRNA

Table 3 Relevant dysregulated circular RNAs associated with alterations in liver metabolism and nonalcoholic fatty liver disease

circRNA	Expression level	Main functional and pathophysiological effects	Ref.
circRNA_0046367	↑	Inhibits hepatic steatosis by preventing hepatotoxicity of lipid peroxidation	[148]
circRNA_0046366	↑	Inhibits hepatic steatosis through miR-34a/PPARα	[149]
circRNA_021412	↑	Associated with hepatic steatosis	[150]
circScd1	↓	Affects steatosis on NAFLD *via* JAK2/STAT5 signaling pathways	[151]
hsa_circ_0048179	↓	Attenuates free fatty acid-induceded steatosis by sponging of miR-188-3p *in vitro*	[152]
mmu_circRNA_29981	↑	Regulatory role in NASH mousee model	[153]
Circ_0057558	↑	Involved in lipogenesis	[156]
		Promotes nonalcoholic fatty liver disease by sponging miR-206	
SCAR	↓	Correlates with steatosis-to-NASH progression	[157]
		In vivo, targeting circRNA SCAR alleviates HFD-induced cirrhosis and insulin resistance	

circRNAs: Circular RNAs; HCC: Hepatocellular carcinoma; HFD: High-fat diet; JAK2: Janus Kinase 2; NAFLD: Nonalcoholic fatty liver disease; NASH: Nonalcoholic steatohepatitis; PPARα: Peroxisome proliferator-activated receptor α; STAT5: Signal transducer and activator of transcription 5.

expression is the trigger or it is just a consequence of other causes such as those associated with lipid metabolism disorder, inflammation and immune system; (2) The role of ncRNAs as mediators of cell and organ crosstalk as well as their impact on different signaling pathways involved in NAFLD pathogenesis are not fully understood. It is now recognized that some ncRNAs are present in the extracellular environment and may be involved in pathophysiological condition. They may act to affect their targets either in an autocrine or paracrine fashion. Hence, special attention should be drawn to further research addressing the role of ncRNAs and their carriers (extracellular vesicles) in mediating potential inter-organ crosstalk in NAFLD condition, and the dynamic interaction of ncRNAs with metabolism cell signaling pathways. While these strategies may seem difficult to carry out and complete, they can be a starting point for increasing our knowledge on the role of circulating ncRNAs in organ crosstalk and may represent an opportunity to better understand how they affect metabolic homeostasis to drive the onset and progression of NAFLD and related pathological conditions; and (3) From a clinical perspective, approaches based on an individual ncRNA targeting or overexpression are what researchers are shooting for. However, each ncRNA has highly redundant roles and multiple functions. Indeed, a previous study revealed that a miRNA can affect a phenotype not only through a simple regulatory process, but *via* multiple targets redundantly and often incoherently, and such a complex regulation is difficult to assemble and control[158]. Indeed, it is becoming evident that it is difficult to diagnose a multifactorial disease such as NAFLD using a single ncRNA. Attempts were conducted to use a combination of serum circulating ncRNAs. Understanding the ncRNA-ncRNA crosstalk and their intricate interplay with different genetic and other epigenetic regulators including DNA methylation, chromatin remodeling, and components of the transcriptional and posttranscriptional machineries to regulate gene networks involved in NAFLD could certainly expand our knowledge on the molecular mechanisms driving this disease. This approach can also lead to a breakdown into NAFLD subtypes which would add resolution and inform about the regulation of molecular processes involved in each stage of the disease by specific ncRNAs.

To sum up, this review highlights the evidence for potential subsets of ncRNAs that are associated with NAFLD and its pathological conditions. The findings from various human and animal studies clearly suggest that dysregulation in ncRNA profiles are critical factors in the initiation and progression of fatty liver diseases, including NAFLD. This may be an appealing argument to further explore the mystery of these RNA molecules and consider their clinical application as biomarkers/therapeutics in the prevention and treatment of NAFLD and its progressive forms.

FOOTNOTES

Author contributions: Zaiou M conducted the literature review and wrote the manuscript.

Conflict-of-interest statement: The author has no conflicts of interest to declare.

Open-Access: This article is an open-access article that was selected by an in-house editor and fully peer-reviewed by external reviewers. It is distributed in accordance with the Creative Commons Attribution NonCommercial (CC BY-NC 4.0) license, which permits others to distribute, remix, adapt, build upon this work non-commercially, and license their derivative works on different terms, provided the original work is properly cited and the use is non-commercial. See: https://creativecommons.org/Licenses/by-nc/4.0/

Country/Territory of origin: France

ORCID number: Mohamed Zaiou 0000-0002-4113-4350.

S-Editor: Gong ZM
L-Editor: A
P-Editor: Gong ZM

REFERENCES

1 **Baffy G**, Brunt EM, Caldwell SH. Hepatocellular carcinoma in non-alcoholic fatty liver disease: an emerging menace. *J Hepatol* 2012; **56**: 1384-1391 [PMID: 22326465 DOI: 10.1016/j.jhep.2011.10.027]
2 **Eslam M**, Sanyal AJ, George J; International Consensus Panel. MAFLD: A Consensus-Driven Proposed Nomenclature for Metabolic Associated Fatty Liver Disease. *Gastroenterology* 2020; **158**: 1999-2014.e1 [PMID: 32044314 DOI: 10.1053/j.gastro.2019.11.312]
3 **Eslam M**, Valenti L, Romeo S. Genetics and epigenetics of NAFLD and NASH: Clinical impact. *J Hepatol* 2018; **68**: 268-279 [PMID: 29122391 DOI: 10.1016/j.jhep.2017.09.003]
4 **Zou B**, Yeo YH, Nguyen VH, Cheung R, Ingelsson E, Nguyen MH. Prevalence, characteristics and mortality outcomes of obese, nonobese and lean NAFLD in the United States, 1999-2016. *J Intern Med* 2020; **288**: 139-151 [PMID: 32319718 DOI: 10.1111/joim.13069]
5 **Leite NC**, Salles GF, Araujo AL, Villela-Nogueira CA, Cardoso CR. Prevalence and associated factors of non-alcoholic fatty liver disease in patients with type-2 diabetes mellitus. *Liver Int* 2009; **29**: 113-119 [PMID: 18384521 DOI: 10.1111/j.1478-3231.2008.01718.x]
6 **Subichin M**, Clanton J, Makuszewski M, Bohon A, Zografakis JG, Dan A. Liver disease in the morbidly obese: a review of 1000 consecutive patients undergoing weight loss surgery. *Surg Obes Relat Dis* 2015; **11**: 137-141 [PMID: 25701959 DOI: 10.1016/j.soard.2014.06.015]
7 **Hardy T**, Oakley F, Anstee QM, Day CP. Nonalcoholic Fatty Liver Disease: Pathogenesis and Disease Spectrum. *Annu Rev Pathol* 2016; **11**: 451-496 [PMID: 26980160 DOI: 10.1146/annurev-pathol-012615-044224]
8 **Rinella ME**. Nonalcoholic fatty liver disease: a systematic review. *JAMA* 2015; **313**: 2263-2273 [PMID: 26057287 DOI: 10.1001/jama.2015.5370]
9 **Mazhar K**. The Future of Nonalcoholic Fatty Liver Disease Treatment. *Med Clin North Am* 2019; **103**: 57-69 [PMID: 30466676 DOI: 10.1016/j.mcna.2018.08.005]
10 **Younossi Z**, Tacke F, Arrese M, Chander Sharma B, Mostafa I, Bugianesi E, Wai-Sun Wong V, Yilmaz Y, George J, Fan J, Vos MB. Global Perspectives on Nonalcoholic Fatty Liver Disease and Nonalcoholic Steatohepatitis. *Hepatology* 2019; **69**: 2672-2682 [PMID: 30179269 DOI: 10.1002/hep.30251]
11 **Angulo P**. Nonalcoholic fatty liver disease. *N Engl J Med* 2002; **346**: 1221-1231 [PMID: 11961152 DOI: 10.1056/NEJMra011775]
12 **Anstee QM**, Daly AK, Day CP. Genetics of alcoholic and nonalcoholic fatty liver disease. *Semin Liver Dis* 2011; **31**: 128-146 [PMID: 21538280 DOI: 10.1055/s-0031-1276643]
13 **Cavalli G**, Heard E. Advances in epigenetics link genetics to the environment and disease. *Nature* 2019; **571**: 489-499 [PMID: 31341302 DOI: 10.1038/s41586-019-1411-0]
14 **Choudhary NS**, Duseja A. Genetic and epigenetic disease modifiers: non-alcoholic fatty liver disease (NAFLD) and alcoholic liver disease (ALD). *Transl Gastroenterol Hepatol* 2021; **6**: 2 [PMID: 33409397 DOI: 10.21037/tgh.2019.09.06]
15 **Pirola CJ**, Sookoian S. Epigenetics factors in nonalcoholic fatty liver disease. *Expert Rev Gastroenterol Hepatol* 2022; **16**: 521-536 [PMID: 32476509 DOI: 10.1080/17474124.2020.1765772]
16 **Zaiou M**, Amrani R, Rihn B, Hajri T. Dietary Patterns Influence Target Gene Expression through Emerging Epigenetic Mechanisms in Nonalcoholic Fatty Liver Disease. *Biomedicines* 2021; **9** [PMID: 34572442 DOI: 10.3390/biomedicines9091256]
17 **Mattick JS**, Makunin IV. Non-coding RNA. *Hum Mol Genet* 2006; **15** Spec No 1: R17-R29 [PMID: 16651366 DOI: 10.1093/hmg/ddl046]
18 **ENCODE Project Consortium**. An integrated encyclopedia of DNA elements in the human genome. *Nature* 2012; **489**: 57-74 [PMID: 22955616 DOI: 10.1038/nature11247]
19 **Djebali S**, Davis CA, Merkel A, Dobin A, Lassmann T, Mortazavi A, Tanzer A, Lagarde J, Lin W, Schlesinger F, Xue C, Marinov GK, Khatun J, Williams BA, Zaleski C, Rozowsky J, Röder M, Kokocinski F, Abdelhamid RF, Alioto T, Antoshechkin I, Baer MT, Bar NS, Batut P, Bell K, Bell I, Chakrabortty S, Chen X, Chrast J, Curado J, Derrien T, Drenkow J, Dumais E, Dumais J, Duttagupta R, Falconnet E, Fastuca M, Fejes-Toth K, Ferreira P, Foissac S, Fullwood MJ, Gao H, Gonzalez D, Gordon A, Gunawardena H, Howald C, Jha S, Johnson R, Kapranov P, King B, Kingswood C, Luo OJ, Park E, Persaud K, Preall JB, Ribeca P, Risk B, Robyr D, Sammeth M, Schaffer L, See LH, Shahab A, Skancke J, Suzuki AM, Takahashi H, Tilgner H, Trout D, Walters N, Wang H, Wrobel J, Yu Y, Ruan X, Hayashizaki Y, Harrow J, Gerstein M, Hubbard T, Reymond A, Antonarakis SE, Hannon G, Giddings MC, Ruan Y, Wold B, Carninci P, Guigó R,

Gingeras TR. Landscape of transcription in human cells. *Nature* 2012; **489**: 101-108 [PMID: 22955620 DOI: 10.1038/nature11233]

20 **Adams BD**, Parsons C, Walker L, Zhang WC, Slack FJ. Targeting noncoding RNAs in disease. *J Clin Invest* 2017; **127**: 761-771 [PMID: 28248199 DOI: 10.1172/JCI84424]

21 **Yamamura S**, Imai-Sumida M, Tanaka Y, Dahiya R. Interaction and cross-talk between non-coding RNAs. *Cell Mol Life Sci* 2018; **75**: 467-484 [PMID: 28840253 DOI: 10.1007/s00018-017-2626-6]

22 **Ganguly N**, Chakrabarti S. Role of long noncoding RNAs and related epigenetic mechanisms in liver fibrosis (Review). *Int J Mol Med* 2021; **47** [PMID: 33495817 DOI: 10.3892/ijmm.2021.4856]

23 **Khalifa O**, Errafii K, Al-Akl NS, Arredouani A. Noncoding RNAs in Nonalcoholic Fatty Liver Disease: Potential Diagnosis and Prognosis Biomarkers. *Dis Markers* 2020; **2020**: 8822859 [PMID: 33133304 DOI: 10.1155/2020/8822859]

24 **Gim JA**, Bang SM, Lee YS, Lee Y, Yim SY, Jung YK, Kim H, Kim BH, Kim JH, Seo YS, Yim HJ, Yeon JE, Um SH, Byun KS. Evaluation of the severity of nonalcoholic fatty liver disease through analysis of serum exosomal miRNA expression. *PLoS One* 2021; **16**: e0255822 [PMID: 34358264 DOI: 10.1371/journal.pone.0255822]

25 **Szabo G**, Csak T. Role of MicroRNAs in NAFLD/NASH. *Dig Dis Sci* 2016; **61**: 1314-1324 [PMID: 26769057 DOI: 10.1007/s10620-015-4002-4]

26 **O'Brien J**, Hayder H, Zayed Y, Peng C. Overview of MicroRNA Biogenesis, Mechanisms of Actions, and Circulation. *Front Endocrinol (Lausanne)* 2018; **9**: 402 [PMID: 30123182 DOI: 10.3389/fendo.2018.00402]

27 **Friedman RC**, Farh KK, Burge CB, Bartel DP. Most mammalian mRNAs are conserved targets of microRNAs. *Genome Res* 2009; **19**: 92-105 [PMID: 18955434 DOI: 10.1101/gr.082701.108]

28 **Mahmoudi A**, Butler AE, Jamialahmadi T, Sahebkar A. The role of exosomal miRNA in nonalcoholic fatty liver disease. *J Cell Physiol* 2022; **237**: 2078-2094 [PMID: 35137416 DOI: 10.1002/jcp.30699]

29 **Ji C**, Guo X. The clinical potential of circulating microRNAs in obesity. *Nat Rev Endocrinol* 2019; **15**: 731-743 [PMID: 31611648 DOI: 10.1038/s41574-019-0260-0]

30 **Hajri T**, Zaiou M, Fungwe TV, Ouguerram K, Besong S. Epigenetic Regulation of Peroxisome Proliferator-Activated Receptor Gamma Mediates High-Fat Diet-Induced Non-Alcoholic Fatty Liver Disease. *Cells* 2021; **10** [PMID: 34072832 DOI: 10.3390/cells10061355]

31 **Lin HY**, Yang YL, Wang PW, Wang FS, Huang YH. The Emerging Role of MicroRNAs in NAFLD: Highlight of MicroRNA-29a in Modulating Oxidative Stress, Inflammation, and Beyond. *Cells* 2020; **9** [PMID: 32331364 DOI: 10.3390/cells9041041]

32 **Liu CH**, Ampuero J, Gil-Gómez A, Montero-Vallejo R, Rojas Á, Muñoz-Hernández R, Gallego-Durán R, Romero-Gómez M. miRNAs in patients with non-alcoholic fatty liver disease: A systematic review and meta-analysis. *J Hepatol* 2018; **69**: 1335-1348 [PMID: 30142428 DOI: 10.1016/j.jhep.2018.08.008]

33 **Gjorgjieva M**, Sobolewski C, Dolicka D, Correia de Sousa M, Foti M. miRNAs and NAFLD: from pathophysiology to therapy. *Gut* 2019; **68**: 2065-2079 [PMID: 31300518 DOI: 10.1136/gutjnl-2018-318146]

34 **Arner P**, Kulyté A. MicroRNA regulatory networks in human adipose tissue and obesity. *Nat Rev Endocrinol* 2015; **11**: 276-288 [PMID: 25732520 DOI: 10.1038/nrendo.2015.25]

35 **Sobolewski C**, Calo N, Portius D, Foti M. MicroRNAs in fatty liver disease. *Semin Liver Dis* 2015; **35**: 12-25 [PMID: 25632931 DOI: 10.1055/s-0034-1397345]

36 **Dongiovanni P**, Meroni M, Longo M, Fargion S, Fracanzani AL. miRNA Signature in NAFLD: A Turning Point for a Non-Invasive Diagnosis. *Int J Mol Sci* 2018; **19** [PMID: 30544653 DOI: 10.3390/ijms19123966]

37 **Arrese M**, Eguchi A, Feldstein AE. Circulating microRNAs: emerging biomarkers of liver disease. *Semin Liver Dis* 2015; **35**: 43-54 [PMID: 25632934 DOI: 10.1055/s-0034-1397348]

38 **Zhang T**, Yang Z, Kusumanchi P, Han S, Liangpunsakul S. Critical Role of microRNA-21 in the Pathogenesis of Liver Diseases. *Front Med (Lausanne)* 2020; **7**: 7 [PMID: 32083086 DOI: 10.3389/fmed.2020.00007]

39 **Dattaroy D**, Pourhoseini S, Das S, Alhasson F, Seth RK, Nagarkatti M, Michelotti GA, Diehl AM, Chatterjee S. Micro-RNA 21 inhibition of SMAD7 enhances fibrogenesis *via* leptin-mediated NADPH oxidase in experimental and human nonalcoholic steatohepatitis. *Am J Physiol Gastrointest Liver Physiol* 2015; **308**: G298-G312 [PMID: 25501551 DOI: 10.1152/ajpgi.00346.2014]

40 **Loyer X**, Paradis V, Hénique C, Vion AC, Colnot N, Guerin CL, Devue C, On S, Scetbun J, Romain M, Paul JL, Rothenberg ME, Marcellin P, Durand F, Bedossa P, Prip-Buus C, Baugé E, Staels B, Boulanger CM, Tedgui A, Rautou PE. Liver microRNA-21 is overexpressed in non-alcoholic steatohepatitis and contributes to the disease in experimental models by inhibiting PPARα expression. *Gut* 2016; **65**: 1882-1894 [PMID: 26338827 DOI: 10.1136/gutjnl-2014-308883]

41 **Pillai SS**, Lakhani HV, Zehra M, Wang J, Dilip A, Puri N, O'Hanlon K, Sodhi K. Predicting Nonalcoholic Fatty Liver Disease through a Panel of Plasma Biomarkers and MicroRNAs in Female West Virginia Population. *Int J Mol Sci* 2020; **21** [PMID: 32933141 DOI: 10.3390/ijms21186698]

42 **Becker PP**, Rau M, Schmitt J, Malsch C, Hammer C, Bantel H, Müllhaupt B, Geier A. Performance of Serum microRNAs -122, -192 and -21 as Biomarkers in Patients with Non-Alcoholic Steatohepatitis. *PLoS One* 2015; **10**: e0142661 [PMID: 26565986 DOI: 10.1371/journal.pone.0142661]

43 **Pawlak M**, Lefebvre P, Staels B. Molecular mechanism of PPARα action and its impact on lipid metabolism, inflammation and fibrosis in non-alcoholic fatty liver disease. *J Hepatol* 2015; **62**: 720-733 [PMID: 25450203 DOI: 10.1016/j.jhep.2014.10.039]

44 **Calo N**, Ramadori P, Sobolewski C, Romero Y, Maeder C, Fournier M, Rantakari P, Zhang FP, Poutanen M, Dufour JF, Humar B, Nef S, Foti M. Stress-activated *miR-21/miR-21** in hepatocytes promotes lipid and glucose metabolic disorders associated with high-fat diet consumption. *Gut* 2016; **65**: 1871-1881 [PMID: 27222533 DOI: 10.1136/gutjnl-2015-310822]

45 **Rodrigues PM**, Afonso MB, Simão AL, Carvalho CC, Trindade A, Duarte A, Borralho PM, Machado MV, Cortez-Pinto H, Rodrigues CM, Castro RE. miR-21 ablation and obeticholic acid ameliorate nonalcoholic steatohepatitis in mice. *Cell Death Dis* 2017; **8**: e2748 [PMID: 28406477 DOI: 10.1038/cddis.2017.172]

46 **Wu H**, Ng R, Chen X, Steer CJ, Song G. MicroRNA-21 is a potential link between non-alcoholic fatty liver disease and

hepatocellular carcinoma *via* modulation of the HBP1-p53-Srebp1c pathway. *Gut* 2016; **65**: 1850-1860 [PMID: 26282675 DOI: 10.1136/gutjnl-2014-308430]

47 **Sun C**, Huang F, Liu X, Xiao X, Yang M, Hu G, Liu H, Liao L. miR-21 regulates triglyceride and cholesterol metabolism in non-alcoholic fatty liver disease by targeting HMGCR. *Int J Mol Med* 2015; **35**: 847-853 [PMID: 25605429 DOI: 10.3892/ijmm.2015.2076]

48 **Meng F**, Henson R, Wehbe-Janek H, Ghoshal K, Jacob ST, Patel T. MicroRNA-21 regulates expression of the PTEN tumor suppressor gene in human hepatocellular cancer. *Gastroenterology* 2007; **133**: 647-658 [PMID: 17681183 DOI: 10.1053/j.gastro.2007.05.022]

49 **Wang XM**, Wang XY, Huang YM, Chen X, Lü MH, Shi L, Li CP. Role and mechanisms of action of microRNA21 as regards the regulation of the WNT/βcatenin signaling pathway in the pathogenesis of nonalcoholic fatty liver disease. *Int J Mol Med* 2019; **44**: 2201-2212 [PMID: 31638173 DOI: 10.3892/ijmm.2019.4375]

50 **Zhao W**, Cheng L, Quek C, Bellingham SA, Hill AF. Novel miR-29b target regulation patterns are revealed in two different cell lines. *Sci Rep* 2019; **9**: 17449 [PMID: 31767948 DOI: 10.1038/s41598-019-53868-x]

51 **Kriegel AJ**, Liu Y, Fang Y, Ding X, Liang M. The miR-29 family: genomics, cell biology, and relevance to renal and cardiovascular injury. *Physiol Genomics* 2012; **44**: 237-244 [PMID: 22214600 DOI: 10.1152/physiolgenomics.00141.2011]

52 **Roderburg C**, Urban GW, Bettermann K, Vucur M, Zimmermann H, Schmidt S, Janssen J, Koppe C, Knolle P, Castoldi M, Tacke F, Trautwein C, Luedde T. Micro-RNA profiling reveals a role for miR-29 in human and murine liver fibrosis. *Hepatology* 2011; **53**: 209-218 [PMID: 20890893 DOI: 10.1002/hep.23922]

53 **Jampoka K**, Muangpaisarn P, Khongnomnan K, Treeprasertsuk S, Tangkijvanich P, Payungporn S. Serum miR-29a and miR-122 as Potential Biomarkers for Non-Alcoholic Fatty Liver Disease (NAFLD). *Microrna* 2018; **7**: 215-222 [PMID: 29848284 DOI: 10.2174/2211536607666180531093302]

54 **Huang C**, Zheng JM, Cheng Q, Yu KK, Ling QX, Chen MQ, Li N. Serum microRNA-29 levels correlate with disease progression in patients with chronic hepatitis B virus infection. *J Dig Dis* 2014; **15**: 614-621 [PMID: 25138057 DOI: 10.1111/1751-2980.12185]

55 **Lambrecht J**, Verhulst S, Reynaert H, van Grunsven LA. The miRFIB-Score: A Serological miRNA-Based Scoring Algorithm for the Diagnosis of Significant Liver Fibrosis. *Cells* 2019; **8** [PMID: 31470644 DOI: 10.3390/cells8091003]

56 **López-Riera M**, Conde I, Tolosa L, Zaragoza Á, Castell JV, Gómez-Lechón MJ, Jover R. New microRNA Biomarkers for Drug-Induced Steatosis and Their Potential to Predict the Contribution of Drugs to Non-alcoholic Fatty Liver Disease. *Front Pharmacol* 2017; **8**: 3 [PMID: 28179883 DOI: 10.3389/fphar.2017.00003]

57 **Yang YL**, Kuo HC, Wang FS, Huang YH. MicroRNA-29a Disrupts DNMT3b to Ameliorate Diet-Induced Non-Alcoholic Steatohepatitis in Mice. *Int J Mol Sci* 2019; **20** [PMID: 30917489 DOI: 10.3390/ijms20061499]

58 **Mattis AN**, Song G, Hitchner K, Kim RY, Lee AY, Sharma AD, Malato Y, McManus MT, Esau CC, Koller E, Koliwad S, Lim LP, Maher JJ, Raffai RL, Willenbring H. A screen in mice uncovers repression of lipoprotein lipase by microRNA-29a as a mechanism for lipid distribution away from the liver. *Hepatology* 2015; **61**: 141-152 [PMID: 25131933 DOI: 10.1002/hep.27379]

59 **Yang YL**, Wang PW, Wang FS, Lin HY, Huang YH. miR-29a Modulates GSK3β/SIRT1-Linked Mitochondrial Proteostatic Stress to Ameliorate Mouse Non-Alcoholic Steatohepatitis. *Int J Mol Sci* 2020; **21** [PMID: 32961796 DOI: 10.3390/ijms21186884]

60 **Najafi-Shoushtari SH**, Kristo F, Li Y, Shioda T, Cohen DE, Gerszten RE, Näär AM. MicroRNA-33 and the SREBP host genes cooperate to control cholesterol homeostasis. *Science* 2010; **328**: 1566-1569 [PMID: 20466882 DOI: 10.1126/science.1189123]

61 **Price NL**, Singh AK, Rotllan N, Goedeke L, Wing A, Canfrán-Duque A, Diaz-Ruiz A, Araldi E, Baldán Á, Camporez JP, Suárez Y, Rodeheffer MS, Shulman GI, de Cabo R, Fernández-Hernando C. Genetic Ablation of miR-33 Increases Food Intake, Enhances Adipose Tissue Expansion, and Promotes Obesity and Insulin Resistance. *Cell Rep* 2018; **22**: 2133-2145 [PMID: 29466739 DOI: 10.1016/j.celrep.2018.01.074]

62 **Lendvai G**, Járomay K, Karácsony G, Halász T, Kovalszky I, Baghy K, Wittmann T, Schaff Z, Kiss A. Elevated miR-33a and miR-224 in steatotic chronic hepatitis C liver biopsies. *World J Gastroenterol* 2014; **20**: 15343-15350 [PMID: 25386083 DOI: 10.3748/wjg.v20.i41.15343]

63 **Erhartova D**, Cahova M, Dankova H, Heczkova M, Mikova I, Sticova E, Spicak J, Seda O, Trunecka P. Serum miR-33a is associated with steatosis and inflammation in patients with non-alcoholic fatty liver disease after liver transplantation. *PLoS One* 2019; **14**: e0224820 [PMID: 31703079 DOI: 10.1371/journal.pone.0224820]

64 **Vega-Badillo J**, Gutiérrez-Vidal R, Hernández-Pérez HA, Villamil-Ramírez H, León-Mimila P, Sánchez-Muñoz F, Morán-Ramos S, Larrieta-Carrasco E, Fernández-Silva I, Méndez-Sánchez N, Tovar AR, Campos-Pérez F, Villarreal-Molina T, Hernández-Pando R, Aguilar-Salinas CA, Canizales-Quinteros S. Hepatic miR-33a/miR-144 and their target gene ABCA1 are associated with steatohepatitis in morbidly obese subjects. *Liver Int* 2016; **36**: 1383-1391 [PMID: 26945479 DOI: 10.1111/liv.13109]

65 **Pan JH**, Cha H, Tang J, Lee S, Lee SH, Le B, Redding MC, Kim S, Batish M, Kong BC, Lee JH, Kim JK. The role of microRNA-33 as a key regulator in hepatic lipogenesis signaling and a potential serological biomarker for NAFLD with excessive dietary fructose consumption in C57BL/6N mice. *Food Funct* 2021; **12**: 656-667 [PMID: 33404569 DOI: 10.1039/d0fo02286a]

66 **Rayner KJ**, Esau CC, Hussain FN, McDaniel AL, Marshall SM, van Gils JM, Ray TD, Sheedy FJ, Goedeke L, Liu X, Khatsenko OG, Kaimal V, Lees CJ, Fernandez-Hernando C, Fisher EA, Temel RE, Moore KJ. Inhibition of miR-33a/b in non-human primates raises plasma HDL and lowers VLDL triglycerides. *Nature* 2011; **478**: 404-407 [PMID: 22012398 DOI: 10.1038/nature10486]

67 **Rotllan N**, Ramírez CM, Aryal B, Esau CC, Fernández-Hernando C. Therapeutic silencing of microRNA-33 inhibits the progression of atherosclerosis in Ldlr-/- mice--brief report. *Arterioscler Thromb Vasc Biol* 2013; **33**: 1973-1977 [PMID: 23702658 DOI: 10.1161/ATVBAHA.113.301732]

68 **Karunakaran D**, Richards L, Geoffrion M, Barrette D, Gotfrit RJ, Harper ME, Rayner KJ. Therapeutic Inhibition of miR-

33 Promotes Fatty Acid Oxidation but Does Not Ameliorate Metabolic Dysfunction in Diet-Induced Obesity. *Arterioscler Thromb Vasc Biol* 2015; **35**: 2536-2543 [PMID: 26427794 DOI: 10.1161/ATVBAHA.115.306404]

69 **Goedeke L**, Salerno A, Ramírez CM, Guo L, Allen RM, Yin X, Langley SR, Esau C, Wanschel A, Fisher EA, Suárez Y, Baldán A, Mayr M, Fernández-Hernando C. Long-term therapeutic silencing of miR-33 increases circulating triglyceride levels and hepatic lipid accumulation in mice. *EMBO Mol Med* 2014; **6**: 1133-1141 [PMID: 25038053 DOI: 10.15252/emmm.201404046]

70 **Allen RM**, Marquart TJ, Jesse JJ, Baldán A. Control of very low-density lipoprotein secretion by N-ethylmaleimide-sensitive factor and miR-33. *Circ Res* 2014; **115**: 10-22 [PMID: 24753547 DOI: 10.1161/CIRCRESAHA.115.303100]

71 **Horie T**, Nishino T, Baba O, Kuwabara Y, Nakao T, Nishiga M, Usami S, Izuhara M, Sowa N, Yahagi N, Shimano H, Matsumura S, Inoue K, Marusawa H, Nakamura T, Hasegawa K, Kume N, Yokode M, Kita T, Kimura T, Ono K. MicroRNA-33 regulates sterol regulatory element-binding protein 1 expression in mice. *Nat Commun* 2013; **4**: 2883 [PMID: 24300912 DOI: 10.1038/ncomms3883]

72 **Cheung O**, Puri P, Eicken C, Contos MJ, Mirshahi F, Maher JW, Kellum JM, Min H, Luketic VA, Sanyal AJ. Nonalcoholic steatohepatitis is associated with altered hepatic MicroRNA expression. *Hepatology* 2008; **48**: 1810-1820 [PMID: 19030170 DOI: 10.1002/hep.22569]

73 **Xu Y**, Zalzala M, Xu J, Li Y, Yin L, Zhang Y. A metabolic stress-inducible miR-34a-HNF4α pathway regulates lipid and lipoprotein metabolism. *Nat Commun* 2015; **6**: 7466 [PMID: 26100857 DOI: 10.1038/ncomms8466]

74 **Miyaaki H**, Ichikawa T, Kamo Y, Taura N, Honda T, Shibata H, Milazzo M, Fornari F, Gramantieri L, Bolondi L, Nakao K. Significance of serum and hepatic microRNA-122 levels in patients with non-alcoholic fatty liver disease. *Liver Int* 2014; **34**: e302-e307 [PMID: 24313922 DOI: 10.1111/liv.12429]

75 **Ding J**, Li M, Wan X, Jin X, Chen S, Yu C, Li Y. Effect of miR-34a in regulating steatosis by targeting PPARα expression in nonalcoholic fatty liver disease. *Sci Rep* 2015; **5**: 13729 [PMID: 26330104 DOI: 10.1038/srep13729]

76 **Simão AL**, Afonso MB, Rodrigues PM, Gama-Carvalho M, Machado MV, Cortez-Pinto H, Rodrigues CMP, Castro RE. Skeletal muscle miR-34a/SIRT1:AMPK axis is activated in experimental and human non-alcoholic steatohepatitis. *J Mol Med (Berl)* 2019; **97**: 1113-1126 [PMID: 31139863 DOI: 10.1007/s00109-019-01796-8]

77 **Ezaz G**, Trivedi HD, Connelly MA, Filozof C, Howard K, L Parrish M, Kim M, Herman MA, Nasser I, Afdhal NH, Jiang ZG, Lai M. Differential Associations of Circulating MicroRNAs With Pathogenic Factors in NAFLD. *Hepatol Commun* 2020; **4**: 670-680 [PMID: 32363318 DOI: 10.1002/hep4.1501]

78 **Salvoza NC**, Klinzing DC, Gopez-Cervantes J, Baclig MO. Association of Circulating Serum miR-34a and miR-122 with Dyslipidemia among Patients with Non-Alcoholic Fatty Liver Disease. *PLoS One* 2016; **11**: e0153497 [PMID: 27077736 DOI: 10.1371/journal.pone.0153497]

79 **Oses M**, Margareto Sanchez J, Portillo MP, Aguilera CM, Labayen I. Circulating miRNAs as Biomarkers of Obesity and Obesity-Associated Comorbidities in Children and Adolescents: A Systematic Review. *Nutrients* 2019; **11** [PMID: 31783635 DOI: 10.3390/nu11122890]

80 **Pirola CJ**, Fernández Gianotti T, Castaño GO, Mallardi P, San Martino J, Mora Gonzalez Lopez Ledesma M, Flichman D, Mirshahi F, Sanyal AJ, Sookoian S. Circulating microRNA signature in non-alcoholic fatty liver disease: from serum non-coding RNAs to liver histology and disease pathogenesis. *Gut* 2015; **64**: 800-812 [PMID: 24973316 DOI: 10.1136/gutjnl-2014-306996]

81 **Hsu SH**, Wang B, Kota J, Yu J, Costinean S, Kutay H, Yu L, Bai S, La Perle K, Chivukula RR, Mao H, Wei M, Clark KR, Mendell JR, Caligiuri MA, Jacob ST, Mendell JT, Ghoshal K. Essential metabolic, anti-inflammatory, and anti-tumorigenic functions of miR-122 in liver. *J Clin Invest* 2012; **122**: 2871-2883 [PMID: 22820288 DOI: 10.1172/JCI63539]

82 **Krützfeldt J**, Rajewsky N, Braich R, Rajeev KG, Tuschl T, Manoharan M, Stoffel M. Silencing of microRNAs in vivo with 'antagomirs'. *Nature* 2005; **438**: 685-689 [PMID: 16258535 DOI: 10.1038/nature04303]

83 **Esau C**, Davis S, Murray SF, Yu XX, Pandey SK, Pear M, Watts L, Booten SL, Graham M, McKay R, Subramaniam A, Propp S, Lollo BA, Freier S, Bennett CF, Bhanot S, Monia BP. miR-122 regulation of lipid metabolism revealed by in vivo antisense targeting. *Cell Metab* 2006; **3**: 87-98 [PMID: 16459310 DOI: 10.1016/j.cmet.2006.01.005]

84 **Tsai WC**, Hsu SD, Hsu CS, Lai TC, Chen SJ, Shen R, Huang Y, Chen HC, Lee CH, Tsai TF, Hsu MT, Wu JC, Huang HD, Shiao MS, Hsiao M, Tsou AP. MicroRNA-122 plays a critical role in liver homeostasis and hepatocarcinogenesis. *J Clin Invest* 2012; **122**: 2884-2897 [PMID: 22820290 DOI: 10.1172/JCI63455]

85 **Cermelli S**, Ruggieri A, Marrero JA, Ioannou GN, Beretta L. Circulating microRNAs in patients with chronic hepatitis C and non-alcoholic fatty liver disease. *PLoS One* 2011; **6**: e23937 [PMID: 21886843 DOI: 10.1371/journal.pone.0023937]

86 **Pirola CJ**, Gianotti TF, Castaño GO, Sookoian S. Circulating MicroRNA-122 signature in nonalcoholic fatty liver disease and cardiovascular disease: a new endocrine system in metabolic syndrome. *Hepatology* 2013; **57**: 2545-2547 [PMID: 23111985 DOI: 10.1002/hep.26116]

87 **Jones A**, Danielson KM, Benton MC, Ziegler O, Shah R, Stubbs RS, Das S, Macartney-Coxson D. miRNA Signatures of Insulin Resistance in Obesity. *Obesity (Silver Spring)* 2017; **25**: 1734-1744 [PMID: 28834285 DOI: 10.1002/oby.21950]

88 **Willeit P**, Skroblin P, Moschen AR, Yin X, Kaudewitz D, Zampetaki A, Barwari T, Whitehead M, Ramírez CM, Goedeke L, Rotllan N, Bonora E, Hughes AD, Santer P, Fernández-Hernando C, Tilg H, Willeit J, Kiechl S, Mayr M. Circulating MicroRNA-122 Is Associated With the Risk of New-Onset Metabolic Syndrome and Type 2 Diabetes. *Diabetes* 2017; **66**: 347-357 [PMID: 27899485 DOI: 10.2337/db16-0731]

89 **Gallo A**, Tandon M, Alevizos I, Illei GG. The majority of microRNAs detectable in serum and saliva is concentrated in exosomes. *PLoS One* 2012; **7**: e30679 [PMID: 22427800 DOI: 10.1371/journal.pone.0030679]

90 **Chen Y**, Siegel F, Kipschull S, Haas B, Fröhlich H, Meister G, Pfeifer A. miR-155 regulates differentiation of brown and beige adipocytes *via* a bistable circuit. *Nat Commun* 2013; **4**: 1769 [PMID: 23612310 DOI: 10.1038/ncomms2742]

91 **Chen JQ**, Papp G, Szodoray P, Zeher M. The role of microRNAs in the pathogenesis of autoimmune diseases. *Autoimmun Rev* 2016; **15**: 1171-1180 [PMID: 27639156 DOI: 10.1016/j.autrev.2016.09.003]

92 **Miller AM**, Gilchrist DS, Nijjar J, Araldi E, Ramirez CM, Lavery CA, Fernández-Hernando C, McInnes IB, Kurowska-Stolarska M. MiR-155 has a protective role in the development of non-alcoholic hepatosteatosis in mice. *PLoS One* 2013;

8: e72324 [PMID: 23991091 DOI: 10.1371/journal.pone.0072324]
93 **Lin X**, Jia J, Du T, Li W, Wang X, Wei J, Lin X, Zeng H, Yao L, Chen X, Zhuang J, Weng J, Liu Y, Lin J, Wu Q, Wang W, Yao K, Xu K, Xiao D. Overexpression of miR-155 in the liver of transgenic mice alters the expression profiling of hepatic genes associated with lipid metabolism. *PLoS One* 2015; **10**: e0118417 [PMID: 25799309 DOI: 10.1371/journal.pone.0118417]
94 **Wang L**, Zhang N, Wang Z, Ai DM, Cao ZY, Pan HP. Decreased MiR-155 Level in the Peripheral Blood of Non-Alcoholic Fatty Liver Disease Patients may Serve as a Biomarker and may Influence LXR Activity. *Cell Physiol Biochem* 2016; **39**: 2239-2248 [PMID: 27832630 DOI: 10.1159/000447917]
95 **Csak T**, Bala S, Lippai D, Kodys K, Catalano D, Iracheta-Vellve A, Szabo G. MicroRNA-155 Deficiency Attenuates Liver Steatosis and Fibrosis without Reducing Inflammation in a Mouse Model of Steatohepatitis. *PLoS One* 2015; **10**: e0129251 [PMID: 26042593 DOI: 10.1371/journal.pone.0129251]
96 **Bala S**, Ganz M, Babuta M, Zhuang Y, Csak T, Calenda CD, Szabo G. Steatosis, inflammasome upregulation, and fibrosis are attenuated in miR-155 deficient mice in a high fat-cholesterol-sugar diet-induced model of NASH. *Lab Invest* 2021; **101**: 1540-1549 [PMID: 34453120 DOI: 10.1038/s41374-021-00626-1]
97 **Ying W**, Riopel M, Bandyopadhyay G, Dong Y, Birmingham A, Seo JB, Ofrecio JM, Wollam J, Hernandez-Carretero A, Fu W, Li P, Olefsky JM. Adipose Tissue Macrophage-Derived Exosomal miRNAs Can Modulate In Vivo and In Vitro Insulin Sensitivity. *Cell* 2017; **171**: 372-384.e12 [PMID: 28942920 DOI: 10.1016/j.cell.2017.08.035]
98 **Coll M**, El Taghdouini A, Perea L, Mannaerts I, Vila-Casadesús M, Blaya D, Rodrigo-Torres D, Affò S, Morales-Ibanez O, Graupera I, Lozano JJ, Najimi M, Sokal E, Lambrecht J, Ginès P, van Grunsven LA, Sancho-Bru P. Integrative miRNA and Gene Expression Profiling Analysis of Human Quiescent Hepatic Stellate Cells. *Sci Rep* 2015; **5**: 11549 [PMID: 26096707 DOI: 10.1038/srep11549]
99 **Tan Y**, Ge G, Pan T, Wen D, Gan J. A pilot study of serum microRNAs panel as potential biomarkers for diagnosis of nonalcoholic fatty liver disease. *PLoS One* 2014; **9**: e105192 [PMID: 25141008 DOI: 10.1371/journal.pone.0105192]
100 **Liu XL**, Pan Q, Cao HX, Xin FZ, Zhao ZH, Yang RX, Zeng J, Zhou H, Fan JG. Lipotoxic Hepatocyte-Derived Exosomal MicroRNA 192-5p Activates Macrophages Through Rictor/Akt/Forkhead Box Transcription Factor O1 Signaling in Nonalcoholic Fatty Liver Disease. *Hepatology* 2020; **72**: 454-469 [PMID: 31782176 DOI: 10.1002/hep.31050]
101 **Wang X**, He Y, Mackowiak B, Gao B. MicroRNAs as regulators, biomarkers and therapeutic targets in liver diseases. *Gut* 2021; **70**: 784-795 [PMID: 33127832 DOI: 10.1136/gutjnl-2020-322526]
102 **Dumortier O**, Fabris G, Pisani DF, Casamento V, Gautier N, Hinault C, Lebrun P, Duranton C, Tauc M, Dalle S, Kerr-Conte J, Pattou F, Prentki M, Van Obberghen E. microRNA-375 regulates glucose metabolism-related signaling for insulin secretion. *J Endocrinol* 2020; **244**: 189-200 [PMID: 31697642 DOI: 10.1530/JOE-19-0180]
103 **Lei L**, Zhou C, Yang X, Li L. Down-regulation of microRNA-375 regulates adipokines and inhibits inflammatory cytokines by targeting AdipoR2 in non-alcoholic fatty liver disease. *Clin Exp Pharmacol Physiol* 2018; **45**: 819-831 [PMID: 29569260 DOI: 10.1111/1440-1681.12940]
104 **Quinn JJ**, Chang HY. Unique features of long non-coding RNA biogenesis and function. *Nat Rev Genet* 2016; **17**: 47-62 [PMID: 26666209 DOI: 10.1038/nrg.2015.10]
105 **Tsai MC**, Manor O, Wan Y, Mosammaparast N, Wang JK, Lan F, Shi Y, Segal E, Chang HY. Long noncoding RNA as modular scaffold of histone modification complexes. *Science* 2010; **329**: 689-693 [PMID: 20616235 DOI: 10.1126/science.1192002]
106 **Wang KC**, Chang HY. Molecular mechanisms of long noncoding RNAs. *Mol Cell* 2011; **43**: 904-914 [PMID: 21925379 DOI: 10.1016/j.molcel.2011.08.018]
107 **Huarte M**. The emerging role of lncRNAs in cancer. *Nat Med* 2015; **21**: 1253-1261 [PMID: 26540387 DOI: 10.1038/nm.3981]
108 **Giovarelli M**, Bucci G, Ramos A, Bordo D, Wilusz CJ, Chen CY, Puppo M, Briata P, Gherzi R. H19 long noncoding RNA controls the mRNA decay promoting function of KSRP. *Proc Natl Acad Sci U S A* 2014; **111**: E5023-E5028 [PMID: 25385579 DOI: 10.1073/pnas.1415098111]
109 **Li X**, Liu R. Long non-coding RNA H19 in the liver-gut axis: A diagnostic marker and therapeutic target for liver diseases. *Exp Mol Pathol* 2020; **115**: 104472 [PMID: 32454104 DOI: 10.1016/j.yexmp.2020.104472]
110 **Liu C**, Yang Z, Wu J, Zhang L, Lee S, Shin DJ, Tran M, Wang L. Long noncoding RNA H19 interacts with polypyrimidine tract-binding protein 1 to reprogram hepatic lipid homeostasis. *Hepatology* 2018; **67**: 1768-1783 [PMID: 29140550 DOI: 10.1002/hep.29654]
111 **Liu J**, Tang T, Wang GD, Liu B. LncRNA-H19 promotes hepatic lipogenesis by directly regulating miR-130a/PPARγ axis in non-alcoholic fatty liver disease. *Biosci Rep* 2019; **39** [PMID: 31064820 DOI: 10.1042/BSR20181722]
112 **Wang H**, Cao Y, Shu L, Zhu Y, Peng Q, Ran L, Wu J, Luo Y, Zuo G, Luo J, Zhou L, Shi Q, Weng Y, Huang A, He TC, Fan J. Long non-coding RNA (lncRNA) H19 induces hepatic steatosis through activating MLXIPL and mTORC1 networks in hepatocytes. *J Cell Mol Med* 2020; **24**: 1399-1412 [PMID: 31809000 DOI: 10.1111/jcmm.14818]
113 **Zhao XY**, Li S, Wang GX, Yu Q, Lin JD. A long noncoding RNA transcriptional regulatory circuit drives thermogenic adipocyte differentiation. *Mol Cell* 2014; **55**: 372-382 [PMID: 25002143 DOI: 10.1016/j.molcel.2014.06.004]
114 **Zhao XY**, Xiong X, Liu T, Mi L, Peng X, Rui C, Guo L, Li S, Li X, Lin JD. Long noncoding RNA licensing of obesity-linked hepatic lipogenesis and NAFLD pathogenesis. *Nat Commun* 2018; **9**: 2986 [PMID: 30061575 DOI: 10.1038/s41467-018-05383-2]
115 **Tang S**, Zhu W, Zheng F, Gui W, Zhang W, Lin X, Li H. The Long Noncoding RNA Blnc1 Protects Against Diet-Induced Obesity by Promoting Mitochondrial Function in White Fat. *Diabetes Metab Syndr Obes* 2020; **13**: 1189-1201 [PMID: 32368112 DOI: 10.2147/DMSO.S248692]
116 **Li D**, Cheng M, Niu Y, Chi X, Liu X, Fan J, Fan H, Chang Y, Yang W. Identification of a novel human long non-coding RNA that regulates hepatic lipid metabolism by inhibiting SREBP-1c. *Int J Biol Sci* 2017; **13**: 349-357 [PMID: 28367099 DOI: 10.7150/ijbs.16635]
117 **Hegele RA**. Plasma lipoproteins: genetic influences and clinical implications. *Nat Rev Genet* 2009; **10**: 109-121 [PMID: 19139765 DOI: 10.1038/nrg2481]

118 **Yan C**, Chen J, Chen N. Long noncoding RNA MALAT1 promotes hepatic steatosis and insulin resistance by increasing nuclear SREBP-1c protein stability. *Sci Rep* 2016; **6**: 22640 [PMID: 26935028 DOI: 10.1038/srep22640]

119 **Leti F**, Legendre C, Still CD, Chu X, Petrick A, Gerhard GS, DiStefano JK. Altered expression of MALAT1 lncRNA in nonalcoholic steatohepatitis fibrosis regulates CXCL5 in hepatic stellate cells. *Transl Res* 2017; **190**: 25-39.e21 [PMID: 28993096 DOI: 10.1016/j.trsl.2017.09.001]

120 **Sookoian S**, Flichman D, Garaycoechea ME, San Martino J, Castaño GO, Pirola CJ. Metastasis-associated lung adenocarcinoma transcript 1 as a common molecular driver in the pathogenesis of nonalcoholic steatohepatitis and chronic immune-mediated liver damage. *Hepatol Commun* 2018; **2**: 654-665 [PMID: 29881817 DOI: 10.1002/hep4.1184]

121 **Lai MC**, Yang Z, Zhou L, Zhu QQ, Xie HY, Zhang F, Wu LM, Chen LM, Zheng SS. Long non-coding RNA MALAT-1 overexpression predicts tumor recurrence of hepatocellular carcinoma after liver transplantation. *Med Oncol* 2012; **29**: 1810-1816 [PMID: 21678027 DOI: 10.1007/s12032-011-0004-z]

122 **Konishi H**, Ichikawa D, Yamamoto Y, Arita T, Shoda K, Hiramoto H, Hamada J, Itoh H, Fujita Y, Komatsu S, Shiozaki A, Ikoma H, Ochiai T, Otsuji E. Plasma level of metastasis-associated lung adenocarcinoma transcript 1 is associated with liver damage and predicts development of hepatocellular carcinoma. *Cancer Sci* 2016; **107**: 149-154 [PMID: 26614531 DOI: 10.1111/cas.12854]

123 **Bu FT**, Wang A, Zhu Y, You HM, Zhang YF, Meng XM, Huang C, Li J. LncRNA NEAT1: Shedding light on mechanisms and opportunities in liver diseases. *Liver Int* 2020; **40**: 2612-2626 [PMID: 32745314 DOI: 10.1111/liv.14629]

124 **Wang X**. Down-regulation of lncRNA-NEAT1 alleviated the non-alcoholic fatty liver disease *via* mTOR/S6K1 signaling pathway. *J Cell Biochem* 2018; **119**: 1567-1574 [PMID: 28771824 DOI: 10.1002/jcb.26317]

125 **Fu X**, Zhu J, Zhang L, Shu J. Long non-coding RNA NEAT1 promotes steatosis *via* enhancement of estrogen receptor alpha-mediated AQP7 expression in HepG2 cells. *Artif Cells Nanomed Biotechnol* 2019; **47**: 1782-1787 [PMID: 31062612 DOI: 10.1080/21691401.2019.1604536]

126 **Chen X**, Tan XR, Li SJ, Zhang XX. LncRNA NEAT1 promotes hepatic lipid accumulation *via* regulating miR-146a-5p/ROCK1 in nonalcoholic fatty liver disease. *Life Sci* 2019; **235**: 116829 [PMID: 31484042 DOI: 10.1016/j.lfs.2019.116829]

127 **Jin SS**, Lin XF, Zheng JZ, Wang Q, Guan HQ. lncRNA NEAT1 regulates fibrosis and inflammatory response induced by nonalcoholic fatty liver by regulating miR-506/GLI3. *Eur Cytokine Netw* 2019; **30**: 98-106 [PMID: 31957704 DOI: 10.1684/ecn.2019.0432]

128 **Zhang Z**, Wen H, Peng B, Weng J, Zeng F. Downregulated microRNA-129-5p by Long Non-coding RNA NEAT1 Upregulates PEG3 Expression to Aggravate Non-alcoholic Steatohepatitis. *Front Genet* 2020; **11**: 563265 [PMID: 33574830 DOI: 10.3389/fgene.2020.563265]

129 **Guo J**, Fang W, Sun L, Lu Y, Dou L, Huang X, Tang W, Yu L, Li J. Ultraconserved element uc.372 drives hepatic lipid accumulation by suppressing miR-195/miR4668 maturation. *Nat Commun* 2018; **9**: 612 [PMID: 29426937 DOI: 10.1038/s41467-018-03072-8]

130 **He Y**, Wu YT, Huang C, Meng XM, Ma TT, Wu BM, Xu FY, Zhang L, Lv XW, Li J. Inhibitory effects of long noncoding RNA MEG3 on hepatic stellate cells activation and liver fibrogenesis. *Biochim Biophys Acta* 2014; **1842**: 2204-2215 [PMID: 25201080 DOI: 10.1016/j.bbadis.2014.08.015]

131 **Huang P**, Huang FZ, Liu HZ, Zhang TY, Yang MS, Sun CZ. LncRNA MEG3 functions as a ceRNA in regulating hepatic lipogenesis by competitively binding to miR-21 with LRP6. *Metabolism* 2019; **94**: 1-8 [PMID: 30711569 DOI: 10.1016/j.metabol.2019.01.018]

132 **Zou D**, Liu L, Zeng Y, Wang H, Dai D, Xu M. LncRNA MEG3 up-regulates SIRT6 by ubiquitinating EZH2 and alleviates nonalcoholic fatty liver disease. *Cell Death Discov* 2022; **8**: 103 [PMID: 35256601 DOI: 10.1038/s41420-022-00889-7]

133 **Zhang L**, Yang Z, Trottier J, Barbier O, Wang L. Long noncoding RNA MEG3 induces cholestatic liver injury by interaction with PTBP1 to facilitate shp mRNA decay. *Hepatology* 2017; **65**: 604-615 [PMID: 27770549 DOI: 10.1002/hep.28882]

134 **Cheng X**, Shihabudeen Haider Ali MS, Moran M, Viana MP, Schlichte SL, Zimmerman MC, Khalimonchuk O, Feinberg MW, Sun X. Long non-coding RNA Meg3 deficiency impairs glucose homeostasis and insulin signaling by inducing cellular senescence of hepatic endothelium in obesity. *Redox Biol* 2021; **40**: 101863 [PMID: 33508742 DOI: 10.1016/j.redox.2021.101863]

135 **Panzitt K**, Tschernatsch MM, Guelly C, Moustafa T, Stradner M, Strohmaier HM, Buck CR, Denk H, Schroeder R, Trauner M, Zatloukal K. Characterization of HULC, a novel gene with striking up-regulation in hepatocellular carcinoma, as noncoding RNA. *Gastroenterology* 2007; **132**: 330-342 [PMID: 17241883 DOI: 10.1053/j.gastro.2006.08.026]

136 **Shen X**, Guo H, Xu J, Wang J. Inhibition of lncRNA HULC improves hepatic fibrosis and hepatocyte apoptosis by inhibiting the MAPK signaling pathway in rats with nonalcoholic fatty liver disease. *J Cell Physiol* 2019; **234**: 18169-18179 [PMID: 30908654 DOI: 10.1002/jcp.28450]

137 **Gandhy SU**, Imanirad P, Jin UH, Nair V, Hedrick E, Cheng Y, Corton JC, Kim K, Safe S. Specificity protein (Sp) transcription factors and metformin regulate expression of the long non-coding RNA HULC. *Oncotarget* 2015; **6**: 26359-26372 [PMID: 26317792 DOI: 10.18632/oncotarget.4560]

138 **Feng W**, Gao C, Bi Y, Wu M, Li P, Shen S, Chen W, Yin T, Zhu D. Randomized trial comparing the effects of gliclazide, liraglutide, and metformin on diabetes with non-alcoholic fatty liver disease. *J Diabetes* 2017; **9**: 800-809 [PMID: 28332301 DOI: 10.1111/1753-0407.12555]

139 **Li P**, Chen X, Lin M, Huang D. Up-regulated HOTAIR induced by fatty acids inhibits PTEN expression and increases triglycerides accumulation in HepG2 cells. *Food Nutr Res* 2017; **61**: 1412794 [DOI: 10.1080/16546628.2017.1412794]

140 **Guo B**, Cheng Y, Yao L, Zhang J, Lu J, Qi H, Chen H. LncRNA HOTAIR regulates the lipid accumulation in non-alcoholic fatty liver disease *via* miR-130b-3p/ROCK1 axis. *Cell Signal* 2022; **90**: 110190 [PMID: 34774989 DOI: 10.1016/j.cellsig.2021.110190]

141 **Yu F**, Chen B, Dong P, Zheng J. HOTAIR Epigenetically Modulates PTEN Expression *via* MicroRNA-29b: A Novel

Mechanism in Regulation of Liver Fibrosis. *Mol Ther* 2017; **25**: 205-217 [PMID: 28129115 DOI: 10.1016/j.ymthe.2016.10.015]

142 **Chen Y**, Huang H, Xu C, Yu C, Li Y. Long Non-Coding RNA Profiling in a Non-Alcoholic Fatty Liver Disease Rodent Model: New Insight into Pathogenesis. *Int J Mol Sci* 2017; **18** [PMID: 28275212 DOI: 10.3390/ijms18010021]

143 **Chen Y**, Chen X, Gao J, Xu C, Xu P, Li Y, Zhu Y, Yu C. Long noncoding RNA FLRL2 alleviated nonalcoholic fatty liver disease through Arntl-Sirt1 pathway. *FASEB J* 2019; **33**: 11411-11419 [PMID: 31311301 DOI: 10.1096/fj.201900643RRR]

144 **Wu YL**, Li HF, Chen HH, Lin H. Emergent Roles of Circular RNAs in Metabolism and Metabolic Disorders. *Int J Mol Sci* 2022; **23** [PMID: 35162956 DOI: 10.3390/ijms23031032]

145 **Zaiou M**. The Emerging Role and Promise of Circular RNAs in Obesity and Related Metabolic Disorders. *Cells* 2020; **9** [PMID: 32560220 DOI: 10.3390/cells9061473]

146 **Xu ZX**, Li JZ, Li Q, Xu MY, Li HY. CircRNA608-microRNA222-PINK1 axis regulates the mitophagy of hepatic stellate cells in NASH related fibrosis. *Biochem Biophys Res Commun* 2022; **610**: 35-42 [PMID: 35436629 DOI: 10.1016/j.bbrc.2022.04.008]

147 **Jin X**, Gao J, Zheng R, Yu M, Ren Y, Yan T, Huang Y, Li Y. Antagonizing circRNA_002581-miR-122-CPEB1 axis alleviates NASH through restoring PTEN-AMPK-mTOR pathway regulated autophagy. *Cell Death Dis* 2020; **11**: 123 [PMID: 32054840 DOI: 10.1038/s41419-020-2293-7]

148 **Guo XY**, Chen JN, Sun F, Wang YQ, Pan Q, Fan JG. circRNA_0046367 Prevents Hepatoxicity of Lipid Peroxidation: An Inhibitory Role against Hepatic Steatosis. *Oxid Med Cell Longev* 2017; **2017**: 3960197 [PMID: 29018509 DOI: 10.1155/2017/3960197]

149 **Guo XY**, Sun F, Chen JN, Wang YQ, Pan Q, Fan JG. circRNA_0046366 inhibits hepatocellular steatosis by normalization of PPAR signaling. *World J Gastroenterol* 2018; **24**: 323-337 [PMID: 29391755 DOI: 10.3748/wjg.v24.i3.323]

150 **Guo XY**, He CX, Wang YQ, Sun C, Li GM, Su Q, Pan Q, Fan JG. Circular RNA Profiling and Bioinformatic Modeling Identify Its Regulatory Role in Hepatic Steatosis. *Biomed Res Int* 2017; **2017**: 5936171 [PMID: 28717649 DOI: 10.1155/2017/5936171]

151 **Li P**, Shan K, Liu Y, Zhang Y, Xu L. CircScd1 Promotes Fatty Liver Disease *via* the Janus Kinase 2/Signal Transducer and Activator of Transcription 5 Pathway. *Dig Dis Sci* 2019; **64**: 113-122 [PMID: 30259280 DOI: 10.1007/s10620-018-5290-2]

152 **Yang W**, Zhao J, Zhao Y, Li W, Zhao L, Ren Y, Ou R, Xu Y. Hsa_circ_0048179 attenuates free fatty acid-induced steatosis *via* hsa_circ_0048179/miR-188-3p/GPX4 signaling. *Aging (Albany NY)* 2020; **12**: 23996-24008 [PMID: 33221744 DOI: 10.18632/aging.104081]

153 **Ou Q**, Zhao Y, Zhou J, Wu X. Comprehensive circular RNA expression profiles in a mouse model of nonalcoholic steatohepatitis. *Mol Med Rep* 2019; **19**: 2636-2648 [PMID: 30720095 DOI: 10.3892/mmr.2019.9935]

154 **Chen Y**, Yuan B, Wu Z, Dong Y, Zhang L, Zeng Z. Microarray profiling of circular RNAs and the potential regulatory role of hsa_circ_0071410 in the activated human hepatic stellate cell induced by irradiation. *Gene* 2017; **629**: 35-42 [PMID: 28774651 DOI: 10.1016/j.gene.2017.07.078]

155 **Zhou Y**, Lv X, Qu H, Zhao K, Fu L, Zhu L, Ye G, Guo J. Preliminary screening and functional analysis of circular RNAs associated with hepatic stellate cell activation. *Gene* 2018; **677**: 317-323 [PMID: 30118889 DOI: 10.1016/j.gene.2018.08.052]

156 **Chen X**, Tan QQ, Tan XR, Li SJ, Zhang XX. Circ_0057558 promotes nonalcoholic fatty liver disease by regulating ROCK1/AMPK signaling through targeting miR-206. *Cell Death Dis* 2021; **12**: 809 [PMID: 34446693 DOI: 10.1038/s41419-021-04090-z]

157 **Zhao Q**, Liu J, Deng H, Ma R, Liao JY, Liang H, Hu J, Li J, Guo Z, Cai J, Xu X, Gao Z, Su S. Targeting Mitochondria-Located circRNA SCAR Alleviates NASH *via* Reducing mROS Output. *Cell* 2020; **183**: 76-93.e22 [PMID: 32931733 DOI: 10.1016/j.cell.2020.08.009]

158 **Liufu Z**, Zhao Y, Guo L, Miao G, Xiao J, Lyu Y, Chen Y, Shi S, Tang T, Wu CI. Redundant and incoherent regulations of multiple phenotypes suggest microRNAs' role in stability control. *Genome Res* 2017; **27**: 1665-1673 [PMID: 28904014 DOI: 10.1101/gr.222505.117]

World Journal of Gastroenterology

Submit a Manuscript: https://www.f6publishing.com

World J Gastroenterol 2022 September 21; 28(35): 5129-5140

DOI: 10.3748/wjg.v28.i35.5129

ISSN 1007-9327 (print) ISSN 2219-2840 (online)

MINIREVIEWS

Combination strategies for pharmacologic treatment of non-alcoholic steatohepatitis

Jaspreet Suri, Sebastian Borja, Joseph K Lim

Specialty type: Gastroenterology and hepatology

Provenance and peer review: Invited article; Externally peer reviewed.

Peer-review model: Single blind

Peer-review report's scientific quality classification

Grade A (Excellent): A
Grade B (Very good): 0
Grade C (Good): C
Grade D (Fair): 0
Grade E (Poor): 0

P-Reviewer: Ji G, China; Radford-Smith DE, Australia

Received: June 24, 2022
Peer-review started: June 24, 2022
First decision: July 11, 2022
Revised: July 26, 2022
Accepted: August 25, 2022
Article in press: August 25, 2022
Published online: September 21, 2022

Jaspreet Suri, Department of Gastroenterology, Norwalk Hospital, Norwalk, CT 06856, United States

Sebastian Borja, Department of Internal Medicine, Norwalk Hospital, Norwalk, CT 06850, United States

Joseph K Lim, Section of Digestive Diseases, Yale University School of Medicine, New Haven, CT 06520, United States

Corresponding author: Joseph K Lim, MD, Professor, Section of Digestive Diseases, Yale University School of Medicine, Yale Liver Center, 333 Cedar Street, LMP 1080, New Haven, CT 06520, United States. joseph.lim@yale.edu

Abstract

Non-alcoholic steatohepatitis (NASH) is defined as hepatic steatosis, inflammation, and hepatocyte injury with or without fibrosis. It has emerged as the second leading indication for liver transplantation with a rising death rate in the non-transplantable population. While there are many drugs in evaluation, currently no approved therapies are on the market for this condition. Given this importance, the Food and Drug Administration has provided formal guidance regarding drug development for stopping or reversing NASH or NASH associated fibrosis. The complex pathogenesis of NASH and its bidirectional relationship with metabolic syndrome has highlighted multiple drugs of interest that address metabolic, inflammatory, and fibrotic factors. A few promising liver specific targets include farnesoid X receptor agonists and peroxisome proliferator-activated receptor agonists. Previously studied drug classes such as glucagon-like peptide-1 analogs or sodium/glucose transport protein 2 inhibitors have also demonstrated ability to improve hepatic steatosis. Here we discuss current rationale, scientific work, and preliminary data in combining multiple drugs for the purposes of a multimodal attack on the pathogenesis of NASH. We highlight multiple Phase 2 and Phase 3 studies that demonstrate the potential to achieve a response rate higher than previously assessed monotherapies for this condition. Ultimately, one of these combination strategies may rise above in its safety and efficacy to become a part of a standardized approach to NASH.

Key Words: Non-alcoholic steatohepatitis; Fatty liver; Combination treatment; Drug therapy; Pharmacologic treatment; Clinical trials

©**The Author(s) 2022.** Published by Baishideng Publishing Group Inc. All rights reserved.

Core Tip: Multimodal combination approaches targeting two or more molecular pathways contributing to steatohepatitis and liver fibrosis are needed to augment efficacy of novel investigational drug regimens to achieve non-alcoholic steatohepatitis (NASH) resolution and NASH fibrosis improvement.

Citation: Suri J, Borja S, Lim JK. Combination strategies for pharmacologic treatment of non-alcoholic steatohepatitis. *World J Gastroenterol* 2022; 28(35): 5129-5140
URL: https://www.wjgnet.com/1007-9327/full/v28/i35/5129.htm
DOI: https://dx.doi.org/10.3748/wjg.v28.i35.5129

INTRODUCTION

Non-alcoholic steatohepatitis (NASH) is defined as the presence of ≥ 5% hepatic steatosis and inflammation with hepatocyte injury with or without fibrosis. Non-alcoholic fatty liver disease (NAFLD) represents a spectrum of pathology encompassing hepatic steatosis, steatohepatitis (NASH), and liver fibrosis, and poses a significant challenge to the medical community as there are currently no Food and Drug Administration (FDA) approved therapies available on the market. The definition of NAFLD includes the lack of secondary causes of hepatic steatosis such as alcohol consumption, steatogenic medication or hereditary liver disease. With NAFLD-associated death rates on the rise and NASH emerging as the second most common indication for liver transplantation, there has been heightened urgency to target various disease pathways in NASH development with the hopes of controlling the global impact of this disease[1,2]. With this rising importance, the FDA has published formal guidance regarding drug development aimed at stopping or reversing NASH and NASH fibrosis. The current drug development pipeline contains many mono-therapeutic options which address a wide range of metabolic, inflammatory, and fibrosis target pathways associated with NASH pathogenesis.

The pathophysiology of NASH is based on a bidirectional relationship between type 2 diabetes mellitus (T2DM), hypertension, obesity and dyslipidemia–or metabolic syndrome. This relationship contributes to excess free fatty acids generated from lipolysis and de novo lipogenesis in the liver, which creates lipotoxic species which induce oxidative stress, inflammasome activation, and fibrinogenesis[3] . Liver specific targets aimed at decreasing histologic inflammation or fibrosis such as farnesoid X receptor (FXR) agonists or peroxisome proliferator-activated receptor (PPAR) agonists are currently being evaluated for the treatment of NASH. These are in addition to drug classes such as glucagon-like peptide-1 (GLP-1) agonists and sodium/glucose transport protein 2 inhibitors that were initially approved for treatment of diabetes but have demonstrated the ability to decrease liver fat content[4,5]. While individually these agents have shown promise in early trials, there has been growing interest in pursuing a multimodal combination approach targeting two or more molecular targets/pathways responsible for NASH and NASH-associated liver fibrosis, particularly in context of modest effects of single agent strategies on histologic endpoints, with fewer than 50% of patients achieving either NASH resolution of fibrosis improvement of one stage or greater[6]. Therefore, this mini review will succinctly summarize the current efforts to examine combination strategies of drugs which may further augment therapeutic response in patients with NASH.

FDA APPROVAL PATHWAY

The FDA generally has two pathways for drug approval. The traditional pathway focuses on clinical benefit endpoints (*i.e.*, morbidity and mortality) and requires long term data. A brief review is provided in Figure 1. The accelerated approval pathway is intended to expedite the process for serious medical conditions with unmet needs. This pathway relies on short term surrogate markers that would reliably predict long term clinical outcomes to support drug approval. To inform clinical trial design for investigational drugs under evaluation for NASH, industry guidance was issued by the FDA in 2018 with a focus on patients with non-cirrhotic NASH with stage 2-3 liver fibrosis[7]. Although histologic endpoints were reinforced as required for assessment of surrogate endpoints for NASH and liver fibrosis, the agency encouraged the development and validation of noninvasive biomarkers in clinical trials to accelerate drug development. NASH was defined as a NAFLD activity score (NAS) greater than or equal to 4 with at least 1 point each in inflammation and ballooning degeneration, plus a NASH Clinical Research Network fibrosis score greater than stage 1 fibrosis but less than stage 4 for enrollment in these trials. Lastly, the primary regulatory endpoints required to support accelerated approval include: (1) NASH resolution on histology (NAS less than 4 with individual components scores of 0 for

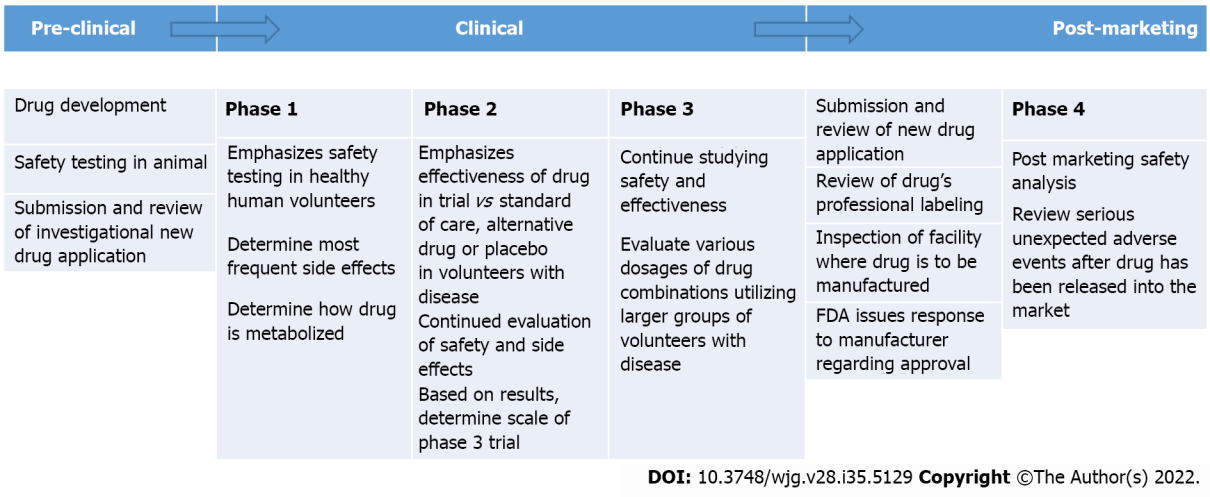


Figure 1 Flow diagram of standard Food and Drug Administration drug approval process.

ballooning degeneration and 0-1 for inflammation) without worsening fibrosis; (2) Improvement in liver fibrosis greater than or equal to one stage without worsening NASH; or (3) NASH resolution and improvement in fibrosis by one stage or greater. Clinical benefit for these drugs was defined as superiority to placebo in delayed disease progression measured by a composite endpoint including progression to cirrhosis, hepatic decompensation, change in MELD score, liver transplantation, or all-cause mortality.

DRUGS IN DEVELOPMENT–PHASE 2

Key phase 2 trials for NASH therapeutics are summarized in Table 1. In brief, one major class being pursued is fibroblast growth factor 21 (FGF21) agonists such as pegbelfermin. FGF21 is endogenously produced by the liver and has a pleiotropic effect on metabolism that may benefit patients with NASH. Endogenous FGF21 concentrations are elevated as much as 10-fold in patients with obesity, NAFLD or NASH, leading to the hypothesis that these may represent an FGF21-resistant state which may benefit from exogenous stimulation to improve insulin sensitivity and lipid metabolism[8] . GLP-1 is an incretin hormone made by intestinal cells post prandially for which receptors are predominantly in the pancreas, adipose tissue and brain. It regulates plasma glucose by stimulating glucose release and inhibiting glucagon secretion. GLP-1 agonists have previously shown to improve hepatic steatosis, decrease liver inflammation, and ameliorate insulin resistance in murine models of fatty liver disease. Semaglutide and liraglutide have shown promising results with statistically significant NASH improvement or resolution compared to placebo[9,10]. Norursodeoxycholic acid is an orally administered side chain-shortened homologue of ursodeoxycholic acid that undergoes hepatic enrichment with hepatoprotective, anti-inflammatory, and antifibrotic activity. It has shown significant reduction of serum alanine aminotransferase (ALT) within 12 wk of treatment when compared with placebo, encouraging further investigation[11]. Aldafermin is an analogue of fibroblast growth factor 19 (FGF19) which regulates bile acid metabolism and fat storage in the liver. FGF19 levels are lower in patients with NAFLD and insulin resistance. Activation of the FGF19 pathway has been shown to improve insulin sensitivity and liver steatosis. In a 24-wk placebo-controlled trial, the aldafermin group experienced a significant reduction in absolute liver fat content compared with placebo (P = 0.002) and fibrosis improvement of at least 1 stage (38% *vs* 18%, P = 0.10)[12]. The currently ongoing phase 2b ALPINE 4 study is designed to assess the efficacy, safety and tolerability of this agent (NCT04210245).

FXR agonists, which bind to the transcription factor FXR to help regulate bile acid metabolism are in multiple phases of clinical trial investigation. The FXR agonist tropifexor has demonstrated a robust and dose-dependent decrease in ALT, hepatic fat fractionation, and body weight with good safety and tolerability after 12 wk of treatment in a phase 2 trial[13]. The PPARα, β/δ and γ, play a central role in the regulation of glucose and lipid metabolism and of the inflammatory and fibrogenic pathways which contribute to NASH pathogenesis. Lanifibranor (IVA337), a pan-PPAR agonist, combines pharmacological effects that could improve fatty acid oxidation, dyslipidemia, and insulin sensitivity, and has demonstrated anti-inflammatory, antifibrotic and hepatoprotective effects in preclinical models and phase 1/2 trials. TVB-2640 is an orally bioavailable, first-in-class fatty acid synthase (FASN) inhibitor. FASN is a key enzyme in the de novo lipogenesis pathway that is responsible for the synthesis of excess fat and activation of fibrogenic and inflammatory mechanisms in the liver of patients with NASH. TVB-2640 demonstrated significant improvement in several NASH endpoints in the FASCINATE-1 trial as

Table 1 Phase 2 trials in non-alcoholic steatohepatitis

Trial name/NCT number	Manufacturer	Drugs	Mechanism of action	Enrollment (targeted)	Study arms	Duration	Primary or relevant end point(s)	Results/SE
NCT03976401	Akero Therapeutics	AKR-001	FGF 21 receptor agonist	80	(1) AKR-001 50 mg QD; and (2) Placebo	112	Change in liver fat fraction measured by MRI-PDFF	Ongoing
NCT04541186	89bio	BIO89-100	FGF 21 receptor agonist	90	(1) BIO89-100 (QW or every 2 wk); and (2) Placebo	112	Change in various lab parameters TG, LDL, HDL, fasting glucose. Change in liver fat fraction measured by MRI-PDFF	Ongoing
NCT02097277	Bristol-Myers Squibb	Pegbelfermin (BMS-986036)	FGF 21 receptor agonist	120	(1) Pegbelfermin 1 mg QD; (2) Pegbelfermin 5 mg QD; (3) Pegbelfermin 20 mg QD; (4) Pegbelfermin 20 mg weekly; and (5) Placebo	84	Safety, tolerability, and change in HbA1c. Change in insulin sensitivity, lipids, adiponectin, and disease progression biomarkers	No significant effects of pegbelfermin versus placebo on HbA1c. Pegbelfermin 20 mg/d significantly improved high-density lipoprotein cholesterol and triglycerides. Most frequent adverse events were injection-site bruising and diarrhea
NCT01237119	Novo Nordisk	Liraglutide	GLP-1analogue	52	(1) Liraglutide 1.8 mg SC QD; and (2) Placebo	336	Resolution of NASH without worsening fibrosis	39% who received liraglutide and underwent end-of-treatment liver biopsy had resolution of definite non-alcoholic steatohepatitis compared with 9% in placebo (P = 0 019). Side efffects diarrhea and loss of appetite
NCT02970942	Novo Nordisk	Semaglutide	GLP-1 analogue	320	(1) Semaglutide 0.1 mg SC QD; (2) Semaglutide 0.2 mg SC QD; (3) Semaglutide 0.4 mg SC QD; and (4) Placebo	504	Resolution of NASH without worsening fibrosis. Improvement in fibrosis, LFTs, A1c level	NASH resolution was achieved in 40% in the 0.1-mg group, 36% in the 0.2-mg group, 59% in the 0.4-mg group, and 17% in the placebo group (P < 0.001 for semaglutide 0.4 mg *vs* placebo). Side effects including nausea, constipation, and vomiting which was higher in the 0.4-mg group
2013-004605-38	Dr Falk Pharma GmbH	Norursodeoxycholic acid	homologue of ursodeoxycholic acid, undergoes hepatic enrichment with hepatoprotective, anti-inflammatory, and antifibrotic activity	198	(1) 500 mg norursodeoxycholic acid QD; (2) 1500 mg norursodeoxycholic acid QD; and (3) Placebo	112	Change in ALT levels	Dose-dependent reduction in ALT with norursodeoxycholic acid versus placebo, with a significant effect in the 1500 mg group (P < 0.0001). Side effects included headache, gastrointestinal disorders, and infections
COHORT 4/NCT02443116	NGM Biopharmaceuticals	Aldafermin	Analog of fibroblast growth factor 19, inhibits bile acid synthesis and regulates metabolic homeostasis	78	(1) aldafermin 1 mg QD; and (2) Placebo	168	Improvement in liver fibrosis of greater or equal to one stage with no worsening of NASH	Aldafermin group with higher rate of liver fat content reduction compared to placebo (7.7% *vs* 2.7%, P = 0.02). Aldafermin produced significantly greater decrease in bile acids, liver enzymes. Fibrosis improvement without worsening NASH higher in aldafermin group (38% *vs* 18%, P = 0.10). NASH resolution without worsening fibrosis higher in aldafermin group (24% *vs* 9%, P = 0.20). Side effects include diarrhea, headache, abdominal distation and peripheral edema

ALPINE 4/NCT04210245	NGM Biopharmaceuticals	Aldafermin	Analog of fibroblast growth factor 19, inhibits bile acid synthesis and regulates metabolic homeostasis	72	(1) Aldafermin 0.3 mg QD; (2) Aldafermin 1 mg QD; (3) Aldafermin 3 mg; and (4) Placebo	168	Improvement in liver fibrosis of greater or equal to one stage with no worsening of NASH	Ongoing
FLIGHT-FXR/NCT02855164	Novartis Pharmaceutical	Tropifexor	FXR agonist	152	(1) TXR 140 g QD; (2) TXR 200gr QD; and (3) Placebo	84	Changes in liver fat fraction, liver enzymes, body weight	End point achieved in TXR 800 mg *vs* 1200 mg *vs* Placebo (51% *vs* 55% *vs* 34%, $P = 0.001$). Side effects include mild pruritus and increase in LDL
NATIVE/NCT03008070	Inventiva	Lanifibranor	PPAR agonist	247	(1) Lanifibranor 800 mg QD; (2) Lanifibranor 1200 mg QD; and (3) Placebo	168	Responder analysis based on the improvement of the SAF activity score	L800 mg *vs* 1200 mg *vs* Placebo (51% *vs* 55% *vs* 34%) $P = 0.0015$. SE weight gain, peripheral edema
FASCINATE-1/NCT03938246	Sagimet Biosciences Inc	TVB-2640	FASN inhibitor	99	(1) TVB2640 25 mg QD; (2) TVB2640 50 mg; and (3) Placebo	84	Change in hepatic fat fraction from baseline in subjects with NASH by proton-density fat fraction by magnetic resonance imaging	Dose-dependent relative changes in liver fat by MRI-PDFF were -28.2% with 50 mg ($P < 0.005$ *vs* placebo), -9.6% with 25 mg, and +4.5% with placebo. 30% relative reduction in liver fat at week 12 were 61% ($P < 0.001$ *vs* placebo)
NCT02856555	Gilead Sciences	Firsocostat	Acetyl-coenzyme A carboxylase Inhibitor	126	(1) Firsocostat 20 mg QD; (2) Firsocostat 5 mg QD; and (3) Placebo	84	Safety and tolerability. Secondary end point efficacy (NASH improvement without fibrosis)	Decrease of at least 30% from baseline in MRI-PDFF occurred in 48% of patients with 20 mg ($P = 0.004$), 23% given 5 mg ($P = 0.43$), and 15% given placebo. SE cause, abdominal pain, diarrhea
VOYAG/LBP20	Viking therapeutics	VK2809	Thyroid beta receptor agonist, selectively cleaved in hepatic tissue	45	(1) VK2809 5 mg QD; (2) VK2809 10 mg QOD; (3) VK280910 mg QD; and (4) Placebo	84	Safety, tolerability and efficacy in reducing liver fat content and LDL	< Liver fat content was 8.7% for 5 mg QD ($P = 0.0014$) *vs* 8.9% 10 mg QOD ($P = 0.013$) *vs* 10.6% for 10 mg QD ($P = 0.0030$), *vs* 1.1% for placebo. 70% in VK2809 therapy showed a ≥ 50%. Reduction in MRI-PDFF ($P = 0.014$)
NCT02912260	Madrigal Pharmaceuticals	Resmetirom (MGL-3196)	Selective thyroid hormone receptor-β agonist	125	(1) Resmetirom 80 mg QD; and (2) Placebo	252	Change in liver fat fraction measured by MRI-PDFF	80 mg *vs* placebo reduction of hepatic fat at week 12 (-32.9% *vs* -10.4%; $P < 0.0001$) and week 36 (-37.3% *vs* -8.5%; $P < 0.0001$)
NCT02784444	Cirius Therapeutics	MSDC-0602K	Insulin sensitizer designed to preferentially target the mitochondrial pyruvate carrier with direct binding to the transcriptional factor PPARγ	392	(1) MSDC-0602K 62.5 mg QD; (2) MSDC-0602K 125 mg QD; (3) MSDC-0602K 250 mg QD; and (4) Placebo	364	Hepatic histological and activity score improvement in either ballooning or lobular inflammationNo increase in fibrosis stage at 12 mo	Primary end point placebo 29.7%, *vs* 62.5 mg 29.8%, *vs* 125 mg 32.9% *vs* 250 mg 39.5% (95%CI: 0.44–1.81) (95%CI: 0.60–2.48), (95%CI: 0.83–3.27)

FGF: Fibroblast growth factor; MRI-PDFF: Magnetic resonance imaging with proton density fat fraction; GLP-1: Glucagon-like peptide-1; FXR: Farnesoid X receptor; PPAR: Peroxisome proliferator-activated receptor; FASN: Fatty acid synthase.

summarized in Table 1[14]. Firsocostat (GS-0976) is an inhibitor of ACC (acetyl-coenzyme A carboxylase) which catalyzes de novo lipogenesis in the liver. In a randomized placebo-controlled trial, firsocostat 20 mg decreased hepatic steatosis and surrogate markers of fibrosis[15]. VK2809 is a small

molecule prodrug of a potent thyroid beta receptor agonist which has demonstrated favorable effects on lipid metabolism and biomarkers of hepatic steatosis and steatohepatitis in a phase 2 trial, supporting its potential role in patients with NASH[16]. MSDC-0602K is a novel insulin sensitizer designed to preferentially target the mitochondrial pyruvate carrier while minimizing direct binding to the transcriptional factor PPARγ. MSDC-0602K did not demonstrate statistically significant effects on primary and secondary histologic endpoints in a phase 2 trial, but favorable effects on liver cell injury and glucose metabolism support further investigation for in patients with type 2 diabetes[17].

DRUGS IN DEVELOPMENT–PHASE 3

Novel investigational agents which have completed are undergoing evaluation in phase 3 trials are summarized in Table 2. Obeticholic acid, an FXR agonist, has been shown to improve the histological features of NASH, with fibrosis improvement in 23% of patients treated with Obeticholic acid compared with 12% in placebo group[18]. Elafibranor, a PPAR agonist, improves liver enzymes, lipids, glucose levels, and markers of systemic inflammation and is being tested in a phase 3 study (NCT02704403)[19]. Aramchol inhibits steroyl-CoA desaturase 1, a key enzyme in hepatic lipogenesis that converts saturated fatty acids into monounsaturated fatty acid. In the phase 2b ARREST trial, aramchol demonstrated liver fat reduction, biochemical improvement, NASH resolution and fibrosis reduction in a dose response pattern[20]. It has since been included in an ongoing phase 3 trial to test its safety and efficacy (NCT04104321). Cenicriviroc is an oral, dual antagonist of C-C motif chemokine receptor (CCR) types 2 and 5. It has shown anti-inflammatory and anti-fibrotic properties, which are mediated by CCR types 2 and 5 (CCR2/CCR5) blockade. In a randomized double-blind phase 2b study of 289 subjects, cenicriviroc was associated with a statistically significant improvement in NASH fibrosis of one stage or greater *vs* placebo (20% *vs* 10%; $P = 0.02$)[21]. A phase 3 randomized, double-blind, placebo-controlled trial (AURORA) is currently ongoing with evaluation of 2000 adults with NASH who are treated with cenicriviroc or placebo for 52 wk[22]. Resmetirom is a liver-directed, orally active, selective thyroid hormone receptor-β agonist designed to improve NASH by increasing hepatic fat metabolism and reducing lipotoxicity. In a phase 2b study, resmetirom treated patients showed a relative reduction of hepatic fat compared with placebo with statistically significant NASH resolution *vs* placebo[23], and is currently under evaluation in a phase 3 registration trial (NCT03900429). GR-MD-02 (belapectin), is an inhibitor of galectin 3 that reduces liver fibrosis and portal hypertension. In a phase 2 trial, belapectin was safe but not associated with significant reduction in hepatic venous pressure gradient (HVPG) or fibrosis. However, in a subgroup analysis of patients without esophageal varices, 2 mg/kg belapectin reduced HVPG and development of varices, suggesting a possible benefit in patients with NASH cirrhosis without esophageal varices[24] . In the phase 3 NAVIGATE trial, the safety and efficacy of belapectin is under evaluation with primary clinical endpoints of development of varices and event-free survival (NCT04365868).

COMBINATION THERAPEUTICS

The rationale of combining two or more strategies for NASH therapy aims to augment rates of NASH resolution and NASH fibrosis improvement. By targeting the development of steatohepatitis, liver fibrosis as well as controlling metabolic syndrome, we may achieve response rates higher than 32% as seen currently *via* trials of drugs as monotherapy[6]. Table 3 is a collection of studies currently underway, and some completed, that evaluate multidrug regimens for the treatment of NASH. FXR agonists, which regulate bile acid metabolism, are one major class of drugs incorporated in many of these trials. Obeticholic acid, a promising drug in this class, has demonstrated the dose-dependent ability to improve liver fibrosis and steatohepatitis in NASH patients with stage F2/F3 fibrosis based on initial and secondary analysis of the REGENERATE trials[18,25]. Cilofexor, another FXR agonist, has been tested in combination with firsocostat, an ACC inhibitor and selonsertib, an ASK1 inhibitor, in the phase 2b ATLAS study that demonstrated improvements in liver enzymes, fibrosis, NAS score on histology and improvements in liver elastography in the cilofexor/firsocostat group compared to placebo[26]. Ongoing studies with tropifexor include combinations with cenicriviroc and LYS0006 with early results still pending and waiting to be reviewed.

By now it is well known that features of metabolic syndrome increase the risk of developing NAFLD. Type 2 diabetes, specifically, is a risk factor for NASH and its presence increases the risk of progression of NASH fibrosis[27,28]. Therefore, some of the ongoing trials in combination therapy for NASH include semaglutide, pioglitazone or licogliflozin; from drug classes that traditionally have been utilized for the management of T2DM. In one randomized, placebo controlled trial in patients with biopsy proven NASH, a GLP-1 analog, liraglutide, was associated with greater improvement in steatohepatitis and lower progression of fibrosis[9]. A proof-of-concept trial is currently underway including semaglutide along with cilofexor and firsocostat. Licogliflozin, which has shown benefit in lowering liver fat content, is being studied as part of a combination trial with tropifexor in the ELIVATE trial.

Table 2 Phase 3 trials in non-alcoholic steatohepatitis

Trial name/NCT number	Manufacturer	Drugs	Mechanism of action	Enrollment (targeted)	Study arms	Duration (weeks)	Primary or relevant end point(s)	Results
REGENERATE/NCT02548351	Intercept Pharmaceuticals	Obeticholic acid	Farnesoid X receptor agonist	2480	(1) Obeticholic acid 10 mg QD; (2) Obeticholic acid 25 mg QD; and (3) Placebo	72-378	Fibrosis improvement (≥ 1 stage) with no worsening of NASH, or NASH resolution with no worsening of fibrosis	Fibrosis improvement endpoint-(12%) placebo, (18%) obeticholic acid 10 mg, (23%) obeticholic acid group 25 mg. Safety most common adverse event was pruritus
RESOLVE-IT/NCT02704403	Genfit	Elafibranor	PPAR agonist	2157	(1) Elafibranor 120 mg QD; and (2) Placebo	72-216	Change in fibrosis. Change in histologic score of NASH	ongoing
ARMOR/NCT0410432	Galmed pharma-ceuticals	Aramchol	SCD-1 inhibitor	247	(1) Aramchol 600 mg QD; (2) Aramchol 400 mg qd; and (3) Placebo	364	(1) Evaluate the safety and efficacy as measured with % change in the liver triglycerides concen-tration; and (2) Safety	Ongoing
AURORA/NCT03028740	Tobira Therapeutics	Cenicriviroc	Dual antagonist of CCR types 2 and 5	2000	(1) Cenicriviroc 150 mg; and (2) Placebo	364	(1) Proportion of subjects with ≥ 1-stage improvement in liver fibrosis and no worsening of steatohepatitis at month 12 relative to screening; and (2) Safety	Ongoing
MAESTRO-NASH/ NCT03900429	Madrigal Pharmaceuticals	Resmetirom	Selective thyroid hormone receptor-β agonist	2000	(1) resmetirom 80 mg QD; (2) resmetirom 100 mg QD; and (3) Placebo	364	NASH resolution, with at least a 2-point reduction in NAS (NASH Activity Score-biopsy), and with no worsening of fibrosis. Secondary end p. (1) Liver fibrosis improvement of at least one stage, with no worsening of NASH; and (2) Lowering of LDL-cholesterol	Ongoing
NAVIGATE/NCT04365868	Galectin Therapeutics	GR-MD-02 (belapectin)	Inhibitor of galectin 3	1010	(1) Belapectin 2 mg/kg intravenously (IV) every other week; (2) Belapectin 4 mg/kg intravenously (IV) every other week; and (3) Placebo	504	Development of new esophageal varices at 78 weeks in the belapectin group Cumulative incidence rate of decompensations and event-free survival by time to first cirrhosis related clinical event	Ongoing

PPAR: Peroxisome proliferator-activated receptor; SCD-1: Steroyl-CoA desaturase 1; CCR: C-C motif chemokine receptor

Numerous trials have already established the benefit of pioglitazone in improving inflammation and fibrosis in patients with biopsy proven NASH and therefore it is included as recommended management for a select group of patients according to the most recent American Association for the Study of Liver Diseases guidelines on NAFLD[29].

Aside from the ability to decrease inflammation and fibrosis in NASH, allowing treatment with lower doses of various drugs in combination or improvement the side effect profile are two alternate motives for pursuing combination therapy. In Wister rat models for NASH, one group was able to demonstrate a synergistic therapeutic effect on inflammation and oxidative stress from combining elafibranor and obeticholic acid at lower doses than with each drug in monotherapy[30]. FXR agonists have been shown to increase low density lipoprotein (LDL) cholesterol concentrations. In the CONTROL study, the

Table 3 Multidrug regimens for the treatment of non-alcoholic steatohepatitis

Trial name/NCT number	Phase	Manufacturer	Drugs	Mechanism of action	Enrollment (targeted)	Study arms	Duration (weeks)	Primary or relevant end point(s)
NCT02781584 (Proof of Concept)	1	Gilead Sciences	Selonsertib, firsocostat, cilofexor, fenofibrate, icosapent ethyl	(1) Selonsertib-selective ASK1 inhibitor; (2) Firsocostat-ACC inhibitor; (3) Cilofexor-FXR agonist; (4) Fenofibrate-PPAR agonist; and (5) Icosapent ethyl-under investigation	220	(1) Selonsertib; (2) Firsocostat; (3) Cilofexor; (4) Selonsertib + cilofexor; (5) Selonsertib + firsocostat; (6) Firsocostat + cilofexor; (7) Firsocostat (cirrhotic patients); (8) Cilofexor (cirrhotic patients); (9) Selonsertib + firsocostat + cilofexor; (10) Firsocostat + fenofibrate 48 mg; (11) Firsocostat + fenofibrate 145 mg; and (12) Icosapent ethyl + firsocostat + cilofexor	12	(1) Adverse events; (2) Serious adverse events; and (3) Lab abnormalities
ATLAS/NCT03449446	2	Gilead Sciences	Selonsertib, firsocostat, cilofexor	(1) Selonsertib-selective ASK1 inhibitor; (2) Firsocostat-ACC inhibitor; and (3) Cilofexor-FXR agonist	395	(1) Selonsertib + firsocostat + placebo; (2) Selonsertib + cilofexor + placebo; (3) Firsocostat + cilofexor + placebo; (4) Selonsertib + placebo + placebo; (5) Firsocostat + placebo + placebo; (6) Cilofexor + placebo + placebo; and (7) 3 placebos	48	(1) Adverse events; (2) Lab abnormalities; and (3) Improvement of ≥ 1-stage in fibrosis without worsening of NASH
NCT03987074	2	Gilead Sciences, Novo Nordisk	Cilofexor, semaglutide, firsocostat	(1) Semaglutide-GLP-1 agonist; (2) Firsocostat-ACC inhibitor; and (3) Cilofexor-FXR agonist	109	(1) Semaglutide; (2) Firsocostat + semaglutide; (3) Semaglutide + cilofexor 30 mg; (4) Semaglutide + cilofexor 100 mg; and (5) Semaglutide + firsocostat + cilofexor	24	(1) Adverse events; (2) Serious adverse events; and (3) Lab abnormalities
ELIVATE/NCT04065841	2	Novartis	Tropifexor, licogli-flozin	(1) Tropifexor-FXR agonist; and (2) Licogliflozin-SGLT1/2 inhibitor	380	(1) Tropifexor + licogliflozin; (2) Tropifexor + placebo; (3) Licogliflozin + placebo; and (4) 2 placebos	48	(1) Improvement of ≥ 1-stage in fibrosis without worsening of NASH; and (2) Resolution of NASH without worsening fibrosis
NCT03776175	2A	Pfizer	PF-05221304, PF-06865571	(1) PF-05221304-ACC inhibitor; and (2) PF-06865571 - DGAT 2 inhibitor	99	(1) ACC inhibitor + placebo; (2) DGAT2 inhibitor + placebo; (3) ACC inhibitor + DGAT2 inhibitor; and (4) 2 placebos	6	Improvement in fat fraction
TANDEM/NCT03517540	2	Novartis, Allergan	Tropifexor, cenicriviroc	(1) Tropifexor-FXR agonist; and (2) Cenicriviroc-CCR2/CCR5 inhibitor	193	(1) Tropifexor; (2) Cenicriviroc; (3) Tropifexor dose 1 + cenicriviroc; and (4) Tropifexor dose 2 + cenicriviroc	48	(1) improvement in fibrosis; and (2) Resolution of steato-hepatitis
CONTROL/NCT02633956	2	Intercept Pharmaceuticals	Obeticholic acid, atorvastatin	(1) Obeticholic acid-FXR agonist; and (2) Atorvastatin-HMG-CoA reductase inhibitor	84	(1) Obeticholic acid 5 mg/10 mg/25 mg + atorvastatin 10 mg/20 mg; and (2) Placebo + atorvastatin 10 mg/20 mg	16	(1) Change in LDL concen-tration; (2) Change in LDL particle size; and (3) Change in LDL particle concentration
NCT04235205	2	Albireo Pharma	Elobixibat, cholestyramine	(1) Elobixibat-IBAT inhibitor; and (2) Cholestyramine-bile acid binding resin	100	(1) Elobixibat + cholestyramine; (2) Elobixibat + placebo; (3) Placebo + cholestyramine; and (4) 2 placebos	16	(1) Change in liver fat fraction measured by MRI-PDFF; and (2) Change in fibrosis measured by MRE
PUVENAFLD/NCT04198805	2	DSM Nutritional Products	Vitamin E, omega-3 fatty acid	(1) Vitamin E-scavenging reactive oxidation species; and (2) Omega 3 FA-competing with omega 6 for cycloox-genase and lipoxygenase-mediated	200	(1) Vitamin E + placebo; (2) Omega-3 fatty acid + placebo; (3) Omega 3-fatty acid + vitamin E; and (4) 2 placebos	24	(1) Change in liver fat fraction measured by MRI-PDFF; (2) Change in liver enzymes; and (3) FIB-4 scores

				inflammatory eicosanoid production, forming anti-inflammatory compounds				
NEXSCOT/NCT04147195	2	Novartis	LYS006, tropifexor	(1) Tropifexor-FXR agonist; and (2) LYS006-leukotriene A4 hydrolase inhibitor	250	(1) LYS006; and (2) LYS006 + tropifexor	21	(1) Change in ELF score; and (2) Change in liver fat fraction measured by MRI-PDFF
NCT02466516	2	Gilead Sciences	Selonsertib, simtuzumab	(1) Selonsertib-selective ASK1 inhibitor; and (2) Simtuzumab-lysyl oxidase-like 2 inhibitor	72	(1) Selonsertib 6 mg; (2) Selonsertib 18 mg; (3) Selonsertib 6 mg + simtuzumab; (4) Selonsertib 18 mg + simtuzumab; and (5) Simtuzumab	24	(1) Adverse events; (2) Serious adverse events; (3) Lab abnormalities; and (4) Number of participants who prematurely discontinued study due to adverse events
NCT01703260	2	AstraZeneca	Roflumilast, pioglitazone	(1) Roflumilast-phosphodiesterase 4 inhibitor; and (2) Pioglitazone-PPAR agonist	16	(1) Roflumilast + pioglitazone; (2) Roflumilast + placebo; and (3) Pioglitazone + placebo	20	(1) Change in liver enzymes; and (2) Change in liver fat fraction measured by MRI-PDFF

ASK1: Apoptosis signal-regulating kinase-1; ACC: Acetyl-coenzyme A carboxylase; FXR: Farnesoid X receptor; PPAR: Peroxisome proliferator-activated receptor; GLP-1: Glucagon-like peptide-1; SGLT: Sodium/glucose transport protein; DGAT: Diacylglycerol acyltransferase; CCR: C-C motif chemokine receptor; IBAT: Ileal bile acid transporter.

authors were able to lower the LDL concentration below baseline with the addition of atorvastatin[31]. In a separate phase 2, proof-of-concept trial, fenofibrate was tested in combination with the ACC inhibitor, firsocostat, to help lower triglyceride levels[32].

CONCLUSION

In this concise review, we have discussed numerous possible therapeutic options for cessation or reversal of NASH and associated fibrosis. It is clear that NASH and particularly NASH fibrosis or cirrhosis is a leading topic garnering much interest in the study of liver diseases today, which would be appropriate considering the clinical impact. Although some of the above targets may seem promising, there are still a few concerns regarding study of this particular topic. Firstly, it is evident by reviewing the endpoints of each of the studies listed above that there is much heterogeneity. This is partly because the gold standard of liver biopsy to prove effectiveness in this endeavor is cumbersome, costly, and generally not favored by patients. The use of surrogates for liver fibrosis and resolution including markers of turnover, inflammation, or non-invasive assessments of liver scarring have not universally been agreed upon in the use of clinical trials. Secondly, for those studies that have utilized liver biopsies are part of their endpoint assessment, there can be considerable inter-observer variability in interpretation of liver biopsy specimens, assuming they are of adequate quality. Additionally, it is apparent that many of the study developers use magnetic resonance imaging with proton density fat fraction for assessment of liver fat content while there are additional tools such as the controlled attenuation parameter of transient elastography systems which might be more acceptable as a point of

care test. Lastly, endoscopic and surgical bariatrics represent an emerging area of therapeutic development for the management of obesity in context of NASH. In one prospective study of 180 patients, bariatric surgery was associated with NASH resolution in 84% of patients with improvement in fibrosis in 70% of patients at the 5 year mark after surgery[33]. Separately, in a 6 mo multi-center study of 85 patients with T2DM undergoing duodenal mucosal resurfacing, not only did their A1c improve, but so did their ALT levels and FIB-4 scores hinting at the possible insulin sensitizing, lipid lowering, anti-inflammatory and antioxidant effects of this procedure[34]. In conclusion, more effective treatments for NASH are urgently needed, and combination pharmacotherapy represents among the most promising approaches in develpoment.

FOOTNOTES

Author contributions: Suri J was responsible for background data review, writing, editing and final review of the manuscript; Borja S was responsible for background data review and writing of the manuscript; Lim JK was responsible for writing, editing and final review of the manuscript.

Conflict-of-interest statement: Suri J, None; Borja S, None; Lim JK, research contract (to Yale University) from Allergan, Celgene, Genfit, Intercept, Pfizer, Viking.

Open-Access: This article is an open-access article that was selected by an in-house editor and fully peer-reviewed by external reviewers. It is distributed in accordance with the Creative Commons Attribution NonCommercial (CC BY-NC 4.0) license, which permits others to distribute, remix, adapt, build upon this work non-commercially, and license their derivative works on different terms, provided the original work is properly cited and the use is non-commercial. See: https://creativecommons.org/Licenses/by-nc/4.0/

Country/Territory of origin: United States

ORCID number: Jaspreet Suri 0000-0002-3897-7234; Joseph K Lim 0000-0003-1037-5773.

S-Editor: Fan JR
L-Editor: A
P-Editor: Fan JR

REFERENCES

1 **Paik JM**, Henry L, De Avila L, Younossi E, Racila A, Younossi ZM. Mortality Related to Nonalcoholic Fatty Liver Disease Is Increasing in the United States. *Hepatol Commun* 2019; **3**: 1459-1471 [PMID: 31701070 DOI: 10.1002/hep4.1419]
2 **Wong RJ**, Aguilar M, Cheung R, Perumpail RB, Harrison SA, Younossi ZM, Ahmed A. Nonalcoholic steatohepatitis is the second leading etiology of liver disease among adults awaiting liver transplantation in the United States. *Gastroenterology* 2015; **148**: 547-555 [PMID: 25461851 DOI: 10.1053/j.gastro.2014.11.039]
3 **Friedman SL**, Neuschwander-Tetri BA, Rinella M, Sanyal AJ. Mechanisms of NAFLD development and therapeutic strategies. *Nat Med* 2018; **24**: 908-922 [PMID: 29967350 DOI: 10.1038/s41591-018-0104-9]
4 **Kuchay MS**, Krishan S, Mishra SK, Farooqui KJ, Singh MK, Wasir JS, Bansal B, Kaur P, Jevalikar G, Gill HK, Choudhary NS, Mithal A. Effect of Empagliflozin on Liver Fat in Patients With Type 2 Diabetes and Nonalcoholic Fatty Liver Disease: A Randomized Controlled Trial (E-LIFT Trial). *Diabetes Care* 2018; **41**: 1801-1808 [PMID: 29895557 DOI: 10.2337/dc18-0165]
5 **Petit JM**, Cercueil JP, Loffroy R, Denimal D, Bouillet B, Fourmont C, Chevallier O, Duvillard L, Vergès B. Effect of Liraglutide Therapy on Liver Fat Content in Patients With Inadequately Controlled Type 2 Diabetes: The Lira-NAFLD Study. *J Clin Endocrinol Metab* 2017; **102**: 407-415 [PMID: 27732328 DOI: 10.1210/jc.2016-2775]
6 **Dufour JF**, Caussy C, Loomba R. Combination therapy for non-alcoholic steatohepatitis: rationale, opportunities and challenges. *Gut* 2020; **69**: 1877-1884 [PMID: 32381514 DOI: 10.1136/gutjnl-2019-319104]
7 **Services USD of H and H**. Noncirrhotic nonalcoholic steatohepatitis with liver fibrosis: developing drugs for treatment. *Guid Ind* 2018 [DOI: 10.1016/b978-0-323-99764-5.00013-5]
8 **Kaufman A**, Abuqayyas L, Denney WS, Tillman EJ, Rolph T. AKR-001, an Fc-FGF21 Analog, Showed Sustained Pharmacodynamic Effects on Insulin Sensitivity and Lipid Metabolism in Type 2 Diabetes Patients. *Cell Rep Med* 2020; **1**: 100057 [PMID: 33205064 DOI: 10.1016/j.xcrm.2020.100057]
9 **Armstrong MJ**, Gaunt P, Aithal GP, Barton D, Hull D, Parker R, Hazlehurst JM, Guo K; LEAN trial team, Abouda G, Aldersley MA, Stocken D, Gough SC, Tomlinson JW, Brown RM, Hübscher SG, Newsome PN. Liraglutide safety and efficacy in patients with non-alcoholic steatohepatitis (LEAN): a multicentre, double-blind, randomised, placebo-controlled phase 2 study. *Lancet* 2016; **387**: 679-690 [PMID: 26608256 DOI: 10.1016/S0140-6736(15)00803-X]
10 **Newsome PN**, Buchholtz K, Cusi K, Linder M, Okanoue T, Ratziu V, Sanyal AJ, Sejling AS, Harrison SA; NN9931-4296 Investigators. A Placebo-Controlled Trial of Subcutaneous Semaglutide in Nonalcoholic Steatohepatitis. *N Engl J Med* 2021; **384**: 1113-1124 [PMID: 33185364 DOI: 10.1056/NEJMoa2028395]

11 **Traussnigg S**, Schattenberg JM, Demir M, Wiegand J, Geier A, Teuber G, Hofmann WP, Kremer AE, Spreda F, Kluwe J, Petersen J, Boettler T, Rainer F, Halilbasic E, Greinwald R, Pröls M, Manns MP, Fickert P, Trauner M; Austrian/German NAFLD-norUDCA study group. Norursodeoxycholic acid versus placebo in the treatment of non-alcoholic fatty liver disease: a double-blind, randomised, placebo-controlled, phase 2 dose-finding trial. *Lancet Gastroenterol Hepatol* 2019; **4**: 781-793 [PMID: 31345778 DOI: 10.1016/S2468-1253(19)30184-0]

12 **Harrison SA**, Neff G, Guy CD, Bashir MR, Paredes AH, Frias JP, Younes Z, Trotter JF, Gunn NT, Moussa SE, Kohli A, Nelson K, Gottwald M, Chang WCG, Yan AZ, DePaoli AM, Ling L, Lieu HD. Efficacy and Safety of Aldafermin, an Engineered FGF19 Analog, in a Randomized, Double-Blind, Placebo-Controlled Trial of Patients With Nonalcoholic Steatohepatitis. *Gastroenterology* 2021; **160**: 219-231.e1 [PMID: 32781086 DOI: 10.1053/j.gastro.2020.08.004]

13 **Tropifexor SA**. A highly potent FXR agonist, produces robust and dose-dependent reductions in hepatic fat and serum alanine aminotransferase in patients with fibrotic NASH after 12 wk of therapy: FLIGH-FXR part C interim results. *Hepatology* 2019; 70 [DOI: 10.1016/j.dld.2019.12.129]

14 **Loomba R**, Rinella M, Harrison S, Wong VW-S, Ratziu V, Mohseni R, Lucas KJ, Perry RG, Rahmini R, Trotter JF. Novel first-in-class, fatty acid synthase inhibitor, TVB-2640 vs. placebo demonstrates clinically significant reduction in liver fat by MRI-PDFF in NASH: a phase 2 randomised controlled trial (FASCINATE-1). *J Hepatol* 2020; **73**: S53-S54 [DOI: 10.1016/s0168-8278(20)30653-x]

15 **Loomba R**, Kayali Z, Noureddin M, Ruane P, Lawitz EJ, Bennett M, Wang L, Harting E, Tarrant JM, McColgan BJ, Chung C, Ray AS, Subramanian GM, Myers RP, Middleton MS, Lai M, Charlton M, Harrison SA. GS-0976 Reduces Hepatic Steatosis and Fibrosis Markers in Patients With Nonalcoholic Fatty Liver Disease. *Gastroenterology* 2018; **155**: 1463-1473.e6 [PMID: 30059671 DOI: 10.1053/j.gastro.2018.07.027]

16 **Loomba R**, Neutel J, Mohseni R, Bernard D, Severance R, Dao M, Saini S, Margaritescu C, Homer K, Tran B, Mancini M, Masamune H, Lian B. LBP-20-VK2809, a Novel Liver-Directed Thyroid Receptor Beta Agonist, Significantly Reduces Liver Fat with Both Low and High Doses in Patients with Non-Alcoholic Fatty Liver Disease: A Phase 2 Randomized, Placebo-Controlled Trial. *J Hepatol* 2019; **70**: e150-1 [DOI: 10.1016/s0618-8278(19)30266-x]

17 **Harrison SA**, Alkhouri N, Davison BA, Sanyal A, Edwards C, Colca JR, Lee BH, Loomba R, Cusi K, Kolterman O, Cotter G, Dittrich HC. Insulin sensitizer MSDC-0602K in non-alcoholic steatohepatitis: A randomized, double-blind, placebo-controlled phase IIb study. *J Hepatol* 2020; **72**: 613-626 [PMID: 31697972 DOI: 10.1016/j.jhep.2019.10.023]

18 **Younossi ZM**, Ratziu V, Loomba R, Rinella M, Anstee QM, Goodman Z, Bedossa P, Geier A, Beckebaum S, Newsome PN, Sheridan D, Sheikh MY, Trotter J, Knapple W, Lawitz E, Abdelmalek MF, Kowdley KV, Montano-Loza AJ, Boursier J, Mathurin P, Bugianesi E, Mazzella G, Olveira A, Cortez-Pinto H, Graupera I, Orr D, Gluud LL, Dufour JF, Shapiro D, Campagna J, Zaru L, MacConell L, Shringarpure R, Harrison S, Sanyal AJ; REGENERATE Study Investigators. Obeticholic acid for the treatment of non-alcoholic steatohepatitis: interim analysis from a multicentre, randomised, placebo-controlled phase 3 trial. *Lancet* 2019; **394**: 2184-2196 [PMID: 31813633 DOI: 10.1016/S0140-6736(19)33041-7]

19 **Ratziu V**, Harrison SA, Francque S, Bedossa P, Lehert P, Serfaty L, Romero-Gomez M, Boursier J, Abdelmalek M, Caldwell S, Drenth J, Anstee QM, Hum D, Hanf R, Roudot A, Megnien S, Staels B, Sanyal A; GOLDEN-505 Investigator Study Group. Elafibranor, an Agonist of the Peroxisome Proliferator-Activated Receptor-α and -δ, Induces Resolution of Nonalcoholic Steatohepatitis Without Fibrosis Worsening. *Gastroenterology* 2016; **150**: 1147-1159.e5 [PMID: 26874076 DOI: 10.1053/j.gastro.2016.01.038]

20 **Ratziu V**, Ladron-De-Guevara L, Safadi R, Poordad F, Fuster F, Flores-Figueroa J, Harrison SA, Arrese M, Fargion S, Ben-Bashat D. One-year results of the global phase 2b randomized placebo-controlled arrest trial of aramchol, a stearoyl CoA desaturase inhibitor, in patients with NASH. In: Hepatology. WILEY 111 RIVER ST, HOBOKEN 07030-5774, NJ United States, 2018: 1448A-1449A

21 **Friedman SL**, Ratziu V, Harrison SA, Abdelmalek MF, Aithal GP, Caballeria J, Francque S, Farrell G, Kowdley KV, Craxi A, Simon K, Fischer L, Melchor-Khan L, Vest J, Wiens BL, Vig P, Seyedkazemi S, Goodman Z, Wong VW, Loomba R, Tacke F, Sanyal A, Lefebvre E. A randomized, placebo-controlled trial of cenicriviroc for treatment of nonalcoholic steatohepatitis with fibrosis. *Hepatology* 2018; **67**: 1754-1767 [PMID: 28833331 DOI: 10.1002/hep.29477]

22 **Anstee QM**, Neuschwander-Tetri BA, Wong VW, Abdelmalek MF, Younossi ZM, Yuan J, Pecoraro ML, Seyedkazemi S, Fischer L, Bedossa P, Goodman Z, Alkhouri N, Tacke F, Sanyal A. Cenicriviroc for the treatment of liver fibrosis in adults with nonalcoholic steatohepatitis: AURORA Phase 3 study design. *Contemp Clin Trials* 2020; **89**: 105922 [PMID: 31881392 DOI: 10.1016/j.cct.2019.105922]

23 **Harrison SA**, Bashir MR, Guy CD, Zhou R, Moylan CA, Frias JP, Alkhouri N, Bansal MB, Baum S, Neuschwander-Tetri BA, Taub R, Moussa SE. Resmetirom (MGL-3196) for the treatment of non-alcoholic steatohepatitis: a multicentre, randomised, double-blind, placebo-controlled, phase 2 trial. *Lancet* 2019; **394**: 2012-2024 [PMID: 31727409 DOI: 10.1016/S0140-6736(19)32517-6]

24 **Chalasani N**, Abdelmalek MF, Garcia-Tsao G, Vuppalanchi R, Alkhouri N, Rinella M, Noureddin M, Pyko M, Shiffman M, Sanyal A, Allgood A, Shlevin H, Horton R, Zomer E, Irish W, Goodman Z, Harrison SA, Traber PG; Belapectin (GR-MD-02) Study Investigators. Effects of Belapectin, an Inhibitor of Galectin-3, in Patients With Nonalcoholic Steatohepatitis With Cirrhosis and Portal Hypertension. *Gastroenterology* 2020; **158**: 1334-1345.e5 [PMID: 31812510 DOI: 10.1053/j.gastro.2019.11.296]

25 **Sanyal AJ**, Ratziu V, Loomba R, Rinella M, Anstee QM, Goodman Z, Bedossa P, Khalili M, Boursier J, Stinton L. Obeticholic acid treatment in patients with non-alcoholic steatohepatitis: a secondary analysis in the regenerate study across fibrosis stages. In: AISF Annual Meeting 2020, 2020: 46–7

26 **Loomba R**, Noureddin M, Kowdley KV, Kohli A, Sheikh A, Neff G, Bhandari BR, Gunn N, Caldwell SH, Goodman Z, Wapinski I, Resnick M, Beck AH, Ding D, Jia C, Chuang JC, Huss RS, Chung C, Subramanian GM, Myers RP, Patel K, Borg BB, Ghalib R, Kabler H, Poulos J, Younes Z, Elkhashab M, Hassanein T, Iyer R, Ruane P, Shiffman ML, Strasser S, Wong VW, Alkhouri N; ATLAS Investigators. Combination Therapies Including Cilofexor and Firsocostat for Bridging Fibrosis and Cirrhosis Attributable to NASH. *Hepatology* 2021; **73**: 625-643 [PMID: 33169409 DOI: 10.1002/hep.31622]

27 **Neuschwander-Tetri BA**, Clark JM, Bass NM, Van Natta ML, Unalp-Arida A, Tonascia J, Zein CO, Brunt EM, Kleiner DE, McCullough AJ, Sanyal AJ, Diehl AM, Lavine JE, Chalasani N, Kowdley KV; NASH Clinical Research Network.

Clinical, laboratory and histological associations in adults with nonalcoholic fatty liver disease. *Hepatology* 2010; **52**: 913-924 [PMID: 20648476 DOI: 10.1002/hep.23784]

28 **Younossi ZM**, Gramlich T, Matteoni CA, Boparai N, McCullough AJ. Nonalcoholic fatty liver disease in patients with type 2 diabetes. *Clin Gastroenterol Hepatol* 2004; **2**: 262-265 [PMID: 15017611 DOI: 10.1016/s1542-3565(04)00014-x]

29 **Chalasani N**, Younossi Z, Lavine JE, Charlton M, Cusi K, Rinella M, Harrison SA, Brunt EM, Sanyal AJ. The diagnosis and management of nonalcoholic fatty liver disease: Practice guidance from the American Association for the Study of Liver Diseases. *Hepatology* 2018; **67**: 328-357 [PMID: 28714183 DOI: 10.1002/hep.29367]

30 **Noel B**, Ratziu V, Harrison S, Rigou G, degallaix nathalie, texier frederic, Brozek J, Daix V, Belanger C, roudot alice, megnien sophie, hum dean, staels bart, Walczak R, sanyal arun. Combination drug therapy allows synergistic therapeutic dosereduction in NASH: A case study of ELAFIBRANOR (GFT505) and an FXR agonist combination in a model of severe NASH. 2017. [cited 10 January 2022]. Available from: https://linkinghub.elsevier.com/retrieve/pii/S0168827817304877

31 **Pockros PJ**, Fuchs M, Freilich B, Schiff E, Kohli A, Lawitz EJ, Hellstern PA, Owens-Grillo J, Van Biene C, Shringarpure R, MacConell L, Shapiro D, Cohen DE. CONTROL: A randomized phase 2 study of obeticholic acid and atorvastatin on lipoproteins in nonalcoholic steatohepatitis patients. *Liver Int* 2019; **39**: 2082-2093 [PMID: 31402538 DOI: 10.1111/liv.14209]

32 **Lawitz EJ**, Neff G, Ruane PJ, Younes Z, Zhang J, Jia C, Chuang J, Huss R, Chung C, Subramanian M. Fenofibrate mitigates increases in serum triglycerides due to the ACC inhibitor firsocostat in patients with advanced fibrosis due to NASH: a phase 2 randomized trial. In: Hepatology. WILEY 111 RIVER ST, HOBOKEN 07030-5774, NJ United States, 2019: 1489A-1490A

33 **Lassailly G**, Caiazzo R, Ntandja-Wandji LC, Gnemmi V, Baud G, Verkindt H, Ningarhari M, Louvet A, Leteurtre E, Raverdy V, Dharancy S, Pattou F, Mathurin P. Bariatric Surgery Provides Long-term Resolution of Nonalcoholic Steatohepatitis and Regression of Fibrosis. *Gastroenterology* 2020; **159**: 1290-1301.e5 [PMID: 32553765 DOI: 10.1053/j.gastro.2020.06.006]

34 **van Baar ACG**, Beuers U, Wong K, Haidry R, Costamagna G, Hafedi A, Deviere J, Ghosh SS, Lopez-Talavera JC, Rodriguez L, Galvao Neto MP, Sanyal A, Bergman JJGHM. Endoscopic duodenal mucosal resurfacing improves glycaemic and hepatic indices in type 2 diabetes: 6-month multicentre results. *JHEP Rep* 2019; **1**: 429-437 [PMID: 32039394 DOI: 10.1016/j.jhepr.2019.10.006]

World Journal of Gastroenterology

Submit a Manuscript: https://www.f6publishing.com

World J Gastroenterol 2022 September 21; 28(35): 5141-5153

DOI: 10.3748/wjg.v28.i35.5141

ISSN 1007-9327 (print) ISSN 2219-2840 (online)

ORIGINAL ARTICLE

Basic Study

Long noncoding RNA negative regulator of antiviral response contributes to pancreatic ductal adenocarcinoma progression *via* targeting miR-299-3p

Hai-Quan Wang, Chun-Hua Qian, Zeng-Ya Guo, Pei-Ming Li, Zheng-Jun Qiu

Specialty type: Medicine, research and experimental

Provenance and peer review: Unsolicited article; Externally peer reviewed.

Peer-review model: Single blind

Peer-review report's scientific quality classification

Grade A (Excellent): 0
Grade B (Very good): B, B
Grade C (Good): C, C
Grade D (Fair): 0
Grade E (Poor): 0

P-Reviewer: Karamarkovic AR, Serbia; Nagaya M, Japan; Nakano H, Japan; Sheykhhasan M, Iran

Received: November 9, 2021
Peer-review started: November 9, 2021
First decision: April 16, 2022
Revised: April 28, 2022
Accepted: September 1, 2022
Article in press: September 1, 2022
Published online: September 21, 2022

Hai-Quan Wang, Zheng-Jun Qiu, Department of General Surgery, Shanghai General Hospital of Nanjing Medical University, Shanghai 200080, China

Hai-Quan Wang, Zeng-Ya Guo, Pei-Ming Li, Zheng-Jun Qiu, Department of General Surgery, Shanghai Jiao Tong University School of Medicine, Shanghai 200080, China

Chun-Hua Qian, Department of Endocrinology and Metabolism, Shanghai Tenth People's Hospital, Shanghai 200072, China

Corresponding author: Zheng-Jun Qiu, MD, Chief Doctor, Director, Surgeon, Department of General Surgery, Shanghai General Hospital of Nanjing Medical University, No. 100 Haining Road, Shanghai 200080, China. qiuzjdoctor@sina.com

Abstract

BACKGROUND

Pancreatic ductal cancer (PDAC) has high malignancy and poor prognosis. Long noncoding RNAs (lncRNAs) are associated with high levels of malignancy, including PDAC. However, the biological and clinical significance of negative regulator of antiviral response (NRAV) in PDAC is unclear.

AIM

To study the regulatory role of lncRNA NRAV in PDAC.

METHODS

GEPIA analyzed lncRNA NRAV and miRNA (miR-299-3p) expression levels in PDAC tissues and measured them in PDAC cells by quantitative measurements in real time. The specific role of NRAV and miR-299-3p in cell proliferation and transfer potential was evaluated by cell formation analysis, Cell Counting Kit-8 and Transwell analysis. The relationship between NRAV and miR-299-3p was studied by predictive bioinformatics, RNA immunoassay, and fluorescence enzyme analysis. *In vivo* experiments included transplantation of simulated tumor cells under naked mice.

RESULTS

The expression level of lncRNA NRAV was higher in both tumor tissues and cell lines of PDAC and was negatively associated with the clinical survival of PDAC

patients. Functionally, overexpression of NRAV promoted cell proliferation and metastasis of PDAC cells, while knockdown of NRAV reversed these effects. Finally, NRAV was performed as a molecular sponge of miR-299-3p. Moreover, overexpression of miR-299-3p could reverse the promoting effects of NRAV on cell proliferation and metastasis of PDAC cells.

CONCLUSION

NRAV facilitates progression of PDAC as a molecular sponge of miR-299-3p and may be a potential molecular marker for diagnosis and treatment of PDAC.

Key Words: Long noncoding RNA; Negative regulator of antiviral response; miR-299-3p; Proliferation; Migration; Invasion; Pancreatic cancer

©The Author(s) 2022. Published by Baishideng Publishing Group Inc. All rights reserved.

Core Tip: In the present research, the expression level of long noncoding RNA negative regulator of antiviral response (NRAV) in pancreatic ductal adenocarcinoma (PDAC) was detected, and the clinicopathological relationship between NRAV and PDAC was demonstrated. Moreover, cell and animal tests were conducted to assess the concrete roles of NRAV in the progression of PDAC. Finally, the existence of potential specific molecular mechanisms that can provide new ideas for finding new molecular markers for the diagnosis and treatment of PDAC is demonstrated.

Citation: Wang HQ, Qian CH, Guo ZY, Li PM, Qiu ZJ. Long noncoding RNA negative regulator of antiviral response contributes to pancreatic ductal adenocarcinoma progression *via* targeting miR-299-3p. *World J Gastroenterol* 2022; 28(35): 5141-5153

URL: https://www.wjgnet.com/1007-9327/full/v28/i35/5141.htm

DOI: https://dx.doi.org/10.3748/wjg.v28.i35.5141

INTRODUCTION

As an extremely malignant tumor, pancreatic ductal adenocarcinoma (PDAC) has shown a rapidly increasing incidence rate in recent years worldwide[1]. According to the latest cancer report in 2021, there are 495773 new cases reported globally every year and about 466003 people die of PDAC annually [2]. Due to insufficient means of early diagnosis and effective treatment, the 5-year survival rate of PDAC patients is only about 8% and will drop to about 3% in patients with advanced PDAC[1]. Therefore, it is urgent to establish a comprehensive pathological mechanism of PDAC and explore a more effective PDAC diagnosis and treatment center.

Long noncoding RNAs (lncRNAs) are new ncRNAs that are composed of > 200 nucleotides, accounting for the largest proportion of the entire human gene transcriptome[3,4]. lncRNAs mainly regulate gene expression in a variety of ways, including chromatin remodeling and transcriptional and post-transcriptional processing, and participate in regulating a variety of biological processes[5,6]. Recently, a large number of researches showed that lncRNAs are dysregulated in most tumors and function as key regulators in the process of tumor growth, metastasis, drug tolerance, and angiogenesis [7,8]. The lncRNA negative regulator of antiviral response (NRAV) is a newly identified lncRNA and is mainly related to immunity[9]. Xu *et al*[10] found that NRAV is highly expressed in the cell system of hepatocytes and regulates the course of hepatocellular carcinoma. However, the statements and specific role of NRAV in PDAC are still unclear.

lncRNAs play an important regulatory role in the occurrence and development of various cancers and may be considered a potential molecular marker. Many studies have shown that RNA plays its biological function of competing with endogenous RNAs[11,12]. Hsa-miR-299-3p plays an important role in the development of many cancers. Many studies describe the regulation of the relationship between miR-299-3p and lncRNAs[13,14]. Many experts conducted in-depth research on the regulation of the relationship between the two and stated that miR-299-3p increased the volume and cellular system and prevented proliferation and metastasis of pancreatic cancer cells with exposure to Notch1 [15]. The relationship between NRAV and miR-299-3p in PDAC has not yet been investigated.

In this study, we tested the expression of NRAV in PDAC and studied its function, and found that NRAV and PDAC have obvious overlaps. The results of functional experiments showed that the level of NRAV expression was directly associated with cell proliferation and metastasis and was closely related to the growth of tumors in naked mice. In addition, we found that NRAV, as a molecular sponge of miR-299-3p, contributes to PDAC progression. Therefore, the results of this study may provide new insights into the role of NRAV in PDAC. It can be a biomarker for the diagnosis and treatment of PDAC.

MATERIALS AND METHODS

Cell lines

PDAC cell lines (PANC-1, AsPC-1, Mia Paca-2 and BxPC-3) and human immortalized normal pancreatic duct epithelial (HPDE) cells were obtained from the American Type Culture Collection (Manassas, VA, United States). The cell lines were cultured at an appropriate concentration in a specific environment in a moistened cell incubator with a CO_2 concentration of 5% at 37 °C. Percentage of 10 fetal serum and 1% penicillin–streptomycin were added to the culture medium, including RPMI-1640 and Dulbecco's modified Eagle's medium.

RNA isolation and quantitative real-time polymerase chain reaction

Total cellular RNA was extracted from cultured cells using Trizol reagent (Invitrogen, Carlsbad, CA, United States). For lncRNA, FastKing gDNA Dispeeling RT Supermix (TIANGEN, China) was selected for reverse transclncRNAn. The specific cDNAs of miRNAs were obtained with a specific kit (miDETECT A Track RT Reagent Kit; RiboBio, China). The quantitative real-time polymerase chain reaction (qRT-PCR) system wasABI 7300 PCR (Foster City, CA, United States). *U6* and *ACTB* were respectively deemed as standardized internal controls of miRNA and lncRNA. The specific sequences of the primers were designed as follows. For NRAV, 5′-GGAGTTGATGCCTCCGAACA-3′ (forward) and 5′-ATGACCGGAGCTGAAAGGTG-3′ (reverse); for β-actin, 5′-TCCCTGGAGAAGAGCTACGA-3′ (forward) and 5′-AGCACTGTGTTGGCGTACAG-3′ (reverse); for miR-299-3p, 5′-ACACTCCAGCTGG-GTATGTGGGATGGTAAAC-3′ (forward) and 5′-GTGCAGGGTCCGAGGT-3′ (reverse); and for U6, 5′-CTCGCTTCGGCAGCACA-3′ (forward) and 5′-AACGCTTCACGAATTTGCGT-3′ (reverse). The relative expression level of each gene was calculated with the $2^{-\Delta\Delta}$Ct method.

Cell transfection

Lipofectamine 2000 kit (Invitrogen) was used to conduct cell transfection. Short hairpin RNAs (shRNAs) targeting NRAV were designed by Genepharma (Shanghai, China). The specific sequences targeting NRAV were designed as follows: For sh-NRAV #1, 5′-CACCTCATCCACAAGTAGGAC-3′; for sh-NRAV #2, 5′-TTGGAGCCAAGGACTGTACTG-3′; and negative control: 5′-TTCTCCGAACGT-GTCACGT-3′. NRAV overexpression plasmid and shRNAs against NRAV were inserted into the pcDNA3.1 vector and pGpU6/GFP/Neo vector, respectively. The miR-299-3p mimic was purchased from RiboBio. qRT-PCR was performed to examine the transfection efficiency.

Cell Counting Kit-8 assay

A 96-well plate was selected, and 2000 tumor cells were cultured in each well. The cells were transfected with different vectors and allowed to stand for 48 h. Cell Counting Kit-8 (CCK-8) solution (10 μL; Mashiki, Japan) was added to each well, and incubated for 2 h. A microplate reader (Winooski, VT, United States) was used to check cell viability.

Colony formation assay

The specific PDAC cells transfected with different plasmids were inoculated into six-well plates and incubated at 37°C for 10 d. Tumor cells were fixed for 20 min in methanol after being washed with phosphate-buffered saline in triplicate. Cell colonies were stained and counted.

Transwell assay

In migration and invasion assays, PDAC cells were added to resuspension after setting a concentration of 10^5 mL in a serum-free environment. Two hundred microliters of cell suspension was added to the upper layer of each Transwell chamber and 600 μL of complete media containing 10% fetal serum was added to the lower layer. To set up the invasion analysis phase, the Matrigel layer (BD Biosciences, United States) was first applied to the chamber membrane, and the cell suspension was placed on top of the transition chamber. A 24-h incubation was followed and the invasive cells were finally fixed and monitored and compared in five random fields.

Tumor xenograft experiments

All animal studies were approved by the Ethics Committee for Animal Studies at Shanghai 10th People's Hospital. Specific PANC-1 cells (2×10^6, 200/L) were transplanted subcutaneously to the right side of naked male mice aged 4 wk. The condition of the mice was monitored daily and the size of the tumor was measured every 5 d. Tumor volume was calculated according to tumor length and length formula volume = length through × wide^2/2. Twenty days after inoculation, mice were killed and the entire tumor removed and weighed.

Immunohistochemical analysis

Mouse tumors were removed for immunohistochemical staining to visualize Ki-67 expression. Paraffin-embedded sections were prepared and wax removed in 100% xylene, followed by rehydration with

various gradients of ethanol and distilled water. The fabric is dyed with a protractor for 1 h at room temperature and removed during washing with distilled water. Tissue sections were incubated for 20 min with secondary antibodies bound to horseradish peroxidase. To facilitate visualization, 3,3'-diaminobenzidine tetrahydrochloride Ki-67 was selected for positive staining.

Nuclear/cytoplasmic fractionation assay

The PARIS Kit (Life Technologies, United States) was used to isolate RNA from the nucleus and cytoplasm. qRT-PCR assays were conducted as described above.

RNA immunoprecipitation assay

RNA immunoprecipitation (RIP) assays were performed by EZ-Magna RNA Immunosuppression Kit (Millipore, United States). The cells were collected and resuspended in an immunodeposition buffer and kept on ice for 30 min. The cell suspension was incubated with a separate RIP buffer containing magnetic beads. Proteinase K was added to the bead state after buffering for further digestion of proteins. All RNA was extracted with Trizol and measured with qRT-PCR.

Dual-luciferase activity assay

According to a special combination of software for network prediction starbes 3.0 and NRAV miR-299-3p (http://starbase.sysu.edu.cn/ b). Other matters according to the V2 specification (enzyme, China), it is a rapid mutation reagent for NRAV, and supplementary DNA and mutant miR-299-3p are added to psicheck2 (US Promega) (NRAV wild and music) satellite. Paycheck-2 and miR-229-3p plasmid samples or miR-229-3p negative control were transferred to PDAC cells. After 48 h, the fluorescent enzyme activity of each well was examined by the Promega reporting system. The relative activity of luciferase is used for normalization.

Statistical analysis

Statistical analysis was performed using GraphPad Prisma 8.2 (LA Jolla, CA, United States) and SPSS 22.0 (IBM, Armonk, NY, United States). Student *t* test was used to compare the differences between the two groups and calculate the *P* value. $P < 0.05$ was statistically significant.

RESULTS

NRAV was significantly upregulated in PDAC and predicted poor prognosis

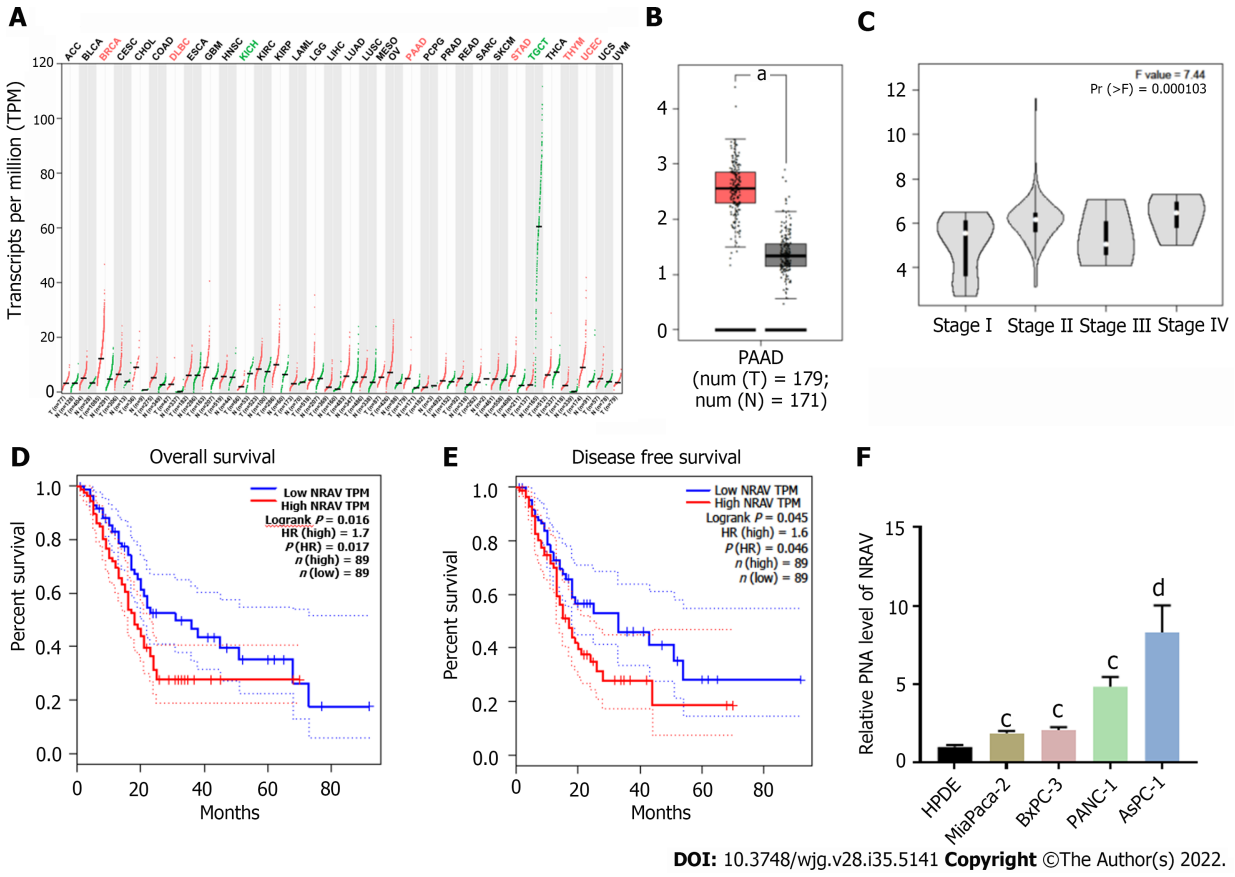
We used GEPIA to determine NRAV expression levels as an online bioinformatics tool for gene expression analysis based on the cancer genome database (TCGA)[16]. NRAV expression of PDAC in tissues was significantly higher than that in nonmedical tissues (Figure 1A and B). The survival curve showed that the total life cycle ($P = 0.034$; Figure 1D) and disease-free life cycle ($P = 0.046$; Figure 1E) of PDAC patients were decreasing. The data of the TCGA database showed that the level of emotional expression was negatively correlated with the level of clinical pathology (Figure 1C). The level of NRAV expression in HPDE cells and four PDAC systems was tested. NRAV in the PDAC cell system was significantly higher than that in HPDE cells (Figure 1F). Based on these data, we believe that NRAV may be a potential carcinogen related to lncRNA.

Knockdown of NRAV inhibited proliferation, migration and invasion of PDAC cells

We studied the biological role of NRAV in the PDAC cell system. We used heterogeneous RNA transplantation to reduce NRAV expression in PANC-1 and AsPC-1 cells. qRT-PCR showed a significant decrease in expression after NRAV (Figure 2A). After showing the results of CCK-8 tests and colony formation, there was a significant reduction after removal of signs of proliferation and abscision of PANC-1 and AsPC-1 cells (Figure 2B and C). We performed Transwell analysis to test whether NRAV affected metastasis and damage to police cells. Similarly, after the removal of PANC-1 and AsPC-1 cells, migration and invasion rates slowed significantly (Figure 2D and E). Knockdown of NRAV inhibited proliferation, migration and invasion of PDAC cells.

Overexpression of NRAV promoted PDAC cell proliferation, migration and invasion

High expression of NRAV in BXPC-3 and Mia PaCa-2 cells used to display exogenous particles confirmed the effectiveness of the expression (Figure 3A). The CCK-8 test and the product reduction test showed that NRAV overexpression significantly supported proliferation and formation of PDAC cells (Figure 3B and C). Transwell analysis found that NRAV overexpression significantly increased displacement and invasion of Mia PaCa-2 and BXPC-3 cells (Figure 3D and E). Overall, the results showed that NRAV promotes proliferation, metastasis and invasion of PDAC cells.



DOI: 10.3748/wjg.v28.i35.5141 **Copyright** ©The Author(s) 2022.

Figure 1 Relative expression of negative regulator of antiviral response in pancreatic cancer tissues and cells and its clinical significance. A: The negative regulator of antiviral response (NRAV) expression profile across all tumor samples and paired normal tissues; B: The NRAV expression of pancreatic adenocarcinoma in tissues was significantly higher than that in normal pancreas tissues; C: Expression of NRAV in patients divided by cancer stages using expression data from The Cancer Genome Atlas (TCGA) database; D: Overall survival analyzed by GEPIA based on the TCGA database; E: Disease-free survival analyzed by GEPIA based on the TCGA database; F: Quantitative real-time polymerase chain reaction analysis measured NRAV expression level in four pancreatic cancer and normal cell lines. $^{c}P < 0.001$; $^{d}P < 0.0001$. PAAD: Pancreatic adenocarcinoma; TPM: Transcripts per million; NRAV: Negative regulator of antiviral response; HR: Hazard ratio.

NRAV ablation inhibited tumor growth in vivo

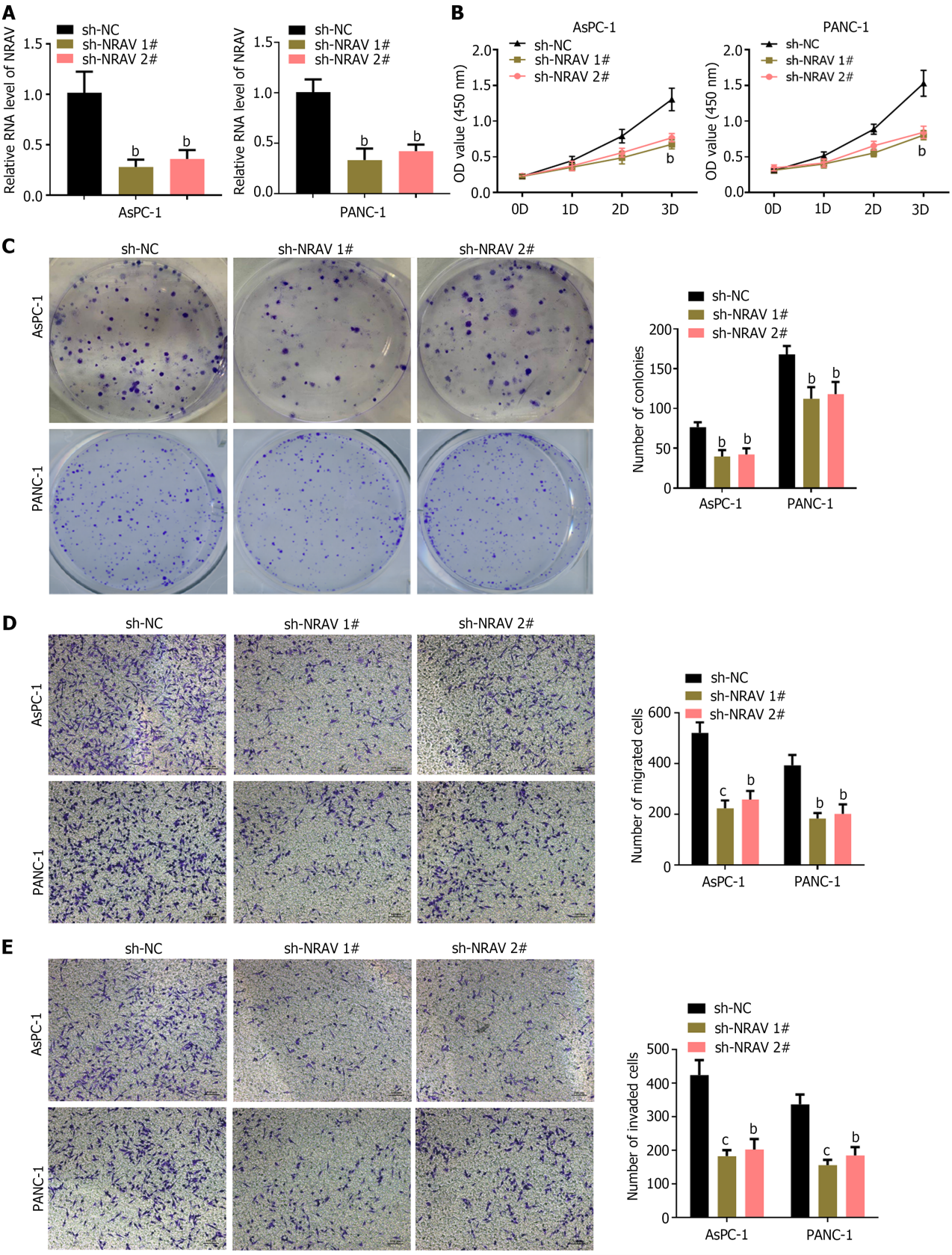
To further investigate whether NRAV supports tumor growth *in vivo*, PANC-1 cells were injected into naked mice treated with sh-NRAV and internal control cells. The tumor volume of the NRAV genotype was significantly lower than the negative control volume (Figure 4A and B). Similarly, the mass of the tumor in the NRAV group (Figure 4C) was significantly reduced compared to the control group. Ki-67 was analyzed for lignin content and immunochemical staining. Reduction of NRAV led to a significant reduction of Ki-67 and inhibition of tumor growth (Figure 4D and E). Overall, these findings suggest that NRAV does not inhibit tumor growth *in vivo*.

NRAV acted as a molecular sponge for miR-299-3p in PDAC

To study how NRAV plays a catalytic role in PDAC, we used the nuclear/cell separation method to determine the location of NRAV in PDAC. Spleen qi was mainly located in cells (Figure 5A), and it can exert its biological function as a competitive endogenous RNA[17,18]. We used starbase V3.0 (http://starbase.sysu.edu.cn/) Interactive Bio information Analysis Software to identify potential miRNAs that may interact with genes. miR-299-3p was selected as the tempered target due to potential point complementarity (Figure 5B). Rip analysis confirms this point[19]. As shown in Overexpression in PDAC cells resulted in significant enrichment of miR-299-3p on ago2 (Figure 5C). The miR-299-3p simulator significantly reduced the fluorescence activity of the wild-type NRAV group, while this change did not occur in the modified NRAV group (Figure 5D). qRT-PCR showed that expression of miR-299-3p in PDAC cells was significantly enhanced after removing the traits (Figure 5E). Spearman's analysis showed that expression of NRAV and miR-299-3p in PDAC tissue was opposite (Figure 5F). Therefore, these results suggest that temper may play the role of molecular sponge miR-299-3p.

miR-299-3p reversed the effect of NRAV on PDAC cells

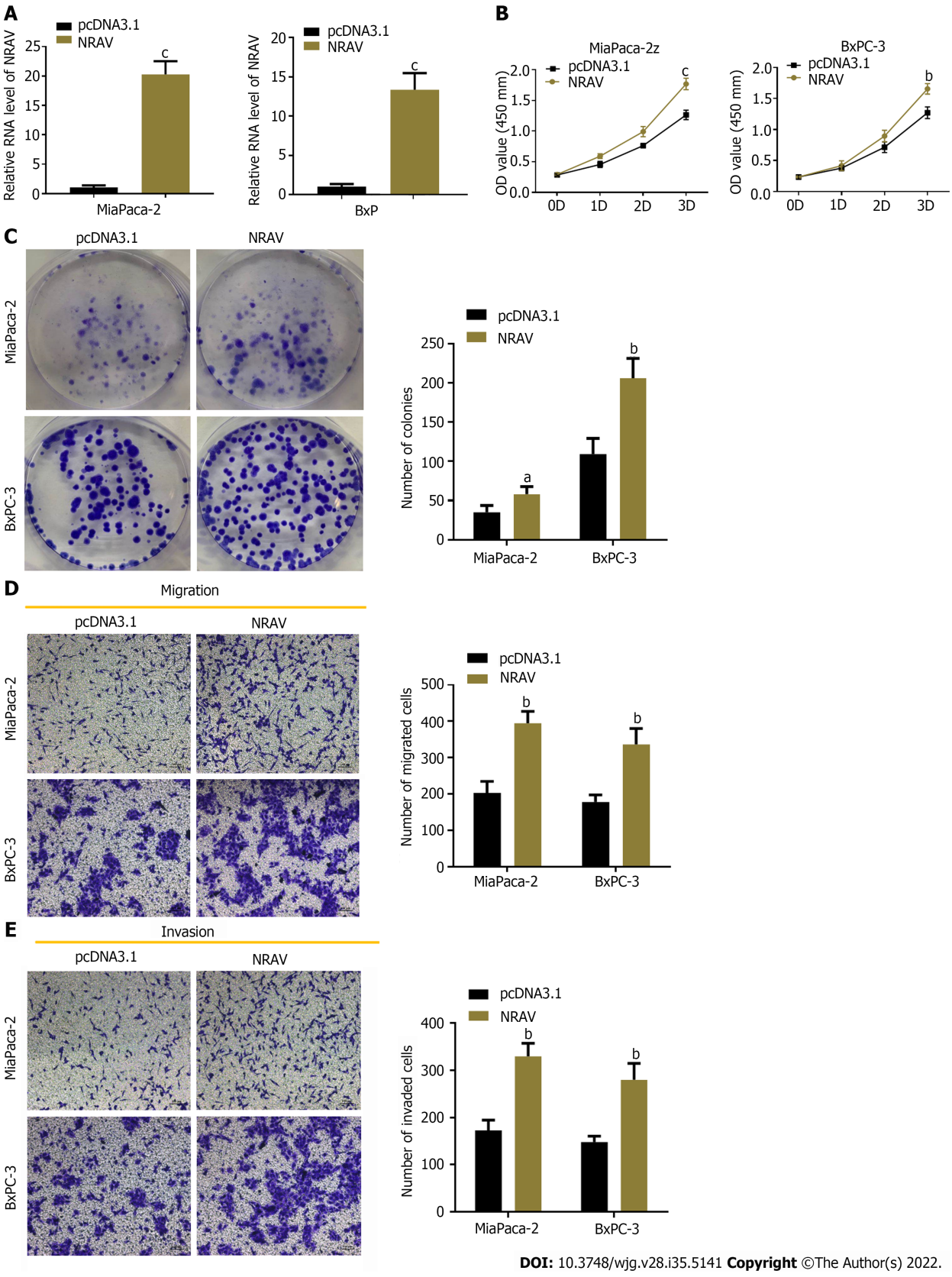
To validate whether NRAV affected proliferation and metastasis of PDAC cells through sponging miR-299-3p, specific miR-299-3p mimic or mimic NC vector was cotransfected into PDAC cells after overex-



DOI: 10.3748/wjg.v28.i35.5141 **Copyright** ©The Author(s) 2022.

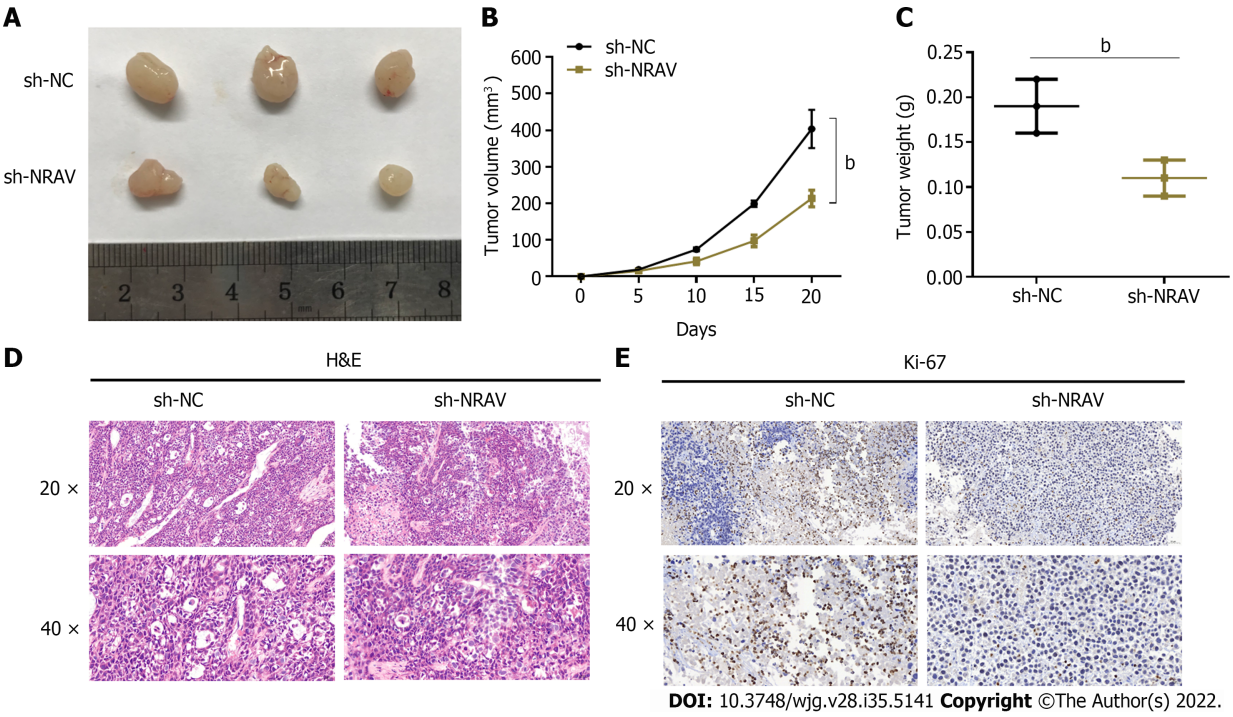
Figure 2 Knockdown of negative regulator of antiviral response inhibited proliferation, migration and invasion of pancreatic cancer cells.

A: Quantitative real-time polymerase chain reaction analysis assessed expression of NRAV in PANC-1 and AsPC-1 cells transfected with shNC, shRNA #1 and shRNA #2 targeting negative regulator of antiviral response; B: Cell Counting Kit-8 analysis showed that compared with the NC group, NRAV gene knockout significantly reduced the proliferation of PANC-1 and AsPC-1 cells; C: The colony formation test showed that NRAV ablation inhibited the colony numbers of PANC-1 and AsPC-1 cells; D: Transwell assays were performed to measure migration of PANC-1 and AsPC-1 cells; E: Transwell assays were performed to measure invasion of PANC-1 and AsPC-1 cells. $^{b}P < 0.01$; $^{c}P < 0.001$. NRAV: Negative regulator of antiviral response; sh: Short hairpin; NC: Negative control.



DOI: 10.3748/wjg.v28.i35.5141 **Copyright** ©The Author(s) 2022.

Figure 3 Overexpression of negative regulator of antiviral response promoted pancreatic cancer cell proliferation, migration and invasion. A: Quantitative real-time polymerase chain reaction measured negative regulator of antiviral response (NRAV) expression in Mia Paca-2 and BxPC-3 cells transfected with pcDNA3.1 empty vector or pcDNA3.1-NRAV; B: Cell Counting Kit-8 was performed to detect proliferation of Mia Paca-2 and BxPC-3 cells; C: Colony formation test showed that NRAV overexpression increased the number of clones of Mia-Paca-2 and BXPC-3 cells; D: Transwell assays were performed to measure migration of Mia Paca-2 and BxPC-3 cells; E: Transwell assays were performed to measure invasion of Mia Paca-2 and BxPC-3 cells. $^{a}P < 0.05$; $^{b}P < 0.01$; $^{c}P < 0.001$. NRAV: Negative regulator of antiviral response.



DOI: 10.3748/wjg.v28.i35.5141 **Copyright** ©The Author(s) 2022.

Figure 4 Negative regulator of antiviral response ablation inhibited tumor growth in a mouse xenograft models. A: Representative images of xenograft tumors after transfection with short hairpin NC or sh-negative regulator of antiviral response (NRAV); B: Tumor volume was measured; C: Tumor weight was measured; D: Representative images of hematoxylin and eosin staining for xenograft tumor tissue samples; E: Expression pattern of Ki-67 in the harvested tumor tissues was detected by immunohistochemical staining. $^{b}P < 0.01$. sh: Short hairpin; NRAV: Negative regulator of antiviral response; NC: Negative control.

pression of NRAV. Subsequently, we evaluated the cell proliferation, migration and invasion of PDAC cells. miR-299-3p mimic reversed the dramatic promotion by overexpression of NRAV on proliferation (Figure 6A and B). Similarly, miR-299-3p mimic inhibited the promoting effects of NRAV overexpression on migration and invasion of PDAC cells (Figure 6C and D). These results indicated that miR-299-3p mediated the promoting effects of NRAV on PDAC cell proliferation, migration and invasion.

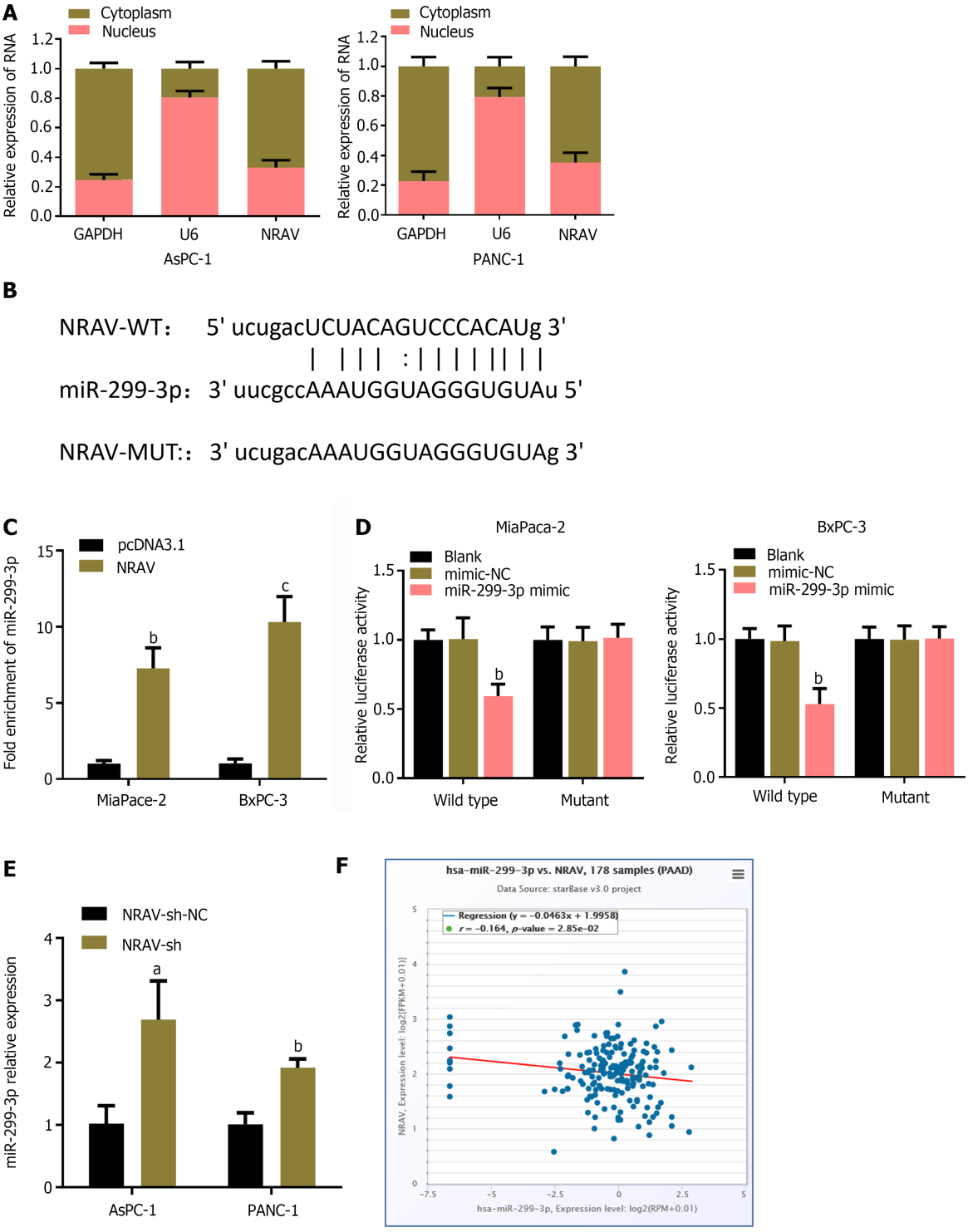
DISCUSSION

An increasing number of studies have shown that lncRNAs play an important role in the development of various malignant tumors. Recent studies have shown that large amounts of lncRNAs are abnormally expressed in PDAC and participate in the tumor process[20,21]. Guo *et al*[22] found that under hypoxia, lncRNAs extract of PDAC *UCA1* cells increased to promote angiogenesis. We used the TCGA database to identify NRAV in PDAC. We confirmed that the code of good conduct is a key element related to the program of action, and that significant progress has been made in the program of action. In addition, in PDAC patients, high levels of NRAV expression inhibit overall and disease-free survival. It is worth noting that NRAV may participate in PDAC progression.

The specific role of NRAV in oncology is not clear due to increased immunization. Recent studies have shown that NRAV expression is significantly increased in liver cancer and myeloma and can play a key role in the development of these two tumors[10,23]. To verify the biological function of NRAV in PDAC, function loss and acquisition studies were carried out. The results of *in vitro* experiments showed that temper has a major contribution to the migration, invasion and reproduction of PDAC cells. In addition, ablation temperament significantly reduced the tumor of the nude mouse model overall, these results show that the NRAV plays an important role in promoting cancer and can be used as a new biometric index for diagnosis and prediction of diseases caused by PDAC.

To further study the potential mechanism of NRAV, nuclear/cell division experiments were carried out in PDAC, and NRAV was mainly in the cytoplasm. Further analysis of the rip report analysis showed that NRAV may play the role of miR-299-3p molecular sponge (Figure 7). In addition, the stimulation effect of NRAV on malignant tumors in PDAC cells was also proved in the rescue experiment. The role of NRAV in promoting progression of PDAC mainly depends on miR-299-3p.

At the beginning of the study, it was emphasized that the significant increase in lncRNA was negatively correlated with overall and disease-free survival in PDAC patients. In addition, it also plays a carcinogenic role by promoting the proliferation and metastasis of cells in the sponge world. Our research shows that NRAV/miR-299-3p play a key role in PDAC and can be used as potential

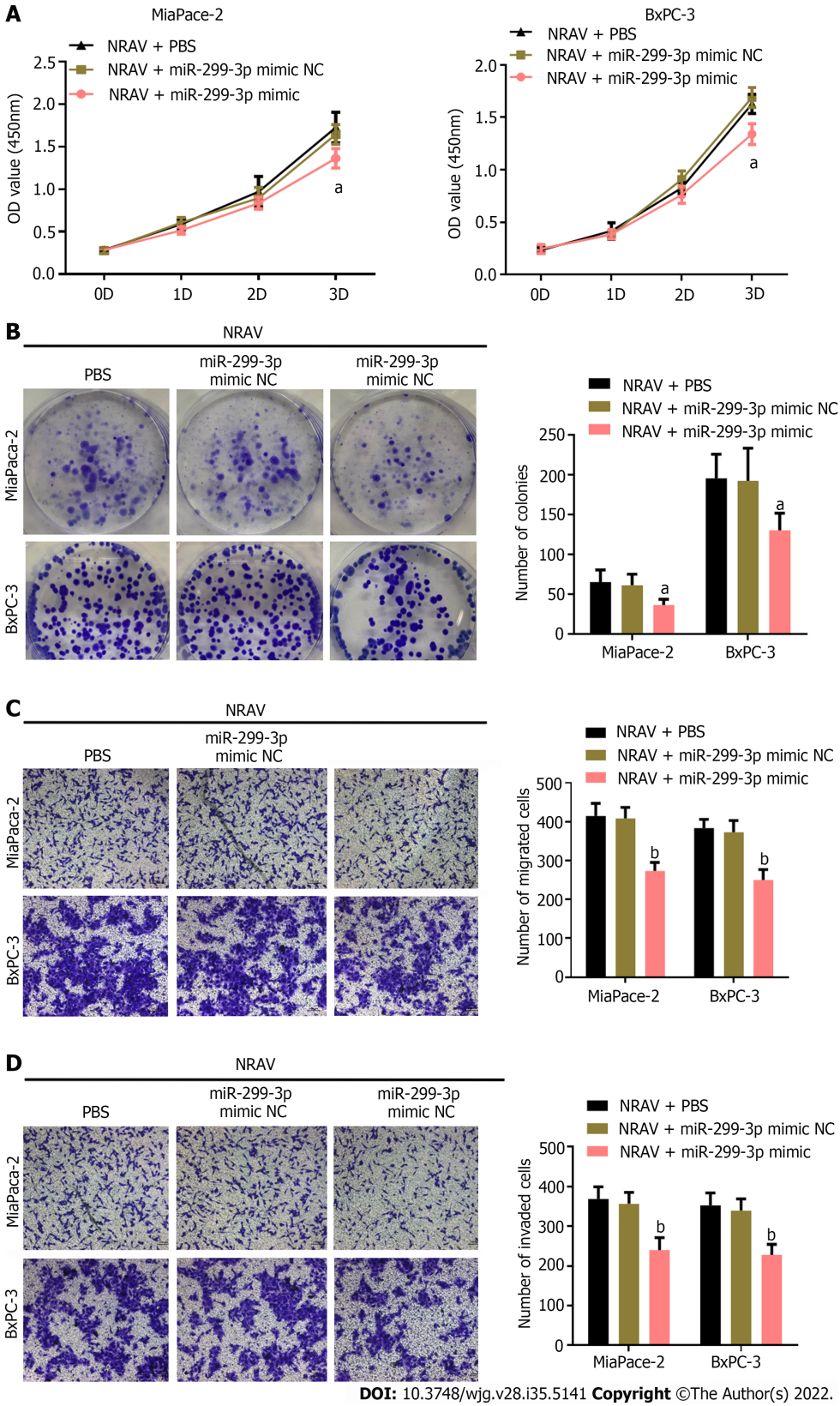


DOI: 10.3748/wjg.v28.i35.5141 **Copyright** ©The Author(s) 2022.

Figure 5 Negative regulator of antiviral response acted as a molecular sponge for miR-299-3p. A: Subcellular fractionation assay was used to determine the subcellular localization of NRAV; B: A complementary binding site of *NRAV* in miR-299-3p was predicted *via* starBase v3.0 online database; C: RNA immunoprecipitation assays were performed to validate whether *NRAV* could interact with miR-299-3p in MiaPaca-2 and BxPC-3 cells; D: Luciferase reporter assays were carried out to verify the direct binding of *NRAV* and miR-299-3p in MiaPaca-2 and BxPC-3 cells; E: Relative expression of miR-299-3p in AsPC-1 and PANC-1 cells following knockdown of *NRAV*; F: Spearman's correlation analysis between *NRAV* and miR-299-3p expression in PAAD by the starBase v3.0 project. $^{a}P < 0.05$; $^{b}P < 0.01$; $^{c}P < 0.001$. NRAV: Negative regulator of antiviral response; MUT: Mutant; NC: Negative control; WT: Wild-type.

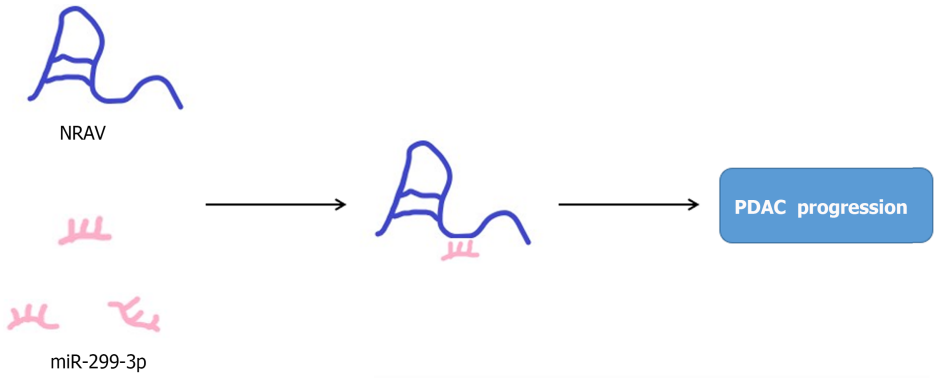
biomarkers for PDAC diagnosis and treatment.

However, because no samples from patients with pancreatic cancer were collected, there was a lack of correlation analysis between temperament expression and PDAC clinicopathological features. In addition, it is also of great significance to study the significance of NRAV and miR-299-3p in PDAC organization.



DOI: 10.3748/wjg.v28.i35.5141 **Copyright** ©The Author(s) 2022.

Figure 6 miR-299-3p reversed the effect of negative regulator of antiviral response on pancreatic cancer cells. A: Viability of MiaPaca-2 and BxPC-3 cells was determined following transfection with pcDNA3.1-*NRAV* and miR-299-3p mimic by Cell Counting Kit-8 assay; B: Proliferation of MiaPaca-2 and BxPC-3 cells was detected by colony formation assay; C: Transwell assays of cell migration was performed in MiaPaca-2 and BxPC-3 cells transfected with pcDNA3.1-*NRAV* and miR-299-3p mimic; D: Transwell assays of cell invasion were performed in MiaPaca-2 and BxPC-3 cells transfected with pcDNA3.1-*NRAV* and miR-299-3p mimic. $^{a}P < 0.05$; $^{b}P < 0.01$. NRAV: Negative regulator of antiviral response; NC: Negative control; PBS: Phosphate-buffered saline.



DOI: 10.3748/wjg.v28.i35.5141 **Copyright** ©The Author(s) 2022.

Figure 7 Negative regulator of antiviral response plays the role of miR-299-3p molecular sponge to promote the progress of pancreatic ductal cancer.

CONCLUSION

NRAV can act as a molecular sponge of miR-299-3p and significantly promote the proliferation and metastasis of PDAC cells.

ARTICLE HIGHLIGHTS

Research background

Pancreatic ductal adenocarcinoma (PDAC) has high malignancy and poor prognosis. Long noncoding RNAs (lnRNAs) are recognized as crucial factors and associated with progression of PDAC. However, the specific biological role and practical clinical significance of lnRNAs and negative regulator of antiviral response (NRAV) in PDAC remain unclear.

Research motivation

Early and timely diagnosis and treatment of PDAC are still scarce. Therefore, it is a matter of urgency to comprehensively understand the pathogenesis of PDAC and explore more effective targets for its diagnosis and treatment.

Research objectives

To study the role of NRAV in the growth and metastasis of PDAC.

Research methods

Real-time polymerase chain reaction detected expression of NRAV and miR-299-3p in PDAC cells. The temperament correction and miR-299-3p in the process of cell proliferation, metastasis and invasion were verified by Cell Counting Kit-8, precipitation test, and Transwell assay. RNA and fluorescent enzyme immunoprecipitation test to test the interaction between NRAV and miR-299-3p. Verify the interaction between NRAV and miR-299-3p.

Research results

According to our data, NRAV in PDAC was significantly increased, which is related to the negative survival rate of PDAC patients. NRAV overexpression was conducive to the proliferation and metastasis of PDAC cells, and NRAV knockout reversed these effects. Finally, in terms of mechanism, NRAV acts as a miR-299-3p molecular sponge. Overexpression of miR-299-3p significantly changed the role of NRAV in the proliferation, metastasis and invasion of PDAC cells.

Research conclusions

NRAV promotes proliferation and metastasis of PDAC by playing the molecule sponge function of miR-299-3p.

Research perspectives

NRAV facilitated the progression of PDAC, which provides a potential biological marker for diagnosis and therapeutic target for PDAC.

FOOTNOTES

Author contributions: Qiu ZJ and Wang HQ designed the experiments and revised the manuscript; Qian CH and Wang HQ performed most of the experiments; Li PM and Guo ZY analyzed the data; Wang HQ and Guo ZY wrote the manuscript; all authors discussed the results and reviewed the manuscript.

Supported by the National Natural Science Foundation of China, No. 81974372.

Institutional animal care and use committee statement: All procedures involving animals were reviewed and approved by the Institutional Animal Care and Use Committee of the Animal Ethics Committee of Shanghai General Hospital, No. SHDSYY-2020-T1663.

Conflict-of-interest statement: There are no conflicts of interest to report.

Data sharing statement: The authors are amenable to data sharing.

ARRIVE guidelines statement: The authors have read the ARRIVE Guidelines, and the manuscript was prepared and revised according to the ARRIVE Guidelines.

Open-Access: This article is an open-access article that was selected by an in-house editor and fully peer-reviewed by external reviewers. It is distributed in accordance with the Creative Commons Attribution NonCommercial (CC BY-NC 4.0) license, which permits others to distribute, remix, adapt, build upon this work non-commercially, and license their derivative works on different terms, provided the original work is properly cited and the use is non-commercial. See: https://creativecommons.org/Licenses/by-nc/4.0/

Country/Territory of origin: China

ORCID number: Hai-Quan Wang 0000-0003-4178-9979; Chun-Hua Qian 0000-0001-5706-2841; Zeng-Ya Guo 0000-0001-8310-5147; Pei-Ming Li 0000-0001-8919-5016; Zheng-Jun Qiu 0000-0002-8318-847X.

S-Editor: Chen YL
L-Editor: Kerr C
P-Editor: Cai YX

REFERENCES

1 **Siegel RL**, Miller KD, Fuchs HE, Jemal A. Cancer Statistics, 2021. *CA Cancer J Clin* 2021; **71**: 7-33 [PMID: 33433946 DOI: 10.3322/caac.21654]
2 **Sung H**, Ferlay J, Siegel RL, Laversanne M, Soerjomataram I, Jemal A, Bray F. Global Cancer Statistics 2020: GLOBOCAN Estimates of Incidence and Mortality Worldwide for 36 Cancers in 185 Countries. *CA Cancer J Clin* 2021; **71**: 209-249 [PMID: 33538338 DOI: 10.3322/caac.21660]
3 **Esteller M**. Non-coding RNAs in human disease. *Nat Rev Genet* 2011; **12**: 861-874 [PMID: 22094949 DOI: 10.1038/nrg3074]
4 **Nagano T**, Fraser P. No-nonsense functions for long noncoding RNAs. *Cell* 2011; **145**: 178-181 [PMID: 21496640 DOI: 10.1016/j.cell.2011.03.014]
5 **Guttman M**, Rinn JL. Modular regulatory principles of large non-coding RNAs. *Nature* 2012; **482**: 339-346 [PMID: 22337053 DOI: 10.1038/nature10887]
6 **Yao RW**, Wang Y, Chen LL. Cellular functions of long noncoding RNAs. *Nat Cell Biol* 2019; **21**: 542-551 [PMID: 31048766 DOI: 10.1038/s41556-019-0311-8]
7 **Bhan A**, Soleimani M, Mandal SS. Long Noncoding RNA and Cancer: A New Paradigm. *Cancer Res* 2017; **77**: 3965-3981 [PMID: 28701486 DOI: 10.1158/0008-5472.CAN-16-2634]
8 **Arun G**, Diermeier SD, Spector DL. Therapeutic Targeting of Long Non-Coding RNAs in Cancer. *Trends Mol Med* 2018; **24**: 257-277 [PMID: 29449148 DOI: 10.1016/j.molmed.2018.01.001]
9 **Ouyang J**, Zhu X, Chen Y, Wei H, Chen Q, Chi X, Qi B, Zhang L, Zhao Y, Gao GF, Wang G, Chen JL. NRAV, a long noncoding RNA, modulates antiviral responses through suppression of interferon-stimulated gene transcription. *Cell Host Microbe* 2014; **16**: 616-626 [PMID: 25525793 DOI: 10.1016/j.chom.2014.10.001]
10 **Xu Q**, Wang Y, Huang W. Identification of immune-related lncRNA signature for predicting immune checkpoint blockade and prognosis in hepatocellular carcinoma. *Int Immunopharmacol* 2021; **92**: 107333 [PMID: 33486322 DOI: 10.1016/j.intimp.2020.107333]
11 **Chan JJ**, Tay Y. Noncoding RNA:RNA Regulatory Networks in Cancer. *Int J Mol Sci* 2018; **19** [PMID: 29702599 DOI: 10.3390/ijms19051310]
12 **Chen W**, Zhang K, Yang Y, Guo Z, Wang X, Teng B, Zhao Q, Huang C, Qiu Z. MEF2A-mediated lncRNA HCP5 Inhibits Gastric Cancer Progression *via* MiR-106b-5p/p21 Axis. *Int J Biol Sci* 2021; **17**: 623-634 [PMID: 33613117 DOI: 10.7150/ijbs.55020]
13 **Duan H**, Li X, Chen Y, Wang Y, Li Z. LncRNA RHPN1-AS1 promoted cell proliferation, invasion and migration in cervical cancer *via* the modulation of miR-299-3p/FGF2 axis. *Life Sci* 2019; **239**: 116856 [PMID: 31525429 DOI: 10.1016/j.lfs.2019.116856]

14 **Bai N**, Ma Y, Zhao J, Li B. Knockdown of lncRNA HCP5 Suppresses the Progression of Colorectal Cancer by miR-299-3p/PFN1/AKT Axis. *Cancer Manag Res* 2020; **12**: 4747-4758 [PMID: 32606965 DOI: 10.2147/CMAR.S255866]

15 **Xu K**, Zhang L. Inhibition of TUG1/miRNA-299-3p Axis Represses Pancreatic Cancer Malignant Progression *via* Suppression of the Notch1 Pathway. *Dig Dis Sci* 2020; **65**: 1748-1760 [PMID: 31655908 DOI: 10.1007/s10620-019-05911-0]

16 **Tang Z**, Li C, Kang B, Gao G, Zhang Z. GEPIA: a web server for cancer and normal gene expression profiling and interactive analyses. *Nucleic Acids Res* 2017; **45**: W98-W102 [PMID: 28407145 DOI: 10.1093/nar/gkx247]

17 **Salmena L**, Poliseno L, Tay Y, Kats L, Pandolfi PP. A ceRNA hypothesis: the Rosetta Stone of a hidden RNA language? *Cell* 2011; **146**: 353-358 [PMID: 21802130 DOI: 10.1016/j.cell.2011.07.014]

18 **Batista PJ**, Chang HY. Long noncoding RNAs: cellular address codes in development and disease. *Cell* 2013; **152**: 1298-1307 [PMID: 23498938 DOI: 10.1016/j.cell.2013.02.012]

19 **Gregory RI**, Chendrimada TP, Cooch N, Shiekhattar R. Human RISC couples microRNA biogenesis and posttranscriptional gene silencing. *Cell* 2005; **123**: 631-640 [PMID: 16271387 DOI: 10.1016/j.cell.2005.10.022]

20 **Wang Y**, Zhou L, Lu J, Jiang B, Liu C, Guo J, Xiao GG. Research progress on long non-coding RNAs and their roles as potential biomarkers for diagnosis and prognosis in pancreatic cancer. *Cancer Cell Int* 2020; **20**: 457 [PMID: 32973402 DOI: 10.1186/s12935-020-01550-y]

21 **Tasaki Y**, Suzuki M, Katsushima K, Shinjo K, Iijima K, Murofushi Y, Naiki-Ito A, Hayashi K, Qiu C, Takahashi A, Tanaka Y, Kawaguchi T, Sugawara M, Kataoka T, Naito M, Miyata K, Kataoka K, Noda T, Gao W, Kataoka H, Takahashi S, Kimura K, Kondo Y. Cancer-Specific Targeting of Taurine-Upregulated Gene 1 Enhances the Effects of Chemotherapy in Pancreatic Cancer. *Cancer Res* 2021; **81**: 1654-1666 [PMID: 33648930 DOI: 10.1158/0008-5472.CAN-20-3021]

22 **Guo Z**, Wang X, Yang Y, Chen W, Zhang K, Teng B, Huang C, Zhao Q, Qiu Z. Hypoxic Tumor-Derived Exosomal Long Noncoding RNA UCA1 Promotes Angiogenesis *via* miR-96-5p/AMOTL2 in Pancreatic Cancer. *Mol Ther Nucleic Acids* 2020; **22**: 179-195 [PMID: 32942233 DOI: 10.1016/j.omtn.2020.08.021]

23 **Maimaiti A**, Jiang L, Wang X, Shi X, Pei Y, Hao Y, Paerhati H, Zibibula Y, Abudujielili A, Kasimu M. Identification and validation of an individualized prognostic signature of lower-grade glioma based on nine immune related long non-coding RNA. *Clin Neurol Neurosurg* 2021; **201**: 106464 [PMID: 33454543 DOI: 10.1016/j.clineuro.2020.106464]

World Journal of Gastroenterology

Submit a Manuscript: https://www.f6publishing.com

World J Gastroenterol 2022 September 21; 28(35): 5154-5174

DOI: 10.3748/wjg.v28.i35.5154

ISSN 1007-9327 (print) ISSN 2219-2840 (online)

ORIGINAL ARTICLE

Basic Study

Alcohol promotes epithelial mesenchymal transformation-mediated premetastatic niche formation of colorectal cancer by activating interaction between laminin-γ2 and integrin-β1

Fei-Fei Nong, Yu-Qi Liang, Shang-Ping Xing, Yin-Fang Xiao, Hui-Hui Chen, Bin Wen

Specialty type: Oncology

Provenance and peer review: Unsolicited article; Externally peer reviewed.

Peer-review model: Single blind

Peer-review report's scientific quality classification

Grade A (Excellent): 0
Grade B (Very good): B
Grade C (Good): 0
Grade D (Fair): D
Grade E (Poor): 0

P-Reviewer: Legaz I, Spain; Spataru A, Canada

Received: May 25, 2022
Peer-review started: May 25, 2022
First decision: July 12, 2022
Revised: July 23, 2022
Accepted: August 22, 2022
Article in press: August 22, 2022
Published online: September 21, 2022

Fei-Fei Nong, Yin-Fang Xiao, Hui-Hui Chen, Bin Wen, Pi-Wei Institute, Science and Technology Innovation Center, Guangzhou University of Chinese Medicine, Guangzhou 510000, Guangdong Province, China

Yu-Qi Liang, The Second Clinical College of Guangzhou University of Chinese Medicine, Guangzhou University of Chinese Medicine, Guangzhou 510000, Guangdong Province, China

Shang-Ping Xing, Guangxi Key Laboratory of Bioactive Molecules Research and Evaluation, School of Pharmacy, Guangxi Medical University, Nanning 530022, Guangxi Zhuang Autonomous Region, China

Corresponding author: Bin Wen, PhD, Academic Research, Full Professor, Pi-Wei Institute, Science and Technology Innovation Center, Guangzhou University of Chinese Medicine, No. 232 Waihuandong Road, Guangzhou 510000, Guangdong Province, China.
wenbin@gzucm.edu.cn

Abstract

BACKGROUND

Colorectal cancer (CRC) is a common malignant tumor. Alcohol consumption is positively correlated with CRC malignant metastasis; however, the mechanism is unclear. The interaction between laminin-γ2 (LAMC2) and integrin-β1 (ITGB1) plays a role in premetastatic niche signaling, which may induce epithelial mesenchymal transformation (EMT) and lead to metastasis.

AIM

To investigate the effects of alcohol on CRC metastasis from the molecular mechanism of the premetastatic niche.

METHODS

The interaction between LAMC2 and ITGB1 was measured by Duolink assay, and the expression levels of LAMC2, ITGB1 and focal adhesion kinase (FAK), snail, fibronectin, N-cadherin and special AT-rich sequence binding protein 1 (SATB1) were measured by quantitative real-time polymerase chain reaction, immunohistochemistry and western blotting. Interleukin-1β (IL-1β), tumor necrosis factor-α (TNF-α) and IL-6 levels were measured *via* enzyme-linked immunosorbent assay, histopathological assessment *via* hematoxylin eosin staining, and determination of

aberrant crypt foci *via* methylene blue.

RESULTS

The lymph node metastasis rate was higher in the alcohol group than non-alcohol group. There was a significant increase in interaction signals between LAMC2 and ITGB1, and an increase in phosphorylate-FAK/FAK, snail, fibronectin, N-cadherin and SATB1, whereas E-cadherin was reduced in the alcohol group compared to the non-alcohol group in both animal and clinical samples. Serum IL-1β, TNF-α and IL-6 were higher in alcohol group than in non-alcohol group. Alcohol may promote CRC metastasis by influencing the molecular mechanism of the premetastatic niche.

CONCLUSION

Our study suggests that alcohol promotes EMT-mediated premetastatic niche formation of CRC by activating the early interaction between LAMC2 and ITGB1 and lead to CRC metastasis.

Key Words: Alcohol; Colorectal cancer; Premetastatic niche; Epithelial mesenchymal transformation; Metastasis

©The Author(s) 2022. Published by Baishideng Publishing Group Inc. All rights reserved.

Core Tip: Our study indicated that alcohol promotes epithelial mesenchymal transformation-mediated premetastatic niche formation of colorectal cancer (CRC) by activating the early interaction between laminin-γ2 and integrin-β1 and lead to CRC metastasis.

Citation: Nong FF, Liang YQ, Xing SP, Xiao YF, Chen HH, Wen B. Alcohol promotes epithelial mesenchymal transformation-mediated premetastatic niche formation of colorectal cancer by activating interaction between laminin-γ2 and integrin-β1. *World J Gastroenterol* 2022; 28(35): 5154-5174

URL: https://www.wjgnet.com/1007-9327/full/v28/i35/5154.htm

DOI: https://dx.doi.org/10.3748/wjg.v28.i35.5154

INTRODUCTION

Colorectal cancer (CRC) is the third most commonly diagnosed malignancy worldwide[1]. A majority of colorectal cancers are associated with the environmental factors such as lifestyle changes including diet, obesity, smoking and alcohol consumption[2,3]. It is reported that long-term alcohol consumption is associated with an increased risk of CRC metastasis[3]. In the presence of concomitant metastasis, the maximum survival rates after surgical intervention do not exceed 20%[4,5]. Therefore, the relationship between alcohol consumption and CRC metastasis should be investigated. However, the mechanism that the alcohol promotes CRC metastasis has not been clearly explained[6,7].

Accumulating evidence suggests that metastasis develops from disseminated cancer cells that can remain dormant, and the dissemination may occur during the early stage of tumor evolution[7,8]. The microenvironment around the early disseminated cancer cells, also known as the premetastatic niche[9,10], may play an important role during the proliferation and migration of disseminated cancer cells in the early stage of tumors[11-13]. The extracellular matrix (ECM) is an important part of the premetastatic niche[14-17].

As an important component of the ECM, laminins are important for adhesion, differentiation, migration, and resistance to apoptosis of various cells, including cancer cells[18-21]. Reports have indicated that laminins are involved in the formation of the premetastatic niche[22,23]. Laminin-γ2 (LAMC2), a subunit of laminin-332, has been reported to be an important component in the survival dependent environment of epithelial cells in CRC and plays a key role in the regulation of tumor cell motility in premetastatic niche formation[24-27]. The interaction between LAMC2 and integrin-β1 (ITGB1) may stimulate the formation of premetastatic focal contacts by activating the premetastatic niche signaling, which promotes the migration of cancer cells[28]. Focal adhesion kinase (FAK) is a premetastatic focal contact involved in LAMC2 and β1 integrin signal transduction[29]. Signaling cascades triggered by integrin-laminin interactions in cells phosphorylate FAK, which induced epithelial mesenchymal transformation (EMT). EMT is a key initiating step during the metastasis and invasion of cancer[30,31] and involved in the formation of the premetastatic niche[32,33].

Alcohol consumption may influence the ECM remodeling and thus induce EMT, which may be closely related to the premetastatic niche[34]. Therefore, we explore its effect on CRC metastasis from the view of the premetastatic niche.

MATERIALS AND METHODS

Antibodies and reagents

The following antibodies were used: LAMC2 monoclonal antibody (YT5379, Immunoway, United States), ITGB1 monoclonal antibody (sc-9970, Santa Cruz, United States), glyceraldehyde-3-phosphate dehydrogenase (GAPDH) monoclonal antibody (ab125247, ABCAM, United Kingdom), phosphorylate-FAK (p-FAK)-Y397 (AP0302, ABclonal, Wuhan, China), FAK monoclonal antibody (A11131, ABclonal, Wuhan, China), snail monoclonal antibody (ab53519, ABCAM, United Kingdom), E-cadherin polyclonal antibody (ab1416, ABCAM, United Kingdom), N-cadherin polyclonal antibody (22018-1-AP, Proteintech, United States), fibronectin polyclonal antibody (A16678, ABclonal, Wuhan, China) and special AT-rich sequence binding protein 1 (SATB1) polyclonal antibody (A5800, ABclonal, Wuhan, China). Secondary antibodies were ab288151 and ab150113 (ABCAM, United Kingdom). Polyvinylidene difluoride membranes with a pore size of 0.45 mm (Millipore, United States) were used. RNAEX reagent (Accurate Biotechnology, Beijing, China), Evo M-MLV RT Premix (Accurate Biotechnology, Beijing, China), SYBR Green Premix Pro Taq HS qPCR Kit (Accurate Biotechnology, China). Interleukin-6 (IL-6), IL-1β and tumor necrosis factor-α (TNF-α) enzyme-linked immunosorbent assay (ELISA) kits (Enzyme-linked Biotechnology Co., LTD, Shanghai, China) were used. Duolink proximity ligation assay (PLA) kits (DUO92012, Merck, United States), Duolink PLA Rabbit PLUS (DUO92002, Merck, United States), and PLA Mouse MINUS (DUO92004, Merck, United States) proximity probes were purchased from Sigma-Aldrich. All above the mentioned antibodies can be used in both in rats and in humans.

Patients and clinical data

A total of 63 patients (26-86 years old) at The First Affiliated Hospital of Guangzhou University of Chinese Medicine (Guangzhou, China) from July 2019 to February 2020 was enrolled in this study. The baseline characteristics were collected, and data on alcohol consumption were collected at baseline using a direct interview method[35]. Participants were asked to answer whether they drank alcoholic beverages ("Yes", "Yes, but not now", or "No" were the answer options to the question, "Have you ever drunk alcohol?"), and for "ever drinkers", consumption frequency and average quantity of one serving over the past year by beverage type was recorded. CRC patients who never drank alcohol were added into the non-alcohol group, and CRC patients who drank alcohol over 3 times a week for more than 5 years were added into the alcohol group. And patients with smoking, family history, blood lipids, obesity, and chronic diseases were excluded. The present study was approved by the Ethics Committee of First Affiliated Hospital of Guangzhou University of Chinese Medicine [No. Y (2019) 172] and carried out in accordance with the "Helsinki Declaration". All CRC patients have sighed informed consent. Patients who received neoadjuvant chemotherapy or radiotherapy or had a history of malignancy were excluded. Clinicopathological data including pathological report, sex, age, macroscopic classification, tumor location, tumor size, tumor differentiation, lymphatic infiltration and invasion depth were collected *via* medical record. The American Joint Council on Cancer tumor, node and metastasis (TNM) staging system is used for the clinical staging of tumors[36].

Animals, induction of CRC and treatments

A total of 32 male Wistar rats, 7 wk old and weighing 200 ± 20 g, were obtained from the Experimental Animal Center of Southern Medical University [Certificate of quality: SCXK (Yue) 2016-0041]. All rats were housed in cages (25 cm × 30 cm × 30 cm, four rats per cage) under specified-pathogens free conditions at 25°C, 40%-60% relative humidity, and a 12-h light/dark cycle in the experimental animal center of Guangzhou University of Chinese Medicine. All rats had ad libitum access to standard rodent chow and filtered water and were acclimatized for 1 wk prior to the initiation of the experiment. The use of laboratory animals was checked by the "Institutional Animal Ethical Committee" and all procedures were approved by the Ethics Committee of Guangzhou University of Chinese Medicine, and performed according to the "Principles of Laboratory Animal Care" as well as specific national laws where applicable. All experimental protocols and handling of the animals followed the guide for the care and use of laboratory animals[37].

A total of 32 rats were randomly divided into two groups: the non-alcohol group and the alcohol group, with 16 rats in each group. Non-alcohol group: The rats were fed water (10 mL/kg b.wt.) every day and from the 6th week on, the rats were administered a subcutaneous injection of 1,2-dimethylhydrazine hydrochloride (DMH) at a dose of 30, 35, 25 or 20 mg/kg b.wt. once a week for 12 wk in order to induce CRC. Alcohol group (DMH + ethanol): The rats were fed 30% ethanol (10 mL/kg b.wt.) every day, and from the 6th week on, they were administered a subcutaneous injection of DMH at a dose of 30, 35, 25 or 20 mg/kg b.wt. once a week for 12 wk in order to induce CRC. The details of the specific modeling method of each group were shown in Figure 1. The blood samples were collected through the posterior orbital venous plexus. And the rats were sacrificed by cervical dislocation, then the colons were removed and used in further experiments.

Hematoxylin and eosin staining and histological evaluation

All specimens were fixed in 4% paraformaldehyde solution for 24 h and embedded in paraffin and

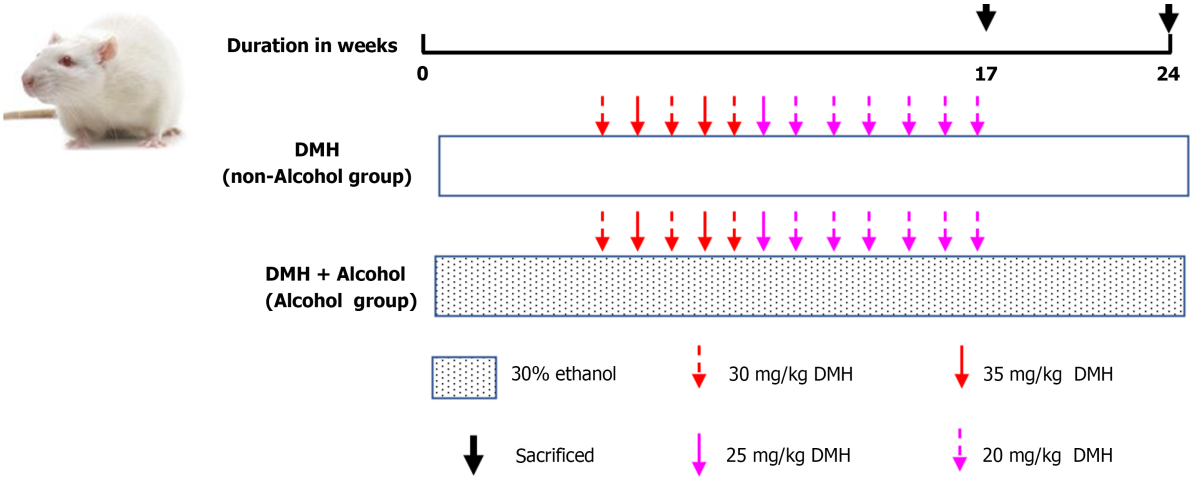


Figure 1 Schematic diagram of animal experimental modeling. DMH: 1,2-Dimethylhydrazine hydrochloride.

processed by standard histological processing techniques. Tissue sections (4-μm thick) were obtained from each sample. The hematoxylin and eosin results were observed under a light microscope at 40× magnifications (Olympus, BX51) to observe the colonic histology differences by the method of Martin B [38].

Determination of aberrant crypt foci

Aberrant crypt foci (ACF) were determined according to the method described by Bird *et al*[39]. Then, the formalin-fixed colon was stained with 0.2% methylene blue for 3 min and observed under light microscope. The diagnosis of colonic pathology and ACF was performed by two pathologists. The number of ACF was counted as described by Sivaranjani *et al*[40].

Cytokines detection by ELISA

Serum samples of rats were collected, and the inflammatory factors (TNF-α, IL-6 and IL-1β) were determined using ELISA kits according to the manufacturers' instructions. The optical density of the colorimetric reaction was measured at 450 nm with a flat microplate reader.

Western blotting

For western blotting, 50 μg of extracted protein was fractionated on a 10% SDS-PAGE gel and then transferred to a polyvinylidene fluoride membrane with a 0.45-mm pore size (Millipore, MA, United States). The membrane was blocked in 5% milk for 3 h at room temperature and probed with antibodies against acetylated LAMC2 (1:1000), integrinβ1 (1:1000), p-FAK (1:1000), FAK (1:1000), snail (1:1000), E-cadherin (1:1000), fibronectin (1:1000) and N-cadherin (1:1000) at 4°C overnight. Horseradish peroxide-conjugated goat anti-rabbit and rabbit anti-mouse was used as the secondary antibodies. FAK and GAPDH (1:8000) were used as loading controls. Band intensity was visualized by ChemiDoc TMXRS+ (Bio-Rad, United States).

Immunohistochemical staining

The immunohistochemical (IHC) was performed by the method described in previous studies[41,42], all colonic tissue were fixed with 4% paraformaldehyde and paraffin embedded, then thin 4μm sections were obtained and deparaffinized in xylene and rehydrated through decreasing grades of alcohol. The sections were placed in a 95°C antigen retrieval solution for 15 min. After cooling the retrieval solutions for 20 min at room temperature, the slides were treated with hydrogen peroxide (H_2O_2) for 10 min to block endogenous peroxidase activity. Then, slides were incubated with primary antibodies against ITGB1 (dilution 1:100), LAMC2 (dilution 1:500), p-FAK (dilution 1:500), snail (dilution 1:500), E-cadherin (dilution 1:100), N-cadherin (dilution 1:800), fibronectin (dilution 1:200), and SATB1 (dilution 1:200) overnight at 4°C. The next day, biotin-conjugated secondary antibody and streptavidin-biotin peroxidase were applied each for 20 min. 3,3'-Diaminobenzidine tetrahydrochloride was used as the substrate, and nuclear contrast was performed using hematoxylin counterstaining. The negative controls for IHC are performed with PBS instead of primary antibody. The results were observed under a light microscope at 40× magnifications (Olympus, BX51). For quantitative analyses, the IHC images were analyzed by Image-Pro Plus 6.0 to calculate the average optical density (AOD), and the following equation: AOD = integrated optical density/area.

Table 1 Primer sequences for quantitative real-time polymerase chain reaction

Gene name	Forward (5'>3')	Reverse (5'>3')
For human		
LAMC2	TTCTACAACGATCCGCACGAC	GAGTTAAAAGCAGCCCTGGT
ITGB1	CCTACTTCTGCACGATGTGATG	CCTTTGCTACGGTTGGTTACATT
FAK	GTCTGCCTTCGCTTCACG	GAATTTGTAACTGGAAGATGCAAG
Snail	CTAGCGAGTGGTTCTTCTGC	GTAGTTAGGCTTCCGATTGGG
E-cadherin	GACCGGTGCAATCTTCAAA	TTGACGCCGAGAGCTACAC
N-cadherin	AGCTTCTCACGGCATACACC	GTGCATGAAGGACAGCCTCT
Fibronectin	GCCTGGTACAGAATA TGTAGTG	ATCCCAGCTGATC AGTAGGCTGGTG
SATB1	GTGGAAGCCTTGGGAATCC	CTGACAGCTCTTCTTCTAGTT
GAPDH	GGAGCGAGATCCCTCCAAAAT	GGCTGTTGTCATACTTCTCATGG
For rats		
LAMC2	GTGAAGCTTCCCTGCAAAAC	CATTTGGCCCCACGTAGT
ITGB1	TCGAAGGACCACTAGACCTGA	TTCCATGGGAACAAAAGGTAA
FAK	TTGGGTTGCAAACTATCTCTAGAAC	TGGTACAAAACTGGCACAGAA
Snail	TTCACATCCGAGTGGGTCTG	ACCCACACTGGTGAGAAGCC
E-cadherin	AAAGCAGGAAGAAAACACCACTC	AAAGGGCACGCTATCAACATTAG
N-cadherin	TCAGTGGCGGAGATCCTAC	GTGCTGAATTCCCTTGGCTA
Fibronectin	TGTCACCCACCACCTTGA	CTGATTGTTCTTCAGTGCGA
SATB1	AGATGCAGGGAGTGCCTTTA	TGCTCCTCCTTGCAATCATA
GAPDH	TGCCCTCATGTTCCTGATAAAT	CATTACATCACAGCTTTCCAGG

ITGB1: Integrin-β1; LAMC2: Laminin-γ2; SATB1: Special AT-rich sequence binding protein 1; FAK: Focal adhesion kinase; GAPDH: Glyceraldehyde-3-phosphate dehydrogenase.

Table 2 Number of rats with mucosal pathological tissue changes in different time periods

Wk	Group	*n*	Normal	Atypical hyperplasia	Adenoma	Adenocarcinoma		With lymphatic metastasis	
						Mucosal carcinoma	Infiltrating carcinoma	Metastasis	Tumor metastasis rate
17	Non-alcohol	8	3	5	0	0	0	0	0.00%
	Alcohol	8	0	6	2	0	0	0	0.00%
24	Non-alcohol	8	0	0	0	6	2	0	0.00%
	Alcohol	8	0	0	0	2	6	3	37.5%

Duolink PLA

The Duolink PLA in situ was used in this study to detect the interaction between LAMC2 and ITGB1 in tissue samples, and it was performed as previously described by Bai *et al*[43]. Briefly, after washing, permeabilizing, and blocking as histological analysis, colon sections were incubated with primary antibodies against LAMC2 (1:200) and ITGB1 (1:400) overnight at 4°C. Then the slides were incubated with Duolink PLA Rabbit MINUS and PLA Mouse PLUS proximity probes for 1 h at 37°C. Ligation and amplification were conducted using the Duolink in situ detection reagent kit according to the protocol. Images were captured under the light microscope (Olympus, BX51).

RNA extraction and quantitative real-time polymerase chain reaction

The total RNA was extracted from tissues using RNAEX reagent (Accurate Biotechnology, China). It

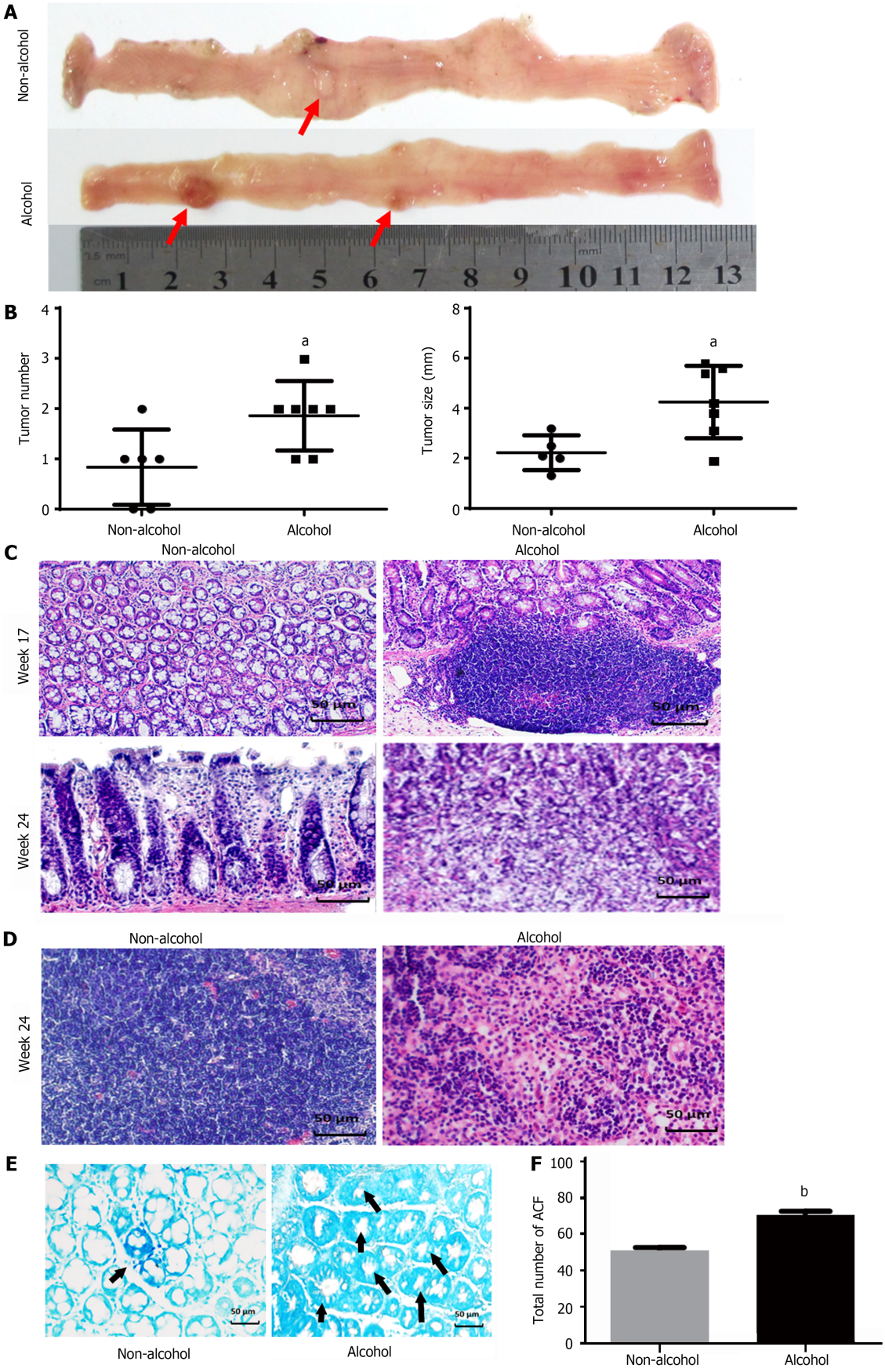


Figure 2 Alcohol consumption promotes colorectal cancer progression. A: Morphological view of colonic tumors; B: Average tumor number and tumor size in each group; C: Colon pathology of different groups (× 400); D: Pathology of colonic lymph node in different groups at the 24th week (× 400); E: Methylene blue staining for aberrant crypt foci (ACF) in the sectioned rat colon (× 400); F: Bar graph of ACF with different crypt multiplicity. The bars represent the mean ± SD (n = 8). Compared with the non-alcohol group: $^{b}P < 0.01$, $^{a}P < 0.05$. ACF: Aberrant crypt foci.

Table 3 Baseline characteristics of colorectal cancer patients

Baseline characteristics	Alcohol group (*n* = 29)	Non-alcohol group (*n* = 34)	*P* value
Gender			
Male, *n* (%)	18 (62.1)	16 (47.1)	0.233
Female, *n* (%)	11 (37.9)	18 (52.9)	
Age (yr old)			
< 55, *n* (%)	10 (34.5)	14 (41.2)	0.586
≥ 55, *n* (%)	19 (65.5)	20 (58.8)	
Differentiation			
Medium, *n* (%)	24 (82.8)	30 (88.2)	0.536
Poor, *n* (%)	5 (17.2)	4 (11.8)	
Clinical stage			
Stage I-II, *n* (%)	12 (41.4)	24 (70.6)	0.020[a]
Stage III-IV, *n* (%)	17 (58.6)	10 (29.4)	
T stage			
T1-T2, *n* (%)	6 (20.7)	12 (35.3)	0.201
T3-T4, *n* (%)	23 (79.3)	22 (64.7)	
Tumor metastasis conditions			
Distant metastasis	12 (41.4)	23 (70.6)	0.046[a]
Lymphatic metastasis	9 (31)	8 (20.6)	
Non-metastasis	8 (27.6)	3 (8.8)	

[a]$P < 0.05$.

was reverse transcribed into cDNA by using Evo M-MLV RT premix (Accurate Biotechnology, China) and quantitative real-time polymerase chain reaction (RT-PCR) system (TaKaRa, Japan). Then a SYBR Green Premix Pro Taq HS qPCR Kit (Accurate Biotechnology, China) was used for PCR. The PCR liquid volume was 20 μL. Quantitative PCR was performed using an RT-PCR system (BioRad, Singapore). At 95°C, 40 cycles were amplified after 90 s of initial denaturation, 10 s desaturation at 95°C, and 34 s of extension at 60°C. GAPDH was used as the reference gene for calculation. And the primer sequences are shown in Table 1.

Statistical analysis

The data were described using the mean (standard deviation), median (range), or frequency (percentage). An independent-samples *t* test or the Mann-Whitney U test was applied for the comparison between two groups (non-alcohol group and alcohol group). The associations between the clinical parameters and immunohistochemical results were analyzed using the χ^2 test. Statistical analyses were conducted using SPSS version 25.0 for Windows (SPSS, Inc.). Statistical analysis was performed: $^{b}P < 0.01$; $^{a}P < 0.05$; $^{ns}P > 0.05$.

RESULTS

Alcohol consumption promoted malignant progression in CRC rats

The total number of ACFs detected in the alcohol group was 70.33 ± 5.16 and 51.6 ± 4.5 in the non-alcohol group (Figure 2E and F), which implied that alcohol consumption may significantly increase considerably raise the risk of precancerous lesions of colorectal cancer ($P < 0.05$). Furthermore, CRC rats in alcohol group had more tumors and larger tumor size was observed in the alcohol group than those in the non-alcohol group (Figure 2A and B). Histopathological analysis revealed that at 17th week, 62.5% of rats in the non-alcohol group showed atypical hyperplasia, and the other 37.5% showed normal colonic tissues. Atypical hyperplasia was seen in 75% of the rats in the alcohol group; however, 25% of the rats in the alcohol group had many heteroepithelial cells in the colonic epithelium and one or more large nucleoli in the pleomorphic cystic nucleus, indicating a carcinoma adenoma. At the 24th week, 25%

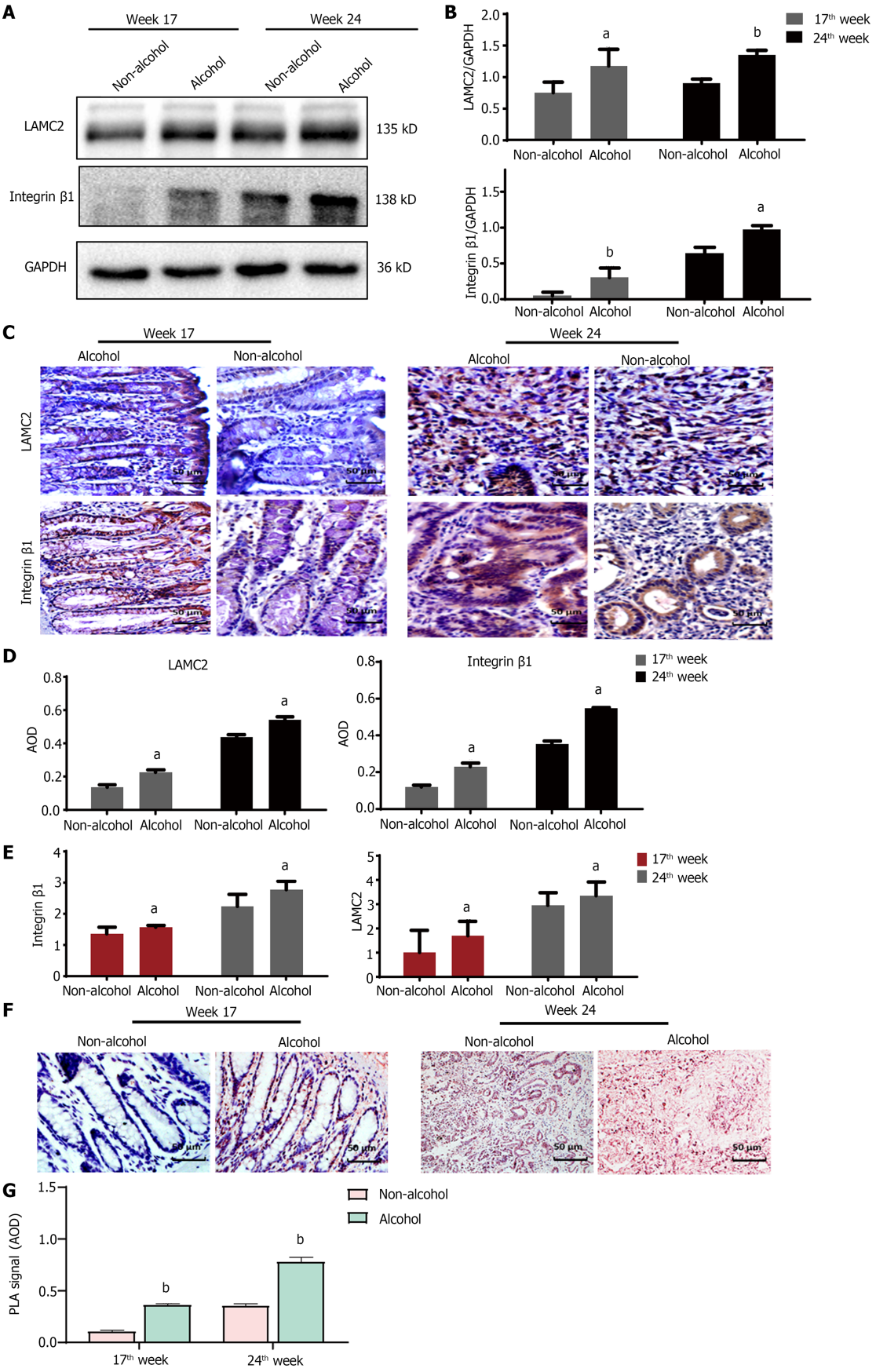


Figure 3 Alcohol consumption regulates the expression and interaction of integrin-β1 and laminin-γ2 in animal samples. The bars represent the mean ± SD (n = 8). A and B: Quantification of the protein levels of integrin-β1 (ITGB1) and laminin-γ2 (LAMC2) detected by western blotting in animal samples; C and D: Quantification of the protein levels of ITGB1 and LAMC2 by immunohistochemical (IHC) in animal samples; E: Quantification of the mRNA levels of ITGB1 and LAMC2 by quantitative real-time polymerase chain reaction in clinical samples; F: Statistical analysis of IHC was performed by counting the average optical density

(AOD). In Duolink proximity ligation assay (PLA), the brown dot particles observed under the microscope represent the interactions between LAMC2 and ITGB1; G: The statistical analysis of PLA positive signals was performed by counting the AOD under a light microscope. Compared with the non-alcohol group: $^{b}P < 0.01$, $^{a}P < 0.05$. ITGB1: Integrin-β1; LAMC2: Laminin-γ2; GAPDH: Glyceraldehyde-3-phosphate dehydrogenase; PLA: Proximity ligation assay; IHC: Immunohistochemical staining; AOD: Average optical density.

of rats in the alcohol group showed intramucosal carcinoma (mucosal carcinoma), which was characterized by less mucus secretion of colonic epithelial cells, compact and irregular arrangement of glandular ducts, and clear invasion of cancer cells into lamina propria in colons. The other 75% of rats in the alcohol group had invasive mucosal infiltrating carcinoma (infiltrating carcinoma), which manifested as abnormal tubular or mucinous structures invading through the muscularis mucosa or deep intestinal wall. In total, 75% and 25% of rats in the non-alcohol group showed mucosal carcinoma and infiltrating carcinoma, respectively. We found no lymphatic metastasis in the non-alcohol group, while cancer cell infiltration was found in the lymph nodes of the alcohol group and the lymph node metastasis rate was 37.5% (Figure 2C and D; Table 2). The abovementioned results indicated that alcohol consumption promoted CRC metastasis.

Alcohol consumption increased the expression of LAMC2, ITGB1 and FAK in CRC rats

The protein levels of LAMC2 and ITGB1 measured by western blotting (Figure 3A and B) and IHC (Figure 3C and D). The result showed that at both of 17th week and 24th week, the protein levels of LAMC2 and ITGB1 in the alcohol group were higher than those in the non-alcohol group ($P < 0.05$). Furthermore, the mRNA levels of LAMC2 and ITGB1 in alcohol group were higher than those in non-alcohol group at both of 17th week and 24th week ($P < 0.05$; Figure 3E). In addition, the protein level of FAK in the alcohol group was higher than that in the non-alcohol group at the 17th and 24th weeks (Figures 4 and 5, $P < 0.05$). However, there was no significant difference in the mRNA level of FAK between the alcohol and non-alcohol group at both of the 17th and 24th week ($P > 0.05$; Figure 6A).

Alcohol consumption enhanced the early interaction between LAMC2 and ITGB1 in CRC rats

Duolink PLA were used to detect the interaction between ITGB1 and LAMC2, and the red spots represent the interactions between LAMC2 and ITGB1. The results revealed that (Figure 3F and G) at 17th week, more early interacting signals between LAMC2 and ITGB1 were found in the alcohol group than that in non-alcohol group. At week 24, the results were consistent with that of week 17. The present study suggested that alcohol consumption may enhance the early interaction between LAMC2 and ITGB1 in CRC rats.

Alcohol consumption increased the expression of the CRC metastasis marker SATB1 in CRC rats

High expression level of SATB1 significantly influenced the malignant phenotypic characteristics of CRC. As shown in Figures 4 and 5, the results of IHC and western blotting indicated that at 17th week, the protein level of SATB1 in the alcohol group was higher than that in non-alcohol group, and the results of qRT-PCR (Figure 6A) showed that the mRNA level of SATB1 was higher than that in non-alcohol group.

Alcohol consumption regulates the protein and mRNA levels of EMT-associated markers in CRC rats

EMT is one of the key events that occur during the formation of premetastatic niche[44]. The results of western blotting (Figure 4A) and IHC (Figure 5) suggested that at the 17th week, long-term alcohol consumption resulted in an increase in the proteins involved in triggering the EMT process including p-FAK, N-cadherin, fibronectin and snail; however, there was a decrease in E-cadherin in the alcohol group. At week 24, the results were similar to those of week 17. In addition, the mRNA levels of FAK, E-cadherin, N-cadherin, fibronectin and snail were measured by qRT-PCR, and the results were consistent with those of protein levels (Figure 6A). The abovementioned results indicated that alcohol consumption may abnormally change the expression levels of EMT biomarkers in CRC rats in early stage.

Alcohol consumption increased the expression of proinflammatory factors associated with premetastatic niche in CRC rats

The results of ELISA (Figure 6B) showed that IL-1β, IL-6 and TNF-α levels in the alcohol group were higher than those in the non-alcohol group at week 17. The results at week 24 were consistent with those at week 17, indicating that the concentrations of IL-1β, IL-6, and TNF-α were higher in the alcohol group than in the non-alcohol group during precancerous lesions, which may be one of the reasons for lymph node metastasis in CRC patients in the alcohol group.

The obtained results showed that in early stages of CRC, the contents of IL-6, IL-1β and TNF-α in the alcohol group were higher than those in the non-alcohol group. This might be one of the explanations for the higher metastatic rate in the alcohol group.

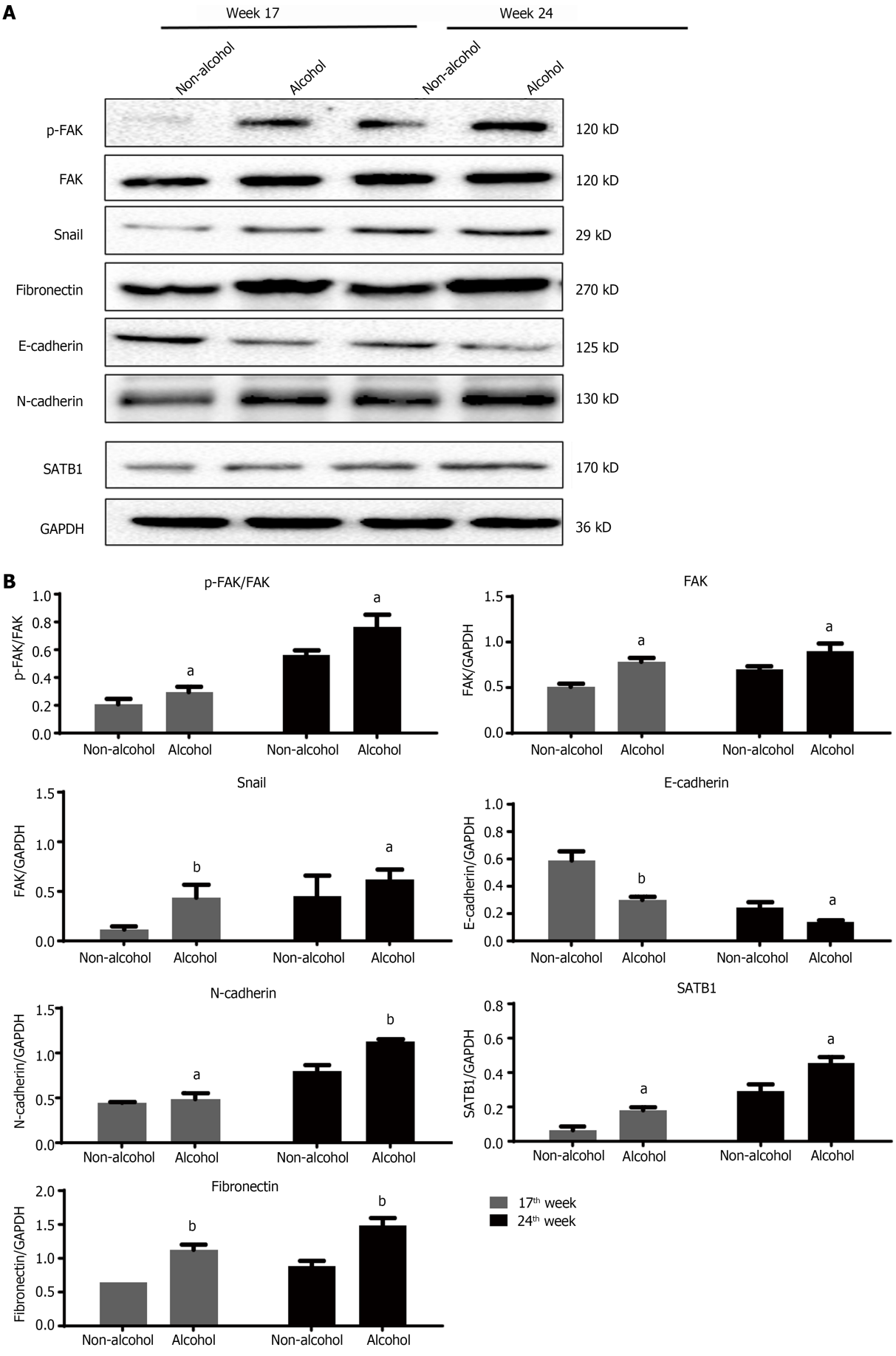


Figure 4 Quantification of the protein levels of epithelial mesenchymal transformation-related markers in colorectal cancer rats by using

western blotting. The bars represent the mean ± SD (*n* = 3). A: The western blotting images of phosphorylate-focal adhesion kinase (p-FAK), FAK, snail, fibronectin, E-cadherin, N-cadherin and special AT-rich sequence binding protein 1 (SATB1) in animal samples; B: Quantification of the protein levels of FAK, p-FAK/FAK, snail, fibronectin, E-cadherin, N-cadherin and SATB1 in animal samples. Compared with the non-alcohol group: $^{b}P < 0.01$, $^{a}P < 0.05$. SATB1: Special AT-rich sequence binding protein 1; FAK: Focal adhesion kinase; p-FAK: Phosphorylate focal adhesion kinase; GAPDH: Glyceraldehyde-3-phosphate dehydrogenase.

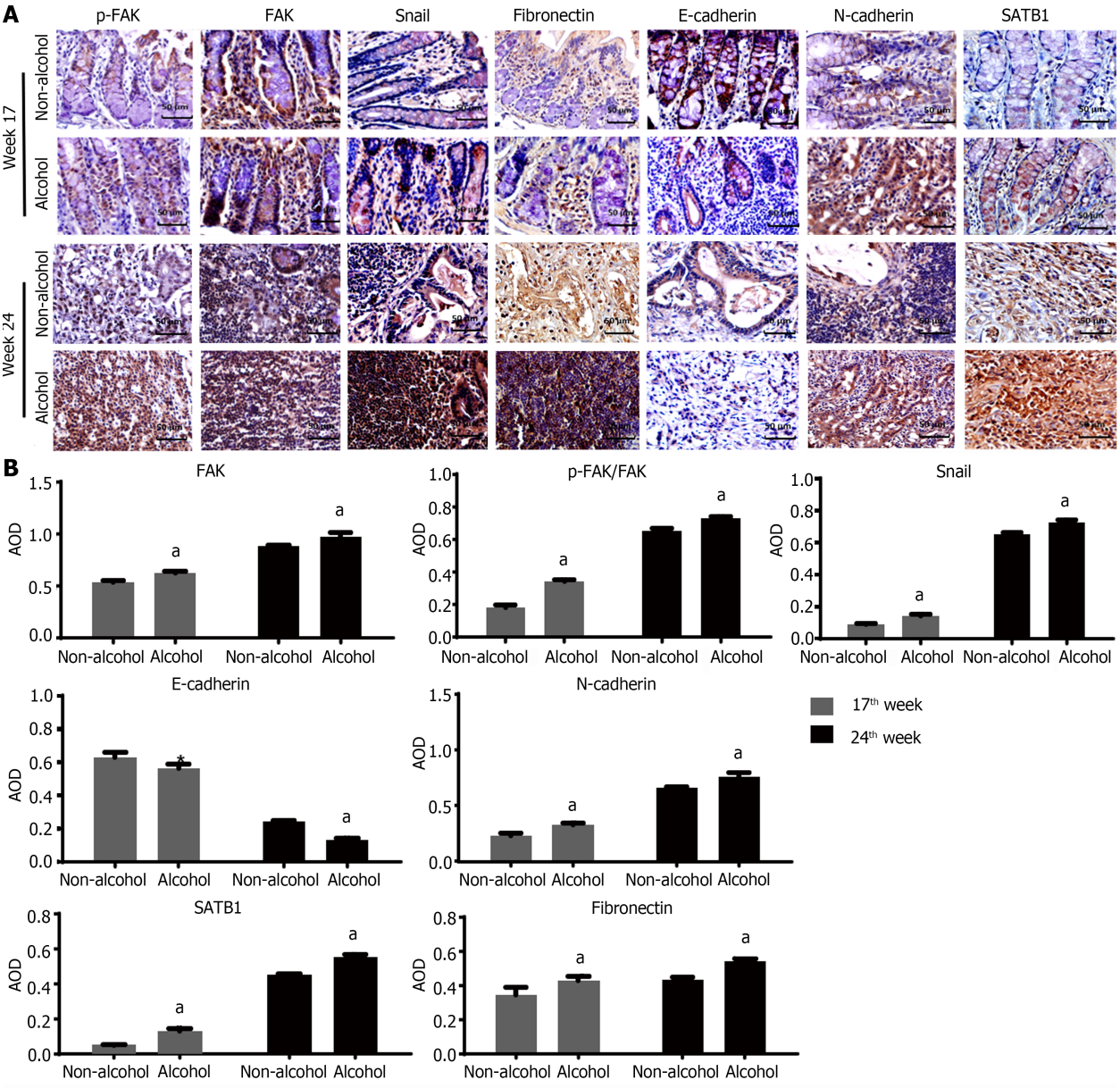


Figure 5 Immunohistochemical staining detected the protein level of epithelial mesenchymal transformation-related markers in colorectal cancer rats. The bars represent the mean ± SD (*n* = 3). A: The images of immunohistochemical (IHC) in animal samples; B: Quantification of the protein levels of focal adhesion kinase (FAK), phosphorylate-FAK (p-FAK)/FAK, snail, Fibronectin, E-cadherin, N-cadherin and special AT-rich sequence binding protein 1 detected by IHC counting the average optical density. Compared with the non-alcohol group: $^{b}P < 0.01$, $^{a}P < 0.05$. SATB1: Special AT-rich sequence binding protein 1; FAK: Focal adhesion kinase; p-FAK: Phosphorylate focal adhesion kinase; qRT-PCR: Quantitative real-time polymerase chain reaction; IHC: Immunohistochemical staining; AOD: Average optical density.

Baseline characteristics of CRC patients

A total of 63 patients with a preliminary diagnosis of colorectal cancer participated in the trial. According to the baseline characteristics and data on alcohol consumption of 63 CRC patients, 29 CRC patients who had been drinking alcohol over 3 times each week for more than 5 years were classified in alcohol group, while the remaining 34 CRC patients who have never drunk alcohol before were classified in non-alcohol group. As shown in Table 3, there are significant differences in clinical stage and tumor metastasis ($P < 0.05$) between alcohol group and non-alcohol group. There were no significant differences in sex, age, degree of differentiation or T stage ($P > 0.05$). The experimental

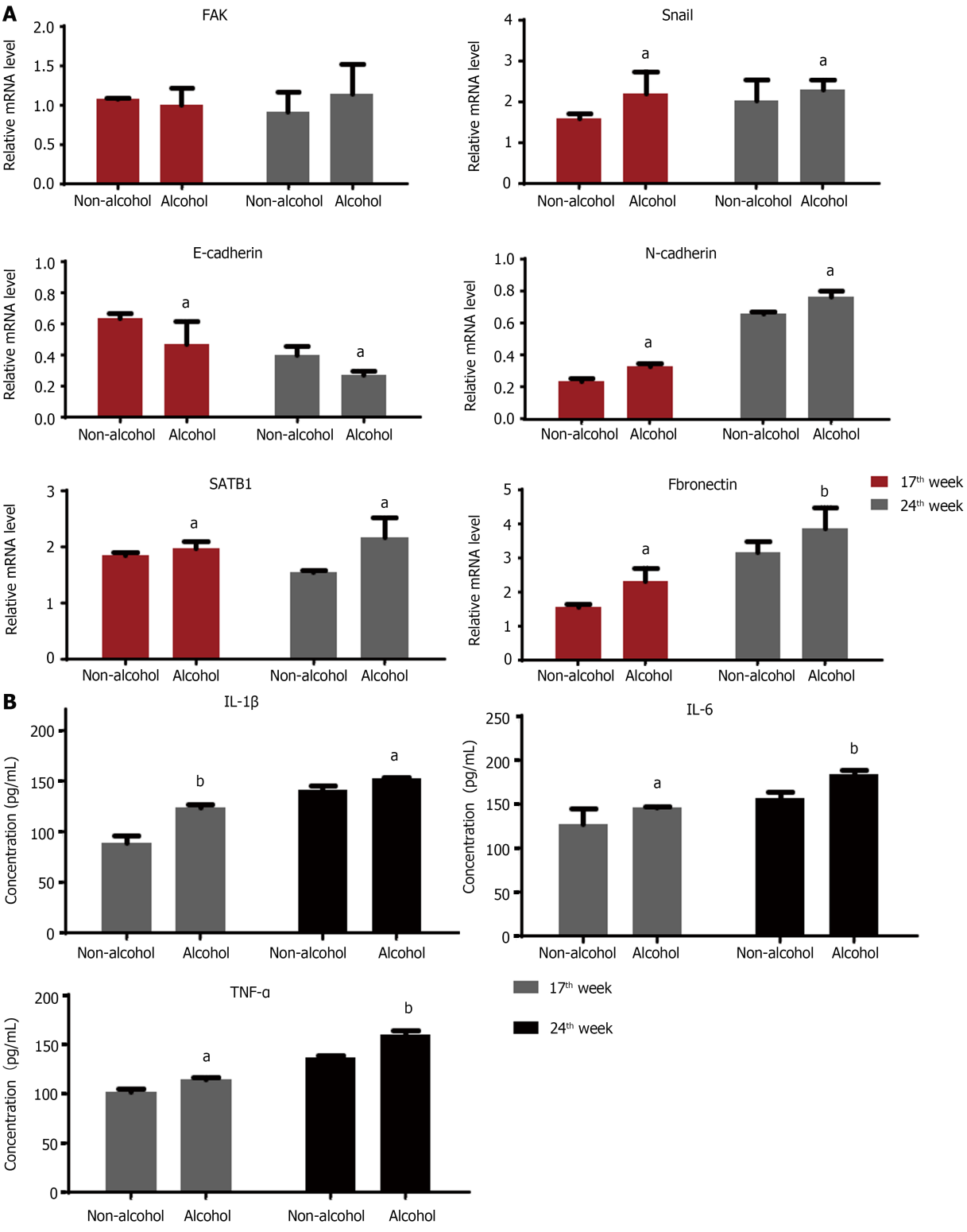


Figure 6 Alcohol consumption regulated the mRNA expression of epithelial mesenchymal transformation-related markers and proinflammatory factors in colorectal cancer rats. The bars represent the mean ± SD (n = 8). A: Quantification of the mRNA levels of snail, focal adhesion kinase, fibronectin, N-cadherin, E-cadherin and special AT-rich sequence binding protein 1 in each group analyzed by quantitative real-time polymerase chain reaction; B: Tumor necrosis factor-α, interleukin-6 (IL-6) and IL-1β levels in each group. Compared with the non-alcohol group: $^{b}P < 0.01$, $^{a}P < 0.05$. SATB1: Special AT-rich sequence binding protein 1; FAK: Focal adhesion kinase; IL-1β: Interleukin-1β; IL-6: Interleukin-6; TNF-α: Tumor necrosis factor-α.

results were consistent with the results of animal experiments. The degree of tumor deterioration in CRC patients in the alcohol group was significantly higher than that in non-alcohol group.

Alcohol consumption increased the expression and interaction of LAMC2 and ITGB1 in CRC patients

The expression of LAMC2 and ITGB1 in clinical samples determined by IHC (shown in Figure 7C and D). In cancer tissues, the mRNA and protein levels of LAMC2 and ITGB1 in alcohol group were significantly higher than those in non-alcohol group (Figure 7B). In addition, according to the survival analysis of 392 CRC patient samples from the GSE39582 dataset, we explored the prognostic significance of LAMC2 and ITGB1. As shown in Figure 7A, the overexpression of LAMC2 and ITGB1 was closely related to poor CRC prognosis. The abovementioned results were consistent with the results of animal experiments. Alcohol consumption may increase the expression levels and the interaction of LAMC2 and ITGB1 in CRC patients.

The interactions of LAMC2-ITGB1 are pivotal in CRC progression. Animal experiments revealed that more interactions between LAMC2 and ITGB1 were found in the alcohol group than in the non-alcohol group in the early stage of CRC. And it has been validated in clinical samples. According to the results of duolink PLA (Figure 7E and F), more interacting signals between LAMC2 and ITGB1 were found in alcohol group than those in non-alcohol group.

Alcohol consumption influenced the protein and mRNA expression of EMT-associated markers in CRC patients

In the animal experiment, we found that alcohol may abnormally change the expression levels of EMT-associated biomarkers in CRC rats in the early stage. To verify the clinical implications of this finding, the levels of EMT biomarkers were detected in clinical samples. The results of IHC (Figure 8A and B) showed that there were significant differences in EMT-associated biomarkers ($P < 0.01$) in cancer tissues between the alcohol and non-alcohol group. In cancer tissues, the protein levels of p-FAK, N-cadherin, fibronectin and snail were significantly higher in alcohol group was significantly higher than that in non-alcohol group; however, the expression of E-cadherin in alcohol group was significantly lower in alcohol group than that in non-alcohol group. The qRT-PCR results (Figure 8C) also showed that the mRNA levels of N-cadherin, fibronectin and snail in the cancer tissues of alcohol group was higher than that in non-alcohol group. The abovementioned findings were consistent with the results of animal experiments. The abnormal expression of EMT biomarkers in CRC patients was different from that in alcohol group, and the abnormal expression of LAMC2 and ITGB1 was more severe in alcohol group.

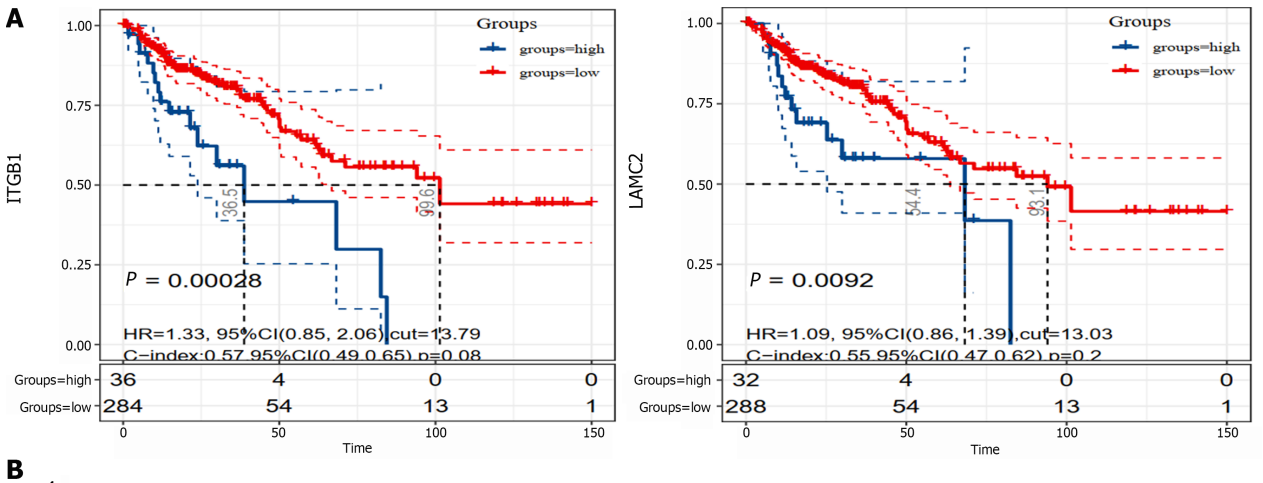
Alcohol consumption increased the expression of the CRC metastasis marker SATB1 in CRC patients

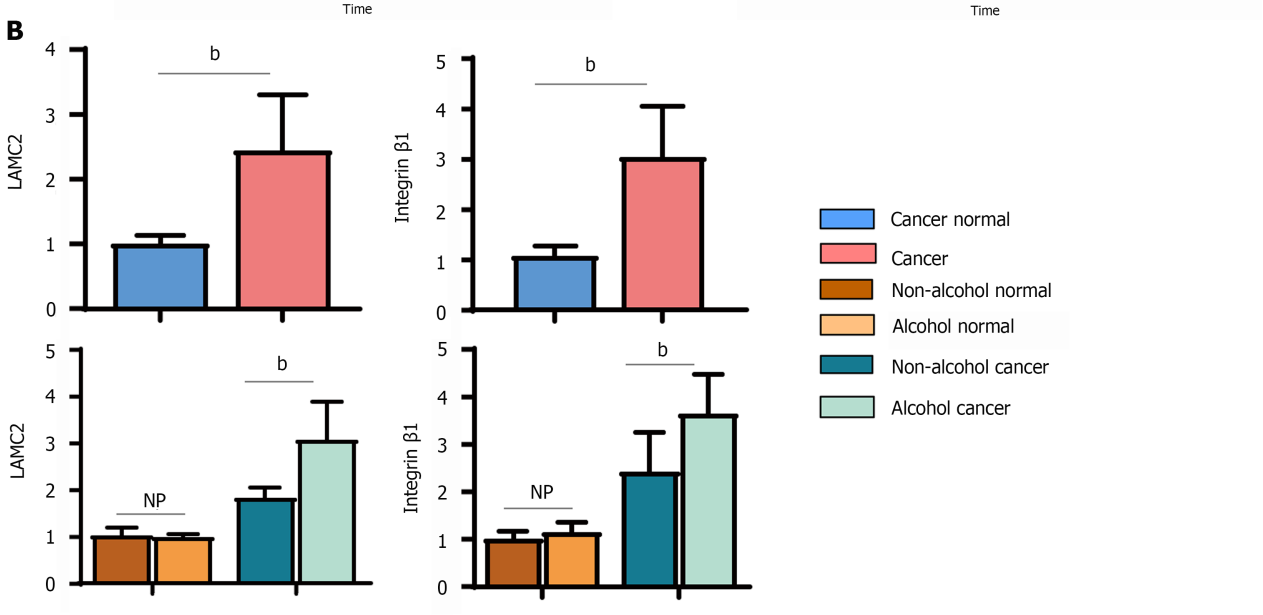
In animal experiments, alcohol consumption was found to increase the expression of SATB1 in CRC rats. IHC and qRT-PCR were used to evaluate the protein and mRNA levels of SATB1 in clinical samples (Figure 8A-C). The obtained results showed that protein and mRNA levels of SATB1 in cancer tissues were significantly higher in alcohol group than that in non-Alcohol group. Our results indicate that the expression of SATB1 is higher in alcohol group than those in non-Alcohol group, which is consistent with the higher metastasis rate of CRC patients who drink alcohol as described by TNM staging. The above results suggest that alcohol consumption may up-regulate the expression of SATB1, thereby induce the early EMT event and leads to malignant metastasis of the tumor[45].

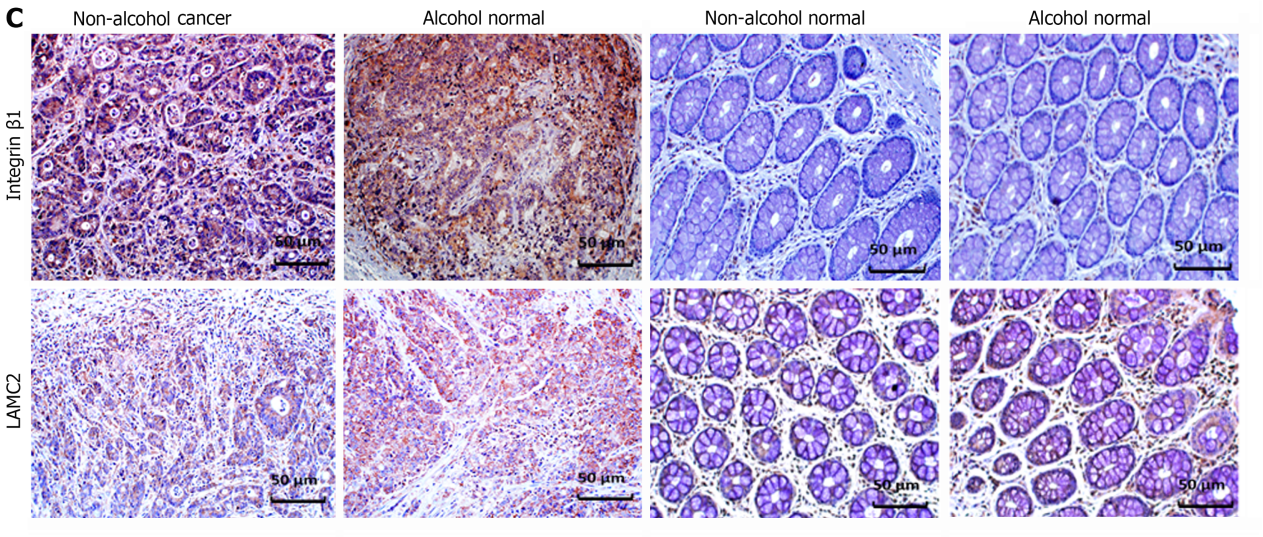
DISCUSSION

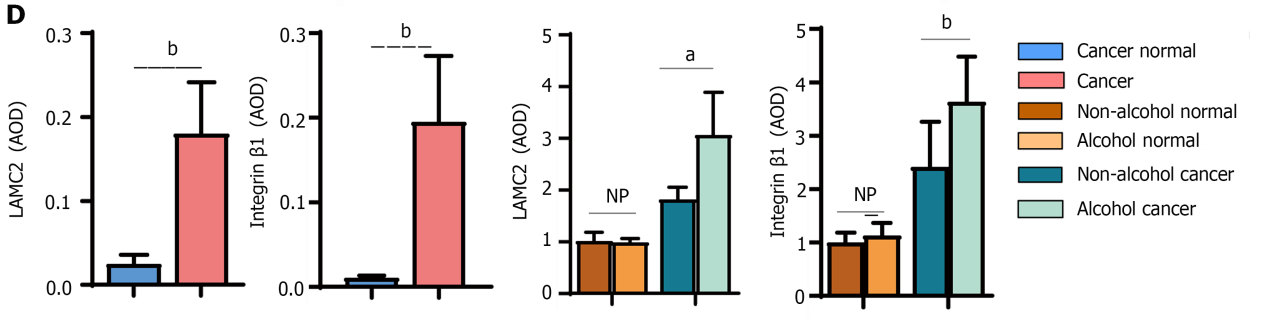
Metastasis is the prominent cause of death in CRC[7]. Chronic alcohol intake has been extensively reported to enhance CRC metastasis; nevertheless, the specific mechanism remains unknown. In the present study, the results of TNM stage, pathological grade and other clinicopathological parameters suggested that the tumor deterioration rate of patients in alcohol group was higher than that in non-alcohol group, and the results were consistent with previous reports[6,7]. The present study demonstrated that the metastasis rate in alcohol group was higher than that in non-alcohol group. Similar to the clinical results, in animal experiments, the number of ACFs in the alcohol group was significantly higher than that in the non-alcohol group, and the pathological evaluation results were similar to the ACF screening results, suggesting that the alcohol group had a higher risk of precolonic lesions in CRC rats. And the number and size of tumors in the alcohol group were higher than those in the non-alcohol group. Lymph node metastasis was found in 37.5% of patients in the alcohol group, while no metastasis was found in the non-alcohol group. The present study indicated a higher risk of precancerous lesions and malignant metastasis of CRC were found in alcohol group compared with the non-alcohol group. Thus, we hypothesized that alcohol may promote the metastasis of CRC, however, the molecular mechanism is still unclear.

A key step in the formation of metastasis is the extravasation of circulating tumor cells to distant organs and their adaptation to the new environment[46,47]. Thus, the interaction between disseminated cancer cells and the microenvironment of the premetastatic niche is necessary for metastasis[10]. Primary tumor cells regulate the metastasis by secreting a variety of molecules that promote the mobilization and recruitment of various cells to the premetastatic niche and alter ECM protein expression and ECM properties in secondary organs[25,48]. The ECM constitutes a scaffold that


A
ITGB1
Groups
groups=high
groups=low
P = 0.00028
HR=1.33, 95%CI(0.85, 2.06),cut=13.79
C-index:0.57,95%CI(0.49,0.65),p=0.08
Groups=high 36 4 0 0
Groups=low 284 54 13 1
Time
LAMC2
P = 0.0092
HR=1.09, 95%CI(0.86, 1.39),cut=13.03
C-index:0.55,95%CI(0.47,0.62),p=0.2
Groups=high 32 4 0 0
Groups=low 288 54 13 1
Time


B
LAMC2
Integrin β1
b
NP
Cancer normal
Cancer
Non-alcohol normal
Alcohol normal
Non-alcohol cancer
Alcohol cancer


C
Non-alcohol cancer
Alcohol normal
Non-alcohol normal
Alcohol normal
Integrin β1
LAMC2
50 μm


D
LAMC2 (AOD)
Integrin β1 (AOD)
b
a
NP
Cancer normal
Cancer
Non-alcohol normal
Alcohol normal
Non-alcohol cancer
Alcohol cancer

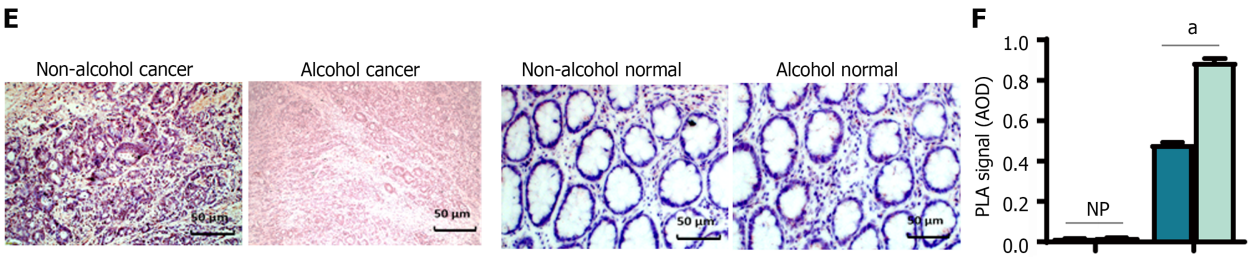


Figure 7 Alcohol consumption increased the expression and interaction of laminin-γ2 and integrin-β1 in colorectal cancer rats. The bars represent the mean ± SD (n = 8). A: Survival analysis of integrin-β1 (ITGB1) and laminin-γ2 (LAMC2) in colorectal cancer; B: The mRNA levels of ITGB1 and LAMC2 determined by quantitative real-time polymerase chain reaction in clinical samples; C: Representative immunohistochemical (IHC) images of ITGB1 and LAMC2 in clinical samples (× 400); D: The quantifications of the protein levels of ITGB1 and LAMC2 determined by IHC in clinical samples; E and F: Duolink proximity ligation assay (PLA) verified the interactions between ITGB1 and LAMC2 in clinical samples. The statistical analysis of PLA positive signals was performed by counting the average optical density under a light microscope. Compared with the non-alcohol group: $^{b}P < 0.01$, $^{a}P < 0.05$. LAMC2: Laminin-γ2; ITGB1: Integrin-β1; qRT-PCR: Quantitative real-time polymerase chain reaction; PLA: Proximity ligation assay; IHC: Immunohistochemical staining; AOD: Average optical density. Cancer normal group: cancer adjacent tissue group. NP: No statistical difference.

supports the attachment and thus reactivation of survival signaling in cancer cells[16]. And the remodeling of ECM is essential during formation of premetastatic niche, which may support cancer cell attachment, metabolism and migration of recruited cells[17,18]. Laminin, as an important component of the ECM and the main structural component of basement membrane, is involved in the formation of pre-metastasis niche[49]. Among them, LAMC2 is an important component of the survival-dependent environment of colorectal cancer epithelial cells and plays a key role in the regulation of tumor cell motility by premetastatic niche formation[50]. LAMC2 plays a role in premetastatic niche signaling by stimulating the formation of premetastatic local contacts and promoting the migration of cancer cells through its interaction with ITGB1[51]. It has been reported that the interaction of ITGB1 and LAMC2 may promote the tumor budding of CRC cells, which leads to malignant metastasis of CRC, and the focal adhesion formed by the interaction of LAMC2 and ITGB1 plays an important role in the prognosis of CRC. This adhesion is not only the basis of cancer cell survival but is also closely related to the migration and metastasis of cancer cells[52]. FAK is involved in LAMC2 and ITGB1 signal transduction, and the overexpression of FAK was found to play a key regulatory role in ITGB1-mediated signal transduction. As the phosphorylated FAK is activated, it transmits signals to the transcription factor snail, thereby inducing EMT[32,33]. The interaction of LAMC2 and ITGB1 and the overexpression of FAK were seen as markers of premetastatic niche formation, which may lead to malignant metastasis of CRC[52]. According to the results of our study, more interacting signals between LAMC2 and ITGB1, and higher level of FAK were found in the alcohol group than those in the non-alcohol group at early stage. In addition, the higher ratio of p-FAK/FAK in the alcohol group in the early stage indicates a higher degree of FAK activation, which may induce early EMT events and promote CRC metastasis.

CRC metastasis depends on EMT, during EMT, epithelial cells lose the connectivity and top-to-base polarity, resulting in a mesenchymal phenotype capability of migration and invasion[32]. There is evidence that some cancer cells may acquire the ability to spread and metastasize before they are fully malignant, which suggests that EMT may be an early event involving in the metastasis[53]. In addition, SATB1 has been found to be associated with early EMT events and can be used as a marker of CRC metastasis[54]. SATB1 was found to be a driver of the malignant phenotype in CRC, and its expression was shown to be positively associated with invasion depth, poor degree of differentiation and advanced TNM stage of CRC. And SATB1 organizes chromatin into spatial rings that provide the necessary "docking sites" for further binding of transcription factors and chromatin modifying enzymes[45]. SATB1 was found to regulate entire genes, even those located on distant chromosomes[55]. The results of the animal experiment suggested that the expression of SATB1 was significantly higher in the alcohol group than that in the non-alcohol group during precancerous lesions, which may predict the early EMT events.

In addition, there is an increasing evidence that proinflammatory cytokines play an important role in the formation of premetastatic niches. Previous studies have shown that the high expression of IL-6 and IL-1β may activate ITGB1[56,57] to stimulate the adhesion of bone marrow cells to endothelial cells, thereby promote the formation of premetastatic niche, and inducing EMT to promote metastasis[58]. Pal *et al*[55] found that TNF-α induces EMT in human HCT116 cells and promotes colorectal cancer invasion and metastasis. According to our study, the levels of the proinflammatory cytokines IL-1β, TNF-α and IL-6 in CRC rats in the alcohol group were significantly increased at the early stage of precancerous lesions, which may serve as paracrine signals to enhance the proliferation and invasion of early disseminated cancer cells. It may help cancer cells change their phenotypes through EMT to enhance metastasis.

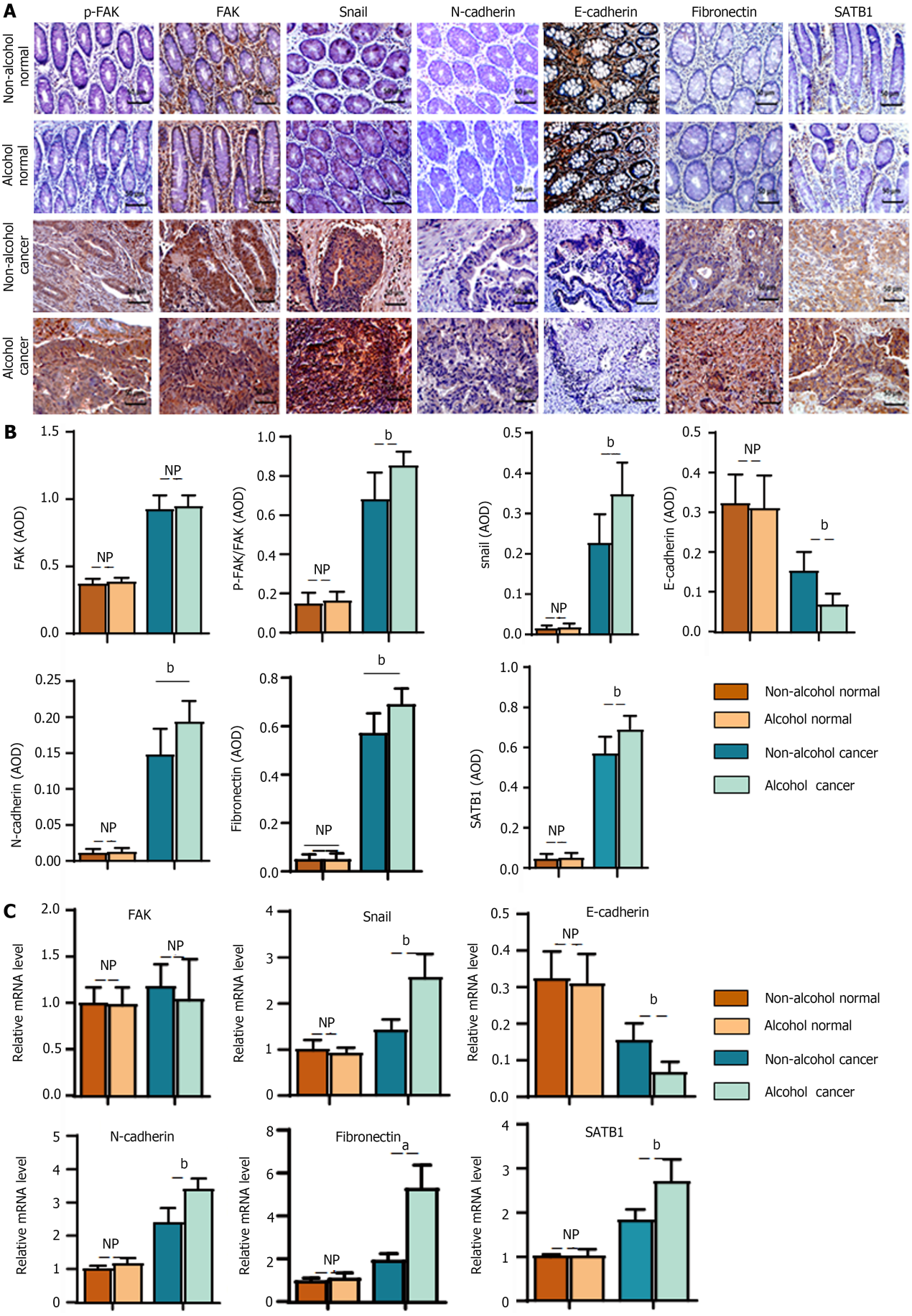


Figure 8 Alcohol consumption influenced the protein and mRNA levels of epithelial mesenchymal transformation -associated markers in

colorectal cancer patients. The bars represent the mean ± SD (n = 8). A: Representative immunohistochemical images of phosphorylate-focal adhesion kinase (p-FAK), FAK, snail, fibronectin, E-cadherin, N-cadherin and special AT-rich sequence binding protein 1 (SATB1) in different groups in clinical samples (× 400); B: Quantification of the protein levels of FAK, p-FAK/FAK, snail, fibronectin, E-cadherin, N-cadherin and SATB1 by counting the average optical density in clinical samples; C: Quantification of the mRNA levels of FAK, snail, fibronectin, E-cadherin, N-cadherin and SATB1 by quantitative real-time polymerase chain reaction in clinical samples. Compared with the non-alcohol group: $^{b}P < 0.01$, $^{a}P < 0.05$. SATB1: Special AT-rich sequence binding protein 1; FAK: Focal adhesion kinase; p-FAK: Phosphorylate focal adhesion kinase; AOD: Average optical density. NP: No statistical difference.

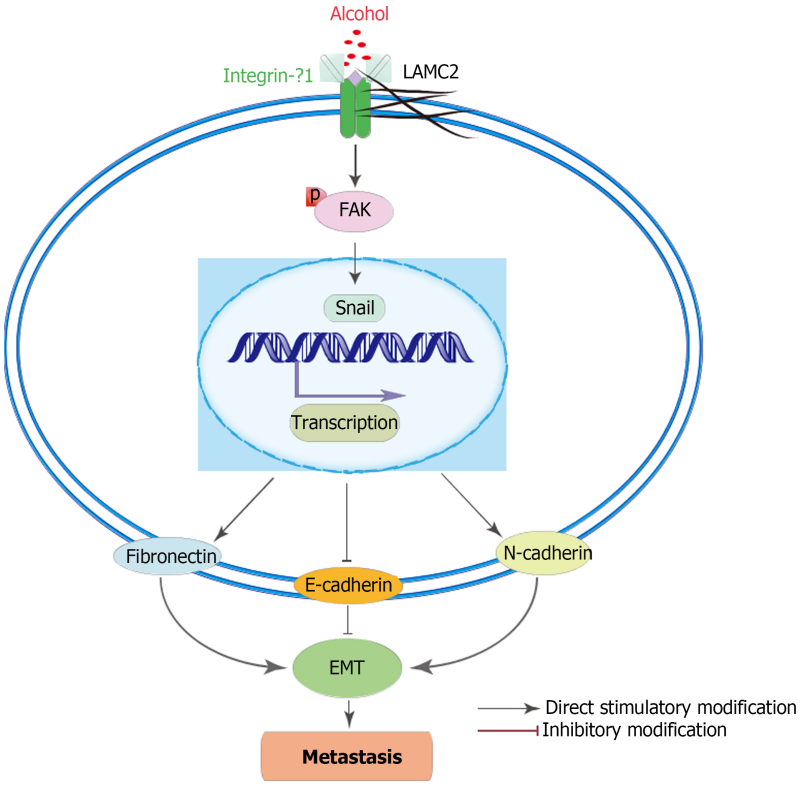


Figure 9 Schematic diagram of the possible signaling pathway regulated by alcohol. EMT: Epithelial mesenchymal transformation; LAMC2: Laminin-γ2; ITGB1: Integrin-β1; FAK: Focal adhesion kinase; p-FAK: Phosphorylate focal adhesion kinase.

The EMT event is also a key event involving in the formation of the premetastatic niche[32,33], which is almost featuring the loss of E-cadherin expression and overexpression of snail, N-cadherin and fibronectin[56,59]. The results of animal experiments suggested that long-term alcohol consumption (shown in Figure 9), as a risk factor of CRC, may further activate p-FAK by enhancing the interaction between LAMC2 and ITGB1 and forming a premetastatic niche, thus upregulating the expression of snail in precancerous lesions. Thus, the expression levels of N-cadherin and fibronectin were increased and the expression level of E-cadherin was downregulated, leading to the mesenchymal phenotype of cancer cells and colorectal cancer metastasis. This may be one of the reasons for the higher metastasis rate of CRC rats in the alcohol group. We found the similar results in clinical samples. The main limitation of the clinical study is the relatively small sample size. Larger-scale functional studies are required to improve our understanding of the effects of alcohol on the premetastatic niche in CRC. However, the obtained results provide some interesting suggestions for future studies with an increased sample size. Based on the abovementioned results, the present study demonstrated that alcohol may promote the formation of premetastatic niche *via* enhancing the EMT event mediated by the LAMC2-ITGB1 interaction, leading to the high incidence of CRC metastasis in the alcohol group.

CONCLUSION

In summary, the present study attempted to examine the nonspecific effect of alcohol on the premetastatic niche of colorectal cancer. Our study suggests that alcohol has an effect on the colorectal carcinogenesis paradigm and may accelerate the malignant metastasis of CRC. The molecular mechanism may involve the effect of alcohol on the early EMT-mediated premetastatic niche of colorectal cancer induced by LAMC2 and ITGB1 interactions.

ACKNOWLEDGMENT

We are very grateful to all the staff of Guangzhou University of Chinese Medicine and The First Affiliated Hospital of Guangxi University of Chinese Medicine for their help in the study.

ARTICLE HIGHLIGHTS

Research background

Colorectal cancer (CRC) is a common malignant tumor.

Research motivation

Alcohol consumption is positively correlated with CRC malignant metastasis; however, the mechanism is unclear.

Research objectives

To investigate the effects of alcohol on CRC metastasis

Research methods

The interaction between laminin-γ2 (LAMC2) and integrin-β1 (ITGB1) was measured by Duolink assay, and the expression levels of LAMC2, ITGB1 and focal adhesion kinase, snail, fibronectin, N-cadherin and special AT-rich sequence binding protein 1 were measured by quantitative real-time polymerase chain reaction, immunohistochemistry and western blotting. Interleukin-1β (IL-1β), tumor necrosis factor-α and IL-6 levels were measured *via* enzyme-linked immunosorbent assay, histopathological assessment *via* hematoxylin eosin staining, and determination of aberrant crypt foci *via* methylene blue.

Research results

Alcohol may promote CRC metastasis by influencing the molecular mechanism of the premetastatic niche.

Research conclusions

Our study suggests that alcohol promotes epithelial mesenchymal transformation-mediated premetastatic niche formation of CRC by activating the early interaction between LAMC2 and ITGB1 and lead to CRC metastasis.

Research perspectives

To explore the effect of alcohol on colorectal cancer metastasis.

FOOTNOTES

Author contributions: Wen B designed the experiments; Nong FF and Liang YQ performed the experiments and wrote the paper; Xing SP revised the paper; Xiao YF and Chen HH analyzed the data; all authors have read and approved this final manuscript.

Supported by the National Natural Science Foundation of China, No. 81673944.

Institutional review board statement: All human subjects were approved by the Ethics Committee of The First Affiliated Hospital of Guangzhou University of Chinese Medicine [No. Y (2019) 172].

Institutional animal care and use committee statement: All animal protocols were approved by the Animal Care and Use Committee of the Guangzhou University of Chinese Medicine (Permit No. 20190801066).

Conflict-of-interest statement: The authors state that the study was conducted in the absence of any business or financial relationships that could be interpreted as potential conflicts of interest.

Data sharing statement: The datasets used and/or analyzed during the present study are available from the corresponding author on reasonable request.

ARRIVE guidelines statement: The authors have read the ARRIVE guidelines, and the manuscript was prepared and revised according to the ARRIVE guidelines.

Open-Access: This article is an open-access article that was selected by an in-house editor and fully peer-reviewed by external reviewers. It is distributed in accordance with the Creative Commons Attribution NonCommercial (CC BY-

NC 4.0) license, which permits others to distribute, remix, adapt, build upon this work non-commercially, and license their derivative works on different terms, provided the original work is properly cited and the use is non-commercial. See: https://creativecommons.org/Licenses/by-nc/4.0/

Country/Territory of origin: China

ORCID number: Fei-Fei Nong 0000-0002-2306-0108; Yu-Qi Liang 0000-0002-7481-116X; Shang-Ping Xing 0000-0001-7252-7176; Yin-Fang Xiao 0000-0001-5196-641X; Hui-Hui Chen 0000-0002-0129-6718; Bin Wen 0000-0001-9096-3115.

S-Editor: Zhang H
L-Editor: A
P-Editor: Cai YX

REFERENCES

1 **Ladabaum U**, Dominitz JA, Kahi C, Schoen RE. Strategies for Colorectal Cancer Screening. *Gastroenterology* 2020; **158**: 418-432 [PMID: 31394083 DOI: 10.1053/j.gastro.2019.06.043]
2 **Akimoto N**, Ugai T, Zhong R, Hamada T, Fujiyoshi K, Giannakis M, Wu K, Cao Y, Ng K, Ogino S. Rising incidence of early-onset colorectal cancer - a call to action. *Nat Rev Clin Oncol* 2021; **18**: 230-243 [PMID: 33219329 DOI: 10.1038/s41571-020-00445-1]
3 **Murphy N**, Moreno V, Hughes DJ, Vodicka L, Vodicka P, Aglago EK, Gunter MJ, Jenab M. Lifestyle and dietary environmental factors in colorectal cancer susceptibility. *Mol Aspects Med* 2019; **69**: 2-9 [PMID: 31233770 DOI: 10.1016/j.mam.2019.06.005]
4 **Zheng K**, Yu J, Chen Z, Zhou R, Lin C, Zhang Y, Huang Z, Yu L, Zhao L, Wang Q. Ethanol promotes alcohol-related colorectal cancer metastasis *via* the TGF-β/RUNX3/Snail axis by inducing TGF-β1 upregulation and RUNX3 cytoplasmic mislocalization. *EBioMedicine* 2019; **50**: 224-237 [PMID: 31757777 DOI: 10.1016/j.ebiom.2019.11.011]
5 **Mohr AM**, Gould JJ, Kubik JL, Talmon GA, Casey CA, Thomas P, Tuma DJ, McVicker BL. Enhanced colorectal cancer metastases in the alcohol-injured liver. *Clin Exp Metastasis* 2017; **34**: 171-184 [PMID: 28168393 DOI: 10.1007/s10585-017-9838-x]
6 **Diao XY**, Peng T, Kong FG, Huang JG, Han S, Shang YS, Liu H. Alcohol consumption promotes colorectal cancer by altering intestinal permeability. *Eur Rev Med Pharmacol Sci* 2020; **24**: 9370-9377 [PMID: 33015778 DOI: 10.26355/eurrev_202009_23020]
7 **Hosseini H**, Obradović MMS, Hoffmann M, Harper KL, Sosa MS, Werner-Klein M, Nanduri LK, Werno C, Ehrl C, Maneck M, Patwary N, Haunschild G, Gužvić M, Reimelt C, Grauvogl M, Eichner N, Weber F, Hartkopf AD, Taran FA, Brucker SY, Fehm T, Rack B, Buchholz S, Spang R, Meister G, Aguirre-Ghiso JA, Klein CA. Early dissemination seeds metastasis in breast cancer. *Nature* 2016; **540**: 552-558 [PMID: 27974799 DOI: 10.1038/nature20785]
8 **Tsai HW**, Yuan CC, Wang PH. Umbilicus as the only site of metastasis in recurrent ovarian cancer. *J Chin Med Assoc* 2006; **69**: 233-235 [PMID: 16835987 DOI: 10.1016/S1726-4901(09)70225-4]
9 **Attaran S**, Bissell MJ. The role of tumor microenvironment and exosomes in dormancy and relapse. *Semin Cancer Biol* 2022; **78**: 35-44 [PMID: 34757184 DOI: 10.1016/j.semcancer.2021.09.008]
10 **Radin DP**, Tsirka SE. Interactions between Tumor Cells, Neurons, and Microglia in the Glioma Microenvironment. *Int J Mol Sci* 2020; **21** [PMID: 33187183 DOI: 10.3390/ijms21228476]
11 **Osipov A**, Saung MT, Zheng L, Murphy AG. Small molecule immunomodulation: the tumor microenvironment and overcoming immune escape. *J Immunother Cancer* 2019; **7**: 224 [PMID: 31439034 DOI: 10.1186/s40425-019-0667-0]
12 **Zhang Z**, Qiao J, Zhang D, Zhu W, Zhu J, Leng X, Li S. Noncoding RNAs Act as Tumor-Derived Molecular Components in Inducing Premetastatic Niche Formation. *Biomed Res Int* 2019; **2019**: 9258075 [PMID: 31309120 DOI: 10.1155/2019/9258075]
13 **Han P**, Cao P, Hu S, Kong K, Deng Y, Zhao B, Li F. Esophageal Microenvironment: From Precursor Microenvironment to Premetastatic Niche. *Cancer Manag Res* 2020; **12**: 5857-5879 [PMID: 32765088 DOI: 10.2147/CMAR.S258215]
14 **Jing B**, Wang T, Sun B, Xu J, Xu D, Liao Y, Song H, Guo W, Li K, Hu M, Zhang S, Ling J, Kuang Y, Zhang T, Zhou BP, Yao F, Deng J. IL6/STAT3 Signaling Orchestrates Premetastatic Niche Formation and Immunosuppressive Traits in Lung. *Cancer Res* 2020; **80**: 784-797 [PMID: 31848193 DOI: 10.1158/0008-5472.CAN-19-2013]
15 **Doglioni G**, Parik S, Fendt SM. Interactions in the (Pre)metastatic Niche Support Metastasis Formation. *Front Oncol* 2019; **9**: 219 [PMID: 31069166 DOI: 10.3389/fonc.2019.00219]
16 **Choi J**, Gyamfi J, Jang H, Koo JS. The role of tumor-associated macrophage in breast cancer biology. *Histol Histopathol* 2018; **33**: 133-145 [PMID: 28681373 DOI: 10.14670/HH-11-916]
17 **Dong Q**, Liu X, Cheng K, Sheng J, Kong J, Liu T. Pre-metastatic Niche Formation in Different Organs Induced by Tumor Extracellular Vesicles. *Front Cell Dev Biol* 2021; **9**: 733627 [PMID: 34616739 DOI: 10.3389/fcell.2021.733627]
18 **Kim H**, Chung H, Kim J, Choi DH, Shin Y, Kang YG, Kim BM, Seo SU, Chung S, Seok SH. Macrophages-Triggered Sequential Remodeling of Endothelium-Interstitial Matrix to Form Pre-Metastatic Niche in Microfluidic Tumor Microenvironment. *Adv Sci (Weinh)* 2019; **6**: 1900195 [PMID: 31179226 DOI: 10.1002/advs.201900195]
19 **Najafi M**, Farhood B, Mortezaee K. Extracellular matrix (ECM) stiffness and degradation as cancer drivers. *J Cell Biochem* 2019; **120**: 2782-2790 [PMID: 30321449 DOI: 10.1002/jcb.27681]
20 **Trapani V**, Bonaldo P, Corallo D. Role of the ECM in notochord formation, function and disease. *J Cell Sci* 2017; **130**: 3203-3211 [PMID: 28883093 DOI: 10.1242/jcs.175950]
21 **Mal'tseva DV**, Makarova YA, Raigorodskaya MP, Rodin SA. Effects of Laminins 332 and 411 on the Epithelial-

Mesenchymal Status of Colorectal Cancer Cells. *Bull Exp Biol Med* 2019; **166**: 377-382 [PMID: 30627897 DOI: 10.1007/s10517-019-04354-x]

22 **Urooj T**, Wasim B, Mushtaq S, Shah SNN, Shah M. Cancer Cell-derived Secretory Factors in Breast Cancer-associated Lung Metastasis: Their Mechanism and Future Prospects. *Curr Cancer Drug Targets* 2020; **20**: 168-186 [PMID: 31858911 DOI: 10.2174/1568009620666191220151856]

23 **Maltseva DV**, Rodin SA. [Laminins in Metastatic Cancer]. *Mol Biol (Mosk)* 2018; B: 411-434 [PMID: 29989574 DOI: 10.7868/S0026898418030059]

24 **Chang YC**, Wang JD, Chang HY, Zhou P, Hahn RA, Gordon MK, Laskin JD, Gerecke DR. Expression of Laminin γ2 Proteolytic Fragments in Murine Skin Following Exposure to Sulfur Mustard. *Anat Rec (Hoboken)* 2020; **303**: 1642-1652 [PMID: 32421930 DOI: 10.1002/ar.24405]

25 **Meireles Da Costa N**, Mendes FA, Pontes B, Nasciutti LE, Ribeiro Pinto LF, Palumbo Júnior A. Potential Therapeutic Significance of Laminin in Head and Neck Squamous Carcinomas. *Cancers (Basel)* 2021; **13** [PMID: 33920762 DOI: 10.3390/cancers13081890]

26 **Tohmatsu Y**, Imura J, Sakai T, Takagi K, Minamisaka T, Tanaka S, Noguchi A, Nakajima T, Nagata T, Makino T, Shimizu T, Fujii T. Expression of laminin-5 gamma 2 chain predicts invasion of extramammary Paget's disease cell. *APMIS* 2021; **129**: 3-8 [PMID: 32996218 DOI: 10.1111/apm.13086]

27 **Huang C**, Chen J. Laminin332 mediates proliferation, apoptosis, invasion, migration and epithelialtomesenchymal transition in pancreatic ductal adenocarcinoma. *Mol Med Rep* 2021; **23** [PMID: 33179081 DOI: 10.3892/mmr.2020.11649]

28 **Wang SH**, Liou GG, Liu SH, Chang JS, Hsiao JR, Yen YC, Chen YL, Wu WL, Chang JY, Chen YW. Laminin γ2-enriched extracellular vesicles of oral squamous cell carcinoma cells enhance in vitro lymphangiogenesis *via* integrin α3-dependent uptake by lymphatic endothelial cells. *Int J Cancer* 2019; **144**: 2795-2810 [PMID: 30485433 DOI: 10.1002/ijc.32027]

29 **Liu CC**, Lin JH, Hsu TW, Hsu JW, Chang JW, Su K, Hsu HS, Hung SC. Collagen XVII/laminin-5 activates epithelial-to-mesenchymal transition and is associated with poor prognosis in lung cancer. *Oncotarget* 2018; **9**: 1656-1672 [PMID: 29416721 DOI: 10.18632/oncotarget.11208]

30 **Brenner H**, Chen C. The colorectal cancer epidemic: challenges and opportunities for primary, secondary and tertiary prevention. *Br J Cancer* 2018; **119**: 785-792 [PMID: 30287914 DOI: 10.1038/s41416-018-0264-x]

31 **Erin N**, Grahovac J, Brozovic A, Efferth T. Tumor microenvironment and epithelial mesenchymal transition as targets to overcome tumor multidrug resistance. *Drug Resist Updat* 2020; **53**: 100715 [PMID: 32679188 DOI: 10.1016/j.drup.2020.100715]

32 **Wang Y**, Shi J, Chai K, Ying X, Zhou BP. The Role of Snail in EMT and Tumorigenesis. *Curr Cancer Drug Targets* 2013; **13**: 963-972 [PMID: 24168186 DOI: 10.2174/15680096113136660102]

33 **Wu X**, Cai J, Zuo Z, Li J. Collagen facilitates the colorectal cancer stemness and metastasis through an integrin/PI3K/AKT/Snail signaling pathway. *Biomed Pharmacother* 2019; **114**: 108708 [PMID: 30913493 DOI: 10.1016/j.biopha.2019.108708]

34 **Wang Y**, Xu M, Ke ZJ, Luo J. Cellular and molecular mechanisms underlying alcohol-induced aggressiveness of breast cancer. *Pharmacol Res* 2017; **115**: 299-308 [PMID: 27939360 DOI: 10.1016/j.phrs.2016.12.005]

35 **Cho S**, Shin A, Park SK, Shin HR, Chang SH, Yoo KY. Alcohol Drinking, Cigarette Smoking and Risk of Colorectal Cancer in the Korean Multi-center Cancer Cohort. *J Cancer Prev* 2015; **20**: 147-152 [PMID: 26151048 DOI: 10.15430/JCP.2015.20.2.147]

36 **Ferretti S**, Patriarca S, Carbone A, Zanetti R. [TNM classification of malignant tumours, VII edition 2009. Changes and practical effects on cancer epidemiology]. *Epidemiol Prev* 2010; **34**: 125-128 [PMID: 20852350]

37 **National Research Council (US) Committee for the Update of the Guide for the Care and Use of Laboratory Animals**. Guide for the Care and Use of Laboratory Animals. 8th edition. Washington (DC): National Academies Press (US); 2011 [PMID: 21595115]

38 **Martin B**, Schäfer E, Jakubowicz E, Mayr P, Ihringer R, Anthuber M, Schenkirsch G, Schaller T, Märkl B. Interobserver variability in the H&E-based assessment of tumor budding in pT3/4 colon cancer: does it affect the prognostic relevance? *Virchows Arch* 2018; **473**: 189-197 [PMID: 29626253 DOI: 10.1007/s00428-018-2341-1]

39 **Bird RP**, Lafave LM. Varying effect of dietary lipids and azoxymethane on early stages of colon carcinogenesis: enumeration of aberrant crypt foci and proliferative indices. *Cancer Detect Prev* 1995; **19**: 308-315 [PMID: 7553672]

40 **Sivaranjani A**, Sivagami G, Nalini N. Chemopreventive effect of carvacrol on 1,2-dimethylhydrazine induced experimental colon carcinogenesis. *J Cancer Res Ther* 2016; **12**: 755-762 [PMID: 27461646 DOI: 10.4103/0973-1482.154925]

41 **Mansour DF**, Abdallah HMI, Ibrahim BMM, Hegazy RR, Esmail RSE, Abdel-Salam LO. The Carcinogenic Agent Diethylnitrosamine Induces Early Oxidative Stress, Inflammation and Proliferation in Rat Liver, Stomach and Colon: Protective Effect of Ginger Extract. *Asian Pac J Cancer Prev* 2019; **20**: 2551-2561 [PMID: 31450931 DOI: 10.31557/APJCP.2019.20.8.2551]

42 **Huang G**, Bao J, Shao X, Zhou W, Wu B, Ni Z, Wang L. Inhibiting pannexin-1 alleviates sepsis-induced acute kidney injury *via* decreasing NLRP3 inflammasome activation and cell apoptosis. *Life Sci* 2020; **254**: 117791 [PMID: 32416166 DOI: 10.1016/j.lfs.2020.117791]

43 **Bai N**, Zhang Q, Zhang W, Liu B, Yang F, Brann D, Wang R. G-protein-coupled estrogen receptor activation upregulates interleukin-1 receptor antagonist in the hippocampus after global cerebral ischemia: implications for neuronal self-defense. *J Neuroinflammation* 2020; **17**: 45 [PMID: 32007102 DOI: 10.1186/s12974-020-1715-x]

44 **Suarez-Carmona M**, Lesage J, Cataldo D, Gilles C. EMT and inflammation: inseparable actors of cancer progression. *Mol Oncol* 2017; **11**: 805-823 [PMID: 28599100 DOI: 10.1002/1878-0261.12095]

45 **Coupland LA**, Parish CR. Platelets, selectins, and the control of tumor metastasis. *Semin Oncol* 2014; **41**: 422-434 [PMID: 25023359 DOI: 10.1053/j.seminoncol.2014.04.003]

46 **Høye AM**, Erler JT. Structural ECM components in the premetastatic and metastatic niche. *Am J Physiol Cell Physiol* 2016; **310**: C955-C967 [PMID: 27053524 DOI: 10.1152/ajpcell.00326.2015]

47 **Zhuyan J**, Chen M, Zhu T, Bao X, Zhen T, Xing K, Wang Q, Zhu S. Critical steps to tumor metastasis: alterations of

tumor microenvironment and extracellular matrix in the formation of pre-metastatic and metastatic niche. *Cell Biosci* 2020; **10**: 89 [PMID: 32742634 DOI: 10.1186/s13578-020-00453-9]

48 **Guo Y**, Ji X, Liu J, Fan D, Zhou Q, Chen C, Wang W, Wang G, Wang H, Yuan W, Ji Z, Sun Z. Effects of exosomes on pre-metastatic niche formation in tumors. *Mol Cancer* 2019; **18**: 39 [PMID: 30857545 DOI: 10.1186/s12943-019-0995-1]

49 **Wang Y**, Shi M, Yang N, Zhou X, Xu L. GPR115 Contributes to Lung Adenocarcinoma Metastasis Associated With LAMC2 and Predicts a Poor Prognosis. *Front Oncol* 2020; **10**: 577530 [PMID: 33330053 DOI: 10.3389/fonc.2020.577530]

50 **Xu L**, Hou Y, Tu G, Chen Y, Du YE, Zhang H, Wen S, Tang X, Yin J, Lang L, Sun K, Yang G, Liu M. Nuclear Drosha enhances cell invasion *via* an EGFR-ERK1/2-MMP7 signaling pathway induced by dysregulated miRNA-622/197 and their targets LAMC2 and CD82 in gastric cancer. *Cell Death Dis* 2017; **8**: e2642 [PMID: 28252644 DOI: 10.1038/cddis.2017.5]

51 **Moon YW**, Rao G, Kim JJ, Shim HS, Park KS, An SS, Kim B, Steeg PS, Sarfaraz S, Changwoo Lee L, Voeller D, Choi EY, Luo J, Palmieri D, Chung HC, Kim JH, Wang Y, Giaccone G. LAMC2 enhances the metastatic potential of lung adenocarcinoma. *Cell Death Differ* 2015; **22**: 1341-1352 [PMID: 25591736 DOI: 10.1038/cdd.2014.228]

52 **Cavaco ACM**, Eble JA. A 3D Spheroid Model as a More Physiological System for Cancer-Associated Fibroblasts Differentiation and Invasion In Vitro Studies. *J Vis Exp* 2019 [PMID: 31449247 DOI: 10.3791/60122]

53 **Wang G**, Yang Q, Li M, Zhang Y, Cai Y, Liang X, Fu Y, Xiao Z, Zhou M, Xie Z, Huang H, Huang Y, Chen Y, He Q, Peng F, Chen Z. Quantitative proteomic profiling of tumor-associated vascular endothelial cells in colorectal cancer. *Biol Open* 2019; **8** [PMID: 31036754 DOI: 10.1242/bio.042838]

54 **Pavan Kumar P**, Purbey PK, Sinha CK, Notani D, Limaye A, Jayani RS, Galande S. Phosphorylation of SATB1, a global gene regulator, acts as a molecular switch regulating its transcriptional activity in vivo. *Mol Cell* 2006; **22**: 231-243 [PMID: 16630892 DOI: 10.1016/j.molcel.2006.03.010]

55 **Pal M**, Bhattacharya S, Kalyan G, Hazra S. Cadherin profiling for therapeutic interventions in Epithelial Mesenchymal Transition (EMT) and tumorigenesis. *Exp Cell Res* 2018; **368**: 137-146 [PMID: 29674112 DOI: 10.1016/j.yexcr.2018.04.014]

56 **Schmid MC**, Avraamides CJ, Foubert P, Shaked Y, Kang SW, Kerbel RS, Varner JA. Combined blockade of integrin-α4β1 plus cytokines SDF-1α or IL-1β potently inhibits tumor inflammation and growth. *Cancer Res* 2011; **71**: 6965-6975 [PMID: 21948958 DOI: 10.1158/0008-5472.CAN-11-0588]

57 **Jones SA**, Jenkins BJ. Recent insights into targeting the IL-6 cytokine family in inflammatory diseases and cancer. *Nat Rev Immunol* 2018; **18**: 773-789 [PMID: 30254251 DOI: 10.1038/s41577-018-0066-7]

58 **Deng Y**, Chakraborty P, Jolly MK, Levine H. A Theoretical Approach to Coupling the Epithelial-Mesenchymal Transition (EMT) to Extracellular Matrix (ECM) Stiffness *via* LOXL2. *Cancers (Basel)* 2021; **13** [PMID: 33807227 DOI: 10.3390/cancers13071609]

59 **Noronha C**, Ribeiro AS, Taipa R, Castro DS, Reis J, Faria C, Paredes J. Cadherin Expression and EMT: A Focus on Gliomas. *Biomedicines* 2021; **9** [PMID: 34680444 DOI: 10.3390/biomedicines9101328]

World Journal of Gastroenterology

Submit a Manuscript: https://www.f6publishing.com

World J Gastroenterol 2022 September 21; 28(35): 5175-5187

DOI: 10.3748/wjg.v28.i35.5175

ISSN 1007-9327 (print) ISSN 2219-2840 (online)

ORIGINAL ARTICLE

Retrospective Cohort Study

Natural history and outcomes of patients with liver cirrhosis complicated by hepatic hydrothorax

Sarah Romero, Andy KH Lim, Gurpreet Singh, Chamani Kodikara, Rachel Shingaki-Wells, Lynna Chen, Samuel Hui, Marcus Robertson

Specialty type: Gastroenterology and hepatology

Provenance and peer review: Unsolicited article; Externally peer reviewed

Peer-review model: Single blind

Peer-review report's scientific quality classification

Grade A (Excellent): 0
Grade B (Very good): B, B, B
Grade C (Good): C
Grade D (Fair): 0
Grade E (Poor): 0

P-Reviewer: Cao HC, China; Gupta T, India; Papadopoulos VP, Greece

Received: January 24, 2022
Peer-review started: January 24, 2022
First decision: April 10, 2022
Revised: April 28, 2022
Accepted: July 25, 2022
Article in press: July 25, 2022
Published online: September 21, 2022

Sarah Romero, Chamani Kodikara, Rachel Shingaki-Wells, Samuel Hui, Marcus Robertson, Department of Gastroenterology, Monash Health, Clayton 3168, Victoria, Australia

Andy KH Lim, Marcus Robertson, Department of General Medicine, School of Clinical Sciences, Monash University, Clayton 3168, Victoria, Australia

Gurpreet Singh, Lynna Chen, Gastroenterology and Liver Transplant Unit, Austin Health, Heidelberg 3084, Victoria, Australia

Corresponding author: Sarah Romero, FRACP, MBBS, Doctor, Department of Gastroenterology, Monash Health, 246 Clayton Road, Clayton 3168, Victoria, Australia. s.romero.md@gmail.com

Abstract

BACKGROUND

Hepatic hydrothorax (HH) is an uncommon and difficult-to-manage complication of cirrhosis with limited treatment options.

AIM

To define the clinical outcomes of patients presenting with HH managed with current standards-of-care and to identify factors associated with mortality.

METHODS

Cirrhotic patients with HH presenting to 3 tertiary centres from 2010 to 2018 were retrospectively identified. HH was defined as pleural effusion in the absence of cardiopulmonary disease. The primary outcomes were overall and transplant-free survival at 12-mo after the index admission. Cox proportional hazards analysis was used to determine factors associated with the primary outcomes.

RESULTS

Overall, 84 patients were included (mean age, 58 years) with a mean model for end-stage liver disease score of 29. Management with diuretics alone achieved long-term resolution of HH in only 12% patients. At least one thoracocentesis was performed in 73.8% patients, transjugular intrahepatic portosystemic shunt insertion in 11.9% patients and 33% patients received liver transplantation within 12-mo of index admission. Overall patient survival and transplant-free survival at 12 mo were 68% and 41% respectively. At multivariable analysis, current smoking

[hazard ratio (HR) = 8.65, 95% confidence interval (CI): 3.43-21.9, $P < 0.001$) and acute kidney injury (AKI) (HR = 2.91, 95%CI: 1.21-6.97, $P = 0.017$) were associated with a significantly increased risk of mortality.

CONCLUSION

Cirrhotic patients with HH are a challenging population with a poor 12-mo survival despite current treatments. Current smoking and episodes of AKI are potential modifiable factors affecting survival. HH is often refractory of diuretic therapy and transplant assessment should be considered in all cases.

Key Words: Cirrhosis; Portal hypertension; Hepatic hydrothorax; Ascites; Liver transplantation

©The Author(s) 2022. Published by Baishideng Publishing Group Inc. All rights reserved.

Core Tip: The development of hepatic hydrothorax (HH) in cirrhotic patients continues to be associated with a very poor prognosis despite current standards-of-care. In one of the largest series to investigate the natural history of patients with hepatic hydrothoraces, a 45-d overall survival rate of 80% and 12-mo transplant-free survival of 41% was observed after index hospitalisation with HH. At multivariate analysis, current smoking and development of acute kidney injury were both independently associated with mortality, and represent important modifiable risk factors.

Citation: Romero S, Lim AK, Singh G, Kodikara C, Shingaki-Wells R, Chen L, Hui S, Robertson M. Natural history and outcomes of patients with liver cirrhosis complicated by hepatic hydrothorax. *World J Gastroenterol* 2022; 28(35): 5175-5187

URL: https://www.wjgnet.com/1007-9327/full/v28/i35/5175.htm

DOI: https://dx.doi.org/10.3748/wjg.v28.i35.5175

INTRODUCTION

Hepatic hydrothorax (HH) is an uncommon but serious complication occurring in patients with decompensated cirrhosis. HH is defined as the accumulation of more than 500 mL of transudative pleural fluid in a patient with cirrhosis and portal hypertension, where primary cardiopulmonary or malignant aetiologies have been excluded[1]. HH has been reported to occur in 5% to 11% of patients with cirrhosis, with more than 90% of cases occurring in Child-Pugh B or C disease[1,2]. HH is thought to arise from direct passage of fluid from the peritoneal cavity to the pleural cavity through diaphragmatic fenestrations[1]. Nuclear medicine studies, using labelled albumin have confirmed unidirectional passage of fluid from the abdominal to the pleural cavity[3], thus supporting a diaphragmatic defect process.

Clinically significant HH develops when accumulation of ascites in the pleural cavity exceeds the absorptive capacity of the pleura and patients typically present with shortness of breath, cough, hypoxia or chest discomfort[1,3]. Most cases occur in patients with appreciable ascites, however ascites may not be a prominent finding in up to 42%[1]. HH is most often unilateral and right-sided (59%-80%), however, there are increasing reports of left-sided (12%-17%) or bilateral (8%-24%) involvement[1,4]. Similar to the development of spontaneous bacterial peritonitis (SBP) in patients with ascites, patients with HH may develop spontaneous infections within the pleural fluid, which are termed spontaneous bacterial empyema (SBEM)[3].

The clinical management of HH remains complex and challenging. Treatment priorities in cirrhotic patients presenting with a pleural effusion include confirming a diagnosis of HH and excluding alternative pathology, relieving symptoms, preventing pulmonary complications and managing the underlying ascites. Diagnostic or therapeutic thoracocentesis is typically performed to confirm the presence of transudative fluid and to exclude SBEM or alternative pathology[5]. Recently developed American Association for the Study of Liver Disease (AASLD) guidelines state that first-line management should include sodium restriction and diuresis[6]. It is recognised, however, that 20%-30% of patients with cirrhosis and HH will develop persistent or recurrent pleural effusion despite these measures[6]. Refractory HH represents a particularly challenging management issue and patients are often considered for repeat therapeutic thoracocentesis and transjugular intrahepatic portosystemic shunt (TIPS) placement. Liver transplantation (LT) is the definitive treatment for HH, and post-transplant outcomes are comparable to outcomes for alternative indications[6].

Currently, there remains a paucity of literature examining the natural history and prognostic significance of HH. No randomised controlled trials have been performed in this population and clinical guidelines were only published for the first time in 2020[6]. Previous small studies have indicated the development of HH is associated with significant morbidity and extremely poor survival in the absence of LT[2,7,8]. The aims of this study were to: (1) Evaluate the probability of survival in a cohort of patients with liver cirrhosis presenting with HH and to examine factors associated with mortality; and (2) Provide a descriptive analysis of the treatments and complications associated with HH treatment during hospitalisation.

MATERIALS AND METHODS

Study design and setting

We conducted a multi-centre retrospective cohort study of patients with cirrhosis and HH presenting to three Australian metropolitan tertiary hospitals, one of which was a liver transplant centre, over a 9-year period from 2010 to 2018. Across all study sites, patients with decompensated cirrhosis were admitted under a specialist gastroenterology or liver transplant unit. Individual patient management was at the discretion of the attending gastroenterologist.

Ethics approval

The Human Research Ethics Committee at Monash Health and Austin Health approved the study as a quality assurance activity and the committee provided a waiver for informed consent (RES-19-0000-343Q).

Study participants

International Classification of Diseases (10th revision) codes for cirrhosis and chronic liver disease (K74, K74.6), HH (J 94.8) and pleural effusion (J90, J91) were used to retrospectively identify eligible patients with cirrhosis and HH[9]. The study eligibility criteria were: (1) Adult patients ≥ 18 years; (2) A confirmed diagnosis of cirrhosis, either biopsy-proven or based on clinical complications of cirrhosis; (3) Confirmed diagnosis of pleural effusion, based on imaging (plain X-ray or computed tomography); (4) Evidence of portal hypertension, as established by the presence of oesophageal varices, ascites and/or thrombocytopenia; and (5) Exclusion of cardiopulmonary or malignant pathology as a cause for the pleural fluid collection. Eligible patients were excluded if they had previously undergone LT. Included patients were followed for 12-mo from the date of the index admission.

Outcomes

The primary outcomes were 12-mo overall and transplant-free patient survival following index hospital admission with HH. Patients were followed-up from the date of first hospital admission with HH to an endpoint of death, LT or end of the study period. We report the 12-mo overall survival using the endpoint of death, censored for LT; and the 12-mo transplant-free survival using a composite endpoint of death and LT. The secondary outcomes included the incidence of specific treatments of HH and associated complications and to determine patient-specific prognostic factors associated with mortality.

HH definition and treatment protocols

HH was defined as the presence of a pleural effusion occurring in a patient with liver cirrhosis where no alternative aetiology was identified. Each patient was reviewed by a specialist hepatologist to ensure that the aetiology of pleural effusion was secondary to HH. Patients were excluded if the pleural effusion was felt to be due to primary infection, cardiopulmonary or malignant pathology.

Paracentesis was performed following radiological marking and thoracocentesis was performed by an interventional radiologist or the unit treating doctor with ultrasound guidance. In all cases, baseline observations were recorded, and the procedure was performed using sterile technique. Intravenous albumin (100 mL of 20% concentrated human albumin) was administered after every 2 liters of ascites or pleural fluid drained as per institutional protocol. Clinical observations were performed every 30 min for the duration of the procedure. Pleural and ascitic fluid was sent for analysis at the discretion of the physician performing the procedure according to indication and specimen viability. Where available, serum-pleural ascites gradient (SPAG) or serum-ascites albumin gradient values were obtained. SPAG greater than 11 g/L is consistent with a transudate[2], and was used to confirm portal hypertensive pathophysiology. SBEM was defined as pleural fluid with polymorphonuclear count of > 500 cells/mm^3 or > 250 cells/mm^3 with a positive culture, where parapneumonic effusion had been excluded[3]. Thoracocentesis without significant fluid drainage (diagnostic aspiration) was not considered in this analysis. TIPS insertion was available at all study centres and was performed by interventional radiology.

Treatment modalities pertaining to HH were categorized as: (1) Medical therapy with diuretics, and/or thoracocentesis; (2) TIPS; and (3) LT. All patients were risk stratified using the model for end-

stage liver disease (MELD) score which was calculated at the time of presentation for each admission. An in-hospital complication was defined as the occurrence of one or more of the following: Infection, procedural complication (hematoma, pneumothorax, death), acute kidney injury (AKI, defined as at least 1.5-1.9 times baseline or ≥ 26.5 mmol/L increase from baseline[10]), and new-onset acute hepatic encephalopathy which was not present on admission.

Data sources

For each patient, baseline demographic data, aetiology of liver disease, comorbidities, medication use, radiology results and laboratory results were extracted from electronic medical records. For patients with recurrent hospital admissions due to HH during the study period, data was collected for each presentation. Death was determined through hospital medical records and confirmed with a patient's Local Medical Officer if required.

Statistical analysis

mean ± SD was used to describe normally distributed continuous data, and median and interquartile range (IQR) for data that was significantly skewed. χ^2 analysis was used to examine the association between categorical variables. For the primary outcome, we used the Cox proportional hazards regression survival model to analyze the time of onset of HH to death. The time at risk begins at the first admission for HH (the index admission, t_0) and patients were censored at the time of LT or study conclusion (365 d after t_0). For transplant-free survival analysis, we omitted censoring LT and treated the transplant date as an outcome event. For each readmission, further clinical data was collected for analysis. The model incorporates enduring baseline variables (age, sex, comorbidities, smoking, alcohol intake, aetiology of cirrhosis) as well as a number of time-varying covariates (MELD score, AKI, encephalopathy, treatment-related complications, functional status, and TIPS).

From the univariable analyses, we included variables with a $P < 0.20$ into the multivariable model. Through backward elimination steps, we retained covariates with a $P < 0.05$ and checked the general model fit using partial Cox-Snell residuals. We used fractional polynomials to assist parameterization of continuous variables. The proportional hazards assumption was tested by examining the Schoenfeld residuals. The DFBETA estimates were used to detect influential observations. To validate our findings, we conducted bootstrapping of the Cox regression analysis with 1000 replications to generate bootstrapped confidence intervals (CIs). All analyses were conducted with STATA 16.1 (StataCorp, TX, United States), and a $P < 0.05$ was considered statistically significant.

RESULTS

Patient characteristics

A total of 246 patients with cirrhosis presenting to hospital with a pleural effusion were identified during the study period, of which 162 were excluded as the pleural effusion did not meet the criteria for HH. The final analysis included 84 patients who had a total of 167 hospital admissions over the study period. The baseline characteristics of the patients are summarized in Table 1. The mean age was 58.3 years, with only 11% patients over the age of 70, and there was a slight predominance of males. All patients had established liver cirrhosis and clinical evidence of portal hypertension. The median MELD score at time of hospital admission was 29 (IQR: 25-33). A diagnosis of hepatocellular carcinoma was present in 27.4% patients.

Across all hospital admissions, 59% of patients were treated with lactulose (13% variation within patients between admissions), 27% of patients were treated with rifaximin (average 12% variation within patients between admissions), and 56% of patients were receiving prophylaxis for SBP (average 12% variation within patients between admissions). Prior to hospital presentation with HH, 93% patients were prescribed diuretic therapy, with median furosemide and spironolactone doses of 40 mg and 100 mg per day respectively and 70% of these patients were receiving dual diuretic treatment.

HH clinical features and management

The clinical features and management of HH are summarized in Table 2. The majority of the hydrothoraces were unilateral on the right side. Of the 167 episodes of HH, 20 (12.0%) were managed solely with increased diuretics. Concurrent treatment with diuretics and ascitic fluid drainage was commonly performed, with abdominal paracentesis performed during 47 (28.1%) presentations, where the median volume of fluid drained was 5 litres. The proportion of patients requiring thoracocentesis, abdominal paracentesis and the complications rates were similar for readmissions compared to the index admission. However, the dose of diuretics used was higher on readmissions than during the index admission.

Thoracocentesis and complications: In total, 115 thoracocentesis procedures were performed in 62 (73.8%) patients with a median of 3 litres drained per procedure. Thoracocentesis was performed in 53 of 84 (63%) patients during the index admission. A further 62 thoracocentesis procedures were

Table 1 Baseline characteristics of patients with cirrhosis during the index hospital admission for hepatic hydrothorax (*n* = 84)

Characteristic	Statistic
Age, mean ± SD, yr	58.3 ± 11.5
Male, *n* (%)	46 (54.8)
Diabetes mellitus, *n* (%)	23 (27.4)
Ischaemic heart disease, *n* (%)	7 (8.3)
Heart failure, *n* (%)	4 (4.8)
Chronic obstructive lung disease, *n* (%)	5 (6.0)
Hepatocellular carcinoma, *n* (%)	23 (27.4)
Other cancer, *n* (%)	3 (3.6)
Chronic kidney disease, *n* (%)	11 (13.1)
Current smoker, *n* (%)	12 (14.3)
Current alcohol drinker, *n* (%)	9 (10.7)
Aetiology of liver disease[1], *n* (%)	
Hepatitis C virus	25 (29.8)
Non-alcoholic fatty liver	17 (20.2)
Alcoholic liver disease	13 (15.5)
Hepatitis B virus	9 (10.7)
Primary biliary cirrhosis/sclerosing cholangitis	7 (8.3)
Cryptogenic	7 (8.3)
Autoimmune hepatitis	6 (7.1)
Budd-Chiari syndrome	3 (3.6)
Metabolic/others[2]	7 (8.3)
MELD score, mean ± SD	26.8 ± 7.1
Platelet count, median (IQR), per nL	103 (65-132)
Platelet count < 50/nL, *n* (%)	9 (10.7)
Anticoagulation, *n* (%)	6 (7.1)
Previous ascitic taps, *n* (%)	69 (82.1)
Beta-blockers, *n* (%)	11 (13.1)
Lactulose, *n* (%)	34 (40.5)
Rifaximin, *n* (%)	14 (16.7)
SBP prophylaxis, *n* (%)	32 (38.1)

[1]Categories are not mutually exclusive as > 1 aetiology may be attributed to each patient.
[2]Hemochromatosis, α1-antitrypsin deficiency, sarcoidosis.
MELD: Model for end-stage liver disease; SBP: Spontaneous bacterial peritonitis; IQR: Interquartile range.

performed in 33 of 43 patients who required one or more readmissions. On average, the probability of receiving another thoracocentesis was 77% during each readmission episode. Sufficient laboratory data to perform pleural/ascitic fluid analysis was available in 31% of procedures. Of these, SBEM was detected in 10 (8.7%) thoracocentesis procedures.

Blood products, including pooled platelets, fresh frozen plasma, cryoprecipitate, were administered in 29% of patients prior to or following thoracocentesis. Sixteen patients received an indwelling intercostal catheter for ongoing drainage rather than simple thoracocentesis in the setting of acute instability (*n* = 4) or refractory disease (*n* = 12). A pneumothorax complicated 17 (15%) thoracocentesis procedures, of which 7 were managed conservatively, 9 required an intercostal catheter insertion, and 1 patient died. Bleeding complications from thoracocentesis were uncommon and we could not determine if blood product infusions (platelets, fresh frozen plasma, cryoprecipitate, or prothrombin complex

Table 2 Clinical features of hepatic hydrothorax, management, and complications

Characteristic	Index admission (*n* = 84)	Readmissions (*n* = 83)
NYHA severity of dyspnoea, *n* (%)		
Class I	13 (15.5)	4 (4.3)
Class II	23 (27.4)	37 (39.4)
Class III	28 (33.3)	22 (23.4)
Class IV	20 (23.8)	31 (33.0)
Distribution of hydrothorax, *n* (%)		
Unilateral, left	13 (15.5)	10 (12.1)
Unilateral, right	68 (81.0)	72 (86.8)
Bilateral	3 (3.6)	1 (1.2)
Admission hepatic encephalopathy, *n* (%)	12 (14.3)	14 (16.9)
De novo hepatic encephalopathy, *n* (%)	11 (13.1)	10 (12.0)
Thoracocentesis performed, *n* (%)	53 (63.1)	62 (74.7)
Pneumothorax, *n* (% of procedures)	6 (11.3)	11 (17.7)
Haematoma, *n* (% of procedures)	2 (3.8)	1 (1.6)
Pre-procedure platelet infusion, *n* (%)	11 (13.3)	6 (7.2)
Pre-procedure blood products[1], *n* (%)	18 (21.7)	12 (14.5)
Pleural fluid drained, mean ± SD, litres	2.8 ± 1.7	3.0 ± 1.5
Indwelling intercostal catheter, *n* (%)	10 (11.9)	8 (9.6)
Infection, *n* (%)	17 (20.2)	14 (16.9)
Acute kidney injury, *n* (%)	30 (35.7)	28 (33.7)
Concurrent ascites drainage, *n* (%)	23 (27.1)	24 (28.9)
Volume drained, mean ± SD, litres	6.0 ± 3.1	5.5 ± 2.1
TIPS performed, *n* (%)	2 (2.4)	8 (9.6)
Furosemide, *n* (%)		
None	27 (32.1)	9 (10.8)
20 to < 100 mg daily	52 (61.9)	60 (72.3)
100 to 240 mg daily	5 (5.6)	14 (16.9)
Spironolactone, *n* (%)		
None	27 (32.1)	18 (21.7)
25 to < 100 mg daily	15 (17.9)	22 (26.5)
100 to 300 mg daily	42 (50.0)	43 (51.8)

[1]One or more of fresh frozen plasma, cryoprecipitate, or prothrombin complex concentrate.
NYHA: New York Heart Association; TIPS: Transjugular intrahepatic portosystemic shunt.

concentrate) reduced procedural complications or affected patient survival.

Other complications: One or more non-pleural complications were recorded in 80 (48%) of HH admissions. The most frequent complications were AKI in 58 (35%) patients, followed by infection in 31 (19%) and new-onset hepatic encephalopathy in 21 (13%). The incidence of these complications was similar for the index admission and readmissions.

TIPS insertion: Ten (12%) patients received a TIPS insertion, with 2 patients receiving TIPS insertion during the index admission, and 8 patients on a readmission. Significantly more females than males received a TIPS (21% *vs* 4%, $P = 0.038$), but age and MELD score did not differ between patients who received TIPS and those who did not. No patient who received a TIPS proceeded to LT within 12 mo of

the index admission.

LT: Forty-seven patients (56%) were referred for liver transplant assessment and 28 patients (33%) were successfully transplanted in the 12-mo following their index admission. The median time to transplantation from the index admission was 105 d (IQR: 55-200 d). The effect of LT on survival could not be estimated as there were no deaths amongst the transplanted patients within the study period.

Hospital length of stay and readmissions

The median hospital length of stay was 8 d (IQR: 4-17) for the index admission and 6 d (IQR: 4-14) for subsequent hospital readmissions. Within 12-mo of the index admission, 22 (26%) patients had 1 readmission, 9 (11%) had 2 readmissions, and 12 (14%) had ≥ 3 readmissions. In the 43 patients who required readmission, the median time interval between the index admission and the first readmission was 32 d (IQR: 12-74 d). The primary reasons for hospital readmissions were recurrent hydrothorax in 24 (38%) patients and decompensated cirrhosis in 26 (41%). There was strong evidence for an association between the New York Health Association (NYHA) functional class of dyspnoea and total number of readmissions (χ^2 = 46.2, P < 0.001) but the strength of the association was weak (Kendall's tau-b = 0.11). Intensive care unit (ICU) admission was required in 13 (15%) patients during the index admission, and 10 (12%) of 83 readmission episodes.

Mortality

There were 23 deaths (27.4% of the cohort) within 12-mo of the index admission. The total time-at-risk was 17850 patient-days with a mortality rate of 1.3 deaths per 1000 patient-days. The Kaplan-Meier survivor functions for overall and transplant-free patient survival are shown in Figure 1. Most deaths occurred early after the index admission, with 30-d overall survival of 87% (95%CI: 78%-93%), 45-d survival of 80% (95%CI: 70%-87%), and 12-mo survival of 68% (95%CI: 56%-78%). For transplant-free survival, the 30-d survival was 85% (95%CI: 75%-91%), 45-d survival of 76% (95%CI: 66%-84%), and 12-mo survival of 41% (95%CI: 30%-51%). Most deaths were due to complications of end-stage liver disease and multiorgan failure (75%) or hepatocellular carcinoma (10%), but a small number were due to cardiovascular events (15%). We noted that the mortality rate for current smokers was 5.58 per 1000 patient-days, compared to non-smokers of 0.86 per 1000 patient-days, giving a mortality rate ratio for current smokers of 6.5 (95%CI: 2.5-16.1, P < 0.001).

Univariable and multivariable Cox regression analysis

The results of univariable analyses are summarised in Table 3. Factors consistently associated with an increased hazard of death were current smoking, episodes of AKI, higher MELD score, and hepatic encephalopathy. In addition, when analysing transplant-free survival, diabetes and TIPS insertion were associated with a lower hazard for death or LT while incident pneumothoraces were associated with greater hazard.

The results of the multivariable analyses are summarised in Table 4. When examining the overall patient survival model, we decided not to include hepatic encephalopathy in the multivariable model as there were only 4 cases of severe encephalopathy on admission which were associated with an increased risk of death. In the transplant-free survival model, age, diabetes, TIPS and incident pneumothoraces were not statistically significant after adjusting for MELD, smoking, AKI, and hepatic encephalopathy. There were no significant statistical interactions between variables in the final models, and the models were a reasonable fit for the data when assessed by partial Cox-Snell residuals.

Due to the cohort size, we conducted bootstrapped analysis to validate our findings (Table 4). The significance of current smoking and AKI remained robust. In the overall survival model, a current smoker had 8.7 times the hazard of death of a non-smoker or ex-smoker; and one or more episodes of AKI was associated with a 2.9-fold increase in the hazard of death, after allowing for age and MELD score. In the transplant-free survival model, a current smoker had 3.1 times the hazard of death of a non-smoker or ex-smoker; and AKI was associated with a 2.2-fold increase in the hazard of death; after allowing for MELD and hepatic encephalopathy. These findings are represented in Figure 2.

Other analysis

To compare with the traditional Cox model, we also performed a competing risks regression analysis (Fine-Gray subdistribution proportional hazards) using the same covariates, with the assumption that all patients were on the active liver transplant waiting list. In this analysis, the effect of smoking and AKI on survival remained significant, and our conclusions remained unchanged. The subhazard ratio (SHR) of smoking on mortality was 6.26 (95%CI: 2.75-14.3), P < 0.001. The SHR of AKI on mortality was 2.60 (95%CI: 1.25-5.36), P = 0.01. The clear effect of smoking can be illustrated by examining the cumulative incidence function for active smokers compared to non-smokers (see Supplementary Figure 1).

Table 3 Univariable Cox regression on patient survival to 12 mo

Enduring variables	Overall[1], 12-mo survival	Transplant-free, 12-mo survival
	HR (95%CI)	HR (95%CI)
Age, per 5-yr	1.13 (0.94-1.35)	0.95 (0.85-1.07)
Male sex	2.05 (0.84-4.99)	1.68 (0.94-3.00)
Diabetes	0.56 (0.25-1.50)	0.39 (0.19-0.81)
Ischaemic heart disease	2.00 (0.68-5.92)	0.80 (0.29-2.23)
Heart failure	0.86 (0.12-6.38)	0.35 (0.05-2.55)
Chronic obstructive lung disease	NE	1.02 (0.32-3.30)
Chronic kidney disease	1.13 (0.38-3.32)	0.82 (0.37-1.83)
Hepatocellular carcinoma	2.11 (0.92-4.81)	1.55 (0.87-2.76)
Hepatitis B	3.36 (1.32-8.53)	1.68 (0.75-3.74)
Hepatitis C	0.81 (0.32-2.05)	1.28 (0.71-2.28)
Alcoholic liver disease	0.76 (0.22-2.55)	0.94 (0.44-2.01)
Non-alcoholic fatty liver	0.51 (0.15-1.73)	0.43 (0.18-1.02)
Current smoking	5.01 (2.15-11.7)	2.27 (1.13-4.56)
Current alcohol intake	0.68 (0.42-1.13)	0.93 (0.68-1.26)
Time varying variables		
MELD score, per 5-points	1.28 (0.93-1.77)	1.82 (1.41-2.34)
NYHA functional class	1.14 (0.74-1.75)	1.09 (0.81-1.46)
TIPS procedure	0.37 (0.05-2.83)	0.13 (0.02-0.96)
Acute kidney injury	2.57 (1.13-5.88)	2.36 (1.35-4.11)
Thoracocentesis	0.51 (0.23-1.16)	1.28 (0.70-2.34)
Pneumothorax	2.37 (0.80-7.00)	2.78 (1.39-5.56)
Intercostal catheter inserted	1.56 (0.53-4.62)	1.85 (0.90-3.82)
Admission hepatic encephalopathy		
None	1.00 (reference)	1.00 (reference)
Mild	0.75 (0.17-3.25)	1.21 (0.54-2.70)
Severe	11.4 (3.28-39.6)	7.93 (2.36-26.6)
Encephalopathy during admission[2]	2.30 (0.84-6.32)	3.20 (1.65-6.24)
Any encephalopathy	2.30 (0.97-5.45)	2.21 (1.22-4.03)

[1]Censored at time of liver transplantation.
[2]New-onset during admission not present on admission, all episodes were mild.
HR: Hazard ratio; CI: Confidence interval; MELD: Model for end-stage liver disease; NYHA: New York Heart Association; TIPS: Transjugular intrahepatic portosystemic shunt; NE: Not estimable.

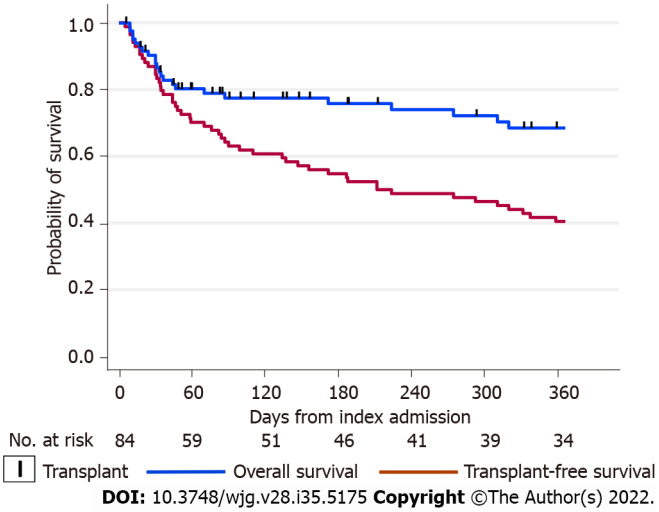
DISCUSSION

HH remains an uncommon but extremely challenging complication in patients with liver cirrhosis. This study represents one of the largest series to analyse the natural history and outcomes of patients with HH and to our knowledge, is the first study to examine factors associated with survival in this population. We demonstrated that development of HH was associated with poor prognosis despite current therapeutic modalities, with a 45-d overall survival of 80% and 12-mo transplant-free survival of 41%. HH is a refractory disease, and the use of diuretics in isolation was rarely effective in this cohort, with 52% of patients experiencing recurrence of HH and rehospitalisation. At multivariable analysis, smoking status and the presence of AKI confer significant additional mortality risk.

Table 4 Multivariable Cox regression on patient survival to 12 mo

Model and variables	AHR (95%CI)	*P* value	Bootstrap CI	*P* value
Overall survival[1]				
Age, per 5-yr increase	1.30 (1.01-1.67)	0.043	0.91-1.85	0.15
MELD score, per 5 points	1.53 (1.06-1.67)	0.025	0.89-2.66	0.13
Current smoking	8.65 (3.43-21.9)	< 0.001	2.54-29.5	0.001
Acute kidney injury	2.91 (1.21-6.97)	0.017	1.04-8.12	0.042
Transplant-free survival				
Hepatic encephalopathy	2.00 (1.08-3.67)	0.030	0.93-4.28	0.078
MELD score, per 5 points	1.78 (1.38-2.29)	< 0.001	1.31-2.44	< 0.001
Current smoking	3.11 (1.49-6.52)	0.003	1.16-8.30	0.024
Acute kidney injury	2.18 (1.20-3.96)	0.011	1.10-4.31	0.026

[1]Censored for liver transplantation.
MELD: Model for end-stage liver disease; AHR: Adjusted hazard ratio; CI: Confidence interval.



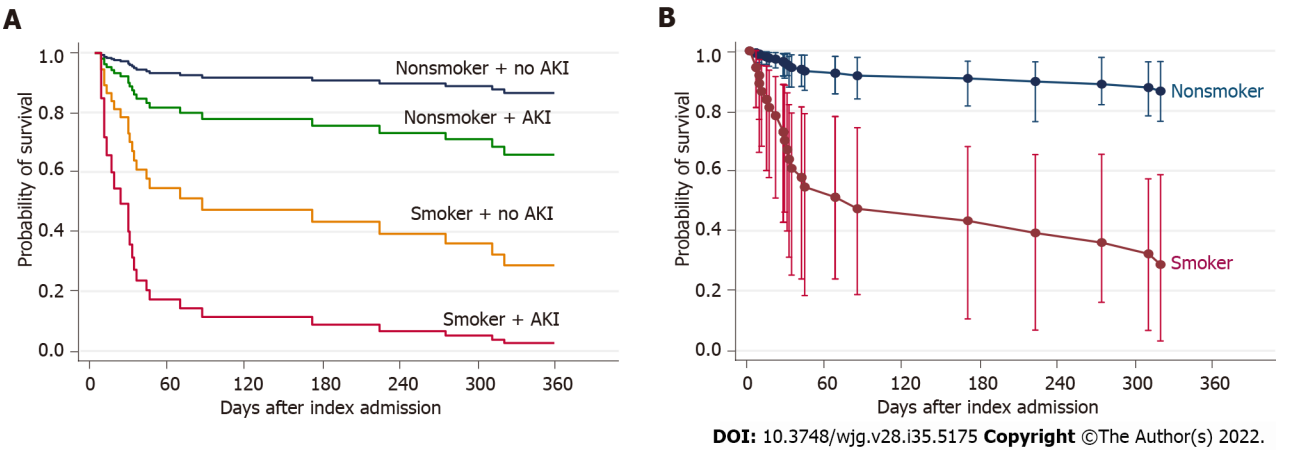
DOI: 10.3748/wjg.v28.i35.5175 **Copyright** ©The Author(s) 2022.

Figure 1 Kaplan-Meier survival curves. Kaplan-Meier survival curves showing transplant-free survival at 12 mo, with liver transplantation and death treated as composite endpoints, and overall patient survival at 12 mo, with patients censored at the time of liver transplantation (ticks on survival curve).

Hospitalisation with symptomatic HH is an uncommon presentation, with 84 patients recruited over a 9-year period to 3 metropolitan tertiary hospitals. The majority of patients presented with a right-sided pleural effusion and concurrent ascites, which is consistent with previous series[1,2,4]. The median MELD score of 29 in our cohort highlights that HH typically occurs in patients with advanced cirrhosis who often have other decompensating events such as hepatic encephalopathy. The median MELD score in our study was higher than that reported in other smaller studies[2,4,11], which may reflect use of data from a LT centre.

Patient management in this study aligns with recent AASLD guidelines, which recommend diuresis as the first-line therapy[6]. Most patients in our study were receiving diuretic therapy at the time of hospital presentation, with 70% receiving 2 diuretic agents, however the median doses of furosemide and spironolactone was well below the recommended maximum doses of 160 mg and 400 mg daily respectively[1]. Nonetheless, only 12% patients achieved long-term resolution of HH with diuretic therapy alone. An important limiting factor in relation to diuretic therapy is the propensity for AKI in patients with advanced cirrhosis. AKI was recorded in nearly one-third of presentations, and this was associated with a significantly higher risk of mortality. This suggests that diuretic therapy should be titrated cautiously in patients with HH with close monitoring of renal function.

There remains no consensus on universal diagnostic thoracocentesis in hospitalised patients with HH. In practice, whilst HH may be suspected on the basis of imaging and clinical presentation, thoracocentesis is useful to confirm transudative fluid and exclude other causes of a pleural effusion. We demonstrated that thoracocentesis in the HH population was associated with a significant higher risk of



DOI: 10.3748/wjg.v28.i35.5175 **Copyright** ©The Author(s) 2022.

Figure 2 Multivariate survival analysis. A: Multivariable Cox regression of overall patient survival (censored for transplantation), showing survival estimates for patients with hepatic hydrothorax by smoking and acute kidney injury status, with age and model for end-stage liver disease (MELD) scores held at the mean values; B: Bootstrapped pointwise confidence intervals for survival functions by active smoking status, in the absence of acute kidney injury and with age and MELD held at the means, demonstrating a robust association between active smoking and mortality in patients with hepatic hydrothorax. AKI: Acute kidney injury.

pneumothorax of 15% compared to the standard pneumothorax risk of 6% in non-cirrhotic populations, despite being performed under ultrasound guidance[12]. Shojaee *et al*[13] reported that repeat thoracocentesis in cirrhotic patients was associated with a higher rate of major complications compared to thoracocentesis for other aetiologies (8% *vs* 0%). In addition, Xiol *et al*[5], observed a pneumothorax rate of 25% in cirrhotic patients undergoing serial therapeutic thoracocentesis. Our analysis suggested that pneumothorax complications were associated with lower transplant-free survival [hazard ratio (HR) = 2.78; 95%CI: 1.39-5.56], however this was not significant in multivariable analysis. Other series have also suggested that HH requiring thoracocentesis independently confers significant morbidity and increased mortality[7,14]. Given the greater complications associated with thoracocentesis in cirrhotic patients, it was concerning that 74.7% of patients who were readmitted underwent repeat thoracocentesis. Further study is needed to elucidate the cause of the high complication rate and strategies to mitigate this risk. For example, it remains unclear if abdominal paracentesis effectively prevents HH recurrence[1].

In relation to other treatment modalities, indwelling intercostal catheter drains are thought to carry substantial risk and are not recommended by current guidelines, with some studies observing complication rates of 80%-90%[11,15]. In our cohort, an indwelling intercostal catheter was placed in 19% of patients, most commonly due to respiratory compromise and rapid re-accumulation of pleural fluid. In contrast, consideration of TIPS insertion is recommended by AASLD guidelines, based on evidence of a 70%-80% response rate in patients with refractory HH[3,6,16-18]. The outcomes following TIPS insertion may be comparable to those for management of refractory ascites and although a survival benefit in HH has not been established[19], the study by Badillo and Rockey[2] suggests a trend toward improved survival in patients proceeding to TIPS. Only 10 (17.9%) of the 56 patients in our cohort who were deemed not suitable for LT received TIPS insertion. No overall survival benefit from TIPS insertion was demonstrated, but transplant-free survival was higher (HR = 0.13; 95%CI: 0.02-0.96), as no patient who had TIPS insertion underwent LT.

Multiple studies have demonstrated that development of HH is associated with a poor prognosis[2,20,21], but mortality is difficult to compare due to heterogeneity between studies[2,4,11,15,21,22]. Our 12-mo transplant-free survival of 41%, however, is comparable to the 12-mo mortality of 57% reported by Badillo and Rockey[2]. In multivariable analysis, increasing age and MELD score, hepatic encephalopathy, development of AKI and active smoking were important factors independently associated with mortality. Given that the majority of deaths in our cohort were observed within 45-d of hospital admission and were most frequently due to complications of end-stage liver disease, we would advocate that in all patients presenting with HH, the appropriateness of transplantation should be considered with early referral for suitable candidates. Indeed, no deaths were recorded in patients who received LT, highlighting the successful outcomes of transplantation in patients with HH.

The strong association between smoking and poor outcomes has not previously been reported in patients with HH. Our study echoes a growing body of literature demonstrating an association between cigarette smoking and poorer outcomes in patients with liver disease[23,24]. Current smokers with cirrhosis have up to a 3.6 times higher mortality risk and cigarette smoking has been linked with progression of fibrosis in non-alcoholic fatty liver disease[24], hepatitis C and primary biliary cholangitis and is associated with an increased incidence of hepatocellular carcinoma[23]. Cigarette smoking represents an important modifiable risk factor that should be actively addressed in all patients with cirrhosis but appears critical in the HH population.

Study strengths and limitations

This is one of the largest, multicentre studies to investigate the prognostic significance of HH requiring hospitalisation in cirrhotic patients. Study inclusion criteria were broad and pragmatic, and represent generalisable real-world data. The Victorian Liver Transplant Centre was established in 1988 and currently performs over 100 transplants annually. The cohort had comprehensive assessments by gastroenterology specialists to confirm HH, which also assured treatment consistent with current standard-of-care practice guidelines. We used multivariable analysis to allow for confounders of mortality, and were able to identify smoking as a novel factor associated with significantly lower 12-mo survival in patients with HH. This study was able to elucidate the less well-described challenges in HH patients, such as need for ICU admission, hospital readmissions, and blood product requirement.

This study is limited by its retrospective design, with the inherent risks of missing information or extraction of inaccurate records. Complete pleural fluid analysis was only available in 31% of patients, which limited our ability to detect complications such as SBEM. SBEM has been associated in other studies with high short-term mortality (20% to 38%)[1]. SBEM was detected in 8.7% of thoracocentesis procedures in our study, which is almost certainly an underrepresentation of the true rate and lower than a study by Xiol *et al*[5], which found SBEM was present in 13% of patients with HH on presentation. Reasons for the low rate of complete pleural fluid analysis included the large number of hospital settings in which thoracocentesis was performed (including the emergency department, ICU, gastroenterology ward, radiology department or other acute hospital wards) with associated heterogeneity in process, incorrect requests for fluid analysis, incorrect tube collection to facilitate fluid analysis, clotting of fluid which precluded analysis, emergency procedures due to patient distress or instability and thoracocentesis performed prior to a diagnosis of HH being made. This reflects the real-world nature of the study and pleural fluid analysis rates were similar across all study sites. As such, we were not able to determine if specific pleural fluid findings were associated with refractory symptoms, rehospitalisation, or poor survival. In addition, factors associated with treatment failure or rehospitalisation such as compliance with diuretics were difficult to discern. The observational nature of the study also limits any causality inferences and eliminates the ability to ensure standardisation, which is particularly relevant to thoracocentesis technique. We could not exclude the possibility that some patients may have been admitted to a non-study hospital, although in practice this would be uncommon, and thus readmissions and complications may be underestimated.

In order to assess if TIPS may have provided clinical benefit apart from survival, we examined the readmissions, thoracocentesis, or ascitic drainage procedures in patients who received TIPS. Four patients had a single readmission post-TIPS, of which 3 occurred < 30 d and one at 6 mo post-TIPS. Thoracocentesis was performed in 3 of 4 of these readmitted patients, and ascitic drainage in 1 of 4 of these readmitted patients. Due to these low frequencies and different timing of TIPS, we cannot provide a meaningful statistical comparison with patients who did not have TIPS.

CONCLUSION

The development of HH is associated with poor transplant-free survival despite current standards-of-care and should prompt consideration of the appropriateness of LT in all patients. HH is often refractory to both conservative and invasive management and patients frequently require repeat hospitalisations. Active smoking and AKI may be important modifiable risk factors to reduce mortality in cirrhotic patients with HH.

ARTICLE HIGHLIGHTS

Research background

Hepatic hydrothorax (HH) is an important complication of cirrhosis, however management is often challenging and the natural history is poorly understood.

Research motivation

HH is a significant complication of cirrhosis, with a paucity of literature studying natural history and factors affecting survival.

Research objectives

This study sought to: (1) Evaluate factors associated with survival in a cohort of patients hospitalised with HH; and (2) Provide descriptive analysis of treatments, complications and outcomes following HH hospitalisation.

Research methods

Cirrhotic patients with HH presenting to three tertiary centres from 2010 to 2018 were retrospectively identified. Patients were followed-up from the date of first hospital admission with HH to an endpoint of death, liver transplantation (LT) or end of the study period. The primary outcomes were overall and transplant free survival at 12 mo after the index admission. The secondary outcomes included the incidence of specific treatments of HH and associated complications and to determine patient-specific prognostic factors associated with mortality.

Research results

Only 12% of patients achieved long-term resolution of HH with diuretic therapy alone. 74% of patients required thoracocentesis, with 15% of procedures being complicated by pneumothorax. 12-mo transplant free survival was 41%. 45-d overall survival was 80%.

Research conclusions

The development of HH is associated with poor transplant-free survival despite current standards-of-care and should prompt consideration of the appropriateness of LT in all patients. HH is often refractory to both conservative and invasive management and patients frequently require repeat hospitalisations. Active smoking and acute kidney injury may be important modifiable risk factors to reduce mortality in cirrhotic patients with HH.

Research perspectives

This study represents one of the largest series examining survival in persons hospitalised with HH, and importantly has identified modifiable risk factors that may alter the natural history in this challenging patient population.

FOOTNOTES

Author contributions: Romero S, Lim AK and Robertson M performed literature review, data analysis and interpretation and manuscript composition and critical revision; Lim AK, Robertson M and Hui S conducted statistical analysis; Romero S, Singh G, Kodikara C, Shangaki-Wells R and Chen L performed data acquisition; Robertson M was responsible for study concept and design; and all authors have read and approved the final manuscript.

Institutional review board statement: The Human Research Ethics Committee at Monash Health and Austin Health approved the study as a quality assurance activity and the committee provided a waiver for informed consent (RES-19-0000-343Q).

Informed consent statement: The informed consent was waived by the Human Research Ethics Committee.

Conflict-of-interest statement: All the authors report no relevant conflicts of interest for this article.

Data sharing statement: Technical appendix, statistical code, and dataset available from the corresponding author at s.romero.md@gmail.com. Patient consent was not obtained for this study, however study data has been anonymised.

STROBE statement: That authors have read the STROBE statement-checklist, and the manuscript was prepared and revised according to the STROBE statement-checklist of items.

Open-Access: This article is an open-access article that was selected by an in-house editor and fully peer-reviewed by external reviewers. It is distributed in accordance with the Creative Commons Attribution NonCommercial (CC BY-NC 4.0) license, which permits others to distribute, remix, adapt, build upon this work non-commercially, and license their derivative works on different terms, provided the original work is properly cited and the use is non-commercial. See: https://creativecommons.org/Licenses/by-nc/4.0/

Country/Territory of origin: Australia

ORCID number: Sarah Romero 0000-0003-2707-6390; Andy KH Lim 0000-0001-7816-4724; Gurpreet Singh 0000-0001-6760-566X; Chamani Kodikara 0000-0002-2381-2875; Rachel Shingaki-Wells 0000-0002-8714-591X; Lynna Chen 0000-0002-7093-2036; Samuel Hui 0000-0002-2839-6209; Marcus Robertson 0000-0002-8848-1771.

S-Editor: Wang JJ
L-Editor: A
P-Editor: Wang JJ

REFERENCES

1 **Chaaban T**, Kanj N, Bou Akl I. Hepatic Hydrothorax: An Updated Review on a Challenging Disease. *Lung* 2019; **197**: 399-405 [PMID: 31129701 DOI: 10.1007/s00408-019-00231-6]

2 **Badillo R**, Rockey DC. Hepatic hydrothorax: clinical features, management, and outcomes in 77 patients and review of the literature. *Medicine (Baltimore)* 2014; **93**: 135-142 [PMID: 24797168 DOI: 10.1097/MD.0000000000000025]

3 **Cardenas A**, Kelleher T, Chopra S. Review article: hepatic hydrothorax. *Aliment Pharmacol Ther* 2004; **20**: 271-279 [PMID: 15274663 DOI: 10.1111/j.1365-2036.2004.02081.x]

4 **Gurung P**, Goldblatt M, Huggins JT, Doelken P, Nietert PJ, Sahn SA. Pleural fluid analysis and radiographic, sonographic, and echocardiographic characteristics of hepatic hydrothorax. *Chest* 2011; **140**: 448-453 [PMID: 21273292 DOI: 10.1378/chest.10-2134]

5 **Xiol X**, Castellote J, Cortes-Beut R, Delgado M, Guardiola J, Sesé E. Usefulness and complications of thoracentesis in cirrhotic patients. *Am J Med* 2001; **111**: 67-69 [PMID: 11448663 DOI: 10.1016/s0002-9343(01)00744-6]

6 **Banini BA**, Alwatari Y, Stovall M, Ogden N, Gershman E, Shah RD, Strife BJ, Shojaee S, Sterling RK. Multidisciplinary Management of Hepatic Hydrothorax in 2020: An Evidence-Based Review and Guidance. *Hepatology* 2020; **72**: 1851-1863 [PMID: 32585037 DOI: 10.1002/hep.31434]

7 **Hung TH**, Tseng CW, Tsai CC, Tseng KC, Hsieh YH. The long-term outcomes of cirrhotic patients with pleural effusion. *Saudi J Gastroenterol* 2018; **24**: 46-51 [PMID: 29451184 DOI: 10.4103/sjg.SJG_336_17]

8 **Yoon JH**, Kim HJ, Jun CH, Cho SB, Jung Y, Choi SK. Various Treatment Modalities in Hepatic Hydrothorax: What Is Safe and Effective? *Yonsei Med J* 2019; **60**: 944-951 [PMID: 31538429 DOI: 10.3349/ymj.2019.60.10.944]

9 **World Health Organization**. ICD-10: international statistical classification of diseases and related health problems: tenth revision, 2nd ed. [cited 12 December 2021]. Available from: https://apps.who.int/iris/handle/10665/42980

10 **Kellum JA**, Lameire N, Aspelin P, Barsoum RS, Burdmann EA, Goldstein SL, Herzog CA, Joannidis M, Kribben A, Levey AS, MacLeod AM, Mehta RL, Murray PT, Naicker S, Opal SM, Schaefer F, Schetz M, Uchino S. Kidney disease: Improving global outcomes (KDIGO) acute kidney injury work group. KDIGO clinical practice guideline for acute kidney injury. *Kidney Int Suppl* 2012; **2**: 1-138 [DOI: 10.1038/kisup.2012.1]

11 **Orman ES**, Lok AS. Outcomes of patients with chest tube insertion for hepatic hydrothorax. *Hepatol Int* 2009; **3**: 582-586 [PMID: 19669710 DOI: 10.1007/s12072-009-9136-z]

12 **Gordon CE**, Feller-Kopman D, Balk EM, Smetana GW. Pneumothorax following thoracentesis: a systematic review and meta-analysis. *Arch Intern Med* 2010; **170**: 332-339 [PMID: 20177035 DOI: 10.1001/archinternmed.2009.548]

13 **Shojaee S**, Khalid M, Kallingal G, Kang L, Rahman N. Repeat Thoracentesis in Hepatic Hydrothorax and Non-Hepatic Hydrothorax Effusions: A Case-Control Study. *Respiration* 2018; **96**: 330-337 [PMID: 29991046 DOI: 10.1159/000490001]

14 **Kallingal G**, Khalid M, Kang L, Shojaee S. Complications Associated With Serial Thoracenteses in Cirrhotic Patients With Hepatic Hydrothorax. Proceedings of the Chest Conference; 2016 Oct 22-26; Los Angeles, USA. Netherlands: Elsevier, 2016: 997A

15 **Liu LU**, Haddadin HA, Bodian CA, Sigal SH, Korman JD, Bodenheimer HC Jr, Schiano TD. Outcome analysis of cirrhotic patients undergoing chest tube placement. *Chest* 2004; **126**: 142-148 [PMID: 15249455 DOI: 10.1378/chest.126.1.142]

16 **Siegerstetter V**, Deibert P, Ochs A, Olschewski M, Blum HE, Rössle M. Treatment of refractory hepatic hydrothorax with transjugular intrahepatic portosystemic shunt: long-term results in 40 patients. *Eur J Gastroenterol Hepatol* 2001; **13**: 529-534 [PMID: 11396532 DOI: 10.1097/00042737-200105000-00011]

17 **Strauss RM**, Martin LG, Kaufman SL, Boyer TD. Transjugular intrahepatic portal systemic shunt for the management of symptomatic cirrhotic hydrothorax. *Am J Gastroenterol* 1994; **89**: 1520-1522 [PMID: 8079930]

18 **Gordon FD**, Anastopoulos HT, Crenshaw W, Gilchrist B, McEniff N, Falchuk KR, LoCicero J 3rd, Lewis WD, Jenkins RL, Trey C. The successful treatment of symptomatic, refractory hepatic hydrothorax with transjugular intrahepatic portosystemic shunt. *Hepatology* 1997; **25**: 1366-1369 [PMID: 9185754 DOI: 10.1002/hep.510250611]

19 **Young S**, Bermudez J, Zhang L, Rostambeigi N, Golzarian J. Transjugular intrahepatic portosystemic shunt (TIPS) placement: A comparison of outcomes between patients with hepatic hydrothorax and patients with refractory ascites. *Diagn Interv Imaging* 2019; **100**: 303-308 [PMID: 30522911 DOI: 10.1016/j.diii.2018.10.006]

20 **Liu WL**, Kuo PH, Ku SC, Huang PM, Yang PC. Impact of therapeutic interventions on survival of patients with hepatic hydrothorax. *J Formos Med Assoc* 2010; **109**: 582-588 [PMID: 20708509 DOI: 10.1016/S0929-6646(10)60095-2]

21 **Mouelhi L**, Daboussi O, Cheffi N, El Jery K, Said Y, Khedher S, Salem M, Dabbèche R, Houissa F, Najjar T. Hepatic hydrothorax: About a hospital serie of 63 cases. *Tunis Med* 2016; **94**: 867 [PMID: 28994887]

22 **Luh SP**, Chen CY. Video-assisted thoracoscopic surgery (VATS) for the treatment of hepatic hydrothorax: Report of twelve cases. *J Zhejiang Univ Sci B* 2009; **10** [DOI: 10.1631/jzus.B0820374]

23 **Rutledge SM**, Asgharpour A. Smoking and Liver Disease. *Gastroenterol Hepatol (N Y)* 2020; **16**: 617-625 [PMID: 34035697]

24 **Carter BD**, Abnet CC, Feskanich D, Freedman ND, Hartge P, Lewis CE, Ockene JK, Prentice RL, Speizer FE, Thun MJ, Jacobs EJ. Smoking and mortality--beyond established causes. *N Engl J Med* 2015; **372**: 631-640 [PMID: 25671255 DOI: 10.1056/NEJMsa1407211]

World Journal of Gastroenterology

Submit a Manuscript: https://www.f6publishing.com

World J Gastroenterol 2022 September 21; 28(35): 5188-5202

DOI: 10.3748/wjg.v28.i35.5188

ISSN 1007-9327 (print) ISSN 2219-2840 (online)

ORIGINAL ARTICLE

Observational Study

Gut microbiota of hepatitis B virus-infected patients in the immune-tolerant and immune-active phases and their implications in metabolite changes

Ya-Nan Li, Na-Ling Kang, Jia-Ji Jiang, Yue-Yong Zhu, Yu-Rui Liu, Da-Wu Zeng, Fei Wang

Specialty type: Infectious diseases

Provenance and peer review: Unsolicited article; Externally peer reviewed.

Peer-review model: Single blind

Peer-review report's scientific quality classification

Grade A (Excellent): 0
Grade B (Very good): B, B
Grade C (Good): C
Grade D (Fair): 0
Grade E (Poor): 0

P-Reviewer: Fraga RS, Brazil; Nath L, India

Received: April 12, 2022
Peer-review started: April 12, 2022
First decision: July 13, 2022
Revised: July 26, 2022
Accepted: August 22, 2022
Article in press: August 22, 2022
Published online: September 21, 2022

Ya-Nan Li, Na-Ling Kang, Jia-Ji Jiang, Yue-Yong Zhu, Yu-Rui Liu, Da-Wu Zeng, Department of Hepatology, Hepatology Research Institute, The First Affiliated Hospital, Fujian Medical University, Fuzhou 350001, Fujian Province, China

Fei Wang, Department of Pharmacy, Fujian Geriatric Hospital, Fuzhou 350001, Fujian Province, China

Corresponding author: Da-Wu Zeng, MD, Associate Chief Physician, Associate Professor, Department of Hepatology, Hepatology Research Institute, The First Affiliated Hospital, Fujian Medical University, No. 20 Chazhong Road, Fuzhou 350001, Fujian Province, China.
zengdw1980@fjmu.edu.cn

Abstract

BACKGROUND

The microbes and metabolomics of microbiota dysbiosis in the gut in the different phases of hepatitis B virus (HBV) infection are not fully understood.

AIM

To investigate the specific gut microbiota and metabolites of the immune-tolerant (IT) and immune-active (IA) phases of chronic hepatitis B (CHB).

METHODS

Clinical fecal samples from healthy individuals and patients in the IT and IA phases of HBV infection were collected. Next, non-target metabolomics, bioinformatics, and 16S rDNA sequencing analyses were performed.

RESULTS

A total of 293 different metabolites in 14 phyla, 22 classes, 29 orders, 51 families, and 190 genera were identified. The four phyla of *Firmicutes*, *Bacteroidetes*, *Actinobacteria*, and *Proteobacteria* were the most abundant, accounting for 99.72%, 99.79%, and 99.55% in the healthy controls, IT-phase patients, and IA-phase patients, respectively. We further identified 16 genera with different richness in the IT phase and IA phase of HBV infection. Of the 134 named metabolites, 57 were upregulated and 77 were downregulated. A total of 101 different metabolic functions were predicted in this study, with 6 metabolic pathways having the highest enrichments, namely carbohydrate metabolism (14.85%), amino acid

metabolism (12.87%), lipid metabolism (11.88%), metabolism of cofactors and vitamins (11.88%), xenobiotic biodegradation (9.9%), and metabolism of terpenoids and polyketides (7.92%).

CONCLUSION

These findings provide observational evidence of compositional alterations of the gut microbiome and some related metabolites in patients with IT-phase or IA-phase HBV infection. Further studies should investigate whether microbiota modulation can facilitate the progression of CHB and the cause-effect relationship between the gut microbiota and CHB.

Key Words: Microbes; Metabolomics; Gut microbiota; Immune-tolerant phase; Hepatitis B virus

©The Author(s) 2022. Published by Baishideng Publishing Group Inc. All rights reserved.

Core Tip: This article provided observational evidence of compositional alterations of gut microbiome and some related metabolite in patients with immune-tolerant phase hepatitis B virus (HBV) infection and immune-active phase HBV infection.

Citation: Li YN, Kang NL, Jiang JJ, Zhu YY, Liu YR, Zeng DW, Wang F. Gut microbiota of hepatitis B virus-infected patients in the immune-tolerant and immune-active phases and their implications in metabolite changes. *World J Gastroenterol* 2022; 28(35): 5188-5202

URL: https://www.wjgnet.com/1007-9327/full/v28/i35/5188.htm

DOI: https://dx.doi.org/10.3748/wjg.v28.i35.5188

INTRODUCTION

As a disease of public health significance, hepatitis B often leads to liver cirrhosis or hepatocellular carcinoma (HCC). Currently, there are few effective treatments and strategies for eliminating hepatitis B virus (HBV) infection. The immune-tolerant (IT) phase is the first stage of HBV infection, and recent studies suggest that HBV-infected patients in this phase suffer from a high risk of HCC and death[1-3]. However, anti-HBV treatment is not generally recommended at this stage. The IT status of patients largely determines the patients' outcomes. Thus, the identification of factors that affect the consequences of HBV infection is crucial for eliminating this disease.

Recent studies indicate that the gut microbiota is involved in chronic hepatitis B (CHB) as well as other liver diseases[4-6]. Some commensal bacteria regulate the host metabolic pathways by improving food-derived energy or modulating the host-derived compounds that alter metabolism[7-9]. In addition, there are various gut microbiota in patients with CHB, hepatitis B-related liver cirrhosis, or HCC[10-12]. To date, information about the gut microbiota in patients at the initial phase of HBV infection remains largely unknown. We believe that studies on the gut microbiota of HBV-infected patients in the IT phase would help to elucidate the underlying mechanism of HBV IT as it will provide valuable information about the immune environment for HBV and its long-term existence.

Most studies on the microbiome have been cross-sectional with samples collected at a single time point, and only some studies have been performed with samples from different stages of HBV infection [12-15]; moreover, few comparisons of HBV-infected patients and healthy individuals have been carried out in these studies. CHB patients may develop recurrent active hepatitis, while the IT phase may change into the immune-active (IA) phase at a later stage in patients[16], which can lead to a substantial change in the composition of the gut microbiota. Therefore, understanding how the gut microbiota change from the IT phase to the IA phase will be important for the development of potential microbiome-targeting therapeutic drugs to combat HBV infection. Furthermore, this dynamic variation in gut microbiota in HBV-infected patients may help us to identify unique bacterial taxa that would contribute to postponing disease progression.

The present study focused on the dynamic profiles of the gut microbiota in IT-phase patients and IA-phase HBV-infected patients without liver fibrosis by 16S rDNA sequencing and analysis. We aimed to identify changes of bacteria involved in the transition from the IT phase to the IA phase in HBV-infected patients and to illustrate the regulation of both microbiota and metabolites. The results will provide a new perspective for the noninvasive diagnosis and treatment of IT-phase HBV-infected patients.

MATERIALS AND METHODS

Recruitment of participants

HBV-infected patients in the IT phase or the IA phase were recruited from The First Affiliated Hospital of Fujian Medical University from January 2018 to December 2020. All HBV-infected patients were at least 18-years-old, hepatitis B surface antigen positive for ≥ 6 mo, and hepatitis B virus e-antigen positive; moreover, the IT patients had a normal alanine aminotransferase level (< 40 IU/L), HBV DNA > 1 million IU/mL, and no fibrosis found by FibroScan analysis[17]. The IA patients had an HBV DNA serum concentration of > 20000 IU/mL as well as elevated alanine aminotransferase and/or aspartate aminotransferase levels[17]. However, patients who suffered from other non-HBV diseases/infections were excluded from the study. Samples from healthy volunteers were blindly collected, and participants who had received antiviral therapy, immunotherapy, probiotics, or antibiotics within 8 wk before enrollment were excluded. Verbal informed consent was provided by all participants. The experimental protocol and participant enrollment procedure were approved by the Ethics Review Committee of the university and were conducted according to the Declaration of Helsinki guidelines.

Clinical measurements

Liver stiffness measurements were conducted using a FibroScan instrument. Measurements with more than ten successful acquisitions were obtained (with a rate > 60% and an interquartile range < 30%). In addition, the alanine aminotransferase, aspartate aminotransferase, glutamyl transpeptidase, total bilirubin, albumin, globulin, and alpha-fetoprotein levels were measured. HBV serological testing was performed with the Architect platform (Abbott Laboratories, Chicago, IL, United States). HBV DNA was tested by a quantitative PCR assay (PG Company, Shenzhen, China).

Sampling, DNA extraction, and PCR

Fecal samples were obtained from all participants, filtered with a 2-mm sieve to remove interferents, and then stored at -80 °C for the following experiments. Total bacterial DNA extraction was performed with a PowerSoil DNA Isolation Kit (MoBio Laboratories, Carlsbad, CA, United States), and the purity and quality of the genomic DNA were checked by electrophoresis on 0.8% agarose gels. The V3-4 hypervariable region of bacterial 16S rDNA was amplified by previously reported conserved primers: 338F (5′-ACTCCTACGGGAGGCAGCAG-3′) and 806R (5′-GGACTACHVGGGTWTCTAAT-3′)[18]. For each sample, the 10-digit barcode sequence was added to the 5′-end of the forward and reverse primers (provided by Allwegene Company, Beijing, China). The PCR was carried out on a Mastercycler Gradient (Eppendorf, Germany) using a reaction volume of 25 μL, containing 12.5 μL of KAPA 2G Robust Hot Start Ready Mix, 1 μL of forward primer (5 μmol/L), 1 μL of reverse primer (5 μmol/L), 5 μL of DNA (total template quantity of 30 ng), and 5.5 μL of H_2O. The cycling parameters were 95 °C for 5 min, followed by 28 cycles of 95 °C for 45 s, 55 °C for 50 s, and 72 °C for 45 s, with a final extension at 72 °C for 10 min.

Three PCR products per sample were pooled to mitigate reaction-level PCR biases. The PCR products were purified using a QIAquick Gel Extraction Kit (QIAGEN, Germany), quantified using real-time PCR, and sequenced at Allwegene Company, Beijing, China. Deep sequencing was done with the Miseq platform at the Allwegene Company (Beijing, China). The raw data were first screened, and sequences were removed from consideration if they were shorter than 200 bp, had a low quality score (≤ 20), contained ambiguous bases, or did not exactly match the primer sequences and barcode tags. Qualified reads were separated using the sample-specific barcode sequences and trimmed with Illumina Analysis Pipeline Version 2.6. Thereafter, the dataset after cleaning was analyzed using the Quantitative Insights into Microbial Ecology (QIIME) platform.

All sequences were clustered into operational taxonomic units (OTUs) at a similarity level of 97%[19] to generate rarefaction curves. The Ribosomal Database Project classifier tool was used to analyze different taxonomic groups[20]. The Venn diagram was built by the R package program. Shared taxa presented in all groups were defined as the core microbiota. Clustering analysis and principal component analysis were performed by using the R package, as described previously[21]. The evolution distances were analyzed with the unweighted pair group method and an arithmetic mean clustering tree[22]. Heatmaps of the top 20 OTUs were generated using Mothur, as described in a previous study [23].

Metabolic pathway and non-target metabolomics

Phylogenetic Investigation of Communities by Reconstruction of Unobserved States (PICRUSt) analysis based on the 16S rDNA was performed. The OTU table derived from QIIME was compared using the Kyoto Encyclopedia of Genes and Genomes and MetaboAnalyst (http://www.metaboanalyst.ca/) databases, and the metabolic function of the gut microbiota was predicted based on the findings. The abundances of functional genes were visualized as heatmaps by the R package.

For metabolite extraction, a 10-μL aliquot of each sample was mixed with 990 μL of the extraction solvent (acetonitrile/methanol/water, 2:2:1), and the mixture was vortexed for 30 s, incubated at -20 °C for 1 h, and then centrifuged at 12000 rpm and 4 °C for 15 min. Finally, the supernatant was diluted 10

times for ultra-high-performance liquid chromatography-tandem mass spectrometry (UHPLC-MS/MS) analysis[24]. UHPLC separation was performed on an Agilent 1290 Infinity II series UHPLC system (Agilent Technologies). Mobile phase A included both 10 mmol/L ammonium formate and 10 mmol/L ammonia, while mobile phase B was acetonitrile. The temperatures for the column and the autosampler were set at 35 °C and 4 °C, respectively[25].

Statistical analysis

One-way analysis of variance was performed to compare continuous variables between two groups. The Wilcoxon signed rank test, Kruskal–Wallis test, χ^2 test, or Student's t test was used to compare categorical variables between groups. All statistical analyses were calculated either in the R package (version 3.6.1) or SPSS (version 26.0). P values less than 0.05 were considered as significant differences.

RESULTS

Overview of gut microbial community shift in patients

To differentiate the characteristics of the gut microbiota in IT-phase HBV-infected patients, IA-phase HBV-infected patients, and healthy individuals, 16S rDNA gene sequencing was performed on the stool samples from 14 IT-phase HBV-infected patients, 10 IA-phase HBV-infected patients, and 13 healthy donors (Table 1). A total of 1521813, 411189, and 1109236 sequences were acquired for the IT, IA, and healthy groups, respectively, after excluding low-quality reads. A total of 19556 clean tags were obtained, of which 824 OTUs were matched. After applying strict trimming criteria to exclude low-quality clean tags, the numbers of OTUs for healthy individuals, IT-phase patients, and IA-phase patients were 633, 662, and 489, respectively, as shown in Table 2. A total of 95, 132, and 27 OTUs existed independently in the healthy controls, IT-phase patients, and IA-phase patients, respectively (Figure 1). There were no significant differences in the Chao1, Shannon, and Simpson indices among the IT, IA, and healthy groups (all P values > 0.05, Table 2). The bacterial communities in the healthy individuals were relatively more heterogeneous than those found in the IT- or IA-phase patients. The IT and IA patients could be separated from the healthy individuals by non-metric multidimensional scaling and principal component analysis (Figure 2A and B). Partial least squares discriminant analysis showed structural differences in the gut bacterial community structure among the groups, indicating that the classification model was effective (Figure 2C).

Predominant bacteria at different levels

To show the abundance of bacteria of all fecal samples, 14 phyla, 22 classes, 29 orders, 51 families, and 190 genera were identified, and the dominant gut microbiota are shown in Supplementary Table 1 and Figure 3. The four phyla of *Firmicutes*, *Bacteroidetes*, *Actinobacteria*, and *Proteobacteria* were the most abundant, accounting for 99.72%, 99.79%, and 99.55% in the healthy controls, IT-phase patients, and IA-phase patients, respectively. In detail, the highest relative abundance of *Actinobacteria*, which reached 7.32%, was found in the healthy group. Meanwhile, compared with the healthy control and the IA-phase patients, the IT patients had the highest abundance of *Bacteroidetes* (33.27%). The IT-phase patients had less *Firmicutes* (61.00%) and *Actinobacteria* (2.71%) than the IA-phase patients. *Clostridiales*, *Bacteroidales*, *Selenomonadales*, *Bifidobacteriales*, *Coriobacteriales*, *Erysipelotrichales*, *Lactobacillales*, and *Enterobacteriales* were the most abundant bacteria at the order level in all three groups.

For the genus level, an abundance of *Bacteroides* (16.19%), *Prevotella 9* (9.04%), and *Megamonas* (7.66%) was found in the IT-phase patients. However, *Blautia* (19.20%) and *Faecalibacterium* (12.68%) were enriched in the IA-phase patients. Interestingly, the healthy groups had more *Eubacterium rectale* (6.69%), *Eubacterium hallii* (4.03%), *Bifidobacterium* (3.87%), and *Dorea* (3.23%). In addition, *Faecalibacterium* and *Blautia* accounted for a high proportion in the IA-phase patients; these bacteria are involved in butyrate short-chain fatty acid metabolism and inhibit inflammation.

Linear discriminant analysis effect size analysis to identify specific microbial taxa related to IT and IA patients

Linear discriminant analysis (LDA) effect size modeling was applied to identify specific bacterial taxa associated with different stages of CHB (Figure 2D and E). There were markedly significant differences in the community compositions in CHB patients compared with the healthy individuals. There were 12 and 6 significantly different taxa in the IT- and IA-phase patients, respectively. The five most enriched genera in the IT-phase patients were *Senegalimassilia* (LDA score = 4.38, $P < 0.05$), *Prevotella 2* (LDA score = 4.24, $P < 0.01$), *Alloprevotella* (LDA score = 4.09, $P < 0.05$), *Sutterella* (LDA score = 3.67, $P < 0.001$), and *Haemophilus* (LDA score = 3.58, $P < 0.05$). The four most enriched genera in the IA-phase patients included *Blautia* (LDA score = 4.78, $P < 0.01$), *Faecalibacterium* (LDA score = 4.51, $P < 0.05$), *Clostridium innocuum* group (LDA score = 4.23, $P < 0.01$), and *Faecalitalea* (LDA score = 3.76, $P < 0.05$) (Supplementary Table 2). These significantly different gut microbial taxa can be used as potential noninvasive biomarkers for the diagnosis of different immune phases of infection in CHB.

Table 1 Basic information and clinical characteristics of healthy individuals, immune-tolerant phase hepatitis B virus infection patients, and immune-active phase hepatitis B virus infection patients

Characteristic	H, *n* = 13	IT, *n* = 14	IA, *n* = 10	*P* value
Sex, M/F	9/4	9/5	7/3	0.949
Age in yr	26.4 ± 0.8	26.9 ± 5.8	36.2 ± 11.3	0.004
HBsAg as log10 IU/mL	NA	4.62 ± 0.18	3.83 ± 0.81	< 0.001
HBeAg as log10 S/Co	NA	3.18 ± 0.08	1.21 ± 1.70	< 0.001
HBV DNA as log10 IU/mL	NA	7.81 ± 0.80	6.28 ± 1.70	< 0.001
AFP in ng/mL	2.06 ± 0.82	2.49 ± 1.05	22.61 ± 40.82	0.045
TBIL in μmol/L	5.9 ± 3.1	12.7 ± 5.3	19.5 ± 9.2	< 0.001
ALB in g/L	48.8 ± 3.5	45.8 ± 2.9	43.0 ± 4.9	0.002
GLO in g/L	24.4 ± 4.0	26.6 ± 4.4	29.3 ± 4.3	0.017
ALT in U/L	22.0 (18.0, 29.0)	29.5 (23.7, 33.0)	277.5 (101.5, 410.8)	< 0.001
AST in U/L	16.0 (12.0, 22.0)	23.0 (19.5, 27.8)	111.0 (67.0, 143.5)	0.006
GGT in U/L	25.7 ± 11.5	18.5 ± 9.4	72.7 ± 64.9	0.001
TBA in μmol/L	2.3 (1.9, 3.4)	5.6 (4.2, 8.4)	13.9 (5.5, 31.1)	0.012
LSM in kPa	4.99 ± 0.99	5.11 ± 1.01	6.38 ± 0.72	0.026

H: Healthy; IT: Immune-tolerant; IA: Immune-active; HBsAg: Hepatitis B surface antigen; HBeAg: Hepatitis B virus e-antigen; HBV: Hepatitis B virus; AFP: Alpha-fetoprotein; TBIL: Total bilirubin; ALB: Albumin; GLO: Globulin; ALT: Alanine aminotransferase; AST: Aspartate aminotransferase; GGT: Gamma glutamyl transpeptidase; TBA: Total bile acid; LSM: Liver stiffness measurement; M: Male; F: Female; NA: Not available.

Table 2 Species richness indices in the fecal samples

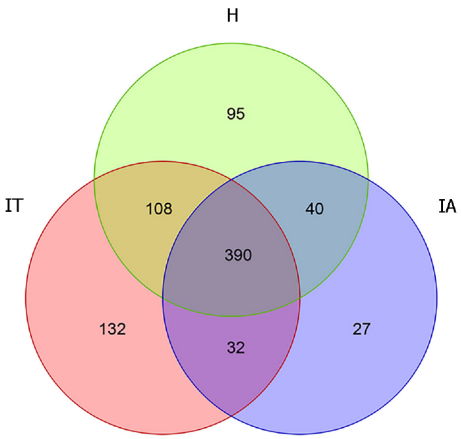
Group	Healthy controls, *n* = 14	IT phase HBV infection, *n* = 13	IA phase HBV infection, *n* = 10	*P* value
OTUs	633	662	489	
α-diversity indexes, median				
Chao1	264.310	233.825	227.000	0.924
Shannon	5.020	4.720	4.705	1.739
Simpson	0.940	0.885	0.915	1.666

IT: Immune-tolerant; IA: Immune-active; HBV: Hepatitis B virus; OTUs: Operational taxonomic units.

Furthermore, the Wilcoxon and Kruskal-Wallis rank sum tests showed the abundance at different taxonomic levels with $P < 0.05$ and FDR $q < 0.1$ (Supplementary Table 3). The top 20 gut microbiota at the genus level consisted of *Bacteroides*, *Prevotella 9*, *Megamonas*, *Blautia*, *Faecalibacterium*, *Roseburia*, *Fusicatenibacter*, *Anaerostipes*, *Prevotella 2*, *Ruminococcus 2*, *Phascolarctobacterium*, *Alloprevotella*, *Bifidobacterium*, *Subdoligranulum*, *Dialister*, *Eubacterium rectale*, *Eubacterium eligens*, *Dorea*, *Eubacterium hallii*, and *Streptococcus*. Moreover, the shared species between the significantly different gut microbiota and the top 20 gut microbiota were *Blautia*, *Faecalibacterium*, *Fusicatenibacter*, *Prevotella 2*, *Alloprevotella*, and *Eubacterium hallii* group, which might be highly associated with the outcomes of CHB in different phases. The differences found in this study revealed the dysbiosis involved in the development of CHB and the aberrant ecological networks of microbial communities during infection.

Longitudinal analysis of patients in the IT phase of HBV infection

Longitudinal follow-up analysis showed that 3 patients progressed from the IT phase to the IA phase and required medical treatments. The change in the microbiota of these 3 patients during treatment was studied. The abundance of *Firmicutes* and *Actinobacteria* increased, while the abundance of *Bacteroidetes* and *Proteobacteria* decreased at the phylum level (Figure 4A). Moreover, *Bacteroides*, *Alistipes*, and *Bilophila* were mostly abundant in the IT phase, while *Actinomyces*, *Adlercreutzia*, and *Streptococcus* were more abundant in the IA phase (Figure 4B and C). A decreased ratio of *Bacteroidetes* to *Firmicutes* was observed, which might be involved in inflammatory disorders in the IA phase.



DOI: 10.3748/wjg.v28.i35.5188 **Copyright** ©The Author(s) 2022.

Figure 1 Operational taxonomic units in healthy controls, immune-tolerant phase patients, and immune-active phase patients. IT: Immune-tolerant; IA: Immune-active; H: Healthy.

Microbial functional dysbiosis in IT and IA patients and co-occurrence network analysis

To identify the bacterial functional alteration in IT and IA patients, we analyzed the functional potential of gut microbiota with PICRUSt analysis. A total of 101 different metabolic functions were predicted in this study, with 6 metabolic pathways having the highest enrichments, namely carbohydrate metabolism (14.85%), amino acid metabolism (12.87%), lipid metabolism (11.88%), metabolism of cofactors and vitamins (11.88%), xenobiotic biodegradation (9.90%), and metabolism of terpenoids and polyketides (7.92%). In addition, the functional roles of the bacteria were highly related to infectious diseases, including bacterial infection (50.00%) and parasitic infection (33.33%) as well as cardiovascular disease (10.00%) and neurodegenerative disease (10.00%) (Supplementary Table 4). The parasitic infectious disease-related gene subgroups (P = 0.03) in the IA-phase patients were highly enriched (Figure 5). The cell motility-related genes were highly enriched in the IA-phase patients (Figure 5A), while the transport and catabolism-related genes (P = 0.03) were significantly enriched in the IT-phase patients. However, signal transduction-related genes were significantly enriched in the healthy controls (P < 0.01) (Figure 5B). The replication repair-related genes and digestive system-related genes in the IT-phase patients were more abundant than in the other groups, but the difference between the three groups was not statistically significant (Figure 5C and E). Moreover, the digestive system disease-related gene subset (P = 0.02) was highly enriched in the IT-phase patients (Figure 5D). Genes that are related to the amino acid metabolism glycosyl biosynthesis cofactors and vitamin metabolism were more enriched in the IT-phase patients than in the healthy controls (P < 0.01) (Figure 5F). These observed results suggested that changes in the bacterial composition can significantly alter gene function, which may contribute to the development of CHB.

As shown in the co-occurrence network analysis using Cytoscape software (Supplementary Figure 1), five genera (Dorea, Bifidobacterium, Bacteroides, Blautia, and Romboutsia) were highly positively correlated. Dorea and Bifidobacterium exhibited the highest degree of linkage, while Dorea and Bacteroides had the least degree of linkage.

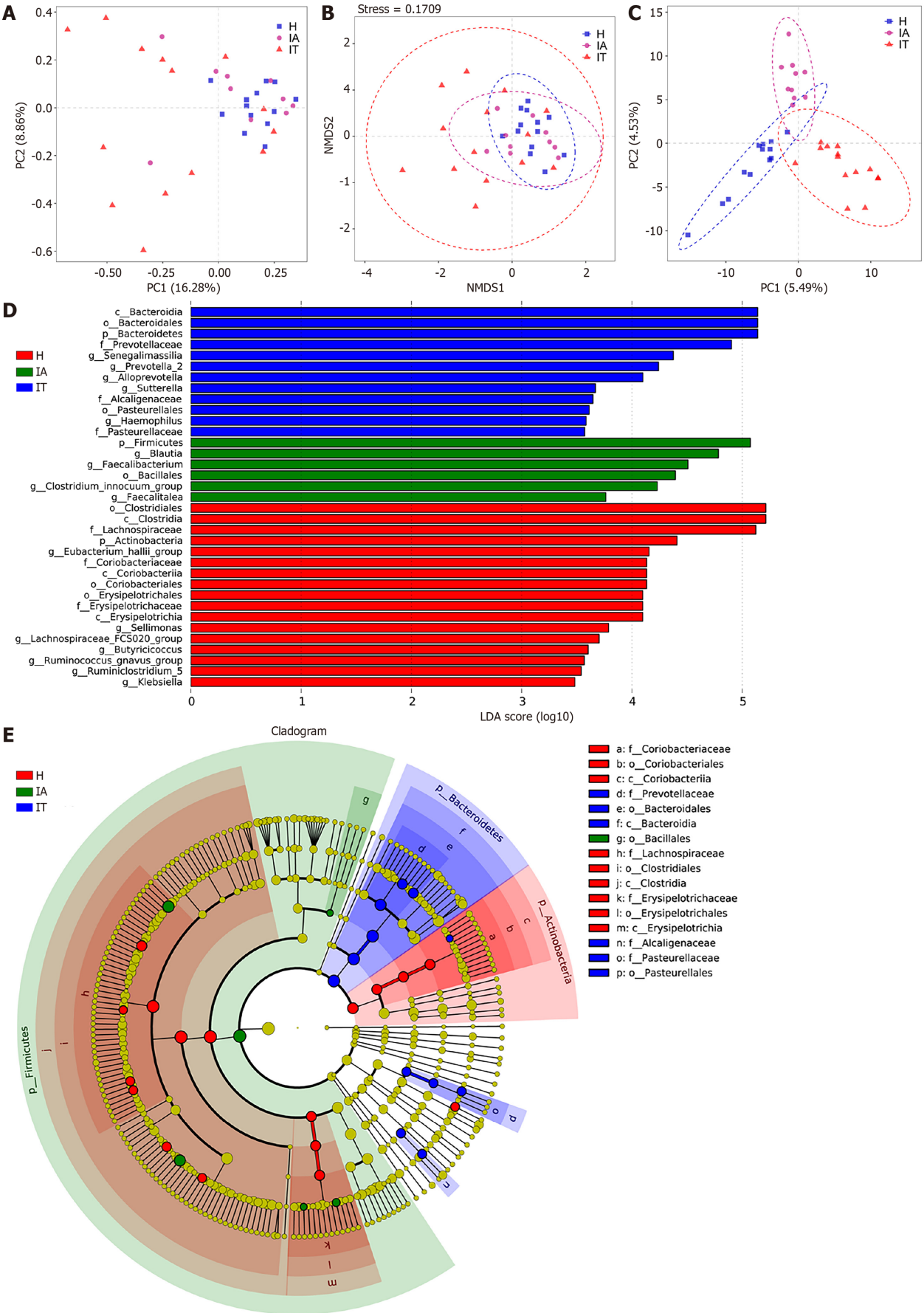
Non-target metabolomics analysis

A total of 293 substantially different metabolites were identified, among which 134 metabolites had an MS2.name provided by the mass spectrometry qualitative matching analysis. A total of 57 metabolites were upregulated, while 77 were downregulated. The different metabolites are shown in Supplementary Table 5.

DISCUSSION

To date, there are limited studies showing the role of dysbiosis of the gut microbiota in HBV-infected patients during the different immune phases of infection. This study revealed the profiles of the gut microbiota during HBV infection from the IT phase to the IA phase. The results suggested that the diversity, composition, and functionality of the microbiota changed from the IT phase to the IA phase and were related to the progression of CHB.

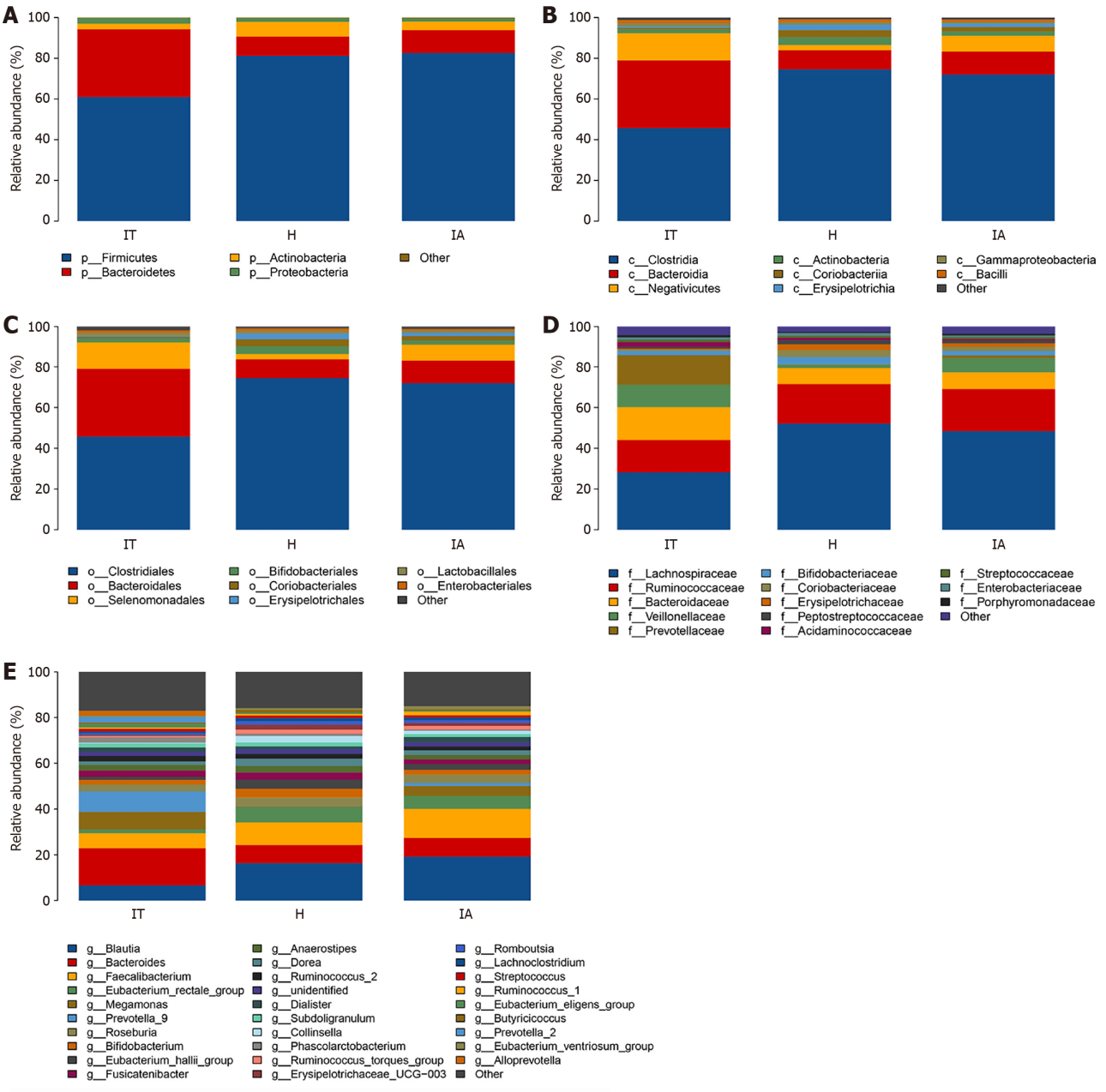
In our study, analysis of α-diversity using the Chao1, Shannon, and Simpson diversity indices showed no significant differences among the three groups. Nevertheless, one study has reported that the α-diversity is increased in cirrhosis patients compared to healthy controls and positively correlated to the Child-Pugh score[26]. In our study, a decreased ratio of *Bacteroidetes* to *Firmicutes* was observed as



DOI: 10.3748/wjg.v28.i35.5188 **Copyright** ©The Author(s) 2022.

Figure 2 Beta-diversity analysis and comparison of variation in microbiota in the three groups using the linear discriminant analysis effect size online tool. A: Principal component analysis on the relative abundance. Each point represents a sample, plotted by the second principal component on

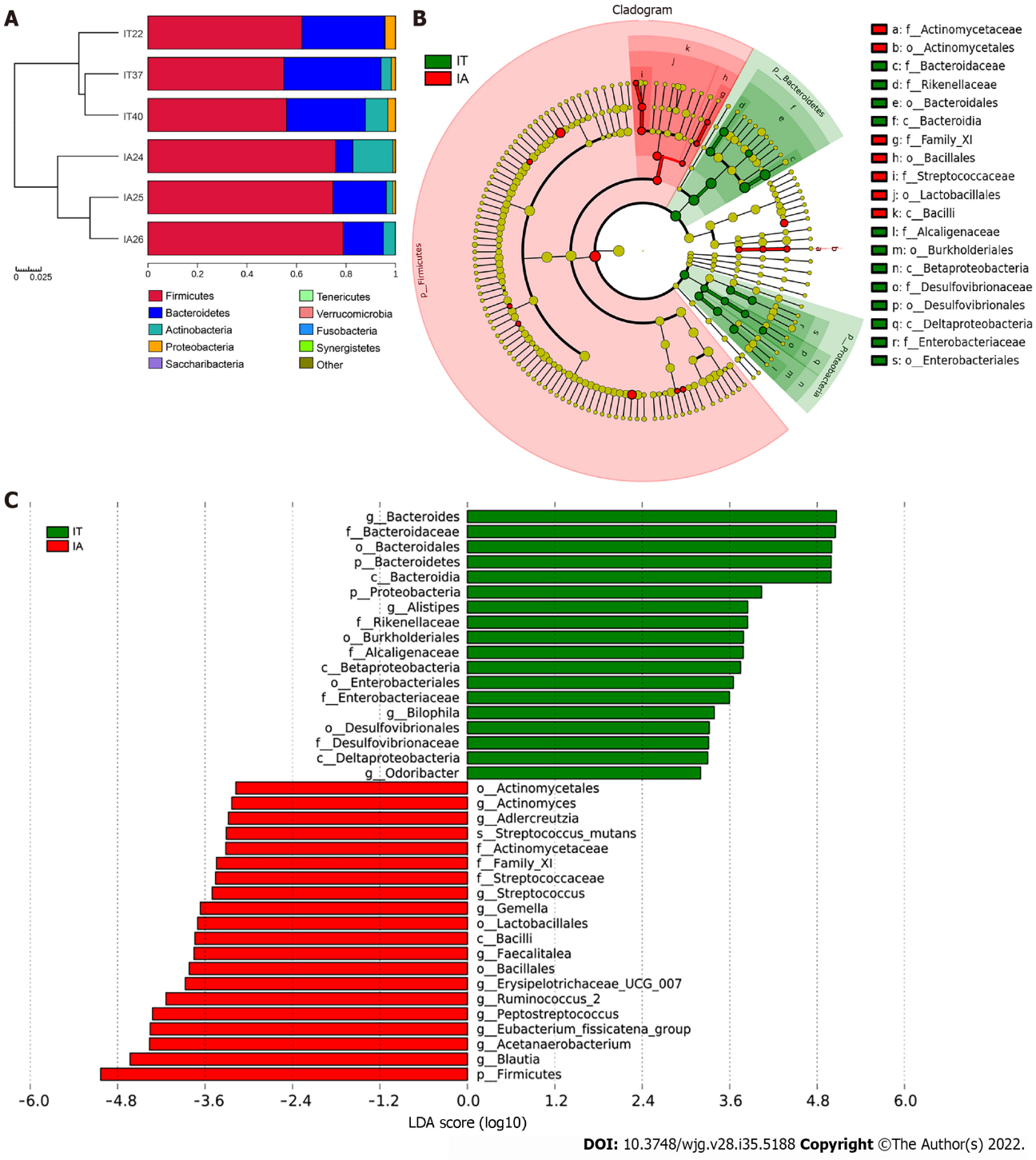
the Y-axis and the first principal component on the X-axis and colored by group; B: Comparison of the sample distribution of different subgroups using weighted non-metric multidimensional scaling analysis. Each sample is represented by a dot; C: Partial least squares discrimination analysis. Each point represents a sample; D: Histogram of the linear discriminant analysis (LDA) scores for differentially abundant genera between groups (a logarithmic LDA score > 3 indicated a higher relative abundance in the corresponding group compared to the other group); E: The taxonomic cladogram obtained from the LDA effect size analysis of 16S sequences and taxonomic representation of statistically significant differences between groups. The diameter of each circle is proportional to the taxon abundance. LDA: Linear discriminant analysis; IT: Immune-tolerant; IA: Immune-active; H: Healthy.



DOI: 10.3748/wjg.v28.i35.5188 **Copyright** ©The Author(s) 2022.

Figure 3 Distribution of the predominant bacteria at different taxonomic levels (phylum, class, order, family, and genus). A-E: Stacked bars of the phylum, class, order, family, and genus level in healthy controls, immune-tolerant phase hepatitis B virus infection, and immune-active phase hepatitis B virus infection. IT: Immune-tolerant; IA: Immune-active; H: Healthy.

patients progressed from the IT phase to the IA phase, while another study has demonstrated that the ratio of *Bacteroidetes* to *Firmicutes* increased in patients with HBV-related cirrhosis compared to that of healthy individuals[27]. These results in different studies indicate that the results may vary greatly depending on the grouping. In addition, our results suggest that the composition of the gut microbiota had changed in the early stages of HBV infection. Furthermore, metabolic changes at different stages of HBV infection were also observed by PICRUSt analysis. Consistent with another study[27], these results suggest that changes in the composition of the gut microbiota can significantly alter gene function,

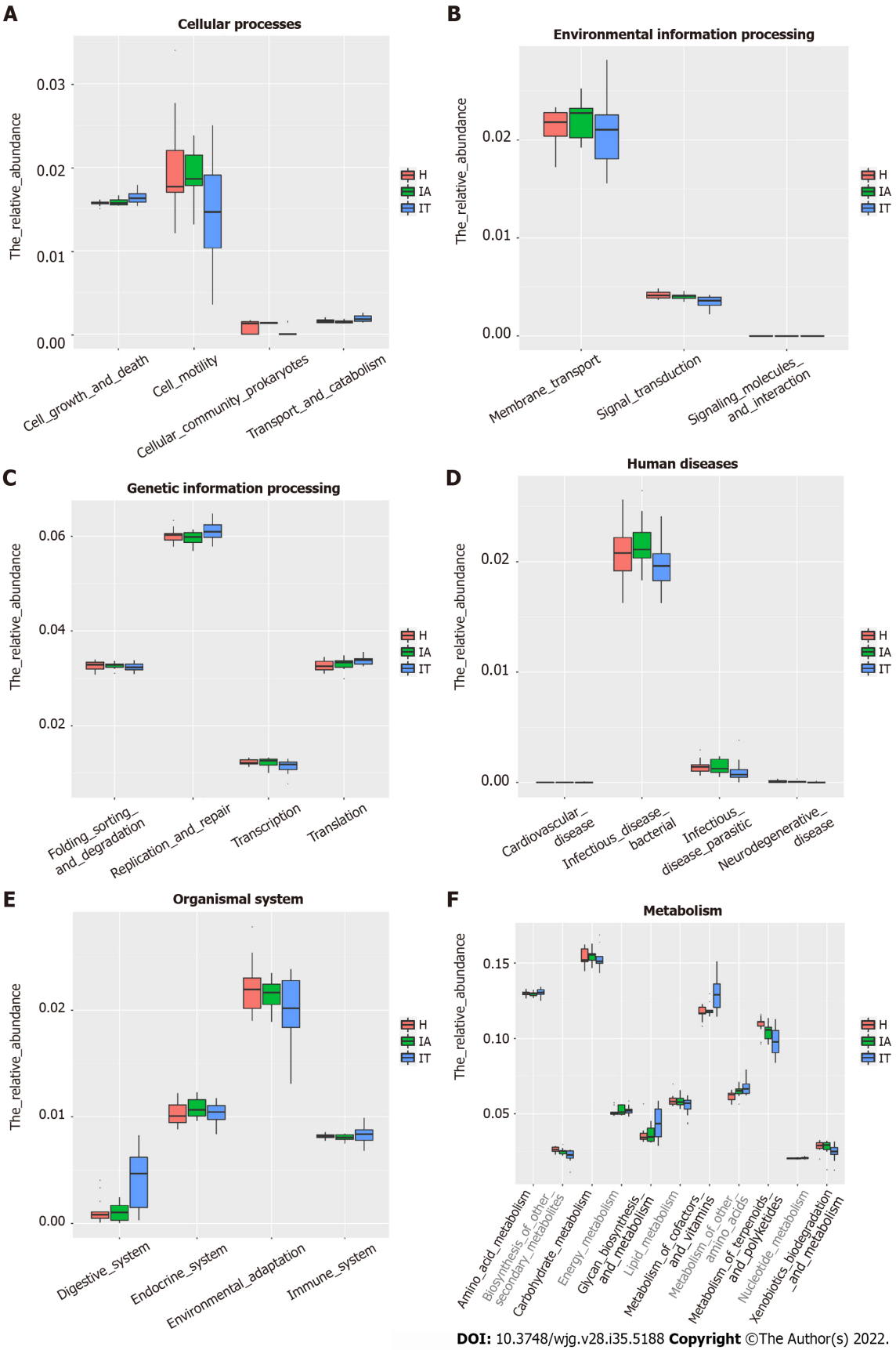


DOI: 10.3748/wjg.v28.i35.5188 **Copyright** ©The Author(s) 2022.

Figure 4 Comparison of variations in the microbiota of 3 patients before and after disease progression using the linear discriminant analysis effect size online tool. A: Distribution of the predominant bacteria at the phylum level in the 3 patients in the immune-tolerant and immune-active phases; B: The taxonomic cladogram obtained from linear discriminant analysis effect size analysis of 16S sequences and taxonomic representation of statistically significant differences between the two groups. The diameter of each circle is proportional to the taxon abundance; C: Histogram of the linear discriminant analysis scores for differentially abundant genera between the two groups (a logarithmic linear discriminant analysis score > 3 indicated a higher relative abundance in the corresponding group compared to the other group). LDA: Linear discriminant analysis; IT: Immune-tolerant; IA: Immune-active.

which may have a potential role in HBV-infected patients.

When compared to the healthy controls, there was a correlation between some gut microbiota in patients at the IT and IA phases. Notably, the IT group presented a high relative abundance of *Senegalimassilia*, *Prevotella 2*, *Alloprevotella*, *Sutterella*, and *Haemophilus*; while the IA group showed a high relative abundance of *Blautia*, *Faecalibacterium*, *Clostridium innocuum* group, and *Faecalitalea*. Some *Prevotella* strains have been reported as potentially clinically important pathobionts in human diseases by increasing the levels of interleukin (IL)-23, IL-1, IL-8, IL-6, and C-C motif chemokine ligand 20[28]. In addition, *Alloprevotella* is enriched in fecal samples from patients with chronic kidney disease[29].



DOI: 10.3748/wjg.v28.i35.5188 **Copyright** ©The Author(s) 2022.

Figure 5 Alteration of the predicted microbial functional composition from the 16S rDNA sequencing data, analyzed using Phylogenetic Investigation of Communities by Reconstruction of Unobserved States. A and B: Representing the differences at the cellular processes among healthy and patients in the immune-tolerant and immune-active phases; C and D: Representing the differences at the genetic information processing and human diseases among healthy and patients in the immune-tolerant and immune-active phases; E and F: Representing the differences at the organismal systems and metabolism among healthy and patients in the immune-tolerant and immune-active phases. IT: Immune-tolerant; IA: Immune-active; H: Healthy.

Moreover, the gut microbiota in prediabetic individuals was found to be aberrant, with decreased *Clostridium* and increased *Sutterella* levels[30]. Furthermore, *Sutterella* has the capacity to degrade IgA, causing failure of therapeutics treating ulcerative colitis[31]. These findings reveal that *Prevotella 2*, *Alloprevotella*, and *Sutterella* are involved in chronic human diseases. Our results also indicate that *Prevotella 2*, *Alloprevotella*, and *Sutterella* are specifically related to HBV infection in the IT phase, suggesting their role of mediating viral escape from the host immune response.

Blautia, *Faecalibacterium*, *Clostridium innocuum* group, and *Faecalitalea* were identified as signature gut microbiota related to HBV infection in the IA phase. Notably, an elevated abundance of *Blautia* has been shown to alleviate the severity of lethal acute graft-versus-host disease[32]. In addition, Benítez-Páez *et al*[33] proposed that *Blautia luti* and *Blautia wexlerae* might help to reduce the inflammation that is linked to obesity-related complications. Moreover, *Blautia* is positively associated with the pathophysiology of type 2 diabetes[34]. Furthermore, *Faecalibacterium prausnitzii*, belonging to *Faecalibacterium*, is a major constituent of the gut microbiota in healthy individuals. This bacterium, which has anti-inflammatory activity, is decreased in patients with inflammatory bowel diseases such as Crohn's disease. Interestingly, *Blautia* and *Faecalibacterium* have been shown to be beneficial in a healthy gut[35]; these bacteria enhance the production of butyrate succinate and lactate, thus providing energy and reducing inflammation[36].

Additionally, a recent finding indicated that in patients with early HBV-related HCC, genera belonging to butyrate-producing bacterial families, including *Ruminococcus*, *Oscillibacter*, *Faecalibacterium* , *Clostridium IV*, and *Coprococcus* decreased, while the lipopolysaccharide-producing bacteria *Klebsiella* and *Haemophilus* increased compared to the levels in cirrhosis patients[37]. Herein, the proportions of *Blautia*, *Faecalibacterium*, and *Clostridium innocuum* group were higher in the IA-phase patients than in the controls, indicating that enrichment of these three signature microbial taxa might be a sign of severe inflammation or exacerbation of disease. Notably, these beneficial gut microbiota might help to clear viral infection in the IA phase, while some gut microbiota in the IT phase might help the virus to escape from host immune responses. Taken together, these findings highlight an important role for the composition of the gut microbiota in the progression of HBV infection, which has significant clinical implications.

Based on the composition and structure of the gut microbiota, the metabolic function of the microflora was further analyzed through PICRUSt. In this study, the genes involved in glycan biosynthesis and metabolism as well as cofactor and vitamin metabolism were more enriched in the IT-phase patients than in the healthy controls. One explanation for this finding is that *Senegalimassilia*, *Prevotella 2*, *Alloprevotella*, *Sutterella*, and *Haemophilus* are enriched in the IT phase and consume glycan as their energy source; the genes found in these bacteria are related to cofactor and vitamin metabolism. In contrast, terpenoid and polyketide metabolism-related genes were more abundant in the IA phase, suggesting that *Senegalimassilia*, *Prevotella 2*, *Alloprevotella*, *Sutterella*, and *Haemophilus* participate in the metabolism of terpenoids and polyketides. These results may indicate that the gut microbiota and metabolites contribute to the abnormal metabolism status in CHB.

Previous research has shown that the gut microbiota composition is closely related to the occurrence of various chronic liver diseases[38-40]. Our current study demonstrated that potential links exist between certain bacteria and different pathological mechanisms during CHB progression from the IT phase to the IA phase.

Studies using mouse models have uncovered that the gut microbiota have a vital role in overcoming the IT phase of viral infection at different ages[41] and that gut microbiota lead to Kupffer cell-mediated T cell suppression, which is associated with HBV persistence[42]. In addition, fecal microbiota transplantation therapy has been shown to improve the clearance rate of HBV antigens in CHB patients after long-term therapy[43]. Our study demonstrated that the gut microbiota composition changed at different phases of HBV infection. Changes in the gut microbiota composition could be a biological factor for the progression of CHB. We believe that the gut microbiome of CHB patients may provide a useful prognostic marker for disease progression, outcome prediction, and treatment and that further microbiome-based study may provide new insights into the pathogenesis of CHB, the etiology of its progression, and novel therapeutic strategies such as the use of probiotics or fecal microbiota transplantation.

Although this study uncovered some insightful findings, some limitations remain. First, all patients enrolled in this study were from different families. Having different genetic backgrounds and dietary habits might affect the gut microbiota composition. In addition, the healthy donors should have had a similar age to the patients; however, the controls were not age-matched to the patients in this study. Second, only 3 patients were followed up from the IT phase to the IA phase. A larger longitudinal sample size will strengthen the results. Third, a real-world cross-sectional study would be beneficial to understand the impact of the microbiota on the progression of liver disease. Fourth, the methods we used have some limitations. Although transcriptomics also contributes to gene expression, the findings could be further confirmed if we used metagenomic sequencing rather than 16S rDNA gene sequencing. Metagenomic sequencing not only sequences the 16S rDNA genes, but it also sequences the whole genome of each bacterium. Thus, only by doing metagenomic sequencing, one can get the complete picture. Fifth, the functional studies of the gut microbiota are based on statistical predictions; therefore, further studies using germ-free animal models and related functional studies are required to investigate

the specific roles of the gut microbiota in CHB. Furthermore, the IT phase is an important phase that needs more attention.

CONCLUSION

These findings provide observational evidence of compositional alterations of the gut microbiome and some related metabolites in patients with IT-phase or IA-phase HBV infection. Further studies should investigate whether microbiota modulation can facilitate the progression of CHB and the cause-effect relationship between the gut microbiota and CHB.

ARTICLE HIGHLIGHTS

Research background

Chronic hepatitis B virus (HBV) infection (CHB) represents a public health problem that may progress to cirrhosis and hepatocellular carcinoma (HCC). HBV-infected individuals in immune tolerance (IT) are generally not recommended for anti-HBV treatment, owing to the absence of curative treatment and the evidence of a low risk of progressive liver injury in the IT patients. However, recent studies indicated hepatocarcinogenesis may occur in IT-phase patients; the body's IT status is a key factor affecting the outcome of the disease. Therefore, finding out the factors that affect the prognosis of HBV infection is of paramount significance for the rapid elimination of virus and the reduction of CHB.

Research motivation

The bacterial diversity level and composition varied between CHB, hepatitis B-related liver cirrhosis, and HCC. Gut microbiota of healthy controls is more consistent, whereas those of CHB, hepatitis B-related liver cirrhosis and HCC varied substantially. As the first phase of HBV progression, IT phase provides a favorable immune environment for HBV invasion and long-term existence, then transitions to immune clearance in the third decade. Therefore, in-depth study of the disease status and changes in the body during the IT phase is conducive to the development of new antiviral treatment methods to break the IT of the body and improve the antiviral efficacy and thus improve the long-term prognosis.

Research objectives

This study aimed to find some potential bacteria, linking different pathological mechanisms of IT phase HBV infection and some related metabolites to the IT phase of CHB infection.

Research methods

Clinical fecal samples from healthy individuals and patients in the IT and IA phases of HBV infection were collected. Next, non-target metabolomics, bioinformatics, and 16S rDNA sequencing analyses were performed.

Research results

A total of 293 different metabolites in 14 phyla, 22 classes, 29 orders, 51 families, and 190 genera were identified. The four phyla of *Firmicutes*, *Bacteroidetes*, *Actinobacteria*, and *Proteobacteria* were the most abundant, accounting for 99.72%, 99.79%, and 99.55% in the healthy controls, IT-phase patients, and IA-phase patients, respectively. We further identified 16 genera with different richness in the IT phase and IA phase of HBV infection. Of the 134 named metabolites, 57 were upregulated and 77 were downregulated. A total of 101 different metabolic functions were predicted in this study, with 6 metabolic pathways having the highest enrichments, namely carbohydrate metabolism (14.85%), amino acid metabolism (12.87%), lipid metabolism (11.88%), metabolism of cofactors and vitamins (11.88%), xenobiotic biodegradation (9.9%), and metabolism of terpenoids and polyketides (7.92%).

Research conclusions

The composition of the gut microbiota changed in the early stages of HBV infection, and changes in the composition of the gut microbiota can significantly alter gene function, which may have a potential role in HBV-infected patients.

Research perspectives

It is relatively difficult to fully understand the causal relationship between gut microbiota and HBV-induced chronic liver disease at different stages in this real-world cross-sectional study. Nevertheless, it should be noted that germ-free animals are good models to study the effect of gut microbiota on human diseases. In a future study, it is imperative to use germ-free animal models and additional biofunctional assays to reveal the cause-effect relationship between gut microbiota and chronic HBV infection.

FOOTNOTES

Author contributions: Zeng DW and Liu YR conceived and designed the experiments; Zeng DW and Li YN performed the experiments; Li YN, Kang NL, and Wang F analyzed the data; Zhu YY and Jiang JJ contributed reagents/materials/analysis tools; Zeng DW and Li YN wrote the manuscript.

Supported by the Fujian Provincial Health Technology Project, No. 2019-ZQN-60; and the Fujian Provincial Department of Science and Technology, No. 2019J01432.

Institutional review board statement: Institutional review board approval of our hospital was obtained for this study.

Informed consent statement: All patients involved in this study gave their informed consent.

Conflict-of-interest statement: The authors declare no conflicts of interest.

Data sharing statement: No additional data are available.

STROBE statement: The authors have read the STROBE statement, and the manuscript was prepared and revised according to the STROBE statement.

Open-Access: This article is an open-access article that was selected by an in-house editor and fully peer-reviewed by external reviewers. It is distributed in accordance with the Creative Commons Attribution NonCommercial (CC BY-NC 4.0) license, which permits others to distribute, remix, adapt, build upon this work non-commercially, and license their derivative works on different terms, provided the original work is properly cited and the use is non-commercial. See: https://creativecommons.org/Licenses/by-nc/4.0/

Country/Territory of origin: China

ORCID number: Ya-Nan Li 0000-0001-8626-9534; Na-Ling Kang 0000-0001-6923-5754; Jia-Ji Jiang 0000-0003-0637-7653; Yue-Yong Zhu 0000-0002-0746-4911; Yu-Rui Liu 0000-0003-0553-846X; Da-Wu Zeng 0000-0003-3818-0062; Fei Wang 0000-0002-4146-5379.

S-Editor: Zhang H
L-Editor: Filipodia
P-Editor: Li X

REFERENCES

1 **Mason WS**, Gill US, Litwin S, Zhou Y, Peri S, Pop O, Hong ML, Naik S, Quaglia A, Bertoletti A, Kennedy PT. HBV DNA Integration and Clonal Hepatocyte Expansion in Chronic Hepatitis B Patients Considered Immune Tolerant. *Gastroenterology* 2016; **151**: 986-998.e4 [PMID: 27453547 DOI: 10.1053/j.gastro.2016.07.012]
2 **Kennedy PTF**, Litwin S, Dolman GE, Bertoletti A, Mason WS. Immune Tolerant Chronic Hepatitis B: The Unrecognized Risks. *Viruses* 2017; **9** [PMID: 28468285 DOI: 10.3390/v9050096]
3 **Kim GA**, Lim YS, Han S, Choi J, Shim JH, Kim KM, Lee HC, Lee YS. High risk of hepatocellular carcinoma and death in patients with immune-tolerant-phase chronic hepatitis B. *Gut* 2018; **67**: 945-952 [PMID: 29055908 DOI: 10.1136/gutjnl-2017-314904]
4 **Xu D**, Huang Y, Wang J. Gut microbiota modulate the immune effect against hepatitis B virus infection. *Eur J Clin Microbiol Infect Dis* 2015; **34**: 2139-2147 [PMID: 26272175 DOI: 10.1007/s10096-015-2464-0]
5 **Wang B**, Li L. Who determines the outcomes of HBV exposure? *Trends Microbiol* 2015; **23**: 328-329 [PMID: 25864882 DOI: 10.1016/j.tim.2015.04.001]
6 **Maslennikov R**, Ivashkin V, Efremova I, Poluektova E, Kudryavtseva A, Krasnov G. Gut dysbiosis and small intestinal bacterial overgrowth as independent forms of gut microbiota disorders in cirrhosis. *World J Gastroenterol* 2022; **28**: 1067-1077 [PMID: 35431497 DOI: 10.3748/wjg.v28.i10.1067]
7 **Tremaroli V**, Bäckhed F. Functional interactions between the gut microbiota and host metabolism. *Nature* 2012; **489**: 242-249 [PMID: 22972297 DOI: 10.1038/nature11552]
8 **Nicholson JK**, Holmes E, Kinross J, Burcelin R, Gibson G, Jia W, Pettersson S. Host-gut microbiota metabolic interactions. *Science* 2012; **336**: 1262-1267 [PMID: 22674330 DOI: 10.1126/science.1223813]
9 **Hernández-Ceballos W**, Cordova-Gallardo J, Mendez-Sanchez N. Gut Microbiota in Metabolic-associated Fatty Liver Disease and in Other Chronic Metabolic Diseases. *J Clin Transl Hepatol* 2021; **9**: 227-238 [PMID: 34007805 DOI: 10.14218/JCTH.2020.00131]
10 **Liu Q**, Li F, Zhuang Y, Xu J, Wang J, Mao X, Zhang Y, Liu X. Alteration in gut microbiota associated with hepatitis B and non-hepatitis virus related hepatocellular carcinoma. *Gut Pathog* 2019; **11**: 1 [PMID: 30675188 DOI: 10.1186/s13099-018-0281-6]
11 **Wang J**, Wang Y, Zhang X, Liu J, Zhang Q, Zhao Y, Peng J, Feng Q, Dai J, Sun S, Zhao L, Zhang Y, Hu Y, Zhang M. Gut Microbial Dysbiosis Is Associated with Altered Hepatic Functions and Serum Metabolites in Chronic Hepatitis B Patients. *Front Microbiol* 2017; **8**: 2222 [PMID: 29180991 DOI: 10.3389/fmicb.2017.02222]
12 **Zeng Y**, Chen S, Fu Y, Wu W, Chen T, Chen J, Yang B, Ou Q. Gut microbiota dysbiosis in patients with hepatitis B virus-

induced chronic liver disease covering chronic hepatitis, liver cirrhosis and hepatocellular carcinoma. *J Viral Hepat* 2020; **27**: 143-155 [PMID: 31600845 DOI: 10.1111/jvh.13216]

13 **Li R**, Yi X, Yang J, Zhu Z, Wang Y, Liu X, Huang X, Wan Y, Fu X, Shu W, Zhang W, Wang Z. Gut Microbiome Signatures in the Progression of Hepatitis B Virus-Induced Liver Disease. *Front Microbiol* 2022; **13**: 916061 [PMID: 35733959 DOI: 10.3389/fmicb.2022.916061]

14 **Chen Z**, Xie Y, Zhou F, Zhang B, Wu J, Yang L, Xu S, Stedtfeld R, Chen Q, Liu J, Zhang X, Xu H, Ren J. Featured Gut Microbiomes Associated With the Progression of Chronic Hepatitis B Disease. *Front Microbiol* 2020; **11**: 383 [PMID: 32265857 DOI: 10.3389/fmicb.2020.00383]

15 **Yang XA**, Lv F, Wang R, Chang Y, Zhao Y, Cui X, Li H, Yang S, Li S, Zhao X, Mo Z, Yang F. Potential role of intestinal microflora in disease progression among patients with different stages of Hepatitis B. *Gut Pathog* 2020; **12**: 50 [PMID: 33117435 DOI: 10.1186/s13099-020-00391-4]

16 **Sarin SK**, Kumar M, Lau GK, Abbas Z, Chan HL, Chen CJ, Chen DS, Chen HL, Chen PJ, Chien RN, Dokmeci AK, Gane E, Hou JL, Jafri W, Jia J, Kim JH, Lai CL, Lee HC, Lim SG, Liu CJ, Locarnini S, Al Mahtab M, Mohamed R, Omata M, Park J, Piratvisuth T, Sharma BC, Sollano J, Wang FS, Wei L, Yuen MF, Zheng SS, Kao JH. Asian-Pacific clinical practice guidelines on the management of hepatitis B: a 2015 update. *Hepatol Int* 2016; **10**: 1-98 [PMID: 26563120 DOI: 10.1007/s12072-015-9675-4]

17 **European Association for the Study of the Liver**. EASL 2017 Clinical Practice Guidelines on the management of hepatitis B virus infection. *J Hepatol* 2017; **67**: 370-398 [PMID: 28427875 DOI: 10.1016/j.jhep.2017.03.021]

18 **Munyaka PM**, Eissa N, Bernstein CN, Khafipour E, Ghia JE. Antepartum Antibiotic Treatment Increases Offspring Susceptibility to Experimental Colitis: A Role of the Gut Microbiota. *PLoS One* 2015; **10**: e0142536 [PMID: 26605545 DOI: 10.1371/journal.pone.0142536]

19 **Edgar RC**. UPARSE: highly accurate OTU sequences from microbial amplicon reads. *Nat Methods* 2013; **10**: 996-998 [PMID: 23955772 DOI: 10.1038/nmeth.2604]

20 **Cole JR**, Wang Q, Cardenas E, Fish J, Chai B, Farris RJ, Kulam-Syed-Mohideen AS, McGarrell DM, Marsh T, Garrity GM, Tiedje JM. The Ribosomal Database Project: improved alignments and new tools for rRNA analysis. *Nucleic Acids Res* 2009; **37**: D141-D145 [PMID: 19004872 DOI: 10.1093/nar/gkn879]

21 **Wang Y**, Sheng HF, He Y, Wu JY, Jiang YX, Tam NF, Zhou HW. Comparison of the levels of bacterial diversity in freshwater, intertidal wetland, and marine sediments by using millions of illumina tags. *Appl Environ Microbiol* 2012; **78**: 8264-8271 [PMID: 23001654 DOI: 10.1128/AEM.01821-12]

22 **Jiang XT**, Peng X, Deng GH, Sheng HF, Wang Y, Zhou HW, Tam NF. Illumina sequencing of 16S rRNA tag revealed spatial variations of bacterial communities in a mangrove wetland. *Microb Ecol* 2013; **66**: 96-104 [PMID: 23649297 DOI: 10.1007/s00248-013-0238-8]

23 **Jami E**, Israel A, Kotser A, Mizrahi I. Exploring the bovine rumen bacterial community from birth to adulthood. *ISME J* 2013; **7**: 1069-1079 [PMID: 23426008 DOI: 10.1038/ismej.2013.2]

24 **Zhou B**, Xiao JF, Tuli L, Ressom HW. LC-MS-based metabolomics. *Mol Biosyst* 2012; **8**: 470-481 [PMID: 22041788 DOI: 10.1039/c1mb05350g]

25 **Dunn WB**, Broadhurst D, Begley P, Zelena E, Francis-McIntyre S, Anderson N, Brown M, Knowles JD, Halsall A, Haselden JN, Nicholls AW, Wilson ID, Kell DB, Goodacre R; Human Serum Metabolome (HUSERMET) Consortium. Procedures for large-scale metabolic profiling of serum and plasma using gas chromatography and liquid chromatography coupled to mass spectrometry. *Nat Protoc* 2011; **6**: 1060-1083 [PMID: 21720319 DOI: 10.1038/nprot.2011.335]

26 **Sanduzzi Zamparelli M**, Rocco A, Compare D, Nardone G. The gut microbiota: A new potential driving force in liver cirrhosis and hepatocellular carcinoma. *United European Gastroenterol J* 2017; **5**: 944-953 [PMID: 29163959 DOI: 10.1177/2050640617705576]

27 **Shu W**, Shanjian C, Jinpiao L, Qishui O. Gut microbiota dysbiosis in patients with hepatitis B virus-related cirrhosis. *Ann Hepatol* 2022; **27**: 100676 [PMID: 35093600 DOI: 10.1016/j.aohep.2022.100676]

28 **Larsen JM**. The immune response to Prevotella bacteria in chronic inflammatory disease. *Immunology* 2017; **151**: 363-374 [PMID: 28542929 DOI: 10.1111/imm.12760]

29 **Li F**, Wang M, Wang J, Li R, Zhang Y. Alterations to the Gut Microbiota and Their Correlation With Inflammatory Factors in Chronic Kidney Disease. *Front Cell Infect Microbiol* 2019; **9**: 206 [PMID: 31245306 DOI: 10.3389/fcimb.2019.00206]

30 **Allin KH**, Tremaroli V, Caesar R, Jensen BAH, Damgaard MTF, Bahl MI, Licht TR, Hansen TH, Nielsen T, Dantoft TM, Linneberg A, Jørgensen T, Vestergaard H, Kristiansen K, Franks PW; IMI-DIRECT consortium, Hansen T, Bäckhed F, Pedersen O. Aberrant intestinal microbiota in individuals with prediabetes. *Diabetologia* 2018; **61**: 810-820 [PMID: 29379988 DOI: 10.1007/s00125-018-4550-1]

31 **Kaakoush NO**. Sutterella Species, IgA-degrading Bacteria in Ulcerative Colitis. *Trends Microbiol* 2020; **28**: 519-522 [PMID: 32544438 DOI: 10.1016/j.tim.2020.02.018]

32 **Jenq RR**, Taur Y, Devlin SM, Ponce DM, Goldberg JD, Ahr KF, Littmann ER, Ling L, Gobourne AC, Miller LC, Docampo MD, Peled JU, Arpaia N, Cross JR, Peets TK, Lumish MA, Shono Y, Dudakov JA, Poeck H, Hanash AM, Barker JN, Perales MA, Giralt SA, Pamer EG, van den Brink MR. Intestinal Blautia Is Associated with Reduced Death from Graft-versus-Host Disease. *Biol Blood Marrow Transplant* 2015; **21**: 1373-1383 [PMID: 25977230 DOI: 10.1016/j.bbmt.2015.04.016]

33 **Benítez-Páez A**, Gómez Del Pugar EM, López-Almela I, Moya-Pérez Á, Codoñer-Franch P, Sanz Y. Depletion of *Blautia* Species in the Microbiota of Obese Children Relates to Intestinal Inflammation and Metabolic Phenotype Worsening. *mSystems* 2020; **5** [PMID: 32209719 DOI: 10.1128/mSystems.00857-19]

34 **Gurung M**, Li Z, You H, Rodrigues R, Jump DB, Morgun A, Shulzhenko N. Role of gut microbiota in type 2 diabetes pathophysiology. *EBioMedicine* 2020; **51**: 102590 [PMID: 31901868 DOI: 10.1016/j.ebiom.2019.11.051]

35 **Lopez-Siles M**, Duncan SH, Garcia-Gil LJ, Martinez-Medina M. Faecalibacterium prausnitzii: from microbiology to diagnostics and prognostics. *ISME J* 2017; **11**: 841-852 [PMID: 28045459 DOI: 10.1038/ismej.2016.176]

36 **Abaidullah M**, Peng S, Kamran M, Song X, Yin Z. Current Findings on Gut Microbiota Mediated Immune Modulation against Viral Diseases in Chicken. *Viruses* 2019; **11** [PMID: 31349568 DOI: 10.3390/v11080681]

37 **Ren Z**, Li A, Jiang J, Zhou L, Yu Z, Lu H, Xie H, Chen X, Shao L, Zhang R, Xu S, Zhang H, Cui G, Sun R, Wen H, Lerut JP, Kan Q, Li L, Zheng S. Gut microbiome analysis as a tool towards targeted non-invasive biomarkers for early hepatocellular carcinoma. *Gut* 2019; **68**: 1014-1023 [PMID: 30045880 DOI: 10.1136/gutjnl-2017-315084]

38 **Aron-Wisnewsky J**, Vigliotti C, Witjes J, Le P, Holleboom AG, Verheij J, Nieuwdorp M, Clément K. Gut microbiota and human NAFLD: disentangling microbial signatures from metabolic disorders. *Nat Rev Gastroenterol Hepatol* 2020; **17**: 279-297 [PMID: 32152478 DOI: 10.1038/s41575-020-0269-9]

39 **Qin N**, Yang F, Li A, Prifti E, Chen Y, Shao L, Guo J, Le Chatelier E, Yao J, Wu L, Zhou J, Ni S, Liu L, Pons N, Batto JM, Kennedy SP, Leonard P, Yuan C, Ding W, Hu X, Zheng B, Qian G, Xu W, Ehrlich SD, Zheng S, Li L. Alterations of the human gut microbiome in liver cirrhosis. *Nature* 2014; **513**: 59-64 [PMID: 25079328 DOI: 10.1038/nature13568]

40 **Albhaisi SAM**, Bajaj JS, Sanyal AJ. Role of gut microbiota in liver disease. *Am J Physiol Gastrointest Liver Physiol* 2020; **318**: G84-G98 [PMID: 31657225 DOI: 10.1152/ajpgi.00118.2019]

41 **Chou HH**, Chien WH, Wu LL, Cheng CH, Chung CH, Horng JH, Ni YH, Tseng HT, Wu D, Lu X, Wang HY, Chen PJ, Chen DS. Age-related immune clearance of hepatitis B virus infection requires the establishment of gut microbiota. *Proc Natl Acad Sci U S A* 2015; **112**: 2175-2180 [PMID: 25646429 DOI: 10.1073/pnas.1424775112]

42 **Zhou W**, Luo J, Xie X, Yang S, Zhu D, Huang H, Yang D, Liu J. Gut Microbiota Dysbiosis Strengthens Kupffer Cell-mediated Hepatitis B Virus Persistence through Inducing Endotoxemia in Mice. *J Clin Transl Hepatol* 2022; **10**: 17-25 [PMID: 35233369 DOI: 10.14218/JCTH.2020.00161]

43 **Ren YD**, Ye ZS, Yang LZ, Jin LX, Wei WJ, Deng YY, Chen XX, Xiao CX, Yu XF, Xu HZ, Xu LZ, Tang YN, Zhou F, Wang XL, Chen MY, Chen LG, Hong MZ, Ren JL, Pan JS. Fecal microbiota transplantation induces hepatitis B virus e-antigen (HBeAg) clearance in patients with positive HBeAg after long-term antiviral therapy. *Hepatology* 2017; **65**: 1765-1768 [PMID: 28027582 DOI: 10.1002/hep.29008]

World Journal of Gastroenterology

Submit a Manuscript: https://www.f6publishing.com

World J Gastroenterol 2022 September 21; 28(35): 5203-5216

DOI: 10.3748/wjg.v28.i35.5203

ISSN 1007-9327 (print) ISSN 2219-2840 (online)

ORIGINAL ARTICLE

Observational Study

Dynamic blood presepsin levels are associated with severity and outcome of acute pancreatitis: A prospective cohort study

Hong-Li Xiao, Guo-Xing Wang, Yan Wang, Zhi-Min Tan, Jie Zhou, Han Yu, Miao-Rong Xie, Chun-Sheng Li

Specialty type: Emergency medicine

Provenance and peer review: Unsolicited article; Externally peer reviewed.

Peer-review model: Single blind

Peer-review report's scientific quality classification

Grade A (Excellent): 0
Grade B (Very good): B
Grade C (Good): C, C
Grade D (Fair): 0
Grade E (Poor): 0

P-Reviewer: Balaban DV, Romania; Ferrarese A, Italy

Received: June 6, 2022
Peer-review started: June 6, 2022
First decision: June 27, 2022
Revised: July 10, 2022
Accepted: September 1, 2022
Article in press: September 1, 2022
Published online: September 21, 2022

Hong-Li Xiao, Guo-Xing Wang, Yan Wang, Zhi-Min Tan, Jie Zhou, Miao-Rong Xie, Chun-Sheng Li, Department of Emergency Medicine, Beijing Friendship Hospital, Capital Medical University, Beijing 100050, China

Han Yu, Department of Emergency Medicine, Beijing Chao-Yang Hospital, Capital Medical University, Beijing 100020, China

Corresponding author: Chun-Sheng Li, MD, Professor, Department of Emergency Medicine, Beijing Friendship Hospital, Capital Medical University, No. 95 Yongan Road, Xicheng District, Beijing 100050, China. lcscyyy@163.com

Abstract

BACKGROUND

Acute pancreatitis (AP) is an inflammatory disorder of the pancreas with an unpredictable course of illness. A major challenge of AP is the early identification of patients at high-risk for organ failure and death. However, scoring systems are complicated and time consuming, and the predictive values for the clinical course are vague.

AIM

To determine whether the dynamic changes in presepsin levels can be used to evaluate the severity of disease and outcome of AP.

METHODS

In this multicentric cohort study, 133 patients with AP were included. Clinical severity was dynamically evaluated using the 2012 revised Atlanta Classification. Blood presepsin levels were measured at days 1, 3, 5 and 7 after admission by chemiluminescent enzyme immunoassay.

RESULTS

The median concentration of presepsin increased and the clearance rate of presepsin decreased with disease severity and organ failure in AP patients. The presepsin levels on days 3, 5 and 7 were independent predictors of moderately severe and severe AP with time-specific area under the curve (AUC) values of 0.827, 0.848 and 0.867, respectively. The presepsin levels positively correlated with bedside index of severity in AP, Ranson, acute physiology and chronic health evaluation II, computed tomography severity index and Marshall scores. Presepsin levels on days 3, 5 and 7 were independent predictors of 28-d mortality of

AP patients with AUC values of 0.781, 0.846 and 0.843, respectively.

CONCLUSION
Blood presepsin levels within 7 d of admission were associated with and may be useful to dynamically predict the severity of disease course and 28-d mortality in AP patients.

Key Words: Presepsin; Acute pancreatitis; Severity; Mortality; Disease severity

©The Author(s) 2022. Published by Baishideng Publishing Group Inc. All rights reserved.

Core Tip: Acute pancreatitis has diverse clinical manifestations with an unpredictable clinical course. A major challenge of acute pancreatitis is the early identification of patients at high-risk for organ failure and death. Scoring systems are complicated and time consuming with limited predictive value for the clinical course. In this study, we investigated the association between the dynamic levels of blood presepsin, a new infection biomarker, and the changes of severity in the early course of acute pancreatitis. We found the predictive value of presepsin for 28-d mortality was similar to the bedside index of severity in acute pancreatitis, Ranson and acute physiology and chronic health evaluation II scores.

Citation: Xiao HL, Wang GX, Wang Y, Tan ZM, Zhou J, Yu H, Xie MR, Li CS. Dynamic blood presepsin levels are associated with severity and outcome of acute pancreatitis: A prospective cohort study. *World J Gastroenterol* 2022; 28(35): 5203-5216
URL: https://www.wjgnet.com/1007-9327/full/v28/i35/5203.htm
DOI: https://dx.doi.org/10.3748/wjg.v28.i35.5203

INTRODUCTION

Acute pancreatitis (AP) is an inflammatory disorder of the pancreas that can lead to systemic inflammatory response syndrome, organ failure and sepsis. AP is one of the most common causes of abdominal emergencies and is associated with mortality rates up to 35%[1,2]. Gallstones and alcohol consumption are the most frequent causes of AP. Irrespective of the etiology, AP has diverse clinical manifestations with an unpredictable clinical course. Various clinical scoring systems such as the bedside index of severity in acute pancreatitis (BISAP) score, Ranson criteria, computed tomography severity index (CTSI) and acute physiology and chronic health evaluation (APACHE) II scores have been developed to predict the illness severity at admission[3]. However, accurate prediction of the clinical course remains difficult[4]. A major challenge of AP is the early identification of patients at high risk for organ failure and death. Moreover, some of these scoring systems are complicated and time consuming with limited predictive value for the clinical course. Therefore, it is necessary to develop simple and convenient biomarkers to dynamically predict the severity of AP in its early course.

Presepsin is a subtype of soluble CD14 formed by a 13 kDa fragment and is an emerging biomarker of infection[5]. CD14 is a glycoprotein receptor for lipopolysaccharide. After lipopolysaccharide binds to CD14, presepsin is released into the blood and cleared by the kidney[6]. Presepsin has been confirmed to predict illness severity[7], number of organs experiencing dysfunction[8] and septic 90-d death rates [9,10]. This study aimed to assess the predictive value of blood presepsin levels for the severity of disease course and outcomes in patients with AP.

MATERIALS AND METHODS

Study population

This prospective, multicentric, and observational cohort study was conducted at the Emergency Departments of Beijing Friendship Hospital and Beijing Chaoyang Hospital affiliated with Capital Medical University. This study was approved by the Beijing Friendship Hospital Ethics Committee (Approval No. 2017-P2-103-02). Written informed consent was obtained from patients or their relatives. Patients diagnosed with AP as per the 2012 revised Atlanta Classification[11] were screened within 24 h of admission and followed up for 28 d. Patients were classified into one of three groups (mild, moderately severe and severe AP) based on the hospital course. Patients with mild AP had neither local complications nor organ failure. Patients with moderately severe AP had transient (< 48 h) organ failure or local complications or both, whereas patients with severe AP had persistent (> 48 h) organ failure. Organ failure was defined as a Marshall score > 2[11]. Patients were subsequently divided into one of

two groups [mild and non-mild (moderately severe and severe) AP] based on their presentation during the first, third, 5th and 7th day of admission. Pregnant women and patients younger than 18 years of age were excluded. All patients received standardized treatment according to the 2012 revised Atlanta Classification[11].

Data collection

The collected data included age, sex, comorbidities, etiologies, scoring, pancreatic imaging and interventions. Abdominal ultrasonography at admission and abdominal computed tomography scans 72 h after symptom onset were performed. The BISAP score, Ranson score, CTSI, APACHE II score, Marshall score and severity of AP were determined at 1, 3, 5 and 7 d post-admission. BISAP and APACHE II scores were evaluated within 24 h. The Ranson score was calculated within 48 h. Levels of the conventional inflammatory biomarkers procalcitonin and C-reactive protein were obtained from the clinical laboratory data. AP patients were classified into survival and non-survival groups based on their 28-d survival.

Determination of blood presepsin concentration

Venous blood samples were collected in tubes containing heparin at days 1, 3, 5 and 7 after admission and stored at 4 °C for analysis within 24 h. Presepsin concentration in the blood was measured using a chemiluminescent enzyme immunoassay[12] with a compact automated immunoanalyzer (PATHFAST; Mitsubishi Chemical Medience Corporation, Tokyo, Japan). The lower and upper detection limits of presepsin concentrations were 20 pg/mL and 200000 pg/mL, respectively.

Statistical analysis

All analyses were performed using SPSS version 25.0 (SPSS, Chicago, IL, United States). With a two-sided $\alpha = 0.05$, a $\beta = 0.2$ and 70% of patients with mild pancreatitis[13], it was determined that 106 patients were required for enrollment, 74 with mild pancreatitis and 32 with non-mild pancreatitis. This study enrolled 137 patients to account for 20% of patients lost to follow-up. The clearance ratio of presepsin was calculated using the following formula: the presepsin level on day 1 minus the presepsin level on days 3, 5 or 7, divided by the presepsin level on day 1 and multiplied by 100%. Data with normal distribution were expressed as mean ± SD and were analyzed by Student's *t* test or variance analysis. Data with non-normal distribution were expressed as the median with quartiles and were analyzed by the Mann-Whitney *U* or Kruskal-Wallis tests. The χ^2 test or Fisher's exact test was used for comparison of frequencies. A receiver operating characteristic (ROC) curve was constructed to assess the predictive value of presepsin for moderate/severe AP and 28-d mortality. Prognostic parameters including sensitivity, specificity, positive predictive value and negative predictive value were calculated based on ROC curve analysis. The areas under the ROC curves (AUCs) were compared by MedCalc version 11.4 (MedCalc Software, Ostend, Belgium). The correlation was analyzed by Spearman rank correlation. Binary logistic regression analyses were used to determine the independent predictors for disease severity and 28-d mortality of AP patients. Cox proportional hazards regression model was used to estimate the independent contribution of presepsin for the prediction of 28-d mortality. All statistical tests were two-tailed, and a P value < 0.05 was considered statistically significant.

RESULTS

Patient characteristics

A total of 137 patients were screened in the emergency departments of the two hospitals from January 2018 to September 2019. Of these, 4 patients were excluded from analysis: 1 patient was diagnosed with pancreatic cancer, and 3 patients were lost to follow-up. Thus, 133 patients were enrolled and classified throughout the course of the disease as mild AP (n = 95 patients), moderately severe AP (n = 21 patients) and severe AP (n = 17 patients) according to the Atlanta 2012 classification. Patient characteristics are described in Table 1. The median age of patients was 65 years. There were 86 males and 47 females. The etiologies of AP included gallstones (63.2%), hypertriglyceridemia (9.0%), post-endoscopic retrograde cholangiopancreatography (11.3%), idiopathic (13.5%) and alcohol (3.0%). The BISAP, Ranson, CTSI and APACHE II scores increased with the severity of disease (all P < 0.01). The incidence of organ failure, mortality and the cost of hospitalization increased with the severity of disease (all P < 0.001).

The role of serial blood presepsin concentration in predicting severity of AP

Compared to patients with mild or moderately severe AP, the presepsin concentration at days 3 and 5 were significantly higher in patients with severe AP (Figure 1A). Compared with the mild group, the presepsin concentration in the moderately severe group at days 5 and 7 and in the severe group at day 7 were significantly higher (Figure 1A). The median clearance rate of presepsin on days 3 and 5 in moderately severe and severe patients were reduced compared to patients in the mild group (Figure 1B).

Table 1 Overall characteristics of the study population

Characteristic	Overall, *n* = 133	Mild, *n* = 95	Moderately severe, *n* = 21	Severe, *n* = 17	*P* value
Demographics					
Male, %	86 (64.7)	56 (58.9)	16 (76.2)	14 (82.4)	0.086
Age, yr	65 (54.0-76.0)	65 (54.0-76.0)	68 (40.5-72.5)	59 (43.0-82.0)	0.860
Comorbidities					
CHF, %	19 (17.4)	16 (18.8)	3 (18.8)	0 (0)	0.402
COPD, %	3 (2.8)	2 (2.4)	0 (0)	1 (12.5)	0.188
Diabetes, %	25 (22.9)	20 (23.5)	3 (18.8)	2 (25.0)	0.907
Immunosuppression, %	8 (7.3)	7 (8.2)	0 (0)	1 (12.5)	0.432
Etiology					0.003
Gallstones, %	84 (63.2)	65 (68.4)	12 (57.1)	7 (41.2)	
Hypertryglyceridemia, %	12 (9.0)	9 (9.5)	0 (0)	3 (17.6)	
Alcohol, %	4 (3.0)	2 (2.1)	2 (9.5)	0 (0)	
Post-ERCP, %	15 (11.3)	13 (13.7)	1 (4.8)	1 (5.9)	
Idiopathic, %	18 (13.5)	6 (6.3)	6 (28.6)	6 (35.3)	
Scoring					
BISAP score at admission	2.0 (1.0-2.0)	1.0 (1.0-2.0)	2.0 (2.0-3.0)	3.0 (2.0-3.0)	< 0.001
Ranson score at 48 h	2.0 (1.0-4.0)	2.0 (1.0-3.0)	3.0 (2.0-5.5)	4.0 (3.5-6.5)	< 0.001
CTSI score	4.0 (2.0-4.0)	2.0 (2.0-4.0)	4.0 (2.0-6.0)	4.0 (4.0-5.0)	0.002
APACHE II score at admission	8.0 (5.0-12.5)	7.0 (3.0-10.0)	9.0 (6.0-15.0)	18.0 (9.0-19.0)	< 0.001
Imaging					
Pancreatic necrosis, %	14 (10.5)	5 (5.3)	6 (28.6)	3 (17.6)	0.013
Mechanical ventilation, %	3 (2.3)	0 (0)	0 (0)	3 (17.6)	< 0.001
CRRT, %	1 (0.8)	0 (0)	0 (0)	1 (5.9)	0.027
Length of hospital stay in d	11.74 ± 5.21	11.08 ± 3.73	13.24 ± 8.40	13.59 ± 6.72	0.067
Outcomes					
Single organ failure, %	30 (22.6)	0 (0)	20 (95.2)	10 (58.8)	< 0.001
Multiple organ failure, %	8 (6.0)	0 (0)	1 (4.8)	7 (41.2)	< 0.001
28-d deaths, %	7 (5.3)	0 (0)	0 (0)	7 (41.2)	< 0.001
Cost in $	5276.14 (3265.34-7739.10)	4482.18 (3127.06-6493.38)	7242.67 (3356.87-8785.31)	11222.04 (7457.31-23045.12)	< 0.001

Data are presented as mean ± SD, *n* (%), or median (25^{th}-75^{th} percentile). CHF: Chronic heart failure; COPD: Chronic obstructive pulmonary disease; BISAP: Bedside index of severity in acute pancreatitis; CTSI: Computed tomography severity index; APACHE: Acute physiology and chronic health evaluation; CRRT: Continuous renal replacement therapy; ERCP: Endoscopic retrograde cholangiopancreatography.

Moreover, presepsin concentration remained significantly higher in the non-mild group compared to the mild group at days 3, 5 and 7 (Figure 1C). The concentrations of presepsin through the 7 d increased progressively with the number of organs failing as defined by the Marshall score (Figure 1D).

Independent predictors of severity of AP

Compared to the mild group, the proportion of patients with biliary etiology in the non-mild group was significantly less (69.4% *vs* 45.7%; $P = 0.013$) and those with idiopathic AP was significantly higher (6.1% *vs* 34.3%; $P < 0.001$). The median presepsin concentration on day 1 in patients with biliary AP was higher compared to those with other etiologies [1154.00 (728.75-2108.50) *vs* 749.00 (474.00-1174.00); $P = 0.001$]. The presepsin concentration on day 1 and etiology were independent predictive factors for non-mild AP on day 1 (Table 2). The presepsin concentrations on days 3, 5 and 7, but not etiology, were

Table 2 Independent factors for time-specific prediction of non-mild (moderately severe and severe) acute pancreatitis

Variable	β	Standard error	Wald statistic	Degrees of freedom	*P* value	Odds ratio	95%CI	
							Lower limit	Upper limit
Non-mild AP day 1								
Etiology	0.456	0.133	11.707	1	0.001	1.578	1.215	2.050
Presepsin day 1	0.000	0.000	5.872	1	0.015	1.001	1.000	1.001
Non-mild AP day 3								
Etiology	0.259	0.178	2.115	1	0.146	1.296	0.914	1.836
Presepsin day 3	0.001	0.000	8.567	1	0.003	1.001	1.000	1.001
Non-mild AP day 5								
Etiology	0.315	0.199	2.502	1	0.114	1.371	0.927	2.026
Presepsin day 5	0.002	0.000	13.141	1	< 0.001	1.002	1.001	1.003
Non-mild AP day 7								
Etiology	0.292	0.215	1.836	1	0.175	1.339	0.878	2.041
Presepsin day 7	0.002	0.000	13.203	1	< 0.001	1.002	1.001	1.003

AP: Acute pancreatitis.

independent predictive factors for non-mild AP on days 3, 5 and 7, respectively (Table 2). Presepsin concentration showed time-specific AUCs of 0.827, 0.848 and 0.867 on days 3, 5 and 7, respectively, in predicting moderately severe and severe AP (Table 3).

Correlation of presepsin concentration with scoring systems and other biomarkers

The Spearman correlation analysis revealed that the presepsin levels through day 7 in AP patients positively correlated with BISAP and Ranson scores (all $P < 0.05$, Figure 2). Positive correlations were also observed between the presepsin concentration on days 5 and 7 with the APACHE II scores. Presepsin levels at days 3, 5 and 7 also positively correlated with CTSI and Marshall scores (all $P < 0.05$, Figure 2). There was a positive correlation between presepsin and procalcitonin levels on days 1 and 3 and between presepsin and C-reactive protein levels on days 3 and 7 (Table 4).

Dynamic changes in presepsin concentrations and clearance rates in survivors and non-survivors

Presepsin levels decreased persistently through the first 7 d after admission in survivors but tended to decrease on day 3 and then increase on day 5 in non-survivors. The presepsin concentration in non-survivors on days 3, 5 and 7 were significantly higher when compared with survivors (Figure 3A). Moreover, the median clearance rate of presepsin on day 3 in the survivors was higher than that in the non-survivors (Figure 3B; $P < 0.01$).

Presepsin concentration for predicting 28-d mortality in patients with AP

The clinical characteristics between survival and non-survival groups are presented in Table 5. The binary logistic regression analysis showed that the presepsin levels on days 3, 5 and 7 and the BISAP, Ranson and APACHE II scores were independent predictors of 28-d mortality in patients with AP (Table 6). The AUC of presepsin for predicting 28-d mortality in AP patients was 0.781 on day 3, 0.846 on day 5 and 0.843 on day 7, which were slightly lower compared to APACHE II (0.955; all $P > 0.05$) and Ranson (0.900; all $P > 0.05$) scores but similar to BISAP (0.811; all $P > 0.05$) scores (Figure 4). The optimal prognostic cutoff values for predicting 28-d mortality on days 3, 5 and 7 were 681.5 pg/mL, 613 pg/mL and 770 pg/mL of presepsin, respectively.

Using the cutoff values determined by ROC curves, the Cox proportional hazards regression model was adjusted for age, sex and etiology to analyze the 28-d survival curves of patients (Figure 5). The hazard ratio (HR) of presepsin at day 3 was 9.475 (95%CI: 1.133-79.226; $P = 0.038$), the HR of presepsin at day 5 was 11.191 (95%CI: 1.297-96.518; $P = 0.028$), and the HR of presepsin at day 7 was 16.495 (95%CI: 2.759-98.615; $P = 0.002$).

Table 3 Time-specific area under the receiver operating characteristic curve of presepsin for prediction of moderately severe and severe acute pancreatitis

Time point	Cutoff (pg/mL)	Sensitivity	Specificity	PPV	NPV	AUROC (95%CI)	*P* value
Day 3	657.5	92.9%	71.4%	76.5%	90.9%	0.827 (0.730-0.923)	< 0.001
Day 5	593.5	84.6%	80.4%	81.2%	83.9%	0.848 (0.751-0.945)	< 0.001
Day 7	601.5	72.7%	89.8%	87.7%	76.7%	0.867 (0.756-0.977)	< 0.001

AUROC: Area under the receiver operating characteristic curve; NPV: Negative predictive value; PPV: Positive predictive value.

Table 4 Correlation between presepsin and procalcitonin or C-reactive protein levels

Variables	Procalcitonin	C-reactive protein
Presepsin day 1	$r = 0.464$	$r = 0.179$
	$P < 0.001$	$P = 0.080$
Presepsin day 3	$r = 0.318$	$r = 0.254$
	$P = 0.002$	$P = 0.016$
Presepsin day 5	$r = 0.208$	$r = 0.183$
	$P = 0.084$	$P = 0.091$
Presepsin day 7	$r = 0.239$	$r = 0.312$
	$P = 0.053$	$P = 0.007$

DISCUSSION

The current findings demonstrated that blood presepsin levels correlated with the severity of AP, and the clearance rate of presepsin was lower in patients with moderately severe or severe AP compared to patients with mild AP. Furthermore, the presepsin levels on days 1, 3, 5 and 7 during the hospital stay independently predicted the severity of AP. High levels of presepsin through the first 7 d after admission were associated with organ failure. It was also found that presepsin positively correlated with the BISAP, Ranson, CTSI, APACHE II, and Marshall scores as well as conventional biomarkers such as procalcitonin and C-reactive protein. Dynamic changes in the concentration of presepsin can be used for ongoing risk stratification of disease course and prediction of 28-d mortality in AP patients. Both presepsin and the clearance rate of presepsin on day 3 may be used as early biomarkers to predict the severity and prognosis of AP.

Recently, the blood presepsin concentration has been shown to be an early biomarker of various infections[14,15] as well as a valuable biomarker for diagnosing the occurrence[16], severity[17] or prognosis[7] of sepsis. Presepsin levels were shown to have good diagnostic and prognostic value for bacterial community-acquired pneumonia (CAP) and intensive care unit (ICU) mortality[18]. Similarly, our previous study showed that presepsin could predict acute respiratory distress syndrome, severe CAP, and 28-d mortality[19]. Recently, Yao *et al*[20] found that presepsin has a better predictive ability than existing biomarkers for bacterial infection following major hepato-biliary-pancreatic surgery. The study of Hiraki *et al*[21] showed that a higher concentration of presepsin in the drainage fluid was an independent predictive marker for clinically relevant postoperative pancreatic fistula after pancreaticoduodenectomy.

For noninfectious diseases, presepsin correlates with the disease activity of autoimmune diseases, such as systemic lupus erythematosus[22]. Higher presepsin levels are associated with renal and liver dysfunction[10]. Presepsin is a 13 kDa peptide that may be cleared by the kidney[6]. Presepsin levels have been shown to increase as the glomerular filtration rate (GFR) decreases and are markedly high in patients with chronic renal failure or receiving hemodialysis[23]. Presepsin concentrations correlate with serum creatinine and GFR levels in patients with chronic kidney disease[24]. Recently, presepsin was found to be a predictor of acute kidney injury and initiation of renal replacement therapy in sepsis patients[25]. Masson *et al*[10] found that presepsin levels are significantly higher in septic patients with shock than those without shock. A gender- and age-matched study on patients with severe AP and healthy volunteers showed that presepsin was an independent predictor of local complications, organ failure and in-hospital mortality[26].

In this study, we observed the dynamic changes of plasma presepsin levels and clearance rate of presepsin with time in patients with mild, moderate and severe AP and found that the presepsin

Table 5 Comparison of clinical characteristics between survival and non-survival groups

Characteristic	28-d survival outcome		*P* value
	Survival (*n* = 126)	Non-survival (*n* = 7)	
Demographics			
Male, %	79 (62.7)	7 (100.0)	0.051
Age, yr	65 (54-75)	75 (54-82)	0.417
Comorbidities			
CHF, %	19 (18.1)	0 (0)	1.000
COPD, %	2 (1.9)	1 (25.0)	0.107
Diabetes, %	24 (22.9)	1 (25.0)	1.000
Immunosuppression, %	7 (6.7)	1 (25.0)	0.266
Etiology			0.634
Gallstones, %	80 (63.5)	4 (57.1)	
Hypertryglyceridemia, %	11 (8.7)	1 (14.3)	
Alcohol, %	4 (3.2)	0 (0.0)	
Post-ERCP, %	15 (11.9)	0 (0.0)	
Idiopathic, %	16 (12.7)	2 (28.6)	
Scoring			
BISAP score at admission	1.0 (1.0-2.0)	3.0 (2.0-4.0)	0.003
Ranson score at 48 h	2.0 (1.0-3.0)	5.0 (4.0-8.0)	< 0.001
CTSI score	2.0 (2.0-4.0)	4.0 (4.0-4.0)	0.181
APACHE II score at admission	8.0 (4.8-11.0)	19.0 (15.0-31.0)	< 0.001
Imaging			
Pancreatic necrosis, %	13 (10.3)	1 (14.3)	0.550
Mechanical ventilation, %	0 (0.0)	3 (42.9)	< 0.001
CRRT, %	0 (0.0)	1 (14.3)	0.053
Length of hospital stay in d	11 (9-14)	13 (5-21)	0.568
Outcomes			
Single organ failure, %	27 (22.1)	3 (100.0)	0.013
Multiple organ failure, %	4 (4.0)	4 (100.0)	< 0.001
Cost in $	4718.99 (3065.47-7104.78)	22243.29 (10432.63-36309.99)	0.001

Data are presented as *n* (%), or median (25^{th}-75^{th} percentile). CHF: Chronic heart failure; COPD: Chronic obstructive pulmonary disease; ERCP: Endoscopic retrograde cholangiopancreatography; BISAP: Bedside index of severity in acute pancreatitis; CTSI: Computed tomography severity index; APACHE: Acute physiology and chronic health evaluation; CRRT: Continuous renal replacement therapy.

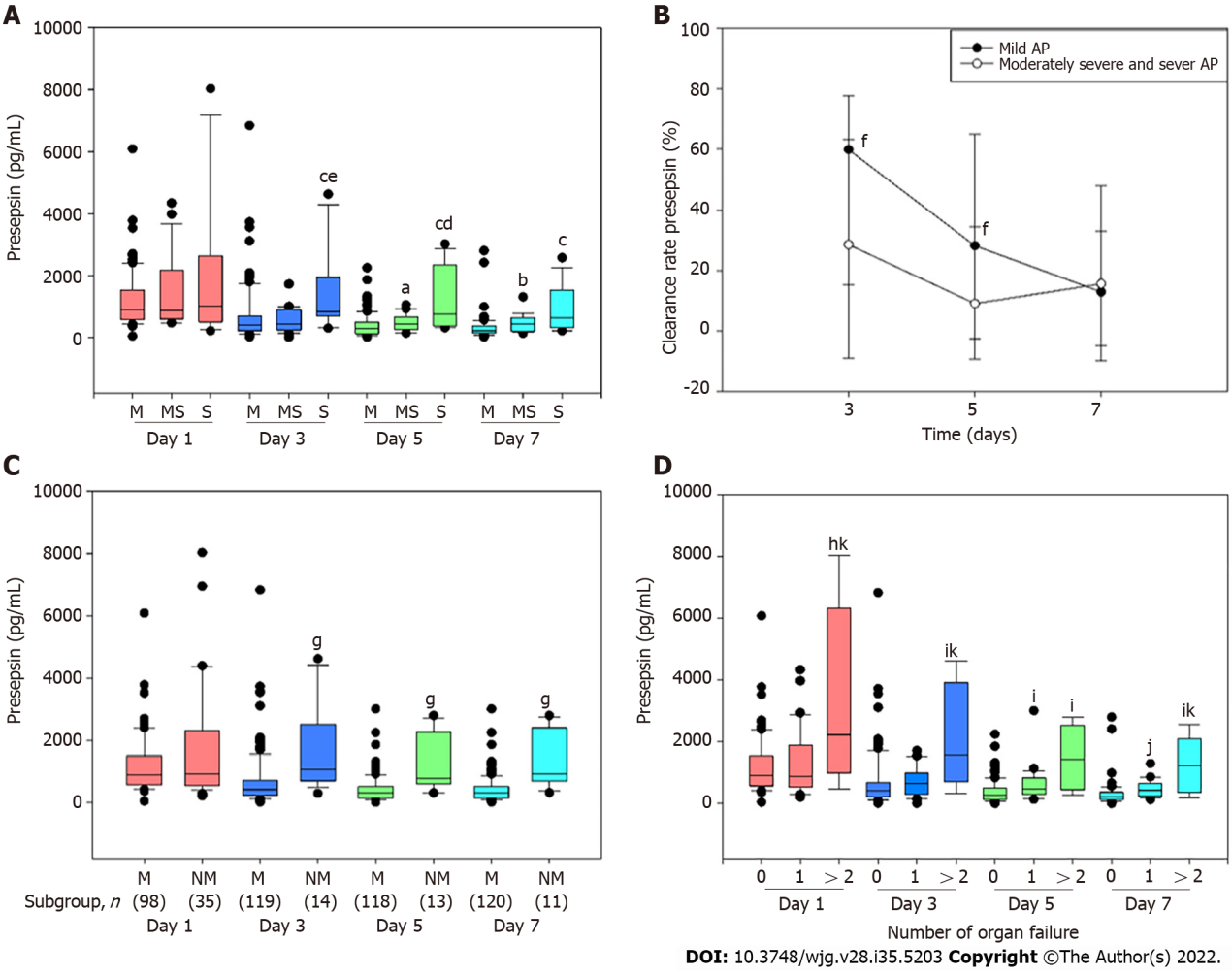
concentrations on days 3, 5 and 7 (but not day 1) increased with the severity of AP. A high presepsin value and low clearance rate of presepsin at day 3 were found to be more valuable in early identification of mild or moderate *vs* severe compared to mild *vs* moderate disease. Inconsistently, the concentrations of presepsin on day 1 through 7 increased significantly with the number of organs experiencing failure.

In most high-income countries, gallstones (45%) and alcohol abuse (20%) are the most frequent causes of AP[27]. In the current study, gallstones (63.2%), but not alcohol (3.0%), was the most common etiology of AP, which is consistent with the conclusion of an 8-year Chinese study by Zhu *et al*[28]. Upon multivariate analysis, after adjusting for the confounding factor of etiology, it was found that presepsin levels were independent predictors for the severity of AP on days 1, 3, 5 and 7. In this study, the proportion of patients with biliary etiology were significantly less, and those with idiopathic AP were significantly higher in the moderately severe or severe AP group compared to the mild AP group. It was shown that the presepsin values on day 1, but not on days 3, 5 or 7, were higher in patients with biliary AP than in other etiologies, which is in line with the procalcitonin values of the study of Modrau

Table 6 Independent factors for the prediction of 28-d mortality in patients with acute pancreatitis

Variable	β	Standard error	Wald statistic	Degrees of freedom	*P* value	Odds ratio	95%CI	
							Lower limit	Upper limit
Presepsin day 3	0.001	0.000	5.013	1	0.025	1.001	1.000	1.001
Presepsin day 5	0.002	0.000	11.406	1	0.001	1.002	1.001	1.003
Presepsin day 7	0.002	0.001	11.672	1	0.001	1.002	1.001	1.003
BISAP score at admission	1.217	0.390	9.700	1	0.002	3.376	1.571	7.255
Ranson score at 48 h	0.868	0.249	12.202	1	< 0.001	2.383	1.464	3.880
APACHE II score at admission	0.477	0.166	8.251	1	0.004	1.611	1.164	2.230

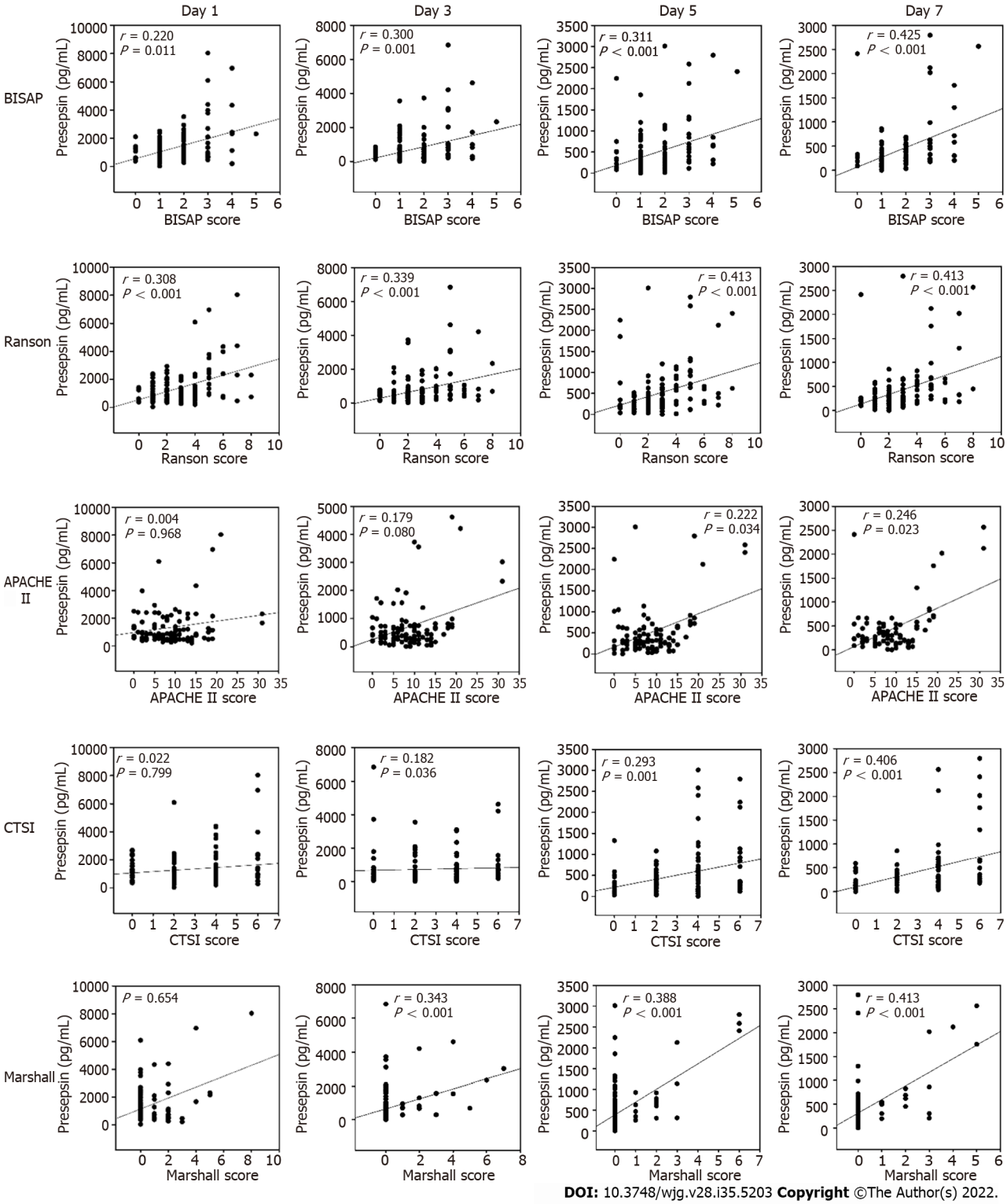
BISAP: Bedside index of severity in acute pancreatitis; APACHE: Acute physiology and chronic health evaluation.



DOI: 10.3748/wjg.v28.i35.5203 **Copyright** ©The Author(s) 2022.

Figure 1 Association between dynamic blood presepsin levels and severity of acute pancreatitis. A: Presepsin levels on days 1, 3, 5 and 7 after admission in mild (M), moderately severe (MS) and severe (S) acute pancreatitis (AP). [a]*P* < 0.05 *vs* M AP; [b]*P* < 0.01 *vs* M AP; [c]*P* < 0.001 *vs* M AP; [d]*P* < 0.05 *vs* MS AP; [e]*P* < 0.01 *vs* MS AP; B: Clearance rate of presepsin in patients with M and non-mild (NM) (MS and S) AP; [f]*P* < 0.05 *vs* MS and S AP; C: Time-specific concentrations of presepsin in patients with M and NM AP; [g]*P* < 0.001 *vs* M AP; D: Correlation between presepsin and organ failure in patients with AP. [h]*P* < 0.05 *vs* no organ failure; [i]*P* < 0.01 *vs* no organ failure; [i]*P* < 0.001 *vs* no organ failure; [k]*P* < 0.05 *vs* 1 organ failure. Lines denote median values, boxes represent 25[th] to 75[th] percentiles, and whiskers indicate the range.

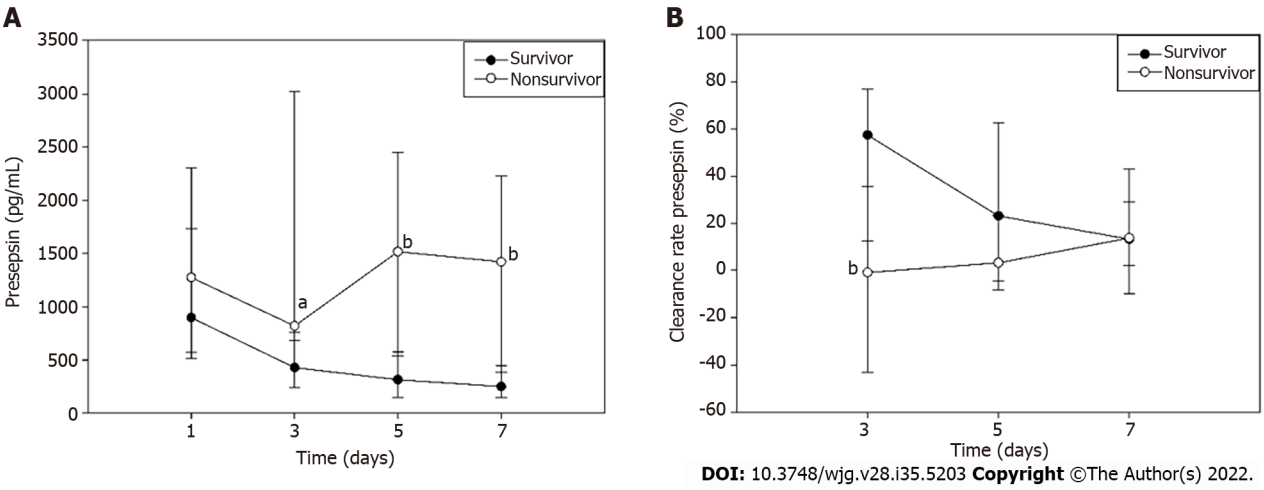
et al[29]. It is likely that the increase in circulating presepsin found in the present study was associated with organ dysfunction and biliary tract infection, though infectious complications are rare during the early course of severe AP[30].



DOI: 10.3748/wjg.v28.i35.5203 **Copyright** ©The Author(s) 2022.

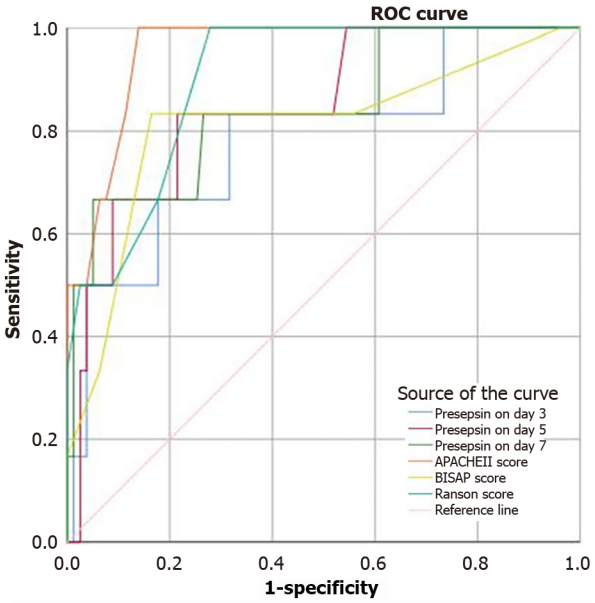
Figure 2 Correlation between presepsin and bedside index of severity in acute pancreatitis, Ranson, acute physiology and chronic health evaluation-II, computed tomography severity index and Marshall scores. BISAP: Bedside index of severity in acute pancreatitis; APACHE: Acute physiology and chronic health evaluation; CTSI: Computed tomography severity index.

Procalcitonin is a sensitive biomarker for the detection of pancreatic infection, and C-reactive protein levels ≥ 150 mg/L at day 3 is a prognostic indicator for severe AP[13]. The current study illustrated that presepsin levels were positively correlated with procalcitonin levels on days 1 and 3 and with C-reactive protein levels on days 3 and 7. There was a positive correlation between the presepsin levels and Marshall scores (including respiratory function, cardiovascular system, renal dysfunction) on days 3, 5 and 7. Meanwhile, the current study found a significant positive correlation between the presepsin levels and other AP scores, such as BISAP, Ranson and APACHE II. In this study, increased presepsin levels were found to be an accurate predictor of disease severity. For the prediction of moderately



DOI: 10.3748/wjg.v28.i35.5203 **Copyright** ©The Author(s) 2022.

Figure 3 Dynamic changes in presepsin concentration and clearance rate in survivors and non-survivors. A: Presepsin concentration; B: Clearance rate. [a]*P* < 0.05 *vs* survivors; [b]*P* < 0.01 *vs* survivors.



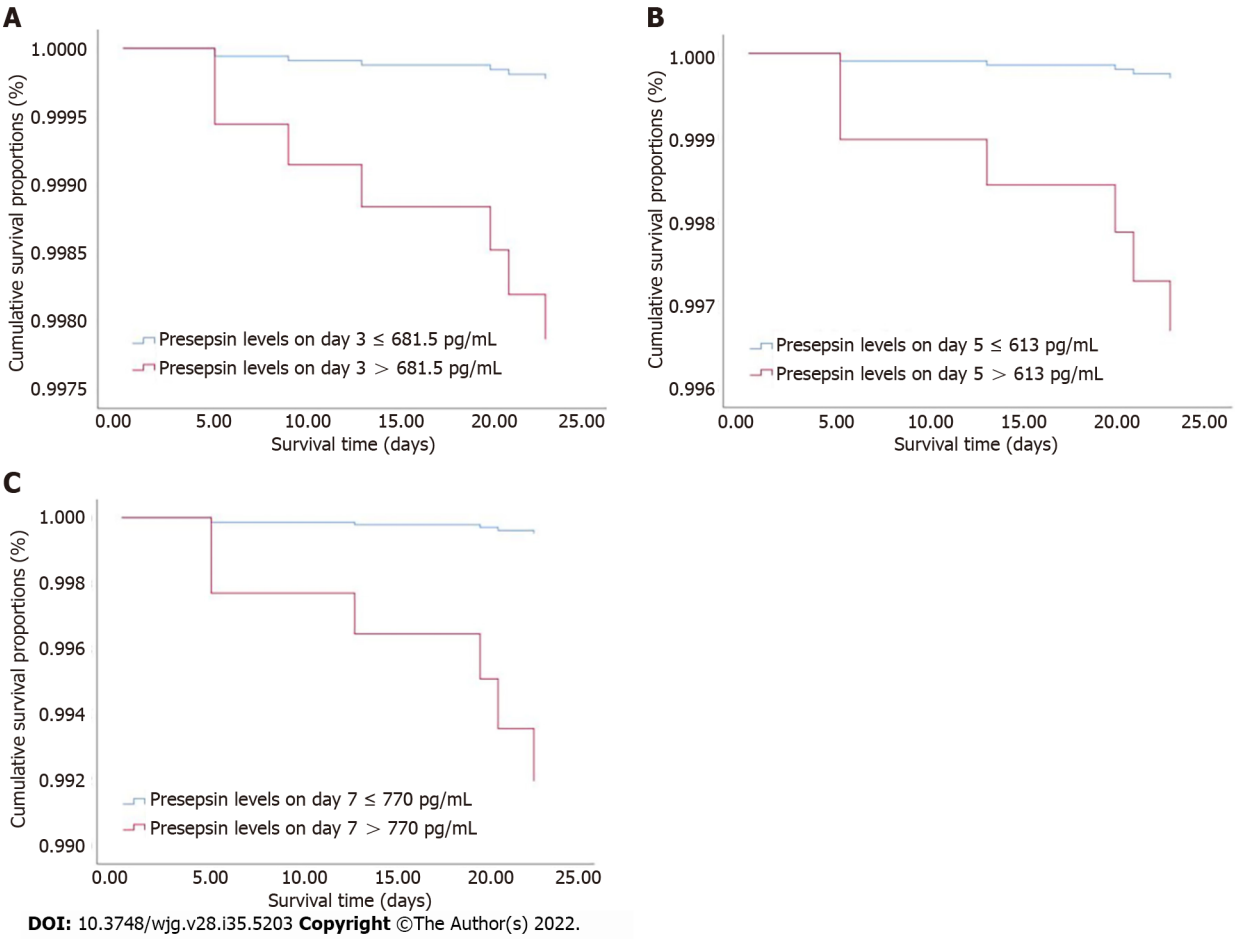
DOI: 10.3748/wjg.v28.i35.5203 **Copyright** ©The Author(s) 2022.

Figure 4 Receiver operating characteristic curves of presepsin, acute physiology and chronic health evaluation-II, index of severity in acute pancreatitis and Ranson scores for 28-d mortality of patients with acute pancreatitis. ROC: Receiver operating characteristic; APACHE: Acute physiology and chronic health evaluation; BISAP: Bedside index of severity in acute pancreatitis.

severe or severe AP, the AUCs of presepsin on days 3, 5 and 7 were 0.827, 0.848 and 0.867, respectively, with high sensitivity and specificity.

The dynamic changes in presepsin were different in survivors and non-survivors of this study. In survivors, presepsin levels showed a decreasing trend over time but in non-survivors presepsin levels first decreased and then increased. Similar trends in presepsin levels have been reported in patients with severe sepsis[31]. In addition, clearance rates of presepsin in non-survivors were lower than that of survivors in the early stage of AP (day 3). Potential explanations involve a reduced clearance of presepsin due to reduced kidney function[22-24] and circulatory dysfunction[10]. The most common organ systems to fail in non-survivors were circulatory [71.4% (5/7 patients)], respiratory [85.7% (6/7 patients)] and renal [42.8% (3/7 patients)] systems. Studies have showed that higher presepsin levels were associated with ICU death and mortality in sepsis[7], CAP[18], cardiac arrest patients after return of spontaneous circulation[32] and severe AP[25]. Interestingly, the presepsin levels on days 3, 5,and 7 were found to independently predict 28-d mortality in AP.

This study has certain limitations. First, the patient population was heterogeneous. Second, the study did not compare presepsin with other biomarkers. Third, the relevance of presepsin during the latter course of AP was not studied. Fourth, the association between presepsin levels and hepatorenal



DOI: 10.3748/wjg.v28.i35.5203 **Copyright** ©The Author(s) 2022.

Figure 5 Cox regression survival curves. A: Acute pancreatitis (AP) patients with presepsin levels higher than 681.5 pg/mL on day 3 had a lower probability of survival at 28 d compared to patients with lower levels; B and C: Similarly, AP patients with presepsin levels on day 5 (B) and day 7 (C) higher than 613 pg/mL and 770 pg/mL, respectively, had a lower probability of survival at 28 d than patients with lower levels. AP: acute pancreatitis.

function was not evaluated. Future multicentric studies with larger cohorts that consider these factors should be conducted to validate the findings of this study.

CONCLUSION

This cohort study found that blood presepsin levels in the first 7 d after admission could accurately predict the severity of disease course and 28-d mortality in patients with AP and may be a promising prognostic marker.

ARTICLE HIGHLIGHTS

Research background

Acute pancreatitis (AP) is one of the most common causes of abdominal emergencies and is associated with sepsis, organ failure and high mortality rates (up to 35%). AP has diverse clinical manifestations with an unpredictable clinical course. It is necessary to predict the severity of AP rapidly and accurately.

Research motivation

A major challenge in AP is the early identification of patients at high-risk for organ failure and death. However, scoring systems are complicated and time consuming with limited predictive value for the clinical course. Biomarkers are promising for the dynamic prediction of disease severity.

Research objectives

To determine whether the dynamic levels of an emerging biomarker, presepsin, can be used to evaluate the severity of disease course and outcome of AP.

Research methods

In this prospective and multicentric cohort study, 133 patients with AP were included from January 2018 to September 2019. Clinical severity (mild, moderately severe and severe AP) was dynamically evaluated using the 2012 revised Atlanta Classification. Blood presepsin levels were measured at days 1, 3, 5 and 7 after admission by chemiluminescent enzyme immunoassay. The patients were followed up for 28 d.

Research results

The median concentration of presepsin increased, and the clearance rate of presepsin decreased with disease severity and organ failure in AP patients. The presepsin levels on days 3, 5 and 7 were independent predictors of moderately severe and severe AP with time-specific area under the curve (AUC) values of 0.827, 0.848 and 0.867, respectively. The presepsin levels positively correlated with bedside index of severity in acute pancreatitis, Ranson, acute physiology and chronic health evaluation-II, computed tomography severity index and Marshall scores and conventional biomarkers such as procalcitonin and C-reactive protein. Presepsin levels on days 3, 5 and 7 were independent predictors of 28-d mortality of AP patients with AUC values of 0.781, 0.846 and 0.843, respectively.

Research conclusions

The blood presepsin levels within 7 d of admission were associated with and may be useful to dynamically predict the severity of disease course and 28-d mortality in AP patients. Both presepsin and clearance rate of presepsin on day 3 may be used as early biomarkers to predict the severity and prognosis of AP.

Research perspectives

Prospective cohort studies report the predictive value of presepsin in the severity of AP. Future research should focus on the guiding significance of presepsin in the treatment of AP, such as antibiotic use.

ACKNOWLEDGEMENTS

We thank Drs. Jian-Dong Zhang, Jie Yang, Shuai Xia, Mei-Ying Zhang, Si-Jia Wang and Zheng Wang for collecting cases. We also thank Dr. Shan-Shan Wu for statistical analyses. We also gratefully acknowledge all health care workers on the front line and all patients involved in the study.

FOOTNOTES

Author contributions: Xiao HL and Wang GX have contributed equally to this work; Li CS and Xie MR contributed to the study conception and design; Xiao HL, Wang GX, Wang Y, Tan ZM, Zhou J and Yu H participated in the material preparation and data collection; Xiao HL and Wang GX performed the analyses; Xiao HL drafted the initial manuscript and revised the article; All authors read and approved the final manuscript.

Supported by Beijing Municipal Administration of Hospitals Clinical Medicine Development of Special Funding Support "Yangfan" Project, No. ZYLX201802; Beijing Municipal Administration of Hospitals' Youth Program, No. QML20170105; and National Natural Science Foundation of China, No. 81374004 and 81773931.

Institutional review board statement: The study was reviewed and approved by the Ethics Commission of Beijing Friendship Hospital affiliated to Capital Medical University (Approval No. 2017-P2-103-02).

Informed consent statement: All study participants, or their legal guardian, provided informed written consent prior to study enrollment.

Conflict-of-interest statement: There are no conflicts of interest to report.

Data sharing statement: No additional data are available.

STROBE statement: The authors have read the STROBE Statement-checklist of items, and the manuscript was prepared and revised according to the STROBE Statement-checklist of items.

Open-Access: This article is an open-access article that was selected by an in-house editor and fully peer-reviewed by external reviewers. It is distributed in accordance with the Creative Commons Attribution NonCommercial (CC BY-NC 4.0) license, which permits others to distribute, remix, adapt, build upon this work non-commercially, and license their derivative works on different terms, provided the original work is properly cited and the use is non-commercial. See: https://creativecommons.org/Licenses/by-nc/4.0/

Country/Territory of origin: China

ORCID number: Hong-Li Xiao 0000-0002-7353-114X; Guo-Xing Wang 0000-0003-1379-5749; Yan Wang 0000-0002-7950-8696; Zhi-Min Tan 0000-0002-8731-4293; Jie Zhou 0000-0003-1298-6789; Han Yu 0000-0002-0529-7152; Miao-Rong Xie 0000-0003-2479-9470; Chun-Sheng Li 0000-0002-3161-4457.

S-Editor: Zhang H
L-Editor: Filipodia
P-Editor: Yu HG

REFERENCES

1 **van Santvoort HC**, Bakker OJ, Bollen TL, Besselink MG, Ahmed Ali U, Schrijver AM, Boermeester MA, van Goor H, Dejong CH, van Eijck CH, van Ramshorst B, Schaapherder AF, van der Harst E, Hofker S, Nieuwenhuijs VB, Brink MA, Kruyt PM, Manusama ER, van der Schelling GP, Karsten T, Hesselink EJ, van Laarhoven CJ, Rosman C, Bosscha K, de Wit RJ, Houdijk AP, Cuesta MA, Wahab PJ, Gooszen HG; Dutch Pancreatitis Study Group. A conservative and minimally invasive approach to necrotizing pancreatitis improves outcome. *Gastroenterology* 2011; **141**: 1254-1263 [PMID: 21741922 DOI: 10.1053/j.gastro.2011.06.073]

2 **van Dijk SM**, Hallensleben NDL, van Santvoort HC, Fockens P, van Goor H, Bruno MJ, Besselink MG; Dutch Pancreatitis Study Group. Acute pancreatitis: recent advances through randomised trials. *Gut* 2017; **66**: 2024-2032 [PMID: 28838972 DOI: 10.1136/gutjnl-2016-313595]

3 **Harshit Kumar A**, Singh Griwan M. A comparison of APACHE II, BISAP, Ranson's score and modified CTSI in predicting the severity of acute pancreatitis based on the 2012 revised Atlanta Classification. *Gastroenterol Rep (Oxf)* 2018; **6**: 127-131 [PMID: 29780601 DOI: 10.1093/gastro/gox029]

4 **Zerem E**. Treatment of severe acute pancreatitis and its complications. *World J Gastroenterol* 2014; **20**: 13879-13892 [PMID: 25320523 DOI: 10.3748/wjg.v20.i38.13879]

5 **Shirakawa K**, Naitou K, Hirose J, Takahashi T, Furusako S. Presepsin (sCD14-ST): development and evaluation of one-step ELISA with a new standard that is similar to the form of presepsin in septic patients. *Clin Chem Lab Med* 2011; **49**: 937-939 [PMID: 21345045 DOI: 10.1515/CCLM.2011.145]

6 **Ackland GL**, Prowle JR. Presepsin: solving a soluble (CD14) problem in sepsis? *Intensive Care Med* 2015; **41**: 351-353 [PMID: 25608923 DOI: 10.1007/s00134-014-3642-8]

7 **Liu B**, Chen YX, Yin Q, Zhao YZ, Li CS. Diagnostic value and prognostic evaluation of Presepsin for sepsis in an emergency department. *Crit Care* 2013; **17**: R244 [PMID: 24138799 DOI: 10.1186/cc13070]

8 **Nakamura Y**, Ishikura H, Nishida T, Kawano Y, Yuge R, Ichiki R, Murai A. Usefulness of presepsin in the diagnosis of sepsis in patients with or without acute kidney injury. *BMC Anesthesiol* 2014; **14**: 88 [PMID: 25309126 DOI: 10.1186/1471-2253-14-88]

9 **Kerr KF**, Wang Z, Janes H, McClelland RL, Psaty BM, Pepe MS. Net reclassification indices for evaluating risk prediction instruments: a critical review. *Epidemiology* 2014; **25**: 114-121 [PMID: 24240655 DOI: 10.1097/EDE.0000000000000018]

10 **Masson S**, Caironi P, Fanizza C, Thomae R, Bernasconi R, Noto A, Oggioni R, Pasetti GS, Romero M, Tognoni G, Latini R, Gattinoni L. Circulating presepsin (soluble CD14 subtype) as a marker of host response in patients with severe sepsis or septic shock: data from the multicenter, randomized ALBIOS trial. *Intensive Care Med* 2015; **41**: 12-20 [PMID: 25319385 DOI: 10.1007/s00134-014-3514-2]

11 **Banks PA**, Bollen TL, Dervenis C, Gooszen HG, Johnson CD, Sarr MG, Tsiotos GG, Vege SS; Acute Pancreatitis Classification Working Group. Classification of acute pancreatitis--2012: revision of the Atlanta classification and definitions by international consensus. *Gut* 2013; **62**: 102-111 [PMID: 23100216 DOI: 10.1136/gutjnl-2012-302779]

12 **Okamura Y**, Yokoi H. Development of a point-of-care assay system for measurement of presepsin (sCD14-ST). *Clin Chim Acta* 2011; **412**: 2157-2161 [PMID: 21839732 DOI: 10.1016/j.cca.2011.07.024]

13 **Leppäniemi A**, Tolonen M, Tarasconi A, Segovia-Lohse H, Gamberini E, Kirkpatrick AW, Ball CG, Parry N, Sartelli M, Wolbrink D, van Goor H, Baiocchi G, Ansaloni L, Biffl W, Coccolini F, Di Saverio S, Kluger Y, Moore E, Catena F. 2019 WSES guidelines for the management of severe acute pancreatitis. *World J Emerg Surg* 2019; **14**: 27 [PMID: 31210778 DOI: 10.1186/s13017-019-0247-0]

14 **Marazzi MG**, Randelli F, Brioschi M, Drago L, Romanò CL, Banfi G, Massaccesi L, Crapanzano C, Morelli F, Corsi Romanelli MM, Galliera E. Presepsin: A potential biomarker of PJI? *Int J Immunopathol Pharmacol* 2018; **31**: 394632017749356 [PMID: 29251000 DOI: 10.1177/0394632017749356]

15 **Chenevier-Gobeaux C**, Borderie D, Weiss N, Mallet-Coste T, Claessens YE. Presepsin (sCD14-ST), an innate immune response marker in sepsis. *Clin Chim Acta* 2015; **450**: 97-103 [PMID: 26164388 DOI: 10.1016/j.cca.2015.06.026]

16 **Kweon OJ**, Choi JH, Park SK, Park AJ. Usefulness of presepsin (sCD14 subtype) measurements as a new marker for the diagnosis and prediction of disease severity of sepsis in the Korean population. *J Crit Care* 2014; **29**: 965-970 [PMID: 25042676 DOI: 10.1016/j.jcrc.2014.06.014]

17 **Behnes M**, Bertsch T, Lepiorz D, Lang S, Trinkmann F, Brueckmann M, Borggrefe M, Hoffmann U. Diagnostic and prognostic utility of soluble CD 14 subtype (presepsin) for severe sepsis and septic shock during the first week of intensive care treatment. *Crit Care* 2014; **18**: 507 [PMID: 25190134 DOI: 10.1186/s13054-014-0507-z]

18 **Klouche K**, Cristol JP, Devin J, Gilles V, Kuster N, Larcher R, Amigues L, Corne P, Jonquet O, Dupuy AM. Diagnostic and prognostic value of soluble CD14 subtype (Presepsin) for sepsis and community-acquired pneumonia in ICU patients. *Ann Intensive Care* 2016; **6**: 59 [PMID: 27389015 DOI: 10.1186/s13613-016-0160-6]

19 **Liu B**, Yin Q, Chen YX, Zhao YZ, Li CS. Role of Presepsin (sCD14-ST) and the CURB65 scoring system in predicting

severity and outcome of community-acquired pneumonia in an emergency department. *Respir Med* 2014; **108**: 1204-1213 [PMID: 24931899 DOI: 10.1016/j.rmed.2014.05.005]

20 **Yao S**, Kaido T, Uozumi R, Hirata M, Iwamura S, Miyachi Y, Macshut M, Sharshar M, Yagi S, Uemoto S. Diagnostic potential of presepsin in bacterial infection following hepato-biliary-pancreatic surgery: A prospective observational study. *J Hepatobiliary Pancreat Sci* 2020; **27**: 756-766 [PMID: 32654388 DOI: 10.1002/jhbp.802]

21 **Hiraki M**, Miyoshi A, Sadashima E, Shinkai Y, Yasunami M, Manabe T, Kitahara K, Noshiro H. The novel early predictive marker presepsin for postoperative pancreatic fistula: A pilot study. *Exp Ther Med* 2020; **20**: 2298-2304 [PMID: 32765708 DOI: 10.3892/etm.2020.8919]

22 **Tanimura S**, Fujieda Y, Kono M, Shibata Y, Hisada R, Sugawara E, Nakamura H, Ohmura K, Shimamura S, Mitani A, Shida H, Watanabe T, Kato M, Oku K, Bohgaki T, Amengual O, Yasuda S, Shimizu C, Atsumi T. Clinical significance of plasma presepsin levels in patients with systemic lupus erythematosus. *Mod Rheumatol* 2018; **28**: 865-871 [PMID: 29239264 DOI: 10.1080/14397595.2017.1408755]

23 **Nagata T**, Yasuda Y, Ando M, Abe T, Katsuno T, Kato S, Tsuboi N, Matsuo S, Maruyama S. Clinical impact of kidney function on presepsin levels. *PLoS One* 2015; **10**: e0129159 [PMID: 26030716 DOI: 10.1371/journal.pone.0129159]

24 **Miyoshi M**, Inoue Y, Nishioka M, Ikegame A, Nakao T, Kishi S, Doi T, Nagai K. Clinical evaluation of presepsin considering renal function. *PLoS One* 2019; **14**: e0215791 [PMID: 31490935 DOI: 10.1371/journal.pone.0215791]

25 **Shimoyama Y**, Umegaki O, Kadono N, Minami T. Presepsin and prognostic nutritional index are predictors of septic acute kidney injury, renal replacement therapy initiation in sepsis patients, and prognosis in septic acute kidney injury patients: a pilot study. *BMC Nephrol* 2021; **22**: 219 [PMID: 34118899 DOI: 10.1186/s12882-021-02422-x]

26 **Lin J**, Li Z, Zheng Y, Zhang Y, Shao C, Liu G, Li J. Elevated Presepsin Levels are Associated with Severity and Prognosis of Severe Acute Pancreatitis. *Clin Lab* 2016; **62**: 1699-1708 [PMID: 28164588 DOI: 10.7754/Clin.Lab.2016.160134]

27 **Roberts SE**, Morrison-Rees S, John A, Williams JG, Brown TH, Samuel DG. The incidence and aetiology of acute pancreatitis across Europe. *Pancreatology* 2017; **17**: 155-165 [PMID: 28159463 DOI: 10.1016/j.pan.2017.01.005]

28 **Zhu Y**, Pan X, Zeng H, He W, Xia L, Liu P, Zhu Y, Chen Y, Lv N. A Study on the Etiology, Severity, and Mortality of 3260 Patients With Acute Pancreatitis According to the Revised Atlanta Classification in Jiangxi, China Over an 8-Year Period. *Pancreas* 2017; **46**: 504-509 [PMID: 28196012 DOI: 10.1097/MPA.0000000000000776]

29 **Modrau IS**, Floyd AK, Thorlacius-Ussing O. The clinical value of procalcitonin in early assessment of acute pancreatitis. *Am J Gastroenterol* 2005; **100**: 1593-1597 [PMID: 15984987 DOI: 10.1111/j.1572-0241.2005.41456.x]

30 **Beger HG**, Bittner R, Block S, Büchler M. Bacterial contamination of pancreatic necrosis. A prospective clinical study. *Gastroenterology* 1986; **91**: 433-438 [PMID: 3522342 DOI: 10.1016/0016-5085(86)90579-2]

31 **Yu H**, Qi Z, Hang C, Fang Y, Shao R, Li C. Evaluating the value of dynamic procalcitonin and presepsin measurements for patients with severe sepsis. *Am J Emerg Med* 2017; **35**: 835-841 [PMID: 28153679 DOI: 10.1016/j.ajem.2017.01.037]

32 **Qi Z**, Zhang Q, Liu B, Shao F, Li C. Presepsin As a Biomarker for Evaluating Prognosis and Early Innate Immune Response of Out-of-Hospital Cardiac Arrest Patients After Return of Spontaneous Circulation. *Crit Care Med* 2019; **47**: e538-e546 [PMID: 30985453 DOI: 10.1097/CCM.0000000000003764]

World Journal of Gastroenterology

Submit a Manuscript: https://www.f6publishing.com

World J Gastroenterol 2022 September 21; 28(35): 5217-5229

DOI: 10.3748/wjg.v28.i35.5217

ISSN 1007-9327 (print) ISSN 2219-2840 (online)

ORIGINAL ARTICLE

Prospective Study

High prevalence of chronic viral hepatitis B and C in Minnesota Somalis contributes to rising hepatocellular carcinoma incidence

Essa A Mohamed, Nasra H Giama, Abubaker O Abdalla, Hassan M Shaleh, Abdul M Oseini, Hamdi A Ali, Fowsiyo Ahmed, Wesam Taha, Hager Ahmed Mohammed, Jessica Cvinar, Ibrahim A Waaeys, Hawa Ali, Loretta K Allotey, Abdiwahab O Ali, Safra A Mohamed, William S Harmsen, Eimad M Ahmmad, Numra A Bajwa, Mohamud D Afgarshe, Abdirashid M Shire, Joyce E Balls-Berry, Lewis R Roberts

Specialty type: Gastroenterology and hepatology

Provenance and peer review: Unsolicited article; Externally peer reviewed.

Peer-review model: Single blind

Peer-review report's scientific quality classification

Grade A (Excellent): 0
Grade B (Very good): B, B
Grade C (Good): C
Grade D (Fair): 0
Grade E (Poor): 0

P-Reviewer: Głuszyńska P, Poland; Pham TTT, Viet Nam; Trifan A, Romania

Received: January 19, 2022
Peer-review started: January 19, 2022
First decision: March 8, 2022
Revised: March 28, 2022
Accepted: August 17, 2022
Article in press: August 17, 2022
Published online: September 21, 2022

Essa A Mohamed, Nasra H Giama, Hassan M Shaleh, Abdul M Oseini, Hamdi A Ali, Fowsiyo Ahmed, Wesam Taha, Hager Ahmed Mohammed, Jessica Cvinar, Hawa Ali, Loretta K Allotey, Eimad M Ahmmad, Numra A Bajwa, Abdirashid M Shire, Lewis R Roberts, Division of Gastroenterology and Hepatology, Mayo Clinic, Rochester, MN 55905, United States

Essa A Mohamed, Joyce E Balls-Berry, Center for Clinical and Translational Science, Mayo Clinic, Rochester, MN 55905, United States

Nasra H Giama, School of Nursing, University of Minnesota, Minneapolis, MN 55455, United States

Abubaker O Abdalla, Division of Digestive Diseases, Emory School of Medicine, Atlanta, GA 30322, United States

Hassan M Shaleh, Ibrahim A Waaeys, Abdiwahab O Ali, Safra A Mohamed, Department of Laboratory Medicine and Pathology, Mayo Clinic, Rochester, MN 55905, United States

Wesam Taha, Department of Internal Medicine, NewYork-Presbyterian Queens, Flushing, NY 11355, United States

Hager Ahmed Mohammed, Department of Pediatrics, University of Nevada Las Vegas, Las Vegas, NV 89154, United States

William S Harmsen, Department of Quantitative Health Sciences, Mayo Clinic, Rochester, MN 55905, United States

Mohamud D Afgarshe, Department of Medicine, Gargar Urgent Care and Clinic, Minneapolis, MN 55406, United States

Abdirashid M Shire, Office of the Director, Shire Scientific, Minneapolis, MN 55405, United States

Joyce E Balls-Berry, Department of Neurology, Washington University School of Medicine in St Louis, St Louis, MO 63130, United States

Joyce E Balls-Berry, Knight Alzheimer Disease Research Center, Washington University School of Medicine, St Louis, MO 63130, United States

Corresponding author: Lewis R Roberts, MBChB, PhD, Professor, Division of Gastroenterology and Hepatology, Mayo Clinic Rochester, 200 First Street SW, Rochester, MN 55905, United States. roberts.lewis@mayo.edu

Abstract

BACKGROUND

Chronic hepatitis B virus (HBV) and hepatitis C virus (HCV) infections are known risk factors for liver disease, cirrhosis and hepatocellular carcinoma (HCC). There is substantial global variation in HBV and HCV prevalence resulting in variations in cirrhosis and HCC. We previously reported high prevalence of HBV and HCV infections in Somali immigrants seen at an academic medical center in Minnesota.

AIM

To determine the prevalence of chronic viral hepatitis in Somali immigrants in Minnesota through a community-based screening program.

METHODS

We conducted a prospective community-based participatory research study in the Somali community in Minnesota in partnership with community advisory boards, community clinics and local mosques between November 2010 and December 2015 (data was analyzed in 2020). Serum was tested for hepatitis B surface antigen, hepatitis B core antibody, hepatitis B surface antibody and anti-HCV antibody.

RESULTS

Of 779 participants, 15.4% tested positive for chronic HBV infection, 50.2% for prior exposure to HBV and 7.6% for chronic HCV infection. Calculated age-adjusted frequencies in males and females for chronic HBV were 12.5% and 11.6%; for prior exposure to HBV were 44.8% and 41.3%; and for chronic HCV were 6.7% and 5.7%, respectively. Seven participants developed incident HCC during follow up.

CONCLUSION

Chronic HBV and HCV are major risk factors for liver disease and HCC among Somali immigrants, with prevalence of both infections substantially higher than in the general United States population. Community-based screening is essential for identifying and providing health education and linkage to care for diagnosed patients.

Key Words: Viral hepatitis; Liver disease; Community engagement; African; Immigrant health

©The Author(s) 2022. Published by Baishideng Publishing Group Inc. All rights reserved.

Core Tip: This prospective community-based study evaluated the prevalence of chronic hepatitis B and C among the immigrant Somali community. Through community partnerships we were able to demonstrate a framework that can be used with other immigrant and/or minority communities at-risk for infectious diseases such as hepatitis B and C.

Citation: Mohamed EA, Giama NH, Abdalla AO, Shaleh HM, Oseini AM, Ali HA, Ahmed F, Taha W, Ahmed Mohammed H, Cvinar J, Waaeys IA, Ali H, Allotey LK, Ali AO, Mohamed SA, Harmsen WS, Ahmmad EM, Bajwa NA, Afgarshe MD, Shire AM, Balls-Berry JE, Roberts LR. High prevalence of chronic viral hepatitis B and C in Minnesota Somalis contributes to rising hepatocellular carcinoma incidence. *World J Gastroenterol* 2022; 28(35): 5217-5229

URL: https://www.wjgnet.com/1007-9327/full/v28/i35/5217.htm

DOI: https://dx.doi.org/10.3748/wjg.v28.i35.5217

INTRODUCTION

Globally, liver cancer ranks 6th in cancer incidence and 4th in cancer mortality[1]. For many years, chronic hepatitis C virus (HCV) infection has been the most common risk factor for hepatocellular carcinoma (HCC) in the United States[2-6]. There is a high prevalence of chronic viral hepatitis in Asia and sub-Saharan Africa[7-11]. Partly due to immigration from high-prevalence countries in Africa and Asia,

hepatitis B virus (HBV) infection remains an important risk factor in the United States[12-15]. Consequently, HCC disproportionately affects individuals of African and Asian ancestry and Hispanic ethnicity[16,17]. Africa has the youngest median [interquartile range (IQR); range] age at HCC diagnosis worldwide [45 (35-57; 8-95)], increasing the burden of years of life lost from chronic viral hepatitis.

Minnesota's foreign-born population constitutes approximately 9% of the state population[18]. From 2008 to 2017, the Minnesota Department of Health reported an age-adjusted incidence rate of liver cancer of 22.4 per 100000 person-years among Black Minnesotans, a 4.3-fold higher rate than the rate of 5.2 per 100000 person-years among white, non-Hispanic Minnesotans[19]. A substantial proportion of Minnesota's Black population are recent African immigrants[18,20-22]. However, due to a general lack of awareness of viral hepatitis, Minnesota's most recent immigrants from Somalia have limited appreciation of their risk from chronic viral hepatitis and its associated complications[23].

To date, few studies have focused on chronic HBV and HCV infection and their sequelae among recent African immigrants to the United States. There is no population-based study of the rates of HBV and HCV infections among Somalis[20,24-28]. We previously conducted a clinic/hospital-based retrospective study of the rates of HBV and/or HCV infections in Somalis seen at Mayo Clinic from July 1996 to October 2009[29]. We found higher frequencies of chronic HBV (13.6%), prior exposure to HBV (55.5%), and chronic HCV (9.1%) in Somali Americans compared to 1.2%, 10.9%, and 2.2% respectively in non-Somali residents of Olmsted County (of whom 90% have European ancestry). Of 30 Somali HCC patients seen, 22 of 29 with available results (76%) were anti-HCV positive, while 5 of 28 with available results (18%) were hepatitis B surface antigen (HBsAg) positive. These results showed high rates of chronic HBV and HCV and revealed that HCV was a primary risk factor for HCC in Somalis[29]. Since clinic/hospital-based studies may overestimate true community disease prevalence, we tested for HBV and HCV in community-resident Somalis through a community-wide screening program.

MATERIALS AND METHODS

Study design

We performed a cross-sectional, community-wide screening study of Somali immigrant adults. Between November 2010 and December 2015, we used a community-based engagement research framework to offer free HBV and HCV screening to Somali immigrant adults living in Minnesota. Eligible individuals who self-identified as: (1) Of Somali descent; (2) ≥ 18 years of age; and (3) Resident in Minnesota received free HBV and HCV serological screening. Screening was provided for both foreign-born and United States-born participants. Study recruitment was carried out in the community. We partnered with three community-based health clinics with large Somali clienteles and faith-based establishments and charter schools, to which participants could come for enrollment and blood draws. In partnership with the Somali Health Advisory Committee (SHAC), a community advisory board based in Rochester and Minneapolis/St Paul, the research team provided educational seminars on viral hepatitis screening and liver disease. In addition, members of SHAC facilitated recruitment through word-of-mouth, advertisements, educational sessions and booths at various community events and health fairs in cities across Minnesota.

Study population

Individuals of Somali heritage who were at least 18 years of age were recruited to participate in the study. Participants provided written informed consent. At the completion of the study, participants received a $20 gift check (remuneration) mailed to their home address. Screening occurred at: (1) The Mayo Clinic Clinical Research and Trials Unit; (2) Community-based clinics; (3) A community-based health center; (4) Religious establishments (*i.e.* mosques); (5) Charter schools; or (6) At various community health-fairs. The study team consented and screened 779 participants aged 18 years to 91 years, of whom 49.9% (389) were male.

Ethical approval

The Mayo Clinic Institutional Review Board approved the study and study related materials including flyers and weekly community outreach program documentation. Study team members conducted outreach field recruitment to inform potential participants about the study in both English and Somali.

Serological tests

Blood samples were processed, stored at -80 °C, and tested for HBsAg, hepatitis B core antibody (HBcAb), hepatitis B surface antibody (HBsAb) and anti-HCV at the Mayo Clinic Department of Laboratory Medicine and Pathology. Participants were administered surveys either in English or in Somali, assessing their age, sex, country of birth, cultural practices and immigration patterns. The screening results were organized into 5 groups depending on the serological test results (Table 1). The first 4 groups defined the hepatitis B infection status, while the fifth reported hepatitis C antibody status. The chronic HBV infected group was defined as those who tested HBsAg positive, HBsAb

Table 1 Antibody and antigen biomarkers for hepatitis B and hepatitis C infections

	Chronic HBV	Resolved HBV	HBV vaccinated	HBV Susceptible	Chronic HCV
HBsAg	Pos	Neg	Neg	Neg	Pos/neg
HBcAb	Pos	Pos	Neg	Neg	Pos/neg
HBsAb	Neg	Pos/indeter/neg	Pos	Neg/indeter	Pos/neg
Anti-HCV	Neg/pos	Neg/pos	Neg/pos	Neg/pos	Pos

HBcAb: Hepatitis B core antibody; HBsAg: Hepatitis B surface antigen; HBsAb: Hepatitis B surface antibody; HBV: Hepatitis B virus; HCV: Hepatitis C virus; Indeter: Indeterminate; Neg: Negative; Pos: Positive.

negative, and HBcAb positive, regardless of anti-HCV status. The resolved HBV group, immune due to exposure to the live virus, was defined as participants who tested HBsAg negative, HBsAb positive and HBcAb positive, regardless of anti-HCV status. Combining the chronic HBV-infected group with the resolved HBV group gives the total number of persons exposed to live HBV infection. The vaccinated group was defined as those who tested HBsAg negative, HBsAb positive, and HBcAb negative, regardless of anti-HCV status. The HBV susceptible group was defined as those who tested HBsAg negative, HBsAb negative and HBcAb negative, regardless of anti-HCV status. Lastly, the chronic HCV infected group was defined as anyone who tested anti-HCV positive, regardless of HBsAg, HBcAb, or HBsAb status. We have previously shown that 93% of anti-HCV antibody-positive individuals in the Somali community also had measurable HCV RNA; thus, the rate of false positive anti-HCV antibody testing in this population is low[29]. Referrals for follow-up testing, health education, counseling, vaccination and treatment were provided to participants depending on their results.

Statistical methods

Descriptive statistics were computed to describe the study population. JMP (v.10; SAS Institute Inc., Cary, NC) was used for statistical analyses. Adjusted frequencies for viral hepatitis infection statuses were standardized using the 2010 United States Census and were stratified based on age and sex[30].

RESULTS

Characteristics of the study population

The study team consented and screened 779 participants aged 18 years to 91 years, of whom 49.9% (389) were male. This number represents 2.3% or 1 in 43 of the estimated 33208 Somalis aged 18 years to 84 years resident in Minnesota between 2013 and 2017[31]. The age distribution of the participants and the primary summary of rates are presented in Table 2.

Proportion of patients with HBV and HCV infections

The crude rates for each age and sex group are shown in Table 2, along with the age-adjusted rate for each group. Of the 779 Somali participants screened, 120 (15.4%) had chronic HBV (HBsAg+, HBcAb+, HBsAb-), and 271 (34.8%) were immune due to prior HBV infection (HBcAb+, HBsAg-, HBsAb+). In addition, a small subset of the patients had HBV and HCV co-infection (n = 5). The crude rates showed that, as is typical for HBV infection in Africa, many participants tested positive for chronic HBV infection by the age of 20. However, the converse was true for HCV, with most positive individuals being over 50 years. The age-adjusted rates for persons with chronic HBV were 12.5% and 11.6% for males and females, respectively. The age-adjusted rates for persons with resolved HBV, characteristic of prior exposure to HBV infection with spontaneous clearance, were 32.3% and 29.7% for males and females, respectively. For prior HBV exposure resulting in either chronic infection or spontaneous clearance, which measures all previous exposure to infectious HBV, the age-adjusted rates were 44.8% for males and 41.3% for females. Lastly, the age-adjusted positive rates for anti-HCV, the marker for HCV infection, were 6.7% for males and 5.7% for females. Of the 59 anti-HCV positive participants, 29 (49.2%) had follow-up testing for HCV RNA, and 28 (96.6%) of the 29 tested positive. This was consistent with the results of our previous retrospective study, in which 93% of anti-HCV-positive Somalis were HCV RNA positive. The most common HCV genotype was 4 (43%) followed by genotype 3 (14%).

Proportion of patients vaccinated or susceptible to HBV infections

Of the 779 Somali participants, 388 (49.8%) had not previously been exposed to HBV. Of these, 195 (25.0% of the total) tested positive for HBsAb only, consistent with immunity due to HBV vaccination. The remaining 193 (24.8%) tested negative for all HBV markers, indicating susceptibility to HBV

Table 2 Frequency of hepatitis B virus- and hepatitis C virus-positive test results in Community Recruited Minnesota Somali Residents

Age group (yr)	Chronic HBV infection		Previous HBV exposure including spontaneous clearance		Chronic HCV infection	
	HBsAg-positive/total males, *n*	HBsAg-positive/total females, *n*	HBcAb-positive/total males, *n*	HBcAb-positive/total females, *n*	Anti-HCV-positive/total males, *n*	Anti-HCV-positive/total females, *n*
≤ 20	0/8 (0)	0/9	1/8	2/9	0/8	0/9
21-30	10/89	6/74	29/89	12/74	3/89	0/74
31-40	20/92	12/92	24/92	29/92	3/92	2/92
41-50	12/72	5/82	32/72	27/82	5/72	1/82
51-60	12/50	10/64	23/50	24/64	3/50	3/64
61-70	6/35	11/40	20/35	16/40	5/35	10/40
> 70	6/43	10/29	20/43	12/29	17/43	7/29
Total	66/389	54/390	149/389	122/390	36/389	23/390
Age-adjusted frequency (per 1000 population)	125	116	323	297	67	57

HBcAb: Hepatitis B core antibody; HBsAg: Hepatitis B surface antigen; HBV: Hepatitis B virus; HCV: Hepatitis C virus.

(Table 3). Remarkably, of the 518 participants from this high prevalence community under age 50, 146 (28.2%) were unvaccinated and susceptible to HBV.

Age and sex group characteristics of HBV and HCV infections

Both age- and sex-specific rates showed differences. The highest proportion of HBsAg in Somalis was observed in females > 70 years of age (34.5%); in males, the highest proportion was in the 51-year-old to 60-year-old age group (24.0%) (Figure 1A). For HBcAb, the highest proportion of positivity for males was in the 61- year-old to 70-year-old age group (57.1%) and for females in the > 70-year-old group (41.4%) (Figure 1B). For anti-HCV, the highest proportion for males was > 70 years of age (39.5%), while the highest proportion for females was in the 61-year-old to 70-year-old age group (25.0%) (Figure 1C).

Follow-up and referral

After completing the serological tests, participants received screening results *via* telephone calls. Participants with positive HBsAg or anti-HCV were referred to their local medical care facility (University of Minnesota Gastroenterology Hepatology and Nutrition or Mayo Clinic Division of Gastroenterology and Hepatology) for subsequent management, surveillance and/or treatment. Participants who were HBsAg negative and anti-HBs negative were referred to their local primary care clinic (Gargar Clinic and Urgent Care or Axis Medical Center) to complete the HBV vaccination series.

Characteristics of participants who developed HCC

After serological tests confirmed positive HBV and/or HCV infection or susceptibility to HBV infection, patients were linked to care for treatment or monitoring of their viral hepatitis, as appropriate, or for HBV vaccination. They were encouraged to notify the study staff if they were diagnosed with advanced liver disease or HCC. Seven individuals were identified by review of the medical records or patient self-report to have HCC in follow-up after testing. Their ages ranged from 43 years to 83 years (mean 69.8 years; IQR 65.8, 76.8). Four were male (57%), and three (43%) were female. The most common etiology was HCV infection (n = 4; 57%); one patient had HBV infection (14%), one had non-alcoholic fatty liver disease without cirrhosis, and one had no known risk factor for HCC. Three of the 4 HCV HCC patients had cirrhosis (Table 4).

Due to the number of participants lost to follow-up, we do not have complete follow-up of the entire cohort of participants over the period and, therefore, were unable to calculate the exact incidence of HCC in the participants of this screening study. However, comparison to our previous retrospective hospital/clinic-based study, in which we found 30 Somali patients with HCC (2.5%) out of a total of 1218 patients tested for any chronic hepatitis markers, shows a lower incidence of 7 HCC cases (0.9%) of the 779 adults tested in this community-recruited cohort. This is not surprising, since the hospital/clinic-based cohort almost certainly had a selection bias for viral hepatitis or more severe chronic liver disease.

Table 3 Rates of hepatitis B virus vaccination and susceptibility in Community Recruited Minnesota Somali Residents

Age group (yr)	HBV vaccinated		HBV susceptible	
	HBV vaccinated[1]/total males, *n*	HBV vaccinated[1]/total females, *n*	HBV susceptible[2]/total males, *n*	HBV susceptible[2]/total females, *n*
≤ 20	4/8	4/9	3/8	3/9
21-30	27/89	37/74	23/89	19/74
31-40	22/92	23/92	26/92	28/92
41-50	15/72	19/82	13/72	31/82
51-60	8/50	13/64	7/50	17/64
61-70	4/35	5/40	5/35	8/40
> 70	10/43	4/29	7/43	3/29
Total	90/389	105/390	84/389	109/390
Age-adjusted frequency (per 1000 population)	299	305	253	282

[1]Vaccinated: Hepatitis B surface antigen negative; anti-HBc negative; anti-HBs positive.
[2]Susceptible: Hepatitis B surface antigen negative; anti-HBc negative; anti-HBc negative.
HBV: Hepatitis B virus.

Table 4 Characteristics of 7 Somali participants who developed hepatocellular carcinoma

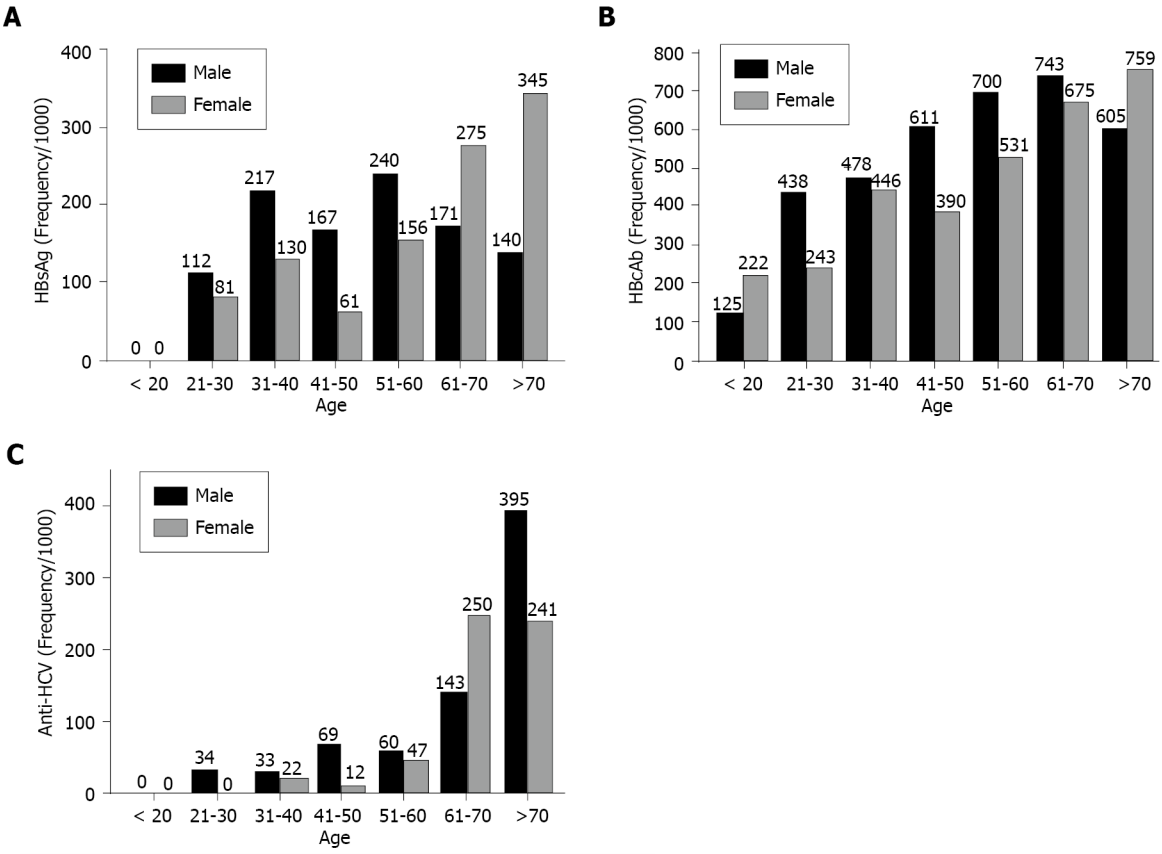
Patient no.	Age	Sex	Etiology	HCV genotype	Cirrhosis	MELD Score	Metastatic HCC	Portal hypertension	Fibrosis staging
1	69	Male	NAFLD	-	No	8	No	No	NR
2	65	Female	HCV	3	Yes	7	No	Yes	NR
3	76	Female	Unknown	-	No	7	No	No	NR
4	75	Male	HCV	4	No	7	Yes	No	2 to 3/4
5	77	Male	HCV	UTG	Yes	11	No	No	4
6	43	Male	HBV	-	No	7	Yes	No	NR
7	83	Female	HCV	UTG	Yes	6	No	No	3 to 4

UTG: Unable to genotype; NR: Not reported; NAFLD: Non-alcoholic fatty liver disease; HCV: Hepatitis C virus; HBV: Hepatitis B virus; MELD: Model for end-stage liver disease; HCC: Hepatocellular carcinoma.

The observed incidence of 7 HCCs in the cohort of 779 adults prospectively tested in this study, albeit with incomplete follow-up over a median of approximately 8 years, is estimated to be 112 per 100000 person-years or 0.11% per year risk of HCC in the entire cohort. This is almost certainly an overestimate as some of the cases may have had unrecognized HCC at the time of initial testing.

DISCUSSION

The primary goal of our study was to examine the prevalence of HBV and HCV viral infections in the immigrant Somali community residing in Minnesota. As a secondary goal, we also ascertained any cases of HCC that developed in study participants by voluntary notification and review of available medical records. This study is the first of its kind to report the results of community-wide screening for HBV and HCV in this immigrant population. We found that 15.4% of participants had chronic HBV infection compared to the estimated United States general population prevalence of 0.4%[32]. HCV prevalence was 7.6%, also significantly higher than the general United States population prevalence of HCV which is less than 2%[33]. In comparison to our previously published results, this prospective study determined that chronic HBV rates are higher than the frequency reported in the 2012 clinic/hospital-based retrospective study[29].



DOI: 10.3748/wjg.v28.i35.5217 **Copyright** ©The Author(s) 2022.

Figure 1 Frequency in Somali Patients Screening. A: Hepatitis B virus (HBV)-positive test results; B: Prior exposure of HBV test results; C: Hepatitis C virus-positive test results. HBcAb: Hepatitis B core antibody; HBsAg: Hepatitis B surface antigen; HCV: Hepatitis C virus.

Somalis in Minnesota are younger than the general population with a median age of 25 years compared to the general population median age of 37 years[34]. Therefore, surveillance for viral hepatitis is important for this community. Given the high prevalence of HBV and HCV infections in Somalia noted in prior studies, a significant number of Somali immigrants are likely to have chronic hepatitis and are at risk for HCC. Yang *et al*[35] reported that African-born individuals diagnosed with HCC in the United States, particularly those of West African ancestry, are diagnosed at a younger age. Most of these individuals have chronic HBV infection, which was acquired in the first few years of life, and it is recommended that HCC surveillance of this group begin at the age of 20 years[5]. The Somali immigrant community may be different; in addition to high rates of chronic HBV infection, there is also a high prevalence of chronic HCV infection, most likely acquired during adulthood. A multi-center, multi-national, retrospective observational cohort study that investigated the current clinical presentation of Africans with HCC showed that in Egypt, where chronic HCV is the major etiology of HCC, the median age of HCC onset was 58 years, compared to 46 years in eight other African countries with a predominance of HBV-induced HCC[6].

While the high level of chronic HBV infection in the immigrant Somali population suggests an elevated risk of maternal-to-child transmission and horizontal transmission of HBV between family members at an early age, it is important to note that about a third of all the individuals we screened had evidence of prior exposure to HBV infection that they had cleared spontaneously. This phenomenon occurs most commonly in adults exposed to HBV infection and suggests substantial transmission of HBV among adolescents and adults in the community. Risk factors associated with these infections need to be identified and addressed. Individuals from areas affected by conflict and displacement are at a greater risk of contracting infectious agents, such as viral hepatitis infections[36]. For instance, Khan *et al* [37] reported that internally displaced individuals have high levels of HBV and HCV infections. This may reflect the lack of basic health infrastructure and services in refugee camps and displaced communities.

Shire *et al*[29] showed an increased frequency of HBV and HCV among Somali patients seen in the hospital/clinic setting, which could potentially have been due to selection bias. However, our community-based screening study of Somali immigrants in Minnesota confirms high rates of chronic HBV and HCV infection rates among this population. The best outcomes for communities with high prevalence of chronic HBV and HCV infections have been shown in Japan and Taiwan, which have

comprehensive programs for screening all adults for chronic viral hepatitis and enrolling those at risk into surveillance programs for HCC. These programs have resulted in ≥ 70% of HCCs being detected at early stages when they are eligible for curative treatment. Consequently, the 5-year survival rate of patients diagnosed with HCC in these countries ranges from 50%-70%, substantially higher than the currently estimated rate of 15% in the United States[38]. Whether HCC surveillance decreases liver disease mortality is still controversial, but almost all international guidelines now recommend surveillance for HCC among high-risk patients using liver ultrasound performed every 6 mo with or without measurement of the serum alpha-fetoprotein[39-45]. There are active efforts underway to develop more sensitive and effective biomarker and imaging technologies for HCC surveillance. We are performing additional studies to assess the stage at diagnosis of HCC in the immigrant Somali community and discern any barriers or disparities in care related to chronic liver disease and HCC.

Furthermore, the observed incidence of 7 HCCs in the cohort of 779 adults prospectively tested in this study is estimated to be 112 per 100000 person-years or 0.11% per year risk of HCC in the entire cohort. This is almost certainly an overestimate as some of the cases may have had unrecognized HCC at the time of initial testing. By comparison, for the time period between 2012 and 2016, the age-standardized rates of liver cancer incidence in Minnesota were 5.7 per 100000 for Non-Hispanic Whites and 24.7 per 100000 for Blacks[46]. Since the total number of Somali adults aged 18-84 in Minnesota, estimated at 33208, represents approximately 23% of the 146020 adults of African descent aged 18-84 who are resident in Minnesota, the Somali immigrant community likely contributes substantially to the overall incidence of HCC in Minnesota[47,48].

The results of this study suggest a need to develop strategies to improve awareness of chronic hepatitis[49], increase screening for chronic HBV and HCV infections in the immigrant Somali community in the United States and promote hepatitis B vaccination in unvaccinated children and adults. These strategies could help prevent chronic liver disease and HCC, increase access to currently available treatments that suppress HBV viral load or cure HCV and substantially reduce the burden of hepatobiliary malignancies observed in Minnesota's non-Hispanic Black population[50-52]. Ahmed Mohammed *et al*[53] reported that visits to gastrointestinal/hepatologist specialists were linked to increased HCC surveillance in Minnesota residents, as compared to primary care practitioner visits. Given the limitations in access to specialist care, efforts to encourage HBV and HCV testing of immigrant Somalis in the primary care setting could improve the early diagnosis of chronic viral hepatitis and appropriate linkage to care.

Limitations

There are several limitations to this study. The first limitation is selection bias and this is due to the nature of the study design. However, through the use of community advisory boards, community-based organizations and clinics, we are confident that our data can be generalizable to the larger Somali community of Minnesota. Second, loss to follow-up was another limitation associated with this study, especially for those individuals who have developed liver cancer and associated co-morbidities. On the contrary, there are several strengths associated with this study. First, the implementation of community-engagement through health education and listening sessions have ensured participants are informed of the goals of the study in a culturally sensitive and responsive framework. Second, building strong partnerships with community-based organizations, charter schools and clinics were instrumental in the success of recruitment and dissemination of information.

CONCLUSION

Chronic HBV and HCV infections are prevalent among Somali immigrants in Minnesota and associated with high rates of HCC. Partnering with community stakeholders helped to improve recruitment rates and to spread awareness of the need for viral hepatitis screening. Community-wide screening is an effective way to identify and provide health education and linkage to care for individuals with or at risk for viral hepatitis. It is important to develop and implement culturally and linguistically acceptable viral hepatitis awareness programs in partnership with communities, in order to promote preventative vaccination, treatment of viral hepatitis and reduction of cancer risk.

ARTICLE HIGHLIGHTS

Research background

Somali immigrants come from regions of the world where viral hepatitis is endemic. Since the start of the Somali civil war in 1991, limited data is available on the impact of viral hepatitis in the community, especially those individuals in the diaspora.

Research motivation

The impetus of this project was communal outcry about community members succumbing to liver disease. In partnership with the community, our research team worked to assess the burden of viral hepatitis in Minnesota. Addressing this pressing communal matter, we were able to connect those who tested positive for hepatitis infections and/or were not vaccinated for hepatitis B virus (HBV) with the needed healthcare.

Research objectives

Our objective was to determine the prevalence of viral hepatitis infections within the community. This is significant because it laid the foundation to start conducting studies on host-viral interactions and the unique development of liver disease among this population. This is relevant to clinical practice because we can use this information to tailor screening practices and treatments for individuals from endemic regions which are historically under studied.

Research methods

In partnership with the community stakeholders, we conducted a prospective study using community-based participatory research from 2010 to 2015. We screened for viral hepatitis infections and reported the results back to the study participant. This is the first study of its kind to screen community based Somali immigrants in Minnesota at a large scale.

Research results

Viral hepatitis infections are a major under recognized disease within the Somali immigrant population. Age-adjusted prevalence rates are high and call for prioritizing responses from health agencies. This data will be used to lobby public health institutions to help address the unique needs of the Minnesota Somali population and for healthcare providers to implement programs to screen community members for both HBV and hepatitis C virus. Furthermore, the follow-up after the patients have enrolled into the study was quite difficult. We should consider effective methods to follow-up patients to assess the potential for development of liver disease sequelae.

Research conclusions

Although there were limitations to the study, we have learned that chronic viral hepatitis infection in the Somali community is high. Effective screening programs need to be implemented in order to prevent suffering and needless death. The use of community-based participatory research was a success and was the first of its kind with this community regarding a disease considered taboo. We will continue this partnership and expand research within this population historically under reported in clinical research.

Research perspectives

We will continue maintaining the partnership and will continue to understand the unique host-viral interactions. We have studies on immunoprofiling as well as examining the influence of the viral genome on liver disease progression. These studies will be used to improve the health of persons from this region of the world.

ACKNOWLEDGEMENTS

The authors would like to thank the study participants and their family members. In addition, the authors would like to thank the community partners who provided their community facilities to recruit, enroll, accrue and disseminate findings (*i.e.* Gargar Urgent Care and Clinic, Axis Medical Center, Masjed Abu Huraira, Masjed Al-Nur, Masjed Abubakr Al-Seddiq, and Mankato Mosque) and the Somali Health Advisory Committee, who ensured that we provided a culturally relevant and responsive manner in our efforts. In addition, the authors would like to thank Dr. Yu Wang, Dr. Chen-Chao Ma, the Mayo Clinic Clinical Trials and Research Unit and Lea Dacy for technical support.

FOOTNOTES

Author contributions: Mohamed EA, Giama NH, Abdalla AO, Shire AM, Shaleh HM, Oseini AM, Ali HA, Ahmed F, Taha W, Ahmed Mohammed H, Cvinar J, Waaeys IA, Ali H, Allotey LK, Ali AO, Mohamed SA, Harmsen WS, Ahmmad EM, Bajwa NA, and Afgarshe MD, Balls-Berry JE, and Roberts LR contributed to the study concept and design, acquisition of data, data analysis and interpretation of data; Mohamed EA, Giama NH, Abdalla AO, and Shire AM drafted the manuscript; Shaleh HM, Oseini AM, Ali HA, Ahmed F, Taha W, Ahmed Mohammed H, Cvinar J, Waaeys IA, Ali H, Allotey LK, Ali AO, Mohamed SA, Harmsen WS, Ahmmad EM, Bajwa NA, Afgarshe MD, Balls-Berry JE, and Roberts LR contributed to the critical revision of the manuscript; All authors contributed to manuscript

revision, read and approved the submitted version.

Supported by the Mayo Clinic Center for Clinical and Translational Science from the National Center for Advancing Translational Sciences (5UL1TR000135-10); the Mayo Clinic Hepatobiliary SPORE from the National Cancer Institute (5P50CA210964-04); the Mayo Clinic Center for Cell Signaling in Gastroenterology (5P30DK084567-14); and Gilead Sciences, Inc. (IN-US-174-0230).

Institutional review board statement: The study was reviewed and approved by the Mayo Clinic Institutional Review Board (19-001670).

Clinical trial registration statement: This study does not include any interventions and is not a randomized controlled trial. The study is registered on ClinicalTrials.Gov (NCT02366286).

Informed consent statement: Written informed consent was obtained from study subjects prior to enrollment.

Conflict-of-interest statement: All the authors report no relevant conflicts of interest for this article.

Data sharing statement: Technical appendix, statistical code, and dataset available from the corresponding author at Roberts.Lewis@mayo.edu. No additional data are available.

CONSORT 2010 statement: The authors have read the CONSORT 2010 Statement, and the manuscript was prepared and revised according to the CONSORT 2010 Statement.

Open-Access: This article is an open-access article that was selected by an in-house editor and fully peer-reviewed by external reviewers. It is distributed in accordance with the Creative Commons Attribution NonCommercial (CC BY-NC 4.0) license, which permits others to distribute, remix, adapt, build upon this work non-commercially, and license their derivative works on different terms, provided the original work is properly cited and the use is non-commercial. See: https://creativecommons.org/Licenses/by-nc/4.0/

Country/Territory of origin: United States

ORCID number: Essa A Mohamed 0000-0002-0307-6241; Nasra H Giama 0000-0003-2764-866X; Abubaker O Abdalla 0000-0002-7022-1074; Hassan M Shaleh 0000-0002-4698-4610; Abdul M Oseini 0000-0003-4079-9825; Hamdi A Ali 0000-0002-2671-0532; Fowsiyo Ahmed 0000-0002-0201-6706; Wesam Taha 0000-0002-6737-3739; Hager Ahmed Mohammed 0000-0002-3731-4332; Jessica Cvinar 0000-0003-4855-6908; Ibrahim A Waaeys 0000-0003-2086-5477; Hawa Ali 0000-0003-4667-5233; Loretta K Allotey 0000-0002-5734-8839; Abdiwahab O Ali 0000-0003-1692-9829; Safra A Mohamed 0000-0001-8408-0017; William S Harmsen 0000-0001-7134-5362; Eimad M Ahmmad 0000-0002-1120-2631; Numra A Bajwa 0000-0002-2727-8710; Mohamud D Afgarshe 0000-0001-9066-0237; Abdirashid M Shire 0000-0002-8216-9971; Joyce E Balls-Berry 0000-0003-3497-1115; Lewis R Roberts 0000-0001-7885-8574.

S-Editor: Wang JJ
L-Editor: Filipodia
P-Editor: Wang JJ

REFERENCES

1 **Global Burden of Disease Cancer Collaboration**, Fitzmaurice C, Allen C, Barber RM, Barregard L, Bhutta ZA, Brenner H, Dicker DJ, Chimed-Orchir O, Dandona R, Dandona L, Fleming T, Forouzanfar MH, Hancock J, Hay RJ, Hunter-Merrill R, Huynh C, Hosgood HD, Johnson CO, Jonas JB, Khubchandani J, Kumar GA, Kutz M, Lan Q, Larson HJ, Liang X, Lim SS, Lopez AD, MacIntyre MF, Marczak L, Marquez N, Mokdad AH, Pinho C, Pourmalek F, Salomon JA, Sanabria JR, Sandar L, Sartorius B, Schwartz SM, Shackelford KA, Shibuya K, Stanaway J, Steiner C, Sun J, Takahashi K, Vollset SE, Vos T, Wagner JA, Wang H, Westerman R, Zeeb H, Zoeckler L, Abd-Allah F, Ahmed MB, Alabed S, Alam NK, Aldhahri SF, Alem G, Alemayohu MA, Ali R, Al-Raddadi R, Amare A, Amoako Y, Artaman A, Asayesh H, Atnafu N, Awasthi A, Saleem HB, Barac A, Bedi N, Bensenor I, Berhane A, Bernabé E, Betsu B, Binagwaho A, Boneya D, Campos-Nonato I, Castañeda-Orjuela C, Catalá-López F, Chiang P, Chibueze C, Chitheer A, Choi JY, Cowie B, Damtew S, das Neves J, Dey S, Dharmaratne S, Dhillon P, Ding E, Driscoll T, Ekwueme D, Endries AY, Farvid M, Farzadfar F, Fernandes J, Fischer F, G/Hiwot TT, Gebru A, Gopalani S, Hailu A, Horino M, Horita N, Husseini A, Huybrechts I, Inoue M, Islami F, Jakovljevic M, James S, Javanbakht M, Jee SH, Kasaeian A, Kedir MS, Khader YS, Khang YH, Kim D, Leigh J, Linn S, Lunevicius R, El Razek HMA, Malekzadeh R, Malta DC, Marcenes W, Markos D, Melaku YA, Meles KG, Mendoza W, Mengiste DT, Meretoja TJ, Miller TR, Mohammad KA, Mohammadi A, Mohammed S, Moradi-Lakeh M, Nagel G, Nand D, Le Nguyen Q, Nolte S, Ogbo FA, Oladimeji KE, Oren E, Pa M, Park EK, Pereira DM, Plass D, Qorbani M, Radfar A, Rafay A, Rahman M, Rana SM, Søreide K, Satpathy M, Sawhney M, Sepanlou SG, Shaikh MA, She J, Shiue I, Shore HR, Shrime MG, So S, Soneji S, Stathopoulou V, Stroumpoulis K, Sufiyan MB, Sykes BL, Tabarés-Seisdedos R, Tadese F, Tedla BA, Tessema GA, Thakur JS, Tran BX, Ukwaja KN, Uzochukwu BSC, Vlassov VV, Weiderpass E, Wubshet Terefe M, Yebyo HG, Yimam HH, Yonemoto N, Younis MZ, Yu C, Zaidi Z, Zaki MES, Zenebe ZM, Murray CJL, Naghavi M. Global, Regional, and National Cancer Incidence, Mortality, Years of Life Lost, Years Lived With Disability, and Disability-

Adjusted Life-years for 32 Cancer Groups, 1990 to 2015: A Systematic Analysis for the Global Burden of Disease Study. *JAMA Oncol* 2017; **3**: 524-548 [PMID: 27918777 DOI: 10.1001/jamaoncol.2016.5688]

2 **McGlynn KA**, Petrick JL, El-Serag HB. Epidemiology of Hepatocellular Carcinoma. *Hepatology* 2021; **73** Suppl 1: 4-13 [PMID: 32319693 DOI: 10.1002/hep.31288]

3 **Yang JD**, Kim WR, Coelho R, Mettler TA, Benson JT, Sanderson SO, Therneau TM, Kim B, Roberts LR. Cirrhosis is present in most patients with hepatitis B and hepatocellular carcinoma. *Clin Gastroenterol Hepatol* 2011; **9**: 64-70 [PMID: 20831903 DOI: 10.1016/j.cgh.2010.08.019]

4 **Razavi H**. Global Epidemiology of Viral Hepatitis. *Gastroenterol Clin North Am* 2020; **49**: 179-189 [PMID: 32389357 DOI: 10.1016/j.gtc.2020.01.001]

5 **Yang JD**, Gyedu A, Afihene MY, Duduyemi BM, Micah E, Kingham TP, Nyirenda M, Nkansah AA, Bandoh S, Duguru MJ, Okeke EN, Kouakou-Lohoues MJ, Abdo A, Awuku YA, Ajayi AO, Omonisi AE, Ocama P, Malu AO, Mustapha S, Okonkwo U, Kooffreh-Ada M, Debes JD, Onyekwere C, Ekere F, Rufina I, Roberts LR; Africa Network for Gastrointestinal and Liver Diseases. Hepatocellular Carcinoma Occurs at an Earlier Age in Africans, Particularly in Association With Chronic Hepatitis B. *Am J Gastroenterol* 2015; **110**: 1629-1631 [PMID: 26618430 DOI: 10.1038/ajg.2015.289]

6 **Yang JD**, Mohamed EA, Aziz AO, Shousha HI, Hashem MB, Nabeel MM, Abdelmaksoud AH, Elbaz TM, Afihene MY, Duduyemi BM, Ayawin JP, Gyedu A, Lohouès-Kouacou MJ, Ndam AW, Moustafa EF, Hassany SM, Moussa AM, Ugiagbe RA, Omuemu CE, Anthony R, Palmer D, Nyanga AF, Malu AO, Obekpa S, Abdo AE, Siddig AI, Mudawi HM, Okonkwo U, Kooffreh-Ada M, Awuku YA, Nartey YA, Abbew ET, Awuku NA, Otegbayo JA, Akande KO, Desalegn HM, Omonisi AE, Ajayi AO, Okeke EN, Duguru MJ, Davwar PM, Okorie MC, Mustapha S, Debes JD, Ocama P, Lesi OA, Odeghe E, Bello R, Onyekwere C, Ekere F, Igetei R, Mah'moud MA, Addissie B, Ali HM, Gores GJ, Topazian MD, Roberts LR; Africa Network for Gastrointestinal and Liver Diseases. Characteristics, management, and outcomes of patients with hepatocellular carcinoma in Africa: a multicountry observational study from the Africa Liver Cancer Consortium. *Lancet Gastroenterol Hepatol* 2017; **2**: 103-111 [PMID: 28403980 DOI: 10.1016/S2468-1253(16)30161-3]

7 **Hassan MA**, Kim WR, Li R, Smith CI, Fried MW, Sterling RK, Ghany MG, Wahed AS, Ganova-Raeva LM, Roberts LR, Lok ASF; Hepatitis B Research Network. Characteristics of US-Born Versus Foreign-Born Americans of African Descent With Chronic Hepatitis B. *Am J Epidemiol* 2017; **186**: 356-366 [PMID: 28525625 DOI: 10.1093/aje/kwx064]

8 **Sonderup MW**, Afihene M, Ally R, Apica B, Awuku Y, Cunha L, Dusheiko G, Gogela N, Lohouès-Kouacou MJ, Lam P, Lesi O, Mbaye PS, Musabeyezu E, Musau B, Ojo O, Rwegasha J, Scholz B, Shewaye AB, Tzeuton C, Kassianides C, Spearman CW; Gastroenterology and Hepatology Association of sub-Saharan Africa (GHASSA). Hepatitis C in sub-Saharan Africa: the current status and recommendations for achieving elimination by 2030. *Lancet Gastroenterol Hepatol* 2017; **2**: 910-919 [PMID: 29132760 DOI: 10.1016/S2468-1253(17)30249-2]

9 **Spearman CW**, Afihene M, Ally R, Apica B, Awuku Y, Cunha L, Dusheiko G, Gogela N, Kassianides C, Kew M, Lam P, Lesi O, Lohouès-Kouacou MJ, Mbaye PS, Musabeyezu E, Musau B, Ojo O, Rwegasha J, Scholz B, Shewaye AB, Tzeuton C, Sonderup MW; Gastroenterology and Hepatology Association of sub-Saharan Africa (GHASSA). Hepatitis B in sub-Saharan Africa: strategies to achieve the 2030 elimination targets. *Lancet Gastroenterol Hepatol* 2017; **2**: 900-909 [PMID: 29132759 DOI: 10.1016/S2468-1253(17)30295-9]

10 **Karuru JW**, Lule GN, Joshi M, Anzala O. Prevalence of HCV and HCV/HIV co-infection among in-patients at the Kenyatta National Hospital. *East Afr Med J* 2005; **82**: 170-172 [PMID: 16122083 DOI: 10.4314/eamj.v82i4.9276]

11 **Karuru JW**, Lule GN, Joshi M, Anzala O. Prevalence of HCV and HIV/HCV co-infection among volunteer blood donors and VCT clients. *East Afr Med J* 2005; **82**: 166-169 [PMID: 16122082 DOI: 10.4314/eamj.v82i4.9275]

12 **Tramuto F**, Maida CM, Colomba GM, Di Carlo P, Mazzola G, Li Vecchi V, Affronti M, Montalto G, Vitale F. Occult hepatitis B infection in the immigrant population of Sicily, Italy. *J Immigr Minor Health* 2013; **15**: 725-731 [PMID: 22875279 DOI: 10.1007/s10903-012-9699-y]

13 **Moore MS**, Bocour A, Tran OC, Qiao B, Schymura MJ, Laraque F, Winters A. Effect of Hepatocellular Carcinoma on Mortality Among Individuals With Hepatitis B or Hepatitis C Infection in New York City, 2001-2012. *Open Forum Infect Dis* 2018; **5**: ofy144 [PMID: 30019001 DOI: 10.1093/ofid/ofy144]

14 **Rossi C**, Shrier I, Marshall L, Cnossen S, Schwartzman K, Klein MB, Schwarzer G, Greenaway C. Seroprevalence of chronic hepatitis B virus infection and prior immunity in immigrants and refugees: a systematic review and meta-analysis. *PLoS One* 2012; **7**: e44611 [PMID: 22957088 DOI: 10.1371/journal.pone.0044611]

15 **Yang JD**, Hainaut P, Gores GJ, Amadou A, Plymoth A, Roberts LR. A global view of hepatocellular carcinoma: trends, risk, prevention and management. *Nat Rev Gastroenterol Hepatol* 2019; **16**: 589-604 [PMID: 31439937 DOI: 10.1038/s41575-019-0186-y]

16 **Ha J**, Yan M, Aguilar M, Bhuket T, Tana MM, Liu B, Gish RG, Wong RJ. Race/ethnicity-specific disparities in cancer incidence, burden of disease, and overall survival among patients with hepatocellular carcinoma in the United States. *Cancer* 2016; **122**: 2512-2523 [PMID: 27195481 DOI: 10.1002/cncr.30103]

17 **Roberts H**, Kruszon-Moran D, Ly KN, Hughes E, Iqbal K, Jiles RB, Holmberg SD. Prevalence of chronic hepatitis B virus (HBV) infection in U.S. households: National Health and Nutrition Examination Survey (NHANES), 1988-2012. *Hepatology* 2016; **63**: 388-397 [PMID: 26251317 DOI: 10.1002/hep.28109]

18 **American Immigration Council**. Immigrants in Minnesota. [cited 15 December 2021]. Available from: https://www.americanimmigrationcouncil.org/research/immigrants-in-minnesota

19 **Minnesota Department of Health**. Liver cancer is increasing in Minnesota. [cited 20 December 2021]. Available from: https://data.web.health.state.mn.us/cancer_liver

20 **Ugwu C**, Varkey P, Bagniewski S, Lesnick T. Sero-epidemiology of hepatitis B among new refugees to Minnesota. *J Immigr Minor Health* 2008; **10**: 469-474 [PMID: 18066661 DOI: 10.1007/s10903-007-9111-5]

21 **Adair R**, Nwaneri O. Communicable disease in African immigrants in Minneapolis. *Arch Intern Med* 1999; **159**: 83-85 [PMID: 9892335 DOI: 10.1001/archinte.159.1.83]

22 **Kim WR**, Benson JT, Therneau TM, Torgerson HA, Yawn BP, Melton LJ 3rd. Changing epidemiology of hepatitis B in a U.S. community. *Hepatology* 2004; **39**: 811-816 [PMID: 14999701 DOI: 10.1002/hep.20098]

23 **Mohamed EA**, Giama NH, Shaleh HM, Kerandi L, Oseini AM, Ahmed Mohammed H, Kerandi H, Allotey LK, Waaeys IA, Ali HA, Ali HM, Mohamed SA, Yang JD, Gaga WO, Tamire LL, Windissa A, Patten CA, Balls-Berry JE, Roberts LR. Knowledge, Attitudes, and Behaviors of Viral Hepatitis Among Recent African Immigrants in the United States: A Community Based Participatory Research Qualitative Study. *Front Public Health* 2020; **8**: 25 [PMID: 32211358 DOI: 10.3389/fpubh.2020.00025]

24 **Bile K**, Mohamud O, Aden C, Isse A, Norder H, Nilsson L, Magnius L. The risk for hepatitis A, B, and C at two institutions for children in Somalia with different socioeconomic conditions. *Am J Trop Med Hyg* 1992; **47**: 357-364 [PMID: 1524149 DOI: 10.4269/ajtmh.1992.47.357]

25 **Bile KM**, Abdirahman M, Aden C, Norder H, Magnius L, Lindberg G, Nilsson LH. Minor role of hepatitis B virus in the causation of chronic liver disease in Somalia indicated by a case-control study. *Trans R Soc Trop Med Hyg* 1991; **85**: 104-108 [PMID: 1712517 DOI: 10.1016/0035-9203(91)90177-z]

26 **Bile KM**, Aden A, Lindberg G, Nilsson L, Lidman K, Norder H, Magnius L. Epidemiology of hepatitis B in Somalia: inference from a cross-sectional survey of serological markers. *Trans R Soc Trop Med Hyg* 1987; **81**: 824-828 [PMID: 3502433 DOI: 10.1016/0035-9203(87)90043-5]

27 **Sebastiani A**, Aceti A, Paparo BS, Pennica A, Ilardi I, Bile K, Mohamud OM. Hepatitis B virus circulation in three different villages of Somalia. *Trans R Soc Trop Med Hyg* 1985; **79**: 162-164 [PMID: 4002285 DOI: 10.1016/0035-9203(85)90323-2]

28 **Hassan-Kadle MA**, Osman MS, Ogurtsov PP. Epidemiology of viral hepatitis in Somalia: Systematic review and meta-analysis study. *World J Gastroenterol* 2018; **24**: 3927-3957 [PMID: 30228786 DOI: 10.3748/wjg.v24.i34.3927]

29 **Shire AM**, Sandhu DS, Kaiya JK, Oseini AM, Yang JD, Chaiteerakij R, Mettler TA, Giama NH, Roberts RO, Therneau TM, Petersen GM, Knutson KL, Roberts LR. Viral hepatitis among Somali immigrants in Minnesota: association of hepatitis C with hepatocellular carcinoma. *Mayo Clin Proc* 2012; **87**: 17-24 [PMID: 22212964 DOI: 10.1016/j.mayocp.2011.08.001]

30 **Howden LM**, Meyer JA. Age and Sex Composition: 2010. In: Bureau USC, editor. Economics and Statistics Administration. United States: Census Bureau, 2011

31 **Minnesota Compass**. Cultural Communities Methodology. [cited 16 December 2021]. Available from: https://www.mncompass.org/topics/demographics/cultural-communities/methodology

32 **Kim WR**. Epidemiology of hepatitis B in the United States. *Hepatology* 2009; **49**: S28-34 [PMID: 19399791 DOI: 10.1002/hep.22975]

33 **Moosavy SH**, Davoodian P, Nazarnezhad MA, Nejatizaheh A, Eftekhar E, Mahboobi H. Epidemiology, transmission, diagnosis, and outcome of Hepatitis C virus infection. *Electron Physician* 2017; **9**: 5646-5656 [PMID: 29238510 DOI: 10.19082/5646]

34 US Department of Commerce. 2020. [cited 16 December 2021]. Available from: https://www.commerce.gov/

35 **Yang JD**, Altekruse SF, Nguyen MH, Gores GJ, Roberts LR. Impact of country of birth on age at the time of diagnosis of hepatocellular carcinoma in the United States. *Cancer* 2017; **123**: 81-89 [PMID: 27571320 DOI: 10.1002/cncr.30246]

36 **Ogunwobi OO**, Dibba O, Zhu L, Ilboudo A, Tan Y, Fraser MA, Ma GX. Hepatitis B Virus Screening and Vaccination in First-generation African Immigrants: A Pilot Study. *J Community Health* 2019; **44**: 1037-1043 [PMID: 31123877 DOI: 10.1007/s10900-019-00668-z]

37 **Khan A**, Qazi J. Risk factors and molecular epidemiology of HBV and HCV in internally displaced persons (IDPs) of North Waziristan Agency, Pakistan. *J Pak Med Assoc* 2018; **68**: 165-169 [PMID: 29479087]

38 **Park JW**, Chen M, Colombo M, Roberts LR, Schwartz M, Chen PJ, Kudo M, Johnson P, Wagner S, Orsini LS, Sherman M. Global patterns of hepatocellular carcinoma management from diagnosis to death: the BRIDGE Study. *Liver Int* 2015; **35**: 2155-2166 [PMID: 25752327 DOI: 10.1111/liv.12818]

39 **Omata M**, Cheng AL, Kokudo N, Kudo M, Lee JM, Jia J, Tateishi R, Han KH, Chawla YK, Shiina S, Jafri W, Payawal DA, Ohki T, Ogasawara S, Chen PJ, Lesmana CRA, Lesmana LA, Gani RA, Obi S, Dokmeci AK, Sarin SK. Asia-Pacific clinical practice guidelines on the management of hepatocellular carcinoma: a 2017 update. *Hepatol Int* 2017; **11**: 317-370 [PMID: 28620797 DOI: 10.1007/s12072-017-9799-9]

40 **Bruix J**, Sherman M; American Association for the Study of Liver Diseases. Management of hepatocellular carcinoma: an update. *Hepatology* 2011; **53**: 1020-1022 [PMID: 21374666 DOI: 10.1002/hep.24199]

41 **Song P**, Tobe RG, Inagaki Y, Kokudo N, Hasegawa K, Sugawara Y, Tang W. The management of hepatocellular carcinoma around the world: a comparison of guidelines from 2001 to 2011. *Liver Int* 2012; **32**: 1053-1063 [PMID: 22432445 DOI: 10.1111/j.1478-3231.2012.02792.x]

42 **European Association for the Study of the Liver**. ; European Association for the Study of the Liver. EASL Clinical Practice Guidelines: Management of hepatocellular carcinoma. *J Hepatol* 2018; **69**: 182-236 [PMID: 29628281 DOI: 10.1016/j.jhep.2018.03.019]

43 **Johnson P**, Berhane S, Kagebayashi C, Satomura S, Teng M, Fox R, Yeo W, Mo F, Lai P, Chan SL, Tada T, Toyoda H, Kumada T. Impact of disease stage and aetiology on survival in hepatocellular carcinoma: implications for surveillance. *Br J Cancer* 2017; **116**: 441-447 [PMID: 28081537 DOI: 10.1038/bjc.2016.422]

44 **Zhang BH**, Yang BH, Tang ZY. Randomized controlled trial of screening for hepatocellular carcinoma. *J Cancer Res Clin Oncol* 2004; **130**: 417-422 [PMID: 15042359 DOI: 10.1007/s00432-004-0552-0]

45 **Mittal S**, Kanwal F, Ying J, Chung R, Sada YH, Temple S, Davila JA, El-Serag HB. Effectiveness of surveillance for hepatocellular carcinoma in clinical practice: A United States cohort. *J Hepatol* 2016; **65**: 1148-1154 [PMID: 27476765 DOI: 10.1016/j.jhep.2016.07.025]

46 **Minnesota Department of Health**. Liver and Intrahepatic Bile Duct Cancer. [cited 20 December 2021]. Available from: https://www.health.state.mn.us/data/mcrs/docs/livercancerfff.pdf

47 **Minnesota Compass**. Somali population. 2020. [cited 20 December 2021]. Available from: https://www.mncompass.org/topics/demographics/cultural-communities/somali

48 **Minnesota Compass**. African American population. 2020. [cited 20 December 2021]. Available from: https://www.mncompass.org/topics/demographics/cultural-communities/african-american

49 **Emeasoba EU**, Omarufilo F, Bosah JN, Sigal SH. Breaking down barriers for hepatitis B screening in the Bronx West African community through education in collaboration with faith-based organizations: A cohort study. *Lancet Regional Health - Americas* 2022; **7**: 100120 [DOI: 10.1016/j.lana.2021.100120]

50 **Minnesota Department of Health**. Cancer in Minnesota 1988-2017. [cited 16 December 2021]. Available from: https://www.health.state.mn.us/data/mcrs/docs/2021bienrpt.pdf

51 **Cohen C**, Moraras K, Jackson M, Kamischke M, Gish RG, Brosgart CL, Toy M, Hutton D, Block TM, Wang S, So S. Letter to the editor: Importance of universal screening for chronic hepatitis B infection in adults in the United States. *Hepatology* 2022; **75**: 1062-1063 [PMID: 34951931 DOI: 10.1002/hep.32304]

52 **Ramrakhiani NS**, Chen VL, Le M, Yeo YH, Barnett SD, Waljee AK, Zhu J, Nguyen MH. Optimizing hepatitis B virus screening in the United States using a simple demographics-based model. *Hepatology* 2022; **75**: 430-437 [PMID: 34496066 DOI: 10.1002/hep.32142]

53 **Ahmed Mohammed HA**, Yang JD, Giama NH, Choi J, Ali HM, Mara KC, Harmsen WS, Wiesner RH, Leise MD, Therneau TM, Roberts LR. Factors Influencing Surveillance for Hepatocellular Carcinoma in Patients with Liver Cirrhosis. *Liver Cancer* 2017; **6**: 126-136 [PMID: 28275579 DOI: 10.1159/000450833]

World Journal of Gastroenterology

Submit a Manuscript: https://www.f6publishing.com

World J Gastroenterol 2022 September 21; 28(35): 5230-5232

DOI: 10.3748/wjg.v28.i35.5230

ISSN 1007-9327 (print) ISSN 2219-2840 (online)

LETTER TO THE EDITOR

Urotensin II level is elevated in inflammatory bowel disease patients

Yan Zhang, Guo-Xun Chen

Specialty type: Gastroenterology and hepatology

Provenance and peer review: Unsolicited article; Externally peer reviewed.

Peer-review model: Single blind

Peer-review report's scientific quality classification

Grade A (Excellent): 0
Grade B (Very good): B
Grade C (Good): C, C
Grade D (Fair): 0
Grade E (Poor): 0

P-Reviewer: Tajra JBM, Brazil; Wen XL, China

Received: January 27, 2022
Peer-review started: January 27, 2022
First decision: April 10, 2022
Revised: April 13, 2022
Accepted: September 1, 2022
Article in press: September 1, 2022
Published online: September 21, 2022

Yan Zhang, Department of Gastroenterology, Affiliated Puren Hospital of Wuhan University of Science and Technology, Wuhan 430081, Hubei Province, China

Guo-Xun Chen, Department of Nutrition, The University of Tennessee, Knoxville, TN 37996, United States

Corresponding author: Guo-Xun Chen, PhD, Associate Professor, Research Scientist, Department of Nutrition, The University of Tennessee, Room 229, Jessie Harris Building, 1512 West Cumberland Avenue, Knoxville, TN 37996, United States. gchen6@utk.edu

Abstract

It was reported that the urotensin II (U-II) level in inflammatory bowel disease (IBD) patients are significantly higher than in controls. To provide future guidance for the management of cardiovascular risk factors in IBD patients, the sample size of the current study appears to be limited, and more clinical samples to compare U-II levels in IBD patients and controls are needed. This will clarify the possible roles of inflammation factors and related signaling pathways (like EPK1/2, NF-κB and Rho/ROCK) in the pathophysiology of IBD. Therefore, large multicenter studies should be done to confirm the findings and underlying mechanisms in the future.

Key Words: Inflammatory bowel disease; Urotensin II; Inflammatory factors; High sensitivity C reactive peptide

©The Author(s) 2022. Published by Baishideng Publishing Group Inc. All rights reserved.

Core Tip: An observational report showed that the level of urotensin II (U-II) in inflammatory bowel disease (IBD) patients was significantly increased compared with that in controls. The authors also reported that blood U-II level was positively correlated with high-sensitivity C-reactive protein, and severe endoscopic features of the disease. This study provides us with a new role of U-II in IBD, which warrants larger, multicenter clinical and basic studies to determine the mechanisms by which U-II triggers inflammatory responses and activates signaling pathways (EPK1/2, NF-κB and Rho/ROCK).

Citation: Zhang Y, Chen GX. Urotensin II level is elevated in inflammatory bowel disease patients. *World J Gastroenterol* 2022; 28(35): 5230-5232
URL: https://www.wjgnet.com/1007-9327/full/v28/i35/5230.htm
DOI: https://dx.doi.org/10.3748/wjg.v28.i35.5230

TO THE EDITOR

We read the observational study reported by Alicic *et al*[1], who have convincingly shown the role of elevated urotensin II (U-II) level in patients with inflammatory bowel disease (IBD). IBD comprising Crohn's disease (CD) and ulcerative colitis (UC) is a multifactorial condition of relapsing chronic inflammation in the gastrointestinal tract with an unpredictable course[2]. In addition, extraintestinal manifestations of IBD cardiovascular risk factors occur frequently and contribute to morbidity and reduced quality of life[3-5].

U-II is a peptide ligand that acts as a potent vasoconstrictor, which was originally discovered four decades ago. The vasoconstriction activity of U-II is 10-fold more potent than that of endothelin-1[6]. Most studies of U-II have been conducted to understand its role in the development of cardiovascular diseases[7]. A growing number of scholars have recognized the links of U-II levels with malignant lesions associated with the liver, pancreas and gut[8]. Whether U-II participates in the initiation and progress of IBD has always intrigued contemporary gastroenterologists. This observational study reported the potential relationship of U-II and IBD, which provides the field with new knowledge and attracted our attention.

Alicic *et al*[1] compared the blood level of U-II in IBD patients and healthy controls, and investigated the association of U-II levels with the anthropometric, clinical and biochemical parameters. The study included 50 adult patients with prediagnosed IBD (24 with UC and 26 with CD) and 50 healthy, age- and gender-matched controls. IBD patients had significantly higher U-II level than control subjects had. Significant positive correlations between serum U-II level and high-sensitivity C-reactive protein (hsCRP) level, UC Endoscopic Index of Severity and Simple Endoscopic Score for CD were observed. Whether these clinical data imply the involvement of U-II in the inflammatory responses and disease outcomes of IBD patients remains to be confirmed.

The action of U-II is mediated by U-II receptor (UTR). UTR is also called GPR14, which is a G-protein-linked receptor[9]. Both U-II and UTR can be found in various cells of the cardiovascular, pulmonary and central nervous systems, kidneys, and other metabolic organs and tissues. The biding of U-II as a ligand activates UTR, which mobilizes calcium in the cytoplasm, induces proliferation of smooth myocytes, and triggers inflammation[10,11]. As expected, the level of inflammatory factor hsCRP in IBD patients is significantly higher than that in healthy controls.

The study by Alicic *et al*[1] is the first clinical study to investigate blood UII level in both UC and CD patients. However, limitations can be seen, which could bolster the authors' conclusions if resolved: (1) This single center study only had 50 subjects each in the IBD and control groups. If more institutions were included in a multicenter investigation and more patients were recruited, the conclusions would become more convincing and relevant. Therefore, large multicenter studies are anticipated in the future; and (2) the results showed that elevation of blood U-II level was associated with disease development and progression, and attributed to the inflammation mediated by hsCRP. However, the levels of other inflammatory factors were not measured (*e.g.*, interleukin-6, interleukin-8, and tumor necrosis factor-α). Their level and involvement in the elevated U-II concentration and inflammatory responses in those patients should be clarified. Regarding the mechanisms, it is possible that U-II as a ligand activates pathways that stimulate the release of inflammatory effectors, such as the cytokines listed above. These cytokines may potently activate signaling pathways consisting of EPK1/2, NF-κB and Rho/ROCK, which regulate a variety of downstream inflammatory responses[12-14]. Whether those cytokines and U-II act against each other or in concert to form a system influencing the host inflammation status remains to be answered. In the future, gastroenterologists should investigate how U-II interacts with other inflammatory mediators, and how U-II modifies those signaling pathways to potentiate IBD severity in various *in vivo* and *in vitro* systems. In so doing, more results could be collected and analyzed, which are needed to form theoretical and practical evidence to guide prevention and treatment of cardiovascular complications in IBD. Additionally, antagonists to the UTR activation system could also be developed, which may counteract any detrimental effects due to increased level of U-II in patients with IBD.

FOOTNOTES

Author contributions: Zhang Y and Chen GX read the commented article, wrote the letter, and revised the letter according to the reviewers' comments; all authors have read and approved the final version of this manuscript.

Conflict-of-interest statement: There are no conflicts of interest to report.

Open-Access: This article is an open-access article that was selected by an in-house editor and fully peer-reviewed by external reviewers. It is distributed in accordance with the Creative Commons Attribution NonCommercial (CC BY-NC 4.0) license, which permits others to distribute, remix, adapt, build upon this work non-commercially, and license their derivative works on different terms, provided the original work is properly cited and the use is non-commercial. See: https://creativecommons.org/Licenses/by-nc/4.0/

Country/Territory of origin: United States

ORCID number: Yan Zhang 0000-0002-0620-5803; Guo-Xun Chen 0000-0001-6226-4050.

S-Editor: Chen YL
L-Editor: Kerr C
P-Editor: Chen YL

REFERENCES

1 **Alicic D**, Martinovic D, Rusic D, Zivkovic PM, Tadin Hadjina I, Vilovic M, Kumric M, Tokic D, Supe-Domic D, Lupi-Ferandin S, Bozic J. Urotensin II levels in patients with inflammatory bowel disease. *World J Gastroenterol* 2021; **27**: 6142-6153 [PMID: 34629825 DOI: 10.3748/wjg.v27.i36.6142]
2 **Zhang YZ**, Li YY. Inflammatory bowel disease: pathogenesis. *World J Gastroenterol* 2014; **20**: 91-99 [PMID: 24415861 DOI: 10.3748/wjg.v20.i1.91]
3 **Bigeh A**, Sanchez A, Maestas C, Gulati M. Inflammatory bowel disease and the risk for cardiovascular disease: Does all inflammation lead to heart disease? *Trends Cardiovasc Med* 2020; **30**: 463-469 [PMID: 31653485 DOI: 10.1016/j.tcm.2019.10.001]
4 **Singh S**, Kullo IJ, Pardi DS, Loftus EV Jr. Epidemiology, risk factors and management of cardiovascular diseases in IBD. *Nat Rev Gastroenterol Hepatol* 2015; **12**: 26-35 [PMID: 25446727 DOI: 10.1038/nrgastro.2014.202]
5 **Zivkovic PM**, Matetic A, Tadin Hadjina I, Rusic D, Vilovic M, Supe-Domic D, Borovac JA, Mudnic I, Tonkic A, Bozic J. Serum Catestatin Levels and Arterial Stiffness Parameters Are Increased in Patients with Inflammatory Bowel Disease. *J Clin Med* 2020; **9** [PMID: 32110996 DOI: 10.3390/jcm9030628]
6 **Svistunov AA**, Tarasov VV, Shakhmardanova SA, Sologova SS, Bagaturiya ET, Chubarev VN, Galenko-Yaroshevsky PA, Avila-Rodriguez MF, Barreto GE, Aliev G. Urotensin II: Molecular Mechanisms of Biological Activity. *Curr Protein Pept Sci* 2018; **19**: 924-934 [PMID: 28875851 DOI: 10.2174/1389203718666170829162335]
7 **Pereira-Castro J**, Brás-Silva C, Fontes-Sousa AP. Novel insights into the role of urotensin II in cardiovascular disease. *Drug Discov Today* 2019; **24**: 2170-2180 [PMID: 31430542 DOI: 10.1016/j.drudis.2019.08.005]
8 **Zappavigna S**, Abate M, Cossu AM, Lusa S, Campani V, Scotti L, Luce A, Yousif AM, Merlino F, Grieco P, De Rosa G, Caraglia M. Urotensin-II-Targeted Liposomes as a New Drug Delivery System towards Prostate and Colon Cancer Cells. *J Oncol* 2019; **2019**: 9293560 [PMID: 31929800 DOI: 10.1155/2019/9293560]
9 **Ross B**, McKendy K, Giaid A. Role of urotensin II in health and disease. *Am J Physiol Regul Integr Comp Physiol* 2010; **298**: R1156-R1172 [PMID: 20421634 DOI: 10.1152/ajpregu.00706.2009]
10 **Sun SL**, Liu LM. Urotensin II: an inflammatory cytokine. *J Endocrinol* 2019 [PMID: 30601760 DOI: 10.1530/joe-18-0505]
11 **Liang DY**, Liu LM, Ye CG, Zhao L, Yu FP, Gao DY, Wang YY, Yang ZW. Inhibition of UII/UTR system relieves acute inflammation of liver through preventing activation of NF-κB pathway in ALF mice. *PLoS One* 2014; **8**: e64895 [PMID: 23755157 DOI: 10.1371/journal.pone.0064895]
12 **Yang Y**, Zhang J, Chen X, Wu T, Xu X, Cao G, Li H, Li Y. UII/GPR14 is involved in NF-κB-mediated colonic inflammation *in vivo* and in vitro. *Oncol Rep* 2016; **36**: 2800-2806 [PMID: 27600191 DOI: 10.3892/or.2016.5069]
13 **Li J**, Zhao PP, Hao T, Wang D, Wang Y, Zhu YZ, Wu YQ, Zhou CH. Urotensin II inhibitor eases neuropathic pain by suppressing the JNK/NF-κB pathway. *J Endocrinol* 2017; **232**: 165-174 [PMID: 27895138 DOI: 10.1530/JOE-16-0255]
14 **Lu D**, Peng F, Li J, Zhao J, Ye X, Li B, Ding W. Urotensin II promotes secretion of LTB_4 through 5-lipoxygenase *via* the UT-ROS-Akt pathway in RAW264.7 macrophages. *Arch Med Sci* 2019; **15**: 1065-1072 [PMID: 31360201 DOI: 10.5114/aoms.2019.85197]

World Journal of Gastroenterology

Submit a Manuscript: https://www.f6publishing.com

World J Gastroenterol 2022 September 21; 28(35): 5233-5236

DOI: 10.3748/wjg.v28.i35.5233

ISSN 1007-9327 (print) ISSN 2219-2840 (online)

LETTER TO THE EDITOR

Hepatitis B viral infection and role of alcohol

Manuel Muro, Aurelia Collados-Ros, Isabel Legaz

Specialty type: Toxicology

Provenance and peer review: Unsolicited article; Externally peer reviewed.

Peer-review model: Single blind

Peer-review report's scientific quality classification

Grade A (Excellent): 0
Grade B (Very good): B, B, B, B
Grade C (Good): C
Grade D (Fair): 0
Grade E (Poor): 0

P-Reviewer: Elfayoumy KN, Egypt; Sahin TT, Turkey; Sira AM, Egypt; Tanaka Y, Japan; Yin GQ, China

Received: May 11, 2022
Peer-review started: May 11, 2022
First decision: June 27, 2022
Revised: July 1, 2022
Accepted: September 1, 2022
Article in press: September 1, 2022
Published online: September 21, 2022

Manuel Muro, Department of Immunology, Clinical University Hospital Virgen de la Arrixaca-IMIB (Murcian Institute of Biomedical Investigation), Murcia 30120, Spain

Aurelia Collados-Ros, Isabel Legaz, Department of Legal and Forensic Medicine, Biomedical Research Institute (IMIB), Regional Campus of International Excellence "Campus Mare Nostrum", Faculty of Medicine, University of Murcia (Spain), Universidad de Murcia, Espinardo 30100, Murcia, Spain

Corresponding author: Isabel Legaz, PhD, Senior Lecturer, Department of Legal and Forensic Medicine, Biomedical Research Institute (IMIB), Regional Campus of International Excellence "Campus Mare Nostrum", Faculty of Medicine, University of Murcia (Spain), Universidad de Murcia, Campus de Espinardo, Facultad de Medicina, Espinardo 30100, Murcia, Spain. isalegaz@um.es

Abstract

End-stage liver disease is frequently caused by hepatitis B virus (HBV) and alcohol consumption. Notably, the mechanism by which alcohol affects the course of HBV-associated liver disease is unknown, and additional research is needed in this area. A reduced immunological response, oxidative stress, endoplasmic reticulum stress, Golgi apparatus stress, and enhanced HBV replication are a few potential causes.

Key Words: Hepatitis B virus; Alcohol; Hepatocarcinoma; Immunity; Liver disease

©The Author(s) 2022. Published by Baishideng Publishing Group Inc. All rights reserved.

Core Tip: In this letter to the editor, we comment on and discuss the combined effects of alcohol consumption and hepatitis B virus (HBV) infection in the progression of liver diseases. In the worst evolution of end-stage liver pathologies, a concordant clinical relationship between alcohol consumption and HBV infection starts to be revealed. There are many potential causes, but some might include increased viral replication, oxidative stress on cellular organelles, and weakened immune responses. Understanding these precepts will open new avenues in managing and treating these patients.

Citation: Muro M, Collados-Ros A, Legaz I. Hepatitis B viral infection and role of alcohol. *World J Gastroenterol* 2022; 28(35): 5233-5236
URL: https://www.wjgnet.com/1007-9327/full/v28/i35/5233.htm
DOI: https://dx.doi.org/10.3748/wjg.v28.i35.5233

TO THE EDITOR

We have read with great attention and special interest the review by Ganesan and collaborators entitled "Role of alcohol in the pathogenesis of hepatitis B virus (HBV) infection"[1]. The authors examine the potential mechanisms by which alcohol results in an increased risk of HBV-associated liver disease. HBV infection combined with alcohol usage accelerates the progression of liver damage[2,3], primarily hepatocellular carcinoma, the fifth most common type of cancer. The mechanisms behind these adverse effects of alcohol in HBV-positive patients are unknown. Chronic alcohol consumption changes the architecture of the liver and reduces its functional capability.

The effects of alcohol metabolism on protein function, DNA, immune system changes, and oxidative stress impact both hepatocytes and other liver cells. Because the liver is the central location for the replication of hepatotropic viruses (HCV and HBV), ethanol metabolism is linked to viral hepatitis[4,5].

Regarding the immune system, the early stages of viral infections result in the generation of interferon (IFN) type 1 and the activation of natural killer (NK) cells. IFN type 1 and other antiviral cytokines, which HBV induces, are not particularly efficient. According to various investigations of persistent HBV infection, NK cells exhibit varying alterations in quantity, phenotype, and/or function. HBV-infected hepatocytes are cleared more quickly when activated NK cells are present. However, when chronic infection progresses, the tolerogenic actions of liver ligands and cytokines can inhibit both NK and T cells, limiting their antiviral activity[6,7]. According to reports, alcohol has an impact on NK cell antiviral activity during acute HBV infection[8].

The large, medium, and small forms of HBsAg, as well as the hepatitis B virus core antigen (HBcAg) and hepatitis B e antigen (HBeAg), can all be targeted by polyclonal antibodies produced by B cells in chronic HBV-infected patients[9]. During acute HBV infection, distinct antibodies are produced against the HBV surface antigen and the HBV core antigen. Anti-HBc is a marker for current or past infection, whereas anti-HBs signifies sickness remission[10]. Alcohol may reduce the number of B cells, decreasing HBV antibodies by weakening B cell immunological responses[11].

The B cell response to acute HBV infection is less well understood, but HBV-specific CD4+ and CD8+ T cell-mediated responses usually become detectable as HBV replication increases exponentially[12,13]. Numerous studies have demonstrated a substantial correlation and link between acute hepatitis, CD4+ T cell response, and viral shedding[14-16].

Cytotoxic T lymphocytes (CTLs) that express particular T cell receptors are in charge of eliminating HBV-infected hepatocytes in HBV infection. CTL activation may be diminished, which thus prevents clearance of HBV-infected hepatocytes when the viral peptide/MHC class I complex display in HBV-infected hepatocytes is compromised[17]. The body's capacity to eliminate HBV may be diminished due to ethanol consumption, allowing the virus to persist and eventually produce end-stage liver disorders such as cirrhosis and hepatocellular carcinoma.

The immune response in the liver is meticulously regulated by signals from the commensal microbiota in the gut. Additionally, drinking alcohol causes the close connections between intestinal epithelial cells to weaken, allowing germs to enter the bloodstream and cause an infection[18-20].

However, hepatic metabolism of ethanol may increase the production of reactive oxygen species (ROS), principally hydrogen peroxide and superoxide anion[21].

Recent studies have shown that the ethanol metabolite acetaldehyde can suppress proteasome activity, which is essential for producing antigenic peptides for MHC class I-restricted antigen presentation and can also cause lipid peroxidation, the formation of protein adducts with 4-hydroxynonenal and malonaldehydes (oxidative stress markers). This reduces the HBV-MHC peptide class I complex exposure to CTL identification and restricts the removal of infected cells[1], which causes HBV persistence and ensuing end-stage liver disease. HBV and alcohol addiction stresses the endoplasmic reticulum (ER), and these two stresses may have additive or synergistic effects. Alcohol has been shown to synergistically cause ER stress when other substances, the environment, or a viral illness are present [22]. The increase in HBV DNA, HbsAg, and HBx protein caused by alcohol may be the mechanism by which alcohol induces ER stress in HBV infection. A strained Golgi apparatus frequently matches a stressed ER.

Further study in this area is required since the interaction of alcohol misuse and HBV infection can be harmful. Future research should examine how alcohol metabolism affects innate IFN responses and IFN-stimulated gene activation throughout the pathogenesis of HBV infection, as well as if IFN therapy might be an effective treatment option for alcoholics with HBV infection.

Additionally, there is a significant gap between the role of alcohol in controlling B cell function and its contribution to the pathogenesis of HBV, necessitating further research in this area. To fully comprehend the processes of alcohol-induced impairment and investigate the effects of ethanol on MHC class II presentation, which is mainly catalyzed by effector cells, additional studies examining the relationship between alcohol and HBV adaptive immune response are required.

FOOTNOTES

Author contributions: Muro M and Legaz I designed the research; Collados-Ros A performed the research; Legaz I, Collados-Ros A, and Muro M wrote the letter; Muro M and Legaz I revised the letter.

Conflict-of-interest statement: There are no conflicts of interest to report.

Open-Access: This article is an open-access article that was selected by an in-house editor and fully peer-reviewed by external reviewers. It is distributed in accordance with the Creative Commons Attribution NonCommercial (CC BY-NC 4.0) license, which permits others to distribute, remix, adapt, build upon this work non-commercially, and license their derivative works on different terms, provided the original work is properly cited and the use is non-commercial. See: https://creativecommons.org/Licenses/by-nc/4.0/

Country/Territory of origin: Spain

ORCID number: Manuel Muro 0000-0001-9987-0994; Isabel Legaz 0000-0002-1140-4313.

S-Editor: Chen YL
L-Editor: Wang TQ
P-Editor: Chen YL

REFERENCES

1 **Ganesan M**, Eikenberry A, Poluektova LY, Kharbanda KK, Osna NA. Role of alcohol in pathogenesis of hepatitis B virus infection. *World J Gastroenterol* 2020; **26**: 883-903 [PMID: 32206001 DOI: 10.3748/wjg.v26.i9.883]
2 **El-Serag HB**. Hepatocellular carcinoma. *N Engl J Med* 2011; **365**: 1118-1127 [PMID: 21992124 DOI: 10.1056/NEJMra1001683]
3 **Sayiner M**, Golabi P, Younossi ZM. Disease Burden of Hepatocellular Carcinoma: A Global Perspective. *Dig Dis Sci* 2019; **64**: 910-917 [PMID: 30835028 DOI: 10.1007/s10620-019-05537-2]
4 **Novo-Veleiro I**, Alvela-Suárez L, Chamorro AJ, González-Sarmiento R, Laso FJ, Marcos M. Alcoholic liver disease and hepatitis C virus infection. *World J Gastroenterol* 2016; **22**: 1411-1420 [PMID: 26819510 DOI: 10.3748/wjg.v22.i4.141]
5 **Shoreibah M**, Anand BS, Singal AK. Alcoholic hepatitis and concomitant hepatitis C virus infection. *World J Gastroenterol* 2014; **20**: 11929-11934 [PMID: 25232227 DOI: 10.3748/wjg.v20.i34.11929]
6 **Maini MK**, Peppa D. NK cells: a double-edged sword in chronic hepatitis B virus infection. *Front Immunol* 2013; **4**: 57 [PMID: 23459859 DOI: 10.3389/fimmu.2013.00057]
7 **Peppa D**, Micco L, Javaid A, Kennedy PT, Schurich A, Dunn C, Pallant C, Ellis G, Khanna P, Dusheiko G, Gilson RJ, Maini MK. Blockade of immunosuppressive cytokines restores NK cell antiviral function in chronic hepatitis B virus infection. *PLoS Pathog* 2010; **6**: e1001227 [PMID: 21187913 DOI: 10.1371/journal.ppat.1001227]
8 **Zhang P**, Bagby GJ, Happel KI, Raasch CE, Nelson S. Alcohol abuse, immunosuppression, and pulmonary infection. *Curr Drug Abuse Rev* 2008; **1**: 56-67 [PMID: 19630706 DOI: 10.2174/1874473710801010056]
9 **Gerlich WH**. Medical virology of hepatitis B: how it began and where we are now. *Virol J* 2013; **10**: 239 [PMID: 23870415 DOI: 10.1186/1743-422X-10-239]
10 **Hoofnagle JH**, Gerety RJ, Barker LF. Antibody to hepatitis-B-virus core in man. *Lancet* 1973; **2**: 869-873 [PMID: 4126916 DOI: 10.1016/s0140-6736(73)92004-7]
11 **Pasala S**, Barr T, Messaoudi I. Impact of Alcohol Abuse on the Adaptive Immune System. *Alcohol Res* 2015; **37**: 185-197 [PMID: 26695744]
12 **Fisicaro P**, Valdatta C, Boni C, Massari M, Mori C, Zerbini A, Orlandini A, Sacchelli L, Missale G, Ferrari C. Early kinetics of innate and adaptive immune responses during hepatitis B virus infection. *Gut* 2009; **58**: 974-982 [PMID: 19201769 DOI: 10.1136/gut.2008.163600]
13 **Webster GJ**, Reignat S, Maini MK, Whalley SA, Ogg GS, King A, Brown D, Amlot PL, Williams R, Vergani D, Dusheiko GM, Bertoletti A. Incubation phase of acute hepatitis B in man: dynamic of cellular immune mechanisms. *Hepatology* 2000; **32**: 1117-1124 [PMID: 11050064 DOI: 10.1053/jhep.2000.19324]
14 **Ferrari C**, Penna A, Bertoletti A, Valli A, Antoni AD, Giuberti T, Cavalli A, Petit MA, Fiaccadori F. Cellular immune response to hepatitis B virus-encoded antigens in acute and chronic hepatitis B virus infection. *J Immunol* 1990; **145**: 3442-3449 [PMID: 2230128]
15 **Jung MC**, Spengler U, Schraut W, Hoffmann R, Zachoval R, Eisenburg J, Eichenlaub D, Riethmüller G, Paumgartner G, Ziegler-Heitbrock HW. Hepatitis B virus antigen-specific T-cell activation in patients with acute and chronic hepatitis B. *J Hepatol* 1991; **13**: 310-317 [PMID: 1808224 DOI: 10.1016/0168-8278(91)90074-l]

16 **Tsui LV**, Guidotti LG, Ishikawa T, Chisari FV. Posttranscriptional clearance of hepatitis B virus RNA by cytotoxic T lymphocyte-activated hepatocytes. *Proc Natl Acad Sci U S A* 1995; **92**: 12398-12402 [PMID: 8618909 DOI: 10.1073/pnas.92.26.12398]
17 **Ganesan M**, Krutik VM, Makarov E, Mathews S, Kharbanda KK, Poluektova LY, Casey CA, Osna NA. Acetaldehyde suppresses the display of HBV-MHC class I complexes on HBV-expressing hepatocytes. *Am J Physiol Gastrointest Liver Physiol* 2019; **317**: G127-G140 [PMID: 31141391 DOI: 10.1152/ajpgi.00064.2019]
18 **Bishehsari F**, Magno E, Swanson G, Desai V, Voigt RM, Forsyth CB, Keshavarzian A. Alcohol and Gut-Derived Inflammation. *Alcohol Res* 2017; **38**: 163-171 [PMID: 28988571]
19 **Lowe PP**, Gyongyosi B, Satishchandran A, Iracheta-Vellve A, Cho Y, Ambade A, Szabo G. Reduced gut microbiome protects from alcohol-induced neuroinflammation and alters intestinal and brain inflammasome expression. *J Neuroinflammation* 2018; **15**: 298 [PMID: 30368255 DOI: 10.1186/s12974-018-1328-9]
20 **Meroni M**, Longo M, Dongiovanni P. Alcohol or Gut Microbiota: Who Is the Guilty? *Int J Mol Sci* 2019; **20** [PMID: 31540133 DOI: 10.3390/ijms20184568]
21 **Iida-Ueno A**, Enomoto M, Tamori A, Kawada N. Hepatitis B virus infection and alcohol consumption. *World J Gastroenterol* 2017; **23**: 2651-2659 [PMID: 28487602 DOI: 10.3748/wjg.v23.i15.2651]
22 **Ji C**. Mechanisms of alcohol-induced endoplasmic reticulum stress and organ injuries. *Biochem Res Int* 2012; **2012**: 216450 [PMID: 22110961 DOI: 10.1155/2012/216450]

World Journal of Gastroenterology

Submit a Manuscript: https://www.f6publishing.com

World J Gastroenterol 2022 September 21; 28(35): 5237-5239

DOI: 10.3748/wjg.v28.i35.5237

ISSN 1007-9327 (print) ISSN 2219-2840 (online)

CORRECTION

Correction to "Inhibiting heme oxygenase-1 attenuates rat liver fibrosis by removing iron accumulation"

Qiu-Ming Wang, Jian-Ling Du, Zhi-Jun Duan, Shi-Bin Guo, Xiao-Yu Sun, Zhen Liu

Specialty type: Gastroenterology and hepatology

Provenance and peer review: Unsolicited article; Externally peer reviewed.

Peer-review model: Single blind

Peer-review report's scientific quality classification

Grade A (Excellent): A
Grade B (Very good): B
Grade C (Good): 0
Grade D (Fair): 0
Grade E (Poor): 0

P-Reviewer: Buechler C, Germany; Gorrell MD, Australia

Received: February 24, 2022
Peer-review started: February 24, 2022
First decision: June 11, 2022
Revised: July 4, 2022
Accepted: August 16, 2022
Article in press: August 16, 2022
Published online: September 21, 2022

Qiu-Ming Wang, Zhi-Jun Duan, Shi-Bin Guo, Xiao-Yu Sun, Zhen Liu, Department of Gastroenterology, The First Affiliated Hospital of Dalian Medical University, Dalian 116011, Liaoning Province, China

Jian-Ling Du, Department of Endocrinology, The First Affiliated Hospital of Dalian Medical University, Dalian 116011, Liaoning Province, China

Corresponding author: Zhi-Jun Duan, MD, Chief Doctor, Department of Gastroenterology, The First Affiliated Hospital of Dalian Medical University, Dalian 116011, Liaoning Province, China. cathydoctor@sina.com

Abstract

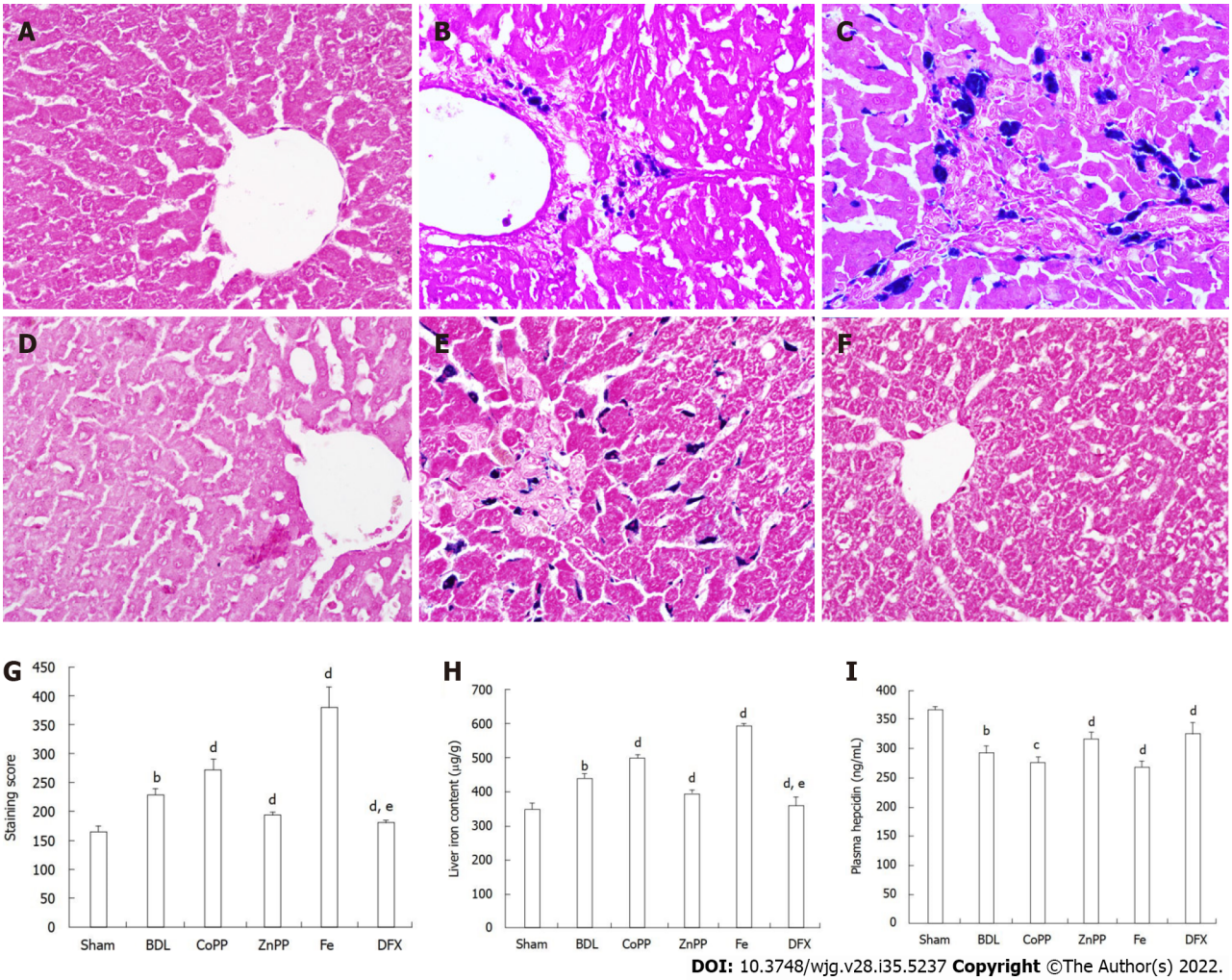
We found a mistake in Figure 6. Panels A (Sham group) and F (DFX group) (180 degrees rotated) is same images. We have replaced the incorrect images (Panels F) with the correct Figure. This error does not change the meaning of the picture or the conclusion of the manuscript. We apologize for our unintentional mistakes, which caused great inconvenience.

Key Words: Heme oxygenase-1; Hepcidin; Iron accumulation; Oxidative stress; Portal vein pressure; Carboxyhemoglobin; Bile duct ligation

©The Author(s) 2022. Published by Baishideng Publishing Group Inc. All rights reserved.

Core Tip: We found a mistake in Figure 6. Panels A (Sham group) and F (DFX group) (180 degrees rotated) is same images. We have replaced the incorrect images (Panels F) with the correct Figure. This error does not change the meaning of the picture or the conclusion of the manuscript. We apologize for our unintentional mistakes, which caused great inconvenience.

Citation: Wang QM, Du JL, Duan ZJ, Guo SB, Sun XY, Liu Z. Correction to "Inhibiting heme oxygenase-1 attenuates rat liver fibrosis by removing iron accumulation". *World J Gastroenterol* 2022; 28(35): 5237-5239
URL: https://www.wjgnet.com/1007-9327/full/v28/i35/5237.htm
DOI: https://dx.doi.org/10.3748/wjg.v28.i35.5237



DOI: 10.3748/wjg.v28.i35.5237 **Copyright** ©The Author(s) 2022.

Figure 1 erl's Prussian blue staining, levels of hepcidin, serum and liver iron. A: No iron accumulated in the Sham group; B: A small amount of iron mainly accumulated on Kupffer cells in the bile duct ligation (BDL) group; C: Much more iron accumulation was found in interlobular and macrophagocytes in the cobalt protoporphyrin (CoPP) group; D and F: Almost no iron accumulation was detected in the zinc protoporphyrin (ZnPP) group and deferoxamine (DFX) group; E: Massive iron accumulation was observed in the Fe group; G and H: There were no differences in the hepatic and serum iron content of these six groups; I: Plasma hepcidin also was measured by enzyme-linked immuno sorbent assay (magnification × 400). Values are expressed as mean ± SE (n = 6). $^{b}P < 0.01$ *vs* Sham group; $^{c}P < 0.05$, $^{d}P < 0.01$ *vs* BDL group; $^{e}P < 0.05$ *vs* ZnPP group.

TO THE EDITOR

We found a mistake in Figure 6. Panels A (Sham group) and F (DFX group) (180 degrees rotated) is same images. We have replaced the incorrect images (Panels F) with the correct Figure 1. We only revised the incorrect figure, and the Manuscript NO: 75978 don't need to revise[1].

FOOTNOTES

Author contributions: Wang QM and Du JL performed the experiments, analyzed the data and wrote the manuscript; Duan ZJ and Wang QM designed the experiments; Wang QM performed the experiments, analyzed the data and wrote the manuscript; Duan ZJ and Guo SB revised the manuscript.

Conflict-of-interest statement: We declare that we have no conflict of interest.

Open-Access: This article is an open-access article that was selected by an in-house editor and fully peer-reviewed by external reviewers. It is distributed in accordance with the Creative Commons Attribution NonCommercial (CC BY-NC 4.0) license, which permits others to distribute, remix, adapt, build upon this work non-commercially, and license their derivative works on different terms, provided the original work is properly cited and the use is non-commercial. See: https://creativecommons.org/Licenses/by-nc/4.0/

Country/Territory of origin: China

ORCID number: Qiu-Ming Wang 0000-0003-1262-6361; Jian-Ling Du 0000-0003-4782-1052; Zhi-Jun Duan 0000-0001-7976-4959; Shi-Bin Guo 0000-0003-2971-3859; Xiao-Yu Sun 0000-0002-4138-6005; Zhen Liu 0000-0002-9899-8184.

S-Editor: Liu JH
L-Editor: A
P-Editor: Liu JH

REFERENCES

1 **Wang QM**, Du JL, Duan ZJ, Guo SB, Sun XY, Liu Z. Inhibiting heme oxygenase-1 attenuates rat liver fibrosis by removing iron accumulation. *World J Gastroenterol* 2013; **19**: 2921-2934 [PMID: 23704825 DOI: 10.3748/wjg.v19.i19.2921]



Published by **Baishideng Publishing Group Inc**
7041 Koll Center Parkway, Suite 160, Pleasanton, CA 94566, USA
Telephone: +1-925-3991568
E-mail: bpgoffice@wjgnet.com
Help Desk: https://www.f6publishing.com/helpdesk
https://www.wjgnet.com



© 2022 Baishideng Publishing Group Inc. All rights reserved.

ISSN 1007-9327 (print)
ISSN 2219-2840 (online)

World Journal of *Gastroenterology*

World J Gastroenterol 2022 September 28; 28(36): 5240-5382



Published by Baishideng Publishing Group Inc

World Journal of Gastroenterology

Contents

Weekly Volume 28 Number 36 September 28, 2022

EDITORIAL

5240 SARS-CoV-2 and the pancreas: What do we know about acute pancreatitis in COVID-19 positive patients?

Brisinda G, Chiarello MM, Tropeano G, Altieri G, Puccioni C, Fransvea P, Bianchi V

REVIEW

5250 Deciphering the role of transforming growth factor-beta 1 as a diagnostic-prognostic-therapeutic candidate against hepatocellular carcinoma

Devan AR, Pavithran K, Nair B, Murali M, Nath LR

5265 P2X7 receptor as the regulator of T-cell function in intestinal barrier disruption

Jiang ZF, Wu W, Hu HB, Li ZY, Zhong M, Zhang L

5280 Liver-specific drug delivery platforms: Applications for the treatment of alcohol-associated liver disease

Warner JB, Guenthner SC, Hardesty JE, McClain CJ, Warner DR, Kirpich IA

MINIREVIEWS

5300 Histopathological assessment of the microscopic activity in inflammatory bowel diseases: What are we looking for?

Fabian O, Bajer L

ORIGINAL ARTICLE

Basic Study

5313 Esophageal magnetic compression anastomosis in dogs

Xu XH, Lv Y, Liu SQ, Cui XH, Suo RY

Retrospective Cohort Study

5324 Impact of sarcopenia on tumor response and survival outcomes in patients with hepatocellular carcinoma treated by trans-arterial (chemo)-embolization

Roth G, Teyssier Y, Benhamou M, Abousalihac M, Caruso S, Sengel C, Seror O, Ghelfi J, Seigneurin A, Ganne-Carrie N, Gigante E, Blaise L, Sutter O, Decaens T, Nault JC

5338 Machine learning-based gray-level co-occurrence matrix signature for predicting lymph node metastasis in undifferentiated-type early gastric cancer

Wei X, Yan XJ, Guo YY, Zhang J, Wang GR, Fayyaz A, Yu J

Observational Study

5351 Early extrahepatic recurrence as a pivotal factor for survival after hepatocellular carcinoma resection: A 15-year observational study

Yoon JH, Choi SK, Cho SB, Kim HJ, Ko YS, Jun CH

5364 Atherogenic index of plasma combined with waist circumference and body mass index to predict metabolic-associated fatty liver disease

Duan SJ, Ren ZY, Zheng T, Peng HY, Niu ZH, Xia H, Chen JL, Zhou YC, Wang RR, Yao SK

LETTER TO THE EDITOR

5380 Nonalcoholic steatohepatitis and hepatocellular carcinoma: Beyond the boundaries of the liver

Gupta T

ABOUT COVER

Editorial Board of *World Journal of Gastroenterology*, Akihiro Tamori, MD, PhD, Professor, Department of Hepatology, Osaka City University Graduate School of Medicine, Osaka 5458585, Japan. tamori-a@omu.ac.jp

AIMS AND SCOPE

The primary aim of *World Journal of Gastroenterology* (*WJG*, *World J Gastroenterol*) is to provide scholars and readers from various fields of gastroenterology and hepatology with a platform to publish high-quality basic and clinical research articles and communicate their research findings online. *WJG* mainly publishes articles reporting research results and findings obtained in the field of gastroenterology and hepatology and covering a wide range of topics including gastroenterology, hepatology, gastrointestinal endoscopy, gastrointestinal surgery, gastrointestinal oncology, and pediatric gastroenterology.

INDEXING/ABSTRACTING

The *WJG* is now abstracted and indexed in Science Citation Index Expanded (SCIE, also known as SciSearch®), Current Contents/Clinical Medicine, Journal Citation Reports, Index Medicus, MEDLINE, PubMed, PubMed Central, Scopus, Reference Citation Analysis, China National Knowledge Infrastructure, China Science and Technology Journal Database, and Superstar Journals Database. The 2022 edition of Journal Citation Reports® cites the 2021 impact factor (IF) for *WJG* as 5.374; IF without journal self cites: 5.187; 5-year IF: 5.715; Journal Citation Indicator: 0.84; Ranking: 31 among 93 journals in gastroenterology and hepatology; and Quartile category: Q2. The *WJG*'s CiteScore for 2021 is 8.1 and Scopus CiteScore rank 2021: Gastroenterology is 18/149.

RESPONSIBLE EDITORS FOR THIS ISSUE

Production Editor: *Yu-Xi Chen*; **Production Department Director:** *Xu Guo*; **Editorial Office Director:** *Jia-Ru Fan*.

NAME OF JOURNAL
World Journal of Gastroenterology

ISSN
ISSN 1007-9327 (print) ISSN 2219-2840 (online)

LAUNCH DATE
October 1, 1995

FREQUENCY
Weekly

EDITORS-IN-CHIEF
Andrzej S Tarnawski

EDITORIAL BOARD MEMBERS
http://www.wjgnet.com/1007-9327/editorialboard.htm

PUBLICATION DATE
September 28, 2022

COPYRIGHT
© 2022 Baishideng Publishing Group Inc

INSTRUCTIONS TO AUTHORS
https://www.wjgnet.com/bpg/gerinfo/204

GUIDELINES FOR ETHICS DOCUMENTS
https://www.wjgnet.com/bpg/GerInfo/287

GUIDELINES FOR NON-NATIVE SPEAKERS OF ENGLISH
https://www.wjgnet.com/bpg/gerinfo/240

PUBLICATION ETHICS
https://www.wjgnet.com/bpg/GerInfo/288

PUBLICATION MISCONDUCT
https://www.wjgnet.com/bpg/gerinfo/208

ARTICLE PROCESSING CHARGE
https://www.wjgnet.com/bpg/gerinfo/242

STEPS FOR SUBMITTING MANUSCRIPTS
https://www.wjgnet.com/bpg/GerInfo/239

ONLINE SUBMISSION
https://www.f6publishing.com

© 2022 Baishideng Publishing Group Inc. All rights reserved. 7041 Koll Center Parkway, Suite 160, Pleasanton, CA 94566, USA
E-mail: bpgoffice@wjgnet.com https://www.wjgnet.com

World Journal of Gastroenterology

Submit a Manuscript: https://www.f6publishing.com

World J Gastroenterol 2022 September 28; 28(36): 5240-5249

DOI: 10.3748/wjg.v28.i36.5240

ISSN 1007-9327 (print) ISSN 2219-2840 (online)

EDITORIAL

SARS-CoV-2 and the pancreas: What do we know about acute pancreatitis in COVID-19 positive patients?

Giuseppe Brisinda, Maria Michela Chiarello, Giuseppe Tropeano, Gaia Altieri, Caterina Puccioni, Pietro Fransvea, Valentina Bianchi

Specialty type: Gastroenterology and hepatology

Provenance and peer review: Unsolicited article; Externally peer reviewed.

Peer-review model: Single blind

Peer-review report's scientific quality classification

Grade A (Excellent): A
Grade B (Very good): B
Grade C (Good): 0
Grade D (Fair): 0
Grade E (Poor): 0

P-Reviewer: Cai J, China; Gonçalves TN, Portugal

Received: May 17, 2022
Peer-review started: May 17, 2022
First decision: June 19, 2022
Revised: June 23, 2022
Accepted: September 8, 2022
Article in press: September 8, 2022
Published online: September 28, 2022

Giuseppe Brisinda, Department of Medical and Surgical Sciences, Fondazione Policlinico Universitario A Gemelli IRCCS, Rome 00168, Italy

Giuseppe Brisinda, Department of Medicine and Surgery, Università Cattolica del Sacro Cuore, Rome 00168, Italy

Maria Michela Chiarello, Department of Surgery, Azienda Sanitaria Provinciale di Cosenza, Cosenza 87100, Italy

Giuseppe Tropeano, Gaia Altieri, Caterina Puccioni, Pietro Fransvea, Valentina Bianchi, Emergency Surgery and Trauma Center, Fondazione Policlinico Universitario A Gemelli IRCCS, Rome 00168, Italy

Corresponding author: Giuseppe Brisinda, MD, Professor, Surgeon, Department of Medical and Surgical Sciences, Fondazione Policlinico Universitario A Gemelli IRCCS, Largo Agostino Gemelli 8, Rome 00168, Italy. gbrisin@tin.it

Abstract

Severe acute respiratory syndrome coronavirus 2 (SARS-CoV-2) can cause pancreatic damage, both directly to the pancreas *via* angiotensin-converting enzyme 2 receptors (the transmembrane proteins required for SARS-CoV-2 entry, which are highly expressed by pancreatic cells) and indirectly through locoregional vasculitis and thrombosis. Despite that, there is no clear evidence that SARS-CoV-2 is an etiological agent of acute pancreatitis. Acute pancreatitis in coronavirus disease 2019 (COVID-19) positive patients often recognizes biliary or alcoholic etiology. The prevalence of acute pancreatitis in COVID-19 positive patients is not exactly known. However, COVID-19 positive patients with acute pancreatitis have a higher mortality and an increased risk of intensive care unit admission and necrosis compared to COVID-19 negative patients. Acute respiratory distress syndrome is the most frequent cause of death in COVID-19 positive patients and concomitant acute pancreatitis. In this article, we reported recent evidence on the correlation between COVID-19 infection and acute pancreatitis.

Key Words: Acute pancreatitis; SARS-CoV-2; Severe acute pancreatitis; Multiparametric scores; Infected necrosis; Step-up approach

©**The Author(s) 2022.** Published by Baishideng Publishing Group Inc. All rights reserved.

Core Tip: The outbreak of severe acute respiratory syndrome coronavirus 2 (SARS-CoV-2), causing a severe acute respiratory syndrome, has rapidly spread from China all over the world, affecting millions of people. Whereas typical presentations of this infection (such as fever, cough, myalgia, fatigue and pneumonia) are well recognized, several studies report a low incidence of gastrointestinal symptoms. The relationship between SARS-CoV-2 infection and acute pancreatitis is controversial. Acute pancreatitis is not specifically caused by SARS-CoV-2. Furthermore, coronavirus disease 2019 positive patients are more likely to develop severe acute pancreatitis and multiple organ failure.

Citation: Brisinda G, Chiarello MM, Tropeano G, Altieri G, Puccioni C, Fransvea P, Bianchi V. SARS-CoV-2 and the pancreas: What do we know about acute pancreatitis in COVID-19 positive patients? *World J Gastroenterol* 2022; 28(36): 5240-5249
URL: https://www.wjgnet.com/1007-9327/full/v28/i36/5240.htm
DOI: https://dx.doi.org/10.3748/wjg.v28.i36.5240

INTRODUCTION

Severe acute respiratory syndrome coronavirus 2 (SARS-CoV-2) secondary to coronavirus disease 2019 (COVID-19) has spread rapidly from China. The disease has affected millions of people[1]. Whereas typical presentations of this infection (such as fever, cough, myalgia, fatigue and pneumonia) are well recognized, few studies reported the incidence of atypical gastrointestinal symptoms[2-5]. COVID-19 is linked to organ damage including lungs, heart and kidneys and can lead to multiple organ failure. Evidence shows that SARS-CoV-2 has a strong tropism for the gastrointestinal tract[6,7]. Moreover, pancreatic injury in COVID-19 has not been common.

Acute pancreatitis is an inflammatory process that originates from the glandular parenchyma, causing damage and/or destruction to the acinar component first and then extending to the surrounding tissues[8-11]. There are several etiological factors contributing to its onset. However, it is possible to ascribe most of the episodes to two main causes, namely gallbladder lithiasis and alcohol abuse. Pharmacological, iatrogenic and viral causes must also be taken into account[12].

The severity of acute pancreatitis does not always correlate with pancreatic structural changes. It is possible to distinguish interstitial pancreatitis when the organ is locally or wholly increased in volume due to the presence of interstitial edema and necrotizing pancreatitis (10%-20% of all cases)[10,13,14]. It is unclear why COVID-19 starts with exclusively gastrointestinal symptoms, albeit in a low percentage of cases. However, acute pancreatic involvement induced by COVID-19 is severe and can develop rapidly. Close monitoring and admission are necessary to offer proper treatment. The following sections of this editorial discuss some of the recent findings and the approaches for a more effective clinical diagnosis and treatment of acute pancreatitis in patients with SARS-CoV-2 infection.

COVID-19 AND THE PANCREAS

Viral RNA has been found in the stools of COVID-19 patients[1,2,15-17]. High replication of the virus has been documented in both the small and large intestines by electron microscopy studies on tissues derived from biopsies and/or autopsy material[7,18,19]. Additionally, fecal-oral transmission has been documented for SARS-CoV-2[20]. Some molecules are receptors for the virus. These determine a specific tropism for different tissues and organs. SARS-CoV-2 uses its surface envelope called the spike glycoprotein. By means of this protein, SARS-CoV-2 interacts and enters host cells. The virus enters the cell *via* the angiotensin-converting enzyme 2 (ACE2) receptor. As such, the spike glycoprotein-ACE2 binding is the determinant for virus entry and propagation and for the transmissibility of COVID-19-related disease. ACE2 is expressed in human pancreatic cells and pancreatic islets and highly represented in pancreas microvasculature pericytes[6,21,22]. As ACE2 is internalized by SARS-CoV-2 binding, an imbalance of the RAS peptides can be established with a rise of angiotensin II and a decrease in angiotensin 1-7. The latter exerts anti-thrombogenic, anti-inflammatory and pro-resolving actions[23]. Laboratory abnormalities, suggesting pancreatic injury, have been noted in 8.0%-17.5% of cases in several studies[24,25], with 7.0% displaying significant pancreatic changes on computed tomography.

The etiopathogenesis of pancreatic injury in SARS-CoV-2 patients is still unclear. Both pancreatic ACE2 expression and drugs taken before the hospitalization might be involved[26]. The inflammation that occurs in the intestine causes the release of cytokines and bacteria. Both cytokines and bacteria can

reach and enter the lung through the bloodstream. At this level, a direct influence on the immune response and inflammation is observed[27-29]. The gut-liver axis is also strongly influenced by damage to the intestinal mucosa and bacterial imbalance[30]. The host and the microbial metabolites present in the intestine are transferred to the liver through the mesenteric-portal circulation; these affect liver function. The liver releases bile acids and bioactive media into the biliary and systemic circulation in order to transport them to the intestine. This could lead to pancreatic function damage in patients and may also explain the abnormality of pancreatic function indicators in COVID-19 patients. It is important not to consider each COVID-19 patient with increased serum amylase level as affected by acute pancreatitis[31]. Elevated levels of pancreatic enzymes may occur during kidney failure or diarrhea in the course of COVID-19[32]. It could be useful to find some criteria that can guide clinical suspicion.

WHAT DO WE KNOW ABOUT ACUTE PANCREATITIS IN COVID-19 POSITIVE PATIENTS?

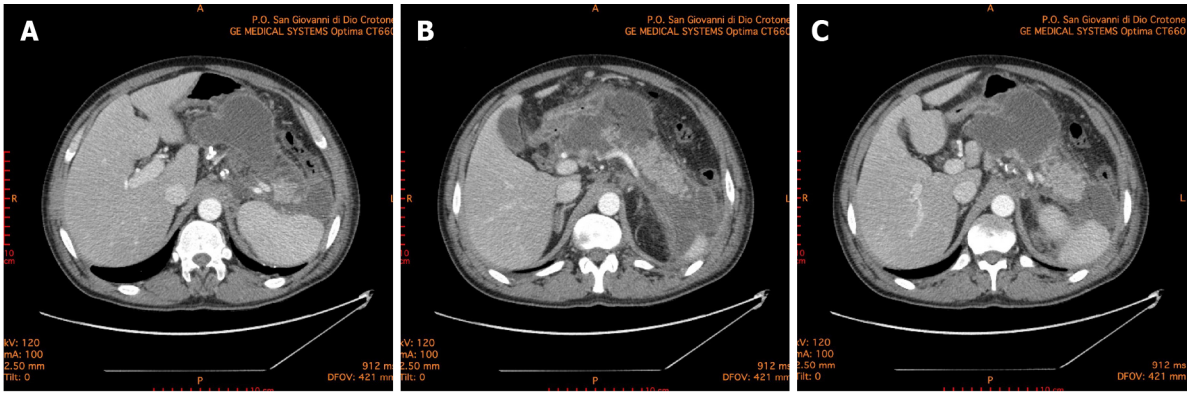
Available literature is not able to determine whether the tissue damage leading to acute pancreatitis occurs as a result of direct SARS-CoV-2 infection or as a results of systemic multiple organ dysfunction with increased levels of amylase and lipase[33,34]. Only a few COVID-19 positive patients also have acute pancreatitis; the association between the two pathologies is infrequent. Only 10% of COVID-19 positive patients show abdominal symptoms exclusively[35]: Usually, these patients have the most severe forms of COVID-19 infections. Furthermore, it has not been demonstrated that an increased incidence of acute pancreatitis occurred during the COVID-19 pandemic period[36]. SARS-CoV-2 cannot be said to be an etiological agent of acute pancreatitis[33,37]. Acute pancreatitis in COVID-19 positive patients is idiopathic in most cases[37], and there is no sufficient evidence showing that COVID-19 can cause acute pancreatitis or negatively impact its prognosis.

The involvement of the pancreatic gland appears possible, in consideration of the fact that ACE2 receptors are present both on exocrine cells and on pancreatic islets[23]. In addition, the ACE2 receptor is expressed more in the pancreatic tissue than in the lungs. Furthermore, SARS-CoV-2 induces the onset of endotheliitis, which results in ischemic damage and that can also occur in the pancreas[38].

In the COVID PAN study, it was documented that acute pancreatitis is more severe in COVID-19 positive patients than in COVID-19 negative patients. In them, the onset of multiple organ failure can be linked to factors other than acute pancreatitis[39]. A greater severity of acute pancreatitis, an increased risk of necrosis, intensive care unit admission, persistent organ failure and the need for mechanical ventilation were observed in COVID-19 positive patients with acute pancreatitis. In this same study, 30-d overall mortality from acute pancreatitis was statistically higher in COVID-19 positive (14.7%) than in COVID-19 negative patients (2.6%, $P < 0.04$)[39]. Furthermore, necrosectomy was more likely to be performed in SARS-CoV-2 positive patients, occurring in 5% compared with 1.3% in the control group ($P < 0.001$).

The predominant organ dysfunction was respiratory failure in the majority of COVID-19 positive patients. In addition, acute pancreatitis with concomitant SARS-CoV-2 was more likely to have poorer outcomes due to double pulmonary damage[40]. Lung involvement is common in severe acute pancreatitis. This involvement can progress to full blown acute respiratory distress syndrome[40]. At present, it could be difficult to stratify the severity of symptoms and the degree of lung involvement. Acute respiratory distress syndrome due to acute pancreatitis can worsen lung injury related to COVID-19 pneumonia. Moreover, changes in the gastrointestinal flora affect the respiratory tract through the common mucosal immune system, the so-called "gut-lung axis"[27,29]. COVID-19 positive patients with gastrointestinal symptoms are more likely to be complicated with acute respiratory distress and pancreatic damage. In these patients the prognosis is poorer. In COVID-19 positive patients with gastrointestinal symptoms, attention should be paid to the patient's gastrointestinal symptoms in the diagnosis and treatment process. It also appears essential to prevent the transmission of the virus *via* the fecal-oral route. In a retrospective cohort study, Inamdar *et al*[37] concluded that pancreatitis should be included in the list of gastrointestinal manifestations of COVID-19.

There are few studies in the literature that investigate the relationship between COVID-19 infection and acute pancreatitis. In their experience, Inamdar *et al*[37] documented 189 cases of acute pancreatitis in 48012 hospitalized patients (0.39%). Thirty-two (17%) of these 189 patients were COVID-19 positive, with a prevalence of 0.27% of acute pancreatitis among the patients hospitalized for COVID-19. Idiopathic forms were more frequent (69%) in this patient group than in COVID-19 negative patients (21%, $P < 0.0001$). Wang *et al*[41] found that of 52 COVID-19 patients enrolled, 17% had pancreatic injury, defined as an abnormal increase of amylase and lipase serum levels. Stephens *et al*[31] showed that COVID-19 patients had an amylase serum peak not always related with acute pancreatitis. They enrolled 234 patients, 158 of which had a serum amylase level three times greater than the normal upper limit, but only 1.7% of the studied population met the revised criteria of Atlanta for diagnosis of acute pancreatitis[31].



DOI: 10.3748/wjg.v28.i36.5240 **Copyright** ©The Author(s) 2022.

Figure 1 Abdominal computed tomography 10 d after the onset of acute pancreatitis. A: Necrotic collection, with a noticeable wall, dislocating stomach; B: Necrotic collection occupying the majority of pancreatic head and compressing the duodenum; C: Multiple collections of fluid and necrosis involving the cephalad portion of the pancreas, multiple peripancreatic collections around the spleen and the left paracolic gutter.

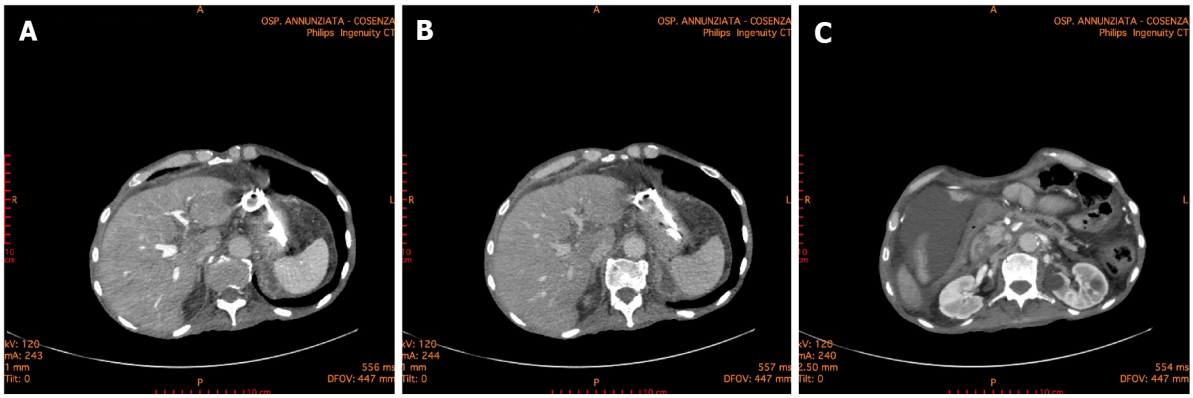
COVID-19 VACCINE AND PANCREATITIS

Vaccines are considered one of the most important public health achievements of the last century. Many vaccines have side effects. One of these adverse events is the onset of pancreatitis. In these cases, it is believed that acute pancreatitis is secondary to an immunologically induced phenomenon as demonstrated by reports in the literature after the administration of vaccines against the hepatitis virus or other viruses[42-44]. The vaccine BNT162b1 developed by Pfizer-BioNTech is a nucleoside-modified mRNA that encodes the receptor binding domain of the SARS-CoV-2 spike protein. The vaccine RNA is formulated in lipid nanoparticles for an efficient delivery into cells after injections[45].

In the literature there are several cases reporting acute pancreatitis after mRNA-based vaccine[46-50]. Although the vaccine has been proven to be effective and safe, vaccine-induced side effects have been observed. There are nausea, diarrhea, decreased appetite, abdominal pain, vomiting, heartburn and constipation among the most frequently reported gastrointestinal side effects. Most of the cases describe mild acute pancreatitis, however Ozaka *et al*[46] and Walter *et al*[47] reported a single case of necrotizing pancreatitis. According to Pfizer's data, 1 case of pancreatitis and 1 case of obstructive pancreatitis as adverse reactions were observed during the phase II/clinical trial of the COVID-19 mRNA vaccine. The trial included about 38000 participants, indicating that such a link between vaccination and pancreatitis is a very rare adverse event[51]. Between December 9, 2020 and July 21, 2021, information obtained from the United Kingdom database showed 275820 adverse reaction reports, which included 18 cases of mild acute pancreatitis and 1 case of necrotizing pancreatitis[52]. In France, out of a total of 42523573 doses, the Agence Nationale de Securité du Medicament et des Produits de Santé reported 57 cases of acute pancreatitis[53]. VigiBase, the World Health Organization global database of individual case safety reports, included 298 cases of acute pancreatitis and 17 cases of necrotizing pancreatitis[54]. The Agenzia Italiana del Farmaco reported 497 gastrointestinal adverse events equal to 14.1% of the total observations in 1 year. The document does not specify the number of cases of acute pancreatitis[55]. Although it is difficult to make conclusions about the likelihood of the vaccine being the etiologic factor of pancreatitis, it is essential to continue monitoring it for possible under-reported side effects until we have extensive long-term data available in post-marketing surveillance for long-term and rare side effects. Surveillance is also necessary because there are currently no conclusive data on the severity of pancreatitis in the population of subjects vaccinated against COVID-19 compared to patients who have not undergone vaccination. Preliminary results would document a reduced incidence of severe forms of acute pancreatitis in subjects vaccinated against SARS-CoV-2.

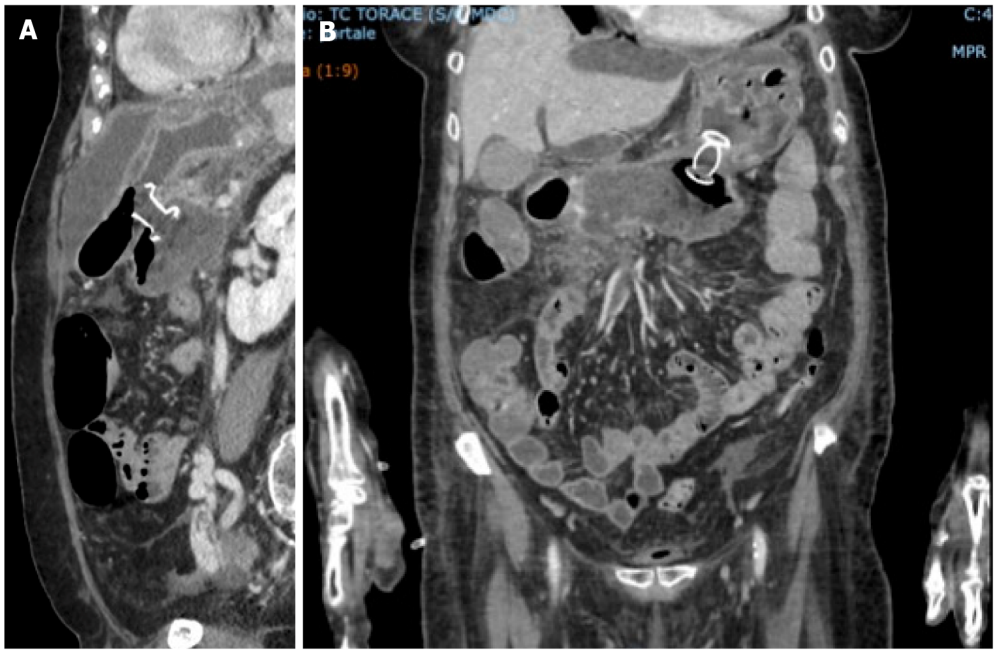
DO WE NEED TO CHANGE THE DIAGNOSTIC AND THERAPEUTIC APPROACH?

Since pancreatitis in COVID-19 positive patients occurs more frequently in severe forms, treatment must be intensive and prompt. It is crucial to define and stratify the severity of illness in patients with acute pancreatitis because of the extreme range of potential clinical courses due to the wide range of organs and tissues that may become involved. It is also fundamental to identify patients with potentially severe pancreatitis who require a multidisciplinary approach and an earlier and more aggressive treatment[56, 57]. Suspected acute pancreatitis can be confirmed with laboratory and instrumental investigations. Increased pancreatic enzymes levels are associated with a poor prognosis in COVID-19 patients. Recent findings show that the increment of pancreatic enzymes are significant in critical COVID-19 patients, but only a few of them progress to acute pancreatitis[58]. The rapid response of C-reactive protein to



DOI: 10.3748/wjg.v28.i36.5240 **Copyright** ©The Author(s) 2022.

Figure 2 Abdominal computed tomography 6 mo after the onset of acute pancreatitis. A and B: The double pigtail stents positioned during the endoscopic necrosectomy through the stomach is highlighted. Endoscopic necrosectomy through the stomach was performed 4 mo prior; C: A necrotic collection is evident in the lower right quadrant of the abdomen.



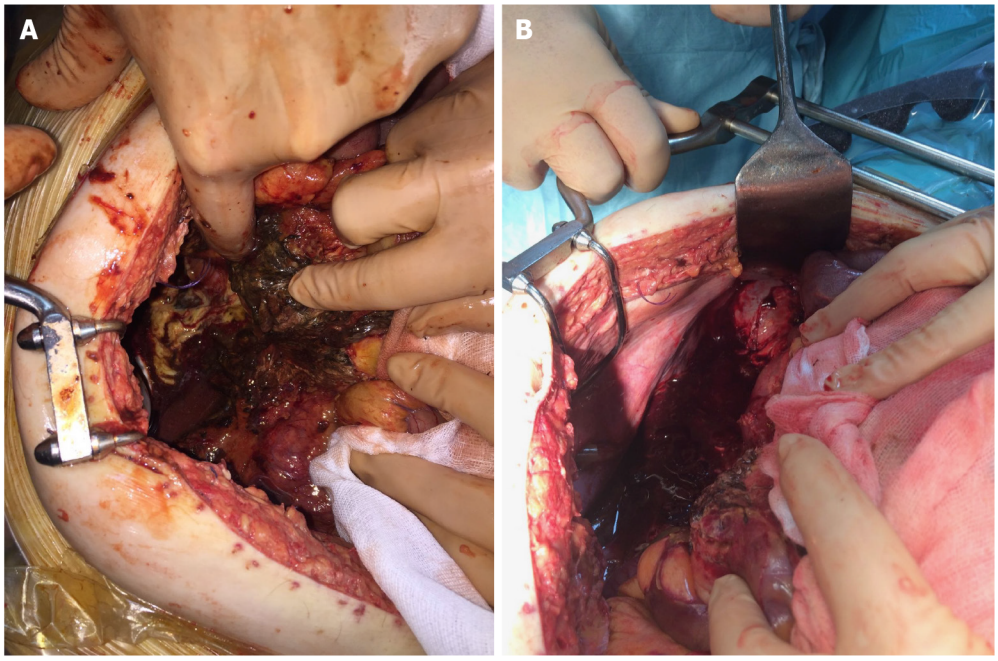
DOI: 10.3748/wjg.v28.i36.5240 **Copyright** ©The Author(s) 2022.

Figure 3 Abdominal computed tomography scan documenting correct placement of lumen-apposing metal stents for the treatment of walled-off necrosis in coronavirus disease 2019 positive patient. A: Sagittal scan; B: Front scan.

changes in the inflammatory process intensity has also suggested its use in the management and monitoring of acute pancreatitis. C-reactive protein is not specific, and although it is correlated with severity, it cannot be used to predict clinical evolution. Serum procalcitonin is also one of the parameters used in predicting the development of severe acute pancreatitis. Its continuous increase correlates with a bacterial superinfection of pancreatic necrosis[59]. In all patients with or without SARS-CoV-2 illness contrast-enhanced computed tomography scan is the gold standard for the diagnosis of acute pancreatitis to evaluate both pancreatic and extrapancreatic alterations (Figure 1).

The revised Atlanta classification provides a good clinical distinction between mild, moderate and severe acute pancreatitis, and it is used in most COVID-19 positive patients with acute pancreatitis[8]. Several scoring systems have been developed to predict the severity of acute pancreatitis; however, none of them represents a gold standard. The scoring systems are without clinical relevance because of their low predictive value[56]. The bedside index for severity in acute pancreatitis failed to identify the severity of acute pancreatitis in COVID-19 positive patients[37].

Early fluid resuscitation is recommended in order to improve tissue perfusion[60], and the maintenance of microcirculation may be associated with resolution of multiple organ failure[61], especially in patients with COVID-19 and acute pancreatitis. Enteral nutrition is safe during acute pancreatitis[62]. Moreover, supplementation of enteral nutrition with probiotics may decrease septic



DOI: 10.3748/wjg.v28.i36.5240 **Copyright** ©The Author(s) 2022.

Figure 4 Intraoperative photos. A: Surgery was performed for severe abdominal hypertension due to acute pancreatitis with necrotic collections in the retroduodenal region; B: Surgery was performed for severe abdominal hypertension due to acute pancreatitis with necrotic collections along the paracolic gutter.

complications. In patients with COVID-19 requiring mechanical ventilation, early enteral nutrition is associated with earlier liberation from ventilator support, shorter intensive care unit and hospital stay and decreased cost[63,64].

Most patients with sterile necrosis can be managed without invasive treatments. Walled off necrotic collections or pseudocysts may cause mechanical obstruction and a step-up approach is indicated. Percutaneous or transmural endoscopic drainage are both appropriate first-line approaches in managing these patients (Figure 2). However, endoscopic drainage is preferred as it avoids the risk of forming a pancreatocutaneous fistula. In the earlier phase of the pandemic, patients with COVID-19, especially with severe pneumonia and considered highly contagious, did not undergo endoscopic ultrasound or endoscopic treatments. In the later stages, patients with COVID-19 and acute pancreatitis were subjected, with necessary precautions, to percutaneous and endoscopic treatments similar to the COVID-19 negative patients (Figure 3).

The step-up approach might reduce the rates of complications and death by minimizing surgical trauma in already critically ill patients[65,66]. Currently, there is general agreement that surgery in severe acute pancreatitis should be performed as late as possible[67]. In the management of necrotizing acute pancreatitis, open operative debridement (Figure 4) maintains a role in cases not amenable to less invasive endoscopic and/or laparoscopic procedures. Open operative debridement was performed in patients with COVID-19 related lung symptoms and lesions.

CONCLUSION

In pandemic times, clinical conditions could be worsened by COVID-19 infection. SARS-CoV-2 cannot be said to be an etiological agent of acute pancreatitis. Acute pancreatitis in COVID-19 positive patients is idiopathic in most cases, and there is no sufficient evidence showing that SARS-CoV-2 can negatively impact prognosis. On the other hand, acute pancreatitis with concomitant SARS-CoV-2 is more likely to have worse outcomes due to double lung damage and greater pancreatic severity. The multiparametric scores could not recognize and stratify the severity of pancreatic diseases and concomitant COVID-19 infection. In these patients, computed tomography is the gold standard for the diagnosis. Management of COVID-19 positive patients with pancreatitis is complex, and it is optimally provided by a multidisciplinary team. Operative treatments should be modulated, preferably, from the least to the most invasive option. Thus, surgical necrosectomy is relegated to the role of "last resort", remembering that necrotizing pancreatitis is a heterogeneous disease with marked variations in extent and course. This also means that one size treatment does not fit all.

FOOTNOTES

Author contributions: Brisinda G and Chiarello MM equally contributed to the drafting of the manuscript and must both be considered first author; Chiarello MM and Brisinda G conceived the original idea; Tropeano G, Alteri G, Puccioni C, Fransvea P and Bianchi V performed a comprehensive review of all available literature and summarized the data; Brisinda G and Chiarello MM meet the criteria for authorship established by the International Committee of Medical Journal Editors and verify the validity of the results reported; and all authors read and approved the final manuscript.

Conflict-of-interest statement: All the authors report no relevant conflicts of interest for this article.

Open-Access: This article is an open-access article that was selected by an in-house editor and fully peer-reviewed by external reviewers. It is distributed in accordance with the Creative Commons Attribution NonCommercial (CC BY-NC 4.0) license, which permits others to distribute, remix, adapt, build upon this work non-commercially, and license their derivative works on different terms, provided the original work is properly cited and the use is non-commercial. See: https://creativecommons.org/Licenses/by-nc/4.0/

Country/Territory of origin: Italy

ORCID number: Giuseppe Brisinda 0000-0001-8820-9471; Maria Michela Chiarello 0000-0003-3455-0062; Giuseppe Tropeano 0000-0001-9006-5040; Gaia Altieri 0000-0002-0324-2430; Caterina Puccioni 0000-0001-6092-7957; Pietro Fransvea 0000-0003-4969-3373; Valentina Bianchi 0000-0002-8817-3760.

S-Editor: Wang JJ
L-Editor: Filipodia
P-Editor: Wang JJ

REFERENCES

1 **Guan WJ**, Ni ZY, Hu Y, Liang WH, Ou CQ, He JX, Liu L, Shan H, Lei CL, Hui DSC, Du B, Li LJ, Zeng G, Yuen KY, Chen RC, Tang CL, Wang T, Chen PY, Xiang J, Li SY, Wang JL, Liang ZJ, Peng YX, Wei L, Liu Y, Hu YH, Peng P, Wang JM, Liu JY, Chen Z, Li G, Zheng ZJ, Qiu SQ, Luo J, Ye CJ, Zhu SY, Zhong NS; China Medical Treatment Expert Group for Covid-19. Clinical Characteristics of Coronavirus Disease 2019 in China. *N Engl J Med* 2020; **382**: 1708-1720 [PMID: 32109013 DOI: 10.1056/NEJMoa2002032]

2 **Henry BM**, de Oliveira MHS, Benoit J, Lippi G. Gastrointestinal symptoms associated with severity of coronavirus disease 2019 (COVID-19): a pooled analysis. *Intern Emerg Med* 2020; **15**: 857-859 [PMID: 32303970 DOI: 10.1007/s11739-020-02329-9]

3 **Nobel YR**, Phipps M, Zucker J, Lebwohl B, Wang TC, Sobieszczyk ME, Freedberg DE. Gastrointestinal Symptoms and Coronavirus Disease 2019: A Case-Control Study From the United States. *Gastroenterology* 2020; **159**: 373-375.e2 [PMID: 32294477 DOI: 10.1053/j.gastro.2020.04.017]

4 **Nayar M**, Varghese C, Kanwar A, Siriwardena AK, Haque AR, Awan A, Balakrishnan A, Rawashdeh A, Ivanov B, Parmar C, Halloran CM, Caruana C, Borg CM, Gomez D, Damaskos D, Karavias D, Finch G, Ebied H, Pine JK, Skipworth JRA, Milburn J, Latif J, Apollos J, El Kafsi J, Windsor JA, Roberts K, Wang K, Ravi K, Coats MV, Hollyman M, Phillips M, Okocha M, Wilson MS, Ameer NA, Kumar N, Shah N, Lapolla P, Magee C, Al-Sarireh B, Lunevicius R, Benhmida R, Singhal R, Balachandra S, Demirli Atıcı S, Jaunoo S, Dwerryhouse S, Boyce T, Charalampakis V, Kanakala V, Abbas Z, Tewari N, Pandanaboyana S; COVIDPAN Collborative Group; COVID Pain Collborative Group. SARS-CoV-2 infection is associated with an increased risk of idiopathic acute pancreatitis but not pancreatic exocrine insufficiency or diabetes: long-term results of the COVIDPAN study. *Gut* 2022; **71**: 1444-1447 [PMID: 34764192 DOI: 10.1136/gutjnl-2021-326218]

5 **Troncone E**, Salvatori S, Sena G, De Cristofaro E, Alfieri N, Marafini I, Paganelli C, Argirò R, Giannarelli D, Monteleone G, Del Vecchio Blanco G. Low Frequency of Acute Pancreatitis in Hospitalized COVID-19 Patients. *Pancreas* 2021; **50**: 393-398 [PMID: 33835971 DOI: 10.1097/MPA.0000000000001770]

6 **Akarsu C**, Karabulut M, Aydin H, Sahbaz NA, Dural AC, Yegul D, Peker KD, Ferahman S, Bulut S, Dönmez T, Asar S, Yasar KK, Adas GT. Association between Acute Pancreatitis and COVID-19: Could Pancreatitis Be the Missing Piece of the Puzzle about Increased Mortality Rates? *J Invest Surg* 2022; **35**: 119-125 [PMID: 33138658 DOI: 10.1080/08941939.2020.1833263]

7 **Cholankeril G**, Podboy A, Aivaliotis VI, Pham EA, Spencer SP, Kim D, Ahmed A. Association of Digestive Symptoms and Hospitalization in Patients With SARS-CoV-2 Infection. *Am J Gastroenterol* 2020; **115**: 1129-1132 [PMID: 32618665 DOI: 10.14309/ajg.0000000000000712]

8 **Banks PA**, Bollen TL, Dervenis C, Gooszen HG, Johnson CD, Sarr MG, Tsiotos GG, Vege SS; Acute Pancreatitis Classification Working Group. Classification of acute pancreatitis--2012: revision of the Atlanta classification and definitions by international consensus. *Gut* 2013; **62**: 102-111 [PMID: 23100216 DOI: 10.1136/gutjnl-2012-302779]

9 **Seppänen H**, Puolakkainen P. Classification, Severity Assessment, and Prevention of Recurrences in Acute Pancreatitis. *Scand J Surg* 2020; **109**: 53-58 [PMID: 32192420 DOI: 10.1177/1457496920910007]

10 **Leppäniemi A**, Tolonen M, Tarasconi A, Segovia-Lohse H, Gamberini E, Kirkpatrick AW, Ball CG, Parry N, Sartelli M, Wolbrink D, van Goor H, Baiocchi G, Ansaloni L, Biffl W, Coccolini F, Di Saverio S, Kluger Y, Moore EE, Catena F. Executive summary: WSES Guidelines for the management of severe acute pancreatitis. *J Trauma Acute Care Surg* 2020;

88: 888-890 [PMID: 32459451 DOI: 10.1097/TA.0000000000002691]
11 **Brisinda G**, Vanella S, Crocco A, Mazzari A, Tomaiuolo P, Santullo F, Grossi U, Crucitti A. Severe acute pancreatitis: advances and insights in assessment of severity and management. *Eur J Gastroenterol Hepatol* 2011; **23**: 541-551 [PMID: 21659951 DOI: 10.1097/MEG.0b013e328346e21e]
12 **Rawla P**, Bandaru SS, Vellipuram AR. Review of Infectious Etiology of Acute Pancreatitis. *Gastroenterology Res* 2017; **10**: 153-158 [PMID: 28725301 DOI: 10.14740/gr858w]
13 **van Dijk SM**, Hallensleben NDL, van Santvoort HC, Fockens P, van Goor H, Bruno MJ, Besselink MG; Dutch Pancreatitis Study Group. Acute pancreatitis: recent advances through randomised trials. *Gut* 2017; **66**: 2024-2032 [PMID: 28838972 DOI: 10.1136/gutjnl-2016-313595]
14 **Brisinda G**, Crocco A, Giustacchini P. Classification of the severity of acute pancreatitis: how much is really needed for a new classification? *Ann Surg* 2015; **261**: e101-e102 [PMID: 24577326 DOI: 10.1097/SLA.0000000000000625]
15 **Du M**, Cai G, Chen F, Christiani DC, Zhang Z, Wang M. Multiomics Evaluation of Gastrointestinal and Other Clinical Characteristics of COVID-19. *Gastroenterology* 2020; **158**: 2298-2301.e7 [PMID: 32234303 DOI: 10.1053/j.gastro.2020.03.045]
16 **Correia de Sá T**, Soares C, Rocha M. Acute pancreatitis and COVID-19: A literature review. *World J Gastrointest Surg* 2021; **13**: 574-584 [PMID: 34194615 DOI: 10.4240/wjgs.v13.i6.574]
17 **Rubin R**. SARS-CoV-2 RNA Can Persist in Stool Months After Respiratory Tract Clears Virus. *JAMA* 2022; **327**: 2175-2176 [PMID: 35583898 DOI: 10.1001/jama.2022.7892]
18 **Hanley B**, Naresh KN, Roufosse C, Nicholson AG, Weir J, Cooke GS, Thursz M, Manousou P, Corbett R, Goldin R, Al-Sarraj S, Abdolrasouli A, Swann OC, Baillon L, Penn R, Barclay WS, Viola P, Osborn M. Histopathological findings and viral tropism in UK patients with severe fatal COVID-19: a post-mortem study. *Lancet Microbe* 2020; **1**: e245-e253 [PMID: 32844161 DOI: 10.1016/S2666-5247(20)30115-4]
19 **Chmielik E**, Jazowiecka-Rakus J, Dyduch G, Nasierowska-Guttmejer A, Michalowski L, Sochanik A, Ulatowska-Bialas M. COVID-19 Autopsies: A Case Series from Poland. *Pathobiology* 2021; **88**: 78-87 [PMID: 33254171 DOI: 10.1159/000512768]
20 **Gu J**, Han B, Wang J. COVID-19: Gastrointestinal Manifestations and Potential Fecal-Oral Transmission. *Gastroenterology* 2020; **158**: 1518-1519 [PMID: 32142785 DOI: 10.1053/j.gastro.2020.02.054]
21 **Dalan R**, Bornstein SR, El-Armouche A, Rodionov RN, Markov A, Wielockx B, Beuschlein F, Boehm BO. The ACE-2 in COVID-19: Foe or Friend? *Horm Metab Res* 2020; **52**: 257-263 [PMID: 32340044 DOI: 10.1055/a-1155-0501]
22 **Shaharuddin SH**, Wang V, Santos RS, Gross A, Wang Y, Jawanda H, Zhang Y, Hasan W, Garcia G Jr, Arumugaswami V, Sareen D. Deleterious Effects of SARS-CoV-2 Infection on Human Pancreatic Cells. *Front Cell Infect Microbiol* 2021; **11**: 678482 [PMID: 34282405 DOI: 10.3389/fcimb.2021.678482]
23 **Liu F**, Long X, Zhang B, Zhang W, Chen X, Zhang Z. ACE2 Expression in Pancreas May Cause Pancreatic Damage After SARS-CoV-2 Infection. *Clin Gastroenterol Hepatol* 2020; **18**: 2128-2130.e2 [PMID: 32334082 DOI: 10.1016/j.cgh.2020.04.040]
24 **Zhou Z**, Zhao N, Shu Y, Han S, Chen B, Shu X. Effect of Gastrointestinal Symptoms in Patients With COVID-19. *Gastroenterology* 2020; **158**: 2294-2297 [PMID: 32199880 DOI: 10.1053/j.gastro.2020.03.020]
25 **Aloysius MM**, Thatti A, Gupta A, Sharma N, Bansal P, Goyal H. COVID-19 presenting as acute pancreatitis. *Pancreatology* 2020; **20**: 1026-1027 [PMID: 32444169 DOI: 10.1016/j.pan.2020.05.003]
26 **Annunziata A**, Coppola A, Andreozzi P, Lanza M, Simioli F, Carannante N, Di Somma C, Di Micco P, Fiorentino G. Acute Pancreatitis and COVID-19: A Single-Center Experience. *J Multidiscip Healthc* 2021; **14**: 2857-2861 [PMID: 34675533 DOI: 10.2147/JMDH.S334835]
27 **Aktas B**, Aslim B. Gut-lung axis and dysbiosis in COVID-19. *Turk J Biol* 2020; **44**: 265-272 [PMID: 32595361 DOI: 10.3906/biy-2005-102]
28 **Dang AT**, Marsland BJ. Microbes, metabolites, and the gut-lung axis. *Mucosal Immunol* 2019; **12**: 843-850 [PMID: 30976087 DOI: 10.1038/s41385-019-0160-6]
29 **Marsland BJ**, Trompette A, Gollwitzer ES. The Gut-Lung Axis in Respiratory Disease. *Ann Am Thorac Soc* 2015; **12** Suppl 2: S150-S156 [PMID: 26595731 DOI: 10.1513/AnnalsATS.201503-133AW]
30 **Albillos A**, de Gottardi A, Rescigno M. The gut-liver axis in liver disease: Pathophysiological basis for therapy. *J Hepatol* 2020; **72**: 558-577 [PMID: 31622696 DOI: 10.1016/j.jhep.2019.10.003]
31 **Stephens JR**, Wong JLC, Broomhead R, Stümpfle R, Waheed U, Patel P, Brett SJ, Soni S. Raised serum amylase in patients with COVID-19 may not be associated with pancreatitis. *Br J Surg* 2021; **108**: e152-e153 [PMID: 33793756 DOI: 10.1093/bjs/znaa168]
32 **Abramczyk U**, Nowaczyński M, Słomczyński A, Wojnicz P, Zatyka P, Kuzan A. Consequences of COVID-19 for the Pancreas. *Int J Mol Sci* 2022; **23** [PMID: 35055050 DOI: 10.3390/ijms23020864]
33 **de-Madaria E**, Capurso G. COVID-19 and acute pancreatitis: examining the causality. *Nat Rev Gastroenterol Hepatol* 2021; **18**: 3-4 [PMID: 33203968 DOI: 10.1038/s41575-020-00389-y]
34 **Suchman K**, Raphael KL, Liu Y, Wee D, Trindade AJ; Northwell COVID-19 Research Consortium. Acute pancreatitis in children hospitalized with COVID-19. *Pancreatology* 2021; **21**: 31-33 [PMID: 33309015 DOI: 10.1016/j.pan.2020.12.005]
35 **Mao R**, Qiu Y, He JS, Tan JY, Li XH, Liang J, Shen J, Zhu LR, Chen Y, Iacucci M, Ng SC, Ghosh S, Chen MH. Manifestations and prognosis of gastrointestinal and liver involvement in patients with COVID-19: a systematic review and meta-analysis. *Lancet Gastroenterol Hepatol* 2020; **5**: 667-678 [PMID: 32405603 DOI: 10.1016/S2468-1253(20)30126-6]
36 **Miró Ò**, Llorens P, Jiménez S, Piñera P, Burillo-Putze G, Martín A, Martín-Sánchez FJ, González Del Castillo J; Spanish Investigators in Emergency Situations TeAm (SIESTA) network. Frequency of five unusual presentations in patients with COVID-19: results of the UMC-19-S_1. *Epidemiol Infect* 2020; **148**: e189 [PMID: 32843127 DOI: 10.1017/S0950268820001910]
37 **Inamdar S**, Benias PC, Liu Y, Sejpal DV, Satapathy SK, Trindade AJ; Northwell COVID-19 Research Consortium. Prevalence, Risk Factors, and Outcomes of Hospitalized Patients With Coronavirus Disease 2019 Presenting as Acute Pancreatitis. *Gastroenterology* 2020; **159**: 2226-2228.e2 [PMID: 32860787 DOI: 10.1053/j.gastro.2020.08.044]

38 **Pons S**, Fodil S, Azoulay E, Zafrani L. The vascular endothelium: the cornerstone of organ dysfunction in severe SARS-CoV-2 infection. *Crit Care* 2020; **24**: 353 [PMID: 32546188 DOI: 10.1186/s13054-020-03062-7]

39 **Pandanaboyana S**, Moir J, Leeds JS, Oppong K, Kanwar A, Marzouk A, Belgaumkar A, Gupta A, Siriwardena AK, Haque AR, Awan A, Balakrishnan A, Rawashdeh A, Ivanov B, Parmar C, M Halloran C, Caruana C, Borg CM, Gomez D, Damaskos D, Karavias D, Finch G, Ebied H, K Pine J, R A Skipworth J, Milburn J, Latif J, Ratnam Apollos J, El Kafsi J, Windsor JA, Roberts K, Wang K, Ravi K, V Coats M, Hollyman M, Phillips M, Okocha M, Sj Wilson M, A Ameer N, Kumar N, Shah N, Lapolla P, Magee C, Al-Sarireh B, Lunevicius R, Benhmida R, Singhal R, Balachandra S, Demirli Atıcı S, Jaunoo S, Dwerryhouse S, Boyce T, Charalampakis V, Kanakala V, Abbas Z, Nayar M; COVID PAN collaborative group. SARS-CoV-2 infection in acute pancreatitis increases disease severity and 30-day mortality: COVID PAN collaborative study. *Gut* 2021; **70**: 1061-1069 [PMID: 33547182 DOI: 10.1136/gutjnl-2020-323364]

40 **Chiarello MM**, Cariati M, Brisinda G. Assessment of severity of acute pancreatitis in a Sars-CoV-2 pandemia. *Br J Surg* 2020; **107**: e379 [PMID: 32779743 DOI: 10.1002/bjs.11818]

41 **Wang K**, Luo J, Tan F, Liu J, Ni Z, Liu D, Tian P, Li W. Acute Pancreatitis as the Initial Manifestation in 2 Cases of COVID-19 in Wuhan, China. *Open Forum Infect Dis* 2020; **7**: ofaa324 [PMID: 32959016 DOI: 10.1093/ofid/ofaa324]

42 **Shlomovitz E**, Davies W, Cairns E, Brintnell WC, Goldszmidt M, Dresser GK. Severe necrotizing pancreatitis following combined hepatitis A and B vaccination. *CMAJ* 2007; **176**: 339-342 [PMID: 17261831 DOI: 10.1503/cmaj.060360]

43 **Adler JB**, Mazzotta SA, Barkin JS. Pancreatitis caused by measles, mumps, and rubella vaccine. *Pancreas* 1991; **6**: 489-490 [PMID: 1876605 DOI: 10.1097/00006676-199107000-00018]

44 **Haviv YS**, Sharkia M, Galun E, Safadi R. Pancreatitis following hepatitis A vaccination. *Eur J Med Res* 2000; **5**: 229-230 [PMID: 10806126]

45 **Sahin U**, Muik A, Derhovanessian E, Vogler I, Kranz LM, Vormehr M, Baum A, Pascal K, Quandt J, Maurus D, Brachtendorf S, Lörks V, Sikorski J, Hilker R, Becker D, Eller AK, Grützner J, Boesler C, Rosenbaum C, Kühnle MC, Luxemburger U, Kemmer-Brück A, Langer D, Bexon M, Bolte S, Karikó K, Palanche T, Fischer B, Schultz A, Shi PY, Fontes-Garfias C, Perez JL, Swanson KA, Loschko J, Scully IL, Cutler M, Kalina W, Kyratsous CA, Cooper D, Dormitzer PR, Jansen KU, Türeci Ö. COVID-19 vaccine BNT162b1 elicits human antibody and T_H1 T cell responses. *Nature* 2020; **586**: 594-599 [PMID: 32998157 DOI: 10.1038/s41586-020-2814-7]

46 **Ozaka S**, Kodera T, Ariki S, Kobayashi T, Murakami K. Acute pancreatitis soon after COVID-19 vaccination: A case report. *Medicine (Baltimore)* 2022; **101**: e28471 [PMID: 35029194 DOI: 10.1097/MD.0000000000028471]

47 **Walter T**, Connor S, Stedman C, Doogue M. A case of acute necrotising pancreatitis following the second dose of Pfizer-BioNTech COVID-19 mRNA vaccine. *Br J Clin Pharmacol* 2022; **88**: 1385-1386 [PMID: 34423463 DOI: 10.1111/bcp.15039]

48 **Meo SA**, Bukhari IA, Akram J, Meo AS, Klonoff DC. COVID-19 vaccines: comparison of biological, pharmacological characteristics and adverse effects of Pfizer/BioNTech and Moderna Vaccines. *Eur Rev Med Pharmacol Sci* 2021; **25**: 1663-1669 [PMID: 33629336 DOI: 10.26355/eurrev_202102_24877]

49 **Rosenblum HG**, Hadler SC, Moulia D, Shimabukuro TT, Su JR, Tepper NK, Ess KC, Woo EJ, Mba-Jonas A, Alimchandani M, Nair N, Klein NP, Hanson KE, Markowitz LE, Wharton M, McNally VV, Romero JR, Talbot HK, Lee GM, Daley MF, Mbaeyi SA, Oliver SE. Use of COVID-19 Vaccines After Reports of Adverse Events Among Adult Recipients of Janssen (Johnson & Johnson) and mRNA COVID-19 Vaccines (Pfizer-BioNTech and Moderna): Update from the Advisory Committee on Immunization Practices - United States, July 2021. *MMWR Morb Mortal Wkly Rep* 2021; **70**: 1094-1099 [PMID: 34383735 DOI: 10.15585/mmwr.mm7032e4]

50 **Parkash O**, Sharko A, Farooqi A, Ying GW, Sura P. Acute Pancreatitis: A Possible Side Effect of COVID-19 Vaccine. *Cureus* 2021; **13**: e14741 [PMID: 34084669 DOI: 10.7759/cureus.14741]

51 **Pfizer**. Pfizer-BioNTech COVID-19 vaccine (BNT162, PF-07302048). Vaccines and related biological products advisory committee. [cited 13 April 2022]. Available from: https://www.fda.gov/media/144246/download

52 COVID-19 mRNA Pfizer-BioNTech vaccine analysis print. All UK spontaneous reports received between 9 December 2020 and 30 June 2021 for mRNA Pfizer/BioNTech vaccine analysis print. 2021. [cited 13 April 2022]. Available from: https://assets.publishing.service.gov.uk/government/uploads/system/uploads/attachment_data/file/1009453/COVID-19_mRNA_Pfizer-BioNTech_Vaccine_Analysis_Print_DPL_28.07.2021

53 **ANSM**. Point de situation sur la surveillance des vaccins contre la COVID-19. [cited 13 April 2022]. Available from: https://ansm.sante.fr/actualites/point-de-situation-sur-la-surveillance-des-vaccins-contre-la-covid-19-7

54 **World Health Organization**. VigiAccess. [cited 13 April 2022]. Available from: http://www.vigiaccess.org

55 **FEDAIISF**. Rapporto annuale sulla sicurezza dei vaccini anti-COVID-19. [cited 13 April 2022]. Available from: https://www.fedaiisf.it/aifa-rapporto-annuale-sulla-sicurezza-dei-vaccini-anti-covid-19/

56 **Boxhoorn L**, Voermans RP, Bouwense SA, Bruno MJ, Verdonk RC, Boermeester MA, van Santvoort HC, Besselink MG. Acute pancreatitis. *Lancet* 2020; **396**: 726-734 [PMID: 32891214 DOI: 10.1016/S0140-6736(20)31310-6]

57 **Bulthuis MC**, Boxhoorn L, Beudel M, Elbers PWG, Kop MPM, van Wanrooij RLJ, Besselink MG, Voermans RP. Acute pancreatitis in COVID-19 patients: true risk? *Scand J Gastroenterol* 2021; **56**: 585-587 [PMID: 33715577 DOI: 10.1080/00365521.2021.1896776]

58 **Ding P**, Song B, Liu X, Fang X, Cai H, Zhang D, Zheng X. Elevated Pancreatic Enzymes in ICU Patients With COVID-19 in Wuhan, China: A Retrospective Study. *Front Med (Lausanne)* 2021; **8**: 663646 [PMID: 34485322 DOI: 10.3389/fmed.2021.663646]

59 **Huang HL**, Nie X, Cai B, Tang JT, He Y, Miao Q, Song HL, Luo TX, Gao BX, Wang LL, Li GX. Procalcitonin levels predict acute kidney injury and prognosis in acute pancreatitis: a prospective study. *PLoS One* 2013; **8**: e82250 [PMID: 24349237 DOI: 10.1371/journal.pone.0082250]

60 **Sarr MG**. Early fluid "resuscitation/therapy" in acute pancreatitis: which fluid? *Ann Surg* 2013; **257**: 189-190 [PMID: 23291660 DOI: 10.1097/SLA.0b013e318280e19e]

61 **Bortolotti P**, Saulnier F, Colling D, Redheuil A, Preau S. New tools for optimizing fluid resuscitation in acute pancreatitis. *World J Gastroenterol* 2014; **20**: 16113-16122 [PMID: 25473163 DOI: 10.3748/wjg.v20.i43.16113]

62 **Arvanitakis M**, Ockenga J, Bezmarevic M, Gianotti L, Krznarić Ž, Lobo DN, Löser C, Madl C, Meier R, Phillips M,

Rasmussen HH, Van Hooft JE, Bischoff SC. ESPEN guideline on clinical nutrition in acute and chronic pancreatitis. *Clin Nutr* 2020; **39**: 612-631 [PMID: 32008871 DOI: 10.1016/j.clnu.2020.01.004]

63 **Haines K**, Parker V, Ohnuma T, Krishnamoorthy V, Raghunathan K, Sulo S, Kerr KW, Besecker BY, Cassady BA, Wischmeyer PE. Role of Early Enteral Nutrition in Mechanically Ventilated COVID-19 Patients. *Crit Care Explor* 2022; **4**: e0683 [PMID: 35464756 DOI: 10.1097/CCE.0000000000000683]

64 **Compher C**, Bingham AL, McCall M, Patel J, Rice TW, Braunschweig C, McKeever L. Guidelines for the provision of nutrition support therapy in the adult critically ill patient: The American Society for Parenteral and Enteral Nutrition. *JPEN J Parenter Enteral Nutr* 2022; **46**: 12-41 [PMID: 34784064 DOI: 10.1002/jpen.2267]

65 **Besselink MG**, van Santvoort HC, Nieuwenhuijs VB, Boermeester MA, Bollen TL, Buskens E, Dejong CH, van Eijck CH, van Goor H, Hofker SS, Lameris JS, van Leeuwen MS, Ploeg RJ, van Ramshorst B, Schaapherder AF, Cuesta MA, Consten EC, Gouma DJ, van der Harst E, Hesselink EJ, Houdijk LP, Karsten TM, van Laarhoven CJ, Pierie JP, Rosman C, Bilgen EJ, Timmer R, van der Tweel I, de Wit RJ, Witteman BJ, Gooszen HG; Dutch Acute Pancreatitis Study Group. Minimally invasive 'step-up approach' *vs* maximal necrosectomy in patients with acute necrotising pancreatitis (PANTER trial): design and rationale of a randomised controlled multicenter trial [ISRCTN13975868]. *BMC Surg* 2006; **6**: 6 [PMID: 16606471 DOI: 10.1186/1471-2482-6-6]

66 **Hollemans RA**, Bakker OJ, Boermeester MA, Bollen TL, Bosscha K, Bruno MJ, Buskens E, Dejong CH, van Duijvendijk P, van Eijck CH, Fockens P, van Goor H, van Grevenstein WM, van der Harst E, Heisterkamp J, Hesselink EJ, Hofker S, Houdijk AP, Karsten T, Kruyt PM, van Laarhoven CJ, Laméris JS, van Leeuwen MS, Manusama ER, Molenaar IQ, Nieuwenhuijs VB, van Ramshorst B, Roos D, Rosman C, Schaapherder AF, van der Schelling GP, Timmer R, Verdonk RC, de Wit RJ, Gooszen HG, Besselink MG, van Santvoort HC; Dutch Pancreatitis Study Group. Superiority of Step-up Approach *vs* Open Necrosectomy in Long-term Follow-up of Patients With Necrotizing Pancreatitis. *Gastroenterology* 2019; **156**: 1016-1026 [PMID: 30391468 DOI: 10.1053/j.gastro.2018.10.045]

67 **Boxhoorn L**, van Dijk SM, van Grinsven J, Verdonk RC, Boermeester MA, Bollen TL, Bouwense SAW, Bruno MJ, Cappendijk VC, Dejong CHC, van Duijvendijk P, van Eijck CHJ, Fockens P, Francken MFG, van Goor H, Hadithi M, Hallensleben NDL, Haveman JW, Jacobs MAJM, Jansen JM, Kop MPM, van Lienden KP, Manusama ER, Mieog JSD, Molenaar IQ, Nieuwenhuijs VB, Poen AC, Poley JW, van de Poll M, Quispel R, Römkens TEH, Schwartz MP, Seerden TC, Stommel MWJ, Straathof JWA, Timmerhuis HC, Venneman NG, Voermans RP, van de Vrie W, Witteman BJ, Dijkgraaf MGW, van Santvoort HC, Besselink MG; Dutch Pancreatitis Study Group. Immediate versus Postponed Intervention for Infected Necrotizing Pancreatitis. *N Engl J Med* 2021; **385**: 1372-1381 [PMID: 34614330 DOI: 10.1056/NEJMoa2100826]

World Journal of Gastroenterology

Submit a Manuscript: https://www.f6publishing.com

World J Gastroenterol 2022 September 28; 28(36): 5250-5264

DOI: 10.3748/wjg.v28.i36.5250

ISSN 1007-9327 (print) ISSN 2219-2840 (online)

REVIEW

Deciphering the role of transforming growth factor-beta 1 as a diagnostic-prognostic-therapeutic candidate against hepatocellular carcinoma

Aswathy R Devan, Keechilat Pavithran, Bhagyalakshmi Nair, Maneesha Murali, Lekshmi R Nath

Specialty type: Gastroenterology and hepatology

Provenance and peer review: Invited article; Externally peer reviewed.

Peer-review model: Single blind

Peer-review report's scientific quality classification

Grade A (Excellent): 0
Grade B (Very good): B
Grade C (Good): C
Grade D (Fair): 0
Grade E (Poor): 0

P-Reviewer: Ghazy A, Egypt; Ying HQ, China

Received: March 9, 2022
Peer-review started: March 9, 2022
First decision: April 11, 2022
Revised: April 30, 2022
Accepted: August 16, 2022
Article in press: August 16, 2022
Published online: September 28, 2022

Aswathy R Devan, Bhagyalakshmi Nair, Maneesha Murali, Lekshmi R Nath, Department of Pharmacognosy, Amrita School of Pharmacy, Amrita Vishwa Vidyapeetham, AIMS Health Science Campus, Kochi 682041, Kerala, India

Keechilat Pavithran, Department of Medical Oncology and Hematology, Amrita Institute of Medical Sciences and Research Centre, Amrita Vishwa Vidyapeetham, Kochi 682041, Kerala, India

Corresponding author: Lekshmi R Nath, PhD, Assistant Professor, Department of Pharmacognosy, Amrita School of Pharmacy, Amrita Vishwa Vidyapeetham, AIMS Health Science Campus, Ponekkara, Kochi 682041, Kerala, India. lekshmirnath@aims.amrita.edu

Abstract

Transforming growth factor-beta (TGF-β) is a multifunctional cytokine that performs a dual role as a tumor suppressor and tumor promoter during cancer progression. Among different ligands of the TGF-β family, TGF-β1 modulates most of its biological outcomes. Despite the abundant expression of TGF-β1 in the liver, steatosis to hepatocellular carcinoma (HCC) progression triggers elevated TGF-β1 levels, contributing to poor prognosis and survival. Additionally, elevated TGF-β1 levels in the tumor microenvironment create an immunosuppressive stage *via* various mechanisms. TGF-β1 has a prime role as a diagnostic and prognostic biomarker in HCC. Moreover, TGF-β1 is widely studied as a therapeutic target either as monotherapy or combined with immune checkpoint inhibitors. This review provides clinical relevance and up-to-date information regarding the potential of TGF-β1 in diagnosis, prognosis, and therapy against HCC.

Key Words: Transforming growth factor-beta 1; Inflammation; Immunosuppression; Fibrogenesis; Hepatocellular carcinoma; Biomarker; Immunotherapy

©The Author(s) 2022. Published by Baishideng Publishing Group Inc. All rights reserved.

Core Tip: Transforming growth factor-beta 1 (TGF-β1) exhibits a progressive elevation throughout hepatic dysfunction starting from hepatitis to hepatocellular carcinoma (HCC) as an inflammatory cytokine, pro-fibrogenic marker, immunosuppressive agent and pro-carcinogenic growth factor. Aberrant TGF-β1 activation in HCC is associated with poor prognosis and survival. TGF-β1 mediated immunosuppression disturbs the anticancer surveillance and the efficacy of the immunotherapeutic agent. This pleiotropic effect of TGF-β1 in the context of HCC makes it ideal as a diagnostic, prognostic, and therapeutic candidate in HCC.

Citation: Devan AR, Pavithran K, Nair B, Murali M, Nath LR. Deciphering the role of transforming growth factor-beta 1 as a diagnostic-prognostic-therapeutic candidate against hepatocellular carcinoma. *World J Gastroenterol* 2022; 28(36): 5250-5264
URL: https://www.wjgnet.com/1007-9327/full/v28/i36/5250.htm
DOI: https://dx.doi.org/10.3748/wjg.v28.i36.5250

INTRODUCTION

Hepatocellular carcinoma, an aggressive and refractory cold tumor

Liver cancer, specifically hepatocellular carcinoma (HCC) is often recognized as an aggressive malignancy, ranking 6th in incidence and 3rd in terms of mortality in 2020, where mortality rates are roughly equivalent to incidence rate[1]. As it develops in the background of chronic inflammation starting from the fatty liver, HCC remains undiagnosed for years until it worsens. The progressive transformation from cirrhosis to HCC also creates longer delays in diagnosis[2]. HCC is commonly diagnosed by liver imaging techniques such as ultrasound, computed tomography and magnetic resonance imaging. Blood biomarkers such as alpha fetoprotein (AFP), protein induced by vitamin K absence or antagonist II levels, and liver biopsy are also used to diagnose HCC[3,4]. Even though the recent guidelines recommend HCC surveillance biannually and antiviral vaccination, the lack of effective surveillance programs significantly contributes to HCC progression to the advanced stage, particularly in high-risk individuals. Once established, HCC cells rapidly proliferate and spread to the extrahepatic site, such as the lungs, portal vein, and lymph nodes. In such cases, in an advanced stage, curative interventions such as liver transplantation, resection, percutaneous ablation, and chemoembolization were not responsive. Systemic drug therapy remains the primary treatment modality[5,6], where immunotherapy and tyrosine kinase inhibitors are the approved treatment options[7]. However, limited response to therapy, the emergence of multidrug resistance, immunosuppressive tumor microenvironment, and lack of validated diagnostic and prognostic biomarkers pose significant obstacles in establishing effective treatment against HCC[8,9].

Transforming growth factor-beta (TGF-β) is a critical homeostasis regulator, which is aberrantly activated during inflammation, fibrosis and carcinogenesis[10]. Among the three isoforms, TGF-β1 is superior in TGF-β signal transduction, especially those related to chronic liver diseases. Since HCC is an inflammation-induced-immunosuppressed malignancy, the role of TGF-β1 signaling in HCC has been extensively evaluated recently[11]. This review presents the potential of the TGF-β superfamily of ligands, specifically TGF-β1, to develop as a therapeutic and prognostic-diagnostic marker candidate against HCC.

TGF-β1 signaling in HCC

TGF-β superfamily of ligands is a dimeric peptide growth factor with more than 30 members in humans, mainly TGF-βs, activins, inhibins, and bone morphogenetic proteins. TGF-βs are categorized into three different isoforms TGF-β1, TGF-β2, and TGF-β3. Of the three isoforms, TGF-β1 is the most evaluated and abundant, found in epithelial, endothelial, hematopoietic, and connective tissue. TGF-β 2 is expressed in epithelial and neuronal cells, while TGF-β3 is found in mesenchymal cells[12]. TGF-βs are implicated in diverse physiological processes, including cell homeostasis and embryonic development[13]. It is a pleiotropic factor that regulates inflammation, fibrogenesis, cell differentiation, proliferation, epithelial-mesenchymal transition (EMT), extracellular matrix (ECM) formation, tumor-suppressive and pro-tumor effect in a cell-context dependent manner[14].

The three isoforms of TGF-β have structural similarity and functional redundancy[15]. However, TGF-β1 is often considered a potent and superior isoform with significant physiological and pathological importance[16]. Importantly, TGF-β1 exerts a cell-context dependent effect in the liver[17,18]. Normal to activated TGF-β1 signature confers a protective effect by inhibiting hepatocyte proliferation and hepatic stellate cells (HSCs) activation, apoptosis induction, preventing fibrosis and improving liver function. While, aberrantly activated TGF-β1 signature manifests as HSC activation and worsening fibrosis to HCC, where tumor cells lose their sensitivity toward the inhibitory effect of TGF-β1[19-21]. Exposure of hepatocytes to various causative factors such as viruses, alcohol, toxicants and

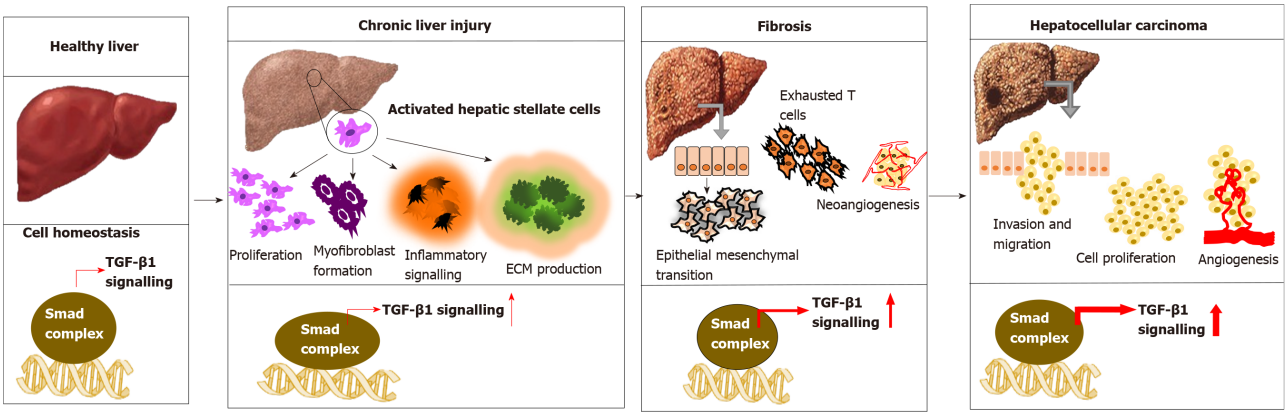
other metabolic disorders leads to the release of TGF-β1. Also, other pro-inflammatory cytokines such as tumor necrosis factor-α and growth factors from non-parenchymal liver cells switch on inflammation, production of ECM, and accumulation of fibrous material that eventually progress to cirrhosis[22,23]. A simultaneous increase in integrins, a vital cell adhesion molecule, is observed as the fibrogenesis continues. These integrins interact with TGF-β1 and other ECM proteins, altering signal transduction pathways[24]. Along with the accumulation of genetic mutations, HSC induces TGF-β and β-catenin-dependent EMT, leading to tumor growth in the liver. TGF-β1 continues to increase, promoting neo-angiogenesis by interacting with other pathways and mediating stromal-tumor cell interaction, conferring aggressive phenotype and metastasis[25] (Figure 1). Wang *et al*[26] demonstrated that both TGF-β1 and TGFβR1 have a crucial role in regulating proliferation, invasion, metastasis and immune response in HCC cells.

TGF-β1 exerts biological and pathological effects *via* Smad and non-Smad pathways. TGF-βs are synthesized in the inactivated form and exist as latent TGF-β complex (LTC) by binding with latency-associated protein. Later, LTC is converted to large latent complex (LLC) by interacting with latent TGF-β binding protein in ECM. Integrin signaling plays a significant role in the activation and subsequent release of TGF-β1 from LLC. It is also mediated by other factors such as pH, protease enzyme *etc.*[27]. In the canonical Smad pathway, activated TGF-β first binds with the extracellular domain of TGF-β receptor type II, which triggers the cross phosphorylation of the kinase domain of TGF-β receptor type I. TGF-β R1 activation leads to the phosphorylation of Smad proteins, Smad 2 and Smad 3. Later Smad-2 and 3 complex bind with the co-Smad, Smad-4 to form a ternary complex. This ternary complex is then translocated into the nucleus, binds to Smad binding elements in DNA, and activates the transcription of TGF-β-dependent genes[28]. Binding of inhibitory Smad, Smad-7 will shut down the activated pathway[29]. In addition to the Canonical Smad pathway, TGF-β can exert biological functions by activating other diverse signalings such as P38, JNK, PI3K/AKT, RAS-ERK, and RHO-ROCK, which constitute the non-Smad pathway of TGF-β signal transduction[30] (Figure 2).

Smad pathway of TGF-β signal transduction also enhances the transcription of FoxP3, predominantly present in T regulatory (Treg) cells[31,32]. A high amount of tumor-infiltrating Treg cells and FoxP3 positive Treg cells in blood is reported in HCC patients, leading to the deterioration of effector T cells such as CD4+ and CD+ cytotoxic T cells lymphocytes, which are pillars of anticancer immunity[33,34]. Together, TGF-β inhibits natural killer (NK) cells, blocks interferon (IFN)-γ secretion, and prevents effector immune cells recruitment to tumor tissue[35,36]. Additionally, TGF-β inhibits IFN-γ secretion by interacting with the activating transcription factor 1[37]. Likewise, TGF-β-RUNX3 transcription factor interaction and co-expression of programmed death ligand 1 (PD-L1) and interleukin-10 promote the transformation of naïve B cells to immunoglobulin A producing B cells, which are crucial in HCC development from non-alcoholic fatty liver[38]. Elevated TGF-β can directly enhance the transcription of PD-1 in HCC. The interaction of PD-1 with PD-L1 causes significant immunosuppression by T cell exhaustion, which manifests as inhibition of T cell activation, proliferation, and cytotoxic action[39,40]. In a recent study, Bao *et al*[41] reported that TGF-β1 trigger the expression of immune checkpoints such as PD-1 and CTLA4 on HCC cells and attenuates T-cell-mediated anti-tumor immune surveillance. Therefore, up-regulated TGF-β mainly isoforms 1 directly affect immune checkpoint inhibition, and it works as an indicator of T cell exhaustion. This evidence suggests the potential of TGF-β1 targeted immunotherapies against HCC. The pivotal role of the TGF-β1 signature in hepatic dysfunction and HCC extends its potential as a biomarker molecule for diagnosis and prognostic prediction and a therapeutic target.

Clinical utility of TGF-β1 as diagnostic marker of HCC

As an inflammatory-fibrogenic cytokine molecule, the involvement of TGF-β1 in all stages of liver injury, starting from fatty liver, steatosis, fibrosis to cirrhosis, and HCC, is evident. Intergromic analysis of TGF-β gene alterations among the 33 cancer types in the TGCA dataset revealed 39% alterations. Gastrointestinal cancers and HCC exhibited prominent mutation compared with other cancer types[42]. Later, in an HCC-specific transcriptomic analysis, 40% of HCC samples were found with mutations in genes of the TGF-β pathway[43]. Higher TGF-β1 levels in HCC correlate with the high rate of extrahepatic metastasis (EHM), poor prognosis, and low survival rate[44]. After acute/chronic liver injury, liver sinusoidal endothelial cells and HSCs secrete TGF-β1 and up-regulate TGF-β receptors[45,46]. Elevated TGF-β1 level was found in viral and alcohol-induced fibrosis[47]. Thus, TGF-β levels can be used to track the response to therapy so that the decrease in TGF-β 1 level followed by IFN treatment in hepatitis B virus (HBV) patients is associated with improved treatment outcomes. Apart from HSC-triggered TGF-β secretion, hepatitis C virus (HCV) infection can also induce TGF-β1 production in hepatocytes[48]. Likewise, proteomic and phospho-proteomic characterization of 110 tumor and non-tumor tissues of early-stage HBV-associated HCC found an increased expression of TGF-β genes compared with the non-tumor tissue[49]. However, the dichromatic role of TGF-β1 on cancer growth *i.e.*, tumor suppressive in early-stage or oncogenic effect in late-stage, is a matter of concern. Another study indicated a comparative functional genomic approach and illustrated the link between TGF-β expression signature and HCC subtypes. The study shows that TGF-β positive HCC clusters can be categorized into two. HCC with early TGF-β signature exhibit physiological responses while HCC associated with late TGF-β signature showed metastasis and poor survival[50]. N-2-fluorenylacetamide-



DOI: 10.3748/wjg.v28.i36.5250 **Copyright** ©The Author(s) 2022.

Figure 1 Involvement of transforming growth factor-beta 1 in various stages of liver dysfunction. Transforming growth factor-beta (TGF-β) regulates cell homeostasis in normal physiological conditions. As an inflammatory-fibrogenic cytokine molecule, the involvement of TGF-β1 in all phases of liver injury, from fatty liver, steatosis, fibrosis to cirrhosis, and hepatocellular carcinoma, is evident. Causative agents like viral infection, alcohol and co-morbidities like diabetes and obesity trigger the release of a pro-inflammatory cytokine such as TGF-β1, which stimulates inflammation, extracellular matrix (ECM) production, and accumulation of fibrous material that eventually progress to cirrhosis. As the fibrosis continues, the interaction of overexpressed TGF-β1 with integrins and other ECM proteins can alter signaling, accumulate gene mutation, and induce epithelial-mesenchymal transition and hepatocarcinogenesis. TGF: Transforming growth factor; ECM: Extracellular matrix; HCC: Hepatocellular carcinoma.

induced rat hepatoma model is used to investigate the association of TGF-β1 expression with different stages of hepatocarcinogenesis and a progressive elevation of hepatic TGF-β1 and TGF-β1 mRNA was found during the transformation of hepatocytes to malignant cells[51]. Another study indicates that elevated plasma TGF-β1 level was found in 89.5% of HCC patients, and interestingly, among these patients, 93.3% had an AFP level less than 400 μg/L[52]. This suggested that TGF-β1 expression can be a more accurate and sensitive biomarker for early diagnosis of HCC for monitoring the disease progression.

The diagnostic importance of TGF-β1 is established significantly earlier itself. In 1997, Tsai *et al*[53] investigated the correlation of urine TGF-β1 level with HCC. They found a significant increase in TGF-β 1 level in HCC patients compared with other healthy control groups, cirrhotic chronic hepatitis patients. They also reported the association of TGF-β 1 levels with poor prognosis and shorter survival[53]. Later, the same team compared the study with another important tumor marker, AFP, and found that disease progression from cirrhosis to HCC is characterized by a typical elevation in both urinary TGF-β1 and serum AFP with a diagnostic accuracy of about 90%[54,55]. These collective data suggest the potential of TGF-β1 be used along with AFP as a complementary tumor marker to differentiate HCC from cirrhosis correctly. Another study investigated the rationale for parallel determination of TGF-β1 and AFP to diagnose HCC. They found that the TGF-β1 level exhibited a stage-dependent increase in all liver diseases where AFP showed HCC-specific elevation[56]. As TGF-β1 estimation tracks the disease progression pattern, TGF-β can be considered a more sensitive diagnostic marker of HCC. Its specificity is higher when it is analyzed along with AFP. To diagnose and select patients for galunisertib (TGF-β inhibitor) therapy, Cao *et al*[57] in 2017 performed next-generation sequencing-based analysis in HCC samples and found that m RNA levels of TGF-β1 along with SKIL and PMEPA1 could be better diagnostic markers as well as to select patients who are more likely to respond with galunisertib.

Another study investigated the association of serum TGF-β1 with disease severity in HCC using 180 subjects in different stages of HCC. Group of cirrhotic patients, as well as healthy control, was also maintained. Consistent with the previous reports, this study also found a significant increase in TGF-β1 level in HCC (1687.47 ± 1462.81 pg/mL) as compared with cirrhotic patients (487.98 ± 344.23 pg/mL) and control (250.16 ± 284.16 pg/mL). Additionally, the serum level of TGF-β1 showed exponential elevation as the disease progressed from early to advanced, *i.e.*, during progression from Barcelona Clinic Liver Cancer stage A to D, TGF-β 1 level increased from 652.83-1668.78 pg/mL[56]. The best cut-off value of TGF-β1 detection was determined as 301.9 pg/mL, comparable with the value (370 pg/mL) reported by Shehata *et al*[58] (Table 1).

Background inflammation and indolent transformation are the critical factors that create a waiting time paradox in diagnosing HCC, making the tumor more aggressive and refractory. Since TGF-β, specifically TGF-β1 plays an essential function from the initial hepatic injury to hepatocarcinogenesis, it holds immense potential to validate as a diagnostic marker of HCC. Though the dual functioning of TGF-β1 is still debatable, the diagnostic relevance of TGF-β1 is well evident, and thus, it warrants further investigations and clinical validation.

Table 1 Research progress on the clinical utility of transforming growth factor-beta 1 as diagnostic marker against hepatocellular carcinoma

Ref.	Sample size HCC/control	Assay type	TGF-β1 level	Sample type	Outcome of the study
[60, 61]	26/20	ELISA	Control: 1.4 ± 0.8 ng/mL HCC: 19.3 ± 1.95 ng/mL (P < 0.05)	Plasma	TGF-β1 level showed a progressive elevation from cirrhotic to HCC patients to normal subjects. No significant association was found between plasma TGF-β1 and serum AFP levels
[62, 63]	70	ELISA	Control: 2.7 ± 0.7 ng/mL HCC: 7.3 ± 4.3 ng/mL (P < 0.05)	Plasma	Elevated plasma TGF-β1 levels in HCC patients are associated with increased tumor size, overexpression of tissue inhibitor of metalloproteinase-1 and tumor severity
[54, 55]	94/50	^{125}I-Radio Immuno Assay Kit	Control: 1.5-33.6 μg-^{1} creatinine Cirrhotic: 4.3-52.5 μg^{-1} creatinine HCC: 3.5-184 μg^{-1} creatinine (P < 0.0001)	Urine	Urinary TGF-β1 and serum AFP levels were higher in HCC than in cirrhotic patients. The study suggested that both TGF-β and AFP can be used as complementary biomarkers to distinguish between HCC and cirrhosis
[64]	54/30	ELISA	TGF-β1 score Control: 0.6 ± 0.2 HCC: 1.6 ± 0.5	Serum	The study team calculated the serum concentration score based on the cut-off limit of 74 pg/mL and 637 pg/mL for TGF-β1 and sFas, respectively. TGF-β1 levels were higher than the cut off value in 23% HCC patients with negative AFP values, suggesting its diagnostic potential in AFP negative HCC
[65]	38/23	ELISA	Control: 300 pg/mL HCC: 954.9 pg/mL (P < 0.0001)	Plasma	Elevated plasma TGF-β1 level can be a useful diagnostic marker in detecting small HCC, with higher sensitivity than AFP
[66]	70/32	ELISA	Control: 2 ng/mL HCC: 7.5 ng/mL (P < 0.0001)	Plasma	Higher circulating TGF-β1 in HCC patients is associated with suppression of anti-tumor immunity and disease progression
[52]	50/30	ELISA	Control: 0.67 ± 0.1 μg/mL HCC: 2.21 ± 1.1 μg/mL (sensitivity = 89.5%, specificity = 94%)	Serum	Aberrant TGF-β1 expression in HCC is associated with differentiation and worsening of HBV infection
		RT-PCR	Overexpression TGF-β1 mRNA in HCC patients, P < 0.0001		Circulating TGF-β1 level and TGF-β1 mRNA expression can be used as sensitive biomarkers for diagnosing HBV induced HCC
[56]	23/40	ELISA	Control: 14.35 ± 8.76 ng/mL HCC: 64.35 ± 33.68 ng/mL (P < 0.05)	Serum	TGF-β1 is a sensitive diagnostic marker for HCC than AFP. Specificity can be increased with combined evaluation of TGF-β1 and AFP levels
[67]	54/30	ELISA	Control: 39.5 ± 9.8 pg/mL HCC: 1194 ± 331 pg/mL (P < 0.0001)	Serum	The study suggested elevated TGF-β1 and EGFR levels as reliable diagnostic markers for HCC induced, AFP negative HCC
[68]	120/30	ELISA	Control: 250.16 ± 284.61 pg/mL Cirrhotic: 487.98 ± 344.23 pg/mL HCC: 1687.47 ± 1642 pg/mL (P < 0.0001)	Serum	TGF-β1 showed progressive elevation during various stages of liver dysfunction. Higher TGF-β1 level in HCC is associated with tumor grade, pathological stage and invasiveness
[69]	100/36	ELISA	Control: 57.29 ± 11.70 ng/mL HCC: 225.82 ± 48.93 ng/mL (P < 0.0001)	Serum	Serum levels of TGF-β were significantly higher in HCC patients than in normal controls

ELISA: Enzyme-linked immunosorbent assay; RT-PCR: Reverse transcription-polymerase chain reaction; HCC: Hepatocellular carcinoma; TGF-β: Transforming growth factor-beta; AFP: Alpha fetoprotein; HBV: Hepatitis B virus; EGFR: Epidermal growth factor receptor.

The clinical utility of TGF-β1 as a prognostic marker of HCC

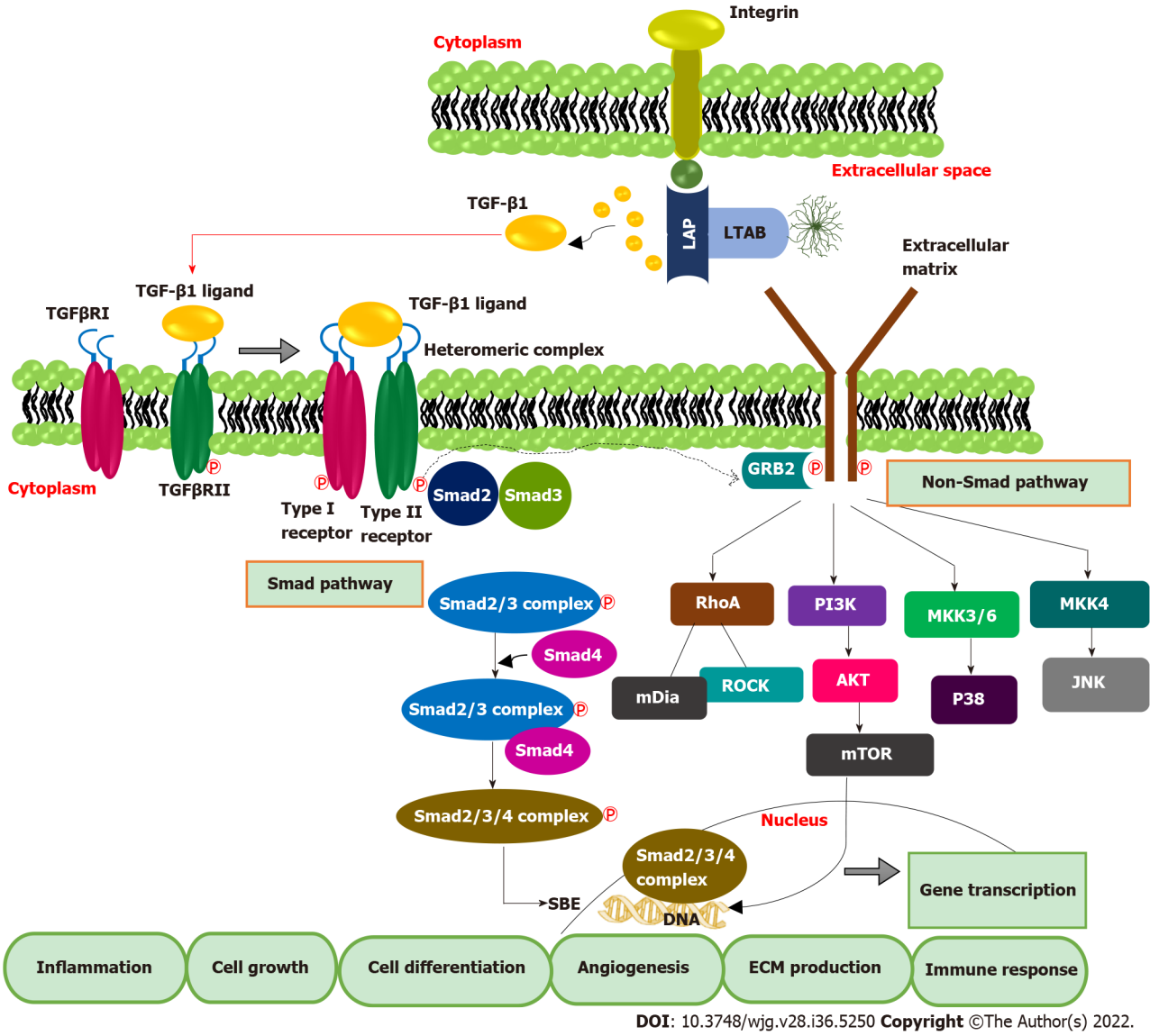
Poor prognostic characteristics of HCC contribute to late detection, aggressiveness and failure of therapeutic interventions[70]. Molecular pathways of hepato-carcinogenesis are still confusing because of the involvement of diverse molecular pathways, genetic alterations and evolution of malignant cells. Thus, this ultimately results in the worst prognosis within the early stage itself[71]. The expression of TGF-β1 is remarkably increased at the advanced stages of HCC and is involved in initiating EMT, regulating tumor proliferation, and promoting immunosuppressive tumor microenvironment during HCC progression under the challenges like liver cirrhosis, HBV and HCV infections. This warrants screening TGF-β1 levels from the early stages of HCC as a tool for evaluating the clinical outcomes. Depending upon the expression profile of TGF-β1, it is effortless to estimate the clinical impact of therapeutic strategies[72].

A research study conducted by Giannelli *et al*[73] proposed that TGF-β1 promotes EMT by stimulating homologous proteins like snail and slug. Secretion of TGF-β1 by HCC invasive cell lines, especially cell lines with α3β1-integrin expression, is significantly higher than in non-invasive and cirrhotic cell lines. The patients at the initial and advanced stages of HCC with a higher profile of TGF-β 1 possess a poor prognostic ratio with lower overall survival (OS) and disease-free survival rate (DFS) [73,74]. Likewise, another notable experimental study by Lee *et al*[75] demonstrated that plasma TGF-β1 is positively correlated with critical conditions like EHM, portal vein thrombosis, EHM, and regional lymph node involvement. Statistical studies involving the detailed examination of overall and cumulative survival rates of HCC patients showed that candidates with abundant levels of plasma TGF-β1 manifested remarkably lower survival rates than the candidates with lower expression of TGF-β1. This evidence points to the usefulness of TGF-β1 as a prognostic marker in HCC.

Wang *et al*[76] elucidated the crucial involvement of TGF-β1 in tumor progression. A total of 180 patients with HCC were selected for the study, and out of 180 HCC patients, 105 patients were found with a solid expression of TGF-β1. This study showed a positive correlation between TGF-β1 and Treg cells. The increased secretion of TGF-β1 at the starting stage of HCC indicates that the tumor may be one of the most critical sources of TGF-β1 in HCC patients. Earlier studies also provided evidence that TGF-β1 promotes the regulatory phenotype and modulates the biological functions of Tregs. By Kaplan-Meier evaluation, HCC patients overexpressing TGF-β1 in neoplastic tissues had a considerably shorter OS and a greater recurrence rate than patients with lower expression[76]. A meta-analysis study conducted by Peng *et al*[77] reported that TGF-β1 implements an unfavorable prognosis on OS rates of HCC patients with a hazard ratio of about 1.71 and 2.29 from both univariate and multivariate analysis. Additionally, the study indicates the worst prognosis of TGF-β1 upon DFS, relapse-free survival and progression-free survival of 1422 patients *via* COX univariate analysis with a hazard ratio of about 1.60. In summary, the results from these studies draw out the negative prognostic impact of high TGF-β1 expression on the OS in HCC patients.

TGF-β1 possesses a dual functional role in malignancy; initially, it acts by blocking epidermal growth and promoting tumor suppression, but in later stages, it appears to be involved in the up-gradation of advanced tumors[78]. Embryonic liver fodrin (ELF), a novel form of β-spectrin is involved as a Smad3/4 adaptor in TGF-β mediated tumor suppression signaling pathway. Miscolocalization of Smad3 and Smad4 caused by the dysregulation of ELF resulted in the disruption of TGF- β signaling pathways[79]. A research study conducted by Ji *et al*[80] investigated the predictive value of both TGF-β1 and ELF in HCC patients after hepatic resection. The expression of TGF-β1 is significantly higher in HCC tissues than in normal liver tissues, while the incidence of ELF is higher in normal liver tissue in contrast with HCC samples. The reports of post-operative survival rates of HCC patients with lower expressions of TGF-β1 showed that DFS and OS rates of HCC patients over 1 (79.4%), 3 (73.5%), and 5 (62.0%) years were significantly higher than the patients with higher expression of TGF-β1 (28.0%, 12.0%, and 12.0%). The study also showed a negative correlation between TGF-β1 and ELF levels. The study also indicates that DFS rates of HCC patients with higher expression of ELF and lower TGF-β1 levels are remarkably more elevated than the HCC patients with low expression of ELF and higher TGF-β1 levels for 1, 3, and 5 years (75.0%, 60.0%, and 57.5% *vs* 25.0%, 15.9%, and 10.2%, respectively), with *P*-value less than 0.001. Data from clinicopathological examination exhibited that TGF-β1 positively relates with hepatitis B surface antigen, tumor size, tumor number, TNM, and recurrence, while ELF is negatively correlated with all metastatic characteristics suggesting that ELF is associated with tumor suppressing features. This research study indicates that both TGF-β1and ELF can be included in the category of relevant biomarkers as prognostic agents for evaluating clinical results after hepatic resection[80].

An experimental approach described the correlation and the possibility of Fibroblast growth factor (FGF) receptor 4 (FGFR4) and TGF-β1 as prognostic biomarkers in HCC. FGFR4 is the most predominant isoform of the FGFRs family and is actively involved in various biological activities, including metastasis, differentiation, embryonic development, proliferation, apoptosis and angiogenesis [81]. Multiple studies showed that FGFR4 plays a clear-cut role in the pathogenesis of HCC and the up-regulation of FGFR4 possesses resistance to various targeted therapies[82]. A clinicopathological examination conducted by Chen *et al*[83] showed that elevated expression of both TGF-β1 and FGFR4 enhances tumors' invasiveness and metastatic nature. Clinicopathologic characteristics revealed that HCC patients at advanced stages with high TGF-β1 and FGFR4 expression were more likely to be at a higher TNM stage. Statistical data showed that the OS of patients over five-year survival rate is about



DOI: 10.3748/wjg.v28.i36.5250 **Copyright** ©The Author(s) 2022.

Figure 2 Transforming growth factor-beta 1 signaling pathway. Smad and non-Smad pathways mainly regulate transforming growth factor-beta 1 (TGF-β 1) signal transduction. Integrin signaling triggers the activation and release of TGF-β1 from LCC (large latent complex). Activated TGF-β1 binds TGF-β type II receptor, leading to phosphorylation of TGF-β type I receptor and associated Smad proteins, mainly Smad-2 and Smad-3. Phosphorylated Smad-2 and 3, complex with the co-Smad, Smad-7, form a ternary complex. This ternary complex then translocates into the nucleus, binds to Smad binding elements and regulates the transcription of TGF-β-related genes. TGF: Transforming growth factor; LAP: Latency associated protein; LTAB: Latent transforming growth factor-beta binding protein; SBE: Smad binding elements; ECM: Extracellular matrix; mTOR: Mammalian target of Rapamycin; PI3K: Phosphoinositide 3-kinase; AKT: AKT serine/threonine kinase 1; MKK: Mitogen-activated protein kinase kinase; JNK: C-Jun N-terminal kinase.

8.5%, and the median survival duration is 32.3 mo in case of TGF-β1 positive cases. In contrast, in TGF-β 1 negative expression cases, the OS of the patient is about 45.6% and the median survival rate is 50.4 mo. Candidates with high TGF-β1 expression had a short OS rate in contrast to those with negative TGF-β1 expression profiles. Likewise in cases of high levels of FGFR4, the OS rate of patients is very low, that is five-year survival rate is only about 8.3%, and median survival rate is 29.4 mo while in the condition of impeded FGFR4 expression, the five-year survival rate is about 70.1% and the median survival period is 51.2 mo. This study showed a positive correlation between TGF-β1 and FGFR4 as prognostic markers in HCC. Additionally, the results from univariate and multivariate analyses showed that both TGF-β1 and FGFR4 are independent and reliable prognostic factors in HCCs for evaluating the therapeutic response in HCC patients, especially after post-operative procedures[83]. The strong correlation between TGF-β1 expression and survival rates of HCC patients suggests its potential as a prognostic biomarker for HCC (Table 2). In addition to the role of TGF-β1 as an effective prognostic marker, it can also be used for targeted therapeutic strategies.

The clinical utility of TGF-β1 as therapeutic target in HCC

Tyrosine kinase inhibitor, Sorafenib was the first approved first-line therapy for advanced HCC. Sorafenib was the first-line therapy for ten years until another tyrosine kinase inhibitor, Levatinib was

Table 2 Research progress on the clinical utility of transforming growth factor-beta 1 as a prognostic marker against hepatocellular carcinoma

Ref.	Sample size HCC/control	Sample and assay type	TGF-β1 level	Survival rate (%), (patients with higher TGF-β1 *vs* patients with lower TGF-β1)	Outcome of the study
[75]	571/551	Plasma ELISA	Control: 3.58 ± 0.17 $\log_{10}$ pg/mL Cirrhotic: 3.20 ± 0.37 $\log_{10}$ pg/mL HCC: 3.83 ± 0.31 $\log_{10}$ pg/mL	1 yr survival (47 *vs* 60) 3 yr survival (28 *vs* 36) $P < 0.05$	Plasma TGF-β1 levels showed a positive correlation with tumor size, invasion and extrahepatic metastasis and inversely correlated with survival rates in HCC patients
[83]	126	Tumor tissue Immunohistochemistry	84% samples (106/126) showed high intra-tumoral TGF-β1 expression 64.3% samples (81/126) showed high peri-tumoral TGF-β1 expression	5 yr survival (8.5 *vs* 45.6)	TGF-β1 and FGFR4 were positively correlated in HCC tumor tissues and showed a significant association with shorter survival rates in patients
[80]	84/20	Tumor tissue Immunohistochemistry	TGF-β1 overexpression found in 59.5% samples (50/84) than that of normal liver tissue	1 yr survival (28 *vs* 79.4) 5 yr survival (12 *vs* 62.6)	TGF-β1 expression was dominant, whereas ELF expression was suppressed in HCC tissues Patients with high TGF-β1 and lower ELF expression are associated with poor overall survival and post-operative disease free survival compared with low TGF-β1 and high ELF group
[76]	184/30	Plasma and tumor tissue ELISA and immunohistochemistry	Elevated plasma TGF-β1 level TGF-β1 was strongly stained in tumor tissue	2 yr survival (51 *vs* 77) 3 yr survival (4 *vs* 68), $P < 0.05$	Higher TGF-β1 expression in tumor tissues triggers Treg cells mediated immunosuppression in tumor microenvironment and contribute to poor prognosis in HCC
[84]	40	Serum ELISA	Before RFA: 63.22 ± 23.61 ng/mL After RFA: 56.33 ± 24.24 ng/mL	NA	Radiofrequency ablation lowered TGF-β1 and AFP L3% expression in HCC patients Low TGF-β1 and AFP L3% levels were observed in the no recurrence group, suggesting its potential as prognostic markers for HCC

ELISA: Enzyme-linked immunosorbent assay; HCC: Hepatocellular carcinoma; TGF-β: Transforming growth factor-beta; AFP: Alpha feto protein; ELF: Embryonic liver fodrin; FGFR: Fibroblast growth factor receptor 4.

approved in 2018. Even though tyrosine kinase inhibitors dominated HCC therapy as first-line or second-line options, the efficacy was only modest, with limited treatment outcome, the emergence of drug resistance, and also relapse[85]. Recently treatment strategies adopted a paradigm shift to immunotherapeutic approaches because of the importance of the immune microenvironment in carcinogenesis.

The liver is the most extensive reticuloendothelial system and peripheral immunomodulatory organ in the human body. Immunotherapy is being extensively evaluated in liver cancer[86]. The liver constitutes a vast repository of immune cells including NK cells, kupffer cells, sinusoidal endothelial cells, and innate T cells[87]. Aberrant immune checkpoint activation makes HCC a cold tumor, where anti-tumor immune surveillance is completely abolished[88]. Combination of immune checkpoint inhibitors (ICIs) such as Nivolumab (PD-1 inhibitor) + Ipilimumab (CTLA4 inhibitor) and Atezolizumab (PD-L1 inhibitor) + Bevacizumab [vascular endothelial growth factor (VEGF) inhibitor] got approval as first-line therapy for various cancer such as non-small cell lung cancer (NSCLC), HCC in 2020[89]. Though ICIs exerted a superior effect to tyrosine inhibitors, current immunotherapeutic drugs failed to establish an effective anticancer immunity against HCC. Though the immunotherapeutic approaches modify effector immune cells functions to elicit anti-tumor immune response, the immunosuppressive tumor microenvironment neutralizes the effects of immunotherapy[90].

Analysis of the TGF-β profile of HCC samples in the TGCA data set revealed four categories with typical TGF-β expression[91]. The cluster with a highly activated TGF-β signature, which accounts for 14.5% of samples, exhibited prominent immune exhaustion and poor prognosis. ICIs may not work well in this cluster. Additionally, anti-inflammatory/anti-fibrotic agents targeting TGF-β can improve the

Table 3 Clinical trials of transforming growth factor-beta 1 blockade with Galunisertib in hepatocellular carcinoma and other cancers

Drug	Title of the study	Treatment	Phase	Status	Trial ID
Galunisertib	A study of Galunisertib on the immune system in participants with cancer	Monotherapy	Phase I	Completed	NCT02304419
Galunisertib	Galunisertib (LY2157299) and stereotactic body radiotherapy in advanced hepatocellular carcinoma	Combination with radiotherapy	Phase I	Completed	NCT02906397
Galunisertib	A study of LY2157299 in participants with unresectable hepatocellular cancer	Combination with Nivolumab	Phase II	Completed	NCT02423343
Galunisertib	A study of LY2157299 in participants with unresectable hepatocellular cancer	Combination with Sorafenib	Phase I	Completed	NCT02240433
Galunisertib	A study of LY2157299 in participants with advanced hepatocellular carcinoma	Combination with Sorafenib	Phase II	Completed	NCT02178358
Galunisertib	A study of LY2157299 in participants with hepatocellular carcinoma	Combination with Sorafenib/Ramucirumumab	Phase II	Completed	NCT01246986
Galunisertib	Galunisertib and Capecitabine in advanced resistant TGF-beta activated colorectal cancer (EORTC1615)	Combination with Capecitabine	Phase II	Withdrawn	NCT03470350
Galunisertib	A study of LY2157299 in participants with pancreatic cancer (advanced or has spread to another part of the body)	Combination with Gemcitabine	Phase I	Completed	NCT02154646
Galunisertib	A study of Galunisertib (LY2157299) and Durvalumab (MEDI4736) in participants with metastatic pancreatic cancer	Combination with Durvalumab	Phase I	Completed	NCT02734160

TGF: Transforming growth factor.

immune milieu[92,93]. The majority of HCC samples belong to a cluster of activated TGF-β signature (45%) and showed a low level of an immune response. Hence, combining a TGF-β inhibitor with an immune checkpoint inhibitor can exert a synergistic effect. 30% of HCC samples showed a normal TGF-β signature associated with active immune surveillance; therefore, immunotherapy will be most suitable for this cluster. The fourth cluster is a minor population (9.9%) that exhibits inactivated TGF-β signature with poor immune cell activation and response[94]. With this evidence, it is clear that TGF-β1 signature can be used to decide the suitable therapy or predict the outcome of immunotherapy.

Several specific and non-specific inhibitors of TGF-β, mainly TGF-β1 and 2 inhibitors, are being developed and evaluated against various tumors, including HCC. Regarding non-specific inhibitors, as the primary molecular target is different, its ability to block the TGF-β pathway offers additional benefits as anticancer agents. One such example is Halofuginone, an alkaloid coccidiostat with reported preclinical activity against HCC. In addition to the prominent inhibition of collagen synthesis, Halofuginone also blocks TGF-β1, inhibits ECM formation and fibroblast proliferation, increases IFN-γ and anti-tumor immune response[95,96]. The effect of Halofuginone against advanced progressive solid tumor has been evaluated in phase I clinical trial (NCT00027677), and in 2000, United States Food and Drug Administration gave orphan drug approval status to Halofuginone for treatment of scleroderma [97]. Histone deacetylase exerts epigenetic regulation of TGF-β1 mediated fibrosis and carcinogenesis [98]. Studies indicate that histone deacetylase inhibitors such as Panobinostat have shown effectiveness in HCC animal models and phase I human trials combined with sorafenib (NCT00823290)[99]. Apart from the non-specific inhibitors, recent preclinical interventions combined TGF-β1 targeting antibodies or TGF-βR1 inhibitor with PD-L1 inhibitors and obtained prominent cytotoxic effect and anticancer immune surveillance in various solid tumors[100,101]. Likewise, M7824 is a bifunctional fusion protein with dual targeting of PD-L1 and TGF-β, which has been evaluated in animal models of various cancers either alone or in combination with vaccines[102]. M7824 exerted a significant inhibitory effect on TGF-β 1[103]. Among the different TGF-β inhibitors, LY2109761 is an orally bioavailable TGF-β receptor type I inhibitor, which exhibited an antitumor effect in various HCC animal models[104]. LY2109761 inhibited TGF-β1 induced migration, invasion, and anoikis in HCC cells[105,106]. Another study suggested the anti-angiogenic potential of LY2109761, which was superior to the typical VEGF inhibitor, Bevacizumab, and the effect was mediated by suppression of VEGF through inhibition of Smad dependent TGF-β1 signaling[107,108]. In addition to this, anti-TGF-β agents targeting other isoforms are also developed. AP-12009 is a TGF-β2 specific antisense oligonucleotide in a clinical trial to treat glioma and anaplastic astrocytoma[109,110]. Likewise, TGF-β1 directed mRNA was developed as AP-11011, which is evaluated against NSCLC, colon cancer in preclinical models[111]. Lordelimumab is a TGF-β2 specific monoclonal antibody with an anti-fibrotic effect[112]. Many preclinical studies investigated different TGF-β inhibitors, yet, Galunisertib (LY2157299), a kinase inhibitor of TGF-β1, is only the one in current clinical trials[113]. Several clinical trials of Galunisertib are ongoing or completed either alone or combined with Sorafenib, ICIs, and alkylating agents (Table 3).

CONCLUSION

TGF-β1 exerts a unique regulatory power on inflammation, fibrogenesis, and immune response in HCC. Among other TGF-β isoforms, significant and progressive expression of TGF-β1 during the entire course of HCC pathogenesis, starting from chronic hepatitis to HCC makes it a sensitive and accurate diagnostic marker of HCC. The specificity and sensitivity of TGF-β1 based diagnosis of HCC by parallel estimation of serum AFP. Even after establishing HCC, TGF-β1 continues to elevate as HCC progresses and is associated with poor prognosis and shorter survival. Since TGF-β1 is the master regulator of the immunosuppressive tumor milieu in HCC, TGF-β1 inhibition could sensitize ICI, tyrosine kinase inhibitors, and other systemic or curative interventions. HCC remains the deadliest-refractory tumor predominantly due to its delayed diagnosis. In that context, TGF-β1 is relevant for early diagnosis, prognosis, and therapy. Even though a plethora of supporting evidence is available, still TGF-β1 is not much studied and evaluated compared with other markers such as AFP. Notably, the dichotomic nature of TGF-β signaling in HCC needs to be defined accurately to establish the clinical utility of TGF-β1. Thus, proper and careful determination of the TGF-β1 profile of patients is necessary to choose the suitable patients for TGF-β1 targeted therapy.

FOOTNOTES

Author contributions: Nath LR conceptualized, designed the review content and revised the draft; Devan AR wrote the draft; Pavithran K revised and proofread; Nair B and Murali M collected the data; and all authors have read and approved the final manuscript.

Supported by the Amrita Vishwa Vidyapeetham SEED grant (K-PHAR-22-662).

Conflict-of-interest statement: All the authors report no relevant conflicts of interest for this article.

Open-Access: This article is an open-access article that was selected by an in-house editor and fully peer-reviewed by external reviewers. It is distributed in accordance with the Creative Commons Attribution NonCommercial (CC BY-NC 4.0) license, which permits others to distribute, remix, adapt, build upon this work non-commercially, and license their derivative works on different terms, provided the original work is properly cited and the use is non-commercial. See: https://creativecommons.org/Licenses/by-nc/4.0/

Country/Territory of origin: India

ORCID number: Aswathy R Devan 0000-0001-8928-8191; Keechilat Pavithran 0000-0002-6129-5709; Bhagyalakshmi Nair 0000-0002-0364-881X; Maneesha Murali 0000-0003-2772-3930; Lekshmi R Nath 0000-0002-7726-7219.

S-Editor: Wang JJ
L-Editor: A
P-Editor: Wang JJ

REFERENCES

1 **McGlynn KA**, Petrick JL, El-Serag HB. Epidemiology of Hepatocellular Carcinoma. *Hepatology* 2021; **73** Suppl 1: 4-13 [PMID: 32319693 DOI: 10.1002/hep.31288]
2 **Patel N**, Yopp AC, Singal AG. Diagnostic delays are common among patients with hepatocellular carcinoma. *J Natl Compr Canc Netw* 2015; **13**: 543-549 [PMID: 25964640 DOI: 10.6004/jnccn.2015.0074]
3 **Bialecki ES**, Di Bisceglie AM. Diagnosis of hepatocellular carcinoma. *HPB (Oxford)* 2005; **7**: 26-34 [PMID: 18333158 DOI: 10.1080/13651820410024049]
4 **Cervello M**, McCubrey JA, Cusimano A, Lampiasi N, Azzolina A, Montalto G. Targeted therapy for hepatocellular carcinoma: novel agents on the horizon. *Oncotarget* 2012; **3**: 236-260 [PMID: 22470194 DOI: 10.18632/oncotarget.466]
5 **Suresh D**, Srinivas AN, Kumar DP. Etiology of Hepatocellular Carcinoma: Special Focus on Fatty Liver Disease. *Front Oncol* 2020; **10**: 601710 [PMID: 33330100 DOI: 10.3389/fonc.2020.601710]
6 **Llovet JM**, Kelley RK, Villanueva A, Singal AG, Pikarsky E, Roayaie S, Lencioni R, Koike K, Zucman-Rossi J, Finn RS. Hepatocellular carcinoma. *Nat Rev Dis Primers* 2021; **7**: 6 [PMID: 33479224 DOI: 10.1038/s41572-020-00240-3]
7 **Kumari R**, Sahu MK, Tripathy A, Uthansingh K, Behera M. Hepatocellular carcinoma treatment: hurdles, advances and prospects. *Hepat Oncol* 2018; **5**: HEP08 [PMID: 31293776 DOI: 10.2217/hep-2018-0002]
8 **Cuestas ML**, Oubina JR, Mathet VL. Hepatocellular carcinoma and multidrug resistance: Past, present and new challenges for therapy improvement. *World J Pharmacol* 2015; **4**: 96-116 [DOI: 10.5497/wjp.v4.i1.96]
9 **Devan AR**, Kumar AR, Nair B, Anto NP, Muraleedharan A, Mathew B, Kim H, Nath LR. Insights into an Immunotherapeutic Approach to Combat Multidrug Resistance in Hepatocellular Carcinoma. *Pharmaceuticals (Basel)* 2021; **14** [PMID: 34358082 DOI: 10.3390/ph14070656]
10 **Prud'homme GJ**. Pathobiology of transforming growth factor beta in cancer, fibrosis and immunologic disease, and

therapeutic considerations. *Lab Invest* 2007; **87**: 1077-1091 [PMID: 17724448 DOI: 10.1038/Labinvest.3700669]
11 **Fabregat I**, Moreno-Càceres J, Sánchez A, Dooley S, Dewidar B, Giannelli G, Ten Dijke P; IT-LIVER Consortium. TGF-β signalling and liver disease. *FEBS J* 2016; **283**: 2219-2232 [PMID: 26807763 DOI: 10.1111/febs.13665]
12 **Katz LH**, Likhter M, Jogunoori W, Belkin M, Ohshiro K, Mishra L. TGF-β signaling in liver and gastrointestinal cancers. *Cancer Lett* 2016; **379**: 166-172 [PMID: 27039259 DOI: 10.1016/j.canlet.2016.03.033]
13 **Ikushima H**, Miyazono K. TGFbeta signalling: a complex web in cancer progression. *Nat Rev Cancer* 2010; **10**: 415-424 [PMID: 20495575 DOI: 10.1038/nrc2853]
14 **Li MO**, Flavell RA. TGF-beta: a master of all T cell trades. *Cell* 2008; **134**: 392-404 [PMID: 18692464 DOI: 10.1016/j.cell.2008.07.025]
15 **Huang J**, Qiu M, Wan L, Wang G, Huang T, Chen Z, Jiang S, Li X, Xie L, Cai L. TGF-β1 Promotes Hepatocellular Carcinoma Invasion and Metastasis *via* ERK Pathway-Mediated FGFR4 Expression. *Cell Physiol Biochem* 2018; **45**: 1690-1699 [PMID: 29490293 DOI: 10.1159/000487737]
16 **Yang AT**, Hu DD, Wang P, Cong M, Liu TH, Zhang D, Sun YM, Zhao WS, Jia JD, You H. TGF-β1 Induces the Dual Regulation of Hepatic Progenitor Cells with Both Anti- and Proliver Fibrosis. *Stem Cells Int* 2016; **2016**: 1492694 [PMID: 26839553 DOI: 10.1155/2016/1492694]
17 **Nair B**, Nath LR. Inevitable role of TGF-β1 in progression of nonalcoholic fatty liver disease. *J Recept Signal Transduct Res* 2020; **40**: 195-200 [PMID: 32054379 DOI: 10.1080/10799893.2020.1726952]
18 **Siegel PM**, Massagué J. Cytostatic and apoptotic actions of TGF-beta in homeostasis and cancer. *Nat Rev Cancer* 2003; **3**: 807-821 [PMID: 14557817 DOI: 10.1038/nrc1208]
19 **Caja L**, Ortiz C, Bertran E, Murillo MM, Miró-Obradors MJ, Palacios E, Fabregat I. Differential intracellular signalling induced by TGF-beta in rat adult hepatocytes and hepatoma cells: implications in liver carcinogenesis. *Cell Signal* 2007; **19**: 683-694 [PMID: 17055226 DOI: 10.1016/j.cellsig.2006.09.002]
20 **Bedossa P**, Peltier E, Terris B, Franco D, Poynard T. Transforming growth factor-beta 1 (TGF-beta 1) and TGF-beta 1 receptors in normal, cirrhotic, and neoplastic human livers. *Hepatology* 1995; **21**: 760-766 [PMID: 7875675 DOI: 10.1002/hep.1840210325]
21 **Zhu T**, Zhang L, Li C, Tan X, Liu J, Huiqin Li, Fan Q, Zhang Z, Zhan M, Fu L, Luo J, Geng J, Wu Y, Zou X, Liang B. The S100 calcium binding protein A11 promotes liver fibrogenesis by targeting TGF-β signaling. *J Genet Genomics* 2022; **49**: 338-349 [PMID: 35240304 DOI: 10.1016/j.jgg.2022.02.013]
22 **Inagaki Y**, Okazaki I. Emerging insights into Transforming growth factor beta Smad signal in hepatic fibrogenesis. *Gut* 2007; **56**: 284-292 [PMID: 17303605 DOI: 10.1136/gut.2005.088690]
23 **Friedman SL**. Mechanisms of hepatic fibrogenesis. *Gastroenterology* 2008; **134**: 1655-1669 [PMID: 18471545 DOI: 10.1053/j.gastro.2008.03.003]
24 **Levine D**, Rockey DC, Milner TA, Breuss JM, Fallon JT, Schnapp LM. Expression of the integrin alpha8beta1 during pulmonary and hepatic fibrosis. *Am J Pathol* 2000; **156**: 1927-1935 [PMID: 10854216 DOI: 10.1016/s0002-9440(10)65066-3]
25 **Mikula M**, Proell V, Fischer AN, Mikulits W. Activated hepatic stellate cells induce tumor progression of neoplastic hepatocytes in a TGF-beta dependent fashion. *J Cell Physiol* 2006; **209**: 560-567 [PMID: 16883581 DOI: 10.1002/jcp.20772]
26 **Wang J**, Xiang H, Lu Y, Wu T. Role and clinical significance of TGFβ1 and TGFβR1 in malignant tumors (Review). *Int J Mol Med* 2021; **47** [PMID: 33604683 DOI: 10.3892/ijmm.2021.4888]
27 **Padua D**, Massagué J. Roles of TGFbeta in metastasis. *Cell Res* 2009; **19**: 89-102 [PMID: 19050696 DOI: 10.1038/cr.2008.316]
28 **Heldin CH**, Moustakas A. Role of Smads in TGFβ signaling. *Cell Tissue Res* 2012; **347**: 21-36 [PMID: 21643690 DOI: 10.1007/s00441-011-1190-x]
29 **Moustakas A**, Heldin CH. Non-Smad TGF-beta signals. *J Cell Sci* 2005; **118**: 3573-3584 [PMID: 16105881 DOI: 10.1242/jcs.02554]
30 **Massagué J**. TGFβ signalling in context. *Nat Rev Mol Cell Biol* 2012; **13**: 616-630 [PMID: 22992590 DOI: 10.1038/nrm3434]
31 **Johnson LD**, Auer R. Commentary on: Jiang B, Zhu F, Cao L, Presley BR, Shen MS, Yang KH. Computational study of fracture characteristics in infant skulls using a simplified finite element model. J Forensic Sci 2017;62(1):39-49. *J Forensic Sci* 2018; **63**: 345-348 [PMID: 29314009 DOI: 10.1111/1556-4029.13706]
32 **Konkel JE**, Zhang D, Zanvit P, Chia C, Zangarle-Murray T, Jin W, Wang S, Chen W. Transforming Growth Factor-β Signaling in Regulatory T Cells Controls T Helper-17 Cells and Tissue-Specific Immune Responses. *Immunity* 2017; **46**: 660-674 [PMID: 28423340 DOI: 10.1016/j.immuni.2017.03.015]
33 **Chen W**, Jin W, Hardegen N, Lei KJ, Li L, Marinos N, McGrady G, Wahl SM. Conversion of peripheral CD4+CD25- naive T cells to CD4+CD25+ regulatory T cells by TGF-beta induction of transcription factor Foxp3. *J Exp Med* 2003; **198**: 1875-1886 [PMID: 14676299 DOI: 10.1084/jem.20030152]
34 **Chen KJ**, Lin SZ, Zhou L, Xie HY, Zhou WH, Taki-Eldin A, Zheng SS. Selective recruitment of regulatory T cell through CCR6-CCL20 in hepatocellular carcinoma fosters tumor progression and predicts poor prognosis. *PLoS One* 2011; **6**: e24671 [PMID: 21935436 DOI: 10.1371/journal.pone.0024671]
35 **David CJ**, Massagué J. Contextual determinants of TGFβ action in development, immunity and cancer. *Nat Rev Mol Cell Biol* 2018; **19**: 419-435 [PMID: 29643418 DOI: 10.1038/s41580-018-0007-0]
36 **de Gramont A**, Faivre S, Raymond E. Novel TGF-**β** inhibitors ready for prime time in onco-immunology. *Oncoimmunology* 2017; **6**: e1257453 [PMID: 28197376 DOI: 10.1080/2162402X.2016.1257453]
37 **Flavell RA**, Sanjabi S, Wrzesinski SH, Licona-Limón P. The polarization of immune cells in the tumour environment by TGFbeta. *Nat Rev Immunol* 2010; **10**: 554-567 [PMID: 20616810 DOI: 10.1038/nri2808]
38 **Shalapour S**, Lin XJ, Bastian IN, Brain J, Burt AD, Aksenov AA, Vrbanac AF, Li W, Perkins A, Matsutani T, Zhong Z, Dhar D, Navas-Molina JA, Xu J, Loomba R, Downes M, Yu RT, Evans RM, Dorrestein PC, Knight R, Benner C, Anstee QM, Karin M. Inflammation-induced IgA+ cells dismantle anti-liver cancer immunity. *Nature* 2017; **551**: 340-345

[PMID: 29144460 DOI: 10.1038/nature24302]

39 **Park BV**, Freeman ZT, Ghasemzadeh A, Chattergoon MA, Rutebemberwa A, Steigner J, Winter ME, Huynh TV, Sebald SM, Lee SJ, Pan F, Pardoll DM, Cox AL. TGFβ1-Mediated SMAD3 Enhances PD-1 Expression on Antigen-Specific T Cells in Cancer. *Cancer Discov* 2016; **6**: 1366-1381 [PMID: 27683557 DOI: 10.1158/2159-8290.CD-15-1347]

40 **Zheng C**, Zheng L, Yoo JK, Guo H, Zhang Y, Guo X, Kang B, Hu R, Huang JY, Zhang Q, Liu Z, Dong M, Hu X, Ouyang W, Peng J, Zhang Z. Landscape of Infiltrating T Cells in Liver Cancer Revealed by Single-Cell Sequencing. *Cell* 2017; **169**: 1342-1356.e16 [PMID: 28622514 DOI: 10.1016/j.cell.2017.05.035]

41 **Bao S**, Jiang X, Jin S, Tu P, Lu J. TGF-β1 Induces Immune Escape by Enhancing PD-1 and CTLA-4 Expression on T Lymphocytes in Hepatocellular Carcinoma. *Front Oncol* 2021; **11**: 694145 [PMID: 34249750 DOI: 10.3389/fonc.2021.694145]

42 **Korkut A**, Zaidi S, Kanchi RS, Rao S, Gough NR, Schultz A, Li X, Lorenzi PL, Berger AC, Robertson G, Kwong LN, Datto M, Roszik J, Ling S, Ravikumar V, Manyam G, Rao A, Shelley S, Liu Y, Ju Z, Hansel D, de Velasco G, Pennathur A, Andersen JB, O'Rourke CJ, Ohshiro K, Jogunoori W, Nguyen BN, Li S, Osmanbeyoglu HU, Ajani JA, Mani SA, Houseman A, Wiznerowicz M, Chen J, Gu S, Ma W, Zhang J, Tong P, Cherniack AD, Deng C, Resar L; Cancer Genome Atlas Research Network, Weinstein JN, Mishra L, Akbani R. A Pan-Cancer Analysis Reveals High-Frequency Genetic Alterations in Mediators of Signaling by the TGF-β Superfamily. *Cell Syst* 2018; **7**: 422-437.e7 [PMID: 30268436 DOI: 10.1016/j.cels.2018.08.010]

43 **Chen J**, Zaidi S, Rao S, Chen JS, Phan L, Farci P, Su X, Shetty K, White J, Zamboni F, Wu X, Rashid A, Pattabiraman N, Mazumder R, Horvath A, Wu RC, Li S, Xiao C, Deng CX, Wheeler DA, Mishra B, Akbani R, Mishra L. Analysis of Genomes and Transcriptomes of Hepatocellular Carcinomas Identifies Mutations and Gene Expression Changes in the Transforming Growth Factor-β Pathway. *Gastroenterology* 2018; **154**: 195-210 [PMID: 28918914 DOI: 10.1053/j.gastro.2017.09.007]

44 **Reichl P**, Haider C, Grubinger M, Mikulits W. TGF-β in epithelial to mesenchymal transition and metastasis of liver carcinoma. *Curr Pharm Des* 2012; **18**: 4135-4147 [PMID: 22630087 DOI: 10.2174/138161212802430477]

45 **Tarantino G**, Conca P, Riccio A, Tarantino M, Di Minno MN, Chianese D, Pasanisi F, Contaldo F, Scopacasa F, Capone D. Enhanced serum concentrations of transforming growth factor-beta1 in simple fatty liver: is it really benign? *J Transl Med* 2008; **6**: 72 [PMID: 19038040 DOI: 10.1186/1479-5876-6-72]

46 **Majumdar A**, Curley SA, Wu X, Brown P, Hwang JP, Shetty K, Yao ZX, He AR, Li S, Katz L, Farci P, Mishra L. Hepatic stem cells and transforming growth factor β in hepatocellular carcinoma. *Nat Rev Gastroenterol Hepatol* 2012; **9**: 530-538 [PMID: 22710573 DOI: 10.1038/nrgastro.2012.114]

47 **Kirmaz C**, Terzioglu E, Topalak O, Bayrak P, Yilmaz O, Ersoz G, Sebik F. Serum tumor growth factor-β1 Levels in patients with cirrhosis, chronic hepatitis B and chronic hepatitis C. *Eur Cytokine Netw* 2004; **15**: 112-116 [DOI: 10.17352/ahr.000019]

48 **Taniguchi H**, Kato N, Otsuka M, Goto T, Yoshida H, Shiratori Y, Omata M. Hepatitis C virus core protein upregulates transforming growth factor-beta 1 transcription. *J Med Virol* 2004; **72**: 52-59 [PMID: 14635011 DOI: 10.1002/jmv.10545]

49 **Jiang Y**, Sun A, Zhao Y, Ying W, Sun H, Yang X, Xing B, Sun W, Ren L, Hu B, Li C, Zhang L, Qin G, Zhang M, Chen N, Huang Y, Zhou J, Liu M, Zhu X, Qiu Y, Sun Y, Huang C, Yan M, Wang M, Liu W, Tian F, Xu H, Wu Z, Shi T, Zhu W, Qin J, Xie L, Fan J, Qian X, He F; Chinese Human Proteome Project (CNHPP) Consortium. Proteomics identifies new therapeutic targets of early-stage hepatocellular carcinoma. *Nature* 2019; **567**: 257-261 [PMID: 30814741 DOI: 10.1038/s41586-019-0987-8]

50 **Coulouarn C**, Factor VM, Thorgeirsson SS. Transforming growth factor-beta gene expression signature in mouse hepatocytes predicts clinical outcome in human cancer. *Hepatology* 2008; **47**: 2059-2067 [PMID: 18506891 DOI: 10.1002/hep.22283]

51 **Dong ZZ**, Yao DF, Zou L, Yao M, Qiu LW, Wu XH, Wu W. [An evaluation of transforming growth factor-beta 1 in diagnosing hepatocellular carcinoma and metastasis]. *Zhonghua Gan Zang Bing Za Zhi* 2007; **15**: 503-508 [PMID: 17669238]

52 **Dong ZZ**, Yao DF, Yao M, Qiu LW, Zong L, Wu W, Wu XH, Yao DB, Meng XY. Clinical impact of plasma TGF-beta1 and circulating TGF-beta1 mRNA in diagnosis of hepatocellular carcinoma. *Hepatobiliary Pancreat Dis Int* 2008; **7**: 288-295 [PMID: 18522884]

53 **Tsai JF**, Chuang LY, Jeng JE, Yang ML, Chang WY, Hsieh MY, Lin ZY, Tsai JH. Clinical relevance of transforming growth factor-beta 1 in the urine of patients with hepatocellular carcinoma. *Medicine (Baltimore)* 1997; **76**: 213-226 [PMID: 9193456 DOI: 10.1097/00005792-199705000-00007]

54 **Tsai JF**, Jeng JE, Chuang LY, Yang ML, Ho MS, Chang WY, Hsieh MY, Lin ZY, Tsai JH. Clinical evaluation of urinary transforming growth factor-beta1 and serum alpha-fetoprotein as tumour markers of hepatocellular carcinoma. *Br J Cancer* 1997; **75**: 1460-1466 [PMID: 9166938 DOI: 10.1038/bjc.1997.250]

55 **Balzarini P**, Benetti A, Invernici G, Cristini S, Zicari S, Caruso A, Gatta LB, Berenzi A, Imberti L, Zanotti C, Portolani N, Giulini SM, Ferrari M, Ciusani E, Navone SE, Canazza A, Parati EA, Alessandri G. Transforming growth factor-beta1 induces microvascular abnormalities through a down-modulation of neural cell adhesion molecule in human hepatocellular carcinoma. *Lab Invest* 2012; **92**: 1297-1309 [PMID: 22732936 DOI: 10.1038/labinvest.2012.94]

56 **Mohd Azamai ES**, Sulaiman S, Mohd Habib SH, Looi ML, Das S, Abdul Hamid NA, Wan Ngah WZ, Mohd Yusof YA. Chlorella vulgaris triggers apoptosis in hepatocarcinogenesis-induced rats. *J Zhejiang Univ Sci B* 2009; **10**: 14-21 [PMID: 19198018 DOI: 10.1631/jzus.B0820168]

57 **Cao Y**, Agarwal R, Dituri F, Lupo L, Trerotoli P, Mancarella S, Winter P, Giannelli G. NGS-based transcriptome profiling reveals biomarkers for companion diagnostics of the TGF-β receptor blocker galunisertib in HCC. *Cell Death Dis* 2017; **8**: e2634 [PMID: 28230858 DOI: 10.1038/cddis.2017.44]

58 **Kohla MA**, Attia A, Darwesh N, Obada M, Taha H, Youssef MF. Association of serum levels of transforming growth factor β1 with disease severity in patients with hepatocellular carcinoma. *Hepatoma Res* 2017; **3**: 294 [DOI: 10.20517/2394-5079.2017.40]

59 **Shehata F**, Abdel Monem N, Sakr M, Kasem S, Balbaa M. Epidermal growth factor, its receptor and transforming growth

factor-β1 in the diagnosis of HCV-induced hepatocellular carcinoma. *Med Oncol* 2013; **30**: 673 [PMID: 23912699 DOI: 10.1007/s12032-013-0673-x]

60 **Shirai Y**, Kawata S, Tamura S, Ito N, Tsushima H, Takaishi K, Kiso S, Matsuzawa Y. Plasma transforming growth factor-β1 in patients with hepatocellular carcinoma. Comparison with chronic liver diseases. *Cancer* 1994; **73**: 2275-2279 [DOI: 10.1002/1097-0142(19940501)73:9<2275::AID-CNCR2820730907>3.0.CO;2-T]

61 **Tu S**, Huang W, Huang C, Luo Z, Yan X. Contextual Regulation of TGF-β Signaling in Liver Cancer. *Cells* 2019; **8** [PMID: 31614569 DOI: 10.3390/cells8101235]

62 **Murawaki Y**, Ikuta Y, Nishimura Y, Koda M, Kawasaki H. Serum markers for fibrosis and plasma transforming growth factor-beta 1 in patients with hepatocellular carcinoma in comparison with patients with liver cirrhosis. *J Gastroenterol Hepatol* 1996; **11**: 443-450 [PMID: 8743916 DOI: 10.1111/j.1440-1746.1996.tb00289.x]

63 **Neuzillet C**, de Gramont A, Tijeras-Raballand A, de Mestier L, Cros J, Faivre S, Raymond E. Perspectives of TGF-β inhibition in pancreatic and hepatocellular carcinomas. *Oncotarget* 2014; **5**: 78-94 [PMID: 24393789 DOI: 10.18632/oncotarget.1569]

64 **Sacco R**, Leuci D, Tortorella C, Fiore G, Marinosci F, Schiraldi O, Antonaci S. Transforming growth factor beta1 and soluble Fas serum levels in hepatocellular carcinoma. *Cytokine* 2000; **12**: 811-814 [PMID: 10843770 DOI: 10.1006/cyto.1999.0650]

65 **Song BC**, Chung YH, Kim JA, Choi WB, Suh DD, Pyo SI, Shin JW, Lee HC, Lee YS, Suh DJ. Transforming growth factor-beta1 as a useful serologic marker of small hepatocellular carcinoma. *Cancer* 2002; **94**: 175-180 [PMID: 11815974 DOI: 10.1002/cncr.10170]

66 **Okumoto K**, Hattori E, Tamura K, Kiso S, Watanabe H, Saito K, Saito T, Togashi H, Kawata S. Possible contribution of circulating transforming growth factor-beta1 to immunity and prognosis in unresectable hepatocellular carcinoma. *Liver Int* 2004; **24**: 21-28 [PMID: 15101997 DOI: 10.1111/j.1478-3231.2004.00882.x]

67 **Divella R**, Daniele A, Gadaleta C, Tufaro A, Venneri MT, Paradiso A, Quaranta M. Circulating transforming growth factor-β and epidermal growth factor receptor as related to virus infection in liver carcinogenesis. *Anticancer Res* 2012; **32**: 141-145 [PMID: 22213299]

68 **Sue SR**, Chari RS, Kong FM, Mills JJ, Fine RL, Jirtle RL, Meyers WC. Transforming growth factor-beta receptors and mannose 6-phosphate/insulin-like growth factor-II receptor expression in human hepatocellular carcinoma. *Ann Surg* 1995; **222**: 171-178 [PMID: 7639583 DOI: 10.1097/00000658-199508000-00009]

69 **An Y**, Gao S, Zhao WC, Qiu BA, Xia NX, Zhang PJ, Fan ZP. Transforming growth factor-β and peripheral regulatory cells are negatively correlated with the overall survival of hepatocellular carcinoma. *World J Gastroenterol* 2018; **24**: 2733-2740 [PMID: 29991878 DOI: 10.3748/wjg.v24.i25.2733]

70 **Llovet JM**, Fuster J, Bruix J. Prognosis of hepatocellular carcinoma. *Hepatogastroenterology* 2002; **49**: 7-11 [PMID: 11941987]

71 **Qin LX**, Tang ZY. The prognostic molecular markers in hepatocellular carcinoma. *World J Gastroenterol* 2002; **8**: 385-392 [PMID: 12046056 DOI: 10.3748/wjg.v8.i3.385]

72 **Matsuzaki K**. Modulation of TGF-beta signaling during progression of chronic liver diseases. *Front Biosci (Landmark Ed)* 2009; **14**: 2923-2934 [PMID: 19273245 DOI: 10.2741/3423]

73 **Giannelli G**, Bergamini C, Fransvea E, Sgarra C, Antonaci S. Laminin-5 with transforming growth factor-beta1 induces epithelial to mesenchymal transition in hepatocellular carcinoma. *Gastroenterology* 2005; **129**: 1375-1383 [PMID: 16285938 DOI: 10.1053/j.gastro.2005.09.055]

74 **Giannelli G**, Fransvea E, Marinosci F, Bergamini C, Colucci S, Schiraldi O, Antonaci S. Transforming growth factor-beta1 triggers hepatocellular carcinoma invasiveness *via* alpha3beta1 integrin. *Am J Pathol* 2002; **161**: 183-193 [PMID: 12107103 DOI: 10.1016/s0002-9440(10)64170-3]

75 **Lee D**, Chung YH, Kim JA, Lee YS, Lee D, Jang MK, Kim KM, Lim YS, Lee HC. Transforming growth factor beta 1 overexpression is closely related to invasiveness of hepatocellular carcinoma. *Oncology* 2012; **82**: 11-18 [PMID: 22269311 DOI: 10.1159/000335605]

76 **Wang Y**, Liu T, Tang W, Deng B, Chen Y, Zhu J, Shen X. Hepatocellular Carcinoma Cells Induce Regulatory T Cells and Lead to Poor Prognosis *via* Production of Transforming Growth Factor-β1. *Cell Physiol Biochem* 2016; **38**: 306-318 [PMID: 26799063 DOI: 10.1159/000438631]

77 **Peng L**, Yuan XQ, Zhang CY, Ye F, Zhou HF, Li WL, Liu ZY, Zhang YQ, Pan X, Li GC. High TGF-β1 expression predicts poor disease prognosis in hepatocellular carcinoma patients. *Oncotarget* 2017; **8**: 34387-34397 [PMID: 28415739 DOI: 10.18632/oncotarget.16166]

78 **Principe DR**, Doll JA, Bauer J, Jung B, Munshi HG, Bartholin L, Pasche B, Lee C, Grippo PJ. TGF-β: duality of function between tumor prevention and carcinogenesis. *J Natl Cancer Inst* 2014; **106**: djt369 [PMID: 24511106 DOI: 10.1093/jnci/djt369]

79 **Wang Z**, Liu F, Tu W, Chang Y, Yao J, Wu W, Jiang X, He X, Lin J, Song Y. Embryonic liver fodrin involved in hepatic stellate cell activation and formation of regenerative nodule in liver cirrhosis. *J Cell Mol Med* 2012; **16**: 118-128 [PMID: 21388516 DOI: 10.1111/j.1582-4934.2011.01290.x]

80 **Ji F**, Fu SJ, Shen SL, Zhang LJ, Cao QH, Li SQ, Peng BG, Liang LJ, Hua YP. The prognostic value of combined TGF-β1 and ELF in hepatocellular carcinoma. *BMC Cancer* 2015; **15**: 116 [PMID: 25880619 DOI: 10.1186/s12885-015-1127-y]

81 **Ho HK**, Pok S, Streit S, Ruhe JE, Hart S, Lim KS, Loo HL, Aung MO, Lim SG, Ullrich A. Fibroblast growth factor receptor 4 regulates proliferation, anti-apoptosis and alpha-fetoprotein secretion during hepatocellular carcinoma progression and represents a potential target for therapeutic intervention. *J Hepatol* 2009; **50**: 118-127 [PMID: 19008009 DOI: 10.1016/j.jhep.2008.08.015]

82 **Lee JJ**, Choo SP. The fibroblast growth factor receptor pathway in hepatocellular carcinoma. *Hepatoma Res* 2018; **4**: 52 [DOI: 10.20517/2394-5079.2018.42]

83 **Chen Z**, Xie B, Zhu Q, Xia Q, Jiang S, Cao R, Shi L, Qi D, Li X, Cai L. FGFR4 and TGF-β1 expression in hepatocellular carcinoma: correlation with clinicopathological features and prognosis. *Int J Med Sci* 2013; **10**: 1868-1875 [PMID: 24324363 DOI: 10.7150/ijms.6868]

84 **El-Ashram S**, Aboelhadid SM, Abdel-Kafy EM, Hashem SA, Mahrous LN, Farghly EM, Kamel AA. Erratum: Saeed, E.-A.; Shawky, M.A.; El-Sayed, M.A.-K.; Shymaa, A.H.; Lilian, N.M.; Eman, M.F.; Asmaa, A.K. Investigation of Pre- and Post-Weaning Mortalities in Rabbits Bred in Egypt, with Reference to Parasitic and Bacterial Causes. *Animals* 2020, *10*, 537. *Animals (Basel)* 2020; **10** [PMID: 32290038 DOI: 10.3390/ani10040650]

85 **Fan G**, Wei X, Xu X. Is the era of sorafenib over? *Ther Adv Med Oncol* 2020; **12**: 1758835920927602 [PMID: 32518599 DOI: 10.1177/1758835920927602]

86 **Giraud J**, Chalopin D, Blanc JF, Saleh M. Hepatocellular Carcinoma Immune Landscape and the Potential of Immunotherapies. *Front Immunol* 2021; **12**: 655697 [PMID: 33815418 DOI: 10.3389/fimmu.2021.655697]

87 **Robinson MW**, Harmon C, O'Farrelly C. Liver immunology and its role in inflammation and homeostasis. *Cell Mol Immunol* 2016; **13**: 267-276 [PMID: 27063467 DOI: 10.1038/cmi.2016.3]

88 **Nishida N**, Kudo M. Immune Phenotype and Immune Checkpoint Inhibitors for the Treatment of Human Hepatocellular Carcinoma. *Cancers (Basel)* 2020; **12** [PMID: 32443599 DOI: 10.3390/cancers12051274]

89 **Xu W**, Liu K, Chen M, Sun JY, McCaughan GW, Lu XJ, Ji J. Immunotherapy for hepatocellular carcinoma: recent advances and future perspectives. *Ther Adv Med Oncol* 2019; **11**: 1758835919862692 [PMID: 31384311 DOI: 10.1177/1758835919862692]

90 **Prieto J**, Melero I, Sangro B. Immunological landscape and immunotherapy of hepatocellular carcinoma. *Nat Rev Gastroenterol Hepatol* 2015; **12**: 681-700 [PMID: 26484443 DOI: 10.1038/nrgastro.2015.173]

91 **Sia D**, Jiao Y, Martinez-Quetglas I, Kuchuk O, Villacorta-Martin C, Castro de Moura M, Putra J, Camprecios G, Bassaganyas L, Akers N, Losic B, Waxman S, Thung SN, Mazzaferro V, Esteller M, Friedman SL, Schwartz M, Villanueva A, Llovet JM. Identification of an Immune-specific Class of Hepatocellular Carcinoma, Based on Molecular Features. *Gastroenterology* 2017; **153**: 812-826 [PMID: 28624577 DOI: 10.1053/j.gastro.2017.06.007]

92 **Chen J**, Gingold JA, Su X. Immunomodulatory TGF-β Signaling in Hepatocellular Carcinoma. *Trends Mol Med* 2019; **25**: 1010-1023 [PMID: 31353124 DOI: 10.1016/j.molmed.2019.06.007]

93 **Pinyol R**, Sia D, Llovet JM. Immune Exclusion-Wnt/CTNNB1 Class Predicts Resistance to Immunotherapies in HCC. *Clin Cancer Res* 2019; **25**: 2021-2023 [PMID: 30617138 DOI: 10.1158/1078-0432.CCR-18-3778]

94 **Meindl-Beinker NM**, Matsuzaki K, Dooley S. TGF-β signaling in onset and progression of hepatocellular carcinoma. *Dig Dis* 2012; **30**: 514-523 [PMID: 23108308 DOI: 10.1159/000341704]

95 **McGaha TL**, Phelps RG, Spiera H, Bona C. Halofuginone, an inhibitor of type-I collagen synthesis and skin sclerosis, blocks transforming-growth-factor-beta-mediated Smad3 activation in fibroblasts. *J Invest Dermatol* 2002; **118**: 461-470 [PMID: 11874485 DOI: 10.1046/j.0022-202x.2001.01690.x]

96 **Taras D**, Blanc JF, Rullier A, Dugot-Senant N, Laurendeau I, Bièche I, Pines M, Rosenbaum J. Halofuginone suppresses the lung metastasis of chemically induced hepatocellular carcinoma in rats through MMP inhibition. *Neoplasia* 2006; **8**: 312-318 [PMID: 16756723 DOI: 10.1593/neo.05796]

97 **Nagler A**, Ohana M, Shibolet O, Shapira MY, Alper R, Vlodavsky I, Pines M, Ilan Y. Suppression of hepatocellular carcinoma growth in mice by the alkaloid coccidiostat halofuginone. *Eur J Cancer* 2004; **40**: 1397-1403 [PMID: 15177499 DOI: 10.1016/j.ejca.2003.11.036]

98 **Glenisson W**, Castronovo V, Waltregny D. Histone deacetylase 4 is required for TGFbeta1-induced myofibroblastic differentiation. *Biochim Biophys Acta* 2007; **1773**: 1572-1582 [PMID: 17610967 DOI: 10.1016/j.bbamcr.2007.05.016]

99 **Di Fazio P**, Schneider-Stock R, Neureiter D, Okamoto K, Wissniowski T, Gahr S, Quint K, Meissnitzer M, Alinger B, Montalbano R, Sass G, Hohenstein B, Hahn EG, Ocker M. The pan-deacetylase inhibitor panobinostat inhibits growth of hepatocellular carcinoma models by alternative pathways of apoptosis. *Cell Oncol* 2010; **32**: 285-300 [PMID: 20208142 DOI: 10.3233/CLO-2010-0511]

100 **Mariathasan S**, Turley SJ, Nickles D, Castiglioni A, Yuen K, Wang Y, Kadel EE III, Koeppen H, Astarita JL, Cubas R, Jhunjhunwala S, Banchereau R, Yang Y, Guan Y, Chalouni C, Ziai J, Şenbabaoğlu Y, Santoro S, Sheinson D, Hung J, Giltnane JM, Pierce AA, Mesh K, Lianoglou S, Riegler J, Carano RAD, Eriksson P, Höglund M, Somarriba L, Halligan DL, van der Heijden MS, Loriot Y, Rosenberg JE, Fong L, Mellman I, Chen DS, Green M, Derleth C, Fine GD, Hegde PS, Bourgon R, Powles T. TGFβ attenuates tumour response to PD-L1 blockade by contributing to exclusion of T cells. *Nature* 2018; **554**: 544-548 [PMID: 29443960 DOI: 10.1038/nature25501]

101 **Tauriello DVF**, Palomo-Ponce S, Stork D, Berenguer-Llergo A, Badia-Ramentol J, Iglesias M, Sevillano M, Ibiza S, Cañellas A, Hernando-Momblona X, Byrom D, Matarin JA, Calon A, Rivas EI, Nebreda AR, Riera A, Attolini CS, Batlle E. TGFβ drives immune evasion in genetically reconstituted colon cancer metastasis. *Nature* 2018; **554**: 538-543 [PMID: 29443964 DOI: 10.1038/nature25492]

102 **Knudson KM**, Hicks KC, Luo X, Chen JQ, Schlom J, Gameiro SR. M7824, a novel bifunctional anti-PD-L1/TGFβ Trap fusion protein, promotes anti-tumor efficacy as monotherapy and in combination with vaccine. *Oncoimmunology* 2018; **7**: e1426519 [PMID: 29721396 DOI: 10.1080/2162402X.2018.1426519]

103 **Lan Y**, Zhang D, Xu C, Hance KW, Marelli B, Qi J, Yu H, Qin G, Sircar A, Hernández VM, Jenkins MH, Fontana RE, Deshpande A, Locke G, Sabzevari H, Radvanyi L, Lo KM. Enhanced preclinical antitumor activity of M7824, a bifunctional fusion protein simultaneously targeting PD-L1 and TGF-β. *Sci Transl Med* 2018; **10** [PMID: 29343622 DOI: 10.1126/scitranslmed.aan5488]

104 **Li HY**, McMillen WT, Heap CR, McCann DJ, Yan L, Campbell RM, Mundla SR, King CH, Dierks EA, Anderson BD, Britt KS, Huss KL, Voss MD, Wang Y, Clawson DK, Yingling JM, Sawyer JS. Optimization of a dihydropyrrolopyrazole series of transforming growth factor-beta type I receptor kinase domain inhibitors: discovery of an orally bioavailable transforming growth factor-beta receptor type I inhibitor as antitumor agent. *J Med Chem* 2008; **51**: 2302-2306 [PMID: 18314943 DOI: 10.1021/jm701199p]

105 **Fransvea E**, Angelotti U, Antonaci S, Giannelli G. Blocking transforming growth factor-beta up-regulates E-cadherin and reduces migration and invasion of hepatocellular carcinoma cells. *Hepatology* 2008; **47**: 1557-1566 [PMID: 18318443 DOI: 10.1002/hep.22201]

106 **Melisi D**, Ishiyama S, Sclabas GM, Fleming JB, Xia Q, Tortora G, Abbruzzese JL, Chiao PJ. LY2109761, a novel transforming growth factor beta receptor type I and type II dual inhibitor, as a therapeutic approach to suppressing

pancreatic cancer metastasis. *Mol Cancer Ther* 2008; **7**: 829-840 [PMID: 18413796 DOI: 10.1158/1535-7163.MCT-07-0337]

107 **Mazzocca A**, Fransvea E, Lavezzari G, Antonaci S, Giannelli G. Inhibition of transforming growth factor beta receptor I kinase blocks hepatocellular carcinoma growth through neo-angiogenesis regulation. *Hepatology* 2009; **50**: 1140-1151 [PMID: 19711426 DOI: 10.1002/hep.23118]

108 **Hau P**, Jachimczak P, Schlingensiepen R, Schulmeyer F, Jauch T, Steinbrecher A, Brawanski A, Proescholdt M, Schlaier J, Buchroithner J, Pichler J, Wurm G, Mehdorn M, Strege R, Schuierer G, Villarrubia V, Fellner F, Jansen O, Straube T, Nohria V, Goldbrunner M, Kunst M, Schmaus S, Stauder G, Bogdahn U, Schlingensiepen KH. Inhibition of TGF-beta2 with AP 12009 in recurrent malignant gliomas: from preclinical to phase I/II studies. *Oligonucleotides* 2007; **17**: 201-212 [PMID: 17638524 DOI: 10.1089/oli.2006.0053]

109 **Vallières L**. Trabedersen, a TGFbeta2-specific antisense oligonucleotide for the treatment of malignant gliomas and other tumors overexpressing TGFbeta2. *IDrugs* 2009; **12**: 445-453 [PMID: 19579166]

110 **Bogdahn U**, Hau P, Stockhammer G, Venkataramana NK, Mahapatra AK, Suri A, Balasubramaniam A, Nair S, Oliushine V, Parfenov V, Poverennova I, Zaaroor M, Jachimczak P, Ludwig S, Schmaus S, Heinrichs H, Schlingensiepen KH; Trabedersen Glioma Study Group. Targeted therapy for high-grade glioma with the TGF-β2 inhibitor trabedersen: results of a randomized and controlled phase IIb study. *Neuro Oncol* 2011; **13**: 132-142 [PMID: 20980335 DOI: 10.1093/neuonc/noq142]

111 **Schlingensiepen KH**, Bischof A, Egger T, Hafner M, Herrmuth H, Jachimczak P, Kielmanowicz M, Niewel M, Zavadova E, Stauder G. The TGF-beta1 antisense oligonucleotide AP 11014 for the treatment of non-small cell lung, colorectal and prostate cancer: Preclinical studies. *J Clin Oncol* 2004; **22**: 3132 [DOI: 10.1200/jco.2004.22.90140.3132]

112 **Mead AL**, Wong TT, Cordeiro MF, Anderson IK, Khaw PT. Evaluation of anti-TGF-beta2 antibody as a new postoperative anti-scarring agent in glaucoma surgery. *Invest Ophthalmol Vis Sci* 2003; **44**: 3394-3401 [PMID: 12882787 DOI: 10.1167/iovs.02-0978]

113 **Rodon J**, Carducci MA, Sepulveda-Sánchez JM, Azaro A, Calvo E, Seoane J, Braña I, Sicart E, Gueorguieva I, Cleverly AL, Pillay NS, Desaiah D, Estrem ST, Paz-Ares L, Holdhoff M, Blakeley J, Lahn MM, Baselga J. First-in-human dose study of the novel transforming growth factor-β receptor I kinase inhibitor LY2157299 monohydrate in patients with advanced cancer and glioma. *Clin Cancer Res* 2015; **21**: 553-560 [PMID: 25424852 DOI: 10.1158/1078-0432.CCR-14-1380]

World Journal of Gastroenterology

Submit a Manuscript: https://www.f6publishing.com

World J Gastroenterol 2022 September 28; 28(36): 5265-5279

DOI: 10.3748/wjg.v28.i36.5265

ISSN 1007-9327 (print) ISSN 2219-2840 (online)

REVIEW

P2X7 receptor as the regulator of T-cell function in intestinal barrier disruption

Zhi-Feng Jiang, Wei Wu, Han-Bing Hu, Zheng-Yang Li, Ming Zhong, Lin Zhang

Specialty type: Critical care medicine

Provenance and peer review: Unsolicited article; Externally peer reviewed.

Peer-review model: Single blind

Peer-review report's scientific quality classification

Grade A (Excellent): A
Grade B (Very good): B, B, B
Grade C (Good): 0
Grade D (Fair): 0
Grade E (Poor): 0

P-Reviewer: Pongcharoen S, Thailand; Zamani M, Iran

Received: March 12, 2022
Peer-review started: March 12, 2022
First decision: June 11, 2022
Revised: June 20, 2022
Accepted: September 1, 2022
Article in press: September 1, 2022
Published online: September 28, 2022

Zhi-Feng Jiang, Han-Bing Hu, Lin Zhang, Center of Emergency & Intensive Care Unit, Jinshan Hospital of Fudan University, Shanghai 201508, China

Wei Wu, Ming Zhong, Department of Critical Care Medicine, Zhongshan Hospital of Fudan University, Shanghai 200032, China

Zheng-Yang Li, Department of Gastroenterology, Jinshan Hospital of Fudan University, Shanghai 201508, China

Corresponding author: Lin Zhang, MD, PhD, Doctor, Center of Emergency & Intensive Care Unit, Jinshan Hospital of Fudan University, No. 1508 Longhang Road, Shanghai 201508, China. linzhang0315@fudan.edu.cn

Abstract

The intestinal mucosa is a highly compartmentalized structure that forms a direct barrier between the host intestine and the environment, and its dysfunction could result in a serious disease. As T cells, which are important components of the mucosal immune system, interact with gut microbiota and maintain intestinal homeostasis, they may be involved in the process of intestinal barrier dysfunction. P2X7 receptor (P2X7R), a member of the P2X receptors family, mediates the effects of extracellular adenosine triphosphate and is expressed by most innate or adaptive immune cells, including T cells. Current evidence has demonstrated that P2X7R is involved in inflammation and mediates the survival and differentiation of T lymphocytes, indicating its potential role in the regulation of T cell function. In this review, we summarize the available research about the regulatory role and mechanism of P2X7R on the intestinal mucosa-derived T cells in the setting of intestinal barrier dysfunction.

Key Words: Intestinal barrier dysfunction; P2X7 receptor; T lymphocyte

©The Author(s) 2022. Published by Baishideng Publishing Group Inc. All rights reserved.

Core Tip: Intestinal barrier dysfunction is usually accompanied by inflammation and the death of epithelial cells, which may lead to an elevated concentration of extracellular adenosine triphosphate and the intestinal immune response. Meanwhile, available studies have demonstrated that P2X7 receptor (P2X7R) can be an important regulatory factor in the activation and differentiation of T cells, suggesting that P2X7R may play a key role in intestinal barrier disruption by regulating T cells. Therefore, in this review, we summarized the recent advances regarding the intestinal barrier, the role of P2X7R and T-cells in the pathophysiology of intestinal barrier disruption, and the role of T cell-derived P2X7R in the pathophysiology of intestinal barrier dysfunction.

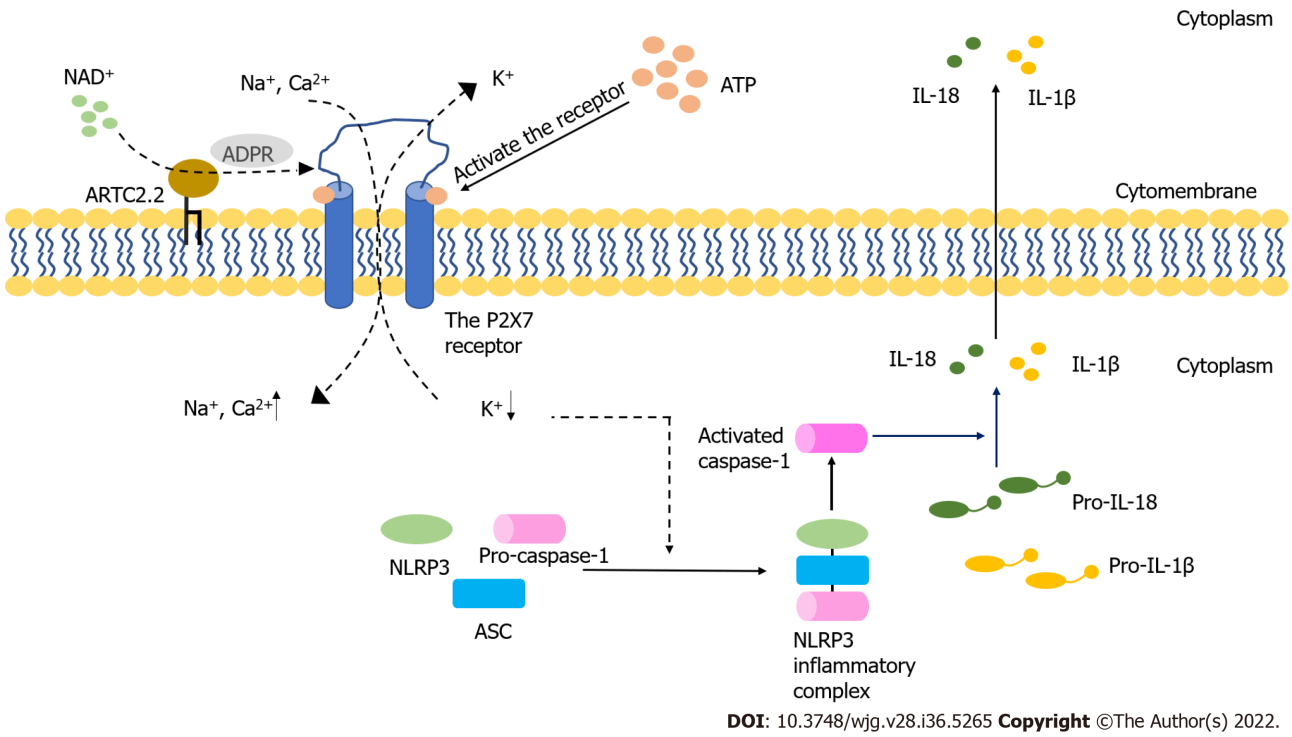
Citation: Jiang ZF, Wu W, Hu HB, Li ZY, Zhong M, Zhang L. P2X7 receptor as the regulator of T-cell function in intestinal barrier disruption. *World J Gastroenterol* 2022; 28(36): 5265-5279
URL: https://www.wjgnet.com/1007-9327/full/v28/i36/5265.htm
DOI: https://dx.doi.org/10.3748/wjg.v28.i36.5265

INTRODUCTION

The intestinal tract is one of the largest interfaces in the human body that directly contacts the external environment[1]. The intestine, a highly specialized and complex organ, plays an important role in absorbing useful substances and presenting potentially harmful substances[2]. The intestinal barrier also maintains the homeostasis of the inner environment and develops the intestinal immune system[3]. The intestinal barrier is composed of several parts, including the microbiological barrier, the chemical barrier, the physical barrier and the immune barrier[4]. Dysfunction of the intestinal barrier increases intestinal permeability and is related to the pathophysiology of several serious diseases[5]. The intestinal tract is exposed to various commensal bacteria, dietary antigens and pathogens that are related to immune tolerance and defense, showing the importance of the immune system in the intestine [6]. The immune barrier mainly includes the lamina propria lymphocytes, dendritic cells (DCs), mast cells, macrophages and lymphocytes — mainly $CD8^+$ T cells — located among epithelial cells[7]. Considering the involvement of T cells in the oral tolerance and immune defense against pathogens in the intestine, it is not surprising that they have an essential role in the pathology of intestinal barrier dysfunction[8,9].

The purinergic signaling pathway is highly conserved and plays a critical role in immune regulatory response[10]. This signaling pathway is mainly mediated by adenosine triphosphate (ATP) and nicotinamide adenine dinucleotide (NAD^+). Purinergic receptors are a group of transmembrane proteins widely expressed in immune cells[11]. According to their different structural properties, these receptors can be divided into the following three families: P2X receptor, P2Y receptor and P1 receptor[12]. Among them, P2X receptors, a class of ligand-gated, cationic-selective channels, are mainly activated by extracellular ATP (eATP)[13]. P2X7 receptors (P2X7R) have a low affinity for ATP and need to be triggered by high concentrations of ATP[14]. When the concentration of ATP is low, P2X7R can act as ion channels for Na^+, K^+ or Ca^{2+}. However, P2X7R can form nonselective and large-conductance pores in settings with high concentrations of ATP, thereby inducing cell apoptosis[14]. Under normal conditions, the cell membrane is impermeable to ATP and other related substances, and the maintenance of low eATP concentration is achieved by the strong degrading activity of ATPases[15,16]. The leakage of intracellular ATP due to the destruction of cell membrane could result in significant elevation of eATP concentration, thereby inducing the activation of the immune system[17-19]. Indeed, an ultrahigh concentration of eATP can be observed at the inflammatory sites[20]. In the process of acute inflammation, ATP activates P2X7R on the Treg cells, inhibiting their activity and viability[21]. P2X receptor channels on effector T cells are stimulated by eATP, facilitating the activation of nuclear factor of activated T cells and the production of IL-2, which could increase the activation of effector T cells[22,23]. The receptor can also be activated by NAD^+ released from damaged cells or activated T cells[24,25]. This NAD^+-dependent process is associated with ecto-ADP-ribosyltransferase ARTC2.2, which is activated by NAD^+ and induces the ADP-ribosylation of P2X7. In the presence of low micromolar concentrations of extracellular NAD^+, this process finally leads to cell death because of the activated P2X7R, a phenomenon known as NAD^+-induced cell death (NICD)[26,27]. In contrast, NAD^+ may be degraded into hydrolysate in the case of high levels of ATP, which would block the NAD^+-dependent process[28,29] (Figure 1). Intestinal barrier dysfunction is usually accompanied by inflammation and the death of epithelial cells, which may lead to an elevated concentration of eATP and the intestinal immune response[30]. Meanwhile, available studies have demonstrated that P2X7R can be an important regulatory factor in the activation and differentiation of T cells[31], suggesting that P2X7R may play a key role in intestinal barrier disruption by regulating T cells.

Therefore, in this review, we summarized the recent advances regarding the intestinal barrier, the role of P2X7R and T-cells in the pathophysiology of intestinal barrier disruption, and the role of T cell-



DOI: 10.3748/wjg.v28.i36.5265 **Copyright** ©The Author(s) 2022.

Figure 1 The activation of the P2X7 receptor and NLRP3 inflammasome. The P2X7 receptor is activated by extracellular ATP and NAD^+ and serves as an ion channel. It can also form non-selective macropores. The activated P2X7 receptor induces the decreasing of intracellular K^+, which initiates NOD-like receptor family pyrin domain containing 3 (NLRP3) inflammasome activation. The activated process of pro-interleukin (IL)-1β and pro-IL-18 are triggered by the active caspase-1 that results from the formation of NLRP3 inflammasome. Mature inflammatory cytokines are released into extracellular space from cells, which finally results in the cell death. ADPR: ADP-ribose; ARTC2.2: ADP-ribosyltransferase 2.2; ASC: Apoptosis-associated speck-like protein containing a CARD; NLRP3: NOD-like receptor family pyrin domain containing 3; IL-18: Interleukin-18; IL-1β: Interleukin-1β.

derived P2X7R in the pathophysiology of intestinal barrier dysfunction.

THE OVERVIEW OF THE INTESTINAL BARRIER

The intestinal barrier, one of the most important biological barriers in the body, is composed of various extracellular and cellular components. It works as a semipermeable membrane that allows nutrients to pass through while limiting the transport of pathogens and noxious substances. This dual function is regulated by the interaction among the four components of the intestinal barrier (the microbiological barrier, the chemical barrier, the physical barrier and the immunological barrier)[2].

There are over 10^{14} microorganisms and about 10000 bacterial species in the human intestine[32]. The microbiological barrier is formed by symbiotic microorganisms in the outermost position of the mucus layer, which effectively prevents harmful substances from entering intestinal epithelial cells[31,33,34]. The chemical barrier, also known as the inner mucus layer, is composed of macromolecules, including proteins, enzymes, peptides and immunoglobulins[35,36]. Mucin2 secreted by goblet cells is the main mucus protein and it serves as a protective barrier[37]. In intestinal crypts, pluripotent stem cells can differentiate into five different cell types, including enterocytes, goblet cells, Paneth cells, enteroendocrine cells and microfold cells[38]. The physical barrier beneath the mucus layer is composed of intestinal epithelial cells which are critical to the physical features of the intestinal barrier[30].

Beneath the intestinal epithelium, the immunological barrier consists of various immune cells, including T lymphocytes, B lymphocytes, dendritic cells, macrophages and plasma cells. This barrier is involved in innate and adaptive immune responses *via* antigen presentation and the secretion of inflammatory mediators and antibodies[39,40]. In addition to immune cells, substances secreted from these cells are also important in the construction of the intestinal immunological barrier. Secretory IgA, another constituent of the immunological barrier, is mainly found at the intestinal mucosal surface, and it provides antipathogen protection by interacting with bacteria[41].

There are several interactions among different components of the intestinal barrier. The physical barrier and the inner mucus layer separate the microbiological barrier and the intestinal immunological barrier, preventing unnecessary conflict and maintaining intestinal homeostasis[42]. The intestinal microbiota induces the functional maturation of innate and adaptive immunity, and instructs immune response through microbiota-derived metabolites and components (such as lipopolysaccharides and

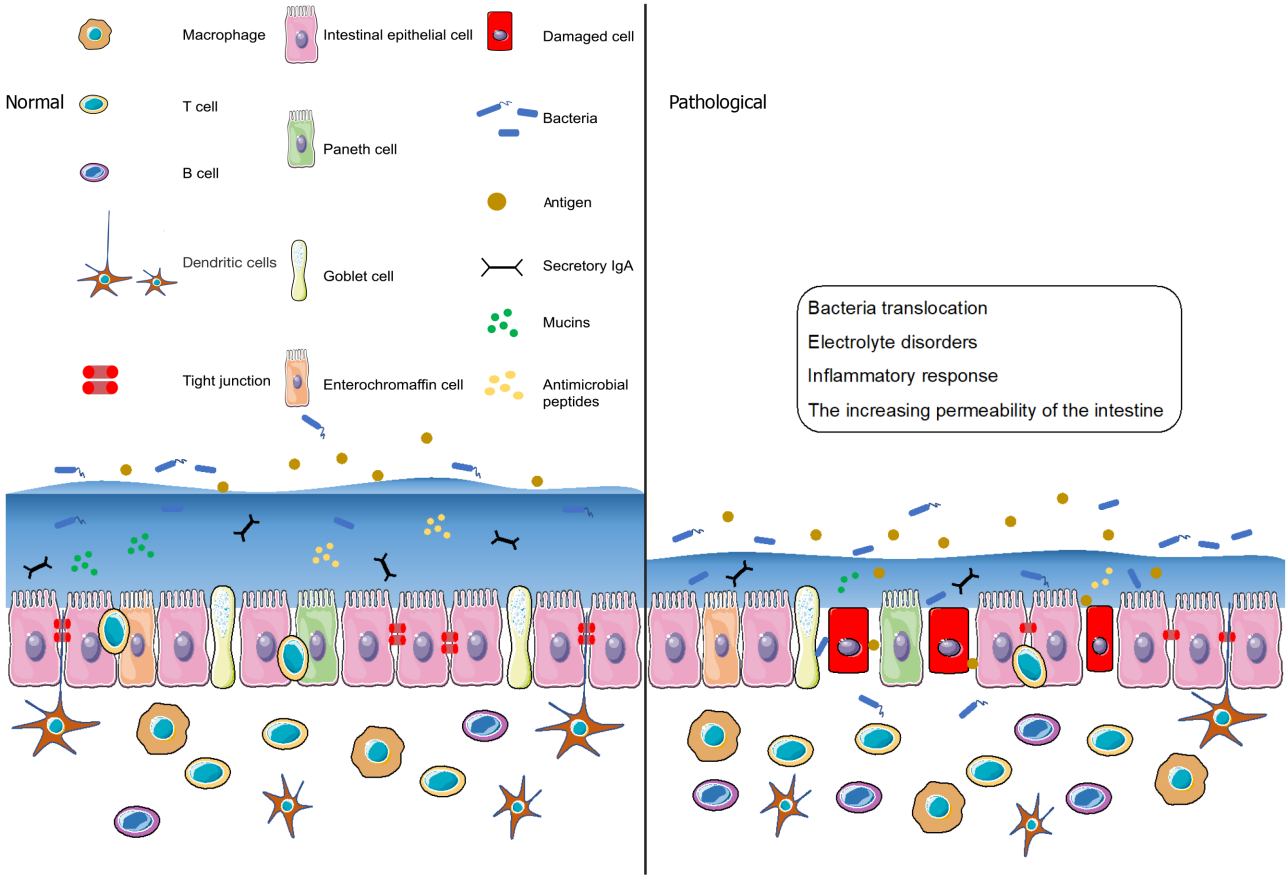
peptidoglycans)[43,44]. The metabolites maintain intestinal homeostasis and regulate inflammation through immune responses, while the components of the microbiota direct immune responses by activating the intestinal TLR pathway[45-47]. For example, the expression of IL17, an inflammatory cytokine produced by γδ T cells, can be inhibited by propionate, a metabolite of intestinal bacteria[48]. Conversely, intestinal immune cells precisely regulate the microbial community both directly and indirectly, thus establishing a sustainable balance between the immune cells and intestinal microbiota [49-51].

The intestinal barrier should be considered a highly dynamic and complex structure that responds to internal and external stimuli[52,53]. Dysfunction of the intestinal barrier often occurs when the damage of the intestinal mucosa is severe and the components of the intestinal barrier change[54]. Under pathological conditions such as stress[55] and ischemia or hypoxia[56], the intestinal barrier is destroyed and the permeability of the intestine increases, thereby inducing bacterial translocation, electrolyte disorders and inflammatory response[57] (Figure 2). With the increasing permeability of the intestine, locally produced ATP is released into the intestinal microenvironment, followed by the activation of immune cells *via* ATP receptors, including P2X7 purinoceptor. When the intestinal immune system is activated, the inflammatory effects may not be regulated, which may lead to the irreversible destruction of the intestinal barrier[58]. More recently, it has been reported that increased ATP concentrations promote T-cell responses by enhancing the expression of the CD86 costimulatory molecule on antigen-presenting cells, an effect mediated through P2X7 purinergic receptor. Thus, the immune system may be the key player in barrier dysfunction and T cells may be involved in adaptive immune responses.

THE ROLE OF T CELLS IN THE INTEGRITY OF THE INTESTINAL BARRIER

T lymphocytes, which are adaptive immune cells, respond to specific antigens and remain the bacterial diversity by complex mechanisms in the homeostatic condition[2]. In the intestine, invariant NKT (iNKT) cells could either enhance or inhibit the immune response, and they might directly or indirectly regulate the microbiota in the intestine[59-62]. $CD8^+$ T cells are the main intraepithelial lymphocytes that monitor and respond to pathogens[63]. $CD4^+$ T cells and T-helper (Th) cells are mainly located in the intestinal lamina propria, and Th1 and Th17 cells can be found in the intestine[64]. Activated intestinal effector T cells could mount immune responses and influence the gut microbiota, and the excess of these cells might induce advanced inflammatory responses and acute or chronic inflammatory diseases[65-67]. In the intestinal adaptive immune response, dendritic cells ingest antigens and activate T cells, and Th cells are induced to differentiate into three different types of Th cells[68]. When lymphocytes respond to different stimuli, they can be divided into different groups based on their cytokine profile, such as Th1, Th2, or Treg cells, which are regulated by P2X7 purinergic receptor, mechanistically[69]. Activated T cells can modulate immune responses by secreting inflammatory cytokines or by interacting with other cells. The function of Th1 cells is to activate and proliferate cytotoxic T cells, thereby inducing the damage of infected intestinal epithelial cells[70]. Th2 cells can release inflammatory cytokines (IL-4, IL-5, and IL-13) and activate B cells to attack the infected cells[71-73]. Transforming growth factor β is capable of suppressing immunoglobulins M and G and promoting their switch to immunoglobulin A. This cytokine is secreted by T cells in Peyer's patches, suggesting the role of T cells in oral tolerance[74]. When intestinal permeability is damaged, antigens can pass through the intestinal epithelial cells and be taken up by macrophages or dendritic cells. Then, the antigens are presented to T cells in the lamina propria by these antigen-presenting cells, which stimulates T cells and induces their proliferation[75, 76]. Some antigens may be taken up by intestinal epithelial cells *via* endocytosis and then be presented to T cells after intracellular processing. This process is based on the classical and nonclassical histocompatibility molecules[77,78]. T cells use both their receptor and a costimulatory signal to recognize antigens[79].

Intestinal barrier disruption is usually accompanied by intestinal inflammation and pathogen invasion. T cells, the key components of adaptive immunity, can effectively limit the invading bacteria and regulate the inflammatory response together with the innate immune system and cytokines[80]. For example, the T helper cell type (Th)1 immune response is necessary in antipathogen protection and is involved in intestinal inflammation[81,82]. In humans, Th17 cells mainly reside in the intestine, where their polarization occurs. Because of the plasticity of Th17 cells, polarized cells have antipathogenic functions and maintain the intestinal epithelial integrity under normal physiological conditions, but they may turn into proinflammatory cells when exposed to IL-23[83]. Th17 cells can mediate inflammation by secreting a proinflammatory cytokine, IL-17A[70]. Peripheral Th17 cells are produced and migrate to the intestine in the case of oral inflammation, which may cause intestinal inflammation[84]. In addition to suppressing the proliferation of Th cells, Treg cells can protect against bacteria and dietary antigens and can produce anti-inflammatory cytokines to exert their anti-inflammatory function, thereby maintaining the homeostasis of the intestinal epithelium[85-87]. With the development of intestinal inflammation, the balance between Th17 cells and Treg cells may be broken up, biasing the function of Th17 cells[88]. In a recent study, it has been found that tissue-resident memory T cells are important in the development of intestinal inflammation, but the role of these cells in this process is not



DOI: 10.3748/wjg.v28.i36.5265 **Copyright** ©The Author(s) 2022.

Figure 2 Intestinal barrier components and the intestinal barrier dysfunction. The normal intestinal barrier is formed by many layers which includes cytokines, bacteria, cells and secretory IgA. The intestinal barrier dysfunction results in the increasing of the intestinal permeability, which subsequently causes the inflammatory response and bacteria translocation.

clear[89]. In summary, T cells are very likely to become effective regulatory targets in the intestinal barrier, and T cell-associated therapy may be used in clinical settings in the future.

THE ROLE OF P2X7R IN THE INTESTINAL BARRIER DYSFUNCTION

Among the members of P2X receptor family, P2X7R (encoded by p2rx7) is the largest (with 595 amino acids in humans). It has special structural and signaling features because of its long intracellular carboxy-terminal, which helps prevent receptor desensitization[90,91]. The monomeric structure of P2X7R has two intracellular domains (C-terminal and N-terminal) and an extracellular ATP-binding domain that separates two transmembrane domains[92]. There were over 1500 single nucleotide polymorphisms (SNPs) reported in NCBI database, and most of them were missense, intronic or nonsynonymous[93]. In highly polymorphic human P2RX7, SNPs play a critical role in the biological process and function of P2X7R. About 10 loss of function SNPs and 3 gain of function SNPs have been identified[12]. For example, the activity of human P2X7R was reduced when Ala replaced Glu 496[94]. When Asn replaced lle-568, the expression of P2X7R was decreased to approximately 50% of normal, and P2X7R became nonfunctional[95]. The mutation of R307Q located in the ATP-binding pocket impaired the binding of ATP to P2X7R[96]. Genetic variants in P2X7R may be involved in the inflammatory response[97,98]. P2X7R function related SNPs played a regulatory role in inflammatory diseases [32]. Unlike other P2X receptors, the complete activation of P2X7R requires a higher concentration of ATP (range from about 0.1 to 2.5 mmol/L)[99]. When activated by ATP, P2X7R not only mediates the uptake of cations and macromolecules, but also leads to the activation of intracellular signaling pathways[100-102]. It has been demonstrated that the formation of macropores requires pannexin-1 channels, and pannexin-1 antagonists can decrease the formation of these pores[103]. However, recent data have suggested that the formation of macropores may be intrinsic to P2X7R without accessory molecules[104-106]. Moreover, P2X7R is associated with the activation of the signaling pathway and transcription factors, including MAP kinases, the cyclic AMP response element[107,108]. P2X7R is widely expressed in immune cells, which suggests its importance in the regulation of both the innate

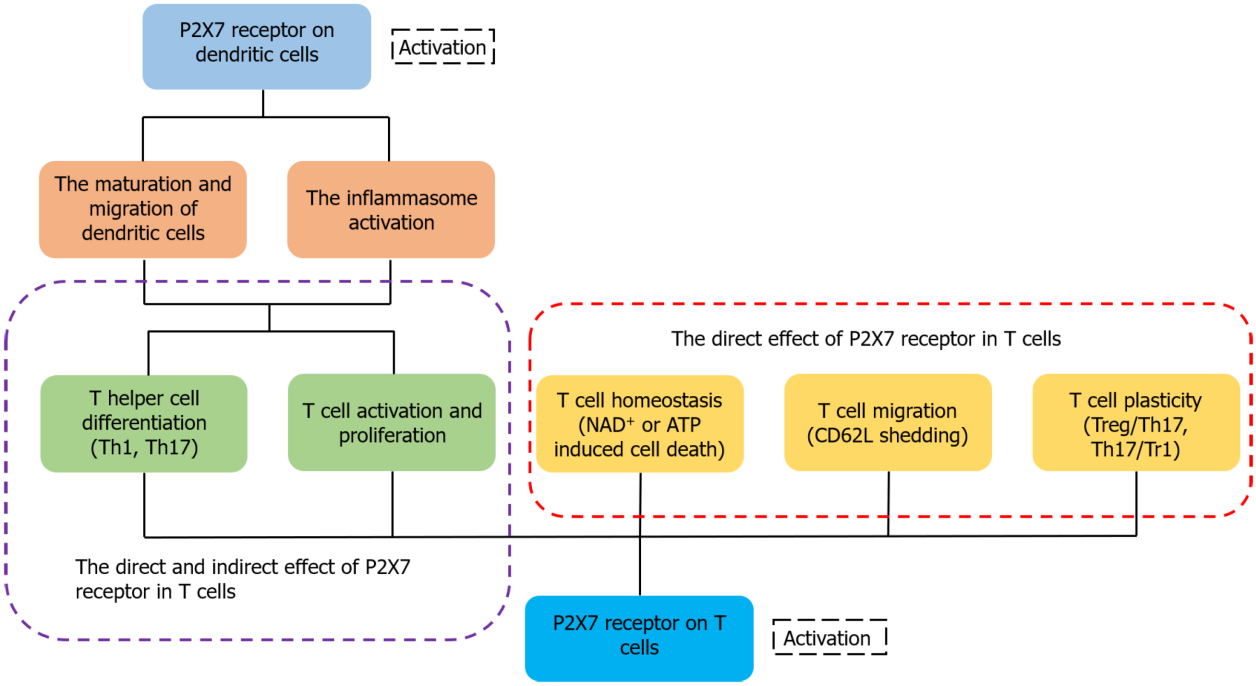
and adaptive immunity, especially in the regulation of inflammation[109,110].

ATP is the most important energy molecule and a common extracellular signaling nucleotide that participates in the regulation of cellular proliferation, differentiation and death[111-113]. In a healthy body, eATP is maintained in a low concentration thanks to ATPases in extracellular spaces. ATP can leak from damaged or distressed cells, and can also be released by nonlytic regulated mechanisms, which increase the concentration of eATP16[114-117]. It has been proven that the concentration of eATP is higher in different inflammatory conditions than in normal conditions[118,119].

The intestinal barrier dysfunction induces the inflammatory response and epithelial cell death[120, 121]. In the acute-inflammatory tissue, high amounts of IL-6 are released, thereby inducing the synthesis and release of ATP from Treg cells exposed to IL-6[122]. The concentration of eATP may increase after intestinal barrier dysfunction, which may activate P2X7R. T follicular helper cells enhance germinal center reactions by deleting P2X7, resisting ATP-mediated immune cell death[123]. When the concentration of eATP produced by the intestinal microbiota is high, commensal-specific IgA responses initiated by intestinal lymphoid tissues are inhibited, which influences the composition of intestinal microbiota[124,125]. Moreover, Perruzza *et al*[126] showed that the blockade of P2X7R could decrease proinflammatory cytokines and protect the intestinal barrier function by inhibiting the activation of macrophages. Nucleotide-binding domain, leucine-rich-repeat receptor, pyrin domain-containing NLR family pyrin domain containing 3 (NLRP3) is a multiprotein complex that participates in the occurrence and development of many inflammatory diseases[127]. The inhibition of NLRP3 can reduce intestinal inflammation and enhance the barrier function[128]. Both NLRP3 and P2X7R are expressed in different immune cells, including T cells, B cells and monocytes[99]. Several signaling pathways induced by activated P2X7R may lead to a decrease in intracellular K^+, an increase in Ca^{2+} and the production of reactive oxygen species, which are key steps in NLRP3 activation[129-132] (Figure 1).

THE ROLE OF T CELL-DERIVED P2X7R IN THE INTESTINAL BARRIER DYSFUNCTION

It has been reported that activated P2X7R can affect several of the biological processes of T cells, including activation, differentiation and death[133]. After recognizing antigens, T cells rapidly release ATP through pannexin channels due to the T cell receptor signaling and co-stimulatory molecules[134, 135]. Because of the highly expressed P2X7 in iNKT cells, they were susceptible to P2X7-mediated cell death and regulated by vitamin A, finally influencing the intestinal homeostasis[136]. ATP released from T cells can activate P2X receptor which increases the expression of the *p2rx7* gene[14,135]. Yip *et al* [135] found that the silencing of P2X7R blocked Ca^{2+} influx and inhibited T cell activation in human $CD4^+$ T cells. These findings suggest that activated P2X7R is essential for the activation of T cells. L-selectin (CD62L) is related to the migration of T cells[137,138]. Low expression of L-selectin is necessary for activated or differentiated T cells to egress from the lymph node[139]. P2X7R activated by ATP can trigger CD62L shedding in human naïve T cells[140]. In a lymph node, activated P2X7R also affects the motility of T cells by inducing their calcium waves[141]. When intracellular ATP and NAD^+ nucleotides are released from cells, they can trigger the activation of P2X7R and induce apoptosis or necrosis[142]. In the case of low micromolar concentration of extracellular NAD^+, ADP ribosylation of P2X7R induces cell death because of persistent P2X7R activation[27]. Under the condition of activated P2X7R, there are two independent ways to induce T cell death: one of them depends on the phosphorylation of ERK1/2, and the other is associated with the nonselective pore[143,144]. In addition, CD62L shedding triggered by the activated P2X7R may induce cell death by apoptosis[145,146]. Compared with native T cells, activated T cells are less sensitive to NICD induced by P2X7R[147]. The expression of P2X7R is different in different populations of T cells. For example, Tregs and follicular helper T cells exhibit high expression of the P2X7 receptor, suggesting that they are more susceptible to cell death than other populations of T cells[148,149]. eATP and P2X7R influence the differentiation of T cells and play a significant role in the metabolism, generation, and memory function of $CD8^+$ T cells[150]. It has been shown that the AMP-activated protein kinase signaling pathway may promote constant efflux of intracellular ATP in memory $CD8^+$ T cells, and is involved in the differentiation and maintenance of memory T cells induced by P2X7R[151,152]. In an inflammatory environment, activated P2X7R drives the differentiation from T cells to Th17 cells[153], and the receptor reduces the differentiation of Tr1 cells with a high expression of IL-10 without Foxp3[21,155]. Activated P2X7R can also regulate the plasticity of Th17 cells and induce Th17 cells to differentiate[156]. In addition to acting directly on T cells, P2X7R can regulate the differentiation of T cells by affecting the physiological functions of dendritic cells[157, 158]. Although ATP may not only reduce the DCs-induced Th1 cell differentiation but can also influence the interaction of DCs with T cells, there is little research on the role of P2X7R during this process[159, 160]. Moreover, activated P2X7R regulates the cytokine secretion and polarization of Th17 cells by influencing dendritic cells[161,162] (Figure 3). Myeloid derived suppressor cells were considered as the regulator of immunosuppression *via* affecting the amounts, functions, or phenotypes of T cells, and the ATP/P2X7R signaling axis may be involved in this process[163].



DOI: 10.3748/wjg.v28.i36.5265 **Copyright** ©The Author(s) 2022.

Figure 3 P2X7 receptor on dendritic cells and T cells influences the fate of T cells indirectly or directly, respectively. The activation of P2X7 receptor on dendritic cells induces the maturation and migration of cells and promotes the inflammasome activation, affecting the activation and differentiation of T cells finally. The activation of P2X7 receptor in T cells can directly regulate the activation, differentiation, migration and homeostasis of T cells[33].

DISCUSSION

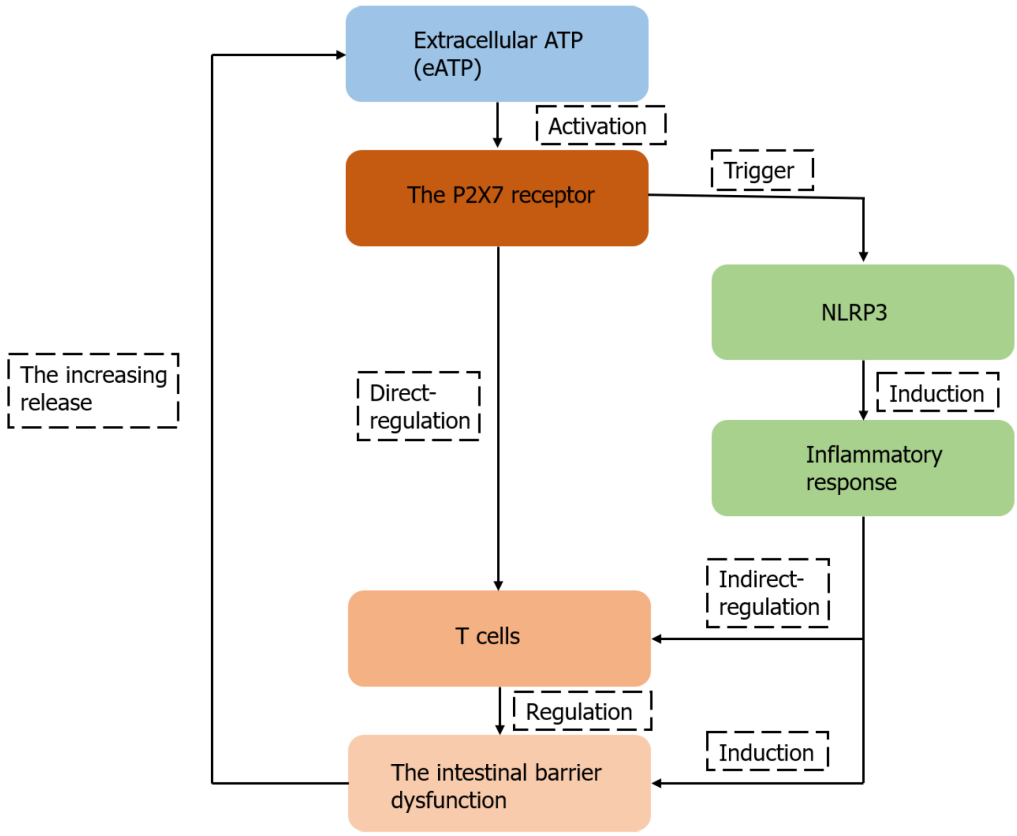
The intestinal barrier dysfunction is a complex and severe pathological condition, which induces the inflammatory response and bacterial invasion. Sepsis is a serious systemic inflammatory disease with high morbidity and mortality in the intensive care unit because it can cause multiple organ failure in patients[164]. Given that the progression and pathogenesis of sepsis have been attributed to intestinal barrier dysfunction, further research on the immune and inflammatory factors of the intestinal barrier dysfunction is necessary[165,166].

According to the above description, T cells are involved in oral tolerance and immune response to antigens in the intestine, and they are the most common lymphocytes that reside in the intestine[167]. Moreover, infiltration by inflammatory T cells is a significant pathological characteristic of intestinal inflammation[168]. Thus, an appropriate number and population of T cells may mitigate the damage of intestinal barrier dysfunction.

P2X7R is widely expressed in T cells and serves as a regulatory factor of their biological processes. Heiss *et al*[169] found that intestinal $CD8^+$ T cells express a high concentration of P2X7R and are highly sensitive to extracellular nucleotides, indicating that P2X7R can regulate intestinal T cell responses. Inflammatory effector T cells can be depleted and intestinal inflammation can be relieved after treatment with NAD^+[170]. P2X7R has been shown to be the trigger for the activation of NLRP3, indicating that this receptor regulates the release of inflammatory cytokines (IL-18, IL-1β) and the initiation of an inflammatory response[171-174]. Therefore, P2X7R may influence inflammation *via* T cells which is indirect. The selectively P2X7 antagonist was proven to significantly inhibit the innate immune cells and upregulate the immunosuppressive-associated T cells, indicating that this antagonist may be a kind of potential treatment[175]. The effect of P2X7-blockade drug has also been demonstrated in the mouse models with advanced tuberculosis[176]. In addition to the above intracellular signaling pathways (MAPK pathway), previous studies verified that P2X7R also regulated MyD88/NF-κB and PI3K/Akt/mTOR signaling pathways in innate and adaptive immune responses, which suggested that the key proteins in these pathways can be considered as novel therapeutic targets[177].

CONCLUSION

In summary, T cells, the key participant in the intestinal barrier dysfunction, are regulated by P2X7R. The roles and mechanisms of P2X7R are associated with T lymphocytes in the intestinal barrier dysfunction and may be a potential research direction, although there have been few studies on this topic (Figure 4). Furthermore, different specific molecules that inhibit the expression of P2X7R may be



DOI: 10.3748/wjg.v28.i36.5265 **Copyright** ©The Author(s) 2022.

Figure 4 The schematic diagram of the hypothesis of the P2X7 receptor as the regulator of T-cell function in intestinal barrier disruption.

potential therapeutic drugs in the future.

FOOTNOTES

Author contributions: Jiang ZF and Wu W contributed equally to this work; Zhong M and Zhang L were co-corresponding authors; Jiang ZF and Wu W wrote the manuscript; Zhang L and Zhong M conceived the topic and reviewed the manuscript; Jiang ZF and Zhang L revised the manuscript; Hu HB and Li ZY reviewed the manuscript; all authors contributed to the article and approved the submitted version.

Supported by The National Natural Science Foundation of China, No. 81801943; Shanghai Pujiang Program, No. 21PJD009; and The Research Grant for Public Health Key Discipline of Shanghai Municipality, China, No. GWV-10.1-XK26.

Conflict-of-interest statement: All the authors report no relevant conflicts of interest for this article.

Open-Access: This article is an open-access article that was selected by an in-house editor and fully peer-reviewed by external reviewers. It is distributed in accordance with the Creative Commons Attribution NonCommercial (CC BY-NC 4.0) license, which permits others to distribute, remix, adapt, build upon this work non-commercially, and license their derivative works on different terms, provided the original work is properly cited and the use is non-commercial. See: https://creativecommons.org/Licenses/by-nc/4.0/

Country/Territory of origin: China

ORCID number: Zhi-Feng Jiang 0000-0003-0714-3453; Lin Zhang 0000-0002-0950-7145.

S-Editor: Gong ZM
L-Editor: Filipodia
P-Editor: Gong ZM

REFERENCES

1 **Takiishi T**, Fenero CIM, Câmara NOS. Intestinal barrier and gut microbiota: Shaping our immune responses throughout life. *Tissue Barriers* 2017; **5**: e1373208 [PMID: 28956703 DOI: 10.1080/21688370.2017.1373208]
2 **Salvo Romero E**, Alonso Cotoner C, Pardo Camacho C, Casado Bedmar M, Vicario M. The intestinal barrier function and its involvement in digestive disease. *Rev Esp Enferm Dig* 2015; **107**: 686-696 [PMID: 26541659 DOI: 10.17235/reed.2015.3846/2015]
3 **Vancamelbeke M**, Vermeire S. The intestinal barrier: a fundamental role in health and disease. *Expert Rev Gastroenterol Hepatol* 2017; **11**: 821-834 [PMID: 28650209 DOI: 10.1080/17474124.2017.1343143]
4 **Huang Z**, Weng Y, Shen Q, Zhao Y, Jin Y. Microplastic: A potential threat to human and animal health by interfering with the intestinal barrier function and changing the intestinal microenvironment. *Sci Total Environ* 2021; **785**: 147365 [PMID: 33933760 DOI: 10.1016/j.scitotenv.2021.147365]
5 **Cui Y**, Wang Q, Chang R, Zhou X, Xu C. Intestinal Barrier Function-Non-alcoholic Fatty Liver Disease Interactions and Possible Role of Gut Microbiota. *J Agric Food Chem* 2019; **67**: 2754-2762 [PMID: 30798598 DOI: 10.1021/acs.jafc.9b00080]
6 **Izcue A**, Coombes JL, Powrie F. Regulatory T cells suppress systemic and mucosal immune activation to control intestinal inflammation. *Immunol Rev* 2006; **212**: 256-271 [PMID: 16903919 DOI: 10.1111/j.0105-2896.2006.00423.x]
7 **Gill N**, Wlodarska M, Finlay BB. Roadblocks in the gut: barriers to enteric infection. *Cell Microbiol* 2011; **13**: 660-669 [PMID: 21392202 DOI: 10.1111/j.1462-5822.2011.01578.x]
8 **Olivares-Villagómez D**, Van Kaer L. Intestinal Intraepithelial Lymphocytes: Sentinels of the Mucosal Barrier. *Trends Immunol* 2018; **39**: 264-275 [PMID: 29221933 DOI: 10.1016/j.it.2017.11.003]
9 **Cheroutre H**, Lambolez F, Mucida D. The light and dark sides of intestinal intraepithelial lymphocytes. *Nat Rev Immunol* 2011; **11**: 445-456 [PMID: 21681197 DOI: 10.1038/nri3007]
10 **Adinolfi E**, Giuliani AL, De Marchi E, Pegoraro A, Orioli E, Di Virgilio F. The P2X7 receptor: A main player in inflammation. *Biochem Pharmacol* 2018; **151**: 234-244 [PMID: 29288626 DOI: 10.1016/j.bcp.2017.12.021]
11 **Di Virgilio F**, Sarti AC, Falzoni S, De Marchi E, Adinolfi E. Extracellular ATP and P2 purinergic signalling in the tumour microenvironment. *Nat Rev Cancer* 2018; **18**: 601-618 [PMID: 30006588 DOI: 10.1038/s41568-018-0037-0]
12 **Di Virgilio F**, Dal Ben D, Sarti AC, Giuliani AL, Falzoni S. The P2X7 Receptor in Infection and Inflammation. *Immunity* 2017; **47**: 15-31 [PMID: 28723547 DOI: 10.1016/j.immuni.2017.06.020]
13 **Niemi K**, Teirilä L, Lappalainen J, Rajamäki K, Baumann MH, Öörni K, Wolff H, Kovanen PT, Matikainen S, Eklund KK. Serum amyloid A activates the NLRP3 inflammasome *via* P2X7 receptor and a cathepsin B-sensitive pathway. *J Immunol* 2011; **186**: 6119-6128 [PMID: 21508263 DOI: 10.4049/jimmunol.1002843]
14 **Junger WG**. Immune cell regulation by autocrine purinergic signalling. *Nat Rev Immunol* 2011; **11**: 201-212 [PMID: 21331080 DOI: 10.1038/nri2938]
15 **Aliagas E**, Muñoz-Esquerre M, Cuevas E, Careta O, Huertas D, López-Sánchez M, Escobar I, Dorca J, Santos S. Is the purinergic pathway involved in the pathology of COPD? *Respir Res* 2018; **19**: 103 [PMID: 29807526 DOI: 10.1186/s12931-018-0793-0]
16 **Linden J**, Koch-Nolte F, Dahl G. Purine Release, Metabolism, and Signaling in the Inflammatory Response. *Annu Rev Immunol* 2019; **37**: 325-347 [PMID: 30676821 DOI: 10.1146/annurev-immunol-051116-052406]
17 **Burnstock G**, Verkhratsky A. Evolutionary origins of the purinergic signalling system. *Acta Physiol (Oxf)* 2009; **195**: 415-447 [PMID: 19222398 DOI: 10.1111/j.1748-1716.2009.01957.x]
18 **Alarcón-Vila C**, Baroja-Mazo A, de Torre-Minguela C, Martínez CM, Martínez-García JJ, Martínez-Banaclocha H, García-Palenciano C, Pelegrin P. CD14 release induced by P2X7 receptor restricts inflammation and increases survival during sepsis. *Elife* 2020; **9** [PMID: 33135636 DOI: 10.7554/eLife.60849]
19 **Cekic C**, Linden J. Purinergic regulation of the immune system. *Nat Rev Immunol* 2016; **16**: 177-192 [PMID: 26922909 DOI: 10.1038/nri.2016.4]
20 **Pelleg A**. Extracellular adenosine 5'-triphosphate in pulmonary disorders. *Biochem Pharmacol* 2021; **187**: 114319 [PMID: 33161021 DOI: 10.1016/j.bcp.2020.114319]
21 **Schenk U**, Frascoli M, Proietti M, Geffers R, Traggiai E, Buer J, Ricordi C, Westendorf AM, Grassi F. ATP inhibits the generation and function of regulatory T cells through the activation of purinergic P2X receptors. *Sci Signal* 2011; **4**: ra12 [PMID: 21364186 DOI: 10.1126/scisignal.2001270]
22 **Wang L**, Jacobsen SE, Bengtsson A, Erlinge D. P2 receptor mRNA expression profiles in human lymphocytes, monocytes and CD34+ stem and progenitor cells. *BMC Immunol* 2004; **5**: 16 [PMID: 15291969 DOI: 10.1186/1471-2172-5-16]
23 **Romio M**, Reinbeck B, Bongardt S, Hüls S, Burghoff S, Schrader J. Extracellular purine metabolism and signaling of CD73-derived adenosine in murine Treg and Teff cells. *Am J Physiol Cell Physiol* 2011; **301**: C530-C539 [PMID: 21593451 DOI: 10.1152/ajpcell.00385.2010]
24 **Scheuplein F**, Rissiek B, Driver JP, Chen YG, Koch-Nolte F, Serreze DV. A recombinant heavy chain antibody approach blocks ART2 mediated deletion of an iNKT cell population that upon activation inhibits autoimmune diabetes. *J Autoimmun* 2010; **34**: 145-154 [PMID: 19796917 DOI: 10.1016/j.jaut.2009.08.012]
25 **Bao L**, Locovei S, Dahl G. Pannexin membrane channels are mechanosensitive conduits for ATP. *FEBS Lett* 2004; **572**: 65-68 [PMID: 15304325 DOI: 10.1016/j.febslet.2004.07.009]
26 **Adriouch S**, Bannas P, Schwarz N, Fliegert R, Guse AH, Seman M, Haag F, Koch-Nolte F. ADP-ribosylation at R125 gates the P2X7 ion channel by presenting a covalent ligand to its nucleotide binding site. *FASEB J* 2008; **22**: 861-869 [PMID: 17928361 DOI: 10.1096/fj.07-9294com]
27 **Seman M**, Adriouch S, Scheuplein F, Krebs C, Freese D, Glowacki G, Deterre P, Haag F, Koch-Nolte F. NAD-induced T cell death: ADP-ribosylation of cell surface proteins by ART2 activates the cytolytic P2X7 purinoceptor. *Immunity* 2003; **19**: 571-582 [PMID: 14563321 DOI: 10.1016/s1074-7613(03)00266-8]

28 **Lee HC**. Structure and enzymatic functions of human CD38. *Mol Med* 2006; **12**: 317-323 [PMID: 17380198 DOI: 10.2119/2006–00086.Lee]

29 **Rissiek B**, Haag F, Boyer O, Koch-Nolte F, Adriouch S. P2X7 on Mouse T Cells: One Channel, Many Functions. *Front Immunol* 2015; **6**: 204 [PMID: 26042119 DOI: 10.3389/fimmu.2015.00204]

30 **Jiang ZF**, Zhang L. LncRNA: A Potential Research Direction in Intestinal Barrier Function. *Dig Dis Sci* 2021; **66**: 1400-1408 [PMID: 32591966 DOI: 10.1007/s10620-020-06417-w]

31 **Rissiek B**, Haag F, Boyer O, Koch-Nolte F, Adriouch S. ADP-ribosylation of P2X7: a matter of life and death for regulatory T cells and natural killer T cells. *Curr Top Microbiol Immunol* 2015; **384**: 107-126 [PMID: 25048544 DOI: 10.1007/82_2014_420]

32 **Javed I**, Cui X, Wang X, Mortimer M, Andrikopoulos N, Li Y, Davis TP, Zhao Y, Ke PC, Chen C. Implications of the Human Gut-Brain and Gut-Cancer Axes for Future Nanomedicine. *ACS Nano* 2020; **14**: 14391-14416 [PMID: 33138351 DOI: 10.1021/acsnano.0c07258]

33 **Paone P**, Cani PD. Mucus barrier, mucins and gut microbiota: the expected slimy partners? *Gut* 2020; **69**: 2232-2243 [PMID: 32917747 DOI: 10.1136/gutjnl-2020-322260]

34 **Donaldson GP**, Lee SM, Mazmanian SK. Gut biogeography of the bacterial microbiota. *Nat Rev Microbiol* 2016; **14**: 20-32 [PMID: 26499895 DOI: 10.1038/nrmicro3552]

35 **Garrett WS**, Gordon JI, Glimcher LH. Homeostasis and inflammation in the intestine. *Cell* 2010; **140**: 859-870 [PMID: 20303876 DOI: 10.1016/j.cell.2010.01.023]

36 **Singh PK**, Parsek MR, Greenberg EP, Welsh MJ. A component of innate immunity prevents bacterial biofilm development. *Nature* 2002; **417**: 552-555 [PMID: 12037568 DOI: 10.1038/417552a]

37 **Zarepour M**, Bhullar K, Montero M, Ma C, Huang T, Velcich A, Xia L, Vallance BA. The mucin Muc2 limits pathogen burdens and epithelial barrier dysfunction during Salmonella enterica serovar Typhimurium colitis. *Infect Immun* 2013; **81**: 3672-3683 [PMID: 23876803 DOI: 10.1128/IAI.00854-13]

38 **Salim SY**, Söderholm JD. Importance of disrupted intestinal barrier in inflammatory bowel diseases. *Inflamm Bowel Dis* 2011; **17**: 362-381 [PMID: 20725949 DOI: 10.1002/ibd.21403]

39 **Mu Q**, Kirby J, Reilly CM, Luo XM. Leaky Gut As a Danger Signal for Autoimmune Diseases. *Front Immunol* 2017; **8**: 598 [PMID: 28588585 DOI: 10.3389/fimmu.2017.00598]

40 **Berin MC**, Li H, Sperber K. Antibody-mediated antigen sampling across intestinal epithelial barriers. *Ann N Y Acad Sci* 2006; **1072**: 253-261 [PMID: 17057205 DOI: 10.1196/annals.1326.002]

41 **Woof JM**, Russell MW. Structure and function relationships in IgA. *Mucosal Immunol* 2011; **4**: 590-597 [PMID: 21937984 DOI: 10.1038/mi.2011.39]

42 **Kayama H**, Okumura R, Takeda K. Interaction Between the Microbiota, Epithelia, and Immune Cells in the Intestine. *Annu Rev Immunol* 2020; **38**: 23-48 [PMID: 32340570 DOI: 10.1146/annurev-immunol-070119-115104]

43 **Round JL**, Mazmanian SK. The gut microbiota shapes intestinal immune responses during health and disease. *Nat Rev Immunol* 2009; **9**: 313-323 [PMID: 19343057 DOI: 10.1038/nri2515]

44 **Rooks MG**, Garrett WS. Gut microbiota, metabolites and host immunity. *Nat Rev Immunol* 2016; **16**: 341-352 [PMID: 27231050 DOI: 10.1038/nri.2016.42]

45 **Park J**, Kim M, Kang SG, Jannasch AH, Cooper B, Patterson J, Kim CH. Short-chain fatty acids induce both effector and regulatory T cells by suppression of histone deacetylases and regulation of the mTOR-S6K pathway. *Mucosal Immunol* 2015; **8**: 80-93 [PMID: 24917457 DOI: 10.1038/mi.2014.44]

46 **Sun M**, Wu W, Chen L, Yang W, Huang X, Ma C, Chen F, Xiao Y, Zhao Y, Yao S, Carpio VH, Dann SM, Zhao Q, Liu Z, Cong Y. Microbiota-derived short-chain fatty acids promote Th1 cell IL-10 production to maintain intestinal homeostasis. *Nat Commun* 2018; **9**: 3555 [PMID: 30177845 DOI: 10.1038/s41467-018-05901-2]

47 **Diehl GE**, Longman RS, Zhang JX, Breart B, Galan C, Cuesta A, Schwab SR, Littman DR. Microbiota restricts trafficking of bacteria to mesenteric lymph nodes by CX(3)CR1(hi) cells. *Nature* 2013; **494**: 116-120 [PMID: 23334413 DOI: 10.1038/nature11809]

48 **Dupraz L**, Magniez A, Rolhion N, Richard ML, Da Costa G, Touch S, Mayeur C, Planchais J, Agus A, Danne C, Michaudel C, Spatz M, Trottein F, Langella P, Sokol H, Michel ML. Gut microbiota-derived short-chain fatty acids regulate IL-17 production by mouse and human intestinal γδ T cells. *Cell Rep* 2021; **36**: 109332 [PMID: 34233192 DOI: 10.1016/j.celrep.2021.109332]

49 **Levy M**, Kolodziejczyk AA, Thaiss CA, Elinav E. Dysbiosis and the immune system. *Nat Rev Immunol* 2017; **17**: 219-232 [PMID: 28260787 DOI: 10.1038/nri.2017.7]

50 **Hoytema van Konijnenburg DP**, Reis BS, Pedicord VA, Farache J, Victora GD, Mucida D. Intestinal Epithelial and Intraepithelial T Cell Crosstalk Mediates a Dynamic Response to Infection. *Cell* 2017; **171**: 783-794.e13 [PMID: 28942917 DOI: 10.1016/j.cell.2017.08.046]

51 **Kogut MH**, Lee A, Santin E. Microbiome and pathogen interaction with the immune system. *Poult Sci* 2020; **99**: 1906-1913 [PMID: 32241470 DOI: 10.1016/j.psj.2019.12.011]

52 **Lee SH**. Intestinal permeability regulation by tight junction: implication on inflammatory bowel diseases. *Intest Res* 2015; **13**: 11-18 [PMID: 25691839 DOI: 10.5217/ir.2015.13.1.11]

53 **Camilleri M**, Madsen K, Spiller R, Greenwood-Van Meerveld B, Verne GN. Intestinal barrier function in health and gastrointestinal disease. *Neurogastroenterol Motil* 2012; **24**: 503-512 [PMID: 22583600 DOI: 10.1111/j.1365-2982.2012.01921.x]

54 **Nalle SC**, Turner JR. Intestinal barrier loss as a critical pathogenic link between inflammatory bowel disease and graft-versus-host disease. *Mucosal Immunol* 2015; **8**: 720-730 [PMID: 25943273 DOI: 10.1038/mi.2015.40]

55 **Ferrier L**, Mazelin L, Cenac N, Desreumaux P, Janin A, Emilie D, Colombel JF, Garcia-Villar R, Fioramonti J, Bueno L. Stress-induced disruption of colonic epithelial barrier: role of interferon-gamma and myosin light chain kinase in mice. *Gastroenterology* 2003; **125**: 795-804 [PMID: 12949725 DOI: 10.1016/s0016-5085(03)01057-6]

56 **Drewe J**, Beglinger C, Fricker G. Effect of ischemia on intestinal permeability of lipopolysaccharides. *Eur J Clin Invest*

2001; **31**: 138-144 [PMID: 11168452 DOI: 10.1046/j.1365-2362.2001.00792.x]
57 **Pan P**, Song Y, Du X, Bai L, Hua X, Xiao Y, Yu X. Intestinal barrier dysfunction following traumatic brain injury. *Neurol Sci* 2019; **40**: 1105-1110 [PMID: 30771023 DOI: 10.1007/s10072-019-03739-0]
58 **Plichta DR**, Graham DB, Subramanian S, Xavier RJ. Therapeutic Opportunities in Inflammatory Bowel Disease: Mechanistic Dissection of Host-Microbiome Relationships. *Cell* 2019; **178**: 1041-1056 [PMID: 31442399 DOI: 10.1016/j.cell.2019.07.045]
59 **Wingender G**, Kronenberg M. Role of NKT cells in the digestive system. IV. The role of canonical natural killer T cells in mucosal immunity and inflammation. *Am J Physiol Gastrointest Liver Physiol* 2008; **294**: G1-G8 [PMID: 17947447 DOI: 10.1152/ajpgi.00437.2007]
60 **Zeissig S**, Kaser A, Dougan SK, Nieuwenhuis EE, Blumberg RS. Role of NKT cells in the digestive system. III. Role of NKT cells in intestinal immunity. *Am J Physiol Gastrointest Liver Physiol* 2007; **293**: G1101-G1105 [PMID: 17717040 DOI: 10.1152/ajpgi.00342.2007]
61 **Wang Y**, Sedimbi S, Löfbom L, Singh AK, Porcelli SA, Cardell SL. Unique invariant natural killer T cells promote intestinal polyps by suppressing TH1 immunity and promoting regulatory T cells. *Mucosal Immunol* 2018; **11**: 131-143 [PMID: 28401935 DOI: 10.1038/mi.2017.34]
62 **Selvanantham T**, Lin Q, Guo CX, Surendra A, Fieve S, Escalante NK, Guttman DS, Streutker CJ, Robertson SJ, Philpott DJ, Mallevaey T. NKT Cell-Deficient Mice Harbor an Altered Microbiota That Fuels Intestinal Inflammation during Chemically Induced Colitis. *J Immunol* 2016; **197**: 4464-4472 [PMID: 27799307 DOI: 10.4049/jimmunol.1601410]
63 **Alonso C**, Vicario M, Pigrau M, Lobo B, Santos J. Intestinal barrier function and the brain-gut axis. *Adv Exp Med Biol* 2014; **817**: 73-113 [PMID: 24997030 DOI: 10.1007/978-1-4939-0897-4_4]
64 **Maynard CL**, Weaver CT. Intestinal effector T cells in health and disease. *Immunity* 2009; **31**: 389-400 [PMID: 19766082 DOI: 10.1016/j.immuni.2009.08.012]
65 **Marrack P**, Scott-Browne J, MacLeod MK. Terminating the immune response. *Immunol Rev* 2010; **236**: 5-10 [PMID: 20636804 DOI: 10.1111/j.1600-065X.2010.00928.x]
66 **Yang Y**, Torchinsky MB, Gobert M, Xiong H, Xu M, Linehan JL, Alonzo F, Ng C, Chen A, Lin X, Sczesnak A, Liao JJ, Torres VJ, Jenkins MK, Lafaille JJ, Littman DR. Focused specificity of intestinal TH17 cells towards commensal bacterial antigens. *Nature* 2014; **510**: 152-156 [PMID: 24739972 DOI: 10.1038/nature13279]
67 **McKinstry KK**, Strutt TM, Swain SL. Regulation of CD4+ T-cell contraction during pathogen challenge. *Immunol Rev* 2010; **236**: 110-124 [PMID: 20636812 DOI: 10.1111/j.1600-065X.2010.00921.x]
68 **Chen Y**, Cui W, Li X, Yang H. Interaction Between Commensal Bacteria, Immune Response and the Intestinal Barrier in Inflammatory Bowel Disease. *Front Immunol* 2021; **12**: 761981 [PMID: 34858414 DOI: 10.3389/fimmu.2021.761981]
69 **Khor B**, Gardet A, Xavier RJ. Genetics and pathogenesis of inflammatory bowel disease. *Nature* 2011; **474**: 307-317 [PMID: 21677747 DOI: 10.1038/nature10209]
70 **Lee SH**, Kwon JE, Cho ML. Immunological pathogenesis of inflammatory bowel disease. *Intest Res* 2018; **16**: 26-42 [PMID: 29422795 DOI: 10.5217/ir.2018.16.1.26]
71 **Chang JT**. Pathophysiology of Inflammatory Bowel Diseases. *N Engl J Med* 2020; **383**: 2652-2664 [PMID: 33382932 DOI: 10.1056/NEJMra2002697]
72 **Armstrong H**, Alipour M, Valcheva R, Bording-Jorgensen M, Jovel J, Zaidi D, Shah P, Lou Y, Ebeling C, Mason AL, Lafleur D, Jerasi J, Wong GK, Madsen K, Carroll MW, Huynh HQ, Dieleman LA, Wine E. Host immunoglobulin G selectively identifies pathobionts in pediatric inflammatory bowel diseases. *Microbiome* 2019; **7**: 1 [PMID: 30606251 DOI: 10.1186/s40168-018-0604-3]
73 **Romagnani S**. Lymphokine production by human T cells in disease states. *Annu Rev Immunol* 1994; **12**: 227-257 [PMID: 8011282 DOI: 10.1146/annurev.iy.12.040194.001303]
74 **Baumgart DC**, Dignass AU. Intestinal barrier function. *Curr Opin Clin Nutr Metab Care* 2002; **5**: 685-694 [PMID: 12394645 DOI: 10.1097/00075197-200211000-00012]
75 **Elson CO**, Cong Y, Iqbal N, Weaver CT. Immuno-bacterial homeostasis in the gut: new insights into an old enigma. *Semin Immunol* 2001; **13**: 187-194 [PMID: 11394961 DOI: 10.1006/smim.2001.0312]
76 **Rescigno M**, Urbano M, Valzasina B, Francolini M, Rotta G, Bonasio R, Granucci F, Kraehenbuhl JP, Ricciardi-Castagnoli P. Dendritic cells express tight junction proteins and penetrate gut epithelial monolayers to sample bacteria. *Nat Immunol* 2001; **2**: 361-367 [PMID: 11276208 DOI: 10.1038/86373]
77 **Shao L**, Serrano D, Mayer L. The role of epithelial cells in immune regulation in the gut. *Semin Immunol* 2001; **13**: 163-176 [PMID: 11394959 DOI: 10.1006/smim.2000.0311]
78 **Telega GW**, Baumgart DC, Carding SR. Uptake and presentation of antigen to T cells by primary colonic epithelial cells in normal and diseased states. *Gastroenterology* 2000; **119**: 1548-1559 [PMID: 11113076 DOI: 10.1053/gast.2000.20168]
79 **Cario E**, Podolsky DK. Differential alteration in intestinal epithelial cell expression of toll-like receptor 3 (TLR3) and TLR4 in inflammatory bowel disease. *Infect Immun* 2000; **68**: 7010-7017 [PMID: 11083826 DOI: 10.1128/iai.68.12.7010-7017.2000]
80 **Holleran G**, Lopetuso L, Petito V, Graziani C, Ianiro G, McNamara D, Gasbarrini A, Scaldaferri F. The Innate and Adaptive Immune System as Targets for Biologic Therapies in Inflammatory Bowel Disease. *Int J Mol Sci* 2017; **18** [PMID: 28934123 DOI: 10.3390/ijms18102020]
81 **Bagheri N**, Salimzadeh L, Shirzad H. The role of T helper 1-cell response in Helicobacter pylori-infection. *Microb Pathog* 2018; **123**: 1-8 [PMID: 29936093 DOI: 10.1016/j.micpath.2018.06.033]
82 **De Carli M**, D'Elios MM, Zancuoghi G, Romagnani S, Del Prete G. Human Th1 and Th2 cells: functional properties, regulation of development and role in autoimmunity. *Autoimmunity* 1994; **18**: 301-308 [PMID: 7858116 DOI: 10.3109/08916939409009532]
83 **Shao L**, Li M, Zhang B, Chang P. Bacterial dysbiosis incites Th17 cell revolt in irradiated gut. *Biomed Pharmacother* 2020; **131**: 110674 [PMID: 32866810 DOI: 10.1016/j.biopha.2020.110674]
84 **Kitamoto S**, Nagao-Kitamoto H, Jiao Y, Gillilland MG 3rd, Hayashi A, Imai J, Sugihara K, Miyoshi M, Brazil JC, Kuffa

P, Hill BD, Rizvi SM, Wen F, Bishu S, Inohara N, Eaton KA, Nusrat A, Lei YL, Giannobile WV, Kamada N. The Intermucosal Connection between the Mouth and Gut in Commensal Pathobiont-Driven Colitis. *Cell* 2020; **182**: 447-462.e14 [PMID: 32758418 DOI: 10.1016/j.cell.2020.05.048]

85 **O'Garra A**, Vieira P. Regulatory T cells and mechanisms of immune system control. *Nat Med* 2004; **10**: 801-805 [PMID: 15286781 DOI: 10.1038/nm0804-801]

86 **Fernandes C**, Wanderley CWS, Silva CMS, Muniz HA, Teixeira MA, Souza NRP, Cândido AGF, Falcão RB, Souza MHLP, Almeida PRC, Câmara LMC, Lima-Júnior RCP. Role of regulatory T cells in irinotecan-induced intestinal mucositis. *Eur J Pharm Sci* 2018; **115**: 158-166 [PMID: 29307857 DOI: 10.1016/j.ejps.2018.01.006]

87 **Geremia A**, Biancheri P, Allan P, Corazza GR, Di Sabatino A. Innate and adaptive immunity in inflammatory bowel disease. *Autoimmun Rev* 2014; **13**: 3-10 [PMID: 23774107 DOI: 10.1016/j.autrev.2013.06.004]

88 **Ueno A**, Jeffery L, Kobayashi T, Hibi T, Ghosh S, Jijon H. Th17 plasticity and its relevance to inflammatory bowel disease. *J Autoimmun* 2018; **87**: 38-49 [PMID: 29290521 DOI: 10.1016/j.jaut.2017.12.004]

89 **Zundler S**, Becker E, Spocinska M, Slawik M, Parga-Vidal L, Stark R, Wiendl M, Atreya R, Rath T, Leppkes M, Hildner K, López-Posadas R, Lukassen S, Ekici AB, Neufert C, Atreya I, van Gisbergen KPJM, Neurath MF. Hobit- and Blimp-1-driven $CD4^+$ tissue-resident memory T cells control chronic intestinal inflammation. *Nat Immunol* 2019; **20**: 288-300 [PMID: 30692620 DOI: 10.1038/s41590-018-0298-5]

90 **Rassendren F**, Buell GN, Virginio C, Collo G, North RA, Surprenant A. The permeabilizing ATP receptor, P2X7. Cloning and expression of a human cDNA. *J Biol Chem* 1997; **272**: 5482-5486 [PMID: 9038151 DOI: 10.1074/jbc.272.9.5482]

91 **McCarthy AE**, Yoshioka C, Mansoor SE. Full-Length $P2X_7$ Structures Reveal How Palmitoylation Prevents Channel Desensitization. *Cell* 2019; **179**: 659-670.e13 [PMID: 31587896 DOI: 10.1016/j.cell.2019.09.017]

92 **Surprenant A**, Rassendren F, Kawashima E, North RA, Buell G. The cytolytic P2Z receptor for extracellular ATP identified as a P2X receptor (P2X7). *Science* 1996; **272**: 735-738 [PMID: 8614837 DOI: 10.1126/science.272.5262.735]

93 **Zhu X**, Li Q, Song W, Peng X, Zhao R. P2X7 receptor: a critical regulator and potential target for breast cancer. *J Mol Med (Berl)* 2021; **99**: 349-358 [PMID: 33486566 DOI: 10.1007/s00109-021-02041-x]

94 **Gu BJ**, Zhang W, Worthington RA, Sluyter R, Dao-Ung P, Petrou S, Barden JA, Wiley JS. A Glu-496 to Ala polymorphism leads to loss of function of the human P2X7 receptor. *J Biol Chem* 2001; **276**: 11135-11142 [PMID: 11150303 DOI: 10.1074/jbc.M010353200]

95 **Wiley JS**, Dao-Ung LP, Li C, Shemon AN, Gu BJ, Smart ML, Fuller SJ, Barden JA, Petrou S, Sluyter R. An Ile-568 to Asn polymorphism prevents normal trafficking and function of the human P2X7 receptor. *J Biol Chem* 2003; **278**: 17108-17113 [PMID: 12586825 DOI: 10.1074/jbc.M212759200]

96 **Gu BJ**, Sluyter R, Skarratt KK, Shemon AN, Dao-Ung LP, Fuller SJ, Barden JA, Clarke AL, Petrou S, Wiley JS. An Arg307 to Gln polymorphism within the ATP-binding site causes loss of function of the human P2X7 receptor. *J Biol Chem* 2004; **279**: 31287-31295 [PMID: 15123679 DOI: 10.1074/jbc.M313902200]

97 **Wesselius A**, Bours MJ, Arts IC, Theunisz EH, Geusens P, Dagnelie PC. The P2X(7) loss-of-function Glu496Ala polymorphism affects *ex vivo* cytokine release and protects against the cytotoxic effects of high ATP-levels. *BMC Immunol* 2012; **13**: 64 [PMID: 23210974 DOI: 10.1186/1471-2172-13-64]

98 **Ide S**, Nishizawa D, Fukuda K, Kasai S, Hasegawa J, Hayashida M, Minami M, Ikeda K. Haplotypes of P2RX7 gene polymorphisms are associated with both cold pain sensitivity and analgesic effect of fentanyl. *Mol Pain* 2014; **10**: 75 [PMID: 25472448 DOI: 10.1186/1744-8069-10-75]

99 **Tao JH**, Cheng M, Tang JP, Dai XJ, Zhang Y, Li XP, Liu Q, Wang YL. Single nucleotide polymorphisms associated with P2X7R function regulate the onset of gouty arthritis. *PLoS One* 2017; **12**: e0181685 [PMID: 28797095 DOI: 10.1371/journal.pone.0181685]

100 **Pelegrin P**. P2X7 receptor and the NLRP3 inflammasome: Partners in crime. *Biochem Pharmacol* 2021; **187**: 114385 [PMID: 33359010 DOI: 10.1016/j.bcp.2020.114385]

101 **Garcia-Marcos M**, Pérez-Andrés E, Tandel S, Fontanils U, Kumps A, Kabré E, Gómez-Muñoz A, Marino A, Dehaye JP, Pochet S. Coupling of two pools of P2X7 receptors to distinct intracellular signaling pathways in rat submandibular gland. *J Lipid Res* 2006; **47**: 705-714 [PMID: 16415476 DOI: 10.1194/jlr.M500408-JLR200]

102 **North RA**. P2X receptors. *Philos Trans R Soc Lond B Biol Sci* 2016; **371** [PMID: 27377721 DOI: 10.1098/rstb.2015.0427]

103 **Virginio C**, MacKenzie A, North RA, Surprenant A. Kinetics of cell lysis, dye uptake and permeability changes in cells expressing the rat P2X7 receptor. *J Physiol* 1999; **519** Pt 2: 335-346 [PMID: 10457053 DOI: 10.1111/j.1469-7793.1999.0335m.x]

104 **Pelegrin P**, Surprenant A. Pannexin-1 mediates large pore formation and interleukin-1beta release by the ATP-gated P2X7 receptor. *EMBO J* 2006; **25**: 5071-5082 [PMID: 17036048 DOI: 10.1038/sj.emboj.7601378]

105 **Schachter J**, Motta AP, de Souza Zamorano A, da Silva-Souza HA, Guimarães MZ, Persechini PM. ATP-induced P2X7-associated uptake of large molecules involves distinct mechanisms for cations and anions in macrophages. *J Cell Sci* 2008; **121**: 3261-3270 [PMID: 18782864 DOI: 10.1242/jcs.029991]

106 **Browne LE**, Compan V, Bragg L, North RA. P2X7 receptor channels allow direct permeation of nanometer-sized dyes. *J Neurosci* 2013; **33**: 3557-3566 [PMID: 23426683 DOI: 10.1523/JNEUROSCI.2235-12.2013]

107 **Jiang LH**, Rassendren F, Mackenzie A, Zhang YH, Surprenant A, North RA. N-methyl-D-glucamine and propidium dyes utilize different permeation pathways at rat P2X(7) receptors. *Am J Physiol Cell Physiol* 2005; **289**: C1295-C1302 [PMID: 16093280 DOI: 10.1152/ajpcell.00253.2005]

108 **Amstrup J**, Novak I. P2X7 receptor activates extracellular signal-regulated kinases ERK1 and ERK2 independently of Ca2+ influx. *Biochem J* 2003; **374**: 51-61 [PMID: 12747800 DOI: 10.1042/bj20030585]

109 **Gavala ML**, Pfeiffer ZA, Bertics PJ. The nucleotide receptor P2RX7 mediates ATP-induced CREB activation in human and murine monocytic cells. *J Leukoc Biol* 2008; **84**: 1159-1171 [PMID: 18625910 DOI: 10.1189/jlb.0907612]

110 **Di Virgilio F**, Sarti AC, Grassi F. Modulation of innate and adaptive immunity by P2X ion channels. *Curr Opin Immunol* 2018; **52**: 51-59 [PMID: 29631184 DOI: 10.1016/j.coi.2018.03.026]

111 **Alarcón-Vila C**, Pizzuto M, Pelegrín P. Purinergic receptors and the inflammatory response mediated by lipids. *Curr Opin Pharmacol* 2019; **47**: 90-96 [PMID: 30952060 DOI: 10.1016/j.coph.2019.02.004]

112 **Burnstock G**. Purinergic signaling and vascular cell proliferation and death. *Arterioscler Thromb Vasc Biol* 2002; **22**: 364-373 [PMID: 11884276 DOI: 10.1161/hq0302.105360]

113 **Burnstock G**. Physiology and pathophysiology of purinergic neurotransmission. *Physiol Rev* 2007; **87**: 659-797 [PMID: 17429044 DOI: 10.1152/physrev.00043.2006]

114 **Surprenant A**, North RA. Signaling at purinergic P2X receptors. *Annu Rev Physiol* 2009; **71**: 333-359 [PMID: 18851707 DOI: 10.1146/annurev.physiol.70.113006.100630]

115 **Sun X**, Zhou R, Lei Y, Hu J, Li X. The ligand-gated ion channel P2X7 receptor mediates NLRP3/caspase-1-mediated pyroptosis in cerebral cortical neurons of juvenile rats with sepsis. *Brain Res* 2020; **1748**: 147109 [PMID: 32905819 DOI: 10.1016/j.brainres.2020.147109]

116 **Bulanova E**, Bulfone-Paus S. P2 receptor-mediated signaling in mast cell biology. *Purinergic Signal* 2010; **6**: 3-17 [PMID: 19921464 DOI: 10.1007/s11302-009-9173-z]

117 **Ruan Z**, Orozco IJ, Du J, Lü W. Structures of human pannexin 1 reveal ion pathways and mechanism of gating. *Nature* 2020; **584**: 646-651 [PMID: 32494015 DOI: 10.1038/s41586-020-2357-y]

118 **Chekeni FB**, Elliott MR, Sandilos JK, Walk SF, Kinchen JM, Lazarowski ER, Armstrong AJ, Penuela S, Laird DW, Salvesen GS, Isakson BE, Bayliss DA, Ravichandran KS. Pannexin 1 channels mediate 'find-me' signal release and membrane permeability during apoptosis. *Nature* 2010; **467**: 863-867 [PMID: 20944749 DOI: 10.1038/nature09413]

119 **Barberà-Cremades M**, Baroja-Mazo A, Gomez AI, Machado F, Di Virgilio F, Pelegrín P. P2X7 receptor-stimulation causes fever *via* PGE2 and IL-1β release. *FASEB J* 2012; **26**: 2951-2962 [PMID: 22490780 DOI: 10.1096/fj.12-205765]

120 **Amores-Iniesta J**, Barberà-Cremades M, Martínez CM, Pons JA, Revilla-Nuin B, Martínez-Alarcón L, Di Virgilio F, Parrilla P, Baroja-Mazo A, Pelegrín P. Extracellular ATP Activates the NLRP3 Inflammasome and Is an Early Danger Signal of Skin Allograft Rejection. *Cell Rep* 2017; **21**: 3414-3426 [PMID: 29262323 DOI: 10.1016/j.celrep.2017.11.079]

121 **Chen WY**, Wang M, Zhang J, Barve SS, McClain CJ, Joshi-Barve S. Acrolein Disrupts Tight Junction Proteins and Causes Endoplasmic Reticulum Stress-Mediated Epithelial Cell Death Leading to Intestinal Barrier Dysfunction and Permeability. *Am J Pathol* 2017; **187**: 2686-2697 [PMID: 28935573 DOI: 10.1016/j.ajpath.2017.08.015]

122 **Sun S**, Duan Z, Wang X, Chu C, Yang C, Chen F, Wang D, Wang C, Li Q, Ding W. Neutrophil extracellular traps impair intestinal barrier functions in sepsis by regulating TLR9-mediated endoplasmic reticulum stress pathway. *Cell Death Dis* 2021; **12**: 606 [PMID: 34117211 DOI: 10.1038/s41419-021-03896-1]

123 **Piconese S**, Gri G, Tripodo C, Musio S, Gorzanelli A, Frossi B, Pedotti R, Pucillo CE, Colombo MP. Mast cells counteract regulatory T-cell suppression through interleukin-6 and OX40/OX40L axis toward Th17-cell differentiation. *Blood* 2009; **114**: 2639-2648 [PMID: 19643985 DOI: 10.1182/blood-2009-05-220004]

124 **Proietti M**, Cornacchione V, Rezzonico Jost T, Romagnani A, Faliti CE, Perruzza L, Rigoni R, Radaelli E, Caprioli F, Preziuso S, Brannetti B, Thelen M, McCoy KD, Slack E, Traggiai E, Grassi F. ATP-gated ionotropic P2X7 receptor controls follicular T helper cell numbers in Peyer's patches to promote host-microbiota mutualism. *Immunity* 2014; **41**: 789-801 [PMID: 25464855 DOI: 10.1016/j.immuni.2014.10.010]

125 **Proietti M**, Perruzza L, Scribano D, Pellegrini G, D'Antuono R, Strati F, Raffaelli M, Gonzalez SF, Thelen M, Hardt WD, Slack E, Nicoletti M, Grassi F. ATP released by intestinal bacteria limits the generation of protective IgA against enteropathogens. *Nat Commun* 2019; **10**: 250 [PMID: 30651557 DOI: 10.1038/s41467-018-08156-z]

126 **Perruzza L**, Gargari G, Proietti M, Fosso B, D'Erchia AM, Faliti CE, Rezzonico-Jost T, Scribano D, Mauri L, Colombo D, Pellegrini G, Moregola A, Mooser C, Pesole G, Nicoletti M, Norata GD, Geuking MB, McCoy KD, Guglielmetti S, Grassi F. T Follicular Helper Cells Promote a Beneficial Gut Ecosystem for Host Metabolic Homeostasis by Sensing Microbiota-Derived Extracellular ATP. *Cell Rep* 2017; **18**: 2566-2575 [PMID: 28297661 DOI: 10.1016/j.celrep.2017.02.061]

127 **Wu X**, Ren J, Chen G, Wu L, Song X, Li G, Deng Y, Wang G, Gu G, Li J. Systemic blockade of P2X7 receptor protects against sepsis-induced intestinal barrier disruption. *Sci Rep* 2017; **7**: 4364 [PMID: 28663567 DOI: 10.1038/s41598-017-04231-5]

128 **Jiang H**, Gong T, Zhou R. The strategies of targeting the NLRP3 inflammasome to treat inflammatory diseases. *Adv Immunol* 2020; **145**: 55-93 [PMID: 32081200 DOI: 10.1016/bs.ai.2019.11.003]

129 **Li M**, Lv R, Wang C, Ge Q, Du H, Lin S. *Tricholoma matsutake*-derived peptide WFNNAGP protects against DSS-induced colitis by ameliorating oxidative stress and intestinal barrier dysfunction. *Food Funct* 2021; **12**: 11883-11897 [PMID: 34738612 DOI: 10.1039/d1fo02806e]

130 **Lee GS**, Subramanian N, Kim AI, Aksentijevich I, Goldbach-Mansky R, Sacks DB, Germain RN, Kastner DL, Chae JJ. The calcium-sensing receptor regulates the NLRP3 inflammasome through Ca2+ and cAMP. *Nature* 2012; **492**: 123-127 [PMID: 23143333 DOI: 10.1038/nature11588]

131 **Tschopp J**, Schroder K. NLRP3 inflammasome activation: The convergence of multiple signalling pathways on ROS production? *Nat Rev Immunol* 2010; **10**: 210-215 [PMID: 20168318 DOI: 10.1038/nri2725]

132 **Hafner-Bratkovič I**, Pelegrín P. Ion homeostasis and ion channels in NLRP3 inflammasome activation and regulation. *Curr Opin Immunol* 2018; **52**: 8-17 [PMID: 29555598 DOI: 10.1016/j.coi.2018.03.010]

133 **Di A**, Xiong S, Ye Z, Malireddi RKS, Kometani S, Zhong M, Mittal M, Hong Z, Kanneganti TD, Rehman J, Malik AB. The TWIK2 Potassium Efflux Channel in Macrophages Mediates NLRP3 Inflammasome-Induced Inflammation. *Immunity* 2018; **49**: 56-65.e4 [PMID: 29958799 DOI: 10.1016/j.immuni.2018.04.032]

134 **Woehrle T**, Yip L, Elkhal A, Sumi Y, Chen Y, Yao Y, Insel PA, Junger WG. Pannexin-1 hemichannel-mediated ATP release together with P2X1 and P2X4 receptors regulate T-cell activation at the immune synapse. *Blood* 2010; **116**: 3475-3484 [PMID: 20660288 DOI: 10.1182/blood-2010-04-277707]

135 **Yip L**, Woehrle T, Corriden R, Hirsh M, Chen Y, Inoue Y, Ferrari V, Insel PA, Junger WG. Autocrine regulation of T-cell activation by ATP release and P2X7 receptors. *FASEB J* 2009; **23**: 1685-1693 [PMID: 19211924 DOI: 10.1096/fj.08-126458]

136 **Liu Q**, Kim CH. Control of Tissue-Resident Invariant NKT Cells by Vitamin A Metabolites and P2X7-Mediated Cell

Death. *J Immunol* 2019; **203**: 1189-1197 [PMID: 31308092 DOI: 10.4049/jimmunol.1900398]
137 **Arbonés ML**, Ord DC, Ley K, Ratech H, Maynard-Curry C, Otten G, Capon DJ, Tedder TF. Lymphocyte homing and leukocyte rolling and migration are impaired in L-selectin-deficient mice. *Immunity* 1994; **1**: 247-260 [PMID: 7534203 DOI: 10.1016/1074-7613(94)90076-0]
138 **Masopust D**, Schenkel JM. The integration of T cell migration, differentiation and function. *Nat Rev Immunol* 2013; **13**: 309-320 [PMID: 23598650 DOI: 10.1038/nri3442]
139 **Mueller SN**, Gebhardt T, Carbone FR, Heath WR. Memory T cell subsets, migration patterns, and tissue residence. *Annu Rev Immunol* 2013; **31**: 137-161 [PMID: 23215646 DOI: 10.1146/annurev-immunol-032712-095954]
140 **Foster JG**, Carter E, Kilty I, MacKenzie AB, Ward SG. Mitochondrial superoxide generation enhances P2X7R-mediated loss of cell surface CD62L on naive human CD4+ T lymphocytes. *J Immunol* 2013; **190**: 1551-1559 [PMID: 23319734 DOI: 10.4049/jimmunol.1201510]
141 **Grassi F**. The P2X7 Receptor as Regulator of T Cell Development and Function. *Front Immunol* 2020; **11**: 1179 [PMID: 32587592 DOI: 10.3389/fimmu.2020.01179]
142 **Wang CM**, Ploia C, Anselmi F, Sarukhan A, Viola A. Adenosine triphosphate acts as a paracrine signaling molecule to reduce the motility of T cells. *EMBO J* 2014; **33**: 1354-1364 [PMID: 24843045 DOI: 10.15252/embj.201386666]
143 **Sluyter R**. The P2X7 Receptor. *Adv Exp Med Biol* 2017; **1051**: 17-53 [PMID: 28676924 DOI: 10.1007/5584_2017_59]
144 **Tsukimoto M**, Maehata M, Harada H, Ikari A, Takagi K, Degawa M. P2X7 receptor-dependent cell death is modulated during murine T cell maturation and mediated by dual signaling pathways. *J Immunol* 2006; **177**: 2842-2850 [PMID: 16920919 DOI: 10.4049/jimmunol.177.5.2842]
145 **Auger R**, Motta I, Benihoud K, Ojcius DM, Kanellopoulos JM. A role for mitogen-activated protein kinase(Erk1/2) activation and non-selective pore formation in P2X7 receptor-mediated thymocyte death. *J Biol Chem* 2005; **280**: 28142-28151 [PMID: 15937334 DOI: 10.1074/jbc.M501290200]
146 **Scheuplein F**, Schwarz N, Adriouch S, Krebs C, Bannas P, Rissiek B, Seman M, Haag F, Koch-Nolte F. NAD+ and ATP released from injured cells induce P2X7-dependent shedding of CD62L and externalization of phosphatidylserine by murine T cells. *J Immunol* 2009; **182**: 2898-2908 [PMID: 19234185 DOI: 10.4049/jimmunol.0801711]
147 **Le Stunff H**, Auger R, Kanellopoulos J, Raymond MN. The Pro-451 to Leu polymorphism within the C-terminal tail of P2X7 receptor impairs cell death but not phospholipase D activation in murine thymocytes. *J Biol Chem* 2004; **279**: 16918-16926 [PMID: 14761980 DOI: 10.1074/jbc.M313064200]
148 **Adriouch S**, Hubert S, Pechberty S, Koch-Nolte F, Haag F, Seman M. NAD+ released during inflammation participates in T cell homeostasis by inducing ART2-mediated death of naive T cells in vivo. *J Immunol* 2007; **179**: 186-194 [PMID: 17579037 DOI: 10.4049/jimmunol.179.1.186]
149 **Hubert S**, Rissiek B, Klages K, Huehn J, Sparwasser T, Haag F, Koch-Nolte F, Boyer O, Seman M, Adriouch S. Extracellular NAD+ shapes the Foxp3+ regulatory T cell compartment through the ART2-P2X7 pathway. *J Exp Med* 2010; **207**: 2561-2568 [PMID: 20975043 DOI: 10.1084/jem.20091154]
150 **Iyer SS**, Latner DR, Zilliox MJ, McCausland M, Akondy RS, Penaloza-Macmaster P, Hale JS, Ye L, Mohammed AU, Yamaguchi T, Sakaguchi S, Amara RR, Ahmed R. Identification of novel markers for mouse CD4(+) T follicular helper cells. *Eur J Immunol* 2013; **43**: 3219-3232 [PMID: 24030473 DOI: 10.1002/eji.201343469]
151 **Borges da Silva H**, Beura LK, Wang H, Hanse EA, Gore R, Scott MC, Walsh DA, Block KE, Fonseca R, Yan Y, Hippen KL, Blazar BR, Masopust D, Kelekar A, Vulchanova L, Hogquist KA, Jameson SC. The purinergic receptor P2RX7 directs metabolic fitness of long-lived memory CD8$^+$ T cells. *Nature* 2018; **559**: 264-268 [PMID: 29973721 DOI: 10.1038/s41586-018-0282-0]
152 **Wanhainen KM**, Jameson SC, da Silva HB. Self-Regulation of Memory CD8 T Cell Metabolism through Extracellular ATP Signaling. *Immunometabolism* 2019; **1** [PMID: 31428464 DOI: 10.20900/immunometab20190009]
153 **Herzig S**, Shaw RJ. AMPK: guardian of metabolism and mitochondrial homeostasis. *Nat Rev Mol Cell Biol* 2018; **19**: 121-135 [PMID: 28974774 DOI: 10.1038/nrm.2017.95]
154 **Roncarolo MG**, Gregori S, Battaglia M, Bacchetta R, Fleischhauer K, Levings MK. Interleukin-10-secreting type 1 regulatory T cells in rodents and humans. *Immunol Rev* 2006; **212**: 28-50 [PMID: 16903904 DOI: 10.1111/j.0105-2896.2006.00420.x]
155 **Mascanfroni ID**, Takenaka MC, Yeste A, Patel B, Wu Y, Kenison JE, Siddiqui S, Basso AS, Otterbein LE, Pardoll DM, Pan F, Priel A, Clish CB, Robson SC, Quintana FJ. Metabolic control of type 1 regulatory T cell differentiation by AHR and HIF1-α. *Nat Med* 2015; **21**: 638-646 [PMID: 26005855 DOI: 10.1038/nm.3868]
156 **Fernández D**, Flores-Santibáñez F, Neira J, Osorio-Barrios F, Tejón G, Nuñez S, Hidalgo Y, Fuenzalida MJ, Meza D, Ureta G, Lladser A, Pacheco R, Acuña-Castillo C, Guixé V, Quintana FJ, Bono MR, Rosemblatt M, Sauma D. Purinergic Signaling as a Regulator of Th17 Cell Plasticity. *PLoS One* 2016; **11**: e0157889 [PMID: 27322617 DOI: 10.1371/journal.pone.0157889]
157 **Del Prete A**, Scutera S, Sozzani S, Musso T. Role of osteopontin in dendritic cell shaping of immune responses. *Cytokine Growth Factor Rev* 2019; **50**: 19-28 [PMID: 31126876 DOI: 10.1016/j.cytogfr.2019.05.004]
158 **de Jong EC**, Smits HH, Kapsenberg ML. Dendritic cell-mediated T cell polarization. *Springer Semin Immunopathol* 2005; **26**: 289-307 [PMID: 15609003 DOI: 10.1007/s00281-004-0167-1]
159 **la Sala A**, Ferrari D, Corinti S, Cavani A, Di Virgilio F, Girolomoni G. Extracellular ATP induces a distorted maturation of dendritic cells and inhibits their capacity to initiate Th1 responses. *J Immunol* 2001; **166**: 1611-1617 [PMID: 11160202 DOI: 10.4049/jimmunol.166.3.1611]
160 **la Sala A**, Sebastiani S, Ferrari D, Di Virgilio F, Idzko M, Norgauer J, Girolomoni G. Dendritic cells exposed to extracellular adenosine triphosphate acquire the migratory properties of mature cells and show a reduced capacity to attract type 1 T lymphocytes. *Blood* 2002; **99**: 1715-1722 [PMID: 11861288 DOI: 10.1182/blood.v99.5.1715]
161 **Li R**, Wang J, Li R, Zhu F, Xu W, Zha G, He G, Cao H, Wang Y, Yang J. ATP/P2X7-NLRP3 axis of dendritic cells participates in the regulation of airway inflammation and hyper-responsiveness in asthma by mediating HMGB1 expression and secretion. *Exp Cell Res* 2018; **366**: 1-15 [PMID: 29545090 DOI: 10.1016/j.yexcr.2018.03.002]

162 **Atarashi K**, Nishimura J, Shima T, Umesaki Y, Yamamoto M, Onoue M, Yagita H, Ishii N, Evans R, Honda K, Takeda K. ATP drives lamina propria T(H)17 cell differentiation. *Nature* 2008; **455**: 808-812 [PMID: 18716618 DOI: 10.1038/nature07240]

163 **Principi E**, Raffaghello L. The role of the P2X7 receptor in myeloid-derived suppressor cells and immunosuppression. *Curr Opin Pharmacol* 2019; **47**: 82-89 [PMID: 30959357 DOI: 10.1016/j.coph.2019.02.010]

164 **Ayala JC**, Grismaldo A, Aristizabal-Pachon AF, Mikhaylenko EV, Nikolenko VN, Mikhaleva LM, Somasundaram SG, Kirkland CE, Aliev G, Morales L. Mitochondrial Dysfunction in Intensive Care Unit Patients. *Curr Pharm Des* 2021; **27**: 3074-3081 [PMID: 33292115 DOI: 10.2174/1381612826666201207112931]

165 **De Winter BY**, De Man JG. Interplay between inflammation, immune system and neuronal pathways: effect on gastrointestinal motility. *World J Gastroenterol* 2010; **16**: 5523-5535 [PMID: 21105185 DOI: 10.3748/wjg.v16.i44.5523]

166 **Tian X**, Li L, Fu G, Wang J, He Q, Zhang C, Qin B. miR-133a-3p regulates the proliferation and apoptosis of intestinal epithelial cells by modulating the expression of TAGLN2. *Exp Ther Med* 2021; **22**: 824 [PMID: 34149870 DOI: 10.3892/etm.2021.10256]

167 **Preza GC**, Yang OO, Elliott J, Anton PA, Ochoa MT. T lymphocyte density and distribution in human colorectal mucosa, and inefficiency of current cell isolation protocols. *PLoS One* 2015; **10**: e0122723 [PMID: 25856343 DOI: 10.1371/journal.pone.0122723]

168 **Tindemans I**, Joosse ME, Samsom JN. Dissecting the Heterogeneity in T-Cell Mediated Inflammation in IBD. *Cells* 2020; **9** [PMID: 31906479 DOI: 10.3390/cells9010110]

169 **Heiss K**, Jänner N, Mähnss B, Schumacher V, Koch-Nolte F, Haag F, Mittrücker HW. High sensitivity of intestinal CD8+ T cells to nucleotides indicates P2X7 as a regulator for intestinal T cell responses. *J Immunol* 2008; **181**: 3861-3869 [PMID: 18768840 DOI: 10.4049/jimmunol.181.6.3861]

170 **Hashimoto-Hill S**, Friesen L, Kim M, Kim CH. Contraction of intestinal effector T cells by retinoic acid-induced purinergic receptor P2X7. *Mucosal Immunol* 2017; **10**: 912-923 [PMID: 27966552 DOI: 10.1038/mi.2016.109]

171 **Shokoples BG**, Paradis P, Schiffrin EL. P2X7 Receptors: An Untapped Target for the Management of Cardiovascular Disease. *Arterioscler Thromb Vasc Biol* 2021; **41**: 186-199 [PMID: 32998520 DOI: 10.1161/ATVBAHA.120.315116]

172 **Zhou J**, Zhou Z, Liu X, Yin HY, Tang Y, Cao X. P2X7 Receptor-Mediated Inflammation in Cardiovascular Disease. *Front Pharmacol* 2021; **12**: 654425 [PMID: 33995071 DOI: 10.3389/fphar.2021.654425]

173 **Sharma D**, Kanneganti TD. The cell biology of inflammasomes: Mechanisms of inflammasome activation and regulation. *J Cell Biol* 2016; **213**: 617-629 [PMID: 27325789 DOI: 10.1083/jcb.201602089]

174 **Rivas-Yáñez E**, Barrera-Avalos C, Parra-Tello B, Briceño P, Rosemblatt MV, Saavedra-Almarza J, Rosemblatt M, Acuña-Castillo C, Bono MR, Sauma D. P2X7 Receptor at the Crossroads of T Cell Fate. *Int J Mol Sci* 2020; **21** [PMID: 32668623 DOI: 10.3390/ijms21144937]

175 **Raffaghello L**, Principi E, Baratto S, Panicucci C, Pintus S, Antonini F, Del Zotto G, Benzi A, Bruzzone S, Scudieri P, Minetti C, Gazzerro E, Bruno C. P2X7 Receptor Antagonist Reduces Fibrosis and Inflammation in a Mouse Model of Alpha-Sarcoglycan Muscular Dystrophy. *Pharmaceuticals (Basel)* 2022; **15** [PMID: 35056146 DOI: 10.3390/ph15010089]

176 **Santiago-Carvalho I**, de Almeida-Santos G, Bomfim CCB, de Souza PC, Silva JCSE, de Melo BMS, Amaral EP, Cione MVP, Lasunskaia E, Hirata MH, Alves-Filho JCF, Nakaya HI, Alvarez JM, D'Império Lima MR. P2x7 Receptor Signaling Blockade Reduces Lung Inflammation and Necrosis During Severe Experimental Tuberculosis. *Front Cell Infect Microbiol* 2021; **11**: 672472 [PMID: 34026666 DOI: 10.3389/fcimb.2021.672472]

177 **Savio LEB**, de Andrade Mello P, da Silva CG, Coutinho-Silva R. The P2X7 Receptor in Inflammatory Diseases: Angel or Demon? *Front Pharmacol* 2018; **9**: 52 [PMID: 29467654 DOI: 10.3389/fphar.2018.00052]

World Journal of Gastroenterology

Submit a Manuscript: https://www.f6publishing.com

World J Gastroenterol 2022 September 28; 28(36): 5280-5299

DOI: 10.3748/wjg.v28.i36.5280

ISSN 1007-9327 (print) ISSN 2219-2840 (online)

REVIEW

Liver-specific drug delivery platforms: Applications for the treatment of alcohol-associated liver disease

Jeffrey Barr Warner, Steven Corrigan Guenthner, Josiah Everett Hardesty, Craig James McClain, Dennis Ray Warner, Irina Andreyevna Kirpich

Specialty type: Gastroenterology and hepatology

Provenance and peer review: Unsolicited article; Externally peer reviewed.

Peer-review model: Single blind

Peer-review report's scientific quality classification

Grade A (Excellent): 0
Grade B (Very good): B, B, B
Grade C (Good): 0
Grade D (Fair): 0
Grade E (Poor): 0

P-Reviewer: Barisani D, Italy; Li H, China; Senchukova M, Russia

Received: June 24, 2022
Peer-review started: June 24, 2022
First decision: August 6, 2022
Revised: August 16, 2022
Accepted: September 6, 2022
Article in press: September 6, 2022
Published online: September 28, 2022

Jeffrey Barr Warner, Steven Corrigan Guenthner, Josiah Everett Hardesty, Craig James McClain, Dennis Ray Warner, Irina Andreyevna Kirpich, Department of Medicine, Division of Gastroenterology, Hepatology and Nutrition, University of Louisville School of Medicine, Louisville, KY 40202, United States

Jeffrey Barr Warner, Irina Andreyevna Kirpich, Department of Pharmacology and Toxicology, University of Louisville School of Medicine, Louisville, KY 40202, United States

Craig James McClain, Irina Andreyevna Kirpich, Alcohol Research Center, University of Louisville School of Medicine, Louisville, KY 40202, United States

Craig James McClain, Irina Andreyevna Kirpich, Hepatobiology and Toxicology Center, University of Louisville School of Medicine, Louisville, KY 40202, United States

Craig James McClain, Veterans Health Administration, Robley Rex Veterans Medical Center, Louisville, KY 40206, United States

Irina Andreyevna Kirpich, Department of Microbiology and Immunology, University of Louisville School of Medicine, Louisville, KY 40202, United States

Corresponding author: Irina Andreyevna Kirpich, MPH, PhD, Associate Professor, Department of Microbiology and Immunology, University of Louisville School of Medicine, 505 S. Hancock St., Louisville, KY 40202, United States. irina.kirpich@louisville.edu

Abstract

Alcohol-associated liver disease (ALD) is a common chronic liver disease and major contributor to liver disease-related deaths worldwide. Despite its prevalence, there are few effective pharmacological options for the severe stages of this disease. While much pre-clinical research attention is paid to drug development in ALD, many of these experimental therapeutics have limitations such as poor pharmacokinetics, poor efficacy, or off-target side effects due to systemic administration. One means of addressing these limitations is through liver-targeted drug delivery, which can be accomplished with different platforms including liposomes, polymeric nanoparticles, exosomes, bacteria, and adeno-associated viruses, among others. These platforms allow drugs to target the liver passively or actively, thereby reducing systemic circulation and increasing the 'effective dose' in the liver. While many studies, some clinical, have applied targeted delivery systems to other liver diseases such as viral hepatitis or hepato-

cellular carcinoma, only few have investigated their efficacy in ALD. This review provides basic information on these liver-targeting drug delivery platforms, including their benefits and limitations, and summarizes the current research efforts to apply them to the treatment of ALD in rodent models. We also discuss gaps in knowledge in the field, which when addressed, may help to increase the efficacy of novel therapies and better translate them to humans.

Key Words: Liver targeted delivery; Nanoparticles; Liposomes; Polymeric nanoparticles; Precision medicine; Alcohol associated liver disease

©The Author(s) 2022. Published by Baishideng Publishing Group Inc. All rights reserved.

Core Tip: Alcohol-associated liver disease (ALD) is a common chronic liver disease and global healthcare burden. While a great deal of pre-clinical research attention is paid to ALD, many experimental therapeutics which are administered systemically suffer from poor pharmacokinetics or poor efficacy. Liver-targeted delivery may address these drawbacks while avoiding extra-hepatic side effects. This article reviews literature applying liver-targeted drug delivery platforms such as liposomes, exosomes, polymeric nanoparticles, viruses, and bioengineered bacteria to the treatment of ALD.

Citation: Warner JB, Guenthner SC, Hardesty JE, McClain CJ, Warner DR, Kirpich IA. Liver-specific drug delivery platforms: Applications for the treatment of alcohol-associated liver disease. *World J Gastroenterol* 2022; 28(36): 5280-5299
URL: https://www.wjgnet.com/1007-9327/full/v28/i36/5280.htm
DOI: https://dx.doi.org/10.3748/wjg.v28.i36.5280

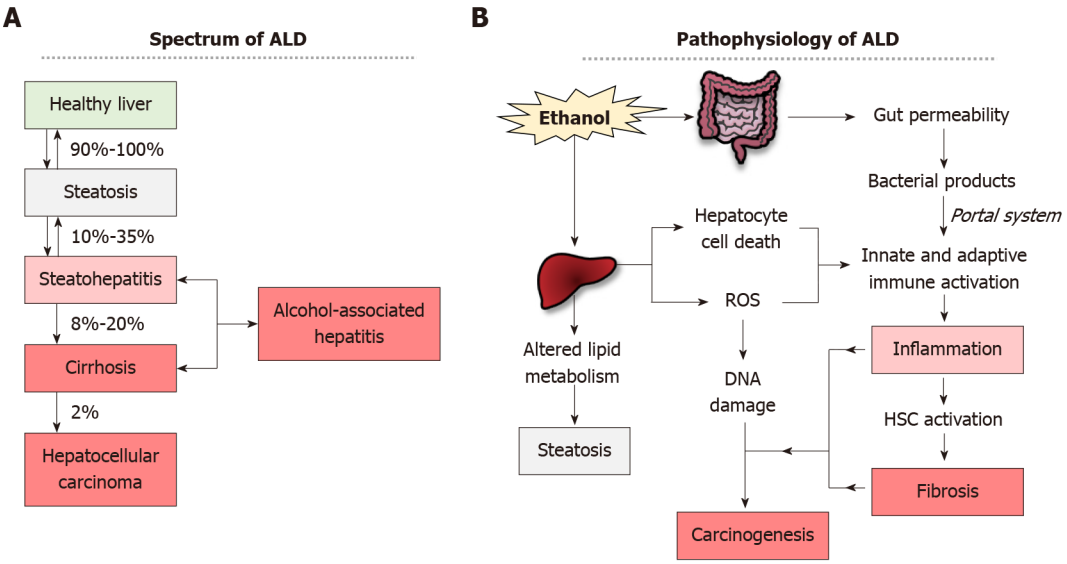
INTRODUCTION

Pathogenesis and pharmacological management of alcohol-associated liver disease

Alcohol-associated liver disease (ALD) is a common chronic liver disease and contributes to the global healthcare burden caused by excess alcohol consumption, which is defined as more than 1 or 2 standard drinks of alcohol per day for females and males, respectively. Globally, nearly half of liver cirrhosis deaths are attributed to alcohol abuse[1]. The pathogenesis of ALD follows a well-described pattern of disease stages beginning with simple liver steatosis progressing to steatohepatitis (steatosis with inflammation), cirrhosis (advanced liver fibrosis), and in some severe cases, hepatocellular carcinoma (HCC) [2] (Figure 1A). In individuals who chronically consume alcohol, binge-drinking episodes may cause acute alcohol-associated hepatitis (AH), a life-threatening condition with high short-term mortality due to infection, severe inflammation, and multi-organ failure[3]. The pathophysiology of ALD is multifactorial and involves a variety of effects of alcohol on multiple organs, including the liver and the gut (Figure 1B). For example, alcohol-induced intestinal permeability and subsequent translocation of gut bacteria and bacteria-derived products into the portal circulation may contribute to inflammation, hepatic stellate cell (HSC) activation, and fibrosis in the liver. Further, direct effects of alcohol on the liver may result in dysregulated lipid signaling, hepatocyte cell death, and production of reactive oxygen species leading to steatosis as well as further inflammation, fibrosis, and ultimately liver cancer (these concepts have been reviewed in detail previously[2]). Most patients with early-to-mid-stage ALD (*i.e.*, hepatic steatosis or mild steatohepatitis) are asymptomatic, therefore a diagnosis of ALD is often not made until later stages of the disease. In those individuals where a diagnosis is made, abstinence and nutrition are key, and indeed, some stages of the disease (*e.g.*, steatosis) are reversible upon alcohol cessation. Limited pharmacological options exist for patients with alcohol-related late-stage liver disease (*e.g.*, cirrhosis or AH), including prednisolone (a corticosteroid) and pentoxifylline (a phosphodiesterase inhibitor used in patients for which corticosteroids are contraindicated or not effective), but importantly, these drugs only reduce short-term mortality[4,5]. There is much research attention being given to drug development in ALD using animal models. These therapies target various pathogenic mechanisms in ALD including oxidative stress (*e.g.*, S-adenosylmethionine, betaine, natural antioxidants), inflammation [*e.g.*, anti-tumor necrosis factor (TNF) therapy, interleukin (IL)-22, glucocorticoids, steroids, IL-1R inhibitors, granulocyte-colony stimulating factor], fibrosis (*e.g.*, transforming growth factor-β inhibitors, phosphodiesterase inhibitors, PPAR agonists), gut barrier dysfunction and microbial dysbiosis (*e.g.*, probiotics and antibiotics), and other processes (these drugs and others are thoroughly reviewed in[6]).

Overview of liver-specific drug delivery systems

While much pre-clinical research attention is given to new drug development for liver diseases,



DOI: 10.3748/wjg.v28.i36.5280 **Copyright** ©The Author(s) 2022.

Figure 1 Spectrum and pathophysiology of alcohol-associated liver disease. A: Schematic diagram describing the spectrum of disease stages in alcohol-associated liver disease (ALD). Percentages represent proportion of chronic drinkers who progress to the indicated disease stage; B: Schematic diagram depicting the pathophysiology of ALD. Ethanol affects both the gut and liver to induce changes in lipid metabolism, generation of reactive oxygen species and hepatocyte cell death, gut permeability, and downstream consequences including inflammation, hepatic stellate cell activation, fibrosis, DNA damage, and carcinogenesis. ALD: Alcohol-associated liver disease; ROS: Reactive oxygen species; HSC: Hepatic stellate cell.

including ALD, many experimental therapeutics relying on systemic drug administration suffer from drawbacks including poor pharmacokinetics or a low margin of safety due to off-target effects in other organs. An example of an early attempt to address some of these drawbacks is covalent conjugation of polyethylene glycol (PEG) to drug molecules (termed 'PEGylation'), a strategy that has been used for many years to lengthen half-life, improve water solubility, and decrease immunogenicity[7]. For instance, PEGylated interferon-α has been the first line treatment for chronic hepatitis B since 2005[8]. However, since that time, advances in nanomedicine have produced numerous liver-specific drug delivery platforms based on lipid vesicles, inorganic nanoparticles, and biological systems which allow: (1) Improved pharmacokinetics for drugs with poor solubility, low bioavailability, rapid metabolism, *etc*.; (2) Reduced systemic side effects by delivering drugs to the liver while avoiding other organs; and (3) Improved efficacy of drugs intended to act in the liver by increasing the 'effective dose'.

There are several types of liver-targeting drug delivery platforms which can be broadly categorized by their composition, including: lipid-based particles (*e.g*., micelles, liposomes, and exosomes, Figure 2A), non-lipid-based particles [*e.g*., polymeric nanoparticles (PNPs), metallic nanoparticles, and ceramic nanoparticles, Figure 2B], and bacterial and viral platforms (*e.g*., bioengineered bacteria and adeno-associated viruses, Figure 2C). These systems are either synthetic or derived from living systems, and have distinct advantages and disadvantages based on their efficacy, pharmacokinetics, and side effects (summarized in Table 1). Briefly, lipid-based particles are composed of endogenous lipids which keep the risk of immunogenicity and toxicity low. Metallic, ceramic, and some PNPs are non-biodegradable and sometimes cytotoxic, but can be modified to reduce toxicity and have additional uses in medical imaging and diagnostics[9]. Bacterial and viral drug delivery platforms benefit from the natural tropism of certain bacteria or viruses for a particular organ or niche but are also potentially immunogenic. These liver-targeting approaches have been used for the treatment of various liver diseases including HCC (*e.g*., liposomal, PEGylated, or PNP-encapsulated anti-cancer compounds[10-12]), viral hepatitis (*e.g*., metal nanoparticles[13] and PEGylated interferon[8]), and liver fibrosis (*e.g*., liposomal vitamin A[14]) with some reaching full FDA approval (*e.g*., Pegasys, Miriplatin, and others)[15].

Biodistribution of liver-targeted drug delivery platforms

The benefits of the liver specific drug delivery platforms stem from their unique ability to biodistribute to the liver while avoiding accumulation in other organs. To better understand the *in vivo* pharmacokinetics of these platforms, a knowledge of the structural organization of the liver and distribution of liver cell types is necessary. A graphical representation of liver structure and cell types can be found in Figure 3. The well-accepted lobular model of liver architecture describes the organ as being divided into discrete hexagonal anatomical units called lobules (Figure 3A)[16]. Surrounding the perimeter of the lobule at each vertex is a portal triad — a vascular bundle composed of a hepatic artery, portal vein, and bile duct. Portal blood and arterial blood fill fenestrated hepatic sinusoids and drain toward the central vein, providing oxygen and nutrients (as well as drugs and nanoparticles) to liver tissue. With regard to

Table 1 Summary of liver-specific drug delivery platforms, including molecular composition, potential modifications, benefits, and limitations

Platform	Composition	Origin	Benefits	Limitations
Lipid-based				
Liposomes	Lipids	Synthetic	Non-immunogenic, non-toxic, modifiable	High clearance by liver/spleen RES
Exosomes	Lipids	Biological	Endogenous cargo (proteins, nucleic acids, *etc.*), but can add additional cargo	Non-standardized isolation methods, potentially immunogenic
Micelles	Lipids	Biological	Non-immunogenic, non-toxic, modifiable	High clearance by liver/spleen RES
Non-lipid-based				
Polymeric nanoparticles	Polymers	Synthetic	Modifiable, capable of controlled drug release	High clearance by liver/spleen RES, potentially immunogenic
Metallic nanoparticles	Gold, silver, aluminum, zinc, iron, gadolinium, copper, rubidium, palladium, titanium	Synthetic	Modifiable, magnetic (iron), anti-microbial (copper, silver, titanium)	Non-biodegradable and potentially cytotoxic, immunogenic, or allergenic
Ceramic nanoparticles	Carbon, silicon with metallic or non-metallic core	Synthetic	Modifiable, resistant to pH change	Potentially cytotoxic or immunogenic, non-biodegradable or lowly biodegradable
Bacterial and viral				
Bacteria	Bacterial cells	Biological	Self-propulsion, chemotaxis, on-site drug production, transfection	Immunogenicity, infection risk
Viral vectors	AAVs, HSVs	Biological	Active liver tropism	Immunogenicity, toxicity, neutralizing antibodies

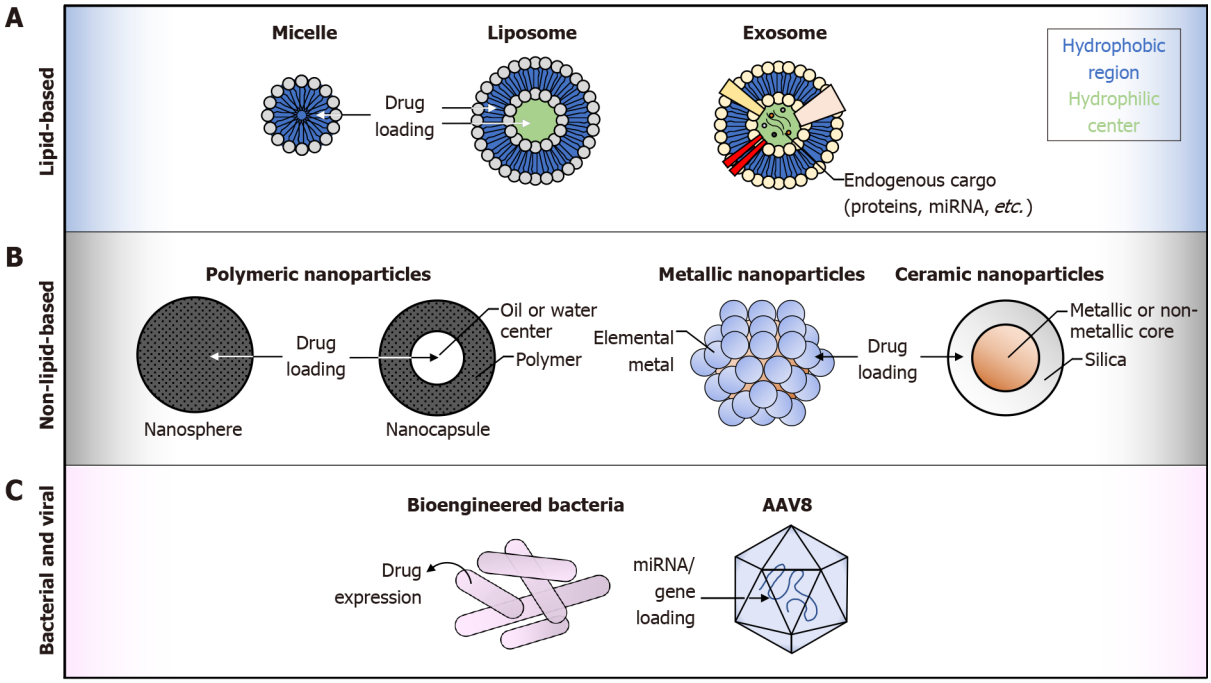
RES: Reticuloendothelial system; AAV: Adeno-associated virus; HSV: Herpes simplex virus.

cellular composition, the liver is divided into parenchymal and non-parenchymal cell types. The parenchymal cells of the liver are the hepatocytes, constituting a majority of cells by both number and volume (60% and 80%, respectively, Figure 3B)[17]. The remaining non-parenchymal cells include liver sinusoidal endothelial cells (LSECs), tissue resident macrophages (Kupffer cells, KCs), HSCs, and intra-hepatic lymphocytes (T cells, B cells, natural killer cells, *etc.*). LSECs form a fenestrated endothelium lacking a basal lamina separating liver sinusoids from the liver parenchyma.

The biodistribution of liver-specific drug delivery platforms in the body after systemic administration is based on the physical properties of the particle. For example, before reaching target liver cells, many particles may be opsonized by binding plasma proteins (*e.g.*, albumin, apolipoproteins, antibodies, complement component proteins) and cleared by the reticuloendothelial system (RES) of the liver and spleen, including by LSECs, particularly if the particles are greater than 200 nm in diameter or carry a negative charge[18]. Particle modifications such as PEGylation help avoid RES surveillance by preventing plasma protein binding, thereby improving *in vivo* half-life. Stealth liposomes, for example, are PEGylated phospholipid particles commonly used to improve the pharmacokinetics of a drug with a short half-life[19]. Particles which avoid RES clearance and have favorable size and charge can pass through the liver sinusoidal fenestrae, which are approximately 100-150 nm in diameter[20], to access HSCs in the space of Disse and the liver parenchyma. Accordingly, particles must have roughly the same or smaller diameter than these fenestrae and carry a charge which is not excessively positive or negative, as high charge magnitude is associated with increased plasma clearance[21]. Controlling these physical properties to allow accumulation of particles in the liver is called passive liver targeting, whereas active liver targeting relies on conjugation of a "homing" ligand whose receptor is expressed in the target organ, and in particular, the specific target cell type. For example, carbohydrate receptors such as the asialoglycoprotein receptor can be targeted to deliver therapeutics to hepatocytes with ligands including galactose, lactose, pullulan, and others (more information regarding active targeting has been reviewed by Kang *et al*[22]).

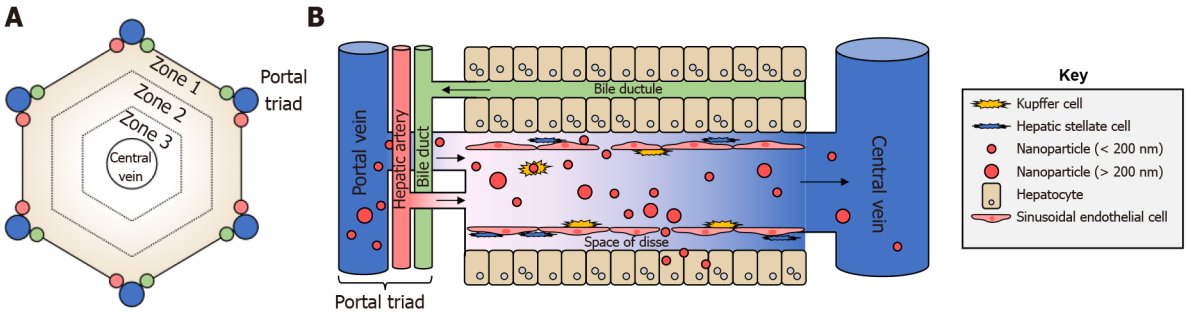
LIVER-SPECIFIC DRUG DELIVERY: IMPLICATIONS FOR ALD

The goal of this review is to summarize pre-clinical research efforts which apply liver-specific drug delivery platforms in various rodent models to prevent or treat ALD, as well as to further discuss the



DOI: 10.3748/wjg.v28.i36.5280 **Copyright** ©The Author(s) 2022.

Figure 2 Graphical representation of targeted drug delivery platforms. A: Lipid-based particles, including micelles, liposomes, and exosomes; B: Non-lipid-based particles, including polymeric nanospheres and nanocapsules, metallic nanoparticles, and ceramic nanoparticles; C: Bioengineered bacteria and adeno-associated virus serotype 8. Graphics are not drawn to scale. miRNA: MicroRNA; AAV8: Adeno-associated virus serotype 8.



DOI: 10.3748/wjg.v28.i36.5280 **Copyright** ©The Author(s) 2022.

Figure 3 Lobular liver architecture and biodistribution of nanoparticles. A: Top-down view of a liver lobule. Portal triads, consisting of a portal vein, hepatic artery, and bile duct, surround a central vein in a hexagonal shape. Concentric hexagons designate zones 1-3 moving from the outside to the inside. Portal and arterial blood flows from the triads toward the central vein, whereas bile travels the opposite direction; B: Side view. With the portal triad on the left, portal blood brings nanoparticles from the digestive tract to the liver sinusoids where they can interact with Kupffer cells, liver sinusoidal endothelial cells, and others. Nanoparticles of sufficiently small size can pass through the liver fenestrae formed by liver sinusoidal endothelial cells to access the Space of Disse, and subsequently, hepatocytes. Images are not drawn to scale.

drug delivery systems themselves, which include liposomes, exosomes, PNPs, bacteria, and adeno-associated viruses. To this end, we searched the PubMed (https://pubmed.ncbi.nlm.nih.gov), Google Scholar (https://scholar.google.com), and Web of Science (https://www.webofscience.com/wos/woscc/basic-search) databases for studies published up to June 1, 2022 using a combination of text keywords "alcohol liver disease" and the following: "liposome(s)", "liposomal", "nanoparticle(s)", "nanoformulated", "polymersome(s)", "polymeric nanoparticle(s)", "micelle(s)", "exosome(s)", "AAV", "adenovirus", "adeno-associated virus", and "bioengineered bacteria". Our search strategy identified 846 unique results, which were screened individually by title and abstract and were included based on relevance to liver-targeted drug delivery in ALD. Studies were not excluded based on date of publication, model organism, funding source, or drug delivery platform used. Based on these criteria, 16 studies were included, and then categorized by drug delivery platform (n = 7 studies related to liposomes, n = 2 related to exosomes, n = 5 related to PNPs, and n = 2 related to bacterial or viral systems). A graphical summary of the search strategy and study categorization can be found in Figure 4. The 16 key studies are described in detail in Table 2. The reader is encouraged to refer to this table for

Table 2 Summary of studies employing a liver-specific drug delivery platform in animal models of alcohol-associated liver disease

Ref.	EtOH feeding model	Platform, route of administration (targeting strategy)	Cargo, paradigm (prevention or treatment)	Physical characterization			Empty particle control	Results	Mechanisms	
				Size (nm)	Charge (mV)	EE%			*In vitro*	*In vivo*
Liposomes										
Ponnappa *et al*[24], 2005	Rat chronic (8-10 wk), males	Liposomes, i.v. (passive)	S-ODN, prevention	N/P	N/P	10%-14%	Yes	↓ Liver injury (ALT)	-	↓ Serum and liver TNFα
Rodriguez *et al*[28], 2019	Mouse acute-on-chronic, males	Fusogenic liposomes, i.p. (passive)	Rolipram, treatment	N/P	N/P	N/P	No	↓ Liver injury (ALT and AST); ↓ Steatosis; ↓ Oxidative stress; ↓ ER Stress; ↓ Liver cell apoptosis	-	↑ Hepatic cAMP; ↑ *Sod1* and *Sod2*; ↓ ATF3, *Atf4*, CHOP, and *Gadd34*; ↑ Bcl-xl; ↓ Caspase activation
Zhao *et al*[32], 2016	Mouse chronic (8 wk), males	Liposomes, i.v. (passive)	Puerarin, Prevention	Approximately 182	Approximately -29.4	93.6% ± 1.7%	Yes	↓ Liver injury (ALT and AST)	-	-
Wu *et al*[35], 2019	Mouse EtOH binge (3 wk), males	Liposomes, i.p. or oral (passive)	Astaxanthin, prevention	225.0 ± 58.3	N/P	98%	Yes	↓ Liver injury (ALT and AST); ↓ Liver fibrosis	-	-
Kumar *et al*[36], 2019	Rat chronic (4 wk *via* 2 × daily gavage), males	Liposomes, oral (passive)	Silymarin, treatment	Approximately 146.9	Approximately -47.4	50.50%	No	↓ Liver injury (ALT and AST); ↑ Liver function (albumin); ↓ Oxidative stress; ↓ Liver inflammation	↓ Apoptosis in Chang cells	↑ SOD, GSH, catalase; ↓ TBARS; ↓ IL-6, MPO, nitrite
Yu *et al*[37], 2021	Mouse acute-on-chronic, males	Liposomes, oral (passive)	Saikosaponin D, prevention	61.66 ± 3.89	-37.18 ± 2.89	92.28% ± 0.84%	Yes	↓ Liver injury (ALT and AST); ↓ Steatosis; ↓ Oxidative stress; ↓ Liver inflammation	-	↓ MDA; ↑ GPx, SOD; ↓ Liver TNFα
Jain *et al*[38], 2013	Rat chronic (8 wk), males and females	Liposomes, oral (passive)	Mangiferin, prevention	980 ± 230	N/P	N/A	No	↓ Oxidative stress	-	↓ MDA; ↑ SOD, GSH, catalase
Exosomes										
Gu *et al*[50], 2021	Mouse acute-on-chronic, males	Exosomes, from LGG, oral (passive)	Endogenous cargo, treatment	75 ± 12.7	N/P	N/A	N/A	↓ Liver injury (ALT and AST); ↓ Steatosis	↓ TNFα, *Il-6*, IL-1β, *Mcp1* in RAW264.7 cells; ↑ AhR activity in gut leukocytes; ↑ ZO-1, occludin, claudin-1, Nrf2 in Caco-2 cells	↓ *Tnf* and *Il-1β*; ↑ *Cyp1a1*, IL-22, *Reg3b*, *Reg3g*; ↓ Hepatic bacteria; ↓ Liver endotoxin; ↑ Nrf2
Zhuang *et al*[57], 2015	Mouse acute-on-chronic, males	Exosomes from ginger, oral (passive)	Endogenous cargo, prevention	Approximately 340.4	Approximately -27.2	N/P	N/A	↓ Liver injury (ALT and AST); ↓ Steatosis	-	↑ Nrf2 activation

Polymeric nanoparticles										
Nag *et al*[64], 2020	Mouse chronic drinking water (16 wk), males	Poly(lactic-co-glycolic acid) nanoparticles, i.p. (passive)	Tannic acid/ vitamin e, treatment	127.5 ± 1.6	-21.2 ± 0.39	Tannic acid: 69.7% ± 2.6%; Vitamin E: 63.7% ± 3.2%	No	↓ Liver injury (ALT, AST, ALP); ↓ Steatosis; ↓ Liver fibrosis; ↓ Oxidative stress; ↓ Liver cell apoptosis; ↓ Liver inflammation; ↑ Cell survival	-	↑ HDL ↓ LDL; ↓ ROS; ↑ Catalase, GPx, Nrf2; ↓ Bax, bad, cytochrome C, caspase activation; ↑ Bcl2; ↓ TFGβ, IL-6, TNFα, IL-1β, iNOS, COX2; ↓ EGF, EGFR, AKT, PI3K, and mTOR
Natarajan *et al*[68], 2019	Mouse chronic (4 wk), males	Poly l-lysine-polyethylene glycol copolymer nanoparticles, i.p. (passive)	Superoxide dismutase, treatment	Approximately 44	N/P	N/P	No	↓ Steatosis; ↓ Liver inflammation	↑ SOD1 and ↓ DCF in E47 Hepatoma cells	↓ SREBP1; ↑ ADH1; ↓ *Cd68*, *Ccl2*, *Mmp12*, MCP1, and CCR2; ↑ P-AMPKα
Gopal *et al*[73], 2020	Mouse chronic (4 wk), males	Poly l-lysine-polyethylene glycol copolymer nanoparticles, i.p. (passive)	Superoxide dismutase 1, treatment	Approximately 44	N/P	N/P	No	↓ Liver injury (ALT); ↓ Steatosis	-	↓ Plasma and liver MCP-1; ↑ *Pparα*, *Acox1*, and *Acot1*; ↑ *Mt2*; ↑ SOD1 activity
Zhang *et al*[75], 2022	Mouse chronic (3 wk) + CCL_4, females	Chol-PCX nanoparticles, i.v. (passive)	PCX and anti-miR-155, Treatment	Approximately 70	Approximately 25	N/P	No	↓ Liver injury (ALT); ↓ Liver fibrosis; ↓ Liver inflammation	↓ LPS-induced miR-155 expression in RAW264.7 cells; ↑ CXCR4 antagonism in U20S cells	↓ *Col1a1*, MMPs, TIMPs, HSC activation; ↓ F480+ cells
Wang *et al*[76], 2020	Mouse EtOH binge (4 d), females	*Angelica sinensis* amphipathic cholesteryl hemisuccinate conjugate nanoparticles, i.v. (passive)	Curcumin, prevention	Approximately 208.4	Approximately -20	54.7%-86.1%	Yes	↓ Liver injury (ALT and AST); ↓ Oxidative stress	-	↑ GSH; ↓ ROS (DHE and MDA)
Bacteria and viruses										
Hendrikx *et al*[83], 2019	Mouse acute-on-chronic, male and females	*L. reuteri*, oral (intestine-targeted)	IL-22, prevention	N/A	N/A	N/A	Yes (regular *L. reuteri*)	↓ Liver injury (ALT); ↓ Steatosis (ORO and TG); ↓ Liver inflammation; ↑ Intestinal barrier defense	-	↓ *Cxcl1*, *Cxcl2*; ↑ Small intestine *Reg3g*; ↓ Hepatic bacteria
Satishchandran *et al* [93], 2018	Mouse chronic (5 wk), females	AAV8, i.v. (active)	*pri-MiR122*, treatment	N/A	N/A	N/A	Yes (scrambled miRNA)	↓ Liver injury (ALT); ↓ Steatosis (TG, ORO); ↓ Liver inflammation; ↓ Liver fibrosis (Sirius red)	-	↓ MCP1, IL-1β; ↓ *Col1a1*

Passive targeting denotes a strategy wherein the physical properties of a particle are modified to target the liver, and active targeting denotes a strategy wherein a particle targets the liver through a ligand/receptor interaction.

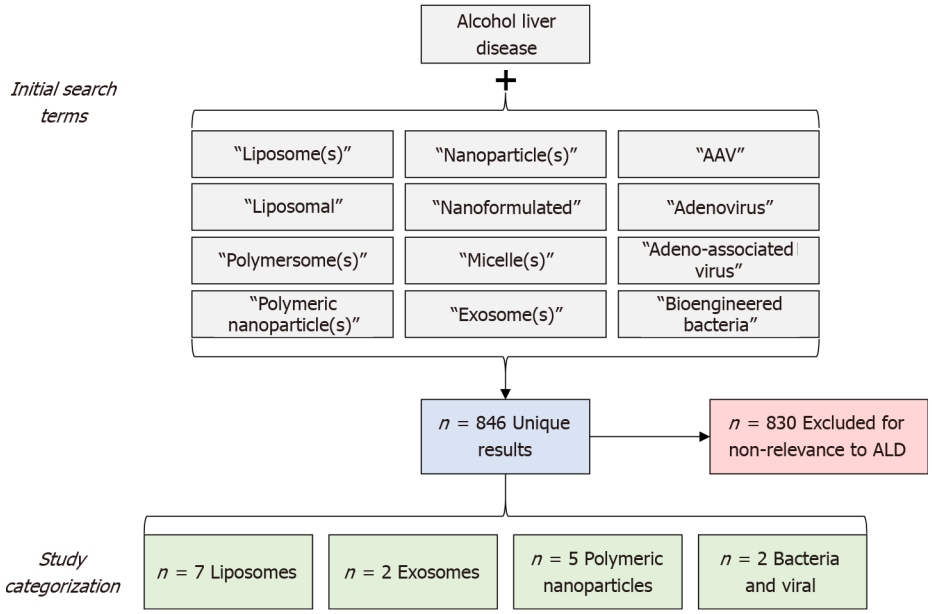
Treatment paradigm denotes models wherein the drug is administered after liver injury has been established (*e.g.*, half-way through the model, at the end of the model, *etc.*), whereas prevention paradigm denotes models wherein the drug is administered for the entire duration of the model. Changes in results/mechanisms columns are in liver unless otherwise stated. AAV8: Adeno-associated Virus Serotype 8; ADH1: Alcohol dehydrogenase 1; AhR: Aryl hydrocarbon receptor; AKT: Protein kinase B; ALP: Alkaline phosphatase; ALT: Alanine aminotransferase; AST: Aspartate aminotransferase; ATF3: Activating transcription factor 3; cAMP: Cyclic adenosine monophosphate; CCl4: Carbon tetrachloride; CCR2: C-C motif chemokine receptor 2; CHOP: C/EBP homologous protein; COX2: Cyclooxygenase 2; DCF: Dichlorodihydrofluorescein; DHE: Dihydroethidium; EE%: Encapsulation efficiency percent; EGF: Epidermal growth factor; EGFR: Epidermal growth factor receptor; ER: Endoplasmic reticulum; GPx: Glutathione peroxidase; GSH: Glutathione; HDL: High density lipoprotein; HSC: Hepatic stellate cell; i.p.: Intraperitoneal injection; i.v.: Intravenous injection; IL: Interleukin ; iNOS: Inducible nitric oxide synthase; LDL: Low density lipoprotein; LGG: Lactobacillus rhamnosus GG; LPS: Lipopolysaccharide; MCP1: Monocyte chemoattractant protein 1; MDA: Malondialdehyde; miR: Micro-RNA; MMPs: Matrix metalloproteinases; MPO: Myeloperoxidase; mTOR: Mechanistic target of rapamycin; N/A: Not applicable; N/P: Not provided; NRF2: Nuclear factor erythroid 2-related factor 2; ORO: Oil red O; P-AMPKα: Phospho-AMP-activated protein kinase alpha; PCX: Polycationic CXCR4 antagonists; PEG: Polyethylene glycol; PG: Propylene glycol; PI3K: Phosphoinositide 3-kinase; RoA: Route of administration; ROS: Reactive oxygen species; SOD: Superoxide dismutase; S-ODN: Antisense phosphorothioate oligodeoxynucleotide; TBARS: Thiobarbituric acid reactive substances; TG: Triglycerides; TGFβ: Transforming growth factor beta; TIMPs: Tissue inhibitors of metalloproteinases; TNFα: Tumor necrosis factor alpha; ZO1: Zonal occludin 1.

information such as the platform employed, the cargo molecule(s), the physical characterization of the particles used (if provided), and the animal model of ALD used, among other information.

Liposome-mediated drug delivery in ALD

Liposomes are one of the most common targeted drug delivery platforms, and indeed, about a third of the studies reviewed here used liposomal drug delivery in some form. Liposomes are vesicles composed of a phospholipid bilayer consisting of one (unilamellar) or more (multilamellar) concentric spherical layers enclosing an aqueous center (Figure 2A, middle panel)[23]. The presence of both aqueous and lipid compartments allows encapsulation or attachment of large quantities of both hydrophilic and lipophilic drugs, respectively (even simultaneously). Liposomes can be modified in many ways to alter their biodistribution *in vivo*, for example by modifying the lipid composition (saturated *vs* unsaturated, positively charged *vs* negatively charged), controlling size, attaching molecules such as PEG to improve stability, or adding proteins, antibodies, peptides, or carbohydrates to facilitate targeting of a specific cell type. The use of naturally occurring phospholipids gives liposomes the advantage of typically being non-immunogenic and non-pharmacologically active when administered alone. A major challenge in using liposomes to deliver drugs to the liver is opsonization and clearance by KCs and LSECs, as well as by RES components in the liver and other organs including the spleen, kidney, lung, bone marrow, and lymph nodes, although the liver is the primary site of liposome retention[23]. Attaching PEG to the liposome surface is an effective way to improve pharmacokinetics and avoid RES clearance, as PEG prevents attachment of opsonizing molecules and subsequent recognition by macrophages[19]. Controlling liposome size and surface charge can also avoid opsonization, as smaller (approximately 200 nm), more neutral liposomes do not as readily bind plasma proteins as larger, more highly charged liposomes.

An early study by Ponnappa *et al*[24] used pH-sensitive liposomes consisting of phosphatidylethanolamine, cholesterol hemisuccinate, and cholesterol to encapsulate an antisense oligonucleotide against *Tnf* mRNA (termed S-ODN) for delivery to the liver in a passive targeting approach. TNF-α is a pro-inflammatory cytokine elevated in ALD which, at high concentrations, sensitizes hepatocytes to cell death signals[25]. Liver macrophages and monocytes are a large source of liver TNF-α production[26]. Given the ability of liposomes to passively target liver macrophages, liposomes were therefore a natural choice of platform for the authors to employ in order to increase delivery of S-ODN to KCs. Intravenous administration of liposomal S-ODNs in a rat chronic ALD model decreased liver *Tnf* mRNA expression



DOI: 10.3748/wjg.v28.i36.5280 **Copyright** ©The Author(s) 2022.

Figure 4 Schematic representation of literature search strategy. Initial search terms included "alcohol liver disease" combined with the boxed terms. Eight hundred and forty-six unique results were generated, screened by title and abstract, and excluded based on relevance to the scope of the review. Sixteen studies were included in the review, broken down into four categories based on drug delivery platform. ALD: Alcohol-associated liver disease; AAV: Adeno-associated virus.

as expected, and subsequently prevented liver injury as demonstrated by plasma ALT[24]. The concentration of S-ODN in KCs was confirmed as being 20-fold higher compared to hepatocytes. In that study, liver-targeted delivery of the therapeutic was necessary to prevent side effects, specifically, to avoid the inhibition of blood coagulation associated with systemic administration (a process already perturbed in liver diseases[27]). A study by Rodriguez *et al*[28] also used a liposomal delivery system to avoid the systemic side effects of the hepato-protective drug rolipram, a phosphodiesterase 4 inhibitor. Previous studies demonstrated the beneficial effects of rolipram for ALD and other liver diseases[29]. However, in humans, rolipram causes significant central nervous system and gastrointestinal side effects (headache, vomiting, *etc*.). To this end, Rodriguez *et al*[28] used fusogenic liposomes composed of 1,2-Dioleoyl-sn-glycerol-3-phosphocholine and 1-palmitoyl-2-oleoyl-sn-glycerol-3-phosphate to passively deliver rolipram to the liver. Fusogenic liposomes differ from conventional liposomes because they avoid endocytosis and lysosomal degradation and instead fuse with the target cell membrane to release the drug cargo into the cytoplasm (for hydrophilic drugs) or membrane (for lipophilic drugs)[30]. Since phosphodiesterase 4 is expressed in the cytoplasm and plasma membrane of HSCs, among other liver cell types[31], the fusogenic liposome platform was an obvious choice for rolipram delivery. Indeed, in an acute-on-chronic mouse model of ALD, rolipram-loaded liposomes reduced liver damage (as determined by plasma ALT/AST activity), steatosis, oxidative stress, and endoplasmic reticulum (ER) stress similar to unencapsulated rolipram. However, encapsulated rolipram prevented liver cell death to a greater degree than un-encapsulated rolipram.

In 2016, Zhao *et al*[32] employed a liposome approach to deliver puerarin to the liver. Unlike the previous two studies, liposomal encapsulation in this study was used to improve pharmacokinetics, because puerarin, a plant-derived isoflavin, is rapidly cleared from the blood by the kidneys (with a half-life of less than one hour[33]). Liposomal encapsulation of this hydrophilic drug was achieved with liposomes composed of phosphatidylcholine, cholesterol, and propylene glycol. The authors demonstrated improved pharmacokinetics when administering puerarin liposomes to mice compared to non-encapsulated puerarin. Specifically, plasma area under the curve and half-life improved by 2.37- and 4.16-fold, respectively, and puerarin was detected most highly in the liver compared to other organs in both preparations. Previous studies supported puerarin as a beneficial molecule in a rat ALD model [34], but liposomal encapsulation improved efficacy further with respect to liver injury (decreased plasma ALT and AST levels) and, to a lesser degree, steatosis. In 2019, Wu *et al*[35] similarly employed a liposomal encapsulation technique to improve the pharmacokinetics of a naturally produced anti-inflammatory carotenoid, astaxanthin. Liposomal astaxanthin was administered to mice either orally or by intraperitoneal injection in an intragastric ethanol feeding model of ALD. Oral and intraperitoneal liposomal astaxanthin ameliorated alcohol-induced liver injury and histological signs of fibrosis. Whereas biodistribution of astaxanthin liposomes was not directly characterized in this study, the physical properties of the drug (low bioavailability, poor water solubility) suggest that liposomal encapsulation was necessary for efficacy. Silymarin is another excellent example of a beneficial

compound with poor pharmacokinetics which can be improved by incorporation into liposomes. Kumar *et al*[36] showed that encapsulation of this hepato-protective flavonolignan in phosphatidylcholine and cholesterol liposomes (either un-modified or PEGylated) improved pharmacokinetics and efficacy. Liposomal encapsulation improved the maximum plasma concentration and plasma area under the curve, while also increasing the solubility of the drug. *In vitro*, silymarin liposomes protected Chang Liver (HeLa) cells against ethanol-induced cell death. *In vivo*, in a rat chronic model of ALD, both un-modified and PEGylated silymarin liposomes ameliorated alcohol-induced liver injury while retaining the anti-inflammatory and antioxidant properties of silymarin. Recently, Yu *et al*[37] encapsulated Saikosaponin D, an anti-inflammatory/anti-oxidant plant-derived compound, in liposomes and demonstrated improved pharmacokinetics and efficacy in a mouse model of ALD compared to the nonencapsulated compound.

Lastly, Jain *et al*[38] employed a liposomal encapsulation approach for a plant-derived molecule, mangiferin. Like silymarin, mangiferin is a natural antioxidant with demonstrated benefits in the treatment of ALD and other diseases[39,40], but is not efficacious when used alone due to low bioavailability and metabolism by gut bacteria, as demonstrated by Jain *et al*[38]. To this end, the authors used a so-called 'herbosome' encapsulation strategy for mangiferin to improve the bioavailability of this compound. Herbosomes are defined as plant-derived compounds encapsulated in phospholipid particles, which in this study consisted of phosphatidylcholine and cholesterol. In a chronic rat model of ALD, unencapsulated mangiferin was able to significantly decrease liver injury, and mangiferin-loaded herbosomes further decreased the liver injury. Mechanistically, the authors attributed this protection to the antioxidant effects of mangiferin, as demonstrated by rescued SOD, catalase, and GSH levels and decreased liver MDA.

These studies support liposomal encapsulation as an effective approach not only for targeting drugs to the liver to avoid systemic side effects, but also for increasing the bioavailability of various compounds. The studies cited herein accomplished these goals by using liposomes composed of various glycerophospholipids including phosphatidylethanolamine, phosphatidyl choline, phosphatidic acid, and lecithin. Selection of certain lipids over others influences membrane fluidity/rigidity, which indirectly alters the permeability of the liposomal bilayer[41]. Certain phospholipids can also be chosen over others to impart fusogenic character, wherein liposomal cargoes can be targeted to the cell cytoplasm by fusing with the plasma membrane while avoiding endocytic degradation[30]. Rodriguez *et al*[28] employed this approach by using liposomes composed of 1,2-dioleoyl-sn-glycero-3-phosphocholine and 1-palmitoyl-2-oleoyl-sn-glycero-3-phosphate to target cytosolic phosphodiesterase. Further, most other groups incorporated cholesterol into their formulation, which can alter the release of the drug cargo and prevent unwanted 'leakage', thereby contributing to the overall stability of the nanoparticle[42].

Exosomes in ALD

Exosomes are another type of lipid-based liver-targeting nanoparticle which have been evaluated pre-clinically as potential therapeutics for ALD as well as potential biomarkers of disease progression in AH [43] (Figure 2A, right panel). Exosomes can be derived from bacteria or food, and are often small (approximately 30-150 nm in diameter) compared to synthetic liposomes (150 nm and larger in the studies cited here)[44]. Because they are products of the host cell membrane which are excreted by exocytosis, they are composed of phospholipids and cholesterol. While originally thought to be used by cells for waste removal, more recent evidence has supported a role in cell signaling, antigen presentation, tissue repair and regeneration, among other processes[44]. Unlike liposomes, exosomes contain numerous surface proteins (*e.g.*, CD63 in eukaryotic exosomes[45]) and internal cargo molecules including lipids, proteins, and nucleic acids. Despite the presence of existing cargo, additional molecules including drugs can be added to exosomes after isolation. The surface proteins present on exosomes mediate their cellular uptake, which has been shown to occur mostly in the liver and spleen, but also to some degree in the kidney, lung, and gastrointestinal tract, although pharmacokinetics depend on the source of the exosomes[46]. Liver macrophages are the cell type thought to be most responsible for exosome uptake through recognition of their charge by scavenging receptors, or recognition of surface signals such as sialic acid or phosphatidyl serine[47,48]. Thus, clearance by macrophages is again a drawback when trying to administer drugs to the liver parenchyma. Another significant consideration is standardization of isolation or purification protocols. Some techniques, for example, fail to completely exclude extraneous types of extracellular vesicles, leading to an impure drug product preparation[49]. Lastly, there are many unanswered questions related to how the choice of cell type from which to isolate exosomes impacts immunogenicity and efficacy.

A study from Gu *et al*[50] aimed to use exosomes derived from the beneficial bacteria *Lactobacillus rhamnosus GG* (LGG) to treat ALD. LGG has previously been demonstrated to be beneficial for ALD as a probiotic supplement which prevents gut permeability, thereby ameliorating liver injury[51,52]. The benefits of LGG probiotic supplementation are mediated, in part, by molecules secreted by LGG, as evidenced by the protective effects of LGG cell culture supernatant[53,54]. These soluble mediators are thought to be released from bacteria in exosomes. Gu *et al*[50] showed that orally administered LGG-derived exosomes (termed LDNPs) ameliorated experimental ALD in an acute-on-chronic mouse model. In contrast to previous studies aiming to deliver drugs to the liver, LDNPs in this study were

designed to ameliorate liver injury *via* the gut-liver axis, by targeting intestinal cells. Fluorescent labeled LDNPs were detectable in the intestine to a much larger extent than in the liver. Mice that received LDNPs were protected from the ethanol-associated reduction in intestinal tight junction protein expression and had boosted expression of intestinal anti-microbial peptides (*e.g.*, *Reg3b*, *Reg3g*) and IL-22. As a result, circulating endotoxin levels were decreased in LDNP-treated mice. Consequently, liver injury, steatosis, and inflammation were attenuated, confirming the critical importance of intestinal barrier defense in preventing ALD pathogenesis. Mechanistically, Gu *et al*[50] showed that the beneficial effects of LDNPs were mediated by the aryl hydrocarbon receptor (AhR), suggesting that the cargo molecules responsible for the benefits of LDNPs are likely AhR ligands.

Foods are another excellent source of exosomes with beneficial endogenous cargo molecules which target the intestinal epithelium or translocate to the bloodstream to target various organs including the liver[55]. Fluorescently labelled milk-derived exosomes, for example, have been shown to localize in the liver after oral administration to mice[56]. Food-derived exosomes from ginger, grapefruit, grape, garlic, ginseng, lemon, and others have been shown to be efficacious in the treatment of numerous diseases by nature of their antioxidant, anti-tumor, or anti-inflammatory cargo[55]. To investigate the efficacy of food-derived exosomes in ALD, Zhuang *et al*[57] used exosomes derived from ginger, a food which has been demonstrated to protect against liver injury of multiple etiologies, including alcohol, *via* antioxidant compounds called gingerols[58]. In an acute-on-chronic mouse model of ALD, daily oral ginger-derived exosome delivery decreased liver injury and steatosis. The antioxidant effects of the exosomes were also demonstrated, with increased expression of antioxidant genes in the liver through activation of NRF2. The authors also analyzed the distribution of the exosomes by fluorescent labeling, showing that the liver was the primary site of accumulation, with no detectable signal in lung, spleen, or other organs. Further, co-localization with albumin-positive cells by immunofluorescence showed that the ginger-derived exosomes primarily associated with hepatocytes, indicating cell-specificity. Collectively, these studies show the utility of exosomes as 'pre-packaged' lipid vesicles which can deliver beneficial cargo molecules from various sources to the liver for the treatment of ALD.

PNP-mediated drug delivery in ALD

PNPs are a class of non-lipid-based nanoparticles composed of natural or synthetic polymers that are gaining popularity in numerous applications, including medicinal and non-medicinal (material science, electronics, ecology, *etc*., Figure 2B, left panel)[59]. PNPs are classified as either nanospheres (composed entirely of polymer matrix) or nanocapsules (a polymer shell with a water or oil center) with an approximate size of 100-250 nm, which can be controlled during synthesis. Poly(lactic-co-glycolic acid) (PLGA) and vinyl monomer-based polymers are commonly used in PNP synthesis (*e.g.*, polystyrene, polyalkyl acrylates), although many other polymers can be used including polyesters, polyurethanes, polysaccharides, polypeptides, and biopolymers (*e.g.*, lignin)[60]. Polymer choice can be adjusted to control stability, particle size, and *in vivo* drug release. As with liposomes, surface modifications can also be made to PNPs to alter their pharmacokinetic profile and biodistribution, such as active targeting moieties or hydrophilic molecules that prevent opsonization (*e.g.*, PEG). Surface modifications can also change the intrinsic negative charge of most PNPs to neutral or positive. PEGylation, for example, shifts the charge to neutral, whereas conjugation of other molecules such as chitosan imparts a positive charge [61,62]. After reaching target cells, PNPs are up taken by pinocytosis or clathrin-mediated endocytosis but can escape lysosomal degradation and enter the cell cytoplasm within 10 min[63]. Other benefits of PNPs include low immunogenicity, low toxicity, and large surface area. As with liposomes, one drawback of PNPs is their susceptibility to opsonization in plasma and rapid clearance by the liver and spleen RES.

Several studies have applied PNPs to the treatment of ALD by attaching various cargo molecules. A study by Nag *et al*[64] used PLGA PNPs to deliver tannic acid and vitamin E to the liver in a chronic mouse model of ALD. These two naturally occurring molecules have previously been established to be beneficial for the treatment of ALD through anti-inflammatory and antioxidant mechanisms[65]. PNP formulation is necessary to ensure extended release of these molecules due to intestinal modification, poor absorption, rapid metabolism, and short half-life[66,67]. Nag *et al*[64] demonstrated that tannic acid/vitamin E PLGA PNPs ameliorated ALD as evaluated by multiple endpoints including reduced liver injury, steatosis, fibrosis, inflammation, oxidative stress, and liver cell apoptosis, as well as increased hepatocyte viability. Importantly, *in vitro* pharmacokinetic analysis showed that the PNPs slowed the movement of tannic acid and vitamin E across a semi-permeable membrane compared to free tannic acid and vitamin E, indicating that this formulation may improve the retention time of these compounds in the liver.

Another study targeting oxidative stress in ALD was conducted by Natarajan *et al*[68], who employed a PNP approach to deliver the enzyme superoxide dismutase (SOD) to the liver. Oxidative stress is a key mechanism in ALD pathogenesis[69]. A previous study in rats demonstrated that increasing hepatic SOD expression (*via* gene therapy) alleviated ALD by scavenging superoxide[70]; however, PNP-mediated SOD delivery is a more favorable translational therapy due to clinical issues surrounding the use of gene therapy (hepatotoxicity and generation of anti-adenovirus antibodies, for example)[71]. Further, previous studies suggest that administration of unencapsulated recombinant SOD does not produce effects that are as long-lasting as those by encapsulated SOD[72]. After establishing successful

delivery of functional SOD *in vitro* in E-47 hepatocytes and protection against ethanol and linoleic acid-induced oxidative stress, the authors administered SOD PNPs to mice by intraperitoneal injection in a chronic model of ALD. Compared to ethanol-treated mice, mice which received ethanol and SOD PNPs had decreased liver steatosis and inflammation as quantified by hematoxylin-eosin staining and decreased liver cytokine expression, respectively. Interestingly, the authors could not detect an increase in SOD in SOD PNP-treated mice, although the authors speculate that the time course of the study may not allow proper detection of elevated SOD levels. In a follow up study by the same research group, Gopal *et al*[73] again assessed the efficacy of intraperitoneal administered SOD PNPs in ALD, although in a modified model where mice are fed a high fat diet prior to the beginning of the ethanol feeding paradigm. Unlike the previous study, here the authors were able to show evidence of increased SOD expression and activity in the livers of mice administered SOD PNPs. Ethanol significantly induced liver injury in control mice, but not in mice administered SOD PNPs, as evidenced by plasma ALT levels. Again, ethanol-induced hepatic steatosis and inflammation were attenuated, corroborating the beneficial effects and mechanisms of protection of liver-specific SOD delivery.

Apart from proteins, another group of novel cargo molecules which can be delivered by PNPs are anti-micro RNAs (anti-MIRs), which are designed to inhibit endogenous MIRs, such as MIR-155, which has been previously shown to play a pathogenic role in ALD[74]. Zhang *et al*[75] aimed to not only block the effects of MIR-155, but also to deliver CXCR4 antagonists (collectively termed polycationic CXCR4 antagonists, or PCX, by the authors), which block alcohol-induced liver fibrosis *via* inhibition of HSC activation. Thus, the group administered synthetic cholesterol-modified polyethyleneimine nanoparticles *via* i.v. injection to mice to target HSCs and KCs in a model of alcohol + CCL_4-induced fibrosis. Indeed, compared to nanoparticles harboring a MIR negative control, the anti-MIR-155/PCX-loaded PNPs significantly reduced liver injury, fibrosis, and inflammation when administered in a treatment paradigm. This study supports the idea that numerous therapeutic cargos are compatible with the PNP platform, even when combined in a dual approach.

In contrast to the synthetic PNPs used in the studies mentioned above, a study by Wang *et al*[76]. used PNPs synthesized from a naturally occurring polysaccharide isolated from *Angelica sinensis* root [*Angelica sinensis* polysaccharide (ASP)]. ASP was combined with cholesterol hemisuccinate to prepare self-assembling ASP-cholesterol hemisuccinate PNPs (termed ACNPs), which were loaded with curcumin, a plant-derived compound with antioxidant effects which has previously shown beneficial effects in ALD[77,78]. The authors used PNPs to improve the delivery of curcumin, which is not readily water-soluble and has low bioavailability due to rapid metabolism[79]. In an intragastric feeding mouse model of ALD, the authors demonstrated that curcumin-loaded ACNPs decreased liver oxidative stress, and consequently, liver injury. Mechanistically, curcumin ACNPs increased NRF2 protein, consistent with other studies implicating NRF2 signaling for the beneficial effects of curcumin[77,80]. These studies show that PNPs, in addition to liposomes, are an effective choice of delivery platform to target drugs to the liver, and importantly, improve the bioavailability of compounds such as tannic acid, vitamin E, and curcumin.

Bacteria and adeno-associated virus-mediated liver-specific delivery in ALD

Certain bacteria have long been considered for their therapeutic potential either as whole organisms (probiotics), colonies of many bacterial species (*i.e.*, fecal transplant), or bacterial products[81]. More recently, genetically engineered bacteria have been developed to facilitate delivery of drugs, proteins, enzymes, and genes for the treatment of numerous pathologies[81] (Figure 2C, left panel). Bacteria as drug delivery systems are beneficial in several ways, including that they can provide their own propulsion and taxis *via* flagella or pili in response to external stimuli (*e.g.*, phototaxis, chemotaxis, thermotaxis, *etc.*), they can be designed to seek a certain molecule (*i.e.*, active targeting), they can produce a desired drug 'on-site' by metabolism, and they can even be designed to transfect host cells. These benefits, and numerous others (described in great detail in[81]), come at the cost of potential host immune response. Use of non-pathogenic bacterial strains, commensal bacteria, or genetic modification can decrease immunogenicity, but there is still considerable risk of septic shock which can result in mortality when targeting sterile body compartments (*e.g.*, blood, abdominal cavity, *etc.*)[82]. Hendrikx *et al*[83], for example, used genetically engineered *Lactobacillus reuteri* (*L. reuteri*), a commensal gut microbe, as a means of increasing intestinal IL-22 for the treatment of ALD in an acute-on-chronic mouse model. This approach aimed to ameliorate alcohol-associated changes in both the intestine and the liver. The gut and liver are connected *via* the so-called gut-liver axis, where alcohol-induced gut permeability allows pro-inflammatory bacteria and bacterial products (*e.g.*, endotoxins) to enter the hepatic portal system and exacerbate liver injury[84]. IL-22 is a cytokine which contributes to gut barrier defense and homeostasis[85], which the authors demonstrated to be decreased in the intestines of ethanol-fed mice. Mice which were enterally provided IL-22-expressing *L. reuteri* throughout the feeding protocol had increased expression of the gut anti-microbial peptide, *Reg3g*, decreased translocation of bacteria to the liver, and consequently, decreased liver injury, steatosis, and inflammation. Increased intestinal IL-22 was confirmed, but there was no increase in plasma IL-22, indicating that a localized increase in gut IL-22 was sufficient to restore gut barrier health and ameliorate liver injury. This engineered bacteria approach may be more clinically useful than simply administering recombinant IL-22 protein systemically, as systemic administration is associated with increased risk of tumor

development in chronic liver disease patients[86-88]. Indeed, bacteria serve as a unique drug delivery system with several key advantages, especially given that liver diseases such as ALD can be targeted indirectly *via* the gut-liver axis.

AAVs (adeno-associated virus) vectors are another biological system with the capability to target specific organs (Figure 2C, right). There exist multiple AAV serotypes with differing capsid proteins (13 in total), which confer serotype-specific functional features, including tropism for different organs[89]. AAV serotype 8 (AAV8), for example, exhibits high liver tropism, since the capsid proteins expressed in this serotype interact with the laminin receptor, which is highly expressed in the liver (for this reason, we have defined AAV8 as 'actively' targeting the liver in Table 2)[90]. This natural ability to target the liver comes at the cost of immunogenicity, liver toxicity, and the production of neutralizing antibodies by the host, several key hurdles for clinical AAV8-based therapy[89]. In contrast to the previous nanoparticle- and bacteria-based delivery systems discussed in this review, AAV vectors are used as a gene delivery vehicle, rather than a carrier of natural or synthetic drugs, based on their ability to transfect host cells[91]. This review will discuss one study using AAV8 as a delivery mechanism for a microRNA; for more information regarding gene therapy for the treatment of liver disease the reader is encouraged to read Kattenhorn *et al*[92]. Satishchandran *et al*[93] employed an AAV8 vector to rescue the ethanol-associated loss of microRNA 122 (MIR-122), which was demonstrated in both human ALD patients and mice in a 5-week chronic model of ALD. Previous work showed that loss of liver *Mir122* alone led to hepatic steatosis with spontaneous development of liver fibrosis and even HCC[94], suggesting a beneficial or homeostatic role of this microRNA in the liver. The authors used the AAV8 serotype to transfect hepatocytes with *pri-MiR122* or a scrambled control vector. Compared to controls, mice receiving AAV8-MIR122 had increased mature liver MIR-122 and, importantly, decreased alcohol-induced liver injury, steatosis, inflammation, and fibrosis. The AAV8 vector was shown to specifically target hepatocytes (as liver mononuclear cells had no increase in MIR122), suggesting this platform may be effective in targeting genes, including microRNAs, to not only the liver, but specifically to hepatocytes.

GAPS IN KNOWLEDGE

Research efforts to apply targeted drug delivery systems for the treatment of ALD are growing, but there are still considerable gaps in knowledge and several barriers to address. First is the lack of use of active targeting strategies, where addition of a ligand to a liposome or nanoparticle targets a drug to a particular liver cell type. Targeting a drug to a particular cell type (*e.g.*, targeting an antioxidant to hepatocytes) may increase efficacy, or produce the same beneficial effect with a lower total dose, thereby reducing the possibility of off-target effects. In additional to hepatocytes, other cell types contribute to ALD, including HSCs and both resident (Kupffer cells) and infiltrating macrophages, thus presenting opportunities to target these non-parenchymal liver cells. In this way, such treatments could target various stages of ALD such as hepatic fibrosis, which is largely driven by these cell types in their activated states (*i.e.*, activated HSCs or M1-polarized KCs)[95]. Fifteen of the 16 studies used a passive targeting approach, where the physical properties of the particle (*i.e.*, size and charge) were controlled in such a way that the particles would passively accumulate in the liver. The Satishchandran *et al*[93] study using AAV8 is one example of biological active targeting, where the AAV8 capsid binds to a particular receptor in the liver. Future research should consider ligand conjugation and active targeting of liposomes and PNPs to improve their drug formulations.

Next, with respect to the paradigm in which drug therapies were administered, in the 16 studies reviewed here, only about half used a so-called 'treatment paradigm', where the drug was given after establishment of liver injury (*i.e.*, half-way through the model or later). The remaining half administered their therapeutics in a 'prevention paradigm', where the drug was given at the start (or even prior to the start) of the alcohol feeding model. Studying the efficacy of a drug in a prevention paradigm certainly provides useful insight into whether the drug has any beneficial effect in ALD. However, this paradigm has limited clinical relevance, since most patients with mild to moderate ALD are asymptomatic, and they would not receive a diagnosis nor treatment until after injury has developed. In the case of studies establishing benefits of a liver-targeted drug in ALD in a prevention paradigm, additional studies should be carried out to determine whether administration of that drug formulation later in the feeding model is still effective. Another issue related to the models used in these studies is the lack of knowledge of the efficacy of these therapies in advanced ALD stages such as fibrosis/cirrhosis. Only one study discussed here (Zhang *et al*[75]), employed a model which is known to produce liver fibrosis, in this case by use of a 'second hit' of carbon tetrachloride superimposed on chronic EtOH feeding. While the authors did note reductions in fibrosis as measured by immunohistochemistry, this is only one study. Most of the studies discussed herein employed chronic, acute-on-chronic, or multiple-binge models which typically produce mild ALD characterized by hepatic steatosis, low-level inflammation, and mild liver injury with elevated ALT but no fibrosis[96,97]. Future studies should investigate the efficacy of nanoformulated drugs in experimental models of more advanced ALD which mimic alcohol-associated cirrhosis or severe AH, especially as better models are developed.

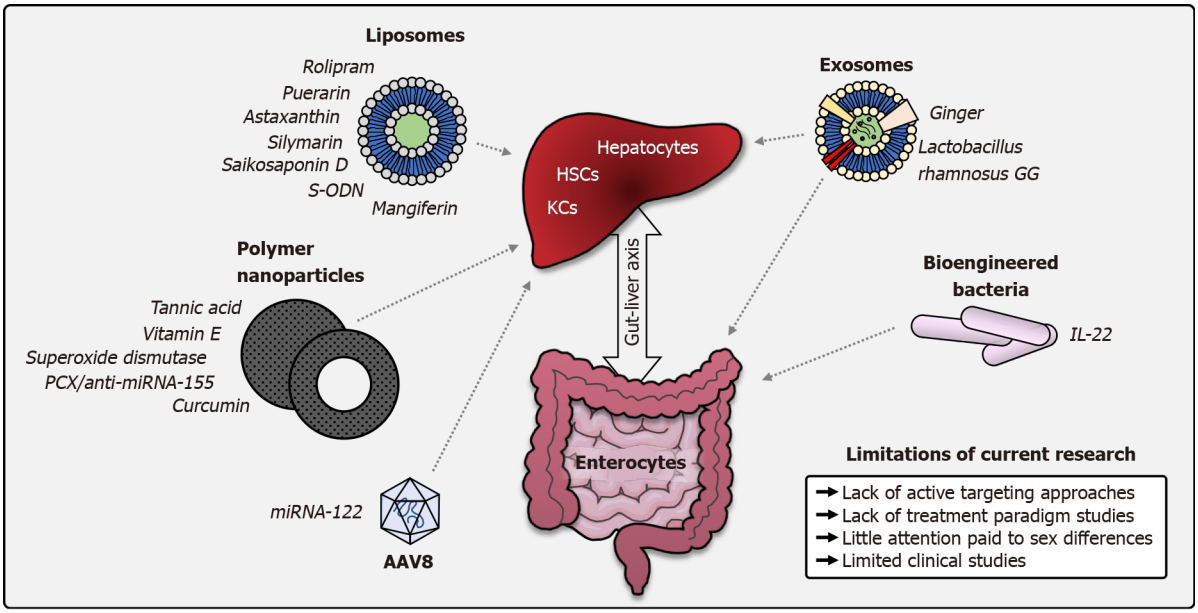
Another consideration with significant clinical implications is the route of administration. The studies reviewed here applied oral (gavage) or injection routes of delivery. Clearly, oral delivery is most attractive from a patient compliance perspective due to ease of self-administration and the absence of potential adverse effects from injections (injection site pain, inflammation, and infection). In general, nanoparticle systems tend to improve the pharmacokinetics of a drug to enable oral delivery in cases where this route would be otherwise unfeasible due to enzymatic digestion or poor absorption[98]. Indeed, many of the studies discussed here employed these platforms with this goal in mind, particularly for poorly soluble plant-derived compounds. However, compared to oral delivery, injection allows the highest level of control over the rate of drug delivery and can bypass any issues associated with first-pass metabolism or poor gastrointestinal absorption, resulting in a bioavailability of 100% and a rapid onset of action[99]. Direct injection of the drug solution into circulation does, however, pose a higher risk of adverse reactions and requires a healthcare professional to administer the treatment. This may be most acceptable in cases where drugs are developed for advanced ALD stages such as AH, where patients are already hospitalized. Regardless, authors should justify their chosen route of administration in the context of their future translational goals.

Additionally, in pre-clinical ALD research, it is important to consider sex differences, since men and women consume and metabolize alcohol differently, have different risk factors contributing to ALD, and ultimately, have different susceptibility to developing the disease[100]. Even in mice, there are sex differences in susceptibility to ALD when controlling for alcohol intake, diet, and other factors[101]. Further, evidence suggests biodistribution of nanoparticles may also differ by sex[102], providing an additional rationale for studying nanoparticle systems in ALD in both sexes. Despite these differences, many of the studies reviewed here (14 of 16) used either only male mice or only female mice, and the remaining two which used both sexes did not report the results for each sex separately.

Lastly, keeping in mind the goal of translating effective therapies to humans for the treatment of ALD, there is a lack of knowledge regarding the efficacy of liver-targeted therapies in humans for this disease. Critically, however, nanoparticle platforms have been used for many years for the treatment of other diseases. For example, liposomes have been used in numerous drug formulations for the treatment of various cancers, fungal and viral infection, pain, and other diseases since 1995 with excellent safety and efficacy[103]. Liposomes are also increasing in popularity as an excellent vaccine delivery system with several benefits over conventional vaccines (*e.g.*, liposomes are used in the Moderna and Pfizer/BioNTech COVID-19 mRNA vaccines)[104]. Although less common than liposomes, PNPs have also undergone clinical evaluation for the treatment of head, neck, lung, and breast cancers[105]. Other platforms not discussed in this review, such as N-acetyl-galactosamine (GalNac) conjugate (commonly used to delivery nucleic acids to hepatocytes by binding the asialoglycoprotein receptor[106]), have also been shown to have favorable safety profiles in clinical trials[107]. Clearly, drug delivery platforms with the capability to deliver drugs to the liver have undergone significant clinical evaluation, although not for the treatment of ALD. Future work should build on the growing pre-clinical data supporting the efficacy of particle therapeutics in ALD and the existing clinical data showing the safety of these systems in humans to move these nanomedicines to the clinic.

CONCLUSION

The research efforts reviewed here employed liver-targeted (or intestine-targeted) drug delivery platforms to improve their drug formulations and more effectively develop pharmacological interventions for ALD (summarized in Figure 5). These platforms, including liposomes, PNPs, exosomes, bacteria, and AAV vectors are aimed at improving a drug's pharmacokinetics, efficacy, and safety by reducing off target effects associated with systemic delivery and increasing the concentration of the drug locally in the liver. The authors of these studies used nanomedicine platforms to deliver phosphodiesterase inhibitors, naturally occurring antioxidants, oligonucleotides, miRNAs, enzymes, and anti-inflammatory cytokines in various rodent models of ALD, showing promising results which will move the pace of drug development for this disease forward toward clinical translation. Future studies should continue to apply and characterize targeted delivery platforms, as well as consider active targeting approaches, drug administration paradigms, and sex-specific differences in the pursuit of supporting future clinical trials in this field.



DOI: 10.3748/wjg.v28.i36.5280 **Copyright** ©The Author(s) 2022.

Figure 5 Summary of studies applying nanoparticle platforms in alcohol-associated liver disease. A graphical summary of nanoparticle platforms which to date have been applied for the treatment or prevention of alcohol-associated liver disease in rodent models. Arrows represent organ targets of each platform. Example cargoes used in research articles discussed in this review are listed next to each platform. Current limitations of the field are described on the lower right. AAV8: Adeno-associated virus serotype 8; HSCs: Hepatic stellate cells; IL-22: Interleukin 22; KCs: Kupffer cells; miRNA: Micro-RNA; PCX: Polycationic CXCR4 antagonists; S-ODN: Antisense phosphorothioate oligodeoxynucleotide.

ACKNOWLEDGEMENTS

We apologize to and acknowledge any authors whose studies were not identified by our literature search strategy. We also acknowledge Marion McClain for manuscript editing support.

FOOTNOTES

Author contributions: Warner JB and Kirpich IA designed and outlined the review; Warner JB wrote the contents of the review; Warner JB and Guenthner SC designed the figures; Guenthner SC, Hardesty JE, McClain CJ, Warner DR, and Kirpich IA edited the manuscript; all authors have read and approve the final manuscript.

Supported by National Institutes of Health, No. R01AA028905-01A1 (to Kirpich IA), No. 1F31AA028423-01A1 (to Warner JB), No. F32AA027950-01A1 (to Hardesty JE) and No. U01AA026934 (to McClain CJ); Jewish Heritage Fund for Excellence Research Enhancement Grant Program at the University of Louisville, as well as an Institutional Development Award (IDeA) from the National Institute of General Medical Sciences of the National Institutes of Health, No. P20GM113226 (to McClain CJ); and National Institute on Alcohol Abuse and Alcoholism of the National Institutes of Health, No. P50AA024337 (to McClain CJ).

Conflict-of-interest statement: All the authors report no relevant conflicts of interest for this article.

Open-Access: This article is an open-access article that was selected by an in-house editor and fully peer-reviewed by external reviewers. It is distributed in accordance with the Creative Commons Attribution NonCommercial (CC BY-NC 4.0) license, which permits others to distribute, remix, adapt, build upon this work non-commercially, and license their derivative works on different terms, provided the original work is properly cited and the use is non-commercial. See: https://creativecommons.org/Licenses/by-nc/4.0/

Country/Territory of origin: United States

ORCID number: Jeffrey Barr Warner 0000-0003-2022-7854; Steven Corrigan Guenthner 0000-0003-3561-9607; Josiah Everett Hardesty 0000-0003-1955-3046; Craig James McClain 0000-0002-7219-8939; Dennis Ray Warner 0000-0002-5303-6870; Irina Andreyevna Kirpich 0000-0002-9545-6451.

S-Editor: Gao CC
L-Editor: A
P-Editor: Gao CC

REFERENCES

1 **Rehm J**, Samokhvalov AV, Shield KD. Global burden of alcoholic liver diseases. *J Hepatol* 2013; **59**: 160-168 [PMID: 23511777 DOI: 10.1016/j.jhep.2013.03.007]
2 **Seitz HK**, Bataller R, Cortez-Pinto H, Gao B, Gual A, Lackner C, Mathurin P, Mueller S, Szabo G, Tsukamoto H. Alcoholic liver disease. *Nat Rev Dis Primers* 2018; **4**: 16 [PMID: 30115921 DOI: 10.1038/s41572-018-0014-7]
3 **Lucey MR**, Mathurin P, Morgan TR. Alcoholic hepatitis. *N Engl J Med* 2009; **360**: 2758-2769 [PMID: 19553649 DOI: 10.1056/NEJMra0805786]
4 **European Association for the Study of the Liver**. EASL Clinical Practice Guidelines: Management of alcohol-related liver disease. *J Hepatol* 2018; **69**: 154-181 [PMID: 29628280 DOI: 10.1016/j.jhep.2018.03.018]
5 **Akriviadis E**, Botla R, Briggs W, Han S, Reynolds T, Shakil O. Pentoxifylline improves short-term survival in severe acute alcoholic hepatitis: a double-blind, placebo-controlled trial. *Gastroenterology* 2000; **119**: 1637-1648 [PMID: 11113085 DOI: 10.1053/gast.2000.20189]
6 **Singh S**, Osna NA, Kharbanda KK. Treatment options for alcoholic and non-alcoholic fatty liver disease: A review. *World J Gastroenterol* 2017; **23**: 6549-6570 [PMID: 29085205 DOI: 10.3748/wjg.v23.i36.6549]
7 **Veronese FM**, Mero A. The impact of PEGylation on biological therapies. *BioDrugs* 2008; **22**: 315-329 [PMID: 18778113 DOI: 10.2165/00063030-200822050-00004]
8 **Woo ASJ**, Kwok R, Ahmed T. Alpha-interferon treatment in hepatitis B. *Ann Transl Med* 2017; **5**: 159 [PMID: 28480195 DOI: 10.21037/atm.2017.03.69]
9 **Mody VV**, Siwale R, Singh A, Mody HR. Introduction to metallic nanoparticles. *J Pharm Bioallied Sci* 2010; **2**: 282-289 [PMID: 21180459 DOI: 10.4103/0975-7406.72127]
10 **Onxeo**. Efficacy and Safety Doxorubicin Transdrug Study in Patients Suffering From Advanced Hepatocellular Carcinoma. [accessed 2022 June 1]. In: ClinicalTrials.gov [Internet]. Canton (OH): U.S. National Library of Medicine. Available from: https://clinicaltrials.gov/ct2/show/study/NCT01655693 ClinicalTrials.gov Identifier: NCT01655693
11 **Zhang L**, Liu M, Jamil S, Han R, Xu G, Ni Y. PEGylation and pharmacological characterization of a potential anti-tumor drug, an engineered arginine deiminase originated from Pseudomonas plecoglossicida. *Cancer Lett* 2015; **357**: 346-354 [PMID: 25462857 DOI: 10.1016/j.canlet.2014.11.042]
12 **Dicerna Pharmaceuticals**. Phase Ib/2, Multicenter, Dose Escalation Study of DCR-MYC in Patients With Hepatocellular Carcinoma. [accessed 2022 June 1]. In: ClinicalTrials.gov [Internet]. Scottsdale (AZ): U.S. National Library of Medicine. Available from: https://clinicaltrials.gov/ct2/show/NCT02314052 ClinicalTrials.gov Identifier: NCT02314052
13 **Li SW**, Zhao Q, Wu T, Chen S, Zhang J, Xia NS. The development of a recombinant hepatitis E vaccine HEV 239. *Hum Vaccin Immunother* 2015; **11**: 908-914 [PMID: 25714510 DOI: 10.1080/21645515.2015.1008870]
14 **Lawitz E**, Tanaka Y, Poordad F, Gutierrez JA, Carr K, Ying WB, Niitsu Y, Maruyama K. Safety, Pharmacokinetics, and Biologic Activity of ND-L02-s0201, a Novel Targeted Lipid-Nanoparticle to Deliver HSP47 siRNA for the Treatment of Patients with Advanced Liver Fibrosis: Interim Results from Clinical Phase 1b/2 Studies. *Hepatology* 2015; **62**: 909a
15 **Ivanenkov YA**, Maklakova SY, Beloglazkina EK, Zyk NV, Nazarenko AG, Tonevitsky AG, Kotelianski VE, Majouga AG. Development of liver cell-targeted drug delivery systems: experimental approaches. *Russian Chem Rev* 2017; **86**
16 **Ben-Moshe S**, Itzkovitz S. Spatial heterogeneity in the mammalian liver. *Nat Rev Gastroenterol Hepatol* 2019; **16**: 395-410 [PMID: 30936469 DOI: 10.1038/s41575-019-0134-x]
17 **Vekemans K**, Braet F. Structural and functional aspects of the liver and liver sinusoidal cells in relation to colon carcinoma metastasis. *World J Gastroenterol* 2005; **11**: 5095-5102 [PMID: 16127736 DOI: 10.3748/wjg.v11.i33.5095]
18 **Shilpi S**, Shivvedi R, Gurnany E, Dixit S, Khatri K, Dwivedi D. Drug targeting strategies for liver cancer and other liver diseases. *Drug Des Devel Ther* 2018; **2**: 171-177 [DOI: 10.15406/mojddt.2018.02.00044]
19 **Immordino ML**, Dosio F, Cattel L. Stealth liposomes: review of the basic science, rationale, and clinical applications, existing and potential. *Int J Nanomedicine* 2006; **1**: 297-315 [PMID: 17717971]
20 **Wisse E**, Jacobs F, Topal B, Frederik P, De Geest B. The size of endothelial fenestrae in human liver sinusoids: implications for hepatocyte-directed gene transfer. *Gene Ther* 2008; **15**: 1193-1199 [PMID: 18401434 DOI: 10.1038/gt.2008.60]
21 **Arvizo RR**, Miranda OR, Moyano DF, Walden CA, Giri K, Bhattacharya R, Robertson JD, Rotello VM, Reid JM, Mukherjee P. Modulating pharmacokinetics, tumor uptake and biodistribution by engineered nanoparticles. *PLoS One* 2011; **6**: e24374 [PMID: 21931696 DOI: 10.1371/journal.pone.0024374]
22 **Kang JH**, Toita R, Murata M. Liver cell-targeted delivery of therapeutic molecules. *Crit Rev Biotechnol* 2016; **36**: 132-143 [PMID: 25025274 DOI: 10.3109/07388551.2014.930017]
23 **Sercombe L**, Veerati T, Moheimani F, Wu SY, Sood AK, Hua S. Advances and Challenges of Liposome Assisted Drug Delivery. *Front Pharmacol* 2015; **6**: 286 [PMID: 26648870 DOI: 10.3389/fphar.2015.00286]
24 **Ponnappa BC**, Israel Y, Aini M, Zhou F, Russ R, Cao QN, Hu Y, Rubin R. Inhibition of tumor necrosis factor alpha secretion and prevention of liver injury in ethanol-fed rats by antisense oligonucleotides. *Biochem Pharmacol* 2005; **69**: 569-577 [PMID: 15670576 DOI: 10.1016/j.bcp.2004.11.011]
25 **Lopetuso LR**, Mocci G, Marzo M, D'Aversa F, Rapaccini GL, Guidi L, Armuzzi A, Gasbarrini A, Papa A. Harmful Effects and Potential Benefits of Anti-Tumor Necrosis Factor (TNF)-α on the Liver. *Int J Mol Sci* 2018; **19** [PMID: 30060508 DOI: 10.3390/ijms19082199]
26 **Yang YM**, Seki E. TNFα in liver fibrosis. *Curr Pathobiol Rep* 2015; **3**: 253-261 [PMID: 26726307 DOI: 10.1007/s40139-015-0093-z]
27 **Lisman T**, Porte RJ. Rebalanced hemostasis in patients with liver disease: evidence and clinical consequences. *Blood* 2010; **116**: 878-885 [PMID: 20400681 DOI: 10.1182/blood-2010-02-261891]
28 **Rodriguez WE**, Wahlang B, Wang Y, Zhang J, Vadhanam MV, Joshi-Barve S, Bauer P, Cannon R, Ahmadi AR, Sun Z, Cameron A, Barve S, Maldonado C, McClain C, Gobejishvili L. Phosphodiesterase 4 Inhibition as a Therapeutic Target

for Alcoholic Liver Disease: From Bedside to Bench. *Hepatology* 2019; **70**: 1958-1971 [PMID: 31081957 DOI: 10.1002/hep.30761]

29 **Wahlang B**, McClain C, Barve S, Gobejishvili L. Role of cAMP and phosphodiesterase signaling in liver health and disease. *Cell Signal* 2018; **49**: 105-115 [PMID: 29902522 DOI: 10.1016/j.cellsig.2018.06.005]

30 **Kube S**, Hersch N, Naumovska E, Gensch T, Hendriks J, Franzen A, Landvogt L, Siebrasse JP, Kubitscheck U, Hoffmann B, Merkel R, Csiszár A. Fusogenic Liposomes as Nanocarriers for the Delivery of Intracellular Proteins. *Langmuir* 2017; **33**: 1051-1059 [PMID: 28059515 DOI: 10.1021/acs.langmuir.6b04304]

31 **Thul PJ**, Åkesson L, Wiking M, Mahdessian D, Geladaki A, Ait Blal H, Alm T, Asplund A, Björk L, Breckels LM, Bäckström A, Danielsson F, Fagerberg L, Fall J, Gatto L, Gnann C, Hober S, Hjelmare M, Johansson F, Lee S, Lindskog C, Mulder J, Mulvey CM, Nilsson P, Oksvold P, Rockberg J, Schutten R, Schwenk JM, Sivertsson Å, Sjöstedt E, Skogs M, Stadler C, Sullivan DP, Tegel H, Winsnes C, Zhang C, Zwahlen M, Mardinoglu A, Pontén F, von Feilitzen K, Lilley KS, Uhlén M, Lundberg E. A subcellular map of the human proteome. *Science* 2017; **356** [PMID: 28495876 DOI: 10.1126/science.aal3321]

32 **Zhao YZ**, Zhang L, Gupta PK, Tian FR, Mao KL, Qiu KY, Yang W, Lv CZ, Lu CT. Using PG-Liposome-Based System to Enhance Puerarin Liver-Targeted Therapy for Alcohol-Induced Liver Disease. *AAPS PharmSciTech* 2016; **17**: 1376-1382 [PMID: 26753818 DOI: 10.1208/s12249-015-0427-5]

33 **Li Y**, Pan WS, Chen SL, Xu HX, Yang DJ, Chan AS. Pharmacokinetic, tissue distribution, and excretion of puerarin and puerarin-phospholipid complex in rats. *Drug Dev Ind Pharm* 2006; **32**: 413-422 [PMID: 16638679 DOI: 10.1080/03639040600559123]

34 **Zhao M**, Du YQ, Yuan L, Wang NN. Protective effect of puerarin on acute alcoholic liver injury. *Am J Chin Med* 2010; **38**: 241-249 [PMID: 20387222 DOI: 10.1142/S0192415X10007816]

35 **Wu YC**, Huang HH, Wu YJ, Manousakas I, Yang CC, Kuo SM. Therapeutic and Protective Effects of Liposomal Encapsulation of Astaxanthin in Mice with Alcoholic Liver Fibrosis. *Int J Mol Sci* 2019; **20** [PMID: 31434227 DOI: 10.3390/ijms20164057]

36 **Kumar N**, Rai A, Reddy ND, Shenoy RR, Mudgal J, Bansal P, Mudgal PP, Arumugam K, Udupa N, Sharma N, Rao CM. Improved *in vitro* and *in vivo* hepatoprotective effects of liposomal silymarin in alcohol-induced hepatotoxicity in Wistar rats. *Pharmacol Rep* 2019; **71**: 703-712 [PMID: 31207432 DOI: 10.1016/j.pharep.2019.03.013]

37 **Yu X**, Pan J, Shen N, Zhang H, Zou L, Miao H, Xing L. Development of Saikosaponin D Liposome Nanocarrier with Increased Hepatoprotective Effect Against Alcoholic Hepatitis Mice. *J Biomed Nanotechnol* 2021; **17**: 627-639 [PMID: 35057889 DOI: 10.1166/jbn.2021.3054]

38 **Jain PK**, Kharya M, Gajbhiye A. Pharmacological evaluation of mangiferin herbosomes for antioxidant and hepatoprotection potential against ethanol induced hepatic damage. *Drug Dev Ind Pharm* 2013; **39**: 1840-1850 [PMID: 23167243 DOI: 10.3109/03639045.2012.738685]

39 **Yoshikawa M**, Ninomiya K, Shimoda H, Nishida N, Matsuda H. Hepatoprotective and antioxidative properties of Salacia reticulata: preventive effects of phenolic constituents on CCl4-induced liver injury in mice. *Biol Pharm Bull* 2002; **25**: 72-76 [PMID: 11824561 DOI: 10.1248/bpb.25.72]

40 **Miura T**, Ichiki H, Hashimoto I, Iwamoto N, Kato M, Kubo M, Ishihara E, Komatsu Y, Okada M, Ishida T, Tanigawa K. Antidiabetic activity of a xanthone compound, mangiferin. *Phytomedicine* 2001; **8**: 85-87 [PMID: 11315760 DOI: 10.1078/0944-7113-00009]

41 **Akbarzadeh A**, Rezaei-Sadabady R, Davaran S, Joo SW, Zarghami N, Hanifehpour Y, Samiei M, Kouhi M, Nejati-Koshki K. Liposome: classification, preparation, and applications. *Nanoscale Res Lett* 2013; **8**: 102 [PMID: 23432972 DOI: 10.1186/1556-276X-8-102]

42 **Ahmed KS**, Hussein SA, Ali AH, Korma SA, Lipeng Q, Jinghua C. Liposome: composition, characterisation, preparation, and recent innovation in clinical applications. *J Drug Target* 2019; **27**: 742-761 [PMID: 30239255 DOI: 10.1080/1061186X.2018.1527337]

43 **Momen-Heravi F**, Saha B, Kodys K, Catalano D, Satishchandran A, Szabo G. Increased number of circulating exosomes and their microRNA cargos are potential novel biomarkers in alcoholic hepatitis. *J Transl Med* 2015; **13**: 261 [PMID: 26264599 DOI: 10.1186/s12967-015-0623-9]

44 **Doyle LM**, Wang MZ. Overview of Extracellular Vesicles, Their Origin, Composition, Purpose, and Methods for Exosome Isolation and Analysis. *Cells* 2019; **8** [PMID: 31311206 DOI: 10.3390/cells8070727]

45 **Kowal J**, Arras G, Colombo M, Jouve M, Morath JP, Primdal-Bengtson B, Dingli F, Loew D, Tkach M, Théry C. Proteomic comparison defines novel markers to characterize heterogeneous populations of extracellular vesicle subtypes. *Proc Natl Acad Sci U S A* 2016; **113**: E968-E977 [PMID: 26858453 DOI: 10.1073/pnas.1521230113]

46 **Morishita M**, Takahashi Y, Nishikawa M, Takakura Y. Pharmacokinetics of Exosomes-An Important Factor for Elucidating the Biological Roles of Exosomes and for the Development of Exosome-Based Therapeutics. *J Pharm Sci* 2017; **106**: 2265-2269 [PMID: 28283433 DOI: 10.1016/j.xphs.2017.02.030]

47 **Matsumoto A**, Takahashi Y, Nishikawa M, Sano K, Morishita M, Charoenviriyakul C, Saji H, Takakura Y. Role of Phosphatidylserine-Derived Negative Surface Charges in the Recognition and Uptake of Intravenously Injected B16BL6-Derived Exosomes by Macrophages. *J Pharm Sci* 2017; **106**: 168-175 [PMID: 27649887 DOI: 10.1016/j.xphs.2016.07.022]

48 **Parada N**, Romero-Trujillo A, Georges N, Alcayaga-Miranda F. Camouflage strategies for therapeutic exosomes evasion from phagocytosis. *J Adv Res* 2021; **31**: 61-74 [PMID: 34194832 DOI: 10.1016/j.jare.2021.01.001]

49 **Li X**, Corbett AL, Taatizadeh E, Tasnim N, Little JP, Garnis C, Daugaard M, Guns E, Hoorfar M, Li ITS. Challenges and opportunities in exosome research-Perspectives from biology, engineering, and cancer therapy. *APL Bioeng* 2019; **3**: 011503 [PMID: 31069333 DOI: 10.1063/1.5087122]

50 **Gu Z**, Li F, Liu Y, Jiang M, Zhang L, He L, Wilkey DW, Merchant M, Zhang X, Deng ZB, Chen SY, Barve S, McClain CJ, Feng W. Exosome-Like Nanoparticles From *Lactobacillus rhamnosus*GG Protect Against Alcohol-Associated Liver Disease Through Intestinal Aryl Hydrocarbon Receptor in Mice. *Hepatol Commun* 2021; **5**: 846-864 [PMID: 34027273 DOI: 10.1002/hep4.1679]

51 **Bruch-Bertani JP**, Uribe-Cruz C, Pasqualotto A, Longo L, Ayres R, Beskow CB, Barth AL, Lima-Morales D, Meurer F, Tayguara Silveira Guerreiro G, da Silveira TR, Álvares-da-Silva MR, Dall'Alba V. Hepatoprotective Effect of Probiotic *Lactobacillus rhamnosus* GG Through the Modulation of Gut Permeability and Inflammasomes in a Model of Alcoholic Liver Disease in Zebrafish. *J Am Coll Nutr* 2020; **39**: 163-170 [PMID: 31241423 DOI: 10.1080/07315724.2019.1627955]

52 **Wang Y**, Kirpich I, Liu Y, Ma Z, Barve S, McClain CJ, Feng W. Lactobacillus rhamnosus GG treatment potentiates intestinal hypoxia-inducible factor, promotes intestinal integrity and ameliorates alcohol-induced liver injury. *Am J Pathol* 2011; **179**: 2866-2875 [PMID: 22093263 DOI: 10.1016/j.ajpath.2011.08.039]

53 **Zhao H**, Zhao C, Dong Y, Zhang M, Wang Y, Li F, Li X, McClain C, Yang S, Feng W. Inhibition of miR122a by Lactobacillus rhamnosus GG culture supernatant increases intestinal occludin expression and protects mice from alcoholic liver disease. *Toxicol Lett* 2015; **234**: 194-200 [PMID: 25746479 DOI: 10.1016/j.toxlet.2015.03.002]

54 **Wang Y**, Liu Y, Sidhu A, Ma Z, McClain C, Feng W. Lactobacillus rhamnosus GG culture supernatant ameliorates acute alcohol-induced intestinal permeability and liver injury. *Am J Physiol Gastrointest Liver Physiol* 2012; **303**: G32-G41 [PMID: 22538402 DOI: 10.1152/ajpgi.00024.2012]

55 **Munir J**, Lee M, Ryu S. Exosomes in Food: Health Benefits and Clinical Relevance in Diseases. *Adv Nutr* 2020; **11**: 687-696 [PMID: 31796948 DOI: 10.1093/advances/nmz123]

56 **Manca S**, Upadhyaya B, Mutai E, Desaulniers AT, Cederberg RA, White BR, Zempleni J. Milk exosomes are bioavailable and distinct microRNA cargos have unique tissue distribution patterns. *Sci Rep* 2018; **8**: 11321 [PMID: 30054561 DOI: 10.1038/s41598-018-29780-1]

57 **Zhuang X**, Deng ZB, Mu J, Zhang L, Yan J, Miller D, Feng W, McClain CJ, Zhang HG. Ginger-derived nanoparticles protect against alcohol-induced liver damage. *J Extracell Vesicles* 2015; **4**: 28713 [PMID: 26610593 DOI: 10.3402/jev.v4.28713]

58 **Mu J**, Zhuang X, Wang Q, Jiang H, Deng ZB, Wang B, Zhang L, Kakar S, Jun Y, Miller D, Zhang HG. Interspecies communication between plant and mouse gut host cells through edible plant derived exosome-like nanoparticles. *Mol Nutr Food Res* 2014; **58**: 1561-1573 [PMID: 24842810 DOI: 10.1002/mnfr.201300729]

59 **Rao JP**, Geckeler KE. Polymer nanoparticles: Preparation techniques and size-control parameters. *Prog Polym Sci* 2011; **36**: 887-913 [DOI: 10.1016/j.progpolymsci.2011.01.001]

60 **Danhier F**, Ansorena E, Silva JM, Coco R, Le Breton A, Préat V. PLGA-based nanoparticles: an overview of biomedical applications. *J Control Release* 2012; **161**: 505-522 [PMID: 22353619 DOI: 10.1016/j.jconrel.2012.01.043]

61 **Danhier F**, Feron O, Préat V. To exploit the tumor microenvironment: Passive and active tumor targeting of nanocarriers for anti-cancer drug delivery. *J Control Release* 2010; **148**: 135-146 [PMID: 20797419 DOI: 10.1016/j.jconrel.2010.08.027]

62 **Tahara K**, Sakai T, Yamamoto H, Takeuchi H, Hirashima N, Kawashima Y. Improved cellular uptake of chitosan-modified PLGA nanospheres by A549 cells. *Int J Pharm* 2009; **382**: 198-204 [PMID: 19646519 DOI: 10.1016/j.ijpharm.2009.07.023]

63 **Vasir JK**, Labhasetwar V. Biodegradable nanoparticles for cytosolic delivery of therapeutics. *Adv Drug Deliv Rev* 2007; **59**: 718-728 [PMID: 17683826 DOI: 10.1016/j.addr.2007.06.003]

64 **Nag S**, Manna K, Saha M, Das Saha K. Tannic acid and vitamin E loaded PLGA nanoparticles ameliorate hepatic injury in a chronic alcoholic liver damage model *via* EGFR-AKT-STAT3 pathway. *Nanomedicine (Lond)* 2020; **15**: 235-257 [PMID: 31789102 DOI: 10.2217/nnm-2019-0340]

65 **Adewusi EA**, Afolayan AJ. Effect of Pelargonium reniforme roots on alcohol-induced liver damage and oxidative stress. *Pharm Biol* 2010; **48**: 980-987 [PMID: 20731548 DOI: 10.3109/13880200903410354]

66 **Carbonaro M**, Grant G, Pusztai A. Evaluation of polyphenol bioavailability in rat small intestine. *Eur J Nutr* 2001; **40**: 84-90 [PMID: 11518204 DOI: 10.1007/s003940170020]

67 **D'Archivio M**, Filesi C, Varì R, Scazzocchio B, Masella R. Bioavailability of the polyphenols: status and controversies. *Int J Mol Sci* 2010; **11**: 1321-1342 [PMID: 20480022 DOI: 10.3390/ijms11041321]

68 **Natarajan G**, Perriotte-Olson C, Casey CA, Donohue TM Jr, Talmon GA, Harris EN, Kabanov AV, Saraswathi V. Effect of nanoformulated copper/zinc superoxide dismutase on chronic ethanol-induced alterations in liver and adipose tissue. *Alcohol* 2019; **79**: 71-79 [PMID: 30611703 DOI: 10.1016/j.alcohol.2018.12.005]

69 **Tan HK**, Yates E, Lilly K, Dhanda AD. Oxidative stress in alcohol-related liver disease. *World J Hepatol* 2020; **12**: 332-349 [PMID: 32821333 DOI: 10.4254/wjh.v12.i7.332]

70 **Wheeler MD**, Kono H, Yin M, Rusyn I, Froh M, Connor HD, Mason RP, Samulski RJ, Thurman RG. Delivery of the Cu/Zn-superoxide dismutase gene with adenovirus reduces early alcohol-induced liver injury in rats. *Gastroenterology* 2001; **120**: 1241-1250 [PMID: 11266387 DOI: 10.1053/gast.2001.23253]

71 **Eto Y**, Yoshioka Y, Mukai Y, Okada N, Nakagawa S. Development of PEGylated adenovirus vector with targeting ligand. *Int J Pharm* 2008; **354**: 3-8 [PMID: 17904316 DOI: 10.1016/j.ijpharm.2007.08.025]

72 **Laursen JB**, Rajagopalan S, Galis Z, Tarpey M, Freeman BA, Harrison DG. Role of superoxide in angiotensin II-induced but not catecholamine-induced hypertension. *Circulation* 1997; **95**: 588-593 [PMID: 9024144 DOI: 10.1161/01.cir.95.3.588]

73 **Gopal T**, Kumar N, Perriotte-Olson C, Casey CA, Donohue TM Jr, Harris EN, Talmon G, Kabanov AV, Saraswathi V. Nanoformulated SOD1 ameliorates the combined NASH and alcohol-associated liver disease partly *via* regulating CYP2E1 expression in adipose tissue and liver. *Am J Physiol Gastrointest Liver Physiol* 2020; **318**: G428-G438 [PMID: 31928222 DOI: 10.1152/ajpgi.00217.2019]

74 **Bala S**, Csak T, Saha B, Zatsiorsky J, Kodys K, Catalano D, Satishchandran A, Szabo G. The pro-inflammatory effects of miR-155 promote liver fibrosis and alcohol-induced steatohepatitis. *J Hepatol* 2016; **64**: 1378-1387 [PMID: 26867493 DOI: 10.1016/j.jhep.2016.01.035]

75 **Zhang C**, Hang Y, Tang W, Sil D, Jensen-Smith HC, Bennett RG, McVicker BL, Oupický D. Dually Active Polycation/miRNA Nanoparticles for the Treatment of Fibrosis in Alcohol-Associated Liver Disease. *Pharmaceutics* 2022; **14** [PMID: 35336043 DOI: 10.3390/pharmaceutics14030669]

76 **Wang K**, Xu J, Liu Y, Cui Z, He Z, Zheng Z, Huang X, Zhang Y. Self-assembled Angelica sinensis polysaccharide

nanoparticles with an instinctive liver-targeting ability as a drug carrier for acute alcoholic liver damage protection. *Int J Pharm* 2020; **577**: 118996 [PMID: 31904402 DOI: 10.1016/j.ijpharm.2019.118996]

77 **Lu C**, Xu W, Zhang F, Shao J, Zheng S. Nrf2 Knockdown Disrupts the Protective Effect of Curcumin on Alcohol-Induced Hepatocyte Necroptosis. *Mol Pharm* 2016; **13**: 4043-4053 [PMID: 27764939 DOI: 10.1021/acs.molpharmaceut.6b00562]

78 **Varatharajalu R**, Garige M, Leckey LC, Reyes-Gordillo K, Shah R, Lakshman MR. Protective Role of Dietary Curcumin in the Prevention of the Oxidative Stress Induced by Chronic Alcohol with respect to Hepatic Injury and Antiatherogenic Markers. *Oxid Med Cell Longev* 2016; **2016**: 5017460 [PMID: 26881029 DOI: 10.1155/2016/5017460]

79 **Yen FL**, Wu TH, Tzeng CW, Lin LT, Lin CC. Curcumin nanoparticles improve the physicochemical properties of curcumin and effectively enhance its antioxidant and antihepatoma activities. *J Agric Food Chem* 2010; **58**: 7376-7382 [PMID: 20486686 DOI: 10.1021/jf100135h]

80 **Ashrafizadeh M**, Ahmadi Z, Mohammadinejad R, Farkhondeh T, Samarghandian S. Curcumin Activates the Nrf2 Pathway and Induces Cellular Protection Against Oxidative Injury. *Curr Mol Med* 2020; **20**: 116-133 [PMID: 31622191 DOI: 10.2174/1566524019666191016150757]

81 **Hosseinidoust Z**, Mostaghaci B, Yasa O, Park BW, Singh AV, Sitti M. Bioengineered and biohybrid bacteria-based systems for drug delivery. *Adv Drug Deliv Rev* 2016; **106**: 27-44 [PMID: 27641944 DOI: 10.1016/j.addr.2016.09.007]

82 **Pawelek JM**, Low KB, Bermudes D. Bacteria as tumour-targeting vectors. *Lancet Oncol* 2003; **4**: 548-556 [PMID: 12965276 DOI: 10.1016/s1470-2045(03)01194-x]

83 **Hendrikx T**, Duan Y, Wang Y, Oh JH, Alexander LM, Huang W, Stärkel P, Ho SB, Gao B, Fiehn O, Emond P, Sokol H, van Pijkeren JP, Schnabl B. Bacteria engineered to produce IL-22 in intestine induce expression of REG3G to reduce ethanol-induced liver disease in mice. *Gut* 2019; **68**: 1504-1515 [PMID: 30448775 DOI: 10.1136/gutjnl-2018-317232]

84 **Szabo G**. Gut-liver axis in alcoholic liver disease. *Gastroenterology* 2015; **148**: 30-36 [PMID: 25447847 DOI: 10.1053/j.gastro.2014.10.042]

85 **Sonnenberg GF**, Fouser LA, Artis D. Border patrol: regulation of immunity, inflammation and tissue homeostasis at barrier surfaces by IL-22. *Nat Immunol* 2011; **12**: 383-390 [PMID: 21502992 DOI: 10.1038/ni.2025]

86 **Park O**, Wang H, Weng H, Feigenbaum L, Li H, Yin S, Ki SH, Yoo SH, Dooley S, Wang FS, Young HA, Gao B. In vivo consequences of liver-specific interleukin-22 expression in mice: Implications for human liver disease progression. *Hepatology* 2011; **54**: 252-261 [PMID: 21465510 DOI: 10.1002/hep.24339]

87 **Waidmann O**, Kronenberger B, Scheiermann P, Köberle V, Mühl H, Piiper A. Interleukin-22 serum levels are a negative prognostic indicator in patients with hepatocellular carcinoma. *Hepatology* 2014; **59**: 1207 [PMID: 23729376 DOI: 10.1002/hep.26528]

88 **Jiang R**, Tan Z, Deng L, Chen Y, Xia Y, Gao Y, Wang X, Sun B. Interleukin-22 promotes human hepatocellular carcinoma by activation of STAT3. *Hepatology* 2011; **54**: 900-909 [PMID: 21674558 DOI: 10.1002/hep.24486]

89 **Pipe S**, Leebeek FWG, Ferreira V, Sawyer EK, Pasi J. Clinical Considerations for Capsid Choice in the Development of Liver-Targeted AAV-Based Gene Transfer. *Mol Ther Methods Clin Dev* 2019; **15**: 170-178 [PMID: 31660419 DOI: 10.1016/j.omtm.2019.08.015]

90 **Akache B**, Grimm D, Pandey K, Yant SR, Xu H, Kay MA. The 37/67-kilodalton laminin receptor is a receptor for adeno-associated virus serotypes 8, 2, 3, and 9. *J Virol* 2006; **80**: 9831-9836 [PMID: 16973587 DOI: 10.1128/JVI.00878-06]

91 **Wang D**, Tai PWL, Gao G. Adeno-associated virus vector as a platform for gene therapy delivery. *Nat Rev Drug Discov* 2019; **18**: 358-378 [PMID: 30710128 DOI: 10.1038/s41573-019-0012-9]

92 **Kattenhorn LM**, Tipper CH, Stoica L, Geraghty DS, Wright TL, Clark KR, Wadsworth SC. Adeno-Associated Virus Gene Therapy for Liver Disease. *Hum Gene Ther* 2016; **27**: 947-961 [PMID: 27897038 DOI: 10.1089/hum.2016.160]

93 **Satishchandran A**, Ambade A, Rao S, Hsueh YC, Iracheta-Vellve A, Tornai D, Lowe P, Gyongyosi B, Li J, Catalano D, Zhong L, Kodys K, Xie J, Bala S, Gao G, Szabo G. MicroRNA 122, Regulated by GRLH2, Protects Livers of Mice and Patients From Ethanol-Induced Liver Disease. *Gastroenterology* 2018; **154**: 238-252.e7 [PMID: 28987423 DOI: 10.1053/j.gastro.2017.09.022]

94 **Hsu SH**, Wang B, Kota J, Yu J, Costinean S, Kutay H, Yu L, Bai S, La Perle K, Chivukula RR, Mao H, Wei M, Clark KR, Mendell JR, Caligiuri MA, Jacob ST, Mendell JT, Ghoshal K. Essential metabolic, anti-inflammatory, and anti-tumorigenic functions of miR-122 in liver. *J Clin Invest* 2012; **122**: 2871-2883 [PMID: 22820288 DOI: 10.1172/JCI63539]

95 **Zhang CY**, Yuan WG, He P, Lei JH, Wang CX. Liver fibrosis and hepatic stellate cells: Etiology, pathological hallmarks and therapeutic targets. *World J Gastroenterol* 2016; **22**: 10512-10522 [PMID: 28082803 DOI: 10.3748/wjg.v22.i48.10512]

96 **Lamas-Paz A**, Hao F, Nelson LJ, Vázquez MT, Canals S, Gómez Del Moral M, Martínez-Naves E, Nevzorova YA, Cubero FJ. Alcoholic liver disease: Utility of animal models. *World J Gastroenterol* 2018; **24**: 5063-5075 [PMID: 30568384 DOI: 10.3748/wjg.v24.i45.5063]

97 **Ghosh Dastidar S**, Warner JB, Warner DR, McClain CJ, Kirpich IA. Rodent Models of Alcoholic Liver Disease: Role of Binge Ethanol Administration. *Biomolecules* 2018; **8** [PMID: 29342874 DOI: 10.3390/biom8010003]

98 **Agrawal U**, Sharma R, Gupta M, Vyas SP. Is nanotechnology a boon for oral drug delivery? *Drug Discov Today* 2014; **19**: 1530-1546 [PMID: 24786464 DOI: 10.1016/j.drudis.2014.04.011]

99 **Chenthamara D**, Subramaniam S, Ramakrishnan SG, Krishnaswamy S, Essa MM, Lin FH, Qoronfleh MW. Therapeutic efficacy of nanoparticles and routes of administration. *Biomater Res* 2019; **23**: 20 [PMID: 31832232 DOI: 10.1186/s40824-019-0166-x]

100 **Kezer CA**, Simonetto DA, Shah VH. Sex Differences in Alcohol Consumption and Alcohol-Associated Liver Disease. *Mayo Clin Proc* 2021; **96**: 1006-1016 [PMID: 33714602 DOI: 10.1016/j.mayocp.2020.08.020]

101 **Wagnerberger S**, Fiederlein L, Kanuri G, Stahl C, Millonig G, Mueller S, Bischoff SC, Bergheim I. Sex-specific differences in the development of acute alcohol-induced liver steatosis in mice. *Alcohol Alcohol* 2013; **48**: 648-656 [PMID: 23969550 DOI: 10.1093/alcalc/agt138]

102 **Hajipour MJ**, Aghaverdi H, Serpooshan V, Vali H, Sheibani S, Mahmoudi M. Sex as an important factor in nanomedicine. *Nat Commun* 2021; **12**: 2984 [PMID: 34017011 DOI: 10.1038/s41467-021-23230-9]

103 **Bulbake U**, Doppalapudi S, Kommineni N, Khan W. Liposomal Formulations in Clinical Use: An Updated Review. *Pharmaceutics* 2017; **9** [PMID: 28346375 DOI: 10.3390/pharmaceutics9020012]

104 **Wang N**, Chen M, Wang T. Liposomes used as a vaccine adjuvant-delivery system: From basics to clinical immunization. *J Control Release* 2019; **303**: 130-150 [PMID: 31022431 DOI: 10.1016/j.jconrel.2019.04.025]

105 **Anselmo AC**, Mitragotri S. Nanoparticles in the clinic: An update. *Bioeng Transl Med* 2019; **4**: e10143 [PMID: 31572799 DOI: 10.1002/btm2.10143]

106 **Springer AD**, Dowdy SF. GalNAc-siRNA Conjugates: Leading the Way for Delivery of RNAi Therapeutics. *Nucleic Acid Ther* 2018; **28**: 109-118 [PMID: 29792572 DOI: 10.1089/nat.2018.0736]

107 **Debacker AJ**, Voutila J, Catley M, Blakey D, Habib N. Delivery of Oligonucleotides to the Liver with GalNAc: From Research to Registered Therapeutic Drug. *Mol Ther* 2020; **28**: 1759-1771 [PMID: 32592692 DOI: 10.1016/j.ymthe.2020.06.015]

World Journal of Gastroenterology

Submit a Manuscript: https://www.f6publishing.com

World J Gastroenterol 2022 September 28; 28(36): 5300-5312

DOI: 10.3748/wjg.v28.i36.5300

ISSN 1007-9327 (print) ISSN 2219-2840 (online)

MINIREVIEWS

Histopathological assessment of the microscopic activity in inflammatory bowel diseases: What are we looking for?

Ondrej Fabian, Lukas Bajer

Specialty type: Gastroenterology and hepatology

Provenance and peer review: Invited article; Externally peer reviewed.

Peer-review model: Single blind

Peer-review report's scientific quality classification

Grade A (Excellent): 0
Grade B (Very good): B
Grade C (Good): C
Grade D (Fair): 0
Grade E (Poor): 0

P-Reviewer: Iizuka M, Japan; Qian N, China

Received: July 1, 2022
Peer-review started: July 1, 2022
First decision: August 1, 2022
Revised: August 11, 2022
Accepted: September 8, 2022
Article in press: September 8, 2022
Published online: September 28, 2022

Ondrej Fabian, Clinical and Transplant Pathology Centre, Institute for Clinical and Experimental Medicine, Prague 14021, Czech Republic

Ondrej Fabian, Department of Pathology and Molecular Medicine, 3rd Faculty of Medicine, Charles University and Thomayer Hospital, Prague 14059, Czech Republic

Lukas Bajer, Hepatogastroenterology Department, Institute for Clinical and Experimental Medicine, Prague 14021, Czech Republic

Lukas Bajer, Institute of Microbiology, Czech Academy of Sciences, Prague 14220, Czech Republic

Corresponding author: Ondrej Fabian, MD, PhD, Assistant Professor, Postdoc, Clinical and Transplant Pathology Centre, Institute for Clinical and Experimental Medicine, Videnska 1958/9, Prague 14021, Czech Republic. ondrej.fabian@ikem.cz

Abstract

Advances in diagnostics of inflammatory bowel diseases (IBD) and improved treatment strategies allowed the establishment of new therapeutic endpoints. Currently, it is desirable not only to cease clinical symptoms, but mainly to achieve endoscopic remission, a macroscopic normalization of the bowel mucosa. However, up to one-third of IBD patients in remission exhibit persisting microscopic activity of the disease. The evidence suggests a better predictive value of histology for the development of clinical complications such as clinical relapse, surgical intervention, need for therapy escalation, or development of colorectal cancer. The proper assessment of microscopic inflammatory activity thus became an important part of the overall histopathological evaluation of colonic biopsies and many histopathological scoring indices have been established. Nonetheless, a majority of them have not been validated and no scoring index became a part of the routine bioptic practice. This review summarizes a predictive value of microscopic disease activity assessment for the subsequent clinical course of IBD, describes the most commonly used scoring indices for Crohn's disease and ulcerative colitis, and comments on current limitations and unresolved issues.

Key Words: Crohn's disease; Microscopy; Predictor; Score; Ulcerative colitis

©The Author(s) 2022. Published by Baishideng Publishing Group Inc. All rights reserved.

Core Tip: Approximately one third of the patients with inflammatory bowel diseases in endoscopic remission show persisting signs of microscopic disease activity. Histology seems to have a predictive value for development of severe clinical complications. Proper assessment of the microscopic activity of the disease using respective scoring indices is thus necessary. This review summarizes the most widely used histological scoring indices, discusses their advantages and limitations and comments persisting unresolved issues from the perspective of gastrointestinal pathologists.

Citation: Fabian O, Bajer L. Histopathological assessment of the microscopic activity in inflammatory bowel diseases: What are we looking for? *World J Gastroenterol* 2022; 28(36): 5300-5312
URL: https://www.wjgnet.com/1007-9327/full/v28/i36/5300.htm
DOI: https://dx.doi.org/10.3748/wjg.v28.i36.5300

INTRODUCTION

The first description of inflammatory bowel disease (IBD) dates back to 1932, when Burrill Bernard Crohn published the article "Regional ileitis: A pathologic and clinical entity"[1]. In the following decades, our understanding of IBD has evolved. Currently, we perceive both Crohn's disease (CD) and ulcerative colitis (UC) as systemic inflammatory conditions showing predilection to the gastrointestinal (GI) tract[2-4]. Despite persisting ominous etiology and poorly understood pathogenesis, substantial advances in diagnostics and therapy of IBD have been made, allowing new therapeutic endpoints to be laid out. At present, we strive not only to cease all clinical symptoms, but mainly to reach the endoscopic remission, defined as normalization of endoscopic mucosal appearance[5,6]. However, normal endoscopic finding does not necessarily reflect normal histology. Correlation between endoscopy and histology is poor and up to 1/3 of both CD and UC patients in endoscopic remission show signs of persisting histological activity[7-10]. There is increasing evidence that histological activity of the disease may be a better predictor of important clinical endpoints such as hospitalization rate, risk of clinical relapse, need for systemic corticosteroid use, or development of colorectal cancer when compared to sole endoscopy[11-16]. This is even more important for certain IBD subtypes such as IBD associated with primary sclerosing cholangitis, currently considered a distinct phenotype of IBD entailing a four times higher risk of a colorectal cancer development compared to conventional IBD[17, 18]. The evaluation of the histological disease activity by reliable scoring indices thus represents an important part of the overall microscopic assessment. Nonetheless, a majority of them lack proper validation and none of them have been established in routine clinical practice. Endoscopy remains a gold standard for the assessment of luminal activity of the disease[5].

The aim of this review is to provide a summary of the most commonly used scoring indices for CD and UC, highlight clinical benefits of the microscopic disease activity assessment and comment on current limitations and unresolved issues from the pathologists' perspective.

BASIC PRINCIPLES OF IBD HISTOPATHOLOGY

To better conceive microscopic features included in histopathological scoring indices, it seems convenient to briefly summarize a basic IBD pathology first. UC is characterized by a continuous inflammation affecting a rectum and progressing towards the proximal colon and terminal ileum. The inflammatory infiltrate is usually confined to the mucosa. Submucosa may be affected in case of severe colitis, but transmural inflammation is not a feature of UC. As far as CD is concerned, the inflammation displays a discontinuous pattern on both macroscopic and microscopic levels. Any part of the GI tract from the oral cavity to the anal region may be affected, while the terminal ileum is the most frequent site of the disease. The inflammation is typically transmural, infiltrating deeper layers of the bowel wall. In both IBD subtypes, the infiltrate is mainly mononuclear, with a predominance of lymphocytes and plasmacytes. The presence of neutrophils is a sign of the disease activity. In case of mildly active disease, they are scarce and confined to lamina propria. With an increasing degree of activity, they tend to infiltrate surface epithelium and colonic crypts (defined as cryptitis). Later on, the crypt walls are disrupted and neutrophils exudate into their lumina forming crypt abscesses. The most severe grade of activity is usually characterized by the presence of erosions and ulcerations. Erosions were traditionally defined as defects confined to the mucosa, whilst ulcerations penetrated deeper into the submucosa, but there is no strict adherence to this criterion in pathological practice. Currently, ulcerations are often recognized rather by the presence of granulation tissue and erosions by fibrinopurulent exudate covering the defect[4,19,20]. The inflammatory infiltrate is often accompanied by numerous eosinophils. However, their proper assessment remains challenging due to the lack of a clearly defined cut-off value for their pathological increase[21]. Their numbers also vary among bowel segments being more

prevalent in the right-sided colon[22] and several studies document their substantial seasonal and geographic oscillation[23,24]. Other characteristic features of IBD are basal plasmacytosis and disrupted mucosal architecture. Basal plasmacytosis is defined as an increased number of plasmacytes between the base of the crypts and muscularis mucosae. It is a strong indicator of IBD and also one of the earliest signs of chronicity[25]. Disrupted mucosal architecture refers to any distortion of the physiological appearance of the crypts. Normally, colonic crypts are straight, parallel, and evenly spaced. In IBD, they show changes such as branching, angulation, dilatation, shortening, or dropout[26]. A hallmark of CD diagnosis is the presence of non-caseating epithelioid granulomas. Although a differential diagnosis of granulomatous colitis is broad, the presence of immune granuloma in IBD patients excludes the diagnosis of UC. Their incidence ranges from 15% to 85% according to various studies[26]. They are more closely tied to an ileocolic form of CD or CD with upper GI involvement[27] and seem to be almost twice as frequent in pediatric CD[28].

A PREDICTIVE VALUE OF MICROSCOPIC DISEASE ACTIVITY FOR THE DEVELOPMENT OF CLINICAL COMPLICATIONS

According to a recent meta-analysis by Gupta *et al*[8] performed on 2677 UC patients in endoscopic remission, the presence of persisting microscopic activity is associated with an increased risk of clinical relapse [odds ratio (OR) 2.41; 95% confidence interval (CI): 1.91-3.04]. These findings are supported by another meta-analysis by Yoon *et al*[29], which showed similar results based on the analysis of 757 UC patients in endoscopic remission. In their cohort, an absence of histological activity of the disease was associated with a 63% lower risk of clinical relapse (risk ratio 0.37; 95%CI: 0.24-0.56). In the study by Hefti *et al*[30], the authors evaluated 561 UC patients with a median follow-up of 21.4 years since the onset of the disease. According to both univariate and multivariate analyses, a mean histological inflammatory activity showed to be a significant predictor of colectomy ($P < 0.001$). Azad *et al*[31] showed that the presence of mucosal neutrophils and eosinophils in clinically and endoscopically quiescent UC was associated with an increased risk of clinical relapse over 12 mo ($P < 0.01$). Last but not least, Bryant *et al*[12] performed a study on 91 UC patients assessing a prognostic value of endoscopic and histological remission for the prediction of corticosteroid use, hospitalization and colectomy in a median 6-year follow-up. In their analysis, a histological remission was a predictor of colectomy and development of an acute severe colitis, in contrast to endoscopy (OR 0.42, 95%CI: 0.2-0.9, $P = 0.02$; OR 0.21, 95%CI: 0.1-0.7, $P = 0.02$ respectively). These results suggest that persisting histological activity of the disease seems to be associated with an adverse clinical course in UC patients.

Studies documenting a prognostic value of histology in CD are still limited in number. However, Christensen *et al*[14] demonstrated that the absence of histologic activity in patients with ileal CD is associated with a lower risk of clinical relapse [hazard ratio (HR) 2.05; 95%CI: 1.07-3.94; $P = 0.031$], corticosteroid use (HR 2.44; 95 % CI 1.17 - 5.09; $P = 0.018$) and medical escalation (HR 2.17; 95%CI: 1.2-3.96; $P = 0.011$) in a 21-mo follow-up. In the study by Brennan *et al*[32], the absence of histological activity was associated with a lower percentage of disease flares at both 12 mo (2.4% *vs* 25.5%, $P = 0.03$) and 24 mo (10.5% *vs* 37.8%, $P = 0.05$) of follow-up, in contrast to endoscopy, where no significant difference between an endoscopically active and an inactive disease was found. On the other hand, the aforementioned meta-analysis by Gupta *et al*[8], which analyzed the predictive value of histology in 2677 UC patients, did not confirm the results, which were displayed by the group of 129 CD patients.

A predictive value of histology for the development of colorectal dysplasia and cancer is of no less importance. A meta-analysis by Flores *et al*[33] performed on 1443 UC patients found that even isolated histologic activity in otherwise endoscopically normal mucosa increased the risk of neoplasia (OR 2.6, 95%CI: 1.49-4.46, $P = 0.01$). In the study by Gupta *et al*[16], the severity of histological inflammation correlated with the risk of progression to an advanced neoplasia (high-grade dysplasia, invasive cancer), with HR being 3.0 (95%CI: 1.4-6.3) for the mean inflammatory score, HR 3.4 (95%CI: 1.1-10.4) for the binary inflammatory score and HR 2.2 [inter-quartile range (IQR) 1.2-4.2] for the maximum inflammatory score. A case-control study of Rutter *et al*[34] included 68 patients with a colorectal neoplasia matched with 136 controls without a neoplasia revealed a highly significant correlation between the histological severity of inflammation and the risk of neoplasia development (OR 4.69, 95%CI: 2.10-10.48, $P < 0.001$). Pai *et al*[35] correlated 52 UC patients with colorectal cancer to 122 patients without cancer. Based on the retrospective re-evaluation of biopsies from the last five years, a mean histological disease activity assessed by two independent histological scores appeared to be a predictor of cancer development, in contrast to endoscopy (HR 7.53, 95%CI: 2.56-12.16, $P < 0.001$ and HR 5.89, 95%CI: 2.18-15.92, $P < 0.001$ respectively). In CD, the predictive value of histology for cancer development is still equivocal. However, in the study by Kirchgesner *et al*[36] assessing a cohort of 398 IBD patients including 237 patients with CD, mean histological disease severity was associated with the risk of cancer development (OR 1.69, 95%CI: 1.29-2.21, $P < 0.001$ per one-unit increase).

In summary, a vast majority of evidence suggests that cessation of microscopic inflammatory activity has a positive impact on the future clinical course of the disease, especially for patients suffering from UC. Assessment of the histological activity should therefore be an integral part of bioptic reports in all

patients with IBD. However, the appropriate extent of the microscopic normalization is still not precisely established. In other words, we still lack a proper definition of histological remission. As a result, establishing it as a primary therapeutic endpoint in clinical practice or clinical trials still lacks validity[6,37,38].

HISTOPATHOLOGIC SCORING INDICES FOR UC

The first histopathological scoring index for UC and the first scoring index for IBD, in general, was established in the 1960s by Truelove and Richards[39]. Since then, up to thirty indices have been proposed according to Cochrane Collaboration review[40], although only a few of them have been fully validated. One of the most widely used remains the Geboes score (GS), established in 2000[41]. This score assesses seven histopathological features including architectural mucosal changes, chronic inflammatory infiltrate, neutrophils and eosinophils in lamina propria, intraepithelial neutrophils, crypt destruction, and mucosal defects. Each of the given variables is further subclassified according to its severity (Table 1). The overall microscopic inflammatory severity should be based on the worst score in the bioptic sample, not on the average grade counted from all samples. Although, such a score may appear overly complicated at the first glance (*i.e.*, grading of the cryptitis severity as < 5%, < 50%, and > 50% of the affected crypts in the sample), it showed surprisingly good interpersonal agreement in preliminary phases of the study, especially when evaluating the presence of disease activity and mucosal defects (Cohen's kappa coefficient κ was above 0.9). A weak agreement was reached for the assessment of an inactive chronic inflammation. The original purpose of the score was a classification scheme, intended to define specific thresholds of the inflammatory severity, such as the presence of the disease activity. In subsequent studies, the score was also used as a continuous scale, assessing treatment efficacy in clinical trials[42,43]. The score seems to have a decent predictive value, being a reliable predictor of a clinical relapse in patients in clinical and endoscopic remission[31,44]. However, it has not been completely validated. In 2017, the Geboes Simplified Score was proposed[45]. The score reduced grading of the inflammatory activity and included the presence of basal plasmacytosis (Table 2). The score shows better overall agreement compared to the original GS (κ 0.56 *vs* 0.4). With regards to individual grades, the best agreement was reached for the detection of the inflammatory activity (κ 0.7). However, the score has not yet been widely used.

Robarts histopathology index (RHI)[46] was established in 2017 and was primarily intended to assess microscopic changes induced by the treatment. The construction process of the index was based on the original GS, from which the histopathological variables with reliable interobserver agreement and good correlation with grades of the inflammatory activity according to Visual Analogue Scale were used and served as a foundation for the final index. The definitive index consists of four histopathological features including chronic inflammatory infiltrate, neutrophils in lamina propria, neutrophils in the epithelium and mucosal defects. Each of the features is further subclassified according to its severity (range 0 to 3), giving the final index range from 0 to 33 points (Table 3). In contrast to GS, RHI exclusively assesses the histologic activity of the disease and excludes the features of chronicity. The agreement among the index grades is very good, with an intraclass correlation coefficient above 0.8. A predictive value of the index is still not fully elucidated. However, the aforementioned study by Pai *et al* [35] showed that a mean index score ≥ 8 during 5 years of observation predicted the development of colorectal cancer.

In the same year, a Nancy histological index (NHI) was proposed[47,48]. It uses five-grade scale based on the presence of chronic and active inflammatory infiltrate and mucosal defects (Table 4 and Figure 1). The final grade is determined by the worst histopathologic feature found in a biopsy sample. Despite the subjective nature of some features making the thresholds between several grades prone to possible higher interobserver variability (*i.e.*, mild *vs* moderate intensity of the chronic inflammatory infiltrate defining grades 0 and 1 respectively), the index shows very good overall interobserver agreement (κ above 0.8) and also a good reciprocal correlation with RHI [49]. The score is fully validated and widely used in clinical practice. With regards to its predictive value, in the study of D'Amico *et al* [49] patients with histologic presence of the inflammation (NHI ≥ 1) had a higher risk of surgical intervention (14% *vs* 0%, $P = 0.01$) and hospitalization (36% *vs* 7.1%, $P = 0.001$) compared to patients in histological remission (NHI grade 0) during a 30-mo median follow-up.

HISTOPATHOLOGIC SCORING INDICES FOR CD

Scoring indices for CD are limited in number. The Cochrane collaboration review mentions 14 indices [50], but the only one used on the larger scale is the Global Histology Activity Score (GHAS)[51]. The score was established by D´Haens *et al* in 1998 with the purpose to assess early postoperative recurrence after ileocecal resection. It includes the following variables: the presence of architectural changes, degree of chronic, neutrophilic and eosinophilic inflammatory infiltration in lamina propria, presence of intraepithelial neutrophils, epithelial damage, mucosal defects, presence of granulomas, and a number of

Table 1 Original Geboes score

Original Geboes score	
Grade 0: Architectural changes	0.0 No abnormality; 0.1 Mild abnormality; 0.2 Mild/moderate diffuse or multifocal abnormalities; 0.3 Severe diffuse or multifocal abnormalities
Grade 1: Chronic inflammatory infiltrate	1.0 No increase; 1.1 Mild but unequivocal increase; 1.2 Moderate increase; 1.3 Marked increase
Grade 2A: Eosinophils in lamina propria	2A.0 No increase; 2A.1 Mild but unequivocal increase; 2A.2 Moderate increase; 2A.3 Marked increase
Grade 2B: Neutrophils in lamina propria	2B.0 No increase; 2B.1 Mild but unequivocal increase; 2B.2 Moderate increase; 2B.3 Marked increase
Grade 3: Neutrophils in epithelium	3.0 None; 3.1 < 5% crypts involved; 3.2 < 50% crypts involved; 3.3 > 50% crypts involved
Grade 4: Crypt destruction	4.0 None; 4.1 Probable: local excess of neutrophils in part of the crypts; 4.2 Probable: marked attenuation; 4.3 Unequivocal crypt destruction
Grade 5: Erosions and ulcerations	5.0 No erosion, ulceration or granulation tissue; 5.1 Recovering epithelium + adjacent inflammation; 5.2 Probable erosion: focally stripped; 5.3 Unequivocal erosion; 5.4 Ulcer or granulation tissue

Table 2 Simplified Geboes score

Simplified Geboes score	
Grade 0: No inflammatory activity	0.0 No abnormalities; 0.1 Presence of architectural changes; 0.2 Presence of architectural changes and chronic mononuclear cell infiltrate
Grade 1: Basal plasma cells	1.0 No increase; 1.1 Mild increase; 1.2 Marked increase
Grade 2A: Eosinophils in lamina propria	2A.0 No increase; 2A.1 Mild increase; 2A.2 Marked increase
Grade 2B: Neutrophils in lamina propria	2B.0 No increase; 2B.1 Mild increase; 2B.2 Marked increase
Grade 3: Neutrophils in epithelium	3.0 None; 3.1 < 50% crypts involved; 3.2 > 50% crypts involved
Grade 4: Epithelial injury (in crypt and surface epithelium)	4.0 None; 4.1 Marked attenuation; 4.2 Probable crypt destruction: probable erosions; 4.3 Unequivocal crypt destruction: unequivocal erosion; 4.4 Ulcer or granulation tissue

Table 3 Robarts histopathology index

Histopathological variable	Grade
Chronic inflammatory infiltrate	0 = No increase; 1 = Mild but unequivocal increase; 2 = Moderate increase; 3 = Marked increase
Lamina propria neutrophils	0 = None; 1 = Mild but unequivocal increase; 2 = Moderate increase; 3 = Marked increase
Neutrophils in epithelium	0 = None; 1 = 50% crypts involved
Erosion or ulceration	0 = No erosion, ulceration or granulation tissue; 1 = Recovering epithelium + adjacent inflammation; 2 = Probable erosion-focally stripped; 3 = Unequivocal erosion; 4 = Ulcer or granulation tissue

affected bowel segments (Table 5). Later on, the score became used separately for terminal ileum and large bowel as Ileal and Colonic GHAS[52]. However, the score is not validated and its utility is limited. Instead of being a continuous scale, it rather represents a sum of present variables, putting minute changes such as architectural distortion or increased mononuclear cells in lamina propria on the same level of importance, for instance mucosal defects. According to a recent multidisciplinary consensus panel[53], the score does not represent a reliable index for the assessment of the inflammatory severity in CD. Its eventual predictive value has not been evidenced.

PRACTICAL ISSUES OF THE MICROSCOPIC ACTIVITY ASSESSMENT

The sole fact that we have been regularly confronted with new indices indirectly implies that we are still struggling to find the perfect one that would satisfy all our demands. A lot of unresolved issues persist

Table 4 Nancy histological index

Grade	Criteria
Grade 0 (no histological significant disease)	No or mild increase in chronic inflammatory infiltrate
Grade 1 (chronic inflammatory infiltrate with no acute inflammatory infiltrate)	Moderate or marked increase in chronic inflammatory infiltrate that is easily apparent. No acute inflammatory infiltrate is present
Grade 2 (mildly active disease)	Few or rare neutrophils in lamina propria or in the epithelium that are difficult to see
Grade 3 (moderately active disease)	Presence of multiple clusters of neutrophils in lamina propria and/or in epithelium that are easily apparent
Grade 4 (severely active disease)	Loss of colonic crypts replaced with "immature" granulation tissue (disorganized blood vessels with extravasated neutrophils) or the presence of fibrinopurulent exudate

Table 5 Global Histology Activity Score

Histopathological variable	Grade
Epithelial damage	0 = Normal; 1 = Focal; 2 = Extensive
Architectural changes	0 = Normal; 1 = Moderate; 2 = Severe
Mononuclear cells in lamina propria	0 = Normal; 1 = Moderate increase; 2 = Severe increase
Neutrophils in lamina propria	0 = Normal; 1 = Moderate increase; 2 = Severe increase
Neutrophils in epithelium	1 = Surface epithelium; 2 = Cryptitis; 3 = Crypt abscess
Erosion or ulceration	0 = No; 1 = Yes
Granuloma	0 = No; 1 = Yes
Number of segmental biopsy specimens affected	1 = < 1/3; 2 = 1/3-2/3; 3 = > 2/3

Each variable is scored independently. The total score is the sum of all individual scores.

throughout the whole diagnostic process, reflecting both the proper biology of the disease and the limitations of given diagnostic modalities.

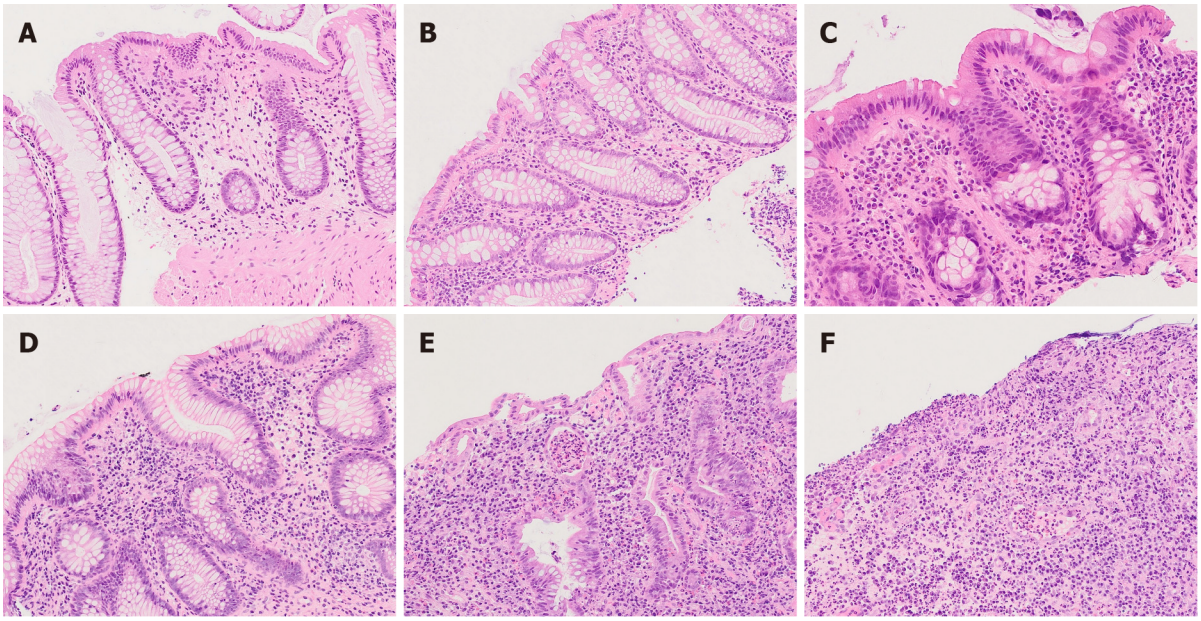
Segmental and transmural character of the inflammation in CD

A correlation between endoscopic and histologic activity in CD is poor due to the segmental nature of the inflammation on both macroscopic and microscopic levels. Indeed, some degree of discrepancy between endoscopy and histology is desirable since the histology should not only confirm the endoscopic findings but represent an additional value by increasing the sensitivity of the inflammatory activity detection. On the other hand, a focal character of the disease may lead to a false underestimation of the histological activity. It is especially true in patients on therapy since treated IBD typically shows a focal and patchy character of the inflammation, even in UC[54].

In CD, a transmural character of the inflammation is one of the defining features, modifying the overall clinical severity of the disease and eventual development of complications. However, both histology and endoscopy provide information exclusively about the luminal activity of the disease. There is thus an increasing effort to establish a reliable scoring index of transmural severity of the disease. The well-known Lemann index[55] represents a clinical score, assessing the cumulative damage of the intestinal wall according to the presence of strictures, penetrating disease (fistulas or abdominal abscesses), previous surgical interventions, and perianal involvement. The majority of histopathological indices of transmural involvement are aimed at the assessment of resection margins of ileocecal resections. Later on, more complex indices were established, evaluating a full spectrum of transmural CD pathology including a degree of inflammatory intensity, fibrosis, smooth muscle changes, or neuronal hypertrophy[56-58]. However, such scores cannot be applied to endoscopic bioptic samples. In some instances, the sample is so superficial, that the basal portion of the mucosa is missing, precluding the assessment of important predictors such as basal plasmacytosis, which is also included in some scoring indices such as Simplified GS.

Upper GI and small intestinal involvement

Both CD and UC are systemic inflammatory conditions capable of affecting any part of the GI tract. This is especially true for pediatric patients, in which the inflammation in the upper GI is more frequent. As defined by the revised Porto criteria for the diagnosis of IBD in children and adolescents[59], pediatric



DOI: 10.3748/wjg.v28.i36.5300 **Copyright** ©The Author(s) 2022.

Figure 1 Microphotographs representing individual grades of Nancy Histopathological Index (hematoxylin and eosin, magnification 100×). A: Grade 0 with no increase in inflammatory cells; B: Grade 0 with mild increase in chronic inflammatory cells; C: Grade 1 with moderate increase in chronic inflammatory cells including more numerous eosinophils, but no neutrophils; D: Grade 2 with scarce neutrophils in lamina propria and epithelium; E: Grade 3 with numerous neutrophils including cryptitis and crypt abscess; F: Grade 4 with completely ulcerated colonic mucosa replaced by granulation tissue.

UC with upper GI involvement is even one of the atypical UC subtypes. However, grading of upper GI inflammatory severity is not a part of any available histological scoring index. In adult patients, a routine esophagogastroduodenoscopy is not even a part of the official recommendations for IBD diagnosis[2,3,59]. A subsequent clinical course may also be aggravated by the persisting inflammatory activity in a small bowel. However, an endoscopy can usually assess only its proximal and distal segments, frequently missing jejunum, and a large portion of the ileum. Key modalities for assessment the small bowel involvement are imaging techniques such as magnetic resonance imaging, computer tomography, ultrasonography or other radiologic procedures[60]. Some of them are also accompanied by respective scoring indices such as Simplified Magnetic Resonance Index of Activity for CD[61]. In recent years, scoring indices for capsule endoscopy were established, with Lewis Score[62] and Capsule Endoscopy Crohn Disease Activity Index[63] being among the most frequently used ones, recommended by both European Crohn's and Colitis Organisation (ECCO) and European Society of Gastrointestinal Endoscopy. Currently, there is no feasible way to sample biopsies during capsule endoscopy.

Number of bioptic samples

According to an official recommendation from the European Society of Pathology and ECCO[4,5], a diagnostic endoscopy should include at least two bioptic samples from at least five or six bowel segments including the terminal ileum and rectum. However, there is still no official recommendation for patients on treatment. Many gastroenterologists still prefer to perform an extensive sampling of severely affected regions and avoid normally appearing segments. This may falsely underestimate an overall histological inflammatory severity and negatively affect some scoring indices such as GHAS, which includes the number of affected regions into a final score.

Assessment of the disease activity in pediatric IBD

A Histopathological scoring index primarily designated for the pediatric population has not been established. Adult indices are used instead, but their feasibility for children is not self-evident. Studies aiming at the predictive value of histology in pediatric IBD are still limited in number. A few years ago, our group performed a retrospective analysis of 63 children with CD[64]. The microscopic severity of the inflammation at the time of diagnosis assessed by GHAS showed moderate correlation with endoscopic activity evaluated by Simple Endoscopic Score for Crohn's Disease (r = 0.48, P = 0.0001), no correlation with clinical activity of the disease, and had no predictive value for the development of defined complications [bowel stricture, intraabdominal or perianal abscess or fistula, initiation of anti-tumor necrosis factor (anti-TNF) therapy] during at least one year of follow-up. On the other hand, endoscopic activity appeared to be a predictor of the complications (HR 3.20, IQR 1.04-4.91, P = 0.037). With regards to pediatric UC, our recently conducted retrospective study[65] including 49 children with

UC showed that microscopic activity of the inflammation assessed by NHI and GS had no predictive value for complications development (acute severe colitis, need of colectomy, initiation of anti-TNF therapy, initiation of systemic 5-aminosalicylic therapy and systemic corticosteroid use). By contrast, levels of fecal calprotectin (FCPT) and clinical activity of the disease assessed by Pediatric Ulcerative Colitis Activity Index (PUCAI) showed to be independent predictors of the systemic 5-aminosalicylic acid induction (FCPT: HR 2.42, IQR 1.042-5.631, P = 0.040; PUCAI: HR 2.98, IQR 1.011-8.787, P = 0.048) and systemic corticosteroid use (FCPT: HR 2.517, IQR 1.115-5.681, P = 0.026; PUCAI: HR 2.98, IQR 1.011-8.787, P = 0.048).

ARE WE ASKING THE RIGHT QUESTION?

Histological activity in IBD is defined by the presence of neutrophils. Hence, strictly speaking, the histological index of the disease activity should be based on the extent of neutrophilic infiltration, their localization (lamina propria, superficial epithelium, cryptitis, crypt abscesses), and the presence of mucosal defects. Grading of the microscopic disease activity thus seems to be apparently straightforward. However, such grading per se is of no use if it does not provide any additional value to other means of disease activity assessment such as endoscopy or non-invasive biomarkers. There is thus a fundamental question about whether histological appearance is predictive of subsequent clinical outcomes. As mentioned before, the bulk of evidence suggests that persisting microscopic activity of the disease harbors an increased risk of development of complications. However, disease activity is not the only microscopic variable associated with an adverse clinical course. Other microscopic features such as basal plasmacytosis or granulomas have proven prognostic value. According to Johnson *et al*[66], the presence of granulomas was associated with increased serum levels of C-reactive protein, higher rates of stricturing and penetrating disease, higher rates of steroid, immunomodulators, biological therapy and narcotic use and higher healthcare utilization. With regards to basal plasmacytosis, the aforementioned meta-analysis by Gupta *et al*[8] demonstrated its predictive value for clinical recurrence in UC patients in endoscopic remission, as well. However, these features represent signs of chronicity rather than activity. Apart from that, there is still unresolved issue regarding the contribution of eosinophils, macrophages and other inflammatory cell types. Therefore, it seems to be more convenient to search for a suitable combination of microscopic features, providing the most accurate prediction for the subsequent clinical course of the disease, with a presence of neutrophils as a sign of the disease activity among the assessed variables. Apropos, the very presence of both chronic lymphoplasmacytic and active neutrophilic inflammatory infiltrate in one scoring index of disease activity may not properly reflect the biology of the process. In a majority of the scoring indices, the presence of isolated chronic inflammatory infiltrate is considered a lower grade of the inflammatory activity, aggravating with the increasing presence of neutrophils and eventually with the appearance of mucosal defects. But the lymphoplasmacytic infiltrate reflects rather chronicity of the process than its activity and these two variables don't necessarily represent a continuum. Such a hypothesis was taken into consideration in the recently established scoring index called Inflammatory Bowel Disease-Distribution, Chronicity, Activity (IBD-DCA) score (Table 6)[67]. The score was proposed at Erlangen International Consensus Conference and consists of three parameters - Distribution (D), Chronicity (C) and, Activity (A), which are assessed in this order. Distribution determines the overall extent of the disease, independently of the presence or absence of the activity. Chronicity is represented by the disrupted mucosal architecture, presence of basal plasmacytosis and increased lymphoplasmacytic infiltration in lamina propria. Activity is marked by the presence of neutrophils. The score thus represents not only a scoring index of the histopathological inflammatory activity, but provides information about the overall microscopic severity of the disease. According to the recent evidence[68], it showed moderate inter-rater reliability for parameter D (median intraclass correlation coefficient 0.645), poor to moderate for parameter C (0.568), and moderate to good for parameter A (0.748) for UC and moderate to good for parameter D and A (0.655 and 0.644 respectively) and poor for parameter C (0.303) for CD. The intra-rater agreement was moderate to excellent for D and C parameters (0.894 and 0.798 respectively) and good to excellent for A (0.909) parameter for UC, whilst CD showed moderate to excellent agreement for parameter D (0.854), poor to excellent for parameter C (0.714) and good to excellent for parameter A (0.888). There is a moderate correlation with NHI and Simplified GS. The unique feature of the score is its versatility, which means that it can be used for both CD and UC, as well as for IBDU, which represents 5%-15% of both adult and pediatric IBD[69-71] and in some cases becomes a definite diagnosis. By this, the score questions the necessity of separate scoring indices for CD and UC. Both diseases share a similar pattern of inflammatory activity and the inferior utility of scoring indices for CD stems rather from the segmental and transmural nature of the disease that from inappropriate assessment of its histological activity. Such a hypothesis is also supported by several studies. In the aforementioned study of Kirchgesner *et al*[36] assessing a predictive value of histology for the development of colorectal cancer, the authors used NHI to evaluate microscopic disease severity for the whole IBD cohort. In both UC and CD, the grade of the NHI correlated with the risk of cancer development. In the study by Löwenberg *et al*[72], the authors evaluated the ability of vedolizumab to induce endoscopic and histological remission in patients with

Table 6 Inflammatory Bowel Disease-Distribution, Chronicity, Activity score

Histopathological variable	Grade
Distribution	0 = Normal; 1 = < 50% of tissue affected per same biopsy site; 2 = > 50% of tissue affected per same biopsy
Chronicity	0 = Normal; 1 = Crypt distortion and/or mild lymphoplasmacytosis; 2 = Marked lymphoplasmacytosis and/or basal plasmacytosis
Activity	0 = Normal; 1 = Two or more neutrophils in lamina propria in one high-power field and/or any presence of intraepithelial neutrophils; 2 = Crypt abscesses, erosions, ulcers

Each variable is scored independently.

CD and the microscopic disease activity in the study was assessed by RHI. Using UC scoring indices for CD patients is suggested also by the recent expert consensus panel[53].

STILL FAR FROM THE HISTOLOGICAL REMISSION

Although achieving deeper mucosal healing is presumably associated with improved clinical course, it is far from synonymous with histological remission. However, establishing its proper definition remains challenging. In previous studies, the definition varied from the absence of active inflammation to the complete normalization of bowel mucosa. A recent position paper from ECCO defines histological remission as a "return to normal". Cessation of the microscopic activity undoubtedly correlates with a lower percentage of future complications. But even a mucosa without a presence of neutrophils may display increased chronic lymphoplasmacytic infiltration or architectonic changes that may aggravate the clinical course of the disease. Returning to the meta-analysis by Gupta *et al*[8] once more, their analysis showed that disrupted mucosal architecture was one of the features independently predicting the disease recurrence (OR 2.22). On the other hand, strict adherence to the histological normalization of the mucosa in each patient in endoscopic and clinical remission could lead to an unreasonable burden of aggressive therapy including all possible side effects. More studies need to be performed until a proper degree of histological normalization with an appropriate cost-benefit ratio will be established. One way or another, a complex histopathological scoring index assessing not only a disease activity but rather an overall microscopical severity seems to be necessary before we finally reach a standardized definition of the histological remission in IBD.

CONCLUSION

A proper assessment of the histological disease activity in IBD represents an essential component of the overall disease severity evaluation and provides important data for the subsequent clinical management of the patients. Many histopathological scoring indices exists, especially for UC, and they seem to be useful tools for the proper objectivization of the microscopic activity. However, their broader validation, subsequent implementation in routine bioptic practice and establishing the universally accepted definition of the histological remission are necessary before we could recognize the absence of the microscopic activity as the primary therapeutic target in IBD.

ACKNOWLEDGEMENTS

We would like to thank Drab D for his contribution during the manuscript revision.

FOOTNOTES

Author contributions: Fabian O collected the data, performed the data analysis and wrote the paper; Bajer L participated in the data analysis and wrote the paper.

Supported by Ministry of Health of the Czech Republic, No. NV18-09-00493 and No. NU21J-06-00027.

Conflict-of-interest statement: All the authors report no relevant conflicts of interest for this article.

Open-Access: This article is an open-access article that was selected by an in-house editor and fully peer-reviewed by external reviewers. It is distributed in accordance with the Creative Commons Attribution NonCommercial (CC BY-NC 4.0) license, which permits others to distribute, remix, adapt, build upon this work non-commercially, and license their derivative works on different terms, provided the original work is properly cited and the use is non-commercial. See: https://creativecommons.org/Licenses/by-nc/4.0/

Country/Territory of origin: Czech Republic

ORCID number: Ondrej Fabian 0000-0002-0393-2415; Lukas Bajer 0000-0002-3815-3120.

S-Editor: Gao CC
L-Editor: A
P-Editor: Gao CC

REFERENCES

1 **Crohn BB**, Ginzburg L, Oppenheimer GD. Regional ileitis; a pathologic and clinical entity. *Am J Med* 1952; **13**: 583-590 [PMID: 12996536 DOI: 10.1016/0002-9343(52)90025-9]
2 **Magro F**, Gionchetti P, Eliakim R, Ardizzone S, Armuzzi A, Barreiro-de Acosta M, Burisch J, Gecse KB, Hart AL, Hindryckx P, Langner C, Limdi JK, Pellino G, Zagórowicz E, Raine T, Harbord M, Rieder F; European Crohn's and Colitis Organisation [ECCO]. Third European Evidence-based Consensus on Diagnosis and Management of Ulcerative Colitis. Part 1: Definitions, Diagnosis, Extra-intestinal Manifestations, Pregnancy, Cancer Surveillance, Surgery, and Ileo-anal Pouch Disorders. *J Crohns Colitis* 2017; **11**: 649-670 [PMID: 28158501 DOI: 10.1093/ecco-jcc/jjx008]
3 **Gomollón F**, Dignass A, Annese V, Tilg H, Van Assche G, Lindsay JO, Peyrin-Biroulet L, Cullen GJ, Daperno M, Kucharzik T, Rieder F, Almer S, Armuzzi A, Harbord M, Langhorst J, Sans M, Chowers Y, Fiorino G, Juillerat P, Mantzaris GJ, Rizzello F, Vavricka S, Gionchetti P; ECCO. 3rd European Evidence-based Consensus on the Diagnosis and Management of Crohn's Disease 2016: Part 1: Diagnosis and Medical Management. *J Crohns Colitis* 2017; **11**: 3-25 [PMID: 27660341 DOI: 10.1093/ecco-jcc/jjw168]
4 **Magro F**, Langner C, Driessen A, Ensari A, Geboes K, Mantzaris GJ, Villanacci V, Becheanu G, Borralho Nunes P, Cathomas G, Fries W, Jouret-Mourin A, Mescoli C, de Petris G, Rubio CA, Shepherd NA, Vieth M, Eliakim R; European Society of Pathology (ESP); European Crohn's and Colitis Organisation (ECCO). European consensus on the histopathology of inflammatory bowel disease. *J Crohns Colitis* 2013; **7**: 827-851 [PMID: 23870728 DOI: 10.1016/j.crohns.2013.06.001]
5 **Annese V**, Daperno M, Rutter MD, Amiot A, Bossuyt P, East J, Ferrante M, Götz M, Katsanos KH, Kießlich R, Ordás I, Repici A, Rosa B, Sebastian S, Kucharzik T, Eliakim R; European Crohn's and Colitis Organisation. European evidence based consensus for endoscopy in inflammatory bowel disease. *J Crohns Colitis* 2013; **7**: 982-1018 [PMID: 24184171 DOI: 10.1016/j.crohns.2013.09.016]
6 **Travis SP**, Higgins PD, Orchard T, Van Der Woude CJ, Panaccione R, Bitton A, O'Morain C, Panés J, Sturm A, Reinisch W, Kamm MA, D'Haens G. Review article: defining remission in ulcerative colitis. *Aliment Pharmacol Ther* 2011; **34**: 113-124 [PMID: 21615435 DOI: 10.1111/j.1365-2036.2011.04701.x]
7 **Peyrin-Biroulet L**, Bressenot A, Kampman W. Histologic remission: the ultimate therapeutic goal in ulcerative colitis? *Clin Gastroenterol Hepatol* 2014; **12**: 929-34.e2 [PMID: 23911875 DOI: 10.1016/j.cgh.2013.07.022]
8 **Gupta A**, Yu A, Peyrin-Biroulet L, Ananthakrishnan AN. Treat to Target: The Role of Histologic Healing in Inflammatory Bowel Diseases: A Systematic Review and Meta-analysis. *Clin Gastroenterol Hepatol* 2021; **19**: 1800-1813.e4 [PMID: 33010406 DOI: 10.1016/j.cgh.2020.09.046]
9 **Chateau T**, Feakins R, Marchal-Bressenot A, Magro F, Danese S, Peyrin-Biroulet L. Histological Remission in Ulcerative Colitis: Under the Microscope Is the Cure. *Am J Gastroenterol* 2020; **115**: 179-189 [PMID: 31809296 DOI: 10.14309/ajg.0000000000000437]
10 **Molander P**, Sipponen T, Kemppainen H, Jussila A, Blomster T, Koskela R, Nissinen M, Rautiainen H, Kuisma J, Kolho KL, Färkkilä M. Achievement of deep remission during scheduled maintenance therapy with TNFα-blocking agents in IBD. *J Crohns Colitis* 2013; **7**: 730-735 [PMID: 23182163 DOI: 10.1016/j.crohns.2012.10.018]
11 **Park S**, Abdi T, Gentry M, Laine L. Histological Disease Activity as a Predictor of Clinical Relapse Among Patients With Ulcerative Colitis: Systematic Review and Meta-Analysis. *Am J Gastroenterol* 2016; **111**: 1692-1701 [PMID: 27725645 DOI: 10.1038/ajg.2016.418]
12 **Bryant RV**, Burger DC, Delo J, Walsh AJ, Thomas S, von Herbay A, Buchel OC, White L, Brain O, Keshav S, Warren BF, Travis SP. Beyond endoscopic mucosal healing in UC: histological remission better predicts corticosteroid use and hospitalisation over 6 years of follow-up. *Gut* 2016; **65**: 408-414 [PMID: 25986946 DOI: 10.1136/gutjnl-2015-309598]
13 **Christensen B**, Hanauer SB, Erlich J, Kassim O, Gibson PR, Turner JR, Hart J, Rubin DT. Histologic Normalization Occurs in Ulcerative Colitis and Is Associated With Improved Clinical Outcomes. *Clin Gastroenterol Hepatol* 2017; **15**: 1557-1564.e1 [PMID: 28238954 DOI: 10.1016/j.cgh.2017.02.016]
14 **Christensen B**, Erlich J, Gibson PR, Turner JR, Hart J, Rubin DT. Histologic Healing Is More Strongly Associated with Clinical Outcomes in Ileal Crohn's Disease than Endoscopic Healing. *Clin Gastroenterol Hepatol* 2020; **18**: 2518-2525.e1 [PMID: 31812654 DOI: 10.1016/j.cgh.2019.11.056]
15 **Rubin DT**, Huo D, Kinnucan JA, Sedrak MS, McCullom NE, Bunnag AP, Raun-Royer EP, Cohen RD, Hanauer SB, Hart J, Turner JR. Inflammation is an independent risk factor for colonic neoplasia in patients with ulcerative colitis: a case-

control study. *Clin Gastroenterol Hepatol* 2013; **11**: 1601-8.e1 [PMID: 23872237 DOI: 10.1016/j.cgh.2013.06.023]
16 **Gupta RB**, Harpaz N, Itzkowitz S, Hossain S, Matula S, Kornbluth A, Bodian C, Ullman T. Histologic inflammation is a risk factor for progression to colorectal neoplasia in ulcerative colitis: a cohort study. *Gastroenterology* 2007; **133**: 1099-105; quiz 1340 [PMID: 17919486 DOI: 10.1053/j.gastro.2007.08.001]
17 **Murasugi S**, Ito A, Omori T, Nakamura S, Tokushige K. Clinical Characterization of Ulcerative Colitis in Patients with Primary Sclerosing Cholangitis. *Gastroenterol Res Pract* 2020; **2020**: 7969628 [PMID: 33224192 DOI: 10.1155/2020/7969628]
18 **Soetikno RM**, Lin OS, Heidenreich PA, Young HS, Blackstone MO. Increased risk of colorectal neoplasia in patients with primary sclerosing cholangitis and ulcerative colitis: a meta-analysis. *Gastrointest Endosc* 2002; **56**: 48-54 [PMID: 12085034 DOI: 10.1067/mge.2002.125367]
19 **Pai RK**, Lauwers GY, Pai RK. Measuring Histologic Activity in Inflammatory Bowel Disease: Why and How. *Adv Anat Pathol* 2022; **29**: 37-47 [PMID: 34879037 DOI: 10.1097/PAP.0000000000000326]
20 **Abraham C**, Cho JH. Inflammatory bowel disease. *N Engl J Med* 2009; **361**: 2066-2078 [PMID: 19923578 DOI: 10.1056/NEJMra0804647]
21 **Conner JR**, Kirsch R. The pathology and causes of tissue eosinophilia in the gastrointestinal tract. *Histopathology* 2017; **71**: 177-199 [PMID: 28370248 DOI: 10.1111/his.13228]
22 **Matsushita T**, Maruyama R, Ishikawa N, Harada Y, Araki A, Chen D, Tauchi-Nishi P, Yuki T, Kinoshita Y. The number and distribution of eosinophils in the adult human gastrointestinal tract: a study and comparison of racial and environmental factors. *Am J Surg Pathol* 2015; **39**: 521-527 [PMID: 25581733 DOI: 10.1097/PAS.0000000000000370]
23 **Polydorides AD**, Banner BF, Hannaway PJ, Yantiss RK. Evaluation of site-specific and seasonal variation in colonic mucosal eosinophils. *Hum Pathol* 2008; **39**: 832-836 [PMID: 18430454 DOI: 10.1016/j.humpath.2007.10.012]
24 **Pascal RR**, Gramlich TL, Parker KM, Gansler TS. Geographic variations in eosinophil concentration in normal colonic mucosa. *Mod Pathol* 1997; **10**: 363-365 [PMID: 9110299]
25 **Villanacci V**, Antonelli E, Reboldi G, Salemme M, Casella G, Bassotti G. Endoscopic biopsy samples of naïve "colitides" patients: role of basal plasmacytosis. *J Crohns Colitis* 2014; **8**: 1438-1443 [PMID: 24931895 DOI: 10.1016/j.crohns.2014.05.003]
26 **Moore M**, Feakins RM, Lauwers GY. Non-neoplastic colorectal disease biopsies: evaluation and differential diagnosis. *J Clin Pathol* 2020; **73**: 783-792 [PMID: 32737191 DOI: 10.1136/jclinpath-2020-206794]
27 **Freeman HJ**. Granuloma-positive Crohn's disease. *Can J Gastroenterol* 2007; **21**: 583-587 [PMID: 17853953 DOI: 10.1155/2007/917649]
28 **Rubio CA**, Orrego A, Nesi G, Finkel Y. Frequency of epithelioid granulomas in colonoscopic biopsy specimens from paediatric and adult patients with Crohn's colitis. *J Clin Pathol* 2007; **60**: 1268-1272 [PMID: 17293387 DOI: 10.1136/jcp.2006.045336]
29 **Yoon H**, Jangi S, Dulai PS, Boland BS, Prokop LJ, Jairath V, Feagan BG, Sandborn WJ, Singh S. Incremental Benefit of Achieving Endoscopic and Histologic Remission in Patients With Ulcerative Colitis: A Systematic Review and Meta-Analysis. *Gastroenterology* 2020; **159**: 1262-1275.e7 [PMID: 32585306 DOI: 10.1053/j.gastro.2020.06.043]
30 **Hefti MM**, Chessin DB, Harpaz NH, Steinhagen RM, Ullman TA. Severity of inflammation as a predictor of colectomy in patients with chronic ulcerative colitis. *Dis Colon Rectum* 2009; **52**: 193-197 [PMID: 19279411 DOI: 10.1007/DCR.0b013e31819ad456]
31 **Azad S**, Sood N, Sood A. Biological and histological parameters as predictors of relapse in ulcerative colitis: a prospective study. *Saudi J Gastroenterol* 2011; **17**: 194-198 [PMID: 21546723 DOI: 10.4103/1319-3767.80383]
32 **Brennan GT**, Melton SD, Spechler SJ, Feagins LA. Clinical Implications of Histologic Abnormalities in Ileocolonic Biopsies of Patients With Crohn's Disease in Remission. *J Clin Gastroenterol* 2017; **51**: 43-48 [PMID: 26927490 DOI: 10.1097/MCG.0000000000000507]
33 **Flores BM**, O'Connor A, Moss AC. Impact of mucosal inflammation on risk of colorectal neoplasia in patients with ulcerative colitis: a systematic review and meta-analysis. *Gastrointest Endosc* 2017; **86**: 1006-1011.e8 [PMID: 28750838 DOI: 10.1016/j.gie.2017.07.028]
34 **Rutter M**, Saunders B, Wilkinson K, Rumbles S, Schofield G, Kamm M, Williams C, Price A, Talbot I, Forbes A. Severity of inflammation is a risk factor for colorectal neoplasia in ulcerative colitis. *Gastroenterology* 2004; **126**: 451-459 [PMID: 14762782 DOI: 10.1053/j.gastro.2003.11.010]
35 **Pai RK**, Hartman DJ, Leighton JA, Pasha SF, Rivers CR, Regueiro M, Binion DG, Pai RK. Validated Indices for Histopathologic Activity Predict Development of Colorectal Neoplasia in Ulcerative Colitis. *J Crohns Colitis* 2021; **15**: 1481-1490 [PMID: 33687061 DOI: 10.1093/ecco-jcc/jjab042]
36 **Kirchgesner J**, Svrcek M, Le Gall G, Landman C, Dray X, Bourrier A, Nion-Larmurier I, Hoyeau N, Sokol H, Seksik P, Cosnes J, Fléjou JF, Beaugerie L; Saint-Antoine Inflammatory Bowel Disease Network. Nancy Index Scores of Chronic Inflammatory Bowel Disease Activity Associate With Development of Colorectal Neoplasia. *Clin Gastroenterol Hepatol* 2020; **18**: 150-157.e1 [PMID: 31085339 DOI: 10.1016/j.cgh.2019.05.002]
37 **D'Haens G**, Sandborn WJ, Feagan BG, Geboes K, Hanauer SB, Irvine EJ, Lémann M, Marteau P, Rutgeerts P, Schölmerich J, Sutherland LR. A review of activity indices and efficacy end points for clinical trials of medical therapy in adults with ulcerative colitis. *Gastroenterology* 2007; **132**: 763-786 [PMID: 17258735 DOI: 10.1053/j.gastro.2006.12.038]
38 **Peyrin-Biroulet L**, Sandborn W, Sands BE, Reinisch W, Bemelman W, Bryant RV, D'Haens G, Dotan I, Dubinsky M, Feagan B, Fiorino G, Gearry R, Krishnareddy S, Lakatos PL, Loftus EV Jr, Marteau P, Munkholm P, Murdoch TB, Ordás I, Panaccione R, Riddell RH, Ruel J, Rubin DT, Samaan M, Siegel CA, Silverberg MS, Stoker J, Schreiber S, Travis S, Van Assche G, Danese S, Panes J, Bouguen G, O'Donnell S, Pariente B, Winer S, Hanauer S, Colombel JF. Selecting Therapeutic Targets in Inflammatory Bowel Disease (STRIDE): Determining Therapeutic Goals for Treat-to-Target. *Am J Gastroenterol* 2015; **110**: 1324-1338 [PMID: 26303131 DOI: 10.1038/ajg.2015.233]
39 **Truelove SC**, Richards WC. Biopsy studies in ulcerative colitis. *Br Med J* 1956; **1**: 1315-1318 [PMID: 13316140 DOI: 10.1136/bmj.1.4979.1315]
40 **Mosli MH**, Parker CE, Nelson SA, Baker KA, MacDonald JK, Zou GY, Feagan BG, Khanna R, Levesque BG, Jairath V.

Histologic scoring indices for evaluation of disease activity in ulcerative colitis. *Cochrane Database Syst Rev* 2017; **5**: CD011256 [PMID: 28542712 DOI: 10.1002/14651858.CD011256.pub2]

41 **Geboes K**, Riddell R, Ost A, Jensfelt B, Persson T, Löfberg R. A reproducible grading scale for histological assessment of inflammation in ulcerative colitis. *Gut* 2000; **47**: 404-409 [PMID: 10940279 DOI: 10.1136/gut.47.3.404]

42 **Lemmens B**, Arijs I, Van Assche G, Sagaert X, Geboes K, Ferrante M, Rutgeerts P, Vermeire S, De Hertogh G. Correlation between the endoscopic and histologic score in assessing the activity of ulcerative colitis. *Inflamm Bowel Dis* 2013; **19**: 1194-1201 [PMID: 23518809 DOI: 10.1097/MIB.0b013e318280e75f]

43 **Jairath V**, Peyrin-Biroulet L, Zou G, Mosli M, Vande Casteele N, Pai RK, Valasek MA, Marchal-Bressenot A, Stitt LW, Shackelton LM, Khanna R, D'Haens GR, Sandborn WJ, Olson A, Feagan BG. Responsiveness of histological disease activity indices in ulcerative colitis: a post hoc analysis using data from the TOUCHSTONE randomised controlled trial. *Gut* 2019; **68**: 1162-1168 [PMID: 30076171 DOI: 10.1136/gutjnl-2018-316702]

44 **Zenlea T**, Yee EU, Rosenberg L, Boyle M, Nanda KS, Wolf JL, Falchuk KR, Cheifetz AS, Goldsmith JD, Moss AC. Histology Grade Is Independently Associated With Relapse Risk in Patients With Ulcerative Colitis in Clinical Remission: A Prospective Study. *Am J Gastroenterol* 2016; **111**: 685-690 [PMID: 26977756 DOI: 10.1038/ajg.2016.50]

45 **Jauregui-Amezaga A**, Geerits A, Das Y, Lemmens B, Sagaert X, Bessissow T, Lobatón T, Ferrante M, Van Assche G, Bisschops R, Geboes K, De Hertogh G, Vermeire S. A Simplified Geboes Score for Ulcerative Colitis. *J Crohns Colitis* 2017; **11**: 305-313 [PMID: 27571771 DOI: 10.1093/ecco-jcc/jjw154]

46 **Mosli MH**, Feagan BG, Zou G, Sandborn WJ, D'Haens G, Khanna R, Shackelton LM, Walker CW, Nelson S, Vandervoort MK, Frisbie V, Samaan MA, Jairath V, Driman DK, Geboes K, Valasek MA, Pai RK, Lauwers GY, Riddell R, Stitt LW, Levesque BG. Development and validation of a histological index for UC. *Gut* 2017; **66**: 50-58 [PMID: 26475633 DOI: 10.1136/gutjnl-2015-310393]

47 **Marchal-Bressenot A**, Salleron J, Boulagnon-Rombi C, Bastien C, Cahn V, Cadiot G, Diebold MD, Danese S, Reinisch W, Schreiber S, Travis S, Peyrin-Biroulet L. Development and validation of the Nancy histological index for UC. *Gut* 2017; **66**: 43-49 [PMID: 26464414 DOI: 10.1136/gutjnl-2015-310187]

48 **Marchal-Bressenot A**, Scherl A, Salleron J, Peyrin-Biroulet L. A practical guide to assess the Nancy histological index for UC. *Gut* 2016; **65**: 1919-1920 [PMID: 27566129 DOI: 10.1136/gutjnl-2016-312722]

49 **D'Amico F**, Guillo L, Baumann C, Danese S, Peyrin-Biroulet L. Histological Disease Activity Measured by the Nancy Index Is Associated with Long-term Outcomes in Patients with Ulcerative Colitis. *J Crohns Colitis* 2021; **15**: 1631-1640 [PMID: 33822915 DOI: 10.1093/ecco-jcc/jjab063]

50 **Novak G**, Parker CE, Pai RK, MacDonald JK, Feagan BG, Sandborn WJ, D'Haens G, Jairath V, Khanna R. Histologic scoring indices for evaluation of disease activity in Crohn's disease. *Cochrane Database Syst Rev* 2017; **7**: CD012351 [PMID: 28731502 DOI: 10.1002/14651858.CD012351.pub2]

51 **D'Haens GR**, Geboes K, Peeters M, Baert F, Penninckx F, Rutgeerts P. Early lesions of recurrent Crohn's disease caused by infusion of intestinal contents in excluded ileum. *Gastroenterology* 1998; **114**: 262-267 [PMID: 9453485 DOI: 10.1016/s0016-5085(98)70476-7]

52 **De Cruz P**, Kamm MA, Prideaux L, Allen PB, Moore G. Mucosal healing in Crohn's disease: a systematic review. *Inflamm Bowel Dis* 2013; **19**: 429-444 [PMID: 22539420 DOI: 10.1002/ibd.22977]

53 **Almradi A**, Ma C, D'Haens GR, Sandborn WJ, Parker CE, Guizzetti L, Borralho Nunes P, De Hertogh G, Feakins RM, Khanna R, Lauwers GY, Mookhoek A, Pai RK, Peyrin-Biroulet L, Riddell R, Rosty C, Schaeffer DF, Valasek MA, Singh S, Crowley E, Feagan BG, Jairath V. An expert consensus to standardise the assessment of histological disease activity in Crohn's disease clinical trials. *Aliment Pharmacol Ther* 2021; **53**: 784-793 [PMID: 33410551 DOI: 10.1111/apt.16248]

54 **MATTS SG**. The value of rectal biopsy in the diagnosis of ulcerative colitis. *Q J Med* 1961; **30**: 393-407 [PMID: 14471445]

55 **Pariente B**, Mary JY, Danese S, Chowers Y, De Cruz P, D'Haens G, Loftus EV Jr, Louis E, Panés J, Schölmerich J, Schreiber S, Vecchi M, Branche J, Bruining D, Fiorino G, Herzog M, Kamm MA, Klein A, Lewin M, Meunier P, Ordas I, Strauch U, Tontini GE, Zagdanski AM, Bonifacio C, Rimola J, Nachury M, Leroy C, Sandborn W, Colombel JF, Cosnes J. Development of the Lémann index to assess digestive tract damage in patients with Crohn's disease. *Gastroenterology* 2015; **148**: 52-63.e3 [PMID: 25241327 DOI: 10.1053/j.gastro.2014.09.015]

56 **Schaeffer DF**, Walsh JC, Kirsch R, Waterman M, Silverberg MS, Riddell RH. Distinctive histopathologic phenotype in resection specimens from patients with Crohn's disease receiving anti-TNF-α therapy. *Hum Pathol* 2014; **45**: 1928-1935 [PMID: 25022570 DOI: 10.1016/j.humpath.2014.05.016]

57 **Chen W**, Lu C, Hirota C, Iacucci M, Ghosh S, Gui X. Smooth Muscle Hyperplasia/Hypertrophy is the Most Prominent Histological Change in Crohn's Fibrostenosing Bowel Strictures: A Semiquantitative Analysis by Using a Novel Histological Grading Scheme. *J Crohns Colitis* 2017; **11**: 92-104 [PMID: 27364949 DOI: 10.1093/ecco-jcc/jjw126]

58 **Pennington L**, Hamilton SR, Bayless TM, Cameron JL. Surgical management of Crohn's disease. Influence of disease at margin of resection. *Ann Surg* 1980; **192**: 311-318 [PMID: 6998388 DOI: 10.1097/00000658-198009000-00006]

59 **Levine A**, Koletzko S, Turner D, Escher JC, Cucchiara S, de Ridder L, Kolho KL, Veres G, Russell RK, Paerregaard A, Buderus S, Greer ML, Dias JA, Veereman-Wauters G, Lionetti P, Sladek M, Martin de Carpi J, Staiano A, Ruemmele FM, Wilson DC; European Society of Pediatric Gastroenterology, Hepatology, and Nutrition. ESPGHAN revised porto criteria for the diagnosis of inflammatory bowel disease in children and adolescents. *J Pediatr Gastroenterol Nutr* 2014; **58**: 795-806 [PMID: 24231644 DOI: 10.1097/MPG.0000000000000239]

60 **Panes J**, Bouhnik Y, Reinisch W, Stoker J, Taylor SA, Baumgart DC, Danese S, Halligan S, Marincek B, Matos C, Peyrin-Biroulet L, Rimola J, Rogler G, van Assche G, Ardizzone S, Ba-Ssalamah A, Bali MA, Bellini D, Biancone L, Castiglione F, Ehehalt R, Grassi R, Kucharzik T, Maccioni F, Maconi G, Magro F, Martín-Comín J, Morana G, Pendsé D, Sebastian S, Signore A, Tolan D, Tielbeek JA, Weishaupt D, Wiarda B, Laghi A. Imaging techniques for assessment of inflammatory bowel disease: joint ECCO and ESGAR evidence-based consensus guidelines. *J Crohns Colitis* 2013; **7**: 556-585 [PMID: 23583097 DOI: 10.1016/j.crohns.2013.02.020]

61 **Ordás I**, Rimola J, Alfaro I, Rodríguez S, Castro-Poceiro J, Ramírez-Morros A, Gallego M, Giner À, Barastegui R, Fernández-Clotet A, Masamunt M, Ricart E, Panés J. Development and Validation of a Simplified Magnetic Resonance

Index of Activity for Crohn's Disease. *Gastroenterology* 2019; **157**: 432-439.e1 [PMID: 30953614 DOI: 10.1053/j.gastro.2019.03.051]

62 **Gralnek IM**, Defranchis R, Seidman E, Leighton JA, Legnani P, Lewis BS. Development of a capsule endoscopy scoring index for small bowel mucosal inflammatory change. *Aliment Pharmacol Ther* 2008; **27**: 146-154 [PMID: 17956598 DOI: 10.1111/j.1365-2036.2007.03556.x]

63 **Gal E**, Geller A, Fraser G, Levi Z, Niv Y. Assessment and validation of the new capsule endoscopy Crohn's disease activity index (CECDAI). *Dig Dis Sci* 2008; **53**: 1933-1937 [PMID: 18034304 DOI: 10.1007/s10620-007-0084-y]

64 **Fabian O**, Hradsky O, Potuznikova K, Kalfusova A, Krskova L, Hornofova L, Zamecnik J, Bronsky J. Low predictive value of histopathological scoring system for complications development in children with Crohn's disease. *Pathol Res Pract* 2017; **213**: 353-358 [PMID: 28216137 DOI: 10.1016/j.prp.2017.01.009]

65 **Fabian O**, Hradsky O, Lerchova T, Mikus F, Zamecnik J, Bronsky J. Limited clinical significance of tissue calprotectin levels in bowel mucosa for the prediction of complicated course of the disease in children with ulcerative colitis. *Pathol Res Pract* 2019; **215**: 152689 [PMID: 31679791 DOI: 10.1016/j.prp.2019.152689]

66 **Johnson CM**, Hartman DJ, Ramos-Rivers C, Rao BB, Bhattacharya A, Regueiro M, Schwartz M, Swoger J, Al Hashash J, Barrie A, Pfanner TP, Dunn M, Koutroubakis IE, Binion DG. Epithelioid Granulomas Associate With Increased Severity and Progression of Crohn's Disease, Based on 6-Year Follow-Up. *Clin Gastroenterol Hepatol* 2018; **16**: 900-907.e1 [PMID: 29277619 DOI: 10.1016/j.cgh.2017.12.034]

67 **Lang-Schwarz C**, Agaimy A, Atreya R, Becker C, Danese S, Fléjou JF, Gaßler N, Grabsch HI, Hartmann A, Kamarádová K, Kühl AA, Lauwers GY, Lugli A, Nagtegaal I, Neurath MF, Oberhuber G, Peyrin-Biroulet L, Rath T, Riddell R, Rubio CA, Sheahan K, Tilg H, Villanacci V, Westerhoff M, Vieth M. Maximizing the diagnostic information from biopsies in chronic inflammatory bowel diseases: recommendations from the Erlangen International Consensus Conference on Inflammatory Bowel Diseases and presentation of the IBD-DCA score as a proposal for a new index for histologic activity assessment in ulcerative colitis and Crohn's disease. *Virchows Arch* 2021; **478**: 581-594 [PMID: 33373023 DOI: 10.1007/s00428-020-02982-7]

68 **Lang-Schwarz C**, Angeloni M, Agaimy A, Atreya R, Becker C, Dregelies T, Danese S, Fléjou JF, Gaßler N, Grabsch HI, Hartmann A, Kamarádová K, Kühl AA, Lauwers GY, Lugli A, Nagtegaal I, Neurath MF, Oberhuber G, Peyrin-Biroulet L, Rath T, Riddell R, Rubio CA, Sheahan K, Siegmund B, Tilg H, Villanacci V, Westerhoff M, Ferrazzi F, Vieth M. Validation of the 'Inflammatory Bowel Disease-Distribution, Chronicity, Activity [IBD-DCA] Score' for Ulcerative Colitis and Crohn´s Disease. *J Crohns Colitis* 2021; **15**: 1621-1630 [PMID: 33773497 DOI: 10.1093/ecco-jcc/jjab055]

69 **Winter DA**, Karolewska-Bochenek K, Lazowska-Przeorek I, Lionetti P, Mearin ML, Chong SK, Roma-Giannikou E, Maly J, Kolho KL, Shaoul R, Staiano A, Damen GM, de Meij T, Hendriks D, George EK, Turner D, Escher JC; Paediatric IBD Porto Group of ESPGHAN. Pediatric IBD-unclassified Is Less Common than Previously Reported; Results of an 8-Year Audit of the EUROKIDS Registry. *Inflamm Bowel Dis* 2015; **21**: 2145-2153 [PMID: 26164665 DOI: 10.1097/MIB.0000000000000483]

70 **Rinawi F**, Assa A, Eliakim R, Mozer-Glassberg Y, Nachmias Friedler V, Niv Y, Rosenbach Y, Silbermintz A, Zevit N, Shamir R. The natural history of pediatric-onset IBD-unclassified and prediction of Crohn's disease reclassification: a 27-year study. *Scand J Gastroenterol* 2017; **52**: 558-563 [PMID: 28128677 DOI: 10.1080/00365521.2017.1282008]

71 **Guindi M**, Riddell RH. Indeterminate colitis. *J Clin Pathol* 2004; **57**: 1233-1244 [PMID: 15563659 DOI: 10.1136/jcp.2003.015214]

72 **Löwenberg M**, Vermeire S, Mostafavi N, Hoentjen F, Franchimont D, Bossuyt P, Hindryckx P, Rispens T, de Vries A, van der Woude CJ, Berends S, Ambarus CA, Mathot R, Clasquin E, Baert F, D'Haens G. Vedolizumab Induces Endoscopic and Histologic Remission in Patients With Crohn's Disease. *Gastroenterology* 2019; **157**: 997-1006.e6 [PMID: 31175865 DOI: 10.1053/j.gastro.2019.05.067]

World Journal of Gastroenterology

Submit a Manuscript: https://www.f6publishing.com

World J Gastroenterol 2022 September 28; 28(36): 5313-5323

DOI: 10.3748/wjg.v28.i36.5313

ISSN 1007-9327 (print) ISSN 2219-2840 (online)

ORIGINAL ARTICLE

Basic Study

Esophageal magnetic compression anastomosis in dogs

Xiang-Hua Xu, Yi Lv, Shi-Qi Liu, Xiao-Hai Cui, Rui-Yang Suo

Specialty type: Gastroenterology and hepatology

Provenance and peer review: Unsolicited article; Externally peer reviewed.

Peer-review model: Single blind

Peer-review report's scientific quality classification
Grade A (Excellent): 0
Grade B (Very good): B, B
Grade C (Good): 0
Grade D (Fair): 0
Grade E (Poor): 0

P-Reviewer: Abass M, Egypt; Tré bol J, Spain

Received: July 14, 2022
Peer-review started: July 14, 2022
First decision: July 31, 2022
Revised: August 11, 2022
Accepted: September 9, 2022
Article in press: September 9, 2022
Published online: September 28, 2022

Xiang-Hua Xu, Yi Lv, Department of Hepatobiliary Surgery, The First Affiliated Hospital of Xi'an Jiaotong University, Xi'an 710061, Shaanxi Province, China

Xiang-Hua Xu, Yi Lv, National Local Joint Engineering Research Center for Precision Surgery and Regenerative Medicine, The First Affiliated Hospital of Xi'an Jiaotong University, Xi'an 710061, Shaanxi Province, China

Shi-Qi Liu, Department of Pediatric Surgery, Xi'an Children's Hospital, Xi'an 710003, Shaanxi Province, China

Xiao-Hai Cui, Department of Thoracic Surgery, The First Affiliated Hospital of Xi'an Jiaotong University, Xi'an 710061, Shaanxi Province, China

Rui-Yang Suo, Zonglian College, Xi'an Jiaotong University Health Science Center, Xi'an 710061, Shaanxi Province, China

Corresponding author: Yi Lv, MD, PhD, Professor, Department of Hepatobiliary Surgery, The First Affiliated Hospital of Xi'an Jiaotong University, No. 277 West Yanta Road, Xi'an 710061, Shaanxi Province, China. luyi169@126.com

Abstract

BACKGROUND

Magnetic compression anastomosis (MCA) is a novel suture-free reconstruction of the digestive tract. It has been used in gastrointestinal anastomosis, jejunal anastomosis, cholangioenteric anastomosis and so on. The traditional operative outcomes of congenital esophageal atresia and benign esophageal stricture are poor, and there are too many complications postoperatively.

AIM

To test MCA technology to reconstruct the esophagus in dogs, prior to studying the feasibility and safety of MCA in humans.

METHODS

Thirty-six dogs were randomized into either the study or control group (n = 18 per group). The dogs in the study group were subjected to end-to-end esophageal anastomosis with the magnetic compression device, while those in the control group underwent hand-sewn anastomosis with 4-0 absorbable multifilament Vicryl. We used interrupted single-layer inverting sutures. The anastomosis time, gross appearance, weight and pathology of the anastomosis were evaluated at one month, three months and six months postoperatively.

RESULTS

The anastomosis time of the MCA group was shorter than that of the hand-sewn group (7.5 ± 1.0 min *vs* 12.5 ± 1.8 min, $P < 0.01$). In the MCA group, X-ray examination was performed every day to locate the magnetic device in the esophagus before the magnetic device fell off from the esophagus. In the hand-sewn group, dogs did not undergo X-ray examination. One month after the surgeries, the mean weight of the dogs in the hand-sewn group had decreased more than that of the dogs in the MCA group (11.63 ± 0.71 kg *vs* 12.73 ± 0.80 kg, $P < 0.05$). At 3 mo and 6 mo after the operation, the dogs' weights were similar between the two groups (13.75 ± 0.84 kg *vs* 14.03 ± 0.82 kg, 14.93 ± 0.80 kg *vs* 15.44 ± 0.47 kg). The number of inflammatory cells in MCA group was lower than that in hand-sewn group on 1 mo after operation.

CONCLUSION

MCA is an effective and safe method for esophageal reconstruction. The anastomosis time of the MCA group was less than that of the hand-sewn group. This study shows that MCA technology may be applied to human esophageal reconstruction, provided these favorable results are confirmed by more publications.

Key Words: Magnetic; Anastomosis; Esophagus; Reconstruction; Hand sewn; Dog

©The Author(s) 2022. Published by Baishideng Publishing Group Inc. All rights reserved.

Core Tip: We used magnetic compression anastomosis (MCA) technology to reconstruct the esophagus. The anastomosis time of the MCA group was shorter than that of the hand-sewn group (7.5 ± 1.0 min *vs* 12.5 ± 1.8 min, $P < 0.01$). One month after the surgeries, the mean weight of the dogs in the hand-sewn group had decreased more than that of the dogs in the MCA group (11.63 ± 0.71 kg *vs* 12.73 ± 0.80 kg, $P < 0.05$). At 3 mo and 6 mo after the operation, the dogs' weights were similar between the two groups. MCA is an effective and safe method for esophageal reconstruction. This study shows that MCA technology may be applied to human esophageal reconstruction, provided these favorable results are confirmed by more publications.

Citation: Xu XH, Lv Y, Liu SQ, Cui XH, Suo RY. Esophageal magnetic compression anastomosis in dogs. *World J Gastroenterol* 2022; 28(36): 5313-5323
URL: https://www.wjgnet.com/1007-9327/full/v28/i36/5313.htm
DOI: https://dx.doi.org/10.3748/wjg.v28.i36.5313

INTRODUCTION

Esophageal atresia (EA) is a serious and fatal gastrointestinal developmental malformation in the neonatal period. It has a worldwide prevalence of 2.4 to 3.8 per 10000 newborns[1-4]. Because of the development of surgical and good neonatal intensive care, the survival is about 90% in those born with EA with severe associated anomalies and is even higher in those born with EA alone[5]. However, the postoperative complications of traditional hand-sewn anastomosis are numerous, and the therapeutic effect is not good. The primary complications during the postoperative period are leakage (incidence 15%-20%), stenosis of the anastomosis (30%-40%), gastroesophageal reflux (40%-65%), esophageal dysmotility, fistula recurrence, scoliosis, deformities of the thoracic wall and respiratory disorders[6-8]. After surgery, children suffer from various complications, which seriously affect their development and quality of life.

Magnetic compression anastomosis (MCA) is a novel suture-free reconstruction of the digestive tract. Since Kanshin *et al*[9] reported using a magnetic device to anastomose gastroduodenal and cecojejunal in dogs in 1978, there have been many reports of this technique using animal experiments and regarding its clinical applications. At present, clinically, it has been used in gastrointestinal anastomosis[10,11], jejunal anastomosis[12,13], cholangioenteric anastomosis[14-16] and so on. Fourteen patients underwent MCA for gastrointestinal anastomosis, and the technical success of MCA was achieved in 100% of the cases. Two patients underwent anastomotic restenosis, and 1 patient had an anastomotic perforation due to balloon dilatation to prevent restenosis. Fifteen patients underwent MCA for jejunal anastomosis, of which five patients had severe systemic disease and underwent complex open urinary reconstruction procedures. The device was successfully placed and effectively formed a side-to-side, functional end-to-end jejunal anastomosis. Forty-seven patients underwent MCA for cholangioenteric anastomosis. Thirty-eight patients had a malignant primary disease, while nine had benign disease. With a median

follow-up of 547.5 d (range 223-1042 d), no patients had biliary fistula, while two developed anastomotic stricture at 4 mo and 14 mo after surgery. Magnetic materials have noncontact suction characteristics that will greatly simplify the process of gastrointestinal anastomosis, especially in the case of gastrointestinal stenosis or atresia. Recently, Kamada *et al*[10] reported that MCA without general anesthesia is a valuable alternative to surgery for gastrointestinal obstruction. Some patients with biliary obstruction are not eligible for conventional endoscopic procedures or are unsuitable for surgery. The MCA technique is an available method for performing choledochocholedochostomy and choledochoenterostomy interventionally[16]. The mean age of the patients in these two reports was above 60 years. Therefore, MCA technology can be designed as a minimally invasive technique and is tolerated by elderly patients.

Because of the many complications of traditional operations and the ability to obtain minimally invasive surgery by MCA, MCA could be a superior method to treat congenital EA. There have been several clinical reports on esophageal reconstruction using MCA[17-19]. Muensterer *et al*[17] reported that they used esophageal MCA for staged EA repair in 3 patients (Gross type A, B, and C) at high risk for conventional surgical repair. Surgeries were all successful, and there were no perioperative complications. Liu *et al*[18] reported that two patients who had severe stricture after simultaneous EA and duodenal obstruction repair underwent magnetic compression stricturoplasty. Magnetic compression stricturoplasty successfully established the patency of the esophagus in these two patients with refractory EA stricture. These two cases required multiple additional procedures, but durable esophageal patency with absence of dysphagia was achieved at 15 or 10 mo after magnetic compression stricturoplasty. Dorman *et al*[19] reported a case in which EA was repaired with a proximal fistula using endoscopic MCA after staged lengthening. Magnetic coupling occurred at 4 d, and after magnet removal at 13 d, an esophagram demonstrated a 10 French channel without leakage. A series of studies on MCA technology have been carried out in our laboratory. The technology has been used in choledochojejunostomy, rectovaginal fistula repair, laparoscopic pancreatoduodenectomy (LPD) and liver transplantation. Twenty-six mongrel dogs underwent choledochojejunostomy magnamosis with different magnetic pressure magnets. The surgical procedures were all successful[20]. There was a comparative study with 12 pigs for rectovaginal fistula repair. Eight animals were in the MCA group, and four animals were in the hand-sewn group. The rectovaginal fistula site was smooth, and healing was complete. This technology was used in one case clinically and achieved success[21]. Seven patients received MCA technology in LPD. LPD was successfully completed in all seven patients, of which seven underwent laparoscopic magnetic compression choledochojejunostomy and two received laparoscopic magnetic compression pancreatojejunostomy. No leakages were observed after the operation. After a median follow-up period of 11 mo (range 4-18 mo), there was no incidence of anastomotic stricture[22]. We also used MCA to reconstruct vessels in liver transplantation. In pig liver transplantation, we used MCA to reconstruct the suprahepatic vena cava, infrahepatic vena cava and portal vein. They were all successful, and the pig lived for over one month[23]. Currently, we want to use MCA technology to treat EA, but there is a paucity of published research data and animal studies. Therefore, the purpose of this study was to study the difference between MCA and hand-sewn anastomosis of the esophagus in dogs.

MATERIALS AND METHODS

Animals

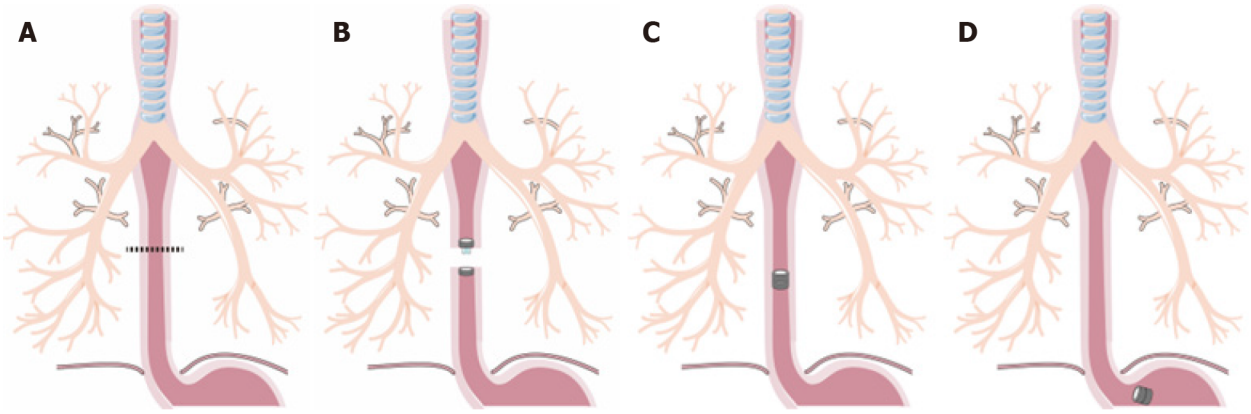
The protocol of the animal study was reviewed and approved by the committee for Ethics of Animal Experiments of Xi'an Jiaotong University (No. XJTULAC2020-1441). Thirty-six mongrel dogs (male = 18, female = 18) with body weights of 10-15 kg were provided by the Laboratory Animal Center of Xi'an Jiaotong University. Dogs were acclimatized to laboratory conditions (23 °C, ad libitum access to food and water) for 2 wk prior to experimentation. In this study, we selected mongrel dogs because the esophagus in the neck is long enough for reconstruction. This purpose is to avoid performing surgery in the thoracic cavity and to improve the survival rate.

Study design

Thirty-six dogs were randomized into either the MCA group or the hand-sewn group, n = 18 per group, with the same male to female ratio. The dogs in the MCA group were subjected to end-to-end esophageal anastomosis with the magnetic device, while those in the hand-sewn group underwent hand-sewn anastomosis with 4-0 absorbable multifilament Vicryl. We used interrupted single-layer sutures. In both groups, there was no surgical left in place. Postoperative complications and weight were observed. The anastomosis time, gross appearance and pathology of the anastomoses were evaluated at one month, three months and six months after the operation.

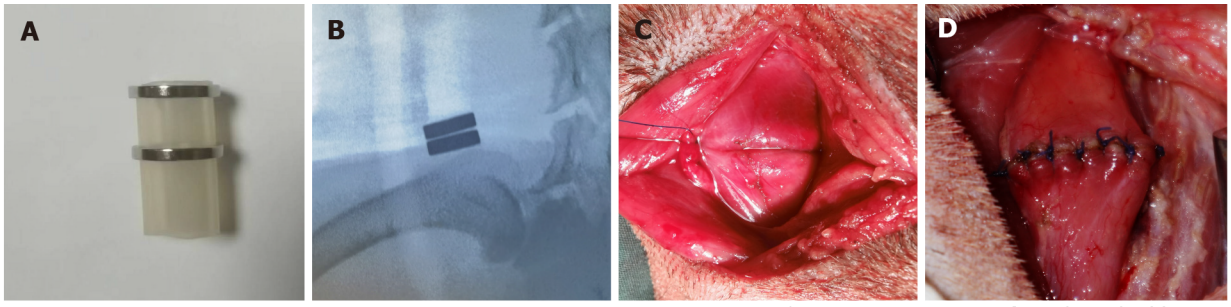
Magnetic anastomosis device

The magnetic anastomosis device used in the study possessed a parent magnetic ring (PMR) and daughter magnetic ring (DMR), which were made of rare earth neodymium iron boron (NdFeB, N40) and plated with nickel from Northwest Institute for Nonferrous Metal Research, Xi'an, China. A special



DOI: 10.3748/wjg.v28.i36.5313 **Copyright** ©The Author(s) 2022.

Figure 1 Surgical procedures of magnetic compress esophagus anastomosis. A: Transecting the esophagus at the diseased region; B: Placing the parent magnetic ring (PMR) and daughter magnetic ring (DMR) on the upper and lower ends of esophagus; C: The PMR and DMR attract each other and create the anastomosis, and the esophagus reconstruction is complete, the dispositive allows food passage; D: The magnetic devices fall off the esophagus into the stomach, and the esophagus lumen is completely open.



DOI: 10.3748/wjg.v28.i36.5313 **Copyright** ©The Author(s) 2022.

Figure 2 The magnetic device and the appearance on X-ray, the esophageal anastomosis of magnetic compression anastomosis and hand-sewn suture. A: The magnetic device, composed of two magnetic rings and one special catheter; B: The magnetic ring position on X-ray postoperatively, and the anastomosis face is smooth; C: Using the magnetic compression anastomosis technology to finish the esophageal anastomosis; D: The anastomosis by hand-sewn suture.

drainage tube was placed between the PMR and DMR, and both the PMR and DMR had outer diameters of 20 mm, inner diameters of 14 mm, and thicknesses of 2 mm. The magnetic force between the PMR and DMR is 30 Newton at zero distance with a magnetic density of 8000 GS.

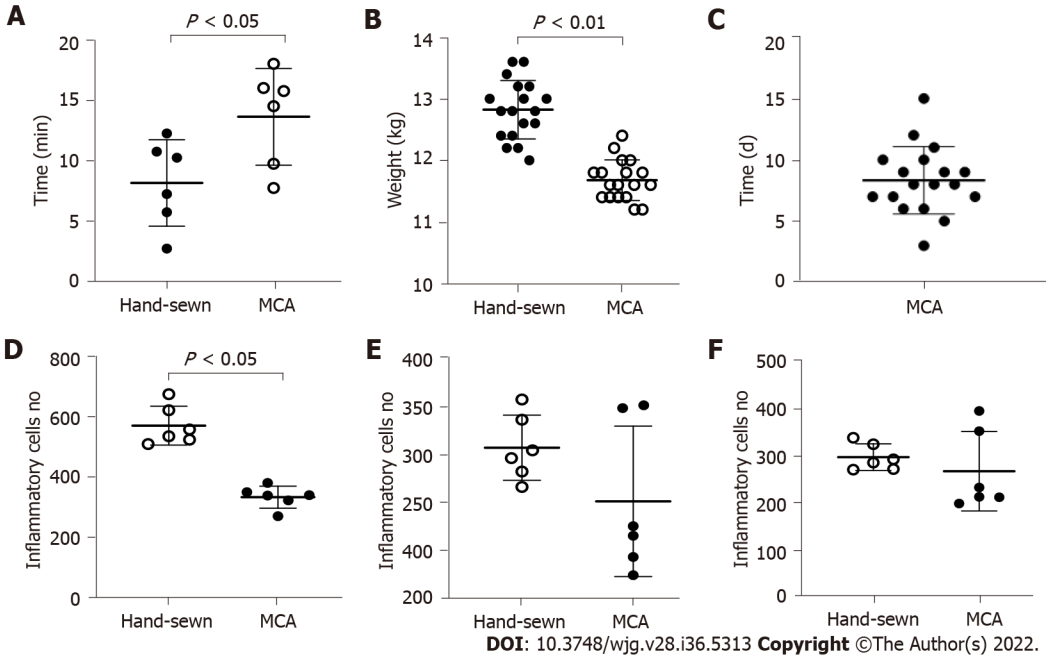
Surgical procedures

The dogs were first anesthetized with an intraperitoneal injection of 30 mg/kg pentobarbital sodium solution. The dogs were anesthetized and then placed in the right lateral position on a temperature-controlled operating table with their cervical region shaved and sterilized. The experimental process is shown in Figure 1. A 5 cm incision was made along the anterior edge of the sternocleidomastoid muscle in the neck. Then, the muscle was separated layer by layer, and a 3 cm long portion of the esophagus was found. Next, the esophagus was transected.

In the MCA group, the PMR and DMR were placed in the upper and lower esophagus, respectively, after transecting the esophagus (Figure 1A). The magnetic anastomosis device was shown in Figure 2A. The upper and lower ends of the esophageal anastomosis were sutured with 4-0 silk thread and tightened to the position of the special drainage tube. Under the action of attraction, the magnetic rings at both ends are attracted to each other automatically and press the anastomotic tissue together, and the esophageal anastomosis is then completed (Figure 2C). When the anastomotic tissue is necrotic and falls off, the magnetic device is discharged into the stomach with the digesta and is discharged out of the body. In the control group, the operation was the same as that in the study group, except that end-to-end anastomosis was performed with 4-0 absorbable sutures (Figure 2D).

Postoperative care

An X-ray (Perlove Medical Equipment incorporated company, Nanjing, China) was performed on the dogs in the study group to confirm the target location and precise mating of the magnetic compression rings (Figure 2B). X-ray was performed every day before the magnets fell off the esophagus. Postoper-



DOI: 10.3748/wjg.v28.i36.5313 **Copyright** ©The Author(s) 2022.

Figure 3 The analysis about anastomosis time, weight changes, the time of the magnetic device fell and the number of inflammatory cells between two groups. A: The anastomosis time of the magnetic compression anastomosis group and hand-sewn group. There were 18 dogs in each group; B: The dogs were weighed at 1 mo, and every group contained 6 dogs. There was a significant difference between the two groups; C: The time when the magnetic device had fallen into the stomach of 18 dogs; D-F: The number of inflammatory cells respectively at 1 mo, 3 mo and 6 mo. MCA: Magnetic compression anastomosis.

atively, every dog was kept in a cage. After the surgery, the dogs in the two groups were fasted for two days and then started on enteral nutrition. However, in the hand-sewn group, dogs generally showed poor appetite and even refused to eat. They started enteral nutrition at 4 d, 5 d, or even longer. During this period, we can only keep them alive with parenteral nutrition. The dogs in the MCA group started enteral nutrition earlier than those in the hand-sewn group. All dogs in both groups were given cefazolin sodium intramuscularly for 3 d postoperatively to prevent infection. Intramuscular injection (0.5 g) was administered twice a day. After a week, dogs were given enteral nutrition, a liquid diet, a semiliquid diet, and a normal diet according to their recovery. Six dogs were randomly selected in each group at 1 mo, 3 mo and 6 mo after the operation. They were weighed and intravenously injected with an overdose of anesthetic.

Specimen collection and histological analysis

All anastomosis segments with a sufficient length were harvested. The anastomotic stoma was found and severed 2 cm above and below the anastomosis. The gross information was observed, and all samples were immersed in 10% buffered formalin overnight. The samples were embedded in paraffin after fixation. Four-micrometer-thick sections were cut at the anastomosis site. Sections were stained with hematoxylin and eosin and Masson's trichrome dye. Then, we observed the changes in the tissue and cells under a light microscope.

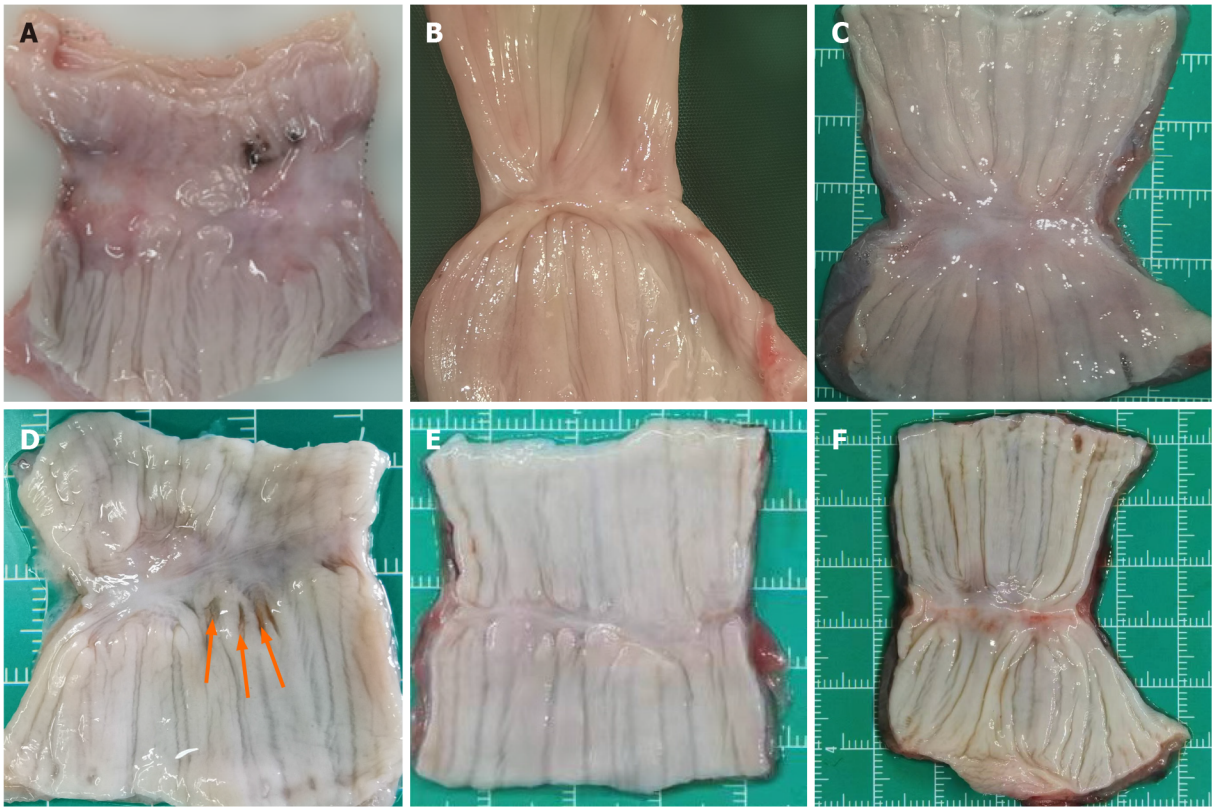
Statistical analysis

Data were analyzed using GraphPad Prism v8 software (GraphPad, La Jolla, CA, United States). Quantitative data are expressed as the mean ± SD, and differences between the two groups were analyzed with the independent samples *t* test. The anastomosis time and weight data conformed to a normal distribution and homogeneity of variance. Statistical significance was set at $P < 0.05$.

RESULTS

Procedural parameters

Anastomosis was successfully created in all dogs. The anastomosis time of the MCA group was shorter than that of the hand-sewn group (7.5 ± 1.0 *vs* 12.5 ± 1.8, $P < 0.01$) (Figure 3A). X-ray examinations showed that the esophagi were all unobstructed and that the contrast agent could pass through the anastomosis in the MCA group. All dogs survived. There was one dog in the hand-sewn group and one dog in the MCA group with stenosis after the operation. These were found when we obtained



DOI: 10.3748/wjg.v28.i36.5313 **Copyright** ©The Author(s) 2022.

Figure 4 Gross appearance of the anastomosis in magnetic compression anastomosis and hand-sewn group. A: The tissue of magnetic compression anastomosis (MCA) group is thin at 1 mo, but the mucous membrane is intact; B: Anastomotic tissue of the MCA group at 3 mo; C: At 6 mo, the tissue becomes smooth and flat in the MCA group. There is little difference from normal tissue; D: The tissue of the hand-sewn anastomotic stoma is incomplete, and the mucous membrane has a small pinhole at 1 mo, which was caused by the suture needle. Red arrow indicates; E: Anastomotic tissue of the hand-sewn group at 3 mo; F: Anastomotic tissue of the hand-sewn group at 6 mo.

anastomotic stoma tissue. We observed one dog in the hand-sewn group who suddenly refused to eat, and the incision skin was red, swollen and purulent 8 d after the operation. We performed surgical exploration and performed a second esophageal reconstruction.

Expulsion time of the magnetic compression rings and weight changes

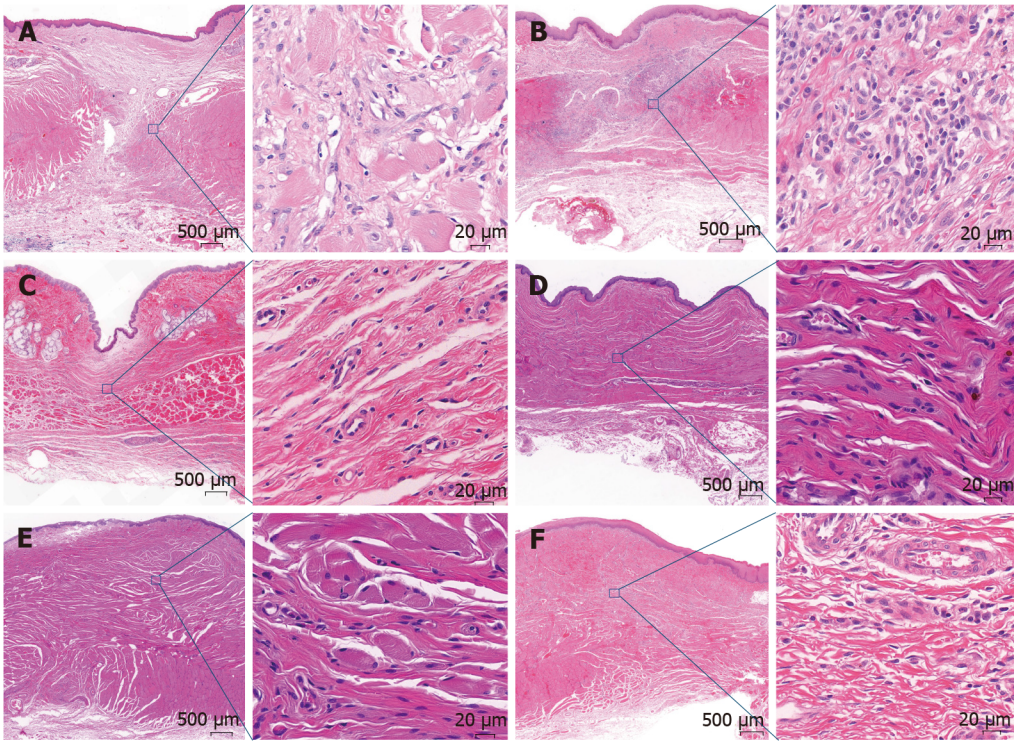
We observed how long the magnetic rings took to fall off into the stomach. The mean time was 8.3 ± 2.7 d (range 3-15 d) (Figure 3C). The weights of dogs in the MCA group (13.87 ± 0.63 kg) and the hand-sewn group (13.98 ± 0.80 kg) were similar at the beginning of the experiment. The difference in weight between the two groups was not statistically significant. However, the weights decreased more in the hand-sewn group than in the MCA group 1 mo after the operation. The mean weight of the MCA group was 12.73 ± 0.80 kg, while the mean weight of the hand-sewn group was 11.63 ± 0.71 kg, $P < 0.05$. At 3 mo and 6 mo after the operation, the dog weights were similar between the two groups (13.75 ± 0.84 kg *vs* 14.03 ± 0.82 kg, 14.93 ± 0.80 kg *vs* 15.44 ± 0.47 kg).

Gross appearance of the anastomosis

The esophagi grew well, and there were no ulcerations or fistulas. The mucosa layers were intact. However, the anastomotic stomas were slightly thinner than the peripheral tissue at 1 mo. We could see that the muscle layer tissues were not completely covered. In the hand-sewn anastomosis group, the suture plots were still visible 1 mo after the operation (Figure 4D). With the passage of time, the submucosa and muscle layers were gradually covered, and the anastomoses became increasingly smooth and flat. However, at 1 mo, 3 mo and 6 mo, the anastomoses of the MCA group were smoother than those of the hand-sewn group.

Histological appearance of the anastomosis

Light microscopy showed that the anastomotic mucosa of the MCA group had grown well during the first month after surgery, while the submucosal and muscular layers were still fractured (Figure 5A). Three months after the operation, the submucosal and muscular layers had completely covered the anastomoses, and the anastomotic tissue was similar to the normal esophageal tissue under light microscopy (Figure 5C). In the hand-sewn group, the mucosa was continuous one month after surgery,



DOI: 10.3748/wjg.v28.i36.5313 **Copyright** ©The Author(s) 2022.

Figure 5 Hematoxylin and eosin dye of the anastomotic tissue in magnetic compression anastomosis and hand-sewn group. Each image consists of two parts, one with a 2 × objective view and the other with a 40 × objective view. A: The anastomotic tissue of the magnetic compression anastomosis (MCA) group at 1 mo. The mucous membrane was intact, but the muscularis was separated; B: The anastomotic tissue of the hand-sewn group at 1 mo. There were more inflammatory cells in the tissue of the hand-sewn group than that of the MCA group; C: The anastomotic tissue of the MCA group at 3 mo. The muscularis became continuous; D: The anastomotic tissue of the hand-sewn group at 3 mo; E: The anastomotic tissue of the MCA group at 6 mo; F: The anastomotic tissue of the hand-sewn group at 6 mo.

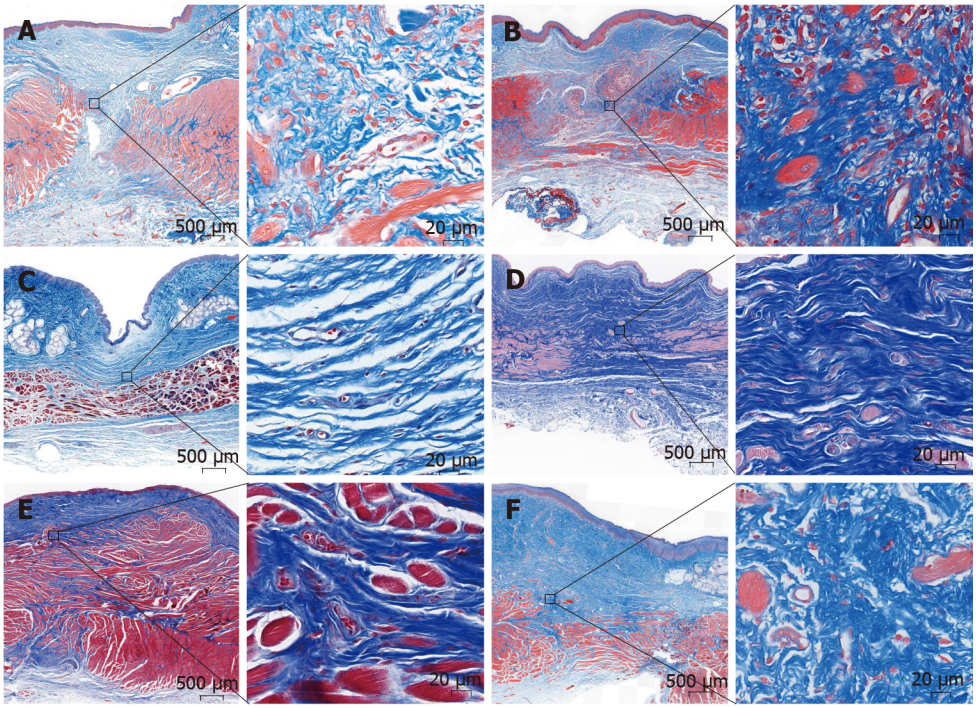
but the submucosa and muscle layers were still broken, similar to the findings in the MCA group at one month (Figure 5B). At 3 mo postoperatively, the anastomotic site was covered by the submucosa and muscularis (Figure 5D). The number of inflammatory cells in the hand-sewn group was greater than that in the MCA group at 1 mo (Figures 5A and B). We counted the number of inflammatory cells in one high-power field (40 ×) in both groups (334 ± 37 *vs* 572 ± 65, $P < 0.01$). At 3 mo and 6 mo, the number of inflammatory cells was less than that at 1 mo. Between the two groups, the number of inflammatory cells was equal at 3 mo and 6 mo (Figures 5C-F). Masson staining showed that the number of collagen fibers in the hand-sewn group was greater than that in the MCA group. The blue fibers are collagen fibers (Figures 6A-F).

DISCUSSION

We studied the tissue status of the anastomotic esophagus after esophageal reconstruction by magnetic anastomosis technology and clarified the safety of MCA surgery. A comparative study was conducted between magnetic anastomosis and hand-sewn anastomosis for esophageal reconstruction to determine whether the effects of MCA were superior to those of the hand-sewn method.

By observing gross specimens and tissue sections at different time periods in the MCA and hand-sewn groups, we found that in both the MCA group and the hand-sewn anastomosis group, the anastomotic tissues were not completely healed at 1 mo after surgery. The mucosal surface of the two groups was smooth without ischemia or necrosis, while some submucosa and muscularis were still missing. After 3 mo, the anastomotic sites of the two groups had healed well, and the mucosal layer, submucosal layer and muscular layer were continuous. Liquid food is still the main diet in the early stage to reduce the stimulation of esophageal mucosa and prevent the occurrence of ulcers. Based on the results of the experiment, we suggest that MCA patients should consume a liquid diet or a semiliquid diet for at least one month.

The tissue healing of the MCA group was faster and better than that of the hand-sewn group. Six months after the operation, the specimens of the MCA group were smoother than those in the hand-sewn group, and a slight amount of scar tissue was observed in the hand-sewn group. There are several reasons for this. Magnetic anastomosis technology applies the mutual attraction between magnetic rings



DOI: 10.3748/wjg.v28.i36.5313 **Copyright** ©The Author(s) 2022.

Figure 6 Masson Thrichrome dye staining of the anastomotic tissue in magnetic compression anastomosis and hand-sewn group. Each image consists of two parts, one with a 2 × objective view and the other with a 40 × objective view. A: The anastomotic tissue of the magnetic compression anastomosis (MCA) group at 1 mo. The mucous membrane was intact, but the muscularis was separated at 1 mo, and the appearance was similar to that of hematoxylin and eosin staining; B: The anastomotic tissue of the hand-sewn group at 1 mo. There were more collagenous fibers than that in MCA group; C: The anastomotic tissue of the MCA group at 3 mo. The muscularis became continuous; D: The anastomotic tissue of the hand-sewn group at 3 mo; E: The anastomotic tissue of the MCA group at 6 mo; F: The anastomotic tissue of the hand-sewn group at 6 mo.

to maintain a constant and balanced pressure on the tissues at the anastomosis, resulting in slow ischemic necrosis of the tissues between the magnetic rings and the growth and healing of the surrounding tissues. This is a slow process that allows time for esophageal compensation to grow. Hand-sewn sutures use Vicryl to quickly tighten the tissues at both ends of the esophagus. There is a certain tension at both ends of the esophagus, which may lead to shearing forces placed on the esophageal tissue from Vicryl. Second, Vicryl, as an absorbable thread, will exist in the tissue for a long time as a foreign body, which may cause infection and scar hyperplasia. The suture material could play an important role in the healing of esophageal anastomosis. Vicryl is an absorbable material, but the time of absorption is more than 1 mo. During this period, Vicryl may act as a foreign body, leading to foreign body granuloma or anastomosis edema. Braided sutures are more prone to infection than monofilament sutures. Vicryl is the braided suture and perhaps in this study Vicryl is not the best selection.

At six months postoperatively, the magnetic anastomosis group grew slightly better than the hand-sewn group. Before surgery, the weights of the dogs in both groups were the same. One month after surgery, the body weight of the hand-sewn group was significantly lower than that of the magnetic anastomosis group. Three months after surgery, the weights of the dogs were similar in both groups. This suggests that MCA may contribute to enhanced recovery after esophageal reconstruction. There are two reasons that may contribute to the enhanced recovery with MCA technology: (1) The magnetic device has a gap in the middle, through which the liquid can enter the stomach, while it will not contact the anastomotic tissue. It may relieve pain and reduce the incidence of infection; and (2) The shedding time of the magnetic device is shorter than the time of the suture being discharged or absorbed by the tissues. The absorbable time of Vicryl RapideR is approximately 40 d[24], while the magnetic device discharge time is approximately 8 d. We observed that the dogs in the MCA group could feed earlier than those in the hand-sewn group. The MCA group of dogs recovered faster and better than the dogs in the hand-sewn group.

During 6 mo of observation, there was 1 stenosis in the MCA group and 1 stenosis and 1 Leakage in the hand-sewn group. Because the sample size was small, there was no statistically significant difference between the two groups. The rate of stenosis and leakage of anastomosis using the traditional hand-sewn operation is high. This has seriously affected the postoperative growth of children. We hope that this novel MCA technology can improve EA. The complication rate needs to be verified by more animal experiments and clinical case reports.

One clinical report showed that anastomosis was achieved in an average of 6 d (range 3 to 7 d) in 5 patients (age 6 mo to 5.9 years) with severe recurrent postsurgical esophageal stenosis refractory to dilatation[25]. Another MCA was achieved on day 36[26]. Clinical reports have shown that the anastomosis time ranges from 3 d to 36 d[26-28]. It involves many factors, such as the age of the child, type of EA, size of the magnetic ring and field strength of the magnetic device. This will be our next experimental purpose. Based on a large amount of experimental and clinical data, a model was established to estimate various parameters of magnetic devices preoperatively.

There are also some limitations of the study. First, our surgery location was on the dog's neck, not in the thoracic cavity. This is not consistent with the clinicopathology. The position of EA is generally flush with the bifurcation of the main bronchus and may have a tracheoesophageal fistula. Second, in this study, we did not consider the effect of different structural sutures on the anastomosis. Does monofilament have less effect on anastomotic healing than multifilament? Third, this is a model of esophageal anastomosis, and not of anastomosis in the setting of an atresia, there are several differences.

CONCLUSION

MCA is an effective and safe method for esophageal reconstruction in dogs. The anastomosis with MCA is faster than the hand-sewn anastomosis. Postoperatively, some aspects of the recovery of the MCA group were faster and better than those of the hand-sewn group. We provide some information useful for the future clinical application of the device in selected cases.

ARTICLE HIGHLIGHTS

Research background

Magnetic compression anastomosis (MCA) is a novel suture-free reconstruction of the digestive tract. It has been used in gastrointestinal anastomosis, jejunal anastomosis, cholangioenteric anastomosis and so on. The traditional operative outcomes of congenital esophageal atresia and benign esophageal stricture are poor, and there are too many complications postoperatively.

Research motivation

There are several case reports of using MCA to treat esophageal stenosis. However, systematic animal experimental studies are scarce. This has restricted further clinical application of MCA.

Research objectives

This study was conducted to demonstrate the feasibility and safety of MCA for esophageal reconstruction and studied the difference between MCA and hand-sewn esophageal reconstruction.

Research methods

Thirty-six dogs were randomized into either the study or control group (n = 18 per group). The dogs in the study group were subjected to end-to-end esophageal anastomosis with the magnetic compression device, while those in the control group underwent hand-sewn anastomosis with 4-0 absorbable multifilament Vicryl. We used interrupted single-layer sutures. The anastomosis time, gross appearance, weight and pathology of the anastomosis were evaluated at one month, three months and six months postoperatively.

Research results

The anastomosis time of the MCA group was shorter than that of the hand-sewn group (7.5 ± 1.0 min *vs* 12.5 ± 1.8 min, $P < 0.01$). One month after the surgeries, the mean weight of the dogs in the hand-sewn group had decreased more than that of the dogs in the MCA group (11.63 ± 0.71 kg *vs* 12.73 ± 0.80 kg, $P < 0.05$). At 3 mo and 6 mo after the operation, the dogs' weights were similar between the two groups (13.75 ± 0.84 kg *vs* 14.03 ± 0.82 kg, 14.93 ± 0.80 kg *vs* 15.44 ± 0.47 kg). Under an optical microscope, the number of inflammatory cells in MCA group was lower than that in hand-sewn group on 1 mo after operation.

Research conclusions

MCA is an effective and safe method for esophageal reconstruction. The anastomosis time of the MCA was less than that of the hand-sewn group. This study shows that MCA technology may be applied to human esophageal reconstruction, provided these favorable results are confirmed by more publications.

Research perspectives

MCA for esophageal reconstruction in the thoracic cavity needs to be tested, and further clinical trials

are needed to test its safety and guide its clinical application.

ACKNOWLEDGEMENTS

The authors would like to acknowledge the Laboratory Animal Center of Xi'an Jiaotong University for skillful technical assistance.

FOOTNOTES

Author contributions: Xu XH, Liu SQ, Lv Y designed and coordinated the study; Xu XH, Liu SQ, Cui XH and Suo RY performed the experiments and acquired and analyzed the data; XH Xu and Lv Y wrote the manuscript; and all authors approved the final version of the article.

Supported by the National Natural Science Foundation of China, No. 82170676; and Natural Science Foundation of Shaanxi Provincial Key Industries Innovation Chain (Cluster)-Social Development Project, No. 2020ZDLSF02-03.

Institutional animal care and use committee statement: All experimental protocols were approved by the Committee on the Ethics of Animal Experiments of Xi'an Jiaotong University (Permit Number: XJTULAC2020-1441).

Conflict-of-interest statement: All the authors report no relevant conflicts of interest for this article.

Data sharing statement: No additional data are available.

ARRIVE guidelines statement: The authors read the ARRIVE guidelines, and the manuscript was prepared and revised according to the ARRIVE guidelines.

Open-Access: This article is an open-access article that was selected by an in-house editor and fully peer-reviewed by external reviewers. It is distributed in accordance with the Creative Commons Attribution NonCommercial (CC BY-NC 4.0) license, which permits others to distribute, remix, adapt, build upon this work non-commercially, and license their derivative works on different terms, provided the original work is properly cited and the use is non-commercial. See: https://creativecommons.org/Licenses/by-nc/4.0/

Country/Territory of origin: China

ORCID number: Xiang-Hua Xu 0000-0001-6144-3938; Yi Lv 0000-0003-3636-6664; Shi-Qi Liu 0000-0002-2274-7880; Xiao-Hai Cui 0000-0002-7856-7117; Rui-Yang Suo 0000-0003-3622-958X.

S-Editor: Wang JJ
L-Editor: A
P-Editor: Wang JJ

REFERENCES

1 **Comella A**, Tan Tanny SP, Hutson JM, Omari TI, Teague WJ, Nataraja RM, King SK. Esophageal morbidity in patients following repair of esophageal atresia: A systematic review. *J Pediatr Surg* 2021; **56**: 1555-1563 [PMID: 33051081 DOI: 10.1016/j.jpedsurg.2020.09.010]
2 **Nassar N**, Leoncini E, Amar E, Arteaga-Vázquez J, Bakker MK, Bower C, Canfield MA, Castilla EE, Cocchi G, Correa A, Csáky-Szunyogh M, Feldkamp ML, Khoshnood B, Landau D, Lelong N, López-Camelo JS, Lowry RB, McDonnell R, Merlob P, Métneki J, Morgan M, Mutchinick OM, Palmer MN, Rissmann A, Siffel C, Sipek A, Szabova E, Tucker D, Mastroiacovo P. Prevalence of esophageal atresia among 18 international birth defects surveillance programs. *Birth Defects Res A Clin Mol Teratol* 2012; **94**: 893-899 [PMID: 22945024 DOI: 10.1002/bdra.23067]
3 **Oddsberg J**, Lu Y, Lagergren J. Aspects of esophageal atresia in a population-based setting: incidence, mortality, and cancer risk. *Pediatr Surg Int* 2012; **28**: 249-257 [PMID: 22020495 DOI: 10.1007/s00383-011-3014-1]
4 **Pedersen RN**, Calzolari E, Husby S, Garne E; EUROCAT Working group. Oesophageal atresia: prevalence, prenatal diagnosis and associated anomalies in 23 European regions. *Arch Dis Child* 2012; **97**: 227-232 [PMID: 22247246 DOI: 10.1136/archdischild-2011-300597]
5 **Smith N**. Oesophageal atresia and tracheo-oesophageal fistula. *Early Hum Dev* 2014; **90**: 947-950 [PMID: 25448787 DOI: 10.1016/j.earlhumdev.2014.09.012]
6 **Pinheiro PF**, Simões e Silva AC, Pereira RM. Current knowledge on esophageal atresia. *World J Gastroenterol* 2012; **18**: 3662-3672 [PMID: 22851858 DOI: 10.3748/wjg.v18.i28.3662]
7 **van Lennep M**, Singendonk MMJ, Dall'Oglio L, Gottrand F, Krishnan U, Terheggen-Lagro SWJ, Omari TI, Benninga MA, van Wijk MP. Oesophageal atresia. *Nat Rev Dis Primers* 2019; **5**: 26 [PMID: 31000707 DOI: 10.1038/s41572-019-0077-0]

8 **Schmedding A**, Wittekindt B, Schloesser R, Hutter M, Rolle U. Outcome of esophageal atresia in Germany. *Dis Esophagus* 2021; **34** [PMID: 32995846 DOI: 10.1093/dote/doaa093]

9 **Kanshin NN**, Permiakov NK, Dzhalagoniia RA, Nikulin BI, Kuznetsov AA. [Sutureless anastomoses in gastrointestinal surgery with and without steady magnetic field (experimental study)]. *Arkh Patol* 1978; **40**: 56-61 [PMID: 365148]

10 **Kamada T**, Ohdaira H, Takeuchi H, Takahashi J, Ito E, Suzuki N, Narihiro S, Yoshida M, Yamanouchi E, Suzuki Y. New Technique for Magnetic Compression Anastomosis Without Incision for Gastrointestinal Obstruction. *J Am Coll Surg* 2021; **232**: 170-177.e2 [PMID: 33190786 DOI: 10.1016/j.jamcollsurg.2020.10.012]

11 **Marrache MK**, Itani MI, Farha J, Fayad L, Sharara SL, Kalloo AN, Khashab MA, Kumbhari V. Endoscopic gastrointestinal anastomosis: a review of established techniques. *Gastrointest Endosc* 2021; **93**: 34-46 [PMID: 32593687 DOI: 10.1016/j.gie.2020.06.057]

12 **Graves CE**, Co C, Hsi RS, Kwiat D, Imamura-Ching J, Harrison MR, Stoller ML. Magnetic Compression Anastomosis (Magnamosis): First-In-Human Trial. *J Am Coll Surg* 2017; **225**: 676-681.e1 [PMID: 28843832 DOI: 10.1016/j.jamcollsurg.2017.07.1062]

13 **Machytka E**, Bužga M, Zonca P, Lautz DB, Ryou M, Simonson DC, Thompson CC. Partial jejunal diversion using an incisionless magnetic anastomosis system: 1-year interim results in patients with obesity and diabetes. *Gastrointest Endosc* 2017; **86**: 904-912 [PMID: 28716404 DOI: 10.1016/j.gie.2017.07.009]

14 **Liu XM**, Li Y, Xiang JX, Ma F, Lu Q, Guo YG, Yan XP, Wang B, Zhang XF, Lv Y. Magnetic compression anastomosis for biliojejunostomy and pancreaticojejunostomy in Whipple's procedure: An initial clinical study. *J Gastroenterol Hepatol* 2019; **34**: 589-594 [PMID: 30278106 DOI: 10.1111/jgh.14500]

15 **Liu XM**, Yan XP, Zhang HK, Ma F, Guo YG, Fan C, Wang SP, Shi AH, Wang B, Wang HH, Li JH, Zhang XG, Wu R, Zhang XF, Lv Y. Magnetic Anastomosis for Biliojejunostomy: First Prospective Clinical Trial. *World J Surg* 2018; **42**: 4039-4045 [PMID: 29947988 DOI: 10.1007/s00268-018-4710-y]

16 **Itoi T**, Kasuya K, Sofuni A, Itokawa F, Tsuchiya T, Kurihara T, Ikeuchi N, Takeuchi M, Nagano T, Iwamoto H, Yamanouchi E, Shimazu M, Tsuchida A. Magnetic compression anastomosis for biliary obstruction: review and experience at Tokyo Medical University Hospital. *J Hepatobiliary Pancreat Sci* 2011; **18**: 357-365 [PMID: 21127913 DOI: 10.1007/s00534-010-0350-9]

17 **Muensterer OJ**, Evans LL, Sterlin A, Sahlabadi M, Aribindi V, Lindner A, König T, Harrison MR. Novel Device for Endoluminal Esophageal Atresia Repair: First-in-Human Experience. *Pediatrics* 2021; **148** [PMID: 34615695 DOI: 10.1542/peds.2020-049627]

18 **Liu S**, Fang Y, Lv Y, Zhao J, Luo R, Cheng J, Yang H, Zhang A, Shen Y, Jiang N. Magnetic compression stricturoplasty in patients with severe stricture after simultaneous esophageal atresia and duodenal obstruction repair: A case report. *Exp Ther Med* 2022; **23**: 93 [PMID: 34976135 DOI: 10.3892/etm.2021.11016]

19 **Dorman RM**, Vali K, Harmon CM, Zaritzky M, Bass KD. Repair of esophageal atresia with proximal fistula using endoscopic magnetic compression anastomosis (magnamosis) after staged lengthening. *Pediatr Surg Int* 2016; **32**: 525-528 [PMID: 27012861 DOI: 10.1007/s00383-016-3889-y]

20 **Xue F**, Guo HC, Li JP, Lu JW, Wang HH, Ma F, Liu YX, Lv Y. Choledochojejunostomy with an innovative magnetic compressive anastomosis: How to determine optimal pressure? *World J Gastroenterol* 2016; **22**: 2326-2335 [PMID: 26900294 DOI: 10.3748/wjg.v22.i7.2326]

21 **She ZF**, Yan XP, Ma F, Wang HH, Yang H, Shi AH, Wang L, Qi X, Xiao B, Zou YL, Lv Y. Treatment of rectovaginal fistula by magnetic compression. *Int Urogynecol J* 2017; **28**: 241-247 [PMID: 27530520 DOI: 10.1007/s00192-016-3097-2]

22 **Li Y**, Liu XM, Zhang HK, Zhang XF, Tang B, Ma F, Lv Y. Magnetic Compression Anastomosis in Laparoscopic Pancreatoduodenectomy: A Preliminary Study. *J Surg Res* 2021; **258**: 162-169 [PMID: 33011447 DOI: 10.1016/j.jss.2020.08.044]

23 **Liu K**, Yang H, Huang G, Shi A, Lu Q, Wang S, Qiao W, Wang H, Ke M, Ding H, Li T, Zhang Y, Yu J, Ren B, Wang R, Wang K, Feng H, Suo Z, Tang J, Lv Y. Adhesive anastomosis for organ transplantation. *Bioact Mater* 2022; **13**: 260-268 [PMID: 35224307 DOI: 10.1016/j.bioactmat.2021.11.003]

24 **Al-Qattan MM**. Vicryl Rapide versus Vicryl suture in skin closure of the hand in children: a randomized prospective study. *J Hand Surg Br* 2005; **30**: 90-91 [PMID: 15620501 DOI: 10.1016/j.jhsb.2004.08.005]

25 **Zaritzky M**, Ben R, Johnston K. Magnetic gastrointestinal anastomosis in pediatric patients. *J Pediatr Surg* 2014; **49**: 1131-1137 [PMID: 24952802 DOI: 10.1016/j.jpedsurg.2013.11.002]

26 **Liu SQ**, Lv Y, Fang Y, Luo RX, Zhao JR, Luo RG, Li YM, Zhang J, Zhang PF, Guo JZ, Li QH, Han MX. Magnetic compression for anastomosis in treating an infant born with long-gap oesophageal atresia: A case report. *Medicine (Baltimore)* 2020; **99**: e22472 [PMID: 33080683 DOI: 10.1097/MD.0000000000022472]

27 **Slater BJ**, Borobia P, Lovvorn HN, Raees MA, Bass KD, Almond S, Hoover JD, Kumar T, Zaritzky M. Use of Magnets as a Minimally Invasive Approach for Anastomosis in Esophageal Atresia: Long-Term Outcomes. *J Laparoendosc Adv Surg Tech A* 2019; **29**: 1202-1206 [PMID: 31524560 DOI: 10.1089/lap.2019.0199]

28 **Woo R**, Wong CM, Trimble Z, Puapong D, Koehler S, Miller S, Johnson S. Magnetic Compression Stricturoplasty For Treatment of Refractory Esophageal Strictures in Children: Technique and Lessons Learned. *Surg Innov* 2017; **24**: 432-439 [PMID: 28745145 DOI: 10.1177/1553350617720994]

World Journal of Gastroenterology

Submit a Manuscript: https://www.f6publishing.com

World J Gastroenterol 2022 September 28; 28(36): 5324-5337

DOI: 10.3748/wjg.v28.i36.5324

ISSN 1007-9327 (print) ISSN 2219-2840 (online)

ORIGINAL ARTICLE

Retrospective Cohort Study

Impact of sarcopenia on tumor response and survival outcomes in patients with hepatocellular carcinoma treated by trans-arterial (chemo)-embolization

Gael Roth, Yann Teyssier, Maxime Benhamou, Mélodie Abousalihac, Stefano Caruso, Christian Sengel, Olivier Seror, Julien Ghelfi, Arnaud Seigneurin, Nathalie Ganne-Carrie, Elia Gigante, Lorraine Blaise, Olivier Sutter, Thomas Decaens, Jean-Charles Nault

Specialty type: Gastroenterology and hepatology

Provenance and peer review: Unsolicited article; Externally peer reviewed.

Peer-review model: Single blind

Peer-review report's scientific quality classification

Grade A (Excellent): 0
Grade B (Very good): 0
Grade C (Good): C, C, C
Grade D (Fair): 0
Grade E (Poor): 0

P-Reviewer: Posa A, Italy; Xi D, China; Zhao G, China

Received: May 2, 2022
Peer-review started: May 2, 2022
First decision: June 19, 2022
Revised: June 22, 2022
Accepted: August 30, 2022
Article in press: August 30, 2022
Published online: September 28, 2022

Gael Roth, Yann Teyssier, Julien Ghelfi, Arnaud Seigneurin, Thomas Decaens, Univ. Grenoble-Alpes, Grenoble 38058, France

Gael Roth, Mélodie Abousalihac, Thomas Decaens, Department of Hepatology, Gastroenterology and Digestive Oncology, CHU Grenoble Alpes, Grenoble 38043, France

Gael Roth, Julien Ghelfi, Thomas Decaens, Institute for Advanced Biosciences, INSERM U1209/CNRS UMR 5309, Grenoble 38043, France

Yann Teyssier, Christian Sengel, Julien Ghelfi, Department of Radiology, CHU Grenoble Alpes, Grenoble 38043, France

Maxime Benhamou, Olivier Seror, Olivier Sutter, Department of Radiology, CHU Avicenne-APHP, Bobigny 93000, France

Stefano Caruso, Olivier Seror, Nathalie Ganne-Carrie, Jean-Charles Nault, Functional Genomics of Solid Tumors Laboratory, Centre de Recherche des Cordeliers-INSERM UMR 1138, Inserm, Université Paris, Paris 75006, France

Olivier Seror, Nathalie Ganne-Carrie, Jean-Charles Nault, Unité de Formation et de Recherche Santé Médecine et Biologie Humaine, Université Paris Nord, Paris 93430, France

Arnaud Seigneurin, Service d'Epidémiologie et Evaluation Médicale, CHU Grenoble Alpes, Grenoble 38043, France

Nathalie Ganne-Carrie, Elia Gigante, Lorraine Blaise, Jean-Charles Nault, Department of Hepatology, CHU Avicenne-APHP, Bobigny 93000, France

Corresponding author: Jean-Charles Nault, MD, PhD, Full Professor, Department of Hepatology, CHU Avicenne-APHP, 125 Rue de Stalingrad, Bobigny 93000, France.
naultjc@gmail.com

Abstract

BACKGROUND

At the diagnosis of hepatocellular carcinoma (HCC), more than 90% of HCC patients present cirrhosis, a clinical condition often associated to malnutrition. Sarcopenia is an indirect marker of malnutrition assessable on computed tomography (CT).

AIM

To evaluate the prognostic value of sarcopenia in patients with HCC treated by trans-arterial (chemo)-embolization.

METHODS

Patients with HCC treated by a first session of trans-arterial (chemo)embolization and an available CT scan before treatment were included. Sarcopenia was assessed using skeletal muscle index at baseline and at the first radiological assessment. Radiological response was recorded after the first session of treatment using mRECIST.

RESULTS

Of 225 patients treated by trans-arterial bland embolization (n = 71) or trans-arterial chemoembolization (n = 154) for HCC between 2007 and 2013, Barcelona Clinic of Liver Cancer stage was A, B, and C in 27.5%, 55%, and 16.8% of cases, respectively. Sarcopenia was present in 57.7% of the patients. Patients with sarcopenia presented a higher rate of progressive disease (19% *vs* 8%, P = 0.0236), a shorter progression-free survival (8.3 *vs* 13.2 mo, P = 0.0035), and a shorter median overall survival (19.4 mo *vs* 35.5 mo, P = 0.0149) compared with non-sarcopenic patients. Finally, patients whose sarcopenia appeared after first transarterial treatment had the worst prognosis (P = 0.0004).

CONCLUSION

Sarcopenia is associated with tumor progression and poor survival outcomes after trans-arterial (chemo)-embolization for HCC.

Key Words: Hepatocellular carcinoma; Transarterial chemoembolization; Bland embolization; Sarcopenia; Skeletal muscle index

©The Author(s) 2022. Published by Baishideng Publishing Group Inc. All rights reserved.

Core Tip: This work evaluated the predictive value of sarcopenia for tumor response and survival outcomes in hepatocellular carcinoma patients treated by transarterial chemoembolization or transarterial embolization. In this study, sarcopenia at imaging was observed in 57.7% of patients. It was associated with a higher rate of progressive disease and a decreased overall survival after adjustment with usual risk factors of death. Sarcopenia is an easy-to-assess radiological biomarker of poor prognosis that should be measured in order to assess prognosis and test a targeted intervention mixing nutritional support and physical activity.

Citation: Roth G, Teyssier Y, Benhamou M, Abousalihac M, Caruso S, Sengel C, Seror O, Ghelfi J, Seigneurin A, Ganne-Carrie N, Gigante E, Blaise L, Sutter O, Decaens T, Nault JC. Impact of sarcopenia on tumor response and survival outcomes in patients with hepatocellular carcinoma treated by trans-arterial (chemo)-embolization. *World J Gastroenterol* 2022; 28(36): 5324-5337

URL: https://www.wjgnet.com/1007-9327/full/v28/i36/5324.htm

DOI: https://dx.doi.org/10.3748/wjg.v28.i36.5324

INTRODUCTION

Liver cancer is the second cause of cancer-related deaths worldwide[1], mostly represented by hepatocellular carcinoma (HCC). At the diagnosis, 70% of HCC patients have only access to palliative treatments, and among intermediate HCC, classified as Barcelona Clinic of Liver Cancer (BCLC)-B[2], transarterial chemoembolization (TACE) and transarterial embolization (TAE) are the best therapeutic options to offer[3-5]. Nonetheless, despite a good level of tumor response, around 50%-55% of patients receiving these treatments suffer from a high level of relapse[6]. It is well demonstrated that TACE presents the best results on patients with a good general status and a low level of liver insufficiency[7], but additional reliable predictive markers are needed to better define which patients will take full benefit of this procedure, and which ones present an increased risk of low efficacy and liver deterioration. At the diagnosis, more than 90% of HCC patients present with cirrhosis, a clinical condition

often associated to malnutrition with sarcopenia. Indeed, sarcopenia, defined as the "progressive loss of muscle mass and strength with a risk of adverse outcomes such as disability, poor quality of life, and death"[8], is a consequence of chronic inflammation, hypercatabolism, and anorexia found in cirrhosis and advanced tumor stages. Sarcopenia has already been described as a poor prognostic factor in HCC patients undergoing surgical resection or treated by systemic therapies[9-12]. Further studies are needed to clarify the predictive value of sarcopenia in other HCC treatment settings, such as TAE or TACE. Indeed, several studies with small numbers of patients showed interesting results on the predictive value of sarcopenia regarding survival outcomes of patients treated by TACE but without clear impact on tumor response[13]. This study aimed to evaluate the predictive value of sarcopenia for tumor response and survival outcomes in a bicentric cohort of HCC patients treated by TACE or TAE.

MATERIALS AND METHODS

Patient selection

Patients were retrospectively included from December 1, 2007 to November 1, 2013 in Jean Verdier Hospital and from June 1, 2011 to December 1, 2014 in Grenoble-Alpes University Hospital. The inclusion criteria were as follow: Age > 18 years, HCC diagnosed by histology or non-invasive criteria [7], first treatment using TAE or TACE, and available pre- and post-therapeutic computed tomography (CT) scan. Transarterial procedures performed for acute bleeding of HCC were excluded.

Transarterial procedures

Patients were treated with transarterial therapy following standard local protocol[14]. Each indication of TACE or TAE was validated during multidisciplinary tumor board including a hepatologist, an interventional radiologist, and a liver surgeon. In case of TACE, chemotherapy was either doxorubicin or idarubicin according to institutional standards of care, as previously described[15]. The choice of chemotherapy was left to the investigator's discretion. Every TACE or TAE was performed by an expert interventional radiologist.

As recommended by European guidelines, TACE could be repeated 2 mo after the first treatment in case of partial response on postoperative scan and preserved liver function after rediscussion in multidisciplinary tumor board[7].

Ethical approval

Written consent was obtained for every patient before transarterial procedures and the study protocol respects the ethical guidelines of the 1975 Declaration of Helsinki (6th revision, 2008). Study ethics was also approved by the independent French ethic committee CERIM (*Comité d'éthique de la recherche en imagerie médicale;* No. CRM-2004-084).

Clinical and paraclinical data collection

Clinical and biological data were recorded before the treatment: Demographic data, body mass index, liver function, platelets, presence of cirrhosis, etiology of the underlying liver disease, alpha-fetoprotein (AFP) level, tumor size, number of nodules, tumor portal invasion, and esophageal varices at the last upper endoscopy.

After the first treatment, all patients were prospectively followed until death or the last recorded visit until June 30, 2018.

Anthropometric measurements

Anthropometric measurements were assessed on the pre-therapeutic CT scan and the first follow-up CT scan realized 1-3 mo after the transarterial treatment by two radiologists (OSu and YT) using the software Image J®. Skeletal muscle and psoas muscle area were measured on a cross-sectional CT image at the level of the 3rd lumbar vertebra. Skeletal muscle index (SMI) was calculated using the total muscle area on the L3 CT slice divided by squared height as previously described[16]. Sarcopenia was defined by SMI < 50 cm^2/m^2 in male and < 39 cm^2/m^2 in female patients as defined by the North American expert statement on sarcopenia in liver transplantation[17]. Psoas muscle index (PMI) defined as the psoas muscle area on height ratio was also assessed as previously described[17].

The following data were recorded on imaging: Liver volume, spleen volume, presence of ascites at imaging, presence of para-umbilical vein, presence of esophageal varices, and presence of splenomegaly defined by a spleen's cranio-caudal diameter superior to 12 cm.

Assessment of tumor response and survival outcomes

All imaging examinations were archived in a picture archiving and communication system and blindly read by two radiologists (OSu and YT). Clinical and paraclinical parameters were extracted from the patient's electronic medical records.

Radiological response was assessed by two radiologists (OSu and YT) comparing the baseline imaging and the imaging available 1-3 mo after the first session of trans-arterial treatment as recommended[7]. Radiological response was classified into complete response, partial response, stable disease, and progressive disease as defined by the modified RECIST criteria[7].

Progression-free survival was defined as the time between the date of the first treatment and the date of death, radiological progression, or the last recorded visit. Patients were censured at the date of liver transplantation. Overall survival (OS) was defined as the time between the date of the first treatment and the date of death or the last recorded visit, with censoring at the date of liver transplantation in transplanted patients.

Statistical analysis

Categorical variables were compared using the Fisher exact test for two groups and Chi squared test for three groups and more. Continuous variables were compared using the Mann-Whitney test. Logistic regression was used to compare the association with radiological response and baseline variables.

Survival outcomes as OS and progression free survival (PFS) were computed using the Kaplan-Meier method, and the Log-rank test was used to compare survival rates. The association between baseline variable and OS and PFS was assessed in univariate analysis using the Cox model. Variables with a P value < 0.05 in the univariate analysis were computed in multivariate analysis using the Cox model. Statistical analyses were performed using Graph Pad (PRISM) and R software.

RESULTS

Description of the population

A total of 225 patients were included in the analysis, including 93 from Jean Verdier Hospital and 132 from Grenoble-Alpes University Hospital (Figure 1). Patients were mainly male (88.8%) with a median age of 65 (58-75) years old. The underlying liver diseases were mainly related to chronic alcohol intake (61%), hepatitis C (28%), and non-alcoholic steatohepatitis (29%) with 81.6% of patients classified as Child-Pugh A.

HCCs were classified as BCLC-A in 27.5%, BCLC-B in 55.5%, and BCLC-C due to segmental portal vein thrombosis in 16.8% of patients. One hundred and fifty-four (68.4%) of the patients were treated by TACE (127 with doxorubicin and 27 with idarubicin; including 87 by lipiodol TACE and 40 by TACE using drug eluting beads). Seventy-one (31.5%) patients were treated by TAE using lipiodol with gelatin sponge. Patients' characteristics are detailed in Table 1.

Anthropometric and portal hypertension assessment at imaging

Anthropometric measurements including the value of total muscle area in L3 and psoas area in L3 are detailed in Table 1. Ascites was identified in 23.5% of the cases at imaging as well as splenomegaly in 57% of the cases, umbilical vein repermeabilization in 36.4%, and esophageal varices in 71.1%. About 57.7% (n = 130) of the patients had sarcopenia based on the SMI. The value of psoas area/squared height (cm^2/m^2) was significantly positively associated with body mass index (BMI), liver volume, albumin, alcohol intake, male, and non-alcoholic steatohepatitis (NASH), and negatively associated with age and hepatitis C virus (Figure 2A). Sarcopenia at imaging (defined by SMI < 50 cm^2/m^2 in male and < 39 cm^2/m^2 in female patients) was observed in 130 (57.7%) patients.

Sarcopenic patients were significantly older (67.5 years old *vs* 62.5 years old; P = 0.0338), with a lower BMI (24.3 *vs* 28.7 P < 0.0001) and a higher median serum AFP level (11.5 ng/mL *vs* 7.7 ng/mL; P = 0.0152) compared to non-sarcopenic patients at imaging (Table 1 and Figure 2B). Sarcopenia was also associated with a higher tumor burden (sum of the size of the 2 main tumors) and a lower BMI, ALAT level, and spleen volume, and was less frequent in alcohol-related cirrhosis and in NASH patients (Figure 2B). At the first radiological assessment, 28.7% of the patients with sarcopenia harbored an increase in Child-Pugh Class (A to B/C or B to C) compared to 24.53% of patients without sarcopenia (P = 0.6862, Fisher exact test). Patients' baseline features as well as treatments following TACE or TAE, according to the presence or not of sarcopenia, are detailed in Table 1.

Relationship between sarcopenia and radiological response

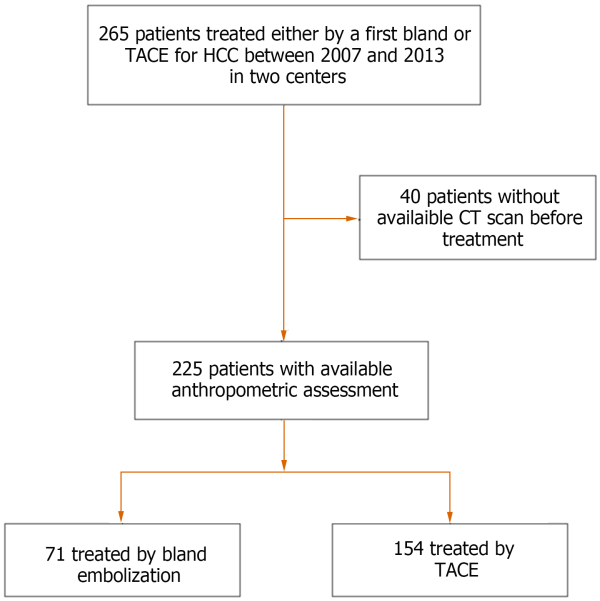
At the first radiological evaluation after TACE or TAE, 23% (n = 52) of patients harbored a complete response, 39% a partial response (n = 88), 23% a stable disease (n = 52), and 15% (n = 33) a progressive disease based on mRECIST criteria. Presence of portal hypertension signs on endoscopy or imaging was not encountered as predictive markers of radiological response. Presence of sarcopenia had a significant impact on progression proportions after TACE (P = 0.0084, Chi square test Figure 3A). Whereas objective tumor response (complete and partial radiological response) was not statistically different in sarcopenic (64%) compared to non-sarcopenic patients (67%, P = 0.66, Fisher exact test), a higher rate of progressive disease was observed in patients with sarcopenia compared to patients without (19% *vs* 8%, P = 0.0236, Fisher exact Test, Figure 3B). In univariate analysis, sarcopenia [odds ratio (OR): 2.59; 95%CI:

Table 1 Description of population features according to presence of sarcopenia or not

	Overall cohort (*n* = 225)	Sarcopenia (*n* = 130)	No sarcopenia (*n* = 95)	*P* value
Clinical and biological features				
Age (years old)[1]	65 (58-75)	67.5 (59.25-76)	62.5 (57-72.5)	0.0338
Gender[2]	200 (88.8%)	120 (92%)	80 (84%)	0.0841
Alcohol[2]	138 (61%)	72 (55%)	66 (69%)	0.04
NASH[2]	66 (29%)	28 (22%)	38 (40%)	0.003
HCV[2]	64 (28%)	42 (32%)	22 (23%)	0.14
HBV[2]	21 (9%)	11 (8%)	10 (11%)	0.65
Cirrhosis[2]	206 (91.5%)	116 (89.2%)	90 (94.7%)	0.1554
Platelets (10^3/mm^3)[1]	123 (83-180)	131 (83.5-198.3)	113 (82-169)	0.1561
Creatinine (μmol/L)	77 (64-89)	77 (64-90)	77 (65-89)	0.93
Total bilirubin (μmol/L)	16 (9.9-22)	15.8 (9-22)	16 (10-22)	0.55
Albumin (g/dL)	36 (32-39)	35 (32-38)	36 (32-40)	0.11
AFP (ng/mL)[1]	10 (4.3-49)	11.5 (5.135-76.5)	7.7 (4-25.5)	0.0152
Child-Pugh A[2]	184 (81.57%)	105 (80.7%)	79 (83.2%)	0.728
MELD	8.7 (7-11)	8.5 (7.6-10)	9.1 (7.3-11)	0.53
BCLC-A[2]	62 (27.5%)	33 (25.3%)	29 (30.5%)	0.1796
BCLC-B[2]	125 (55.5%)	70 (53.8%)	55 (57.89%)	
BCLC-C[2]	38 (16.8%)	27 (20.76%)	11 (11.57%)	
Segmental portal vein thrombosis[2]	34 (15.1%)	24 (18.46%)	10 (10.5%)	0.1314
Type of treatment				
TACE[2]	154 (68.4%)	86 (66.6%)	68 (71.5%)	0.4681
Bland embolization[2]	71 (31.5%)	43 (33.3%)	27 (28.4%)	0178
Number of procedures *per* patient[1]	2 (1-3)	2 (1-2)	2 (1-3)	0.0178
Body mass index[1]	26.4 (23.5-29.18)	24.3 (22.3-26.9)	28.7 (26.4-32.33)	< 0.0001
Oesophageal varices[2]	107 (49.3%)	61 (48.4%)	46 (50.5%)	0.784
Radiological features				
Size of the largest nodule (mm)[1]	37 (24-61)	40 (24-70)	34 (23-53)	0.0665
Multiples nodules[2]	169 (75.1%)	99 (76.1%)	70 (73.7%)	0.7552
Skeletal muscle index (cm^2/m^2)[1]	47.12 (41.75-53.2)	42.85 (38.61-46.79)	54.19 (51.38-58.27)	< 0.0001
Psoas muscle index (cm^2/m^2)[1]	10 (8.575-11.94)	9.205. (8.087-10.97)	11.51 (9.679-14.26)	< 0.0001
Psoas L3 (cm^2)[1]	17 (14.72-37.27)	15.95 (13.95-18.7)	19.8 (16.6-23.8)	< 0.0001
Muscle L3 (cm^2)[1]	137 (119.3-155.4)	125.8 (113.8-138.1)	156.2 (145-176)	< 0.0001
Umbilical vein repermeabilization[2]	82 (36.4%)	51 (39.2%)	31 (32.6%)	0.3292
Oesophageal varices[2]	160 (71.1%)	91 (70%)	69 (72%)	0.7661
Ascites[2]	53 (23.5%)	29 (22.3%)	24 (25.2%)	0.6355
Liver/spleen volume ratio[1]	4.346 (2.885-6.798)	4.562 (2.927-7.205)	3.797 (2.605-6.187)	0.1085
Liver volume (cm^3)[1]	1715 (1430-2071)	1701 (1407-1978)	1800 (1461-2142)	0.0833
Spleen volume (cm^3)[1]	414 (252-606)	382 (230.5-573.3)	480 (308-634)	0.0283
Splenomegaly[2]	129 (57.6%)	71 (55%)	58 (61%)	0.4127
Treatments following TAE/TACE				

Curative-intent			
Liver resection	2 (0.9%)	1 (0.8%)	1 (1.1%)
RFA/Microwaves/Alcoholization	27 (12.0%)	14 (10.8%)	13 (13.7%)
Liver transplantation	46 (20.4%)	19 (14.6%)	27 (28.4%)
Palliative-intent			
SIRT	2 (0.9%)	2 (1.5%)	0
Sorafenib	44 (19.6%)	28 (21.5%)	16 (16.8%)
Other systemic treatments	8 (3.6%)	4 (3.1%)	4 (4.2%)
No additional treatment	82 (36.4%)	50 (38.5%)	32 (33.7%)

[1]Median (25^{th}-75^{th} percentiles).
[2]Numbers (percentages).
AFP: Alpha-fetoprotein; BCLC: Barcelona clinic liver cancer staging system; HCV: Hepatitis C virus; HBV: Hepatitis B virus; NASH: Non-alcoholic steatohepatitis; RFA: Radiofrequency ablation; SIRT: Selective internal radiation therapy; TACE: Trans-arterial chemoembolization.



DOI: 10.3748/wjg.v28.i36.5324 **Copyright** ©The Author(s) 2022.

Figure 1 Flowchart of the study. TACE: Transarterial chemoembolization; CT: Computed tomography; HCC: Hepatocellular carcinoma.

1.16-6.40, P = 0.0274], serum AFP level (OR: 1.00029; 95%CI: 1.00008-1.0006, P = 0.0226), and BCLC-C stage (OR: 2.22; 95%CI: 1.25-4.05; P = 0.00758) were related to progressive disease at imaging. In multivariate analysis, only BCLC-C stage (OR: 1.98; 95%CI: 1.038-3.88, P = 0.0416) remained independently associated with a higher rate of progressive disease.

Relationship between sarcopenia before TACE and survival

The median progression-free survival was 9.4 mo. Patients with sarcopenia had a lower median PFS compared to patients without (8.3 mo *vs* 13.2 mo, P = 0.0035, log rank test, Figure 4A). In univariate analysis, sarcopenia, tumor portal vein thrombosis, size of the largest nodule, serum AFP level, and platelet level were significantly associated with a lower PFS (Table 2). In multivariate analysis, sarcopenia [hazard ratio (HR): 1.62; 95%CI: 1.15-2.28], tumor portal vein thrombosis (HR: 1.77; 95%CI: 1.11-2.83), size of the largest nodule (HR: 1.008; 95%CI: 1.002-1.013), and platelet level (HR: 1.002; 95%CI: 1.002; 95%CI: 1.0001-1.005) remained independently associated with a lower PFS (Table 2).

The median OS was 24.3 mo. OS was shorter in patients with sarcopenia compared to patients without (19.4 mo *vs* 35.5 mo, P = 0.0149, log rank test, Figure 4B). Sarcopenia, ascites at imaging, size of the largest nodule, serum AFP level, Child-Pugh score, and BMI were associated with OS at univariate analysis (Table 3). In multivariate analysis, sarcopenia (HR: 1.68; 95%CI: 1.04-2.72), AFP level (HR: 1.0001; 95%CI: 1.00001-1.002), and size of the largest nodule (HR: 1.007, 95%CI: 1.0015-1.013) were independently associated with a higher risk of death (Table 3).

Table 2 Univariate and multivariate Cox analyses of baseline variables associated with progression-free survival

Variable	Univariate analysis			Multivariate analysis		
	HR	95%CI	*P* value	HR	95%CI	*P* value
Sarcopenia (yes *vs* no, imaging)	1.58	1.17-2.15	0.003	1.62	1.15-2.28	0.006
Skeletal muscle index (imaging)[1]	0.91	0.98-1.01	0.306			
Psoas muscle index (imaging)[1]	0.97	0.92-1.02	0.18			
Paraombilical vein (imaging)	1.21	0.88-1.65	0.24			
Esophageal varices (imaging)	0.94	0.68-1.30	0.72			
Ascites (imaging)	1.38	0.97-1.97	0.07			
Liver/spleen ratio (imaging)[1]	1.02	0.98-1.07	0.21			
Liver volume (imaging)[1]	1.00	1.00-1.00	0.062			
Spleen volume (imaging)[1]	0.99	0.99-1.00	0.54			
Splenomegaly (imaging)	1.18	0.87-1.60	0.28			
BCLC stage	1.24	0.98-1.58	0.068			
Multiple nodules	1.03	0.73-1.45	0.88			
Portal vein thrombosis	1.58	1.05-2.39	0.03	1.77	1.11-2.83	0.02
Size of the largest nodule[1]	1.01	1.00-1.01	0.0003	1.008	1.002-1.013	0.006
Esophageal varices at endoscopy	0.98	0.72-1.33	0.88			
Serum AFP[1]	1.00	1.00-1.00	0.0007	1.0001	1.00001-1.00002	0.07
Platelets[1]	1.00	1.00-1.01	0.002	1.002	1.0001-1.005	0.04
Child Pugh B7	1.02	0.67-1.56	0.93			
Creatinin[1]	1.00	0.99-1.01	0.097			
Prothrombin time[1]	1.00	0.99-1.01	0.68			
Total bilirubin[1]	0.99	0.99-1.01	0.99			
Albumin[1]	0.99	0.97-1.03	0.84			
Clinical ascites	1.00	0.63-1.59	0.99			
Cirrhosis	0.87	0.53-1.45	0.60			
NASH	1.21	0.60-1.14	0.24			
HCV	0.85	0.61-1.18	0.32			
HBV	0.73	0.41-1.28	0.27			
Alcohol intake	1.013	0.75-1.37	0.93			
Body mass index[1]	0.98	0.95-1.01	0.21			
Gender (Male)	1.37	0.86-2.19	0.19			
Age (years old)[1]	1.00	0.99-1.02	0.68			

[1]Parameters expressed as continuous variables.
Sarcopenia was analyzed as a categoric factor (yes *vs* no). AFP: Alpha-fetoprotein; BCLC: Barcelona clinic liver cancer; HCV: Hepatitis C virus; HBV: Hepatitis B virus; NASH: Non alcoholic steatohepatitis.

Evolution of sarcopenia after TACE and its impact on OS

Post-TACE SMI was assessed by CT scan at the first radiological assessment in 218 patients in order to assess the evolution of sarcopenia after treatment. Among the patients without sarcopenia at baseline, 71 were still non-sarcopenic, and 22 became sarcopenic. Among the 22 patients who became sarcopenic, 19 had a progressive disease at the first radiological assessment.

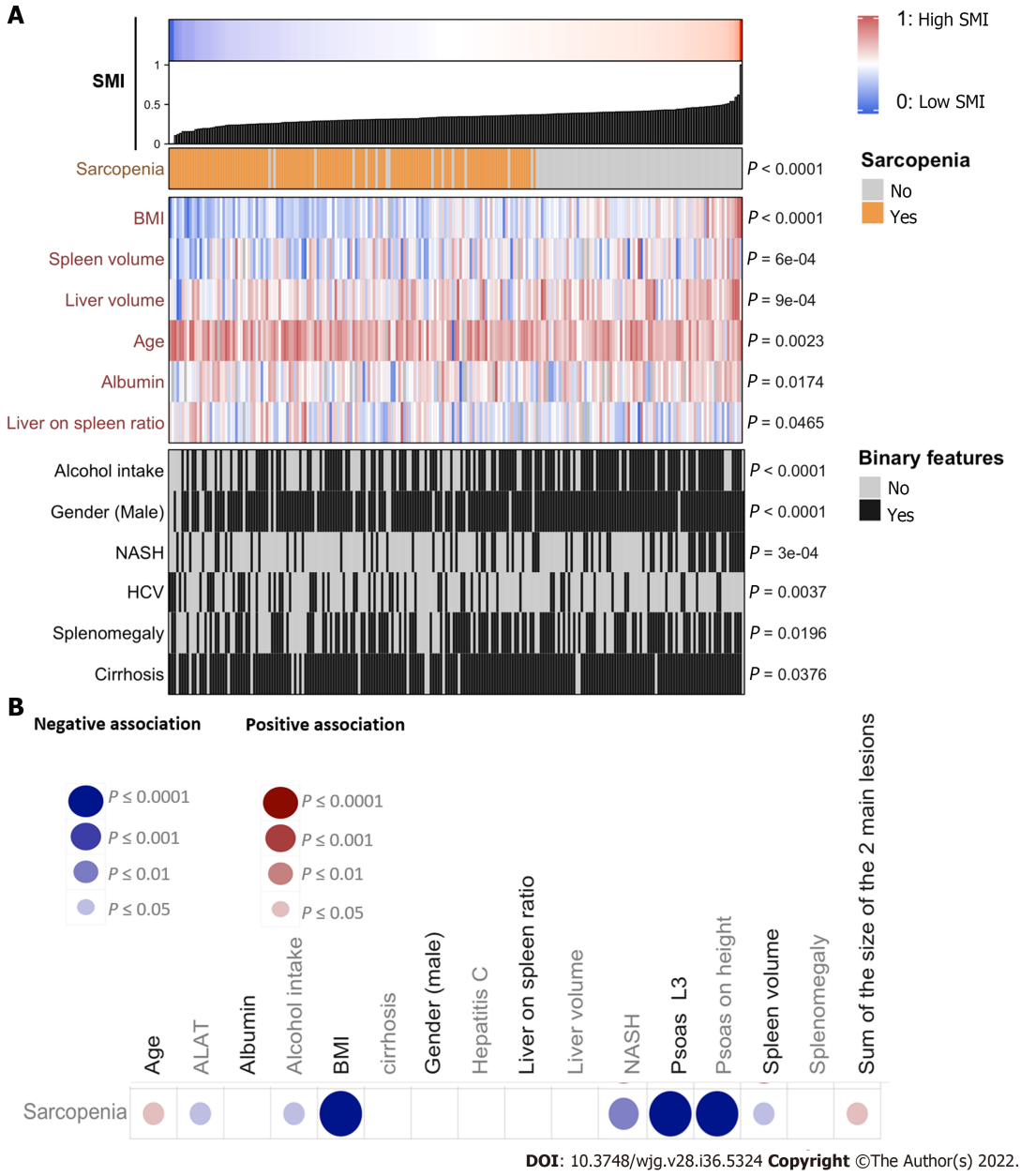
Patients with post-TACE sarcopenia presented a shorter median OS (n = 147, 18.15 mo) compared with non-sarcopenic patients (n = 71, 35.7 mo, P = 0.0019) (Figure 4C).

Table 3 Univariate and multivariate Cox analyses of baseline variables associated with overall survival

Variable	Univariate analysis			Multivariate analysis		
	HR	95%CI	*P* value	HR	95%CI	*P* value
Sarcopenia (yes *vs* no, imaging)	1.57	1.09-2.27	0.016	1.68	1.04- 2.72	0.03
Skeletal muscle index (imaging)[1]	0.99	0.97-1.01	0.19			
Psoas muscle index (imaging)[1]	0.95	0.89-1.01	0.14			
Paraombilical vein (imaging)	1.16	0.80-1.66	0.43			
Esophageal varices (imaging)	1.09	0.75-1.61	0.63			
Ascites (imaging)	1.74	1.16-2.60	0.007	1.59	0.97-2.60	0.07
Liver/spleen ratio (imaging)[1]	1.03	0.98-1.08	0.13			
Liver volume (imaging)[1]	1.00	0.99-1.00	0.86			
Spleen volume (imaging)[1]	0.99	0.99-1.00	0.19			
Splenomegaly (imaging)	0.95	0.66-1.35	0.77			
BCLC stage	1.28	0.97-1.68	0.08			
Multiple nodule	0.83	0.56-1.22	0.34			
Portal vein thrombosis	1.52	0.98-2.38	0.06			
Size of the largest nodule[1]	1.01	1.00-1.01	0.003	1.007	1.0015-1.013	0.014
Esophageal varices (endoscopy)	1.17	0.82-1.69	0.38			
AFP[1]	1.00	1.00-1.00	0.00018	1.0001	1.00001-1.0002	0.006
Platelet[1]	1.00	0.99-1.00	0.170			
Child-Pugh B7	2.04	1.21-3.45	0.007	1.59	0.86-2.96	0.14
Creatinin[1]	1.00	0.99-1.00	0.18			
Prothrombin time[1]	1.01	0.98-1.01	0.45			
Total bilirubin[1]	1.02	1.00-1.03	0.035			
Albumin[1]	0.94	0.91-0.98	0.003			
Clinical ascites	1.46	0.88-2.42	0.143			
Cirrhosis	1.27	0.71-2.26	0.42			
NASH	0.70	0.47- 1.04	0.075			
HCV	1.32	0.89-1.95	0.17			
HBV	0.71	0.33-1.54	0.39			
Alcohol intake	1.05	0.67-1.37	0.80			
Age (years old)[1]	1.00	0.99-1.02	0.79			
BMI[1]	0.96	0.93-0.99	0.026	0.99	0.95-1.040	0.75
Gender (Male)	1.08	0.63-1.85	0.79			

[1]Parameters expressed as continuous variables.
Sarcopenia was analyzed as a categoric factor (yes *vs* no). AFP: Alpha-fetoprotein; BCLC: Barcelona clinic liver cancer; HCV: Hepatitis C virus; HBV: Hepatitis B virus; NASH: Non alcoholic steatohepatitis; BMI: Body mass index.

In non-sarcopenic patients at baseline, emergence of a post-TACE sarcopenia was associated with a significant shorter median OS of 17 mo when compared with already sarcopenic patients before TACE (19.3 mo) and patients who stayed non-sarcopenic along TACE procedure (36.43 mo, P = 0.0004) (Figure 4D).

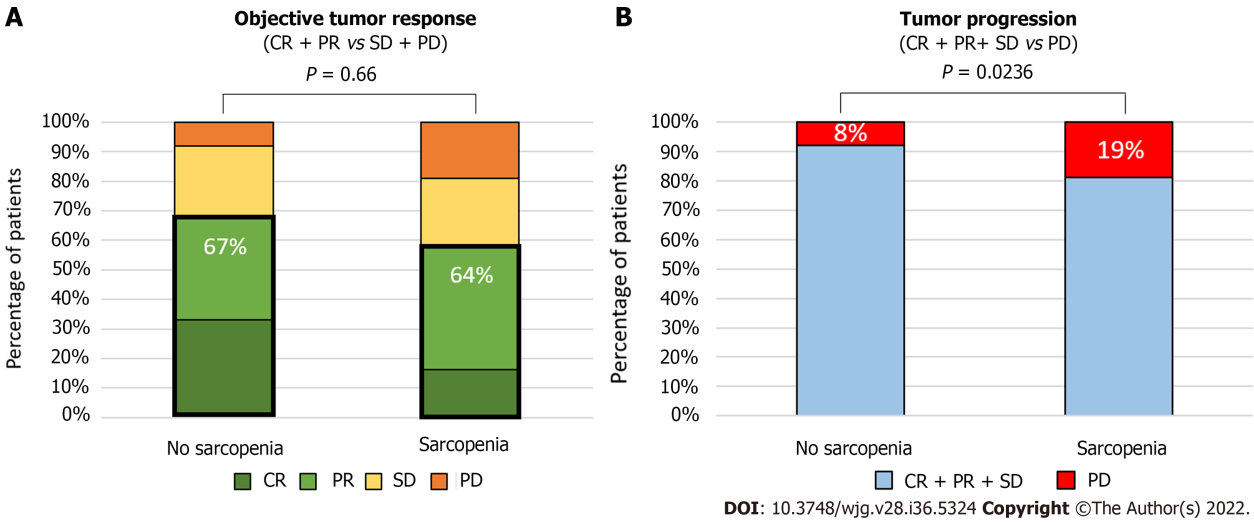


DOI: 10.3748/wjg.v28.i36.5324 **Copyright** ©The Author(s) 2022.

Figure 2 Correlation of biological and clinical features with sarcopenia. A: Association of clinical, biological, and radiological features with skeletal muscle index expressed as a continuous variable; B: Association of clinical, biological, and radiological features with the presence or not of sarcopenia. Comparison of a continuous variable in two or more than two groups was performed using Wilcoxon signed-rank test or Kruskal-Wallis test, respectively. Qualitative data were compared using the Fisher's exact test. Correlation analysis between continuous variables was performed using Spearman's rank-order correlation. All tests were two-tailed and a *P*-value < 0.05 was considered significant. BMI: Body mass index; HCV: Hepatitis C virus; NASH: Non-alcoholic steatohepatitis; SMI: Skeletal muscle index.

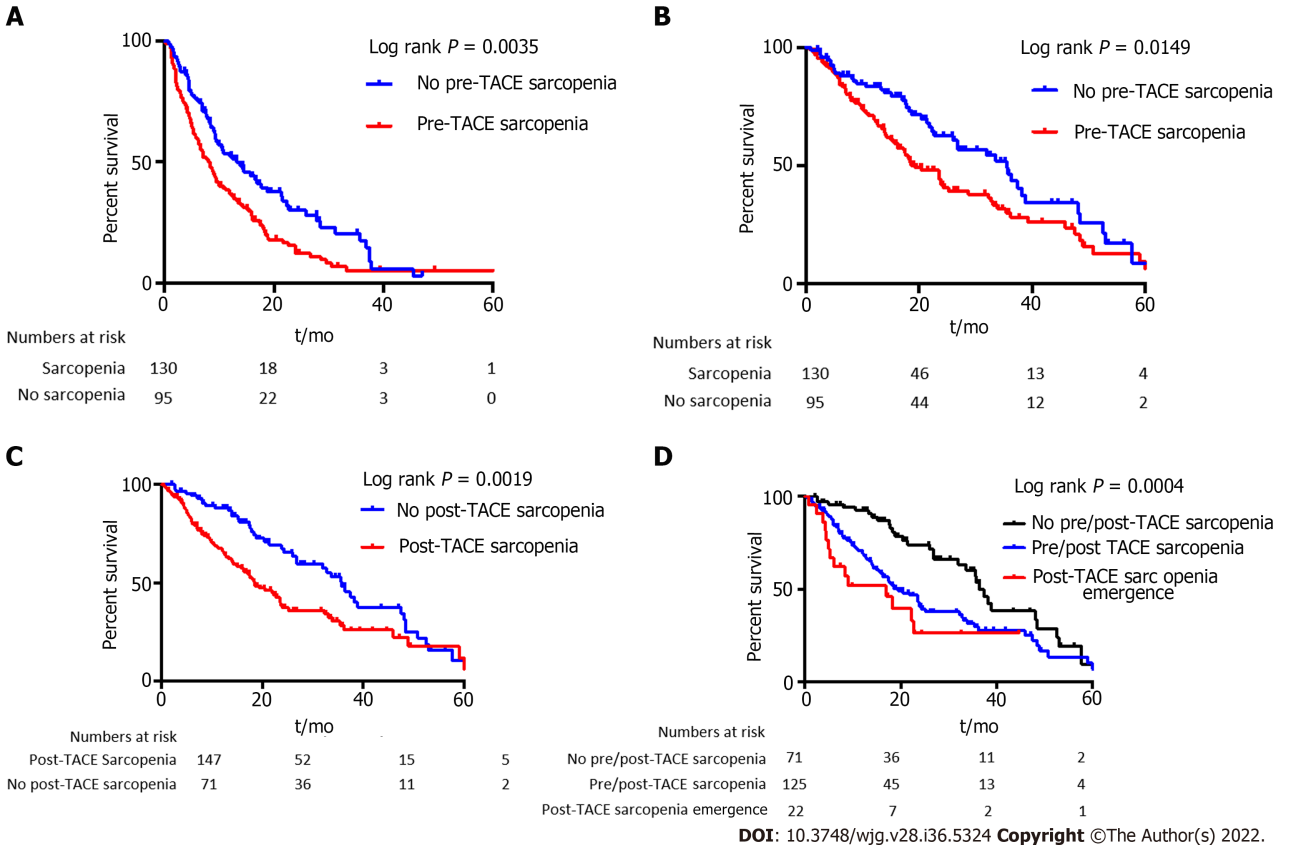
DISCUSSION

This study is the largest multicentric cohort study exploring the impact of sarcopenia on tumor response and survival outcomes in patients with HCC treated by TACE or TAE. Sarcopenia represents a major challenge in chronic diseases and especially in the treatment of cancers in which the general status is classically altered, and aggressive treatments with poor tolerance profiles are frequent. Sarcopenia in cirrhosis has already been described as impacting survival, confirming the need of a global approach with a close nutritional support of these patients. Sarcopenia measures were assessed on the open-access software Image J®, which has been proved as equivalently efficient as other commercial programs, meaning that radiological assessment of sarcopenia is accessible to every center[18]. The use of SMI was preferred to methods only based on the measurement of PMI or the transverse psoas muscle thickness. Even though the two latter are simple to assess and showed interesting results in term of survival in HCC patients treated by TACE in previous studies, SMI seems to offer a more robust and complete measurement of the muscle mass in cirrhotic patients. Besides, PMI may identify fewer patients at risk of an increased mortality and presents a higher inter-observer variability. To finish, SMI is easy to use



DOI: 10.3748/wjg.v28.i36.5324 **Copyright** ©The Author(s) 2022.

Figure 3 Radiological response according to presence of sarcopenia. A: Complete response *vs* partial response *vs* stable disease *vs* progressive disease assessed using the mRECIST criteria after the first session of treatment; B: Complete and partial response and stable disease *vs* progressive disease assessed using the mRECIST criteria after the first session of treatment. Statistical analysis was performed using the chi square test. CR: Complete response; PR: Partial response; SD: Stable disease; PD: Progressive disease; TACE: Trans-arterial chemoembolization.



DOI: 10.3748/wjg.v28.i36.5324 **Copyright** ©The Author(s) 2022.

Figure 4 Survival according to presence of sarcopenia before and after trans-arterial chemoembolization. A and B: Progression free survival (A) and overall survival (OS) (B) according to the presence or not of sarcopenia before trans-arterial chemoembolization (TACE); C: OS according to presence or not of sarcopenia after TACE; D: OS according to the presence or not of sarcopenia before TACE, and appearance of sarcopenia after TACE designated as post-TACE sarcopenia. Results were computed using the Kaplan-Meier method and compared by the log rank test. The patients at risk are represented under the x-axis.

and recommended by the North American Expert Opinion Statement on Sarcopenia in Liver Transplantation[17,19,20]. In this study, measures were performed by only one radiologist *per* center, which limits bias induced by potential interobserver variability. This also constitutes a limit as interobserver variability should be studied to improve result exportability and better evaluate their reproducibility.

In this study, a high prevalence of sarcopenia (57%) in patients with HCC treated by transarterial treatment was observed despite the predominance of Child-Pugh A patients and intermediate stage tumors (BCLC-B). This is consistent with a recent HCC cohort study exploring the impact of sarcopenia on survival in patients treated by hepatectomy where 54% of patients were sarcopenic, as well as published data in liver transplantation[17]. Even if patients with sarcopenia have a lower BMI than patients without, most of patients with sarcopenia harbored a normal BMI (median value of 24). Moreover, with the increase of overweight and obesity which represents 15%-20% of the worldwide population[21], BMI is even less sensitive to detect malnutrition in patients with chronic diseases and especially liver diseases. These elements suggest that sarcopenia measured by performant radiological methods reflect more precisely the nutritional state and the protein catabolism of these patients. Nonetheless, other markers that could impact the outcomes after trans-arterial (chemo)embolization such as patient's daily activities and diet are not collected in this study due to its retrospective character. As well, this study lacked of other frailty parameters such as grip strength or walking speed. It constitutes another limit that cannot be addressed due to the retrospective character of the study.

One of the main strengths of this study is the radiological reviewing of radiological response using mRECIST criteria. This analysis revealed that sarcopenia was associated with a higher risk of progressive disease after trans-arterial treatment but without any difference on objective tumor response. Nevertheless, in multivariate analysis, only BCLC-C (segmental portal thrombosis) was independently associated with progressive disease. Sarcopenia was also associated with a shorter PFS together with tumor size in multivariate analysis. These data suggest that a subgroup of patients with advanced tumor stage and sarcopenia have a more aggressive disease which is more prone to resist to trans-arterial treatments. Indeed, sarcopenia may reflect the consequences of an intense hypercatabolism due to a particularly aggressive disease. In these patients, transarterial treatment may be deleterious in addition to be less effective as it could lead to liver failure and decrease the possibility of using systemic treatments after progression. Besides, the increased rate of radiological response obtained with the recent combination atezolizumab-bevacizumab forces us to better select the optimal treatment for patients between TACE and systemic treatments[22]. However, as sarcopenia has also been associated with poorer survival outcomes in patients under systemic therapies[10], it remains to be studied if sarcopenic patients with a high tumor burden benefit more from systemic treatments than trans-arterial procedures. In any case, sarcopenia needs to be detected as early as possible to initiate a medical intervention using nutritional support and physical activity to reverse sarcopenia and potentially improve survival. Indeed, muscle restoration before starting these treatments showed interesting results in terms of survival[10,23], and this type of intervention should be tested in a randomized controlled trial as up to 60% of patients treated by TACE harbored sarcopenia.

Sarcopenia was also associated with a shorter OS independently of tumor burden, suggesting that undernutrition and loss of muscle are key prognostic factors in patients with HCC treated by TACE or TAE. As sarcopenia is easily assessable using a CT scan in clinical practice, it could be useful to stratify patients in clinical trials. This study showed that sarcopenia assessed at the first radiological evaluation after TACE was also associated with a shorter OS, underlying the robustness of this association. Moreover, a subset of patients rapidly developed sarcopenia at the first radiological assessment which was particularly associated with a poor OS. Almost all these patients presented a progressive disease at the first evaluation, suggesting that they harbored an aggressive tumoral disease potentially responsible for the fast development of sarcopenia.

CONCLUSION

In conclusion, sarcopenia is associated with a higher rate of tumor progression and shorter survival in patients with HCC treated by TACE or TAE. Moreover, sarcopenia is an easy-to-assess radiological biomarker of poor prognosis that should be measured in order to better estimate prognosis and test a targeted intervention mixing nutritional support and physical activity.

ARTICLE HIGHLIGHTS

Research background

At the diagnosis of hepatocellular carcinoma (HCC), more than 90% of HCC patients present a cirrhosis, a clinical condition often associated to malnutrition. Sarcopenia has been associated with a lower tumor response or poorer survival of patients undergoing various treatments such as surgery or systemic therapies. Transarterial chemoembolization is the treatment of choice for intermediate HCC and is largely used worldwide, but the impact of sarcopenia on its results was poorly studied.

Research motivation

Finding easy ways to detect sarcopenia within daily practice should benefit to patients by better charac-

terizing their prognosis and taking their nutritional status into account in therapeutic decisions.

Research objectives

This study aimed to evaluate the prognostic value of sarcopenia in patients with HCC treated by transarterial (chemo)-embolization based on baseline computed tomography (CT) findings and study its impact on objective tumor response and survival outcomes.

Research methods

Sarcopenia is easy to assess on CT by measuring the skeletal muscle index. A skeletal muscle index (SMI) < 50 cm^2/m^2 in male and < 39 cm^2/m^2 in female patients corresponding to sarcopenia was observed in 57.7% of the patients.

Research results

Based on SMI analysis measured on baseline imaging, sarcopenia was observed in 57.7% of the patients. After full review of radiological response using mRECIST criteria, sarcopenia was associated with a higher rate of progressive disease. It was also associated with a decrease overall survival even after adjustment with usual risk factors of death.

Research conclusions

Sarcopenia is an easy-to-assess radiological biomarker of poor prognosis that should be measured in order to better assess prognosis of HCC patients.

Research perspectives

Sarcopenia should be systematically detected at baseline, and induce a targeted intervention mixing nutritional support and physical activity. Further studies are needed to assess the benefit of these strategies in HCC patients.

FOOTNOTES

Author contributions: Roth G, Teyssier Y, Decaens T, and Nault JC equivalently contributed to this work; Roth G, Decaens T, and Nault JC contributed to the conceptualization; Roth G and Nault JC contributed to the methodology; Roth G, Teyssier Y, Benhamou M, Abousalihac M, Sengel C, Seror O, Ghelfi J, Ganne-Carrié N, Gigante E, Blaise L, Sutter O, Decaens T, and Nault JC contributed to the investigation; Roth G, Benhamou M, Teyssier Y, Abousalihac M, and Nault JC contributed to the formal analysis; Roth G, Nault JC, Seigneurin A, and Caruso S contributed to the data curation; Nault JC, Seigneurin A, and Caruso S contributed to the statistical analysis; Roth G, Teyssier Y, Benhamou M, Caruso S, Seigneurin A, Abousalihac M, Sengel C, Seror O, Ghelfi J, Ganne-Carrié N, Gigante E, Blaise L, Sutter O, Decaens T, and Nault JC contributed to the validation; Decaens T and Nault JC contributed to the resources; Roth G and Nault JC wrote the original draft; Roth G, Teyssier Y, Benhamou M, Seigneurin A, Abousalihac M, Sengel C, Seror O, Ghelfi J, Ganne-Carrié N, Gigante E, Blaise L, Sutter O, Decaens T, and Nault JC reviewed and edited the manuscript; Roth G, Decaens T, and Nault JC contributed to the supervision; all authors have read and approved the manuscript.

Institutional review board statement: The study was conducted according to the guidelines of the Declaration of Helsinki. Study ethics was approved by the independent French ethic committee CERIM (Comité d'éthique de la recherche en imagerie médicale) (approval date May 25 2020; No. CRM-2004-084).

Informed consent statement: Patients gave their written consent before TACE procedures as in routine care practice. No specific consent statement was required regarding the retrospective analysis of data as they were anonymously used.

Conflict-of-interest statement: All the authors report no relevant conflicts of interest for this article.

Data sharing statement: No additional data are available.

STROBE statement: The authors have read the STROBE Statement—checklist of items, and the manuscript was prepared and revised according to the STROBE Statement—checklist of items.

Open-Access: This article is an open-access article that was selected by an in-house editor and fully peer-reviewed by external reviewers. It is distributed in accordance with the Creative Commons Attribution NonCommercial (CC BY-NC 4.0) license, which permits others to distribute, remix, adapt, build upon this work non-commercially, and license their derivative works on different terms, provided the original work is properly cited and the use is non-commercial. See: https://creativecommons.org/Licenses/by-nc/4.0/

Country/Territory of origin: France

ORCID number: Gael Roth 0000-0001-5822-4320; Yann Teyssier 0000-0002-9785-8729; Maxime Benhamou 0000-0002-8590-5161; Mélodie Abousalihac 0000-0002-0661-1684; Stefano Caruso 0000-0002-6319-3642; Christian Sengel 0000-0001-9004-256X; Olivier Seror 0000-0001-6680-8991; Julien Ghelfi 0000-0002-9039-6488; Arnaud Seigneurin 0000-0002-2168-1672; Nathalie Ganne-Carrie 0000-0002-7351-5027; Elia Gigante 0000-0002-5455-2308; Lorraine Blaise 0000-0001-5344-1625; Olivier Sutter 0000-0002-2802-9652; Thomas Decaens 0000-0003-0928-0048; Jean-Charles Nault 0000-0002-4875-9353.

S-Editor: Fan JR
L-Editor: Wang TQ
P-Editor: Cai YX

REFERENCES

1 **Bray F**, Ferlay J, Soerjomataram I, Siegel RL, Torre LA, Jemal A. Global cancer statistics 2018: GLOBOCAN estimates of incidence and mortality worldwide for 36 cancers in 185 countries. *CA Cancer J Clin* 2018; **68**: 394-424 [PMID: 30207593 DOI: 10.3322/caac.21492]
2 **Reig M**, Forner A, Rimola J, Ferrer-Fàbrega J, Burrel M, Garcia-Criado Á, Kelley RK, Galle PR, Mazzaferro V, Salem R, Sangro B, Singal AG, Vogel A, Fuster J, Ayuso C, Bruix J. BCLC strategy for prognosis prediction and treatment recommendation: The 2022 update. *J Hepatol* 2022; **76**: 681-693 [PMID: 34801630 DOI: 10.1016/j.jhep.2021.11.018]
3 **Llovet JM**, Bruix J. Systematic review of randomized trials for unresectable hepatocellular carcinoma: Chemoembolization improves survival. *Hepatology* 2003; **37**: 429-442 [PMID: 12540794 DOI: 10.1053/jhep.2003.50047]
4 **Sieghart W**, Hucke F, Peck-Radosavljevic M. Transarterial chemoembolization: modalities, indication, and patient selection. *J Hepatol* 2015; **62**: 1187-1195 [PMID: 25681552 DOI: 10.1016/j.jhep.2015.02.010]
5 **Blanc JF**, Debaillon-Vesque A, Roth G, Barbare JC, Baumann AS, Boige V, Boudjema K, Bouattour M, Crehange G, Dauvois B, Decaens T, Dewaele F, Farges O, Guiu B, Hollebecque A, Merle P, Selves J, Aparicio T, Ruiz I, Bouché O; Thésaurus National de Cancérologie Digestive (TNCD); Société Nationale Française de Gastroentérologie (SNFGE); Fédération Francophone de Cancérologie Digestive (FFCD); Groupe Coopérateur multidisciplinaire en Oncologie (GERCOR); Fédération Nationale des Centres de Lutte Contre le Cancer (UNICANCER); Société Française de Chirurgie Digestive (SFCD); Société Française d'Endoscopie Digestive (SFED); Société Française de Radiothérapie Oncologique (SFRO); Association Française pour l'Etude du Foie (AFEF). Hepatocellular carcinoma: French Intergroup Clinical Practice Guidelines for diagnosis, treatment and follow-up (SNFGE, FFCD, GERCOR, UNICANCER, SFCD, SFED, SFRO, AFEF, SIAD, SFR/FRI). *Clin Res Hepatol Gastroenterol* 2021; **45**: 101590 [PMID: 33780876 DOI: 10.1016/j.clinre.2020.101590]
6 **Lencioni R**, de Baere T, Soulen MC, Rilling WS, Geschwind JF. Lipiodol transarterial chemoembolization for hepatocellular carcinoma: A systematic review of efficacy and safety data. *Hepatology* 2016; **64**: 106-116 [PMID: 26765068 DOI: 10.1002/hep.28453]
7 **European Association for the Study of the Liver**. EASL Clinical Practice Guidelines: Management of hepatocellular carcinoma. *J Hepatol* 2018; **69**: 182-236 [PMID: 29628281 DOI: 10.1016/j.jhep.2018.03.019]
8 **Fielding RA**, Vellas B, Evans WJ, Bhasin S, Morley JE, Newman AB, Abellan van Kan G, Andrieu S, Bauer J, Breuille D, Cederholm T, Chandler J, De Meynard C, Donini L, Harris T, Kannt A, Keime Guibert F, Onder G, Papanicolaou D, Rolland Y, Rooks D, Sieber C, Souhami E, Verlaan S, Zamboni M. Sarcopenia: an undiagnosed condition in older adults. Current consensus definition: prevalence, etiology, and consequences. International working group on sarcopenia. *J Am Med Dir Assoc* 2011; **12**: 249-256 [PMID: 21527165 DOI: 10.1016/j.jamda.2011.01.003]
9 **Voron T**, Tselikas L, Pietrasz D, Pigneur F, Laurent A, Compagnon P, Salloum C, Luciani A, Azoulay D. Sarcopenia Impacts on Short- and Long-term Results of Hepatectomy for Hepatocellular Carcinoma. *Ann Surg* 2015; **261**: 1173-1183 [PMID: 24950264 DOI: 10.1097/SLA.0000000000000743]
10 **Nishikawa H**, Nishijima N, Enomoto H, Sakamoto A, Nasu A, Komekado H, Nishimura T, Kita R, Kimura T, Iijima H, Nishiguchi S, Osaki Y. Prognostic significance of sarcopenia in patients with hepatocellular carcinoma undergoing sorafenib therapy. *Oncol Lett* 2017; **14**: 1637-1647 [PMID: 28789390 DOI: 10.3892/ol.2017.6287]
11 **Fujiwara N**, Nakagawa H, Kudo Y, Tateishi R, Taguri M, Watadani T, Nakagomi R, Kondo M, Nakatsuka T, Minami T, Sato M, Uchino K, Enooku K, Kondo Y, Asaoka Y, Tanaka Y, Ohtomo K, Shiina S, Koike K. Sarcopenia, intramuscular fat deposition, and visceral adiposity independently predict the outcomes of hepatocellular carcinoma. *J Hepatol* 2015; **63**: 131-140 [PMID: 25724366 DOI: 10.1016/j.jhep.2015.02.031]
12 **Marasco G**, Serenari M, Renzulli M, Alemanni LV, Rossini B, Pettinari I, Dajti E, Ravaioli F, Golfieri R, Cescon M, Festi D, Colecchia A. Clinical impact of sarcopenia assessment in patients with hepatocellular carcinoma undergoing treatments. *J Gastroenterol* 2020; **55**: 927-943 [PMID: 32748172 DOI: 10.1007/s00535-020-01711-w]
13 **Loosen SH**, Schulze-Hagen M, Bruners P, Tacke F, Trautwein C, Kuhl C, Luedde T, Roderburg C. Sarcopenia Is a Negative Prognostic Factor in Patients Undergoing Transarterial Chemoembolization (TACE) for Hepatic Malignancies. *Cancers (Basel)* 2019; **11** [PMID: 31597337 DOI: 10.3390/cancers11101503]
14 **Roth GS**, Benhamou M, Teyssier Y, Seigneurin A, Abousalihac M, Sengel C, Seror O, Ghelfi J, Ganne-Carrié N, Blaise L, Sutter O, Decaens T, Nault JC. Comparison of Trans-Arterial Chemoembolization and Bland Embolization for the Treatment of Hepatocellular Carcinoma: A Propensity Score Analysis. *Cancers (Basel)* 2021; **13** [PMID: 33672012 DOI: 10.3390/cancers13040812]
15 **Roth GS**, Teyssier Y, Abousalihac M, Seigneurin A, Ghelfi J, Sengel C, Decaens T. Idarubicin *vs* doxorubicin in transarterial chemoembolization of intermediate stage hepatocellular carcinoma. *World J Gastroenterol* 2020; **26**: 324-334 [PMID: 31988592 DOI: 10.3748/wjg.v26.i3.324]
16 **Prado CM**, Lieffers JR, McCargar LJ, Reiman T, Sawyer MB, Martin L, Baracos VE. Prevalence and clinical implications

of sarcopenic obesity in patients with solid tumours of the respiratory and gastrointestinal tracts: a population-based study. *Lancet Oncol* 2008; **9**: 629-635 [PMID: 18539529 DOI: 10.1016/S1470-2045(08)70153-0]

17 **Carey EJ**, Lai JC, Sonnenday C, Tapper EB, Tandon P, Duarte-Rojo A, Dunn MA, Tsien C, Kallwitz ER, Ng V, Dasarathy S, Kappus M, Bashir MR, Montano-Loza AJ. A North American Expert Opinion Statement on Sarcopenia in Liver Transplantation. *Hepatology* 2019; **70**: 1816-1829 [PMID: 31220351 DOI: 10.1002/hep.30828]

18 **Long DE**, Villasante Tezanos AG, Wise JN, Kern PA, Bamman MM, Peterson CA, Dennis RA. A guide for using NIH Image J for single slice cross-sectional area and composition analysis of the thigh from computed tomography. *PLoS One* 2019; **14**: e0211629 [PMID: 30730923 DOI: 10.1371/journal.pone.0211629]

19 **Lanza E**, Masetti C, Messana G, Muglia R, Pugliese N, Ceriani R, Lleo de Nalda A, Rimassa L, Torzilli G, Poretti D, D'Antuono F, Politi LS, Pedicini V, Aghemo A; Humanitas HCC Multidisciplinary Group. Sarcopenia as a predictor of survival in patients undergoing bland transarterial embolization for unresectable hepatocellular carcinoma. *PLoS One* 2020; **15**: e0232371 [PMID: 32555707 DOI: 10.1371/journal.pone.0232371]

20 **Beer L**, Bastati N, Ba-Ssalamah A, Pötter-Lang S, Lampichler K, Bican Y, Lauber D, Hodge J, Binter T, Pomej K, Simbrunner B, Semmler G, Trauner M, Mandorfer M, Reiberger T. MRI-defined sarcopenia predicts mortality in patients with chronic liver disease. *Liver Int* 2020; **40**: 2797-2807 [PMID: 32816394 DOI: 10.1111/liv.14648]

21 **Tao W**, Lagergren J. Clinical management of obese patients with cancer. *Nat Rev Clin Oncol* 2013; **10**: 519-533 [PMID: 23856746 DOI: 10.1038/nrclinonc.2013.120]

22 **Finn RS**, Qin S, Ikeda M, Galle PR, Ducreux M, Kim TY, Kudo M, Breder V, Merle P, Kaseb AO, Li D, Verret W, Xu DZ, Hernandez S, Liu J, Huang C, Mulla S, Wang Y, Lim HY, Zhu AX, Cheng AL; IMbrave150 Investigators. Atezolizumab plus Bevacizumab in Unresectable Hepatocellular Carcinoma. *N Engl J Med* 2020; **382**: 1894-1905 [PMID: 32402160 DOI: 10.1056/NEJMoa1915745]

23 **Cheng TY**, Lee PC, Chen YT, Chao Y, Hou MC, Huang YH. Pre-sarcopenia determines post-progression outcomes in advanced hepatocellular carcinoma after sorafenib failure. *Sci Rep* 2020; **10**: 18375 [PMID: 33110117 DOI: 10.1038/s41598-020-75198-z]

World Journal of Gastroenterology

Submit a Manuscript: https://www.f6publishing.com

World J Gastroenterol 2022 September 28; 28(36): 5338-5350

DOI: 10.3748/wjg.v28.i36.5338

ISSN 1007-9327 (print) ISSN 2219-2840 (online)

ORIGINAL ARTICLE

Retrospective Cohort Study

Machine learning-based gray-level co-occurrence matrix signature for predicting lymph node metastasis in undifferentiated-type early gastric cancer

Xin Wei, Xue-Jiao Yan, Yu-Yan Guo, Jie Zhang, Guo-Rong Wang, Arsalan Fayyaz, Jiao Yu

Specialty type: Gastroenterology and hepatology

Provenance and peer review: Unsolicited article; Externally peer reviewed.

Peer-review model: Single blind

Peer-review report's scientific quality classification

Grade A (Excellent): A, A
Grade B (Very good): B
Grade C (Good): 0
Grade D (Fair): 0
Grade E (Poor): 0

P-Reviewer: He D, China; Pantelis AG, Greece; Toyoshima O, Japan

Received: July 20, 2022
Peer-review started: July 20, 2022
First decision: August 6, 2022
Revised: August 14, 2022
Accepted: September 6, 2022
Article in press: September 6, 2022
Published online: September 28, 2022

Xin Wei, Department of Oncology, Shaanxi Provincial People's Hospital, Xi'an 710068, Shaanxi Province, China

Xue-Jiao Yan, Department of Magnetic Resonance, Shaanxi Provincial People's Hospital, Xi'an 710068, Shaanxi Province, China

Yu-Yan Guo, Department of Radiotherapy, The Second Affiliated Hospital of Xi'an Jiaotong University, Xi'an 710004, Shaanxi Province, China

Jie Zhang, Department of Gastrointestinal Surgery, Shaanxi Provincial Tumour Hospital, Xi'an 710068, Shaanxi Province, China

Guo-Rong Wang, Department of General Surgery, Shaanxi Provincial People's Hospital, Xi'an 710068, Shaanxi Province, China

Arsalan Fayyaz, School of Management, Northwestern Polytechnical University, Xi'an 710072, Shaanxi Province, China

Jiao Yu, Department of Radiotherapy, Shaanxi Provincial People's Hospital, Xi'an 710068, Shaanxi Province, China

Corresponding author: Jiao Yu, MD, Radiologist, Department of Radiotherapy, Shaanxi Provincial People's Hospital, No. 256 Youyi West Road, Beilin District, Xi'an 710068, Shaanxi Province, China. shawn170215@163.com

Abstract

BACKGROUND

The most important consideration in determining treatment strategies for undifferentiated early gastric cancer (UEGC) is the risk of lymph node metastasis (LNM). Therefore, identifying a potential biomarker that predicts LNM is quite useful in determining treatment.

AIM

To develop a machine learning (ML)-based integral procedure to construct the LNM gray-level co-occurrence matrix (GLCM) prediction model.

METHODS

We retrospectively selected 526 cases of UEGC confirmed through pathological examination after radical gastrectomy without endoscopic treatment in four tertiary hospitals between January 2015 to December 2021. We extracted GLCM-based features from grayscale images and applied ML to the classification of candidate predictive variables. The robustness and clinical utility of each model were evaluated based on the following factors: Receiver operating characteristic curve (ROC), decision curve analysis, and clinical impact curve.

RESULTS

GLCM-based feature extraction significantly correlated with LNM. The top 7 GLCM-based factors included inertia value 0° (IV_0), inertia value 45° (IV_45), inverse gap 0° (IG_0), inverse gap 45° (IG_45), inverse gap full angle (IG_all), Haralick 30° (Haralick_30), Haralick full angle (Haralick_all), and Entropy. The areas under the ROC curve (AUCs) of the random forest classifier (RFC) model, support vector machine, eXtreme gradient boosting, artificial neural network, and decision tree ranged from 0.805 [95% confidence interval (CI): 0.258-1.352] to 0.925 (95%CI: 0.378-1.472) in the training set and from 0.794 (95%CI: 0.237-1.351) to 0.912 (95%CI: 0.355-1.469) in the testing set, respectively. The RFC (training set: AUC: 0.925, 95%CI: 0.378-1.472; testing set: AUC: 0.912, 95%CI: 0.355-1.469) model that incorporates Entropy, Haralick_all, Haralick_30, IG_all, IG_45, IG_0, and IV_45 had the highest predictive accuracy.

CONCLUSION

The evaluation results indicate that the method of selecting radiological and textural features becomes more effective in the LNM discrimination against UEGC patients. Additionally, the ML-based prediction model developed using the RFC can be used to derive treatment options and identify LNM, which can hence improve clinical outcomes.

Key Words: Undifferentiated early gastric cancer; Machine learning; Lymph node metastasis; Gray-level co-occurrence matrix; Feature selection; Prediction

©The Author(s) 2022. Published by Baishideng Publishing Group Inc. All rights reserved.

Core Tip: Gray-level co-occurrence matrix-based feature extraction can be a robust and promising tool to improve the efficiency in predicting lymph node metastasis of individual undifferentiated early gastric cancer patients. Additionally, machine learning adopts more optimized algorithms and more clear feature extraction. Models developed using random forest classifier have the highest predictive accuracy in terms of Entropy, Haralick full angle, Haralick 30°, inverse gap full angle, inverse gap 45°, inverse gap 0°, and inertia value 45°. Further research is required to develop these models for clinical practice.

Citation: Wei X, Yan XJ, Guo YY, Zhang J, Wang GR, Fayyaz A, Yu J. Machine learning-based gray-level co-occurrence matrix signature for predicting lymph node metastasis in undifferentiated-type early gastric cancer. *World J Gastroenterol* 2022; 28(36): 5338-5350

URL: https://www.wjgnet.com/1007-9327/full/v28/i36/5338.htm

DOI: https://dx.doi.org/10.3748/wjg.v28.i36.5338

INTRODUCTION

Gastric cancer (GC) is one of the most common and fatal malignancies worldwide and is an important part of the global cancer burden[1,2]. In GC, undifferentiated early GC (UEGC) differs from differentiated-type GC in terms of clinical features and disease state, and their treatment and prognosis vary[3]. Therefore, UEGC should be identified and diagnosed early.

The incidence of lymphatic vessel invasion and risk of lymph node metastasis (LNM) in UEGC are high in surgical specimens of GC[4,5]. Endoscopic resection (ER), including endoscopic mucosal resection (EMR) and endoscopic submucosal dissection (ESD), has been considered a minimally invasive treatment option for early GC with negligible risk of LNM[6,7]. Nevertheless, indication or curability evaluation has not been conducted for ESD of undifferentiated GC (*e.g.*, poorly differentiated adenocarcinoma, signet ring cell carcinoma, or mucinous adenocarcinoma) due to the potential risk of LNM. Although ER can be used as painless treatment, the LNM incidence after non-curative ER can be as low as 5.1% and as high as 12.2%[8-10]. Additionally, ESD is only applicable to intramucosal cancer with a tumor diameter of ≤ 20 mm and without ulcer lesions; thus, treating lesions that meet the ESD indications through surgery is unnecessary[11,12]. That is, when resection beyond the expanded

standard is considered ineffective, the potential risk of LNM cannot be ignored. Hence, additional surgical resection and lymph node dissection should be performed. Unlike differentiated early GC, ER indications of UEGC are limited. Therefore, to address this challenging problem, a precise tool that can predict LNM must be explored.

Previous studies have mainly focused on risk factors for LNM or distant metastasis of differentiated-type early GC[13-15]. However, for UEGC, LNM has different risk factors. Thus, objective and universal evaluation indicators for evaluating its risk are lacking. In this study, we clarified the LNM risk factors of patients with UEGC who underwent surgical resection. Subsequently, we analyzed clinical-pathological factors by introducing gray-level co-occurrence matrix (GLCM) image feature extraction mining to classify LNM risk groups according to the combination of risk factors. This study aims to provide a reference for clinical diagnosis and treatment.

MATERIALS AND METHODS

Patient selection

The clinical records of 526 patients who were diagnosed with UEGC were confirmed through pathological examination after radical gastrectomy without endoscopic treatment at four tertiary hospitals. These hospitals are Shaanxi Provincial People's Hospital, Shaanxi Provincial Tumour Hospital, the First Affiliated Hospital of Xi'an Jiaotong University, and the Second Affiliated Hospital of Xi'an Jiaotong University. The clinical records were between January 2015 to December 2021 and were retrospectively reviewed. The following were the inclusion criteria: (1) Imaging examination was performed; (2) Patients have a complete set of medical data; (3) Primary lesion was resected either *via* open surgery or laparoscopic surgery and not *via* EMR or ESD; and (4) The status of infiltrating lymph nodes was assessed through routine hematoxylin-eosin staining. To minimize the confounding effect of unnecessary variables, the following were the exclusion criteria: (1) Sufficient information cannot be extracted or mismatched clinical data of patients; and (2) Patients without complete magnetic resonance imaging (MRI) plain scan or the MRI image quality being unacceptable. This study complies with the provisions of the Helsinki Declaration (revised in 2013) and was approved by the Institutional Review Committee of Shaanxi Provincial People's Hospital (2021-Y024). Figure 1 presents in detail the patient screening steps and modeling process.

Construction strategy of the GLCM

All texture parameter post-processing was conducted on Omni dynamics software (GE pharmaceuticals, Shanghai). Two radiologists who have vast experience in gastrointestinal diagnosis referred to the MRI images to sketch the lesions on the ADC map. First, they manually sketch the entire area with cancer on each layer of the map, avoiding the gas in the intestine, until the whole tumor volume was cut out. Second, the software automatically generates the texture features. In this study, the following are the selected texture parameters of the GLCM: Total frequency, energy value, entropy, inertia value, correlation coefficient, inverse moment, cluster shadow, and cluster prominence.

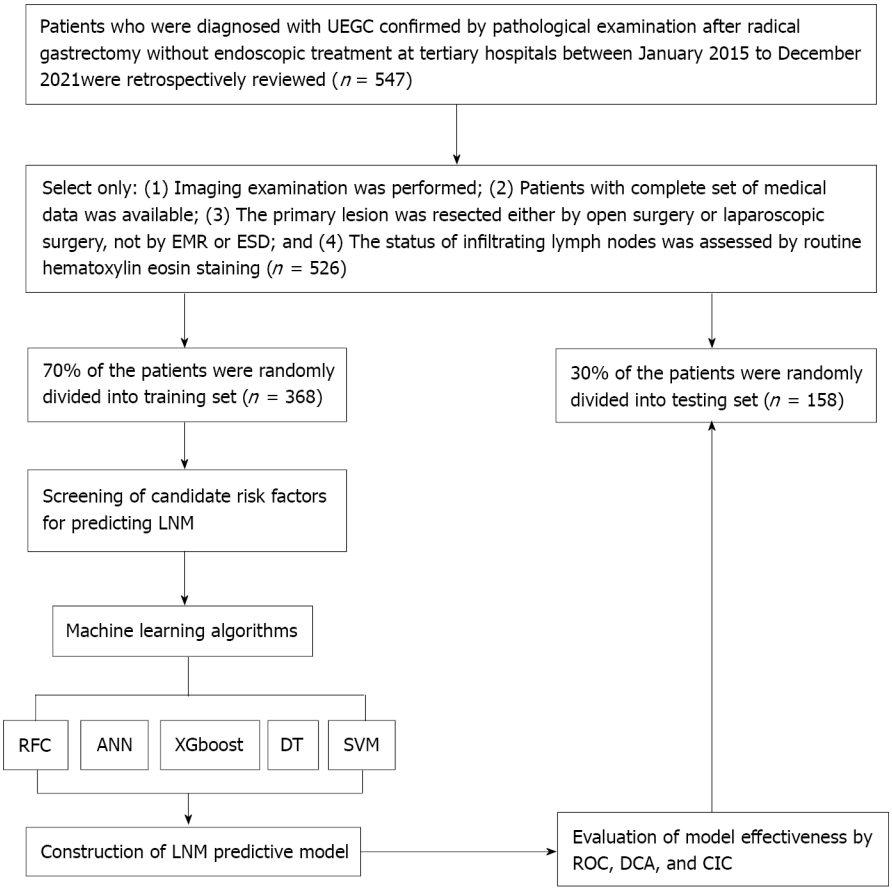
Data extraction and quality assessment

For variables with missing values (often this missing value is less than 10%), the variable's mean value should be filled. If ≥ 10% of the given variables are missing, this value is excluded from the variable screening of the final model. Similarly, this study adopted unit feature interpolation for the missing values that meet the interpolation requirements. That is, the missing values can be interpolated using the constant values provided or using the statistical data of each column where these missing values are located (*e.g.*, average value, median value, or the most frequently occurring value)[16,17].

Construction and effectiveness evaluation of the LNM model

Based on the machine learning (ML) algorithm, the commonly used iterative algorithm models are included: Random forest classifier (RFC), decision tree (DT), support vector machine (SVM), eXtreme gradient boosting (XGBoost), and artificial neural network (ANN). The RFC is an integrated method that forms a cumulative effect by integrating multiple relatively simple evaluators. Random forest is an integrated learning tool based on DT. The SVM is a type of a generalized linear classifier that categorizes data binary through supervised learning. The ANN is a nonlinear equation transformation output algorithm comprising input, hidden, and output layers. Finally, XGBoost is an additive model. In each iteration, only the sub-models in the current step are optimized. In this study, we refer to the guide proposed by Luo *et al*[18] for the best use of prediction models in biomedical research, that is, the Delphi method, which is used to generate the list of reported items.

For the screening of candidate variables, we mainly rely on the principle of "bag repeatedly put back and extract", sort according to variables' weight, and finally obtain the final predictor of the prediction model from the top 10 variables[19]. For the effectiveness evaluation of the prediction model, the receiver operating characteristic (ROC) curve is used to evaluate the accuracy of the model. Meanwhile,



DOI: 10.3748/wjg.v28.i36.5338 **Copyright** ©The Author(s) 2022.

Figure 1 Flowchart of patient selection and data processing. UEGC: Undifferentiated early gastric cancer; EMR: Endoscopic mucosal resection; ESD: Endoscopic submucosal dissection; RFC: Random forest classifier; SVM: Support vector machine; DT: Decision tree; ANN: Artificial neural network; XGboost: Extreme gradient boosting; ROC: Receiver operating characteristic; DCA: Decision curve analysis; CIC: Clinical impact curve; LNM: Lymph node metastasis.

the decision curve analysis and clinical impact curve (CIC) were used to evaluate the model's robustness and differentiation, respectively.

Statistical analysis

The measurement and counting data in this study are expressed by interquartile spacing (25%, 75%) and percentage (%), respectively. For the comparison between groups, the continuous variables adopt the *t*-test or Mann-Whitney *U* test of independent samples (provided that it does not conform to the normal distribution). The counting data adopt the chi-square goodness-of-fit test. Values of Bonferroni corrected probability are used to compare the qualitative data[20]. The prediction model visualization and other data analysis are performed using R software (version 4.0.4, http://www.r-project.org/). For the comparison between groups, P value < 0.05 is considered statistically significant and vice versa.

RESULTS

Comparison of baseline data between LNM and non-LNM queues

Table 1 summarizes the baseline characteristics of 526 hospitalized patients with UEGC. For internal validation, the patients were randomly divided into two sets using the caret package: Training set (n = 368, 70%) and validation set (n = 158, 30%). Regarding the LNM rate, the training and validation cohorts were 62 (16.85%) and 29 (18.35%), respectively. In addition to the previously reported clinical-related indicators (*e.g.*, tumor size, infiltration depth, vascular_invasion, and vascular tumor thrombus), significant differences exist between the LNM and non-LNM groups. We found that GLCM-based texture acquisition features also have significant statistical differences between the two groups.

Feature correlation and potential predictors

We conducted a correlation analysis on the variables with significant differences based on the statistical difference analysis of baseline data. As shown in Figure 2A, the correlation matrix (based on Pearson

Table 1 Patient baseline population and image index characteristic

Variables	Training set				Testing set			
	Overall (*n* = 368)	Yes (*n* = 62)	No (*n* = 306)	*P* value	Overall (*n* = 158)	Yes (*n* = 29)	No (*n* = 129)	*P* value
Age (median, IQR), yr	51.00 (40.75, 61.00)	52.50 (40.25, 64.50)	51.00 (41.00, 60.00)	0.185	47.00 (37.25, 58.75)	53.00 (39.00, 63.00)	46.00 (37.00, 57.00)	0.215
Sex (%)								
Male	266 (72.3)	48 (77.4)	218 (71.2)	0.404	123 (77.8)	21 (72.4)	102 (79.1)	0.594
Female	102 (27.7)	14 (22.6)	88 (28.8)		35 (22.2)	8 (27.6)	27 (20.9)	
Site (%)								
Nearly 1/3	81 (22.0)	10 (16.1)	71 (23.2)	0.384	37 (23.4)	9 (31.0)	28 (21.7)	0.138
Medium 1/3	73 (19.8)	15 (24.2)	58 (19.0)		23 (14.6)	1 (3.4)	22 (17.1)	
Far 1/3	214 (58.2)	37 (59.7)	177 (57.8)		98 (62.0)	19 (65.5)	79 (61.2)	
Ulcer (%)								
Yes	103 (28.0)	21 (33.9)	82 (26.8)	0.329	45 (28.5)	11 (37.9)	34 (26.4)	0.308
No	265 (72.0)	41 (66.1)	224 (73.2)		113 (71.5)	18 (62.1)	95 (73.6)	
Gross_type (%)								
Uplift	98 (26.6)	14 (22.6)	84 (27.5)	0.587	56 (35.4)	8 (27.6)	48 (37.2)	0.227
Flat	72 (19.6)	11 (17.7)	61 (19.9)		27 (17.1)	8 (27.6)	19 (14.7)	
Sunken	198 (53.8)	37 (59.7)	161 (52.6)		75 (47.5)	13 (44.8)	62 (48.1)	
Tumor_size (%)								
≤ 2 cm	296 (80.4)	18 (29.0)	278 (90.8)	< 0.001	120 (75.9)	6 (20.7)	114 (88.4)	< 0.001
> 2 cm	72 (19.6)	44 (71.0)	28 (9.2)		38 (24.1)	23 (79.3)	15 (11.6)	
Infiltration_depth (%)								
Mucosal layer	267 (72.6)	12 (19.4)	255 (83.3)	< 0.001	113 (71.5)	9 (31.0)	104 (80.6)	< 0.001
Submucosa	101 (27.4)	50 (80.6)	51 (16.7)		45 (28.5)	20 (69.0)	25 (19.4)	
Vascular_invasion (%)								
Yes	124 (33.7)	42 (67.7)	82 (26.8)	< 0.001	56 (35.4)	21 (72.4)	35 (27.1)	< 0.001
No	244 (66.3)	20 (32.3)	224 (73.2)		102 (64.6)	8 (27.6)	94 (72.9)	
VTT (%)								
Yes	124 (33.7)	45 (72.6)	79 (25.8)	< 0.001	44 (27.8)	23 (79.3)	21 (16.3)	< 0.001
No	244 (66.3)	17 (27.4)	227 (74.2)		114 (72.2)	6 (20.7)	108 (83.7)	
TF (median, IQR)	3.78 (3.56, 3.99)	4.13 (3.97, 4.27)	3.70 (3.51, 3.90)	< 0.001	3.79 (3.52, 4.01)	4.16 (4.00, 4.31)	3.70 (3.49, 3.93)	< 0.001
EV (median, IQR)	0.88 (0.64, 1.12)	0.60 (0.49, 0.68)	0.98 (0.72, 1.20)	< 0.001	0.85 (0.65, 1.09)	0.64 (0.54, 0.70)	0.92 (0.72, 1.16)	< 0.001
Entropy (median, IQR)	8.68 (8.37, 8.98)	10.51 (10.07, 10.88)	8.57 (8.33, 8.83)	< 0.001	8.79 (8.43, 9.02)	10.44 (10.16, 10.96)	8.65 (8.38, 8.89)	< 0.001
IG_all (median, IQR)	2.16 (1.76, 2.47)	3.04 (2.64, 3.62)	2.03 (1.69, 2.30)	< 0.001	2.12 (1.75, 2.47)	2.94 (2.70, 3.54)	1.97 (1.64, 2.31)	< 0.001
IG_0 (median, IQR)	2.26 (1.75, 2.66)	3.34 (2.72, 3.80)	2.10 (1.69, 2.48)	< 0.001	2.41 (1.90, 2.79)	3.70 (3.16, 4.18)	2.22 (1.77, 2.62)	< 0.001
IG_45 (median, IQR)	1.88 (1.54, 2.18)	2.85 (2.32, 3.26)	1.78 (1.47, 2.04)	< 0.001	1.85 (1.48, 2.18)	2.73 (2.31, 3.11)	1.74 (1.40, 2.03)	< 0.001
IG_90 (median, IQR)	2.34 (1.85, 2.85)	3.36 (2.89, 3.84)	2.20 (1.75, 2.63)	< 0.001	2.42 (1.94, 2.78)	3.27 (3.03, 3.61)	2.25 (1.75, 2.61)	< 0.001
IV_all (median, IQR)	176.90 (148.98, 207.25)	134.80 (109.30, 163.02)	182.00 (156.00, 210.75)	< 0.001	175.50 (143.25, 200.75)	133.50 (105.80, 155.70)	183.00 (154.00, 206.00)	< 0.001
IV_all_SD (median, IQR)	4584.00 (3148.00, 6602.50)	2166.50 (1340.50, 3535.00)	5025.00 (3747.00, 7011.75)	< 0.001	4940.50 (2987.25, 6682.00)	2849.00 (1841.00, 3428.00)	5618.00 (3813.00, 6897.00)	< 0.001

IV_0 (median, IQR)	149.85 (122.75, 186.75)	96.40 (78.95, 125.82)	163.20 (134.00, 195.65)	< 0.001	146.70 (112.78, 185.57)	74.10 (65.60, 90.60)	158.40 (131.40, 196.20)	< 0.001
IV_45 (median, IQR)	239.55 (201.40, 284.75)	164.40 (123.83, 188.62)	254.30 (220.67, 290.60)	< 0.001	226.25 (201.25, 266.67)	157.40 (133.90, 193.80)	243.90 (214.30, 273.50)	< 0.001
IV_90 (median, IQR)	129.00 (103.00, 154.00)	101.00 (77.75, 119.00)	134.00 (109.25, 159.00)	< 0.001	124.50 (109.00, 150.75)	105.00 (77.00, 118.00)	133.00 (117.00, 156.00)	< 0.001
Haralick_all (median, IQR)	0.10 (0.09, 0.10)	0.12 (0.11, 0.13)	0.09 (0.09, 0.10)	< 0.001	0.10 (0.09, 0.10)	0.12 (0.12, 0.14)	0.09 (0.09, 0.10)	< 0.001
Haralick_30 (median, IQR)	0.10 (0.09, 0.11)	0.14 (0.12, 0.15)	0.10 (0.09, 0.11)	< 0.001	0.10 (0.09, 0.11)	0.14 (0.13, 0.15)	0.10 (0.09, 0.11)	< 0.001
Haralick_45 (median, IQR)	0.09 (0.08, 0.10)	0.11 (0.10, 0.12)	0.09 (0.08, 0.10)	< 0.001	0.09 (0.08, 0.10)	0.11 (0.10, 0.13)	0.09 (0.08, 0.10)	< 0.001
Haralick_90 (median, IQR)	0.11 (0.10, 0.13)	0.14 (0.12, 0.16)	0.11 (0.09, 0.12)	< 0.001	0.12 (0.10, 0.13)	0.15 (0.12, 0.16)	0.11 (0.09, 0.13)	< 0.001
CSV (median, IQR)	106.00 (102.00, 111.00)	108.00 (105.00, 111.00)	106.00 (101.00, 111.00)	0.001	107.00 (102.25, 111.00)	109.00 (105.00, 113.00)	107.00 (102.00, 111.00)	0.007
CP (median, IQR)	65.50 (60.00, 70.00)	68.00 (66.00, 71.00)	64.00 (59.00, 70.00)	< 0.001	64.00 (60.00, 68.00)	67.00 (64.00, 68.00)	63.00 (59.00, 68.00)	0.002

IQR: Interquartile range; TF: Total frequency; EV: Energy value; IV_0: Inertia value 0°; IV_45: Inertia value 45°; IV_90: Inertia value 90°; IG_0: Inverse gap 0°; IG_45: Inverse gap 45°; IG_90: Inverse gap 90°; IG_all: Inverse gap full angle; Haralick_30: Haralick 30°; Haralick_45: Haralick 45°; Haralick_90: Haralick 90°; Haralick_all: Haralick full angle; CSV: Cluster shadow value; CP: Cluster prominence.

correlation analysis) indicates that the characteristic variables in the GLCM and LNM had a strong correlation degree ($r > 0.6$). For example, Entropy, Haralick full angle (Haralick_all), Haralick 30° (Haralick_30), Inverse gap full angle (IG_all), Inverse gap 45° (IG_45), Inverse gap 0° (IG_0), *etc.* were highly correlated with LNM. This suggests that these potential candidate variables can be used as LNM predictors and for the construction of subsequent models. Interestingly, in the subsequent models developed based on ML algorithms, we found that Entropy, Haralick_all, Haralick_30, IG_all, IG_45, IG_0, and Inertia value 45° (IV_45) occupied high weights as the top 7 GLCM-based factors (Figure 2B). Specifically, Entropy has the largest weight among these factors.

Establishment and performance evaluation of the LNM prediction model

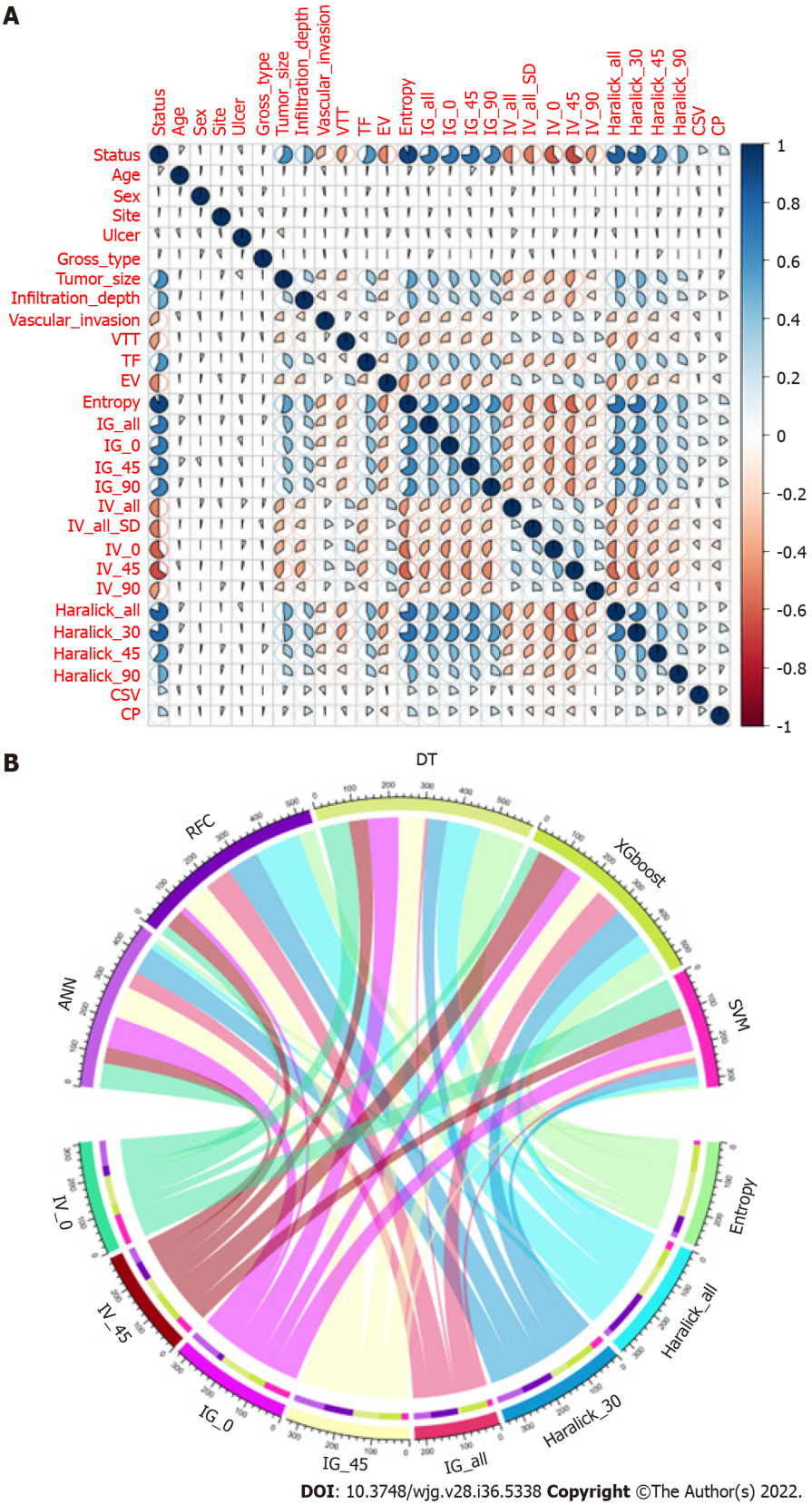
When constructing the RFC model [training set: Areas under the ROC curve (AUC): 0.925, 95% confidence interval (CI): 0.378-1.472; testing set: AUC: 0.912, 95%CI: 0.355-1.469], we repeatedly randomly selected *N* samples from the original training set *N* to generate the new training set DT and then generate *M* DTs to form a random forest according to the above steps. As shown in Figure 3A and Supplementary Table 1, the smallest Gini index after splitting was selected, including that for Entropy, Haralick_all, Haralick_30, IG_all, IG_45, IG_0, and IV_45. Similarly, Haralick_30 and IG_all served as important weight at DT branches (training set: AUC: 0.856, 95%CI: 0.309-1.403; testing set: AUC: 0.813, 95%CI: 0.256-1.370) (Figure 3B). In the ANN model (Figure 4), the accuracy of the prediction model developed using the prediction variables in the GLCM can also reach 0.887 (95%CI: 0.340-1.434) and 0.837 (95%CI: 0.280-1.394) in the training and verification sets, respectively. Although this accuracy is slightly inferior to that of the RFC model, it is better than those of other prediction models (*i.e.*, DT, XGBoost, and SVM). Table 2, Supplementary Table 1, and Figure 5 summarize the predictive performance of ML-based models. In general, the prediction model constructed by using any ML algorithm was better than the logistic regression algorithm in predicting LNM, further confirming the superiority of ML algorithm, especially the robustness of the RFC.

Internal validation of the optimal RFC predictive model

The prediction efficiency of the RFC model was the best in the process of precise stratification of LNM patients. To further evaluate the "stratification effect" of the RFC, results of CIC analysis indicate that high-risk LNM was accurately distinguished using the RFC model, and "cross-linking" did not occur in the stratification process. The results of this model for the validation and training sets were consistent (Supplementary Table 2), implying that the robustness and LNM discrimination of the RFC model were satisfactory.

DISCUSSION

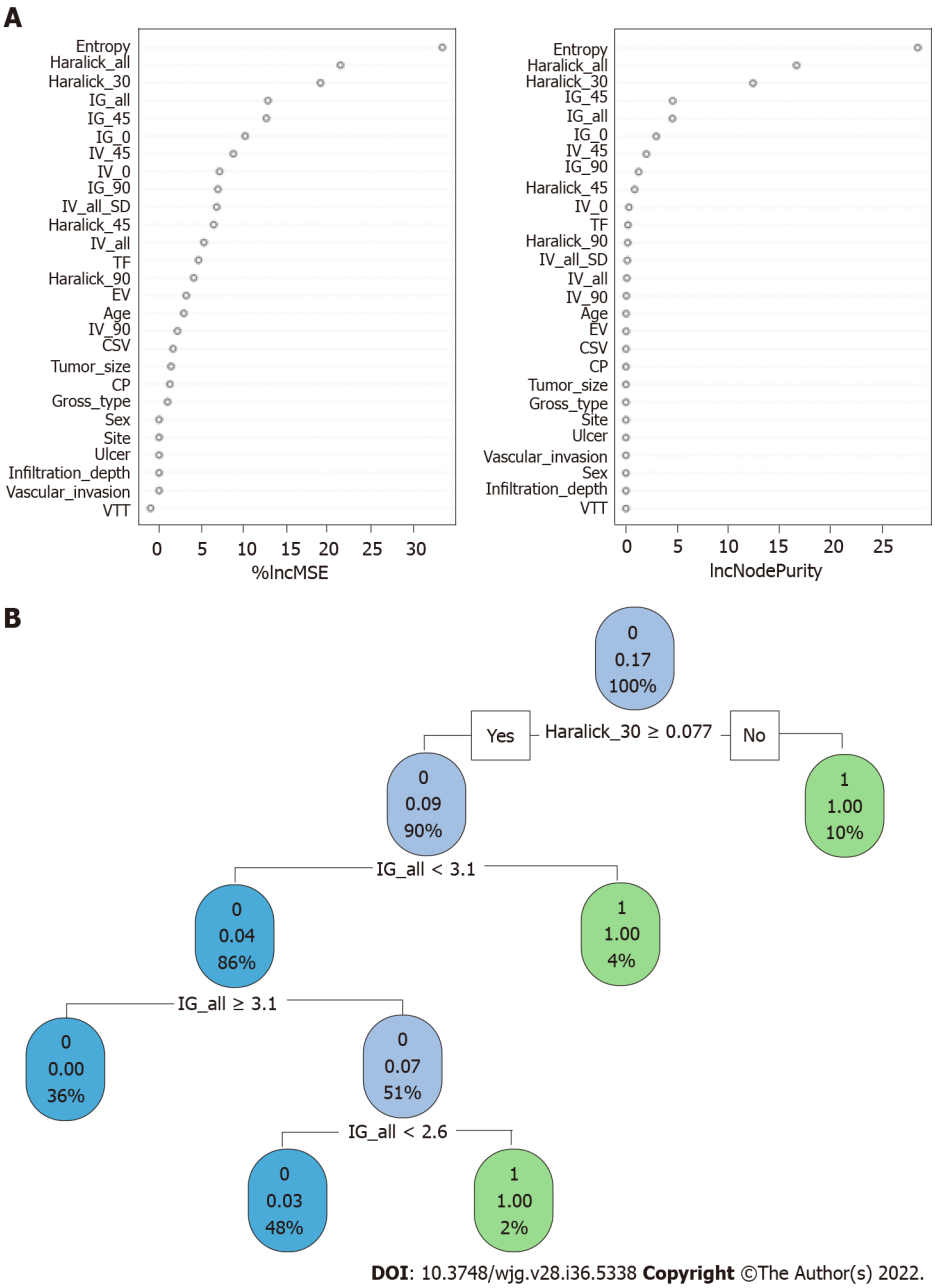
The standard treatment for early GC is surgery. However, recently, ER has become the standard local



DOI: 10.3748/wjg.v28.i36.5338 **Copyright** ©The Author(s) 2022.

Figure 2 Variable screening and weight allocation. A: Correlation matrix analysis of candidate features; B: Weight distribution of candidate variables for each mL based model. RFC: Random forest classifier; SVM: Support vector machine; DT: Decision tree; ANN: Artificial neural network; XGboost: Extreme gradient boosting.

treatment for some patients with early GC without LNM[21]. For a long time, it has been used to treat differentiated-type early GC limited to the mucosa, with a diameter of < 2 cm[22,23]. Recent studies have shown that ER indications have been expanded in many studies, even including UEGC and ≤ 2 cm diameter, without ulcer or lymphatic vessel invasion[24]. However, whether UEGC can accept the

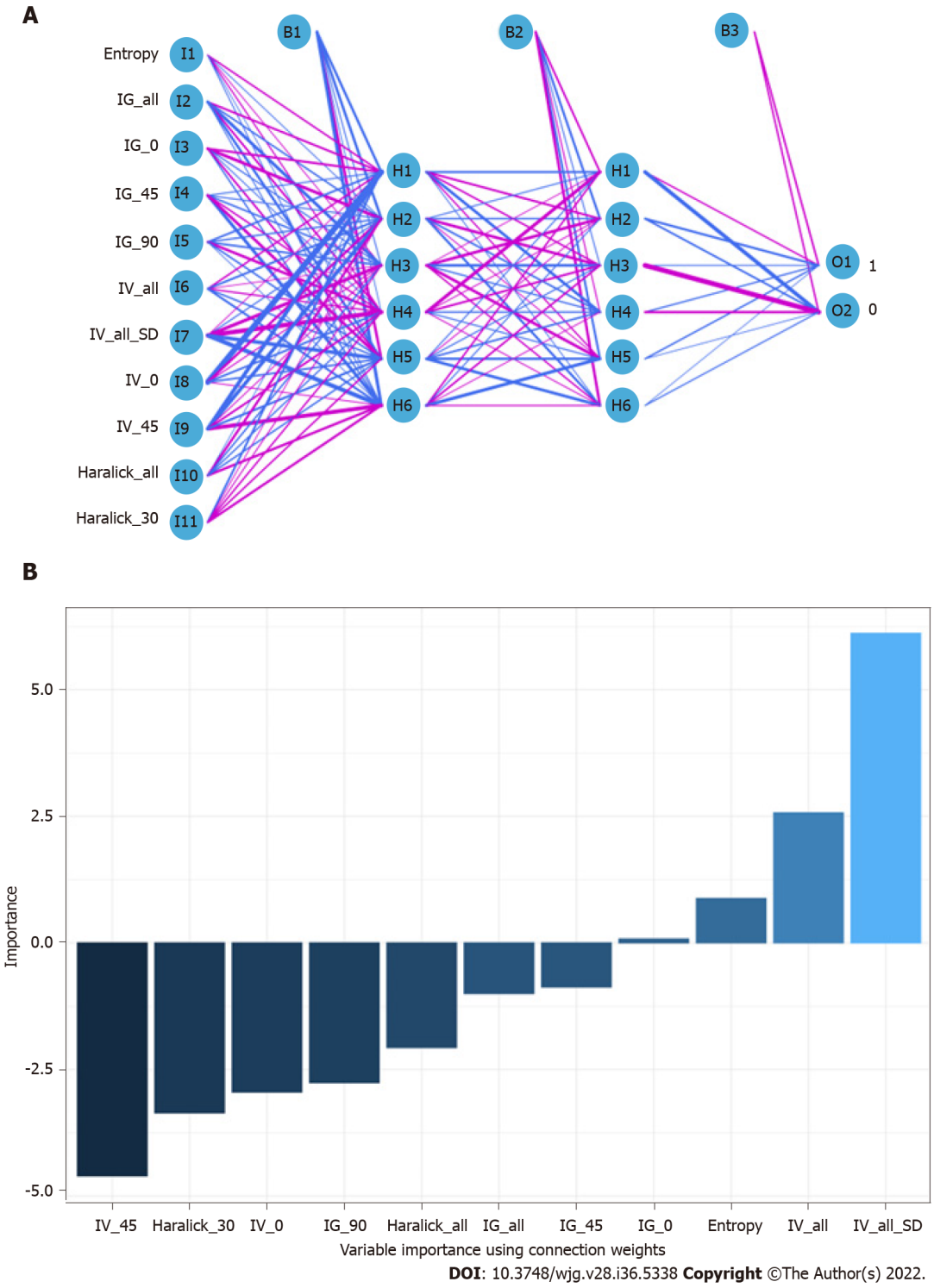


DOI: 10.3748/wjg.v28.i36.5338 **Copyright** ©The Author(s) 2022.

Figure 3 Visualization model prediction based on machine learning based algorithm. A: Random forest classifier model; B: Decision tree model. Candidate factors associated with fracture risk are named through random forest classifier algorithm, and prediction nodes and weights are assigned by the decision tree algorithm.

standard treatment of ER remains a subject of debate. That is, additional surgery should be performed if curability is considered questionable. Given this situation, the risk factors of LNM or distant metastasis and mortality after non-curative ER of UEGC should be investigated. Previous studies have also shown that patients with two or more risk factors (*e.g.*, ulcer, submucosal invasion, and positive vertical margin) benefit greatly from surgical resection after ER that cannot be cured by UEGC[14,25]. However, due to the heterogeneity of clinical characteristics, risk stratification based on these predictions provides a simple prediction, which is challenging to apply in clinical practice.

The potential application of the GLCM in the prediction of LNM of UEGC has not been systematically explored thus far. In this study, GLCM-based features were extracted from underlying grayscale images collected through MRI. We developed an LNM risk prediction model for patients with UEGC using an ML-based algorithm. The following are the two important findings of our study. First, the accurate risk stratification of UEGC patients who should undergo additional surgery depends on the added value of the GLCM. Second, a new ML-based prediction model was used to identify patients and whether they have LNM. According to previous studies[26], texture analysis can quantify the spatial differences of pixels and the subtle differences reflected in gray values, which is consistent with the conclusion of this study. To some extent, we used GLCM features to gather spatial information and reduced the



DOI: 10.3748/wjg.v28.i36.5338 **Copyright** ©The Author(s) 2022.

Figure 4 Visualization of prediction models based on artificial neural network algorithm. A: Artificial neural network model; B: Importance of variables using connection weights. Candidate factors associated with lymph node metastasis are ordered *via* artificial neural network (ANN) algorithm and prediction nodes, and weights are assigned *via* an ANN algorithm. IV_0: Inertia value 0°; IV_45: Inertia value 45°; IG_0: Inverse gap 0°; IG_45: Inverse gap 45°; IG_all: Inverse gap full angle; Haralick_30: Haralick 30°; Haralick_all: Haralick full angle.

overfitting effect by replacing the softmax layer with the ML-based algorithm.

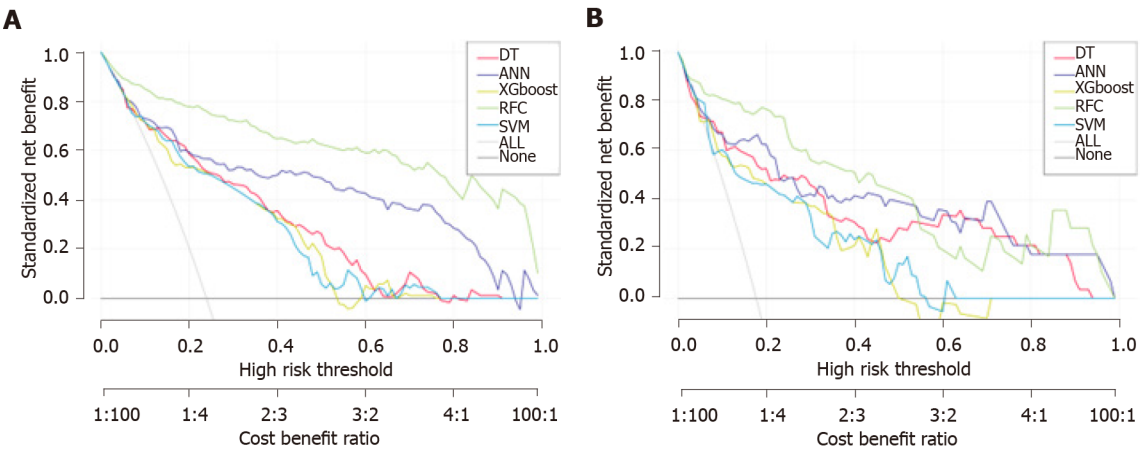
In this study, we created five types of ML-based models (*i.e.*, RFC, ANN, DT, XGBoost, and SVM), which used GLCM features to predict LNM. Interestingly, there were differences in the prediction efficiency obtained by ML-based models of different algorithms. For example, the RFC model had the highest predictive accuracy, which was achieved by incorporating Entropy, Haralick_all, Haralick_30, IG_all, IG_45, IG_0, and IV_45. Meanwhile, the ANN, DT, XGBoost, and SVM exhibited an inferior performance compared with the RFC. This suggests that the accuracy of the RFC in predicting LNM is superior to that of the ML model. A previous study indicated that a random forest algorithm is more

Table 2 Receiver operating characteristic curve analysis of lymph node metastasis in each mL based model

Model	Training set		Testing set		Variables[1]
	AUC mean	AUC 95%CI	AUC mean	AUC 95%CI	
RFC	0.925	0.378-1.472	0.912	0.355-1.469	Entropy, Haralick_all, Haralick_30, IG_all, IG_45, IG_0, IV_45
ANN	0.887	0.340-1.434	0.837	0.280-1.394	Entropy, IG_all, IG_0, IG_45, IG_90, IV_all, IV_all_SD, IV_0, IV_45, Haralick_all, Haralick_30
DT	0.856	0.309-1.403	0.813	0.256-1.370	Entropy, Haralick_all, Haralick_30, IG_all, IG_45, IG_0, IV_45
XGboost	0.814	0.267-1.361	0.807	0.250-1.364	Entropy, Haralick_all, Haralick_30, IG_all, IG_45, IG_0, IV_45, IG_90
SVM	0.805	0.258-1.352	0.794	0.237-1.351	Entropy, Haralick_all, Haralick_30, IG_all, IG_45, IG_0, IV_45
GLM	0.796	0.229-1.362	0.799	0.233-1.365	Entropy, Haralick_all, Haralick_30, IG_all, IG_45, IG_0, IV_45
Radiologist	0.789	0.242-1.336	0.801	0.254-1.348	-

[1]Variables are included in the model.

RFC: Random forest classifier; SVM: Support vector machine; DT: Decision tree; ANN: Artificial neural network; XGboost: Extreme gradient boosting; GLM; Generalized linear model; AUC: Area under the receiver operating characteristic curve; 95%CI: 95% confidence interval; IV_0: Inertia value 0°; IV_45: Inertia value 45°; IV_90: Inertia value 90°; IG_0: Inverse gap 0°; IG_45: Inverse gap 45°; IG_90: Inverse gap 90°; IG_all: Inverse gap full angle; Haralick_30: Haralick 30°.



DOI: 10.3748/wjg.v28.i36.5338 **Copyright** ©The Author(s) 2022.

Figure 5 Predictive performance of candidate models based on machine learning based algorithm. A: Decision curve analysis (DCA) for five mL based models in training sets; B: DCA for five ml based models in test sets. RFC: Random forest classifier; SVM: Support vector machine; DT: Decision tree; ANN: Artificial neural network; XGboost: Extreme gradient boosting.

efficient in processing classification problems, which is consistent with the results of this study[27]. Meanwhile, DT is not as good as the RFC in terms of fitting, and the low prediction ability of the ANN model indicates that an "overfitting" phenomenon may occur. In general, different ML models show consistent accuracy, indicating that the prediction performance of ML can be improved through data processing.

Our results confirm a GLCM-based LNM classification, which has an ideal predictive effect on the diagnosis and treatment of patients with UEGC. However, the following problems were inevitably encountered in this study. First, because this study involved a retrospective analysis, the case inclusion criteria may have a certain bias on the results, which remains to be confirmed by a large sample of prospective studies in the future. Second, there were relatively few selected cases in this study, and only some parameters of the GLCM were extracted. Thus, the results of its prediction model should be verified by external data. Third, when data from multi-center and large sample studies are available in the future, it is crucial to predict the presence or absence of LNM. Additionally, the GLCM is an important imaging sequence of UEGC, and hence we will further perform other image texture analyses

in subsequent research.

CONCLUSION

GLCM-based feature extraction could, in general, serve as a robust and promising tool to improve predictive efficiency for LNM in individual UEGC patients. ML adopts the algorithm of "classification and pruning" and clearer feature extraction, leading to better data fitting than the conventional prediction model. The model constructed using the RFC had the highest predictive accuracy, with the following being the most important predictors: Entropy, Haralick_all, Haralick_30, IG_all, IG_45, IG_0, and IV_45. In the future, we are still required to validate and optimize these prediction models using datasets of various scenarios to better apply them to clinical practice.

ARTICLE HIGHLIGHTS

Research background

Gray-level co-occurrence matrix (GLCM) based feature extraction could serve as a robust and promising tool to improve the predictive efficiency for lymph node metastasis (LNM) of individual undifferentiated early gastric cancer (UEGC) patients. Additionally, machine learning (ML) adopts more optimized algorithms and more clear feature extraction. Models built using random forest classifier (RFC) have the highest predictive accuracy in Entropy, Haralick full angle (Haralick_all), Haralick 30° (Haralick_30), Inverse gap full angle (IG_all), Inverse gap 45° (IG_45), Inverse gap 0° (IG_0), and Inertia value 45° (IV_45). Further research is needed to develop these models for clinical practice.

Research motivation

The evaluation results indicate that the method of selecting radiological and textural features becomes more effective in the discrimination of LNM from UEGC patients. In addition, an ML-based prediction model developed using RFC can be used to derive treatment options and identify LNM that can improve clinical outcomes.

Research objectives

GLCM based feature extraction significantly correlated with LNM. The top 7 GLCM based factors included Inertia value 0°, IV_45, IG_0, IG_45, IG_all, Haralick_30, Haralick_all, and Entropy. The areas under the receiver operating characteristic (ROC) curve (AUCs) of the RFC model, support vector machine (SVM), eXtreme gradient boosting (XGBoost), artificial neural network (ANN), and decision tree (DT) ranged from 0.805 [95% confidence interval (CI): 0.258-1.352] to 0.925 (95%CI: 0.378-1.472) in the training set and from 0.794 (95%CI: 0.237-1.351) to 0.912 (95%CI: 0.355-1.469) in the testing set, respectively. The RFC (training set: AUC: 0.925, 95%CI: 0.378-1.472; testing set: AUC: 0.912, 95%CI: 0.355-1.469) model incorporating Entropy, Haralick_all, Haralick_30, IG_all, IG_45, IG_0, and IV_45 had the highest predictive accuracy.

Research methods

We retrospectively selected 526 cases of UEGC confirmed by pathological examination after radical gastrectomy without endoscopic treatment in four tertiary hospitals between January 2015 to December 2021. GLCM-based features were extracted from grayscale images and ML was applied to the classification of candidate predictive variables. In order to evaluate robustness and clinical utility of each model, the following were made: ROC, decision curve analysis, and clinical impact curve.

Research results

Identifying a potential biomarker that predicts LNM is proven to be very useful in determining treatment.

Research conclusions

To develop a ML-based integral procedure to construct the LNM gray level co-occurrence matrix (GLCM) prediction model.

Research perspectives

The risk of LNM is the most important consideration in determining treatment strategies for UEGC. Therefore, identifying a potential biomarker that predicts LNM is proven to be very useful in determining treatment.

ACKNOWLEDGEMENTS

The authors thank all study participants for consenting to the use of their medical records.

FOOTNOTES

Author contributions: Yu J and Wei X conceived and designed the study and wrote the manuscript; Yan XJ, Guo YY, Zhang J, Wang GR, and Arsalan F collected the data, performed the data analysis, and interpreted the outcomes; and all authors critically reviewed the content of the manuscript and helped with the drafts.

Supported by the General Project-Social Development Field of Shaanxi Province Science and Technology Department, No. 2021SF-313; and Innovation Capability Support Plan of Shaanxi Science and Technology Department - Science and Technology Innovation Team, No. 2020TD-048.

Institutional review board statement: This study was approved by the Institutional Review Committee of Shaanxi Provincial People's Hospital (2021-Y024).

Informed consent statement: Written informed consent was not required given the retrospective nature of the study from chart review.

Conflict-of-interest statement: All the authors report no relevant conflicts of interest for this article.

Data sharing statement: No additional data are available.

STROBE statement: The authors have read the STROBE Statement-a checklist of items is provided. The manuscript was prepared and revised according to the STROBE Statement-a checklist of items is provided.

Open-Access: This article is an open-access article that was selected by an in-house editor and fully peer-reviewed by external reviewers. It is distributed in accordance with the Creative Commons Attribution NonCommercial (CC BY-NC 4.0) license, which permits others to distribute, remix, adapt, build upon this work non-commercially, and license their derivative works on different terms, provided the original work is properly cited and the use is non-commercial. See: https://creativecommons.org/Licenses/by-nc/4.0/

Country/Territory of origin: China

ORCID number: Jiao Yu 0000-0002-8707-8606.

S-Editor: Wang JJ
L-Editor: A
P-Editor: Wang JJ

REFERENCES

1 **Puliga E**, Corso S, Pietrantonio F, Giordano S. Microsatellite instability in Gastric Cancer: Between lights and shadows. *Cancer Treat Rev* 2021; **95**: 102175 [PMID: 33721595 DOI: 10.1016/j.ctrv.2021.102175]
2 **Karimi P**, Islami F, Anandasabapathy S, Freedman ND, Kamangar F. Gastric cancer: descriptive epidemiology, risk factors, screening, and prevention. *Cancer Epidemiol Biomarkers Prev* 2014; **23**: 700-713 [PMID: 24618998 DOI: 10.1158/1055-9965.EPI-13-1057]
3 **Lee A**, Chung H. Endoscopic Resection of Undifferentiated-type Early Gastric Cancer. *J Gastric Cancer* 2020; **20**: 345-354 [PMID: 33425437 DOI: 10.5230/jgc.2020.20.e37]
4 **Horiuchi Y**, Fujisaki J, Yamamoto N, Ishizuka N, Ishiyama A, Yoshio T, Hirasawa T, Yamamoto Y, Nagahama M, Takahashi H, Tsuchida T. Undifferentiated-type predominant mixed-type early gastric cancer is a significant risk factor for requiring additional surgeries after endoscopic submucosal dissection. *Sci Rep* 2020; **10**: 6748 [PMID: 32317768 DOI: 10.1038/s41598-020-63781-3]
5 **Ono H**, Kondo H, Gotoda T, Shirao K, Yamaguchi H, Saito D, Hosokawa K, Shimoda T, Yoshida S. Endoscopic mucosal resection for treatment of early gastric cancer. *Gut* 2001; **48**: 225-229 [PMID: 11156645 DOI: 10.1136/gut.48.2.225]
6 **Lee JH**, Kim JJ. Endoscopic mucosal resection of early gastric cancer: Experiences in Korea. *World J Gastroenterol* 2007; **13**: 3657-3661 [PMID: 17659722 DOI: 10.3748/wjg.v13.i27.3657]
7 **Ohkuwa M**, Hosokawa K, Boku N, Ohtu A, Tajiri H, Yoshida S. New endoscopic treatment for intramucosal gastric tumors using an insulated-tip diathermic knife. *Endoscopy* 2001; **33**: 221-226 [PMID: 11293753 DOI: 10.1055/s-2001-12805]
8 **Zhao X**, Cai A, Xi H, Chen L, Peng Z, Li P, Liu N, Cui J, Li H. Predictive Factors for Lymph Node Metastasis in Undifferentiated Early Gastric Cancer: a Systematic Review and Meta-analysis. *J Gastrointest Surg* 2017; **21**: 700-711 [PMID: 28120275 DOI: 10.1007/s11605-017-3364-7]

9 **Kato M**, Nishida T, Yamamoto K, Hayashi S, Kitamura S, Yabuta T, Yoshio T, Nakamura T, Komori M, Kawai N, Nishihara A, Nakanishi F, Nakahara M, Ogiyama H, Kinoshita K, Yamada T, Iijima H, Tsujii M, Takehara T. Scheduled endoscopic surveillance controls secondary cancer after curative endoscopic resection for early gastric cancer: a multicentre retrospective cohort study by Osaka University ESD study group. *Gut* 2013; **62**: 1425-1432 [PMID: 22914298 DOI: 10.1136/gutjnl-2011-301647]

10 **Hahn KY**, Park JC, Kim EH, Shin S, Park CH, Chung H, Shin SK, Lee SK, Lee YC. Incidence and impact of scheduled endoscopic surveillance on recurrence after curative endoscopic resection for early gastric cancer. *Gastrointest Endosc* 2016; **84**: 628-638.e1 [PMID: 26996290 DOI: 10.1016/j.gie.2016.03.1404]

11 **Nasu J**, Doi T, Endo H, Nishina T, Hirasaki S, Hyodo I. Characteristics of metachronous multiple early gastric cancers after endoscopic mucosal resection. *Endoscopy* 2005; **37**: 990-993 [PMID: 16189772 DOI: 10.1055/s-2005-870198]

12 **Nakajima T**, Oda I, Gotoda T, Hamanaka H, Eguchi T, Yokoi C, Saito D. Metachronous gastric cancers after endoscopic resection: how effective is annual endoscopic surveillance? *Gastric Cancer* 2006; **9**: 93-98 [PMID: 16767364 DOI: 10.1007/s10120-006-0372-9]

13 **Kawata N**, Kakushima N, Takizawa K, Tanaka M, Makuuchi R, Tokunaga M, Tanizawa Y, Bando E, Kawamura T, Sugino T, Kusafuka K, Shimoda T, Nakajima T, Terashima M, Ono H. Risk factors for lymph node metastasis and long-term outcomes of patients with early gastric cancer after non-curative endoscopic submucosal dissection. *Surg Endosc* 2017; **31**: 1607-1616 [PMID: 27495338 DOI: 10.1007/s00464-016-5148-7]

14 **Suzuki H**, Oda I, Abe S, Sekiguchi M, Nonaka S, Yoshinaga S, Saito Y, Fukagawa T, Katai H. Clinical outcomes of early gastric cancer patients after noncurative endoscopic submucosal dissection in a large consecutive patient series. *Gastric Cancer* 2017; **20**: 679-689 [PMID: 27722825 DOI: 10.1007/s10120-016-0651-z]

15 **Hirasawa T**, Gotoda T, Miyata S, Kato Y, Shimoda T, Taniguchi H, Fujisaki J, Sano T, Yamaguchi T. Incidence of lymph node metastasis and the feasibility of endoscopic resection for undifferentiated-type early gastric cancer. *Gastric Cancer* 2009; **12**: 148-152 [PMID: 19890694 DOI: 10.1007/s10120-009-0515-x]

16 **Donders AR**, van der Heijden GJ, Stijnen T, Moons KG. Review: a gentle introduction to imputation of missing values. *J Clin Epidemiol* 2006; **59**: 1087-1091 [PMID: 16980149 DOI: 10.1016/j.jclinepi.2006.01.014]

17 **Carpenter JR**, Smuk M. Missing data: A statistical framework for practice. *Biom J* 2021; **63**: 915-947 [PMID: 33624862 DOI: 10.1002/bimj.202000196]

18 **Luo W**, Phung D, Tran T, Gupta S, Rana S, Karmakar C, Shilton A, Yearwood J, Dimitrova N, Ho TB, Venkatesh S, Berk M. Guidelines for Developing and Reporting Machine Learning Predictive Models in Biomedical Research: A Multidisciplinary View. *J Med Internet Res* 2016; **18**: e323 [PMID: 27986644 DOI: 10.2196/jmir.5870]

19 **Fan J**, Lv J. A Selective Overview of Variable Selection in High Dimensional Feature Space. *Stat Sin* 2010; **20**: 101-148 [PMID: 21572976]

20 **Armstrong RA**. When to use the Bonferroni correction. *Ophthalmic Physiol Opt* 2014; **34**: 502-508 [PMID: 24697967 DOI: 10.1111/opo.12131]

21 **Goto O**, Fujishiro M, Kodashima S, Ono S, Omata M. Outcomes of endoscopic submucosal dissection for early gastric cancer with special reference to validation for curability criteria. *Endoscopy* 2009; **41**: 118-122 [PMID: 19214889 DOI: 10.1055/s-0028-1119452]

22 **Gotoda T**, Yanagisawa A, Sasako M, Ono H, Nakanishi Y, Shimoda T, Kato Y. Incidence of lymph node metastasis from early gastric cancer: estimation with a large number of cases at two large centers. *Gastric Cancer* 2000; **3**: 219-225 [PMID: 11984739 DOI: 10.1007/pl00011720]

23 **Kojima T**, Parra-Blanco A, Takahashi H, Fujita R. Outcome of endoscopic mucosal resection for early gastric cancer: review of the Japanese literature. *Gastrointest Endosc* 1998; **48**: 550-4; discussion 554 [PMID: 9831855 DOI: 10.1016/s0016-5107(98)70108-7]

24 **Soetikno R**, Kaltenbach T, Yeh R, Gotoda T. Endoscopic mucosal resection for early cancers of the upper gastrointestinal tract. *J Clin Oncol* 2005; **23**: 4490-4498 [PMID: 16002839 DOI: 10.1200/JCO.2005.19.935]

25 **Kim ER**, Lee H, Min BH, Lee JH, Rhee PL, Kim JJ, Kim KM, Kim S. Effect of rescue surgery after non-curative endoscopic resection of early gastric cancer. *Br J Surg* 2015; **102**: 1394-1401 [PMID: 26313295 DOI: 10.1002/bjs.9873]

26 **Naik A**, Edla DR, Dharavath R. Prediction of Malignancy in Lung Nodules Using Combination of Deep, Fractal, and Gray-Level Co-Occurrence Matrix Features. *Big Data* 2021; **9**: 480-498 [PMID: 34191590 DOI: 10.1089/big.2020.0190]

27 **Li J**, Tian Y, Zhu Y, Zhou T, Li J, Ding K. A multicenter random forest model for effective prognosis prediction in collaborative clinical research network. *Artif Intell Med* 2020; **103**: 101814 [PMID: 32143809 DOI: 10.1016/j.artmed.2020.101814]

World Journal of Gastroenterology

Submit a Manuscript: https://www.f6publishing.com

World J Gastroenterol 2022 September 28; 28(36): 5351-5363

DOI: 10.3748/wjg.v28.i36.5351

ISSN 1007-9327 (print) ISSN 2219-2840 (online)

ORIGINAL ARTICLE

Observational Study

Early extrahepatic recurrence as a pivotal factor for survival after hepatocellular carcinoma resection: A 15-year observational study

Jae Hyun Yoon, Sung Kyu Choi, Sung Bum Cho, Hee Joon Kim, Yang Seok Ko, Chung Hwan Jun

Specialty type: Gastroenterology and hepatology

Provenance and peer review: Unsolicited article; Externally peer reviewed.

Peer-review model: Single blind

Peer-review report's scientific quality classification

Grade A (Excellent): 0
Grade B (Very good): B, B
Grade C (Good): C
Grade D (Fair): 0
Grade E (Poor): 0

P-Reviewer: Ding J, China; Manrai M, India; Posa A, Italy

Received: May 11, 2022
Peer-review started: May 11, 2022
First decision: August 1, 2022
Revised: August 11, 2022
Accepted: September 8, 2022
Article in press: September 8, 2022
Published online: September 28, 2022

Jae Hyun Yoon, Sung Kyu Choi, Department of Gastroenterology and Hepatology, Chonnam National University Hospital and College of Medicine, Gwangju 61469, South Korea

Sung Bum Cho, Department of Gastroenterology and Hepatology, Hwasun Chonnam National University Hospital and College of Medicine, Hwasun 58128, South Korea

Hee Joon Kim, Department of Surgery, Chonnam National University Hospital and College of Medicine, Gwangju 61469, South Korea

Yang Seok Ko, Department of Surgery, Hwasun Chonnam National University Hospital and College of Medicine, Hwasun 58128, South Korea

Chung Hwan Jun, Department of Internal Medicine, Mokpo Hankook Hospital, Mokpo 58643, South Korea

Corresponding author: Sung Kyu Choi, MD, PhD, Professor, Department of Gastroenterology and Hepatology, Chonnam National University Hospital and College of Medicine, Jebongroe 42, Gwangju 61469, South Korea. choisk@jnu.ac.kr

Abstract

BACKGROUND

Surgical resection is one of the most widely used modalities for the treatment of hepatocellular carcinoma (HCC). Early extrahepatic recurrence (EHR) of HCC after surgical resection is considered to be closely associated with poor prognosis. However, data regarding risk factors and survival outcomes of early EHR after surgical resection remain scarce.

AIM

To investigate the clinical features and risk factors of early EHR and elucidate its association with survival outcomes.

METHODS

From January 2004 to December 2019, we enrolled treatment-naïve patients who were ≥ 18 years and underwent surgical resection for HCC in two tertiary academic centers. After excluding patients with tumor types other than HCC and/or ineligible data, this retrospective study finally included 779 patients. Surgical resection of HCC was performed according to the physicians' decisions and the EHR was diagnosed based on contrast-enhanced computed tomography

or magnetic resonance imaging, and pathologic confirmation was performed in selected patients. Multivariate Cox regression analysis was performed to identify the variables associated with EHR.

RESULTS

Early EHR within 2 years after surgery was diagnosed in 9.5% of patients during a median follow-up period of 4.4 years. The recurrence-free survival period was 5.2 mo, and the median time to EHR was 8.8 mo in patients with early EHR. In 52.7% of patients with early EHR, EHR occurred as the first recurrence of HCC after surgical resection. On multivariate analysis, serum albumin < 4.0 g/dL, serum alkaline phosphatase > 100 U/L, surgical margin involvement, venous and/or lymphatic involvement, satellite nodules, tumor necrosis detected by pathology, tumor size ≥ 7 cm, and macrovascular invasion were determined as risk factors associated with early EHR. After sub-categorizing the patients according to the number of risk factors, the rates of both EHR and survival showed a significant correlation with the risk of early EHR. Furthermore, multivariate analysis revealed that early EHR was associated with substantially worse survival outcomes (Hazard ratio, 6.77; 95% confidence interval, 4.81-9.52; $P < 0.001$).

CONCLUSION

Early EHR significantly deteriorates the survival of patients with HCC, and our identified risk factors may predict the clinical outcomes and aid in postoperative strategies for improving survival.

Key Words: Early extrahepatic recurrence; Hepatocellular carcinoma; Prognosis; Surgery; Survival

©The Author(s) 2022. Published by Baishideng Publishing Group Inc. All rights reserved.

Core Tip: Surgical resection of hepatocellular carcinoma is effective and curative treatment modality. However, early extrahepatic recurrence (EHR) after resection is related to poor prognosis. This study indicates the close correlation between the early EHR and survival outcome (hazard ratio 6.77, 95% confidence interval 4.81-9.52). The time to EHR was 8.8 mo and in 52.7% of early EHR group, EHR occurred as the first recurrence. On multivariate analysis, serum albumin < 4.0 g/dL, serum alkaline phosphatase > 100 U/L, surgical margin involvement, venous and/or lymphatic involvement, satellite nodules, tumor necrosis, tumor size ≥ 7 cm, and macrovascular invasion were associated risk factors with early EHR.

Citation: Yoon JH, Choi SK, Cho SB, Kim HJ, Ko YS, Jun CH. Early extrahepatic recurrence as a pivotal factor for survival after hepatocellular carcinoma resection: A 15-year observational study. *World J Gastroenterol* 2022; 28(36): 5351-5363

URL: https://www.wjgnet.com/1007-9327/full/v28/i36/5351.htm

DOI: https://dx.doi.org/10.3748/wjg.v28.i36.5351

INTRODUCTION

Surgical resection remains one of the best options for treating early hepatocellular carcinoma (HCC), along with liver transplantation and radiofrequency ablation[1-3]. With the development of surgical techniques and medical devices, surgical resection of tumors has been performed for a wide spectrum of patients with HCC. Nonetheless, HCC recurrence after surgery leads to an unfavorable prognosis and is still a major issue, with the 2-year recurrence rate ranging from 30.0% to 43.0%[4,5].

HCC recurrence after surgical resection mostly occurs inside the liver (intrahepatic), but recurrence outside the liver (extrahepatic) can also occur[2,6]. Most cases of extrahepatic recurrence (EHR) of HCC generally have an aggressive phenotype, and this contributes to poor survival outcomes[7]. Taketomi *et al*[6] reported the 3-, 5-, and 10-year cumulative survival rates of EHR as 60.3%, 24.0%, and 6.0%, respectively, which were lower than those in patients with intrahepatic recurrence (IHR) (74.5%, 57.7%, and 23.1%, respectively; $P = 0.004$). Although IHR of HCC can be managed by various loco-regional treatment modalities and systemic therapies, there are only limited methods for the treatment of EHR. However, despite an expected poor prognosis, favorable outcomes in selected patients with limited EHR have been reported with treatment modalities, such as metastasectomy[8]. Therefore, predicting the risk of EHR is essential, and better outcomes can be accomplished by predicting high-risk patients and monitoring these patients with close follow-up surveillance for early detection of EHR and/or timely postoperative adjuvant therapy.

We have reported simple parameters for predicting EHR after hepatectomy[9], and in that study, approximately 49.2% of the patients with EHR (31 of 63 patients) showed early EHR and demonstrated poorer recurrence-free survival (RFS) and overall survival rates. There have been many reports regarding the risk factors and predictive models for early recurrence mostly concerning IHR of HCC after surgery[10-12]; however, there are limited data regarding the risk factors and survival outcomes related to early EHR after surgical resection of HCC. Moreover, the clinical characteristics and survival outcomes of patients with early EHR in comparison with those with a later onset of EHR have not been examined. Hence, we aimed to investigate the characteristics and potential risk factors of early EHR after curative surgical resection for HCC and explore the relationship between early EHR and survival outcomes.

MATERIALS AND METHODS

Patients

This study enrolled 890 patients who underwent surgery for HCC from January 2004 to December 2019 at two tertiary hospitals. Patients with tumor types other than HCC, previous treatment experience, and ineligible data were excluded. Finally, 779 patients were enrolled for this study and were analyzed. Surgical resection of HCC was determined by a physician's decision regarding the tumor stage, liver function, and the patient's physical status. There had been no changes in the keynote of surgical resection during the study period in both centers. To exclude potential bias regarding surgical technique and concentrate on EHR development and survival rate based on tumor findings, patients who developed EHR prior to the completion of the post-surgical duration of 60 d were excluded.

Baseline HCC staging, surgical resection, and follow-up

HCC was diagnosed according to the guidelines of the Korean Liver Cancer Study Group and the National Cancer Center[13]. HCC staging at the time of diagnosis was determined using the modified Union for International Cancer Control (mUICC) staging system[14] and the Barcelona Clinic Liver Cancer (BCLC) classification system[3]. Milan criteria were based on radiologic findings at initial the diagnosis of HCC[15]. Abdominal computed tomography (CT) or magnetic resonance imaging (MRI) and assessment of serological tumor markers were routinely performed 1 mo after surgical resection and at each 3-6-month follow-up visit.

The tumor sizes were measured by radiologic modalities with CT or MRI. The histological differentiation of HCC was graded according to the criteria of Edmondson and Steiner[16]. The presence of macrovascular invasion was defined as vascular invasion of HCC detected on CT imaging or MRI while microvascular invasion was defined as invasion of vascular structures on microscopic analysis of resected tumor specimens. Lymph node metastasis, serosal invasion, bile duct invasion, capsule formation, multicentricity, satellite nodule, intrahepatic metastasis, tumor necrosis, tumor hemorrhage, and fatty changes within tumors were all confirmed from pathological findings of resected specimens. Overall survival was defined as the time interval in days between the date of diagnosis of HCC and the date of death or last follow-up examination. The cause of death of each patient is presented in Supplementary Table 1.

Diagnosis of recurrence and EHR

The diagnosis of EHR was confirmed by contrast-enhanced CT or MRI, and pathological examination was performed only for selected patients as decided by the physician. In addition, chest radiographs, bone scintigraphy, positron emission tomography-CT, and brain MR or CT imaging were used when new signs suggesting tumor metastasis manifested. Early EHR was defined as EHR that developed within 2 years after initial surgical resection. Most cases of EHR were diagnosed during the routine follow-up studies, with a few cases diagnosed during the evaluation of new-onset symptoms or based on significant elevation in alpha-fetoprotein (AFP) or serial AFP elevation without definite intra-hepatic lesions.

Ethics statement

This study was approved by the Institutional Review Board of Chonnam National University Hospital (IRB No. CNUH-2019-203). Because of the retrospective design of our study and the use of de-identified data, the requirement for informed consent was waived under the approval of the Institutional Review Board of Chonnam National University Hospital. The study was performed in compliance with the tenets of the 1975 Helsinki Declaration.

Statistical analysis

The data are presented as means ± SD or as medians and ranges, as appropriate, for the data type and distribution. Univariate analyses were performed using the chi-squared test or Student's *t*-test, as appropriate. Variables with a P value of < 0.05 on univariate analyses were included in a multivariate

logistic regression analysis to identify factors predictive of EHR. A multivariate Cox regression model was built using a stepwise backward selection of variables, and variables with a P value of < 0.05 were retained as predictive factors. The risk levels of EHR were defined based on the number of risk factors present, and Kaplan-Meier survival curves were constructed for each risk level. All statistical analyses were performed using SPSS software version 27.0 (IBM Corp., Armonk, NY, United States). The statistical methods of this study were reviewed by Cho Hee Hwang from the Biomedical research institute of Chonnam National University Hospital.

RESULTS

Baseline characteristics of the enrolled patients

The baseline characteristics of patients with early EHR were assessed (Table 1). These patients were younger, had lower serum albumin levels, and higher initial serum AFP concentration > 400 (IU/mL) than those without early EHR. Additionally, patients with early EHR showed more advanced tumor stage with respect to tumor size, BCLC stage, mUICC stage, and beyond Milan criteria. The patients in the early EHR group presented higher rates of macrovascular invasion and longer duration of hospital stay after liver resection. Furthermore, when we subdivided the patients into those without EHR, those with non-early EHR, and those with early EHR, the following factors exhibited a close relationship to the interval of EHR development: younger age, ALP levels, albumin levels, preoperative serum AFP > 1500 IU/mL, tumor size, tumor numbers, tumor stages, and the presence of macrovascular invasion (Supplementary Table 2).

Comparison of clinicopathological findings and clinical outcomes

We analyzed the surgical findings of tumor specimens categorized by the presence of early EHR (Table 2). Patients with early EHR had more metastatic lymph nodes, microvascular invasion, and satellite nodules (0.1% *vs* 4.1%, 16.3% *vs* 44.6%, and 12.2% *vs* 23.0%, respectively). Furthermore, the tumor specimens in the early EHR group showed a higher probability of tumor necrosis, hemorrhages, and absence of fatty changes (41.5% *vs* 82.4%, 43.0% *vs* 62.2%, and 36.0% *vs* 20.5%, respectively). On subgroup analysis stratifying patients with EHR into the early EHR and non-early EHR groups, microvascular invasion, serosal invasion, presence of satellite nodules, tumor necrosis, hemorrhages, and absence of fatty changes still showed consistent significance (Supplementary Table 3).

When comparing the findings on the first recurrence between the early and non-early EHR groups, the proportion of patients with serum AFP > 400 IU/mL was higher (10.2% *vs* 31.0%, P < 0.001) (Table 2) and the RFS was shorter (32.4 *vs* 5.21 mo, P < 0.001) in the early EHR group. These trends for serum AFP and RFS also showed consistency when we compared all patients with non-early EHR and early EHR (Supplementary Table 1). Furthermore, the mUICC stage at first recurrence was more advanced in the early EHR group (38.7% *vs* 75.7% with mUICC stage ≥ 3, P < 0.001), and 52.7% of patients developed EHR as the first recurrence after surgical resection.

Analysis of factors associated with early EHR

We performed Cox regression analysis to assess multiple factors relevant to EHR after surgical resection of HCC (Table 3). Among various risk factors, eight were proven to be closely associated with EHR, including serum albumin < 4.0 g/dL [Hazard ratio (HR), 2.12; P < 0.001], serum ALP > 100 U/L (HR, 1.586; P = 0.018), surgical margin involvement (HR, 2.53; P = 0.032), venous and/or lymphatic involvement (HR, 1.900; P = 0.002), satellite nodules (HR, 1.73; P = 0.011), tumor necrosis (HR, 1.92; P = 0.001), sum of tumor size ≥ 7 cm (HR, 1.84; P = 0.004), and macrovascular invasion (HR, 2.30; P = 0.008).

Analysis of factors associated with overall survival

We conducted Cox regression analysis to determine the risk factors associated with survival after surgical resection of HCC and to assess the relationship between early EHR and survival. On multivariate analysis, serum albumin < 4.0 g/dL (HR, 2.44; P < 0.001), serum ALP > 100 U/L (HR, 1.61; P = 0.001), major Edmondson-Steiner grade ≥ 3 (HR, 1.45; P = 0.008), pathological mUICC stage III or IVa (HR, 1.63; P = 0.002), satellite nodules (HR, 1.92; P < 0.011), tumor necrosis (HR, 1.35; P = 0.030), and early EHR (HR, 6.77; P < 0.001) were identified as factors related to survival outcome.

Cumulative rates of early EHR and overall survival

Among the 779 patients enrolled, 136 (17.5%) developed EHR during a median follow-up period of 4.41 years, and 74 (54.4%) exhibited early EHR after surgical resection of HCC. Both the cumulative rates of recurrence and the overall survival rates after surgical resection of HCC showed stepwise correlations with the interval to EHR (Figure 1). The 1-, 3-, 5-, and 10-year cumulative rates of recurrence were 15.8%, 35.4%, 46.5%, and 60.1% in the non-EHR group and were 32.3%, 64.5%, 85.5%, and 100.0% in the non-early EHR group. The early EHR group had a 1-year recurrence rate of 83.8% and 100.0% from the 2nd year after surgical resection (Figure 1A). The 1-, 3-, 5-, and 10-year cumulative rates of overall

Table 1 Baseline characteristics of the enrolled patients

	Patients without early EHR (*n* = 705)	Patients with early EHR (*n* = 74)	*P* value
Age (yr)	59.49 ± 10.08	56.51 ± 10.37	**0.020**
Male sex (*n*, %)	603 (85.5)	64 (86.5)	0.824
BMI (kg/m^2)	23.89 ± 3.03	24.10 ± 2.98	0.790
Etiology of hepatitis, *n* (%)			0.569
HBV/HCV	425 (63.2)/55 (8.2)	53 (73.6)/8 (11.1)	
Alcohol/combined	40 (10.4)/49 (7.0)	5 (6.9)/2 (2.8)	
NASH/unknown	1 (0.1)/73 (10.8)	0/4 (5.6)	
ALP (U/L)	89.25 ± 44.04	113.23 ± 106.76	0.059
Albumin (mg/dL)	4.36 ± 0.45	4.19 ± 0.48	**0.002**
ALBI grade ≥ 2, *n* (%)	97 (13.8)	16 (21.9)	0.063
ICG R15	12.02 ± 7.29	12.58 ± 7.62	0.566
Preoperative serum AFP > 400 (IU/mL)	127 (18.6)	24 (32.9)	**0.004**
Sum of tumor size	4.17 ± 2.44	6.06 ± 3.38	**< 0.001**
Tumor numbers	1.19 ± 0.54	1.32 ± 0.82	0.176
BCLC stage, *n* (%)			**< 0.001**
0/A/≥ B	89 (12.7)/491 (69.9)/122 (17.4)	3 (4.1)/44 (59.5)/27 (36.5)	
Pathological mUICC stage, *n* (%)			**< 0.001**
I/II/≥ III	111 (15.8)/431 (61.4)/160 (22.8)	2 (2.7)/32 (43.2)/40 (54.1)	
Radiological mUICC stage, *n* (%)			**< 0.001**
I/II/≥ III	112 (15.9%)/463 (66.0%)/127 (18.1%)	4 (5.4)/43 (58.1)/27 (36.5)	
Beyond Milan criteria, *n* (%)	179 (25.4)	40 (54.1)	**< 0.001**
Macrovascular invasion, *n* (%)	32 (4.6)	11 (14.9)	**< 0.001**
Hospital stay, days (median, range)	13.3 ± 7.1	15.6 ± 75.6	**0.049**
Follow-up duration, years (median, range)	4.8 (0.23-15.36)	1.8 (0.31-1.43)	**< 0.001**

Values are presented as mean ± SD. SD: Standard deviation; EHR: Extrahepatic recurrence; BMI: Body mass index; HBV: Hepatitis B virus; HCV: Hepatitis C virus; AST: Aspartate transaminase; ALT: Alanine transaminase; ALP: Alkaline phosphatase; AFP: Alpha-fetoprotein; BCLC: Barcelona Clinic Liver Cancer; mUICC: Modified Union for International Cancer Control.

survival were as follows: 97.8%, 90.2%, 80.9%, and 66.8% for the non-EHR group; 100.0%, 90.3%, 67.2%, and 9.9% for the non-early EHR group; and 74.9%, 23.0%, 15.2%, and 10.8% for the early EHR group (Figure 1B).

Cumulative rates of early EHR and survival categorized by risk factors

Depending on the eight factors proven to be associated with early EHR, we categorized the patients according to the number of risk factors. The cumulative rates of early EHR onset and survival were analyzed in the sub-categorized patients, and both rates showed stepwise correlations according to the number of risk factors (Figure 2A and B). Consequently, we stratified the patients into three categories: a low-risk group with 0-1 risk factor, an intermediate-risk group with 2-3 risk factors, and a high-risk group with ≥ 4 risk factors. The rates of EHR and survival exhibited a significant correlation with the risk stratification model (Figure 2C and D). The 1-, 2-, 3-, 5-, and 10-year cumulative rates of EHR in each group were as follows: 0.5%, 2.0%, 3.4%, 6.2%, and 16.8% in the low-risk group; 10.3%, 16.1%, 18.6%, 23.8%, and 42.8% in the intermediate-risk group; and 31.7%, 44.0%, 50.2%, 66.2%, and 77.5% in the high-risk group. The 1-, 3-, 5-, and 10-year overall survival rates in each group were as follows: 98.9%, 94.7%, 89.5%, and 70.0% in the low-risk group; 93.9%, 75.7%, 59.3%, and 38.1% in the intermediate-risk group; and 78.8%, 47.7%, 31.2%, and 12.5% in the high-risk group.

Table 2 Comparison of surgical findings and clinical outcomes in patients with and without extrahepatic recurrence

	Patients without early EHR (*n* = 705)	Patients with early EHR (*n* = 74)	*P* value
Margin involvement, *n* (%)	16 (2.3%)	4 (5.5%)	0.104
Metastatic lymph nodes, *n* (%)	1 (0.1)	3 (4.1)	**< 0.001**
Microvascular invasion, *n* (%)	114 (16.3)	33 (44.6)	**< 0.001**
Serosal invasion, *n* (%)	13 (1.9)	4 (5.4)	0.052
Bile duct invasion, *n* (%)	9 (1.3)	1 (1.4)	0.975
Capsule formation, *n* (%)	456 (66.7)	53 (71.6)	0.389
Multicentricity, *n* (%)	54 (7.8)	8 (10.8)	0.372
Satellite nodule, *n* (%)	84 (12.2)	17 (23.0)	**0.009**
Intrahepatic metastasis, *n* (%)	8 (1.2)	2 (2.7)	0.268
Necrosis, *n* (%)	286 (41.5)	61 (82.4)	**< 0.001**
Haemorrhage, *n* (%)	296 (43.0)	46 (62.2)	**0.002**
Fatty change, *n* (%)	246 (36.0)	15 (20.5)	**0.008**
Major Edmondson-Steiner grade, *n* (%)			0.243
1/2	30 (4.4)/352 (51.8)	2 (2.7)/30 (41.1)	
3/4	274 (40.3)/24 (3.5)	38 (52.1)/3 (4.1)	
Worst Edmondson-Steiner grade, *n* (%)			0.094
1/2	8 (1.1)/130 (18.9)	1 (1.4)/5 (6.8)	
3/4	357 (51.8)/194 (28.2)	40 (54.1)/28 (37.8)	
Serum AFP > 400 IU/mL on first recurrence	34 (10.2)	22 (31.0)	**< 0.001**
Recurrence-free survival, mo (median, range)	32.4 (2.24-177.34)	5.21 (2.04-20.28)	**< 0.001**
mUICC T stage on first recurrence, *n* (%)			**< 0.001**
0/1	6 (1.8)/144 (43.6)	10 (13.7)/23 (31.5)	
2/3	131 (39.7)/39 (11.8)	14 (19.2)/20 (27.4)	
4	10 (3.0)	6 (8.2)	
Second treatment modality			0.070
Surgery/RFA	46 (6.5)/95 (13.5)	9 (12.2)/10 (13.5)	
TACE/RFA + TACE	156(22.1)/14 (2.0)	13 (17.6)/6 (8.1)	
RT/systemic chemotherapy/BSC	20 (2.8)/11 (1.5)/20 (2.8)	3 (4.1)/1 (1.4)	

AFP: Alpha-fetoprotein; mUICC: Modified Union for International Cancer Control stage; RFA: Radiofrequency ablation; TACE: Trans-arterial chemoembolization; RT: Radiotherapy; BSC: Best supportive care.

DISCUSSION

EHR of HCC is a well-known predictive marker of poor survival outcomes, and EHR after surgical resection of HCC is deemed to be a pivotal factor for grave prognosis[7,9,17,18]. In this large-scale 15-year observational study conducted at two academic tertiary hospitals, EHR and early EHR occurred in 17.5% and 9.5% of 779 patients with HCC, respectively. Patients with early EHR had a rapid recurrence of HCC after surgical resection and poor survival outcomes. Furthermore, we elucidated the potential risk factors for early EHR after curative surgical resection of HCC.

Since the proportion of IHR cases is higher than that of EHR cases after surgical resection of HCC, previous studies have analyzed various risk factors associated with IHR alone, previous studies have analyzed various risk factors associated with IHR. Portolani *et al*[19] examined the early and late recurrence of HCC after liver resection and showed that the survival rates in the early recurrence group were significantly lower than those in the late recurrence group (25.7% *vs* 4.5% at 5 years). Moreover, similar results were demonstrated in a large-scale multicenter study conducted in China by Yan *et al*[20] comprising 1426 patients, where patients in the early recurrence group showed poor post-recurrence

Table 3 Univariate and multivariate analyses of factors associated with early extrahepatic recurrence

	Univariate analysis		Multivariate analysis	
	HR (95%CI)	*P* value	HR (95%CI)	*P* value
Serum albumin < 4.0 g/dL	2.27 (1.56-3.29)	< 0.001	**2.19 (1.45-3.31)**	**< 0.001**
Serum ALP > 100 U/L	1.76 (1.24-2.52)	0.002	**1.59 (1.08-2.32)**	**0.018**
ALBI grade ≥ 2	1.71 (1.12-2.59)	0.012		
Surgical margin involvement	2.30 (1.07-4.93)	0.032	**2.53 (1.09-5.90)**	**0.032**
Pathological mUICC stage (III, IVa)	2.94 (2.09-4.12)	< 0.001		
Multiple tumors[1]	3.21 (1.57-6.56)	0.002		
Venous/lymphatic involvement[2]	2.98 (2.09-4.25)	< 0.001	**1.90 (1.28-2.83)**	**0.002**
Serosa invasion	2.86 (1.33-6.12)	0.007		
Bile duct invasion	3.25 (1.20-8.83)	0.020		
Satellite nodule	2.69 (1.83-3.94)	< 0.001	**1.73 (1.14-2.63)**	**0.011**
Intrahepatic metastasis	2.99 (1.10-8.09)	0.032		
Tumor necrosis	3.18 (2.20-4.61)	<0.001	**1.92 (1.29-2.79)**	**0.001**
Tumor hemorrhage	1.81 (1.28-2.55)	0.001		
Sum of tumor size ≥ 7 cm	3.25 (2.23-4.73)	< 0.001	**1.84 (1.21-2.77)**	**0.004**
Macrovascular invasion	2.48 (1.37-4.50)	0.003	**2.30 (1.24-4.26)**	**0.008**
Serum AFP > 1500 IU/mL	1.99 (1.27-3.12)	0.003		

[1]Number of tumors examined during pathological evaluation.
[2]Confirmed findings during pathological evaluation.
HR: Hazards ratio; CI: Confidence interval; ALP: Alkaline phosphatase; ALBI: Albumin-bilirubin; mUICC: Modified Union for International Cancer Control; AFP: Alpha-fetoprotein.

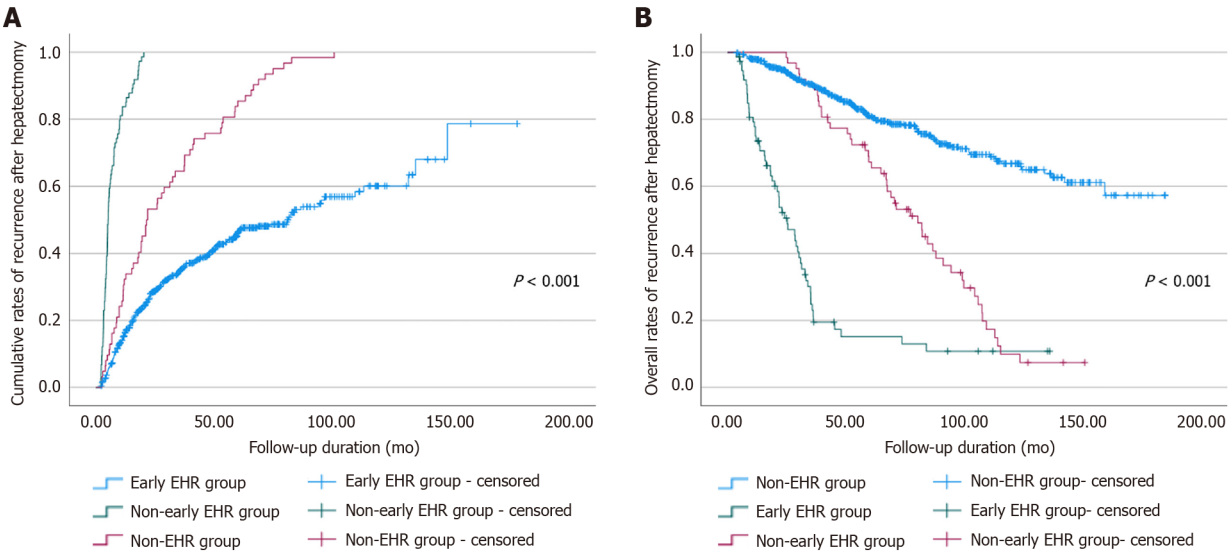


Figure 1 Both the cumulative rates of recurrence and the overall survival rates after surgical resection of hepatocellular carcinoma showed stepwise correlations with the interval to extrahepatic recurrence. A: Cumulative rate of the first recurrence of hepatocellular carcinoma after curative surgical resection; B: Overall survival rates stratified by the characteristics of extrahepatic recurrence. EHR: Extrahepatic recurrence.

survival (13.5 *vs* 36.6 mo, $P < 0.001$). Furthermore, Yang *et al*[21] stated that recurrent HCC cases with multicentric recurrence may have had greater survival than intrahepatic metastasis cases. In contrast, Byeon *et al*[22] compared the outcomes of 111 patients with IHR and 41 patients with EHR who had undergone surgical resection for HCC and found that patients in the EHR group showed significantly lower 5-year survival rates than those in the IHR group (21.5% *vs* 36.3%, $P < 0.001$). Considering the

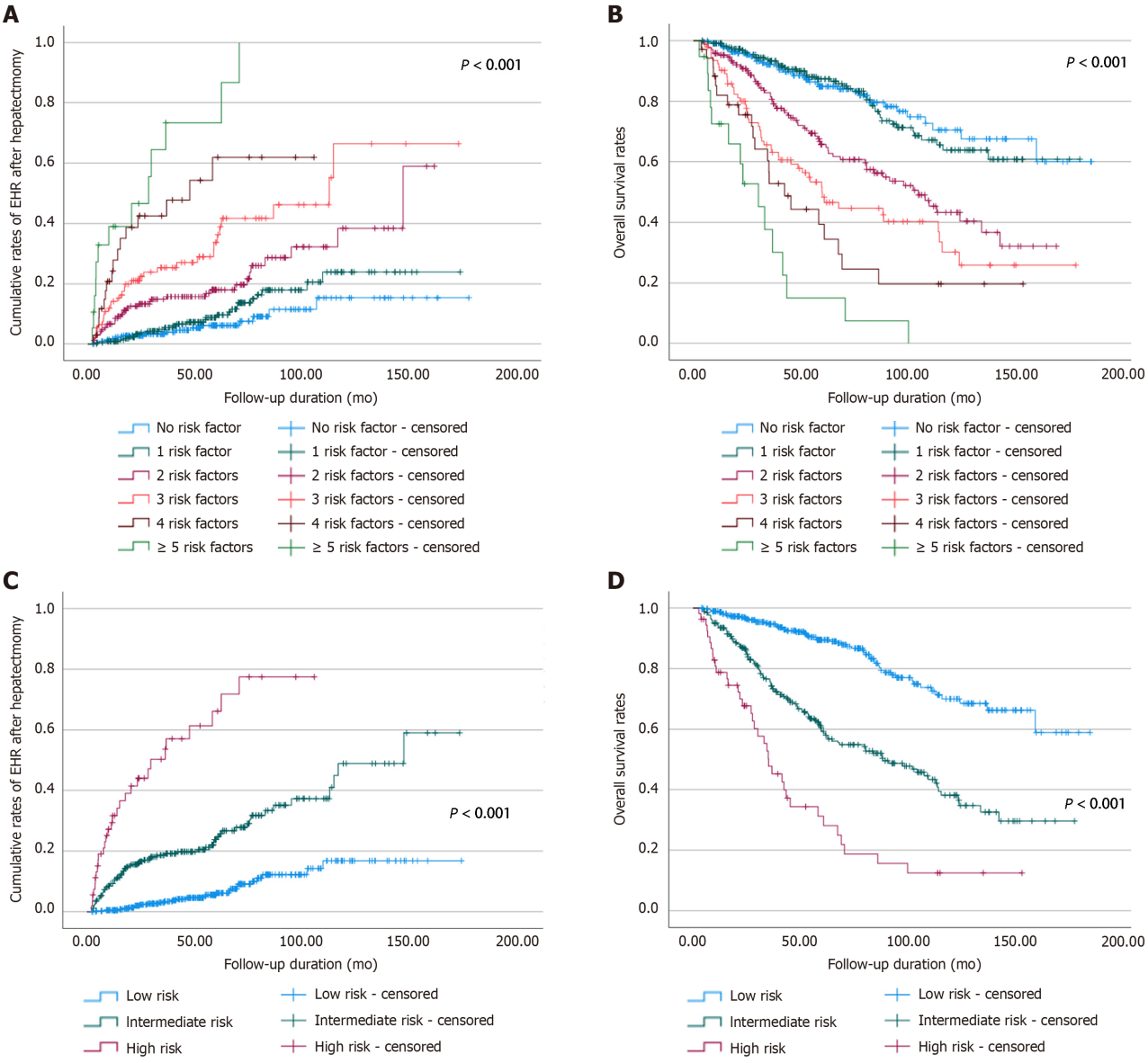


Figure 2 Patients were classified according to the number of eight risk factors related to early extrahepatic recurrence, and the probability of extrahepatic recurrence and overall survival rate was evaluated. A: Cumulative rates of extrahepatic recurrence; B: Cumulative rates of overall survival after surgical resection; C: The cumulative rates of extrahepatic recurrence; D: The cumulative rates of overall survival. EHR: Extrahepatic recurrence.

non-negligible rates of EHR after surgical resection of HCC and the dismal prognosis of patients with EHR, risk stratification and prediction of early EHR may have been of great importance in improving the clinical outcome.

In 52.7% of the patients with early EHR, EHR was the first recurrence of HCC after surgical resection (Supplementary Table 1), and both interval to first recurrence and EHR were significantly shorter in the early EHR group compared with that in the non-early EHR group (5.2 *vs* 21.6 mo, $P < 0.001$; and 8.81 *vs* 58.57 mo, $P < 0.001$). Moreover, a higher proportion of patients with early EHR showed an advanced stage at first recurrence (mUICC stage ≥ 3, 75.7% *vs* 38.7%, $P < 0.001$), and 43.2% of patients had no intrahepatic HCC (mUICC T stage 0) at EHR. This suggests that EHR may occur within a very short interval after surgical resection of HCC with an advanced tumor stage while intrahepatic HCC is not exhibited. Considering the aggressive nature of the tumors in patients with early EHR, adjuvant therapy after surgical resection or meticulous postoperative surveillance may be highly required in a specific group of patients to prompt detection of EHR. In addition, with respect to the high proportion of patients with EHR as their first recurrence (52.7%), pre- and/or peri-operative factors are considered to play critical roles in predicting early EHR.

Among the several factors associated with early EHR, serum albumin < 4.0 g/dL, serum ALP > 100 U/L, surgical margin involvement, venous and/or lymphatic involvement, satellite nodules, tumor necrosis, tumor size ≥ 7 cm, and the presence of macrovascular invasion confirmed on radiologic examination were identified as risk factors related to early EHR, as determined by multivariate Cox regression analysis (Table 3). The concentrations of albumin and/or ALP alone or in combination with

other parameters have been proposed as useful markers for predicting recurrence after surgical removal of HCC in previous studies[23-26]. Li *et al*[27] showed the prognostic value of the albumin-to-ALP ratio in patients with HCC who received liver transplants, whereas Yu *et al*[26] determined ALP concentration as an independent factor influencing disease-free survival and overall survival that aids in the prediction of recurrence in high-risk patients with HCC. Additionally, involvement of the surgical margins was related to poor clinical outcomes, as shown by a previous study[28] and a meta-analysis conducted by Zhong *et al*[29], which is consistent with the findings of our study. Chen *et al*[30] reported a poorer prognosis related to microvascular invasion in solitary small HCC in their meta-analysis, while Hasegawa *et al*[31] reported the association between lymphatic system involvement and patient survival after surgical resection of HCC, which are consistent with our findings. In a large-scale study of 734 patients who underwent surgery for HCC, satellite nodules, tumor size (> 5 cm), and the presence of macrovascular invasion were closely related to late recurrence of HCC in multivariate analysis (HR, 1.59, 1.49, and 4.63, respectively), and these findings are concordant with our study[32]. A recent study by Wei *et al*[33] reported that tumor necrosis was associated with the prognosis of patients undergoing surgery for HCC with regard to overall survival and RFS and advanced tumor characteristics, and Ling *et al*[34] also reported tumor necrosis as a potential parameter of the aggressiveness of HCC. Concordant with these previous study results, our study also demonstrated a significant association between tumor necrosis and early EHR.

In addition, we analyzed multiple factors associated with overall survival after surgical resection of HCC and identified that serum albumin < 4.0 g/dL, serum ALP > 100 U/L, major Edmondson-Steiner grade ≥ 3, pathological mUICC stage III or IVa, satellite nodules, tumor necrosis, and early EHR were related to survival (Table 4). Most risk factors exhibited similar results in the multivariate analysis of factors associated with early EHR (serum albumin < 4.0 g/dL, serum ALP > 100 U/L, satellite nodules, and tumor necrosis). The Edmondson-Steiner grade has been previously reported as a crucial predictor of recurrence and survival by Zhou *et al*[31] and Martins-Filho *et al*[32], and our study also showed poor survival outcomes in patients with major Edmondson-Steiner grade ≥ 3. Finally, early EHR showed a significant association with poor survival and increased the risk of death more than six times (HR, 6.77; 95%CI, 4.81-9.52; $P < 0.001$).

The cumulative rates of first recurrence and overall survival were correlated with the development of EHR and the interval to EHR (Figure 1). In particular, patients with early EHR showed substantially worse survival outcomes (HR, 6.77; 95%CI, 4.81-9.52; $P < 0.001$). Furthermore, considering the heterogeneity of patient characteristics regarding the tumor nature, degree of liver cirrhosis, and diverse disease courses after surgical resection, predictive markers of early EHR within 2 years after surgical resection with preoperative and/or operative factors may well reflect the initial state of the tumor.

We categorized the patients by the number of eight risk factors associated with early EHR and assessed the probability rates of EHR and overall survival. As demonstrated in Figure 2, there was a significant relationship between the number of the risk factors and the cumulative rates of both EHR and overall survival ($P < 0.001$). For a simple and intuitive predictive model of EHR, we subgrouped the patients into three categories: a low-risk group with 0-1 risk factor, an intermediate-risk group with 2-3 risk factors, and a high-risk group with ≥ 4 risk factors. The rates of both EHR and survival showed a substantial correlation with these risk stratifications. Hence, the prediction of early EHR after surgical resection of HCC may be regarded as essential, especially for high-risk patients.

Our study had several limitations. First, this study was retrospective and included patients with heterogenous clinical courses and outcomes. The postoperative surveillance methods, schedule, and treatment methods for recurrence of HCC were not fully standardized. To minimize the potential bias owing to the design of this study, we strived to enroll a large number of patients in multiple tertiary academic hospitals. Furthermore, the fact that more than half of the patients (52.7%) developed EHR as their first recurrence highlighted the importance of preoperative and operative factors. Second, although pathological confirmation of EHR was performed for a few patients, most instances of EHR were solely identified at the physician's discretion using imaging diagnostic modalities. Finally, owing to patient geographic characteristics, the majority of patients had chronic hepatitis B as the etiology of liver cirrhosis and HCC. Further studies are warranted to investigate characteristics and risk factors for early EHR in patients with diverse chronic hepatitis by using a standardized study protocol. Especially, the use of radiomic tumor features for the prediction of recurrence after HCC treatment can be considered as an additional tool for prompt detection of early EHR[35,36]. Using an accurate tool for the prediction of early EHR, the prognosis of patients with a high risk of early EHR may be improved with the utilization of adjunctive post-operative therapy.

CONCLUSION

Patients with early EHR showed rapid recurrence of HCC after surgical resection and significantly worse survival outcomes. . We derived several risk factors associated with early EHR and the numbers of risk factors correlated with not only with cumulative rates of EHR but also with survival rates. In terms of poor prognosis associated with early EHR, patients who undergo surgical resection for HCC

Table 4 Univariate and multivariate analysis of factors associated with overall survival

	Univariate analysis		Multivariate analysis	
	HR (95%CI)	*P* value	HR (95%CI)	*P* value
Serum albumin < 4.0 g/dL	2.14 (1.61-2.85)	< 0.001	**2.44 (1.79-3.32)**	**< 0.001**
ALBI grade ≥ 2	1.84 (1.36-2.51)	< 0.001		
Serum ALP > 100 U/L	1.84 (1.41-2.41)	< 0.001	**1.62 (1.22-2.16)**	**0.001**
Single tumor[1]	1.87 (1.21-2.91)	0.005		
Major Edmondson-Steiner grade ≥ 3	1.64 (1.26-2.13)	< 0.001	**1.45 (1.10-1.90)**	**0.008**
Venous/lymphatic involvement[2]	2.44 (1.84-3.22)	< 0.001		
Pathological mUICC stage (III, IVa)	2.59 (2.00-3.35)	< 0.001	**1.63 (1.21-2.22)**	**0.002**
Bile duct invasion	2.72 (1.21-6.13)	0.016		
Intrahepatic metastasis	3.66 (1.72-7.77)	0.001		
Multicentricity	1.91 (1.29-2.82)	0.001		
Satellite nodule	2.45 (1.82-3.30)	< 0.001	**1.92 (1.38-2.69)**	**< 0.001**
Tumor necrosis	2.12 (1.63-2.77)	< 0.001	**1.35 (1.030-1.78)**	**0.030**
Tumor hemorrhage	1.58 (1.21-2.05)	0.001		
Sum of tumor size ≥ 7 cm	2.21 (1.63-3.00)	< 0.001		
Beyond Milan criteria	1.79 (1.38-2.33)	< 0.001		
Serum AFP > 1500 IU/mL	1.47 (1.01-2.15)	0.046		
Early extrahepatic recurrence	7.72 (5.67-10.51)	< 0.001	**6.77 (4.81-9.52)**	**< 0.001**

[1]Number of tumors examined during pathological evaluation.
[2]Confirmed findings during pathological evaluation.
HR: Hazards ratio; CI: Confidence interval; ALBI: Albumin-bilirubin; ALP: Alkaline phosphatase; mUICC: Modified Union for International Cancer Control; AFP: Alpha-fetoprotein.

can be stratified by the risk of EHR with our model, and meticulous postoperative surveillance and adjuvant therapies may be required for timely EHR detection and positive clinical outcomes.

ARTICLE HIGHLIGHTS

Research background

Surgical resection is one of the most widely used modalities for the treatment of hepatocellular carcinoma (HCC). Early extrahepatic recurrence (EHR) of HCC after surgical resection is considered to be closely associated with poor prognosis.

Research motivation

Data regarding risk factors and survival outcomes of early EHR after surgical resection remain scarce.

Research objectives

We decided to investigate the clinical features and risk factors of early EHR and elucidate its association with survival outcomes.

Research methods

From January 2004 to December 2019, we enrolled treatment-naïve patients who were ≥ 18 years and underwent surgical resection for HCC in two tertiary academic centers. After excluding patients with tumor types other than HCC and/or ineligible data, this retrospective study finally included 779 patients. Surgical resection of HCC was performed according to the physicians' decisions and the EHR was diagnosed based on contrast-enhanced computed tomography or magnetic resonance imaging, and pathologic confirmation was performed in selected patients. Multivariate Cox regression analysis was performed to identify the variables associated with EHR.

Research results

Early EHR within 2 years after surgery was diagnosed in 9.5% of patients during a median follow-up period of 4.4 years. The recurrence-free survival period was 5.2 mo, and the median time to EHR was 8.8 mo in patients with early EHR. In 52.7% of patients with early EHR, EHR occurred as the first recurrence of HCC after surgical resection. On multivariate analysis, serum albumin < 4.0 g/dL, serum alkaline phosphatase > 100 U/L, surgical margin involvement, venous and/or lymphatic involvement, satellite nodules, tumor necrosis detected by pathology, tumor size ≥ 7 cm, and macrovascular invasion were determined as risk factors associated with early EHR. After sub-categorizing the patients according to the number of risk factors, the rates of both EHR and survival showed a significant correlation with the risk of early EHR. Furthermore, multivariate analysis revealed that early EHR was associated with substantially worse survival outcomes (hazard ratio, 6.77; 95% confidence interval, 4.81-9.52; $P < 0.001$).

Research conclusions

Early EHR significantly deteriorates the survival of patients with HCC, and our identified risk factors may predict the clinical outcomes and aid in postoperative strategies for improving survival.

Research perspectives

Further studies are warranted to investigate characteristics and risk factors for early EHR in patients with diverse chronic hepatitis by using a standardized study protocol. Using an accurate tool for the prediction of early EHR, the prognosis of patients with a high risk of early EHR may be improved with the utilization of adjunctive post-operative therapy.

FOOTNOTES

Author contributions: Yoon JH wrote the manuscript; Choi SK, Cho SB, and Jun CH designed the concept of the study; Yoon JH, Kim HJ, and Ko YS collected and analyzed the data on baseline patient characteristics and recurrence of HCC; Yoon JH interpreted the data; Choi SK, Cho SB, and Jun CH supervised the project.

Supported by Research Supporting Program of the Korean Association for the Study of the Liver and the Korean Liver Foundation, No. KASLKLF2019-06; and Chonnam National University Hospital Biomedical Research Institute, No. BCRI121007.

Institutional review board statement: This study was approved by the Institutional Review Board of Chonnam National University Hospital (IRB No. CNUH-2019-203).

Informed consent statement: Owing to the retrospective design of our study and the use of de-identified data, the requirement for informed consent was waived under the approval of the Institutional Review Board of Chonnam National University Hospital.

Conflict-of-interest statement: The authors declare no competing interests.

Data sharing statement: Data available on additional request.

STROBE statement: The authors have read the STROBE Statement—checklist of items, and the manuscript was prepared and revised according to the STROBE Statement—checklist of items.

Open-Access: This article is an open-access article that was selected by an in-house editor and fully peer-reviewed by external reviewers. It is distributed in accordance with the Creative Commons Attribution NonCommercial (CC BY-NC 4.0) license, which permits others to distribute, remix, adapt, build upon this work non-commercially, and license their derivative works on different terms, provided the original work is properly cited and the use is non-commercial. See: https://creativecommons.org/Licenses/by-nc/4.0/

Country/Territory of origin: South Korea

ORCID number: Jae Hyun Yoon 0000-0002-4993-2496; Sung Kyu Choi 0000-0002-6878-3385; Sung Bum Cho 0000-0001-9816-3446; Hee Joon Kim 0000-0002-8636-5726; Yang Seok Ko 0000-0000-0368-5389; Chung Hwan Jun 0000-0002-7136-8350.

S-Editor: Wu YXJ
L-Editor: A
P-Editor: Li X

REFERENCES

1 **Villanueva A**. Hepatocellular Carcinoma. *N Engl J Med* 2019; **380**: 1450-1462 [PMID: 30970190 DOI: 10.1056/NEJMra1713263]
2 **Torimura T**, Iwamoto H. Optimizing the management of intermediate-stage hepatocellular carcinoma: Current trends and prospects. *Clin Mol Hepatol* 2021; **27**: 236-245 [PMID: 33317248 DOI: 10.3350/cmh.2020.0204]
3 **Reig M**, Forner A, Rimola J, Ferrer-Fàbrega J, Burrel M, Garcia-Criado Á, Kelley RK, Galle PR, Mazzaferro V, Salem R, Sangro B, Singal AG, Vogel A, Fuster J, Ayuso C, Bruix J. BCLC strategy for prognosis prediction and treatment recommendation: The 2022 update. *J Hepatol* 2022; **76**: 681-693 [PMID: 34801630 DOI: 10.1016/j.jhep.2021.11.018]
4 **Chan AWH**, Zhong J, Berhane S, Toyoda H, Cucchetti A, Shi K, Tada T, Chong CCN, Xiang BD, Li LQ, Lai PBS, Mazzaferro V, García-Fiñana M, Kudo M, Kumada T, Roayaie S, Johnson PJ. Development of pre and post-operative models to predict early recurrence of hepatocellular carcinoma after surgical resection. *J Hepatol* 2018; **69**: 1284-1293 [PMID: 30236834 DOI: 10.1016/j.jhep.2018.08.027]
5 **Kim J**, Kang W, Sinn DH, Gwak GY, Paik YH, Choi MS, Lee JH, Koh KC, Paik SW. Substantial risk of recurrence even after 5 recurrence-free years in early-stage hepatocellular carcinoma patients. *Clin Mol Hepatol* 2020; **26**: 516-528 [PMID: 32911589 DOI: 10.3350/cmh.2020.0016]
6 **Taketomi A**, Toshima T, Kitagawa D, Motomura T, Takeishi K, Mano Y, Kayashima H, Sugimachi K, Aishima S, Yamashita Y, Ikegami T, Gion T, Uchiyama H, Soejima Y, Maeda T, Shirabe K, Maehara Y. Predictors of extrahepatic recurrence after curative hepatectomy for hepatocellular carcinoma. *Ann Surg Oncol* 2010; **17**: 2740-2746 [PMID: 20411432 DOI: 10.1245/s10434-010-1076-2]
7 **Uka K**, Aikata H, Takaki S, Shirakawa H, Jeong SC, Yamashina K, Hiramatsu A, Kodama H, Takahashi S, Chayama K. Clinical features and prognosis of patients with extrahepatic metastases from hepatocellular carcinoma. *World J Gastroenterol* 2007; **13**: 414-420 [PMID: 17230611 DOI: 10.3748/wjg.v13.i3.414]
8 **Wang L**, Ye G, Zhan C, Sun F, Lin Z, Jiang W, Wang Q. Clinical Factors Predictive of a Better Prognosis of Pulmonary Metastasectomy for Hepatocellular Carcinoma. *Ann Thorac Surg* 2019; **108**: 1685-1691 [PMID: 31445050 DOI: 10.1016/j.athoracsur.2019.06.086]
9 **Yoon JH**, Lee WJ, Kim SM, Kim KT, Cho SB, Kim HJ, Ko YS, Kook HY, Jun CH, Choi SK, Kim BS, Cho SY, You HS, Lee Y, Son S. Simple parameters predicting extrahepatic recurrence after curative hepatectomy for hepatocellular carcinoma. *Sci Rep* 2021; **11**: 12984 [PMID: 34155324 DOI: 10.1038/s41598-021-92503-6]
10 **Li WF**, Yen YH, Liu YW, Wang CC, Yong CC, Lin CC, Cheng YF, Wang JH, Lu SN. Preoperative predictors of early recurrence after resection for hepatocellular carcinoma. *Am J Surg* 2022; **223**: 945-950 [PMID: 34399978 DOI: 10.1016/j.amjsurg.2021.08.012]
11 **Beumer BR**, Takagi K, Vervoort B, Buettner S, Umeda Y, Yagi T, Fujiwara T, Steyerberg EW, IJzermans JNM. Prediction of Early Recurrence After Surgery for Liver Tumor (ERASL): An International Validation of the ERASL Risk Models. *Ann Surg Oncol* 2021; **28**: 8211-8220 [PMID: 34235600 DOI: 10.1245/s10434-021-10235-3]
12 **Saito A**, Toyoda H, Kobayashi M, Koiwa Y, Fujii H, Fujita K, Maeda A, Kaneoka Y, Hazama S, Nagano H, Mirza AH, Graf HP, Cosatto E, Murakami Y, Kuroda M. Prediction of early recurrence of hepatocellular carcinoma after resection using digital pathology images assessed by machine learning. *Mod Pathol* 2021; **34**: 417-425 [PMID: 32948835 DOI: 10.1038/s41379-020-00671-z]
13 **Llovet JM**, Di Bisceglie AM, Bruix J, Kramer BS, Lencioni R, Zhu AX, Sherman M, Schwartz M, Lotze M, Talwalkar J, Gores GJ; Panel of Experts in HCC-Design Clinical Trials. Design and endpoints of clinical trials in hepatocellular carcinoma. *J Natl Cancer Inst* 2008; **100**: 698-711 [PMID: 18477802 DOI: 10.1093/jnci/djn134]
14 **Kudo M**, Kitano M, Sakurai T, Nishida N. General Rules for the Clinical and Pathological Study of Primary Liver Cancer, Nationwide Follow-Up Survey and Clinical Practice Guidelines: The Outstanding Achievements of the Liver Cancer Study Group of Japan. *Dig Dis* 2015; **33**: 765-770 [PMID: 26488173 DOI: 10.1159/000439101]
15 **Mazzaferro V**, Regalia E, Doci R, Andreola S, Pulvirenti A, Bozzetti F, Montalto F, Ammatuna M, Morabito A, Gennari L. Liver transplantation for the treatment of small hepatocellular carcinomas in patients with cirrhosis. *N Engl J Med* 1996; **334**: 693-699 [PMID: 8594428 DOI: 10.1056/NEJM199603143341104]
16 **EDMONDSON HA**, STEINER PE. Primary carcinoma of the liver: a study of 100 cases among 48,900 necropsies. *Cancer* 1954; **7**: 462-503 [PMID: 13160935 DOI: 10.1002/1097-0142(195405)7:3<462::aid-cncr2820070308>3.0.co;2-e]
17 **Yoon JH**, Goo YJ, Lim CJ, Choi SK, Cho SB, Shin SS, Jun CH. Features of extrahepatic metastasis after radiofrequency ablation for hepatocellular carcinoma. *World J Gastroenterol* 2020; **26**: 4833-4845 [PMID: 32921960 DOI: 10.3748/wjg.v26.i32.4833]
18 **Natsuizaka M**, Omura T, Akaike T, Kuwata Y, Yamazaki K, Sato T, Karino Y, Toyota J, Suga T, Asaka M. Clinical features of hepatocellular carcinoma with extrahepatic metastases. *J Gastroenterol Hepatol* 2005; **20**: 1781-1787 [PMID: 16246200 DOI: 10.1111/j.1440-1746.2005.03919.x]
19 **Portolani N**, Coniglio A, Ghidoni S, Giovanelli M, Benetti A, Tiberio GA, Giulini SM. Early and late recurrence after liver resection for hepatocellular carcinoma: prognostic and therapeutic implications. *Ann Surg* 2006; **243**: 229-235 [PMID: 16432356 DOI: 10.1097/01.sla.0000197706.21803.a1]
20 **Yan WT**, Li C, Yao LQ, Qiu HB, Wang MD, Xu XF, Zhou YH, Wang H, Chen TH, Gu WM. Predictors and long-term prognosis of early and late recurrence for patients undergoing hepatic resection of hepatocellular carcinoma: a large-scale multicenter study. *Hepatobiliary Surg Nutr* 2021 [DOI: 10.21037/hbsn-21-288]
21 **Yang SL**, Luo YY, Chen M, Zhou YP, Lu FR, Deng DF, Wu YR. A systematic review and meta-analysis comparing the prognosis of multicentric occurrence and vs. intrahepatic metastasis in patients with recurrent hepatocellular carcinoma after hepatectomy. *HPB (Oxford)* 2017; **19**: 835-842 [PMID: 28734693 DOI: 10.1016/j.hpb.2017.06.002]
22 **Byeon J**, Cho EH, Kim SB, Choi DW. Extrahepatic recurrence of hepatocellular carcinoma after curative hepatic resection. *Korean J Hepatobiliary Pancreat Surg* 2012; **16**: 93-97 [PMID: 26388915 DOI: 10.14701/kjhbps.2012.16.3.93]
23 **He W**, Peng B, Tang Y, Yang J, Zheng Y, Qiu J, Zou R, Shen J, Li B, Yuan Y. Nomogram to Predict Survival of Patients With Recurrence of Hepatocellular Carcinoma After Surgery. *Clin Gastroenterol Hepatol* 2018; **16**: 756-764.e10 [PMID:

29246702 DOI: 10.1016/j.cgh.2017.12.002]

24 **Jeng LB**, Li TC, Hsu SC, Chan WL, Teng CF. Association of Low Serum Albumin Level with Higher Hepatocellular Carcinoma Recurrence in Patients with Hepatitis B Virus Pre-S2 Mutant after Curative Surgical Resection. *J Clin Med* 2021; **10** [PMID: 34575311 DOI: 10.3390/jcm10184187]

25 **Ekpanyapong S**, Philips N, Loza BL, Abt P, Furth EE, Tondon R, Khungar V, Olthoff K, Shaked A, Hoteit MA, Reddy KR. Predictors, Presentation, and Treatment Outcomes of Recurrent Hepatocellular Carcinoma After Liver Transplantation: A Large Single Center Experience. *J Clin Exp Hepatol* 2020; **10**: 304-315 [PMID: 32655233 DOI: 10.1016/j.jceh.2019.11.003]

26 **Yu MC**, Chan KM, Lee CF, Lee YS, Eldeen FZ, Chou HS, Lee WC, Chen MF. Alkaline phosphatase: does it have a role in predicting hepatocellular carcinoma recurrence? *J Gastrointest Surg* 2011; **15**: 1440-1449 [PMID: 21541770 DOI: 10.1007/s11605-011-1537-3]

27 **Li H**, Wang L, Chen L, Zhao H, Cai J, Yao J, Zheng J, Yang Y, Wang G. Prognostic Value of Albumin-to-Alkaline Phosphatase Ratio in Hepatocellular Carcinoma Patients Treated with Liver Transplantation. *J Cancer* 2020; **11**: 2171-2180 [PMID: 32127944 DOI: 10.7150/jca.39615]

28 **Wang H**, Yu H, Qian YW, Cao ZY, Wu MC, Cong WM. Impact of Surgical Margin on the Prognosis of Early Hepatocellular Carcinoma (≤5 cm): A Propensity Score Matching Analysis. *Front Med (Lausanne)* 2020; **7**: 139 [PMID: 32478080 DOI: 10.3389/fmed.2020.00139]

29 **Zhong FP**, Zhang YJ, Liu Y, Zou SB. Prognostic impact of surgical margin in patients with hepatocellular carcinoma: A meta-analysis. *Medicine (Baltimore)* 2017; **96**: e8043 [PMID: 28906395 DOI: 10.1097/MD.0000000000008043]

30 **Chen ZH**, Zhang XP, Wang H, Chai ZT, Sun JX, Guo WX, Shi J, Cheng SQ. Effect of microvascular invasion on the postoperative long-term prognosis of solitary small HCC: a systematic review and meta-analysis. *HPB (Oxford)* 2019; **21**: 935-944 [PMID: 30871805 DOI: 10.1016/j.hpb.2019.02.003]

31 **Hasegawa K**, Makuuchi M, Kokudo N, Izumi N, Ichida T, Kudo M, Ku Y, Sakamoto M, Nakashima O, Matsui O, Matsuyama Y; Liver Cancer Study Group of Japan. Impact of histologically confirmed lymph node metastases on patient survival after surgical resection for hepatocellular carcinoma: report of a Japanese nationwide survey. *Ann Surg* 2014; **259**: 166-170 [PMID: 23532111 DOI: 10.1097/SLA.0b013e31828d4960]

32 **Xu XF**, Xing H, Han J, Li ZL, Lau WY, Zhou YH, Gu WM, Wang H, Chen TH, Zeng YY, Li C, Wu MC, Shen F, Yang T. Risk Factors, Patterns, and Outcomes of Late Recurrence After Liver Resection for Hepatocellular Carcinoma: A Multicenter Study From China. *JAMA Surg* 2019; **154**: 209-217 [PMID: 30422241 DOI: 10.1001/jamasurg.2018.4334]

33 **Wei T**, Zhang XF, Bagante F, Ratti F, Marques HP, Silva S, Soubrane O, Lam V, Poultsides GA, Popescu I, Grigorie R, Alexandrescu S, Martel G, Workneh A, Guglielmi A, Hugh T, Aldrighetti L, Endo I, Pawlik TM. Tumor Necrosis Impacts Prognosis of Patients Undergoing Curative-Intent Hepatocellular Carcinoma. *Ann Surg Oncol* 2021; **28**: 797-805 [PMID: 33249525 DOI: 10.1245/s10434-020-09390-w]

34 **Ling YH**, Chen JW, Wen SH, Huang CY, Li P, Lu LH, Mei J, Li SH, Wei W, Cai MY, Guo RP. Tumor necrosis as a poor prognostic predictor on postoperative survival of patients with solitary small hepatocellular carcinoma. *BMC Cancer* 2020; **20**: 607 [PMID: 32600297 DOI: 10.1186/s12885-020-07097-5]

35 **Wang F**, Chen Q, Zhang Y, Chen Y, Zhu Y, Zhou W, Liang X, Yang Y, Hu H. CT-Based Radiomics for the Recurrence Prediction of Hepatocellular Carcinoma After Surgical Resection. *J Hepatocell Carcinoma* 2022; **9**: 453-465 [PMID: 35646748 DOI: 10.2147/JHC.S362772]

36 **Iezzi R**, Casà C, Posa A, Cornacchione P, Carchesio F, Boldrini L, Tanzilli A, Cerrito L, Fionda B, Longo V, Miele L, Lancellotta V, Cellini F, Tran HE, Ponziani FR, Giuliante F, Rapaccini GL, Grieco A, Pompili M, Gasbarrini A, Valentini V, Gambacorta MA, Tagliaferri L, Manfredi R. Project for interventional Oncology LArge-database in liveR Hepatocellular carcinoma - Preliminary CT-based radiomic analysis (POLAR Liver 1.1). *Eur Rev Med Pharmacol Sci* 2022; **26**: 2891-2899 [PMID: 35503635 DOI: 10.26355/eurrev_202204_28620]

World Journal of Gastroenterology

Submit a Manuscript: https://www.f6publishing.com

World J Gastroenterol 2022 September 28; 28(36): 5364-5379

DOI: 10.3748/wjg.v28.i36.5364

ISSN 1007-9327 (print) ISSN 2219-2840 (online)

ORIGINAL ARTICLE

Observational Study

Atherogenic index of plasma combined with waist circumference and body mass index to predict metabolic-associated fatty liver disease

Shao-Jie Duan, Zhi-Ying Ren, Tao Zheng, Hong-Ye Peng, Zuo-Hu Niu, Hui Xia, Jia-Liang Chen, Yuan-Chen Zhou, Rong-Rui Wang, Shu-Kun Yao

Specialty type: Gastroenterology and hepatology

Provenance and peer review: Unsolicited article; Externally peer reviewed.

Peer-review model: Single blind

Peer-review report's scientific quality classification

Grade A (Excellent): 0
Grade B (Very good): 0
Grade C (Good): C, C
Grade D (Fair): 0
Grade E (Poor): 0

P-Reviewer: Cumhur Cure M, Turkey; Lin WR, Taiwan

Received: June 26, 2022
Peer-review started: June 26, 2022
First decision: August 1, 2022
Revised: August 9, 2022
Accepted: September 8, 2022
Article in press: September 8, 2022
Published online: September 28, 2022

Shao-Jie Duan, Zhi-Ying Ren, Tao Zheng, Hong-Ye Peng, Zuo-Hu Niu, Hui Xia, Rong-Rui Wang, Graduate School, Beijing University of Chinese Medicine, Beijing 100029, China

Jia-Liang Chen, Center of Integrative Medicine, Beijing Ditan Hospital, Capital Medical University, Beijing 100015, China

Yuan-Chen Zhou, Graduate school, Peking University China-Japan Friendship School of Clinical Medicine, Beijing 100029, China

Shu-Kun Yao, Department of Gastroenterology, China-Japan Friendship Hospital, Beijing 100029, China

Corresponding author: Shu-Kun Yao, MD, Professor, Department of Gastroenterology, China-Japan Friendship Hospital, No. 2 Yinghua East Street, Chaoyang District, Beijing 100029, China. shukunyao@126.com

Abstract

BACKGROUND

Early identification of metabolic-associated fatty liver disease (MAFLD) is urgent. Atherogenic index of plasma (AIP) is a reference predictor of obesity-related diseases, but its predictive value for MAFLD remains unclear. No studies have reported whether its combination with waist circumference (WC) and body mass index (BMI) can improve the predictive performance for MAFLD.

AIM

To systematically explore the relationship between AIP and MAFLD and evaluate its predictive value for MAFLD and to pioneer a novel noninvasive predictive model combining AIP, WC, and BMI while validating its predictive performance for MAFLD.

METHODS

This cross-sectional study consecutively enrolled 864 participants. Multivariate logistic regression analysis and receiver operating characteristic curve were used to evaluate the relationship between AIP and MAFLD and its predictive power for MAFLD. The novel prediction model A-W-B combining AIP, WC, and BMI to

predict MAFLD was established, and internal verification was completed by magnetic resonance imaging diagnosis.

RESULTS

Subjects with higher AIP exhibited a significantly increased risk of MAFLD, with an odds ratio of 12.420 (6.008-25.675) for AIP after adjusting for various confounding factors. The area under receiver operating characteristic curve of the A-W-B model was 0.833 (0.807-0.858), which was significantly higher than that of AIP, WC, and BMI (all $P < 0.05$). Subgroup analysis illustrated that the A-W-B model had significantly higher area under receiver operating characteristic curves in female, young and nonobese subgroups (all $P < 0.05$). The best cutoff values for the A-W-B model to predict MAFLD in males and females were 0.5932 and 0.4105, respectively. Additionally, in the validation set, the area under receiver operating characteristic curve of the A-W-B model to predict MAFLD was 0.862 (0.791-0.916). The A-W-B level was strongly and positively associated with the liver proton density fat fraction ($r = 0.630$, $P < 0.001$) and significantly increased with the severity of MAFLD ($P < 0.05$).

CONCLUSION

AIP was strongly and positively associated with the risk of MAFLD and can be a reference predictor for MAFLD. The novel prediction model A-W-B combining AIP, WC, and BMI can significantly improve the predictive ability of MAFLD and provide better services for clinical prediction and screening of MAFLD.

Key Words: Atherogenic index of plasma; Metabolic-associated fatty liver disease; Receiver operating characteristic curve; Predictor

©The Author(s) 2022. Published by Baishideng Publishing Group Inc. All rights reserved.

Core Tip: Metabolic-associated fatty liver disease (MAFLD) is the most common chronic liver disease, and early identification of MAFLD is urgent. This study demonstrated that the atherogenic index of plasma was strongly and positively associated with the risk of MAFLD, and it can be a reference predictor for MAFLD. Then, we pioneered a novel noninvasive prediction model, A-W-B, combining atherogenic index of plasma, waist circumference, and body mass index and validated its excellent predictive performance for MAFLD. Furthermore, we also pointed out the optimal cutoff values of the A-W-B model to predict MAFLD in males and females, which will facilitate early clinical identification of MAFLD in different sex populations. This study is highly innovative, and the noninvasive prediction model, A-W-B, is convenient, affordable, and easy to obtain, which can provide better services for clinical prediction and screening of MAFLD and metabolic-related diseases.

Citation: Duan SJ, Ren ZY, Zheng T, Peng HY, Niu ZH, Xia H, Chen JL, Zhou YC, Wang RR, Yao SK. Atherogenic index of plasma combined with waist circumference and body mass index to predict metabolic-associated fatty liver disease. *World J Gastroenterol* 2022; 28(36): 5364-5379
URL: https://www.wjgnet.com/1007-9327/full/v28/i36/5364.htm
DOI: https://dx.doi.org/10.3748/wjg.v28.i36.5364

INTRODUCTION

Metabolic-associated fatty liver disease (MAFLD), formerly known as nonalcoholic fatty liver disease, is a common disease closely related to genetic, obesity, and metabolic abnormalities and has become a global public health problem[1,2]. In recent decades, obesity has become increasingly widespread owing to huge changes in dietary structure and living habits[3,4]. The prevalence of MAFLD has risen rapidly, and patients tend to be younger[5]. Notably, MAFLD can not only progress to hepatitis, liver cirrhosis, and liver cancer[6] but also increase the occurrence and development of diabetes[7] and cardiovascular diseases[8,9], which seriously endangers individual health and increases the social and medical economic burden[10]. Therefore, it is necessary to predict and screen MAFLD at an early stage to intervene in a timely manner.

The occurrence and development of MAFLD are closely related to lipid metabolism disorders and dyslipidemia caused by the accumulation of visceral fat[11]. Patients with fatty liver usually have elevated triglycerides (TG) and generally lower high-density lipoprotein cholesterol (HDL-C) than healthy people[12]. Waist circumference (WC) and body mass index (BMI) are commonly used as

indicators to assess obesity, and it has been shown that elevated WC and BMI can significantly increase the risk of fatty liver disease. However, they have certain limitations in accurately reflecting the accumulation of visceral fat[13].

Recently, the atherogenic index of plasma (AIP), calculated from the logarithm of the ratio of TG to HDL-C[14], has been proven to be closely related to abdominal obesity, and it can sensitively reflect the accumulation of visceral fat and effectively predict the risk of atherosclerosis and cardiovascular disease [15,16]. Previous studies indicate that AIP is significantly higher in patients with fatty liver and may be a potential indicator for identifying fatty liver disease[17]. However, few studies have systematically reported the predictive value of AIP for MAFLD and whether AIP combined with WC and BMI can improve the predictive ability for MAFLD is unclear.

Therefore, the two main objectives of this study were: (1) To systematically assess the relationship between AIP and MAFLD and evaluate its predictive value for MAFLD; and (2) To establish a novel noninvasive prediction model combining AIP, WC and BMI and validate its predictive performance for MAFLD.

MATERIALS AND METHODS

Study design and participants

This study was conducted in Beijing, China. Among the adults who underwent a physical examination for health at China-Japan Friendship Hospital in Beijing from September 2018 to October 2021, we consecutively recruited 943 participants who completed the standardized questionnaire, finished anthropometric and laboratory tests, and underwent liver ultrasonography. All subjects agreed to participate in this study voluntarily and submitted informed consent forms.

According to quality control, after excluding pregnant and lactating women, subjects who had a history of any severe brain, heart, lung, kidney, or blood diseases, mental illness, infectious diseases, malignant tumors, *etc* as well as the subjects with incomplete data, a total of 864 subjects were finally included (Figure 1), with 624 males and 240 females, aged from 20-years-old to 78-years-old.

This study was approved by the Clinical Research Ethics Committee of China-Japan Friendship Hospital (2018-110-K79-1).

Data collection and definition

The physical examination was performed in the morning in a fasting state. Anthropometric indicators were measured by professionally trained doctors. Height, weight, and waist circumference were measured while subjects were naturally standing barefoot with lightweight clothes. After 10 min of rest, the blood pressure was measured with an upper arm electronic sphygmomanometer. Peripheral blood was drawn into an EDTA-containing tube and subjected to biochemical experiments within 2 h. The relevant laboratory indicators were obtained through the electronic database of this physical examination center, including alanine aminotransferase (ALT), aspartate aminotransferase (AST), total cholesterol, TG, HDL-C, low-density lipoprotein cholesterol, fasting blood glucose (FBG), serum uric acid (SUA) and so on.

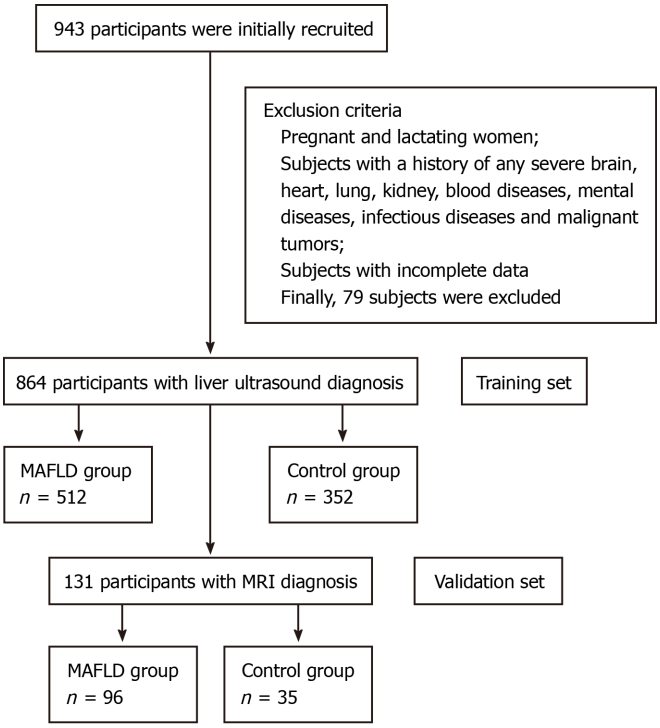
BMI was calculated as the body weight (in kilograms) divided by the square of the height (in meters). WC referred to the waist circumference at the level of the flat navel. AIP was calculated as the logarithmic transformation of the ratio of TG to HDL-C [log (TG/HDL-C)].

Diagnostic criteria and detection methods of MAFLD

The diagnostic criteria of MAFLD refer to the consensus of international experts in 2020 that in addition to the evidence of hepatic steatosis[18], one of the following three criteria, namely, overweight/obesity, type 2 diabetes, or metabolic dysregulation, needs to be met[19,20]. Among them, metabolic dysregulation refer to the existence of at least two of the following metabolic risk criteria: (1) Waist circumference ≥ 102/88 cm in Caucasian males and females, respectively, or ≥ 90/80 cm in Asian males and females; (2) Blood pressure ≥ 130/85 mmHg or specific drug treatment; (3) Plasma TG ≥ 1.70 mmol/L or specific drug treatment; (4) Plasma HDL-C < 1.0 mmol/L for males and < 1.3 mmol/L for females or specific drug treatment; (5) Prediabetes (*i.e.* fasting glucose levels 5.6 to 6.9 mmol/L or 2-h post load glucose levels 7.8 to 11.0 mmol or glycated hemoglobin 5.7% to 6.4%; (6) Homeostasis model assessment-insulin resistance score ≥ 2.5; and (7) Plasma high-sensitivity C-reactive protein level > 2 mg/L.

In the training set, fatty liver (hepatic steatosis) was defined by liver ultrasound examination based on at least two of the following three abnormal findings: (1) Diffusely increased echogenicity of the liver relative to the kidney or spleen; (2) Ultrasound beam attenuation; and (3) Poor visualization of intrahepatic structures.

In the validation set, the proton density fat fraction (PDFF) based on magnetic resonance spectroscopy and magnetic resonance imaging (MRI) was used to diagnose fatty liver and to evaluate the severity of MAFLD[21]. PDFF < 5% was defined as no fatty liver, PDFF 5.0%-14.0% was defined as mild MAFLD, and PDFF > 14.0% was defined as moderate to severe MAFLD.



DOI: 10.3748/wjg.v28.i36.5364 **Copyright** ©The Author(s) 2022.

Figure 1 Flow chart of the study subjects. MAFLD: Metabolic-associated fatty liver disease; MRI: Magnetic resonance imaging.

Statistical analysis

First, the baseline characteristics of the MAFLD and non-MAFLD groups were compared. The independent samples *t* test was used for comparing normally or approximately normally distributed quantitative data between groups, expressed as the mean and standard deviation (SD). The Mann-Whitney *U* test was used for comparing nonnormally distributed quantitative data between groups, represented as medians and quartiles. The χ^2 test was used for comparing categorical data between groups, represented as numbers and percentages.

Then, multivariate logistic regression analysis was conducted to calculate the odds ratios (ORs) and 95% confidence intervals of AIP for MAFLD under different adjustment conditions. The logistic regression prediction model A-W-B combining AIP, WC, and BMI was established. The Hosmer-Lemeshow test and the receiver operating characteristic (ROC) curve were used to evaluate the calibration and discrimination of this model. The DeLong test was used to compare the predictive ability of the AIP, WC, BMI, and A-W-B model for MAFLD. Spearman's correlation analysis was used to explore the correlation between parameters. Finally, the internal verification was completed with MRI as the diagnostic standard.

All statistical tests were two-tailed and were considered significant for *P* less than 0.05 ($P < 0.05$). Statistical analyses were performed using Statistical Package for the Sciences (SPSS, version 25.0) and MedCalc statistical software (version 19.6.4).

RESULTS

Characteristics of participants

The demographics, anthropometrics, and laboratory test characteristics of 864 subjects are presented in Table 1. The prevalence of male and young patients (age < 40-years-old) and the percentage of smoking history, drinking history, overweight, obesity, elevated ALT, and elevated ALT in MAFLD subjects were significantly higher than those in the non-MAFLD subjects (all $P < 0.05$). Participants with MAFLD had dramatically higher WC, BMI, SBP, DBP, ALT, AST, total cholesterol, TG, low-density lipoprotein cholesterol, FBG, and SUA and significantly lower AST/ALT and HDL-C (all $P < 0.05$). In addition, a significant association between AIP and MAFLD was initially demonstrated.

Multivariate logistic regression analysis of AIP on the risk of MAFLD

Multivariate logistic regression analyses were conducted to further explore the relationship between AIP and MAFLD, and the results are shown in Table 2. AIP had a strong association with the risk of MAFLD, and the OR for a 1-SD increase in AIP was 50.286 (26.953-93.819) without adjustment (Model

Table 1 Baseline characteristics of the study subjects

Variable	Non-MAFLD, *n* = 352	MAFLD, *n* = 512	Statistics[1]	*P* value
Demographics				
Sex			χ^2 = 14.020	< 0.001
Male	230 (65.3)	394 (77.0)		
Female	122 (34.7)	118 (23.0)		
Age in yr	37.750 ± 10.736	41.240 ± 10.852	*t* = -4.634	< 0.001
Age ≥ 40 yr	115 (32.7)	254 (49.6)	χ^2 = 24.461	< 0.001
Age < 40 yr	237 (67.3)	258 (40.4)		
Smoking history	81 (23.0)	174 (34.0)	χ^2= 12.073	< 0.001
Drinking history	76 (21.6)	145 (28.3)	χ^2= 4.962	0.027
Anthropometrics				
WC in cm	86.240 ± 9.893	96.790 ± 8.618	*t* = -16.219	< 0.001
BMI in kg/m^2	24.436 ± 3.169	28.028 ± 3.221	*t* = -16.228	< 0.001
SBP in mmHg	125.880 ± 14.883	133.610 ± 16.859	*t* = -6.908	< 0.001
DBP in mmHg	77.500 ± 11.658	82.950 ± 12.525	*t* = -6.461	< 0.001
Laboratory tests				
ALT in U/L	21.0 (15.0, 30.0)	34.0 (24.0, 54.0)	*Z* = -12.276	< 0.001
AST in U/L	19.0 (17.0, 23.0)	23.0 (19.0, 29.0)	*Z* = -9.058	< 0.001
TC in mmol/L	4.539 ± 0.847	4.783 ± 0.902	*t* = -4.104	< 0.001
TG in mmol/L	1.1 (0.7, 1.5)	1.8 (1.3, 2.6)	*Z* = -13.650	< 0.001
HDL-C in mmol/L	1.351 ± 0.283	1.191 ± 0.256	*t* = 8.321	< 0.001
LDL-C in mmol/L	2.645 ± 0.708	2.906 ± 0.884	*t* = -4.568	< 0.001
FBG in mmol/L	5.2 (4.9, 5.4)	5.4 (5.1, 5.9)	*Z* = -7.637	< 0.001
SUA in μmol/L	332.722 ± 86.289	377.836 ± 85.859	*t* = -7.590	< 0.001
AIP	-0.11 (-0.30, 0.08)	0.20 (0.03, 0.39)	*Z* = -14.006	< 0.001

[1]Comparison of significant differences between the two groups; χ2 value calculated by the χ2 test; *Z* value calculated by the Mann-Whitney *U* test; *t* value calculated by the independent samples *t* test. Data are presented as median and interquartile range, mean and standard deviation or frequency (percentage). MAFLD: Metabolic-associated fatty liver disease; WC: Waist circumference; BMI: Body mass index; SBP: Systolic blood pressure; DBP: Diastolic blood pressure; ALT: Alanine aminotransferase; AST: Aspartate aminotransferase; TC: Total cholesterol; TG: Triglyceride; HDL-C: High-density lipoprotein cholesterol; LDL-C: Low-density lipoprotein cholesterol; FBG: Fasting blood glucose; SUA: Serum uric acid; AIP: Atherogenic index of plasma.

1). After adjusting for sex and age, the OR for a 1-SD increase in AIP was 48.874 (26.087-91.569) (Model 2). After further adjusting for smoking history, drinking history, WC, and BMI, the degree of this association changed but was still strong; the OR for a 1-SD increase in AIP was 16.184 (7.961-32.902) (Model 3). Further adjusting for SBP, DBP, ALT, AST, total cholesterol, TG, HDL-C, low-density lipoprotein cholesterol, FBG, and SUA attenuated the association but only slightly; there was still a 12.420-fold (6.008-25.675) higher risk for MAFLD with a 1-SD increase in AIP (Model 4).

After dividing AIP into quartiles, the risk of MAFLD increased robustly with higher AIP quartiles. When comparing the top quartiles with the bottom categories, the risk of MAFLD increased 16.882-fold to 7.160-fold from Model 1 to Model 4. The *P* values for the linear trend were less than 0.01, signifying that linear trends from the lowest to the highest quartiles were eminent.

Predictive ability of AIP for MAFLD in different subgroups

The ROC curve of AIP for predicting MAFLD in different sex, age, and weight subgroups was plotted, and the DeLong test was used to compare the area under the ROC curve (AUC) between the subgroups. As shown in Figure 2, the AUC of AIP for MAFLD in the young was significantly higher than that in middle-age and elderly subjects [0.816 (0.779-0.849) *vs* 0.726 (0.678-0.771), $P < 0.05$]. The AUC of AIP for MAFLD in nonobese subjects was significantly higher than that in obese subjects [0.783 (0.747-0.816) *vs* 0.579 (0.519-0.638), $P < 0.0001$]. However, there was no significant difference between males and females

Table 2 Multivariate logistic regression of atherogenic index of plasma for the risk of metabolic-associated fatty liver disease

Variable		β	SE	Wald χ^2	*P* value	OR (95%CI)
Model 1	AIP level (per change in SD)	3.918	0.318	151.599	< 0.001	50.286 (26.953-93.819)
	Quartiles of AIP					
	A1 (≤ -0.1265)	-	-	-	-	1 (Ref)
	A2 (-0.1265-0.0947)	1.241	0.209	35.108	< 0.001	3.460 (2.295-5.217)
	A3 (0.0947-0.3023)	2.323	0.226	105.794	< 0.001	10.204 (6.554-15.885)
	A4 (> 0.3022)	2.826	0.245	132.611	< 0.001	16.882 (10.436-27.311)
Model 2	AIP level (per change in SD)	3.889	0.32	147.414	< 0.001	48.874 (26.087-91.569)
	Quartiles of AIP					
	A1 (≤ -0.1265)	-	-	-	-	1 (Ref)
	A2 (-0.1265-0.0947)	0.847	0.241	12.347	< 0.001	3.218 (2.124-4.876)
	A3 (0.0947-0.3023)	1.690	0.260	42.107	< 0.001	9.774 (6.256-15.270)
	A4 (> 0.3022)	2.103	0.281	55.913	< 0.001	16.514 (10.176-26.799)
Model 3	AIP level (per change in SD)	2.784	0.362	59.147	< 0.001	16.184 (7.961-32.902)
	Quartiles of AIP					
	A1 (≤ -0.1265)	-	-	-	-	1 (Ref)
	A2 (-0.1265-0.0947)	0.847	0.241	12.347	< 0.001	2.334 (1.455-3.744)
	A3 (0.0947-0.3023)	1.690	0.260	42.107	< 0.001	5.421 (3.253-9.032)
	A4 (> 0.3022)	2.103	0.281	55.913	< 0.001	8.194 (4.721-14.22)
Model 4	AIP level (per change in SD)	2.519	0.371	46.230	< 0.001	12.420 (6.008-25.675)
	Quartiles of AIP					
	A1 (≤ -0.1265)	-	-	-	-	1 (Ref)
	A2 (-0.1265-0.0947)	0.828	0.249	11.088	0.001	2.288 (1.4063-725)
	A3 (0.0947-0.3023)	1.642	0.268	37.636	< 0.001	5.167 (3.058-8.732)
	A4 (> 0.3022)	1.969	0.289	46.343	< 0.001	7.160 (4.062-12.62)

Model 1: Unadjusted. Model 2: Adjusted for age and sex. Model 3: Adjusted for age, sex, smoking history, drinking history, waist circumference and body mass index. Model 4: Adjusted for age, sex, smoking history, drinking history, waist circumference, body mass index, systolic blood pressure, diastolic blood pressure, alanine aminotransferase, aspartate aminotransferase, total cholesterol, triglyceride, high-density lipoprotein cholesterol, low-density lipoprotein cholesterol, fasting blood glucose, and serum uric acid. AIP: Atherogenic index of plasma; SE: Standard error; OR: Odds ratio; CI: Confidence interval; SD: Standard deviation.

(P = 0.0639).

In addition, the best cutoff values for AIP to predict MAFLD in males and females were 0.0821 and -0.1390, respectively. The AUCs of AIP, WC, and BMI for predicting total MAFLD were 0.780 (0.751-0.807), 0.790 (0.761-0.817), and 0.788 (0.759-0.814), respectively, with no significant difference among the three (Table 3).

Establishment of the A-W-B model for better predicting MAFLD

To further improve the predictive ability of MAFLD, we combined AIP, WC, and BMI and put them into the binary logistic regression model to construct a new logistic regression prediction model, A-W-B. The regression equation was logit (A-W-B) = -8.782 + 2.560 × AIP + 0.049 × WC + 0.170 × BMI (Table 4).

The Hosmer-Lemeshow test and ROC curve analysis were used to evaluate the calibration and discrimination of the A-W-B model. Figure 3A illustrated the calibration line graph of the A-W-B model, and the result of the Hosmer-Lemeshow test showed that χ^2 = 8.5901, P = 0.3780 > 0.05, indicating that the A-W-B model had a good calibration ability for MAFLD. Figure 3B illustrated the ROC curve of the A-W-B model, with the AUC of 0.833 (0.807-0.858), indicating that the A-W-B model had a good

Table 3 Results analysis of the receiver operating characteristic curves

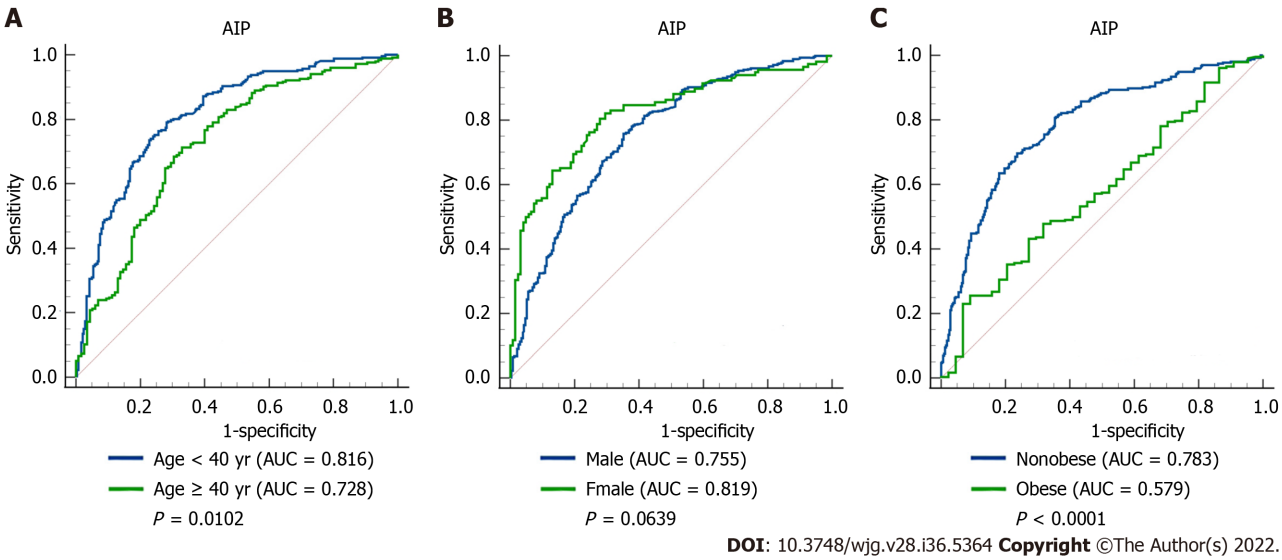
Variable	AUC (95%CI)	*P* value	Sensitivity (%)	Specificity (%)	Youden index	Cutoff value
Total						
AIP	0.780 (0.751-0.807)	< 0.0001	75.20	69.89	0.4508	0.0340
WC in cm	0.790 (0.761-0.817)	< 0.0001	85.94	58.52	0.4446	88.00
BMI in kg/m^2	0.788 (0.759-0.814)	< 0.0001	83.20	59.09	0.4229	25.10
A-W-B	0.833 (0.807-0.858)[1,2,3]	< 0.0001	86.13	68.47	0.5460	0.5019
Male						
AIP	0.755 (0.719-0.788)	< 0.0001	75.89	64.78	0.4067	0.0821
WC in cm	0.770 (0.735-0.803)	< 0.0001	72.59	67.39	0.3998	92.50
BMI in kg/m^2	0.773 (0.738-0.805)	< 0.0001	72.34	68.70	0.4103	26.32
A-W-B	0.814 (0.781-0.843)[1,2,3]	< 0.0001	82.99	65.65	0.4865	0.5932
Female						
AIP	0.819 (0.764-0.865)	< 0.0001	82.2	70.49	0.5270	-0.1390
WC in cm	0.820 (0.765-0.866)	< 0.0001	81.36	69.67	0.5103	85.50
BMI in kg/m^2	0.804 (0.748-0.852)	< 0.0001	88.98	58.20	0.4718	23.34
A-W-B	0.874 (0.826-0.914)[1,2,3]	< 0.0001	78.81	83.61	0.6242	0.4105
Age ≥ 40 yr						
AIP	0.726 (0.678-0.771)	< 0.0001	71.26	66.96	0.3822	0.0367
WC in cm	0.736 (0.688-0.780)	< 0.0001	82.68	52.17	0.3485	88.00
BMI in kg/m^2	0.736 (0.688-0.780)	< 0.0001	71.26	66.96	0.3822	26.03
A-W-B	0.787 (0.742-0.828)[1,2,3]	< 0.0001	77.56	69.57	0.4712	0.5574
Age < 40 yr						
AIP	0.816 (0.779-0.849)	< 0.0001	73.64	77.22	0.5086	0.0814
WC in cm	0.824 (0.787-0.856)	< 0.0001	89.15	61.60	0.5075	88.00
BMI in kg/m^2	0.820 (0.783-0.853)	< 0.0001	83.72	66.24	0.4997	25.31
A-W-B	0.863 (0.830-0.892)[1,2,3]	< 0.0001	89.92	71.73	0.6165	0.4947
BMI ≥ 28 kg/m^2						
AIP	0.579 (0.519-0.638)	0.0849	25.63	90.91	0.1654	0.4140
WC in cm	0.597 (0.688-0.780)	0.0303	36.97	79.55	0.1652	104.50
BMI in kg/m^2	0.648 (0.589-0.704)	0.0005	65.13	68.18	0.3331	29.38
A-W-B	0.644 (0.585-0.700)[1]	0.0007	43.28	84.09	0.2737	0.9009
BMI < 28 kg/m^2						
AIP	0.783 (0.747-0.816)[3]	< 0.0001	69.71	76.30	0.4601	0.0340
WC in cm	0.754 (0.717-0.789)	< 0.0001	78.1	63.31	0.4141	87.50
BMI in kg/m^2	0.733 (0.695-0.768)	< 0.0001	77.37	59.42	0.3679	24.56
A-W-B	0.822 (0.789-0.852)[1,2,3]	< 0.0001	80.66	72.08	0.5273	0.4531

[1]Indicates significantly larger compared with atherogenic index of plasma.
[2]Indicates significantly larger as compared with waist circumference.
[3]Indicates significantly larger as compared with body mass index.
AUC: Area under the receiver operating characteristic curve; AIP: Atherogenic index of plasma; WC: Waist circumference; BMI: Body mass index; A-W-B: Prediction model combining atherogenic index of plasma, waist circumference, and body mass index; CI: Confidence interval.

Table 4 Establishment of the logistic regression prediction model A-W-B combined with the atherogenic index of plasma, waist circumference, and body mass index

Variable	β	SE	Wald χ^2	*P* value	OR (95%CI)
AIP	2.560	0.345	55.017	< 0.001	12.939 (6.578-25.45)
WC	0.049	0.017	7.951	0.005	1.050 (1.015-1.087)
BMI	0.170	0.051	11.087	0.001	1.186 (1.073-10311)
Constant	-8.782	1.003	76.689		

AIP: Atherogenic index of plasma; WC: Waist circumference; BMI: Body mass index; SE: Standard error; OR: Odds ratio; CI: Confidence interval.



DOI: 10.3748/wjg.v28.i36.5364 **Copyright** ©The Author(s) 2022.

Figure 2 Receiver operating characteristic curves of atherogenic index of plasma in predicting metabolic-associated fatty liver disease in different subgroups. A: Comparison between the young (age < 40 years) and middle-age and elderly (age ≥ 40 years) subjects (*P* = 0.0102); B: Comparison between male and female subjects (*P* = 0.0639); C: Comparison between nonobese and obese subjects (*P* < 0.0001). AIP: Atherogenic index of plasma; AUC: Area under the receiver operating characteristic curve.

discrimination ability for MAFLD.

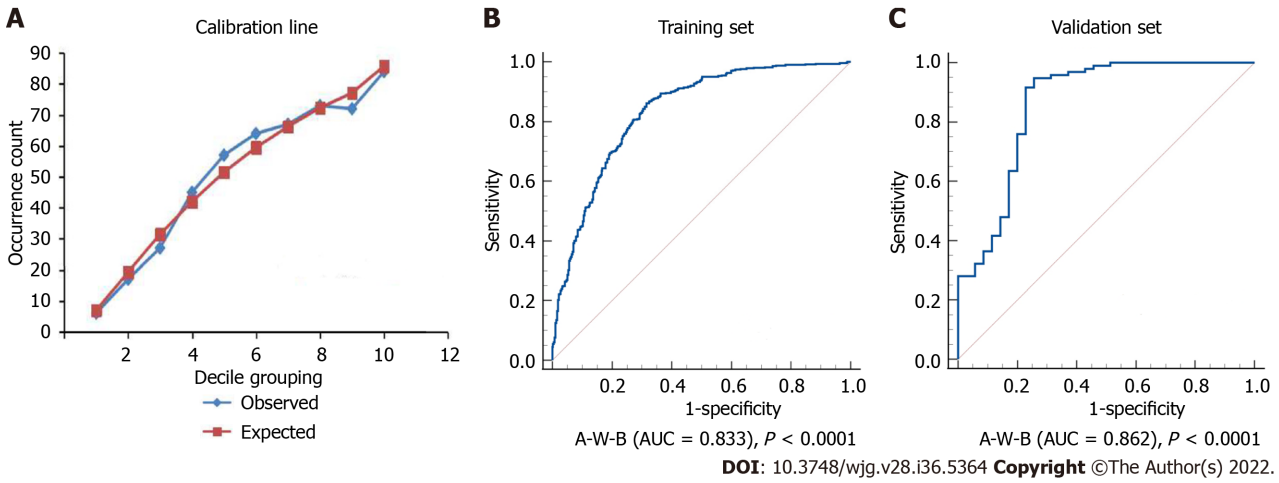
Predictive ability of the A-W-B model for MAFLD in different subgroups

To further evaluate the predictive power of the A-W-B model for MAFLD in different populations, we performed a subgroup analysis. As shown in Figure 4, the AUCs of A-W-B for MAFLD in female, young, and nonobese subjects were 0.874 (0.826-0.914), 0.863 (0.830-0.892), and 0.822 (0.789-0.852), respectively, which were significantly higher than those in male [0.814 (0.781-0.843)], middle-aged and elderly [0.787 (0.742-0.828)], and obese subjects [0.644 (0.585-0.700)] (all $P < 0.05$). These results indicated that the A-W-B model had stronger predictive power for MAFLD in female, young, and nonobese subjects. Furthermore, the results in Table 3 showed that the best cutoff values for A-W-B to predict MAFLD in males and females were 0.5932 and 0.4105, respectively.

Comparison of the A-W-B model and AIP, WC, and BMI for predicting MAFLD

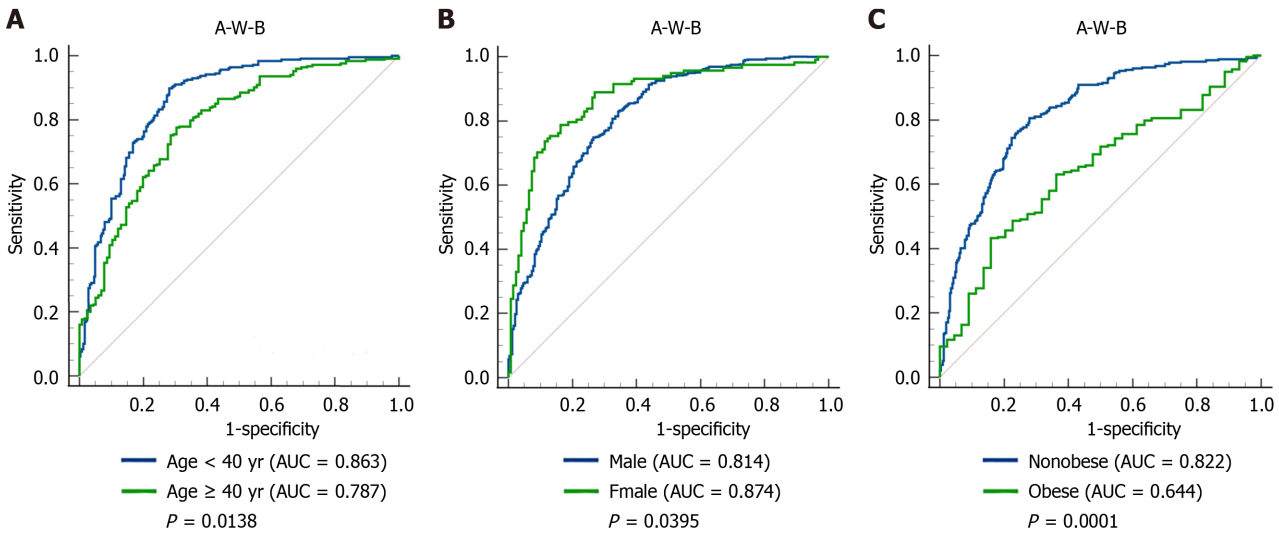
The DeLong test was used to compare the predictive ability of the A-W-B model and AIP, WC, and BMI. The AUC of the A-W-B model for MAFLD was 0.833 (0.807-0.858), which was significantly higher than that of AIP, WC, and BMI ($P < 0.05$). The sensitivity, specificity, Youden index, and cutoff value of the A-W-B model were 86.13%, 68.47%, 0.5460, and 0.5019, respectively (Table 3).

As shown in Figure 5A-E, subgroup analysis showed that the AUCs of the A-W-B model were significantly higher than those of AIP, WC, and BMI in male, female, young, middle-aged and elderly, and nonobese subjects (all $P < 0.01$), demonstrating that the A-W-B model has a higher ability to predict MAFLD than AIP, WC, and BMI in different age, sex, and nonobese subjects. However, as shown in Figure 5F, among obese subjects, the predictive ability of the A-W-B model for MAFLD was only better than that of AIP. In addition, the Z values between the AIP, WC, BMI, and the A-W-B model in different subgroups were illustrated in Supplementary Table 1.



DOI: 10.3748/wjg.v28.i36.5364 **Copyright** ©The Author(s) 2022.

Figure 3 Calibration line and receiver operating characteristic curves of the A-W-B model. A: Calibration line of the prediction model combining atherogenic index of plasma, waist circumference, and body mass index (A-W-B) model (Hosmer-Lemeshow test: χ^2 = 8.5901, P = 0.3780); B: Receiver operating characteristic curve of the A-W-B model in the training set (area under the receiver operating characteristic curve [AUC] = 0.833); C: Receiver operating characteristic curve of the A-W-B model in the validation set (AUC = 0.862).



DOI: 10.3748/wjg.v28.i36.5364 **Copyright** ©The Author(s) 2022.

Figure 4 Receiver operating characteristic curves of the A-W-B model to predict metabolic-associated fatty liver disease in different subgroups. A: Comparison between young (age < 40 years) and middle-age and elderly (age ≥ 40 years) subjects (P = 0.0138); B: Comparison between male and female subjects (P = 0.0395); C: Comparison between nonobese and obese subjects (P = 0.0001); AUC: Area under the receiver operating characteristic curve; A-W-B: Prediction model combining atherogenic index of plasma, waist circumference, and body mass index.

The concrete ROC curve results of the AIP, WC, BMI, and A-W-B model for predicting MAFLD in different subgroups were illustrated in Table 3. Compared to AIP, WC, and BMI, the A-W-B model had the best sensitivity in male, young and nonobese subjects, which may be more conducive to identifying patients with positive MAFLD to reduce the missed diagnosis rate. Meanwhile, the A-W-B model had the best specificity in female and middle-aged and elderly subjects, which may be more beneficial to identifying people without MAFLD and reducing the misdiagnosis rate.

Moreover, Spearman's correlations between A-W-B, AIP, WC, BMI, and various physical and chemical indicators are illustrated in Table 5. Compared with AIP, WC, and BMI, the A-W-B model had a higher positive association with SBP, DBP, ALT, AST, FBG, and SUA.

Validation of the A-W-B model

To further validate the diagnostic performance of the A-W-B model for MAFLD, we randomly selected approximately 15% of the subjects (131 cases) from the overall subjects as the validation set and used MRI to diagnose MAFLD. Among them, 35 cases were in the control group, 67 cases were mild MAFLD, and 29 cases were moderate to severe MAFLD. The data comparison between the training set and validation set was shown in Table 6. There was no statistically significant difference in age, sex, and

Table 5 Spearman's correlation analysis results between various indicators (*r* value)

Variable	AIP	WC	BMI	A-W-B
SBP in mmHg	0.299[b]	0.358[b]	0.362[b]	0.392[b]
DBP in mmHg	0.327[b]	0.325[b]	0.315[b]	0.375[b]
ALT in U/L	0.470[b]	0.455[b]	0.451[b]	0.530[b]
AST in U/L	0.306[b]	0.307[b]	0.304[b]	0.351[b]
TC in mmol/L	0.193[b]	0.070[a]	0.056	0.132[b]
TG in mmol/L	0.954[b]	0.455[b]	0.430[b]	0.763[b]
HDL-C in mmol/L	-0.617[b]	-0.365[b]	-0.373[b]	-0.543[b]
LDL-C in mmol/L	0.253[b]	0.128[b]	0.105[b]	0.190[b]
FBG in mmol/L	0.294[b]	0.280[b]	0.274[b]	0.334[b]
SUA in μmol/L	0.462[b]	0.375[b]	0.358[b]	0.469[b]

[a]$P < 0.05$.
[b]$P < 0.01$.
SBP: Systolic blood pressure; DBP: Diastolic blood pressure; ALT: Alanine aminotransferase; AST: Aspartate aminotransferase; TC: Total cholesterol; TG: Triglyceride; HDL-C: High-density lipoprotein cholesterol; LDL-C: Low-density lipoprotein cholesterol; FBG: Fasting blood glucose; SUA: Serum uric acid; AIP: Atherogenic index of plasma; WC: Waist circumference; BMI: Body mass index; A-W-B: Prediction model combining atherogenic index of plasma, waist circumference, and body mass index.

various indicators between the two groups (all $P > 0.05$).

Figure 3C illustrated the ROC curve of the A-W-B model in the validation set, with the AUC of 0.862 (0.791-0.916), indicating that the A-W-B model also exhibited outstanding discrimination for MAFLD in the validation set. In addition, Figure 6 shows that the A-W-B level was strongly and positively associated with the PDFF ($r = 0.630$, $P < 0.001$). With the degree of severity of MAFLD increased, the A-W-B level also increased significantly ($P < 0.05$).

DISCUSSION

In this study, the relationship between AIP and MAFLD was systematically assessed, and it was confirmed that AIP had a strong and positive association with the risk of MAFLD and can be used as a reference predictor for MAFLD. Then, to further improve the predictive power for MAFLD, we combined AIP, WC, and BMI to pioneer a novel noninvasive prediction model, A-W-B, and confirmed that it had a better predictive value for MAFLD than AIP, WC, and BMI. At the same time, we also pointed out the optimal cutoff values of the A-W-B model to predict MAFLD in males and females, which will facilitate early clinical identification of MAFLD in different sex populations. Finally, we internally validated the model with MRI as the diagnostic standard, further affirming its outstanding predictive performance for MAFLD, which provided a new tool for the early prevention and screening of MAFLD.

As a new type of body fat index calculated as the logarithmic transformation of the ratio of TG to HDL-C, AIP is more sensitive to visceral fat accumulation than WC and BMI and has shown predictive potential for fatty liver in previous studies[15]. Xie *et al*[17] found that a higher AIP level was positively associated with fatty liver, which might be a novel and strong predictor associated with fatty liver in the Chinese Han population. In this study, the multivariate logistic regression results showed that the subjects with higher AIP still exhibited a significantly increased risk of MAFLD after adjusting for age, sex, smoking history, drinking history, WC, BMI, and various physical and chemical indicators, indicating that AIP was strongly and positively associated with the risk of MAFLD.

Visceral fat accumulation has been proven to increase the prevalence of a variety of cardiovascular risk factors, including insulin resistance and dyslipidemia, which also play a tremendously crucial role in the pathogenesis of fatty liver disease[16]. It is widely accepted that the increased TG caused by liver lipid accumulation is a prerequisite for MAFLD and that insulin resistance is a key factor during its development. Previous studies demonstrated that increasing levels of TG and decreasing concentrations of HDL-C could reduce sensitivity to insulin, and higher TG/HDL-C usually indicates insulin resistance [22], which may explain the close relationship between AIP and MAFLD. In addition, this study also pointed out the optimal cutoff values of AIP for predicting MAFLD in males and females, which provided a new idea for the early prevention of MAFLD. People with AIP levels above this cutoff point may be at higher risk for MAFLD and require more attention to liver conditions.

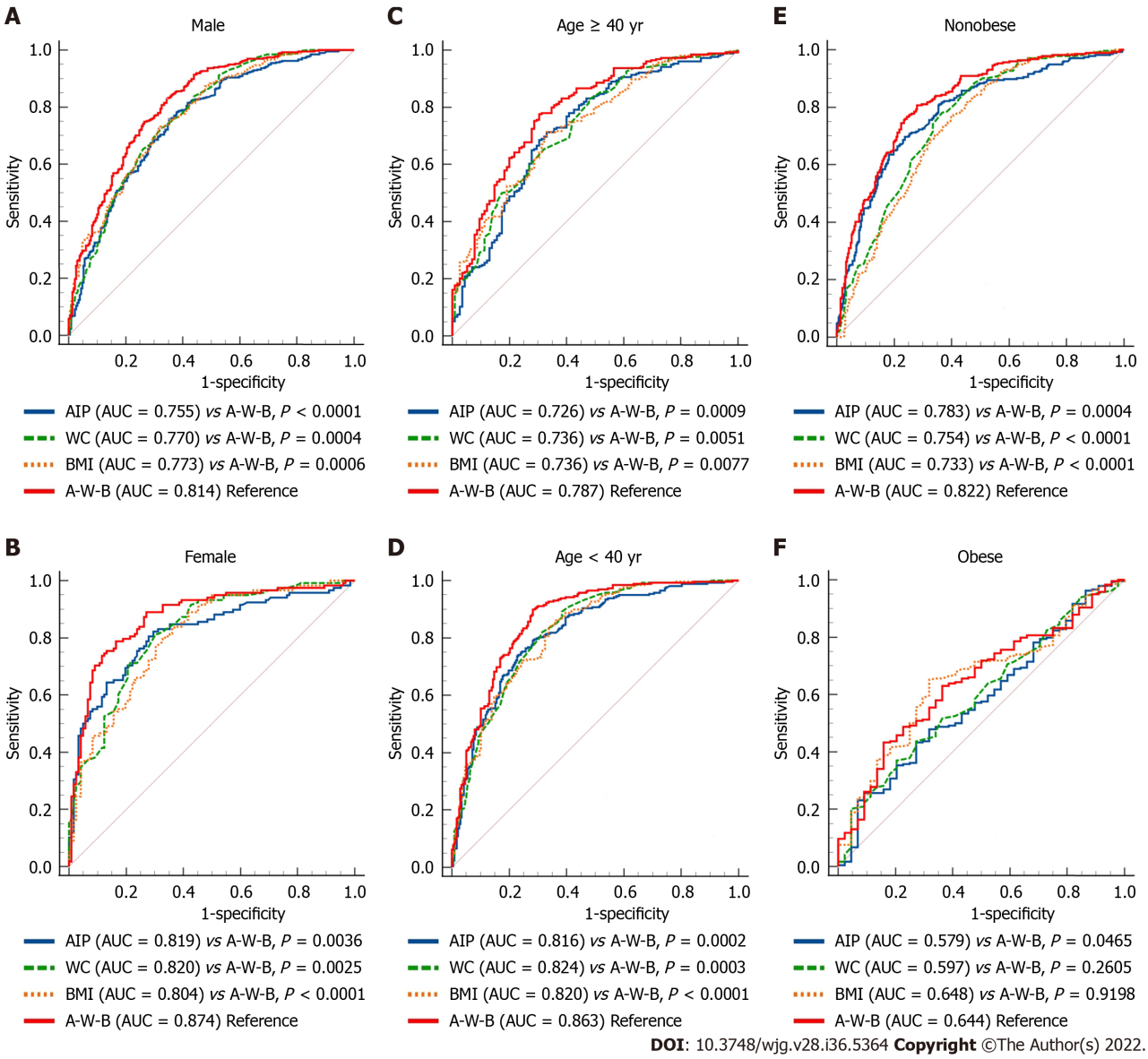
Table 6 Data comparison between training set and validation set

Variable	Training set, *n* = 864	Validation set, *n* = 131	*P* value
Sex, female	240 (27.8)	38 (29.0)	0.770
Age in yr	39.820 ± 10.934	39.660 ± 10.861	0.885
Smoking history	255 (29.5)	38 (29.0)	0.906
Drinking history	221 (25.6)	24 (18.3)	0.072
WC in cm	92.490 ± 10.522	93.690 ± 10.759	0.057
BMI in kg/m^2	26.563 ± 3.653	27.055 ± 3.772	0.155
SBP in mmHg	130.460 ± 16.517	129.090 ± 16.822	0.386
DBP in mmHg	80.730 ± 12.464	78.560 ± 12.192	0.063
ALT in U/L	28.0 (19.0, 42.0)	28.0 (19.0, 43.0)	0.837
AST in U/L	21.0 (18.0, 26.0)	22.0 (18.0, 26.0)	0.612
TC in mmol/L	4.683 ± 0.888	4.607 ± 0.865	0.349
TG in mmol/L	1.5 (1.0, 2.2)	1.6 (1.0, 2.5)	0.307
HDL-C in mmol/L	1.256 ± 0.279	1.241 ± 0.293	0.533
LDL-C in mmol/L	2.800 ± 0.826	2.763 ± 0.769	0.651
FBG in mmol/L	5.3 (5.0, 5.7)	5.2 (4.9, 5.8)	0.326
SUA in μmol/L	359.434 ± 88.800	342.901 ± 88.448	0.052
AIP	0.09 (-0.13, 0.30)	0.12 (-0.13, 0.33)	0.306

Data are presented as median and interquartile range, mean ± SD, or *n* (%). WC: Waist circumference; BMI: Body mass index; SBP: Systolic blood pressure; DBP: Diastolic blood pressure; ALT: Alanine aminotransferase; AST: Aspartate aminotransferase; TC: Total cholesterol; TG: Triglyceride; HDL-C: High-density lipoprotein cholesterol; LDL-C: Low-density lipoprotein cholesterol; FBG: Fasting blood glucose; SUA: Serum uric acid; AIP: Atherogenic index of plasma.

Xie *et al*[17] indicated that the ORs of AIP on the risk of fatty liver disease in women and young adults increased faster. This study showed that the AIP had a better predictive ability for MAFLD in young subjects, which may be related to the higher excessive fat accumulation of young people caused by dietary irregularities and insufficient exercise. However, there was no significant difference between males and females. Wang *et al*[23] and Dong *et al*[24] studied the predictive value of AIP for nonalcoholic fatty liver disease in obese and nonobese populations separately, with AUCs of 0.718 and 0.803, respectively. It seems that the predictive ability of AIP in the nonobese population might be better, but no studies have directly compared the ability of AIP in identifying MAFLD between different weights. Fortunately, our study filled this gap, and confirmed that the AIP had a remarkably higher predictive ability for MAFLD in nonobese subjects. A cohort study demonstrated that visceral obesity was dose-dependently associated with nonalcoholic fatty liver disease[25]. It is worth noting that lean people with unhealthy metabolism may have a greater accumulation of visceral fat[26], and nonobese MAFLD patients with unhealthy metabolism usually exhibit higher liver damage and cardiovascular risks[27]. AIP, as a sensitive indicator that reflects the accumulation of visceral fat, might have a stronger association with nonobese MAFLD patients and thus might have a better predictive ability for MAFLD in nonobese populations.

WC and BMI are common indicators for obesity evaluation and have been proven to be good predictors of fatty liver[17]. This study confirmed that they also had good predictive ability for MAFLD, with no significant difference compared to AIP. However, no previous study has assessed the predictive power of AIP combined with WC and BMI for MAFLD. Therefore, another focus of this study was to explore whether AIP combined with WC and BMI can improve the ability to identify MAFLD. The results showed that the logistic regression prediction Model A-W-B established by AIP combined with WC and BMI had excellent calibration and discrimination for MAFLD and had a significantly better ability to identify MAFLD. At the same time, it also had an outstanding ability to identify MAFLD in the validation, further affirming its outstanding predictive performance for MAFLD. Interestingly, we also found that the level of A-W-B was positively correlated with the liver fat content and the degree of severity of MAFLD in the validation, which may be objective evidence explaining the positive association and excellent predictive ability of the A-W-B model for MAFLD.

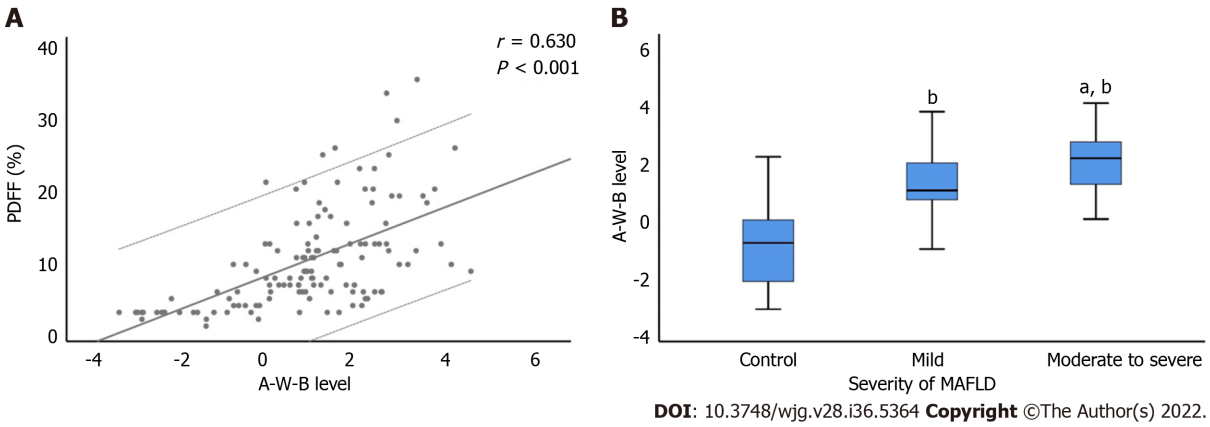


DOI: 10.3748/wjg.v28.i36.5364 **Copyright** ©The Author(s) 2022.

Figure 5 Receiver operating characteristic curves of atherogenic index of plasma, waist circumference, body mass index, and A-W-B model to predict metabolic-associated fatty liver disease in different subgroups. A-E: The area under the receiver operating characteristic curve (AUC) of the prediction model combining atherogenic index of plasma, waist circumference (WC), and body mass index (BMI) (A-W-B) model was significantly higher than that of A-W-B in male, female, young, middle-aged and elderly, and nonobese subjects (all $P < 0.01$); F: The AUC of the A-W-B model was only better than atherogenic index of plasma (AIP) in obese subjects ($P = 0.0465$).

The Spearman's correlation analysis showed that AIP, WC, and BMI were all positively associated with SBP, DBP, ALT, AST, FBG, and SUA. Notably, these physical and chemical indicators were also risk factors for MAFLD, and compared with AIP, WC, and BMI, the A-W-B model had a higher correlation with SBP, DBP, ALT, AST, FBG, and SUA, which may indirectly explain the better correlation and predictive ability of the A-W-B model for MAFLD. Furthermore, this study also pointed out that the optimal cutoff values of the A-W-B model to predict MAFLD in males and females were 0.5932 and 0.4105, respectively, which will facilitate early clinical identification of MAFLD in different sex populations. When the A-W-B level of the subject is above the cutoff point, it can be preliminarily identified as MAFLD.

In summary, compared with other studies, this study has the following advantages. First, this study confirmed that AIP was strongly and positively associated with the risk of MAFLD, and it can be a reference predictor for MAFLD and determined the optimal cutoff values of AIP for predicting MAFLD in males and females, providing a new idea for early prevention of MAFLD. Then, we pioneered a novel noninvasive prediction model A-W-B combining AIP, WC, and BMI that can significantly improve the predictive ability for MAFLD and determined its optimal cutoff values of the A-W-B model to predict MAFLD in males and females. Furthermore, we also validated the model with MRI as the diagnostic standard, further affirming its outstanding predictive performance for MAFLD. This study is highly innovative, and this noninvasive prediction model A-W-B is convenient, affordable, and easy to obtain,



DOI: 10.3748/wjg.v28.i36.5364 **Copyright** ©The Author(s) 2022.

Figure 6 Correlation between A-W-B levels with liver proton density fat fraction and the severity of metabolic-associated fatty liver disease. A: The prediction model combining atherogenic index of plasma, waist circumference, and body mass index (A-W-B) level was strongly and positively associated with liver proton density fat fraction (PDFF) (r = 0.630, P < 0.001); B: Compared with the control group, ^{b}P < 0.001; compared with the mild group, ^{a}P < 0.01. MAFLD: Metabolic-associated fatty liver disease.

which can provide better services for clinical prediction and screening of MAFLD and metabolic-related diseases.

However, there are still some limitations. First, to avoid subject recall bias, this study did not collect confounding factors, such as specific dietary structure and physical activity, and mainly focused on objective laboratory indicators and basic demographic indicators, which may slightly affect the results of multiple logistic regression analysis. Second, the subjects in this study were limited to a single physical examination center, which may cause selection bias. Third, fatty liver in the training set of this study was diagnosed by abdominal ultrasonography, and we did not use ultrasonography to accurately classify the severity of MAFLD. Therefore, the relationship between AIP, A-W-B model, and the severity of fatty liver by ultrasonography was unclear. Notably, we found that the A-W-B levels were positively correlated with MRI-diagnosed MAFLD severity in the validation set. However, due to limited funds, the number of validation sets using MRI as the diagnostic standard was relatively small. Therefore, further multicenter, large-sample prospective cohort studies are needed in the future to verify and explore the predictive value of AIP and A-W-B for MAFLD and differential severity.

CONCLUSION

AIP was strongly and positively associated with MAFLD, and it can be a reference predictor for MAFLD. The novel noninvasive prediction model A-W-B combining AIP, WC, and BMI can significantly improve the predictive ability for MAFLD and provide better services for clinical prediction and screening of MAFLD.

ARTICLE HIGHLIGHTS

Research background

Metabolic-associated fatty liver disease (MAFLD) is the most common chronic liver disease and poses great harm to people's health. Early identification of MAFLD is imminent.

Research motivation

Atherogenic index of plasma (AIP) is a reference predictor of obesity-related diseases, but its predictive value for MAFLD remains unclear. No studies have reported whether its combination with waist circumference (WC) and body mass index (BMI) can improve the predictive performance for MAFLD.

Research objectives

This study had two main objectives: (1) To systematically explore the relationship between AIP and MAFLD and evaluate its predictive value for MAFLD; and (2) To pioneer a novel prediction model combining AIP, WC, and BMI and validate its predictive performance for MAFLD.

Research methods

This cross-sectional study consecutively enrolled 864 participants. Multivariate logistic regression analysis and receiver operating characteristic curve were used to evaluate the relationship between AIP and MAFLD and its predictive power for MAFLD. The novel prediction model A-W-B combining AIP, WC, and BMI to predict MAFLD was established, and internal verification was completed by magnetic resonance imaging diagnosis.

Research results

Subjects with higher AIP exhibited a significantly increased risk of MAFLD, with an odds ratio of 12.420 (6.008-25.675) for AIP after adjusting for various confounding factors. The area under receiver operating characteristic curve of the A-W-B model was 0.833 (0.807-0.858), which was significantly higher than that of AIP, WC, and BMI (all P <0.05). The best cutoff values for the A-W-B model to predict MAFLD in males and females were 0.5932 and 0.4105, respectively. Additionally, in the validation set the area under receiver operating characteristic curve of A-W-B model to predict MAFLD was 0.862 (0.791-0.916). The A-W-B level was strongly and positively associated with the liver proton density fat fraction (r = 0.630, P < 0.001) and significantly increased with the severity of MAFLD (P < 0.05).

Research conclusions

AIP was strongly and positively associated with MAFLD and can be a reference predictor for MAFLD. The novel noninvasive prediction model A-W-B combining AIP, WC, and BMI can significantly improve the predictive ability for MAFLD and provide better services for clinical prediction and screening of MAFLD.

Research perspectives

Studies that may be conducted in the future should further explore the predictive value of AIP and the A-W-B model for different severities of MAFLD and other related metabolic diseases.

ACKNOWLEDGEMENTS

We thank all staff for helping recruit the subjects. We thank English language expert Liang JT for the English language revision.

FOOTNOTES

Author contributions: Duan SJ designed and performed the study, analyzed the data, and drafted the manuscript; Ren ZY, Zheng T, Peng HY, Niu ZH, and Wang RR collected the samples and clinical data of the patients; Xia H, Chen JL, and Zhou YC took part in designing the study and analyzing the data; Yao SK designed the study, supervised the study performance, and revised the manuscript.

Institutional review board statement: This study was approved by the Clinical Research Ethics Committee of China-Japan Friendship Hospital (2018-110-K79-1).

Informed consent statement: All study participants provided informed written consent prior to study enrollment.

Conflict-of-interest statement: All the authors report no relevant conflicts of interest for this article.

Data sharing statement: No additional data are available.

STROBE statement: The authors have read the STROBE Statement checklist of items, and the manuscript was prepared and revised according to the STROBE Statement checklist of items.

Open-Access: This article is an open-access article that was selected by an in-house editor and fully peer-reviewed by external reviewers. It is distributed in accordance with the Creative Commons Attribution NonCommercial (CC BY-NC 4.0) license, which permits others to distribute, remix, adapt, build upon this work non-commercially, and license their derivative works on different terms, provided the original work is properly cited and the use is non-commercial. See: https://creativecommons.org/Licenses/by-nc/4.0/

Country/Territory of origin: China

ORCID number: Shao-Jie Duan 0000-0002-6022-5039; Zhi-Ying Ren 0000-0001-7834-0556; Tao Zheng 0000-0002-4241-5584; Hong-Ye Peng 0000-0001-7980-683X; Zuo-Hu Niu 0000-0001-5215-8318; Hui Xia 0000-0001-7481-673X; Jia-Liang Chen 0000-0002-3007-0451; Yuan-Chen Zhou 0000-0001-6024-6246; Rong-Rui Wang 0000-0001-5279-5472; Shu-Kun Yao 0000-0002-8512-2589.

S-Editor: Gong ZM
L-Editor: Filipodia
P-Editor: Gong ZM

REFERENCES

1 **Loomba R**, Sanyal AJ. The global NAFLD epidemic. *Nat Rev Gastroenterol Hepatol* 2013; **10**: 686-690 [PMID: 24042449 DOI: 10.1038/nrgastro.2013.171]
2 **Younossi ZM**, Koenig AB, Abdelatif D, Fazel Y, Henry L, Wymer M. Global epidemiology of nonalcoholic fatty liver disease-Meta-analytic assessment of prevalence, incidence, and outcomes. *Hepatology* 2016; **64**: 73-84 [PMID: 26707365 DOI: 10.1002/hep.28431]
3 **Caballero B**. Humans against Obesity: Who Will Win? *Adv Nutr* 2019; **10**: S4-S9 [PMID: 30721956 DOI: 10.1093/advances/nmy055]
4 **Ogden CL**, Fakhouri TH, Carroll MD, Hales CM, Fryar CD, Li X, Freedman DS. Prevalence of Obesity Among Adults, by Household Income and Education - United States, 2011-2014. *MMWR Morb Mortal Wkly Rep* 2017; **66**: 1369-1373 [PMID: 29267260 DOI: 10.15585/mmwr.mm6650a1]
5 **Sarin SK**, Kumar M, Eslam M, George J, Al Mahtab M, Akbar SMF, Jia J, Tian Q, Aggarwal R, Muljono DH, Omata M, Ooka Y, Han KH, Lee HW, Jafri W, Butt AS, Chong CH, Lim SG, Pwu RF, Chen DS. Liver diseases in the Asia-Pacific region: a Lancet Gastroenterology & Hepatology Commission. *Lancet Gastroenterol Hepatol* 2020; **5**: 167-228 [PMID: 31852635 DOI: 10.1016/S2468-1253(19)30342-5]
6 **Dulai PS**, Singh S, Patel J, Soni M, Prokop LJ, Younossi Z, Sebastiani G, Ekstedt M, Hagstrom H, Nasr P, Stal P, Wong VW, Kechagias S, Hultcrantz R, Loomba R. Increased risk of mortality by fibrosis stage in nonalcoholic fatty liver disease: Systematic review and meta-analysis. *Hepatology* 2017; **65**: 1557-1565 [PMID: 28130788 DOI: 10.1002/hep.29085]
7 **Dewidar B**, Kahl S, Pafili K, Roden M. Metabolic liver disease in diabetes - From mechanisms to clinical trials. *Metabolism* 2020; **111S**: 154299 [PMID: 32569680 DOI: 10.1016/j.metabol.2020.154299]
8 **Lee H**, Lee YH, Kim SU, Kim HC. Metabolic Dysfunction-Associated Fatty Liver Disease and Incident Cardiovascular Disease Risk: A Nationwide Cohort Study. *Clin Gastroenterol Hepatol* 2021; **19**: 2138-2147.e10 [PMID: 33348045 DOI: 10.1016/j.cgh.2020.12.022]
9 **Stahl EP**, Dhindsa DS, Lee SK, Sandesara PB, Chalasani NP, Sperling LS. Nonalcoholic Fatty Liver Disease and the Heart: JACC State-of-the-Art Review. *J Am Coll Cardiol* 2019; **73**: 948-963 [PMID: 30819364 DOI: 10.1016/j.jacc.2018.11.050]
10 **Wong MCS**, Huang JLW, George J, Huang J, Leung C, Eslam M, Chan HLY, Ng SC. The changing epidemiology of liver diseases in the Asia-Pacific region. *Nat Rev Gastroenterol Hepatol* 2019; **16**: 57-73 [PMID: 30158570 DOI: 10.1038/s41575-018-0055-0]
11 **Ipsen DH**, Lykkesfeldt J, Tveden-Nyborg P. Molecular mechanisms of hepatic lipid accumulation in non-alcoholic fatty liver disease. *Cell Mol Life Sci* 2018; **75**: 3313-3327 [PMID: 29936596 DOI: 10.1007/s00018-018-2860-6]
12 **Katsiki N**, Mikhailidis DP, Mantzoros CS. Non-alcoholic fatty liver disease and dyslipidemia: An update. *Metabolism* 2016; **65**: 1109-1123 [PMID: 27237577 DOI: 10.1016/j.metabol.2016.05.003]
13 **Eslam M**, Sarin SK, Wong VW, Fan JG, Kawaguchi T, Ahn SH, Zheng MH, Shiha G, Yilmaz Y, Gani R, Alam S, Dan YY, Kao JH, Hamid S, Cua IH, Chan WK, Payawal D, Tan SS, Tanwandee T, Adams LA, Kumar M, Omata M, George J. The Asian Pacific Association for the Study of the Liver clinical practice guidelines for the diagnosis and management of metabolic associated fatty liver disease. *Hepatol Int* 2020; **14**: 889-919 [PMID: 33006093 DOI: 10.1007/s12072-020-10094-2]
14 **Dobiásová M**. Atherogenic index of plasma [log(triglycerides/HDL-cholesterol)]: theoretical and practical implications. *Clin Chem* 2004; **50**: 1113-1115 [PMID: 15229146 DOI: 10.1373/clinchem.2004.033175]
15 **Zhu X**, Yu L, Zhou H, Ma Q, Zhou X, Lei T, Hu J, Xu W, Yi N, Lei S. Atherogenic index of plasma is a novel and better biomarker associated with obesity: a population-based cross-sectional study in China. *Lipids Health Dis* 2018; **17**: 37 [PMID: 29506577 DOI: 10.1186/s12944-018-0686-8]
16 **Shen SW**, Lu Y, Li F, Yang CJ, Feng YB, Li HW, Yao WF, Shen ZH. Atherogenic index of plasma is an effective index for estimating abdominal obesity. *Lipids Health Dis* 2018; **17**: 11 [PMID: 29334966 DOI: 10.1186/s12944-018-0656-1]
17 **Xie F**, Zhou H, Wang Y. Atherogenic index of plasma is a novel and strong predictor associated with fatty liver: a cross-sectional study in the Chinese Han population. *Lipids Health Dis* 2019; **18**: 170 [PMID: 31511022 DOI: 10.1186/s12944-019-1112-6]
18 **Eslam M**, Sanyal AJ, George J; International Consensus Panel. MAFLD: A Consensus-Driven Proposed Nomenclature for Metabolic Associated Fatty Liver Disease. *Gastroenterology* 2020; **158**: 1999-2014.e1 [PMID: 32044314 DOI: 10.1053/j.gastro.2019.11.312]
19 **Shiha G**, Korenjak M, Eskridge W, Casanovas T, Velez-Moller P, Högström S, Richardson B, Munoz C, Sigurðardóttir S, Coulibaly A, Milan M, Bautista F, Leung NWY, Mooney V, Obekpa S, Bech E, Polavarapu N, Hamed AE, Radiani T, Purwanto E, Bright B, Ali M, Dovia CK, McColaugh L, Koulla Y, Dufour JF, Soliman R, Eslam M. Redefining fatty liver disease: an international patient perspective. *Lancet Gastroenterol Hepatol* 2021; **6**: 73-79 [PMID: 33031758 DOI: 10.1016/S2468-1253(20)30294-6]
20 **Eslam M**, Newsome PN, Sarin SK, Anstee QM, Targher G, Romero-Gomez M, Zelber-Sagi S, Wai-Sun Wong V, Dufour JF, Schattenberg JM, Kawaguchi T, Arrese M, Valenti L, Shiha G, Tiribelli C, Yki-Järvinen H, Fan JG, Grønbæk H, Yilmaz Y, Cortez-Pinto H, Oliveira CP, Bedossa P, Adams LA, Zheng MH, Fouad Y, Chan WK, Mendez-Sanchez N, Ahn SH, Castera L, Bugianesi E, Ratziu V, George J. A new definition for metabolic dysfunction-associated fatty liver disease: An international expert consensus statement. *J Hepatol* 2020; **73**: 202-209 [PMID: 32278004 DOI:

10.1016/j.jhep.2020.03.039]
21 **Kromrey ML**, Ittermann T, Berning M, Kolb C, Hoffmann RT, Lerch MM, Völzke H, Kühn JP. Accuracy of ultrasonography in the assessment of liver fat compared with MRI. *Clin Radiol* 2019; **74**: 539-546 [PMID: 30955836 DOI: 10.1016/j.crad.2019.02.014]
22 **Li YW**, Kao TW, Chang PK, Chen WL, Wu LW. Atherogenic index of plasma as predictors for metabolic syndrome, hypertension and diabetes mellitus in Taiwan citizens: a 9-year longitudinal study. *Sci Rep* 2021; **11**: 9900 [PMID: 33972652 DOI: 10.1038/s41598-021-89307-z]
23 **Wang Q**, Zheng D, Liu J, Fang L, Li Q. Atherogenic index of plasma is a novel predictor of non-alcoholic fatty liver disease in obese participants: a cross-sectional study. *Lipids Health Dis* 2018; **17**: 284 [PMID: 30545385 DOI: 10.1186/s12944-018-0932-0]
24 **Dong BY**, Mao YQ, Li ZY, Yu FJ. The value of the atherogenic index of plasma in non-obese people with non-alcoholic fatty liver disease: a secondary analysis based on a cross-sectional study. *Lipids Health Dis* 2020; **19**: 148 [PMID: 32576204 DOI: 10.1186/s12944-020-01319-2]
25 **Kim D**, Chung GE, Kwak MS, Seo HB, Kang JH, Kim W, Kim YJ, Yoon JH, Lee HS, Kim CY. Body Fat Distribution and Risk of Incident and Regressed Nonalcoholic Fatty Liver Disease. *Clin Gastroenterol Hepatol* 2016; **14**: 132-8.e4 [PMID: 26226099 DOI: 10.1016/j.cgh.2015.07.024]
26 **Stefan N**, Schick F, Häring HU. Causes, Characteristics, and Consequences of Metabolically Unhealthy Normal Weight in Humans. *Cell Metab* 2017; **26**: 292-300 [PMID: 28768170 DOI: 10.1016/j.cmet.2017.07.008]
27 **Fracanzani AL**, Petta S, Lombardi R, Pisano G, Russello M, Consonni D, Di Marco V, Cammà C, Mensi L, Dongiovanni P, Valenti L, Craxì A, Fargion S. Liver and Cardiovascular Damage in Patients With Lean Nonalcoholic Fatty Liver Disease, and Association With Visceral Obesity. *Clin Gastroenterol Hepatol* 2017; **15**: 1604-1611.e1 [PMID: 28554682 DOI: 10.1016/j.cgh.2017.04.045]

World Journal of Gastroenterology

Submit a Manuscript: https://www.f6publishing.com

World J Gastroenterol 2022 September 28; 28(36): 5380-5382

DOI: 10.3748/wjg.v28.i36.5380

ISSN 1007-9327 (print) ISSN 2219-2840 (online)

LETTER TO THE EDITOR

Nonalcoholic steatohepatitis and hepatocellular carcinoma: Beyond the boundaries of the liver

Tarana Gupta

Specialty type: Gastroenterology and hepatology

Provenance and peer review: Unsolicited article; Externally peer reviewed.

Peer-review model: Single blind

Peer-review report's scientific quality classification

Grade A (Excellent): 0
Grade B (Very good): 0
Grade C (Good): C, C, C
Grade D (Fair): D
Grade E (Poor): 0

P-Reviewer: Kao JT, Taiwan; Protopapas AA, Greece; Sempokuya T, United States; Tsoulfas G, Greece

Received: May 8, 2022
Peer-review started: May 8, 2022
First decision: June 8, 2022
Revised: June 20, 2022
Accepted: September 12, 2022
Article in press: September 12, 2022
Published online: September 28, 2022

Tarana Gupta, Department of Medicine, Pandit Bhagwat Dayal Sharma Post Graduate Institute of Medical Sciences, Rohtak 124001, Haryana, India

Corresponding author: Tarana Gupta, Doctor, MBBS, MD, DM Hepatology, Professor, Department of Medicine, Pandit Bhagwat Dayal Sharma Post Graduate Institute of Medical Sciences, Medical Mor, Rohtak 124001, Haryana, India. taranagupta@gmail.com

Abstract

The burden of non-alcoholic steatohepatitis (NASH) related hepatocellular carcinoma (HCC) is drawing attention due to the emerging epidemic of obesity and metabolic syndrome and is expected to increase in the near future. Antidiabetic medications, air pollutants, and newer genetic mutations are latest concerns as risk factors for HCC development in patients with NASH. Although molecular signatures are very accurate, they are not cost-effective and cannot be applied in larger population due to logistic issues. We need multicentric longitudinal studies including diverse geographical areas to evaluate the complex interplay of different risk factors and genetics in these patients.

Key Words: Non-alcoholic steatohepatitis; Hepatocellular carcinoma; Cirrhosis; Genetic factors; Lifestyle factors; Surveillance

©The Author(s) 2022. Published by Baishideng Publishing Group Inc. All rights reserved.

Core Tip: Nonalcoholic steatohepatitis (NASH) is a metabolic liver disease which also involves multiple organs like the heart, lungs, and kidneys. NASH may arise primarily, followed by involvement of other organs, or it may come late in the course of metabolic syndrome. The multidisciplinary approach is needed towards a patient with diabetes, obesity, and metabolic syndrome to address all issues related to the liver, heart, *etc.* Genetic and molecular signatures have provided a ray of hope for estimating risk in these patients; however, it has many practical issues. The impact of environmental pollutants and toxins as a causative factor in NASH, especially lean patient population, should also be considered. We need population based studies from different geographical areas for estimation of metabolic, environmental, and genetic risk factors.

Citation: Gupta T. Nonalcoholic steatohepatitis and hepatocellular carcinoma: Beyond the boundaries of the liver. *World J Gastroenterol* 2022; 28(36): 5380-5382
URL: https://www.wjgnet.com/1007-9327/full/v28/i36/5380.htm
DOI: https://dx.doi.org/10.3748/wjg.v28.i36.5380

TO THE EDITOR

Chrysavgis *et al*[1] have extensively reviewed the literature on non-alcoholic steatohepatitis (NASH) related hepatocellular carcinoma (HCC) with regard to its risk stratification, screening, and surveillance strategies. Metabolic syndrome is a systemic disease involving the heart, kidneys, lungs, and liver, *etc.* NASH is the liver manifestation of metabolic syndrome. With the emerging epidemic of obesity and metabolic syndrome, NASH is expected to supersede all other etiologies of liver cirrhosis as well as HCC. In various studies as discussed by Chrysavgis *et al*[1], the prevalence of HCC in non-cirrhotic non-alcoholic fatty liver disease (NAFLD) patients ranges from 15%-55%. Factors like age, male sex, concomitant smoking and alcohol intake, obesity, and type 2 diabetes mellitus have been shown to increase the risk of HCC in non-cirrhotic NASH. Recently, use of insulin and sulfonylureas has also been shown to increase the long-term risk of HCC in patients with diabetes. In an Italian study[2], an increased HCC risk with an odds ratio of 3.7 for insulin, 1.3 for sulfonylureas, and 2.1 for repaglinide was found in patients with diabetes. Even the duration of treatment with insulin, though not with other therapies, increased the risk of HCC. The same has also been confirmed in a nationwide nested case-control study[3] in Korea which showed an increased HCC risk with glimepiride instead of other sulfonylureas. And yet we do not have long-term data for GLP-1 agonists and DPP4 inhibitors. Chinese data[4] recently showed an increased association of air pollutants of particulate matter (PM) with an aerodynamic diameter of < 1 (PM_1), < 2.5 ($PM_{2.5}$), and < 10 μm (PM_{10}) with metabolic associated fatty liver disease. The role of intestinal dysbiosis has also been investigated in animal models and found to be associated with an increased risk of NASH and HCC.

In a multicentric trial, Pinyol *et al*[5] collected samples from NASH-HCC and NASH patients, performed expression array and whole exome sequencing, and compared it with HCC from non-NASH etiologies like viral/alcohol. They found *TERT* promoter, *CTNNB1*, *TP53*, and *ACVR2A* most frequently to be present in NASH-HCC patients. The *ACVR2A* (activin type 2 receptor gene) mutation was found in a higher number of patients with NASH-HCC as compared to those with HCC of other etiologies. The molecular signature revealed higher expression of bile acid and fatty acid signaling pathways. The Wnt/TGF-β proliferation subclass was more common in NASH-HCC. The upcoming data suggests that the molecular signature of NASH-HCC is different from that of HCC due to other etiologies. Collectively, the development of NAFLD-HCC results from a complex interplay of multiple factors related to unhealthy life style, environment, and genetics of an individual.

The authors have included abbreviated magnetic resonance imaging (MRI) in their suggested algorithm for HCC surveillance in NAFLD due to a poor window of ultrasound in obese patients. We have concerns regarding this strategy. First, a large number of individuals would need surveillance, so its cost-effectiveness, availability on large scale, and practicality need to be addressed. Second, how frequently MRI would have to be repeated is a practical issue. Third, when during the clinical course of NASH, screening should be performed. Although authors have included HCC risk model as suggested by Ioannou *et al*[6] in their algorithm, we believe that future prospective longitudinal studies are needed to determine the weightage of different risk factors in determining HCC risk in patients with cirrhotic and non-cirrhotic NAFLD, separately. The role of extracellular vesicles (EVs) for molecular characterization of HCC in patients with NASH may further be evaluated for HCC surveillance also. NAFLD is a risk factor not only for HCC but also for colorectal and breast cancers. Instead of screening for each carcinoma separately, we need to have studies on a common platform targeting the molecular signatures in blood for surveillance of different carcinomas in the body which share the pathogenetic mechanisms or pathways. The challenges involved are large population-based studies in different geographical regions, mapping of molecular signatures, and implementation. It has to be cost-effective, easily accessible, and readily available.

In patients with NAFLD, all-cause mortality includes mortality related to issues of the liver, heart, kidneys, lungs, *etc.* It is time to recognise the need for multidisciplinary approach towards a patient with diabetes, obesity, and metabolic syndrome to address all issues related to the liver, heart, kidneys, *etc.* Large prospective, multicentric studies including diverse geographical regions and dietary habits are needed to evaluate for risk stratification in these patients regarding need for HCC surveillance.

FOOTNOTES

Author contributions: Gupta T wrote and critically revised the manuscript.

Conflict-of-interest statement: There are no conflicts of interest to report.

Open-Access: This article is an open-access article that was selected by an in-house editor and fully peer-reviewed by external reviewers. It is distributed in accordance with the Creative Commons Attribution NonCommercial (CC BY-NC 4.0) license, which permits others to distribute, remix, adapt, build upon this work non-commercially, and license their derivative works on different terms, provided the original work is properly cited and the use is non-commercial. See: https://creativecommons.org/Licenses/by-nc/4.0/

Country/Territory of origin: India

ORCID number: Tarana Gupta 0000-0003-3453-2040.

Corresponding Author's Membership in Professional Societies: American Association for the Study of Liver Diseases, 226223.

S-Editor: Chen YL
L-Editor: Wang TQ
P-Editor: Chen YL

REFERENCES

1 **Chrysavgis L**, Giannakodimos I, Diamantopoulou P, Cholongitas E. Non-alcoholic fatty liver disease and hepatocellular carcinoma: Clinical challenges of an intriguing link. *World J Gastroenterol* 2022; **28**: 310-331 [PMID: 35110952 DOI: 10.3748/wjg.v28.i3.310]

2 **Bosetti C**, Franchi M, Nicotra F, Asciutto R, Merlino L, La Vecchia C, Corrao G. Insulin and other antidiabetic drugs and hepatocellular carcinoma risk: a nested case-control study based on Italian healthcare utilization databases. *Pharmacoepidemiol Drug Saf* 2015; **24**: 771-778 [PMID: 26013675 DOI: 10.1002/pds.3801]

3 **Lee JY**, Jang SY, Nam CM, Kang ES. Incident Hepatocellular Carcinoma Risk in Patients Treated with a Sulfonylurea: A Nationwide, Nested, Case-Control Study. *Sci Rep* 2019; **9**: 8532 [PMID: 31189966 DOI: 10.1038/s41598-019-44447-1]

4 **Guo B**, Guo Y, Nima Q, Feng Y, Wang Z, Lu R, Baimayangji, Ma Y, Zhou J, Xu H, Chen L, Chen G, Li S, Tong H, Ding X, Zhao X; China Multi-Ethnic Cohort (CMEC) collaborative group. Exposure to air pollution is associated with an increased risk of metabolic dysfunction-associated fatty liver disease. *J Hepatol* 2022; **76**: 518-525 [PMID: 34883157 DOI: 10.1016/j.jhep.2021.10.016]

5 **Pinyol R**, Torrecilla S, Wang H, Montironi C, Piqué-Gili M, Torres-Martin M, Wei-Qiang L, Willoughby CE, Ramadori P, Andreu-Oller C, Taik P, Lee YA, Moeini A, Peix J, Faure-Dupuy S, Riedl T, Schuehle S, Oliveira CP, Alves VA, Boffetta P, Lachenmayer A, Roessler S, Minguez B, Schirmacher P, Dufour JF, Thung SN, Reeves HL, Carrilho FJ, Chang C, Uzilov AV, Heikenwalder M, Sanyal A, Friedman SL, Sia D, Llovet JM. Molecular characterisation of hepatocellular carcinoma in patients with non-alcoholic steatohepatitis. *J Hepatol* 2021; **75**: 865-878 [PMID: 33992698 DOI: 10.1016/j.jhep.2021.04.049]

6 **Ioannou GN**, Green P, Kerr KF, Berry K. Models estimating risk of hepatocellular carcinoma in patients with alcohol or NAFLD-related cirrhosis for risk stratification. *J Hepatol* 2019; **71**: 523-533 [PMID: 31145929 DOI: 10.1016/j.jhep.2019.05.008]



Published by **Baishideng Publishing Group Inc**
7041 Koll Center Parkway, Suite 160, Pleasanton, CA 94566, USA
Telephone: +1-925-3991568
E-mail: bpgoffice@wjgnet.com
Help Desk: https://www.f6publishing.com/helpdesk
https://www.wjgnet.com



© 2022 Baishideng Publishing Group Inc. All rights reserved.

ISSN 1007-9327 (print)
ISSN 2219-2840 (online)

World Journal of *Gastroenterology*

World J Gastroenterol 2022 October 7; 28(37): 5383-5514



Published by Baishideng Publishing Group Inc

World Journal of Gastroenterology

Contents

Weekly Volume 28 Number 37 October 7, 2022

STANDARD AND CONSENSUS

5383 Baishideng's *Reference Citation Analysis* database announces the first *Journal Article Influence Index* of 101 core journals and a list of high-quality academic journals in gastroenterology and hepatology

Wang JL, Ma YJ, Ma L, Ma N, Guo DM, Ma LS

OPINION REVIEW

5395 Milestones in the discovery of hepatitis C

Campollo O, Amaya G, McCormick PA

REVIEW

5403 Immunotherapy-based novel nanoparticles in the treatment of gastrointestinal cancer: Trends and challenges

Ding YN, Xue M, Tang QS, Wang LJ, Ding HY, Li H, Gao CC, Yu WP

ORIGINAL ARTICLE

Basic Study

5420 Lentivirus-mediated short hairpin RNA interference of CENPK inhibits growth of colorectal cancer cells with overexpression of Cullin 4A

Li X, Han YR, Xuefeng X, Ma YX, Xing GS, Yang ZW, Zhang Z, Shi L, Wu XL

Retrospective Cohort Study

5444 Prognostic performance of an index based on lactic dehydrogenase and transaminases for patients with liver steatosis and COVID-19

Macías-Rodríguez RU, Solís-Ortega AA, Ornelas-Arroyo VJ, Ruiz-Margáin A, González-Huezo MS, Urdiales-Morán NA, Román-Calleja BM, Mayorquín-Aguilar JM, González-Regueiro JA, Campos-Murguía A, Toledo-Coronado IV, Chapa-Ibargüengoitia M, Valencia-Peña B, Martínez-Cabrera CF, Flores-García NC

Retrospective Study

5457 Efficacy of endoscopic ultrasound in the evaluation of small gastrointestinal stromal tumors

Ge QC, Wu YF, Liu ZM, Wang Z, Wang S, Liu X, Ge N, Guo JT, Sun SY

5469 Online calculator for predicting the risk of malignancy in patients with pancreatic cystic neoplasms: A multicenter, retrospective study

Jiang D, Chen ZX, Ma FX, Gong YY, Pu T, Chen JM, Liu XQ, Zhao YJ, Xie K, Hou H, Wang C, Geng XP, Liu FB

Observational Study

5483 Application of an artificial intelligence system for endoscopic diagnosis of superficial esophageal squamous cell carcinoma

Meng QQ, Gao Y, Lin H, Wang TJ, Zhang YR, Feng J, Li ZS, Xin L, Wang LW

5494 Insights into hepatitis E virus epidemiology in Croatia

Jelicic P, Ferenc T, Mrzljak A, Jemersic L, Janev-Holcer N, Milosevic M, Bogdanic M, Barbic L, Kolaric B, Stevanovic V, Vujica M, Jurekovic Z, Pavicic Saric J, Vilibic M, Vilibic-Cavlek T

CASE REPORT

5506 Massive bleeding from gastric submucosal arterial collaterals secondary to splenic artery thrombosis: A case report

Martino A, Di Serafino M, Zito FP, Maglione F, Bennato R, Orsini L, Iacobelli A, Niola R, Romano L, Lombardi G

World Journal of Gastroenterology

Weekly Volume 28 Number 37 October 7, 2022

Contents

ABOUT COVER

Editorial Board Member of *World Journal of Gastroenterology*, Masahiro Iizuka, MD, PhD, Director, Akita Health Care Center, Akita Red Cross Hospital, 3-4-23 Nakadori, Akita-shi, Akita 010-0001, Japan. maiizuka@woody.ocn.ne.jp

AIMS AND SCOPE

The primary aim of *World Journal of Gastroenterology* (*WJG*, *World J Gastroenterol*) is to provide scholars and readers from various fields of gastroenterology and hepatology with a platform to publish high-quality basic and clinical research articles and communicate their research findings online. *WJG* mainly publishes articles reporting research results and findings obtained in the field of gastroenterology and hepatology and covering a wide range of topics including gastroenterology, hepatology, gastrointestinal endoscopy, gastrointestinal surgery, gastrointestinal oncology, and pediatric gastroenterology.

INDEXING/ABSTRACTING

The *WJG* is now abstracted and indexed in Science Citation Index Expanded (SCIE, also known as SciSearch®), Current Contents/Clinical Medicine, Journal Citation Reports, Index Medicus, MEDLINE, PubMed, PubMed Central, Scopus, Reference Citation Analysis, China National Knowledge Infrastructure, China Science and Technology Journal Database, and Superstar Journals Database. The 2022 edition of Journal Citation Reports® cites the 2021 impact factor (IF) for *WJG* as 5.374; IF without journal self cites: 5.187; 5-year IF: 5.715; Journal Citation Indicator: 0.84; Ranking: 31 among 93 journals in gastroenterology and hepatology; and Quartile category: Q2. The *WJG*'s CiteScore for 2021 is 8.1 and Scopus CiteScore rank 2021: Gastroenterology is 18/149.

RESPONSIBLE EDITORS FOR THIS ISSUE

Production Editor: *Ying-Yi Yuan*; **Production Department Director:** *Xiang Li*; **Editorial Office Director:** *Jia-Ru Fan.*

NAME OF JOURNAL
World Journal of Gastroenterology

ISSN
ISSN 1007-9327 (print) ISSN 2219-2840 (online)

LAUNCH DATE
October 1, 1995

FREQUENCY
Weekly

EDITORS-IN-CHIEF
Andrzej S Tarnawski

EDITORIAL BOARD MEMBERS
http://www.wjgnet.com/1007-9327/editorialboard.htm

PUBLICATION DATE
October 7, 2022

COPYRIGHT
© 2022 Baishideng Publishing Group Inc

INSTRUCTIONS TO AUTHORS
https://www.wjgnet.com/bpg/gerinfo/204

GUIDELINES FOR ETHICS DOCUMENTS
https://www.wjgnet.com/bpg/GerInfo/287

GUIDELINES FOR NON-NATIVE SPEAKERS OF ENGLISH
https://www.wjgnet.com/bpg/gerinfo/240

PUBLICATION ETHICS
https://www.wjgnet.com/bpg/GerInfo/288

PUBLICATION MISCONDUCT
https://www.wjgnet.com/bpg/gerinfo/208

ARTICLE PROCESSING CHARGE
https://www.wjgnet.com/bpg/gerinfo/242

STEPS FOR SUBMITTING MANUSCRIPTS
https://www.wjgnet.com/bpg/GerInfo/239

ONLINE SUBMISSION
https://www.f6publishing.com

© 2022 Baishideng Publishing Group Inc. All rights reserved. 7041 Koll Center Parkway, Suite 160, Pleasanton, CA 94566, USA
E-mail: bpgoffice@wjgnet.com https://www.wjgnet.com

World Journal of Gastroenterology

Submit a Manuscript: https://www.f6publishing.com

World J Gastroenterol 2022 October 7; 28(37): 5383-5394

DOI: 10.3748/wjg.v28.i37.5383

ISSN 1007-9327 (print) ISSN 2219-2840 (online)

STANDARD AND CONSENSUS

Baishideng's *Reference Citation Analysis* database announces the first *Journal Article Influence Index* of 101 core journals and a list of high-quality academic journals in gastroenterology and hepatology

Jin-Lei Wang, Yu-Jie Ma, Li Ma, Na Ma, Diao-Mei Guo, Lian-Sheng Ma

Specialty type: Gastroenterology and hepatology

Provenance and peer review: Unsolicited article; Externally peer reviewed.

Peer-review model: Single blind

Peer-review report's scientific quality classification

Grade A (Excellent): 0
Grade B (Very good): B
Grade C (Good): 0
Grade D (Fair): 0
Grade E (Poor): 0

P-Reviewer: Morozov S, Russia

Received: August 16, 2022
Peer-review started: August 16, 2022
First decision: August 25, 2022
Revised: September 6, 2022
Accepted: September 21, 2022
Article in press: September 21, 2022
Published online: October 7, 2022

Jin-Lei Wang, Yu-Jie Ma, Li Ma, Na Ma, Diao-Mei Guo, Lian-Sheng Ma, Baishideng Publishing Group Inc, Pleasanton, CA 94566, United States

Corresponding author: Lian-Sheng Ma, Doctor, Founder and CEO, Baishideng Publishing Group Inc, 7041 Koll Center Parkway, Suite 160, Pleasanton, CA 94566, United States. l.s.ma@baishideng.com

Abstract

After three rounds of rigorous evaluation of core journals in gastroenterology and hepatology conducted by the *Reference Citation Analysis* (*RCA*) editorial team of Baishideng Publishing Group (Baishideng), the *RCA* database of Baishideng officially released the 2022 *Journal Article Influence Index* (2022 *JAII*) of 101 core journals in gastroenterology and hepatology, for the first time. The list of 101 core journals can be found at: https://www.referencecitationanalysis.com/Search-Journal. Among them, the highest 2022 *JAII* is 48.014 and the lowest is 3.900. This article highlights the top 20 journals, describes the calculation method for the 2022 *JAII*, the evaluation process, and the inclusion principles for journals in the *RCA*. These steps are the underpinning of the *RCA*'s empirical journal academic evaluation service by which the digital platform addresses the needs of authors to select reliable journals for submission, readers to select high-quality literature for reading, and editors to track their own journal citation performance. As such, the *RCA* core journal list will serve as a useful Find-a-Journal tool. Any interested party is welcome to use this journal list and recommend it to their peers.

Key Words: *Reference Citation Analysis*; *Journal Article Influence Index*; Gastroenterology and hepatology; Journal list; Find a journal; Announcement

©The Author(s) 2022. Published by Baishideng Publishing Group Inc. All rights reserved.

Core Tip: The *Reference Citation Analysis* (*RCA*) database of Baishideng Publishing Group officially released the 2022 *Journal Article Influence Index* (2022 *JAII*) of 101 core journals in gastroenterology and hepatology, for the first time. This article highlights the top 20 journals, describes the calculation method for the 2022 *JAII*, evaluation process and inclusion principles. The *RCA* journal academic evaluation service platform addresses the needs of authors to select reliable journals for submission, readers to select high-quality literature for reading, and editors to track their own journal citation performance, effectively serving as a useful Find-a-Journal tool. You are welcome to use this journal list and recommend it to your peers.

Citation: Wang JL, Ma YJ, Ma L, Ma N, Guo DM, Ma LS. Baishideng's *Reference Citation Analysis* database announces the first *Journal Article Influence Index* of 101 core journals and a list of high-quality academic journals in gastroenterology and hepatology. *World J Gastroenterol* 2022; 28(37): 5383-5394
URL: https://www.wjgnet.com/1007-9327/full/v28/i37/5383.htm
DOI: https://dx.doi.org/10.3748/wjg.v28.i37.5383

INTRODUCTION

We are very pleased to announce that the *Reference Citation Analysis* (*RCA*) database of Baishideng Publishing Group (Baishideng) has, for the first time, officially released the 2022 *Journal Article Influence Index* (2022 *JAII*) of 101 core journals in the field of gastroenterology and hepatology on August 8, 2022. A total of 101 core journals in gastroenterology and hepatology can be found at: https://www.referencecitationanalysis.com/SearchJournal.

RCA is an artificial intelligence technology-based open multidisciplinary citation analysis database. It was carefully designed to lead the development of wisdom, knowledge innovation, and emerging disciplines[1]. As such, the functions of *RCA* include: Find an Article (54753299), Find a Category (254), Find a Journal (14087), Find a Scholar (631), and Find an Academic Assistant (15). *RCA* updates its list of journals daily, according to relevant data including total number of articles, total citations, and the *JAII*. *RCA* acquires newly released abstracts and references from Crossref and adds them to the *RCA* database weekly. *RCA* also acquires abstracts and references released within the calendar year from Crossref and adds them to the *RCA* database monthly, and then updates the total number of articles, citations, and *JAII* accordingly. Herein, we introduce the top 20 2022 *JAII* from the total 101 core journals in the field of gastroenterology and hepatology included in *RCA*, the calculation method for the 2022 *JAII*, and the evaluation process and the inclusion principles of *RCA* journals.

TOP 20 2022 *JAII* JOURNALS IN THE FIELD OF GASTROENTEROLOGY AND HEPATOLOGY INCLUDED IN THE *RCA*

The *RCA* classifies academic journals with a *JAII* of 20.0 or above as high quality academic journals, which will be highly recommended to authors and readers. There are 101 core journals in the field of gastroenterology and hepatology in the *RCA*, of which 20 were identified to be high quality academic journals, accounting for 19.8%. These 20 journals are listed below.

2022 JAII and rankings of Seminars in Liver Disease

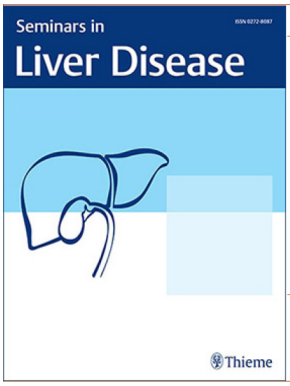
In the *RCA* database, the 2022 *JAII* for *Seminars in Liver Disease* is 48.014, ranking 1st among 101 core journals in the field of gastroenterology and hepatology included in the *RCA*, with a total of 83641 citations (28/101) and a total of 1742 articles (50/101) (Figure 1). For more information on *Seminars in Liver Disease*, please visit: https://www.referencecitationanalysis.com/SearchJournal.

2022 JAII and rankings of Hepatology

In the *RCA* database, the 2022 *JAII* for *Hepatology* is 43.054, ranking 2nd among 101 core journals in the field of gastroenterology and hepatology included in the *RCA*, with a total of 1169100 citations (2/101) and a total of 27154 articles (2/101) (Figure 2). For more information on *Hepatology*, please visit: https://www.referencecitationanalysis.com/SearchJournal.

2022 JAII and rankings of Gastroenterology

In the *RCA* database, the 2022 *JAII* for *Gastroenterology* is 37.170, ranking 3rd among 101 core journals in the field of gastroenterology and hepatology included in the *RCA*, with a total of 1711173 citations (1/101) and a total of 46037 articles (1/101) (Figure 3). For more information on *Gastroenterology*, please



SEMINARS IN LIVER DISEASE

Category Rank: Gastroenterology & Hepatology

Total View: 19 (2/101)

Journal Article Influence Index: 48.014 (1/101)

Total Citations: 83641 (28/101)

Cited by in F6Publishing: 73076 (26/101)

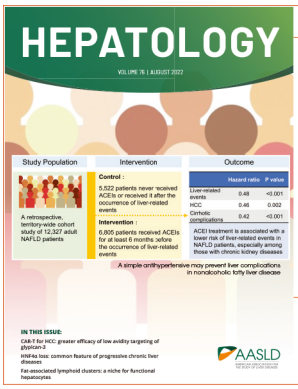
Total Articles: 1742 (50/101)

Number of Years: 41 (15/101)

Peer-Reviewed Journal: Yes

DOI: 10.3748/wjg.v28.i37.5383 **Copyright** ©The Author(s) 2022.

Figure 1 2022 *Journal Article Influence Index* and rankings of *Seminars in Liver Disease*. The image of the journal cover is originally from the home page of the journal: https://www.thieme.in/seminars-in-liver-disease.



HEPATOLOGY

Category Rank: Gastroenterology & Hepatology

Total View: 10 (3/101)

Journal Article Influence Index: 43.054 (2/101)

Total Citations: 1169100 (2/101)

Cited by in F6Publishing: 1041533 (2/101)

Total Articles: 27154 (2/101)

Number of Years: 41 (14/101)

Peer-Reviewed Journal: Yes

DOI: 10.3748/wjg.v28.i37.5383 **Copyright** ©The Author(s) 2022.

Figure 2 2022 *Journal Article Influence Index* and rankings of *Hepatology*. The image of the journal cover is originally from the home page of the journal: https://aasldpubs.onlinelibrary.wiley.com/journal/15273350.



GASTROENTEROLOGY

Category Rank: Gastroenterology & Hepatology

Total View: 5 (11/101)

Journal Article Influence Index: 37.170 (3/101)

Total Citations: 1711173 (1/101)

Cited by in F6Publishing: 1096503 (1/101)

Total Articles: 46037 (1/101)

Number of Years: 73 (2/101)

Peer-Reviewed Journal: Yes

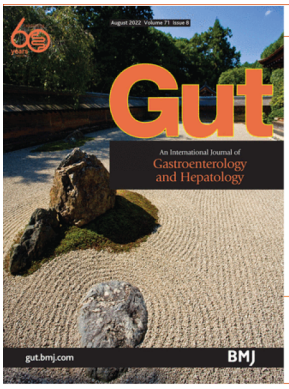
DOI: 10.3748/wjg.v28.i37.5383 **Copyright** ©The Author(s) 2022.

Figure 3 2022 *Journal Article Influence Index* and rankings of *Gastroenterology*. The image of the journal cover is originally from the home page of the journal: https://www.gastrojournal.org/.

visit: https://www.referencecitationanalysis.com/SearchJournal.

2022 JAII and rankings of Gut

In the *RCA* database, the 2022 *JAII* for *Gut* is 36.751, ranking 4th among 101 core journals in the field of gastroenterology and hepatology included in the *RCA*, with a total of 914769 citations (3/101) and a total of 24891 articles (3/101) (Figure 4). For more information on *Gut*, please visit: https://www.referencecitationanalysis.com/SearchJournal.



GUT
Category Rank: Gastroenterology & Hepatology
Total View: 2 (57/101)
Journal Article Influence Index: 36.751 (4/101)
Total Citations: 914769 (3/101)
Cited by in F6Publishing: 809970 (3/101)
Total Articles: 24891 (3/101)
Number of Years: 62 (4/101)
Peer-Reviewed Journal: Yes

DOI: 10.3748/wjg.v28.i37.5383 **Copyright** ©The Author(s) 2022.

Figure 4 2022 *Journal Article Influence Index* and rankings of *Gut*. The image of the journal cover is originally from the home page of the journal: http://gut.bmj.com/.

2022 JAII and rankings of Nature Reviews Gastroenterology & Hepatology

In the *RCA* database, the 2022 *JAII* for *Nature Reviews Gastroenterology & Hepatology* is 35.473, ranking 5th among 101 core journals in the field of gastroenterology and hepatology included in the *RCA*, with a total of 100601 citations (24/101) and a total of 2836 articles (40/101) (Figure 5). For more information on *Nature Reviews Gastroenterology & Hepatology*, please visit: https://www.referencecitationanalysis.com/SearchJournal.

2022 JAII and rankings of Gut Microbes

In the *RCA* database, the 2022 *JAII* for *Gut Microbes* is 31.557, ranking 6th among 101 core journals in the field of gastroenterology and hepatology included in the *RCA*, with a total of 38720 citations (41/101) and a total of 1227 articles (64/101) (Figure 6). For more information on *Gut Microbes*, please visit: https://www.referencecitationanalysis.com/SearchJournal.

2022 JAII and rankings of Alimentary Pharmacology & Therapeutics

In the *RCA* database, the 2022 *JAII* for *Alimentary Pharmacology & Therapeutics* is 28.725, ranking 7th among 101 core journals in the field of gastroenterology and hepatology included in the *RCA*, with a total of 323707 citations (10/101) and a total of 11269 articles (13/101) (Figure 7). For more information on *Alimentary Pharmacology & Therapeutics*, please visit: https://www.referencecitationanalysis.com/SearchJournal.

2022 JAII and rankings of Journal of Hepatology

In the *RCA* database, the 2022 *JAII* for *Journal of Hepatology* is 28.725, ranking 8th among 101 core journals in the field of gastroenterology and hepatology included in the *RCA*, with a total of 556699 citations (4/101) and a total of 19575 articles (7/101) (Figure 8). For more information on *Journal of Hepatology*, please visit: https://www.referencecitationanalysis.com/SearchJournal.

2022 JAII and rankings of Best Practice & Research Clinical Gastroenterology

In the *RCA* database, the 2022 *JAII* for *Best Practice & Research Clinical Gastroenterology* is 28.428, ranking 9th among 101 core journals in the field of gastroenterology and hepatology included in the *RCA*, with a total of 44917 citations (36/101) and a total of 1580 articles (54/101) (Figure 9). For more information on *Best Practice & Research Clinical Gastroenterology*, please visit: https://www.referencecitationanalysis.com/SearchJournal.

2022 JAII and rankings of Diseases of the Colon & Rectum

In the *RCA* database, the 2022 *JAII* for *Diseases of the Colon & Rectum* is 26.946, ranking 10th among 101 core journals in the field of gastroenterology and hepatology included in the *RCA*, with a total of 344714 citations (9/101) and a total of 12793 articles (10/101) (Figure 10). For more information on *Diseases of the Colon & Rectum*, please visit: https://www.referencecitationanalysis.com/SearchJournal.

2022 JAII and rankings of Liver Transplantation

In the *RCA* database, the 2022 *JAII* for *Liver Transplantation* is 26.872, ranking 11th among 101 core journals in the field of gastroenterology and hepatology included in the *RCA*, with a total of 159891 citations (18/101) and a total of 5950 articles (25/101) (Figure 11). For more information on *Liver Transplantation*, please visit: https://www.referencecitationanalysis.com/SearchJournal.



NATURE REVIEWS GASTROENTEROLOGY & HEPATOLOGY

Category Rank: Gastroenterology & Hepatology
Total View: 4 (17/101)
Journal Article Influence Index: 35.473 (5/101)
Total Citations: 100601 (24/101)
Cited by in F6Publishing: 88228 (23/101)
Total Articles: 2836 (40/101)
Number of Years: 13 (69/101)

Peer-Reviewed Journal: Yes

DOI: 10.3748/wjg.v28.i37.5383 **Copyright** ©The Author(s) 2022.

Figure 5 2022 *Journal Article Influence Index* and rankings of *Nature Reviews Gastroenterology & Hepatology*. The image of the journal cover is originally from the home page of the journal: https://www.nature.com/nrgastro/.



GUT MICROBES

Category Rank: Gastroenterology & Hepatology
Total View: 4 (18/101)
Journal Article Influence Index: 31.557 (6/101)
Total Citations: 38720 (41/101)
Cited by in F6Publishing: 33614 (39/101)
Total Articles: 1227 (64/101)
Number of Years: 12 (71/101)

Peer-Reviewed Journal: Yes
Free Access: Open

DOI: 10.3748/wjg.v28.i37.5383 **Copyright** ©The Author(s) 2022.

Figure 6 2022 *Journal Article Influence Index* and rankings of *Gut Microbes*. The image of the journal cover is originally from the home page of the journal: http://www.tandfonline.com/kgmi.



ALIMENTARY PHARMACOLOGY & THERAPEUTICS

Category Rank: Gastroenterology & Hepatology
Total View: 1 (68/101)
Journal Article Influence Index: 28.725 (7/101)
Total Citations: 323707 (10/101)
Cited by in F6Publishing: 288471 (7/101)
Total Articles: 11269 (13/101)
Number of Years: 35 (26/101)

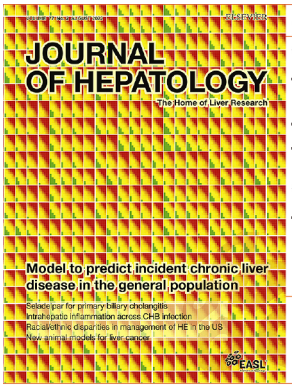
Peer-Reviewed Journal: Yes

DOI: 10.3748/wjg.v28.i37.5383 **Copyright** ©The Author(s) 2022.

Figure 7 2022 *Journal Article Influence Index* and rankings of *Alimentary Pharmacology & Therapeutics*. The image of the journal cover is originally from the home page of the journal: https://onlinelibrary.wiley.com/journal/13652036.

2022 JAII and rankings of Gastric Cancer

In the *RCA* database, the 2022 *JAII* for *Gastric Cancer* is 24.105, ranking 12th among 101 core journals in the field of gastroenterology and hepatology included in the *RCA*, with a total of 45558 citations (35/101) and a total of 1890 articles (49/101) (Figure 12). For more information on *Gastric Cancer*, please visit: https://www.referencecitationanalysis.com/SearchJournal.



JOURNAL OF HEPATOLOGY

Category Rank: Gastroenterology & Hepatology

Total View: 2 (56/101)

Journal Article Influence Index: 28.439 (8/101)

Total Citations: 556699 (4/101)

Cited by in F6Publishing: 379065 (6/101)

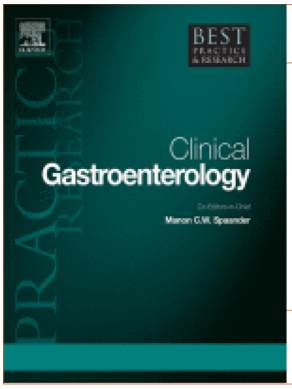
Total Articles: 19575 (7/101)

Number of Years: 37 (20/101)

Peer-Reviewed Journal: Yes

DOI: 10.3748/wjg.v28.i37.5383 **Copyright** ©The Author(s) 2022.

Figure 8 2022 *Journal Article Influence Index* and rankings of *Journal of Hepatology*. The image of the journal cover is originally from the home page of the journal: https://www.sciencedirect.com/journal/journal-of-hepatology.



BEST PRACTICE & RESEARCH CLINICAL GASTROENTEROLOGY

Category Rank: Gastroenterology & Hepatology

Total View: 1 (66/101)

Journal Article Influence Index: 28.428 (9/101)

Total Citations: 44917 (36/101)

Cited by in F6Publishing: 35508 (37/101)

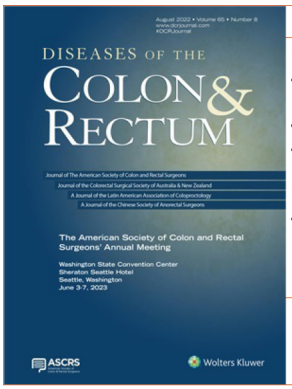
Total Articles: 1580 (54/101)

Number of Years: 23 (43/101)

Peer-Reviewed Journal: Yes

DOI: 10.3748/wjg.v28.i37.5383 **Copyright** ©The Author(s) 2022.

Figure 9 2022 *Journal Article Influence Index* and rankings of *Best Practice & Research Clinical Gastroenterology*. The image of the journal cover is originally from the home page of the journal: http://www.sciencedirect.com/science/journal/15216918.



DISEASES OF THE COLON & RECTUM

Category Rank: Gastroenterology & Hepatology

Total View: 1 (67/101)

Journal Article Influence Index: 26.946 (10/101)

Total Citations: 344714 (9/101)

Cited by in F6Publishing: 124064 (18/101)

Total Articles: 12793 (10/101)

Number of Years: 64 (3/101)

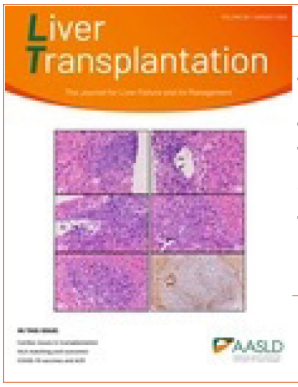
Peer-Reviewed Journal: Yes

DOI: 10.3748/wjg.v28.i37.5383 **Copyright** ©The Author(s) 2022.

Figure 10 2022 *Journal Article Influence Index* and rankings of *Diseases of the Colon & Rectum*. The image of the journal cover is originally from the home page of the journal: https://journals.lww.com/dcrjournal/pages/default.aspx.

2022 JAII and rankings of The American Journal of Gastroenterology

In the *RCA* database, the 2022 *JAII* for *The American Journal of Gastroenterology* is 23.563, ranking 13th among 101 core journals in the field of gastroenterology and hepatology included in the *RCA*, with a total of 476726 citations (5/101) and a total of 20232 articles (6/101) (Figure 13). For more information on *The American Journal of Gastroenterology*, please visit: https://www.referencecitationanalysis.com/SearchJournal.



LIVER TRANSPLANTATION

Category Rank: Gastroenterology & Hepatology

Total View: 5 (10/101)

Journal Article Influence Index: 26.872 (11/101)

Total Citations: 159891 (18/101)

Cited by in F6Publishing: 134312 (16/101)

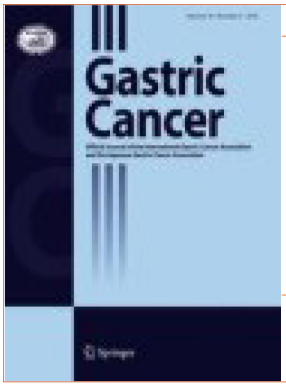
Total Articles: 5950 (25/101)

Number of Years: 25 (40/101)

Peer-Reviewed Journal: Yes

DOI: 10.3748/wjg.v28.i37.5383 **Copyright** ©The Author(s) 2022.

Figure 11 2022 *Journal Article Influence Index* and rankings of *Liver Transplantation*. The image of the journal cover is originally from the home page of the journal: https://aasldpubs.onlinelibrary.wiley.com/journal/15276473.



GASTRIC CANCER

Category Rank: Gastroenterology & Hepatology

Total View: 1 (79/101)

Journal Article Influence Index: 24.105 (12/101)

Total Citations: 45558 (35/101)

Cited by in F6Publishing: 40701 (34/101)

Total Articles: 1890 (49/101)

Number of Years: 24 (41/101)

Peer-Reviewed Journal: Yes

DOI: 10.3748/wjg.v28.i37.5383 **Copyright** ©The Author(s) 2022.

Figure 12 2022 *Journal Article Influence Index* and rankings of *Gastric Cancer*. The image of the journal cover is originally from the home page of the journal: https://link.springer.com/journal/10120.



THE AMERICAN JOURNAL OF GASTROENTEROLOGY

Category Rank: Gastroenterology & Hepatology

Total View: 3 (24/101)

Journal Article Influence Index: 23.563 (13/101)

Total Citations: 476726 (5/101)

Cited by in F6Publishing: 414976 (5/101)

Total Articles: 20232 (6/101)

Number of Years: 47 (9/101)

Peer-Reviewed Journal: Yes

DOI: 10.3748/wjg.v28.i37.5383 **Copyright** ©The Author(s) 2022.

Figure 13 2022 *Journal Article Influence Index* and rankings of *the American Journal of Gastroenterology*. The image of the journal cover is originally from the home page of the journal: https://journals.lww.com/ajg/pages/default.aspx.

2022 JAII and rankings of Lancet Gastroenterology & Hepatology

In the *RCA* database, the 2022 *JAII* for *Lancet Gastroenterology & Hepatology* is 23.470, ranking 14th among 101 core journals in the field of gastroenterology and hepatology included in the *RCA*, with a total of 30276 citations (48/101) and a total of 1290 articles (63/101) (Figure 14). For more information on *Lancet Gastroenterology & Hepatology*, please visit: https://www.referencecitationanalysis.com/SearchJournal.



DOI: 10.3748/wjg.v28.i37.5383 **Copyright** ©The Author(s) 2022.

Figure 14 2022 *Journal Article Influence Index* and rankings of *Lancet Gastroenterology & Hepatology*. The image of the journal cover is originally from the home page of the journal: https://www.thelancet.com/journals/langas/home.

2022 JAII and rankings of Journal of Gastroenterology

In the *RCA* database, the 2022 *JAII* for *Journal of Gastroenterology* is 22.837, ranking 15th among 101 core journals in the field of gastroenterology and hepatology included in the *RCA*, with a total of 110941 citations (22/101) and a total of 4858 articles (28/101) (Figure 15). For more information on *Journal of Gastroenterology*, please visit: https://www.referencecitationanalysis.com/SearchJournal.

2022 JAII and rankings of Neurogastroenterology and Motility

In the *RCA* database, the 2022 *JAII* for *Neurogastroenterology and Motility* is 22.335, ranking 16th among 101 core journals in the field of gastroenterology and hepatology included in the *RCA*, with a total of 93695 citations (26/101) and a total of 4195 articles (30/101) (Figure 16). For more information on *Neurogastroenterology and Motility*, please visit: https://www.referencecitationanalysis.com/SearchJournal.

2022 JAII and rankings of Clinical Gastroenterology and Hepatology

In the *RCA* database, the 2022 *JAII* for *Clinical Gastroenterology and Hepatology* is 22.295, ranking 17th among 101 core journals in the field of gastroenterology and hepatology included in the *RCA*, with a total of 223108 citations (13/101) and a total of 10007 articles (17/101) (Figure 17). For more information on *Clinical Gastroenterology and Hepatology*, please visit: https://www.referencecitationanalysis.com/SearchJournal.

2022 JAII and rankings of World Journal of Gastroenterology

In the *RCA* database, the 2022 *JAII* for *World Journal of Gastroenterology* is 21.914, ranking 18th among 101 core journals in the field of gastroenterology and hepatology included in the *RCA*, with a total of 471463 citations (4/101) and a total of 21514 articles (5/101) (Figure 18). For more information on *World Journal of Gastroenterology*, please visit: https://www.referencecitationanalysis.com/00000009.

2022 JAII and rankings of American Journal of Physiology-Gastrointestinal and Liver Physiology

In the *RCA* database, the 2022 *JAII* for *American Journal of Physiology-Gastrointestinal and Liver Physiology* is 21.406, ranking 19th among 101 core journals in the field of gastroenterology and hepatology included in the *RCA*, with a total of 230179 citations (11/101) and a total of 10753 articles (14/101) (Figure 19). For more information on *American Journal of Physiology-Gastrointestinal and Liver Physiology*, please visit: https://www.referencecitationanalysis.com/SearchJournal.

2022 JAII and rankings of Journal of Gastrointestinal Surgery

In the *RCA* database, the 2022 *JAII* for *Journal of Gastrointestinal Surgery* is 20.714, ranking 20th among 101 core journals in the field of gastroenterology and hepatology included in the *RCA*, with a total of 138742 citations (20/101) and a total of 6698 articles (22/101) (Figure 20). For more information on *Journal of Gastrointestinal Surgery*, please visit: https://www.referencecitationanalysis.com/SearchJournal.

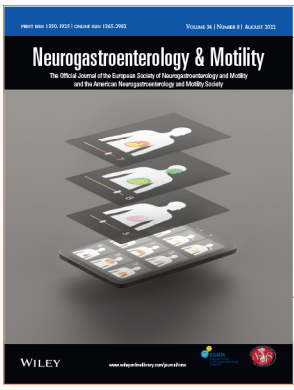
RCA'S MISSION

The mission of *RCA* is to provide a high quality academic article evaluation service platform for various categories. At present, there are many evaluation methods for academic articles, but their calculation methods are complicated. The *RCA* is a new method of evaluating the quality of academic articles,



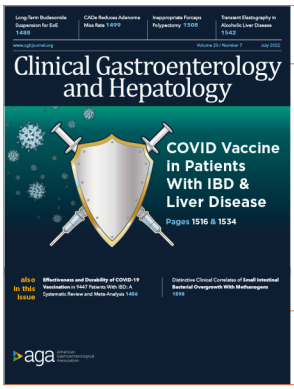
DOI: 10.3748/wjg.v28.i37.5383 **Copyright** ©The Author(s) 2022.

Figure 15 2022 *Journal Article Influence Index* and rankings of *Journal of Gastroenterology*. The image of the journal cover is originally from the home page of the journal: https://link.springer.com/journal/535.



DOI: 10.3748/wjg.v28.i37.5383 **Copyright** ©The Author(s) 2022.

Figure 16 2022 *Journal Article Influence Index* and rankings of *Neurogastroenterology and Motility*. The image of the journal cover is originally from the home page of the journal: https://onlinelibrary.wiley.com/journal/13652982.



DOI: 10.3748/wjg.v28.i37.5383 **Copyright** ©The Author(s) 2022.

Figure 17 2022 *Journal Article Influence Index* and rankings of *Clinical Gastroenterology and Hepatology*. The image of the journal cover is originally from the home page of the journal: http://www.sciencedirect.com/science/journal/15423565.

which allows academic evaluation of journals, scholars, institutions, drugs, medical devices, and publishers based on the *JAII* of each article in the citation analysis database, thus greatly enriching the academic evaluation systems across different disciplines and guiding the healthy development of the academic community[2].



WORLD JOURNAL OF GASTROENTEROLOGY

Category Rank: Gastroenterology & Hepatology

Total View: 30 (1/101)

Journal Article Influence Index: 21.914 (18/101)

Total Citations: 471463 (6/101)

Cited by in F6Publishing: 431655 (4/101)

Total Articles: 21514 (5/101)

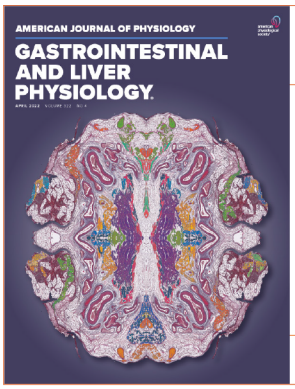
Number of Years: 27 (34/101)

Peer-Reviewed Journal: Yes

Free Access: Open

DOI: 10.3748/wjg.v28.i37.5383 **Copyright** ©The Author(s) 2022.

Figure 18 2022 *Journal Article Influence Index* and rankings of *World Journal of Gastroenterology*. The image of the journal cover is originally from the home page of the journal: http://www.wjgnet.com/1007-9327/index.htm.



AMERICAN JOURNAL OF PHYSIOLOGY-GASTROINTESTINAL AND LIVER PHYSIOLOGY

Category Rank: Gastroenterology & Hepatology

Total View: 3 (25/101)

Journal Article Influence Index: 21.406 (19/101)

Total Citations: 230179 (11/101)

Cited by in F6Publishing: 219030 (9/101)

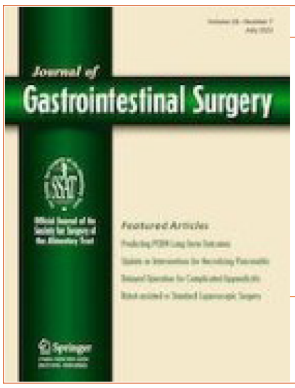
Total Articles: 10753 (14/101)

Number of Years: 42 (12/101)

Peer-Reviewed Journal: Yes

DOI: 10.3748/wjg.v28.i37.5383 **Copyright** ©The Author(s) 2022.

Figure 19 2022 *Journal Article Influence Index* and rankings of *American Journal of Physiology-Gastrointestinal and Liver Physiology*. The image of the journal cover is originally from the home page of the journal: https://journals.physiology.org/journal/ajpgi.



JOURNAL OF GASTROINTESTINAL SURGERY

Category Rank: Gastroenterology & Hepatology

Total View: 2 (48/101)

Journal Article Influence Index: 20.714 (20/101)

Total Citations: 138742 (20/101)

Cited by in F6Publishing: 103502 (19/101)

Total Articles: 6698 (22/101)

Number of Years: 25 (37/101)

Peer-Reviewed Journal: Yes

DOI: 10.3748/wjg.v28.i37.5383 **Copyright** ©The Author(s) 2022.

Figure 20 2022 *Journal Article Influence Index* and rankings of *Journal of Gastrointestinal Surgery*. The image of the journal cover is originally from the home page of the journal: https://link.springer.com/journal/11605.

OPENNESS AND TRANSPARENCY OF RCA EVALUATION

RCA is unique in its objective, impartial, fair, and transparent release of citation analysis data of important academic journals to authors and readers, including evaluation data, evaluation indices, evaluation methods, and evaluation results, in order to ensure the reliability of academic evaluation[2].

CALCULATION METHOD FOR 2022 *JAII*

The 2022 *JAII*, calculated as Total citations/Total articles, is not a 2-year or 5-year average of citations, but is an average of citations for all articles since the journal was assigned its DOI number. Article types are not only limited to original articles and review articles, but for all types of articles. In this way, it is a more objective, fair, and transparent calculation of the academic influence index of an academic journal. Furthermore, the journal list itself is evaluated dynamically, its bibliographic metrics being updated daily, including total number of articles, total citations, and *JAII*[2].

EVALUATION PROCESS OF *RCA* JOURNALS

The journals included in the *RCA* core journal list need to undergo three rounds of strict evaluation. The evaluation process is as follows[2]:

First-round evaluation: Verify the basic information on the journal, including Journal Name, Abbreviated Title, Print ISSN, Online ISSN, Language, Category, Peer-Reviewed Journal, Ownership, Publisher, Journal Website, Editorial Board Members, Submit a Manuscript, and Indexed by.

Second-round evaluation: Verify the activity of the journal, including Total Articles, Total Citations, Cited by in F6Publishing, and the *JAII*.

Third-round evaluation: Based on the reliability of journal information, the activity of publication data, whether the journal is a peer-reviewed journal or not, and *JAII*, the editorial team evaluates every journal, makes the decision to accept or reject the journal, and creates a list of core journals by discipline. The function of the list of core academic journals is to classify journals according to categories and rank them according to various bibliometrics, including Total Views, *JAII*, Total Citations, Cited by in F6Publishing, Total Articles, and Number of Years.

INCLUSION PRINCIPLES OF *RCA* JOURNAL

The *RCA* editorial team of Baishideng conducted three rounds of rigorous evaluation on core journals in gastroenterology and hepatology. The resultant *RCA* core journal list for the field of gastroenterology and hepatology includes a total of 101 journals, among which the highest 2022 *JAII* is 48.014 and the lowest *JAII* is 3.900, the highest total number of citations is 1711173 and the lowest is 698, and the highest total number of articles is 46037 and the lowest is 133. The *RCA* core journal list does not include any journals with a *JAII* lower than 3.0. We implement dynamic evaluation inclusively for the *RCA* core journal list. Evaluation is initiated once an *RCA*-nonincluded journal receives a *JAII* over 3.0. Similarly, if a journal included in the *RCA* core journal list receives a *JAII* lower than 3.0, it will be excluded[2]. The *RCA* core journal list is designed by publishers, scientific editors, and engineers for use by readers, authors, and editorial offices, and is free-of-charge to users.

Upon completion of the three rounds of rigorous evaluation on core journals in gastroenterology and hepatology by the *RCA* editorial team, all data in each journal are organized for public consumption according to category rank, including the 2022 *JAII*, total citations, cited by in F6Publishing, total articles, and the 2021 Journal Impact Factor™. All information in each journal, including Journal Name, Print ISSN, Online ISSN, Language, Free Access, Peer-Reviewed Journal, Ownership, Publisher, Journal Website, Editorial Board Members, Submit a Manuscript, and Indexed by are made available in *RCA*. Moreover, the citations of each journal can be then ranked in *RCA* by the *Impact Index Per Article*, Cited by in Crossref, and Cited by in F6Publishing parameters. Results analysis available for each journal includes Year Published Analysis, Article Type Analysis, Journal Title Analysis, and Category Analysis. The references of each journal are also refined by Year Published and Article Type. Each reference's citation information is displayed, including PMID, DOI, Cited by in Crossref, *Impact Index Per Article*, *RCA*, and Track Full Text[2].

CONCLUSION

The ultimate purpose of *RCA* is to provide an open, objective, fair, and reliable academic evaluation service platform for readers, authors, and journal editors. The *RCA* journal academic evaluation service platform is designed and actively maintained to address the needs of authors to select reliable journals for submission, readers to select high-quality literature for reading, and editors to track their own journal citation performance. The *RCA* core journal list itself will serve as a useful Find-a-Journal tool. Any interested party is welcome to use this journal list and recommend it to their peers.

FOOTNOTES

Author contributions: Wang JL analyzed the data and drafted the manuscript; Ma YJ participated in the data collection; Ma LS revised the manuscript for important intellectual content; and all authors participated in manuscript revision.

Conflict-of-interest statement: The authors are employees of the Baishideng Publishing Group Inc, and declare that they have no other real or potential conflicts of interest to disclose.

Open-Access: This article is an open-access article that was selected by an in-house editor and fully peer-reviewed by external reviewers. It is distributed in accordance with the Creative Commons Attribution NonCommercial (CC BY-NC 4.0) license, which permits others to distribute, remix, adapt, build upon this work non-commercially, and license their derivative works on different terms, provided the original work is properly cited and the use is non-commercial. See: https://creativecommons.org/Licenses/by-nc/4.0/

Country/Territory of origin: United States

ORCID number: Jin-Lei Wang 0000-0002-5197-3051; Lian-Sheng Ma 0000-0002-1430-4844.

S-Editor: Wang JJ
L-Editor: Webster JR
P-Editor: Wang JJ

REFERENCES

1 **Baishideng Publishing Group Inc**. Welcome to the Reference Citation Analysis. Available from: https://www.referencecitationanalysis.com
2 **Baishideng Publishing Group Inc**. Reference Citation Analysis's evaluation process for inclusion of academic journals. Available from: https://www.wjgnet.com/bpg/GerInfo/303

World Journal of Gastroenterology

Submit a Manuscript: https://www.f6publishing.com

World J Gastroenterol 2022 October 7; 28(37): 5395-5402

DOI: 10.3748/wjg.v28.i37.5395

ISSN 1007-9327 (print) ISSN 2219-2840 (online)

OPINION REVIEW

Milestones in the discovery of hepatitis C

Octavio Campollo, Gerardo Amaya, P Aiden McCormick

Specialty type: Gastroenterology and hepatology

Provenance and peer review: Invited article; Externally peer reviewed.

Peer-review model: Single blind

Peer-review report's scientific quality classification

Grade A (Excellent): A
Grade B (Very good): B, B, B
Grade C (Good): 0
Grade D (Fair): D
Grade E (Poor): 0

P-Reviewer: Ballestín SS, Spain; Lo SY, Taiwan; Villela-Nogueira CA, Brazil; Yu ML, Taiwan

Received: March 4, 2022
Peer-review started: March 4, 2022
First decision: March 27, 2022
Revised: April 11, 2022
Accepted: August 16, 2022
Article in press: August 16, 2022
Published online: October 7, 2022

Octavio Campollo, Center of Studies on Alcohol and Addictions, Antiguo Hospital Civil de Guadalajara, Department of Medical Clinics, Universidad de Guadalajara, Guadalajara 44280, Jalisco, Mexico

Gerardo Amaya, Medical Clinics, CUCS, Universidad de Guadalajara, Guadalajara 44280, Jalisco, Mexico

P Aiden McCormick, Department of Hepatology, Saint Vincent's University Hospital, National Liver Transplant Unit, Dublin D04, Ireland

Corresponding author: Octavio Campollo, MD, PhD, Full Professor, Center of Studies on Alcohol and Addictions, Antiguo Hospital Civil de Guadalajara, Department of Medical Clinics, Universidad de Guadalajara, Calle Hospital 278, Col. El Retiro, Guadalajara 44280, Jalisco, Mexico. renaceboy@hotmail.com

Abstract

The discovery of hepatitis C has been a landmark in public health as it brought the opportunity to save millions of lives through the diagnosis, prevention and cure of the disease. The combined work of three researchers, Alter H, Houghton M and Rice C, which set the basis for the diagnosis, treatment and prevention of hepatitis C apart from laying the ground work for a new approach to study infections in general and developing new antiviral agents. This is a story of a transfusion-associated infection. A series of clinical studies demonstrated the existence of an infectious agent associated with hepatitis. That was followed by the identification of what was later known to be the hepatitis C virus (HCV) and the development of diagnostic tests. It all preceded the full molecular identification and demonstration of a causal effect. Finally it ended up with the development and discovery of a new class of therapeutic drugs, the direct acting antivirals, which are now used not only to cure the disease but most probably, to eliminate the problem. This work started with Dr Alter H who demonstrated that a new virus was responsible for the majority of post-transfusion hepatitis followed by Houghton M who cloned the virus and developed the blood test to identify those cases that carried the virus. Finally, the work of Rice C demonstrated that a cloned HCV produced after applying molecular biology techniques could cause long-standing infection and cause the same disease as the one observed in humans.

Key Words: Hepatitis C; Nobel prize; Discovery; Diagnosis; Treatment; Elimination; World Health Organization initiative

©The Author(s) 2022. Published by Baishideng Publishing Group Inc. All rights reserved.

Core Tip: The discovery of hepatitis C has been a landmark in public health as it brought the opportunity to save millions of lives through the diagnosis, prevention and cure of a disease that was perhaps noticed 5000 years ago. It was through the combined work of three researchers, Alter H, Houghton M and Rice C, which set the basis for the diagnosis, treatment and prevention of hepatitis C apart from laying the ground work for a new approach to study infections in general and developing new antiviral agents.

Citation: Campollo O, Amaya G, McCormick PA. Milestones in the discovery of hepatitis C. *World J Gastroenterol* 2022; 28(37): 5395-5402
URL: https://www.wjgnet.com/1007-9327/full/v28/i37/5395.htm
DOI: https://dx.doi.org/10.3748/wjg.v28.i37.5395

INTRODUCTION

"*The methodological studies of transfusion-associated hepatitis by Harvey J. Alter demonstrated that an unknown virus was a common cause of chronic hepatitis. Michael Houghton used an untested strategy to isolate the genome of the new virus that was named Hepatitis C virus. Charles M. Rice provided the final evidence showing that Hepatitis C virus alone could cause hepatitis.*" Nobel Prize assembly, 2020[1].

THE DISCOVERY OF HEPATITIS C VIRUS WAS A LANDMARK IN PUBLIC HEALTH

The prolonged campaign to discover and treat the various causes of viral hepatitis is a major medical success story as it brought about the opportunity to save thousands of lives through the diagnosis, prevention and cure of the disease, sparing lives that would be lost to chronic hepatitis C and its complications. It was through the combined work of three researchers starting with Dr Alter H working at National Institutes of Health (NIH) who demonstrated that a new virus was responsible for the majority of post-transfusion hepatitis. That was followed by Houghton M who cloned the virus and developed the blood test to identify those cases that carried the virus. And finally, Rice C demonstrated that a cloned hepatitis C virus (HCV), produced after applying molecular biology techniques (a virion), could cause long-standing infection and cause the same disease as the one observed in humans[2]. These scientific breakthroughs enabled the World Health Organization (WHO) to set the, once unthinkable, goal for HCV elimination by 2030[3]. The implications of this work are not limited to hepatitis C as the new diagnostic techniques and methods of drug development may be applicable to other viral pathogens. Furthermore, the complete new approach to treatment based on the study and new knowledge of the HCV genetics and lifecycle together with the molecular biology approach attacking many targets directly (in the HCV lifecycle) *i.e.*, protease inhibitors, polymerase inhibitors and NS5A inhibitors[4-6], the former being the most successful prodrug developed and currently used in the WHO policy for world elimination of hepatitis C aimed at either[6,7], virion processing, RNA replication and virion assembly in the liver cell[6,8].

For those of us who grew up in the hepatology field when non-A non-B hepatitis (what a strange name!) was a common topic of discussion in the clinic and the laboratory, the award of the Nobel prize for the discovery of HCV in 2020 marked a fitting end to a long saga. This is the second Nobel prize awarded to investigators in viral hepatitis recognizing the major advances in this field of clinical and laboratory research [the first Nobel prize was awarded to Blumberg B in 1976 for the discovery of hepatitis B virus (HBV)][9]. Initially viral hepatitis was regarded as an epidemic disease which was a major problem in congregated settings such as residential schools and military establishments. It became a major issue in time of war when epidemics reduced the effectiveness of armies in the field. Much important early research was funded by the military. Only later did it become apparent that chronic viral hepatitis could lead to cirrhosis and hepatocellular carcinoma (HCC). Many millions of people were infected making it one of the leading causes of morbidity and mortality in some parts of the world. In the early 2000's it was estimated that chronic viral hepatitis was responsible for over one million deaths annually[10]. The development of vaccines for hepatitis B and effective anti-viral therapy for hepatitis B and C have been dramatically effective and offer the prospect of banishing these diseases to the sidelines of human history.

BRIEF HISTORY OF HEPATITIS

The hepatitis problem was perhaps noticed 5000 years ago when epidemics of jaundice were attributed to a devil called "Ahhazu" by the Sumerians[11] and many years later were described by Hippocrates in the 5th century BC in his book "Epidemics". They were particular noted in armies during time of war, hence the term "campaign jaundice". The cause of jaundice was not understood and up till the outbreak of the second world war many clinicians accepted Virchow's theory that a mucous plug at the mouth of the common bile duct caused "catarrhal jaundice"[12]. The large number of hepatitis cases and the impact it had on battle readiness acted as a major stimulus to understanding hepatitis. Most of the subsequent advances in knowledge were described in the British and American literature. Up until D-day in 1944 the British army was mainly engaged in fighting in the Mediterranean theatre. Hepatitis, with malaria and venereal disease were the three most important medical conditions afflicting the troops there[13]. On the other side of the Atlantic ocean, 28585 United States servicemen developed jaundice after receiving the yellow fever vaccine[14]. Clinical, epidemiological and transmission studies established that there were two distinct forms of hepatitis, characterized as infectious or serum hepatitis. Infectious hepatitis was transmitted by the fecal-oral route whereas serum hepatitis was transmitted by injection or blood products[15].

Stokes and Neff of the United States Army Medical Corps had been using concentrated gamma globulin to prevent or attenuate measles infection. Despite several thousand treatments they recorded no cases of hepatitis[16]. They reasoned that there may be neutralizing antibodies in gamma globulin prepared from large pools of adult plasma and suggested that gamma globulin could be useful in the treatment of viral hepatitis. The hypothesis was tested when there was a large epidemic of hepatitis in a summer camp for boys and girls in September 1944. There was sufficient gamma globulin to treat 45 children, who were compared to 246 controls. Hepatitis was subsequently documented in 16% (7/45) treated compared to (70%) 172/246 controls. None of those treated developed clinical jaundice thus demonstrating that gamma globulin could prevent or attenuate infectious hepatitis[17]. Many of the subsequent transmission studies on viral hepatitis of questionable procedures were performed in the Willowbrook State School in New York for children with mental disorders which had a major problem with endemic infectious hepatitis[15]. The investigators clearly demonstrated two types of hepatitis, with different incubation periods and no cross-immunity, subsequently proven to be hepatitis A and hepatitis B. The ethics of that program have since been questioned[18].

The problem of hepatitis continued up until modern times when many cases of un-explained jaundice continued to puzzle clinicians until some 51 years ago when Holland, Schmidt, Purcell, Walsh and Alter began to study what was called "Transfusion-associated hepatitis" in 1969[19]. It would take some 20 years more until the infectious agent, HCV, was discovered[20]. Those of us who grew up in the hepatology field when non-A non-B hepatitis was a common topic for discussion in clinical meetings and on the wards remember the cases of unexplained post-transfusion hepatitis. In addition there were many cases of "nosocomial" hepatitis[21] and cryptogenic hepatitis and a lack of diagnostic tests. The journey to unravel this problem took another 39 years, 14 years from the identification of non-A non-B hepatitis to the discovery of the HCV and 25 years from the discovery of HCV in 1989 to the approval of one of the most prescribed direct acting antiviral agents (DAA) Sofosbuvir in 2013 for the treatment of hepatitis C[22]. In all, those 39 years don't seem too bad now when we look at the progress made from those early clinical and epidemiologic studies by Alter and others up to the incredibly creative and imaginative pharmacological approach to therapy involving the design of DAA that inhibit HCV infection by blocking viral assembly and replication at the present time[22].

Currently, it is estimated, that there are more than 71 million people around the world infected with HCV. Complications of end-stage liver disease due to hepatitis C make it one of the world's most important causes of death with 400000 cases a year[23]. It is well-known that HCV can cause chronic hepatitis C, a silent but progressive condition which may progress to cirrhosis and HCC over decades. Hepatitis C is transmitted by the parenteral route. As blood products for transfusion have become increasingly safe due to effective viral testing, the main route of transmission in most countries is through intravenous drug use. Eradication of hepatitis C requires effective harm reduction strategies for intravenous drug use in addition to antiviral therapy[7,20].

Interest in this problem (now known as hepatitis C) was renewed almost 70 years ago when there was a high incidence of chronic hepatitis after blood transfusions or use of blood products. At that time it was impossible to know who of the donors carried the disease. In 1960, Alter[24] started his search for the "source" of post-transfusion hepatitis having previously worked with Blumberg B with whom he had observed a "precipitin line … that stained intensely red" in a reaction between blood from a patient with hemophilia and blood from an Australian aborigine which they called initially the "Australia antigen". That was later identified as the surface protein of the HBV (HBsAg). Blumberg continued his research on the Australia antigen to establish the link with HBV for which he won the Nobel prize in Medicine in 1976[11]. In his studies, Alter[19] found that even if hepatitis B contaminated blood was excluded from use most post-transfusional hepatitis remained. He tested the blood supplies for the presence of suspected known viruses and followed up patients who developed hepatitis after receiving a blood transfusion and found that an incredible high number of cases could not be explained. Alter[19] and other researchers suspected there was another infectious agent. In 1978, Alter[24] demonstrated that

plasma from those patients with post-transfusion hepatitis could infect chimpanzees who developed clinical and laboratory signs of hepatitis suggesting that the cause of that liver inflammation was infectious. Further studies by Alter[24] showed that the causative agent had characteristics of a virus. The next goal was the search for the virus which took lots of effort and time *i.e.*, years! Nevertheless Alter[19] had learnt from Blumberg to work with tenacity and perseverance to carry on with his work. Robert Purcell and Steve Feinstone at the NIH[19] and Alfred Prince in New York noted that most cases of post-transfusion hepatitis were HBsAg negative and hepatitis A virus negative[11]. At that time they started calling it non-A non-B hepatitis (NANBH)[11]. Another important step was the observation that infectivity titers in chimps studied by Purcell were almost identical to the genomic titers in a patient with severe acute NANBH studied by Alter[19]. Alter[19] worked with the assumption that genetic material would be present in pools of DNA sequences isolated from those animals infected with hepatitis, and on the other hand that serum from humans with this form of hepatitis would have specific antibodies against that virus that would bind to some proteins or viral particles and could then be used to identify those samples with the virus. Together with Purcell he attempted every serological approach known at the time to identify the virus without success.

In 1989, Houghton[25] at Chiron Laboratories in California (now part of Novartis) tried a combination of molecular biology and immunology methods. They extracted nucleic acid from plasma and cloned it in an expression vector (GT11) creating a phage expression library. This technique enabled them to identify the first epitope characteristic of the HCV envelope in 1989[11]. They later named it HCV. Houghton rapidly came up with the idea of developing immunoassays to detect antibodies to protein products of those clones establishing a blood test for HCV which he evaluated using Alter's blood samples' collection at NIH[26]. They correctly identified all samples which were thought to be infected with the virus as well as all negative controls. This was a major milestone for medicine and public health. It allowed blood banks to screen all blood supplies resulting in an immediate and dramatic drop in the incidence of post-transfusion hepatitis.

At this point there was another crucial question, that is whether this virus could reproduce infection if inoculated into an experimental model, hence probing that the now called HCV was the causative agent of the formerly known NANBH. Rice C a researcher at the University of Washington who had been working with molecular virology of *Flavivirus*[22] focused on dissecting HCV gene expression using blood from infected chimpanzees to introduce DNA fragments into bacteria to express individual protein fragments. Those products were then screened with the antiviral antibodies until they could isolate one positive clone. The positive clone encoded a sequence that was very similar to sequences of the virus family of flaviviruses. Next, Rice started investigating what was needed for the molecularly cloned HCV to be reproduced *in vitro*. In 1996, he and his group identified the conserved 3'-terminal region of the HCV genomic RNA which was previously unknown[27], and was crucial for recovery of infectious HCV cDNA clones. However, initially they could not produce infection when injected into the liver of animals speculating that there could be some inactivating random mutations in the genome produced during the replication of the virus[28]. That meant that some individual clones may be defective. He sequenced many clones and compared them with each other and found that some of these clones contained potentially inactivating mutations which he thought could be removed with genetic engineering[29]. He later combined that repaired viral genome with the 3'-end of the genomic RNA hoping he would obtain a functional virus. When he injected this genome into the liver of chimpanzees clinical signs of hepatitis ensued and there was virus present in the blood producing now the evidence that the clone of the HCV could produce the disease associated with hepatitis infection[22,30]. That was a very important advance because the development of HCV replicons provided a live HCV system in the laboratory where viral replication, pathogenesis and evolution in culture could be studied in a viable *in vitro* replication system[22]. Later on newer constructs were obtained with higher replicative ability *in vitro*[22]. This was another milestone. Within 1 year of the cloning of HCV the nucleotide sequence of the entire viral genome was determined and the agent was characterized as a single-stranded positive-sense RNA virus of about 9600 nucleotides in length[2,31]. The advent of functional replicons also enabled the assay development for antiviral drug development which made the search for effective anti-viral drugs much easier[22]. Another collaborator of Rice, Ralf Bartenschlager, a molecular biologist who had previously worked with HBV, successfully replicated HCV genomic RNA in a human hepatoma cell line Huh7[32]. Confirmatory reports from various groups worldwide all corroborated that replicons were robust *in vitro* replication (subgenomic HCV replication system) systems that set the basis for production of infectious virus particles in cell cultures[22,32]. That improved the HCV RNA replicon system model was used in collaboration with Michael Sofia to design the new DAA[22]. One of those developed, DAA PSI-7797 (Sofosbuvir), had a very effective antiviral effect with broader genotype coverage and fewer side effects on a shorter duration treatment[11,22]. This prodrug enters the hepatocyte readily where it is metabolized to produce a triphosphate derivative which is a potent viral replication inhibitor[20,22]. It has just recently been announced that it can cure up to 95% of patients infected with HCV[33]. Different prodrugs were tested in genotype-specific cell lines that have been used in preclinical studies to select and validate novel targets for HCV. Those included NS3-4A protease inhibitors, nucleoside analogue viral polymerase inhibitors, non-nucleoside inhibitors of the viral RNA polymerase, NS5A inhibitors, host targeted agents (HTA), cyclophilin inhibitors and a cellular miRNA antagonist[4]. The discovery of over 30 new DAAs and HTAs revolutionized the treatment of chronic

HCV[8]. The swift development of interferon-free protocols using DAA monotherapy or the combined administration of two or three DAAs or HTAs, administered for 8-12 and up to 24 wk, led to sustained virological response (SVR) rates between 90% and 100%[8,33,34].

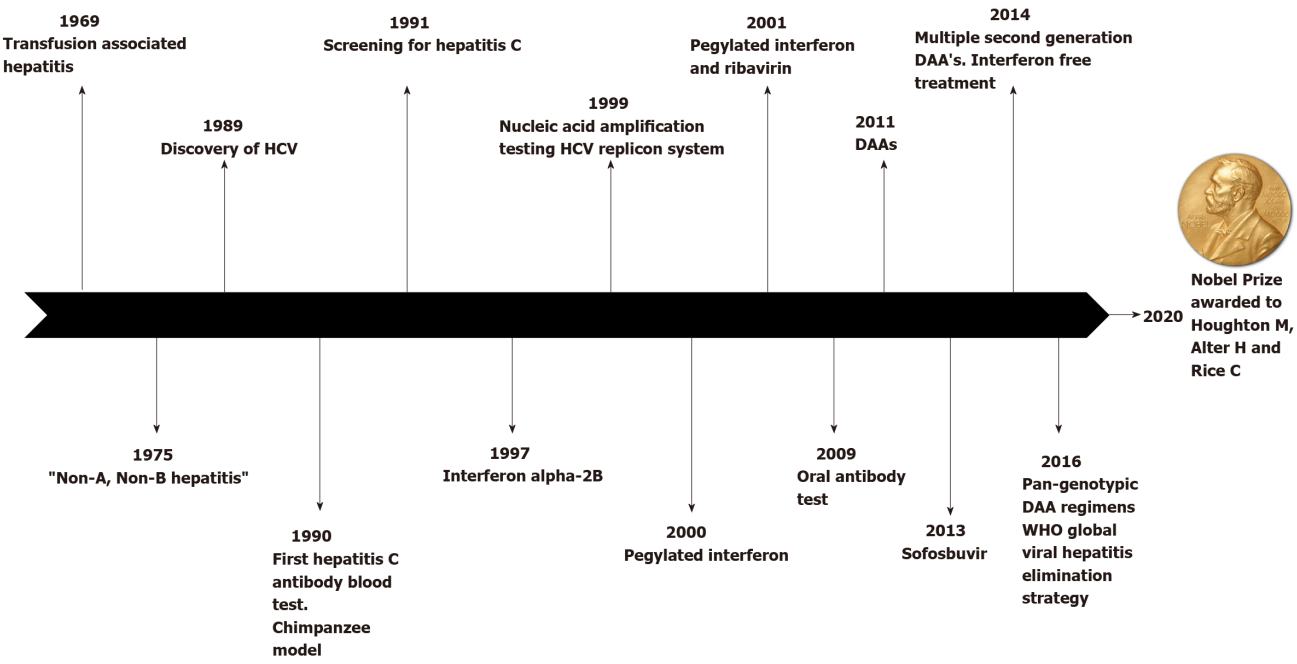
With the widespread use of DAAs many countries are now reporting a reduction in mortality associated with chronic hepatitis C and it's complications such as liver cirrhosis and HCC[3]. A strategy of "treatment as prevention" has been proposed with the aim of reducing the population prevalence, interrupting the chain of viral transmission and ultimately leading to elimination of HCV infection[11,20], although patients with HCV infection with cirrhosis or decompensated liver disease present special challenges such as post-SVR complications including HCV reinfection, HCC risk, residual HCC which should be addressed by early detection and treatment, combination and multiple DAA therapy avoiding the use of protease inhibitors and risk reduction counseling[7,34]. As epidemiologists, infectious diseases and liver specialists analyze the natural history, epidemiology and public health figures, world experts have proposed a rationale towards hepatitis C elimination based on infection control and disease elimination and eradication[7,20].

ELIMINATION OF HEPATITIS C

Viral hepatitis is a global health burden affecting 325 million people globally of which 71 million have hepatitis C with 1.5 million infections occurring per year and 542316 global HCV related deaths[3,20]. In 2016, the WHO set the Global health sector strategy for viral hepatitis proposing to eliminate viral hepatitis as a public health problem by 2030[3]. That is a 90% reduction in incidence and a 65% reduction in mortality by 2030 and a new guidance was released in June 2021[35]. These targets are achievable with the tools now at our disposal as demonstrated for hepatitis B in Taiwan[36] and hepatitis C in Egypt[37]. The main global strategies are to increase HCV testing, improve clinical education of providers, utilize simple models for HCV care and provide universal access to antiviral treatment at affordable cost. While there have been technical, geographic and policy limitations such as limited funding, lack of transparency and high in-country process, fragmented procurement, HCV diagnostics inefficiencies[3] and most recently the severe acute respiratory syndrome coronavirus 2 pandemic to mention a few there have been many examples around the globe showing that the goals are feasible[35]. In Egypt the cost of hepatitis C antiviral therapy fell from $1650 to $85 United States dollars between 2015 and 2018. A nationwide screening and treatment program identified 1.15 million infected individuals. By September 2019 over 1.05 million had commenced treatment with sustained virological clearance rates of 98.8%[37]. In spite of those challenges mentioned above, the future of mankind looks promising as millions of people will have the chance of a life free of hepatitis virus.

CONCLUSION

We have summarized the contributions of several groups of medical researchers starting with Dr Alter H who demonstrated that a new virus was responsible for the majority of post-transfusion hepatitis followed by Houghton M who cloned the virus and developed the blood test to identify those cases that carried the virus. That was continued with the work of Rice C that demonstrated that a cloned HCV produced after applying molecular biology techniques could produce long-standing infection and cause the same disease in animals as the one observed in humans[2] (Figure 1). That is a milestone not only in the diagnosis, treatment and prevention of hepatitis C, but in the approach to study infections in general apart from contributing to the understanding of the role genetic and environmental factors play in the development of this infection. In all, that set the basis for the production of new antivirals which are central for hepatitis C control and elimination. Of note, the cloning of HCV in 1989 was a remarkable accomplishment that has not only saved a large number of human lives but also demonstrated the power of molecular biology in unearthing new infectious agents. The discovery of HCV, the first virus ever discovered by molecular cloning technology, with its accompanying development of new methodologies such as new generation sequencing and new generation diagnostic automated systems[38], is also a landmark in public health. The discovery of HCV provides the opportunity to save thousands of lives through prevention and now, cure of the disease, which would otherwise be lost to chronic hepatitis C and its complications.



DOI: 10.3748/wjg.v28.i37.5395 **Copyright** ©The Author(s) 2022.

Figure 1 Timeline of the events leading and following the discovery of the hepatitis C virus. DAAs: Direct-acting antivirals; HCV: Hepatitis C virus; WHO: World Health Organization.

ACKNOWLEDGEMENTS

We thank Octavio Guadalupe Campollo for the art work.

FOOTNOTES

Author contributions: Campollo O conceived the idea of the article, discussed and collaborated with the authors, answered the reviewers comments and reviewed the final version; Amaya G reviewed the literature and updated the references, made contributions to the manuscript, reviewed and corrected the drafts, and answered the reviewers comments; McCormick PA wrote several sections of earlier and final versions of the manuscript, reviewed and corrected the final draft, and, reviewed the English language.

Conflict-of-interest statement: All the authors report no relevant conflicts of interest for this article.

Open-Access: This article is an open-access article that was selected by an in-house editor and fully peer-reviewed by external reviewers. It is distributed in accordance with the Creative Commons Attribution NonCommercial (CC BY-NC 4.0) license, which permits others to distribute, remix, adapt, build upon this work non-commercially, and license their derivative works on different terms, provided the original work is properly cited and the use is non-commercial. See: https://creativecommons.org/Licenses/by-nc/4.0/

Country/Territory of origin: Mexico

ORCID number: Octavio Campollo 0000-0003-1812-4207; Gerardo Amaya 0000-0002-6747-1881; P Aiden McCormick 0000-0002-5994-6023.

S-Editor: Wang JJ
L-Editor: Webster JR
P-Editor: Wang JJ

REFERENCES

1 **Masaccio MG**, Hedestam GK. The discovery of Hepatitis C virus. The Nobel assembly at Karolinska Institutet. [cited 12 February 2022]. Available from: https://www.nobelprize.org/prizes/medicine/2020/advanced-information/
2 **Farci P**. Choo QL, Kuo G, Weiner AJ, Overby LR, Bradley DW, Houghton M. Isolation of a cDNA clone derived from a blood-borne non-A, non-B viral hepatitis genome [Science 1989; 244: 359-362]. *J Hepatol* 2002; **36**: 582-585 [PMID:

11983439 DOI: 10.1016/s0168-8278(02)00051-X]
3 **World Health Organization**. Global health sector strategy on viral hepatitis 2016-2021. Towards ending viral hepatitis. [cited 15 February 2022]. Available from: https:// www.who.int/publications/i/item/WHO-HIV-2016.06
4 **Johnson KA**, Dangerfield T. Mechanisms of inhibition of viral RNA replication by nucleotide analogs. *Enzymes* 2021; **49**: 39-62 [PMID: 34696838 DOI: 10.1016/bs.enz.2021.07.001]
5 **European Association for the Study of the Liver**. Clinical Practice Guidelines Panel: Chair:; EASL Governing Board representative:; Panel members:. EASL recommendations on treatment of hepatitis C: Final update of the series☆. *J Hepatol* 2020; **73**: 1170-1218 [PMID: 32956768 DOI: 10.1016/j.jhep.2020.08.018]
6 **Manns MP**, Buti M, Gane E, Pawlotsky JM, Razavi H, Terrault N, Younossi Z. Hepatitis C virus infection. *Nat Rev Dis Primers* 2017; **3**: 17006 [PMID: 28252637 DOI: 10.1038/nrdp.2017.6]
7 **Ghany MG**, Morgan TR; AASLD-IDSA Hepatitis C Guidance Panel. Hepatitis C Guidance 2019 Update: American Association for the Study of Liver Diseases-Infectious Diseases Society of America Recommendations for Testing, Managing, and Treating Hepatitis C Virus Infection. *Hepatology* 2020; **71**: 686-721 [PMID: 31816111 DOI: 10.1002/hep.31060]
8 **Webster DP**, Klenerman P, Dusheiko GM. Hepatitis C. *Lancet* 2015; **385**: 1124-1135 [PMID: 25687730 DOI: 10.1016/S0140-6736(14)62401-6]
9 **Gerlich WH**. Medical virology of hepatitis B: how it began and where we are now. *Virol J* 2013; **10**: 239 [PMID: 23870415 DOI: 10.1186/1743-422X-10-239]
10 **Stanaway JD**, Flaxman AD, Naghavi M, Fitzmaurice C, Vos T, Abubakar I, Abu-Raddad LJ, Assadi R, Bhala N, Cowie B, Forouzanfour MH, Groeger J, Hanafiah KM, Jacobsen KH, James SL, MacLachlan J, Malekzadeh R, Martin NK, Mokdad AA, Mokdad AH, Murray CJL, Plass D, Rana S, Rein DB, Richardus JH, Sanabria J, Saylan M, Shahraz S, So S, Vlassov VV, Weiderpass E, Wiersma ST, Younis M, Yu C, El Sayed Zaki M, Cooke GS. The global burden of viral hepatitis from 1990 to 2013: findings from the Global Burden of Disease Study 2013. *Lancet* 2016; **388**: 1081-1088 [PMID: 27394647 DOI: 10.1016/S0140-6736(16)30579-7]
11 **Trepo C**. A brief history of hepatitis milestones. *Liver Int* 2014; **34** Suppl 1: 29-37 [PMID: 24373076 DOI: 10.1111/liv.12409]
12 **MacCallum FO**. 1971 International Symposium on Viral Hepatitis. Historical perspectives. *Can Med Assoc J* 1972; **106** Suppl: 423-Suppl:426 [PMID: 4552628]
13 **Witts LJ**. Some Problems of Infective Hepatitis. *Br Med J* 1944; **1**: 739-743 [PMID: 20785459 DOI: 10.1136/bmj.1.4352.739]
14 **Reuben A**. The thin red line. *Hepatology* 2002; **36**: 770-773 [PMID: 12198682 DOI: 10.1002/hep.510360341]
15 **Krugman S**, Giles JP, Hammond J. Infectious hepatitis. Evidence for two distinctive clinical, epidemiological, and immunological types of infection. *JAMA* 1967; **200**: 365-373 [PMID: 4164595 DOI: 10.1001/jama.1967.03120180053006]
16 **Stokes J**, Maris EP, Gellis SS. Chemical, clinical, and immunological studies on the products of human plasma fractionation. xi. the use of concentrated normal human serum gamma globulin (human immune serum globulin) in the prophylaxis and treatment of measles. *J Clin Invest* 1944; **23**: 531-540 [PMID: 16695129 DOI: 10.1172/JCI101518]
17 **Stokes JJ**, Neefe JR. Prevention and attenuation of infectious hepatitis by gamma globulin: preliminary note. *JAMA* 1945; **127**: 144-145 [DOI: 10.1001/jama.1945.02860030016004]
18 **Rothman DJ**. Were Tuskegee & Willowbrook 'studies in nature'? *Hastings Cent Rep* 1982; **12**: 5-7 [PMID: 7096065 DOI: 10.2307/3561798]
19 **Alter HJ**. The road not taken or how I learned to love the liver: a personal perspective on hepatitis history. *Hepatology* 2014; **59**: 4-12 [PMID: 24123147 DOI: 10.1002/hep.26787]
20 **Ward JW**. Hepatitis C virus: the 25-year journey from discovery to cure. *Hepatology* 2014; **60**: 1479-1482 [PMID: 25131647 DOI: 10.1002/hep.27377]
21 **Campollo O**, Valencia-Salinas JJ, Berumen-Arellano A, Pérez-Aranda MA, Panduro-Cerda A, Segura-Ortega J. [Epidemiological characteristics of liver cirrhosis at the Hospital Civil of Guadalajara]. *Salud Publica Mex* 1997; **39**: 195-200 [PMID: 9304222 DOI: 10.1590/S0036-36341997000300004]
22 **Zhao Q**, Xia N. The 2016 Lasker-DeBakey Clinical Medical Research Award: Innovative hepatitis C virus (HCV) replicons leading to drug development for hepatitis C cure. *Sci China Life Sci* 2016; **59**: 1198-1201 [PMID: 27785725 DOI: 10.1007/s11427-016-0313-9]
23 **EASL**. EASL Policy Statement on Hepatitis C Elimination. [cited 15 February 2022]. Available from: https://easl.eu/wp-content/uploads/2019/04/EASL-Policy-Statement-on-Hepatitis-C-Elimination.pdf
24 **Alter HJ**, Purcell RH, Holland PV, Popper H. Transmissible agent in non-A, non-B hepatitis. *Lancet* 1978; **1**: 459-463 [PMID: 76017 DOI: 10.1016/s0140-6736(78)90131-9]
25 **Houghton M**. The long and winding road leading to the identification of the hepatitis C virus. *J Hepatol* 2009; **51**: 939-948 [PMID: 19781804 DOI: 10.1016/j.jhep.2009.08.004]
26 **Kuo G**, Choo QL, Alter HJ, Gitnick GL, Redeker AG, Purcell RH, Miyamura T, Dienstag JL, Alter MJ, Stevens CE. An assay for circulating antibodies to a major etiologic virus of human non-A, non-B hepatitis. *Science* 1989; **244**: 362-364 [PMID: 2496467 DOI: 10.1126/science.2496467]
27 **Kolykhalov AA**, Feinstone SM, Rice CM. Identification of a highly conserved sequence element at the 3' terminus of hepatitis C virus genome RNA. *J Virol* 1996; **70**: 3363-3371 [PMID: 8648666 DOI: 10.1128/JVI.70.6.3363-3371.1996]
28 **Harak C**, Meyrath M, Romero-Brey I, Schenk C, Gondeau C, Schult P, Esser-Nobis K, Saeed M, Neddermann P, Schnitzler P, Gotthardt D, Perez-Del-Pulgar S, Neumann-Haefelin C, Thimme R, Meuleman P, Vondran FW, De Francesco R, Rice CM, Bartenschlager R, Lohmann V. Tuning a cellular lipid kinase activity adapts hepatitis C virus to replication in cell culture. *Nat Microbiol* 2016; **2**: 16247 [PMID: 27991882 DOI: 10.1038/nmicrobiol.2016.247]
29 **Saeed M**, Andreo U, Chung HY, Espiritu C, Branch AD, Silva JM, Rice CM. SEC14L2 enables pan-genotype HCV replication in cell culture. *Nature* 2015; **524**: 471-475 [PMID: 26266980 DOI: 10.1038/nature14899]
30 **Kolykhalov AA**, Agapov EV, Blight KJ, Mihalik K, Feinstone SM, Rice CM. Transmission of hepatitis C by intrahepatic inoculation with transcribed RNA. *Science* 1997; **277**: 570-574 [PMID: 9228008 DOI: 10.1126/science.277.5325.570]

31 **Choo QL**, Kuo G, Weiner AJ, Overby LR, Bradley DW, Houghton M. Isolation of a cDNA clone derived from a blood-borne non-A, non-B viral hepatitis genome. *Science* 1989; **244**: 359-362 [PMID: 2523562 DOI: 10.1126/science.2523562]

32 **Lohmann V**, Körner F, Koch J, Herian U, Theilmann L, Bartenschlager R. Replication of subgenomic hepatitis C virus RNAs in a hepatoma cell line. *Science* 1999; **285**: 110-113 [PMID: 10390360 DOI: 10.1126/science.285.5424.110]

33 **Shouval D**, Friedman SL. Focusing on the past, present, and future of hepatology. *J Hepatol* 2014; **61**: 1196-1198 [PMID: 25195549 DOI: 10.1016/j.jhep.2014.08.039]

34 **Huang CF**, Yu ML. Unmet needs of chronic hepatitis C in the era of direct-acting antiviral therapy. *Clin Mol Hepatol* 2020; **26**: 251-260 [PMID: 32188235 DOI: 10.3350/cmh.2020.0018]

35 **World Health Organization**. Interim guidance for country validation of viral hepatitis elimination. [cited 15 February 2022]. Available from: https://www.who.int/publications/i/item/9789240028395

36 **Chang MH**, You SL, Chen CJ, Liu CJ, Lai MW, Wu TC, Wu SF, Lee CM, Yang SS, Chu HC, Wang TE, Chen BW, Chuang WL, Soon MS, Lin CY, Chiou ST, Kuo HS, Chen DS; Taiwan Hepatoma Study Group. Long-term Effects of Hepatitis B Immunization of Infants in Preventing Liver Cancer. *Gastroenterology* 2016; **151**: 472-480.e1 [PMID: 27269245 DOI: 10.1053/j.gastro.2016.05.048]

37 **Waked I**, Esmat G, Elsharkawy A, El-Serafy M, Abdel-Razek W, Ghalab R, Elshishiney G, Salah A, Abdel Megid S, Kabil K, El-Sayed MH, Dabbous H, El Shazly Y, Abo Sliman M, Abou Hashem K, Abdel Gawad S, El Nahas N, El Sobky A, El Sonbaty S, El Tabakh H, Emad E, Gemeah H, Hashem A, Hassany M, Hefnawy N, Hemida AN, Khadary A, Labib K, Mahmoud F, Mamoun S, Marei T, Mekky S, Meshref A, Othman A, Ragab O, Ramadan E, Rehan A, Saad T, Saeed R, Sharshar M, Shawky H, Shawky M, Shehata W, Soror H, Taha M, Talha M, Tealaab A, Zein M, Hashish A, Cordie A, Omar Y, Kamal E, Ammar I, AbdAlla M, El Akel W, Doss W, Zaid H. Screening and Treatment Program to Eliminate Hepatitis C in Egypt. *N Engl J Med* 2020; **382**: 1166-1174 [PMID: 32187475 DOI: 10.1056/NEJMsr1912628]

38 **Panduro A**. Viruses and the Liver 2020: Before COVID-19 and the beginning of a new age in medicine. *Ann Hepatol* 2021; **20**: 100293 [PMID: 33388122 DOI: 10.1016/j.aohep.2020.100293]

World Journal of Gastroenterology

Submit a Manuscript: https://www.f6publishing.com

World J Gastroenterol 2022 October 7; 28(37): 5403-5419

DOI: 10.3748/wjg.v28.i37.5403

ISSN 1007-9327 (print) ISSN 2219-2840 (online)

REVIEW

Immunotherapy-based novel nanoparticles in the treatment of gastrointestinal cancer: Trends and challenges

Yi-Nan Ding, Ming Xue, Qiu-Sha Tang, Li-Jun Wang, Hui-Yan Ding, Han Li, Cheng-Cheng Gao, Wei-Ping Yu

Specialty type: Gastroenterology and hepatology

Provenance and peer review: Invited article; Externally peer reviewed.

Peer-review model: Single blind

Peer-review report's scientific quality classification

Grade A (Excellent): 0
Grade B (Very good): B
Grade C (Good): C
Grade D (Fair): 0
Grade E (Poor): 0

P-Reviewer: Manojlovic N, Serbia; Serban ED, Romania

Received: July 21, 2022
Peer-review started: July 21, 2022
First decision: August 19, 2022
Revised: August 27, 2022
Accepted: September 15, 2022
Article in press: September 15, 2022
Published online: October 7, 2022

Yi-Nan Ding, Qiu-Sha Tang, Li-Jun Wang, Hui-Yan Ding, Department of Pathophysiology, College of Medicine, Southeast University, Nanjing 210000, Jiangsu Province, China

Ming Xue, Department of Critical Care Medicine, Zhongda Hospital, School of Medicine, Southeast University, Nanjing 210000, Jiangsu Province, China

Han Li, Department of Tuberculosis, The Second Hospital of Nanjing, Nanjing University of Chinese Medicine, Nanjing 210000, Jiangsu Province, China

Cheng-Cheng Gao, Department of Radiology, Affiliated Hangzhou First People's Hospital, Zhejiang University School of Medicine, Hangzhou 310000, Zhejiang Province, China

Wei-Ping Yu, Medical School, Southeast University, Nanjing 210009, Jiangsu Province, China

Corresponding author: Wei-Ping Yu, MD, PhD, Doctor, Professor, Medical School, Southeast University, No. 87 Dingjiaqiao, Nanjing 210009, Jiangsu Province, China.
wpylg@hotmail.com

Abstract

Gastrointestinal cancer (GIC) is the most common cancer with a poor prognosis. Currently, surgery is the main treatment for GIC. However, the high rate of postoperative recurrence leads to a low five-year survival rate. In recent years, immunotherapy has received much attention. As the only immunotherapy drugs approved by the Food and Drug Administration (FDA), immune checkpoint blockade (ICB) drugs have great potential in cancer therapy. Nevertheless, the efficacy of ICB treatment is greatly limited by the low immunogenicity and immunosuppressive microenvironment of GIC. Therefore, the targets of immunotherapy have expanded from ICB to increasing tumor immunogenicity, increasing the recruitment and maturation of immune cells and reducing the proportion of inhibitory immune cells, such as M2-like macrophages, regulatory T cells and myeloid-derived suppressor cells. Moreover, with the development of nanotechnology, a variety of nanoparticles have been approved by the FDA for clinical therapy, so novel nanodrug delivery systems have become a research focus for anticancer therapy. In this review, we summarize recent advances in the application of immunotherapy-based nanoparticles in GICs, such as gastric cancer, hepatocellular carcinoma, colorectal cancer and pancreatic cancer, and described the existing challenges and future trends.

Key Words: Gastrointestinal cancer; Gastric cancer; Hepatocellular carcinoma; Colorectal cancer; Pancreatic cancer; Immunotherapy-based novel nanoparticles

©The Author(s) 2022. Published by Baishideng Publishing Group Inc. All rights reserved.

Core Tip: Recently, immunotherapy has received substantial attention. Although there are several Food and Drug Administration-approved immune checkpoint blockade (ICB) drugs, the efficacy remains limited, and the response rate is less than 20%. Because gastrointestinal cancer (GIC) is a group of immunosuppressive cancers, the efficacy of ICB treatment is also limited. Therefore, enhancing the immunogenicity of GIC or reversing the immunosuppressive microenvironment of GIC have become potential approaches for GIC immunotherapy. There are many studies on nanoparticle-based cancer therapy. However, there are only a few studies on immunotherapy-based nanoparticles in GIC. Here, we summarize recent advances in the application of immunotherapy-based nanoparticles in GIC and present our thoughts about this topic.

Citation: Ding YN, Xue M, Tang QS, Wang LJ, Ding HY, Li H, Gao CC, Yu WP. Immunotherapy-based novel nanoparticles in the treatment of gastrointestinal cancer: Trends and challenges. *World J Gastroenterol* 2022; 28(37): 5403-5419
URL: https://www.wjgnet.com/1007-9327/full/v28/i37/5403.htm
DOI: https://dx.doi.org/10.3748/wjg.v28.i37.5403

INTRODUCTION

Gastrointestinal cancer (GIC) has been among the most commonly diagnosed cancers in recent decades [1-3]. In recent reports, the incidence and mortality rates have gradually decreased for gastric cancer (GC), hepatocellular carcinoma (HCC) and esophageal cancer in China; in contrast, the rates for colorectal cancer (CRC) have increased[4]. Regardless of the changes in the incidence and mortality rates of GIC, the disease has greatly affected the quality of life of many individuals.

Similar to other types of cancer, GIC has several therapies available. As the most conventional means of cancer treatment, surgery, chemotherapy and radiotherapy play important roles. Although traditional therapies effectively prolong survival for patients with GIC, there are still many drawbacks that cannot be ignored[5]. Surgery, especially minimally invasive surgery and radiotherapy, can effectively shrink the tumor and even make the local tumor disappear; chemotherapy can be administered systematically to kill cancer cells[6-8]. However, these treatments cannot prevent recurrence. Moreover, for GICs, the side effects of radiotherapy and chemotherapy on the digestive system seriously affect the quality of life of patients and cannot be ignored[9-11]. To improve the therapeutic effect and reduce the occurrence of adverse reactions, clinicians often try a variety of therapeutic combinations to achieve complementary advantages[12,13].

With progress in the concept of cancer treatment and the development of diagnosis and treatment technology, various precision treatment methods, such as targeted therapy, photodynamic therapy (PDT), photothermal therapy (PTT) and immunotherapy, have emerged as new sources of hope for patients[14-19]. Some scholars believe that the characteristics of the GIC immune microenvironment are related to the high mortality of patients with GIC; therefore, treatments that target the GIC immune microenvironment are gradually being recognized[20]. As one of the therapeutic methods that targets the cancer immune microenvironment, immune checkpoint blockade (ICB) treatment has achieved great success in clinical practice, laying a good foundation for the development of cancer immunotherapy[21].

Recently, a variety of nanobased drugs (such as Eligard[22], Marqibo[23], Onivyde[24], Doxil[25], Abraxane[26], Ontak[27] and Nanotherm[28]) have been widely used in clinical practice due to several characteristics, including their low toxicity, long circulation and passive targeting ability[29,30]. However, most of the nanobased drugs mentioned above are liposomes. In addition to liposomes, there are also other types of nanoparticles that possess the same potential for clinical translation. Similar to liposomes, small extracellular vesicles and cell membrane vesicles also have lipid bilayers, and they have better biocompatibility than liposomes due to their origin[31-34]. Furthermore, due to their simple production process and high drug loading efficiency, polymersomes are also considered candidate nanoparticles for clinical translation[35-37]. There are also many kinds of novel nanoparticles, such as gold nanoparticles, manganese dioxide nanoparticles, upconversion nanoparticles (UCNPs), metal organic framework nanoparticles and mesoporous silica nanoparticles (MSNPs), which can also play important roles in different diseases or cancers through their own characteristics[38-42]. Here, among the GICs, we focus on GC, HCC, CRC and pancreatic cancer and summarize the application trends of immunotherapy-based novel nanoparticles in these cancers as well as the challenges and opportunities

in the future.

IMMUNOTHERAPY-BASED NOVEL NANOPARTICLES IN GC

GC remains one of the most common causes of cancer-related death globally. Although a variety of treatments have been developed, the main treatment for GC is still surgery or endoscopic resection. The probability of patients experiencing recurrence after surgery is approximately 60%[43]. Currently, the median overall survival time with fluoropyrimidine-based combination chemotherapy is less than one year. In general, the overall clinical therapeutic effect of GC is not satisfactory[44,45]. In addition, immunotherapy for GC will become an important treatment option in the future, and nanoparticles, as highly efficient drug carriers, have played an important role in clinical practice[46-48]. Whether the combination of immunotherapy and nanoparticles can produce improved therapeutic effects is also worth examining.

Immune checkpoint inhibitors (ICIs), such as anti-programmed death receptor-1 (anti-PD-1) antibody and anti-programmed death receptor-ligand 1 (anti-PD-L1) antibody, can effectively block the PD-1/PD-L1 pathway and enhance the anticancer immune response[49]. Based on ICI treatment, Xu *et al*[50] prepared a novel nanoparticle named docetaxel (DOC)-PEG-PCL-monoclonal antibody (mAb) NP, which contained DOC as the chemotherapeutic drug and conjugated PD-L1 mAb on the surface of the nanoparticle. This nanodrug delivery system (NDDS) can effectively improve drug delivery efficiency and the solubility of hydrophobic drugs such as DOC. In addition, the system can target PD-L1-positive GC cells, exhibiting clinical translation potential. Recently, scientists found that a gradually acquired heritable *de novo* methylation program inhibited T-cell proliferation and clonal diversity during PD-1 blockade therapy[51]. Inspired by this study, Hu *et al*[52] designed copolymers loaded with the epigenetic agent 5-Aza-20-deoxycytidine (DAC), and an anti-PD-1 antibody was conjugated to the surface of the nanoparticles. The nanoparticles increased the stability of DAC and improved the therapeutic effect of ICI treatment *in vivo*.

Due to the characteristics of the cancer immune microenvironment, T-cell infiltration in GC patients is insufficient, which limits the effect of ICB treatment in GC[53]. Guo *et al*[54] constructed an NDDS named HMON@IR820/Pt-NPs, which coencapsulated platinum nanoparticles (chemo-prodrugs) and IR820 (photosensitizer) into hollow mesoporous organosilica nanoparticles. IR820-mediated PDT can lead to the release of oxidative mitochondrial DNA (mitoDNA). In addition, this oxidative process can oxidize Pt(0) to cytotoxic Pt(II), which can lead to the dysfunction of nuclear DNA (nDNA). The dual damage of mitoDNA and nDNA can activate the c-GAS/stimulator of interferon genes (STING) pathway, which can directly stimulate innate immunity and increase the infiltration of $CD8^+$ T cells, thus improving the efficacy of immunotherapy for GC.

Multiple studies have confirmed that tumor-associated macrophages (TAMs) are also involved in the composition of the tumor immune microenvironment. Moreover, M2-like macrophages can inhibit tumor immunity and promote tumor immune escape[55,56]. Zhang *et al*[57]'s group designed a novel human serum albumin (HSA)-Au(III) thiosemicarbazone agent nanoparticle delivery system for chemotherapy and immunotherapy in GC. This NDDS can simultaneously directly kill GC cells and polarize TAMs into M1-like macrophages, providing a new immunotherapy strategy for clinical translation.

The majority of cancer patients are often unable to activate adequate levels of anticancer immunity, whereas therapeutic tumor vaccines can help patients proactively generate adequate anticancer immune responses against tumor-specific antigens (TSAs) and tumor-associated antigens[58]. Among the different types of tumor vaccines, dendritic cell (DC)-based tumor vaccines have been explored in clinical experiments[59,60]. Kohnepoushi *et al*[61] prepared poly(lactic-co-glycolic) acid nanoparticles to protect the human gastric tumor antigen against proteolytic enzymes. In addition, nanoparticles that contain human gastric tumor antigen can facilitate DC maturation and further enhance the efficacy of DC vaccines in clinical practice.

In addition to ICB treatment and other therapies that can improve the cancer immune microenvironment, immunoadjuvants can act as a potential adjunctive therapy to stimulate anticancer immunity [62,63]. Zhang *et al*[64] developed a gold nanoshell-based NDDS that can convert near-infrared (NIR) light into thermal energy, enabling PTT. Moreover, high temperature can also break thiol bonds to release gene therapy agents and oligooxynucleotides that contain cytosine-guanine (CpG) motifs (which are also known as immunoadjuvants). This study designed a novel NDDS combined with hyperthermia, gene therapy and immunotherapy, which exhibited encouraging anticancer efficacy against GC *in vitro* and *in vivo* (Table 1).

IMMUNOTHERAPY-BASED NOVEL NANOPARTICLES IN HCC

Primary liver cancer is among the most commonly diagnosed cancers, most of which are HCC[65,66]. Due to the high infection rate of hepatitis B virus, the incidence of HCC in China remains high[67].

Table 1 Overview of immunotherapy-based novel nanoparticles in the treatment of gastric cancer [PubMed Search (immunotherapy) AND (nanoparticle) AND (gastric cancer)]

Type of nanoparticle	Treatment strategy	Drugs or active substance involved	The main involvement of immune cells	Ref.
Copolymers	ICIs, chemotherapy	DOC, PD-L1 mAb	T cells	Xu *et al*[50]
Copolymers	ICIs, epigenetic treatment	DAC, nivolumab	$PD1^+CD8^+$ TILs	Hu *et al*[52]
Hollow mesoporous organosilica nanoparticles	Dual-damage to nDNA and mitoDNA activates the c-GAS/STING pathway to stimulate innate immunity	Platinum, IR820	$CD8^+$ T cells, DCs	Guo *et al*[54]
HSA nanoparticles	Targeted chemotherapy and immunotherapy	Au(III) thiosemicarbazone agent	TAMs	Zhang *et al*[57]
Polymers	DC vaccine	Human gastric tumor antigens	DCs	Kohnepoushi *et al*[61]
Gold nanoshell	Gene therapy, hyperthermia and immunoadjuvants therapy	HER-2 targeted siRNA, gold, CpG	DCs, T cells	Zhang *et al*[64]

ICIs: Immune checkpoint inhibitors; DOC: Docetaxel; PD-L1: Programmed cell death ligand 1; mAb: Monoclonal antibody; DAC: 5-Aza-20-deoxycytidine; TILs: Tumor-infiltrating T cells; DCs: Dendritic cells; HSA: Human serum albumin; TAMs: Tumor-associated macrophages; HER-2: Human epidermal growth factor receptor-2; CpG: Cytosine–guanine.

Surgical resection of the liver is the main treatment for HCC. However, the prognosis after surgery is still poor. Recently, the development of molecular targeted therapy and immunotherapy for HCC has gained recognition in clinical studies[68]. Moreover, NDDSs can improve the efficiency of drug delivery into the tumor area and reduce side effects[69-71]. At present, a large number of studies using immunotherapy-based NDDSs have shown great potential for clinical translation.

ICB treatment has also emerged as a new option for advanced HCC[72]. However, ICB treatment alone has limited efficacy against HCC. Therefore, how to combine other kinds of therapies to improve the efficiency of ICB treatment has become a new academic topic. For example, Food and Drug Administration (FDA)-approved sorafenib-experienced patients used ipilimumab (anti-CTLA-4) combined with nivolumab (anti-PD-1) in March 2020[73]. In the last two decades, scientists have found that chemotherapeutic drugs, radiotherapy, PDT and some other treatments can induce immunogenic cell death (ICD), which can lead to the release of TSAs and increase tumor antigenicity[74]. Hence, ICD can improve the efficacy of ICB treatment by increasing tumor immunogenicity. According to the therapeutic strategies mentioned above, Xu *et al*[75] designed a cyclic arginine-glycine-aspartic acid peptide-modified self-assembling polymer-based NDDS. Cancer cells were damaged by PDT and chemotherapy, while induced ICD and enhanced tumor immunogenicity provided a suitable immune microenvironment for ICB treatment. Previous studies found that a lack of the p53 tumor suppressor gene leads to tumorigenesis and drug resistance[76-78]. With the development of research on the p53 tumor suppressor gene, an increasing body of evidence indicates that the p53 protein plays an important role in anticancer immunity by regulating the cancer immune microenvironment[79-81]. Furthermore, a recent study suggested that ICD induced by cytotoxic agents, such as chemotherapy drugs, may be involved in the activation of the p53 pathway[82]. Xiao *et al*[83] developed a novel lipid-polymer hybrid nanoplatform for mRNA delivery that can induce the expression of p53, effectively reprogramming the immune microenvironment of HCC. Moreover, combination with anti-PD-1 therapy can reverse the inhibitory immune microenvironment of HCC. To solve the problem of HCC recurrence after surgery, Li *et al*[84] designed a bionic NDDS consisting of MSNPs loaded with anti-PD-L1 and sorafenib and coated with platelet membranes at the surface of the MSNPs. This NDDS can target wounds and generate potent anti-HCC immunity, providing a new therapeutic idea for preventing recurrence in postsurgery HCC patients.

As we mentioned before, chemotherapy-based ICD can cause cancer cells to be more easily recognized by the immune system. However, the effect of single-drug-mediated ICD is very limited. Some studies have attempted to enhance the effect of ICD by combining two different ICD inducers to solve this problem. Yu *et al*[85] evaluated the potential of icaritin as an ICD inducer and utilized NDDS to deliver low doses of icaritin and doxorubicin simultaneously to the tumor area. This NDDS can reprogram the immune microenvironment and induce satisfactory anti-HCC effects. Furthermore, NDDS can lower the dose of chemotherapy to reduce the side effects.

TAMs play a major role in the immunosuppressive microenvironment of HCC[86]. Wang *et al*[87] screened chemokine C-C motif ligand (CCL)2 and CCL5 as two major chemokines responsible for the polarization of M2-like macrophages and designed a CCL2 and CCL5 dual-target lipid nanoparticle system. The combination of TAMs targeting lipid nanoparticles with ICB treatment achieved long-term survival in HCC mice. Similarly, as a common feature of the tumor microenvironment, hypoxia is also

common in HCC. Hypoxia can lead to radioresistance and the formation of an immunosuppressive microenvironment, including the accumulation of TAMs and depletion of effector T cells, which are closely related to the occurrence and development of cancer[88-90]. Dai *et al*[91] synthesized polydopamine-nanoparticle-stabilized oxygen microcapsules that can deliver oxygen to the tumor region and rapidly increase the concentration of oxygen. In this study, oxygen microcapsules increased HCC sensitivity to radiotherapy and polarized M2-like macrophages into M1-like macrophages, consequently activating anti-HCC immunity. In addition to conventional immune cells, liver sinusoidal endothelial cells (LSECs) can also play a significant role in immunosuppressive regulation[92]. Yu *et al*[93] designed a simvastatin-loaded NDDS to target LSECs in HCC patients. This NDDS can reduce the capillarization of LSECs to improve the stromal microenvironment and recruit natural killer T cells to inhibit tumor progression.

Cationic lipid nanoparticles have been suggested to be suitable delivery vectors for RNA, and several messenger RNA vaccines are based on lipid nanotechnology that was approved by the FDA during the severe acute respiratory syndrome coronavirus 2 (SARS-CoV-2) pandemic[94-97]. Zhang *et al*[98] developed a total HCC-derived RNA-loaded lipid nanoparticle vaccine to target DCs and activate anticancer immunity (Figure 1 and Table 2).

IMMUNOTHERAPY-BASED NOVEL NANOPARTICLES IN CRC

CRC is the third leading cause of cancer-related deaths globally[99]. CRC is the only cancer that can be reduced by screening. Most CRC patients can be screened by flexible sigmoidoscopy or guaiac-based fecal occult blood tests[100]. However, approximately 25% of CRC patients are at stage 4, and the 5-year survival rate is only 11%[101,102]. To improve the survival rate of advanced CRC patients, immunotherapy and nanoparticle-based drug delivery systems have become the focus of basic and clinical research for the past few years[103-105].

Similar to GC and HCC, ICB treatment is more widely used in CRC patients, but its curative effect is extremely limited, especially for mismatch repair-proficient/microsatellite stability/microsatellite instability-low CRC patients[106]. As we reported earlier, ICB treatment combined with ICD can achieve a "1 + 1 > 2" effect. A similar treatment strategy has also been applied in CRC research. For example, Yuan *et al*[107] utilized the ability of PDT to induce ICD and developed a photosensitive NDDS combined with ICB treatment that can enhance the response rate of anti-PD-L1 therapy in CRC. Zhu *et al*[108] also designed an oxaliplatin prodrug-conjugated photosensitive NDDS that can be stimulated by the NIR-II window (1000-1700 nm) for PTT, which is a proven to induce ICD. Moreover, oxaliplatin, a chemotherapy drug, is also known as an ICD inducer. This novel NDDS can induce ICD through both PTT and chemotherapy, which may provide a promising immunotherapy strategy for advanced CRC treatment. Shikonin (SK), a major active ingredient isolated from traditional Chinese medicine, has also been proven to induce ICD. Li *et al*[109] designed a versatile nanoparticle that can deliver knockdown siRNA for both the ICD inducer SK and PD-L1, which presents potential for CRC immunotherapy. Recently, ferroptosis was discovered as a nonapoptotic form of regulated cell death [110]. In addition, Duan *et al*[111]'s group proved that dihydroartemisinin (DHA), as a reactive oxygen species (ROS)-producing drug and ferroptosis inducer, can also induce ICD to potentiate anticancer immunity. Therefore, the same research group developed a Zn-pyrophosphate core-shell NDDS codeliver DHA and pyropheophorbide-iron (pyro-Fe). Glutathione and other thiol-based reductants in cancer cells can reduce Pyro-Fe^{III} to Pyro-Fe^{II}, which can catalyze the decomposition of DHA to induce ICD and ferroptosis. This novel NDDS overcame the deficiency of iron in solid tumors, enhanced the ability of DHA to induce ferroptosis and ICD, and increased the infiltration of $CD8^+$ T cells in CRC.

In addition to actively increasing the immunogenicity of CRC, stimulating immune cells can also activate anti-CRC immunity. Immune cells can be activated by stimulating toll-like receptors (TLRs), such as DCs and macrophages. Several TLR agonists have been approved by the FDA. However, none are currently approved for CRC treatment. The major problem for TLR agonists is the small size of the drugs, which allows the drugs to spread rapidly from the administration site and cause severe systemic side effects (Figure 2)[112]. Fortunately, nanoparticle-based delivery systems can solve this problem. Bahmani *et al*[113] prepared a platelet membrane-coated nanoparticle loaded with the TLR7 agonist R848. This biomimetic NDDS enhanced the retention of the drug in the tumor and effectively stimulated the maturation of DCs, resulting in complete tumor eradication in a murine model of CRC.

Notably, long noncoding RNAs (lncRNAs) have recently been reported to be involved in the formation of the immunosuppressive cancer microenvironment and have become a potential immunotherapy target[114-116]. Liu *et al*[117] designed a bioscaffold loaded with a lncRNA-targeting biomimetic NDDS that modulated the cancer immune microenvironment against CRC recurrence after surgery. The biomimetic NDDS coated with a CRC membrane, which provides NDDS with a tumor-homing capacity and carries TSAs into the tumor area, promotes the maturation of DCs. Moreover, a plasmid-encoding short hairpin RNA against Pvt1 was encapsulated inside the NDDS to enhance ICD and ameliorate granulocytic-myeloid-derived suppressor cell (G-MDSC)-mediated immunosuppression. This work provides a new perspective for NDDS-based lncRNA-targeted immunotherapy.

Table 2 Overview of Immunotherapy-based novel nanoparticles in the treatment of hepatocellular carcinoma [PubMed Search (immunotherapy) AND (nanoparticle) AND (hepatocellular carcinoma)]

Type of nanoparticle	Treatment strategy	Drugs or active substance involved	The main involvement of immune cells	Ref.
Nano-micelles	ICD, chemotherapy, PDT	PTX, TPABDTO	CTLs, MDSCs, Tregs, DCs	Xu *et al*[75]
Polymers	p53 gene reprograms the immune microenvironment	p53 mRNA	T cells, NK cells	Xiao *et al*[83]
MSNPs	Anti-angiogenic drugs, ICIs	Sorafenib, PD-L1 antibody	T cells	Li *et al*[84]
Copolymers	ICD, chemotherapy	Icaritin, DOX	T cells, DCs	Yu *et al*[85]
Lipid nanoparticle	CCL2 and CCL5 dual-target	BisCCL2/5i mRNA	TAMs	Wang *et al*[87]
Microcapsules	Improving hypoxia	Oxygen	TAMs	Dai *et al*[91]
Copolymers	Mitigates LSEC capillarization	Simvastatin	NKT cells	Yu *et al*[93]
LNPs	Antigen specific vaccine	Tumor-derived RNA	T cells, DCs	Zhang *et al*[98]

ICD: Immunogenic cell death; PDT: Photodynamic therapy; CTLs: Cytotoxic T lymphocytes; PTX: Paclitaxel; MDSCs: Myeloid-derived suppressor cells; DCs: Dendritic cells; CCL2: Chemokine C-C motif ligand 2; CCL5: Chemokine C-C motif ligand 5; DOX: Doxorubicin; PD-L1: Programmed cell death ligand 1; NK cells: Natural killer cells; TAMs: Tumor-associated macrophages; Tregs: Regulatory T lymphocytes; MSNPs: Mesoporous silica nanoparticles; LSEC: Liver sinusoidal endothelial cells; LNPs: Lipid nanoparticles; NKT: Natural killer T.

In recent years, as an important component of the immunosuppressive cancer microenvironment, MDSCs have also been identified as potential targets for cancer immunotherapy. Additionally, recent studies reported that MDSCs could be selectively enlarged because of the enrichment of *Fusobacterium nucleatum* (Fn) in CRC tissue, resulting in a cancer immunosuppressive microenvironment[118-121]. Dong *et al*[122] proposed a phage-based antibacterial system that used the broad-spectrum antibacterial effect of silver nanoparticles (AgNPs) for antibacterial activity and then transported phage M13 into the tumor and utilized the recognition mechanism of phages to selectively kill Fn, thus preventing the recruitment of MDSCs. In addition, phages are highly immunogenic and can directly stimulate the maturation of DCs and promote the activation of M1-like macrophages, significantly enhancing the anti-CRC immune response.

Over the years, CRC vaccines have been a focus of scientific research. Zhang *et al*[123] designed an in situ cancer vaccine. They reported a supramolecular assembled programmable immune activation nanomedicine (PIAN) that can produce strong and durable anticancer immunity in situ. PIAN entered the tumor area through enhanced permeability and retention (EPR) after tail vein injection and was then disassembled by the high ROS within the tumor tissue. The release of poly-[(N-2-hydroxyethyl)-aspartamide]-Pt(IV)/beta-cyclodextrin simultaneously mediated tumor cell death and antigen release. In addition, CpG/polyamidoamine (CpG/PAMAM) captured the released antigen and entered the tumor draining lymph node to stimulate DC maturation, thus activating anti-CRC-specific immunity. This excellent work provides a new idea for designing nanomedicine-based programmable *in situ* cancer vaccines for cancer immunotherapy (Table 3).

IMMUNOTHERAPY-BASED NOVEL NANOPARTICLES IN PANCREATIC CANCER

As one of the most aggressive and fatal cancers, pancreatic cancer has been the leading cause of cancer-related deaths worldwide in the last few decades[124,125]. Most patients experience no obvious symptoms during the development of the disease. Therefore, it is difficult to diagnose the disease in the early stage, and patients often miss the optimal treatment time after they have been diagnosed with pancreatic cancer. Moreover, the majority of patients eventually relapse, even if they receive potentially radical treatment[126]. In contrast to other malignant tumors, stromal hyperplasia is the main feature of the pancreatic cancer microenvironment[127]. As a result, pancreatic cancer does not have a sufficient blood supply, so antiangiogenic drugs are not suitable for pancreatic cancer[128]. In addition, the tumor stroma of pancreatic cancer acts as a natural physical barrier between the tumor tissue and the body's immune system, which also limits the application of immunotherapy[129,130]. Until now, most phase I and II clinical trials of immunotherapy in pancreatic cancer have failed. Interestingly, ICB treatment combined with chemotherapy and/or radiotherapy has shown encouraging clinical efficacy[131]. In recent years, with the continuous development of nanotechnology, scientists have proposed a variety of nanodelivery systems aimed at the unique pathological characteristics of pancreatic cancer. They attempted to utilize NDDSs to achieve synergistic therapy and improve the tumor microenvironment to reverse the current situation of pancreatic cancer[132].

Table 3 Overview of Immunotherapy-based novel nanoparticles in the treatment of colorectal cancer [PubMed Search (immunotherapy) AND (nanoparticle) AND (colorectal cancer)]

Type of nanoparticle	Treatment strategy	Drugs or active substance involved	The main involvement of immune cells	Ref.
Copolymers	PDT induces HIF-1α expression, leading to the upregulation of PD-L1 expression, ICIs	Photosensitizer, PD-L1 antibody	DCs, $CD8^+$T cells, memory T cells	Yuan *et al*[107]
Polymeric nanoparticle	PTT, chemotherapy, ICD	PBOXA, donor–spacer–acceptor–spacer–donor type fluorophore	DCs, T cells, CTLs	Zhu *et al*[108]
Copolymers	ICD, ICIs	SK, PD-L1 knockdown siRNA	DCs, TAMs, Tregs, T cells	Li *et al*[109]
Polymers	ICD, ferroptosis	DHA	DCs, T cells	Duan *et al*[111]
Platelet membrane-coated nanoparticle	TLR7 treatment	R848	DCs	Bahmani *et al* [113]
Liposomes with cell membrane	ICD, chemotherapy, lncRNA-targeting therapy	Oxaliplatin, shPvt1	DCs, MDSCs, $CD8^+$T cells	Liu *et al*[117]
Silver nanoparticles	Anti-Fn	Phage M13	MDSCs, DCs, TAMs	Dong *et al*[122]
Supramolecular assembled programmable immune activation nanomedicine	*In-situ* cancer vaccine, ICD	PPCD, CpG/PAMAM	DCs, $CD8^+$T cells	Zhang *et al*[123]

ICIs: Immune checkpoint inhibitors; HIF-1α: Hypoxia-inducible factor 1α; PDT: Photodynamic therapy; PTT: Photothermal therapy; ICD: Immunogenic cell death; PD-L1: Programmed cell death ligand 1; PBOXA: Oxaliplatin prodrug; SK: Shikonin, DHA: Dihydroartemisinin; TLR: Toll-like receptor; shPvt1: Short hair-pinned RNA against Pvt1; Fn: *Fusobacterium nucleatum*; PPCD: Poly-[(N-2-hydroxyethyl)-aspartamide]-Pt(IV)/beta-cyclodextrin; PAMAM: Polyamidoamine; MDSCs: Myeloid-derived suppressor cells; DCs: Dendritic cells; CTLs: Cytotoxic T lymphocytes; TAMs: Tumor-associated macrophages; Tregs: Regulatory T lymphocytes; MDSCs: Myeloid-derived suppressor cells.

As we mentioned above, the tumor stroma of pancreatic cancer limits the efficacy of immunotherapy. Wang *et al*[133] reported a pH-responsive clustered nanoparticle (iCluster) loaded with both siPD-L1 and transforming growth factor-β (TGF-β) receptor inhibitors (LY2157299). iCluster can deliver siPD-L1 and LY2157299 to tumor blood vessels and then release small PAMAM at acidic tumor extracellular pH (pH_e). Therefore, siPD-L1 can penetrate into tumor tissue as deeply as possible to activate anticancer immunity, and a TGF-β receptor inhibitor can reduce the barrier function of the tumor stroma to help more drugs penetrate into the tumor tissue, further promoting the activation of anticancer immunity. Similarly, Yu *et al*[134] designed a size-adjustable nanoparticle consisting of IR780 containing the thermosensitive ICB drug (BMS-202) conjugated to HSA-BMS. Under mild hyperthermia therapy, this novel nanoparticle releases the small HSA-BMS into the tumor site and relieves the immunosuppressive environment to normalize immunity. In recent years, some studies have reported that RNA interference (RNAi) has emerged as a better agent for inducing anticancer immunity than antibodies or small molecules *in vivo*[135]. PLGA polymers have been proven to be a potentially excellent siRNA delivery vector exhibiting low toxicity, sustained release and the EPR effect[136,137]. Jung *et al*[138] developed a poly(lactic-co-glycolic) acid (PLGA)-based siRNA nanoparticle named siPD-L1@PLGA. siPD-L1@PLGA increased the infiltration of $CD8^+$ T cells and significantly inhibited tumor growth.

The poor immunogenicity and excessive immunosuppressive cancer microenvironment of pancreatic cancer result in a lack of adequate antigen-presenting cells in the tumor microenvironment. Lorkowski *et al*[139] reported a dual-immunostimulatory nanoparticle that was simultaneously loaded with a STING agonist and TLR4 agonist. These dual-immunostimulatory nanoparticles can be taken up by DCs in the tumor site to significantly increase the number of mature DCs and activate anticancer immunity in pancreatic cancer. Theoretically, cancer immunosuppressive cells mainly include TAMs, MDSCs and regulatory T cells (Tregs). Recent studies have shown that MDSCs are the major inhibitory immune cells in the immunosuppressive microenvironment of pancreatic cancer[140]. A previous study found that low-molecular-weight heparin-D-α-tocopheryl (LMWH) could significantly inhibit G-MDSC recruitment[141]. Therefore, Lu *et al*[142] designed a paclitaxel-loaded 3-aminophenylboronic acid-modified LMWH-based nanoparticle. This novel LMWH-based nanoparticle can inhibit the recruitment of MDSCs and weaken the immunosuppressive state.

Pyroptosis is a mode of programmed cell death[143]. Recent studies have shown that pyrophosis can induce powerful anticancer immunity[144-146]. However, pyrophosis is usually induced by chemotherapeutic drugs, which limits the applications of pyrophosis in drug-resistant tumors[147]. Ding *et al* [148] designed biodegradable K3ZrF7:Yb/Er UCNPs (ZrNPs) as self-therapeutic agents and pyrophosis

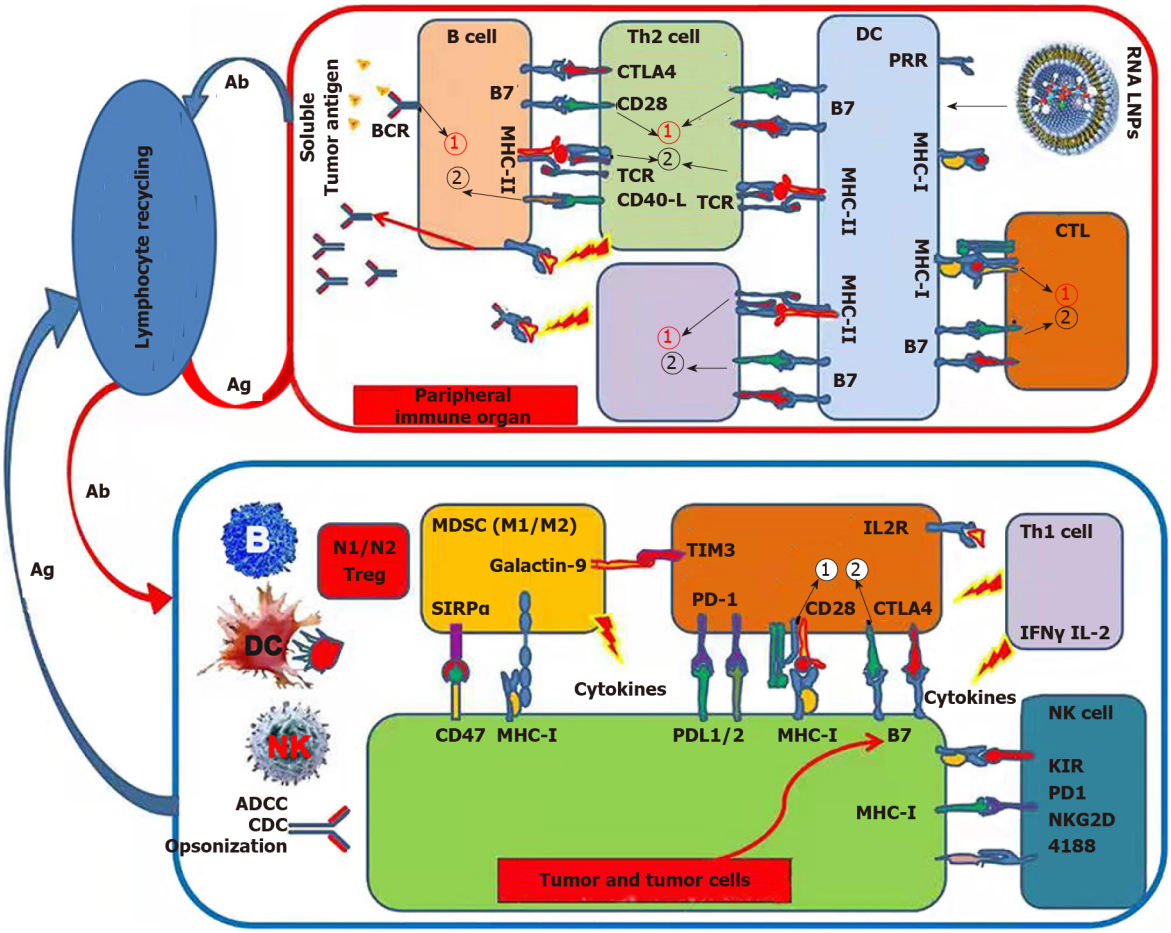


Figure 1 Tumor vaccine and tumor immunotherapy. Total tumor RNA was extracted and mixed with an immune adjuvant to formulate tumor vaccine. Tumor antigen was expressed and presented or cross-presented to Th and Tc cells by antigen presenting cells in lymph node to generate specific anti-tumor response. Citation: Zhang Y, Xie F, Yin Y, Zhang Q, Jin H, Wu Y, Pang L, Li J, Gao J. Immunotherapy of Tumor RNA-Loaded Lipid Nanoparticles Against Hepatocellular Carcinoma. Int J Nanomedicine 2021; 16: 1553-1564. Copyright ©The Authors 2011. Published by Dove Medical Press. The authors have obtained the permission for figure using from the Dove Medical Press Publishing Group (Supplementary material). Ab: Antibody; Ag: Antigen; BCR: B cell receptor; TCR: T-cell receptor; MHC: Major histocompatibility complex; PRR: Pattern recognition receptors; Th1/2: T helper type 1/2; CTL: Cytotoxic T-lymphocyte; CTLA4: Cytotoxic T-lymphocyte-associated protein 4; Treg: Regulatory T cell; DC: Dendritic cell; NK: Natural killer cell; MDSC: Mmyeloid-derived suppressor cell; ADCC: Antibody-dependent cellular cytotoxicity; CDC: Complement-dependent cytotoxicity; SIRPα: Signal regulatory protein α; LILRB1: Leukocyte immunoglobulin like receptor B1; TIM-3: T-cell immunoglobulin and mucin domain-3; PD1: Programmed cell death protein 1; PD-L1: Programmed death-ligand 1; IL-2: Interleukin-2; IFNγ: Interferon γ; KIR: Killer cell immunoglobulin-like receptor; NKG2D: Natural killer group 2 member D.

inducers for the first time. ZrNP can lead to osmotic pressure disorder and further result in an increase in ROS, the activation of caspase-1 protein, the cleavage of gasdermin, the maturation of interleukin-1β, and ultimately cytolysis. ZrNP-induced pyrophosis can lead to DC maturation and activate effector memory T cells, as well as inhibit tumor growth and metastasis.

Gemcitabine is among the most effective FDA-approved chemotherapy drugs to prolong survival in patients with pancreatic cancer. However, the immunosuppressive cancer microenvironment, especially the presence of TAMs, significantly weakens the efficacy of gemcitabine. It has even been reported that gemcitabine can induce an increase in TAMs and promote the establishment of a tumor-suppressive immune microenvironment, which further increases gemcitabine drug resistance[149]. Furthermore, gemcitabine can even induce an increase in TAMs and promote the establishment of an immunosuppressive tumor microenvironment, which further leads to gemcitabine drug resistance[150]. Thus, Wang *et al*[151] developed a biomimetic nanoparticle named PG@KMCM consisting of gemcitabine-loaded PLGA nanoparticles coated with stable M2-like macrophage targeting peptides (M2pep). Pancreatic cancer cell membranes can deliver PG@KMCM to pancreatic cancer and target M2-like macrophages by M2pep to reprogram TAMs and reverse gemcitabine drug resistance. Cao *et al*[152] also considered TAMs to be a therapeutic target and reported a reduction-responsive RNAi NDDS to regulate the function of TAMs and reprogram tumor lipid metabolism. On the one hand, this novel NDDS can block the activity of monoacylglycerol lipase (MGLL) by MGLL siRNA to reduce the production of free fatty acids and thus cut off the tumor's nutrition supply. On the other hand, MGLL blockade may lead to the accumulation of 2-arachidonoylglycerol, which can be secreted into the cancer microenvironment and activate the endocannabinoid receptor-2 (CB-2), which can transform TAMs into M2-like macrophages.

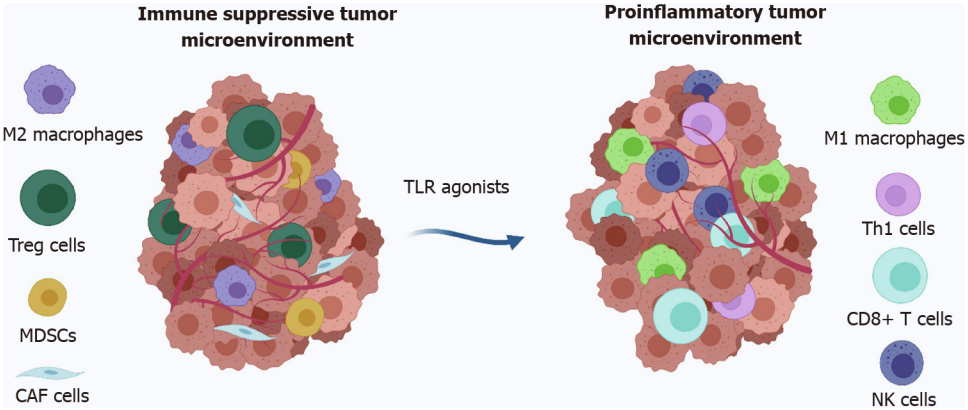


Figure 2 Altering an immunosuppressive tumor microenvironment into a pro-inflammatory microenvironment with the use of toll-like receptor agonists. Citation: Haegebaert RMS, Kempers M, Ceelen W, Lentacker I, Remaut K. Nanoparticle mediated targeting of toll-like receptors to treat colorectal cancer. Eur J Pharm Biopharm 2022; 172: 16-30. Copyright ©The Authors 2022. Published by Elsevier. The authors have obtained the permission for figure using from the Elsevier Publishing Group (Supplementary material). Treg: T regulatory cell; MDSCs: Myeloid-derived suppressor cells; CAF: Cancer-associated fibroblast; Th1: T-helper 1; $CD8^+$ T cells: Cytotoxic T cells; NK: Natural killer; TLR: Toll-like receptor.

Therefore, they prepared CB-2 siRNA to block CB-2 expression, preventing the transition of M2-like macrophages. The dual-RNAi NDDS developed in this research shows significant enhancement of the immunological environment in pancreatic cancer.

PTT has achieved satisfactory results in animal experiments, but it is difficult to apply widely in the clinic. The main reason is poor light penetration. It is harder to achieve the desired therapeutic effect for pancreatic cancer due to the depth of pancreatic cancer and the presence of the tumor stroma. To solve this conundrum, Wang *et al*[153] proposed magnetic resonance imaging (MRI)-guided interventional PTT (IPTT). They designed an iron oxide-based nanoparticle loaded with indocyanine green for PTT and imiquimod (IMQ) as an immunostimulant. IPTT can induce *in situ* cancer vaccination, which can be amplified by IMQ. In addition, iron oxide is a widely used MRI contrast agent. A recent study reported that iron oxide can modulate the cancer microenvironment by transforming M2-like macrophages into M1-like macrophages[154]. Overall, these novel iron oxide-based nanoparticles can improve therapeutic effects by directly killing cancer cells and activating the long-lasting immune effect by *in situ* vaccination and regulation of the immune microenvironment (Table 4).

FUTURE DIRECTIONS

In recent years, the increased development of immunotherapy has provided hope to patients with advanced cancer. Several ICB drugs have been approved by the FDA for clinical application in cancer treatment. However, due to the immunosuppressive microenvironment, only approximately 20% of patients can benefit from ICB treatment. In addition to ICB treatment, some conventional therapies, such as chemotherapy and radiotherapy, are also closely related to the immunosuppressive tumor microenvironment. The facts we mentioned above also exist in GIC. Therefore, we believe that in addition to ICB treatment, we should focus on reversing the immunosuppressive microenvironment in the future. Moreover, advances in nanotechnology have made drug delivery more efficient, allowing us to deliver drugs at specific times and locations based on the characteristics of the cancer and the drugs. We wondered whether the combination of nanotechnology and immunotherapy could achieve satisfactory therapeutic efficacy in GIC. Here, we summarize recent advances in immunotherapy-based novel nanoparticles in the treatment of GIC.

Since GC, HCC and CRC share similar tumor immune microenvironments, we will discuss the application of immunotherapy-based nanoparticles in these three kinds of GICs in the following paragraphs. Due to the limited monotherapy effect of ICB treatment, nanoparticles, as drug delivery vehicles, cannot significantly improve the therapeutic effect of ICB treatment. Thus, basically all ICB-based nanoparticles are combined with other therapeutic strategies. ICB treatment can reverse tumor immune escape from T cells. However, the low immunogenicity of the tumor results in insufficient T-cell infiltration in the tumor tissue. Hence, most studies have attempted to promote the therapeutic effect of ICB-based nanoparticles by inducing ICD.

ICD can increase tumor immunogenicity, but similar to ICB treatment, the immune-stimulating effect of ICD is limited. To amplify the ICD effect, some studies utilized the drug-loading capacity of nanoparticles and adopted a combination of multiple ICD inducers to enhance the immune response. Even so, we still do not recommend the combination of multiple ICD inducers to promote anticancer immunity. On the one hand, this strategy does not solve the problem of insufficient T-cell infiltration; on

Table 4 Overview of Immunotherapy-based novel nanoparticles in the treatment of pancreatic cancer [PubMed Search (immunotherapy) AND (nanoparticle) AND (pancreatic cancer)]

Type of nanoparticle	Treatment strategy	Drugs or active substance involved	The main involvement of immune cells	Ref.
Clustered nanoparticle	ICIs, TGF-β receptor inhibitors	LY2157299, siPD-L1	T cells	Wang *et al*[133]
HAS-Liposomes	ICD, ICIs, PTT	BMS-202, IR780	DCs, CTLs, T cells	Yu *et al*[134]
Copolymers	ICIs	siPD-L1	$CD8^+$T cells, NK cells	Jung *et al*[138]
LNPs	STING and TLR4 therapy	STING agonist, R4 agonist	DCs, Tregs, TAMs	Lorkowski *et al*[139]
Micellar nanoparticle	Inhibit G-MDSCs recruitment, chemotherapy	LMWH, PTX	G-MDSC, $CD8^+$T cells, $CD4^+$T cells	Lu *et al*[142]
UCNPs	Pyroptosis	K3ZrF7:Yb/Er UCNPs	DCs, memory T cells	Ding *et al*[148]
Cancer cell membrane with copolymers	ICIs, M2-macrophages targeting	M2pep, TAAs, PD-L1 antibody	TAMs, $CD8^+$T cells	Wang *et al*[151]
PDSA-based nanoplatform	Suppression of FFAs, repolarization of TAMs	siMGLL, siCB-2	TAMs	Cao *et al*[152]
Copolymers	PTT, immunotherapy	ICG, IMQ, IONs	TAMs, $CD8^+$T cells, $CD4^+$T cells, $CD4^+$T cells	Wang *et al*[153]
IONs	Repolarization of TAMs	Ferumoxytol	TAMs	Zanganeh *et al*[154]

ICIs: Immune checkpoint inhibitors; PD-L1: Programmed cell death ligand 1; TGF-β: Transforming growth factor-β; ICD: Immunogenic cell death; DCs: Dendritic cells; STING: Stimulator of interferon genes; LMWH: Low molecular weight heparin; MDSCs: Myeloid-derived suppressor cells; G-MDSCs: Granulocytic myeloid-derived suppressor cells; UCNPs: Upconversion nanoparticles; M2pep: Peptides targeting M2-like macrophages; TAAs: Tumor-associated antigens; PDSA: Poly (disulfide amide); FFAs: Free fatty acids; siMGLL: MGLL siRNA; siCB-2: CB-2 siRNA; ICG Indocyanine green; IMQ: Imiquimod; IONs: Iron oxide nanoparticles; PTX: Paclitaxel; PTT: Photothermal therapy; TAMs: Tumor-associated macrophages; Tregs: Regulatory T lymphocytes; TLR: Toll-like receptor.

the other hand, ICD inducers themselves can directly kill tumor cells. It is difficult to determine whether tumor inhibition is due to cytotoxicity or ICD-induced anticancer immunity.

Compared with ICD and ICB treatment, we believe that reprogramming the immunosuppressive tumor microenvironment by targeting inhibitory immune cells (*e.g.*, TAMs, Tregs and MDSCs) will be a revolutionary breakthrough in cancer immunotherapy in the future. Recently, many studies have attempted to successfully reprogram the tumor immune microenvironment by polarizing M2-like macrophages into M1-like macrophages. However, few reports have designed NDDSs to target Tregs and MDSCs in the tumor microenvironment. Therefore, it is of great significance to develop NDDSs for Tregs and MDSCs. In addition, the relationship between the intestinal flora and the immunosuppressive microenvironment of CRC also deserves future attention.

TLR agonists have also emerged as a promising treatment for cancer immunotherapy. However, due to the lack of targeting of TLR agonists, free TLR agonists often lead to serious systemic side effects. Therefore, it is necessary to deliver TLR agonists by nanoparticles. Numerous TLR agonists have been proven to be effective in stimulating anticancer immunity. In addition, combination therapies of TLR agonists with other immunotherapies are also anticipated. However, how to deliver TLR agonists to the tumor site stably and accurately and reduce serious systemic side effects are still problems that need prompt solutions.

With the successful large-scale clinical application of SARS-CoV-2 mRNA vaccines, research on cancer vaccines is also imminent. Due to the high heterogeneity of cancer, RNA vaccines are the best option. However, RNA is highly unstable. Liposomes, as mature NDDSs, can prepare cancer vaccines by encapsulating RNA. In addition, to improve the vaccine effect, NDDSs can be encapsulated with immune adjuvants to promote immune activation. RNA-based cancer vaccines, as a personalized cancer treatment strategy, can effectively improve anticancer immunity.

Next, we will discuss the application of immunotherapy-based nanoparticles in pancreatic cancer. Pancreatic cancer has several characteristics that are not found in other kinds of GICs, including the following: (1) Pancreatic cancer is surrounded by a tumor stroma, resulting in a physical barrier that isolates pancreatic cancer from the surrounding immune microenvironment; (2) Due to the anatomic position of the pancreas, pancreatic cancer is located deep in the abdominal cavity and therefore is not sensitive to PDT and PTT; and (3) Unlike other GICs, pancreatic cancer lacks blood supply and can adapt to nutrient deficiency and in a long-term hypoxic state.

To pass through the physical barrier of pancreatic cancer, size-adjusted NDDSs are the best option. Due to the deep location of pancreatic cancer, PTT has limited efficacy. Inspired by a previous study, we believe that IPTT and interventional PDT can be widely applied in the treatment of pancreatic cancer.

Additionally, interventional light-mediated therapy can be extended to GC, esophageal cancer and CRC, as well as HCC.

Compared with GC, HCC and CRC, pancreatic cancer has a similar immunosuppressive microenvironment, and the immunosuppressive situation is even worse. Most of the treatment strategies mentioned in GC, HCC and CRC can also be applied in pancreatic cancer. In previous reports, immunotherapy-based nanoparticles mainly used liposomes and copolymer nanoparticles, which are chemical synthesis products. Therefore, the nanoparticles can be designed according to demand. To increase biocompatibility and deliver tumor antigens, some literature has used tumor cell membranes to prepare biomimetic NDDSs, which have also achieved good results. In addition to the abovementioned nanoparticles, we particularly recommend small extracellular vesicles (also known as exosomes) as immunotherapy-based nanoparticles. First, exosomes are naturally nanosized. Second, similar to cell membrane vesicles, exosomes derived from tumor cells can carry tumor antigens. Third, exosomes can use surface modification to achieve biological functions, such as targeting. Last, exosomes have a certain drug delivery capacity. Thus, exosomes are potential immunotherapy-based nanoparticles for GIC that have not been reported in previous studies.

CONCLUSION

GIC is a common tumor worldwide. The immune microenvironments of GC, HCC, CRC and pancreatic cancer have similarities and differences. There are still many mechanisms of immune escape in GIC that are not well understood. Therefore, we need an in-depth understanding of the characteristics of each kind of GIC to take advantage of its characteristics and design immunotherapy-based nanoparticles.

FOOTNOTES

Author contributions: Ding YN and Ding HY wrote the paper; Ding YN, Li H, Gao CC and Wang LJ carried out reference searching; Yu WP and Tang QS made review and final editing; and all authors have read and agree to the published version of the manuscript.

Supported by the National Natural Science Foundation of China, No. 82102303; and Natural Science Foundation of Jiangsu Province, China, No. BK20210231.

Conflict-of-interest statement: All the authors report no relevant conflicts of interest for this article.

Open-Access: This article is an open-access article that was selected by an in-house editor and fully peer-reviewed by external reviewers. It is distributed in accordance with the Creative Commons Attribution NonCommercial (CC BY-NC 4.0) license, which permits others to distribute, remix, adapt, build upon this work non-commercially, and license their derivative works on different terms, provided the original work is properly cited and the use is non-commercial. See: https://creativecommons.org/Licenses/by-nc/4.0/

Country/Territory of origin: China

ORCID number: Yi-Nan Ding 0000-0002-1010-2874; Ming Xue 0000-0002-5178-6424; Qiu-Sha Tang 0000-0001-5701-0996; Li-Jun Wang 0000-0002-0208-0273; Hui-Yan Ding 0000-0002-5850-8080; Han Li 0000-0003-4174-8480; Cheng-Cheng Gao 0000-0002-9482-9535; Wei-Ping Yu 0000-0003-3968-3104.

S-Editor: Wang JJ
L-Editor: A
P-Editor: Wang JJ

REFERENCES

1 **Huang F**, Wang BR, Wu YQ, Wang FC, Zhang J, Wang YG. Oncolytic viruses against cancer stem cells: A promising approach for gastrointestinal cancer. *World J Gastroenterol* 2016; **22**: 7999-8009 [PMID: 27672294 DOI: 10.3748/wjg.v22.i35.7999]
2 **Siegel RL**, Miller KD, Fuchs HE, Jemal A. Cancer statistics, 2022. *CA Cancer J Clin* 2022; **72**: 7-33 [PMID: 35020204 DOI: 10.3322/caac.21708]
3 **Ferlay J**, Colombet M, Soerjomataram I, Parkin DM, Piñeros M, Znaor A, Bray F. Cancer statistics for the year 2020: An overview. *Int J Cancer* 2021 [PMID: 33818764 DOI: 10.1002/ijc.33588]
4 **Xia C**, Dong X, Li H, Cao M, Sun D, He S, Yang F, Yan X, Zhang S, Li N, Chen W. Cancer statistics in China and United States, 2022: profiles, trends, and determinants. *Chin Med J (Engl)* 2022; **135**: 584-590 [PMID: 35143424 DOI: 10.1097/CM9.0000000000002108]

5 **Neumann PA**, Berlet MW, Friess H. Surgical oncology in the age of multimodality therapy for cancer of the upper and lower gastrointestinal tract. *Expert Rev Anticancer Ther* 2021; **21**: 511-522 [PMID: 33355020 DOI: 10.1080/14737140.2021.1868991]

6 **Hamed OH**, Gusani NJ, Kimchi ET, Kavic SM. Minimally invasive surgery in gastrointestinal cancer: benefits, challenges, and solutions for underutilization. *JSLS* 2014; **18** [PMID: 25489209 DOI: 10.4293/JSLS.2014.00134]

7 **Pofahl WE**, Pories WJ. Current status and future directions of geriatric general surgery. *J Am Geriatr Soc* 2003; **51**: S351-S354 [PMID: 12823667 DOI: 10.1046/j.1365-2389.2003.51347.x]

8 **Ciabatti S**, Cammelli S, Frakulli R, Arcelli A, Macchia G, Deodato F, Cilla S, Giaccherini L, Buwenge M, Morganti AG. Radiotherapy of pancreatic cancer in older patients: A systematic review. *J Geriatr Oncol* 2019; **10**: 534-539 [PMID: 30270196 DOI: 10.1016/j.jgo.2018.09.007]

9 **Grabenbauer GG**, Holger G. Management of radiation and chemotherapy related acute toxicity in gastrointestinal cancer. *Best Pract Res Clin Gastroenterol* 2016; **30**: 655-664 [PMID: 27644912 DOI: 10.1016/j.bpg.2016.06.001]

10 **Sipaviciute A**, Sileika E, Burneckis A, Dulskas A. Late gastrointestinal toxicity after radiotherapy for rectal cancer: a systematic review. *Int J Colorectal Dis* 2020; **35**: 977-983 [PMID: 32296933 DOI: 10.1007/s00384-020-03595-x]

11 **Marin JJ**, Romero MR, Blazquez AG, Herraez E, Keck E, Briz O. Importance and limitations of chemotherapy among the available treatments for gastrointestinal tumours. *Anticancer Agents Med Chem* 2009; **9**: 162-184 [PMID: 19199863 DOI: 10.2174/187152009787313828]

12 **Kelly RJ**. Emerging Multimodality Approaches to Treat Localized Esophageal Cancer. *J Natl Compr Canc Netw* 2019; **17**: 1009-1014 [PMID: 31390584 DOI: 10.6004/jnccn.2019.7337]

13 **Metzger R**, Bollschweiler E, Hölscher AH, Warnecke-Eberz U. ERCC1: impact in multimodality treatment of upper gastrointestinal cancer. *Future Oncol* 2010; **6**: 1735-1749 [PMID: 21142660 DOI: 10.2217/fon.10.140]

14 **Tazawa H**, Kagawa S, Fujiwara T. MicroRNAs as potential target gene in cancer gene therapy of gastrointestinal tumors. *Expert Opin Biol Ther* 2011; **11**: 145-155 [PMID: 21219233 DOI: 10.1517/14712598.2011.542749]

15 **Rosenbaum MW**, Gonzalez RS. Targeted therapy for upper gastrointestinal tract cancer: current and future prospects. *Histopathology* 2021; **78**: 148-161 [PMID: 33382497 DOI: 10.1111/his.14244]

16 **Yano T**, Wang KK. Photodynamic Therapy for Gastrointestinal Cancer. *Photochem Photobiol* 2020; **96**: 517-523 [PMID: 31886891 DOI: 10.1111/php.13206]

17 **Hao M**, Kong C, Jiang C, Hou R, Zhao X, Li J, Wang Y, Gao Y, Zhang H, Yang B, Jiang J. Polydopamine-coated Au-Ag nanoparticle-guided photothermal colorectal cancer therapy through multiple cell death pathways. *Acta Biomater* 2019; **83**: 414-424 [PMID: 30366131 DOI: 10.1016/j.actbio.2018.10.032]

18 **Lee SY**, Shieh MJ. Platinum(II) Drug-Loaded Gold Nanoshells for Chemo-Photothermal Therapy in Colorectal Cancer. *ACS Appl Mater Interfaces* 2020; **12**: 4254-4264 [PMID: 31927943 DOI: 10.1021/acsami.9b18855]

19 **Ding Y**, Yang R, Yu W, Hu C, Zhang Z, Liu D, An Y, Wang X, He C, Liu P, Tang Q, Chen D. Chitosan oligosaccharide decorated liposomes combined with TH302 for photodynamic therapy in triple negative breast cancer. *J Nanobiotechnology* 2021; **19**: 147 [PMID: 34011362 DOI: 10.1186/s12951-021-00891-8]

20 **Zhang Y**, Xu J, Zhang N, Chen M, Wang H, Zhu D. Targeting the tumour immune microenvironment for cancer therapy in human gastrointestinal malignancies. *Cancer Lett* 2019; **458**: 123-135 [PMID: 31121212 DOI: 10.1016/j.canlet.2019.05.017]

21 **He M**, Yang T, Wang Y, Wang M, Chen X, Ding D, Zheng Y, Chen H. Immune Checkpoint Inhibitor-Based Strategies for Synergistic Cancer Therapy. *Adv Healthc Mater* 2021; **10**: e2002104 [PMID: 33709564 DOI: 10.1002/adhm.202002104]

22 **Sartor O**. Eligard: leuprolide acetate in a novel sustained-release delivery system. *Urology* 2003; **61**: 25-31 [PMID: 12667884 DOI: 10.1016/s0090-4295(02)02396-8]

23 FDA approves liposomal vincristine (Marqibo) for rare leukemia. *Oncology (Williston Park)* 2012; **26**: 841 [PMID: 23061340]

24 **Frampton JE**. Liposomal Irinotecan: A Review in Metastatic Pancreatic Adenocarcinoma. *Drugs* 2020; **80**: 1007-1018 [PMID: 32557396 DOI: 10.1007/s40265-020-01336-6]

25 **Safra T**, Muggia F, Jeffers S, Tsao-Wei DD, Groshen S, Lyass O, Henderson R, Berry G, Gabizon A. Pegylated liposomal doxorubicin (doxil): reduced clinical cardiotoxicity in patients reaching or exceeding cumulative doses of 500 mg/m^2. *Ann Oncol* 2000; **11**: 1029-1033 [PMID: 11038041 DOI: 10.1023/a:1008365716693]

26 **Yardley DA**. nab-Paclitaxel mechanisms of action and delivery. *J Control Release* 2013; **170**: 365-372 [PMID: 23770008 DOI: 10.1016/j.jconrel.2013.05.041]

27 **Duvic M**, Talpur R. Optimizing denileukin diftitox (Ontak) therapy. *Future Oncol* 2008; **4**: 457-469 [PMID: 18684057 DOI: 10.2217/14796694.4.4.457]

28 **Rivera Gil P**, Hühn D, del Mercato LL, Sasse D, Parak WJ. Nanopharmacy: Inorganic nanoscale devices as vectors and active compounds. *Pharmacol Res* 2010; **62**: 115-125 [PMID: 20097288 DOI: 10.1016/j.phrs.2010.01.009]

29 **Ding Y**, Wang L, Li H, Miao F, Zhang Z, Hu C, Yu W, Tang Q, Shao G. Application of lipid nanovesicle drug delivery system in cancer immunotherapy. *J Nanobiotechnology* 2022; **20**: 214 [PMID: 35524277 DOI: 10.1186/s12951-022-01429-2]

30 DaunoXome approved. *AIDS Patient Care STDS* 1996; **10**: 263 [PMID: 11361607]

31 **Bost JP**, Barriga H, Holme MN, Gallud A, Maugeri M, Gupta D, Lehto T, Valadi H, Esbjörner EK, Stevens MM, El-Andaloussi S. Delivery of Oligonucleotide Therapeutics: Chemical Modifications, Lipid Nanoparticles, and Extracellular Vesicles. *ACS Nano* 2021; **15**: 13993-14021 [PMID: 34505766 DOI: 10.1021/acsnano.1c05099]

32 **Zou S**, Wang B, Wang C, Wang Q, Zhang L. Cell membrane-coated nanoparticles: research advances. *Nanomedicine (Lond)* 2020; **15**: 625-641 [PMID: 32098564 DOI: 10.2217/nnm-2019-0388]

33 **Huang R**, Cai GQ, Li J, Li XS, Liu HT, Shang XL, Zhou JD, Nie XM, Gui R. Platelet membrane-camouflaged silver metal-organic framework drug system against infections caused by methicillin-resistant Staphylococcus aureus. *J Nanobiotechnology* 2021; **19**: 229 [PMID: 34348721 DOI: 10.1186/s12951-021-00978-2]

34 **Jing B**, Qian R, Jiang D, Gai Y, Liu Z, Guo F, Ren S, Gao Y, Lan X, An R. Extracellular vesicles-based pre-targeting strategy enables multi-modal imaging of orthotopic colon cancer and image-guided surgery. *J Nanobiotechnology* 2021; **19**: 151 [PMID: 34022897 DOI: 10.1186/s12951-021-00888-3]

35 **Moulahoum H**, Ghorbanizamani F, Zihnioglu F, Timur S. Surface Biomodification of Liposomes and Polymersomes for Efficient Targeted Drug Delivery. *Bioconjug Chem* 2021; **32**: 1491-1502 [PMID: 34283580 DOI: 10.1021/acs.bioconjchem.1c00285]

36 **He C**, Ding H, Chen J, Ding Y, Yang R, Hu C, An Y, Liu D, Liu P, Tang Q, Zhang Z. Immunogenic Cell Death Induced by Chemoradiotherapy of Novel pH-Sensitive Cargo-Loaded Polymersomes in Glioblastoma. *Int J Nanomedicine* 2021; **16**: 7123-7135 [PMID: 34712045 DOI: 10.2147/IJN.S333197]

37 **He C**, Zhang Z, Ding Y, Xue K, Wang X, Yang R, An Y, Liu D, Hu C, Tang Q. LRP1-mediated pH-sensitive polymersomes facilitate combination therapy of glioblastoma *in vitro* and in vivo. *J Nanobiotechnology* 2021; **19**: 29 [PMID: 33482822 DOI: 10.1186/s12951-020-00751-x]

38 **Han Y**, An Y, Jia G, Wang X, He C, Ding Y, Tang Q. Facile assembly of upconversion nanoparticle-based micelles for active targeted dual-mode imaging in pancreatic cancer. *J Nanobiotechnology* 2018; **16**: 7 [PMID: 29378593 DOI: 10.1186/s12951-018-0335-4]

39 **Xu W**, Qing X, Liu S, Chen Z, Zhang Y. Manganese oxide nanomaterials for bacterial infection detection and therapy. *J Mater Chem B* 2022; **10**: 1343-1358 [PMID: 35129557 DOI: 10.1039/d1tb02646a]

40 **Connor DM**, Broome AM. Gold Nanoparticles for the Delivery of Cancer Therapeutics. *Adv Cancer Res* 2018; **139**: 163-184 [PMID: 29941104 DOI: 10.1016/bs.acr.2018.05.001]

41 **Zhang X**, Lu Y, Jia D, Qiu W, Ma X, Zhang X, Xu Z, Wen F. Acidic microenvironment responsive polymeric MOF-based nanoparticles induce immunogenic cell death for combined cancer therapy. *J Nanobiotechnology* 2021; **19**: 455 [PMID: 34963499 DOI: 10.1186/s12951-021-01217-4]

42 **Iranpour S**, Bahrami AR, Nekooei S, Sh Saljooghi A, Matin MM. Improving anti-cancer drug delivery performance of magnetic mesoporous silica nanocarriers for more efficient colorectal cancer therapy. *J Nanobiotechnology* 2021; **19**: 314 [PMID: 34641857 DOI: 10.1186/s12951-021-01056-3]

43 **Smyth EC**, Nilsson M, Grabsch HI, van Grieken NC, Lordick F. Gastric cancer. *Lancet* 2020; **396**: 635-648 [PMID: 32861308 DOI: 10.1016/S0140-6736(20)31288-5]

44 **Menges M**, Hoehler T. Current strategies in systemic treatment of gastric cancer and cancer of the gastroesophageal junction. *J Cancer Res Clin Oncol* 2009; **135**: 29-38 [PMID: 18523800 DOI: 10.1007/s00432-008-0425-z]

45 **Sasaki Y**, Nishina T, Yasui H, Goto M, Muro K, Tsuji A, Koizumi W, Toh Y, Hara T, Miyata Y. Phase II trial of nanoparticle albumin-bound paclitaxel as second-line chemotherapy for unresectable or recurrent gastric cancer. *Cancer Sci* 2014; **105**: 812-817 [PMID: 24716542 DOI: 10.1111/cas.12419]

46 **Avgustinovich AV**, Bakina OV, Afanas'ev SG, Cheremisina OV, Spirina LV, Dobrodeev AY, Buldakov M, Choynzonov EL. Nanoparticles in Gastric Cancer Management. *Curr Pharm Des* 2021; **27**: 2436-2444 [PMID: 33222664 DOI: 10.2174/1381612826666201120155120]

47 **Zhao Q**, Cao L, Guan L, Bie L, Wang S, Xie B, Chen X, Shen X, Cao F. Immunotherapy for gastric cancer: dilemmas and prospect. *Brief Funct Genomics* 2019; **18**: 107-112 [PMID: 30388190 DOI: 10.1093/bfgp/ely019]

48 **Nakamura M**, Ojima T, Katsuda M, Hayata K, Kitadani J, Nakamori M, Yamaue H. Phase 1 Study of Combined Chemotherapy of Nab-Paclitaxel, S-1, and Oxaliplatin for Gastric Cancer with Peritoneal Metastasis (NSOX Study). *Oncology* 2021; **99**: 57-61 [PMID: 32877909 DOI: 10.1159/000509396]

49 **Han Y**, Liu D, Li L. PD-1/PD-L1 pathway: current researches in cancer. *Am J Cancer Res* 2020; **10**: 727-742 [PMID: 32266087]

50 **Xu S**, Cui F, Huang D, Zhang D, Zhu A, Sun X, Cao Y, Ding S, Wang Y, Gao E, Zhang F. PD-L1 monoclonal antibody-conjugated nanoparticles enhance drug delivery level and chemotherapy efficacy in gastric cancer cells. *Int J Nanomedicine* 2019; **14**: 17-32 [PMID: 30587982 DOI: 10.2147/IJN.S175340]

51 **Sharma P**, Allison JP. Immune checkpoint targeting in cancer therapy: toward combination strategies with curative potential. *Cell* 2015; **161**: 205-214 [PMID: 25860605 DOI: 10.1016/j.cell.2015.03.030]

52 **Hu N**, Li W, Hong Y, Zeng Z, Zhang J, Wu X, Zhou K, Wu F. A PD1 targeted nano-delivery system based on epigenetic alterations of T cell responses in the treatment of gastric cancer. *Mol Ther Oncolytics* 2022; **24**: 148-159 [PMID: 35024441 DOI: 10.1016/j.omto.2021.12.006]

53 **Kumagai S**, Togashi Y, Sakai C, Kawazoe A, Kawazu M, Ueno T, Sato E, Kuwata T, Kinoshita T, Yamamoto M, Nomura S, Tsukamoto T, Mano H, Shitara K, Nishikawa H. An Oncogenic Alteration Creates a Microenvironment that Promotes Tumor Progression by Conferring a Metabolic Advantage to Regulatory T Cells. *Immunity* 2020; **53**: 187-203.e8 [PMID: 32640259 DOI: 10.1016/j.immuni.2020.06.016]

54 **Guo W**, Chen Z, Li Z, Huang H, Ren Y, Zhao B, Li G, Hu Y. Improved immunotherapy for gastric cancer by nanocomposites with capability of triggering Dual-Damage of Nuclear/Mitochondrial DNA and cGAS/STING-Mediated innate immunity. *Chem Eng J* 2022; **443**: 136428 [DOI: 10.1016/j.cej.2022.136428]

55 **Pan Y**, Yu Y, Wang X, Zhang T. Tumor-Associated Macrophages in Tumor Immunity. *Front Immunol* 2020; **11**: 583084 [PMID: 33365025 DOI: 10.3389/fimmu.2020.583084]

56 **Cheng N**, Bai X, Shu Y, Ahmad O, Shen P. Targeting tumor-associated macrophages as an antitumor strategy. *Biochem Pharmacol* 2021; **183**: 114354 [PMID: 33279498 DOI: 10.1016/j.bcp.2020.114354]

57 **Zhang J**, Jiang M, Li S, Zhang Z, Sun H, Yang F, Liang H. Developing a Novel Anticancer Gold(III) Agent to Integrate Chemotherapy and Immunotherapy. *J Med Chem* 2021; **64**: 6777-6791 [PMID: 34000198 DOI: 10.1021/acs.jmedchem.1c00050]

58 **Morse MA**, Gwin WR 3rd, Mitchell DA. Vaccine Therapies for Cancer: Then and Now. *Target Oncol* 2021; **16**: 121-152 [PMID: 33512679 DOI: 10.1007/s11523-020-00788-w]

59 **Liu BY**, Chen XH, Gu QL, Li JF, Yin HR, Zhu ZG, Lin YZ. Antitumor effects of vaccine consisting of dendritic cells pulsed with tumor RNA from gastric cancer. *World J Gastroenterol* 2004; **10**: 630-633 [PMID: 14991927 DOI: 10.3748/wjg.v10.i5.630]

60 **Wu Y**, Wang L, Zhang Y. Dendritic cells as vectors for immunotherapy of tumor and its application for gastric cancer therapy. *Cell Mol Immunol* 2004; **1**: 351-356 [PMID: 16285894]

61 **Kohnepoushi C**, Nejati V, Delirezh N, Biparva P. Poly Lactic-co-Glycolic Acid Nanoparticles Containing Human Gastric Tumor Lysates as Antigen Delivery Vehicles for Dendritic Cell-Based Antitumor Immunotherapy. *Immunol Invest* 2019; **48**: 794-808 [PMID: 31094258 DOI: 10.1080/08820139.2019.1610889]

62 **Banstola A**, Jeong JH, Yook S. Immunoadjuvants for cancer immunotherapy: A review of recent developments. *Acta Biomater* 2020; **114**: 16-30 [PMID: 32777293 DOI: 10.1016/j.actbio.2020.07.063]

63 **Bode C**, Zhao G, Steinhagen F, Kinjo T, Klinman DM. CpG DNA as a vaccine adjuvant. *Expert Rev Vaccines* 2011; **10**: 499-511 [PMID: 21506647 DOI: 10.1586/erv.10.174]

64 **Zhang J**, Zhao T, Han F, Hu Y, Li Y. Photothermal and gene therapy combined with immunotherapy to gastric cancer by the gold nanoshell-based system. *J Nanobiotechnology* 2019; **17**: 80 [PMID: 31277667 DOI: 10.1186/s12951-019-0515-x]

65 **Xu XF**, Xing H, Han J, Li ZL, Lau WY, Zhou YH, Gu WM, Wang H, Chen TH, Zeng YY, Li C, Wu MC, Shen F, Yang T. Risk Factors, Patterns, and Outcomes of Late Recurrence After Liver Resection for Hepatocellular Carcinoma: A Multicenter Study From China. *JAMA Surg* 2019; **154**: 209-217 [PMID: 30422241 DOI: 10.1001/jamasurg.2018.4334]

66 **Wang DX**, Yang X, Lin JZ, Bai Y, Long JY, Yang XB, Seery S, Zhao HT. Efficacy and safety of lenvatinib for patients with advanced hepatocellular carcinoma: A retrospective, real-world study conducted in China. *World J Gastroenterol* 2020; **26**: 4465-4478 [PMID: 32874058 DOI: 10.3748/wjg.v26.i30.4465]

67 **Lou T**, Li B, Xiong P, Jin C, Chen Y. External validation of hepatocellular carcinoma risk scores in patients with chronic hepatitis B virus infection in China. *J Viral Hepat* 2021; **28**: 1373-1380 [PMID: 34218498 DOI: 10.1111/jvh.13569]

68 **Qing X**, Xu W, Zong J, Du X, Peng H, Zhang Y. Emerging treatment modalities for systemic therapy in hepatocellular carcinoma. *Biomark Res* 2021; **9**: 64 [PMID: 34419152 DOI: 10.1186/s40364-021-00319-3]

69 **Kumari P**, Ghosh B, Biswas S. Nanocarriers for cancer-targeted drug delivery. *J Drug Target* 2016; **24**: 179-191 [PMID: 26061298 DOI: 10.3109/1061186X.2015.1051049]

70 **Jia G**, Han Y, An Y, Ding Y, He C, Wang X, Tang Q. NRP-1 targeted and cargo-loaded exosomes facilitate simultaneous imaging and therapy of glioma in vitro and in vivo. *Biomaterials* 2018; **178**: 302-316 [PMID: 29982104 DOI: 10.1016/j.biomaterials.2018.06.029]

71 **An Y**, Yang R, Wang X, Han Y, Jia G, Hu C, Zhang Z, Liu D, Tang Q. Facile Assembly of Thermosensitive Liposomes for Active Targeting Imaging and Synergetic Chemo-/Magnetic Hyperthermia Therapy. *Front Bioeng Biotechnol* 2021; **9**: 691091 [PMID: 34422777 DOI: 10.3389/fbioe.2021.691091]

72 **Lee YH**, Tai D, Yip C, Choo SP, Chew V. Combinational Immunotherapy for Hepatocellular Carcinoma: Radiotherapy, Immune Checkpoint Blockade and Beyond. *Front Immunol* 2020; **11**: 568759 [PMID: 33117354 DOI: 10.3389/fimmu.2020.568759]

73 **Yau T**, Kang Y-K, Kim T-Y, El-Khoueiry AB, Santoro A, Sangro B, Melero I, Kudo M, Hou M-M, Matilla A, Tovoli F, Knox JJ, He AR, El-Rayes BF, Acosta-Rivera M, Neely J, Shen Y, Baccan C, Cruz CMD, Hsu C. Nivolumab (NIVO) + ipilimumab (IPI) combination therapy in patients (pts) with advanced hepatocellular carcinoma (aHCC): Results from CheckMate 040. *J Clin Oncol* 2019; **37**: 4012-4012 [DOI: 10.1200/JCO.2019.37.15_suppl.4012]

74 **Galluzzi L**, Vitale I, Warren S, Adjemian S, Agostinis P, Martinez AB, Chan TA, Coukos G, Demaria S, Deutsch E, Draganov D, Edelson RL, Formenti SC, Fucikova J, Gabriele L, Gaipl US, Gameiro SR, Garg AD, Golden E, Han J, Harrington KJ, Hemminki A, Hodge JW, Hossain DMS, Illidge T, Karin M, Kaufman HL, Kepp O, Kroemer G, Lasarte JJ, Loi S, Lotze MT, Manic G, Merghoub T, Melcher AA, Mossman KL, Prosper F, Rekdal Ø, Rescigno M, Riganti C, Sistigu A, Smyth MJ, Spisek R, Stagg J, Strauss BE, Tang D, Tatsuno K, van Gool SW, Vandenabeele P, Yamazaki T, Zamarin D, Zitvogel L, Cesano A, Marincola FM. Consensus guidelines for the definition, detection and interpretation of immunogenic cell death. *J Immunother Cancer* 2020; **8** [PMID: 32209603 DOI: 10.1136/jitc-2019-000337]

75 **Xu J**, Zheng Q, Cheng X, Hu S, Zhang C, Zhou X, Sun P, Wang W, Su Z, Zou T, Song Z, Xia Y, Yi X, Gao Y. Chemo-photodynamic therapy with light-triggered disassembly of theranostic nanoplatform in combination with checkpoint blockade for immunotherapy of hepatocellular carcinoma. *J Nanobiotechnology* 2021; **19**: 355 [PMID: 34717654 DOI: 10.1186/s12951-021-01101-1]

76 **Chang F**, Syrjänen S, Syrjänen K. Implications of the p53 tumor-suppressor gene in clinical oncology. *J Clin Oncol* 1995; **13**: 1009-1022 [PMID: 7707100 DOI: 10.1200/JCO.1995.13.4.1009]

77 **Harris CC**. Structure and function of the p53 tumor suppressor gene: clues for rational cancer therapeutic strategies. *J Natl Cancer Inst* 1996; **88**: 1442-1455 [PMID: 8841019 DOI: 10.1093/jnci/88.20.1442]

78 **Xu L**, Pirollo KF, Chang EH. Tumor-targeted p53-gene therapy enhances the efficacy of conventional chemo/radiotherapy. *J Control Release* 2001; **74**: 115-128 [PMID: 11489488 DOI: 10.1016/s0168-3659(01)00324-8]

79 **Cui Y**, Guo G. Immunomodulatory Function of the Tumor Suppressor p53 in Host Immune Response and the Tumor Microenvironment. *Int J Mol Sci* 2016; **17** [PMID: 27869779 DOI: 10.3390/ijms17111942]

80 **Blagih J**, Buck MD, Vousden KH. p53, cancer and the immune response. *J Cell Sci* 2020; **133** [PMID: 32144194 DOI: 10.1242/jcs.237453]

81 **Bezzi M**, Seitzer N, Ishikawa T, Reschke M, Chen M, Wang G, Mitchell C, Ng C, Katon J, Lunardi A, Signoretti S, Clohessy JG, Zhang J, Pandolfi PP. Diverse genetic-driven immune landscapes dictate tumor progression through distinct mechanisms. *Nat Med* 2018; **24**: 165-175 [PMID: 29309058 DOI: 10.1038/nm.4463]

82 **Guo G**, Yu M, Xiao W, Celis E, Cui Y. Local Activation of p53 in the Tumor Microenvironment Overcomes Immune Suppression and Enhances Antitumor Immunity. *Cancer Res* 2017; **77**: 2292-2305 [PMID: 28280037 DOI: 10.1158/0008-5472.CAN-16-2832]

83 **Xiao Y**, Chen J, Zhou H, Zeng X, Ruan Z, Pu Z, Jiang X, Matsui A, Zhu L, Amoozgar Z, Chen DS, Han X, Duda DG, Shi J. Combining p53 mRNA nanotherapy with immune checkpoint blockade reprograms the immune microenvironment for effective cancer therapy. *Nat Commun* 2022; **13**: 758 [PMID: 35140208 DOI: 10.1038/s41467-022-28279-8]

84 **Li B**, Zhang X, Wu Z, Chu T, Yang Z, Xu S, Wu S, Qie Y, Lu Z, Qi F, Hu M, Zhao G, Wei J, Zhao Y, Nie G, Meng H, Liu R, Li S. Reducing Postoperative Recurrence of Early-Stage Hepatocellular Carcinoma by a Wound-Targeted

Nanodrug. *Adv Sci (Weinh)* 2022; **9**: e2200477 [PMID: 35524631 DOI: 10.1002/advs.202200477]
85 **Yu Z**, Guo J, Hu M, Gao Y, Huang L. Icaritin Exacerbates Mitophagy and Synergizes with Doxorubicin to Induce Immunogenic Cell Death in Hepatocellular Carcinoma. *ACS Nano* 2020; **14**: 4816-4828 [PMID: 32188241 DOI: 10.1021/acsnano.0c00708]
86 **Li Z**, Wu T, Zheng B, Chen L. Individualized precision treatment: Targeting TAM in HCC. *Cancer Lett* 2019; **458**: 86-91 [PMID: 31129147 DOI: 10.1016/j.canlet.2019.05.019]
87 **Wang Y**, Tiruthani K, Li S, Hu M, Zhong G, Tang Y, Roy S, Zhang L, Tan J, Liao C, Liu R. mRNA Delivery of a Bispecific Single-Domain Antibody to Polarize Tumor-Associated Macrophages and Synergize Immunotherapy against Liver Malignancies. *Adv Mater* 2021; **33**: e2007603 [PMID: 33945178 DOI: 10.1002/adma.202007603]
88 **Kabakov AE**, Yakimova AO. Hypoxia-Induced Cancer Cell Responses Driving Radioresistance of Hypoxic Tumors: Approaches to Targeting and Radiosensitizing. *Cancers (Basel)* 2021; **13** [PMID: 33806538 DOI: 10.3390/cancers13051102]
89 **Manoochehri Khoshinani H**, Afshar S, Najafi R. Hypoxia: A Double-Edged Sword in Cancer Therapy. *Cancer Invest* 2016; **34**: 536-545 [PMID: 27824512 DOI: 10.1080/07357907.2016.1245317]
90 **Boutilier AJ**, Elsawa SF. Macrophage Polarization States in the Tumor Microenvironment. *Int J Mol Sci* 2021; **22** [PMID: 34209703 DOI: 10.3390/ijms22136995]
91 **Dai X**, Ruan J, Guo Y, Sun Z, Liu J, Bao X, Zhang H, Li Q, Ye C, Wang X, Zhao CX, Zhou F, Sheng J, Chen D, Zhao P. Enhanced radiotherapy efficacy and induced anti-tumor immunity in HCC by improving hypoxia microenvironment using oxygen microcapsules. *Chem Eng J* 2021; **422**: 130109 [DOI: 10.1016/j.cej.2021.130109]
92 **Yang M**, Zhang C. The role of liver sinusoidal endothelial cells in cancer liver metastasis. *Am J Cancer Res* 2021; **11**: 1845-1860 [PMID: 34094657]
93 **Yu Z**, Guo J, Liu Y, Wang M, Liu Z, Gao Y, Huang L. Nano delivery of simvastatin targets liver sinusoidal endothelial cells to remodel tumor microenvironment for hepatocellular carcinoma. *J Nanobiotechnology* 2022; **20**: 9 [PMID: 34983554 DOI: 10.1186/s12951-021-01205-8]
94 **Kon E**, Elia U, Peer D. Principles for designing an optimal mRNA lipid nanoparticle vaccine. *Curr Opin Biotechnol* 2022; **73**: 329-336 [PMID: 34715546 DOI: 10.1016/j.copbio.2021.09.016]
95 **Gebre MS**, Brito LA, Tostanoski LH, Edwards DK, Carfi A, Barouch DH. Novel approaches for vaccine development. *Cell* 2021; **184**: 1589-1603 [PMID: 33740454 DOI: 10.1016/j.cell.2021.02.030]
96 **Huang H**, Zhang C, Yang S, Xiao W, Zheng Q, Song X. The investigation of mRNA vaccines formulated in liposomes administrated in multiple routes against SARS-CoV-2. *J Control Release* 2021; **335**: 449-456 [PMID: 34029632 DOI: 10.1016/j.jconrel.2021.05.024]
97 **Szebeni J**, Storm G, Ljubimova JY, Castells M, Phillips EJ, Turjeman K, Barenholz Y, Crommelin DJA, Dobrovolskaia MA. Applying lessons learned from nanomedicines to understand rare hypersensitivity reactions to mRNA-based SARS-CoV-2 vaccines. *Nat Nanotechnol* 2022; **17**: 337-346 [PMID: 35393599 DOI: 10.1038/s41565-022-01071-x]
98 **Zhang Y**, Xie F, Yin Y, Zhang Q, Jin H, Wu Y, Pang L, Li J, Gao J. Immunotherapy of Tumor RNA-Loaded Lipid Nanoparticles Against Hepatocellular Carcinoma. *Int J Nanomedicine* 2021; **16**: 1553-1564 [PMID: 33658783 DOI: 10.2147/IJN.S291421]
99 **Siegel RL**, Miller KD, Jemal A. Cancer statistics, 2020. *CA Cancer J Clin* 2020; **70**: 7-30 [PMID: 31912902 DOI: 10.3322/caac.21590]
100 **Ladabaum U**, Dominitz JA, Kahi C, Schoen RE. Strategies for Colorectal Cancer Screening. *Gastroenterology* 2020; **158**: 418-432 [PMID: 31394083 DOI: 10.1053/j.gastro.2019.06.043]
101 **Sagaert X**, Vanstapel A, Verbeek S. Tumor Heterogeneity in Colorectal Cancer: What Do We Know So Far? *Pathobiology* 2018; **85**: 72-84 [PMID: 29414818 DOI: 10.1159/000486721]
102 **Siegel RL**, Miller KD, Fedewa SA, Ahnen DJ, Meester RGS, Barzi A, Jemal A. Colorectal cancer statistics, 2017. *CA Cancer J Clin* 2017; **67**: 177-193 [PMID: 28248415 DOI: 10.3322/caac.21395]
103 **Bai J**, Chen H, Bai X. Relationship between microsatellite status and immune microenvironment of colorectal cancer and its application to diagnosis and treatment. *J Clin Lab Anal* 2021; **35**: e23810 [PMID: 33938589 DOI: 10.1002/jcla.23810]
104 **Krasteva N**, Georgieva M. Promising Therapeutic Strategies for Colorectal Cancer Treatment Based on Nanomaterials. *Pharmaceutics* 2022; **14** [PMID: 35745786 DOI: 10.3390/pharmaceutics14061213]
105 **Liu H**, Xu C, Meng M, Li S, Sheng S, Zhang S, Ni W, Tian H, Wang Q. Metal-organic framework-mediated multifunctional nanoparticles for combined chemo-photothermal therapy and enhanced immunotherapy against colorectal cancer. *Acta Biomater* 2022; **144**: 132-141 [PMID: 35307591 DOI: 10.1016/j.actbio.2022.03.023]
106 **Wangmo D**, Premsrirut PK, Yuan C, Morris WS, Zhao X, Subramanian S. ACKR4 in Tumor Cells Regulates Dendritic Cell Migration to Tumor-Draining Lymph Nodes and T-Cell Priming. *Cancers (Basel)* 2021; **13** [PMID: 34638505 DOI: 10.3390/cancers13195021]
107 **Yuan Z**, Fan G, Wu H, Liu C, Zhan Y, Qiu Y, Shou C, Gao F, Zhang J, Yin P, Xu K. Photodynamic therapy synergizes with PD-L1 checkpoint blockade for immunotherapy of CRC by multifunctional nanoparticles. *Mol Ther* 2021; **29**: 2931-2948 [PMID: 34023507 DOI: 10.1016/j.ymthe.2021.05.017]
108 **Zhu Q**, Sun F, Li T, Zhou M, Ye J, Ji A, Wang H, Ding C, Chen H, Xu Z, Yu H. Engineering Oxaliplatin Prodrug Nanoparticles for Second Near-Infrared Fluorescence Imaging-Guided Immunotherapy of Colorectal Cancer. *Small* 2021; **17**: e2007882 [PMID: 33690984 DOI: 10.1002/smll.202007882]
109 **Li J**, Zhao M, Sun M, Wu S, Zhang H, Dai Y, Wang D. Multifunctional Nanoparticles Boost Cancer Immunotherapy Based on Modulating the Immunosuppressive Tumor Microenvironment. *ACS Appl Mater Interfaces* 2020; **12**: 50734-50747 [PMID: 33124808 DOI: 10.1021/acsami.0c14909]
110 **Liang C**, Zhang X, Yang M, Dong X. Recent Progress in Ferroptosis Inducers for Cancer Therapy. *Adv Mater* 2019; **31**: e1904197 [PMID: 31595562 DOI: 10.1002/adma.201904197]
111 **Duan X**, Chan C, Han W, Guo N, Weichselbaum RR, Lin W. Immunostimulatory nanomedicines synergize with checkpoint blockade immunotherapy to eradicate colorectal tumors. *Nat Commun* 2019; **10**: 1899 [PMID: 31015397 DOI: 10.1038/s41467-019-09221-x]

112 **Haegebaert RMS**, Kempers M, Ceelen W, Lentacker I, Remaut K. Nanoparticle mediated targeting of toll-like receptors to treat colorectal cancer. *Eur J Pharm Biopharm* 2022; **172**: 16-30 [PMID: 35074555 DOI: 10.1016/j.ejpb.2022.01.002]

113 **Bahmani B**, Gong H, Luk BT, Haushalter KJ, DeTeresa E, Previti M, Zhou J, Gao W, Bui JD, Zhang L, Fang RH, Zhang J. Intratumoral immunotherapy using platelet-cloaked nanoparticles enhances antitumor immunity in solid tumors. *Nat Commun* 2021; **12**: 1999 [PMID: 33790276 DOI: 10.1038/s41467-021-22311-z]

114 **Luo Y**, Yang J, Yu J, Liu X, Yu C, Hu J, Shi H, Ma X. Long Non-coding RNAs: Emerging Roles in the Immunosuppressive Tumor Microenvironment. *Front Oncol* 2020; **10**: 48 [PMID: 32083005 DOI: 10.3389/fonc.2020.00048]

115 **Huang D**, Chen J, Yang L, Ouyang Q, Li J, Lao L, Zhao J, Liu J, Lu Y, Xing Y, Chen F, Su F, Yao H, Liu Q, Su S, Song E. NKILA lncRNA promotes tumor immune evasion by sensitizing T cells to activation-induced cell death. *Nat Immunol* 2018; **19**: 1112-1125 [PMID: 30224822 DOI: 10.1038/s41590-018-0207-y]

116 **Zheng Y**, Tian X, Wang T, Xia X, Cao F, Tian J, Xu P, Ma J, Xu H, Wang S. Long noncoding RNA Pvt1 regulates the immunosuppression activity of granulocytic myeloid-derived suppressor cells in tumor-bearing mice. *Mol Cancer* 2019; **18**: 61 [PMID: 30925926 DOI: 10.1186/s12943-019-0978-2]

117 **Liu F**, Dai Z, Cheng Q, Xu L, Huang L, Liu Z, Li X, Wang N, Wang G, Wang L, Wang Z. LncRNA-targeting bio-scaffold mediates triple immune effects for postoperative colorectal cancer immunotherapy. *Biomaterials* 2022; **284**: 121485 [PMID: 35367839 DOI: 10.1016/j.biomaterials.2022.121485]

118 **Tilg H**, Adolph TE, Gerner RR, Moschen AR. The Intestinal Microbiota in Colorectal Cancer. *Cancer Cell* 2018; **33**: 954-964 [PMID: 29657127 DOI: 10.1016/j.ccell.2018.03.004]

119 **Louis P**, Hold GL, Flint HJ. The gut microbiota, bacterial metabolites and colorectal cancer. *Nat Rev Microbiol* 2014; **12**: 661-672 [PMID: 25198138 DOI: 10.1038/nrmicro3344]

120 **Kostic AD**, Chun E, Robertson L, Glickman JN, Gallini CA, Michaud M, Clancy TE, Chung DC, Lochhead P, Hold GL, El-Omar EM, Brenner D, Fuchs CS, Meyerson M, Garrett WS. Fusobacterium nucleatum potentiates intestinal tumorigenesis and modulates the tumor-immune microenvironment. *Cell Host Microbe* 2013; **14**: 207-215 [PMID: 23954159 DOI: 10.1016/j.chom.2013.07.007]

121 **Chen T**, Li Q, Wu J, Wu Y, Peng W, Li H, Wang J, Tang X, Peng Y, Fu X. Fusobacterium nucleatum promotes M2 polarization of macrophages in the microenvironment of colorectal tumours *via* a TLR4-dependent mechanism. *Cancer Immunol Immunother* 2018; **67**: 1635-1646 [PMID: 30121899 DOI: 10.1007/s00262-018-2233-x]

122 **Dong X**, Pan P, Zheng DW, Bao P, Zeng X, Zhang XZ. Bioinorganic hybrid bacteriophage for modulation of intestinal microbiota to remodel tumor-immune microenvironment against colorectal cancer. *Sci Adv* 2020; **6**: eaba1590 [PMID: 32440552 DOI: 10.1126/sciadv.aba1590]

123 **Zhang Y**, Ma S, Liu X, Xu Y, Zhao J, Si X, Li H, Huang Z, Wang Z, Tang Z, Song W, Chen X. Supramolecular Assembled Programmable Nanomedicine As In Situ Cancer Vaccine for Cancer Immunotherapy. *Adv Mater* 2021; **33**: e2007293 [PMID: 33448050 DOI: 10.1002/adma.202007293]

124 **GBD 2017 Pancreatic Cancer Collaborators**. The global, regional, and national burden of pancreatic cancer and its attributable risk factors in 195 countries and territories, 1990-2017: a systematic analysis for the Global Burden of Disease Study 2017. *Lancet Gastroenterol Hepatol* 2019; **4**: 934-947 [PMID: 31648972 DOI: 10.1016/S2468-1253(19)30347-4]

125 **Klein AP**. Pancreatic cancer epidemiology: understanding the role of lifestyle and inherited risk factors. *Nat Rev Gastroenterol Hepatol* 2021; **18**: 493-502 [PMID: 34002083 DOI: 10.1038/s41575-021-00457-x]

126 **Zhao Z**, Liu W. Pancreatic Cancer: A Review of Risk Factors, Diagnosis, and Treatment. *Technol Cancer Res Treat* 2020; **19**: 1533033820962117 [PMID: 33357065 DOI: 10.1177/1533033820962117]

127 **Nishida T**, Yoshitomi H, Takano S, Kagawa S, Shimizu H, Ohtsuka M, Kato A, Furukawa K, Miyazaki M. Low Stromal Area and High Stromal Microvessel Density Predict Poor Prognosis in Pancreatic Cancer. *Pancreas* 2016; **45**: 593-600 [PMID: 26495781 DOI: 10.1097/MPA.0000000000000499]

128 **Li S**, Xu HX, Wu CT, Wang WQ, Jin W, Gao HL, Li H, Zhang SR, Xu JZ, Qi ZH, Ni QX, Yu XJ, Liu L. Angiogenesis in pancreatic cancer: current research status and clinical implications. *Angiogenesis* 2019; **22**: 15-36 [PMID: 30168025 DOI: 10.1007/s10456-018-9645-2]

129 **Selvanesan BC**, Meena K, Beck A, Meheus L, Lara O, Rooman I, Gravekamp C. Nicotinamide combined with gemcitabine is an immunomodulatory therapy that restrains pancreatic cancer in mice. *J Immunother Cancer* 2020; **8** [PMID: 33154149 DOI: 10.1136/jitc-2020-001250]

130 **Rocha FG**. Landmark Series: Immunotherapy and Targeted Therapy for Pancreatic Cancer. *Ann Surg Oncol* 2021; **28**: 1400-1406 [PMID: 33386541 DOI: 10.1245/s10434-020-09367-9]

131 **Schizas D**, Charalampakis N, Kole C, Economopoulou P, Koustas E, Gkotsis E, Ziogas D, Psyrri A, Karamouzis MV. Immunotherapy for pancreatic cancer: A 2020 update. *Cancer Treat Rev* 2020; **86**: 102016 [PMID: 32247999 DOI: 10.1016/j.ctrv.2020.102016]

132 **Jia M**, Zhang D, Zhang C, Li C. Nanoparticle-based delivery systems modulate the tumor microenvironment in pancreatic cancer for enhanced therapy. *J Nanobiotechnology* 2021; **19**: 384 [PMID: 34809634 DOI: 10.1186/s12951-021-01134-6]

133 **Wang Y**, Gao Z, Du X, Chen S, Zhang W, Wang J, Li H, He X, Cao J. Co-inhibition of the TGF-β pathway and the PD-L1 checkpoint by pH-responsive clustered nanoparticles for pancreatic cancer microenvironment regulation and anti-tumor immunotherapy. *Biomater Sci* 2020; **8**: 5121-5132 [PMID: 32820750 DOI: 10.1039/d0bm00916d]

134 **Yu Q**, Tang X, Zhao W, Qiu Y, He J, Wan D, Li J, Wang X, He X, Liu Y, Li M, Zhang Z, He Q. Mild hyperthermia promotes immune checkpoint blockade-based immunotherapy against metastatic pancreatic cancer using size-adjustable nanoparticles. *Acta Biomater* 2021; **133**: 244-256 [PMID: 34000465 DOI: 10.1016/j.actbio.2021.05.002]

135 **Wang C**, Shi X, Song H, Zhang C, Wang X, Huang P, Dong A, Zhang Y, Kong D, Wang W. Polymer-lipid hybrid nanovesicle-enabled combination of immunogenic chemotherapy and RNAi-mediated PD-L1 knockdown elicits antitumor immunity against melanoma. *Biomaterials* 2021; **268**: 120579 [PMID: 33278683 DOI: 10.1016/j.biomaterials.2020.120579]

136 **Danhier F**, Ansorena E, Silva JM, Coco R, Le Breton A, Préat V. PLGA-based nanoparticles: an overview of biomedical applications. *J Control Release* 2012; **161**: 505-522 [PMID: 22353619 DOI: 10.1016/j.jconrel.2012.01.043]

137 **Allavena P**, Palmioli A, Avigni R, Sironi M, La Ferla B, Maeda A. PLGA Based Nanoparticles for the Monocyte-Mediated Anti-Tumor Drug Delivery System. *J Biomed Nanotechnol* 2020; **16**: 212-223 [PMID: 32252882 DOI: 10.1166/jbn.2020.2881]

138 **Jung JY**, Ryu HJ, Lee SH, Kim DY, Kim MJ, Lee EJ, Ryu YM, Kim SY, Kim KP, Choi EY, Ahn HJ, Chang S. siRNA Nanoparticle Targeting PD-L1 Activates Tumor Immunity and Abrogates Pancreatic Cancer Growth in Humanized Preclinical Model. *Cells* 2021; **10** [PMID: 34685714 DOI: 10.3390/cells10102734]

139 **Lorkowski ME**, Atukorale PU, Bielecki PA, Tong KH, Covarrubias G, Zhang Y, Loutrianakis G, Moon TJ, Santulli AR, Becicka WM, Karathanasis E. Immunostimulatory nanoparticle incorporating two immune agonists for the treatment of pancreatic tumors. *J Control Release* 2021; **330**: 1095-1105 [PMID: 33188827 DOI: 10.1016/j.jconrel.2020.11.014]

140 **Porembka MR**, Mitchem JB, Belt BA, Hsieh CS, Lee HM, Herndon J, Gillanders WE, Linehan DC, Goedegebuure P. Pancreatic adenocarcinoma induces bone marrow mobilization of myeloid-derived suppressor cells which promote primary tumor growth. *Cancer Immunol Immunother* 2012; **61**: 1373-1385 [PMID: 22215137 DOI: 10.1007/s00262-011-1178-0]

141 **Long Y**, Lu Z, Xu S, Li M, Wang X, Zhang Z, He Q. Self-Delivery Micellar Nanoparticles Prevent Premetastatic Niche Formation by Interfering with the Early Recruitment and Vascular Destruction of Granulocytic Myeloid-Derived Suppressor Cells. *Nano Lett* 2020; **20**: 2219-2229 [PMID: 31823615 DOI: 10.1021/acs.nanolett.9b03883]

142 **Lu Z**, Long Y, Wang Y, Wang X, Xia C, Li M, Zhang Z, He Q. Phenylboronic acid modified nanoparticles simultaneously target pancreatic cancer and its metastasis and alleviate immunosuppression. *Eur J Pharm Biopharm* 2021; **165**: 164-173 [PMID: 34020022 DOI: 10.1016/j.ejpb.2021.05.014]

143 **Yu P**, Zhang X, Liu N, Tang L, Peng C, Chen X. Pyroptosis: mechanisms and diseases. *Signal Transduct Target Ther* 2021; **6**: 128 [PMID: 33776057 DOI: 10.1038/s41392-021-00507-5]

144 **Li J**, Anraku Y, Kataoka K. Self-Boosting Catalytic Nanoreactors Integrated with Triggerable Crosslinking Membrane Networks for Initiation of Immunogenic Cell Death by Pyroptosis. *Angew Chem Int Ed Engl* 2020; **59**: 13526-13530 [PMID: 32383236 DOI: 10.1002/anie.202004180]

145 **Liu Y**, Zhen W, Wang Y, Song S, Zhang H. $Na_2S_2O_8$ Nanoparticles Trigger Antitumor Immunotherapy through Reactive Oxygen Species Storm and Surge of Tumor Osmolarity. *J Am Chem Soc* 2020; **142**: 21751-21757 [PMID: 33337859 DOI: 10.1021/jacs.0c09482]

146 **Zhao P**, Wang M, Chen M, Chen Z, Peng X, Zhou F, Song J, Qu J. Programming cell pyroptosis with biomimetic nanoparticles for solid tumor immunotherapy. *Biomaterials* 2020; **254**: 120142 [PMID: 32485591 DOI: 10.1016/j.biomaterials.2020.120142]

147 **Fan JX**, Deng RH, Wang H, Liu XH, Wang XN, Qin R, Jin X, Lei TR, Zheng D, Zhou PH, Sun Y, Zhang XZ. Epigenetics-Based Tumor Cells Pyroptosis for Enhancing the Immunological Effect of Chemotherapeutic Nanocarriers. *Nano Lett* 2019; **19**: 8049-8058 [PMID: 31558023 DOI: 10.1021/acs.nanolett.9b03245]

148 **Ding B**, Sheng J, Zheng P, Li C, Li D, Cheng Z, Ma P, Lin J. Biodegradable Upconversion Nanoparticles Induce Pyroptosis for Cancer Immunotherapy. *Nano Lett* 2021; **21**: 8281-8289 [PMID: 34591494 DOI: 10.1021/acs.nanolett.1c02790]

149 **D'Errico G**, Alonso-Nocelo M, Vallespinos M, Hermann PC, Alcalá S, García CP, Martin-Hijano L, Valle S, Earl J, Cassiano C, Lombardia L, Feliu J, Monti MC, Seufferlein T, García-Bermejo L, Martinelli P, Carrato A, Sainz B Jr. Tumor-associated macrophage-secreted 14-3-3ζ signals *via* AXL to promote pancreatic cancer chemoresistance. *Oncogene* 2019; **38**: 5469-5485 [PMID: 30936462 DOI: 10.1038/s41388-019-0803-9]

150 **Bulle A**, Dekervel J, Deschuttere L, Nittner D, Libbrecht L, Janky R, Plaisance S, Topal B, Coosemans A, Lambrechts D, Van Cutsem E, Verslype C, van Pelt J. Gemcitabine Recruits M2-Type Tumor-Associated Macrophages into the Stroma of Pancreatic Cancer. *Transl Oncol* 2020; **13**: 100743 [PMID: 32145636 DOI: 10.1016/j.tranon.2020.01.004]

151 **Wang M**, Hu Q, Huang J, Zhao X, Shao S, Zhang F, Yao Z, Ping Y, Liang T. Engineered a dual-targeting biomimetic nanomedicine for pancreatic cancer chemoimmunotherapy. *J Nanobiotechnology* 2022; **20**: 85 [PMID: 35177078 DOI: 10.1186/s12951-022-01282-3]

152 **Cao S**, Saw PE, Shen Q, Li R, Liu Y, Xu X. Reduction-responsive RNAi nanoplatform to reprogram tumor lipid metabolism and repolarize macrophage for combination pancreatic cancer therapy. *Biomaterials* 2022; **280**: 121264 [PMID: 34823884 DOI: 10.1016/j.biomaterials.2021.121264]

153 **Wang M**, Li Y, Wang M, Liu K, Hoover AR, Li M, Towner RA, Mukherjee P, Zhou F, Qu J, Chen WR. Synergistic interventional photothermal therapy and immunotherapy using an iron oxide nanoplatform for the treatment of pancreatic cancer. *Acta Biomater* 2022; **138**: 453-462 [PMID: 34757232 DOI: 10.1016/j.actbio.2021.10.048]

154 **Zanganeh S**, Hutter G, Spitler R, Lenkov O, Mahmoudi M, Shaw A, Pajarinen JS, Nejadnik H, Goodman S, Moseley M, Coussens LM, Daldrup-Link HE. Iron oxide nanoparticles inhibit tumour growth by inducing pro-inflammatory macrophage polarization in tumour tissues. *Nat Nanotechnol* 2016; **11**: 986-994 [PMID: 27668795 DOI: 10.1038/nnano.2016.168]

World Journal of Gastroenterology

Submit a Manuscript: https://www.f6publishing.com

World J Gastroenterol 2022 October 7; 28(37): 5420-5443

DOI: 10.3748/wjg.v28.i37.5420

ISSN 1007-9327 (print) ISSN 2219-2840 (online)

ORIGINAL ARTICLE

Basic Study

Lentivirus-mediated short hairpin RNA interference of CENPK inhibits growth of colorectal cancer cells with overexpression of Cullin 4A

Xian Li, Yi-Ru Han, Xuefeng Xuefeng, Yong-Xiang Ma, Guo-Sheng Xing, Zhi-Wen Yang, Zhen Zhang, Lin Shi, Xin-Lin Wu

Specialty type: Gastroenterology and hepatology

Provenance and peer review: Unsolicited article; Externally peer reviewed.

Peer-review model: Single blind

Peer-review report's scientific quality classification

Grade A (Excellent): 0
Grade B (Very good): B, B
Grade C (Good): 0
Grade D (Fair): 0
Grade E (Poor): 0

P-Reviewer: Fouad MA, Egypt; Mohamed SY, Egypt

Received: November 22, 2021
Peer-review started: November 22, 2021
First decision: January 11, 2022
Revised: January 24, 2022
Accepted: September 12, 2022
Article in press: September 12, 2022
Published online: October 7, 2022

Xian Li, Clinical Medical Research Center, The Affiliated Hospital of Inner Mongolia Medical University, Hohhot 010050, Inner Mongolia Autonomous Region, China

Yi-Ru Han, Xuefeng Xuefeng, Yong-Xiang Ma, Guo-Sheng Xing, Zhi-Wen Yang, Zhen Zhang, Xin-Lin Wu, Department of Gastrointestinal Surgery, The Affiliated Hospital of Inner Mongolia Medical University, Hohhot 010050, Inner Mongolia Autonomous Region, China

Lin Shi, Department of Pathology, The Affiliated Hospital of Inner Mongolia Medical University, Hohhot 010050, Inner Mongolia Autonomous Region, China

Corresponding author: Xin-Lin Wu, Doctor, Chief Doctor, Department of Gastrointestinal Surgery, The Affiliated Hospital of Inner Mongolia Medical University, No. 1 North Street, Hohhot 010050, Inner Mongolia Autonomous Region, China. wuxinlin@126.com

Abstract

BACKGROUND

Colorectal cancer (CRC) is one of the most common malignant tumors worldwide. The identification of novel diagnostic and prognostic biomarkers for CRC is a key research imperative. Immunohistochemical analysis has revealed high expression of centromere protein K (CENPK) in CRC. However, the role of CENPK in the progression of CRC is not well characterized.

AIM

To evaluate the effects of knockdown of CENPK and overexpression of Cullin 4A (CUL4A) in RKO and HCT116 cells.

METHODS

Human colon cancer samples were collected and tested using a human gene expression chip. We identified CENPK as a potential oncogene for CRC based on bioinformatics analysis. *In vitro* experiments verified the function of this gene. We investigated the expression of CENPK in RKO and HCT116 cells using quantitative polymerase chain reaction (qPCR), western blot, and flow cytometry. The effect of short hairpin RNA (shRNA) virus-infected RKO cells on tumor growth was evaluated *in vivo* using quantitative analysis of fluorescence imaging. To evaluate the effects of knockdown of CENPK and overexpression of CUL4A in

RKO and HCT116 cells, we performed a series of *in vitro* experiments, using qPCR, western blot, MTT assay, and flow cytometry.

RESULTS

We demonstrated overexpression of CENPK in human colon cancer samples. CENPK was an independent risk factor in patients with CRC. The downstream genes FBX32, CUL4A, and Yes-associated protein isoform 1 were examined to evaluate the regulatory action of CENPK in RKO cells. Significantly delayed xenograft tumor emergence, slower growth rate, and lower final tumor weight and volume were observed in the CENPK short hairpin RNA virus infected group compared with the CENPK negative control group. The CENPK gene interference inhibited the proliferation of RKO cells *in vitro* and *in vivo*. The lentivirus-mediated shRNA interference of CENPK inhibited the proliferation of RKO and HCT116 colon cancer cells, with overexpression of the CUL4A.

CONCLUSION

We indicated a potential role of CENPK in promoting tumor proliferation, and it may be a novel diagnostic and prognostic biomarker for CRC.

Key Words: Colorectal cancer; Centromere protein K; Bioinformatics analysis; Lentivirus-mediated short hairpin RNA interference; Cullin 4A

©The Author(s) 2022. Published by Baishideng Publishing Group Inc. All rights reserved.

Core Tip: High expression of centromere protein K (CENPK) in colorectal cancer (CRC) was found by immunohistochemistry. We demonstrated overexpression of CENPK in human colon cancer samples. CENPK was an independent risk factor in patients with CRC. Our findings indicate a potential role of CENPK in promoting tumor proliferation. CENPK may serve as a novel diagnostic and prognostic biomarker in patients with CRC.

Citation: Li X, Han YR, Xuefeng X, Ma YX, Xing GS, Yang ZW, Zhang Z, Shi L, Wu XL. Lentivirus-mediated short hairpin RNA interference of CENPK inhibits growth of colorectal cancer cells with overexpression of Cullin 4A. *World J Gastroenterol* 2022; 28(37): 5420-5443

URL: https://www.wjgnet.com/1007-9327/full/v28/i37/5420.htm

DOI: https://dx.doi.org/10.3748/wjg.v28.i37.5420

INTRODUCTION

Colorectal cancer (CRC) is the third most common cancer in the Western Hemisphere, and the incidence increases with age. RNA interference has been developed to silence genes of interest. Short hairpin RNA (shRNA) expression vectors are useful in gene silencing[1]. The shRNA-mediated silencing of MASTL expression in colon cancer cells induced cell cycle arrest and apoptosis *in vitro* and xenograft-tumor growth *in vivo*[2]. Emerging studies have suggested that shRNAs play a crucial role in CRC tumorigenesis and progression[3]. Inducible gene knockdown systems based on lentivirus-mediated gene transfer were developed to regulate colon cancer progression[1]. This property of the shRNA system offers unique applications to study gene function in animals that cannot be achieved using knockout technologies[4]. Although lentivirus vectors have been used for several years, the use of Tet-on lentiviral vectors expressing shRNA as a therapeutic tool for CRC has not been clearly explored[5].

The role of centromere protein K (CENPK) in cancer is an emerging research hotspot. CENPK is overexpressed in several tumor types, and it promotes tumor progression. Research on the role of CENPK in the progression of hepatocellular carcinoma (HCC) has shown that CENPK knockdown significantly inhibits proliferation, migration, invasion, and epithelial-mesenchymal transition in HCC cells[6]. The expression of CENPK has been silenced and promoted *via* lentivirus-mediated transfection with shRNA sequences in differentiated thyroid carcinomas, such as two pore channel 1 and FTC-133 cells[7]. CENPK is specifically upregulated in ovarian cancer tissues and cell lines, and its overexpression is associated with a poor prognosis in patients with ovarian cancer[8]. Overexpression of CENPK promotes expression of oncogenic cell cycle regulators[9]. However, there has been little research on the role of CENPK in the progression of CRC.

The ubiquitin ligase Cullin 4A (CUL4A) is highly expressed in CRC. CUL4A promotes proliferation and inhibits apoptosis of CRC cells by regulating the Hippo pathway[10]. CUL4A significantly promotes the migration of CRC cells *in vitro*, which suggests that CUL4A acts as an oncogene in CRC

and may become a potential therapeutic target[11]. Therefore, CUL4A expression positively correlates with the prognosis of CRC[12]. Despite extensive fundamental studies, the role of CUL4A expression and lentivirus-mediated transfection with shRNA for CENPK in CRC is not clear. The present study identified CENPK as a novel proto-oncogene in CRC. Increased CENPK levels were found in CRC specimens and negatively correlated with survival rate. Knockdown of CENPK in RKO and HCT116 CRC cells induced apoptosis and suppressed cell proliferation and xenograft tumor formation. Lentivirus-mediated transfection with shRNA for CENPK and CUL4A overexpression played major regulatory roles in CRC.

MATERIALS AND METHODS

Patient information and immunohistochemistry

Fourteen patients with CRC were enrolled from 2016 to 2019, and five tumor-adjacent normal tissues were taken from an area > 10 cm away from the primary neoplasm. The median age of the patients was 59 years (range: 49-68 years) at the time of surgery, and the median follow-up was 31 mo postoperatively (range: 25-37 mo). The Ethics Committee of The Affiliated Hospital of Inner Mongolia Medical University approved the study. Written informed consent was obtained from all patients.

The expression and localization of CENPK protein in 14 cancerous and five noncancerous tissue samples were detected using immunohistochemistry. An antibody against CENPK (26208-1-AP, 1:100; SIGMA) was used for analysis. Vulcan Fast Red Chromogen kit 2 staining was performed for 15-20 min to stop the reaction until 3,3-diaminobenzidine staining was performed to obtain a yellow color to complete the reaction. The staining intensity and positive rate of cytosolic and membrane staining of the antibody (0/1+/2+/3+) in the cancer and adjacent tissue (epithelium) were interpreted. The intensity of the staining score was 0 (negative), 1 (weak), 2 (middle), and 3 (strong). The positive rate of staining was as follows: 0 (negative), 1 (1%-25%), 2 (26%-50%), 3 (51%-75%), and 4 (76%-100%).

Primeview human gene expression array of PathArray™

Gene expression in a human colon cancer tissue chip (C06161) was detected. The sample was divided into male (age < 57 years) and female (age > 57 years) groups by T stage, N stage, pathological grade, and clinical stage. For the chip assay, total RNA was extracted from tissue using the TRIzol method and measured using a Nanodrop 2000. Qualified samples were used in the chip experiment. The quality checking standard was 1.7 < A260/A280 < 2.2 on Thermo NanoDrop 2000 and RNA integrity number (RIN) ≥ 7.0 and 28S/18S > 0.7 on the Agilent 2100 Bioanalyzer. The quality check results are shown in Table 1. The human gene expression chip type was GeneChip PrimeView Human (100 format, 902487; Affymetrix). Chip hybridization was performed in a GeneChip Hybridization Oven 645 ChIP, washing and dyeing were performed using a GeneChip Fluidics Station 450, and ChIP scanning was performed using a GeneChip Scanner 3000. The reagent used was a GeneChip Hybridization Wash and Stain Kit.

For the chip detection, gradient dilution of poly-A RNA controls was prepared to synthesize the first-chain cDNA and second-chain cDNA, and then cRNA of synthetic markers was synthesized *via* transcription *in vitro*, which was followed by cRNA purification and quantification to obtain cRNA fragment markers. The expression analysis of the CENPK gene in human colon cancer tissue in the chip (C06161) and clinical data are shown in Table 2. A statistical analysis of CRC tissue chips was performed.

Cell culture

The human CRC cell lines RKO and HCT 116 were cultured in RPMI 1640 medium (Invitrogen) supplemented with 10% fetal bovine serum (FBS) (Corning) and 1% penicillin and streptomycin solution (Corning) at 37 °C with 5% CO_2[13].

Quantitative polymerase chain reaction

Total RNA was extracted from RKO cells with TRIzol reagent (Thermo Fisher Scientific). A 1-mg RNA sample was reverse transcribed into first-strand cDNA using the Revert Aid First Strand cDNA Synthesis kit (Thermo Fisher Scientific). Quantitative polymerase chain reaction (qPCR) was performed using the Taq-Man Gene Expression assay (Thermo Fisher Scientific) on an Mx3000P real-time PCR system (Agilent Technologies). The primer pairs were designed and synthesized by Sangon Biotech (GAPDH: Forward, TGACTTCAACAGCGACACCCA and reverse, CACCCTGTTGCTGTAGCCAAA; CENPK: Forward, ATGGTACTGTCCACTAAGGAGTC and reverse, TGTTCATCCAACCACCGTTGT). The mRNA levels were normalized to the internal reference gene GAPDH, with the mRNA relative expression calculated using the $2^{-\Delta\Delta Ct}$ method.

Western blot analysis

After protein extraction from RKO cells, the protein concentrations of different groups were quantified using a commercial BCA kit. Electrophoresis was performed for 2 h at 4 °C and 300 mA, and the protein

Table 1 Quality check results

Order number	Sample number	Sample name	Thermo NanoDrop 2000		2100 result		Results
			Concentration (ng/μL)	A260/A280	RIN	28S/18S	
1	Y9148-1	NC	739.969	1.951	10	2.1	Pass
2	Y9148-2	NC	688.748	1.979	10	2.1	Pass
3	Y9148-3	NC	668.435	1.944	10	1.9	Pass
4	Y9149-1	KD	676.797	1.93	10	1.7	Pass
5	Y9149-2	KD	697.671	1.958	10	1.7	Pass
6	Y9149-3	KD	678.338	1.971	10	1.7	Pass

NC: RKO cells infected with centromere protein K negative control virus; KD: RKO cells with centromere protein K gene short hairpin RNA virus infection.

Table 2 Clustering of clinical data

Number	Variable	Group 1	Group 2
1	Age (yr)	< 57	> 57
2	Sex	Male	Female
3	T stage	T1/2/3	T4
4	N metastasis	N0	N1/2
5	Pathological grade	1/2	3
6	Clinical stage	I/II	III/IV

was transferred to polyvinylidene fluoride (PVDF) membranes (IPVH00010; Millipore) for immunostaining. The PVDF membranes were incubated in TBST solution containing 5% skimmed milk at room temperature for 1 h. The antibodies were diluted in the blocking solution and then incubated with the PVDF membranes for 2 h at room temperature. The antibodies applied in the present study included those against Yes-associated protein isoform 1 (YAP1) (ab52771; Abcam), CENPK (ab13939; Abcam), CUL4A (ab92554; Abcam), F-box protein 32 (FBX32) (ab168372; Abcam), X chromosome-linked inhibitor of apoptosis (XIAP) (ab28151; Abcam), heat shock protein 90 family class A member 1 (HSP90AA1) (4877; Cell Signaling Technology), class III-tubulin (TUBB3) (#5568; Abcam), and mitogen-activated protein kinase kinase kinase 7 (MAP3K7) (ab109526; Abcam). After primary antibody incubation, the membranes were washed three times with TBST (10 min each) and incubated with the secondary antibodies mouse immunoglobulin G (IgG) (1:2000, sc-2005; Santa Cruz Biotechnology) and rabbit IgG (1:2000, sc-2004; Santa Cruz Biotechnology) at room temperature for 2 h. The Pierce ECL Western Blotting Substrate kit (Thermo) was used for X-ray photography.

Establishment and examination of a tumor model

The Ethics Committee of The Affiliated Hospital of Inner Mongolia Medical University approved the study. RKO cells with sufficient logarithmic growth were digested with trypsin and suspended in culture medium with the final cell density adjusted to 2.0×10^7/mL. To establish the tumor model, 4.0×10^6 cells were subcutaneously injected into mice. The tumor size and animal body weight were measured 5-20 d later. The tumor volume was calculated as $\pi/6 \times L \times W \times W$, where L represents the long diameter, and W and W represent the short diameter. Cancer progression was imaged at 10 d after tumor formation (animals were fasted for 1 d in advance to reduce fluorescence interference) with intraperitoneal injection of 10 μL/g D-luciferin (Bench Mark 15 mg/mL) into mice. After anesthesia by intraperitoneal injection of 10 μL/g pentobarbital solution (BM 7 mg/mL), the mice underwent imaging examination, quantitative analysis, and total fluorescence examination to determine the CENPK function *in vivo*. After imaging, the experimental animals were killed with an overdose of 2% sodium pentobarbital (0.5 mL) and were in a complete coma before removal of the cervical spine to confirm death. Animals were dissected with medical scissors and tweezers to observe the lungs, liver, and other organs and tissues, which were removed for imaging to observe biological changes and measure the fluorescence.

Construction and packaging of lentiviral vectors

293T cells for lentivirus packaging were cultured in Dulbecco's modified Eagle's medium supplemented with 10% FBS. The scramble order for the RNAi negative control was TTCTCCGAACGTGTCACGT. Vector enzyme digestion products were obtained for agarose gel electrophoresis to recover bands of interest. The framework of the viral vector was constructed, and single-strand primers were synthesized. Double-stranded DNA was formed by annealing the primer to the vector. After transformation, the bacterial colonies were assessed by PCR. Identified positive carbendazim transformants were inoculated into Luria-Bertani (LB) liquid medium containing an appropriate amount of antibiotics, and an appropriate amount of bacterial solution was incubated at 37 °C for 12-16 h. The incubated bacterial solution was transferred to 10 mL LB liquid medium containing the corresponding antibiotics for culture at 37 °C overnight. The plasmid was extracted with the small medium-lift kit from Tiangen, and the qualified plasmid was extracted for the following experiments.

Lentiviral infection

The lentivirus-infected HCT116 cells are shown in Table 3. RKO and HCT 116 cells (2×10^5 cell/mL) were cultured in RPMI 1640 medium containing 10% FBS with polybrene in six-well plates. The following experimental groups were used: (1) Cells (RKO or HCT 116 cells) infected with CENPK negative control virus [NC (KD)]; (2) Cells with lentivirus-mediated shRNA interference of CENPK (KD); (3) Cells with overexpression and negative control virus interference [NC (OE)]; (4) Cells virally infected with CUL4A (OE); (5) Cells with shRNA interference of CENPK and overexpression of negative control virus [KD + NC (OE)]; and (6) Cells with lentivirus-mediated shRNA interference of CENPK and CUL4A (KD + OE).

For the lentiviral infection, media for adherent cell inoculation and viral infection were used at a 1:1 ratio in 96-well plates. The culture medium was replaced, and the optimal amount of virus was added for the infection. The most appropriate time point after infection was selected for the replacement of conventional medium and continued culture, 8-12 h after infection. When fluorescently labeled lentiviral infection occurred, the green fluorescent protein reporter signal was observed by fluorescence microscopy 72 h after infection. After infection efficiency reached 80%, 0.5 mL of puromycin was used for cell function experiments. Western blot and qPCR analysis were performed to confirm the knockdown of CENPK.

Detection of cell growth

The proliferation potential of RKO and HCT 116 cells was analyzed by cell growth curve and MTT assay. For the cell growth curve assay, RKO and HCT 116 cells of different groups [shCtrl and shCENPK or NC, NC (KD), NC (OE), OE, KD + NC (OE), and KD + OE] were collected, replated in 24-well plates at 2000 cells/well, and cultured at 37 °C in a 5% CO_2 incubator for 5 d. Beginning on day 2, the optical absorption value of each group was checked once daily and the number of fluorescent cells calculated. A growth curve was drawn to show cell proliferation.

For the MTT assay, RKO and HCT 116 cells were replated in 24-well plates at 2000 cells/well and cultured at 37 °C in a 5% CO_2 incubator for 24 h. Subsequently, 20 μL MTT (5 mg/mL) was added to the wells. After incubation for 4 h, reactions were stopped with 100 μL DMSO. After shaking for 2-5 min, the OD value at 490/570 nm was determined (M2009PR, Tecan Infinite).

Apoptosis detection

Apoptosis was analyzed by flow cytometry (fluorescence-activated cell sorting; FACS) with a commercial Annexin V-APC kit (88-8007, eBioscience). RKO and HCT 116 cells of each group were collected after washing in 1 × binding buffer, and centrifuged at 1300 rpm for 3 min. After centrifugation, the cell suspension was prepared by adding 200 μL of 1 × binding buffer. Subsequently, 10 μL of Annexin V-APC staining solution was added to the suspension. After incubation in the dark at room temperature for 10-15 min, 400 μL of 1 × binding buffer was added to the cell suspension, and FACS was conducted for apoptosis detection.

Caspase 3/7 detection

Caspases 3/7 were detected in RKO and HCT 116 cells using a commercial Caspase-Glo3/7 detection kit (G8091, Promega). For the preparation of Caspase-Glo reaction solution, 10 mL of caspase-Glo3/7 buffer was added and vortexed until the dissolve of substrates. After collection and counting, the RKO and HCT 116 cells at a final density of 10^4 cells/well were replated in 96-well plates, and an empty control group containing culture medium without RKO or HCT 116 cells was established. Next, 100 μL of Caspase-Glo reaction solution was added to each well and shaken for 30 min at 500 rpm at room temperature for 2 h. The signal strength was measured using a microplate reader (M2009PR, Tecan Infinite).

PathScan® array detection

RKO cells were incubated with 1 mL of 1 × cell lysis buffer (Cell Signaling Technology) containing 1 mmol/L PMSF on ice for 2 min. Then, 100 μL of blocking solution was added to RKO cells with the cell

Table 3 Lentiviral-infected HCT 116 cells

Virus number	Experimental group	Virus titer	Virus infection dose
psc3741	NC (KD)	2.0E + 08 TU/mL	10.00 μL
LVpGCSIL-004PSC45249-1	KD	3.0E + 08 TU/mL	6.67 μL
KL9688-21	NC (OE)	4.0E + 8 TU/mL	5.00 μL
LVKL6733-2	OE	2.0E + 08 TU/mL	10.00 μL
LVpGCSIL-004PSC45249-1+ KL9688-21	KD+NC (OE)	3.0E + 08 + 2E + 8 TU/mL	3.33 + 5.00 μL
LVpGCSIL-004PSC45249-1+ LVKL6733-2	KD+OE	3.0E + 08 + 2E + 8 TU/mL	3.33 + 5.00 μL

NC: HCT 116 cells infected with centromere protein K negative control virus; KD: HCT 116 cells with centromere protein K gene short hairpin RNA virus infection; OE: HCT 116 cells virally infected with Cullin 4A.

lysate samples shaken at room temperature for 15 min. After incubation at room temperature for 2 h, the cell lysate samples were washed with 1 × cleaning solution on a horizontal shaker for 5 min. After three washes, 75 μL of 1 × antibody was added to the cell lysate samples and incubated on a horizontal shaker for 1 h. Then, 75 μL of 1 × HRP-linked streptavidin solution was added, followed by incubation on a horizontal shaker for 1 h. 1 × array cleaning solution was added to the cell lysate samples, which were then washed on a horizontal shaking bed four times (5 min each). The slides were placed in 1 × cleaning solution and then in exposure liquid (9 mL deionized water + 0.5 mL lumiGlo + 0.5 mL hydrogen peroxide) for 1-2 s, followed by observation with a chemiluminescence imaging system (ChemiScope 5300; Clinx Science Instruments).

Statistical analysis

Statistical analyses were performed using SPSS version 19.0 (IBM Corp.). Data are presented as the mean ± SD. Data comparing two samples were analyzed using student's *t*-test. Comparisons of datasets containing > 3 groups were evaluated by one-way repeated-measures ANOVA followed by the Bonferroni *post hoc* test. Gene expression of cancer and noncancer tissue groups was evaluated by the Mann-Whitney *U* test. $P < 0.05$ was considered to indicate a significant difference.

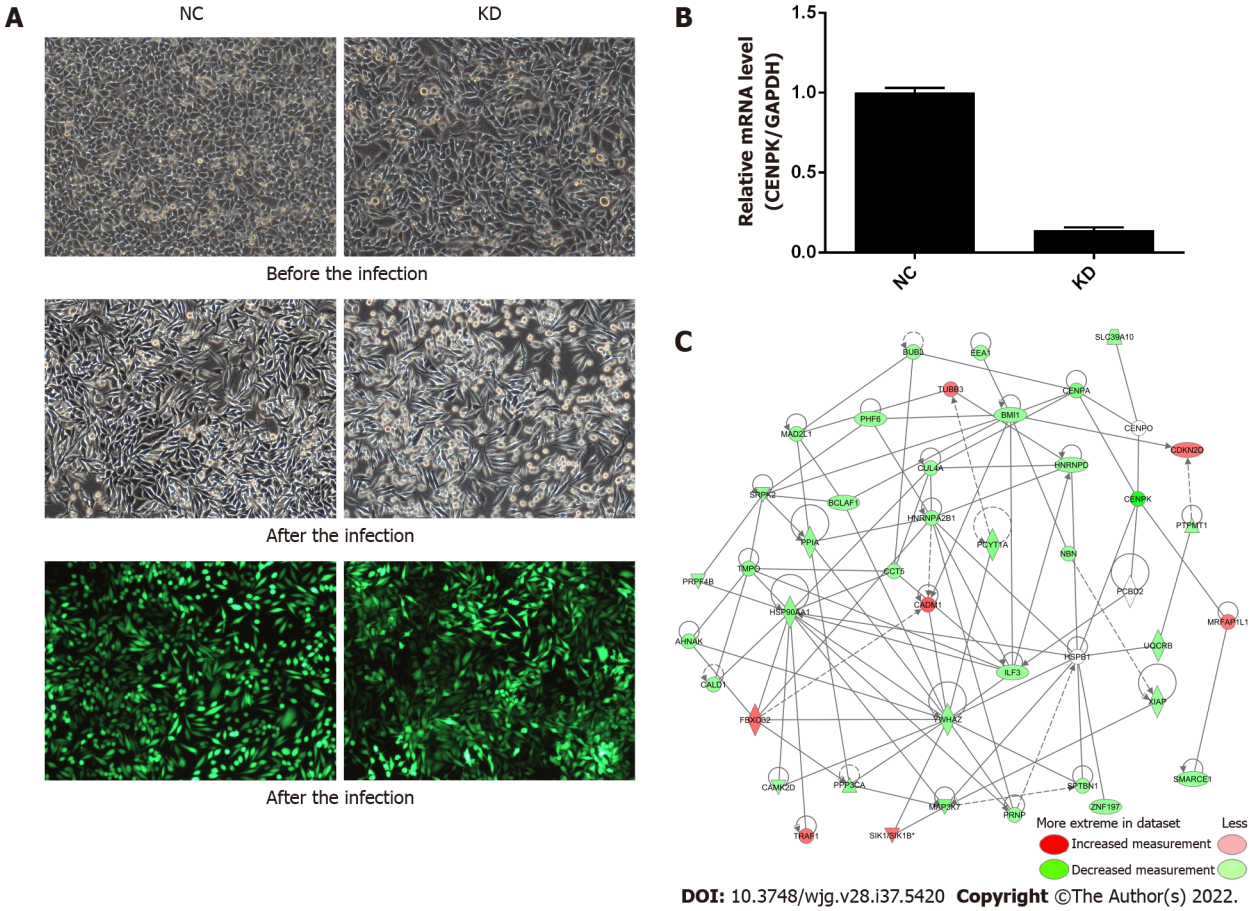
RESULTS

Lentivirus infection for inducing CENPK knockdown

For lentiviral infection marked with antibiotic resistance genes, the antibiotics (such as puromycin) were used to screen cells after 72 h, and the infection efficiency was approximately 80% for fluorescence labeled lentivirus infection (Figure 1A). CENPK knockdown efficiency in RKO cells in the KD group reached 86.1% compared to the NC group (23.4%) (Figure 1B). This analysis revealed the genes related to tumor cell proliferation and invasion. The genes that inhibited tumor cell proliferation or tumor invasion were selected, together with the target genes of concern, to develop a gene relationship network diagram. This analysis suggested that CENPK affected the proliferation and invasion of cells by acting on YWHAZ and BMI1, which affected the performance of downstream genes. The gene interaction network diagram shows a network of interaction relationships between molecules within a determined functional region. Different shapes represent genes, proteins, and chemicals in the network maps (Figure 1C).

Screening of target genes CENPK by chip detection

The original quality evaluation for the quality control data and the remaining data meeting the filter standards, including significant difference analysis and functional analysis of differential genes, was used to evaluate the tumor occurrence, development, metastasis, and other molecular mechanisms using chip information analysis for target screening and drug design. Figure 2A shows the signal strength distribution of the entire chip probes. Better signal intensity distribution curves of different samples indicated higher reliability of the chip experiment. The average *Z* score of all samples within one signal strength range was < 2, which supported the reliability of all chip results meeting the continuing analysis criteria. Figure 2B shows the distribution of the relative logarithmic signal strength for all chips. Closer distribution of the relative logarithmic signal strength box diagram indicated better repeatability of the data. The median *Z* score for all samples was < 2, which indicated good repeatability of the chip experiments in the project that met the continued analysis criteria. The Pearson correlation coefficient distribution diagram shows the level of correlation of the signal strength between all chips, where each lattice represents the degree of correlation between two samples corresponding to the

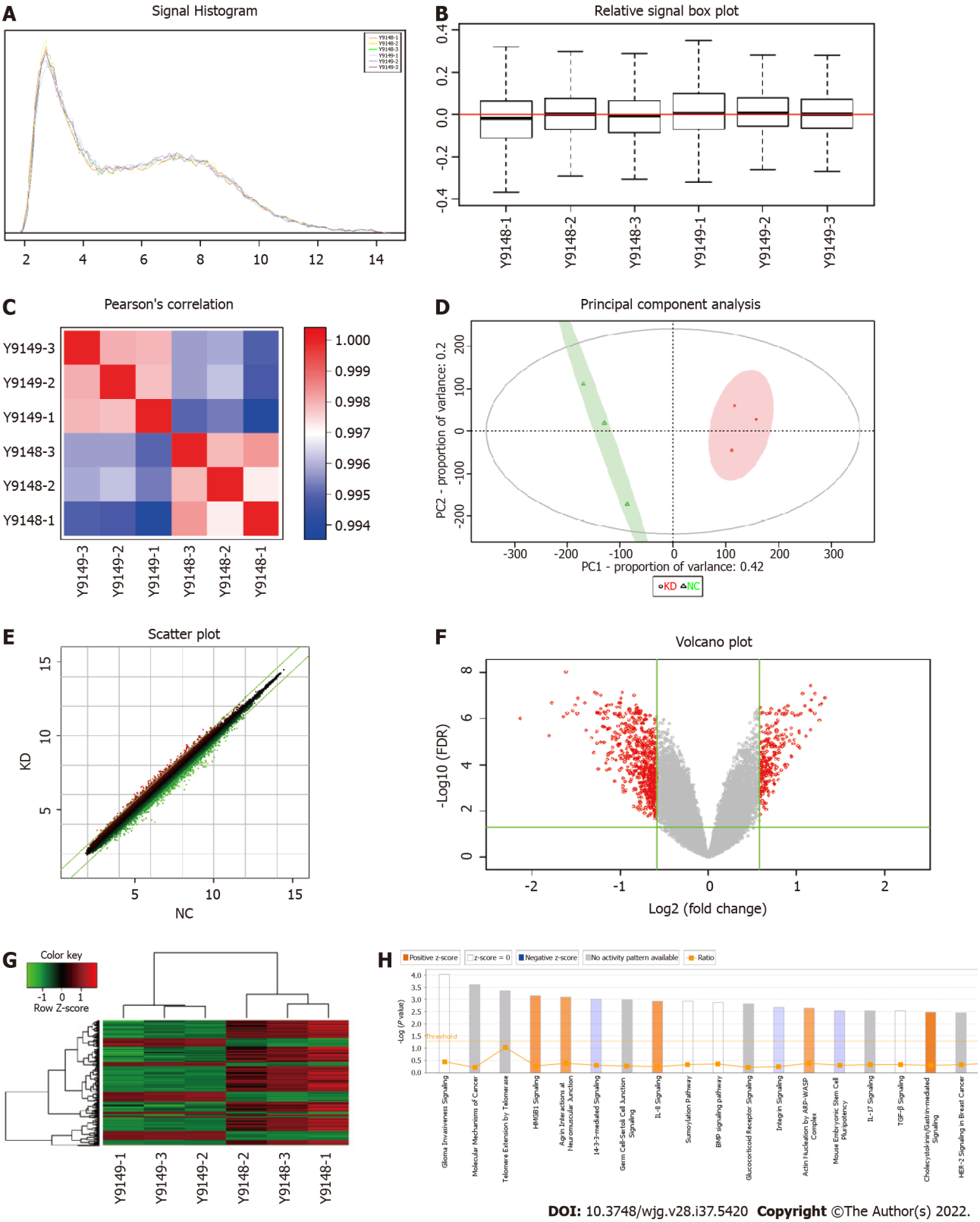


DOI: 10.3748/wjg.v28.i37.5420 **Copyright** ©The Author(s) 2022.

Figure 1 Centromere protein K affects the proliferation and invasion of colorectal cancer cells by acting on downstream genes. A: Morphology of RKO cells in NC and KD groups before and after lentivirus infection as well as infection efficiency assessed using fluorescence microscopy (× 100 magnification); B: Relative expression level of centromere protein K by quantitative polymerase chain reaction in NC and KD groups; C: Gene interaction network diagram. Genes, proteins, and chemicals are represented by different shapes; color labeling of molecules is shown in the illustration. NC: RKO cells infected with centromere protein K negative control virus; KD: RKO cells with lentivirus-mediated short hairpin RNA interference of centromere protein K; CENPK: Centromere protein K.

ordinate and transverse (Figure 2C). The group sample gene expression patterns were typically similar and demonstrated a high correlation coefficient, as shown in red in the correlation coefficient distribution diagram. The gene expression pattern difference between groups demonstrated a low correlation coefficient, which is shown in blue in the correlation coefficient distribution diagram. The correlation coefficient in the KD and NC groups was > 0.99, which indicated a high similarity of gene expression in the same group. The intergroup correlation coefficient was significantly lower than the group correlation coefficient, which indicated a large difference between groups that met the continuing analysis standard.

From the PCA score chart (Figure 2D), there was an obvious sample aggregation trend in the PC1 and PC2 dimensions in the KD and NC groups and an obvious intergroup separation trend, which indicated similar samples and significant differences between groups that met the standard of the continuing analysis. The cross ordinate of each point in Figure 2E represents the signal strength of a probe group in the NC and KD groups. The parallel green solid line is the reference line difference, and the points in the interval within the reference line represent the probe group without a significant change. The red point outside the interval represents the relatively elevated probe group in the KD group, and the green point represents the relatively elevated probe group in the NC group. A volcano graph was drawn using gene expression differences (fold change) and false discovery rate (FDR) tests between the two samples to show the significant differences between the two samples (Figure 2F). Thermal mapping of KD and NC samples was performed using the differential expression spectrum of genes screened by |fold change| ≥ 1.5 and FDR < 0.05 (Figure 2G). Figure 2H shows the significant enrichment of differentially expressed genes in the classical pathway. The orange notation indicates an activated pathway ($Z > 0$); the blue label indicates inhibition of the pathway ($Z < 0$); shades of orange and blue (or absolute Z values) represent the degree of activation or inhibition ($Z \geq 2$ represents a significant activation and standard, and $Z \leq -2$ denotes significant suppression); and the ratio represents the ratio of the difference of the gene number in this signaling pathway to all genes contained in the pathway. G1/S checkpoint regulation was activated in the cell cycle, and Z was 2.236.



DOI: 10.3748/wjg.v28.i37.5420 **Copyright** ©The Author(s) 2022.

Figure 2 Screening of target genes by chip detection. A: Signal strength distribution curve diagram, with the cross coordinates representing the probe signal strength range and the longitudinal coordinates representing the number of probe sets within the signal strength range; B: Relative line ram of the logarithmic signal strength, with the horizontal coordinate representing the sample name, the vertical coordinate indicating the relative logarithmic signal strength, the red line in the middle representing the average of the relative logarithmic signal strength of all samples, and the upper and lower horizontal lines representing the 90% confidence interval. The upper and lower edges represent the upper and lower quartiles, and the black line in the middle represents the median; C: Distribution diagram of the Pearson correlation coefficient among samples. The correlation coefficient indicates a positive correlation of the expression mode of genes in two subjects, and a negative value indicates an expression mode with a negative correlation. As the absolute value of the correlation coefficient approaches 1.0, the correlation increases; D: Principal component analysis. Red dots represent normal purpose cells with centromere protein K (CENPK) gene short hairpin RNA virus infection (KD) samples, and green dots represent normal purpose cells infected with CENPK negative control virus (NC) samples; E: Scatter diagram. The cross

coordinate represents the NC group, and the vertical coordinate represents the KD group; F: Volcano map, where the cross coordinate is a difference multiple (the logarithmic change in the bottom 2); longitudinal significance false discovery rate (FDR) (of the difference in the bottom 10 Logarithmic change); significantly different genes screened by |fold change| ≥ 1.5 and FDR < 0.05 in red, and other genes with no significant difference in gray; G: Cluster analysis results. Each column represents a sample, and each row represents a differentially expressed gene; H: Statistics for the classical pathway enrichment analysis. The transverse coordinate is the path name and the longitudinal significance level of enrichment (negative logarithmic transformation in the bottom 10).

G1/S checkpoint regulation was significantly activated. Red represents significant upregulation, and green represents the genes. Figure 3A shows the changing trend of gene expression in the pathway, which provided the basis for the study of the molecular mechanisms involved in the changes between sample groups. The upstream regulator network diagram (Figure 3B) shows the interaction between upstream regulators and downstream molecules that were directly associated in the dataset. Let-7 significantly suppressed SOX9 mRNA levels, and consistent trends were observed between let-7 and signal sequence receptor 1. Figure 3C shows the significant enrichment of differentially expressed genes in disease and function. According to the internal algorithms and standards of IPA, $Z \geq 2$ denoted significant activation of the disease or function, and $Z \leq -2$ indicated significant suppression of the disease or function. Significantly activated diseases or functions included morbidity or mortality ($Z = 4.216$) and organismal death ($Z = 4.164$). Significantly suppressed diseases or functions included infection by human immunodeficiency virus 1 ($Z = -3.335$) and viral infection ($Z = -3.2$) (Figure 3D). The network contains all the differentially expressed genes associated with the specified disease or function, and demonstrates possible interactions and changes in expression trends between genes based on the ingenuity knowledge base (Figure 3E). The top ranked regulatory network in this regulatory effect analysis suggested that the dataset was inhibitory due to the regulator miR-8 in the binding of tumor cell lines and the proliferation of stem cells *via* BMI1, COMMD3-BMI1, HMGB1, and YAP1 (Figure 3F). The network of interactions between molecules of a disease or function-related relationship is shown in Figure 3G.

Based on the above biological analysis, we speculated that CENPK was more likely to function in CRC by regulating the expression of the above-mentioned genes. Therefore, these genes were selected for western blot validation. Western blot analyses and qPCR showed that expression of FBX32 was upregulated, and CUL4A and YAP1 were downregulated (Figures 4A-D). Taken together, these results suggested that CENPK played a role in CRC by regulating FBX32, CUL4A, YAP1, and other genes in RKO cells.

High expression of CENPK in CRC

The expression of CENPK in CRC tissue was measured using immunohistochemistry to detect target protein expression and localization in tissue cells. Expression of CENPK was higher in cancerous than in paracancerous tissues (Figure 5A). Positive expression of CENPK in the cancerous and noncancerous tissues exhibited a differential multiple of 2.61, which was a significant difference (Figure 5B). Expression and proportional statistics of the CENPK gene in cancerous and noncancerous tissue are shown in Table 4.

CENPK gene expression in cancerous and noncancerous tissues is shown in Table 5. The differential expression of CENPK gene in cancerous and noncancerous tissues was analyzed using the Mann-Whitney *U* test. The significantly higher expression of CENPK in cancerous than in noncancerous tissues ($P < 0.05$) supports CENPK as an effective diagnostic marker for CRC. The expression and proportion of CENPK genes in cancerous tissues are shown in Table 6. The CENPK gene expression in different types of clinical experiment, including sex, age, T stage, and N metastases, was analyzed to compare its low expression and high expression. Expression of CENPK gene in cancerous tissue differed significantly according to T stage, N stage, and clinical stage, which suggested that CENPK expression was associated with these pathological indicators. The correlation between CENPK expression and clinical data (T stage, N stage, and clinical stage) in cancerous tissues was examined using Spearman's test, and the potential role of these clinical data in the development of CRC was examined (Table 7). Expression of the CENPK gene in cancerous tissues was positively correlated with T stage, N stage, and clinical stage, which suggested that low CENPK expression in the early stage of cancer gradually increased with the disease course.

shRNA lentivirus infects RKO cells and inhibits the growth of tumor cells

RKO cells infected by viruses were subcutaneously injected into nude mice for analysis of tumor growth conditions (Figure 6). RKO cells were infected with lentivirus, and there was no significant cell death, especially in the NC group, which was comparable to the control group. In contrast, the infection efficiency reached approximately 80% in the KD group (Figure 6A). The infection efficiency in the target screening experiment was > 90% in the KD group. Therefore, the good cell conditions and qualified infection efficiency up to 80% were used for downstream testing. Here, RKO cells were injected subcutaneously into the nude mice to analyze the tumor growth conditions and detect the infection efficiency of RKO cells. Based on the PCR results, CENPK gene knockdown efficiency in RKO cells reached 83.2% in the KD group compared to the NC group. The tumor status (the tumor formed and

Table 4 Expression and proportional statistics of the centromere protein K gene in cancerous and noncancerous tissue by immunohistochemical staining.

	Case group		*P* value
	Cancerous tissues	Noncancerous tissue	
Higher expression	4	5	0.008
Lower expression	10	0	

Table 5 Tissue type group * gene expression group using the Mann-Whitney *U* test

		CENPK gene expression group		Total	*P* value
		Low expression	High expression		
Tissue type group	Cancerous tissues	146	160	306	
	Noncancerous tissue	27	1	28	0.000
Total		173	161	334	

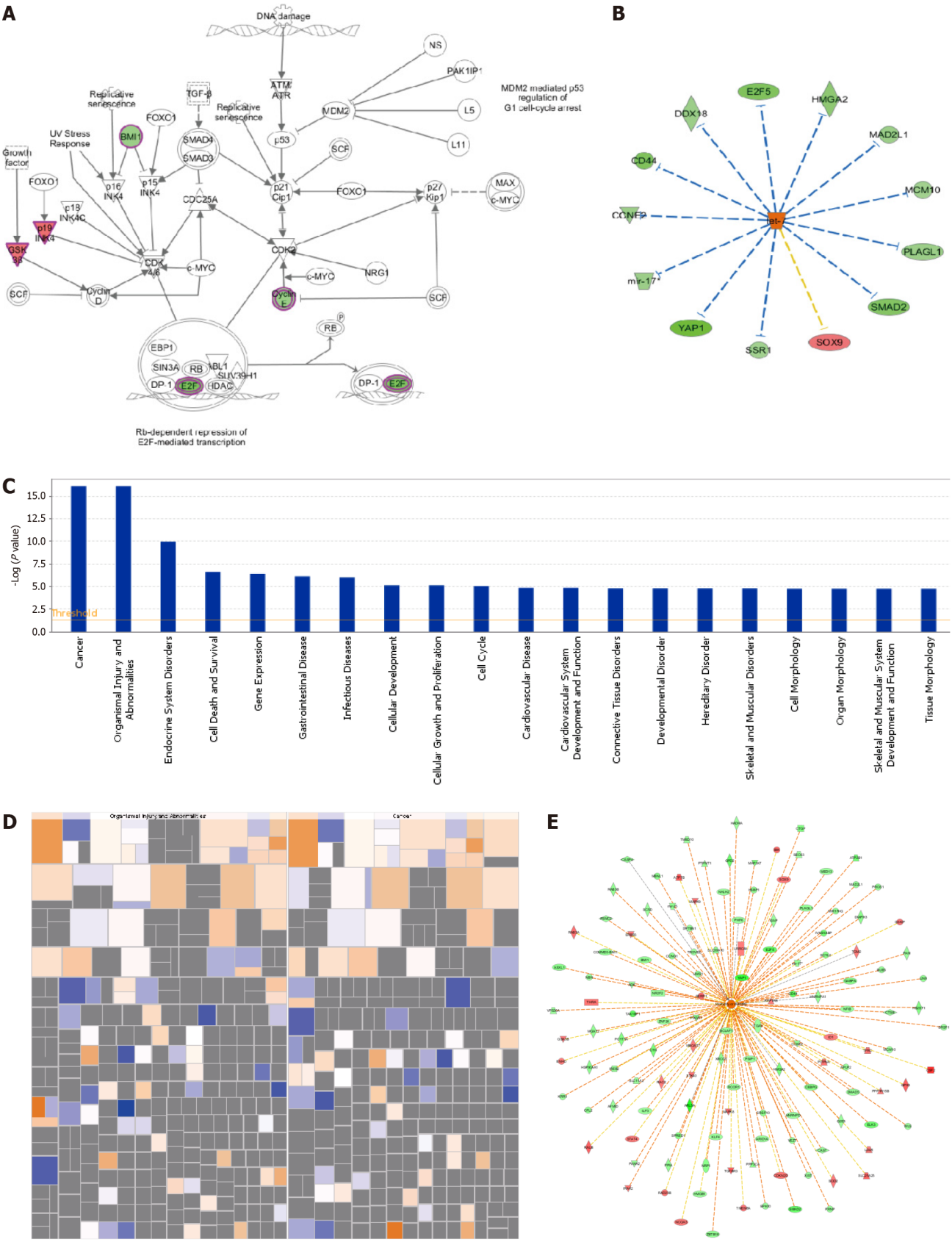
CENPK: Centromere protein K.

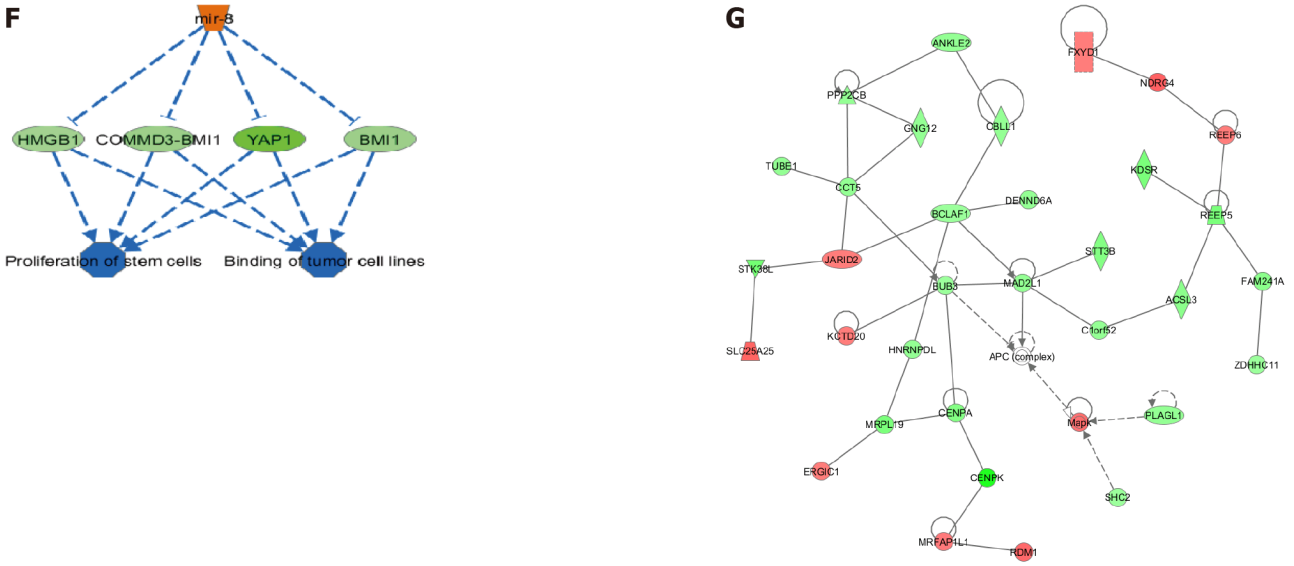
Table 6 Clinical data * gene expression group analysis using the Mann-Whitney *U* test

		CENPK gene expression group		Total	*P* value
		Low expression	High expression		
Sex	Male	88	103	191	0.460
	Female	58	57	115	
Total		146	160	306	
Age	< 57	75	82	157	0.983
	> 57	71	78	149	
Total		146	160	306	
T stage	T1/2/3	108	98	206	0.018
	T4	38	62	100	
Total		146	160	306	
N metastasis	N0	117	108	225	0.012
	N1/2	29	52	81	
Total		146	160	306	
Pathological grade	1/2	111	114	225	0.130
	3	29	45	74	
Total		140	159	299	
Clinical stage	I/II	116	108	224	0.019
	III/IV	30	52	82	
Total		146	160	306	

CENPK: Centromere protein K.

size) was good 1 d after subcutaneous injection. Over 20 d, the tumors gradually decreased and even disappeared in the KD group, but they persisted in the NC group (Figure 6C). Tumors in mice were analyzed using live imaging. The total fluorescence expression volume in ten nude mice in the KD and NC groups was measured *via* quantitative analysis of fluorescence (Figures 6D and 6E). Total fluorescence expression in the region was significantly decreased in the KD group compared to the NC


A
DNA damage
ATM/ATR
NS
PAK1IP1
MDM2
L5
L11
MDM2 mediated p53 regulation of G1 cell-cycle arrest
p53
SCF
Replicative senescence
TGF-β
FOXO1
BMI1
SMAD4
SMAD3
UV Stress Response
Growth factor
p16 INK4
p15 INK4
p18 INK4C
p19 INK4
GSK 3β
CDC25A
p21 Cip1
FOXO1
p27 Kip1
MAX
c-MYC
CDK 4/6
CDK2
c-MYC
NRG1
Cyclin D
Cyclin E
SCF
RB
P
EBP1
SIN3A
RB
HDAC
SUV39H1
DP-1
E2F
Rb-dependent repression of E2F-mediated transcription
B
E2F5
HMGA2
DDX18
MAD2L1
CD44
MCM10
CCNF
PLAGL1
miR-17
SMAD2
YAP1
SOX9
SSR1
C
-Log (P value)
15.0
12.5
10.0
7.5
5.0
2.5
0.0
Threshold
Cancer
Organismal Injury and Abnormalities
Endocrine System Disorders
Cell Death and Survival
Gene Expression
Gastrointestinal Disease
Infectious Diseases
Cellular Development
Cellular Growth and Proliferation
Cell Cycle
Cardiovascular Disease
Cardiovascular System Development and Function
Connective Tissue Disorders
Developmental Disorder
Hereditary Disorder
Skeletal and Muscular Disorders
Cell Morphology
Organ Morphology
Skeletal and Muscular System Development and Function
Tissue Morphology
D
E



DOI: 10.3748/wjg.v28.i37.5420 **Copyright** ©The Author(s) 2022.

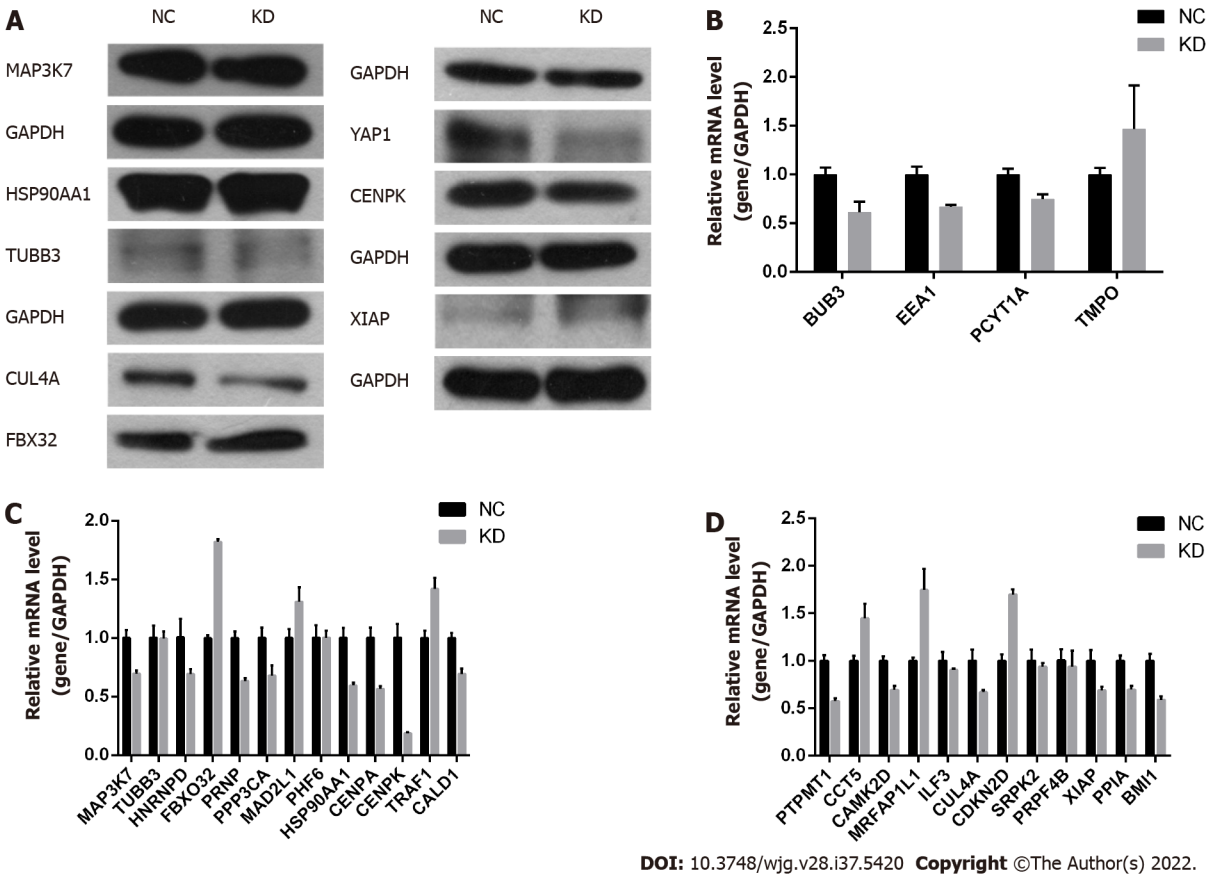
Figure 3 Centromere protein K functions in colon cancer by regulating the expression of related genes. A: Trend of molecules in the experimental results in the classical pathway; B: Upstream regulator network diagram (the orange line indicates consistent activation of upstream regulators and genes, the blue line indicates consistent upstream regulators and gene inhibition, the yellow line indicates inconsistent expression trends between upstream regulators and genes, and the gray line indicates that there is no prediction information related to the expression state in the dataset); C: Analysis and statistics of disease and functional enrichment (the transverse coordinate is the path name and the longitudinal coordinate is significance level of enrichment (negative logarithmic transformation in the bottom 10); D: Disease and functional heatmap of the effect of disease and functional changes at gene expression levels; E: Activation and inhibition relationship between genes and disease or function; F: Interplay between genes and regulators and function in the dataset; G: Network of interaction relationships between molecules of a disease or function-related relationship. TGF-β: Transforming growth factor beta; FOXO: Forkhead box O; SMAD: Suppressor of mothers against decapentaplegic; MDM: Mouse double minute; ATM: Ataxia telangiectasia mutated; ATR: Ataxia telangiectasia and Rad3 related; PAK: p21 activated kinases; NS: Non-structural; MAX: MYC associated factor X; c-MYC: Cellular myelocytomatosis oncogene; SCF: Stem cell factor; INK: CDKN2A, cyclin dependent kinase inhibitor 2A; BMI 1: BMI1 proto-oncogene; GSK: Guanosine kinase; CDK: Cyclin-dependent kinase; NRG: Neuregulin; EBP1: ErbB3-binding protein 1; SIN3A: Suppressor interacting 3a; SUV39H1: SUV39H1 histone lysine methyltransferase; DP-1: Dodeca-satellite-binding protein 1; E2F: Early region 2 binding factor; RB: Retinoblastoma; HDAC: Histone deacetylase; CD44: Cluster of differentiation-44; DDX18: DEAD-box helicase 18; HMGA: High mobility group A; MAD2L1: Mitotic arrest deficient 2 like 1; MCM: Mei-mini-chromosome maintenance; PLAGL: Pleiomorphic adenoma gene-like; SOX: SRY-box transcription factor; SSR: Signal sequence receptor subunit; YAP1: Yes1 associated transcriptional regulator; CCNE2: Cyclin E2; COMMD3: COMM domain containing 3.

group (Figure 6H). Tumor weight and volume were significantly decreased in the KD group compared to the NC group ($P < 0.05$) (Figures 6F and 6G). Therefore, lentiviral infection of RKO cells inhibited the growth of tumor cells *in vivo*.

Effect of CENPK on proliferation of RKO cells

Expression of CENPK gene in CRC cells is shown in Figure 7A, and the target gene expression abundance was relatively low. Based on the mRNA level, the CENPK gene reduction efficiency was examined using qPCR. Expression of the CENPK gene in RKO and HCT116 cells in the experimental group was inhibited after 3 d of shRNA lentivirus infection (Figures 7B and 7C). Target reduction of foreign proteins due to CENPK gene expression was detected using western blot, which showed that shCENPK had a significant knockdown effect on the exogenous expression of CENPK gene at the protein level in 293T cells (Figure 7D). Endogenous protein expression of CENPK showed that shCENPK had a significant knockdown effect on endogenous CENPK expression at the protein level in RKO cells (Figure 7D). Endogenous expression of CENPK was knocked down at the protein level in HCT116 cells (Figure 7D).

After 3 d of shRNA lentivirus infection, 1500 cells were seeded in 96-well plates. The effect of CENPK on cell proliferation *via* Celigo detection showed that proliferation of RKO cells was significantly inhibited in the experimental group. Celigo continuous detection for 5 d suggested that the CENPK gene was significantly associated with RKO and HCT116 cell proliferation (Figures 7E-H). To examine the effects of gene reduction on cell proliferation after 3 d of shRNA lentivirus infection, the cells were seeded in 96-well plates. After 5 d, the proliferation rate of RKO and HCT116 cells in the experimental group was significantly inhibited, which suggests a significant correlation between CENPK gene and RKO and HCT116 cell proliferation (Figure 7G). Detection of the effect of CENPK gene reduction on apoptosis using FACS showed that after 5 d of shRNA lentivirus infection, RKO and HCT116 cells in the experimental group increased significantly, which suggested that the CENPK gene was significantly related to apoptosis of RKO and HCT116 cells (Figure 7J, Supplementary Figures 1 and 2). Based on the detection of CENPK for apoptosis, caspase 3/7 activity was increased after 3 d of shRNA lentivirus infection in the experimental group, which suggested that CENPK gene was significantly related to



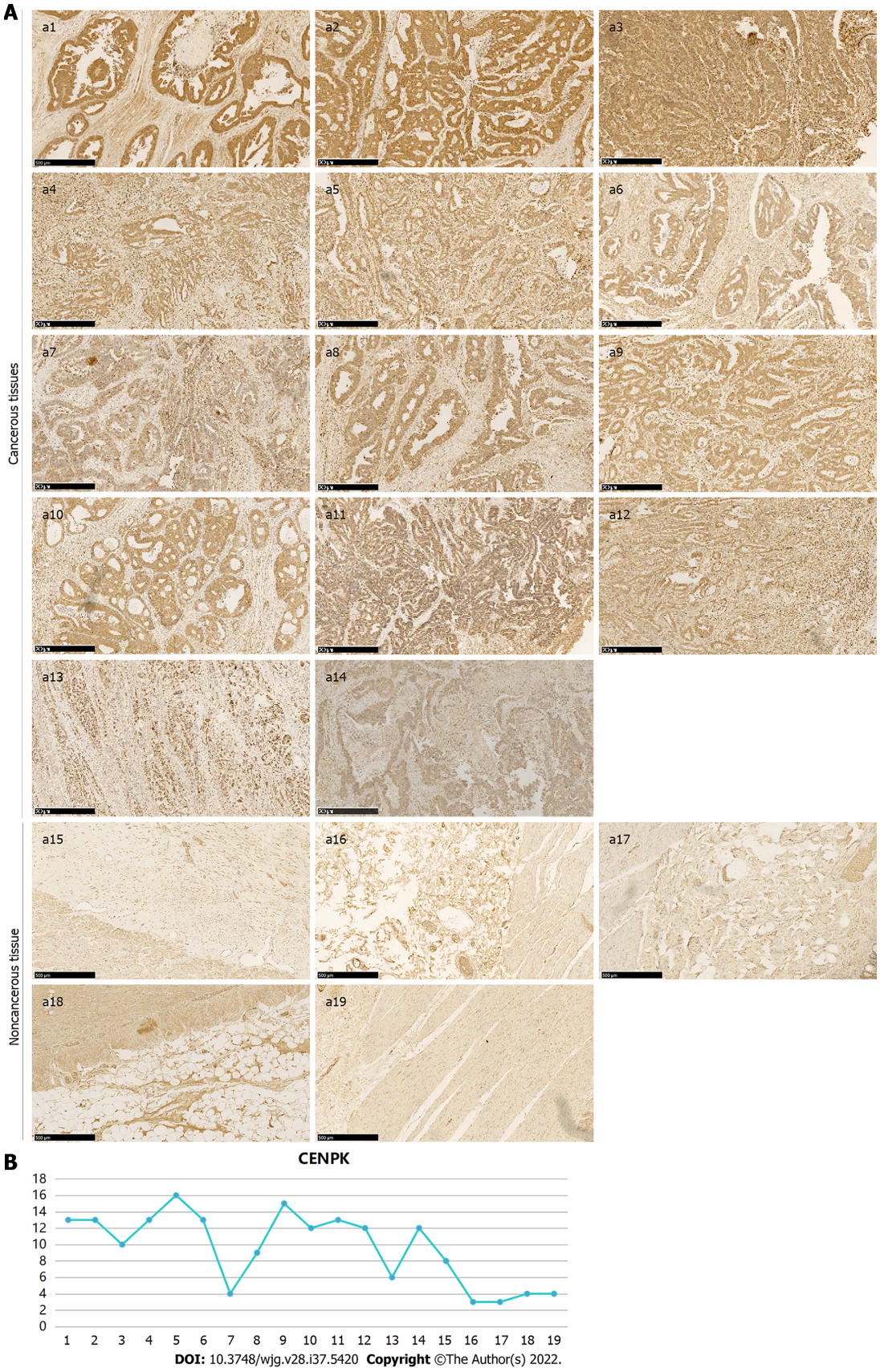
DOI: 10.3748/wjg.v28.i37.5420 **Copyright** ©The Author(s) 2022.

Figure 4 Centromere protein K plays a role by regulating F-box protein 32, Cullin 4A, Yes-associated protein isoform 1, and other genes in RKO cells. A: Downstream gene (Yes-associated protein isoform 1, centromere protein K, Cullin 4A, F-box protein 32, X chromosome-linked inhibitor of apoptosis, heat shock protein 90 alpha family class A member 1, class III-tubulin, and mitogen-activated protein kinase kinase kinase 7) testing using western blot analysis in NC and KD groups; B-D: Relative gene expression detected using quantitative polymerase chain reaction in NC and KD groups. F-box protein 32 was upregulated, while Cullin 4A and Yes-associated protein isoform 1 were downregulated. FBX32: F-box protein 32; YAP1: Yes-associated protein isoform 1; CENPK: Centromere protein K; CUL4A: Cullin 4A; XIAP: X chromosome-linked inhibitor of apoptosis; HSP90AA1: Heat shock protein 90 alpha family class A member 1; TUBB3: Class III-tubulin; MAP3K7: Mitogen-activated protein kinase kinase kinase 7; BUB3: BUB3 mitotic checkpoint protein; EEA1: Early endosomal antigen 1; PCYT1A: Phosphate cytidylyltransferase 1A; TMPO: Thymopoietin; HNRNPD: Heterogeneous nuclear ribonucleoprotein D; PRNP: Prion protein; PPP3CA: Protein phosphatase 3 catalytic subunit alpha; MAD2L1: Mitotic arrest deficient 2 like 1; PHF6: PHD finger protein 6; CENPA: Centromere protein A; TRAF1: TNF receptor associated factor 1; CALD1: Caldesmon 1; PTPMT1: Protein tyrosine phosphatase mitochondrial 1; CCT5: Chaperonin containing TCP1 subunit 5; CAMK2D: Calcium/calmodulin dependent protein kinase II delta; MRFAP1L1: Morf4 family associated protein 1 like 1; ILF3: Interleukin enhancer binding factor 3; CDKN2D: Cyclin dependent kinase inhibitor 2D; SRPK2: SRSF protein kinase 2; PRPF4B: Pre-mRNA processing factor 4B; PPIA: Peptidylprolyl isomerase A; BMI1: BMI1 proto-oncogene; GAPDH: Glyceraldehyde-3-phosphate dehydrogenase. NC: RKO cells infected with CENPK negative control virus; KD: RKO cells with lentivirus-mediated short hairpin RNA interference of CENPK.

apoptosis of RKO and HCT116 cells (Figure 7I). Therefore, CENPK gene inhibited proliferation of RKO cells. After RNAi of the CENPK gene in RKO cells, associated genes in the signaling pathway were detected using PathScan. The protein expression levels in the p-ERK1/2, p-Stat1, p-Stat3, p-Akt (Ser473), p-HSP27, p-p70 S6 kinase, p-PRAS40, and p-p38 signaling pathways were significantly different ($P < 0.05$) (Figure 7K).

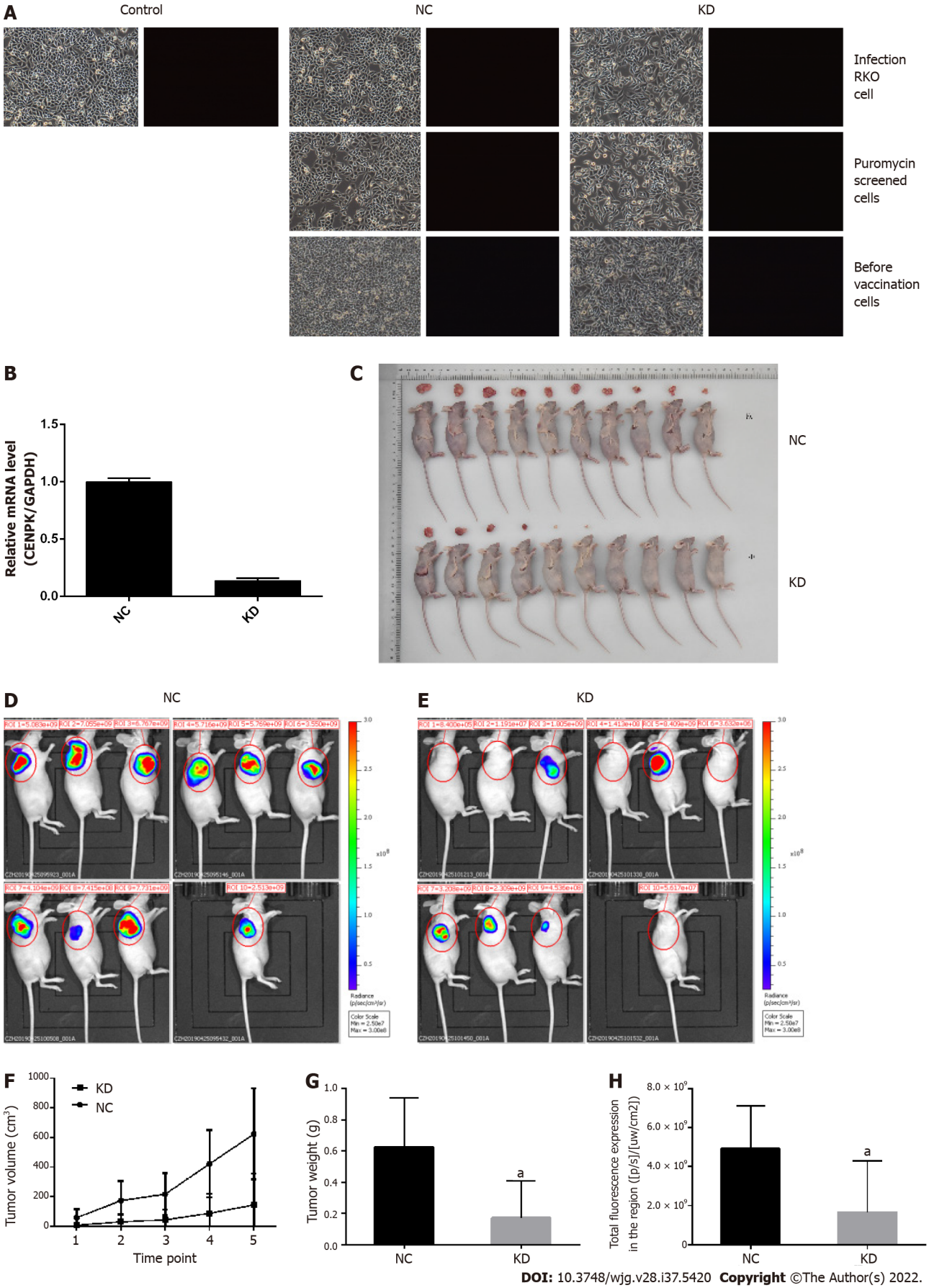
Inhibition of RKO and HCT116 cells by abrogation of CENPK and overexpression of CUL4A

Lentivirus-mediated shRNA interference of CENPK in HCT116 cells and RKO cells was observed (Figure 8). The control and target lentivirus-infected cells (HCT116 cells and RKO cells) were observed after 72 h under a microscope, and cell infection efficiency reached > 80%, and the cell state was normal. The effects of CENPK gene reduction and CUL4A gene overexpression on HCT 116 and RKO cell proliferation using Celigo detection are shown in Figures 9A-D. At 3 d after lentiviral infection, the number of HCT 116 cells was 1000, and the number of RKO cells was 2000. After 5 d, the KD group exhibited slower cell proliferation compared to the NC (KD) group. Cell proliferation increased rapidly in the KD + OE and NC (OE) groups compared to the KD + NC (OE) and OE groups in HCT 116 cells (Figures 8A and 8B, Supplementary Figures 3 and 4) and RKO cells (Figures 6C and 6D). HCT 116 and RKO cell proliferation was measured using the MTT assay (Figures 9E-H). Cell proliferation increased slowly in the KD group compared to the NC (KD) group, but it increased rapidly in the OE group compared to the NC (OE) group. However, RKO cell proliferation was not consistently increased in the KD + OE



DOI: 10.3748/wjg.v28.i37.5420 **Copyright** ©The Author(s) 2022.

Figure 5 Expression of centromere protein K in colon cancer tissue and noncancerous tissue detected using immunohistochemistry. A: Centromere protein K (CENPK) expression in cancerous (a1-a14) and noncancerous tissue (a15-a19) using immunohistochemistry (Scale bar: 500 μm) with VULCAN FAST RED CHROMOGEN kit 2; B: Positive expression of CENPK in cancerous and noncancerous tissues. CENPK: Centromere protein K.



DOI: 10.3748/wjg.v28.i37.5420 **Copyright** ©The Author(s) 2022.

Figure 6 Analysis of tumor growth in nude mice subcutaneously injected with lentivirus-infected RKO cells. A: Control lentivirus-infected RKO cells, RKO cells infected with centromere protein K (CENPK) negative control virus (NC), and RKO cells with CENPK gene short hairpin RNA virus infection (KD); puromycin-screened cells in the NC and KD groups; and RKO cells in the NC and KD groups before inoculation are shown (× 100 magnification). On the left and right

are bright field and fluorescence images, respectively; B: Real-time polymerase chain reaction detection of CENPK mRNA expression in RKO cells; C: Tumor status in nude mice subcutaneously injected with lentivirus-infected RKO cells in the NC and KD groups. D: Isoflurane gas anesthesia was applied for live imaging under a live imager in the NC group; E: Isoflurane gas anesthesia was applied for live imaging under a live imager in the KD group; F: Tumor volume of lentivirus-infected RKO cells examined in nude mice in the NC and KD groups; G: Tumor weight of lentivirus-infected RKO cells were examined in nude mice in the NC and KD groups; H: Regional total fluorescence expression in the NC and KD groups. $^{a}P < 0.05$, compared with RKO cells infected with centromere protein K negative control virus. CENPK: Centromere protein K; NC: RKO cells infected with centromere protein K negative control virus; KD: RKO cells with lentivirus-mediated short hairpin RNA interference of centromere protein K.

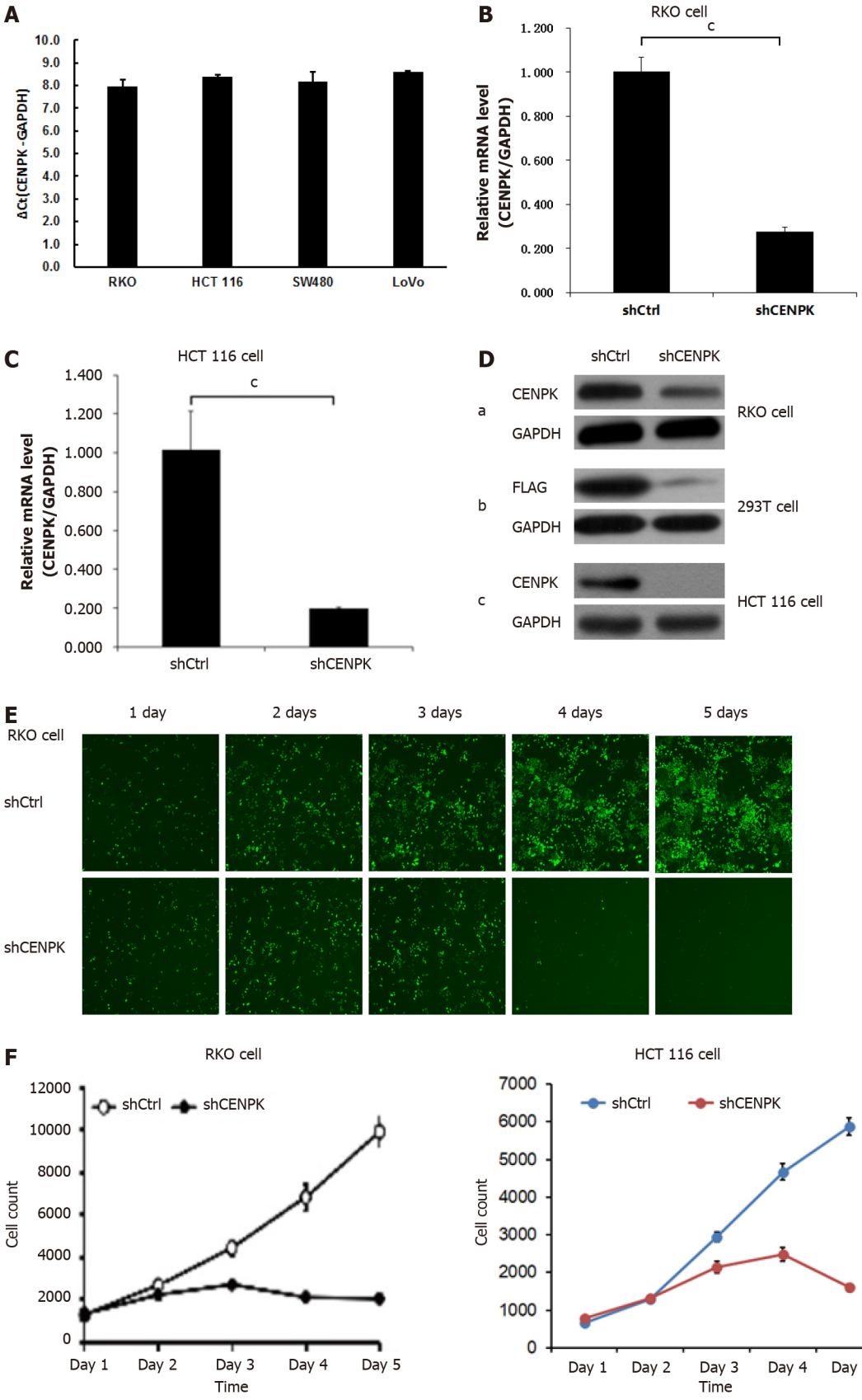
group compared with the KD + NC (OE) group, and HCT 116 cell proliferation was obviously increased in the KD + OE group. HCT 116 and RKO cell apoptosis was induced by CENPK gene reduction and CUL4A gene overexpression; therefore, caspase 3/7 activity and apoptotic cells were measured after lentiviral infection for 5 d. Based on the findings for HCT 116 and RKO cells shown in Figure 9I, caspase 3/7 activity and apoptotic cells were increased in the KD group compared to the NC (KD) group. Caspase 3/7 activity did not change significantly in the OE group, and apoptotic cells did not change significantly compared with the NC (OE) group. Similar to the KD + NC (OE) group, the KD + OE groups exhibited decreased caspase 3/7 activity and apoptosis. HCT 116 and RKO cell apoptosis *via* CENPK gene reduction and CUL4A gene overexpression was detected using FACS (Figure 9K, Supplementary Figures 5 and 6). HCT 116 and RKO cell apoptosis was increased significantly in the KD group ($P < 0.01$) compared to the NC (KD) group. Apoptosis was decreased significantly in the KD + OE group ($P < 0.01$) compared to the KD + NC (OE) group. However, no significant change in apoptosis occurred in the OE group. The FLAG protein level after CUL4A overexpression was detected using western blot (Figure 9J). The proliferation rate in the OE group compared to the NC group after CUL4A overexpression in HCT116 and RKO cells was detected by FLAG. These results suggested that lentivirus-mediated shRNA interference of CENPK inhibited the proliferation of RKO and HCT116 cells, and overexpression of the CUL4A gene reversed this effect in RKO and HCT 116 cells with CENPK gene knockdown.

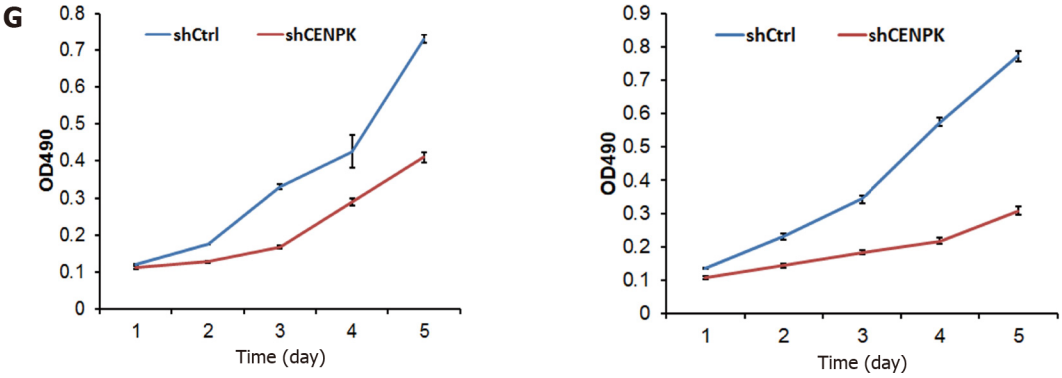
DISCUSSION

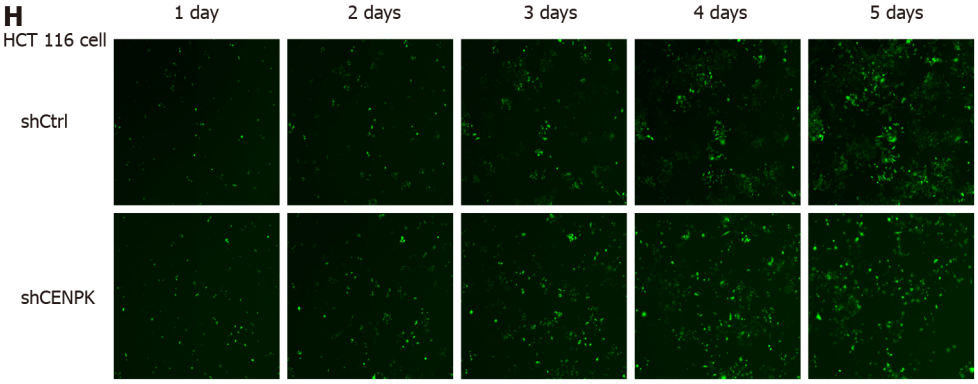
CRC is one of the most common malignant tumors. Increasing evidence suggests that CENPK plays a key role in promoting carcinogenesis[14]. To the best of our knowledge, this study is the first to clarify the clinical value of CENPK in human CRC tissues. However, the underlying mechanism is largely unknown. The expression of CENPK in CRC tissues was quantified using western blot and quantitative real-time PCR. CENPK was highly expressed in CRC tissue and positively correlated with large tumor size and advanced tumor stage. CENPK was found to be frequently downregulated in CRC primary tumor samples compared to adjacent normal tissues, using bioinformatics analysis and experiments *in vivo*. Expression of the CENPK gene was significantly different in cancerous and noncancerous tissues, which supports the use of CENPK for diagnosis of CRC and patient selection for therapy. Tissue chip detection showed that CENPK expression was associated with pathological indicators, such as T stage, N stage, and clinical stage. This confirmed the low level of CENPK expression in early cancer and increasing expression during the course of the disease. We used *in vitro* and *in vivo* models to demonstrate that lentivirus-mediated shRNA interference of CENPK regulated the proliferation of CRC cells. The CENPK gene may affect the expression of a series of downstream genes by acting on YWHAZ and BMI1, which affect cell proliferation and invasion. Therefore, CENPK gene functions in the progression of CRC by altering the expression of CUL4A, CENPK, XIAP, FBX32, YAP1, MAP3K7, TUBB3, and HSP90AA1. Western blot analysis showed that FBX32 was upregulated and CUL4A and YAP1 were downregulated.

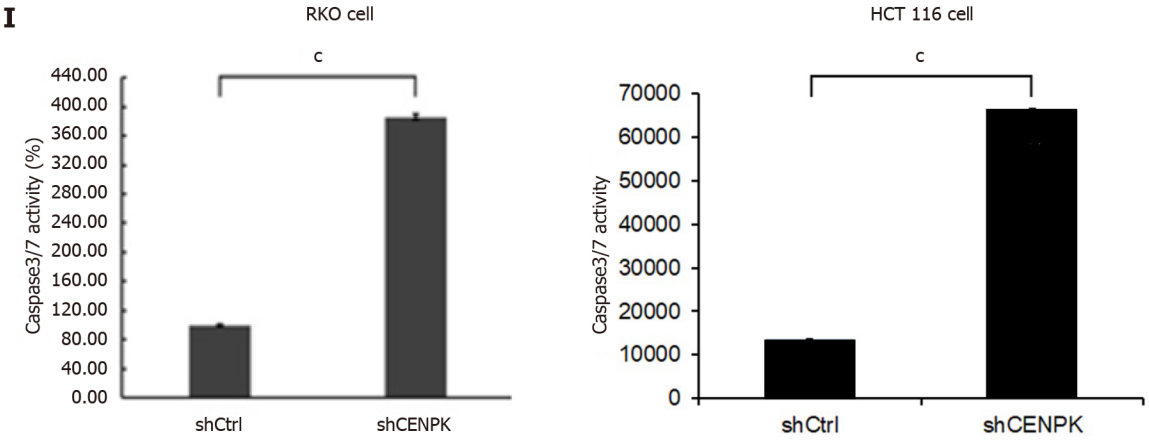
YAP1 is an effector of the Hippo pathway, which is critical for regulating organ size, cell proliferation, and tumor growth in mammals[15]. Research on YAP1 expression in CRC tissues showed the effect of silencing expression of the YAP1 gene on the proliferation and invasion of SW620 CRC cells [16]. Another study showed that FBX32 and the mRNA levels of several proteasome-related genes were significantly upregulated by methionine limitation[17]. Moreover, CUL4A is highly expressed in colon cancer and promotes the proliferation and inhibits the apoptosis of colon cancer cells by regulating the Hippo pathway[10]. Therefore, the mechanism of the effect of CUL4A expression on cell proliferation and apoptosis in CRC by regulating the CENPK pathway was further investigated.

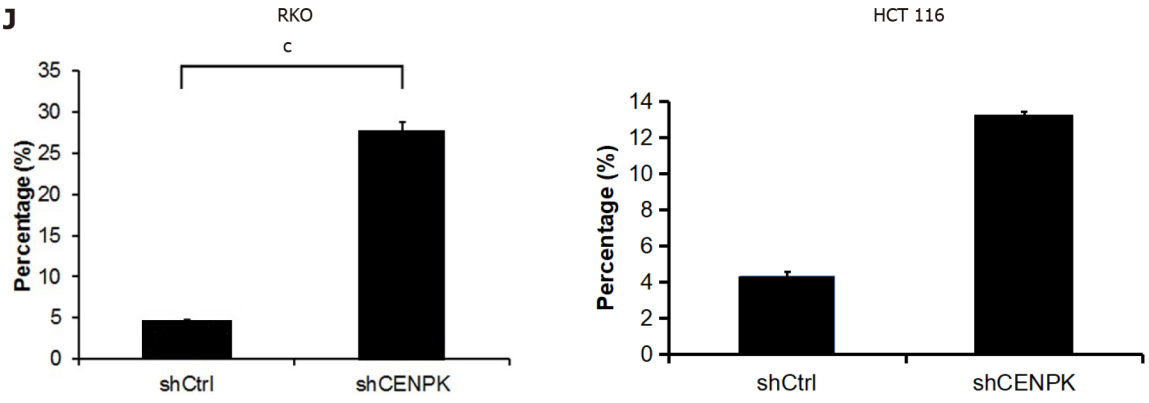
Lentivirus-mediated shRNA interference of CENPK was successfully and stably induced in RKO cells, which lays a foundation for further study of the role of the CENPK gene in the carcinogenesis and progression of CRC. With regard to therapeutic options for CRC, increased CENPK expression inhibited CRC cell proliferation and induced apoptosis of RKO cells with lentiviral infection, which suggests that CENPK inhibits CRC progression. A xenograft mouse model also confirmed the tumor-suppressive function of CENPK. We used RKO cells with lentiviral infection to control these processes and inhibit tumor growth. Specifically, we found that the CENPK gene regulated tumor growth, and the total

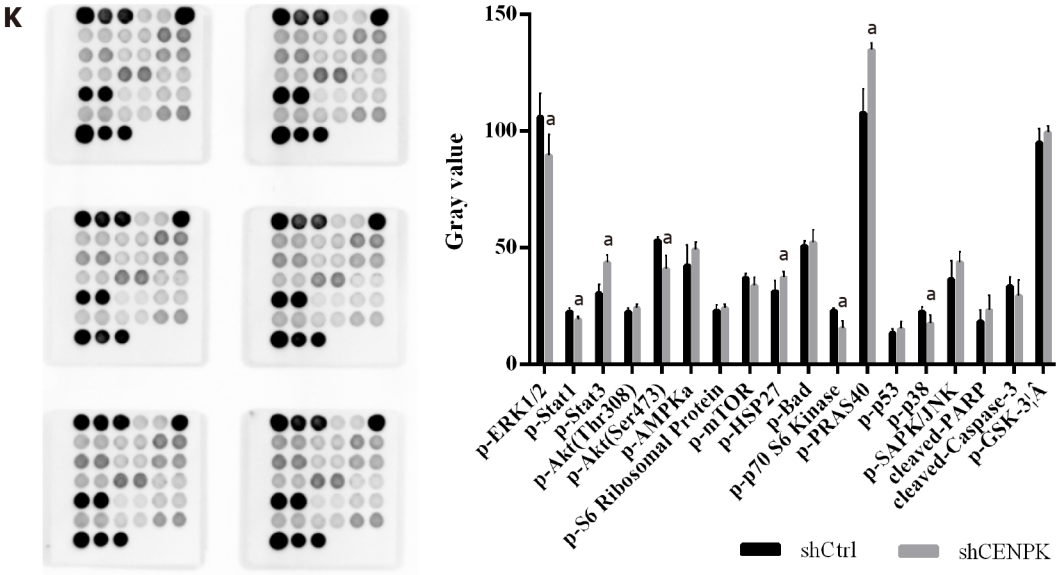

A
ΔCt(CENPK-GAPDH)
10.0
9.0
8.0
7.0
6.0
5.0
4.0
3.0
2.0
1.0
0.0
RKO
HCT 116
SW480
LoVo
B
RKO cell
c
Relative mRNA level (CENPK/GAPDH)
1.200
1.000
0.800
0.600
0.400
0.200
0.000
shCtrl
shCENPK
C
HCT 116 cell
c
Relative mRNA level (CENPK/GAPDH)
1.400
1.200
1.000
0.800
0.600
0.400
0.200
0.000
shCtrl
shCENPK
D
shCtrl
shCENPK
a
CENPK
GAPDH
RKO cell
b
FLAG
GAPDH
293T cell
c
CENPK
GAPDH
HCT 116 cell
E
1 day
2 days
3 days
4 days
5 days
RKO cell
shCtrl
shCENPK
F
RKO cell
shCtrl
shCENPK
Cell count
12000
10000
8000
6000
4000
2000
0
Day 1
Day 2
Day 3
Day 4
Day 5
Time
HCT 116 cell
shCtrl
shCENPK
Cell count
7000
6000
5000
4000
3000
2000
1000
0
Day 1
Day 2
Day 3
Day 4
Day 5
Time


G
shCtrl
shCENPK
OD490
Time (day)
shCtrl
shCENPK
OD490
Time (day)


H
1 day
2 days
3 days
4 days
5 days
HCT 116 cell
shCtrl
shCENPK


I
RKO cell
HCT 116 cell
c
Caspase3/7 activity (%)
Caspase3/7 activity
shCtrl
shCENPK


J
RKO
HCT 116
c
Percentage (%)
shCtrl
shCENPK



DOI: 10.3748/wjg.v28.i37.5420 **Copyright** ©The Author(s) 2022.

Figure 7 Effects of centromere protein K on proliferation of RKO cells. A: Expression of the centromere protein K (CENPK) gene in colon cancer cells; B and C: CENPK mRNA level reduction in RKO and HCT116 cells; D: Exogenous expression of CENPK protein in RKO cells (a), 293T cells (b), and HCT116 cells (c); E and F: Effects of CENPK gene reduction on RKO cell proliferation by Celigo detection; G: Effects of CENPK gene reduction on RKO and HCT116 cell proliferation detected by MTT assay; H: Effects of CENPK gene reduction on HCT116 cell proliferation by Celigo detection; I: Effects of CENPK gene reduction on RKO and HCT116 cell apoptosis by caspases 3/7 detection; J: Effects of CENPK gene reduction on RKO and HCT116 cell apoptosis by FACS detection; K: Chemiluminescence analysis in the shCtrl and shCENPK groups. $^{a}P < 0.01$, compared with shCtrl; $^{b}P < 0.05$, shCtrl compared to the short hairpin RNA lentivirus treatment group; $^{c}P < 0.01$, shCtrl compared to the short hairpin RNA lentivirus treatment group. CENPK: Centromere protein K.

fluorescence in the tumor was significantly decreased compared to the controls. We analyzed whether lentivirus-mediated shRNA interference of CENPK was involved in cell proliferation and apoptosis. The results indicated that interference with the CENPK gene inhibited RKO cell proliferation. Taken together, these findings support the hypothesis that lentivirus-mediated shRNA suppresses CENPK expression *via* lentivirus epigenetically. Overexpression of CENPK has been observed in various tumor types[8,18,19].

CUL4A plays a critical role in cellular proliferation and tumor invasion[20,21]. *In vitro* experiments were performed to verify the function of the CUL4A gene. To investigate whether CUL4A gene was involved in CENPK-induced CRC cell proliferation, we performed rescue experiments, which indicated that knockdown of CENPK and overexpression of CUL4A partially rescued proliferation in RKO and HCT116 cells. These findings support the hypothesis that interference with the CENPK gene inhibits RKO and HCT116 cell proliferation. Overexpression of CUL4A had a response effect on RKO and HCT 116 cells.

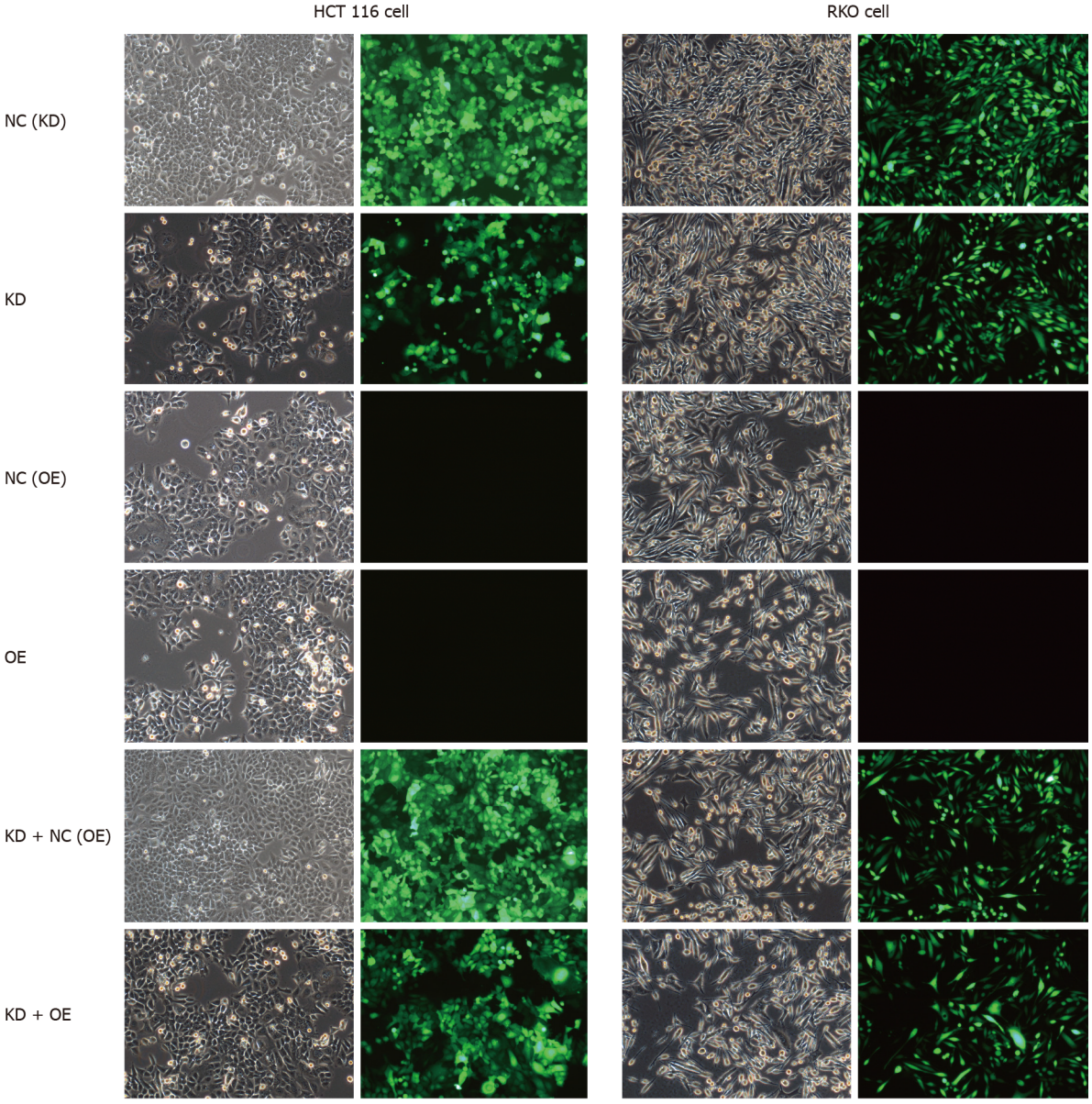
The functional effects of CUL4A proteins on their targets have been well characterized and are involved in the proliferation of cancer cells[22]. CUL4A may be a prognostic marker of precancerous lesions and a potential therapeutic target in cancer[23]. Consistent with these reports, overexpression of CUL4A was observed in 20 pairs of CRC tissues, and knockdown of CUL4A inhibited cell proliferation. A previous study showed that CUL4A was highly expressed in CRC and promoted proliferation and inhibited apoptosis of CRC cells by regulating the Hippo pathway[10]. Our study demonstrated that restoration of CUL4A expression suppressed CRC cell proliferation. These results indicate that CUL4A acts as a tumor suppressor in CRC. It has been found that high CUL4A protein expression is an independent prognostic marker in CRC[12].

CONCLUSION

Our study demonstrated that overexpression of CUL4A led to CRC tumorigenesis, and knockdown of the CENPK gene affected CRC progression and development in target cells. To the best of our knowledge, this study is the first to investigate CUL4A protein expression and its potential interference with CENPK gene interactions in CRC. We demonstrated the critical role of the CUL4A gene in the progression of CRC. However, due to the complexity of shRNA biological function, further analysis is required to achieve a more comprehensive understanding of CRC diagnosis and therapy.

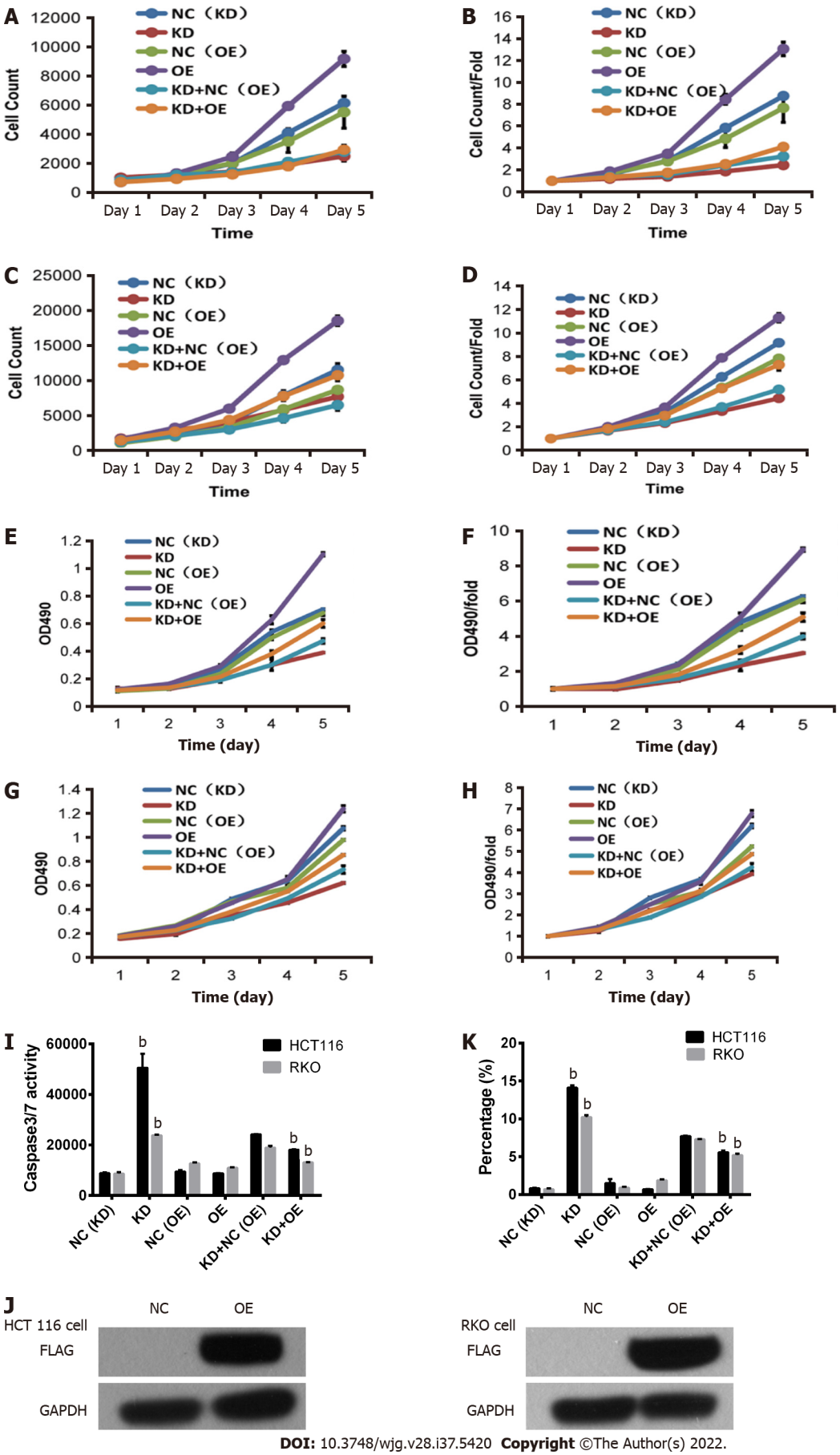
Table 7 Correlation between centromere protein K gene expression and clinical data in cancerous tissues

		Gene expression	T stage	N metastasis	Pathological grade
Gene expression	Correlation coefficient	1.000	0.135	0.143	0.135
	Significance (two-tailed)	0.000	0.018	0.012	0.018
T stage	Correlation coefficient	0.135	1.000	0.000	0.000
	Significance (two-tailed)	0.018	0.000	0.000	0.000
N metastasis	Correlation coefficient	0.143	0.000	1.000	0.000
	Significance (two-tailed)	0.012	0.000	0.000	0.000
Pathological grade	Correlation coefficient	0.135	0.000	0.000	1.000
	Significance (two-tailed)	0.018	0.000	0.000	0.000



DOI: 10.3748/wjg.v28.i37.5420 **Copyright** ©The Author(s) 2022.

Figure 8 Lentivirus-mediated short hairpin RNA interference of centromere protein K in HCT116 and RKO cells. Bright field (left) and fluorescence images (right) are shown. NC: RKO or HCT 116 cells infected with centromere protein K negative control virus; KD: RKO or HCT 116 cells with centromere protein K gene short hairpin RNA virus infection; OE: RKO or HCT 116 cells virally infected with Cullin 4A.



DOI: 10.3748/wjg.v28.i37.5420 **Copyright** ©The Author(s) 2022.

Figure 9 Inhibition of RKO and HCT116 colon cancer cells by abrogation of centromere protein K and overexpression of Cullin 4A. A and B: Effects of centromere protein K (CENPK) knockdown and Cullin 4A (CUL4A) overexpression on HCT116 cell proliferation detected by Celigo assay; C and D:

Effects of CENPK knockdown and CUL4A overexpression on RKO cell proliferation detected by Celigo assay; E and F: Effects of CENPK knockdown and CUL4A overexpression on HCT116 cell proliferation detected by MTT assay; G and H: Effects of CENPK knockdown and CUL4A overexpression on RKO cell proliferation detected by MTT assay; I: HCT116 and RKO cell apoptosis after CENPK knockdown and CUL4A overexpression detected by caspases 3/7; J: FLAG protein expression levels after CUL4A overexpression detected using western blot; K: HCT116 and RKO cell apoptosis. $^{b}P < 0.01$, shCtrl compared to short hairpin RNA lentivirus treatment group. NC: RKO or HCT 116 cells infected with centromere protein K negative control virus; KD: RKO or HCT 116 cells with centromere protein K gene short hairpin RNA virus infection; OE: RKO or HCT 116 cells virally infected with Cullin 4A.

ARTICLE HIGHLIGHTS

Research background

Colorectal cancer (CRC) is one of the most common malignant tumors worldwide. Immunohistochemistry has found high expression of centromere protein (CENPK) in CRC. However, the role of CENPK in the progression of CRC is not well characterized.

Research motivation

To explore the role of Cullin (CUL)4A expression and lentivirus-mediated transfection with short hairpin RNA (shRNA) for CENPK in CRC.

Research objectives

We performed a series of *in vitro* experiments, such as quantitative polymerase chain reaction (qPCR), western blot, MTT assay, and flow cytometry, to evaluate the knockdown behavior of CENPK and overexpression of CUL4A in RKO and HCT 116 CRC cells.

Research methods

We identified CENPK as a potential new oncogene for CRC based on bioinformatics analysis. *In vitro* experiments verified the function of this gene. We investigated the expression of CENPK in RKO and HCT 116 cells using virus infection and analyzed datasets from qPCR, western blot, and flow cytometry. The effect of RKO cells infected with virus on tumor growth was evaluated *in vivo* using quantitative analysis of fluorescence imaging.

Research results

The downstream genes FBX32, CUL4A, and YAP1 were examined to evaluate the regulatory action of CENPK in RKO cells. Significantly delayed xenograft emergence, slower growth, and lower final tumor weight and volume were observed in the RKO and HCT 116 with lentivirus-mediated shRNA interference of CENPK. Interference of CENPK inhibited the proliferation rate of RKO cells *in vitro* and *in vivo*. The shRNA interference of CENPK inhibited the proliferation of RKO and HCT 116 cells, and overexpression of CUL4A gene responded to RKO and HCT 116 cells with CENPK silencing.

Research conclusions

Our findings indicate a potential role of CENPK in promoting tumor proliferation, and it may serve as a novel diagnostic and prognostic biomarker in patients with CRC.

Research perspectives

An investigation for lentivirus-mediated transfection with shRNA for CENPK and overexpression of CUL4A demonstrated major regulatory roles in CRC. Further analysis is required to achieve a more comprehensive understanding of CRC diagnosis and therapy.

FOOTNOTES

Author contributions: Wu XL analyzed and interpreted the patient data; Han YR, XueFeng X, Ma YX, Xing GS, Yang ZW, Zhang Z, and Shi L did the experiments; Li X was a major contributor in writing the manuscript. All the authors read and approved the final manuscript.

Supported by the National Natural Science Foundation of China, No. 81860416 and No. 22168028; Inner Mongolia Autonomous Region Grassland Talent Innovation Talent Team Fund, No. 2019; and Inner Mongolia Natural Science Fund, No. 2021MS02005.

Institutional review board statement: The study was reviewed and approved by the Ethics Committee of The Affiliated Hospital of Inner Mongolia Medical University Institutional Review Board (Approval No. WZ 2021045).

Conflict-of-interest statement: All the authors report no relevant conflicts of interest for this article.

Data sharing statement: No additional data are available.

Open-Access: This article is an open-access article that was selected by an in-house editor and fully peer-reviewed by external reviewers. It is distributed in accordance with the Creative Commons Attribution NonCommercial (CC BY-NC 4.0) license, which permits others to distribute, remix, adapt, build upon this work non-commercially, and license their derivative works on different terms, provided the original work is properly cited and the use is non-commercial. See: https://creativecommons.org/Licenses/by-nc/4.0/

Country/Territory of origin: China

ORCID number: Xian Li 0000-0002-9107-5096; Yi-Ru Han 0000-0001-8245-9533; Xuefeng Xuefeng 0000-0002-5058-5735; Yong-Xiang Ma 0000-0002-1027-0093; Guo-Sheng Xing 0000-0002-5183-7607; Zhi-Wen Yang 0000-0001-6502-3850; Zhen Zhang 0000-0002-5281-7067; Lin Shi 0000-0001-6543-8650; Xin-Lin Wu 0000-0002-2860-4477.

S-Editor: Wang JJ
L-Editor: Wang TQ
P-Editor: Wang JJ

REFERENCES

1 **Matsushita N**, Matsushita S, Hirakawa S, Higashiyama S. Doxycycline-dependent inducible and reversible RNA interference mediated by a single lentivirus vector. *Biosci Biotechnol Biochem* 2013; **77**: 776-781 [PMID: 23563548 DOI: 10.1271/bbb.120917]
2 **Uppada SB**, Gowrikumar S, Ahmad R, Kumar B, Szeglin B, Chen X, Smith JJ, Batra SK, Singh AB, Dhawan P. MASTL induces Colon Cancer progression and Chemoresistance by promoting Wnt/β-catenin signaling. *Mol Cancer* 2018; **17**: 111 [PMID: 30068336 DOI: 10.1186/s12943-018-0848-3]
3 **Li Y**, Yang Z, Wu N, Xu L and Leng Z. Effects and Mechanism of shRNA Interfering with KLF4 Expression on the Migration and Invasion of Lgr5 + Colorectal Cancer Stem Cells. *Med J Wuhan University* 2018; **39**: 899-904 [DOI: 10.14188/j.1671-8852.2018.0509]
4 **Sacca R**, Engle SJ, Qin W, Stock JL, McNeish JD. Genetically engineered mouse models in drug discovery research. *Methods Mol Biol* 2010; **602**: 37-54 [PMID: 20012391 DOI: 10.1007/978-1-60761-058-8_3]
5 **Zhao B**, Yang C, Yang S, Gao Y, Wang J. Construction of conditional lentivirus-mediated shRNA vector targeting the human Mirk gene and identification of RNAi efficiency in rhabdomyosarcoma RD cells. *Int J Oncol* 2013; **43**: 1253-1259 [PMID: 23913162 DOI: 10.3892/ijo.2013.2048]
6 **Wang J**, Li H, Xia C, Yang X, Dai B, Tao K, Dou K. Downregulation of CENPK suppresses hepatocellular carcinoma malignant progression through regulating YAP1. *Onco Targets Ther* 2019; **12**: 869-882 [PMID: 30774374 DOI: 10.2147/OTT.S190061]
7 **Li Q**, Liang J, Zhang S, An N, Xu L, Ye C. Overexpression of centromere protein K (CENPK) gene in Differentiated Thyroid Carcinoma promote cell Proliferation and Migration. *Bioengineered* 2021; **12**: 1299-1310 [PMID: 33904381 DOI: 10.1080/21655979.2021.1911533]
8 **Lee YC**, Huang CC, Lin DY, Chang WC, Lee KH. Overexpression of centromere protein K (CENPK) in ovarian cancer is correlated with poor patient survival and associated with predictive and prognostic relevance. *PeerJ* 2015; **3**: e1386 [PMID: 26587348 DOI: 10.7717/peerj.1386]
9 **Jia B**, Dao J, Han J, Huang Z, Sun X, Zheng X, Xiang S, Zhou H, Liu S. LINC00958 promotes the proliferation of TSCC *via* miR-211-5p/CENPK axis and activating the JAK/STAT3 signaling pathway. *Cancer Cell Int* 2021; **21**: 147 [PMID: 33658048 DOI: 10.1186/s12935-021-01808-z]
10 **Yi LJ**, Yi LJ, Ding N, Ren J. CUL4A promotes proliferation and inhibits apoptosis of colon cancer cells *via* regulating Hippo pathway. *Eur Rev Med Pharmacol Sci* 2020; **24**: 10518-10525 [PMID: 33155207 DOI: 10.26355/eurrev_202010_23404]
11 **Sui X**, Zhou H, Zhu L, Wang D, Fan S, Zhao W. CUL4A promotes proliferation and metastasis of colorectal cancer cells by regulating H3K4 trimethylation in epithelial-mesenchymal transition. *Onco Targets Ther* 2017; **10**: 735-743 [PMID: 28223829 DOI: 10.2147/OTT.S118897]
12 **Li C**, Bu J, Liao Y, Zhang J, Han J, Zhang H, Xing H, Li Z, Wu H, Liang L, Wang M, Qin W, Yang T. High Expressions of CUL4A and TP53 in Colorectal Cancer Predict Poor Survival. *Cell Physiol Biochem* 2018; **51**: 2829-2842 [PMID: 30562757 DOI: 10.1159/000496013]
13 **Wu XL**, Yang ZW, He L, Dong PD, Hou MX, Meng XK, Zhao HP, Wang ZY, Wang F, Baoluri, Wurenqimuge, Agudamu, Jia YF, Shi L. RRS1 silencing suppresses colorectal cancer cell proliferation and tumorigenesis by inhibiting G2/M progression and angiogenesis. *Oncotarget* 2017; **8**: 82968-82980 [PMID: 29137316 DOI: 10.18632/oncotarget.20897]
14 **Wang Y**, Wang Y, Ren C, Wang H, Zhang Y, Xiu Y. Upregulation of centromere protein K is crucial for lung adenocarcinoma cell viability and invasion. *Adv Clin Exp Med* 2021; **30**: 691-699 [PMID: 34118147 DOI: 10.17219/acem/133820]
15 **Ou C**, Sun Z, Li X, Ren W, Qin Z, Zhang X, Yuan W, Wang J, Yu W, Zhang S, Peng Q, Yan Q, Xiong W, Li G, Ma J. Corrigendum to "MiR-590-5p, a density-sensitive microRNA, inhibits tumorigenesis by targeting YAP1 in colorectal cancer", [Canc. Lett. 399 (2017) 53-63]. *Cancer Lett* 2018; **420**: 260 [PMID: 29429755 DOI: 10.1016/j.canlet.2018.01.073]
16 **Zhao YP**, Han ZW, Xie Y. Expression and significance of YAP1 in colorectal cancer tissues. *Chin J Curr Advan Gene Sur*

2019 [DOI: 10.11569/wcjd.v22.i2.273]

17 **Belghit I**, Skiba-Cassy S, Geurden I, Dias K, Surget A, Kaushik S, Panserat S, Seiliez I. Dietary methionine availability affects the main factors involved in muscle protein turnover in rainbow trout (Oncorhynchus mykiss). *Br J Nutr* 2014; **112**: 493-503 [PMID: 24877663 DOI: 10.1017/S0007114514001226]

18 **Huang H**, Cheng S, Ding M, Wen Y, Ma M, Zhang L, Li P, Cheng B, Liang X, Liu L, Du Y, Zhao Y, Kafle OP, Han B, Zhang F. Integrative analysis of transcriptome-wide association study and mRNA expression profiles identifies candidate genes associated with autism spectrum disorders. *Autism Res* 2019; **12**: 33-38 [PMID: 30561910 DOI: 10.1002/aur.2048]

19 **Parolin C**, Corso AD, Alberghina L, Porro D, Branduardi P. Heterologous production of five Hepatitis C virus-derived antigens in three Saccharomyces cerevisiae host strains. *J Biotechnol* 2005; **120**: 46-58 [PMID: 16039743 DOI: 10.1016/j.jbiotec.2005.05.025]

20 **Wang Y**, Wen M, Kwon Y, Xu Y, Liu Y, Zhang P, He X, Wang Q, Huang Y, Jen KY, LaBarge MA, You L, Kogan SC, Gray JW, Mao JH, Wei G. CUL4A induces epithelial-mesenchymal transition and promotes cancer metastasis by regulating ZEB1 expression. *Cancer Res* 2014; **74**: 520-531 [PMID: 24305877 DOI: 10.1158/0008-5472.CAN-13-2182]

21 **Pan Y**, Wang B, Yang X, Bai F, Xu Q, Li X, Gao L, Ma C, Liang X. CUL4A facilitates hepatocarcinogenesis by promoting cell cycle progression and epithelial-mesenchymal transition. *Sci Rep* 2015; **5**: 17006 [PMID: 26593394 DOI: 10.1038/srep17006]

22 **Ashok C**, Owais S, Srijyothi L, Selvam M, Ponne S, Baluchamy S. A feedback regulation of CREB activation through the CUL4A and ERK signaling. *Med Oncol* 2019; **36**: 20 [PMID: 30666499 DOI: 10.1007/s12032-018-1240-2]

23 **Feng M**, Wang Y, Bi L, Zhang P, Wang H, Zhao Z, Mao JH, Wei G. CRL4A^{DTL} degrades DNA-PKcs to modulate NHEJ repair and induce genomic instability and subsequent malignant transformation. *Oncogene* 2021; **40**: 2096-2111 [PMID: 33627782 DOI: 10.1038/s41388-021-01690-z]

World Journal of Gastroenterology

Submit a Manuscript: https://www.f6publishing.com

World J Gastroenterol 2022 October 7; 28(37): 5444-5456

DOI: 10.3748/wjg.v28.i37.5444

ISSN 1007-9327 (print) ISSN 2219-2840 (online)

ORIGINAL ARTICLE

Retrospective Cohort Study

Prognostic performance of an index based on lactic dehydrogenase and transaminases for patients with liver steatosis and COVID-19

Ricardo Ulises Macías-Rodríguez, Alberto Adrián Solís-Ortega, Victoria J Ornelas-Arroyo, Astrid Ruiz-Margáin, Maria Sarai González-Huezo, Nestor A Urdiales-Morán, Berenice M Román-Calleja, Juan M Mayorquín-Aguilar, José A González-Regueiro, Alejandro Campos-Murguía, Israel Vicente Toledo-Coronado, Mónica Chapa-Ibargüengoitia, Bernardo Valencia-Peña, Carlos Fernando Martínez-Cabrera, Nayelli C Flores-García

Specialty type: Gastroenterology and hepatology

Provenance and peer review: Invited article; Externally peer reviewed.

Peer-review model: Single blind

Peer-review report's scientific quality classification

Grade A (Excellent): 0
Grade B (Very good): B, B
Grade C (Good): 0
Grade D (Fair): 0
Grade E (Poor): 0

P-Reviewer: Hasabo EA, Sudan; Mamom J, Thailand

Received: June 22, 2022
Peer-review started: June 22, 2022
First decision: August 1, 2022
Revised: August 16, 2022
Accepted: September 13, 2022
Article in press: September 13, 2022
Published online: October 7, 2022

Ricardo Ulises Macías-Rodríguez, Alberto Adrián Solís-Ortega, Victoria J Ornelas-Arroyo, Astrid Ruiz-Margáin, Berenice M Román-Calleja, Juan M Mayorquín-Aguilar, José A González-Regueiro, Alejandro Campos-Murguía, Bernardo Valencia-Peña, Carlos Fernando Martínez-Cabrera, Nayelli C Flores-García, Department of Gastroenterology, Instituto Nacional de Ciencias Médicas y Nutrición Salvador Zubirán, Mexico City 14080, Mexico

Maria Sarai González-Huezo, Nestor A Urdiales-Morán, Department of Gastroenterology, Centro Médico ISSEMYM, Toluca 52140, Mexico

Israel Vicente Toledo-Coronado, Mónica Chapa-Ibargüengoitia, Department of Radiology, Instituto Nacional de Ciencias Médicas y Nutrición Salvador Zubirán, Mexico City 14080, Mexico

Corresponding author: Ricardo Ulises Macías-Rodríguez, MD, MSc, PhD, Assistant Professor, Department of Gastroenterology, Instituto Nacional de Ciencias Médicas y Nutrición Salvador Zubirán, Vasco de Quiroga 15, Col. Belisario Domínguez Sección XVI, Liver Fibrosis and Nutrition Lab, MICTLÁN Network: Mechanisms of Liver Injury, Cell Death and Translational Nutrition in Liver Diseases-Research Network, Mexico City 14080, Mexico.
ricardomacro@yahoo.com.mx

Abstract

BACKGROUND

Metabolic associated fatty liver disease (MAFLD) is associated with complications and mortality in patients with coronavirus disease 2019 (COVID-19). However, there are no prognostic scores aimed to evaluate the risk of severe disease specifically in patients with MAFLD, despite its high prevalence. Lactate dehydrogenase, aspartate aminotransferase and alanine aminotransferase have been used as markers of liver damage. Therefore, we propose an index based on lactate dehydrogenase, aspartate aminotransferase and alanine aminotransferase for the prediction of complications and mortality in patients with MAFLD and COVID-19.

AIM

To evaluate the prognostic performance of an index based on lactate dehydro-

genase and transaminases (aspartate aminotransferase/alanine aminotransferase) in patients with COVID-19 and MAFLD [liver fibrosis and nutrition (LNF)-COVID-19 index].

METHODS

In this retrospective cohort study, two cohorts from two different tertiary centers were included. The first was the derivation cohort to obtain the score cutoffs, and the second was the validation cohort. We included hospitalized patients with severe COVID-19 and MAFLD. Liver steatosis was evaluated by computed tomography scan. Area under the receiver operating characteristic (ROC) curve analysis and survival analysis were used.

RESULTS

In the derivation cohort, 44.6% had MAFLD; ROC curve analysis yielded a LFN-COVID-19 index > 1.67 as the best cutoff, with a sensitivity of 78%, specificity of 63%, negative predictive value of 91% and an area under the ROC curve of 0.77. In the multivariate analysis, the LFN-COVID-19 index > 1.67 was independently associated with the development of acute kidney injury (odds ratio: 1.8, 95% confidence interval: 1.3-2.5, $P < 0.001$), orotracheal intubation (odds ratio: 1.9, 95% confidence interval: 1.4-2.4, $P < 0.001$), and death (odds ratio: 2.86, 95% confidence interval: 1.6-4.5, $P < 0.001$) in both cohorts.

CONCLUSION

LFN-COVID-19 index has a good performance to predict prognosis in patients with MAFLD and COVID-19, which could be useful for the MAFLD population.

Key Words: COVID-19; Metabolic associated fatty liver disease; Lactate dehydrogenase; Transaminases; Prognosis; Nonalcoholic fatty liver disease

©The Author(s) 2022. Published by Baishideng Publishing Group Inc. All rights reserved.

Core Tip: The liver fibrosis and nutrition-coronavirus disease 2019 (LFN-COVID-19) index that includes lactate dehydrogenase and transaminases is a new prognostic index for patients with metabolic associated fatty liver disease and COVID-19; it was developed to specifically predict adverse clinical outcomes, including mortality, in this population with both conditions. The variables included in this index allow an easy, quick and reliable risk assessment in this population with simple markers, allowing for broad implementation.

Citation: Macías-Rodríguez RU, Solís-Ortega AA, Ornelas-Arroyo VJ, Ruiz-Margáin A, González-Huezo MS, Urdiales-Morán NA, Román-Calleja BM, Mayorquín-Aguilar JM, González-Regueiro JA, Campos-Murguía A, Toledo-Coronado IV, Chapa-Ibargüengoitia M, Valencia-Peña B, Martínez-Cabrera CF, Flores-García NC. Prognostic performance of an index based on lactic dehydrogenase and transaminases for patients with liver steatosis and COVID-19. *World J Gastroenterol* 2022; 28(37): 5444-5456

URL: https://www.wjgnet.com/1007-9327/full/v28/i37/5444.htm

DOI: https://dx.doi.org/10.3748/wjg.v28.i37.5444

INTRODUCTION

The severe acute respiratory syndrome coronavirus 2 (SARS-CoV-2) pandemic (coronavirus disease 2019, COVID-19) still affects the entire world. As of June 15, 2022, 536720870 people have been infected, of whom 6312601 have died[1].

Different risk factors associated with the development of complications and mortality in patients with COVID-19 have been identified, including age > 60 years, the presence of cirrhosis, diabetes, immunodeficiencies, obesity, cardiovascular disease, chronic kidney disease and chronic obstructive pulmonary disease, among others[2-4]. Metabolic dysfunction associated fatty liver disease (MAFLD), regarded as the hepatic manifestation of metabolic syndrome, has a controversial role in the prognosis of patients with COVID-19. Some studies have reported a poor prognosis in patients with MAFLD, while others have only showed this finding when fibrosis was present. This could be explained by a more pronounced baseline systemic inflammatory profile and activation of the immune response in patients with liver fibrosis, which contributes to increased inflammation when SARS-CoV-2 infection is added[5, 6].

Acute respiratory distress syndrome is the major complication in patients with severe COVID-19; other complications such as cardiac or cardiovascular, renal and secondary infections may occur[7]. These patients, mainly those admitted to the intensive care unit, may present with laboratory abnormalities, such as leukopenia, lymphopenia (< 800 mm^3 at admission), elevated prothrombin time, elevated serum levels of D-dimer (> 1000 ng/mL), elevated inflammatory markers (ferritin > 300 μg/L), elevated lactate dehydrogenase (LDH), elevated liver enzymes, elevated creatine phosphokinase (twice the upper limit of normal) and elevated troponin I[7-9].

In patients with pneumonia associated with SARS-CoV-2 infection, high LDH levels correlate with lung damage, severe disease and mortality at day 30[10-13]. In the study by Yan *et al*[14], LDH (> 365 U/L), lymphocyte count (< 14.7%) and C-reactive protein (> 41.2 mg/L) were identified as the three laboratory abnormalities that predicted mortality risk with 90% accuracy, which represented a simple way to promptly recognize severe illness.

Likewise, in patients with acute liver injury (non-COVID-19 related), an increase in LDH levels has been reported, secondary to endothelial damage induced by macrophages during acute inflammation, conditioning microcirculation alterations and hypoxia. Thus, it has been suggested that LDH may have a discriminatory role in identifying the etiology of liver damage. As a marker of damage due to liver ischemia, it must be taken into account that LDH has a shorter half-life. Therefore, a faster fall occurs when the damage disappears, and it has been suggested as a parameter to monitor the evolution of patients with acute liver injury. The ubiquitous nature of LHD in the human body makes it a nonspecific but sensitive biomarker, which in the context of organ damage can provide information with diagnostic and prognostic potential. In the same way, increase in alanine aminotransferase (ALT), aspartate aminotransferase (AST) and the AST/ALT ratio has been associated to adverse clinical outcomes including mortality in patients with COVID-19[10-13,15].

Identifying factors associated with poor prognosis that may be related to a pathophysiological mechanism is ideal in patients with COVID-19 since those patients at risk of progressing to a severe illness could be identified promptly. Therefore, measures could be taken to influence the outcomes of those patients. In this sense, having a prognostic index specific for patients with MAFLD who develop COVID-19 may be useful to identify individuals at risk of developing adverse clinical outcomes.

Therefore, the aim of this study was to evaluate the performance of a prognostic index based on LDH, AST and ALT in patients with MAFLD and COVID-19 and its association with the development of adverse clinical outcomes and mortality.

MATERIALS AND METHODS

This was a retrospective cohort study performed at two third-level hospitals in Mexico, (INCMNSZ and ISSEMYM) from March 2020 to July 2020, during the first phase of the COVID-19 pandemic and before steroids became a standard of care for severe COVID-19. The study was carried out according to the Declaration of Helsinki and was approved by the institutional Ethics Committee, ref. No. 3777).

Validation process

This study consisted of two phases. Phase 1, a derivation/training cohort, (its methods are described below) used to create and evaluate the newly proposed prognostic index. This cohort was derived from a tertiary care center hospital in Mexico City (INCMNSZ). Phase 2, the validation cohort aimed to evaluate the diagnostic performance of the proposed index in patients with COVID-19 and liver steatosis at a different center. This cohort was derived from a tertiary care center hospital in Toluca, in the center of Mexico (ISSEMYM).

Patients

All patients admitted during the period of study, > 18 years of age, either sex and with a confirmed diagnosis of SARS-CoV-2 infection by RT-PCR and with severe disease (pneumonia + respiratory rate > 30/respiratory distress/SaO_2 < 90%), were included in the study[19]. Patients without an adequate follow-up were excluded from the analysis (*e.g.*, those requiring referral to another hospital, those with insufficient information in the clinical records, *etc*). Follow-up and evaluation of the clinical outcomes were conducted through revision of electronic clinical records.

Biochemical tests

Upon admission, a blood sample was drawn for determination of the following tests: complete blood count, glucose, creatinine, electrolytes, ferritin, C-reactive protein, LDH, liver chemistry, creatine phosphokinase, arterial blood gases, D-dimer, troponin I and fibrinogen. HIV (human Immunodeficiency virus) and viral hepatitis panel (HCV and HBV) were performed in all participants. All the tests met the quality standards from our central laboratory, accredited by the College of American Pathologists.

Computed tomography scan

In order to evaluate the severity of pulmonary involvement, all patients underwent a pulmonary computed tomography scan, where a portion of the liver was also evaluated for the presence of steatosis. The methodology was previously described from our group[16]. Briefly, an expert radiologist blinded to the patient´s clinical status evaluated computed tomography scans to detect liver steatosis, according to the following criteria: (1) Attenuation coefficient ≤ 40 Hounsfield units in the liver (segments VII and VIII); and (2) Attenuation coefficient ≥ 10 Hounsfield units between the splenic and liver parenchyma.

Estimation of the LFN-COVID-19 index

The liver fibrosis and nutrition (LNF)-COVID-19 index was calculated according to the following formula:

LFN-COVID-19 index = (AST/ALT) × (LDH/LDH_{ULN}).

Where AST/ALT ratio included transaminase levels expressed in U/L and was multiplied by the times above the upper limit of normal value for LDH (U/L). The final value was included in the statistical analysis for characterization of clinical outcomes.

Statistical analysis

Sample size estimation considered a hypothetical area under the receiver operating characteristic curve (AUROC) of 0.8 for LFN-COVID-19 index and 0.7 as null hypothesis. Considering an alpha error of 0.05 and beta 0.20 and a negative/positive ratio of 1/1, estimation yielded 81 negative/positive cases (162 patients in total).

Normality of the data was evaluated with Kolmogorov-Smirnov test. Data was presented as mean ± standard deviation, median (P25-P75) or absolute frequencies. Comparisons between the groups were made through Mann-Whitney *U* or Student's *t* test. ROC curve analysis was performed to obtain the best cutoff from the LFN-COVID-19 index for mortality, through the Youden index as well as sensitivity, specificity, positive and negative predictive values and likelihood ratios.

Clinical outcomes were evaluated by logistic regression and a time-dependent survival analysis, including Kaplan-Meier and Cox regression (Cox proportional-hazards model) for 28-d mortality and general mortality. Statistical analysis was carried out with the statistics software SPSS version 20.0 (IBM, Armonk, NY, United States) and ROC analysis with MedCalc Statistical Software version 19.4.1 (MedCalc Software Ltd, Ostend, Belgium).

RESULTS

In the validation cohort a total of 457 patients were included in the final analysis (Figure 1), after excluding those without an adequate follow-up, those with computed tomography scan issues (artifacts, unable to evaluate liver or spleen tissue, post-surgical changes) or those with known autoimmune liver diseases, HIV, hepatitis C or B chronic infection or cancer.

Participant's characteristics

General characteristics of the study population, with and without MAFLD are presented in Table 1. Mean age in the total population was 50.4 ± 13.3 years, most of the patients were male (65.2%), and the mean body mass index (BMI) was 30.1 ± 5.6 kg/m^2. In general, in the group of patients with MAFLD there was a higher prevalence of overweight and obese patients, they were younger than those without MAFLD, and they had a higher prevalence of diabetes and metabolic syndrome.

Biochemical tests

Biochemical tests related to proinflammatory status, such as LDH, creatine phosphokinase, lymphocytes and neutrophil/lymphocyte ratio, were higher in the MAFLD group, as well as liver chemistry abnormalities, glucose, triglycerides and prognostic scores (SOFA: sequential organ failure assessment;).

Index diagnostic performance

In the group of patients with MAFLD, diagnostic yield of the LFN-COVID-19 index [(AST/ALT) × (LDH/LDH_{ULN})] was investigated through the AUROC analysis to determine the prognostic value of the index as a prognostic marker in patients with COVID-19. Characteristics related to diagnostic yield of the LFN-COVID-19 index are shown in Table 2. According to Youden's index, the best cutoff value of the LFN-COVID-19 index for mortality in patients with MAFLD was > 1.67. This cutoff value showed an AUROC of 0.77 [95% confidence interval (CI): 0.709-0.823, $P < 0.0001$], with a sensitivity of 78.7% and specificity of 63.8% (Figure 2A). In general, the AUROC in this group of patients was better than in patients without MAFLD (AUROC: 0.703, 95%CI: 0.647-0.755, $P < 0.0001$) (Figure 2B).

Table 3 shows the characteristics of patients with MAFLD according to the LFN-COVID-19 index. Similitudes in both groups regarding metabolic syndrome and BMI were observed, while other

Table 1 Baseline characteristics of the total population and according to metabolic associated fatty liver disease presence

Characteristics	All, *n* = 457	No MAFLD, *n* = 253	MAFLD, *n* = 204	*P* value
Demographic features				
Sex as male/female, %	65.2/34.8	63.6/36.4	67.2/32.8	0.432
Age in yr	50.4 ± 13.3	52.4 ± 14.0	47.8 ± 11.8	< 0.0001
BMI in kg/m^2	30.1 ± 5.6	28.7 ± 4.9	31.8 ± 5.8	< 0.0001
Comorbidities, n (%)				
Malnutrition	10 (2.8)	7 (3.4)	3 (1.9)	< 0.0001
Normal weight	49 (13.6)	43 (21.0)	6 (3.9)	
Overweight	136 (37.9)	82 (40.0)	54 (35.1)	
Obesity G1	110 (30.6)	51 (24.9)	59 (38.3)	
Obesity G2	36 (10.0)	16 (7.8)	20 (13.0)	
Obesity G3	18 (5.0)	6 (2.9)	12 (7.8)	
T2DM	107 (23.5)	47 (18.7)	60 (29.6)	0.006
Hypertension	122 (26.8)	60 (23.8)	62 (30.5)	0.107
Chronic kidney disease	8 (1.8)	6 (2.4)	2 (1.0)	0.225
Pulmonary obstructive disease	4 (0.9)	1 (0.4)	3 (1.5)	0.235
Autoimmune disease	6 (1.3)	3 (1.2)	3 (1.5)	0.551
Immunosuppression	3 (0.7)	3 (1.2)	0 (0)	0.169
Metabolic syndrome	155 (36.0)	61 (25.5)	94 (49.0)	< 0.0001
Prognostic scores				
qSOFA	1 (0-1)	1 (0-1)	1 (0-1)	0.800
SOFA	2 (1-2)	2 (1-2)	2 (1-2)	0.034
NEWS	6.7 ± 2.3	6.6 ± 2.3	6.8 ± 2.2	0.190
PSI/PORT	62 (50-80)	62 (50-82)	61 (49-77)	0.316
SMART COP	3 (2-4)	3 (2-4)	3 (2-4)	0.091
Biochemical values				
CRP, ref: 0-1 mg/dL	13.2 (6.6-20.7)	13.1 (6.6-20.0)	13.7 (6.2-21.5)	0.286
Ferritin, ref: 11.0-306.8 ng/mL	747.8 ± 665.0	717.2 ± 662.0	784.0 ± 668.0	0.290
D-dimer, ref: 0-500 ng/mL	707 (426-1146)	699 (413-1138)	721 (451-1182)	0.418
LDH, ref: 120-246 U/L	388 ± 160	374 ± 149	406 ± 173	0.032
Troponin, ref: < 15 pg/mL	4.7 (3.2-8.2)	4.7 (3.1-10.4)	4.6 (3.2-7.1)	0.525
CPK, ref: 30-233 U/L	110 (59-242)	98 (55-210)	133 (66-311)	0.006
Bilirubin, ref: 0/3-1 mg/dL	0.68 ± 0.49	0.66 ± 0.54	0.69 ± 0.43	0.593
ALT, ref: 7-52 U/L	37.5 (25.0-56.0)	33.0 (23.8-54.7)	41.0 (28.0-59.0)	0.004
AST, ref: 13-39 U/L	42.0 (30.0-62.0)	40.0 (29.0-58.0)	43.9 (32.9-64.3)	0.051
Globulins, ref: 1.9-3.7 g/dL	3.2 ± 0.4	3.2 ± 0.4	3.2 ± 0.4	0.560
Albumin, ref: 3.5-5.7 g/dL	3.7 ± 0.4	3.6 ± 0.4	3.7 ± 0.4	0.051
ALP, ref: 34-104 U/L	86 (70-111)	86 (70-113)	85 (69-109)	0.505
Creatinine, ref: 0.6-1.2 mg/dL	0.9 (0.8-1.1)	0.9 (0.8-1.1)	0.9 (0.7-1.1)	0.877
Glucose, ref: 70-99 mg/dL	116 (102-144)	110 (99-131)	124 (105-184)	< 0.0001
Leukocytes, ref: 4-12 × 10^3/μL	7.6 (5.6-10.0)	7.2 (5.4-9.8)	7.9 (5.7-10.3)	0.191
Lymphocytes, ref: 1-3.9 × 10^3/μL	881.6 ± 509.0	835.0 ± 352.0	938.0 ± 649.0	0.043

Platelets, ref: 150-450 K/μL	239 ± 88	248 ± 95	227 ± 78	0.012
25 (HO) vitamin D, ref: 30-100 ng/mL	21.5 ± 8.0	21.6 ± 8.1	21.5 ± 8.0	0.917
Triglycerides, ref: < 150 mg/dL	159 ± 85	155 ± 60	165 ± 110	0.264
CT scan results, pulmonary involvement				
Mild, < 20%	91 (20.0)	51 (20.3)	40 (19.6)	0.281
Moderate, 20%-50%	172 (37.8)	102 (40.6)	70 (34.3)	
Severe, > 50%	192 (42.2)	98 (39.0)	94 (46.1)	
Treatment, n (%)				
Antibiotics	402 (88.4)	228 (90.8)	174 (85.3)	0.096
Antimalarials	132 (28.9)	72 (28.5)	60 (29.4)	0.823
Tocilizumab	51 (11.2)	26 (10.3)	25 (12.3)	0.504
Remdesivir	9 (2.0)	7 (2.8)	2 (1.0)	0.152
PaO2/FiO2 ratio	233.9 ± 109.9	239.0 ± 91.0	227.0 ± 130.0	0.011
Neutrophil/lymphocyte ratio	7.0 (4.4-11.6)	7.2 (4.5-12.0)	6.7 (4.0-10.8)	0.860
Days between the beginning of symptoms and hospitalization	8.2 ± 4.4	8.6 ± 4.6	7.8 ± 4.0	0.110

BMI: Body mass index; T2DM: Type 2 diabetes mellitus; q-SOFA: Quick sequential organ failure assessment; SOFA: Sequential organ failure assessment; NEWS: National early warning score; PSI/PORT: Pneumonia severity index; CRP: C-reactive protein; LDH: Lactate dehydrogenase; CPK: Creatine phosphokinase; ALT: Alanine aminotransferase; AST: Aspartate aminotransferase; ALP: Alkaline phosphatase; CT: Computed tomography; MAFLD: Metabolic associated fatty liver disease; PaO2/FiO2 ratio: Ratio of arterial oxygen partial pressure to fractional inspired oxygen.

Table 2 Diagnostic yield of the LFN-COVID-19 index in patients with metabolic associated fatty liver disease

Diagnostic yield	
Sensitivity	0.787 (0.643-0.893)
Specificity	0.638 (0.563-0.709)
Positive predictive value, %	0.360 (0.273-0.468)
Negative predictive value, %	0.910 (0.855-0.960)
+ Likelihood ratio	2.18 (1.70-2.80)
- Likelihood ratio	0.33 (0.20-0.60)
AUROC	0.770 (0.709-0.823), $P < 0.0001$
Youden index	0.4257

AUROC: Area under the receiver operating characteristic.

variables including age, prognostic scores, and biomarkers related to proinflammatory and prothrombotic status, severe COVID-19 (PaO_2/FiO_2 < 100 mmHg), orotracheal intubation and other clinical outcomes, including mortality, were higher in the > 1.67 group.

Prognostic performance

In order to determine if the LFN-COVID-19 index was independently associated with the presence of acute kidney injury or orotracheal intubation during hospitalization, a logistic regression was performed, observing that a value of > 1.67 was associated to adverse clinical outcomes, independently of metabolic factors, severity scores and demographic variables (Table 4).

A marker of mortality was studied by a 28-d Kaplan-Meier survival analysis (Figure 3), observing that patients with a value > 1.67 have a lower survival than those with a value < 1.67 ($P < 0.001$). The influence of other variables on mortality was evaluated through univariate and multivariate Cox proportional hazard analysis. Table 5 summarized the variables that were significant in the univariate analysis, with the results subjected to the multivariate analysis where the variables that were independently associated with mortality were the LFN-COVID-19 index, the neutrophil/lymphocyte

Table 3 Characteristics and outcomes in patients with metabolic associated fatty liver disease according to the LFN-COVID-19 index

	< 1.67, *n* = 115	> 1.67, *n* = 89	*P* value
Demographic features			
Sex as male/female, %	63.5/36.5	71.9/28.1	0.203
Age in yr	46 ± 10	50 ± 12	0.011
BMI in kg/m^2	31.1 ± 4.8	32.5 ± 6.9	0.111
Prognostic scores			
qSOFA	1 (0-1)	1 (1-1)	0.007
SOFA	2 (1-2)	2 (2-3)	0.004
NEWS	7 (5-8)	7 (6-9)	0.035
PSI/PORT	56 (47-69)	66 (53-85)	< 0.0001
SMART COP	3 (2-4)	4 (3-4)	0.012
Biochemical values			
CRP, ref: 0-1 mg/dL	8.5 (4.2-18.1)	17.2 (11.6-23.8)	< 0.0001
Ferritin, ref: 11.0-306.8 ng/mL	503 (266-970)	795 (412-1114)	0.003
D-dimer, ref: 0-500 ng/mL	587 (399-962)	967 (606-1549)	< 0.0001
LDH, ref: 120-246 µ/L	312 ± 86	529 ± 180	< 0.0001
Troponin, ref: < 15 pg/mL	3.7 (2.9-5.7)	6.1 (3.8-10.9)	< 0.0001
CPK, ref: 30-223 µ/L	107 (58-222)	190 (78-414)	0.001
Bilirubin, ref: 0/3-1 mg/dL	0.62 ± 0.30	0.78 ± 0.54	0.017
ALT, ref: 7-52 U/L	43.2 (31.0-61.2)	37.0 (26.3-52.8)	0.026
AST, ref: 13-39 U/L	38.3 (27.8-52.2)	52.4 (42.0-73.7)	< 0.0001
Globulins, ref: 1.9-3.7 g/dL	3.22 ± 0.39	3.29 ± 0.43	0.259
Albumin, ref: 3.5-5.7 g/dL	3.90 ± 0.42	3.50 ± 0.40	< 0.0001
ALP, ref: 34-104 µ/L	85 (70-109)	85 (67-110.5)	0.786
Creatinine, ref: 0.6-1.2 mg/dL	0.85 (0.69-1.00)	0.95 (0.79-1.16)	0.005
Glucose, ref: 70-99 mg/dL	118 (102-180)	135 (114-187)	0.03
Leukocytes, ref: 4-12 × 10^3/µL	7.6 (5.6-9.9)	8.3 (6.3-10.8)	0.089
Lymphocytes, ref: 1-3.9 × 10^3/µL	937 (693-1210)	715 (510-967)	< 0.0001
Platelets, ref: 150-450 K/µL	228 ± 78	226 ± 79	0.827
25 (HO) vitamin D, ref: 30-100 ng/mL	21.9 ± 7.8	20.9 ± 8.3	0.488
Triglycerides, ref: < 150 mg/dL	151 (118-187)	137 (111-184)	0.13
PaO2/FiO2 ratio	240 (161-287)	159 (96-245)	< 0.0001
Neutrophil/lymphocyte ratio	5.9 (3.5-9.9)	9.6 (6.4-13.7)	< 0.0001
Other, *n* (%)			
Metabolic syndrome	49.0 (46.2)	45.0 (52.3)	0.401
Severe COVID-19, PaO_2/FiO_2 < 100 mmHg	9 (8.2)	23 (26.7)	< 0.0001
Orotracheal intubation	13 (11.3)	36 (40.9)	< 0.0001
Acute kidney injury	11 (11)	26 (34.7)	< 0.0001
Thrombotic event	1 (1.0)	2 (2.7)	0.576
Death	6 (5.3)	25 (29.8)	< 0.0001
Days between the beginning of symptoms and hospitalization	7.2 ± 3.4	8.6 ± 4.9	0.027

Length of hospital stay in days	7 (4-10)	8 (6-10)	0.131
Days in ICU	7 (5-12)	12 (6-13)	0.395
Days between ICU requirement and death	7 (6-7)	5 (3-7)	0.203

BMI: Body mass index; q-SOFA: Quick-sequential organ failure assessment; SOFA: Sequential organ failure assessment; NEWS: National early warning score; PSI/PORT: Pneumonia severity index; CRP: C-reactive protein; LDH: Lactate dehydrogenase; CPK: Creatine phosphokinase; ALT: Alanine aminotransferase; AST: Aspartate aminotransferase; ALP: Alkaline phosphatase; COVID-19: Coronavirus disease 2019; ICU: Intensive care unit; PaO2/FiO2 ratio: Ratio of arterial oxygen partial pressure to fractional inspired oxygen.

Table 4 Logistic regression analysis to evaluate the association between LFN-COVID-19 index and clinical outcomes

	Orotracheal intubation				Acute kidney injury			
	OR	95%CI	B coefficient	*P* value	OR	95%CI	B coefficient	*P* value
LFN-COVID-19 index	1.900	1.481-2.437	0.642	0.000	1.849	1.366-2.504	0.615	0.000
Sex	0.605	0.288-1.271	-0.502	0.185	0.280	0.103-0.765	-1.272	0.013
Age	0.966	0.939-0.993	-0.035	0.015	1.021	0.988-1.054	0.021	0.209
BMI	1.054	0.997-1.114	0.053	0.061	1.085	1.011-1.164	0.081	0.023

OR: Odds ratio; CI: Confidence interval; BMI: Body mass index; COVID-19: Coronavirus disease 2019.

Table 5 Cox proportional hazard multivariate analysis for mortality in patients with metabolic associated fatty liver disease according to the LFN-COVID-19 index

	OR	B coefficient	*P* value	95%CI
LFN-COVID-19 index	0.241	-1.422	0.013	0.079-0.741
PaO_2/FiO_2 ratio	1.000	0.000	0.877	0.996-1.004
Neutrophil/lymphocyte ratio	1.043	0.042	0.030	1.004-1.083
Creatine phosphokinase	1.001	0.001	0.340	0.999-1.002
Body mass index in kg/m^2	1.093	0.089	0.002	1.033-1.157

OR: Odds ratio; CI: Confidence interval; COVID-19: Coronavirus disease 2019; PaO2/FiO2 ratio: Ratio of arterial oxygen partial pressure to fractional inspired oxygen.

ratio and BMI.

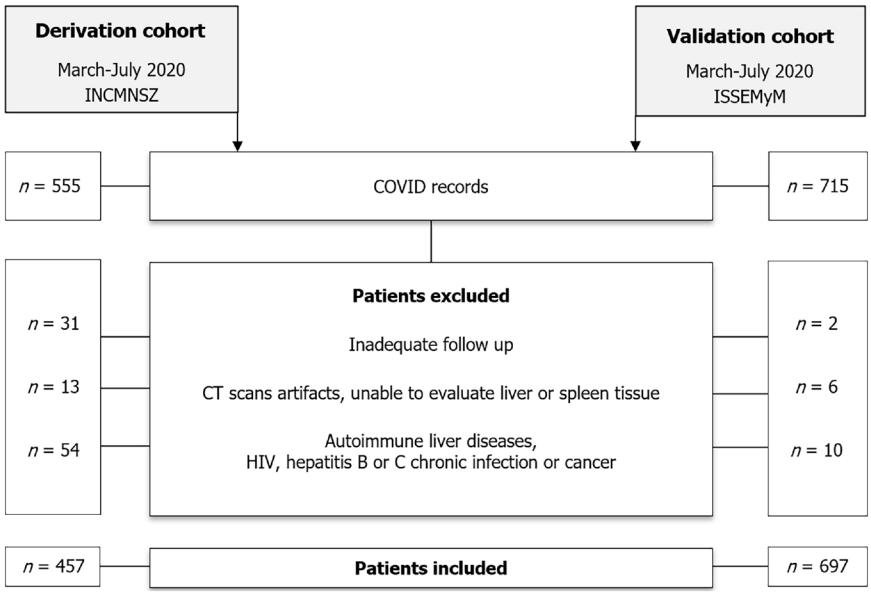
In this analysis, a LFN-COVID-19 index > 1.67 was associated independently to other variables of mortality, including severity markers, prognostic scores and general characteristics (Figure 4).

Validation cohort

From the 697 patients included in the validation cohort, 104 had MAFLD (15.0%). In general, patients with MAFLD were younger and had higher degrees of obesity and mild abnormalities in liver chemistry (Supplementary Table 1). The MAFLD group was further analyzed according to the LFN-COVID-19 index, finding higher levels of C-reactive protein and D-dimer in the group > 1.67, with little changes in the rest of the variables (Supplementary Table 2). Interestingly, mechanical intubation and clinical outcomes including mortality, were more frequent in the > 1.67 group, as was found in the initial cohort (Supplementary Table 3). These same findings in another cohort and in a different hospital highlight the validity of the LFN-COVID-19 index.

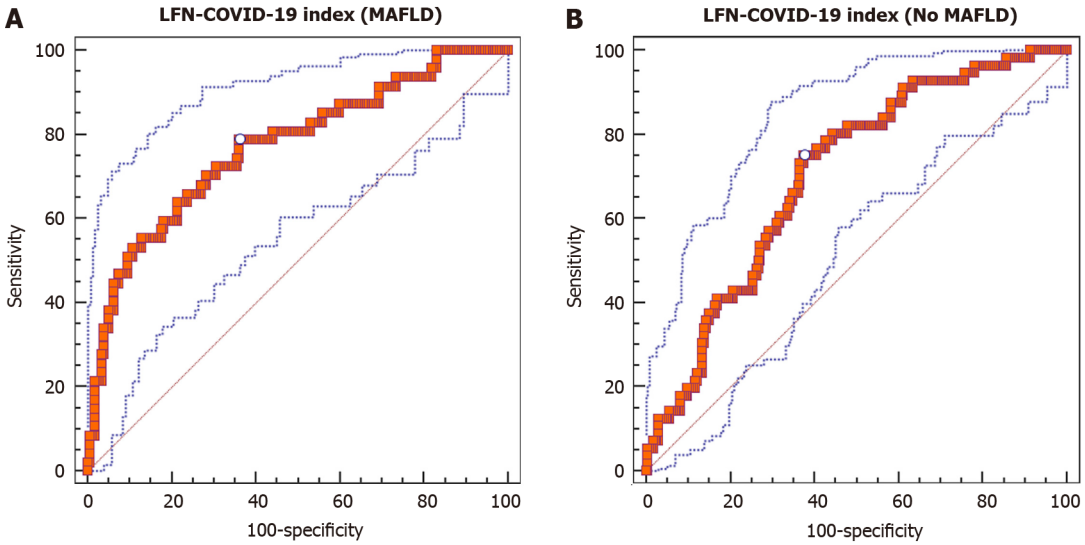
DISCUSSION

MAFLD is currently the main etiology of chronic liver disease in the world. The main associated risk factors are obesity, type 2 diabetes, dyslipidemia and metabolic syndrome, all factors with a growing incidence. Both risk factors for MAFLD and MAFLD itself have also been shown to have prognostic value in COVID-19, associating their presence with higher severity and mortality. However, it remains



DOI: 10.3748/wjg.v28.i37.5444 **Copyright** ©The Author(s) 2022.

Figure 1 Flowchart of participants in both cohorts. COVID: Coronavirus disease 2019; CT: Computed tomography; HIV: Human Immunodeficiency virus.

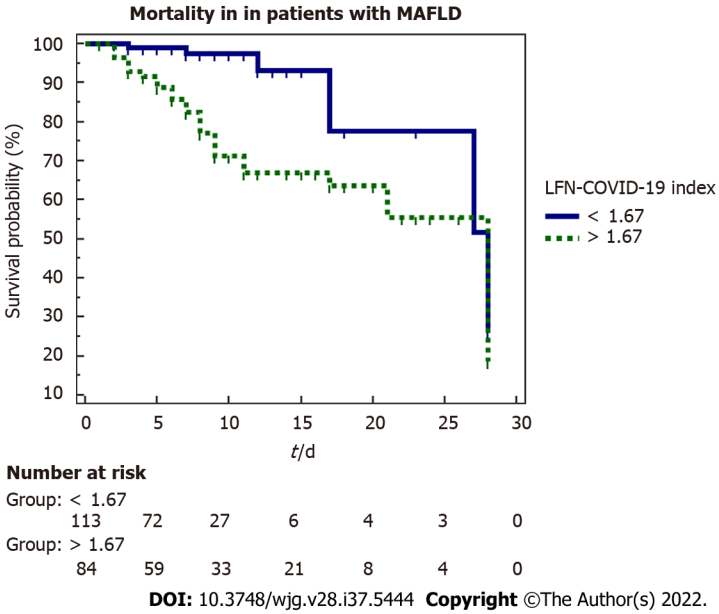


DOI: 10.3748/wjg.v28.i37.5444 **Copyright** ©The Author(s) 2022.

Figure 2 Area under the receiver operating characteristic curve for the LFN-coronavirus disease 2019 index to predict mortality. A: Patients with metabolic associated fatty liver disease and coronavirus disease 2019; B: Patients without metabolic associated fatty liver disease and coronavirus disease 2019. MAFLD: Metabolic associated fatty liver disease; COVID-19: Coronavirus disease 2019; LFN: Liver fibrosis and nutrition.

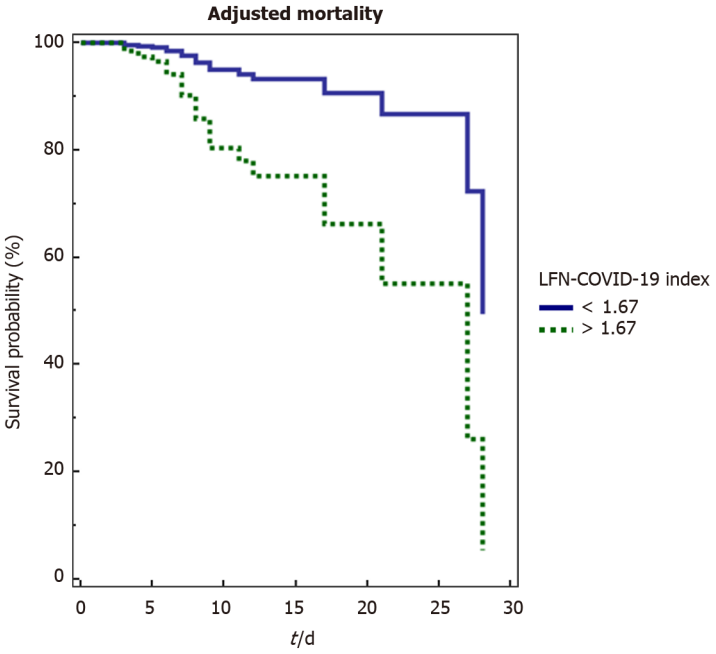
controversial whether all patients within the spectrum of MAFLD have a worse prognosis or only those who, in addition to steatosis, have fibrosis[16].

Evidence pointing to MAFLD as a prognostic factor emerged from different studies around the world. A retrospective study in patients with COVID-19 found an association of MAFLD with higher intensive care unit admittance (OR: 2.3, 95%CI: 1.27-4.17), mechanical ventilation (2.08, 95%CI: 1.2-3.6) and in patients with cirrhosis with higher mortality (12.5, 95%CI: 2.16-72.5)[6]. In a cohort study in patients with COVID-19 and chronic liver disease (42% MAFLD), the authors observed a relative risk of 2.8 (95%CI: 1.9-4.0) for death in this group of patients, regardless of age, race, BMI, presence of hypertension or diabetes[12]. Another study conducted in Zhejiang, China found that hospitalized COVID-19 patients who had MAFLD with fibrosis (evaluated through FIB-4 and NFS - nonalcoholic fatty liver disease fibrosis score) were at increased risk of severe disease, regardless of other comorbidities[5]. Lastly, a study conducted by Lucifora *et al*[17] showed that patients with COVID-19 and MAFLD had a higher prevalence of alterations in the liver biochemistry test as well as a longer viral clearance time compared with patients without MAFLD.



DOI: 10.3748/wjg.v28.i37.5444 **Copyright** ©The Author(s) 2022.

Figure 3 Kaplan-Meier curve for 28-d mortality according to the LFN-coronavirus disease 2019 index. MAFLD: Metabolic associated fatty liver disease; COVID-19: Coronavirus disease 2019; LFN: Liver fibrosis and nutrition.



DOI: 10.3748/wjg.v28.i37.5444 **Copyright** ©The Author(s) 2022.

Figure 4 Adjusted mortality analysis (Cox regression) for 28-d mortality according to LFN-coronavirus disease 2019 index. COVID-19: Coronavirus disease 2019; LFN: Liver fibrosis and nutrition.

Considering the evidence mentioned above, it is possible that the synergism between the baseline proinflammatory state of patients with MAFLD together with the body's inflammatory response to COVID-19 could be the pathophysiological support that explains greater severity and worse prognosis in these patients. Another important component in multiorgan damage in COVID-19, is the state of hypoxemia, cell death and hypoperfusion reflected by biomarkers such as LDH, which correlates positively with worse clinical outcomes (including mortality). Although it is not specific for liver damage, it can be a sensitive and dynamic marker of hypoxic tissue damage due to its short half-life, together with other well-known markers of liver damage, such as AST, ALT and the AST/ALT ratio[10].

Due to the link between MAFLD and COVID-19 and the higher risk of mortality and adverse clinical outcomes, we conceived a prognostic index intended to be used in patients with MAFLD, including variables reflecting the pathophysiology of liver damage, mainly hepatocyte cell death induced by the factors previously mentioned, and associating it with hard clinical outcomes, including mortality[18].

The LFN-COVID-19 index includes the AST/ALT ratio as well as LDH levels normalized by the laboratory's upper limit of normal, facilitating the implementation of the index by non-restricting its usefulness to a specific cutoff value (AST, ALT or LDH). This overcomes the problem of regional variations in laboratory values. The use of this index has potential implications in clinical practice establishing a prognosis of patients. On the other hand, the simplicity of the index allows easy calculation and includes widely available, cheap and reliable laboratory tests.

In the present study, we found a good diagnostic performance of the LFN-COVID-19 index in hospitalized patients with MAFLD and COVID-19. In the ROC curve analysis, a cutoff value of > 1.67 was associated with adverse clinical outcomes including the need for mechanical ventilation, acute kidney injury and higher mortality. This was reproduced in the validation cohort performed at a different center finding this cutoff point as the best for predicting these outcomes[19].

An interesting finding was that there were no differences in the days of stay in the intensive care unit based on this cutoff point. The same length of stay in the intensive care unit could be explained by the severity of the disease, where those with an index below 1.67 were discharged from the critical care area earlier and those with an index above 1.67 present earlier mortality.

Among the weaknesses of this study was the fact that the diagnosis of hepatic steatosis was made with computed tomography. However, given the high risk of transmission of SARS-CoV-2 to healthcare workers, this safer approach was chosen in order to reduce the exposure involved in carrying out a study such as transient hepatic elastography or magnetic resonance imaging requiring more time to perform it. Another aspect to highlight is that patients with COVID-19 usually present with elevated transaminases and LDH from multifactorial causes. Nevertheless, both biomarkers have been widely used as markers of hepatocyte cell death and may reflect liver damage occurring during SARS-CoV-2 infection and exacerbated in patients with MAFLD.

This study has several strengths. The sample size was adequate and sufficient due to the fact that the study was carried out in a center fully converted for the care of COVID-19 patients and included the general population in a country with a highest prevalence of MAFLD and a genetic profile that predisposes the population to the development of metabolic diseases such as type 2 diabetes mellitus, obesity and metabolic syndrome. In addition, we included an external validation cohort, where the results were replicated, enhancing the validity of the LFN-COVID-19 index.

CONCLUSION

Based on the findings of this study, we propose a new prognostic index based on markers of liver damage and severity in patients with MAFLD and COVID-19, which can be used in clinical practice to stratify the risk of adverse outcomes in MAFLD patients. Timely actions to reduce the associated morbidity and mortality in this population could be achieved through the implementation of this index.

ARTICLE HIGHLIGHTS

Research background

This article was conceived considering the high prevalence of metabolic associated fatty liver disease (MAFLD) in the general population amid the coronavirus disease 2019 (COVID-19) pandemic and the risk of these patients in clinical settings with limited resources.

Research motivation

The growing evidence showing worse clinical outcomes in patients with metabolic diseases and COVID-19, including those with fatty liver disease, and the lack of a specific index to specifically stratify patients with both conditions motivated the creation of an index capable of discriminating those patients with an unfavorable outcome.

Research objectives

To evaluate the diagnostic yield of the liver fibrosis and nutrition (LNF)-COVID-19 index (includes lactate dehydrogenase, aspartate aminotransferase and alanine aminotransferase values), to predict adverse clinical outcomes, including mortality, in patients with both COVID-19 and MAFLD.

Research methods

Data from a derivation cohort, including patients admitted with a diagnosis of severe COVID-19 and meeting the MAFLD criteria identified the best LFN-COVID-19 index cutoff value for risk stratification. The results were evaluated using a validation cohort.

Research results

The LFN-COVID-19 index with a cutoff point > 1.67 was associated with higher mortality ($P < 0.001$) with an area under the curve of 0.77 (95% confidence interval: 0.709-0.823), sensitivity of 78.7% and specificity of 63.8%. It was independently associated with worse outcomes such as higher mortality, intubation rate and acute kidney injury in both cohorts.

Research conclusions

The LFN-COVID-19 index with a cutoff point > 1.67 showed good discrimination capability in patients with severe COVID-19 and MAFLD, identifying patients with an unfavorable prognosis associated with the need for mechanical ventilation, acute kidney injury and higher mortality.

Research perspectives

The use of this prognostic index will allow timely identification of patients with MAFLD and COVID-19 at higher risk of adverse clinical outcomes, leading to better therapeutic decision-making and resource allocation.

FOOTNOTES

Author contributions: Macías-Rodríguez RU contributed to conception and design of the study; Macías-Rodríguez RU, Solís-Ortega AA and Ornelas-Arroyo VJ contributed with data extraction, literature review and writing; Macías-Rodríguez RU, Ruiz-Margáin A and Román-Calleja BM contributed with writing and analysis of data; Macías-Rodríguez RU, Solís-Ortega AA, Ornelas-Arroyo VJ, Ruiz-Margáin A, Román-Calleja BM, González-Huezo MS, Urdiales-Morán NA, Mayorquín-Aguilar JM, González-Regueiro JA, Campos-Murguía A, Toledo-Coronado IV, Chapa-Ibargüengoitia M, Valencia-Peña B, Martínez-Cabrera CF and Flores-García NC contributed to drafting, critical revision, supervision and editing of the content of the manuscript.

Institutional review board statement: The study was reviewed and approved by the Instituto Nacional de Ciencias Médicas y Nutrición Salvador Zubirán Institutional Review Board (approval No. 3777).

Informed consent statement: Due to the retrospective nature of the study, no informed consent was needed.

Conflict-of-interest statement: All the authors report no relevant conflicts of interest for this article.

Data sharing statement: No additional data are available.

STROBE statement: The authors have read the STROBE Statement-checklist of items, and the manuscript was prepared and revised according to the STROBE Statement-checklist of items.

Open-Access: This article is an open-access article that was selected by an in-house editor and fully peer-reviewed by external reviewers. It is distributed in accordance with the Creative Commons Attribution NonCommercial (CC BY-NC 4.0) license, which permits others to distribute, remix, adapt, build upon this work non-commercially, and license their derivative works on different terms, provided the original work is properly cited and the use is non-commercial. See: https://creativecommons.org/Licenses/by-nc/4.0/

Country/Territory of origin: Mexico

ORCID number: Ricardo Ulises Macías-Rodríguez 0000-0002-7637-4477; Alberto Adrián Solís-Ortega 0000-0003-2715-503X; Berenice M Román-Calleja 0000-0001-7624-9679; Juan M Mayorquín-Aguilar 0000-0002-5805-1455; José A González-Regueiro 0000-0001-5211-4710; Alejandro Campos-Murguía 0000-0002-2178-302X; Israel Vicente Toledo-Coronado 0000-0002-5479-3953; Mónica Chapa-Ibargüengoitia 0000-0001-7178-0073; Carlos Fernando Martínez-Cabrera 0000-0002-5549-5763; Nayelli C Flores-García 0000-0003-3930-2682.

S-Editor: Gao CC
L-Editor: Filipodia
P-Editor: Li X

REFERENCES

1 **Johns Hopkins University**. COVID-19 Dashboard by the Center for Systems Science and Engineering (CSSE) at Johns Hopkins University (JHU). *JHU* 2022; 1-2 [DOI: 10.21203/rs.3.rs-15447/v1]

2 **Guan WJ**, Ni ZY, Hu Y, Liang WH, Ou CQ, He JX, Liu L, Shan H, Lei CL, Hui DSC, Du B, Li LJ, Zeng G, Yuen KY, Chen RC, Tang CL, Wang T, Chen PY, Xiang J, Li SY, Wang JL, Liang ZJ, Peng YX, Wei L, Liu Y, Hu YH, Peng P, Wang JM, Liu JY, Chen Z, Li G, Zheng ZJ, Qiu SQ, Luo J, Ye CJ, Zhu SY, Zhong NS; China Medical Treatment Expert Group for Covid-19. Clinical Characteristics of Coronavirus Disease 2019 in China. *N Engl J Med* 2020; **382**: 1708-1720

[PMID: 32109013 DOI: 10.1056/NEJMoa2002032]
3 **Santoso A**, Pranata R, Wibowo A, Al-Farabi MJ, Huang I, Antariksa B. Cardiac injury is associated with mortality and critically ill pneumonia in COVID-19: A meta-analysis. *Am J Emerg Med* 2021; **44**: 352-357 [PMID: 32331955 DOI: 10.1016/j.ajem.2020.04.052]
4 **Shi S**, Qin M, Shen B, Cai Y, Liu T, Yang F, Gong W, Liu X, Liang J, Zhao Q, Huang H, Yang B, Huang C. Association of Cardiac Injury With Mortality in Hospitalized Patients With COVID-19 in Wuhan, China. *JAMA Cardiol* 2020; **5**: 802-810 [PMID: 32211816 DOI: 10.1001/jamacardio.2020.0950]
5 **Targher G**, Mantovani A, Byrne CD, Wang XB, Yan HD, Sun QF, Pan KH, Zheng KI, Chen YP, Eslam M, George J, Zheng MH. Risk of severe illness from COVID-19 in patients with metabolic dysfunction-associated fatty liver disease and increased fibrosis scores. *Gut* 2020; **69**: 1545-1547 [PMID: 32414813 DOI: 10.1136/gutjnl-2020-321611]
6 **Hashemi N**, Viveiros K, Redd WD, Zhou JC, McCarty TR, Bazarbashi AN, Hathorn KE, Wong D, Njie C, Shen L, Chan WW. Impact of chronic liver disease on outcomes of hospitalized patients with COVID-19: A multicentre United States experience. *Liver Int* 2020; **40**: 2515-2521 [PMID: 32585065 DOI: 10.1111/liv.14583]
7 **Zhang G**, Hu C, Luo L, Fang F, Chen Y, Li J, Peng Z, Pan H. Clinical features and short-term outcomes of 221 patients with COVID-19 in Wuhan, China. *J Clin Virol* 2020; **127**: 104364 [PMID: 32311650 DOI: 10.1016/j.jcv.2020.104364]
8 **Huang C**, Wang Y, Li X, Ren L, Zhao J, Hu Y, Zhang L, Fan G, Xu J, Gu X, Cheng Z, Yu T, Xia J, Wei Y, Wu W, Xie X, Yin W, Li H, Liu M, Xiao Y, Gao H, Guo L, Xie J, Wang G, Jiang R, Gao Z, Jin Q, Wang J, Cao B. Clinical features of patients infected with 2019 novel coronavirus in Wuhan, China. *Lancet* 2020; **395**: 497-506 [PMID: 31986264 DOI: 10.1016/S0140-6736(20)30183-5]
9 **Siordia JA Jr**. Epidemiology and clinical features of COVID-19: A review of current literature. *J Clin Virol* 2020; **127**: 104357 [PMID: 32305884 DOI: 10.1016/j.jcv.2020.104357]
10 **Chaudhary A**, Chauhan V. Lactate dehydrogenase as an indicator of liver diseases. *J Adv Med Dental Sci Res* 2015; **3** [DOI: 10.12980/jclm.3.2015j5-54]
11 **Kotoh K**, Enjoji M, Kato M, Kohjima M, Nakamuta M, Takayanagi R. A new parameter using serum lactate dehydrogenase and alanine aminotransferase level is useful for predicting the prognosis of patients at an early stage of acute liver injury: a retrospective study. *Comp Hepatol* 2008; **7**: 6 [PMID: 18700988 DOI: 10.1186/1476-5926-7-6]
12 **Singh S**, Khan A. Clinical Characteristics and Outcomes of Coronavirus Disease 2019 Among Patients With Preexisting Liver Disease in the United States: A Multicenter Research Network Study. *Gastroenterology* 2020; **159**: 768-771.e3 [PMID: 32376408 DOI: 10.1053/j.gastro.2020.04.064]
13 **Cassidy WM**, Reynolds TB. Serum lactic dehydrogenase in the differential diagnosis of acute hepatocellular injury. *J Clin Gastroenterol* 1994; **19**: 118-121 [PMID: 7963356 DOI: 10.1097/00004836-199409000-00008]
14 **Yan L**, Zhang HT, Xiao Y, Wang M, Guo Y, Sun C, Liang J, Li S, Zhang M, Tang X, Cao H, Tan X, Huang NN, Jiao B, Luo A, Cao Z, Xu H, Yuan Y. Prediction of criticality in patients with severe Covid-19 infection using three clinical features: a machine learning-based prognostic model with clinical data in Wuhan. 2020 Preprint. Available from: medRxiv:20028027 [DOI: 10.1101/2020.02.27.20028027]
15 **Li X**, Xu S, Yu M, Wang K, Tao Y, Zhou Y, Shi J, Zhou M, Wu B, Yang Z, Zhang C, Yue J, Zhang Z, Renz H, Liu X, Xie J, Xie M, Zhao J. Risk factors for severity and mortality in adult COVID-19 inpatients in Wuhan. *J Allergy Clin Immunol* 2020; **146**: 110-118 [PMID: 32294485 DOI: 10.1016/j.jaci.2020.04.006]
16 **Ruiz-Margáin A**, Campos-Murguía A, González-Regueiro JA, Román-Calleja BM, Delint DK, Macías-Rodríguez RU. Reply to: "Liver fibrosis and adverse outcomes in COVID-19". *Dig Liver Dis* 2021; **53**: 800 [PMID: 33947641 DOI: 10.1016/j.dld.2021.04.001]
17 **Lucifora J**, Michelet M, Rivoire M, Protzer U, Durantel D, Zoulim F. Two-dimensional-cultures of primary human hepatocytes allow efficient HBV infection: Old tricks still work! *J Hepatol* 2020; **73**: 449-451 [PMID: 32423632 DOI: 10.1016/j.jhep.2020.03.042]
18 **Wynants L**, Van Calster B, Collins GS, Riley RD, Heinze G, Schuit E, Bonten MMJ, Dahly DL, Damen JAA, Debray TPA, de Jong VMT, De Vos M, Dhiman P, Haller MC, Harhay MO, Henckaerts L, Heus P, Kammer M, Kreuzberger N, Lohmann A, Luijken K, Ma J, Martin GP, McLernon DJ, Andaur Navarro CL, Reitsma JB, Sergeant JC, Shi C, Skoetz N, Smits LJM, Snell KIE, Sperrin M, Spijker R, Steyerberg EW, Takada T, Tzoulaki I, van Kuijk SMJ, van Bussel B, van der Horst ICC, van Royen FS, Verbakel JY, Wallisch C, Wilkinson J, Wolff R, Hooft L, Moons KGM, van Smeden M. Prediction models for diagnosis and prognosis of covid-19: systematic review and critical appraisal. *BMJ* 2020; **369**: m1328 [PMID: 32265220 DOI: 10.1136/bmj.m1328]
19 **World Health Organization**. Clinical management of COVID-19: evolutionary guidelines, January 25, 2021. [cited 16 Jun 2022]. In: World Health Organization [Internet]. Available from: https://apps.who.int/iris/handle/10665/338882

World Journal of Gastroenterology

Submit a Manuscript: https://www.f6publishing.com

World J Gastroenterol 2022 October 7; 28(37): 5457-5468

DOI: 10.3748/wjg.v28.i37.5457

ISSN 1007-9327 (print) ISSN 2219-2840 (online)

ORIGINAL ARTICLE

Retrospective Study

Efficacy of endoscopic ultrasound in the evaluation of small gastrointestinal stromal tumors

Qi-Chao Ge, Yu-Fan Wu, Zi-Ming Liu, Zhe Wang, Sheng Wang, Xiang Liu, Nan Ge, Jin-Tao Guo, Si-Yu Sun

Specialty type: Gastroenterology and hepatology

Provenance and peer review: Unsolicited article; Externally peer reviewed.

Peer-review model: Single blind

Peer-review report's scientific quality classification

Grade A (Excellent): A, A
Grade B (Very good): B
Grade C (Good): 0
Grade D (Fair): 0
Grade E (Poor): 0

P-Reviewer: Kim HJ, South Korea; Sundaram S, India; Villa E, United States

Received: June 22, 2022
Peer-review started: June 22, 2022
First decision: September 2, 2022
Revised: September 14, 2022
Accepted: September 20, 2022
Article in press: September 20, 2022
Published online: October 7, 2022

Qi-Chao Ge, Yu-Fan Wu, Zi-Ming Liu, Sheng Wang, Xiang Liu, Nan Ge, Jin-Tao Guo, Si-Yu Sun, Department of Gastroenterology, Shengjing Hospital of China Medical University, Shenyang 110004, Liaoning Province, China

Zhe Wang, Department of Pathology, Shengjing Hospital of China Medical University, Shenyang 110004, Liaoning Province, China

Corresponding author: Jin-Tao Guo, MD, PhD, Professor, Department of Gastroenterology, Shengjing Hospital of China Medical University, No. 36 Sanhao Street, Shenyang 110004, Liaoning Province, China. guojt@sj-hospital.org

Abstract

BACKGROUND

Gastrointestinal stromal tumors (GISTs) with a diameter of < 2 cm are called small GISTs. Currently, endoscopic ultrasound (EUS) is widely used as a regular follow-up method for GISTs, which can also provide a preliminary basis for judging the malignancy potential of lesions. However, there are no studies on the accuracy of EUS to assess the malignant potential of small GISTs.

AIM

To evaluate the efficacy of EUS in the diagnosis and risk assessment of small GISTs.

METHODS

We collected data from patients with small GISTs who were admitted to Shengjing Hospital of China Medical University between October 2014 and July 2019. The accurate diagnosis and risk classifications of patients were based on the pathological assessment according to the modified National Institute of Health criteria after endoscopic resection or laparoscopic surgery. Preoperative EUS features (marginal irregularity, cystic changes, homogeneity, ulceration, and strong echogenic foci) were retrospectively analyzed. The assessment results based on EUS features were compared with the pathological features.

RESULTS

A total of 256 patients (69 men and 187 women) were enrolled. Pathological results included 232, 16, 7, and 1 very low-, low-, intermediate-, and high-risk cases, respectively. The most frequent tumor location was the gastric fundus (78.1%), and mitoses were calculated as > 5/50 high power field in 8 (3.1%)

patients. Marginal irregularity, ulceration, strong echo foci, and heterogeneity were detected in 1 (0.4%), 2 (0.8%), 22 (8.6%), and 67 (65.1%) patients, respectively. However, cystic changes were not detected. Tumor size was positively correlated with the mitotic index ($P < 0.001$). Receiver operating curve analysis identified 1.48 cm as the best cut-off value to predict malignant potential (95% confidence interval: 0.824–0.956). EUS heterogeneity with tumor diameters > 1.48 cm was associated with higher risk classification ($P < 0.05$).

CONCLUSION

Small GISTs (diameters > 1.48 cm) with positive EUS features should receive intensive surveillance or undergo endoscopic surgery. EUS and dissection are efficient diagnostic and therapeutic approaches for small GISTs.

Key Words: Gastrointestinal stromal tumors; Endoscopic ultrasound; Diagnosis; Risk classification

©The Author(s) 2022. Published by Baishideng Publishing Group Inc. All rights reserved.

Core Tip: Endoscopic ultrasound (EUS) has been the recommended follow-up method for small gastrointestinal stromal tumors (GISTs); however, it is not clear whether positive EUS features can predict the malignant potential of small GISTs. Besides, undergoing close follow-up is an economic and mental burden on patients with small GISTs. This study illustrates an optimal cut-off value for the tumor size (1.48 cm) of small GISTs and uses heterogeneity to evaluate risk prediction. Overall, small GISTs with diameters > 1.48 cm with positive EUS features should receive more intensive follow-up or undergo endoscopic surgery.

Citation: Ge QC, Wu YF, Liu ZM, Wang Z, Wang S, Liu X, Ge N, Guo JT, Sun SY. Efficacy of endoscopic ultrasound in the evaluation of small gastrointestinal stromal tumors. *World J Gastroenterol* 2022; 28(37): 5457-5468

URL: https://www.wjgnet.com/1007-9327/full/v28/i37/5457.htm

DOI: https://dx.doi.org/10.3748/wjg.v28.i37.5457

INTRODUCTION

Gastrointestinal stromal tumors (GISTs) are the most common mesenchy-derived tumors of the gastrointestinal tract[1,2]. They occur most frequently in the stomach, accounting for approximately 60% of all cases[3,4]. Most GISTs contain mutations that activate the c-kit or platelet-derived growth factor receptor α gene[5,6]. The golden standard for the diagnosis of GISTs relies on pathological features assessed by methods, such as hematoxylin and eosin (H&E) and immunohistochemical staining. Currently, the risk classification of GISTs is mainly based on the National Institute of Health (NIH) 2008 (modified) or Fletcher criteria[7,8], which include tumor size (2, 5, and 10 cm), mitotic index, primary tumor sites, and tumor rupture.

GISTs with a diameter of < 2 cm are called small GISTs[9]. Currently, the management of small GISTs is controversial. There is no consensus on the treatment of GIST with a diameter of < 2 cm in the latest guidelines of the National Comprehensive Cancer Network (NCCN) (United States), European Society for Medical Oncology (ESMO), and Chinese Society of Clinical Oncology (CSCO)[10-12]. Most small GISTs are discovered incidentally during regular endoscopic scanning, and they are now easier to be detected than before using endoscopic ultrasound (EUS). EUS has been the widely recommended surveillance method for small GISTs. In addition, EUS elastography, contrast-enhanced EUS, and EUS-guided fine needle aspiration and biopsy (EUS-FNA/FNB) have further improved their diagnostic accuracy[13-16]. Furthermore, EUS features have been used in some studies to predict the risk degree of GISTs[17-19]. However, the management of small GISTs remains controversial, and endoscopic resection *via* endoscopic submucosal dissection (ESD) or endoscopic full-thickness resection (EFTR) is not recommended as a routine treatment. Conversely, no study has focused on the positive EUS features for determining the degree of risk for small GISTs. Therefore, in this study, we aimed to identify the efficiency of EUS in the risk assessment and safety of endoscopic dissection for small GISTs.

MATERIALS AND METHODS

Patients

Data on consecutive patients with pathologically confirmed GISTs who were admitted to Shengjing Hospital of China Medical University between September 2014 and July 2019 were collected. The study included patients who underwent endoscopic resection and were pathologically or genotypically diagnosed with GISTs with a diameter of ≤ 2 cm. All the patients underwent preoperative EUS examination. Patients with other sarcomatous malignancies and/or with incomplete data were excluded. This study was approved by the Institutional Review Board and the Ethics Committee of China Medical University (No. 2022PS009K), and all the patients provided informed consent to participate in the study.

EUS examination

Linear EUS (EG3870UT; Pentax, Tokyo, Japan) was used for the examination. Two experienced endoscopists, who were blinded to the pathological results of these lesions, retrospectively evaluated the characteristics of the EUS images to determine whether there were positive features, including irregular borders, cystic changes, ulcerations, strong echogenic foci, heterogeneity, and the presence of an exogenous type of development (Figures 1 and 2). According to the NCCN guidelines, one or more positive EUS features indicate the malignant potential of small GISTs.

Endoscopic resection procedure

The equipment and accessories used during the endoscopic procedure included a standard single-channel gastroscope (EG29-i10, Pentax, Tokyo, Japan) and a transparent cap. Triangle- (TT knife, Olympus Corporation, Tokyo, Japan) and insulation- tipped knifes (IT knife, Olympus Corporation, Tokyo, Japan) were used for the dissection and resection of tumors. During the procedure, hot biopsy forceps (FD-410LR, Olympus Corporation, Tokyo, Japan) were used for hemostasis. Metal clips (Boston Resolution™, Boston, United States) and an over-the-scope clips (OTSC) (Ovesco Endoscopy GmbH, Tuebingen, Germany) were used for the closure of defects.

All endoscopic resections were performed by skilled gastroenterologists, following the standard endoscopic treatment regimen. All procedures were performed using propofol sedation under continuous cardiorespiratory monitoring. Ligation-assisted endoscopic resection, ESD, and EFTR were performed to resect gastric GISTs.

Pathological examination

All resected GIST specimens were routinely processed using a standard surgical pathology protocol after overnight fixation in 10% neutral buffered formalin solution. The details of the tumor site, size, shape, surface color, and consistency were documented by a surgical pathologist. Conventional immunochemistry with a panel of antibodies, such as CD117 (c-kit), CD34, Dog-1, S-100, and smooth muscle actin, was used to support the histopathological diagnosis of GIST. Based on the modified NIH criteria, patients with GISTs were divided into very low-, low-, intermediate-, and high-risk groups (Table 1).

Follow-up strategy

All the patients were routinely followed-up with conventional endoscopic surveillance at 1, 3, 6, and 12 mo after resection. This was followed by annual abdominal computed tomography (CT) for 3 years to rule out recurrence and metastasis. If no residual tumor or tumor recurrence was observed, endoscopic examinations were performed once every 2 years. The follow-up period was up to October 2020. If residual tumor or tumor recurrence was detected, endoscopic resection or surgery could be performed.

Statistical analysis

Data processing was performed using the SPSS statistical software (SPSS 23.0, Chicago, IL, United States). Continuous data are expressed as the mean ± SD, and categorical data are displayed as number (*n*) or percentage (%). The accuracy of the diagnostic test was evaluated by sensitivity, specificity, false negative and positive rates, positive and negative likelihood ratios, and Youden's index. The Chi-square test was applied for intergroup comparisons. A receiver operating characteristic (ROC) curve was performed to determine the optimal tumor diameter for predicting malignant potential. Lesions with positive EUS features or mitoses more than 5/50 high power field (HPF) were defined as true positives. P value < 0.05 was considered statistically significant.

RESULTS

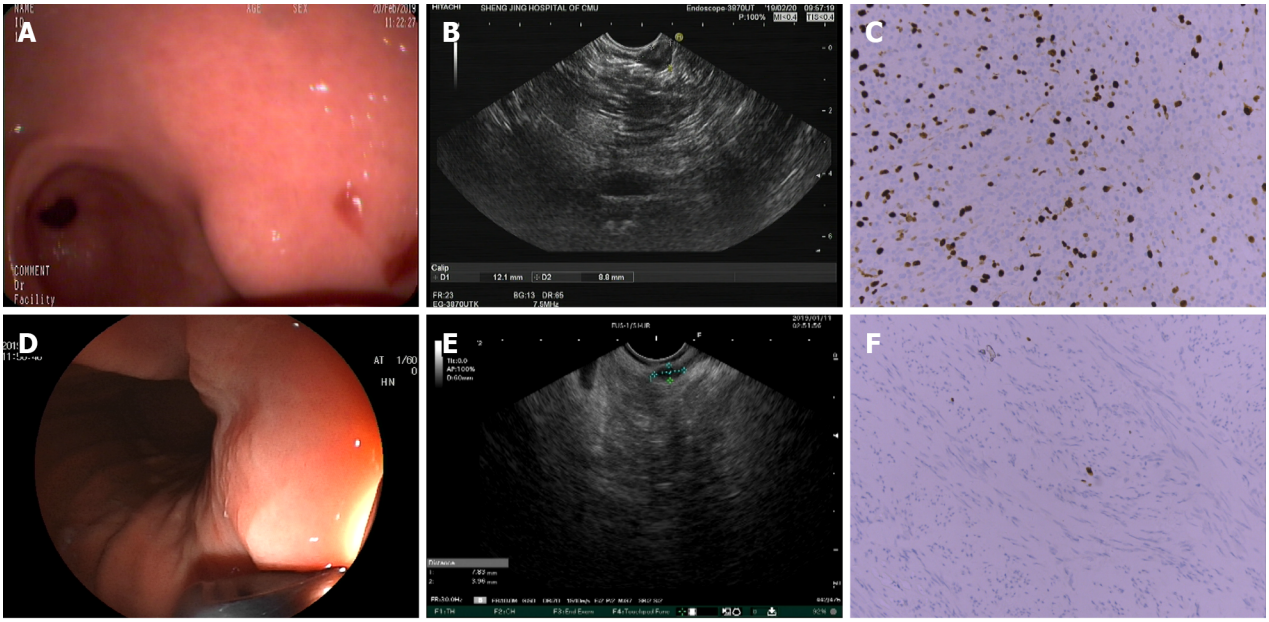
Clinical and pathological features of small gastric GISTs

A total of 256 patients, including 69 men (27%) and 187 women (73%), were enrolled in the study

Table 1 The modified National Institute of Health risk classification of small Gastrointestinal stromal tumors

Risk classification	Tumor diameter (d/cm)	Mitotic count (number/50 HPF)
Very-low	D ≤ 2	Mitotic ≤ 5
Intermediate	D ≤ 2	5 < mitotic ≤ 10
High	D ≤ 2	Mitotic > 10

HPF: High power field.



DOI: 10.3748/wjg.v28.i37.5457 **Copyright** ©The Author(s) 2022.

Figure 1 Endoscopic ultrasound imaging features were consistent with the postoperative pathological results. A: A lesion with a diameter of approximately 1.2 cm was observed in the gastric antrum using an endoscope; B: Heterogeneity was observed as a characteristic of endoscopic ultrasound (EUS) imaging; C: Gastric stromal tumor (intermediate risk). The spindle of the tumor cells is arranged in sheets and bundles with nuclear division of approximately 8-9/50 high power field. Immunohistochemistry: CD117 (+); CD34 (-); Desmin (-); Dog1 (+); Ki-67 (35%+); smooth muscle actin (+); and S-100 (-); D: A lesion with a diameter of approximately 0.6 cm was observed in the gastric fundus using an endoscope; E: EUS images were characterized by a hypoechoic mass in the muscularis propria; F: Gastric stromal tumor (very low risk). The spindle of the tumor cells is arranged in spindle and bundles without obvious nuclear division. Immunohistochemistry: CD117 (+); CD34 (-); Desmin (-); Dog1 (+); Ki-67 (< 1%+); smooth muscle actin (-); and S-100 (-).

(Table 2), with an average age of 57.4 ± 8.6 years. The most frequent locations of the tumors were the gastric fundus (78.1%) and body (17.2%), and the average diameter of all lesions was 1.05 cm (range, 0.30–2.00 cm). These patients were eventually diagnosed with GISTs mainly based on pathological standards, such as H&E and immunohistochemistry staining. According to the modified NIH criterion, mitoses were calculated as > 5/50 HPF and ≤ 5/50 HPF in 8 (3.1%) and 248 (96.9%) patients, respectively. The patients' features in the EUS images are shown in Table 2, illustrating that 67 (65.1%) and 22 (8.6%) cases were identified with heterogenous and hyperechoic foci, respectively. However, a lobular border and ulceration were detected in only 3 cases (1.2%).

ROC curve analysis

To determine a suitable cut-off value for predicting the higher risk potential of small GISTs, aggressive biological behaviors were expanded to mitoses more than 5/50 HPF. Lesions with mitoses more than 5/50 HPF were defined as true positives. A tumor diameter of 1.48 cm was finally identified as the optimal cut-off value, with the area under the curve (AUC) being 0.89 (95% confidence interval: 0.824–0.956; P < 0.001) (Figure 3A), a sensitivity of 0.875, and a specificity of 0.828 (Figure 3B). Subsequently, 208 and 48 patients were classified into groups with tumor size ≤ 1.48 cm and > 1.48 cm, respectively. The comparison of the clinicopathological characteristics between the two groups is presented in Table 3. In the > 1.48 cm group, a higher percentage of patients had more than 5 mitotic indexes/50 HPFs compared to those in the ≤ 1.48 cm group (14.58% *vs* 0.48%, P < 0.001). Moreover, patients with larger tumor diameter tended to display positive EUS features (56.25% *vs* 31.25%, P = 0.002).

Table 2 Clinicopathological characteristics of the patients

Characteristics	Cases (*n* = 256)
Age (year)	57.4 ± 8.6
Sex, *n* (%)	
Male	69 (27.0)
Female	187 (73.0)
Tumor location, *n* (%)	
Cardia	6 (2.3)
Fundus	200 (78.1)
Body	44 (17.2)
Antrum	6 (2.4)
Endoscopic resection, *n* (%)	
ESD	136 (53.1)
EFTR	120 (46.9)
Tumor size (cm), *n* (%)	
≤ 1.48	208 (81.3)
>1.48	48 (18.7)
Mitotic index (/50HPF), *n* (%)	
≤ 5	248 (96.9)
> 5	8 (3.1)
Modified NIH classification, *n* (%)	
Very-low	232 (90.6)
Low	16 (6.3)
Intermediate	7 (2.7)
High	1 (0.4)
Positive EUS features, *n* (%)	
Heterogenous	67 (65.1)
Hyperechoic foci	22 (8.6)
Lobular border	1 (0.4)
Ulceration	2 (0.8)

ESD: Endoscopic submucosal dissection; EFTR: Endoscopic full-thickness resection; EUS: Endoscopic ultrasound; HPF: High power field; NIH: National Institute of Health.

Comparison of non-low-risk and low-risk GISTs in terms of EUS features

We compared the consistency of positive EUS features and pathological risk classification of small GISTs, and found that intermediate- and very low-risk cases presented with heterogeneous (Figure 1A-C) and hypoechoic (Figure 1D-F) EUS findings, respectively. This suggests that EUS imaging features were consistent with the postoperative pathological results. However, some cases showed that EUS imaging features were inconsistent with the postoperative pathological results [intermediate-risk case with hypoechoic mass (Figure 2A-C) and very-low-risk case with strong echogenic foci (Figure 2D-F)]. To further identify the efficiency of positive EUS features in the risk assessment of small GISTs, we divided these patients into non-low-risk and low-risk groups (Table 4). Five of eight patients with non-low-risk GISTs (62.5%) and 62 of 248 patients with low-risk GISTs (25%) had heterogeneous features. There was a significant difference (P = 0.031) in the heterogeneous features between low- and high-grade risk GISTs. However, there was no statistical difference in hyperechoic foci and ulceration between low- and high-grade risk GISTs. Hyperechoic foci were found in 0 of 8 (0%) and 22 of 248 (8.87%) non-low- and low-risk groups, respectively. The ulcerative appearance was found in 0 of 8 (0%) and 2 of 248 (0.8%) non-low- and low-risk groups, respectively. Furthermore, other positive EUS

Table 3 Comparisons of clinicopathological and endoscopic ultrasonographic features between ≤ 1.48 cm and > 1.48 cm groups

Characteristic	Tumor size		
	≤ 1.48 cm group	> 1.48 cm group	*P* value
Age (year)	57.3 ± 8.6	58.2 ± 8.4	0.49
Sex			0.368
Men	59	10	
Women	149	38	
Tumor location			0.01
Fundus	168	32	
Body	34	10	
Antrum	4	2	
Cardia	2	4	
Mitotic index (/50 HPFs)			< 0.001
≤ 5	207	41	
>5	1	7	
Positive EUS features[1]			0.002
Yes	65	25	
No	143	23	

[1]Marginal irregularity, cystic changes, ulcers, strong echo foci, and heterogeneity. EUS: Endoscopic ultrasound; HPF: High power field.

Table 4 Comparisons of positive endoscopic ultrasonographic features between the pathologically non-low-risk group and low-risk group

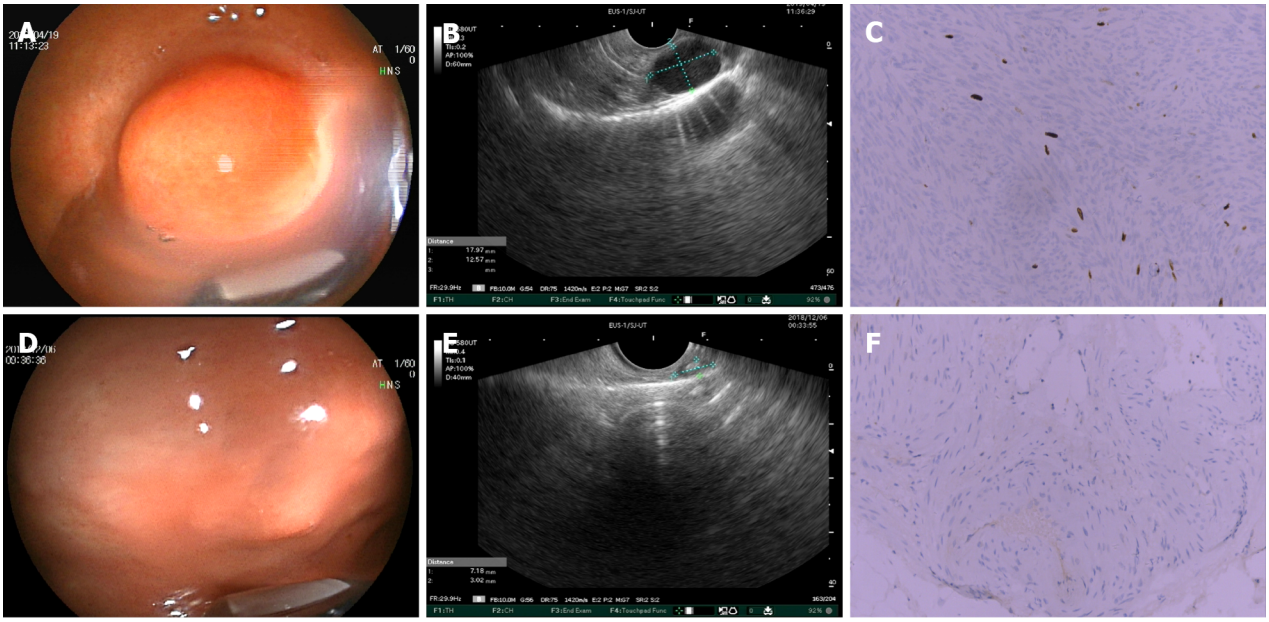
Positive EUS features	Risk classification		
	Intermediate/high	Very low/low	*P* value
Heterogeneous			0.031
Yes	5	62	
No	3	186	
Hyperechoic foci			NS
Yes	0	22	
No	8	226	
Ulcers			NS
Yes	0	2	
No	8	246	

EUS: Endoscopic ultrasound; NS: No significant.

features, such as marginal irregularity and cystic changes, were not detected in small GISTs.

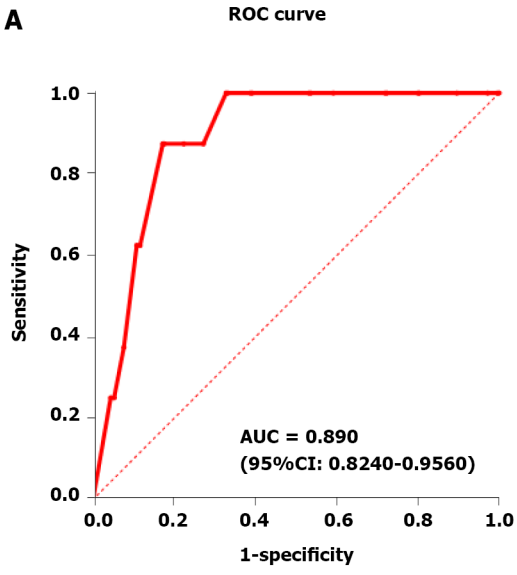
DISCUSSION

The incidence of GIST ranges from 6 to 22 cases *per* 10^6 individuals *per* year[20,21], while that of small GISTs might be higher as more cases of asymptomatic small GISTs have been detected clinically due to the growing popularity of endoscopy in the recent years. Currently, there is no consensus on whether small GISTs (≤ 2 cm) require resection or yearly surveillance in the latest guidelines, including NCCN, ESMO, and CSCO[10-12,22]. However, the ESMO recommends that resection should be the standard



DOI: 10.3748/wjg.v28.i37.5457 **Copyright** ©The Author(s) 2022.

Figure 2 Endoscopic ultrasound imaging features were inconsistent with the postoperative pathological results. A: A lesion with a diameter of approximately 2 cm was observed in the gastric fundus using an endoscope; B: Endoscopic ultrasound (EUS) images were characterized by a hypoechoic mass in the muscularis propria; C: Gastric stromal tumor (intermediate risk). The spindle of the tumor cells is arranged in a spindle and braided pattern with nuclear division of approximately 8/50 high power field. Immunohistochemistry: CD117 (+); CD34 (-); Desmin (-); Dog1 (+); Ki-67 (10%+); smooth muscle actin (-); and S-100 (-); D: A lesion with a diameter of approximately 0.6 cm was observed in the gastric fundus using an endoscope; E: Strong echogenic foci and heterogeneity were observed as characteristics of EUS imaging; F: Gastric stromal tumor (very low risk). The spindle of the tumor cells is arranged in spindle and bundles without obvious nuclear division. Some tissues calcify. Immunohistochemistry: CD117 (+); CD34 (+); Desmin (-); Ki-67 (1%+); smooth muscle actin (+); and S-100 (-).



B

Optimal cut-off value

Positive if ≥ cm	Sensitivity	Specificity	Youden index
> 0.3500	1	0.004	0.004
> 0.4500	1	0.028	0.028
> 0.5500	1	0.104	0.104
> 0.6250	1	0.196	0.196
> 0.6750	1	0.2	0.2
> 0.7200	1	0.276	0.276
> 0.7700	1	0.28	0.28
> 0.8500	1	0.408	0.408
> 0.9250	1	0.464	0.464
> 0.9750	1	0.468	0.468
> 1.020	1	0.608	0.608
> 1.070	1	0.612	0.612
> 1.105	1	0.668	0.668
> 1.155	1	0.672	0.672
> 1.250	0.875	0.728	0.603
> 1.350	0.875	0.776	0.651
> 1.430	0.875	0.824	0.699
> 1.480	0.875	0.828	0.703
> 1.550	0.625	0.884	0.509
> 1.650	0.625	0.892	0.517
> 1.750	0.375	0.924	0.299
> 1.850	0.25	0.948	0.198
> 1.950	0.25	0.956	0.206

DOI: 10.3748/wjg.v28.i37.5457 **Copyright** ©The Author(s) 2022.

Figure 3 Receiver operating characteristic curve. A: The receiver operating characteristic curve of the cut-off (1.48 cm); B: The optimal cut-off (1.48 cm) with a sensitivity of 0.875 and a specificity of 0.828. ROC: Receiver operating characteristic; AUC: Area under the curve.

treatment for histologically confirmed small GISTs[21]. Small GISTs are generally considered to have a low malignant potential, and few of them may progress to clinically relevant tumors. However, a population-based study reviewed 378 patients with small GISTs found that approximately 11.4% of small GISTs were accompanied by local progression or even distant metastasis when first diagnosed and claimed that small GISTs might progress and become life-threatening, with a mortality of 12% at 5 years[23]. Additionally, some scholars believe that the conservative observational methods for small GISTs can only evaluate whether the tumor diameter has increased, which will cause psychological

burden and risk to patients as clinicians would only passively wait for the tumor size to increase before performing surgical resection[24]. Therefore, it is critical to choose optimal approaches for accurately evaluating the clinical features and providing risk suggestions for small GISTs before their progression.

EUS has been recommended as an optimal method for the diagnosis and follow-up of small GISTs, while its efficacy in risk assessment of small GISTs is still not clear. The NCCN guidelines recommend that conservative follow-up should be performed in small GISTs lacking high-risk EUS features (marginal irregularity, cystic changes, ulcers, strong echo foci, and heterogeneity)[10]. Moreover, in recent years, many studies have shown that EUS can provide a preliminary basis for assessing the malignant potential of lesions. Palazzo *et al*[25] showed that EUS was reliable in predicting the malignant potential of GISTs, including three most predictive EUS features (one or more of the following: Irregular border, cystic changes, and lymph nodes with a malignant pattern) with a sensitivity of 91% and a specificity of 88%[25]. Jeon *et al*[26] found that the best predictor of high-risk GISTs was the combination of endoscopic and EUS features, including a tumor diameter > 3 cm, irregular border, mucosal ulceration, and a non-oval shape[26]. Concerning small GISTs, Gao *et al*[18] studied 69 patients suspected to have GISTs as indicated by EUS and concluded that the tumor size of > 9.5 mm was significantly correlated with tumor progression, which was of great value in predicting the malignant potential of the GISTs[18]. Wang *et al*[27] examined 648 cases of small GISTs and concluded that GISTs with a diameter of < 1.45 cm had an overall good prognosis; however, those with a diameter > 1.45 cm required intensive monitoring or had to undergo endoscopic surgery[27,28].

Our study enrolled a total of 256 patients who underwent ESD or EFTR during 2014–2019 in Shengjing Hospital including 248 very low- or low-risk cases and 8 intermediate/high-risk cases based on the modified NIH classification. We generated a ROC curve based on the potential malignancy predictor (mitoses more than 5/50 HPF) to determine the optimal cut-off value of tumor size. A tumor diameter of 1.48 cm was identified as the optimal cutoff value, with a sensitivity of 87.5%, a specificity of 82.8%, and an AUC of 0.89. Of all the 256 patients with small gastric GISTs included in our study, EUS features for malignancy prediction were studied retrospectively. Heterogenous, hyperechoic foci, lobular border, and ulceration were detected in 67 (65.1%), 22 (8.6%), 1 (0.4%) and 2 (0.8%) patients, respectively. According to the optimal cut-off value, patients were subsequently divided into two groups: ≤ 1.48 cm and >1.48 cm. We identified that tumors with a diameter > 1.48 cm were more likely to present positive EUS features (P = 0.002). To further identify whether positive EUS features can predict the malignant potential of small GISTs, we compared EUS features between the non-low- and low-risk groups. The results showed that there was a significant difference between the two groups regarding the heterogeneity, which might suggest that patients with GISTs experiencing this EUS feature should be followed-up more frequently while considering endoscopic surgery when regular follow-up is not feasible or EUS-guided tissue acquisition for pathological assessment. However, there was no statistical difference in hyperechoic foci and ulceration features between the two groups. We believed that limited cases with these two EUS features might have resulted in a partial evaluation. Therefore, a larger scale study is needed to further comprehensively evaluate the efficacy of EUS for the risk prediction of small GISTs.

Other studies have shown that contrast-enhanced harmonic EUS and EUS-elastography can distinguish GISTs from other submucosal tumors, but the risk grade of GISTs cannot be evaluated[14,29]. Moreover, another study suggests that EUS-FNA/FNB can be used to obtain tissue for assessing the malignancy risk of tumors[30]. However, for small GISTs, the diagnostic rate of EUS-FNA is low, and due to the small size of the lesion and certain mobility limitations, puncturing the tumor is difficult and the possibility of obtaining sufficient samples is low[31,32]. A study of 53 patients[33] showed that the successful diagnostic rate of an adequate specimen was related to the lesion size: Only 71% of lesions measuring < 20 mm had complications led by repeated needle puncture[34,35]. In contrast, with the advance of endoscopic techniques, complete treatment has become possible *via* endoscopic surgery, such as ESD and EFTR. ESD is currently the most widely used endoscopic treatment for resecting GISTs. Studies have shown that ESD is safe and effective for treating GISTs that originate from the muscularis propria layer, with a diameter ≤3 cm and without extra-gastrointestinal invasion or abdominal metastasis[36-38]. The main adverse events of this technique are bleeding and perforation[39,40]. EFTR is mainly suitable for patients whose lesions are located in the deep muscularis propria layer and are closely connected to the serosal layer, in which metal clips, OTSCs, and other methods are used for rapid closure of defects to prevent pneumoperitoneum and peritonitis. In this study, only one patient treated with endoscopy developed delayed bleeding; however, the patient recovered well after endoscopic hemostasis was performed. Furthermore, all patients who underwent endoscopic resection had no recurrence or metastasis during a mean follow-up period of 40 mo (range, 15–72 mo), suggesting that endoscopic surgery is feasible and safe for small GISTs.

This study had a few limitations. First, the results of this retrospective study may be affected by selection bias. Second, the follow-up period was relatively short, which may result in missing cases of recurrence. Third, limited samples may affect the comprehensive evaluation of positive EUS features for risk classification. Therefore, multicenter randomized controlled trials should be conducted in the future to enhance the robustness of these conclusions.

CONCLUSION

In conclusion, partial EUS features, such as heterogeneity, can be applied to predict higher-risk small GISTs with a diameter > 1.48 cm. These tumors with diameters > 1.48 cm should undergo more intensive surveillance. Endoscopic surgery should be strongly recommended for small GISTs if regular follow-up is infeasible for low recurrence rate and metastatic rate.

ARTICLE HIGHLIGHTS

Research background

Small gastrointestinal stromal tumors (GISTs) have a high incidence, and their prognosis and treatment remain controversial.

Research motivation

Endoscopic ultrasound (EUS) plays a pivotal role in the diagnosis of GISTs, but its ability to assess the prognosis of small GISTs remains to be explored.

Research objectives

To evaluate the efficacy of EUS in the diagnosis and risk assessment of small GISTs.

Research methods

We collected data from patients with small GISTs, the diagnosis and risk classifications of which were based on the pathological assessment according to the modified National Institute of Health criteria after endoscopic resection or laparoscopic surgery. The assessment results based on EUS features (marginal irregularity, cystic changes, homogeneity, ulceration, and strong echogenic foci) were compared with the pathological features.

Research results

A total of 256 patients (69 men and 187 women) were enrolled. Tumor size was positively correlated with the mitotic index ($P < 0.001$). Receiver operating curve analysis identified 1.48 cm as the best cut-off value to predict malignant potential (95% confidence interval: 0.824–0.956). EUS heterogeneity with tumor diameters > 1.48 cm was associated with higher risk classification ($P < 0.05$).

Research conclusions

Small GISTs (diameters, > 1.48 cm) with positive EUS features should receive intensive surveillance or undergo endoscopic surgery. EUS and dissection are efficient diagnostic and therapeutic approaches for small GISTs.

Research perspectives

EUS provides reference evidence for the precise assessment and early risk assessment of small GISTs.

ACKNOWLEDGEMENTS

We thank Professor Si-Yu Sun, for his support and guidance during this study. We also thank all other doctors who participated in this study.

FOOTNOTES

Author contributions: Ge QC wrote a majority portion of manuscript, prepared the figures and tables, and performed statistical analysis; Wu YF collected the data of patients; Liu ZM helped with the statistical analysis and manuscript writing; Wang Z provided and confirmed the pathological data of all the patients; Wang S, Liu X, and Ge N took part in the design of the study outline and performed tumor dissection; Guo JT and Sun SY were responsible for the revision of the manuscript for important intellectual content and supervised the study; all the authors read and gave their final approval for the manuscript to be submitted.

Supported by National Natural Science Foundation of China, No. 81900601; The University Innovation Team and Innovative Talent Support Program of Liaoning Province, No. LR2019073; and Shenyang Young and Middle-aged Science and Technology Innovation Talent Support Program, No. RC200438.

Institutional review board statement: This study was approved by the Ethics Review Committee of Shengjing

Hospital of China Medical University, No. 2022PS009K.

Informed consent statement: All the individual involved gave their informed consent prior to study inclusion.

Conflict-of-interest statement: All the authors report no relevant conflicts of interest for this article.

Data sharing statement: No additional data are available.

Open-Access: This article is an open-access article that was selected by an in-house editor and fully peer-reviewed by external reviewers. It is distributed in accordance with the Creative Commons Attribution NonCommercial (CC BY-NC 4.0) license, which permits others to distribute, remix, adapt, build upon this work non-commercially, and license their derivative works on different terms, provided the original work is properly cited and the use is non-commercial. See: https://creativecommons.org/Licenses/by-nc/4.0/

Country/Territory of origin: China

ORCID number: Qi-Chao Ge 0000-0003-3412-2033; Yu-Fan Wu 0000-0003-4290-8263; Zi-Ming Liu 0000-0001-6123-4466; Zhe Wang 0000-0003-1877-826X; Sheng Wang 0000-0002-1531-7655; Nan Ge 0000-0002-5764-7054; Jin-Tao Guo 0000-0001-5722-6359; Si-Yu Sun 0000-0002-7308-0473.

S-Editor: Fan JR
L-Editor: A
P-Editor: Fan JR

REFERENCES

1 **Di Vita M**, Zanghì A, Cavallaro A, Cardì F, Uhlig M, Ursi P, Lo Menzo E, Panebianco V, Cappellani A. Gastric GIST and prognostic models. Which is the best to predict survival after surgery? *Ann Ital Chir* 2019; **90**: 31-40 [PMID: 30942768]
2 **Xu C**, Han H, Wang J, Zhang B, Shao Y, Zhang L, Wang H, Wu Y, Li X, Li R, Tian Y. Diagnosis value of CD117 and PDGFRA, alone or in combination DOG1, as biomarkers for gastrointestinal stromal tumors. *Ann Transl Med* 2015; **3**: 308 [PMID: 26697468 DOI: 10.3978/j.issn.2305-5839.2015.10.07]
3 **Søreide K**, Sandvik OM, Søreide JA, Giljaca V, Jureckova A, Bulusu VR. Global epidemiology of gastrointestinal stromal tumours (GIST): A systematic review of population-based cohort studies. *Cancer Epidemiol* 2016; **40**: 39-46 [PMID: 26618334 DOI: 10.1016/j.canep.2015.10.031]
4 **Wang M**, Xu J, Zhang Y, Tu L, Qiu WQ, Wang CJ, Shen YY, Liu Q, Cao H. Gastrointestinal stromal tumor: 15-years' experience in a single center. *BMC Surg* 2014; **14**: 93 [PMID: 25403624 DOI: 10.1186/1471-2482-14-93]
5 **Corless CL**, Barnett CM, Heinrich MC. Gastrointestinal stromal tumours: origin and molecular oncology. *Nat Rev Cancer* 2011; **11**: 865-878 [PMID: 22089421 DOI: 10.1038/nrc3143]
6 **Hirota S**, Isozaki K, Moriyama Y, Hashimoto K, Nishida T, Ishiguro S, Kawano K, Hanada M, Kurata A, Takeda M, Muhammad Tunio G, Matsuzawa Y, Kanakura Y, Shinomura Y, Kitamura Y. Gain-of-function mutations of c-kit in human gastrointestinal stromal tumors. *Science* 1998; **279**: 577-580 [PMID: 9438854 DOI: 10.1126/science.279.5350.577]
7 **Murphey MD**. World Health Organization classification of bone and soft tissue tumors: modifications and implications for radiologists. *Semin Musculoskelet Radiol* 2007; **11**: 201-214 [PMID: 18260031 DOI: 10.1055/s-2008-1038310]
8 **Fletcher CD**, Berman JJ, Corless C, Gorstein F, Lasota J, Longley BJ, Miettinen M, O'Leary TJ, Remotti H, Rubin BP, Shmookler B, Sobin LH, Weiss SW. Diagnosis of gastrointestinal stromal tumors: A consensus approach. *Hum Pathol* 2002; **33**: 459-465 [PMID: 12094370 DOI: 10.1053/hupa.2002.123545]
9 **Demetri GD**, von Mehren M, Antonescu CR, DeMatteo RP, Ganjoo KN, Maki RG, Pisters PW, Raut CP, Riedel RF, Schuetze S, Sundar HM, Trent JC, Wayne JD. NCCN Task Force report: update on the management of patients with gastrointestinal stromal tumors. *J Natl Compr Canc Netw* 2010; **8** Suppl 2: S1-41; quiz S42 [PMID: 20457867 DOI: 10.6004/jnccn.2010.0116]
10 **von Mehren M**, Randall RL, Benjamin RS, Boles S, Bui MM, Ganjoo KN, George S, Gonzalez RJ, Heslin MJ, Kane JM, Keedy V, Kim E, Koon H, Mayerson J, McCarter M, McGarry SV, Meyer C, Morris ZS, O'Donnell RJ, Pappo AS, Paz IB, Petersen IA, Pfeifer JD, Riedel RF, Ruo B, Schuetze S, Tap WD, Wayne JD, Bergman MA, Scavone JL. Soft Tissue Sarcoma, Version 2.2018, NCCN Clinical Practice Guidelines in Oncology. *J Natl Compr Canc Netw* 2018; **16**: 536-563 [PMID: 29752328 DOI: 10.6004/jnccn.2018.0025]
11 **ESMO/European Sarcoma Network Working Group**. Gastrointestinal stromal tumours: ESMO Clinical Practice Guidelines for diagnosis, treatment and follow-up. *Ann Oncol* 2014; **25** Suppl 3: iii21-iii26 [PMID: 25210085 DOI: 10.1093/annonc/mdu255]
12 **Li J**, Ye Y, Wang J, Zhang B, Qin S, Shi Y, He Y, Liang X, Liu X, Zhou Y, Wu X, Zhang X, Wang M, Gao Z, Lin T, Cao H, Shen L; Chinese Society Of Clinical Oncology Csco Expert Committee On Gastrointestinal Stromal Tumor. Chinese consensus guidelines for diagnosis and management of gastrointestinal stromal tumor. *Chin J Cancer Res* 2017; **29**: 281-293 [PMID: 28947860 DOI: 10.21147/j.issn.1000-9604.2017.04.01]
13 **Hu J**, Ge N, Wang S, Liu X, Guo J, Wang G, Sun S. The Role of Endoscopic Ultrasound and Endoscopic Resection for Gastric Glomus: A Case Series and Literature Review. *J Transl Int Med* 2019; **7**: 149-154 [PMID: 32010601 DOI: 10.2478/jtim-2019-0030]
14 **Kovacevic B**, Vilmann P. EUS tissue acquisition: From A to B. *Endosc Ultrasound* 2020; **9**: 225-231 [PMID: 32655082

DOI: 10.4103/eus.eus_21_20]

15 **Fabbri C**, Fornelli A, Fuccio L, Giovanelli S, Tarantino I, Antonini F, Liotta R, Frazzoni L, Gusella P, La Marca M, Barresi L, Macarri G, Traina M, De Biase D, Fiorino S, Jovine E, Larghi A, Cennamo V. High diagnostic adequacy and accuracy of the new 20G procore needle for EUS-guided tissue acquisition: Results of a large multicentre retrospective study. *Endosc Ultrasound* 2019; **8**: 261-268 [PMID: 31115386 DOI: 10.4103/eus.eus_14_19]

16 **Ang TL**, Li JW, Kwek ABE, Thurairajah PH, Wang LM. The difference in histological yield between 19G EUS-FNA and EUS-fine-needle biopsy needles. *Endosc Ultrasound* 2019; **8**: 255-260 [PMID: 31115385 DOI: 10.4103/eus.eus_12_19]

17 **Săftoiu A**, Vilmann P, Ciurea T. Utility of endoscopic ultrasound for the diagnosis and treatment of submucosal tumors of the upper gastrointestinal tract. *Rom J Gastroenterol* 2003; **12**: 215-229 [PMID: 14502323]

18 **Gao Z**, Wang C, Xue Q, Wang J, Shen Z, Jiang K, Shen K, Liang B, Yang X, Xie Q, Wang S, Ye Y. The cut-off value of tumor size and appropriate timing of follow-up for management of minimal EUS-suspected gastric gastrointestinal stromal tumors. *BMC Gastroenterol* 2017; **17**: 8 [PMID: 28077094 DOI: 10.1186/s12876-016-0567-4]

19 **Kim GH**, Kim KB, Lee SH, Jeon HK, Park DY, Jeon TY, Kim DH, Song GA. Digital image analysis of endoscopic ultrasonography is helpful in diagnosing gastric mesenchymal tumors. *BMC Gastroenterol* 2014; **14**: 7 [PMID: 24400772 DOI: 10.1186/1471-230X-14-7]

20 **Kim HJ**, Lim SJ, Park K, Yuh YJ, Jang SJ, Choi J. Multiple gastrointestinal stromal tumors with a germline c-kit mutation. *Pathol Int* 2005; **55**: 655-659 [PMID: 16185297 DOI: 10.1111/j.1440-1827.2005.01885.x]

21 **Sanborn RE**, Blanke CD. Gastrointestinal stromal tumors and the evolution of targeted therapy. *Clin Adv Hematol Oncol* 2005; **3**: 647-657 [PMID: 16167051]

22 **Casali PG**, Abecassis N, Aro HT, Bauer S, Biagini R, Bielack S, Bonvalot S, Boukovinas I, Bovee JVMG, Brodowicz T, Broto JM, Buonadonna A, De Álava E, Dei Tos AP, Del Muro XG, Dileo P, Eriksson M, Fedenko A, Ferraresi V, Ferrari A, Ferrari S, Frezza AM, Gasperoni S, Gelderblom H, Gil T, Grignani G, Gronchi A, Haas RL, Hassan B, Hohenberger P, Issels R, Joensuu H, Jones RL, Judson I, Jutte P, Kaal S, Kasper B, Kopeckova K, Krákorová DA, Le Cesne A, Lugowska I, Merimsky O, Montemurro M, Pantaleo MA, Piana R, Picci P, Piperno-Neumann S, Pousa AL, Reichardt P, Robinson MH, Rutkowski P, Safwat AA, Schöffski P, Sleijfer S, Stacchiotti S, Sundby Hall K, Unk M, Van Coevorden F, van der Graaf WTA, Whelan J, Wardelmann E, Zaikova O, Blay JY; ESMO Guidelines Committee and EURACAN. Gastrointestinal stromal tumours: ESMO-EURACAN Clinical Practice Guidelines for diagnosis, treatment and follow-up. *Ann Oncol* 2018; **29**: iv68-iv78 [PMID: 29846513 DOI: 10.1093/annonc/mdy095]

23 **Coe TM**, Fero KE, Fanta PT, Mallory RJ, Tang CM, Murphy JD, Sicklick JK. Population-Based Epidemiology and Mortality of Small Malignant Gastrointestinal Stromal Tumors in the USA. *J Gastrointest Surg* 2016; **20**: 1132-1140 [PMID: 27025710 DOI: 10.1007/s11605-016-3134-y]

24 **Fang YJ**, Cheng TY, Sun MS, Yang CS, Chen JH, Liao WC, Wang HP. Suggested cutoff tumor size for management of small EUS-suspected gastric gastrointestinal stromal tumors. *J Formos Med Assoc* 2012; **111**: 88-93 [PMID: 22370287 DOI: 10.1016/j.jfma.2011.01.002]

25 **Palazzo L**, Landi B, Cellier C, Cuillerier E, Roseau G, Barbier JP. Endosonographic features predictive of benign and malignant gastrointestinal stromal cell tumours. *Gut* 2000; **46**: 88-92 [PMID: 10601061 DOI: 10.1136/gut.46.1.88]

26 **Jeon SW**, Park YD, Chung YJ, Cho CM, Tak WY, Kweon YO, Kim SK, Choi YH. Gastrointestinal stromal tumors of the stomach: endosonographic differentiation in relation to histological risk. *J Gastroenterol Hepatol* 2007; **22**: 2069-2075 [PMID: 18031362 DOI: 10.1111/j.1440-1746.2006.04767.x]

27 **Wang M**, Xue A, Yuan W, Gao X, Fu M, Fang Y, Wang L, Shu P, Li H, Hou Y, Shen K, Sun Y, Qin X. Clinicopathological Features and Prognosis of Small Gastric Gastrointestinal Stromal Tumors (GISTs). *J Gastrointest Surg* 2019; **23**: 2136-2143 [PMID: 31012047 DOI: 10.1007/s11605-018-04070-3]

28 **Tsuji Y**, Kusano C, Gotoda T, Itokawa F, Fukuzawa M, Sofuni A, Matsubayashi J, Nagao T, Itoi T, Moriyasu F. Diagnostic potential of endoscopic ultrasonography-elastography for gastric submucosal tumors: A pilot study. *Dig Endosc* 2016; **28**: 173-178 [PMID: 26530730 DOI: 10.1111/den.12569]

29 **Pesenti C**, Bories E, Caillol F, Ratone JP, Godat S, Monges G, Poizat F, Raoul JL, Ries P, Giovannini M. Characterization of subepithelial lesions of the stomach and esophagus by contrast-enhanced EUS: A retrospective study. *Endosc Ultrasound* 2019; **8**: 43-49 [PMID: 30264741 DOI: 10.4103/eus.eus_89_17]

30 **Kuwatani M**, Sakamoto N. Evolution and a promising role of EUS-FNA in gene and future analyses. *Endosc Ultrasound* 2020; **9**: 151-153 [PMID: 32584309 DOI: 10.4103/eus.eus_29_20]

31 **Okubo K**, Yamao K, Nakamura T, Tajika M, Sawaki A, Hara K, Kawai H, Yamamura Y, Mochizuki Y, Koshikawa T, Inada K. Endoscopic ultrasound-guided fine-needle aspiration biopsy for the diagnosis of gastrointestinal stromal tumors in the stomach. *J Gastroenterol* 2004; **39**: 747-753 [PMID: 15338368 DOI: 10.1007/s00535-004-1383-0]

32 **Attila T**, Aydın Ö. Lesion size determines diagnostic yield of EUS-FNA with onsite cytopathologic evaluation for upper gastrointestinal subepithelial lesions. *Turk J Gastroenterol* 2018; **29**: 436-441 [PMID: 30249558 DOI: 10.5152/tjg.2018.17876]

33 **Akahoshi K**, Sumida Y, Matsui N, Oya M, Akinaga R, Kubokawa M, Motomura Y, Honda K, Watanabe M, Nagaie T. Preoperative diagnosis of gastrointestinal stromal tumor by endoscopic ultrasound-guided fine needle aspiration. *World J Gastroenterol* 2007; **13**: 2077-2082 [PMID: 17465451 DOI: 10.3748/wjg.v13.i14.2077]

34 **Hunt GC**, Smith PP, Faigel DO. Yield of tissue sampling for submucosal lesions evaluated by EUS. *Gastrointest Endosc* 2003; **57**: 68-72 [PMID: 12518134 DOI: 10.1067/mge.2003.34]

35 **Sepe PS**, Moparty B, Pitman MB, Saltzman JR, Brugge WR. EUS-guided FNA for the diagnosis of GI stromal cell tumors: sensitivity and cytologic yield. *Gastrointest Endosc* 2009; **70**: 254-261 [PMID: 19482280 DOI: 10.1016/j.gie.2008.11.038]

36 **Levy MJ**, Jondal ML, Clain J, Wiersema MJ. Preliminary experience with an EUS-guided trucut biopsy needle compared with EUS-guided FNA. *Gastrointest Endosc* 2003; **57**: 101-106 [PMID: 12518144 DOI: 10.1067/mge.2003.49]

37 **Bai J**, Wang Y, Guo H, Zhang P, Ling X, Zhao X. Endoscopic resection of small gastrointestinal stromal tumors. *Dig Dis Sci* 2010; **55**: 1950-1954 [PMID: 20204697 DOI: 10.1007/s10620-010-1168-7]

38 **Yu C**, Liao G, Fan C, Yu J, Nie X, Yang S, Bai J. Long-term outcomes of endoscopic resection of gastric GISTs. *Surg*

Endosc 2017; **31**: 4799-4804 [PMID: 28424911 DOI: 10.1007/s00464-017-5557-2]

39 **Li B**, Chen T, Qi ZP, Yao LQ, Xu MD, Shi Q, Cai SL, Sun D, Zhou PH, Zhong YS. Efficacy and safety of endoscopic resection for small submucosal tumors originating from the muscularis propria layer in the gastric fundus. *Surg Endosc* 2019; **33**: 2553-2561 [PMID: 30478693 DOI: 10.1007/s00464-018-6549-6]

40 **An W**, Sun PB, Gao J, Jiang F, Liu F, Chen J, Wang D, Li ZS, Shi XG. Endoscopic submucosal dissection for gastric gastrointestinal stromal tumors: a retrospective cohort study. *Surg Endosc* 2017; **31**: 4522-4531 [PMID: 28374257 DOI: 10.1007/s00464-017-5511-3]

World Journal of Gastroenterology

Submit a Manuscript: https://www.f6publishing.com

World J Gastroenterol 2022 October 7; 28(37): 5469-5482

DOI: 10.3748/wjg.v28.i37.5469

ISSN 1007-9327 (print) ISSN 2219-2840 (online)

ORIGINAL ARTICLE

Retrospective Study

Online calculator for predicting the risk of malignancy in patients with pancreatic cystic neoplasms: A multicenter, retrospective study

Dong Jiang, Zi-Xiang Chen, Fu-Xiao Ma, Yu-Yong Gong, Tian Pu, Jiang-Ming Chen, Xue-Qian Liu, Yi-Jun Zhao, Kun Xie, Hui Hou, Cheng Wang, Xiao-Ping Geng, Fu-Bao Liu

Specialty type: Gastroenterology and hepatology

Provenance and peer review: Unsolicited article; Externally peer reviewed.

Peer-review model: Single blind

Peer-review report's scientific quality classification

Grade A (Excellent): 0
Grade B (Very good): B, B, B
Grade C (Good): C
Grade D (Fair): D
Grade E (Poor): 0

P-Reviewer: Cheng H, China; Ghareeb WM, China; Luo J, China; Tsujinaka S, Japan

Received: June 16, 2022
Peer-review started: June 16, 2022
First decision: July 12, 2022
Revised: July 25, 2022
Accepted: September 8, 2022
Article in press: September 8, 2022
Published online: October 7, 2022

Dong Jiang, Zi-Xiang Chen, Fu-Xiao Ma, Yu-Yong Gong, Tian Pu, Jiang-Ming Chen, Xue-Qian Liu, Yi-Jun Zhao, Kun Xie, Xiao-Ping Geng, Fu-Bao Liu, Department of General Surgery, The First Affiliated Hospital of Anhui Medical University, Hefei 230000, Anhui Province, China

Hui Hou, Department of General Surgery, The Second Affiliated Hospital of Anhui Medical University, Hefei 230000, Anhui Province, China

Cheng Wang, Department of General Surgery, The First Affiliated Hospital of University of Science and Technology of China, Hefei 230000, Anhui Province, China

Corresponding author: Fu-Bao Liu, MD, PhD, Chief Doctor, Professor, Department of General Surgery, The First Affiliated Hospital of Anhui Medical University, No. 81 Meishan Road, Hefei 230000, Anhui Province, China. lancetlfb@126.com

Abstract

BACKGROUND

Efficient and practical methods for predicting the risk of malignancy in patients with pancreatic cystic neoplasms (PCNs) are lacking.

AIM

To establish a nomogram-based online calculator for predicting the risk of malignancy in patients with PCNs.

METHODS

In this study, the clinicopathological data of target patients in three medical centers were analyzed. The independent sample t-test, Mann–Whitney U test or chi-squared test were used as appropriate for statistical analysis. After univariable and multivariable logistic regression analysis, five independent factors were screened and incorporated to develop a calculator for predicting the risk of malignancy. Finally, the concordance index (C-index), calibration, area under the curve, decision curve analysis and clinical impact curves were used to evaluate the performance of the calculator.

RESULTS

Enhanced mural nodules [odds ratio (OR): 4.314; 95% confidence interval (CI): 1.618–11.503, $P = 0.003$], tumor diameter ≥ 40 mm (OR: 3.514; 95%CI: 1.138–10.849, $P = 0.029$), main pancreatic duct dilatation (OR: 3.267; 95%CI: 1.230–8.678, $P =$

0.018), preoperative neutrophil-to-lymphocyte ratio ≥ 2.288 (OR: 2.702; 95%CI: 1.008–7.244, P = 0.048], and preoperative serum CA19-9 concentration ≥ 34 U/mL (OR: 3.267; 95%CI: 1.274–13.007, P = 0.018) were independent risk factors for a high risk of malignancy in patients with PCNs. In the training cohort, the nomogram achieved a C-index of 0.824 for predicting the risk of malignancy. The predictive ability of the model was then validated in an external cohort (C-index: 0.893). Compared with the risk factors identified in the relevant guidelines, the current model showed better predictive performance and clinical utility.

CONCLUSION

The calculator demonstrates optimal predictive performance for identifying the risk of malignancy, potentially yielding a personalized method for patient selection and decision-making in clinical practice.

Key Words: Pancreatic cystic neoplasms; Risk of malignancy; Nomogram; Model; Prediction; Calculator

©The Author(s) 2022. Published by Baishideng Publishing Group Inc. All rights reserved.

Core Tip: A nomogram-based online calculator for predicting the risk of malignancy in patients with pancreatic cystic neoplasms was developed. The calculator demonstrates optimal predictive performance for identifying the risk of malignancy, potentially yielding a personalized method for patient selection and decision-making in clinical practice.

Citation: Jiang D, Chen ZX, Ma FX, Gong YY, Pu T, Chen JM, Liu XQ, Zhao YJ, Xie K, Hou H, Wang C, Geng XP, Liu FB. Online calculator for predicting the risk of malignancy in patients with pancreatic cystic neoplasms: A multicenter, retrospective study. *World J Gastroenterol* 2022; 28(37): 5469-5482
URL: https://www.wjgnet.com/1007-9327/full/v28/i37/5469.htm
DOI: https://dx.doi.org/10.3748/wjg.v28.i37.5469

INTRODUCTION

Pancreatic cystic neoplasms (PCNs) are estimated to be present in 2%–45% of the general population[1-3]. With rapid advancements in medical examination technologies over the past decades, the use of these technologies in the identification of PCNs has dramatically increased. Moreover, PCNs are frequently discovered in asymptomatic patients[4]. Consequently, centers with high volumes of patients undergoing pancreatic surgery are evaluating an increasing number of PCNs cases annually. Nevertheless, how to properly manage patients with PCNs remains a topic of debate.

PCNs are usually divided into serous cystic neoplasms (SCNs), mucinous cystic neoplasms (MCNs), intraductal papillary mucinous neoplasms (IPMNs) and other rare cystic lesions, such as solid pseudopapillary tumors (SPTs) and cystic neuroendocrine tumors (cNET) which show biological behavior ranging from benign to malignant[5,6]. Moreover, the main controversy regarding the treatment of PCNs is related to the inability to precisely determine their histopathological diagnosis without surgical resection[7,8], thereby precluding the accurate identification of different subtypes of PCNs. Consequently, clinicians are challenged to maintain a difficult balance between avoiding excessive surgical treatment and keeping a malignant lesion under surveillance.

Although previous studies have focused on the identification of different types of PCNs[9-11], only a few of these studies have emphasized the judgment or prediction of malignancy risk in PCNs. Thus, identifying a method that can accurately and preoperatively predict the risk of malignancy in PCNs is of great significance. Nomograms are effective statistical tools that enable the simultaneous consideration of various factors for clinicians to visualize the malignant probability of a neoplasm, allowing the formulation of an optimal therapeutic schedule. Nomogram possess other advantages including ease of comprehension, user-friendliness and personalized evaluation[12]. Therefore, this study aimed to establish a novel clinical online nomogram-based calculator to predict the risk of malignancy in PCNs.

MATERIALS AND METHODS

The clinical and pathological data of patients with PCNs who underwent surgery at the Department of General Surgery in three medical centers between January 2015 and December 2021 were collected and analyzed. Patients from the First Affiliated Hospital of Anhui Medical University and Second Affiliated

Hospital of Anhui Medical University were set as the training cohort, while those from the First Affiliated Hospital of the University of Science and Technology of China were set as the validation cohort. All hospitals were high-volume surgical centers that employed similar therapeutic approaches for PCNs. Pathological diagnosis was confirmed by postoperative specimen examinations by two experienced pathologists. According to the histological classification of PCNs proposed by the World Health Organization (2019) and the Baltimore consensus meeting, PCNs are classified as those with low- or intermediate-grade dysplasia and those with high-grade dysplasia or invasive carcinoma[13,14]. Patients from the three centers who met the following criteria were included: (1) Patients who underwent surgical treatment and were confirmed as showing SCNs, IPMNs or MCNs in postoperative pathological examinations; (2) Patients with complete clinical data, including medical history and laboratory test data; and (3) Patients who underwent preoperative imaging examinations. The following patients were excluded: (1) Patients who were pathologically confirmed as having other rare cystic lesions such as SPTs and cNET; (2) Patients who were pathologically confirmed as having other uncommon and undefined cystic tumors of the pancreas; and (3) Patients with a history of pancreatic surgery, radiotherapy or chemotherapy. All clinical data were screened and collected in a computerized database by a professional research assistant. In this study, patients were categorized as showing low-risk (low- or intermediate-grade dysplasia) or high-risk (high-grade dysplasia or invasive carcinoma) disease based on the pathological diagnosis. The appearance of high-risk disease was characterized as a study endpoint. Figure 1 depicts a flowchart of patient enrollment and the inclusion process. This study was conducted in accordance with the Declaration of Helsinki and was approved by the institutional ethics committee (Quick-PJ2022-06-26). All included patients or their relatives provided written informed consent before their data were analyzed.

Perioperative management

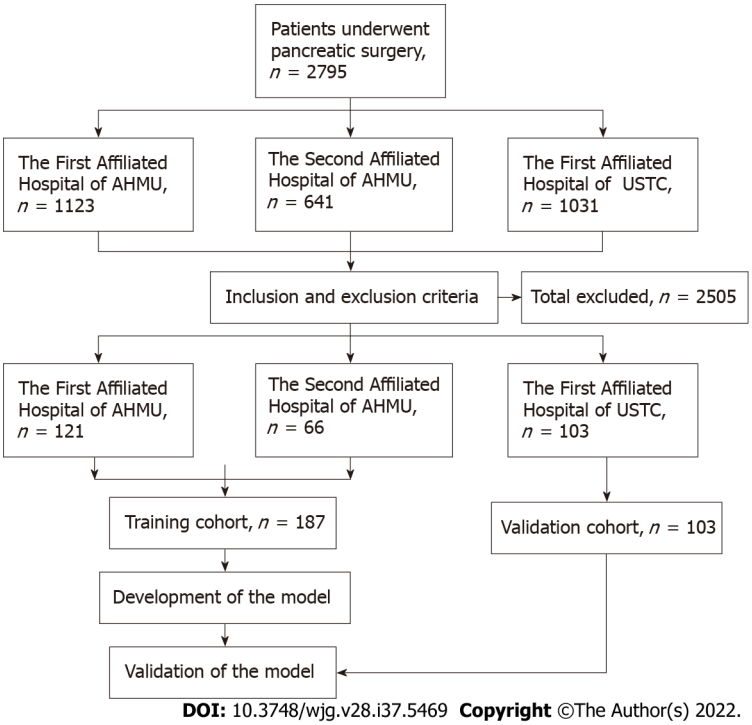
In accordance with the similar preoperative evaluation protocol at all centers, all patients were routinely examined using blood tests, including routine blood counts and analysis of blood biochemistry, hemostatic function, immunological markers and tumor markers. Moreover, all patients underwent at least two preoperative imaging examinations through ultrasound (US), computed tomography (CT), magnetic resonance imaging or 2-^{18}F-fluoro-2-deoxy-d-glucose positron emission tomography-CT, which provided information about the size, number, location and internal condition of the lesions. Definitive planning of the procedure was performed according to the examination results and the patient's age, comorbidities and preferences.

Surgical procedures, including pancreatoduodenectomy, total pancreatectomy, partial pancreatectomy and distal pancreatectomy with or without splenic preservation, were performed depending on the tumor location and characteristics. Experienced pancreatic surgeons performed all surgical procedures. Meanwhile, the balance between the benefits of oncological clearance and the risks of inadequate parenchymal preservation was carefully considered.

Normative and meticulous postoperative care including monitoring of vital signs, maintenance of moderate tissue perfusion and support for nutritional needs was implemented for every patient at the initial stage.

Statistical analysis

All data, including demographic data, preoperative imaging data and clinical and pathological data were recorded in detail using a special recorder. Continuous variables were expressed as mean ± SD for normally distributed variables or median (interquartile range) for non-normally distributed variables and statistical tests were used as appropriate (the independent sample t-test or the Mann–Whitney U test). Categorical variables were expressed as numbers (n) and proportions (%) and compared appropriately *via* Fisher's exact test or the chi-squared test. The cutoff values of continuous parameters were derived from the Youden index[15]. Univariable logistic regression analysis was performed on the training cohort to screen for risk factors associated with malignancy. On the basis of the univariable analysis, multivariable logistic regression analysis was conducted using variables that had statistical significance. A nomogram for the prediction of malignancy in patients with PCNs was developed based on the multivariable logistic regression model. The performance of the nomogram was evaluated using a concordance index (C-index) and calibration plots based on bootstrap validation method (n = 1000) to reduce overfitting bias. The area under the curve (AUC) of the receiver operating characteristic (ROC) curves and the quality indices such as sensitivity, specificity, accuracy, positive predictive value and negative predictive value with the associated 95% confidence intervals (CIs) of the model applied to the training and external validation cohorts were obtained. This allowed assessment of the predictive efficiency of the model in comparison with those of the risk factors identified in the relevant guidelines. The clinical usefulness of the nomogram was examined by determining the net benefit using decision curve analysis (DCA)[16]. DCA can assess the utility of models for decision making by plotting net benefit at a range of clinically reasonable risk thresholds. The predictive accuracy and clinical usefulness of the nomogram were demonstrated by clinical impact curves. Based on the sensitivity, specificity and predictive values, the optimal cutoff value was evaluated for accuracy. An online calculator for public use was created through shinyapps.io by RStudio to facilitate the use of the model in clinical practice. Statistical analyses were performed using R version 4.0.5 (http://www.r-project.org/, R Development



DOI: 10.3748/wjg.v28.i37.5469 **Copyright** ©The Author(s) 2022.

Figure 1 Flowchart of patient recruitment and diagnosis. AHMU: Anhui Medical University; USTC: University of Science and Technology of China.

Core Team) and SPSS version 23.0 (SPSS Inc, Armonk, NY, United States. In this study, the packages rms, nomogramFormula, DynNom and rmda were utilized for statistical analysis and figure drawing. A two-tailed P value < 0.05 was considered significant.

RESULTS

Patient cohorts and clinicopathologic features

The clinicopathologic data of 1764 consecutive patients who underwent pancreatic surgery at the First Affiliated Hospital of Anhui Medical University and the Second Affiliated Hospital of Anhui Medical University between January 2015 and December 2021 were collected. Among them, 246 patients (13.9%) who were pathologically confirmed as having IPMNs, MCNs or SCNs were classified as the initial target population. Of these 246 patients, 59 (24.0%) who did not fulfill the inclusion criteria were excluded, including 19 patients with incomplete clinical or imaging data, nine with a history of pancreatic surgery, 25 with mixed pathological characteristics and 6 with a history of radiotherapy or chemotherapy. Ultimately, 187 patients (76.0%) were included in the training cohort. Based on the same criteria, an independent group consisting of 103 patients from the First Affiliated Hospital of University of Science and Technology of China who were eligible for inclusion in the same period was included in the present study and served as an external validation cohort. The two cohorts showed no significant differences in baseline characteristics (P > 0.05; Tables 1 and 2).

Univariable and multivariable analysis in the training cohort

The results of the univariable and multivariable analyses of variables concerning malignancy in the training cohort were listed in Table 3. The optimal cutoff values of the neutrophil-to-lymphocyte ratio (NLR) was 2.288. Factors that significantly affected the risk of malignancy in the univariable analysis were then included in the multivariable analysis, which demonstrated that the presence of enhanced mural nodules [odds ratio (OR): 4.314; 95%CI: 1.618–11.503, P = 0.003], tumor diameter ≥ 40 mm (OR: 3.514; 95%CI: 1.138–10.849, P = 0.029), main pancreatic duct dilatation (OR: 3.267; 95%CI: 1.230–8.678, P = 0.018), preoperative NLR ≥ 2.288 (OR: 2.702; 95%CI: 1.008–7.244, P = 0.048) and preoperative serum CA19-9 concentration ≥ 34 U/mL (OR: 3.267; 95%CI: 1.274–13.007, P = 0.018) were independent risk factors for a high risk of malignancy in patients with PCNs.

Development and evaluation of the predictive model

The factors that were proven to be related to a high risk of malignancy were utilized to establish a nomogram for evaluating the probability of malignancy (Figure 2). The model obtained using this approach showed good predictive capacity for estimating the risk of malignancy in patients with PCNs

Table 1 Preoperative clinical characteristics of patients with pancreatic cystic neoplasms

Characteristics	Training cohort	Validation cohort	*P* value
	n = 187 (64.5%)	*n* = 103 (35.5%)	
Sex			0.190
Male	126 (67.4)	77 (74.8)	
Female	61 (32.6)	26 (25.2)	
Age in yr			0.344
< 60	123 (65.8)	62 (60.2)	
≥ 60	64 (34.2)	41 (39.8)	
BMI	23.25 ± 3.37	23.00 ± 3.53	0.561
Weight loss			0.830
No	165 (88.2)	90 (87.4)	
Yes	22 (11.8)	13 (12.6)	
Alcohol			0.378
No	168 (89.8)	89 (86.4)	
Yes	19 (10.2)	14 (13.6)	
Symptomatic			0.602
No	74 (39.6)	44 (42.7)	
Yes	113 (60.4)	59 (57.3)	
NLR			0.510
< 2.288	134 (71.7)	70 (68.0)	
≥ 2.288	53 (28.3)	33 (32.0)	
TB in μmol/L			0.763
< 34.2	181 (96.8)	99 (96.1)	
≥ 34.2	6 (3.2)	4 (3.9)	
CEA in ng/mL			0.901
< 5	175 (93.6%)	96 (96.0%)	
≥ 5	12 (6.4)	7 (7.0)	
CA19-9 in U/mL			0.135
< 34	163 (87.2)	83 (80.6)	
≥ 34	24 (12.8)	20 (19.4)	
GGT in IU/L			0.287
< 150	174 (93.0)	99 (96.1)	
≥ 150	13 (7.0)	4 (3.9)	
ALP in IU/L			0.556
< 200	179 (95.7)	97 (94.2)	
≥ 200	8 (4.3)	6 (5.8)	

ALP: Alkaline phosphatase; BMI: Body mass index; CA19-9: Carbohydrate antigen 19-9; CEA: Carcinoembryonic antigen; GGT: γ-glutamyl transpeptidase; NLR: Neutrophil-to-lymphocyte; TB: Total bilirubin.

(training cohort: C-index, 0.824; 95%CI: 0.735–0.914, *vs* validation cohort: C-index, 0.893; 95%CI: 0.823–0.963). The calibration plots demonstrated good consistency between the observed and predicted probabilities in both the internal and external validations. Both predicted and reference curves were approximately aligned which indicates good performance of the nomogram (Figure 3). Overall performance was scored at 0.091 using Brier's score which measured the difference between observed

Table 2 Preoperative imaging characteristics of patients with pancreatic cystic neoplasms

Characteristic	Training cohort	Validation cohort	*P* value
	n = 187 (64.5%)	*n* = 103 (35.5%)	
Tumor involve the head of pancreas			0.239
Yes	65 (34.8)	43 (41.7)	
No	122 (65.2)	60 (58.3)	
Bile duct dilation			0.106
No	174 (93.0)	90 (87.4)	
Yes	13 (7.0)	13 (12.6)	
Tumor size in mm			0.254
< 40	158 (84.5)	92 (89.3)	
≥ 40	29 (15.5)	11 (10.7)	
Intratumoral septum			0.264
No	76 (40.6)	35 (34.0)	
Yes	111 (59.4)	68 (66.0)	
Cyst wall enhancement			0.244
No	118 (63.1)	72 (69.9)	
Yes	69 (36.9)	31 (30.1)	
Cyst wall thickening			0.709
No	178 (95.2)	97 (94.2)	
Yes	9 (4.8)	6 (5.8)	
Enhanced mural nodules			0.126
No	148 (79.1)	89 (86.4)	
Yes	39 (20.9)	14 (13.6)	
Intracapsular calcification			0.117
No	162 (86.6)	82 (79.6)	
Yes	25 (13.4)	21 (20.4)	
Main pancreatic duct dilatation			0.419
No	122 (65.2)	72 (69.9)	
Yes	65 (34.8)	31 (30.1)	

and predicted values (values closer to 0 indicate better predictive ability). A calibration slope of 1.0 was obtained to assess the agreement between observed and predicted values (values closer to 1.0 indicate better performance)[17]. An online calculator for predicting the risk of malignancy was created and was freely available at https://ahmuptt.shinyapps.io/JDYX/.

Comparison of the performance of the nomogram and the risk factors identified in the relevant guidelines

Using ROC analyses, the diagnostic performance of the nomogram established in this study was compared with those of the risk factors identified in the relevant guidelines[6,18], including tumor diameter ≥ 40 mm, enhanced mural nodules and main pancreatic duct dilatation (Figure 4). In the training cohort, the AUC values and 95%CIs of the nomogram and the three factors (tumor diameter ≥ 40 mm, enhanced mural nodules and main pancreatic duct dilatation) were 0.824 (0.735–0.914), 0.619 (0.496–0.742), 0.692 (0.575–0.810) and 0.653 (0.540–0.766), respectively. In the validation cohort, these values were 0.893 (0.823–0.963), 0.718 (0.560–0.876), 0.665 (0.506–0.824) and 0.672 (0.524–0.820), respectively. In both cohorts, significant statistical differences were found between the nomogram and the three factors ($P < 0.05$). The training cohort had an accuracy, sensitivity, specificity, positive predictive value and negative predictive value of 0.829, 0.643, 0.862, 0.451 and 0.932, respectively. In the validation cohort, these values were 0.925, 0.882, 0.826, 0.501 and 0.973, respectively. Thus, the

Table 3 Univariable and multivariable logistic regression analyses of the risk factors for high risk of malignancy in patients with pancreatic cystic neoplasms

Variable	OR comparisons	Univariable analysis		Multivariable analysis	
		OR (95%CI)	*P* value	OR (95%CI)	*P* value
Sex	Female *vs* Male	2.383 (1.054-5.386)	0.037[a]	0.716 (0.232-2.213)	0.562
Age in yr	≥ 60 *vs* < 60	2.180 (0.967-4.915)	0.060		
BMI		0.986 (0.874-1.111)	0.816		
Weight loss	Yes *vs* No	2.437 (0.861-6.897)	0.093		
Alcohol	Yes *vs* No	2.252 (0.741-6.845)	0.153		
Symptomatic	Yes *vs* No	1.774 (0.737-4.271)	0.201		
Tumor involve the head of pancreas	Yes *vs* No	1.148 (0.487-2.705)	0.753		
Bile duct dilation	Yes *vs* No	1.788 (0.460-6.952)	0.402		
Tumor diameter in mm	≥ 40 *vs* < 40	4.094 (1.649-10.165)	0.002[a]	3.514 (1.138-10.849)	0.029[a]
Intratumoral septum	Yes *vs* No	0.539 (0.240-1.211)	0.135		
Cyst wall enhancement	Yes *vs* No	1.127 (0.494-2.569)	0.777		
Cyst wall thickening	Yes *vs* No	1.670 (0.329-8.488)	0.536		
Enhanced mural nodules	Yes *vs* No	6.490 (2.746-15.342)	< 0.001[a]	4.314 (1.618-11.503)	0.003[a]
Intracapsular calcification	Yes *vs* No	0.208 (0.027-1.606)	0.132		
Main pancreatic duct dilatation	Yes *vs* No	3.574 (1.558-8.201)	0.003[a]	3.267 (1.230-8.678)	0.018[a]
NLR	≥ 2.288 *vs* < 2.288	3.077 (1.350-7.015)	0.008[a]	2.702 (1.008-7.244)	0.048[a]
TB in μmol/L	≥ 34.2 *vs* < 34.2	6.240 (1.192-32.657)	0.030[a]	0.870 (0.050-15.020)	0.924
ALP in IU/L	≥ 200 *vs* < 200	9.420 (1.499-59.213)	0.017[a]	0.632 (0.064-6.285)	0.695
GGT in IU/L	≥ 150 *vs* < 150	2.925 (0.931-9.189)	0.066		
CEA in ng/mL	≥ 5 *vs* < 5	6.955 (2.060-23.477)	0.002[a]	3.798 (0.825-17.482)	0.087
CA199 in U/mL	≥ 34 *vs* < 34	4.547 (1.750-11.816)	0.002[a]	3.267 (1.274-13.007)	0.018[a]

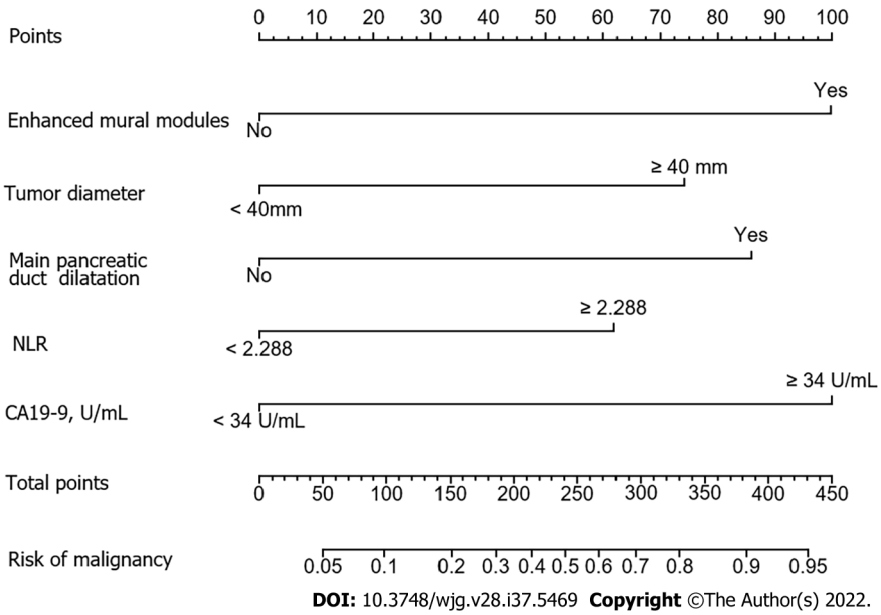
[a]*P* < 0.05.

ALP: Alkaline phosphatase; BMI: Body mass index; CA19-9: Carbohydrate antigen 19-9; CEA: Carcinoembryonic antigen; CI: Confidence interval; GGT: γ-glutamyl transpeptidase; NLR: Neutrophil-to-lymphocyte; OR: Odds ratio; TB: Total bilirubin.

nomogram showed high accuracy in predicting the risk of malignancy in patients with PCNs. When considering the maximum Youden index value, the optimal cutoff value of the nomogram was 160.8 in the ROC curve and the sensitivity and specificity for differentiating between high and low risk were 64.3% and 86.2%, respectively. This cut off value is used to categorize patients with total nomogram score of < 160.8 points or ≥ 160.8 points as either low- or high-risk group, respectively. In the training cohort, DCA showed that using the nomogram to predict the risk of malignancy had a greater net benefit than the other three factors when the threshold probability ranged from 0.2 to 1.0. In the validation cohort, DCA showed that the nomogram had a greater net benefit when the threshold probability ranged from 0.0 to 0.4 (Figure 5). Figure 6 depicts the number of high-risk patients (solid red line) and the number of high-risk patients with the outcome (black dotted line) at different threshold probabilities within a given population. In both the training and validation cohorts, the solid red and black dotted lines show a great fit indicating that the model has remarkable predictive ability.

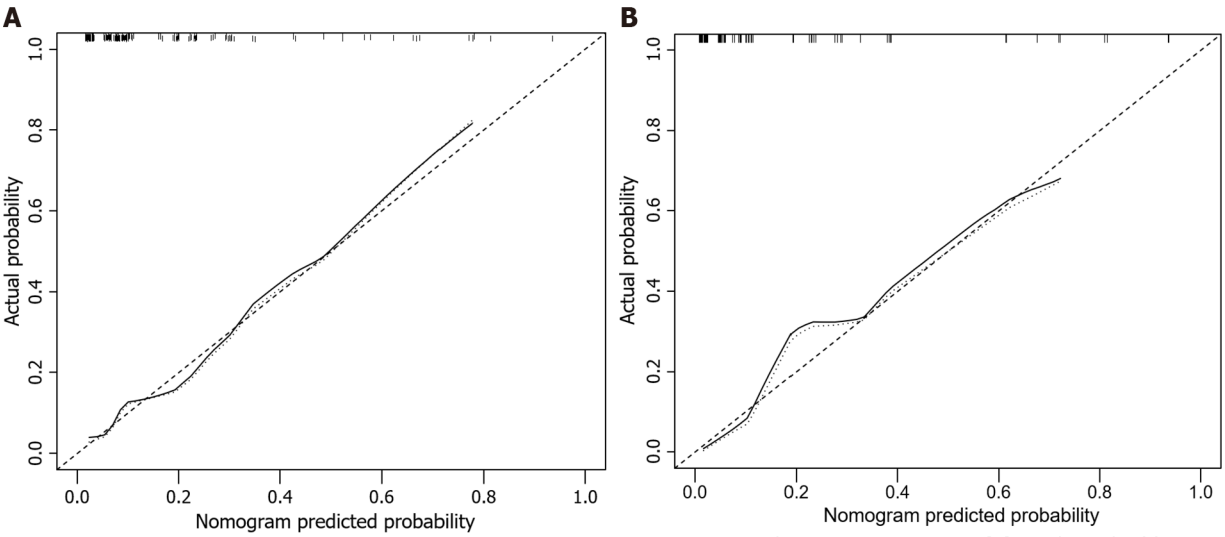
DISCUSSION

The increasing use of high-resolution cross-sectional imaging techniques has resulted in more frequent detection of PCNs in recent years[19]. However, accurate prediction of the risk of malignancy of PCNs as early as possible is of great value in developing more appropriate individualized treatment strategies. In the current study, we developed and validated a preoperative clinical model that strongly predicted the risk of high-grade dysplasia or invasive cancer in patients with PCNs.



DOI: 10.3748/wjg.v28.i37.5469 **Copyright** ©The Author(s) 2022.

Figure 2 Nomogram for predicting risk of malignancy in the training cohort. NLR: Neutrophil-to-lymphocyte ratio.

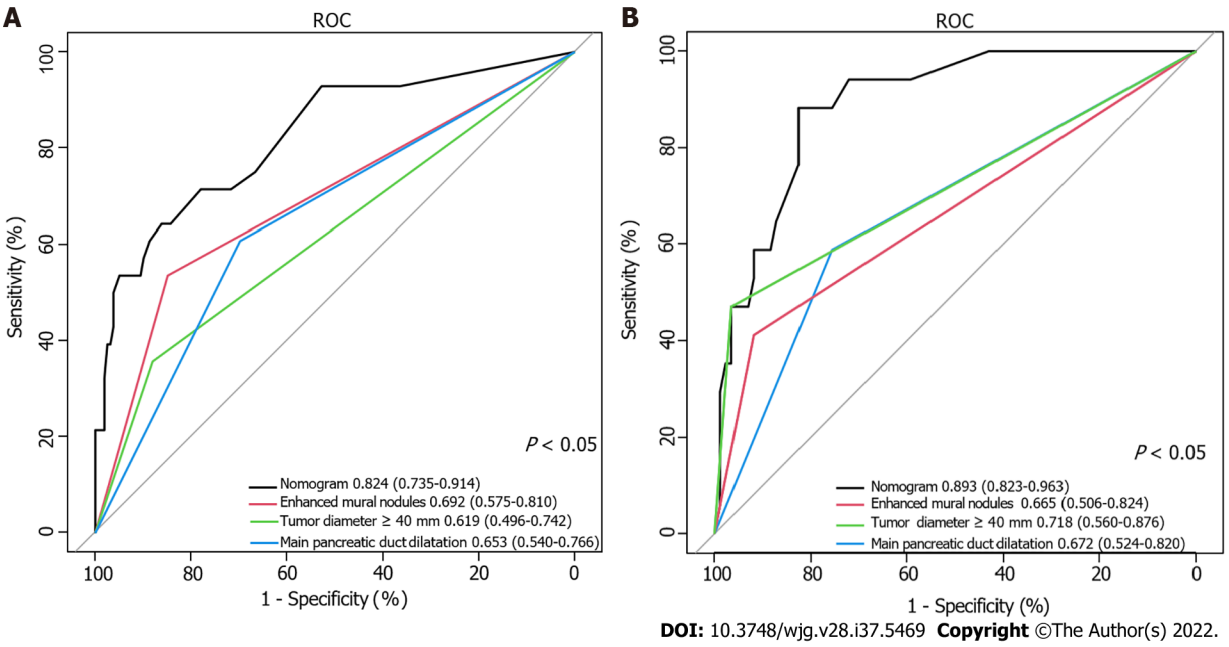


DOI: 10.3748/wjg.v28.i37.5469 **Copyright** ©The Author(s) 2022.

Figure 3 Calibration curves for predicting the risk of malignancy. The nomogram had concordance index values of 0.824 and 0.893 in the training and validation cohort, respectively. A: Training cohort; B: Validation cohort.

As shown in Tables 1 and 2, our study analyzed dozens of objective factors, and the findings indicated that for patients with PCNs, lesions with enhanced mural nodules, tumor diameter ≥ 40 mm, main pancreatic duct dilatation, preoperative NLR ≥ 2.288 and preoperative serum CA19-9 levels ≥ 34 U/mL were significant independent predictors. These factors were combined with patients' preoperative imaging and serological data to quantify the risk of malignancy concisely and spontaneously. The sufficient statistical power of the model for predicting the risk of malignancy was verified based on multiple validation methods. The C-index of the model in the validation cohort was 0.893 (0.823–0.963), highlighting the ability of the model to distinguish low-risk disease from high-risk disease in a large group of patients. In addition, we used an independent validation dataset that effectively decreased the risk of overfitting the model to an individual dataset. The similarity between the C-index of the training [0.824 (0.735–0.914)] and validation [0.893 (0.823–0.963)] cohorts suggested that this model was widely applicable. In addition, a mobile-friendly online version of the nomogram was programmed to eliminate the inconvenience of traditional nomograms in clinical use.

The latest guidelines, including the European evidence-based guidelines on PCNs and the International Association of Pancreatology guidelines of 2017, have described the management strategies for different subtypes of PCNs in detail[6,18]. In addition, many published nomogram models for predicting malignancy in patients with a specific subtype of PCNs, such as IPMNs, have been



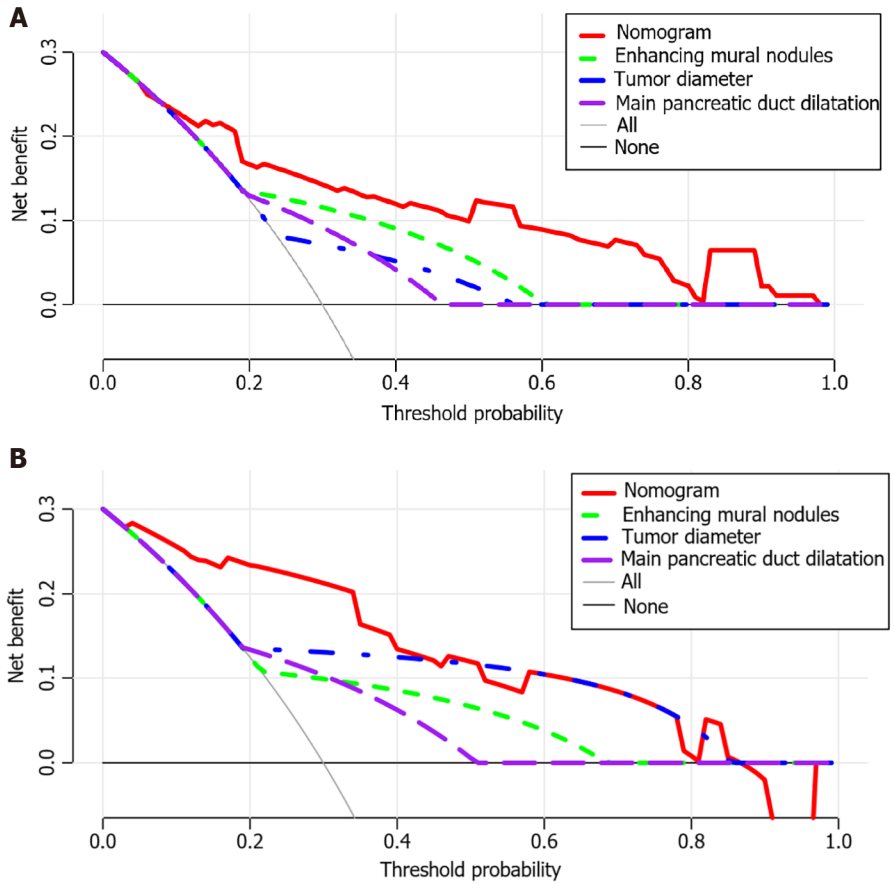
DOI: 10.3748/wjg.v28.i37.5469 **Copyright** ©The Author(s) 2022.

Figure 4 Receiver operating characteristic curve of the nomogram and other three risk factors identified in guidelines. A: Training cohort; B: Validation cohort. AUC: Area under the curve.

established to facilitate the preoperative prediction of malignant lesions[20-22]. Nevertheless, real-world preoperative diagnosis of the different PCN subtypes remains difficult due to their similarities in both clinical and imaging features. In particular, accurate diagnosis of pathological neoplasms and preoperative assessments of the benign or malignant status of some lesions with atypical manifestations are even more difficult[23]. Previous studies have reported differing probabilities for the accurate preoperative identification of each subtype. Salvia *et al*[24] found that in 476 patients with PCNs, 78% showed postoperative pathological examination results consistent with the preoperative diagnosis[24]. Furthermore, a multicenter study of 2251 patients in China showed that the preoperative diagnosis was not always accurate for a specific subtype with a correct diagnosis rate of only 33%[25]. Meanwhile, the risk factors proposed to be associated with malignant lesions in the guidelines lack universality, efficiency and accuracy in clinical applications to a certain extent. In this study, a model with strong practicability and high predictive efficiency was constructed by analyzing PCNs showing similar clinical and imaging manifestations across subtypes. Therefore, this model can help clinicians predict the risk of lesion malignancy when they are unable to accurately determine the PCN subtype or have difficulties in confirming the nature of the tumor.

NLR was also included as a laboratory indicator in the nomogram. Researches have shown that inflammation contributes to the occurrence and progression of tumors by releasing cytokines and other inflammatory mediators[26,27]. NLR measurement can serve as a simple and convenient way to assess the systemic inflammatory response and many recent studies have confirmed that inflammatory markers play an important role in predicting benign and malignant PCNs[28-30]. In the current study, a significant correlation was found between NLR and high-risk groups by multivariable analysis and the cutoff value of NLR was calculated as 2.43 which was rarely studied and reported in previous studies. We believe that neutrophils can recruit and activate inflammatory cells by producing cytokines and chemokines thus acting on the tumor microenvironment. In addition, reactive oxygen species and proteases produced by neutrophils can regulate tumor cell proliferation, angiogenesis and metastasis [31]. Thus, an increase in NLR may indicate a macroscopic withdrawal of inflammatory and immune responses in the local tumor microenvironment.

The nomogram was chosen to establish the model mainly because of its ability to assign risk probabilities on a continuous scale as an individualized risk score, rather than simply dividing patients into malignant and benign groups. This allows for additional risk stratification and may help patients and doctors tailor treatment decisions based on patients' individual risks. In addition, as shown in Figure 2, the nomogram showed that the model score for cases with serum CA19-9 levels ≥ 34 U/mL (100 points) was significantly higher than that for cases with an NLR of ≥ 2.288 (61 points), suggesting that serum CA19-9 levels ≥ 34 U/mL increase the possibility of a malignant lesion significantly. Moreover, the additive effect of several risk factors is important clinically. In this context, the patient-specific quantitative estimation of risk is valuable. Therefore, in cases where benign and malignant PCNs cannot be easily distinguished, clinicians can calculate the total nomogram scores using this predictive model. We propose that surgical treatment should be considered as the first choice for patients with a total nomogram score ≥ 160.

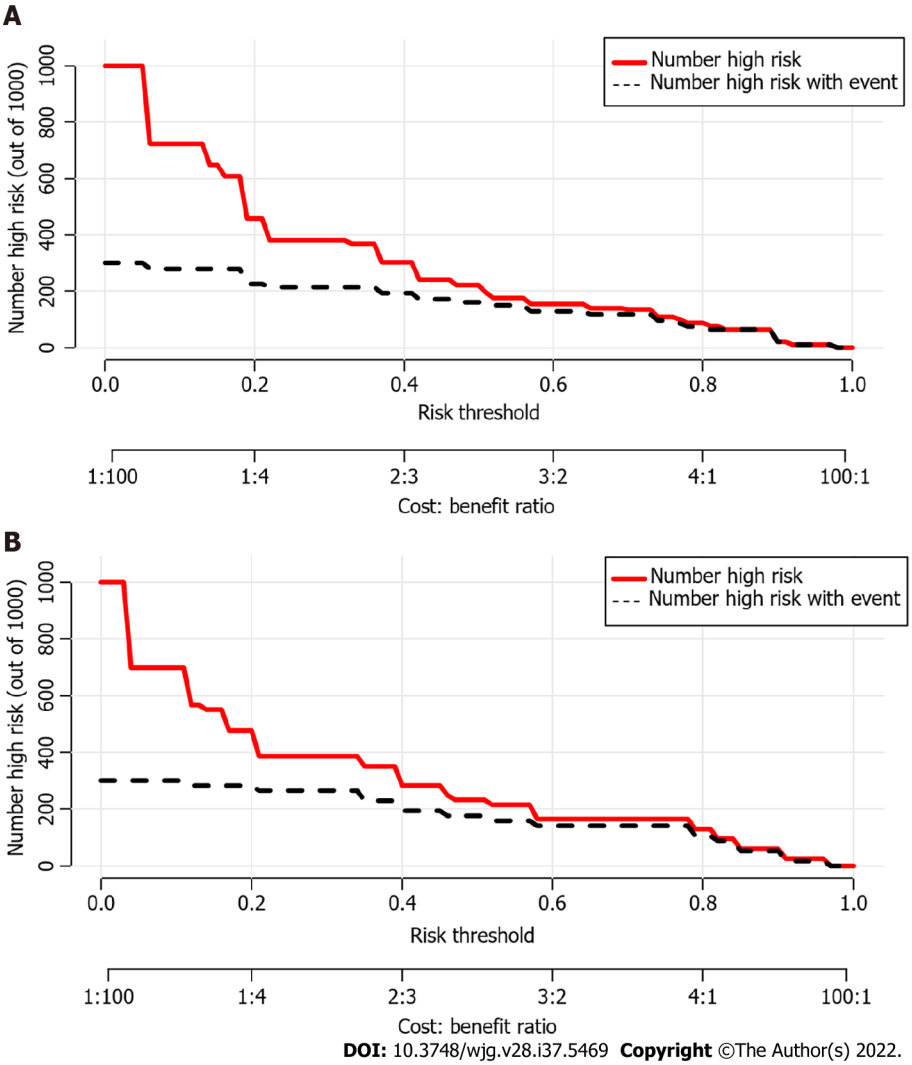


DOI: 10.3748/wjg.v28.i37.5469 **Copyright** ©The Author(s) 2022.

Figure 5 Decision curve analysis of the nomogram and other three risk factors identified in guidelines. The x-axis represents the threshold probability and the y-axis represents the net benefit. In the training cohort, the nomogram adds more net benefit than the other three factors when the threshold probability ranged from 0.2 to 1.0. In the validation cohort, the nomogram adds more net benefit than the other three factors when the threshold probability ranged from 0.0 to 0.4. A: In the training cohort; B: In the validation cohort.

In recent years, machine learning has rapidly developed as a tool with promising results and improved usability[32]. Machine learning addresses many preexisting and novel medical challenges and is widely discussed by researchers and practitioners alike. Machine learning algorithms have many advantages, such as improved flexibility and scalability when compared with traditional statistical methods. This makes machine learning advantageous for many tasks, including risk stratification, diagnosis, classification and survival predictions. Another advantage of machine learning is the ability to analyze diverse data types (*e.g.*, demographic data, laboratory findings, imaging data and doctors' free-text notes) and to incorporate them into predictions for disease risk, diagnosis, prognosis and appropriate treatment[33]. Despite these advantages, the application of machine learning in healthcare delivery also presents unique challenges, including the need for data pre-processing, model training and refinement of the system with respect to the actual clinical problem. Also crucial are ethical considerations which include medico-legal implications, doctors' understanding of machine learning tools, and data privacy and security[34]. In summary, attempts can be made to refine the model further using advanced machine learning in the future.

The present study had several limitations that merit discussion. First, endoscopic US (EUS) helps identify PCNs with features that may indicate the need for surgical resection[6]. However, in our study, only less than 10% of the patients underwent EUS. This may be attributable to the considerable interobserver variation in EUS-based diagnoses. On the other hand, data on EUS-based differentiation between benign and malignant PCNs are inconsistent[35,36]. Moreover, economic affordability is an important consideration, especially for most patients from rural areas. Second, heterogeneity in pathological diagnosis to determine the grade of dysplasia or malignancy and heterogeneity between different imaging examinations may exist. Third, this was a retrospective study considering only patients who underwent surgery which meant that it had inherent limitations resulting from potential selection biases; prospective validation is therefore required to confirm the value of the findings.



DOI: 10.3748/wjg.v28.i37.5469 **Copyright** ©The Author(s) 2022.

Figure 6 Clinical impact curves of the nomogram. At different threshold probabilities within a given population, the number of high-risk patients (solid red line) and the number of high-risk patients with the outcome (black dotted line) are shown. In both training and validation cohort, the solid red line and black dotted line show a great fit. A: In the training cohort; B: In the validation cohort.

CONCLUSION

In conclusion, we developed and validated a novel online calculator using a nomogram based on widely available data to predict the risk of malignancy in patients with PCNs dynamically. The calculator is user-friendly, highly accurate and well validated. Clinicians can use it to alert patients at high risk of malignancy at early stages and to design individual therapy for them.

ARTICLE HIGHLIGHTS

Research background

Efficient and practical methods for predicting the risk of malignancy in patients with pancreatic cystic neoplasms (PCNs) are currently lacking.

Research motivation

Currently, there is no effective clinical prediction model for patients with PCNs and no large study has been conducted to predict malignant risk.

Research objectives

The aim of this study was to identify the risk factors influencing the malignant risk of PCNs and develop a prediction model that is useful for clinical surgeons when making decisions regarding surgical interventions.

Research methods

Data collected in three major medical centers were analyzed to identify independent risk parameters and propose a calculator for patients with PCNs. A number of statistical indices, such as concordance index, calibration curves, area under the curve, decision curve analysis, CIC and others were used to evaluate the performance of the nomogram.

Research results

Five factors, including enhanced mural nodules, tumor diameter ≥ 40 mm, main pancreatic duct dilatation, preoperative neutrophil-to-lymphocyte ratio ≥ 2.288 and preoperative serum CA19-9 concentration ≥ 34 U/mL were found to independently influencing the risk of malignancy. As a result, the model we constructed has a greater predictive value than the factors identified in relevant guidelines.

Research conclusions

For the first time, a model was developed to predict the malignant risk of PCNs and an online calculator was further established to guide decision-making.

Research perspectives

More medical centers included, more data collection and application of "Artificial Intelligence".

ACKNOWLEDGEMENTS

We would like to thank Prof. Faming Pan (Department of Epidemiology and Biostatistics, School of Public Health, Anhui Medical University), who has made valuable support to the data quality and data analysis which ensured the reliability of the study.

FOOTNOTES

Author contributions: Jiang D, Chen JM, Chen ZX and Ma FX contributed to the data analysis and participated in drafting the article; Liu XQ, Gong YY, and Pu T extracted the clinical data and calculated the clinical correlations; Xie K and Zhao YJ interpreted the results and revised the manuscript; Liu FB, Hou H, Wang C and Geng XP gave final approval of the version to be published; All authors contributed to the design and interpretation of the study and to further drafts and approved the final version to be published.

Supported by University Natural Science Research Project of Anhui Province, No. KJ2021ZD0021.

Institutional review board statement: The study was reviewed and approved by the Institutional ethics committees of the First Affiliated Hospital of Anhui Medical University (Approval Quick-PJ2022-06-26).

Informed consent statement: All study participants or their legal guardian provided informed written consent prior to study enrollment.

Conflict-of-interest statement: All the authors report no relevant conflicts of interest for this article.

Data sharing statement: No additional data are available.

Open-Access: This article is an open-access article that was selected by an in-house editor and fully peer-reviewed by external reviewers. It is distributed in accordance with the Creative Commons Attribution NonCommercial (CC BY-NC 4.0) license, which permits others to distribute, remix, adapt, build upon this work non-commercially, and license their derivative works on different terms, provided the original work is properly cited and the use is non-commercial. See: https://creativecommons.org/Licenses/by-nc/4.0/

Country/Territory of origin: China

ORCID number: Dong Jiang 0000-0003-3372-6062; Tian Pu 0000-0002-6961-0814; Jiang-Ming Chen 0000-0003-4683-5866; Yi-Jun Zhao 0000-0001-9082-8861; Kun Xie 0000-0002-2491-4988; Hui Hou 0000-0002-5997-1229; Cheng Wang 0000-0001-7899-2079; Xiao-Ping Geng 0000-0002-6219-6366; Fu-Bao Liu 0000-0003-3431-2187.

S-Editor: Fan JR
L-Editor: Filipodia
P-Editor: Yu HG

REFERENCES

1 **de Jong K**, Nio CY, Hermans JJ, Dijkgraaf MG, Gouma DJ, van Eijck CH, van Heel E, Klass G, Fockens P, Bruno MJ. High prevalence of pancreatic cysts detected by screening magnetic resonance imaging examinations. *Clin Gastroenterol Hepatol* 2010; **8**: 806-811 [PMID: 20621679 DOI: 10.1016/j.cgh.2010.05.017]

2 **Girometti R**, Intini S, Brondani G, Como G, Londero F, Bresadola F, Zuiani C, Bazzocchi M. Incidental pancreatic cysts on 3D turbo spin echo magnetic resonance cholangiopancreatography: prevalence and relation with clinical and imaging features. *Abdom Imaging* 2011; **36**: 196-205 [PMID: 20473669 DOI: 10.1007/s00261-010-9618-4]

3 **Ip IK**, Mortele KJ, Prevedello LM, Khorasani R. Focal cystic pancreatic lesions: assessing variation in radiologists' management recommendations. *Radiology* 2011; **259**: 136-141 [PMID: 21292867 DOI: 10.1148/radiol.10100970]

4 **Laffan TA**, Horton KM, Klein AP, Berlanstein B, Siegelman SS, Kawamoto S, Johnson PT, Fishman EK, Hruban RH. Prevalence of unsuspected pancreatic cysts on MDCT. *AJR Am J Roentgenol* 2008; **191**: 802-807 [PMID: 18716113 DOI: 10.2214/AJR.07.3340]

5 **Kern SE**, Hruban RH, Hidalgo M, Yeo CJ. An introduction to pancreatic adenocarcinoma genetics, pathology and therapy. *Cancer Biol Ther* 2002; **1**: 607-613 [PMID: 12642681 DOI: 10.4161/cbt.307]

6 **European Study Group on Cystic Tumours of the Pancreas**. European evidence-based guidelines on pancreatic cystic neoplasms. *Gut* 2018; **67**: 789-804 [PMID: 29574408 DOI: 10.1136/gutjnl-2018-316027]

7 **Kim SY**, Lee JM, Kim SH, Shin KS, Kim YJ, An SK, Han CJ, Han JK, Choi BI. Macrocystic neoplasms of the pancreas: CT differentiation of serous oligocystic adenoma from mucinous cystadenoma and intraductal papillary mucinous tumor. *AJR Am J Roentgenol* 2006; **187**: 1192-1198 [PMID: 17056905 DOI: 10.2214/AJR.05.0337]

8 **Wang GX**, Wang ZP, Chen HL, Zhang D, Wen L. Discrimination of serous cystadenoma from mucinous cystic neoplasm and branch duct intraductal papillary mucinous neoplasm in the pancreas with CT. *Abdom Radiol (NY)* 2020; **45**: 2772-2778 [PMID: 32705313 DOI: 10.1007/s00261-020-02664-7]

9 **Chen S**, Ren S, Guo K, Daniels MJ, Wang Z, Chen R. Preoperative differentiation of serous cystic neoplasms from mucin-producing pancreatic cystic neoplasms using a CT-based radiomics nomogram. *Abdom Radiol (NY)* 2021; **46**: 2637-2646 [PMID: 33558952 DOI: 10.1007/s00261-021-02954-8]

10 **Yang J**, Guo X, Ou X, Zhang W, Ma X. Discrimination of Pancreatic Serous Cystadenomas From Mucinous Cystadenomas With CT Textural Features: Based on Machine Learning. *Front Oncol* 2019; **9**: 494 [PMID: 31245294 DOI: 10.3389/fonc.2019.00494]

11 **Dmitriev K**, Kaufman AE, Javed AA, Hruban RH, Fishman EK, Lennon AM, Saltz JH. Classification of Pancreatic Cysts in Computed Tomography Images Using a Random Forest and Convolutional Neural Network Ensemble. *Med Image Comput Comput Assist Interv* 2017; **10435**: 150-158 [PMID: 29881827 DOI: 10.1007/978-3-319-66179-7_18]

12 **Balachandran VP**, Gonen M, Smith JJ, DeMatteo RP. Nomograms in oncology: more than meets the eye. *Lancet Oncol* 2015; **16**: e173-e180 [PMID: 25846097 DOI: 10.1016/S1470-2045(14)71116-7]

13 **Nagtegaal ID**, Odze RD, Klimstra D, Paradis V, Rugge M, Schirmacher P, Washington KM, Carneiro F, Cree IA; WHO Classification of Tumours Editorial Board. The 2019 WHO classification of tumours of the digestive system. *Histopathology* 2020; **76**: 182-188 [PMID: 31433515 DOI: 10.1111/his.13975]

14 **Basturk O**, Hong SM, Wood LD, Adsay NV, Albores-Saavedra J, Biankin AV, Brosens LA, Fukushima N, Goggins M, Hruban RH, Kato Y, Klimstra DS, Klöppel G, Krasinskas A, Longnecker DS, Matthaei H, Offerhaus GJ, Shimizu M, Takaori K, Terris B, Yachida S, Esposito I, Furukawa T; Baltimore Consensus Meeting. A Revised Classification System and Recommendations From the Baltimore Consensus Meeting for Neoplastic Precursor Lesions in the Pancreas. *Am J Surg Pathol* 2015; **39**: 1730-1741 [PMID: 26559377 DOI: 10.1097/PAS.0000000000000533]

15 **Youden WJ**. Index for rating diagnostic tests. *Cancer* 1950; **3**: 32-35 [PMID: 15405679 DOI: 10.1002/1097-0142(1950)3:1<32::aid-cncr2820030106>3.0.co;2-3]

16 **Vickers AJ**, Cronin AM, Elkin EB, Gonen M. Extensions to decision curve analysis, a novel method for evaluating diagnostic tests, prediction models and molecular markers. *BMC Med Inform Decis Mak* 2008; **8**: 53 [PMID: 19036144 DOI: 10.1186/1472-6947-8-53]

17 **Semenkovich TR**, Yan Y, Subramanian M, Meyers BF, Kozower BD, Nava R, Patterson GA, Kreisel D, Puri V. A Clinical Nomogram for Predicting Node-positive Disease in Esophageal Cancer. *Ann Surg* 2021; **273**: e214-e221 [PMID: 31274650 DOI: 10.1097/SLA.0000000000003450]

18 **Tanaka M**, Fernández-Del Castillo C, Kamisawa T, Jang JY, Levy P, Ohtsuka T, Salvia R, Shimizu Y, Tada M, Wolfgang CL. Revisions of international consensus Fukuoka guidelines for the management of IPMN of the pancreas. *Pancreatology* 2017; **17**: 738-753 [PMID: 28735806 DOI: 10.1016/j.pan.2017.07.007]

19 **Gaujoux S**, Brennan MF, Gonen M, D'Angelica MI, DeMatteo R, Fong Y, Schattner M, DiMaio C, Janakos M, Jarnagin WR, Allen PJ. Cystic lesions of the pancreas: changes in the presentation and management of 1,424 patients at a single institution over a 15-year time period. *J Am Coll Surg* 2011; **212**: 590-600; discussion 600 [PMID: 21463795 DOI: 10.1016/j.jamcollsurg.2011.01.016]

20 **Attiyeh MA**, Fernández-Del Castillo C, Al Efishat M, Eaton AA, Gönen M, Batts R, Pergolini I, Rezaee N, Lillemoe KD, Ferrone CR, Mino-Kenudson M, Weiss MJ, Cameron JL, Hruban RH, D'Angelica MI, DeMatteo RP, Kingham TP, Jarnagin WR, Wolfgang CL, Allen PJ. Development and Validation of a Multi-institutional Preoperative Nomogram for Predicting Grade of Dysplasia in Intraductal Papillary Mucinous Neoplasms (IPMNs) of the Pancreas: A Report from The Pancreatic Surgery Consortium. *Ann Surg* 2018; **267**: 157-163 [PMID: 28079542 DOI: 10.1097/SLA.0000000000002015]

21 **Jang JY**, Park T, Lee S, Kim Y, Lee SY, Kim SW, Kim SC, Song KB, Yamamoto M, Hatori T, Hirono S, Satoi S, Fujii T, Hirano S, Hashimoto Y, Shimizu Y, Choi DW, Choi SH, Heo JS, Motoi F, Matsumoto I, Lee WJ, Kang CM, Han HS, Yoon YS, Sho M, Nagano H, Honda G, Kim SG, Yu HC, Chung JC, Nagakawa Y, Seo HI, Yamaue H. Proposed Nomogram Predicting the Individual Risk of Malignancy in the Patients With Branch Duct Type Intraductal Papillary Mucinous Neoplasms of the Pancreas. *Ann Surg* 2017; **266**: 1062-1068 [PMID: 27607098 DOI: 10.1097/SLA.0000000000001985]

22 **Shimizu Y**, Hijioka S, Hirono S, Kin T, Ohtsuka T, Kanno A, Koshita S, Hanada K, Kitano M, Inoue H, Itoi T, Ueki T,

Matsuo K, Yanagisawa A, Yamaue H, Sugiyama M, Okazaki K. New Model for Predicting Malignancy in Patients With Intraductal Papillary Mucinous Neoplasm. *Ann Surg* 2020; **272**: 155-162 [PMID: 30499803 DOI: 10.1097/SLA.0000000000003108]

23 **Sahani DV**, Kadavigere R, Saokar A, Fernandez-del Castillo C, Brugge WR, Hahn PF. Cystic pancreatic lesions: a simple imaging-based classification system for guiding management. *Radiographics* 2005; **25**: 1471-1484 [PMID: 16284129 DOI: 10.1148/rg.256045161]

24 **Salvia R**, Malleo G, Marchegiani G, Pennacchio S, Paiella S, Paini M, Pea A, Butturini G, Pederzoli P, Bassi C. Pancreatic resections for cystic neoplasms: from the surgeon's presumption to the pathologist's reality. *Surgery* 2012; **152**: S135-S142 [PMID: 22766364 DOI: 10.1016/j.surg.2012.05.019]

25 **Pancreatic Surgery of Chinese Academic Society of Young Surgeons**. [The current status of diagnosis and treatment of pancreatic cystic neoplasm in China: a report of 2 251 cases]. *Zhonghua Wai Ke Za Zhi* 2018; **56**: 24-29 [PMID: 29325350 DOI: 10.3760/cma.j.issn.0529-5815.2018.01.007]

26 **Bausch D**, Pausch T, Krauss T, Hopt UT, Fernandez-del-Castillo C, Warshaw AL, Thayer SP, Keck T. Neutrophil granulocyte derived MMP-9 is a VEGF independent functional component of the angiogenic switch in pancreatic ductal adenocarcinoma. *Angiogenesis* 2011; **14**: 235-243 [PMID: 21442180 DOI: 10.1007/s10456-011-9207-3]

27 **Gong L**, Cumpian AM, Caetano MS, Ochoa CE, De la Garza MM, Lapid DJ, Mirabolfathinejad SG, Dickey BF, Zhou Q, Moghaddam SJ. Promoting effect of neutrophils on lung tumorigenesis is mediated by CXCR2 and neutrophil elastase. *Mol Cancer* 2013; **12**: 154 [PMID: 24321240 DOI: 10.1186/1476-4598-12-154]

28 **Zhou W**, Rong Y, Kuang T, Xu Y, Shen X, Ji Y, Lou W, Wang D. The value of systemic inflammatory markers in identifying malignancy in mucinous pancreatic cystic neoplasms. *Oncotarget* 2017; **8**: 115561-115569 [PMID: 29383181 DOI: 10.18632/oncotarget.23310]

29 **Gemenetzis G**, Bagante F, Griffin JF, Rezaee N, Javed AA, Manos LL, Lennon AM, Wood LD, Hruban RH, Zheng L, Zaheer A, Fishman EK, Ahuja N, Cameron JL, Weiss MJ, He J, Wolfgang CL. Neutrophil-to-lymphocyte Ratio is a Predictive Marker for Invasive Malignancy in Intraductal Papillary Mucinous Neoplasms of the Pancreas. *Ann Surg* 2017; **266**: 339-345 [PMID: 27631774 DOI: 10.1097/SLA.0000000000001988]

30 **Goh BK**, Tan DM, Chan CY, Lee SY, Lee VT, Thng CH, Low AS, Tai DW, Cheow PC, Chow PK, Ooi LL, Chung AY. Are preoperative blood neutrophil-to-lymphocyte and platelet-to-lymphocyte ratios useful in predicting malignancy in surgically-treated mucin-producing pancreatic cystic neoplasms? *J Surg Oncol* 2015; **112**: 366-371 [PMID: 26280242 DOI: 10.1002/jso.23997]

31 **Gregory AD**, Houghton AM. Tumor-associated neutrophils: new targets for cancer therapy. *Cancer Res* 2011; **71**: 2411-2416 [PMID: 21427354 DOI: 10.1158/0008-5472.CAN-10-2583]

32 **Harish KB**, Price WN, Aphinyanaphongs Y. Open-Source Clinical Machine Learning Models: Critical Appraisal of Feasibility, Advantages, and Challenges. *JMIR Form Res* 2022; **6**: e33970 [PMID: 35404258 DOI: 10.2196/33970]

33 **Sendak M**, Gao M, Nichols M, Lin A, Balu S. Machine Learning in Health Care: A Critical Appraisal of Challenges and Opportunities. *EGEMS (Wash DC)* 2019; **7**: 1 [PMID: 30705919 DOI: 10.5334/egems.287]

34 **Decherchi S**, Pedrini E, Mordenti M, Cavalli A, Sangiorgi L. Opportunities and Challenges for Machine Learning in Rare Diseases. *Front Med (Lausanne)* 2021; **8**: 747612 [PMID: 34676229 DOI: 10.3389/fmed.2021.747612]

35 **Donahue TR**, Hines OJ, Farrell JJ, Tomlinson JS, Eibl G, Reber HA. Cystic neoplasms of the pancreas: results of 114 cases. *Pancreas* 2010; **39**: 1271-1276 [PMID: 20717069 DOI: 10.1097/MPA.0b013e3181e1d6f4]

36 **Kim JH**, Eun HW, Park HJ, Hong SS, Kim YJ. Diagnostic performance of MRI and EUS in the differentiation of benign from malignant pancreatic cyst and cyst communication with the main duct. *Eur J Radiol* 2012; **81**: 2927-2935 [PMID: 22227264 DOI: 10.1016/j.ejrad.2011.12.019]

World Journal of Gastroenterology

Submit a Manuscript: https://www.f6publishing.com

World J Gastroenterol 2022 October 7; 28(37): 5483-5493

DOI: 10.3748/wjg.v28.i37.5483

ISSN 1007-9327 (print) ISSN 2219-2840 (online)

ORIGINAL ARTICLE

Observational Study

Application of an artificial intelligence system for endoscopic diagnosis of superficial esophageal squamous cell carcinoma

Qian-Qian Meng, Ye Gao, Han Lin, Tian-Jiao Wang, Yan-Rong Zhang, Jian Feng, Zhao-Shen Li, Lei Xin, Luo-Wei Wang

Specialty type: Gastroenterology and hepatology

Provenance and peer review: Unsolicited article; Externally peer reviewed.

Peer-review model: Single blind

Peer-review report's scientific quality classification

Grade A (Excellent): A, A
Grade B (Very good): B
Grade C (Good): 0
Grade D (Fair): 0
Grade E (Poor): 0

P-Reviewer: Shiroma S, Japan; Sudou K, Japan; Tsoulfas G, Greece

Received: June 2, 2022
Peer-review started: June 2, 2022
First decision: August 1, 2022
Revised: August 9, 2022
Accepted: September 20, 2022
Article in press: September 20, 2022
Published online: October 7, 2022

Qian-Qian Meng, Ye Gao, Han Lin, Tian-Jiao Wang, Yan-Rong Zhang, Zhao-Shen Li, Lei Xin, Luo-Wei Wang, Department of Gastroenterology, Changhai Hospital, Shanghai 200433, China

Jian Feng, Qingdao Medcare Digital Engineering Co. Ltd., Qingdao Medcare Digital Engineering Co. Ltd., Qingdao 26600, Shandong Province, China

Corresponding author: Luo-Wei Wang, MD, Chief Doctor, Department of Gastroenterology, Changhai Hospital, No. 168 Changhai Road, Yangpu District, Shanghai 200433, China. wangluoweimd@126.com

Abstract

BACKGROUND

Upper gastrointestinal endoscopy is critical for esophageal squamous cell carcinoma (ESCC) detection; however, endoscopists require long-term training to avoid missing superficial lesions.

AIM

To develop a deep learning computer-assisted diagnosis (CAD) system for endoscopic detection of superficial ESCC and investigate its application value.

METHODS

We configured the CAD system for white-light and narrow-band imaging modes based on the YOLO v5 algorithm. A total of 4447 images from 837 patients and 1695 images from 323 patients were included in the training and testing datasets, respectively. Two experts and two non-expert endoscopists reviewed the testing dataset independently and with computer assistance. The diagnostic performance was evaluated in terms of the area under the receiver operating characteristic curve, accuracy, sensitivity, and specificity.

RESULTS

The area under the receiver operating characteristics curve, accuracy, sensitivity, and specificity of the CAD system were 0.982 [95% confidence interval (CI): 0.969-0.994], 92.9% (95%CI: 89.5%-95.2%), 91.9% (95%CI: 87.4%-94.9%), and 94.7% (95%CI: 89.0%-97.6%), respectively. The accuracy of CAD was significantly higher than that of non-expert endoscopists (78.3%, $P < 0.001$ compared with CAD) and comparable to that of expert endoscopists (91.0%, $P = 0.129$ compared with CAD). After referring to the CAD results, the accuracy of the non-expert endoscopists

significantly improved (88.2% *vs* 78.3%, $P < 0.001$). Lesions with Paris classification type 0-IIb were more likely to be inaccurately identified by the CAD system.

CONCLUSION

The diagnostic performance of the CAD system is promising and may assist in improving detectability, particularly for inexperienced endoscopists.

Key Words: Computer-aided diagnosis; Artificial intelligence; Deep learning; Esophageal squamous cell carcinoma; Early detection of cancer; Upper gastrointestinal endoscopy

©The Author(s) 2022. Published by Baishideng Publishing Group Inc. All rights reserved.

Core Tip: Esophageal squamous cell carcinoma (ESCC) poses a heavy burden to high-risk areas, and screening using upper gastrointestinal endoscopy is an established strategy for early detection and prognosis improvement. However, endoscopic detection of superficial-ESCC can be challenging and depends greatly on operator experience. We developed and validated a novel computer-assisted diagnostic system with a deep neural network algorithm to detect superficial ESCC using upper endoscopy with white-light and narrow-band imaging. The system demonstrated high diagnostic accuracy, which is comparable to that of expert endoscopists. The diagnostic performance of non-expert endoscopists was significantly improved under the assistance of this system.

Citation: Meng QQ, Gao Y, Lin H, Wang TJ, Zhang YR, Feng J, Li ZS, Xin L, Wang LW. Application of an artificial intelligence system for endoscopic diagnosis of superficial esophageal squamous cell carcinoma. *World J Gastroenterol* 2022; 28(37): 5483-5493

URL: https://www.wjgnet.com/1007-9327/full/v28/i37/5483.htm

DOI: https://dx.doi.org/10.3748/wjg.v28.i37.5483

INTRODUCTION

Esophageal cancer is the seventh most common and sixth most fatal malignancy[1], and esophageal squamous cell carcinoma (ESCC) is the most prevalent histological type[2]. Screening high-risk populations using upper gastrointestinal endoscopy may facilitate early detection and treatment[3], and markedly improve the prognosis of ESCC[4]. However, due to its subtlety and flat appearance under white light imaging (WLI) or image-enhanced endoscopy, identification of early stage ESCC may be especially difficult for inexperienced endoscopists[5-7]. A recent multicenter cohort study found that 6.4% of all esophageal cancers were missed during upper gastrointestinal endoscopy, which was associated with poor survival[8].

In recent years, artificial intelligence (AI)-aided endoscopy has garnered attention, and several studies have heralded this technique as a promising tool for improving the detection of early ESCC[9-12]. A systematic review showed that the pooled sensitivity and specificity of AI for ESCC diagnosis were 0.95 and 0.92, respectively, and AI performed better than endoscopists, although the differences were not statistically significant[13]. However, few computer-assisted diagnosis (CAD) systems for ESCC that support WLI and narrow-band imaging (NBI) have been applied in clinical practice. We developed and validated a novel CAD system with a deep neural network algorithm to detect superficial ESCC using upper endoscopy with WLI and NBI. Moreover, we assessed its value for endoscopists with differing experience levels of superficial ESCC detection and investigated the characteristics of lesions that were inaccurately identified by the CAD system.

MATERIALS AND METHODS

Preparation of datasets for training and testing

Static and non-magnified WLI or NBI images used for CAD system training and testing for superficial ESCC were retrospectively retrieved from endoscopic databases of four general hospitals in mainland China between January 2016 and April 2019. For the training dataset, 1503 WLI images and 2100 NBI images from 622 cases of superficial ESCC and high-grade intraepithelial neoplasia (HGIN), and 523 WLI images and 321 NBI images from 215 non-cancerous cases (including normal, esophagitis, submucosal lesion, and leukoplakia) were obtained from the First Affiliated Hospital of Zhengzhou University, Xingtai First Hospital, and Tangyin People's Hospital. For the independent testing dataset,

577 WLI images and 793 NBI images from 209 cases of superficial ESCC and HGIN, and 209 WLI images and 116 NBI images from 114 non-cancerous cases were obtained from Changhai Hospital. All images were captured using an Olympus gastroscope (GIF-H260, GIF-H260Z, GIF-H290, GIF-Q260J, or GIF-HQ290; Olympus, Tokyo, Japan). Poor-quality images, including blurred images, and those with mucus or foam that prevented adequate mucosal inspection were excluded from the study. The personal data of the patients in the images were hidden. This study was approved by the ethics committee of Shanghai Changhai Hospital (No. CHEC2019-002).

All superficial ESCC and HGIN images were obtained from patients who underwent subsequent endoscopic submucosal dissection. Additionally, histologic results including margin status and invasion depth of endoscopic submucosal dissection specimens were retrieved. Three experienced gastrointestinal (GI) pathologists conducted histological assessments. Histological images were first reviewed by two independent pathologists who determined the final pathological result through diagnostic consensus. In case of disagreement, images were reviewed by a third pathologist, and the final decision was discussed. Non-cancerous images were confirmed by three experienced endoscopists (all with > 15 years of experience), before inclusion in training and testing datasets.

All images were annotated by the three endoscopists mentioned above. The first endoscopist reviewed and marked the WLI and NBI images (margins of the lesion) using specific frames. The second endoscopist reviewed the annotations of the first, and if in agreement, the annotation was completed. Alternately, the images were reviewed by a third endoscopist, and the final decision was made in unison. Paris classification subtypes of lesions were also recorded[14].

Development of the CAD system

CAD system development was based on the YOLO v5 deep-learning algorithm. YOLO v5 employs cross stage partial network as the backbone for feature extraction and path aggregation network to generate a feature pyramid network to perform feature aggregation and pass it to the prediction mode. YOLO v5 demonstrated increased efficiency and efficacy compared to previous versions. To improve network accuracy, we modified the loss function of YOLO V5 and introduced the mapping distance of the aspect ratio. The input of this network was esophageal images, and the output was an indicator frame that captured the rectangular region of interest, together with the predicted quantitative level of confidence for ESCC above the frame (Figure 1).

Testing of the CAD system

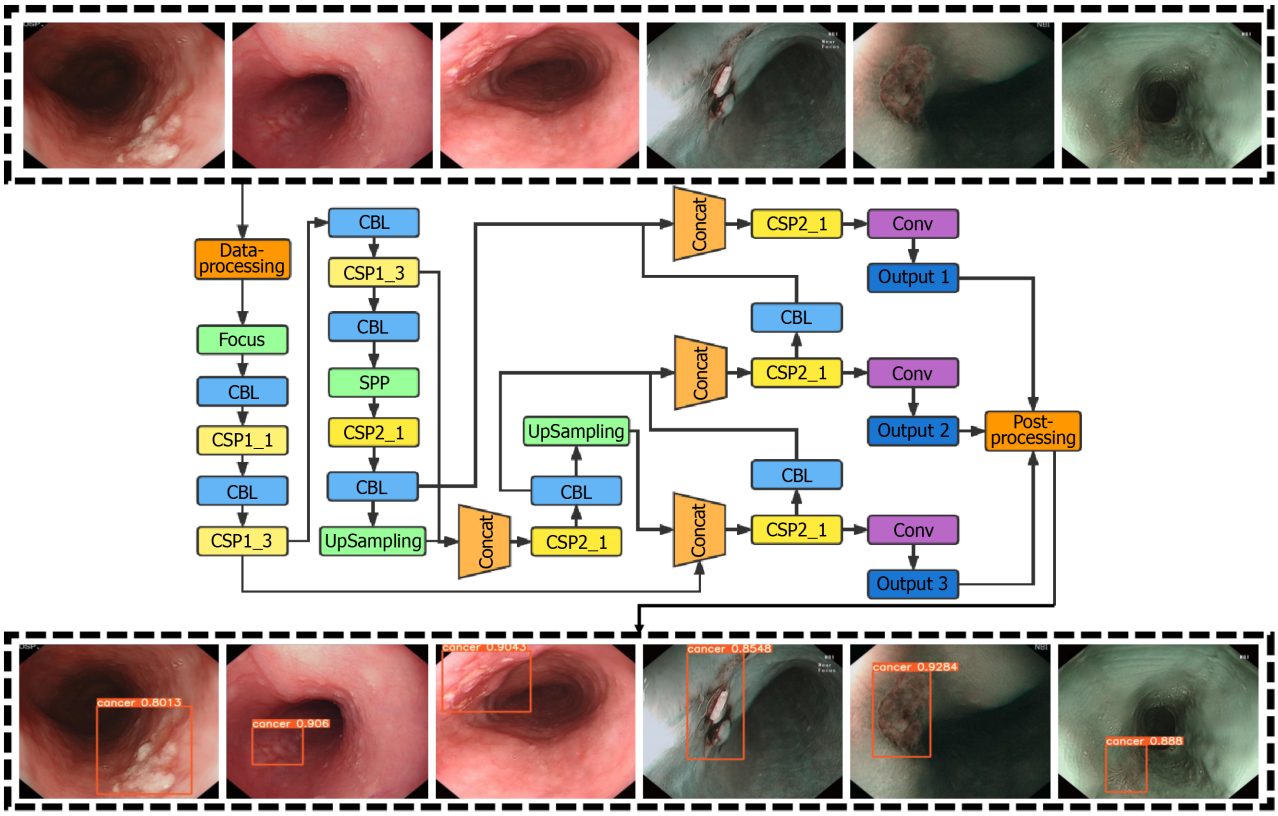
The diagnostic accuracy of the CAD system was validated using a previously established independent testing dataset. To compare the performance of the CAD system with that of endoscopists and investigate its added value, four endoscopists from Changhai Hospital were invited to review the images in the testing dataset, independently and with the assistance from the CAD system. Two experts (endoscopy experience ≥ 10 years) and two non-expert endoscopists (endoscopy experience > 1 year but < 5 years) participated. None were involved in the selection and annotation of images. All images in the testing dataset, including 598 WLI and 817 NBI cancerous and 209 WLI and 116 NBI non-cancerous images, were randomly sequenced, and all participating endoscopists independently reviewed the images and made diagnoses within one day. After a washout period of one month, the images were randomly re-sequenced, and endoscopists reviewed the images using the results of the CAD system as a reference. Throughout the study, participating endoscopists were unaware of the correct endoscopic and histologic diagnoses, their own performance, and the diagnostic accuracy of the CAD system.

Outcome measures

Primary outcome measures included the area under the receiver operating characteristic curve (AUROC), accuracy, sensitivity, and specificity of the CAD system. Secondary outcome measures included positive predictive value (PPV) and negative predictive value (NPV) of the CAD system; diagnostic performance of participating endoscopists; and improvement in diagnostic accuracy, sensitivity, and specificity in the expert and non-expert groups, after referring to the CAD system results.

Statistical analysis

AUROC, accuracy, sensitivity, specificity, PPV, and NPV were calculated, and the binominal 95% confidence intervals (CI) were estimated using the CAD-predicted confidence ≥ 0.5, as the prespecified criteria for testing positive. The Delong test was used to compare different AUROCs. A two-sided McNemar test was used to compare differences in accuracy, sensitivity, and specificity. Differences in more than three groups were compared using Cochran's Q test. Additionally, the McNemar test was used for post-hoc comparisons of P values adjusted using Bonferroni's method. Pearson's chi-squared test, t test, and Mann-Whitney U test were used wherever applicable. Superficial ESCC lesions with a CAD-predicted confidence < 0.5 and an intersection over union (IoU) value < 0.45 were defined as inaccurately identified. A P value < 0.05 was considered statistically significant. All statistical analyses were performed using SPSS 26.0 (SPSS Inc., Chicago, IL, United States). The statistical methods of this study were reviewed by XFY from Department of Health Statistics, Naval Medical University.



DOI: 10.3748/wjg.v28.i37.5483 **Copyright** ©The Author(s) 2022.

Figure 1 The architecture of the computer-assisted diagnosis system. The input of this network was the esophageal images, and the output was an indicator frame that captured the interest region, together with the predicted quantitative level of confidence for esophageal squamous cell carcinoma.

RESULTS

Characteristics of subjects and lesions in test dataset

Table 1 summarizes the characteristics of the patients and lesions in the testing dataset. For 209 cases of superficial ESCC, the lesion size was 2.0 (1.2-4.0) cm and most (82.3%) were located in the middle thoracic esophagus. Flat-type (0-IIb) lesions accounted for 53.6%, and most lesions involved < 25% of the esophageal circumference. Regarding histologic depth of invasion, 165 Lesions (78.9%) were limited to the lamina propria (LPM), 38 (18.2%) invaded the muscularis mucosa or superficial submucosa, and 6 (2.9%) extended beyond the superficial submucosa. Of the 114 non-cancerous cases, 23 were diagnosed with gastroesophageal reflux disease, five were diagnosed with esophageal submucosal lesions, and 86 were judged to be normal on upper gastrointestinal endoscopy.

Diagnostic performance of the CAD system

The receiver operating characteristic (ROC) curve of the CAD system is shown in Figure 2. The AUROC of the WLI, NBI, and combined modes were 0.970, 0.988, and 0.982, respectively. The AUROC of WLI, NBI, and the combined mode did not differ significantly. The diagnostic performance measures of the CAD system in the testing dataset are summarized in Table 2. In per-patient analysis, the accuracy, sensitivity, specificity, PPV, and NPV of the CAD system were 92.9%, 91.9%, 94.7%, 97.0%, and 86.4%, respectively. The accuracy ($P < 0.001$), sensitivity ($P < 0.001$), and specificity ($P = 0.015$) of the CAD system were significantly different among the different imaging modes. In post-hoc comparisons, the accuracy of the NBI (adjusted $P < 0.001$) and combined modes (adjusted $P = 0.002$) was significantly higher than that of the WLI mode. Furthermore, the sensitivity of NBI (adjusted $P < 0.001$) and combined modes (adjusted $P = 0.014$) was significantly higher than that of the WLI mode. No statistically significant differences in specificity were found in post-hoc comparisons between the two imaging modes. The results of the per-imaging analysis are presented in Table 2.

Comparison between the CAD system and endoscopists

Figure 3 compares the diagnostic performance of the CAD system under the combined WLI and NBI modes, among endoscopists with different experience levels. The accuracy (91.0% *vs* 78.3%, $P < 0.001$), sensitivity (90.0% *vs* 76.1%, $P < 0.001$), and specificity (93.0% *vs* 82.5%, $P = 0.002$) were significantly higher for expert endoscopists than for non-expert endoscopists. The diagnostic performance of the

Table 1 Characteristics of subjects and lesions involved in the testing dataset

Characteristics	Values
Cancerous cases (*n* = 209)	
Age (yr), mean ± SD	62.0 ± 7.2
Sex, Male/Female	158/51
Lesion location, Ce/Ut/Mt/Lt/Ae	2/21/172/14/0
Lesion size (cm), median (Q1, Q3)	2.0 (1.2-4.0)
Paris classification, 0-I/IIa/IIb/IIc/IIa+IIc/III	6/43/112/26/20/2
Circumference, < 1/4, 1/4-1/2, 1/2-3/4, > 3/4	117/63/18/11
Depth of invasion, EP-LPM/MM-SM1/SM2	165/38/6
Non-Cancerous cases (*n* = 114)	
Age (yr), mean ± SD	63.2 ± 5.3
Sex, male/female	65/49
Endoscopic diagnosis, GERD/submucosal lesion/normal	23/5/86

SD: Standard deviation; Ce: Cervical esophagus; Ut: Upper thoracic esophagus; Mt: Middle thoracic esophagus; Lt: Lower thoracic esophagus; Ae, Abdominal esophagus; Q1: Lower quartile; Q3: Upper quartile; EP-LPM: Epithelium or lamina propria; MM-SM1: Muscularis mucosa or submucosal invasion < 200 μm; SM2: Submucosal invasion > 200 μm; GERD: Gastroesophageal reflux disease.

Table 2 Diagnostic performance of the computer-assisted diagnosis system in the testing dataset

	Per-patient analysis				Per-image analysis			
	Overall (%)	WLI (%)	NBI (%)	*P* value	Overall (%)	WLI (%)	NBI (%)	*P* value
Accuracy (95%CI)	92.9 (89.5-95.2)	89.2 (85.3-92.1)	94.7 (91.7-96.7)	< 0.001	87.5 (85.9-89.0)	85.9 (83.3-88.1)	89.0 (86.8-90.9)	0.156
Sensitivity (95%CI)	91.9 (87.4-94.9)	88.0 (82.9-91.8)	94.3 (90.2-96.7)	< 0.001	86.6 (84.7-88.3)	84.1 (80.8-86.8)	88.4 (86.0-90.4)	0.067
Specificity (95%CI)	94.7 (89.0-97.6)	91.2 (84.6-95.2)	95.6 (90.1-98.1)	0.015	91.7 (88.2-94.3)	90.9 (86.2-94.1)	93.4 (87.0-96.8)	0.750
PPV (95%CI)	97.0 (93.5-98.6)	94.8 (90.8-97.2)	97.7 (94.3-98.9)	0.316	97.9 (96.9-98.5)	96.2 (94.2-97.6)	99.0 (98.0-99.5)	0.004
NPV (95%CI)	86.4 (79.3-91.3)	80.6 (73.0-86.5)	90.1 (83.5-94.2)	0.099	61.1 (56.6-65.4)	67.4 (61.7-72.6)	51.8 (44.8-58.8)	0.003

WLI: White-light imaging; NBI: Narrow-band imaging; PPV: Positive predictive value; NPV: Negative predictive value.

CAD system was significantly higher than that of non-expert endoscopists ($P < 0.001$) and similar to that of expert endoscopists.

Improvement after referring to CAD

Figure 4 depicts improved diagnostic performance of endoscopists for superficial ESCC after referring to the results of the CAD system. The accuracy (88.2% *vs* 78.3%, $P < 0.001$), sensitivity (87.6% *vs* 76.1%, $P < 0.001$), and specificity (89.5% *vs* 82.5%, $P = 0.039$) of the non-expert endoscopists were all significantly improved after using the CAD system, whereas the diagnostic performances of expert endoscopists did not differ significantly between the two stages. After referring to the CAD system, the accuracy (88.2% *vs* 93.2%, $P < 0.001$) and sensitivity (87.6% *vs* 92.3%, $P = 0.013$) of the non-experts were still significantly lower than those of the experts, while the disparities were markedly decreased. The specificity (89.5% *vs* 94.7%, $P = 0.124$) was similar between experts and non-experts after referring to the CAD.

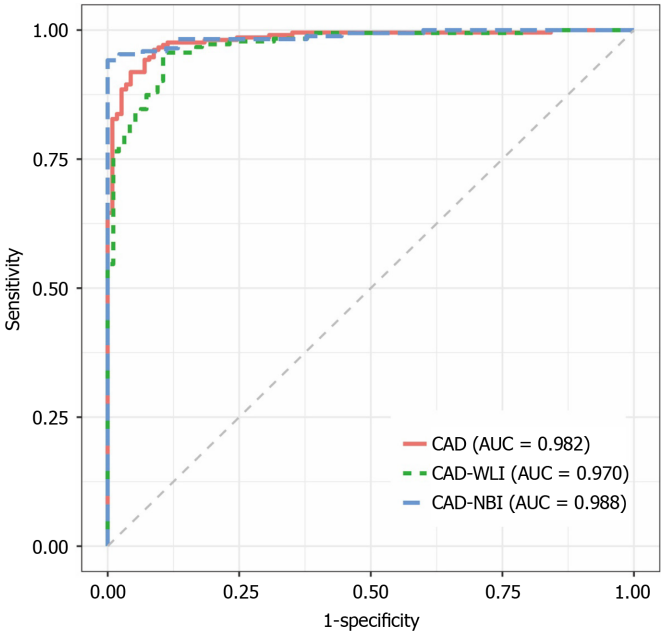
Inaccurately identified lesions

Under the prespecified definition, 23 (11.0%) lesions were inaccurately identified. Table 3 compares the characteristics of lesions with accurate and inaccurate identifications. The proportion of type 0-IIb lesions was significantly higher in inaccurately identified lesions (73.9% *vs* 51.1%, $P = 0.038$), and the proportion of lesions limited to the LPM was higher in the inaccurate identification group, although not significantly so (91.3% *vs* 77.4%, $P = 0.123$).

Table 3 Characteristics of lesions that were inaccurately identified by the computer-assisted diagnosis system

Characteristics	Accurate identification (*n* = 186)	Inaccurate identification (*n* = 23)	*P* value
Lesion location, *n* (%)			1.000
Ce	2 (1.1)	0 (0)	
Ut	13 (7.0)	2 (8.7)	
Mt	152 (81.7)	20 (87.0)	
Lt	19 (10.2)	1 (4.3)	
Lesion size (cm), median (Q1, Q3)	2.0 (1.1-4.0)	3 (1.5-3.0)	0.476
Paris classification, *n* (%)			0.038
Type 0-IIb	95 (51.1)	17 (73.9)	
Other non-flat types	91 (48.9)	6 (26.1)	
Circumference, *n* (%)			0.591
< 1/4	107 (57.4)	10 (43.5)	
1/4-1/2	54 (29.0)	9 (39.1)	
1/2-3/4	16 (8.6)	2 (8.7)	
> 3/4	9 (4.8)	2 (8.7)	
Depth of invasion, *n* (%)			0.123
EP-LPM	144 (77.4)	21 (91.3)	
MM and deeper	42 (22.6)	2 (8.7)	

Ce: Cervical esophagus; Ut: Upper thoracic esophagus; Mt: Middle thoracic esophagus; Lt: Lower thoracic esophagus; Q1: Lower quantile; Q3: Upper quantile; EP-LPM: Epithelium or lamina propria; MM: Muscularis mucosa.

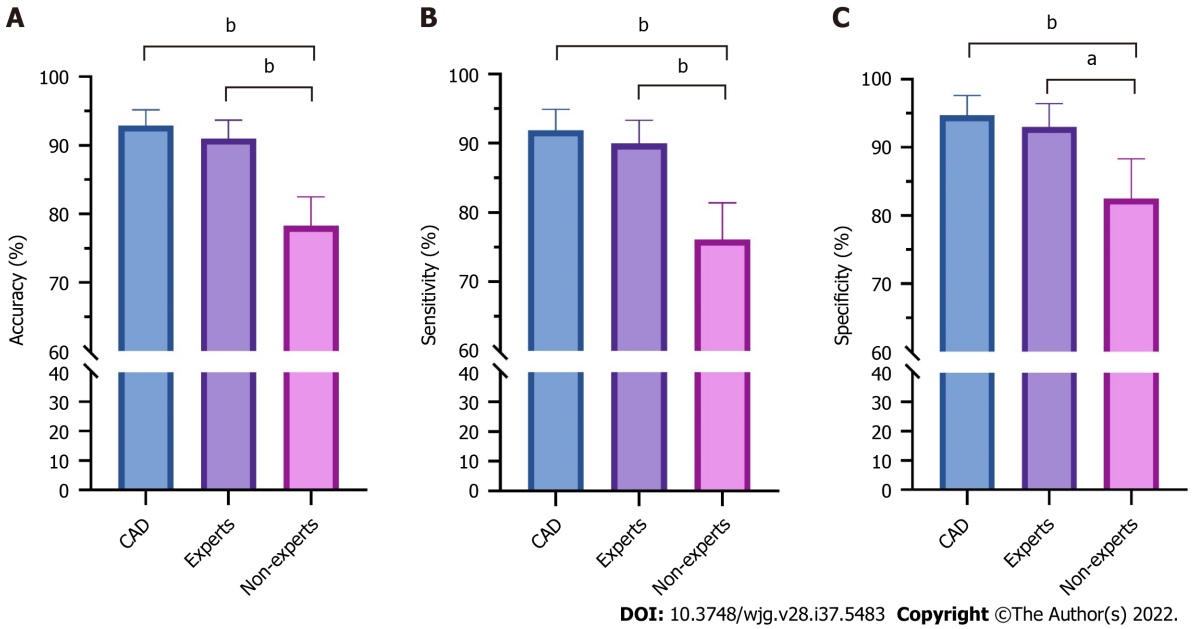


DOI: 10.3748/wjg.v28.i37.5483 **Copyright** ©The Author(s) 2022.

Figure 2 Receiver operating characteristic curve for the computer-assisted diagnosis system in the testing dataset. CAD: Computer-assisted diagnosis; AUC: Area under the curve; WLI: White light imaging; NBI: Narrow-band imaging.

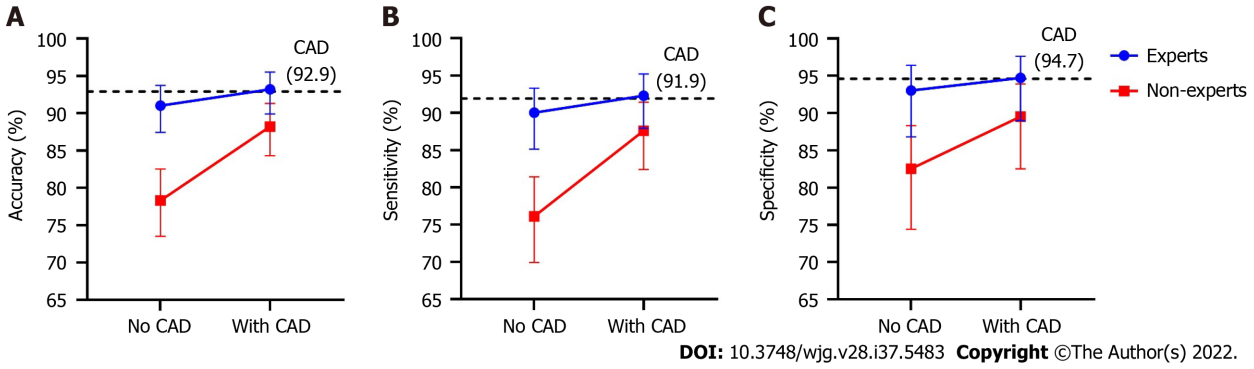
DISCUSSION

Upper gastrointestinal endoscopy is critical for screening and early diagnosis of ESCC. However, the subtle endoscopic appearance of most superficial ESCC types is challenging for early detection and



DOI: 10.3748/wjg.v28.i37.5483 **Copyright** ©The Author(s) 2022.

Figure 3 Comparison of diagnostic performances between the computer-assisted diagnosis system and endoscopists for superficial esophageal squamous cell carcinoma. A: Accuracy; B: Sensitivity; C: Specificity. [a]*P* < 0.05; [b]*P* < 0.01. CAD: Computer-assisted diagnosis.



DOI: 10.3748/wjg.v28.i37.5483 **Copyright** ©The Author(s) 2022.

Figure 4 The improvements in the diagnostic performance of endoscopists after referring to the results of computer-assisted diagnosis system. A: Accuracy; B: Sensitivity; C: Specificity. CAD: Computer-assisted diagnosis.

relies greatly on the skills and experience of endoscopists. Herein, we developed and validated a novel deep-learning-based CAD system for the detection of superficial ESCC in the WLI and NBI modes of upper gastrointestinal endoscopy. The AUROC, accuracy, sensitivity, and specificity of the CAD system were 0.982, 92.9%, 91.9%, and 94.7%, respectively. The diagnostic performance was significantly superior to that of non-experts and comparable to that of expert endoscopists. After referring to the results of the CAD system, the detectability of non-expert endoscopists significantly improved, and disparities between experts and non-experts markedly decreased. This system may assist in improving the detectability of superficial ESCC, particularly for inexperienced endoscopists and in undeveloped areas with limited resources.

Horie *et al*[9] developed a deep learning-based CAD system for superficial ESCC, with a sensitivity of 98% and low PPV of 40%. Zhao *et al*[15] developed an AI-based model for magnifying NBI images for automated classification of intrapapillary capillary loops, with a mean diagnostic accuracy of 89.6%. In a recent study by Guo *et al*[16], the authors developed a CAD system for real-time automated diagnosis of precancerous lesions and ESCC based on endoscopic video datasets, which achieved a per-lesion sensitivity of 100%. A systematic review by Visaggi *et al*[13] reported that the AUROC, sensitivity, and specificity of AI in diagnosing ESCC were 0.97, 0.95, and 0.92, respectively. However, few existing systems can support WLI and NBI, both of which are indispensable to the diagnosis of superficial ESCC under the same algorithm framework. We developed the current system under the updated YOLO v5 algorithm network supporting WLI and NBI, and achieved an AUROC, accuracy, sensitivity, and specificity of 0.982, 92.9%, 91.9%, and 94.7%, respectively, which was comparable to the best performance reported in previous studies. Esophageal endoscopic imaging is affected by factors such as

esophageal peristalsis, contraction, and imaging quality. Therefore, to supplement data by mimicking the above influencing factors, we added undistorted imaging correction enhancement based on the original data enhancement method of YOLO v5.

Superficial ESCC is difficult to inspect under WLI; however, NBI may significantly improve detectability with similar sensitivity and higher specificity than Lugol chromoendoscopy[6]. This may explain the demonstrated decrease in the accuracy and sensitivity of the CAD system, without NBI. Cai *et al*[10] reported on a deep neural network (DNN)-based system that utilizes WLI with high accuracy and sensitivity, for early ESCC detection. They subsequently developed a CAD-NBI system and found that its accuracy (94.3% *vs* 89.5%, $P = 0.028$) and specificity (96.7% *vs* 83.1%, $P < 0.001$) were significantly better than those of the CAD-WLI system[12]. By using CAD-WLI and CAD-NBI, endoscopists can significantly improve their diagnostic efficacy. Taken together, we recommend the combined implementation of NBI with other image-enhancing techniques for the detection of superficial ESCC, even under the CAD system.

To assess the clinical application value of the CAD system, endoscopists of varying experience reviewed the entire testing dataset independently and after referring to the diagnostic results of the CAD system. During the independent review, non-expert endoscopists showed significantly lower accuracy, sensitivity, and specificity than the experts, which highlighted the difficulty of novices in detecting superficial ESCC and disparities in detectability among endoscopists. The diagnostic performance of the non-experts significantly improved after referring to the CAD system. This suggests that the results of the CAD system provide useful references for non-expert endoscopists and facilitate further inspection and evaluation of potentially malignant lesions. The improved diagnostic performance of non-experts remained unequal to that of the CAD system, suggesting that endoscopists had made independent decisions, rather than relying completely on CAD. Similar results were reported in previous studies[10,12,17]. In the current study, although the performance of non-experts was still inferior to that of the experts after referring to the CAD system, the disparity markedly decreased. This suggests that the CAD system can homogenize the performance of endoscopists by overcoming the differences among endoscopists with different experience levels. In clinical practice, the usefulness of high-definition and imaging-enhanced endoscopy may be jeopardized by the inadequate number of highly trained endoscopists. In contrast, the CAD system does not require additional training and has instead been found to improve the performance of non-expert endoscopists by approximating the level of expertise. Thus, the CAD system may be especially useful in resource-limited areas, to improve the quality of endoscopic services and patient outcomes.

To our knowledge, this is the first study to analyze the characteristics of inaccurately identified lesions. We defined cases of inaccurate identification based on the predicted confidence and accuracy of the location frame. Endoscopists should be aware that flat-type and earlier-stage lesions limited to the LPM may be associated with an increased risk of inaccurate identification. To avoid a missed diagnosis of superficial ESCC, we recommend the use of Lugol's staining or magnifying endoscopy for flat-type lesions that are difficult to distinguish even under CAD.

In clinical practice, the CAD system automatically captures images as endoscopists inspect the esophagus, once integrated into an endoscopy workstation. Additionally, images frozen by endoscopists were input into the CAD system for analysis and detection of potential lesions. The CAD system then address potential malignant lesions with an indicator frame and a predicted quantitative level of confidence. Lesions with a predicted confidence ≥ 0.5 are strongly suggested for further evaluation and endoscopic biopsy. Other lesions may also be further evaluated or biopsied based on endoscopists' discretion. The diagnostic accuracy for ESCC is significantly improved after referring to the CAD system, particularly for non-expert endoscopists. Moreover, an updated CAD system that can process real-time videos or images with suboptimal quality is in development and may further facilitate clinical practice. In future, both endoscopists and patients may benefit from the increasing application of AI in endoscopy.

Our study had several limitations. First, the number of included endoscopists was relatively small, and the representation might be inadequate. Second, only still and non-magnified images were included; thus, the identification of videos and types of intrapapillary capillary loops could not be achieved. Third, the numbers and angles of lesions in NBI and WLI images were not identical in the testing dataset, and biases may exist in the comparison of diagnostic performance among the different modes of the CAD system.

CONCLUSION

We developed and validated a deep-learning CAD system, for the endoscopic detection of superficial ESCC, that achieved a high diagnostic accuracy comparable to that of expert endoscopists and could significantly improve the detecting ability of non-expert endoscopists.

ARTICLE HIGHLIGHTS

Research background

Esophageal squamous cell carcinoma (ESCC) is a leading cause of cancer-related morbidity and mortality worldwide. Upper gastrointestinal endoscopy is critical for ESCC detection; however, endoscopists require long-term training to avoid missing superficial lesions. Artificial intelligence (AI) has been increasingly investigated to assist endoscopic diagnosis.

Research motivation

AI has shown promising results for endoscopic diagnosis of superficial ESCC. However, few AI-based computer-assisted diagnosis (CAD) systems for ESCC that support white-light and narrow-band imaging have been applied in clinical practice.

Research objectives

We aimed to develop a CAD system for endoscopic detection of superficial ESCC and investigate its application value.

Research methods

We configured the CAD system for white-light and narrow-band imaging modes based on the YOLO v5 algorithm. A total of 4447 images from 837 patients and 1695 images from 323 patients were included in the training and testing datasets, respectively. Two experts and two non-expert endoscopists reviewed the testing dataset independently and with computer assistance. The diagnostic performance was evaluated in terms of the area under the receiver operating characteristic curve, accuracy, sensitivity, and specificity.

Research results

The area under the receiver operating characteristics curve, accuracy, sensitivity, and specificity of the CAD system were 0.982 [95% confidence interval (CI): 0.969-0.994], 92.9% (95%CI: 89.5%-95.2%), 91.9% (95%CI: 87.4%-94.9%), and 94.7% (95%CI: 89.0%-97.6%), respectively. The accuracy of CAD was significantly higher than that of non-expert endoscopists (78.3%, $P < 0.001$ compared with CAD) and comparable to that of expert endoscopists (91.0%, $P = 0.129$ compared with CAD). After referring to the CAD results, the accuracy of the non-expert endoscopists significantly improved (88.2% *vs* 78.3%, $P < 0.001$).

Research conclusions

The diagnostic performance of the CAD system is promising and may assist in improving detectability, particularly for inexperienced endoscopists.

Research perspectives

An updated CAD system that can process real-time videos or images with suboptimal quality is in development. Randomized controlled trials are warranted to investigate the clinical pragmaticality.

FOOTNOTES

Author contributions: Wang LW was the guarantor and designed the study; Lin H, Wang TJ, Zhang YR, Feng J participated in the acquisition, analysis, and interpretation of the data; Gao Y, Meng QQ drafted the initial manuscript; Xin L, Li ZS revised the article critically for important intellectual content; Meng QQ, Gao Y and Lin H contributed equally to this article.

Supported by Shanghai Science and Technology Innovation Action Program, No. 21Y31900100; and 234 Clinical Research Fund of Changhai Hospital, No. 2019YXK006.

Institutional review board statement: The study was reviewed and approved by the Shanghai Changhai Hospital Ethical Committee.

Informed consent statement: All study participants, or their legal guardian, provided informed written consent prior to study enrollment.

Conflict-of-interest statement: Dr. Wang reports grants from The Science and Technology Commission of Shanghai Municipality during the conduct of the study. Other authors report no relevant conflicts of interest for this article.

Data sharing statement: No additional data are available.

STROBE statement: The authors have read the STROBE Statement—checklist of items, and the manuscript was

prepared and revised according to the STROBE Statement—checklist of items.

Open-Access: This article is an open-access article that was selected by an in-house editor and fully peer-reviewed by external reviewers. It is distributed in accordance with the Creative Commons Attribution NonCommercial (CC BY-NC 4.0) license, which permits others to distribute, remix, adapt, build upon this work non-commercially, and license their derivative works on different terms, provided the original work is properly cited and the use is non-commercial. See: https://creativecommons.org/Licenses/by-nc/4.0/

Country/Territory of origin: China

ORCID number: Qian-Qian Meng 0000-0003-4719-1425; Ye Gao 0000-0002-6338-9602; Han Lin 0000-0002-0137-5176; Tian-Jiao Wang 0000-0002-7537-8089; Yan-Rong Zhang 0000-0002-5779-3828; Jian Feng 0000-0001-9022-462X; Zhao-Shen Li 0000-0002-1650-4014; Lei Xin 0000-0002-0495-8780; Luo-Wei Wang 0000-0002-6588-0542.

S-Editor: Gong ZM
L-Editor: A
P-Editor: Gong ZM

REFERENCES

1 **Bray F**, Ferlay J, Soerjomataram I, Siegel RL, Torre LA, Jemal A. Global cancer statistics 2018: GLOBOCAN estimates of incidence and mortality worldwide for 36 cancers in 185 countries. *CA Cancer J Clin* 2018; **68**: 394-424 [PMID: 30207593 DOI: 10.3322/caac.21492]
2 **Arnold M**, Ferlay J, van Berge Henegouwen MI, Soerjomataram I. Global burden of oesophageal and gastric cancer by histology and subsite in 2018. *Gut* 2020; **69**: 1564-1571 [PMID: 32606208 DOI: 10.1136/gutjnl-2020-321600]
3 **Chen R**, Liu Y, Song G, Li B, Zhao D, Hua Z, Wang X, Li J, Hao C, Zhang L, Liu S, Wang J, Zhou J, Zhang Y, Li Y, Feng X, Li L, Dong Z, Wei W, Wang G. Effectiveness of one-time endoscopic screening programme in prevention of upper gastrointestinal cancer in China: a multicentre population-based cohort study. *Gut* 2021; **70**: 251-260 [PMID: 32241902 DOI: 10.1136/gutjnl-2019-320200]
4 **Hölscher AH**, Bollschweiler E, Schröder W, Metzger R, Gutschow C, Drebber U. Prognostic impact of upper, middle, and lower third mucosal or submucosal infiltration in early esophageal cancer. *Ann Surg* 2011; **254**: 802-7; discussion 807 [PMID: 22042472 DOI: 10.1097/SLA.0b013e3182369128]
5 **Lee YC**, Wang CP, Chen CC, Chiu HM, Ko JY, Lou PJ, Yang TL, Huang HY, Wu MS, Lin JT, Hsiu-Hsi Chen T, Wang HP. Transnasal endoscopy with narrow-band imaging and Lugol staining to screen patients with head and neck cancer whose condition limits oral intubation with standard endoscope (with video). *Gastrointest Endosc* 2009; **69**: 408-417 [PMID: 19019362 DOI: 10.1016/j.gie.2008.05.033]
6 **Morita FH**, Bernardo WM, Ide E, Rocha RS, Aquino JC, Minata MK, Yamazaki K, Marques SB, Sakai P, de Moura EG. Narrow band imaging versus lugol chromoendoscopy to diagnose squamous cell carcinoma of the esophagus: a systematic review and meta-analysis. *BMC Cancer* 2017; **17**: 54 [PMID: 28086818 DOI: 10.1186/s12885-016-3011-9]
7 **Ishihara R**, Takeuchi Y, Chatani R, Kidu T, Inoue T, Hanaoka N, Yamamoto S, Higashino K, Uedo N, Iishi H, Tatsuta M, Tomita Y, Ishiguro S. Prospective evaluation of narrow-band imaging endoscopy for screening of esophageal squamous mucosal high-grade neoplasia in experienced and less experienced endoscopists. *Dis Esophagus* 2010; **23**: 480-486 [PMID: 20095991 DOI: 10.1111/j.1442-2050.2009.01039.x]
8 **Rodríguez de Santiago E**, Hernanz N, Marcos-Prieto HM, De-Jorge-Turrión MÁ, Barreiro-Alonso E, Rodríguez-Escaja C, Jiménez-Jurado A, Sierra-Morales M, Pérez-Valle I, Machado-Volpato N, García-Prada M, Núñez-Gómez L, Castaño-García A, García García de Paredes A, Peñas B, Vázquez-Sequeiros E, Albillos A. Rate of missed oesophageal cancer at routine endoscopy and survival outcomes: A multicentric cohort study. *United European Gastroenterol J* 2019; **7**: 189-198 [PMID: 31080603 DOI: 10.1177/2050640618811477]
9 **Horie Y**, Yoshio T, Aoyama K, Yoshimizu S, Horiuchi Y, Ishiyama A, Hirasawa T, Tsuchida T, Ozawa T, Ishihara S, Kumagai Y, Fujishiro M, Maetani I, Fujisaki J, Tada T. Diagnostic outcomes of esophageal cancer by artificial intelligence using convolutional neural networks. *Gastrointest Endosc* 2019; **89**: 25-32 [PMID: 30120958 DOI: 10.1016/j.gie.2018.07.037]
10 **Cai SL**, Li B, Tan WM, Niu XJ, Yu HH, Yao LQ, Zhou PH, Yan B, Zhong YS. Using a deep learning system in endoscopy for screening of early esophageal squamous cell carcinoma (with video). *Gastrointest Endosc* 2019; **90**: 745-753.e2 [PMID: 31302091 DOI: 10.1016/j.gie.2019.06.044]
11 **Luo H**, Xu G, Li C, He L, Luo L, Wang Z, Jing B, Deng Y, Jin Y, Li Y, Li B, Tan W, He C, Seeruttun SR, Wu Q, Huang J, Huang DW, Chen B, Lin SB, Chen QM, Yuan CM, Chen HX, Pu HY, Zhou F, He Y, Xu RH. Real-time artificial intelligence for detection of upper gastrointestinal cancer by endoscopy: a multicentre, case-control, diagnostic study. *Lancet Oncol* 2019; **20**: 1645-1654 [PMID: 31591062 DOI: 10.1016/S1470-2045(19)30637-0]
12 **Li B**, Cai SL, Tan WM, Li JC, Yalikong A, Feng XS, Yu HH, Lu PX, Feng Z, Yao LQ, Zhou PH, Yan B, Zhong YS. Comparative study on artificial intelligence systems for detecting early esophageal squamous cell carcinoma between narrow-band and white-light imaging. *World J Gastroenterol* 2021; **27**: 281-293 [PMID: 33519142 DOI: 10.3748/wjg.v27.i3.281]
13 **Visaggi P**, Barberio B, Gregori D, Azzolina D, Martinato M, Hassan C, Sharma P, Savarino E, de Bortoli N. Systematic review with meta-analysis: artificial intelligence in the diagnosis of oesophageal diseases. *Aliment Pharmacol Ther* 2022; **55**: 528-540 [PMID: 35098562 DOI: 10.1111/apt.16778]

14 **Endoscopic Classification Review Group**. Update on the paris classification of superficial neoplastic lesions in the digestive tract. *Endoscopy* 2005; **37**: 570-578 [PMID: 15933932 DOI: 10.1055/s-2005-861352]
15 **Zhao YY**, Xue DX, Wang YL, Zhang R, Sun B, Cai YP, Feng H, Cai Y, Xu JM. Computer-assisted diagnosis of early esophageal squamous cell carcinoma using narrow-band imaging magnifying endoscopy. *Endoscopy* 2019; **51**: 333-341 [PMID: 30469155 DOI: 10.1055/a-0756-8754]
16 **Guo L**, Xiao X, Wu C, Zeng X, Zhang Y, Du J, Bai S, Xie J, Zhang Z, Li Y, Wang X, Cheung O, Sharma M, Liu J, Hu B. Real-time automated diagnosis of precancerous lesions and early esophageal squamous cell carcinoma using a deep learning model (with videos). *Gastrointest Endosc* 2020; **91**: 41-51 [PMID: 31445040 DOI: 10.1016/j.gie.2019.08.018]
17 **Yang XX**, Li Z, Shao XJ, Ji R, Qu JY, Zheng MQ, Sun YN, Zhou RC, You H, Li LX, Feng J, Yang XY, Li YQ, Zuo XL. Real-time artificial intelligence for endoscopic diagnosis of early esophageal squamous cell cancer (with video). *Dig Endosc* 2021; **33**: 1075-1084 [PMID: 33275789 DOI: 10.1111/den.13908]

World Journal of Gastroenterology

Submit a Manuscript: https://www.f6publishing.com

World J Gastroenterol 2022 October 7; 28(37): 5494-5505

DOI: 10.3748/wjg.v28.i37.5494

ISSN 1007-9327 (print) ISSN 2219-2840 (online)

ORIGINAL ARTICLE

Observational Study

Insights into hepatitis E virus epidemiology in Croatia

Pavle Jelicic, Thomas Ferenc, Anna Mrzljak, Lorena Jemersic, Natasa Janev-Holcer, Milan Milosevic, Maja Bogdanic, Ljubo Barbic, Branko Kolaric, Vladimir Stevanovic, Mateja Vujica, Zeljka Jurekovic, Jadranka Pavicic Saric, Maja Vilibic, Tatjana Vilibic-Cavlek

Specialty type: Gastroenterology and hepatology

Provenance and peer review: Invited article; Externally peer reviewed.

Peer-review model: Single blind

Peer-review report's scientific quality classification

Grade A (Excellent): 0
Grade B (Very good): 0
Grade C (Good): C, C
Grade D (Fair): 0
Grade E (Poor): 0

P-Reviewer: Jackson K, Australia; Zhou C, China

Received: July 16, 2022
Peer-review started: July 16, 2022
First decision: August 6, 2022
Revised: August 15, 2022
Accepted: September 16, 2022
Article in press: September 16, 2022
Published online: October 7, 2022

Pavle Jelicic, Natasa Janev-Holcer, Department of Environmental Health, Croatian Institute of Public Health, Zagreb 10000, Croatia

Thomas Ferenc, Department of Radiology, Merkur University Hospital, Zagreb 10000, Croatia

Anna Mrzljak, Department of Gastroenterology and Hepatology, University Hospital Center Zagreb, Zagreb 10000, Croatia

Anna Mrzljak, Tatjana Vilibic-Cavlek, School of Medicine, University of Zagreb, Zagreb 10000, Croatia

Lorena Jemersic, Department of Virology, Croatian Veterinary Institute, Zagreb 10000, Croatia

Natasa Janev-Holcer, Department of Social Medicine and Epidemiology, Faculty of Medicine University of Rijeka, Rijeka 51000, Croatia

Milan Milosevic, Department of Occupational and Environmental Health, Andrija Stampar School of Public Health, Zagreb 10000, Croatia

Maja Bogdanic, Tatjana Vilibic-Cavlek, Department of Virology, Croatian Institute of Public Health, Zagreb 10000, Croatia

Ljubo Barbic, Vladimir Stevanovic, Department of Microbiology and Infectious Diseases with Clinic, Faculty of Veterinary Medicine University of Zagreb, Zagreb 10000, Croatia

Branko Kolaric, Department of Gerontology and Social Medicine, Andrija Stampar Teaching Institute of Public Health, Zagreb 10000, Croatia

Mateja Vujica, Institute of Emergency Medicine of Krapina-Zagorje County, Krapina 49000, Croatia

Zeljka Jurekovic, Department of Nephrology, Merkur University Hospital, Zagreb 10000, Croatia

Jadranka Pavicic Saric, Department of Anesthesiology, University Hospital Merkur, Zagreb 10000, Croatia

Maja Vilibic, Department for Social Psychiatry, Psychotherapy and Psychodiagnostics, University Clinical Hospital Center "Sestre Milosrdnice", Zagreb 10000, Croatia

Corresponding author: Anna Mrzljak, FEBG, PhD, Adjunct Professor, Associate Professor, Department of Gastroenterology and Hepatology, University Hospital Center Zagreb, Kispaticeva 12, Zagreb 10000, Croatia. anna.mrzljak@gmail.com

Abstract

BACKGROUND

Hepatitis E virus (HEV) is an emerging virus of global health concern. The seroprevalence rates differ greatly according to geographic region and population group.

AIM

To analyze the seroprevalence of HEV in exposed (animal-related professions) and nonexposed populations, as well as solid organ and hematopoietic stem cell transplant patients.

METHODS

Forestry workers (n = 93), hunters (n = 74), and veterinarians (n = 151) represented the exposed population. The general population (n = 126) and pregnant women (n = 118) constituted the control group. Transplant patients included liver transplant recipients (LTRs) (n = 83), kidney transplant recipients (KTRs) (n = 43), and hematopoietic stem cell transplant recipients (HSCRs) (n = 39). HEV immunoglobulin G antibodies were detected using the enzyme-linked immunosorbent assay and confirmed by the immunoblot test.

RESULTS

The HEV seroprevalence significantly differed between groups: Veterinarians 15.2%, hunters 14.9%, forestry workers 6.5%, general population 7.1%, and pregnant women 1.7%. In transplant patients, the seropositivity was highest in LTRs (19.3%), while in KTRs and HSCRs, the seroprevalence was similar to the general population (6.9% and 5.1%, respectively). A significant increase in seropositivity with age was observed from 2.9% in individuals less than 30 years to 23.5% in those older than 60 years. Sociodemographic characteristics (sex, educational level, area of residence, and number of household members), eating habits (game meat, offal, and pork products consumption), and environmental and housing conditions (drinking water supply, type of water drainage/sewer, waste disposal, domestic animals) were not associated with HEV seropositivity. However, individuals who reported a pet ownership were more often seropositive compared to those who did not have pet animals (12.5% *vs* 7.0%).

CONCLUSION

The results of this study showed that individuals in professional contact with animals and LTRs are at higher risk for HEV infection. In addition, age is a significant risk factor for HEV seropositivity.

Key Words: Hepatitis E virus; Seroprevalence; Veterinarians; Hunters; Forestry workers; Transplant patients; Croatia

©The Author(s) 2022. Published by Baishideng Publishing Group Inc. All rights reserved.

Core Tip: Hepatitis E virus (HEV) is an emerging viral pathogen of public health concern. We analyzed the epidemiological characteristics of HEV infection in different groups in Croatia. The highest seroprevalence was reported in professionally exposed individuals such as veterinarians, hunters, and liver transplant recipients. Seropositivity was similar in the general population, forestry workers, kidney transplant patients, and hematopoietic stem cell transplant patients. The lowest seroprevalence was recorded in pregnant women. A significant increase in seroprevalence with age was observed. Pet ownership was also associated with HEV seropositivity. Sex, environmental and housing conditions, and eating habits were not associated with HEV seroprevalence.

Citation: Jelicic P, Ferenc T, Mrzljak A, Jemersic L, Janev-Holcer N, Milosevic M, Bogdanic M, Barbic L, Kolaric B, Stevanovic V, Vujica M, Jurekovic Z, Pavicic Saric J, Vilibic M, Vilibic-Cavlek T. Insights into hepatitis E virus epidemiology in Croatia. *World J Gastroenterol* 2022; 28(37): 5494-5505

URL: https://www.wjgnet.com/1007-9327/full/v28/i37/5494.htm

DOI: https://dx.doi.org/10.3748/wjg.v28.i37.5494

INTRODUCTION

Hepatitis E virus (HEV) is an emerging viral pathogen of global health concern. It is a nonenveloped RNA virus, a member of the *Hepeviridae* family, genus *Orthohepevirus*[1]. Along with hepatitis B and hepatitis C virus (1.5 million new infections per year for each virus)[2,3], HEV is a major cause of viral hepatitis worldwide with approximately 20 million documented infections annually, over three million symptomatic cases, and 60-70000 fatal outcomes[4]. East and South Asia account for more than 60% of all reported cases[5]. There are eight known HEV genotypes. HEV-1 and HEV-2 are confined to humans and mainly cause infections in developing countries of tropical and subtropical regions[4-6]. HEV-3 and HEV-4 have been isolated from humans and different animal species (pigs, wild boars, deer, rabbits, goats, cows), primarily causing sporadic, autochthonous human infections in the developed world[5,7]. HEV-5 and HEV-6 have been restricted to wild boars only, while genotypes 7 and 8 have been isolated in dromedary and Bactrian camels[7,8]. In low-income countries, the main mode of HEV transmission is the fecal-oral route (contaminated drinking water, poor hygiene), whereas in more industrialized countries people are getting infected through zoonotic transmission (uncooked or undercooked animal products, mainly infected meat, and milk)[6,7]. Pigs are the main HEV animal reservoir. Almost 13% of domestic pigs and 9.5% of wild boars are actively infected by HEV with 10% of commercial pork products being HEV-RNA-positive[9]. Several other foods have also been proposed as a potential source of HEV infection in humans, *e.g.*, shellfish, mussels, and oysters[6]. One study found that HEV maintains infectivity for up to 21 d at 37 °C and up to 28 d at usual room temperature[8]. The virus can also be transmitted through blood transfusion, intravenous drug use, solid organ transplantation (SOT), hemodialysis, or maternal-fetal interaction[5,7]. In most cases, HEV presents as a self-limiting acute illness with low mortality rates (1%-2%) in immunocompetent individuals. However, genotypes 3, 4, and 7 may induce chronic infection and subsequent cirrhosis in immunocompromised patients, especially in SOT recipients, and human immunodeficiency virus-positive individuals[4]. Pregnant women are more susceptible to rapid disease progression such as fulminant hepatic and extrahepatic manifestations and obstetric complications leading to high mortality rates (15%-25%) compared to the non-pregnant population[4,5]. Professionally exposed individuals (*e.g.*, forestry workers, veterinarians, hunters, farmers) are also at increased risk of getting infected by HEV. Detected HEV seroprevalence rates in professionally exposed workers differ greatly between countries: Forestry workers (2.2%-31.0%)[10-13], hunters (3.81%-22.2%)[13-15], and veterinarians (10.2%-43.7%)[16,17]. In the transplant population, HEV seroprevalence rates were reportedly between 6.0% and 29.6%[18].

The seroepidemiological studies have shown that HEV is widespread in Croatia with seroprevalence rates ranging from 2.7% in healthcare professionals to 24.4% in liver transplant patients and up to 43.5% in hemodialysis patients[19,20]. However, only preliminary data are available on the HEV seroprevalence in animal-related professions. The aim of this study was to analyze the HEV epidemiology in different professionally exposed (animal-related) and nonexposed population groups in Croatia.

MATERIALS AND METHODS

Study participants

From October 2016 to September 2017, serum samples collected from Croatian residents were tested for the presence of HEV immunoglobulin G (IgG) antibodies. Samples were obtained from different exposed and nonexposed population groups. Forestry workers, hunters, and veterinarians represented the exposed population. The general population and pregnant women constituted the control group. In addition, from January 2021 to December 2021, a total of 165 serum samples were collected from SOT recipients [liver transplant recipients (LTRs) and kidney transplant recipients (KTRs)] and hematopoietic stem cell transplant recipients (HSCRs). None of the participants showed symptoms of acute hepatitis or reported a recent febrile disease. The distribution of study participants according to the population group is presented in Table 1.

Methods

HEV IgG antibodies were detected using a commercial enzyme-linked immunosorbent assay (ELISA) based on recombinant antigens of HEV genotypes 1 and 3 (anti-hepatitis E virus IgG ELISA; Euroimmun, Lübeck, Germany). Reactive samples were tested for the presence of HEV IgM antibodies (anti-hepatitis E virus IgM ELISA; Euroimmun). Additionally, ELISA IgG-positive samples were confirmed by a commercial immunoblot (IB) assay using highly purified recombinant HEV antigens: O2N genotype 1/3, O2C genotype 1/3, O2M genotype 1, O3 genotype 1/3 (HEV Recomline; Mikrogen, Neuried, Germany). IB-positive samples were further retested using a second assay (Euroline anti-hepatitis E virus IgG, Euroimmun, Lübeck, Germany) based on the recombinant HEV genotypes 1-4 antigens (ORF2). For the IB, the manufacturer states a diagnostic sensitivity of 96.6% and specificity of 97.1% (Mikrogen) and 100% (Euroimmun).

Table 1 Exposed and nonexposed population groups included in the study

Population	*n*	Median age, yr	IQR, yr
Exposed group			
Hunters	74	55	41-60
Veterinarians	151	46	36-55.5
Forestry workers	93	43	31-51
Non-exposed group			
General population	126	48	33-62
Pregnant women	118	31.5	29-35
Transplant patients			
Liver transplant recipients	83	60	49-65.5
Kidney transplant recipients	43	52.5	42-62
Hematopoietic stem cell recipients	39	55	51-64

IQR: Interquartile range.

Table 2 Hepatitis E virus immunoglobulin G prevalence in exposed and nonexposed populations

Population group	Tested, *n* (%)	HEV IgG, *n* (%)	95%CI	*P* value
Hunters	74	11 (14.9)	8.2-14.2	0.003
Veterinarians	151	23 (15.2)	10.2-21.6	
Forestry workers	93	6 (6.5)	2.7-12.8	
General population	126	9 (7.1)	3.3-13.1	
Pregnant women	118	2 (1.7)	0.2-5.9	
Liver transplant recipients	83	16 (19.3)	11.4-29.4	
Kidney transplant recipients	43	3 (6.9)	1.5-19.1	
Hematopoietic stem cell recipients	39	2 (5.1)	0.6-7.3	

CI: Confidence interval; HEV: Hepatitis E virus; IgG: Immunoglobulin G.

To identify potential risk factors that may be associated with HEV infection, for animal-related professions (exposed group) and nonexposed group, data on demographic characteristics and potential risk factors (eating habits, environmental and housing conditions, traveling history, and blood transfusion) were collected using a questionnaire. The modified Health-Environment-Life Style questionnaire created by the Andrija Stampar School of Public Health, School of Medicine, University of Zagreb was used in the study.

Statistical analysis

The HEV IgG prevalence is presented as a percentage with 95% confidence intervals (CIs). Differences in categorical variables between HEV seropositive and seronegative participants were tested using the Fisher's exact or Fisher-Freeman-Halton test. Odds ratio (OR) and relative risk (RR) were also calculated. Variables with statistical significance in a bivariate analysis were analyzed in multivariate regression analysis (binary logistic regression). $P < 0.05$ was considered statistically significant. Statistical analysis was performed using MedCalc® Statistical Software version 20.022 (MedCalc Software Ltd., Ostend, Belgium; https://www.medcalc.org; 2021).

RESULTS

HEV IgG antibodies were detected in 72/727 (9.9%; 95%CI: 7.8-12.3) participants: 40/278 (12.6%; 95%CI: 9.3-16.6) in the exposed group, 11/244 (4.3%; 95%CI: 2.3-7.3) in the nonexposed group, and 12/165

Table 3 Hepatitis E virus immunoglobulin G prevalence according to sociodemographic characteristics

Characteristic	Subjects[1], *n*	HEV IgG, *n* (%)	95%CI	*P* value
Sex				0.065
Male	238	29 (10.9)	7.6-15.0	
Female	282	22 (7.2)	4.7-10.6	
Age group in yr				< 0.001
< 30	99	3 (2.9)	0.8-7.6	
30-39	147	11 (7.0)	3.8-11.7	
40-49	94	5 (5.1)	2.0-10.7	
50-59	90	11 (10.9)	5.9-18.1	
60 +	62	19 (23.5)	15.3-33.5	
Area of residence				0.144
Rural	151	16 (9.6)	5.8-14.7	
Suburban	54	11 (16.9)	9.3-27.4	
Urban	255	24 (8.6)	5.7-12.3	
Number of household members				0.301
≤ 3	258	22 (7.9)	5.1-11.4	
> 3	177	21 (10.6)	6.9-15.5	
Educational level				0.467
Primary school	58	5 (7.9)	3.1-16.5	
High school	254	25 (9.0)	6.0-12.7	

[1]Subjects who filled a questionnaire.

CI: Confidence interval; HEV: Hepatitis E virus; IgG: Immunoglobulin G.

(12.7%; 95%CI: 8.1-18.8) in transplant patients. None of the participants were HEV IgM-positive. There were significant differences in the IgG seroprevalence rates among population groups (Table 2). In animal-related professions, the seropositivity was higher (14.9% in hunters and 15.2% in veterinarians) than in pregnant women (1.7%) and the general population (7.1%). Seroprevalence in transplant populations was highest in LTR (19.3%), followed by KTR (6.9%) and HSCR (5.1%).

A significant increase in seroprevalence was observed according to age. Participants in the age group 60 + years and 50-59 years showed higher seropositivity rates (23.5% and 10.9%, respectively) compared to younger age groups (2.9%-7.0%). There was no difference in HEV seroprevalence according to sex, area of residence, number of household members, and educational level (Table 3). HEV seropositivity did not differ regarding to the frequency of game meat, offal, and pork products consumption. However, there was a difference in the seroprevalence rates according to the frequency of shellfish consumption (Table 4).

Analyzing the environmental and housing conditions of the study participants and HEV seropositivity (Table 5), no significant difference was found according to drinking water supply, type of water drainage/sewer, and waste disposal. However, participants who reported having pet animals had a higher seroprevalence rate compared to those who did not have pet animals (12.5% *vs* 7.0%). Travel history as well as previous blood transfusion, surgical procedure, and tattoo/piercing were not associated with HEV seroprevalence (Table 6).

Risk analysis showed that animal-related professions and liver transplant patients were more likely to be HEV seropositive than other tested groups: Hunters OR = 3.873, 95%CI: 1.605-9.341; RR = 3.445, 95%CI: 1.556-7.628; veterinarians OR = 3.985, 95%CI: 1.883-8.435; RR = 3.531, 95%CI: 1.771-7.038; LTRs OR = 5.058, 95%CI: 2.240-11.420; RR = 4.276, 95%CI: 2.068-8.839 (Table 7).

DISCUSSION

The zoonotic risk of HEV transmission is well established, while exact transmission routes remain to be determined. The HEV seroprevalence rates vary greatly according to geographical region and study

Table 4 Hepatitis E virus immunoglobulin G prevalence according to eating habits

Eating habits	Subjects[1], *n*	HEV IgG, *n* (%)	95%CI	*P* value
Shellfish consumption				0.004
Never	60	15 (25.0)	14.4-37.0	
Rarely	374	32 (8.6)	6.0-11.7	
Once a month	16	2 (12.5)	2.7-34.4	
Every week	2	0 (0)	0-84.1[2]	
Game meat consumption				0.104
Never	20	1 (5.0)	0.5-21.1	
Rarely	324	30 (9.3)	6.5-12.8	
Once a month	89	14 (15.7)	9.3-24.3	
Every week	19	4 (21.1)	7.6-42.6	
Offal consumption (liver)				0.070
Never	25	0 (0)	0-13.7[2]	
Rarely	296	29 (9.8)	6.8-13.6	
Once a month	120	18 (15.0)	9.5-22.2	
Every week	11	2 (18.2)	4-46.7	
Pork products consumption				0.216
No	204	18 (8.8)	5.5-13.3	
Yes	249	31 (12.4)	8.8-17.0	

[1]Subjects who filled a questionnaire.
[2]One-sided 97.5% confidence interval.
CI: Confidence interval; HEV: Hepatitis E virus; IgG: Immunoglobulin G.

cohorts. The proposed transmission routes linked to professional exposures include frequent contact with the zoonotic HEV reservoirs, such as pigs and other wildlife species (mainly wild boar)[12]. Forestry workers, hunters, and veterinarians represented risk populations in this study. The HEV seroprevalence was significantly higher in the exposed population (12.6%) compared to the nonexposed population (4.3%). In the exposed group, seroprevalence was similar in the veterinarians (15.2%) and hunters (14.9%), while it was lower in the forestry workers (6.5%).

HEV seropositivity in forestry workers included in this study was similar to the seroprevalence in the Croatian general population (7.1%). Seroepidemiological studies conducted among forestry workers in Europe showed seropositivity of 31% in France (2002-2003)[11] and 18% in Germany (Brandenburg, 2008)[21]. In more recent studies, HEV antibodies were detected in 2.2% of forest rangers from western Poland (Poznan, 2014)[10], 5% of forestry workers from eastern Poland (Lubelskie Voivodship, 2014-2015)[13], and 14% of forestry workers in Italy (Trentino-Alto Adige Region, 2014-2015)[12]. Although forestry workers have been identified as being at risk of HEV infection in several studies, the French study revealed for the first time that woodcutters are at a particularly high risk of infection. Among woodcutters, 37.2% were found to be seropositive compared to game and fishing keepers/rangers and silviculturists (20.0% and 24.8% seropositive, respectively)[11]. Close contact with wild boar stools in the forest environment could be an additional source of HEV infection in this risk population.

HEV seropositivity in the Croatian hunters included (14.9%) was two times higher than that in the general population. Two studies conducted among Polish hunters from 2010 to 2012 showed a HEV seropositivity of 25%[22] and 22.2%, respectively[14]. A similar seroprevalence rate (25%) was detected in Italian hunters from the Latium Region tested during the hunting season[23] and German hunters (21%) from Central Germany tested in 2013[15]. By contrast, only 4.2% of hunters from nine Estonian counties were seropositive to HEV in 2013[24] as well as 3.81% of Polish hunters from the Lubelskie Voivodship (eastern Poland) tested from 2014 to 2015[13].

In 2009, serum samples were collected from participants of the National Veterinary Congress in Helsinki. Finnish veterinarians commonly have HEV antibodies with a seroprevalence of 10.2%. The highest seroprevalence rate of 17.8% was unexpectedly detected in small animal practitioners[17]. A study from Norway in 2013 found IgG seroprevalence of 14%. When stratifying by work experience, HEV seroprevalence in Norwegian veterinarians working with swine was more than two times higher

Table 5 Hepatitis E virus immunoglobulin G prevalence according to environmental and housing conditions

Characteristics	Subjects[1], *n* (%)	HEV IgG, *n* (%)	95%CI	*P* value
Drinking water supply				0.694
Public water supply	431	43 (10.0)	7.4-13.1	
Private water well	70	7 (10.0)	4.6-18.6	
Bottled water	4	0 (0)	0-60.2[2]	
Others	4	1 (25.0)	2.8-71.6	
Type of water drainage/sewer				0.781
Public sewer	320	33 (10.3)	7.3-14	
Septic tank	185	18 (9.7)	6.1-14.6	
Others	4	0 (0)	0-60.2[2]	
Waste disposal				1.000
Public	501	51 (10.2)	7.8-13.1	
Burning	5	0 (0)	0-52.2[2]	
Slurry	2	0 (0)	0-84.1[2]	
Having pet animals				0.039
Yes	265	33 (12.5)	8.9-16.8	
No	243	17 (7.0)	4.3-10.7	
Having domestic animals				0.629
Yes	140	16 (11.4)	7.0-17.5	
No	348	35 (10.1)	7.2-13.5	
Rodent control in the basement				0.670
Yes	264	28 (10.6)	7.3-14.7	
No	243	23 (9.5)	6.3-13.6	
Storing food in the basement				0.346
Yes	122	15 (12.3)	7.4-19.0	
No	385	36 (9.4)	6.7-12.6	

[1]Subjects who filled a questionnaire.
[2]One-sided 97.5% confidence interval.
CI: Confidence interval; HEV: Hepatitis E virus; IgG: Immunoglobulin G.

compared to those who did not work with swine (22% *vs* 9%)[25]. Chinese studies conducted from 2003 to 2017 demonstrated high IgG seropositivity in veterinarians ranging from 26.7%[16] to 43.7%[26]. In addition, a high seroprevalence rate of 23% was notified in swine veterinarians in the United States[27].

By contrast, a Thai study found no association between HEV seroprevalence and frequent direct occupational pig contact[28]. A very low HEV seropositivity (2.6%) was found in Estonian veterinarians. All antibody-positive veterinarians worked in small animal clinics and some of them were cat or dog owners[29]. The majority of veterinarians included in this study are small animal practitioners and showed seropositivity to HEV of 15.2%. In some countries, significant regional differences in the HEV seroprevalence were observed. In Polish hunters, seroprevalence varied from 10% to 42.4%[14].

A recent meta-analysis of 14626 transplant recipients showed that anti-HEV seroprevalence ranges from 6%-29.6%[18]. This wide HEV seroprevalence range reflects the differences in viral circulation within different geographical regions and the impact of assays used in the particular study. In our transplant cohort, LTRs showed the highest seroprevalence rate of 19.3%, and in the risk analysis for HEV IgG seropositivity exhibited the highest OR of 5.058 among tested groups. This supports the hypothesis that HEV in combination with other factors may promote chronic inflammation and even be a cofactor in hepatocellular carcinoma occurrence leading to liver transplant candidacy[30]. Chronicity of HEV infection is of emerging relevance in transplant recipients; however, there are still conflicting viewpoints on the overall anti-HEV seroprevalence and rate of chronic HEV infection in immunocompromised patients[31].

Table 6 Hepatitis E virus immunoglobulin G prevalence according to other potential risk factors

Characteristics	Subjects[1], *n*	HEV IgG, *n* (%)	95%CI	*P* value
Traveling abroad				0.621
Yes	119	11 (9.2)	5-15.4	
No	369	40 (10.8)	8-14.3	
Blood transfusion				0.120
Yes	44	8 (18.2)	9-31.4	
No	410	41 (10)	7.4-13.2	
Surgical procedure				0.570
Yes	230	23 (10)	6.6-14.4	
No	223	26 (11.7)	7.9-16.4	
Tattoo and piercing				0.540
Yes	72	6 (8.3)	3.6-16.4	
No	378	43 (11.4)	8.5-14.9	

[1]Subjects who filled a questionnaire.
CI: Confidence interval; HEV: Hepatitis E virus; IgG: Immunoglobulin G.

Table 7 Risk analysis for hepatitis E virus immunoglobulin G seropositivity

Population group	OR	95%CI	*P* value	RR	95%CI	*P* value
General population	Ref			Ref		
Hunters	3.873	1.605-9.341	0.002	3.445	1.556-7.628	0.002
Veterinarians	3.985	1.883-8.435	< 0.001	3.531	1.771-7.038	< 0.001
Forestry workers	1.529	0.549-4.261	0.416	1.495	0.569-3.929	0.414
Liver transplant recipients	5.058	2.240-11.420	< 0.001	4.276	2.068-8.839	< 0.001
Kidney transplant recipients	1.588	0.424-5.946	0.491	1.547	0.450-5.320	0.488
Hematopoietic stem cell recipients	1.145	0.244-5.373	0.863	1.137	0.262-4.938	0.863

CI: Confidence interval; OR: Odds ratio; RR: Relative risk.

Several studies have found sex variations in HEV seropositivity, with males having higher seropositivity compared to women[14,32]. This study found no significant difference in the seropositivity between men (10.9%) and women (7.2%). Similarly, a German study found no sex differences in the HEV seropositivity[15]. An increase in HEV seroprevalence with age, which is likely to reflect cumulative exposure to HEV over time was observed in many studies[11,12,14,27]. In this study, the highest seropositivity (23.5%) was observed in the age group 60 + years compared to 2.9%-10.9% in other age groups. By contrast, one German study conducted in forestry workers did not find a statistically significant association between seropositivity and age[21]. Similarly, no association of HEV seroprevalence with age was observed in Norwegian veterinarians[25].

Working with a septic tank was identified as a strong risk factor for HEV infection in the Netherlands [33]. Additionally, using a stream or well as a source of water has been identified as a risk factor for HEV infection in some countries[34]. Similar to a previous Croatian study[35], in this study, we found no difference in the HEV seroprevalence regarding the type of drainage/sewer, type of water supply, and waste disposal.

Eating habits were associated with HEV seropositivity in some studies. Eating internal pig organs more than twice a week was linked to a higher seroprevalence of anti-HEV IgG in a rural community in Thailand[28]. In France, the presence of anti-HEV IgG was associated with the consumption of pork meat, pork liver sausages, game meat, offal, and oysters[36]. The association between HEV seroprevalence and consumption of stewed offal was also confirmed among Polish hunters[12]. In Italy, many seropositive individuals reported consumption of raw or undercooked food, particularly shellfish (mussels) and unbottled drinking water[37]. This study found no association between offal consumption

and HEV seropositivity. Although participants who reported eating pork liver every week showed a higher seroprevalence rate (18.2%) compared to those who did not eat or ate pork liver rarely (0%-15.0%), this difference was not significant. In addition, there was no difference in the seropositivity regarding pork meat and game meat consumption. Similar to our results, a German study showed that wild boar meat consumption was not associated with HEV seroprevalence. However, HEV RNA was detected in muscle specimens from wild boar, suggesting this is a possible HEV transmission route[15]. Surprisingly, there was a significant difference in the seroprevalence regarding shellfish consumption in our study, with the highest seroprevalence in participants who reported to never eat shellfish. However, due to a very small number in the tested subgroups regarding the frequency of shellfish consumption, this limitation should be considered when interpreting the results.

In this study, a pet ownership was associated with HEV seroprevalence with a seropositivity rate of 12.5% in individuals who reported having a cat/dog compared to 7.0% in those who did not have pet animals. Animal ownership, including both domestic and pet animals, was not found to be a risk factor for HEV infection in a Jordanian study[38]. The use of a self-reported questionnaire in the study is a limitation that should be addressed. In addition, data on the risk factors in the transplant patients were not available.

CONCLUSION

The results of this study showed that individuals in professional contact with animals are at higher risk for HEV infection. Identification of people at risk for HEV infection is essential to implement preventive measures and educate these groups about modes of HEV transmission and prevention. Since immunocompromised populations such as SOT are at risk of chronic hepatitis E, such individuals should be counseled regarding the risk of HEV before and after transplantation.

ARTICLE HIGHLIGHTS

Research background

Hepatitis E virus (HEV) seroprevalence rates differ greatly according to the geographic region and population group.

Research motivation

Only preliminary data are available on the HEV seroprevalence in some population groups in Croatia.

Research objectives

To determine the HEV seroprevalence in different populations (animal-related professions, transplant patients, general population).

Research methods

HEV immunoglobulin G antibodies were detected using an enzyme-linked immunosorbent assay. Initially, reactive samples were confirmed by immunoblot test.

Research results

Significant differences in HEV seropositivity were observed among the population groups: Veterinarians 15.2%, hunters 14.9%, forestry workers 6.5%, general population 7.1%, pregnant women 1.7%, liver transplant recipients 19.3%, kidney transplant recipients 6.9%, and hematopoietic stem cell recipients 5.1%. Older age was a significant risk factor for HEV seropositivity. In addition, pet ownership was associated with HEV seroprevalence. Sociodemographic characteristics, eating habits, and environmental and housing conditions were not associated with the HEV seropositivity.

Research conclusions

Professional contact with animals and older age are significant risk factors for HEV infection.

Research perspectives

Further studies on a large sample of exposed and nonexposed population are needed to determine the HEV RNA prevalence/seroprevalence and clinical significance of HEV infection in the Croatian population.

FOOTNOTES

Author contributions: Jelicic P and Vilibic-Cavlek T conceived the study and wrote the original draft; Ferenc T, Mrzljak A, and Vilibic-Cavlek T wrote the original draft; Janev-Holcer N, Bogdanic M, Mrzljak A, Barbic L, Stevanovic V, Vujica M, Jurekovic Z, Pavicic Saric J, and Vilibic M were involved in the data collection and analysis; Milosevic M and Kolaric B performed the statistical analyses; Jemersic L and Vilibic-Cavlek T revised the manuscript critically; and all authors approved the final version of the manuscript.

Supported by the Croatian Science Foundation (Emerging and Neglected Hepatotropic Viruses after Solid Organ and Hematopoietic Stem Cell Transplantation to Mrzljak A), No. IP-2020-02-7407.

Institutional review board statement: The study was approved by the Ethic Committee of the Croatian Institute of Public Health (protocol code 80327/1-16, approved on 12 February 2016) and School of Medicine University of Zagreb (protocol code 641-01/20-02/01, approved on 22 October 2020).

Informed consent statement: Written informed consent was obtained from all participants included in the study.

Conflict-of-interest statement: All the authors report no relevant conflicts of interest for this article.

Data sharing statement: Data sharing available upon request.

STROBE statement: The authors have read the STROBE Statement-checklist of items, and the manuscript was prepared and revised according to the STROBE Statement-checklist of items.

Open-Access: This article is an open-access article that was selected by an in-house editor and fully peer-reviewed by external reviewers. It is distributed in accordance with the Creative Commons Attribution NonCommercial (CC BY-NC 4.0) license, which permits others to distribute, remix, adapt, build upon this work non-commercially, and license their derivative works on different terms, provided the original work is properly cited and the use is non-commercial. See: https://creativecommons.org/Licenses/by-nc/4.0/

Country/Territory of origin: Croatia

ORCID number: Pavle Jelicic 0000-0003-3200-1596; Thomas Ferenc 0000-0002-4917-9270; Anna Mrzljak 0000-0001-6270-2305; Lorena Jemersic 0000-0002-8379-4787; Natasa Janev-Holcer 0000-0002-2584-6681; Milan Milosevic 0000-0001-9008-7645; Maja Bogdanic 0000-0002-8236-3205; Ljubo Barbic 0000-0002-5170-947X; Branko Kolaric 0000-0002-0884-4043; Vladimir Stevanovic 0000-0002-9572-8760; Mateja Vujica 0000-0001-7766-5113; Zeljka Jurekovic 0000-0003-0690-2577; Jadranka Pavicic Saric 0000-0003-4124-8056; Maja Vilibic 0000-0002-5357-5890; Tatjana Vilibic-Cavlek 0000-0002-1877-5547.

S-Editor: Wang JJ
L-Editor: Filipodia
P-Editor: Wang JJ

REFERENCES

1 **Webb GW**, Dalton HR. Hepatitis E: an underestimated emerging threat. *Ther Adv Infect Dis* 2019; **6**: 2049936119837162 [PMID: 30984394 DOI: 10.1177/2049936119837162]
2 **World Health Organization**. Hepatitis B. [cited 10 June 2022]. Available from: https://www.who.int/news-room/fact-sheets/detail/hepatitis-b
3 **World Health Organization**. Hepatitis C. [cited 10 June 2022]. Available from: https://www.who.int/news-room/fact-sheets/detail/hepatitis-c
4 **Nimgaonkar I**, Ding Q, Schwartz RE, Ploss A. Hepatitis E virus: advances and challenges. *Nat Rev Gastroenterol Hepatol* 2018; **15**: 96-110 [PMID: 29162935 DOI: 10.1038/nrgastro.2017.150]
5 **Raji YE**, Toung OP, Taib NM, Sekawi ZB. Hepatitis E Virus: An emerging enigmatic and underestimated pathogen. *Saudi J Biol Sci* 2022; **29**: 499-512 [PMID: 35002446 DOI: 10.1016/j.sjbs.2021.09.003]
6 **Doceul V**, Bagdassarian E, Demange A, Pavio N. Zoonotic Hepatitis E Virus: Classification, Animal Reservoirs and Transmission Routes. *Viruses* 2016; **8** [PMID: 27706110 DOI: 10.3390/v8100270]
7 **Primadharsini PP**, Nagashima S, Okamoto H. Mechanism of Cross-Species Transmission, Adaptive Evolution and Pathogenesis of Hepatitis E Virus. *Viruses* 2021; **13** [PMID: 34069006 DOI: 10.3390/v13050909]
8 **Ferri G**, Vergara A. Hepatitis E Virus in the Food of Animal Origin: A Review. *Foodborne Pathog Dis* 2021; **18**: 368-377 [PMID: 33784472 DOI: 10.1089/fpd.2020.2896]
9 **Li P**, Ji Y, Li Y, Ma Z, Pan Q. Estimating the global prevalence of hepatitis E virus in swine and pork products. *One Health* 2022; **14**: 100362 [PMID: 34977322 DOI: 10.1016/j.onehlt.2021.100362]
10 **Bura M**, Bukowska A, Michalak M, Bura A, Nawrocki MJ, Karczewski M, Mozer-Lisewska I. Exposure to hepatitis E virus, hepatitis A virus and Borrelia spp. infections in forest rangers from a single forest district in western Poland. *Adv Clin Exp Med* 2018; **27**: 351-355 [PMID: 29533542 DOI: 10.17219/acem/65787]

11 **Carpentier A**, Chaussade H, Rigaud E, Rodriguez J, Berthault C, Boué F, Tognon M, Touzé A, Garcia-Bonnet N, Choutet P, Coursaget P. High hepatitis E virus seroprevalence in forestry workers and in wild boars in France. *J Clin Microbiol* 2012; **50**: 2888-2893 [PMID: 22718947 DOI: 10.1128/JCM.00989-12]

12 **Monini M**, Ostanello F, Dominicis A, Tagliapietra V, Vaccari G, Rizzoli A, Trombetta CM, Montomoli E, Di Bartolo I. Seroprevalence of Hepatitis E Virus in Forestry Workers from Trentino-Alto Adige Region (Northern Italy). *Pathogens* 2020; **9** [PMID: 32674277 DOI: 10.3390/pathogens9070568]

13 **Weiner M**, Tokarska-Rodak M, Plewik D, Pańczuk A, Szepeluk A, Krajewska M. The Serological Surveillance of Hepatitis E virus among Hunters and Foresters in Eastern Poland. *Pol J Microbiol* 2017; **66**: 277-279 [PMID: 28735306 DOI: 10.5604/01.3001.0010.7882]

14 **Baumann-Popczyk A**, Popczyk B, Gołąb E, Rożej-Bielicka W, Sadkowska-Todys M. A cross-sectional study among Polish hunters: seroprevalence of hepatitis E and the analysis of factors contributing to HEV infections. *Med Microbiol Immunol* 2017; **206**: 367-378 [PMID: 28776194 DOI: 10.1007/s00430-017-0515-0]

15 **Schielke A**, Ibrahim V, Czogiel I, Faber M, Schrader C, Dremsek P, Ulrich RG, Johne R. Hepatitis E virus antibody prevalence in hunters from a district in Central Germany, 2013: a cross-sectional study providing evidence for the benefit of protective gloves during disembowelling of wild boars. *BMC Infect Dis* 2015; **15**: 440 [PMID: 26493830 DOI: 10.1186/s12879-015-1199-y]

16 **Kang YH**, Cong W, Zhang XY, Wang CF, Shan XF, Qian AD. Hepatitis E virus seroprevalence among farmers, veterinarians and control subjects in Jilin province, Shandong province and Inner Mongolia Autonomous Region, China. *J Med Virol* 2017; **89**: 872-877 [PMID: 27664799 DOI: 10.1002/jmv.24693]

17 **Kantala T**, Kinnunen PM, Oristo S, Jokelainen P, Vapalahti O, Maunula L. Hepatitis E Virus Antibodies in Finnish Veterinarians. *Zoonoses Public Health* 2017; **64**: 232-238 [PMID: 27621202 DOI: 10.1111/zph.12312]

18 **Buescher G**, Ozga AK, Lorenz E, Pischke S, May J, Addo MM, Horvatits T. Hepatitis E seroprevalence and viremia rate in immunocompromised patients: a systematic review and meta-analysis. *Liver Int* 2021; **41**: 449-455 [PMID: 33034121 DOI: 10.1111/liv.14695]

19 **Mrzljak A**, Dinjar-Kujundzic P, Vilibic-Cavlek T, Jemersic L, Prpic J, Dakovic-Rode O, Kolaric B, Vince A. Hepatitis E seroprevalence and associated risk factors in Croatian liver transplant recipients. *Rev Soc Bras Med Trop* 2019; **52**: e20190302 [PMID: 31618309 DOI: 10.1590/0037-8682-0302-2019]

20 **Mrzljak A**, Dinjar-Kujundzic P, Knotek M, Kudumija B, Ilic M, Gulin M, Zibar L, Hrstic I, Jurekovic Z, Kolaric B, Jemersic L, Prpic J, Tomljenovic M, Vilibic-Cavlek T. Seroepidemiology of hepatitis E in patients on haemodialysis in Croatia. *Int Urol Nephrol* 2020; **52**: 371-378 [PMID: 31894559 DOI: 10.1007/s11255-019-02363-3]

21 **Dremsek P**, Wenzel JJ, Johne R, Ziller M, Hofmann J, Groschup MH, Werdermann S, Mohn U, Dorn S, Motz M, Mertens M, Jilg W, Ulrich RG. Seroprevalence study in forestry workers from eastern Germany using novel genotype 3- and rat hepatitis E virus-specific immunoglobulin G ELISAs. *Med Microbiol Immunol* 2012; **201**: 189-200 [PMID: 22179131 DOI: 10.1007/s00430-011-0221-2]

22 **Sadkowska-Todys M**, Baumann-Popczyk A, Wnukowska N, Popczyk B, Kucharczyk B, Gołąb E. Occurrence and prevalence of selected zoonotic agents: Echinococcus multilocularis, Trichinella spiralis and hepatitis E virus (HEV) in the population of Polish hunters--results of the study conducted in 2010-2012. *Przegl Epidemiol* 2015; **69**: 673-678, 823 [PMID: 27139343]

23 **Montagnaro S**, De Martinis C, Sasso S, Ciarcia R, Damiano S, Auletta L, Iovane V, Zottola T, Pagnini U. Viral and Antibody Prevalence of Hepatitis E in European Wild Boars (Sus scrofa) and Hunters at Zoonotic Risk in the Latium Region. *J Comp Pathol* 2015; **153**: 1-8 [PMID: 26025105 DOI: 10.1016/j.jcpa.2015.04.006]

24 **Ivanova A**, Tefanova V, Reshetnjak I, Kuznetsova T, Geller J, Lundkvist Å, Janson M, Neare K, Velström K, Jokelainen P, Lassen B, Hütt P, Saar T, Viltrop A, Golovljova I. Hepatitis E Virus in Domestic Pigs, Wild Boars, Pig Farm Workers, and Hunters in Estonia. *Food Environ Virol* 2015; **7**: 403-412 [PMID: 26141050 DOI: 10.1007/s12560-015-9210-8]

25 **Lange H**, Øverbø J, Borgen K, Dudman S, Hoddevik G, Urdahl AM, Vold L, Sjurseth SK. Hepatitis E in Norway: seroprevalence in humans and swine. *Epidemiol Infect* 2017; **145**: 181-186 [PMID: 27671461 DOI: 10.1017/S0950268816002144]

26 **Yue N**, Wang Q, Zheng M, Wang D, Duan C, Yu X, Zhang X, Bao C, Jin H. Prevalence of hepatitis E virus infection among people and swine in mainland China: A systematic review and meta-analysis. *Zoonoses Public Health* 2019; **66**: 265-275 [PMID: 30884147 DOI: 10.1111/zph.12555]

27 **Meng XJ**, Wiseman B, Elvinger F, Guenette DK, Toth TE, Engle RE, Emerson SU, Purcell RH. Prevalence of antibodies to hepatitis E virus in veterinarians working with swine and in normal blood donors in the United States and other countries. *J Clin Microbiol* 2002; **40**: 117-122 [PMID: 11773103 DOI: 10.1128/JCM.40.1.117-122.2002]

28 **Hinjoy S**, Nelson KE, Gibbons RV, Jarman RG, Mongkolsirichaikul D, Smithsuwan P, Fernandez S, Labrique AB, Patchanee P. A cross-sectional study of hepatitis E virus infection in healthy people directly exposed and unexposed to pigs in a rural community in northern Thailand. *Zoonoses Public Health* 2013; **60**: 555-562 [PMID: 23280251 DOI: 10.1111/zph.12030]

29 **Lassen B**, Janson M, Neare K, Tallo T, Reshetnjak I, Kuznetsova T, Viltrop A, Golovljova I, Jokelainen P. Prevalence of Antibodies Against Hepatitis E Virus in Veterinarians in Estonia. *Vector Borne Zoonotic Dis* 2017; **17**: 773-776 [PMID: 28933680 DOI: 10.1089/vbz.2017.2122]

30 **Colson P**, Borentain P, Gérolami R. Hepatitis E virus as an agent of hepatocellular carcinoma. *Int J Infect Dis* 2019; **80**: 62-63 [PMID: 30634042 DOI: 10.1016/j.ijid.2018.12.015]

31 **Kamar N**, Garrouste C, Haagsma EB, Garrigue V, Pischke S, Chauvet C, Dumortier J, Cannesson A, Cassuto-Viguier E, Thervet E, Conti F, Lebray P, Dalton HR, Santella R, Kanaan N, Essig M, Mousson C, Radenne S, Roque-Afonso AM, Izopet J, Rostaing L. Factors associated with chronic hepatitis in patients with hepatitis E virus infection who have received solid organ transplants. *Gastroenterology* 2011; **140**: 1481-1489 [PMID: 21354150 DOI: 10.1053/j.gastro.2011.02.050]

32 **Joon A**, Rao P, Shenoy SM, Baliga S. Prevalence of Hepatitis A virus (HAV) and Hepatitis E virus (HEV) in the patients presenting with acute viral hepatitis. *Indian J Med Microbiol* 2015; **33** Suppl: 102-105 [PMID: 25657123 DOI: 10.4103/0255-0857.150908]

33 **Tulen AD**, Vennema H, van Pelt W, Franz E, Hofhuis A. A case-control study into risk factors for acute hepatitis E in the Netherlands, 2015-2017. *J Infect* 2019; **78**: 373-381 [PMID: 30738918 DOI: 10.1016/j.jinf.2019.02.001]

34 **Meng QF**, You HL, Wang WL, Zhou N, Dong W, Cong W. Seroprevalence and risk factors of hepatitis E virus infection among children in China. *J Med Virol* 2015; **87**: 1573-1577 [PMID: 25940435 DOI: 10.1002/jmv.24203]

35 **Vilibic-Cavlek T**, Vilibic M, Kolaric B, Jemersic L, Kucinar J, Barbic L, Bagaric A, Stevanovic V, Tabain I, Sviben M, Jukic V, Mlinaric-Galinovic G. Seroepidemiology of Hepatitis E in Selected Population Groups in Croatia: A Prospective Pilot Study. *Zoonoses Public Health* 2016; **63**: 494-502 [PMID: 26776465 DOI: 10.1111/zph.12254]

36 **Mansuy JM**, Gallian P, Dimeglio C, Saune K, Arnaud C, Pelletier B, Morel P, Legrand D, Tiberghien P, Izopet J. A nationwide survey of hepatitis E viral infection in French blood donors. *Hepatology* 2016; **63**: 1145-1154 [PMID: 27008201 DOI: 10.1002/hep.28436]

37 **La Fauci V**, Facciolà A, Riso R, Calimeri S, Lo Giudice D, Squeri R. Seroprevalence of hev antibodies in a sample of pregnant women in the city of Messina. *Ann Ig* 2017; **29**: 232-238 [PMID: 28383615 DOI: 10.7416/ai.2017.2151]

38 **Obaidat MM**, Roess AA. Seroprevalence and risk factors of Hepatitis E infection in Jordan's population: First report. *Int J Infect Dis* 2018; **66**: 121-125 [PMID: 29146513 DOI: 10.1016/j.ijid.2017.11.015]

World Journal of Gastroenterology

Submit a Manuscript: https://www.f6publishing.com

World J Gastroenterol 2022 October 7; 28(37): 5506-5514

DOI: 10.3748/wjg.v28.i37.5506

ISSN 1007-9327 (print) ISSN 2219-2840 (online)

CASE REPORT

Massive bleeding from gastric submucosal arterial collaterals secondary to splenic artery thrombosis: A case report

Alberto Martino, Marco Di Serafino, Francesco Paolo Zito, Franco Maglione, Raffaele Bennato, Luigi Orsini, Alessandro Iacobelli, Raffaella Niola, Luigia Romano, Giovanni Lombardi

Specialty type: Gastroenterology and hepatology

Provenance and peer review: Unsolicited article; Externally peer reviewed.

Peer-review model: Single blind

Peer-review report's scientific quality classification

Grade A (Excellent): A
Grade B (Very good): B
Grade C (Good): 0
Grade D (Fair): 0
Grade E (Poor): 0

P-Reviewer: Chang A, Thailand; Tieranu CG, Romania

Received: June 18, 2022
Peer-review started: June 18, 2022
First decision: July 11, 2022
Revised: July 17, 2022
Accepted: September 8, 2022
Article in press: September 8, 2022
Published online: October 7, 2022

Alberto Martino, Francesco Paolo Zito, Raffaele Bennato, Luigi Orsini, Giovanni Lombardi, Department of Gastroenterology and Digestive Endoscopy, AORN "Antonio Cardarelli", Napoli 80131, Italy

Marco Di Serafino, Luigia Romano, Department of General and Emergency Radiology, AORN "Antonio Cardarelli", Napoli 80131, Italy

Franco Maglione, Department of Radiology, Sanatrix Clinic, Napoli 80127, Italy

Alessandro Iacobelli, Department of Pathology, AORN "Antonio Cardarelli", Napoli 80131, Italy

Raffaella Niola, Department of Interventional Radiology, AORN "Antonio Cardarelli", Napoli 80131, Italy

Corresponding author: Alberto Martino, MD, Staff Physician, Department of Gastroenterology and Digestive Endoscopy, AORN "Antonio Cardarelli", Via Antonio Cardarelli 9, Napoli 80131, Italy. albertomartinomd@gmail.com

Abstract

BACKGROUND

Gastric submucosal arterial collaterals (GSAC) secondary to splenic artery occlusion is an extraordinary rare and potentially life-threatening cause of acute upper gastrointestinal bleeding. Here, we report a case of massive bleeding from GSAC successfully treated by means of a multidisciplinary minimally invasive approach.

CASE SUMMARY

A 60-year-old non-cirrhotic gentleman with a history of arterial hypertension was admitted due to hematemesis. Emergent esophagogastroduodenoscopy revealed pulsating and tortuous varicose shaped submucosal vessels in the gastric fundus along with a small erosion overlying one of the vessels. In order to characterize the fundic lesion, pre-operative emergent computed tomography-angiography was performed showing splenic artery thrombosis (SAT) and tortuous arterial structures arising from the left gastric artery and the left gastroepiploic artery in the gastric fundus. GSAC was successfully treated by means of a minimally invasive step-up approach consisting in endoscopic clipping followed by transcatheter arterial embolization (TAE).

CONCLUSION
This was a previously unreported case of bleeding GSAC secondary to SAT successfully managed by means of a multidisciplinary minimally invasive approach consisting in endoscopic clipping for the luminal bleeding control followed by elective TAE for the definitive treatment.

Key Words: Upper gastrointestinal bleeding; Non variceal upper gastrointestinal bleeding; Acute upper gastrointestinal bleeding; Gastric submucosal arterial collaterals; Splenic artery thrombosis; Case report

©The Author(s) 2022. Published by Baishideng Publishing Group Inc. All rights reserved.

Core Tip: Gastric submucosal arterial collaterals (GSAC) secondary to splenic artery occlusion is an extremely rare cause of severe non variceal upper gastrointestinal bleeding. Herein, we describe a previously unreported case of massive bleeding from GSAC secondary to splenic artery thrombosis effectively treated by endoscopic mechanical hemostasis followed by endovascular embolization.

Citation: Martino A, Di Serafino M, Zito FP, Maglione F, Bennato R, Orsini L, Iacobelli A, Niola R, Romano L, Lombardi G. Massive bleeding from gastric submucosal arterial collaterals secondary to splenic artery thrombosis: A case report. *World J Gastroenterol* 2022; 28(37): 5506-5514
URL: https://www.wjgnet.com/1007-9327/full/v28/i37/5506.htm
DOI: https://dx.doi.org/10.3748/wjg.v28.i37.5506

INTRODUCTION

Acute upper gastrointestinal bleeding (UGIB) is a common gastroenterological emergency associated with significant morbidity and mortality. Reported hospitalization rate is 61-78 cases *per* 100.000 adults *per* year[1-3], whereas estimated overall mortality is around 10%[4,5]. Peptic ulcers are the most common cause of acute UGIB, followed by oesophageal varices, Mallory-Weiss syndrome and neoplasms[1,3,4]. Acute UGIB caused by gastric submucosal arterial collaterals (GSAC) secondary to splenic artery occlusion (SAO) is extremely rare, with only few cases reported worldwide up to date. Herein, we describe a previously unreported case of bleeding GSAC secondary to splenic artery thrombosis (SAT) successfully treated by means of endoscopic mechanical hemostasis followed by endovascular embolization.

CASE PRESENTATION

Chief complaints

A 60-year-old non-cirrhotic gentleman was admitted to our dedicated bleed unit for severe anemia (hemoglobin 4.8 g/dL on admission) and recent onset of hematemesis and melena with unstable hemodynamic parameters.

History of present illness

One attack of hematemesis and two episodes of melena occurred two and 24 h prior to the hospital admission, respectively.

History of past illness

The patient had a history of arterial hypertension. He denied any history of, or risk factors for, liver disease, pancreatitis, abdominal trauma and hypercoagulable states.

Personal and family history

The patient denied personal and family history.

Physical examination

At admission, the patient was hemodynamically unstable (pulse of 110 bpm, blood pressure of 100/50 mmHg). He was afebrile, with respiratory rate of 15 rpm and oxygen saturation of 98%. His physical examination was negative for any evidence of portal hypertension or other stigmata of chronic liver disease. Abdominal examination revealed non-distended, non-tender abdomen with normoactive bowel sounds. The digital rectal examination showed black terry feces.

Laboratory examinations

Complete blood count revealed a hemoglobin level of 4.8 g/dL and hematocrit of 14.6%. All other laboratoristic exams, including coagulation, liver and renal function tests, were within normal values.

Imaging examinations

Following high-dose intravenous proton pump inhibitor administration, blood transfusion and hemodynamic stabilization, emergent esophagogastroduodenoscopy (EGD) under monitored anaesthesia care was performed. A moderate amount of fresh blood within the stomach was noted and fully aspirated. The retroflexion maneuver revealed varicose shaped pulsating and tortuous submucosal vessels in the gastric fundus without active bleeding. A small erosion overlying one of the vessels consistent with an area of recent healed rupture was noted (Figure 1). Given the absence of clinical or laboratory signs of portal hypertension, we decided to perform emergent computed tomography-angiography (CTA) in order to further characterize the fundic lesion and to look for signs of portal hypertension. SAT and tortuous arterial structures emerging from the left gastric artery (LGA) and the left gastroepiploic artery (LGEA) in the gastric fundus were showed. No signs of active bleeding were observed (Figure 2).

Further hospital course

Given the high-risk of massive early rebleeding due to the presence of a small erosion overlying one of the GSAC vessels, we decided to attempt therapeutic EGD in order to provide definitive treatment in a more stable non-emergent setting. The patient was informed that in case of luminal bleeding control failure, emergent transcatheter arterial embolization (TAE) would be performed by the pre-alerted interventional radiologist. Immediately after the first endoclip application downstream to the mucosal erosion, spurting bleeding started. Hemostasis was achieved by means of two endoclips placement upstream to the mucosal defect. Finally, two endoclips were further prophylactically positioned (Figure 3 and Video 1).

MULTIDISCIPLINARY EXPERT CONSULTATION

No rebleeding was observed following the endoscopic treatment. However, the patient refused splenectomy for definitive treatment. Therefore, after multidisciplinary evaluation, involving GI endoscopist, surgeon, diagnostic and interventional radiologist, a minimally-invasive approach with elective TAE was planned.

FINAL DIAGNOSIS

Non variceal acute UGIB from GSAC secondary to SAT.

TREATMENT

Operative angiography showed SAT with multiple collateral arteries arising from the LGA and the LGEA and projecting in the gastric fundus (Figure 4). Selective TAE of the LGA collaterals with trisacryl gelatin microspheres (Embospheres, Guerbet Biomedical, Louvres, France) was effectively realized.

OUTCOME AND FOLLOW-UP

Post-operative stay was complicated by splenic infarction, responsive to conservative treatment (Figure 5). The patient underwent hematology consultation and thrombophilic disorders were excluded. No rebleeding occurred. The patient was discharged with stable haemoglobin value (9.1 g/dL) on post-operative day 18. No rebleeding was observed at 12-mo follow-up.

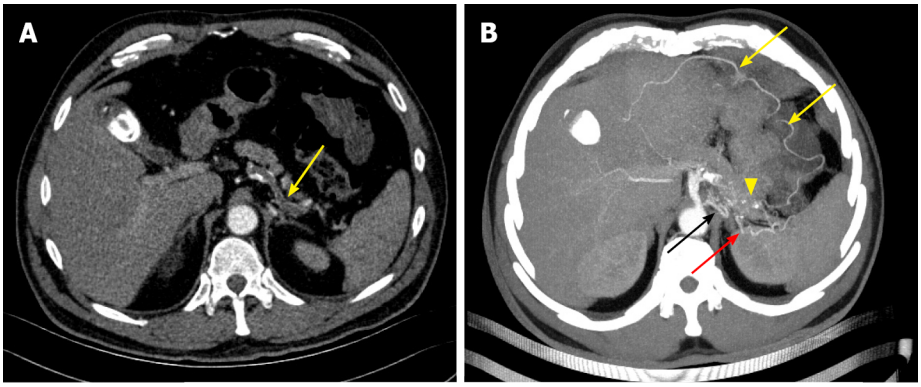
DISCUSSION

GSAC are an extraordinary rare cause of massive UGIB. They are not related to portal hypertension, resulting from either occlusion or congenital absence of the SA. SAO may be congenital, idiopathic, or secondary to various conditions such as surgery, endovascular procedure, trauma and extrinsic compression. In the case of SAO, in order to provide splenic blood supply, extensive collaterals may



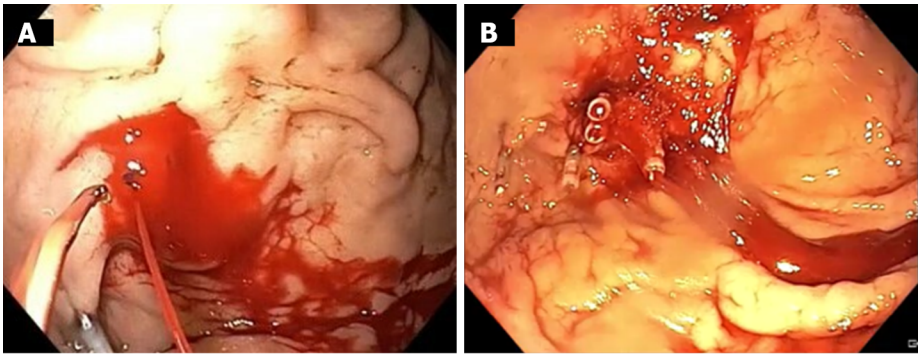
DOI: 10.3748/wjg.v28.i37.5506 **Copyright** ©The Author(s) 2022.

Figure 1 Emergent esophagogastroduodenoscopy: Retroflexed view of the gastric fundus showing varicose-shaped submucosal vessels with a small erosion (arrow).



DOI: 10.3748/wjg.v28.i37.5506 **Copyright** ©The Author(s) 2022.

Figure 2 Emergent computed tomography angiography: Axial view. A: Arterial phase showing complete splenic artery thrombosis (arrow); B: Arterial phase curved-multiplanar reconstruction showing splenic artery collateral vessels (yellow arrows) with an arterial cluster at the gastric fundus (arrowhead) arising from the left gastric artery (black arrow) and the left gastroepiploic artery (red arrow).



DOI: 10.3748/wjg.v28.i37.5506 **Copyright** ©The Author(s) 2022.

Figure 3 Therapeutic esophagogastroduodenoscopy. A: Spurting active bleeding of the gastric submucosal arterial collaterals after first endoclip application; B: Successful mechanical hemostasis achievement.

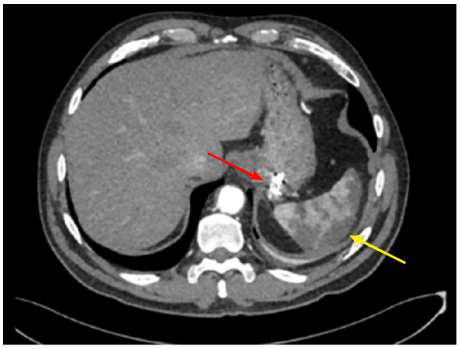
arise from adjacent proximal patent arteries, such as the pancreatic, left gastric, gastroepiploic, and short gastric arteries and pass through the gastric wall[6]. Collateral supply may be clinically asymptomatic or may less frequently present with massive UGIB from erosion of GSAC.

The differential diagnosis of GSAC includes mainly isolated gastric varices (IGV). Gastric vascular lesions due to collaterization of an occluded splenic artery may have a very similar endoscopic appearance to IGV and can be easily misinterpreted on EGD. However, they are, as opposed to GSAC, due to cirrhotic portal hypertension or splenic vein obstruction resulting in left-sided portal hypertension[7,8]. Therefore, an accurate differential diagnosis between these two entities is crucial. Indeed, endoscopic cyanoacrylate glue injection (ECGI), currently recommended as the first-line treatment for



DOI: 10.3748/wjg.v28.i37.5506 **Copyright** ©The Author(s) 2022.

Figure 4 Operative angiography showing a cluster of collateral arterial vessels emerging from the left gastric artery (red arrow) and the left gastroepiploic artery (yellow arrow) projecting into the gastric fundus. It also shows previously placed endoclips on the submucosal collateral arteries of the gastric fundus without active contrast extravasation (arrowhead).



DOI: 10.3748/wjg.v28.i37.5506 **Copyright** ©The Author(s) 2022.

Figure 5 Post-operative computed tomography angiography: Axial view showing collateral arteries of the gastric fundus treated by endoscopic clipping plus microspheres embolization (red arrow) and splenic infarction (yellow arrow).

bleeding IGV[9], is associated with a significant risk of systemic embolization and life-threatening adverse events in case of direct arterial injection of cyanoacrylate[10-12]. Finally, fatal arterial embolic complications in hepatolienogastric blood supply have been reported during ECGI to a non-variceal bleeding source[13-16]. A high level of diagnostic certainty is thus required before proceeding with ECGI.

We performed a comprehensive literature search of PubMed/MEDLINE and EMBASE electronic databases up to March 2022, identifying 10 case reports of GSAC secondary to SAO (Table 1).

In 1984, Spriggs[17] first reported a case of severe UGIB due to GSAC secondary to SA congenital absence[17]. The diagnosis was made by arteriography and the treatment consisted in splenectomy followed by partial gastrectomy due to rebleeding. Later on, a similar case was reported, effectively treated by means of splenectomy after ligation of the LGA[18].

In 2000, Baron *et al*[19] reported a case of bleeding GSAC secondary to post-traumatic SAO. It was diagnosed by operative angiography and successfully treated by splenectomy and partial gastric devascularization[19]. Subsequently, Worthley and colleagues described a case of UGIB secondary to SAO due to previous SA aneurysmectomy. As previously reported, it was managed by angiography followed by splenectomy with ligation of the splenic vein and artery together with the left gastric and short gastric arteries[20].

In 2004, Cyrany *et al*[21,22] illustrated the first case of massive UGIB from GSAC secondary to SAT successfully managed endoscopically. Of interest, pre-operative diagnosis was made by endoscopy only, and treatment consisted in ECGI alone. No rebleeding was observed. However, post-procedural stay was complicated by the occurrence of splenic infarction, treated conservatively[21,22].

Later on, the first case of bleeding GSAC successfully treated by endovascular embolization alone was reported by Mnatzakanian *et al*[23] Pre-operative accurate diagnosis was made by CTA followed by

Table 1 Summary of case reports reporting acute upper gastrointestinal bleeding from gastric submucosal arterial collaterals secondary to occlusion or congenital absence of the splenic artery

Case	Ref.	Age/sex	Presentation	SAO etiology	Diagnosis	Treatment	Major AEs	Outcome	Follow-up (months)
1	Spriggs[17], 1984	31/M	Hematemesis	SA congenital absence	Angiography	Splenectomy + partial gastrectomy (due to rebleeding)	Severe respiratory distress	Alive–no rebleeding	-
2	Durrans *et al* [18], 1985	13/M	Hematemesis	SA congenital absence	Angiography	LGA ligation + splenectomy	None	Alive–no rebleeding	-
3	Baron *et al*[19], 2000	36/M	Hematemesis	Blunt abdominal trauma	Angiography	Splenectomy + partial gastric devascular-ization	None	Alive–no rebleeding	18
4	Worthley *et al* [20], 2003	68/F	Melena	Iatrogenic(SA aneurysmectomy)	Angiography	Splenectomy + ligation of SV and SA with LGA and SGA	None	Alive–no rebleeding	-
5	Cyrany *et al* [21], 2004	59/M	Hematemesis and melena	SAT	CTA + angiography	ECGI	Splenic infarction	Alive–no rebleeding	9
6	Mnatzakanian *et al*[23], 2008	66/M	Melena	-	CTA + angiography	TAE (coils and pledgets)	None	Alive–no rebleeding	-
7	von Trotha *et al* [26], 2011	69/M	-	SAT	CTA + angiography + EUS	ECGI + endoscopic clipping + splenectomy and SGA collaterals dissection	Splenic infarction	Alive–no rebleeding	6
8	Saddekni *et al* [24], 2012	23/F	Hematemesis and melena	Iatrogenic (SA ligation)	CTA + angiography	TAE (coils)	None	Alive–no rebleeding	8
9	Arslan *et al* [27], 2017	52/M	Hematemesis	SAT	CTA	-	-	Death	-
10	Al-Balas *et al* [25], 2021	49/M	Hematemesis	SAT	CTA + angiography	TAE (coils) + splenectomy and bleeding gastric vessel ligation (due to rebleeding)	None	Alive–no rebleeding	18
11	Our case	60/M	Hematemesis and melena	SAT	CTA + angiography	Endoscopic clipping + TAE (microspheres)	Splenic infarction	Alive–no rebleeding	12

SAO: Splenic artery occlusion; AEs: Adverse events; SA: Splenic artery; LGA: Left gastric artery; SGA: Short gastric arteries; SAT: Splenic artery thrombosis; CTA: Computed tomography angiography; ECGI: Endoscopic cyanoacrylate glue injection; TAE: Transcatheter arterial embolization; EUS: Endoscopic ultrasound.

angiogram, in order to rule out IGV. No procedure-related major adverse events were observed[23]. Few years later, another case successfully managed in a very similar manner was described[24]. Conversely, Al-Balas *et al*[25] recently reported a case of bleeding GSAC initially managed *via* TEA and subsequently requiring emergency laparotomy with ligation of a bleeding gastric vessel and splenectomy due to severe rebleeding occurrence[25].

In 2011, von Trotha *et al*[26] reported a case of bleeding GSAC secondary to idiopathic SAT. GSAC was endoscopically misdiagnosed as type 1 IGV and ECGI with subsequent clipping was performed in order to control active bleeding. Of note, the authors did not clarify the choice for endoscopic clipping adoption in the setting of supposed IGV. Furthermore, as previously reported by Cyrany and colleagues, ECGI was complicated by splenic infarction. A proper diagnosis was subsequently made by CTA and conventional angiography. Interestingly, endoscopic color doppler ultrasonography was adopted to secure the diagnosis and laparoscopic splenectomy was finally provided for the definitive treatment[26].

Up to date, one case only of fatal UGIB due to GSAC has been reported. In this istance, urgent EGD failed to identify the source of bleeding. CTA examination was then performed showing GSAC due to SAT, in the absence of active bleeding. However, after diagnosis, no treatment was provided and death due to recurrent bleeding occurred[27].

Our case is the first report in which bleeding GSAC was effectively treated with endoscopic mechanical hemostasis alone for the luminal bleeding control and subsequent elective TAE for the definitive treatment. Given the absence of active bleeding and portal hypertension signs or history, emergent CTA was performed prior to endoscopic treatment in order to properly characterize the gastric vascular lesion. Following endoscopic treatment neither adverse events nor rebleeding signs

occurred. The patient refused splenectomy with or without partial gastrectomy for the definitive treatment. Thus, following multidisciplinary evaluation, elective TAE was planned and effectively realized. Post-operative stay was complicated by splenic ischemia, effectively treated by conservative medical treatment. In our case, the presumed etiology of GSAC was idiopathic SAT. Given the formation of an extensive collateral pathway preserving the splenic perfusion, complete SAO likely occurred gradually.

CONCLUSION

Gastroenterologists should be aware of this potentially life-threatening, albeit extraordinary rare, source of massive upper gastrointestinal hemorrhage, in order to allow proper management. In our opinion, endoscopic mechanical hemostasis seems to be a safe and effective method for the luminal bleeding control across referral centers. Conversely, we may not recommend ECGI adoption given the potential occurrence of fatal adverse events due to arterial embolization. CTA appears to be the best modality for a prompt differential diagnosis, and should be performed in all UGIB patients with endoscopic evidence of gastric varicose shaped submucosal vessels and no signs or history of portal hypertension. For the definitive treatment of bleeding GSAC, either a minimally invasive approach with TAE or a standard approach with splenectomy may be provided, taking into account patient preference and status.

ACKNOWLEDGEMENTS

We are grateful to Velia De Magistris for English editing.

FOOTNOTES

Author contributions: Martino A was responsible for the conception of the paper, execution of the endoscopic procedures, drafting of the article, interpretation of the data and final approval of the article; Di Serafino M was responsible for conception of the paper, execution of the diagnostic radiological examinations, drafting of the article and final approval of the article; Zito FP was responsible for the conception of the paper, drafting of the article, interpretation of data and final approval of the article; Maglione F and Niola R were responsible for execution of the interventional radiological procedures, drafting of the article, interpretation of the data and final approval of the article; Bennato R, Orsini L and Iacobelli A were responsible for drafting of the article, interpretation of data and final approval of the article; Romano L and Lombardi G were responsible for the analysis and interpretation of data, revision of the manuscript for important intellectual content and final approval of the article.

Informed consent statement: Informed consent was obtained from the patient for the publication of this report and any accompanying images.

Conflict-of-interest statement: All the authors report no relevant conflicts of interest for this article.

CARE Checklist (2016) statement: The authors have read the CARE Checklist (2016), and the manuscript was prepared and revised according to the CARE Checklist (2016).

Open-Access: This article is an open-access article that was selected by an in-house editor and fully peer-reviewed by external reviewers. It is distributed in accordance with the Creative Commons Attribution NonCommercial (CC BY-NC 4.0) license, which permits others to distribute, remix, adapt, build upon this work non-commercially, and license their derivative works on different terms, provided the original work is properly cited and the use is non-commercial. See: https://creativecommons.org/Licenses/by-nc/4.0/

Country/Territory of origin: Italy

ORCID number: Alberto Martino 0000-0002-8759-6518; Marco Di Serafino 0000-0001-6972-1859; Francesco Paolo Zito 0000-0002-1084-3373; Raffaele Bennato 0000-0002-8343-8205; Luigi Orsini 0000-0001-7029-3994; Raffaella Niola 0000-0002-6668-5669; Luigia Romano 0000-0002-5201-547X; Giovanni Lombardi 0000-0002-5957-3132.

Corresponding Author's Membership in Professional Societies: Società Italiana Di Gastroenterologia Ed Endoscopia Digestiva; Associazione Italiana Gastroenterologi Ed Endoscopisti Digestivi Ospedalieri; European Society of Gastrointestinal Endoscopy.

S-Editor: Fan JR
L-Editor: A
P-Editor: Fan JR

REFERENCES

1 **Laine L**, Yang H, Chang SC, Datto C. Trends for incidence of hospitalization and death due to GI complications in the United States from 2001 to 2009. *Am J Gastroenterol* 2012; **107**: 1190-5; quiz 1196 [PMID: 22688850 DOI: 10.1038/ajg.2012.168]

2 **Abougergi MS**, Travis AC, Saltzman JR. The in-hospital mortality rate for upper GI hemorrhage has decreased over 2 decades in the United States: a nationwide analysis. *Gastrointest Endosc* 2015; **81**: 882-8.e1 [PMID: 25484324 DOI: 10.1016/j.gie.2014.09.027]

3 **Wuerth BA**, Rockey DC. Changing Epidemiology of Upper Gastrointestinal Hemorrhage in the Last Decade: A Nationwide Analysis. *Dig Dis Sci* 2018; **63**: 1286-1293 [PMID: 29282637 DOI: 10.1007/s10620-017-4882-6]

4 **Hearnshaw SA**, Logan RF, Lowe D, Travis SP, Murphy MF, Palmer KR. Acute upper gastrointestinal bleeding in the UK: patient characteristics, diagnoses and outcomes in the 2007 UK audit. *Gut* 2011; **60**: 1327-1335 [PMID: 21490373 DOI: 10.1136/gut.2010.228437]

5 **Nahon S**, Hagège H, Latrive JP, Rosa I, Nalet B, Bour B, Faroux R, Gower P, Arpurt JP, Denis J, Henrion J, Rémy AJ, Pariente A; Groupe des Hémorragies Digestives Hautes de l'ANGH. Epidemiological and prognostic factors involved in upper gastrointestinal bleeding: results of a French prospective multicenter study. *Endoscopy* 2012; **44**: 998-1008 [PMID: 23108771 DOI: 10.1055/s-0032-1310006]

6 **Stolze T**, Wienbeck M. [The collateral circulation in the chronic occlusion of the splenic artery]. *Rofo* 1976; **124**: 386-387 [PMID: 131773 DOI: 10.1055/s-0029-1230356]

7 **Sarin SK**, Jain AK, Lamba GS, Gupta R, Chowdhary A. Isolated gastric varices: prevalence, clinical relevance and natural history. *Dig Surg* 2003; **20**: 42-47 [PMID: 12637804 DOI: 10.1159/000068865]

8 **Köklü S**, Coban S, Yüksel O, Arhan M. Left-sided portal hypertension. *Dig Dis Sci* 2007; **52**: 1141-1149 [PMID: 17385040 DOI: 10.1007/s10620-006-9307-x]

9 **de Franchis R**, Bosch J, Garcia-Tsao G, Reiberger T, Ripoll C; Baveno VII Faculty. Baveno VII - Renewing consensus in portal hypertension. *J Hepatol* 2022; **76**: 959-974 [PMID: 35120736 DOI: 10.1016/j.jhep.2021.12.022]

10 **Lee CW**, Liu KL, Wang HP, Chen SJ, Tsang YM, Liu HM. Transcatheter arterial embolization of acute upper gastrointestinal tract bleeding with N-butyl-2-cyanoacrylate. *J Vasc Interv Radiol* 2007; **18**: 209-216 [PMID: 17327553 DOI: 10.1016/j.jvir.2006.12.003]

11 **Jae HJ**, Chung JW, Jung AY, Lee W, Park JH. Transcatheter arterial embolization of nonvariceal upper gastrointestinal bleeding with N-butyl cyanoacrylate. *Korean J Radiol* 2007; **8**: 48-56 [PMID: 17277563 DOI: 10.3348/kjr.2007.8.1.48]

12 **Kim BS**, Do HM, Razavi M. N-butyl cyanoacrylate glue embolization of splenic artery aneurysms. *J Vasc Interv Radiol* 2004; **15**: 91-94 [PMID: 14709694 DOI: 10.1097/01.rvi.0000099537.29957.13]

13 **Lee GH**, Kim JH, Lee KJ, Yoo BM, Hahm KB, Cho SW, Park YS, Moon YS. Life-threatening intraabdominal arterial embolization after histoacryl injection for bleeding gastric ulcer. *Endoscopy* 2000; **32**: 422-424 [PMID: 10817185 DOI: 10.1055/s-2000-9002]

14 **Lee KJ**, Kim JH, Hahm KB, Cho SW, Park YS. Randomized trial of N-butyl-2-cyanoacrylate compared with injection of hypertonic saline-epinephrine in the endoscopic treatment of bleeding peptic ulcers. *Endoscopy* 2000; **32**: 505-511 [PMID: 10917181 DOI: 10.1055/s-2000-3816]

15 **Kobilica N**, Flis V, Sojar V. Major complication after Histoacryl injection for endoscopic treatment of bleeding peptic ulcer. *Endoscopy* 2012; **44** Suppl 2 UCTN: E204-E205 [PMID: 22622746 DOI: 10.1055/s-0032-1308923]

16 **Vallieres E**, Jamieson C, Haber GB, Mackenzie RL. Pancreatoduodenal necrosis after endoscopic injection of cyanoacrylate to treat a bleeding duodenal ulcer: a case report. *Surgery* 1989; **106**: 901-903 [PMID: 2814823]

17 **Spriggs DW**. Congenital absence of the splenic artery. *Cardiovasc Intervent Radiol* 1984; **7**: 303-305 [PMID: 6335674 DOI: 10.1007/BF02625116]

18 **Durrans D**, Fawcitt RA, Taylor TV. Congenital absence of the splenic artery associated with major gastric bleeding in adolescence. *Br J Surg* 1985; **72**: 456-457 [PMID: 3874675 DOI: 10.1002/bjs.1800720618]

19 **Baron PW**, Sindram D, Suhocki P, Webb DD, Clavien PA. Upper gastrointestinal bleeding from gastric submucosal arterial collaterals secondary to splenic artery occlusion: treatment by splenectomy and partial gastric devascularization. *Am J Gastroenterol* 2000; **95**: 3003-3004 [PMID: 11051401 DOI: 10.1111/j.1572-0241.2000.03228.x]

20 **Worthley DL**, Rayner CK, Devitt PG, Fraser R. Gastric hemorrhage as a late complication of splenic artery aneurysm repair: a dramatic way to vent one's spleen. *J Gastroenterol Hepatol* 2003; **18**: 604-605 [PMID: 12702057 DOI: 10.1046/j.1440-1746.2003.03012.x]

21 **Cyrany J**, Kopáčová M, Rejchrt S, Krajina A, Bureš J. Gastric arterial bleeding secondary to chronic occlusion of the splenic artery. *Folia Gastroenterol Hepatol* 2004; **2**: 92-98

22 **Cyrany J**, Kopacova M, Rejchrt S, Jirkovsky V, Al-Tashi M, Bures J. Gastric arterial bleeding secondary to chronic occlusion of the splenic artery (with video). *Gastrointest Endosc* 2010; **71**: 1335; author reply 1336 [PMID: 20598266 DOI: 10.1016/j.gie.2009.09.039]

23 **Mnatzakanian G**, Smaggus A, Wang CS, Common AA, Jeejeebhoy KN. Splenic artery collaterals masquerading as gastric fundal varices on endoscopy: a sticky situation. *Gastrointest Endosc* 2008; **67**: 751-755 [PMID: 18206881 DOI: 10.1016/j.gie.2007.09.044]

24 **Saddekni S**, Abdel-Aal AK, Oser RF, Underwood E, Bag A. Transcatheter embolization of extensive left gastric artery collaterals presenting with massive upper gastrointestinal bleed. *Vasc Endovascular Surg* 2012; **46**: 480-483 [PMID: 22669265 DOI: 10.1177/1538574412449908]

25 **Al-Balas H**, Metwalli ZA, Sada DM. Chronic splenic artery occlusion with gastric wall arterial ectasia, an unusual cause of massive upper gastrointestinal hemorrhage. *BJR Case Rep* 2021; **7**: 20200194 [PMID: 34131504 DOI: 10.1259/bjrcr.20200194]

26 **von Trotha KT**, Binnebösel M, Truong S, Behrendt FF, Wasmuth HE, Neumann UP, Jansen M. Severe gastric variceal haemorrhage due to splenic artery thrombosis and consecutive arterial bypass. *BMC Surg* 2011; **11**: 14 [PMID: 21711534 DOI: 10.1186/1471-2482-11-14]

27 **Arslan S**, Onur MR, Akpınar E. A rare cause of upper gastrointestinal hemorrhage: chronic thrombosis of the splenic artery. *Turk J Gastroenterol* 2017; **28**: 221-222 [PMID: 28316323 DOI: 10.5152/tjg.2017.16745]



Published by **Baishideng Publishing Group Inc**
7041 Koll Center Parkway, Suite 160, Pleasanton, CA 94566, USA
Telephone: +1-925-3991568
E-mail: bpgoffice@wjgnet.com
Help Desk: https://www.f6publishing.com/helpdesk
https://www.wjgnet.com

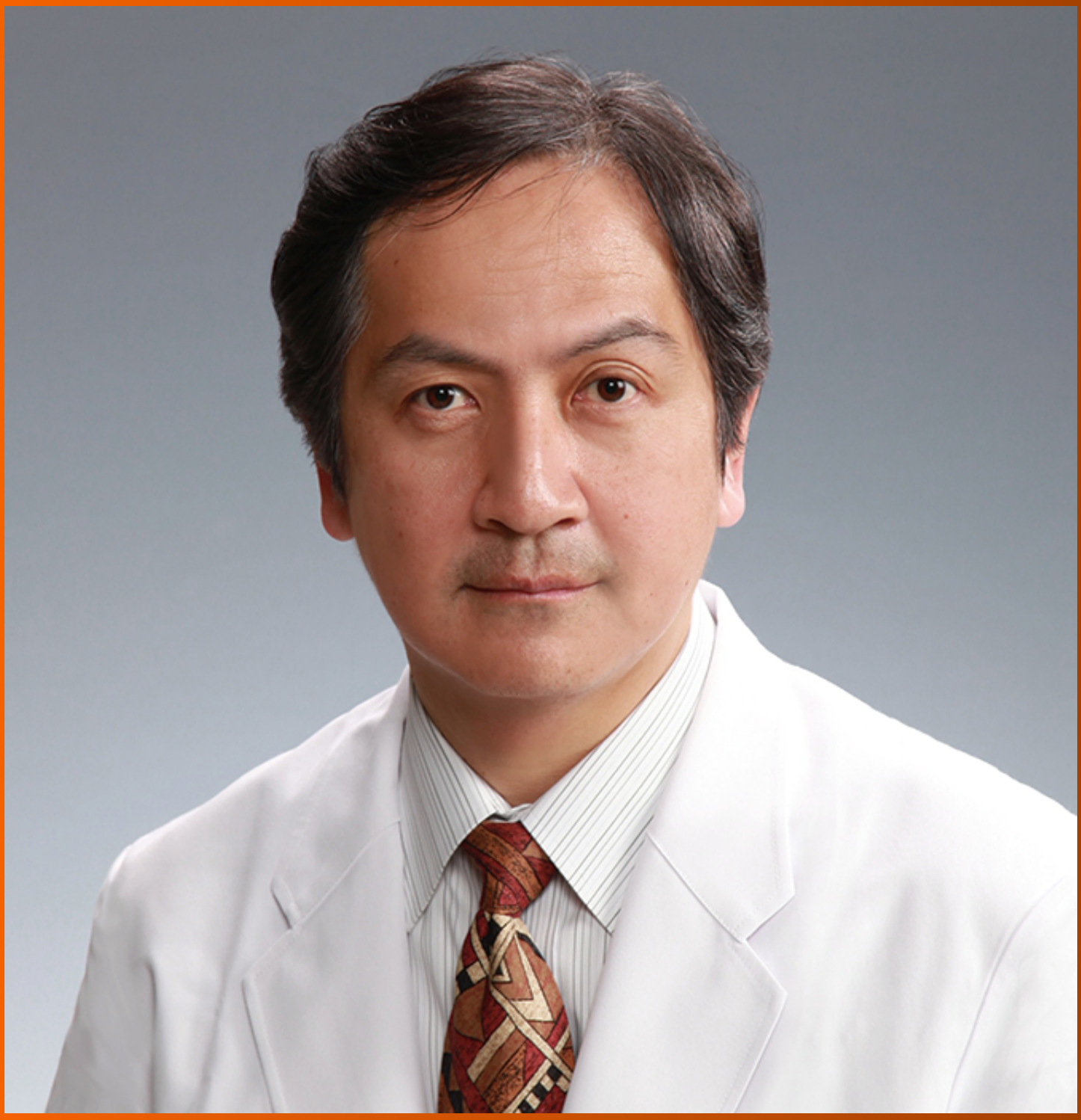


© 2022 Baishideng Publishing Group Inc. All rights reserved.

ISSN 1007-9327 (print)
ISSN 2219-2840 (online)

World Journal of *Gastroenterology*

World J Gastroenterol 2022 October 14; 28(38): 5515-5657



Published by Baishideng Publishing Group Inc

World Journal of Gastroenterology

Contents

Weekly Volume 28 Number 38 October 14, 2022

REVIEW

5515 Gastrointestinal and liver disease in patients with schizophrenia: A narrative review

Grant RK, Brindle WM, Donnelly MC, McConville PM, Stroud TG, Bandieri L, Plevris JN

MINIREVIEWS

5530 Ultrasound-based artificial intelligence in gastroenterology and hepatology

Liu JQ, Ren JY, Xu XL, Xiong LY, Peng YX, Pan XF, Dietrich CF, Cui XW

5547 Oxidative stress bridges the gut microbiota and the occurrence of frailty syndrome

Chen SY, Wang TY, Zhao C, Wang HJ

ORIGINAL ARTICLE

Basic Study

5557 Effect of low-dose radiation on thyroid function and the gut microbiota

Tong JY, Jiang W, Yu XQ, Wang R, Lu GH, Gao DW, Lv ZW, Li D

5573 Hypoxia inducible factor 1α promotes interleukin-1 receptor antagonist expression during hepatic ischemia-reperfusion injury

Wang ZY, Liu Y, Li SP, Li JJ, Zhang Z, Xiao XC, Ou Y, Wang H, Cai JZ, Yang S

Retrospective Cohort Study

5589 No long-term survival benefit with sustained-release 5-fluorouracil implants in patients with stages II and III gastric cancer

Wu YZ, Wu M, Zheng XH, Wang BZ, Xue LY, Ding SK, Yang L, Ren JS, Tian YT, Xie YB

5602 Timing of endoscopic retrograde cholangiopancreatography in the treatment of acute cholangitis of different severity

Huang YC, Wu CH, Lee MH, Wang SF, Tsou YK, Lin CH, Sung KF, Liu NJ

Retrospective Study

5614 Clearance of the liver remnant predicts short-term outcome in patients undergoing resection of hepatocellular carcinoma

Miki A, Sakuma Y, Ohzawa H, Saito A, Meguro Y, Watanabe J, Morishima K, Endo K, Sasanuma H, Shimizu A, Lefor AK, Yasuda Y, Sata N

5626 A new scoring system to evaluate adjuvant chemotherapy for patients with T2N0M0 gastric cancer after D2 gastrectomy

Xu Q, Kang WZ, Xiong JP, Shao XX, Li WK, Hu HT, Tian YT

World Journal of Gastroenterology

Weekly Volume 28 Number 38 October 14, 2022

Contents

Observational Study

5636 Red blood cell distribution width derivatives in alcohol-related liver cirrhosis and metabolic-associated fatty liver disease

Michalak A, Guz M, Kozicka J, Cybulski M, Jeleniewicz W, Lach T, Cichoż-Lach H

SCIENTOMETRICS

5648 Comparison of evaluation indexes for Gastroenterology and Hepatology journals in different databases

Li JY, Yan ZH, Xiang Z, Gao C, Wu J

ABOUT COVER

Editorial Board of *World Journal of Gastroenterology*, Shunji Fujimori, AGAF, MD, PhD, Director, Department of Gastroenterology, Chiba Hokusoh Hospital, Nippon Medical School, Chiba 270-1694, Japan. s-fujimori@nms.ac.jp

AIMS AND SCOPE

The primary aim of *World Journal of Gastroenterology* (*WJG*, *World J Gastroenterol*) is to provide scholars and readers from various fields of gastroenterology and hepatology with a platform to publish high-quality basic and clinical research articles and communicate their research findings online. *WJG* mainly publishes articles reporting research results and findings obtained in the field of gastroenterology and hepatology and covering a wide range of topics including gastroenterology, hepatology, gastrointestinal endoscopy, gastrointestinal surgery, gastrointestinal oncology, and pediatric gastroenterology.

INDEXING/ABSTRACTING

The *WJG* is now abstracted and indexed in Science Citation Index Expanded (SCIE, also known as SciSearch®), Current Contents/Clinical Medicine, Journal Citation Reports, Index Medicus, MEDLINE, PubMed, PubMed Central, Scopus, Reference Citation Analysis, China National Knowledge Infrastructure, China Science and Technology Journal Database, and Superstar Journals Database. The 2022 edition of Journal Citation Reports® cites the 2021 impact factor (IF) for *WJG* as 5.374; IF without journal self cites: 5.187; 5-year IF: 5.715; Journal Citation Indicator: 0.84; Ranking: 31 among 93 journals in gastroenterology and hepatology; and Quartile category: Q2. The *WJG*'s CiteScore for 2021 is 8.1 and Scopus CiteScore rank 2021: Gastroenterology is 18/149.

RESPONSIBLE EDITORS FOR THIS ISSUE

Production Editor: *Hua-Ge Yu*; **Production Department Director:** *Xu Guo*; **Editorial Office Director:** *Jia-Ru Fan.*

NAME OF JOURNAL
World Journal of Gastroenterology

ISSN
ISSN 1007-9327 (print) ISSN 2219-2840 (online)

LAUNCH DATE
October 1, 1995

FREQUENCY
Weekly

EDITORS-IN-CHIEF
Andrzej S Tarnawski

EDITORIAL BOARD MEMBERS
http://www.wjgnet.com/1007-9327/editorialboard.htm

PUBLICATION DATE
October 14, 2022

COPYRIGHT
© 2022 Baishideng Publishing Group Inc

INSTRUCTIONS TO AUTHORS
https://www.wjgnet.com/bpg/gerinfo/204

GUIDELINES FOR ETHICS DOCUMENTS
https://www.wjgnet.com/bpg/GerInfo/287

GUIDELINES FOR NON-NATIVE SPEAKERS OF ENGLISH
https://www.wjgnet.com/bpg/gerinfo/240

PUBLICATION ETHICS
https://www.wjgnet.com/bpg/GerInfo/288

PUBLICATION MISCONDUCT
https://www.wjgnet.com/bpg/gerinfo/208

ARTICLE PROCESSING CHARGE
https://www.wjgnet.com/bpg/gerinfo/242

STEPS FOR SUBMITTING MANUSCRIPTS
https://www.wjgnet.com/bpg/GerInfo/239

ONLINE SUBMISSION
https://www.f6publishing.com

© 2022 Baishideng Publishing Group Inc. All rights reserved. 7041 Koll Center Parkway, Suite 160, Pleasanton, CA 94566, USA

E-mail: bpgoffice@wjgnet.com https://www.wjgnet.com

World Journal of Gastroenterology

Submit a Manuscript: https://www.f6publishing.com

World J Gastroenterol 2022 October 14; 28(38): 5515-5529

DOI: 10.3748/wjg.v28.i38.5515

ISSN 1007-9327 (print) ISSN 2219-2840 (online)

REVIEW

Gastrointestinal and liver disease in patients with schizophrenia: A narrative review

Rebecca K Grant, William M Brindle, Mhairi C Donnelly, Pauline M McConville, Thomas G Stroud, Lorenzo Bandieri, John N Plevris

Specialty type: Gastroenterology and hepatology

Provenance and peer review: Unsolicited article; Externally peer reviewed.

Peer-review model: Single blind

Peer-review report's scientific quality classification

Grade A (Excellent): A
Grade B (Very good): B
Grade C (Good): 0
Grade D (Fair): 0
Grade E (Poor): 0

P-Reviewer: Garbuzenko DV, Russia; Radhakrishnan R, New Zealand

Received: July 18, 2022
Peer-review started: July 18, 2022
First decision: August 19, 2022
Revised: August 29, 2022
Accepted: September 21, 2022
Article in press: September 21, 2022
Published online: October 14, 2022

Rebecca K Grant, William M Brindle, Mhairi C Donnelly, John N Plevris, The Centre for Liver and Digestive Disorders, Royal Infirmary of Edinburgh, Edinburgh, EH16 4SA, United Kingdom

Pauline M McConville, Thomas G Stroud, Lorenzo Bandieri, General Adult Psychiatry, Royal Edinburgh Hospital, Edinburgh, EH10 5HF, United Kingdom

Corresponding author: Rebecca K Grant, BSc, MA, MBChB, MSc, The Centre for Liver and Digestive Disorders, Royal Infirmary of Edinburgh, 51 Little France Cres, Old Dalkeith Rd, Edinburgh, EH16 4SA, United Kingdom. rebecca.x.grant@nhs.scot

Abstract

Schizophrenia is a severe mental illness which can have a devastating impact on an individual's quality of life. Comorbidities are high amongst patients and life expectancy is approximately 15 years less than the general population. Despite the well-known increased mortality, little is known about the impact of gastrointestinal and liver disease on patients with schizophrenia. We aimed to review the literature and to make recommendations regarding future care. Literature searches were performed on PubMed to identify studies related to gastrointestinal and liver disease in patients with schizophrenia. High rates of chronic liver disease were reported, with Non-Alcoholic Fatty Liver Disease being of particular concern; antipsychotics and metabolic syndrome were contributing factors. Rates of acute liver failure were low but have been associated with antipsychotic use and paracetamol overdose. Coeliac disease has historically been linked to schizophrenia; however, recent research suggests that a causal link is yet to be proven. Evidence is emerging regarding the relationships between schizophrenia and peptic ulcer disease, inflammatory bowel disease and irritable bowel syndrome; clinical vigilance regarding these conditions should be high. Patients with schizophrenia poorly engage with bowel cancer screening programmes, leading to late diagnosis and increased mortality. Clozapine induced constipation is a significant issue for many patients and requires close monitoring. There is a significant burden of gastrointestinal and liver disease amongst patients with schizophrenia. Better levels of support from all members of the medical team are essential to ensure that appropriate, timely care is provided.

Key Words: Schizophrenia; Gastrointestinal disease; Liver disease; Mental health

©The Author(s) 2022. Published by Baishideng Publishing Group Inc. All rights reserved.

Core Tip: We report significant rates of liver disease, particularly Non-alcoholic Fatty Liver Disease, in patients with schizophrenia, in addition to emerging evidence regarding the prevalence of lower gastrointestinal disease and peptic ulcer disease. We have clearly demonstrated the importance of a multidisciplinary approach to management and propose recommendations to ameliorate future care of this vulnerable group of patients.

Citation: Grant RK, Brindle WM, Donnelly MC, McConville PM, Stroud TG, Bandieri L, Plevris JN. Gastrointestinal and liver disease in patients with schizophrenia: A narrative review. *World J Gastroenterol* 2022; 28(38): 5515-5529
URL: https://www.wjgnet.com/1007-9327/full/v28/i38/5515.htm
DOI: https://dx.doi.org/10.3748/wjg.v28.i38.5515

INTRODUCTION

Schizophrenia is a complex and frequently devastating illness, worldwide prevalence of which is estimated to be at 0.32%[1]. It is well established that patients with schizophrenia often suffer from a large number of comorbidities, with high rates of alcohol and substance misuse[2]. Life expectancy amongst patients has also been demonstrated to be approximately 15 years shorter than that of the general population[3].

Although the general rate of comorbidities is acknowledged to be high, no comprehensive review currently exists regarding the burden and distribution of gastrointestinal and liver disease amongst this cohort. This is particularly relevant in light of the coronavirus disease 2019 pandemic, as already marginalised patients may have become more isolated from services and only present when seriously unwell. This subject is of importance to gastroenterologists and hepatologists, in addition to general medical physicians, in order to better understand the particular risks associated with these patients and to help ensure that optimal inpatient and outpatient care is provided. It is also relevant to community and inpatient psychiatric teams to highlight when prompt referrals to specialists may be required.

In this review we summarise the available evidence regarding different aspects of gastrointestinal and liver disease in patients with schizophrenia (Figure 1) in a clear and systematic manner, highlighting key findings, and suggesting recommendations (Table 1) regarding the management of each illness to better inform the future care of this vulnerable group of patients. All articles referenced in this review were identified following a PubMed search for literature specifically considering both gastrointestinal and/or liver disease in patients who had a diagnosis of schizophrenia.

CHRONIC LIVER DISEASE

Chronic liver disease (CLD) has consistently been demonstrated to have a higher prevalence amongst those with schizophrenia than amongst the general population. Carney *et al*[2] reported that people with schizophrenia were 4.42 times more likely than healthy controls to have a diagnosis of CLD; amongst a population of veterans, Fuller *et al*[4] reported an eightfold (8.73) increased likelihood of CLD, and Hsu *et al*[5] have also noted a significantly higher prevalence and incidence of CLD than in the general population. Furthermore, mild and severe liver disease were reported in a Danish study[6] (along with dementia) to have the highest incidence rate ratio amongst nineteen somatic chronic diseases in a cohort of 16,079 patients with schizophrenia who were hospitalised between 1995-2007. Only one study[7] has recorded no elevated risk of liver disease, however the results were adjusted for substance use disorders, which undoubtedly will have had a significant effect on results.

Given such findings, it is essential to reflect on the potential aetiology of the reported results. CLD primarily comprises non-alcoholic fatty liver disease (NAFLD), chronic viral hepatitis and alcohol related liver disease; each will presently be considered and their individual relevance to patients with schizophrenia reviewed.

Non-alcoholic fatty liver disease

Metabolic syndrome: Prior to focusing specifically on NAFLD, the importance of the broader role of metabolic syndrome must be acknowledged. Metabolic syndrome is defined as insulin resistance, impaired glucose tolerance, abdominal obesity, reduced high-density lipoprotein cholesterol levels, elevated triglycerides, and hypertension[8]. A significant association has been widely reported[9,10]

Table 1 Key recommendations

Gastrointestinal/liver disease	Recommendations
NAFLD	Regular monitoring of body mass index and triglycerides
	Encouragement of lifestyle modification
	Liver function tests performed and Fibrosis-4 scores calculated in all psychiatric inpatients and outpatients
Viral hepatitis	Routine screening for viral hepatitis during contact with mental health services
	Integrated approach between mental health, sexual health, substance misuse and specialist hepatology services
ALD	Integrated approach between mental health, substance misuse and hepatology
	Long term studies prospective studies required to fully comprehend burden of ALD
ALF	Clinicians prescribing clozapine should be aware of the potential risk of ALF and have a low threshold for checking liver enzymes and prothrombin time
	Psychiatric review of all patients presenting with POD
	For patients presenting with POD who have a pre-existing psychiatric diagnosis prompt communication must be made with community mental health teams, and appropriate follow-up arranged for those with a new diagnosis
	Decisions regarding liver transplant in patients with schizophrenia must involve the multidisciplinary team and be made on a patient-by-patient basis
PUD	Encouragement of lifestyle modification, particular smoking cessation and alcohol reduction
	Physicians to have a high suspicion for *Helicobacter pylori* infection
Coeliac disease	Large-scale studies amongst diverse population required
	Diagnosis to be considered in patients with schizophrenia presenting with malabsorption
Colorectal cancer	Supporting patients to participate in screening programmes and to attend follow-up appointments is key
IBD	Increased vigilance amongst clinicians regarding a potential diagnosis of IBD is central in enabling prompt diagnosis and maintenance of remission
IBS	Patients should be directly questioned concerning IBS symptoms when undergoing physical health review as many cases may go unrecognised
Clozapine induced constipation	Lifestyle advice to reduce risk
	Regular screening and escalation to GP/secondary care as appropriate
	Physicians to be aware of clozapine as potential cause of constipation and to discuss with psychiatry if considering dose adjustment/cessation

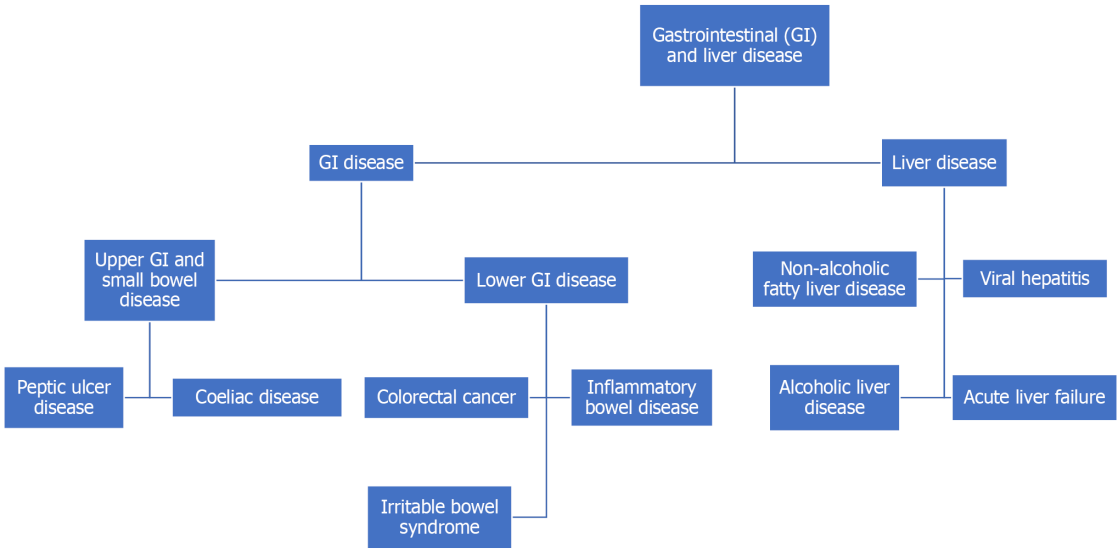
NAFLD: Non-alcoholic fatty liver disease; ALD: Alcohol related liver disease; ALF: Acute liver failure; POD: Paracetamol overdose; PUD: Peptic ulcer disease; IBD: Inflammatory bowel disease; IBS: Irritable bowel syndrome; GP: General practitioner.

between major psychiatric disorders and metabolic syndrome; a prevalence of 32.5% was recorded in a 2013 meta-analysis[11] of patients with schizophrenia and related disorders. An unhealthy lifestyle[12] and use of antipsychotics[13] have been cited as contributing factors to its development in this group.

Definition: The development of NAFLD is associated with obesity, insulin resistance, and type 2 diabetes mellitus and it therefore may be viewed as the hepatic manifestation of metabolic syndrome. NAFLD is characterised by excessive hepatic fat accumulation, which is defined as the presence of steatosis in > 5% of hepatocytes[9]. For a diagnosis of NAFLD to be made, steatosis secondary to factors including hepatitis C, alcohol use, genetics, medications and toxins must first be excluded. NAFLD is reported to have a prevalence amongst the general population of 20% to 30%[14].

Role of antipsychotic medications: The metabolic side effects of antipsychotic medications are well-established, with clozapine and olanzapine in particular being related to weight gain, hyperglycaemia and dyslipidaemia[15]. Understandably, therefore, much of the research into NAFLD and schizophrenia has focused on the potential role of these medications in its development.

A 2016 prospective Spanish study[16] involving 191 patients with a first episode of schizophrenia (94.2% of which were antipsychotic naïve), reported that 25.1% (48/191) of patients demonstrated a fatty liver index (FLI) result suggestive of the presence of steatosis after three years of antipsychotic treatment; none of the included patients had steatosis at index abdominal ultrasound scan (AUSS). The patients in the study were randomised to aripiprazole, risperidone, quetiapine and ziprasidone; the



DOI: 10.3748/wjg.v28.i38.5515 **Copyright** ©The Author(s) 2022.

Figure 1 Summary of gastrointestinal and liver disease in patients with schizophrenia. GI: Gastrointestinal.

dose and type of antipsychotic changed throughout the follow-up period and results were not stratified according to medications. There was no control group. This study is unique in that it prospectively demonstrated the development of NAFLD following the initiation of antipsychotics; the other studies considered hereafter have focused on NAFLD in patients already established on treatment regimes.

In a cohort of 253 patients with schizophrenia, Koreki *et al*[17] reported that 42.7% (108/253) were found to have steatosis on AUSS. All patients included in this study were on at least one antipsychotic treatment (duration was not specified); on univariate analysis total antipsychotic dose (all daily doses were calculated based on chlorpromazine equivalents) was noted to be significantly associated with the presence of steatosis (P = 0.009). On regression analysis, doses of antipsychotic medications recognised as carrying an increased risk of metabolic syndrome and hyperprolactinaemia were significantly associated with NAFLD (P = 0.049 and P = 0.041 respectively). A comparably high prevalence of NAFLD was also reported in a 2017 Chinese study[18] which compared 202 male patients aged 18-35 with schizophrenia and on antipsychotics for at least one month to 149 controls. 49.5% (100/202) of the schizophrenia group had steatosis on AUSS, compared with 20.1% (30/149) of the control group. Although NAFLD prevalence amongst inpatients with schizophrenia was not as high (22.44%) as in the aforementioned studies, in another 2021 Chinese study[19] comprising 66,273 patients with "mental disorders", it was still higher than amongst those with bipolar affective disorder (17.89%), depressive disorder (12.62%) and other mental disorders (12.99%) and was demonstrated to be associated with antipsychotic treatment.

The highest reported prevalence of NAFLD was recorded in a 2021 Taiwanese study[20] which considered 182 patients with schizophrenia who had been hospitalised for at least two years and been on antipsychotic treatment for at least one year. 70.8% (129/182) were diagnosed with steatosis on AUSS; results were stratified according to antipsychotic generation and cumulative dose (using chlorpromazine equivalents), however no significant association between these and NAFLD were demonstrated. Given the reported increased association of NAFLD with second generation antipsychotics[15], the authors attribute the disparity in their results to population demographics and sample size. Interestingly, antipsychotic treatment duration, potentially the biggest contributor to the reported results in this cohort, was not reported in the results.

Rates of NAFLD have also been reported in studies not specifically considering antipsychotic therapies. In a population of veterans in the United States[4], those with a diagnosis of schizophrenia were significantly more likely to be diagnosed with NAFLD ($P \leq 0.001$) and in a cross-sectional Danish study[21] 21.4% (31/145) were diagnosed with moderate-severe steatosis on non-enhanced CT. In these studies, significant associations were however demonstrated with metabolic syndrome, suggesting (although not confirming due to lack of data) that antipsychotics may also be potentially playing a role in these reported results.

Lifestyle and negative symptoms: While research has predominantly focused on the close links between antipsychotics and NAFLD, it is also important to briefly consider potential alternative aetiologies that have been proposed.

Patients with schizophrenia are acknowledged as being at higher risk of an unhealthy lifestyle compared to the general population[17]. They may have an unbalanced diet, poor self-care, avoid certain foods due to paranoid delusions or hallucinations, and withdraw from physical and social

activities, leading to a lack of exercise[22]. Yan *et al*[18] in their 2017 study emphasised the role of negative symptoms in young men with schizophrenia and NAFLD; a negative factor score in the Positive and Negative Syndrome Scale (PANSS) was significantly associated with a NAFLD diagnosis ($P = 0.025$). It is not challenging to understand how the negative symptoms of anhedonia, poor attention, low motivation, apathy and social withdrawal may lead to obesity and the associated sequelae of metabolic syndrome.

Recommendations: It is evident that a diagnosis of schizophrenia carries with it a significant risk of developing NAFLD, both due to treatment with antipsychotics and also due to the intrinsic nature of the illness itself. In order to prevent progression to cirrhosis and its associated complications it is necessary to increase awareness of this risk and consider how it may be ameliorated. At the very least, body mass index (BMI) and triglycerides should be monitored regularly in all patients with schizophrenia and psychiatrists and general medical physicians should make every effort to support patients in modifying their lifestyles. Furthermore, all patients admitted to psychiatric hospitals and attending outpatient psychiatry appointments ought to have liver function tests performed and Fibrosis-4 (Fib-4) scores calculated to determine if a referral to hepatology is necessary.

Chronic viral hepatitis-hepatitis B and hepatitis C

People with serious mental illness (including schizophrenia) have been shown to be at increased risk of blood borne viruses (BBVs)[23]. A significant minority of patients with schizophrenia engage in risky behaviour (unprotected sex with multiple partners, sex work, and intravenous drug use) putting them at risk of infection; they are also more likely to live in shared accommodation and may share personal equipment such as razors and toothbrushes, carrying a potential increased risk of hepatitis B and C transmission[23]. Patients with hepatitis B and C have an increased risk of developing hepatocellular carcinoma[24], therefore adequate treatment and monitoring of the conditions is vital.

In 2017 a Swedish study[25] considered the prevalence and risk factors for BBVs amongst people with severe mental illness; when compared with healthy controls, those with schizophrenia were significantly more likely to have either a diagnosis of hepatitis B ($P \leq 0.001$) or hepatitis C ($P \leq 0.001$). A history of substance misuse was noted as having contributed the most to the risk of developing a BBV ($P \leq 0.001$). Increased prevalence of hepatitis C was also shown in a study of veterans[4] diagnosed with schizophrenia when compared to controls ($P \leq 0.001$). Substance use disorder and alcohol use disorder were identified as significant risk factors for development of schizophrenia ($P \leq 0.001$ and $P \leq 0.001$ respectively). A small study performed in Boston[26] identified eight patients with hepatitis C out of a total cohort of 98 patients (8.2%) treated with clozapine; one was a confirmed intravenous drug user, three had a history of polysubstance misuse and in the remaining four patients no risk factors were identified. A further small Canadian study[27] reported a hepatitis C rate of 2.7% (3/110) of clozapine-treated patients. Two of the three patients diagnosed with hepatitis C had a history of intravenous drug use.

Outcomes in patients with schizophrenia diagnosed with hepatitis C and hepatitis B were considered in a 2021 Chinese study[24]. From a total cohort of 15,914 patients with newly diagnosed schizophrenia between 2007 and 2013, 614 patients were identified with viral hepatitis and were matched with 1228 controls. The primary outcome measure was the incidence and risk of "severe hepatic outcomes" (SHOs), including liver cancer, failure and decompensation. The viral hepatitis group were significantly more likely to develop SHOs ($P \leq 0.001$) than the control group; a total of 26 patients with viral hepatitis developed SHOs (20/26 Liver decompensation, 3/26 Liver failure, and 3/26 Liver cancer).

Recommendations: While the risk of viral hepatitis amongst people with schizophrenia cannot be disputed, optimal management of it is challenging. Routine screening for viral hepatitis during contact with mental health services would allow an opportunity for discussion about safe sex and drug use, it may also prompt consent to other tests (such as HIV), leading to the discovery of potentially treatable illnesses, and, crucially, a positive result may allow prevention of further liver damage[26]. If diagnosed, encouragement of treatment adherence in this population may be difficult, therefore an integrated approach between mental health, sexual health, substance misuse[25] and specialist hepatology services would be required to aid optimal patient outcomes.

Alcohol related liver disease

A high prevalence of alcohol use disorder (AUD) has been demonstrated in patients with schizophrenia, with a recent meta-analysis reporting a lifetime prevalence of AUD of 24.3%[28]. A number of hypotheses have been put forward to explain this association, including genetic polymorphisms, poor cognitive development, poor social functioning, the effects of poverty, poor social environments and "self-medication" to gain relief from distressing symptoms[29].

Despite such a high prevalence of AUD in patients with schizophrenia, research into alcohol related liver disease (ALD) in this cohort is relatively limited with variable results. The most common manifestations of ALD are alcoholic fatty liver, acute alcoholic hepatitis and alcohol related cirrhosis of the liver. In 2014 Hsu *et al*[5] reported an increased risk of alcohol related fatty liver in patients with schizophrenia when compared with the general population ($P = 0.007$); risk of alcoholic hepatitis and cirrhosis

did not vary significantly between the two cohorts. In a 2022 Scottish study[30] of patients with schizophrenia admitted to a general hospital under the care of gastroenterology, 42.5% (17/40) of patients had a background of cirrhosis (88.2% of which had a background of alcohol excess) and 60.0% (24/40) of all patients had a history of alcohol excess. Interestingly, Fuller *et al*[4], in their 2011 study, reported schizophrenia being a protective factor (odds ratio = 0.53) in the diagnosis of alcohol related cirrhosis when a group of veterans with schizophrenia were compared to those without.

Recommendations: In common with viral hepatitis, an integrated approach between mental health, substance misuse services and specialist hepatology services is key in supporting patients with schizophrenia and alcohol use disorder. Further research, including long term prospective studies, is also required to better comprehend the burden of ALD amongst patients with schizophrenia.

ACUTE LIVER FAILURE

Acute liver failure (ALF) is a rare clinical syndrome in which the onset of liver injury, with coagulopathy and hepatic encephalopathy, occurs in a patient with no underlying CLD and previously normal liver function. The associations between ALF and schizophrenia can be considered under the following categories: ALF arising as a result of pharmacological treatment for schizophrenia, ALF arising as a consequence of mental state alteration in patients with schizophrenia and finally the implications of a diagnosis of schizophrenia on decision making around emergency liver transplantation for ALF.

Pharmacological treatments

In patients with treatment resistant schizophrenia (*i.e.*, following the failure of at least two antipsychotics, including a second-generation antipsychotic) prompt initiation of clozapine, the only remaining evidence-based treatment, is required to reduce symptoms and risk of relapse[31,32]. Clozapine acts as a dopamine and serotonin receptor antagonist. The most recognised and feared side effect of clozapine is agranulocytosis, however there are now case reports of clozapine induced ALF[33,34]. The mechanism of liver injury in this scenario is unclear, but it is idiosyncratic. A modest elevation in liver enzymes occurs in up to two thirds of patients treated with clozapine, and often resolves spontaneously[35]. Clinically apparent liver injury (with jaundice) occurs in approximately 1 in 2000 patients treated with clozapine[35] and progression to ALF (and death, or the need for emergency liver transplant) is now reported. ALF secondary to clozapine is extremely rare however, with less than five reported cases in the literature[33,34,36]. ALF has also been reported as a rare side effect of quetiapine therapy[37]; no cases of ALF have been reported with olanzapine or risperidone. Most treatment guidelines do not give clear recommendations on monitoring liver function tests in patients on clozapine and other antipsychotics, in part due to the fact that the vast majority of liver enzyme abnormalities secondary to these drugs do resolve spontaneously. Clinicians prescribing clozapine should be aware of the risk of ALF and could consider checking liver enzymes and prothrombin time when performing blood work monitoring for agranulocytosis.

Paracetamol overdose

Schizophrenia is associated with suicidal ideation[38]. In the United Kingdom, intentional paracetamol overdose is the most frequent cause of ALF. There is no clear evidence that schizophrenia is associated with an increased risk of paracetamol overdose resulting in ALF compared with the general population or patients with other psychiatric diagnoses. Scottish data have shown that of 472 patients with paracetamol overdose requiring admission to the Scottish Liver Transplant Unit who underwent formal inpatient assessment by psychiatry, schizophrenia was diagnosed or recorded in 2.8% of patients [Personal communication: Dr Roger Smyth, Consultant Liaison Psychiatrist, Royal Infirmary of Edinburgh]. In comparison, affective disorders were recorded in 16.1% and personality disorders in 6.9% of patients. One Danish study assessed the association between paracetamol (and other weak analgesic) poisoning and the subsequent diagnosis of a psychiatric disorder[39]. The risk of an admission with schizophrenia increased 3.9-fold after paracetamol poisoning and 2-fold after non-paracetamol poisoning compared with matched population controls. Patients with a previous psychiatric admission were excluded, but it is possible that patients with schizophrenia who had not required prior hospitalisation (*i.e.*, but who already had an established diagnosis) were included in the study. Furthermore, the admission with poisoning is likely to have prompted a psychiatric review and subsequent diagnosis. These data suggest that poisoning is a risk marker for a psychiatric disorder, rather than there being a causative association. Clinicians assessing patients presenting with paracetamol overdose should be aware of the risk of underlying psychiatric disorder and ensure appropriate assessments are arranged.

Interestingly, in addition to its role in treatment of paracetamol overdose, there is ongoing research into the reduction of negative symptoms and anti-suicidal properties of N-acetyl cysteine (NAC) in the treatment of schizophrenia. Chen *et al*[40] identified two placebo-controlled, double-blind, randomised

clinical trials of NAC in schizophrenia and reported that NAC may be efficacious in reducing the negative and general symptoms of schizophrenia. A meta-analysis by Zheng *et al*[41], which included three randomized control trials with 307 (N-acetylcysteine: 153, placebo: 154) participants, showed that NAC significantly improved total symptom scores in schizophrenia. Other related systematic reviews, including a Cochrane review on antioxidant treatment for schizophrenia, have also found NAC to be a promising add-on treatment for schizophrenia[42].

Emergency liver transplantation

Emergency liver transplantation may be required in patients with ALF if spontaneous recovery of sufficient liver function is deemed unlikely. Psychiatric disorders can be relative or absolute contraindications to liver transplantation, particularly if the disorder is deemed "untreatable" and may be graft threatening. A diagnosis of a psychiatric condition such as schizophrenia is relevant if it affects the prospect of survival post-transplant or affects compliance with medication and clinic follow-up. In a Scottish cohort of patients with ALF secondary to paracetamol overdose, 56.6% of patients who were rejected for listing for liver transplantation were rejected on the basis of psychiatric contraindications [43]. As described above, schizophrenia is associated with an increased risk of suicide, and this must be taken into account when considering the role of transplantation in an illness potentially arising from self-harm or parasuicide such as paracetamol overdose; the consequences of further suicidal intent must be reviewed. Specific to severe psychiatric disorders such as schizophrenia, absolute contraindications to liver transplantation include chronic, severe illness with a poor prognosis, especially if refractory to appropriate treatment. The potential impact of a diagnosis of schizophrenia on substance misuse, compliance with immunosuppression and clinic follow-up must be considered. Therefore, patients with schizophrenia being considered for emergency liver transplantation for ALF should be assessed by the wider multi-disciplinary team and decisions made on a highly individualised basis.

Recommendations: While cases of ALF are rare in patients treated with clozapine, prescribing clinicians should be aware of the potential risk and have a low threshold for checking liver enzymes and prothrombin time, particularly in patients presenting with possible symptoms of liver dysfunction such as nausea, vomiting and/or anorexia[44].

Regarding paracetamol overdose, it is essential that treating physicians are aware of the risk of a diagnosis of a psychiatric disorder and ensure patients are reviewed by psychiatric teams during their admission. For patients who have a pre-existing diagnosis prompt communication must be made with community mental health teams (CMHT), and appropriate follow-up arranged for those with a new diagnosis. The use of NAC in the treatment of schizophrenia is an emerging area of research and further evidence is required regarded its potential.

The assessment of patients with schizophrenia for liver transplant is complex. Decisions must involve the multidisciplinary team (MDT) and be made on a patient-by-patient basis.

UPPER GASTROINTESTINAL AND SMALL BOWEL DISEASE

Peptic ulcer disease and upper gastrointestinal bleeding

Upper gastrointestinal bleeding (UGIB) is the consequence of often readily treatable digestive conditions such as gastroduodenal ulcers and reflux oesophagitis progressing to a potentially fatal event; in patients with schizophrenia the risk may be heightened due to high rates of alcohol misuse, smoking and non-steroidal anti-inflammatory drug use, in addition to reluctance to present to medical services. There are relatively limited studies which have considered incidence of peptic ulcer disease (PUD) and UGI bleeds in this cohort, with evidence being inconclusive, and, at times, contradictory.

Helicobacter pylori (*H. pylori*) infection is recognised[45] as a major contributor to PUD and consequently UGIBs. Following a 1997 study by De Hert *et al*[46] and a 2005 study by Yilmaz *et al*[47] (both of which reported high rates of *H. pylori* infection in patients with schizophrenia), a Turkish group [47] discussed the role of *H. pylori* as a possible environmental contributor to the pathogenesis of schizophrenia in genetically predisposed individuals. The authors identified four mechanisms to support this theory: (1) Dopaminergic dysfunction; (2) inflammation; (3) polyunsaturated fatty acids; and (4) hyperhomocysteinaemia. With regard to dopaminergic dysfunction specifically, the authors propose that dopamine antagonists (such as commonly used antipsychotics) promote ulcer formation favouring the growth of *H. pylori*; this is a theory which is supported by Ozdemir[48] in their 2007 paper in which they propose that the lesser prevalence of PUD in their cohort of patients with schizophrenia was due to the over expression (and subsequent protective effect) of dopamine.

The reduced prevalence of PUD in patients with schizophrenia reported by Ozdemir *et al*[48] is in contrast to results reported in other studies. In 1968 Hussar[49] proposed that the incidence of PUD was at least as high amongst long term institutionalised patients with schizophrenia compared with the general population and, more recently, in 2014, Liao *et al*[50] reported an incidence of PUD that was 1.27 times higher in patients with schizophrenia than in the general population. An American study in 2014 [51] of 224,361 patients with schizophrenia, reported an incidence of bleeding ulcers amongst this cohort

as being 1.4 per 1000 person years, compared to 1.2 per 1000 person years in those without schizophrenia. Similarly increased risk of UGIB was also noted in a 2018 Danish study[52] of 39,998 patients with schizophrenia; the authors acknowledge the role that increased rates of *H. pylori* infectivity amongst patients with schizophrenia may have played in the observed results.

Recommendations: It is challenging to draw definitive conclusions regarding biological links between the aetiology of PUD and schizophrenia and more research is required before such links are established. However, it important to acknowledge the increased risk of PUD those patients with schizophrenia has due to lifestyle factors, and, as a result, ensures that help is given to aid modification. Suspicion regarding the presence of *H. pylori* should also be high, particularly as it may have the potential to contribute to mortality through a catastrophic UGIB or the development of gastric cancer[53].

Coeliac disease

Coeliac disease is an autoimmune disease which is triggered by gluten peptides in wheat, rye, barley and other grains. Histologically it is characterised by villous atrophy, hypertrophy of intestinal crypts and increased lymphocytes in the epithelium and lamina propria[54]. This results in malabsorption and the associated bloating, pain and diarrhoea in sufferers. Current prevalence of coeliac disease is estimated at 1% of the general population[54].

Historical perspective: A potential association between coeliac disease (or gluten intolerance) and schizophrenia is one which has long since interested researchers[55], with Bender[56] first reporting in 1953 that children with schizophrenia were more likely to have coeliac disease. This was then followed by the publication of a case series on five patients with schizophrenia with coeliac disease who were admitted to a psychiatric hospital during the same year[57]. Dohan was particularly prolific in the publication of papers regarding coeliac disease and schizophrenia, with results variably showing reduced prevalence of schizophrenia in areas of low grain consumption and an improvement in the symptoms of schizophrenia following the initiation of a gluten free diet[58-62].

Current status: More recent research has focused on the risk of patients with coeliac disease developing schizophrenia as opposed to prevalence of coeliac disease amongst those with schizophrenia; nevertheless, the strength of an association between the two conditions may be extrapolated from the available evidence. A 2018 meta-analysis[63] of the four most recent epidemiological studies[64-67] reported a significantly higher risk (two-fold) of schizophrenia in those with coeliac disease when compared with controls. Of the four studies, three[64,66,67] reported a significant association and one [65] did not (in common with an earlier British study[68]). The authors of the meta-analysis acknowledge that the mechanism underlying this association is unclear, however propose the following potential explanations: (1) There is high prevalence of folate deficiency in individuals with coeliac disease, given the important role of folate in DNA methylation, aberrant methylation may contribute to the development of schizophrenia; (2) schizophrenia may share a genetic diathesis with coeliac disease; and (3) diagnoses of schizophrenia in patients with coeliac disease may be resulting from surveillance bias as those with coeliac will present more often to physicians due to their chronic illness requiring regular follow-up. Since the publication of the meta-analysis, a small study[69] of 16 patients with IgG antigliadin antibodies (raised in coeliac disease) has also demonstrated an improvement in psychiatric patients with schizophrenia or schizoaffective disorder with a gluten free diet; a larger scale clinical trial is planned.

Recommendations: While research into a possible link between coeliac disease and schizophrenia has previously relied on relatively small case reports and series, more recently trial evidence has emerged to strengthen the association. Proof of a causal relationship between the two remains unclear and further large-scale studies, amongst more diverse populations, are required. Nevertheless, current evidence does serve to increase awareness of the likelihood of a diagnosis of coeliac disease amongst patients with schizophrenia presenting with symptoms of malabsorption.

LOWER GASTROINTESTINAL DISEASE

Colorectal cancer

Evidence regarding rates of cancer mortality in patients with schizophrenia has historically been contradictory, with some studies reporting lower or similar risk of cancer mortality compared to the general population[70-72], while others have reported higher rates[73-75]. Regarding colorectal cancer, however, a recent systematic review and meta-analysis[76] found that patients with schizophrenia had a significantly higher risk of mortality, with male patients having a relative risk of 1.90 and female patients 2.42. Increased risk of colorectal cancer[77] was also reported in a 2007 study. As in the general population, screening is vital in promoting earlier diagnosis and reducing mortality; a 2018 Japanese study[78] reported a rate of participation in colorectal cancer screening of 13.4% in patients with schizophrenia (in contrast to 47.8% of men and 40.9% of women in the general population[79]). The benefit of

case management interventions, in the form of three counselling sessions to support adherence to screening, was demonstrated in a 2021 Japanese study[79], which showed a 35.3% increase in participation amongst the case management group.

Recommendations: As reported in the 2021 study[79], participation in screening programmes is key to reducing mortality from colorectal cancer amongst patients with schizophrenia to be in line with the general population. Supporting patients to participate in screening and attend potential follow-up procedures is essential to address the disparity between colorectal cancer mortality in this cohort when compared to the general population.

Inflammatory bowel disease

Crohn's disease (CD) and ulcerative colitis (UC) are the two main types of inflammatory bowel disease (IBD) and are characterised by chronic inflammation - in the case of UC it is limited to the mucosa of colon and rectum, and, in CD, it is transmural and extends potentially to the whole GI tract. Symptoms of both conditions include diarrhoea, abdominal pain and extreme fatigue. Prevalence of IBD is increasing and is projected to reach 1% by 2028[80].

The relationship between IBD and schizophrenia has been explored in a small number of studies, with variable results. Bernstein *et al*[81] reported an increased incidence of schizophrenia amongst patients with CD but not with UC, whereas no increased risk in either form of IBD was demonstrated by West *et al*[68]; a Swedish study actually noted a diminished risk of schizophrenia in those with IBD[82].

In contrast to earlier studies which focused on risk of schizophrenia in IBD patients, a recent study from Taiwan[83] considered risk of a new IBD diagnosis amongst patients with a diagnosis of schizophrenia. It included 116,164 patients with schizophrenia and 464,656 matched controls and concluded that overall incidence of IBD was significantly higher amongst the schizophrenia cohort (1.14% *vs* 0.25%); risk was also higher amongst those with more severe schizophrenia. These findings are potentially supportive of research suggestive of shared genetic susceptibility between the two conditions[84,85], although the role of diet and microbiota remain important confounding factors.

Recommendations: CD and UC are challenging conditions to manage, this risk is heightened in vulnerable patients with schizophrenia as engagement with health services is essential for positive outcomes. As recommended by the authors of the recent Taiwanese study[83], increased vigilance amongst clinicians and other members of the MDT regarding potential cases of IBD may prove vital in enabling prompt diagnoses and maintenance of remission.

Irritable bowel syndrome

Irritable bowel syndrome (IBS) is a functional gastrointestinal disorder characterised by abdominal pain, bloating and a change in bowel habit [either constipation (IBS-C), or, more commonly, diarrhoea (IBS-D)]; diagnosis is made based on the Rome IV criteria. Current prevalence of IBS in the United Kingdom is estimated to be at 14%[86].

The first study to consider IBS in patients with schizophrenia was published in 1997[87]. The authors reported that 19% of the patients with schizophrenia met the diagnostic criteria for IBS, compared with 2.5% of those in the control group. It must however be acknowledged that the study only included 87 patients in total. Interestingly, it was noted that the patients with schizophrenia did not complain of symptoms of IBS, unlike when the authors considered a group of patients with anxiety and depressive disorder; the authors attributed this to a preoccupation with delusions and hallucinations or being due to apathy resulting from negative symptoms.

A further study[88] comprising 134 patients with schizophrenia reported IBS in 48.8%; the study also reported higher rates of IBS-D in patients presenting with positive symptoms of schizophrenia, IBS-C and alternating IBS-D/C were more common in those with negative symptoms. The group was not compared to a control, which makes conclusions limited.

Recommendations: Research suggests that there may be an under-reporting of IBS symptoms amongst patients with schizophrenia. Consideration should therefore be given to IBS symptomatology in patients with schizophrenia undergoing physical health review as many cases may go unrecognized unless patients are directly questioned. Addressing diet and lifestyle factors are also important in improving the quality of life in patients with schizophrenia and IBS symptoms.

Clozapine induced constipation

Whilst recognising it as a side effect of clozapine treatment as opposed to a disease in itself, it is necessary to acknowledge the risk of clozapine induced constipation in patients with schizophrenia. Risk of constipation is greatest in the first four months following treatment initiation, however may occur at any time[89]. A 2016 systematic review and meta-analysis[90] of 11 studies reported a prevalence of clozapine induced constipation of 31.2%. The authors attribute increased risk of constipation to the anti-muscarinic and anti-histaminergic effects of the drug, as well as to a sedentary lifestyle, dehydration, obesity and a diet which is low in fibre. Complications of constipation such as bowel obstruction, ileus (a Danish study[91] reported a 0.8% incidence of ileus in clozapine treated

patients) and toxic megacolon may be life threatening; in severe constipation the case fatality rate has been documented at approximately 20%-30%[89]. Following the aforementioned systematic review and meta-analysis[90], subsequent studies and case reports[92-96] have also reported similarly high incidence of clozapine induced constipation and gastrointestinal hypomotility, highlighting the ongoing significance of this issue.

Recommendations: Given the high prevalence of clozapine-induced constipation, all patients on clozapine should be given lifestyle advice to help prevent the development of constipation. It is crucial to screen for its presence during CMHT review (regular attendance at clozapine blood monitoring may help to facilitate this) and it is particularly important to ask directly about it as incidence may be underreported by patients. Patients may be referred to their general practitioner (GP) for prescription of laxatives and ongoing monitoring if constipation is present, in addition to plasma clozapine levels being reviewed by the CMHT; if there are features concerning for obstruction prompt referral to secondary care is required.

Caution should be exercised in the prescription of anti-cholinergics for hypersalivation (a known side effect of clozapine) due to their potential to contribute to constipation; other regular medications with constipating side effects should also be kept under close review. For secondary care physicians it is important to be aware of clozapine as a potential cause of constipation and essential to seek advice from colleagues in psychiatry if dose adjustment or treatment cessation is being considered.

GUT MICROBIOME AND SCHIZOPHRENIA

In consideration of gastrointestinal disease in schizophrenia it is important lastly to acknowledge an emerging area of active research - the gut microbiome. The gut microbiome in humans comprises a diverse population of microbes, the most numerous of which are reported to be Bacteroidetes and Firmicutes[97]. Factors such as diet, smoking and social circumstances have been suggested to influence the composition of an individual's developing microbiome. While each microbiome is unique, when the microbial composition differs significantly from controls, it is referred to as dysbiosis. Alterations in gut microbiota have been demonstrated to be implicated in several psychiatric illnesses, including depression, addiction and eating disorders. Evidence is now emerging regarding the potential role of gut dysbiosis in the aetiology of schizophrenia and the use of pre and probiotics in treatment pathways is also being explored.

In 2020 Szeligowski *et al*[98] performed a narrative review of research considering the differences in microbiome between healthy controls and patients with schizophrenia; six studies were identified. The authors reported only one consistent finding between the studies-that patients with schizophrenia had significantly elevated Lactobacilli, which also correlated with symptom severity. As Lactobacilli are typically thought to be beneficial for gut health, this finding was attributed to the existence of different subtypes. The authors conclude that different exclusion criteria, stage of illness and treatments make definitive conclusions regarding the role of dysbiosis in schizophrenia challenging and further larger scale prospective studies are required.

Pre and probiotics are also being investigated for their ability to reduce the effect of antipsychotic medications on the microbiome which can lead to potentially life- threatening constipation and significant weight gain. Results of small studies which have been reported in reviews of the literature [98-101] are encouraging, for example co-administration of prebiotics to olanzapine treated rats led to attenuation of weight gain[102]. As with the role of dysbiosis in the aetiology of schizophrenia, more detailed studies in human subjects are of course needed but early results do suggest this may be a promising area for future treatment.

CONCLUSION

Gastrointestinal and liver disease have been shown to have a profound impact on patients with schizophrenia. The scale of liver disease, and metabolic syndrome in particular, in this population, is perhaps the most significant finding upon review of the literature. Optimal management of these conditions deserves close consideration from psychiatrists, hepatologists and all members of the MDT involved in the care of patients with schizophrenia. A recurring theme from consideration of all gastrointestinal and liver diseases is that patients with schizophrenia need appropriate additional levels of support from care providers to ensure that their physical health receives the attention it requires and which they, as individuals, deserve.

FOOTNOTES

Author contributions: Grant RK and Brindle WM conceived the study; Grant RK performed the literature review and drafted all sections of the manuscript except for the section on acute liver failure; Donnelly MC performed the literature review and drafted the section on acute liver failure; Brindle WM, Donnelly MC, McConville PM, Stroud TG, and Bandieri L critically revised the manuscript; Plevris JN was senior author and critically revised the manuscript for important intellectual content.

Conflict-of-interest statement: There are no conflicts of interest to report.

Open-Access: This article is an open-access article that was selected by an in-house editor and fully peer-reviewed by external reviewers. It is distributed in accordance with the Creative Commons Attribution NonCommercial (CC BY-NC 4.0) license, which permits others to distribute, remix, adapt, build upon this work non-commercially, and license their derivative works on different terms, provided the original work is properly cited and the use is non-commercial. See: https://creativecommons.org/Licenses/by-nc/4.0/

Country/Territory of origin: United Kingdom

ORCID number: Rebecca K Grant 0000-0002-9440-1192; William M Brindle 0000-0002-8972-0332; Mhairi C Donnelly 0000-0001-7655-7284; Pauline M McConville 0000-0002-4655-2367; Thomas G Stroud 0000-0003-1701-898X; John N Plevris 0000-0001-8863-8778.

Corresponding Author's Membership in Professional Societies: British Society of Gastroenterology, No. BSG64199.

S-Editor: Chen YL
L-Editor: A
P-Editor: Chen YL

REFERENCES

1 **World Health Organization**. Schizophrenia. [cited 2022 May 23]. Available from: https://www.who.int/news-room/fact-sheets/detail/schizophrenia
2 **Carney CP**, Jones L, Woolson RF. Medical comorbidity in women and men with schizophrenia: a population-based controlled study. *J Gen Intern Med* 2006; **21**: 1133-1137 [PMID: 17026726 DOI: 10.1111/j.1525-1497.2006.00563.x]
3 **Hjorthøj C**, Stürup AE, McGrath JJ, Nordentoft M. Years of potential life lost and life expectancy in schizophrenia: a systematic review and meta-analysis. *Lancet Psychiatry* 2017; **4**: 295-301 [PMID: 28237639 DOI: 10.1016/S2215-0366(17)30078-0]
4 **Fuller BE**, Rodriguez VL, Linke A, Sikirica M, Dirani R, Hauser P. Prevalence of liver disease in veterans with bipolar disorder or schizophrenia. *Gen Hosp Psychiatry* 2011; **33**: 232-237 [PMID: 21601719 DOI: 10.1016/j.genhosppsych.2011.03.006]
5 **Hsu JH**, Chien IC, Lin CH, Chou YJ, Chou P. Increased risk of chronic liver disease in patients with schizophrenia: a population-based cohort study. *Psychosomatics* 2014; **55**: 163-171 [PMID: 23932529 DOI: 10.1016/j.psym.2013.06.001]
6 **Laursen TM**, Munk-Olsen T, Gasse C. Chronic somatic comorbidity and excess mortality due to natural causes in persons with schizophrenia or bipolar affective disorder. *PLoS One* 2011; **6**: e24597 [PMID: 21935426 DOI: 10.1371/journal.pone.0024597]
7 **Crump C**, Winkleby MA, Sundquist K, Sundquist J. Comorbidities and mortality in persons with schizophrenia: a Swedish national cohort study. *Am J Psychiatry* 2013; **170**: 324-333 [PMID: 23318474 DOI: 10.1176/appi.ajp.2012.12050599]
8 **BMJ Best Practice**. Metabolic Syndrome. [cited 2022 Apr 30]. Available from: https://bestpractice.bmj.com/topics/en-gb/212
9 **Soto-Angona Ó**, Anmella G, Valdés-Florido MJ, De Uribe-Viloria N, Carvalho AF, Penninx BWJH, Berk M. Non-alcoholic fatty liver disease (NAFLD) as a neglected metabolic companion of psychiatric disorders: common pathways and future approaches. *BMC Med* 2020; **18**: 261 [PMID: 32998725 DOI: 10.1186/s12916-020-01713-8]
10 **Papanastasiou E**. The prevalence and mechanisms of metabolic syndrome in schizophrenia: a review. *Ther Adv Psychopharmacol* 2013; **3**: 33-51 [PMID: 23983991 DOI: 10.1177/2045125312464385]
11 **Mitchell AJ**, Vancampfort D, Sweers K, van Winkel R, Yu W, De Hert M. Prevalence of metabolic syndrome and metabolic abnormalities in schizophrenia and related disorders--a systematic review and meta-analysis. *Schizophr Bull* 2013; **39**: 306-318 [PMID: 22207632 DOI: 10.1093/schbul/sbr148]
12 **Pérez-Iglesias R**, Martínez-García O, Pardo-Garcia G, Amado JA, Garcia-Unzueta MT, Tabares-Seisdedos R, Crespo-Facorro B. Course of weight gain and metabolic abnormalities in first treated episode of psychosis: the first year is a critical period for development of cardiovascular risk factors. *Int J Neuropsychopharmacol* 2014; **17**: 41-51 [PMID: 24103107 DOI: 10.1017/S1461145713001053]
13 **Bobes J**, Arango C, Aranda P, Carmena R, Garcia-Garcia M, Rejas J; CLAMORS Study Collaborative Group. Cardiovascular and metabolic risk in outpatients with schizophrenia treated with antipsychotics: results of the CLAMORS Study. *Schizophr Res* 2007; **90**: 162-173 [PMID: 17123783 DOI: 10.1016/j.schres.2006.09.025]
14 **NICE**. Non-alcoholic fatty liver disease (NAFLD): assessment and management. [cited 2022 May 2]. Available from: https://www.nice.org.uk/guidance/ng49/chapter/Context

15 **Xu H**, Zhuang X. Atypical antipsychotics-induced metabolic syndrome and nonalcoholic fatty liver disease: a critical review. *Neuropsychiatr Dis Treat* 2019; **15**: 2087-2099 [PMID: 31413575 DOI: 10.2147/NDT.S208061]

16 **Morlán-Coarasa MJ**, Arias-Loste MT, Ortiz-García de la Foz V, Martínez-García O, Alonso-Martín C, Crespo J, Romero-Gómez M, Fábrega E, Crespo-Facorro B. Incidence of non-alcoholic fatty liver disease and metabolic dysfunction in first episode schizophrenia and related psychotic disorders: a 3-year prospective randomized interventional study. *Psychopharmacology (Berl)* 2016; **233**: 3947-3952 [PMID: 27620899 DOI: 10.1007/s00213-016-4422-7]

17 **Koreki A**, Mori H, Nozaki S, Koizumi T, Suzuki H, Onaya M. Risk of Nonalcoholic Fatty Liver Disease in Patients With Schizophrenia Treated With Antipsychotic Drugs: A Cross-sectional Study. *J Clin Psychopharmacol* 2021; **41**: 474-477 [PMID: 34086626 DOI: 10.1097/JCP.0000000000001421]

18 **Yan J**, Hou C, Liang Y. The prevalence and risk factors of young male schizophrenics with non-alcoholic fatty liver disease. *Neuropsychiatr Dis Treat* 2017; **13**: 1493-1498 [PMID: 28652750 DOI: 10.2147/NDT.S137183]

19 **Ma Q**, Yang F, Ma B, Jing W, Liu J, Guo M, Li J, Wang Z, Liu M. Prevalence of nonalcoholic fatty liver disease in mental disorder inpatients in China: an observational study. *Hepatol Int* 2021; **15**: 127-136 [PMID: 33512644 DOI: 10.1007/s12072-020-10132-z]

20 **Lee TC**, Wu BJ, Yu CH, Wang TJ. Nonalcoholic fatty liver disease among long-term hospitalized patients with schizophrenia in a public psychiatric hospital. *Taiwanese J of Psychiatr* 2021; **35**: 197 [DOI: 10.4103/TPSY.TPSY_38_21]

21 **Aarøe ASK**, Odgaard Maeng K, Leifsdottir Jacobsen R, Eggert Jensen S, Graff C, Polcwiartek C, Bolvig Mark E, Dalsgaard AB, Tranekaer Hostrup C, Veiss-Pedersen P, Frøkjaer JB, Aagaard J, Nielsen RE. Hepatic steatosis in patients with schizophrenia: a clinical cross-sectional study. *Nord J Psychiatry* 2022; **76**: 114-119 [PMID: 34289326 DOI: 10.1080/08039488.2021.1939779]

22 **Kim SR**, Kim JY, Kim HY, Nho JH, Kim YH, Min SY. Factors related to malnutrition in community-dwelling patients with schizophrenia. *Perspect Psychiatr Care* 2019; **55**: 415-423 [PMID: 30430589 DOI: 10.1111/ppc.12327]

23 **Hughes E**, Bassi S, Gilbody S, Bland M, Martin F. Prevalence of HIV, hepatitis B, and hepatitis C in people with severe mental illness: a systematic review and meta-analysis. *Lancet Psychiatry* 2016; **3**: 40-48 [PMID: 26620388 DOI: 10.1016/S2215-0366(15)00357-0]

24 **Chang CH**, Liu CY, Chen SJ, Tsai HC. Hepatitis C virus and hepatitis B virus in patients with schizophrenia. *Medicine (Baltimore)* 2021; **100**: e26218 [PMID: 34087899 DOI: 10.1097/MD.0000000000026218]

25 **Bauer-Staeb C**, Jörgensen L, Lewis G, Dalman C, Osborn DPJ, Hayes JF. Prevalence and risk factors for HIV, hepatitis B, and hepatitis C in people with severe mental illness: a total population study of Sweden. *Lancet Psychiatry* 2017; **4**: 685-693 [PMID: 28687481 DOI: 10.1016/S2215-0366(17)30253-5]

26 **Freudenreich O**, Gandhi RT, Walsh JP, Henderson DC, Goff DC. Hepatitis C in schizophrenia: screening experience in a community-dwelling clozapine cohort. *Psychosomatics* 2007; **48**: 405-411 [PMID: 17878499 DOI: 10.1176/APPI.PSY.48.5.405]

27 **Sockalingam S**, Shammi C, Powell V, Barker L, Remington G. Determining rates of hepatitis C in a clozapine treated cohort. *Schizophr Res* 2010; **124**: 86-90 [PMID: 20605572 DOI: 10.1016/j.schres.2010.06.005]

28 **Hunt GE**, Large MM, Cleary M, Lai HMX, Saunders JB. Prevalence of comorbid substance use in schizophrenia spectrum disorders in community and clinical settings, 1990-2017: Systematic review and meta-analysis. *Drug Alcohol Depend* 2018; **191**: 234-258 [PMID: 30153606 DOI: 10.1016/j.drugalcdep.2018.07.011]

29 **Archibald L**, Brunette MF, Wallin DJ, Green AI. Alcohol Use Disorder and Schizophrenia or Schizoaffective Disorder. *Alcohol Res* 2019; **40** [PMID: 31886105 DOI: 10.35946/arcr.v40.1.06]

30 **Grant R**, Brindle W, Plevris J. P262 Outcomes in patients with schizophrenia admitted under gastroenterology. Gut. 2022;71(A168). [Abstract only] [DOI: 10.1136/gutjnl-2022-BSG.316]

31 SIGN. SIGN 131 Management of schizophrenia [Internet]. 2013 [cited 2022 Jun 13]. Available from: https://www.sign.ac.uk/assets/sign131.pdf

32 **NICE Quality Standard [QS80]**. Psychosis and schizophrenia in adults-Quality Statement 4: Treatment with clozapine. 2015 [cited 2022 Jun 13]. Available from: https://www.nice.org.uk/guidance/qs80/chapter/quality-statement-4-treatment-with-clozapine#:~:text=Clozapine%20is%20the%20only%20drug intolerant%20of%2C%20conventional%20antipsychotic%20drugs.

33 **Macfarlane B**, Davies S, Mannan K, Sarsam R, Pariente D, Dooley J. Fatal acute fulminant liver failure due to clozapine: a case report and review of clozapine-induced hepatotoxicity. *Gastroenterology* 1997; **112**: 1707-1709 [PMID: 9136851 DOI: 10.1016/s0016-5085(97)70054-4]

34 **Chang A**, Krygier DS, Chatur N, Yoshida EM. Clozapine-induced fatal fulminant hepatic failure: a case report. *Can J Gastroenterol* 2009; **23**: 376-378 [PMID: 19440569 DOI: 10.1155/2009/503916]

35 Clozapine. 2017 Oct 16. In: LiverTox: Clinical and Research Information on Drug-Induced Liver Injury [Internet]. Bethesda (MD): National Institute of Diabetes and Digestive and Kidney Diseases; 2012– [PMID: 31643731]

36 **Chaplin AC**, Curley MA, Wanless IR. Re: Recent case report of clozapine-induced acute hepatic failure. *Can J Gastroenterol* 2010; **24**: 739-40; author reply 741 [PMID: 21165382 DOI: 10.1155/2010/535026]

37 Quetiapine. 2018 May 15. In: LiverTox: Clinical and Research Information on Drug-Induced Liver Injury [Internet]. Bethesda (MD): National Institute of Diabetes and Digestive and Kidney Diseases; 2012– [PMID: 31643928]

38 **Bai W**, Liu ZH, Jiang YY, Zhang QE, Rao WW, Cheung T, Hall BJ, Xiang YT. Worldwide prevalence of suicidal ideation and suicide plan among people with schizophrenia: a meta-analysis and systematic review of epidemiological surveys. *Transl Psychiatry* 2021; **11**: 552 [PMID: 34716297 DOI: 10.1038/s41398-021-01671-6]

39 **Jepsen P**, Qin P, Nørgård B, Agerbo E, Mortensen PB, Vilstrup H, Sørensen HT. The association between admission for poisoning with paracetamol or other weak analgesics and subsequent admission for psychiatric disorder: a Danish nationwide case-control study. *Aliment Pharmacol Ther* 2005; **22**: 645-651 [PMID: 16181304 DOI: 10.1111/j.1365-2036.2005.02638.x]

40 **Chen AT**, Chibnall JT, Nasrallah HA. Placebo-controlled augmentation trials of the antioxidant NAC in schizophrenia: A review. *Ann Clin Psychiatry* 2016; **28**: 190-196 [PMID: 27490835]

41 **Zheng W**, Zhang QE, Cai DB, Yang XH, Qiu Y, Ungvari GS, Ng CH, Berk M, Ning YP, Xiang YT. N-acetylcysteine for major mental disorders: a systematic review and meta-analysis of randomized controlled trials. *Acta Psychiatr Scand* 2018; **137**: 391-400 [PMID: 29457216 DOI: 10.1111/acps.12862]

42 **Deepmala**, Slattery J, Kumar N, Delhey L, Berk M, Dean O, Spielholz C, Frye R. Clinical trials of N-acetylcysteine in psychiatry and neurology: A systematic review. *Neurosci Biobehav Rev* 2015; **55**: 294-321 [PMID: 25957927 DOI: 10.1016/j.neubiorev.2015.04.015]

43 **Simpson KJ**, Bates CM, Henderson NC, Wigmore SJ, Garden OJ, Lee A, Pollok A, Masterton G, Hayes PC. The utilization of liver transplantation in the management of acute liver failure: comparison between acetaminophen and non-acetaminophen etiologies. *Liver Transpl* 2009; **15**: 600-609 [PMID: 19479803 DOI: 10.1002/lt.21681]

44 **Clozaril Connect**. Clozapine and liver function. 2018 [cited 2022 Jun 13]. Available from: https://www.hcpinfo.clozaril.co.uk/-/media/clozarilcouk/pdf/download/00812_01_clozapine_and_liver_function_v1.pdf

45 **Siau K**, Chapman W, Sharma N, Tripathi D, Iqbal T, Bhala N. Management of acute upper gastrointestinal bleeding: an update for the general physician. *J R Coll Physicians Edinb* 2017; **47**: 218-230 [PMID: 29465096 DOI: 10.4997/JRCPE.2017.303]

46 **De Hert M**, Hautekeete M, De Wilde D, Peuskens J. High prevalence of Helicobacter pylori in institutionalized schizophrenic patients. *Schizophr Res* 1997; **26**: 243-244 [PMID: 9323357 DOI: 10.1016/s0920-9964(97)00069-8]

47 **Yilmaz Y**, Gul CB, Arabul M, Eren MA. Helicobacter pylori: a role in schizophrenia? *Med Sci Monit* 2008; **14**: HY13-HY16 [PMID: 18591925]

48 **Ozdemir V**, Jamal MM, Osapay K, et al Cosegregation of Gastrointestinal Ulcers and Schizophrenia in a Large National Inpatient Discharge Database. Journal of Investigative Medicine. 2007;55(6):315-320.

49 **Hussar AE**. Peptic ulcer in long-term institutionalized schizophrenic patients. *Psychosom Med* 1968; **30**: 374-377 [PMID: 5672039 DOI: 10.1097/00006842-196807000-00002]

50 **Liao CH**, Chang CS, Chang SN, Muo CH, Lane HY, Sung FC, Kao CH. The association of peptic ulcer and schizophrenia: a population-based study. *J Psychosom Res* 2014; **77**: 541-546 [PMID: 25199406 DOI: 10.1016/j.jpsychores.2014.08.005]

51 **Foskett N**, Curkendall S, Princic N, Lenhart G, Balas B, Milosavljevic-Ristic S. Upper Gastrointestinal Bleeding in Patients with Schizophrenia in the United States. *Pharmacoepidemiol Drug Saf* 2014; **23**: 276

52 **Cotton CC**, Farkas DK, Foskett N, Sørensen HT, Milosavljevic-Ristic S, Balas B, Ehrenstein V. Risk of Upper Gastrointestinal Bleeding and Gastroduodenal Ulcers in Persons With Schizophrenia: A Danish Cohort Study. *Clin Transl Gastroenterol* 2019; **10**: e00005 [PMID: 30829916 DOI: 10.14309/ctg.0000000000000005]

53 **Gao J**, Wang Y, Jia Z, Zhou T, Zhang X, Zu G. Incidence of Gastric Cancer in the Patients with Schizophrenia: A Meta-analysis. *Inter J of Gastroenterol* 2021; **5**: 48-52 [DOI: 10.11648.J.IJG.20210502.12]

54 **BMJ Best Practice**. Coeliac disease [Internet]. [cited 2022 May 3]. Available from: https://bestpractice.bmj.com/topics/en-gb/636

55 **Kalaydjian AE**, Eaton W, Cascella N, Fasano A. The gluten connection: the association between schizophrenia and celiac disease. *Acta Psychiatr Scand* 2006; **113**: 82-90 [PMID: 16423158 DOI: 10.1111/j.1600-0447.2005.00687.x]

56 **Bender L**. Childhood schizophrenia. *Psychiatr Q* 1953; **27**: 663-681 [PMID: 13112324 DOI: 10.1007/BF01562517]

57 **GRAFF H**, HANDFORD A. Celiac syndrome in the case histories of five schizophrenics. *Psychiatr Q* 1961; **35**: 306-313 [PMID: 13707687 DOI: 10.1007/BF01566581]

58 **Dohan FC**. Wheat "consumption" and hospital admissions for schizophrenia during World War II. A preliminary report. *Am J Clin Nutr* 1966; **18**: 7-10 [PMID: 5900428 DOI: 10.1093/ajcn/18.1.7]

59 **Dohan FC**, Grasberger JC. Relapsed schizophrenics: earlier discharge from the hospital after cereal-free, milk-free diet. *Am J Psychiatry* 1973; **130**: 685-688 [PMID: 4739849 DOI: 10.1176/ajp.130.6.685]

60 **Dohan FC**, Levitt DR, Kushnir LD. Abnormal behavior after intracerebral injection of polypeptides from wheat gliadin: possible relevance to schizophrenia. *Pavlov J Biol Sci* 1978; **13**: 73-82 [PMID: 567316 DOI: 10.1007/BF03000668]

61 **Dohan FC**, Harper EH, Clark MH, Rodrigue RB, Zigas V. Is schizophrenia rare if grain is rare? *Biol Psychiatry* 1984; **19**: 385-399 [PMID: 6609726]

62 **Dohan FC**, Grasberger JC, Lowell FM, Johnston HT Jr, Arbegast AW. Relapsed schizophrenics: more rapid improvement on a milk- and cereal-free diet. *Br J Psychiatry* 1969; **115**: 595-596 [PMID: 5820122 DOI: 10.1192/bjp.115.522.595]

63 **Wijarnpreecha K**, Jaruvongvanich V, Cheungpasitporn W, Ungprasert P. Association between celiac disease and schizophrenia: a meta-analysis. *Eur J Gastroenterol Hepatol* 2018; **30**: 442-446 [PMID: 29280918 DOI: 10.1097/MEG.0000000000001048]

64 **Eaton W**, Mortensen PB, Agerbo E, Byrne M, Mors O, Ewald H. Coeliac disease and schizophrenia: population based case control study with linkage of Danish national registers. *BMJ* 2004; **328**: 438-439 [PMID: 14976100 DOI: 10.1136/bmj.328.7437.438]

65 **Ludvigsson JF**, Osby U, Ekbom A, Montgomery SM. Coeliac disease and risk of schizophrenia and other psychosis: a general population cohort study. *Scand J Gastroenterol* 2007; **42**: 179-185 [PMID: 17327937 DOI: 10.1080/00365520600863472]

66 **Benros ME**, Nielsen PR, Nordentoft M, Eaton WW, Dalton SO, Mortensen PB. Autoimmune diseases and severe infections as risk factors for schizophrenia: a 30-year population-based register study. *Am J Psychiatry* 2011; **168**: 1303-1310 [PMID: 22193673 DOI: 10.1176/appi.ajp.2011.11030516]

67 **Chen SJ**, Chao YL, Chen CY, Chang CM, Wu EC, Wu CS, Yeh HH, Chen CH, Tsai HJ. Prevalence of autoimmune diseases in in-patients with schizophrenia: nationwide population-based study. *Br J Psychiatry* 2012; **200**: 374-380 [PMID: 22442099 DOI: 10.1192/bjp.bp.111.092098]

68 **West J**, Logan RF, Hubbard RB, Card TR. Risk of schizophrenia in people with coeliac disease, ulcerative colitis and Crohn's disease: a general population-based study. *Aliment Pharmacol Ther* 2006; **23**: 71-74 [PMID: 16393282 DOI: 10.1111/j.1365-2036.2006.02720.x]

69 **Kelly DL**, Demyanovich HK, Rodriguez KM, Cináková D, Talor MV, McMahon RP, Richardson CM, Vyas G, Adams HA, August SM, Fasano A, Cascella NG, Feldman SM, Liu F, Sayer MA, Powell MM, Wehring HJ, Buchanan RW, Gold

JM, Carpenter WT, Eaton WW. Randomized controlled trial of a gluten-free diet in patients with schizophrenia positive for antigliadin antibodies (AGA IgG): a pilot feasibility study. *J Psychiatry Neurosci* 2019; **44**: 269-276 [PMID: 30938127 DOI: 10.1503/jpn.180174]

70 **Mortensen PB**, Juel K. Mortality and causes of death in first admitted schizophrenic patients. *Br J Psychiatry* 1993; **163**: 183-189 [PMID: 8075909 DOI: 10.1192.bjp.163.2.183]

71 **Saku M**, Tokudome S, Ikeda M, Kono S, Makimoto K, Uchimura H, Mukai A, Yoshimura T. Mortality in psychiatric patients, with a specific focus on cancer mortality associated with schizophrenia. *Int J Epidemiol* 1995; **24**: 366-372 [PMID: 7635598 DOI: 10.1093/ije/24.2.366]

72 **Perini G**, Grigoletti L, Hanife B, Biggeri A, Tansella M, Amaddeo F. Cancer mortality among psychiatric patients treated in a community-based system of care: a 25-year case register study. *Soc Psychiatry Psychiatr Epidemiol* 2014; **49**: 693-701 [PMID: 24092521 DOI: 10.1007/s00127-013-0765-0]

73 **Tran E**, Rouillon F, Loze JY, Casadebaig F, Philippe A, Vitry F, Limosin F. Cancer mortality in patients with schizophrenia: an 11-year prospective cohort study. *Cancer* 2009; **115**: 3555-3562 [PMID: 19548261 DOI: 10.1002/cncr.24383]

74 **Olfson M**, Gerhard T, Huang C, Crystal S, Stroup TS. Premature Mortality Among Adults With Schizophrenia in the United States. *JAMA Psychiatry* 2015; **72**: 1172-1181 [PMID: 26509694 DOI: 10.1001/jamapsychiatry.2015.1737]

75 **Kisely S**, Crowe E, Lawrence D. Cancer-related mortality in people with mental illness. *JAMA Psychiatry* 2013; **70**: 209-217 [PMID: 23247556 DOI: 10.1001/jamapsychiatry.2013.278]

76 **Ni L**, Wu J, Long Y, Tao J, Xu J, Yuan X, Yu N, Wu R, Zhang Y. Mortality of site-specific cancer in patients with schizophrenia: a systematic review and meta-analysis. *BMC Psychiatry* 2019; **19**: 323 [PMID: 31660909 DOI: 10.1186/s12888-019-2332-z]

77 **Hippisley-Cox J**, Vinogradova Y, Coupland C, Parker C. Risk of malignancy in patients with schizophrenia or bipolar disorder: nested case-control study. *Arch Gen Psychiatry* 2007; **64**: 1368-1376 [PMID: 18056544 DOI: 10.1001/archpsyc.64.12.1368]

78 **Inagaki M**, Fujiwara M, Nakaya N, Fujimori M, Higuchi Y, Hayashibara C, So R, Kakeda K, Kodama M, Uchitomi Y, Yamada N. Low Cancer Screening Rates among Japanese People with Schizophrenia: A Cross-Sectional Study. *Tohoku J Exp Med* 2018; **244**: 209-218 [PMID: 29540627 DOI: 10.1620/tjem.244.209]

79 **Fujiwara M**, Yamada Y, Shimazu T, Kodama M, So R, Matsushita T, Yoshimura Y, Horii S, Fujimori M, Takahashi H, Nakaya N, Kakeda K, Miyaji T, Hinotsu S, Harada K, Okada H, Uchitomi Y, Yamada N, Inagaki M. Encouraging participation in colorectal cancer screening for people with schizophrenia: A randomized controlled trial. *Acta Psychiatr Scand* 2021; **144**: 318-328 [PMID: 34242396 DOI: 10.1111/acps.13348]

80 **Jones GR**, Lyons M, Plevris N, Jenkinson PW, Bisset C, Burgess C, Din S, Fulforth J, Henderson P, Ho GT, Kirkwood K, Noble C, Shand AG, Wilson DC, Arnott ID, Lees CW. IBD prevalence in Lothian, Scotland, derived by capture-recapture methodology. *Gut* 2019; **68**: 1953-1960 [PMID: 31300515 DOI: 10.1136/gutjnl-2019-318936]

81 **Bernstein CN**, Hitchon CA, Walld R, Bolton JM, Sareen J, Walker JR, Graff LA, Patten SB, Singer A, Lix LM, El-Gabalawy R, Katz A, Fisk JD, Marrie RA; CIHR Team in Defining the Burden and Managing the Effects of Psychiatric Comorbidity in Chronic Immunoinflammatory Disease. Increased Burden of Psychiatric Disorders in Inflammatory Bowel Disease. *Inflamm Bowel Dis* 2019; **25**: 360-368 [PMID: 29986021 DOI: 10.1093/ibd/izy235]

82 **Ludvigsson JF**, Olén O, Larsson H, Halfvarson J, Almqvist C, Lichtenstein P, Butwicka A. Association Between Inflammatory Bowel Disease and Psychiatric Morbidity and Suicide: A Swedish Nationwide Population-Based Cohort Study With Sibling Comparisons. *J Crohns Colitis* 2021; **15**: 1824-1836 [PMID: 33640971 DOI: 10.1093/ecco-jcc/jjab039]

83 **Sung KY**, Zhang B, Wang HE, Bai YM, Tsai SJ, Su TP, Chen TJ, Hou MC, Lu CL, Wang YP, Chen MH. Schizophrenia and risk of new-onset inflammatory bowel disease: a nationwide longitudinal study. *Aliment Pharmacol Ther* 2022; **55**: 1192-1201 [PMID: 35261051 DOI: 10.1111/apt.16856]

84 **Qian L**, He X, Gao F, Fan Y, Zhao B, Ma Q, Yan B, Wang W, Ma X, Yang J. Estimation of the bidirectional relationship between schizophrenia and inflammatory bowel disease using the mendelian randomization approach. *Schizophrenia (Heidelb)* 2022; **8**: 31 [PMID: 35347152 DOI: 10.1038/s41537-022-00244-w]

85 **Uellendahl-Werth F**, Maj C, Borisov O, Juzenas S, Wacker EM, Jørgensen IF, Steiert TA, Bej S, Krawitz P, Hoffmann P, Schramm C, Wolkenhauer O, Banasik K, Brunak S, Schreiber S, Karlsen TH, Degenhardt F, Nöthen M, Franke A, Folseraas T, Ellinghaus D. Cross-tissue transcriptome-wide association studies identify susceptibility genes shared between schizophrenia and inflammatory bowel disease. *Commun Biol* 2022; **5**: 80 [PMID: 35058554 DOI: 10.1038/s42003-022-03031-6]

86 **NICE**. Irritable Bowel Syndrome in Adults. [cited 2022 May 23]. Available from: https://www.nice.org.uk/guidance/qs114/documents/irritable-bowel-syndrome-in-adults-qs-briefing-paper2

87 **Gupta S**, Masand PS, Kaplan D, Bhandary A, Hendricks S. The relationship between schizophrenia and irritable bowel syndrome (IBS). *Schizophr Res* 1997; **23**: 265-268 [PMID: 9075306 DOI: 10.1016/s0920-9964(96)00099-0]

88 **Kashani SA**, Mari MU, Ilyas M, Rasool G, Rumi J, Ali H, Nasir A, Kakar Z, Chand R. Frequency of subtypes of irritable bowel syndrome in subtypes of schizophrenia. *J of Psychol & Clini Psychiat***7**: 11-12 [DOI: 10.15406.jpcpy.2017.07.00458]

89 **Taylor DM**, Barnes TRE, Young AH. The Maudsley Prescribing Guidelines in Psychiatry. 13th ed. Wiley Blackwell, 2018: 193

90 **Shirazi A**, Stubbs B, Gomez L, Moore S, Gaughran F, Flanagan RJ, MacCabe JH, Lally J. Prevalence and Predictors of Clozapine-Associated Constipation: A Systematic Review and Meta-Analysis. *Int J Mol Sci* 2016; **17** [PMID: 27271593 DOI: 10.3390/ijms17060863]

91 **Nielsen J**, Meyer JM. Risk factors for ileus in patients with schizophrenia. *Schizophr Bull* 2012; **38**: 592-598 [PMID: 21112965 DOI: 10.1093/schbul/sbq137]

92 **Chougule A**, Praharaj SK, Bhat SM, Sharma PSVN. Prevalence and Factors Associated With Clozapine-Related Constipation: An Observational Study. *J Clin Psychopharmacol* 2018; **38**: 42-46 [PMID: 29257785 DOI:

10.1097/JCP.0000000000000824]
93 **Every-Palmer S**, Inns SJ, Grant E, Ellis PM. Effects of Clozapine on the Gut: Cross-Sectional Study of Delayed Gastric Emptying and Small and Large Intestinal Dysmotility. *CNS Drugs* 2019; **33**: 81-91 [PMID: 30456745 DOI: 10.1007/s40263-018-0587-4]
94 **Blackman G**, Kapila A, Grosskopf CM, Dratcu L. Focussing on the fundaments - assessing and treating Clozapine Induced Gastrointestinal Hypomotility. *Int J Psychiatry Clin Pract* 2020; **24**: 18-19 [PMID: 31910056 DOI: 10.1080/13651501.2019.1710538]
95 **Kapur M**, Shah RA, Ferro A, Basyuni S, Brassett C, Santhanam V. Re: Sexual dimorphism and geographical variance: their impact on the reliability of the antilingula as a landmark in human mandibular surgery. *Br J Oral Maxillofac Surg* 2022; **60**: 370-371 [PMID: 35164985 DOI: 10.1016/j.bjoms.2022.01.001]
96 **Patel RS**, Veluri N, Suchorab A, Shah K, Verma G. Clozapine-Induced Constipation: A Case Report and Review of Current Management Guidelines. *Cureus* 2021; **13**: e14846 [PMID: 34123610 DOI: 10.7759/cureus.14846]
97 **Arumugam M**, Raes J, Pelletier E, Le Paslier D, Yamada T, Mende DR, Fernandes GR, Tap J, Bruls T, Batto JM, Bertalan M, Borruel N, Casellas F, Fernandez L, Gautier L, Hansen T, Hattori M, Hayashi T, Kleerebezem M, Kurokawa K, Leclerc M, Levenez F, Manichanh C, Nielsen HB, Nielsen T, Pons N, Poulain J, Qin J, Sicheritz-Ponten T, Tims S, Torrents D, Ugarte E, Zoetendal EG, Wang J, Guarner F, Pedersen O, de Vos WM, Brunak S, Doré J; MetaHIT Consortium, Antolín M, Artiguenave F, Blottiere HM, Almeida M, Brechot C, Cara C, Chervaux C, Cultrone A, Delorme C, Denariaz G, Dervyn R, Foerstner KU, Friss C, van de Guchte M, Guedon E, Haimet F, Huber W, van Hylckama-Vlieg J, Jamet A, Juste C, Kaci G, Knol J, Lakhdari O, Layec S, Le Roux K, Maguin E, Mérieux A, Melo Minardi R, M'rini C, Muller J, Oozeer R, Parkhill J, Renault P, Rescigno M, Sanchez N, Sunagawa S, Torrejon A, Turner K, Vandemeulebrouck G, Varela E, Winogradsky Y, Zeller G, Weissenbach J, Ehrlich SD, Bork P. Enterotypes of the human gut microbiome. *Nature* 2011; **473**: 174-180 [PMID: 21508958 DOI: 10.1038/nature09944]
98 **Szeligowski T**, Yun AL, Lennox BR, Burnet PWJ. The Gut Microbiome and Schizophrenia: The Current State of the Field and Clinical Applications. *Front Psychiatry* 2020; **11**: 156 [PMID: 32226399 DOI: 10.3389/fpsyt.2020.00156]
99 **Patrono E**, Svoboda J, Stuchlík A. Schizophrenia, the gut microbiota, and new opportunities from optogenetic manipulations of the gut-brain axis. *Behav Brain Funct* 2021; **17**: 7 [PMID: 34158061 DOI: 10.1186/s12993-021-00180-2]
100 **Kelly JR**, Minuto C, Cryan JF, Clarke G, Dinan TG. The role of the gut microbiome in the development of schizophrenia. *Schizophr Res* 2021; **234**: 4-23 [PMID: 32336581 DOI: 10.1016/j.schres.2020.02.010]
101 **Munawar N**, Ahsan K, Muhammad K, Ahmad A, Anwar MA, Shah I, Al Ameri AK, Al Mughairbi F. Hidden Role of Gut Microbiome Dysbiosis in Schizophrenia: Antipsychotics or Psychobiotics as Therapeutics? *Int J Mol Sci* 2021; **22** [PMID: 34299291 DOI: 10.3390/ijms22147671]
102 **Kao AC**, Spitzer S, Anthony DC, Lennox B, Burnet PWJ. Prebiotic attenuation of olanzapine-induced weight gain in rats: analysis of central and peripheral biomarkers and gut microbiota. *Transl Psychiatry* 2018; **8**: 66 [PMID: 29540664 DOI: 10.1038/s41398-018-0116-8]

World Journal of Gastroenterology

Submit a Manuscript: https://www.f6publishing.com

World J Gastroenterol 2022 October 14; 28(38): 5530-5546

DOI: 10.3748/wjg.v28.i38.5530

ISSN 1007-9327 (print) ISSN 2219-2840 (online)

MINIREVIEWS

Ultrasound-based artificial intelligence in gastroenterology and hepatology

Ji-Qiao Liu, Jia-Yu Ren, Xiao-Lan Xu, Li-Yan Xiong, Yue-Xiang Peng, Xiao-Fang Pan, Christoph F Dietrich, Xin-Wu Cui

Specialty type: Gastroenterology and hepatology

Provenance and peer review: Invited article; Externally peer reviewed.

Peer-review model: Single blind

Peer-review report's scientific quality classification

Grade A (Excellent): 0
Grade B (Very good): B, B
Grade C (Good): C
Grade D (Fair): 0
Grade E (Poor): 0

P-Reviewer: Amin A, United Arab Emirates; Surani S, United States

Received: July 1, 2022
Peer-review started: July 1, 2022
First decision: July 13, 2022
Revised: August 12, 2022
Accepted: September 22, 2022
Article in press: September 22, 2022
Published online: October 14, 2022

Ji-Qiao Liu, Jia-Yu Ren, Xiao-Lan Xu, Li-Yan Xiong, Xin-Wu Cui, Department of Medical Ultrasound, Tongji Hospital, Tongji Medical College, Huazhong University of Science and Technology, Wuhan 430030, Hubei Province, China

Yue-Xiang Peng, Department of Ultrasound, Wuhan Third Hospital, Tongren Hospital of Wuhan University, Wuhan 430030, Hubei Province, China

Xiao-Fang Pan, Health Medical Department, Dalian Municipal Central Hospital, Dalian 116000, Liaoning Province, China

Christoph F Dietrich, Department Allgemeine Innere Medizin, Kliniken Hirslanden Beau Site, Salem und Permanence, Bern 3003, Switzerland

Corresponding author: Xin-Wu Cui, MD, PhD, Professor, Director, Department of Medical Ultrasound, Tongji Hospital, Tongji Medical College, Huazhong University of Science and Technology, No. 1095 Jiefang Avenue, Wuhan 430030, Hubei Province, China.
cuixinwu@live.cn

Abstract

Artificial intelligence (AI), especially deep learning, is gaining extensive attention for its excellent performance in medical image analysis. It can automatically make a quantitative assessment of complex medical images and help doctors to make more accurate diagnoses. In recent years, AI based on ultrasound has been shown to be very helpful in diffuse liver diseases and focal liver lesions, such as analyzing the severity of nonalcoholic fatty liver and the stage of liver fibrosis, identifying benign and malignant liver lesions, predicting the microvascular invasion of hepatocellular carcinoma, curative transarterial chemoembolization effect, and prognoses after thermal ablation. Moreover, AI based on endoscopic ultrasonography has been applied in some gastrointestinal diseases, such as distinguishing gastric mesenchymal tumors, detection of pancreatic cancer and intraductal papillary mucinous neoplasms, and predicting the preoperative tumor deposits in rectal cancer. This review focused on the basic technical knowledge about AI and the clinical application of AI in ultrasound of liver and gastroenterology diseases. Lastly, we discuss the challenges and future perspectives of AI.

Key Words: Artificial intelligence; Ultrasound; Liver; Gastroenterology; Deep learning

©The Author(s) 2022. Published by Baishideng Publishing Group Inc. All rights reserved.

Core Tip: Artificial intelligence (AI) based on ultrasound has been confirmed to be helpful in diagnosing diffuse liver diseases and focal liver lesions, such as analyzing the severity of nonalcoholic fatty liver and the stage of liver fibrosis, identifying benign and malignant liver lesions, predicting microvascular invasion of hepatocellular carcinoma, curative transarterial chemoembolization effect, and prognoses after thermal ablation. AI based on endoscopic ultrasonography has been applied in some gastrointestinal diseases. We focused on basic technical knowledge about AI and the aforementioned clinical application in the ultrasound of liver and gastroenterology. Additionally, we discuss the challenges and future perspectives of AI.

Citation: Liu JQ, Ren JY, Xu XL, Xiong LY, Peng YX, Pan XF, Dietrich CF, Cui XW. Ultrasound-based artificial intelligence in gastroenterology and hepatology. *World J Gastroenterol* 2022; 28(38): 5530-5546
URL: https://www.wjgnet.com/1007-9327/full/v28/i38/5530.htm
DOI: https://dx.doi.org/10.3748/wjg.v28.i38.5530

INTRODUCTION

Liver disease causes two million deaths per year in the world among which cirrhosis is the 11th leading cause of death in the world and liver cancer is the 16th leading cause of death[1]. The prevalence of nonalcoholic fatty liver disease (NAFLD) is 25.0% and is estimated to be 33.5% by 2030[2]. Gastrointestinal diseases affect an estimated 60 to 70 million American citizens annually. It is reported that pancreatic cancer (PC) is one of the top five causes of death from cancer, and colorectal cancer accounts for 8.5% of cancer-related deaths[3-5]. Therefore, it is of great importance to pay attention to these diseases.

In clinical practice, many imaging techniques such as X-ray, computed tomography (CT), magnetic resonance imaging (MRI), and ultrasound have played a vital role in the detection and treatment of diseases[6]. Ultrasound, a noninvasive and real-time diagnostic technique, is the most commonly used method for detecting and diagnosing human digestive diseases[7]. However, the interpretation and analysis of ultrasound images depend deeply on the subjective judgment and experience of human experts. Radiologists may make mistakes due to exhaustion when dealing with a large number of images[8].

Artificial intelligence (AI) is defined as computer algorithms created by humans and improved with analogs of the thoughts, judgments, and reactions that take place in the human brain. In recent years, radiologists have increasingly embraced the aid of AI-powered diagnoses. AI can make a quantitative analysis by recognizing the information of images automatically and is widely applied in the medical images of ultrasound in diffuse liver diseases, focal liver lesions, PC, and colorectal cancer. In this review, we described the development of AI-based ultrasound in the aforementioned applications. In addition, we also discussed the future opportunities and challenges of AI-based ultrasound.

AI

Currently, the algorithms of AI used in medical images mainly include traditional machine learning algorithms and deep learning.

Machine learning

Machine learning is described as a kind of data science that offers computers with the capacity to study without being programmed with specific rules[9]. It focuses on computer algorithms that are studied from the training model and give predictions on another model[10]. Machine learning depends primarily on the predefined characteristics that display the regular patterns inherent in models acquired from regions of interest with explicit parameters on the basis of expert experience. Then, other medical image features, such as various mass shape, size, and echo, can be quantified.

Radiomics, which belongs to traditional machine learning, is a popular field of study related to the acquisition and assessment of patterns within medical images, including CT, MRI, and ultrasound. These patterns include complicated patterns that are difficult to recognize or analyze by the human eye [11].

Deep learning

Deep learning is at the leading edge of AI and is developing rapidly. Deep learning is described as a group of artificial neural network (ANN) algorithms, which include many hidden layers. Namely, deep learning depends on a subset of algorithms that try to model high-level abstractions[12].

Recently, convolutional neural networks (CNNs) are the preferred type of deep learning architecture in the assessment of medical images[13]. CNNs consist of an input layer, multiple hidden layers, and an output layer (Figure 1). The hidden layers include convolutional layers, pooling layers, connected layers, and normalization layers. Convolutional layers and pooling layers can complete feature extraction and aggregation[9].

APPLICATION OF ULTRASOUND-BASED AI IN HEPATOLOGY

Diffuse liver diseases

Diffuse liver diseases display a failure in the metabolic and synthesis processes of the liver[14]. Liver biopsy is the gold standard for the diagnosis of fibrosis and NAFLD. However, liver biopsy is an invasive process that has many complications such as hemorrhage, biliary peritonitis, and pneumothorax[15]. In addition, liver biopsy is not feasible for the long-term management of patients with chronic liver diseases. Noninvasive liver imaging methods such as CT, MRI, and ultrasound have been extensively studied. Ultrasound is one of most common methods to diagnose liver diseases due to its noninvasiveness, inexpensive price, and real-time ability. Machine learning algorithms based on ultrasound have been applied for analysis of steatosis and the staging of liver fibrosis. Table 1 shows the application of ultrasound-based AI in diffuse liver disease.

Fatty liver diseases: An excess amount of fat in the liver cells is found in fatty liver diseases (FLD). The main causes of FLD include obesity, alcoholism, diabetes, nonalcoholic steatohepatitis, drugs, and toxins [16,17]. FLD is related to the growing risk of cirrhosis and liver cancer. The most common cause of FLD is NAFLD, which ranges in prevalence from 25% to 45%[18]. Several noninvasive imaging methods such as CT, MRI, and ultrasound can diagnose NAFLD[19]. Ultrasound is the cheapest diagnostic method with 93% sensitivity, while hepatic steatosis is greater than 33%[18].

Conventional ultrasound is commonly used for NAFLD evaluation, but its qualitative nature, doctor dependency, and unsatisfactory accuracy limits the application. Moreover, the ultrasound images of fatty liver and early cirrhosis have many common features, making it hard to distinguish the two diseases by the human eye[20].

In recent years, ultrasound-based AI has demonstrated high accuracy for detection of steatosis and represents excellent reproducibility and reliability.

Byra *et al*[21] created a CNN model to acquire features from B-mode ultrasound image. It was reported that they could assess the amount of steatosis present in the liver with the area under the receiver operating characteristic curve (AUC) of 0.98, and their approach may assist the doctors in automatically assessing the amount of fat in the liver clinically[21].

Biswas *et al*[22] revealed that a deep learning-based algorithm reached a superior performance for FLD identification and risk stratification with 100% accuracy and AUC of 1.0 when compared with a conventional machine learning system support vector machine (SVM) (accuracy: 82%, AUC: 0.79) and extreme learning machine (accuracy: 92%, AUC: 0.92).

Deep learning has also been applied to quantitatively evaluate NAFLD. The radiofrequency data of ultrasound displays much more information of hepatic microstructure than that of gray-scale B-mode images[23]. Han *et al*[24] developed a deep learning algorithm that used radiofrequency data for NAFLD assessment. The results revealed that the sensitivity, specificity, and positive predictive value (PPV) for NAFLD diagnosis were 97%, 94%, and 97%, respectively. They confirmed that the quantitative analysis of raw radiofrequency ultrasound signals showed the potential of identifying NAFLD and quantifying hepatic fat fraction[24].

Liver fibrosis and cirrhosis: Patients with chronic liver disease may have no clinical symptoms for an extended period, or it may develop to fibrosis and cirrhosis[25]. The activation of the resting hepatic stellate cell into an activated myofibroblast plays an important role in the progression of liver fibrosis. The activated myofibroblast expresses abundant a-smooth muscle actin and collagen[26].

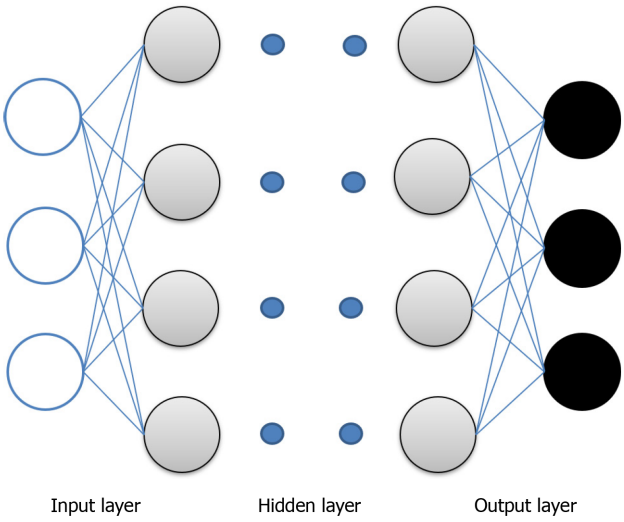
Cirrhosis, which consists of various nodules and is harder than the normal liver, is the advanced period of fibrosis[27]. Liver fibrosis and early cirrhosis are confirmed to be partly reversible. Therefore, the precise diagnosis of liver fibrosis is vital for the treatment and management of chronic liver disease patients.

In clinical practice, liver biopsy is the gold standard for the diagnosis of liver fibrosis. Various noninvasive modalities such as ultrasound and elastography have been used as alternatives to liver biopsy. Some studies suggest that AI models based on ultrasound and elastography have great potential for the classification of liver fibrosis.

Table 1 Application of ultrasound-based artificial intelligence in diffuse liver diseases

Ref.	Diseases: number of cases	Type of ultrasound	Algorithm of AI	Performance
Byra *et al*[21]	Severely obese patients: 55	B-mode	CNN	Sensitivity: 100%
				Specificity: 88%
				Accuracy: 96%
	Fatty liver disease: 38			AUC: 0.98
Biswas *et al*[22]	Normal patients: 27	B-mode	Deep learning	Accuracy: 100%
	Fatty liver disease: 36			AUC: 1.0
Han *et al*[24]	NAFLD: 140	B-mode	CNN	Sensitivity: 97%
				Specificity: 94%
	Control: 64			Accuracy: 96%
				AUC: 0.98
Yeh *et al*[28]	Postsurgical human liver samples: 20	B-mode	SVM	F2 accuracy: 91%
				F3 accuracy: 85%
				F4 accuracy: 81%
				F6 accuracy: 72%
Zhang *et al*[29]	Liver fibrosis or cirrhosis: 239	Duplex	ANN	Sensitivity: 95%
	Training group: 179			Specificity: 85%
	Validation group: 60			Accuracy: 88%
Gao *et al*[30]	S0: 4	B-mode	ANN	S0 accuracy: 100%
	S1: 16			S1 accuracy: 90%
				S2 accuracy: 70%
				S3 accuracy: 90%
	S2: 8			S4 accuracy: 100%
	S3: 5			
	S4: 4			
Lee *et al*[31]	Patients: 3446	B-mode	CNN	AUC: 0.86
	Internal validation set: 263			
	Internal test set: 266			
	External test set: 572			
Gatos *et al*[34,35]	Chronic liver disease: 70	Shear-wave elastography	SVM	Sensitivity: 94%
	Healthy: 56			Specificity: 81%
				Accuracy: 87%
Wang *et al*[36]	Liver fibrosis: 398	Shear-wave elastography	Deep learning radiomic	F4 AUC: 0.97
	Training group: 266			
	Validation group: 132			F3 AUC: 0.98
				F2 AUC: 0.85
Xue *et al*[38]	Liver fibrosis: 401	Elastography	CNN by TL radiomics	S2 AUC: 0.95
	Patient without fibrosis: 65			S3 AUC: 0.93
				S4 AUC: 0.93

AI: Artificial intelligence; ANN: Artificial neural network; AUC: Area under the receiver operating characteristic curve; CNN: Convolutional neural network; NAFLD: Nonalcoholic fatty liver disease; SVM: Support vector machine; TL: Transfer learning.



DOI: 10.3748/wjg.v28.i38.5530 **Copyright** ©The Author(s) 2022.

Figure 1 Framework of convolutional neural networks. Blue dots represent multiple hidden layers.

AI based on conventional ultrasound: AI based on conventional ultrasound has been applied to improve their performance for the diagnosis and grading of liver fibrosis.

Yeh *et al*[28] built an SVM model to analyze liver fibrosis. B-mode images of 20 fresh postsurgical human livers were used to assess ultrasound capacity in evaluating the stage of fibrosis. The study indicated the best classification accuracy of two, three, four, and six classes were 91%, 85%, 81%, and 72%, respectively[28]. The results confirmed that the SVM model may be suggested to assess diverse liver fibrosis stage.

Other than the B-mode ultrasound, duplex ultrasound has also been applied to diagnose liver fibrosis. Using an ANN model based on duplex ultrasound, Zhang *et al*[29] demonstrated that their model reached the accuracy, sensitivity, and specificity were 88.3%, 95.0%, and 85.0%, respectively. The ANN model included five ultrasonographic parameters: thickness of spleen, liver vein waveform, the hepatic parenchyma, liver artery pulsatile index, and hepatic damping index. The study suggested that their ANN model has the potential to diagnose liver fibrosis noninvasively[29].

Studies confirmed that radiomics show great performance in the grading of liver fibrosis. By the use of texture analysis to analyze ultrasound liver images, the study found the accuracies of S0-S4 were 100%, 90%, 70%, 90%, and 100%, respectively[30].

It was reported that deep learning has great potential for liver fibrosis evaluation. Lee *et al*[31] built a deep CNN and trained a four-class model (F0 *vs* F1 *vs* F23 *vs* F4) to predict METAVIR scores. They used 13608 ultrasound images of 3446 patients who accepted surgery, liver biopsy, or transient elastography to train the deep CNN model. The model achieved a higher AUC of 0.857 for the classification of cirrhosis compared with five radiologists (AUC range, 0.656-0.816; $P < 0.05$) using the external test set [31].

AI based on ultrasound elastography: ultrasound elastography has been performed to acquire quantitative assessment of liver tissue stiffness, which is related to the grades of fibrosis. These technologies include strain elastography and shear wave elastography (SWE)[32]. Recently, some studies confirmed that the AI based on SWE has great value to identify and stage liver fibrosis.

Compared to conventional radiomics, a multiparametric ultrasonic model using machine learning algorithms demonstrated better manifestation in fibrosis assessment[33]. By quantifying color information from SWE images, Gatos *et al*[34,35] created an SVM model that could differentiate patients with liver diseases from controls with accuracy, sensitivity, and specificity of 87.3%, 93.5% and 81.2%, respectively.

Deep learning has also been applied in the assessment of liver fibrosis. A multicenter study used deep learning radiomics on 2D-SWE ultrasound images for the classification of liver fibrosis[36]. 2D-SWE ultrasound images had higher AUCs of 0.97 for F4, 0.98 for ≥ F3, and 0.85 for ≥ F2 fibrosis when compared with standard 2D-SWE.

It is necessary to contain a large training dataset for deep learning. However, it is difficult and expensive to get abundant medical images in clinics. One method to solve this problem is the employment of transfer learning (TL), which can enhance the performance by TL from other areas to the ultrasound area[37]. A study developed a CNN model by TL radiomics to assess ultrasound images of gray-scale modality and elastogram modality for the grade of accurate liver fibrosis. TL in gray-scale modality and elastogram modality revealed much higher diagnostic accuracy of AUCs compared with non-TL. Multimodal gray-scale modality + elastogram modality was confirmed to be the most precise diagnostic model with AUCs of 0.930, 0.932, and 0.950 for classifying ≥ S2, ≥ S3, and S4, respectively. It

was suggested that this TL model had excellent performance in liver fibrosis staging in clinical applications[38].

Focal liver lesion

Focal liver lesions (FLLs) are described as an abnormal part of the liver mainly coming from hepatocytes, biliary epithelium, and mesenchymal tissue[39]. Due to its cheap price, noninvasiveness, and real-time imaging, ultrasound is the preferred method for the diagnosis of FLLs. Based on this trend, the AI models using ultrasound images have more advantages over CT and MRI in routine clinical applications[40]. Table 2 shows the application of ultrasound-based AI in FLLs.

The application of AI in the diagnosis of benign and malignant FLLs: Hepatocellular carcinoma (HCC) is the fifth most common malignancy worldwide and accounts for the second leading cause of cancer-related deaths[41]. It is vital to identify benign and malignant FLLs for patients in the early stage.

AI based on conventional ultrasound: deep learning based on B-mode ultrasound has been demonstrated to be helpful in the diagnosis of benign and malignant FLLs. A CNN model was used to distinguish benign and malignant FLLs and achieved a higher accuracy than two experts[42]. Yang *et al*[43] developed a multicenter study to improve the B-mode ultrasound diagnostic performance for FLLs. The CNN of ultrasound performed high sensitivity and specificity in detecting FLLs, and it may be helpful for less-experienced doctors to enhance their judgment in liver cancer diagnosis.

AI based on B-mode ultrasound images has also been applied for the diagnosis of primary or secondary malignant liver tumors. A study proposed machine learning for discriminating HCC and metastatic liver tumors using SVM. The results revealed a classification accuracy of 91.6% with a sensitivity of 90.0% for HCCs and 93.3% for metastatic liver tumors[44].

AI based on contrast-enhanced ultrasound (CEUS): Recently, CEUS has become a commonly used ultrasound modality for the detection of FLLs[45]. Many studies have indicated that CEUS images had better sensitivity and specificity for the differentiation of malignant and benign tumors compared with B-mode images. One of the advantages of CEUS is that the images can be analyzed quantitatively. Time intensity curve (TIC) is a common quantitative analysis tool for CEUS[46]. Recently, AI based on CEUS images was reported to have great performance for the discrimination of FLLs.

Gatos *et al*[47] created a pretrained SVM algorithm to distinguish benign and malignant FLLs. In this model, a complex segmentation method based on TIC was used to detect lesions and process contours of 52 CEUS images. The accuracy, sensitivity, and specificity were 90.3%, 93.1%, and 86.9%, respectively [47]. Another study using SVM revealed that the sensitivity, specificity, and accuracy of benign and malignant grading were 94.0%, 87.1%, and 91.8%, respectively, while the classification accuracy of HCC, metastatic liver tumor, and benign were 85.7%, 87.7%, and 84.4%, respectively[46].

In addition to TIC, extracting features except TICs from a region of interest on CEUS images and videos was also applied in AI. A two-stage multiview learning framework, which was the integration of deep canonical correlation analysis and multiple kernel learning for CEUS-based computer-aided diagnosis, was proposed to identify liver tumors. The deep canonical correlation analysis-multiple kernel learning framework achieved performance for discriminating benign from malignant liver tumors with the accuracy, sensitivity, and specificity of 90.4%, 93.6%, and 86.8%, respectively[48].

The application of AI for the differential diagnosis of FLLs: With the development of AI, AI based on B-mode ultrasound images has great performance on the diagnosis of different FLLs. Hwang *et al*[49] extracted hybrid textural features from ultrasound images and used an ANN to diagnose FLLs. They indicated that the model revealed enormous potential with the diagnosis accuracy of over 96% among all FLLs groups (hemangioma *vs* malignant, cyst *vs* hemangioma, and cyst *vs* malignant)[49].

Deep learning was also applied in the distinction of different FLLs. Schmauch *et al*[50] created an algorithm that simultaneously detected and characterized FLLs. Although the amount of training data was relatively small, the average AUC of FLL detection and characterization was 0.935 and 0.916, respectively.

A CNN model was developed and validated for tumor detection and 6-class discrimination (HCC, focal fatty sparing, focal fatty infiltration, hemangiomas, and cysts)[51]. This model reached 87.0% detection rate, 83.9% sensitivity, and 97.1% specificity in the internal evaluation. In external validation groups, the model achieved 75.0% detection rate, 84.9% sensitivity, and 97.1% specificity.

CEUS also had excellent potential for AI to distinguish different FLLs. An ANN was applied to study the role of TIC analysis parameters of 4-class discrimination of liver tumors. The neural network had 94.45% training accuracy and 87.12% testing accuracy. The automatic classification process registered 93.2% sensitivity and 89.7% specificity[52].

Căleanu *et al*[53] reported the 5-class classification of liver tumors using deep neural networks with an accuracy of 88%. In this study, deep neural network algorithms were compared with state-of-the-art architectures, and a novel leave-one-patient-out evaluation procedure was presented.

All these studies indicated that AI based on conventional ultrasound and CEUS played a vital role in the detection and distinction of FLLs.

The application of AI in the management of HCC patients: Because of the development of new treatments, the management of HCC patients has become much more complicated. Radiomics can offer

Table 2 Application of ultrasound-based artificial intelligence in focal liver lesions

Ref.	Diseases: number of cases	Type of ultrasound	Algorithm of AI	Performance
Xi *et al*[42]	Benign lesions: 300	B-mode	CNN	All lesions
				Accuracy: 84%
				Uncertain set of lesions
	Malignant lesions: 296			Accuracy: 79%
Yang *et al*[43]	Benign tumor: 427	B-mode	CNN	AUC for EV: 0.924
	Malignant tumor: 1786			Sensitivity: 86.5%
				Specificity: 85.5%
Virmani *et al*[44]	HCC: 27	B-mode	SVM	Accuracy of HCC: 91.6%
				Sensitivity
	Metastatic liver tumor: 24			HCC: 90%
				Metastatic liver tumor: 93.3%
Hwang *et al*[49]	Cyst: 29	B-mode	ANN	Accuracy: 96%
				Cyst *vs* hemangioma
	Hemangioma: 37			Cyst *vs* malignant
	Malignant: 33			Hemangioma *vs* malignant
Schmauch *et al*[50]	Non-tumorous liver: 258	B-mode	CNN	AUC
	Hemangioma: 17			FLL detection: 0.935
	Metastasis: 48			
	HCC: 6			FLL discrimination: 0.916
	Cyst: 30			
	FNH: 8			
Tiyarattanachai *et al*[51]	HCC: 2414	B-mode	CNN	Detection rate: 87.0%
	Cyst: 6600			Sensitivity: 83.9%
	Hemangioma: 5374			Specificity: 97.1%
	Focal fatty sparing: 5110			
	Focal fatty infiltration: 934			
Gatos *et al*[47]	Benign FLL: 30	CEUS	SVM	Accuracy: 90.3%
				Sensitivity: 93.1%
	Malignant FLL: 22			Specificity: 86.9%
Kondo *et al*[46]	Benign FLL: 31	CEUS	SVM	Benign *vs* malignant
				Accuracy: 91.8%
				Sensitivity: 94%
				Specificity: 87.1%
	Malignant FLL: 67			Accuracy
				Benign: 84.4%
				HCC: 87.7%
				Metastatic liver tumor: 85.7%
Guo *et al*[48]	Benign FLL: 46	CEUS	Deep canonical correlation analysis and multiple kernel learning	Accuracy: 90.4%
				Sensitivity: 93.6%

	Malignant FLL: 47			Specificity: 86.8%
Streba *et al*[52]	HCC: 41	CEUS	ANN	Training accuracy: 94.5%
	Hypervascular liver metastasis: 20			Testing accuracy: 87.1%
	Hypovascular liver metastasis: 12			Sensitivity: 93.2%
	Hemangioma: 16			Specificity: 89.7%
	Focal fatty changes: 23			
Căleanu *et al*[53]	HCC: 30	CEUS	Deep neural network	Accuracy: 88%
	Hypervascular liver metastasis: 11			
	Hypovascular liver metastasis: 11			
	Hemangioma: 23			
	FNH: 16			
Dong *et al*[56]	HCC: 322	B-mode	Radiomics	AUC: 0.81
Hu *et al*[57]	HCC: 482	CEUS	Radiomics	AUC: 0.731
	Training cohort: 341			
	Validation cohort: 141			
Zhang *et al*[58]	HCC: 313	CEUS	Radiomics	AUC
	Primary cohort: 192			Primary dataset: 0.849
	Validation cohort: 121			Validation dataset: 0.788
Liu *et al*[63]	HCC: 130	CEUS	Deep learning radiomics	AUC: 0.93
	Training cohort: 89			
	Validation cohort: 41			
Ma *et al*[66]	HCC: 318	CEUS	Radiomics	AUC: 0.89
	Training cohort: 255			
	Validation cohort: 63			
Liu *et al*[69]	HCC: 419	CEUS	Deep learning radiomics	C-index
	RFA: 214			RFA: 0.726
	SR: 205			SR: 0.741

AI: Artificial intelligence; ANN: Artificial neural network; AUC: Area under the receiver operating characteristic curve; CEUS: Contrast-enhanced ultrasound; CNN: Convolutional neural network; EV: External validation; HCC: Hepatocellular carcinoma; FNH: Focal nodular hyperplasia; FLL: Focal liver lesion; RFA: Radiofrequency ablation; SR: Surgical resection; SVM: Support vector machine.

accurate assessment of great numbers of image features from medical images. These features that are difficult to detect by the human eye can be detected by machine learning or deep learning. AI models based on radiomics has also been reported to be applicable for the management of HCC, such as the prediction of microvascular invasion (MVI), curative transarterial chemoembolization (TACE) effect, recurrence after thermal ablation, and prognosis.

Predicting MVI: MVI is described as the invasion of tumor cells within a vascular space lined by endothelium. It has been proven that MVI is a predictor of early recurrence of HCC and poor survival outcomes[54]. The only way to confirm MVI is *via* histopathology after surgery. Patients with HCC can receive a great benefit when MVI is identified noninvasively and accurately before surgery[55]. The application of AI based on gray-scale ultrasound images and CEUS indicated good performance in predicting preoperative MVI.

A study indicated that the radiological features of gray-scale ultrasound images of gross tumoral area predicted preoperative MVI of HCC with an AUC of 0.81[56]. A CEUS-based radiomics score was built for preoperative prediction of MVI in HCC[57]. The radiomics nomogram revealed great potential in the detection of MVI with an AUC of 0.731 compared with the clinical nomogram with an AUC of 0.634. It

was indicated that the radiomics data based on ultrasound was a single predictor of MVI in HCC. Our group created a radiomics model based on CEUS to evaluate MVI of HCC patients before surgery. The model revealed a better detection in the primary group with an AUC of 0.849 *vs* 0.690 as well as the validation group with an AUC of 0.788 *vs* 0.661 when compared with the clinical model. We confirmed that the portal venous phase, delay phase, tumor size, rad-score, and alpha-fetoprotein level were single predictors related to MVI[58].

Predicting curative TACE effect: Pathways participating in important cancer-related progression, such as cell proliferation and angiogenesis, are major goals for the treatment of HCC patients. Additionally, transcription factors and cell cycle regulators are also considered to be interesting for anti-HCC drugs[59].

TACE is a widely used first-line therapy for HCC patients diagnosed at the intermediate stage. The tumor response to the first TACE treatment is highly different and obviously related to the subsequent therapies as well as the patients' survival[60]. Hence, the exact prediction of HCC responses after the first TACE treatment is vital for patients.

The prediction of tumor responses to TACE heavily depends on MRI and serological biomarkers[61,62]. But these methods achieved unsatisfactory accuracy of prediction. The application of AI based on both B-mode ultrasound and CEUS demonstrated better prediction efficacy.

An AI-based radiomics was established and validated to predict the personalized responses of HCC to the first TACE session. The deep learning radiomics-based CEUS model showed better performance compared with the machine learning radiomics-based B-mode model and machine learning radiomics-based time intensity curve of CEUS model with AUCs of 0.93, 0.80, and 0.81, respectively[63]. They suggested that the deep learning-based radiomics could benefit TACE candidates in clinical work.

Predicting recurrence after thermal ablation: Thermal ablation has been confirmed to be an available therapy for early-stage HCC patients who are unsuitable for operation or recurrence after surgery[64]. In addition, the recent 2-year recurrence rates of HCC patients who underwent thermal ablation were reported as 2%-18%[65]. The accurate preoperative prediction of thermal ablation outcomes is of great importance for HCC patients. Compared with other imaging modalities, CEUS is radiation-free and has better temporal resolution when revealing the blood supply of the tumor. The application of AI based on CEUS could be performed for the preoperative prediction of thermal ablation outcomes.

A radiomics model was created to predict the early and late recurrence of HCC patients who accepted thermal ablation[66]. The combined model including CEUS, ultrasound radiomics, and clinical factors showed better performance for early recurrence with an AUC of 0.89 and for late recurrence prediction with a C-index of 0.77.

Predicting the prognoses: Surgical resection (SR) and radiofrequency ablation (RFA) are common curative strategies for HCC patients diagnosed at the early stage[64]. Some studies have compared the long-term survival of RFA and SR for early-stage HCC patients[67,68]. However, the conclusions were sharply different. Hence, it is necessary to find useful predictive means to select the optimal patients who are suitable for RFA or SR before surgery. AI models based on CEUS had great performance for the prediction of progression-free survival (PFS).

A deep learning-based radiomics from CEUS images was built to predict the PFS of SR and RFA for HCC patients. Both SR and RFA models achieved high prediction accuracy of 2-year PFS. They also identified that a higher average probability of 2-year PFS may be acquired while some RFA and SR patients exchange their choices[69]. By utilizing conventional ultrasound images and CEUS, these AI prediction models can be applied in the individualized management of HCC patients.

APPLICATION OF ULTRASOUND-BASED AI IN UPPER GASTROINTESTINAL DISEASE

Gastric mesenchymal tumors

The majority of gastric mesenchymal tumors are occasionally found during routine esophagogastroduodenoscopy examinations. The incidence of gastric mesenchymal tumors is uncertain, but the prevalence of subepithelial tumors identified under endoscopy in Korea was reported as 1.7%[70]. Most gastric mesenchymal tumors are gastrointestinal stromal tumors (GISTs), which may metastasize to the liver and peritoneum after surgery[71,72]. Hence, distinguishing GISTs from benign mesenchymal tumors such as leiomyomas or schwannomas is of great importance in clinic practice. Endoscopic ultrasonography (EUS) is a common method to assess gastric mesenchymal tumors. It helps doctors evaluate the detailed size, shape, origin, and border of the lesions[73-75]. But the interpretation of EUS images by endoscopists is subjective and has poor interobserver agreement. Recently, EUS image interpretation using AI has developed rapidly and is applied to distinguish GISTs from benign mesenchymal tumors.

A convolutional neural network computer-aided diagnosis (CNN-CAD) model based on EUS images was developed to assess gastric mesenchymal tumors. They reported the model distinguished GISTs from non-GIST tumors with 83.0% sensitivity, 75.5% specificity, and 79.2% accuracy[76]. The CNN-CAD model had the potential to provide diagnostic assistance to endoscopists in the future.

Pancreatic diseases

EUS is currently a common tool to diagnose pancreatic diseases in clinical practice. However, the specificity for the diagnosis of pancreatic diseases using EUS images is low and deeply depends on the subjective judgment of endoscopists. Studies have confirmed that AI based on EUS improves their performance for the diagnosis of pancreatic diseases. Recently, AI using EUS images has been applied in the differential diagnosis of PC, distinguishing intraductal papillary mucinous neoplasms (IPMNs) and detecting pancreatic segmentation.

Pancreatic cancer: PC is relatively uncommon, with an incidence of 8-12 per 100000 per year. PC is attributed to hereditary germline or somatic acquired mutations in some genes such as tumor suppressor genes and cell cycle genes. These mutations are also associated with the progression and metastasis of PC. Moreover, shortened telomerase, cell turnover, and genomic instability have an important role in the development of PC[77].

The early diagnosis and surgery of PC, especially for lesions less than 1 cm, can achieve long-term prognoses with a 5-year survival rate of 80.4%[78]. However, PC is most frequently detected at an advanced stage, and the 5-year survival rate remains as low as 3%-15%[79]. Hence, early detection is vital for the treatment of PC patients. Studies have reported that AI based on EUS has great performance for the diagnosis of PC.

AI based on B-mode EUS: AI models based on B-mode EUS have been applied to improve their performance for the diagnosis of PC. Norton *et al*[80] first reported the use of CAD utilizing EUS images in pancreatic diseases in 2001. The study included 14 patients with focal chronic pancreatitis and 21 patients with PC. They showed the diagnostic sensitivity of the two diseases was 89%, and the overall accuracy was 80%[80]. However, this study cannot be referred to as AI-CAD in current applications as the number of patients was limited and the resolution of images were very low.

With the development of AI, ANN and SVM presented good performance in the diagnosis of PC[81-83]. Das *et al*[81] developed an ANN model to distinguish chronic pancreatitis from PC. The results achieved 93% sensitivity, 92% specificity, 87% PPV, 96% negative predictive value (NPV), and 0.93 AUC [81]. By using a multilayered neural network, the study confirmed the first machine learning results for the EUS images of the pancreas. But the sample size was small and lacked pathological evidence in the chronic pancreatitis and normal pancreas groups.

By selecting better texture features that included multifractal dimensional features, a quantitative measure of fractality (self-similarity), and complexity from EUS images, a SVM prediction model was created to identify PC and non-PC patients[83]. The model reached 97.98% accuracy, 94.32% sensitivity, 99.45% specificity, 98.65% PPV, and 97.77% NPV. The study demonstrated that SVM using EUS images is a useful tool for diagnosing PC and pancreatic diseases.

It was reported that AI was also applied for the age-dependent pancreatic changes on EUS images of PC cases. Ozkan *et al*[84] suggested a high-performance CAD model applying ANN to discriminate PC and noncancer patients in three age groups. In the under 40-year-old group, the accuracy, sensitivity and specificity were 92.0%, 87.5%, and 94.1%, respectively. In the 40-year-old to 60-year-old group, the accuracy, sensitivity, and specificity were 88.5%, 85.7%, and 91.7%, respectively. In the > 60-year-old group, the accuracy, sensitivity, and specificity were 91.7%, 93.3%, and 88.9%, respectively. The total performance of this model showed the accuracy, sensitivity, and specificity were 87.5%, 83.3%, and 93.3%, respectively.

Besides machine learning, deep learning has been applied to B-mode EUS images for analysis of PC. A CNN model using EUS images was developed for the detection of PC[85]. The sensitivity, specificity, PPV, and NPV were 90.2%, 74.9%, 80.1%, and 88.7%, respectively. The CNN model included six normalization layers, seven convolution layers, four max-pooling layers, and six activation layers. The EUS-CNN application was first reported to have the potential to detect PC from EUS images.

AI based on EUS elastography: Real-time EUS elastography can provide more information about the features of pancreatic masses by the use of strain assessment. It was reported that EUS elastography has been applied in the differential diagnosis of pancreatic lesions. However, the accuracy and reproducibility were unstable[86,87].

The application of AI improves their performance in the diagnosis of PC. A prospective, blinded, multicentric study using EUS elastography by ANN was performed in focal pancreatic lesions[88]. They demonstrated the sensitivity, specificity, PPV, and NPV values for the diagnosis of PC were 87.59%, 82.94%, 96.25%, and 57.22%, respectively. The study suggested that the ANN model may provide fast and accurate diagnoses in the clinical.

AI based on contrast-enhanced EUS: Contrast-enhanced EUS has been used to enhance the detection of pancreatic lesions[89]. AI based on contrast-enhanced EUS has great performance for the diagnosis of PC. An ANN model based on the TIC analysis from contrast-enhanced EUS images was designed to diagnose PC and chronic pancreatitis. The study reached 94.64% sensitivity, 94.44% specificity, 97.24% PPV, and 89.47% NPV[90]. The study suggested that the model could provide additional diagnostic value to CEUS interpretation and EUS fine needle aspiration results.

IPMNs: IPMNs are considered to be precursor lesions of pancreatic adenocarcinoma. Early surgical resection of IPMNs can provide a survival benefit for patients[91]. EUS is often used to assess the

malignancy of IPMNs in clinics. Several predictive techniques were used to diagnose the malignancy of IPMNs with no satisfactory results (70%-80%)[92,93].

Compared with human diagnosis and conventional EUS features, AI *via* deep learning algorithms was confirmed to be a more exact and objective way for the differential diagnosis of malignant IPMNs. Kuwahara *et al*[94] performed a predictive CNN model using EUS images to detect malignant IPMNs. The model reached 95.7% sensitivity, 94.0% accuracy, and 92.6% specificity. The accuracy was higher compared with the diagnosis of a radiologist (56.0%). The author suggested that the application of AI can evaluate malignant IPMNs before surgery.

Pancreatic segmentation: AI using EUS images has also been applied in pancreatic segmentation. A deep learning-based classification system was created to utilize the "station approach" in EUS of pancreas[95]. The system obtained 90.0% accuracy in classification and 0.770 and 0.813 in blood vessel and pancreas segmentation, respectively. The results were similar to that of EUS experts. Thus, this study revealed that AI has the feasibility to detect the station and segmentation of the pancreas.

APPLICATION OF ULTRASOUND-BASED AI IN LOWER GASTROINTESTINAL DISEASE

Colorectal tumors

Colorectal cancer is the third most common cancer worldwide and accounts for the second leading cause of cancer-related deaths. Moreover, a growing number of patients diagnosed with rectal cancer are under 50-years-old[96]. Colorectal cancer is attributed to gene mutations of epithelial cells, such as oncogenes, tumor suppressor genes, and DNA repair genes. The specific molecular mechanisms implicated in this type of cancer may include the instability of chromosomes and microsatellites[97].

Recently, some researchers studied tumor deposits (TDs) of rectal cancer. TDs are described as focal aggregates of adenocarcinoma located in the surrounding fat of the colon or rectum. They are discontinuous with the primary tumor and unrelated to a lymph node[98,99].

It was reported that a patient who is TD-positive has more malignant tumors, with decreased disease-free survival and overall survival[100]. However, TDs are often diagnosed by pathology only after surgery. Hence, the noninvasive preoperative prediction of TDs is important for rectal cancer patients. EUS is currently a common tool to detect rectal masses. Recently, ultrasound-based radiomics have been applied to predict the status of TDs.

Chen *et al*[101] developed an ANN system using ultrasound radiomics and clinical factors to predict TDs. Endorectal ultrasound and SWE examinations were conducted for 127 patients with rectal cancer. The accuracy was 75.0% in the validation group. The model reached 72.7% sensitivity, 75.9% specificity, and 0.743 AUC. The study suggested that ultrasound-based radiomics has the potential for the prediction of TDs before treatment. Table 3 shows the application of ultrasound-based AI in gastrointestinal disease.

CONCLUSION

In recent years, AI models using ultrasound images have developed rapidly. They can offer a more precise and efficient diagnosis and ease the burden of doctors. AI based on ultrasound has been confirmed to be helpful in diffuse liver diseases and FLLs, such as assessing the severity of NAFLD and the grade of liver fibrosis, distinguishing benign and malignant liver lesions, predicting the MVI of HCC, curative TACE effect, and prognoses after thermal ablation. In addition, AI based on EUS has great performance in gastrointestinal diseases, such as distinguishing gastric mesenchymal tumors, differential diagnosis of PC, distinguishing IPMNs, and predicting the status of TDs in rectal cancer.

However, the application of AI based on ultrasound in clinical practice has some limitations. The main reason may be due to the high variability between radiologists in ultrasound image acquisition and interpretation[102]. Hence, it is necessary to unify the ultrasonic image acquisition process as well as the standard of ultrasonic data measurement during the ultrasound examination.

In addition, some studies of AI-powered ultrasound were retrospective and trained on limited data offered by a single hospital with potential data selection bias, and the amount of data in the training set was not enough. Abundant multicenter prospective studies should assure the efficiency and stability of these AI models. Additionally, deep learning needs a large number of images, so it is necessary to establish an abundant database with common collaborative efforts.

In addition, the application of AI based on EUS has some limitations. The number of EUS examinations is overwhelmingly low compared to other examinations such as endoscopy and CT, especially in gastrointestinal diseases.

In the future, AI based on ultrasound may be used to develop highly accurate and more efficient models for more digestive diseases such as peptic ulcers, stomach neoplasms, inflammatory bowel disease, and so on. These models may heavily reduce the workload for doctors by automatic identi-

Table 3 Application of ultrasound-based artificial intelligence in gastrointestinal disease

Ref.	Diseases: number of cases	Type of ultrasound	Algorithm of AI	Performance
Kim *et al*[76]	GISTs: 125	B-mode EUS	CNN	Sensitivity: 83.0%
	Leiomyomas: 33			Specificity: 75.5%
	Schwannomas: 21			Accuracy: 79.2%
Norton *et al*[80]	Chronic pancreatitis: 14	B-mode EUS	Basic neural network	Sensitivity: 89%
	Pancreatic cancer: 21			Accuracy: 80%
Das *et al*[81]	Chronic pancreatitis: 12	B-mode EUS	ANN	Sensitivity: 93%
	Pancreatic cancer: 22			Specificity: 92%
	Normal patient: 22			AUC: 0.93
Zhu *et al*[82]	Chronic pancreatitis: 126	B-mode EUS	SVM	Sensitivity: 96.25%
				Specificity: 93.38%
	Pancreatic cancer: 262			Accuracy: 94.2%
Zhang *et al*[83]	Pancreatic cancer: 153	B-mode EUS	SVM	Sensitivity: 94.32%
	Normal patient: 63			Specificity: 99.45%
				Accuracy: 97.98%
Ozkan *et al*[84]	Pancreatic cancer: 202	B-mode EUS	ANN	Sensitivity: 83.3%
				Specificity: 93.3%
	Normal patient: 130			Accuracy: 87.5%
Tonozuka *et al*[85]	Chronic pancreatitis: 34	B-mode EUS	CNN	Sensitivity: 90.2%
	Pancreatic cancer: 76			
	Normal patient: 29			Specificity: 74.9%
Săftoiu *et al*[88]	Chronic pancreatitis: 47	EUS elastography	ANN	Sensitivity: 87.59%
	Pancreatic cancer: 211			Specificity: 82.94%
Săftoiu *et al*[90]	Chronic pancreatitis: 55	Contrast-enhanced EUS	ANN	Sensitivity: 94.64%
	Pancreatic cancer: 122			Specificity: 94.44%
Kuwahara *et al*[94]	IPMN: 50	B-mode EUS	CNN	Sensitivity: 95.7%
				Specificity: 92.6%
				Accuracy: 94.0%
Zhang *et al*[95]	Training: 291	B-mode EUS	CNN	Accuracy: 90.0%
	Testing: 181			
Chen *et al*[101]	Rectal cancer: 127	Endorectal ultrasound	ANN	Sensitivity: 72.7%
		Shear-wave elastography		Specificity: 75.9%
				AUC: 0.743

AI: Artificial intelligence; ANN: Artificial neural network; CNN: Convolutional neural network; GISTs: Gastrointestinal stromal tumors; IPMN: Intraductal papillary mucinous neoplasm; EUS: Endoscopic ultrasonography; SVM: Support vector machine.

fication of disease on radiologic and histopathologic images. Moreover, the application of AI can enable building individual management for patients as well as predicting disease progression and complications in clinics. Additionally, AI may improve distance teaching by remote monitoring and enhance medical services in undeveloped areas.

FOOTNOTES

Author contributions: Cui XW and Dietrich CF established the design and conception of the paper; Liu JQ, Ren JY, Xu XL, Xiong LY, Peng YX, Pan XF, Cui XW, and Dietrich CF explored the literature data; Liu JQ provided the first draft of the manuscript, which was discussed and revised critically for intellectual content by Ren JY, Xu XL, Xiong LY, Peng YX, Pan XF, Cui XW, and Dietrich CF; All authors discussed the statement and conclusions and approved the final version to be published.

Supported by the National Natural Science Foundation of China, No. 82071953; and Medical Youth Top-notch Talent Project of Hubei Province.

Conflict-of-interest statement: All the authors report no relevant conflicts of interest for this article.

Open-Access: This article is an open-access article that was selected by an in-house editor and fully peer-reviewed by external reviewers. It is distributed in accordance with the Creative Commons Attribution NonCommercial (CC BY-NC 4.0) license, which permits others to distribute, remix, adapt, build upon this work non-commercially, and license their derivative works on different terms, provided the original work is properly cited and the use is non-commercial. See: https: //creativecommons.org/Licenses/by-nc/4.0/

Country/Territory of origin: China

ORCID number: Christoph F Dietrich 0000-0001-6382-6377; Xin-Wu Cui 0000-0003-3890-6660.

S-Editor: Gong ZM
L-Editor: Filipodia
P-Editor: Gong ZM

REFERENCES

1 **Asrani SK**, Devarbhavi H, Eaton J, Kamath PS. Burden of liver diseases in the world. *J Hepatol* 2019; **70**: 151-171 [PMID: 30266282 DOI: 10.1016/j.jhep.2018.09.014]
2 **Araújo AR**, Rosso N, Bedogni G, Tiribelli C, Bellentani S. Global epidemiology of non-alcoholic fatty liver disease/non-alcoholic steatohepatitis: What we need in the future. *Liver Int* 2018; **38** Suppl 1: 47-51 [PMID: 29427488 DOI: 10.1111/liv.13643]
3 **Torre LA**, Bray F, Siegel RL, Ferlay J, Lortet-Tieulent J, Jemal A. Global cancer statistics, 2012. *CA Cancer J Clin* 2015; **65**: 87-108 [PMID: 25651787 DOI: 10.3322/caac.21262]
4 **Peery AF**, Dellon ES, Lund J, Crockett SD, McGowan CE, Bulsiewicz WJ, Gangarosa LM, Thiny MT, Stizenberg K, Morgan DR, Ringel Y, Kim HP, DiBonaventura MD, Carroll CF, Allen JK, Cook SF, Sandler RS, Kappelman MD, Shaheen NJ. Burden of gastrointestinal disease in the United States: 2012 update. *Gastroenterology* 2012; **143**: 1179-1187.e3 [PMID: 22885331 DOI: 10.1053/j.gastro.2012.08.002]
5 **Yadav D**, Lowenfels AB. The epidemiology of pancreatitis and pancreatic cancer. *Gastroenterology* 2013; **144**: 1252-1261 [PMID: 23622135 DOI: 10.1053/j.gastro.2013.01.068]
6 **Brody H**. Medical imaging. *Nature* 2013; **502**: S81 [PMID: 24187698 DOI: 10.1038/502s81a]
7 **Tchelepi H**, Ralls PW, Radin R, Grant E. Sonography of diffuse liver disease. *J Ultrasound Med* 2002; **21**: 1023-32; quiz 1033 [PMID: 12216750 DOI: 10.7863/jum.2002.21.9.1023]
8 **Vicas C**, Lupsor M, Badea R, Nedevschi S. Usefulness of textural analysis as a tool for noninvasive liver fibrosis staging. *J Med Ultrason (2001)* 2011; **38**: 105-117 [PMID: 27278498 DOI: 10.1007/s10396-011-0307-x]
9 **Wang S**, Summers RM. Machine learning and radiology. *Med Image Anal* 2012; **16**: 933-951 [PMID: 22465077 DOI: 10.1016/j.media.2012.02.005]
10 **Chen H**, Sung JJY. Potentials of AI in medical image analysis in Gastroenterology and Hepatology. *J Gastroenterol Hepatol* 2021; **36**: 31-38 [PMID: 33140875 DOI: 10.1111/jgh.15327]
11 **Mayerhoefer ME**, Materka A, Langs G, Häggström I, Szczypiński P, Gibbs P, Cook G. Introduction to Radiomics. *J Nucl Med* 2020; **61**: 488-495 [PMID: 32060219 DOI: 10.2967/jnumed.118.222893]
12 **LeCun Y**, Bengio Y, Hinton G. Deep learning. *Nature* 2015; **521**: 436-444 [PMID: 26017442 DOI: 10.1038/nature14539]
13 **Litjens G**, Kooi T, Bejnordi BE, Setio AAA, Ciompi F, Ghafoorian M, van der Laak JAWM, van Ginneken B, Sánchez CI. A survey on deep learning in medical image analysis. *Med Image Anal* 2017; **42**: 60-88 [PMID: 28778026 DOI: 10.1016/j.media.2017.07.005]
14 **Ros PR**, Mortele KJ. Diffuse liver disease. *Clin Liver Dis* 2002; **6**: 181-201 [PMID: 11933589 DOI: 10.1016/s1089-3261(03)00072-2]
15 **Piccinino F**, Sagnelli E, Pasquale G, Giusti G. Complications following percutaneous liver biopsy. A multicentre retrospective study on 68,276 biopsies. *J Hepatol* 1986; **2**: 165-173 [PMID: 3958472 DOI: 10.1016/s0168-8278(86)80075-7]
16 **Farrell GC**, Larter CZ. Nonalcoholic fatty liver disease: from steatosis to cirrhosis. *Hepatology* 2006; **43**: S99-S112 [PMID: 16447287 DOI: 10.1002/hep.20973]
17 **Sriraam N**, Roopa J, Saranya M, Dhanalakshmi M. Performance evaluation of computer aided diagnostic tool (CAD) for detection of ultrasonic based liver disease. *J Med Syst* 2009; **33**: 267-274 [PMID: 19697693 DOI: 10.1007/s10916-008-9187-z]

18 **Rinella ME**. Nonalcoholic fatty liver disease: a systematic review. *JAMA* 2015; **313**: 2263-2273 [PMID: 26057287 DOI: 10.1001/jama.2015.5370]

19 **Acharya UR**, Raghavendra U, Fujita H, Hagiwara Y, Koh JE, Jen Hong T, Sudarshan VK, Vijayananthan A, Yeong CH, Gudigar A, Ng KH. Automated characterization of fatty liver disease and cirrhosis using curvelet transform and entropy features extracted from ultrasound images. *Comput Biol Med* 2016; **79**: 250-258 [PMID: 27825038 DOI: 10.1016/j.compbiomed.2016.10.022]

20 **Mathiesen UL**, Franzén LE, Aselius H, Resjö M, Jacobsson L, Foberg U, Frydén A, Bodemar G. Increased liver echogenicity at ultrasound examination reflects degree of steatosis but not of fibrosis in asymptomatic patients with mild/moderate abnormalities of liver transaminases. *Dig Liver Dis* 2002; **34**: 516-522 [PMID: 12236486 DOI: 10.1016/s1590-8658(02)80111-6]

21 **Byra M**, Styczynski G, Szmigielski C, Kalinowski P, Michałowski Ł, Paluszkiewicz R, Ziarkiewicz-Wróblewska B, Zieniewicz K, Sobieraj P, Nowicki A. Transfer learning with deep convolutional neural network for liver steatosis assessment in ultrasound images. *Int J Comput Assist Radiol Surg* 2018; **13**: 1895-1903 [PMID: 30094778 DOI: 10.1007/s11548-018-1843-2]

22 **Biswas M**, Kuppili V, Edla DR, Suri HS, Saba L, Marinhoe RT, Sanches JM, Suri JS. Symtosis: A liver ultrasound tissue characterization and risk stratification in optimized deep learning paradigm. *Comput Methods Programs Biomed* 2018; **155**: 165-177 [PMID: 29512496 DOI: 10.1016/j.cmpb.2017.12.016]

23 **Oelze ML**, Mamou J. Review of Quantitative Ultrasound: Envelope Statistics and Backscatter Coefficient Imaging and Contributions to Diagnostic Ultrasound. *IEEE Trans Ultrason Ferroelectr Freq Control* 2016; **63**: 336-351 [PMID: 26761606 DOI: 10.1109/TUFFC.2015.2513958]

24 **Han A**, Byra M, Heba E, Andre MP, Erdman JW Jr, Loomba R, Sirlin CB, ''Brien WD Jr. Noninvasive Diagnosis of Nonalcoholic Fatty Liver Disease and Quantification of Liver Fat with Radiofrequency Ultrasound Data Using One-dimensional Convolutional Neural Networks. *Radiology* 2020; **295**: 342-350 [PMID: 32096706 DOI: 10.1148/radiol.2020191160]

25 **Ishak K**, Baptista A, Bianchi L, Callea F, De Groote J, Gudat F, Denk H, Desmet V, Korb G, MacSween RN. Histological grading and staging of chronic hepatitis. *J Hepatol* 1995; **22**: 696-699 [PMID: 7560864 DOI: 10.1016/0168-8278(95)80226-6]

26 **Amin A**, Mahmoud-Ghoneim D. Texture analysis of liver fibrosis microscopic images: a study on the effect of biomarkers. *Acta Biochim Biophys Sin (Shanghai)* 2011; **43**: 193-203 [PMID: 21258076 DOI: 10.1093/abbs/gmq129]

27 **Bharti P**, Mittal D, Ananthasivan R. Computer-aided Characterization and Diagnosis of Diffuse Liver Diseases Based on Ultrasound Imaging: A Review. *Ultrason Imaging* 2017; **39**: 33-61 [PMID: 27097589 DOI: 10.1177/0161734616639875]

28 **Yeh WC**, Huang SW, Li PC. Liver fibrosis grade classification with B-mode ultrasound. *Ultrasound Med Biol* 2003; **29**: 1229-1235 [PMID: 14553797 DOI: 10.1016/s0301-5629(03)01010-x]

29 **Zhang L**, Li QY, Duan YY, Yan GZ, Yang YL, Yang RJ. Artificial neural network aided non-invasive grading evaluation of hepatic fibrosis by duplex ultrasonography. *BMC Med Inform Decis Mak* 2012; **12**: 55 [PMID: 22716936 DOI: 10.1186/1472-6947-12-55]

30 **Gao S**, Peng Y, Guo H, Liu W, Gao T, Xu Y, Tang X. Texture analysis and classification of ultrasound liver images. *Biomed Mater Eng* 2014; **24**: 1209-1216 [PMID: 24212015 DOI: 10.3233/BME-130922]

31 **Lee JH**, Joo I, Kang TW, Paik YH, Sinn DH, Ha SY, Kim K, Choi C, Lee G, Yi J, Bang WC. Deep learning with ultrasonography: automated classification of liver fibrosis using a deep convolutional neural network. *Eur Radiol* 2020; **30**: 1264-1273 [PMID: 31478087 DOI: 10.1007/s00330-019-06407-1]

32 **Gatos I**, Tsantis S, Spiliopoulos S, Karnabatidis D, Theotokas I, Zoumpoulis P, Loupas T, Hazle JD, Kagadis GC. Temporal stability assessment in shear wave elasticity images validated by deep learning neural network for chronic liver disease fibrosis stage assessment. *Med Phys* 2019; **46**: 2298-2309 [PMID: 30929260 DOI: 10.1002/mp.13521]

33 **Li W**, Huang Y, Zhuang BW, Liu GJ, Hu HT, Li X, Liang JY, Wang Z, Huang XW, Zhang CQ, Ruan SM, Xie XY, Kuang M, Lu MD, Chen LD, Wang W. Multiparametric ultrasomics of significant liver fibrosis: A machine learning-based analysis. *Eur Radiol* 2019; **29**: 1496-1506 [PMID: 30178143 DOI: 10.1007/s00330-018-5680-z]

34 **Gatos I**, Tsantis S, Spiliopoulos S, Karnabatidis D, Theotokas I, Zoumpoulis P, Loupas T, Hazle JD, Kagadis GC. A new computer aided diagnosis system for evaluation of chronic liver disease with ultrasound shear wave elastography imaging. *Med Phys* 2016; **43**: 1428-1436 [PMID: 26936727 DOI: 10.1118/1.4942383]

35 **Gatos I**, Tsantis S, Spiliopoulos S, Karnabatidis D, Theotokas I, Zoumpoulis P, Loupas T, Hazle JD, Kagadis GC. A Machine-Learning Algorithm Toward Color Analysis for Chronic Liver Disease Classification, Employing Ultrasound Shear Wave Elastography. *Ultrasound Med Biol* 2017; **43**: 1797-1810 [PMID: 28634041 DOI: 10.1016/j.ultrasmedbio.2017.05.002]

36 **Wang K**, Lu X, Zhou H, Gao Y, Zheng J, Tong M, Wu C, Liu C, Huang L, Jiang T, Meng F, Lu Y, Ai H, Xie XY, Yin LP, Liang P, Tian J, Zheng R. Deep learning Radiomics of shear wave elastography significantly improved diagnostic performance for assessing liver fibrosis in chronic hepatitis B: a prospective multicentre study. *Gut* 2019; **68**: 729-741 [PMID: 29730602 DOI: 10.1136/gutjnl-2018-316204]

37 **Liu S**, Wang Y, Yang X, Lei B, Liu L, Li SX, Ni D, Wang T. Deep Learning in Medical Ultrasound Analysis: A Review. *Engineering* 2019; **5**: 261-275 [DOI: 10.1016/j.eng.2018.11.020]

38 **Xue LY**, Jiang ZY, Fu TT, Wang QM, Zhu YL, Dai M, Wang WP, Yu JH, Ding H. Transfer learning radiomics based on multimodal ultrasound imaging for staging liver fibrosis. *Eur Radiol* 2020; **30**: 2973-2983 [PMID: 31965257 DOI: 10.1007/s00330-019-06595-w]

39 **Bruix J**, Sherman M; American Association for the Study of Liver Diseases. Management of hepatocellular carcinoma: an update. *Hepatology* 2011; **53**: 1020-1022 [PMID: 21374666 DOI: 10.1002/hep.24199]

40 **Nishida N**, Kudo M. Artificial Intelligence in Medical Imaging and Its Application in Sonography for the Management of Liver Tumor. *Front Oncol* 2020; **10**: 594580 [PMID: 33409151 DOI: 10.3389/fonc.2020.594580]

41 **Heimbach JK**, Kulik LM, Finn RS, Sirlin CB, Abecassis MM, Roberts LR, Zhu AX, Murad MH, Marrero JA. AASLD guidelines for the treatment of hepatocellular carcinoma. *Hepatology* 2018; **67**: 358-380 [PMID: 28130846 DOI:

10.1002/hep.29086]
42 **Xi IL**, Wu J, Guan J, Zhang PJ, Horii SC, Soulen MC, Zhang Z, Bai HX. Deep learning for differentiation of benign and malignant solid liver lesions on ultrasonography. *Abdom Radiol (NY)* 2021; **46**: 534-543 [PMID: 32681268 DOI: 10.1007/s00261-020-02564-w]
43 **Yang Q**, Wei J, Hao X, Kong D, Yu X, Jiang T, Xi J, Cai W, Luo Y, Jing X, Yang Y, Cheng Z, Wu J, Zhang H, Liao J, Zhou P, Song Y, Zhang Y, Han Z, Cheng W, Tang L, Liu F, Dou J, Zheng R, Yu J, Tian J, Liang P. Improving B-mode ultrasound diagnostic performance for focal liver lesions using deep learning: A multicentre study. *eBioMedicine* 2020; **56**: 102777 [PMID: 32485640 DOI: 10.1016/j.ebiom.2020.102777]
44 **Virmani J**, Kumar V, Kalra N, Khandelwal N. Characterization of primary and secondary malignant liver lesions from B-mode ultrasound. *J Digit Imaging* 2013; **26**: 1058-1070 [PMID: 23412917 DOI: 10.1007/s10278-013-9578-7]
45 **Claudon M**, Cosgrove D, Albrecht T, Bolondi L, Bosio M, Calliada F, Correas JM, Darge K, Dietrich C, ''Onofrio M, Evans DH, Filice C, Greiner L, Jäger K, Jong Nd, Leen E, Lencioni R, Lindsell D, Martegani A, Meairs S, Nolsøe C, Piscaglia F, Ricci P, Seidel G, Skjoldbye B, Solbiati L, Thorelius L, Tranquart F, Weskott HP, Whittingham T. Guidelines and good clinical practice recommendations for contrast enhanced ultrasound (CEUS)–- update 2008. *Ultraschall Med* 2008; **29**: 28-44 [PMID: 18270887 DOI: 10.1055/s-2007-963785]
46 **Kondo S**, Takagi K, Nishida M, Iwai T, Kudo Y, Ogawa K, Kamiyama T, Shibuya H, Kahata K, Shimizu C. Computer-Aided Diagnosis of Focal Liver Lesions Using Contrast-Enhanced Ultrasonography With Perflubutane Microbubbles. *IEEE Trans Med Imaging* 2017; **36**: 1427-1437 [PMID: 28141517 DOI: 10.1109/TMI.2017.2659734]
47 **Gatos I**, Tsantis S, Spiliopoulos S, Skouroliakou A, Theotokas I, Zoumpoulis P, Hazle JD, Kagadis GC. A new automated quantification algorithm for the detection and evaluation of focal liver lesions with contrast-enhanced ultrasound. *Med Phys* 2015; **42**: 3948-3959 [PMID: 26133595 DOI: 10.1118/1.4921753]
48 **Guo LH**, Wang D, Qian YY, Zheng X, Zhao CK, Li XL, Bo XW, Yue WW, Zhang Q, Shi J, Xu HX. A two-stage multi-view learning framework based computer-aided diagnosis of liver tumors with contrast enhanced ultrasound images. *Clin Hemorheol Microcirc* 2018; **69**: 343-354 [PMID: 29630528 DOI: 10.3233/CH-170275]
49 **Hwang YN**, Lee JH, Kim GY, Jiang YY, Kim SM. Classification of focal liver lesions on ultrasound images by extracting hybrid textural features and using an artificial neural network. *Biomed Mater Eng* 2015; **26** Suppl 1: S1599-S1611 [PMID: 26405925 DOI: 10.3233/BME-151459]
50 **Schmauch B**, Herent P, Jehanno P, Dehaene O, Saillard C, Aubé C, Luciani A, Lassau N, Jégou S. Diagnosis of focal liver lesions from ultrasound using deep learning. *Diagn Interv Imaging* 2019; **100**: 227-233 [PMID: 30926443 DOI: 10.1016/j.diii.2019.02.009]
51 **Tiyarattanachai T**, Apiparakoon T, Marukatat S, Sukcharoen S, Geratikornsupuk N, Anukulkarnkusol N, Mekaroonkamol P, Tanpowpong N, Sarakul P, Rerknimitr R, Chaiteerakij R. Development and validation of artificial intelligence to detect and diagnose liver lesions from ultrasound images. *pLoS One* 2021; **16**: e0252882 [PMID: 34101764 DOI: 10.1371/journal.pone.0252882]
52 **Streba CT**, Ionescu M, Gheonea DI, Sandulescu L, Ciurea T, Saftoiu A, Vere CC, Rogoveanu I. Contrast-enhanced ultrasonography parameters in neural network diagnosis of liver tumors. *World J Gastroenterol* 2012; **18**: 4427-4434 [PMID: 22969209 DOI: 10.3748/wjg.v18.i32.4427]
53 **Căleanu CD**, Sîrbu CL, Simion G. Deep Neural Architectures for Contrast Enhanced Ultrasound (CEUS) Focal Liver Lesions Automated Diagnosis. *Sensors (Basel)* 2021; **21** [PMID: 34208548 DOI: 10.3390/s21124126]
54 **Lim KC**, Chow PK, Allen JC, Chia GS, Lim M, Cheow PC, Chung AY, Ooi LL, Tan SB. Microvascular invasion is a better predictor of tumor recurrence and overall survival following surgical resection for hepatocellular carcinoma compared to the Milan criteria. *Ann Surg* 2011; **254**: 108-113 [PMID: 21527845 DOI: 10.1097/SLA.0b013e31821ad884]
55 **Banerjee S**, Wang DS, Kim HJ, Sirlin CB, Chan MG, Korn RL, Rutman AM, Siripongsakun S, Lu D, Imanbayev G, Kuo MD. A computed tomography radiogenomic biomarker predicts microvascular invasion and clinical outcomes in hepatocellular carcinoma. *Hepatology* 2015; **62**: 792-800 [PMID: 25930992 DOI: 10.1002/hep.27877]
56 **Dong Y**, Zhou L, Xia W, Zhao XY, Zhang Q, Jian JM, Gao X, Wang WP. Preoperative Prediction of Microvascular Invasion in Hepatocellular Carcinoma: Initial Application of a Radiomic Algorithm Based on Grayscale Ultrasound Images. *Front Oncol* 2020; **10**: 353 [PMID: 32266138 DOI: 10.3389/fonc.2020.00353]
57 **Hu HT**, Wang Z, Huang XW, Chen SL, Zheng X, Ruan SM, Xie XY, Lu MD, Yu J, Tian J, Liang P, Wang W, Kuang M. Ultrasound-based radiomics score: a potential biomarker for the prediction of microvascular invasion in hepatocellular carcinoma. *Eur Radiol* 2019; **29**: 2890-2901 [PMID: 30421015 DOI: 10.1007/s00330-018-5797-0]
58 **Zhang D**, Wei Q, Wu GG, Zhang XY, Lu WW, Lv WZ, Liao JT, Cui XW, Ni XJ, Dietrich CF. Preoperative Prediction of Microvascular Invasion in Patients With Hepatocellular Carcinoma Based on Radiomics Nomogram Using Contrast-Enhanced Ultrasound. *Front Oncol* 2021; **11**: 709339 [PMID: 34557410 DOI: 10.3389/fonc.2021.709339]
59 **Juaid N**, Amin A, Abdalla A, Reese K, Alamri Z, Moulay M, Abdu S, Miled N. Anti-Hepatocellular Carcinoma Biomolecules: Molecular Targets Insights. *Int J Mol Sci* 2021; **22** [PMID: 34639131 DOI: 10.3390/ijms221910774]
60 **Kim BK**, Kim SU, Kim KA, Chung YE, Kim MJ, Park MS, Park JY, Kim DY, Ahn SH, Kim MD, Park SI, Won JY, Lee DY, Han KH. Complete response at first chemoembolization is still the most robust predictor for favorable outcome in hepatocellular carcinoma. *J Hepatol* 2015; **62**: 1304-1310 [PMID: 25637785 DOI: 10.1016/j.jhep.2015.01.022]
61 **Loosen SH**, Schulze-Hagen M, Leyh C, Benz F, Vucur M, Kuhl C, Trautwein C, Tacke F, Bruners P, Roderburg C, Luedde T. IL-6 and IL-8 Serum Levels Predict Tumor Response and Overall Survival after TACE for Primary and Secondary Hepatic Malignancies. *Int J Mol Sci* 2018; **19** [PMID: 29899223 DOI: 10.3390/ijms19061766]
62 **Lahrsow M**, Albrecht MH, Bickford MW, Vogl TJ. Predicting Treatment Response of Colorectal Cancer Liver Metastases to Conventional Lipiodol-Based Transarterial Chemoembolization Using Diffusion-Weighted MR Imaging: Value of Pretreatment Apparent Diffusion Coefficients (ADC) and ADC Changes Under Therapy. *Cardiovasc Intervent Radiol* 2017; **40**: 852-859 [PMID: 28357571 DOI: 10.1007/s00270-017-1634-0]
63 **Liu D**, Liu F, Xie X, Su L, Liu M, Kuang M, Huang G, Wang Y, Zhou H, Wang K, Lin M, Tian J. Accurate prediction of responses to transarterial chemoembolization for patients with hepatocellular carcinoma by using artificial intelligence in contrast-enhanced ultrasound. *Eur Radiol* 2020; **30**: 2365-2376 [PMID: 31900703 DOI: 10.1007/s00330-019-06553-6]

64 **European Association for the Study of the Liver**. EASL Clinical Practice Guidelines: Management of hepatocellular carcinoma. *J Hepatol* 2018; **69**: 182-236 [PMID: 29628281 DOI: 10.1016/j.jhep.2018.03.019]

65 **European Association For The Study Of The Liver**. European Organisation For Research And Treatment Of Cancer. EASL-EORTC clinical practice guidelines: management of hepatocellular carcinoma. *J Hepatol* 2012; **56**: 908-943 [PMID: 22424438 DOI: 10.1016/j.jhep.2011.12.001]

66 **Ma QP**, He XL, Li K, Wang JF, Zeng QJ, Xu EJ, He XQ, Li SY, Kun W, Zheng RQ, Tian J. Dynamic Contrast-Enhanced Ultrasound Radiomics for Hepatocellular Carcinoma Recurrence Prediction After Thermal Ablation. *Mol Imaging Biol* 2021; **23**: 572-585 [PMID: 33483803 DOI: 10.1007/s11307-021-01578-0]

67 **Chen MS**, Li JQ, Zheng Y, Guo RP, Liang HH, Zhang YQ, Lin XJ, Lau WY. A prospective randomized trial comparing percutaneous local ablative therapy and partial hepatectomy for small hepatocellular carcinoma. *Ann Surg* 2006; **243**: 321-328 [PMID: 16495695 DOI: 10.1097/01.sla.0000201480.65519.b8]

68 **Feng K**, Yan J, Li X, Xia F, Ma K, Wang S, Bie P, Dong J. A randomized controlled trial of radiofrequency ablation and surgical resection in the treatment of small hepatocellular carcinoma. *J Hepatol* 2012; **57**: 794-802 [PMID: 22634125 DOI: 10.1016/j.jhep.2012.05.007]

69 **Liu F**, Liu D, Wang K, Xie X, Su L, Kuang M, Huang G, Peng B, Wang Y, Lin M, Tian J. Deep Learning Radiomics Based on Contrast-Enhanced Ultrasound Might Optimize Curative Treatments for Very-Early or Early-Stage Hepatocellular Carcinoma Patients. *Liver Cancer* 2020; **9**: 397-413 [PMID: 32999867 DOI: 10.1159/000505694]

70 **Lee JH**, Lee HL, Ahn YW, Lee KN, Jun DW, Lee OY, Han DS, Yoon BC, Choi HS. Prevalence of Gastric Subepithelial Tumors in Korea: A Single Center Experience. *Korean J Gastroenterol* 2015; **66**: 274-276 [PMID: 26586350 DOI: 10.4166/kjg.2015.66.5.274]

71 **Blay JY**, Bonvalot S, Casali P, Choi H, Debiec-Richter M, Dei Tos AP, Emile JF, Gronchi A, Hogendoorn PC, Joensuu H, Le Cesne A, McClure J, Maurel J, Nupponen N, Ray-Coquard I, Reichardt P, Sciot R, Stroobants S, van Glabbeke M, van Oosterom A, Demetri GD; GIST consensus meeting panelists. Consensus meeting for the management of gastrointestinal stromal tumors. Report of the GIST Consensus Conference of 20-21 March 2004, under the auspices of ESMO. *Ann Oncol* 2005; **16**: 566-578 [PMID: 15781488 DOI: 10.1093/annonc/mdi127]

72 **Miettinen M**, Sobin LH, Lasota J. Gastrointestinal stromal tumors of the stomach: a clinicopathologic, immunohistochemical, and molecular genetic study of 1765 cases with long-term follow-up. *Am J Surg Pathol* 2005; **29**: 52-68 [PMID: 15613856 DOI: 10.1097/01.pas.0000146010.92933.de]

73 **Chak A**, Canto MI, Rösch T, Dittler HJ, Hawes RH, Tio TL, Lightdale CJ, Boyce HW, Scheiman J, Carpenter SL, Van Dam J, Kochman ML, Sivak MV Jr. Endosonographic differentiation of benign and malignant stromal cell tumors. *Gastrointest Endosc* 1997; **45**: 468-473 [PMID: 9199902 DOI: 10.1016/s0016-5107(97)70175-5]

74 **Palazzo L**, Landi B, Cellier C, Cuillerier E, Roseau G, Barbier JP. Endosonographic features predictive of benign and malignant gastrointestinal stromal cell tumours. *Gut* 2000; **46**: 88-92 [PMID: 10601061 DOI: 10.1136/gut.46.1.88]

75 **Kim GH**, Park DY, Kim S, Kim DH, Choi CW, Heo J, Song GA. Is it possible to differentiate gastric GISTs from gastric leiomyomas by EUS? *World J Gastroenterol* 2009; **15**: 3376-3381 [PMID: 19610138 DOI: 10.3748/wjg.15.3376]

76 **Kim YH**, Kim GH, Kim KB, Lee MW, Lee BE, Baek DH, Kim DH, Park JC. Application of A Convolutional Neural Network in The Diagnosis of Gastric Mesenchymal Tumors on Endoscopic Ultrasonography Images. *J Clin Med* 2020; **9** [PMID: 33003602 DOI: 10.3390/jcm9103162]

77 **Goral V**. Pancreatic Cancer: Pathogenesis and Diagnosis. *Asian Pac J Cancer Prev* 2015; **16**: 5619-5624 [PMID: 26320426 DOI: 10.7314/apjcp.2015.16.14.5619]

78 **Egawa S**, Toma H, Ohigashi H, Okusaka T, Nakao A, Hatori T, Maguchi H, Yanagisawa A, Tanaka M. Japan Pancreatic Cancer Registry; 30th year anniversary: Japan Pancreas Society. *Pancreas* 2012; **41**: 985-992 [PMID: 22750974 DOI: 10.1097/MPA.0b013e318258055c]

79 **Pereira SP**, Oldfield L, Ney A, Hart PA, Keane MG, Pandol SJ, Li D, Greenhalf W, Jeon CY, Koay EJ, Almario CV, Halloran C, Lennon AM, Costello E. Early detection of pancreatic cancer. *Lancet Gastroenterol Hepatol* 2020; **5**: 698-710 [PMID: 32135127 DOI: 10.1016/S2468-1253(19)30416-9]

80 **Norton ID**, Zheng Y, Wiersema MS, Greenleaf J, Clain JE, Dimagno EP. Neural network analysis of EUS images to differentiate between pancreatic malignancy and pancreatitis. *Gastrointest Endosc* 2001; **54**: 625-629 [PMID: 11677484 DOI: 10.1067/mge.2001.118644]

81 **Das A**, Nguyen CC, Li F, Li B. Digital image analysis of EUS images accurately differentiates pancreatic cancer from chronic pancreatitis and normal tissue. *Gastrointest Endosc* 2008; **67**: 861-867 [PMID: 18179797 DOI: 10.1016/j.gie.2007.08.036]

82 **Zhu M**, Xu C, Yu J, Wu Y, Li C, Zhang M, Jin Z, Li Z. Differentiation of pancreatic cancer and chronic pancreatitis using computer-aided diagnosis of endoscopic ultrasound (EUS) images: a diagnostic test. *pLoS One* 2013; **8**: e63820 [PMID: 23704940 DOI: 10.1371/journal.pone.0063820]

83 **Zhang MM**, Yang H, Jin ZD, Yu JG, Cai ZY, Li ZS. Differential diagnosis of pancreatic cancer from normal tissue with digital imaging processing and pattern recognition based on a support vector machine of EUS images. *Gastrointest Endosc* 2010; **72**: 978-985 [PMID: 20855062 DOI: 10.1016/j.gie.2010.06.042]

84 **Ozkan M**, Cakiroglu M, Kocaman O, Kurt M, Yilmaz B, Can G, Korkmaz U, Dandil E, Eksi Z. Age-based computer-aided diagnosis approach for pancreatic cancer on endoscopic ultrasound images. *Endosc Ultrasound* 2016; **5**: 101-107 [PMID: 27080608 DOI: 10.4103/2303-9027.180473]

85 **Tonozuka R**, Itoi T, Nagata N, Kojima H, Sofuni A, Tsuchiya T, Ishii K, Tanaka R, Nagakawa Y, Mukai S. Deep learning analysis for the detection of pancreatic cancer on endosonographic images: a pilot study. *J Hepatobiliary Pancreat Sci* 2021; **28**: 95-104 [PMID: 32910528 DOI: 10.1002/jhbp.825]

86 **Iglesias-Garcia J**, Larino-Noia J, Abdulkader I, Forteza J, Dominguez-Munoz JE. EUS elastography for the characterization of solid pancreatic masses. *Gastrointest Endosc* 2009; **70**: 1101-1108 [PMID: 19647248 DOI: 10.1016/j.gie.2009.05.011]

87 **Iglesias-Garcia J**, Larino-Noia J, Abdulkader I, Forteza J, Dominguez-Munoz JE. Quantitative endoscopic ultrasound elastography: an accurate method for the differentiation of solid pancreatic masses. *Gastroenterology* 2010; **139**: 1172-

1180 [PMID: 20600020 DOI: 10.1053/j.gastro.2010.06.059]
88 **Săftoiu A**, Vilmann P, Gorunescu F, Janssen J, Hocke M, Larsen M, Iglesias-Garcia J, Arcidiacono P, Will U, Giovannini M, Dietrich CF, Havre R, Gheorghe C, McKay C, Gheonea DI, Ciurea T; European EUS Elastography Multicentric Study Group. Efficacy of an artificial neural network-based approach to endoscopic ultrasound elastography in diagnosis of focal pancreatic masses. *Clin Gastroenterol Hepatol* 2012; **10**: 84-90.e1 [PMID: 21963957 DOI: 10.1016/j.cgh.2011.09.014]
89 **Dietrich CF**, Braden B, Hocke M, Ott M, Ignee A. Improvedharacterizationn of solitary solid pancreatic tumours using contrast enhanced transabdominal ultrasound. *J Cancer Res Clin Oncol* 2008; **134**: 635-643 [PMID: 17952469 DOI: 10.1007/s00432-007-0326-6]
90 **Săftoiu A**, Vilmann P, Dietrich CF, Iglesias-Garcia J, Hocke M, Seicean A, Ignee A, Hassan H, Streba CT, Ioncică AM, Gheonea DI, Ciurea T. Quantitative contrast-enhanced harmonic EUS in differential diagnosis of focal pancreatic masses (with videos). *Gastrointest Endosc* 2015; **82**: 59-69 [PMID: 25792386 DOI: 10.1016/j.gie.2014.11.040]
91 **Moris D**, Damaskos C, Spartalis E, Papalampros A, Vernadakis S, Dimitroulis D, Griniatsos J, Felekouras E, Nikiteas N. Updates and Critical Evaluation on Novel Biomarkers for the Malignant Progression of Intraductal Papillary Mucinous Neoplasms of the Pancreas. *Anticancer Res* 2017; **37**: 2185-2194 [PMID: 28476781 DOI: 10.21873/anticanres.11553]
92 **Shimizu Y**, Hijioka S, Hirono S, Kin T, Ohtsuka T, Kanno A, Koshita S, Hanada K, Kitano M, Inoue H, Itoi T, Ueki T, Matsuo K, Yanagisawa A, Yamaue H, Sugiyama M, Okazaki K. New Model for Predicting Malignancy in Patients With Intraductal Papillary Mucinous Neoplasm. *Ann Surg* 2020; **272**: 155-162 [PMID: 30499803 DOI: 10.1097/SLA.0000000000003108]
93 **Shimizu Y**, Yamaue H, Maguchi H, Yamao K, Hirono S, Osanai M, Hijioka S, Hosoda W, Nakamura Y, Shinohara T, Yanagisawa A. Predictors of malignancy in intraductal papillary mucinous neoplasm of the pancreas: analysis of 310 pancreatic resection patients at multiple high-volume centers. *Pancreas* 2013; **42**: 883-888 [PMID: 23508017 DOI: 10.1097/MPA.0b013e31827a7b84]
94 **Kuwahara T**, Hara K, Mizuno N, Okuno N, Matsumoto S, Obata M, Kurita Y, Koda H, Toriyama K, Onishi S, Ishihara M, Tanaka T, Tajika M, Niwa Y. Usefulness of Deep Learning Analysis for the Diagnosis of Malignancy in Intraductal Papillary Mucinous Neoplasms of the Pancreas. *Clin Transl Gastroenterol* 2019; **10**: 1-8 [PMID: 31117111 DOI: 10.14309/ctg.0000000000000045]
95 **Zhang J**, Zhu L, Yao L, Ding X, Chen D, Wu H, Lu Z, Zhou W, Zhang L, An P, Xu B, Tan W, Hu S, Cheng F, Yu H. Deep learning-based pancreas segmentation and station recognition system in EUS: development and validation of a useful training tool (with video). *Gastrointest Endosc* 2020; **92**: 874-885.e3 [PMID: 32387499 DOI: 10.1016/j.gie.2020.04.071]
96 **Keller DS**, Berho M, Perez RO, Wexner SD, Chand M. The multidisciplinary management of rectal cancer. *Nat Rev Gastroenterol Hepatol* 2020; **17**: 414-429 [PMID: 32203400 DOI: 10.1038/s41575-020-0275-y]
97 **Alzahrani SM**, Al Doghaither HA, Al-Ghafari AB. General insight into cancer: An overview of colorectal cancer (Review). *Mol Clin Oncol* 2021; **15**: 271 [PMID: 34790355 DOI: 10.3892/mco.2021.2433]
98 **Greene FL**. Tumor deposits in colorectal cancer: a moving target. *Ann Surg* 2012; **255**: 214-215 [PMID: 22202583 DOI: 10.1097/SLA.0b013e3182430eaa]
99 **Tong LL**, Gao P, Wang ZN, Song YX, Xu YY, Sun Z, Xing CZ, Xu HM. Is the seventh edition of the UICC/AJCC TNM staging system reasonable for patients with tumor deposits in colorectal cancer? *Ann Surg* 2012; **255**: 208-213 [PMID: 21527844 DOI: 10.1097/SLA.0b013e31821ad8a2]
100 **Nagtegaal ID**, Knijn N, Hugen N, Marshall HC, Sugihara K, Tot T, Ueno H, Quirke P. Tumor Deposits in Colorectal Cancer: Improving the Value of Modern Staging-A Systematic Review and Meta-Analysis. *J Clin Oncol* 2017; **35**: 1119-1127 [PMID: 28029327 DOI: 10.1200/JCO.2016.68.9091]
101 **Chen LD**, Li W, Xian MF, Zheng X, Lin Y, Liu BX, Lin MX, Li X, Zheng YL, Xie XY, Lu MD, Kuang M, Xu JB, Wang W. Preoperative prediction of tumour deposits in rectal cancer by an artificial neural network-based US radiomics model. *Eur Radiol* 2020; **30**: 1969-1979 [PMID: 31828415 DOI: 10.1007/s00330-019-06558-1]
102 **Akkus Z**, Cai J, Boonrod A, Zeinoddini A, Weston AD, Philbrick KA, Erickson BJ. A Survey of Deep-Learning Applications in Ultrasound: Artificial Intelligence-Powered Ultrasound for Improving Clinical Workflow. *J Am Coll Radiol* 2019; **16**: 1318-1328 [PMID: 31492410 DOI: 10.1016/j.jacr.2019.06.004]

World Journal of Gastroenterology

Submit a Manuscript: https://www.f6publishing.com

World J Gastroenterol 2022 October 14; 28(38): 5547-5556

DOI: 10.3748/wjg.v28.i38.5547

ISSN 1007-9327 (print) ISSN 2219-2840 (online)

MINIREVIEWS

Oxidative stress bridges the gut microbiota and the occurrence of frailty syndrome

Si-Yue Chen, Tong-Yao Wang, Chao Zhao, Hui-Jing Wang

Specialty type: Gastroenterology and hepatology

Provenance and peer review: Invited article; Externally peer reviewed.

Peer-review model: Single blind

Peer-review report's scientific quality classification

Grade A (Excellent): 0
Grade B (Very good): B
Grade C (Good): C, C, C
Grade D (Fair): 0
Grade E (Poor): 0

P-Reviewer: Almeida C, Portugal; Amedei A, Italy; Konopelski P, Poland; Yi B, China

Received: August 1, 2022
Peer-review started: August 1, 2022
First decision: August 19, 2022
Revised: August 31, 2022
Accepted: September 23, 2022
Article in press: September 23, 2022
Published online: October 14, 2022

Si-Yue Chen, Hui-Jing Wang, Laboratory of Neuropsychopharmacology, College of Fundamental Medicine, Shanghai University of Medicine & Health Science, Shanghai 201318, China

Tong-Yao Wang, Chao Zhao, Key Laboratory of Medical Molecular Virology, School of Basic Medical Sciences, Shanghai Medical College & National Clinical Research Center for Aging and Medicine, Huashan Hospital, Shanghai Medical College, Fudan University, Shanghai 200032, China

Chao Zhao, Shanghai Frontiers Science Center of Pathogenic Microbes and Infection, Shanghai Frontiers Science Center, Shanghai 200032, China

Corresponding author: Hui-Jing Wang, PhD, Associate Professor, Laboratory of Neuropsychopharmacology, College of Fundamental Medicine, Shanghai University of Medicine & Health Science, No. 279, Zhouzhu Highway, Pudong New Area, Shanghai 201318, China. wanghj@sumhs.edu.cn

Abstract

The incidence of frailty gradually increases with age. This condition places a heavy burden on modern society, of which the aging population is increasing. Frailty is one of the most complicated clinical syndromes; thus, it is difficult to uncover its underlying mechanisms. Oxidative stress (OS) is involved in frailty in multiple ways. The association between the gut microbiota (GM) and frailty was recently reported. Herein, we propose that OS is involved in the association between the GM and the occurrence of frailty syndrome. An imbalance between oxidation and antioxidants can eventually lead to frailty, and the GM probably participates in this process through the production of reactive oxygen species. On the other hand, OS can disturb the GM. Such dysbiosis consequently induces or exacerbates tissue damage, leading to the occurrence of frailty syndrome. Finally, we discuss the possibility of improving frailty by intervening in the vicious cycle between the imbalance of OS and dysbiosis.

Key Words: Oxidative stress; Gut microbiota; Frail syndrome; Traditional Chinese medicine

©The Author(s) 2022. Published by Baishideng Publishing Group Inc. All rights reserved.

Core Tip: Frailty is defined as a decrease in the reserve and restoring capacity of the body. It is recognized that oxidative stress (OS) is involved in frailty in multiple ways; however, the underlying mechanisms are still unknown. The association between the gut microbiota (GM) and frailty was recently reported. Herein, we propose that OS is involved in the association between the GM and the occurrence of frailty syndrome. The role of the imbalance between OS and dysbiosis is discussed in this review.

Citation: Chen SY, Wang TY, Zhao C, Wang HJ. Oxidative stress bridges the gut microbiota and the occurrence of frailty syndrome. *World J Gastroenterol* 2022; 28(38): 5547-5556
URL: https://www.wjgnet.com/1007-9327/full/v28/i38/5547.htm
DOI: https://dx.doi.org/10.3748/wjg.v28.i38.5547

INTRODUCTION

Frailty is one of the most complicated clinical syndromes and is defined as a decrease in the reserve and restoring capacity of the body[1]. For frail people, a slight irritant can result in strong responses, which require a longer period to recover. Thus, frailty can also be regarded as a decline in the ability to maintain homeostasis. Multiple organs and systems, such as the skeletal muscle, immune, endocrine, hematopoiesis, and cardiovascular systems, are involved in the process of frailty[2]. Patients with frailty have a high risk of developing age-related diseases, including neurodegenerative diseases (such as dementia), type II diabetes, atherosclerosis, and chronic heart failure[3]. Frailty places a heavy burden on modern society, which has an extensive elderly population.

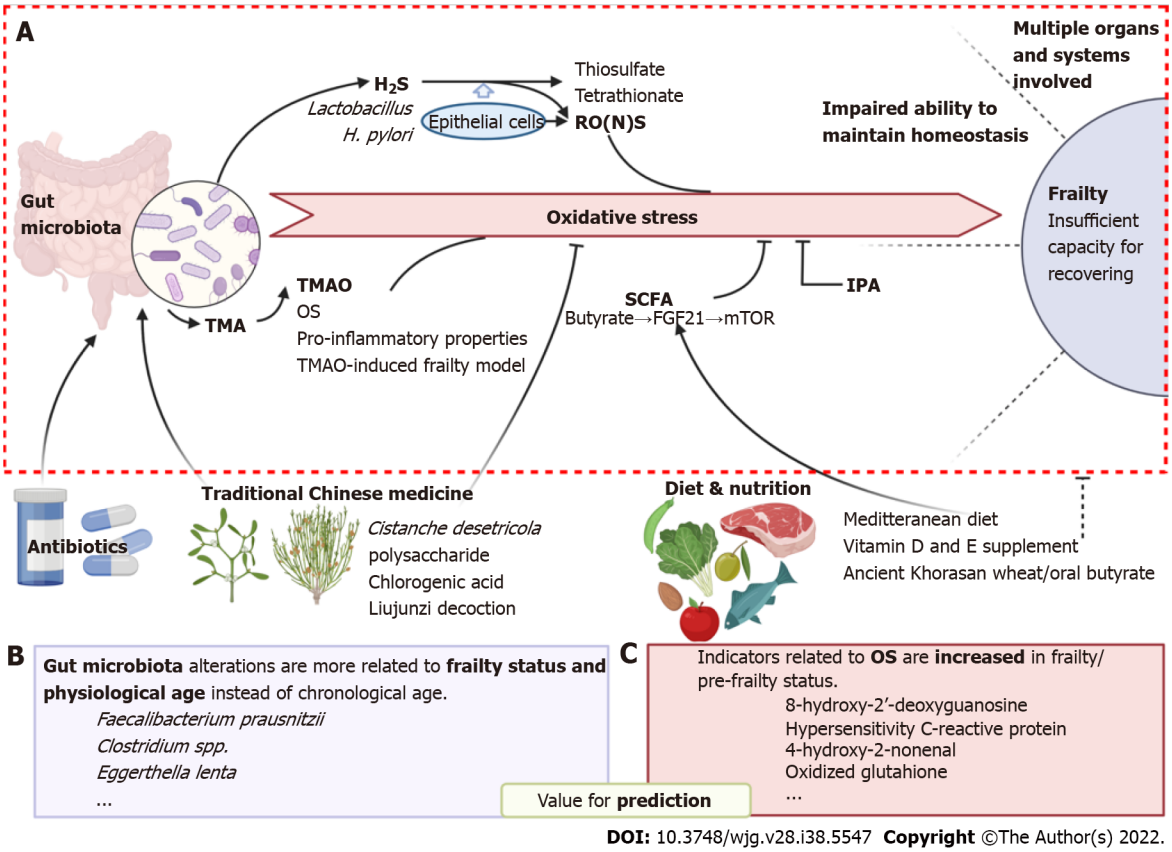
Although there are a few hypotheses at present, the mechanisms involved in frailty remain unknown. Researchers have different opinions about the origin of frailty. It is generally accepted that frailty is related to aging. According to Jayanama *et al*'s survey[4], among 9030 volunteers over the age of 20, the average age with a frailty index score of less than 0.1 was 39.7 years old. Moreover, those who had an average age of 65.3 years had a frailty index score of more than 0.3. Miller *et al*[5] reported that 75.4% of 18- to 64-year-old people have an simplified, 5-item frailty index (sFI) = 0, which means they are considered nonfrail. In contrast, 20.1% of the 80 to 89-year-old age group had an sFI ≥ 3, and thus, this age group can be referred to as a frail population. There were 9252 patients included in this analysis.

The incidence of frailty increases with age. However, frailty is not necessarily related to aging. According to an investigation by Xing and Guo[6], 43.2% of 683 older people (≥ 60 years old) from Beijing did not have frailty, while the incidence of prefrailty was 45.7%, and 11.1% of the cohort was frail. These data suggest that healthy aging could be achieved by preventing and improving frailty status.

With the increasing focus on frailty, emerging evidence has increased our understanding of this syndrome. Findings from centenarians suggest that specific gut microbiota (GM) constituents may contribute to healthy aging. For example, *Escherichia*, *Ruminococcus*[7], and *Clostridioides leptum* are increased, whereas *Faecalibacterium prausnitzii* and other species are decreased in centenarians[8]. Biagi *et al*[8] also showed that the proportion of *Clostridioides* cluster XIVa was significantly lower in centenarians than in elderly and younger adults. Furthermore, the diversity and abundance of the GM vary between elderly adults and centenarians. However, the bridge between the GM and the occurrence of frailty remains unclear. In this review, we proposed the possible mechanisms involved in frailty from the perspective of the GM and oxidative stress (OS). The correlations and potential causality among these factors are discussed. The idea of using GM biomarkers to predict frailty is then proposed prospectively. Notably, frailty is not an irreversible status[9]. Timely interventions have the potential to revert the prefrailty or frailty state to a nonfrailty state. According to existing research, dietary interventions are the most commonly used treatment for frailty[10]. Moreover, traditional Chinese medicine (TCM) is a unique application for the treatment of frailty (Figure 1). Achieving healthy aging is becoming a core goal of future research.

THE GM AND FRAILTY

The abundance and diversity of the GM changes with aging. Alterations in the GM partially lead to individual differences in the health status of elderly people by interacting with the host immune system [11]. Evidence has shown that the elderly population has higher abundances of *Clostridioides* cluster XIVa, *Faecalibacterium prauanitzii, Actinomycetes* (mainly *Bifidobacterium*) and *Proteobacteria* than those of young adults[12]. Biagi *et al*[8] showed that the abundance of *Clostridioides* cluster XIVa was significantly higher in the elderly population (49%) than in the centenarians (34%) and the young population (44%). There was no significant difference in the abundance of *Clostridioides* cluster IV among these three age groups, but the subgroups had a different tendency to change. The abundance of *Faecalibacterium*



DOI: 10.3748/wjg.v28.i38.5547 **Copyright** ©The Author(s) 2022.

Figure 1 Oxidative stress is involved in the association between the gut microbiota and frailty syndrome. A: Involving molecular and pathways of how oxidative stress bridges gut microbiota and frailty; B and C: Potential bacterial species and oxidative markers which are valuable for prediction of frailty are listed in B and C, respectively. In addition, possible intervene strategies including traditional Chinese medicine and diet & nutrition are shown at the bottom of the figure. Created with BioRender.com. OS: Oxidative stress; TMA: Trimethylamine; SCFA: Short-chain fatty acid; FGF21: Fibroblast growth factor 21; IPA: Indole-3-propionic acid; RONS: Reactive oxygen and nitrogen species; 8-OdG: 8-hydroxy-2'-deoxyguanosine; 4-HNE: 4-hydroxy-2-nonenal; GSSG: Glutathione.

prausnitzii et rel. decreased in centenarians, and the abundance of *Clostridioides leptum et rel.* was increased. Centenarians had the highest abundance of *Bacilli* (12%) and *Proteobacteria* (2.6%), and the young population and the old population had similar proportions of *Bacilli* (5%) and *Proteobacteria* (1.2%). Jackson *et al*[13] studied the relationship between frailty and the composition of the GM. They found that frailty was negatively correlated with the abundance of *Clostridioides* (in which it accounted for the largest proportion of the GM). Moreover, frailty was positively correlated with the abundance of *Eggerthella lenta*. Centenarians, who are regarded as the "healthy aging" population, have a different GM composition than the aged population. This finding indicates that the GM is not entirely chronological age-correlated but that it is more closely related to the frailty status of the body.

In addition to chronological age, physiological age may better reflect the correlation between frailty and the GM (Figure 1B). In the study by Maffei *et al*[14], 85 volunteers aged 43-79 years were divided into low, medium and upper groups according to either physiological age or chronological age. The chronological age is the number of years from birth to the present. Physiological age was assessed by 34 items of the frailty index (frailty index 34, FI_{34}). According to the FI_{34} value, there were significant differences in the abundance and diversity of the GM among the three age groups. Excluding the effect of sex, body mass index, antibiotic usage, and other confounders, *Eggerthella, Rumen coccus* and *Coprobacillus* were the three main species with the greatest influence. According to the Rockwood FI value, *Faecalibacterium prausnitzii* was negatively correlated with age, while *Eubacterium dolichum* and *Eggerthella lenta* were positively correlated with age[15]. However, there was no significant difference in the GM among the three groups according to chronological age. Although there are contradictory changes in certain strains in the gut, it can be concluded that the change in *Clostridioides* abundance with age is the most remarkable. All the experiments mentioned above suggest that the GM changes with frailty status and that there is a potential link between the GM and frailty syndrome.

In frailty, the most significant change in the GM is a decrease in diversity. In the frail aged population, the microbiota shifts toward a predomination by *Bacteroidetes*, especially in the genus *Prevotella* and its subspecies. Changes in microbiota diversity affect the influence of the metabolites and pathways related to the microbiota. For instance, the GM regulates estrogen levels by secreting β-glucuronidase. β-glucuronidase is an enzyme that can deconjugate estrogen into the active form. Low levels of estrogen downregulate physiological functions that affect neural development, cardiovascular

health, bone density and neoplastic diseases[16]. Scientific evidence suggests that estrogen supplementation could improve physiological functions that prevent or reverse frailty[17]. Said *et al*[18] found that diarylpropionitrile, an estrogen receptor β agonist, had longevity-promoting properties and could reverse frailty.

THE ROLE OF OS IN FRAILTY

OS was regarded as one of the main causes of frailty as early as the 1950s. Harman[19] first proposed the free radical theory of aging; according to this theory, oxygen free radicals damage cell components and intercellular substances, causing the deterioration of body functions and age-related diseases. In the 1980s, OS was discovered. The advent of OS indicates that the balance between oxidation and antioxidation is inclined toward oxidation. This leads to neutrophil inflammatory infiltration, an increase in protease secretion, and the generation of a large number of oxidative intermediates. The study by Viña *et al*[20] suggested that OS was an important negative factor that led to aging and diseases, such as cardiovascular disease, neurodegenerative disease, chronic obstructive pulmonary disease or cancer and other illnesses in aged individuals. Some researchers have thought that oxidative damage may be due to the imbalance between antioxidation defenses and reactive oxygen and nitrogen species (RONS), thus inducing cell apoptosis. This imbalance would lead to alterations in the expression of a number of transcription factors and then cause chemical modifications in macromolecular substances, such as lipids, proteins and DNA[21,22].

Since the free radical theory of aging was proposed, increasing concern has been given to the influence of OS on frailty (Figure 1C). Wu *et al*[23] screened 90 volunteers who were older than 65 years old, dividing them into a frailty group, a prefrailty group and a nonfrailty group according to Fried's phenotype. The serum levels of OS biomarkers such as 8-hydroxy-2′-deoxyguanosine (8-OdG), metabolic markers such as albumin, and inflammatory markers such as hypersensitivity C-reactive protein (hs-CRP) were measured by competitive enzyme-linked immunosorbent assay. The results demonstrated that the serum albumin and hs-CRP levels in the frail group were higher than those in the other two groups. Furthermore, the levels of 8-OdG and hs-CRP increased with the progression of frailty. Serviddio *et al*[24] compared the levels of oxidized glutathione (GSSG), tumor necrosis factor-α, malondialdehyde (MDA), 4-hydroxy-2-nonenal (4-HNE), and other OS-related indicators in patients with frailty syndrome with those in nonfrail individuals. The data suggested that these indicators of OS were all significantly increased in frail individuals.

In addition to the direct evaluation of the frailty index, OS was also found to be related to sarcopenia. Severe sarcopenia in the elderly was defined as the prophase of frailty by the European Working Group on Sarcopenia. Bernabeu-Wittel *et al*[25] found that in 444 polypathological patients, 97 patients had sarcopenia. The number of patients with a combination of sarcopenia and frailty was 80. The authors also reported that OS markers were significantly increased in patients with sarcopenia, frailty or both. OS was evaluated by the levels of catalase, GSSG reductase, total antioxidant capacity to reactive oxygen species (ROS), and superoxide dismutase (SOD). Coto Montes *et al*[26] found that sarcopenia was closely related to lipid peroxidation. Significant increases in biomarkers such as MDA and 4-HNE were observed in 200 independent 80-year-old persons who had been diagnosed with sarcopenia. Liu *et al*[27] also discovered that the incidence of frailty increased with a rise in the levels of interleukin-6 (IL-6), isoprostaglandin and lipoprotein phosphorylation A2. These studies suggested a correlation between frailty and OS. OS-related biomarkers in serum may be potential biomarkers for predicting frailty. This possibility needs further study.

THE UNDERLYING MECHANISM OF THE INFLUENCE OF THE GM ON FRAILTY SYNDROME WAS ANALYZED BY OS

OS is affected by many factors *in vivo* and *in vitro*. The GM plays a role as "environmental factors" which regulates ROS levels in plasma and maintaining the functions of the digestive, endocrine, immune, skeletal, cardiovascular, and nervous systems. The stability of the GM is fragile and easily affected by external factors, including diet, heavy use of drugs, geographic position, individual lifestyle, and the genetic background of the host[28]. Once the GM is disturbed ("dysbiosis"), it may cause a series of related illnesses, such as inflammatory bowel diseases, obesity, and type II diabetes. These diseases can also affect the oxidative balance, thus forming a vicious cycle.

For example, a variety of colon bacteria, such as *Fusobacterium*, *Clostridioides*, *Escherichia*, *Salmonella*, *Klebsiella*, *Streptococcus*, *Desulfovibrio* and *Enterobacter*, can convert sulfide to hydrogen sulfide (H_2S)[29]. Intestinal epithelial cells protect themselves by converting H_2S into thiosulfate ($S_2O_3^{2-}$). Thiosulfate can be oxidized to tetrathionate ions ($S_4O_6^{2-}$) in the case of intestinal inflammation (Figure 1A). This process is accompanied by the formation of RONS. In both anaerobic and microaerobic environments, tetrathionate can specifically promote the proliferation of *Salmonella enterica Typhimurium* model strains

[30]. It has also been reported that certain GM can cause a sharp increase in ROS. *Lactobacillus* is a strong inducer of ROS. It can stimulate the production of ROS by enhancing the ability to pass through the mucous membrane or increasing the secretion of mucus. Additionally, it can interact with certain cellular receptors, such as formylated peptide receptors or Toll-like receptors[31,32]. In addition, *Lactobacilli* promotes the oxidation of soluble redox proteins, such as GSSG and thioredoxin, and it facilitates the transcription of redox regulatory factors by activating the nuclear factor erythroid 2-related factor 2 pathway[32]. The pathogenic mechanisms of action of *Helicobacter pylori* (*H. pylori*) may also be related to its promotion of ROS production. *H. pylori* can induce severe white blood cell tissue infiltration and release virulence factors that stimulate epithelial cells to produce ROS and secrete myeloperoxidase, chemokines, and proinflammatory cytokines. Consequently, *H. pylori* results in gastrointestinal microbiome dysbiosis and induces nonalcoholic fatty liver disease (NAFLD)[33]. The antioxidant enzyme SOD can be used to treat NAFLD. SOD can convert superoxide anion into hydrogen peroxide and molecular oxygen, thus preventing the accumulation of ROS[34]. In addition to *H. pylori*, the GM has been proposed to be strongly associated with the development and progression of metabolic diseases, including NAFLD[33]. NAFLD patients showed lower fecal microbial diversity than that of healthy controls in one study[35]. At the taxonomic and functional levels, another recent study showed that *Lactobacilli* inhibited the incidence and development of NAFLD by improving hepatic mitochondria and lipid metabolism by promoting the production of the antioxidant GSSG[36].

These studies indicate that the activation of OS by the GM is a possible mechanism of frailty. For example, gut microbes metabolize choline, L-carnitine and betaine in the daily diet to trimethylamine (TMA). These substances are mainly found in red meat, meat products, eggs, and shellfish[37,38]. Nine GM strains can convert choline to TMA: *Anaerococcus hydrogenalis*, *Clostridioides asparagiforme*, *Clostridioides hathewayi*, *Clostridioides sporogenes*, *Escherichia fergusonii*, *Proteus penneri*, *Providencia rettgeri*, *Edwardsiella tarda* and *Providencia rustiganii*. These species belong to *Firmicutes* and *Proteobacteria*[39]. Liver enzymes further convert TMA to TMAO through the flavin-containing monooxygenase (FMO) family members FMO1 and FMO3[37]. Researchers have found that the level of TMAO was increased in the aged population and that TMAO was independently associated with frailty. Nam *et al*[40] reported that the average levels of TMAO were 3.21 μM and 4.04 μM in nonfrail and frail participants, respectively. Moreover, participants who had the highest plasma TMAO levels showed a significant 3.7-fold increase in the incidence of frailty syndrome. A high level of plasma TMAO can increase the risk of stroke, atrial fibrillation, diabetes, congestive heart failure, chronic kidney disease, coronary artery disease, peripheral artery disease and other cardiovascular diseases, which are associated with frailty [40]. Moreover, TMAO significantly increases OS, inflammatory conditions and endothelial dysfunction. TMAO stimulates the TXNIP-NLRP3 inflammasome and activates the release of the inflammatory cytokines IL-1β and IL-18. However, it inhibits the production of endothelial nitric oxide (NO) synthase and NO[41]. It has also been reported that TMAO can promote inflammatory hepatocellular carcinoma by inducing ROS and activating ILK/AKT/mammalian target of rapamycin (mTOR) signaling *via* POSTN[42]. Our previous studies showed that administration of TMAO produced a novel model of frailty in mice[43]. In this TMAO-induced frailty model, the abundance of *Firmicutes* was decreased slightly, while the abundance of *Bacteroidetes* was significantly increased in the gut. The ratio of *Firmicutes* to *Bacteroidetes* (F/B) was significantly decreased. Relevantly, the F/B ratio is reported to be a potential marker of obesity and GM disorder[44], both of which are potential factors of frailty[45,46]. According to an investigation, obese females have higher FI values than those of nonobese females. In addition to TMAO, short-chain fatty acids (SCFAs) are also common metabolites of the GM that are converted from undigested carbohydrates, such as starch and pectin (Figure 1A). Butyrate is a SCFA product. Studies have shown that there is a significant association between SCFAs/butyrate and gut/celiac diseases[47,48]. It is transcriptionally activated by peroxisome proliferator-activated receptor α by replacing histone deacetylase 3 on the fibroblast growth factor 21 (FGF21) promoter. This reaction actives FGF21 and induces the expression and secretion of FGF21[46]. FGF21 regulates the adenosine monophosphate-activated protein kinase-Sirtuin1-mTOR pathway, which is associated with longevity. FGF21 can also alleviate various diseases related to aging[49,50]. In addition, the GM can affect the levels of inflammation by regulating the immune system and can affect insulin resistance by regulating the metabolomic system[51].

In addition to these metabolites, indole-3-propionic acid (IPA), another microbiota-derived metabolite of tryptophan, has been proven to have a positive impact at the cellular level by preventing OS injury and lipoperoxidation and inhibiting the synthesis of proinflammatory cytokines[52], suggesting that IPA may be a promising new target for improving frailty.

The GM and metabolites changes with frailty. Scientific evidence also shows that some antibiotics can reverse frailty. This action may be due to the effect of antibiotics changing the composition of the GM. For example, rapamycin is a broad-spectrum antibiotic. It also acts as an immunosuppressor. Rapamycin regulates protein synthesis and redox reactions. Animal studies have shown that rapamycin prolongs lifespan and improves frailty[50]. These results indicate that the GM plays an important role in the process of frailty *via* OS.

POTENTIAL INTERVENTIONS FOR FRAILTY

By understanding the role of the GM and OS in frailty, several interventions have been proposed to improve this syndrome and to achieve the goal of healthy aging.

Effect of diet on frailty

One possible intervention is to regulate the GM *via* the daily diet. Data from short-lived organisms, such as yeast, worms and fruit flies, showed that diet had an anti-senescence effect and prolonged the lives of these organisms by enhancing stress resistance, reliance on lipid fuel use, and the activation of proteostatic mechanisms[53]. Such effects of diet and nutrition on aging can also be reproduced in humans [54]. For example, the Mediterranean diet can improve frailty. The Mediterranean diet is characterized by an increase in the consumption of vegetables, legumes, fruits, nuts, olive oil and fish[55]. At the same time, the consumption of meat and unsaturated fatty acids is reduced. The Mediterranean diet provides a higher intake of micronutrients, such as antioxidant nutrients, polyphenols and plant bioactive compounds[56]. Ghosh *et al*[57] found that one year of Mediterranean diet intervention can change the composition of the GM and alleviate frailty. Some of the GM that belong to the "diet positive" taxa increased, including *Faecalibacterium prausnitzii*, *Roseburia*, *Eubacterium* (*E. rectale, E. eligens,* and *E. xylanophilum*), *Bacteroides thetaiotaomicron*, *Prevotella copri* and *Anaerostipes hadrus*. An increase in these microbiotas facilitates the production of SCFAs and the enhancement of the anti-inflammatory capacity. On the other hand, the microbiota deemed to be "diet negative" taxa, such as *Ruminococcus torques*, *Collinsella aerofaciens*, *Coprococcus comes*, *Dorea formicigenerans*, *Clostridioides ramosum*, *Veillonella dispar*, *Flavonifractor plautii* and *Actinomyces lingnae*, were reduced. These "diet negative" taxa are associated with type II diabetes, colorectal cancer, atherosclerosis, cirrhosis and inflammatory bowel disease. With the progressive aggravation of frailty symptoms, the "diet-positive" taxa decreased, and the "diet-negative" taxa increased. Proper nutritional supplements can improve frailty. Bo conducted a double-blind experiment and found that mixed supplementation with whey protein, vitamin D and vitamin E can significantly improve muscle mass and strength (handgrip strength)[58]. It was also used to treat elderly individuals with sarcopenia, and the supplementation improved frailty and quality of life. Moreover, the Mediterranean diet was found to tend to increase the plasma concentration of IPA[52]. IPA could reduce the level of OS in the body and help to improve frailty.

In addition to the Mediterranean diet, some other diet regimens can also improve GM and OS. For example, the replacement diet based on ancient Khorasan wheat results in beneficial GM compositional and functional modifications that positively correlate with an improvement in fibromyalgia symptomatology[59]. A habitual diet supplemented with oral butyrate could reduce the production of ROS in leukocytes[60]. Whether these diet regimens could improve frailty remains to be further investigated.

Effect of TCM on frailty

With an increasing number of studies on TCM, many effective monomers and prescription preparations of TCM have been found to improve frailty by regulating the GM and OS. For example, *Cistanche deserticola* and *Eucommia ulmoides* are common TCM with a tonifying effect on the kidneys, which are important organs for aging[61-63]. Modern pharmacological investigations have demonstrated that both TCMs can regulate the GM and OS. *Cistanche deserticola* polysaccharide is one of the main active components of *Cistanche deserticola*. It can produce antiaging effects by scavenging free radicals, reducing telomerase activity, improving mitochondrial antioxidant capacity and improving mitochondrial energy metabolism[64]. Moreover, *Cistanche deserticola* polysaccharide can inhibit the growth of a variety of gut pathogenic bacteria and can promote the growth of probiotics. These effects help to maintain the health of the GM[65]. Chlorogenic acid is one of the main effective components of *Eucommia ulmoides*, and it has strong anti-inflammatory and antioxidant effects. It can reduce OS and improve mitochondrial dysfunction[66]. Furthermore, chlorogenic acid and its hydrolytic form, which is called caffeic acid, have been demonstrated to alleviate inflammation and OS by improving the GM[67]. This effect is manifested by an increase in the content of *Ackermann* bacteria and the restoration of the abundance of GM[68]. It can increase the expression of tight junction proteins in intestinal epithelial cells to repair the intestinal barrier and reduce permeability[69]. These actions may contribute to the antiaging effect of chlorogenic acid[69] and further prolong the lifespan in experiments with *Caenorhabditis elegans*[70]. Liujunzi decoction, a TCM prescription consisting of Dangshen, Tuckahoe, Atracylodes macrocephala, Licorice, Pinellia ternata and Orange peel, was found to significantly improve the frailty state of elderly patients with stable chronic obstructive pulmonary disease. This effect was significantly better than that of tiotropium bromide[71]. In addition, administration of Liujunzi decoction for eight weeks increased the muscle weight and exercise endurance of the frail patients. Supplementation with Chinese medicinal plant extracts from *Lonicera hypoglauca* and *Scutellaria baicalensis*, as well as *Dihydroquercetin* supplementation, could mitigate colonic inflammation by regulating OS and the GM[72,73].

Since TCM is popular in China, Japan and other East Asian regions, most of the available literature to date is limited to the data obtained from Asian populations. However, considering that most modern pharmacological studies are performed with standard experimental animals, the anti-frailty effect of

these TCMs may potentially be extended to Western populations based on these basic research data. However, these medicines still need to be more widely investigated in studies involving a larger population.

CONCLUSION

In summary, the abundance and diversity of the GM were found to change with age. Specific GMs and their metabolites stimulate the production of ROS and affect OS in the body, leading to damage to multiple biological macromolecules. The occurrence of OS may be the intermediate process of the GM that leads to frailty, producing a direct action on the body. This may be one of the precipitating factors of frailty syndrome. Thus, the GM and its metabolites can be used as biomarkers of frailty syndrome. Regulating the GM and OS by diet or TCM could help to improve frailty. Additionally, there is increasing evidence indicating that circadian rhythms may also play important roles in mediating the impact of the GM on chronic diseases[74]. Clarifying the mechanisms involved in frailty from the perspective of the GM may be important to achieving the goal of healthy aging.

FOOTNOTES

Author contributions: Chen SY and Wang TY wrote the paper; Zhao C and Wang HJ supervised the writing and editing the manuscript.

Supported by the National Key Research and Development Program of China, No. 2018YFC2002000 and 2018YFC2000500/03; and Shanghai Natural Science Foundation, No. 21ZR1409200.

Conflict-of-interest statement: All the authors report no relevant conflicts of interest for this article.

Open-Access: This article is an open-access article that was selected by an in-house editor and fully peer-reviewed by external reviewers. It is distributed in accordance with the Creative Commons Attribution NonCommercial (CC BY-NC 4.0) license, which permits others to distribute, remix, adapt, build upon this work non-commercially, and license their derivative works on different terms, provided the original work is properly cited and the use is non-commercial. See: https://creativecommons.org/Licenses/by-nc/4.0/

Country/Territory of origin: China

ORCID number: Tong-Yao Wang 0000-0002-8998-5509; Chao Zhao 0000-0001-7349-306X; Hui-Jing Wang 0000-0002-4246-233X.

S-Editor: Wang JJ
L-Editor: A
P-Editor: Wang JJ

REFERENCES

1 **Clegg A**, Young J, Iliffe S, Rikkert MO, Rockwood K. Frailty in elderly people. *Lancet* 2013; **381**: 752-762 [PMID: 23395245 DOI: 10.1016/S0140-6736(12)62167-9]
2 **Fulop T**, McElhaney J, Pawelec G, Cohen AA, Morais JA, Dupuis G, Baehl S, Camous X, Witkowski JM, Larbi A. Frailty, Inflammation and Immunosenescence. *Interdiscip Top Gerontol Geriatr* 2015; **41**: 26-40 [PMID: 26301977 DOI: 10.1159/000381134]
3 **Fülöp T**, Dupuis G, Witkowski JM, Larbi A. The Role of Immunosenescence in the Development of Age-Related Diseases. *Rev Invest Clin* 2016; **68**: 84-91 [PMID: 27103044]
4 **Jayanama K**, Theou O, Blodgett JM, Cahill L, Rockwood K. Frailty, nutrition-related parameters, and mortality across the adult age spectrum. *BMC Med* 2018; **16**: 188 [PMID: 30360759 DOI: 10.1186/s12916-018-1176-6]
5 **Miller SM**, Wolf J, Katlic M, D'Adamo CR, Coleman J, Ahuja V. Frailty is a better predictor than age for outcomes in geriatric patients with rectal cancer undergoing proctectomy. *Surgery* 2020; **168**: 504-508 [PMID: 32665144 DOI: 10.1016/j.surg.2020.05.027]
6 **Xing X**, Guo G. Research on the current situation of frailty and its influencing factors among the elderly in the community. *Chinese Nursing Management* 2014; **12**: 1315-1319
7 **Rampelli S**, Candela M, Turroni S, Biagi E, Collino S, Franceschi C, O'Toole PW, Brigidi P. Functional metagenomic profiling of intestinal microbiome in extreme ageing. *Aging (Albany NY)* 2013; **5**: 902-912 [PMID: 24334635 DOI: 10.18632/aging.100623]
8 **Biagi E**, Nylund L, Candela M, Ostan R, Bucci L, Pini E, Nikkïla J, Monti D, Satokari R, Franceschi C, Brigidi P, De Vos W. Through ageing, and beyond: gut microbiota and inflammatory status in seniors and centenarians. *PLoS One* 2010; **5**: e10667 [PMID: 20498852 DOI: 10.1371/journal.pone.0010667]

9 **Ulley J**, Abdelhafiz AH. Frailty predicts adverse outcomes in older people with diabetes. *Practitioner* 2017; **261**: 17-20 [PMID: 29023081]

10 **Salminen KS**, Suominen MH, Kautiainen H, Pitkälä KH. Associations between Nutritional Status, Frailty and Health-Related Quality of Life among Older Long-Term Care Residents in Helsinki. *J Nutr Health Aging* 2020; **24**: 319-324 [PMID: 32115614 DOI: 10.1007/s12603-019-1320-9]

11 **Wu YL**, Xu J, Rong XY, Wang F, Wang HJ, Zhao C. Gut microbiota alterations and health status in aging adults: From correlation to causation. *Aging Med (Milton)* 2021; **4**: 206-213 [PMID: 34553118 DOI: 10.1002/agm2.12167]

12 **Salazar N**, Valdés-Varela L, González S, Gueimonde M, de Los Reyes-Gavilán CG. Nutrition and the gut microbiome in the elderly. *Gut Microbes* 2017; **8**: 82-97 [PMID: 27808595 DOI: 10.1080/19490976.2016.1256525]

13 **Jackson MA**, Jeffery IB, Beaumont M, Bell JT, Clark AG, Ley RE, O'Toole PW, Spector TD, Steves CJ. Signatures of early frailty in the gut microbiota. *Genome Med* 2016; **8**: 8 [PMID: 26822992 DOI: 10.1186/s13073-016-0262-7]

14 **Maffei VJ**, Kim S, Blanchard E 4th, Luo M, Jazwinski SM, Taylor CM, Welsh DA. Biological Aging and the Human Gut Microbiota. *J Gerontol A Biol Sci Med Sci* 2017; **72**: 1474-1482 [PMID: 28444190 DOI: 10.1093/gerona/glx042]

15 **Ticinesi A**, Lauretani F, Milani C, Nouvenne A, Tana C, Del Rio D, Maggio M, Ventura M, Meschi T. Aging Gut Microbiota at the Cross-Road between Nutrition, Physical Frailty, and Sarcopenia: Is There a Gut-Muscle Axis? *Nutrients* 2017; **9** [PMID: 29189738 DOI: 10.3390/nu9121303]

16 **Baker JM**, Al-Nakkash L, Herbst-Kralovetz MM. Estrogen-gut microbiome axis: Physiological and clinical implications. *Maturitas* 2017; **103**: 45-53 [PMID: 28778332 DOI: 10.1016/j.maturitas.2017.06.025]

17 **Schwartz E**, Holtorf K. Hormone replacement therapy in the geriatric patient: current state of the evidence and questions for the future. Estrogen, progesterone, testosterone, and thyroid hormone augmentation in geriatric clinical practice: part 1. *Clin Geriatr Med* 2011; **27**: 541-559 [PMID: 22062440 DOI: 10.1016/j.cger.2011.07.013]

18 **Said SA**, Isedowo R, Guerin C, Nar NN, Lillie L, Bukovac S, Simone JJ, Green MR, McCormick CM, Stuart JA. Effects of long-term dietary administration of estrogen receptor-beta agonist diarylpropionitrile on ovariectomized female ICR (CD-1) mice. *Geroscience* 2018; **40**: 393-403 [PMID: 30099673 DOI: 10.1007/s11357-018-0038-7]

19 **Harman D**. Aging: a theory based on free radical and radiation chemistry. *J Gerontol* 1956; **11**: 298-300 [PMID: 13332224 DOI: 10.1093/geronj/11.3.298]

20 **Viña J**, Borras C, Gomez-Cabrera MC. A free radical theory of frailty. *Free Radic Biol Med* 2018; **124**: 358-363 [PMID: 29958933 DOI: 10.1016/j.freeradbiomed.2018.06.028]

21 **Liguori I**, Russo G, Curcio F, Bulli G, Aran L, Della-Morte D, Gargiulo G, Testa G, Cacciatore F, Bonaduce D, Abete P. Oxidative stress, aging, and diseases. *Clin Interv Aging* 2018; **13**: 757-772 [PMID: 29731617 DOI: 10.2147/CIA.S158513]

22 **Soysal P**, Isik AT, Carvalho AF, Fernandes BS, Solmi M, Schofield P, Veronese N, Stubbs B. Oxidative stress and frailty: A systematic review and synthesis of the best evidence. *Maturitas* 2017; **99**: 66-72 [PMID: 28364871 DOI: 10.1016/j.maturitas.2017.01.006]

23 **Wu IC**, Shiesh SC, Kuo PH, Lin XZ. High oxidative stress is correlated with frailty in elderly chinese. *J Am Geriatr Soc* 2009; **57**: 1666-1671 [PMID: 19682113 DOI: 10.1111/j.1532-5415.2009.02392.x]

24 **Serviddio G**, Romano AD, Greco A, Rollo T, Bellanti F, Altomare E, Vendemiale G. Frailty syndrome is associated with altered circulating redox balance and increased markers of oxidative stress. *Int J Immunopathol Pharmacol* 2009; **22**: 819-827 [PMID: 19822098 DOI: 10.1177/039463200902200328]

25 **Bernabeu-Wittel M**, Gómez-Díaz R, González-Molina Á, Vidal-Serrano S, Díez-Manglano J, Salgado F, Soto-Martín M, Ollero-Baturone M, On Behalf Of The Proteo Researchers. Oxidative Stress, Telomere Shortening, and Apoptosis Associated to Sarcopenia and Frailty in Patients with Multimorbidity. *J Clin Med* 2020; **9** [PMID: 32824789 DOI: 10.3390/jcm9082669]

26 **Coto Montes A**, Boga JA, Bermejo Millo C, Rubio González A, Potes Ochoa Y, Vega Naredo I, Martínez Reig M, Romero Rizos L, Sánchez Jurado PM, Solano JJ, Abizanda P, Caballero B. Potential early biomarkers of sarcopenia among independent older adults. *Maturitas* 2017; **104**: 117-122 [PMID: 28923171 DOI: 10.1016/j.maturitas.2017.08.009]

27 **Liu CK**, Lyass A, Larson MG, Massaro JM, Wang N, D'Agostino RB Sr, Benjamin EJ, Murabito JM. Biomarkers of oxidative stress are associated with frailty: the Framingham Offspring Study. *Age (Dordr)* 2016; **38**: 1 [PMID: 26695510 DOI: 10.1007/s11357-015-9864-z]

28 **Casati M**, Ferri E, Azzolino D, Cesari M, Arosio B. Gut microbiota and physical frailty through the mediation of sarcopenia. *Exp Gerontol* 2019; **124**: 110639 [PMID: 31226349 DOI: 10.1016/j.exger.2019.110639]

29 **Blachier F**, Beaumont M, Kim E. Cysteine-derived hydrogen sulfide and gut health: a matter of endogenous or bacterial origin. *Curr Opin Clin Nutr Metab Care* 2019; **22**: 68-75 [PMID: 30461448 DOI: 10.1097/MCO.0000000000000526]

30 **Winter SE**, Thiennimitr P, Winter MG, Butler BP, Huseby DL, Crawford RW, Russell JM, Bevins CL, Adams LG, Tsolis RM, Roth JR, Bäumler AJ. Gut inflammation provides a respiratory electron acceptor for Salmonella. *Nature* 2010; **467**: 426-429 [PMID: 20864996 DOI: 10.1038/nature09415]

31 **Jones RM**, Mercante JW, Neish AS. Reactive oxygen production induced by the gut microbiota: pharmacotherapeutic implications. *Curr Med Chem* 2012; **19**: 1519-1529 [PMID: 22360484 DOI: 10.2174/092986712799828283]

32 **Jones RM**, Neish AS. Redox signaling mediated by the gut microbiota. *Free Radic Biol Med* 2017; **105**: 41-47 [PMID: 27989756 DOI: 10.1016/j.freeradbiomed.2016.10.495]

33 **Han H**, Jiang Y, Wang M, Melaku M, Liu L, Zhao Y, Everaert N, Yi B, Zhang H. Intestinal dysbiosis in nonalcoholic fatty liver disease (NAFLD): focusing on the gut-liver axis. *Crit Rev Food Sci Nutr* 2021; 1-18 [PMID: 34404276 DOI: 10.1080/10408398.2021.1966738]

34 **Borrelli A**, Bonelli P, Tuccillo FM, Goldfine ID, Evans JL, Buonaguro FM, Mancini A. Role of gut microbiota and oxidative stress in the progression of non-alcoholic fatty liver disease to hepatocarcinoma: Current and innovative therapeutic approaches. *Redox Biol* 2018; **15**: 467-479 [PMID: 29413959 DOI: 10.1016/j.redox.2018.01.009]

35 **Del Chierico F**, Nobili V, Vernocchi P, Russo A, De Stefanis C, Gnani D, Furlanello C, Zandonà A, Paci P, Capuani G, Dallapiccola B, Miccheli A, Alisi A, Putignani L. Gut microbiota profiling of pediatric nonalcoholic fatty liver disease and obese patients unveiled by an integrated meta-omics-based approach. *Hepatology* 2017; **65**: 451-464 [PMID: 27028797

DOI: 10.1002/hep.28572]
36 **Rodrigues RR**, Gurung M, Li Z, García-Jaramillo M, Greer R, Gaulke C, Bauchinger F, You H, Pederson JW, Vasquez-Perez S, White KD, Frink B, Philmus B, Jump DB, Trinchieri G, Berry D, Sharpton TJ, Dzutsev A, Morgun A, Shulzhenko N. Transkingdom interactions between Lactobacilli and hepatic mitochondria attenuate western diet-induced diabetes. *Nat Commun* 2021; **12**: 101 [PMID: 33397942 DOI: 10.1038/s41467-020-20313-x]
37 **Yang S**, Li X, Yang F, Zhao R, Pan X, Liang J, Tian L, Liu L, Xing Y, Wu M. Gut Microbiota-Dependent Marker TMAO in Promoting Cardiovascular Disease: Inflammation Mechanism, Clinical Prognostic, and Potential as a Therapeutic Target. *Front Pharmacol* 2019; **10**: 1360 [PMID: 31803054 DOI: 10.3389/fphar.2019.01360]
38 **He W**, Luo Y, Liu JP, Sun N, Guo D, Cui LL, Zheng PP, Yao SM, Yang JF, Wang H. Trimethylamine N-Oxide, a Gut Microbiota-Dependent Metabolite, is Associated with Frailty in Older Adults with Cardiovascular Disease. *Clin Interv Aging* 2020; **15**: 1809-1820 [PMID: 33061331 DOI: 10.2147/CIA.S270887]
39 **Romano KA**, Vivas EI, Amador-Noguez D, Rey FE. Intestinal microbiota composition modulates choline bioavailability from diet and accumulation of the proatherogenic metabolite trimethylamine-N-oxide. *mBio* 2015; **6**: e02481 [PMID: 25784704 DOI: 10.1128/mBio.02481-14]
40 **Nam HS**. Gut Microbiota and Ischemic Stroke: The Role of Trimethylamine N-Oxide. *J Stroke* 2019; **21**: 151-159 [PMID: 31161760 DOI: 10.5853/jos.2019.00472]
41 **Sun X**, Jiao X, Ma Y, Liu Y, Zhang L, He Y, Chen Y. Trimethylamine N-oxide induces inflammation and endothelial dysfunction in human umbilical vein endothelial cells *via* activating ROS-TXNIP-NLRP3 inflammasome. *Biochem Biophys Res Commun* 2016; **481**: 63-70 [PMID: 27833015 DOI: 10.1016/j.bbrc.2016.11.017]
42 **Wu Y**, Rong X, Pan M, Wang T, Yang H, Chen X, Xiao Z, Zhao C. Integrated Analysis Reveals the Gut Microbial Metabolite TMAO Promotes Inflammatory Hepatocellular Carcinoma by Upregulating POSTN. *Front Cell Dev Biol* 2022; **10**: 840171 [PMID: 35676936 DOI: 10.3389/fcell.2022.840171]
43 **Chen SY**, Rong XY, Sun XY, Zou YR, Zhao C, Wang HJ. A Novel Trimethylamine Oxide-Induced Model Implicates Gut Microbiota-Related Mechanisms in Frailty. *Front Cell Infect Microbiol* 2022; **12**: 803082 [PMID: 35360115 DOI: 10.3389/fcimb.2022.803082]
44 **Grigor'eva IN**. Gallstone Disease, Obesity and the Firmicutes/Bacteroidetes Ratio as a Possible Biomarker of Gut Dysbiosis. *J Pers Med* 2020; **11** [PMID: 33375615 DOI: 10.3390/jpm11010013]
45 **Li G**, Compston JE, Leslie WD, Thabane L, Papaioannou A, Lau A, Wang X, Qin C, Chen B, Chen M, Adachi JD. Relationship Between Obesity and Risk of Major Osteoporotic Fracture in Postmenopausal Women: Taking Frailty Into Consideration. *J Bone Miner Res* 2020; **35**: 2355-2362 [PMID: 32717113 DOI: 10.1002/jbmr.4139]
46 **Michaud M**, Balardy L, Moulis G, Gaudin C, Peyrot C, Vellas B, Cesari M, Nourhashemi F. Proinflammatory cytokines, aging, and age-related diseases. *J Am Med Dir Assoc* 2013; **14**: 877-882 [PMID: 23792036 DOI: 10.1016/j.jamda.2013.05.009]
47 **Baldi S**, Menicatti M, Nannini G, Niccolai E, Russo E, Ricci F, Pallecchi M, Romano F, Pedone M, Poli G, Renzi D, Taddei A, Calabrò AS, Stingo FC, Bartolucci G, Amedei A. Free Fatty Acids Signature in Human Intestinal Disorders: Significant Association between Butyric Acid and Celiac Disease. *Nutrients* 2021; **13**: 742 [PMID: 33652681 DOI: 10.3390/nu13030742]
48 **Niccolai E**, Baldi S, Ricci F, Russo E, Nannini G, Menicatti M, Poli G, Taddei A, Bartolucci G, Calabrò AS, Stingo FC, Amedei A. Evaluation and comparison of short chain fatty acids composition in gut diseases. *World J Gastroenterol* 2019; **25**: 5543-5558 [PMID: 31576099 DOI: 10.3748/wjg.v25.i36.5543]
49 **Finlay BB**, Pettersson S, Melby MK, Bosch TCG. The Microbiome Mediates Environmental Effects on Aging. *Bioessays* 2019; **41**: e1800257 [PMID: 31157928 DOI: 10.1002/bies.201800257]
50 **Salminen A**, Kaarniranta K, Kauppinen A. Regulation of longevity by FGF21: Interaction between energy metabolism and stress responses. *Ageing Res Rev* 2017; **37**: 79-93 [PMID: 28552719 DOI: 10.1016/j.arr.2017.05.004]
51 **Ma L**, Sha G, Zhang Y, Li Y. Elevated serum IL-6 and adiponectin levels are associated with frailty and physical function in Chinese older adults. *Clin Interv Aging* 2018; **13**: 2013-2020 [PMID: 30410318 DOI: 10.2147/CIA.S180934]
52 **Konopelski P**, Mogilnicka I. Biological Effects of Indole-3-Propionic Acid, a Gut Microbiota-Derived Metabolite, and Its Precursor Tryptophan in Mammals' Health and Disease. *Int J Mol Sci* 2022; **23**: 1222 [PMID: 35163143 DOI: 10.3390/ijms23031222]
53 **Palliyaguru DL**, Moats JM, Di Germanio C, Bernier M, de Cabo R. Frailty index as a biomarker of lifespan and healthspan: Focus on pharmacological interventions. *Mech Ageing Dev* 2019; **180**: 42-48 [PMID: 30926563 DOI: 10.1016/j.mad.2019.03.005]
54 **Longo VD**, Anderson RM. Nutrition, longevity and disease: From molecular mechanisms to interventions. *Cell* 2022; **185**: 1455-1470 [PMID: 35487190 DOI: 10.1016/j.cell.2022.04.002]
55 **Davis C**, Bryan J, Hodgson J, Murphy K. Definition of the Mediterranean Diet; a Literature Review. *Nutrients* 2015; **7**: 9139-9153 [PMID: 26556369 DOI: 10.3390/nu7115459]
56 **Ni Lochlainn M**, Cox NJ, Wilson T, Hayhoe RPG, Ramsay SE, Granic A, Isanejad M, Roberts HC, Wilson D, Welch C, Hurst C, Atkins JL, Mendonça N, Horner K, Tuttiett ER, Morgan Y, Heslop P, Williams EA, Steves CJ, Greig C, Draper J, Corish CA, Welch A, Witham MD, Sayer AA, Robinson S. Nutrition and Frailty: Opportunities for Prevention and Treatment. *Nutrients* 2021; **13** [PMID: 34371858 DOI: 10.3390/nu13072349]
57 **Ghosh TS**, Rampelli S, Jeffery IB, Santoro A, Neto M, Capri M, Giampieri E, Jennings A, Candela M, Turroni S, Zoetendal EG, Hermes GDA, Elodie C, Meunier N, Brugere CM, Pujos-Guillot E, Berendsen AM, De Groot LCPGM, Feskins EJM, Kaluza J, Pietruszka B, Bielak MJ, Comte B, Maijo-Ferre M, Nicoletti C, De Vos WM, Fairweather-Tait S, Cassidy A, Brigidi P, Franceschi C, O'Toole PW. Mediterranean diet intervention alters the gut microbiome in older people reducing frailty and improving health status: the NU-AGE 1-year dietary intervention across five European countries. *Gut* 2020; **69**: 1218-1228 [PMID: 32066625 DOI: 10.1136/gutjnl-2019-319654]
58 **Bo Y**, Liu C, Ji Z, Yang R, An Q, Zhang X, You J, Duan D, Sun Y, Zhu Y, Cui H, Lu Q. A high whey protein, vitamin D and E supplement preserves muscle mass, strength, and quality of life in sarcopenic older adults: A double-blind randomized controlled trial. *Clin Nutr* 2019; **38**: 159-164 [PMID: 29395372 DOI: 10.1016/j.clnu.2017.12.020]

59 **Baldi S**, Pagliai G, Dinu M, Di Gloria L, Nannini G, Curini L, Pallecchi M, Russo E, Niccolai E, Danza G, Benedettelli S, Ballerini G, Colombini B, Bartolucci G, Ramazzotti M, Sofi F, Amedei A. Effect of ancient Khorasan wheat on gut microbiota, inflammation, and short-chain fatty acid production in patients with fibromyalgia. *World J Gastroenterol* 2022; **28**: 1965-1980 [PMID: 35664958 DOI: 10.3748/wjg.v28.i18.1965]

60 **Emmi G**, Bettiol A, Niccolai E, Ramazzotti M, Amedei A, Pagliai G, Taddei N, Sofi F, Fiorillo C, Prisco D, Becatti M. Butyrate-Rich Diets Improve Redox Status and Fibrin Lysis in Behçet's Syndrome. *Circ Res* 2021; **128**: 278-280 [PMID: 33198585 DOI: 10.1161/CIRCRESAHA.120.317789]

61 **Wang T**, Zhang X, Xie W. Cistanche deserticola Y. C. Ma, "Desert ginseng": a review. *Am J Chin Med* 2012; **40**: 1123-1141 [PMID: 23227786 DOI: 10.1142/S0192415X12500838]

62 **Hussain T**, Tan B, Liu G, Oladele OA, Rahu N, Tossou MC, Yin Y. Health-Promoting Properties of Eucommia ulmoides: A Review. *Evid-Based Compl Alt* 2016 [DOI: 10.1155/2016/5202908]

63 **Huang L**, Lyu Q, Zheng W, Yang Q, Cao G. Traditional application and modern pharmacological research of Eucommia ulmoides Oliv. *Chin Med* 2021; **16**: 73 [PMID: 34362420 DOI: 10.1186/s13020-021-00482-7]

64 **Gao X**, Chen J, Peng Y. Research Situation of Pharmacological Effects of Cistanche Deserticol Polysaccharides. *Food Drug* 2015; **17**: 136-139

65 **Deng N**, Shen Y, Ding H, Song X, Zhang L. Research Progress on Pharmacological Action of Polysaccharides in Cistanche Deserticola. *J Liaoning University Tradition Chin Med* 2020; **22**: 67-71 [DOI: 10.13194/j.issn.1673-842x.2020.06.018]

66 **Wang Q**, Du T, Zhang Z, Ji M, Hu H, Chen X. Advances in research on the pharmacological effects and mechanism of action of chlorogenic acid. *Acta Pharmaceutica Sinica* 2020; **55**: 2273-2280 [DOI: 10.16438/j.0513-4870.2020-0423]

67 **Wan F**, Zhong R, Wang M, Zhou Y, Chen Y, Yi B, Hou F, Liu L, Zhao Y, Chen L, Zhang H. Caffeic Acid Supplement Alleviates Colonic Inflammation and Oxidative Stress Potentially Through Improved Gut Microbiota Community in Mice. *Front Microbiol* 2021; **12**: 784211 [PMID: 34867926 DOI: 10.3389/fmicb.2021.784211]

68 **Wu X**. Studies on the regulation of UC inflammatory response and intestinal flora by chlorogenic acid. Proceedings of the Science and Technology Salon of the Youth Committee of the Chinese Toxicology Society; 2019 Jun 13; Hulunbuir, Nei Mongol, China: China Academic Journal Electronic Publishing House

69 **Mi S**. Chlorogenic Acid Attenuates Intestinal Barrier Damage in Colitis Rats. Nanchang University, 2014

70 **Zheng SQ**, Huang XB, Xing TK, Ding AJ, Wu GS, Luo HR. Chlorogenic Acid Extends the Lifespan of Caenorhabditis elegans *via* Insulin/IGF-1 Signaling Pathway. *J Gerontol A Biol Sci Med Sci* 2017; **72**: 464-472 [PMID: 27378235 DOI: 10.1093/gerona/glw105]

71 **Han W**. Clinical Benifit study of Senile COPD Patients in Stationary Phase Combined with Frailty with the Lung and Spleen Qi Deficiency Syndrome Treated with Liujunzi Decoction Combined Comprehensive Therapy. *Chengdu University Tradition Chin Med* 2021; **65**

72 **Wan F**, Wang M, Zhong R, Chen L, Han H, Liu L, Zhao Y, Lv H, Hou F, Yi B, Zhang H. Supplementation With Chinese Medicinal Plant Extracts From Lonicera hypoglauca and Scutellaria baicalensis Mitigates Colonic Inflammation by Regulating Oxidative Stress and Gut Microbiota in a Colitis Mouse Model. *Front Cell Infect Microbiol* 2022; **11**: 798052 [PMID: 35059326 DOI: 10.3389/fcimb.2021.798052]

73 **Wan F**, Han H, Zhong R, Wang M, Tang S, Zhang S, Hou F, Yi B, Zhang H. Dihydroquercetin supplement alleviates colonic inflammation potentially through improved gut microbiota community in mice. *Food Function* 2021; **12**: 11420-11434 [DOI: 10.1039/D1FO01422F]

74 **Wang T**, Rong X, Zhao C. Circadian Rhythms Coordinated With Gut Microbiota Partially Account for Individual Differences in Hepatitis B-Related Cirrhosis. *Front Cell Infect Microbiol* 2022; **12**: 936815 [PMID: 35846774 DOI: 10.3389/fcimb.2022.936815]

World Journal of Gastroenterology

Submit a Manuscript: https://www.f6publishing.com

World J Gastroenterol 2022 October 14; 28(38): 5557-5572

DOI: 10.3748/wjg.v28.i38.5557

ISSN 1007-9327 (print) ISSN 2219-2840 (online)

ORIGINAL ARTICLE

Basic Study

Effect of low-dose radiation on thyroid function and the gut microbiota

Jun-Yu Tong, Wen Jiang, Xia-Qing Yu, Ru Wang, Gang-Hua Lu, Ding-Wei Gao, Zhong-Wei Lv, Dan Li

Specialty type: Microbiology

Provenance and peer review: Unsolicited article; Externally peer reviewed.

Peer-review model: Single blind

Peer-review report's scientific quality classification

Grade A (Excellent): 0
Grade B (Very good): B
Grade C (Good): C, C
Grade D (Fair): 0
Grade E (Poor): 0

P-Reviewer: Bairwa DBL, India; Eccher A, Italy; Lee KS, South Korea

Received: May 11, 2022
Peer-review started: May 11, 2022
First decision: June 19, 2022
Revised: June 21, 2022
Accepted: September 8, 2022
Article in press: September 8, 2022
Published online: October 14, 2022

Jun-Yu Tong, Wen Jiang, Xia-Qing Yu, Ru Wang, Gang-Hua Lu, Ding-Wei Gao, Zhong-Wei Lv, Nuclear Medicine, Shanghai Tenth People's Hospital, Tongji University School of Medicine, Shanghai 200072, China

Dan Li, Department of Nuclear Medicine, Sun Yat-sen Memorial Hospital, Sun Yat-sen University, Guangzhou 200072, Guangdong Province, China

Corresponding author: Dan Li, PhD, Professor, Department of Nuclear Medicine , Sun Yat-sen Memorial Hospital, Sun Yat-sen University, No. 107 Yanjiangxi Road, Guangzhou 200072, Guangdong Province, China. plumredlinda@163.com

Abstract

BACKGROUND

The thyroid-gut axis has a great influence on the maintenance of human health; however, we know very little about the effects of low-dose ionizing radiation (LDR) on thyroid hormone levels and gut microbiota composition.

AIM

To investigate the potential effects of low-dose X-ray radiation to male C57BL/6J mice.

METHODS

Peripheral blood was collected for enzyme-linked immunosorbent assay (ELISA), and stool samples were taken for 16S ribosomal RNA (rRNA) gene sequencing after irradiation.

RESULTS

We found that LDR caused changes in thyroid stimulating hormone (TSH) levels in the irradiated mice, suggesting a dose-dependent response in thyroid function to ionizing radiation. No changes in the diversity and richness of the gut microbiota were observed in the LDR-exposed group in comparison to the controls. The abundance of *Moraxellaceae* and *Enterobacteriaceae* decreased in the LDR-exposed groups compared with the controls, and the *Lachnospiraceae* abundance increased in a dose-dependent manner in the radiated groups. And the abundances of *uncultured_bacterium_g_Acinetobacter*, *uncultured_bacterium_o_Mollicutes_RF39*, *uncultured_bacterium_g_Citrobacter*, and *uncultured_bacterium_g_Lactococcus* decreased in the radiated groups at the genus level, which showed a correlation with radiation exposure and diagnostic efficacy. Analysis of

functional metabolic pathways revealed that biological metabolism was predicted to have an effect on functional activities, such as nucleotide metabolism, carbohydrate metabolism, and glycan biosynthesis and metabolism. Furthermore, Kyoto Encyclopedia of Genes and Genomes pathway annotation also suggested that changes in the gut microbiota were related to processing functions, including translation, replication and repair.

CONCLUSION

LDR can change thyroid function and the gut microbiota, and changes in the abundances of bacteria are correlated with the radiation dose.

Key Words: Low-dose ionizing radiation; Thyroid; Gut microbiota; Thyroid-gut axis

©The Author(s) 2022. Published by Baishideng Publishing Group Inc. All rights reserved.

Core Tip: In this study, we administered low-dose X-ray radiation to male C57BL/6J mice to investigate the potential effects. Peripheral blood was collected for enzyme-linked immunosorbent assay, and stool samples were taken for 16S ribosomal RNA gene sequencing after irradiation. We found that LDR caused changes in TSH levels in the irradiated mice and the gut microbiota, and changes in the abundances of bacteria are correlated with the radiation dose. Our research aims to explore the influence of LDR on homeostasis from the "thyroid-gut axis" perspective for the first time.

Citation: Tong JY, Jiang W, Yu XQ, Wang R, Lu GH, Gao DW, Lv ZW, Li D. Effect of low-dose radiation on thyroid function and the gut microbiota. *World J Gastroenterol* 2022; 28(38): 5557-5572
URL: https://www.wjgnet.com/1007-9327/full/v28/i38/5557.htm
DOI: https://dx.doi.org/10.3748/wjg.v28.i38.5557

INTRODUCTION

According to microecological theory, the ecological balance of the nervous system, endocrine system, metabolic system, microbial system and immune system is the essence of life[1]. The thyroid is an important endocrine gland that regulates multiple metabolic pathways by producing thyroid hormones and has a great impact on the regulation of the internal environment[2]. Several investigations have indicated that the gut microbiota may indirectly participate in disease development and might become a promising biomarker for immune-related adverse events[3]. Studies have found that intestinal flora are related to various thyroid diseases, and the "thyroid-gut axis" theory has been proposed accordingly[4, 5]. The mechanism by which the thyroid-gut axis maintains homeostasis under external stimulation deserves further study.

As one of the environmental stressors affecting people worldwide, low-dose ionizing radiation (LDR) exposure is usually from medical radiotherapy, radiation-contaminated areas and human space exploration[6,7]. The studies previously reported have indicated that the biological responses of LDR exposure on epidemiology, animals, and cells are paradoxical due to discrepancies in the dose rate[8]. The role of LDR in inducing apoptosis, stimulating antioxidant capacity and repairing DNA damage has been well established[9]. Conversely, LDR exposure from radiotherapy for the treatment of autoimmune diseases or carcinoma is associated with an increasing risk of cardiovascular disease or secondary carcinoma[10]. For the thyroid, the levels of thyroid stimulating hormone (TSH), free triiodothyronine (fT3) and free thyroxine (fT4) have been reported to be affected by LDR exposure[11]. In addition, changes between external irradiation and the gut microbiota have been preliminarily confirmed[12]. Thus, we want to know how the thyroid-gut axis responds to radiation exposure and what roles the thyroid and gut microbiota play in an individual's response to radiation injury.

The objective of our research was to investigate changes in thyroid hormone levels and gut microbiota composition in LDR-exposed mice by enzyme-linked immunosorbent assay (ELISA) and 16S rRNA gene sequencing, respectively. Our research revealed the abundances of microbial species in the gut ecosystem following dose-modulated LDR exposure. These investigations predicted possible LDR-induced gut microbiota disorders based on variations in microbial species abundance. Our research aims to explore the influence of LDR on homeostasis from the "thyroid-gut axis" perspective for the first time and may provide a concrete conceptual and analytical basis for the additional study into the long-term impact of LDR on human health.

MATERIALS AND METHODS

Mice and samples

Thirty 6-wk-old female wild-type C57BL/6J mice were divided equally into five groups after one week of adaptive feeding at the Science and Innovation Center of Shanghai Tenth People's Hospital (ID Number: SHDSYY-2022-4381). The low-dose irradiation conditions were as follows: Dose rate, 0.05 Gy/min; 1 min/time; and once every other day. Irradiation was completed by the Irradiation Center of the Institute of Radiation Medicine, Tongji University (160 keV, 1 mA). The two groups were the test group and control group. And the test group was further divided into four groups according to the radiation dose, namely, the 0.05 Gy group, 0.10 Gy group, 0.15 Gy group, and 0.20 Gy group. The general condition of the mice was observed during the experiment.

Assays of thyroid function and acquisition of thyroid tissue

Peripheral blood was collected from the mouse tail vein to measure thyroid hormone levels when the mice completed the planned dose of radiation exposure within 24 h. Serum levels of TSH, fT4, and fT3 were assayed by an ELISA kit (Rayto RT-6100). Histological sections of mouse thyroid tissue were prepared by paraffin embedding and stained with hematoxylin and eosin (HE).

DNA extraction and 16S rRNA gene sequencing

Stool samples were stored in a sterile container and snap-frozen with liquid nitrogen following collection at -80 °C (Sarstedt, 80.734.311, Germany). Using the E.Z.N.A. Soil Kit for DNA extraction (Omega, Bio-Tek, Norcross, GA, United States) and using a Nanodrop 2000 to measure the concentration of bacterial DNA (Thermo Scientific, Wilmington, United States). All the fecal samples were stored at -20 °C until ready for sequencing. Then, the V3-V4 region of the bacterial 16S rRNA was amplified by polymerase chain reaction with barcode index primers using TransStart FastPfu DNA Polymerase (TransGen BioTech, AP221-02, Beijing, China) on an ABI GeneAmp 9700 polymerase chain reaction system (United States). Amplicons were then purified by gel extraction (AxyPrep DNA Gel Extraction Kit, Axygen Biosciences, United States) and quantified using QuantiFluor-ST (Promega, United States). The adapter sequences were added to the purified amplicons using a TruSeq™ DNA Sample Prep Kit (Illumina, San Diego, United States), and paired-end sequencing was performed using an Illumina MiSeq instrument (Illumina, San Diego, United States) (Figure 1).

Microbial analysis

The paired-end readings obtained by MiSeq were first merged by overlapping sequences. Filtering and quality control allow the sequences to be optimized. Operational taxonomic units (OTUs) were clustered using a 97% similarity cutoff with UPARSE (version 10.0). Cohort was randomly generated for a cross-sectional study that included 24 mice exposed to radiation and 6 controls. The alpha diversity was analyzed in terms of the species richness, including CHAO, ACE, SHANNON, and SIMPSON indices. Beta diversity was used to calculate structural variation by principal coordinates analysis (PCoA) and nonmetric multidimensional scaling (NMDS) and was mapped from principal coordinate analysis. Functional pathway analysis was conducted in accordance with the Kyoto Encyclopedia of Genes and Genomes (KEGG) database based on our microbial information.

Statistical analysis

Data that fit the normal distribution are expressed as the mean ± SD, and nonnormally distributed data are expressed as the median (interquartile). The t test or rank-sum test was used for comparing the thyroid hormone levels between the control group (n = 6) and test group (n = 24). Significant differences in the diversity index and microbial abundance between groups was determined by the Mann-Whitney U test. The microbial taxa with differences between the two groups were identified by linear discriminant analysis (LDA) effect size (LEfSe), with an LDA threshold value of > 2.0. The correlation between microbiota abundance and thyroid function was analyzed by Spearman correlation coefficient. The area under the curve (AUC) reflected the diagnostic accuracy of the bacterial indicators based on the receiver operating characteristic (ROC) curve. Unless otherwise stated, all analyses were performed using SPSS Statistics (Version 20.0). Statistical significance was set at $P < 0.05$ for analyses.

RESULTS

LDR caused changes in TSH levels in the mice

To understand changes in thyroid function in the irradiated mice, the levels of thyroid hormones in peripheral blood were determined by ELISA, including TSH, fT3, and fT4. As shown in Figure 2A, the TSH level of mice in the test mice (1.487 ± 0.347 mU/L) was obviously lower than the control mice (1.799 ± 0.289 mU/L), t = 2.188, P = 0.037). The level of TSH was the lowest in the 0.05 Gy group (1.262 ± 0.254 mU/L), which was the lowest among the four test subgroups, and in the 0.20 Gy group, it was the

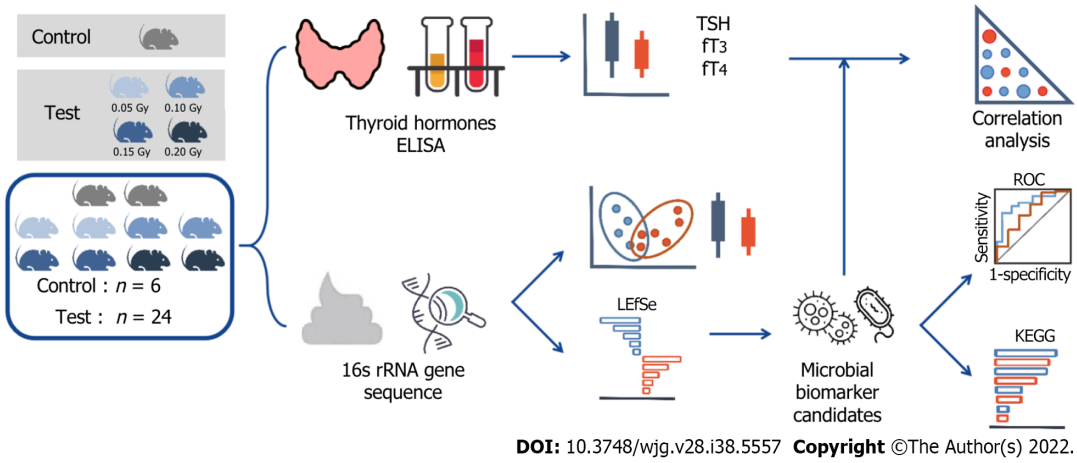


Figure 1 Graphical abstract. Schematic showing sample workflow from sequencing to analysis. TSH: Thyroid stimulating hormone; ELISA: Enzyme-linked immunosorbent assay; ROC: Receiver operating characteristic; KEGG: Kyoto Encyclopedia of Genes and Genomes; LEfSe: Linear discriminant analysis effect size.

highest (1.664 ± 0.264 mU/L) (Figure 2A and B). The change in thyroid hormone levels increased with increasing radiation dose and was consistent with TSH regulation in the test mice. The average levels of fT3 and fT4 in the test mice [386.560 (323.973, 442.594) ng/mL and 6.211 (5.018, 8.536) ng/mL, respectively] were higher than those in the control groups [372.664 (260.701, 384.492) ng/mL and 4.428 (3.175, 6.781) ng/mL, respectively]; nevertheless, the difference was not statistically confirmed between the two groups (Figure 2C and E). Moreover, the changes in fT3 and fT4 Levels from the different dose groups were consistent with the regulation of TSH (Figure 2D and F). Figure 3 shows thyroid tissue from the different groups of mice, and there were no obvious structural abnormalities.

Overview of the 16S rRNA gene sequencing data

An overview of the thyroid hormone levels and taxonomic data of all mice is visualized in Figure 4. High-throughput sequencing results of the 16S rRNA V3-V4 hypervariable regions obtained from stool samples revealed that the tested taxa were abundant, including 11 phyla, 50 families, 110 genera, and 424 OTUs. Rank-abundance curves according to OTU levels indicated that the species were distributed evenly and richly (Figure 5A). Figure 5B indicates that the curves flattened as increasing the sample size, demonstrating that the sequencing data were adequate and appropriately capturing microbial diversity.

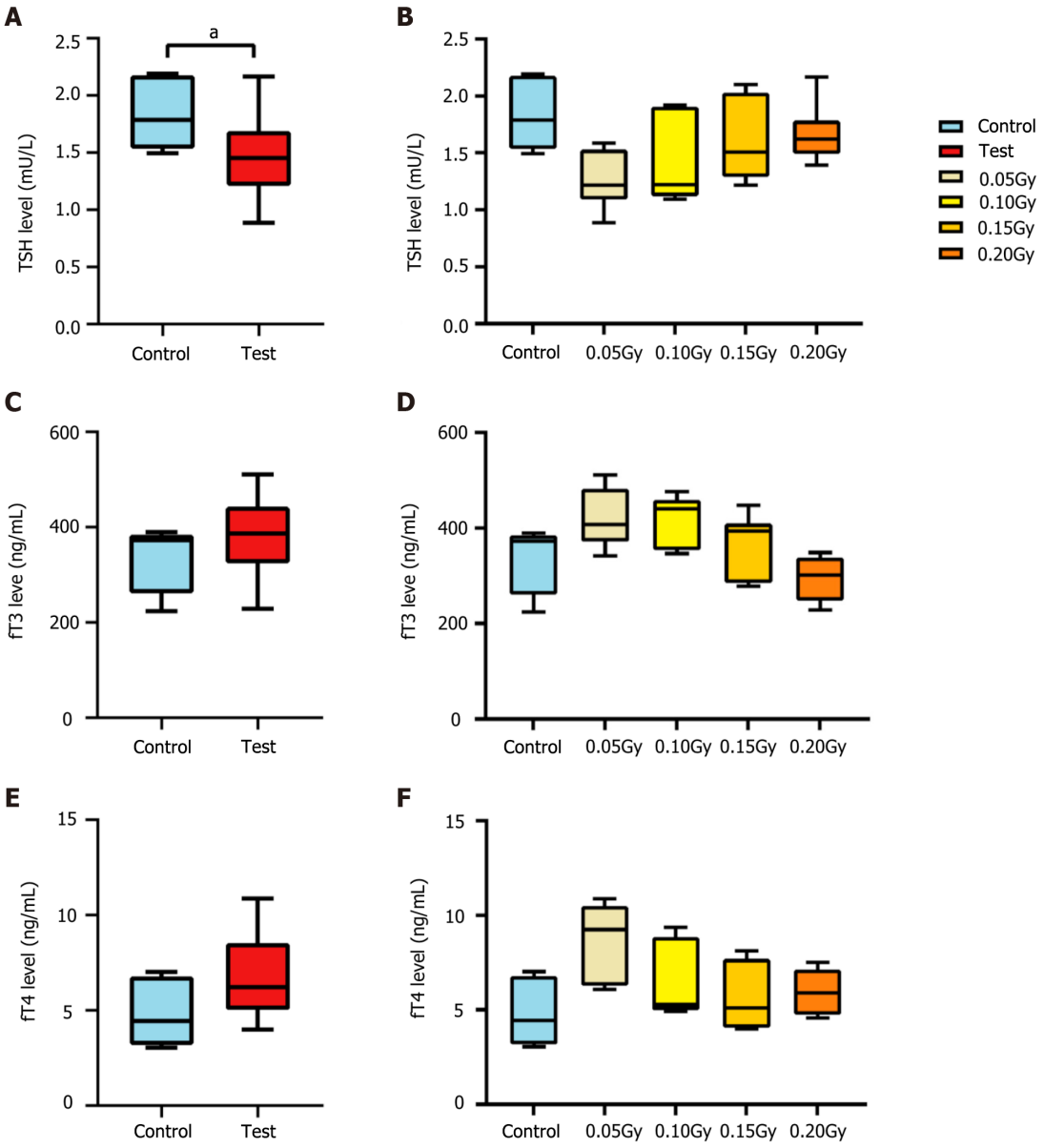
LDR does not cause gut microbiota diversity changes in irradiated mice

According to the outcome of alpha diversity analysis, the results showed that the test group had no differences in the diversity and abundances of certain microbes compared with the control group. The Chao and Ace indices, reflecting richness, indicated no considerable difference was found between the two groups ($P > 0.05$) (Figure 5C and D). Moreover, the Shannon and Simpson indices, which represent alpha diversity, indicated no meaningful difference between the two groups ($P > 0.05$, Figure 5E and F). Figure 5G-J shows the Chao, Ace, Shannon and Simpson indices among the different subgroups from the test group.

PCoA and NMDS analyses of the unweighted UniFrac distance were conducted on evaluation the overall microbiota diversity. PCoA indicated that there were no statistically significant variation in diversity of the microbiota between the test and control mice (R = -0.065, $P = 0.715$, Figure 5K). The NMDS results demonstrated no differences between the two groups (R = -0.065, $P = 0.695$, Figure 5L). Figure 5M and N show the results of the PCoA and NMDS analyses in the four test subgroups. These findings suggest that LDR in this study does not lead to altered microbiota diversity.

Changes in the composition of the gut microbiota in irradiated mice

The taxon compositions were further determined in the two groups. Eleven phyla, 50 families, and 110 genera were present in the samples from both groups. Figure 6A shows that *Firmicutes*, *Bacteroidetes*, *Patescibacteria*, and *Deferribacteres* were the four dominant phyla, with total abundances accounting for 97.83% ± 1.23% and 97.68% ± 0.75% of the microbiota of the test and control groups, respectively. The two dominant phyla were Firmicutes and *Bacteroidetes* in both the test and control group. At the phylum level, no meaningful variation in the relative abundances of the microorganisms was observed between the two groups (Figure 6B). We found that the *Firmicutes*-to-*Bacteroidetes* (F/B) ratio in the test group (median = 1.623 ± 0.679) was higher than controls (median = 1.266 ± 0.345), the differences were not confirmed by statistics. In addition, the microbiota was further analyzed according to the distribution at the family and genus levels.

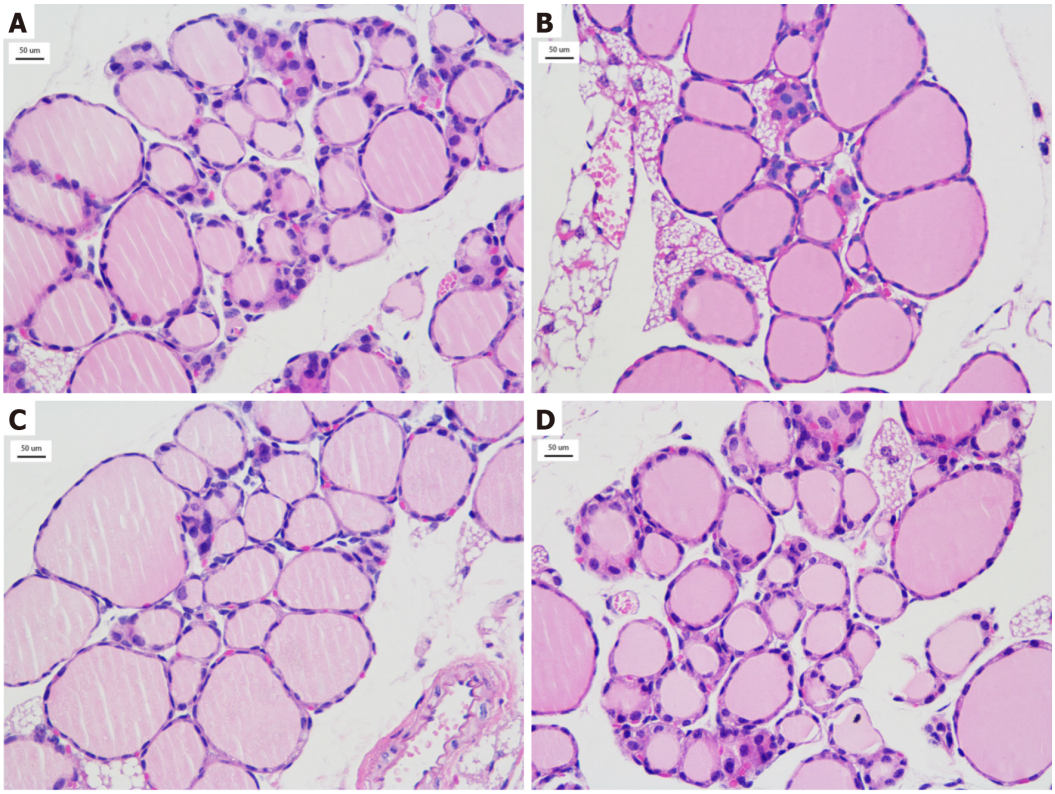


DOI: 10.3748/wjg.v28.i38.5557 **Copyright** ©The Author(s) 2022.

Figure 2 The level of thyroid hormone in mice exposed to radiation. A: Box and whisker plots of the levels of thyroid stimulating hormone (TSH) in the control (n = 6) and test (n = 24) groups. The TSH level of the mice in the test group was lower than that in the control mice (t = 2.188, P = 0.037); B: Histogram of the levels of TSH from the control and test groups. Statistically significant differences were not confirmed between the two groups; C: Box and whisker plots of the level of fT3 in the control (n = 6) and test groups (n = 24); D: Histogram of the level of fT3 in the control and test subgroups; E: Box and whisker plots of the level of fT4 in the control (n = 6) and test groups (n = 24); F: Histogram of the level of fT4 in the control and test subgroups. TSH: Thyroid stimulating hormone. $^{a}P < 0.05$.

LEfSe analysis results indicated that the control group had relatively high abundance in two families and four genera (LDA > 2, $P < 0.05$, Figure 7A). *Muribaculaceae*, *Lachnospiraceae*, *Ruminococcaceae*, *Lactobacillaceae* and *Bacteroidaceae* were the five dominant families, with total abundances accounting for 83.04% ± 4.59% and 80.68% ± 6.93% of the microbiomes of the test group and control group, respectively (Figure 7A). At the family level, the test group had significantly lower levels of *Moraxellaceae* and *Enterobacteriaceae* (all $P < 0.05$, Figure 7B). We also found that the abundance of *Lachnospiraceae* in the test group (20.05% ± 10.79%) was significantly higher than that in the controls (15.08% ± 10.02%), which increased in a dose-dependent manner following LDR exposure (Figure 7B and C).

Uncultured_bacterium_f_Muribaculaceae, *Lactobacillus*, *uncultured_bacterium_f_Lachnospiraceae*, *Bacteroides*, and *uncultured_bacterium_g_Ruminococcaceae_UCG-014* were the five dominant genera, with total abundances accounting for 59.87% ± 11.92% and 67.05% ± 10.38% of the microbiomes of the test group and control group, respectively (Figure 6C and D). At the genus level, the test group had significantly lower levels of *uncultured_bacterium_g_Acinetobacter*, *uncultured_bacterium_o_Mollicutes_RF39*, *uncultured_bacterium_g_Citrobacter*, and *uncultured_bacterium_g_Lactococcus* (all $P < 0.05$, Figure 7D).



DOI: 10.3748/wjg.v28.i38.5557 **Copyright** ©The Author(s) 2022.

Figure 3 Thyroid tissue from the mice exposed to radiation (HE, × 400). A-D: Thyroid tissue of radiation-exposed mice from the 0.05 Gy group, 0.10 Gy group, 0.15 Gy group, and 0.20 Gy group. TSH: Thyroid stimulating hormone.

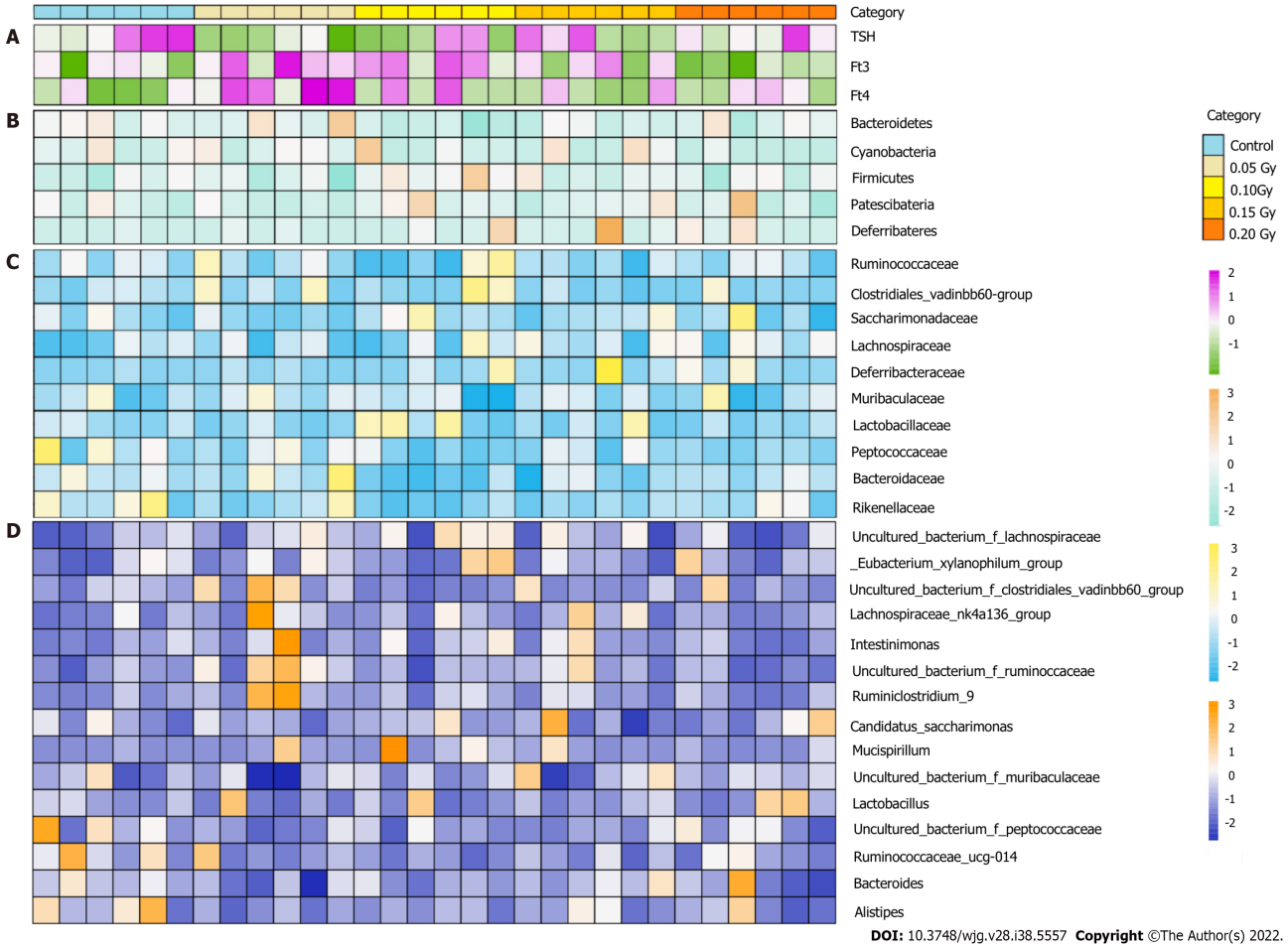
ROC curve analysis reveals the diagnostic value of specific intestinal microbiota

Based on the altered gut microbiota composition between the test and control groups, we found that six kinds of bacteria might serve as diagnostic biomarkers. At the family level, *Moraxellaceae* and *Enterobacteriaceae* are the two different bacteria between the two groups, and we selected them to serve as diagnostic biomarkers. ROC curves were generated to evaluate the diagnostic accuracy of these two families [AUC value of 0.819 (95% confidence interval: 0.640-0.999)] (Figure 8A).

At the genus level, we found four different bacteria and selected them to serve as diagnostic biomarkers, including *uncultured_bacterium_g_Acinetobacter*, *uncultured_bacterium_o_Mollicutes_RF39*, *uncultured_bacterium_g_Citrobacter*, and *uncultured_bacterium_g_Lactococcus*. ROC curves were generated to evaluate the diagnostic accuracy of these four genera [AUC value of 0.882 (confidence interval: 0.728-1.000)]. At the same time, the accuracy of the prognostic variables of two families and four genera was also analyzed by ROC curves [AUC value of 0.854 (confidence interval: 0.673-1.000)] (Figure 8).

The test groups included the 0.05 Gy group, 0.10 Gy group, 0.15 Gy group, and 0.20 Gy group according to the total radiation dose the mice received. On the basis of these results, we investigated the following relationships among thyroid function tests, absorbed dose, and levels of the gut microorganisms: *f_Moraxellaceae*, *f_Enterobacteriaceae*, *uncultured_bacterium_g_Acinetobacter*, *uncultured_bacterium_o_Mollicutes_RF39*, *uncultured_bacterium_g_Citrobacter*, and *uncultured_bacterium_g_Lactococcus*. We made an attempt to demarcate the functional influence of these flora according to the KEGG database to determine which biological pathways they may participate. Spearman correlation coefficient testing showed that *Moraxellaceae* (r = -0.789, P = 7.75E-7), *Enterobacteriaceae* (r=-0.662, P = 2.92E-4), *uncultured_bacterium_g_Acinetobacter* (r = -0.789, P = 7.75E-7), *uncultured_bacterium_o_Mollicutes_RF39* (r = -0.365, P = 0.0106), and *uncultured_bacterium_g_Lactococcus* (r = -0.667, P = 4.77E-3) levels were significantly negatively correlated with the absorbed dose (Figure 9).

The OTU abundance table was standardized to acquire information about the prediction of metabolic function in the KEGG pathway (Figure 10). According to the effect size, the top five pathways included carbohydrate metabolism, nucleotide metabolism, glycan biosynthesis and metabolism, xenobiotics biodegradation and metabolism, and metabolism of other amino acids. The effect size of the genetic information processing function is second only to metabolic function, which includes translation, replication and repair, folding, sorting and degradation, and transcription.



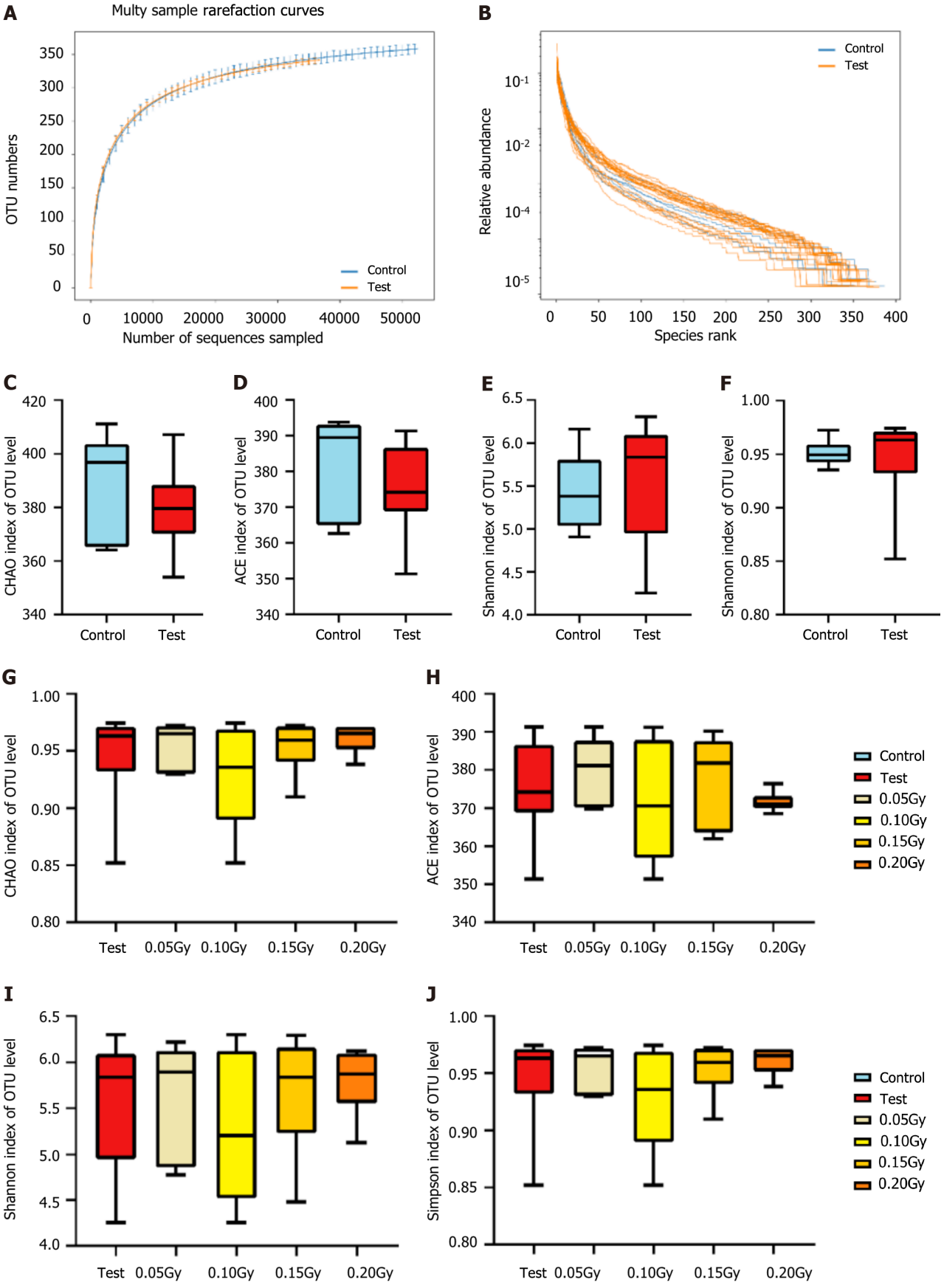
DOI: 10.3748/wjg.v28.i38.5557 **Copyright** ©The Author(s) 2022.

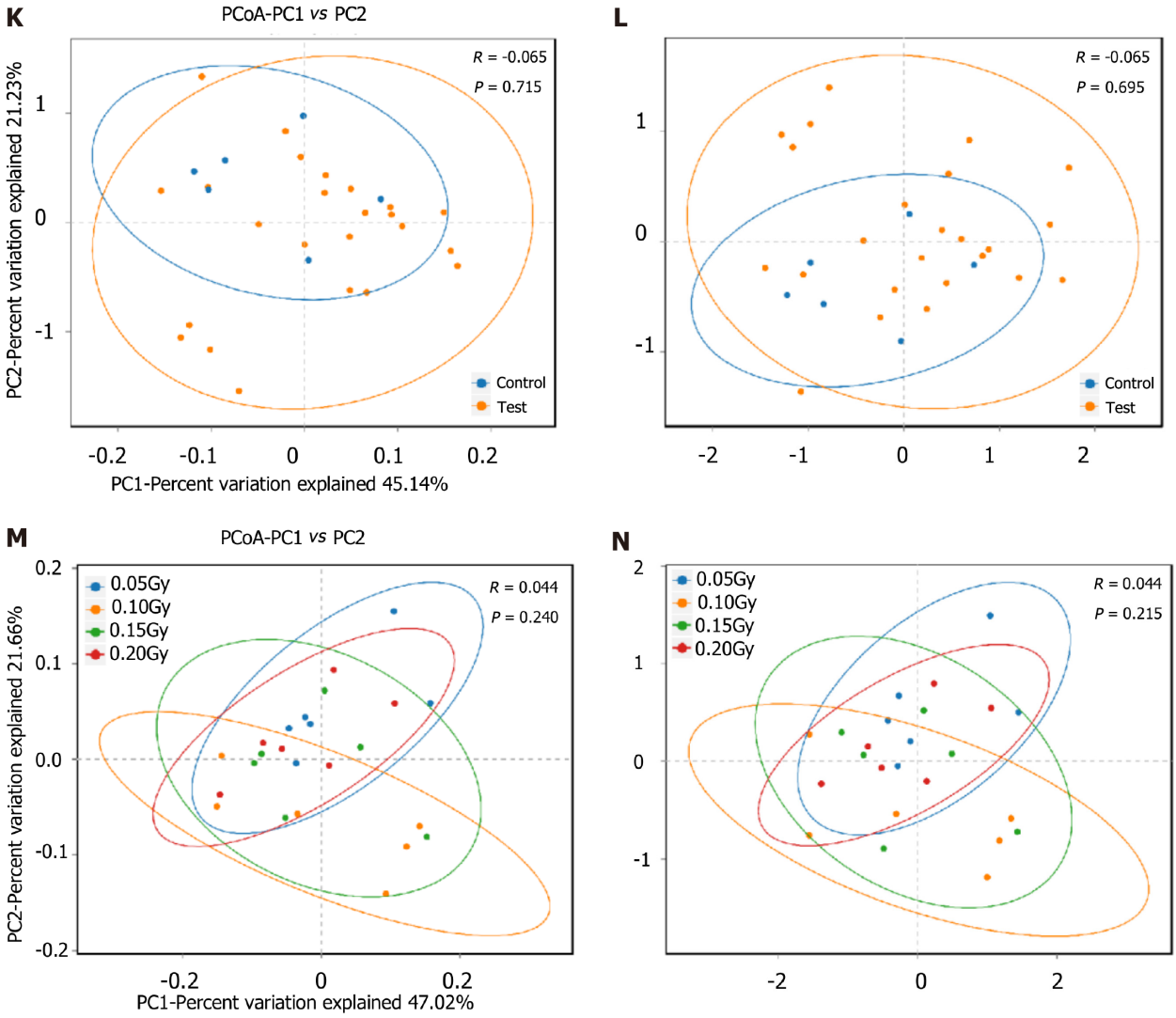
Figure 4 Taxonomic features of the thyroid hormone level and gut microbiota in the control mice (*n* = 6) and radiation-exposed group (*n* = 24). A-D: The thyroid hormone level for all subjects (A), with an overview of the 5 most abundant phyla (B), 10 most abundant families (C) and 15 most abundant genera (D) in fecal samples identified by 16S rRNA gene sequencing. The taxa levels were determined by summing the operational taxonomic units and are presented by relative abundance.

DISCUSSION

As an important organ of the endocrine system, the thyroid participates in homeostatic regulation. Recent studies demonstrated that the gut microbiota, a sophisticated and metabolically active community, is closely related to homeostasis in the host[13]. Although LDR exposure has been demonstrated to induce contradictory effects previously, *i.e.*, beneficial or harmful, the impacts of LDR exposure on the "thyroid-gut axis" have yet to be clarified. Therefore, we analyzed the association among LDR exposure, thyroid function and the gut microbiota in mice in this research. Our group indicated that as the LDR radiation dose increased, subclinical thyroid hyperthyroidism appeared in mice, and the observed species and OTU abundances showed no obvious changes in the radiated groups compared with the controls. It was thought that the low doses of radiation applied in this paper have an influence on the thyroid function of mice but are unable to alter the richness of the intestinal flora.

The thyroid is a radiation-sensitive organ, and internal radionuclide contamination external radiation and exposure (such as therapeutic radiation) may lead to thyroid dysfunction[14,15]. Our research found that the TSH level in the test mice was lower than the controls. Double-strand breaks can lead to cytotoxic, mutagenic and carcinogenic effects if unrepaired or misrepaired, although they only constitute a minority of DNA lesions induced by LDR, which will affect cell function[16,17]. Ishizaki *et al*[18] demonstrated a very small increase in γH2AX-positive foci in a human diploid cell line after exposure to LDR, which indicates the presence of DNA double-strand breaks. Some studies have also suggested that radiation-induced thyroid dysfunction is induced by damage to small thyroid vessels and to the gland capsule, the mechanisms of which include direct thyroid cell injury from radiation damage[19]. Because of the low thyroid dose in patients treated with total body irradiation, the incidence of Graves' disease accompanying this management was also reported in a total body irradiation series[20]. Strikingly, our results indicate pronounced modulation of the TSH level in mice exposed to 0.05 Gy and 0.10 Gy, while those exposed to a much higher dose (0.20 Gy) consistently


A
Multy sample rarefaction curves
OTU numbers
Number of sequences sampled
Control
Test
B
Relative abundance
Species rank
Control
Test
C
CHAO index of OTU level
Control
Test
D
ACE index of OTU level
Control
Test
E
Shannon index of OTU level
Control
Test
F
Shannon index of OTU level
Control
Test
G
CHAO index of OTU level
Test
0.05Gy
0.10Gy
0.15Gy
0.20Gy
H
ACE index of OTU level
Test
0.05Gy
0.10Gy
0.15Gy
0.20Gy
Control
Test
0.05Gy
0.10Gy
0.15Gy
0.20Gy
I
Shannon index of OTU level
Test
0.05Gy
0.10Gy
0.15Gy
0.20Gy
J
Simpson index of OTU level
Test
0.05Gy
0.10Gy
0.15Gy
0.20Gy
Control
Test
0.05Gy
0.10Gy
0.15Gy
0.20Gy



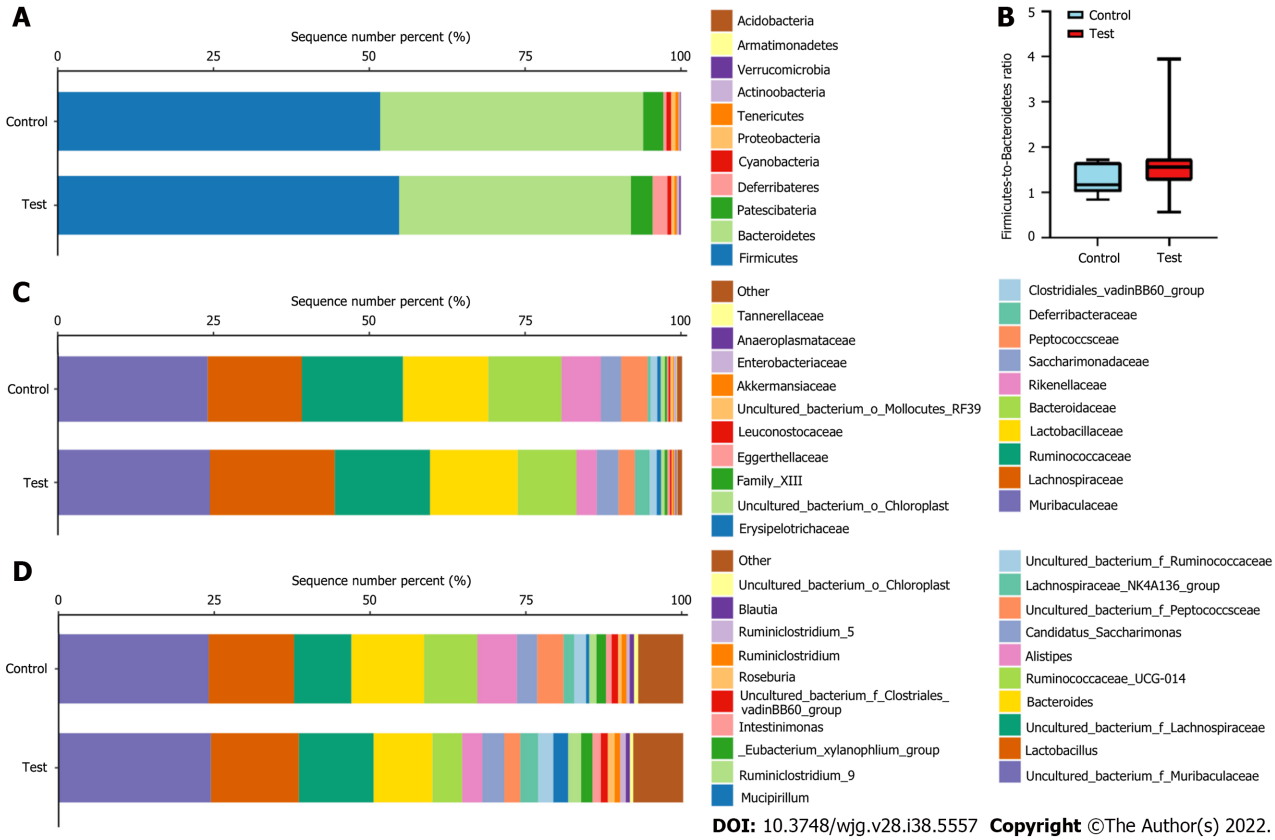
DOI: 10.3748/wjg.v28.i38.5557 **Copyright** ©The Author(s) 2022.

Figure 5 Bioinformatic analysis of 16S rRNA gene sequencing data in the exploratory cohort at the operational taxonomic units level. A and B: Rank-abundance curves and rarefaction curves (SOB index) of the gut microbiota; C-F: Box and whisker plots of the alpha diversity indices for richness (Chao index and Ace index) and diversity (Shannon index and Simpson index) of the bacterial communities in control mice (n = 6) and the test mice (n = 24); G-J: Box and whisker plots of the alpha diversity indices for richness (Chao index and Ace index) and diversity (Shannon index and Simpson index) of the bacterial communities among the test subgroups (0.05 Gy, 0.10 Gy, 0.15 Gy, and 0.20 Gy; n = 6 in each group); K and L: Principal coordinates analysis (PCoA) and nonmetric multidimensional scaling (NMDS) analyses indicated that the microbial diversity differed nonsignificantly between the control and test groups based on the unweighted UniFrac distance (PCoA, R = -0.065, P = -0.715; NMDS, R = -0.065, P = 0.695); M and N: PCoA and NMDS analyses indicated that the microbial diversity differed nonsignificantly among the test subgroups based on the unweighted UniFrac distance (PCoA, R = 0.004, P = 0.24; NMDS, R = 0.215, P = 0.695).

clustered with controls in terms of thyroid hormone levels. We speculate that there is an intricate dose-dependent response in thyroid function to ionizing radiation, with enhanced sensitivity for the lowest doses employed here. Therefore, thyroid function and microbial communities might be directly affected by LDR exposure.

Firmicutes and *Bacteroidetes* were the two dominant microbiota in these two groups. We found that the *Firmicutes* proportion in the irradiated group was higher than in the controls, while the *Bacteroidetes* proportion was lower in the irradiated group. One study about environmental radionuclides on the gut microbiota from Lavrinienko came to similar conclusions that the F/B ratio was increased almost 2-fold compared with an unirradiated group[21]. Previous investigation have also revealed that patients with metabolic diseases such as obesity, diabetes, and nonalcoholic fatty liver disease have a reduced F/B ratio compared to healthy individuals[22-24]. Recently, our group demonstrated that thyroid diseases, including Graves' disease and thyroid carcinoma, can cause changes in the F/B ratio[25,26]. Therefore, we speculate that the composition and function of microbial communities might be affected by LDR exposure directly or indirectly through changes in thyroid function.

Compared with the controls, the abundances of *Moraxellaceae* and *Enterobacteriaceae* were decreased in the test group at the family level. Obvious differences in the levels of four species were observed between the two groups at the genus level, and *uncultured_bacterium_g_Acinetobacter*, *uncultured_*



DOI: 10.3748/wjg.v28.i38.5557 **Copyright** ©The Author(s) 2022.

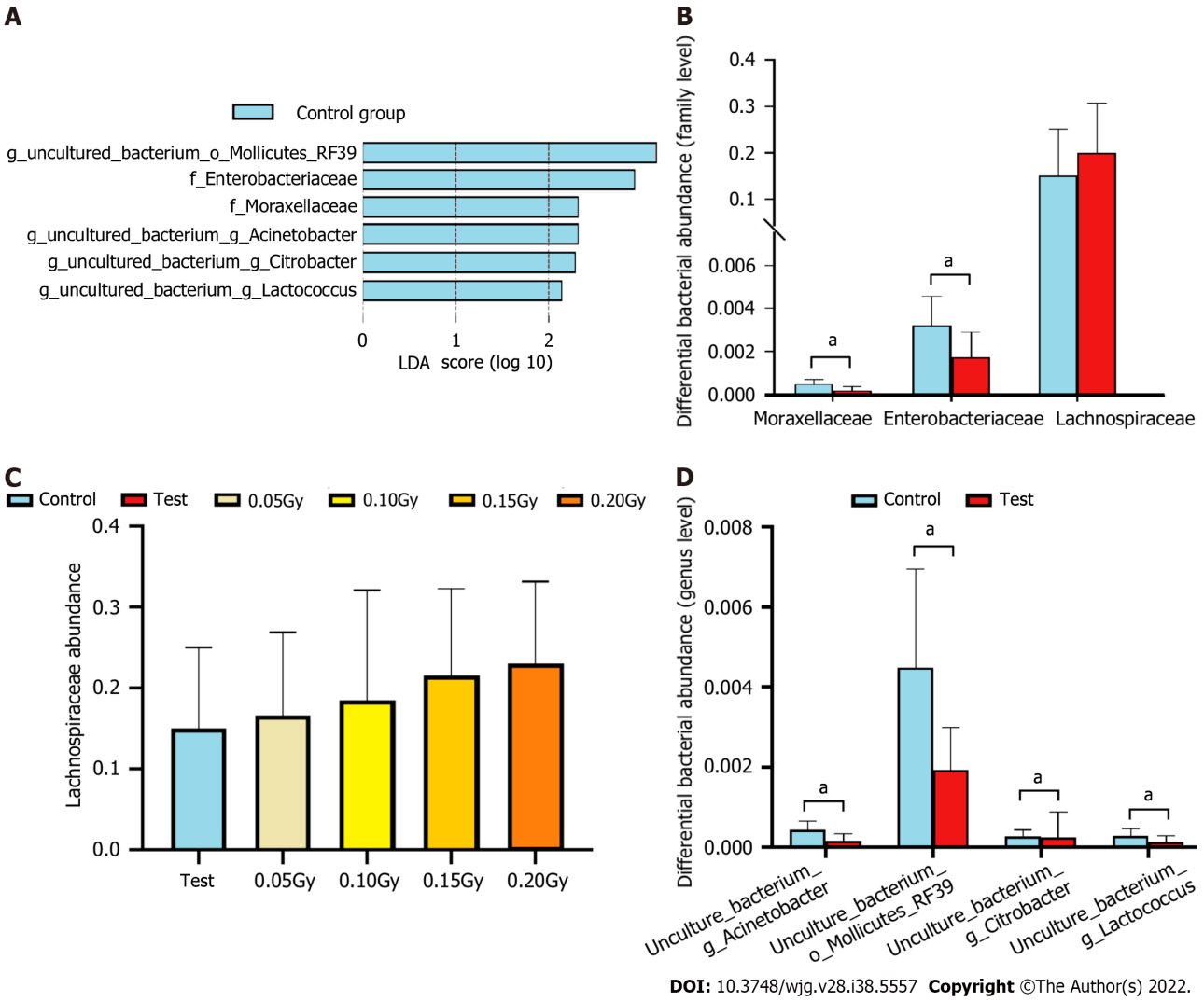
Figure 6 The gut microbiota composition in the control and test groups. A: Bar plots show the gut microbiota composition at the phylum level; B: Box and whisker plots of the *Firmicutes/Bacteroidetes* ratio in the control (n = 6) and test groups (n = 24), and there was no difference between the groups; C: Bar plots show the gut microbiota composition at the family level; D: Bar plots show the gut microbiota composition at the genus level.

bacterium_o_Mollicutes_RF39, *uncultured_bacterium_g_Citrobacter* and *uncultured_bacterium_g_Lactococcus* were reduced in the test group. On the one hand, the decreased abundance of the bacterium might be directly caused by radiation damage. On the other hand, changes in microbial abundance inhibit the development of gastrointestinal mucositis and promote intestinal repair mechanisms[27]. We hypothesize that metabolites from bacteria impair intestinal barrier function. By regulating bacterial abundance and reducing the release of proinflammatory factors, the intestinal barrier could repair the damage from LDR exposure. Another significant finding in this research was that the abundance of *Lachnospiraceae* increased in a dose-dependent manner following LDR exposure, which was in accordance with the performance outcome of the group of mice that have recovered from high-dose radiation to live a normal life span[28].

The synthesis of short-chain fatty acids (SCFAs) by fermenting polysaccharides in food has made members of the *Lachnospira* family well known[29]. SCFAs are essential substrates for the maintenance of the intestinal epithelium, regulation of the immune system and inflammatory response[30,31]. Broad inhibition of systemic inflammation, through reduction the levels of proinflammatory cytokines or through induction of anti-inflammatory cytokine interleukin-10, mediated by SCFAs may also potentially provide radioprotection. Elevated abundances of *Lachnospiraceae* have been shown to be connected with the repair of gastrointestinal after exposure to radiation[32].

Additionally, we employed KEGG pathway analysis to characterize changes in the gut microbiota associated with the stress from LDR exposure. KEGG pathway analysis based on OTU abundance indicated that biological metabolism was predicted to influence functional activities, including carbohydrate metabolism, glycan biosynthesis and metabolism, and nucleotide metabolism. The gut microbiota composition and metabolic pathways were influenced by LDR exposure. Moreover, processing functions were second only to metabolic functions according to the effect size, including translation, replication and repair. As the most significant influence of radiation, base modifications are a common type of DNA lesion[33]. KEGG pathway analysis may suggest a relationship between radiation damage and functional repair. Nevertheless, our observations provide circumstantial the proof of host-microbiome interactions; more investigations are required to uncover the crosstalk within LDR-responsive alterations and host-derived targets or signals.

Our research did not consider the following issues, and these limitations will also become the focus of follow-up research. First, the effects of exposure dose and recovery time on the thyroid and gut microbiota in the mice were not considered. Second, this was a descriptive study in nature and lacked



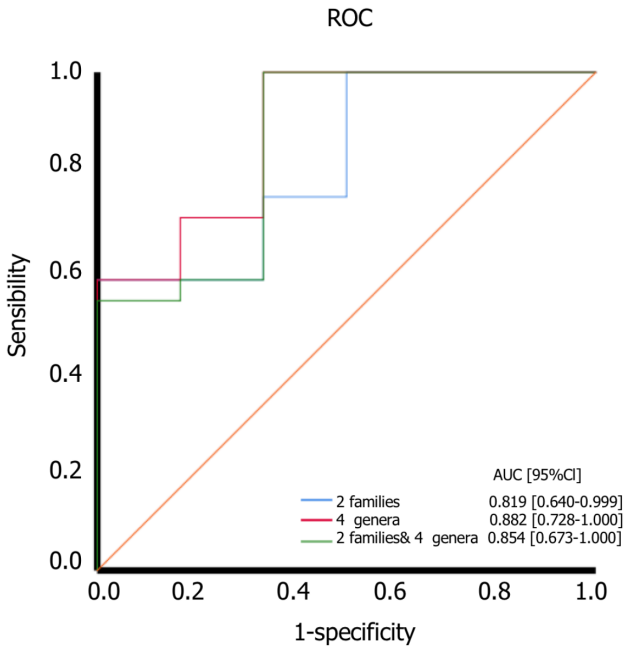
DOI: 10.3748/wjg.v28.i38.5557 **Copyright** ©The Author(s) 2022.

Figure 7 Altered gut microbiota composition in the radiation-exposed group compared with the control group. A: Identification of the significantly different species in the radiation-exposed group and controls at the family and genus levels as determined by linear discriminant analysis (LDA) effect size (LEfSe). Only taxa meeting a significant linear discriminant analysis threshold value of > 2.0 and $P < 0.05$ are shown; B: Comparison of *Moraxellaceae*, *Enterobacteriaceae, and Lachnospiraceae* abundances between the test group and control group at the family level; C: Histogram of the abundance of *Lachnospiraceae* in the control and test subgroups; D: Comparison of the differential bacterial abundances between the test group and controls at the genus level, including *uncultured_bacterium_g_Acinetobacter*, *uncultured_bacterium_o_Mollicutes_RF39*, *uncultured_bacterium_g_Citrobacter*, and *uncultured_bacterium_g_Lactococcus*. $^{a}P < 0.05$.

evidence regarding the underlying mechanisms of the responses to LDR exposure, which could be used to determine the alterations in metabolites from the gut microbiota. Finally, our experiment was a single-center study that lacked external validation. Despite these limitations, our research is one of the few to indicate the effects of LDR on homeostasis from the "thyroid-gut axis" perspective. In summary, our study constitutes a baseline analysis that can not only be used to further study the effects of LDR on human health but also provide potential targets for preventing or predicting radiation damage.

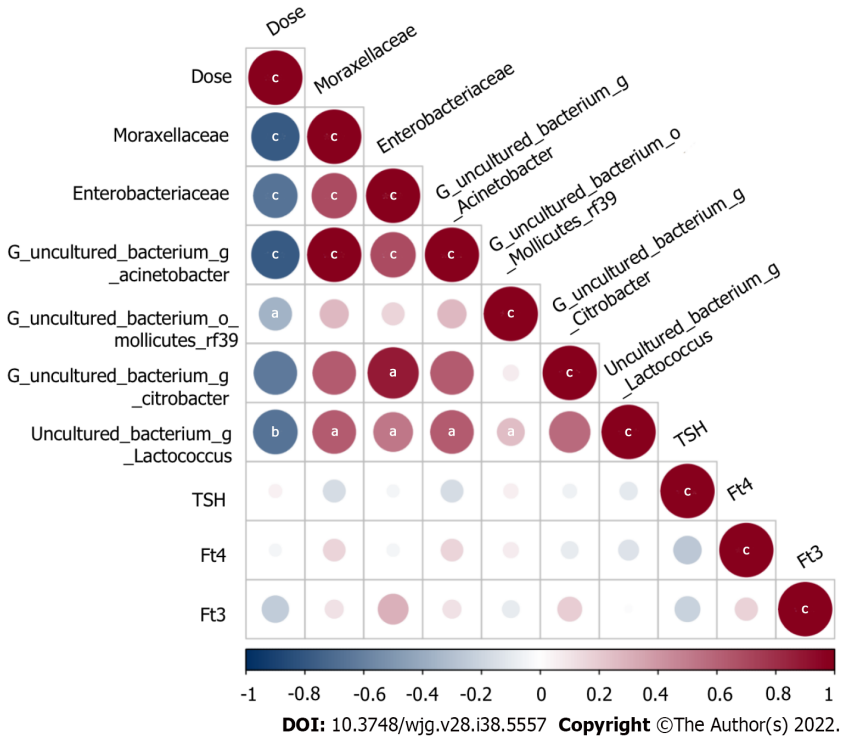
CONCLUSION

LDR can change the thyroid function and gut microbiota of mice, and changes in the abundances of bacteria are correlated with the radiation dose.



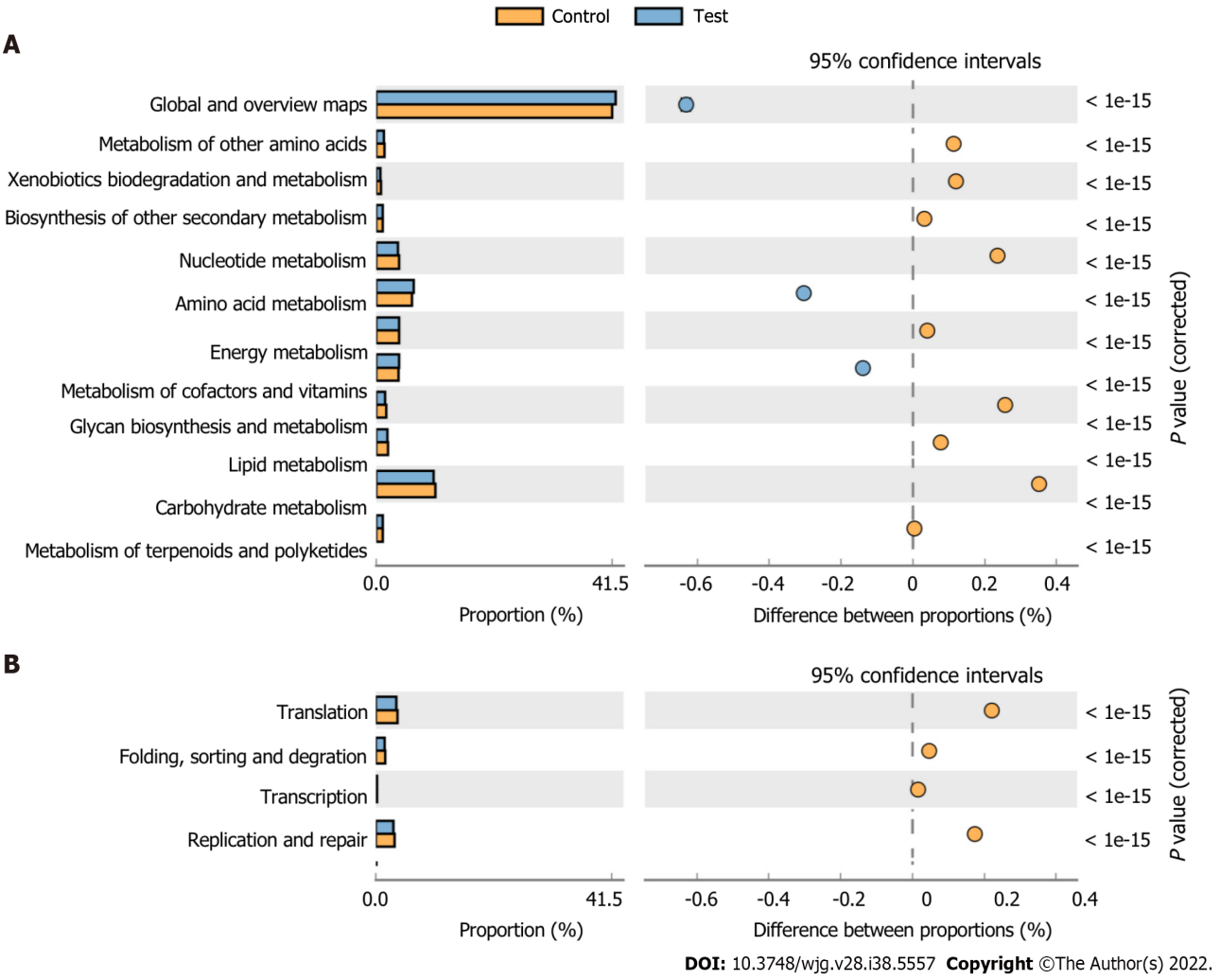
DOI: 10.3748/wjg.v28.i38.5557 **Copyright** ©The Author(s) 2022.

Figure 8 The diagnostic accuracy of the bacteria based on the linear discriminant analysis effect size results. ROC: Receiver operating characteristic.



DOI: 10.3748/wjg.v28.i38.5557 **Copyright** ©The Author(s) 2022.

Figure 9 The relationship between the dose and predictive bacteria as well as thyroid function tests. Positive correlations are represented in red, negative correlations are colored in blue. [a]$P < 0.05$; [b]$P < 0.01$; [c]$P < 0.001$.



DOI: 10.3748/wjg.v28.i38.5557 **Copyright** ©The Author(s) 2022.

Figure 10 The histogram shows the Kyoto Encyclopedia of Genes and Genomes categories that differed significantly between the test group and controls. A: Metabolic function; B: Processing function.

ARTICLE HIGHLIGHTS

Research background

The thyroid-gut axis has a great influence on the maintenance of human health.

Research motivation

We know very little about the effects of low-dose ionizing radiation (LDR) on thyroid hormone levels and gut microbiota composition.

Research objectives

To investigate the potential effects by administering low-dose X-ray radiation to male C57BL/6J mice.

Research methods

Peripheral blood was collected for enzyme-linked immunosorbent assay (ELISA), and stool samples were taken for 16S ribosomal RNA (rRNA) gene sequencing after irradiation.

Research results

We found that LDR caused changes in thyroid stimulating hormone (TSH) levels in the irradiated mice, suggesting a dose-dependent response in thyroid function to ionizing radiation. No changes in the diversity and richness of the gut microbiota were observed in the LDR-exposed group in comparison to the controls. The abundance of *Moraxellaceae* and *Enterobacteriaceae* decreased in the LDR-exposed groups compared with the controls, and the *Lachnospiraceae* abundance increased in a dose-dependent manner in the radiated groups. And the abundances of *uncultured_bacterium_g_Acinetobacter*, *uncultured_bacterium_o_Mollicutes_RF39*, *uncultured_bacterium_g_Citrobacter*, and *uncul-tured_*

bacterium_g_Lactococcus decreased in the radiated groups at the genus level, which showed a correlation with radiation exposure and diagnostic efficacy. Analysis of functional metabolic pathways revealed that biological metabolism was predicted to have an effect on functional activities, such as nucleotide metabolism, carbohydrate metabolism, and glycan biosynthesis and metabolism. Furthermore, KEGG pathway annotation also suggested that changes in the gut microbiota were related to processing functions, including translation, replication and repair.

Research conclusions

LDR can change thyroid function and the gut microbiota, and changes in the abundances of bacteria are correlated with the radiation dose.

Research perspectives

We administered low-dose X-ray radiation to male C57BL/6J mice to investigate the potential effects. Peripheral blood was collected for ELISA, and stool samples were taken for 16S rRNA gene sequencing after irradiation.

FOOTNOTES

Author contributions: Tong JY performed the statistical analysis and drafted this manuscript; Jiang W designed and performed the experiments; Yu XQ, Wang R, Lu CH, and Gao DW contributed to data collection; Lv ZW and Li D conceived the project and reviewed the manuscript; all authors approved the final version of the manuscript; Tong JY and Jiang W contributed equally to this work.

Supported by the Natural Science Foundation of Shanghai, No. 21ZR1449600; Shanghai Tenth People's Hospital, Tongji University School of Medicine, No. 2021SYPDRC064; and the Natural Science Foundation of China, No. 82071964.

Institutional animal care and use committee statement: All procedures involving animals were reviewed and approved by the Shanghai Tenth People's Hospital institutional review board (Approval No. SHDSYY-2022-4381).

Conflict-of-interest statement: The authors declared no potential conflicts of interest with respect to the research, authorship, and/or publication of this article.

Data sharing statement: No additional data are available.

ARRIVE guidelines statement: The authors have read the ARRIVE Guidelines, and the manuscript was prepared and revised according to the ARRIVE Guidelines.

Open-Access: This article is an open-access article that was selected by an in-house editor and fully peer-reviewed by external reviewers. It is distributed in accordance with the Creative Commons Attribution NonCommercial (CC BY-NC 4.0) license, which permits others to distribute, remix, adapt, build upon this work non-commercially, and license their derivative works on different terms, provided the original work is properly cited and the use is non-commercial. See: https://creativecommons.org/Licenses/by-nc/4.0/

Country/Territory of origin: China

ORCID number: Dan Li 0000-0002-9815-1792.

S-Editor: Chen YL
L-Editor: A
P-Editor: Chen YX

REFERENCES

1 **Fröhlich E**, Wahl R. Microbiota and Thyroid Interaction in Health and Disease. *Trends Endocrinol Metab* 2019; **30**: 479-490 [PMID: 31257166 DOI: 10.1016/j.tem.2019.05.008]
2 **Baş Y**, Hassan HA, Adıgüzel C, Bulur O, Ibrahim İA, Soydan S. The distribution of cancer cases in Somalia. *Semin Oncol* 2017; **44**: 178-186 [PMID: 29248129 DOI: 10.1053/j.seminoncol.2017.10.007]
3 **von Itzstein MS**, Khan S, Gerber DE. Investigational Biomarkers for Checkpoint Inhibitor Immune-Related Adverse Event Prediction and Diagnosis. *Clin Chem* 2020; **66**: 779-793 [PMID: 32363387 DOI: 10.1093/clinchem/hvaa081]
4 **Knezevic J**, Starchl C, Tmava Berisha A, Amrein K. Thyroid-Gut-Axis: How Does the Microbiota Influence Thyroid Function? *Nutrients* 2020; **12** [PMID: 32545596 DOI: 10.3390/nu12061769]
5 **Samimi H**, Haghpanah V. Gut Microbiome and Radioiodine-Refractory Papillary Thyroid Carcinoma Pathophysiology.

Trends Endocrinol Metab 2020; **31**: 627-630 [PMID: 32273149 DOI: 10.1016/j.tem.2020.03.005]
6 **Huang R**, Zhou P. Double-edged effects of noncoding RNAs in responses to environmental genotoxic insults: Perspectives with regards to molecule-ecology network. *Environ Pollut* 2019; **247**: 64-71 [PMID: 30654255 DOI: 10.1016/j.envpol.2019.01.014]
7 **Liu X**, Zhou Y, Wang S, Guan H, Hu S, Huang R, Zhou P. Impact of Low-dose Ionising Radiation on the Composition of the Gut Microbiota of Mice. *Toxicol Sci* 2019 [PMID: 31236581 DOI: 10.1093/toxsci/kfz144]
8 **Ebrahimian TG**, Beugnies L, Surette J, Priest N, Gueguen Y, Gloaguen C, Benderitter M, Jourdain JR, Tack K. Chronic Exposure to External Low-Dose Gamma Radiation Induces an Increase in Anti-inflammatory and Anti-oxidative Parameters Resulting in Atherosclerotic Plaque Size Reduction in ApoE$^{-/-}$ Mice. *Radiat Res* 2018; **189**: 187-196 [PMID: 29227739 DOI: 10.1667/RR14823.1]
9 **Farooque A**, Mathur R, Verma A, Kaul V, Bhatt AN, Adhikari JS, Afrin F, Singh S, Dwarakanath BS. Low-dose radiation therapy of cancer: role of immune enhancement. *Expert Rev Anticancer Ther* 2011; **11**: 791-802 [PMID: 21554054 DOI: 10.1586/era.10.217]
10 **Skov KA**. Radioresponsiveness at low doses: hyper-radiosensitivity and increased radioresistance in mammalian cells. *Mutat Res* 1999; **430**: 241-253 [PMID: 10631339 DOI: 10.1016/s0027-5107(99)00136-0]
11 **Cioffi DL**, Fontana L, Leso V, Dolce P, Vitale R, Vetrani I, Galdi A, Iavicoli I. Low dose ionizing radiation exposure and risk of thyroid functional alterations in healthcare workers. *Eur J Radiol* 2020; **132**: 109279 [PMID: 32950799 DOI: 10.1016/j.ejrad.2020.109279]
12 **Li Y**, Dong J, Xiao H, Zhang S, Wang B, Cui M, Fan S. Gut commensal derived-valeric acid protects against radiation injuries. *Gut Microbes* 2020; **11**: 789-806 [PMID: 31931652 DOI: 10.1080/19490976.2019.1709387]
13 **Virili C**, Centanni M. "With a little help from my friends" - The role of microbiota in thyroid hormone metabolism and enterohepatic recycling. *Mol Cell Endocrinol* 2017; **458**: 39-43 [PMID: 28167127 DOI: 10.1016/j.mce.2017.01.053]
14 **Sassolas G**, Hafdi-Nejjari Z, Casagranda L, Berger C, Bournaud C, Decaussin-Petrucci M, Berger N, Borson-Chazot F. Thyroid cancers in children, adolescents, and young adults with and without a history of childhood exposure to therapeutic radiation for other cancers. *Thyroid* 2013; **23**: 805-810 [PMID: 23286372 DOI: 10.1089/thy.2011.0370]
15 **Bang HS**, Choi MH, Kim CS, Choi SJ. Gene expression profiling in undifferentiated thyroid carcinoma induced by high-dose radiation. *J Radiat Res* 2016; **57**: 238-249 [PMID: 27006382 DOI: 10.1093/jrr/rrw002]
16 **Asaithamby A**, Chen DJ. Mechanism of cluster DNA damage repair in response to high-atomic number and energy particles radiation. *Mutat Res* 2011; **711**: 87-99 [PMID: 21126526 DOI: 10.1016/j.mrfmmm.2010.11.002]
17 **Bhattacharya S**, Asaithamby A. Ionizing radiation and heart risks. *Semin Cell Dev Biol* 2016; **58**: 14-25 [PMID: 26849909 DOI: 10.1016/j.semcdb.2016.01.045]
18 **Ishizaki K**, Hayashi Y, Nakamura H, Yasui Y, Komatsu K, Tachibana A. No induction of p53 phosphorylation and few focus formation of phosphorylated H2AX suggest efficient repair of DNA damage during chronic low-dose-rate irradiation in human cells. *J Radiat Res* 2004; **45**: 521-525 [PMID: 15635261 DOI: 10.1269/jrr.45.521]
19 **Jereczek-Fossa BA**, Alterio D, Jassem J, Gibelli B, Tradati N, Orecchia R. Radiotherapy-induced thyroid disorders. *Cancer Treat Rev* 2004; **30**: 369-384 [PMID: 15145511 DOI: 10.1016/j.ctrv.2003.12.003]
20 **Thomas O**, Mahé M, Campion L, Bourdin S, Milpied N, Brunet G, Lisbona A, Le Mevel A, Moreau P, Harousseau J, Cuillière J. Long-term complications of total body irradiation in adults. *Int J Radiat Oncol Biol Phys* 2001; **49**: 125-131 [PMID: 11163505 DOI: 10.1016/s0360-3016(00)01373-0]
21 **Lavrinienko A**, Mappes T, Tukalenko E, Mousseau TA, Møller AP, Knight R, Morton JT, Thompson LR, Watts PC. Environmental radiation alters the gut microbiome of the bank vole Myodes glareolus. *ISME J* 2018; **12**: 2801-2806 [PMID: 29988064 DOI: 10.1038/s41396-018-0214-x]
22 **Riva A**, Borgo F, Lassandro C, Verduci E, Morace G, Borghi E, Berry D. Pediatric obesity is associated with an altered gut microbiota and discordant shifts in Firmicutes populations. *Environ Microbiol* 2017; **19**: 95-105 [PMID: 27450202 DOI: 10.1111/1462-2920.13463]
23 **Loomba R**, Seguritan V, Li W, Long T, Klitgord N, Bhatt A, Dulai PS, Caussy C, Bettencourt R, Highlander SK, Jones MB, Sirlin CB, Schnabl B, Brinkac L, Schork N, Chen CH, Brenner DA, Biggs W, Yooseph S, Venter JC, Nelson KE. Gut Microbiome-Based Metagenomic Signature for Non-invasive Detection of Advanced Fibrosis in Human Nonalcoholic Fatty Liver Disease. *Cell Metab* 2017; **25**: 1054-1062.e5 [PMID: 28467925 DOI: 10.1016/j.cmet.2017.04.001]
24 **Brown CT**, Davis-Richardson AG, Giongo A, Gano KA, Crabb DB, Mukherjee N, Casella G, Drew JC, Ilonen J, Knip M, Hyöty H, Veijola R, Simell T, Simell O, Neu J, Wasserfall CH, Schatz D, Atkinson MA, Triplett EW. Gut microbiome metagenomics analysis suggests a functional model for the development of autoimmunity for type 1 diabetes. *PLoS One* 2011; **6**: e25792 [PMID: 22043294 DOI: 10.1371/journal.pone.0025792]
25 **Jiang W**, Yu X, Kosik RO, Song Y, Qiao T, Tong J, Liu S, Fan S, Luo Q, Chai L, Lv Z, Li D. Gut Microbiota May Play a Significant Role in the Pathogenesis of Graves' Disease. *Thyroid* 2021; **31**: 810-820 [PMID: 33234057 DOI: 10.1089/thy.2020.0193]
26 **Yu X**, Jiang W, Kosik RO, Song Y, Luo Q, Qiao T, Tong J, Liu S, Deng C, Qin S, Lv Z, Li D. Gut microbiota changes and its potential relations with thyroid carcinoma. *J Adv Res* 2022; **35**: 61-70 [PMID: 35003794 DOI: 10.1016/j.jare.2021.04.001]
27 **Touchefeu Y**, Montassier E, Nieman K, Gastinne T, Potel G, Bruley des Varannes S, Le Vacon F, de La Cochetière MF. Systematic review: the role of the gut microbiota in chemotherapy- or radiation-induced gastrointestinal mucositis - current evidence and potential clinical applications. *Aliment Pharmacol Ther* 2014; **40**: 409-421 [PMID: 25040088 DOI: 10.1111/apt.12878]
28 **Guo H**, Chou WC, Lai Y, Liang K, Tam JW, Brickey WJ, Chen L, Montgomery ND, Li X, Bohannon LM, Sung AD, Chao NJ, Peled JU, Gomes ALC, van den Brink MRM, French MJ, Macintyre AN, Sempowski GD, Tan X, Sartor RB, Lu K, Ting JPY. Multi-omics analyses of radiation survivors identify radioprotective microbes and metabolites. *Science* 2020; **370** [PMID: 33122357 DOI: 10.1126/science.aay9097]
29 **Reichardt N**, Duncan SH, Young P, Belenguer A, McWilliam Leitch C, Scott KP, Flint HJ, Louis P. Phylogenetic distribution of three pathways for propionate production within the human gut microbiota. *ISME J* 2014; **8**: 1323-1335

[PMID: 24553467 DOI: 10.1038/ismej.2014.14]

30 **Smith PM**, Howitt MR, Panikov N, Michaud M, Gallini CA, Bohlooly-Y M, Glickman JN, Garrett WS. The microbial metabolites, short-chain fatty acids, regulate colonic Treg cell homeostasis. *Science* 2013; **341**: 569-573 [PMID: 23828891 DOI: 10.1126/science.1241165]

31 **Arpaia N**, Campbell C, Fan X, Dikiy S, van der Veeken J, deRoos P, Liu H, Cross JR, Pfeffer K, Coffer PJ, Rudensky AY. Metabolites produced by commensal bacteria promote peripheral regulatory T-cell generation. *Nature* 2013; **504**: 451-455 [PMID: 24226773 DOI: 10.1038/nature12726]

32 **Xiao HW**, Cui M, Li Y, Dong JL, Zhang SQ, Zhu CC, Jiang M, Zhu T, Wang B, Wang HC, Fan SJ. Gut microbiota-derived indole 3-propionic acid protects against radiation toxicity *via* retaining acyl-CoA-binding protein. *Microbiome* 2020; **8**: 69 [PMID: 32434586 DOI: 10.1186/s40168-020-00845-6]

33 **Cadet J**, Delatour T, Douki T, Gasparutto D, Pouget JP, Ravanat JL, Sauvaigo S. Hydroxyl radicals and DNA base damage. *Mutat Res* 1999; **424**: 9-21 [PMID: 10064846 DOI: 10.1016/s0027-5107(99)00004-4]

World Journal of Gastroenterology

Submit a Manuscript: https://www.f6publishing.com

World J Gastroenterol 2022 October 14; 28(38): 5573-5588

DOI: 10.3748/wjg.v28.i38.5573

ISSN 1007-9327 (print) ISSN 2219-2840 (online)

ORIGINAL ARTICLE

Basic Study

Hypoxia inducible factor 1α promotes interleukin-1 receptor antagonist expression during hepatic ischemia-reperfusion injury

Zhao-Yang Wang, Yu Liu, Shi-Peng Li, Jian-Jun Li, Zhen Zhang, Xue-Chun Xiao, Yang Ou, Hang Wang, Jin-Zhen Cai, Shuang Yang

Specialty type: Gastroenterology and hepatology

Provenance and peer review: Unsolicited article; Externally peer reviewed.

Peer-review model: Single blind

Peer-review report's scientific quality classification

Grade A (Excellent): 0
Grade B (Very good): 0
Grade C (Good): C, C
Grade D (Fair): D
Grade E (Poor): 0

P-Reviewer: Katada K, Japan; Tzeng IS, Taiwan

Received: May 30, 2022
Peer-review started: May 30, 2022
First decision: August 1, 2022
Revised: August 16, 2022
Accepted: September 21, 2022
Article in press: September 21, 2022
Published online: October 14, 2022

Zhao-Yang Wang, Jian-Jun Li, Xue-Chun Xiao, Yang Ou, Hang Wang, Tianjin Key Laboratory of Tumor Microenvironment and Neurovascular Regulation, Medical College of Nankai University, Tianjin 300071, China

Yu Liu, Department of Internal Medicine, Wangdingdi Hospital, Tianjin 300071, China

Shi-Peng Li, Liver Transplant Center of Beijing Friendship Hospital, Capital Medical University, Beijing 100050, China

Zhen Zhang, Institute of Clinical Medicine, Jiangxi Provincial People's Hospital Affiliated to Nanchang University, Nanchang 330006, Jiangxi Province, China

Jin-Zhen Cai, Organ Transplantation Center, Affiliated Hospital of Qingdao University, Qingdao 266000, Shandong Province, China

Shuang Yang, Institute of Transplantation Medicine, Tianjin First Central Hospital, Nankai University, Tianjin 300071, China

Corresponding author: Shuang Yang, PhD, Professor, Institute of Transplantation Medicine, Tianjin First Central Hospital, Nankai University, No. 94 Weijin Road, Nankai District, Tianjin 300071, China. yangshuang@mail.nankai.edu.cn

Abstract

BACKGROUND

Ischemia-reperfusion injury (IRI) is a major risk associated with liver surgery and transplantation, and its pathological mechanism is complex. Interleukin-1 receptor antagonist (IL-1ra) can protect the liver from IRI. However, the regulatory mechanism of IL-1ra expression is still unclear.

AIM

To identify the mechanism that could protect the liver in the early stage of IRI.

METHODS

To screen the key genes in hepatic IRI, we performed RNA sequencing and gene enrichment analysis on liver tissue from mice with hepatic IRI. Subsequently, we verified the expression and effect of IL-1ra in hepatic IRI. We also used promoter mutagenesis and chromatin immunoprecipitation assay to search for the trans-

criptional regulatory sites of hypoxia-inducible factor (HIF)-1α. Finally, to explore the protective mechanism of ischemic preconditioning (IP), we examined the expression of HIF-1α and IL-1ra after IP.

RESULTS

We identified IL-1ra as a key regulator in hepatic IRI. The expression of IL-1ra was significantly upregulated after hepatic IRI both *in vivo* and *in vitro*. Furthermore, we found that HIF-1α regulated *Il-1ra* transcription in response to hypoxia. Increased HIF-1α accumulation promoted IL-1ra expression, whereas inhibition of HIF-1α exhibited the opposite effect. We also confirmed a predominant role for hypoxia response element in the regulation of *Il1ra* transcription by HIF-1α activation. Of note, we demonstrated that IP protects against hepatic IRI by inducing IL-1ra expression, which is mediated through HIF-1α.

CONCLUSION

We demonstrated that ischemia or hypoxia leads to increased expression of IL-1ra through HIF-1α. Importantly, IP protects the liver from IRI *via* the HIF-1α–IL-1ra pathway.

Key Words: Hepatic ischemia-reperfusion injury; Interleukin-1 receptor antagonist; Hypoxia inducible factor 1α; Ischemic preconditioning

©The Author(s) 2022. Published by Baishideng Publishing Group Inc. All rights reserved.

Core Tip: Ischemia-reperfusion injury (IRI) is a major risk associated with liver surgery and transplantation, and its pathological mechanism is complex. Interleukin-1 receptor antagonist (IL-1ra) can protect the liver from IRI. The expression of IL-1ra was significantly upregulated after IRI in mice. Hypoxia promoted the expression of IL-1ra. Hypoxia-inducible factor (HIF)-1α accumulation contributed to increased *Il-1ra* transcription. Ischemic preconditioning protected the liver from IRI *via* the HIF-1α-IL-1ra pathway.

Citation: Wang ZY, Liu Y, Li SP, Li JJ, Zhang Z, Xiao XC, Ou Y, Wang H, Cai JZ, Yang S. Hypoxia inducible factor 1α promotes interleukin-1 receptor antagonist expression during hepatic ischemia-reperfusion injury. *World J Gastroenterol* 2022; 28(38): 5573-5588
URL: https://www.wjgnet.com/1007-9327/full/v28/i38/5573.htm
DOI: https://dx.doi.org/10.3748/wjg.v28.i38.5573

INTRODUCTION

Hepatic ischemia (IS)-reperfusion injury (IRI) is a common complication in liver surgery and transplantation[1]. IRI usually results from restoration of the blood supply after brief IS[2]. The sterile inflammatory response induced by hypoxic stress leads to hepatic IRI[3]. The pathogenesis of hepatic IRI is complex and affected by various factors[4,5], which involve the damage-associated molecular patterns, innate immune response, and inflammation. Among them, the inflammation caused by interleukin (IL)-1β plays an important role[6,7]. During hepatic IRI, injured cells activate the inflammasome pathway, allowing the IL-1β precursor to be cleaved into its mature form by caspase-1 and subsequently released. Mature IL-1β is a broad-acting proinflammatory cytokine that increases the recruitment of endothelial adhesion molecules to innate immune cells and promotes the development of inflammatory phenotypes[8]. However, blocking the action of IL-1 can reduce hepatic damage[9,10]. As a natural anti-inflammatory factor, IL-1 receptor antagonist (IL-1ra) is highly expressed in a variety of inflammatory diseases and is closely related to the occurrence and progression of inflammation[11-14]. Several studies have shown a potential protective effect of IL-1ra in inflammation. For example, IL-1ra competes with IL-1β to bind to IL-1 receptor I, thus playing an anti-inflammatory role[15]. However, the transcriptional regulatory mechanism of IL-1ra during IRI remains unclear.

As a transcription factor, hypoxia-inducible factor (HIF)-1α is an important molecule for cell regulation in the hypoxic environment[16,17]. There have been a few reports confirming that HIF-1α plays an irreplaceable role in hepatic IRI[18]. HIF-1α can regulate the expression of multiple genes in cells after hypoxia[19], and consequently reduce organ IRI by regulating metabolism[20]. Furthermore, the mechanism of HIF-1α protection against hepatic IRI deserves further study.

Ischemic preconditioning (IP) was first reported by Murry *et al*[21] in 1986, who demonstrated that multiple IP reduces cell death after coronary artery occlusion. Although the protective effect of IP on hepatic IRI has been subsequently reported[22], its mechanism of action remains unclear. Therefore, it is

necessary to confirm the mechanism underlying this protective effect, which would be of great clinical significance. In the present study, we found that IL-1ra was expressed in hepatic tissue during IRI and was regulated by IS-induced HIF-1α. We also confirmed that the protective effect of IP was exerted precisely *via* the HIF-1α–IL-1ra pathway, leading to inhibition of IL-1β signaling and subsequent reduction in hepatic IRI.

MATERIALS AND METHODS

Reagents and antibodies

2-MeOE2 (S1233) and DMOG (S7483) were purchased from Selleck (China). Percoll (17089101) was purchased from GE Healthcare (United States). Collagenase IV (C8160) was purchased from Solarbio (China). Mouse monoclonal antibody for β-actin (sc-47778) was purchased from Santa Cruz Biotechnology (Santa Cruz, CA, United States). A rabbit monoclonal antibody for IL-1ra (ab124962) was purchased from Abcam (Cambridge, MA, United States). Rabbit antibodies for HIF-1α (36169), BAX (14796), Bcl-2 (3498), and cleaved caspase-3 (9664) were purchased from Cell Signaling Technology (Danvers, MA, United States). ELISA kits for detecting mouse alanine transaminase (ALT) (JL12668), aspartate transaminase (AST) (JL13793), and IL-1ra (JL20255) were purchased from Jonln (China). Recombinant IL-1ra (200-01RA) was purchased from PeproTech (United States).

Animals

Wild-type male C57BL/6 mice, aged 6-8 wk, were purchased from Beijing HFK Bioscience (Beijing, China). The mice were raised in standard conditions[23] and received humanitarian care. The mice were acclimated to the rearing environment for 3-4 d before experimentation.

Animal experiments

Mice were randomly grouped and marked. The mice were weighed and anesthetized with 1% pentobarbital (50 mg/kg). For the hepatic IR experiments, mice were divided into six groups (n = 5 each): Sham group: The portal vein was exposed, and no blood vessels were clamped; ischemia reperfusion (IS) 1.5 h group: We only clamped the left and middle lobe vessels for 1.5 h; IR 3-24 h group: Reperfusion was performed for the corresponding time after the vessels had been clamped for 1.5 h; IP group: We briefly clamped the vessel for 10 min and released it for 10 min before IS; this was named an IP cycle; sh*Il1ra* group: Adenovirus carrying *Il1ra* shRNA was injected *via* the tail vein 48 h before IR. At the end of the experiment, the ischemic hepatic lobes were isolated for subsequent processing or stored at -80 °C. The animal study protocol was approved by the Animal Ethical and Welfare Committee (protocol code: IRM-DWLL-2020173 and date of approval: September 15, 2020).

Nonparenchymal cell and hepatocyte isolation

Nonparenchymal cells (NPCs) and hepatocytes were isolated from mice by collagenase digestion and differential centrifugation using Percoll, as previously described[24].

Histological examination of liver tissue

The left lobe samples of mouse livers were fixed in formaldehyde solution, dehydrated, paraffin-embedded, and cut into 4-μm-thick sections. The IL-1ra levels were determined by immunohistochemistry. The histological analysis was performed using the histochemistry score. A section was selected from the left lobe in every liver, and five views (200 ×) were captured for calculation in each section.

Cell culture

Mouse liver parenchymal cells, AML12 (SCSP-550; American Type Culture Collection, Manassas, VA, United States), were cultured in Dulbecco's modified Eagle's medium (DMEM)/F12 (11965092; Gibco) supplemented with 10% fetal bovine serum (FBS) (10099133; Gibco) and 1% penicillin/streptomycin at 37 °C in an atmosphere containing 5% CO_2. HEK293T cells were cultured in DMEM (11320033; Gibco) supplemented with 10% FBS, 1% sodium pyruvate, 1% non-essential amino acids, and 2% glutamine.

Cell experiment

AML12 cells were subjected to hypoxia and reoxygenation to simulate the ischemic and reperfusion environment *in vivo*. During hypoxia, cells were cultured in a 37 °C incubator with 95% N_2 and 5% CO_2. After a specific time period, cells were removed and placed back into the 37 °C incubator with 5% CO_2. To interfere with HIF-1α, cells were treated with DMOG or 2-MeOE2 at a concentration of 100 μM for 6 h before subsequent experiments were performed.

Table 1 Primer sequences

Gene	Forward sequence	Reverse sequence
Il1ra	TCTTGGGCATCCACGGG	GAGGCTCACAGGACGGTCAG
β-actin	GTGACGTTGACATCCGTAAAGA	GCCGGACTCATCGTACTCC
Il1ra pro-2.1K	CGGAGCTCGCCAGCAAGATTTTAAGTGATTCT	CCAGATCTGGGTGAGCTAAACAGGACACAAGGT
Il1ra pro-1.5K	CGGAGCTCCCCAACAACTTCCAGACTTCCCTC	CCAGATCTGGGTGAGCTAAACAGGACACAAGGT
Il1ra pro-1.1K	CGGAGCTCATCAGTCTAAGGCTGGGCAGGGAG	CCAGATCTGGGTGAGCTAAACAGGACACAAGGT
Il1ra pro-0.6K	CGGAGCTCCCCAGCTCAAATGCCACCATTCTC	CCAGATCTGGGTGAGCTAAACAGGACACAAGGT
Il1ra Mut1	TTTATGCACATTCCCTCTTTCAGC	AGAGGGAATGTGCATAAACTTGT
Il1ra Mut2	GATATGGACTTGCCATTTTGACTC	AAATGGCAAGTCCATATCTTTCTT

Plasmid construction

The mouse *Il1ra* promoter (-2113/+143) sequences were obtained by polymerase chain reaction (PCR) from mouse genomic DNA and cloned into the pGL3-basic vector (Promega, Madison, WI, United States). Mutagenesis of HRE-I and HRE-II in the mouse *Il1ra* promoter was performed using a QuickChange® Lightning Site-Directed Mutagenesis Kit (Stratagene, La Jolla, CA, United States). The primer sequences are listed in Table 1. The mouse *Il1ra* shRNA plasmid was purchased from Hanbio Biotechnology (Shanghai, China), and packaged into adenoviral particles.

RNA extraction and quantitative qPCR

Total RNA from liver tissue and AML12 cells was extracted using Trizol (Life Technologies, Carlsbad, CA, United States). cDNA was synthesized using reverse transcriptase (Takara, Japan). The specific product of *Il1ra* was amplified by qPCR using the TransStart Green Q-PCR SuperMix Kit (TransGen, China). β-Actin was used as a normalization control. The primer sequences are listed in Table 1.

Immunoblotting assay

Tissues and cell lysates were prepared in RIPA buffer with protease and phosphatase inhibitors. The immunoblotting procedures can be found in the literature[25].

Luciferase assay

Cells were transfected with wild-type or mutant mouse *Il1ra* promoters, followed by treatment with DMOG or 2-MeOE2 under hypoxia in 24-well plates. Lysates were prepared 48 h after transfection, and the luciferase activity was measured using the Dual-Luciferase Reporter Assay System (Promega). The luciferase activity was normalized to the values for Renilla luciferase.

Chromatin immunoprecipitation

Chromatin immunoprecipitation (ChIP) assays were performed using an EZ-ChIP kit (Millipore, Billerica, MA, United States). The primers and antibodies used in these experiments are shown in Table 1.

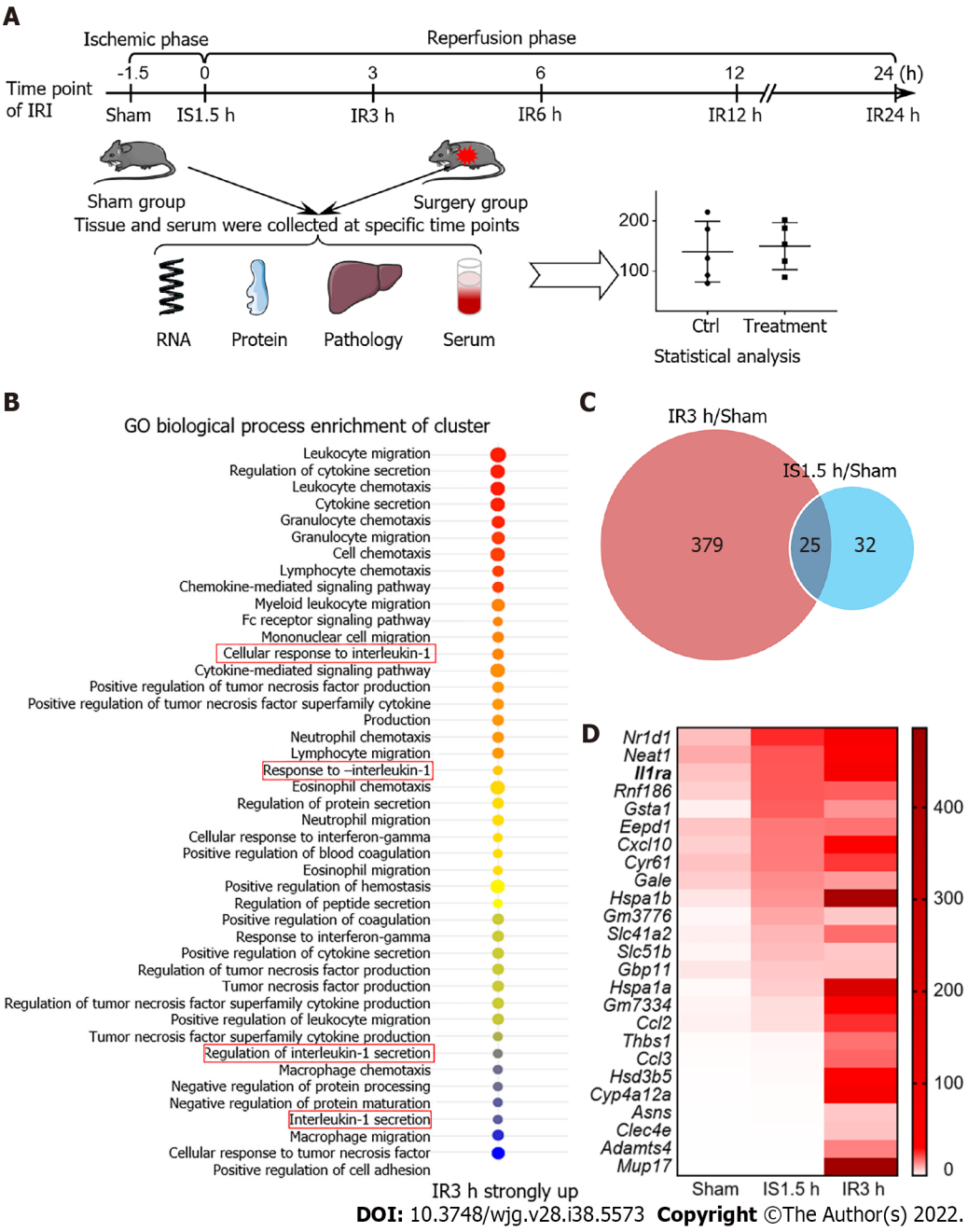
Statistical analysis

Statistical analyses were performed using GraphPad Prism 7.0 (San Diego, CA, United States). All the data are presented as the mean ± SEM and represent three or five independent experiments. One-way analysis of variance was used to compare means among treatment groups. Student's *t*-test for unpaired observations was applied. $P < 0.05$ was considered significant.

RESULTS

Screening of protective genes during hepatic IRI

To screen key genes that potentially play protective roles in the liver in IRI, we constructed a mouse model of hepatic IRI and performed transcriptome sequencing using mRNAs of the liver from the Sham, IS 1.5 h, and IR 3 h groups (Figure 1A). Gene enrichment analysis showed that, after IR 3h, a group of genes enriched in the IL-1 pathway were upregulated (Figure 1B). Expression of 25 genes was significantly increased (> 2-fold) in both IS and IR periods (Figure 1C). These genes were then ranked in descending order of ischemic expression abundance, and *Il1ra*, as a key antagonist of the IL-1 signaling, was shown to be one of the highly differentially expressed genes (Figure 1D). Thus, we chose *Il1ra* for further investigation on its regulatory mechanism in the hepatic IRI.



DOI: 10.3748/wjg.v28.i38.5573 **Copyright** ©The Author(s) 2022.

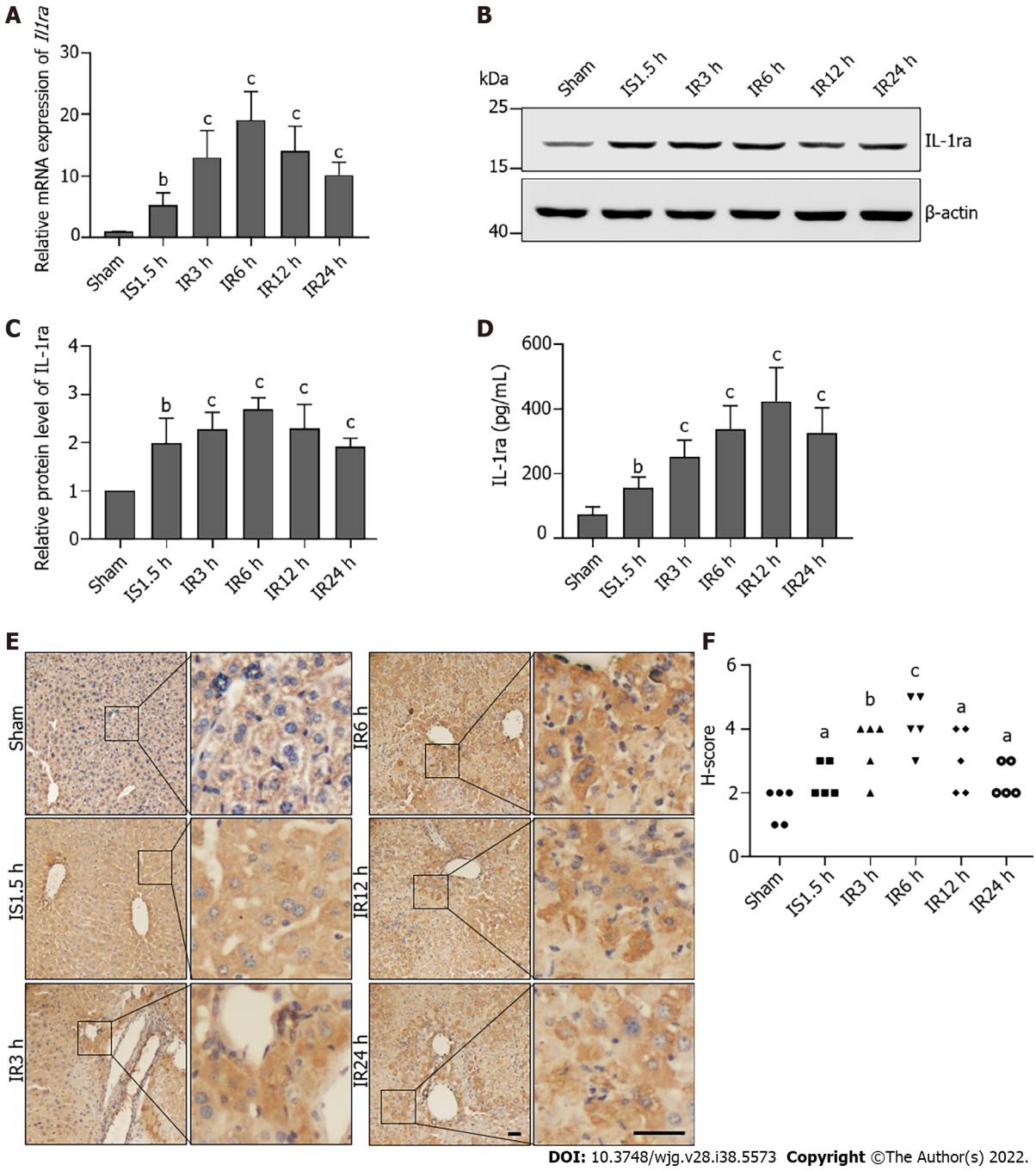
Figure 1 Construction of a mouse model of hepatic ischemia-reperfusion injury and gene enrichment analysis. A: Model of ischemia-reperfusion injury (IRI) in mice; B: GO enrichment analysis upon IR for 3 h; C: Venn diagram shows that the expression of genes for IR 3 h and ischemia (IS) 1.5 h was more than 2-fold than that in the Sham group; D: Twenty-five genes were elevated in both IR 3 h and IS 1.5 h groups according to IS 1.5 h expression level. IS: Ischemia; IR: Ischemia-reperfusion; IRI: Ischemia-reperfusion injury.

IL-1ra expression is elevated during hepatic IRI

We detected IL-1ra expression in mice with IRI. This confirmed that mRNA expression of *Il1ra* was increased in mice that experienced hepatic IRI as compared with the Sham group (Figure 2A). Upregulation of IL-1ra in liver tissue was confirmed at the protein level by immunoblotting (Figures 2B and C), ELISA (Figure 2D), and immunohistochemistry (Figures 2E and F), demonstrating that expression of IL-1ra is significantly elevated in response to hepatic IRI in mice.

Hepatocytes and hepatic NPCs both express high levels of IL-1ra after IRI

The liver is composed of several different embryonic-derived cell types, including hepatocytes, bile duct epithelial cells, stellate cells, Kupffer cells, and sinusoidal endothelial cells[26]. The liver consists of 80% hepatocytes, and 20% of the other cells are collectively called NPCs. Hepatocytes are the major epithelial cell population of the liver and perform various physiological functions. Therefore, we aimed to identify whether there is a difference in the expression of IL-1ra in hepatocytes and NPCs after IRI. To do so, gradient centrifugation was used to separate hepatocytes and NPCs from mouse liver tissue, and

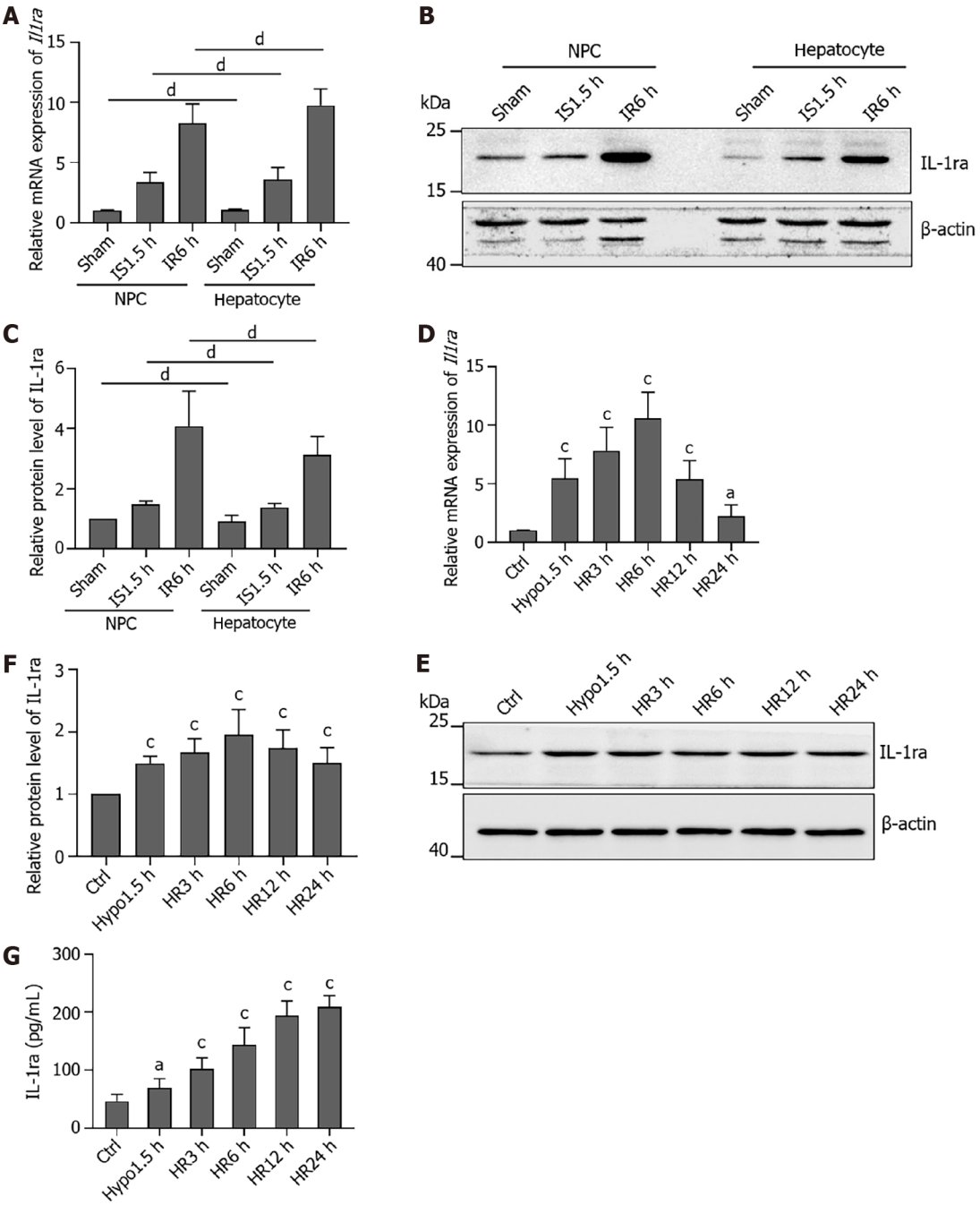


DOI: 10.3748/wjg.v28.i38.5573 **Copyright** ©The Author(s) 2022.

Figure 2 Interleukin-1 receptor antagonist expression is elevated after hepatic ischemia-reperfusion injury in mice. A: Relative mRNA levels of interleukin-1 receptor antagonist (*Il1ra*) in the liver upon ischemia-reperfusion injury (IRI); B: Protein levels of IL-1ra in the liver upon IRI; C: Statistical analysis of protein levels of IL-1Ra upon IRI; D: Protein content of IL-1ra in serum upon IRI; E. Representative images of immunohistochemical staining for IL-1ra in the liver upon IRI. Scale bars, 100 μm; F: Statistical analysis of immunohistochemical scores. Indicated *P* values were calculated using a two-tailed unpaired Student's *t*-test. Data are presented as the mean ± SEM. Data are representative of five independent experiments. $^{a}P < 0.05$, $^{b}P < 0.01$, $^{c}P < 0.001$. IS: Ischemia; IR: Ischemia-reperfusion; IL-1ra: Interleukin-1 receptor antagonist.

expression of IL-1ra was detected. There was no significant difference in the expression of IL-1ra at both the mRNA (Figure 3A) and protein (Figures 3B and C) levels between hepatocytes and NPCs after IR treatment.

To confirm these results *in vitro*, we performed the hypoxia–reoxygenation experiments in the mouse hepatic cell line AML12 to simulate IRI. We found that the mRNA (Figure 3D) and protein (Figures 3E and F) expression of IL-1ra was increased in AML12 cells upon hypoxia and reoxygenation. Similarly, the content of IL-1ra in the culture medium of the hypoxia-reoxygenation group was significantly higher than that in the control group (Figure 3G). Together, these data suggested that IL-1ra is highly expressed in both hepatocytes and NPCs after IRI.



DOI: 10.3748/wjg.v28.i38.5573 **Copyright** ©The Author(s) 2022.

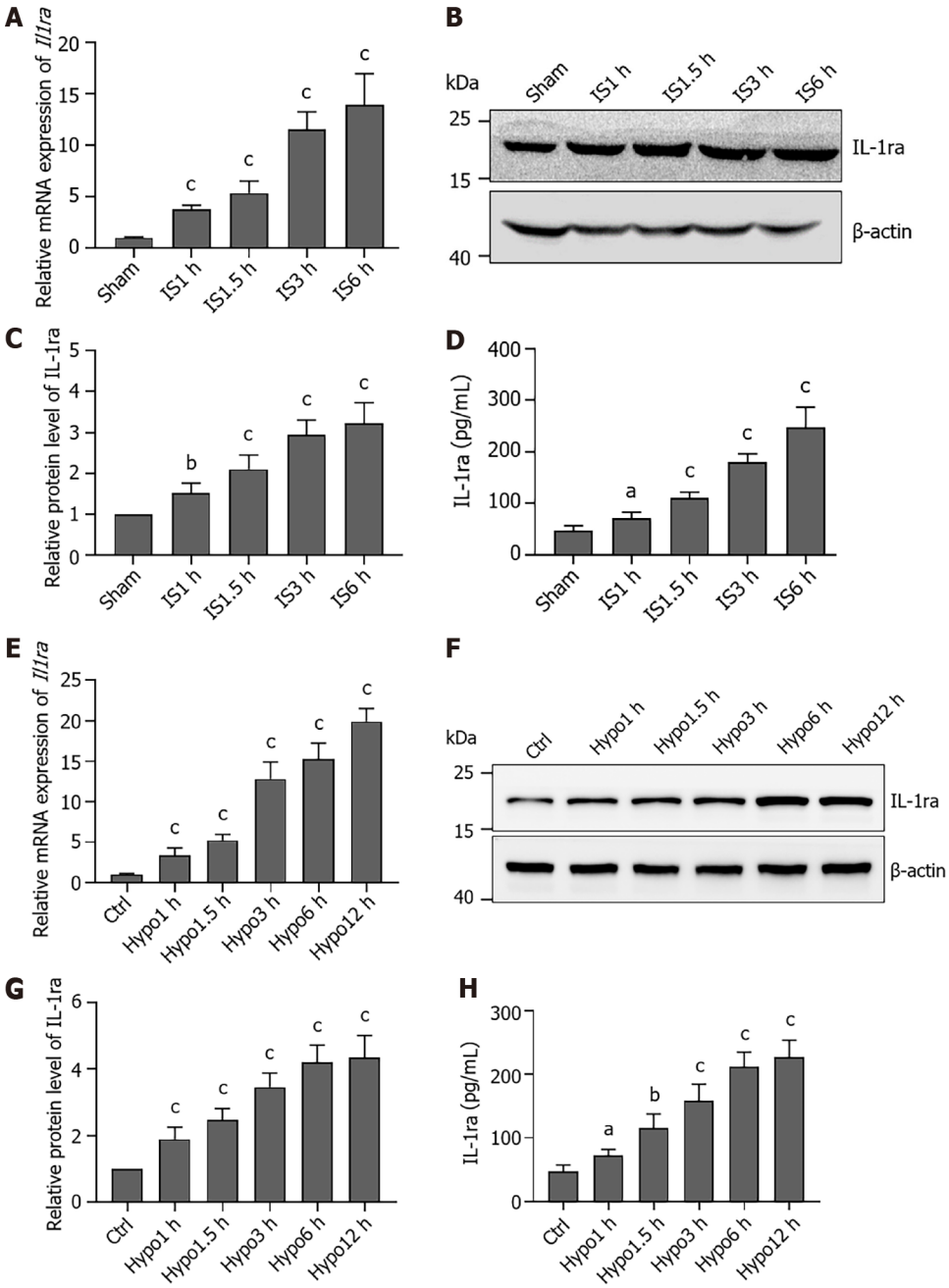
Figure 3 Interleukin-1 receptor antagonist is expressed in both mouse hepatocytes and nonparenchymal cells. A: Relative mRNA levels of interleukin-1 receptor antagonist (*Il1ra*) in hepatocytes and nonparenchymal cells (NPCs) after ischemia-reperfusion injury (IRI); B: Protein levels of IL-1ra in hepatocytes and NPCs after IRI; C: Statistical analysis of protein levels of IL-1Ra in hepatocytes and NPCs after IRI; D: Relative mRNA levels of *Il1ra* in AML12 cells upon hypoxia-reoxygenation (HR); E: Protein levels of IL-1ra in AML12 cells upon HR; F: Statistical analysis of protein levels of IL-1Ra in AML12 cells upon HR; G: Protein content of IL-1ra in culture medium upon HR. Indicated *P* values were calculated using two-tailed unpaired Student's *t*-tests. Data are presented as the mean ± SEM. Data are representative of five independent experiments. $^{ns}P > 0.05$, $^{a}P < 0.05$, $^{b}P < 0.001$. HR: Hypoxia-reoxygenation; NPCs: Nonparenchymal cells; IL-1ra: Interleukin-1 receptor antagonist.

IL-1ra expression is upregulated upon IS and hypoxia

To verify the regulation of IL-1ra expression in the early stage of hepatic IRI, we constructed hypoxic models at different time points *in vivo* and *in vitro*. Compared with the Sham group, ischemic treatment in mice increased IL-1ra expression in a time-dependent manner at both the mRNA (Figure 4A) and protein (Figures 4B-D) levels. Similar results were also revealed in AML12 cells (Figures 4E-H), demonstrating that IS and hypoxia could promote the expression of IL-1ra.

HIF-1α promotes IL-1ra expression under hypoxic conditions

HIF-1α, as a transcriptional regulator, plays an important role under hypoxic conditions. Therefore, we

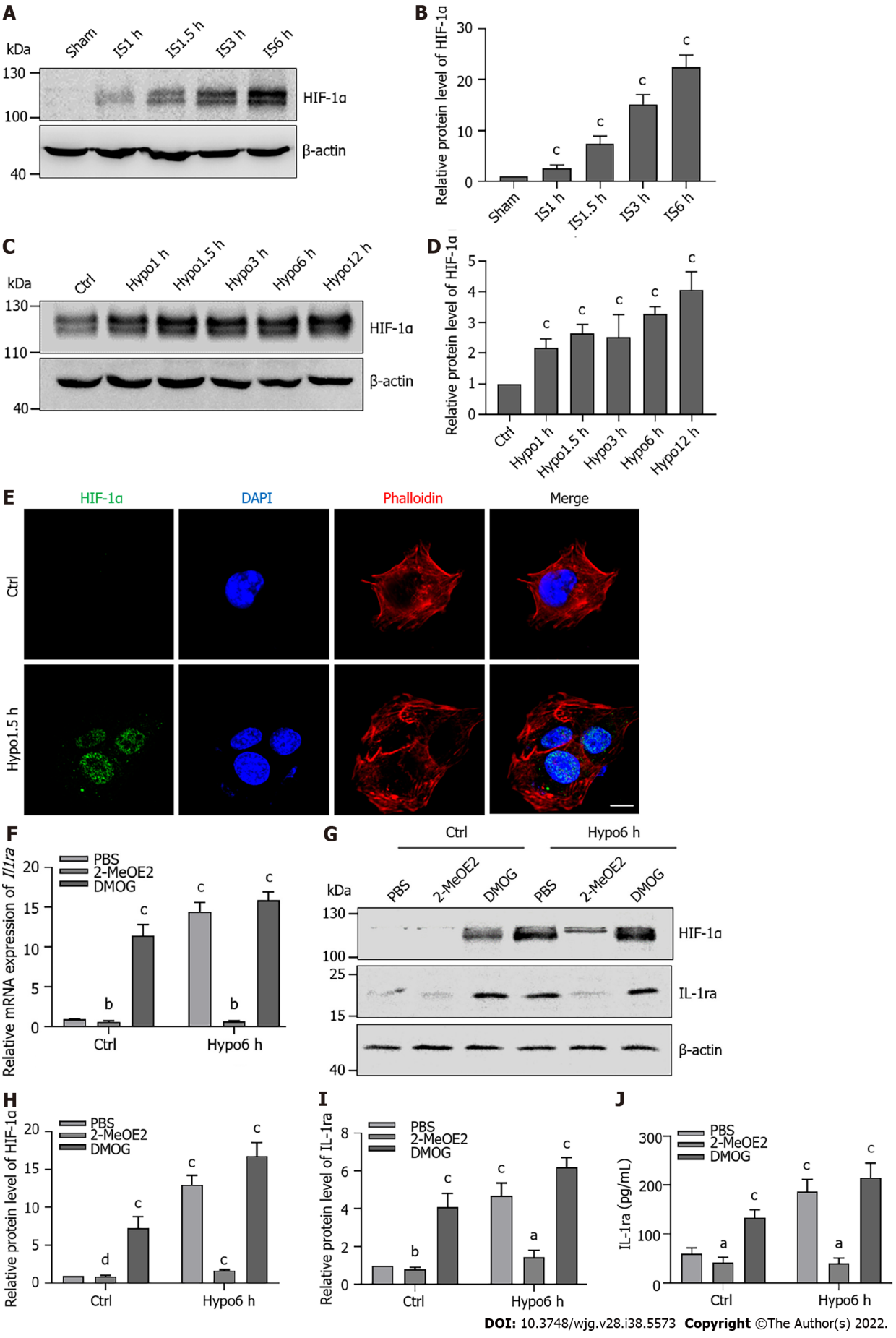


DOI: 10.3748/wjg.v28.i38.5573 **Copyright** ©The Author(s) 2022.

Figure 4 Interleukin-1 receptor antagonist expression is elevated during ischemia or hypoxia. A: Relative mRNA levels of interleukin-1 receptor antagonist (*Il1ra*) in the liver upon ischemia; B: Protein levels of IL-1ra in the liver upon ischemia; C: Statistical analysis of protein levels of IL-1ra upon ischemia; D: Protein content of IL-1ra in serum upon ischemia; E: Relative mRNA levels of *Il1ra* in AML12 cells upon hypoxia; F: Protein levels of IL-1ra in AML12 cells upon hypoxia; G: Statistical analysis of protein levels of IL-1Ra in AML12 cells upon hypoxia; H: Protein content of IL-1ra in culture medium upon ischemia. Indicated *P* values were calculated using two-tailed unpaired Student's *t*-tests. Data are presented as the mean ± SEM. Data are representative of five independent experiments. $^{a}P < 0.05$, $^{b}P < 0.01$, $^{c}P < 0.001$. Hypo: Hypoxia; IS: Ischemia; IL-1ra: Interleukin-1 receptor antagonist.

speculated that HIF-1α would regulate the expression of IL-1ra. Thus, we moved to evaluate the relationship between HIF-1α and IL-1ra expression in hepatic IRI. Increased expression of HIF-1α was observed upon ischemic treatment in mice in a time-dependent manner (Figures 5A and B). Similar results were confirmed in AML12 cells (Figures 5C and D). Immunofluorescence analysis indicated that HIF-1α was localized in the nuclei of AML12 cells after 1.5 h of hypoxia (Figure 5E).

We treated AML12 cells with 2-MeOE2 (a specific HIF-1α inhibitor) or DMOG (a specific HIF-1α agonist). 2-MeOE2 reduced the expression of *Il-1ra* mRNA during hypoxia, while DMOG increased *Il-1ra* expression under normoxia (Figure 5F). Immunoblotting (Figures 5G-I) and ELISA (Figure 5J) confirmed that 2-MeOE2 reduced the protein levels of HIF-1α and IL-1ra in AML12 cells; however, DMOG had the opposite effect. These results indicated that HIF-1α independently promotes the expression of IL-1ra.



DOI: 10.3748/wjg.v28.i38.5573 **Copyright** ©The Author(s) 2022.

Figure 5 Hypoxia-inducible factor-1α promotes the expression of interleukin-1 receptor antagonist during ischemia or hypoxia. A: Protein

levels of hypoxia-inducible factor (HIF)-1α in the liver upon ischemia; B: Statistical analysis of protein levels of HIF-1α in the liver upon ischemia; C: Protein levels of HIF-1α in AML12 cells upon hypoxia; D: Statistical analysis of protein levels of HIF-1α in AML12 cells upon hypoxia; E: Immunofluorescence staining for HIF-1α in AML12 cells upon hypoxia for 1.5 h. Scale bars, 10 μm; F: Relative mRNA levels of interleukin-1 receptor antagonist (*Il1ra*) in AML12 cells treated with 2-MeOE2 (100 μM) and DMOG (100 μM) upon hypoxia; G: Protein levels of HIF-1α and IL-1ra in AML12 cells treated with 2-MeOE2 and DMOG upon hypoxia; H: Statistical analysis of protein levels of HIF-1α in AML12 cells treated with 2-MeOE2 and DMOG upon hypoxia; I: Statistical analysis of protein levels of IL-1ra in AML12 cells treated with 2-MeOE2 and DMOG upon hypoxia; J: Protein content of IL-1ra in culture medium of in AML12 cells treated with 2-MeOE2 and DMOG upon hypoxia. Indicated *P*-values were calculated using two-tailed unpaired Student's *t*-tests. Data are presented as the mean ± SEM. Dots depict individual samples. $^{ns}P > 0.05$, $^{a}P < 0.05$, $^{b}P < 0.01$, $^{c}P < 0.001$. Hypo: Hypoxia; IS: Ischemia; HIF: Hypoxia-inducible factor; IL-1ra: Interleukin-1 receptor antagonist; IgG: Immunoglobulin G.

HIF-1α transcriptionally upregulates IL-1ra expression

To investigate the regulatory mechanism of IL-1ra by HIF-1α, we transfected a mouse *Il1ra* promoter-reporter construct into AML12 cells (Figure 6A). Upon treatment with hypoxia, we found that *Il1ra* promoter activity was significantly increased (Figure 6B). To explore the transcriptional regulatory elements of the *Il1ra* promoter in response to hypoxia, we generated a series of truncated *Il1ra* promoter–reporter constructs. *Il1ra*-p-2.1k promoter activity was significantly increased upon hypoxic treatment, while the truncated promoter activity of *Il1ra*-p-1.5k, *Il1ra*-p-1.1k, and *Il1ra*-p-0.6k was not altered by hypoxia (Figure 6C).

We used the JASPAR database to predict the binding site of HIF-1α on the *Il1ra*-p-2.1k promoter and found two possible binding elements, HRE I (-2018/-2011) and HRE II (-1895/-1888) (Figure 6D). Site-directed mutagenesis showed that mutation of HRE II did not affect hypoxia-induced activation of the *Il1ra* promoter, while mutation of either HRE I or HRE I + II eliminated this effect (Figure 6D). Importantly, we used the ChIP assay to verify that HIF-1α was able to be recruited to the HRE I element in the *Il1ra* promoter (Figures 6E and F).

IP protects the liver from IRI via the HIF-1α-IL-1ra pathway

It has been reported that IP can alleviate hepatic IRI[27]. However, the protective mechanism of IP is not yet clear. Here, we speculated that IL-1ra might play a potential role in the regulation of IP. Thus, the mice were subjected to IP with the indicated cycles. Compared with the control group, the IP group had significantly lower ALT and AST levels in their serum, which were further reduced by increased IP cycles (Figures 7A and B). Similar results of IL-1ra upregulation were observed by immunoblotting (Figures 7C and D) and ELISA (Figure 7E).

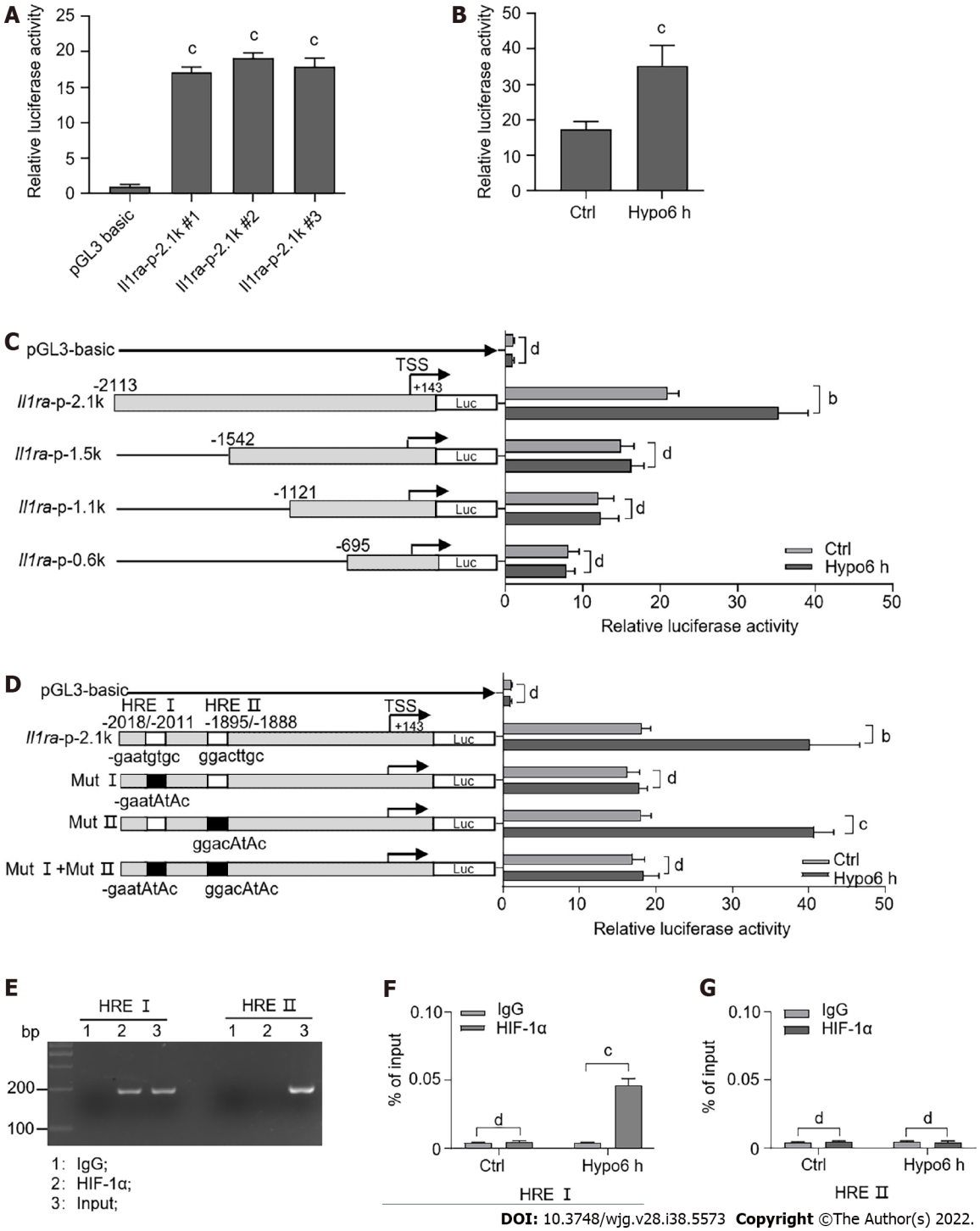
To verify whether IL-1ra plays a protective role in IP, we injected adenovirus carrying *Il1ra* shRNA *via* the tail vein to knock down the expression of IL-1ra in mice. Expression of IL-1ra in the liver and serum of mice injected with adenovirus was significantly decreased (Figures 7F-H). The ALT and AST levels were increased by knockdown of IL-1ra in the liver (Figures 7I and J).

It has been reported that HIF-1α plays an important role in IP[28], and we thus speculated that the expression of IL-1ra in IP is regulated by HIF-1α. We found that IP induced accumulation of HIF-1α in the liver (Figures 7K-M); however, 2-MeOE2 significantly attenuated this effect (Figures 7M-P). These results collectively suggested that IP might exert a protective effect on the liver from IRI through regulating the HIF-1α–IL-1ra signaling.

DISCUSSION

Hepatic IRI is a common complication of liver surgery. Previous studies have demonstrated that the IL-1 signaling pathway plays a pivotal role in the regulation of hepatic IRI. Here, we extended the study, showing that the expression of IL-1ra, an inhibitor of the IL-1 signaling pathway, is increased in response to hepatic IRI, especially in the ischemic stage. Mechanistically, hypoxia induces the transcriptional expression of IL-1ra through HIF-1α accumulation. Of note, we proved that IP could protect the liver from IRI by promoting IL-1ra expression in a HIF-1α-dependent manner. Thus, our study has provided additional evidence for the regulatory mechanism of IL-1ra during IS, indicating a practical strategy for alleviating hepatic IRI.

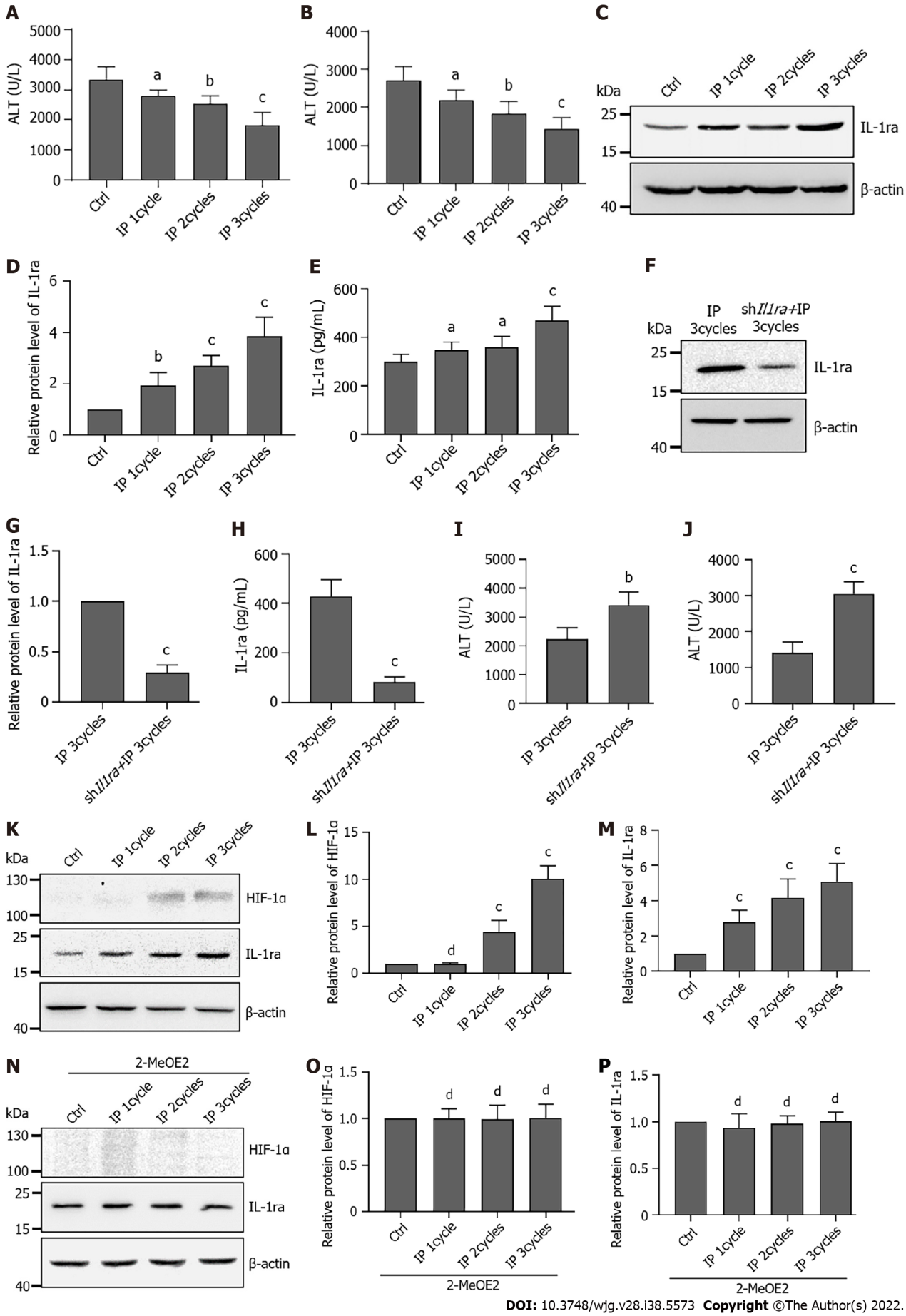
Previous studies have shown that hepatic IRI not only causes damage to the liver itself, but also leads to the abnormal functioning of various organs, and induces systemic inflammatory response syndrome [29]. Therefore, the question of how to reduce or even eliminate hepatic IRI has received constant attention among clinicians and researchers. Hepatic IRI is a complex pathophysiological process with numerous and relational influencing factors. Among them, the early inflammatory response plays a crucial role in the occurrence and development of hepatic IRI[30], because it is located in the upstream region of the injury response chain. Upon activation, downstream factors often promote each other and thus aggravate the injury[31]. If the activation of early inflammation can be reduced or even blocked, it may be possible to prevent the occurrence and development of hepatic IRI at source.



DOI: 10.3748/wjg.v28.i38.5573 **Copyright** ©The Author(s) 2022.

Figure 6 Hypoxia-inducible factor transcriptionally upregulates interleukin-1 receptor antagonist expression. A: Luciferase assay for the wild-type promoter (-2113/+143) of interleukin-1 receptor antagonist (*Il1ra*) in AML12 cells; B: Luciferase assay for the wild-type promoter of *Il1ra* in AML12 cells upon hypoxia; C: Luciferase assay for wild-type and truncated promoters of *Il1ra* in AML12 cells upon hypoxia; D: Luciferase assay for wild-type (-2113/+143) and HRE-mutated promoters of *Il1ra* upon hypoxia; E: Chromatin immunoprecipitation assay for hypoxia-inducible factor (HIF)-1α binding to HRE sites upon hypoxia; F and G: Quantitative polymerase chain reaction analysis for the recruitment of HIF-1α to the endogenous *Il1ra* promoter in AML12 cells upon hypoxia. Indicated *P*-values were calculated using two-tailed unpaired Student's *t*-tests. Data are presented as the mean ± SEM. Data are representative of independent experiments. $^{ns}P > 0.05$, $^{a}P < 0.01$, $^{b}P < 0.001$. Hypo: Hypoxia; IS: Ischemia; HIF: Hypoxia-inducible factor; IL-1ra: Interleukin-1 receptor antagonist; IgG: Immunoglobulin G.

Current studies have shown that many proinflammatory cytokines are released in the early stage of hepatic IRI[4]. For example, blocking the activation of proinflammatory IL-1 signaling significantly prevents IRI[32]. IL-1 is a major inflammatory response mediator[33]. Experimental results have shown that large amounts of IL-1β and tumor necrosis factor-α are produced in the tissue after hepatic IS and reperfusion[34]. At the same time, this can also stimulate the secretion of inflammatory cells, leading to the inflammatory destruction of local tissues. IL-1β and the nucleotide-binding and leucine-rich repeat protein 3 (NLRP3) inflammasome play a role through high mobility group box 1 protein[35], nuclear



DOI: 10.3748/wjg.v28.i38.5573 **Copyright** ©The Author(s) 2022.

Figure 7 Ischemic preconditioning protects the liver by promoting interleukin-1 receptor antagonist expression *via* hypoxia-inducible

factor-1α. A: Serum alanine transaminase (ALT) levels in mice undergoing ischemia-reperfusion injury (IRI) after different ischemic preconditioning (IP) cycles; B: Serum aspartate transaminase (AST) levels in mice undergoing IRI after different IP cycles; C: Protein levels of interleukin-1 receptor antagonist (IL-1ra) in the liver after different IP cycles; D: Statistical analysis of protein levels of IL-1ra after different IP cycles; E: Protein content of IL-1ra in serum after different IP cycles; F: Protein levels of IL-1ra in the liver with sh*Il1ra* injection after three IP cycles; G: Statistical analysis of protein levels of IL-1ra with sh*Il1ra* injection after three IP cycles; H: Protein content of IL-1ra in serum with sh*Il1ra* injection after three IP cycles; I: Serum ALT levels in mice with sh*Il1ra* injection after three IP cycles; J: Serum AST levels in mice with sh*Il1ra* injection after three IP cycles; K: Protein levels of hypoxia-inducible factor (HIF)-1α and IL-1ra in the liver after different IP cycles; L: Statistical analysis of protein levels of HIF-1α after different IP cycles; M: Statistical analysis of protein levels of IL-1ra after different IP cycles; N: Protein levels of HIF-1α and IL-1ra in the liver with 2-MeOE2 treatment after different IP cycles; O: Statistical analysis of protein levels of HIF-1α with 2-MeOE2 treatment after different IP cycles; P: Statistical analysis of protein levels of IL-1ra with 2-MeOE2 treatment after different IP cycles; Indicated *P* values were calculated using two-tailed unpaired Student's *t*-tests. Data are presented as the mean ± SEM. Data are representative of five independent experiments. $^{ns}P > 0.05$, $^{a}P < 0.05$, $^{b}P < 0.01$, $^{c}P < 0.001$. IP: Ischemic preconditioning; AST: Aspartate transaminase; ALT: Alanine transaminase; IL-1ra: Interleukin-1 receptor antagonist; HIF: Hypoxia-inducible factor.

factor-κB and Toll-like receptor 4 in lesions caused by warm IRI[7]. Of note, NLRP3 may be involved in IRI independently of the inflammasome pathway by recruiting neutrophils. Macrophages secrete pro-IL-1β, which is subsequently cleaved and activated by neutrophil-derived proteases in a mouse model. Mature IL-1β is required to induce inflammation during hepatic IR, and the interaction between macrophages and neutrophils is essential in this process[6]. Therefore, the antagonism of proinflammatory IL-1 cytokines has important therapeutic potential for reducing IRI.

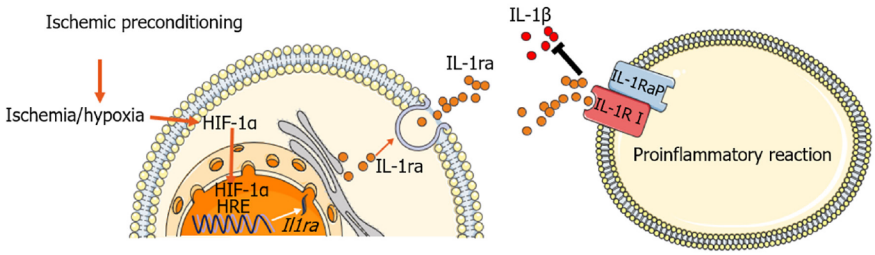
IL-1ra is a naturally occurring polypeptide. Recent research has focused on the role of IL-1ra in various pathophysiological states or the effects of recombinant IL-1ra administration in animals and humans[36]. It has been reported that the delivery of the *Il-1ra* gene to the rat liver *via* the adenovirus vector or lipofection can significantly reduce IR-induced proinflammatory cytokine production and hepatocyte injury[15]. This is consistent with our results showing that the knockdown of IL-1ra significantly increased the damage during hepatic IRI, suggesting a potential inhibitory effect of IL-1ra on inflammation in response to hepatic IR.

In the process of IRI, IS is a prerequisite. It is precisely regulated because the depletion of oxygen and energy in the ischemic period cause a series of injuries in the subsequent reperfusion period. In the state of hepatic IS, the metabolic mode switches from aerobic to anaerobic, the redox process in hepatocytes is blocked, the ATP-dependent cellular metabolic activity gradually stops, and the intracellular ATP is rapidly depleted. At the same time, the absence of oxygen causes HIF-1α to gradually accumulate. The increased transport of HIF-1α into the nucleus triggers the expression of genes involved in oxygen transport, oxygen utilization, glycolytic metabolism, cell death, cell survival, and other processes that affect cell survival during IS. Recent studies have demonstrated that HIF-1α can alleviate IRI by regulating the expression of inducible NO synthase[37]. HIF-1α may also enhance tissue anti-inflammatory effects by increasing heme oxygenase-1 expression, thereby reducing damage[38]. In this study, we further showed that HIF-1α, as an important protective factor in IRI, could protect the liver from injury by promoting the expression of IL-1ra and subsequently inhibiting activation of the IL-1 signaling pathway. In terms of the mechanism, we found that HIF-1α recognizes and binds to the basic helix-loop-helix protein sequence in the *Il1ra* promoter region, resulting in the increased transcription of *Il1ra*.

Recent studies have shown that IP has broad protective effects against IRI[39]. However, due to the complexity of IRI, the underlying cellular and molecular mechanisms of IP remain largely unknown. In the present study, we provided evidence that IP promotes the expression and release of IL-1ra into the hepatic microenvironment, thus blocking the downstream activation of IL-1β and protecting the liver from the cascading effects of inflammatory factors. We demonstrated that IP can induce the accumulation of HIF-1α, which increases with the number of IP cycles. These results would explain the protective effect of IP at a mechanistic level and lay a theoretical foundation for the better application of IP.

CONCLUSION

Our study demonstrated a protective effect of IL-1ra on hepatic IRI through the transcriptional regulation of IL-1ra by HIF-1α. Importantly, we found that IP can regulate the expression of IL-1ra through HIF-1α at early stage of hepatic IRI, thereby blocking the inflammatory IL-1 signaling pathway to protect the liver from IRI (Figure 8).



DOI: 10.3748/wjg.v28.i38.5573 **Copyright** ©The Author(s) 2022.

Figure 8 Model of ischemic preconditioning-induced hypoxia-inducible factor-1α-interleukin-1 receptor antagonist signaling to alleviate hepatic ischemia-reperfusion injury. Ischemic preconditioning promotes the accumulation of hypoxia-inducible factor (HIF)-1α, which subsequently increases HIF-1α entry into the nucleus and promotes the transcriptional expression of interleukin-1 receptor antagonist (IL-1ra). In turn, this inhibits the pro-inflammatory effects of IL-1β and eventually protects against hepatic ischemia-reperfusion injury. HIF: Hypoxia-inducible factor; IL-1ra: Interleukin-1 receptor antagonist.

ARTICLE HIGHLIGHTS

Research background

Ischemia-reperfusion injury (IRI) is associated with transplant failures, graft dysfunction, and a relatively poor prognosis. Interleukin-1 receptor antagonists (IL-1ra) play an important role in protecting the liver from IRI. However, the mechanism of its regulatory expression remains unclear.

Research motivation

Inhibition of hepatic inflammation by promoting the expression of IL-1ra is one of the key targets for the treatment of hepatic IRI.

Research objectives

To investigate the regulatory mechanism of hepatocyte-derived IL-1ra expression in the process of hepatic IRI to provide a therapeutic target for hepatic IRI.

Research methods

A 70% hepatic IRI model was established in mice, and AML12 cells were subjected to hypoxia/reoxygenation for the simulation of IRI *in vitro*. The *Il-1ra* promoter-reporter system was constructed to detect the regulatory effect of hypoxia. The ischemic preconditioning (IP) model was established to investigate its regulatory effect on IL-1ra.

Research results

IL-1ra is a key regulator of hepatic IRI. Il-1ra expression was significantly up-regulated after hepatic IRI *in vivo* and *in vitro*. Hypoxia inducible factor (HIF)-1α regulates *Il-1ra* transcription during hypoxia. IP prevents hepatic IRI by inducing the expression of IL-1ra, which is mediated by HIF-1α.

Research conclusions

Ischemia or hypoxia leads to increased IL-1ra expression through HIF-1α. In addition, IP protects the hepatic tissue from IRI through the HIF-1α-IL-1ra pathway.

Research perspectives

HIF-1α-IL-1ra pathway is a potential mechanism of hepatic protection during hepatic IRI, and also a key target for the treatment of hepatic IRI.

ACKNOWLEDGEMENTS

The authors would like to thank Yi Shi and Wei Sun (Medical College of Nankai University) for their skillful technical assistance.

FOOTNOTES

Author contributions: Wang ZY, Li SP, Cai JZ, and Yang S designed and coordinated the study; Wang ZY, Liu Y, Li JJ, Zhang Z, Xiao XC, Ou Y, and Wang H performed the experiments, and acquired and analyzed the data; Wang ZY and Yang S interpreted the data; Wang ZY and Yang S wrote the manuscript; and all authors approved the final

version of the article.

Supported by the National Natural Science Foundation of China, No. 81670600.

Institutional animal care and use committee statement: The animal study protocol was approved by the Animal Ethical and Welfare Committee (protocol code: IRM-DWLL-2020173 and date of approval: September 15, 2020).

Conflict-of-interest statement: All the authors report no relevant conflicts of interest for this article.

Data sharing statement: No additional data are available.

ARRIVE guidelines statement: The authors have reviewed the ARRIVE guidelines, and the manuscript was prepared and revised according to the ARRIVE guidelines.

Open-Access: This article is an open-access article that was selected by an in-house editor and fully peer-reviewed by external reviewers. It is distributed in accordance with the Creative Commons Attribution NonCommercial (CC BY-NC 4.0) license, which permits others to distribute, remix, adapt, build upon this work non-commercially, and license their derivative works on different terms, provided the original work is properly cited and the use is non-commercial. See: https://creativecommons.org/Licenses/by-nc/4.0/

Country/Territory of origin: China

ORCID number: Zhao-Yang Wang 0000-0001-7618-5353; Yu Liu 0000-0003-1657-2946; Shi-Peng Li 0000-0001-8615-2440; Zhen Zhang 0000-0002-6400-6052; Jin-Zhen Cai 0000-0001-5414-1050; Shuang Yang 0000-0002-4779-8553.

S-Editor: Wang JJ
L-Editor: Wang TQ
P-Editor: Yu HG

REFERENCES

1 **Asrani SK**, Devarbhavi H, Eaton J, Kamath PS. Burden of liver diseases in the world. *J Hepatol* 2019; **70**: 151-171 [PMID: 30266282 DOI: 10.1016/j.jhep.2018.09.014]
2 **Jennings RB**, Sommers HM, Smyth GA, Flack HA, Linn H. Myocardial necrosis induced by temporary occlusion of a coronary artery in the dog. *Arch Pathol* 1960; **70**: 68-78 [PMID: 14407094]
3 **Ji H**, Liu Y, Zhang Y, Shen XD, Gao F, Busuttil RW, Kuchroo VK, Kupiec-Weglinski JW. T-cell immunoglobulin and mucin domain 4 (TIM-4) signaling in innate immune-mediated liver ischemia-reperfusion injury. *Hepatology* 2014; **60**: 2052-2064 [PMID: 25066922 DOI: 10.1002/hep.27334]
4 **Peralta C**, Jiménez-Castro MB, Gracia-Sancho J. Hepatic ischemia and reperfusion injury: effects on the liver sinusoidal milieu. *J Hepatol* 2013; **59**: 1094-1106 [PMID: 23811302 DOI: 10.1016/j.jhep.2013.06.017]
5 **Zhai Y**, Petrowsky H, Hong JC, Busuttil RW, Kupiec-Weglinski JW. Ischaemia-reperfusion injury in liver transplantation--from bench to bedside. *Nat Rev Gastroenterol Hepatol* 2013; **10**: 79-89 [PMID: 23229329 DOI: 10.1038/nrgastro.2012.225]
6 **Sadatomo A**, Inoue Y, Ito H, Karasawa T, Kimura H, Watanabe S, Mizushina Y, Nakamura J, Kamata R, Kasahara T, Horie H, Sata N, Takahashi M. Interaction of Neutrophils with Macrophages Promotes IL-1β Maturation and Contributes to Hepatic Ischemia-Reperfusion Injury. *J Immunol* 2017; **199**: 3306-3315 [PMID: 28972095 DOI: 10.4049/jimmunol.1700717]
7 **Kamo N**, Ke B, Ghaffari AA, Shen XD, Busuttil RW, Cheng G, Kupiec-Weglinski JW. ASC/caspase-1/IL-1β signaling triggers inflammatory responses by promoting HMGB1 induction in liver ischemia/reperfusion injury. *Hepatology* 2013; **58**: 351-362 [PMID: 23408710 DOI: 10.1002/hep.26320]
8 **Sims JE**, Smith DE. The IL-1 family: regulators of immunity. *Nat Rev Immunol* 2010; **10**: 89-102 [PMID: 20081871 DOI: 10.1038/nri2691]
9 **Gehrke N**, Hövelmeyer N, Waisman A, Straub BK, Weinmann-Menke J, Wörns MA, Galle PR, Schattenberg JM. Hepatocyte-specific deletion of IL1-RI attenuates liver injury by blocking IL-1 driven autoinflammation. *J Hepatol* 2018; **68**: 986-995 [PMID: 29366909 DOI: 10.1016/j.jhep.2018.01.008]
10 **Dinarello CA**, Simon A, van der Meer JW. Treating inflammation by blocking interleukin-1 in a broad spectrum of diseases. *Nat Rev Drug Discov* 2012; **11**: 633-652 [PMID: 22850787 DOI: 10.1038/nrd3800]
11 **Arend WP**. The balance between IL-1 and IL-1Ra in disease. *Cytokine Growth Factor Rev* 2002; **13**: 323-340 [PMID: 12220547 DOI: 10.1016/s1359-6101(02)00020-5]
12 **Arend WP**, Malyak M, Guthridge CJ, Gabay C. Interleukin-1 receptor antagonist: role in biology. *Annu Rev Immunol* 1998; **16**: 27-55 [PMID: 9597123 DOI: 10.1146/annurev.immunol.16.1.27]
13 **Thompson RC**, Dripps DJ, Eisenberg SP. Interleukin-1 receptor antagonist (IL-1ra) as a probe and as a treatment for IL-1 mediated disease. *Int J Immunopharmacol* 1992; **14**: 475-480 [PMID: 1535616 DOI: 10.1016/0192-0561(92)90178-n]
14 **Dayer JM**. Evidence for the biological modulation of IL-1 activity: the role of IL-1Ra. *Clin Exp Rheumatol* 2002; **20**: S14-S20 [PMID: 14989424]
15 **Harada H**, Wakabayashi G, Takayanagi A, Shimazu M, Matsumoto K, Obara H, Shimizu N, Kitajima M. Transfer of the interleukin-1 receptor antagonist gene into rat liver abrogates hepatic ischemia-reperfusion injury. *Transplantation* 2002;

74: 1434-1441 [PMID: 12451245 DOI: 10.1097/00007890-200211270-00016]
16 **McGettrick AF**, O'Neill LAJ. The Role of HIF in Immunity and Inflammation. *Cell Metab* 2020; **32**: 524-536 [PMID: 32853548 DOI: 10.1016/j.cmet.2020.08.002]
17 **Schumacker PT**. Hypoxia-inducible factor-1 (HIF-1). *Crit Care Med* 2005; **33**: S423-S425 [PMID: 16340411 DOI: 10.1097/01.ccm.0000191716.38566.e0]
18 **Guo Y**, Feng L, Zhou Y, Sheng J, Long D, Li S, Li Y. Systematic review with meta-analysis: HIF-1α attenuates liver ischemia-reperfusion injury. *Transplant Rev (Orlando)* 2015; **29**: 127-134 [PMID: 26007634 DOI: 10.1016/j.trre.2015.05.001]
19 **Zhang H**, Bosch-Marce M, Shimoda LA, Tan YS, Baek JH, Wesley JB, Gonzalez FJ, Semenza GL. Mitochondrial autophagy is an HIF-1-dependent adaptive metabolic response to hypoxia. *J Biol Chem* 2008; **283**: 10892-10903 [PMID: 18281291 DOI: 10.1074/jbc.M800102200]
20 **Semenza GL**. Oxygen sensing, homeostasis, and disease. *N Engl J Med* 2011; **365**: 537-547 [PMID: 21830968 DOI: 10.1056/NEJMra1011165]
21 **Murry CE**, Jennings RB, Reimer KA. Preconditioning with ischemia: a delay of lethal cell injury in ischemic myocardium. *Circulation* 1986; **74**: 1124-1136 [PMID: 3769170 DOI: 10.1161/01.cir.74.5.1124]
22 **Liu A**, Fang H. Ischemic Preconditioning on Liver Ischemia Reperfusion Injury: How Far is the Bedside from the Bench? *J Invest Surg* 2020; **33**: 884-885 [PMID: 30885026 DOI: 10.1080/08941939.2019.1578443]
23 **Ferreira-Silva M**, Faria-Silva C, Carvalheiro MC, Simões S, Marinho HS, Marcelino P, Campos MC, Metselaar JM, Fernandes E, Baptista PV, Fernandes AR, Corvo ML. Quercetin Liposomal Nanoformulation for Ischemia and Reperfusion Injury Treatment. *Pharmaceutics* 2022; **14** [PMID: 35057000 DOI: 10.3390/pharmaceutics14010104]
24 **Alchera E**, Chandrashekar BR, Clemente N, Borroni E, Boldorini R, Carini R. Ischemia/Reperfusion Injury of Fatty Liver Is Protected by A2AR and Exacerbated by A1R Stimulation through Opposite Effects on ASK1 Activation. *Cells* 2021; **10** [PMID: 34831394 DOI: 10.3390/cells10113171]
25 **Jiang H**, Zhou C, Zhang Z, Wang Q, Wei H, Shi W, Li J, Wang Z, Ou Y, Wang W, Wang H, Zhang Q, Sun W, Sun P, Yang S. Jagged1-Notch1-deployed tumor perivascular niche promotes breast cancer stem cell phenotype through Zeb1. *Nat Commun* 2020; **11**: 5129 [PMID: 33046710 DOI: 10.1038/s41467-020-18860-4]
26 **Malik R**, Selden C, Hodgson H. The role of non-parenchymal cells in liver growth. *Semin Cell Dev Biol* 2002; **13**: 425-431 [PMID: 12468243 DOI: 10.1016/s1084952102001301]
27 **Lloris-Carsí JM**, Cejalvo D, Toledo-Pereyra LH, Calvo MA, Suzuki S. Preconditioning: effect upon lesion modulation in warm liver ischemia. *Transplant Proc* 1993; **25**: 3303-3304 [PMID: 8266552]
28 **Cai Z**, Zhong H, Bosch-Marce M, Fox-Talbot K, Wang L, Wei C, Trush MA, Semenza GL. Complete loss of ischaemic preconditioning-induced cardioprotection in mice with partial deficiency of HIF-1 alpha. *Cardiovasc Res* 2008; **77**: 463-470 [PMID: 18006459 DOI: 10.1093/cvr/cvm035]
29 **Quesnelle KM**, Bystrom PV, Toledo-Pereyra LH. Molecular responses to ischemia and reperfusion in the liver. *Arch Toxicol* 2015; **89**: 651-657 [PMID: 25566829 DOI: 10.1007/s00204-014-1437-x]
30 **Beg AA**. Endogenous ligands of Toll-like receptors: implications for regulating inflammatory and immune responses. *Trends Immunol* 2002; **23**: 509-512 [PMID: 12401394 DOI: 10.1016/s1471-4906(02)02317-7]
31 **Suzuki S**, Toledo-Pereyra LH, Rodriguez FJ, Cejalvo D. Neutrophil infiltration as an important factor in liver ischemia and reperfusion injury. Modulating effects of FK506 and cyclosporine. *Transplantation* 1993; **55**: 1265-1272 [PMID: 7685932 DOI: 10.1097/00007890-199306000-00011]
32 **Zhu P**, Duan L, Chen J, Xiong A, Xu Q, Zhang H, Zheng F, Tan Z, Gong F, Fang M. Gene silencing of NALP3 protects against liver ischemia-reperfusion injury in mice. *Hum Gene Ther* 2011; **22**: 853-864 [PMID: 21128730 DOI: 10.1089/hum.2010.145]
33 **Wang J**, Yu S, Li J, Li H, Jiang H, Xiao P, Pan Y, Zheng J, Yu L, Jiang J. Protective role of *N*-acetyl-l-tryptophan against hepatic ischemia-reperfusion injury *via* the RIP2/caspase-1/IL-1β signaling pathway. *Pharm Biol* 2019; **57**: 385-391 [PMID: 31184936 DOI: 10.1080/13880209.2019.1617750]
34 **Saleh H**, El-Shorbagy HM. Chitosan protects liver against ischemia-reperfusion injury *via* regulating Bcl-2/Bax, TNF-α and TGF-β expression. *Int J Biol Macromol* 2020; **164**: 1565-1574 [PMID: 32735924 DOI: 10.1016/j.ijbiomac.2020.07.212]
35 **Zhong W**, Rao Z, Rao J, Han G, Wang P, Jiang T, Pan X, Zhou S, Zhou H, Wang X. Aging aggravated liver ischemia and reperfusion injury by promoting STING-mediated NLRP3 activation in macrophages. *Aging Cell* 2020; **19**: e13186 [PMID: 32666684 DOI: 10.1111/acel.13186]
36 **Carter DB**, Deibel MR Jr, Dunn CJ, Tomich CS, Laborde AL, Slightom JL, Berger AE, Bienkowski MJ, Sun FF, McEwan RN. Purification, cloning, expression and biological characterization of an interleukin-1 receptor antagonist protein. *Nature* 1990; **344**: 633-638 [PMID: 2139180 DOI: 10.1038/344633a0]
37 **Xi L**, Taher M, Yin C, Salloum F, Kukreja RC. Cobalt chloride induces delayed cardiac preconditioning in mice through selective activation of HIF-1alpha and AP-1 and iNOS signaling. *Am J Physiol Heart Circ Physiol* 2004; **287**: H2369-H2375 [PMID: 15284066 DOI: 10.1152/ajpheart.00422.2004]
38 **Ockaili R**, Natarajan R, Salloum F, Fisher BJ, Jones D, Fowler AA 3rd, Kukreja RC. HIF-1 activation attenuates postischemic myocardial injury: role for heme oxygenase-1 in modulating microvascular chemokine generation. *Am J Physiol Heart Circ Physiol* 2005; **289**: H542-H548 [PMID: 15805230 DOI: 10.1152/ajpheart.00089.2005]
39 **Suzuki S**, Inaba K, Konno H. Ischemic preconditioning in hepatic ischemia and reperfusion. *Curr Opin Organ Transplant* 2008; **13**: 142-147 [PMID: 18685294 DOI: 10.1097/MOT.0b013e3282f6a164]

World Journal of Gastroenterology

Submit a Manuscript: https://www.f6publishing.com

World J Gastroenterol 2022 October 14; 28(38): 5589-5601

DOI: 10.3748/wjg.v28.i38.5589

ISSN 1007-9327 (print) ISSN 2219-2840 (online)

ORIGINAL ARTICLE

Retrospective Cohort Study

No long-term survival benefit with sustained-release 5-fluorouracil implants in patients with stages II and III gastric cancer

Yun-Zi Wu, Ming Wu, Xiao-Hao Zheng, Bing-Zhi Wang, Li-Yan Xue, Shi-Kang Ding, Lin Yang, Jian-Song Ren, Yan-Tao Tian, Yi-Bin Xie

Specialty type: Gastroenterology and hepatology

Provenance and peer review: Unsolicited article; Externally peer reviewed.

Peer-review model: Single blind

Peer-review report's scientific quality classification

Grade A (Excellent): A
Grade B (Very good): B, B
Grade C (Good): 0
Grade D (Fair): D, D, D
Grade E (Poor): 0

P-Reviewer: Liu YQ, United States; Mishra TS, India; Sempokuya T, United States; Socea B, Romania

Received: June 8, 2022
Peer-review started: June 8, 2022
First decision: September 2, 2022
Revised: September 10, 2022
Accepted: September 23, 2022
Article in press: September 23, 2022
Published online: October 14, 2022

Yun-Zi Wu, Xiao-Hao Zheng, Shi-Kang Ding, Yan-Tao Tian, Yi-Bin Xie, Department of Pancreatic and Gastric Surgery, National Cancer Center/National Clinical Research Center for Cancer/Cancer Hospital, Chinese Academy of Medical Sciences and Peking Union Medical College, Beijing 100021, China

Ming Wu, Department of Gastrointestinal Surgery, Yun Cheng Center Hospital, Yuncheng 044000, Shanxi Province, China

Bing-Zhi Wang, Li-Yan Xue, Department of Pathology, National Cancer Center/National Clinical Research Center/Cancer Hospital, Chinese Academy of Medical Sciences and Peking Union Medical College, Beijing 100021, China

Lin Yang, Department of Medical Oncology, National Cancer Center/National Clinical Research Center/Cancer Hospital, Chinese Academy of Medical Sciences and Peking Union Medical College, Beijing 100021, China

Jian-Song Ren, Office of Cancer Screening, National Cancer Center/National Clinical Research Center for Cancer/Cancer Hospital, Chinese Academy of Medical Sciences and Peking Union Medical College, Beijing 100021, China

Yi-Bin Xie, Department of Pancreatic and Gastric Surgery, National Cancer Center/National Clinical Research Center for Cancer/Hebei Cancer Hospital, Chinese Academy of Medical Sciences, Langfang 065001, Hebei Province, China

Corresponding author: Yi-Bin Xie, MD, Doctor, Department of Pancreatic and Gastric Surgery, National Cancer Center/National Clinical Research Center for Cancer/Cancer Hospital, Chinese Academy of Medical Sciences and Peking Union Medical College, No. 17 Panjiayuan South Lane, Chaoyang District, Beijing 100021, China. yibinxie_2003@163.com

Abstract

BACKGROUND

The prognosis of gastric cancer in an advanced stage remains poor. The exact efficacy of the use of intraoperative sustained-release chemotherapy with 5-fluorouracil (5-FU) in advanced-stage gastric cancer is still unelucidated.

AIM

To explore the long-term survival benefit of using sustained-release 5-FU implants

in stage II and stage III gastric cancer patients.

METHODS

Patients with gastric cancer in a locally advanced stage and who underwent an R0 radical resection between Jan 2014, to Dec 2016, in this single institution were included. Patients with pathological diagnoses other than adenocarcinoma were excluded. All included patients were grouped according to whether intraoperative sustained-release (SR) chemotherapy with 5-FU was used or not (NSR). The primary end-point was 5-year overall survival. Kaplan–Meier method with log-rank test was used to analyze the overall survival of patients and Cox analysis was used to analyze prognosis factors of these patients.

RESULTS

In total, there were 563 patients with gastric cancer with locally advanced stage, who underwent an R0 radical resection. 309 patients were included in the final analysis. 219 (70.9%) were men, with an average age of 58.25 years. Furthermore, 56 (18.1%) received neoadjuvant chemotherapy, and 191 (61.8%) were in TNM stage III. In addition, 158 patients received intraoperative sustained-release chemotherapy with 5-FU and were included in the SR group, while the other 161 patients were included in the NSR group. The overall complication rate was 12.94% in the whole group and 10.81%, 16.46% in SR and NSR groups, respectively. There were no significant differences between the two groups in overall survival and complication rate ($P > 0.05$). The multivariate cox analysis indicated that only N Stage and neoadjuvant therapy were independent influencing factors of survival.

CONCLUSION

Intraoperative sustained-release chemotherapy usage with 5-FU, did not improve the survival of patients who underwent an R0 radical resection in locally advanced stage of gastric cancer.

Key Words: Sustained-release 5-fluorouracil implants; Gastric cancer; 5-year survival rate; Safety; Prognostic factor; R0 radical resection

©The Author(s) 2022. Published by Baishideng Publishing Group Inc. All rights reserved.

Core Tip: Intraoperative drug administration shows promise in preventing the recurrence of gastric cancer. Sustained-release 5-fluorouracil (5-FU) implant is a new convenient and continuous drug release method that ensures locally high drug concentration for approximately 1 mo. 5-FU implants are widely used to treat various gastric tumors. However, presently, only retrospective research and a small-scale clinical study conducted in China have reported on its use in patients with gastric cancer. In our real-world study, we collected complete datasets, making this the largest study in China. Unfortunately, 5-FU implants did not improve the long-term survival of gastric cancer patients.

Citation: Wu YZ, Wu M, Zheng XH, Wang BZ, Xue LY, Ding SK, Yang L, Ren JS, Tian YT, Xie YB. No long-term survival benefit with sustained-release 5-fluorouracil implants in patients with stages II and III gastric cancer. *World J Gastroenterol* 2022; 28(38): 5589-5601

URL: https://www.wjgnet.com/1007-9327/full/v28/i38/5589.htm

DOI: https://dx.doi.org/10.3748/wjg.v28.i38.5589

INTRODUCTION

Gastric cancer is the fifth most common newly diagnosed cancer and the third most common cause of cancer mortality worldwide[1-3]. In China, there are approximately 400000 new patients with gastric cancer, and nearly 300000 people die of gastric cancer every year[4]. At present, locally advanced gastric cancer with the American Joint Committee on Cancer TNM stages II and III accounts for the majority of these cases[5]. For locally-advanced gastric cancer patients, the current standard treatment is D2 gastrectomy, followed by adjuvant chemotherapy[6]. However, even in those who received standard treatment, 30–60% of them may relapse either locally or distantly[7].

Patients with stages II and III gastric cancer have been found to have a tendency to relapse after treatment[8]. According to the findings of a study by Yago *et al*[9], the 5-year recurrence-free survival rate was 88.3% for stage IIA, 73.8% for stage IIB, 67.4% for stage IIIA, 55.7% for stage IIIB, and 29.9% for stage IIIC. Of the three major recurrence patterns namely hematogenous, peritoneal, and lymph nodal

recurrences after curative gastrectomy, the latter two account for the majority of the cases[10-13]. In order to decrease local recurrence after resection, methods, such as extended peritoneal lavage[14], hyperthermic intraperitoneal perfusion chemotherapy[15], peritoneal lavage with 5-FU, and continuous intraperitoneal chemotherapy using a retained tube or pump, have been developed[16]. Furthermore, it has been reported that intraoperative intraperitoneal chemotherapy can reduce the mortality risk[17]. In addition, increasing the temperature of chemotherapeutic drugs has a synergistic effect with the increase of intraperitoneal chemotherapy. The CYTO-CHIP study group reported that compared with the routine method of cytoreductive surgery combined with hyperthermic intraperitoneal chemotherapy, it can improve median overall survival time and increase the 3-and 5-year overall survival rates [18]. In another study, the use of catheter-based intraperitoneal chemotherapy showed similar results of increased the 5-year overall survival rate and reduced the peritoneal recurrence rate[19]. The use of sustained-release 5-FU implants intraoperatively is a relatively newly developed method and has been used widely in almost all types of digestive tract cancer in China[20]. When this drug was placed intraoperatively into the tumor bed, it was released continuously, and it maintained a locally high drug concentration for approximately 1 mo[21]. The potential remnant tumor tends to grow quickly in the first year after resection owing to the decreased immunity and absence of adjuvant chemotherapy[9]. This is the theoretical basis for the use of sustained-release 5-FU implants.

Moreover, optimistic results concerning the use of sustained-release 5-FU implants in the treatment of gastric cancer have been shown. Recently, a multi-center, randomized, open-label, controlled clinical study showed that for cTNM stage III gastric cancer patients, the use of intraoperative 5-FU implants, combined with postoperative adjuvant chemotherapy, may reduce the risk of peritoneal recurrence and prolong progression-free survival significantly[22]. Another retrospective study with 5-FU implants in advanced gastric cancer patients showed that the use of 5-FU implants may improve 5-years overall survival (OS) and progression-free survival rates after surgery in gastric cancer patients[21]. However, these studies had limitations. The sample size of these studies was limited, the follow-up times were insufficient, and the rate of loss of follow-up was extremely high. In order to explore the long-term survival benefit of the use of sustained-release 5-FU implants, we conducted a real-world study using our own clinical data from a single institution.

MATERIALS AND METHODS

Data Collection and Primary Outcomes

In total, we treated 563 stages II and III gastric cancer patients between January 2014 and December 2016. The inclusion criteria were the presence of clinical TNM stage II and stage III, pathologically diagnosed adenocarcinoma of the stomach, a complete record of history, and age between 18–80 years. The exclusion criteria were the presence of gastric remnant cancer, distant metastases, positive peritoneal cytology, palliative resection, and any unsuitable condition for 5-FU chemotherapy. The primary clinical outcome was 5-year OS. Information on the patients' age, sex, body mass index, tumor (TNM Stage, Borrmann classification, Lauren classification, pathological classification, differentiation, number of resected lymph nodes, number of positive lymph nodes, as well as the extent of nerve invasion, and presence of a vascular tumor thrombus), treatment (resections, neoadjuvant therapy, and use of 5-FU implants), postoperative complications (pulmonary infections, anastomotic fistulas, bleeding, abdominal infections, intestinal obstructions, and admissions to the intensive care unit), and their follow-up results were extracted from our hospital's electronic records.

Treatment methods

All our patients underwent a standard D2 gastric resection with or without neoadjuvant therapy. In addition, all the patients received 6–8 cycles of adjuvant chemotherapy with an S-1 + oxaliplatin regimen. In the sustained-release (SR) group, sustained-release 5-FU implants in a fixed dosage of 1000 mg were placed intraoperatively near the tumor bed after resection. Other patients were divided into non-sustained-release (NSR) group. The placement of 5-FU implants near vessels and anastomotic stoma should be avoided.

Statistical analyses

The continuous variables were presented as central tendencies (means or medians) and dispersions (standard deviations or interquartile ranges). For the group comparisons of the numeric variables, the Student's *t*-test was used when the data were normally distributed, and the Mann–Whitney test for the variables in which distribution was not normal. When the categorical predictors were compared between the groups, we used Pearson's χ^2 test or Fisher's exact test. The survival analysis included the use of the Kaplan–Meier estimator for OS. A Cox regression analysis was performed to obtain the crude and adjusted hazard ratios for OS. Significance level for all tests was reached when the two-tailed P value was < 0.05. Statistical analyzes were performed using the IBM SPSS Statistics (version 26.0, IBM Inc., Armonk, NY, United States), and Prism software (version 9, GraphPad Software Inc., San Diego, CA, United States).

RESULTS

Clinicopathological characteristics

In total, 241 patients with incomplete data and 13 patients with a pathological diagnosis of gastric neuroendocrine tumor were excluded. Finally, 309 patients were included in this study, and they were divided into two groups according to whether sustained-release 5-FU was used or not. Therefore, there were 158 patients in the SR group and 164 patients in the NSR group (Figure 1).

The average age of the whole group was 58.25 ± 11.2 years, with male patients being the majority (70.9%). All the patients were diagnosed pathologically as having a stomach adenocarcinoma of TNM stages II and III. Furthermore, 32.4% of patients had signet ring cell carcinoma. All of the patients underwent an R0 resection surgery. As shown in Table 1, we compared the differences in the clinicopathological characteristics between the two patient cohorts. There were no significant differences between the two groups with respect to age, sex, body mass index, and TNM stage. Similarly, there were no differences between the two groups with respect to their pathological characteristics such as the Borrmann classification, Lauren classification, and differentiation. Although the number of resected lymph nodes in the SR group was higher than that in the NSR (P = 0.0145), the number of positive lymph nodes number was similar (P = 0.2319). Lymph node dissection was satisfactory in both groups, even though there was a gap between the two groups (Table 1).

Postoperative complications in patients

Table 2 shows the major postoperative complications, such as pulmonary inflections, anastomotic fistulas, postoperative bleeding, abdominal infections, and intestinal obstructions. There were no significant differences between the two groups with respect to the incidence of postoperative complications (P > 0.05).

Prognostic factors in gastric cancer patients

Figure 2 shows the results of the univariate and multivariate Cox analyses. From the univariate analysis, N stage (P < 0.001), T stage (P = 0.001), TNM stage (P < 0.001) neoadjuvant therapy (P < 0.001), Borrmann classification (P = 0.001), and resection type (P = 0.002) were found to be influencing prognostic factors in this group of patients. As per the multivariate Cox analysis, only N stage (P = 0.030) and neoadjuvant therapy were found to be independent influencing prognostic factors (Figure 2 and Table 3). The use of sustained-release 5-FU implants was not an independent influencing prognostic factor in this group (P = 0.786).

Survival outcomes

The 5-years OS rate of the SR and NSR groups were 68.2% and 67.9%, respectively (P = 0.9850). The median survival time for both groups was not obtained, as patient mortality numbers were too low to calculate. Furthermore, we performed subgroup comparisons according to the patient's age, sex, and TNM stage. There were no significant differences in any of the subgroups (P > 0.05) (Figures 3 and 4, Table 3).

DISCUSSION

Gastric cancer remains one of the most lethal cancers in China[23,24]. Almost 70% of the relapses occur within 2 years and more than 90% within 5 years[7,25]. In clinical practice, the recurrence patterns are classified as locoregional, peritoneal, and hematogenous. As reported by Wu, approximately all of the recurrences (99.5%) occurred within 7 years after the surgery, with 53.5% having had peritoneal dissemination, 43.3% hematogenous metastases, and 28.6% distant lymphatic spread[26]. The locoregional and peritoneal recurrences, which usually occur in gastric cancer patients, were found to be a critical problem. Peritoneal recurrence has been reported as the most common recurrence pattern in locally advanced gastric cancer patients, which accounts for 50% of the cases and occurs within 2 years after surgery[27]. In another study, almost 60% of the gastric cancer patients experienced a recurrence, which included 32.4% locoregional recurrences, 13.7% peritoneal metastases, and 44.3% distant metastases[28].

To reduce locoregional recurrences, intraperitoneal chemotherapy has been used widely worldwide. Different from other methods, the use of intraoperative sustained-release 5-FU is promising because of the convenient usage and a long effective time of approximately 1 mo. The use of sustained-release 5-FU implants has shown survival benefits in different types of digestive system tumors such as colon cancer and primary hepatic cellular cancer[29,30]. Furthermore, a few studies on the treatment of gastric cancer, which showed similar results, were also reported by Chinese researchers[21,22]. However, P values of survival benefits obtained in previous studies on gastric cancer were lower, but close to 0.05. Therefore, we conducted this real-world study to confirm the findings.

In the present study, the use of sustained-release 5-FU implants did not improve the long-term survival of gastric cancer patients with either TNM stage II or III. The estimated 5-year survival of patients with gastric cancer with TNM stage III in SR and NSR group was 50% and 49%, respectively (P

Table 1 Clinicopathological characteristics of different gastric cancer group

	SR group (*n* = 148)	NSR group (*n* =161)	*P* value
Age (yr)	57.15 ± 10.71	59.27 ± 11.52	0.2917
Gender, *n* (%)			0.781
Male	106 (71.6)	113 (70.2)	
Female	42 (28.4)	48 (29.8)	
BMI (kg/m^2)	23.97 ± 3.591	23.68 ± 3.488	0.9716
Neoadjuvant therapy, *n* (%)			0.52
Yes	29 (19.6)	27 (16.8)	
No	119 (80.4)	134 (83.2)	
Cardiovascular disease, *n* (%)			0.503
Yes	32 (21.6)	40 (24.8)	
No	116 (78.4)	121 (75.2)	
Diabetes, *n* (%)			0.093
Yes	10 (6.8)	20 (12.4)	
No	138 (93.2)	141 (87.6)	
T stage, *n* (%)			0.699
T1 and T2	23 (15.5)	21 (13.0)	
T3 and T4	96 (64.9)	113 (70.2)	
yp T1 and T2	5 (3.4)	3 (1.9)	
yp T3 and T4	24 (16.2)	24 (14.9)	
N stage, *n* (%)			0.533
N0 and N1	44 (29.7)	51 (31.7)	
N2 and N3	75 (50.7)	83 (51.6)	
yp N0 and yp N1	11 (7.4)	15 (9.3)	
yp N2 and yp N3	18 (12.2)	12 (7.5)	
M stage, *n* (%)			> 0.999
M0	148 (100.00)	161 (100)	
TNM stage, *n* (%)			0.91
Stage II	57 (38.5)	61 (37.9)	
Stage III	91 (61.5)	100 (62.1)	
Borrmann classification, *n* (%)			0.207
Superficial type	3 (2.0)	1 (0.6)	
Type I	10 (6.8)	9 (5.6)	
Type II	41 (27.7)	36 (22.4)	
Type III	73 (49.3)	78 (48.4)	
Type IV	2 (1.4)	9 (5.6)	
NA	19 (12.8)	28 (17.4)	
Lauren classification, *n* (%)			0.782
Intestinal type	42 (28.4)	48 (29.8)	
Diffuse type	64 (43.2)	69 (42.9)	
Mixed type	34 (23.0)	39 (24.2)	
NA	8 (5.4)	5 (3.1)	

Differentiation, *n* (%)			0.666
Low	88 (59.5)	91 (56.5)	
Low-medium	36 (24.3)	39 (24.2)	
Medium	19 (12.8)	26 (16.1)	
Medium-high and high	2 (1.4)	4 (2.5)	
NA	3 (2.0)	1 (0.6)	
Nerve invasion, *n* (%)			0.26
Yes	73 (49.3)	92 (57.1)	
No	24 (16.2)	27 (16.8)	
NA	51 (34.5)	42 (26.1)	
Vascular tumor thrombus, *n* (%)			0.23
Yes	57 (38.5)	57 (38.5)	
No	40 (27.0)	54 (33.5)	
NA	51 (34.5)	42 (26.1)	
Pathological classification, *n* (%)			0.481
Signet-ring cell carcinoma	45 (30.4)	55 (34.2)	
Another adenocarcinoma	103 (69.6)	106 (65.8)	
Resection type, *n* (%)			0.057
Total gastrectomy	53 (35.8)	54 (33.5)	
Proximal gastrectomy	7 (4.7)	20 (12.4)	
Distal gastrectomy	88 (59.5)	87 (54.0)	
R0 resection	148 (100.00)	161 (100)	> 0.999
Resected lymph nodes number	39.21 ± 14.13	35.73 ± 13.53	0.0145
Positive lymph nodes number	7.393 ± 8.864	6.856 ± 9.743	0.2319

SR: Sustained-release; NSR: Not sustained-release; BMI: Body mass index; NA: Not available.

Table 2 Postoperative complications in patients

	SR group (*n* = 148), *n* (%)	NSR group (*n* = 161), *n* (%)	*P* value
Pulmonary infection	3 (2.0)	6 (3.8)	0.583
Anastomotic fistula	6 (4.0)	6 (3.8)	0.882
Postoperative bleeding	1 (0.7)	3 (1.9)	0.675
Abdominal infection	3 (2.0)	9 (5.6)	0.105
Intestinal obstruction	3 (2.0)	1 (0.6)	0.556

SR: Sustained-release; NSR: Not sustained-release.

= 0.775), slightly higher than that of previous studies[31,32]. This may have been due to the R0 radical resection decreasing the risk of local-regional recurrence and compromising the effects of the sustained-release drug. Therefore, we may hypothesize that in cases of incomplete resections, such as an R1 resection, or if the lymph node dissection did not reach the D2 resection standard, the use of a sustained-release drug may improve survival. Previous results of drug use in the treatment of unresectable tumors, such as pancreatic cancer and colorectal cancer, provided evidence for this hypothesis[33].

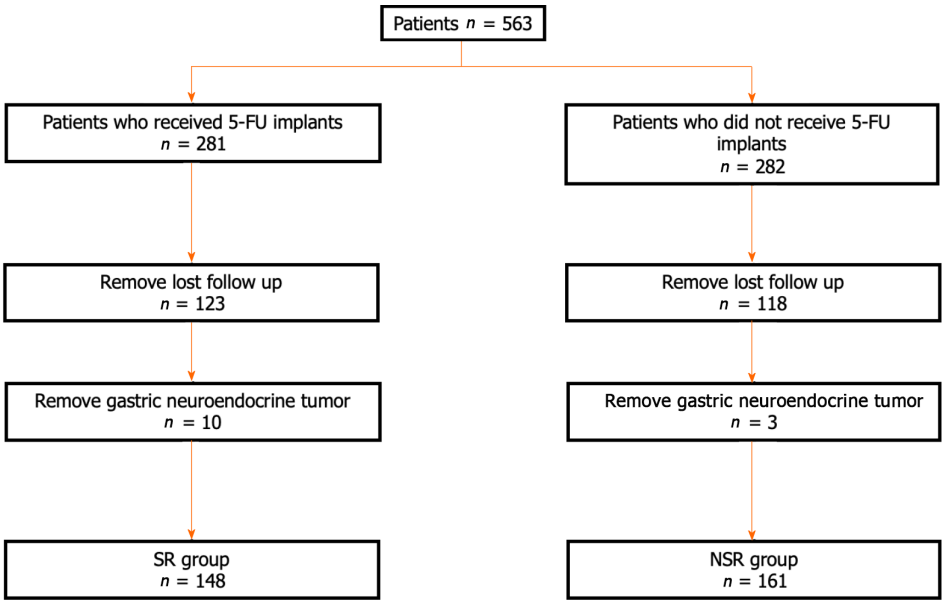
Similar to the findings of previous studies, the use of the sustained-release 5-FU implants did not increase postoperative complications, and systemic toxicity was rare in the present study. The use of 5-FU implants is usually recommended in gastric cancer patients, particularly at TNM stage T4 or N1–3

Table 3 Univariate and multivariate Cox analysis of patients

	Univariate analysis			Multivariate analysis		
Characteristics	**HR**	**95%CI**	***P* value**	**HR**	**95%CI**	***P* value**
Gender						
Male	Reference					
Female	1.058	0.712-1.572	0.781			
Age, yr						
< 60	Reference					
≥ 60	1.03	0.717-1.481	0.872			
Neoadjuvant therapy						
No	Reference					
Yes	2.188	1.448-3.306	< 0.001	2.118	1.194-3.759	0.01
BMI						
Normal < 24	Reference					
Abnormal ≥ 24	0.752	0.516-1.098	0.14			
Cardiovascular disease						
No	Reference					
Yes	0.943	0.606-1.467	0.794			
Diabetes						
No	Reference					
Yes	0.891	0.479-1.658	0.715			
Drug administration						
No	Reference					
Yes	1.052	0.731-1.513	0.786			
Resection type						
Total gastrectomy	Reference					
Partial gastrectomy	0.558	0.387-0.804	0.002	0.663	0.428-1.027	0.066
Borrmann classification						
Superficial type, Type I and II	Reference					
Type III and IV	2.203	1.378-3.522	0.001	1.562	0.951-2.566	0.078
Lauren classification						
Intestinal type	Reference					
Others	1.158	0.762-1.762	0.492			
Differentiation type						
Low	Reference					
Others	0.874	0.535-1.430	0.593			
TNM stage						
Stage II	Reference					
Stage III	3.12	1.977-4.926	< 0.001	1.315	0.561-3.084	0.528
T stage						
T1 and T2	Reference					
T3 and T4	3.382	1.649-6.937	0.001	1.9	0.777-4.645	0.159
N stage						

N0 and N1	Reference					
N2 and N3	2.516	1.636-3.869	< 0.001	2.224	1.082-4.572	0.03
Signet-ring cell carcinoma						
Yes	Reference					
No	1.188	0.736-1.916	0.481			
Nerve invasion						
No	Reference					
Yes	1.703	0.938-3.093	0.08			
Vascular tumor thrombus						
No	Reference					
Yes	1.099	0.701-1.722	0.681			

HR: Hazard ratio; CI: Confidence interval; BMI: Body mass index.



DOI: 10.3748/wjg.v28.i38.5589 **Copyright** ©The Author(s) 2022.

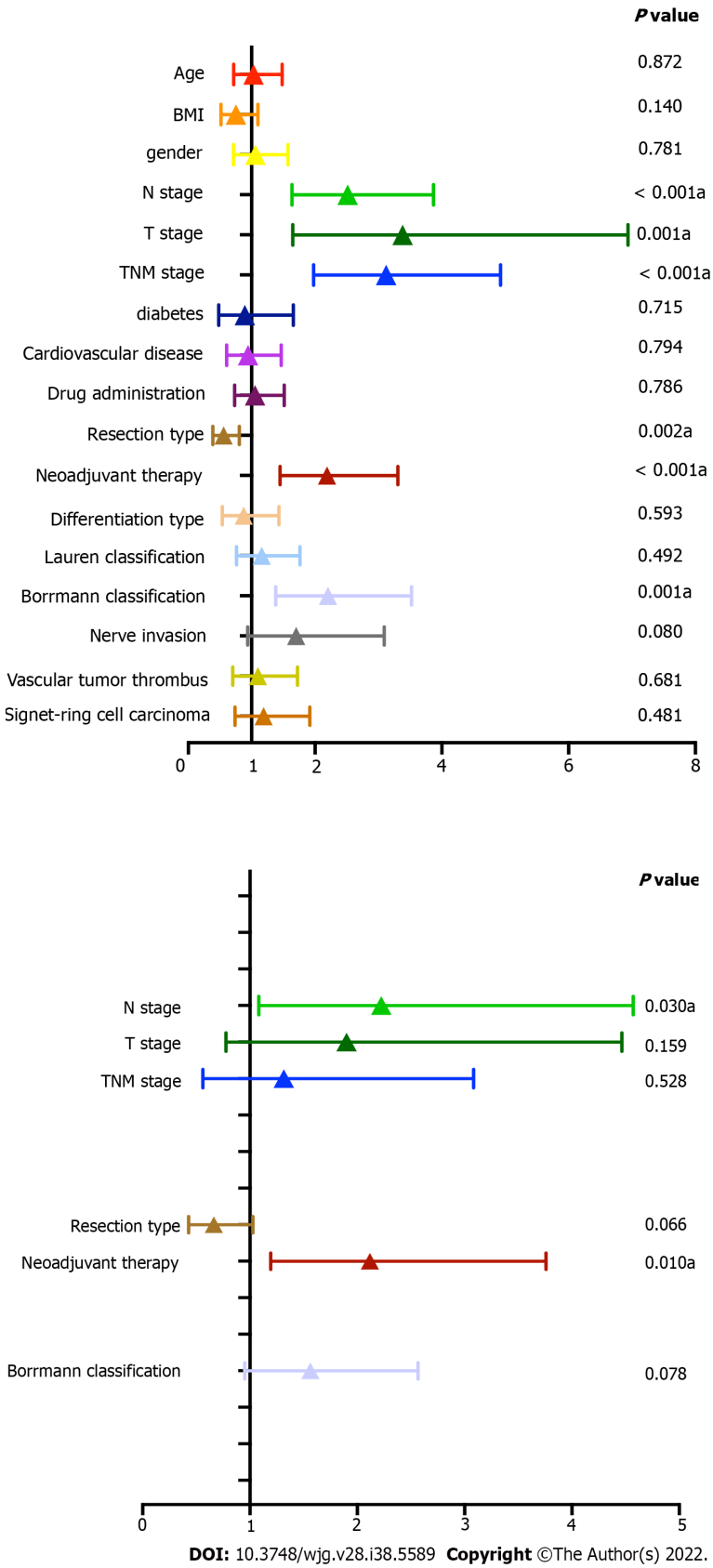
Figure 1 Flowchart of the selection of gastric cancer patients. 5-FU: 5-fluorouracil; NSR: Non-sustained-release.

[34]. In our study, the selection criteria were based on preoperative image examinations. Patients treated with 5-FU implants were in stage II and III, which is in accordance with the recommendations from the Chinese expert consensus[34].

Our study had some limitations. First, the sample size was insufficient. However, to date it remains the largest group studied. Second, selection biases existed. Many patients had incomplete history records, which may have contributed to a contrary result. Finally, the exact relapse time and the first site of recurrence were recorded incompletely. Owing to a lack of analysis of the relapses, the results were compromised. In order to understand the survival benefit of the sustained-release 5-FU plants on gastric cancer, a randomized controlled large-scale study is needed.

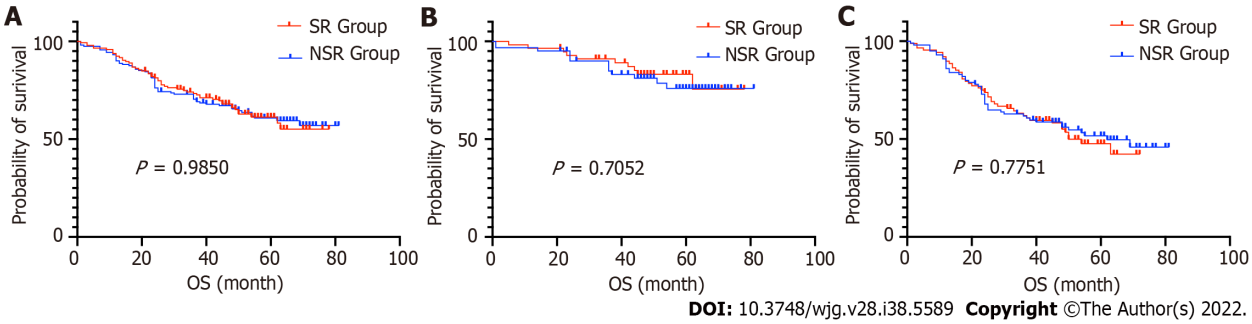
CONCLUSION

While the use of intraoperative sustained-release chemotherapy with 5-FU did not improve the survival of patients in an advanced stage of gastric cancer who underwent an R0 radical resection, it was a safe method, and it did not increase the complication rate.



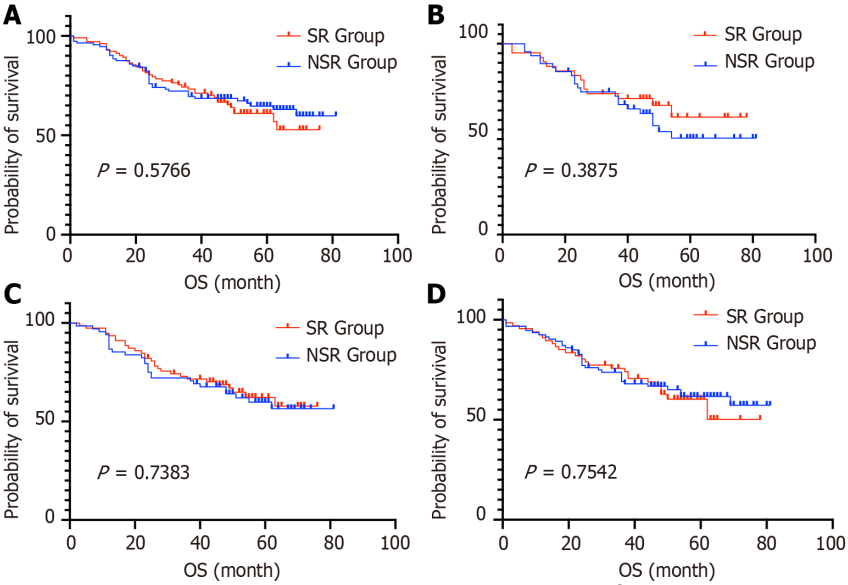
DOI: 10.3748/wjg.v28.i38.5589 **Copyright** ©The Author(s) 2022.

Figure 2 Univariate and Multivariate Cox analyses of prognostic factors of 5-year survival in this group. N stage (N0 and N1 *vs* N2 and N3), T stage (T1 and T2 *vs* T3 and T4), TNM stage (stage II and stage III), surgery type (Total gastrectomy *vs* Partial gastrectomy), Neoadjuvant therapy (No *vs* Yes) and Borrmann classification (Superficial Type, Type I and Type II *vs* Type III and Type IV) are the prognosis factor of gastric cancer patients.



DOI: 10.3748/wjg.v28.i38.5589 **Copyright** ©The Author(s) 2022.

Figure 3 Survival Outcomes in gastric cancer patients. A: Overall survival analysis in all gastric cancer patients; B: Overall survival analysis in stage II gastric cancer patients; C: Overall survival analysis in stage III gastric cancer patients. NSR: Non-sustained-release.



DOI: 10.3748/wjg.v28.i38.5589 **Copyright** ©The Author(s) 2022.

Figure 4 Survival analysis in the age and gender subgroups. A: Survival analysis in male gastric cancer patients; B: Survival analysis in female gastric cancer patients; C: Survival analysis in gastric cancer patients less than 60 years old; D: Survival analysis in gastric cancer patients is mor than 60 years old. NSR: Non-sustained-release.

ARTICLE HIGHLIGHTS

Research background

The prognosis of gastric cancer in an advanced stage remains poor. The exact efficacy of the use of intraoperative sustained-release chemotherapy with 5-fluorouracil (5-FU) in advanced-stage gastric cancer is still unelucidated.

Research motivation

To explore the long-term survival benefit of using sustained-release 5-FU implants in stage II and stage III gastric cancer patients.

Research objectives

To explore the long-term survival benefit of using sustained-release 5-FU implants in stage II and stage III gastric cancer patients.

Research methods

All included patients were grouped according to whether intraoperative sustained-release (SR) chemotherapy with 5-FU was used or not (NSR). The primary end-point was 5-year overall survival. Kaplan–Meier method with log-rank test was used to analyze the overall survival of patients and Cox analysis was used to analyze prognosis factors of these patients.

Research results

309 patients were included in the final analysis. In addition, 158 patients received intraoperative sustained-release chemotherapy with 5-FU and were included in the SR group, while the other 161 patients were included in the NSR group. The overall complication rate was 12.94% in the whole group and 10.81%, 16.46% in SR and NSR groups, respectively. There were no significant differences between the two groups in overall survival and complication rate ($P > 0.05$).

Research conclusions

Intraoperative sustained-release chemotherapy usage with 5-FU, did not improve the survival of patients who underwent an R0 radical resection in locally advanced stage of gastric cancer.

Research perspectives

5-FU implants did not improve survival.

FOOTNOTES

Author contributions: Wu YZ and Xie YB contributed to the manuscript writing; Wu YZ, Zheng XH, Ming Wu, and Ding SK contributed to the data collection; Wu YZ and Ren JS contributed to the data analysis; Wang BZ and Xue LY contributed to the pathological diagnosis; Xie YB, Tian YT, and Yang L contributed to the clinical treatment and manuscript modification; all the authors contributed to the manuscript and approved the submitted version.

Supported by the CAMS Initiative for Innovative Medicine, No. 2016-I2M-1-007.

Institutional review board statement: This study was approved by the ethics committee of the National Cancer Center/National Clinical Research Center for Cancer/Cancer Hospital, Chinese Academy of Medical Sciences, and Peking Union Medical College.

Informed consent statement: Informed consent from patients was waived by the ethics committee of the National Cancer Center/National Clinical Research Center for Cancer/Cancer Hospital, Chinese Academy of Medical Sciences, and Peking Union Medical College.

Conflict-of-interest statement: The authors declare that the research was conducted in the absence of any commercial or financial relationships that could be construed as a potential conflict of interest.

Data sharing statement: The datasets generated during and/or analyzed during the current study are available from the corresponding author on reasonable request.

STROBE statement: The authors have read the STROBE Statement—checklist of items, and the manuscript was prepared and revised according to the STROBE Statement—checklist of items.

Open-Access: This article is an open-access article that was selected by an in-house editor and fully peer-reviewed by external reviewers. It is distributed in accordance with the Creative Commons Attribution NonCommercial (CC BY-NC 4.0) license, which permits others to distribute, remix, adapt, build upon this work non-commercially, and license their derivative works on different terms, provided the original work is properly cited and the use is non-commercial. See: https://creativecommons.org/Licenses/by-nc/4.0/

Country/Territory of origin: China

ORCID number: Yun-Zi Wu 0000-0002-8254-8998; Ming Wu 0000-0002-1172-1351; Xiao-Hao Zheng 0000-0002-0282-1684; Bing-Zhi Wang 0000-0001-9622-7151; Li-Yan Xue 0000-0001-5185-0126; Shi-Kang Ding 0000-0001-5578-2845; Lin Yang 0000-0002-4829-3119; Jian-Song Ren 0000-0002-6445-0153; Yan-Tao Tian 0000-0001-6479-7547; Yi-Bin Xie 0000-0002-0255-3018.

S-Editor: Wu YXJ
L-Editor: A
P-Editor: Zhang XD

REFERENCES

1 **Sung H**, Ferlay J, Siegel RL, Laversanne M, Soerjomataram I, Jemal A, Bray F. Global Cancer Statistics 2020: GLOBOCAN Estimates of Incidence and Mortality Worldwide for 36 Cancers in 185 Countries. *CA Cancer J Clin* 2021; **71**: 209-249 [PMID: 33538338 DOI: 10.3322/caac.21660]
2 **Wong MCS**, Huang J, Chan PSF, Choi P, Lao XQ, Chan SM, Teoh A, Liang P. Global Incidence and Mortality of Gastric

Cancer, 1980-2018. *JAMA Netw Open* 2021; **4**: e2118457 [PMID: 34309666 DOI: 10.1001/jamanetworkopen.2021.18457]
3 **Lin Y**, Zheng Y, Wang HL, Wu J. Global Patterns and Trends in Gastric Cancer Incidence Rates (1988-2012) and Predictions to 2030. *Gastroenterology* 2021; **161**: 116-127.e8 [PMID: 33744306 DOI: 10.1053/j.gastro.2021.03.023]
4 **Zheng R**, Zhang S, Zeng H, Wang S, Sun K, Chen R, Li L, Wei W, He J. Cancer incidence and mortality in China, 2016. *Guojia Aizheng Zhongxin Zazhi* 2022 [DOI: 10.1016/j.jncc.2022.02.002]
5 **Sano T**, Coit DG, Kim HH, Roviello F, Kassab P, Wittekind C, Yamamoto Y, Ohashi Y. Proposal of a new stage grouping of gastric cancer for TNM classification: International Gastric Cancer Association staging project. *Gastric Cancer* 2017; **20**: 217-225 [PMID: 26897166 DOI: 10.1007/s10120-016-0601-9]
6 **Wang FH**, Zhang XT, Li YF, Tang L, Qu XJ, Ying JE, Zhang J, Sun LY, Lin RB, Qiu H, Wang C, Qiu MZ, Cai MY, Wu Q, Liu H, Guan WL, Zhou AP, Zhang YJ, Liu TS, Bi F, Yuan XL, Rao SX, Xin Y, Sheng WQ, Xu HM, Li GX, Ji JF, Zhou ZW, Liang H, Zhang YQ, Jin J, Shen L, Li J, Xu RH. The Chinese Society of Clinical Oncology (CSCO): Clinical guidelines for the diagnosis and treatment of gastric cancer, 2021. *Cancer Commun (Lond)* 2021; **41**: 747-795 [PMID: 34197702 DOI: 10.1002/cac2.12193]
7 **Li JH**, Zhang SW, Liu J, Shao MZ, Chen L. Review of clinical investigation on recurrence of gastric cancer following curative resection. *Chin Med J (Engl)* 2012; **125**: 1479-1495 [PMID: 22613657]
8 **Nakauchi M**, Vos E, Tang LH, Gonen M, Janjigian YY, Ku GY, Ilson DH, Maron SB, Yoon SS, Brennan MF, Coit DG, Strong VE. Outcomes of Neoadjuvant Chemotherapy for Clinical Stages 2 and 3 Gastric Cancer Patients: Analysis of Timing and Site of Recurrence. *Ann Surg Oncol* 2021; **28**: 4829-4838 [PMID: 33566242 DOI: 10.1245/s10434-021-09624-5]
9 **Yago A**, Haruta S, Ueno M, Hamada Y, Ogawa Y, Ohkura Y, Urabe M, Udagawa H. Adequate period of surveillance in each stage for curatively resected gastric cancer: analyzing the time and rates of recurrence. *Gastric Cancer* 2021; **24**: 752-761 [PMID: 33400037 DOI: 10.1007/s10120-020-01147-4]
10 **Roviello F**, Marrelli D, De Manzoni G, Morgagni P, Di Leo A, Saragoni L, De Stefano A. Prospective study of peritoneal recurrence after curative surgery for gastric cancer. *Br J Surg* 2003; **90**: 1113-1119
11 **Yoo CH**, Noh SH, Shin DW, Choi SH, Min JS. Recurrence following curative resection for gastric carcinoma. *Br J Surg* 2000; **87**: 236-242 [PMID: 10671934 DOI: 10.1046/j.1365-2168.2000.01360.x]
12 **Nakanishi Y**, Ohara M, Domen H, Shichinohe T, Hirano S, Ishizaka M. Differences in risk factors between patterns of recurrence in patients after curative resection for advanced gastric carcinoma. *World J Surg Oncol* 2013; **11**: 98 [PMID: 23683476 DOI: 10.1186/1477-7819-11-98]
13 **D'Angelica M**, Gonen M, Brennan MF, Turnbull AD, Bains M, Karpeh MS. Patterns of initial recurrence in completely resected gastric adenocarcinoma. *Ann Surg* 2004; **240**: 808-816 [PMID: 15492562 DOI: 10.1097/01.sla.0000143245.28656.15]
14 **Li S**, Li L, Tan B, Wang J, Xue S. The benefits of surgery plus extensive intraoperative peritoneal lavage (EIPL) for patients with gastric cancer compared with surgery alone: a systematic review and meta-analysis. *Updates Surg* 2022; **74**: 65-72 [PMID: 34170498 DOI: 10.1007/s13304-021-01120-5]
15 **Zhang JF**, Lv L, Zhao S, Zhou Q, Jiang CG. Hyperthermic Intraperitoneal Chemotherapy (HIPEC) Combined with Surgery: A 12-Year Meta-Analysis of this Promising Treatment Strategy for Advanced Gastric Cancer at Different Stages. *Ann Surg Oncol* 2022; **29**: 3170-3186 [PMID: 35175455 DOI: 10.1245/s10434-021-11316-z]
16 **Joshi SS**, Badgwell BD. Current treatment and recent progress in gastric cancer. *CA Cancer J Clin* 2021; **71**: 264-279 [PMID: 33592120 DOI: 10.3322/caac.21657]
17 **Huang JY**, Xu YY, Sun Z, Zhu Z, Song YX, Guo PT, You Y, Xu HM. Comparison different methods of intraoperative and intraperitoneal chemotherapy for patients with gastric cancer: a meta-analysis. *Asian Pac J Cancer Prev* 2012; **13**: 4379-4385 [PMID: 23167347 DOI: 10.7314/apjcp.2012.13.9.4379]
18 **Bonnot PE**, Piessen G, Kepenekian V, Decullier E, Pocard M, Meunier B, Bereder JM, Abboud K, Marchal F, Quenet F, Goere D, Msika S, Arvieux C, Pirro N, Wernert R, Rat P, Gagnière J, Lefevre JH, Courvoisier T, Kianmanesh R, Vaudoyer D, Rivoire M, Meeus P, Passot G, Glehen O; FREGAT and BIG-RENAPE Networks. Cytoreductive Surgery With or Without Hyperthermic Intraperitoneal Chemotherapy for Gastric Cancer With Peritoneal Metastases (CYTO-CHIP study): A Propensity Score Analysis. *J Clin Oncol* 2019; **37**: 2028-2040 [PMID: 31084544 DOI: 10.1200/JCO.18.01688]
19 **Kwon OK**, Chung HY, Yu W. Early postoperative intraperitoneal chemotherapy for macroscopically serosa-invading gastric cancer patients. *Cancer Res Treat* 2014; **46**: 270-279 [PMID: 25038762 DOI: 10.4143/crt.2014.46.3.270]
20 **Li L**, Li C, Zhou J. Effective sustained release of 5-FU-loaded PLGA implant for improving therapeutic index of 5-FU in colon tumor. *Int J Pharm* 2018; **550**: 380-387 [PMID: 30040972 DOI: 10.1016/j.ijpharm.2018.07.045]
21 **Ge J**, Liu T, Lei T, Li X, Song K, Azizi S, Liu H, Tang M. Retrospective Cohort Study of Intraoperative Administration of Sustained-Release 5-Fluorouracil Implants in Advanced Gastric Cancer Patients. *Front Pharmacol* 2021; **12**: 659258 [PMID: 33927633 DOI: 10.3389/fphar.2021.659258]
22 **Xu Y**, Zhang R, Li C, Sun Z, Deng J, Wang X, Ding X, Wang B, Xue Q, Ke B, Zhan H, Liu N, Liu Y, Liang H, Xue Y, Xu H. Intraperitoneal Chemotherapy Using Fluorouracil Implants Combined With Radical Resection and Postoperative Adjuvant Chemotherapy for Stage III Gastric Cancer: A Multi-Center, Randomized, Open-Label, Controlled Clinical Study. *Front Oncol* 2021; **11**: 670651 [PMID: 34307140 DOI: 10.3389/fonc.2021.670651]
23 **Gao K**, Wu J. National trend of gastric cancer mortality in China (2003-2015): a population-based study. *Cancer Commun (Lond)* 2019; **39**: 24 [PMID: 31046840 DOI: 10.1186/s40880-019-0372-x]
24 **Zeng H**, Ran X, An L, Zheng R, Zhang S, Ji JS, Zhang Y, Chen W, Wei W, He J; HBCR Working Group. Disparities in stage at diagnosis for five common cancers in China: a multicentre, hospital-based, observational study. *Lancet Public Health* 2021; **6**: e877-e887 [PMID: 34838194 DOI: 10.1016/S2468-2667(21)00157-2]
25 **Smyth EC**, Nilsson M, Grabsch HI, van Grieken NC, Lordick F. Gastric cancer. *Lancet* 2020; **396**: 635-648 [DOI: 10.1016/S0140-6736(20)31288-5]
26 **Wu CW**, Lo SS, Shen KH, Hsieh MC, Chen JH, Chiang JH, Lin HJ, Li AF, Lui WY. Incidence and factors associated with recurrence patterns after intended curative surgery for gastric cancer. *World J Surg* 2003; **27**: 153-158 [PMID: 12616428 DOI: 10.1007/s00268-002-6279-7]

27 **Maehara Y**, Hasuda S, Koga T, Tokunaga E, Kakeji Y, Sugimachi K. Postoperative outcome and sites of recurrence in patients following curative resection of gastric cancer. *Br J Surg* 2000; **87**: 353-357 [PMID: 10718807 DOI: 10.1046/j.1365-2168.2000.01358.x]

28 **Liu D**, Lu M, Li J, Yang Z, Feng Q, Zhou M, Zhang Z, Shen L. The patterns and timing of recurrence after curative resection for gastric cancer in China. *World J Surg Oncol* 2016; **14**: 305 [PMID: 27931221 DOI: 10.1186/s12957-016-1042-y]

29 **Yuan H**, Zheng B, Tu S. Clinical research of intraperitoneal implantation of sustained-release 5-fluorouracil in advanced colorectal cancer. *World J Surg Oncol* 2015; **13**: 320 [PMID: 26596801 DOI: 10.1186/s12957-015-0737-9]

30 **Chen J**, Zhang J, Wang C, Yao K, Hua L, Zhang L, Ren X. Safety of implanting sustained-release 5-fluorouracil into hepatic cross-section and omentum majus after primary liver cancer resection. *Int J Immunopathol Pharmacol* 2016; **29**: 475-479 [PMID: 27207445 DOI: 10.1177/0394632016648176]

31 **Liang Y**, Zhao L, Chen H, Lin T, Chen T, Zhao M, Hu Y, Yu J, Liu H, Li G. Survival analysis of elderly patients over 65 years old with stage II/III gastric cancer treated with adjuvant chemotherapy after laparoscopic D2 gastrectomy: a retrospective cohort study. *BMC Cancer* 2021; **21**: 196 [PMID: 33632161 DOI: 10.1186/s12885-021-07919-0]

32 **Huang H**, Wang W, Chen Z, Jin JJ, Long ZW, Cai H, Liu XW, Zhou Y, Wang YN. Prognostic factors and survival in patients with gastric stump cancer. *World J Gastroenterol* 2015; **21**: 1865-1871 [PMID: 25684953 DOI: 10.3748/wjg.v21.i6.1865]

33 **Shim IK**, Yi HJ, Yi HG, Lee CM, Lee YN, Choi YJ, Jeong SY, Jun E, Hoffman RM, Cho DW, Kim SC. Locally-applied 5-fluorouracil-loaded slow-release patch prevents pancreatic cancer growth in an orthotopic mouse model. *Oncotarget* 2017; **8**: 40140-40151 [PMID: 28498800 DOI: 10.18632/oncotarget.17370]

34 **Chen HQ**, Gong JP, He YL, Huang CM, Liang H, Meng XL, Xu HM, Xue YW, Yan M, Zhou ZW. Expert consensus on intraoperative regional sustained-release chemotherapy for advanced gastric cancer. *Zhonghua Wichang Waike Zazhi* 2012; **15**: 981-983

World Journal of Gastroenterology

Submit a Manuscript: https://www.f6publishing.com

World J Gastroenterol 2022 October 14; 28(38): 5602-5613

DOI: 10.3748/wjg.v28.i38.5602

ISSN 1007-9327 (print) ISSN 2219-2840 (online)

ORIGINAL ARTICLE

Retrospective Cohort Study

Timing of endoscopic retrograde cholangiopancreatography in the treatment of acute cholangitis of different severity

Yao-Chi Huang, Chi-Huan Wu, Mu Hsien Lee, Sheng Fu Wang, Yung-Kuan Tsou, Cheng-Hui Lin, Kai-Feng Sung, Nai-Jen Liu

Specialty type: Gastroenterology and hepatology

Provenance and peer review: Unsolicited article; Externally peer reviewed.

Peer-review model: Single blind

Peer-review report's scientific quality classification

Grade A (Excellent): A
Grade B (Very good): 0
Grade C (Good): C
Grade D (Fair): 0
Grade E (Poor): 0

P-Reviewer: Isogai M, Japan; Liao JX, China

Received: June 27, 2022
Peer-review started: June 27, 2022
First decision: August 1, 2022
Revised: August 12, 2022
Accepted: September 23, 2022
Article in press: September 23, 2022
Published online: October 14, 2022

Yao-Chi Huang, Yung-Kuan Tsou, Department of Medicine, College of Medicine, Chang Gung University, Taoyuan 333, Taiwan

Chi-Huan Wu, Mu Hsien Lee, Sheng Fu Wang, Yung-Kuan Tsou, Cheng-Hui Lin, Kai-Feng Sung, Nai-Jen Liu, Department of Gastroenterology and Hepatology, Chang Gung Memorial Hospital, Taoyuan 333, Taiwan

Corresponding author: Yung-Kuan Tsou, MD, Associate Professor, Doctor, Department of Gastroenterology and Hepatology, Chang Gung Memorial Hospital, No. 5 Fu-Shin Street, Kweishan, Taoyuan 333, Taiwan. flying@adm.cgmh.org.tw

Abstract

BACKGROUND

The optimal timing of endoscopic retrograde cholangiopancreatography (ERCP) in acute cholangitis (AC) is uncertain, especially in patients with AC of varying severity.

AIM

To report whether the timing of ERCP is associated with outcomes in AC patients with different severities.

METHODS

According to the 2018 Tokyo guidelines, 683 patients who met the definite diagnostic criteria for AC were retrospectively identified. The results were first compared between patients receiving ERCP ≤ 24 h and > 24 h and then between patients receiving ERCP ≤ 48 h and > 48 h. Subgroup analyses were performed in patients with grade I, II or III AC. The primary outcome was 30-d mortality. Secondary outcomes were intensive care unit (ICU) admission rate, length of hospital stay (LOHS) and 30-d readmission rate.

RESULTS

Taking 24 h as the critical value, compared with ERCP > 24 h, malignant biliary obstruction as a cause of AC was significantly less common in the ERCP ≤ 24 h group (5.2% *vs* 11.5%). The proportion of cardiovascular dysfunction (11.2% *vs* 2.6%), respiratory dysfunction (14.2% *vs* 5.3%), and ICU admission (11.2% *vs* 4%) in the ERCP ≤ 24 h group was significantly higher, while the LOHS was significantly shorter (median, 6 d *vs* 7 d). Stratified by the severity of AC, higher ICU

admission was only observed in grade III AC and shorter LOHS was only observed in grade I and II AC. There were no significant differences in 30-d mortality between groups, either in the overall population or in patients with grade I, II or III AC. With 48 h as the critical value, compared with ERCP > 48 h, the proportion of choledocholithiasis as the cause of AC was significantly higher in the ERCP ≤ 48 h group (81.5% *vs* 68.3%). The ERCP ≤ 48 h group had significantly lower 30-d mortality (0 *vs* 1.9%) and shorter LOHS (6 d *vs* 8 d). Stratified by AC severity, lower 30-d mortality (0 *vs* 6.1%) and higher ICU admission rates (22.2% *vs* 10.2%) were only observed in grade III AC, and shorter LOHS was only observed in grade I and II AC. In the multivariate analysis, cardiovascular dysfunction and time to ERCP were two independent factors associated with 30-d mortality.

CONCLUSION

ERCP ≤ 48 h conferred a survival benefit in patients with grade III AC. Early ERCP shortened the LOHS in patients with grade I and II AC.

Key Words: Acute cholangitis; Endoscopic retrograde cholangiopancreatography; severity; Timing; Thirty-day mortality; Length of hospital stay

©The Author(s) 2022. Published by Baishideng Publishing Group Inc. All rights reserved.

Core Tip: Compared with endoscopic retrograde cholangiopancreatography (ERCP) > 24 h, ERCP ≤ 24 h group had a significantly higher intensive care unit (ICU) admission rate and shorter length of hospital stay (LOHS). Subgroup analysis showed higher ICU admission rate was only in grade III acute cholangitis (AC); shorter LOHS was only in grade II and I AC. Compared with ERCP > 48 h, ERCP ≤ 48 h group had significantly lower 30-d mortality and shorter LOHS. Subgroup analysis revealed lower 30-d mortality was only in grade III AC; shorter LOHS was only in grade II and I AC. We concluded that ERCP ≤ 48 h conferred a survival benefit in grade III AC; early ERCP shortened LOHS in grade II and I AC.

Citation: Huang YC, Wu CH, Lee MH, Wang SF, Tsou YK, Lin CH, Sung KF, Liu NJ. Timing of endoscopic retrograde cholangiopancreatography in the treatment of acute cholangitis of different severity. *World J Gastroenterol* 2022; 28(38): 5602-5613

URL: https://www.wjgnet.com/1007-9327/full/v28/i38/5602.htm

DOI: https://dx.doi.org/10.3748/wjg.v28.i38.5602

INTRODUCTION

Without treatment, patients with acute cholangitis (AC) may progress to septicemia and organ failure resulting in mortality[1,2]. Over the past two decades, endoscopic retrograde cholangiopancreatography (ERCP) has been generally accepted as a first-line treatment for AC[3,4]. Although delayed biliary drainage may not affect the risk of complications in patients who respond well to antibiotics, some patients with AC require early ERCP to avoid (persistent) organ failure or mortality[2,5,6]. Despite consensus on the need for biliary drainage, the optimal timing for early ERCP remains unclear due to mixed results in the literature[7]. Different definitions of early ERCP have been used in the literature, ranging from 12 h to 72 h[2,5,8-11]. The varied definitions among studies have led to inconsistent conclusions. In addition, the definitions of AC are not uniform across studies. More importantly, most studies did not define the timing of ERCP by stratifying the severity of AC[7]. In this context, the recently published Tokyo Guidelines 2018 (TG18) provide not only a diagnosis of AC but also a severity grading, which is important for predicting prognosis and determining treatment strategies[3]. However, although TG18 recommends early or urgent biliary drainage for moderate or severe cholangitis, there is no specific timing for early or urgent ERCP. Therefore, this study aims to investigate whether the timing of ERCP is associated with improved outcomes in AC patients with different severities.

MATERIALS AND METHODS

This was a retrospective study conducted at Chang Gung Memorial Hospital Linkou Center. At our center, ERCP has been the first-line of treatment for patients with AC for the past two decades. This study was reviewed and approved by the Ethics Committee of the Chang Gung Memorial Hospital (IRB No. 202200881B0). Since this was a retrospective study using routine clinical treatment or diagnostic

medical records, the Chang Gung Medical Foundation Institutional Review Board approved the waiver of the participant's consent. All methods were carried out under relevant guidelines and regulations.

Definition of acute cholangitis

The diagnostic criteria for AC were based on the 2018 Tokyo Guidelines, including systemic inflammation, cholestasis and imaging findings[3]. Systemic inflammation included fever (body temperature > 38 °C) or evidence of an inflammatory response [white blood cell (WBC) count < 4000 or > 10000/μL or C-reactive protein ≥ 1 mg/dL]. Cholestasis included jaundice (serum total bilirubin ≥ 2 mg/dL) or abnormal liver function tests (serum alkaline phosphatase, r-glutamyl transferase, aspartate aminotransferase, or alanine aminotransferase > 1.5 times the upper limit of the normal value). Imaging findings included bile duct dilatation or imaging evidence of etiology such as strictures, stones or stents. A definite diagnosis of AC was defined as one item in systemic inflammation, one item in cholestasis and one item in imaging findings.

Definition of the severity of acute cholangitis

AC severity was divided into three grades based on the 2018 Tokyo Guidelines[3]. Grade III (severe) AC was AC associated with the onset of dysfunction in at least one of the following organs/systems: cardiovascular dysfunction (defined as hypotension requiring dopamine ≥ 5 μg/kg per min, or any dose of norepinephrine), neurological dysfunction (presence of conscious disturbance), respiratory dysfunction (defined as PaO_2/FiO_2 ratio < 300), renal dysfunction (oliguria, serum creatinine > 2.0 mg/dL), hepatic dysfunction [defined as prothrombin time-international normalized ratio (PT-INR) > 1.5] or hematological dysfunction (defined as platelet count < 100 × 10^3/μL). Grade II (moderate) AC was AC associated with any two of the following conditions: abnormal WBC count (> 12000/μL or < 4000/μL), high fever (≥ 39 °C), old age (≥ 75 years), hyperbilirubinemia (serum total bilirubin ≥ 5 mg/dL), or hypoalbuminemia (< lower limit of normal value × 0.7). Grade I (mild) AC was AC that did not meet the criteria of "Grade III" or "Grade II" AC at initial diagnosis.

Definition of time to ERCP

Time to ERCP was defined as the time from the emergency department visit to the commencement of ERCP.

Patient selection and clinical variables

The study flow chart is shown in Figure 1. Between 2016 and 2017, 2121 patients who underwent ERCP in our center were retrospectively collected from the computer database of the Therapeutic Endoscopy Center. The inclusion criteria were patients who met the TG18/TG13 criteria for a definite diagnosis of AC. The exclusion criteria were: (1) Patients who did not meet the criteria for a definite diagnosis of AC; (2) inpatients who developed AC after hospitalization; and (3) patients who received ERCP 7 or more days after an emergency department visit. For patients readmitted for AC during the study period, we included only the first admission and the ERCP procedure.

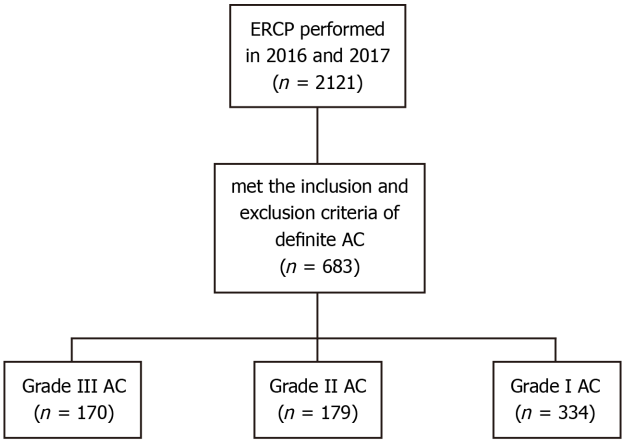
Medical records were reviewed, and the following data were obtained: sex; age; clinical manifestations, including body temperature, systolic blood pressure, heart rate, saturation, respiratory rate and urine output; laboratory values including WBC count, platelet count, PT-INR, C-reactive protein, creatinine, bilirubin, alkaline phosphatase, r-glutamyl transferase, aspartate aminotransferase, alanine aminotransferase and albumin; diagnosis and treatment of ERCP, including causes of obstruction (such as stones, malignant strictures or stent dysfunction); and the timing of ERCP.

Outcome assessments

The primary outcome was 30-d mortality. Secondary outcomes were ICU admission rate, length of hospital stay (LOHS) and 30-d readmission rate. The results were first compared for patients receiving ERCP ≤ 24 h *vs* > 24 h and then for patients receiving ERCP ≤ 48 h *vs* > 48 h. Subgroup analyses were also performed in patients with grade I, II, and III AC.

Statistical analysis

Continuous variable data are represented by the median and interquartile range (IQR); categorical variables are presented as a number (%). For comparisons, the Kruskal-Wallis test was used for continuous variable data and the chi-square test or Fisher's exact test was used for suitable categorical variables. Logistic regression analysis was performed to identify factors associated with 30-d mortality. Only variables with a P value < 0.05 in the univariate analysis were included in the multivariate analysis. Two-tailed P values < 0.05 were considered statistically significant and P values = 0.05 were considered marginally significant. Statistical analysis was performed using SPSS software (version 22.0; SPSS, Inc., Chicago, IL, United States).



DOI: 10.3748/wjg.v28.i38.5602 **Copyright** ©The Author(s) 2022.

Figure 1 Study flow chart. AC: Acute cholangitis; ERCP: Endoscopic retrograde cholangiopancreatography.

RESULTS

A total of 683 patients who met the eligibility criteria were included in the study. Among them, there were 170 (24.9%) grade III AC patients, 179 grade II AC patients (26.4%) and 334 grade I AC patients (48.9%).

Patient characteristics

The baseline characteristics of the patients are presented in Table 1. The median (IQR) age of the patients was 66 (53-78) years; 57.2% were male. The median body temperature was 37.5 (36.8-38.4) °C and 58.4% of patients had abnormal WBC counts. The median platelet count was 198 × 10^3 (148 × 10^3-251 × 10^3)/μL. The median serum levels of aspartate aminotransferase, alanine aminotransferase and alkaline phosphatase were 150 U/L, 166 U/L and 265 U/L, respectively. Serum amylase and lipase data were available for 307 (44.9%) and 487 (71.3%) patients with median levels of 65 U/L and 37 U/L, respectively. The median serum bilirubin level was 3.7 (2.3-6.3) mg/dL and the median creatine level was 0.93 (0.73-1.24) mg/dL. The median PT/INR was 1.1 (1.1-1.2). Only 133 (19.5%) patients had data on serum albumin and the median level was 3.56 (3.05-3.98) g/dL. Twenty-nine (4.2%) patients had cardiovascular dysfunction, 35 (5.1%) patients had neurological dysfunction and 48 (7%) patients had respiratory dysfunction.

Comparisons between ERCP ≤ 24 h and ERCP > 24 h: Compared with ERCP > 24 h, patients with ERCP ≤ 24 h had significantly lower body temperature (median, 37.2 °C *vs* 37.5 °C. P = 0.003), significantly higher serum alanine aminotransferase (median, 194 U/L *vs* 156 U/L, P = 0.02) and serum creatinine levels (median, 0.96 *vs* 0.93, P = 0.004), and significantly higher proportions of abnormal WBC counts (70.9% *vs* 55.4%, P = 0.001), cardiovascular dysfunction (11.2% *vs* 2.6%, P < 0.001) and respiratory dysfunction (14.2% *vs* 5.3%, P < 0.001).

Comparisons between ERCP ≤ 48 h and ERCP > 48 h: Compared with ERCP > 48 h, patients with ERCP ≤ 48 h had significantly lower body temperature (median, 37.4 °C *vs* 37.6 °C, P = 0.009), significantly higher serum alanine aminotransferase levels (median, 188 U/L *vs* 142 U/L, P = 0.004) and significantly lower PT/INR (median, 1.1 *vs* 1.2, P = 0.001).

ERCP characteristics and causes of AC

The characteristics of ERCP are listed in Table 2. Causes of AC included common bile duct stones (CBDS, 74.4%), malignant biliary obstruction (MBO, 10.2%), biliary stent dysfunction (8.9%), benign biliary stricture (4.5%) and others (1.9%). ERCP failed in 1% of patients. For patients with successful ERCP, endoscopic treatments during ERCP included endoscopic sphincterotomy (81.7%), endoscopic papillary balloon dilatation (0.7%), bile duct stone retrieval (73.5%), stone-free bile duct clearance (5.4%), removal of old biliary stents (8.8%), insertion of new biliary stents (27.4%), dilation of biliary strictures (1%) and others (0.4%).

Comparisons between ERCP ≤ 24 h and ERCP > 24 h: The median time to ERCP was 17.7 (9.0-20.4) h in the ERCP ≤ 24 h group and 67.6 (43.6-98.9) h in the ERCP > 24 h group. Only malignant biliary obstruction as a cause of AC was significantly less common in the ERCP ≤ 24 h group (5.2% *vs* 11.5%, P = 0.032). In therapeutic ERCP, bile duct stone retrieval was higher in the ERCP ≤ 24 h group (80.6% *vs* 71.8%, P = 0.038) whereas the old biliary stent removal rate was lower (4.5% *vs* 9.8%, P = 0.049).

Table 1 Characteristics of the patients

Patient characteristics	Total, *n* = 683	Time to ERCP divided by 24 h			Time to ERCP divided by 48 h		
		ERCP ≤ 24 h, *n* = 134	ERCP > 24 h, *n* = 549	*P* value	ERCP ≤ 48 h, *n* = 314	ERCP > 48 h, *n* = 369	*P* value
Age in yr[1]	66 (53-78)	64 (56-75.5)	66 (52-78)	0.803	65 (54-79)	66 (51-79)	0.518
Male sex, *n* (%)	391 (57.2)	76 (56.7)	315 (57.4)	0.890	171 (54.5)	220 (59.6)	0.174
Body temperature in °C[1]	37.5 (36.8-38.4)	37.2 (36.7-38.1)	37.5 (36.9-38.5)	0.003	37.4 (36.8-38.28)	37.6 (36.9-38.5)	0.009
Abnormal WBC count[2], *n* (%)	399 (58.4)	95 (70.9)	304 (55.4)	0.001	195 (62.1)	204 (55.3)	0.072
Platelet count as /μL[1]	198 (148-251)	205 (142-256)	196.5 (149-250)	0.806	195 (148-249.8)	200 (148-251.5)	0.844
AST in U/L[1]	150 (83-305)	175 (97-406)	145 (80-289)	0.063	164 (95-311)	139 (76-302)	0.08
ALT in U/L[1]	166 (82-300)	194 (118-337)	156 (79-292)	0.02	188 (101-311)	142 (69-277)	0.004
ALK-P in U/L[1]	205 (133-327)	198 (123-321)	209 (133-327)	0.486	190 (123-329)	211 (140-324)	0.208
Amylase in U/L[1]	65 (41-170) (*n* = 307)	68 (42-634) (*n* = 66)	65 (40-145) (*n* = 241)	0.126	68 (41-367) (*n* = 138)	62 (40-139) (*n* = 169)	0.118
Lipase in U/L[1]	37 (26-144) (*n* = 487)	46 (25-1297) (*n* = 97)	36 (26-99) (*n* = 390)	0.104	41 (26-339) (*n* = 232)	35 (26-76) (*n* = 255)	0.094
Bilirubin in mg/dL[1]	3.7 (2.3-6.3)	4.1 (2.6-5.8)	3.7 (2.3-6.3)	0.395	3.8 (2.4-6.2)	3.7 (2.3-6.5)	0.878
PT/INR[1]	1.1 (1.1-1.2)	1.1 (1.1-1.3)	1.1 (1.1-1.2)	0.685	1.1 (1.1-1.2)	1.2 (1.1-1.3)	0.001
Creatinine in mg/dL[1]	0.93 (0.73-1.24)	0.96 (0.78-1.45)	0.93 (0.72-1.20)	0.040	0.95 (0.75-1.28)	0.93 (0.72-1.21)	0.389
Albumin in g/dL[1]	3.56 (3.05-3.98) (*n* = 133)	3.83 (3.24-4.0) (*n* = 23)	3.48 (3.05-3.98) (*n* = 110)	0.218	3.69 (3.21-3.96) (*n* = 43)	3.46 (2.98-3.99) (*n* = 90)	0.334
Cardiovascular dysfunction, *n* (%)	29 (4.2)	15 (11.2)	14 (2.6)	< 0.001	18 (5.7)	11 (3.0)	0.076
Neurological disturbance, *n* (%)	35 (5.1)	9 (6.7)	26 (4.7)	0.351	16 (5.1)	19 (5.1)	0.975
Respiratory dysfunction, *n* (%)	48 (7)	19 (14.2)	29 (5.3)	< 0.001	24 (7.6)	24 (6.5)	0.562

[1]Expressed as median (interquartile range).
[2]Abnormal WBC count is defined as WBC < 4000/μL or > 12000/μL.
ALK-P: Alkaline phosphatase; ALT: Alanine aminotransferase; AST: Aspartate aminotransferase; BT: Body temperature; ERCP: Endoscopic retrograde cholangiopancreatography; PT/INR: Prothrombin time/international normalized ratio; WBC: White blood cell count.

Comparisons between ERCP ≤ 48 h and ERCP > 48 h: The median time to ERCP was 26.0 (18.8-40.1) h in the ERCP ≤ 48 h group and 88.5 (67.2-114.6) h in the ERCP > 48 h group. Regarding indications for ERCP, CBDS was more common in the ERCP ≤ 48 h group (81.5% *vs* 68.3%, $P < 0.001$) whereas malignant biliary obstruction (6.1% *vs* 13.8%, $P < 0.001$) and stent dysfunction were less common (5.4% *vs* 11.9%, $P = 0.003$). In therapeutic ERCP, endoscopic sphincterotomy (85.7% *vs* 78.3%, $P = 0.013$) and bile duct stone retrieval (79.6% *vs* 68.3%, $P = 0.001$) were more frequent in the ERCP ≤ 48 h group whereas the removal of old biliary stents (5.4% *vs* 11.7%, $P = 0.004$) and the insertion of new biliary stents (22.3% *vs* 31.7%, $P = 0.006$) were less frequent.

Primary and secondary outcomes

The primary and secondary outcomes are summarized in Table 3.

Overall patients: Overall, the 30-d mortality rate was 1.02% (or 7/683). The ICU admission rate was 5.4%; the median LOHS was 7 (5-10) d; and the 30-d readmission rate was 12.7%.

(1) Comparisons between ERCP ≤ 24 h and ERCP > 24 h: The overall 30-d mortality rate was 0 in the ERCP ≤ 24 h group and 1.3% in the ERCP > 24 h group. However, the difference did not reach statistical significance ($P = 0.356$). Regarding secondary outcomes, the ERCP ≤ 24 h group had significantly higher ICU admission rates (11.2% *vs* 4.0%, $P = 0.001$) and shorter LOHS (median, 6 d *vs* 7 d, $P = 0.018$).

(2) Comparisons between ERCP ≤ 48 h and ERCP > 48 h: Overall, the 30-d mortality rate was significantly lower in the ERCP ≤ 48 h group than in the ERCP > 48 h group (0 *vs* 1.9%, $P = 0.017$). For secondary outcomes, the ERCP ≤ 48 h group had a significantly shorter LOHS (median, 6 d *vs* 8 d, $P <$

Table 2 Characteristics of endoscopic retrograde cholangiopancreatography

Patient characteristics	Total, *n* = 683	Time to ERCP divided by 24 h			Time to ERCP divided by 48 h		
		ERCP ≤ 24 h, *n* = 134	ERCP > 24 h, *n* = 549	*P* value	ERCP ≤ 48 h, *n* = 314	ERCP > 48 h, *n* = 369	*P* value
Time to ERCP in h[1]	53.8 (28.4-90.7)	17.7 (9.0-20.4)	67.6 (43.6-98.9)	-	26.0 (18.8-40.1)	88.5 (67.2-114.6)	
Indications of ERCP, *n* (%)							
Common bile duct stones	508 (74.4)	107 (79.9)	401 (73)	0.106	256 (81.5)	252 (68.3)	< 0.001
Malignant obstruction	70 (10.2)	7 (5.2)	63 (11.5)	0.032	19 (6.1)	51 (13.8)	< 0.001
Stent dysfunction	61 (8.9)	8 (6.0)	53 (9.7)	0.180	17 (5.4)	44 (11.9)	0.003
Benign stricture	31 (4.5)	8 (6.0)	23 (4.2)	0.375	15 (4.8)	16 (4.3)	0.783
Others	13 (1.9)	4 (3.0)	9 (1.6)	0.296	7 (2.2)	6 (1.6)	0.565
Treatment during ERCP, *n* (%)							
ES	558 (81.7)	112 (83.6)	446 (81.2)	0.529	269 (85.7)	289 (78.3)	0.013
EPBD	5 (0.7)	0	5 (0.9)	0.589	2 (0.6)	3 (0.8)	1
Stone retrieval	502 (73.5)	108 (80.6)	394 (71.8)	0.038	250 (79.6)	252 (68.3)	0.001
Clearance without stone	37 (5.4)	5 (3.7)	32 (5.8)	0.336	16 (5.1)	21 (5.7)	0.732
Removal of old stents	60 (8.8)	6 (4.5)	54 (9.8)	0.049	17 (5.4)	43 (11.7)	0.004
Stent insertion	187 (27.4)	35 (26.1)	152 (27.7)	0.715	70 (22.3)	117 (31.7)	0.006
Biliary stricture dilatation	7 (1.0)	1 (0.7)	6 (1.1)	1	1 (0.3)	6 (1.6)	0.132
Others	3 (0.4)	0	3 (0.5)	1	0	3 (0.8)	0.254
ERCP failure, *n* (%)	7 (1.0)	0	7 (1.3)	0.356	1 (0.3)	6 (1.6)	0.132

[1]Expressed as median (interquartile range). EPBD: Endoscopic papillary balloon dilation; ERCP: Endoscopic retrograde cholangiopancreatography; ES: Endoscopic sphincterotomy.

0.001).

Patients with Grade III AC: The 30-d mortality rate was 3.5% (or 6/170) for patients with grade III AC. The ICU admission rate was 15.3%; the median LOHS was 7 (7-14) d; and the 30-d readmission rate was 13.5% in this patient group.

(1) Comparisons between ERCP ≤ 24 h and ERCP > 24 h: The 30-d mortality rate for grade III AC patients was 0 in the ERCP ≤ 24 h group and 4.6% in the ERCP > 24 h group. However, the difference did not reach statistical significance ($P = 0.338$). Regarding secondary outcomes, the ERCP ≤ 24 h group had significantly higher ICU admission rates (9.0% *vs* 2.6%, $P = 0.002$).

(2) Comparisons between ERCP ≤ 48 h and ERCP > 48 h: Among grade III AC patients, the 30-d mortality rate was significantly lower in the ERCP ≤ 48 h group than in the ERCP > 48 h group (0 *vs* 6.1%, $P = 0.039$). Regarding secondary outcomes, the ERCP ≤ 48 h group had significantly higher ICU admission rates (22.2% *vs* 10.2%, $P = 0.031$).

Patients with Grade II AC: The 30-d mortality rate was 0 for patients with grade II AC. The ICU admission rate was 2.8%; the median LOHS was 7 (5-10) d; and the 30-d readmission rate was 13.4% in this patient group.

(1) Comparisons between ERCP ≤ 24 h and ERCP > 24 h: The only significant finding in grade II AC patients was that the LOHS was shorter (median, 6 d *vs* 7 d, $P = 0.047$) in the ERCP ≤ 24 h group.

(2) Comparisons between ERCP ≤ 48 h and ERCP > 48 h: Among grade II AC patients, the only significant finding was that the LOHS was shorter (median, 6 d *vs* 8 d, $P = 0.001$) in the ERCP ≤ 48 h group.

Patients with Grade I AC: The 30-d mortality rate was 0.3% (or 1/334) for patients with grade I AC. The ICU admission rate was 1.8%; the median LOHS was 6 (5-9) d; and the 30-d readmission rate was 12% in this patient group.

(1) Comparisons between ERCP ≤ 24 h and ERCP > 24 h: The only significant finding in grade I AC patients was that the LOHS was shorter (median, 6 d *vs* 7 d, $P = 0.005$) in the ERCP ≤ 24 h group.

Table 3 Primary and secondary outcomes

Outcomes	Total	Time to ERCP divided by 24 h			Time to ERCP divided by 48 h		
		ERCP ≤ 24 h	ERCP > 24 h	*P* value	ERCP ≤ 48 h	ERCP > 48 h	*P* value
Overall	*n* = 683	*n* = 134	*n* = 549		*n* = 314	*n* = 369	
30-d mortality, *n* (%)	7 (1.02)	0	7 (1.3)	0.356	0	7 (1.9)	0.017
ICU admission, *n* (%)	37 (5.4)	15 (11.2)	22 (4)	0.001	22 (7.0)	15 (4.07)	0.091
LOHS in d[1]	7 (5-10)	6 (4-10)	7 (5-10)	0.018	6 (4-9)	8 (6-11)	< 0.001
30-d readmission, *n* (%)	87 (12.7)	16 (11.9)	71 (12.9)	0.757	40 (12.7)	47 (12.7)	0.999
Grade III AC	*n* = 170	*n* = 39	*n* = 131		*n* = 72	*n* = 98	
30-d mortality, *n* (%)	6 (3.5)	0	6 (4.6)	0.338	0	6 (6.1)	0.039
ICU admission, *n* (%)	26 (15.3)	12 (9.0)	14 (2.6)	0.002	16 (22.2)	10 (10.2)	0.031
LOHS in d[1]	7 (7-14)	10 (6-16.5)	9 (7-12)	0.637	9 (6-15)	9 (7-12)	0.448
30-d readmission, *n* (%)	23 (13.5)	4 (3)	19 (14.5)	0.602	10 (13.9)	13 (13.3)	0.906
Grade II AC	*n* = 179	*n* = 39	*n* = 140		*n* = 88	*n* = 91	
30-d mortality, *n* (%)	0	0	0	-	0	0	-
ICU admission, *n* (%)	5 (2.8)	2 (5.1)	3 (2.1)	0.299	3 (3.4)	2 (2.2)	0.679
LOHS in d[1]	7 (5-10)	6 (4-9.5)	7 (5.8-10)	0.047	6 (4.8-9)	8 (6-11)	0.001
30-d readmission, *n* (%)	24 (13.4)	4 (10.3)	20 (14.3)	0.514	8 (9.1)	16 (17.6)	0.096
Grade I AC	*n* = 334	*n* = 56	*n* = 278		*n* = 154	*n* = 180	
30-d mortality, *n* (%)	1 (0.3)	0	1 (0.36)	1	0	1 (0.56)	1
ICU admission, *n* (%)	6 (1.8)	1 (1.8)	5 (1.8)	1	3 (1.9)	3 (1.7)	1
LOHS in d[1]	6 (5-9)	6 (4-8.3)	7 (5-9.8)	0.005	6 (4-7)	7 (6-11)	< 0.001
30-d readmission, *n* (%)	40 (12)	8 (14.3)	32 (11.5)	0.56	22 (14.3)	18	0.229

[1]Expressed as median (interquartile range). AC: Acute cholangitis; ERCP: Endoscopic retrograde cholangiopancreatography; ICU: Intensive care unit; LOHS: Length of hospital stay.

(2) Comparisons between ERCP ≤ 48 h and ERCP > 48 h: Among grade I AC patients, the only significant finding was that the LOHS was shorter (median, 6 d *vs* 7 d, $P < 0.001$) in the ERCP ≤ 48 h group.

Factors associated with 30-d mortality

The results of the univariate and multivariate analyses are listed in Table 4. The univariate analysis revealed that malignant biliary obstruction (OR: 6.817, 95%CI: 1.494-31.109, $P = 0.013$), hepatic dysfunction (OR: 8.896, 95%CI: 1.645-48.119, $P = 0.011$), respiratory dysfunction (OR: 10.517, 95%CI: 2.284-48.431, $P = 0.003$), neurological dysfunction (OR: 15.094, 95%CI: 3.241-70.298, $P = 0.001$), cardiovascular dysfunction (OR: 18.750, 95%CI: 3.990-88.112, $P < 0.001$), severity of AC (severe *vs* moderate + mild, OR: 18.732, 95%CI: 2.239-156.728, $P = 0.007$), ICU admission (OR: 7.326, 95%CI: 1.373-39.101, $P = 0.02$), and time to ERCP (every 1-d delay, OR: 1.950, 95%CI: 1.252-3.038, $P = 0.003$) were associated with 30-d mortality. The multivariate analysis revealed that time to ERCP (every 1-d delay, OR: 2.081, 95%CI: 1.154-3.753, $P = 0.015$) was the only independent factor associated with 30-d mortality. However, cardiovascular dysfunction (OR: 17.756, 95%CI: 0.994-317.241, $P = 0.050$) was of marginal significance.

DISCUSSION

Kiriyama *et al*[3] reported that early or urgent ERCP significantly reduced 30-d mortality only in patients with grade II AC compared with patients who did not receive early or urgent ERCP. This result may be due to the lack of well-defined timing for early or urgent ERCP. In a meta-analysis published in 2020, Du *et al*[7] reported that early ERCP reduced in-hospital mortality regardless of whether it was defined as < 24 h, < 48 h or < 72 h. In the present study, we found that ERCP ≤ 48 h but not ERCP ≤ 24 h

Table 4 Univariate and multivariate analyses of the factors associated with 30-d mortality

Variables		Univariate analysis		Multivariate analysis	
		OR (95%CI)	*P* value	OR (95%CI)	*P* value
Age	≥ 75 yr	1.772 (0.393-7.991)	0.456		
	< 75 yr	Reference			
Common bile duct stones	Yes	0.254 (0.056-1.146)	0.075		
	No	Reference			
Malignant biliary obstruction	Yes	6.817 (1.494-31.109)	0.013	7.718 (0.664-89.660)	0.102
	No	Reference			
Fever, BT ≥ 39 °C	Yes	1.045 (0.124-8.777)	0.968		
	No	Reference			
Abnormal WBC count	Yes	1.789 (0.345-9.289)	0.489		
	No	Reference			
Hyperbilirubinemia, ≥ 5 mg/dL	Yes	1.382 (0.307-6.228)	0.673		
	No	Reference			
Hepatic dysfunction, PT-INR > 1.5	Yes	8.896 (1.645-48.119)	0.011	2.257 (0.275-18.553)	0.449
	No	Reference			
Hematological dysfunction, PLT < 100 × 10^3/μL	Yes	4.885 (0.919-25.649)	0.063		
	No	Reference			
Renal dysfunction, Cr > 2.0 mg/dL	Yes	4.548 (0.862-23.998)	0.074		
	No	Reference			
Respiratory dysfunction, PaO_2/FiO_2 ratio > 300	Yes	10.517 (2.284-48.431)	0.003	1.644 (0.172-15.676)	0.666
	No	Reference			
Neurological dysfunction, conscious disturbance	Yes	15.094 (3.241-70.298)	0.001	2.773 (0.380-20.238)	0.315
	No	Reference			
Cardiovascular dysfunction[1]	Yes	18.750 (3.990-88.112)	< 0.001	17.756 (0.994-317.241)	0.050
	No	Reference			
Severity of AC	Grade III	18.732 (2.239-156.728)	0.007	3.603 (0.274-47.356)	0.329
	Grade II + I	Reference			
ICU admission	Yes	7.326 (1.373-39.101)	0.02	2.463 (0.204-29.703)	0.478
	No	Reference			
Time to ERCP	Every 1-d delay	1.950 (1.252-3.038)	0.003	2.081 (1.154-3.753)	0.015

[1]Defined as hypotension requiring dopamine ≥ 5 μg/kg per min, or any dose of norepinephrine. AC: Acute cholangitis; BT: Body temperature; ERCP: Endoscopic retrograde cholangiopancreatography; ICU: Intensive care unit; PT/INR: Prothrombin time/international normalized ratio; WBC: White blood cell count.

significantly reduced 30-d mortality. Our results were consistent with the 2021 American Society for Gastrointestinal Endoscopy guidelines recommending ERCP ≤ 48 h in AC patients[12]. In that study, however, the data were insufficient to stratify by disease severity. In a subgroup analysis, we found that the same survival benefit was observed only in patients with grade III AC but not in patients with grade II or I AC. These results were because patients with grade III AC had significantly higher 30-d mortality than those with grade II or I AC (3.5% *vs* 0 *vs* 0.3%, $P = 0.001$). Hakuta *et al*[10] reported that time to ERCP was not associated with clinical outcomes (including in-hospital mortality) in patients with non-grade III AC. Therefore, we recommend emergent ERCP (≤ 48 h) for patients with grade III AC in terms of survival benefit.

However, 30-d mortality in AC has been reported to range from 1% to 16% between studies, which may be one of the reasons leading to inconsistent conclusions about the optimal timing of ERCP[11,13-

15]. Differences in mortality may be due to different patient populations in different studies, *e.g.*, patients with AC due to CBDS and MBO may have different clinical courses and prognoses. Kiriyama *et al*[14] reported that patients with AC associated with MBO had a higher 30-d mortality rate than those with AC associated with CBDS. In our univariate analysis, MBO was a factor associated with 30-d mortality. Therefore, one of the reasons for the low 30-d mortality in our study was the low proportion of patients with MBO (10.2%). In contrast, Tan *et al*[11] included 43% of MBO patients in their study and reported a 30-d mortality rate of 16%. However, Park *et al*[15] included only patients with AC associated with distal MBO and reported an overall 30-d mortality rate of 4.8%. Therefore, there may be some other factors associated with 30-d mortality between studies.

Of the five organ failure criteria used to diagnose grade III AC, cardiovascular dysfunction was the only independent factor associated with 30-d mortality in the current study. Therefore, among grade III AC patients, those with cardiovascular dysfunction may need to be treated differently[16,17]. Karvellas *et al*[17] reported an overall mortality rate of 37% in 260 patients with AC-related septic shock. They found that delayed biliary decompression > 12 h from the onset of shock was one of three independent factors associated with mortality. The 2019 European Society of Gastrointestinal Endoscopy guidelines recommend biliary drainage (preferably endoscopic) within 12 h of shock onset for AC patients with CBDS-related septic shock[16]. Therefore, cardiovascular dysfunction should be weighed when developing new guidelines in the future.

Some studies found no survival benefit but did find early ERCP to reduce the LOHS[18-21]. Hou *et al*[20] reported that in a multivariate analysis, the LOHS increased by 1.44 d for every 1-d delay in ERCP ($P < 0.001$). Similar results were seen in the study by Zhu *et al*[18]: LOHS increased by 1.49 d for every 1-d delay in biliary drainage ($P < 0.0001$). However, these findings were not stratified by disease severity. Although we did not perform a multivariate analysis of the LOHS, our results suggested that the LOHS could be significantly reduced regardless of ERCP ≤ 24 h or ≤ 48 h. In subgroup analyses stratified by disease severity, this benefit was only observed in patients with grade I or II AC. The benefit of early ERCP in shortening the LOHS might be offset by higher ICU admission rates in grade III AC patients. Similar findings were found by Jang *et al*[19], who recommended urgent ERCP (≤ 24 h) for patients with grade I or II AC because it can shorten the LOHS.

This study has several limitations. First, this retrospective, single-center study might have inherent selection bias. Patients with cardiovascular dysfunction and respiratory dysfunction tended to receive ERCP ≤ 24 h. Therefore, caution is required when interpreting the results of this subgroup analysis. Second, we identified patients from the endoscopy database. AC patients who died before receiving ERCP might not have been included in this study, resulting in an underestimation of 30-d mortality. Third, data on albumin, one of the criteria for class II AC, were available in only 19.5% of patients. Therefore, some patients with grade II AC may be misclassified as grade I AC and vice versa.

CONCLUSION

ERCP ≤ 48 h but not ≤ 24 h has a survival benefit in AC patients; this benefit is only observed in patients with grade III AC. Early ERCP is also recommended for patients with grade I or II AC because it shortens the LOHS.

ARTICLE HIGHLIGHTS

Research background

The optimal timing of endoscopic retrograde cholangiopancreatography (ERCP) for acute cholangitis has been inconsistently reported and there are few studies on the timing of ERCP in acute cholangitis of varying severity.

Research motivation

On the one hand, unnecessary emergent ERCP increases medical costs and the burden on physicians and technicians; on the other hand, delayed ERCP may increase morbidity and mortality in patients with acute cholangitis. The findings of this study may guide the avoidance of unnecessary urgent and delayed ERCP for acute cholangitis.

Research objectives

This study aims to answer the optimal timing of ERCP for acute cholangitis of different severity according to 30-d mortality after ERCP. Answering this question can serve as important evidence for future guideline development.

Research methods

The retrospective cohort study included 683 patients who met the diagnostic criteria for acute cholangitis defined by the 2018 Tokyo Guidelines. Among them, there were 170 (24.9%) grade III acute cholangitis patients, 179 grade II acute cholangitis patients (26.4%) and 334 grade I acute cholangitis patients (48.9%). Results are first compared between patients receiving ERCP ≤ 24 h and > 24 h, and then between patients receiving ERCP ≤ 48 h and > 48 h. Subgroup analyses are performed on patients with grade III, II or I acute cholangitis.

Research results

When 24 h was considered a critical value for ERCP timing, we found that patients with malignant biliary obstruction received ERCP ≤ 24 h less frequently when compared with ERCP > 24 h (5.2% *vs* 11.5%). Patients with organ dysfunction such as cardiovascular dysfunction (11.2% *vs* 2.6%) and respiratory dysfunction (14.2% *vs* 5.3%) or those admitted to the ICU (11.2% *vs* 4%) tended to receive ERCP ≤ 24 h. Patients with ERCP ≤ 24 h had significantly shorter hospital stays (median, 6 d *vs* 7 d). Stratified by the severity of acute cholangitis, higher ICU admission was only observed in grade III acute cholangitis and a shorter length of hospital stay was only observed in grade I and II acute cholangitis. Regarding 30-d mortality, the results of ERCP ≤ 24 h and > 24 h were not significantly different, either in the overall population or in patients with grade I, II or III acute cholangitis. When 48 h was considered a critical value for ERCP timing, patients with choledocholithiasis received ERCP ≤ 48 h more frequently (81.5% *vs* 68.3%). Patients who received ERCP ≤ 48 h had significantly lower 30-d mortality (0 *vs* 1.9%) and shorter hospital stays (6 d *vs* 8 d). Stratified by the severity of acute cholangitis, lower 30-d mortality (0 *vs* 6.1%) and higher ICU admission rates (22.2% *vs* 10.2%) were only observed in grade III acute cholangitis and a shorter length of hospital stay was only observed in grade I and II acute cholangitis. In the multivariate analysis, cardiovascular dysfunction and time to ERCP were two independent factors associated with 30-d mortality.

Research conclusions

ERCP ≤ 48 h but not ≤ 24 h has a survival benefit in acute cholangitis patients; this benefit is only observed in patients with grade III acute cholangitis. Early ERCP is also recommended for patients with grade I and II acute cholangitis because it shortens the length of hospital stay.

Research perspectives

Of the five organ failure criteria used to diagnose grade III AC, cardiovascular dysfunction was the only independent factor associated with 30-d mortality in the current study. Therefore, cardiovascular dysfunction should be weighed more heavily in the development of new guidelines in the future.

FOOTNOTES

Author contributions: Huang YC contributed to the conceptualization of the study and original manuscript; Wu CH, Lee MH and Wang SF contributed to data planning, interpretation and formal analysis; Lin CH and Sung KF contributed to data collection; Tsou YK is committed to the conceptualization of the study, manuscript writing, review and editing; Liu NJ contributed to revising the final version of the manuscript for submission.

Institutional review board statement: This study was reviewed and approved by the Ethics Committee of the Chang Gung Memorial Hospital (IRB No. 202200881B0).

Informed consent statement: Since this was a retrospective study using clinical routine treatment or diagnostic medical records, the Chang Gung Medical Foundation Institutional Review Board approved the waiver of the participant's consent.

Conflict-of-interest statement: All the authors report no relevant conflicts of interest for this article.

Data sharing statement: Technical appendix, statistical code and dataset available from the corresponding author at flying@adm.cgmh.org.tw.

STROBE statement: The authors have read the STROBE Statement-checklist of items, and the manuscript was prepared and revised according to the STROBE Statement-checklist of items.

Open-Access: This article is an open-access article that was selected by an in-house editor and fully peer-reviewed by external reviewers. It is distributed in accordance with the Creative Commons Attribution NonCommercial (CC BY-NC 4.0) license, which permits others to distribute, remix, adapt, build upon this work non-commercially, and license their derivative works on different terms, provided the original work is properly cited and the use is non-commercial. See: https://creativecommons.org/Licenses/by-nc/4.0/

Country/Territory of origin: Taiwan

ORCID number: Chi-Huan Wu 0000-0002-3913-8010; Mu Hsien Lee 0000-0003-3664-5313; Sheng Fu Wang 0000-0002-7856-2957; Yung-Kuan Tsou 0000-0002-7254-7369; Cheng-Hui Lin 0000-0001-8102-0625; Kai-Feng Sung 0000-0001-6118-0234; Nai-Jen Liu 0000-0002-7992-0234.

S-Editor: Gong ZM
L-Editor: Filipodia
P-Editor: Gong ZM

REFERENCES

1 **Mosler P**. Diagnosis and management of acute cholangitis. *Curr Gastroenterol Rep* 2011; **13**: 166-172 [PMID: 21207254 DOI: 10.1007/s11894-010-0171-7]
2 **Lee F**, Ohanian E, Rheem J, Laine L, Che K, Kim JJ. Delayed endoscopic retrograde cholangiopancreatography is associated with persistent organ failure in hospitalised patients with acute cholangitis. *Aliment Pharmacol Ther* 2015; **42**: 212-220 [PMID: 25997554 DOI: 10.1111/apt.13253]
3 **Kiriyama S**, Kozaka K, Takada T, Strasberg SM, Pitt HA, Gabata T, Hata J, Liau KH, Miura F, Horiguchi A, Liu KH, Su CH, Wada K, Jagannath P, Itoi T, Gouma DJ, Mori Y, Mukai S, Giménez ME, Huang WS, Kim MH, Okamoto K, Belli G, Dervenis C, Chan ACW, Lau WY, Endo I, Gomi H, Yoshida M, Mayumi T, Baron TH, de Santibañes E, Teoh AYB, Hwang TL, Ker CG, Chen MF, Han HS, Yoon YS, Choi IS, Yoon DS, Higuchi R, Kitano S, Inomata M, Deziel DJ, Jonas E, Hirata K, Sumiyama Y, Inui K, Yamamoto M. Tokyo Guidelines 2018: diagnostic criteria and severity grading of acute cholangitis (with videos). *J Hepatobiliary Pancreat Sci* 2018; **25**: 17-30 [PMID: 29032610 DOI: 10.1002/jhbp.512]
4 **Xu MM**, Carr-Locke DL. Early ERCP for severe cholangitis? *Gastrointest Endosc* 2018; **87**: 193-195 [PMID: 29241849 DOI: 10.1016/j.gie.2017.06.008]
5 **Khashab MA**, Tariq A, Tariq U, Kim K, Ponor L, Lennon AM, Canto MI, Gurakar A, Yu Q, Dunbar K, Hutfless S, Kalloo AN, Singh VK. Delayed and unsuccessful endoscopic retrograde cholangiopancreatography are associated with worse outcomes in patients with acute cholangitis. *Clin Gastroenterol Hepatol* 2012; **10**: 1157-1161 [PMID: 22507875 DOI: 10.1016/j.cgh.2012.03.029]
6 **Iqbal U**, Khara HS, Hu Y, Khan MA, Ovalle A, Siddique O, Sun H, Shellenberger MJ. Emergent versus urgent ERCP in acute cholangitis: a systematic review and meta-analysis. *Gastrointest Endosc* 2020; **91**: 753-760.e4 [PMID: 31628955 DOI: 10.1016/j.gie.2019.09.040]
7 **Du L**, Cen M, Zheng X, Luo L, Siddiqui A, Kim JJ. Timing of Performing Endoscopic Retrograde Cholangiopancreatography and Inpatient Mortality in Acute Cholangitis: A Systematic Review and Meta-Analysis. *Clin Transl Gastroenterol* 2020; **11**: e00158 [PMID: 32352721 DOI: 10.14309/ctg.0000000000000158]
8 **Navaneethan U**, Gutierrez NG, Jegadeesan R, Venkatesh PG, Sanaka MR, Vargo JJ, Parsi MA. Factors predicting adverse short-term outcomes in patients with acute cholangitis undergoing ERCP: A single center experience. *World J Gastrointest Endosc* 2014; **6**: 74-81 [PMID: 24634711 DOI: 10.4253/wjge.v6.i3.74]
9 **Nishino T**, Hamano T, Mitsunaga Y, Shirato I, Shirato M, Tagata T, Shimada M, Yoshida S, Mitsunaga A. Clinical evaluation of the Tokyo Guidelines 2013 for severity assessment of acute cholangitis. *J Hepatobiliary Pancreat Sci* 2014; **21**: 841-849 [PMID: 25410528 DOI: 10.1002/jhbp.189]
10 **Hakuta R**, Hamada T, Nakai Y, Kogure H, Uchino R, Takahara N, Mizuno S, Suzuki T, Sato T, Takeda T, Ishigaki K, Saito K, Saito T, Tada M, Isayama H, Koike K. No Association of Timing of Endoscopic Biliary Drainage with Clinical Outcomes in Patients with Non-severe Acute Cholangitis. *Dig Dis Sci* 2018; **63**: 1937-1945 [PMID: 29663264 DOI: 10.1007/s10620-018-5058-8]
11 **Tan M**, Schaffalitzky de Muckadell OB, Laursen SB. Association between early ERCP and mortality in patients with acute cholangitis. *Gastrointest Endosc* 2018; **87**: 185-192 [PMID: 28433613 DOI: 10.1016/j.gie.2017.04.009]
12 **Buxbaum JL**, Buitrago C, Lee A, Elmunzer BJ, Riaz A, Ceppa EP, Al-Haddad M, Amateau SK, Calderwood AH, Fishman DS, Fujii-Lau LL, Jamil LH, Jue TL, Kwon RS, Law JK, Lee JK, Naveed M, Pawa S, Sawhney MS, Schilperoort H, Storm AC, Thosani NC, Qumseya BJ, Wani S. ASGE guideline on the management of cholangitis. *Gastrointest Endosc* 2021; **94**: 207-221.e14 [PMID: 34023065 DOI: 10.1016/j.gie.2020.12.032]
13 **On W**, Watters C, Dwyer L, Hood S, Saleem R, Sturgess R, Stern N. P55 Timing of ERCP and outcomes in patients with acute gallstone cholangitis graded by severity. *Gut* 2021; **70** (Suppl 1): A69 [DOI: 10.1136/gutjnl-2020-bsgcampus.130]
14 **Kiriyama S**, Takada T, Hwang TL, Akazawa K, Miura F, Gomi H, Mori R, Endo I, Itoi T, Yokoe M, Chen MF, Jan YY, Ker CG, Wang HP, Wada K, Yamaue H, Miyazaki M, Yamamoto M. Clinical application and verification of the TG13 diagnostic and severity grading criteria for acute cholangitis: an international multicenter observational study. *J Hepatobiliary Pancreat Sci* 2017; **24**: 329-337 [PMID: 28419764 DOI: 10.1002/jhbp.458]
15 **Park N**, Lee SH, You MS, Kim JS, Huh G, Chun JW, Cho IR, Paik WH, Ryu JK, Kim YT. Optimal timing of endoscopic retrograde cholangiopancreatography for acute cholangitis associated with distal malignant biliary obstruction. *BMC Gastroenterol* 2021; **21**: 175 [PMID: 33865307 DOI: 10.1186/s12876-021-01755-z]
16 **Manes G**, Paspatis G, Aabakken L, Anderloni A, Arvanitakis M, Ah-Soune P, Barthet M, Domagk D, Dumonceau JM, Gigot JF, Hritz I, Karamanolis G, Laghi A, Mariani A, Paraskeva K, Pohl J, Ponchon T, Swahn F, Ter Steege RWF, Tringali A, Vezakis A, Williams EJ, van Hooft JE. Endoscopic management of common bile duct stones: European Society of Gastrointestinal Endoscopy (ESGE) guideline. *Endoscopy* 2019; **51**: 472-491 [PMID: 30943551 DOI: 10.1055/a-0862-0346]
17 **Karvellas CJ**, Abraldes JG, Zepeda-Gomez S, Moffat DC, Mirzanejad Y, Vazquez-Grande G, Esfahani EK, Kumar A;

Cooperative Antimicrobial Therapy of Septic Shock (CATSS) Database Research Group. The impact of delayed biliary decompression and anti-microbial therapy in 260 patients with cholangitis-associated septic shock. *Aliment Pharmacol Ther* 2016; **44**: 755-766 [PMID: 27506331 DOI: 10.1111/apt.13764]

18 **Zhu Y**, Tu J, Zhao Y, Jing J, Dong Z, Pan W. Association of Timing of Biliary Drainage with Clinical Outcomes in Severe Acute Cholangitis: A Retrospective Cohort Study. *Int J Gen Med* 2021; **14**: 2953-2963 [PMID: 34234525 DOI: 10.2147/IJGM.S315306]

19 **Jang SE**, Park SW, Lee BS, Shin CM, Lee SH, Kim JW, Jeong SH, Kim N, Lee DH, Park JK, Hwang JH. Management for CBD stone-related mild to moderate acute cholangitis: urgent versus elective ERCP. *Dig Dis Sci* 2013; **58**: 2082-2087 [PMID: 23456495 DOI: 10.1007/s10620-013-2595-z]

20 **Hou LA**, Laine L, Motamedi N, Sahakian A, Lane C, Buxbaum J. Optimal Timing of Endoscopic Retrograde Cholangiopancreatography in Acute Cholangitis. *J Clin Gastroenterol* 2017; **51**: 534-538 [PMID: 27875357 DOI: 10.1097/MCG.0000000000000763]

21 **Aboelsoud M**, Siddique O, Morales A, Seol Y, Al-Qadi M. Early biliary drainage is associated with favourable outcomes in critically-ill patients with acute cholangitis. *Prz Gastroenterol* 2018; **13**: 16-21 [PMID: 29657606 DOI: 10.5114/pg.2018.74557]

World Journal of Gastroenterology

Submit a Manuscript: https://www.f6publishing.com

World J Gastroenterol 2022 October 14; 28(38): 5614-5625

DOI: 10.3748/wjg.v28.i38.5614

ISSN 1007-9327 (print) ISSN 2219-2840 (online)

ORIGINAL ARTICLE

Retrospective Study

Clearance of the liver remnant predicts short-term outcome in patients undergoing resection of hepatocellular carcinoma

Atsushi Miki, Yasunaru Sakuma, Hideyuki Ohzawa, Akira Saito, Yoshiyuki Meguro, Jun Watanabe, Kazue Morishima, Kazuhiro Endo, Hideki Sasanuma, Atsushi Shimizu, Alan Kawarai Lefor, Yoshikazu Yasuda, Naohiro Sata

Specialty type: Gastroenterology and hepatology

Provenance and peer review: Unsolicited article; Externally peer reviewed.

Peer-review model: Single blind

Peer-review report's scientific quality classification

Grade A (Excellent): A
Grade B (Very good): 0
Grade C (Good): C
Grade D (Fair): 0
Grade E (Poor): 0

P-Reviewer: Ali SNH, Jordan; Finotti M, Italy

Received: November 16, 2021
Peer-review started: November 16, 2021
First decision: May 10, 2022
Revised: May 21, 2022
Accepted: August 16, 2022
Article in press: August 16, 2022
Published online: October 14, 2022

Atsushi Miki, Yasunaru Sakuma, Hideyuki Ohzawa, Akira Saito, Yoshiyuki Meguro, Jun Watanabe, Kazue Morishima, Kazuhiro Endo, Hideki Sasanuma, Atsushi Shimizu, Alan Kawarai Lefor, Yoshikazu Yasuda, Naohiro Sata, Department of Surgery, Jichi Medical University, Shimotsuke 329-0498, Tochigi, Japan

Corresponding author: Atsushi Miki, MD, PhD, Assistant Professor, Department of Surgery, Jichi Medical University, 3311-1 Yakushiji, Shimotsuke 329-0498, Tochigi, Japan.
amiki@jichi.ac.jp

Abstract

BACKGROUND

Estimation of the functional reserve of the remnant liver is important to reduce morbidity and mortality.

AIM

To estimate the functional reserve of the remnant liver in patients with hepatocellular carcinoma (HCC).

METHODS

We reviewed the medical records of 199 patients who underwent resection of HCC. Hepatic clearance of the remnant liver was calculated using fusion images of ^{99m}Tc-labelled galactosyl-human serum albumin liver scintigraphy and computed tomography. Posthepatectomy liver failure (PHLF) was classified according to the International Study Group of Liver Surgery. Complications was classified according to Clavien–Dindo classification. We analyzed by the risk factors for PHLF, morbidity and mortality with multivariate analysis.

RESULTS

Twenty-seven (30%) patients had major complications and 23 (12%) developed PHLF. The incidence of major complications increased with increasing albumin–bilirubin (ALBI) grade. The area under the curve values for hepatic clearance of the remnant liver, liver to heart-plus-liver radioactivity at 15 min (LHL15), and ALBI score predicting PHLF were 0.868, 0.629, and 0.655, respectively. The area under the curve for hepatic clearance of the remnant liver, LHL15, and ALBI score predicting major complications were 0.758, 0.594, and

0.647, respectively. The risk factors for PHLF and major complications were hepatic clearance of the remnant liver and intraoperative bleeding.

CONCLUSION
The measurement of hepatic clearance may predict PHLF and major complications for patients undergoing resection of HCC.

Key Words: Liver function; Hepatectomy; Cirrhosis; Fusion image; Complication; Mortality

©The Author(s) 2022. Published by Baishideng Publishing Group Inc. All rights reserved.

Core tip: Little is known about the association of remnant hepatic clearance with morbidity and mortality. The aim of present study was to evaluate the effectiveness of measuring hepatic clearance of the remnant liver and to determine its association with morbidity and mortality in patients undergoing hepatectomy for hepatocellular carcinoma. Risk factors significantly associated with morbidity and mortality were remnant liver clearance and intraoperative blood loss. Hepatic clearance was associated with posthepatectomy liver failure and the development of major complications. The estimation of hepatic clearance of the remnant liver may provide guidance for determining the extent of resection in a patient-specific manner.

Citation: Miki A, Sakuma Y, Ohzawa H, Saito A, Meguro Y, Watanabe J, Morishima K, Endo K, Sasanuma H, Shimizu A, Lefor AK, Yasuda Y, Sata N. Clearance of the liver remnant predicts short-term outcome in patients undergoing resection of hepatocellular carcinoma. *World J Gastroenterol* 2022; 28(38): 5614-5625
URL: https://www.wjgnet.com/1007-9327/full/v28/i38/5614.htm
DOI: https://dx.doi.org/10.3748/wjg.v28.i38.5614

INTRODUCTION

Advances in surgical technique and postoperative care have improved the outcomes of patients undergoing hepatectomy. However, posthepatectomy liver failure (PHLF) can lead to increased rates of morbidity and mortality in patients with hepatocellular carcinoma (HCC) especially in patients with chronic liver damage[1]. Major hepatectomy must be performed to preserve the maximal remnant liver function. However, adequate hepatectomy must be performed to ensure adequate surgical margins around the tumor[2]. Therefore, preoperative assessment of remnant liver function reserve is important to determine the appropriate surgical procedure.

An algorithm including the presence of ascites, serum bilirubin, serum albumin concentration, prothrombin time and encephalopathy is commonly used to determine the indications for resection of HCC. The indocyanine green (ICG) test is the most commonly used test and is considered relatively reliable for assessment of liver functional reserve[3]. However, the Child–Pugh score and ICG test do not accurately predict the development of PHLF[4]. A simple method using conventional data has been reported. The albumin–bilirubin (ALBI) score is an effective predictor of PHLF in patients with HCC compared to that of ICG test[5].

Computed tomography (CT) volumetry can accurately determine the regional liver volume, and has been used to estimate remnant liver function[6]. However, CT volumetry can never reflect the function of the remnant liver. The liver function of each lobe varies with progression of chronic liver disease or steatosis, which indicate that liver function is not distributed homogeneously[7]. Liver function is unevenly modified, resulting from impaired blood circulation[8], biliary stenosis, or induction by the tumor[9]. Changes in portal hemodynamics and a regional reduction in liver function must be considered to determine the optimal surgical procedure[7,10]. A novel method is needed to preoperatively plan for hepatic resection.

Taniguchi *et al*[11] described that ^{99m}Tc-labelled galactosyl-human serum albumin (GSA) hepatic clearance strongly correlates with the degree of liver fibrosis and conventional liver function tests. GSA scintigraphy is widely used to evaluate liver function[10,12-16]. Asialoglycoprotein receptors exist predominantly in the liver on the surface of hepatocytes and are responsible for the metabolism of serum glycoproteins[17]. The receptor density in the liver is closely related to serum asialoglycoprotein level and hepatocyte function[18]. However, little is known about the clinical utility of hepatic clearance for the prediction of PHLF, morbidity and mortality. The aim of present study was to evaluate the effectiveness of measuring hepatic clearance of the remnant liver and to verify risk factors based on the standardized PHLF criteria and complications in patients undergoing hepatectomy.

MATERIALS AND METHODS

Patients

We included patients who underwent hepatectomy between July 2011 and March 2021 at Jichi Medical University (Shimotsuke, Tochigi, Japan). The protocol for this research project was approved by a suitably constituted Ethics Committee of the institution and it conformed to the provision of the Declaration of Helsinki (Committees of Jichi Medical University, Approval No. A21-029). Blood samples obtained preoperatively were analyzed for conventional liver tests.

The procedures for hepatectomy were categorized according to the Brisbane Nomenclature from the International Hepato-Pancreato-Biliary Association[19]. The anatomical resection was defined as resection of the tumor together with the related portal vein branches and the corresponding hepatic territory. The procedure was classified as a hemihepatectomy, an extended hemihepatectomy (hepatectomy plus removal of additional contiguous segments), a sectionectomy (resection of two Couinaud subsegments), or segmentectomy (resection of one Couinaud subsegment). All other nonanatomical procedures were classified as limited resections.

Contrast-enhanced CT

A three-phase enhanced helical CT scan of the liver was used to confirm tumor location and margins before surgery. A 16-row multi-detector CT scan was performed at 3 mm intervals with 100 mL iohexol (Omnipaque 300; Daiichi Sankyo, Tokyo, Japan) (3 mL/s) injected intravenously.

GSA single photon emission CT image

Patients underwent preoperative GSA scintigraphy using a dual-head rotating gamma camera system and a dedicated data processing unit (Prism Axis; Picker Prism International, Cleveland, OH, USA). A single bolus of 3 mg GSA (185 MBq; Nihon Medi-Physics, Tokyo, Japan) was injected intravenously. After confirmation that the detector covered the area in the liver and heart, acquisition of planar images was begun with an acquisition time of 15 s each for 16 min immediately after injection. After acquisition of planar images, dynamic single photon emission CT (SPECT) acquisition was started with an acquisition time of 20 s every 5 min. To generate a set of images equivalent to static SPECT images, projection data from dynamic SPECT were merged. Total liver function was calculated as the total liver GSA clearance, expressed as mL/min by the Patlak plot method.

Region of interest (ROI) was also generated over the entire liver on the tomographic images using isocount methods (25% cutoff of minimal count) to estimate the liver functional volume (mL). Functional liver volume does not include function parameters.

Estimation of function of the remnant liver

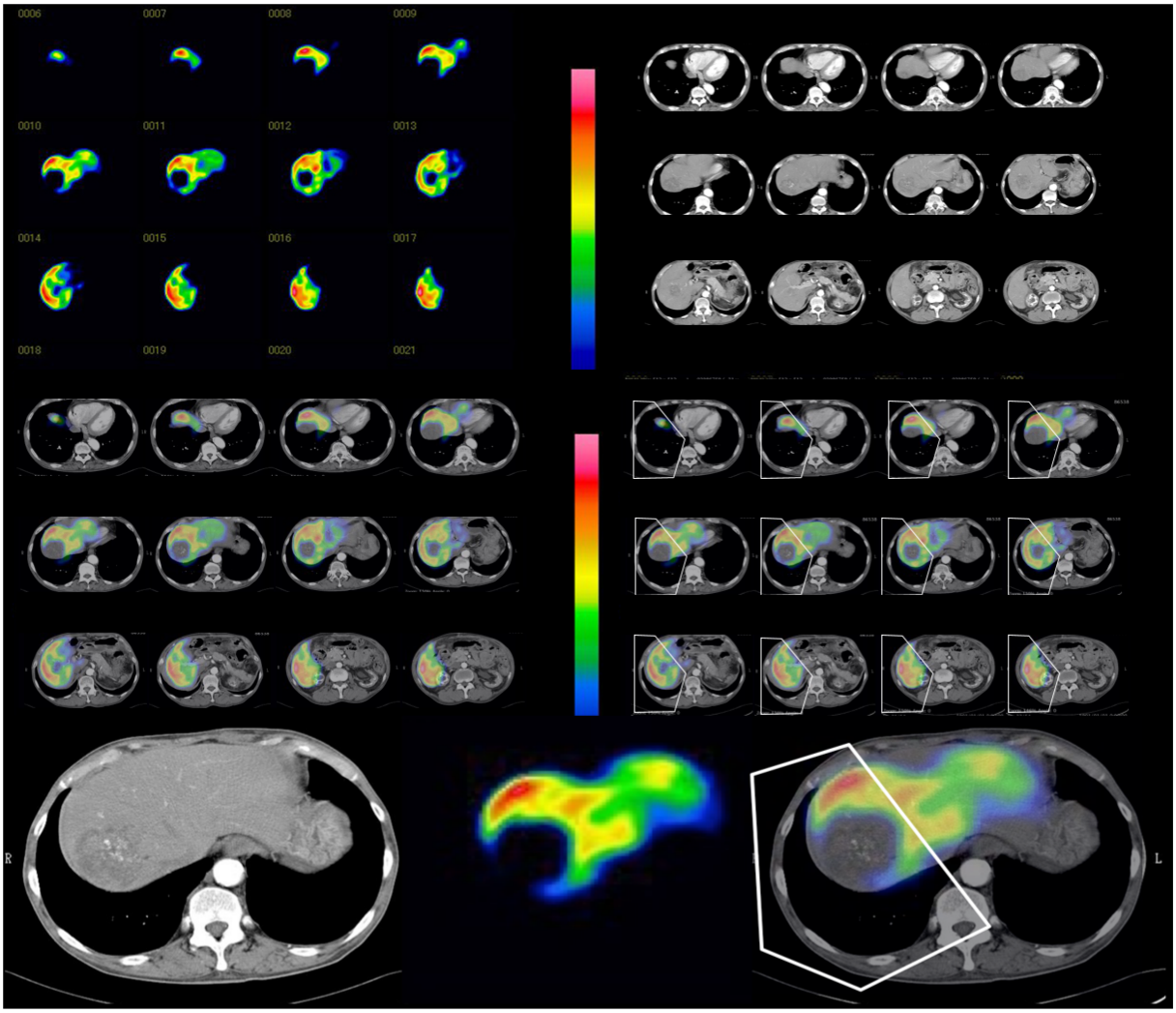
Hepatic clearance and functional volume of the remnant liver were estimated from the fusion with CT scan images (Figure 1). Images from the CT scan were aligned with the slice of the liver SPECT image with reference to the hepatic vein on every 3-mm liver cross-slice as a landmark on contrast-enhanced helical CT (Figure 1). After the transection line was set on the SPECT images based on the surgical procedure, the remnant liver with the resection line was determined manually. Remnant liver function was calculated from the proportional allocation of voxel count in static SPECT by the Patlak plot method and expressed by GSA clearance (mL/min). Regional functional liver volume (mL) was also calculated from the SPECT data by the outline extraction method[7].

Definition of major complication and PHLF

Postoperative complications were defined according to the Clavien–Dindo classification[20]. A major complication was defined as grade IIIa or higher. Postoperative mortality was defined as death within 30 d after surgery. PHLF was defined following the definition of the International Study Group of Liver Surgery[21]. Patients with increased prothrombin time–international normalized ratio (PT-INR) and hyperbilirubinemia (according to the normal cut-off levels defined by the local laboratory) on or after postoperative day 5 were considered to have PHLF. PHLF Grade A resulted in abnormal laboratory parameters and required no change in clinical management. Grade B was a deviation from the regular, postoperative clinical pathway, but patients could be managed without invasive treatment. Grade C resulted in deviation from the regular clinical management and required invasive treatment.

Statistical analysis

Continuous variables were expressed as mean ± standard deviation. All categorical data were analyzed by Pearson's χ^2 test. Normally distributed values were analyzed by Student's t test. Non-normally distributed values were analyzed using the Mann–Whitney U test. We analyzed the power for the prediction of PHLF, morbidity and mortality with the parameters of GSA scintigraphy with the area under the receiver-operating characteristic (ROC) curves, and the area under the ROC curve was calculated. In multivariate analysis, risk factors for PHLF were determined by logistic regression multivariate analysis with JMP statistical software (version 13; SAS, Inc. Cary, NC, USA). The level of statistical significance was set at $P < 0.05$.



DOI: 10.3748/wjg.v28.i38.5614 **Copyright** ©The Author(s) 2022.

Figure 1 Schematic model for analysis of regional hepatic clearance with computed tomography fusion images. The images of ^{99m}Tc-galactosyl serum albumin scintigraphy single photon emission computed tomography and computed tomography scans were merged using software. The cutting line was set based on tumor location and size on each fusion image. The liver function was calculated automatically as ^{99m}Tc-galactosyl serum albumin scintigraphy parameters. CT: Computed tomography; SPECT: Single photon emission computed tomography.

RESULTS

Clinicopathological characteristics

A total of consecutive 199 patients with HCC were included, including 156 men and 43 women, with a median age of 70 (range, 24–87 years) (Table 1). Among the 199 patients, 94 (47%) had hepatitis C virus infection and 22 (11%) had hepatitis B virus infection. Most patients were Child–Pugh class A (197/199, 99%) and the remaining patients were class B (2/199, 1%). According to ALBI grade, 68% (135/199) of patients were stratified into Grade 1, 32% (64/199) Grade 2, and 1% (2/199) Grade 3. There were 6% of ALBI Grade 1 patients who developed major complications and 18% ALBI Grade 2 patients had major complications (P = 0.04).

Postoperative morbidity, PHLF and mortality

Among the 199 patients, 41 (21%) developed postoperative complications (Table 2). The most common complication was PHLF (12%, 23/199), followed by wound infection (5.0%, 10/199). Thirty-three (17%) patients developed minor complications, including Grade I complications in 25 (13%) patients and Grade II complications in eight (4.0%) patients. Major complications occurred in 27 (14%) patients, including Grade IIIa (11%, 21/199), Grade IIIb (1.5%, 3/199), Grade IVa (0.5%, 1/199) and Grade V (1%, 2/199). Eleven patients (5%) had PHLF Grade A, eight (4%) had PHLF Grade B, and four (2%) had PHLF Grade C. Two patients died of PHLF within 30 d after surgery, for a postoperative mortality rate of 1% (Table 2).

Table 1 Patient characteristics

Variables	All patients (*n* = 199)	No PHLF < Grade B (*n* = 187)	PHLF ≥ Grade B (*n* = 12)	*P* value
General				
Age (yr)	69.1 ± 9.0	69.2 ± 9.12	66.9 ± 7.05	0.53
Gender (male : female)	154 : 45	144 : 43	10 : 2	0.61
Child–Pugh class (A : B : C)	196 : 3 :0	184 : 3 : 0	12 : 0 : 0	0.31
Preoperative laboratory tests				
Total bilirubin (mg/dL)	0.85 ± 0.38	0.82 ± 0.38	1.06 ± 0.32	0.01
PT-INR	1.12 ± 0.20	1.12 ± 0.21	1.13 ± 0.08	0.70
Albumin (mg/dL)	4.1 ± 0.5	4.1 ± 0.5	3.9 ± 0.4	0.16
AST (IU/L)	43 ± 41	41 ± 40	56 ± 47	0.11
ALT (IU/L)	40 ± 34	39 ± 33	47 ± 40	0.31
Choline esterase(U/L)	262 ± 77	267 ± 76	226 ± 73	0.02
PNI score	48.6 ± 6.0	48.9 ± 6.0	46.4 ± 5.6	0.08
ALBI score	-2.76 ± 0.4	-2.78 ± 0.4	-2.57 ± 0.35	0.14
NLR	2.48 ± 2.03	2.50 ± 2.12	2.31 ± 1.07	0.82
PLR	0.12 ± 0.08	0.13 ± 0.09	0.10 ± 0.05	0.29
Procedure-related factors				
Limited resection	80 (39.8%)	77 (38.7%)	3 (1.5%)	0.43
Segmentectomy	57 (28.4%)	51 (25.6%)	6 (3.0%)	
Secteionectomy	36 (17.9%)	33 (16.6%)	1 (0.5%)	
Hemihepatectomy	24 (11.9%)	22 (11.1%)	2 (1.0%)	
Trisectionectomy	4 (2.0%)	4 (2.1%)	0 (0%)	
Operative time (min)	304 ± 109	299 ± 104	345 ± 135	0.06
Intraoperative blood loss (mL)	848 ±1006	743 ± 889	1604 ± 1456	< 0.001
Liver function tests				
Total Liver hepatic clearance (mL/min)	285 ± 98	315 ± 106	258 ± 91	0.02
Total Liver Functional volume (mL)	1321 ± 280	1340 ± 278	1202 ± 270	0.04
Hepatic clearance of the remnant liver (mL/min)	248 ± 95	261 ± 91	149 ± 47	< 0.001
Functional volume of the remnant liver (mL)	1057 ± 334	1104 ± 317	710 ± 239	< 0.001
LHL15	0.92 ± 0.03	0.925 ± 0.03	0.906 ± 0.05	0.02
HH15	0.60 ± 0.07	0.602 ± 0.07	0.651 ± 0.07	0.01
Surgical outcome				
PHLF grade (0 : A : B : C)	176 : 11 : 8 : 4	176 : 11 : 0 : 0	0 : 0 : 8 : 4	-
Hospital length of stay (d)	15 (7-119)	14 (7-119)	25 (12-74)	< 0.001

PNI: Prognostic nutrition index; ALBI: Albumin–bilirubin; NLR: Neutrophil–lymphocyte ratio; PLR: Platelet-to-lymphocyte ratio; LHL15: liver to heart-plus-liver radioactivity at 15 min; PHLF: Posthepatectomy liver failure; AST: Aspartate aminotransferase; ALT: Alanine aminotransferase; PT-INR: Prothrombin time international normalized ratio.

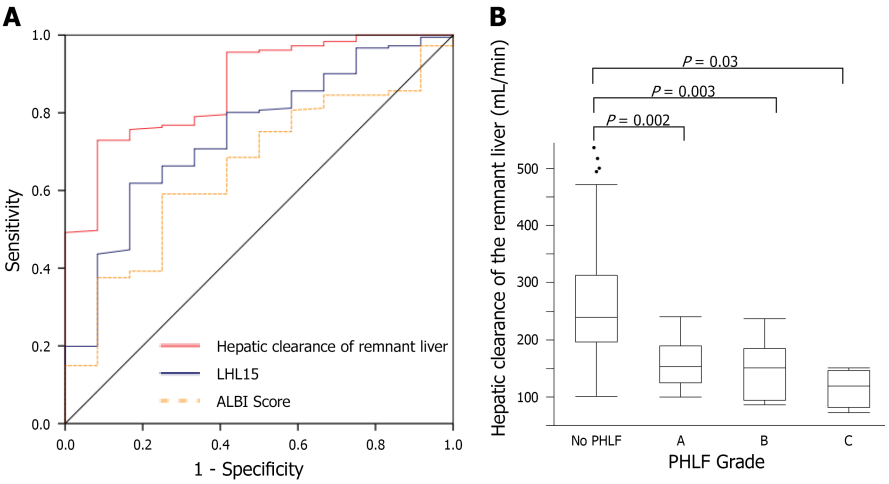
Correlations between hepatic clearance of the remnant liver and PHLF

ROC curve analysis of hepatic clearance of the remnant liver, liver to heart-plus-liver radioactivity at 15 min (LHL15), and ALBI score were used to predict the risk of developing PHLF (Figure 2A). The area under the ROC curve for hepatic clearance of the remnant liver, LHL15, and ALBI score for predicting

Table 2 Postoperative morbidity in patients with hepatocellular carcinoma

Complication	Clavien–Dindo classification							Total (%)
	I	II	IIIa	IIIb	IVa	IVb	V	
Pleural effusion or ascites	6		1					7 (3.5)
Pneumonia		1	1					2 (1.0)
Biliary leakage		1	5					6 (3.0)
Arrhythmia	1							1 (1.0)
Wound infection	10							10 (5.0)
Intra-abdominal abscess		1	8					9 (4.5)
Intra-abdominal hemorrhage			1	1				2 (1.0)
PHLF	8	5	5	2	1		2	23 (11.6)
Total (%)	25 (12.5)	8 (4.0)	21 (10.6)	3 (1.5)	1 (0.5)	0	2 (1.0)	60 (30.0)

PHLF: Posthepatectomy liver failure.



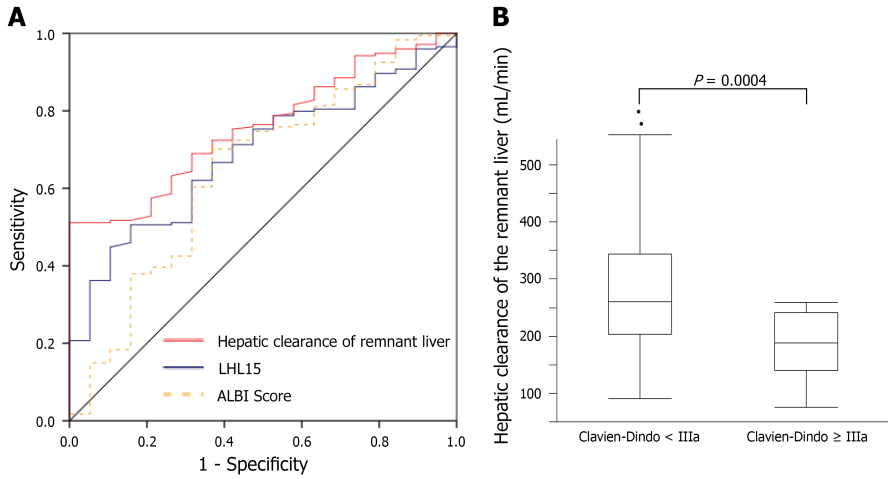
DOI: 10.3748/wjg.v28.i38.5614 **Copyright** ©The Author(s) 2022.

Figure 2 Analysis of hepatic clearance for post hepatectomy liver failure. A: Receiver-operating characteristic curve analysis of hepatic clearance of the remnant liver, LHL15, and albumin–bilirubin (ALBI) score in predicting PHLF. The area under the receiver-operating characteristic curve values for analysis of hepatic clearance of the remnant liver, LHL15, and ALBI score in predicting PHLF were 0.868, 0.629, and 0.655, respectively; B: Hepatic clearance of the remnant liver for each PHLF. The median hepatic clearances of the remnant liver were 239, 153, 150.5, and 119.5 mL/min for normal, Grades A, B, and C, respectively. LHL15: liver to heart-plus-liver radioactivity at 15 min; ALBI score: Albumin–bilirubin score; PHLF: Post hepatectomy liver failure.

the development of PHLF were 0.868, 0.629, and 0.655, respectively. Hepatic clearance of the remnant liver had the highest area under the curve for predicting the development of PHLF. The cutoff values for predicting PHLF with highest sensitivity and specificity were 192 mL/min (sensitivity, 87.0%; specificity, 76.1%) for hepatic clearance of the remnant liver, 0.91 (sensitivity, 47.8%; specificity, 73.3%) for LHL15, 2.96 (sensitivity, 34.9%; specificity, 95.7%) for ALBI score. The relationship between hepatic clearance of the remnant liver and PHLF grade was evaluated (Figure 2B). The median hepatic clearances of the remnant liver were 239, 153, 150.5 and 119.5 mL/min for no PHLF, Grades A, B and C, respectively. The differences were significant for no PHLF and Grade A (P = 0.002), no PHLF and Grade B (P = 0.003), and no PHLF and Grade C (P = 0.02).

Correlation between hepatic clearance of remnant liver and morbidity and mortality

ROC curve analysis of hepatic clearance of the remnant liver, LHL15, and ALBI score were used to predict the risk of developing major complications (Figure 3A). The area under ROC curves for hepatic clearance of the remnant liver, LHL15, and ALBI score for predicting major complications were 0.758, 0.594, and 0.647, respectively. Hepatic clearance of the remnant liver had the highest area under the curve for predicting the development of major complications. The cutoff values for predicting PHLF with highest sensitivity and specificity were 237 mL/min (sensitivity, 100%; specificity, 51.9%) for



DOI: 10.3748/wjg.v28.i38.5614 **Copyright** ©The Author(s) 2022.

Figure 3 Analysis of hepatic clearance for morbidity and mortality. A: Receiver operating characteristic curve analysis of hepatic clearance of the remnant liver, LHL15, and albumin–bilirubin (ALBI) score in predicting major morbidity. The area under the receiver operating characteristic curve analysis of hepatic clearance of the remnant liver, LHL15, and ALBI score in predicting major morbidity were 0.758, 0.594, and 0.647, respectively; B: Hepatic clearance of the remnant liver for Clavien–Dindo classification. The median hepatic clearances of the remnant liver were 238 and 179 mL/min for Clavien–Dindo < III and Clavien–Dindo ≥ III. LHL15: liver to heart-plus-liver radioactivity at 15 min; ALBI score: Albumin–bilirubin score.

hepatic clearance of the remnant liver, 0.94 (sensitivity, 84.2%; specificity, 36.2%) for LHL15, 2.63 (sensitivity, 69.3%; specificity, 63.2%) for ALBI score. The relationship between hepatic clearance of the remnant liver and Clavien–Dindo classification was evaluated (Figure 3B). The median hepatic clearances of the remnant liver were 238 and 179 mL/min for Clavien–Dindo < IIIa and Clavien–Dindo ≥ IIIa. The differences were significant for Clavien–Dindo < IIIa and Clavien–Dindo ≥ IIIa (P = 0.0004).

Multivariate analysis for PHLF Grade B or C

Multivariate regression analysis was performed between variables, with statistically significant differences following the univariate analysis regarding PHLF Grade B or C (Table 3). Hepatic clearance of the remnant liver [P = 0.001, odds ratio (OR): 0.973, 95% confidence interval (CI): 0.952–0.995] and intraoperative blood loss (P = 0.006, OR: 1.001, 95%CI: 1.0002–1.002) were independent risk factors for PHLF Grade B or C.

Multivariate analysis for major complication and mortality

Multivariate regression analysis was performed between variables, with significant differences following the univariate analysis regarding major complications (Table 4). Hepatic clearance of the remnant liver (P = 0.004, OR: 0.988, 95%CI: 0.979–0.999) and intraoperative blood loss (P = 0.005, OR: 1.0005, 95%CI: 1.0002–1.0014) were independent risk factors for developing major complications.

DISCUSSION

Hepatic clearance was associated with PHLF and major complications. The independent risk factors for developing PHLF and major complications were the hepatic clearance of the remnant liver, and intraoperative blood loss. The results of this study show that the measurement of hepatic clearance of the remnant liver is reliable for predicting the development of PHLF and major complications.

The results of this study support the use of hepatic clearance of the remnant liver, LHL15, and ALBI score for predicting the development of PHLF and postoperative major complications in patient with HCC. LHL15 and HH15, which are hepatic uptake and blood clearance ratios in GSA scintigraphy, are the most popular and widely used in many institutions. However, they may be insufficient for accurately estimating the degree of liver function because these indices are calculated from planar scintigraphic images, which do not correctly reflect hepatocyte volume[11]. In contrast, hepatic clearance measured by SPECT analysis contains volumetric information and may correctly estimate the hepatocyte volume[11]. LHL15 reflects the function of the whole liver, but the hepatic clearance of remnant liver shows the liver function of remnant liver, therefore, hepatic clearance may reflect functional reserve and short term outcome.

Many studies have investigated the relationship between GSA scintigraphy and PHLF. However, this is the first report comparing residual liver function and major complications using GSA scintigraphy. Patients with lower remnant liver function are at higher risk for PHLF, morbidity and mortality. The

Table 3 Predictive factors for post-hepatectomy liver failure in grade B, or C

	Univariate analysis			Multivariate analysis		
	P	OR	95%CI	*P*	OR	95%CI
Age (yr)	0.53	1.02	0.96-1.08			
Gender (male : female)	0.59	0.67	0.10-2.66			
Child–Pugh class	0.47	1.63	0.06-1.63			
PT-INR	0.86	0.79	0.05-11.0			
AST	0.34	0.99	0.98-1.00			
ALT	0.14	0.99	0.98-1.00			
Choline Esterase	0.24	1.00	0.99-1.01			
ALBI score	0.15	0.37	0.09-1.41	0.375	3.31	0.37-29.3
Operation time	0.02	1.01	0.99-1.00	0.110	1.010	0.99-1.01
Intraoperative blood loss	0.001	1.0007	1.0003-1.0012	0.033	1.001	1.0002-1.002
Hepatic clearance of the remnant liver	< 0.001	0.972	0.958-0.987	0.002	0.973	0.952-0.995
Functional volume of the remnant liver	0.002	0.997	0.994-0.999	0.351	0.998	0.995-1.00
LHL15	0.02	52	2.03-1382	0.362	9.597	0.08-1211

AST: Aspartate aminotransferase; ALT: Alanine aminotransferase; PT-INR: Prothrombin time international normalized ratio; ALBI: Albumin-bilirubin; LHL15: liver to heart-plus-liver radioactivity at 15 min; OR: Odds ratio; CI: Confidence interval.

quality and volume of the postoperative remnant liver have been shown to be associated with postoperative outcomes[22]. Surgeons should emphasize the remnant liver functional reserve rather than the resected liver volume[12,23]. Elevation of serum bilirubin and PT-INR are associated with morbidity and mortality, regardless of the extent of resection[24]. Liver failure after limited resection can develop. Patients with reduced reserve of the remnant liver are at higher risk for the development of PHLF and major complications[22,25,26]. The extent of surgery should be considered to preserve as much liver function as possible. Moreover PHLF grade C is most severe types of liver failure that may lead to in-hospital death[24]. In ROC curve analysis, the cutoff line of PHLF grade C was 151 mL/min (sensitivity 87.5%, specificity 100%). Patients below the cutoff line should be given special consideration by surgeons before surgery and may not be ideal candidates for hepatic resection. Hepatic clearance of the remnant liver below 100 mL/min is associated with a high mortality rate. Therefore, PTPE should be performed when hepatic clearance of the remnant liver is below 100 mL/min, and surgery should be considered when the clearance is above 100 mL/min. In addition, if hepatic clearance of the remnant liver is greater than 100 mL/min preoperatively, unnecessary PTPE can be avoided.

The risk for developing PHLF and major complications is determined by patient and surgical factors. Intraoperative blood loss is a well-known risk factor for morbidity and mortality after hepatic resection [25,27-30]. Hemorrhage can lead to the development of metabolic acidosis as a consequence of intracellular derangements in oxygen and substrate utilization[29]. Reduced levels of cytokines and humoral factors, such as interleukin-6, hepatocyte growth factors, and growth hormone after extensive blood loss may result in decreased liver regeneration because of loss of growth factors needed for regeneration[28].

The present study had some limitations, including a retrospective design, and being a single center study. Preoperative GSA scintigraphy was routinely performed to estimate total liver function in this hospital. Total liver function, remnant liver function, laboratory data, and liver failure were objectively assessed in advance, which limited the risk of observation bias. Prospective multicenter trials are needed to validate the results of this study.

CONCLUSION

Lower functional reserve of the remnant liver results in a higher risk of developing PHLF and major complications in patients undergoing resection of HCC. The estimation of hepatic clearance of the remnant liver may provide guidance for determining the extent of resection in a patient-specific manner.

Table 4 Predictive factors for morbidity (Clavien–Dindo classification ≥ IIIa)

	Univariate analysis			Multivariate analysis		
	P	OR	95%CI	*P*	OR	95%CI
Age (yr)	0.68	1.01	0.96-1.06			
Gender (male : female)	0.69	0.80	0.27-2.36			
Child–Pugh class	0.89	1.09	0.29-2.91			
PT-INR	0.97	1.03	0.09-11.6			
AST	0.27	0.99	0.98-1.00			
ALT	0.11	0.99	0.98-1.00			
Cholinesterase	0.58	1.00	0.99-1.01			
ALBI score	0.02	3.57	1.19-10.7	0.790	1.22	0.286-5.19
Operation time	0.01	1.01	1.00-1.01	0.166	1.004	0.991-1.015
Intraoperative blood loss	0.001	1.0006	1.0002-1.001	0.005	1.0005	1.0002-1.0014
Hepatic clearance of the remnant liver	< 0.001	0.986	0.978-0.994	0.004	0.988	0.979-0.999
Functional volume of the remnant liver	0.003	0.998	0.996-0.999	0.329	0.99	0.997-1.00
LHL15	0.13	9.9	0.53-183	0.914	1.27	0.02-99.2

AST: Aspartate aminotransferase; ALT: Alanine aminotransferase; PT-INR: Prothrombin time international normalized ratio; ALBI: Albumin-bilirubin; LHL15: liver to heart-plus-liver radioactivity at 15 min; OR: Odds ratio; CI: Confidence interval.

ARTICLE HIGHLIGHTS

Research background

Preoperative assessment of liver function is important to reduce the rate of complications.

Research motivation

Few studies evaluate the relationship of residual liver function to complications and prognosis using hepatic clearance.

Research objectives

To measure hepatic clearance of the remnant liver using ^{99m}Tc-galactosyl serum albumin (GSA) scintigraphy, single photon emission computed tomography, to elucidate the association between residual liver function and morbidity and mortality, and to identify risk factors for those factors.

Research methods

We collected data from 199 patients who underwent resection of hepatocellular carcinoma. Hepatic clearance of the remnant liver was measured using fusion images of ^{99m}Tc-labelled GSA liver scintigraphy and computed tomography scans. Risk factors were determined using logistic regression multivariate analysis.

Research results

Risk factors for posthepatectomy liver failure, morbidity, and mortality were low hepatic clearance of the remnant liver and intra-operative bleeding.

Research conclusions

Lower residual liver function is associated with a poor short-term prognosis.

Research perspectives

Preoperative estimation of remnant liver function is useful to determine the surgical approach.

ACKNOWLEDGEMENTS

I especially thank Michio Ashizaki for helping patient data acquisition.

FOOTNOTES

Author contributions: Miki A, Sakuma Y, Shimizu A and Yasuda Y designated the overall concept and outline the manuscript; Ohzawa H, Saito A, Meguro Y, Watanabe J, Morishima K, Endo K, Sasanuma H, and Sata N contributed to the discussion and design of the manuscript; Miki A and Lefor AK contributed to the writing, editing the manuscript, illustrations, and review of literature.

Institutional review board statement: The study was reviewed and approved by the Institutional Review Board of Jichi Medical University, Approval No. A21-029.

Informed consent statement: Written informed consent from any patient for data collection in a prospectively collected data base is available. However, the need for written informed consent for this study was waived by the Institutional Review Board of Jichi Medical University in view of the retrospective design of the study, based on national and local guidelines such as the fact that all clinical/ laboratory measurements and procedures were part of routine care.

Conflict-of-interest statement: The authors declare no conflicts of interest for this study.

Data sharing statement: The database contains highly confidential data which may provide insight in clinical and personnel information about patients and lead to their identification. Therefore, according to organizational restrictions and regulations these data cannot be made publicly available. However, the datasets used and/or analyzed during the current study are available from the corresponding author on reasonable request.

Open-Access: This article is an open-access article that was selected by an in-house editor and fully peer-reviewed by external reviewers. It is distributed in accordance with the Creative Commons Attribution NonCommercial (CC BY-NC 4.0) license, which permits others to distribute, remix, adapt, build upon this work non-commercially, and license their derivative works on different terms, provided the original work is properly cited and the use is non-commercial. See: https://creativecommons.org/Licenses/by-nc/4.0/

Country/Territory of origin: Japan

ORCID number: Atsushi Miki 0000-0002-2908-0177; Yasunaru Sakuma 0000-0003-3633-3221; Hideyuki Ohzawa 0000-0001-9422-2840; Akira Saito 0000-0002-3247-7845; Yoshiyuki Meguro 0000-0003-4328-1909; Jun Watanabe 0000-0003-4477-4238; Kazue Morishima 0000-0002-7837-3742; Kazuhiro Endo 0000-0002-2845-3533; Hideki Sasanuma 0000-0002-9758-7295; Atsushi Shimizu 0000-0001-6249-4489; Alan Kawarai Lefor 0000-0001-6673-5630; Yoshikazu Yasuda 0000-0002-4101-6629; Naohiro Sata 0000-0002-6689-5623.

S-Editor: Chang KL
L-Editor: Kerr C
P-Editor: Chang KL

REFERENCES

1 **Shimada M**, Takenaka K, Fujiwara Y, Gion T, Shirabe K, Yanaga K, Sugimachi K. Risk factors linked to postoperative morbidity in patients with hepatocellular carcinoma. *Br J Surg* 1998; **85**: 195-198 [PMID: 9501814 DOI: 10.1046/j.1365-2168.1998.00567.x]
2 **Huang J**, Hernandez-Alejandro R, Croome KP, Zeng Y, Wu H, Chen Z. Hepatic resection for huge (>15 cm) multinodular HCC with macrovascular invasion. *J Surg Res* 2012; **178**: 743-750 [PMID: 22656039 DOI: 10.1016/j.jss.2012.04.058]
3 **Wang YY**, Zhao XH, Ma L, Ye JZ, Wu FX, Tang J, You XM, Xiang BD, Li LQ. Comparison of the ability of Child-Pugh score, MELD score, and ICG-R15 to assess preoperative hepatic functional reserve in patients with hepatocellular carcinoma. *J Surg Oncol* 2018; **118**: 440-445 [PMID: 30259515 DOI: 10.1002/jso.25184]
4 **Tomimaru Y**, Eguchi H, Gotoh K, Kawamoto K, Wada H, Asaoka T, Noda T, Yamada D, Ogawa H, Umeshita K, Nagano H, Doki Y, Mori M. Platelet count is more useful for predicting posthepatectomy liver failure at surgery for hepatocellular carcinoma than indocyanine green clearance test. *J Surg Oncol* 2016; **113**: 565-569 [PMID: 26751258 DOI: 10.1002/jso.24166]
5 **Park HJ**, Seo KI, Kim SJ, Lee SU, Yun BC, Han BH, Shin DH, Choi YI, Moon HH. Effectiveness of Albumin-bilirubin Score as a Predictor of Post-hepatectomy Liver Failure in Patients with Hepatocellular Carcinoma. *Korean J Gastroenterol* 2021; **77**: 115-122 [PMID: 33658474 DOI: 10.4166/kjg.2020.148]
6 **Kubota K**, Makuuchi M, Kusaka K, Kobayashi T, Miki K, Hasegawa K, Harihara Y, Takayama T. Measurement of liver volume and hepatic functional reserve as a guide to decision-making in resectional surgery for hepatic tumors. *Hepatology*

1997; **26**: 1176-1181 [PMID: 9362359 DOI: 10.1053/jhep.1997.v26.pm0009362359]
7 **Sugahara K**, Togashi H, Takahashi K, Onodera Y, Sanjo M, Misawa K, Suzuki A, Adachi T, Ito J, Okumoto K, Hattori E, Takeda T, Watanabe H, Saito K, Saito T, Sugai Y, Kawata S. Separate analysis of asialoglycoprotein receptors in the right and left hepatic lobes using Tc-GSA SPECT. *Hepatology* 2003; **38**: 1401-1409 [PMID: 14647051 DOI: 10.1016/j.hep.2003.09.031]
8 **Akaki S**, Okumura Y, Sasai N, Sato S, Tsunoda M, Kuroda M, Kanazawa S, Hiraki Y. Hepatectomy simulation discrepancy between radionuclide receptor imaging and CT volumetry: influence of decreased unilateral portal venous flow. *Ann Nucl Med* 2003; **17**: 23-29 [PMID: 12691127 DOI: 10.1007/BF02988255]
9 **Li XF**, Taki J, Kinuya S, Higuchi T, Konishi S, Hwang EH, Shuke N, Nakajima K, Tonami N. Asialoglycoprotein receptor concentration in tumor-bearing livers and its fate early after their sectorial resection. *Ann Nucl Med* 2003; **17**: 489-493 [PMID: 14575385 DOI: 10.1007/BF03006440]
10 **Iimuro Y**, Kashiwagi T, Yamanaka J, Hirano T, Saito S, Sugimoto T, Watanabe S, Kuroda N, Okada T, Asano Y, Uyama N, Fujimoto J. Preoperative estimation of asialoglycoprotein receptor expression in the remnant liver from CT/99mTc-GSA SPECT fusion images correlates well with postoperative liver function parameters. *J Hepatobiliary Pancreat Sci* 2010; **17**: 673-681 [PMID: 20703846 DOI: 10.1007/s00534-010-0264-6]
11 **Taniguchi M**, Okizaki A, Watanabe K, Imai K, Uchida K, Einama T, Shuke N, Miyokawa N, Furukawa H. Hepatic clearance measured with (99m)Tc-GSA single-photon emission computed tomography to estimate liver fibrosis. *World J Gastroenterol* 2014; **20**: 16714-16720 [PMID: 25469042 DOI: 10.3748/wjg.v20.i44.16714]
12 **Yumoto Y**, Yagi T, Sato S, Nouso K, Kobayashi Y, Ohmoto M, Yumoto E, Nagaya I, Nakatsukasa H. Preoperative estimation of remnant hepatic function using fusion images obtained by (99m)Tc-labelled galactosyl-human serum albumin liver scintigraphy and computed tomography. *Br J Surg* 2010; **97**: 934-944 [PMID: 20474004 DOI: 10.1002/bjs.7025]
13 **Ha-Kawa SK**, Tanaka Y, Hasebe S, Kuniyasu Y, Koizumi K, Ishii Y, Yamamoto K, Kashiwagi T, Ito A, Kudo M, Ikekubo K, Tsuda T, Murase K. Compartmental analysis of asialoglycoprotein receptor scintigraphy for quantitative measurement of liver function: a multicentre study. *Eur J Nucl Med* 1997; **24**: 130-137 [PMID: 9021109 DOI: 10.1007/BF02439544]
14 **Harada K**, Mizuguchi T, Katagiri Y, Kawamoto M, Nakamura Y, Meguro M, Ota S, Sasaki S, Miyanishi K, Sonoda T, Mori M, Shinomura Y, Kato J, Hirata K. Area between the hepatic and heart curves of (99m)Tc-galactosyl-human serum albumin scintigraphy represents liver function and disease progression for preoperative evaluation in hepatocellular carcinoma patients. *J Hepatobiliary Pancreat Sci* 2012; **19**: 667-673 [PMID: 22179579 DOI: 10.1007/s00534-011-0486-2]
15 **Shuke N**, Okizaki A, Kino S, Sato J, Ishikawa Y, Zhao C, Kinuya S, Watanabe N, Yokoyama K, Aburano T. Functional mapping of regional liver asialoglycoprotein receptor amount from single blood sample and SPECT. *J Nucl Med* 2003; **44**: 475-482 [PMID: 12621017]
16 **Kwon AH**, Ha-Kawa SK, Uetsuji S, Inoue T, Matsui Y, Kamiyama Y. Preoperative determination of the surgical procedure for hepatectomy using technetium-99m-galactosyl human serum albumin (99mTc-GSA) liver scintigraphy. *Hepatology* 1997; **25**: 426-429 [PMID: 9021958 DOI: 10.1002/hep.510250228]
17 **Kwon AH**, Ha-Kawa SK, Uetsuji S, Kamiyama Y, Tanaka Y. Use of technetium 99m diethylenetriamine-pentaacetic acid-galactosyl-human serum albumin liver scintigraphy in the evaluation of preoperative and postoperative hepatic functional reserve for hepatectomy. *Surgery* 1995; **117**: 429-434 [PMID: 7716725 DOI: 10.1016/s0039-6060(05)80063-7]
18 **Sawamura T**, Kawasato S, Shiozaki Y, Sameshima Y, Nakada H, Tashiro Y. Decrease of a hepatic binding protein specific for asialoglycoproteins with accumulation of serum asialoglycoproteins in galactosamine-treated rats. *Gastroenterology* 1981; **81**: 527-533 [PMID: 7250640]
19 **Pang YY**. The Brisbane 2000 terminology of liver anatomy and resections. HPB 2000; 2:333-39. *HPB (Oxford)* 2002; **4**: 99; author reply 99-99; author reply100 [PMID: 18332933 DOI: 10.1080/136518202760378489]
20 **Dindo D**, Demartines N, Clavien PA. Classification of surgical complications: a new proposal with evaluation in a cohort of 6336 patients and results of a survey. *Ann Surg* 2004; **240**: 205-213 [PMID: 15273542 DOI: 10.1097/01.sla.0000133083.54934.ae]
21 **Rahbari NN**, Garden OJ, Padbury R, Brooke-Smith M, Crawford M, Adam R, Koch M, Makuuchi M, Dematteo RP, Christophi C, Banting S, Usatoff V, Nagino M, Maddern G, Hugh TJ, Vauthey JN, Greig P, Rees M, Yokoyama Y, Fan ST, Nimura Y, Figueras J, Capussotti L, Büchler MW, Weitz J. Posthepatectomy liver failure: a definition and grading by the International Study Group of Liver Surgery (ISGLS). *Surgery* 2011; **149**: 713-724 [PMID: 21236455 DOI: 10.1016/j.surg.2010.10.001]
22 **Safiri S**, Ayubi E. Comments on combining albumin-bilirubin score with future liver remnant predicts posthepatectomy liver failure in HBV-associated HCC patients. *Liver Int* 2018; **38**: 761 [PMID: 28792643 DOI: 10.1111/liv.13542]
23 **Vauthey JN**, Chaoui A, Do KA, Bilimoria MM, Fenstermacher MJ, Charnsangavej C, Hicks M, Alsfasser G, Lauwers G, Hawkins IF, Caridi J. Standardized measurement of the future liver remnant prior to extended liver resection: methodology and clinical associations. *Surgery* 2000; **127**: 512-519 [PMID: 10819059 DOI: 10.1067/msy.2000.105294]
24 **Reissfelder C**, Rahbari NN, Koch M, Kofler B, Sutedja N, Elbers H, Büchler MW, Weitz J. Postoperative course and clinical significance of biochemical blood tests following hepatic resection. *Br J Surg* 2011; **98**: 836-844 [PMID: 21456090 DOI: 10.1002/bjs.7459]
25 **Kokudo N**, Vera DR, Tada K, Koizumi M, Seki M, Matsubara T, Ohta H, Yamaguchi T, Takahashi T, Nakajima T, Muto T. Predictors of successful hepatic resection: prognostic usefulness of hepatic asialoglycoprotein receptor analysis. *World J Surg* 2002; **26**: 1342-1347 [PMID: 12297928 DOI: 10.1007/s00268-002-6262-3]
26 **Torizuka K**, Ha-Kawa SK, Kudo M, Kubota Y, Yamamoto K, Itoh K, Nagao K, Uchiyama G, Koizumi K, Sasaki Y. [Phase III multi-center clinical study on 99mTc-GSA, a new agent for functional imaging of the liver]. *Kaku Igaku* 1992; **29**: 159-181 [PMID: 1564788]
27 **Yang T**, Zhang J, Lu JH, Yang GS, Wu MC, Yu WF. Risk factors influencing postoperative outcomes of major hepatic resection of hepatocellular carcinoma for patients with underlying liver diseases. *World J Surg* 2011; **35**: 2073-2082 [PMID: 21656309 DOI: 10.1007/s00268-011-1161-0]
28 **Shirabe K**, Motomura T, Takeishi K, Morita K, Kayashima H, Taketomi A, Ikegami T, Soejima Y, Yoshizumi T, Maehara Y. Human early liver regeneration after hepatectomy in patients with hepatocellular carcinoma: special reference to age.

Scand J Surg 2013; **102**: 101-105 [PMID: 23820685 DOI: 10.1177/1457496913482250]

29 **Cucchetti A**, Siniscalchi A, Ercolani G, Vivarelli M, Cescon M, Grazi GL, Faenza S, Pinna AD. Modification of acid-base balance in cirrhotic patients undergoing liver resection for hepatocellular carcinoma. *Ann Surg* 2007; **245**: 902-908 [PMID: 17522516 DOI: 10.1097/01.sla.0000256356.23026.9f]

30 **Jarnagin WR**, Gonen M, Fong Y, DeMatteo RP, Ben-Porat L, Little S, Corvera C, Weber S, Blumgart LH. Improvement in perioperative outcome after hepatic resection: analysis of 1,803 consecutive cases over the past decade. *Ann Surg* 2002; **236**: 397-406; discussion 406 [PMID: 12368667 DOI: 10.1097/01.SLA.0000029003.66466.B3]

World Journal of Gastroenterology

Submit a Manuscript: https://www.f6publishing.com

World J Gastroenterol 2022 October 14; 28(38): 5626-5635

DOI: 10.3748/wjg.v28.i38.5626

ISSN 1007-9327 (print) ISSN 2219-2840 (online)

ORIGINAL ARTICLE

Retrospective Study

A new scoring system to evaluate adjuvant chemotherapy for patients with T2N0M0 gastric cancer after D2 gastrectomy

Quan Xu, Wen-Zhe Kang, Jian-Ping Xiong, Xin-Xin Shao, Wei-Kun Li, Hai-Tao Hu, Yan-Tao Tian

Specialty type: Oncology

Provenance and peer review: Unsolicited article; Externally peer reviewed.

Peer-review model: Single blind

Peer-review report's scientific quality classification

Grade A (Excellent): A
Grade B (Very good): B, B
Grade C (Good): C
Grade D (Fair): D, D
Grade E (Poor): E

P-Reviewer: Acikgoz Y, Turkey; Dumitraşcu T, Romania; Hsu JT, Taiwan; Hwang GS, South Korea; Liu YQ, United States; Ntavatzikos A, Greece

Received: June 9, 2022
Peer-review started: June 9, 2022
First decision: August 1, 2022
Revised: August 19, 2022
Accepted: September 21, 2022
Article in press: September 21, 2022
Published online: October 14, 2022

Quan Xu, Wen-Zhe Kang, Jian-Ping Xiong, Xin-Xin Shao, Wei-Kun Li, Hai-Tao Hu, Yan-Tao Tian, Department of Pancreatic and Gastric Surgery, National Cancer Center/National Clinical Research Center for Cancer/Cancer Hospital, Chinese Academy of Medical Sciences and Peking Union Medical College, Beijing 100021, China

Corresponding author: Yan-Tao Tian, PhD, Professor, Department of Pancreatic and Gastric Surgery, National Cancer Center/National Clinical Research Center for Cancer/Cancer Hospital, Chinese Academy of Medical Sciences and Peking Union Medical College, No. 17 Panjiayuan Nanli, Chaoyang District, Beijing 100021, China. tianyantao@cicams.ac.cn

Abstract

BACKGROUND

At present, there is insufficient medical evidence to determine whether adjuvant chemotherapy is necessary for T2N0M0 gastric cancer.

AIM

To obtain a risk score to assess the need for adjuvant chemotherapy in patients with T2N0M0 gastric cancer.

METHODS

We identified 325 patients with pathological T2N0M0 stage primary gastric cancer at the National Cancer Center between 2011 and 2018. Univariate and multivariate Cox regression analyses were performed to predict factors affecting prognosis. Vascular invasion, tumor site, and body mass index were assessed, and a scoring system was established. We compared the survival outcomes and benefits of adjuvant chemotherapy between the different subgroups.

RESULTS

Five-year survival rates of the score 0, 1, 2, and 3 groups were 92%, 95%, 80%, and 50%, respectively ($P < 0.001$). In the score 2-3 group, five-year survival rates for patients in the adjuvant chemotherapy group and postoperative observation group were 95% and 61%, respectively ($P = 0.021$).

CONCLUSION

For patients with T2N0M0 stage gastric cancer and two or more risk factors, adjuvant chemotherapy after D2 gastrectomy may have a survival benefit.

Key Words: Gastric cancer; Risk score; T2N0M0; Adjuvant chemotherapy; D2

gastrectomy; Survival

©The Author(s) 2022. Published by Baishideng Publishing Group Inc. All rights reserved.

Core Tip: It is controversial whether adjuvant chemotherapy is necessary for stage T2N0M0 gastric cancer. In our study, we assessed the risk score of patients with pathologic T2N0M0 gastric cancer after D2 gastrectomy, based on clinicopathological factors, and identified a high-risk subgroup that could benefit from adjuvant chemotherapy. For patients with T2N0M0 stage gastric cancer with two or more risk factors, adjuvant chemotherapy after D2 gastrectomy may have a survival benefit.

Citation: Xu Q, Kang WZ, Xiong JP, Shao XX, Li WK, Hu HT, Tian YT. A new scoring system to evaluate adjuvant chemotherapy for patients with T2N0M0 gastric cancer after D2 gastrectomy. *World J Gastroenterol* 2022; 28(38): 5626-5635
URL: https://www.wjgnet.com/1007-9327/full/v28/i38/5626.htm
DOI: https://dx.doi.org/10.3748/wjg.v28.i38.5626

INTRODUCTION

Gastric cancer is one of the most common malignancies worldwide[1-3]. D2 gastrectomy combined with postoperative adjuvant chemotherapy is the main treatment modality for advanced gastric cancer[4-8]. According to the 8th edition of the American Joint Committee on Cancer (AJCC) guidelines for gastric cancer, T2 was defined as tumor invasion of the muscularis propria[9]. It is controversial whether adjuvant chemotherapy is necessary for stage T2N0M0 gastric cancer[10-16]. Previous studies have suggested that patients with stage I gastric cancer cannot benefit from adjuvant chemotherapy[17]. However, there are some risk factors for recurrence of T2N0M0 gastric cancer, such as lymphatic and/or blood vessel invasion, tumor diameter, perineural invasion, proximal tumor location, and poor differentiation[14,18]. Postoperative adjuvant chemotherapy may inhibit the recurrence in these patients. To further clarify the indications for the use of postoperative adjuvant chemotherapy in T2N0M0 gastric cancer, we reviewed 325 patients with T2N0M0 gastric cancer admitted to the National Cancer Center between 2011 and 2018. In this study, we assessed the risk score of patients with pathologic T2N0M0 gastric cancer after D2 gastrectomy based on clinicopathological factors and identified a high-risk subgroup that could benefit from postoperative adjuvant chemotherapy.

MATERIALS AND METHODS

Patient selection

We identified 402 patients with pathological T2N0M0 stage primary gastric carcinoma and gastroesophageal junction carcinoma (as defined by the AJCC guidelines, 8th edition) who were admitted to the Department of Pancreatic and Gastric Surgery, National Cancer Center, from 2011 to 2018. Three hundred and twenty-five patients were included in our study, all of whom underwent D2 gastrectomy. A total of 63 patients received post-operative adjuvant chemotherapy. The major chemotherapy regimens included platinum + 5-FU; paclitaxel + platinum + 5-FU; and others. Adjuvant chemotherapy is usually performed for 4-6 cycles. Exclusion criteria included loss to follow-up, lack of adenocarcinoma, neoadjuvant chemotherapy, adjuvant radiotherapy, Siewert I type/Siewert II type gastroesophageal junction carcinoma invading the dentate line, and postoperative survival time < 1 mo. Patients were followed-up by telephone. The follow-up was completed on April 30, 2020. The median follow-up time was 65.4 mo.

Statistical analyses

Univariate and multivariate Cox regression analyses were performed to screen for prognostic variables. Variables with a P value < 0.05 and < 0.25 in the univariate and multivariable Cox regression analyses were included in the study. Three variables were included in total: Vascular invasion, tumor site, and body mass index (BMI). The tumor site was classified as cardiac or non-cardiac. Cardiac cancer refers to Siewert type II gastroesophageal junction carcinoma that does not invade the dentate line and Siewert type III gastroesophageal junction carcinoma. BMI of < 18.5 or > 23.9, positive result of vascular invasion, and cardiac cancer were defined as risk factors. Each risk factor was assigned one point, and a total of four groups were obtained, which were defined as scores 0, 1, 2, and 3, respectively. We found that patients with a score ≥ 2 had a poor prognosis, and chemotherapy significantly improved

Table 1 Clinicopathologic variables of 325 T2N0M0 gastric cancer patients

Variable	Overall	Adjuvant chemotherapy group	Postoperative observation group	*P* value
	325	63	262	
Age (yr) *n* (%)				0.609
< 40	20 (6.2)	3 (4.8)	17 (6.5)	
≥ 40	305 (93.8)	60 (95.2)	245 (93.5)	
Sex, *n* (%)				0.878
Male	250 (76.9)	48 (76.2)	202 (77.1)	
Female	75 (23.1)	15 (23.8)	60 (22.9)	
Smoking history, *n* (%)				0.363
Yes	169 (52.0)	36 (57.1)	133 (50.8)	
No	156 (48.0)	27 (42.9)	129 (49.2)	
Family history of gastric cancer, *n* (%)				0.852
Yes	24 (7.4)	5 (7.9)	19 (7.3)	
No	301 (92.6)	58 (92.1)	243 (92.7)	
BMI, *n* (%)				0.150
< 18.5 or > 23.9	176 (54.2)	29 (46.0)	147 (56.1)	
18.5-23.9	149 (45.8)	34 (54.0)	115 (43.9)	
Postoperative hospital stay, *n* (%)				0.747
≤ 14 d	285 (87.7)	56 (88.9)	229 (87.4)	
> 14 d	40 (12.3)	7 (11.1)	33 (12.6)	
Tumor site, *n* (%)				0.004
Cardia cancer	105 (32.3)	30 (47.6)	75 (28.6)	
Non-cardia gastric cancer	220 (67.7)	33 (52.4)	187 (71.4)	
The degree of differentiation, *n* (%)				0.571
Poorly differentiated	121 (37.2)	24 (38.1)	97 (37.0)	
Moderately differentiated	178 (54.8)	36 (57.1)	142 (54.2)	
Highly differentiated	26 (8.0)	3 (4.8)	23 (8.8)	
Vascular invasion, *n* (%)				0.014
Yes	54 (16.6)	17 (27.0)	37 (14.1)	
No	271 (83.4)	46 (73.0)	225 (85.9)	

BMI: Body mass index.

prognosis. According to the study results, scores of 2-3 were defined as the high-risk group. The Kaplan-Meier method was used to calculate the 5-year survival rate and compare the overall survival (OS) between the different score groups.

Statistical analysis was performed using the R software 4.0.5 (R Foundation for Statistical Computing, Vienna, Austria) and the SPSS 22.0 software (SPSS Inc., Chicago, IL, United States). Each test was bilateral, and statistical significance was set at $P < 0.05$.

RESULTS

Clinicopathological characteristics, univariate and multivariable cox regression analyses

A total of 325 patients were recruited for this study. Table 1 summarizes the clinicopathological characteristics of the patients enrolled in this study. Univariate Cox regression analysis demonstrated that the tumor site ($P = 0.022$, Table 2), vascular invasion ($P < 0.001$, Table 2), and BMI ($P = 0.036$, Table 2) were

Table 2 Univariate Cox Proportional Hazards Modeling for overall survival

Clinicopathological features	HR (95%CI)	*P* value
Sex		
Male	Reference	
Female	0.278 (0.066-1.172)	$P = 0.081$
Smoking history		
Yes	Reference	
No	0.605 (0.276-1.323)	$P = 0.208$
Family history of gastric cancer		
Yes	Reference	
No	0.550 (0.075-4.057)	$P = 0.558$
BMI		
18.5-23.9	Reference	
> 23.9 or < 18.5	2.509 (1.060-5.937)	$P = 0.036$
Postoperative hospital stay		
≤ 14 d	Reference	
> 14 d	0.990 (0.298-3.292)	$P = 0.987$
Tumor site		
Cardia cancer	Reference	
Non-cardia gastric cancer	0.411 (0.192-0.878)	$P = 0.022$
The degree of differentiation		
Poorly differentiated	Reference	
Moderately differentiated	1.330 (0.574-3.082)	$P = 0.507$
Highly differentiated	0.857 (0.182-4.043)	$P = 0.846$
Vascular invasion		
Yes	Reference	
No	0.097 (0.044-0.212)	$P < 0.001$

BMI: Body mass index; HR: Hazard ratio; 95%CI: 95% confidence interval.

significant risk factors for OS. Multivariate Cox regression analysis demonstrated that vascular invasion was an independent risk factor for OS ($P < 0.001$, Table 3).

Vascular invasion, tumor site, and BMI were assessed in the study, and a scoring system was established.

Survival results of different groups

Figure 1A summarizes the survival curves of patients with scores of 0, 1, 2, and 3. There were significant differences among all groups except for the score 0 and 1 groups (score 0 group *vs* score 1 group, $P = 0.537$; score 0 group *vs* score 2 group, $P = 0.049$; score 0 group *vs* score 3 group, $P < 0.001$; score 1 group *vs* score 2 group, $P = 0.003$; score 1 group *vs* score 3 group, $P < 0.001$; score 2 group *vs* score 3 group, $P = 0.008$). For all patients, 5-year survival rates of the adjuvant chemotherapy and postoperative observation groups were 96% and 90%, respectively ($P = 0.676$, Table 4). Five-year survival rates of the score 0, 1, 2, and 3 groups were 92%, 95%, 80%, and 50%, respectively ($P < 0.001$, Table 4). In the score 0 and score 1 groups, there were no differences in the 5-year survival rates between the postoperative observation and adjuvant chemotherapy groups. In the score 2-3 group, 5-year survival rates for patients in the adjuvant chemotherapy group and postoperative observation group were 95% and 61%, respectively ($P = 0.021$, Table 4).

Figure 1B-D summarizes the survival curves of patients with scores of 0, 1, and score 2-3 T2N0M0 gastric cancer in the adjuvant chemotherapy and postoperative observation groups. Table 5 summarizes the distribution of the different risk factors in each risk score group.

Table 3 Multivariable Cox Proportional Hazards Modeling for overall survival

Clinicopathological features	HR (95%CI)	*P* value
Sex		
Male	Reference	
Female	0.390 (0.076-1.988)	*P* = 0.257
Smoking history		
Yes	Reference	
No	0.725 (0.308-1.710)	*P* = 0.463
Family history of gastric cancer		
Yes	Reference	
No	0.495 (0.058-4.224)	*P* = 0.521
BMI		
18.5-23.9	Reference	
> 23.9 or < 18.5	1.848 (0.760-4.490)	*P* = 0.175
Postoperative hospital stay		
≤ 14 d	Reference	
> 14 d	1.198 (0.350-4.100)	*P* = 0.960
Tumor site		
Cardia cancer	Reference	
Non-cardia gastric cancer	0.620 (0.277-1.390)	*P* = 0.246
The degree of differentiation		
Poorly differentiated	Reference	
Moderately differentiated	0.517 (0.206-1.300)	*P* = 0.161
Highly differentiated	0.390 (0.077-1.960)	*P* = 0.305
Vascular invasion		
Yes	Reference	
No	0.106 (0.045-0.246)	*P* < 0.001

HR: Hazard ratio; 95%CI: 95% confidence interval.

DISCUSSION

Our study found that adjuvant chemotherapy is necessary for the treatment of T2N0M0 gastric cancer patients with two or more risk factors. The risk factors included vascular invasion, BMI, and tumor site. Based on these results, we obtained a simple risk score to assess the need for adjuvant chemotherapy in patients with T2N0M0 gastric cancer. Patients with a score 2-3 were assigned to the high-risk group.Previous studies have shown that adjuvant chemotherapy can prolong OS in advanced gastric cancer and reduce recurrence[19]. However, evidence of the survival benefits of adjuvant chemotherapy for early gastric cancer is lacking. Although there is no lymph node metastasis in T2N0M0 gastric cancer, some patients still experience recurrence[10-16]. Therefore, it is important to identify patients with stage T2N0M0 gastric cancer who are at high risk of recurrence and may require adjuvant chemotherapy. Univariate Cox regression analysis demonstrated that tumor site (P = 0.022, Table 2), vascular invasion (P < 0.001, Table 2), and BMI (P = 0.036, Table 2) were significant risk factors for OS in patients with T2N0M0 disease. Multivariate Cox regression analysis showed that vascular invasion was an independent prognostic indicator in patients with T2N0M0 disease[14]. Tumor site has been reported to be a prognostic risk factor for stage IB gastric cancer[11]. The 5-year OS rate of patients with stage IB gastric cancer whose tumors are located in the upper third of the stomach is only 81.8%, which is lower than that of patients with stage II disease receiving S-1 adjuvant chemotherapy[5]. Another study that followed 532 patients reported poorer long-term survival in patients with proximal gastric cancer than in those with distal gastric cancer[20]. Proximal gastric cancer has a higher proportion of undifferentiated tumors, and tumors located in this region can metastasize to almost all lymph nodes, except in the

Table 4 Five-year survival rates of different groups

	Group	*n*	5-year survival rate	Log rank test
All patients				$P = 0.676$
	Adjuvant chemotherapy	63	96%	
	Postoperative observation	262	90%	
Risk score				$P < 0.001$
	Score 0 group	98	92%	
	Score 1 group	152	95%	
	Score 2 group	69	80%	
	Score 3 group	6	50%	
Score 0 group				$P = 0.825$
	Adjuvant chemotherapy	13	92%	
	Postoperative observation	85	92%	
Score 1 group				$P = 0.308$
	Adjuvant chemotherapy	22	92%	
	Postoperative observation	130	96%	
Score 2-3 group				$P = 0.021$
	Adjuvant chemotherapy	28	95%	
	Postoperative observation	47	61%	

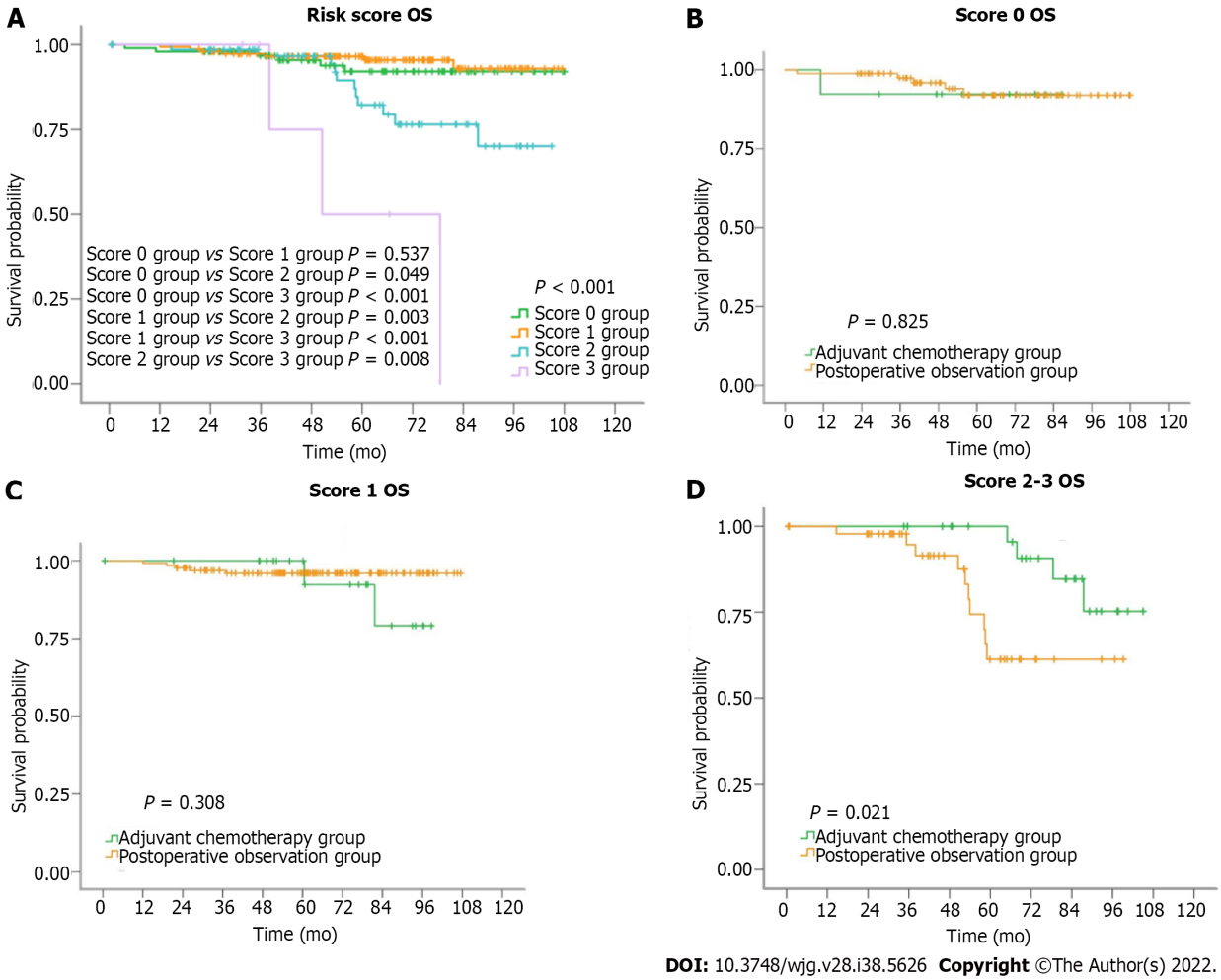
Table 5 Distribution of three different risk factors in each score group

	BMI < 18.5 or > 23.9	Vascular invasion	Cardia cancer
All	149	54	105
Score 0 group	0	0	0
Score 1 group	92	15	45
Score 2 group	51	33	54
Score 3 group	6	6	6

BMI: Body mass index.

five groups[11]. These factors may account for the lower survival rates of patients with proximal gastric cancer. Several studies have shown that BMI affects the prognosis of patients with gastric cancer[21-26]. Low BMI was associated with malnutrition, whereas high BMI was associated with a higher risk of surgery and a higher rate of postoperative complications. A high BMI also increases the risk of stomach cancer[27]. The degree of tumor differentiation was not included in the study, possibly because poorly differentiated tumors do not show significant aggressiveness in the early stages of tumor development.

Based on these findings, we developed a scoring system to assess the need for the use of adjuvant chemotherapy in patients with T2N0M0 gastric cancer. Patients with no or only one risk factor had good prognosis after D2 gastrectomy and did not require adjuvant chemotherapy. Patients in the score 2-3 group had a significantly worse prognosis and could benefit from adjuvant chemotherapy. Our study may help to provide targeted treatment for patients with stage T2N0M0 gastric cancer.This study had some limitations. This was a single-center retrospective study with a lower level of evidence than that of a prospective study. We did not classify the patients into subgroups based on the number of lymph nodes removed. The number of lymph node dissections has a significant effect on OS. For patients with stage T1-2 node-negative gastric cancer, the 5-year survival rate increased by 7.6% for every 10 Lymph nodes examined[28]. No recurrence-free survival or recurrence pattern was observed. We did not discuss the genetic characteristics of patients with gastric cancer included in the study. Genetic characteristics of patients with gastric cancer may influence the efficacy of adjuvant chemotherapy.



DOI: 10.3748/wjg.v28.i38.5626 **Copyright** ©The Author(s) 2022.

Figure 1 Survival curves. A: The survival curves of score 0 group, score 1 group, score 2 group and score 3 group patients; B: The survival curves of score 0 T2N0M0 gastric cancer patients in adjuvant chemotherapy group and postoperative observation group; C: The survival curves of score 1 T2N0M0 gastric cancer patients in adjuvant chemotherapy group and postoperative observation group; D: The survival curves of score 2-3 T2N0M0 gastric cancer patients in adjuvant chemotherapy group and postoperative observation group. OS: Overall survival.

CONCLUSION

For patients with T2N0M0 stage gastric cancer and two or more risk factors, adjuvant chemotherapy after D2 gastrectomy may have a survival benefit. Individualized treatment should be adopted according to examination and pathological results in patients with T2N0M0 gastric cancer.

ARTICLE HIGHLIGHTS

Research background

It is controversial whether adjuvant chemotherapy is necessary for stage T2N0M0 gastric cancer.

Research motivation

To further clarify the indications for the use of postoperative adjuvant chemotherapy in patients with T2N0M0 gastric cancer.

Research objectives

To obtain a risk score to assess the need for adjuvant chemotherapy in patients with T2N0M0 gastric cancer.

Research methods

Univariate and multivariate Cox regression analyses were performed to predict factors affecting prognosis. Vascular invasion, tumor site, and BMI were assessed, and a scoring system was established.

We compared the survival outcomes and benefits of adjuvant chemotherapy between the different subgroups.

Research results

Five-year survival rates of the score 0, 1, 2, and 3 groups were 92%, 95%, 80%, and 50%, respectively ($P < 0.001$). In the score 2-3 group, five-year survival rates for patients in the adjuvant chemotherapy group and postoperative observation group were 95% and 61%, respectively ($P = 0.021$).

Research conclusions

For patients with T2N0M0 stage gastric cancer and two or more risk factors, adjuvant chemotherapy after D2 gastrectomy may have a survival benefit.

Research perspectives

Individualized treatment should be adopted according to examination and pathological results in patients with T2N0M0 gastric cancer.

FOOTNOTES

Author contributions: Xu Q and Kang WZ contributed equally to this work; Tian YT and Xu Q designed the research; Kang WZ, Xiong JP, and Shao XX analyzed the data and wrote the paper; Li WK and Hu HT collected the patient's clinical data.

Supported by the National Natural Science Foundation of China, No. 82072734.

Institutional review board statement: The study was reviewed and approved by the National Cancer Center/National Clinical Research Center for Cancer/Cancer Hospital, Chinese Academy of Medical Sciences and Peking Union Medical College Institutional Review Board (Approval No. 17-156/1412).

Conflict-of-interest statement: All the authors report no relevant conflicts of interest for this article.

Data sharing statement: Dataset available from the author at kwz@whu.edu.cn.

Open-Access: This article is an open-access article that was selected by an in-house editor and fully peer-reviewed by external reviewers. It is distributed in accordance with the Creative Commons Attribution NonCommercial (CC BY-NC 4.0) license, which permits others to distribute, remix, adapt, build upon this work non-commercially, and license their derivative works on different terms, provided the original work is properly cited and the use is non-commercial. See: https://creativecommons.org/Licenses/by-nc/4.0/

Country/Territory of origin: China

ORCID number: Quan Xu 0000-0001-6177-9503; Wen-Zhe Kang 0000-0001-9965-8109; Jian-Ping Xiong 0000-0001-6593-6377; Xin-Xin Shao 0000-0002-1826-3832; Wei-Kun Li 0000-0002-3883-1497; Hai-Tao Hu 0000-0003-0585-6070; Yan-Tao Tian 0000-0001-6479-7547.

S-Editor: Chen YL
L-Editor: A
P-Editor: Chen YL

REFERENCES

1 **Sung H**, Ferlay J, Siegel RL, Laversanne M, Soerjomataram I, Jemal A, Bray F. Global Cancer Statistics 2020: GLOBOCAN Estimates of Incidence and Mortality Worldwide for 36 Cancers in 185 Countries. *CA Cancer J Clin* 2021; **71**: 209-249 [PMID: 33538338 DOI: 10.3322/caac.21660]

2 **Chen W**, Zheng R, Baade PD, Zhang S, Zeng H, Bray F, Jemal A, Yu XQ, He J. Cancer statistics in China, 2015. *CA Cancer J Clin* 2016; **66**: 115-132 [PMID: 26808342 DOI: 10.3322/caac.21338]

3 **Smyth EC**, Nilsson M, Grabsch HI, van Grieken NC, Lordick F. Gastric cancer. *Lancet* 2020; **396**: 635-648 [PMID: 32861308 DOI: 10.1016/S0140-6736(20)31288-5]

4 **Bang YJ**, Kim YW, Yang HK, Chung HC, Park YK, Lee KH, Lee KW, Kim YH, Noh SI, Cho JY, Mok YJ, Ji J, Yeh TS, Button P, Sirzén F, Noh SH; CLASSIC trial investigators. Adjuvant capecitabine and oxaliplatin for gastric cancer after D2 gastrectomy (CLASSIC): a phase 3 open-label, randomised controlled trial. *Lancet* 2012; **379**: 315-321 [PMID: 22226517 DOI: 10.1016/S0140-6736(11)61873-4]

5 **Sasako M**, Sakuramoto S, Katai H, Kinoshita T, Furukawa H, Yamaguchi T, Nashimoto A, Fujii M, Nakajima T, Ohashi Y. Five-year outcomes of a randomized phase III trial comparing adjuvant chemotherapy with S-1 versus surgery alone in stage II or III gastric cancer. *J Clin Oncol* 2011; **29**: 4387-4393 [PMID: 22010012 DOI: 10.1200/JCO.2011.36.5908]

6 **Yoshida K**, Kodera Y, Kochi M, Ichikawa W, Kakeji Y, Sano T, Nagao N, Takahashi M, Takagane A, Watanabe T, Kaji M, Okitsu H, Nomura T, Matsui T, Yoshikawa T, Matsuyama J, Yamada M, Ito S, Takeuchi M, Fujii M. Addition of Docetaxel to Oral Fluoropyrimidine Improves Efficacy in Patients With Stage III Gastric Cancer: Interim Analysis of JACCRO GC-07, a Randomized Controlled Trial. *J Clin Oncol* 2019; **37**: 1296-1304 [PMID: 30925125 DOI: 10.1200/JCO.18.01138]

7 **Yoshikawa T**, Terashima M, Mizusawa J, Nunobe S, Nishida Y, Yamada T, Kaji M, Fukushima N, Hato S, Choda Y, Yabusaki H, Yoshida K, Ito S, Takeno A, Yasuda T, Kawachi Y, Katayama H, Fukuda H, Boku N, Sano T, Sasako M. Four courses versus eight courses of adjuvant S-1 for patients with stage II gastric cancer (JCOG1104 [OPAS-1]): an open-label, phase 3, non-inferiority, randomised trial. *Lancet Gastroenterol Hepatol* 2019; **4**: 208-216 [PMID: 30679107 DOI: 10.1016/S2468-1253(18)30383-2]

8 **Noh SH**, Park SR, Yang HK, Chung HC, Chung IJ, Kim SW, Kim HH, Choi JH, Kim HK, Yu W, Lee JI, Shin DB, Ji J, Chen JS, Lim Y, Ha S, Bang YJ; CLASSIC trial investigators. Adjuvant capecitabine plus oxaliplatin for gastric cancer after D2 gastrectomy (CLASSIC): 5-year follow-up of an open-label, randomised phase 3 trial. *Lancet Oncol* 2014; **15**: 1389-1396 [PMID: 25439693 DOI: 10.1016/S1470-2045(14)70473-5]

9 **Amin MB**, Edge S, Greene F, Byrd DR, Brookland RK, Washington MK, Gershenwald JE, Compton CC, Hess KR, Sullivan DC, Jessup JM, Brierley JD, Gaspar LE, Schilsky RL, Balch CM, Winchester DP, Asare EA, Madera M, Gress DM, Meyer LR. AJCC Cancer Staging Manual. 8th ed. New York: Springer

10 **Yu B**, Park JY, Park KB, Kwon OK, Lee SS, Chung HY. Prognostic Factors in Stage IB Gastric Cancer after Surgical Resection. *J Gastric Cancer* 2020; **20**: 328-336 [PMID: 33024588 DOI: 10.5230/jgc.2020.20.e30]

11 **Aoyama T**, Yoshikawa T, Fujikawa H, Hayashi T, Ogata T, Cho H, Yamada T, Hasegawa S, Tsuchida K, Yukawa N, Oshima T, Oba MS, Morita S, Rino Y, Masuda M. Prognostic factors in stage IB gastric cancer. *World J Gastroenterol* 2014; **20**: 6580-6585 [PMID: 24914380 DOI: 10.3748/wjg.v20.i21.6580]

12 **Wang Z**, Yan J, Hu W, Zhang J, Huo B. Adjuvant chemotherapy provided survival benefit for stage T2N0 gastric cancer with high-risk factors. *Neoplasma* 2018; **65**: 592-598 [PMID: 29940758 DOI: 10.4149/neo_2018_170620N436]

13 **In H**, Kantor O, Sharpe SM, Baker MS, Talamonti MS, Posner MC. Adjuvant Therapy Improves Survival for T2N0 Gastric Cancer Patients with Sub-optimal Lymphadenectomy. *Ann Surg Oncol* 2016; **23**: 1956-1962 [PMID: 26753752 DOI: 10.1245/s10434-015-5075-1]

14 **Du C**, Zhou Y, Huang K, Zhao G, Fu H, Shi Y. Defining a high-risk subgroup of pathological T2N0 gastric cancer by prognostic risk stratification for adjuvant therapy. *J Gastrointest Surg* 2011; **15**: 2153-2158 [PMID: 21938559 DOI: 10.1007/s11605-011-1684-6]

15 **Saito H**, Murakami Y, Miyatani K, Kuroda H, Matsunaga T, Fukumoto Y, Osaki T, Ikeguchi M. Predictive factors for recurrence in T2N0 and T3N0 gastric cancer patients. *Langenbecks Arch Surg* 2016; **401**: 823-828 [PMID: 27460840 DOI: 10.1007/s00423-016-1480-6]

16 **Gabriel E**, Attwood K, Narayanan S, Brady M, Nurkin S, Hochwald S, Kukar M. Does neoadjuvant/perioperative chemotherapy improve overall survival for T2N0 gastric adenocarcinoma? *J Surg Oncol* 2018; **117**: 659-670 [PMID: 29127704 DOI: 10.1002/jso.24894]

17 **Coburn NG**, Govindarajan A, Law CH, Guller U, Kiss A, Ringash J, Swallow CJ, Baxter NN. Stage-specific effect of adjuvant therapy following gastric cancer resection: a population-based analysis of 4,041 patients. *Ann Surg Oncol* 2008; **15**: 500-507 [PMID: 18026800 DOI: 10.1245/s10434-007-9640-0]

18 **Jin LX**, Moses LE, Squires MH 3rd, Poultsides GA, Votanopoulos K, Weber SM, Bloomston M, Pawlik TM, Hawkins WG, Linehan DC, Strasberg SM, Schmidt C, Worhunsky DJ, Acher AW, Cardona K, Cho CS, Kooby DA, Levine E, Winslow ER, Saunders ND, Spolverato G, Maithel SK, Fields RC. Factors Associated With Recurrence and Survival in Lymph Node-negative Gastric Adenocarcinoma: A 7-Institution Study of the US Gastric Cancer Collaborative. *Ann Surg* 2015; **262**: 999-1005 [PMID: 25607760 DOI: 10.1097/SLA.0000000000001084]

19 **Jiang Z**, Sun Y, Zhang W, Cui C, Yang L, Zhou A. Comparison of S-1 plus oxaliplatin (SOX) and capecitabine plus oxaliplatin (XELOX) as adjuvant chemotherapies for stage II and III gastric cancer after D2 resection: A single-center retrospective study. *Asia Pac J Clin Oncol* 2020; **16**: 180-186 [PMID: 32077628 DOI: 10.1111/ajco.13321]

20 **Piso P**, Werner U, Lang H, Mirena P, Klempnauer J. Proximal versus distal gastric carcinoma--what are the differences? *Ann Surg Oncol* 2000; **7**: 520-525 [PMID: 10947021 DOI: 10.1007/s10434-000-0520-0]

21 **Wada T**, Kunisaki C, Ono HA, Makino H, Akiyama H, Endo I. Implications of BMI for the Prognosis of Gastric Cancer among the Japanese Population. *Dig Surg* 2015; **32**: 480-486 [PMID: 26529523 DOI: 10.1159/000440654]

22 **Guo ZQ**, Yu JM, Li W, Fu ZM, Lin Y, Shi YY, Hu W, Ba Y, Li SY, Li ZN, Wang KH, Wu J, He Y, Yang JJ, Xie CH, Song XX, Chen GY, Ma WJ, Luo SX, Chen ZH, Cong MH, Ma H, Zhou CL, Wang W, Luo Q, Shi YM, Qi YM, Jiang HP, Guan WX, Chen JQ, Chen JX, Fang Y, Zhou L, Feng YD, Tan RS, Li T, Ou JW, Zhao QC, Wu JX, Deng L, Lin X, Yang LQ, Yang M, Wang C, Song CH, Xu HX, Shi HP; Investigation on the Nutrition Status and Clinical Outcome of Common Cancers (INSCOC) Group. Survey and analysis of the nutritional status in hospitalized patients with malignant gastric tumors and its influence on the quality of life. *Support Care Cancer* 2020; **28**: 373-380 [PMID: 31049672 DOI: 10.1007/s00520-019-04803-3]

23 **Chen S**, Nie RC, OuYang LY, Li YF, Xiang J, Zhou ZW, Chen Y, Peng J. Body mass index (BMI) may be a prognostic factor for gastric cancer with peritoneal dissemination. *World J Surg Oncol* 2017; **15**: 52 [PMID: 28228146 DOI: 10.1186/s12957-016-1076-1]

24 **Lianos GD**, Bali CD, Glantzounis GK, Katsios C, Roukos DH. BMI and lymph node ratio may predict clinical outcomes of gastric cancer. *Future Oncol* 2014; **10**: 249-255 [PMID: 24490611 DOI: 10.2217/fon.13.188]

25 **Feng F**, Zheng G, Guo X, Liu Z, Xu G, Wang F, Wang Q, Guo M, Lian X, Zhang H. Impact of body mass index on surgical outcomes of gastric cancer. *BMC Cancer* 2018; **18**: 151 [PMID: 29409475 DOI: 10.1186/s12885-018-4063-9]

26 **Tsekrekos A**, Lovece A, Chrysikos D, Ndegwa N, Schizas D, Kumagai K, Rouvelas I. Impact of obesity on the outcomes after gastrectomy for gastric cancer: A meta-analysis. *Asian J Surg* 2022; **45**: 15-26 [PMID: 33965317 DOI: 10.1016/j.asjsur.2021.04.033]

27 **Hirabayashi M**, Inoue M, Sawada N, Saito E, Abe SK, Hidaka A, Iwasaki M, Yamaji T, Shimazu T, Shibuya K, Tsugane

S; JPHC Study Group. Effect of body-mass index on the risk of gastric cancer: A population-based cohort study in A Japanese population. *Cancer Epidemiol* 2019; **63**: 101622 [PMID: 31654882 DOI: 10.1016/j.canep.2019.101622]

28 **Smith DD**, Schwarz RR, Schwarz RE. Impact of total lymph node count on staging and survival after gastrectomy for gastric cancer: data from a large US-population database. *J Clin Oncol* 2005; **23**: 7114-7124 [PMID: 16192595 DOI: 10.1200/JCO.2005.14.621]

World Journal of Gastroenterology

Submit a Manuscript: https://www.f6publishing.com

World J Gastroenterol 2022 October 14; 28(38): 5636-5647

DOI: 10.3748/wjg.v28.i38.5636

ISSN 1007-9327 (print) ISSN 2219-2840 (online)

ORIGINAL ARTICLE

Observational Study

Red blood cell distribution width derivatives in alcohol-related liver cirrhosis and metabolic-associated fatty liver disease

Agata Michalak, Małgorzata Guz, Joanna Kozicka, Marek Cybulski, Witold Jeleniewicz, Tomasz Lach, Halina Cichoż-Lach

Specialty type: Gastroenterology and hepatology

Provenance and peer review: Unsolicited article; Externally peer reviewed.

Peer-review model: Single blind

Peer-review report's scientific quality classification

Grade A (Excellent): 0
Grade B (Very good): B
Grade C (Good): C, C
Grade D (Fair): D
Grade E (Poor): 0

P-Reviewer: Hu BL, China; Xu RY, China; Zhu CW, China

Received: July 4, 2022
Peer-review started: July 4, 2022
First decision: July 31, 2022
Revised: August 7, 2022
Accepted: September 21, 2022
Article in press: September 21, 2022
Published online: October 14, 2022

Agata Michalak, Joanna Kozicka, Halina Cichoż-Lach, Department of Gastroenterology, Medical University of Lublin, Lublin 20-954, Poland

Małgorzata Guz, Marek Cybulski, Witold Jeleniewicz, Department of Biochemistry and Molecular Biology, Medical University of Lublin, Lublin 20-093, Poland

Tomasz Lach, Department of Orthopedics and Traumatology, Medical University of Lublin, Lublin 20-954, Poland

Corresponding author: Halina Cichoż-Lach, PhD, Professor, Department of Gastroenterology, Medical University of Lublin, Jaczewski Str. 8, Lublin 20-954, Poland. lach.halina@wp.pl

Abstract

BACKGROUND

Looking for undiscovered blood markers of liver fibrosis and steatosis still remains an issue worth exploring. There are still plenty of unresolved issues related to the actual role of hematological indices as potential markers of liver function.

AIM

To study red blood cell distribution width (RDW), RDW-to-platelet ratio (RPR) and RDW-to-lymphocyte ratio (RLR) in alcohol-related liver cirrhosis (ALC) and metabolic-associated fatty liver disease (MAFLD).

METHODS

The study group was composed of 302 people: 142 patients with ALC and 92 with MAFLD; 68 persons were included as controls. RDW, RPR and RLR were measured in each person. Indirect and direct parameters of liver fibrosis were also assessed [aspartate transaminase to alkaline transaminase ratio, aspartate transaminase to platelet ratio index (APRI), fibrosis-4 (FIB-4), gamma-glutamyl transpeptidase to platelet ratio (GPR), procollagen I carboxyterminal propeptide, procollagen III aminoterminal propeptide, transforming growth factor-α, platelet-derived growth factor AB, laminin]. MELD score in ALC patients and non-alcoholic fatty liver disease (NAFLD) fibrosis score together with BARD score were obtained in the MAFLD group. The achieved results were compared to controls. Then a correlation between assessed markers was done. Diagnostic value of each investigated parameter and its suggested cut-off in the research group

were evaluated with area under the curve (AUC).

RESULTS

RDW, RPR and RLR values turned out to be significantly higher in ALC and MAFLD groups compared to controls (ALC: $P < 0.0001$; NAFLD: $P < 0.05$, $P < 0.0001$ and $P < 0.0001$, respectively). RPR correlated positively with MELD score ($P < 0.01$) and indirect indices of liver fibrosis (FIB-4 and GPR; $P < 0.0001$) in ALC patients; negative correlations were found between PDGF-AB and both: RDW and RPR ($P < 0.01$ and $P < 0.0001$, respectively). RPR correlated positively with NAFLD fibrosis score and APRI ($P < 0.0001$) in the MAFLD group; a positive relationship was observed between RDW and FIB-4, too ($P < 0.05$). AUC values and suggested cut-offs for RDW, RPR and RLR in ALC patients were: 0.912 (> 14.2%), 0.965 (> 0.075) and 0.914 (> 8.684), respectively. AUC values and suggested cut-offs for RDW, RPR and RLR in MAFLD patients were: 0.606 (> 12.8%), 0.724 (> 0.047) and 0.691 (> 6.25), respectively.

CONCLUSION

RDW with its derivatives appear to be valuable diagnostic markers in patients with ALC. They can also be associated with a deterioration of liver function in this group.

Key Words: Hematological indices; Alcohol-related liver cirrhosis; Metabolic-associated liver disease; Red blood cell distribution width; Red blood cell distribution width-to-platelet ratio; Red blood cell distribution width-to-lymphocyte ratio

©The Author(s) 2022. Published by Baishideng Publishing Group Inc. All rights reserved.

Core Tip: Red blood cell distribution width (RDW), RDW-to-platelet ratio (RPR) and RDW-to-lymphocyte ratio (RLR) remain uninvestigated in Polish patients suffering from alcohol-related liver cirrhosis (ALC) and metabolic-associated liver disease. Based on the available literature, association between RDW, RPR, RLR and serological (indirect and direct) indices of liver fibrosis have never been explored in a single study to date. We consider RPR as a potential reliable diagnostic tool in the assessment of ALC patients, corresponding with MELD score and serous markers of liver cirrhosis. Hematological parameters could be perceived as possible indices in the noninvasive evaluation of people with liver disorders.

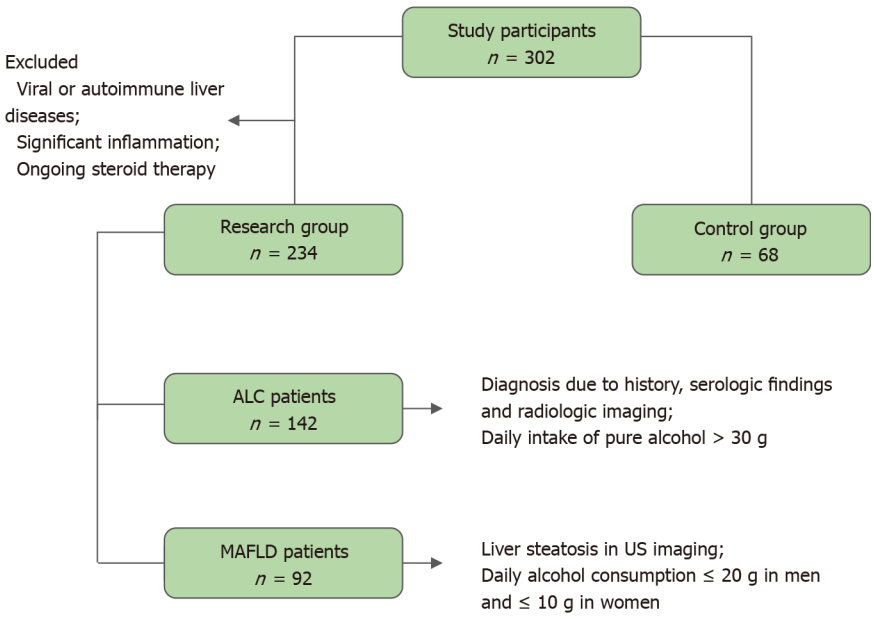
Citation: Michalak A, Guz M, Kozicka J, Cybulski M, Jeleniewicz W, Lach T, Cichoż-Lach H. Red blood cell distribution width derivatives in alcohol-related liver cirrhosis and metabolic-associated fatty liver disease. *World J Gastroenterol* 2022; 28(38): 5636-5647

URL: https://www.wjgnet.com/1007-9327/full/v28/i38/5636.htm

DOI: https://dx.doi.org/10.3748/wjg.v28.i38.5636

INTRODUCTION

Alcohol-related liver cirrhosis (ALC) and metabolic-associated fatty liver disease (MAFLD) belong to pathologies with an undeniable global impact. Their monitoring and prediction of a possible outcome are of crucial importance. Due to the progress in hepatology and increased access to new imaging techniques, the evaluation of advanced liver fibrosis (even without a biopsy) turned out to be available. Nevertheless, liver elastography in an ultrasound or magnetic resonance mode are not commonly accessible tools in all medical centers. Direct and indirect markers of liver fibrosis obtained from the blood still remain quite trustworthy indices, but they are not perfect, either. Thus, looking for potentially novel parameters of liver disease progression is a key goal in the field of hepatology[1-4]. The most meaningful and valuable future diagnostic tools are new noninvasive blood markers of liver fibrosis; red blood cell distribution width (RDW) together with RDW-to-platelet ratio (RPR) were suggested to be such probable indices. Nevertheless, their probable role in the course of liver steatosis has been poorly explored. RDW reflects the diversity of red blood cells in volume and size. It is obtained from automated hematology analyzers in everyday clinical practice. In the past, RDW was clinically applied only to diagnose anemia or related maladies. Nowadays the spectrum of its possible clinical performance has been significantly broadened. RDW and RPR have already been proven to achieve higher levels in the course of the neoplastic process, being connected with an overall poor survival (*e.g.*, in the course of cervical, colorectal and prostate cancers), as well[5-7]. Cardiovascular disorders and stroke constitute other pathologies that were explored in the context of RDW. Its high level was even



DOI: 10.3748/wjg.v28.i38.5636 **Copyright** ©The Author(s) 2022.

Figure 1 Flow chart demonstrating the selection of study participants. ALC: Alcohol-related liver cirrhosis; MAFLD: Metabolic-associated fatty liver disease; US: Ultrasound.

proved to be associated with a 3-mo poor functional outcome in the course of thrombolytic therapy due to acute ischemic stroke. RDW was additionally described as a marker of acutely decompensated chronic heart failure and an indicator of increased mortality among critically ill patients with myocardial infarction[8-11]. Of note, except for RDW derivatives, hematocrit was found to be inseparably connected with the development of atherosclerosis (evaluated as internal carotid intima-media thickness) in MAFLD patients, suggesting a common potential role of hematological markers - not only in MAFLD, but also due to MAFLD-followed cardiovascular disorders[12]. Thus, RDW derivatives can be perceived as systemic markers of various pathologies. Moreover, according to previously conducted studies, RDW and RPR can even correlate with MELD score and are suggested to behave as markers of poor survival in patients with chronic liver pathologies. RDW-to-lymphocyte ratio (RLR) appears to be a relatively uninvestigated parameter in patients with liver disorders[13-16]. We suspect that no survey to date has explored the diagnostic role of RDW derivatives and their relationships with serological indices of liver fibrosis in the course of ALC and MAFLD. Furthermore, our investigation appears to be the first one performed on Polish patients to evaluate existing dependences between hematological indices and serological markers of liver fibrosis.

MATERIALS AND METHODS

The survey was accepted by the local ethics committee of the Medical University of Lublin (No. KE-0254/86/2016) and all participants signed an informed written consent on the basis of the Helsinki Declaration for the procedures they followed.

Materials

The investigation was conducted retrospectively on 302 persons. The study group was formed by 142 patients with ALC and 92 with MAFLD. The control group was represented by 68 healthy volunteers. Figure 1 displays the selection of the participants included in the survey. Table 1 shows clinical features of the study population. The diagnosis of liver cirrhosis (LC) was established in accordance with commonly used criteria. The doppler mode abdominal ultrasound examination was applied to confirm the presence of portal hypertension (diameter of portal vein ≥ 13 mm). Different underlying factors leading to portal hypertension were ruled out. Panendoscopy was performed in each of the 142 persons belonging to the ALC group - in 126 of them varices in the esophagus or stomach of the different stages were visualized. Ascites was found in 92 of the ALC patients, leading consequently to the paracentesis in 84 of them. None from the study group suffered from hepatic encephalopathy or spontaneous bacterial peritonitis. All persons enrolled to the survey were given 0/9 points on the CHESS scale. Alcohol-related etiology of LC was figured out due to the proven daily intake of pure ethanol more than 30 g. A detailed history of alcohol addiction was obtained directly from the patients or their trustworthy family members. In addition, all included in the study of ALC patients got positive results on the

Table 1 Clinical characteristics of study participants

Parameter	ALC, *n* = 142	MAFLD, *n* = 92	Controls, *n* = 68	Together, *n* = 302
Sex (F/M)	36/106	33/59	36/32	105/197
Age (yr), (mean ± SD; median; min-max)	54 ± 12; 55; 31-84	60 ± 15; 61; 22-90	46 ± 16; 45; 20-85	54 ± 15; 55; 20-90
BMI (kg/m^2) (mean ± SD; median; min-max)	25.89 ± 9.31; 25.91; 16.7-36.71	29.49 ± 4.9; 28.7; 16.26-43.01	21.95 ± 2.62; 22.45; 16.18-24.86	-
DM type 2	0/142	22/92	-	-
AH	32/142	46/92	-	-

F: Female; M: Male; min: Minimum; max: Maximum; BMI: Body mass index; DM: Diabetes mellitus; AH: Arterial hypertension.

conducted CAGE test. On the other hand, MAFLD was diagnosed according to the previous history, physical examination, laboratory findings and ultrasound imaging. A daily alcohol consumption amount was not greater than 20 g in men and 10 g in women. Disorders potentially responsible for the development of liver steatosis (celiac disease, Wilson's disease, hepatobiliary infections and alpha-1-antitrypsin deficiency) had been ruled out. Diabetes mellitus type 2 was identified among 22 persons. The presence of diabetes mellitus type 1 caused the exclusion from the survey. None of the MAFLD patients was diagnosed with impaired fasting glucose. Forty six of them were found to suffer from arterial hypertension; 84 persons presented features of metabolic syndrome. Viral/autoimmune liver diseases, clinically relevant inflammatory process and anemia constituted other excluding criteria. None of the survey participants was on steroid therapy.

Procedures

Venous blood samples obtained from peripheral blood were collected from all study participants. EDTA was applied to evaluate hematological indices and citrate to evaluate clotting. Biochemical indices were obtained from the blood samples without an anticoagulant. We collected the blood after at least 12 h of fasting. Hematological and biochemical procedures were performed 4 h after blood sample collection. All of the measurements were conducted in the laboratory of Clinical Hospital Number 4, Lublin, Poland. The remaining part of the blood samples, without an anticoagulant, were centrifuged at the speed of 2000 *g* for 10 min within 15 min after blood collection. The obtained serum was then stored in 1 mL Eppendorf test tubes at the temperature of -80 °C until the evaluation of direct markers of liver fibrosis with ELISA. Among morphotic parameters of the blood, the RDW, RPR and RLR were obtained. The evaluation of indirect indices of liver cirrhosis concerned: Aspartate transaminase to alkaline transaminase ratio (AAR), aspartate transaminase to platelet ratio index (APRI), FIB-4 (fibrosis-4) and gamma-glutamyl transpeptidase to platelet ratio (GPR) (GGT to PLT Ratio). MELD score was assessed in the ALC patients and non-alcoholic fatty liver disease (NAFLD) fibrosis score and BARD score were applied to the MAFLD group. Procollagen I carboxyterminal propeptide (PICP), procollagen III aminoterminal propeptide (PIIINP), platelet-derived growth factor AB (PDGF-AB), transforming growth factor-α (TGF-α) and laminin belonged to direct indices of liver fibrosis that were measured. Laboratory procedures were performed in the Department of Biochemistry and Molecular Biology, Medical University of Lublin according to the recommended indications. The assessment of PICP and PIIINP was conducted with quantitative ELISA tests. PDGF-AB and TGF-α were evaluated with the use of R&D Systems Quantikine ELISA Kits. Finally, the measurement of the concentration of laminin was possible because of the Takara Laminin EIA Kit without Sulphuric Acid.

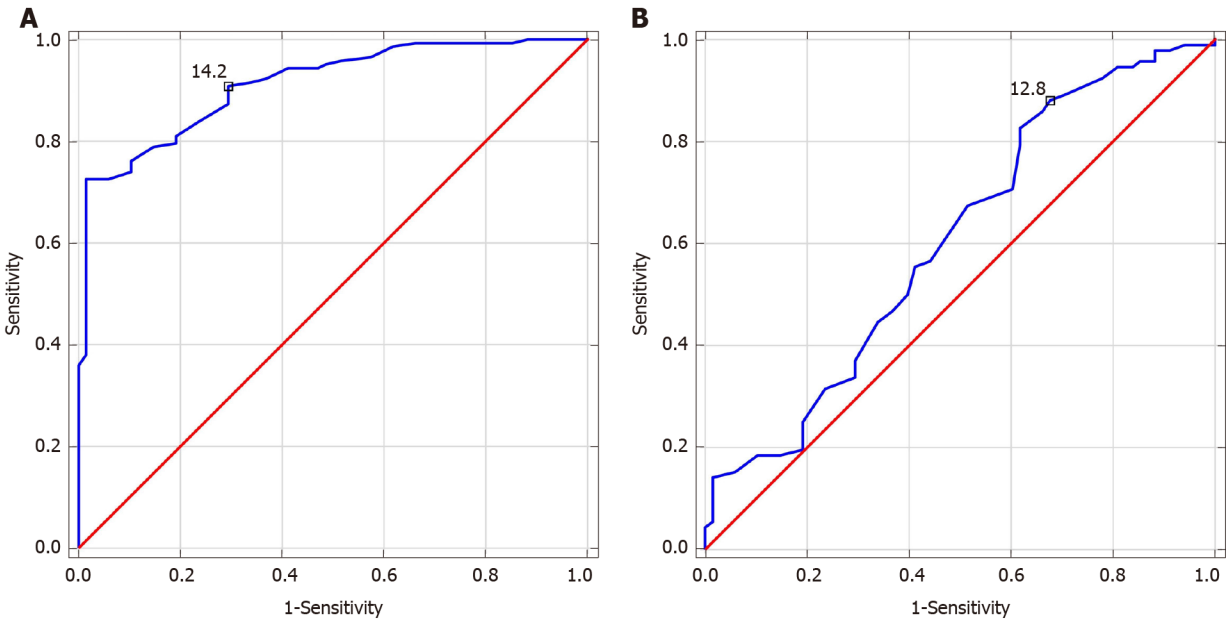
Statistical analysis

Statistical analysis of the results was carried out with Statistica 13.0 (StatSoft Polska Sp. z o.o., Kraków, Poland) for Windows system. The demographic characteristics of study participants and findings of laboratory investigations were shown as the mean ± SD and Student's *t* test was applied to compare these data. Deviation from normality was assessed with the use of Kolmogorov-Smirnov test. Data collected in the study were shown as the median and range (minimum–maximum). The Mann-Whitney *U* test was applied for between-group comparisons due to non-normal distribution. The correlations were verified with Spearman correlation analyses. All probability values were two-tailed, and a value of *P* less than 0.05 was perceived as statistically significant. Receiver operating characteristic (ROC) curves and area under the curve (AUC) values were used to evaluate the sensitivity and specificity of investigated indices and to verify suggested cut-offs of tested markers in ALC and MAFLD patients.

Table 2 Results of used scores in research group

Score	ALC				MAFLD			
	mean ± SD	Median	Min	Max	mean ± SD	Median	Min	Max
MELD	17 ± 8	16	6	45	-	-	-	-
BARD	-	-	-	-	2 ± 1	2	0	4
NAFLD fibrosis score	-	-	-	-	-1.36 ± 1.5	-1.16	-5.83	1.74

Min: Minimum; Max: Maximum; MELD: Model for end-stage liver disease; NAFLD: Non-alcoholic fatty liver disease.

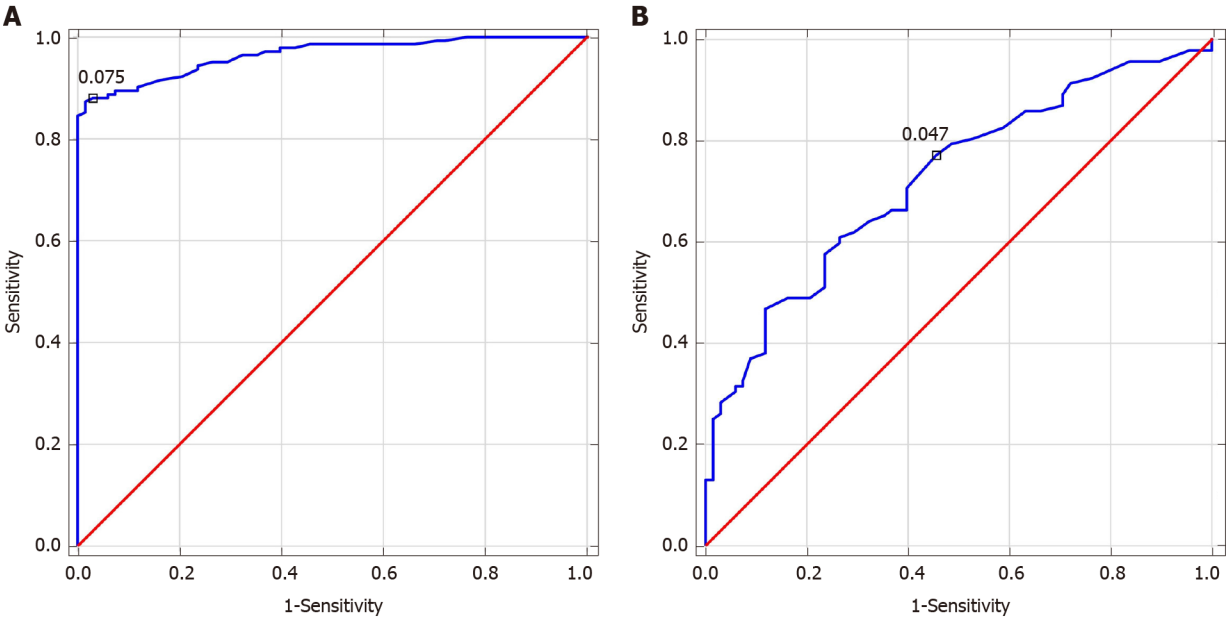


DOI: 10.3748/wjg.v28.i38.5636 **Copyright** ©The Author(s) 2022.

Figure 2 Receiver operating characteristics for red blood cell distribution width. A: Alcohol-related liver cirrhosis (ALC), area under the curve (AUC) = 0.912 (cut-off > 14.2%); B: Metabolic-associated fatty liver disease (MAFLD), AUC = 0.606 (cut-off > 12.8%). Youden index cut-off for red blood cell distribution width in ALC and MAFLD groups = 15.1% and 13%, respectively.

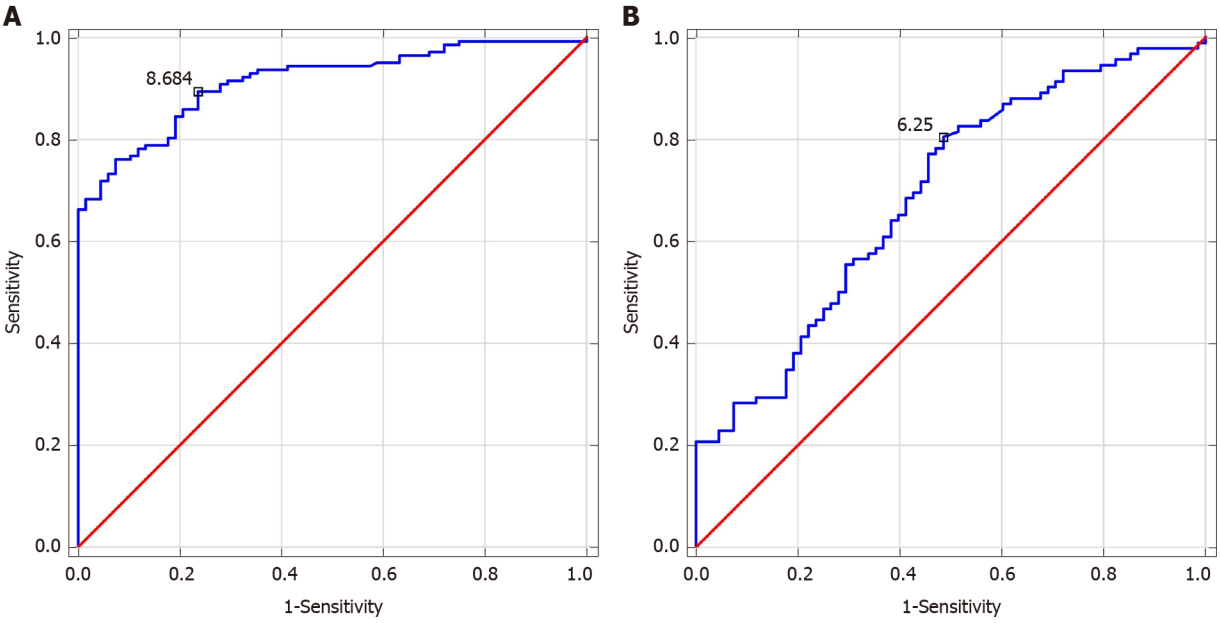
RESULTS

Table 2 presents results of applied scores in the research group. Results of hematological parameters are presented in Table 3. The RDW level was above the reference range in both the ALC and MAFLD groups; its level was significantly higher in comparison to the controls ($P < 0.0001$ and $P < 0.05$, respectively). RPR and RLR values turned out to be significantly higher among ALC and MAFLD patients compared to the control group ($P < 0.0001$). Table 3 presents results of indirect and direct indices of liver fibrosis, as well. The medians of AAR, APRI, FIB-4 and GPR were shown to be significantly higher within the ALC group in comparison to the controls ($P < 0.0001$). Excluding AAR, patients with MAFLD were observed to present notably higher values of all the enumerated above indirect markers of liver fibrosis compared to the control group ($P < 0.0001$). According to the direct parameters of liver fibrosis, laminin value in the course of ALC was importantly higher than in the control group ($P < 0.05$). Except for PICP, medians of PIIINP, PDGF-AB and TGF-α had notably lower levels ($P < 0.01$, $P < 0.001$, $P < 0.0001$, respectively). Concentrations of TGF-α and laminin in MAFLD patients in comparison to controls were found to be remarkably lower ($P < 0.0001$). PICP, PIIINP and PDGF-AB medians did not differ in a significant pattern. Table 4 presents noted correlations between evaluated indices in ALC and MAFLD groups. We observed meaningful positive dependences between RPR and indirect parameters of liver cirrhosis - FIB-4 and GPR ($P < 0.0001$) in the ALC patients. RDW and RPR correlated in a negative pattern with PDGF-AB ($P < 0.01$ and $P < 0.0001$, respectively). A positive correlation was found between RPR and MELD scores ($P < 0.01$). Other positive dependences were observed between: RDW and FIB-4 ($P < 0.05$), and between RPR and APRI ($P < 0.0001$), in the MAFLD group. RPR correlated positively with the NAFLD fibrosis scores ($P < 0.0001$), as well. Table 5 shows diagnostic accuracy of evaluated hematological markers. ROCs describing investigated parameters in the ALC and MAFLD groups are shown below in Figures 2-4. AUC values with



DOI: 10.3748/wjg.v28.i38.5636 **Copyright** ©The Author(s) 2022.

Figure 3 Receiver operating characteristics for red blood cell distribution width-to-platelet ratio. A: Alcohol-related liver cirrhosis (ALC), area under the curve (AUC) = 0.965 (cut off > 0.075); B: Metabolic-associated fatty liver disease (MAFLD), AUC = 0.724 (cut-off > 0.047). Youden index cut-off for red blood cell distribution width-to-platelet ratio in ALC and MAFLD groups = 0.08 and 0.06, respectively.



DOI: 10.3748/wjg.v28.i38.5636 **Copyright** ©The Author(s) 2022.

Figure 4 Receiver operating characteristics for red blood cell distribution width-to-lymphocyte ratio. A: Alcohol-related liver cirrhosis (ALC), area under the curve (AUC) = 0.914 (cut-off > 8.684); B: Metabolic-associated fatty liver disease (MAFLD), AUC = 0.691 (cut-off > 6.25). Youden index cut-off for red blood cell distribution width-to-lymphocyte ratio in ALC and MAFLD groups = 11.16 and 6.25, respectively.

suggested cut-offs for RDW, RPR and RLR in ALC patients were: 0.912 (> 14.2%), 0.965 (> 0.075) and 0.914 (> 8.684), respectively. AUC values and proposed cut-offs for RDW, RPR and RLR in the MAFLD groups were: 0.606 (> 12.8%), 0.724 (> 0.047) and 0.691 (> 6.25), respectively.

DISCUSSION

New reliable blood markers required in the evaluation of liver fibrosis and clinical prognosis of cirrhosis are permanently in the interest of scientists. Several years ago, basic hematological indices, used in

Table 3 Results of indirect and direct markers of liver fibrosis together with hematological markers in examined patients

Parameter (reference range)	ALC				MAFLD				Controls			
	mean ± SD	Median	Min	Max	mean ± SD	Median	Min	Max	mean ± SD	Median	Min	Max
RDW (11%-15%)	17.27 ± 3.26	**16.7**[d]	12.2	27.9	14.25 ± 2.52	**13.85**[a]	4.2	25	13.45 ± 1.1	**13.4**	11.1	15
RPR	0.26 ± 0.37	**0.18**[d]	0.04	3.55	0.06 ± 0.02	**0.06**[d]	0.02	0.18	0.05 ± 0.01	**0.05**	0.03	0.08
RLR	19.14 ± 12.27	**15.73**[d]	1.6	79.23	10.89 ± 8.55	**8.13**[d]	0.66	60	7.09 ± 2.48	**6.24**	3.38	12.5
FIB-4	11.67 ± 25.46	**6.34**[d]	0.69	287.59	1.92 ± 1.63	**1.57**[d]	0.23	11.58	0.85 ± 0.54	**0.71**	0.28	3.27
GPR	15.73 ± 28.54	**6.65**[d]	0.18	188.71	2.76 ± 5.57	**0.54**[d]	0.13	35.41	0.25 ± 0.1	**0.24**	0.06	0.63
PICP (ng/mL)	63.32 ± 31.53	**60.53**	6.15	161.12	52.14 ± 27.56	**46.08**	10.10	147.27	58.26 ± 37.39	**44.18**	0	202.89
PIIINP (ng/mL)	9.28 ± 4.33	**8.4**[b]	2.43	28.65	11.41 ± 3.99	**11.00**	2.18	25.35	11.07 ± 5.61	**10.25**	4.35	43.63
PDGF-AB (pg/mL)	18280.47 ± 8061.06	**17343.71**[c]	1925.68	42823.84	26858.68 ± 7335.09	**26682.83**	10821.02	49808.07	23579.28 ± 10068.8	**25623.2**	1638.2	47758.7
TGF-α (pg/mL)	24 ± 45.33	**13.77**[d]	0.872	507.09	17.89 ± 19.18	**12.09**[d]	1.39	142.63	28.44 ± 17.21	**24.59**	1.31	93.55
Laminin (ng/mL)	976.34 ± 705.29	**832.06**[a]	101.933	3301.00	48 ± 230.24	**375.23**[d]	72.87	1335.92	718.24 ± 386.1	**663.27**	140.88	1813.88

[a]$P < 0.05$.
[b]$P < 0.01$.
[c]$P < 0.001$.
[d]$P < 0.0001$.

ALC: Alcoholic liver cirrhosis; MAFLD: Metabolic associated fatty liver disease; Min: Minimum; Max: Maximum; AAR: Aspartate transaminase to alkaline transaminase ratio; APRI: Aspartate transaminase to platelet ratio index; FIB-4: Fibrosis-4; GPR: Gamma-glutamyl transpeptidase to platelet ratio; PICP: Procollagen I carboxyterminal propeptide; PIIINP: Procollagen III aminoterminal propeptide; PDGF-AB: Platelet-derived growth factor AB; TGF-α: Transforming growth factor-α; RDW: Red blood cell distribution width; RPR: Red blood cell distribution width-to-platelet ratio; RLR: Red blood cell distribution width-to-lymphocyte ratio.

everyday life, were proposed as potential candidates in this area, *e.g.*, mean platelet volume, platelet crit and RDW. It is assumed that their linkage with liver disorders is due to the inflammation and the release of interleukin-6, interfering hemolytic anemia, hypersplenism and bone marrow activation. The greatest number of surveys in this area of hepatology seems to concern hepatitis B virus- and hepatitis C virus-related cirrhosis; the ALC and MAFLD patients were not explored as much[17-20]. Moreover, a quick diagnosis and further staging of liver steatosis is also a crucial goal nowadays, due to the global prevalence of MAFLD together with its possible severe consequences. RDW derivatives require further investigations in the context of liver disorders. Being the marker of red blood cells heterogeneity, RDW was commonly used as an indicator of anemia. However, it turned out that its potential role can be even more complex. Former surveys proved that the progression of liver cirrhosis is accompanied by an increase in RDW and its elevation might even be a marker of poor prognosis. Similar observations were made with reference to its derivative - RPR. Recent meta-analyses by Cai *et al*[21] and Milas *et al*[22] confirmed these data. RDW and RPR were even found to be markers of increased mortality in ALC

Table 4 Correlations between examined parameters in examined alcohol-related liver cirrhosis and metabolic-associated fatty liver disease patients

Pair	R Spearman	*P* value
ALC		
RPR *vs* FIB-4	0.733	$P < 0.0001$
RPR *vs* GPR	0.398	$P < 0.0001$
RPR *vs* MELD	0.267	$P < 0.01$
RDW *vs* PDGF-AB	-0.257	$P < 0.01$
RPR *vs* PDGF-AB	-0.380	$P < 0.0001$
MAFLD		
RDW *vs* FIB-4	0.215	$P < 0.05$
RPR *vs* APRI	0.469	$P < 0.0001$
RPR *vs* NFS	0.688	$P < 0.0001$

ALC: Alcoholic liver cirrhosis; MAFLD: Metabolic-associated fatty liver disease; RDW: Red blood cell distribution width; RPR: Red blood cell distribution width-to-platelet ratio; MELD: Model of end stage liver disease; APRI: Aspartate transaminase to platelet ratio index; FIB-4: Fibrosis-4; GPR: Gamma-glutamyl transpeptidase to platelet ratio; PDGF-AB: Platelet-derived growth factor AB; NFS: NAFLD fibrosis score.

patients - independently of MELD score. Lately, RDW elevation was found to accompany severe inflammation and liver fibrosis in three independent studies on autoimmune hepatitis patients[23-25]. RDW was even proposed as a prognostic marker in the course of hepatocellular carcinoma[26,27]. What is more, recently a higher level of RLR has been explored as a potential marker of its recurrence[28]. In our ALC group, RPR correlated positively with MELD score and the diagnostic accuracy of both: RDW and RPR turned out to be high (AUC = 0.912 and AUC = 0.965, respectively). A close relationship between RDW derivatives and indirect indices of liver fibrosis in the course of cirrhosis was already established and our results support this association. However, it seems that previous surveys did not explore relationships between RDW derivatives and indirect parameters of liver fibrosis. According to the available literature, we are the first to note a negative correlation between PDGF-AB concentration and both: RDW and RPR levels in the course of ALC. RLR appears to be explored so far, among liver pathologies, only in the course of primary biliary cholangitis (PBC) and in people affected with acute hepatitis E virus (HEV) infection. Its diagnostic accuracy in the assessment of liver fibrosis in PBC patients and in the diagnosis of HEV infection in symptomatic patients was better compared to APRI, FIB-4 and RPR[29-31]. Our study appears to be the first one concentrating on the role of RLR in ALC and MAFLD. Interestingly, its diagnostic accuracy in the ALC patients turned out to be very high (AUC = 0.914). The data on RDW derivatives in MAFLD patients are very limited. However, previous research observed that elevation in RDW can be assumed as a sign of the progression of simple steatosis to steatohepatitis and the progression of liver fibrosis in the course of MAFLD[32-36]. In our examined MAFLD patients, RPR correlated positively with indirect parameters of liver fibrosis and NAFLD fibrosis score, however, its diagnostic accuracy was quite disappointing (AUC = 0.606). In our survey, we did not aim to perform the comparison of selected hematological markers between the ALC and MAFLD patients. The purpose of our study was to find out whether deviations in certain hematological parameters might accompany an isolated liver steatosis. Our investigation focused on the population of people with MAFLD without the evaluation of possible features of hepatitis in liver biopsy. In the future, we would like to differentiate patients with a simple steatosis and already developed steatohepatitis confirmed by liver biopsy in the context of potential deviations among hematological markers.

CONCLUSION

In conclusion, our study gives a new insight into the tight relationship between serological indices of liver fibrosis and RDW derivatives in patients with liver pathologies. Especially, RLR seems to be a valuable unexplored parameter in the course of ALC. Its high diagnostic accuracy in our ALC patients is a promising message for subsequent studies. Undoubtedly, this direction of research should be continued to define a potential role of commonly accessible RDW derivatives as indicators of liver disorders in everyday clinical life.

Table 5 Diagnostic accuracy of hematological indices in examined alcohol-related liver cirrhosis and metabolic-associated fatty liver disease patients

Parameter	ALC								MAFLD							
	Diagnostic accuracy								Diagnostic accuracy							
	AUC	Sensitivity (%)	Specificity (%)	PPV (%)	NPV (%)	PLR	NLR	*P* value	AUC	Sensitivity (%)	Specificity (%)	PPV (%)	NPV (%)	PLR	NLR	*P* value
RDW	**0.912**	91	71	87	79	3.14	0.13	$P < 0.0001$	**0.606**	88	32	64	67	1.29	0.38	$P < 0.05$
RPR	**0.965**	88	97	98	80	29.33	0.12	$P < 0.0001$	**0.724**	77	54	70	64	1.67	0.43	$P < 0.0001$
RLR	**0.914**	89	77	89	78	3,87	0,14	$P < 0.0001$	**0.691**	80	52	69	66	1.67	0.38	$P < 0.0001$

ALC: Alcoholic liver cirrhosis; MAFLD: Metabolic-associated fatty liver disease; AUC: Area under the curve; PPV: Positive predictive value; NPV: Negative predictive value; PLR: Positive likelihood; NLR: Negative likelihood ratio.

ARTICLE HIGHLIGHTS

Research background

The most meaningful and valuable future diagnostic tools are new noninvasive blood markers of liver fibrosis, and red blood cell distribution width (RDW) together with RDW-to-platelet-(PLT)-ratio (RPR) were suggested to be such probable indices. Their potential role in the course of liver disorders still requires further elucidation.

Research motivation

In light of the above, we decided to study the diagnostic role of RDW derivatives and their relationships with direct and indirect indices of liver fibrosis in patients with alcohol-related liver cirrhosis (ALC) and metabolic-associated fatty liver disease (MAFLD). It seems to be the first investigation performed among Polish patients to evaluate the potential dependences between hematological parameters and serological markers of liver fibrosis.

Research objectives

The aim of the study was the evaluation of RDW, RPR and RDW-to-lymphocyte ratio (RLR) in ALC and MAFLD patients.

Research methods

The study group was comprised of 302 persons: 142 patients with ALC, 92 with MAFLD and 68 volunteers as controls. RDW, RPR and RLR were assessed in each participant. Indirect and direct indices of liver fibrosis were also measured [aspartate transaminase to alkaline transaminase ratio, aspartate transaminase to platelet ratio index (APRI), fibrosis-4 (FIB-4), gamma-glutamyl transpeptidase to platelet ratio (GPR), procollagen I carboxyterminal propeptide, procollagen III aminoterminal propeptide, transforming growth factor-α, platelet-derived growth factor AB, laminin]. MELD score in the ALC patients and NAFLD fibrosis score together with BARD score were obtained in the MAFLD

group. The achieved results were compared to controls. Then a correlation between investigated parameters was done. Diagnostic value of each evaluated marker together with suggested cut-off in the research group were assessed with area under the curve (AUC).

Research results

RDW, RPR and RLR values were significantly higher in ALC and MAFLD patients in comparison to controls. RPR correlated positively with MELD score and indirect parameters of liver fibrosis in the ALC group. RPR correlated positively with the NAFLD fibrosis score and APRI in the MAFLD patients; a positive dependency was noted between the RDW and FIB-4. The AUC values and suggested cut-offs for RDW, RPR and RLR in ALC patients were: 0.912 (> 14.2%), 0.965 (> 0.075) and 0.914 (> 8.684), respectively. AUC values and proposed cut-offs for RDW, RPR and RLR in MAFLD patients were: 0.606 (> 12.8%), 0.724 (> 0.047) and 0.691 (> 6.25), respectively.

Research conclusions

Our study gives a new insight into the tight relationship between serological indices of liver fibrosis and RDW derivatives in ALC and MAFLD patients. RLR seems to be a valuable unexplored parameter in the course of ALC patients. Its high diagnostic accuracy in ALC is a promising message for subsequent studies. Undoubtedly, this direction of research should be continued to define a potential role of commonly accessible RDW derivatives as indicators of liver disorders in everyday clinical life.

Research perspectives

It seems that our results have important clinical implications and could be applied in everyday diagnostics of patients with liver disorders.

FOOTNOTES

Author contributions: Michalak A, Lach T and Cichoż-Lach H prepared data; Michalak A and Cichoż-Lach H invented and conducted the study; Guz M, Kozicka J and Jeleniewicz W applied the experiments, gained and interpreted data; Cybulski M statistically analyzed the data; Michalak A and Cichoż-Lach H wrote the article; All authors accepted the current version of the manuscript.

Institutional review board statement: The survey was accepted by the local ethics committee of the Medical University of Lublin (No. KE-0254/86/2016).

Informed consent statement: All study participants, or their legal guardian, provided informed written consent prior to study enrollment.

Conflict-of-interest statement: All the authors report no relevant conflicts of interest for this article.

Data sharing statement: No additional data are available.

STROBE statement: The authors have read the STROBE Statement-checklist of items, and the manuscript was prepared and revised according to the STROBE Statement-checklist of items.

Open-Access: This article is an open-access article that was selected by an in-house editor and fully peer-reviewed by external reviewers. It is distributed in accordance with the Creative Commons Attribution NonCommercial (CC BY-NC 4.0) license, which permits others to distribute, remix, adapt, build upon this work non-commercially, and license their derivative works on different terms, provided the original work is properly cited and the use is non-commercial. See: https://creativecommons.org/Licenses/by-nc/4.0/

Country/Territory of origin: Poland

ORCID number: Agata Michalak 0000-0003-4426-6321; Małgorzata Guz 0000-0001-6783-8017; Joanna Kozicka 0000-0002-3094-8789; Marek Cybulski 0000-0003-0540-1199; Witold Jeleniewicz 0000-0003-1423-0504; Tomasz Lach 0000-0003-1370-7657; Halina Cichoż-Lach 0000-0002-7337-835X.

S-Editor: Gao CC
L-Editor: Filipodia
P-Editor: Gao CC

REFERENCES

1 **Lackner C**, Tiniakos D. Fibrosis and alcohol-related liver disease. *J Hepatol* 2019; **70**: 294-304 [PMID: 30658730 DOI:

10.1016/j.jhep.2018.12.003]
2 **Sookoian S**, Pirola CJ. Review article: shared disease mechanisms between non-alcoholic fatty liver disease and metabolic syndrome - translating knowledge from systems biology to the bedside. *Aliment Pharmacol Ther* 2019; **49**: 516-527 [PMID: 30714632 DOI: 10.1111/apt.15163]
3 **Grgurevic I**, Podrug K, Mikolasevic I, Kukla M, Madir A, Tsochatzis EA. Natural History of Nonalcoholic Fatty Liver Disease: Implications for Clinical Practice and an Individualized Approach. *Can J Gastroenterol Hepatol* 2020; **2020**: 9181368 [PMID: 32051820 DOI: 10.1155/2020/9181368]
4 **Gustot T**, Jalan R. Acute-on-chronic liver failure in patients with alcohol-related liver disease. *J Hepatol* 2019; **70**: 319-327 [PMID: 30658733 DOI: 10.1016/j.jhep.2018.12.008]
5 **Orabi H**, Howard L, Amling CL, Aronson WJ, Cooperberg MR, Kane CJ, Terris MK, Klaassen Z, Janes JL, Freedland SJ, Polascik TJ. Red Blood Cell Distribution Width Is Associated with All-cause Mortality but Not Adverse Cancer-specific Outcomes in Men with Clinically Localized Prostate Cancer Treated with Radical Prostatectomy: Findings Based on a Multicenter Shared Equal Access Regional Cancer Hospital Registry. *Eur Urol Open Sci* 2022; **37**: 106-112 [PMID: 35243395 DOI: 10.1016/j.euros.2022.01.003]
6 **Li Y**, Li Z, Zhang G. Clinical Utility of Red Blood Cell Distribution Width for the Diagnosis and Prognosis of Cervical Cancer. *Int J Gen Med* 2022; **15**: 2597-2606 [PMID: 35282652 DOI: 10.2147/IJGM.S354569]
7 **Cheng KC**, Lin YM, Liu CC, Wu KL, Lee KC. High Red Cell Distribution Width Is Associated with Worse Prognosis in Early Colorectal Cancer after Curative Resection: A Propensity-Matched Analysis. *Cancers (Basel)* 2022; **14** [PMID: 35205691 DOI: 10.3390/cancers14040945]
8 **Zhang Y**, Xing Z, Zhou K, Jiang S. The Predictive Role of Systemic Inflammation Response Index (SIRI) in the Prognosis of Stroke Patients. *Clin Interv Aging* 2021; **16**: 1997-2007 [PMID: 34880606 DOI: 10.2147/CIA.S339221]
9 **Kim DY**, Hong DY, Kim SY, Park JJ, Kim JW, Park SO, Lee KR, Baek KJ. Prognostic value of red blood cell distribution width in predicting 3-month functional outcome of patients undergoing thrombolysis treatment for acute ischemic stroke. *Medicine (Baltimore)* 2021; **100**: e27255 [PMID: 34664873 DOI: 10.1097/MD.0000000000027255]
10 **Xanthopoulos A**, Tryposkiadis K, Dimos A, Bourazana A, Zagouras A, Iakovis N, Papamichalis M, Giamouzis G, Vassilopoulos G, Skoularigis J, Triposkiadis F. Red blood cell distribution width in elderly hospitalized patients with cardiovascular disease. *World J Cardiol* 2021; **13**: 503-513 [PMID: 34621495 DOI: 10.4330/wjc.v13.i9.503]
11 **Chen M**, Liao L, Yan J, Lin FQ. Predictive Value of Red Blood Cell Distribution Width for 1-Year All-Cause Mortality in Critically Ill Patients with Acute Myocardial Infarction. *Int J Gen Med* 2022; **15**: 465-471 [PMID: 35046707 DOI: 10.2147/IJGM.S345109]
12 **Tarantino G**, Barrea L, Capone D, Citro V, Mosca T, Savastano S. Hematocrit Values Predict Carotid Intimal-Media Thickness in Obese Patients With Non-Alcoholic Fatty Liver Disease: A Cross-Sectional Study. *Front Endocrinol (Lausanne)* 2018; **9**: 203 [PMID: 29760679 DOI: 10.3389/fendo.2018.00203]
13 **Moreno C**, Mueller S, Szabo G. Non-invasive diagnosis and biomarkers in alcohol-related liver disease. *J Hepatol* 2019; **70**: 273-283 [PMID: 30658728 DOI: 10.1016/j.jhep.2018.11.025]
14 **Hsu C**, Caussy C, Imajo K, Chen J, Singh S, Kaulback K, Le MD, Hooker J, Tu X, Bettencourt R, Yin M, Sirlin CB, Ehman RL, Nakajima A, Loomba R. Magnetic Resonance *vs* Transient Elastography Analysis of Patients With Nonalcoholic Fatty Liver Disease: A Systematic Review and Pooled Analysis of Individual Participants. *Clin Gastroenterol Hepatol* 2019; **17**: 630-637.e8 [PMID: 29908362 DOI: 10.1016/j.cgh.2018.05.059]
15 **Jiang H**, Zheng T, Duan T, Chen J, Song B. Non-invasive *in vivo* Imaging Grading of Liver Fibrosis. *J Clin Transl Hepatol* 2018; **6**: 198-207 [PMID: 29951365 DOI: 10.14218/JCTH.2017.00038]
16 **Wang H**, Xu H, Qu L, Wang X, Wu R, Gao X, Jin Q, Niu J. Red blood cell distribution width and globulin, noninvasive indicators of fibrosis and inflammation in chronic hepatitis patients. *Eur J Gastroenterol Hepatol* 2016; **28**: 997-1002 [PMID: 27167453 DOI: 10.1097/MEG.0000000000000662]
17 **Wang J**, Huang R, Yan X, Li M, Chen Y, Xia J, Liu Y, Jia B, Zhu L, Zhang Z, Zhu C, Wu C. Red blood cell distribution width: A promising index for evaluating the severity and long-term prognosis of hepatitis B virus-related diseases. *Dig Liver Dis* 2020; **52**: 440-446 [PMID: 32008975 DOI: 10.1016/j.dld.2019.12.144]
18 **Yuyun D**, Zhihua T, Haijun W, Zhaoping L, Xiaoli Z, Wenfang X, Faxiang J, Hongmei L. Predictive value of the red blood cell distribution width-to-platelet ratio for hepatic fibrosis. *Scand J Gastroenterol* 2019; **54**: 81-86 [PMID: 30663454 DOI: 10.1080/00365521.2018.1558786]
19 **Lu W**, Zhang YP, Zhu HG, Zhang T, Zhang L, Gao N, Chang DY, Yin J, Zhou XY, Li MY, Li YT, Li ZZ, He Q, Geng Y. Evaluation and comparison of the diagnostic performance of routine blood tests in predicting liver fibrosis in chronic hepatitis B infection. *Br J Biomed Sci* 2019; **76**: 137-142 [PMID: 31062646 DOI: 10.1080/09674845.2019.1615717]
20 **Fan X**, Deng H, Wang X, Fu S, Liu Z, Sang J, Zhang X, Li N, Han Q. Association of red blood cell distribution width with severity of hepatitis B virus-related liver diseases. *Clin Chim Acta* 2018; **482**: 155-160 [PMID: 29627486 DOI: 10.1016/j.cca.2018.04.002]
21 **Cai Y**, Liu D, Cui J, Sha Y, Zhou H, Tang N, Wang N, Huang A, Xia J. Diagnostic accuracy of red blood cell distribution width to platelet ratio for predicting staging liver fibrosis in chronic liver disease patients: A systematic review and meta-analysis. *Medicine (Baltimore)* 2019; **98**: e15096 [PMID: 30946368 DOI: 10.1097/MD.0000000000015096]
22 **Milas GP**, Karageorgiou V, Cholongitas E. Red cell distribution width to platelet ratio for liver fibrosis: a systematic review and meta-analysis of diagnostic accuracy. *Expert Rev Gastroenterol Hepatol* 2019; **13**: 877-891 [PMID: 31389726 DOI: 10.1080/17474124.2019.1653757]
23 **Wang H**, Wang J, Huang R, Xia J, Zuo L, Yan X, Yang Y, Wu C. Red blood cell distribution width for predicting significant liver inflammation in patients with autoimmune hepatitis. *Eur J Gastroenterol Hepatol* 2019; **31**: 1527-1532 [PMID: 31107736 DOI: 10.1097/MEG.0000000000001447]
24 **Liu L**, Cao J, Zhong Z, Guo Z, Jiang Y, Bai Y, Xu J. Noninvasive indicators predict advanced liver fibrosis in autoimmune hepatitis patients. *J Clin Lab Anal* 2019; **33**: e22922 [PMID: 31115929 DOI: 10.1002/jcla.22922]
25 **Zeng T**, Yu J, Tan L, Wu Y, Tian Y, Wu Q, Duan X, Yu L. Noninvasive indices for monitoring disease course in Chinese patients with autoimmune hepatitis. *Clin Chim Acta* 2018; **486**: 135-141 [PMID: 30036523 DOI:

10.1016/j.cca.2018.07.030]
26 **Goyal H**, Hu ZD. Prognostic value of red blood cell distribution width in hepatocellular carcinoma. *Ann Transl Med* 2017; **5**: 271 [PMID: 28758097 DOI: 10.21037/atm.2017.06.30]
27 **Jing JS**, Fu XL, Zhao W, Kong LB. Red Cell Distribution Width as a Prognostic Factor in Patients with Hepatocellular Carcinoma. *Clin Lab* 2020; **66** [PMID: 32658432 DOI: 10.7754/Clin.Lab.2019.191027]
28 **Chu W**, Li P, Wu X, Zhang P, Zhou H, Niu B. Risk factors for recurrence beyond Milan criteria after radiofrequency ablation in transplantable small hepatocellular carcinoma. *Rev Esp Enferm Dig* 2022 [PMID: 35042367 DOI: 10.17235/reed.2022.8592/2022]
29 **Meng J**, Xu H, Liu X, Wu R, Niu J. Increased red cell width distribution to lymphocyte ratio is a predictor of histologic severity in primary biliary cholangitis. *Medicine (Baltimore)* 2018; **97**: e13431 [PMID: 30508955 DOI: 10.1097/MD.0000000000013431]
30 **Wu J**, Zhang X, Liu H, Guo N, Pan Q, Wang Y. RDW, NLR and RLR in predicting liver failure and prognosis in patients with hepatitis E virus infection. *Clin Biochem* 2019; **63**: 24-31 [PMID: 30502317 DOI: 10.1016/j.clinbiochem.2018.11.012]
31 **Wang H**, Xu H, Wang X, Wu R, Gao X, Jin Q, Niu J. Red Blood Cell Distribution Width to Platelet Ratio is Related to Histologic Severity of Primary Biliary Cirrhosis. *Medicine (Baltimore)* 2016; **95**: e3114 [PMID: 26986159 DOI: 10.1097/MD.0000000000003114]
32 **Cengiz M**, Candır BA, Yılmaz G, Akyol G, Ozenirler S. Is increased red cell distribution width an indicating marker of nonalcoholic steatohepatitis and fibrotic stage? *World J Gastroenterol* 2013; **19**: 7412-7418 [PMID: 24259972 DOI: 10.3748/wjg.v19.i42.7412]
33 **Yang W**, Huang H, Wang Y, Yu X, Yang Z. High red blood cell distribution width is closely associated with nonalcoholic fatty liver disease. *Eur J Gastroenterol Hepatol* 2014; **26**: 174-178 [PMID: 24025980 DOI: 10.1097/MEG.0b013e328365c403]
34 **Cengiz M**, Ozenirler S. Comparative diagnostic accuracy of red cell distribution width-to-platelet ratio *vs* noninvasive fibrosis scores for the diagnosis of liver fibrosis in biopsy-proven nonalcoholic fatty liver disease. *Eur J Gastroenterol Hepatol* 2015; **27**: 1293-1299 [PMID: 26302023 DOI: 10.1097/MEG.0000000000000445]
35 **Farah R**, Khamisy-Farah R. Significance of MPV, RDW with the Presence and Severity of Metabolic Syndrome. *Exp Clin Endocrinol Diabetes* 2015; **123**: 567-570 [PMID: 26372846 DOI: 10.1055/s-0035-1564072]
36 **Zhou WJ**, Yang J, Zhang G, Hu ZQ, Jiang YM, Yu F. Association between red cell distribution width-to-platelet ratio and hepatic fibrosis in nonalcoholic fatty liver disease: A cross-sectional study. *Medicine (Baltimore)* 2019; **98**: e16565 [PMID: 31348282 DOI: 10.1097/MD.0000000000016565]

World Journal of Gastroenterology

Submit a Manuscript: https://www.f6publishing.com

World J Gastroenterol 2022 October 14; 28(38): 5648-5657

DOI: 10.3748/wjg.v28.i38.5648

ISSN 1007-9327 (print) ISSN 2219-2840 (online)

SCIENTOMETRICS

Comparison of evaluation indexes for Gastroenterology and Hepatology journals in different databases

Jia-Yuan Li, Zhi-Han Yan, Ze Xiang, Ce Gao, Jian Wu

Specialty type: Scientific journal

Provenance and peer review: Invited article; Externally peer reviewed.

Peer-review model: Single blind

Peer-review report's scientific quality classification

Grade A (Excellent): A
Grade B (Very good): B
Grade C (Good): 0
Grade D (Fair): 0
Grade E (Poor): 0

P-Reviewer: Mansour AM, Lebanon; Santos BS, Brazil

Received: August 9, 2022
Peer-review started: August 9, 2022
First decision: August 25, 2022
Revised: September 4, 2022
Accepted: September 21, 2022
Article in press: September 21, 2022
Published online: October 14, 2022

Jia-Yuan Li, Ze Xiang, Zhejiang University School of Medicine, Zhejiang University, Hangzhou 310009, Zhejiang Province, China

Zhi-Han Yan, Department of Hepatology, Wuxi Fifth People's Hospital Affiliated to Jiangnan University, Wuxi 214005, Jiangsu Province, China

Ce Gao, Jian Wu, Department of Clinical Laboratory, The Affiliated Suzhou Hospital of Nanjing Medical University, Suzhou Municipal Hospital, Gusu School, Nanjing Medical University, Suzhou 215008, Jiangsu Province, China

Corresponding author: Jian Wu, MD, PhD, Professor, Department of Clinical Laboratory, The Affiliated Suzhou Hospital of Nanjing Medical University, Suzhou Municipal Hospital, Gusu School, Nanjing Medical University, No. 242 Guangji Road, Suzhou 215008, Jiangsu Province, China. wujianglinxing@163.com

Abstract

BACKGROUND

Accurate assessment of the quality of academic journals is of great significance. While Journal Impact Factor (JIF), calculated by Clarivate and based upon the Web of Science literature database, and CiteScore (CS), developed by Elseiver and based upon the Scopus database, have enjoyed high uptake worldwide, efforts continue towards creation of other scientometric indexes that will provide ever-greater qualitative insights into journal impact. Such efforts have yielded the newly-launched *Journal Article Influence Index* (*JAII*), which is based on the *Reference Citation Analysis* (*RCA*) database, an open multidisciplinary citation analysis database based on artificial intelligence technology.

AIM

To evaluate and summarize the similarities and differences between *JAII* and JIF/CS as journal evaluation indicators, and provide an intuitive method for visual representation of the related data.

METHODS

We searched the Journal Citation Reports to obtain the 2021 JIF list, downloaded the CS list updated in July on the Scopus website, and collected the comprehensive list of 2022 *JAII*s from the *RCA* database (www.referencecitationanalysis.com).

RESULTS

Our research results revealed that by breaking through the time limit of mainstream journal evaluation methods, the *JAII* is able to perform well in data reliability, establishing its benefit as a complementary scientometric index to JIF and CS.

CONCLUSION

JAII provides comprehensive assessment of the quality and performance of journals.

Key Words: *Journal Article Influence Index*; Journal Impact Factor; CiteScore; Gastroenterology and Hepatology; Scientometric index

©The Author(s) 2022. Published by Baishideng Publishing Group Inc. All rights reserved.

Core Tip: Compared with Journal Impact Factor (JIF) and CiteScore (CS), the newly-launched *Journal Article Influence Index* (*JAII*) breaks through the time limit feature of the former indexes. A key benefit of the *JAII* is that it does not require the temporal path (wait-time) of JIF and CS to accurately evaluate a journal's impact. As such, *JAII* is immediately useful for assessing the performance of journals and the drawbacks of time randomness are overcome. Here, we describe the features of *JAII* as a comprehensive assessment of the quality and performance of journals, in its functionality based upon the *Reference Citation Analysis* (*RCA*) database that covers some more specific journals than other literature databases.

Citation: Li JY, Yan ZH, Xiang Z, Gao C, Wu J. Comparison of evaluation indexes for Gastroenterology and Hepatology journals in different databases. *World J Gastroenterol* 2022; 28(38): 5648-5657
URL: https://www.wjgnet.com/1007-9327/full/v28/i38/5648.htm
DOI: https://dx.doi.org/10.3748/wjg.v28.i38.5648

INTRODUCTION

The quality assessment of peer-reviewed published research is important for the reputation, substance and growth of various professional associations, individual scientists, and academic institutions, as well as the funding organizations that evaluate and support them[1]. The quality of scientific contributions is primarily assessed on a temporal basis, with quantitative evaluation of the long-term impact in a field or discipline. The impact of an individual scientific article can be inferred from the citations that it receives. A similar principle is applied to evaluation of the journals that publish these scientific articles[2]. These long-standing efforts have led to researchers proposing various methods that improve the assessment of the quality of scientific journals[3,4]. What most of these methods have in common, though, is the use of complex mathematical algorithms to analyze networks of scientific papers to estimate citation quality.

First proposed by Eugene Garfield in 1955, the Scientific Citation Index, Journal Citation Reports [(JCR); published by the Institute for Scientific Information (ISI)] aims to rank, evaluate, classify, and compare journals[5]. The involved metrics are calculated based on the number of articles published by a journal and the number of times that a journal is cited. Moreover, they have been widely adopted as tools to evaluate researchers and research work in a wide range of scientific settings. One of the most prominent among such indicators is the Journal Impact Factor (JIF).

In addition to the JIF, other metrics provided by the ISI include total citation frequency, immediacy index, number of source entries published in the current year, frequency of citations in the previous 2 years, cited half-life, and the ratio of different citations for each article. The ISI introduced a simplified system in 1974, along with a list of topic categories and an accompanying catalog of the total 176 JCR journals. In recent decades, the different journal categories have been subjected to many holistic analyses. The resultant definitions of the common characteristics that underpin particular types of journals and relate to the JIF have served as a useful tool for researchers, both in the scientometric field and in general as contributing authors, to better evaluate journal impact[6,7]. To this day, journals are ranked by JIF within their assigned category. The journals listed in the JCR are further subgrouped by the ranking of JIF-related indicators (*i.e.* JIF variation coefficient, *etc*); this greater detailed categorization has allowed scholars to perlustrate the impact factor values more intuitively from a holistic and comprehensive perspective.

JIF has been the most widely used indicator of quality of scientific journals over the past decades[8]. However, in accordance with the 1999 announcement by the ISI/JCR that the accuracy of JIF is not fully guaranteed[9], it is important to note that the methodological considerations in the JIF calculation still include a lack of assessment of the quality of citations, the inclusion of self-citations, poor comparability between different scientific fields, and an analysis of publications mainly in English[10]. This is in addition to the fact that JIFs of journals representing different disciplines are not comparable to each

other.

On December 8, 2016, Scopus launched the CiteScore (CS) quality metric, in direct competition of JIF but which was developed specifically for journals indexed by Scopus. Over the past few years, the number of journals assigned a CS has increased dramatically, especially for journals that are not included in the JIF annual assignments. Scientometric studies evaluating the relationship between CS and JIF have revealed that although there is a strong correlation between the two metrics, there are also obvious complex differences[11,12]. While CS may be more balanced and most certainly is more transparent[13], it also shares some key limitations with the JIF[14,15].

Reference Citation Analysis (*RCA*) is a very recently launched open multidisciplinary citation analysis database based on artificial intelligence technology. This database covers a wide array of seemingly disparate disciplines such as business, economics and management, chemistry and materials science, engineering and computer science, health and medical sciences, humanities, literature and arts, life sciences and earth sciences, physics and mathematics, and social sciences. Users can search the collective literature based on fields such as author, category, DOI, ISSN, keyword, ORCID number, publication name, PubMed ID, and title to track original innovative research results and cutting-edge progress; they can also sort results by an article impact index metric. Importantly, the results analysis functionality culminates in a comprehensive and customizable report of the retrieved results.

Based on the *RCA* database, the *Journal Article Influence Index* (*JAII*) metric is officially available as a new indicator of journal quality that is calculated *via* the normal approach of quantifiable citations. Systematically comparing this new metric to traditional journal evaluation metrics will help ensure the accuracy of *JAII*. With acknowledgement of the continuous deepening of research in the field of Gastroenterology and Hepatology of recent years[16], we performed such a comparative analysis to determine the similarities and differences between *JAII* and JIF/CS as journal evaluation indicators, with the ultimate aim of providing an intuitive method for visual representation of the related data.

MATERIALS AND METHODS

Data sources

The raw data for this study was obtained in July 2022 from the official websites of the institutions that released each metric under consideration. We searched the JCR to obtain the 2021 JIF list, downloaded the CS list updated in July from the Scopus website, and collected the 2022 *JAII* list from the *RCA* database (www.referencecitationanalysis.com). In addition, we also searched for information related to the characteristics of these scientific journal quality indexes for reference.

Besides, based on the results of *RCA* search by the Gastroenterology and Hepatology category, we compared *JAII* to JIF and CS respectively. The resultant data from the *RCA* database were used as the matching benchmark, and the matching method was based on ISSN, EISSN, and journal name.

RESULTS

Statistical analysis and visualization

The Gastroenterology and Hepatology-categorized journals identified in each database are presented in Table 1 (grouped by the evaluation indicator and in descending order according to the respective quality metric value). In total, 102 journals carried a *JAII*, 81 carried a JIF, and 76 carried a CS (all assigned in 2021).

Next, in order to make an intuitive comparison between the three evaluation indicators, we drew a scatter distribution plot for JIF-*JAII* (Figure 1A) and CS-*JAII* (Figure 1B), and plotted a single-timepoint uniform curve using the least squares method[17]. In this case, we took an intersection, considering that some journals with *JAII* have no JIF or CS. It can be seen from the figure that in the evaluation of lower-quality journals, the linearity of *JAII* and JIF/CS has greater overlap, but in the evaluation of higher-quality journals, the randomness of the data is greater. Journals with a large deviation between JIF and *JAII* include *Nature Reviews Gastroenterology & Hepatology*, *Lancet Gastroenterology & Hepatology*, *Seminars in Liver Disease*, and so on. Journals with a large deviation between CS and *JAII* include *Gut*, *Journal of Hepatology*, *Gastroenterology*, and so on.

The results of the combined analysis of the three journal evaluation indicators are visualized in Figure 2A-C[18]. Figure 2A gives a comparison of the values between the three evaluation indicators of the same journal (73 in total, taking the intersection). Figure 2B gives the JIF-*JAII* ratio and CS-*JAII* ratio for each journal. Figure 2C gives the values of JIF and CS in descending *JAII* order.

Finally, we combined the three journal evaluation indicators together, and through a histogram (Figure 2D), we can more clearly see the impact of the joint evaluation of the three on the ranking of journals without weight. This can also be used as a reference evaluation method.

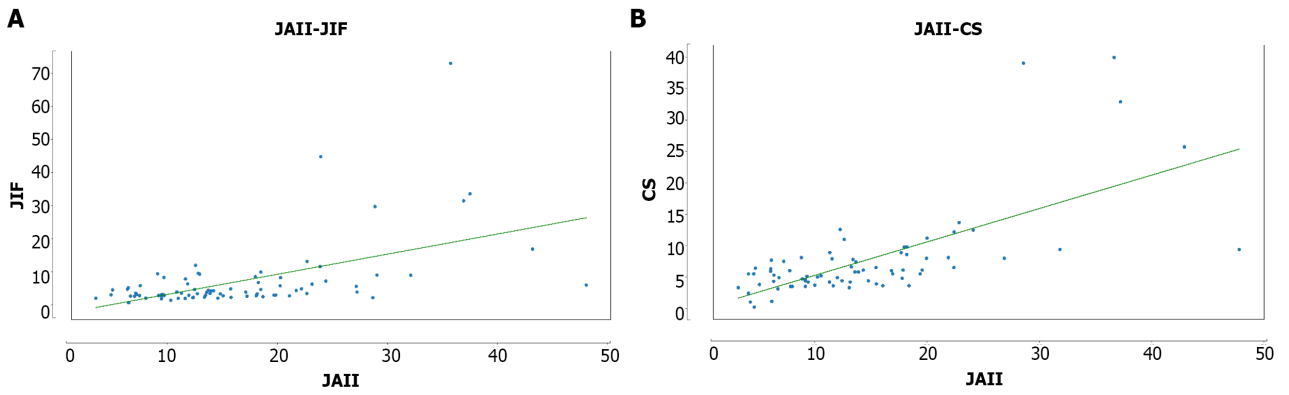
Table 1 Comparison of *Journal Article Influence Index*, Journal Impact Factor, and CiteScore in decreasing order of *Journal Article Influence Index* values

Journal name	2022 *JAII*	2021 JIF	2021 CS
Seminars in Liver Disease	48.011	6.512	9.4
Hepatology	43.087	17.298	25.8
Gastroenterology	37.347	33.883	33
Gut	36.77	31.793	40.1
Nature Reviews Gastroenterology & Hepatology	35.564	73.082	-
Gut Microbes	31.922	9.434	9.4
Alimentary Pharmacology & Therapeutics	28.815	9.524	-
Journal of Hepatology	28.63	30.083	39.2
Best Practice & Research Clinical Gastroenterology	28.443	2.695	-
Diseases of the Colon & Rectum	26.986	4.412	-
Liver Transplantation	26.916	6.112	8
Gastric Cancer	24.132	7.701	12.5
Lancet Gastroenterology & Hepatology	23.661	45.042	-
The American Journal of Gastroenterology	23.599	12.045	-
Journal of Gastroenterology	22.863	6.772	13.7
Clinical Gastroenterology and Hepatology	22.413	13.576	12.2
Neurogastroenterology and Motility	22.381	3.96	6.5
World Journal of Gastroenterology	21.897	5.374	8.1
American Journal of Physiology-Gastrointestinal and Liver Physiology	21.407	4.871	-
Journal of Gastrointestinal Surgery: Official Journal of the Society for Surgery of the Alimentary Tract	20.787	3.267	-
Liver International	19.971	8.754	11.2
Clinics in Liver Disease	19.939	6.265	8
Journal of Viral Hepatitis	19.545	3.517	6.1
Digestive Diseases and Sciences	19.37	3.487	5.5
World Journal of Gastrointestinal Pathophysiology	18.735	-	-
Scandinavian Journal of Gastroenterology	18.364	3.027	3.6
Gastrointestinal Endoscopy	18.175	10.396	9.8
Helicobacter	18.162	5.182	8.6
Inflammatory Bowel Diseases	17.936	7.29	9.8
Gastroenterology Clinics of North America	17.833	3.867	6.1
Journal of Pediatric Gastroenterology and Nutrition	17.742	3.288	4.8
Hepatology International	17.664	9.029	8.9
Journal of Clinical Gastroenterology	16.888	3.174	5.5
Journal of Gastroenterology and Hepatology	16.793	4.369	6
World Journal of Hepatology	16.007	-	3.6
International Journal of Colorectal Disease	15.433	2.796	3.9
Gut Pathogens	15.39	5.324	6.5
World Journal of Gastrointestinal Pharmacology and Therapeutics	14.797	-	-
Pancreas	14.71	3.243	4.4
HPB: The Official Journal of the International Hepato Pancreato Biliary Association	14.453	3.842	-

International Journal of Hepatology	14.249	-	6.1
European Journal of Gastroenterology & Hepatology	14.227	2.586	-
Therapeutic Advances in Gastroenterology	13.823	4.802	5.8
Journal of Neurogastroenterology and Motility	13.594	4.725	7.4
Pancreatology	13.497	3.977	5.8
Hepatology Research	13.332	4.942	7.8
Gut and Liver	13.193	4.321	6.6
Digestive Diseases	13.081	3.421	4.2
BMC Gastroenterology	12.991	2.847	3.3
Endoscopy	12.541	9.776	11
Journal of Crohn's & Colitis	12.432	10.02	
Colorectal Disease	12.341	3.917	4.4
Liver Cancer	12.174	12.43	12.6
Digestive and Liver Disease: Official Journal of the Italian Society of Gastroenterology and the Italian Association for the Study of the Liver	12.096	5.165	-
Diseases of the Esophagus: Official Journal of the International Society for Diseases of the Esophagus	11.969	2.822	-
Current Opinion in Gastroenterology	11.929	2.741	4.9
World Journal of Gastrointestinal Oncology	11.552	3.404	3.6
United European Gastroenterology Journal	11.453	6.866	7.9
Clinical and Molecular Hepatology	11.251	8.337	8.9
Digestive Surgery	11.226	2.459	4.2
Expert Review of Gastroenterology & Hepatology	10.885	4.095	-
World Journal of Gastrointestinal Endoscopy	10.598	-	-
World Journal of Gastrointestinal Surgery	10.579	2.505	-
Clinical and Translational Gastroenterology	10.45	4.396	5.2
Clinical and Experimental Gastroenterology	10.149	-	5
Gastroenterology Research and Practice	9.902	1.919	3.7
Journal of Digestive Diseases	9.302	3.366	4.2
Cellular and Molecular Gastroenterology and Hepatology	9.277	8.797	-
Digestion	9.189	3.672	5.1
Clinics in Colon and Rectal Surgery	9.059	2.403	3.5
Techniques in Coloproctology	9.056	3.699	4.6
Journal of Gastric Cancer	9.031	3.197	4.4
Hepatic Medicine: Evidence and Research	8.847	-	-
Annals of Hepatology	8.782	3.388	4.7
JHEP Reports	8.693	9.917	8.1
BMJ Open Gastroenterology	7.884	-	3.5
Clinical Endoscopy	7.72	-	3.5
Intestinal Research	7.651	-	6
Canadian Journal of Gastroenterology & Hepatology	7.615	2.605	-
Digestive Endoscopy	7.111	6.337	7.5
Hepatobiliary & Pancreatic Diseases International	7.052	3.355	-
Esophagus: Official Journal of the Japan Esophageal Society	6.775	3.671	-

Endoscopy International Open	6.725	-	-
Gastroenterology Report	6.685	4.063	4.9
Clinics and Research in Hepatology and Gastroenterology	6.59	3.189	3.1
Journal of Clinical and Experimental Hepatology	6.236	-	5.3
Saudi Journal of Gastroenterology	6.205	3.214	4.3
Hepatitis Monthly	6.037	1.214	1.1
Hepatology Communications	6.006	5.701	7.7
Liver Research	5.941	-	6.3
Endoscopic Ultrasound	5.932	5.275	5.9
Gastrointestinal Tumors	5.556	-	-
Indian Journal of Gastroenterology: Official Journal of the Indian Society of Gastroenterology	5.311	-	-
Frontline Gastroenterology	4.933	-	3.8
Journal of Clinical and Translational Hepatology	4.562	5.065	6.4
Inflammatory Intestinal Diseases	4.474	-	0.2
Annals of Gastroenterological Surgery	4.427	3.583	5.5
Case Reports in Gastroenterology	4.117	-	1
Annals of Coloproctology	3.946	-	2.4
Translational Gastroenterology and Hepatology	3.945	-	5.5
Clinical Liver Disease	3.934	-	2.4
Journal of Gastrointestinal Oncology	3.029	2.587	3.3

CS: CiteScore; *JAII*: *Journal Article Influence Index*; JIF: Journal Impact Factor. "-" denotes lack of score assigned by the corresponding institution/database.



DOI: 10.3748/wjg.v28.i38.5648 **Copyright** ©The Author(s) 2022.

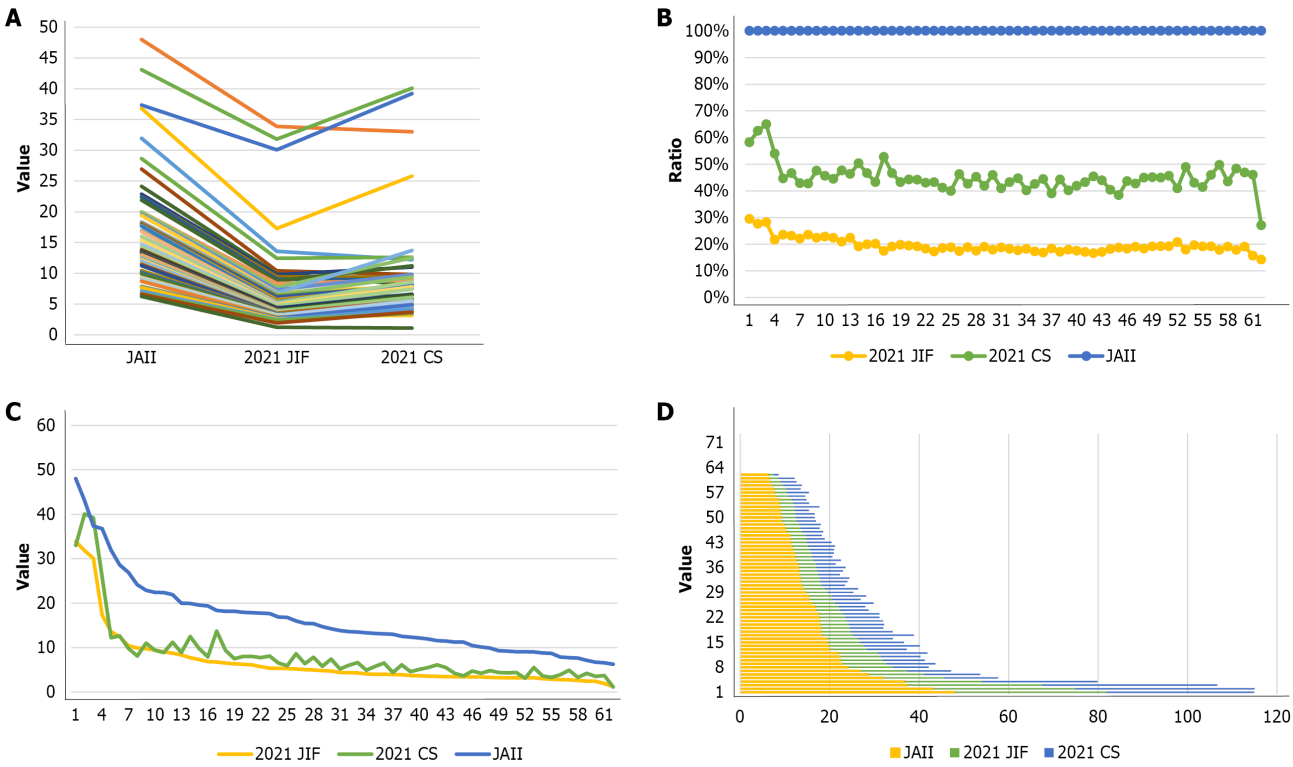
Figure 1 Scatter distribution plots for Journal Impact Factor-*Journal Article Influence Index* and CiteScore-*Journal Article Influence Index*.
A: Journal Impact Factor-*Journal article influence index* (*JAII*); B: CiteScore-*JAII*. JIF: Journal Impact Factor; CS: CiteScore; *JAII*: *Journal Article Influence Index*.

DISCUSSION

Comparison of databases and calculation principles

JIF: JIFs are obtained through the Web of Knowledge database using the Science Edition of JCR which collects citation data from more than 7300 science and technology journals worldwide. The IF of a T-year journal is defined as the number of times that the journal has been cited in years T-1 and T-2 divided by the number of documents that can be cited in the journal in years T-1 and T-2[19].

CS: CSs are calculated using data from the Scopus database. CS has a publication window of 3 years before the 1-year reference window and counts the references from one document type to another[20]. In other words, CS calculates the average number of citations of papers published in a journal for 3



DOI: 10.3748/wjg.v28.i38.5648 **Copyright** ©The Author(s) 2022.

Figure 2 Visualization of the three journal evaluation indicators. A: Comparison of the values obtained upon application of the three evaluation indicators; B: Journal Impact Factor (JIF)-*Journal Article Influence Index* (*JAII*) and CiteScore (CS)-*JAII* ratios for each journal; C: Values of JIF and CS in descending *JAII* order; D: Histogram combining the three journal evaluation indicators together. JIF: Journal Impact Factor; CS: CiteScore; *JAII*: *Journal Article Influence Index*.

consecutive years in the 4th year. In a given year, CS is calculated as the amount of times that documents published in the previous 3 years were cited in that year divided by the number of documents published in those 3 years that were included in the Scopus database.

JAII: *JAII*s, calculated as total citations divided by total articles, are based on journals and their citations included in the *RCA* database.

Advantages and disadvantages of JAII

It is undeniable that the *JAII* metric has its merits as a journal evaluation indicator. (1) Compared with JIF and CS, *JAII* is able to break through the time limit disadvantage of the first two. Journals do not need to meet the waiting-time thresholds of JIF and CS to be accurately evaluated. As such, *JAII* is able to evaluate more journals accurately in a near-real time manner, which explains why there are more journals with a *JAII* than those with a JIF/CS. (2) Compared with JIF and CS, *JAII* is useful for assessing the performance of journals immediately upon its creation. Moreover, since a small number of articles in journals will result in a high JIF and CS at a given time, *JAII* relieves the chance of biased evaluation of journals. *JAII* is also more conducive to a comprehensive assessment of the quality and performance of journals. And (3), compared with JIF and CS, *JAII* is more conducive to high-quality journal evaluation. In addition to these advantages, *JAII* has a high degree of compliance with JIF and CS in the evaluation of journals with a lower impact.

Another important feature related to the *JAII* is that the *RCA* database, upon which it is based, can enable queries to journals by category, such as focused query of Gastroenterology and Hepatology, representing a ready convenience to researchers.

There exist disadvantages in the *JAII*. These include the lack of statistical timeliness, a feature by which *JAII* is slightly inferior to JIF and CS, and the lack of consideration to different developments of the same journal in different periods. *JAII* also shares some of the drawbacks of both JIF and CS, such as the lack of evaluation of citation quality and the inclusion of self-citations.

Non-linearity interpretation

As we have shown in Figure 1 and described textually in the "Results" section above, the linearity of *JAII*-JIF-CS was clear for lower-quality journals but failed to match each other perfectly for higher-quality journals.

Our explanation is that JIF and CS are subject to changes in citation frequency and number of published articles in different years, and their correlation with time exacerbates the influence of human manipulability[21]. *JAII* reduces this time randomness. In addition, the JIF and CS of high-quality journals may be more susceptible to this effect, and their fluctuations can be effectively explained.

Threats to validity

In addition to the lack of evaluation of citation quality and self-citation, other factors may threaten the effectiveness of the evaluation parameters in use. Research on JIF, CS and other statistical standards for journal quality has shown that there are still many statistical violations at play, including those related to and arising from reliability, incomplete reporting of validity, insignificant results, insignificant effect sizes, and hypothesis checking, as well as uncorrected inferences and multiple comparisons from descriptive statistics[22]. *JAII* is also inevitably affected by the same, to at least some extent, and this limitation cannot be ignored.

CONCLUSION

The main differences between *JAII* and JIF/CS come from the differences in the scientific databases used as the cited sources, as well as the differences in the evaluation methods underpinning each of these indicators. Due to the JIF/CS time factor limitation, the *JAII* method based on the *RCA* database is able to evaluate more journals. Besides, *JAII* provides more focused quantitative insight by considering categories of journal papers. In terms of practicality, the novelty introduced by the *JAII* indicator is its open-accessibility to users (as opposed to a subscription service to select users). To summarize, *JAII* is a reliable index to evaluate the quality of journals in near-real time.

In the future, scientometric researchers can focus on the differences of the different journal evaluation indexes to aid in their studies on the origin of nonlinear characteristics in order to put forward a more perfect journal evaluation standard. Meanwhile, researchers in general can exploit the distinct advantages of each as they currently stand to better understand journal quality and promote the impact of their own scientific communications.

ARTICLE HIGHLIGHTS

Research background

The evaluation of journal quality is very important for researchers. Journal Impact Factor (JIF) and CiteScore (CS) are two of the most popular and authoritative journal evaluation indicators. With the ongoing scientometric research into their advantages and disadvantages, there is a consequent emergence of new journal evaluation indicators. The logical next-step is comparative judgement of the reliability and innovative novelty of such new journal evaluation indexes.

Research motivation

The recently-launched *Reference Citation Analysis* database of Baishideng Publishing Group is an open multidisciplinary citation analysis database founded in artificial intelligence technology. Based on this database, *Journal Article Influence Index* (*JAII*) has been proposed as a new journal evaluation indicator.

Research objectives

To compare the advantages and disadvantages of *JAII* with those of JIF and CS.

Research methods

For comparisons between *JAII* and 2021 JIF/2021 CS, we conducted statistical analyses and provided an intuitive method for visual representation of the related data.

Research results

For lower-quality journals, *JAII*, 2021 JIF, and 2021 CS had a good linear correlation. However, their results of assessments of higher-quality journals varied widely. These three evaluation indexes have their own advantages and disadvantages, including the avoidance of time randomness and ability for near-real time evaluation of the *JAII*.

Research conclusions

JAII is a comprehensive assessment tool to assess the quality and performance of journals.

Research perspectives

In the future, we hope to better explain the current existent nonlinear relationship among the three evaluation indexes, and combine a variety of journal evaluation indicators to allow for more comprehensive evaluation of journal quality by scientometric-focused and general researchers.

FOOTNOTES

Author contributions: Wu J designed the study and revised the manuscript; Li JY and Yan ZH performed the data analysis and manuscript drafting; Xiang Z and Gao C searched the literature and collected the data; Li JY wrote the paper; Wu J reviewed the results and made critical comments on the manuscript; All authors reviewed and approved the final version; Li JY and Yan ZH contributed equally to this work.

Supported by the Youth Medical Talent of Jiangsu Province, No. QNRC2016475.

Conflict-of-interest statement: The authors declare that there are no competing interests associated with this manuscript.

PRISMA 2009 Checklist statement: The authors have read the PRISMA 2009 Checklist, and the manuscript was prepared and revised according to the PRISMA 2009 Checklist.

Open-Access: This article is an open-access article that was selected by an in-house editor and fully peer-reviewed by external reviewers. It is distributed in accordance with the Creative Commons Attribution NonCommercial (CC BY-NC 4.0) license, which permits others to distribute, remix, adapt, build upon this work non-commercially, and license their derivative works on different terms, provided the original work is properly cited and the use is non-commercial. See: https://creativecommons.org/Licenses/by-nc/4.0/

Country/Territory of origin: China

ORCID number: Jian Wu 0000-0003-0087-3744.

S-Editor: Chen YL
L-Editor: Wang TQ
P-Editor: Chen YL

REFERENCES

1 **Azer SA**, Holen A, Wilson I, Skokauskas N. Impact factor of medical education journals and recently developed indices: Can any of them support academic promotion criteria? *J Postgrad Med* 2016; **62**: 32-39 [PMID: 26732194 DOI: 10.4103/0022-3859.173202]
2 **Brezgov S**. Misleading Metrics. Sch. 2022. Available from: https://scholarlyoa.com/misleading-metrics/
3 **Valderrama P**, Jiménez-Contreras E, Escabias M, Valderrama MJ. Introducing a bibliometric index based on factor analysis. *Scientometrics* 2022; **127**: 509-522 [DOI: 10.1007/s11192-021-04195-4]
4 **Abramo G**, D'Angelo CA, Felici G. Predicting publication long-term impact through a combination of early citations and journal impact factor. *J Informetr* 2019; **13**: 32-49 [DOI: 10.1016/j.joi.2018.11.003]
5 **Garfield E**. The history and meaning of the journal impact factor. *JAMA* 2006; **295**: 90-93 [PMID: 16391221 DOI: 10.1001/jama.295.1.90]
6 **Solari A**, Magri M-H. A New Approach to the SCI Journal Citation Reports, a System for Evaluating Scientific Journals. *Scientometrics* 2000; **47**: 605-625 [DOI: 10.1023/a:1005680202961]
7 **Pichappan P**. Identification of mainstream journals of science speciality: A method using the discipline-contribution score. *Scientometrics* 1993; **27**: 179-193 [DOI: 10.1007/bf02016549]
8 **Callaway E**. Beat it, impact factor! *Nature* 2016; **535**: 210-211 [PMID: 27411614 DOI: 10.1038/nature.2016.20224]
9 **Moed H**, Leeuwen TV, Reedijk J. Towards appropriate indicators of journal impact. *Scientometrics* 2006; **46**: 575-589 [DOI: 10.1007/bf02459613]
10 **Falagas ME**, Kouranos VD, Arencibia-Jorge R, Karageorgopoulos DE. Comparison of SCImago journal rank indicator with journal impact factor. *FASEB J* 2008; **22**: 2623-2628 [PMID: 18408168 DOI: 10.1096/fj.08-107938]
11 **Okagbue HI**, Teixeira da Silva JA. Correlation between the CiteScore and Journal Impact Factor of top-ranked library and information science journals. *Scientometrics* 2020; **124**: 797-801 [DOI: 10.1007/s11192-020-03457-x]
12 **Fu BS**, Yu Z, Tiwari K. New Release of 2020 Impact Factor (Web of Science) and Cite Score (Scopus). *J Orthop Translat* 2021; **29**: A3 [PMID: 34466383 DOI: 10.1016/j.jot.2021.07.003]
13 **Teixeira da Silva JA**, Memon AR. CiteScore: A cite for sore eyes, or a valuable, transparent metric? *Scientometrics* 2017; **111**: 553-556 [DOI: 10.1007/s11192-017-2250-0]
14 **Teixeira da Silva JA**. CiteScore: Advances, Evolution, Applications, and Limitations. *Publ Res Q* 2020; **36**: 459-468 [DOI: 10.1007/s12109-020-09736-y]
15 **Teixeira da Silva JA**. CiteScore: Risk of copy-cat, fake and misleading metrics. *Scientometrics* 2021; **126**: 1859-1862

[DOI: 10.1007/s11192-020-03791-0]

16 **Zhao Z**, Tang H, Li F. Measles-Associated Severe Pneumonia in a Patient with HBeAg-Negative Chronic Hepatitis B: A Case Report. *Zoonoses* 2022; **2**: 3 [DOI: 10.15212/zoonoses-2021-0013]

17 **Axelsson O**. A generalized conjugate gradient, least square method. *Numer Math* 1987; **51**: 209-227 [DOI: 10.1007/bf01396750]

18 **Gleicher M**, Albers D, Walker R, Jusufi I, Hansen CD, Roberts JC. Visual comparison for information visualization. *Inf Vis* 2011; **10**: 289-309 [DOI: 10.1177/1473871611416549]

19 **McGinnis R**. Research tool. *Science* 1980; **207**: 972 [PMID: 17830451 DOI: 10.1126/science.207.4434.972]

20 **James C**, Colledge L, Meester W, Azoulay N, Plume A. CiteScore metrics: Creating journal metrics from the Scopus citation index. *ArXiv Prepr ArXiv181206871* 2018 [DOI: 10.1002/Leap.1246]

21 **Kiesslich T**, Weineck SB, Koelblinger D. Reasons for Journal Impact Factor Changes: Influence of Changing Source Items. *PLoS One* 2016; **11**: e0154199 [PMID: 27105434 DOI: 10.1371/journal.pone.0154199]

22 **Al-Hoorie AH**, Vitta JP. The seven sins of L2 research: A review of 30 journals' statistical quality and their CiteScore, SJR, SNIP, JCR Impact Factors. *Lang Teach Res* 2019; **23**: 727-744 [DOI: 10.1177/1362168818767191]



Published by **Baishideng Publishing Group Inc**
7041 Koll Center Parkway, Suite 160, Pleasanton, CA 94566, USA
Telephone: +1-925-3991568
E-mail: bpgoffice@wjgnet.com
Help Desk: https://www.f6publishing.com/helpdesk
https://www.wjgnet.com



© 2022 Baishideng Publishing Group Inc. All rights reserved.

ISSN 1007-9327 (print)
ISSN 2219-2840 (online)

World Journal of *Gastroenterology*

World J Gastroenterol 2022 October 21; 28(39): 5658-5783



Published by Baishideng Publishing Group Inc

World Journal of Gastroenterology

Contents

Weekly Volume 28 Number 39 October 21, 2022

OPINION REVIEW

5658 Risk factors for small intestinal adenocarcinomas that are common in the proximal small intestine

Fujimori S, Hamakubo R, Hoshimoto A, Nishimoto T, Omori J, Akimoto N, Tanaka S, Tatsuguchi A, Iwakiri K

REVIEW

5666 COVID-19 and hepatorenal syndrome

Wu HHL, Athwal VS, Kalra PA, Chinnadurai R

5679 Receptor of advanced glycation end-products axis and gallbladder cancer: A forgotten connection that we should reconsider

Rojas A, Lindner C, Schneider I, Gonzàlez I, Morales MA

5691 Interplay between metabolic dysfunction-associated fatty liver disease and chronic kidney disease: Epidemiology, pathophysiologic mechanisms, and treatment considerations

Theofilis P, Vordoni A, Kalaitzidis RG

MINIREVIEWS

5707 Pitfalls and promises of bile duct alternatives: A narrative review

Miyazawa M, Aikawa M, Takashima J, Kobayashi H, Ohnishi S, Ikada Y

5723 SARS-CoV-2-induced liver injury: A review article on the high-risk populations, manifestations, mechanisms, pathological changes, management, and outcomes

Payus AO, Mohd Noh M, Azizan N, Muthukaruppan Chettiar R

ACADEMIC WRITING

5731 All journals should include a correspondence section

Papanas N, Mikhailidis DP, Mukherjee D

ORIGINAL ARTICLE

Retrospective Cohort Study

5735 Effects of COVID-19 on the liver: The experience of a single center

Liakina V, Stundiene I, Milaknyte G, Bytautiene R, Reivytyte R, Puronaite R, Urbanoviciute G, Kazenaite E

Retrospective Study

5750 Immune checkpoint inhibitor-mediated colitis is associated with cancer overall survival

Weingarden AR, Gubatan J, Singh S, Balabanis TC, Patel A, Sharma A, Habtezion A

Observational Study

5764 Serum metabolic profiling of targeted bile acids reveals potentially novel biomarkers for primary biliary cholangitis and autoimmune hepatitis

Ma ZH, Wang XM, Wu RH, Hao DL, Sun LC, Li P, Niu JQ

ABOUT COVER

Editorial Board of *World Journal of Gastroenterology*, Raquel Rocha, PhD, MD, Professor, Department of Sciences of Nutrition, School of Nutrition, Federal University of Bahia, Salvador 40.110-907, BA, Brazil. raquelrocha@ufba.br

AIMS AND SCOPE

The primary aim of *World Journal of Gastroenterology* (*WJG*, *World J Gastroenterol*) is to provide scholars and readers from various fields of gastroenterology and hepatology with a platform to publish high-quality basic and clinical research articles and communicate their research findings online. *WJG* mainly publishes articles reporting research results and findings obtained in the field of gastroenterology and hepatology and covering a wide range of topics including gastroenterology, hepatology, gastrointestinal endoscopy, gastrointestinal surgery, gastrointestinal oncology, and pediatric gastroenterology.

INDEXING/ABSTRACTING

The *WJG* is now abstracted and indexed in Science Citation Index Expanded (SCIE, also known as SciSearch®), Current Contents/Clinical Medicine, Journal Citation Reports, Index Medicus, MEDLINE, PubMed, PubMed Central, Scopus, Reference Citation Analysis, China National Knowledge Infrastructure, China Science and Technology Journal Database, and Superstar Journals Database. The 2022 edition of Journal Citation Reports® cites the 2021 impact factor (IF) for *WJG* as 5.374; IF without journal self cites: 5.187; 5-year IF: 5.715; Journal Citation Indicator: 0.84; Ranking: 31 among 93 journals in gastroenterology and hepatology; and Quartile category: Q2. The *WJG*'s CiteScore for 2021 is 8.1 and Scopus CiteScore rank 2021: Gastroenterology is 18/149.

RESPONSIBLE EDITORS FOR THIS ISSUE

Production Editor: *Yi-Xuan Cai*; **Production Department Director:** *Xiang Li*; **Editorial Office Director:** *Jia-Ru Fan.*

NAME OF JOURNAL
World Journal of Gastroenterology

ISSN
ISSN 1007-9327 (print) ISSN 2219-2840 (online)

LAUNCH DATE
October 1, 1995

FREQUENCY
Weekly

EDITORS-IN-CHIEF
Andrzej S Tarnawski

EDITORIAL BOARD MEMBERS
http://www.wjgnet.com/1007-9327/editorialboard.htm

PUBLICATION DATE
October 21, 2022

COPYRIGHT
© 2022 Baishideng Publishing Group Inc

INSTRUCTIONS TO AUTHORS
https://www.wjgnet.com/bpg/gerinfo/204

GUIDELINES FOR ETHICS DOCUMENTS
https://www.wjgnet.com/bpg/GerInfo/287

GUIDELINES FOR NON-NATIVE SPEAKERS OF ENGLISH
https://www.wjgnet.com/bpg/gerinfo/240

PUBLICATION ETHICS
https://www.wjgnet.com/bpg/GerInfo/288

PUBLICATION MISCONDUCT
https://www.wjgnet.com/bpg/gerinfo/208

ARTICLE PROCESSING CHARGE
https://www.wjgnet.com/bpg/gerinfo/242

STEPS FOR SUBMITTING MANUSCRIPTS
https://www.wjgnet.com/bpg/GerInfo/239

ONLINE SUBMISSION
https://www.f6publishing.com

© 2022 Baishideng Publishing Group Inc. All rights reserved. 7041 Koll Center Parkway, Suite 160, Pleasanton, CA 94566, USA

E-mail: bpgoffice@wjgnet.com https://www.wjgnet.com

World Journal of Gastroenterology

Submit a Manuscript: https://www.f6publishing.com

World J Gastroenterol 2022 October 21; 28(39): 5658-5665

DOI: 10.3748/wjg.v28.i39.5658

ISSN 1007-9327 (print) ISSN 2219-2840 (online)

OPINION REVIEW

Risk factors for small intestinal adenocarcinomas that are common in the proximal small intestine

Shunji Fujimori, Ryohei Hamakubo, Aitoshi Hoshimoto, Takayoshi Nishimoto, Jun Omori, Naohiko Akimoto, Shu Tanaka, Atsushi Tatsuguchi, Katsuhiko Iwakiri

Specialty type: Gastroenterology and hepatology

Provenance and peer review: Invited article; Externally peer reviewed

Peer-review model: Single blind

Peer-review report's scientific quality classification

Grade A (Excellent): 0
Grade B (Very good): B
Grade C (Good): C
Grade D (Fair): D
Grade E (Poor): 0

P-Reviewer: Philipose J, United States; Saif U, China; Thongon N, Thailand

Received: August 5, 2022
Peer-review started: August 5, 2022
First decision: September 8, 2022
Revised: September 18, 2022
Accepted: October 11, 2022
Article in press: October 11, 2022
Published online: October 21, 2022

Shunji Fujimori, Ryohei Hamakubo, Department of Gastroenterology, Chiba Hokusoh Hospital, Nippon Medical School, Chiba 270-1694, Japan

Aitoshi Hoshimoto, Takayoshi Nishimoto, Jun Omori, Naohiko Akimoto, Atsushi Tatsuguchi, Katsuhiko Iwakiri, Department of Gastroenterology, Nippon Medical School, Graduate School of Medicine, Tokyo 113-8603, Japan

Shu Tanaka, Department of Gastroenterology, Tama-Nagayama Hospital, Nippon Medical School, Tokyo 206-0025, Japan

Corresponding author: Shunji Fujimori, AGAF, MD, PhD, Director, Department of Gastroenterology, Chiba Hokusoh Hospital, Nippon Medical School, 1715 Kamagari, Inzai-City, Chiba 270-1694, Japan. s-fujimori@nms.ac.jp

Abstract

The frequency of primary small intestinal adenocarcinoma is increasing but is still low. Its frequency is approximately 3% of that of colorectal adenocarcinoma. Considering that the small intestine occupies 90% of the surface area of the gastrointestinal tract, small intestinal adenocarcinoma is very rare. The main site of small intestinal adenocarcinoma is the proximal small intestine. Based on this characteristic, dietary animal proteins/lipids and bile concentrations are implicated and reported to be involved in carcinogenesis. Since most nutrients are absorbed in the proximal small intestine, the effect of absorbable intestinal content is a suitable explanation for why small intestinal adenocarcinoma is more common in the proximal small intestine. The proportion of aerobic bacteria is high in the proximal small intestine, but the absolute number of bacteria is low. In addition, the length and density of villi are greater in the proximal small intestine. However, the involvement of villi is considered to be low because the number of small intestinal adenocarcinomas is much smaller than that of colorectal adenocarcinomas. On the other hand, the reason for the low incidence of small intestinal adenocarcinoma in the distal small intestine may be that immune organs reside there. Genetic and disease factors increase the likelihood of small intestinal adenocarcinoma. In carcinogenesis experiments in which the positions of the small and large intestines were exchanged, tumors still occurred in the large intestinal mucosa more often. In other words, the influence of the intestinal contents is small, and there is a large difference in epithelial properties between the small intestine and the large intestine. In conclusion, small intestinal adenocar-

cinoma is rare compared to large intestinal adenocarcinoma due to the nature of the epithelium. It is reasonable to assume that diet is a trigger for small intestinal adenocarcinoma.

Key Words: Small intestine; Large intestine; Adenocarcinoma; Risk factor; Carcinogenesis

©The Author(s) 2022. Published by Baishideng Publishing Group Inc. All rights reserved.

Core Tip: When investigating the risk factors for small intestinal adenocarcinoma, an important point to note is that small intestinal adenocarcinoma is often found in the proximal small intestine. Intestinal contents remain in the ileum longer than in the jejunum, so poorly absorbed food is unlikely to be a carcinogenic factor. Animal proteins and lipids, bile concentrations, and aerobic bacteria, which are thought to be concentrated in the proximal small intestine, may be carcinogens in the small intestine. Since small intestinal adenocarcinoma is much rarer than colorectal adenocarcinoma, it is unlikely that small intestinal villi are involved in carcinogenesis.

Citation: Fujimori S, Hamakubo R, Hoshimoto A, Nishimoto T, Omori J, Akimoto N, Tanaka S, Tatsuguchi A, Iwakiri K. Risk factors for small intestinal adenocarcinomas that are common in the proximal small intestine. *World J Gastroenterol* 2022; 28(39): 5658-5665
URL: https://www.wjgnet.com/1007-9327/full/v28/i39/5658.htm
DOI: https://dx.doi.org/10.3748/wjg.v28.i39.5658

INTRODUCTION

Although the small intestine occupies 75% of the gastrointestinal tract length and 90% of the mucosal surface area, primary small intestinal cancer accounts for less than 5% of gastrointestinal cancers[1]. During the last century, enteroscopy was a difficult procedure to perform, and thus, the elucidation of small intestinal cancer was delayed compared to that of other gastrointestinal cancers. However, in this century, capsule endoscopy and balloon-assisted endoscopy have made it easier than ever to examine the small intestine. The frequency of small intestinal cancer has been increasing since 2000 or earlier and continues to rise with the addition of improved diagnostic power *via* new endoscopes[2]. Especially in patients with anemia of unknown cause, cases of small intestinal cancer diagnosed as a bleeding source are increasing[3]. In addition, many cases are diagnosed by positron emission tomography or computed tomography. The frequency of small intestinal adenocarcinoma is still on the rise, partly due to the widespread performance of small intestinal examinations[4].

According to a 2006 French report, the incidence of primary small intestinal malignancies in both men and women was approximately four times that 30 years ago (1.2 males and 0.8 females per 100000 in 2006)[5]. Primary small intestinal malignancies include neuroendocrine tumors, sarcomas, and lymphomas in addition to adenocarcinomas. A report of 10946 primary malignancies of the small intestine, mainly in Europe, showed that adenocarcinomas accounted for 37% of cases, carcinoid tumors accounted for 37% of cases, sarcomas accounted for 12% of cases, and malignant lymphomas accounted for 4% of cases[6]. In the United States, 40% of primary malignancies of the small intestine are reported to be adenocarcinomas, and 36% are carcinoid tumors[7].

According to the cancer statistics published yearly by the American Cancer Society, 5420 small intestinal malignancies and 145290 colorectal malignancies were predicted to develop in the United States in 2005[8]. The frequency of small intestinal malignancies was only 3.7% of that of colorectal malignancies. In 2019, the predicted number of colorectal malignancies was almost 145600 cases. However, the number of small bowel malignancies was 10590, which is 7.3% of the number of colorectal malignancies. Additionally, this percentage is twofold higher than that reported in 2005[9]. In the United States, colorectal adenocarcinomas account for 98% of colorectal malignancies, but small intestinal adenocarcinomas account for only approximately 30%-40% of small intestinal malignancies [10]. Therefore, regarding adenocarcinoma at present, the number of cases of small intestinal adenocarcinoma is approximately 3% of that of large intestinal adenocarcinoma cases. Considering that the small intestinal villi and circular folds have even been reported to occupy 98% of the intestinal surface area [11], the frequency of small intestinal adenocarcinoma per surface area is extremely low compared to that of colorectal adenocarcinoma.

In the 1970s, an experiment was performed in which azoxymethane, a carcinogen, was intravascularly administered to rats. The results showed that adenocarcinomas appeared in the proximal small intestine, which corresponds to the duodenum, and the large intestine. However, no adenocarcinoma appeared in the jejunum/ileum[12]. It is worth noting that in this experiment, in rats in which a part of the small intestine or large intestine had been replaced, tumors still appeared in the large intestine and

not the small intestine, regardless of the position in the digestive tract. In other words, the content of the intestinal tract did not significantly influence the development of tumors in the intestinal tract, and this experiment showed that the properties of the intestinal tract are involved in the development of tumors. This azoxymethane administration experiment was conducted again recently, and the results did not show carcinogenicity in the small intestine[13]. In the 1980s, an experiment was conducted in which dimethylhydrazine was administered to rats to examine the reproducibility of the above experiment, and the results were similar[14]. Based on this fact, many tumors can develop in the proximal small intestine (probably in the papilla of Vater) and in the large intestine, regardless of the position in the digestive tract. However, tumor development is less common in the jejunum and ileum. In other words, there is a decisive difference between the small and large intestines.

Differences between the small and large intestines are mainly the presence or absence of villi, intestinal contents, intestinal content retention time, intestinal flora, intestinal epithelial turnover, mucosal properties, and genetic factors. There are very few adenocarcinomas in the small intestine compared to the large intestine, but small intestinal adenocarcinomas are more common in the jejunum than in the ileum, as shown below. Here, we would like to consider the risk factors for small intestinal adenocarcinoma.

RISK FACTORS FOR SMALL INTESTINAL ADENOCARCINOMA IN THE PROXIMAL SMALL INTESTINE

Table 1 summarizes the reports of small intestinal adenocarcinoma according to site, namely, the duodenum, jejunum, and ileum. The majority of reports show that adenocarcinoma is the most common malignancy in the duodenum. The oral side of the duodenum can usually be explored endoscopically, which is why many malignancies are diagnosed in this area. However, these reports may include cancer of the papilla of Vater. The only Chinese report on this topic does not show a high cancer incidence rate in the duodenum. In this report, 160 cases of cancer of the papilla of Vater were excluded from 202 cases of all small intestinal adenocarcinomas, and adenocarcinomas were more common in the jejunum than in other parts of the small intestine[15]. When we examined the adenocarcinomas of the small intestine that were diagnosed at our institution only in patients in whom a normal papilla of Vater was observed, the jejunum was the most common site. This finding is in agreement with that reported in China. Because the duodenum is short, this result may be appropriate in assessments of the small intestine alone. In recent years, the papilla of Vater has been suggested to have characteristics different from those of the duodenum[16,17]. A mixture of bile and pancreatic juice passes through the papilla of Vater, and the bile and pancreatic ducts themselves have different carcinogenic properties. It is natural to think that the carcinogenic origin in the papilla of Vater is different from that in the small intestinal mucosa. We did not examine cancer of the papilla of Vater here.

When comparing the jejunum and the ileum and excluding the duodenum, adenocarcinoma was more common in the jejunum than in the ileum in all reports. Based on these results, it seems clear that there are more small intestinal adenocarcinomas in the proximal small intestine than in the distal small intestine. According to a report summarizing small intestinal gastrointestinal stromal tumors (GISTs), the jejunum has more GISTs than the ileum[18]. In addition, reports of small intestinal neuroendocrine tumors are often reported in the jejunum within 1 m from the ileocecal valve[19]. Differences in the site of occurrence are observed depending on the type of tumor. Here, since small intestinal adenocarcinoma is more common in the proximal small intestine, we would like to determine the risk factors for adenocarcinoma of the small intestine by considering the difference between the proximal side of the small intestine and the distal side.

Food

Most absorbable dietary components are absorbed in the duodenum and jejunum[20]. In other words, undegraded proteins and unabsorbed lipids flow in the proximal part of the small intestine. Diets containing high volumes of animal fat and protein have been reported to have a high risk of small intestinal adenocarcinoma, with correlation coefficients of 0.61 and 0.75, respectively[21]. Lipids and even small amounts of large peptides penetrate the cell membrane, which may be involved in carcinogenesis. Most proteins and lipids are absorbed in the proximal intestine and rarely reach the ileum, so there is no contradiction in this respect. Therefore, they may be involved in the carcinogenesis of the small intestine.

Bile and pancreatic juice

The proximal part of the small intestine has higher levels of bile and pancreatic juice than the distal part. A review of the literature on the effects of bile and pancreatic juice reveals that bile may be converted to carcinogenic deoxycholic acid by bacteria and that cholecystectomy reduces the incidence of small intestinal cancer[22,23]. In other words, bile may be involved in small intestinal carcinogenesis. However, it is difficult to judge the validity of the results because there are few reports on the effects of

Table 1 Regions where small intestinal adenocarcinoma was reported

Country	Year	Number[1]	Duodenum		Jejunum		Ileum		Ref.
France	2020	347	210	60.6%	72	20.7%	65	18.7%	[31]
China	2020	42	11[2]	26.2%	29	69.0%	2	4.8%	[15]
Japan	2015	47	14	29.8%	21	44.7%	12	25.5%	[32]
United States	2010	421	230	54.6%	142	33.7%	49	11.7%	[33]
China	2010	197	108	54.8%	59	29.9%	30	15.3%	[34]
United States	2006	460	272	59.1%	98	21.3%	90	19.6%	[35]
United States	2005	195	113	57.9%	54	27.7%	28	14.4%	[7]
United States	1996	1404	777	55.3%	376	26.8%	251	17.9%	[2]
Japan	Our cases	50[3]	20	40.0%	26	52.0%	4	8.0%	N/A

[1]Number excludes cases of unknown site.
[2]A total of 160 cases of primary cancer in the papilla of Vater were excluded.
[3]Only patients with a normal papilla of Vater were included.
N/A: Not applicable.

bile on the small intestine.

Intestinal chemicals

The contents of the intestinal tract include chemicals contained in the diet and various chemical substances produced by bacteria. As mentioned above, chemical carcinogenesis occurs when the large intestine comes into contact with chemical substances. However, since the transit time of the intestinal contents into the small intestine is approximately 4 h, which is considerably shorter than that of the large intestine, the effect of chemical substances in the intestine is thought to be smaller than that of the large intestine. In addition, if carcinogenesis due to dietary or bacterial chemical substances is the main cause of adenocarcinoma, more adenocarcinomas would be likely to develop in the ileum, where the intestinal contents stagnate longer than in the jejunum. However, if the carcinogen is absorbed in the oral side of the small intestine, this is not inconceivable.

Intestinal flora

Intestinal bacteria influence the intestinal tract through various means. Among the various chemicals produced by intestinal bacteria, those that not only cause inflammation but also have a direct carcinogenic effect and those that delay or prevent cell division of the intestinal epithelium have been reported[24]. Delaying epithelial turnover may be beneficial for bacteria directly involved in the epithelium. This delay in turnover is considered to be a factor that increases the possibility of cancer cell engraftment. There is a high possibility that intestinal bacteria are involved in carcinogenesis in the large intestine. However, it is difficult to explain why the number of jejunal adenocarcinomas is larger than that of ilial adenocarcinomas if intestinal bacteria are strongly associated with carcinogenesis in the small intestine. This is because it is difficult to explain why there are few bacteria in the proximal small intestine but many small intestinal adenocarcinomas in that area. However, the proximal small intestine is characterized by a relatively large number of aerobic bacteria, although the absolute number of bacteria is small. Therefore, given that small intestinal adenocarcinoma predominantly occurs in the proximal small intestine and aerobic bacteria are abundant in the proximal small intestine, the role of aerobic bacteria in small intestinal adenocarcinoma must be considered.

Immunity

To absorb and excrete various substances, the cell membrane of the small intestine needs to have direct contact with the outside environment of the body. Therefore, the intestinal lumen needs to protect itself against bacteria, viruses, and many substances that invade the body using various types of immune mechanisms. The small intestine has the highest levels of immunity in the body. Additionally, the lymphatic system within the small intestine is stronger in the distal small intestine, where cancer may be strongly eliminated by immune mechanisms. Benzopyrene, for example, has been reported to suppress mouse immunity and thus, in the presence of carcinogens, lead to adenocarcinoma development in the proximal small intestine[25]. However, it remains unclear whether immunity can explain why cancer is overwhelmingly less common in the small intestine than in the large intestine because there are few reports on this topic.

Table 2 Risk factors for small intestinal adenocarcinoma

Factor	Disease	Risks of small intestinal adenocarcinoma	Ref.
Animal fat		Correlation coefficient of 0.61	[21]
Animal protein		Correlation coefficient of 0.75	[21]
		2–3-fold higher risk	[36]
Bile salts		Bile salts may transform into carcinogenic deoxycholic acid	[22]
Hereditary polyposis	FAP	APC mutation; 5% is small bowel adenocarcinoma and half is duodenal adenocarcinoma	[27]
		The incidence is 330 times higher than that in the general population	[28]
	HNPCC	MMR gene mutation; lifetime risk is at approximately 1% in a French registry	[29]
	PJS	STK11 mutation; incidence is 520 times higher than that in the general population	[30]
Disease	Crohn's disease	The incidence is 17.4 times higher than that in the general population	[37]
		The incidence is almost 3 times higher than that in the average American	[38]
	Celiac disease	It is implicated in 8%-13% of small bowel adenocarcinoma cases	[39,40]

FAP: Familial adenomatous polyposis; APC: Adenoma polyposis coli; HNPCC: Hereditary nonpolyposis colorectal cancer; MMR: Mismatch repair: PJS: Peutz-Jeghers syndrome; STK 11: Serine/threonine kinase 1.

Villus length

The small intestine has villi and crypts, and the large intestine has only crypts and no villi. The lifespan of cells that have migrated to the villi is short, and the small intestinal epithelium is thought to be renewed every 3-5 d[26]. The proximal small intestine has longer and denser villi than the distal part. Therefore, the rate of epithelial turnover in the proximal small intestine may be longer than that in the distal part. This may be the reason why small intestinal adenocarcinoma is more common in the proximal small intestine. However, considering that many cancers develop in the large intestine, which has only crypts, it is unlikely that villi are significantly involved in cancer development.

SUMMARY OF SMALL INTESTINAL ADENOCARCINOMA RISK FACTORS

Based on the above rationale and considering that the number of small intestinal adenocarcinomas in the proximal small intestine is larger than that in the distal small intestine, the possible causes of carcinogenesis are the effects of diet, bile concentration, aerobic bacteria, and intestinal immunity, in the order described. However, none of the above causes is definitive. Table 2 briefly summarizes the reported risk factors for small intestinal adenocarcinoma. In addition to the above causes, genetic factors and inflammatory diseases have been added to the table. Papillary carcinoma is increased in patients with familial adenomatous polyposis due to a mutation in adenoma polyposis coli, but it is less associated with the jejunum and ileum[27,28]. Small intestinal adenocarcinoma also occurs in hereditary nonpolyposis colorectal cancer patients due to mismatch repair mutations, but it is much less frequent than colorectal adenocarcinoma[29]. Small intestinal adenocarcinoma occurs 520-fold more often in patients with Peutz-Jeghers syndrome than in healthy individuals, but the population with small intestinal adenocarcinoma was originally small[30]. An increase in small intestinal adenocarcinoma is also observed in patients with Crohn's disease and celiac disease, which are thought to be related to inflammatory carcinogenesis. Therefore, it is understandable that genetic factors and disease factors are involved in small intestinal adenocarcinoma.

CONCLUSION

Small intestinal adenocarcinoma is characterized by its predominance in the proximal small intestine. Animal proteins and lipids, bile concentrations, aerobic bacteria, and intestinal immunity were discussed as factors playing a role in small intestinal adenocarcinoma. Of these, it is highly possible that the dietary content absorbed in the proximal part of the small intestine is a risk factor for small intestinal adenocarcinoma. However, since the number of small intestinal adenocarcinomas is small, there are few reports, and none of the results are definitive. Moreover, in small intestine/large intestine replacement

experiments, at least in rats, the results show that the contents of the intestine are rarely involved in carcinogenesis. It seems that the nature of the organs is strongly related to susceptibility to carcinogenesis. Future studies are expected.

FOOTNOTES

Author contributions: Fujimori S contributed to the writing of this paper; Hamakubo R, Hoshimoto A, Nishimoto T, Omori J, and Tanaka S performed the small intestinal examinations; Akimoto N and Tatsuguchi A conducted the pathological examinations; Iwakiri K gave advice for the writing of the paper.

Conflict-of-interest statement: All the authors report no relevant conflicts of interest for this article.

Open-Access: This article is an open-access article that was selected by an in-house editor and fully peer-reviewed by external reviewers. It is distributed in accordance with the Creative Commons Attribution NonCommercial (CC BY-NC 4.0) license, which permits others to distribute, remix, adapt, build upon this work non-commercially, and license their derivative works on different terms, provided the original work is properly cited and the use is non-commercial. See: https://creativecommons.org/Licenses/by-nc/4.0/

Country/Territory of origin: Japan

ORCID number: Shunji Fujimori 0000-0002-6214-2595; Ryohei Hamakubo 0000-0003-1205-3866; Aitoshi Hoshimoto 0000-0002-6883-4795; Takayoshi Nishimoto 0000-0002-5147-0665; Jun Omori 0000-0002-4375-5070; Naohiko Akimoto 0000-0001-9880-4143; Shu Tanaka 0000-0003-4121-5553; Atsushi Tatsuguchi 0000-0002-8499-8837; Katsuhiko Iwakiri 0000-0002-5558-6104.

S-Editor: Wang JJ
L-Editor: A
P-Editor: Wang JJ

REFERENCES

1 **Neugut AI**, Jacobson JS, Suh S, Mukherjee R, Arber N. The epidemiology of cancer of the small bowel. *Cancer Epidemiol Biomarkers Prev* 1998; **7**: 243-251 [PMID: 9521441]
2 **Severson RK**, Schenk M, Gurney JG, Weiss LK, Demers RY. Increasing incidence of adenocarcinomas and carcinoid tumors of the small intestine in adults. *Cancer Epidemiol Biomarkers Prev* 1996; **5**: 81-84 [PMID: 8850266]
3 **Fujimori S**, Seo T, Gudis K, Tanaka S, Mitsui K, Kobayashi T, Ehara A, Yonezawa M, Tatsuguchi A, Sakamoto C. Diagnosis and treatment of obscure gastrointestinal bleeding using combined capsule endoscopy and double balloon endoscopy: 1-year follow-up study. *Endoscopy* 2007; **39**: 1053-1058 [PMID: 18072055 DOI: 10.1055/s-2007-967014]
4 **Qubaiah O**, Devesa SS, Platz CE, Huycke MM, Dores GM. Small intestinal cancer: a population-based study of incidence and survival patterns in the United States, 1992 to 2006. *Cancer Epidemiol Biomarkers Prev* 2010; **19**: 1908-1918 [PMID: 20647399 DOI: 10.1158/1055-9965.EPI-10-0328]
5 **Lepage C**, Bouvier AM, Manfredi S, Dancourt V, Faivre J. Incidence and management of primary malignant small bowel cancers: a well-defined French population study. *Am J Gastroenterol* 2006; **101**: 2826-2832 [PMID: 17026561 DOI: 10.1111/j.1572-0241.2006.00854.x]
6 **Scélo G**, Boffetta P, Hemminki K, Pukkala E, Olsen JH, Andersen A, Tracey E, Brewster DH, McBride ML, Kliewer EV, Tonita JM, Pompe-Kirn V, Chia KS, Jonasson JG, Martos C, Colin D, Brennan P. Associations between small intestine cancer and other primary cancers: an international population-based study. *Int J Cancer* 2006; **118**: 189-196 [PMID: 16003748 DOI: 10.1002/ijc.21284]
7 **Dabaja BS**, Suki D, Pro B, Bonnen M, Ajani J. Adenocarcinoma of the small bowel: presentation, prognostic factors, and outcome of 217 patients. *Cancer* 2004; **101**: 518-526 [PMID: 15274064 DOI: 10.1002/cncr.20404]
8 **Jemal A**, Murray T, Ward E, Samuels A, Tiwari RC, Ghafoor A, Feuer EJ, Thun MJ. Cancer statistics, 2005. *CA Cancer J Clin* 2005; **55**: 10-30 [PMID: 15661684 DOI: 10.3322/canjclin.55.1.10]
9 **Siegel RL**, Miller KD, Jemal A. Cancer statistics, 2019. *CA Cancer J Clin* 2019; **69**: 7-34 [PMID: 30620402 DOI: 10.3322/caac.21551]
10 **Schottenfeld D**, Beebe-Dimmer JL, Vigneau FD. The epidemiology and pathogenesis of neoplasia in the small intestine. *Ann Epidemiol* 2009; **19**: 58-69 [PMID: 19064190 DOI: 10.1016/j.annepidem.2008.10.004]
11 **Gabos S**, Berkel J, Band P, Robson D, Whittaker H. Small bowel cancer in western Canada. *Int J Epidemiol* 1993; **22**: 198-206 [PMID: 8505174 DOI: 10.1093/ije/22.2.198]
12 **Gennaro AR**, Villanueva R, Sukonthaman Y, Vathanophas V, Rosemond GP. Chemical carcinogenesis in transposed intestinal segments. *Cancer Res* 1973; **33**: 536-541 [PMID: 4689902]
13 **Metzger R**, Maruskova M, Krebs S, Janssen KP, Krug AB. Increased Incidence of Colon Tumors in AOM-Treated *Apc*$^{1638N/+}$ Mice Reveals Higher Frequency of Tumor Associated Neutrophils in Colon Than Small Intestine. *Front Oncol* 2019; **9**: 1001 [PMID: 31681563 DOI: 10.3389/fonc.2019.01001]
14 **Celik C**, Mittelman A, Paolini NS Jr, Lewis D, Evans JT. Effects of 1,2-symmetrical dimethylhydrazine on jejunocolic transposition in Sprague-Dawley rats. *Cancer Res* 1981; **41**: 2908-2911 [PMID: 7248950]

15 **Tian J**, Liu J, Guo C, Yang X, Yang Y, Gou H, Qiu M, Cao D. Prognostic factors and treatment outcomes in patients with non-ampullary small bowel adenocarcinoma: Long-term analysis. *Medicine (Baltimore)* 2019; **98**: e15381 [PMID: 31027129 DOI: 10.1097/MD.0000000000015381]

16 **Kimura W**, Futakawa N, Zhao B. Neoplastic diseases of the papilla of Vater. *J Hepatobiliary Pancreat Surg* 2004; **11**: 223-231 [PMID: 15368105 DOI: 10.1007/s00534-004-0894-7]

17 **Chandrasegaram MD**, Gill AJ, Samra J, Price T, Chen J, Fawcett J, Merrett ND. Ampullary cancer of intestinal origin and duodenal cancer - A logical clinical and therapeutic subgroup in periampullary cancer. *World J Gastrointest Oncol* 2017; **9**: 407-415 [PMID: 29085567 DOI: 10.4251/wjgo.v9.i10.407]

18 **Misawa S**, Takeda M, Sakamoto H, Kirii Y, Ota H, Takagi H. Spontaneous rupture of a giant gastrointestinal stromal tumor of the jejunum: a case report and literature review. *World J Surg Oncol* 2014; **12**: 153 [PMID: 24885725 DOI: 10.1186/1477-7819-12-153]

19 **Tran CG**, Sherman SK, Howe JR. The Landmark Series: Management of Small Bowel Neuroendocrine Tumors. *Ann Surg Oncol* 2021; **28**: 2741-2751 [PMID: 33452604 DOI: 10.1245/s10434-020-09566-4]

20 **Fujimori S**. Capsule endoscopy for investigating the digestion process. *VideoGIE* 2020; **5**: 14-15 [PMID: 31922073 DOI: 10.1016/j.vgie.2019.10.009]

21 **Lowenfels AB**, Sonni A. Distribution of small bowel tumors. *Cancer Lett* 1977; **3**: 83-86 [PMID: 890689 DOI: 10.1016/s0304-3835(77)94394-4]

22 **Delaunoit T**, Neczyporenko F, Limburg PJ, Erlichman C. Pathogenesis and risk factors of small bowel adenocarcinoma: a colorectal cancer sibling? *Am J Gastroenterol* 2005; **100**: 703-710 [PMID: 15743371 DOI: 10.1111/j.1572-0241.2005.40605.x]

23 **Nogueira L**, Freedman ND, Engels EA, Warren JL, Castro F, Koshiol J. Gallstones, cholecystectomy, and risk of digestive system cancers. *Am J Epidemiol* 2014; **179**: 731-739 [PMID: 24470530 DOI: 10.1093/aje/kwt322]

24 **Mandal P**. Molecular mechanistic pathway of colorectal carcinogenesis associated with intestinal microbiota. *Anaerobe* 2018; **49**: 63-70 [PMID: 29277623 DOI: 10.1016/j.anaerobe.2017.12.008]

25 **Nebert DW**, Shi Z, Gálvez-Peralta M, Uno S, Dragin N. Oral benzo[a]pyrene: understanding pharmacokinetics, detoxication, and consequences--Cyp1 knockout mouse lines as a paradigm. *Mol Pharmacol* 2013; **84**: 304-313 [PMID: 23761301 DOI: 10.1124/mol.113.086637]

26 **Bellafante E**, Morgano A, Salvatore L, Murzilli S, Di Tullio G, D'Orazio A, Latorre D, Villani G, Moschetta A. PGC-1β promotes enterocyte lifespan and tumorigenesis in the intestine. *Proc Natl Acad Sci U S A* 2014; **111**: E4523-E4531 [PMID: 25288742 DOI: 10.1073/pnas.1415279111]

27 **Jagelman DG**, DeCosse JJ, Bussey HJ. Upper gastrointestinal cancer in familial adenomatous polyposis. *Lancet* 1988; **1**: 1149-1151 [PMID: 2896968 DOI: 10.1016/s0140-6736(88)91962-9]

28 **Shenoy S**. Genetic risks and familial associations of small bowel carcinoma. *World J Gastrointest Oncol* 2016; **8**: 509-519 [PMID: 27326320 DOI: 10.4251/wjgo.v8.i6.509]

29 **Bonadona V**, Bonaïti B, Olschwang S, Grandjouan S, Huiart L, Longy M, Guimbaud R, Buecher B, Bignon YJ, Caron O, Colas C, Noguès C, Lejeune-Dumoulin S, Olivier-Faivre L, Polycarpe-Osaer F, Nguyen TD, Desseigne F, Saurin JC, Berthet P, Leroux D, Duffour J, Manouvrier S, Frébourg T, Sobol H, Lasset C, Bonaïti-Pellié C; French Cancer Genetics Network. Cancer risks associated with germline mutations in MLH1, MSH2, and MSH6 genes in Lynch syndrome. *JAMA* 2011; **305**: 2304-2310 [PMID: 21642682 DOI: 10.1001/jama.2011.743]

30 **Giardiello FM**, Brensinger JD, Tersmette AC, Goodman SN, Petersen GM, Booker SV, Cruz-Correa M, Offerhaus JA. Very high risk of cancer in familial Peutz-Jeghers syndrome. *Gastroenterology* 2000; **119**: 1447-1453 [PMID: 11113065 DOI: 10.1053/gast.2000.20228]

31 **Aparicio T**, Henriques J, Manfredi S, Tougeron D, Bouché O, Pezet D, Piessen G, Coriat R, Zaanan A, Legoux JL, Terrebone E, Pocard M, Gornet JM, Lecomte T, Lombard-Bohas C, Perrier H, Lecaille C, Lavau-Denes S, Vernerey D, Afchain P; NADEGE Investigators. Small bowel adenocarcinoma: Results from a nationwide prospective ARCAD-NADEGE cohort study of 347 patients. *Int J Cancer* 2020; **147**: 967-977 [PMID: 31912484 DOI: 10.1002/ijc.32860]

32 **Kumagai R**, Kohashi K, Takahashi S, Yamamoto H, Hirahashi M, Taguchi K, Nishiyama K, Oda Y. Mucinous phenotype and CD10 expression of primary adenocarcinoma of the small intestine. *World J Gastroenterol* 2015; **21**: 2700-2710 [PMID: 25759539 DOI: 10.3748/wjg.v21.i9.2700]

33 **Halfdanarson TR**, McWilliams RR, Donohue JH, Quevedo JF. A single-institution experience with 491 cases of small bowel adenocarcinoma. *Am J Surg* 2010; **199**: 797-803 [PMID: 20609724 DOI: 10.1016/j.amjsurg.2009.05.037]

34 **Chang HK**, Yu E, Kim J, Bae YK, Jang KT, Jung ES, Yoon GS, Kim JM, Oh YH, Bae HI, Kim GI, Jung SJ, Gu MJ, Kim JY, Jang KY, Jun SY, Eom DW, Kwon KW, Kang GH, Park JB, Hong S, Lee JS, Park JY, Hong SM; Korean Small Intestinal Cancer Study Group. Adenocarcinoma of the small intestine: a multi-institutional study of 197 surgically resected cases. *Hum Pathol* 2010; **41**: 1087-1096 [PMID: 20334897 DOI: 10.1016/j.humpath.2010.01.006]

35 **Verma D**, Stroehlein JR. Adenocarcinoma of the small bowel: a 60-yr perspective derived from M. D. Anderson Cancer Center Tumor Registry. *Am J Gastroenterol* 2006; **101**: 1647-1654 [PMID: 16863573 DOI: 10.1111/j.1572-0241.2006.00625.x]

36 **Chow WH**, Linet MS, McLaughlin JK, Hsing AW, Chien HT, Blot WJ. Risk factors for small intestine cancer. *Cancer Causes Control* 1993; **4**: 163-169 [PMID: 8481495 DOI: 10.1007/bf00053158]

37 **Bernstein CN**, Blanchard JF, Kliewer E, Wajda A. Cancer risk in patients with inflammatory bowel disease: a population-based study. *Cancer* 2001; **91**: 854-862 [PMID: 11241255 DOI: 10.1002/1097-0142(20010215)91:4<854::aid-cncr1073>3.0.co;2-z]

38 **Shaukat A**, Virnig DJ, Howard D, Sitaraman SV, Liff JM, Lederle FA. Crohn's disease and small bowel adenocarcinoma: a population-based case-control study. *Cancer Epidemiol Biomarkers Prev* 2011; **20**: 1120-1123 [PMID: 21467236 DOI: 10.1158/1055-9965.EPI-10-1281]

39 **Swinson CM**, Slavin G, Coles EC, Booth CC. Coeliac disease and malignancy. *Lancet* 1983; **1**: 111-115 [PMID: 6129425 DOI: 10.1016/s0140-6736(83)91754-3]

40 **Askling J**, Linet M, Gridley G, Halstensen TS, Ekström K, Ekbom A. Cancer incidence in a population-based cohort of

individuals hospitalized with celiac disease or dermatitis herpetiformis. *Gastroenterology* 2002; **123**: 1428-1435 [PMID: 12404215 DOI: 10.1053/gast.2002.36585]

World Journal of Gastroenterology

Submit a Manuscript: https://www.f6publishing.com

World J Gastroenterol 2022 October 21; 28(39): 5666-5678

DOI: 10.3748/wjg.v28.i39.5666

ISSN 1007-9327 (print) ISSN 2219-2840 (online)

REVIEW

COVID-19 and hepatorenal syndrome

Henry H L Wu, Varinder S Athwal, Philip A Kalra, Rajkumar Chinnadurai

Specialty type: Gastroenterology and hepatology

Provenance and peer review: Invited article; Externally peer reviewed.

Peer-review model: Single blind

Peer-review report's scientific quality classification

Grade A (Excellent): 0
Grade B (Very good): B
Grade C (Good): C, C
Grade D (Fair): 0
Grade E (Poor): 0

P-Reviewer: Gupta A, India; Shariati MBH, Iran; Wang MK, China

Received: September 4, 2022
Peer-review started: September 4, 2022
First decision: September 19, 2022
Revised: September 21, 2022
Accepted: September 30, 2022
Article in press: September 30, 2022
Published online: October 21, 2022

Henry H L Wu, Renal Research, Kolling Institute of Medical Research, Royal North Shore Hospital, Sydney 2065, New South Wales, Australia

Varinder S Athwal, Faculty of Biology, Medicine & Health (Division of Diabetes, Metabolism & Gastroenterology), The University of Manchester, Manchester M13 9PL, United Kingdom

Philip A Kalra, Rajkumar Chinnadurai, Department of Renal Medicine, Northern Care Alliance NHS Foundation Trust, Salford M6 8HD, United Kingdom

Corresponding author: Henry H L Wu, MBChB, Academic Editor, Academic Fellow, Doctor, Honorary Research Fellow, Renal Research, Kolling Institute of Medical Research, Royal North Shore Hospital, Reserve Road, 2065 St. Leonards NSW, Sydney 2065, New South Wales, Australia. honlinhenry.wu@health.nsw.gov.au

Abstract

Coronavirus disease 2019 (COVID-19) is a highly infectious disease which emerged into a global pandemic. Although it primarily causes respiratory symptoms for affected patients, COVID-19 was shown to have multi-organ manifestations. Elevated liver enzymes appear to be commonly observed during the course of COVID-19, and there have been numerous reports of liver injury secondary to COVID-19 infection. It has been established that patients with pre-existing chronic liver disease (CLD) are more likely to have poorer outcomes following COVID-19 infection compared to those without CLD. Co-morbidities such as diabetes, hypertension, obesity, cardiovascular and chronic kidney disease frequently co-exist in individuals living with CLD, and a substantial population may also live with some degree of frailty. The mechanisms of how COVID-19 induces liver injury have been postulated. Hepatorenal syndrome (HRS) is the occurrence of kidney dysfunction in patients with severe CLD/fulminant liver failure in the absence of another identifiable cause, and is usually a marker of severe decompensated liver disease. Select reports of HRS following acute COVID-19 infection have been presented, although the risk factors and pathophysiological mechanisms leading to HRS in COVID-19 infection or following COVID-19 treatment remain largely unestablished due to the relative lack and novelty of published data. Evidence discussing the management of HRS in high-dependency care and intensive care contexts is only emerging. In this article, we provide an overview on the speculative pathophysiological me-chanisms of COVID-19 induced HRS and propose strategies for clinical diagnosis and management to optimize outcomes in this scenario.

Key Words: COVID-19; Hepatorenal syndrome; Pathophysiology; Clinical assessment;

Management; Prognosis

©The Author(s) 2022. Published by Baishideng Publishing Group Inc. All rights reserved.

Core Tip: There have been numerous reviews evaluating the causative relationship between coronavirus disease 2019 (COVID-19) and liver pathology, given an emerging number of cases reporting COVID-19 induced liver injury. There are few reports noting the onset of hepatorenal syndrome (HRS) in the face of COVID-19 infection. Occurrence of HRS in any circumstance is typically an indicator of severe and perhaps life-threatening disease, potentially requiring liver transplantation. With a paucity in literature compilation on the associations between COVID-19 and HRS, we provide a review which discusses the purported pathophysiological mechanisms of COVID-19 induced HRS, and propose clinical assessment and management approaches in this scenario.

Citation: Wu HHL, Athwal VS, Kalra PA, Chinnadurai R. COVID-19 and hepatorenal syndrome. *World J Gastroenterol* 2022; 28(39): 5666-5678
URL: https://www.wjgnet.com/1007-9327/full/v28/i39/5666.htm
DOI: https://dx.doi.org/10.3748/wjg.v28.i39.5666

INTRODUCTION

The impact of coronavirus disease 2019 (COVID-19) has been tremendous since the initial case was reported in December 2019, and COVID-19 subsequently spiraled into a global pandemic which is affecting populations and societies significantly up to this day[1-3]. The severity of COVID-19 could be wide ranging from mild to severe disease[4]. This depends on various intrinsic and environmental factors for each individual[4,5]. The manifestations of COVID-19 are thought to be primarily respiratory, with severe COVID-19 infection leading to acute respiratory distress syndrome potentially progressing towards life-threatening septic shock and multi-organ failure[6,7]. There is emerging evidence on the multi-systemic effects of COVID-19 outside of the respiratory system. It is suggested that COVID-19 has direct associations with acute disease processes across the neurological, cardiovascular, renal and gastroenterological systems amongst other organ systems, but the pathophysiology of how COVID-19 affects these organs has not been fully established in most instances[8-12].

Liver injury secondary to COVID-19 has been investigated, with its incidence ranging between 15% and 53%[13]. In most patients, the effect of COVID-19 on the liver is a transient reaction with elevation of transaminases which resolves and most patients achieve recovery back to their normal baseline[14]. However, individuals with underlying cirrhosis and chronic liver disease (CLD) were found to have significantly greater 30-day mortality and lengthier hospitalization, and poorer prognosis following acute recovery from COVID-19 induced liver injury[15]. Histological damage to hepatocytes and bile duct cells was found in patients testing positive for COVID-19[16].

Hepatorenal syndrome (HRS) is a state of kidney function deterioration (usually profound oliguria and sodium retention) in patients with advanced cirrhosis or acute liver failure[17,18]. The decline in kidney function could be rapid (Type I) or gradual (Type II), dependent on the etiology of HRS[18]. In cirrhosis, Type 1 and Type 2 HRS has been replaced with newer terminology and HRS is now defined as either acute (HRS-AKI), sub-acute (HRS-AKD) or chronic (HRS-CKD)[19]. HRS is a diagnosis of exclusion in which other causes of kidney dysfunction are not identified, and where the kidneys were not found to be structurally damaged[17,18]. The dominant theory to explain for the pathophysiology of HRS is significant constriction of blood vessels which perfuse the kidneys, most likely mediated by splanchnic vasodilation (leading to central hypovolemia) and hepatorenal reflex mechanisms as a result of portal hypertension[17,18]. HRS is most likely seen in the context of advanced stage cirrhosis. The most common etiologies of cirrhosis include alcohol, non-alcoholic steatohepatitis and chronic viral hepatitis[20]. Multiple triggers of HRS have been recognized and spontaneous bacterial peritonitis (SBP) in patients with ascites from decompensated cirrhosis is a leading cause[21]. HRS is a marker of poor prognosis in hepatology, and the risk of death is very high unless prompt liver transplantation or acute dialysis can be provided[22].

There were select case reports of liver injury following COVID-19 infection where acute kidney dysfunction was found, suggesting the potential manifestation of COVID-19 induced HRS[23,24]. Evidence of the pathophysiology, optimal strategies for clinical assessment and management of COVID-19 induced HRS is seldom discussed at present due to a relative lack of cases. In this review, we will explore the speculative pathophysiological mechanisms of HRS following COVID-19 infection based on early evidence, and propose potential clinical assessment and management strategies to optimize HRS outcomes in this scenario.

POTENTIAL PATHOPHYSIOLOGICAL MECHANISMS OF COVID-19 INDUCED HRS

Current perspectives on the potential pathophysiological mechanisms of COVID-19 induced HRS are that of a multifactorial process (Figure 1). COVID-19 induced liver injury can be the result of direct viral cytopathic hepatocyte injury, systemic inflammatory cytokine storms causing hepatocyte cell death, endothelitis and dysfunction of the liver vasculature leading to widespread cell damage and ischemia, and drug-associated exacerbations in COVID-19 induced liver injury[25,26]. Subsequently, these multiple pathways of liver injury may result in circulatory dysfunction, progressing to HRS with vasoconstriction and hypoperfusion of the kidneys amongst other mechanisms[17-19].

Direct COVID-19 infection of hepatocytes

Direct viral cytopathic injury to the liver, similar to how various organs are affected by COVID-19 infection, should be considered as the major pathophysiological mechanism. Ultrastructural histological examination identified severe acute respiratory syndrome coronavirus-2 (SARS-CoV-2) particles in the cytoplasm of hepatocytes[27]. Features of cellular viral invasion such as conspicuous mitochondrial swelling, decreased glycogen granules, and endoplasmic reticulum dilatation were observed in SARS-CoV-2-infected hepatocytes[27]. The presence of binuclear hepatocytes, central lobular necrosis and hepatocyte apoptosis were observed features of liver damage following COVID-19 infection[27]. Induction of hepatocyte apoptosis from COVID-19 infection could be the result of p7a overexpression [26,28]. p7a is a protein which can be expressed in cells infected by SARS-CoV-2, and induces apoptosis in cell lines derived from organs including the lungs, liver and kidneys *via* a caspase-dependent pathway[29]. This mechanism confirms the pathway of how SARS-CoV-2 can directly attack liver tissues and cause damage.

The extent of viral tropism is typically dependent on the availability of viral receptors at the surface of host cells in specific tissues[30]. The spike (S) protein of SARS-CoV-2 mediates cellular entry of SARS-CoV-2. S protein is cleaved by transmembrane serine protease 2/transmembrane serine protease 4 and interacts with the angiotensin converting enzyme 2 (ACE2) protein in host cells specifically[30]. In normal circumstances, ACE2 would only be expressed in bile duct epithelial cells, central hepatic vein and portal vein endothelial cells within the hepatobiliary system, being almost absent in hepatocytes [31]. The level of ACE2 expression in bile duct epithelial cells is comparable to that of alveolar epithelial cells in the lungs (commonly recognized to have the greatest expression of ACE2 in the body)[31]. The compensatory differentiation and proliferation of liver parenchymal cells derived from bile duct cells during diseased states may explain the underlying pathophysiological mechanisms of how SARS-CoV-2 induces liver injury[32]. The degree of ACE2 expression in hepatocytes is regulated by multiple factors. Histological studies in mice and humans identified greater ACE2 expression in subjects with cirrhosis [33]. The degree of hypoxia is also shown to correlate with ACE2 expression in hepatocytes, and notably the affinity of S protein towards the ACE2 receptor is increased with hypoxia due to trypsin activation, trypsin being a protein commonly expressed in liver epithelial cells[34,35]. These findings may explain why the effects of COVID-19 infection would tend to be more severe in patients living with underlying CLD and other hypoxic conditions.

Systemic inflammatory cytokine storms in COVID-19 induced liver injury

Another purported pathway of COVID-19 induced liver injury is an excessive immune response triggered by the virus causing a systemic inflammatory cytokine storm[36]. During a systemic inflammatory cytokine storm stimulated by COVID-19 induced liver injury, complement and interleukin-23 (IL-23) are released into the bloodstream, activating kupffer cells and inducing their production of tumor necrosis factor α (TNF-α)[37,38]. As an inflammatory cytokine, TNF-α aggravates the responses of inflammation by upregulating the expression of endothelial cell adhesion molecules and inducing hepatocytes to secrete chemokines[39]. Under the induction of chemokines, $CD4^+$ T cells and neutrophils are rapidly recruited to the liver, in which $CD4^+$ T cells assist mucosal molecules to promote neutrophil entry into the liver parenchyma[40,41]. Neutrophils directly damage hepatocytes by releasing oxidants and proteases, resulting in cell necrosis[41]. In patients who are severely affected or critically ill following COVID-19 infection, much higher plasma levels of inflammatory cytokines and lower lymphocyte counts were observed[42]. Previous studies note that an increase in IL-6 and IL-10 and a decrease in $CD4^+$ T cells were independent risk factors related to severe liver damage, and lymphopenia and C-reactive protein levels were found to be independently associated with the degree of liver injury [43].

The inflammatory storm response from COVID-19 infection is usually mild in the early stages of COVID-19 infection, but patients may clinically deteriorate rapidly if appropriate management of COVID-19 is not administered in a timely manner, with the inflammatory storm response occurring more strongly during the post-viral inflammatory phase[6]. For patients living with decompensated CLD complications, notably ascites, their threshold to develop systemic inflammatory storm responses following COVID-19 infection would even be lower than those without CLD due to underlying pro-inflammatory risks with SBP[44,45].

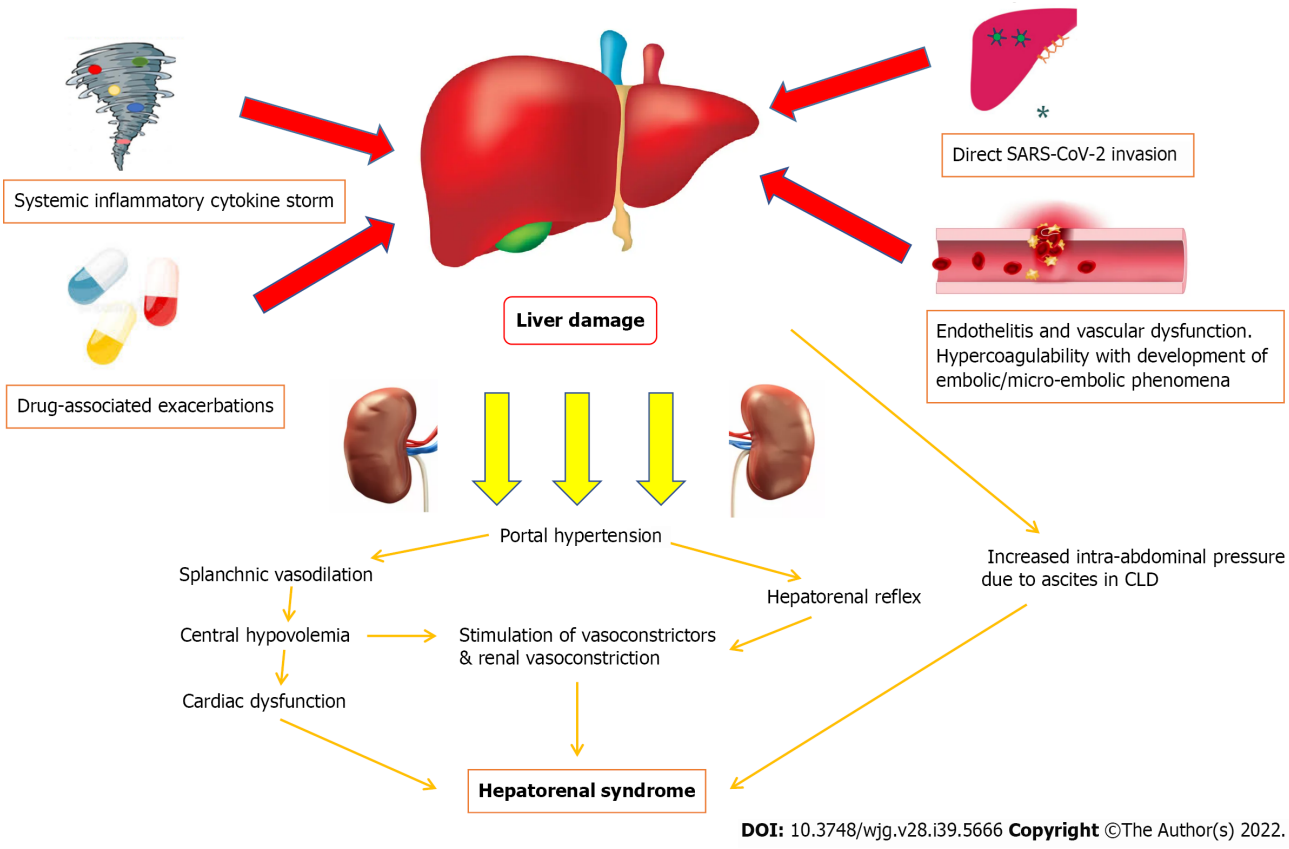


Figure 1 Potential pathophysiological mechanisms of COVID-19 induced hepatorenal syndrome. SARS-CoV-2: Severe acute respiratory syndrome coronavirus 2.

Endothelitis and vascular dysfunction in COVID-19 induced liver injury

The impact of COVID-19 towards thrombo-inflammation in endothelial tissues is significant. The ACE2 protein, which is present in many organs across the body, facilitates SARS-CoV-2 entry into endothelial cells *via* endocytosis with its binding to the ACE2 protein[46]. Viral infection and immune-mediated inflammatory responses occur within endothelial cells, leading to vascular dysfunction, especially in capillaries[47-49]. Subsequently, vascular dysfunction progresses to a hypercoagulable state and the development of embolic/micro-embolic phenomena, tissue edema, and organ ischemia[47-49]. In the liver, ischemia reperfusion injury which occurs typically after rapid recovery of blood circulation following events of vascular dysfunction leading to ischemia, has been touted as an underlying pathophysiological mechanism of COVID-19 induced liver injury[48,49]. Reperfusion following ischemia activates neutrophils, kupffer cells, and platelets within the cellular surroundings, leading to a series of destructive cellular reactions such as reactive oxygen species and calcium overload, which manifests towards widespread inflammatory response and cell damage[48,49]. Eventually, increased anaerobic glycolysis leads to reduced adenosine triphosphate production, which ultimately results in hepatocyte cell death from inhibition of hepatocyte signal transduction[42,48,49].

Drug-associated exacerbations in COVID-19 induced liver injury

In addition to the direct viral and systemic inflammatory mechanisms of liver injury following COVID-19 infection, the impact of various drugs received during acute hospitalization in patients with COVID-19 associated liver injury has been discussed. There has been debate whether these drugs (drugs trialed/used for COVID-19 treatment-antivirals such as Lopinavir/Ritonavir, Remdesivir, Favipiravir, Arbidol, Oseltamivir and others; antibiotics such as Doxycycline and Azithromycin; chloroquines; steroids; non-steroidal anti-inflammatory drugs) play a greater pathophysiological role in causing liver injury compared to COVID-19 infection itself[50].

Several studies have evaluated antivirals targeting COVID-19 infection in the midst of liver injury. For example, Lopinavir is a protease inhibitor conventionally used to treat human immunodeficiency virus infection in combination with a low dose of Ritonavir, another protease inhibitor, which enhances its biological half-life[51]. If high doses of Ritonavir (> 1 g daily) are taken, severe hepatotoxicity may ensue[52]. Recent studies show that Lopinavir/Ritonavir, when prescribed with or without ribavirin, interferon beta, and/or corticosteroids, was independently associated with increased levels of serum alanine transaminase (ALT) and aspartate transaminase (AST) in patients with positive COVID-19

status[53]. It was demonstrated from a retrospective observational study by Jiang and colleagues that Lopinavir/Ritonavir use in COVID-19 patients is associated with liver injury and abnormal liver function, particularly for patients in a non-critical state[54]. Ultimately, considering the fact that there is yet to be a completely effective antiviral therapy for COVID-19 and that antiviral drugs may cause abnormal liver function, there should be careful consideration of whether to prescribe antivirals, in particular for patients with CLD and/or metabolic diseases[52].

Antibiotics, particularly those of tetracycline-class and Azithromycin, have been shown to exacerbate liver damage in the context of COVID-19 induced liver injury[55]. For example, Doxycycline chelates zinc, which is required by the matrix metalloproteinases involved in COVID-19 infection, and inhibits SARS-CoV-2 RNA polymerase activity and direct viral entry[56,57]. Whilst generally safe to use with its anti-inflammatory effects, Doxycycline use may contribute towards hepatotoxicity and has been linked to occasional bile duct injuries[55]. There should be caution when prescribing Doxycycline alongside other potential hepatotoxic drugs, given reports of fulminant liver failure and hepatocellular necrosis occurring following the prescription of Doxycycline in these scenarios[55].

At a molecular level, there has been focused discussion on cytochrome P450 (CYP450) in the context of drug-associated exacerbations in COVID-19 induced liver injury. CYP450 is a superfamily of monooxygenase enzymes that mediate drug interactions during various pathological conditions[58]. It is presumed the metabolic activity of CYP450 would be altered by the effects of acute COVID-19 infection[57]. Liver injury in the context of COVID-19 infection complicates our understanding of how and to what extent CYP450 would be affected, and further work is needed in this area. Nevertheless, it is suggested that there would be clearance-associated pharmacokinetic interactions with antivirals and other drugs that are administered in this situation[57-61]. Common drugs affected by alterations in the CYP450 pathway could include Remdesivir, which is extensively metabolized by CYP450s, particularly CYP3A4, as well as Chloroquine and Colchicine which are both included in clinical trials researching COVID-19 treatment regimes[57-61].

Pathogenesis of HRS in COVID-19 induced liver injury

The multifactorial components of COVID-19 induced liver injury leads to the development of splanchnic vasodilation, with or without portal hypertension[62]. Splanchnic vasodilation is recognized as one of the major causative factors of HRS and occurs as the result of a plethora of vasodilatory responses[63]. With increased severities of hepatic damage, there is increased production of nitrous oxide in the splanchnic bed with reduced production in liver sinusoidal cells, which lead to increased portal gradient pressures[64]. Greater levels of other vasodilating peptides such as calcitonin gene-related peptide and adrenomedullin are also observed, as a result of increased production and reduced hepatic clearance[65].

Splanchnic vasodilation creates a state of hypovolemia in the central circulation, as splanchnic vasodilation combined with restricted portal blood flow causes blood to pool in the splanchnic circulation[66,67]. The body's physiological response to central hypovolemia will eventually lead to dysregulation of blood pressure, due to abnormalities in the baroreflex and cardiovascular responses to angiotensin II, norepinephrine, and vasopressin[68]. Central circulatory dysfunction can cause cardiomyopathy affecting both systolic and diastolic heart function. There will be electrophysiological alterations, which includes QT interval prolongation and electromechanical dyssynchrony[63,64]. The ability of the heart to respond to inotropic and chronotropic stimuli is reduced. Because of decreased systemic vascular resistance, cardiac output (in absolute terms) would be maintained at a high level initially[63,64]. However, the impaired cardiac function due to the aforementioned cardiac physiological changes will become clinically apparent with normalization of systemic vascular resistance and when there are further stress stimuluses[62-64].

Ultimately, renal perfusion pressure and blood flow to the kidneys will be reduced as a result of the various mechanisms which cause central circulatory dysfunction[68,69]. Overactivation of the sympathetic system as a homeostatic response could initially increase the kidney's reliance on blood pressure levels to maintain its perfusion[68]. Reduced blood flow to the kidneys would lead to more active stimulation of both β-adrenergic and subsequently α-adrenergic receptors, which results in afferent and efferent arteriole constriction[69]. The pathophysiological process of kidney damage is exacerbated by an inability of the liver in HRS to degrade renin, which will lead to persistent stimulation of the renin-angiotensin-aldosterone axis[70].

There are other theories of how HRS may manifest following severe liver injury from COVID-19 infection. One relates to the impact of reduced hepatic blood flow to kidneys *via* the hepatorenal reflex and exacerbated further by cytokine-induced vasoconstriction, which alters kidney hemodynamics[62,71]. Animal studies have highlighted that an acute increase in portal vein pressure results in increased renal nerve activity, although this phenomenon does not occur when the liver is denervated[71]. In studies assessing empirical treatment of HRS, a lumbar sympathetic block has been shown to improve kidney function [sodium excretion, blood flow and estimated glomerular filtration rate (eGFR) were shown to be improved][72]. This may explain why medical procedures such as transjugular intrahepatic portosystemic shunt (TIPS) improve HRS in many patients *via* reduction of portal pressure gradients. Another theory explaining the development of HRS in this context may relate to the direct effects of intra-abdominal ascitic pressure, in patients with underlying decompensated CLD where the ascites

may be exacerbated following COVID-19 infection[73]. Increased intra-abdominal ascitic pressure can lead to venous congestion and stimulation of the renin-angiotensin-aldosterone system, resulting in further kidney function decline and histopathological changes[73].

CLINICAL ASSESSMENT AND MANAGEMENT STRATEGIES IN COVID-19 INDUCED HRS

Key components of clinical assessment and management in COVID-19 induced HRS are summarized in Table 1. Clinical assessment of patients presenting with COVID-19 induced HRS should encompass a holistic understanding of an individual's medical history. This should be followed by physical examination to elicit specific signs, before urine, serum and imaging investigations are conducted, with these investigations forming the crux of the diagnostic criteria. Management strategies in this scenario should focus on achieving spontaneous recovery of liver function and resolution of HRS *via* medical management and only if this fails, then to consider the potential for liver transplantation.

Clinical assessment of COVID-19 induced HRS

Our current understanding of the typical signs and symptoms which appear with COVID-19 induced liver injury and HRS remains premature, and there are likely non-specific presentations in most instances. It is reasonable to suggest patients who develop acute liver injury following a positive COVID-19 diagnosis would likely have a COVID-19 infection severe enough to present as such[74]. From a thoroughly taken medical history, clinicians should aim to determine the likely course of COVID-19 infection and rule out other differentials more likely to explain the development of acute liver injury/fulminant liver failure[57]. There should be close observation for systemic (*i.e.*, septic symptoms, monitor hemodynamic stability as likely to have low mean arterial pressure) as well as respiratory-specific signs and symptoms[57]. It has been reported from prospective studies conducted in China that risks of severe liver injury is greater in patients who develop gastrointestinal symptoms such as diarrhea, nausea and vomiting, anorexia and abdominal pain (OR 2.71, 95%CI 1.52-4.83, $P < 0.05$) following acute COVID-19 infection[75]. Given patients with underlying CLD such as cirrhosis are more likely to develop HRS regardless of COVID-19 status, classical features of CLD/decompensated liver disease including jaundice, altered mental status, malnutrition, and ascites (ascites resistant to the use of diuretic medications is characteristic of type 2 HRS) should be meticulously monitored[76]. Whilst there is relative clarity regarding hepatic signs and symptoms in HRS, the same cannot be said for renal-specific signs and symptoms. Both oliguria and normal levels of urine output have been observed for patients diagnosed with HRS[62]. Due to inability in establishing definitive renal symptoms in HRS, there is wide opinion that HRS should be diagnosed mainly on the basis of laboratory results rather than symptomatic presentation.

The utilization of diagnostic tests should initially confirm COVID-19 status *via* a real-time reverse-transcriptase-polymerase chain reaction (rRT-PCR) test and determine the severity of disease through chest imaging (*i.e.*, chest X-ray or computed tomography)[77]. Serum tests evaluating the systemic inflammatory state (*i.e.*, full blood cell count, C-reactive protein, interleukin-6 Levels) should follow alongside tests to identify the presence of liver pathology, typically indicated by the rise in serum ALT, AST, total bilirubin, gamma-glutamyl transferase (GGT), alkaline phosphatase (ALP) levels and reduction in serum albumin[78]. Recent observational data reported the pooled prevalence of the elevated liver enzymes ALT, AST, and total bilirubin in COVID-19 positive patients to be 18% (95%CI 13%-25%), 21% (95%CI 14%-29%), and 6%(95%CI 3%-11%), respectively[79]. These serum tests may prove to be a strong marker of poor prognosis, as a fatal outcome with COVID-19 induced liver disease is estimated to be between 58% and 78%[80]. The presence of hypoalbuminemia also signifies a more severe disease process with poorer prognosis[81,82]. Liver ultrasound could also be a useful front-line diagnostic imaging tool to detect the presence of any acutely developed liver lesions.

Investigations to ascertain kidney function in confirming a HRS diagnosis should encompass urinalysis, a serum urea & electrolytes screen and other renal panel testing to rule out differential diagnoses[83-86]. Important results to look out for in urinalysis is concentrated urine with low urine sodium (< 10 mmol/L) where there is usually no proteinuria or hematuria[85,86]. There would be absence or few granular (hyaline or muddy-brown) casts identified in urine microscopy, in contrast to acute tubular necrosis (ATN) which is a known renal complication of cirrhosis[84]. ATN in the context of liver injury most likely occurs as a result of exposure to toxic medications or the development of decreased blood pressure, and proximal tubular cells are unable to reabsorb sodium from urine[62,84,85]. Because of this, urinary sodium levels in ATN would be expected to be higher than that of HRS[84]. It is expected that there is marked reduction in eGFR with HRS, with no improvements in kidney function despite treatment with intravenous fluids (kidney function improvements are observed in most other causes of pre-renal kidney failure following intravenous fluid administration with reduction in serum creatinine and increased sodium excretion) due to the intra-renal vasoconstricted state[87]. Serum sodium concentration would be low due to retention of fluid together with sodium leading to dilutional hyponaetremia[88]. Plasma renin activity would be elevated considering the metabolic changes in HRS [89]. Kidney ultrasound would rule out obstruction of the kidney outflow tract.

Table 1 Key components of clinical assessment and management in COVID-19 induced hepatorenal syndrome

Clinical Assessment of HRS	Management of HRS
Medical history: (1) Identify likely course of disease progression; and (2) rule out other causes of acute liver injury/fulminant liver failure	Minimize potential drug-induced hepato- and nephron-toxicities: (1) Monitor response to immunosuppressive treatments; (2) monitor response to antivirals and other COVID-19 treatment regimes; and (3) aim to prescribe these medications through a dose-dependent approach
Clinical examination: (1) Identify signs of systemic and/or respiratory decompensation; (2) identify evidence of cirrhosis/decompensated liver disease; and (3) monitor for oliguria	Medical management strategies in COVID-19 induced HRS: (1) Extracorporeal membrane support therapy & dialysis; (2) potential utilization of MARS or other liver support devices; (3) TIPSS to reduce portal vein pressure (if renal function allows and known CLD); (4) adding intravenous albumin to other procedural/medical therapies to expand plasma volume; and (5) combined use of Midodrine (α-agonist) and Octreotide (somatostatin analogue) to regulate blood vessel tone in the gastrointestinal tract and act as systemic vasoconstrictors to inhibit splanchnic vasodilation. Terlipressin may be used as an alternative
Laboratory and imaging tests: (1) Confirm positive COVID-19 status; (2) assess systemic hemodynamic stability through basic observations; (3) chest imaging to assess degree of COVID-19 severity for the respiratory system; (4) serum tests to evaluate the degree of inflammation; (5) liver pathology could be evaluated *via* serum markers (*e.g.*, increased ALT, AST, total bilirubin, GGT and ALP, reduction in albumin) and liver ultrasound; (6) urinalysis to identify low urine sodium *i.e.*, < 10 mmol/L, proteinuria, hematuria and urinary casts seen in ATN; (7) serum eGFR reductions, low serum sodium (dilutional hyponatremia) and elevated plasma renin would be classically observed in HRS; and (8) kidney ultrasound should be performed to rule out obstruction of the kidney outflow tract	Consider liver transplantation if kidney function and hepatic recovery is unlikely with medical management

AKI: Acute kidney injury; ALP: Alkaline phosphatase; ALT: Alanine transaminase; AST: Aspartate transaminase; ATN: Acute tubular necrosis; COVID-19: Coronavirus disease 2019; eGFR: Estimated glomerular filtration rate; GGT: Gamma-glutamyl transferase; HRS: Hepatorenal syndrome; MARS: Molecular adsorbents recirculation systems; TIPS: Transjugular intrahepatic portosystemic shunt.

Management strategies in COVID-19 induced HRS

The mainstay of treatment in HRS from either acute liver failure or cirrhosis, whether the cause is COVID-19 related or not, is usually medical management to aim for gradual liver recovery and resolution of HRS, with supportive dialysis or haemofiltration if required. Liver transplantation would not be indicated if recovery of liver function and resolution of HRS is achieved solely through medical management, with this usually resulting in the best outcome for patients. A key priority is to limit drug-induced hepato- and nephrotoxicity through a dose-dependent adjustment approach of managing immunosuppressive medications, antivirals and other COVID-19 treatment regimes if and when COVID-19 treatment is indicated[57].

The combination of extracorporeal membrane support and dialysis in HRS demonstrated significant effects in removing toxins from the circulation, including systemic inflammatory molecules generated from COVID-19 infection[83,90-92]. There has been greater use of molecular adsorbents recirculation systems in HRS as both a supportive treatment option or as a bridging therapy to liver transplantation if indicated, though wider work is needed to improve accessibility with this technology still being relatively novel[93]. Close haemodynamic monitoring during hemodialysis is recommended, given concerns that this may further deteriorate blood pressure stability in HRS, increasing the risk of mortality[94]. TIPS involves decompressing the high pressures in the portal circulation by placing a small stent between a portal and hepatic vein, *via* placement of a radiologically-guided catheter passed into the hepatic vein either through the internal jugular vein or the femoral vein[95]. This will theoretically reduce portal vein pressure, which as discussed in the previous section is a key factor in the hemodynamic process leading up to HRS[17,18,62,95]. Previous studies in patients with cirrhosis largely noted improvements in kidney function when TIPS is performed, particularly as a bridging treatment if liver transplantation might be indicated[96].

Intravenous albumin can expand plasma volume, and provide other benefits in the form of its immunological, antioxidant, endothelial protective functions. Combining intravenous albumin with other medical and/or procedural treatments displayed better outcomes compared to administering intravenous albumin alone[97]. Other pharmacological options which have demonstrated efficacy across all forms of HRS may include the combined use of Midodrine, an α agonist with somatostatin analogues such as Octreotide[98,99]. In Europe, Terlispressin and albumin are recommended in the best practice guidelines[100]. These drugs regulate blood vessel tone in the gastrointestinal tract, and also systemic vasoconstrictors which inhibit splanchnic vasodilation[97]. Interestingly, these drugs were only found to be effective when used in combination and not when independently prescribed[100]. There is preliminary data that other vasopressin analogues (*e.g.*, Ornipressin), Pentoxifylline, Acetylcysteine and Misoprostol amongst other treatments are potentially useful treatments in HRS, but this will require

further study[101-103].

Liver transplantation would be the ideal treatment in HRS, if renal function cannot be corrected with medical management and hepatic recovery is unlikely with conservative management alone. These situations mostly occur in patients with CLD, where the medical management options aforementioned serve as bridging therapies towards transplantation[17,18,20,62]. The optimal strategy would usually observe effects from treatment of the underlying cause of HRS first before planning for liver transplantation. During the COVID-19 pandemic, most hepatology societies advised the deferral of liver transplantation in stabilized patients[104]. There has been continuous debate throughout the pandemic on how to optimize the procedures of liver transplantation for patients with COVID-19 positive status, such as those with active COVID-19 infection inducing HRS[105]. Currently, there is only one reported case of liver transplantation in HRS with COVID-19 infection, performed 28 d after hospital admission [23]. Individuals with HRS who receive liver transplantation almost universally achieve recovery in kidney function[91]. Previous studies have demonstrated that survival rates at 3-year follow-up for liver transplant recipients in HRS are comparable to liver transplant recipients for other causes of liver disease[106]. Although differences in long-term outcomes are significant between patients who receive liver transplantation and those who do not, acute mortality rates after liver transplantation were found to be up to 25% in the first month[107]. Patients who present with further decline in liver and kidney function following liver transplantation are at higher risk[17]. Kidney function decline following liver transplantation in HRS is usually transient and most likely attributed to drug-induced nephrotoxicity, specifically the introduction of immunosuppressants such as Tacrolimus and Cyclosporine which are known to affect kidney function[17,105].

CONCLUSION

There is increased attention towards the extra-respiratory manifestations of COVID-19 as the pandemic continues to affect billions of lives. Hepatic consequences of COVID-19 infection are now recognized as an important complication of COVID-19. The development of HRS following COVID-19 induced liver injury suggests severe and perhaps life-threatening disease, particularly for individuals with multi-morbidities including pre-existing CLD. The prognosis of HRS is largely dependent on whether liver transplantation would be viable and accessible for the patient. Confounding effects of drug-induced hepato- and nephrotoxicity in exacerbating the systemic damage from COVID-19 induced HRS should always be considered and avoided if possible. A greater understanding of the multi-faceted pathophysiological mechanisms which result in HRS following acute COVID-19 infection is important to guide clinical decisions in a timely manner for the optimization of patient outcomes.

FOOTNOTES

Author contributions: Wu HHL performed the majority of the writing, prepared the figures and tables; Athwal VS, Kalra PA, and Chinnadurai R provided review of the draft versions of the paper prior to submission of the final version; Wu HHL and Chinnadurai R designed the outline and coordinated the writing of the paper.

Conflict-of-interest statement: The authors report no conflicts of interest associated with the work presented in this manuscript.

Open-Access: This article is an open-access article that was selected by an in-house editor and fully peer-reviewed by external reviewers. It is distributed in accordance with the Creative Commons Attribution NonCommercial (CC BY-NC 4.0) license, which permits others to distribute, remix, adapt, build upon this work non-commercially, and license their derivative works on different terms, provided the original work is properly cited and the use is non-commercial. See: https://creativecommons.org/Licenses/by-nc/4.0/

Country/Territory of origin: Australia

ORCID number: Henry H L Wu 0000-0002-4561-0844; Varinder S Athwal 0000-0002-1684-721X; Philip A Kalra 0000-0001-7652-1572; Rajkumar Chinnadurai 0000-0003-3973-6595.

S-Editor: Chen YL
L-Editor: A
P-Editor: Chen YL

REFERENCES

1 **World Health Organization**. Pneumonia of Unknown Cause. [Cited 31 December 2020]. Available from: https://www.who.int/emergencies/diseaseoutbreak-news/item/2020-DON229
2 **World Health Organization**. WHO Coronavirus disease (COVID-19) dashboard. [Cited 6 July 2022]. Available from: https://covid19.who.int/
3 **Verma AK**, Prakash S. Impact of covid-19 on environment and society. *J Global Biosci* 2020; **9**: 7352-7363
4 **Yuki K**, Fujiogi M, Koutsogiannaki S. COVID-19 pathophysiology: A review. *Clin Immunol* 2020; **215**: 108427 [PMID: 32325252 DOI: 10.1016/j.clim.2020.108427]
5 **Jordan RE**, Adab P, Cheng KK. Covid-19: risk factors for severe disease and death. *BMJ* 2020; **368**: m1198 [PMID: 32217618 DOI: 10.1136/bmj.m1198]
6 **Xu Z**, Shi L, Wang Y, Zhang J, Huang L, Zhang C, Liu S, Zhao P, Liu H, Zhu L, Tai Y, Bai C, Gao T, Song J, Xia P, Dong J, Zhao J, Wang FS. Pathological findings of COVID-19 associated with acute respiratory distress syndrome. *Lancet Respir Med* 2020; **8**: 420-422 [PMID: 32085846 DOI: 10.1016/S2213-2600(20)30076-X]
7 **Mokhtari T**, Hassani F, Ghaffari N, Ebrahimi B, Yarahmadi A, Hassanzadeh G. COVID-19 and multiorgan failure: A narrative review on potential mechanisms. *J Mol Histol* 2020; **51**: 613-628 [PMID: 33011887 DOI: 10.1007/s10735-020-09915-3]
8 **Varatharaj A**, Thomas N, Ellul MA, Davies NWS, Pollak TA, Tenorio EL, Sultan M, Easton A, Breen G, Zandi M, Coles JP, Manji H, Al-Shahi Salman R, Menon DK, Nicholson TR, Benjamin LA, Carson A, Smith C, Turner MR, Solomon T, Kneen R, Pett SL, Galea I, Thomas RH, Michael BD; CoroNerve Study Group. Neurological and neuropsychiatric complications of COVID-19 in 153 patients: a UK-wide surveillance study. *Lancet Psychiatry* 2020; **7**: 875-882 [PMID: 32593341 DOI: 10.1016/S2215-0366(20)30287-X]
9 **Rey JR**, Caro-Codón J, Rosillo SO, Iniesta ÁM, Castrejón-Castrejón S, Marco-Clement I, Martín-Polo L, Merino-Argos C, Rodríguez-Sotelo L, García-Veas JM, Martínez-Marín LA, Martínez-Cossiani M, Buño A, Gonzalez-Valle L, Herrero A, López-Sendón JL, Merino JL; CARD-COVID Investigators. Heart failure in COVID-19 patients: prevalence, incidence and prognostic implications. *Eur J Heart Fail* 2020; **22**: 2205-2215 [PMID: 32833283 DOI: 10.1002/ejhf.1990]
10 **Jeyalan V**, Storrar J, Wu HHL, Ponnusamy A, Sinha S, Kalra PA, Chinnadurai R. Native and transplant kidney histopathological manifestations in association with COVID-19 infection: A systematic review. *World J Transplant* 2021; **11**: 480-502 [PMID: 34868898 DOI: 10.5500/wjt.v11.i11.480]
11 **Ye Q**, Wang B, Zhang T, Xu J, Shang S. The mechanism and treatment of gastrointestinal symptoms in patients with COVID-19. *Am J Physiol Gastrointest Liver Physiol* 2020; **319**: G245-G252 [PMID: 32639848 DOI: 10.1152/ajpgi.00148.2020]
12 **He W**, Chen L, Yuan G, Fang Y, Chen W, Wu D, Liang B, Lu X, Ma Y, Li L, Wang H, Chen Z, Li Q, Gale RP. COVID-19 in persons with haematological cancers. *Leukemia* 2020; **34**: 1637-1645 [PMID: 32332856 DOI: 10.1038/s41375-020-0836-7]
13 **Velarde-Ruiz Velasco JA**, García-Jiménez ES, Remes-Troche JM. Hepatic manifestations and impact of COVID-19 on the cirrhotic patient. *Rev Gastroenterol Mex (Engl Ed)* 2020; **85**: 303-311 [PMID: 32553772 DOI: 10.1016/j.rgmx.2020.05.002]
14 **Yu D**, Du Q, Yan S, Guo XG, He Y, Zhu G, Zhao K, Ouyang S. Liver injury in COVID-19: clinical features and treatment management. *Virol J* 2021; **18**: 121 [PMID: 34108015 DOI: 10.1186/s12985-021-01593-1]
15 **Galiero R**, Pafundi PC, Simeon V, Rinaldi L, Perrella A, Vetrano E, Caturano A, Alfano M, Beccia D, Nevola R, Marfella R, Sardu C, Coppola C, Scarano F, Maggi P, De Lucia Sposito P, Vocciante L, Rescigno C, Sbreglia C, Fraganza F, Parrella R, Romano A, Calabria G, Polverino B, Pagano A, Bologna C, Amitrano M, Esposito V, Coppola N, Maturo N, Adinolfi LE, Chiodini P, Sasso FC; COVOCA Study Group. Impact of chronic liver disease upon admission on COVID-19 in-hospital mortality: Findings from COVOCA study. *PLoS One* 2020; **15**: e0243700 [PMID: 33301529 DOI: 10.1371/journal.pone.0243700]
16 **Zghal M**, Bouhamed M, Mellouli M, Triki M, Kallel R, Ayedi L, Boudawara TS, Makni S. Liver injury in COVID-19: pathological findings. *Pan Afr Med J* 2022; **41**: 56 [PMID: 35317475 DOI: 10.11604/pamj.2022.41.56.31114]
17 **Ginès P**, Solà E, Angeli P, Wong F, Nadim MK, Kamath PS. Hepatorenal syndrome. *Nat Rev Dis Primers* 2018; **4**: 23 [PMID: 30213943 DOI: 10.1038/s41572-018-0022-7]
18 **Francoz C**, Durand F, Kahn JA, Genyk YS, Nadim MK. Hepatorenal Syndrome. *Clin J Am Soc Nephrol* 2019; **14**: 774-781 [PMID: 30996046 DOI: 10.2215/CJN.12451018]
19 **Angeli P**, Garcia-Tsao G, Nadim MK, Parikh CR. News in pathophysiology, definition and classification of hepatorenal syndrome: A step beyond the International Club of Ascites (ICA) consensus document. *J Hepatol* 2019; **71**: 811-822 [PMID: 31302175 DOI: 10.1016/j.jhep.2019.07.002]
20 **Amin AA**, Alabsawy EI, Jalan R, Davenport A. Epidemiology, Pathophysiology, and Management of Hepatorenal Syndrome. *Semin Nephrol* 2019; **39**: 17-30 [PMID: 30606404 DOI: 10.1016/j.semnephrol.2018.10.002]
21 **Biggins SW**, Angeli P, Garcia-Tsao G, Ginès P, Ling SC, Nadim MK, Wong F, Kim WR. Diagnosis, Evaluation, and Management of Ascites, Spontaneous Bacterial Peritonitis and Hepatorenal Syndrome: 2021 Practice Guidance by the American Association for the Study of Liver Diseases. *Hepatology* 2021; **74**: 1014-1048 [PMID: 33942342 DOI: 10.1002/hep.31884]
22 **Nassar M**, Nso N, Medina L, Ghernautan V, Novikov A, El-Ijla A, Soliman KM, Kim Y, Alfishawy M, Rizzo V, Daoud A. Liver Kidney Crosstalk: Hepatorenal Syndrome. *World J Hepatol* 2021; **13**: 1058-1068 [PMID: 34630874 DOI: 10.4254/wjh.v13.i9.1058]
23 **Große K**, Kramer M, Trautwein C, Bruns T. SARS-CoV-2 as an extrahepatic precipitator of acute-on-chronic liver failure. *Liver Int* 2020; **40**: 1792-1793 [PMID: 32436600 DOI: 10.1111/liv.14540]
24 **Airoldi A**, Perricone G, De Nicola S, Molisano C, Tarsia P, Belli LS. COVID-19-related thrombotic microangiopathy in a cirrhotic patient. *Dig Liver Dis* 2020; **52**: 946 [PMID: 32641274 DOI: 10.1016/j.dld.2020.06.019]
25 **Wu J**, Song S, Cao HC, Li LJ. Liver diseases in COVID-19: Etiology, treatment and prognosis. *World J Gastroenterol*

2020; **26**: 2286-2293 [PMID: 32476793 DOI: 10.3748/wjg.v26.i19.2286]
26 **Cai Y**, Ye LP, Song YQ, Mao XL, Wang L, Jiang YZ, Que WT, Li SW. Liver injury in COVID-19: Detection, pathogenesis, and treatment. *World J Gastroenterol* 2021; **27**: 3022-3036 [PMID: 34168405 DOI: 10.3748/wjg.v27.i22.3022]
27 **Wang Y**, Liu S, Liu H, Li W, Lin F, Jiang L, Li X, Xu P, Zhang L, Zhao L, Cao Y, Kang J, Yang J, Li L, Liu X, Li Y, Nie R, Mu J, Lu F, Zhao S, Lu J, Zhao J. SARS-CoV-2 infection of the liver directly contributes to hepatic impairment in patients with COVID-19. *J Hepatol* 2020; **73**: 807-816 [PMID: 32437830 DOI: 10.1016/j.jhep.2020.05.002]
28 **Tan YJ**, Fielding BC, Goh PY, Shen S, Tan TH, Lim SG, Hong W. Overexpression of 7a, a protein specifically encoded by the severe acute respiratory syndrome coronavirus, induces apoptosis *via* a caspase-dependent pathway. *J Virol* 2004; **78**: 14043-14047 [PMID: 15564512 DOI: 10.1128/JVI.78.24.14043-14047.2004]
29 **Shroff A**, Nazarko TY. The Molecular Interplay between Human Coronaviruses and Autophagy. *Cells* 2021; **10** [PMID: 34440791 DOI: 10.3390/cells10082022]
30 **Hoffmann M**, Kleine-Weber H, Schroeder S, Krüger N, Herrler T, Erichsen S, Schiergens TS, Herrler G, Wu NH, Nitsche A, Müller MA, Drosten C, Pöhlmann S. SARS-CoV-2 Cell Entry Depends on ACE2 and TMPRSS2 and Is Blocked by a Clinically Proven Protease Inhibitor. *Cell* 2020; **181**: 271-280.e8 [PMID: 32142651 DOI: 10.1016/j.cell.2020.02.052]
31 **Pirola CJ**, Sookoian S. SARS-CoV-2 virus and liver expression of host receptors: Putative mechanisms of liver involvement in COVID-19. *Liver Int* 2020; **40**: 2038-2040 [PMID: 32352224 DOI: 10.1111/liv.14500]
32 **Letko M**, Marzi A, Munster V. Functional assessment of cell entry and receptor usage for SARS-CoV-2 and other lineage B betacoronaviruses. *Nat Microbiol* 2020; **5**: 562-569 [PMID: 32094589 DOI: 10.1038/s41564-020-0688-y]
33 **Paizis G**, Tikellis C, Cooper ME, Schembri JM, Lew RA, Smith AI, Shaw T, Warner FJ, Zuilli A, Burrell LM, Angus PW. Chronic liver injury in rats and humans upregulates the novel enzyme angiotensin converting enzyme 2. *Gut* 2005; **54**: 1790-1796 [PMID: 16166274 DOI: 10.1136/gut.2004.062398]
34 **Huang Q**, Xie Q, Shi CC, Xiang XG, Lin LY, Gong BD, Zhao GD, Wang H, Jia NN. Expression of angiotensin-converting enzyme 2 in CCL4-induced rat liver fibrosis. *Int J Mol Med* 2009; **23**: 717-723 [PMID: 19424597 DOI: 10.3892/ijmm_00000185]
35 **Mohammed FF**, Khokha R. Thinking outside the cell: proteases regulate hepatocyte division. *Trends Cell Biol* 2005; **15**: 555-563 [PMID: 16150595 DOI: 10.1016/j.tcb.2005.08.009]
36 **Qin C**, Zhou L, Hu Z, Zhang S, Yang S, Tao Y, Xie C, Ma K, Shang K, Wang W, Tian DS. Dysregulation of Immune Response in Patients With Coronavirus 2019 (COVID-19) in Wuhan, China. *Clin Infect Dis* 2020; **71**: 762-768 [PMID: 32161940 DOI: 10.1093/cid/ciaa248]
37 **Maggi E**, Canonica GW, Moretta L. COVID-19: Unanswered questions on immune response and pathogenesis. *J Allergy Clin Immunol* 2020; **146**: 18-22 [PMID: 32389590 DOI: 10.1016/j.jaci.2020.05.001]
38 **Costela-Ruiz VJ**, Illescas-Montes R, Puerta-Puerta JM, Ruiz C, Melguizo-Rodríguez L. SARS-CoV-2 infection: The role of cytokines in COVID-19 disease. *Cytokine Growth Factor Rev* 2020; **54**: 62-75 [PMID: 32513566 DOI: 10.1016/j.cytogfr.2020.06.001]
39 **Tacke F**, Luedde T, Trautwein C. Inflammatory pathways in liver homeostasis and liver injury. *Clin Rev Allergy Immunol* 2009; **36**: 4-12 [PMID: 18600481 DOI: 10.1007/s12016-008-8091-0]
40 **Chaudhry S**, Emond J, Griesemer A. Immune Cell Trafficking to the Liver. *Transplantation* 2019; **103**: 1323-1337 [PMID: 30817405 DOI: 10.1097/TP.0000000000002690]
41 **Robinson MW**, Harmon C, O'Farrelly C. Liver immunology and its role in inflammation and homeostasis. *Cell Mol Immunol* 2016; **13**: 267-276 [PMID: 27063467 DOI: 10.1038/cmi.2016.3]
42 **Zhang H**, Liao YS, Gong J, Liu J, Zhang H. Clinical characteristics and risk factors for liver injury in COVID-19 patients in Wuhan. *World J Gastroenterol* 2020; **26**: 4694-4702 [PMID: 32884226 DOI: 10.3748/wjg.v26.i31.4694]
43 **Zhan K**, Liao S, Li J, Bai Y, Lv L, Yu K, Qiu L, Li C, Yuan G, Zhang A, Mei Z. Risk factors in patients with COVID-19 developing severe liver injury during hospitalisation. *Gut* 2021; **70**: 628-629 [PMID: 32571973 DOI: 10.1136/gutjnl-2020-321913]
44 **Ali FEM**, Mohammedsaleh ZM, Ali MM, Ghogar OM. Impact of cytokine storm and systemic inflammation on liver impairment patients infected by SARS-CoV-2: Prospective therapeutic challenges. *World J Gastroenterol* 2021; **27**: 1531-1552 [PMID: 33958841 DOI: 10.3748/wjg.v27.i15.1531]
45 **Brozat JF**, Hanses F, Haelberger M, Stecher M, Dreher M, Tometten L, Ruethrich MM, Vehreschild JJ, Trautwein C, Borgmann S, Vehreschild MJGT, Jakob CEM, Stallmach A, Wille K, Hellwig K, Isberner N, Reuken PA, Geisler F, Nattermann J, Bruns T; LEOSS study group. COVID-19 mortality in cirrhosis is determined by cirrhosis-associated comorbidities and extrahepatic organ failure: Results from the multinational LEOSS registry. *United European Gastroenterol J* 2022; **10**: 409-424 [PMID: 35482663 DOI: 10.1002/ueg2.12232]
46 **Wang Q**, Zhang Y, Wu L, Niu S, Song C, Zhang Z, Lu G, Qiao C, Hu Y, Yuen KY, Wang Q, Zhou H, Yan J, Qi J. Structural and Functional Basis of SARS-CoV-2 Entry by Using Human ACE2. *Cell* 2020; **181**: 894-904.e9 [PMID: 32275855 DOI: 10.1016/j.cell.2020.03.045]
47 **Krüger-Genge A**, Blocki A, Franke RP, Jung F. Vascular Endothelial Cell Biology: An Update. *Int J Mol Sci* 2019; **20** [PMID: 31500313 DOI: 10.3390/ijms20184411]
48 **Antoniak S**, Mackman N. Multiple roles of the coagulation protease cascade during virus infection. *Blood* 2014; **123**: 2605-2613 [PMID: 24632711 DOI: 10.1182/blood-2013-09-526277]
49 **Antoniak S**. The coagulation system in host defense. *Res Pract Thromb Haemost* 2018; **2**: 549-557 [PMID: 30046760 DOI: 10.1002/rth2.12109]
50 **Yang Z**, Xu M, Yi JQ, Jia WD. Clinical characteristics and mechanism of liver damage in patients with severe acute respiratory syndrome. *Hepatobiliary Pancreat Dis Int* 2005; **4**: 60-63 [PMID: 15730921]
51 **Cao B**, Wang Y, Wen D, Liu W, Wang J, Fan G, Ruan L, Song B, Cai Y, Wei M, Li X, Xia J, Chen N, Xiang J, Yu T, Bai T, Xie X, Zhang L, Li C, Yuan Y, Chen H, Li H, Huang H, Tu S, Gong F, Liu Y, Wei Y, Dong C, Zhou F, Gu X, Xu J, Liu Z, Zhang Y, Shang L, Wang K, Li K, Zhou X, Dong X, Qu Z, Lu S, Hu X, Ruan S, Luo S, Wu J, Peng L, Cheng F,

Pan L, Zou J, Jia C, Liu X, Wang S, Wu X, Ge Q, He J, Zhan H, Qiu F, Guo L, Huang C, Jaki T, Hayden FG, Horby PW, Zhang D, Wang C. A Trial of Lopinavir-Ritonavir in Adults Hospitalized with Severe Covid-19. *N Engl J Med* 2020; **382**: 1787-1799 [PMID: 32187464 DOI: 10.1056/NEJMoa2001282]

52 **Sulkowski MS**, Mehta SH, Chaisson RE, Thomas DL, Moore RD. Hepatotoxicity associated with protease inhibitor-based antiretroviral regimens with or without concurrent ritonavir. *AIDS* 2004; **18**: 2277-2284 [PMID: 15577540 DOI: 10.1097/00002030-200411190-00008]

53 **Yip TC**, Lui GC, Wong VW, Chow VC, Ho TH, Li TC, Tse YK, Hui DS, Chan HL, Wong GL. Liver injury is independently associated with adverse clinical outcomes in patients with COVID-19. *Gut* 2021; **70**: 733-742 [PMID: 32641471 DOI: 10.1136/gutjnl-2020-321726]

54 **Jiang S**, Wang R, Li L, Hong D, Ru R, Rao Y, Miao J, Chen N, Wu X, Ye Z, Hu Y, Xie M, Zuo M, Lu X, Qiu Y, Liang T. Liver Injury in Critically Ill and Non-critically Ill COVID-19 Patients: A Multicenter, Retrospective, Observational Study. *Front Med (Lausanne)* 2020; **7**: 347 [PMID: 32656222 DOI: 10.3389/fmed.2020.00347]

55 **Heaton PC**, Fenwick SR, Brewer DE. Association between tetracycline or doxycycline and hepatotoxicity: a population based case-control study. *J Clin Pharm Ther* 2007; **32**: 483-487 [PMID: 17875115 DOI: 10.1111/j.1365-2710.2007.00853.x]

56 **Sodhi M**, Etminan M. Therapeutic Potential for Tetracyclines in the Treatment of COVID-19. *Pharmacotherapy* 2020; **40**: 487-488 [PMID: 32267566 DOI: 10.1002/phar.2395]

57 **Sivandzadeh GR**, Askari H, Safarpour AR, Ejtehadi F, Raeis-Abdollahi E, Vaez Lari A, Abazari MF, Tarkesh F, Bagheri Lankarani K. COVID-19 infection and liver injury: Clinical features, biomarkers, potential mechanisms, treatment, and management challenges. *World J Clin Cases* 2021; **9**: 6178-6200 [PMID: 34434987 DOI: 10.12998/wjcc.v9.i22.6178]

58 **Storelli F**, Samer C, Reny JL, Desmeules J, Daali Y. Complex Drug-Drug-Gene-Disease Interactions Involving Cytochromes P450: Systematic Review of Published Case Reports and Clinical Perspectives. *Clin Pharmacokinet* 2018; **57**: 1267-1293 [PMID: 29667038 DOI: 10.1007/s40262-018-0650-9]

59 **Montastruc F**, Thuriot S, Durrieu G. Hepatic Disorders With the Use of Remdesivir for Coronavirus 2019. *Clin Gastroenterol Hepatol* 2020; **18**: 2835-2836 [PMID: 32721580 DOI: 10.1016/j.cgh.2020.07.050]

60 **Gao J**, Tian Z, Yang X. Breakthrough: Chloroquine phosphate has shown apparent efficacy in treatment of COVID-19 associated pneumonia in clinical studies. *Biosci Trends* 2020; **14**: 72-73 [PMID: 32074550 DOI: 10.5582/bst.2020.01047]

61 **Deftereos SG**, Siasos G, Giannopoulos G, Vrachatis DA, Angelidis C, Giotaki SG, Gargalianos P, Giamarellou H, Gogos C, Daikos G, Lazanas M, Lagiou P, Saroglou G, Sipsas N, Tsiodras S, Chatzigeorgiou D, Moussas N, Kotanidou A, Koulouris N, Oikonomou E, Kaoukis A, Kossyvakis C, Raisakis K, Fountoulaki K, Comis M, Tsiachris D, Sarri E, Theodorakis A, Martinez-Dolz L, Sanz-Sánchez J, Reimers B, Stefanini GG, Cleman M, Filippou D, Olympios CD, Pyrgakis VN, Goudevenos J, Hahalis G, Kolettis TM, Iliodromitis E, Tousoulis D, Stefanadis C. The Greek study in the effects of colchicine in COvid-19 complications prevention (GRECCO-19 study): Rationale and study design. *Hellenic J Cardiol* 2020; **61**: 42-45 [PMID: 32251729 DOI: 10.1016/j.hjc.2020.03.002]

62 **Erly B**, Carey WD, Kapoor B, McKinney JM, Tam M, Wang W. Hepatorenal Syndrome: A Review of Pathophysiology and Current Treatment Options. *Semin Intervent Radiol* 2015; **32**: 445-454 [PMID: 26622108 DOI: 10.1055/s-0035-1564794]

63 **Zardi EM**, Abbate A, Zardi DM, Dobrina A, Margiotta D, Van Tassell BW, Afeltra A, Sanyal AJ. Cirrhotic cardiomyopathy. *J Am Coll Cardiol* 2010; **56**: 539-549 [PMID: 20688208 DOI: 10.1016/j.jacc.2009.12.075]

64 **Møller S**, Henriksen JH, Bendtsen F. Pathogenetic background for treatment of ascites and hepatorenal syndrome. *Hepatol Int* 2008; **2**: 416-428 [PMID: 19669317 DOI: 10.1007/s12072-008-9100-3]

65 **Ruiz-del-Arbol L**, Urman J, Fernández J, González M, Navasa M, Monescillo A, Albillos A, Jiménez W, Arroyo V. Systemic, renal, and hepatic hemodynamic derangement in cirrhotic patients with spontaneous bacterial peritonitis. *Hepatology* 2003; **38**: 1210-1218 [PMID: 14578859 DOI: 10.1053/jhep.2003.50447]

66 **Stadlbauer V**, Wright GA, Banaji M, Mukhopadhya A, Mookerjee RP, Moore K, Jalan R. Relationship between activation of the sympathetic nervous system and renal blood flow autoregulation in cirrhosis. *Gastroenterology* 2008; **134**: 111-119 [PMID: 18166350 DOI: 10.1053/j.gastro.2007.10.055]

67 **Møller S**, Henriksen JH. Review article: pathogenesis and pathophysiology of hepatorenal syndrome--is there scope for prevention? *Aliment Pharmacol Ther* 2004; **20** Suppl 3: 31-41; discussion 42 [PMID: 15335398 DOI: 10.1111/j.1365-2036.2004.02112.x]

68 **Møller S**, Iversen JS, Henriksen JH, Bendtsen F. Reduced baroreflex sensitivity in alcoholic cirrhosis: relations to hemodynamics and humoral systems. *Am J Physiol Heart Circ Physiol* 2007; **292**: H2966-H2972 [PMID: 17293491 DOI: 10.1152/ajpheart.01227.2006]

69 **Ginès P**, Guevara M, Perez-Villa F. Management of hepatorenal syndrome: another piece of the puzzle. *Hepatology* 2004; **40**: 16-18 [PMID: 15239080 DOI: 10.1002/hep.20313]

70 **Epstein M**, Berk DP, Hollenberg NK, Adams DF, Chalmers TC, Abrams HL, Merrill JP. Renal failure in the patient with cirrhosis. The role of active vasoconstriction. *Am J Med* 1970; **49**: 175-185 [PMID: 5452940 DOI: 10.1016/s0002-9343(70)80073-0]

71 **Jalan R**, Forrest EH, Redhead DN, Dillon JF, Hayes PC. Reduction in renal blood flow following acute increase in the portal pressure: evidence for the existence of a hepatorenal reflex in man? *Gut* 1997; **40**: 664-670 [PMID: 9203948 DOI: 10.1136/gut.40.5.664]

72 **Mohmand H**, Goldfarb S. Renal dysfunction associated with intra-abdominal hypertension and the abdominal compartment syndrome. *J Am Soc Nephrol* 2011; **22**: 615-621 [PMID: 21310818 DOI: 10.1681/ASN.2010121222]

73 **de Laet IE**, Malbrain M. Current insights in intra-abdominal hypertension and abdominal compartment syndrome. *Med Intensiva* 2007; **31**: 88-99 [PMID: 17433187 DOI: 10.1016/s0210-5691(07)74781-2]

74 **Jiehao C**, Jin X, Daojiong L, Zhi Y, Lei X, Zhenghai Q, Yuehua Z, Hua Z, Ran J, Pengcheng L, Xiangshi W, Yanling G, Aimei X, He T, Hailing C, Chuning W, Jingjing L, Jianshe W, Mei Z. A Case Series of Children With 2019 Novel Coronavirus Infection: Clinical and Epidemiological Features. *Clin Infect Dis* 2020; **71**: 1547-1551 [PMID: 32112072 DOI: 10.1093/cid/ciaa198]

75 **Lee IC**, Huo TI, Huang YH. Gastrointestinal and liver manifestations in patients with COVID-19. *J Chin Med Assoc* 2020; **83**: 521-523 [PMID: 32243269 DOI: 10.1097/JCMA.0000000000000319]

76 **Agarwal A**, Chen A, Ravindran N, To C, Thuluvath PJ. Gastrointestinal and Liver Manifestations of COVID-19. *J Clin Exp Hepatol* 2020; **10**: 263-265 [PMID: 32405183 DOI: 10.1016/j.jceh.2020.03.001]

77 **Sun Z**, Zhang N, Li Y, Xu X. A systematic review of chest imaging findings in COVID-19. *Quant Imaging Med Surg* 2020; **10**: 1058-1079 [PMID: 32489929 DOI: 10.21037/qims-20-564]

78 **Jothimani D**, Venugopal R, Abedin MF, Kaliamoorthy I, Rela M. COVID-19 and the liver. *J Hepatol* 2020; **73**: 1231-1240 [PMID: 32553666 DOI: 10.1016/j.jhep.2020.06.006]

79 **Mao R**, Qiu Y, He JS, Tan JY, Li XH, Liang J, Shen J, Zhu LR, Chen Y, Iacucci M, Ng SC, Ghosh S, Chen MH. Manifestations and prognosis of gastrointestinal and liver involvement in patients with COVID-19: a systematic review and meta-analysis. *Lancet Gastroenterol Hepatol* 2020; **5**: 667-678 [PMID: 32405603 DOI: 10.1016/S2468-1253(20)30126-6]

80 **Zhang B**, Zhou X, Qiu Y, Song Y, Feng F, Feng J, Song Q, Jia Q, Wang J. Clinical characteristics of 82 cases of death from COVID-19. *PLoS One* 2020; **15**: e0235458 [PMID: 32645044 DOI: 10.1371/journal.pone.0235458]

81 **Zhang Y**, Zheng L, Liu L, Zhao M, Xiao J, Zhao Q. Liver impairment in COVID-19 patients: A retrospective analysis of 115 cases from a single centre in Wuhan city, China. *Liver Int* 2020; **40**: 2095-2103 [PMID: 32239796 DOI: 10.1111/Liv.14455]

82 **Richardson S**, Hirsch JS, Narasimhan M, Crawford JM, McGinn T, Davidson KW; the Northwell COVID-19 Research Consortium, Barnaby DP, Becker LB, Chelico JD, Cohen SL, Cookingham J, Coppa K, Diefenbach MA, Dominello AJ, Duer-Hefele J, Falzon L, Gitlin J, Hajizadeh N, Harvin TG, Hirschwerk DA, Kim EJ, Kozel ZM, Marrast LM, Mogavero JN, Osorio GA, Qiu M, Zanos TP. Presenting Characteristics, Comorbidities, and Outcomes Among 5700 Patients Hospitalized With COVID-19 in the New York City Area. *JAMA* 2020; **323**: 2052-2059 [PMID: 32320003 DOI: 10.1001/jama.2020.6775]

83 **Simonetto DA**, Gines P, Kamath PS. Hepatorenal syndrome: pathophysiology, diagnosis, and management. *BMJ* 2020; **370**: m2687 [PMID: 32928750 DOI: 10.1136/bmj.m2687]

84 **Bucsics T**, Krones E. Renal dysfunction in cirrhosis: acute kidney injury and the hepatorenal syndrome. *Gastroenterol Rep (Oxf)* 2017; **5**: 127-137 [PMID: 28533910 DOI: 10.1093/gastro/gox009]

85 **Tsien CD**, Rabie R, Wong F. Acute kidney injury in decompensated cirrhosis. *Gut* 2013; **62**: 131-137 [PMID: 22637695 DOI: 10.1136/gutjnl-2011-301255]

86 **Angeli P**, Gines P, Wong F, Bernardi M, Boyer TD, Gerbes A, Moreau R, Jalan R, Sarin SK, Piano S, Moore K, Lee SS, Durand F, Salerno F, Caraceni P, Kim WR, Arroyo V, Garcia-Tsao G; International Club of Ascites. Diagnosis and management of acute kidney injury in patients with cirrhosis: revised consensus recommendations of the International Club of Ascites. *Gut* 2015; **64**: 531-537 [PMID: 25631669 DOI: 10.1136/gutjnl-2014-308874]

87 **Lenz K**, Buder R, Kapun L, Voglmayr M. Treatment and management of ascites and hepatorenal syndrome: an update. *Therap Adv Gastroenterol* 2015; **8**: 83-100 [PMID: 25729433 DOI: 10.1177/1756283X14564673]

88 **Mohanty A**, Garcia-Tsao G. Hyponatremia and Hepatorenal Syndrome. *Gastroenterol Hepatol (N Y)* 2015; **11**: 220-229 [PMID: 27099594]

89 **Pasqualetti P**, Casale R. The atrial natriuretic peptide-renin-aldosterone system in hepatorenal syndrome. *Riv Eur Sci Med Farmacol* 1996; **18**: 137-141 [PMID: 9177611]

90 **Husain-Syed F**, Ricci Z, Brodie D, Vincent JL, Ranieri VM, Slutsky AS, Taccone FS, Gattinoni L, Ronco C. Extracorporeal organ support (ECOS) in critical illness and acute kidney injury: from native to artificial organ crosstalk. *Intensive Care Med* 2018; **44**: 1447-1459 [PMID: 30043276 DOI: 10.1007/s00134-018-5329-z]

91 **Mitzner SR**, Stange J, Klammt S, Risler T, Erley CM, Bader BD, Berger ED, Lauchart W, Peszynski P, Freytag J, Hickstein H, Loock J, Löhr JM, Liebe S, Emmrich J, Korten G, Schmidt R. Improvement of hepatorenal syndrome with extracorporeal albumin dialysis MARS: results of a prospective, randomized, controlled clinical trial. *Liver Transpl* 2000; **6**: 277-286 [PMID: 10827226 DOI: 10.1002/Lt.500060326]

92 **Wu WK**, Grogan WM, Ziogas IA, Patel YJ, Bacchetta M, Alexopoulos SP. Extracorporeal membrane oxygenation in patients with hepatopulmonary syndrome undergoing liver transplantation: A systematic review of the literature. *Transplant Rev (Orlando)* 2022; **36**: 100693 [PMID: 35413506 DOI: 10.1016/j.trre.2022.100693]

93 **MacDonald AJ**, Subramanian RM, Olson JC, Speiser JL, Durkalski-Mauldin VL, Abraldes JG, Bigam DL, Flynn MM, Rapaka B, Shropshire BM, Vora RS, Karvellas CJ; U. S. Acute Liver Failure Study Group. Use of the Molecular Adsorbent Recirculating System in Acute Liver Failure: Results of a Multicenter Propensity Score-Matched Study. *Crit Care Med* 2022; **50**: 286-295 [PMID: 34259656 DOI: 10.1097/CCM.0000000000005194]

94 **Shawwa K**, Kompotiatis P, Jentzer JC, Wiley BM, Williams AW, Dillon JJ, Albright RC, Kashani KB. Hypotension within one-hour from starting CRRT is associated with in-hospital mortality. *J Crit Care* 2019; **54**: 7-13 [PMID: 31319348 DOI: 10.1016/j.jcrc.2019.07.004]

95 **Rajesh S**, George T, Philips CA, Ahamed R, Kumbar S, Mohan N, Mohanan M, Augustine P. Transjugular intrahepatic portosystemic shunt in cirrhosis: An exhaustive critical update. *World J Gastroenterol* 2020; **26**: 5561-5596 [PMID: 33088154 DOI: 10.3748/wjg.v26.i37.5561]

96 **Song T**, Rössle M, He F, Liu F, Guo X, Qi X. Transjugular intrahepatic portosystemic shunt for hepatorenal syndrome: A systematic review and meta-analysis. *Dig Liver Dis* 2018; **50**: 323-330 [PMID: 29422242 DOI: 10.1016/j.dld.2018.01.123]

97 **Martín-Llahí M**, Pépin MN, Guevara M, Díaz F, Torre A, Monescillo A, Soriano G, Terra C, Fábrega E, Arroyo V, Rodés J, Ginès P; TAHRS Investigators. Terlipressin and albumin vs albumin in patients with cirrhosis and hepatorenal syndrome: a randomized study. *Gastroenterology* 2008; **134**: 1352-1359 [PMID: 18471512 DOI: 10.1053/j.gastro.2008.02.024]

98 **Esrailian E**, Pantangco ER, Kyulo NL, Hu KQ, Runyon BA. Octreotide/Midodrine therapy significantly improves renal function and 30-day survival in patients with type 1 hepatorenal syndrome. *Dig Dis Sci* 2007; **52**: 742-748 [PMID: 17235705 DOI: 10.1007/s10620-006-9312-0]

99 **Skagen C**, Einstein M, Lucey MR, Said A. Combination treatment with octreotide, midodrine, and albumin improves survival in patients with type 1 and type 2 hepatorenal syndrome. *J Clin Gastroenterol* 2009; **43**: 680-685 [PMID: 19238094 DOI: 10.1097/MCG.0b013e318188947c]

100 **European Association for the Study of the Liver**. EASL Clinical Practice Guidelines for the management of patients with decompensated cirrhosis. *J Hepatol* 2018; **69**: 406-460 [PMID: 29653741 DOI: 10.1016/j.jhep.2018.03.024]

101 **Diaconescu D**, Pantea Stoian A, Socea LI, Stanescu AM, Iancu MA, Socea B, Pituru S, Bratu O, Diaconu C. Hepatorenal syndrome: a review. *Arch Balk Med Union* 2018; **53**: 239-45 [DOI: 10.2139/ssrn.3299050]

102 **Stine JG**, Wang J, Cornella SL, Behm BW, Henry Z, Shah NL, Caldwell SH, Northup PG. Treatment of Type-1 Hepatorenal Syndrome with Pentoxifylline: A Randomized Placebo Controlled Clinical Trial. *Ann Hepatol* 2018; **17**: 300-306 [PMID: 29469046 DOI: 10.5604/01.3001.0010.8660]

103 **Izzedine H**, Kheder-Elfekih R, Deray G, Thabut D. Endothelin-receptor antagonist/N-acetylcysteine combination in type 1 hepatorenal syndrome. *J Hepatol* 2009; **50**: 1055-1056 [PMID: 19328583 DOI: 10.1016/j.jhep.2009.02.002]

104 **American Association for the Study of Liver Diseases**. Clinical Best Practice Advice for Hepatology and Liver Transplant Providers During the COVID-19 Pandemic: AASLD Expert Panel Consensus Statement. 2 Nov 2021. [Cited 6 July 2022]. Available from: https://www.aasld.org/sites/default/files/2021-11/AASLD%20COVID-19%20Expert%20Panel%20Consensus%20Statement%20Update%2011.02.2021.pdf

105 **Kidson KM**, Park J, Charles MK, Omar M, Krajden M, Wright AJ, Hussaini T, Kim PTW, Chung SW, Yoshida EM. Successful Liver Transplantation in a Patient With Acute COVID-19 Infection and Acute Liver Failure: A Case Report. *Transplant Direct* 2021; **7**: e747 [PMID: 34476292 DOI: 10.1097/TXD.0000000000001210]

106 **Ng CK**, Chan MH, Tai MH, Lam CW. Hepatorenal syndrome. *Clin Biochem Rev* 2007; **28**: 11-17 [PMID: 17603637]

107 **Boyer TD**, Sanyal AJ, Garcia-Tsao G, Regenstein F, Rossaro L, Appenrodt B, Gülberg V, Sigal S, Bexon AS, Teuber P; Terlipressin Study Group. Impact of liver transplantation on the survival of patients treated for hepatorenal syndrome type 1. *Liver Transpl* 2011; **17**: 1328-1332 [PMID: 21837734 DOI: 10.1002/Lt.22395]

World Journal of Gastroenterology

Submit a Manuscript: https://www.f6publishing.com

World J Gastroenterol 2022 October 21; 28(39): 5679-5690

DOI: 10.3748/wjg.v28.i39.5679

ISSN 1007-9327 (print) ISSN 2219-2840 (online)

REVIEW

Receptor of advanced glycation end-products axis and gallbladder cancer: A forgotten connection that we should reconsider

Armando Rojas, Cristian Lindner, Iván Schneider, Ileana Gonzàlez, Miguel Angel Morales

Specialty type: Gastroenterology and hepatology

Provenance and peer review: Invited article; Externally peer reviewed.

Peer-review model: Single blind

Peer-review report's scientific quality classification

Grade A (Excellent): 0
Grade B (Very good): B
Grade C (Good): C
Grade D (Fair): 0
Grade E (Poor): 0

P-Reviewer: Shalaby MN, Egypt; Yasukawa K, Japan

Received: June 27, 2022
Peer-review started: June 27, 2022
First decision: August 1, 2022
Revised: August 5, 2022
Accepted: September 9, 2022
Article in press: September 9, 2022
Published online: October 21, 2022

Armando Rojas, Ileana Gonzàlez, Biomedical Research Laboratories, Catholic University of Maule, Talca 34600000, Maule, Chile

Cristian Lindner, Iván Schneider, Medicine Faculty, Catholic University of Maule, Talca 34600000, Maule, Chile

Miguel Angel Morales, Department of Molecular and Clinical Pharmacology Program, Institute of Biomedical Sciences, University of Chile, Santiago 8320000, Santiago, Chile

Corresponding author: Armando Rojas, PhD, Full Professor, Senior Scientist, Biomedical Research Labs, Catholic University of Maule, 3605, San Miguel Ave., Talca 34600000, Maule, Chile. arojasr@ucm.cl

Abstract

Compelling evidence derived from clinical and experimental research has demonstrated the crucial contribution of chronic inflammation in the development of neoplasms, including gallbladder cancer. In this regard, data derived from clinical and experimental studies have demonstrated that the receptor of advanced glycation end-products (RAGE)/AGEs axis plays an important role in the onset of a crucial and long-lasting inflammatory milieu, thus supporting tumor growth and development. AGEs are formed in biological systems or foods, and food-derived AGEs, also known as dietary AGEs are known to contribute to the systemic pool of AGEs. Once they bind to RAGE, the activation of multiple and crucial signaling pathways are triggered, thus favoring the secretion of several proinflammatory cytokines also involved in the promotion of gallbladder cancer invasion and migration. In the present review, we aimed to highlight the relevance of the association between high dietary AGEs intakes and high risk for gallbladder cancer, and emerging data supporting that dietary intervention to reduce gallbladder cancer risk is a very attractive approach that deserves much more research efforts.

Key Words: Gallbladder cancer; Advanced glycation end-products; Receptor of advanced glycation end-products; Chronic inflammation; Nutrition

©The Author(s) 2022. Published by Baishideng Publishing Group Inc. All rights reserved.

Core tip: A growing body of data has demonstrated a positive association between the risk of gallbladder cancer and high dietary intake of advanced glycation end-products (AGEs). These noxious compounds are important contributors to the onset of a chronic inflammatory response, through the activation of the receptor of AGEs (RAGE). We herein discuss how RAGE activation is crucial in the development of gallbladder cancer and the relevance of new incoming data supporting the role of dietary interventions to reduce the risk of gallbladder cancer.

Citation: Rojas A, Lindner C, Schneider I, Gonzàlez I, Morales MA. Receptor of advanced glycation end-products axis and gallbladder cancer: A forgotten connection that we should reconsider. *World J Gastroenterol* 2022; 28(39): 5679-5690
URL: https://www.wjgnet.com/1007-9327/full/v28/i39/5679.htm
DOI: https://dx.doi.org/10.3748/wjg.v28.i39.5679

INTRODUCTION

Gallbladder cancer development is linked to both genetic and environmental factors, and where the onset of chronic inflammation is a crucial contributor to gallbladder carcinogenesis. This chronic inflammatory condition can be triggered by several factors including not only chronic infection by *Salmonella* spp., or *Helicobacter pylori*[1-4] but also some dietary habits or metabolic conditions[5-9], which are associated with an overactivation of the receptor of advanced glycation end-products (RAGE).

At present, the onset of many of both age- and diet-related noncommunicable diseases, including different cancer types, is widely associated with the chronicity of low-grade inflammation[10,11]. At this point, the diet is widely recognized as an important modulator of this chronic and systemic inflammation[12,13], particularly the western-type dietary patterns[14].

One common and important element in this unhealthy diet is the advanced glycation end-products (AGEs), which are a large and heterogeneous group of compounds that were initially recognized in the Maillard reaction, but they can also form by other reactions, including the oxidation of sugars, lipids, and amino acids[15,16].

Food-derived AGEs, also known as dietary AGEs, substantially contribute to the systemic pool of AGEs. Their intake has been linked in humans and mice to an increased level of oxidative stress and inflammation, thus playing an important role in the onset and development of several health disorders [17,18].

The pathogenic mechanisms of dietary AGEs are the same as those endogenously produced, either by activation of the RAGE or by covalent crosslinking of proteins, thus altering protein structure and function. The receptor-dependent and receptor-independent mechanisms are recognized as important contributors to tumor growth and development[19,20].

In the present review, we aim to highlight the burden of RAGE axis activation on gallbladder cancer, its therapeutic potential, as well as the significance of lowering dietary consumption of AGEs in subjects at risk.

THE RAGE/AGEs AXIS AND GALLBLADDER CANCER: NEW INCOMING PIECES OF EVIDENCE

There is growing evidence supporting the key role of dietary AGEs as major contributors to the systemic pool of AGEs[21], which notably increase oxidative stress and chronic/acute inflammation, contributing to the pathophysiology of many human inflammatory and malignant diseases[18,22,23].

Since the multicenter prospective European Prospective Investigation into Cancer and Nutrition (EPIC) cohort study, which investigated the relationship of dietary and environmental factors with the incidence of cancer and other chronic diseases[24-27], a growing body of evidence has revealed strong findings to support that a proinflammatory diet with high levels of dietary AGEs intake increases the risk of several types of cancer[28], such as breast, skin and those originating from the digestive tract[29-31].

Recently, Mayén *et al*[32] conducted a multinational cohort study using the EPIC database to characterize the daily dietary intake (mg/d) of three AGEs including Nε-[carboxymethyl] lysine (CML), Nε-[1-carboxyethyl] lysine (CEL), and Nδ-[5-hydro-5-methyl-4-imidazolon-2-yl]-ornithine (MG-H1) for each study participant, to assess AGE consumption with hepatobiliary cancer risk. In this study, the authors found a positive association between the risk of gallbladder cancer and high dietary intake of CML [hazard ratio (HR) = 1.30, 95% confidence interval (CI): 1.07–1.57] and MG-H1 (HR = 1.26, 95%CI: 1.06–1.50), and thus suggesting that higher intakes of dietary AGEs may increase the risk of gallbladder

cancer.

Although the study of Mayen *et al*[32] has some limitations, particularly in estimating dietary AGEs exposure, other epidemiological studies have revealed an increased tumor progression and mortality of gallbladder cancer patients, with inflammatory comorbidities related to overactivation of the RAGE axis, such as high-fat diet consumption[33], metabolic syndrome[34], and diabetes mellitus [35-38], due to the increased endogenous formation of AGEs reported in these entities.

Some studies have shown increased expression of RAGE in gallbladder cancer cells, which were directly in concordance with the invasive ability of the neoplastic cell lines[39]. Additionally, compelling evidence has been reported of a strong increase in AGEs formation under hyperglycemic conditions[40, 41]. Noteworthy, the gallbladder accumulation of AGEs is significantly higher in the gallbladder of diabetic mice when compared to control animals. These findings support the role of the RAGE/AGEs axis activation in gallbladder carcinogenesis[42].

Furthermore, other *in vivo* analyses of adenocarcinoma cells treated under a hyperglycemic milieu, a condition favoring the increased accumulation of AGEs, have been revealed to promote tumor cell proliferation and migration[43].

Emerging *in vitro* and *in vivo* analyses have revealed overexpression of several RAGE ligands such as high mobility group B1 (HMGB1) and members of the S100P protein family in malignant gallbladder epithelial cells compared to benign tissue[44,45].

This increased expression of those RAGE ligands in gallbladder cancer cells has been closely correlated with malignant progression and therefore may then be considered an independent risk factor for poor prognosis and proliferation in gallbladder cancer[45-47].

A key consequence of RAGE binding with its ligands is the activation of multiple and crucial signaling pathways[48], that are involved in gallbladder carcinogenesis, such as reactive oxygen species (ROS)[49], Erk1/2 (p44/42) mitogen-activated protein kinases (MAPKs)[50], C-Jun n-terminal kinase and p38 MAPK[51], and phosphatidylinositol 3-kinase pathways[52].

These signals trigger important downstream inflammatory and procarcinogenic consequences such as activation of signal transducer and activator of transcription 3[53,54], activator protein-1[55], and nuclear factor (NF)-κB pathways[49,54,56-58], favoring the secretion of several proinflammatory cytokines also involved in the promotion of gallbladder cancer invasion and migration such as tumor necrosis factor-α[59,60]. Hence, this proinflammatory milieu continuously fuels chronic inflammation in gallbladder carcinogenesis in a RAGE-dependent manner[19,61].

THERAPEUTIC POTENTIAL OF THE RAGE/AGEs AXIS IN TUMOR BIOLOGY

RAGE is recognized as a pattern recognition receptor, and its activation plays a pivotal role in the propagation of immune responses and inflammatory reactions[62]. It is expressed at low levels in most differentiated adult cells in a regulated manner. However, upregulation of RAGE expression is associated with many inflammation-related pathological entities, including cancer[63].

RAGE engagement subsequently converts transient cellular stimulation into a sustained cellular dysfunctional state driven by long-term activation of NF-κB[64]. There is compelling evidence that RAGE activation promotes many crucial steps during tumorigenesis, from DNA damage and genetic instability to supporting many phenotypic changes in tumor cells favoring their growth and dissemination[65].

Since the work by Taguchi *et al*[66], which experimentally reported that *in vivo* blockade of the RAGE–amphotericin axis suppresses tumor growth and dissemination, intense research efforts have been focused towards the development of new therapeutic approaches to modulate both deleterious proinflammatory and procarcinogenesis effects of RAGE axis activation[67,68].

The use of novel RAGE-targeting antibodies and blocking peptides derived from RAGE ligands such as S100P and HMGB1 has demonstrated to block the ability of ligands to stimulate RAGE activation in cancer cells both *in vitro* and *in vivo* models, thus inhibiting tumor growth, metastasis, and inflammation [69], as well as significant reductions in tumor growth with acceptable toxicity levels in several *in vivo* mouse adenocarcinoma models[70,71]. Furthermore, the treatment of cancer cell lines with anti-RAGE antibodies demonstrates that RAGE blocking may even enhance the chemotherapeutic effects of antineoplastic drugs[72,73].

Recent evidence has also revealed that the antibody targeting of RAGE ligands such as HMGB1 and AGEs may effectively decrease tumor progression in solid malignancies[74]. This approach can even enhance the antitumoral response of cancer immunotherapies by remobilizing the antitumor immune response[75].

Another emerging therapeutic approach is based on the high binding affinity to RAGE of some members of the family of glycosaminoglycans such as chondroitin sulfate, heparan sulfate (HS), and low molecular weight and semisynthetic glycosaminoglycan[76]. These molecules have been reported to be involved in effectively inhibiting RAGE signaling pathways in *both in vitro* and *in vivo* models[71,77].

Strikingly, new evidence has revealed that HS acts as a crucial element for RAGE signaling, leading to the formation of stable RAGE–HS complexes, which drive the RAGE oligomerization and subsequent

downstream functional signaling[78,79].

These observations have revealed a new strategy for treating RAGE-associated diseases by hindering RAGE oligomerization.

The use of synthetic compounds with both anticarcinogenic and anti-inflammatory activities based on their capacities to interfere with the HMGB1–RAGE axis seems to be a promising strategy for several cancer types, including gallbladder cancer[80,81].

A novel molecule, recently discovered by Tanuma *et al*[82], 7-methoxy-3-hydroxy-styrylchromone (c6), is not only an effective suppressor of cell cycle/proliferation but also an initiator of apoptosis in cancer cells, and a promising potentiator of the anticancer effects of DNA-damaging antineoplastic agents.

RAGE gene silencing has been demonstrated to significantly downregulate AGE-induced inflammation and RAGE-dependent release of proinflammatory cytokines in normal human cells[83], while in malignant cells, *RAGE* gene silencing can decrease the colony-forming ability, proliferation, migration, and the invasive potential of cancer cells, through inhibiting RAGE-dependent mechanisms that sustain cancer cell progression and invasion[84].

The requirement of the cytoplasmic tail of RAGE to interact with its molecular effector DIAPH1 to mediate downstream signal transduction has been highlighted as a promising approach to inhibit RAGE signaling[85-87].

This novel screening strategy of searching for molecules able to block protein–protein interactions has been demonstrated to be successful to inhibit the RAGE-mediated expression of inflammatory genes in diabetes complications[88,89] and atherosclerosis[90].

A growing body of experimental data using the DNA-aptamer technology against RAGE has demonstrated that this novel approach can inhibit the inflammatory reactions triggered by activation of the RAGE axis in different *in vivo* models[91-93].

Experimental research has reported interesting results in different cancer types, as revealed in tumor-bearing mice treated with RAGE-aptamers, where marked inhibition of tumor growth was achieved [94]. The use of this technology on tumor-bearing mice is also able to inhibit macrophage infiltration and neoangiogenesis through the inhibition of RAGE/NF-κB/VEGF-A-dependent signaling pathways [94-96] (Figure 1).

In many clinical entities where the activation of the RAGE/AGEs axis is crucial in the underlying pathogenic mechanisms, restriction of dietary AGEs has been extensively studied in clinical trials[97-101]. Under the same rationale, and based on the active role of RAGE-mediated mechanisms in tumor biology, different interventional clinical studies already published[102-107] (Table 1), or in progress, have supported the use of restriction of AGEs intake in human cancers, as documented on the website ClinicalTrials.gov (ClinicalTrials.gov identifier: NCT03712371, NCT04716764, NCT02946996, NCT03092635, NCT01820299, NCT01363141, NCT03147339). However, it must be emphasized that therapeutic interventions, including dietary interventional actions on the RAGE axis, have been focused on achieving clinical improvements in disease course, including dietary interventional actions, and therefore the potential of modulating RAGE activation in terms of cancer prevention is still controversial.

REDUCING DIETARY AGEs INTAKE IN SUBJECTS AT RISK OF GALLBLADDER CANCER. A HOPEFUL APPROACH?

International consensus estimates that almost 40% of cancer cases are preventable through a healthy lifestyle[108]. Compelling evidence derived from epidemiological studies of different cancer types suggests that lifestyle changes, including dietary habits, may play a crucial role in determining the risk of various cancers[109-113].

Currently, the western diet is considered a major driver of chronic, low-grade, metabolic inflammation, which is a crosswise element in the pathogenesis of many human diseases, including cancer [114]. Data derived from preclinical investigations, and observational and interventional studies, has provided conclusive evidence that the western diet is associated with an increased incidence of many malignancies, such as colorectal, pancreatic, prostate and breast cancers[115-118].

In modern society, dietary AGE consumption – as a component of modern westernized diets – is markedly increased. Therefore, dietary AGE restriction is now recognized as a useful intervention, as demonstrated in several pathologies[119-123].

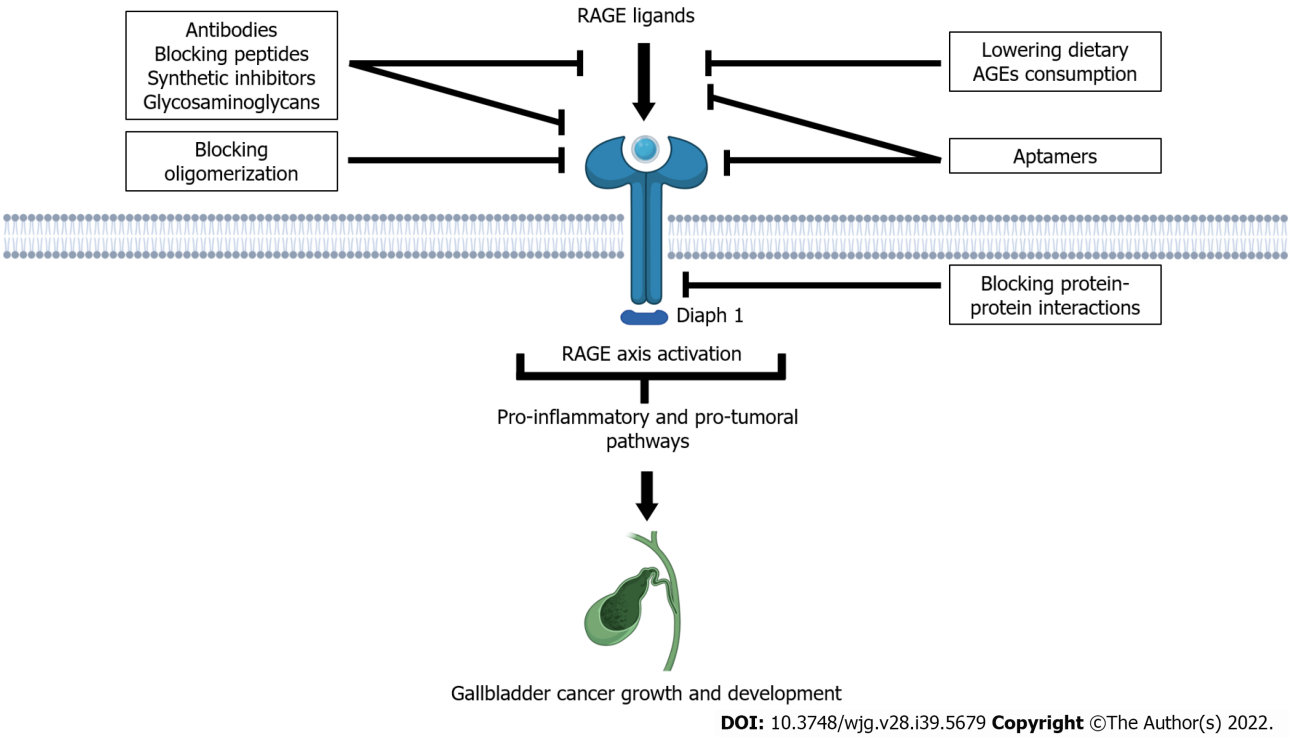
Western diet generally contains large amounts of fructose, thus promoting AGE formation[124]. This diet is also an important source of AGE precursors, such as methylglyoxal and glyoxal[125]. In light of these findings, dietary AGEs have gained particular importance due to their capacity to support the onset of many human diseases, including cancer, mainly due to their proinflammatory and pro-oxidant properties[17,18].

The role of RAGE/AGEs axis activation has emerged as a crucial element in the tumor microenvironment to promote cancer cell migration, invasion, survival, and even resistance to chemotherapy[19]. Additionally, the accumulation of AGEs in tissues can promote protein structural damage and

Table 1 Some clinical trials supporting the usefulness of restriction of advanced glycation end-products intake in human cancers

Ref.	Year	Condition	Outcome
Jiao *et al*[102]	2015	Pancreatic cancer	Increased risk of pancreatic cancer
Peterson *et al*[103]	2020	Breast cancer	Increased breast cancer risk in postmenopausal women
Omofuma *et al*[104]	2020	Breast cancer	Increased risk of breast cancer
Aglago *et al*[105]	2021	Colorectal cancer	Increased risk of CRC
Mao *et al*[106]	2021	Colorectal cancer	Increased CRC mortality in non-T2D patients
Omofuma *et al*[107]	2021	Breast cancer	Increased breast cancer mortality
Mayén *et al*[32]	2021	Hepatobiliary cancers	Increased risk of gallbladder cancer

CRC: Colorectal cancer; T2D: Type 2 diabetes.



DOI: 10.3748/wjg.v28.i39.5679 **Copyright** ©The Author(s) 2022.

Figure 1 Different therapeutic approaches used to inhibit the consequences of the receptor of advanced glycation end-products axis activation in cancer. RAGE: Receptor of advanced glycation end-products; AGEs: Advanced glycation end-products.

modification of the mechanical and physiological functions of the extracellular matrix, thus contributing to carcinogenesis and inflammation[20].

Therefore, the report recently published by Mayén *et al*[32] showed a positive association between dietary AGEs and the risk of gallbladder cancer in the EPIC cohort, which deserves special attention. We believe that actions such as dietary recommendations for the reduction of dietary AGEs intake to individuals at risk of gallbladder cancer will be beneficial. In this regard, it is important to highlight that some pre-existing clinical conditions such as diabetes mellitus and metabolic syndrome are risk factors for the development of gallbladder cancer[34,35-38]. Additionally, the demonstrated links between genetic ancestry and gallbladder cancer development may represent another risk factor for some populations[126,127]. Other recommendations that focus on reducing the RAGE/AGEs axis activation are attractive, particularly the consumption of polyphenol-rich foods due to the inhibitory activities of polyphenols on the RAGE/AGEs axis at different levels, such as by inhibition of ROS formation during glycation reactions, chelation of transition metal ions, trapping dicarbonyls, and activation of AGE detoxification pathways[128].

CONCLUSION

Gallbladder cancer is an aggressive and rare neoplasm with an unusual geographic distribution. Most patients are diagnosed in the advanced stages of the disease, and therefore the life expectancy is low. Compelling evidence supports the role of several risk factors, which are linked to the onset, and chronicity of an inflammatory reaction. The report of Taguchi *et al*[66] represented a critical point in understanding the role of the RAGE axis in tumor biology, and highlighting the potential of therapeutic interventions on a hyperactive cellular signaling pathway that causes disease, as the RAGE axis is[129].

The role of RAGE axis activation in gallbladder cancer is supported by its active contribution to the pathogenic framework of the main risk factors associated with this neoplasm, such as infectious agents [130,131], some metabolic conditions[132,133], and dietary habits[32].

Although much research is needed, lowering dietary AGEs intake as well as increasing the consumption of foods rich in polyphenols in subjects at risk of gallbladder cancer, either by pre-existing metabolic conditions or genetic ancestry, seems to be a plausible recommendation, to avoid the hyperactivation of the RAGE/AGEs axis.

FOOTNOTES

Author contributions: All authors contributed to the original ideas and writing of this paper; Rojas A designed the report and wrote the paper; Lindner C artwork and data acquisition, drafting and revising the manuscript; Schneider I, Gonzalez I, and Morales MA, data acquisition, drafting and revising the manuscript.

Conflict-of-interest statement: All the authors report no relevant conflicts of interest for this article.

Open-Access: This article is an open-access article that was selected by an in-house editor and fully peer-reviewed by external reviewers. It is distributed in accordance with the Creative Commons Attribution NonCommercial (CC BY-NC 4.0) license, which permits others to distribute, remix, adapt, build upon this work non-commercially, and license their derivative works on different terms, provided the original work is properly cited and the use is non-commercial. See: https://creativecommons.org/Licenses/by-nc/4.0/

Country/Territory of origin: Chile

ORCID number: Armando Rojas 0000-0001-9911-7142; Cristian Lindner 0000-0002-2642-4288; Iván Schneider 0000-0001-5294-5995; Ileana Gonzàlez 0000-0002-2488-9380; Miguel Angel Morales 0000-0001-7698-9669.

S-Editor: Gong ZM
L-Editor: Kerr C
P-Editor: Gong ZM

REFERENCES

1 **Dutta U**, Garg PK, Kumar R, Tandon RK. Typhoid carriers among patients with gallstones are at increased risk for carcinoma of the gallbladder. *Am J Gastroenterol* 2000; **95**: 784-787 [PMID: 10710075 DOI: 10.1111/j.1572-0241.2000.01860.x]
2 **Leong RW**, Sung JJ. Review article: Helicobacter species and hepatobiliary diseases. *Aliment Pharmacol Ther* 2002; **16**: 1037-1045 [PMID: 12030944 DOI: 10.1046/j.1365-2036.2002.01282.x]
3 **Nath G**, Gulati AK, Shukla VK. Role of bacteria in carcinogenesis, with special reference to carcinoma of the gallbladder. *World J Gastroenterol* 2010; **16**: 5395-5404 [PMID: 21086555 DOI: 10.3748/wjg.v16.i43.5395]
4 **Scanu T**, Spaapen RM, Bakker JM, Pratap CB, Wu LE, Hofland I, Broeks A, Shukla VK, Kumar M, Janssen H, Song JY, Neefjes-Borst EA, te Riele H, Holden DW, Nath G, Neefjes J. Salmonella Manipulation of Host Signaling Pathways Provokes Cellular Transformation Associated with Gallbladder Carcinoma. *Cell Host Microbe* 2015; **17**: 763-774 [PMID: 26028364 DOI: 10.1016/j.chom.2015.05.002]
5 **Strom BL**, Soloway RD, Rios-Dalenz JL, Rodriguez-Martinez HA, West SL, Kinman JL, Polansky M, Berlin JA. Risk factors for gallbladder cancer. An international collaborative case-control study. *Cancer* 1995; **76**: 1747-1756 [PMID: 8625043 DOI: 10.1002/1097-0142(19951115)76:10<1747::aid-cncr2820761011>3.0.co;2-l]
6 **Zatonski WA**, Lowenfels AB, Boyle P, Maisonneuve P, Bueno de Mesquita HB, Ghadirian P, Jain M, Przewozniak K, Baghurst P, Moerman CJ, Simard A, Howe GR, McMichael AJ, Hsieh CC, Walker AM. Epidemiologic aspects of gallbladder cancer: a case-control study of the SEARCH Program of the International Agency for Research on Cancer. *J Natl Cancer Inst* 1997; **89**: 1132-1138 [PMID: 9262251 DOI: 10.1093/jnci/89.15.1132]
7 **Kato K**, Akai S, Tominaga S, Kato I. A case-control study of biliary tract cancer in Niigata Prefecture, Japan. *Jpn J Cancer Res* 1989; **80**: 932-938 [PMID: 2515177 DOI: 10.1111/j.1349-7006.1989.tb01629.x]
8 **Larsson SC**, Wolk A. Obesity and the risk of gallbladder cancer: a meta-analysis. *Br J Cancer* 2007; **96**: 1457-1461 [PMID: 17375043 DOI: 10.1038/sj.bjc.6603703]
9 **Park JH**, Hong JY, Park YS, Kang G, Han K, Park JO. Association of prediabetes, diabetes, and diabetes duration with

biliary tract cancer risk: A nationwide cohort study. *Metabolism* 2021; **123**: 154848 [PMID: 34371066 DOI: 10.1016/j.metabol.2021.154848]

10 **Duncan BB**, Schmidt MI, Pankow JS, Ballantyne CM, Couper D, Vigo A, Hoogeveen R, Folsom AR, Heiss G; Atherosclerosis Risk in Communities Study. Low-grade systemic inflammation and the development of type 2 diabetes: the atherosclerosis risk in communities study. *Diabetes* 2003; **52**: 1799-1805 [PMID: 12829649 DOI: 10.2337/diabetes.52.7.1799]

11 **Furman D**, Campisi J, Verdin E, Carrera-Bastos P, Targ S, Franceschi C, Ferrucci L, Gilroy DW, Fasano A, Miller GW, Miller AH, Mantovani A, Weyand CM, Barzilai N, Goronzy JJ, Rando TA, Effros RB, Lucia A, Kleinstreuer N, Slavich GM. Chronic inflammation in the etiology of disease across the life span. *Nat Med* 2019; **25**: 1822-1832 [PMID: 31806905 DOI: 10.1038/s41591-019-0675-0]

12 **Minihane AM**, Vinoy S, Russell WR, Baka A, Roche HM, Tuohy KM, Teeling JL, Blaak EE, Fenech M, Vauzour D, McArdle HJ, Kremer BH, Sterkman L, Vafeiadou K, Benedetti MM, Williams CM, Calder PC. Low-grade inflammation, diet composition and health: current research evidence and its translation. *Br J Nutr* 2015; **114**: 999-1012 [PMID: 26228057 DOI: 10.1017/S0007114515002093]

13 **Ricordi C**, Garcia-Contreras M, Farnetti S. Diet and Inflammation: Possible Effects on Immunity, Chronic Diseases, and Life Span. *J Am Coll Nutr* 2015; **34** Suppl 1: 10-13 [PMID: 26400428 DOI: 10.1080/07315724.2015.1080101]

14 **Malesza IJ**, Malesza M, Walkowiak J, Mussin N, Walkowiak D, Aringazina R, Bartkowiak-Wieczorek J, Mądry E. High-Fat, Western-Style Diet, Systemic Inflammation, and Gut Microbiota: A Narrative Review. *Cells* 2021; **10** [PMID: 34831387 DOI: 10.3390/cells10113164]

15 **Twarda-Clapa A**, Olczak A, Białkowska AM, Koziołkiewicz M. Advanced Glycation End-Products (AGEs): Formation, Chemistry, Classification, Receptors, and Diseases Related to AGEs. *Cells* 2022; **11** [PMID: 35455991 DOI: 10.3390/cells11081312]

16 **Ruiz HH**, Ramasamy R, Schmidt AM. Advanced Glycation End Products: Building on the Concept of the "Common Soil" in Metabolic Disease. *Endocrinology* 2020; **161** [PMID: 31638645 DOI: 10.1210/endocr/bqz006]

17 **Garay-Sevilla ME**, Rojas A, Portero-Otin M, Uribarri J. Dietary AGEs as Exogenous Boosters of Inflammation. *Nutrients* 2021; **13** [PMID: 34444961 DOI: 10.3390/nu13082802]

18 **Uribarri J**, del Castillo MD, de la Maza MP, Filip R, Gugliucci A, Luevano-Contreras C, Macías-Cervantes MH, Markowicz Bastos DH, Medrano A, Menini T, Portero-Otin M, Rojas A, Sampaio GR, Wrobel K, Garay-Sevilla ME. Dietary advanced glycation end products and their role in health and disease. *Adv Nutr* 2015; **6**: 461-473 [PMID: 26178030 DOI: 10.3945/an.115.008433]

19 **Rojas A**, Figueroa H, Morales E. Fueling inflammation at tumor microenvironment: the role of multiligand/RAGE axis. *Carcinogenesis* 2010; **31**: 334-341 [PMID: 20028726 DOI: 10.1093/carcin/bgp322]

20 **Rojas A**, Añazco C, González I, Araya P. Extracellular matrix glycation and receptor for advanced glycation end-products activation: a missing piece in the puzzle of the association between diabetes and cancer. *Carcinogenesis* 2018; **39**: 515-521 [PMID: 29373651 DOI: 10.1093/carcin/bgy012]

21 **Davis KE**, Prasad C, Vijayagopal P, Juma S, Adams-Huet B, Imrhan V. Contribution of dietary advanced glycation end products (AGE) to circulating AGE: role of dietary fat. *Br J Nutr* 2015; **114**: 1797-1806 [PMID: 26392152 DOI: 10.1017/S0007114515003487]

22 **Gill V**, Kumar V, Singh K, Kumar A, Kim JJ. Advanced Glycation End Products (AGEs) May Be a Striking Link Between Modern Diet and Health. *Biomolecules* 2019; **9** [PMID: 31861217 DOI: 10.3390/biom9120888]

23 **Ahmad S**, Khan H, Siddiqui Z, Khan MY, Rehman S, Shahab U, Godovikova T, Silnikov V, Moinuddin. AGEs, RAGEs and s-RAGE; friend or foe for cancer. *Semin Cancer Biol* 2018; **49**: 44-55 [PMID: 28712719 DOI: 10.1016/j.semcancer.2017.07.001]

24 **Riboli E**, Hunt KJ, Slimani N, Ferrari P, Norat T, Fahey M, Charrondière UR, Hémon B, Casagrande C, Vignat J, Overvad K, Tjønneland A, Clavel-Chapelon F, Thiébaut A, Wahrendorf J, Boeing H, Trichopoulos D, Trichopoulou A, Vineis P, Palli D, Bueno-De-Mesquita HB, Peeters PH, Lund E, Engeset D, González CA, Barricarte A, Berglund G, Hallmans G, Day NE, Key TJ, Kaaks R, Saracci R. European Prospective Investigation into Cancer and Nutrition (EPIC): study populations and data collection. *Public Health Nutr* 2002; **5**: 1113-1124 [PMID: 12639222 DOI: 10.1079/PHN2002394]

25 **Bingham S**, Riboli E. Diet and cancer--the European Prospective Investigation into Cancer and Nutrition. *Nat Rev Cancer* 2004; **4**: 206-215 [PMID: 14993902 DOI: 10.1038/nrc1298]

26 **Riboli E**, Kaaks R. The EPIC Project: rationale and study design. European Prospective Investigation into Cancer and Nutrition. *Int J Epidemiol* 1997; **26** Suppl 1: S6-14 [PMID: 9126529 DOI: 10.1093/ije/26.suppl_1.s6]

27 **Hainaut P**, Vozar B, Rinaldi S, Riboli E, Caboux E. The European Prospective Investigation into Cancer and Nutrition biobank. *Methods Mol Biol* 2011; **675**: 179-191 [PMID: 20949388 DOI: 10.1007/978-1-59745-423-0_7]

28 **Ubago-Guisado E**, Rodríguez-Barranco M, Ching-López A, Petrova D, Molina-Montes E, Amiano P, Barricarte-Gurrea A, Chirlaque MD, Agudo A, Sánchez MJ. Evidence Update on the Relationship between Diet and the Most Common Cancers from the European Prospective Investigation into Cancer and Nutrition (EPIC) Study: A Systematic Review. *Nutrients* 2021; **13** [PMID: 34684583 DOI: 10.3390/nu13103582]

29 **Agudo A**, Cayssials V, Bonet C, Tjønneland A, Overvad K, Boutron-Ruault MC, Affret A, Fagherazzi G, Katzke V, Schübel R, Trichopoulou A, Karakatsani A, La Vecchia C, Palli D, Grioni S, Tumino R, Ricceri F, Panico S, Bueno-de-Mesquita B, Peeters PH, Weiderpass E, Skeie G, Nøst TH, Lasheras C, Rodríguez-Barranco M, Amiano P, Chirlaque MD, Ardanaz E, Ohlsson B, Dias JA, Nilsson LM, Myte R, Khaw KT, Perez-Cornago A, Gunter M, Huybrechts I, Cross AJ, Tsilidis K, Riboli E, Jakszyn P. Inflammatory potential of the diet and risk of gastric cancer in the European Prospective Investigation into Cancer and Nutrition (EPIC) study. *Am J Clin Nutr* 2018; **107**: 607-616 [PMID: 29635497 DOI: 10.1093/ajcn/nqy002]

30 **Aglago EK**, Schalkwijk CG, Freisling H, Fedirko V, Hughes DJ, Jiao L, Dahm CC, Olsen A, Tjønneland A, Katzke V, Johnson T, Schulze MB, Aleksandrova K, Masala G, Sieri S, Simeon V, Tumino R, Macciotta A, Bueno-de-Mesquita B, Skeie G, Gram IT, Sandanger T, Jakszyn P, Sánchez MJ, Amiano P, Colorado-Yohar SM, Gurrea AB, Perez-Cornago A,

Mayén AL, Weiderpass E, Gunter MJ, Heath AK, Jenab M. Plasma concentrations of advanced glycation end-products and colorectal cancer risk in the EPIC study. *Carcinogenesis* 2021; **42**: 705-713 [PMID: 33780524 DOI: 10.1093/carcin/bgab026]

31 **González CA**, Jakszyn P, Pera G, Agudo A, Bingham S, Palli D, Ferrari P, Boeing H, del Giudice G, Plebani M, Carneiro F, Nesi G, Berrino F, Sacerdote C, Tumino R, Panico S, Berglund G, Simán H, Nyrén O, Hallmans G, Martinez C, Dorronsoro M, Barricarte A, Navarro C, Quirós JR, Allen N, Key TJ, Day NE, Linseisen J, Nagel G, Bergmann MM, Overvad K, Jensen MK, Tjonneland A, Olsen A, Bueno-de-Mesquita HB, Ocke M, Peeters PH, Numans ME, Clavel-Chapelon F, Boutron-Ruault MC, Trichopoulou A, Psaltopoulou T, Roukos D, Lund E, Hemon B, Kaaks R, Norat T, Riboli E. Meat intake and risk of stomach and esophageal adenocarcinoma within the European Prospective Investigation Into Cancer and Nutrition (EPIC). *J Natl Cancer Inst* 2006; **98**: 345-354 [PMID: 16507831 DOI: 10.1093/jnci/djj071]

32 **Mayén AL**, Aglago EK, Knaze V, Cordova R, Schalkwijk CG, Wagner KH, Aleksandrova K, Fedirko V, Keski-Rahkonen P, Leitzmann MF, Katzke V, Srour B, Schulze MB, Masala G, Krogh V, Panico S, Tumino R, Bueno-de-Mesquita B, Brustad M, Agudo A, Chirlaque López MD, Amiano P, Ohlsson B, Ramne S, Aune D, Weiderpass E, Jenab M, Freisling H. Dietary intake of advanced glycation endproducts and risk of hepatobiliary cancers: A multinational cohort study. *Int J Cancer* 2021 [PMID: 33899229 DOI: 10.1002/ijc.33612]

33 **Pérez-Moreno P**, Riquelme I, García P, Brebi P, Roa JC. Environmental and Lifestyle Risk Factors in the Carcinogenesis of Gallbladder Cancer. *J Pers Med* 2022; **12** [PMID: 35207722 DOI: 10.3390/jpm12020234]

34 **Borena W**, Edlinger M, Bjørge T, Häggström C, Lindkvist B, Nagel G, Engeland A, Stocks T, Strohmaier S, Manjer J, Selmer R, Tretli S, Concin H, Hallmans G, Jonsson H, Stattin P, Ulmer H. A prospective study on metabolic risk factors and gallbladder cancer in the metabolic syndrome and cancer (Me-Can) collaborative study. *PLoS One* 2014; **9**: e89368 [PMID: 24586723 DOI: 10.1371/journal.pone.0089368]

35 **Jing C**, Wang Z, Fu X. Effect of diabetes mellitus on survival in patients with gallbladder Cancer: a systematic review and meta-analysis. *BMC Cancer* 2020; **20**: 689 [PMID: 32709224 DOI: 10.1186/s12885-020-07139-y]

36 **Tsilidis KK**, Kasimis JC, Lopez DS, Ntzani EE, Ioannidis JP. Type 2 diabetes and cancer: umbrella review of meta-analyses of observational studies. *BMJ* 2015; **350**: g7607 [PMID: 25555821 DOI: 10.1136/bmj.g7607]

37 **Pearson-Stuttard J**, Papadimitriou N, Markozannes G, Cividini S, Kakourou A, Gill D, Rizos EC, Monori G, Ward HA, Kyrgiou M, Gunter MJ, Tsilidis KK. Type 2 Diabetes and Cancer: An Umbrella Review of Observational and Mendelian Randomization Studies. *Cancer Epidemiol Biomarkers Prev* 2021; **30**: 1218-1228 [PMID: 33737302 DOI: 10.1158/1055-9965.EPI-20-1245]

38 **Gu J**, Yan S, Wang B, Shen F, Cao H, Fan J, Wang Y. Type 2 diabetes mellitus and risk of gallbladder cancer: a systematic review and meta-analysis of observational studies. *Diabetes Metab Res Rev* 2016; **32**: 63-72 [PMID: 26111736 DOI: 10.1002/dmrr.2671]

39 **Hirata K**, Takada M, Suzuki Y, Kuroda Y. Expression of receptor for advanced glycation end products (RAGE) in human biliary cancer cells. *Hepatogastroenterology* 2003; **50**: 1205-1207 [PMID: 14571699]

40 **Berg TJ**, Snorgaard O, Faber J, Torjesen PA, Hildebrandt P, Mehlsen J, Hanssen KF. Serum levels of advanced glycation end products are associated with left ventricular diastolic function in patients with type 1 diabetes. *Diabetes Care* 1999; **22**: 1186-1190 [PMID: 10388987 DOI: 10.2337/diacare.22.7.1186]

41 **Bellier J**, Nokin MJ, Lardé E, Karoyan P, Peulen O, Castronovo V, Bellahcène A. Methylglyoxal, a potent inducer of AGEs, connects between diabetes and cancer. *Diabetes Res Clin Pract* 2019; **148**: 200-211 [PMID: 30664892 DOI: 10.1016/j.diabres.2019.01.002]

42 **Swartz-Basile DA**, Lu D, Tran KQ, Graewin S, Nakeeb A, Pitt HA. Advanced glycation end products accumulate in the diabetic gallbladder. *J Surg Res* 2006; **130**: 302 [DOI: 10.1016/j.jss.2005.11.410]

43 **Liao YF**, Yin S, Chen ZQ, Li F, Zhao B. High glucose promotes tumor cell proliferation and migration in lung adenocarcinoma *via* the RAGENOXs pathway. *Mol Med Rep* 2018; **17**: 8536-8541 [PMID: 29693146 DOI: 10.3892/mmr.2018.8914]

44 **Wang W**, Ai KX, Yuan Z, Huang XY, Zhang HZ. Different expression of S100A8 in malignant and benign gallbladder diseases. *Dig Dis Sci* 2013; **58**: 150-162 [PMID: 22806545 DOI: 10.1007/s10620-012-2307-0]

45 **Shi Z**, Huang Q, Chen J, Yu P, Wang X, Qiu H, Chen Y, Dong Y. Correlation of HMGB1 expression to progression and poor prognosis of adenocarcinoma and squamous cell/adenosquamous carcinoma of gallbladder. *Am J Transl Res* 2015; **7**: 2015-2025 [PMID: 26692945]

46 **Li Z**, Chen Y, Wang X, Zhang H, Zhang Y, Gao Y, Weng M, Wang L, Liang H, Li M, Zhang F, Zhao S, Liu S, Cao Y, Shu Y, Bao R, Zhou J, Liu X, Yan Y, Zhen L, Dong Q, Liu Y. LASP-1 induces proliferation, metastasis and cell cycle arrest at the G2/M phase in gallbladder cancer by down-regulating S100P *via* the PI3K/AKT pathway. *Cancer Lett* 2016; **372**: 239-250 [PMID: 26797416 DOI: 10.1016/j.canlet.2016.01.008]

47 **Liu BX**, Tang CT, Dai XJ, Zeng L, Cheng F, Chen Y, Zeng C. Prognostic Value of S100P Expression in Patients With Digestive System Cancers: A Meta-Analysis. *Front Oncol* 2021; **11**: 593728 [PMID: 33747914 DOI: 10.3389/fonc.2021.593728]

48 **Rojas A**, Delgado-López F, González I, Pérez-Castro R, Romero J, Rojas I. The receptor for advanced glycation end-products: a complex signaling scenario for a promiscuous receptor. *Cell Signal* 2013; **25**: 609-614 [PMID: 23200851 DOI: 10.1016/j.cellsig.2012.11.022]

49 **Yu J**, Shi L, Lin W, Lu B, Zhao Y. UCP2 promotes proliferation and chemoresistance through regulating the NF-κB/β-catenin axis and mitochondrial ROS in gallbladder cancer. *Biochem Pharmacol* 2020; **172**: 113745 [PMID: 31811866 DOI: 10.1016/j.bcp.2019.113745]

50 **Tang H**, Shi X, Zhu P, Guo W, Li J, Yan B, Zhang S. Melatonin inhibits gallbladder cancer cell migration and invasion *via* ERK-mediated induction of epithelial-to-mesenchymal transition. *Oncol Lett* 2021; **22**: 609 [PMID: 34188711 DOI: 10.3892/ol.2021.12870]

51 **Liu S**, Chu B, Cai C, Wu X, Yao W, Wu Z, Yang Z, Li F, Liu Y, Dong P, Gong W. DGCR5 Promotes Gallbladder Cancer by Sponging MiR-3619-5p *via* MEK/ERK1/2 and JNK/p38 MAPK Pathways. *J Cancer* 2020; **11**: 5466-5477 [PMID: 32742494 DOI: 10.7150/jca.46351]

52 **Tong C**, Wang Y, Li J, Cen W, Zhang W, Zhu Z, Yu J, Lu B. Pterostilbene inhibits gallbladder cancer progression by suppressing the PI3K/Akt pathway. *Sci Rep* 2021; **11**: 4391 [PMID: 33623100 DOI: 10.1038/s41598-021-83924-4]

53 **Pan MS**, Wang H, Ansari KH, Li XP, Sun W, Fan YZ. Gallbladder cancer-associated fibroblasts promote vasculogenic mimicry formation and tumor growth in gallbladder cancer *via* upregulating the expression of NOX4, a poor prognosis factor, through IL-6-JAK-STAT3 signal pathway. *J Exp Clin Cancer Res* 2020; **39**: 234 [PMID: 33153467 DOI: 10.1186/s13046-020-01742-4]

54 **Nakada S**, Kuboki S, Nojima H, Yoshitomi H, Furukawa K, Takayashiki T, Takano S, Miyazaki M, Ohtsuka M. Roles of Pin1 as a Key Molecule for EMT Induction by Activation of STAT3 and NF-κB in Human Gallbladder Cancer. *Ann Surg Oncol* 2019; **26**: 907-917 [PMID: 30610554 DOI: 10.1245/s10434-018-07132-7]

55 **Hong H**, He C, Zhu S, Zhang Y, Wang X, She F, Chen Y. CCR7 mediates the TNF-α-induced lymphatic metastasis of gallbladder cancer through the "ERK1/2 - AP-1" and "JNK - AP-1" pathways. *J Exp Clin Cancer Res* 2016; **35**: 51 [PMID: 27009073 DOI: 10.1186/s13046-016-0318-y]

56 **Zhang DC**, Liu JL, Ding YB, Xia JG, Chen GY. Icariin potentiates the antitumor activity of gemcitabine in gallbladder cancer by suppressing NF-κB. *Acta Pharmacol Sin* 2013; **34**: 301-308 [PMID: 23274410 DOI: 10.1038/aps.2012.162]

57 **Bao D**, Yuan RX, Zhang Y. Effects of lncRNA MEG3 on proliferation and apoptosis of gallbladder cancer cells through regulating NF-κB signaling pathway. *Eur Rev Med Pharmacol Sci* 2020; **24**: 6632-6638 [PMID: 32633352 DOI: 10.26355/eurrev_202006_21649]

58 **Ouyang B**, Pan N, Zhang H, Xing C, Ji W. miR146b5p inhibits tumorigenesis and metastasis of gallbladder cancer by targeting Tolllike receptor 4 *via* the nuclear factorκB pathway. *Oncol Rep* 2021; **45** [PMID: 33649824 DOI: 10.3892/or.2021.7966]

59 **Zhu G**, Du Q, Wang X, Tang N, She F, Chen Y. TNF-α promotes gallbladder cancer cell growth and invasion through autocrine mechanisms. *Int J Mol Med* 2014; **33**: 1431-1440 [PMID: 24676340 DOI: 10.3892/ijmm.2014.1711]

60 **Hong H**, Jiang L, Lin Y, He C, Zhu G, Du Q, Wang X, She F, Chen Y. TNF-alpha promotes lymphangiogenesis and lymphatic metastasis of gallbladder cancer through the ERK1/2/AP-1/VEGF-D pathway. *BMC Cancer* 2016; **16**: 240 [PMID: 26992854 DOI: 10.1186/s12885-016-2259-4]

61 **Li Y**, Zhang J, Ma H. Chronic inflammation and gallbladder cancer. *Cancer Lett* 2014; **345**: 242-248 [PMID: 23981574 DOI: 10.1016/j.canlet.2013.08.034]

62 **González I**, Romero J, Rodríguez BL, Pérez-Castro R, Rojas A. The immunobiology of the receptor of advanced glycation end-products: trends and challenges. *Immunobiology* 2013; **218**: 790-797 [PMID: 23182709 DOI: 10.1016/j.imbio.2012.09.005]

63 **Palanissami G**, Paul SFD. RAGE and Its Ligands: Molecular Interplay Between Glycation, Inflammation, and Hallmarks of Cancer-a Review. *Horm Cancer* 2018; **9**: 295-325 [PMID: 29987748 DOI: 10.1007/s12672-018-0342-9]

64 **Bierhaus A**, Humpert PM, Morcos M, Wendt T, Chavakis T, Arnold B, Stern DM, Nawroth PP. Understanding RAGE, the receptor for advanced glycation end products. *J Mol Med (Berl)* 2005; **83**: 876-886 [PMID: 16133426 DOI: 10.1007/s00109-005-0688-7]

65 **Rojas A**, Schneider I, Lindner C, Gonzalez I, Morales MA. The RAGE/multiligand axis: a new actor in tumor biology. *Biosci Rep* 2022; **42** [PMID: 35727208 DOI: 10.1042/BSR20220395]

66 **Taguchi A**, Blood DC, del Toro G, Canet A, Lee DC, Qu W, Tanji N, Lu Y, Lalla E, Fu C, Hofmann MA, Kislinger T, Ingram M, Lu A, Tanaka H, Hori O, Ogawa S, Stern DM, Schmidt AM. Blockade of RAGE-amphoterin signalling suppresses tumour growth and metastases. *Nature* 2000; **405**: 354-360 [PMID: 10830965 DOI: 10.1038/35012626]

67 **Rojas A**, Morales M, Gonzalez I, Araya P. Inhibition of RAGE Axis Signaling: A Pharmacological Challenge. *Curr Drug Targets* 2019; **20**: 340-346 [PMID: 30124149 DOI: 10.2174/1389450119666180820105956]

68 **Shen CY**, Lu CH, Wu CH, Li KJ, Kuo YM, Hsieh SC, Yu CL. The Development of Maillard Reaction, and Advanced Glycation End Product (AGE)-Receptor for AGE (RAGE) Signaling Inhibitors as Novel Therapeutic Strategies for Patients with AGE-Related Diseases. *Molecules* 2020; **25** [PMID: 33261212 DOI: 10.3390/molecules25235591]

69 **Arumugam T**, Ramachandran V, Gomez SB, Schmidt AM, Logsdon CD. S100P-derived RAGE antagonistic peptide reduces tumor growth and metastasis. *Clin Cancer Res* 2012; **18**: 4356-4364 [PMID: 22718861 DOI: 10.1158/1078-0432.CCR-12-0221]

70 **Healey GD**, Pan-Castillo B, Garcia-Parra J, Davies J, Roberts S, Jones E, Dhar K, Nandanan S, Tofazzal N, Piggott L, Clarkson R, Seaton G, Frostell A, Fagge T, McKee C, Margarit L, Conlan RS, Gonzalez D. Antibody drug conjugates against the receptor for advanced glycation end products (RAGE), a novel therapeutic target in endometrial cancer. *J Immunother Cancer* 2019; **7**: 280 [PMID: 31665084 DOI: 10.1186/s40425-019-0765-z]

71 **Mizumoto S**, Takahashi J, Sugahara K. Receptor for advanced glycation end products (RAGE) functions as receptor for specific sulfated glycosaminoglycans, and anti-RAGE antibody or sulfated glycosaminoglycans delivered *in vivo* inhibit pulmonary metastasis of tumor cells. *J Biol Chem* 2012; **287**: 18985-18994 [PMID: 22493510 DOI: 10.1074/jbc.M111.313437]

72 **Zhao Z**, Wang H, Zhang L, Mei X, Hu J, Huang K. Receptor for advanced glycation end product blockade enhances the chemotherapeutic effect of cisplatin in tongue squamous cell carcinoma by reducing autophagy and modulating the Wnt pathway. *Anticancer Drugs* 2017; **28**: 187-196 [PMID: 27831944 DOI: 10.1097/CAD.0000000000000451]

73 **Swami P**, O'Connell KA, Thiyagarajan S, Crawford A, Patil P, Radhakrishnan P, Shin S, Caffrey TC, Grunkemeyer J, Neville T, Vetter SW, Hollingsworth MA, Leclerc E. Inhibition of the Receptor for Advanced Glycation End Products Enhances the Cytotoxic Effect of Gemcitabine in Murine Pancreatic Tumors. *Biomolecules* 2021; **11** [PMID: 33915939 DOI: 10.3390/biom11040526]

74 **Wendel U**, Persson N, Risinger C, Bengtsson E, Nodin B, Danielsson L, Welinder C, Nordin Fredrikson G, Jansson B, Blixt O. A novel monoclonal antibody targeting carboxymethyllysine, an advanced glycation end product in atherosclerosis and pancreatic cancer. *PLoS One* 2018; **13**: e0191872 [PMID: 29420566 DOI: 10.1371/journal.pone.0191872]

75 **Hubert P**, Roncarati P, Demoulin S, Pilard C, Ancion M, Reynders C, Lerho T, Bruyere D, Lebeau A, Radermecker C, Meunier M, Nokin MJ, Hendrick E, Peulen O, Delvenne P, Herfs M. Extracellular HMGB1 blockade inhibits tumor

growth through profoundly remodeling immune microenvironment and enhances checkpoint inhibitor-based immunotherapy. *J Immunother Cancer* 2021; **9** [PMID: 33712445 DOI: 10.1136/jitc-2020-001966]

76 **Mizumoto S**, Sugahara K. Glycosaminoglycans are functional ligands for receptor for advanced glycation end-products in tumors. *FEBS J* 2013; **280**: 2462-2470 [PMID: 23360476 DOI: 10.1111/febs.12156]

77 **Takeuchi A**, Yamamoto Y, Munesue S, Harashima A, Watanabe T, Yonekura H, Yamamoto H, Tsuchiya H. Low molecular weight heparin suppresses receptor for advanced glycation end products-mediated expression of malignant phenotype in human fibrosarcoma cells. *Cancer Sci* 2013; **104**: 740-749 [PMID: 23421467 DOI: 10.1111/cas.12133]

78 **Xu D**, Young JH, Krahn JM, Song D, Corbett KD, Chazin WJ, Pedersen LC, Esko JD. Stable RAGE-heparan sulfate complexes are essential for signal transduction. *ACS Chem Biol* 2013; **8**: 1611-1620 [PMID: 23679870 DOI: 10.1021/cb4001553]

79 **Li M**, Ong CY, Langouët-Astrié CJ, Tan L, Verma A, Yang Y, Zhang X, Shah DK, Schmidt EP, Xu D. Heparan sulfate-dependent RAGE oligomerization is indispensable for pathophysiological functions of RAGE. *Elife* 2022; **11** [PMID: 35137686 DOI: 10.7554/eLife.71403]

80 **Li ML**, Wang XF, Tan ZJ, Dong P, Gu J, Lu JH, Wu XS, Zhang L, Ding QC, Wu WG, Rao LH, Mu JS, Yang JH, Weng H, Ding Q, Zhang WJ, Chen L, Liu YB. Ethyl pyruvate administration suppresses growth and invasion of gallbladder cancer cells *via* downregulation of HMGB1-RAGE axis. *Int J Immunopathol Pharmacol* 2012; **25**: 955-965 [PMID: 23298486 DOI: 10.1177/039463201202500413]

81 **Yang Y**, Zhao LH, Huang B, Wang RY, Yuan SX, Tao QF, Xu Y, Sun HY, Lin C, Zhou WP. Pioglitazone, a PPARγ agonist, inhibits growth and invasion of human hepatocellular carcinoma *via* blockade of the rage signaling. *Mol Carcinog* 2015; **54**: 1584-1595 [PMID: 25307746 DOI: 10.1002/mc.22231]

82 **Tanuma SI**, Oyama T, Okazawa M, Yamazaki H, Takao K, Sugita Y, Amano S, Abe T, Sakagami H. A Dual Anti-Inflammatory and Anti-Proliferative 3-Styrylchromone Derivative Synergistically Enhances the Anti-Cancer Effects of DNA-Damaging Agents on Colon Cancer Cells by Targeting HMGB1-RAGE-ERK1/2 Signaling. *Int J Mol Sci* 2022; **23** [PMID: 35408786 DOI: 10.3390/ijms23073426]

83 **Ramya R**, Coral K, Bharathidevi SR. RAGE silencing deters CML-AGE induced inflammation and TLR4 expression in endothelial cells. *Exp Eye Res* 2021; **206**: 108519 [PMID: 33639133 DOI: 10.1016/j.exer.2021.108519]

84 **Yu YX**, Pan WC, Cheng YF. Silencing of advanced glycosylation and glycosylation and product-specific receptor (RAGE) inhibits the metastasis and growth of non-small cell lung cancer. *Am J Transl Res* 2017; **9**: 2760-2774 [PMID: 28670367]

85 **Hudson BI**, Kalea AZ, Del Mar Arriero M, Harja E, Boulanger E, D'Agati V, Schmidt AM. Interaction of the RAGE cytoplasmic domain with diaphanous-1 is required for ligand-stimulated cellular migration through activation of Rac1 and Cdc42. *J Biol Chem* 2008; **283**: 34457-34468 [PMID: 18922799 DOI: 10.1074/jbc.M801465200]

86 **Hofmann MA**, Drury S, Fu C, Qu W, Taguchi A, Lu Y, Avila C, Kambham N, Bierhaus A, Nawroth P, Neurath MF, Slattery T, Beach D, McClary J, Nagashima M, Morser J, Stern D, Schmidt AM. RAGE mediates a novel proinflammatory axis: a central cell surface receptor for S100/calgranulin polypeptides. *Cell* 1999; **97**: 889-901 [PMID: 10399917 DOI: 10.1016/s0092-8674(00)80801-6]

87 **Touré F**, Fritz G, Li Q, Rai V, Daffu G, Zou YS, Rosario R, Ramasamy R, Alberts AS, Yan SF, Schmidt AM. Formin mDia1 mediates vascular remodeling *via* integration of oxidative and signal transduction pathways. *Circ Res* 2012; **110**: 1279-1293 [PMID: 22511750 DOI: 10.1161/CIRCRESAHA.111.262519]

88 **Manigrasso MB**, Pan J, Rai V, Zhang J, Reverdatto S, Quadri N, DeVita RJ, Ramasamy R, Shekhtman A, Schmidt AM. Small Molecule Inhibition of Ligand-Stimulated RAGE-DIAPH1 Signal Transduction. *Sci Rep* 2016; **6**: 22450 [PMID: 26936329 DOI: 10.1038/srep22450]

89 **Manigrasso MB**, Rabbani P, Egaña-Gorroño L, Quadri N, Frye L, Zhou B, Reverdatto S, Ramirez LS, Dansereau S, Pan J, Li H, D'Agati VD, Ramasamy R, DeVita RJ, Shekhtman A, Schmidt AM. Small-molecule antagonism of the interaction of the RAGE cytoplasmic domain with DIAPH1 reduces diabetic complications in mice. *Sci Transl Med* 2021; **13**: eabf7084 [PMID: 34818060 DOI: 10.1126/scitranslmed.abf7084]

90 **Leerach N**, Munesue S, Harashima A, Kimura K, Oshima Y, Kawano S, Tanaka M, Niimura A, Sakulsak N, Yamamoto H, Hori O, Yamamoto Y. RAGE signaling antagonist suppresses mouse macrophage foam cell formation. *Biochem Biophys Res Commun* 2021; **555**: 74-80 [PMID: 33813279 DOI: 10.1016/j.bbrc.2021.03.139]

91 **Koga Y**, Sotokawauchi A, Higashimoto Y, Nishino Y, Hashizume N, Kakuma T, Akiba J, Tanaka Y, Matsui T, Yagi M, Yamagishi SI. DNA-Aptamer Raised against Receptor for Advanced Glycation End Products Improves Survival Rate in Septic Mice. *Oxid Med Cell Longev* 2021; **2021**: 9932311 [PMID: 34413930 DOI: 10.1155/2021/9932311]

92 **Sotokawauchi A**, Matsui T, Higashimoto Y, Nishino Y, Koga Y, Yagi M, Yamagishi SI. DNA aptamer raised against receptor for advanced glycation end products suppresses renal tubular damage and improves insulin resistance in diabetic mice. *Diab Vasc Dis Res* 2021; **18**: 1479164121990533 [PMID: 33535822 DOI: 10.1177/1479164121990533]

93 **Kaida Y**, Fukami K, Matsui T, Higashimoto Y, Nishino Y, Obara N, Nakayama Y, Ando R, Toyonaga M, Ueda S, Takeuchi M, Inoue H, Okuda S, Yamagishi S. DNA aptamer raised against AGEs blocks the progression of experimental diabetic nephropathy. *Diabetes* 2013; **62**: 3241-3250 [PMID: 23630304 DOI: 10.2337/db12-1608]

94 **Ojima A**, Matsui T, Maeda S, Takeuchi M, Inoue H, Higashimoto Y, Yamagishi S. DNA aptamer raised against advanced glycation end products inhibits melanoma growth in nude mice. *Lab Invest* 2014; **94**: 422-429 [PMID: 24514068 DOI: 10.1038/labinvest.2014.5]

95 **Zheng J**, Zhu W, He F, Li Z, Cai N, Wang HH. An Aptamer-Based Antagonist against the Receptor for Advanced Glycation End-Products (RAGE) Blocks Development of Colorectal Cancer. *Mediators Inflamm* 2021; **2021**: 9958051 [PMID: 34035661 DOI: 10.1155/2021/9958051]

96 **Nakamura N**, Matsui T, Ishibashi Y, Sotokawauchi A, Fukami K, Higashimoto Y, Yamagishi SI. RAGE-aptamer Attenuates the Growth and Liver Metastasis of Malignant Melanoma in Nude Mice. *Mol Med* 2017; **23**: 295-306 [PMID: 29387865 DOI: 10.2119/molmed.2017.00099]

97 **Lotan R**, Ganmore I, Shelly S, Zacharia M, Uribarri J, Beisswenger P, Cai W, Troen AM, Schnaider Beeri M. Long Term Dietary Restriction of Advanced Glycation End-Products (AGEs) in Older Adults with Type 2 Diabetes Is Feasible and

Efficacious-Results from a Pilot RCT. *Nutrients* 2020; **12** [PMID: 33076217 DOI: 10.3390/nu12103143]

98 **Yacoub R**, Nugent M, Cai W, Nadkarni GN, Chaves LD, Abyad S, Honan AM, Thomas SA, Zheng W, Valiyaparambil SA, Bryniarski MA, Sun Y, Buck M, Genco RJ, Quigg RJ, He JC, Uribarri J. Advanced glycation end products dietary restriction effects on bacterial gut microbiota in peritoneal dialysis patients; a randomized open label controlled trial. *PLoS One* 2017; **12**: e0184789 [PMID: 28931089 DOI: 10.1371/journal.pone.0184789]

99 **Berdún R**, Jové M, Sol J, Cai W, He JC, Rodriguez-Mortera R, Martin-Garí M, Pamplona R, Uribarri J, Portero-Otin M. Restriction of Dietary Advanced Glycation End Products Induces a Differential Plasma Metabolome and Lipidome Profile. *Mol Nutr Food Res* 2021; **65**: e2000499 [PMID: 34599622 DOI: 10.1002/mnfr.202000499]

100 **Goudarzi R**, Sedaghat M, Hedayati M, Hekmatdoost A, Sohrab G. Low advanced Glycation end product diet improves the central obesity, insulin resistance and inflammatory profiles in Iranian patients with metabolic syndrome: a randomized clinical trial. *J Diabetes Metab Disord* 2020; **19**: 1129-1138 [PMID: 33520830 DOI: 10.1007/s40200-020-00614-0]

101 **Gutierrez-Mariscal FM**, Cardelo MP, de la Cruz S, Alcala-Diaz JF, Roncero-Ramos I, Guler I, Vals-Delgado C, López-Moreno A, Luque RM, Delgado-Lista J, Perez-Martinez P, Yubero-Serrano EM, Lopez-Miranda J. Reduction in Circulating Advanced Glycation End Products by Mediterranean Diet Is Associated with Increased Likelihood of Type 2 Diabetes Remission in Patients with Coronary Heart Disease: From the Cordioprev Study. *Mol Nutr Food Res* 2021; **65**: e1901290 [PMID: 32529753 DOI: 10.1002/mnfr.201901290]

102 **Jiao L**, Stolzenberg-Solomon R, Zimmerman TP, Duan Z, Chen L, Kahle L, Risch A, Subar AF, Cross AJ, Hollenbeck A, Vlassara H, Striker G, Sinha R. Dietary consumption of advanced glycation end products and pancreatic cancer in the prospective NIH-AARP Diet and Health Study. *Am J Clin Nutr* 2015; **101**: 126-134 [PMID: 25527756 DOI: 10.3945/ajcn.114.098061]

103 **Peterson LL**, Park S, Park Y, Colditz GA, Anbardar N, Turner DP. Dietary advanced glycation end products and the risk of postmenopausal breast cancer in the National Institutes of Health-AARP Diet and Health Study. *Cancer* 2020; **126**: 2648-2657 [PMID: 32097496 DOI: 10.1002/cncr.32798]

104 **Omofuma OO**, Turner DP, Peterson LL, Merchant AT, Zhang J, Steck SE. Dietary Advanced Glycation End-products (AGE) and Risk of Breast Cancer in the Prostate, Lung, Colorectal and Ovarian Cancer Screening Trial (PLCO). *Cancer Prev Res (Phila)* 2020; **13**: 601-610 [PMID: 32169887 DOI: 10.1158/1940-6207.CAPR-19-0457]

105 **Aglago EK**, Mayén AL, Knaze V, Freisling H, Fedirko V, Hughes DJ, Jiao L, Eriksen AK, Tjønneland A, Boutron-Ruault MC, Rothwell JA, Severi G, Kaaks R, Katzke V, Schulze MB, Birukov A, Palli D, Sieri S, Santucci de Magistris M, Tumino R, Ricceri F, Bueno-de-Mesquita B, Derksen JWG, Skeie G, Gram IT, Sandanger T, Quirós JR, Luján-Barroso L, Sánchez MJ, Amiano P, Chirlaque MD, Gurrea AB, Johansson I, Manjer J, Perez-Cornago A, Weiderpass E, Gunter MJ, Heath AK, Schalkwijk CG, Jenab M. Dietary Advanced Glycation End-Products and Colorectal Cancer Risk in the European Prospective Investigation into Cancer and Nutrition (EPIC) Study. *Nutrients* 2021; **13** [PMID: 34579010 DOI: 10.3390/nu13093132]

106 **Mao Z**, Aglago EK, Zhao Z, Schalkwijk C, Jiao L, Freisling H, Weiderpass E, Hughes DJ, Eriksen AK, Tjønneland A, Severi G, Rothwell J, Boutron-Ruault MC, Katzke V, Kaaks R, Schulze MB, Birukov A, Krogh V, Panico S, Tumino R, Ricceri F, Bueno-de-Mesquita HB, Vermeulen RCH, Gram IT, Skeie G, Sandanger TM, Quirós JR, Crous-Bou M, Sánchez MJ, Amiano P, Chirlaque MD, Barricarte Gurrea A, Manjer J, Johansson I, Perez-Cornago A, Jenab M, Fedirko V. Dietary Intake of Advanced Glycation End Products (AGEs) and Mortality among Individuals with Colorectal Cancer. *Nutrients* 2021; **13** [PMID: 34959986 DOI: 10.3390/nu13124435]

107 **Omofuma OO**, Peterson LL, Turner DP, Merchant AT, Zhang J, Thomson CA, Neuhouser ML, Snetselaar LG, Caan BJ, Shadyab AH, Saquib N, Banack HR, Uribarri J, Steck SE. Dietary Advanced Glycation End-Products and Mortality after Breast Cancer in the Women's Health Initiative. *Cancer Epidemiol Biomarkers Prev* 2021; **30**: 2217-2226 [PMID: 34583965 DOI: 10.1158/1055-9965.EPI-21-0610]

108 **Islami F**, Goding Sauer A, Miller KD, Siegel RL, Fedewa SA, Jacobs EJ, McCullough ML, Patel AV, Ma J, Soerjomataram I, Flanders WD, Brawley OW, Gapstur SM, Jemal A. Proportion and number of cancer cases and deaths attributable to potentially modifiable risk factors in the United States. *CA Cancer J Clin* 2018; **68**: 31-54 [PMID: 29160902 DOI: 10.3322/caac.21440]

109 **Du H**, Cao T, Lu X, Zhang T, Luo B, Li Z. Mediterranean Diet Patterns in Relation to Lung Cancer Risk: A Meta-Analysis. *Front Nutr* 2022; **9**: 844382 [PMID: 35495942 DOI: 10.3389/fnut.2022.844382]

110 **Long T**, Liu K, Long J, Li J, Cheng L. Dietary glycemic index, glycemic load and cancer risk: a meta-analysis of prospective cohort studies. *Eur J Nutr* 2022; **61**: 2115-2127 [PMID: 35034169 DOI: 10.1007/s00394-022-02797-z]

111 **Papadimitriou N**, Markozannes G, Kanellopoulou A, Critselis E, Alhardan S, Karafousia V, Kasimis JC, Katsaraki C, Papadopoulou A, Zografou M, Lopez DS, Chan DSM, Kyrgiou M, Ntzani E, Cross AJ, Marrone MT, Platz EA, Gunter MJ, Tsilidis KK. An umbrella review of the evidence associating diet and cancer risk at 11 anatomical sites. *Nat Commun* 2021; **12**: 4579 [PMID: 34321471 DOI: 10.1038/s41467-021-24861-8]

112 **Kazemi A**, Barati-Boldaji R, Soltani S, Mohammadipoor N, Esmaeilinezhad Z, Clark CCT, Babajafari S, Akbarzadeh M. Intake of Various Food Groups and Risk of Breast Cancer: A Systematic Review and Dose-Response Meta-Analysis of Prospective Studies. *Adv Nutr* 2021; **12**: 809-849 [PMID: 33271590 DOI: 10.1093/advances/nmaa147]

113 **Key TJ**, Allen NE, Spencer EA, Travis RC. The effect of diet on risk of cancer. *Lancet* 2002; **360**: 861-868 [PMID: 12243933 DOI: 10.1016/S0140-6736(02)09958-0]

114 **Kopp W**. How Western Diet And Lifestyle Drive The Pandemic Of Obesity And Civilization Diseases. *Diabetes Metab Syndr Obes* 2019; **12**: 2221-2236 [PMID: 31695465 DOI: 10.2147/DMSO.S216791]

115 **Benninghoff AD**, Hintze KJ, Monsanto SP, Rodriguez DM, Hunter AH, Phatak S, Pestka JJ, Wettere AJV, Ward RE. Consumption of the Total Western Diet Promotes Colitis and Inflammation-Associated Colorectal Cancer in Mice. *Nutrients* 2020; **12** [PMID: 32093192 DOI: 10.3390/nu12020544]

116 **Zheng J**, Guinter MA, Merchant AT, Wirth MD, Zhang J, Stolzenberg-Solomon RZ, Steck SE. Dietary patterns and risk of pancreatic cancer: a systematic review. *Nutr Rev* 2017; **75**: 883-908 [PMID: 29025004 DOI: 10.1093/nutrit/nux038]

117 **Fabiani R**, Minelli L, Bertarelli G, Bacci S. A Western Dietary Pattern Increases Prostate Cancer Risk: A Systematic

Review and Meta-Analysis. *Nutrients* 2016; **8** [PMID: 27754328 DOI: 10.3390/nu8100626]

118 **Xiao Y**, Xia J, Li L, Ke Y, Cheng J, Xie Y, Chu W, Cheung P, Kim JH, Colditz GA, Tamimi RM, Su X. Associations between dietary patterns and the risk of breast cancer: a systematic review and meta-analysis of observational studies. *Breast Cancer Res* 2019; **21**: 16 [PMID: 30696460 DOI: 10.1186/s13058-019-1096-1]

119 **Uribarri J**, Peppa M, Cai W, Goldberg T, Lu M, He C, Vlassara H. Restriction of dietary glycotoxins reduces excessive advanced glycation end products in renal failure patients. *J Am Soc Nephrol* 2003; **14**: 728-731 [PMID: 12595509 DOI: 10.1097/01.asn.0000051593.41395.b9]

120 **Vlassara H**, Cai W, Crandall J, Goldberg T, Oberstein R, Dardaine V, Peppa M, Rayfield EJ. Inflammatory mediators are induced by dietary glycotoxins, a major risk factor for diabetic angiopathy. *Proc Natl Acad Sci U S A* 2002; **99**: 15596-15601 [PMID: 12429856 DOI: 10.1073/pnas.242407999]

121 **Vlassara H**, Cai W, Goodman S, Pyzik R, Yong A, Chen X, Zhu L, Neade T, Beeri M, Silverman JM, Ferrucci L, Tansman L, Striker GE, Uribarri J. Protection against loss of innate defenses in adulthood by low advanced glycation end products (AGE) intake: role of the antiinflammatory AGE receptor-1. *J Clin Endocrinol Metab* 2009; **94**: 4483-4491 [PMID: 19820033 DOI: 10.1210/jc.2009-0089]

122 **Luévano-Contreras C**, Garay-Sevilla ME, Wrobel K, Malacara JM. Dietary advanced glycation end products restriction diminishes inflammation markers and oxidative stress in patients with type 2 diabetes mellitus. *J Clin Biochem Nutr* 2013; **52**: 22-26 [PMID: 23341693 DOI: 10.3164/jcbn.12-40]

123 **de Courten B**, de Courten MP, Soldatos G, Dougherty SL, Straznicky N, Schlaich M, Sourris KC, Chand V, Scheijen JL, Kingwell BA, Cooper ME, Schalkwijk CG, Walker KZ, Forbes JM. Diet low in advanced glycation end products increases insulin sensitivity in healthy overweight individuals: a double-blind, randomized, crossover trial. *Am J Clin Nutr* 2016; **103**: 1426-1433 [PMID: 27030534 DOI: 10.3945/ajcn.115.125427]

124 **Gugliucci A**. Formation of Fructose-Mediated Advanced Glycation End Products and Their Roles in Metabolic and Inflammatory Diseases. *Adv Nutr* 2017; **8**: 54-62 [PMID: 28096127 DOI: 10.3945/an.116.013912]

125 **Aragno M**, Mastrocola R. Dietary Sugars and Endogenous Formation of Advanced Glycation Endproducts: Emerging Mechanisms of Disease. *Nutrients* 2017; **9**: 385 [PMID: 28420091 DOI: 10.3390/nu9040385]

126 **Lorenzo Bermejo J**, Boekstegers F, González Silos R, Marcelain K, Baez Benavides P, Barahona Ponce C, Müller B, Ferreccio C, Koshiol J, Fischer C, Peil B, Sinsheimer J, Fuentes Guajardo M, Barajas O, Gonzalez-Jose R, Bedoya G, Cátira Bortolini M, Canizales-Quinteros S, Gallo C, Ruiz Linares A, Rothhammer F. Subtypes of Native American ancestry and leading causes of death: Mapuche ancestry-specific associations with gallbladder cancer risk in Chile. *PLoS Genet* 2017; **13**: e1006756 [PMID: 28542165 DOI: 10.1371/journal.pgen.1006756]

127 **Boekstegers F**, Marcelain K, Barahona Ponce C, Baez Benavides PF, Müller B, de Toro G, Retamales J, Barajas O, Ahumada M, Morales E, Rojas A, Sanhueza V, Loader D, Rivera MT, Gutiérrez L, Bernal G, Ortega A, Montalvo D, Portiño S, Bertrán ME, Gabler F, Spencer L, Olloquequi J, González Silos R, Fischer C, Scherer D, Jenab M, Aleksandrova K, Katzke V, Weiderpass E, Moradi T, Fischer K, Bossers W, Brenner H, Hveem K, Eklund N, Völker U, Waldenberger M, Fuentes Guajardo M, Gonzalez-Jose R, Bedoya G, Bortolini MC, Canizales S, Gallo C, Ruiz Linares A, Rothhammer F, Lorenzo Bermejo J. ABCB1/4 gallbladder cancer risk variants identified in India also show strong effects in Chileans. *Cancer Epidemiol* 2020; **65**: 101643 [PMID: 32058310 DOI: 10.1016/j.canep.2019.101643]

128 **González I**, Morales MA, Rojas A. Polyphenols and AGEs/RAGE axis. Trends and challenges. *Food Res Int* 2020; **129**: 108843 [PMID: 32036875 DOI: 10.1016/j.foodres.2019.108843]

129 **Liotta LA**, Clair T. Cancer. Checkpoint for invasion. *Nature* 2000; **405**: 287-288 [PMID: 10830943 DOI: 10.1038/35012728]

130 **Rojas A**, González I, Rodríguez B, Romero J, Figueroa H, Llanos J, Morales E, Pérez-Castro R. Evidence of involvement of the receptor for advanced glycation end-products (RAGE) in the adhesion of Helicobacter pylori to gastric epithelial cells. *Microbes Infect* 2011; **13**: 818-823 [PMID: 21609778 DOI: 10.1016/j.micinf.2011.04.005]

131 **Yamamoto Y**, Harashima A, Saito H, Tsuneyama K, Munesue S, Motoyoshi S, Han D, Watanabe T, Asano M, Takasawa S, Okamoto H, Shimura S, Karasawa T, Yonekura H, Yamamoto H. Septic shock is associated with receptor for advanced glycation end products ligation of LPS. *J Immunol* 2011; **186**: 3248-3257 [PMID: 21270403 DOI: 10.4049/jimmunol.1002253]

132 **Garay-Sevilla ME**, Gomez-Ojeda A, González I, Luévano-Contreras C, Rojas A. Contribution of RAGE axis activation to the association between metabolic syndrome and cancer. *Mol Cell Biochem* 2021; **476**: 1555-1573 [PMID: 33398664 DOI: 10.1007/s11010-020-04022-z]

133 **Rojas A**, González I, Morales E, Pérez-Castro R, Romero J, Figueroa H. Diabetes and cancer: Looking at the multiligand/RAGE axis. *World J Diabetes* 2011; **2**: 108-113 [PMID: 21860695 DOI: 10.4239/wjd.v2.i7.108]

World Journal of Gastroenterology

Submit a Manuscript: https://www.f6publishing.com

World J Gastroenterol 2022 October 21; 28(39): 5691-5706

DOI: 10.3748/wjg.v28.i39.5691

ISSN 1007-9327 (print) ISSN 2219-2840 (online)

REVIEW

Interplay between metabolic dysfunction-associated fatty liver disease and chronic kidney disease: Epidemiology, pathophysiologic mechanisms, and treatment considerations

Panagiotis Theofilis, Aikaterini Vordoni, Rigas G Kalaitzidis

Specialty type: Gastroenterology and hepatology

Provenance and peer review: Invited article; Externally peer reviewed.

Peer-review model: Single blind

Peer-review report's scientific quality classification

Grade A (Excellent): A
Grade B (Very good): B
Grade C (Good): 0
Grade D (Fair): 0
Grade E (Poor): 0

P-Reviewer: Dong Z, China; Popovic DS, Serbia

Received: August 12, 2022
Peer-review started: August 12, 2022
First decision: August 29, 2022
Revised: September 6, 2022
Accepted: September 19, 2022
Article in press: September 19, 2022
Published online: October 21, 2022

Panagiotis Theofilis, Aikaterini Vordoni, Rigas G Kalaitzidis, Center for Nephrology "G. Papadakis," General Hospital of Nikaia-Piraeus "Agios Panteleimon," Nikaia 18454, Greece

Corresponding author: Panagiotis Theofilis, MD, Doctor, Researcher, Center for Nephrology "G. Papadakis," General Hospital of Nikaia-Piraeus "Agios Panteleimon," Piraeus, Nikaia 18454, Greece. panos.theofilis@hotmail.com

Abstract

The recently proposed nomenclature change from non-alcoholic fatty liver disease to metabolic dysfunction-associated fatty liver disease (MAFLD) has resulted in the reappraisal of epidemiological trends and associations with other chronic diseases. In this context, MAFLD appears to be tightly linked to incident chronic kidney disease (CKD). This association may be attributed to multiple shared risk factors including type 2 diabetes mellitus, arterial hypertension, obesity, dyslipidemia, and insulin resistance. Moreover, similarities in their molecular pathophysiologic mechanisms can be detected, since inflammation, oxidative stress, fibrosis, and gut dysbiosis are highly prevalent in these pathologic states. At the same time, lines of evidence suggest a genetic predisposition to MAFLD due to gene polymorphisms, such as the *PNPLA3* rs738409 G allele polymorphism, which may also propagate renal dysfunction. Concerning their management, available treatment considerations for obesity (bariatric surgery) and novel antidiabetic agents (glucagon-like peptide 1 receptor agonists, sodium-glucose co-transporter 2 inhibitors) appear beneficial in preclinical and clinical studies of MAFLD and CKD modeling. Moreover, alternative approaches such as melatonin supplementation, farnesoid X receptor agonists, and gut microbiota modulation may represent attractive options in the future. With a look to the future, additional adequately sized studies are required, focusing on preventing renal complications in patients with MAFLD and the appropriate management of individuals with concomitant MAFLD and CKD.

Key Words: Metabolic dysfunction-associated fatty liver disease; Chronic kidney disease; Hepatic steatosis; inflammation; Type 2 diabetes mellitus; Obesity

©The Author(s) 2022. Published by Baishideng Publishing Group Inc. All rights reserved.

Core Tip: Metabolic dysfunction-associated fatty liver disease (MAFLD) is a recently defined pathological state aiming to identify individuals at increased risk of adverse prognosis. Numerous epidemiological studies propose that chronic kidney disease may be among its complications. Their shared risk factors, molecular mechanisms, and genetic predisposition represent the basis for this relationship. Accordingly, treatment approaches with combined efficacy in MAFLD and chronic renal impairment are expected to positively impact the natural history of this deleterious interaction, which remains to be confirmed in future studies.

Citation: Theofilis P, Vordoni A, Kalaitzidis RG. Interplay between metabolic dysfunction-associated fatty liver disease and chronic kidney disease: Epidemiology, pathophysiologic mechanisms, and treatment considerations. *World J Gastroenterol* 2022; 28(39): 5691-5706
URL: https://www.wjgnet.com/1007-9327/full/v28/i39/5691.htm
DOI: https://dx.doi.org/10.3748/wjg.v28.i39.5691

INTRODUCTION

Metabolic abnormalities, namely obesity and type 2 diabetes mellitus (T2DM) constitute contemporary pandemics with a high prevalence and rising incidence[1,2]. Although cardiovascular diseases remain the most prominent complication of metabolic derangement, hepatic insult is frequent, as documented in recently reported epidemiologic trends of non-alcoholic fatty liver disease (NAFLD) and non-alcoholic steatohepatitis (NASH)[3,4]. However, the existing NAFLD definition required the exclusion of other forms of liver disease instead of providing positive criteria for the diagnosis of metabolic dysfunction-associated fatty liver disease (MAFLD). A recent expert consensus tried to resolve this gap in evidence by providing a simple and comprehensive MAFLD definition and diagnostic criteria[5]. These included the presence of steatosis along with a main metabolic abnormality (overweight/obesity or T2DM) or at least two metabolic risk factors.

The establishment of MAFLD as an entity may promote the need for intense research in this field to define its epidemiology better, identify predisposing and prognostic factors, and evaluate effective therapeutic approaches. Moreover, investigating the association between MAFLD and other pathological states, primarily cardiac and renal diseases, will improve our understanding of this complex entity. Even though the link between MAFLD and cardiovascular disease has been the most extensively studied[6], ample evidence suggests the relationship between MAFLD and chronic kidney disease (CKD).

In this narrative review, we elaborate on this interaction by assessing its epidemiological features, the involved pathophysiologic pathways, and the potential therapeutic interventions.

MAFLD AND CKD; EPIDEMIOLOGICAL TRENDS

Due to the recent change in terminology and diagnostic criteria, we are now beginning to reevaluate the epidemiological characteristics of MAFLD. In a recently reported study that followed a meta-analytic approach, the prevalence of MAFLD in overweight or obese subjects was 50.7%[7]. The authors pointed to potential geographic variations in MAFLD prevalence, with South American populations exhibiting the highest prevalence rates (approximately 71%). Moreover, they detected a significantly higher prevalence in male subjects and in obese compared to overweight. No differences according to age or income were reported. Finally, T2DM and metabolic syndrome prevalence was 19.7% and 57.5%, respectively. A similar prevalence (47%) was detected in a cross-sectional study of the Mexican population, with male sex, older age, and increasing body mass index (BMI) being predictive factors[8]. Other than high prevalence rates, there is an association between MAFLD and all-cause mortality, which extends to cancer- and cardiovascular disease-related mortality[9]. Moreover, a higher risk of atherosclerotic disease, heart failure, obstructive sleep apnea, and malignancy has been reported[9].

According to the available evidence, MAFLD is tied to a higher incidence of CKD. To begin with, in an analysis of approximately 270000 individuals that underwent National Health Insurance Service health examinations, MAFLD was associated with an increased risk of incident CKD compared to non-metabolic NAFLD (adjusted hazard ratio 1.18, 95% confidence interval [CI]: 1.01-1.39; P = 0.04)[10]. In the study by Tanaka *et al*[11] in a sizeable Japanese population followed up for 10 years, MAFLD was a determinant of incident CKD irrespective of age, sex, smoking, coronary artery disease, estimated glomerular filtration rate (eGFR), and metabolic risk factors (diabetes mellitus [DM], hypertension, hyperlipidemia, obesity). Notably, such observations were not made for the presence of NAFLD or only fatty liver[11]. In a Chinese cohort of 6873 participants with a 4.6-year follow-up, the investigators noted a higher risk of CKD in MAFLD subjects (risk ratio 1.64, 95%CI: 1.39-1.94)[12]. Last but not least, the

authors of a recently published systematic review and meta-analysis found a potent association between a MAFLD diagnosis and new onset of CKD (hazard ratio 1.53, 95%CI: 1.38-1.68)[9]. Contradictory to the findings mentioned above, in an analysis of the National Health and Nutrition Examination Surveys of the United States 2017-2018, the relationship between MAFLD and CKD was not statistically significant after the propensity score matching[13]. Scientific interest is intense in this field due to the recently proposed change in the nomenclature of NAFLD into MAFLD. Future studies are eagerly awaited to assess the association between MAFLD and CKD and the prognosis of individuals with concomitant CKD and MAFLD.

Concerning the interplay between MAFLD and CKD, the use of transient elastography is of great importance. Ciardullo *et al*[14], in their meta-analysis of seven cross-sectional studies, detected an association of non-invasively assessed liver fibrosis with increased urinary albumin-to-creatinine ratio (UACR) (odds ratio [OR] 1.98, 95%CI: 1.29-3.05; $P = 0.002$) and incident CKD (OR 2.49, 95%CI: 1.89-3.29; $P < 0.001$). The study by Freitas *et al*[15] further stressed the role of transient elastography. Liver fibrosis, assessed by the liver stiffness measurements (LSM), was associated with early kidney dysfunction, characterized by the development of microalbuminuria (UACR 30-300 mg/g) or a drop in eGFR to < 60 mL/min/1.73 m^2 in MAFLD individuals[15]. LSM values of over 6.1 kPa were predictive of the endpoint, with a sensitivity and specificity of 85.7% and 67.6%, respectively[15]. It appears that Fibroscan-derived controlled attenuated parameter (CAP) may be a more crucial predictor of prevalent CKD in subjects with MAFLD than LSM. Specifically, CAP values of 353 dB/m were associated with CKD, even after multivariable adjustment (OR 1.07, 95%CI: 1.00-1.20; $P = 0.01$)[16].

PATHOPHYSIOLOGIC PATHWAYS LINKING MAFLD WITH CKD

According to those recently published reports, it is evident that MAFLD is a growing pandemic due to the constantly rising prevalence of its underlying risk factors. Moreover, the association between MAFLD and incident CKD is remarkable but unsurprising, due to the common pathophysiologic mechanisms surrounding those entities (Figure 1). To begin with, the main risk factors for CKD development, T2DM and arterial hypertension[17-19], are among the established diagnostic criteria for MAFLD. The same could be argued for obesity, prediabetes, dyslipidemia, and insulin resistance since studies have proposed an independent association between the risk factors mentioned above and incident CKD[17,19-21].

Inflammatory hypothesis in MAFLD and CKD

Regarding the involved molecular mechanisms, we should stress the role of inflammation. We know that inflammation is among the cardinal features of MAFLD, with elevations of high-sensitivity C reactive protein (hsCRP) being among the criteria of metabolic dysregulation. hsCRP elevation was correlated with the extent of liver steatosis and fibrosis in 393 obese individuals with MAFLD, even after adjustment for confounding factors[22]. Chronic, low-grade inflammation may propagate oxidative stress and endothelial dysfunction in MAFLD[23,24]. Ultimately, liver fibrosis ensues due to extracellular matrix formation and collagen deposition[25], potentially progressing to cirrhosis and hepatocellular carcinoma. Intriguingly, this pro-inflammatory state could facilitate the development of CKD, with nuclear factor kappa B (NF-κB) mediating the activation of endothelial cells, mesangial cells, podocytes, and tubular epithelial cells, resulting in increased permeability, the release of inflammatory mediators, and proteinuria[26]. In this deleterious setting, the additional extracellular matrix remodeling, epithelial-to-mesenchymal transition, and interstitial fibrosis contribute to the progression of CKD[27]. We should also stress that the contribution of MAFLD and CKD to the systemic inflammatory milieu could have deleterious cardiovascular implications[28-32].

Obesity and adipokines

Obesity, another shared risk factor for MAFLD and CKD, is also pivotal in their development. Adipose tissue is a known endocrine organ with critical regulatory functions on satiety, insulin sensitivity, inflammation, and the renin-angiotensin system through the secretion of adipokines[33,34]. The most well-characterized hazardous adipokine in FLD, leptin, by interacting with its primary receptor Ob-Rb, results in Janus kinase 2 phosphorylation, in turn leading to the upregulation of the Akt/mammalian target of rapamycin (mTOR), signal transducer and activator of transcription 5, and mitogen-activated protein kinase (MAPK) pathways[35]. This may aid in the development and progression of hepatic steatosis, steatohepatitis, and liver fibrosis. By contrast, low levels of the protective adipokine adiponectin are significantly associated with advanced fibrosis[36]. Moreover, an increased leptin-to-adiponectin ratio is positively correlated with the increasing severity of steatosis[37]. The imbalance in leptin and adiponectin may influence the development of CKD, as leptin could induce sympathetic nervous system activation and blood pressure increases[38], as well as transforming growth factor-β synthesis[39]. A recently reported longitudinal study of 2646 Koreans without CKD showed that higher plasma leptin was predictive of incident CKD after a 2.8-year mean follow-up[40]. On the other hand, adiponectin could have renoprotective effects by ameliorating renal inflammation, oxidative stress, and

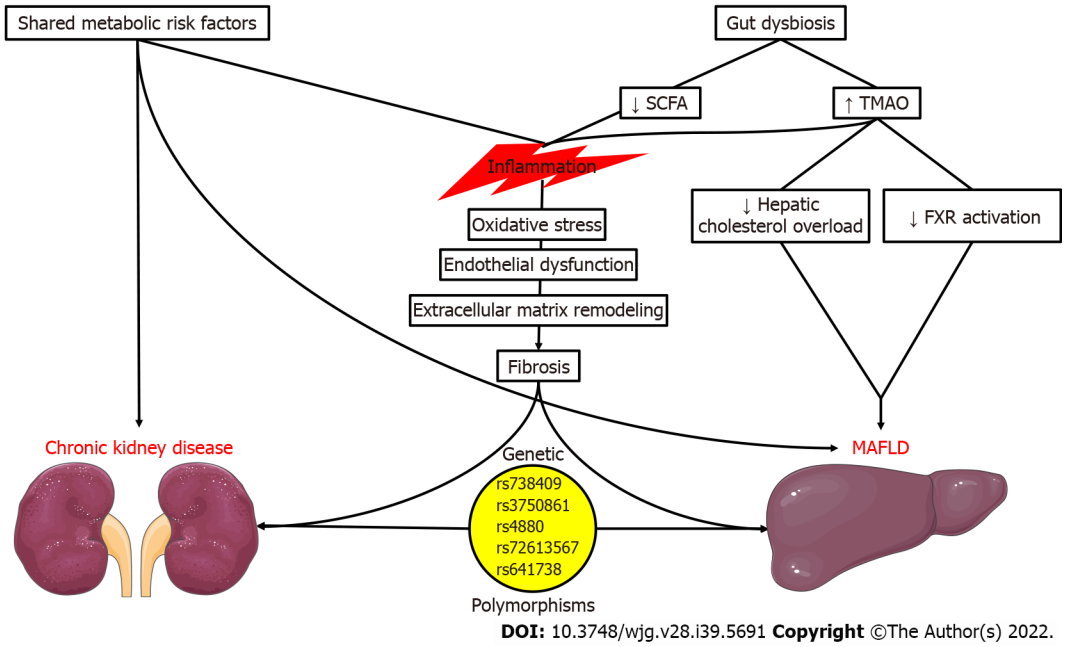


Figure 1 Common pathophysiologic mechanisms in metabolic dysfunction-associated fatty liver disease and chronic kidney disease.
FXR: Farnesoid X receptor; MAFLD: Metabolic dysfunction-associated fatty liver disease; SCFA: Short-chain fatty acid; TMAO: Trimethylamine N-oxide.

fibrosis[41]. However, multiple studies have shown that high adiponectin levels are inversely associated with eGFR in individuals with CKD[42] and were predictive of renal function deterioration in subjects without CKD[43].

Gut dysbiosis

The role of the gut microbiome in human health and disease is a highly relevant field of scientific interest. Therefore, potential associations of gut dysbiosis with MAFLD and CKD have been suggested in the past years, strengthening the importance of the gut-liver-kidney axis. In altered gut microbiome synthesis, hazardous metabolites such as trimethylamine N-oxide (TMAO), p-cresyl sulfate, and indoxyl sulfate may be formed.

TMAO is the most extensively studied metabolite regarding its health implications[44]. According to preclinical studies, it may aggravate hepatic steatosis and steatohepatitis by modulating bile acid metabolism, inhibiting farnesoid X receptor activation, and reducing hepatic cholesterol overload[45,46]. NAFLD presence and severity were correlated with circulating TMAO in a study of Chinese individuals[47]. The levels of TMAO were higher in individuals with obesity and NASH, only in the presence of T2DM[48]. TMAO was also associated with all-cause mortality only in NAFLD patients in the Prevention of Renal and Vascular End-stage Disease cohort study, even after adjustment for confounders[49]. Regarding the kidney, TMAO may exert deleterious effects, such as promoting inflammation and fibrosis[50-52]. In a meta-analysis of kidney function indices involving 32 clinical studies with 42062 participants, TMAO concentration was associated with advanced CKD, inversely correlated with eGFR, and positively correlated with UACR, serum creatinine, and serum cystatin C[53]. Circulating TMAO was predictive of all-cause and cardiovascular mortality in a recently reported systematic review and meta-analysis, with this finding being irrespective of kidney function and common risk factors (DM, hypertension, dyslipidemia, inflammation)[54].

Depletion of bacteria responsible for the production of beneficial short-chain fatty acids (SCFAs), such as acetate, propionate, and butyrate, in the setting of a disrupted gut microbiome may lead to deleterious effects in the liver and kidney. These SCFAs could promote anti-inflammatory and anti-oxidative actions by limiting neutrophil recruitment, macrophage secretion of pro-inflammatory mediators, and histone deacetylase-induced NF-κB activation while promoting anti-inflammatory interleukin-10 formation by T regulatory cells[55]. Increased availability of SCFA-producing bacteria or SCFA treatment in clinical studies of patients on hemodialysis patients has resulted in lowering inflammatory markers and ameliorating renal function[56,57]. SCFAs are also helpful in the prevention of MAFLD due to the effects mentioned above, together with hepatic AMP-activated protein kinase (AMPK) activation and glucagon-like peptide 1 receptor (GLP1-R) activation, promotion of satiety, and abrogation of insulin resistance[58].

Gene polymorphisms

Polymorphisms in a few NAFLD-associated genes may also be associated with CKD. *PNPLA3* rs738409

G allele polymorphism is the most well-studied and correlated with NAFLD risk and severity[59]. Its potential association with renal outcomes has been investigated with conflicting evidence, as it may propagate podocyte activation and lipid nephrotoxicity. Initially, Sun *et al*[60] found a significant link between the G/G *PNPLA3* genotype with glomerular and tubular injury. In a United Kingdom Biobank analysis, the rs738409 single nucleotide polymorphism was associated with decreased eGFR, independently of metabolic risk factors[61]. Patients homozygous for the *PNPLA3* rs738409 had a higher prevalence of CKD and lower eGFR irrespective of liver stiffness and other risk factors in the study of Mantovani *et al*[62]. This study also found similar expression of *PNPLA3* in podocytes, hepatocytes, and hepatic stellate cells[62]. The same study group had previously proven the independent association of the G/G *PNPLA3* rs738409 polymorphism phenotype with eGFR and CKD in post-menopausal women with T2DM[63]. However, no associations between *PNPLA3* rs738409 gene polymorphism and kidney function were detected in other studies[64-67].

Other polymorphisms have also been investigated, albeit to a lesser degree. Risk alleles for *KLF6* rs3750861 and *SOD2* rs4880 polymorphisms correlate with kidney function in MAFLD[65]. Moreover, in a population of biopsy-proven NAFLD, the *HSD17B13* rs72613567 A alleles were protective against albuminuria but not eGFR decline[68]. Lastly, an association between the *MBOAT7-TMC4* rs641738 T/T genotype and lower eGFR was detected in a cohort of Asian individuals with biopsy-proven NAFLD [67]. While the genetic predisposition of kidney dysfunction in FLD represents an exciting hypothesis, further studies are required to improve our understanding of this link.

THERAPEUTIC APPROACHES

Treating patients with MAFLD and CKD requires therapeutic interventions to ameliorate their prognosis by targeting their shared risk factors and pathophysiology. Although studies have not explicitly assessed this subgroup of patients, we may assume that interventions with documented efficacy in MAFLD[69-81] and CKD[82-90] could lead to positive outcomes in this combination of diseases (Table 1). Moreover, due to the recent change in the nomenclature with the introduction of MAFLD, we should stress that most of the available clinical evidence discussed below is derived from studies of NAFLD patients. Therefore, future appropriately designed studies considering the novel MAFLD diagnostic criteria will shed additional light on managing this entity.

Bariatric surgery

Since obesity is among the main risk factors for the development of MAFLD, the role of bariatric surgery may be crucial in carefully selected eligible individuals. Initially, we should state that the prevalence of MAFLD may be exceptionally high in those morbidly obese patients that are eligible for bariatric surgery. Ciardullo *et al*[91] have demonstrated this association in a study of 434 potential candidates for bariatric surgery, with the prevalence of steatosis and fibrosis being 76.7% and 23.1%, respectively. In the only study assessing bariatric surgery in MAFLD patients, Meneses *et al*[69] prospectively enrolled 52 subjects whose MAFLD status was evaluated *via* liver biopsy. Those with a histological diagnosis of steatohepatitis were followed up with an additional biopsy 12 mo after the index procedure. Most subjects with steatohepatitis did not experience any disease progression, while a significant proportion (56.5%) exhibited complete resolution. Additionally, fibrosis and fibrotic scores were improved, highlighting a non-negligible benefit of bariatric surgery in this small-scale study.

Bearing in mind the increased prevalence (~80%) of steatosis in morbidly obese patients (BMI > 40 kg/m^2)[92], several clinical implications can be made regarding kidney outcomes. To begin with, compared with individuals who have undergone a bariatric surgery procedure, severely obese subjects had greater odds of having stage III CKD (OR 3.10, 95%CI: 3.05-3.14, $P < 0.001$) and end-stage renal disease (OR 1.13, 95%CI: 1.09-1.18, $P < 0.001$). This finding was consistent even after adjustment for CKD risk factors[93]. The performance of sleeve gastrectomy could have renoprotective effects, as shown in a retrospective analysis of 1330 individuals undergoing this procedure. The investigators noted a greater improvement of eGFR in subjects with impaired kidney function 12 mo after the procedure[82]. A rise in eGFR, together with albuminuria reduction, was observed by Wee *et al*[83] in their retrospective study of 557 Asian patients after metabolic bariatric surgery. Importantly, the CKD stage improved in 12.9% of the study participants, while the prevalence of albuminuria (UACR > 3.5 mg/mmol) decreased from 24.8% to 1.9% at the 1-year follow-up[83]. Fathy *et al*[84] also noted an astonishing albuminuria remission rate (83%) in 137 non-diabetic, non-hypertensive, severely obese subjects with albuminuria who underwent bariatric surgery. Moreover, in another study, subjects undergoing bariatric surgery had a lesser incidence of kidney disease than the control group (hazard ratio 0.46, 95%CI: 0.22-0.92)[85]. A systematic review and meta-analysis of 19 studies revealed that bariatric surgery led to ameliorated eGFR and lesser odds of incident albuminuria[94]. The observed benefits may be attributed to enhanced glomerular hyperfiltration, reduction in detrimental adipocyte-derived mediators such as leptin, and alterations in pro-inflammatory and pro-fibrotic molecule expression[95].

Table 1 Selected human studies assessing various treatment approaches in metabolic dysfunction-associated fatty liver disease and chronic kidney disease

Study	Treatment	Finding
MAFLD		
Meneses *et al*[69]	Bariatric surgery	Stabilization of fibrosis or complete resolution; ↓ NAFLD fibrosis score
Li *et al*[70]	GLP1-RA	↓ Liver fat
Morieri *et al*[71]	GLP1-RA	↓ MAFLD prevalence
Jianping *et al*[72]	GLP1-RA	Improvement in histological MAFLD features
Akuta *et al*[73]	Canagliflozin	↓ Histological steatosis, lobular inflammation, and fibrosis stage
Takahashi *et al*[74]	Ipragliflozin	↓ Hepatic fibrosis; Steatohepatitis resolution
Pakravan *et al*[75]	Melatonin	↓ Inflammation; Improvement of ultrasonographic fatty liver grade
Akhavan *et al*[76]	Melatonin	↓ Hepatic enzyme levels
Rinella *et al*[77]	Obeticholic acid	↓ Hepatic enzyme levels↓ Liver fibrosis
Neuschwander-Tetri *et al*[78]	Obeticholic acid	Improvement in histological features
Mohamad Nor *et al*[79]	Probiotics	↔ Elastography-derived hepatic steatosis and fibrosis
Derosa *et al*[80]	Probiotics	↓ Hepatic steatosis index; ↓ Ultrasonographic steatosis
Musazadeh *et al*[81]	Probiotics	↓ Hepatic enzyme levels
CKD		
Funes *et al*[82]	Bariatric surgery	↑ eGFR
Wee *et al*[83]	Bariatric surgery	↑ eGFR↓ Albuminuria
Fathy *et al*[84]	Bariatric surgery	↓ Albuminuria
Dash *et al*[85]	Bariatric surgery	↓ Kidney disease incidence
Shaman *et al*[86]	GLP1-RAs	↓ Albuminuria; Halted eGFR decline
Perkovic *et al*[87]	Canagliflozin	Reduction in the renal outcome (ESKD, doubling of serum creatinine, or renal death) by 34%
Heerspink *et al*[88]	Dapagliflozin	Reduction in the renal outcome (decline in eGFR of ≥ 50%, ESKD, or renal death) by 44%
Bhatt *et al*[89]	Sotagliflozin	Reduction in the renal outcome (decline in eGFR of ≥ 50%, ESKD, renal transplantation) by 29%
Wang *et al*[90]	Probiotic	Halted eGFR decline; ↓ Inflammation

↑: Increase; ↓: Decrease; ↔: No change. CKD: Chronic kidney disease; eGFR: Estimated glomerular filtration rate; ESKD: End-stage kidney disease; GLP1-RA: Glucagon-like peptide 1 receptor agonist; MAFLD: Metabolic dysfunction-associated fatty liver disease; NAFLD: Non-alcoholic fatty liver disease.

GLP1-R agonists

GLP1-R agonists (GLP1-RAs) are novel potent antidiabetic agents with proven efficacy in reducing major adverse cardiovascular events. Besides their glucose-lowering action, their beneficial hepatic effects may be related to the influence on the AMPK/mTOR pathway, as shown by Reis-Barbosa *et al*[96] in obese C57BL/6 mice treated with subcutaneous semaglutide. Other inflammatory and oxidative pathways in the liver could be inhibited by GLP1-RAs, such as the receptor for advanced glycation end products/nicotinamide-adenine dinucleotide phosphate oxidase 2, limiting liver injury and fibrosis in mice on a high-fat diet[97]. Concerning human studies, patients with MAFLD treated with GLP1-RAs have exhibited a significant reduction in liver fat, which may be positively correlated to fibroblast growth factor 21[70]. The use of GLP1-RAs also resulted in a significant reduction of MAFLD prevalence (defined based on hepatic steatosis index > 36) during a 24-mo follow-up[71]. Interestingly, the effect was evident only in subjects on human-based GLP1-RAs[71]. Moreover, in a meta-analysis of 4 randomized clinical trials, semaglutide was associated with significant decreases in body weight, alanine aminotransferase, liver steatosis, and stiffness[98]. GLP1-RAs may also improve histologic features on MAFLD, such as liver fat deposition, steatohepatitis, and fibrosis, as shown by the systematic review and meta-analysis of Jianping *et al*[72].

GLP1-RAs have shown benefits in preventing the development or halting the progression of CKD. As demonstrated above, their effect in ameliorating steatosis and promoting anti-oxidative and anti-inflammatory actions may be among the determining factors in this renoprotective effect, together with weight loss, blood pressure, and glucose-lowering[99]. Other speculated mechanisms include glomerular hyperfiltration, the regulation of the renin-angiotensin system, sodium-hydrogen exchanger-3, and renal endothelial vasodilation[100]. Regarding clinical evidence, and as recently shown in a pooled analysis of the SUSTAIN 6 and LEADER trials of patients with T2DM, semaglutide and liraglutide diminished albuminuria and eGFR decline, especially in subjects with CKD (eGFR < 60 mL/min/1.73 m^2)[86]. Moreover, efpeglenatide, an exendin-4-based GLP1-RA, also led to favorable renal outcomes compared to placebo in the AMPLITUDE-O trial of individuals with T2DM, irrespective of eGFR and concurrent sodium-glucose co-transporter-2 (SGLT2) inhibitor use[101,102]. As far as head-to-head comparisons, the renoprotective effects of GLP1-RAs were of greater magnitude compared with dipeptidyl peptidase-4 inhibitors[103], whereas SGLT2 inhibitors may promote increased renal benefits[104,105].

Dual GLP1 and glucose-dependent insulinotropic peptide receptor agonists have recently emerged into the spotlight owing to the results of the SURMOUNT-1 clinical trial of tirzepatide for the treatment of obesity[106]. Regarding FLD, the administration of a hybrid agonist by the name of 19W in C57BL/6J on a high-fat diet decreased the area of liver fibrosis[107]. Moreover, dual GLP1/2 receptor agonists may also ameliorate NASH prognosis, as shown in C57BL/6J mice on a high-fat diet/high fructose and sucrose solution through an improvement in liver fibrosis[108]. However, these concepts need further validation in preclinical settings. Concerning clinical evidence, tirzepatide dose-dependently ameliorated biomarkers of NASH such as alanine transaminase, aspartate aminotransferase, keratin-18, and procollagen III compared to placebo. At the same time, it was associated with an increase in adiponectin[109]. Lastly, in a recently published substudy of the SURPASS-3 MRI clinical trial, administration of tirzepatide in patients with T2DM decreased the liver fat content along with the volume of visceral and abdominal subcutaneous adipose tissue, compared to insulin degludec[110].

SGLT2 inhibitors

SGLT2 inhibitors have been at the forefront of scientific research owing to the remarkable reduction in the rate of heart failure hospitalization and their ability to impact cardiac remodeling[111,112]. Their pleiotropic mechanisms of action have been a topic of continuous investigation[111,113], and their therapeutic indications are constantly expanding. In the field of MAFLD, specifically in obese, diabetic mice with FLD treated with empagliflozin, Kurtz *et al*[114] documented a reduction in hepatic steatosis, which was correlated with the whitening of the adipose tissue. Empagliflozin may also attenuate hepatocyte lipotoxicity through the calcium/calmodulin dependent protein kinase beta/AMPKα pathway[115]. Another SGLT2 inhibitor, ipragliflozin, ameliorated the progression of MAFLD in STAM mice with β cell depletion, evidenced by decreased histologic steatosis, hepatocyte ballooning, inflammation, and fibrosis[116]. This effect was accompanied by antioxidant and mitochondrial transport-related gene upregulation, and overexpression of miR-19b-3p[116]. Additionally, dapagliflozin reduced liver fat accumulation in male NIH mice on a high-fat diet by acting on the AMPK/mTOR pathway [117]. Moving to clinical evidence, empagliflozin may lessen liver fibrosis, insulin resistance, and hepatic enzyme concentrations, as shown by the systematic review and meta-analysis of Zhang *et al* [118]. An interesting study on the importance of SGLT2 inhibition in MAFLD was performed by Akuta *et al*[73], who retrospectively reviewed patients with T2DM and FLD initiated on canagliflozin with consequent biopsy results over a period of 5 years. Compared to pre-treatment biopsy, the investigators noted a histologic improvement in 50% of the participants and a decrease in steatosis, lobular inflammation, and fibrosis stage in 67%, 33%, and 33%, respectively, at the 5th year. In line with this study, ipragliflozin use in patients with T2DM and FLD led to significant improvements in hepatic fibrosis and greater rates of steatohepatitis resolution compared to the control group[74]. According to the available evidence, we can assume that SGLT2 inhibitors will become an essential tool in the prevention and treatment of MAFLD.

While the use of SGLT2 inhibitors in MAFLD is gaining ground, this drug class is an established treatment option for CKD. Among the putative nephroprotective mechanisms are the regulation of autophagy and the resulting inflammation, oxidative stress, endothelial dysfunction, fibrosis, and apoptosis, the reduction of intraglomerular and blood pressure, and the improvement of podocytopathy. Large-scale randomized clinical trials on CKD patients such as CREDENCE[87], DAPA-CKD [88], and SCORED[89] demonstrated the unequivocal benefit of SGLT2 inhibition in reducing the rate of adverse renal outcomes and eGFR decline. The upcoming EMPA-KIDNEY trial was stopped early due to clear efficacy detected in the interim analysis, and the detailed results are eagerly awaited. Subanalyses of the abovementioned trials stressed the effect of SGLT2 inhibitors on kidney outcomes independently of T2DM status, baseline hemoglobin A1c, CKD etiology, and stage[119-122]. The upcoming revision of existing CKD guidelines should incorporate this option in CKD treatment algorithms.

Melatonin

Melatonin, a crucial hormone produced in response to darkness, could be an additional approach to managing MAFLD and CKD due to its pleiotropic effects, as we have previously reviewed[123]. Starting

with its impact on MAFLD, fine particulate matter-induced hepatic steatosis was ameliorated with the administration of melatonin in apolipoprotein E knockout (ApoE$^{-/-}$) mice through anti-oxidative mechanisms involving protein tyrosine phosphatase 1B and nuclear factor erythroid 2-related factor 2 signaling pathways[124]. Furthermore, melatonin promoted anti-inflammatory actions by modulating NACHT, LRR, and PYD domain-containing protein 3 inflammasome activation and downregulating the toll-like receptor 4/NF-κB pathway in C57BL/6 mice models of high-fat diet-induced steatohepatitis [125]. This resulted in histopathological improvement of steatosis, ballooning, inflammation, fibrosis, and overall disease score[125]. In clinical studies, the administration of oral melatonin thrice daily for 3 mo ameliorated metabolic and inflammatory indices, as well as ultrasonography fatty liver grade, in patients with histologically proven NAFLD[75]. In a meta-analysis of studies with NAFLD patients, alanine transaminase, alkaline phosphatase, gamma-glutamyl transferase, triglycerides, and total cholesterol were significantly reduced after melatonin supplementation[76]. However, more clinical trials are needed to improve our understanding of the importance of melatonin treatment in MAFLD development, progression, and prognosis.

Melatonin supplementation has also been attempted in CKD, both preclinically and clinically. Based on experimental studies, several mechanisms of nephroprotection have been suggested, including anti-oxidative, anti-inflammatory, anti-fibrotic, and anti-apoptotic[123]. Although there is no reliable clinical evidence concerning CKD prognosis after melatonin therapy, human trials have proven an anti-oxidative and anti-inflammatory effect, paired with improved glycemia[126,127]. Moreover, ameliorating mitochondrial damage and promoting autophagy could represent other putative effects of melatonin treatment[123].

Farnesoid X receptor agonists

Farnesoid X receptor agonists have demonstrated efficacy both in fatty liver disease regression and kidney disease. The most commonly used agent of this drug class, obeticholic acid, at a dose of 25 mg, led to significant improvement in liver function tests, elastography-derived and histologically proven liver fibrosis in patients with steatohepatitis and liver fibrosis (F2-F3)[77]. Based on the results of the FLINT trial of patients with non-cirrhotic, non-alcoholic steatohepatitis, obeticholic acid 25 mg administration led to an improvement in liver histology in 45% of the participants compared to in the control group (relative risk 1.9, 95%CI: 1.3-2.8)[78]. Although the dosage of 25 mg may be more efficacious than 10 mg, it may be met with a more significant burden of side effects and possibly higher discontinuation rates[128]. Preclinical evidence has suggested the potential of farnesoid X receptor agonists in experimental kidney disease by abrogating inflammation, oxidative stress, fibrosis, and apoptosis[129-132]. Due to the lack of clinical data, the efficacy of farnesoid X receptor agonists in CKD remains speculative to date.

Gut microbiome modulation

Targeting the gut microbiome may represent an appealing approach to the holistic management of MAFLD and CKD. Probiotics such as *Bifidobacterium animalis, B. bifidum, B. adolescentis, Lactobacillus paracasei, L. plantarum, L. reuteri,* and *Weissella cibaria* have been assessed in preclinical FLD models and may alter gut permeability, ultimately affecting the processes of inflammation and oxidative stress among others[133-138]. Unfortunately, a probiotic supplement containing six different Lactobacillus and Bifidobacterium species for 6 mo did not improve hepatic steatosis and fibrosis evaluated by elastography in ultrasonography-diagnosed NAFLD subjects[79]. By contrast, a high-concentration probiotic combination of *Streptococcus thermophilus*, multiple *Bifidobacteria* and *Lactobacilli* led to a reduction of hepatic steatosis index as well as ultrasonographic steatosis in a double-blind, placebo-controlled, randomized clinical trial of NAFLD patients[80]. A recently reported umbrella systematic review and meta-analysis also suggested liver biochemical improvement through the administration of probiotics in NAFLD patients[81]. Although probiotics appear helpful in experimental FLD settings, more clinical trials are required to improve our understanding of their importance in human MAFLD.

Moving to CKD, *L. rhamnosus* administration for 14 wk in 5/6 nephrectomized mice diminished gut-derived uremic toxins and systemic inflammatory markers by restoring intestinal integrity and protecting against renal fibrosis[139]. Anti-inflammatory, anti-apoptotic, and anti-fibrotic effects with *L. rhamnosus* were demonstrated in cisplatin-induced CKD rat models by acting on the MAPK/NF-κB/cyclooxygenase-2, the p53/B-cell lymphoma 2-associated X protein/caspase-3, and the signal transducer and activator of 3 pathway[140]. Moreover, a lactobacillus mixture consisting of *L. paracasei* and *L. plantarum* led to attenuated kidney injury, inflammation, and fibrosis in adenine-induced CKD mouse models, while also restoring gut microbial composition[141]. Translating these findings in a clinical setting of patients with advanced CKD, 6 mo of treatment with a probiotic formulation containing *L. acidophilus*, *B. longum*, and *B. bifidum* significantly halted the eGFR decline, together with lowering of inflammatory markers[90].

Although still experimental, TMAO inhibitors may represent a possible approach to modulating gut microbiota. Using 3,3-dimethyl-1-butanol, a trimethylamine formation inhibitor, decreased plasma TMAO levels and attenuated renal inflammation, oxidative stress, and fibrosis in C57BL/6 mice on a high-fat diet[142]. Importantly, no changes in blood pressure and weight adiposity parameters were noted[142]. Iodomethylcholine (IMC), a selective gut microbial choline TMA-lyase inhibitor, was also

able to diminish TMAO production and revert the renal function decline and tubulointerstitial fibrosis in isoproterenol-induced CKD mouse models on a choline diet[143]. Similar observations were made in ApoE$^{-/-}$ mouse models with adenine-induced CKD treated with IMC, together with ameliorated microalbuminuria, cardiac hypertrophy, and vascular inflammation indices[144]. These molecules have not been assessed yet in FLD, and upcoming studies evaluating their efficacy are awaited.

CONCLUSION

In conclusion, it has become evident that the newly defined MAFLD is associated with high prevalence and mortality rates and is an independent predictor of CKD. The degree of hepatic steatosis and fibrosis in this group of patients correlates with kidney function indices such as urinary albumin-to-creatinine ratio and estimated glomerular filtration rate. This interaction is unsurprising, as these entities have shared risk factors and deleterious molecular mechanisms such as inflammation, oxidative stress, and gut dysbiosis. At the same time, gene polymorphisms associated with fatty liver disease predisposition may also propagate renal dysfunction. In the field of treatment, pharmacologic interventions have demonstrated considerable preclinical and clinical efficacy in ameliorating surrogate disease markers and clinical outcomes in these pathological states. Future studies should aim at the subpopulation of MAFLD patients with renal impairment to appropriately determine their prognosis and the impact of treatment approaches.

FOOTNOTES

Author contributions: Theofilis P contributed to conceiving the study; Theofilis P and Vordoni A contributed to the investigation; Theofilis P contributed to the visualization; Kalaitzidis RG contributed to the supervision; Theofilis P and Vordoni A wrote the original draft; Kalaitzidis RG edited the original draft; All authors have read and agreed to the published version of the manuscript.

Conflict-of-interest statement: The authors have no conflicts of interest to declare.

Open-Access: This article is an open-access article that was selected by an in-house editor and fully peer-reviewed by external reviewers. It is distributed in accordance with the Creative Commons Attribution NonCommercial (CC BY-NC 4.0) license, which permits others to distribute, remix, adapt, build upon this work non-commercially, and license their derivative works on different terms, provided the original work is properly cited and the use is non-commercial. See: https://creativecommons.org/Licenses/by-nc/4.0/

Country/Territory of origin: Greece

ORCID number: Panagiotis Theofilis 0000-0001-9260-6306; Aikaterini Vordoni 0000-0002-4532-0206; Rigas G Kalaitzidis 0000-0002-7773-7575.

S-Editor: Zhang H
L-Editor: Filipodia
P-Editor: Zhang H

REFERENCES

1 **Blüher M**. Obesity: global epidemiology and pathogenesis. *Nat Rev Endocrinol* 2019; **15**: 288-298 [PMID: 30814686 DOI: 10.1038/s41574-019-0176-8]
2 **Wang L**, Li X, Wang Z, Bancks MP, Carnethon MR, Greenland P, Feng YQ, Wang H, Zhong VW. Trends in Prevalence of Diabetes and Control of Risk Factors in Diabetes Among US Adults, 1999-2018. *JAMA* 2021 [PMID: 34170288 DOI: 10.1001/jama.2021.9883]
3 **Le MH**, Yeo YH, Li X, Li J, Zou B, Wu Y, Ye Q, Huang DQ, Zhao C, Zhang J, Liu C, Chang N, Xing F, Yan S, Wan ZH, Tang NSY, Mayumi M, Liu X, Rui F, Yang H, Yang Y, Jin R, Le RHX, Xu Y, Le DM, Barnett S, Stave CD, Cheung R, Zhu Q, Nguyen MH. 2019 Global NAFLD Prevalence: A Systematic Review and Meta-analysis. *Clin Gastroenterol Hepatol* 2021 [PMID: 34890795 DOI: 10.1016/j.cgh.2021.12.002]
4 **Younossi ZM**, Golabi P, de Avila L, Paik JM, Srishord M, Fukui N, Qiu Y, Burns L, Afendy A, Nader F. The global epidemiology of NAFLD and NASH in patients with type 2 diabetes: A systematic review and meta-analysis. *J Hepatol* 2019; **71**: 793-801 [PMID: 31279902 DOI: 10.1016/j.jhep.2019.06.021]
5 **Eslam M**, Newsome PN, Sarin SK, Anstee QM, Targher G, Romero-Gomez M, Zelber-Sagi S, Wai-Sun Wong V, Dufour JF, Schattenberg JM, Kawaguchi T, Arrese M, Valenti L, Shiha G, Tiribelli C, Yki-Järvinen H, Fan JG, Grønbæk H, Yilmaz Y, Cortez-Pinto H, Oliveira CP, Bedossa P, Adams LA, Zheng MH, Fouad Y, Chan WK, Mendez-Sanchez N, Ahn SH, Castera L, Bugianesi E, Ratziu V, George J. A new definition for metabolic dysfunction-associated fatty liver

disease: An international expert consensus statement. *J Hepatol* 2020; **73**: 202-209 [PMID: 32278004 DOI: 10.1016/j.jhep.2020.03.039]

6 **Lee H**, Lee YH, Kim SU, Kim HC. Metabolic Dysfunction-Associated Fatty Liver Disease and Incident Cardiovascular Disease Risk: A Nationwide Cohort Study. *Clin Gastroenterol Hepatol* 2021; **19**: 2138-2147.e10 [PMID: 33348045 DOI: 10.1016/j.cgh.2020.12.022]

7 **Liu J**, Ayada I, Zhang X, Wang L, Li Y, Wen T, Ma Z, Bruno MJ, de Knegt RJ, Cao W, Peppelenbosch MP, Ghanbari M, Li Z, Pan Q. Estimating Global Prevalence of Metabolic Dysfunction-Associated Fatty Liver Disease in Overweight or Obese Adults. *Clin Gastroenterol Hepatol* 2022; **20**: e573-e582 [PMID: 33618024 DOI: 10.1016/j.cgh.2021.02.030]

8 **Ruiz-Manriquez J**, Olivas-Martinez A, Chávez-García LC, Fernández-Ramírez A, Moctezuma-Velazquez C, Kauffman-Ortega E, Castro-Narro G, Astudillo-García F, Escalona-Nandez I, Aguilar-Salinas CA, Navarro-Alvarez N, Torre A. Prevalence of Metabolic-associated Fatty Liver Disease in Mexico and Development of a Screening Tool: The MAFLD-S Score. *Gastro Hep Advances* 2022; **1**: 352-358 [DOI: 10.1016/j.gastha.2021.12.011]

9 **Quek J**, Ng CH, Tang ASP, Chew N, Chan M, Khoo CM, Wei CP, Chin YH, Tay P, Lim G, Tan DJH, Lim WH, Chan KE, Teng M, Tan E, Tamaki N, Huang DQ, Siddiqui MS, Young DY, Noureddin M, Muthiah MD. Metabolic Associated Fatty Liver Disease Increases the Risk of Systemic Complications and Mortality. A Meta-Analysis and Systematic Review of 12 620 736 Individuals. *Endocr Pract* 2022; **28**: 667-672 [PMID: 35364328 DOI: 10.1016/j.eprac.2022.03.016]

10 **Jung CY**, Koh HB, Park KH, Joo YS, Kim HW, Ahn SH, Park JT, Kim SU. Metabolic dysfunction-associated fatty liver disease and risk of incident chronic kidney disease: A nationwide cohort study. *Diabetes Metab* 2022; **48**: 101344 [PMID: 35346856 DOI: 10.1016/j.diabet.2022.101344]

11 **Tanaka M**, Mori K, Takahashi S, Higashiura Y, Ohnishi H, Hanawa N, Furuhashi M. Metabolic dysfunction-associated fatty liver disease predicts new onset of chronic kidney disease better than does fatty liver or nonalcoholic fatty liver disease. *Nephrol Dial Transplant* 2022 [PMID: 35612975 DOI: 10.1093/ndt/gfac188]

12 **Liang Y**, Chen H, Liu Y, Hou X, Wei L, Bao Y, Yang C, Zong G, Wu J, Jia W. Association of MAFLD With Diabetes, Chronic Kidney Disease, and Cardiovascular Disease: A 4.6-Year Cohort Study in China. *J Clin Endocrinol Metab* 2022; **107**: 88-97 [PMID: 34508601 DOI: 10.1210/clinem/dgab641]

13 **Deng Y**, Zhao Q, Gong R. Association Between Metabolic Associated Fatty Liver Disease and Chronic Kidney Disease: A Cross-Sectional Study from NHANES 2017-2018. *Diabetes Metab Syndr Obes* 2021; **14**: 1751-1761 [PMID: 33911888 DOI: 10.2147/DMSO.S292926]

14 **Ciardullo S**, Ballabeni C, Trevisan R, Perseghin G. Liver Stiffness, Albuminuria and Chronic Kidney Disease in Patients with NAFLD: A Systematic Review and Meta-Analysis. *Biomolecules* 2022; **12** [PMID: 35053253 DOI: 10.3390/biom12010105]

15 **Freitas M**, Macedo Silva V, Xavier S, Magalhães J, Marinho C, Cotter J. Early Kidney Dysfunction in Metabolic-Associated Fatty Liver Disease: Is Transient Elastography Useful as a Screening Method? *Dig Dis* 2021; **39**: 653-662 [PMID: 33508843 DOI: 10.1159/000514811]

16 **Marc L**, Mihaescu A, Lupusoru R, Grosu I, Gadalean F, Bob F, Chisavu L, Olariu N, Tucicovschi V, Timar B, Sporea I, Timar R, Schiller A. Liver Steatosis: Better Predictor of CKD in MAFLD Than Liver Fibrosis as Determined by Transient Elastography With Controlled Attenuation Parameter. *Front Med (Lausanne)* 2021; **8**: 788881 [PMID: 35096879 DOI: 10.3389/fmed.2021.788881]

17 **Duan J**, Wang C, Liu D, Qiao Y, Pan S, Jiang D, Zhao Z, Liang L, Tian F, Yu P, Zhang Y, Zhao H, Liu Z. Prevalence and risk factors of chronic kidney disease and diabetic kidney disease in Chinese rural residents: a cross-sectional survey. *Sci Rep* 2019; **9**: 10408 [PMID: 31320683 DOI: 10.1038/s41598-019-46857-7]

18 **Alkerwi A**, Sauvageot N, El Bahi I, Delagardelle C, Beissel J, Noppe S, Roderick PJ, Mindell JS, Stranges S. Prevalence and related risk factors of chronic kidney disease among adults in Luxembourg: evidence from the observation of cardiovascular risk factors (ORISCAV-LUX) study. *BMC Nephrol* 2017; **18**: 358 [PMID: 29221436 DOI: 10.1186/s12882-017-0772-6]

19 **Ordunez P**, Martinez R. Belize population-based survey confirms the high prevalence of Chronic Kidney Disease and its risk factors in Central America. *Lancet Reg Health Am* 2021; **1**: None [PMID: 34568864 DOI: 10.1016/j.lana.2021.100035]

20 **Kim GS**, Oh HH, Kim SH, Kim BO, Byun YS. Association between prediabetes (defined by $HbA1_C$, fasting plasma glucose, and impaired glucose tolerance) and the development of chronic kidney disease: a 9-year prospective cohort study. *BMC Nephrol* 2019; **20**: 130 [PMID: 30992067 DOI: 10.1186/s12882-019-1307-0]

21 **Chen J**, Muntner P, Hamm LL, Fonseca V, Batuman V, Whelton PK, He J. Insulin resistance and risk of chronic kidney disease in nondiabetic US adults. *J Am Soc Nephrol* 2003; **14**: 469-477 [PMID: 12538749 DOI: 10.1097/01.asn.0000046029.53933.09]

22 **Zhu C**, Huang D, Ma H, Qian C, You H, Bu L, Qu S. High-Sensitive CRP Correlates With the Severity of Liver Steatosis and Fibrosis in Obese Patients With Metabolic Dysfunction Associated Fatty Liver Disease. *Front Endocrinol (Lausanne)* 2022; **13**: 848937 [PMID: 35620390 DOI: 10.3389/fendo.2022.848937]

23 **Theofilis P**, Vordoni A, Nakas N, Kalaitzidis RG. Endothelial Dysfunction in Nonalcoholic Fatty Liver Disease: A Systematic Review and Meta-Analysis. *Life (Basel)* 2022; **12** [PMID: 35629385 DOI: 10.3390/Life12050718]

24 **Masarone M**, Rosato V, Dallio M, Gravina AG, Aglitti A, Loguercio C, Federico A, Persico M. Role of Oxidative Stress in Pathophysiology of Nonalcoholic Fatty Liver Disease. *Oxid Med Cell Longev* 2018; **2018**: 9547613 [PMID: 29991976 DOI: 10.1155/2018/9547613]

25 **Qu W**, Ma T, Cai J, Zhang X, Zhang P, She Z, Wan F, Li H. Liver Fibrosis and MAFLD: From Molecular Aspects to Novel Pharmacological Strategies. *Front Med (Lausanne)* 2021; **8**: 761538 [PMID: 34746195 DOI: 10.3389/fmed.2021.761538]

26 **Stenvinkel P**, Chertow GM, Devarajan P, Levin A, Andreoli SP, Bangalore S, Warady BA. Chronic Inflammation in Chronic Kidney Disease Progression: Role of Nrf2. *Kidney Int Rep* 2021; **6**: 1775-1787 [PMID: 34307974 DOI: 10.1016/j.ekir.2021.04.023]

27 **Raj DS**, Pecoits-Filho R, Kimmel PL. Chapter 17 - Inflammation in Chronic Kidney Disease. In: Kimmel PL, Rosenberg

ME. Chronic Renal Disease. San Diego: Academic Press, 2015: 199-212
28 **Sagris M**, Theofilis P, Antonopoulos AS, Oikonomou E, Paschaliori C, Galiatsatos N, Tsioufis K, Tousoulis D. Inflammation in Coronary Microvascular Dysfunction. *Int J Mol Sci* 2021; **22** [PMID: 34948272 DOI: 10.3390/ijms222413471]
29 **Sagris M**, Theofilis P, Antonopoulos AS, Tsioufis C, Oikonomou E, Antoniades C, Crea F, Kaski JC, Tousoulis D. Inflammatory Mechanisms in COVID-19 and Atherosclerosis: Current Pharmaceutical Perspectives. *Int J Mol Sci* 2021; **22** [PMID: 34205487 DOI: 10.3390/ijms22126607]
30 **Oikonomou E**, Leopoulou M, Theofilis P, Antonopoulos AS, Siasos G, Latsios G, Mystakidi VC, Antoniades C, Tousoulis D. A link between inflammation and thrombosis in atherosclerotic cardiovascular diseases: Clinical and therapeutic implications. *Atherosclerosis* 2020; **309**: 16-26 [PMID: 32858395 DOI: 10.1016/j.atherosclerosis.2020.07.027]
31 **Theofilis P**, Sagris M, Oikonomou E, Antonopoulos AS, Siasos G, Tsioufis C, Tousoulis D. Inflammatory Mechanisms Contributing to Endothelial Dysfunction. *Biomedicines* 2021; **9** [PMID: 34356845 DOI: 10.3390/biomedicines9070781]
32 **Theofilis P**, Sagris M, Antonopoulos AS, Oikonomou E, Tsioufis C, Tousoulis D. Inflammatory Mediators of Platelet Activation: Focus on Atherosclerosis and COVID-19. *Int J Mol Sci* 2021; **22** [PMID: 34681830 DOI: 10.3390/ijms222011170]
33 **Stojsavljević S**, Gomerčić Palčić M, Virović Jukić L, Smirčić Duvnjak L, Duvnjak M. Adipokines and proinflammatory cytokines, the key mediators in the pathogenesis of nonalcoholic fatty liver disease. *World J Gastroenterol* 2014; **20**: 18070-18091 [PMID: 25561778 DOI: 10.3748/wjg.v20.i48.18070]
34 **Rüster C**, Wolf G. Adipokines promote chronic kidney disease. *Nephrol Dial Transplant* 2013; **28** Suppl 4: iv8-i14 [PMID: 24179016 DOI: 10.1093/ndt/gft191]
35 **Jiménez-Cortegana C**, García-Galey A, Tami M, Del Pino P, Carmona I, López S, Alba G, Sánchez-Margalet V. Role of Leptin in Non-Alcoholic Fatty Liver Disease. *Biomedicines* 2021; **9** [PMID: 34209386 DOI: 10.3390/biomedicines9070762]
36 **Savvidou S**, Hytiroglou P, Orfanou-Koumerkeridou H, Panderis A, Frantzoulis P, Goulis J. Low serum adiponectin levels are predictive of advanced hepatic fibrosis in patients with NAFLD. *J Clin Gastroenterol* 2009; **43**: 765-772 [PMID: 19525862 DOI: 10.1097/MCG.0b013e31819e9048]
37 **Mikami K**, Endo T, Sawada N, Igarashi G, Kimura M, Hasegawa T, Iino C, Tomita H, Sawada K, Nakaji S, Matsuzaka M, Torok NJ, Fukuda S. Leptin/adiponectin ratio correlates with hepatic steatosis but not arterial stiffness in nonalcoholic fatty liver disease in Japanese population. *Cytokine* 2020; **126**: 154927 [PMID: 31756645 DOI: 10.1016/j.cyto.2019.154927]
38 **Ma D**, Feitosa MF, Wilk JB, Laramie JM, Yu K, Leiendecker-Foster C, Myers RH, Province MA, Borecki IB. Leptin is associated with blood pressure and hypertension in women from the National Heart, Lung, and Blood Institute Family Heart Study. *Hypertension* 2009; **53**: 473-479 [PMID: 19204185 DOI: 10.1161/HYPERTENSIONAHA.108.118133]
39 **Kümpers P**, Gueler F, Rong S, Mengel M, Tossidou I, Peters I, Haller H, Schiffer M. Leptin is a coactivator of TGF-beta in unilateral ureteral obstructive kidney disease. *Am J Physiol Renal Physiol* 2007; **293**: F1355-F1362 [PMID: 17686962 DOI: 10.1152/ajprenal.00003.2007]
40 **Park YC**, Lee S, Kim YS, Park JM, Han K, Lee H, Hong KW, Kim JK, Cho ES, Chung TH, Kim BT, Koh SB. Serum leptin level and incidence of CKD: a longitudinal study of adult enrolled in the Korean genome and epidemiology study(KoGES). *BMC Nephrol* 2022; **23**: 197 [PMID: 35619087 DOI: 10.1186/s12882-022-02795-7]
41 **Zhao D**, Zhu X, Jiang L, Huang X, Zhang Y, Wei X, Zhao X, Du Y. Advances in understanding the role of adiponectin in renal fibrosis. *Nephrology (Carlton)* 2021; **26**: 197-203 [PMID: 33073881 DOI: 10.1111/nep.13808]
42 **Song SH**, Oh TR, Choi HS, Kim CS, Ma SK, Oh KH, Ahn C, Kim SW, Bae EH. High serum adiponectin as a biomarker of renal dysfunction: Results from the KNOW-CKD study. *Sci Rep* 2020; **10**: 5598 [PMID: 32221363 DOI: 10.1038/s41598-020-62465-2]
43 **Fumeron F**, El Boustany R, Bastard JP, Fellahi S, Balkau B, Marre M, Venteclef N, Velho G, Roussel R. Plasma total adiponectin and changes in renal function in a cohort from the community: the prospective Data from an Epidemiological Study on the Insulin Resistance Syndrome study. *Nephrol Dial Transplant* 2021; **36**: 2058-2065 [PMID: 33141880 DOI: 10.1093/ndt/gfaa228]
44 **Li D**, Lu Y, Yuan S, Cai X, He Y, Chen J, Wu Q, He D, Fang A, Bo Y, Song P, Bogaert D, Tsilidis K, Larsson SC, Yu H, Zhu H, Theodoratou E, Zhu Y, Li X. Gut microbiota-derived metabolite trimethylamine-N-oxide and multiple health outcomes: an umbrella review and updated meta-analysis. *Am J Clin Nutr* 2022; **116**: 230-243 [PMID: 35348578 DOI: 10.1093/ajcn/nqac074]
45 **Tan X**, Liu Y, Long J, Chen S, Liao G, Wu S, Li C, Wang L, Ling W, Zhu H. Trimethylamine N-Oxide Aggravates Liver Steatosis through Modulation of Bile Acid Metabolism and Inhibition of Farnesoid X Receptor Signaling in Nonalcoholic Fatty Liver Disease. *Mol Nutr Food Res* 2019; **63**: e1900257 [PMID: 31095863 DOI: 10.1002/mnfr.201900257]
46 **Zhao ZH**, Xin FZ, Zhou D, Xue YQ, Liu XL, Yang RX, Pan Q, Fan JG. Trimethylamine N-oxide attenuates high-fat high-cholesterol diet-induced steatohepatitis by reducing hepatic cholesterol overload in rats. *World J Gastroenterol* 2019; **25**: 2450-2462 [PMID: 31171889 DOI: 10.3748/wjg.v25.i20.2450]
47 **Chen YM**, Liu Y, Zhou RF, Chen XL, Wang C, Tan XY, Wang LJ, Zheng RD, Zhang HW, Ling WH, Zhu HL. Associations of gut-flora-dependent metabolite trimethylamine-N-oxide, betaine and choline with non-alcoholic fatty liver disease in adults. *Sci Rep* 2016; **6**: 19076 [PMID: 26743949 DOI: 10.1038/srep19076]
48 **León-Mimila P**, Villamil-Ramírez H, Li XS, Shih DM, Hui ST, Ocampo-Medina E, López-Contreras B, Morán-Ramos S, Olivares-Arevalo M, Grandini-Rosales P, Macías-Kauffer L, González-González I, Hernández-Pando R, Gómez-Pérez F, Campos-Pérez F, Aguilar-Salinas C, Larrieta-Carrasco E, Villarreal-Molina T, Wang Z, Lusis AJ, Hazen SL, Huertas-Vazquez A, Canizales-Quinteros S. Trimethylamine N-oxide levels are associated with NASH in obese subjects with type 2 diabetes. *Diabetes Metab* 2021; **47**: 101183 [PMID: 32791310 DOI: 10.1016/j.diabet.2020.07.010]
49 **Flores-Guerrero JL**, Post A, van Dijk PR, Connelly MA, Garcia E, Navis G, Bakker SJL, Dullaart RPF. Circulating trimethylamine-N-oxide is associated with all-cause mortality in subjects with nonalcoholic fatty liver disease. *Liver Int*

2021; **41**: 2371-2382 [PMID: 33993608 DOI: 10.1111/liv.14963]
50 **Fang Q**, Zheng B, Liu N, Liu J, Liu W, Huang X, Zeng X, Chen L, Li Z, Ouyang D. Trimethylamine N-Oxide Exacerbates Renal Inflammation and Fibrosis in Rats With Diabetic Kidney Disease. *Front Physiol* 2021; **12**: 682482 [PMID: 34220546 DOI: 10.3389/fphys.2021.682482]
51 **Kapetanaki S**, Kumawat AK, Persson K, Demirel I. The Fibrotic Effects of TMAO on Human Renal Fibroblasts Is Mediated by NLRP3, Caspase-1 and the PERK/Akt/mTOR Pathway. *Int J Mol Sci* 2021; **22** [PMID: 34769294 DOI: 10.3390/ijms222111864]
52 **Lai Y**, Tang H, Zhang X, Zhou Z, Zhou M, Hu Z, Zhu F, Zhang L, Nie J. Trimethylamine-N-Oxide Aggravates Kidney Injury *via* Activation of p38/MAPK Signaling and Upregulation of HuR. *Kidney Blood Press Res* 2022; **47**: 61-71 [PMID: 34788763 DOI: 10.1159/000519603]
53 **Zeng Y**, Guo M, Fang X, Teng F, Tan X, Li X, Wang M, Long Y, Xu Y. Gut Microbiota-Derived Trimethylamine N-Oxide and Kidney Function: A Systematic Review and Meta-Analysis. *Adv Nutr* 2021; **12**: 1286-1304 [PMID: 33751019 DOI: 10.1093/advances/nmab010]
54 **Zhou Z**, Jin H, Ju H, Sun M, Chen H, Li L. Circulating Trimethylamine-N-Oxide and Risk of All-Cause and Cardiovascular Mortality in Patients With Chronic Kidney Disease: A Systematic Review and Meta-Analysis. *Front Med (Lausanne)* 2022; **9**: 828343 [PMID: 35433743 DOI: 10.3389/fmed.2022.828343]
55 **Magliocca G**, Mone P, Di Iorio BR, Heidland A, Marzocco S. Short-Chain Fatty Acids in Chronic Kidney Disease: Focus on Inflammation and Oxidative Stress Regulation. *Int J Mol Sci* 2022; **23** [PMID: 35628164 DOI: 10.3390/ijms23105354]
56 **Jia L**, Dong X, Li X, Jia R, Zhang HL. Benefits of resistant starch type 2 for patients with end-stage renal disease under maintenance hemodialysis: a systematic review and meta-analysis. *Int J Med Sci* 2021; **18**: 811-820 [PMID: 33437217 DOI: 10.7150/ijms.51484]
57 **Marzocco S**, Fazeli G, Di Micco L, Autore G, Adesso S, Dal Piaz F, Heidland A, Di Iorio B. Supplementation of Short-Chain Fatty Acid, Sodium Propionate, in Patients on Maintenance Hemodialysis: Beneficial Effects on Inflammatory Parameters and Gut-Derived Uremic Toxins, A Pilot Study (PLAN Study). *J Clin Med* 2018; **7** [PMID: 30274359 DOI: 10.3390/jcm7100315]
58 **Wang TY**, Wang RF, Bu ZY, Targher G, Byrne CD, Sun DQ, Zheng MH. Association of metabolic dysfunction-associated fatty liver disease with kidney disease. *Nat Rev Nephrol* 2022; **18**: 259-268 [PMID: 35013596 DOI: 10.1038/s41581-021-00519-y]
59 **Xu R**, Tao A, Zhang S, Deng Y, Chen G. Association between patatin-like phospholipase domain containing 3 gene (PNPLA3) polymorphisms and nonalcoholic fatty liver disease: a HuGE review and meta-analysis. *Sci Rep* 2015; **5**: 9284 [PMID: 25791171 DOI: 10.1038/srep09284]
60 **Sun DQ**, Zheng KI, Xu G, Ma HL, Zhang HY, Pan XY, Zhu PW, Wang XD, Targher G, Byrne CD, Chen YP, Yuan WJ, Zheng MH. PNPLA3 rs738409 is associated with renal glomerular and tubular injury in NAFLD patients with persistently normal ALT levels. *Liver Int* 2020; **40**: 107-119 [PMID: 31519069 DOI: 10.1111/liv.14251]
61 **Park S**, Lee S, Kim Y, Cho S, Kim K, Chul Kim Y, Han SS, Lee H, Lee JP, Joo KW, Lim CS, Kim YS, Kim DK. Causal effects from non-alcoholic fatty liver disease on kidney function: A Mendelian randomization study. *Liver Int* 2022; **42**: 412-418 [PMID: 34843158 DOI: 10.1111/liv.15118]
62 **Mantovani A**, Taliento A, Zusi C, Baselli G, Prati D, Granata S, Zaza G, Colecchia A, Maffeis C, Byrne CD, Valenti L, Targher G. PNPLA3 I148M gene variant and chronic kidney disease in type 2 diabetic patients with NAFLD: Clinical and experimental findings. *Liver Int* 2020; **40**: 1130-1141 [PMID: 32125756 DOI: 10.1111/liv.14419]
63 **Mantovani A**, Zusi C, Sani E, Colecchia A, Lippi G, Zaza GL, Valenti L, Byrne CD, Maffeis C, Bonora E, Targher G. Association between PNPLA3rs738409 polymorphism decreased kidney function in postmenopausal type 2 diabetic women with or without non-alcoholic fatty liver disease. *Diabetes Metab* 2019; **45**: 480-487 [PMID: 30763699 DOI: 10.1016/j.diabet.2019.01.011]
64 **Baratta F**, D'Erasmo L, Di Costanzo A, Umbro I, Pastori D, Angelico F, Del Ben M. Metabolic Syndrome but Not Fatty Liver-Associated Genetic Variants Correlates with Glomerular Renal Function Decline in Patients with Non-Alcoholic Fatty Liver Disease. *Biomedicines* 2022; **10** [PMID: 35327522 DOI: 10.3390/biomedicines10030720]
65 **Villani R**, Magnati GP, De Girolamo G, Sangineto M, Romano AD, Cassano T, Serviddio G. Genetic Polymorphisms and Clinical Features in Diabetic Patients With Fatty Liver: Results From a Single-Center Experience in Southern Italy. *Front Med (Lausanne)* 2021; **8**: 737759 [PMID: 34746177 DOI: 10.3389/fmed.2021.737759]
66 **Seko Y**, Yano K, Takahashi A, Okishio S, Kataoka S, Okuda K, Mizuno N, Takemura M, Taketani H, Umemura A, Nishikawa T, Yamaguchi K, Moriguchi M, Okanoue T, Itoh Y. FIB-4 Index and Diabetes Mellitus Are Associated with Chronic Kidney Disease in Japanese Patients with Non-Alcoholic Fatty Liver Disease. *Int J Mol Sci* 2019; **21** [PMID: 31881781 DOI: 10.3390/ijms21010171]
67 **Koo BK**, An JN, Joo SK, Kim D, Lee S, Bae JM, Park JH, Kim JH, Chang MS, Kim W. Association Between a Polymorphism in MBOAT7 and Chronic Kidney Disease in Patients With Biopsy-Confirmed Nonalcoholic Fatty Liver Disease. *Clin Gastroenterol Hepatol* 2020; **18**: 2837-2839.e2 [PMID: 31546054 DOI: 10.1016/j.cgh.2019.09.017]
68 **Sun DQ**, Wang TY, Zheng KI, Zhang HY, Wang XD, Targher G, Byrne CD, Chen YP, Yuan WJ, Jin Y, Zheng MH. The HSD17B13 rs72613567 variant is associated with lower levels of albuminuria in patients with biopsy-proven nonalcoholic fatty liver disease. *Nutr Metab Cardiovasc Dis* 2021; **31**: 1822-1831 [PMID: 33853719 DOI: 10.1016/j.numecd.2021.02.018]
69 **Meneses D**, Olveira A, Corripio R, Méndez MD, Romero M, Calvo-Viñuelas I, González-Pérez-de-Villar N, de-Cos-Blanco AI. The Benefit of Bariatric Surgery on Histological Features of Metabolic Associated Fatty Liver Disease Assessed Through Noninvasive Methods. *Obes Surg* 2022; **32**: 2682-2695 [PMID: 35697996 DOI: 10.1007/s11695-022-06153-2]
70 **Li X**, Wu X, Jia Y, Fu J, Zhang L, Jiang T, Liu J, Wang G. Liraglutide Decreases Liver Fat Content and Serum Fibroblast Growth Factor 21 Levels in Newly Diagnosed Overweight Patients with Type 2 Diabetes and Nonalcoholic Fatty Liver Disease. *J Diabetes Res* 2021; **2021**: 3715026 [PMID: 34660809 DOI: 10.1155/2021/3715026]
71 **Morieri ML**, Targher G, Lapolla A, D'Ambrosio M, Tadiotto F, Rigato M, Frison V, Paccagnella A, Simioni N, Avogaro

A, Fadini GP. Changes in markers of hepatic steatosis and fibrosis in patients with type 2 diabetes during treatment with glucagon-like peptide-1 receptor agonists. A multicenter retrospective longitudinal study. *Nutr Metab Cardiovasc Dis* 2021; **31**: 3474-3483 [PMID: 34629258 DOI: 10.1016/j.numecd.2021.08.049]

72 **Jianping W**, Xuelian Z, Anjiang W, Haiying X. Efficacy and Safety of Glucagon-like Peptide-1 Receptor Agonists in the Treatment of Metabolic Associated Fatty Liver Disease: A Systematic Review and Meta-analysis. *J Clin Gastroenterol* 2021; **55**: 586-593 [PMID: 34039937 DOI: 10.1097/MCG.0000000000001556]

73 **Akuta N**, Kawamura Y, Fujiyama S, Saito S, Muraishi N, Sezaki H, Hosaka T, Kobayashi M, Arase Y, Ikeda K, Suzuki F, Suzuki Y, Kumada H. Favorable impact of long-term SGLT2 inhibitor for NAFLD complicated by diabetes mellitus: A 5-year follow-up study. *Hepatol Commun* 2022; **6**: 2286-2297 [PMID: 35581956 DOI: 10.1002/hep4.2005]

74 **Takahashi H**, Kessoku T, Kawanaka M, Nonaka M, Hyogo H, Fujii H, Nakajima T, Imajo K, Tanaka K, Kubotsu Y, Isoda H, Oeda S, Kurai O, Yoneda M, Ono M, Kitajima Y, Tajiri R, Takamori A, Kawaguchi A, Aishima S, Kage M, Nakajima A, Eguchi Y, Anzai K. Ipragliflozin Improves the Hepatic Outcomes of Patients With Diabetes with NAFLD. *Hepatol Commun* 2022; **6**: 120-132 [PMID: 34558835 DOI: 10.1002/hep4.1696]

75 **Pakravan H**, Ahmadian M, Fani A, Aghaee D, Brumanad S, Pakzad B. The Effects of Melatonin in Patients with Nonalcoholic Fatty Liver Disease: A Randomized Controlled Trial. *Adv Biomed Res* 2017; **6**: 40 [PMID: 28503495 DOI: 10.4103/2277-9175.204593]

76 **Akhavan Rezayat A**, Ghasemi Nour M, Bondarsahebi Y, Hozhabrossadati SA, Amirkhanlou F, Akhavan Rezayat S, Kiani M, Imani B. The effects of melatonin therapy on the treatment of patients with Non-alcoholic steatohepatitis: A systematic review and Meta-analysis on clinical trial studies. *Eur J Pharmacol* 2021; **905**: 174154 [PMID: 34058202 DOI: 10.1016/j.ejphar.2021.174154]

77 **Rinella ME**, Dufour JF, Anstee QM, Goodman Z, Younossi Z, Harrison SA, Loomba R, Sanyal AJ, Bonacci M, Trylesinski A, Natha M, Shringarpure R, Granston T, Venugopal A, Ratziu V. Non-invasive evaluation of response to obeticholic acid in patients with NASH: Results from the REGENERATE study. *J Hepatol* 2022; **76**: 536-548 [PMID: 34793868 DOI: 10.1016/j.jhep.2021.10.029]

78 **Neuschwander-Tetri BA**, Loomba R, Sanyal AJ, Lavine JE, Van Natta ML, Abdelmalek MF, Chalasani N, Dasarathy S, Diehl AM, Hameed B, Kowdley KV, McCullough A, Terrault N, Clark JM, Tonascia J, Brunt EM, Kleiner DE, Doo E; NASH Clinical Research Network. Farnesoid X nuclear receptor ligand obeticholic acid for non-cirrhotic, non-alcoholic steatohepatitis (FLINT): a multicentre, randomised, placebo-controlled trial. *Lancet* 2015; **385**: 956-965 [PMID: 25468160 DOI: 10.1016/S0140-6736(14)61933-4]

79 **Mohamad Nor MH**, Ayob N, Mokhtar NM, Raja Ali RA, Tan GC, Wong Z, Shafiee NH, Wong YP, Mustangin M, Nawawi KNM. The Effect of Probiotics (MCP® BCMC® Strains) on Hepatic Steatosis, Small Intestinal Mucosal Immune Function, and Intestinal Barrier in Patients with Non-Alcoholic Fatty Liver Disease. *Nutrients* 2021; **13** [PMID: 34579068 DOI: 10.3390/nu13093192]

80 **Derosa G**, Guasti L, D'Angelo A, Martinotti C, Valentino MC, Di Matteo S, Bruno GM, Maresca AM, Gaudio GV, Maffioli P. Probiotic Therapy With VSL#3® in Patients With NAFLD: A Randomized Clinical Trial. *Front Nutr* 2022; **9**: 846873 [PMID: 35685888 DOI: 10.3389/fnut.2022.846873]

81 **Musazadeh V**, Roshanravan N, Dehghan P, Ahrabi SS. Effect of Probiotics on Liver Enzymes in Patients With Non-alcoholic Fatty Liver Disease: An Umbrella of Systematic Review and Meta-Analysis. *Front Nutr* 2022; **9**: 844242 [PMID: 35677540 DOI: 10.3389/fnut.2022.844242]

82 **Funes DR**, Montorfano L, Blanco DG, Cobos MS, Lo Menzo E, Szomstein S, Agrawal N, Rosenthal RJ. Sleeve gastrectomy in patients with severe obesity and baseline chronic kidney disease improves kidney function independently of weight loss: a propensity score matched analysis. *Surg Obes Relat Dis* 2022; **18**: 772-778 [PMID: 35331642 DOI: 10.1016/j.soard.2022.02.006]

83 **Wee Z**, Ganguly S, Tham KW, Lim CH, Tan JTH, Lee PC. Renal Outcomes 1 Year After Metabolic Bariatric Surgery in a Multi-ethnic Asian Cohort. *Obes Surg* 2021; **31**: 5358-5366 [PMID: 34586568 DOI: 10.1007/s11695-021-05732-z]

84 **Fathy E**, Aisha HAA, Abosayed AK, ElAnsary AMSEO, Al Aziz AA. Effect of Bariatric Surgery on Albuminuria in Non-Diabetic Non-Hypertensive Patients with Severe Obesity: a Short-Term Outcome. *Obes Surg* 2022; **32**: 2397-2402 [PMID: 35524905 DOI: 10.1007/s11695-022-06091-z]

85 **Dash S**, Everett K, Jackson T, Okrainec A, Urbach DR, Sockalingam S, Shah BR, Farkouh ME. Cardiorenal outcomes in eligible patients referred for bariatric surgery. *Obesity (Silver Spring)* 2021; **29**: 2035-2043 [PMID: 34724336 DOI: 10.1002/oby.23294]

86 **Shaman AM**, Bain SC, Bakris GL, Buse JB, Idorn T, Mahaffey KW, Mann JFE, Nauck MA, Rasmussen S, Rossing P, Wolthers B, Zinman B, Perkovic V. Effect of the Glucagon-Like Peptide-1 Receptor Agonists Semaglutide and Liraglutide on Kidney Outcomes in Patients With Type 2 Diabetes: Pooled Analysis of SUSTAIN 6 and LEADER. *Circulation* 2022; **145**: 575-585 [PMID: 34903039 DOI: 10.1161/CIRCULATIONAHA.121.055459]

87 **Perkovic V**, Jardine MJ, Neal B, Bompoint S, Heerspink HJL, Charytan DM, Edwards R, Agarwal R, Bakris G, Bull S, Cannon CP, Capuano G, Chu PL, de Zeeuw D, Greene T, Levin A, Pollock C, Wheeler DC, Yavin Y, Zhang H, Zinman B, Meininger G, Brenner BM, Mahaffey KW; CREDENCE Trial Investigators. Canagliflozin and Renal Outcomes in Type 2 Diabetes and Nephropathy. *N Engl J Med* 2019; **380**: 2295-2306 [PMID: 30990260 DOI: 10.1056/NEJMoa1811744]

88 **Heerspink HJL**, Stefánsson BV, Correa-Rotter R, Chertow GM, Greene T, Hou FF, Mann JFE, McMurray JJV, Lindberg M, Rossing P, Sjöström CD, Toto RD, Langkilde AM, Wheeler DC; DAPA-CKD Trial Committees and Investigators. Dapagliflozin in Patients with Chronic Kidney Disease. *N Engl J Med* 2020; **383**: 1436-1446 [PMID: 32970396 DOI: 10.1056/NEJMoa2024816]

89 **Bhatt DL**, Szarek M, Pitt B, Cannon CP, Leiter LA, McGuire DK, Lewis JB, Riddle MC, Inzucchi SE, Kosiborod MN, Cherney DZI, Dwyer JP, Scirica BM, Bailey CJ, Díaz R, Ray KK, Udell JA, Lopes RD, Lapuerta P, Steg PG; SCORED Investigators. Sotagliflozin in Patients with Diabetes and Chronic Kidney Disease. *N Engl J Med* 2021; **384**: 129-139 [PMID: 33200891 DOI: 10.1056/NEJMoa2030186]

90 **Wang IK**, Yen TH, Hsieh PS, Ho HH, Kuo YW, Huang YY, Kuo YL, Li CY, Lin HC, Wang JY. Effect of a Probiotic

Combination in an Experimental Mouse Model and Clinical Patients With Chronic Kidney Disease: A Pilot Study. *Front Nutr* 2021; **8**: 661794 [PMID: 34136518 DOI: 10.3389/fnut.2021.661794]

91 **Ciardullo S**, Pizzi M, Pizzi P, Oltolini A, Muraca E, Perseghin G. Prevalence of Elevated Liver Stiffness Among Potential Candidates for Bariatric Surgery in the United States. *Obes Surg* 2022; **32**: 712-719 [PMID: 34988895 DOI: 10.1007/s11695-021-05885-x]

92 **Hillenbrand A**, Kiebler B, Schwab C, Scheja L, Xu P, Henne-Bruns D, Wolf AM, Knippschild U. Prevalence of non-alcoholic fatty liver disease in four different weight related patient groups: association with small bowel length and risk factors. *BMC Res Notes* 2015; **8**: 290 [PMID: 26138508 DOI: 10.1186/s13104-015-1224-7]

93 **Funes DR**, Blanco DG, Hong L, Lo Menzo E, Szomstein S, Rosenthal RJ. Prevalence of chronic kidney disease and end-stage renal disease in a bariatric *vs* nonbariatric population: a retrospective analysis of the U.S. National Inpatient Sample database. *Surg Obes Relat Dis* 2022; **18**: 281-287 [PMID: 34756566 DOI: 10.1016/j.soard.2021.09.021]

94 **Lee Y**, Anvari S, Chu MM, Lovrics O, Khondker A, Malhan R, Aditya I, Doumouras AG, Walsh M, Hong D. Improvement of kidney function in patients with chronic kidney disease and severe obesity after bariatric surgery: A systematic review and meta-analysis. *Nephrology (Carlton)* 2022; **27**: 44-56 [PMID: 34375462 DOI: 10.1111/nep.13958]

95 **Morales E**, Porrini E, Martin-Taboada M, Luis-Lima S, Vila-Bedmar R, González de Pablos I, Gómez P, Rodríguez E, Torres L, Lanzón B, Rodríguez AE, Maíz M, Medina-Gómez G, Praga M. Renoprotective role of bariatric surgery in patients with established chronic kidney disease. *Clin Kidney J* 2021; **14**: 2037-2046 [PMID: 34476090 DOI: 10.1093/ckj/sfaa266]

96 **Reis-Barbosa PH**, Marcondes-de-Castro IA, Marinho TS, Aguila MB, Mandarim-de-Lacerda CA. The mTORC1/AMPK pathway plays a role in the beneficial effects of semaglutide (GLP-1 receptor agonist) on the liver of obese mice. *Clin Res Hepatol Gastroenterol* 2022; **46**: 101922 [PMID: 35427802 DOI: 10.1016/j.clinre.2022.101922]

97 **Ji J**, Feng M, Huang Y, Niu X. Liraglutide inhibits receptor for advanced glycation end products (RAGE)/reduced form of nicotinamide-adenine dinucleotide phosphate (NAPDH) signaling to ameliorate non-alcoholic fatty liver disease (NAFLD) *in vivo* and vitro. *Bioengineered* 2022; **13**: 5091-5102 [PMID: 35164657 DOI: 10.1080/21655979.2022.2036902]

98 **Dutta D**, Kumar M, Shivaprasad KS, Kumar A, Sharma M. Impact of semaglutide on biochemical and radiologic measures of metabolic-dysfunction associated fatty liver disease across the spectrum of glycaemia: A meta-analysis. *Diabetes Metab Syndr* 2022; **16**: 102539 [PMID: 35709586 DOI: 10.1016/j.dsx.2022.102539]

99 **Tommerdahl KL**, Kendrick J, Bjornstad P. The Role of Glucagon-Like Peptide 1 (GLP-1) Receptor Agonists in the Prevention and Treatment of Diabetic Kidney Disease: Insights from the AMPLITUDE-O Trial. *Clin J Am Soc Nephrol* 2022; **17**: 905-907 [PMID: 35396319 DOI: 10.2215/CJN.00020122]

100 **Górriz JL**, Soler MJ, Navarro-González JF, García-Carro C, Puchades MJ, D'Marco L, Martínez Castelao A, Fernández-Fernández B, Ortiz A, Górriz-Zambrano C, Navarro-Pérez J, Gorgojo-Martinez JJ. GLP-1 Receptor Agonists and Diabetic Kidney Disease: A Call of Attention to Nephrologists. *J Clin Med* 2020; **9** [PMID: 32235471 DOI: 10.3390/jcm9040947]

101 **Gerstein HC**, Sattar N, Rosenstock J, Ramasundarahettige C, Pratley R, Lopes RD, Lam CSP, Khurmi NS, Heenan L, Del Prato S, Dyal L, Branch K; AMPLITUDE-O Trial Investigators. Cardiovascular and Renal Outcomes with Efpeglenatide in Type 2 Diabetes. *N Engl J Med* 2021; **385**: 896-907 [PMID: 34215025 DOI: 10.1056/NEJMoa2108269]

102 **Lam CSP**, Ramasundarahettige C, Branch KRH, Sattar N, Rosenstock J, Pratley R, Del Prato S, Lopes RD, Niemoeller E, Khurmi NS, Baek S, Gerstein HC. Efpeglenatide and Clinical Outcomes With and Without Concomitant Sodium-Glucose Cotransporter-2 Inhibition Use in Type 2 Diabetes: Exploratory Analysis of the AMPLITUDE-O Trial. *Circulation* 2022; **145**: 565-574 [PMID: 34775781 DOI: 10.1161/CIRCULATIONAHA.121.057934]

103 **Chen JJ**, Wu CY, Jenq CC, Lee TH, Tsai CY, Tu HT, Huang YT, Yen CL, Yen TH, Chen YC, Tian YC, Yang CW, Yang HY. Association of Glucagon-Like Peptide-1 Receptor Agonist *vs* Dipeptidyl Peptidase-4 Inhibitor Use With Mortality Among Patients With Type 2 Diabetes and Advanced Chronic Kidney Disease. *JAMA Netw Open* 2022; **5**: e221169 [PMID: 35254430 DOI: 10.1001/jamanetworkopen.2022.1169]

104 **Lui DTW**, Au ICH, Tang EHM, Cheung CL, Lee CH, Woo YC, Wu T, Tan KCB, Wong CKH. Kidney outcomes associated with sodium-glucose cotransporter 2 inhibitors *vs* glucagon-like peptide 1 receptor agonists: A real-world population-based analysis. *EClinicalMedicine* 2022; **50**: 101510 [PMID: 35784442 DOI: 10.1016/j.eclinm.2022.101510]

105 **Cao H**, Liu T, Wang L, Ji Q. Comparative efficacy of novel antidiabetic drugs on cardiovascular and renal outcomes in patients with diabetic kidney disease: A systematic review and network meta-analysis. *Diabetes Obes Metab* 2022; **24**: 1448-1457 [PMID: 35665989 DOI: 10.1111/dom.14702]

106 **Jastreboff AM**, Aronne LJ, Ahmad NN, Wharton S, Connery L, Alves B, Kiyosue A, Zhang S, Liu B, Bunck MC, Stefanski A; SURMOUNT-1 Investigators. Tirzepatide Once Weekly for the Treatment of Obesity. *N Engl J Med* 2022; **387**: 205-216 [PMID: 35658024 DOI: 10.1056/NEJMoa2206038]

107 **Ma T**, Lu W, Wang Y, Qian P, Tian H, Gao X, Yao W. An oral GLP-1 and GIP dual receptor agonist improves metabolic disorders in high fat-fed mice. *Eur J Pharmacol* 2022; **914**: 174635 [PMID: 34800466 DOI: 10.1016/j.ejphar.2021.174635]

108 **Kim ER**, Park JS, Kim JH, Oh JY, Oh IJ, Choi DH, Lee YS, Park IS, Kim S, Lee DH, Cheon JH, Bae JW, Lee M, Cho JW, An IB, Nam EJ, Yang SI, Lee MS, Bae SH, Lee YH. A GLP-1/GLP-2 receptor dual agonist to treat NASH: Targeting the gut-liver axis and microbiome. *Hepatology* 2022; **75**: 1523-1538 [PMID: 34773257 DOI: 10.1002/hep.32235]

109 **Hartman ML**, Sanyal AJ, Loomba R, Wilson JM, Nikooienejad A, Bray R, Karanikas CA, Duffin KL, Robins DA, Haupt A. Effects of Novel Dual GIP and GLP-1 Receptor Agonist Tirzepatide on Biomarkers of Nonalcoholic Steatohepatitis in Patients With Type 2 Diabetes. *Diabetes Care* 2020; **43**: 1352-1355 [PMID: 32291277 DOI: 10.2337/dc19-1892]

110 **Gastaldelli A**, Cusi K, Fernández Landó L, Bray R, Brouwers B, Rodríguez Á. Effect of tirzepatide *vs* insulin degludec on liver fat content and abdominal adipose tissue in people with type 2 diabetes (SURPASS-3 MRI): a substudy of the randomised, open-label, parallel-group, phase 3 SURPASS-3 trial. *Lancet Diabetes Endocrinol* 2022; **10**: 393-406 [PMID: 35468325 DOI: 10.1016/S2213-8587(22)00070-5]

111 **Theofilis P**, Sagris M, Oikonomou E, Antonopoulos AS, Siasos G, Tsioufis K, Tousoulis D. Pleiotropic effects of SGLT2 inhibitors and heart failure outcomes. *Diabetes Res Clin Pract* 2022; **188**: 109927 [PMID: 35577035 DOI: 10.1016/j.diabres.2022.109927]

112 **Theofilis P**, Antonopoulos AS, Katsimichas T, Oikonomou E, Siasos G, Aggeli C, Tsioufis K, Tousoulis D. The impact of SGLT2 inhibition on imaging markers of cardiac function: A systematic review and meta-analysis. *Pharmacol Res* 2022; **180**: 106243 [PMID: 35523389 DOI: 10.1016/j.phrs.2022.106243]

113 **Theofilis P**, Sagris M, Oikonomou E, Antonopoulos AS, Siasos G, Tsioufis K, Tousoulis D. The impact of SGLT2 inhibitors on inflammation: A systematic review and meta-analysis of studies in rodents. *Int Immunopharmacol* 2022; **111**: 109080 [PMID: 35908505 DOI: 10.1016/j.intimp.2022.109080]

114 **Kurtz R**, Libby A, Jones BA, Myakala K, Wang X, Lee Y, Knoer G, Lo Cascio JN, McCormack M, Nguyen G, Choos END, Rodriguez O, Rosenberg AZ, Ranjit S, Albanese C, Levi M, Ecelbarger CM, Shepard BD. Empagliflozin Treatment Attenuates Hepatic Steatosis by Promoting White Adipose Expansion in Obese TallyHo Mice. *Int J Mol Sci* 2022; **23** [PMID: 35628485 DOI: 10.3390/ijms23105675]

115 **Wang Y**, Ding Y, Sun P, Zhang W, Xin Q, Wang N, Niu Y, Chen Y, Luo J, Lu J, Zhou J, Xu N, Zhang Y, Xie W. Empagliflozin-Enhanced Antioxidant Defense Attenuates Lipotoxicity and Protects Hepatocytes by Promoting FoxO3a- and Nrf2-Mediated Nuclear Translocation *via* the CAMKK2/AMPK Pathway. *Antioxidants (Basel)* 2022; **11** [PMID: 35624663 DOI: 10.3390/antiox11050799]

116 **Morishita A**, Tadokoro T, Fujihara S, Iwama H, Oura K, Fujita K, Tani J, Takuma K, Nakahara M, Shi T, Haba R, Okano K, Nishiyama A, Ono M, Himoto T, Masaki T. Ipragliflozin attenuates non-alcoholic steatohepatitis development in an animal model. *PLoS One* 2022; **17**: e0261310 [PMID: 35192632 DOI: 10.1371/journal.pone.0261310]

117 **Luo J**, Sun P, Wang Y, Chen Y, Niu Y, Ding Y, Xu N, Zhang Y, Xie W. Dapagliflozin attenuates steatosis in livers of high-fat diet-induced mice and oleic acid-treated L02 cells *via* regulating AMPK/mTOR pathway. *Eur J Pharmacol* 2021; **907**: 174304 [PMID: 34224699 DOI: 10.1016/j.ejphar.2021.174304]

118 **Zhang Y**, Liu X, Zhang H, Wang X. Efficacy and Safety of Empagliflozin on Nonalcoholic Fatty Liver Disease: A Systematic Review and Meta-Analysis. *Front Endocrinol (Lausanne)* 2022; **13**: 836455 [PMID: 35282455 DOI: 10.3389/fendo.2022.836455]

119 **Wheeler DC**, Stefánsson BV, Jongs N, Chertow GM, Greene T, Hou FF, McMurray JJV, Correa-Rotter R, Rossing P, Toto RD, Sjöström CD, Langkilde AM, Heerspink HJL; DAPA-CKD Trial Committees and Investigators. Effects of dapagliflozin on major adverse kidney and cardiovascular events in patients with diabetic and non-diabetic chronic kidney disease: a prespecified analysis from the DAPA-CKD trial. *Lancet Diabetes Endocrinol* 2021; **9**: 22-31 [PMID: 33338413 DOI: 10.1016/S2213-8587(20)30369-7]

120 **Jardine MJ**, Zhou Z, Mahaffey KW, Oshima M, Agarwal R, Bakris G, Bajaj HS, Bull S, Cannon CP, Charytan DM, de Zeeuw D, Di Tanna GL, Greene T, Heerspink HJL, Levin A, Neal B, Pollock C, Qiu R, Sun T, Wheeler DC, Zhang H, Zinman B, Rosenthal N, Perkovic V; CREDENCE Study Investigators. Renal, Cardiovascular, and Safety Outcomes of Canagliflozin by Baseline Kidney Function: A Secondary Analysis of the CREDENCE Randomized Trial. *J Am Soc Nephrol* 2020; **31**: 1128-1139 [PMID: 32354987 DOI: 10.1681/ASN.2019111168]

121 **Bakris G**, Oshima M, Mahaffey KW, Agarwal R, Cannon CP, Capuano G, Charytan DM, de Zeeuw D, Edwards R, Greene T, Heerspink HJL, Levin A, Neal B, Oh R, Pollock C, Rosenthal N, Wheeler DC, Zhang H, Zinman B, Jardine MJ, Perkovic V. Effects of Canagliflozin in Patients with Baseline eGFR <30 mL/min per 1.73 m^2: Subgroup Analysis of the Randomized CREDENCE Trial. *Clin J Am Soc Nephrol* 2020; **15**: 1705-1714 [PMID: 33214158 DOI: 10.2215/CJN.10140620]

122 **Cannon CP**, Perkovic V, Agarwal R, Baldassarre J, Bakris G, Charytan DM, de Zeeuw D, Edwards R, Greene T, Heerspink HJL, Jardine MJ, Levin A, Li JW, Neal B, Pollock C, Wheeler DC, Zhang H, Zinman B, Mahaffey KW. Evaluating the Effects of Canagliflozin on Cardiovascular and Renal Events in Patients With Type 2 Diabetes Mellitus and Chronic Kidney Disease According to Baseline HbA1c, Including Those With HbA1c <7%: Results From the CREDENCE Trial. *Circulation* 2020; **141**: 407-410 [PMID: 31707795 DOI: 10.1161/CIRCULATIONAHA.119.044359]

123 **Theofilis P**, Vordoni A, Kalaitzidis RG. The Role of Melatonin in Chronic Kidney Disease and Its Associated Risk Factors: A New Tool in Our Arsenal? *Am J Nephrol* 2022; **53**: 565-574 [PMID: 35767942 DOI: 10.1159/000525441]

124 **Du Z**, Liang S, Li Y, Zhang J, Yu Y, Xu Q, Sun Z, Duan J. Melatonin Alleviates $PM_{2.5}$-Induced Hepatic Steatosis and Metabolic-Associated Fatty Liver Disease in $ApoE^{-/-}$ Mice. *Oxid Med Cell Longev* 2022; **2022**: 8688643 [PMID: 35720187 DOI: 10.1155/2022/8688643]

125 **Saha M**, Manna K, Das Saha K. Melatonin Suppresses NLRP3 Inflammasome Activation *via* TLR4/NF-κB and P2X7R Signaling in High-Fat Diet-Induced Murine NASH Model. *J Inflamm Res* 2022; **15**: 3235-3258 [PMID: 35668917 DOI: 10.2147/JIR.S343236]

126 **Satari M**, Bahmani F, Reiner Z, Soleimani A, Aghadavod E, Kheiripour N, Asemi Z. Metabolic and Anti-inflammatory Response to Melatonin Administration in Patients with Diabetic Nephropathy. *Iran J Kidney Dis* 2021; **1**: 22-30 [PMID: 33492301]

127 **Ostadmohammadi V**, Soleimani A, Bahmani F, Aghadavod E, Ramezani R, Reiter RJ, Mansournia MA, Banikazemi Z, Soleimani M, Zaroudi M, Asemi Z. The Effects of Melatonin Supplementation on Parameters of Mental Health, Glycemic Control, Markers of Cardiometabolic Risk, and Oxidative Stress in Diabetic Hemodialysis Patients: A Randomized, Double-Blind, Placebo-Controlled Trial. *J Ren Nutr* 2020; **30**: 242-250 [PMID: 31597622 DOI: 10.1053/j.jrn.2019.08.003]

128 **Kulkarni AV**, Tevethia HV, Arab JP, Candia R, Premkumar M, Kumar P, Sharma M, Reddy DN, Padaki NR. Efficacy and safety of obeticholic acid in liver disease-A systematic review and meta-analysis. *Clin Res Hepatol Gastroenterol* 2021; **45**: 101675 [PMID: 33722778 DOI: 10.1016/j.clinre.2021.101675]

129 **Wang XX**, Jiang T, Shen Y, Adorini L, Pruzanski M, Gonzalez FJ, Scherzer P, Lewis L, Miyazaki-Anzai S, Levi M. The farnesoid X receptor modulates renal lipid metabolism and diet-induced renal inflammation, fibrosis, and proteinuria. *Am J Physiol Renal Physiol* 2009; **297**: F1587-F1596 [PMID: 19776172 DOI: 10.1152/ajprenal.00404.2009]

130 **Bae EH**, Choi HS, Joo SY, Kim IJ, Kim CS, Choi JS, Ma SK, Lee J, Kim SW. Farnesoid X receptor ligand prevents cisplatin-induced kidney injury by enhancing small heterodimer partner. *PLoS One* 2014; **9**: e86553 [PMID: 24475141 DOI: 10.1371/journal.pone.0086553]

131 **Wang XX**, Wang D, Luo Y, Myakala K, Dobrinskikh E, Rosenberg AZ, Levi J, Kopp JB, Field A, Hill A, Lucia S, Qiu L,

Jiang T, Peng Y, Orlicky D, Garcia G, Herman-Edelstein M, D'Agati V, Henriksen K, Adorini L, Pruzanski M, Xie C, Krausz KW, Gonzalez FJ, Ranjit S, Dvornikov A, Gratton E, Levi M. FXR/TGR5 Dual Agonist Prevents Progression of Nephropathy in Diabetes and Obesity. *J Am Soc Nephrol* 2018; **29**: 118-137 [PMID: 29089371 DOI: 10.1681/ASN.2017020222]

132 **Zhu JB**, Xu S, Li J, Song J, Luo B, Song YP, Zhang ZH, Chen YH, Xie DD, Yu DX, Xu DX. Farnesoid X receptor agonist obeticholic acid inhibits renal inflammation and oxidative stress during lipopolysaccharide-induced acute kidney injury. *Eur J Pharmacol* 2018; **838**: 60-68 [PMID: 30196109 DOI: 10.1016/j.ejphar.2018.09.009]

133 **Choi SI**, You S, Kim S, Won G, Kang CH, Kim GH. *Weissella cibaria* MG5285 and *Lactobacillus reuteri* MG5149 attenuated fat accumulation in adipose and hepatic steatosis in high-fat diet-induced C57BL/6J obese mice. *Food Nutr Res* 2021; **65** [PMID: 34776827 DOI: 10.29219/fnr.v65.8087]

134 **Wang Y**, Zhang Y, Yang J, Li H, Wang J, Geng W. *Lactobacillus plantarum* MA2 Ameliorates Methionine and Choline-Deficient Diet Induced Non-Alcoholic Fatty Liver Disease in Rats by Improving the Intestinal Microecology and Mucosal Barrier. *Foods* 2021; **10** [PMID: 34945677 DOI: 10.3390/foods10123126]

135 **Long X**, Liu D, Gao Q, Ni J, Qian L, Ni Y, Fang Q, Jia W, Li H. *Bifidobacterium adolescentis* Alleviates Liver Steatosis and Steatohepatitis by Increasing Fibroblast Growth Factor 21 Sensitivity. *Front Endocrinol (Lausanne)* 2021; **12**: 773340 [PMID: 35035378 DOI: 10.3389/fendo.2021.773340]

136 **Wang L**, Jiao T, Yu Q, Wang J, Wang L, Wang G, Zhang H, Zhao J, Chen W. *Bifidobacterium bifidum* Shows More Diversified Ways of Relieving Non-Alcoholic Fatty Liver Compared with *Bifidobacterium adolescentis*. *Biomedicines* 2021; **10** [PMID: 35052765 DOI: 10.3390/biomedicines10010084]

137 **Liu Z**, Zhou X, Wang W, Gu L, Hu C, Sun H, Xu C, Hou J, Jiang Z. *Lactobacillus paracasei* 24 Attenuates Lipid Accumulation in High-Fat Diet-Induced Obese Mice by Regulating the Gut Microbiota. *J Agric Food Chem* 2022; **70**: 4631-4643 [PMID: 35377154 DOI: 10.1021/acs.jafc.1c07884]

138 **Do MH**, Oh MJ, Lee HB, Kang CH, Yoo G, Park HY. *Bifidobacterium animalis* ssp. *lactis* MG741 Reduces Body Weight and Ameliorates Nonalcoholic Fatty Liver Disease *via* Improving the Gut Permeability and Amelioration of Inflammatory Cytokines. *Nutrients* 2022; **14** [PMID: 35565930 DOI: 10.3390/nu14091965]

139 **Tungsanga S**, Katavetin P, Panpetch W, Udompornpitak K, Saisorn W, Praditpornsilpa K, Eiam-Ong S, Tungsanga K, Tumwasorn S, Leelahavanichkul A. Lactobacillus rhamnosus L34 attenuates chronic kidney disease progression in a 5/6 nephrectomy mouse model through the excretion of anti-inflammatory molecules. *Nephrol Dial Transplant* 2022; **37**: 1429-1442 [PMID: 35138387 DOI: 10.1093/ndt/gfac032]

140 **Tsai YS**, Chen YP, Lin SW, Chen YL, Chen CC, Huang GJ. Lactobacillus rhamnosus GKLC1 ameliorates cisplatin-induced chronic nephrotoxicity by inhibiting cell inflammation and apoptosis. *Biomed Pharmacother* 2022; **147**: 112701 [PMID: 35131657 DOI: 10.1016/j.biopha.2022.112701]

141 **Huang H**, Li K, Lee Y, Chen M. Preventive Effects of *Lactobacillus* Mixture against Chronic Kidney Disease Progression through Enhancement of Beneficial Bacteria and Downregulation of Gut-Derived Uremic Toxins. *J Agric Food Chem* 2021; **69**: 7353-7366 [PMID: 34170659 DOI: 10.1021/acs.jafc.1c01547]

142 **Sun G**, Yin Z, Liu N, Bian X, Yu R, Su X, Zhang B, Wang Y. Gut microbial metabolite TMAO contributes to renal dysfunction in a mouse model of diet-induced obesity. *Biochem Biophys Res Commun* 2017; **493**: 964-970 [PMID: 28942145 DOI: 10.1016/j.bbrc.2017.09.108]

143 **Gupta N**, Buffa JA, Roberts AB, Sangwan N, Skye SM, Li L, Ho KJ, Varga J, DiDonato JA, Tang WHW, Hazen SL. Targeted Inhibition of Gut Microbial Trimethylamine N-Oxide Production Reduces Renal Tubulointerstitial Fibrosis and Functional Impairment in a Murine Model of Chronic Kidney Disease. *Arterioscler Thromb Vasc Biol* 2020; **40**: 1239-1255 [PMID: 32212854 DOI: 10.1161/ATVBAHA.120.314139]

144 **Zhang W**, Miikeda A, Zuckerman J, Jia X, Charugundla S, Zhou Z, Kaczor-Urbanowicz KE, Magyar C, Guo F, Wang Z, Pellegrini M, Hazen SL, Nicholas SB, Lusis AJ, Shih DM. Inhibition of microbiota-dependent TMAO production attenuates chronic kidney disease in mice. *Sci Rep* 2021; **11**: 518 [PMID: 33436815 DOI: 10.1038/s41598-020-80063-0]

World Journal of Gastroenterology

Submit a Manuscript: https://www.f6publishing.com

World J Gastroenterol 2022 October 21; 28(39): 5707-5722

DOI: 10.3748/wjg.v28.i39.5707

ISSN 1007-9327 (print) ISSN 2219-2840 (online)

MINIREVIEWS

Pitfalls and promises of bile duct alternatives: A narrative review

Mitsuo Miyazawa, Masayasu Aikawa, Junpei Takashima, Hirotoshi Kobayashi, Shunsuke Ohnishi, Yoshito Ikada

Specialty type: Gastroenterology and hepatology

Provenance and peer review: Unsolicited article; Externally peer reviewed.

Peer-review model: Single blind

Peer-review report's scientific quality classification

Grade A (Excellent): 0
Grade B (Very good): B, B
Grade C (Good): C, C
Grade D (Fair): 0
Grade E (Poor): 0

P-Reviewer: Feier F, Brazil; Ferreira GSA, Brazil; Qin J, China

Received: May 24, 2022
Peer-review started: May 24, 2022
First decision: August 1, 2022
Revised: August 18, 2022
Accepted: September 22, 2022
Article in press: September 22, 2022
Published online: October 21, 2022

Mitsuo Miyazawa, Junpei Takashima, Hirotoshi Kobayashi, Department of Surgery, Teikyo University Mizonokuch Hospital, Kanagawa 213-8507, Japan

Masayasu Aikawa, Department of Surgery, Saitama Medical University International Medical Center, Saitama 350-1298, Japan

Shunsuke Ohnishi, Department of Gastroenterology and Hepatology, Hokkaido University Faculty of Medicine and Graduate School of Medicine, Sapporo 060-8638, Japan

Yoshito Ikada, Department of Bioenvironmental Medicine, Nara Medical University, Nara 634-8521, Japan

Corresponding author: Mitsuo Miyazawa, FACS, MD, PhD, Professor, Department of Surgery, Teikyo University Mizonokuch Hospital, 5-1-1 Futago, Takatsu-ku, Kawasaki-shi, Kanagawa 213-8507, Japan. mmiyazawa@med.teikyo-u.ac.jp

Abstract

Biliodigestive anastomosis between the extrahepatic bile duct and the intestine for bile duct disease is a gastrointestinal reconstruction that abolishes duodenal papilla function and frequently causes retrograde cholangitis. This chronic inflammation can cause liver dysfunction, liver abscess, and even bile duct cancer. Although research has been conducted for over 100 years to directly repair bile duct defects with alternatives, no bile duct substitute (BDS) has been developed. This narrative review confirms our understanding of why bile duct alternatives have not been developed and explains the clinical applicability of BDSs in the near future. We searched the PubMed electronic database to identify studies conducted to develop BDSs until December 2021 and identified studies in English. Two independent reviewers reviewed studies on large animals with 8 or more cases. Four types of BDSs prevail: Autologous tissue, non-bioabsorbable material, bioabsorbable material, and others (decellularized tissue, 3D-printed structures, *etc.*). In most studies, BDSs failed due to obstruction of the lumen or stenosis of the anastomosis with the native bile duct. BDS has not been developed primarily because control of bile duct wound healing and regeneration has not been elucidated. A BDS expected to be clinically applied in the near future incorporates a bioabsorbable material that allows for regeneration of the bile duct outside the BDS.

Key Words: Bile duct alternative; Bile duct substitute; Biliary regeneration; Bile duct reconstruction; Peribiliary gland; Bioabsorbable polymer

©The Author(s) 2022. Published by Baishideng Publishing Group Inc. All rights reserved.

Core Tip: The bile duct-intestinal anastomosis eliminating the function of the papilla of Vater causes chronic inflammation due to the reflux of bile and is not an ideal reconstruction method. Bile duct alternatives for bile duct defects have not been developed for over 100 years. In the present situation where the wound healing of the bile duct defect cannot be controlled, only the use of a bioabsorbable material, such as a scaffold, and the regeneration of the bile duct outside the scaffold can be expected as a bile duct substitute.

Citation: Miyazawa M, Aikawa M, Takashima J, Kobayashi H, Ohnishi S, Ikada Y. Pitfalls and promises of bile duct alternatives: A narrative review. *World J Gastroenterol* 2022; 28(39): 5707-5722
URL: https://www.wjgnet.com/1007-9327/full/v28/i39/5707.htm
DOI: https://dx.doi.org/10.3748/wjg.v28.i39.5707

INTRODUCTION

The treatment of gastrointestinal diseases in the 21st century involves robotic and endoscopic surgeries, which aim to minimize potential risks and side effects[1-3]. Minimally invasive endoscopic treatments have been developed to facilitate functional preservation[4,5]. For diseases of the biliary system, the use of laparoscopic cholecystectomy as a treatment for cholelithiasis has become widespread, and minimally invasive approaches have been pursued[6]. In contrast, the incidence of severe iatrogenic extrahepatic bile duct injury due to laparoscopic cholecystectomy has increased significantly worldwide compared to that due to laparotomy surgery[7]. With regard to bile duct injuries, there is currently no bile duct substitute (BDS) for partially defective or damaged parts of the bile duct. Reconstruction by anastomosis of the hepatic bile duct and intestine is typically performed[8].

Bile duct-intestinal anastomosis is a biliary tract reconstruction procedure that was first performed by von Winiwater in 1880[9]. However, liver abscess, cirrhosis, and liver dysfunction were often observed in patients who underwent this anastomosis. In the early 20th century, retrograde cholangitis tended to cause chronic inflammation if duodenal papilla function was not preserved[10,11]. The suboptimal nature of this approach resulted in attempts to preserve papilla function and to develop alternatives for addressing bile duct defects and injury. Chronic inflammation caused by abnormal pancreatic-bile duct junctions, intrahepatic stones[12,13], and exposure to organic solvents from the printing industry is considered a high-risk factor for cholangiocarcinoma[14]. Therefore, the development of BDS has emerged as a critical, unmet need. To date, various alternatives, including autologous tissue[10,15-18], non-bioabsorbable[19-23], bioabsorbable materials[24-28], and decellularized tissue[29,30], have been investigated. Nevertheless, BDSs with widespread clinical applications have not yet been developed. In this review, we discuss potential factors underpinning the failure to develop clinically usable products despite efforts to develop BDSs for more than a century. Furthermore, we highlight the types of BDSs that may be clinically applied in the near future.

MATERIALS AND METHODS

We searched the PubMed electronic database to identify studies conducted to develop bile duct alternatives until December 2021 and identified studies in English. The following search items for the data relevant to "why has a product that can replace bile ducts not been developed?" were included: "bile duct alternative", "bile duct substitute", "bile duct regeneration", "biliary alternative", "extrahepatic bile duct", "biliary regeneration", and "bile duct reconstruction". Studies using large animals such as dogs, pigs, and goats were included, whereas studies using small animals such as rats and mice were excluded. To evaluate the efficacy of the BDS, the "type of substitute", "shape and length of substitute", "method of reconstruction of the bile duct by substitute", and "observation period" were included as search terms. The items to be examined were "presence or absence of regeneration process", "localization of regenerated bile duct to substitute", "number of large animals that could be sacrificed and killed intentionally", and "cause of narrowing of substitute". We also cited high-quality articles in *Reference Citation Analysis* (https://www.referencecitationanalysis.com).

For studies in which the items could be determined from the abstract or text, the number of experimental large animals used was eight or more. The full text was reviewed by two researchers (Miyazawa M, Takashima J). In each of these studies, the cases in which BDS transplantation was successful were as follows: These cases were sacrificed as planned before BDS transplantation, no stenosis was observed at the anastomotic site between the BDS transplantation site and the natural bile duct, and there was no

liver dysfunction after BDS transplantation.

Animal type

In small animals, such as rats, jaundice is unlikely to occur even if the extrahepatic bile duct is narrowed, and liver dysfunction may be difficult to evaluate. As such, BDS transplantation may be difficult[31]. Accordingly, only large-animal studies were considered.

Size of BDS

If the length of the BDS implantation segment was less than 1 cm, tissues such as the omentum may migrate around it after inserting the T-tube into the defective bile duct segment[32]. Therefore, BDSs ≤ 1 cm and > 1 cm in length were considered separately. For the same reason, patch-like or circular implantation of the BDS was examined separately. Regarding the implantation method, the site of BDS implantation (between the common bile duct or between the common bile duct and intestine) was examined separately because it affects the patency of the BDS lumen.

Observation period after BDS implantation

Early after BDS transplantation, stenosis of the BDS may not occur in the event of retrograde cholangitis or severe inflammation at the alternative transplant site. After chronic inflammation, the bile duct becomes narrowed due to the gradual hyperplasia of connective tissue around the substitute[33]. After stent insertion into the BDS, bile may flow through the stent and a bile plug may not be formed in the BDS in the early stage of BDS transplantation[34]. As anastomotic stenosis was considered less likely to occur when a stent was inserted, the observation period after BDS transplantation was included in the examination items.

Bile duct regeneration

After the formation of connective tissue in the shape of the bile duct, the BDS lumen does not become completely stenotic early after BDS transplantation, even if bile duct regeneration does not occur and bile remains in the lumen. However, stenosis tends to occur after a prolonged period[35]. Tissue regeneration in the defective bile duct area occurs due to wound healing[35]. The mature bile duct takes time (3 mo or more) to regenerate from bile duct stem cells[25,36,37] (Figure 1). Therefore, to examine the effectiveness of BDS for inducing bile duct regeneration, histological images of bile duct regeneration at the BDS transplantation site were included in the examination. If the study did not report neo-bile duct regeneration and the histology was similar to that of the native bile duct, the tissue was excluded from evaluation. The histology of the anastomotic site between the BDS and native bile duct was examined because the bile duct epithelium is continuous at the anastomotic site if stenosis of the anastomotic site does not occur[38].

Localization of bile duct regeneration with respect to BDS implants

We did not identify any reports of bile duct regeneration on the inner surface of the T-tube when it was placed in the injured part of the bile duct. This suggests that the bile duct does not regenerate on the inner surface of non-bioabsorbable BDSs. However, it is important from the viewpoint of wound healing whether the localization of the regenerated bile duct is the outer surface of the BDS, the part of the BDS itself, or the inner surface of the BDS (only the bile passage surface). For these reasons, the site where the regenerated bile duct regenerates was included in the examination items for the BDS transplantation site. When the localization of bile duct regeneration was not specified, it was judged from the BDS implantation site and bile passage position in the paper.

Causes of stenosis

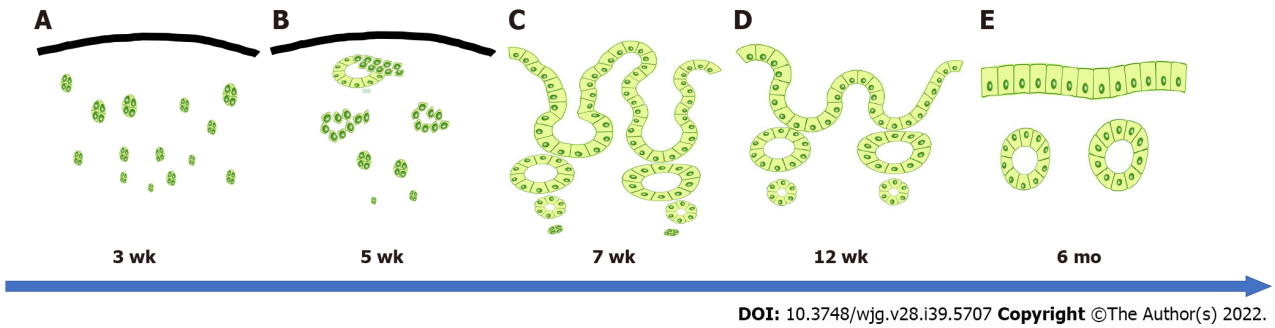
Narrowing of the anastomotic site between the BDS and the native bile duct or the BDS lumen was evaluated as a separate cause of wound healing. We also examined the stenotic tissue type. For BDS lumen and anastomotic site stenosis, scar contraction was considered to occur over a prolonged period if granulation or connective tissue growth was reported[35,39,40].

BDS REPORTED TO DATE

The literature search enabled the classification of BDSs into four categories: Autologous tissues[10,15-18], non-bioabsorbable materials[19-23], bioabsorbable materials[24-28], and others (decellularized tissues[29,30], structures made with 3D printers[41,42], *etc.*).

BDS using autologous tissue

Tissues with a similar morphology to that of the extrahepatic bile duct and lumen have been investigated as BDSs. In practice, arteries[43], veins[15,17-19,44], ureters[45], skin[46], and jejunum[16] have been used as grafts. Due to the thickness of the extrahepatic bile duct and wall, the femoral vein was



DOI: 10.3748/wjg.v28.i39.5707 **Copyright** ©The Author(s) 2022.

Figure 1 Ideal bile duct regeneration process. A: Bile duct regeneration at approximately 3 wk. Numerous cell masses appear in the stroma that are thought to form peribiliary glands; B: Bile duct regeneration at approximately 5 wk. A ring-shaped peribiliary gland-like structure is observed, in which cell masses that are thought to form peribiliary glands are fused; C: Bile duct regeneration at approximately 7 wk. Numerous bile duct-attached glandular structures are observed on the bile passage surface, and the epithelial surface exhibits a high papillary morphology; D: Bile duct regeneration at approximately 12 wk. The number of peribiliary glands on the bile passage surface is decreased, the peribiliary glands become fused, and the epithelial surface becomes more even; E: Approximately 6 mo after bile duct regeneration. Similar to the native bile duct, the epithelial surface becomes a single layer of cubic columnar epithelium.

often used. In BDSs using these autologous tissues, necrosis of the substitute in the early stage of transplantation and obstruction due to attachment of the bile plug to the substitute in the middle stage of transplantation were common[10,17,18,44,47]. In the long term, scar contraction occurs due to the growth of connective tissue around the substitute and at the anastomotic site[10,17-19,44]. To address these issues, attempts have been made to wrap the omentum around the substitute to supply blood flow or to use stents and cuffs to prevent obstruction of the BDS lumen and anastomotic site[17,48,49]. As the BDS did not regenerate to the extent of the native bile duct, few BDSs were successful, and no clinically usable product was developed[48,49]. The localization of neo-bile ducts to the BDS, which attempted to promote bile duct regeneration, formed a part of the autologous tissue itself.

The most commonly used species in these studies was dog. Pearce *et al*[10] investigated autologous alternative veins as a BDS and concluded that 1 in 32 successful cases over 3 mo was insufficient for the use of autologous tissue as a BDS. A study by Dunphy and Stephens[19] using large animals (44 sheep and 8 pigs) evaluated autologous arteries, veins, and homozygous arteries. Only sheep that received autologous arteries as a BDS survived for 6 mo or more, but bile duct dilation on the liver side was observed. Myers *et al*[18] conducted a circular transplantation experiment using autologous bile ducts, arteries, veins, and genomic grafts to treat bile duct defects in 28 dogs. All homografts were rejected, and the dogs that received transplants died within 13 d.

Even in transplantations using autologous tissue, histological assessment revealed that the bile duct epithelium did not regenerate on the epithelial surface, fibrous connective tissue was increased on the epithelial surface, and the BDS transplantation site became stenotic. The authors concluded that self-organization is not possible in BDS. In 2009, Palmes *et al*[48] reported a high success rate of transplantation of the external jugular vein and a bioabsorbable stent as a BDS in pigs. However, histological changes in the bile ducts of autologous veins have not been reported (Table 1).

Due to the lack of blood supply in autologous tissue BDSs, the tissue becomes necrotic, and the anastomotic site is scar-contracted. A BDS capable of allowing bile to flow freely into the duodenum over a prolonged period has not yet been developed. It is unlikely that autologous tissue will resemble the native bile duct in the context of wound healing[40,50,51]. Stenting through the anastomotic site was effective in preventing narrowing[17,48,49]. High success rates have been reported when bioabsorbable stents are placed in the venous lumen; however, it is unclear how autologous venous tissue is induced for good bile duct regeneration. These findings suggested that autologous tissue cannot be used as a BDS.

BDS using non-bioabsorbable material

Since the 1930s, polyvinyl sponge[20], polytetrafluorethylene[22,23], Teflon[19,52], Dacron[53], and polyethylene[54,55] have been used as non-bioabsorbable BDS materials. These alternatives were used experimentally as patches or rings, but most studies reported high rejection rates early in transplantation and varying degrees of cholangitis, narrowing of the alternative lumen, and stenosis of the anastomotic site with the native bile duct[19,27,28]. Although partial success has been reported, the bile duct epithelium failed to regenerate on either the medial side (bile passage surface) or lateral side of these alternatives[29,30]. As a result, the perimeter of these BDSs was covered with fibrous connective tissue, and the luminal surface was clogged with bile plugs[19-22]. This resulted in stenosis of the anastomosis with the native bile duct, which prevented bile passage. As such, research on cyclic BDS made solely from non-bioabsorbable materials has ceased.

Sherman *et al*[21] transplanted a BDS made from acrylamide into dogs. In the stented group, 7 of the 33 cases were successful over 3 mo. However, bile duct regeneration has not been reported. Bergan *et al*

Table 1 Bile duct substitute using autologous tissue

Ref.	Journal	Substitute (*n*)	Stent (*n*)	Animal type (*n*)	Size of BDS (cm)	Method of reconstruction of bile duct by BDS (*n*)	Observation period after implantation	Localization of regenerated bile duct	Causes of stenosis	Note (planned sacrificial death and epithelialization)
Shea and Hubay[15], 1948	*Ann Surg*	Femoral vein (21)	Vitallium tube	Dog (21)	Ring (1.5)	CBC (21)	Maximum 208 d	BDS itself	Necrosis of BDS itself, narrowing of the BDS lumen, and narrowing of the anastomosis with the native bile duct	Although 14 out of 21 dogs were intentionally killed, the tissue of the regenerated bile duct was shown only as a result, and the process of bile duct regeneration was not demonstrated
Kirby and Fitts[16], 1950	*Arch Surg* (1920)	Jejunum (9)	T-tube	Dog (9)	Jejunum (2.5)	GBC (5); CBC (4)	Maximum 13 mo	BDS itself	BDS stenosis was not observed when the T-tube was inserted	Seven out of nine dogs were intentionally killed; however, no epithelial regeneration was observed at the anastomotic site. The procedure was too complicated
Pearce *et al* [10], 1951	*Ann Surg*	Femoral vein (32)	Lord and blakemore tube	Dog (32)	Ring (1.0)	CBC (10); CBJ (20); GBC (2)	Maximum 6 mo	BDS itself	Necrosis of autologous tissue, narrowing of the lumen of autologous tissue, narrowing of the anastomosis with the native bile duct, necrosis of BDS itself, narrowing of the BDS lumen, and narrowing of the anastomosis with the native bile duct	Only 1 of the 32 dogs survived for more than 6 mo. It was investigated in 32 dogs; however, in the end, fibrosis of the vein and stenosis of the anastomotic site with the native site occurred, and bile duct epithelial regeneration was not observed. It was concluded that the vein was not suitable for BDS
Ulin *et al* [17], 1955	*Ann Surg*	Vascularised jugular vein (10)	Polyethylene tube	Dog (10)	Ring (2.0-5.0)	CBC (10)	Maximum 10 mo	BDS itself	Necrosis of autologous tissue, narrowing of the lumen of autologous tissue, narrowing of the anastomosis with the native bile duct, necrosis of BDS itself, narrowing of the lumen of BDS, and narrowing of the anastomosis with the native bile duct	The omentum was used to maintain blood flow to the BDS, but in some cases, it functioned as a BDS only during the period when the stent was in place (6 out of 10 dogs). Bile duct regeneration process was not studied. No regeneration of the bile duct epithelium was observed
Myers *et al* [18], 1960	*Ann Surg*	Femoral vein and artery, bile duct (17), and homologous bile duct (6)	Polyethylene tube	Dog (28)	Ring (unknown)	CBC (23)	Maximum 449 d	BDS itself	Necrosis of autologous tissue, narrowing of the lumen of autologous tissue, narrowing of the anastomosis with the native bile duct, necrosis of BDS itself, narrowing of the BDS lumen, and narrowing of the anastomosis with the native bile duct	BDS using autologous veins, arteries, or allogeneic arteries also narrowed shortly after transplantation. No bile duct epithelial regeneration was observed
Dunphy and Stephens [19], 1962	*Ann Surg*	Autologous vein and artery (20), and homologous artery (32)	T-tube	Goat (44), dog (8)	Ring (1.0)	CBC (52)	Maximum 9 mo	BDS itself	Necrosis of autologous tissue, narrowing of the lumen of autologous tissue, narrowing of the anastomosis with the native bile duct, necrosis of BDS itself, narrowing of the BDS lumen, and narrowing of the anastomosis	In an experiment using autologous veins and T-tube as BDS, 2 dogs survived for more than 6 mo; however, both dogs demonstrated dilation of the bile duct on the liver side. No bile duct epithelial regeneration was observed

									with the native bile duct	
Belzer *et al* [44], 1965	*Ann Surg*	Femoral vein (20)	T-tube	Goat (20)	Patch (3.0-4.0)	Patch (20)	Maximum 11 mo	BDS itself	Necrosis of autologous tissue, narrowing of the lumen of autologous tissue, narrowing of the anastomosis with the native bile duct, necrosis of BDS itself, narrowing of the BDS lumen, and narrowing of the anastomosis with the native bile duct	Only 3 out of 20 dogs were intentionally killed, but no good bile duct epithelial regeneration was observed
Lindenauer and Child [47], 1966	*Ann Surg*	Vascularized jugular vein (14)	(-)	Dog (14)	Ring (unknown)	CBC (14)	Maximum 18 mo	BDS itself	The omentum increased blood flow to the BDS; however, it resulted in scar contraction. Necrosis of BDS itself, narrowing of the BDS lumen, and narrowing of the anastomosis with the native bile duct	No dog survived for more than 3.5 mo, although the omentum was used to maintain BDS blood flow
Palmes *et al* [48], 2009	*J Invest Surg*	External jugular vein (18)	PLA stent (12)	Pig (18)	Ring (2.0)	CBC (18)	Maximum 6 mo	BDS itself	When the stent was not inserted, the BDS was necrotic. When the stent was inserted, the BDS lumen was preserved, but eventually, it became necrotic and narrowed	Of the 18 dogs, all 12 stented dogs were deliberately killed. However, the process of regeneration of veins into the bile duct was not reported
Liang *et al* [49], 2012	*World J Gastroenterol*	Omentum (8)	Bioabsorbable stent	Pig (8)	Ring (0.5-1.0)	CBC (8)	Maximum 4 mo	BDS itself	The BDS lumen was preserved when the stent was inserted	The bile duct defect was repaired with an omentum, which was similar to inserting a T-tube into the defect. Bile duct regeneration was also poorly demonstrated

BDS: Bile duct substitute; CBC: Common bile duct to bile duct substitute to common bile duct; CBJ: Common bile duct to bile duct substitute to jejunum; GBC: Gallbladder to bile duct substitute to common bile duct; PLA: Polylactide acid.

[20] attached blood vessels to a BDS composed of polyvinyl sponge in dogs. Of the 12 dogs examined, 4 survived for more than 60 d, but the transplant was ultimately unsuccessful due to the formation of bile plugs inside the substitute. Dunphy and Stephens[19] examined Teflon as a BDS in four dogs and four sheep, but all failed because of severe rejection early in the transplantation. Recently, Gómez *et al*[23] investigated Gore-Tex as a BDS in 12 dogs and reported that 11 cases were successful. However, BDS was surrounded by strong fibrotic tissue and exhibited narrowing, indicating that it was not clinically usable in the long term (Table 2).

Currently, cyclic non-absorbable materials, such as polytetrafluoroethylene, are used clinically as artificial blood vessels. Anticoagulants are used to prevent blood from coagulating in artificial blood vessels when the blood vessel diameter is small[56]. Compared to blood, bile is more viscous and has a slower flow velocity. The bile duct diameter is similar to that of small blood vessels[57]. As such, this material may be unsuitable because the BDS lumen may be blocked by a bile plug[21,22]. In addition, the epithelium does not regenerate continuously at the anastomotic site between the BDS and native bile duct, scar contraction occurs in the long term after transplantation[38]. A bile plug may form if a tubular stent is inserted to secure bile passage, even when using non-bioabsorbable materials. This phenomenon

Table 2 Bile duct substitute using non-bioabsorbable material

Ref.	Journal	Substitute (*n*)	Stent	Animal type (*n*)	Size of BDS (cm)	Method of reconstruction of bile duct by BDS (*n*)	Observation period after implantation	Localization of regenerated bile duct	Causes of stenosis	Note (planned sacrificial death and epithelialization)
Dunphy and Stephens[19], 1962	*Ann Surg*	Teflon (8)	(-)	Dog (4), goat (4)	Ring (1.0)	CBC (8)	Maximum 7 wk	BDS outside	Narrowing of the anastomosis with the native bile duct; narrowing of the lumen of BDS	In all cases, the hepatobiliary enzyme levels increased, and no survivors were observed for more than 7 wk after transplantation
Bergan *et al*[20], 1962	*Arch Surg*	Vascularized polyvinyl sponge (21)	(-)	Dog (21)	Ring (0.5)	CBC (21)	Maximum 14 mo	BDS outside	Narrowing of the anastomosis with the native bile duct; narrowing of the lumen of BDS	Four out of 21 dogs survived for > 60 d after transplantation, and four of them had stenosis of BDS
Sherman *et al* [21], 1963	*Ann Surg*	Acrylamide with Dacron (33)	(-)	Dog (33)	Ring (1.5-3.5)	CBC (33)	Maximum 31 mo	BDS outside	Narrowing of the anastomosis with the native bile duct; narrowing of the lumen of BDS	Twenty-six out of 33 dogs died within 3 mo. In all cases, fibrotic thickening around the BDS and severe scar contraction had occurred at the site of anastomosis
Mendelowitz *et al*[22], 1982	*Am J Surg*	Gore-Tex (6), dacron (2)	(-)	Dog (8)	Ring (2.0-3.0), patch (2.0 cm × 1.0 cm)	Patch (Gore-Tex) (2), CBJ (Gore-Tex) (2), CBC (Gore-Tex) (1), CBC (Dacron) (2), GBJ (Gore-Tex) (1)	Maximum 40 d	BDS outside	Narrowing of the anastomosis with the native bile duct; narrowing of the lumen of BDS	In all cases, a bile plug was found in the lumen of the BDS, and a high degree of fibrotic thickening was found around the site of anastomosis
Gómez *et al*[23], 2002	*J Gastrointest Surg*	Gore-Tex (12)	(-)	Dog (12)	Ring (2.0-3.0)	CBC (12)	Maximum 3 mo	BDS outside	Narrowing of the lumen of BDS	Eleven out of 12 dogs were intentionally killed, but severe fibrotic thickening was observed around the BDS

BDS: Bile duct substitute; CBC: Common bile duct to bile duct substitute to common bile duct; CBJ: Common bile duct to bile duct substitute to jejunum; GBJ: Gallbladder to bile duct substitute to jejunum.

is similar to current endoscopic stenting for bile duct stenosis[58,59].

BDS using bioabsorbable material

Due to the failure to develop clinically applicable BDSs made from autologous tissue or non-bioabsorbable materials, increasing focus has been placed on bioabsorbable materials as BDSs. This concept is based on the technique of tissue engineering proposed by Langer and Vacanti[60] in 1993 for bile duct regeneration. The complex formed by the bioabsorbable material and cells attached to the material is absorbed in the body while the bioabsorbable material acts as a scaffold to maintain the environment and shape of the organ[60,61]. Concurrently, the cells attached to the scaffold regenerate the target organ. Natural polymers (particularly collagen)[24,27,28] and engineered synthetic polymers [25,26,62-64] have been investigated as BDSs based on bioabsorbable materials.

BDS using natural polymers

Alternative natural polymers to collagen have been investigated, such as the small intestinal submucosa (SIS) using porcine submucosa. Using this SIS, Rosen *et al*[24] reported that 9 cases of patch-like transplantation and 6 cases of circular transplantation were performed as BDS, and 13 of them were successful. However, bile duct regeneration was not observed as a pathological finding. On the other hand, in another study using SIS as a BDS, scar contraction was high[65]. As such, this material has not been clinically applied as a BDS (Table 3).

Nakashima *et al*[66] reported the successful use of collagen as a BDS in consideration of cell adhesion. However, collagen was attached to a non-bioabsorbable material (polypropylene) to maintain the hardness of this BDS; therefore, it may not be a strictly bioabsorbable BDS. The BDS scaffold was sutured to the native bile duct. As bile passes through the lumen, the scaffold must maintain an annular shape and therefore a degree of hardness. Collagen tends to lose its shape when immersed in water[66, 67]. Collagen-based BDSs require hardness in other substances to maintain the scaffold hardness, resulting in an absorption period longer than several months. For this reason, SIS uses collagen and submucosal tissue to maintain hardness[24].

To promote bile duct regeneration within the bioabsorbable material itself, the period of *in vivo* absorption of the bioabsorbable material is important for suppressing scar contraction. In the case of artificial skin using collagen for skin regeneration, it has been reported that the half-life of the bioabsorbable material, which most strongly suppresses scar contraction, is approximately 14 d[67]. If a BDS made of a bioabsorbable material has a half-life of 3-4 wk or more, scar contraction may be high. When bioabsorbable materials other than the skin are used as alternatives for bile duct regeneration, the absorption period of such materials must also be considered, but this is not the case for SIS[24].

In collagen-based BDSs, the density of the material ligand is important for cell adhesion to promote bile duct regeneration[68]. However, there is a paucity of research in this area. If attempts are made for bile duct regeneration within the bioabsorbable material itself, scar contraction of the BDS part cannot be suppressed after transplantation unless these points are taken into consideration.

BDS using synthetic polymers

BDSs based on synthetic polymers are predominantly composed of polyglycolic acid (PGA)[26] and polycaprolactone[24,62], BDSs produced using PGA fibers may fail to maintain their radial shape. In many studies, the major axis of the bile duct has been replaced by approximately 1 cm. The absorption period of PGA is approximately 3 mo; as such, chronic inflammation occurs, and bile duct regeneration occurs at the implanted site. As such, attempts to regenerate the bile duct epithelium on the inner surface (bile passage surface) of this BDS eventually cause scar contraction similar to that of non-bioabsorbable BDS, and previous efforts have been unsuccessful[24,61].

Studies employing polycaprolactone-based BDSs have reported good bile duct regeneration outside the BDS implant. The material in these studies comprised a 50:50 copolymer of lactic acid and caprolactone, which was reinforced with latticed PGA fibers to facilitate suturing[25]. Generally, the absorption period is 6-8 wk, and the material becomes vulnerable *in vivo* for approximately 3 wk. After the BDS becomes fragile and sheds into the duodenum, a bile duct thicker than the outer circumference of the BDS regenerates outside the BDS. Cells migrating to the BDS as a foreign body reaction may promote bile duct regeneration[25]. Previous studies have reported good results, including BDS experiments in infectious reservoirs[69]. The occurrence of bile duct regeneration on the outside of the BDS resembles bile duct regeneration after insertion of a T-tube into a defective bile duct followed by T-tube removal (Table 3).

As BDSs using synthetic polymers can be engineered, the period of absorption in the body can be adjusted[70]. However, if the BDS is hard to maintain the shape of the bile duct, the absorption period may be prolonged. As BDS results in longer chronic inflammation due to a foreign body reaction, the results are likely to be similar to those of non-bioabsorbable materials. In contrast, if the absorption period is too short, the BDS transplantation site becomes fragile and is destroyed after transplantation. Bile may flow out of the BDS transplantation site, making this material unsuitable for BDS. With regard to cell adhesion, the scaffold itself (for example, PGA only) has lower cell adhesion compared to collagen-based scaffolds owing to the lack of receptors for cell adhesion[38]. Therefore, to regenerate the scaffold itself within the bile duct, materials in which receptors are added to the scaffold have been investigated[38]. Failure of the bile duct to regenerate in the scaffold part while being absorbed prevents clinical application as a BDS; hence, these materials remain in the development stage.

BDS made of other materials

In recent years, attempts have been made to utilize decellularized tissues as BDSs because of the lack of an immune reaction when transplanted into a living organism[29,30]. The use of decellularized tissues as scaffolds for liver regeneration has been investigated. The bile was reported to drain into the duodenum as a tube for a prolonged period and functioned while the stent was inserted. However, reports of long-term bile duct regeneration and function after stent removal are lacking.

Scaffolds of the same shape as that of the extrahepatic bile duct have been produced using 3D printing[41,42]. The extrahepatic bile duct has been reported to regenerate in a ring shape, but no

Table 3 Bile duct substitute using bioabsorbable material

Ref.	Journal	Substitute	Stent	Animal type (*n*)	Size of BDS (cm)	Method of reconstruction of bile duct by BDS (*n*)	Observation period after implantation	Localization of regenerated bile duct	Causes of stenosis	Note (planned sacrificial death and epithelialization)
Rosen *et al* [24], 2002	*Surgery*	SIS	(-)	Dog (15)	Patch: (2.0 cm × 1.0 cm), ring: (2.0-3.0)	Patch (9), CBC (6)	Maximum 5 mo	BDS itself	Scar contraction at the site of anastomosis on the duodenal side	Thirteen out of 15 dogs were intentionally killed. The regenerated bile duct tissue was shown consequently, and the process of regenerating the bile duct was not shown
Miyazawa *et al*[25], 2005	*Am J Transplant*	P (CL/LLA) with PGA	(-)	Pig (18)	Ring (3.0)	CBJ (18)	Maximum 6 mo	BDS outside	No narrowed BDS	All pigs were intentionally killed. A good bile duct regeneration process was shown
Nau *et al* [26], 2011	*HPB (Oxford)*	PGA and TMC	5 Fr pancreatic stent	Dog (11)	Ring (1.0)	CBC (11)	Maximum 12 mo	BDS itself	Narrowing of the BDS lumen	Ten out of 11 dogs were intentionally killed. No good bile duct epithelial regeneration was observed
Li *et al*[27], 2012	*Biomaterials*	Collagen with bFGF	(-)	Pig (26)	Patch (2.0 cm × 1.0 cm)	Patch (26)	Maximum 6 mo	BDS itself	No narrowed BDS	All pigs were intentionally killed. The regenerated bile duct tissue was shown consequently, while the process of regenerating the bile duct was not shown
Tao *et al*[28], 2015	*Artif Organs*	Collagen	Plastic stent	Pig (20)	Patch (2.0 cm × 0.6 cm)	Patch (12)	Maximum 12 wk	BDS itself	No narrowed BDS	All pigs were intentionally killed. The regenerated bile duct tissue was observed consequently, while the process of regenerating the bile duct was not shown
Tanimoto *et al*[62], 2016	*Langenbecks Arch Surg*	P (CL/LLA)	T-tube	Pig (11)	Ring (2.0)	CBC (11)	Maximum 6 mo	BDS itself	No narrowed BDS	All pigs were intentionally killed. A high degree of fibrosis was observed in the regenerated bile duct tissue
de Abreu *et al*[63], 2020	*J Biomater Appl*	Bacterial cellulose film	T-tube	Pig (10)	Patch (2.0 cm × 1.0 cm)	CBC (20)	Maximum 330 d	BDS itself	No narrowed BDS	All pigs were intentionally killed. No process of bile duct regeneration was shown

BDS: Bile duct substitute; bFGF: Basic fibroblast growth factor; CBC: Common bile duct to bile duct substitute to common bile duct; CBJ: Common bile duct to bile duct substitute to jejunum; P(CL/LLA): Polyε-caprolactone/poly l-lactide; PGA: Polyglycolic acid; SIS: Small intestinal submucosa; TMC: Trimethylene carbonate.

studies to date have examined bile duct regeneration using these BDSs. Furthermore, there have been efforts to develop an actual bile duct as an organoid *in vitro* for transplantation[70]. However, it has not been possible to produce organoids of a certain length in the longitudinal direction for clinical use and with a length that can be sutured.

FACTORS TO CONSIDER FOR BDS DEVELOPMENT

Below, we discuss the factors that should be considered in the development of clinically applicable BDSs.

Bile duct wound healing

Bile duct regeneration must occur concurrently with wound healing[40,50,51]. Notably, the natural course of wound healing involves scar contraction. Therefore, if the BDS does not reduce scar contraction, the migrating cell mass results in scar contraction and lumen narrowing after removal of the BDS or decomposition and absorption[35,51]. For the BDS to promote bile duct regeneration, the BDS implant must be guided into the regeneration process while maintaining the shape of the bile duct rather than increasing scarring of the cell mass[40]. As such, which allows the cell mass that regenerates the bile duct to maintain the shape of the bile duct when the BDS is absorbed or removed.

A BDS made of a non-bioabsorbable material that has been present in the body for a prolonged period retains its shape until the BDS is removed, but the lumen is prone to clogging by bile plugs[20-22]. Further, the anastomotic site with the native bile duct will be narrowed due to connective tissue growth[50,51]. Current bile duct regeneration methods using BDSs suggest that after the cell mass gathers around the foreign body and the BDS forms the shape of the bile duct, the cell mass regenerates as a bile duct after BDS removal[25]. If the BDS cannot maintain the shape of the bile duct, a stent may be used instead.

Studies have demonstrated that bone marrow-derived and adipose-derived cells are effective in suppressing scar contraction[72,73]. In addition, it has been reported that fibrosis is suppressed by controlling the function of macrophages that have migrated to the injured region during the remodeling period of wound healing[40,51]. However, methods for reliably suppressing scar contraction have yet to be developed[72,73]. For bile duct regeneration and retention of normal tissue structure, it is necessary for the dynamics and function of multiple types of cells that have migrated around the BDS to be tightly regulated and to reduce scar contraction.

Bile properties

Compared to blood, bile is more viscous and has a slower velocity[57]. If a BDS is not absorbed in the body, a bile plug may adhere to the BDS at the anastomosis site with the lumen or native bile duct. This results in impaired bile flow and narrowing of the lumen. In studies using Teflon (a non-bioabsorbable material) as a BDS, anticoagulants are often used even for blood. Therefore, further measures are required to prevent bile plug formation. This resembles the insertion of metal or tube stents for the treatment of bile duct stenosis, which often clogs the stent with a bile plug[58,59].

Bile duct regeneration

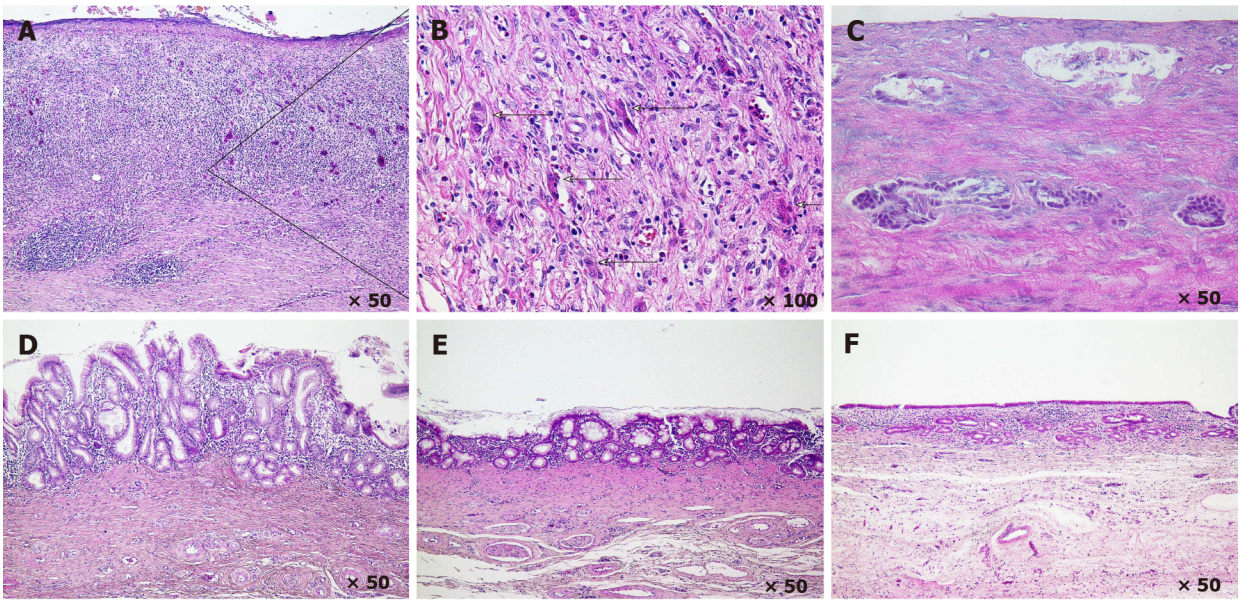
The extrahepatic bile duct is a component of the digestive tract, and the mature bile duct is regenerated *via* a regeneration process similar to that of the stomach and intestine[36,74,75]. In pigs, it takes approximately 6 mo for bile duct stem/progenitor cells to undergo regeneration to form a mature bile duct similar to the native bile duct. Furthermore, the bile duct epithelium is covered with a layer of cubic columnar epithelial cells[25] (Figures 1 and 2). Therefore, it is controversial in studies that do not show the process of bile duct regeneration, even if BDS transplantation is reported to be successful. For example, in the subsequent regeneration of the T-tube insertion site, the portion of the hole with the T-tube inserted reproduced well without any narrowing. This suggests that small partial bile duct regeneration often occurs without stenosis even if a patch of omentum or blood vessel is applied externally[76]. However, if bile duct defects are extensive and the BDS is placed between the native bile ducts, the cell mass must undergo substantial regeneration from the early stage of bile duct regeneration to regenerate the bile duct without stenosis. Studies have demonstrated that cells attached to the bioabsorbable material regenerate the bile ducts, but the mechanisms by which these cells undergo bile duct regeneration in the presence of the bioabsorbable material remain unclear[24].

Immature cells attached to the scaffold migrate using the scaffold of the BDS as a foreign substance [40,50]. These cell masses first form an assembly of the peribiliary gland[25,74,75]. When good bile duct regeneration is achieved approximately 2 mo after the initial stage of regeneration, a tall papillary shape is formed on the inner surface through which bile passes. In pigs, after approximately 3 mo of bile duct regeneration, these peribiliary glands fuse and the epithelial cells become shorter; within approximately 6 mo, these structures mature into bile ducts that are similar to native bile ducts (Figures 1 and 2)[25].

With regard to the mechanisms of bile duct regeneration in the injured part of the bile duct, activated bile duct cells mobilize immune cells, vascular cells, and mesenchymal cells to the inflamed region as a ductular reaction during bile duct ligation and inflammation[77]. This process is involved in regeneration of the inflamed area. Inflammation-activated bile duct cells secrete chemokines, cytokines, and angiogenic factors, which are involved in wound healing[35,50,51]. Furthermore, reactive ductal cells generated *via* complex mechanisms depend on the nature and intensity of bile duct injury[35,50,51]. However, further investigations of bile duct regeneration mechanisms in various bile duct injuries, such as circular transplantation of BDS, are required to develop effective BDSs.

Regeneration of anastomotic site

When the anastomosis between a BDS and the native bile duct is narrowed, the flow of bile into the duodenum is obstructed, which limits the clinical application of the BDS. In a normal gastrointestinal anastomosis, a large anastomotic hole and fixed shape that does not experience deformation are



DOI: 10.3748/wjg.v28.i39.5707 **Copyright** ©The Author(s) 2022.

Figure 2 Histology of bile duct regeneration on the outside of the short-term absorption type bile duct substitute. A and B: At 3 wk after bile duct substitute (BDS) implantation, a cell population in the stroma that may comprise the origin of the peribiliary gland is observed; C: At 5 wk after BDS implantation, a ring-shaped biliary gland-like structure is observed in which cell masses that are thought to form peribiliary glands are fused; D: At 7 wk after BDS implantation, many bile duct appendages are observed on the bile passage surface, and the epithelial surface exhibits a high papillary morphology; E: At 12 wk after BDS implantation, the number of peribiliary gland on the bile passage surface is decreased, the appendages begin to fuse, and the epithelial surface becomes more even; F: At 6 mo after BDS implantation, the epithelial surface becomes a single layer of cubic columnar epithelium, similar to the native bile duct.

prerequisites to prevent narrowing of the anastomosis[78]. Therefore, in surgical practice, a stent is inserted when the anastomotic hole is small[78]. For BDSs made from non-bioabsorbable materials, the extrahepatic bile duct is thin; hence, the anastomotic site with the native bile duct is likely to be narrowed by connective tissue in the absence of stent insertion. To prevent anastomotic stenosis between the BDS and the native bile duct, it may be necessary to insert a stent through the anastomotic site to maintain its shape. Even for BDSs made from bioabsorbable materials, it may be difficult to maintain the shape of the anastomotic site and stent insertion is recommended to prevent stenosis.

Localization of bile duct regeneration to BDS

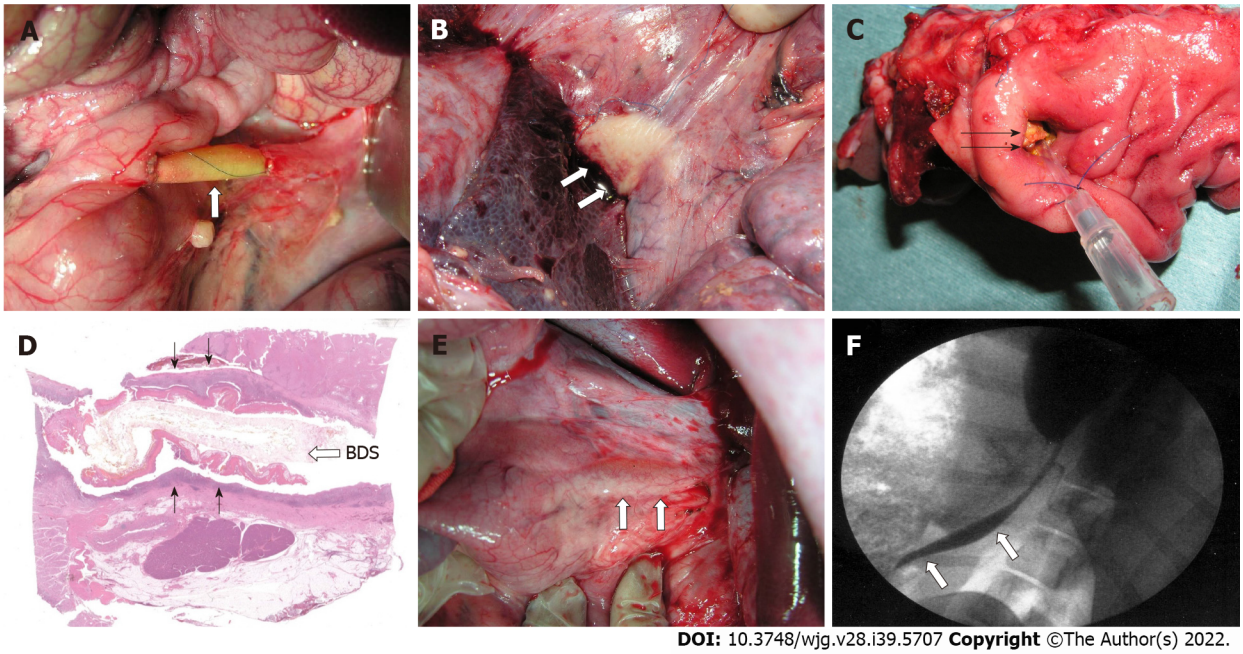
Three regenerative localizations of the neo-bile duct with respect to the BDS have been identified: Outside the BDS, within part of the BDS itself, and inside the BDS (bile passage surface). If the BDS is present for a prolonged period, chronic inflammation will persist[50,51]. As such, it is unlikely that the cell mass that has migrated due to detection of the BDS as a foreign substance will regenerate into a structure similar to the native bile duct at the site of the BDS in the context of wound healing[20-22,51].

If the BDS is present for a prolonged period, the bile duct does not regenerate outside the BDS or as part of the BDS itself. Bile duct stem cells do not appear to adhere to the luminal surface of non-living non-absorbable materials, such as T-tubes. Given that the bile duct does not tend to narrow after T-tube removal, a cell mass that has migrated outside the BDS is formed. In the absence of BDS, the cell mass is exposed to fresh bile and regenerates as a bile duct, which may promote good bile duct regeneration at the BDS transplant site[25] (Figures 3 and 4).

The use of decellularized tissue as a BDS is thought to promote bile duct regeneration by cell adhesion to the luminal surface or inside the scaffold[29,30]. For BDSs made of bioabsorbable materials with a short absorption period, cell clusters contributing to bile duct regeneration migrate to the outside of the BDS and regenerate the bile duct. This bioabsorbable material may become fragile in approximately 3 wk and shed to the duodenal side, after which the cells surrounding the BDS regenerate the bile duct[25] (Figures 3 and 4). Although further research is needed, the extant literature suggests that the cell mass forms a ring-shaped structure more rapidly than during chronic inflammation and subsequently disappears from the site. Collectively, these findings suggest that bioabsorbable materials that induce good bile duct regeneration may be harnessed as effective BDSs.

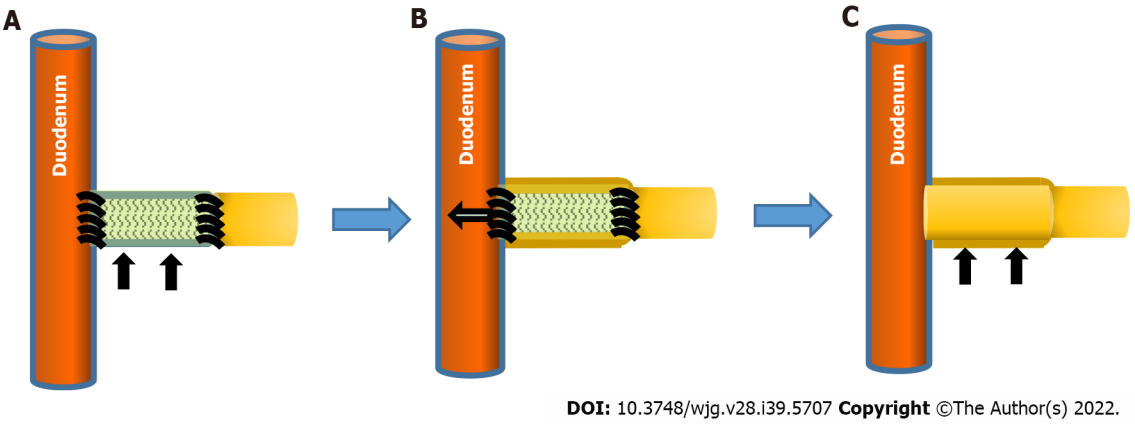
RESEARCH LIMITATIONS

One study reported that when a stent was placed in the BDS, bile flowed through the stent for a certain period, resulting in a successful BDS. However, the study did not demonstrate bile duct regeneration.



DOI: 10.3748/wjg.v28.i39.5707 **Copyright** ©The Author(s) 2022.

Figure 3 Bile duct substitutes using bioabsorbable material (synthetic polymer with short absorption period). A: A bile duct substitute (BDS) using bioabsorbable material is implanted to bypass the extrahepatic bile duct (3 cm in size). Three weeks post-BDS implantation; B: White cell clusters are observed on the outside of the BDS; C: A vulnerable BDS is observed from the duodenal side; D: Dark purple connective tissue is noted on the outside of the BDS; E: At 6 mo after BDS implantation, the neo-bile duct is macroscopically similar to the natural common bile duct have been regenerated (arrow); F: Cholangiography (6 mo after BDS implantation). The BDS implant and anastomotic site become unknown, and the contrast medium flows smoothly into the duodenum (white arrows).



DOI: 10.3748/wjg.v28.i39.5707 **Copyright** ©The Author(s) 2022.

Figure 4 Regeneration of the neo-bile duct outside the short-term absorption type bile duct substitute. A: Bile duct substitute (BDS) (black arrows) is anastomosed to the native extrahepatic bile duct; B: Immature cells attach around the BDS, forming a cylindrical cell mass outside the BDS. The bioabsorbable polymer that comprise BDS becomes fragile in the living body from approximately 3 wk and sheds to the duodenal side; C: After BDS is no longer present at the transplant site, immature cell clusters mature as bile duct cells and the bile ducts are regenerated as tissue (black arrows).

This process is similar to that of stent insertion during the treatment of benign bile duct stenosis. Nevertheless, the alternative portion eventually becomes stenotic and clinically unusable over a prolonged period. Our analysis was unable to identify these issues accurately. Although numerous studies using various BDSs have been conducted, the lack of success highlights the limitations of the field. Moreover, we did not analyze successful cases in small animals or studies using a small number of large animals.

FUTURE PERSPECTIVES

Extant research has provided novel insights into the mechanisms of repair after tissue damage[75]. If the injured area does not undergo normal repair, a high degree of fibrosis will occur in the injured area, resulting in scar formation at the site. For bile duct injuries, the injured area or the BDS implant may

become stenotic. For the regeneration of a bile duct similar to the native bile duct at the injury site, cells that have migrated to the bile duct injury site must suppress scar contraction, similar to the regeneration of other organs. In this regard, it is necessary to create a niche for bile duct regeneration similar to that of the native bile duct[73,75]. In addition, chronic inflammation is associated with prolonged and severe fibrosis, resulting in scar formation. Therefore, a BDS should not remain at the transplantation site for a prolonged period.

Based on these caveats, two methods can be considered for regenerating a bile duct similar to the native bile duct at the BDS transplantation site. The first involves the use of a short-term absorption type of bioabsorbable BDS, in which cells that have migrated to repair bile duct injury (BDS transplantation site) form the shape of the bile duct *via* a foreign body reaction. Ultimately, the BDS will no longer be present at that site and chronic inflammation does not occur (*i.e.*, the bile duct regenerates outside the BDS)[25] (Figure 4). The second method involves bile duct stem/progenitor cells adhering to part of the BDS itself, and wound healing is regulated such that bile duct regeneration progresses well while the BDS is being absorbed. Therefore, it is necessary to develop a method to control wound healing so that the scaffold portion of the decellularized tissue and adhering cells do not cause scar contraction. In summary, bioabsorbable BDSs for bile duct regeneration outside the bile duct constitute a promising development that will be clinically useful in the future.

CONCLUSION

To date, successful BDSs have not been developed. This is predominantly due to poor mechanistic understanding and lack of methods for regulating bile duct wound healing and bile duct regeneration. As an alternative to the extrahepatic bile duct, bioabsorbable materials can be used to form the shape of the bile duct, and the cell mass forming the shape of the bile duct can migrate to the external surface of this structure. Once the cell mass was able to maintain the shape of the bile duct, the BDS acting as a scaffold was removed. The development of BDSs that enable this process will permit the treatment of a wide range of bile duct defects.

ACKNOWLEDGEMENTS

The authors would like to thank Dr. Naoe Akimoto for her excellent technical assistance.

FOOTNOTES

Author contributions: Miyazawa M designed and carried out the data analyses, prepared the figures, and wrote the manuscript; Aikawa M, Takashima J, and Ohnishi S performed data analysis; Ikada Y contributed to the design of the polymer and supervised the project.

Supported by the Japan Society for the Promotion of Science, No. 21K08786.

Conflict-of-interest statement: All the authors report no relevant conflicts of interest for this article.

Open-Access: This article is an open-access article that was selected by an in-house editor and fully peer-reviewed by external reviewers. It is distributed in accordance with the Creative Commons Attribution NonCommercial (CC BY-NC 4.0) license, which permits others to distribute, remix, adapt, build upon this work non-commercially, and license their derivative works on different terms, provided the original work is properly cited and the use is non-commercial. See: https://creativecommons.org/Licenses/by-nc/4.0/

Country/Territory of origin: Japan

ORCID number: Mitsuo Miyazawa 0000-0002-7364-6086; Masayasu Aikawa 0000-0002-6706-8734; Junpei Takashima 0000-0002-1231-482X; Hirotoshi Kobayashi 0000-0002-4381-0439; Shunsuke Ohnishi 0000-0003-1194-4149; Yoshito Ikada 000-0002-9677-3993.

S-Editor: Wang JJ
L-Editor: A
P-Editor: Wang JJ

REFERENCES

1 **Asbun HJ**, Moekotte AL, Vissers FL, Kunzler F, Cipriani F, Alseidi A, D'Angelica MI, Balduzzi A, Bassi C, Björnsson B, Boggi U, Callery MP, Del Chiaro M, Coimbra FJ, Conrad C, Cook A, Coppola A, Dervenis C, Dokmak S, Edil BH, Edwin B, Giulianotti PC, Han HS, Hansen PD, van der Heijde N, van Hilst J, Hester CA, Hogg ME, Jarufe N, Jeyarajah DR, Keck T, Kim SC, Khatkov IE, Kokudo N, Kooby DA, Korrel M, de Leon FJ, Lluis N, Lof S, Machado MA, Demartines N, Martinie JB, Merchant NB, Molenaar IQ, Moravek C, Mou YP, Nakamura M, Nealon WH, Palanivelu C, Pessaux P, Pitt HA, Polanco PM, Primrose JN, Rawashdeh A, Sanford DE, Senthilnathan P, Shrikhande SV, Stauffer JA, Takaori K, Talamonti MS, Tang CN, Vollmer CM, Wakabayashi G, Walsh RM, Wang SE, Zinner MJ, Wolfgang CL, Zureikat AH, Zwart MJ, Conlon KC, Kendrick ML, Zeh HJ, Hilal MA, Besselink MG; International Study Group on Minimally Invasive Pancreas Surgery (I-MIPS). The Miami International Evidence-based Guidelines on Minimally Invasive Pancreas Resection. *Ann Surg* 2020; **271**: 1-14 [PMID: 31567509 DOI: 10.1097/SLA.0000000000003590]

2 **Suda K**, Nakauchi M, Inaba K, Ishida Y, Uyama I. Minimally invasive surgery for upper gastrointestinal cancer: Our experience and review of the literature. *World J Gastroenterol* 2016; **22**: 4626-4637 [PMID: 27217695 DOI: 10.3748/wjg.v22.i19.4626]

3 **Hui VW**, Guillem JG. Minimal access surgery for rectal cancer: an update. *Nat Rev Gastroenterol Hepatol* 2014; **11**: 158-165 [PMID: 24192606 DOI: 10.1038/nrgastro.2013.203]

4 **di Pietro M**, Canto MI, Fitzgerald RC. Endoscopic Management of Early Adenocarcinoma and Squamous Cell Carcinoma of the Esophagus: Screening, Diagnosis, and Therapy. *Gastroenterology* 2018; **154**: 421-436 [PMID: 28778650 DOI: 10.1053/j.gastro.2017.07.041]

5 **Mönig S**, Chevallay M, Niclauss N, Zilli T, Fang W, Bansal A, Hoeppner J. Early esophageal cancer: the significance of surgery, endoscopy, and chemoradiation. *Ann N Y Acad Sci* 2018; **1434**: 115-123 [PMID: 30138532 DOI: 10.1111/nyas.13955]

6 **Strasberg SM**. A three-step conceptual roadmap for avoiding bile duct injury in laparoscopic cholecystectomy: an invited perspective review. *J Hepatobiliary Pancreat Sci* 2019; **26**: 123-127 [PMID: 30828991 DOI: 10.1002/jhbp.616]

7 **Rystedt J**, Lindell G, Montgomery A. Bile Duct Injuries Associated With 55,134 Cholecystectomies: Treatment and Outcome from a National Perspective. *World J Surg* 2016; **40**: 73-80 [PMID: 26530691 DOI: 10.1007/s00268-015-3281-4]

8 **Rose JB**, Bilderback P, Raphaeli T, Traverso W, Helton S, Ryan JA Jr, Biehl T. Use the duodenum, it's right there: a retrospective cohort study comparing biliary reconstruction using either the jejunum or the duodenum. *JAMA Surg* 2013; **148**: 860-865 [PMID: 23884401 DOI: 10.1001/jamasurg.2013.2701]

9 **Horgan E**. Reconstruction of the Common Bile Duct by end-to-end Anastomosis. *Ann Surg* 1931; **93**: 1162-1166 [PMID: 17866582 DOI: 10.1097/00000658-193106000-00010]

10 **Pearce AE**, Ulin AW, Entine JH, Froio GF. Experimental reconstruction of the extrahepatic biliary system using free venous grafts. *Ann Surg* 1951; **134**: 808-814 [PMID: 14885945 DOI: 10.1097/00000658-195111000-00003]

11 **Brewer GE**. VIII. Hepaticoduodenal Anastomosis. *Ann Surg* 1910; **51**: 830-833 [PMID: 17862542 DOI: 10.1097/00000658-191006000-00008]

12 **Clements O**, Eliahoo J, Kim JU, Taylor-Robinson SD, Khan SA. Risk factors for intrahepatic and extrahepatic cholangiocarcinoma: A systematic review and meta-analysis. *J Hepatol* 2020; **72**: 95-103 [PMID: 31536748 DOI: 10.1016/j.jhep.2019.09.007]

13 **Tocchi A**, Mazzoni G, Liotta G, Lepre L, Cassini D, Miccini M. Late development of bile duct cancer in patients who had biliary-enteric drainage for benign disease: a follow-up study of more than 1,000 patients. *Ann Surg* 2001; **234**: 210-214 [PMID: 11505067 DOI: 10.1097/00000658-200108000-00011]

14 **Kubo S**, Kinoshita M, Takemura S, Tanaka S, Shinkawa H, Nishioka T, Hamano G, Ito T, Abue M, Aoki M, Nakagawa K, Unno M, Hijioka S, Fujiyoshi T, Shimizu Y, Mizuguchi T, Shirabe K, Nishie A, Oda Y, Takenaka K, Kobarai T, Hisano T, Saiura A, Numao H, Toda M, Kuwae Y, Nakanuma Y, Endo G. Characteristics of printing company workers newly diagnosed with occupational cholangiocarcinoma. *J Hepatobiliary Pancreat Sci* 2014; **21**: 809-817 [PMID: 25088751 DOI: 10.1002/jhbp.137]

15 **Shea PC Jr**, Hubay CA. Experimental Repair of Common Duct Defects Utilizing a Free Vein Graft Over Blakemore-Lord Tubes. *Ann Surg* 1948; **128**: 21-29 [PMID: 17859179 DOI: 10.1097/00000658-194807000-00005]

16 **Kirby CK**, Fitts WT Jr. Reconstruction of the bile ducts with an isolated segment of jejunum; an experimental study. *Arch Surg (1920)* 1950; **61**: 462-468 [PMID: 15433726 DOI: 10.1001/archsurg.1950.01250020467006]

17 **Ulin AW**, Shoemaker WC, Entine JH. Vascularized venous grafts in the experimental reconstruction of the common bile duct. *Ann Surg* 1955; **142**: 279-282 [PMID: 13239064 DOI: 10.1097/00000658-195508000-00016]

18 **Myers RT**, Meredith JH, Rhodes J, Gilbert JW. The fate of free grafts in the common bile duct. *Ann Surg* 1960; **151**: 776-782 [PMID: 14425624]

19 **Dunphy JE**, Stephens FO. Experimental Study of the Effect of Grafts in the Common Duct on Biliary and Hepartic Function. *Ann Surg* 1962; **155**: 906-919 [PMID: 17859703 DOI: 10.1097/00000658-196206000-00011]

20 **Bergan JJ**, Anderson MC, Lounsbury BF. Vascularized polyvinyl sponge prosthesis. Its use to replace the canine common bile duct. *Arch Surg* 1962; **84**: 301-305 [PMID: 13867620 DOI: 10.1001/archsurg.1962.01300210035007]

21 **Sherman RT**, Jackson TM, Nielson CA, Wilson H. Reconstruction of the common bile duct with an acrylate-amide prosthesis. *Ann Surg* 1963; **158**: 420-430 [PMID: 14061708 DOI: 10.1097/00000658-196309000-00010]

22 **Mendelowitz DS**, Beal JM. Expanded polytetrafluoroethylene in reconstruction of the canine biliary system. *Am J Surg* 1982; **143**: 221-224 [PMID: 7058992 DOI: 10.1016/0002-9610(82)90073-3]

23 **Gómez NA**, Alvarez LR, Mite A, Andrade JP, Alvarez JR, Vargas PE, Tomalá NE, Vivas AF, Zapatier JA. Repair of bile duct injuries with Gore-Tex vascular grafts: experimental study in dogs. *J Gastrointest Surg* 2002; **6**: 116-120 [PMID: 11986027 DOI: 10.1016/s1091-255x(01)00038-5]

24 **Rosen M**, Ponsky J, Petras R, Fanning A, Brody F, Duperier F. Small intestinal submucosa as a bioscaffold for biliary tract regeneration. *Surgery* 2002; **132**: 480-486 [PMID: 12324762 DOI: 10.1067/msy.2002.126505]

25 **Miyazawa M**, Torii T, Toshimitsu Y, Okada K, Koyama I, Ikada Y. A tissue-engineered artificial bile duct grown to

resemble the native bile duct. *Am J Transplant* 2005; **5**: 1541-1547 [PMID: 15888066 DOI: 10.1111/j.1600-6143.2005.00845.x]

26 **Nau P**, Liu J, Ellison EC, Hazey JW, Henn M, Muscarella P, Narula VK, Melvin WS. Novel reconstruction of the extrahepatic biliary tree with a biosynthetic absorbable graft. *HPB (Oxford)* 2011; **13**: 573-578 [PMID: 21762301 DOI: 10.1111/j.1477-2574.2011.00337.x]

27 **Li Q**, Tao L, Chen B, Ren H, Hou X, Zhou S, Zhou J, Sun X, Dai J, Ding Y. Extrahepatic bile duct regeneration in pigs using collagen scaffolds loaded with human collagen-binding bFGF. *Biomaterials* 2012; **33**: 4298-4308 [PMID: 22429981 DOI: 10.1016/j.biomaterials.2012.03.003]

28 **Tao L**, Li Q, Ren H, Chen B, Hou X, Mou L, Zhou S, Zhou J, Sun X, Dai J, Ding Y. Repair of extrahepatic bile duct defect using a collagen patch in a Swine model. *Artif Organs* 2015; **39**: 352-360 [PMID: 25345752 DOI: 10.1111/aor.12388]

29 **Cheng Y**, Xiong XZ, Zhou RX, Deng YL, Jin YW, Lu J, Li FY, Cheng NS. Repair of a common bile duct defect with a decellularized ureteral graft. *World J Gastroenterol* 2016; **22**: 10575-10583 [PMID: 28082809 DOI: 10.3748/wjg.v22.i48.10575]

30 **Chakhunashvili K**, Kiladze M, G Chakhunashvili D, Karalashvili L, Kakabadze Z. A three-dimensional scaffold from decellularized human umbilical artery for bile duct reconstruction. *Ann Ital Chir* 2019; **90**: 165-173 [PMID: 30530984]

31 **Rodríguez-Garay EA**, Agüero RM, Pisani G, Trbojevich RA, Farroni A, Viglianco RA. Rat model of mild stenosis of the common bile duct. *Res Exp Med (Berl)* 1996; **196**: 105-116 [PMID: 8739800 DOI: 10.1007/BF02576832]

32 **Şahiner İT**, Kendirci M. Retrospective Clinical Study of the Effects of T-Tube Placement for Bile Duct Stricture. *Med Sci Monit* 2017; **23**: 4328-4333 [PMID: 28883388 DOI: 10.12659/msm.906630]

33 **Singhi AD**, Nikiforova MN, Chennat J, Papachristou GI, Khalid A, Rabinovitz M, Das R, Sarkaria S, Ayasso MS, Wald AI, Monaco SE, Nalesnik M, Ohori NP, Geller D, Tsung A, Zureikat AH, Zeh H, Marsh JW, Hogg M, Lee K, Bartlett DL, Pingpank JF, Humar A, Bahary N, Dasyam AK, Brand R, Fasanella KE, McGrath K, Slivka A. Integrating next-generation sequencing to endoscopic retrograde cholangiopancreatography (ERCP)-obtained biliary specimens improves the detection and management of patients with malignant bile duct strictures. *Gut* 2020; **69**: 52-61 [PMID: 30971436 DOI: 10.1136/gutjnl-2018-317817]

34 **Bill JG**, Mullady DK. Stenting for Benign and Malignant Biliary Strictures. *Gastrointest Endosc Clin N Am* 2019; **29**: 215-235 [PMID: 30846150 DOI: 10.1016/j.giec.2018.12.001]

35 **Wynn TA**, Ramalingam TR. Mechanisms of fibrosis: therapeutic translation for fibrotic disease. *Nat Med* 2012; **18**: 1028-1040 [PMID: 22772564 DOI: 10.1038/nm.2807]

36 **Cardinale V**, Wang Y, Carpino G, Mendel G, Alpini G, Gaudio E, Reid LM, Alvaro D. The biliary tree--a reservoir of multipotent stem cells. *Nat Rev Gastroenterol Hepatol* 2012; **9**: 231-240 [PMID: 22371217 DOI: 10.1038/nrgastro.2012.23]

37 **Sutton ME**, op den Dries S, Koster MH, Lisman T, Gouw AS, Porte RJ. Regeneration of human extrahepatic biliary epithelium: the peribiliary glands as progenitor cell compartment. *Liver Int* 2012; **32**: 554-559 [PMID: 22171992 DOI: 10.1111/j.1478-3231.2011.02721.x]

38 **Barber WH**. Choledocho-enterostomy and postoperative dilation of the bile-ducts: An experimental study. *Ann Surg* 1919; **70**: 530-534 [PMID: 17864188 DOI: 10.1097/00000658-191911000-00004]

39 **Yannas IV**, Tzeranis DS, So PTC. Regeneration of injured skin and peripheral nerves requires control of wound contraction, not scar formation. *Wound Repair Regen* 2017; **25**: 177-191 [PMID: 28370669 DOI: 10.1111/wrr.12516]

40 **Gurtner GC**, Werner S, Barrandon Y, Longaker MT. Wound repair and regeneration. *Nature* 2008; **453**: 314-321 [PMID: 18480812 DOI: 10.1038/nature07039]

41 **Li H**, Yin Y, Xiang Y, Liu H, Guo R. A novel 3D printing PCL/GelMA scaffold containing USPIO for MRI-guided bile duct repair. *Biomed Mater* 2020; **15**: 045004 [PMID: 32092713 DOI: 10.1088/1748-605X/ab797a]

42 **Dhir V**, Itoi T, Fockens P, Perez-Miranda M, Khashab MA, Seo DW, Yang AM, Lawrence KY, Maydeo A. Novel ex vivo model for hands-on teaching of and training in EUS-guided biliary drainage: creation of "Mumbai EUS" stereolithography/3D printing bile duct prototype (with videos). *Gastrointest Endosc* 2015; **81**: 440-446 [PMID: 25475900 DOI: 10.1016/j.gie.2014.09.011]

43 **Santos M**, Smith ML, Hughes CW, Riley PA Jr. Reconstruction of the bile ducts: an experimental study using free arterial grafts and nylon mesh tubes. *Surgery* 1957; **42**: 462-473 [PMID: 13467600]

44 **Belzer FO**, Watts JM, Ross HB, Dunphy JE. Auto-reconstruction of the common bile duct after venous patch graft. *Ann Surg* 1965; **162**: 346-355 [PMID: 5318669 DOI: 10.1097/00000658-196509000-00004]

45 **Rieger IT**, Wahl FJ, Hass GM. Experimental substitution of the common bile duct with an autologous ureteral graft. *J Urol* 1953; **69**: 487-491 [PMID: 13053611 DOI: 10.1016/s0022-5347(17)68099-6]

46 **Schatten WE**, Cramer LM, Herbsman H, Swarm RL. Experimental reconstruction of the common bile duct with split thickness skin grafts. *Surg Gynecol Obstet* 1957; **105**: 747-753 [PMID: 13495840]

47 **Lindenauer SM**, Child CG 3rd. Vascularized venous autografts in common bile duct reconstruction. *Arch Surg* 1966; **92**: 749-751 [PMID: 5934220 DOI: 10.1001/archsurg.1966.01320230097018]

48 **Palmes D**, Wolters H, Spiegel HU, M Ller E, Minin E, Heistermann HP. Morphological changes during creation of a neo-bile duct using a vein and a biodegradable endoluminal stent. *J Invest Surg* 2009; **22**: 435-444 [PMID: 20001814 DOI: 10.3109/08941930903410791]

49 **Liang YL**, Yu YC, Liu K, Wang WJ, Ying JB, Wang YF, Cai XJ. Repair of bile duct defect with degradable stent and autologous tissue in a porcine model. *World J Gastroenterol* 2012; **18**: 5205-5210 [PMID: 23066314 DOI: 10.3748/wjg.v18.i37.5205]

50 **Roehlen N**, Crouchet E, Baumert TF. Liver Fibrosis: Mechanistic Concepts and Therapeutic Perspectives. *Cells* 2020; **9** [PMID: 32260126 DOI: 10.3390/cells9040875]

51 **Tomasek JJ**, Gabbiani G, Hinz B, Chaponnier C, Brown RA. Myofibroblasts and mechano-regulation of connective tissue remodelling. *Nat Rev Mol Cell Biol* 2002; **3**: 349-363 [PMID: 11988769 DOI: 10.1038/nrm809]

52 **Thomas JP**, Metropol HJ, Myers RT. Teflon patch graft for reconstruction of the extrahepatic bile ducts. *Ann Surg* 1964; **160**: 967-970 [PMID: 14246149 DOI: 10.1097/00000658-196412000-00004]

53 **Cochran EB**, Ferguson EF Jr, Moseley T. Reconstruction of the common bile duct with a collagen-dacron prosthesis: mucosal regeneration in dogs. *Am Surg* 1966; **32**: 757-761 [PMID: 5926852]

54 **Grindlay JH**. Method of making tubes of polyethylene film for use in anastomosis of the common bile duct, trachea, and pelvic colon. *Surgery* 1948; **24**: 22-29 [PMID: 18872831]

55 **Reynolds RM**, Reynolds RP. Choledochoduodenostomy using a polyethylene tube prosthesis. *J Mich State Med Soc* 1958; **57**: 1724-1726 [PMID: 13621181]

56 **Abir F**, Barkhordarian S, Sumpio BE. Efficacy of dextran solutions in vascular surgery. *Vasc Endovascular Surg* 2004; **38**: 483-491 [PMID: 15592628 DOI: 10.1177/153857440403800601]

57 **Minh NN**, Obara H. Porcine bile viscosity is proportional to density. *Biorheology* 2020; **57**: 27-36 [PMID: 32333577 DOI: 10.3233/BIR-190238]

58 **Schreuder AM**, Busch OR, Besselink MG, Ignatavicius P, Gulbinas A, Barauskas G, Gouma DJ, van Gulik TM. Long-Term Impact of Iatrogenic Bile Duct Injury. *Dig Surg* 2020; **37**: 10-21 [PMID: 30654363 DOI: 10.1159/000496432]

59 **van Berkel AM**, van Marle J, Groen AK, Bruno MJ. Mechanisms of biliary stent clogging: confocal laser scanning and scanning electron microscopy. *Endoscopy* 2005; **37**: 729-734 [PMID: 16032491 DOI: 10.1055/s-2005-870131]

60 **Langer R**, Vacanti JP. Tissue engineering. *Science* 1993; **260**: 920-926 [PMID: 8493529 DOI: 10.1126/science.8493529]

61 **Zhang L**, Hui L. Bioengineering: Bile ducts regenerated. *Nature* 2017; **547**: 171-172 [PMID: 28703183 DOI: 10.1038/547171a]

62 **Tanimoto Y**, Tashiro H, Mikuriya Y, Kuroda S, Hashimoto M, Kobayashi T, Taniura T, Ohdan H. Radiopaque biodegradable stent for duct-to-duct biliary reconstruction in pigs. *Langenbecks Arch Surg* 2016; **401**: 513-517 [PMID: 27138018 DOI: 10.1007/s00423-016-1442-z]

63 **de Abreu GF**, Batista LL, Adeodato DC, de Albuquerque AV, Ferraz-Carvalho RS, de Lima RP, de Souza VS, de Carvalho GL, Aguiar J. Use of bacterial cellulose film for repair of bile duct injury in pigs. *J Biomater Appl* 2020; **35**: 331-341 [PMID: 32501137 DOI: 10.1177/0885328220928221]

64 **Pérez Alonso AJ**, Del Olmo Rivas C, Romero IM, Cañizares Garcia FJ, Poyatos PT. Tissue-engineering repair of extrahepatic bile ducts. *J Surg Res* 2013; **179**: 18-21 [PMID: 23010513 DOI: 10.1016/j.jss.2012.08.035]

65 **Gómez NA**, Zapatier JA, Vargas PE. Re: "Small intestinal submucosa as a bioscaffold for biliary tract regeneration". *Surgery* 2004; **135**: 460 [PMID: 15041976 DOI: 10.1016/j.surg.2003.06.004]

66 **Nakashima S**, Nakamura T, Miyagawa K, Yoshikawa T, Kin S, Kuriu Y, Nakase Y, Sakakura C, Otsuji E, Hagiwara A, Yamagishi H. In situ tissue engineering of the bile duct using polypropylene mesh-collagen tubes. *Int J Artif Organs* 2007; **30**: 75-85 [PMID: 17295195 DOI: 10.1177/039139880703000110]

67 **Takimoto Y**, Dixit V, Arthur M, Gitnick G. De novo liver tissue formation in rats using a novel collagen-polypropylene scaffold. *Cell Transplant* 2003; **12**: 413-421 [PMID: 12911129 DOI: 10.3727/000000003108746966]

68 **Yannas IV**, Tzeranis D, So PT. Surface biology of collagen scaffold explains blocking of wound contraction and regeneration of skin and peripheral nerves. *Biomed Mater* 2015; **11**: 014106 [PMID: 26694657 DOI: 10.1088/1748-6041/11/1/014106]

69 **Miyazawa M**, Aikawa M, Okada K, Watanabe Y, Okamoto K, Santosh S, Yamaguchi S, Koyama I, Ikada Y. An Artificial Bile Duct Made of Bioabsorbable Polymer: A Viable Substitute for Narrowed Portion of the Extrahepatic Bile Duct. *Int Surg* 2015; **100**: 1408-1413 [DOI: 10.9738/INTSURG-D-15-00037.1]

70 **Langer R**. Implantable controlled release systems. *Pharmacol Ther* 1983; **21**: 35-51 [PMID: 6353438 DOI: 10.1016/0163-7258(83)90066-9]

71 **Sampaziotis F**, Muraro D, Tysoe OC, Sawiak S, Beach TE, Godfrey EM, Upponi SS, Brevini T, Wesley BT, Garcia-Bernardo J, Mahbubani K, Canu G, Gieseck R 3rd, Berntsen NL, Mulcahy VL, Crick K, Fear C, Robinson S, Swift L, Gambardella L, Bargehr J, Ortmann D, Brown SE, Osnato A, Murphy MP, Corbett G, Gelson WTH, Mells GF, Humphreys P, Davies SE, Amin I, Gibbs P, Sinha S, Teichmann SA, Butler AJ, See TC, Melum E, Watson CJE, Saeb-Parsy K, Vallier L. Cholangiocyte organoids can repair bile ducts after transplantation in the human liver. *Science* 2021; **371**: 839-846 [PMID: 33602855 DOI: 10.1126/science.aaz6964]

72 **Fu X**, Liu G, Halim A, Ju Y, Luo Q, Song AG. Mesenchymal Stem Cell Migration and Tissue Repair. *Cells* 2019; **8** [PMID: 31357692 DOI: 10.3390/cells8080784]

73 **Ding BS**, Cao Z, Lis R, Nolan DJ, Guo P, Simons M, Penfold ME, Shido K, Rabbany SY, Rafii S. Divergent angiocrine signals from vascular niche balance liver regeneration and fibrosis. *Nature* 2014; **505**: 97-102 [PMID: 24256728 DOI: 10.1038/nature12681]

74 **de Jong IEM**, Matton APM, van Praagh JB, van Haaften WT, Wiersema-Buist J, van Wijk LA, Oosterhuis D, Iswandana R, Suriguga S, Overi D, Lisman T, Carpino G, Gouw ASH, Olinga P, Gaudio E, Porte RJ. Peribiliary Glands Are Key in Regeneration of the Human Biliary Epithelium After Severe Bile Duct Injury. *Hepatology* 2019; **69**: 1719-1734 [PMID: 30506902 DOI: 10.1002/hep.30365]

75 **Carpino G**, Nevi L, Overi D, Cardinale V, Lu WY, Di Matteo S, Safarikia S, Berloco PB, Venere R, Onori P, Franchitto A, Forbes SJ, Alvaro D, Gaudio E. Peribiliary Gland Niche Participates in Biliary Tree Regeneration in Mouse and in Human Primary Sclerosing Cholangitis. *Hepatology* 2020; **71**: 972-989 [PMID: 31330051 DOI: 10.1002/hep.30871]

76 **Wang AW**, Prieto JM, Cauvi DM, Bickler SW, De Maio A. The Greater Omentum-A Vibrant and Enigmatic Immunologic Organ Involved in Injury and Infection Resolution. *Shock* 2020; **53**: 384-390 [PMID: 31389904 DOI: 10.1097/SHK.0000000000001428]

77 **Alvaro D**, Mancino MG, Glaser S, Gaudio E, Marzioni M, Francis H, Alpini G. Proliferating cholangiocytes: a neuroendocrine compartment in the diseased liver. *Gastroenterology* 2007; **132**: 415-431 [PMID: 17241889 DOI: 10.1053/j.gastro.2006.07.023]

78 **Peng SY**, Wang JW, Hong DF, Liu YB, Wang YF. Binding pancreaticoenteric anastomosis: from binding pancreaticojejunostomy to binding pancreaticogastrostomy. *Updates Surg* 2011; **63**: 69-74 [PMID: 21442343 DOI: 10.1007/s13304-011-0067-6]

World Journal of Gastroenterology

Submit a Manuscript: https://www.f6publishing.com

World J Gastroenterol 2022 October 21; 28(39): 5723-5730

DOI: 10.3748/wjg.v28.i39.5723

ISSN 1007-9327 (print) ISSN 2219-2840 (online)

MINIREVIEWS

SARS-CoV-2-induced liver injury: A review article on the high-risk populations, manifestations, mechanisms, pathological changes, management, and outcomes

Alvin Oliver Payus, Malehah Mohd Noh, Nornazirah Azizan, Raman Muthukaruppan Chettiar

Specialty type: Gastroenterology and hepatology

Provenance and peer review: Invited article; Externally peer reviewed

Peer-review model: Single blind

Peer-review report's scientific quality classification

Grade A (Excellent): A
Grade B (Very good): B
Grade C (Good): 0
Grade D (Fair): D
Grade E (Poor): 0

P-Reviewer: Floreani A, Italy; Hernandez-Caballero A, Mexico; Nooripour R, Iran

Received: July 16, 2022
Peer-review started: July 16, 2022
First decision: August 19, 2022
Revised: August 24, 2022
Accepted: October 10, 2022
Article in press: October 10, 2022
Published online: October 21, 2022

Alvin Oliver Payus, Malehah Mohd Noh, Department of Medicine, Faculty of Medicine and Health Sciences, Universiti Malaysia Sabah, Kota Kinabalu 88400, Sabah, Malaysia

Nornazirah Azizan, Department of Pathobiology and Medical Diagnostic, Faculty of Medicine and Health Sciences, Universiti Malaysia Sabah, Kota Kinabalu 88400, Malaysia

Raman Muthukaruppan Chettiar, Department of Medicine, Hospital Queen Elizabeth I, 13a, Jalan Penampang, Kota Kinabalu 88200, Malaysia

Corresponding author: Alvin Oliver Payus, MD, MRCP, Senior Lecturer, Department of Medicine, Faculty of Medicine and Health Sciences, Universiti Malaysia Sabah, Jalan UMS, Kota Kinabalu 88400, Sabah, Malaysia. dralvinpayus@ums.edu.my

Abstract

The novel coronavirus disease 2019 is an infection caused by severe acute respiratory syndrome coronavirus 2 (SARS-CoV-2) and was declared a global pandemic with more than 500 million reported cases and more than 6 million deaths worldwide to date. Although it has transitioned into the endemic phase in many countries, the mortality rate and overall prognosis of the disease are still abysmal and need further improvement. There has been evidence that shows the significance of SARS-CoV-2-related liver injury. Here, we review the literature on the various spectrum of SARS-CoV-2 infection-induced liver injury and the possible mechanisms of damage to the hepatobiliary system. This review aimed to illustrate the latest understanding regarding SARS-CoV-2-induced liver injury including the high-risk populations, the characteristic clinical manifestations, the possible pathogenic mechanism, the pathological changes, the current suggestions for clinical treatment for various spectrum of populations, and the prognosis of the condition. In conclusion, SARS-CoV-2 patients with a liver injury warrant close monitoring as it is associated with the more severe and poorer outcome of the infection.

Key Words: COVID-19; SARS-CoV-2; Pandemic; Liver injury; Pandemics; Prognosis

©The Author(s) 2022. Published by Baishideng Publishing Group Inc. All rights reserved.

Core Tip: There are several reviews in the literature that discuss the pathophysiology, management, and outcomes of liver injury in coronavirus disease 2019 (COVID-19). Here, we reviewed the current understanding on various aspects of COVID-19-related liver injury, including the high-risk populations, the characteristic clinical manifestations, the possible pathogenic mechanism, the pathological changes, the current suggestions for clinical treatment for the spectrum of populations, and the prognosis of the condition.

Citation: Payus AO, Mohd Noh M, Azizan N, Muthukaruppan Chettiar R. SARS-CoV-2-induced liver injury: A review article on the high-risk populations, manifestations, mechanisms, pathological changes, management, and outcomes. *World J Gastroenterol* 2022; 28(39): 5723-5730
URL: https://www.wjgnet.com/1007-9327/full/v28/i39/5723.htm
DOI: https://dx.doi.org/10.3748/wjg.v28.i39.5723

INTRODUCTION

Severe acute respiratory syndrome coronavirus 2 (SARS-CoV-2) is the name given to the newly emerged zoonotic virus that causes coronavirus disease 2019 (COVID-19)[1]. It was first reported in Wuhan, China on December 29, 2019 and was declared a global pandemic on March 11, 2020[2]. SARS-CoV-2 is an enveloped, single-stranded positive-sense RNA genome virus that harbors the largest genome among currently known RNA viruses, with a genome length of around 26 to 32 kb. It has an oval shape and an average size of 100 nm in diameter. Electron microscopy revealed large club-shaped spikes of glycoprotein membrane on the viral surface making the viral particles appear like a typical crown-like shape[3].

COVID-19 is a syndrome with various systemic and respiratory symptoms such as fever, fatigue, dry cough, and breathing difficulties. It can be critical, causing severe pneumonia and cardiorespiratory failure that requires specialized management in intensive care units[4]. SARS-CoV-2 can also affect other systems, namely the nervous system causing headache, anosmia, paresthesia, and altered consciousness[5]. Abnormal liver function parameters are commonly found in patients with SARS-CoV-2 infection, indicating that SARS-COV-2 infection is associated with liver injury and even failure. Apart from that, several studies suggested that liver injury has a significant role in determining the severity and mortality rate of the disease. Considering the ongoing global threat of SARS-CoV-2 infection and the necessity to improve the prognosis of the disease, the treating physicians need to be aware of the association and significance of SARS-CoV-2 infection-related liver injury not only for the severity of the disease but also for the mortality rate and prognosis as a whole. Therefore, this review aimed to elucidate the importance of hepatobiliary involvement in SARS-CoV-2 infections and provide helpful information for managing the condition and improving the overall prognosis of the disease.

HIGH RISK POPULATIONS OF SARS-COV-2-INDUCED LIVER INJURY

Since the beginning of the pandemic, it was reported that patients with severe SARS-CoV-2 infection tended to develop liver injury compared to mild infection. Cai *et al*[6] reported that male patients of older age and higher body mass index have a higher tendency to develop liver injury during the course of the disease. A similar finding was seen in a study on 79 non-hospitalized SARS-CoV-2 patients by Xie *et al*[7], who reported that liver injury was more common among male patients. The authors also said that patients with an underlying severe chronic lung disease have a higher rate of liver injury, which was also reported by Zhang *et al*[8]. Cai *et al*[6] and Singh and Khan[9] both found that liver injury was more common among patients with underlying liver disease. According to Da *et al*[10], the common etiology of chronic liver disease that is prone to developing worsening liver injury during the infection is alcohol-related liver disease. Patients with nonalcoholic fatty liver disease and nonalcoholic steatohepatitis are usually associated with additional metabolic risk factors, such as obesity, that can increase the susceptibility to the infection and is commonly associated with a more severe presentation[11].

There has been significant concern about the increased susceptibility to SARS-CoV-2 infection among solid organ transplant recipients. In a systematic review by Piedade and Pereira[12], patients with liver transplant were not associated with an increased risk of SARS-CoV-2 infection. The risk is highly dependent on the sex, age, body mass index, history of hepatocellular carcinoma, and the immunosuppression drug dose of the patient. However, the prevalence of severe infection was higher among liver transplanted patients. A study by Becchetti *et al*[13] found that alterations in liver enzymes among liver transplanted patients with SARS-CoV-2 occurs more commonly among hospitalized patients. In addition, Ali Malekhosseini *et al*[14] showed that the admission rate of liver transplanted patients to the intensive care unit was as high as 33.3%.

No evidence shows that pregnancy increases susceptibility to SARS-CoV-2-induced liver injury. Nevertheless, a retrospective cohort study involving 122 pregnant patients with confirmed SARS-CoV-2 infection by Can *et al*[15] found that 13.9% developed an abnormal liver function that was generally mild, where most of them were critically ill and had a longer stay in the hospital compared to the normal liver function group.

THE CHARACTERISTIC MANIFESTATIONS OF SARS-COV-2-INDUCED LIVER INJURY

The most common manifestations of SARS-CoV-2 induced liver injury was the elevation of liver enzymes, such as alanine transaminase (ALT), aspartate aminotransferase (AST), gamma-glutamyl transferase, and alkaline phosphatase. In a meta-analysis completed in the first few months of the pandemic by Cai *et al*[6], about 25% of SARS-CoV-2 patients had increased liver enzyme levels, which showed a direct association with the disease activity. The prevalence of increased AST was higher than ALT levels and was positively correlated with the severity of cases, where the level was higher in patients with severe cases[7,8,15]. Lei *et al*[16] reported a significant association between inpatient mortality in SARS-CoV-2 infected patients and liver injury based on liver enzymes, specifically AST elevation.

In a study on 417 SARS-CoV-2 infected patients by Cai *et al*[6], 41.0% of patients had abnormal liver tests, and 5.0% had liver injury upon presentation to the hospital. Throughout hospitalization, 76.3% developed some form of abnormal liver function, and it was high enough to be considered liver injury in 21.5% of patients. A similar finding was reported by Fan *et al*[17], who conducted a retrospective single center study on 148 patients with SARS-CoV-2 infection, where 37.2% had an abnormal liver function at hospital admission. Patients with the abnormal liver function were also found to have an extended hospital stays. A retrospective study of 79 patients with SARS-CoV-2 by Xie *et al*[7] found that patients with an abnormal liver test had an extended stay in the hospital.

Phipps *et al*[18] reported that 21.0% of 2273 patients with SARS-CoV-2 infection had a moderate liver injury, which was defined as elevated liver enzymes two to five times above the upper limit of normal, and 6.4% had severe liver injury, which was defined as liver enzymes more than five times the upper limit of normal. In this study, 69% of the patients with liver injury required intensive care unit care. The reports also mentioned that severe liver injury was associated with elevated inflammation markers, including ferritin and interleukin 6 (IL-6).

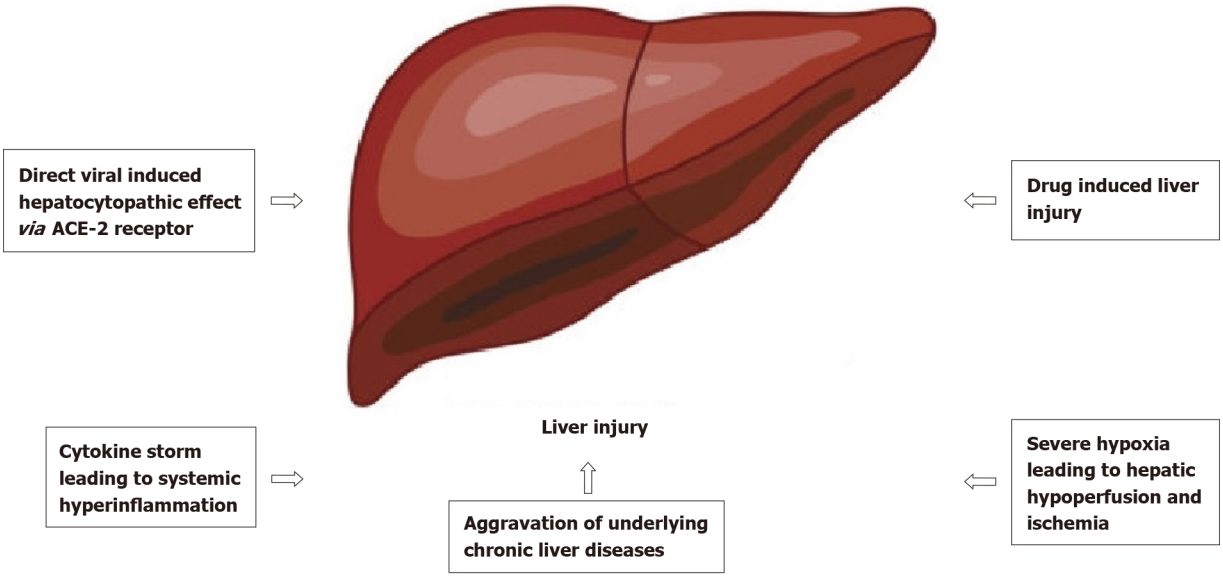
PROPOSED PATHOPHYSIOLOGICAL MECHANISM OF SARS-COV-2-INDUCED LIVER INJURY

The exact pathophysiological mechanism of SARS-CoV-2-induced liver injury is still poorly understood, but evidence has shown it to be multifactorial (as shown in Figure 1). One of the factors is direct invasion of SARS-CoV-2, which has been suggested in several studies. The primary receptor for SARS-CoV-2 cellular entry is the angiotensin-converting enzyme 2 (ACE2) receptors, which are found not only in the lung parenchyma but also in other parts of the body[19], such as the brain[5], gastrointestinal tract, biliary tree, and liver epithelia[20]. Zhou *et al*[21] stated that SARS-CoV-2 patients with gastrointestinal symptoms had higher AST and ALT levels, which reflected that ACE2 receptor was expressed within the gastrointestinal tract and the biliary tree. However, even though the ACE2 receptor is expressed more within the biliary tree than the liver parenchyma, most studies showed a predominant pattern of parenchymal liver injury based on the elevated levels of AST and ALT rather than the damage to the bile ducts, which was reflected by increased gamma-glutamyl transferase and alkaline phosphatase[22].

Wu *et al*[23] found that almost 50% of SARS-CoV-2 infected patients who recovered from the disease had persistent virus shedding in their fecal specimens for more than 10 d after viral detection in respiratory tract samples became negative. This may further support the possibility of viral replication in the hepatobiliary system. Similarly, the previous SARS-CoV strains that caused an outbreak from 2002 to 2004 have also been shown to directly injure the liver parenchyma causing lobular inflammation and apoptosis of hepatocytes[24].

Apart from the direct viral-induced hepatocytopathic hypothesis, autoinflammatory mediated injury to the liver is another plausible explanation. Immune dysregulation can occur in severe SARS-CoV-2 infection, which the overactivation of the immune system will lead to systemic hyperinflammation in extreme conditions. This condition is called 'cytokine storm syndrome', which is a phenomenon that will not only cause pulmonary inflammation but also multiorgan involvement, including the nervous system causing encephalitis[25] and peripheral neuritis[26] and the liver causing acute hepatitis and even failure[27,28].

Drug-induced liver injury is also common in SARS-CoV-2 patients, as the medications used to treat the infection can be hepatotoxic. These include lopinavir/ritonavir, remdesivir, tocilizumab, and others



DOI: 10.3748/wjg.v28.i39.5723 **Copyright** ©The Author(s) 2022.

Figure 1 Possible pathophysiological mechanisms of liver injury induced by severe acute respiratory syndrome coronavirus 2 infection.
ACE 2: Angiotensin-converting enzyme 2.

[29]. A study of 148 cases of SARS-CoV-2 infected patients in Shanghai by Li *et al*[30] found that the utilization rate of lopinavir/ritonavir among patients with abnormal liver function was higher than the patients with normal liver function. There was no significant difference in the pre-hospital medication between the two groups of patients. The exact mechanism of how lopinavir/ritonavir induces liver injury is still uncertain, but there is evidence that it activates the endoplasmic reticulum stress pathway in the liver and induces hepatocytes apoptosis[31].

Ritonavir is also widely metabolized by the liver through the cytochrome P450 system, where the production of toxic intermediates of any drugs that are metabolized by the system will have the potential of causing liver injury[32]. Tocilizumab, which is an IL-6 inhibitor that is used to reduce overactive inflammation, has been reported to cause drug-induced liver injury and liver failure, which in some cases requires a liver transplant[33]. The exact mechanism is still unknown but may be due to its inhibitory effect on the IL-6 pathway, which is essential for liver regeneration.

SARS-CoV-2 patients with underlying chronic liver diseases are more likely to suffer from liver injury. This may suggest that SARS-CoV-2 infection can aggravate underlying liver diseases. In addition, there is a possibility that the liver damage may be caused by the viral reactivation of existing liver diseases in SARS-CoV-2 infection. Some biological medications such as tocilizumab and baricitinib may cause reactivation of viral hepatitis B, which causes deterioration of liver function[34].

Another simpler hypothesis is that prolonged hypoxia and tissue ischemia in critically ill SARS-CoV-2 patients who suffer from severe pneumonia and acute respiratory distress syndrome can also be one of the mechanisms of liver injury and even failure[35]. This occurs due to prolonged tissue hypoperfusion leading to ischemia, including in the liver. The anaerobic metabolism and lactic acidosis will further depress the cardiorespiratory effort, which will cause the continuation of the vicious circle[36].

PATHOLOGICAL CHANGES IN SARS-COV-2-INDUCED LIVER INJURY

The first post-mortem autopsy on a patient who succumbed to SARS-CoV-2 infection was reported by Xu *et al*[37]. The liver histology showed a moderate degree of microvesicular steatosis with mild lobular and portal vein activity in the study. Ji *et al*[38] reported overactivation of T cells, suggesting viral-induced cytotoxic T cell liver damage. Liu *et al*[39] described various hepatic lesions, including focal lobular necrosis, lobular lymphocytic and monocytic infiltration, ballooning degeneration of liver cells, and sinusoidal congestion with microthrombosis. A study on 48 liver autopsies by Sonzogni *et al*[40] reported focal portal and lobular lymphocytic infiltrates with multiple vascular changes, which are suggestive of hepatic vascular involvement.

Tian *et al*[41] also reported a similar autopsy finding of mild lobular lymphocytic infiltration, with sinusoidal expansion of the central lobule and patchy necrosis in the periportal and centrilobular areas. There was no significant inflammatory cell infiltration around the portal tracts, which is consistent with the mode of acute liver injury. Autopsy reports on 7 SARS-CoV-2 infected patients who died noted multiple platelet-fibrin microthrombi in the hepatic sinusoids[42]. Wang *et al*[43] and Wang *et al*[44]

reported massive hepatic apoptosis, microvesicular steatosis, and inflammatory cell infiltration over the portal systems. In addition, there was a large amount of viral SARS-CoV-2 RNA titers detected in the liver *via* reverse transcriptase-polymerase chain reaction[41,45].

CURRENT MANAGEMENT OF SARS-COV-2-INDUCED LIVER INJURY IN VARIOUS POPULATIONS

Liver injury is a severe complication of SARS-CoV-2 infection and can significantly affect the outcome of the patient. Multiple studies have suggested regular monitoring of liver function parameters in SARS-CoV-2-infected patients. Based on the consensus statement of the American Association for the Study of Liver Diseases[46], it is recommended to consider etiologies outside SARS-CoV-2, such as other viral hepatitis. This has been proven in a case reported by Hambali *et al*[47], where a patient with SARS-CoV-2 infection presented with abnormal liver function and high IL-6, which was due to hepatocellular carcinoma. It is also essential to consider other indirect causes of liver injury such as myositis, cardiac injury, ischemia, and cytokine release syndrome. Patients with liver enzymes more than five times the upper limit of normal may be excluded but not contraindicated from using medications such as remdesivir, tocilizumab, and hydroxychloroquine. Every patient receiving the medications, especially remdesivir and tocilizumab should be regularly monitored for liver biochemical indicators regardless of baseline values. It should not be assumed that patients with autoimmune hepatitis and liver transplantation have a sudden onset of disease or acute cellular rejection without biopsy confirmation. Patients who are immunocompromised or are treated with immunosuppressive drugs should be considered at increased risk for SARS-CoV-2 infection and should be prioritized for testing[46].

SARS-CoV-2-infected patients with ongoing antiviral treatment for hepatitis B or C should be continued, but the initiation of antiviral treatment for hepatitis C may need to be delayed. Patients with an underlying liver disease requiring immunosuppressants should be continued in cases of mild infection, but in moderate to severe infection, the treatment dosage of calcineurin inhibitors should be reduced. The position statement from the European Association for the Study of the Liver-European Society of Clinical Microbiology and Infectious Diseases recommended that the dose of immunosuppressant drugs can be adjusted according to antiviral treatment regimens because the drugs in both regimens will likely interact with each other[48].

THE OUTCOME OF SARS-COV-2-INDUCED LIVER INJURY AND PREDICTORS OF INFECTION SEVERITY

The biomarkers of liver injury were significantly higher in severe cases of SARS-CoV-2 infection. In a meta-analysis by Henry *et al*[49], the severity and mortality rate of SARS-CoV-2 infection was related to the biomarkers of liver functions, which suggests that liver injury has a strong correlation with the severity of SARS-CoV-2 infection. A retrospective study that compared the clinical spectrum between patients with and without liver injury by Xie *et al*[7] found the hospitalization time was significantly longer in patients with liver injury. Lei *et al*[16] reported that abnormal AST in SARS-CoV-2 infection was associated with a higher risk of death during hospitalization than other indicators of liver injury.

Kulkarni *et al*[50] stated that the severity of elevated liver enzyme markers determined the outcome of SARS-CoV-2 infection, with the incidence of liver injury as high as 58%-78% among the death cases. A multicenter study involving 2780 SARS-CoV-2 infected patients by Singh and Khan[9] found that patients with underlying liver disease had higher mortality and hospitalization. In addition to the abnormal liver biochemistry, hypoalbuminemia during the illness is an important indicator of the severity of the SARS-CoV-2 infection. Both studies by Gong *et al*[51] and Huang *et al*[52] showed that hypoalbuminemia was associated with severe infection and an independent risk factor for death.

CONCLUSION

In conclusion, this review illuminated the significance of liver injury in SARS-CoV-2 infection based on the descriptions from the scientific literature. Although it is common and mild in the majority of cases, it is a strong predictor of the severity and a significant risk factor for the mortality rate of the disease, especially if it is associated with male sex, older age, the presence of other comorbidities or underlying chronic liver disease, and in severe respiratory symptoms. Therefore, it is prudent to monitor SARS-CoV-2-infected patients with liver injury and to individualize treatment for patients with an underlying disease who developed liver injury to improve the prognosis by delivering the appropriate management.

ACKNOWLEDGEMENTS

The authors would like to thank all who were involved in writing this review article.

FOOTNOTES

Author contributions: Payus AO designed the study, prepared the figure, and performed the majority of the writing; Azizan N provided input for the article and contributed to writing; Mohd Noh M and Muthukaruppan Chettiar R were both supervisors and contributed to the final revision of the manuscript; and all authors have read and approved the final manuscript.

Conflict-of-interest statement: All the authors report no relevant conflicts of interest for this article.

Open-Access: This article is an open-access article that was selected by an in-house editor and fully peer-reviewed by external reviewers. It is distributed in accordance with the Creative Commons Attribution NonCommercial (CC BY-NC 4.0) license, which permits others to distribute, remix, adapt, build upon this work non-commercially, and license their derivative works on different terms, provided the original work is properly cited and the use is non-commercial. See: https://creativecommons.org/Licenses/by-nc/4.0/

Country/Territory of origin: Malaysia

ORCID number: Alvin Oliver Payus 0000-0003-4675-103X; Malehah Mohd Noh 0000-0002-8166-7119; Nornazirah Azizan 0000-0002-5831-3734; Raman Muthukaruppan Chettiar 0000-0003-1506-6021.

S-Editor: Wang JJ
L-Editor: Filipodia
P-Editor: Wang JJ

REFERENCES

1 **Zhu N**, Zhang D, Wang W, Li X, Yang B, Song J, Zhao X, Huang B, Shi W, Lu R, Niu P, Zhan F, Ma X, Wang D, Xu W, Wu G, Gao GF, Tan W; China Novel Coronavirus Investigating and Research Team. A Novel Coronavirus from Patients with Pneumonia in China, 2019. *N Engl J Med* 2020; **382**: 727-733 [PMID: 31978945 DOI: 10.1056/NEJMoa2001017]
2 **Li Q**, Guan X, Wu P, Wang X, Zhou L, Tong Y, Ren R, Leung KSM, Lau EHY, Wong JY, Xing X, Xiang N, Wu Y, Li C, Chen Q, Li D, Liu T, Zhao J, Liu M, Tu W, Chen C, Jin L, Yang R, Wang Q, Zhou S, Wang R, Liu H, Luo Y, Liu Y, Shao G, Li H, Tao Z, Yang Y, Deng Z, Liu B, Ma Z, Zhang Y, Shi G, Lam TTY, Wu JT, Gao GF, Cowling BJ, Yang B, Leung GM, Feng Z. Early Transmission Dynamics in Wuhan, China, of Novel Coronavirus-Infected Pneumonia. *N Engl J Med* 2020; **382**: 1199-1207 [PMID: 31995857 DOI: 10.1056/NEJMoa2001316]
3 **Schoeman D**, Fielding BC. Coronavirus envelope protein: current knowledge. *Virol J* 2019; **16**: 69 [PMID: 31133031 DOI: 10.1186/s12985-019-1182-0]
4 **Huang C**, Wang Y, Li X, Ren L, Zhao J, Hu Y, Zhang L, Fan G, Xu J, Gu X, Cheng Z, Yu T, Xia J, Wei Y, Wu W, Xie X, Yin W, Li H, Liu M, Xiao Y, Gao H, Guo L, Xie J, Wang G, Jiang R, Gao Z, Jin Q, Wang J, Cao B. Clinical features of patients infected with 2019 novel coronavirus in Wuhan, China. *Lancet* 2020; **395**: 497-506 [PMID: 31986264 DOI: 10.1016/S0140-6736(20)30183-5]
5 **Payus AO**, Liew Sat Lin C, Mohd Noh M, Jeffree MS, Ali RA. SARS-CoV-2 infection of the nervous system: A review of the literature on neurological involvement in novel coronavirus disease-(COVID-19). *Bosn J Basic Med Sci* 2020; **20**: 283-292 [PMID: 32530389 DOI: 10.17305/bjbms.2020.4860]
6 **Cai Q**, Huang D, Yu H, Zhu Z, Xia Z, Su Y, Li Z, Zhou G, Gou J, Qu J, Sun Y, Liu Y, He Q, Chen J, Liu L, Xu L. COVID-19: Abnormal liver function tests. *J Hepatol* 2020; **73**: 566-574 [PMID: 32298767 DOI: 10.1016/j.jhep.2020.04.006]
7 **Xie H**, Zhao J, Lian N, Lin S, Xie Q, Zhuo H. Clinical characteristics of non-ICU hospitalized patients with coronavirus disease 2019 and liver injury: A retrospective study. *Liver Int* 2020; **40**: 1321-1326 [PMID: 32239591 DOI: 10.1111/liv.14449]
8 **Zhang Y**, Zheng L, Liu L, Zhao M, Xiao J, Zhao Q. Liver impairment in COVID-19 patients: A retrospective analysis of 115 cases from a single centre in Wuhan city, China. *Liver Int* 2020; **40**: 2095-2103 [PMID: 32239796 DOI: 10.1111/liv.14455]
9 **Singh S**, Khan A. Clinical Characteristics and Outcomes of Coronavirus Disease 2019 Among Patients With Preexisting Liver Disease in the United States: A Multicenter Research Network Study. *Gastroenterology* 2020; **159**: 768-771.e3 [PMID: 32376408 DOI: 10.1053/j.gastro.2020.04.064]
10 **Da BL**, Im GY, Schiano TD. Coronavirus Disease 2019 Hangover: A Rising Tide of Alcohol Use Disorder and Alcohol-Associated Liver Disease. *Hepatology* 2020; **72**: 1102-1108 [PMID: 32369624 DOI: 10.1002/hep.31307]
11 **Zheng KI**, Gao F, Wang XB, Sun QF, Pan KH, Wang TY, Ma HL, Chen YP, Liu WY, George J, Zheng MH. Letter to the Editor: Obesity as a risk factor for greater severity of COVID-19 in patients with metabolic associated fatty liver disease. *Metabolism* 2020; **108**: 154244 [PMID: 32320741 DOI: 10.1016/j.metabol.2020.154244]
12 **Piedade J**, Pereira G. COVID-19 in liver transplant recipients. *J Liver Transplant* 2021; **3**: 100026 [DOI:

10.1016/j.liver.2021.100026]
13 **Becchetti C**, Zambelli MF, Pasulo L, Donato MF, Invernizzi F, Detry O, Dahlqvist G, Ciccarelli O, Morelli MC, Fraga M, Svegliati-Baroni G, van Vlierberghe H, Coenraad MJ, Romero MC, de Gottardi A, Toniutto P, Del Prete L, Abbati C, Samuel D, Pirenne J, Nevens F, Dufour JF; COVID-LT group. COVID-19 in an international European liver transplant recipient cohort. *Gut* 2020; **69**: 1832-1840 [PMID: 32571972 DOI: 10.1136/gutjnl-2020-321923]
14 **Ali Malekhosseini S**, Nikoupour H, Gholami S, Shamsaeefar A, Arasteh P, Kazemi K, Dehghani M, Eghlimi H, Raeisi Shahraki H, Roozbeh J, Rezaianzadeh A, Nikeghbalian S. A Report of 85 Cases of COVID-19 and Abdominal Transplantation From a Single Center: What Are the Associated Factors With Death Among Organ Transplantation Patients. *Transplantation* 2021; **105**: 90-99 [PMID: 32976364 DOI: 10.1097/TP.0000000000003470]
15 **Can E**, Oğlak SC, Ölmez F. Abnormal liver function tests in pregnant patients with COVID-19 - a retrospective cohort study in a tertiary center. *Ginekol Pol* 2022 [PMID: 35072238 DOI: 10.5603/GP.a2021.0182]
16 **Lei F**, Liu YM, Zhou F, Qin JJ, Zhang P, Zhu L, Zhang XJ, Cai J, Lin L, Ouyang S, Wang X, Yang C, Cheng X, Liu W, Li H, Xie J, Wu B, Luo H, Xiao F, Chen J, Tao L, Cheng G, She ZG, Zhou J, Wang H, Lin J, Luo P, Fu S, Ye P, Xiao B, Mao W, Liu L, Yan Y, Chen G, Huang X, Zhang BH, Yuan Y. Longitudinal Association Between Markers of Liver Injury and Mortality in COVID-19 in China. *Hepatology* 2020; **72**: 389-398 [PMID: 32359177 DOI: 10.1002/hep.31301]
17 **Fan Z**, Chen L, Li J, Cheng X, Yang J, Tian C, Zhang Y, Huang S, Liu Z, Cheng J. Clinical Features of COVID-19-Related Liver Functional Abnormality. *Clin Gastroenterol Hepatol* 2020; **18**: 1561-1566 [PMID: 32283325 DOI: 10.1016/j.cgh.2020.04.002]
18 **Phipps MM**, Barraza LH, LaSota ED, Sobieszczyk ME, Pereira MR, Zheng EX, Fox AN, Zucker J, Verna EC. Acute Liver Injury in COVID-19: Prevalence and Association with Clinical Outcomes in a Large U.S. Cohort. *Hepatology* 2020; **72**: 807-817 [PMID: 32473607 DOI: 10.1002/hep.31404]
19 **Arima Y**, Yoshimoto K, Namera A, Makita R, Murata K, Nagao M. The Sarin-like Organophosphorus Agent bis (isopropyl methyl)phosphonate Induces Apoptotic Cell Death and COX-2 Expression in SK-N-SH Cells. *Hiroshima J Med Sci* 2016; **65**: 1-8 [PMID: 27348899]
20 **Chai X**, Hu L, Zhang Y, Han W, Lu Z, Ke A, Zhou J, Shi G, Fang N, Fan J, Cai J, Lan F. Specific ACE2 expression in cholangiocytes may cause liver damage after 2019-nCoV infection. 2020 Preprint. Available from: bioRxiv: 2020.02.03.931766 [DOI: 10.1101/2020.02.03.931766]
21 **Zhou Z**, Zhao N, Shu Y, Han S, Chen B, Shu X. Effect of Gastrointestinal Symptoms in Patients With COVID-19. *Gastroenterology* 2020; **158**: 2294-2297 [PMID: 32199880 DOI: 10.1053/j.gastro.2020.03.020]
22 **Wijarnpreecha K**, Ungprasert P, Panjawatanan P, Harnois DM, Zaver HB, Ahmed A, Kim D. COVID-19 and liver injury: a meta-analysis. *Eur J Gastroenterol Hepatol* 2021; **33**: 990-995 [PMID: 32639420 DOI: 10.1097/MEG.0000000000001817]
23 **Wu Y**, Guo C, Tang L, Hong Z, Zhou J, Dong X, Yin H, Xiao Q, Tang Y, Qu X, Kuang L, Fang X, Mishra N, Lu J, Shan H, Jiang G, Huang X. Prolonged presence of SARS-CoV-2 viral RNA in faecal samples. *Lancet Gastroenterol Hepatol* 2020; **5**: 434-435 [PMID: 32199469 DOI: 10.1016/S2468-1253(20)30083-2]
24 **Chau TN**, Lee KC, Yao H, Tsang TY, Chow TC, Yeung YC, Choi KW, Tso YK, Lau T, Lai ST, Lai CL. SARS-associated viral hepatitis caused by a novel coronavirus: report of three cases. *Hepatology* 2004; **39**: 302-310 [PMID: 14767982 DOI: 10.1002/hep.20111]
25 **Payus AO**, Jeffree MS, Ohn MH, Tan HJ, Ibrahim A, Chia YK, Raymond AA. Immune-mediated neurological syndrome in SARS-CoV-2 infection: a review of literature on autoimmune encephalitis in COVID-19. *Neurol Sci* 2022; **43**: 1533-1547 [PMID: 34853897 DOI: 10.1007/s10072-021-05785-z]
26 **Payus AO**, Jan T, Ibrahim A, Raymond AA. Autoimmune polyradiculopathy In SARS-CoV-2: a narrative review of Guillain-Barre syndrome in novel coronavirus disease (COVID-19). *Acta Med* 2020 [DOI: 10.19193/0393-6384_2020_6_599]
27 **Liu J**, Li S, Liu J, Liang B, Wang X, Wang H, Li W, Tong Q, Yi J, Zhao L, Xiong L, Guo C, Tian J, Luo J, Yao J, Pang R, Shen H, Peng C, Liu T, Zhang Q, Wu J, Xu L, Lu S, Wang B, Weng Z, Han C, Zhu H, Zhou R, Zhou H, Chen X, Ye P, Zhu B, Wang L, Zhou W, He S, He Y, Jie S, Wei P, Zhang J, Lu Y, Wang W, Zhang L, Li L, Zhou F, Wang J, Dittmer U, Lu M, Hu Y, Yang D, Zheng X. Longitudinal characteristics of lymphocyte responses and cytokine profiles in the peripheral blood of SARS-CoV-2 infected patients. *EBioMedicine* 2020; **55**: 102763 [PMID: 32361250 DOI: 10.1016/j.ebiom.2020.102763]
28 **Alqahtani SA**, Schattenberg JM. Liver injury in COVID-19: The current evidence. *United European Gastroenterol J* 2020; **8**: 509-519 [PMID: 32450787 DOI: 10.1177/2050640620924157]
29 **Spearman CW**, Aghemo A, Valenti L, Sonderup MW. COVID-19 and the liver: A 2021 update. *Liver Int* 2021; **41**: 1988-1998 [PMID: 34152690 DOI: 10.1111/liv.14984]
30 **Li J**, Gong X, Wang Z, Chen R, Li T, Zeng D, Li M. Clinical features of familial clustering in patients infected with 2019 novel coronavirus in Wuhan, China. *Virus Res* 2020; **286**: 198043 [PMID: 32502551 DOI: 10.1016/j.virusres.2020.198043]
31 **Zha BS**, Wan X, Zhang X, Zha W, Zhou J, Wabitsch M, Wang G, Lyall V, Hylemon PB, Zhou H. HIV protease inhibitors disrupt lipid metabolism by activating endoplasmic reticulum stress and inhibiting autophagy activity in adipocytes. *PLoS One* 2013; **8**: e59514 [PMID: 23533630 DOI: 10.1371/journal.pone.0059514]
32 **Cao R**, Hu Y, Wang Y, Gurley EC, Studer EJ, Wang X, Hylemon PB, Pandak WM, Sanyal AJ, Zhang L, Zhou H. Prevention of HIV protease inhibitor-induced dysregulation of hepatic lipid metabolism by raltegravir *via* endoplasmic reticulum stress signaling pathways. *J Pharmacol Exp Ther* 2010; **334**: 530-539 [PMID: 20472667 DOI: 10.1124/jpet.110.168484]
33 **Ferrara F**, Granata G, Pelliccia C, La Porta R, Vitiello A. The added value of pirfenidone to fight inflammation and fibrotic state induced by SARS-CoV-2 : Anti-inflammatory and anti-fibrotic therapy could solve the lung complications of the infection? *Eur J Clin Pharmacol* 2020; **76**: 1615-1618 [PMID: 32594204 DOI: 10.1007/s00228-020-02947-4]
34 **Sun J**, Aghemo A, Forner A, Valenti L. COVID-19 and liver disease. *Liver Int* 2020; **40**: 1278-1281 [PMID: 32251539 DOI: 10.1111/liv.14470]
35 **Ghoda A**, Ghoda M. Liver Injury in COVID-19 Infection: A Systematic Review. *Cureus* 2020; **12**: e9487 [PMID:

32879813 DOI: 10.7759/cureus.9487]
36 **Yang L**, Wang W, Wang X, Zhao J, Xiao L, Gui W, Fan H, Xia J, Li Z, Yan J, Alasbahi A, Zhu Q, Hou X. Creg in Hepatocytes Ameliorates Liver Ischemia/Reperfusion Injury in a TAK1-Dependent Manner in Mice. *Hepatology* 2019; **69**: 294-313 [PMID: 30076625 DOI: 10.1002/hep.30203]
37 **Xu Z**, Shi L, Wang Y, Zhang J, Huang L, Zhang C, Liu S, Zhao P, Liu H, Zhu L, Tai Y, Bai C, Gao T, Song J, Xia P, Dong J, Zhao J, Wang FS. Pathological findings of COVID-19 associated with acute respiratory distress syndrome. *Lancet Respir Med* 2020; **8**: 420-422 [PMID: 32085846 DOI: 10.1016/S2213-2600(20)30076-X]
38 **Ji D**, Qin E, Xu J, Zhang D, Cheng G, Wang Y, Lau G. Non-alcoholic fatty liver diseases in patients with COVID-19: A retrospective study. *J Hepatol* 2020; **73**: 451-453 [PMID: 32278005 DOI: 10.1016/j.jhep.2020.03.044]
39 **Liu Q**, Wang RS, Qu GQ, Wang YY, Liu P, Zhu YZ, Fei G, Ren L, Zhou YW, Liu L. Gross examination report of a COVID-19 death autopsy. *Fa Yi Xue Za Zhi* 2020; **36**: 21-23 [PMID: 32198987 DOI: 10.12116/j.issn.1004-5619.2020.01.005]
40 **Sonzogni A**, Previtali G, Seghezzi M, Grazia Alessio M, Gianatti A, Licini L, Morotti D, Zerbi P, Carsana L, Rossi R, Lauri E, Pellegrinelli A, Nebuloni M. Liver histopathology in severe COVID 19 respiratory failure is suggestive of vascular alterations. *Liver Int* 2020; **40**: 2110-2116 [PMID: 32654359 DOI: 10.1111/liv.14601]
41 **Tian S**, Xiong Y, Liu H, Niu L, Guo J, Liao M, Xiao SY. Pathological study of the 2019 novel coronavirus disease (COVID-19) through postmortem core biopsies. *Mod Pathol* 2020; **33**: 1007-1014 [PMID: 32291399 DOI: 10.1038/s41379-020-0536-x]
42 **Rapkiewicz AV**, Mai X, Carsons SE, Pittaluga S, Kleiner DE, Berger JS, Thomas S, Adler NM, Charytan DM, Gasmi B, Hochman JS, Reynolds HR. Megakaryocytes and platelet-fibrin thrombi characterize multi-organ thrombosis at autopsy in COVID-19: A case series. *EClinicalMedicine* 2020; **24**: 100434 [PMID: 32766543 DOI: 10.1016/j.eclinm.2020.100434]
43 **Wang XX**, Shao C, Huang XJ, Sun L, Meng LJ, Liu H, Zhang SJ, Li HJ, Lv FD. Histopathological features of multiorgan percutaneous tissue core biopsy in patients with COVID-19. *J Clin Pathol* 2021; **74**: 522-527 [PMID: 32848014 DOI: 10.1136/jclinpath-2020-206623]
44 **Wang Y**, Liu S, Liu H, Li W, Lin F, Jiang L, Li X, Xu P, Zhang L, Zhao L, Cao Y, Kang J, Yang J, Li L, Liu X, Li Y, Nie R, Mu J, Lu F, Zhao S, Lu J, Zhao J. SARS-CoV-2 infection of the liver directly contributes to hepatic impairment in patients with COVID-19. *J Hepatol* 2020; **73**: 807-816 [PMID: 32437830 DOI: 10.1016/j.jhep.2020.05.002]
45 **Wichmann D**, Sperhake JP, Lütgehetmann M, Steurer S, Edler C, Heinemann A, Heinrich F, Mushumba H, Kniep I, Schröder AS, Burdelski C, de Heer G, Nierhaus A, Frings D, Pfefferle S, Becker H, Bredereke-Wiedling H, de Weerth A, Paschen HR, Sheikhzadeh-Eggers S, Stang A, Schmiedel S, Bokemeyer C, Addo MM, Aepfelbacher M, Püschel K, Kluge S. Autopsy Findings and Venous Thromboembolism in Patients With COVID-19: A Prospective Cohort Study. *Ann Intern Med* 2020; **173**: 268-277 [PMID: 32374815 DOI: 10.7326/M20-2003]
46 **Fix OK**, Hameed B, Fontana RJ, Kwok RM, McGuire BM, Mulligan DC, Pratt DS, Russo MW, Schilsky ML, Verna EC, Loomba R, Cohen DE, Bezerra JA, Reddy KR, Chung RT. Clinical Best Practice Advice for Hepatology and Liver Transplant Providers During the COVID-19 Pandemic: AASLD Expert Panel Consensus Statement. *Hepatology* 2020; **72**: 287-304 [PMID: 32298473 DOI: 10.1002/hep.31281]
47 **Hambali NL**, Mohd Noh M, Paramasivam S, Chua TH, Hayati F, Payus AO, Tee TY, Rosli KT, Abd Rachman Isnadi MF, Manin BO. A Non-severe Coronavirus Disease 2019 Patient With Persistently High Interleukin-6 Level. *Front Public Health* 2020; **8**: 584552 [PMID: 33304877 DOI: 10.3389/fpubh.2020.584552]
48 **Sahin TT**, Akbulut S, Yilmaz S. COVID-19 pandemic: Its impact on liver disease and liver transplantation. *World J Gastroenterol* 2020; **26**: 2987-2999 [PMID: 32587443 DOI: 10.3748/wjg.v26.i22.2987]
49 **Henry BM**, de Oliveira MHS, Benoit S, Plebani M, Lippi G. Hematologic, biochemical and immune biomarker abnormalities associated with severe illness and mortality in coronavirus disease 2019 (COVID-19): a meta-analysis. *Clin Chem Lab Med* 2020; **58**: 1021-1028 [PMID: 32286245 DOI: 10.1515/cclm-2020-0369]
50 **Kulkarni AV**, Kumar P, Tevethia HV, Premkumar M, Arab JP, Candia R, Talukdar R, Sharma M, Qi X, Rao PN, Reddy DN. Systematic review with meta-analysis: liver manifestations and outcomes in COVID-19. *Aliment Pharmacol Ther* 2020; **52**: 584-599 [PMID: 32638436 DOI: 10.1111/apt.15916]
51 **Gong J**, Ou J, Qiu X, Jie Y, Chen Y, Yuan L, Cao J, Tan M, Xu W, Zheng F, Shi Y, Hu B. A Tool for Early Prediction of Severe Coronavirus Disease 2019 (COVID-19): A Multicenter Study Using the Risk Nomogram in Wuhan and Guangdong, China. *Clin Infect Dis* 2020; **71**: 833-840 [PMID: 32296824 DOI: 10.1093/cid/ciaa443]
52 **Huang J**, Cheng A, Kumar R, Fang Y, Chen G, Zhu Y, Lin S. Hypoalbuminemia predicts the outcome of COVID-19 independent of age and co-morbidity. *J Med Virol* 2020; **92**: 2152-2158 [PMID: 32406952 DOI: 10.1002/jmv.26003]

World Journal of Gastroenterology

Submit a Manuscript: https://www.f6publishing.com

World J Gastroenterol 2022 October 21; 28(39): 5731-5734

DOI: 10.3748/wjg.v28.i39.5731

ISSN 1007-9327 (print) ISSN 2219-2840 (online)

ACADEMIC WRITING

All journals should include a correspondence section

Nikolaos Papanas, Dimitri P Mikhailidis, Debabrata Mukherjee

Specialty type: Medical informatics

Provenance and peer review: Invited article; Externally peer reviewed.

Peer-review model: Single blind

Peer-review report's scientific quality classification

Grade A (Excellent): 0
Grade B (Very good): B
Grade C (Good): C
Grade D (Fair): 0
Grade E (Poor): 0

P-Reviewer: Kurtcehajic A, Bosnia and Herzegovina; Ravindran V, India

Received: July 3, 2022
Peer-review started: July 3, 2022
First decision: August 1, 2022
Revised: September 3, 2022
Accepted: October 1, 2022
Article in press: October 1, 2022
Published online: October 21, 2022

Nikolaos Papanas, Diabetes Centre, Second Department of Internal Medicine, Democritus Univ Thrace, Alexandroupolis 68100, Greece

Dimitri P Mikhailidis, Department of Surgical Biotechnology, Division of Surgery and Interventional Science, and Department of Clinical Biochemistry, University College London Medical School, Royal Free Hosp Campus, London NW3 2QG, United Kingdom

Debabrata Mukherjee, Department of Internal Medicine, Texas Tech University, Health Science Central, El Paso, TX 79905, United States

Corresponding author: Dimitri P Mikhailidis, MSc, MD, FRCPath, FRCP, Hon. Professor, Department of Surgical Biotechnology, Division of Surgery and Interventional Science, and Department of Clinical Biochemistry, University College London Medical School, Royal Free Hosp Campus, Pond St, London NW3 2QG, United Kingdom. mikhailidis@aol.com

Abstract

Letters to the editor can provide useful scientific information and evaluation of published work as well as acting as an additional level of peer review. Furthermore, letters are good reading material, especially if they involve a debate between authors. Finally, letters are relatively short. Therefore, inexperienced career researchers can use such an opportunity to practice putting together a cogent argument. However, it is far from an ideal situation if letters are the only (or main) type of article on which to base an academic career.

Key Words: Correspondence; Journals; Letters to the editor; Medical writing; Peer review; Debate

©The Author(s) 2022. Published by Baishideng Publishing Group Inc. All rights reserved.

Core tip: Letters provide another level of worldwide peer review. Three editors express their opinions regarding the scientific value and structure of correspondence sections in journals.

Citation: Papanas N, Mikhailidis DP, Mukherjee D. All journals should include a correspondence section. *World J Gastroenterol* 2022; 28(39): 5731-5734
URL: https://www.wjgnet.com/1007-9327/full/v28/i39/5731.htm
DOI: https://dx.doi.org/10.3748/wjg.v28.i39.5731

INTRODUCTION

In this brief overview, three editors express their opinions regarding the scientific value and structure of correspondence sections in journals. Interpretations and suggestions are based on experience and the literature.

THE NEED FOR A CORRESPONDENCE SECTION

We propose that a correspondence section is an essential part of all journals. The reasons are summarised as follows[1-3]: Letters provide an additional level in the peer review process. Essentially, anyone worldwide can comment on a publication. Letters often promote good reading, especially when they involve a debate between authors. This is especially true for journals that have letters openly available. Given that letters are short, they are relatively easy to write. Therefore, they provide a training opportunity for inexperienced authors. Letters do not count as items when the Clarivate journal impact factor is calculated but if they are cited, these citations count. Thus, any citations of a letter may prove helpful for journals. However, we also need to consider that most letters are probably not highly cited.

TIPS ON WRITING A LETTER

A general rule would be a short text (the shorter, the better); brevity is important[1,2]. Therefore, letters need to focus on a restricted number of topics. Most journals impose limits on the word count and number of references. Some journals allow inclusion of a figure or table in a letter[1,2]. However, some editors provide substantial flexibility. Most letters are usually related to publications in the same journal [1-3]. Indeed, some editors do not consider letters unless they relate to material published in their journal. There are broadly two types of letters[1].

Correspondence

This is the commonest type. Such letters aim at one of the following goals[1-3]: (1) To contradict a published finding, for example by citing omitted studies or presenting unpublished results. Letter authors may also wish to highlight methodological or statistical flaws in a published study; (2) To reinterpret a published finding; for example based on additional findings; and (3) To support a published finding; for example on the basis of additional findings, possibly unpublished. This may include indirect evidence (*e.g.*, involving a different gender, ethnicity, species, methodology or related disease).

Early unpublished findings or a case report/series

More rarely, letters present early (unpublished) findings or a case report/series[1,2]. Such letters are miniatures of full studies or case reports. Their main advantages for the authors include rapid publication and the ability to present data on smaller patient series[1,2]. Full papers take longer to be published and processed. This may even take several months and it is possible that during that time more recent and relevant findings become available. For the journals, a potential advantage of full papers (and reviews) is that they are likely to have a higher citation rate than letters.

One final tip for academics and clinicians: avoid exclusively writing letters to the editor without also authoring original or review articles[4]. Indeed, it has already been noted that some authors try to build their career solely on letters published in high-ranking journals[4]. This will be noticed by others and will not be to the authors' benefit.

SUGGESTIONS FOR JOURNAL EDITORS REGARDING MANAGING A CORRESPONDENCE SECTION

We suggest that all journals could benefit from a correspondence section as a peer review "safety net". One of us has resigned as Associate Editor from two journals, because they would not introduce a correspondence section on the grounds that it would require too much editorial work.

A dedicated editor for the correspondence section would be ideal. However, this may be impractical for some journals. One of us has recently experienced a 5-mo delay regarding a decision on a 300-word letter. In our opinion, this represents completely unacceptable standards by the editorial staff of this journal. However, this is probably and hopefully, a rare event.

Letters provide an opportunity for a rapid response by journal editors[1,2]. Based on our experience both as editors and authors, this may be, at least ideally, a matter of a few days. When letters refer to a specific publication, the authors of the latter usually provide a response, pointing out every possible

error.

What to do if authors decline to respond to a letter commenting on their work? There is no simple answer. Possibly, if a letter is highly critical of a study, it may be published together with an editorial message, stating that the authors of the original work declined to respond. It would be unfortunate if some authors avoid criticism just by refusing to respond to valid points raised in a letter. Again, this has happened to us, although the definition of valid comments is based on our knowledge/views. Nevertheless, in our opinion they were obvious. That is why, in similar circumstances, we prefer to underline that the letter containing criticisms will be published, whether the authors of the original work respond or not. Editors must not suppress valid criticism of a publication thinking that it may suggest an oversight of errors by the peer reviewers and editors involved. This is an example of how correspondence provides another valuable level of peer review. One of us is currently involved in resolving such a problem. Obviously, any improvements in peer reviewing are welcome, and are still being sought[5-7].

In defence of authors who refuse to respond to comments in a letter, we need to consider that responding may require considerable additional work, which they do not wish to carry out or would like to reserve for their next publication. In such circumstances, honesty is the best policy. The authors can just state why they cannot provide a detailed response at this time, but they will do so in their forthcoming work. However, the comments will remain in the literature. If they are not covered by future work, this deficiency may be pointed out. Citing an older letter to show that the queries raised were answered is not only professional behaviour, but will also suit the journal where the letter was published by delivering a citation.

Other editorial issues include whether to allow more than one round of exchanges regarding the same publication. The time allowed between publication of an item and the submission of related letters needs to be clearly stated in the instructions for authors.

Finally, in the event of an interesting but too long letter, an option may be to convert it to a commentary or brief communication.

CONCLUSION

Letters to the editor are useful for authors, readers and journals. They provide training for younger researchers and are another valuable level of peer review. For all these reasons, in our opinion as editors, a correspondence section is likely to be a useful part of all scientific journals.

FOOTNOTES

Author contributions: Papanas N, Mikhailidis DP, and Mukherjee D contributed to: (1) Substantial contributions to conception and design, or acquisition of data, or analysis and interpretation of data; (2) drafting the article or revising it critically for important intellectual content; and (3) final approval of the version to be published.

Conflict-of-interest statement: The authors declare that they have no conflict of interest.

Open-Access: This article is an open-access article that was selected by an in-house editor and fully peer-reviewed by external reviewers. It is distributed in accordance with the Creative Commons Attribution NonCommercial (CC BY-NC 4.0) license, which permits others to distribute, remix, adapt, build upon this work non-commercially, and license their derivative works on different terms, provided the original work is properly cited and the use is non-commercial. See: https://creativecommons.org/Licenses/by-nc/4.0/

Country/Territory of origin: United Kingdom

ORCID number: Nikolaos Papanas 0000-0002-7320-785X; Dimitri P Mikhailidis 0000-0002-9566-2263; Debabrata Mukherjee 0000-0002-5131-3694.

S-Editor: Chen YL
L-Editor: Kerr C
P-Editor: Chen YL

REFERENCES

1 **Papanas N**, Georgiadis GS, Maltezos E, Lazarides MK. Letters to the editor: definitely not children of a lesser god. *Int Angiol* 2009; **28**: 418-420 [PMID: 19935598]

2 **Tierney E**, O'Rourke C, Fenton JE. What is the role of 'the letter to the editor'? *Eur Arch Otorhinolaryngol* 2015; **272**: 2089-2093 [PMID: 25231709 DOI: 10.1007/s00405-014-3289-7]

3 **Peh WC**, Ng KH. Writing a letter to the Editor. *Singapore Med J* 2010; **51**: 532-535 [PMID: 20730391]
4 **Neghina R**, Neghina AM. How to build a scientific publishing career based on hundreds of letters-to-the-editor: "The Art of Loss". *Account Res* 2011; **18**: 247-249 [PMID: 21707416 DOI: 10.1080/08989621.2011.584761]
5 **Lazarides MK**, Georgiadis GS, Papanas N. Do's and Don'ts for a Good Reviewer of Scientific Papers: A Beginner's Brief Decalogue. *Int J Low Extrem Wounds* 2020; **19**: 227-229 [PMID: 32525721 DOI: 10.1177/1534734620924349]
6 **Papanas N**, Mikhailidis DP. Alice through the Looking-glass: Can We Improve Peer Review? *Int J Low Extrem Wounds* 2022; 15347346221084784 [PMID: 35253507 DOI: 10.1177/15347346221084784]
7 **Papanas N**, Mikhailidis DP. A Call to Encourage Participation in the Reviewing Process: The REFEREE Acrostic. *Int J Low Extrem Wounds* 2022; 15347346221102645 [PMID: 35578539 DOI: 10.1177/15347346221102645]

World Journal of Gastroenterology

Submit a Manuscript: https://www.f6publishing.com

World J Gastroenterol 2022 October 21; 28(39): 5735-5749

DOI: 10.3748/wjg.v28.i39.5735

ISSN 1007-9327 (print) ISSN 2219-2840 (online)

ORIGINAL ARTICLE

Retrospective Cohort Study

Effects of COVID-19 on the liver: The experience of a single center

Valentina Liakina, Ieva Stundiene, Gabriele Milaknyte, Ramune Bytautiene, Rosita Reivytyte, Roma Puronaite, Gintare Urbanoviciute, Edita Kazenaite

Specialty type: Gastroenterology and hepatology

Provenance and peer review: Invited article; Externally peer reviewed.

Peer-review model: Single blind

Peer-review report's scientific quality classification

Grade A (Excellent): A
Grade B (Very good): B
Grade C (Good): C, C
Grade D (Fair): 0
Grade E (Poor): 0

P-Reviewer: Al-Ani RM, Iraq; Nooripour R, Iran

Received: June 22, 2022
Peer-review started: June 22, 2022
First decision: August 1, 2022
Revised: August 12, 2022
Accepted: September 21, 2022
Article in press: September 21, 2022
Published online: October 21, 2022

Valentina Liakina, Ieva Stundiene, Gabriele Milaknyte, Ramune Bytautiene, Edita Kazenaite, Centre of Hepatology, Gastroenterology and Dietetics, Clinic of Gastroenterology, Nephrourology and Surgery, Institute of Clinical Medicine, Faculty of Medicine, Vilnius University, Vilnius 01513, Lithuania

Valentina Liakina, Department of Chemistry and Bioengineering, Faculty of Fundamental Sciences, VILNIUS TECH, Vilnius 10223, Lithuania

Rosita Reivytyte, Gintare Urbanoviciute, Faculty of Medicine, Vilnius University, Vilnius 01513, Lithuania

Roma Puronaite, Clinic of Cardiac and Vascular Diseases, Institute of Clinical Medicine, Faculty of Medicine, Vilnius University, Vilnius 01513, Lithuania

Roma Puronaite, Institute of Data Science and Digital Technologies, Faculty of Mathematics and Informatics, Vilnius University, Vilnius 01513, Lithuania

Edita Kazenaite, Department of Pathology, Forensic Medicine and Pharmacology, Institute of Biomedical Sciences, Faculty of Medicine, Vilnius University, Vilnius 01513, Lithuania

Corresponding author: Valentina Liakina, PhD, Senior Research Fellow, Centre of Hepatology, Gastroenterology and Dietetics, Clinic of Gastroenterology, Nephrourology and Surgery, Institute of Clinical Medicine, Faculty of Medicine, Vilnius University, 3 Universiteto Street, Vilnius 01513, Lithuania. valentina.liakina@santa.lt

Abstract

BACKGROUND

The coronavirus disease 2019 (COVID-19) was perhaps the most severe global health crisis in living memory. Alongside respiratory symptoms, elevated liver enzymes, abnormal liver function, and even acute liver failure were reported in patients suffering from severe acute respiratory disease coronavirus 2 pneumonia. However, the precise triggers of these forms of liver damage and how they affect the course and outcomes of COVID-19 itself remain unclear.

AIM

To analyze the impact of liver enzyme abnormalities on the severity and outcomes of COVID-19 in hospitalized patients.

METHODS

In this study, 684 depersonalized medical records from patients hospitalized with COVID-19 during the 2020-2021 period were analyzed. COVID-19 was diagnosed according to the guidelines of the National Institutes of Health (2021). Patients were assigned to two groups: those with elevated liver enzymes (Group 1: 603 patients), where at least one out of four liver enzymes were elevated (following the norm of hospital laboratory tests: alanine aminotransferase (ALT) ≥ 40, aspartate aminotransferase (AST) ≥ 40, gamma-glutamyl transferase ≥ 36, or alkaline phosphatase ≥ 150) at any point of hospitalization, from admission to discharge; and the control group (Group 2: 81 patients), with normal liver enzymes during hospitalization. COVID-19 severity was assessed according to the interim World Health Organization guidance (2022). Data on viral pneumonia complications, laboratory tests, and underlying diseases were also collected and analyzed.

RESULTS

In total, 603 (88.2%) patients produced abnormal liver test results. ALT and AST levels were elevated by a factor of less than 3 in 54.9% and 74.8% of cases with increased enzyme levels, respectively. Patients in Group 1 had almost double the chance of bacterial viral pneumonia complications [odds ratio (OR) = 1.73, P = 0.0217], required oxygen supply more often, and displayed higher biochemical inflammation indices than those in Group 2. No differences in other COVID-19 complications or underlying diseases were observed between groups. Preexisting hepatitis of a different etiology was rarely documented (in only 3.5% of patients), and had no impact on the severity of COVID-19. Only 5 (0.73%) patients experienced acute liver failure, 4 of whom died. Overall, the majority of the deceased patients (17 out of 20) had elevated liver enzymes, and most were male. All deceased patients had at least one underlying disease or combination thereof, and the deceased suffered significantly more often from heart diseases, hypertension, and urinary tract infections than those who made recoveries. Alongside male gender (OR = 1.72, P = 0.0161) and older age (OR = 1.02, P = 0.0234), diabetes (OR = 3.22, P = 0.0016) and hyperlipidemia (OR = 2.67, P = 0.0238), but not obesity, were confirmed as independent factors associated with more a severe COVID-19 infection in our cohort.

CONCLUSION

In our study, the presence of liver impairment allows us to predict a more severe inflammation with a higher risk of bacterial complication and worse outcomes of COVID-19. Therefore, patients with severe disease forms should have their liver tests monitored regularly and their results should be considered when selecting treatment to avoid further liver damage or even insufficiency.

Key Words: COVID-19; SARS-CoV-2; Liver enzymes; Complications; Underlying disease; Disease severity

©The Author(s) 2022. Published by Baishideng Publishing Group Inc. All rights reserved.

Core Tip: In our study, elevated liver enzymes were detected in 88.2% of patients hospitalized with coronavirus disease 2019 (COVID-19). Alanine aminotransferase and aspartate aminotransferase were elevated by a factor of less than 3 in 54.9% and 74.8% of cases, respectively. Regardless of underlying diseases, including hepatitis, these patients had higher biochemical indices of inflammation, required an O_2 supply, and exhibited bacterial pneumonia complications more often than those with normal liver tests. Male gender, older age, diabetes, and hyperlipidemia were confirmed as independent factors associated with a more severe course of COVID-19. All deceased patients (2.9%) had underlying diseases - most often heart disease, hypertension, and urinary tract infections.

Citation: Liakina V, Stundiene I, Milaknyte G, Bytautiene R, Reivytyte R, Puronaite R, Urbanoviciute G, Kazenaite E. Effects of COVID-19 on the liver: The experience of a single center. *World J Gastroenterol* 2022; 28(39): 5735-5749

URL: https://www.wjgnet.com/1007-9327/full/v28/i39/5735.htm

DOI: https://dx.doi.org/10.3748/wjg.v28.i39.5735

INTRODUCTION

In addition to the most common symptoms of coronavirus disease 2019 (COVID-19) - such as fever, dyspnea, sore throat, dry cough, headache, fatigue, restlessness, myalgia, anosmia, dysgeusia, and chest pain with ground-glass opacities seen on radiological investigations[1] - approximately half of patients

suffer from gastrointestinal symptoms such as a lack of appetite, nausea, and vomiting[2]. In some cases, gastrointestinal symptoms may precede respiratory symptoms or even occur as the sole symptom of COVID-19[3]. A wealth of evidence suggesting that elevated liver enzymes are also a common finding in COVID-19 pneumonia has already been published[4]. Depending on the population studied, elevated levels of liver enzymes– alanine aminotransferase (ALT) and aspartate aminotransferase (AST) - in the blood have been detected in the range of 14%-76%[5,6]. In patients with severe COVID-19, gamma-glutamyl transferase (GGT) and hypoalbuminemia have also been documented[7]. Although liver injury is often transient and is usually normalized without special treatment in mild cases of disease[8], in severe and critical cases it can be the first sign of life-threatening upcoming events such as acute liver failure[9].

However, the exact triggers of liver damage, how it affects patients, and whether it could predict the course and outcomes of COVID-19 itself remain unclear. To address this issue, this study examines liver enzyme abnormalities in patients hospitalized with COVID-19.

MATERIALS AND METHODS

Study design and participants

This is a retrospective cohort study of patients hospitalized at Vilnius University Hospital's Santaros Clinics during the 2020-2021 severe acute respiratory disease coronavirus 2 (SARS-CoV-2) viral pneumonia pandemic. The inclusion criteria for patients were as follows: documented SARS-CoV-2 infection, diagnosed according to NIH guidelines[10] based on manifestations of clinical pneumonia; positive real-time reverse transcription SARS-CoV-2 polymerase chain reaction (RT-PCR) test from nasopharynx swab specimens (MagMAX™ Viral/Pathogen II Nucleic Acid Isolation Kit and TaqPath COVID-19 CE-IVD kit, Applied Biosystems); radiologically confirmed viral pneumonia; and age over 18 years.

Thus, exclusion criteria were: Age ≤ 18 years; patients with incomplete medical records, and negative SARS-CoV-2 test from nasopharyngeal swab specimen.

The depersonalized data of 684 patients were analyzed. Patients were assigned to two groups according to the results of liver tests: those with elevated liver enzymes (603 patients), where at least one of four liver enzymes were elevated (ALT ≥ 40, AST ≥ 40, GGT ≥ 36, or alkaline phosphatase (ALP) ≥ 150; following the norm of hospital laboratory tests) at any point of hospitalization from admission to discharge; or the control group (81 patients), with all four liver enzymes within normal range during hospitalization (Table 1). Depending on the severity of SARS-CoV-2 pneumonia - which was evaluated by radiological observation of lung damage (lung infiltration, pleura infiltration, ground glass opacities), level of respiratory failure (SpO_2, respiratory rate), and the overall clinical picture of the case – patients were assigned to the groups of moderate, severe, or critical COVID-19 pneumonia following the NIH COVID-19 disease guide (2022)[11].

Data collection

Depersonalized electronic medical records - including symptoms and clinical characteristics of COVID-19, laboratory and instrumental tests, therapeutic interventions, and outcome data - were collected for each patient. Demographic data included only age and gender. Underlying diseases were also recorded for all patients.

To confirm the diagnosis and evaluate the severity of COVID-19, the following tests were performed for all patients upon admission, and were repeated during treatment as required: throat roentgenogram; SARS-CoV-2 RT-PCR of nasopharyngeal swab; routine hematologic (full blood cell formula) and biochemical blood tests (troponin I, glucose, creatinine, blood urea nitrogen test, ferritin, procalcitonin, lactate, eGFR (CKD-EPI), ALT, AST, ALP, GGT, lactate dehydrogenase (LDH), bilirubin, C-reactive protein (CRP), interleukine-6 (IL-6), blood electrolyte tests (K, Na, Mg, Ca, Cl), coagulation tests (ADTL, Stago prothrombin assay, international normalized ratio, fibrinogen, D-dimers); and urea tests. In particular cases, an arterial blood analysis (pH, pCO_2, pO_2, HCO_3, SBC, ABE, SBE) was also performed, as well as additional instrumental, biochemical, and microbiological tests of blood and urea.

Hepatitis B and C markers, together with human immunodeficiency virus, cytomegalovirus, and Epstein-Barr virus markers as required, were also performed on admitted patients.

Statistical analysis

Quantitative data were presented as mean ± SD and range. Qualitative data were presented as numbers and percentages. The characteristics of the data distribution were evaluated using the Shapiro-Wilk test. Depending on data distribution normality, the difference in continuous variables between the groups of patients with elevated and normal liver enzymes was assessed using the Welch two independent sample *t*-test or the nonparametric Mann-Witney-Wilcoxon test. Pearson's chi-squared test was used to compare categorical variables between groups.

Table 1 Characteristics of the studied patients

Variables	Group 1 (with elevated liver enzymes)		Group 2 (with normal liver enzymes)		*P* value
		Number of tested		Number of tested	
n/%	603/88.2	603	81/11.8	81	
Male, *n*/%	356/59.0	356	28/34.6	28	< 0.0001
Female, *n*/%	247/41.0	247	53/65.4	53	
Age, yr ± SD	50.7 ± 9.5	603	51.9 ± 12.4	81	0.5075
Hospitalization, d ± SD	9.7 ± 5.9	603	8.7 ± 6.5	81	0.2039
ALT, U/L, range	149 ± 115, 40-728	603	22 ± 9, 7-39	81	< 0.0001
AST, U/L, range	90 ± 77, 3-818	552	22 ± 7, 11-39	70	< 0.0001
GGT, U/L, range	114 ± 125, 8-820	550	22 ± 8, 7-35	72	< 0.0001
ALP, U/L, range	101 ± 128, 29-1183	93	77 ± 25, 45-131	10	0.128
Bilirubin, μmol/L, range	9.1 ± 5.5, 3-67.1	460	7.6 ± 3.2, 3.2-18.5	61	0.0028
SPA, %, range	96.1 ± 19.5, 5-176	500	98.6 ± 21.9, 39-154	64	0.3868
INR, range	1.04 ± 0.18, 0.83-3.87	506	1.03 ± 0.11, 0.86-1.6	68	0.4728

ALT: Alanine aminotransferase; AST: Aspartate aminotransferase; GGT: Gamma-glutamyl transferase; ALP: Alkaline phosphatase; INR: International normalized ratio; SPA: Stago prothrombin assay.

Univariate and multivariate logistic regression analysis was performed to assess the likelihood of the cohesion of the variables.

Data were considered statistically significant when the *P* value was < 0.05 for the confidence interval set at 95%. All statistical analysis was performed with the R software, version 4.1.2 (The R Project for Statistical Computing, r-project.org).

RESULTS

Elevated liver enzymes, especially ALT, were detected in the majority of patients hospitalized with SARS-CoV-2 pneumonia (603 out of 684). ALT and AST were elevated by a factor of less than 3 in 54.9% and 74.8% of cases with increased enzyme levels, respectively. Only 9.3% of the cases of elevated ALT, 2.7% of AST, and 11.2% of GGT were in concentrations higher than 300 U/L (Table 1).

In most patients (432, 71.6%), elevated ALT in the range of 41-728 U/L was detected on the first day of hospitalization. In almost half (209) of these patients, ALT increased to 80 U/L; in 91 patients, up to 120 U/L; and in only 17 patients did the level of ALT increase to more than 300 U/L (Table 1). ALT tended to rise during hospitalization and pneumonia treatment, and in some cases its level did not recede to the normal range even after SARS-CoV-2 infection recovery and discharge.

AST levels were elevated in 449 (72.1%) patients overall: for 241 (53.7%) of these patients, AST was found to be elevated in the range of 41-351 U/L on the first day of hospitalization; 159 patients had an up to two-fold elevation of AST; 50 patients up to 120 U/L; and only two patients had AST levels over 300 U/L (Table 1). Similarly to ALT, AST levels were prone to increase during the treatment of SARS-CoV-2 pneumonia, but for most patients, these levels returned to their normal range by the time of discharge.

GGT levels in the range of 40-820 U/L were detected in 438 (70.4%) of the patients tested, and in 353 (80.6%) patients, elevated GGT was detected on the first day of hospitalization. Up to two-fold elevated GGT was detected in 198 patients; 71 patients displayed CGT levels up to 120 U/L; and 25 patients displayed CGT levels over 300 U/L (Table 1). Like ALT, GGT tends to increase during hospitalization and slowly normalizes after patients recover from viral pneumonia.

ALP level was tested for only 103 patients, and most cases 89 (86.4%) were in the normal range (Table 1). Only 7 (6.8%) patients had up to three-fold elevated ALP, and in one patient with a critical course of COVID-19 ALP increased dramatically to 1183 U/L, along with ALT 162 U/L and AST 223 U/L. This patient suffered from acute liver and kidney failure, electrolyte and alkaline-acid imbalance, and sepsis aggravated by resistance to beta-lactam antibiotics, from which they did not recover.

Only 24 patients (3.5%) of the studied cohort had preexisting hepatitis of different etiologies (including two patients with chronic hepatitis C and two patients with chronic hepatitis B), and only two of these patients (8.3%), with hepatitis B in long-term remission, had normal levels of liver enzymes

at admission and during hospitalization. The other 22 (91.7%) patients had elevated liver enzymes, including two patients (8.3%) with chronic hepatitis C. Most patients with preexisting liver diseases had a moderate course of COVID-19 pneumonia (20, 83.3%), three (12.5%) had severe cases, and one patient (4.7%) had a critical course of COVID-19. Only one female patient in this group died of COVID-19. No differences in other comorbidities or COVID-19 complications were observed in the remainder of the patients with preexisting liver disease.

Comparison of patient groups with elevated liver enzymes versus normal liver enzymes

When comparing patients who showed signs of liver impairment with those who did not, the main difference was the severity of inflammation. Patients with elevated liver enzymes (Group 1) more often demanded oxygen, and all biochemical inflammation indices were higher than in those with normal enzymes (Group 2). Of the 684 patients studied, 209 (30.5%) required O_2 supply due to respiratory failure, mostly belonging to Group 1 (Table 2). In addition, these patients required a longer duration of supportive O_2 due to low blood O_2 saturation because of severe lung infiltration.

For most patients, Il-6 blood concentration was in the range of 2-626 ng/L. Only one 62-year-old male with a critical course of pneumonia and elevated liver enzymes had an Il-6 as high as 2499 ng/L. This patient died after the manifestation of a cytokine storm (Table 2).

The level of LDH in the blood was in the range of 134 U/L–979 U/L for most patients. Only one patient (a 72-year-old male), who had normal liver enzyme levels during all stages of the disease, had LDH 1304 U/L and died of critical COVID-19.

Patients with elevated liver enzymes had almost double the chance of bacterial complications of viral pneumonia (univariate logistic regression: odds ratio (OR) = 1.73 (1.087–2.789), P = 0.0217). The incidences of other complications were largely similar in both groups (Table 3).

Underlying diseases - including hypertension, the most common - did not substantially prevail in patients with elevated liver enzymes (Table 4).

Analysis of the association of variables with the seriousness of SARS-CoV-2 pneumonia

A moderate course of SARS-CoV-2 pneumonia was diagnosed in 500 (73.1%) patients; a severe course in 148 (21.6%); and a critical course of SARS-CoV-2 pneumonia was diagnosed in 36 (5.3%) patients. There were no significant differences in the distribution of severity between the two groups of patients studied (Table 2).

To clarify which factors predispose a patient toward a more severe course of COVID-19, univariate (Tables 5 and 6) and multivariate (Table 7) analyses were performed.

The age of patients had almost no influence on the course of the disease, while male patients had forms of COVID-19 that were almost 1.5 times more severe and critical (Table 5). Multivariate logistic regression analysis also confirmed that the male gender was independently associated with more severe COVID-19 (Table 7). Acute kidney failure, but not acute liver failure, was also found to be associated with a more severe course of the disease (Table 5).

Neither the underlying disease that was most frequently presented - primary hypertension - nor less frequent lung diseases, cancers, or obesity were confirmed to be associated with a more severe course of COVID-19. Only heart disease of various etiologies, type 2 diabetes, and hyperlipidemia were prone to aggravate COVID-19 (Table 6). Diabetes and hyperlipidemia, but not heart disease, were also independently confirmed to be associated with more severe COVID-19 (Table 7).

Multivariate logistic regression analysis included age, gender, underlying diseases, and complications of pneumonia. Among the pneumonia complications analyzed, only sepsis, increased respiratory rate, and respiratory failure were independently associated with the severity of COVID-19 (Table 7).

Analysis of patients with liver failure

In our study, five patients, all of whom were male, experienced acute liver failure (0.73%) (Table 8). Septic shock developed in four patients, who did not recover despite all efforts to stabilize their condition. Two patients experienced rapid progression of the disease, and died after three days (a 50-year-old male with angioblastic T lymphoma) and eight days (an 84-year-old male with intracranial abscess, epilepsy, and chronic heart disease) of hospitalization.

Disease outcome analysis

Twenty patients died from COVID-19, 85% of whom (17 patients) had elevated liver enzymes. When comparing between patients with elevated and normal liver enzymes, no significant differences were found in mortality rate - 2.8% for those with abnormal liver test results, and 3.7% for those with normal liver test results.

Most of the deceased patients were older males who experienced much more severe SARS-CoV-2 pneumonia, with more life-threatening complications than recovered patients (Table 9). All deceased patients had at least one underlying disease or a combination thereof, and suffered significantly more often from heart disease, hypertension, and urinary tract infections than patients who made recoveries (Table 9). It should be noted that despite the fact that deceased patients were characterized by developing resistance to antibiotics more often than recovered patients, bacterial complications of viral

Table 2 Coronavirus disease 2019 pneumonia severity indices of patients with elevated liver enzymes (group 1) versus normal liver enzymes (group 2)

	Group 1 (n = 603)		Group 2 (n = 81)		*P* value
		Number of tested		Number of tested	
Moderate COVID, n/%	436/72.2	603	64/79.0	81	0.4341
Severe COVID, n/%	134/22.4		14/17.3		
Critical COVID, n/%	33/5.4		3/3.7		
O_2 demand, n/%	188/31.2	603	21/25.9	81	0.3354
SpO_2, %, range	94.4 ± 3.5, 68-100	594	95.3 ± 2.9, 84-99	76	0.0169
Respiratory rate, n/min, range	18.4 ± 3.2, 14-40	543	17.7 ± 2.4, 14-28	72	0.0291
Mortality, total, n/%	17/2.8	603	3/3.7	81	0.6573
CRP, mg/L, range	72.3 ± 68.9, 0.4-459.0	571	54.2 ± 56.1, 0.6-327.0	70	0.0151
IL-6, ng/L, range	50.3 ± 120.0, 3-2499	546	35.7 ± 38.9, 2-188	65	0.0402
LDH, U/L, range	357.9 ± 134.0, 167-979	435	299.0 ± 173.4, 134-1304	49	0.0254

COVID: Coronavirus disease; CRP: C-reactive protein; LDH: Lactate dehydrogenase; IL-6: Interleukin-6.

Table 3 Comparison of coronavirus disease 2019 pneumonia complications in patients with (group 1) and without (group 2) elevated liver enzymes

	Group 1	Group 2	*P* value
Bacterial complication, n/%	335/55.6	34/42.0	0.0213
Sepsis, n/%	14/2.3	4/4.9	0.1672
Respiratory failure, n/%	63/10.4	7/8.6	0.6146
Acid-alkaline imbalance, n/%	11/1.8	0	0.2204
Electrolyte imbalance, n/%	67/11.1	8/9.9	0.7385
Hyperkalemia, n/%	10/1.7	0	0.2426
Hypokalemia, n/%	40/6.6	7/8.6	0.5023
Hypernatremia, n/%	1/0.2	2/2.5	0.0032
Hyponatremia, n/%	13/2.2	0	0.1821
Blood volume decrease, n/%	15/2.5	3/3.7	0.5209
Blood clotting disorder, n/%	6/1.0	3/3.7	0.0446
Acute kidney failure, n/%	15/2.5	1/1.2	0.4836
Acute liver failure, n/%	5/0.8	0	0.3672
Antibiotic resistance, n/%	18/3.0	1/1.2	0.3681

pneumonia were less frequently documented in this group. Only two deceased patients were obese (2, or 10%, *vs* 15, or 2.26%, of recovered patients).

DISCUSSION

In our cohort, 88.2% of hospitalized COVID-19 patients had elevated liver enzymes - most often ALT (88.2%) followed by AST (71.6%) and GGT (70.4%). Similar results were found in the Cai *et al*[7], where 76.3% of hospitalized patients displayed abnormal liver test results. On the contrary, the Hao study reported that 79.2% of hospitalized patients displayed normal liver tests[5].

An increase in LDH level was observed in patients with severe forms of COVID-19, and was associated with a poor prognosis. In the acute liver failure group, four patients had elevated LDH in the

Table 4 Prevalence of underlying diseases in patients with (group 1) and without (group 2) elevated liver enzymes

	Group 1	Group 2	*P* value
Hospitalization, d, *n* ± SD	9.7 ± 5.9	8.7 ± 6.5	0.2039
Primary hypertension, *n*/%	193/32.0	21/25.9	0.2638
Heart disease, *n*/%	32/5.3	6/7.4	0.4430
Lung disease, *n*/%	19/3.2	5/6.2	0.1652
Diabetes, *n*/%	50/8.3	9/11.1	0.4015
Obesity, *n*/%	14/2.3	3/3.7	0.4532
Hyperlipidemia, *n*/%	31/5.1	5/6.2	0.6962
Podagra, *n*/%	12/2.0	0	0.2002
Kidney disease, *n*/%	16/2.7	4/4.9	0.2518
Prostate disease, *n*/%	9/1.5	1/1.2	0.8546
Urinary tract disease, *n*/%	39/6.5	6/7.4	0.7487
Thyroiditis and goiter, *n*/%	21/3.5	4/4.9	0.5121
Gastrointestinal disease, *n*/%	32/5.3	3/3.7	0.5387
Liver disease, *n*/%	22/3.7	2/2.5	0.5865
Nervous and mental diseases, *n*/%	27/4.5	1/1.2	0.1666
Cancers, *n*/%	17/2.8	5/6.2	0.1098

Table 5 The association of the severity of coronavirus pneumonia with the demographic characteristics of patients and critical disease outcomes (data from univariate logistic regression analysis)

	OR	95% confidence interval	*P* value
Gender: male *vs* female	1.5989137	1.1317308-2.2732760	0.0083
Age	1.0260275	1.0116249-1.0409474	0.0004
Respiratory rate	1.1588882	1.0942282-1.2311821	< 0.0001
Acute respiratory failure	3.3114884	2.0001907-5.4967193	< 0.0001
O_2 demand	3.9476028	2.7654860-5.6573094	< 0.0001
Sepsis	7.4825581	2.7778683-23.601933	0.0002
Acute kidney failure	6.2586207	2.2427771-20.097089	0.0008
Antibiotic resistance	3.8879310	1.5485304-10.193077	0.0041
Mortality	26.8383223	7.6407747-169.97850	< 0.0001

OR: Odds ratio.

range of 448-900 U/L. One patient with normal liver enzymes had an LDH of 1304 U/L. These patients died during treatment. Our findings are consistent with data from an Indonesian meta-analysis in which an association between increased LDH levels and mortality was observed (OR = 4.22, $P < 0.001$)[12].

It should be noted that the proportion of patients with abnormal liver test results varies between published COVID-19 studies for several reasons. As in our case, some studies are restricted only to hospitalized patients[5,7,13,14], whereas other studies include all positive cases of COVID-19[9]. Moreover, the liver test norms that apply in particular hospitals vary, making it somewhat difficult to compare data. In our study, ALT and AST below 40 U/L, GGT below 36 U/L, and ALP below 150 U/L were considered normal for both male and female patients, as in the Cai *et al*[7], while in other studies the normal limits of liver tests were set lower. In the Hao study, the ALT norm for males was 35 U/L, while for females it was 25 U/L[5]; in the Wishniewska study, ALT and AST norms for males were 41 U/L, and for females they were 32 U/L[15].

In general, some reviews provide elevated liver enzymes for COVID-19 patients in the range of 14.8%-53%[16], while others consider 50%-78% to be elevated[6].

Table 6 The association of the severity of coronavirus pneumonia with underlying diseases (data from univariate logistic regression analysis)

	OR	95% confidence interval	*P* value
Diabetes	2.3041738	1.3274753-3.9642971	0.0027
Heart disease	2.5760479	1.3198252-4.9960747	0.0050
Hyperlipidemia	2.2857140	1.1426635-4.5048434	0.0173

OR: Odds ratio.

Table 7 Independent factors associated with the severity of coronavirus disease 2019 (data from multivariate logistic regression analysis)

	OR	95% confidence interval	*P* value
Age	1.0227924	1.0032076-1.0431564	0.0234
Gender: male *vs* female	1.7233575	1.1114172-2.7017507	0.0161
Respiratory rate	1.1444804	1.0724480-1.2254639	< 0.0001
Respiration failure	2.1878906	1.1163265-4.2384266	0.0209
Sepsis	14.923604	1.6112025-359.53433	0.0352
Diabetes	3.2206335	1.5539799-6.6834759	0.0016
Hyperlipidemia	2.6652639	1.1327787-6.2794095	0.0238

OR: Odds ratio.

Table 8 Data from patients with acute liver failure

Gender	Age	Outcome	COVID severity	Respiratory failure, SpO_2, respiratory rate	O_2	Laboratory tests	COVID complications	Comorbidities
Male	84	Deceased	Critical	Yes, 83%, 18/min	No	ALT 107, ALP 117, GGT 107, LDH 743, Alb 29.3	Sepsis; Electrolytes imbalance; Hypokalemia; Acid-alkaline imbalance	Heart disease; Epilepsy
Male	55	Deceased	Critical	Yes, 91%, 34/min	Yes	CRP 111, IL-6 87, ALT 115, AST 344, ALP 40, LDH 448, Alb 28.1	Sepsis; Hypokalemia; Hyponatremia; Blood coagulation disorder	Primary hypertension; Obesity; Antibiotic resistance
Male	44	Recovered	Moderate	No, 94%, 16/min	No	CRP 98, IL-6 54, ALT 113, AST 193, ALP 73, GGT 355, LDH 399	Hypokalemia	Primary hypertension; Heart disease; Kidney disease
Male	42	Deceased	Critical	Yes, 80%, 30/min	Yes	CRP 459, IL-6 99, ALT 162, AST 183, ALP 1183, GGT 67, LDH 900, Alb 16.6	Acute kidney failure; Sepsis; Bacterial pneumonia complication; Hypokalemia; Blood coagulation disorder	Urinary tract infection; Anemia; Antibiotic resistance
Male	50	Deceased	Moderate	No, 98%, 22/min	No	CRP 221, IL-6 626, ALT 521, AST 53, ALP 296, GGT 559, LDH 546, Alb 16.5	Acute kidney failure; Sepsis; Blood coagulation disorder; Hypokalemia	Heart disease; Cancer (lymphoma)

COVID: Coronavirus disease; CRP: C-reactive protein; LDH: Lactate dehydrogenase; IL-6: Interleukin-6; ALT: Alanine aminotransferase; AST: Aspartate aminotransferase; GGT: Gamma-glutamyl transferase; ALP: Alkaline phosphatase; Alb: Albumin.

Despite the aforementioned discrepancies, abnormalities in liver tests deserve the attention of clinicians due to the wealth of evidence suggesting that patients with elevated liver enzymes, especially ALT and AST, generally have more severe SARS-CoV-2 pneumonia[6,7,17-20]. In different studies, elevated transaminases are associated with a 2–9-fold increased probability of poor outcomes of COVID-19[19,21].

Table 9 Analysis of patients hospitalized with coronavirus disease 2019 depending on the outcome of the disease

	Deceased	Recovered	*P* value
Total number, *n*/%	20/2.9	664/97.1	
Male/female ratio	17/3	367/297	0.0081
Age, yr ± SD	64.3±11.9	50.45	0.0004
With normal enzymes, *n*/%	3/15.0	78/11.7	0.6554
With elevated enzymes, *n*/%	17/85.0	586/88.3	
Moderate COVID, *n*/%	2/10.0	498/75.0	< 0.0001
Severe COVID, *n*/%	5/25.0	143/21.5	
Critical COVID, *n*/%	13/65.0	23/3.5	
Respiratory failure, *n*/%	17/85.0	53/8.0	< 0.0001
Respiratory rate, *n*/min ± SD	22.3 ± 5.6	18.2 ± 2.9	0.0099
SpO_2, % ± SD	88.7 ± 6.3	94.6 ± 3.2	0.0010
O_2 demand, *n*/%	11/55.0	198/29.8	0.0158
Bacterial pneumonia complication, *n*/%	5/25.0	364/54.8	0.0084
Sepsis, *n*/%	13/65.0	5/0.8	< 0.0001
Acute liver failure, *n*/%	4/20.0	1/0.15	< 0.0001
Acute kidney failure, *n*/%	10/50.0	6/0.9	< 0.0001
Electrolytes imbalance, *n*/%	11/55.0	64/9.6	< 0.0001
Antibiotic resistance, *n*/%	7/35.0	12/1.8	< 0.0001
Urinary tract infections, *n*/%	5/25.0	40/6.0	0.0007
Primary hypertension, *n*/%	10/50.0	204/30.7	0.0669
Heart disease, *n*/%	10/50.0	28/4.2	< 0.0001

COVID: Coronavirus disease.

In our study, moderate pneumonia was more frequent in patients with normal liver enzymes, while critical pneumonia prevailed in patients with elevated liver test results. Furthermore, the majority of the deceased patients had elevated liver enzymes. Despite this, it should be noted that we have not proved that abnormal liver test results are directly related with the likelihood of more severe COVID-19.

The broader field of research has no consensus on the pathological mechanism by which SARS-CoV-2 infection damages the liver because the histological view of liver injury rarely presents. In the Cai *et al* [7], postmortem histological liver analysis showed neither lesions of the lobular architecture nor portal tract infiltration - only slight vesicular steatosis, watery degeneration of hepatocytes with minimal plasma cells, and neutrophil infiltration of hepatic sinuses[7]. Such alterations prompted the formulation of a hypothesis of ischemic/hypoxic hepatitis due to altered O_2 blood saturation, and cardiac failure in critically affected cases[22].

However, the pattern of increase in transaminase in patients with COVID-19 was different from hypoxic hepatitis, suggesting that this was not the case. ALT and AST were elevated by a factor of less than 3 in 54.9% and 74.8%, respectively, of cases of abnormal liver test results in this study. Only 9.3% of the cases of elevated ALT, 2.7% of AST, and 11.2% of GGT were in concentrations greater than 300 U/L. Other studies also emphasize that transaminases rarely increase by a factor of more than 2-3 in COVID-19 patients[19,23].

It should also be borne in mind that elevated transaminases do not always originate exclusively from the liver; therefore, other causes such as myositis, ischemia, and cytokine release syndrome must be excluded to draw a definitive conclusion regarding liver injury in COVID-19 patients[24]. ACE-2, responsible for the virus entry receptor, is expressed not only in respiratory tract epithelium cells but also in vascular endothelium, cardiovascular tissue, renal tissue, and intestinal epithelia, which is why the possibility for the entry and replication of SARS-CoV-2 theoretically exists in practically all vasculated tissues of the human body[25]. Histopathological analysis of autopsies confirmed inflammatory infiltration of the lamina propria; epithelium of the digestive tract, skin, and kidney blood vessels; features of viral myocarditis; and hypoxic brain injury[26]. Furthermore, other research has established that SARS-CoV-2 can persist in the intestines of infected subjects even longer than in the

respiratory tract[27-29].

Abnormal liver test results are more likely to reflect the severity of COVID-19 in general than a particular liver injury[21]. A comprehensive meta-analysis of 35 studies with more than 10000 total participants concluded that COVID-19, despite its severity, has a minor impact on the liver[4]. We agree with this conclusion.

Patients with elevated liver enzymes also displayed increased indices of inflammation, such as CRP and IL-6 levels. Elevated serum levels of CRP, IL-1, IL-6, and the tumor necrosis factor were reported in several other studies, and this was associated with a non-favorable course of liver injury[30]. Additionally, the bacterial complication of SARS-CoV-2 pneumonia, which contributes to the systemic inflammatory response, was diagnosed more frequently in patients with increased liver enzymes (OR = 1.73, P = 0.0217).

In our study, resistance to antibiotics, most often beta-lactams, was found to be associated with more severe COVID-19 (OR = 3.89, P = 0.004) and was documented more frequently in deceased patients. This issue is rarely discussed in COVID-19-related studies and needs more careful evaluation, as only very few studies with a small number of patients have been published[31,32]. Although concerns that the pandemic has led to an increase in antibiotic resistance due to self-medication of this viral infection have already been raised[33,34], it is necessary to elucidate how resistance to antibiotics modulates COVID-19 itself as very little comprehensive analysis has been published so far.

It also appeared that male patients in our cohort were more likely to have elevated liver enzymes than female patients. Furthermore, the male gender was confirmed as an independent factor associated with more severe COVID-19. This finding is consistent with previous data which highlights the male gender as one of the indicators of liver affliction[7,35]. With some disagreements, the protective effect of estrogen is often mentioned in relation to liver diseases[36], but the specific reasons that males suffer from more severe COVID-19 should be elucidated in more studies involving not only clinical but also detailed epidemiological data.

Weber and co-authors reported that only rare cases of acute liver failure were diagnosed in infected patients[37]. Our findings are in line with this: only five (0.72%) patients experienced acute liver failure, all of whom were male. In four of those patients, sepsis developed, leading to death. Males also prevailed among the total number of deceased patients (20, or 2.9%), most of whom (17, or 85%) displayed abnormal liver test results. Other similar results have been posted elsewhere which suggest that the majority (58%-78%) of deceased COVID-19 patients had liver injuries[38,39]. However, a comprehensive meta-analysis of 158 studies involving 78798 patients drew the conclusion that elevated liver enzymes, despite being a common finding in COVID-19 patients, had no effect on mortality or the critical course of the disease[20].

It should be emphasized that none of the patients in our study who experienced liver failure during the course of COVID-19 had an underlying liver disease. Furthermore, there was no association of elevated liver enzymes with preexisting liver disease.

Overall, 3.5% of patients had underlying liver disease, the majority of whom (91.7%) exhibited abnormal liver test results during the course of COVID-19. Only 12.5% of these patients had severe COVID-19, and one female died of critical COVID-19.

Although chronic comorbid liver diseases are reported in 2.6%-11% of patients[19], it seems that in most cases this does not influence COVID-19-associated liver injury, severe COVID-19 infection, or poor patient outcomes. This was confirmed in our study, was also shown in a nationwide matched cohort study[40], and has been approved in several reviews[19,41]. However, in one publication with 99 patients, preexisting hepatitis B infection was reported as a condition for more severe COVID-19 infection compared to patients without hepatitis B[42]. It is assumed that the immunosuppressive effect of the SARS-CoV-2 virus may lead to the reactivation of the hepatitis B virus[43]. We could neither confirm nor deny this, as our cohort included only two patients with chronic hepatitis B in remission and two patients with chronic hepatitis C.

There is an opinion that the SARS-CoV-2 virus itself could be responsible for liver injury during COVID-19, but the histopathological mechanism remains uncertain[41]. In the liver, the majority of abandonment of ACE-2 expression is determined in cholangiocytes, but in patients with COVID-19, the cytopathic, not cholestatic, profile of elevated enzymes prevails. On the other hand, the level of expression of ACE-2 receptors in hepatocytes is believed to be regulated by the virus. There may also be additional ACE receptors or co-receptors[44]. Thus, we agree with the conclusion that COVID-19-associated liver injury usually occurs as a result of the progression of COVID-19 itself[45].

We did not find any differences between the groups of patients with and without elevated liver enzymes concerning the prevalence of underlying diseases. Therefore, we cannot predict nor draw any conclusions regarding how underlying diseases contribute to liver damage during COVID-19. However, patients with diabetes, heart diseases of various etiologies, and hyperlipidemia, but not obesity, have an increased likelihood of suffering from more severe SARS-CoV-2 pneumonia. Furthermore, diabetes and hyperlipidemia were independently confirmed to be associated with more severe COVID-19 (OR = 3.2, P = 0.0016, and OR = 2.7, P = 0.0238, respectively). Thus, concomitant pathology appeared to be more likely to affect the severity of COVID-19 than the probability of liver damage in our study. Many studies also mention cardiovascular and renal diseases, diabetes, obesity, and hypertension as factors that worsen the course of COVID-19[20].

In summary, elevated liver enzymes are often found in patients with COVID-19. This may be due to a variety of factors, including the effects of medications used to treat the disease, concomitant liver pathology, and the influence of the virus itself. In the cases that we examined, there were significantly more patients with hepatic impairment than with normal liver function, and hepatic-impaired patients had both a higher risk of bacterial complications and a more severe course of viral pneumonia, with increased oxygen demand. This is most likely due to the effects of the SARS-CoV-2 virus, which causes more damage not only to the respiratory system but also to other organs, including the liver, due to more pathogenicity and increased cytopathic aggression which causes a greater storm of cytokines.

Because we only examined inpatients with moderate to severe and critical COVID-19, we cannot compare the frequency of hepatic impairment in mild cases of COVID-19.

Limitations of the study

We must consider several limitations of our study. Because we studied only patients with COVID-19 who needed hospitalization, and outpatients were omitted, the groups of patients differed in size by a factor of almost 8: the group with elevated liver enzymes consisted of 603 patients, and the group with normal liver enzymes consisted of 81 patients. This circumstance perhaps prevented us from statistically proving an association between liver impairment and severity of COVID-19 course - although direct damage of the liver tissue by the SARS-CoV-2 virus itself should be proved histologically, since elevated transaminases do not entirely arise from damage to the liver tissue.

Our study featured no groups with asymptomatic or mild COVID-19; their liver enzymes would likely have been in the normal range. Thus, the group with normal enzymes could be larger. This circumstance is also necessary to consider when evaluating data on the impact of preexisting diseases on COVID-19 severity. We also have not followed up with patients after discharge, which is why we do not know how quickly signs of liver impairment are resolved after the recovery of patients from COVID-19 pneumonia.

CONCLUSION

Despite a wealth of published data analyzing liver tests in COVID-19 patients, it is still difficult to draw inferences not only about the cause of such an effect of the SARS-CoV-2 virus infection on the liver, but also about the prevalence of elevated liver enzymes in such patients.

In summarizing our results, we can conclude that liver impairment allows a more severe inflammation to be predicted, with a higher risk of bacterial complications and worse outcomes in patients with SARS-CoV-2 pneumonia. Because several drugs with potentially hepatotoxic effects are used in severe cases, patients with more aggressive forms of COVID-19 should have their liver enzymes monitored regularly; their results should be considered when selecting a treatment to avoid further hepatic impairment or even insufficiency.

ARTICLE HIGHLIGHTS

Research background

Alongside respiratory symptoms, elevated liver enzymes, abnormal liver function, and even acute liver failure were reported in patients suffering from severe acute respiratory disease coronavirus 2 (SARS-CoV-2) pneumonia. However, the exact triggers of liver damage, how it affects patients, and whether it could predict the course and outcomes of coronavirus disease 2019 (COVID-19) itself remain unclear.

Research motivation

Although liver injury in patients with COVID-19 is often transient and is usually normalized without special treatment in mild cases of the disease, it can be the first sign of life-threatening events such as acute liver failure in severe and critical cases. Therefore, it is essential for everyday clinical practice to have a more precise view of how the liver impairment affects the course and outcomes of SARS-CoV-2 infection itself. Our study contributes to this goal.

Research objectives

This study aims to analyze the impact of liver enzyme abnormalities on the severity and outcomes of COVID-19 in hospitalized patients to have a clearer view of how to evaluate the risk of severe liver impairment from elevated enzyme tests.

Research methods

In this study, 684 depersonalized medical records from patients hospitalized with COVID-19 during the 2020-2021 period were analyzed. Patients were assigned to two groups: those with elevated liver

enzymes, where at least one out of four liver enzymes were elevated at any point of hospitalization, from admission to discharge; and the control group, with normal liver enzymes during hospitalization. COVID-19 severity was assessed according to the interim World Health Organization guidance (2022). Data on viral pneumonia complications, laboratory tests, and underlying diseases were also collected and analyzed.

Research results

In total, 88.2% of patients with SARS-CoV-2 infection produced abnormal liver test results. Alanine aminotransferase and aspartate aminotransferase levels were elevated by a factor of less than 3 in 54.9% and 74.8% of cases with increased enzyme levels, respectively. Patients in Group 1 had almost double the chance of bacterial viral pneumonia complications, required oxygen supply more often, and displayed higher biochemical inflammation indices than those in Group 2. Like in other research, our patients rarely experienced acute liver failure. The majority of the deceased patients had at least one underlying disease or a combination thereof, and most were male. Alongside male gender and older age, diabetes and hyperlipidemia, but not obesity, were confirmed as independent factors associated with more a severe COVID-19 infection in our cohort.

Research conclusions

In our study, the presence of liver impairment allows us to predict a more severe inflammation with a higher risk of bacterial complication and worse outcomes of COVID-19. Therefore, monitoring liver enzyme levels should be a part of the qualitative care of patients with SARS-CoV-2 pneumonia.

Research perspectives

To find out more precisely the sources of increased liver enzymes in patients with COVID-19, it would be beneficial to elucidate whether the SARS-CoV-2 virus can enter and replicate in hepatocytes. For this purpose, an experimental study on the cell line of the liver origin or virus detection in hepatocytes during a histological analysis of autopsies could be promising.

ACKNOWLEDGEMENTS

We are grateful to the collaborators of the Centre for Informatics and the Development of Vilnius University Hospital's Santaros Clinics for their valuable assistance in the data collection process. Our special thanks go to Ulbinas P, whose patience and competence allowed us to perform impersonalized data extraction in the most efficient and relevant manner.

FOOTNOTES

Author contributions: Puronaite R, Milaknyte G, Reivytyte R and Urbanoviciute G performed raw data collection; Liakina V, Stundiene I, Bytautiene R and Kazenaite E revised collected data for relevance and sufficiency; Liakina V, Stundiene I, Milaknyte G and Bytautiene R wrote the manuscript draft; Liakina V edited draft and prepared the final version of the manuscript; Kazenaite E revised manuscript for important intellectual content.

Institutional review board statement: The study was reviewed and approved by the Vilnius Regional Biomedical Research Ethics Committee and by Institutional Review Board (approval No. 2022/2-1411-882).

Informed consent statement: Patients were not required to give informed consent to the study because the analysis used anonymous data that were obtained after each patients agreed to treatment by written consent.

Conflict-of-interest statement: All the authors report no relevant conflicts of interest for this article.

Data sharing statement: No additional data are available.

STROBE statement: The authors have read the STROBE Statement-checklist of items, and the manuscript was prepared and revised according to the STROBE Statement-checklist of items.

Open-Access: This article is an open-access article that was selected by an in-house editor and fully peer-reviewed by external reviewers. It is distributed in accordance with the Creative Commons Attribution NonCommercial (CC BY-NC 4.0) license, which permits others to distribute, remix, adapt, build upon this work non-commercially, and license their derivative works on different terms, provided the original work is properly cited and the use is non-commercial. See: https://creativecommons.org/Licenses/by-nc/4.0/

Country/Territory of origin: Lithuania

ORCID number: Valentina Liakina 0000-0001-8685-1292; Ieva Stundiene 0000-0002-2569-3638; Gabriele Milaknyte 0000-0001-9343-6345; Ramune Bytautiene 0000-0002-6071-9688; Rosita Reivytyte 0000-0002-9140-227X; Roma Puronaite 0000-0001-7571-4989; Gintare Urbanoviciute 0000-0001-8392-3019; Edita Kazenaite 0000-0002-7127-1399.

Corresponding Author's Membership in Professional Societies: Lithuanian Society of Immunology; Lithuanian Society of Gastroenterology; European Association of the Study of the Liver.

S-Editor: Gao CC
L-Editor: A
P-Editor: Gao CC

REFERENCES

1 **Frediansyah A**, Nainu F, Dhama K, Mudatsir M, Harapan H. Remdesivir and its antiviral activity against COVID-19: A systematic review. *Clin Epidemiol Glob Health* 2021; **9**: 123-127 [PMID: 32838064 DOI: 10.1016/j.cegh.2020.07.011]
2 **Zhong P**, Xu J, Yang D, Shen Y, Wang L, Feng Y, Du C, Song Y, Wu C, Hu X, Sun Y. COVID-19-associated gastrointestinal and liver injury: clinical features and potential mechanisms. *Signal Transduct Target Ther* 2020; **5**: 256 [PMID: 33139693 DOI: 10.1038/s41392-020-00373-7]
3 **Marasco G**, Cremon C, Barbaro MR, Salvi D, Cacciari G, Kagramanova A, Bordin D, Drug V, Miftode E, Fusaroli P, Mohamed SY, Ricci C, Bellini M, Rahman MM, Melcarne L, Santos J, Lobo B, Bor S, Yapali S, Akyol D, Sapmaz FP, Urun YY, Eskazan T, Celebi A, Kacmaz H, Ebik B, Binicier HC, Bugdayci MS, Yağcı MB, Pullukcu H, Kaya BY, Tureyen A, Hatemi İ, Koc ES, Sirin G, Calıskan AR, Bengi G, Alıs EE, Lukic S, Trajkovska M, Hod K, Dumitrascu D, Pietrangelo A, Corradini E, Simren M, Sjolund J, Tornkvist N, Ghoshal UC, Kolokolnikova O, Colecchia A, Serra J, Maconi G, De Giorgio R, Danese S, Portincasa P, Di Stefano M, Maggio M, Philippou E, Lee YY, Venturi A, Borghi C, Zoli M, Gionchetti P, Viale P, Stanghellini V, Barbara G; GI-COVID19 Study Group. Prevalence of Gastrointestinal Symptoms in Severe Acute Respiratory Syndrome Coronavirus 2 Infection: Results of the Prospective Controlled Multinational GI-COVID-19 Study. *Am J Gastroenterol* 2022; **117**: 147-157 [PMID: 34751672 DOI: 10.14309/ajg.0000000000001541]
4 **Bzeizi K**, Abdulla M, Mohammed N, Alqamish J, Jamshidi N, Broering D. Effect of COVID-19 on liver abnormalities: a systematic review and meta-analysis. *Sci Rep* 2021; **11**: 10599 [PMID: 34012016 DOI: 10.1038/s41598-021-89513-9]
5 **Hao SR**, Zhang SY, Lian JS, Jin X, Ye CY, Cai H, Zhang XL, Hu JH, Zheng L, Zhang YM, Jia HY, Yu GD, Wang XY, Gu JQ, Lu YF, Yu XP, Yu L, Xiang DR, Jin CL, Qiu YQ, Li LJ, Sheng JF, Liang TB, Yang YD. Liver Enzyme Elevation in Coronavirus Disease 2019: A Multicenter, Retrospective, Cross-Sectional Study. *Am J Gastroenterol* 2020; **115**: 1075-1083 [PMID: 32618658 DOI: 10.14309/ajg.0000000000000717]
6 **Xu L**, Liu J, Lu M, Yang D, Zheng X. Liver injury during highly pathogenic human coronavirus infections. *Liver Int* 2020; **40**: 998-1004 [PMID: 32170806 DOI: 10.1111/liv.14435]
7 **Cai Q**, Huang D, Yu H, Zhu Z, Xia Z, Su Y, Li Z, Zhou G, Gou J, Qu J, Sun Y, Liu Y, He Q, Chen J, Liu L, Xu L. COVID-19: Abnormal liver function tests. *J Hepatol* 2020; **73**: 566-574 [PMID: 32298767 DOI: 10.1016/j.jhep.2020.04.006]
8 **Zhang C**, Shi L, Wang FS. Liver injury in COVID-19: management and challenges. *Lancet Gastroenterol Hepatol* 2020; **5**: 428-430 [PMID: 32145190 DOI: 10.1016/S2468-1253(20)30057-1]
9 **Phipps MM**, Barraza LH, LaSota ED, Sobieszczyk ME, Pereira MR, Zheng EX, Fox AN, Zucker J, Verna EC. Acute Liver Injury in COVID-19: Prevalence and Association with Clinical Outcomes in a Large U.S. Cohort. *Hepatology* 2020; **72**: 807-817 [PMID: 32473607 DOI: 10.1002/hep.31404]
10 **National Institutes of Health**. Treatment Guidelines Panel. Coronavirus Disease 2019 (COVID-19). [cited 15 May 2022]. In: National Institutes of Health [Internet]. Available from: www.covid19treatmentguidelines.nih.gov
11 **World Health Organization**. Public Health Surveillance for COVID-19. Interim guidance 2022. [cited 15 May 2022]. In: World Health Organization [Internet]. Available from: www.who.int/publications/i/item/WHO-2019-nCoV-SurveillanceGuidance-2022.2
12 **Martha JW**, Wibowo A, Pranata R. Prognostic value of elevated lactate dehydrogenase in patients with COVID-19: a systematic review and meta-analysis. *Postgrad Med J* 2022; **98**: 422-427 [PMID: 33452143 DOI: 10.1136/postgradmedj-2020-139542]
13 **Hundt MA**, Deng Y, Ciarleglio MM, Nathanson MH, Lim JK. Abnormal Liver Tests in COVID-19: A Retrospective Observational Cohort Study of 1,827 Patients in a Major U.S. Hospital Network. *Hepatology* 2020; **72**: 1169-1176 [PMID: 32725890 DOI: 10.1002/hep.31487]
14 **Mendizabal M**, Piñero F, Ridruejo E, Anders M, Silveyra MD, Torre A, Montes P, Urzúa A, Pages J, Toro LG, Díaz J, Gonzalez Ballerga E, Miranda-Zazueta G, Peralta M, Gutiérrez I, Michelato D, Venturelli MG, Varón A, Vera-Pozo E, Tagle M, García M, Tassara A, Brutti J, Ruiz García S, Bustios C, Escajadillo N, Macias Y, Higuera-de la Tijera F, Gómez AJ, Dominguez A, Castillo-Barradas M, Contreras F, Scarpin A, Schinoni MI, Toledo C, Girala M, Mainardi V, Sanchez A, Bessone F, Rubinstein F, Silva MO. Prospective Latin American cohort evaluating outcomes of patients with COVID-19 and abnormal liver tests on admission. *Ann Hepatol* 2021; **21**: 100298 [PMID: 33359234 DOI: 10.1016/j.aohep.2020.100298]
15 **Wiśniewska H**, Skonieczna-Żydecka K, Parczewski M, Niścigorska-Olsen J, Karpińska E, Hornung M, Jurczyk K, Witak-Jędra M, Laurans Ł, Maciejewska K, Socha Ł, Leonciuk A, Bander D, Karasińska-Cieślak M, Aksak-Wąs B, Wawrzynowicz-Syczewska M. Hepatotropic Properties of SARS-CoV-2-Preliminary Results of Cross-Sectional Observational Study from the First Wave COVID-19 Pandemic. *J Clin Med* 2021; **10** [PMID: 33572429 DOI:

10.3390/jcm10040672]
16 **Morgan K**, Samuel K, Vandeputte M, Hayes PC, Plevris JN. SARS-CoV-2 Infection and the Liver. *Pathogens* 2020; **9** [PMID: 32486188 DOI: 10.3390/pathogens9060430]
17 **Guan WJ**, Ni ZY, Hu Y, Liang WH, Ou CQ, He JX, Liu L, Shan H, Lei CL, Hui DSC, Du B, Li LJ, Zeng G, Yuen KY, Chen RC, Tang CL, Wang T, Chen PY, Xiang J, Li SY, Wang JL, Liang ZJ, Peng YX, Wei L, Liu Y, Hu YH, Peng P, Wang JM, Liu JY, Chen Z, Li G, Zheng ZJ, Qiu SQ, Luo J, Ye CJ, Zhu SY, Zhong NS; China Medical Treatment Expert Group for Covid-19. Clinical Characteristics of Coronavirus Disease 2019 in China. *N Engl J Med* 2020; **382**: 1708-1720 [PMID: 32109013 DOI: 10.1056/NEJMoa2002032]
18 **Bloom PP**, Meyerowitz EA, Reinus Z, Daidone M, Gustafson J, Kim AY, Schaefer E, Chung RT. Liver Biochemistries in Hospitalized Patients With COVID-19. *Hepatology* 2021; **73**: 890-900 [PMID: 32415860 DOI: 10.1002/hep.31326]
19 **Sharma A**, Jaiswal P, Kerakhan Y, Saravanan L, Murtaza Z, Zergham A, Honganur NS, Akbar A, Deol A, Francis B, Patel S, Mehta D, Jaiswal R, Singh J, Patel U, Malik P. Liver disease and outcomes among COVID-19 hospitalized patients - A systematic review and meta-analysis. *Ann Hepatol* 2021; **21**: 100273 [PMID: 33075578 DOI: 10.1016/j.aohep.2020.10.001]
20 **Shehab M**, Alrashed F, Shuaibi S, Alajmi D, Barkun A. Gastroenterological and hepatic manifestations of patients with COVID-19, prevalence, mortality by country, and intensive care admission rate: systematic review and meta-analysis. *BMJ Open Gastroenterol* 2021; **8** [PMID: 33664052 DOI: 10.1136/bmjgast-2020-000571]
21 **Wang MY**, Zhao R, Gao LJ, Gao XF, Wang DP, Cao JM. SARS-CoV-2: Structure, Biology, and Structure-Based Therapeutics Development. *Front Cell Infect Microbiol* 2020; **10**: 587269 [PMID: 33324574 DOI: 10.3389/fcimb.2020.587269]
22 **Li Y**, Xiao SY. Hepatic involvement in COVID-19 patients: Pathology, pathogenesis, and clinical implications. *J Med Virol* 2020; **92**: 1491-1494 [PMID: 32369204 DOI: 10.1002/jmv.25973]
23 **Lei HY**, Ding YH, Nie K, Dong YM, Xu JH, Yang ML, Liu MQ, Wei L, Nasser MI, Xu LY, Zhu P, Zhao MY. Potential effects of SARS-CoV-2 on the gastrointestinal tract and liver. *Biomed Pharmacother* 2021; **133**: 111064 [PMID: 33378966 DOI: 10.1016/j.biopha.2020.111064]
24 **Boettler T**, Marjot T, Newsome PN, Mondelli MU, Maticic M, Cordero E, Jalan R, Moreau R, Cornberg M, Berg T. Impact of COVID-19 on the care of patients with liver disease: EASL-ESCMID position paper after 6 mo of the pandemic. *JHEP Rep* 2020; **2**: 100169 [PMID: 32835190 DOI: 10.1016/j.jhepr.2020.100169]
25 **Lopes-Pacheco M**, Silva PL, Cruz FF, Battaglini D, Robba C, Pelosi P, Morales MM, Caruso Neves C, Rocco PRM. Pathogenesis of Multiple Organ Injury in COVID-19 and Potential Therapeutic Strategies. *Front Physiol* 2021; **12**: 593223 [PMID: 33584343 DOI: 10.3389/fphys.2021.593223]
26 **Tabary M**, Khanmohammadi S, Araghi F, Dadkhahfar S, Tavangar SM. Pathologic features of COVID-19: A concise review. *Pathol Res Pract* 2020; **216**: 153097 [PMID: 32825963 DOI: 10.1016/j.prp.2020.153097]
27 **Zhang W**, Du RH, Li B, Zheng XS, Yang XL, Hu B, Wang YY, Xiao GF, Yan B, Shi ZL, Zhou P. Molecular and serological investigation of 2019-nCoV infected patients: implication of multiple shedding routes. *Emerg Microbes Infect* 2020; **9**: 386-389 [PMID: 32065057 DOI: 10.1080/22221751.2020.1729071]
28 **Holshue ML**, DeBolt C, Lindquist S, Lofy KH, Wiesman J, Bruce H, Spitters C, Ericson K, Wilkerson S, Tural A, Diaz G, Cohn A, Fox L, Patel A, Gerber SI, Kim L, Tong S, Lu X, Lindstrom S, Pallansch MA, Weldon WC, Biggs HM, Uyeki TM, Pillai SK; Washington State 2019-nCoV Case Investigation Team. First Case of 2019 Novel Coronavirus in the United States. *N Engl J Med* 2020; **382**: 929-936 [PMID: 32004427 DOI: 10.1056/NEJMoa2001191]
29 **Xiao F**, Tang M, Zheng X, Liu Y, Li X, Shan H. Evidence for Gastrointestinal Infection of SARS-CoV-2. *Gastroenterology* 2020; **158**: 1831-1833.e3 [PMID: 32142773 DOI: 10.1053/j.gastro.2020.02.055]
30 **Mehta P**, McAuley DF, Brown M, Sanchez E, Tattersall RS, Manson JJ; HLH Across Speciality Collaboration, UK. COVID-19: consider cytokine storm syndromes and immunosuppression. *Lancet* 2020; **395**: 1033-1034 [PMID: 32192578 DOI: 10.1016/S0140-6736(20)30628-0]
31 ESICM LIVES 2021: Part 1. *Intensive Care Med Exp* 2021; **9**: 51 [PMID: 34633565 DOI: 10.1186/s40635-021-00413-8]
32 ESICM LIVES 2020. *Intensive Care Med Exp* 2020; **8**: 73 [PMID: 33313986 DOI: 10.1186/s40635-020-00354-8]
33 **Balasegaram M**. Learning from COVID-19 to Tackle Antibiotic Resistance. *ACS Infect Dis* 2021; **7**: 693-694 [PMID: 33683857 DOI: 10.1021/acsinfecdis.1c00079]
34 **Vinoth R**, Sambath Kumar R, Venkateswaramurthy N. Misuse of Antibiotic during COVID 19 Outbreaks. *J Drug Deliv Ther* 2021; **11**: 181-187 [DOI: 10.22270/jddt.v11i6-s.5102]
35 **Lei F**, Liu YM, Zhou F, Qin JJ, Zhang P, Zhu L, Zhang XJ, Cai J, Lin L, Ouyang S, Wang X, Yang C, Cheng X, Liu W, Li H, Xie J, Wu B, Luo H, Xiao F, Chen J, Tao L, Cheng G, She ZG, Zhou J, Wang H, Lin J, Luo P, Fu S, Ye P, Xiao B, Mao W, Liu L, Yan Y, Chen G, Huang X, Zhang BH, Yuan Y. Longitudinal Association Between Markers of Liver Injury and Mortality in COVID-19 in China. *Hepatology* 2020; **72**: 389-398 [PMID: 32359177 DOI: 10.1002/hep.31301]
36 **Ezhilarasan D**. Critical role of estrogen in the progression of chronic liver diseases. *Hepatobiliary Pancreat Dis Int* 2020; **19**: 429-434 [PMID: 32299655 DOI: 10.1016/j.hbpd.2020.03.011]
37 **Weber S**, Mayerle J, Irlbeck M, Gerbes AL. Severe liver failure during SARS-CoV-2 infection. *Gut* 2020; **69**: 1365-1367 [PMID: 32327526 DOI: 10.1136/gutjnl-2020-321350]
38 **Zhou F**, Yu T, Du R, Fan G, Liu Y, Liu Z, Xiang J, Wang Y, Song B, Gu X, Guan L, Wei Y, Li H, Wu X, Xu J, Tu S, Zhang Y, Chen H, Cao B. Clinical course and risk factors for mortality of adult inpatients with COVID-19 in Wuhan, China: a retrospective cohort study. *Lancet* 2020; **395**: 1054-1062 [PMID: 32171076 DOI: 10.1016/S0140-6736(20)30566-3]
39 **Zhang B**, Zhou X, Qiu Y, Song Y, Feng F, Feng J, Song Q, Jia Q, Wang J. Clinical characteristics of 82 cases of death from COVID-19. *PLoS One* 2020; **15**: e0235458 [PMID: 32645044 DOI: 10.1371/journal.pone.0235458]
40 **Simon TG**, Hagström H, Sharma R, Söderling J, Roelstraete B, Larsson E, Ludvigsson JF. Risk of severe COVID-19 and mortality in patients with established chronic liver disease: a nationwide matched cohort study. *BMC Gastroenterol* 2021; **21**: 439 [PMID: 34814851 DOI: 10.1186/s12876-021-02017-8]
41 **Marjot T**, Webb GJ, Barritt AS 4th, Moon AM, Stamataki Z, Wong VW, Barnes E. COVID-19 and liver disease:

mechanistic and clinical perspectives. *Nat Rev Gastroenterol Hepatol* 2021; **18**: 348-364 [PMID: 33692570 DOI: 10.1038/s41575-021-00426-4]

42 **Chen N**, Zhou M, Dong X, Qu J, Gong F, Han Y, Qiu Y, Wang J, Liu Y, Wei Y, Xia J, Yu T, Zhang X, Zhang L. Epidemiological and clinical characteristics of 99 cases of 2019 novel coronavirus pneumonia in Wuhan, China: a descriptive study. *Lancet* 2020; **395**: 507-513 [PMID: 32007143 DOI: 10.1016/S0140-6736(20)30211-7]

43 **Xu Z**, Shi L, Wang Y, Zhang J, Huang L, Zhang C, Liu S, Zhao P, Liu H, Zhu L, Tai Y, Bai C, Gao T, Song J, Xia P, Dong J, Zhao J, Wang FS. Pathological findings of COVID-19 associated with acute respiratory distress syndrome. *Lancet Respir Med* 2020; **8**: 420-422 [PMID: 32085846 DOI: 10.1016/S2213-2600(20)30076-X]

44 **Wang Y**, Liu S, Liu H, Li W, Lin F, Jiang L, Li X, Xu P, Zhang L, Zhao L, Cao Y, Kang J, Yang J, Li L, Liu X, Li Y, Nie R, Mu J, Lu F, Zhao S, Lu J, Zhao J. SARS-CoV-2 infection of the liver directly contributes to hepatic impairment in patients with COVID-19. *J Hepatol* 2020; **73**: 807-816 [PMID: 32437830 DOI: 10.1016/j.jhep.2020.05.002]

45 **Sun J**, Aghemo A, Forner A, Valenti L. COVID-19 and liver disease. *Liver Int* 2020; **40**: 1278-1281 [PMID: 32251539 DOI: 10.1111/liv.14470]

World Journal of Gastroenterology

Submit a Manuscript: https://www.f6publishing.com

World J Gastroenterol 2022 October 21; 28(39): 5750-5763

DOI: 10.3748/wjg.v28.i39.5750

ISSN 1007-9327 (print) ISSN 2219-2840 (online)

ORIGINAL ARTICLE

Retrospective Study

Immune checkpoint inhibitor-mediated colitis is associated with cancer overall survival

Alexa R Weingarden, John Gubatan, Sundeep Singh, Tatiana Clorice Balabanis, Akshar Patel, Arpita Sharma, Aida Habtezion

Specialty type: Immunology

Provenance and peer review: Invited article; Externally peer reviewed.

Peer-review model: Single blind

Peer-review report's scientific quality classification

Grade A (Excellent): A
Grade B (Very good): 0
Grade C (Good): C, C, C
Grade D (Fair): 0
Grade E (Poor): 0

P-Reviewer: Chen YH, China; Rizzo A, Italy; Zhang XJ, China

Received: July 2, 2022
Peer-review started: July 2, 2022
First decision: August 1, 2022
Revised: September 24, 2022
Accepted: October 10, 2022
Article in press: October 10, 2022
Published online: October 21, 2022

Alexa R Weingarden, John Gubatan, Sundeep Singh, Tatiana Clorice Balabanis, Akshar Patel, Arpita Sharma, Aida Habtezion, Medicine, Division of Gastroenterology and Hepatology, Stanford University School of Medicine, Stanford, CA 94305, United States

Corresponding author: Alexa R Weingarden, MD, PhD, Academic Fellow, Consultant Physician-Scientist, Medicine, Division of Gastroenterology and Hepatology, Stanford University School of Medicine, Alway Building, Room M211, 300 Pasteur Drive, Stanford, CA 94305, United States. aweingar@stanford.edu

Abstract

BACKGROUND

Immune checkpoint inhibitor-mediated colitis (IMC) is a common adverse event following immune checkpoint inhibitor (ICI) therapy for cancer. IMC has been associated with improved overall survival (OS) and progression-free survival (PFS), but data are limited to a single site and predominantly for melanoma patients.

AIM

To determine the association of IMC with OS and PFS and identify clinical predictors of IMC.

METHODS

We performed a retrospective case-control study including 64 ICI users who developed IMC matched according to age, sex, ICI class, and malignancy to a cohort of ICI users without IMC, from May 2011 to May 2020. Using univariate and multivariate logistic regression, we determined association of presence of IMC on OS, PFS, and clinical predictors of IMC. Kaplan-Meier curves were gen-erated to compare OS and PFS between ICI users with and without IMC.

RESULTS

IMC was significantly associated with a higher OS (mean 24.3 mo *vs* 17.7 mo, P = 0.05) but not PFS (mean 13.7 mo *vs* 11.9 mo, P = 0.524). IMC was significantly associated with OS greater than 12 mo [Odds ratio (OR) 2.81, 95% confidence interval (CI) 1.17-6.77]. Vitamin D supplementation was significantly associated with increased risk of IMC (OR 2.48, 95%CI 1.01-6.07).

CONCLUSION

IMC was significantly associated with OS greater than 12 mo. In contrast to prior work, we found that vitamin D use may be a risk factor for IMC.

Key Words: Immune checkpoint inhibitors; Immune checkpoint inhibitor-mediated colitis; Immune-related adverse events

©The Author(s) 2022. Published by Baishideng Publishing Group Inc. All rights reserved.

Core Tip: Immune checkpoint inhibitor-mediated colitis (IMC) is a common adverse event following immune checkpoint inhibitor (ICI) therapy for cancer. We sought to determine the association of IMC with overall survival (OS) and progression-free survival (PFS) among cancer patients treated with ICI and identify clinical predictors of IMC. We performed a retrospective case-control study including 64 ICI users who developed IMC. In multivariate logistic regression analysis, IMC was significantly associated with a higher OS but not PFS. IMC was significantly associated with OS greater than 12 mo. Vitamin D supplementation was associated with increased risk of IMC.

Citation: Weingarden AR, Gubatan J, Singh S, Balabanis TC, Patel A, Sharma A, Habtezion A. Immune checkpoint inhibitor-mediated colitis is associated with cancer overall survival. *World J Gastroenterol* 2022; 28(39): 5750-5763
URL: https://www.wjgnet.com/1007-9327/full/v28/i39/5750.htm
DOI: https://dx.doi.org/10.3748/wjg.v28.i39.5750

INTRODUCTION

Immune checkpoint inhibitors (ICI) have dramatically changed the landscape of cancer therapy. Early studies showed significantly prolonged survival in patients with metastatic melanoma compared to standard chemotherapy[1], and evidence now exists for improved outcomes in a variety of tumors ranging from lung cancers to urothelial carcinoma to breast cancer[2-5]. Although these are powerful treatments in our armamentarium against malignancy, ICI can cause immune-related adverse events (irAE) characterized by autoimmune-like inflammation in a variety of non-tumor organs, leading to increased morbidity for patients[6].

One of the most common irAE is immune checkpoint inhibitor-mediated colitis (IMC). IMC may occur in up to 40% of patients treated with ipilimumab, an antibody targeting CTLA-4, 11%-17% of patients treated with antibodies against anti-PD-1 or anti-PD-L1, such as nivolumab, pembrolizumab, or atezolizumab, and around 32% of patients treated with a combination of anti-CTLA-4 and anti-PD-1[7]. Prior retrospective analyses of patients with IMC have attempted to identify characteristics associated with development of IMC, including type of malignancy, ICI class, dose of ICI, cancer stage, and vitamin D use[8-11]. Intriguingly, two prior studies have suggested that development of IMC may positively correlate with improved progression-free survival (PFS) and overall survival (OS)[9,10]. One of these studies controlled for confounding effects of ICI class *via* frequency matching, but was limited to patients with melanoma, hindering wider applicability of their findings[10]. These findings also conflict with data suggesting that use of steroids and the anti-TNF antibody infliximab in patients treated with ICI are associated with worse cancer outcomes[12,13]. These discrepancies represent a significant knowledge gap that impedes our ability to evaluate and manage IMC and ICI use.

Here we present data from a retrospective study of patients treated with ICI at our institution who developed IMC across malignancy types. We compare this cohort to a matched control cohort to determine whether IMC was associated with improved progression-free survival and overall survival. We also evaluate which clinical characteristics increase the risk of developing IMC, including severe IMC.

MATERIALS AND METHODS

Study design and population

We conducted a retrospective case-control single-center study after obtaining approval from the Institutional Review Board at Stanford University (IRB 57125, approved 6/30/2020). Our primary aim was to determine the association of presence and severity of IMC on OS and PFS in ICI users. Our secondary aim was to identify clinical variables which predicted development of IMC in ICI users. We evaluated all patients over the age of 18 who had been treated with immune checkpoint inhibitors (ICI) for

malignancy at Stanford Health Care from May 2011 to May 2020, including anti-CTLA-4 (ipilimumab), anti-PD-1 (nivolumab, pembrolizumab), and anti-PD-L1 (atezolizumab, avelumab, durvalumab), with follow up through October 2020. Using the Stanford Research Repository tool, we screened patients treated with ICI who were assigned International Classification of Diseases (ICD) 9 and ICD 10 codes associated with non-infectious colitis and diarrhea (Supplementary Table 1). Each chart which passed the initial screen was further screened by review of clinic notes to confirm diagnosis of immune checkpoint inhibitor-related colitis by oncology providers. Any patient found to have other explanations for their clinical presentation was excluded from the study.

Control patients were matched one to one with each IMC patient for sex, age, malignancy, type of ICI used, prior ICI exposure, and duration of ICI exposure (matched to number of doses from initiation of ICI to development of colitis in study cohort). Control patients were initially screened by those lacking the above ICD codes and were confirmed *via* direct evaluation of each chart to lack diarrhea and/or colitis ascribable to ICI per their treating oncologist.

We extracted clinical data on IMC and control patient charts including demographics (age at time of ICI initiation, sex, body mass index, race per patient report), medical history (presence of prior non-liver and non-upper gastrointestinal disease, personal history of autoimmune disease, family history of autoimmune disease), and cancer history (type of malignancy, tumor stage at ICI initiation, prior chemotherapy, prior radiation therapy, type of ICI used, duration of ICI use, OS and PFS) (Supplementary Table 2). OS was determined as time from initiation of ICI to death, while PFS was determined as time from initiation of ICI to death or progression of disease as determined by oncology providers, based on radiographic evidence of progression. IMC severity was graded using commonly accepted determinants of IMC and irAE grading[14]. We specifically noted prior use of therapies designed to increase immune responses [interleukin (IL)-2, interferon (IFN)-γ, toll-like receptor (TLR)-9 agonist, tebentafusp, or anti-CD47 antibody]. Vitamin D and non-steroidal anti-inflammatory (NSAID) use were defined as vitamin D supplement or NSAID medication, respectively, noted in the history of present illness or on the patient's medication list at the clinic visit closest to their date of ICI initiation.

We collected data on IMC diagnosis including number of patients who received endoscopy (flexible sigmoidoscopy or colonoscopy), findings on endoscopy, and fecal calprotectin (Supplementary Table 3). Data on management of IMC included treatment with anti-diarrheal medications, mesalamine, steroids (prednisone, budesonide, dexamethasone), infliximab, and vedolizumab.

Statistical analysis

The rate of the primary outcomes (OS > 12 mo and PFS > 6 mo among all ICI users, OS > 12 mo and PFS > 6 mo in patients with IMC) and secondary outcomes (risks of IMC among patients with malignancy using ICI, IMC severity), predictive value of clinical variables on primary and secondary outcomes, odds ratio (OR) with its 95% confidence interval (CI), and *P* values were calculated using Statistics/Data Analysis (Stata/IC 15.1 for Windows, College Station, TX, United States). Dichotomous variables were analyzed for outcomes using the chi-squared test or the Fisher's exact test where appropriate, and continuous variables were analyzed using Student's *t*-tests if normally distributed, or the Wilcoxon signed-rank test for non-normal data. For our multivariate analyses, model building was based on forward stepwise logistic regression, with a *P* value of 0.05 required for entry, and known predictors were also included. We constructed Kaplan Meier curves for the outcomes of OS and PFS between patients with and without IMC and patients with mild *vs* severe IMC using GraphPad Prism (version 8.3; GraphPad Software, Inc., La Jolla, CA, United States). All authors had access to the study data and reviewed and approved the final manuscript.

RESULTS

Clinical characteristics associated with IMC

We identified a total of 314 patients treated with ICI at Stanford Health Care from May 2011 to May 2020 who had ICD codes matching our query (Supplementary Table 1). Of these, 64 had a diagnosis of IMC per review of Oncology providers' notes, after excluding patients with alternative diagnoses for their symptoms. 24 (37.5%) of these IMC patients underwent an endoscopy (colonoscopy or flexible sigmoidoscopy) during workup, of which seven (29.2%) had a normal endoscopic appearance, consistent with prior reports demonstrating that approximately one third of patients with IMC related to anti-PD-1 therapy have microscopic colitis[15] (Supplementary Table 3). An additional 14 patients (21.9%) had imaging findings suggestive of IMC while 3 patients (4.69%) without imaging or endoscopy had an elevated calprotectin or fecal lactoferrin.

These 64 patients were manually matched 1:1 with control patients based on age, sex, malignancy, type of ICI, whether or not the patient had prior ICI exposure, and duration of ICI use. We compared clinical characteristics of patients from the IMC cohort and the control cohort (Table 1). None of the matched characteristics were significantly different between the two cohorts. The mean age across the combined cohorts was 66.6 years, with an average age of 67.4 in the cohort with IMC compared with 65.8 in the control cohort ($P = 0.42$). 57.81% of patients in each group were male ($P = 1.00$). Patients were

Table 1 Baseline characteristics of patients with immune checkpoint inhibitor use

Clinical variables	All patients (*n* = 128)		Patients with IMC (*n* = 64)		Patients without IMC (*n* = 64)		*P* value
Age, yr (mean ± SD)[1]	66.6 (± 11.5)		67.4 (± 11.7)		65.8 (± 11.3)		0.420
Sex[1]							
Male, *n* (%)	74	57.81%	37	57.81%	37	57.81%	1.000
Female, *n* (%)	54	42.19%	27	42.19%	27	42.19%	
Race							
White, *n* (%)	102	79.69%	52	81.25%	50	78.13%	0.660
Black, *n* (%)	4	3.13%	2	3.13%	2	3.13%	1.000
Asian, *n* (%)	9	7.03%	4	6.25%	5	7.81%	0.730
Type of malignancy[1]							
Melanoma, *n* (%)	66	51.56%	33	51.56%	33	51.56%	1.000
RCC, *n* (%)	15	11.72%	8	12.50%	7	10.94%	0.783
NSCLC, *n* (%)	12	9.38%	6	9.38%	6	9.38%	1.000
Sarcoma, *n* (%)	11	8.59%	5	7.81%	6	9.38%	0.752
Head and neck SCC, *n* (%)	7	5.47%	3	4.69%	4	6.25%	0.697
Other, *n* (%)	17	13.28%	9	14.06%	8	12.50%	0.795
Stage IV malignancy, *n* (%)	114	89.07%	56	87.50%	58	90.63%	0.778
Type of immune checkpoint inhibitor[1]							
Ipilimumab plus nivolumab, *n* (%)	48	37.50%	24	37.50%	24	37.50%	1.000
Ipilimumab, *n* (%)	22	17.19%	11	17.19%	11	17.19%	1.000
Nivolumab, *n* (%)	12	9.38%	6	9.38%	6	9.38%	1.000
Pembrolizumab, *n* (%)	38	29.69%	19	29.69%	19	29.69%	1.000
Atezolizumab, *n* (%)	8	6.25%	4	6.25%	4	6.25%	1.000
Number of Infusions[a] (mean ± SD)[1]	6.91 (± 8.40)		6.09 (± 7.20)		7.73 (± 9.40)		0.268
Dose of ICI (mg/kg) (mean ± SD)	2.47 (± 1.30)		2.63 (± 1.60)		2.31 (± 1.00)		0.318
Prior ICI use[1]	19	14.84%	10	15.63%	9	14.06%	0.500
Medical history, *n* (%)							
Non-liver, non-upper GI disease[b], *n* (%)	28	21.88%	18	28.13%	10	15.63%	0.087
Personal history of autoimmune disease[b], *n* (%)	30	23.44%	20	31.25%	10	15.63%	0.037
Prior irAE[b], *n* (%)	8	12.50%	7	10.90%	1	1.56%	0.062
Family history of autoimmune disease[b], *n* (%)	10	7.81%	8	12.50%	2	3.13%	0.048
Prior immune-enhancing therapy[b], *n* (%)	11	8.59%	2	3.13%	9	14.06%	0.027
Prior interferon-γ therapy, *n* (%)	7	5.47%	1	1.56%	6	9.38%	0.115
Vitamin D use, *n* (%)	38	29.69%	25	39.06%	13	20.31%	0.020
Smoking (current or prior), *n* (%)	61	47.66%	33	51.56%	28	43.75%	0.376
NSAID use, *n* (%)	21	16.41%	10	15.63%	11	17.19%	0.811
Any vaccine, *n* (%)	25	19.53%	9	14.06%	16	25.00%	0.119
Flu vaccine, *n* (%)	19	14.84%	7	10.94%	12	18.75%	0.214

Pneumonia vaccine, *n* (%)	11	8.59%	4	6.25%	7	10.94%	0.344
Other vaccine, *n* (%)	2	1.56%	1	1.56%	1	1.56%	1.000
Weight at start of ICI (kg) (mean ± SD)	78.1 (± 17.4)		79.4 (± 16.9)		76.8 (± 17.9)		0.396
Medications							
Steroid at start of ICI, *n* (%)	20	15.63%	11	17.19%	9	14.06%	0.626
Steroid duration (d)	N/A		107.7 (± 164.2)		N/A		
Infliximab use, *n* (%)	N/A		10	15.63%	N/A		
Vedolizumab use, *n* (%)	N/A		1	1.56%	N/A		
Malignancy outcomes							
Mean PFS (mo)	12.8 (± 15.3)		13.7 (± 14.9)		11.9 (± 15.8)		0.524
PFS > 6 mo, *n* (%)	63	49.22%	35	54.69%	28	43.75%	0.216
OS (mo)	21.0 (± 18.9)		24.3 (± 19.4)		17.7 (± 18.0)		0.050
OS > 12 mo, *n* (%)	72.0	56.25%	42	65.63%	30	46.88%	0.025
Death, *n* (%)	20	15.63%	6	9.38%	14	21.88%	0.051

[1]Variable matched between cases and controls.
[a]Number of infusions of immune checkpoint inhibitor prior to immune checkpoint inhibitor-mediated colitis diagnosis (cases) or total (controls).
[b]See Supplementary Table 2.
IMC: Immune checkpoint inhibitor-mediated colitis; ICI: Immune checkpoint inhibitor; SD: Standard deviation; RCC: Renal cell carcinoma; NSCLC: Non-small cell lung cancer; SCC: Squamous cell carcinoma; PFS: Progression-Free Survival; irAE: Immune related adverse event; OS: Overall survival.

predominantly white in both groups, with 52 (81.25%) white individuals in the IMC cohort compared to 50 (78.13%) in the control group (P = 0.66). The most common malignancy in each group was melanoma [33 (51.56%) in both cohorts], followed by renal cell carcinoma [8 (12.5%) in the IMC cohort and 7 (10.94%) in the control cohort] and non-small cell lung cancer [6 (9.38%) in both cohorts]. Both groups had similar numbers of patients with stage IV malignancy [56 (87.5%) in the IMC cohort and 58 (90.63%) in the control cohort, P = 0.778]. Combination ipilimumab and nivolumab was the most commonly used checkpoint therapy [24 (37.5%) of patients in each cohort], followed by nivolumab monotherapy [19 (29.69%) of each cohort] and ipilimumab monotherapy [11 (17.19%) of each cohort].

Among the remainder of the clinical characteristics evaluated, personal history of autoimmune disease (including prior irAE) and family history of autoimmune disease were significantly more common in patients with IMC (P = 0.037 and 0.048, respectively). Intriguingly, prior use of a therapy designed to increase immune responses was more common in the control cohort without IMC (P = 0.027). In contrast to prior data[11], use of vitamin D supplementation at the time of first dose of ICI was significantly more prevalent in patients with IMC (P = 0.020). Neither smoking status, NSAID use at time of ICI initiation, steroid use at the time of ICI initiation, nor recent vaccination were significantly more common in IMC patients compared to controls.

IMC significantly increases overall survival

As IMC has previously been associated with increased OS and PFS in cancer patients[9,10], we evaluated whether this association was seen in our study. We found that OS was significantly longer in patients who developed IMC compared to those who did not, with a mean OS of 24.3 mo in patients with IMC and 17.7 mo in control (P = 0.05, Table 1). OS at 12 mo following ICI initiation was significantly higher in patients who developed IMC compared to those who did not (P = 0.02, Figure 1). However, in contrast to prior findings, our study did not find a significant difference in PFS between IMC patients and controls, with a mean PFS 13.7 mo in IMC patients and 11.9 mo in controls (P = 0.524) (Table 1). PFS also did not differ between patients who developed mild *vs* severe IMC (P = 0.690, Supplementary Table 5).

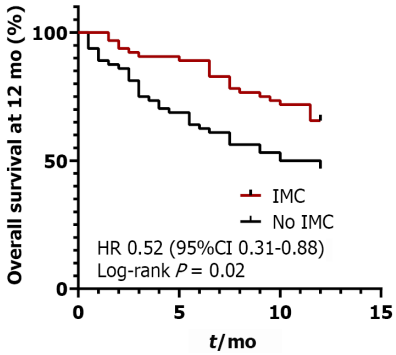
Across both cohorts, we identified clinical characteristics significantly associated with OS greater than 12 mo and PFS greater than 6 mo, which are correlated with cancer outcomes in patients treated with ICI[16] (Tables 2 and 3) (Supplementary Tables 4 and 5). IMC was significantly and independently associated with OS > 12 mo in the multivariate model (OR 2.81, 95%CI 1.17-6.77, P = 0.021) (Table 2). Number of ICI infusions was also positively associated with OS > 12 mo (OR 1.23, 95%CI 1.09-1.40), while sarcoma as underlying malignancy was significantly associated with OS < 12 mo (OR 0.17, 95%CI 0.029-0.947). Within the IMC cohort, nivolumab use was associated with OS < 12 mo in the univariate analysis (OR 0.09, 95%CI 0.01-0.83), while only age was associated with OS < 12 mo in multivariate analysis (OR 0.93, 95%CI 0.88-0.99) (Table 3). No individual malignancy was significantly associated

Table 2 Univariate and multivariate predictors of overall survival > 12 mo among patients with malignancy using immune checkpoint inhibitor (*n* = 128)

Clinical variables	Univariate predictors			Multivariate predictors		
	OR	95%CI	*P* value	OR	95%CI	*P* value
Demographics						
Age (yr)	1.00	0.97-1.03	0.970			
Male	0.92	0.45-1.87	0.822			
Female	1.08	0.53-2.20	0.822			
Race						
White	1.37	0.58-3.25	0.473			
Black	2.39	0.24-23.6	0.456			
Asian	0.97	0.25-3.79	0.965			
Other	0.45	0.14-1.45	0.181			
Type of malignancy						
Melanoma	0.87	0.43-1.74	0.688			
RCC	1.65	0.53-5.12	0.390			
NSCLC	2.52	0.65-9.80	0.181			
Sarcoma	0.15	0.03-0.72	0.018	0.17	0.03-0.95	0.043
Head and neck SCC	1.04	0.22-4.84	0.961			
Other	1.50	0.52-4.35	0.453			
Presence of IMC	2.16	1.06-4.41	0.034	2.81	1.17-6.77	0.021
Presence of high grade IMC	0.47	0.16-1.38	0.167			
Stage IV malignancy	0.48	0.14-1.61	0.233			
Type of Immune Checkpoint Inhibitor						
Ipilimumab plus nivolumab	1.32	0.30-5.77	0.714			
Ipilimumab	0.74	0.29-1.85	0.517			
Nivolumab	1.63	0.46-5.70	0.448			
Pembrolizumab	2.93	1.27-6.73	0.011	1.06	0.38-2.98	0.911
Atezolizumab	1.32	0.30-5.77	0.714			
Number of ICI infusions[a]	1.19	1.08-1.32	0.001	1.23	1.09-1.40	0.001
Dose of ICI (mg/kg)	1.33	0.86-2.05	0.198			
Prior ICI use	0.51	0.19-1.37	0.183			
Medical history						
Non-liver, non-upper GI disease[b]	0.87	0.38-2.02	0.747			
Personal history of autoimmune disease[b]	1.47	0.63-3.40	0.373			
Family history of autoimmune disease[b]	1.03	0.32-4.41	0.804			
Prior irAE	2.84	0.31 - 25.9	0.356			
Prior immune-enhancing therapy[b]	0.62	0.18-2.15	0.454			
Vitamin D use	0.60	0.28-1.29	0.190			
Smoking (current or prior)	0.74	0.37-1.50	0.410			
NSAID use	1.04	0.41-2.69	0.928			
Any vaccine	0.36	0.14-0.89	0.026	1.03	0.16-6.70	0.972

Flu vaccine	0.22	0.08-0.67	0.007	0.30	0.04-2.31	0.248
Pneumonia vaccine	0.41	0.11-1.48	0.175			
Other vaccine	0.77	0.05-12.66	0.858			
Weight at start of ICI (kg)	0.99	0.97-1.01	0.207			
Medications						
Steroid at start of ICI	0.74	0.29-1.93	0.541			
Steroid duration (d)	1.00	0.997-1.01	0.368			
Infliximab use	0.76	0.21-2.77	0.226			
Vedolizumab use	1.00	0.99-1.01	1.000			

[a]Number of infusions of immune checkpoint inhibitor prior to immune checkpoint inhibitor-mediated colitis diagnosis (cases) or total (controls).
[b]See Supplementary Table 2.
ICI: Immune checkpoint inhibitor; IMC: Immune checkpoint inhibitor-mediated colitis; OR: Odds ratios; CI: Confidence interval; SD: Standard deviation; RCC: Renal cell carcinoma; NSCLC: Non-small cell lung cancer; SCC: Squamous cell carcinoma; irAE: Immune related adverse event.



DOI: 10.3748/wjg.v28.i39.5750 **Copyright** ©The Author(s) 2022.

Figure 1 Overall survival at 12 mo in patients with and without immune checkpoint inhibitor-mediated colitis. Kaplan-Meier curve of overall survival at 12 mo in patients with immune checkpoint inhibitor-mediated colitis (IMC, red) and without IMC (black). IMC: Immune checkpoint inhibitor-mediated colitis; HR: Hazard ratio.

with OS > 12 mo within the IMC cohort (Table 3).

Significant risk factors for developing IMC and severe IMC

As certain clinical characteristics were significantly more common in patients with IMC compared to controls, we evaluated whether any of these clinical characteristics were associated with risk of developing IMC (Table 4). In univariate analysis, history of autoimmune disease and vitamin D use were both significantly associated with increased risk of IMC (OR 2.45, 95%CI 1.04-5.78, P = 0.040 for autoimmune disease; OR 2.51, 95%CI 1.14-5.54, P = 0.022 for vitamin D use). Interestingly, the use of vitamin D supplementation has previously been associated with a decreased risk of IMC, in contrast to our findings here[11]. Prior use of an immune-enhancing therapy (Supplementary Table 2) was associated with a significantly decreased risk of IMC (OR 0.20, 95%CI 0.04-0.95, P = 0.043). In the multivariate model which incorporated these characteristics, only the use of immune-enhancing therapy remained significantly associated with decreased risk of IMC, with an OR of 0.20 (95%CI 0.04-1.00, P = 0.050).

We next determined if any variables were associated with an increased risk of severe IMC. Consistent with prior studies of irAE in ICI[17-19], we defined grade 1-2 IMC as mild and grade 3 or higher IMC as severe. In our study, 38 of the 64 patients (59.4%) had severe IMC (Supplementary Table 3). In the univariate model, ipilimumab and vitamin D supplementation were significantly associated with development of severe IMC (OR 8.93, 95%CI 1.07-74.8, P = 0.043 for ipilimumab; OR 3.33, 95%CI 1.10-10.14, P = 0.034 for vitamin D) (Supplementary Table 6). Combination therapy (ipilimumab plus nivolumab) trended towards an increased risk of severe IMC but did not reach significance (P = 0.053). In contrast, pembrolizumab was significantly associated with a decreased risk of severe IMC (OR 0.26, 95%CI 0.09-0.81, P = 0.020). In the multivariate model no characteristic reached significance for association with severe IMC, although both combination therapy and ipilimumab monotherapy approached significance for increased risk of severe IMC (P = 0.058 and 0.060, respectively).

Table 3 Univariate and multivariate predictors of overall survival > 12 mo among patients with immune checkpoint inhibitor colitis (*n* = 64)

Clinical variables	Univariate predictors			Multivariate predictors		
	OR	95%CI	*P* value	OR	95%CI	*P* value
Demographics						
Age (yr)	0.96	0.92-1.01	0.103	0.93	0.88-0.99	0.023
Male	0.82	0.29-2.32	0.711			
Female	1.22	0.43-3.44	0.711			
Race						
White	0.87	0.23-3.27	0.835			
Black	1.00	0.90-1.34	0.996			
Asian	0.54	0.07-4.10	0.550			
Other	1.07	0.97-1.11	0.912			
Type of malignancy						
Melanoma	1.26	0.45-3.51	0.654			
RCC	0.51	0.12-2.28	0.381			
NSCLC	0.53	0.10-2.85	0.456			
Sarcoma	2.38	0.25-22.65	0.451			
Head and neck SCC	1.05	0.89-1.10	0.865			
Other	5.33	0.62-45.68	0.127			
Stage IV malignancy	0.60	0.11-3.26	0.554			
Presence of high grade IMC	0.91	0.32-2.57	0.855			
Type of immune checkpoint inhibitor						
Ipilimumab plus nivolumab	0.95	0.31-2.88	0.922			
Ipilimumab	0.98	0.25-3.77	0.974			
Nivolumab	0.09	0.01-0.83	0.033	0.13	0.01-1.43	0.096
Pembrolizumab	2.74	0.78-9.58	0.114	3.46	0.84-14.19	0.084
Atezolizumab	1.74	0.17-17.73	0.641			
Number of ICI infusions[a]	0.28	0.04-1.82	0.183			
Dose of ICI (mg/kg)	1.88	0.36-9.83	0.457			
Prior ICI use	0.46	0.12-1.80	0.265			
Medical history						
Non-liver, non-upper GI disease[b]	1.67	0.51-5.49	0.397			
Personal history of autoimmune disease[b]	0.78	0.26-2.31	0.648			
Family history of autoimmune disease[b]	0.93	0.20-4.29	0.922			
Prior immune-enhancing therapy[b]	0.55	0.03-9.23	0.678			
Prior interferon-g therapy	1.00	0.99-1.10	0.976			
Vitamin D use	2.45	0.80-7.46	0.116	2.77	0.75-10.20	0.124
Smoking (current or prior)	1.66	0.59-5.65	0.334			
NSAID use	2.55	0.49-13.16	0.265			
Any vaccine	5.33	0.62-45.68	0.127			
Flu vaccine	1.46	0.26-8.19	0.668			

Pneumonia vaccine	1.00	0.99-1.05	0.995
Other vaccine	1.00	1.00-1.01	0.941
Weight at start of ICI (kg)	1.02	0.98-1.05	0.329
Medications			
Steroid at start of ICI	0.98	0.25-3.77	0.974
Steroid duration (d)	1.00	1.00-1.01	0.736
Infliximab use	2.55	0.49-13.16	0.265
Vedolizumab use	1.00	1.00-1.01	0.936

[a]Number of infusions of immune checkpoint inhibitor prior to immune checkpoint inhibitor-mediated colitis diagnosis (cases) or total (controls).
[b]See Supplementary Table 2.
ICI: Immune checkpoint inhibitor; IMC: Immune checkpoint inhibitor-mediated colitis; SD: Standard deviation; RCC: Renal cell carcinoma; NSCLC: Non-small cell lung cancer; SCC: Squamous cell carcinoma; irAE: Immune related adverse event.

DISCUSSION

In our study, development of IMC following ICI use was associated with improved overall survival, although not improved progression-free survival, compared to ICI users without IMC. This is similar to findings at another center demonstrating both improved OS and PFS in patients with IMC[9,10]. We also found that vitamin D supplementation at the start of ICI treatment is a risk factor for developing IMC, in contrast to other research suggesting vitamin D use is associated with lower risk of IMC[11]. Our results, therefore, provide critical additional information on these previous associations and present a need for prospective studies.

Both publications showing improved survival in patients with IMC were retrospective analyses performed at the same center[9,10]. One study noted that ICI class was significantly associated with development of IMC[9], a finding that has been demonstrated several times in retrospective work[8,17,18,20-23]. However, unlike our work, this study did not match control patients to account for this likely confounder, as ICI class has been associated with differences in PFS in some malignancies[24,25]. The second study at this center examined survival in melanoma patients with IMC, compared to our work across multiple malignancies, although frequency matching was performed to account for use of different ICI classes[10]. Since our study is the first to examine survival in patients with IMC at a different center, our work here reinforces that IMC may be associated with increased overall survival and prompts a need for prospective studies.

The only other independent factor in our study positively associated with OS > 12 mo was number of ICI doses. This finding may be due to trivial length-time bias, as patients who survive longer are more likely to receive more doses of ICI. It is also possible that patients who required cessation of ICI due to IMC had worse outcomes, although prior work has suggested that patients still derive equivalent long-term benefit from ICI even if stopped due to irAE[26]. Type of underlying malignancy (sarcoma) was independently associated with OS < 12 mo in our study. These findings are not unexpected, as most advanced soft tissue sarcomas have a median OS of less than one year[27].

In contrast to prior work, we found a positive association between vitamin D supplementation and development of IMC[11]. It is unclear if this is related to low serum vitamin D levels or negative impact of the supplementation itself, as vitamin D levels near the time of ICI initiation were not recorded in most patients. Additionally, the prior report on vitamin D in IMC was in melanoma patients only, which may partially account for discrepancies with our study. As this association did not remain significant in our multivariate analysis, it is possible that another confounding factor may explain the association between vitamin D supplementation and IMC in our study.

In addition to challenging existing findings, we report here on additional novel risk factors for IMC. We are the first to report that prior use of immune-enhancing medications prior to ICI, such as IL-2 or interferon-γ, is significantly and independently associated with decreased risk of IMC. Much more work should be done to evaluate the relationship between these medications and future risk of IMC.

Finally, our study is the first to examine risk factors for severe IMC. In addition to increasing risk for IMC overall, we find that vitamin D supplementation may also be a risk factor for severe IMC. Similarly, our results suggest that the use of ipilimumab may be associated with increased risk of severe IMC, while pembrolizumab may be associated with decreased risk of severe IMC in patients who develop this syndrome. As ipilimumab has previously been associated with increased risk of IMC overall, while anti-PD-1, including pembrolizumab, are associated with lower risk of IMC overall[8,9], these findings emphasize that ICI class may affect severity of IMC.

Our findings may significantly impact clinical practice by identifying novel risks for IMC and severe IMC that clinicians, including oncologists and gastroenterologists, should be aware of, while also potentially providing reassurance to physicians and patients that development of IMC may be a positive

Table 4 Univariate and multivariate predictors of immune checkpoint inhibitor-mediated colitis among patients using immune checkpoint inhibitor (*n* = 128)

Clinical variables	Univariate predictors			Multivariate predictors		
	OR	95%CI	*P* value	OR	95%CI	*P* value
Demographics						
Age (yr)	1.01	0.98-1.04	0.417			
Male	1.00	0.50-2.02	1.000			
Female	1.00	0.50-2.02	1.000			
Race						
White	1.21	0.51-2.88	0.661			
Black	1.00	0.14-7.33	1.000			
Asian	0.79	0.20-3.07	0.730			
Other	0.84	0.27-2.66	0.770			
Type of malignancy						
Melanoma	1.00	0.50-2.00	1.000			
RCC	1.16	0.40-3.42	0.784			
NSCLC	1.00	0.30-3.28	1.000			
Sarcoma	0.82	0.24-2.83	0.753			
Head and neck SCC	0.74	0.16-3.44	0.698			
Other	1.15	0.41-3.18	0.795			
Stage IV malignancy	0.72	0.24-2.22	0.572			
Type of Immune Checkpoint Inhibitor						
Ipilimumab plus nivolumab	1.00	0.49-2.05	1.000			
Ipilimumab	1.00	0.40-2.51	1.000			
Nivolumab	1.00	0.30-3.28	1.000			
Pembrolizumab	1.00	0.47-2.13	1.000			
Atezolizumab	1.00	0.24-4.18	1.000			
Number of Infusions[a]	0.98	0.93-1.02	0.273			
Dose of ICI (mg/kg)	1.23	0.82-1.84	0.327			
Medical History						
Non-liver, non-upper GI[b]	2.11	0.89-5.03	0.091			
Autoimmune disease[b]	2.45	1.04-5.78	0.040	1.87	0.74-4.74	0.186
Prior irAE	7.74	0.92-64.82	0.059			
Family history of autoimmune disease[b]	4.43	0.90-21.74	0.067	3.98	0.74-21.38	0.107
Prior immune-enhancing therapy[b]	0.20	0.04-0.95	0.043	0.19	0.04-1.01	0.052
Prior interferon-γ therapy	0.15	0.018-1.31	0.087			
Vitamin D use	2.51	1.14-5.54	0.022	2.48	1.01-6.07	0.047
Smoking (current or prior)	1.37	0.68-2.74	0.377			
NSAID use	0.89	0.35-2.28	0.811			
Any vaccine	0.49	0.20-1.21	0.123			
Flu vaccine	0.53	0.19-1.45	0.219			
Pneumonia vaccine	0.54	0.15-1.95	0.350			

Other vaccine	1.00	0.06-16.34	1.000
Weight at start of ICI (kg)	1.01	0.99-1.03	0.393

[a]Number of infusions of immune checkpoint inhibitor prior to immune checkpoint inhibitor-mediated colitis diagnosis (cases) or total (controls).
[b]See Supplementary Table 2.
ICI: Immune checkpoint inhibitor; IMC: Immune checkpoint inhibitor-mediated colitis; RCC: Renal cell carcinoma; NSCLC: Non-small cell lung cancer; SCC: Squamous cell carcinoma; irAE: Immune related adverse event.

prognosticator for cancer survival. Neither prior work nor ours found that treatment of IMC, including steroids or infliximab, negatively impacts OS[9,10], and therefore appropriate treatment of IMC should be pursued early on to minimize morbidity and mortality. Both steroid and infliximab use have been suggested to worsen survival in ICI users[12,13], but all current evidence suggests that use of these medications for IMC specifically does not impair cancer outcomes. Our work also cautions against supplementation with vitamin D in ICI users, as this may increase risk of IMC and severe IMC, although carefully designed studies with vitamin D measurements should be performed.

Our work has several strengths. We performed robust cohort matching to minimize confounding effects of ICI class and malignancy. This is also the first study to explore risk factors associated with severe IMC. However, there are limitations to our work. As a retrospective, observational study, it is subject to recall bias and cannot evaluate causation, and may also be subject to immortal time bias (ITB). Patients may have longer exposure to checkpoint inhibitors before developing IMC, compared to patients who do not manifest this irAE, leading to a period where they must survive for long enough to develop IMC and are therefore "immortal"[28]. We found that OS > 12 mo was significantly associated with greater numbers of ICI infusions (Table 2), which is likely due to ITB. However, greater numbers of infusions were not associated with IMC (Table 4). This suggests that the association between OS > 12 mo and IMC is likely independent of the number of ICI infusions, limiting this as a source of ITB in our study.

Other weaknesses of our work include selection of patients based on clinical criteria for IMC, including those who did not undergo endoscopy or other objective testing for intestinal inflammation, and therefore may not have had a true colitis. Like prior work, this is also a single-center study, and our results may not be widely generalizable, particularly since we identified fewer patients compared to prior work and our patient population is highly variable, including individuals with several different underlying malignancies. We did not exclude patients with prior non-GI irAEs in either group, although the presence of these was not independently associated with increased OS in our study. We also have not accounted for other factors which may be potential predictors of ICI response, including tumor PD-L1 expression burden, tumor mutational burden, gut microbial composition, proton pump inhibitor use, and combination treatment with tyrosine kinase inhibitors[29-34].

CONCLUSION

In conclusion, our findings suggest presence of IMC is associated with improved OS in cancer patients when cases were matched closely to controls. We also found that vitamin D supplementation was significantly associated with development of both IMC and severe IMC, while immune-enhancing medications were significantly associated with decreased risk of IMC. Future work should focus on broader populations to resolve the discrepancies raised in our work, and to confirm the association between IMC and increased cancer survival. Closely involving gastroenterologists with the workup and management of IMC will be crucial to ensuring the best care possible for these patients.

ARTICLE HIGHLIGHTS

Research background

Immune checkpoint inhibitor-mediated colitis (IMC) is a common immune-related side effect (irAE) of checkpoint inhibitor treatment for cancer. Prior work has suggested that IMC may be associated with increased survival from cancer.

Research motivation

We sought to determine if IMC was associated with increased overall survival (OS) in a cohort of patients at our institution. These findings could expand existing data on IMC and cancer outcomes and might suggest a common immunological underpinning between the efficacy of checkpoint inhibitors and certain irAEs.

Research objectives
We performed a retrospective case-control study of individuals treated with immune checkpoint inhibitors at our institution who developed IMC, closely matched to a cohort of patients treated with checkpoint inhibitors without IMC. Using univariate and multivariate logistic regression, we determined significant clinical predictors of IMC and the association of presence of IMC on OS.

Research methods
We found that IMC was significantly associated with a higher OS as well as OS greater than 12 mo. In contrast to previous findings, vitamin D supplementation was significantly associated with development of both IMC and severe IMC. However, prior treatment with immune-enhancing medications was significantly associated with decreased risk of IMC.

Research results
In multivariate logistic regression analysis, IMC was significantly associated with a higher OS but not PFS. IMC was significantly associated with OS greater than 12 mo. Vitamin D supplementation was associated with increased risk of IMC.

Research conclusions
Our findings lend strength to the idea that IMC is associated with improved cancer outcomes with checkpoint inhibitor treatment. This may suggest common immunologic underpinnings between IMC and the anti-tumor effects of checkpoint inhibitors. These results also emphasize the importance of involving gastroenterologists with the management of IMC.

Research perspectives
Future research in this area should seek to expand current knowledge of the relationship between IMC and cancer survival. In particular, future work should focus on broadening the type and number of patients treated with immune checkpoint inhibitors and on tracking patients prior to initiating checkpoint inhibitors to determine if this relationship remains significant prospectively.

FOOTNOTES

Author contributions: Weingarden AR and Habtezion A designed the research study; Weingarden AR, Balabanis T, Patel A, and Sharma A performed data collection; Gubatan J analyzed data; Weingarden AR, Gubatan J, Singh S, and Habtezion A wrote and edited the manuscript; all authors have read and approve the final manuscript.

Institutional review board statement: The study was reviewed and approved by the Institutional Review Board at Stanford University (Approval No. IRB 57125).

Conflict-of-interest statement: None of the authors have any potential conflicts of interest to disclose.

Data sharing statement: Data availability upon request from authors.

Open-Access: This article is an open-access article that was selected by an in-house editor and fully peer-reviewed by external reviewers. It is distributed in accordance with the Creative Commons Attribution NonCommercial (CC BY-NC 4.0) license, which permits others to distribute, remix, adapt, build upon this work non-commercially, and license their derivative works on different terms, provided the original work is properly cited and the use is non-commercial. See: https://creativecommons.org/Licenses/by-nc/4.0/

Country/Territory of origin: United States

ORCID number: Alexa R Weingarden 0000-0002-1567-1320; John Gubatan 0000- 0001- 6037-2883; Tatiana Clorice Balabanis 0000-0002-9475-6989; Akshar Patel 0000-0002-2524-6061; Aida Habtezion 0000-0002-4473-006X.

S-Editor: Chen YL
L-Editor: A
P-Editor: Chen YL

REFERENCES

1 **Hodi FS**, O'Day SJ, McDermott DF, Weber RW, Sosman JA, Haanen JB, Gonzalez R, Robert C, Schadendorf D, Hassel JC, Akerley W, van den Eertwegh AJ, Lutzky J, Lorigan P, Vaubel JM, Linette GP, Hogg D, Ottensmeier CH, Lebbé C, Peschel C, Quirt I, Clark JI, Wolchok JD, Weber JS, Tian J, Yellin MJ, Nichol GM, Hoos A, Urba WJ. Improved survival with ipilimumab in patients with metastatic melanoma. *N Engl J Med* 2010; **363**: 711-723 [PMID: 20525992 DOI:

10.1056/NEJMoa1003466]
2 **Le DT**, Uram JN, Wang H, Bartlett BR, Kemberling H, Eyring AD, Skora AD, Luber BS, Azad NS, Laheru D, Biedrzycki B, Donehower RC, Zaheer A, Fisher GA, Crocenzi TS, Lee JJ, Duffy SM, Goldberg RM, de la Chapelle A, Koshiji M, Bhaijee F, Huebner T, Hruban RH, Wood LD, Cuka N, Pardoll DM, Papadopoulos N, Kinzler KW, Zhou S, Cornish TC, Taube JM, Anders RA, Eshleman JR, Vogelstein B, Diaz LA Jr. PD-1 Blockade in Tumors with Mismatch-Repair Deficiency. *N Engl J Med* 2015; **372**: 2509-2520 [PMID: 26028255 DOI: 10.1056/NEJMoa1500596]
3 **Borghaei H**, Paz-Ares L, Horn L, Spigel DR, Steins M, Ready NE, Chow LQ, Vokes EE, Felip E, Holgado E, Barlesi F, Kohlhäufl M, Arrieta O, Burgio MA, Fayette J, Lena H, Poddubskaya E, Gerber DE, Gettinger SN, Rudin CM, Rizvi N, Crinò L, Blumenschein GR Jr, Antonia SJ, Dorange C, Harbison CT, Graf Finckenstein F, Brahmer JR. Nivolumab *vs* Docetaxel in Advanced Nonsquamous Non-Small-Cell Lung Cancer. *N Engl J Med* 2015; **373**: 1627-1639 [PMID: 26412456 DOI: 10.1056/NEJMoa1507643]
4 **Bellmunt J**, de Wit R, Vaughn DJ, Fradet Y, Lee JL, Fong L, Vogelzang NJ, Climent MA, Petrylak DP, Choueiri TK, Necchi A, Gerritsen W, Gurney H, Quinn DI, Culine S, Sternberg CN, Mai Y, Poehlein CH, Perini RF, Bajorin DF; KEYNOTE-045 Investigators. Pembrolizumab as Second-Line Therapy for Advanced Urothelial Carcinoma. *N Engl J Med* 2017; **376**: 1015-1026 [PMID: 28212060 DOI: 10.1056/NEJMoa1613683]
5 **Schmid P**, Cortes J, Pusztai L, McArthur H, Kümmel S, Bergh J, Denkert C, Park YH, Hui R, Harbeck N, Takahashi M, Foukakis T, Fasching PA, Cardoso F, Untch M, Jia L, Karantza V, Zhao J, Aktan G, Dent R, O'Shaughnessy J; KEYNOTE-522 Investigators. Pembrolizumab for Early Triple-Negative Breast Cancer. *N Engl J Med* 2020; **382**: 810-821 [PMID: 32101663 DOI: 10.1056/NEJMoa1910549]
6 **Postow MA**, Sidlow R, Hellmann MD. Immune-Related Adverse Events Associated with Immune Checkpoint Blockade. *N Engl J Med* 2018; **378**: 158-168 [PMID: 29320654 DOI: 10.1056/NEJMra1703481]
7 **Collins M**, Soularue E, Marthey L, Carbonnel F. Management of Patients With Immune Checkpoint Inhibitor-Induced Enterocolitis: A Systematic Review. *Clin Gastroenterol Hepatol* 2020; **18**: 1393-1403.e1 [PMID: 32007539 DOI: 10.1016/j.cgh.2020.01.033]
8 **Khoja L**, Day D, Wei-Wu Chen T, Siu LL, Hansen AR. Tumour- and class-specific patterns of immune-related adverse events of immune checkpoint inhibitors: a systematic review. *Ann Oncol* 2017; **28**: 2377-2385 [PMID: 28945858 DOI: 10.1093/annonc/mdx286]
9 **Wang Y**, Abu-Sbeih H, Mao E, Ali N, Ali FS, Qiao W, Lum P, Raju G, Shuttlesworth G, Stroehlein J, Diab A. Immune-checkpoint inhibitor-induced diarrhea and colitis in patients with advanced malignancies: retrospective review at MD Anderson. *J Immunother Cancer* 2018; **6**: 37 [PMID: 29747688 DOI: 10.1186/s40425-018-0346-6]
10 **Abu-Sbeih H**, Ali FS, Qiao W, Lu Y, Patel S, Diab A, Wang Y. Immune checkpoint inhibitor-induced colitis as a predictor of survival in metastatic melanoma. *Cancer Immunol Immunother* 2019; **68**: 553-561 [PMID: 30666357 DOI: 10.1007/s00262-019-02303-1]
11 **Grover S**, Dougan M, Tyan K, Giobbie-Hurder A, Blum SM, Ishizuka J, Qazi T, Elias R, Vora KB, Ruan AB, Martin-Doyle W, Manos M, Eastman L, Davis M, Gargano M, Haq R, Buchbinder EI, Sullivan RJ, Ott PA, Hodi FS, Rahma OE. Vitamin D intake is associated with decreased risk of immune checkpoint inhibitor-induced colitis. *Cancer* 2020; **126**: 3758-3767 [PMID: 32567084 DOI: 10.1002/cncr.32966]
12 **Michot JM**, Bigenwald C, Champiat S, Collins M, Carbonnel F, Postel-Vinay S, Berdelou A, Varga A, Bahleda R, Hollebecque A, Massard C, Fuerea A, Ribrag V, Gazzah A, Armand JP, Amellal N, Angevin E, Noel N, Boutros C, Mateus C, Robert C, Soria JC, Marabelle A, Lambotte O. Immune-related adverse events with immune checkpoint blockade: a comprehensive review. *Eur J Cancer* 2016; **54**: 139-148 [PMID: 26765102 DOI: 10.1016/j.ejca.2015.11.016]
13 **Verheijden RJ**, May AM, Blank CU, Aarts MJB, van den Berkmortel FWPJ, van den Eertwegh AJM, de Groot JWB, Boers-Sonderen MJ, van der Hoeven JJM, Hospers GA, Piersma D, van Rijn RS, Ten Tije AJ, van der Veldt AAM, Vreugdenhil G, van Zeijl MCT, Wouters MWJM, Haanen JBAG, Kapiteijn E, Suijkerbuijk KPM. Association of Anti-TNF with Decreased Survival in Steroid Refractory Ipilimumab and Anti-PD1-Treated Patients in the Dutch Melanoma Treatment Registry. *Clin Cancer Res* 2020; **26**: 2268-2274 [PMID: 31988197 DOI: 10.1158/1078-0432.CCR-19-3322]
14 **National Cancer Institute**. Common Terminology Criteria for Adverse Events (CTCAE) v5.0. Available from: https://ctep.cancer.gov/20protocoldevelopment/electronic_applications/%20docs/CTCAE_v5_Quick_Reference_8.5x11.pdf [DOI: 10.32388/erjxiq]
15 **Collins M**, Michot JM, Danlos FX, Mussini C, Soularue E, Mateus C, Loirat D, Buisson A, Rosa I, Lambotte O, Laghouati S, Chaput N, Coutzac C, Voisin AL, Soria JC, Marabelle A, Champiat S, Robert C, Carbonnel F. Inflammatory gastrointestinal diseases associated with PD-1 blockade antibodies. *Ann Oncol* 2017; **28**: 2860-2865 [PMID: 29045560 DOI: 10.1093/annonc/mdx403]
16 **Kok PS**, Cho D, Yoon WH, Ritchie G, Marschner I, Lord S, Friedlander M, Simes J, Lee CK. Validation of Progression-Free Survival Rate at 6 Months and Objective Response for Estimating Overall Survival in Immune Checkpoint Inhibitor Trials: A Systematic Review and Meta-analysis. *JAMA Netw Open* 2020; **3**: e2011809 [PMID: 32897371 DOI: 10.1001/jamanetworkopen.2020.11809]
17 **Wang DY**, Ye F, Zhao S, Johnson DB. Incidence of immune checkpoint inhibitor-related colitis in solid tumor patients: A systematic review and meta-analysis. *Oncoimmunology* 2017; **6**: e1344805 [PMID: 29123955 DOI: 10.1080/2162402X.2017.1344805]
18 **Bishay K**, Tandon P, Bourassa-Blanchette S, Laurie SA, McCurdy JD. The risk of diarrhea and colitis in patients with lung cancer treated with immune checkpoint inhibitors: a systematic review and meta-analysis. *Curr Oncol* 2020; **27**: e486-e494 [PMID: 33173388 DOI: 10.3747/co.27.6251]
19 **De Velasco G**, Je Y, Bossé D, Awad MM, Ott PA, Moreira RB, Schutz F, Bellmunt J, Sonpavde GP, Hodi FS, Choueiri TK. Comprehensive Meta-analysis of Key Immune-Related Adverse Events from CTLA-4 and PD-1/PD-L1 Inhibitors in Cancer Patients. *Cancer Immunol Res* 2017; **5**: 312-318 [PMID: 28246107 DOI: 10.1158/2326-6066.CIR-16-0237]
20 **Soularue E**, Lepage P, Colombel JF, Coutzac C, Faleck D, Marthey L, Collins M, Chaput N, Robert C, Carbonnel F. Enterocolitis due to immune checkpoint inhibitors: a systematic review. *Gut* 2018; **67**: 2056-2067 [PMID: 30131322 DOI: 10.1136/gutjnl-2018-316948]

21 **Tandon P**, Bourassa-Blanchette S, Bishay K, Parlow S, Laurie SA, McCurdy JD. The Risk of Diarrhea and Colitis in Patients With Advanced Melanoma Undergoing Immune Checkpoint Inhibitor Therapy: A Systematic Review and Meta-Analysis. *J Immunother* 2018; **41**: 101-108 [PMID: 29401166 DOI: 10.1097/CJI.0000000000000213]

22 **Komaki Y**, Komaki F, Yamada A, Micic D, Ido A, Sakuraba A. Meta-Analysis of the Risk of Immune-Related Adverse Events With Anticytotoxic T-Lymphocyte-Associated Antigen 4 and Antiprogrammed Death 1 Therapies. *Clin Pharmacol Ther* 2018; **103**: 318-331 [PMID: 28118483 DOI: 10.1002/cpt.633]

23 **Yao J**, Li M, Zhang H, Ge Y, Weygant N, An G. Differential risks of immune-related colitis among various immune checkpoint inhibitor regimens. *Int Immunopharmacol* 2020; **87**: 106770 [PMID: 32702598 DOI: 10.1016/j.intimp.2020.106770]

24 **Schachter J**, Ribas A, Long GV, Arance A, Grob JJ, Mortier L, Daud A, Carlino MS, McNeil C, Lotem M, Larkin J, Lorigan P, Neyns B, Blank C, Petrella TM, Hamid O, Zhou H, Ebbinghaus S, Ibrahim N, Robert C. Pembrolizumab *vs* ipilimumab for advanced melanoma: final overall survival results of a multicentre, randomised, open-label phase 3 study (KEYNOTE-006). *Lancet* 2017; **390**: 1853-1862 [PMID: 28822576 DOI: 10.1016/S0140-6736(17)31601-X]

25 **Robert C**, Ribas A, Schachter J, Arance A, Grob JJ, Mortier L, Daud A, Carlino MS, McNeil CM, Lotem M, Larkin JMG, Lorigan P, Neyns B, Blank CU, Petrella TM, Hamid O, Su SC, Krepler C, Ibrahim N, Long GV. Pembrolizumab *vs* ipilimumab in advanced melanoma (KEYNOTE-006): post-hoc 5-year results from an open-label, multicentre, randomised, controlled, phase 3 study. *Lancet Oncol* 2019; **20**: 1239-1251 [PMID: 31345627 DOI: 10.1016/S1470-2045(19)30388-2]

26 **Larkin J**, Chiarion-Sileni V, Gonzalez R, Grob JJ, Rutkowski P, Lao CD, Cowey CL, Schadendorf D, Wagstaff J, Dummer R, Ferrucci PF, Smylie M, Hogg D, Hill A, Márquez-Rodas I, Haanen J, Guidoboni M, Maio M, Schöffski P, Carlino MS, Lebbé C, McArthur G, Ascierto PA, Daniels GA, Long GV, Bastholt L, Rizzo JI, Balogh A, Moshyk A, Hodi FS, Wolchok JD. Five-Year Survival with Combined Nivolumab and Ipilimumab in Advanced Melanoma. *N Engl J Med* 2019; **381**: 1535-1546 [PMID: 31562797 DOI: 10.1056/NEJMoa1910836]

27 **Savina M**, Le Cesne A, Blay JY, Ray-Coquard I, Mir O, Toulmonde M, Cousin S, Terrier P, Ranchere-Vince D, Meeus P, Stoeckle E, Honoré C, Sargos P, Sunyach MP, Le Péchoux C, Giraud A, Bellera C, Le Loarer F, Italiano A. Patterns of care and outcomes of patients with METAstatic soft tissue SARComa in a real-life setting: the METASARC observational study. *BMC Med* 2017; **15**: 78 [PMID: 28391775 DOI: 10.1186/s12916-017-0831-7]

28 **Yadav K**, Lewis RJ. Immortal Time Bias in Observational Studies. *JAMA* 2021; **325**: 686-687 [PMID: 33591334 DOI: 10.1001/jama.2020.9151]

29 **Rizzo A**, Mollica V, Santoni M, Ricci AD, Rosellini M, Marchetti A, Montironi R, Ardizzoni A, Massari F. Impact of Clinicopathological Features on Survival in Patients Treated with First-line Immune Checkpoint Inhibitors Plus Tyrosine Kinase Inhibitors for Renal Cell Carcinoma: A Meta-analysis of Randomized Clinical Trials. *Eur Urol Focus* 2022; **8**: 514-521 [PMID: 33714725 DOI: 10.1016/j.euf.2021.03.001]

30 **Mollica V**, Santoni M, Matrana MR, Basso U, De Giorgi U, Rizzo A, Maruzzo M, Marchetti A, Rosellini M, Bleve S, Maslov D, Tawagi K, Philon E, Blake Z, Massari F. Concomitant Proton Pump Inhibitors and Outcome of Patients Treated with Nivolumab Alone or Plus Ipilimumab for Advanced Renal Cell Carcinoma. *Target Oncol* 2022; **17**: 61-68 [PMID: 34894318 DOI: 10.1007/s11523-021-00861-y]

31 **Rizzo A**, Ricci AD. PD-L1, TMB, and other potential predictors of response to immunotherapy for hepatocellular carcinoma: how can they assist drug clinical trials? *Expert Opin Investig Drugs* 2022; **31**: 415-423 [PMID: 34429006 DOI: 10.1080/13543784.2021.1972969]

32 **Routy B**, Le Chatelier E, Derosa L, Duong CPM, Alou MT, Daillère R, Fluckiger A, Messaoudene M, Rauber C, Roberti MP, Fidelle M, Flament C, Poirier-Colame V, Opolon P, Klein C, Iribarren K, Mondragón L, Jacquelot N, Qu B, Ferrere G, Clémenson C, Mezquita L, Masip JR, Naltet C, Brosseau S, Kaderbhai C, Richard C, Rizvi H, Levenez F, Galleron N, Quinquis B, Pons N, Ryffel B, Minard-Colin V, Gonin P, Soria JC, Deutsch E, Loriot Y, Ghiringhelli F, Zalcman G, Goldwasser F, Escudier B, Hellmann MD, Eggermont A, Raoult D, Albiges L, Kroemer G, Zitvogel L. Gut microbiome influences efficacy of PD-1-based immunotherapy against epithelial tumors. *Science* 2018; **359**: 91-97 [PMID: 29097494 DOI: 10.1126/science.aan3706]

33 **Matson V**, Fessler J, Bao R, Chongsuwat T, Zha Y, Alegre ML, Luke JJ, Gajewski TF. The commensal microbiome is associated with anti-PD-1 efficacy in metastatic melanoma patients. *Science* 2018; **359**: 104-108 [PMID: 29302014 DOI: 10.1126/science.aao3290]

34 **Gopalakrishnan V**, Spencer CN, Nezi L, Reuben A, Andrews MC, Karpinets TV, Prieto PA, Vicente D, Hoffman K, Wei SC, Cogdill AP, Zhao L, Hudgens CW, Hutchinson DS, Manzo T, Petaccia de Macedo M, Cotechini T, Kumar T, Chen WS, Reddy SM, Szczepaniak Sloane R, Galloway-Pena J, Jiang H, Chen PL, Shpall EJ, Rezvani K, Alousi AM, Chemaly RF, Shelburne S, Vence LM, Okhuysen PC, Jensen VB, Swennes AG, McAllister F, Marcelo Riquelme Sanchez E, Zhang Y, Le Chatelier E, Zitvogel L, Pons N, Austin-Breneman JL, Haydu LE, Burton EM, Gardner JM, Sirmans E, Hu J, Lazar AJ, Tsujikawa T, Diab A, Tawbi H, Glitza IC, Hwu WJ, Patel SP, Woodman SE, Amaria RN, Davies MA, Gershenwald JE, Hwu P, Lee JE, Zhang J, Coussens LM, Cooper ZA, Futreal PA, Daniel CR, Ajami NJ, Petrosino JF, Tetzlaff MT, Sharma P, Allison JP, Jenq RR, Wargo JA. Gut microbiome modulates response to anti-PD-1 immunotherapy in melanoma patients. *Science* 2018; **359**: 97-103 [PMID: 29097493 DOI: 10.1126/science.aan4236]

World Journal of Gastroenterology

Submit a Manuscript: https://www.f6publishing.com

World J Gastroenterol 2022 October 21; 28(39): 5764-5783

DOI: 10.3748/wjg.v28.i39.5764

ISSN 1007-9327 (print) ISSN 2219-2840 (online)

ORIGINAL ARTICLE

Observational Study

Serum metabolic profiling of targeted bile acids reveals potentially novel biomarkers for primary biliary cholangitis and autoimmune hepatitis

Zhen-Hua Ma, Xiao-Mei Wang, Rui-Hong Wu, Da-Lin Hao, Li-Chao Sun, Pan Li, Jun-Qi Niu

Specialty type: Gastroenterology and hepatology

Provenance and peer review: Unsolicited article; Externally peer reviewed.

Peer-review model: Single blind

Peer-review report's scientific quality classification

Grade A (Excellent): 0
Grade B (Very good): B, B
Grade C (Good): 0
Grade D (Fair): 0
Grade E (Poor): 0

P-Reviewer: Liakina V, Lithuania; Velikova TV, Bulgaria

Received: June 28, 2022
Peer-review started: June 28, 2022
First decision: August 19, 2022
Revised: September 7, 2022
Accepted: September 23, 2022
Article in press: September 23, 2022
Published online: October 21, 2022

Zhen-Hua Ma, Da-Lin Hao, Li-Chao Sun, Department of Infection and Hepatology, The Affiliated Hospital of Beihua University, Jilin 132011, Jilin Province, China

Xiao-Mei Wang, Rui-Hong Wu, Jun-Qi Niu, Department of Hepatology, The First Hospital of Jilin University, Changchun 130061, Jilin Province, China

Pan Li, Department of Pathology, The Affiliated Hospital of Beihua University, Jilin 132011, Jilin Province, China

Corresponding author: Jun-Qi Niu, MMed, Professor, Department of Hepatology, The First Hospital of Jilin University, No. 1 Xinmin Dajie, Chaoyang District, Changchun 130061, Jilin Province, China. junqiniu@jlu.edu.cn

Abstract

BACKGROUND

Primary biliary cholangitis (PBC) and autoimmune hepatitis (AIH) are two unexplained immune diseases. The golden standard for diagnosis of these diseases requires a liver biopsy. Liver biopsy is not widely accepted by patients because of its invasive nature, and atypical liver histology can confuse diagnosis. In view of the lack of effective diagnostic markers for PBC and AIH, combined with the increasingly mature metabolomics technologies, including full-contour metabolomics and target.

AIM

To determine non-invasive, reliable, and sensitive biochemical markers for the differential diagnosis of PBC and AIH.

METHODS

Serum samples from 54 patients with PBC, 26 patients with AIH and 30 healthy controls were analyzed by Ultra-high performance liquid chromatography-tandem mass spectrometry serum metabolomics. The metabolites and metabolic pathways were identified, and the metabolic changes, metabolic pathways and inter-group differences between PBC and AIH were analyzed. Fifteen kinds of target metabolites of bile acids (BAs) were quantitatively analyzed by SRM, and the differential metabolites related to the diagnosis of PBC were screened by receiver operating characteristic curve analysis.

RESULTS

We found the changes in the levels of amino acids, BAs, organic acids, phospholipids, choline, sugar, and sugar alcohols in patients with PBC and AIH. Furthermore, the SRM assay of BAs revealed the increased levels of chenodeoxycholic acid, lithocholic acid (LCA), taurolithocholic acid (TLCA), and LCA + TLCA in the PBC group compared with those in the AIH group. The levels of BAs may be used as biomarkers to differentiate PBC from AIH diseases. The levels of glycochenodeoxycholic acid, glycochenodeoxycholic sulfate, and taurodeoxycholic acid were gradually elevated with the increase of Child-Pugh class, which was correlated with the severity of disease.

CONCLUSION

The results demonstrated that the levels of BAs could serve as potential biomarkers for the early diagnosis and assessment of the severity of PBC and AIH.

Key Words: Primary biliary cholangitis; Autoimmune hepatitis; Biomarkers; Serum metabolic profiling; Bile acids; Ultra-performance liquid chromatography-quadrupole time-of-flight mass spectrometry

©The Author(s) 2022. Published by Baishideng Publishing Group Inc. All rights reserved.

Core Tip: Using full-contour metabolomics and SRM, to determine non-invasive, reliable, and sensitive biochemical markers for the differential diagnosis of primary biliary cholangitis (PBC) and autoimmune hepatitis (AIH). We revealed the increased levels of chenodeoxycholic acid, lithocholic acid (LCA), taurolithocholic acid (TLCA), and LCA + TLCA in the PBC group compared with those in the AIH group. The levels of glycochenodeoxycholic acid, glycochenodeoxycholic sulfate, and taurodeoxycholic acid were gradually elevated with the increase of Child-Pugh class, which was correlated with the severity of disease. The levels of BAs could serve as potential biomarkers for the early diagnosis and assessment of the severity of PBC and AIH.

Citation: Ma ZH, Wang XM, Wu RH, Hao DL, Sun LC, Li P, Niu JQ. Serum metabolic profiling of targeted bile acids reveals potentially novel biomarkers for primary biliary cholangitis and autoimmune hepatitis. *World J Gastroenterol* 2022; 28(39): 5764-5783

URL: https://www.wjgnet.com/1007-9327/full/v28/i39/5764.htm

DOI: https://dx.doi.org/10.3748/wjg.v28.i39.5764

INTRODUCTION

Primary biliary cholangitis (PBC) and autoimmune hepatitis (AIH) are two unexplained immune diseases[1]. Although advanced methods have been presented for diagnosing PBC and AIH, 5%-10% of PBC patients have anti-mitochondrial antibody-negative, and missed diagnosis or misdiagnosis mainly occurs in clinical practice[2]. For some patients with anti-mitochondrial antibody-positive, rather than significant changes in hepatic histology and function, long-term follow-up revealed that these patients eventually developed to PBC. Thus, early diagnosis of these patients is a clinical challenge. Clinical manifestations of AIH may have similarities to other autoimmune liver diseases, such as drug-induced hepatitis, alcoholic liver disease, inherited metabolic disorders, and hepatitis C virus infection, such as regardless of the cause of liver disease, patients may present with fatigue, abdominal distention, skin and sclera yellow staining, laboratory test show liver dysfunction. Because of the complexity and difficulty of diagnosing, leading to the delayed diagnosis of several AIH patients. Liver biopsy remains the golden standard for the diagnosis of autoimmune liver diseases, while it is an invasive, painful, and costly method that is associated with the possibility of sampling error and variability in interpretation. Therefore, identification of novel and accurate noninvasive biomarkers for the diagnosis and assessment of severity is of great importance.

As one of the emerging 'omics' platforms, metabolomics enables the qualitative and quantitative analyses of metabolites in complex biological samples[3]. As products of cellular adjustment processes, metabolites are regarded as the ultimate readouts that reflect genetic or environmental changes in biological systems[4,5] High-throughput metabolic profiling has been successfully used for the identification of novel diagnostic molecules and disease-related pathways, as well as development of new therapeutic targets for some diseases (*e.g.*, cancer, non-alcoholic fatty liver disease, non-alcoholic steatohepatitis, and PBC)[6-10]. Thus, it is essential to identify specific metabolomic markers, and to establish a diagnostic model for AIH or PBC.

In the present study, we aimed to identify serum biomarkers for the differential diagnosis of PBC and AIH using ultra-performance liquid chromatography-quadrupole time-of-flight mass spectrometry (UPLC-QTOF-MS). UPLC-QTOF-MS is a newly developed technique that provides rapid and efficient access to detailed information pertaining to the nature of specific components within complex multicomponent mixtures. Compared with traditional high-performance liquid chromatography (HPLC), UPLC possesses the advantages of ultra-high resolution, high-speed scanning, and high sensitivity. Furthermore, bile acids (BAs) are crucial for the diagnosis, follow-up, and prognosis of liver and intestinal disorders, as well as diseases affecting BA metabolism. We applied a targeted metabolomic approach to quantify and compare 15 BA metabolites in PBC/AIH patients with those in healthy controls (HCs). The findings of the present study may reveal potentially novel biomarkers for the diagnosis of PBC and AIH. This study also aimed to compare metabolic profiles between PBC/AIH patients and HCs.

MATERIALS AND METHODS

Patients and study design

A total of 54 PBC and 26 AIH patients who were admitted to the First Hospital of Jilin University (Changchun, China) between May 2009 and November 2013 were respectively recruited in the present study. The study protocol was carefully reviewed and approved by the Institutional Review Board of The First Hospital of Jilin University. All the eligible patients and HCs signed the written informed consent form prior to enrollment. Patients with AIH were diagnosed according to the revised criteria presented by the International Autoimmune Hepatitis Group in 1999[11]. Patients with PBC were diagnosed according to the criteria released by the American Association for the Study of Liver Diseases [12]. Patients taking medication or supplements, or those with gallstones or other factors that might cause cholestatic liver diseases were excluded. In both groups, patients with primary sclerosing cholangitis (PSC), overlap syndromes (*e.g.*, PBC and AIH or AIH and PSC), hepatitis virus infection, human immunodeficiency virus co-infection, hepatocellular carcinoma, or diabetes were excluded. In total, 30 HCs who were admitted to our hospital for physical check-ups were enrolled. These HCs exhibited normal liver functions and had no evidence of disease. No statistically significant differences were found in age and gender among the PBC, AIH, and control groups (Table 1, $P > 0.05$).

Blood samples at the fasting state were collected from the eligible PBC patients, AIH patients, and HCs, in which 1 mL of serum was collected and stored at -80 °C for subsequent metabolic profiling. Participants' baseline characteristics are summarized in Table 1.

Reagents

HPLC-grade acetonitrile was purchase from Merck Inc. (Kenilworth, NJ, United States). HPLC-grade formic acid was obtained from Sigma-Aldrich (St. Louis, MO, United States). These two reagents were used for the preparation of mobile phases in HPLC. Milli-Q water was used, and obtained by filtering distilled water through a Milli-Q system (Millipore, Bedford, MA, United States). The chemical standards for the validation of molecular structure were obtained from Sigma-Aldrich.

Sample preparation and serum metabolic profiling

In the present study, 100 μL of each serum sample was mixed with 400 μL of cold acetonitrile for protein precipitation, followed by centrifugation at 14000 g for 10 min at 4 °C. Then, 400 μL of the supernatant was subsequently collected and lyophilized, and the residue was resolved in 100 μL of 20% acetonitrile. Equal aliquot of each serum sample was pooled together and mixed thoroughly by vortex for 1 min, which was used as the quality control (QC) sample. A QC sample was prepared after preparation of 10 real samples, and QC samples served to assess the repeatability of sample pretreatment and to monitor the stability of the UPLC-QTOF-MS system at the sequence analysis.

The UPLC-QTOF-MS approach was employed to perform serum metabolic profiling of samples obtained from PBC patients, AIH patients, and HCs, as previously described[13]. In brief, 5 μL of the reconstituted solution was carefully injected into the ACQUITY-UPLC system (Waters Corp., Milford, MA, United States) for separation using chromatography. Then, MS signals were acquired *via* the QTOF-MS system (Micromass, Manchester, United Kingdom), which was equipped with an electrospray source operating in both positive and negative ion modes. During the acquisition of MS signals, the m/z scan was set to a range of 100-1000[14]. Then, the AC18 column (2.1 mm × 100 mm, 1.7 μm), which was purchased from Waters Corp., was used for the separation of small molecular compounds at an elution speed of 0.35 mL/min. The gradient was set to 95% formic acid (0.1%, V/V), and maintained for 1 min. Subsequently, elution strength linearly increased to 100% acetonitrile for 22 min, and was kept for 3 min. The total duration was 30 min, which included equilibration for 1 min.

Analysis of BAs

All samples prepared with GCA-d5 as the internal standard and blood samples were resolved in 100 μL

Table 1 Characteristics of enrolled population in the metabolic profiling study

Clinical parameters	PBC (*n* = 54)	AIH (*n* = 26)	Control (*n* = 30)	*P* value (PBC *vs* control)	*P* value (AIH *vs* control)	*P* value (PBC *vs* AIH)
Age (mean, range) (yr), *n*	56 (38-73)	54.6 (17-75)	54.9(34-70)	0.922	0.805	0.890
Sex (Male/Female), *n*	7/47	3/23	4/26	-	-	-
AST (U/L) median, range	113.3 (14-1300)	168.8 (23-961)	23.3 (7-38)	< 0.001	< 0.001	0.423
ALT (U/L) median, range	95.9 (12-734)	153.3 (10-780)	19.0 (7-39)	< 0.001	< 0.001	0.125
ALP (U/L) median, range	292.4 (55-953)	240.1 (46-795)	73.6 (32-116)	< 0.001	< 0.001	0.123
γ-GT (U/L) median, range	299.4 (32-1631)	245.2 (26-957)	21.1 (9-77)	< 0.001	< 0.001	0.377
TBA (μmol/L) median, range	60.0 (2.7-295.7)	126.0 (1.1-1335)	-	-	-	0.696
TBiL (μmol/L) median, range	65.5 (5.6-825.8)	89.1 (6.5-543.9)	10.9 (6.3-19.5)	< 0.001	< 0.001	0.481
DBIL (μmol/L) median range	35.9 (2.4-407.4)	52.9 (2.1-300.8)	3.3 (0.4-6)	< 0.001	< 0.001	0.648
Liver cirrhosis (%)	65 (35/54)	62 (16/26)	-	-	-	-
Liver biopsy (%)	18 (10/54)	53 (14/26)	-	-	-	-
Positive of AMA (%)	81 (44/54)	0 (0/26)	-	-	-	-
Positive of ANA (%)	61 (33/54)	100 (26/26)	-	-	-	-

PBC: Primary biliary cirrhosis; AIH: Autoimmune hepatitis; AST: Aspartatetransaminase; ALT: Alanine aminotransferase; ALP: Alkaline phosphatase; γ-GT: γ-glutamyl transpeptidase; TBiL: Totalbilirubin; DBiL: Direct bilirubin; TBA: Total bile acid; AMA: Anti-mitochondrial antibody; ANA: Anti-nuclear antibody. All data are presented as median and range. Statistically significant differences between controls and patients were determined by the rank sums Mann-Whitney.

of 25% ACN aqueous solution. The LC-MS parameters were as follows: 20 μL of the reconstituted solution was carefully injected into an ACQUITY UPLC C8 column with a particle size of 1.7 μm (Waters Corp.), and the SRM signals were obtained using an Agilent 6460 Triple Quadruple MS system (Agilent Technologies, Inc., Chicago, IL, United States), which was equipped with an electrospray source operating in the negative ion mode. The column was eluted with 10 mmol/L NH_4HCO_3 (solution A) and acetonitrile (solution B) in a linear gradient, in which the initial gradient was set to 75% solution A. Subsequently, after 9.0 min of elution, the strength was linearly elevated to 90% solution B, which lasted for 4 min. Then, this was returned to the initial gradient after 13.5 min of elution. Along with an equilibration of 1.5 min, the total running time was approximately 15 min. The following MS parameters were set in this study: Gas flow rate, 8 L/min; gas temperature, 350 °C; sheath gas temperature, 400 °C; nebulizer gas pressure, 40 psi; capillary voltage, 3500 V; sheath gas flow rate, 8 L/min; nozzle voltage, 400 V. The precursor and product ion pairs were acquired as follows: Cholic acid (CA) (407.5→407.5), glycocholic acid (GCA) (464.2→74.1), taurocholic acid (TCA) (514.2→80.1), ursodeoxycholic acid (UDCA) (391.4→391.4), glycoursodeoxycholic acid (GUDCA) (448.3→74.1), tauroursodeoxycholic acid (TUDCA) (498.3→80.1), chenodeoxycholic acid (CDCA) (391.4→391.4), glycochenodeoxycholic acid (GCDCA) (448.3→74.1), tauroursodeoxycholic acid (TCDCA) (498.2→80.1), glycochenodeoxycholic sulfate (GCDCS) (528.3→448.3), deoxycholic acid (DCA) (391.2→391.2), glycodeoxycholic acid (GDCA) (448.2→74.1), taurodeoxycholic acid (TDCA) (498.3→80.2), lithocholic acid (LCA) (375.3→375.3), taurolithocholic acid (TLCA) (482.1→80.1), and GCA-d5 (469.2→74.1).

Bioinformatics and statistical analyses

The raw data were imported into Databridge (MassHunter Quantitative Analysis software; Agilent Technologies, Inc.), followed by the peak extraction and alignment on the obtained NetCDF files using XCMS 18.0 software. The alignment parameters were set as follows: The retention time window was 7, the full width at half maximum was 14, and the remaining parameters were set as default. Subsequently, the peaks with the paired m/z, as well as their corresponding peak intensities and retention time were exported into the Excel software. Prior to univariate and multivariate logistic regression analyses, each peak area was initially normalized to the total peak area. In the multivariate logistic regression analysis, the principal component analysis (PCA) in combination with the partial least squares-discriminant analysis (PLS-DA) was conducted by SIMCA-P 11.0 software (Umetrics AB, Umea, Sweden) using the prepared data. After scaling for PCA to unit variance, the data provided an overview of the repeatability of the QC samples. Additionally, the data were Pareto scaled for PLS-DA to assess

the performance of the classification models, and to identify variables for the corresponding model.

In the univariate analysis, data were statistically analyzed by SPSS 18.0 software (IBM, Armonk, NY, United States). The biochemical data and the concentrations of BAs were log-transformed to approximately normalize their distributions. $P < 0.05$ was considered statistically significant. Nonparametric statistical analysis was conducted using GraphPad Prism 5.0 software (GraphPad Software Inc., San Diego, CA, United States) for making comparison between two groups.

RESULTS

Patients' baseline clinical characteristics

Patients' baseline clinical characteristics are summarized in Table 1. Previous epidemiological studies have demonstrated that women were more frequently affected by PBC and AIH than men. Consistently, the incidence rates of PBC and AIH were higher in women than in men in our study. Furthermore, to avoid the influences of drugs on the metabolomics analysis, no patient had received any treatment, including traditional Chinese medicine. The mean age of patients with PBC and AIH, and HCs was 56 (range, 38-73), 54.6 (range, 17-75), and 54.9 (range, 30-76) years old, respectively. There were no significant differences in age, parity, and gender among patients with PBC and AIH, and HCs ($P > 0.05$). Besides, 10 cases from the PBC group and 14 cases from the AIH group were newly diagnosed by biopsy. Other cases from the PBC group were diagnosed by M2-positive, and other cases from the AIH group were diagnosed by pathological scores (> 12).

There were 26 cases of Child-Pugh class A, 19 cases of Child-Pugh class B, and 9 cases of Child-Pugh class C in PBC patients. There were 17 Child-Pugh grade A and 9 Child-Pugh grade B patients with AIH. The levels of globulin, transaminases, and specific autoantibodies in the sera are presented in Table 2.

Serum metabolic profiling

A total of 110 serum samples obtained from 54 patients with PBC, 26 patients with AIH, and 30 HCs were analyzed using UPLC-QTOF-MS in both positive and negative ion modes. As shown in Supplementary Figures 1 and 2, a typical base peak chromatogram was detected by MS in positive and negative ion modes, respectively. After the peaks were aligned, 1133 peaks of positive ions and 963 peaks of negative ions were identified using MassLynx and the same acquisition method. The data were transformed into SIMCA-P11 software for PCA. Plots of the PCA scores in positive and negative ion modes are illustrated in Figure 1A, Figure 2A, Figure 3A, Figure 4A, Figure 5A and Figure 6A. Distinct clustering was observed between PBC patients and HCs, and between AIH patients and HCs. No distinct clustering was found between PBC patients and AIH patients. The QC samples were tightly clustered (Figure 1A, Figure 2A, Figure 3A, Figure 4A, Figure 5A and Figure 6A), ensuring the repeatability of the information[13].

Identification of serum metabolites specific to PBC and AIH

To find out the differentially expressed metabolites, *P*-values ($P < 0.05$) in the t-test were combined with variable importance in the projection (VIP) values in the PLS-DA model. The PLS-DA score charts are shown in Figure 1B, Figure 2B, Figure 3B, Figure 4B, Figure 5B and Figure 6B. We also conduct sorting verification on the model to check whether the model is "over-fitting". The results are shown in Figure 1C, Figure 2C, Figure 3C, Figure 4C, Figure 5C and Figure 6C. As can be seen from the sorting test figure, Figure 1C, Figure 2C, Figure 5C and Figure 6C, there is no "over-fitting" in these models. Figure 3C and Figure 4C show that the two models are "overfitted". We only established the discriminant analysis model of multivariate analysis between PBC/Control and AIH/Control, but failed to establish the discriminant analysis model of PBC/AIH. The PBC and AIH samples of the two groups overlaps on the PCA score plot (as shown in Figure 3A and Figure 6A), and the supervised PLS-DA (as shown in Figure 3B and Figure 6B) still failed to distinguish them significantly, indicating that there was little difference in metabolic profile between the two groups of different autoimmune liver diseases.

The METLIN metabolomics database (http://metlin.scripps.edu/) was used to facilitate metabolite annotation through MS analysis. The data of differentially expressed are presented in Tables 3 and 4. Fold-change (FC) was used to indicate changes in potential PBC- and AIH-specific biomarkers, and the chosen FC values were > 2 and < 0.5.

Identification of serum metabolites specific to PBC

As presented in Table 3 the levels of 17 of 26 potential biomarkers identified were elevated in the serum samples of patients with PBC, while the levels of 9 of these 26 potential biomarkers were reduced in the serum samples of patients with PBC compared with those in HCs. Among these biomarkers, the levels of TDCA, GUDCA, tetracosahexaenoic acid, bilirubin, sphinganine, phytosphingosine, L-phenylalanine, L-proline, TCA, LysoPC [18:3 (6Z, 9Z, 12Z)], TUDCA, GCA, LysoPE [0:0/18:4 (6Z, 9Z, 12Z, 15Z)], LysoPE [20:3 (11Z, 14Z, 17Z)/0:0], L-urobilinogen, L-urobilin, and DCA significantly increased in patients with PBC compared with those in HCs ($P < 0.5$). The levels of 12-ketodeoxycholic acid, α-

Table 2 Characteristics of classified enrolled population according to Child-Pugh in the metabolic profiling study

Clinical parameters	PBC-A (*n* = 26)	PBC-B (*n* = 19)	PBC-C (*n* = 9)	AIH-A (*n* = 17)	AIH-B (*n* = 9)
Age (mean, range) (yr), *n*	54 (38, 68)	57.11 (40, 73)	59.33 (51, 67)	52.35 (17, 75)	59.11 (36, 73)
Sex (Male/Female), *n*	6/20	3/16	0/9	2/15	1/8
AST (U/L) median, range	62.77 (20, 210)	182.62 (14, 1300)	113.27 (35, 235)	122.28 (23, 961)	256.78 (64, 472)
ALT (U/L) median, range	74.18 (15, 293)	130.32 (12, 734)	84.51 (17, 236)	100.54 (10, 780)	253.11 (103, 598)
ALP (U/L) median, range	276.41 (75, 53)	352.73 (79, 913)	211.43 (55, 483)	230.33 (57, 795)	258.78 (46, 738)
γ-GT (U/L) median, range	380.18 (40, 631)	281.77 (40, 744)	103.49 (32, 235)	166.46 (26, 654)	393.89 (73, 957)
TBA (μmol/L) median, range	31.04 (2.9, 09.3)	75.16 (2.7, 295.7)	127.37 (23.4, 267.5)	116.46 (1, 1335)	144.29 (15, 379)
TBiL (μmol/L) median, range	19.7 (5.6, 48.8)	81.0 (11.3, 306.5)	181.62 (17.7, 825.8)	48.33 (6.5, 229.5)	166.23 (50.0, 543.9)
DBIL (μmol/L) median, range	9.18 (2.4, 32.0)	48.3 (4.1, 207.9)	99.71 (6.6, 407.4)	27.40 (2.1, 139.3)	101.24 (30.6, 300.8)
Liver cirrhosis (%)	0.38 (10/26)	0.84 (16/19)	1 (9/9)	0.47 (8/17)	0.33 (3/9)
Liver biopsy (%)	0.35 (9/26)	0.05 (1/19)	0 (0/9)	0.64 (11/17)	0.33 (3/9)
Positive of AMA (%)	80 (21/26)	80 (15/19)	89 (8/9)	0 (0/17)	0 (0/9)
Positive of ANA (%)	73 (19/26)	52 (10/19)	44 (4/9)	100 (17/17)	100 (9/9)

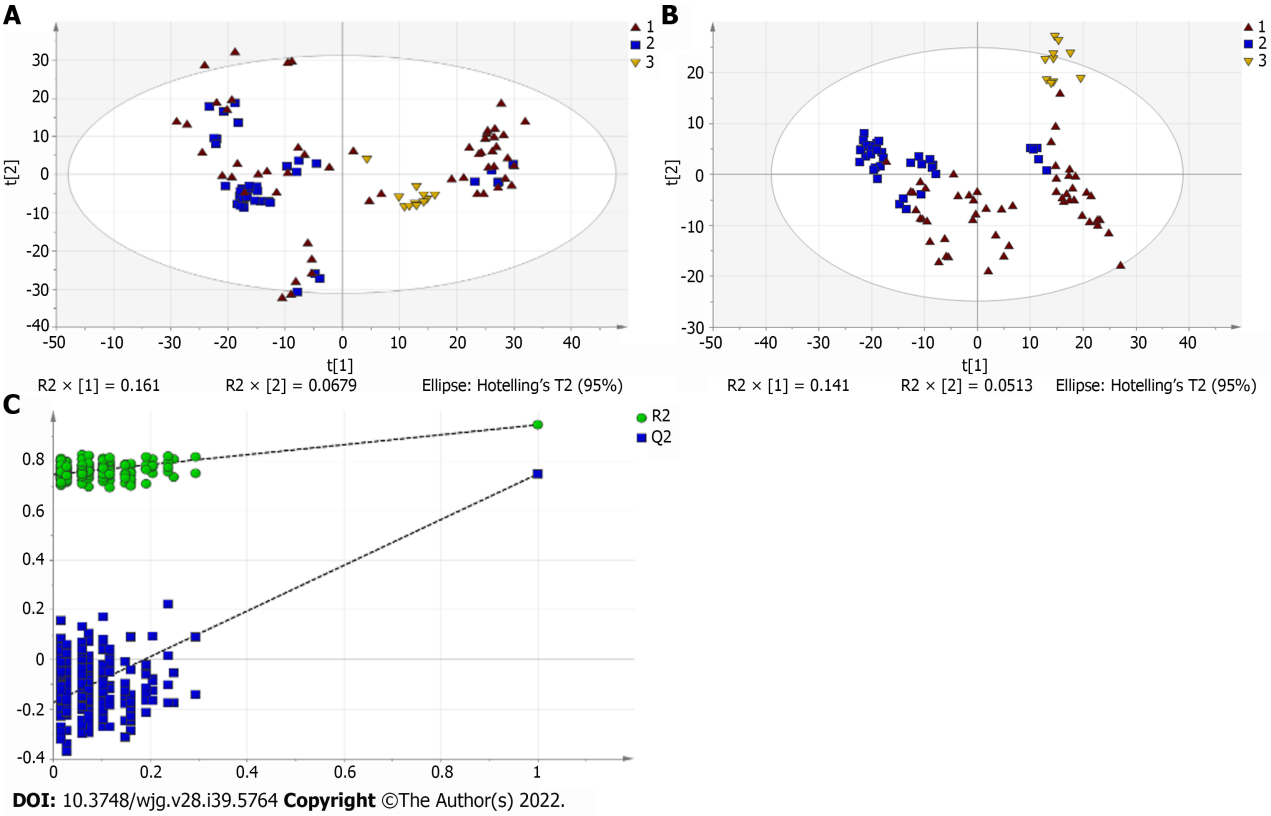
PBC: Primary biliary cirrhosis; AIH: Autoimmune hepatitis; AST: Aspartatetransaminase; ALT: Alanine aminotransferase; ALP: Alkaline phosphatase; γ-GT: γ-glutamyl transpeptidase; TBiL: Totalbilirubin; DBiL: Direct bilirubin; TBA: Total bile acid; AMA: Anti-mitochondrial antibody; ANA: Anti-nuclear antibody. All data are presented as median and range. Statistically significant differences between controls and patients were determined by the rank sums Mann-Whitney.

Table 3 Potential serum biomarkers for primary biliary cirrhosis compared to healthy control in positive and negative ions model

Name	VIP	MZ	Time	PBC/control	
				t-test	Fold change (P/C)
ESI+					
Taurodeoxycholic acid	1.747	500.3033	10.598	0.001	8.146
Glycodeoxycholate	2.175	450.3207	12.146	0.000	4.558
Tetracosahexaenoic acid	1.100	357.2786	9.333	0.045	3.490
Bilirubin	1.511	585.2701	10.218	0.006	3.334
Sphinganine	1.953	302.3052	12.792	0.000	3.285
Phytosphingosine	2.482	318.2999	10.734	0.000	3.039
L-Phenylalanine	1.690	166.0860	2.037	0.002	0.372
L-Proline	1.194	116.0706	0.725	0.030	0.180
12-Ketodeoxycholic acid	1.573	391.2842	15.210	0.004	-0.324
ESI-					
Taurocholic acid	1.493	514.2805	9.146	0.000	6.634
LysoPC [18:3(6Z, 9Z, 12Z)]	1.184	516.3064	13.057	0.001	5.263
Tauroursodeoxycholic acid	1.843	498.2861	10.456	0.000	4.627
Glycocholic Acid	1.866	464.2988	9.957	0.000	3.644
LysoPE [0:0/18:4 (6Z, 9Z, 12Z, 15Z)]	1.316	472.2430	9.798	0.000	3.274
LysoPE [20:3 (11Z, 14Z, 17Z)/0:0]	1.882	500.2947	10.456	0.000	3.225
L-Urobilinogen	1.027	595.3478	11.784	0.003	3.202
L-Urobilin	1.032	593.3315	11.665	0.003	2.411

Deoxycholic acid	1.032	391.2833	11.641	0.003	2.121
α-ketoisovaleric acid	1.040	115.0399	1.831	0.003	-0.348
Pyroglutamic acid	1.252	128.0350	0.931	0.000	-0.392
Lactic acid	1.548	89.0242	0.938	0.000	-0.402
Hypoxanthine	1.384	135.0308	0.886	0.000	-0.431
LysoPE [0:0/20:2 (11Z, 14Z)]	1.335	504.3072	14.333	0.000	-0.453
Ketoleucine	1.392	129.0555	4.110	0.000	-0.486
LysoPE [0:0/22:4 (7Z, 10Z, 13Z, 16Z)]	1.333	528.2850	13.617	0.000	-0.544
MG [0:0/18:4 (6Z, 9Z, 12Z, 15Z)/0:0]	2.060	349.2373	8.969	0.000	-2.181

PBC: Primary biliary cirrhosis; VIP: Variable importance in the projection.



DOI: 10.3748/wjg.v28.i39.5764 **Copyright** ©The Author(s) 2022.

Figure 1 Multivariate statistical analysis on serum profiling data in positive ions between primary biliary cholangitis and control. A: Plots of principal component analysis (PCA) in positive ion mode. (1) Primary biliary cholangitis (PBC); (2) Control; and (3) Quality control (QC); B: Scatter plots of partial least squares-discriminant analysis (PLS-DA) with a positive model of serum from patients with PBC, autoimmune hepatitis and healthy controls. (1) PBC; (2) Control; and (3) QC; C: Validation plot of the original PLS-DA with a positive model, strongly indicating that the original model is valid and shows signs of overfitting. The permutation test was repeated 200 times in the cross-validation plot.

ketoisovaleric acid, pyroglutamic acid, lactic acid, hypoxanthine, LysoPE [0:0/20:2 (11Z, 14Z)], ketoleucine, LysoPE [0:0/22:4 (7Z, 10Z, 13Z, 16Z)], and MG [0:0/18:4 (6Z, 9Z, 12Z, 15Z)/0:0] in patients with PBC were significantly reduced compared with those in HCs.

Identification of serum metabolites specific to AIH

As shown in Table 4. The levels of 17 of 25 potential biomarkers identified were elevated in the serum samples of the patients with AIH, while the levels of 8 of these 25 potential biomarkers were reduced in the serum samples of patients with AIH compared with those in HCs. Among these biomarkers, the levels of TDCA, GUDCA, L-Urobilin, sphinganine, phytosphingosine, I-Urobilin, bilirubin, stearamide, kynurenine, L-threonine, L-phenylalanine, urea, TCA, LysoPC [18:3 (6Z, 9Z, 12Z)], TDCA, GCA, and LysoPE [20:3 (11Z, 14Z, 17Z)/0:0] significantly increased in patients with AIH compared with those in HCs. The levels of 12-ketodeoxycholic acid, uric acid, pyroglutamic acid, LysoPE [0:0/20:2 (11Z, 14Z)],

Table 4 Potential serum biomarkers for autoimmune hepatitis compared to healthy control

Name	VIP	MZ	Time	AIH/control	
				t-test	Fold change (A/C)
ESI+					
Taurodeoxycholic acid	1.900	500.3033	10.598	0.000	8.791
Glycodeoxycholate	1.912	450.3207	12.146	0.000	5.217
L-Urobilin	1.442	595.3484	7.835	0.007	5.164
Sphinganine	2.308	302.3052	12.792	0.000	4.509
Phytosphingosine	2.344	318.2999	10.734	0.000	4.118
I-Urobilin	1.454	591.3169	7.628	0.006	3.661
Bilirubin	1.876	585.2701	10.218	0.000	3.578
Kynurenine	2.279	209.0919	1.944	0.000	0.592
L-Threonine	1.446	120.0655	0.708	0.007	0.386
L-Phenylalanine	1.551	166.0860	2.037	0.004	0.262
Urea	1.160	61.0395	0.730	0.032	0.113
12-Ketodeoxycholic acid	1.125	391.2842	15.210	0.037	-0.270
Uric acid	1.208	169.0354	1.035	0.025	-0.265
Pyroglutamic acid	2.489	130.0499	1.029	0.000	-0.517
ESI-					
Taurocholic acid	1.605	514.281	9.146	0.000	7.368
LysoPC [18:3 (6Z, 9Z, 12Z)]	1.454	516.306	13.057	0.000	6.614
Tauroursodeoxycholic acid	1.807	498.286	10.456	0.000	5.151
Glycocholic Acid	1.961	464.299	9.957	0.000	3.946
LysoPE [20:3 (11Z, 14Z, 17Z)/0:0]	1.807	500.295	10.456	0.000	3.670
LysoPE [0:0/20:2 (11Z, 14Z)]	1.234	504.307	14.333	0.001	-0.471
Lactic acid	1.489	89.024	0.938	0.000	-0.489
Hypoxanthine	1.380	135.031	0.886	0.000	-0.562
CPA (16:0/0:0)	1.629	391.224	26.118	0.000	-2.159
MG [0:0/18:4 (6Z, 9Z, 12Z, 15Z)/0:0]	1.771	349.237	8.969	0.000	-2.464

AIH: Autoimmune hepatitis; VIP: Variable importance in the projection.

Table 5 Changes of the serum bile acid profile between primary biliary cirrhosis, autoimmune hepatitis and controls

	AIH (mean ± SD)	PBC (mean ± SD)	Control (mean ± SD)	PBC/AIH	AIH/control	PBC/control
				P value	*P* value	*P* value
CA	2.38 ± 0.69	2.26 ± 0.85	1.60 ± 0.51	0.53	< 0.001[b]	< 0.001[a]
GCA	3.00 ± 1.02	2.91 ± 0.91	1.33 ± 0.50	0.69	< 0.001[b]	< 0.001[a]
TCA	2.12 ± 1.23	2.12 ± 0.93	0.03 ± 0.46	0.99	< 0.001[b]	< 0.001[a]
UDCA	2.41 ± 1.03	2.60 ± 1.05	2.05 ± 0.36	0.62	0.2	0.01[a]
GUDCA	2.59 ± 1.17	3.04 ± 1.14	1.64 ± 0.50	0.09	< 0.001[b]	< 0.001[a]
TUDCA	1.48 ± 1.07	1.84 ± 1.09	0.13 ± 0.25	0.15	< 0.001[b]	< 0.001[a]
CDCA	2.88 ± 0.39	3.07 ± 0.48	2.63 ± 0.38	0.046[c]	0.01[b]	< 0.001[a]

GCDCA	3.78 ± 0.80	3.79 ± 0.67	2.93 ± 0.33	0.96	< 0.001[b]	< 0.001[a]
TCDCA	2.73 ± 0.40	2.84 ± 0.44	2.49 ± 0.57	0.27	0.09	0.004[a]
GCDCS	2.39 ± 0.82	2.42 ± 0.70	1.08 ± 0.39	0.95	< 0.001[b]	< 0.001[a]
DCA	2.76 ± 0.35	2.75 ± 0.40	2.76 ± 0.18	0.87	0.7	0.59
GDCA	3.18 ± 0.58	3.14 ± 0.53	2.64 ± 0.32	0.8	< 0.001[b]	< 0.001[a]
TDCA	3.32 ± 0.64	3.16 ± 0.50	2.57 ± 0.19	0.33	< 0.001[b]	< 0.001[a]
LCA	0.94 ± 0.68	1.28 ± 0.66	0.72 ± 0.43	0.04[c]	0.14	< 0.001[a]
TLCA	0.30 ± 0.41	0.48 ± 0.47	0.02 ± 0.06	0.07	< 0.001[b]	< 0.001[a]
LCA + TLCA	1.25 ± 0.18	1.75 ± 0.14	0.74 ± 0.07	0.034[c]	0.031[b]	< 0.001[a]
CDCA/CA	1.30 ± 0.35	1.56 ± 0.65	1.74 ± 0.42	0.26	< 0.001[b]	< 0.001[a]
pBA	3.11 ± 0.45	3.17 ± 0.51	2.67 ± 0.38	0.98	< 0.001[b]	< 0.001[a]
sBA	3.14 ± 0.52	3.19 ± 0.61	2.87 ± 0.17	0.75	0.003[b]	0.002[a]
pBA/sBA	1.02 ± 0.18	1.01 ± 0.17	1.08 ± 0.13	0.85	0.087	< 0.001
sBA	2.77 ± 0.35	2.79 ± 0.40	2.77 ± 0.18	0.81	0.02[b]	0.003[a]
G-BA	4.14 ± 0.70	4.12 ± 0.64	3.16 ± 0.31	0.97	< 0.001[b]	< 0.001[a]
T-BA	3.58 ± 0.54	3.47 ± 0.46	2.89 ± 0.27	0.34	< 0.001[b]	< 0.001[a]
G-BA/T-BA	0.55 ± 0.34	0.65 ± 0.34	0.27 ± 0.30	0.25	< 0.001[b]	< 0.001[a]
total BA	36.31 ± 6.00	37.69 ± 7.40	24.80 ± 3.12	0.41	< 0.001[b]	0.026[a]

[a]$P < 0.05$ Primary biliary cirrhosis (PBC) *vs* control.
[b]$P < 0.05$ Autoimmune hepatitis (AIH) *vs* control.
[c]$P < 0.05$ PBC *vs* AIH
Bile acid (BA) levels are expressed in log10 concentrations. Statistically significant differences in BA concentrations between controls and patients were determined by the rank sums Mann-Whitney test. CA: Cholic acid; CDCA: Chenodeoxycholic acid; DCA: Deoxycholic acid; GCA: Glycocholic acid; GCDCA: Glycochenodeoxycholic acid; GCDCS: Glycochenodeoxycholic sulfate; GDCA: Glycodeoxycholic acid; GUDCA: Glycoursodeoxycholic acid; LCA: Lithocholic acid; TCA: Taurocholic acid; TCDCA: Taurochenodeoxycholic acid; TDCA: Taurodeoxycholic acid; TLCA: Taurolithocholic acid; TUDCA: Tauroursodeoxycholic acid; UDCA: Ursodeoxycholic acid; PBA: Primary bile acid; PBC: Primary biliary cirrhosis; AIH: Autoimmune hepatitis.

lactic acid, pyroglutamic acid, hypoxanthine, CPA (16:0/0:0), and MG [0:0/18:4 (6Z, 9Z, 12Z, 15Z)/0:0] significantly decreased in patients with AIH compared with those in HCs.

Quantification of targeted BAs specific to PBC and AIH

Recently, BAs have been shown to be potentially more effective biomarkers for PBC and AIH. Regarding the most abundant BAs in humans, the following 15 BAs were selected: CA, GCA, TCA, UDCA, GUDCA, TUDCA, CDCA, GCDCA, TCDCA, GCDCS, DCA, GDCA, TDCA, LCA, and TLCA. The levels of these 15 BAs were measured using the UPLC-QTOF-MS. The levels of all BAs in the disease group were higher than those in the control group, and the levels of glycine-bound cholic acid and tauro-bound cholic acid were elevated, shown in Supplementary Table 1.

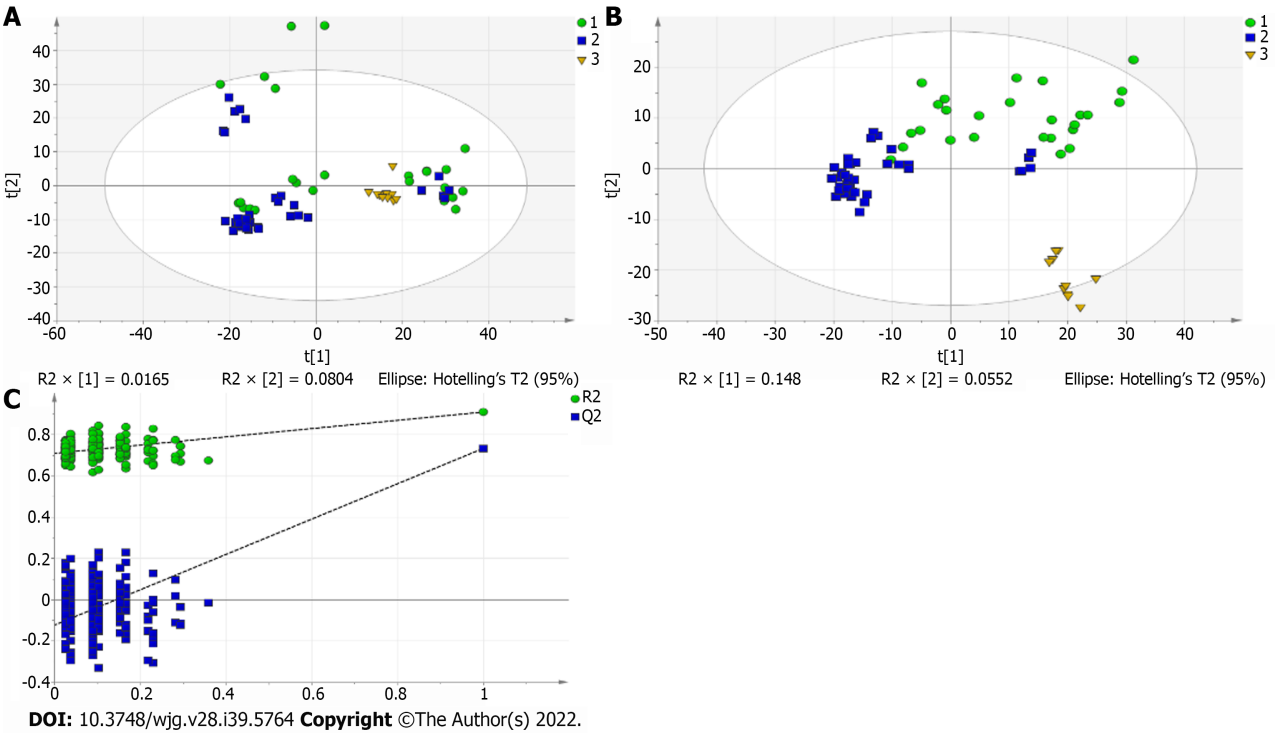
Furthermore, the levels of BAs in patients with PBC and AIH were compared with the corresponding levels in HCs, show in Table 5. It was revealed that the levels of BAs were elevated in patients with PBC and AIH. The levels of CDCA, LCA, TLCA, and LCA + TLCA in PBC patients were higher than those in AIH patients, in which a significant difference was found in the levels of CDCA and LCA ($P < 0.05$; for TLCA, $P = 0.0767$).The differences in the levels of CDCA, LCA, and LCA + TLCA among the three groups were statistically show in Figure 7. The levels of CDCA, LCA, and LCA + TLCA significantly increased in PBC patients compared with those in AIH patients ($P < 0.05$). Moreover, the CDCA-to-CA ratio decreased in PBC and AIH patients compared with that in HCs.

The receiver operating characteristic curve analysis of BAs with differences between the PBC and AIH groups showed that the area under the curve values of CDCA, LCA, and TLCA were greater than 0.7, and sensitivity was higher than 70%, indicating a high sensitivity, while a low specificity was noted in identification of patients with PBC and AIH (Figure 8 and Table 6). Compared with sensitivity and specificity of the traditional biochemical indicators, such as alanine transaminase, aspartate transaminase, gamma glutamyl transpeptidase, alkaline phosphatase, total bilirubin, direct bilirubin, and total bile acid, sensitivity and specificity of CDCA, LCA and TLCA were higher than the traditional markers of liver injury, which are of great significance for clinical diagnosis and can be further verified by enlarging the sample size. Thus, BAs can be potentially considered as markers for the diagnosis of PBC and AIH.

Table 6 Area under the curve, sensitivity and specificity of difference bile acids, conventional biochemical indicators in primary biliary cirrhosis, autoimmune hepatitis and control group

	AUC	Sensitivity	Specificity
LCA	0.68	0.82	0.50
LCA + TLCA	0.73	0.74	0.46
CDCA	0.74	0.74	0.54
AST	0.54	0.67	0.58
ALT	0.61	0.64	0.61
ALP	0.41	0.56	0.35
GGT	0.43	0.50	0.46
TBiL	0.53	0.59	0.42
DBiL	0.47	0.44	0.62
TBA	0.52	0.52	0.42

CDCA: Chenodeoxycholic acid; LCA: Lithocholic acid; TLCA: Taurolithocholic acid; ALT: Alanine transaminase; AST: Aspartate transaminase; GGT: Gamma glutamyl transpeptidase; ALP: Alkaline phosphatase; TBiL: Total bilirubin; DBiL: Direct bilirubin; TBA: Total bile acid; AUC: Area under the curve.

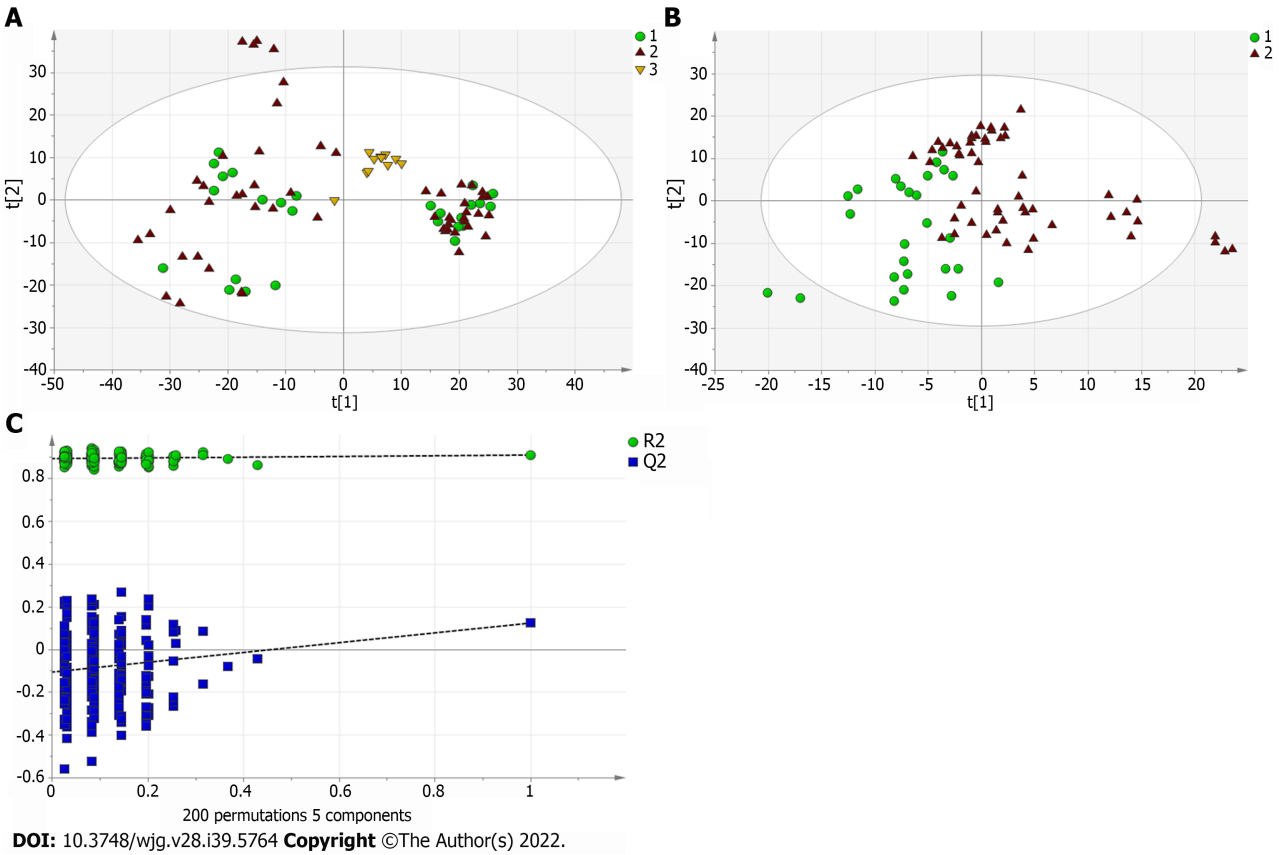


DOI: 10.3748/wjg.v28.i39.5764 **Copyright** ©The Author(s) 2022.

Figure 2 Multivariate statistical analysis on serum profiling data in positive ions between autoimmune hepatitis and control. A: Plots of principal component analysis in positive ion mode. (1) Autoimmune hepatitis (AIH); (2) Control; and (3) Quality control (QC); B: Scatter plots of partial least squares-discriminant analysis (PLS-DA) with a positive model of serum from patients with primary biliary cholangitis (PBC), AIH and healthy controls. (1) PBC; (2) Control; and (3) QC; C: Validation plot of the original PLS-DA with a positive model, strongly indicating that the original model is valid and shows signs of overfitting. The permutation test was repeated 200 times in the cross-validation plot.

DISCUSSION

In the present study, we established a diagnostic model for PBC and AIH using the UPLC-QTOF-MS. Besides, VIP values from PLS-DA were calculated to describe a quantitative estimation of the discriminatory power of each individual feature. We found changes in the levels of amino acids, BAs, organic acids, phospholipids, sugar, and sugar alcohols in patients with PBC and AIH, and in HCs. These substances are mainly involved in lipid metabolism, BA metabolism, and bilirubin metabolism, which



DOI: 10.3748/wjg.v28.i39.5764 **Copyright** ©The Author(s) 2022.

Figure 3 Multivariate statistical analysis on serum profiling data in positive ions between primary biliary cholangitis and autoimmune hepatitis. A: Plots of principal component analysis in positive ion mode. (1) Autoimmune hepatitis (AIH); (2) Primary biliary cholangitis (PBC); and (3) Quality control; B: Scatter plots of partial least squares-discriminant analysis (PLS-DA) with a positive model of serum from patients with PBC, AIH and healthy controls. (1) PBC; and (2) AIH; C: Validation plot of the original PLS-DA with a positive model, strongly indicating that the original model is valid and shows signs of overfitting. The permutation test was repeated 200 times in the cross-validation plot.

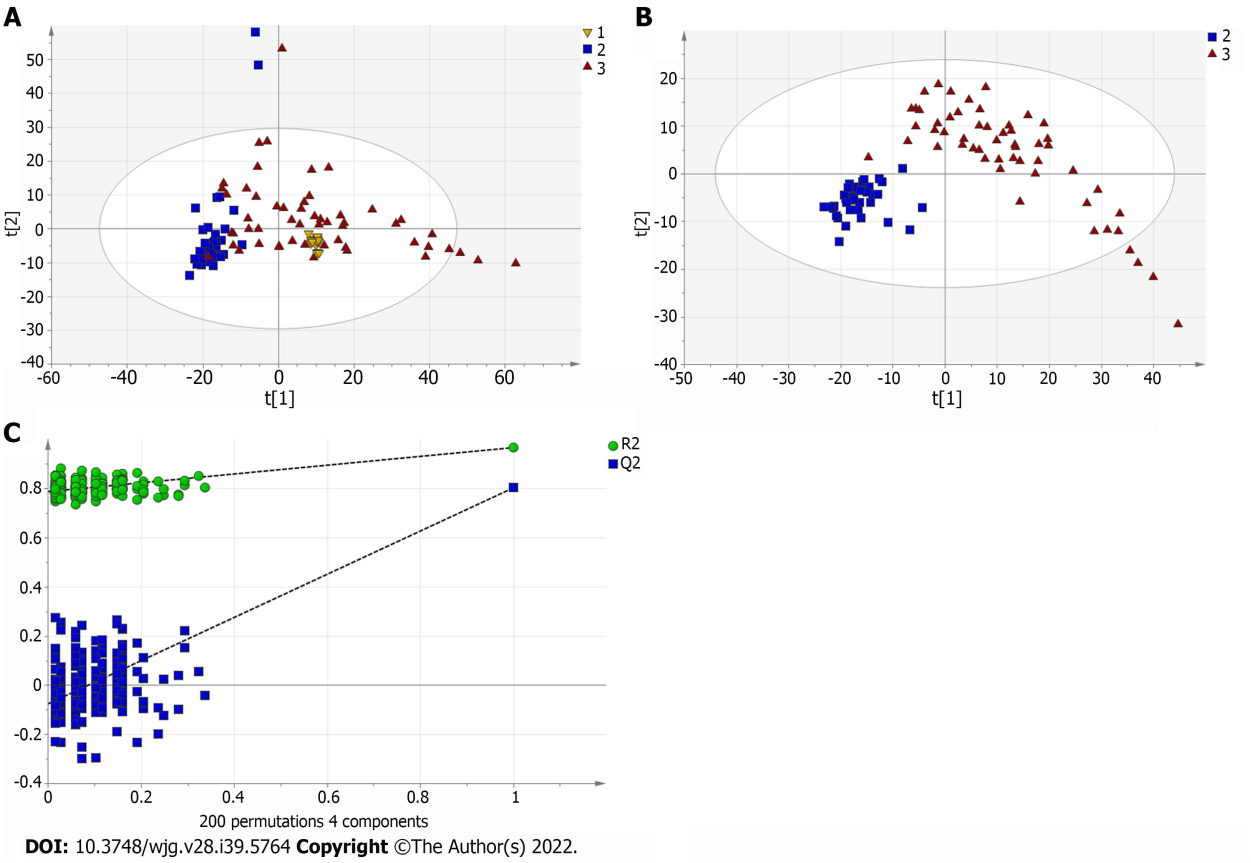
are related to metabolic functions of the liver and inflammatory reactions. These compound classes are also associated with key hepatic metabolic pathways. Importantly, our findings are consistent with those reported previously; for instance, BAs have been identified as a significant factor contributing to PBC[14-16]. When liver injury occurs, intrahepatic clearance rate of BAs decreases and serum BA level increases. BAs have long been used as markers of liver dysfunction. In recent studies, elevated serum levels of BAs have been found to be closely associated with liver diseases[17-21].

The levels of lysophosphatidylcholine (LPC) and lysophosphatidylethanolamine (LPE) significantly changed in patients with PBC and AIH. To date, no study has used lysophospholipids in the diagnosis of PBC and AIH. Lysophospholipids are biologically active lipids that are involved in a variety of important processes, including cell proliferation, cell migration, angiogenesis, and inflammation[22]. Our results also provided important clues to further explore the pathogenesis of PBC and AIH.

A discriminatory diagnostic model of PBC/AIH could not be established using the UPLC/MS/MS, suggesting that the changes of terminal metabolites in serum samples of patients with PBC and AIH were no special differences. Failure in the establishment of a discriminatory diagnostic model of PBC/AIH could be related to the sample size. Therefore, BAs were quantitatively analyzed according to the differences found between PBC/control and AIH/control groups.

BA is the general term used for a class of bisexual molecules produced by the metabolism of cholesterol. The liver has an effective clearance effect on BAs, and BAs are kept at low levels, confirming the low levels of BAs in the human peripheral blood plasma. In the human liver, cholesterol is metabolized into primary BAs, including CA and CDCA, and then into the intestine, followed by into the corresponding secondary show in Figure 9.

The results of our targeted metabolomic study of BAs showed that the levels of BAs increased in patients with PBC and AIH compared with those in HCs, and the levels of CDCA, LCA, and LCA + TLCA in PBC patients were significantly higher than those in AIH patients. It is noteworthy that CA and CDCA, the two major human BAs, are synthesized from cholesterol in a series of reactions catalyzed by enzymes located in the endoplasmic reticulum, mitochondria, cytosol, and peroxisomes, suggesting that there were significant differences in the levels of BAs in PBC patients, providing clues for the future study on the pathogenesis of PBC. In autoimmune liver diseases, the dysfunction of BA metabolism occurs after liver injury, which may be related to bile stasis after liver injury, especially in



DOI: 10.3748/wjg.v28.i39.5764 **Copyright** ©The Author(s) 2022.

Figure 4 Multivariate statistical analysis on serum profiling data in negative ions between primary biliary cholangitis and control. A: Plots of principal component analysis in negative ion mode. (1) Primary biliary cholangitis (PBC); (2) Control; and (3) Quality control (QC); B: Scatter plots of partial least squares-discriminant analysis (PLS-DA) with a negative model of serum from patients with PBC, autoimmune hepatitis and healthy controls. (1) PBC; (2) Control; and (3) QC; C: Validation plot of the original PLS-DA with a negative model, strongly indicating that the original model is valid and shows signs of overfitting. The permutation test was repeated 200 times in the cross-validation plot.

PBC, which is more drastic, and is related to the pathogenesis of PBC. After bile duct obstruction and sclerosis, BAs cannot be transported and metabolized normally. Patients may present with jaundice and itchy skin.

Therefore, determination of the levels of BAs in plasma can reflect the synthesis, ingestion, and secretion of hepatocytes. Abnormalities in the levels of BAs not only reflect the extent of liver damage, but also indirectly indicate the conditions of blood-bile barrier in the liver.

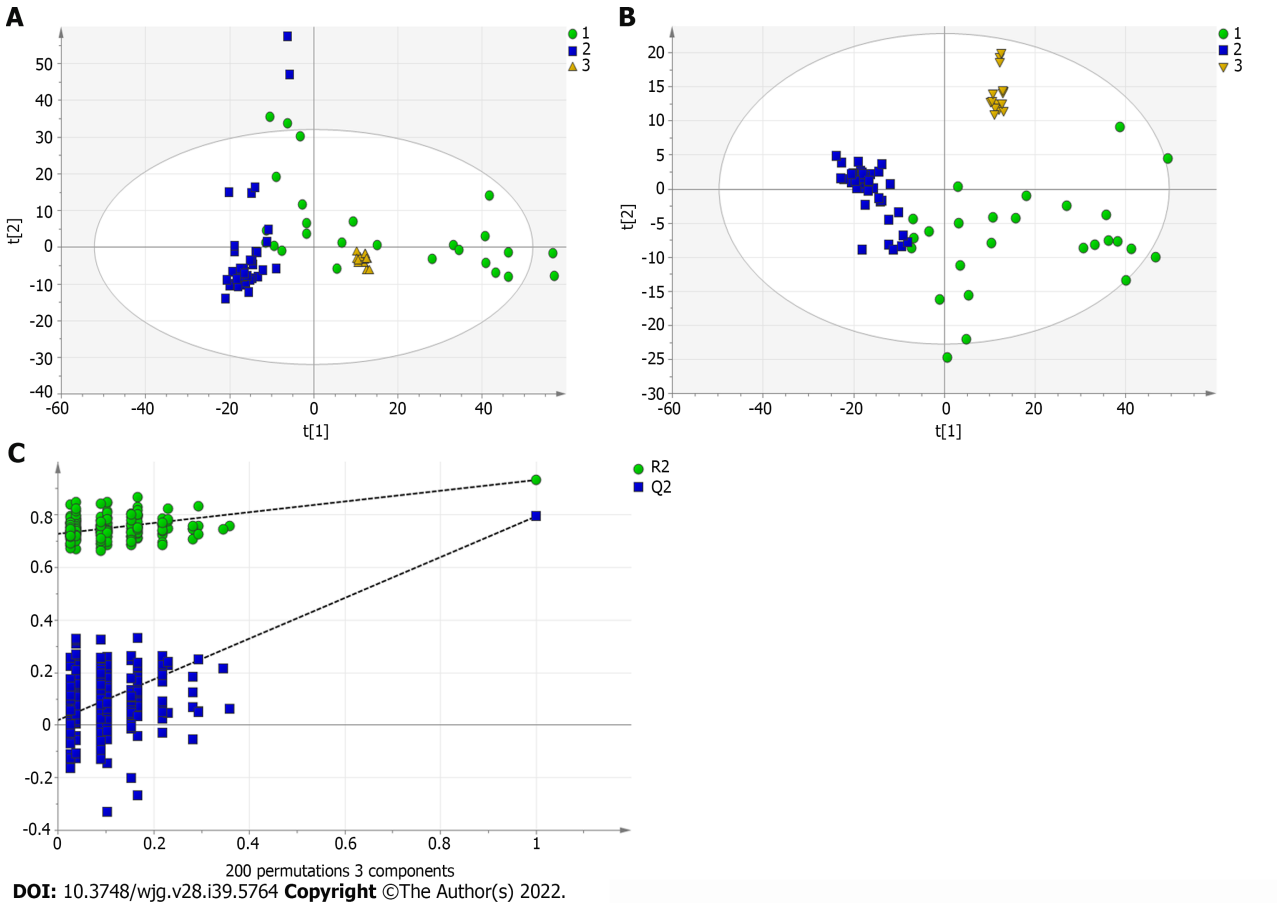
To our knowledge, this is the first study that used serum metabolic profiling for diagnosing patients with PBC and AIH.

LCA is an endogenous compound associated with hepatic toxicity during cholestasis. A previous study[23] revealed that LCA induced disruption of phospholipid/ sphingolipid homeostasis through the transforming growth factor-β signaling pathway and serum LPC could be a biomarker for biliary injury.

The hepatic level of LCA was reported to elevate in patients with cholestatic liver disease[24,25]. This result is consistent with our finding, in which the levels of CDCA, LCA, TLCA, and LCA + TLCA were higher in PBC patients than those in AIH patients.

Previous studies[26,27] indicated that the activation of cytochrome P450 is correlated with Farnesoid X receptor (FXR). Mammalian FXR, which is a transcription regulatory factor in bile salt synthesis, is activated by BAs, such as CDCA or LCA[28,29]. The derangements of lipid metabolism are weakened in FXR-null mice compared with those in wild-type mice after LCA exposure[30,31]. As a cholestatic liver disease, the high levels of BAs may induce FXR gene transcription in PBC patients. Therefore, we hypothesized that these pathways may lead to LCA poisoning in PBC patients, and LCA metabolic pathway plays an important role in the incidence of PBC. Lian *et al*[14] used the untargeted metabolomic method of UPLC-MS, and clarified the relationship between LCA level and PBC incidence, as well as the relationship between LCA level and the incidence of lipid metabolism disorders. Our study also revealed the abnormal levels of LPC and LPE in PBC patients.

However, the retention of hydrophobic BAs in pathophysiological conditions, such as cholestatic diseases, plays an important role in liver injury by inducing apoptosis or necrosis of hepatocytes[32]. The retention and accumulation of hydrophobic Bas (*e.g.*, CDCA and DCA)inside hepatocytes during cholestasis have long been implicated as a major cause of liver dysfunction[32].



DOI: 10.3748/wjg.v28.i39.5764 **Copyright** ©The Author(s) 2022.

Figure 5 Multivariate statistical analysis on serum profiling data in negative ions between autoimmune hepatitis and control. A: Plots of principal component analysis in negative ion mode. (1) Autoimmune hepatitis (AIH); (2) Control; and (3) Quality control (QC); B: Scatter plots of partial least squares-discriminant analysis (PLS-DA) with a negative model of serum from patients with Primary biliary cholangitis, AIH and healthy controls. (1) Autoimmune hepatitis (AIH); (2) Control; and (3) QC; C: Validation plot of the original PLS-DA with a negative model, strongly indicating that the original model is valid and shows signs of overfitting. The permutation test was repeated 200 times in the cross-validation plot.

The hydrophobicity of BAs is an important determinant of the toxicity and protection of BAs. Under normal conditions, the levels of BAs undergoing further biotransformations to dianionic glucuronidated or sulfated derivatives are negligible, although they may become important in cholestasis[33].

Several mechanisms may be involved in the cytotoxicity associated with the most hydrophobic BAs in cholestatic liver diseases[32]. BAs could disrupt cell membranes through their detergent action on lipid components[34] and promote the generation of reactive oxygen species that, in turn, oxidatively modify lipids, proteins, and nucleic acids, and eventually cause hepatocyte apoptosis[35].

As shown in Figure 9 CDCA/LCA/TLCA are all related to the decomposition and hydrolysis of bacteria in the intestine. CDCA is decomposed into LCA through bacteria in the intestine, and then, synthesizes TLCA through the intestinal bacteria. Intestinal bacteria may play a key role in this process. Therefore, we can hypothesize that dysfunction of intestinal bacteria may increase the incidence of autoimmune liver diseases, including PBC. Lv *et al*[36] and Zheng *et al*[37] found that the interaction of intestinal microflora with metabolism and immunity is crucial for the occurrence or development of PBC.

The Child-Pugh scoring system was used to classify PBC and AIH patients according to their Child-Pugh scores, show in Supplementary Table 2 and the levels of BAs in these patients with Child-Pugh scores were statistically show in Table 7. It was found that the levels of GCA, TCA, GCDCA, GCDCS, TDCA, and tauro-conjugated BAs were gradually elevated with the increase of Child-Pugh scores. The levels of BAs in PBC patients with Child-Pugh class C were significantly different from those in PBC patients with Child-Pugh class A ($P < 0.05$). The levels of BAs in AIH patients with Child-Pugh class B were significantly different from those in PBC patients with Child-Pugh class A ($P < 0.05$). The levels of GCA, GCDCS, and TDCA significantly differed in PBC and AIH patients with Child-Pugh class B (Figure 10). These BAs are all conjugated BAs, suggesting that the levels of conjugated BAs are elevated in patients with severe liver injury. The determination of BA level can not only reflect liver damage, but also indicate the degree of liver damage, which is similar to the results of our previous study on drug-induced liver injury (DILI)[38]. The increase in the levels of GCA, TCA, TUDCA, GCDCA, GCDCS, and TDCA was corresponded to a higher degree of DILI. Tang *et al*[15] used UPLC/Q-TOF-MS to analyze

Table 7 Changes of the serum bile acid profile between primary biliary cirrhosis and autoimmune hepatitis in different grade of Child-Pugh

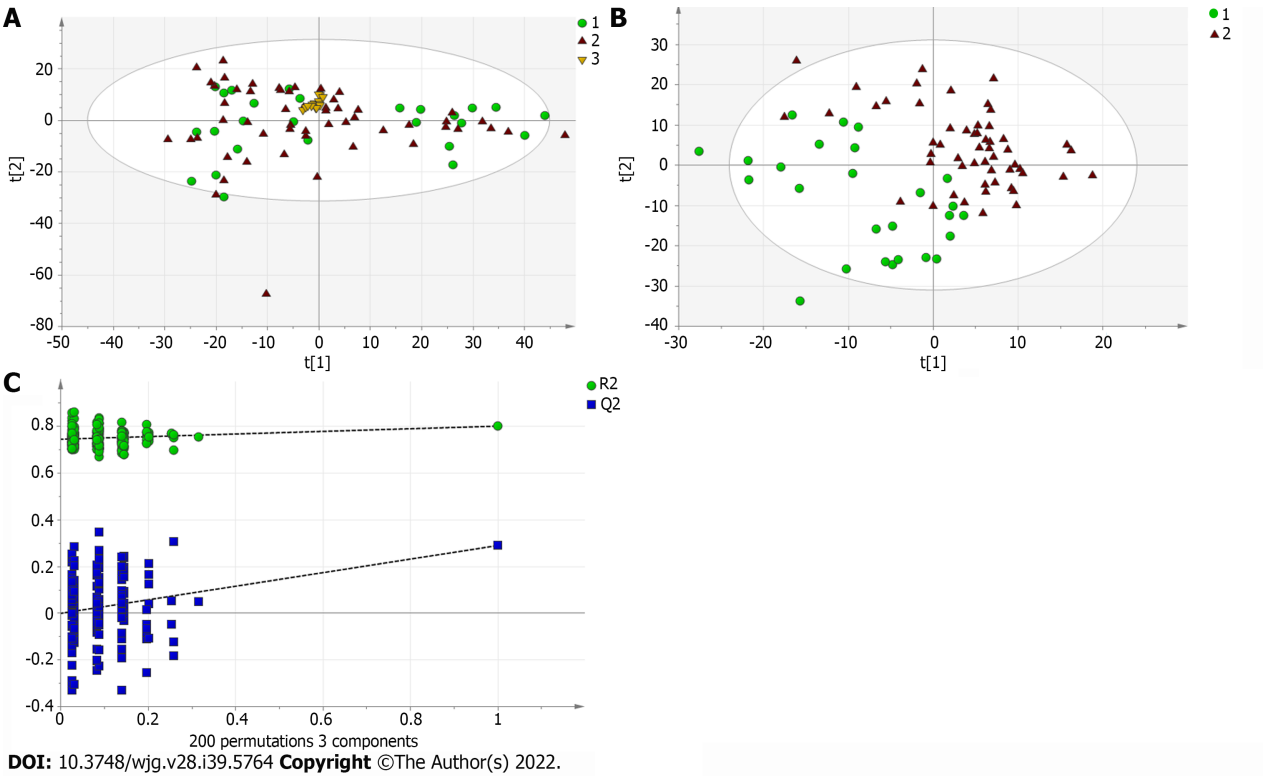
	AIH-A/PBC/A	AIH-B/PBC-B	AIH-A/AIH-B	PBC-A/PBC-B	PBC-B/PBC-C	PBC-A/PBC-C	AIH-A/control	AIH-B/control	PBC-A/control	PBC-B/control	PBC-C/control
	P value	*P* value	*P* value	*P* value	*P* value	*P* value	*P* value	*P* value	*P* value	*P* value	*P* value
CA	0.75	0.34	0.24	0.67	0.82	0.50	< 0.001	< 0.001	< 0.001	< 0.001	0.03
GCA	0.79	0.03	< 0.001	0.07	0.43	0.02	< 0.001	< 0.001	< 0.001	< 0.001	< 0.001
TCA	0.79	0.03	< 0.001	0.0522	0.71	0.0567	< 0.001	< 0.001	< 0.001	< 0.001	< 0.001
UDCA	0.77	0.26	0.07	0.70	0.30	0.38	< 0.001	0.52	<0.001	0.05	< 0.001
GUDCA	0.60	0.33	0.40	0.58	0.21	0.06	< 0.001	0.13	< 0.001	< 0.001	< 0.001
TUDCA	0.97	0.22	1.00	0.10	0.29	0.02	< 0.001	< 0.001	< 0.001	< 0.001	< 0.001
CDCA	0.26	0.09	0.07	0.30	0.44	0.78	< 0.001	0.47	< 0.001	< 0.001	< 0.001
GCDCA	0.89	0.19	0.01	0.06	0.17	< 0.001	< 0.001	< 0.001	< 0.001	< 0.001	< 0.001
TCDCA	0.82	0.20	0.31	0.34	0.92	0.26	0.05	0.48	0.02	0.01	0.04
GCDCS	0.33	0.04	< 0.001	0.15	0.24	0.01	< 0.001	< 0.001	< 0.001	< 0.001	< 0.001
DCA	0.71	0.26	0.02	0.13	0.66	0.38	0.24	0.01	0.64	0.21	0.45
GDCA	0.50	0.08	0.09	0.37	0.09	0.11	< 0.001	< 0.001	< 0.001	0.01	< 0.001
TDCA	0.69	0.03	< 0.001	0.01	0.33	< 0.001	< 0.001	< 0.001	< 0.001	< 0.001	< 0.001
LCA	0.29	0.13	0.57	0.82	0.24	0.33	0.08	0.51	< 0.001	< 0.001	< 0.001
TLCA	0.07	0.88	0.05	0.13	0.74	0.29	0.01	< 0.001	< 0.001	< 0.001	< 0.001
CDCA/CA	0.46	0.04	0.04	0.66	0.50	0.27	< 0.001	< 0.001	< 0.001	0.06	0.26
Primary bile acid	0.75	0.81	0.96	0.42	0.70	0.96	< 0.001	0.02	< 0.001	< 0.001	< 0.001
Secondary bile acid	0.92	0.80	0.20	0.33	0.20	0.45	< 0.001	0.45	< 0.001	0.15	< 0.001
Secondary/primary	0.61	0.99	0.32	0.27	0.23	0.44	0.30	0.05	0.06	0.01	0.78
Secondary bile acid	0.89	0.91	0.08	0.05	0.24	0.79	0.13	0.08	0.09	0.12	0.35
Glycoconjugates	0.53	0.16	< 0.001	0.21	0.16	< 0.001	< 0.001	< 0.001	< 0.001	< 0.001	< 0.001
Tauroconjugted	0.48	0.08	< 0.001	0.02	0.42	< 0.001	< 0.001	< 0.001	< 0.001	< 0.001	< 0.001
Glyco/tauro	0.21	0.56	0.23	0.63	0.07	0.18	0.01	< 0.001	< 0.001	< 0.001	< 0.001
Total BA	0.62	0.72	0.05	0.26	0.19	0.01	< 0.001	< 0.001	< 0.001	< 0.001	< 0.001

Bile acid (BA) levels are expressed in log10 concentrations. Statistically significant differences in BA concentrations between controls and patients were determined by the rank sums Mann-Whitney test. CA: Cholic acid; CDCA: Chenodeoxycholic acid; DCA: Deoxycholic acid; GCA: Glycocholic acid; GCDCA: Glycochenodeoxycholic acid; GCDCS: Glycochenodeoxycholic sulfate; GDCA: Glycodeoxycholic acid; GUDCA: Glycoursodeoxycholic acid; LCA: Lithocholic acid; TCA: Taurocholic acid; TCDCA: Taurochenodeoxycholic acid; TDCA: Taurodeoxycholic acid; TLCA: Taurolithocholic acid; TUDCA: Tauroursodeoxycholic acid; UDCA: Ursodeoxycholic acid; PBA: Primary bile acid; PBC: Primary biliary cirrhosis; AIH: Autoimmune hepatitis.

the metabolic groups of blood and urine in 32 pairs of PBC patients and HCs. It was found that the BA level increased with the PBC progression, while the higher accuracy of our findings was confirmed. Elevated levels of BAs are correlated with severity of a variety of diseases. BAs can be used as a factor to judge the severity of the disease and as a basis for the diagnosis of the disease. It is necessary to further expand the sample size for research.

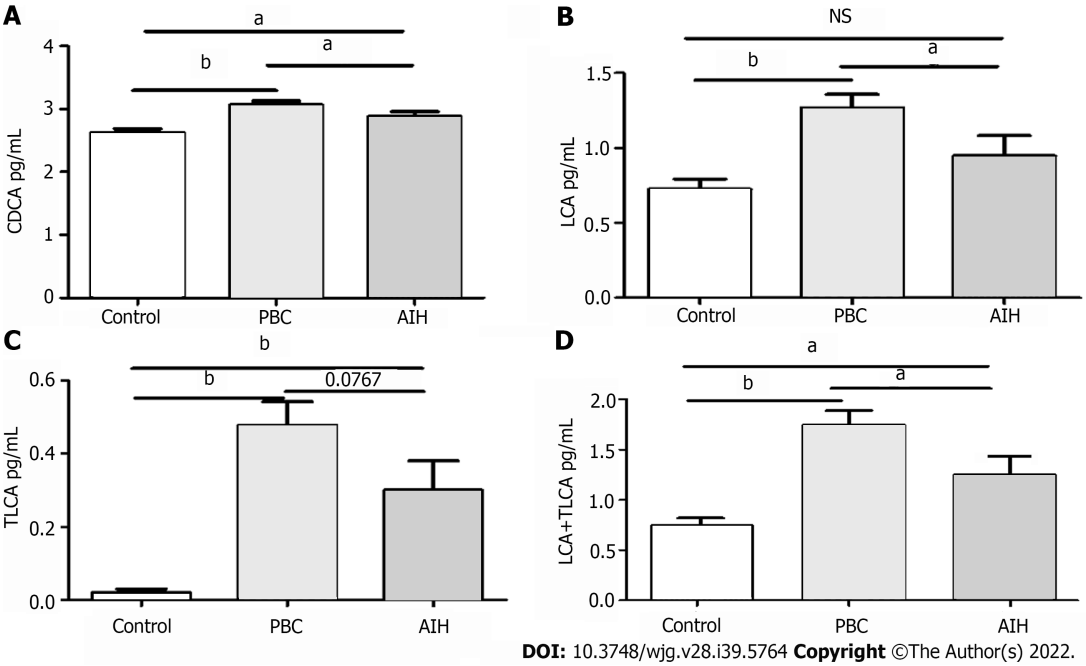
CONCLUSION

A discriminatory diagnostic model for PBC and AIH using UPLC-QTOF-MS was established. Besides, differential metabolomics analysis was conducted using the PLS-DA model to screen the differentially expressed substances in the different groups. The changes in the levels of BAs, LPC, LPE, bilirubin, and



DOI: 10.3748/wjg.v28.i39.5764 **Copyright** ©The Author(s) 2022.

Figure 6 Multivariate statistical analysis on serum profiling data in negative ions between primary biliary cholangitis and autoimmune hepatitis. A: Plots of principal component analysis in negative ion mode. (1) Autoimmune hepatitis (AIH); (2) Primary biliary cholangitis (PBC); and (3) Quality control; B: Scatter plots of partial least squares-discriminant analysis (PLS-DA) with a negative model of serum from patients with PBC, AIH and healthy controls. (1) AIH; and (2) PBC; C: Validation plot of the original PLS-DA with a negative model, strongly indicating that the original model is valid and shows signs of overfitting. The permutation test was repeated 200 times in the cross-validation plot.

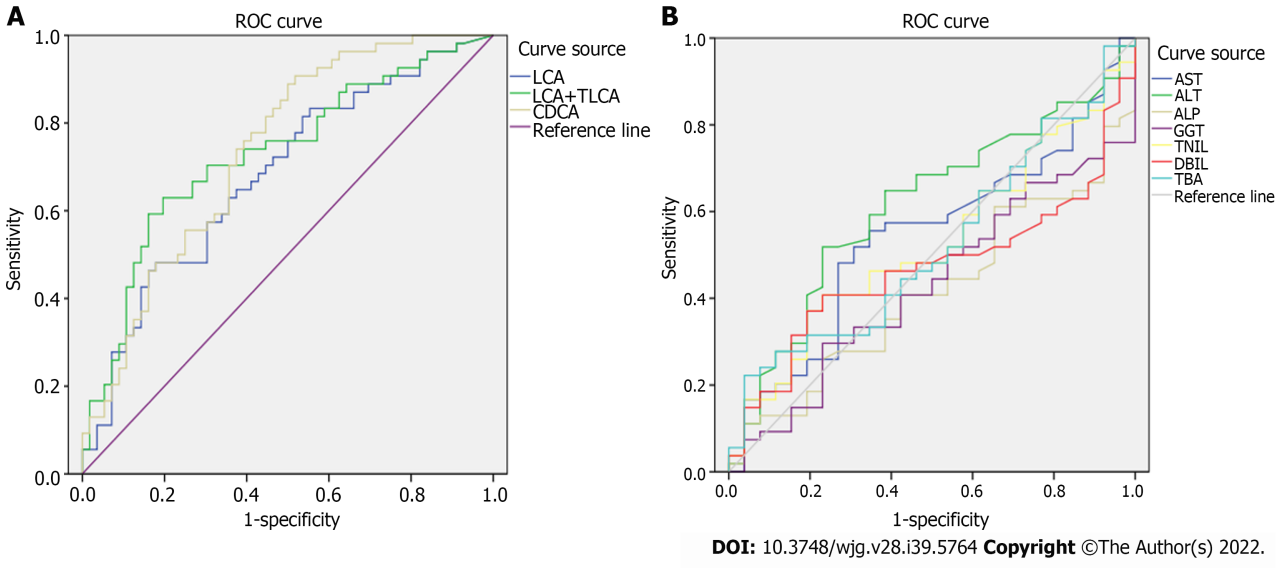


DOI: 10.3748/wjg.v28.i39.5764 **Copyright** ©The Author(s) 2022.

Figure 7 Comparative analysis of alterations in serum bile acid levels in patients in the mild and severe injury groups, and in healthy controls. A: Chenodeoxycholic acid; B: Lithocholic acid (LCA); C: Taurolithocholic acid (TLCA); D: LCA + TLCA; $^{a}P < 0.05$; $^{b}P < 0.0001$; NS: Not significant.

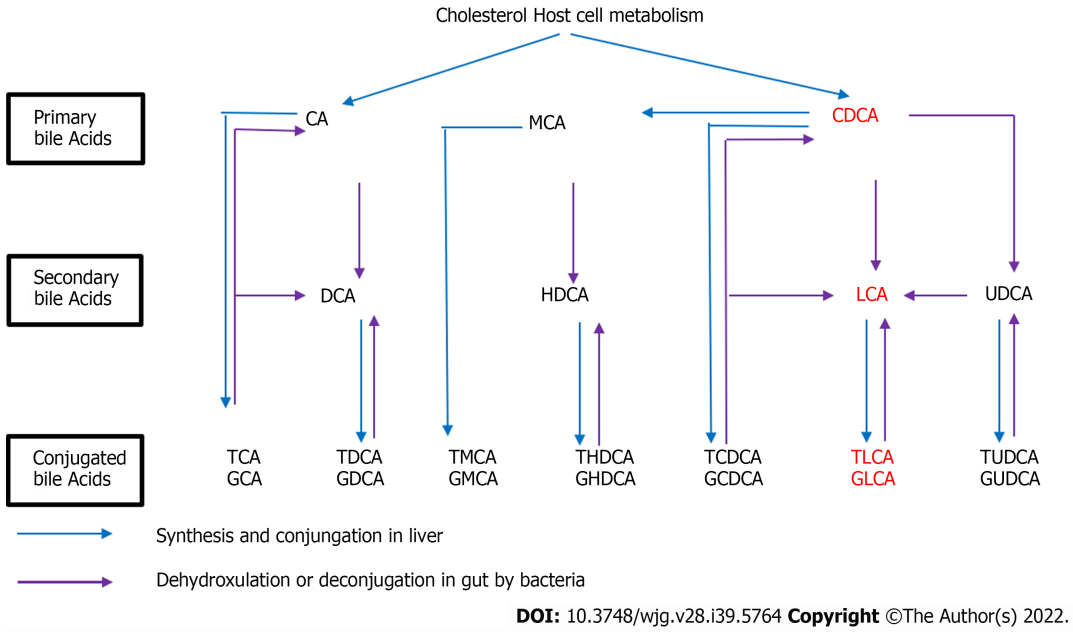
phytosphingosine in PBC and AIH patients and HCs were compared.

The levels of CDCA, LCA, TLCA, and LCA + TLCA significantly increased in the PBC group compared with those in the AIH group. These results suggested that the levels of BAs can be used as a marker to differentiate PBC from AIH, and the results may be advantageous to study the pathogenesis



DOI: 10.3748/wjg.v28.i39.5764 **Copyright** ©The Author(s) 2022.

Figure 8 Receiver operating characteristic curve analysis. A: Lithocholic acid (LCA), sum of LCA and taurolithocholic acid, chenodeoxycholic acid; B: Common clinical biochemical indicators.

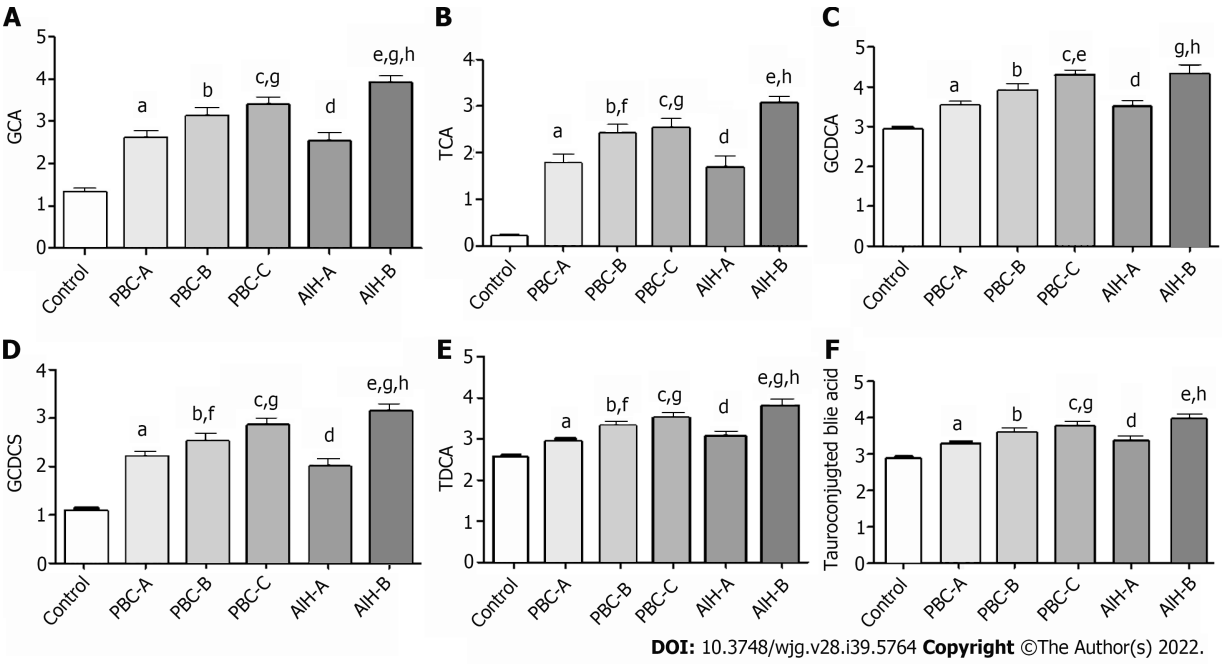


DOI: 10.3748/wjg.v28.i39.5764 **Copyright** ©The Author(s) 2022.

Figure 9 Cholesterol host cell metabolism. CA: Cholic acid; CDCA: Chenodeoxycholic acid; DCA: Deoxycholic acid; TCA: Taurocholic acid; GCA: Glycocholic acid; TDCA: Taurodeoxycholic acid; GDCA: Glycodeoxycholic acid; TCDCA: Taurochenodeoxycholic acid; TLCA: Taurolithocholic acid; TUDCA: Tauroursodeoxycholic acid.

of PBC/AIH in the future.

In conclusion, this study revealed that in patients with PBC and AIH, there were significant differences in serum levels of BAs. However, due to the existence of some limitations (*i.e.*, the small sample size, the lack of staging methods for PBC and AIH, and phenotypic information), further study with a larger sample size is required to eliminate the above-mentioned limitations and to confirm the findings.



DOI: 10.3748/wjg.v28.i39.5764 **Copyright** ©The Author(s) 2022.

Figure 10 Bile acid levels are expressed in log10 concentrations. Statistically significant differences in bile acid concentrations between controls and patients were determined by the rank sums Mann-Whitney test. Primary biliary cholangitis (PBC)-A *vs* control, $^{a}P < 0.05$; PBC-B *vs* control, $^{b}P < 0.05$; PBC-C *vs* control, $^{c}P < 0.05$; autoimmune hepatitis (AIH)-A *vs* control, $^{d}P < 0.05$; AIH-B *vs* control, $^{e}P < 0.05$; PBC-A *vs* PBC-B, $^{f}P < 0.05$; PBC-A *vs* PBC-C, $^{g}P < 0.05$; AIH-A *vs* AIH-B, $^{h}P < 0.05$; PBC-A *vs* AIH-A. A: Glycocholic acid; B: Taurocholic acid; C: Glycochenodeoxycholic acid; D: Glycochenodeoxycholic sulfate; E: Taurodeoxycholic acid; F: Tauroconjugted bile acid. GCDCA: Glycochenodeoxycholic acid; GCDCS: Glycochenodeoxycholic sulfate; TDCA: Taurodeoxycholic acid; GCA: Glycocholic acid; TCA: Taurocholic acid.

ARTICLE HIGHLIGHTS

Research background

Primary biliary cholangitis (PBC) and autoimmune hepatitis (AIH) are two unexplained immune diseases. It is difficult to identify and Liver biopsy should be done.

Research motivation

Avoid liver perforation and relieve the pain of patient, to improve the diagnostic rate of PBC and AIH.

Research objectives

To determine non-invasive, reliable, and sensitive biochemical markers for the differential diagnosis of PBC and AIH.

Research methods

Metabolomics technologies, including full-contour metabolomics and target.

Research results

We revealed the increased levels of chenodeoxycholic acid, lithocholic acid (LCA), taurolithocholic acid (TLCA), and LCA + TLCA in the PBC group compared with those in the AIH group. The levels of glycochenodeoxycholic acid, glycochenodeoxycholic sulfate, and taurodeoxycholic acid were gradually elevated with the increase of Child-Pugh class, which was correlated with the severity of disease.

Research conclusions

The levels of bile acids could serve as potential biomarkers for the early diagnosis and assessment of the severity of PBC and AIH.

Research perspectives

It is necessary to further expand the sample size for research and search for the mechanism for the changes.

ACKNOWLEDGEMENTS

Thanks to Dalian Chemical Institute for providing the test site and technical guidance.

FOOTNOTES

Author contributions: Niu JQ contributed to conception and design of the research, review and editing; Ma ZH, Sun LC, and Li P contributed to investigation and wrote the manuscript; Ma ZH, Wang XM, and Wu RH contributed to acquisition of data and statistical analysis; Hao DL contributed to funding acquisition; all authors have read and approve the final manuscript.

Supported by Health and Family Planning Commission Project of Jilin Province, No. 2016Q043; and Health and Hygiene Committee Project of Jilin Province, No. 2021LC082.

Institutional review board statement: The study protocol was carefully reviewed and approved by the Institutional Review Board (IRB) of the Affiliated Hospital of the Medical School of Jilin University, No. 2009-017.

Informed consent statement: All the eligible patients and HCs signed the written informed consent form prior to enrollment.

Conflict-of-interest statement: All the authors report no relevant conflicts of interest for this article.

Data sharing statement: No additional data are available.

STROBE statement: The authors have read the STROBE Statement—checklist of items, and the manuscript was prepared and revised according to the STROBE Statement—checklist of items.

Open-Access: This article is an open-access article that was selected by an in-house editor and fully peer-reviewed by external reviewers. It is distributed in accordance with the Creative Commons Attribution NonCommercial (CC BY-NC 4.0) license, which permits others to distribute, remix, adapt, build upon this work non-commercially, and license their derivative works on different terms, provided the original work is properly cited and the use is non-commercial. See: https://creativecommons.org/Licenses/by-nc/4.0/

Country/Territory of origin: China

ORCID number: Xiao-Mei Wang 0000-0003-2606-4013; Jun-Qi Niu 0000-0001-5415-2024.

S-Editor: Fan JR
L-Editor: A
P-Editor: Cai YX

REFERENCES

1 **Biewenga M**, Farina Sarasqueta A, Tushuizen ME, de Jonge-Muller ESM, van Hoek B, Trouw LA. The role of complement activation in autoimmune liver disease. *Autoimmun Rev* 2020; **19**: 102534 [PMID: 32234403 DOI: 10.1016/j.autrev.2020.102534]
2 **He XS**, Ansari AA, Ridgway WM, Coppel RL, Gershwin ME. New insights to the immunopathology and autoimmune responses in primary biliary cirrhosis. *Cell Immunol* 2006; **239**: 1-13 [PMID: 16765923 DOI: 10.1016/j.cellimm.2006.04.006]
3 **Dumas ME**, Davidovic L. Metabolic Profiling and Phenotyping of Central Nervous System Diseases: Metabolites Bring Insights into Brain Dysfunctions. *J Neuroimmune Pharmacol* 2015; **10**: 402-424 [PMID: 25616565 DOI: 10.1007/s11481-014-9578-5]
4 **Clayton TA**, Lindon JC, Cloarec O, Antti H, Charuel C, Hanton G, Provost JP, Le Net JL, Baker D, Walley RJ, Everett JR, Nicholson JK. Pharmaco-metabonomic phenotyping and personalized drug treatment. *Nature* 2006; **440**: 1073-1077 [PMID: 16625200 DOI: 10.1038/nature04648]
5 **Blow N**. Metabolomics: Biochemistry's new look. *Nature* 2008; **455**: 697-700 [PMID: 18833281 DOI: 10.1038/455697a]
6 **Yin P**, Wan D, Zhao C, Chen J, Zhao X, Wang W, Lu X, Yang S, Gu J, Xu G. A metabonomic study of hepatitis B-induced liver cirrhosis and hepatocellular carcinoma by using RP-LC and HILIC coupled with mass spectrometry. *Mol Biosyst* 2009; **5**: 868-876 [PMID: 19603122 DOI: 10.1039/b820224a]
7 **Tokushige K**, Hashimoto E, Kodama K, Tobari M, Matsushita N, Kogiso T, Taniai M, Torii N, Shiratori K, Nishizaki Y, Ohga T, Ohashi Y, Sato T. Serum metabolomic profile and potential biomarkers for severity of fibrosis in nonalcoholic fatty liver disease. *J Gastroenterol* 2013; **48**: 1392-1400 [PMID: 23478936 DOI: 10.1007/s00535-013-0766-5]
8 **Barr J**, Caballería J, Martínez-Arranz I, Domínguez-Díez A, Alonso C, Muntané J, Pérez-Cormenzana M, García-Monzón C, Mayo R, Martín-Duce A, Romero-Gómez M, Lo Iacono O, Tordjman J, Andrade RJ, Pérez-Carreras M, Le Marchand-Brustel Y, Tran A, Fernández-Escalante C, Arévalo E, García-Unzueta M, Clement K, Crespo J, Gual P, Gómez-Fleitas M,

Martínez-Chantar ML, Castro A, Lu SC, Vázquez-Chantada M, Mato JM. Obesity-dependent metabolic signatures associated with nonalcoholic fatty liver disease progression. *J Proteome Res* 2012; **11**: 2521-2532 [PMID: 22364559 DOI: 10.1021/pr201223p]

9 **Hao J**, Yang T, Zhou Y, Gao GY, Xing F, Peng Y, Tao YY, Liu CH. Serum Metabolomics Analysis Reveals a Distinct Metabolic Profile of Patients with Primary Biliary Cholangitis. *Sci Rep* 2017; **7**: 784 [PMID: 28400566 DOI: 10.1038/s41598-017-00944-9]

10 **Sreekumar A**, Poisson LM, Rajendiran TM, Khan AP, Cao Q, Yu J, Laxman B, Mehra R, Lonigro RJ, Li Y, Nyati MK, Ahsan A, Kalyana-Sundaram S, Han B, Cao X, Byun J, Omenn GS, Ghosh D, Pennathur S, Alexander DC, Berger A, Shuster JR, Wei JT, Varambally S, Beecher C, Chinnaiyan AM. Metabolomic profiles delineate potential role for sarcosine in prostate cancer progression. *Nature* 2009; **457**: 910-914 [PMID: 19212411 DOI: 10.1038/nature07762]

11 **Alvarez F**, Berg PA, Bianchi FB, Bianchi L, Burroughs AK, Cancado EL, Chapman RW, Cooksley WG, Czaja AJ, Desmet VJ, Donaldson PT, Eddleston AL, Fainboim L, Heathcote J, Homberg JC, Hoofnagle JH, Kakumu S, Krawitt EL, Mackay IR, MacSween RN, Maddrey WC, Manns MP, McFarlane IG, Meyer zum Büschenfelde KH, Zeniya M. International Autoimmune Hepatitis Group Report: review of criteria for diagnosis of autoimmune hepatitis. *J Hepatol* 1999; **31**: 929-938 [PMID: 10580593 DOI: 10.1016/s0168-8278(99)80297-9]

12 **Silveira MG**, Brunt EM, Heathcote J, Gores GJ, Lindor KD, Mayo MJ. American Association for the Study of Liver Diseases endpoints conference: design and endpoints for clinical trials in primary biliary cirrhosis. *Hepatology* 2010; **52**: 349-359 [PMID: 20578151 DOI: 10.1002/hep.23637]

13 **Yin P**, Zhao X, Li Q, Wang J, Li J, Xu G. Metabonomics study of intestinal fistulas based on ultraperformance liquid chromatography coupled with Q-TOF mass spectrometry (UPLC/Q-TOF MS). *J Proteome Res* 2006; **5**: 2135-2143 [PMID: 16944924 DOI: 10.1021/pr060256p]

14 **Lian JS**, Liu W, Hao SR, Chen DY, Wang YY, Yang JL, Jia HY, Huang JR. A serum metabolomic analysis for diagnosis and biomarker discovery of primary biliary cirrhosis and autoimmune hepatitis. *Hepatobiliary Pancreat Dis Int* 2015; **14**: 413-421 [PMID: 26256087 DOI: 10.1016/s1499-3872(15)60393-9]

15 **Tang YM**, Wang JP, Bao WM, Yang JH, Ma LK, Yang J, Chen H, Xu Y, Yang LH, Li W, Zhu YP, Cheng JB. Urine and serum metabolomic profiling reveals that bile acids and carnitine may be potential biomarkers of primary biliary cirrhosis. *Int J Mol Med* 2015; **36**: 377-385 [PMID: 26046127 DOI: 10.3892/ijmm.2015.2233]

16 **Chen W**, Wei Y, Xiong A, Li Y, Guan H, Wang Q, Miao Q, Bian Z, Xiao X, Lian M, Zhang J, Li B, Cao Q, Fan Z, Zhang W, Qiu D, Fang J, Gershwin ME, Yang L, Tang R, Ma X. Comprehensive Analysis of Serum and Fecal Bile Acid Profiles and Interaction with Gut Microbiota in Primary Biliary Cholangitis. *Clin Rev Allergy Immunol* 2020; **58**: 25-38 [PMID: 30900136 DOI: 10.1007/s12016-019-08731-2]

17 **Yang L**, Xiong A, He Y, Wang Z, Wang C, Li W, Yang L, Hu Z. Bile acids metabonomic study on the CCl4- and alpha-naphthylisothiocyanate-induced animal models: quantitative analysis of 22 bile acids by ultraperformance liquid chromatography-mass spectrometry. *Chem Res Toxicol* 2008; **21**: 2280-2288 [PMID: 19053324 DOI: 10.1021/tx800225q]

18 **Monte MJ**, Marin JJ, Antelo A, Vazquez-Tato J. Bile acids: chemistry, physiology, and pathophysiology. *World J Gastroenterol* 2009; **15**: 804-816 [PMID: 19230041 DOI: 10.3748/wjg.15.804]

19 **Perez MJ**, Briz O. Bile-acid-induced cell injury and protection. *World J Gastroenterol* 2009; **15**: 1677-1689 [PMID: 19360911 DOI: 10.3748/wjg.15.1677]

20 **Gilat T**, Leikin-Frenkel A, Goldiner I, Juhel C, Lafont H, Gobbi D, Konikoff FM. Prevention of diet-induced fatty liver in experimental animals by the oral administration of a fatty acid bile acid conjugate (FABAC). *Hepatology* 2003; **38**: 436-442 [PMID: 12883488 DOI: 10.1053/jhep.2003.50348]

21 **Kobayashi N**, Katsumata H, Uto Y, Goto J, Niwa T, Kobayashi K, Mizuuchi Y. A monoclonal antibody-based enzyme-linked immunosorbent assay of glycolithocholic acid sulfate in human urine for liver function test. *Steroids* 2002; **67**: 827-833 [PMID: 12231118 DOI: 10.1016/s0039-128x(02)00036-3]

22 **Goetzl EJ**. Pleiotypic mechanisms of cellular responses to biologically active lysophospholipids. *Prostaglandins Other Lipid Mediat* 2001; **64**: 11-20 [PMID: 11324701 DOI: 10.1016/s0090-6980(01)00104-6]

23 **Matsubara T**, Tanaka N, Patterson AD, Cho JY, Krausz KW, Gonzalez FJ. Lithocholic acid disrupts phospholipid and sphingolipid homeostasis leading to cholestasis in mice. *Hepatology* 2011; **53**: 1282-1293 [PMID: 21480330 DOI: 10.1002/hep.24193]

24 **Fischer S**, Beuers U, Spengler U, Zwiebel FM, Koebe HG. Hepatic levels of bile acids in end-stage chronic cholestatic liver disease. *Clin Chim Acta* 1996; **251**: 173-186 [PMID: 8862472 DOI: 10.1016/0009-8981(96)06305-x]

25 **Setchell KD**, Rodrigues CM, Clerici C, Solinas A, Morelli A, Gartung C, Boyer J. Bile acid concentrations in human and rat liver tissue and in hepatocyte nuclei. *Gastroenterology* 1997; **112**: 226-235 [PMID: 8978363 DOI: 10.1016/s0016-5085(97)70239-7]

26 **Akiyama TE**, Gonzalez FJ. Regulation of P450 genes by liver-enriched transcription factors and nuclear receptors. *Biochim Biophys Acta* 2003; **1619**: 223-234 [PMID: 12573481 DOI: 10.1016/s0304-4165(02)00480-4]

27 **Krasowski MD**, Ni A, Hagey LR, Ekins S. Evolution of promiscuous nuclear hormone receptors: LXR, FXR, VDR, PXR, and CAR. *Mol Cell Endocrinol* 2011; **334**: 39-48 [PMID: 20615451 DOI: 10.1016/j.mce.2010.06.016]

28 **Eloranta JJ**, Kullak-Ublick GA. The role of FXR in disorders of bile acid homeostasis. *Physiology (Bethesda)* 2008; **23**: 286-295 [PMID: 18927204 DOI: 10.1152/physiol.00020.2008]

29 **Hofmann AF**. Detoxification of lithocholic acid, a toxic bile acid: relevance to drug hepatotoxicity. *Drug Metab Rev* 2004; **36**: 703-722 [PMID: 15554243 DOI: 10.1081/dmr-200033475]

30 **Bogdanos DP**, Invernizzi P, Mackay IR, Vergani D. Autoimmune liver serology: current diagnostic and clinical challenges. *World J Gastroenterol* 2008; **14**: 3374-3387 [PMID: 18528935 DOI: 10.3748/wjg.14.3374]

31 **Kitada H**, Miyata M, Nakamura T, Tozawa A, Honma W, Shimada M, Nagata K, Sinal CJ, Guo GL, Gonzalez FJ, Yamazoe Y. Protective role of hydroxysteroid sulfotransferase in lithocholic acid-induced liver toxicity. *J Biol Chem* 2003; **278**: 17838-17844 [PMID: 12637555 DOI: 10.1074/jbc.M210634200]

32 **Attili AF**, Angelico M, Cantafora A, Alvaro D, Capocaccia L. Bile acid-induced liver toxicity: relation to the hydrophobic-hydrophilic balance of bile acids. *Med Hypotheses* 1986; **19**: 57-69 [PMID: 2871479 DOI: 10.1016/0306-9877(86)90137-4]

33 **Javitt NB**. Cholesterol, hydroxycholesterols, and bile acids. *Biochem Biophys Res Commun* 2002; **292**: 1147-1153 [PMID: 11969205 DOI: 10.1006/bbrc.2001.2013]

34 **Billington D**, Evans CE, Godfrey PP, Coleman R. Effects of bile salts on the plasma membranes of isolated rat hepatocytes. *Biochem J* 1980; **188**: 321-327 [PMID: 7396866 DOI: 10.1042/bj1880321]

35 **Sokol RJ**, Straka MS, Dahl R, Devereaux MW, Yerushalmi B, Gumpricht E, Elkins N, Everson G. Role of oxidant stress in the permeability transition induced in rat hepatic mitochondria by hydrophobic bile acids. *Pediatr Res* 2001; **49**: 519-531 [PMID: 11264436 DOI: 10.1203/00006450-200104000-00014]

36 **Lv LX**, Fang DQ, Shi D, Chen DY, Yan R, Zhu YX, Chen YF, Shao L, Guo FF, Wu WR, Li A, Shi HY, Jiang XW, Jiang HY, Xiao YH, Zheng SS, Li LJ. Alterations and correlations of the gut microbiome, metabolism and immunity in patients with primary biliary cirrhosis. *Environ Microbiol* 2016; **18**: 2272-2286 [PMID: 27243236 DOI: 10.1111/1462-2920.13401]

37 **Zheng Y**, Ran Y, Zhang H, Wang B, Zhou L. The Microbiome in Autoimmune Liver Diseases: Metagenomic and Metabolomic Changes. *Front Physiol* 2021; **12**: 715852 [PMID: 34690796 DOI: 10.3389/fphys.2021.715852]

38 **Ma Z**, Wang X, Yin P, Wu R, Zhou L, Xu G, Niu J. Serum metabolome and targeted bile acid profiling reveals potential novel biomarkers for drug-induced liver injury. *Medicine (Baltimore)* 2019; **98**: e16717 [PMID: 31374067 DOI: 10.1097/MD.0000000000016717]



Published by **Baishideng Publishing Group Inc**
7041 Koll Center Parkway, Suite 160, Pleasanton, CA 94566, USA
Telephone: +1-925-3991568
E-mail: bpgoffice@wjgnet.com
Help Desk: https://www.f6publishing.com/helpdesk
https://www.wjgnet.com



© 2022 Baishideng Publishing Group Inc. All rights reserved.

ISSN 1007-9327 (print)
ISSN 2219-2840 (online)

World Journal of *Gastroenterology*

World J Gastroenterol 2022 October 28; 28(40): 5784-5892



Published by Baishideng Publishing Group Inc

World Journal of Gastroenterology

Contents

Weekly Volume 28 Number 40 October 28, 2022

MINIREVIEWS

5784 Heterogeneity of immune control in chronic hepatitis B virus infection: Clinical implications on immunity with interferon-α treatment and retreatment

Yin GQ, Chen KP, Gu XC

5801 Interaction between gut microbiota and COVID-19 and its vaccines

Leung JSM

5807 Improving the prognosis before and after liver transplantation: Is muscle a game changer?

Goffaux A, Delorme A, Dahlqvist G, Lanthier N

5818 Management of liver diseases: Current perspectives

Ray G

5827 Pancreatic acinar cell carcinoma: A comprehensive review

Calimano-Ramirez LF, Daoud T, Gopireddy DR, Morani AC, Waters R, Gumus K, Klekers AR, Bhosale PR, Virarkar MK

ORIGINAL ARTICLE

Basic Study

5845 Expression of the methylcytosine dioxygenase ten-eleven translocation-2 and connexin 43 in inflammatory bowel disease and colorectal cancer

El-Harakeh M, Saliba J, Sharaf Aldeen K, Haidar M, El Hajjar L, Awad MK, Hashash JG, Shirinian M, El-Sabban M

5865 Curcumin alleviates experimental colitis *via* a potential mechanism involving memory B cells and Bcl-6-Syk-BLNK signaling

Wei SY, Wu TT, Huang JQ, Kang ZP, Wang MX, Zhong YB, Ge W, Zhou BG, Zhao HM, Wang HY, Liu DY

Observational Study

5881 Liver transplantation is beneficial regardless of cirrhosis stage or acute-on-chronic liver failure grade: A single-center experience

Cervantes-Alvarez E, Vilatoba M, Limon-de la Rosa N, Mendez-Guerrero O, Kershenobich D, Torre A, Navarro-Alvarez N

World Journal of Gastroenterology

Weekly Volume 28 Number 40 October 28, 2022

Contents

ABOUT COVER

Editorial Board of *World Journal of Gastroenterology*, Julio Mayol, MD, PhD, Professor, Surgeon, Department of Surgery, Universidad Complutense de Madrid Medical School, Hospital Clinico San Carlos, Madrid 28040, Spain. jmayol@ucm.es

AIMS AND SCOPE

The primary aim of *World Journal of Gastroenterology* (*WJG*, *World J Gastroenterol*) is to provide scholars and readers from various fields of gastroenterology and hepatology with a platform to publish high-quality basic and clinical research articles and communicate their research findings online. *WJG* mainly publishes articles reporting research results and findings obtained in the field of gastroenterology and hepatology and covering a wide range of topics including gastroenterology, hepatology, gastrointestinal endoscopy, gastrointestinal surgery, gastrointestinal oncology, and pediatric gastroenterology.

INDEXING/ABSTRACTING

The *WJG* is now abstracted and indexed in Science Citation Index Expanded (SCIE, also known as SciSearch®), Current Contents/Clinical Medicine, Journal Citation Reports, Index Medicus, MEDLINE, PubMed, PubMed Central, Scopus, Reference Citation Analysis, China National Knowledge Infrastructure, China Science and Technology Journal Database, and Superstar Journals Database. The 2022 edition of Journal Citation Reports® cites the 2021 impact factor (IF) for *WJG* as 5.374; IF without journal self cites: 5.187; 5-year IF: 5.715; Journal Citation Indicator: 0.84; Ranking: 31 among 93 journals in gastroenterology and hepatology; and Quartile category: Q2. The *WJG*'s CiteScore for 2021 is 8.1 and Scopus CiteScore rank 2021: Gastroenterology is 18/149.

RESPONSIBLE EDITORS FOR THIS ISSUE

Production Editor: *Yu-Xi Chen*; **Production Department Director:** *Xu Guo*; **Editorial Office Director:** *Jia-Ru Fan*.

NAME OF JOURNAL
World Journal of Gastroenterology

ISSN
ISSN 1007-9327 (print) ISSN 2219-2840 (online)

LAUNCH DATE
October 1, 1995

FREQUENCY
Weekly

EDITORS-IN-CHIEF
Andrzej S Tarnawski

EDITORIAL BOARD MEMBERS
http://www.wjgnet.com/1007-9327/editorialboard.htm

PUBLICATION DATE
October 28, 2022

COPYRIGHT
© 2022 Baishideng Publishing Group Inc

INSTRUCTIONS TO AUTHORS
https://www.wjgnet.com/bpg/gerinfo/204

GUIDELINES FOR ETHICS DOCUMENTS
https://www.wjgnet.com/bpg/GerInfo/287

GUIDELINES FOR NON-NATIVE SPEAKERS OF ENGLISH
https://www.wjgnet.com/bpg/gerinfo/240

PUBLICATION ETHICS
https://www.wjgnet.com/bpg/GerInfo/288

PUBLICATION MISCONDUCT
https://www.wjgnet.com/bpg/gerinfo/208

ARTICLE PROCESSING CHARGE
https://www.wjgnet.com/bpg/gerinfo/242

STEPS FOR SUBMITTING MANUSCRIPTS
https://www.wjgnet.com/bpg/GerInfo/239

ONLINE SUBMISSION
https://www.f6publishing.com

© 2022 Baishideng Publishing Group Inc. All rights reserved. 7041 Koll Center Parkway, Suite 160, Pleasanton, CA 94566, USA
E-mail: bpgoffice@wjgnet.com https://www.wjgnet.com

World Journal of Gastroenterology

Submit a Manuscript: https://www.f6publishing.com

World J Gastroenterol 2022 October 28; 28(40): 5784-5800

DOI: 10.3748/wjg.v28.i40.5784

ISSN 1007-9327 (print) ISSN 2219-2840 (online)

MINIREVIEWS

Heterogeneity of immune control in chronic hepatitis B virus infection: Clinical implications on immunity with interferon-α treatment and retreatment

Guo-Qing Yin, Ke-Ping Chen, Xiao-Chun Gu

Specialty type: Gastroenterology and hepatology

Provenance and peer review: Unsolicited article; Externally peer reviewed.

Peer-review model: Single blind

Peer-review report's scientific quality classification

Grade A (Excellent): 0
Grade B (Very good): 0
Grade C (Good): C, C
Grade D (Fair): 0
Grade E (Poor): 0

P-Reviewer: Jha P, United States; Leowattana W, Thailand

Received: May 10, 2022
Peer-review started: May 10, 2022
First decision: August 20, 2022
Revised: September 8, 2022
Accepted: October 9, 2022
Article in press: October 9, 2022
Published online: October 28, 2022

Guo-Qing Yin, Ke-Ping Chen, Xiao-Chun Gu, Center of Hepatology, Zhong-Da Hospital, Southeast University, Nanjing 210009, Jiangsu Province, China

Corresponding author: Guo-Qing Yin, MD, PhD, Chief Doctor, Chief Physician, Center of Hepatology, Zhong-Da Hospital, Southeast University, No. 87 Dingjiaqiao, Nanjing 210009, Jiangsu Province, China. yingq62@sina.com

Abstract

Hepatitis B virus (HBV) infection is a global public health issue. Interferon-α (IFN-α) treatment has been used to treat hepatitis B for over 20 years, but fewer than 5% of Asians receiving IFN-α treatment achieve functional cure. Thus, IFN-α retreatment has been introduced to enhance antiviral function. In recent years, immune-related studies have found that the complex interactions between immune cells and cytokines could modulate immune response networks, including both innate and adaptive immunity, triggering immune responses that control HBV replication. However, heterogeneity of the immune system to control HBV infection, particularly HBV-specific $CD8^+$ T cell heterogeneity, has consequential effects on T cell-based immunotherapy for treating HBV infection. Altogether, the host's genetic variants, negative-feedback regulators and HBV components affecting the immune system's ability to control HBV. In this study, we reviewed the literature on potential immune mechanisms affecting the immune control of HBV and the clinical effects of IFN-α treatment and retreatment.

Key Words: Hepatitis B virus; Chronic; Functional cure; Heterogeneity; Immunity; Immune control; Interferon-α; Retreatment

©The Author(s) 2022. Published by Baishideng Publishing Group Inc. All rights reserved.

Core Tip: Hepatitis B virus (HBV)-specific immune control is characterized by distinct phenotypical and functional profiles. Owing to the negative feedback associated with all immune responses in an infected host, immunomodulators regulating a single immune pathway are unlikely to fully restore antiviral immunity. Interferon-α (IFN-α) treatment was shown to simultaneously affect multiple immune pathways and various immune cell populations in the host and integrate signals toward improving HBV-specific immune control. In addition, IFN-α retreatment was shown to improved functional cure rates, indicating that could gradually enhance the overall immune control.

Citation: Yin GQ, Chen KP, Gu XC. Heterogeneity of immune control in chronic hepatitis B virus infection: Clinical implications on immunity with interferon-α treatment and retreatment. *World J Gastroenterol* 2022; 28(40): 5784-5800
URL: https://www.wjgnet.com/1007-9327/full/v28/i40/5784.htm
DOI: https://dx.doi.org/10.3748/wjg.v28.i40.5784

INTRODUCTION

Hepatitis B virus (HBV) infection is a major global health problem. It is estimated that over 257 million people are suffering from chronic hepatitis B (CHB) infection[1]. After being infected by HBV, the virus transfers its genome into the nucleus of hepatocytes, where it is converted into covalently closed circular DNA (cccDNA), which has two major roles: Acting as a template for virus replication and acting as a reservoir for long-term virus preservation. Some studies have found that cccDNA persists in the hepatocytes of patients even decades after HBV infection has been resolved[2]. Further, it was shown that part of the viral genome remained integrated into the genomic DNA of the host's hepatocytes. Therefore, targeted eradication of cccDNA and viral genome in hepatocytes is regarded as the holy grail for curing HBV[3-5], which has not yet been achieved with current therapies.

HBV infection induces various immune responses that lead to heterogeneous immune control associated with the HBV infection[5,6]. Acute HBV infection can be terminated by the host's adaptive immune responses, characterized by multi-specific and vigorous HBV-specific $CD8^+$ T cell responses. In contrast, during CHB infection, the adaptive immune responses are severely depressed due to exhausted or reduced HBV-specific $CD8^+$ T-cells[6,7] and dysfunctions in HBV-specific B cells[7-9]. Researchers have noticed different outcomes from HBV infection in different populations and races.

Most CHB cases in the Asian population occur during infancy or childhood. However, asymptomatic infection during childhood makes it very challenging for authorities to determine when the infection actually occurred. Further, due to the uncertain timing of hepatitis flares and disease phases, there is little research on this topic in past literature, and little is known about hepatitis flares and intrahepatic immunity. Recently, studies on the partial immune mechanism in CHB have been performed, and important discoveries were made[2-6].

Currently, CHB is treated with nucleoside/nucleotide analogs (NAs) or interferon-α (IFN-α). NAs can target HBV polymerase/reverse transcriptase, inhibit HBV replication and are better tolerated by patients, but they cannot target cccDNA and unavoidably often results in NAs resistance and associated mutations. Since NAs do not directly influence immune response, functional cure with NAs is rarely achieved. In contrast, IFN-α treatment enhances HBV-specific immune control and can result in a partial or functional cure. However, due to poor efficacy with single course IFN-α treatment, since 1996, researchers have begun using IFN-α retreatment to improve the antiviral efficacy in CHB patients[10-15] or sufferers from NAs multi-drugs resistance[15-18].

In this present article, we reviewed the complex interactions between immune cells and cytokines of the immune response network against HBV, the correlation between host genetic variations and hepatitis B, the interplay between HBV components and HBV-specific immune control, and the heterogeneity of HBV-specifical immune control. Based on this foundation, we also discussed the underlying mechanism of IFN-α treatment and retreatment for improved HBV-specific immune control.

HETEROGENEOUS IMMUNITIES DURING HBV INFECTION

The innate and adaptive immunity work together to control immune responses against HBV. Innate immunity is not HBV antigen-specific but still produces T-cell polarizing and inflammatory cytokines that alter the intrahepatic microenvironment for presenting HBV antigens to naïve T cells to establish HBV-specific immunity. In recent years, researchers have recognized adaptive immunity as a crucial player for persistent and efficient immune control of HBV infection, which comprises a complex web of effector cell types. HBV-specific T cells help clearing HBV-infected hepatocytes and reduce the levels of circulating virus, while B cells neutralize viral particles and prevent reinfection[3,19-22]. Thus, their

levels ultimately determine the outcome of the disease.

The liver is an immunologically tolerant organ in which most immune cells are suppressed to limit hypersensitivity of immune responses against organ damage and local antigens. Thus, in a healthy state, the proportion of immune cells within the liver is much lower than in the peripheral blood. The difference in immune statuses between the liver and peripheral blood is defined as "immune compartmentalization". Investigations into the effects of costimulation have shown that Toll-like receptors (TLRs) and Treg cells participate in the intrahepatic immunopathogenesis in patients with HBV infection[3,23-25].

Recognition of HBV components by the innate immunity

Non-specific recognition of HBV components occurs at the molecular/subcellular level by innate immunosensors, namely pathogen-recognition receptors (PRRs) that recognize pathogen-associated molecular patterns (PAMP). The main PRRs that sense viral infection consists of retinoic acid-inducible gene I (RIG-I)-like receptors, nucleotide-binding oligomerization domain-containing protein-like receptors, TLRs, DNA-sensing receptors and C-type Lectin. These PRRs are expressed in epithelial cells, endothelial cells and immune cells. When PRRs interact with their cognate PAMP, downstream signaling pathways cascade, including adaptor/co-adaptor molecules, kinases and transcription factors are activated. This leads to the expression of interferon-stimulated genes (ISGs) and NFκB-inducible or pro-inflammatory genes, and various inflammatory cytokines are secreted. Primary cytokines include various classes of IFNs, pro-inflammatory cytokines and chemokines. These cytokines recruit various immune cells to the HBV-infected site, causing direct or indirect antiviral actions. These immune responses induce T cell proliferation and increase the efficiency of HBV-specific CD8+ T cells[21,26,27]. In particular, TLRs in hepatocytes and hepatic non-parenchymal cells (NPCs) have been shown to play vital roles in antiviral immunity. Currently, the use of TLR agonists as therapeutic agents to treat CHB is being validated[7].

In addition to cytokines, innate effector cells also participate in the control of HBV infection. Innate effector cells, including natural killer (NK) cells, γδT cells and mucosal-associated invariant T cells, can restrain the virus but are not specific for controlling HBV. Activated NK cells can induce inflammation in the liver, while activated T cells can be killed by NK cells, thereby reducing HBV-specific T cells. Although NK cells can suppress HBV replication, their activity was shown to be inhibited by transforming growth factor β (TGF-β) and IL-10 in CHB patients[3]. In addition, hepatic PCs, such as KCs and liver sinusoidal endothelial cells, can stimulate innate and adaptive immunity against HBV infection[28,29].

In short, the activation of innate immunity can lead to the production of cytokines, enhance antigen presentation, alter the intrahepatic microenvironment and trigger adaptive immunity (Figure 1).

HBV infection and adaptive immunity

HBV-specific T cells play a vital role in controlling HBV infection, and their immune responses can lead to the resolution of HBV replication. In acute hepatitis B patients, spontaneous viral clearance can occur *via* multi-specific $CD8^+$ T cell responses against HBV components[3,30]. In contrast, in CHB, the patients suffer from the exhaustion of HBV-specific $CD8^+$ T-cell responses throughout the HBV infection. Thus, most research on immune dysfunction focus on the activity of T cells, including $CD8^+$ and $CD4^+$ T-cells.

CHB is associated with the exhaustion of HBV-specific $CD8^+$ T-cells, marked by compromising functionality, such as reduced production of antiviral cytokines and immunodulatory cytokines and impaired proliferative capacities, defined as T-cell exhaustion[31,32]. HBV-specific $CD8^+$ T-cell exhaustion can be induced by: (1) Gradual aggravation of $CD8^+$ T-cells dysfunction and decreasing inflammatory cytokines production; (2) Increase in checkpoint inhibitors and immunosuppressive cytokines; (3) Epigenetic alterations leading to unrecoverable $CD8^+$ T-cell functions; (4) Alterations in $CD8^+$ T-cell phenotype; (5) Mitochondrial dysfunction and glycolysis downregulation, (6) Decrease in cell detection rate; and (7) Terminal exhaustion and physical deletion of HBV-specific $CD8^+$ T-cells.

In acute hepatitis B, $CD4^+$ T-cells have an important but indirect role in cleaning the virus. Th1-polarized $CD4^+$ T-cells regulate and maintain $CD8^+$ T-cell responses, contributing to HBV clearance. In contrast, during chronic HBV infection, the activation and upregulation of $CD4^+CD25^+$ Treg-cells suppress effective antiviral immune responses by inhibiting IFN-γ secretion, which inhibits the proliferation and cytokine secretion of $CD4^+$ and $CD8^+$ T-cells[7,30]. Figure 1 illustrates the complex interactions between immune cells and cytokine within the immune response network. The immune cells and their related cytokines are presented in Table 1.

HBV components inhibit innate and acquired immunity

HBV is believed to have existed in the human population for thousands of years and evolved with humans. During this evolution process, HBV has developed a particular lifecycle based on its unique replication mode through cccDNA and viral components that can adapt and suppress its host's immunity. Although the innate immunity can differentiate between different HBV components, HBV virion, antigens and peptides are still able to attack the TLR signaling pathway, resulting in negligible ISGs or IFNs secretions[4,7].

Table 1 Immune cells and their corresponding cytokines released

Immune cells	Released cytokines
NK cells	IFN-γ, TNF-α, IL-10
NKT cells	IFN-γ, IL-4, IL-13
Monocytes	IFN-γ, TNF-α, IL-10
Macrophages	IFN-γ, IL-6, MCP-1, IL-1β, TNF-α, CXCL10
γδT cells	IL-17, TNF-α
HSCs	IL-1β, IL-6, TGF-β
Kupffer cells	IL-10, TGF-β, IL-12, IL-6, TNF-α
$CD8^+$ T cells	IFN-γ, TNF-α, IL-2, IL-10, IL-17, IL-21
CD4+ T cells	IFN-γ, IL-21,IL-17
Regulatory T cells	IL-10, TGF-β, IL-35
Regulatory B cells	IL-10

HSCs: Hepatic stellate cells; IL: Interleukin; TGF-β: Transforming growth factor β; TNF-α: Tumor necrosis factor-α; IFN-γ: Interferon-γ; NK: Natural killer.

Among the ISGs is the apolipoprotein B editing complex (APOBEC) gene. APOBEC3A/B has been shown to cause cccDNA degradation, while APOBEC3G can inhibit HBV replication. However, APOBEC3G expression is often reduced by HBsAg[32].

A viral protein known for influencing HBV replication is HBx. It can interact with the cellular proteins in hepatocytes to increase viral replication by impairing IFN signaling and enhancing HBV gene expression[33-35]. Further, it was shown that HBV antigens could inhibit $CD8^+$ T-cell efficiency. Antagonist functions may provide a means for HBV to escape immune detection. Considering that certain $CD8^+$ T-cell epitopes in hepatitis B core antigen (HBcAg) or HBsAg can act as T-cell receptor (TCR) antagonists, their binding to TCR can lead to the suppression of $CD8^+$ T-cell response, thus decreasing their efficiency (Figure 2). In addition, the chronicity of HBV infection was shown to be promoted by HBeAg *via* the induction of $CD8^+$ T-cell tolerance[36].

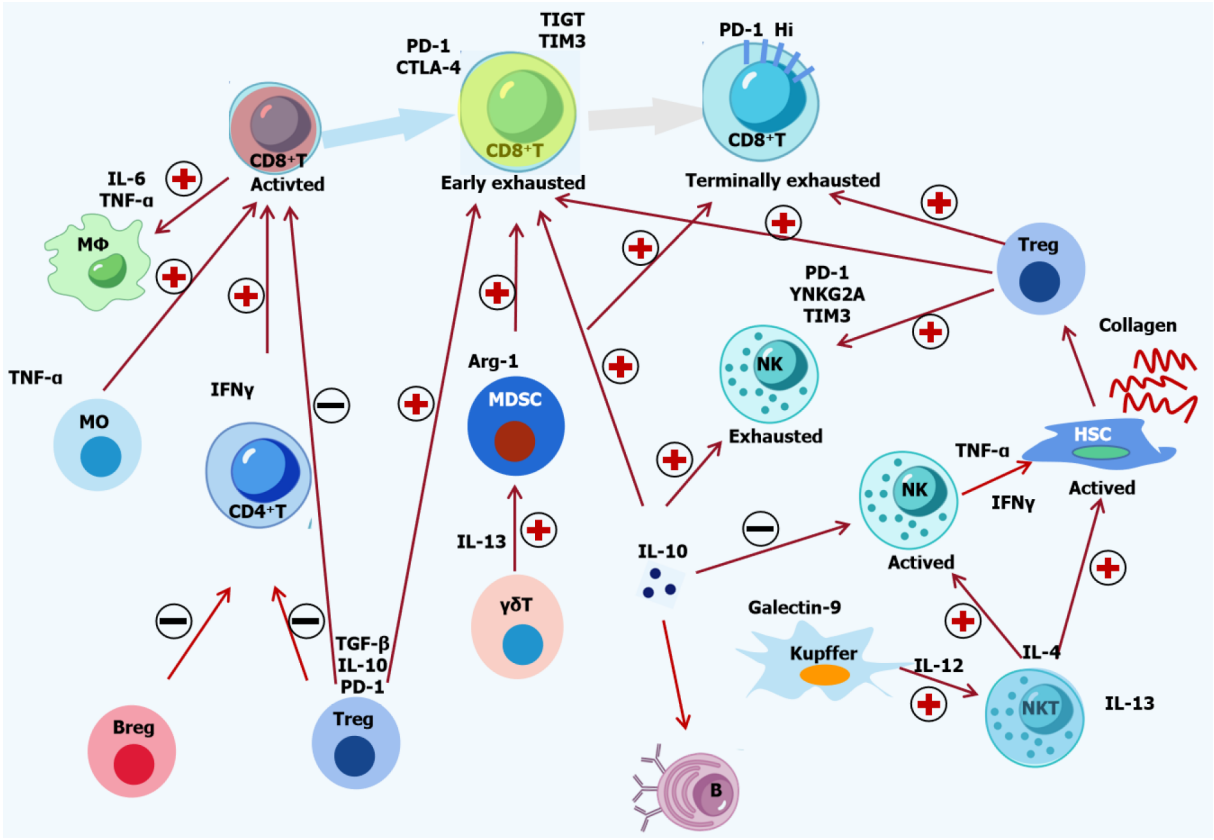
Mechanisms of immune escape in antigen-presenting cells/HBV specific-$CD8^+$ T-cells

When the HBV protein is swallowed by antigen-presenting cells (APCs), this protein is digested into tiny pieces, which are transferred onto human leukocyte antigen (HLA) antigens. The HLA antigen complex on APCs is then displayed to T cells, which produce effector molecules to eliminate HBV. However, when HBV enters a hepatocyte, it enhances intracellular survival at the expense of higher levels of HBV replication. Thus, HBV-infected hepatocytes produce a large number of HBV antigens that can, in turn, inhibit HBV antigen processing and presentation in APCs. Further, amino acids flanking the viral epitopes in APCs play a critical role in antigen processing. Mutations at these regions in HBV infection harm the proteasomal processing of epitopes and lead to $CD8^+$ T-cell escape[30].

HLA genes are critical for the immune system as they control pathogens and clear infections. Host HLA polymorphisms have been demonstrated to influence disease progression in HBV infection[37]. Studies found that changes in the surface expression of HLA class I complexes on APCs were associated with HBV replication and persistence. Lower HLA class I expression led to early HBeAg seroconversion, while down-regulation of HLA class II molecules led to pre-core mutants of HBcAg[38]. Lumley *et al*[30] focused on the interplay between the immune escape of HBV and the selective mutation of HLA-binding residues. They reported that this selective mutation of HLA-binding residues in $CD8^+$ epitopes could induce the immune escape of HBV, which is one of the most commonly identified mechanisms for HBV-specific $CD8^+$ immune escape[30].

N-linked glycosylation (NLG) is a post-translational modification that can impact the infectivity and antigenicity of HBV. It can mask immune epitopes, leading to immune escape and interfering with the antibody recognition of hepatitis B surface antigen. NLG can also affect the ability through which the envelope protein of HBV interacts with the surface of capsids to drive HBV virion secretion[30].

The connection between TCR on T-cell and HLA class I/peptide complexes induces the activation of $CD8^+$ T-cells, but alterations in TCR recognition, *i.e.*, epitope mutations in TCR contact residues, can lead to the immune escape of $CD8^+$ T-cells. Immunodominance of HBV epitopes is ensured by the amino acid sequence of the peptide and its concentration and binding affinity with T cell clones. In different $CD8^+$ T-cell clones, the same viral peptide can induce different signaling cascades[22]. Figure 2 illustrates the immune escape of HBV, which can occur through multiple pathways. This has a vital role in HBV infection that can last for decades, with some T cell defects being irreversible.



DOI: 10.3748/wjg.v28.i40.5784 **Copyright** ©The Author(s) 2022.

Figure 1 Crosstalk among immune cells and cytokines in hepatitis B virus infection. The complex interactions among immune cells and cytokines in chronic hepatitis B are shown. Hepatitis B virus (HBV)-specific CD8$^+$ T-cells are activated by monocytes and CD4$^+$ T-cells, followed by recruitment and activation of macrophages by active CD8$^+$ T-cells. The activation of natural killer (NK) T-cells is induced by Kupffer cells, which activate NK cells and hepatic stellate cells (HSCs). Suppressive Tregs, Bregs and Kupffer cells induce the functional impairment of CD8$^+$ T cells, CD4$^+$ T-cells and NK cells. Moreover, Treg cells, Kupffer cells and myeloid-derived suppressor cells can lead to the exhaustion of CD8$^+$ T-cells and NK cells. Inflammatory and inhibitory cytokines, including Monocyte chemoattractant protein-1, tumor necrosis factor-α, interferon-γ, interleukin (IL)-4, IL-6, IL-12, IL-13, IL-17, IL-10, and transforming growth factor-β, are involved in the crosstalk among immune cells. The activation of HSCs in sinusoids is induced by a complement protein such as C5a. Finally, decreasing epigenetic modification and function of HBV-specific CD8$^+$ T-cells inhibits the immune control of HBV. PD-1: Programmed death 1; CTLA-4: Cytotoxic T-lymphocyte antigen-4; IL: Interleukin; TNF-α: Tumor necrosis factor-α; TGF-β: Transforming growth factor β; IFN-γ: Interferon-γ; HSC: Hepatic stellate cell; MDSC: Myeloid-derived suppressor cells; NK: Natural killer.

Negative feedback regulation in immune response pathways

Negative feedback regulations commonly occur in immune response pathways. These regulations include negative regulation of immune signal pathways (*i.e.*, negative feedback regulation in TLRs pathway), activation of immune checkpoints, expression of inhibitory cytokines, and activation of inhibitory immune cells. An active innate immunity can induce the secretion of cytokines with antiviral activity, enhance the efficiency of APCs and alter the microenvironment of the liver. However, inflammatory cytokines such as IFNs and tumor necrosis factor-α (TNF-α) can induce immune tolerance[39-41]. Many immune cells and signaling pathways in the liver contribute to immune responses against HBV infection. These immune responses are contact-dependent and can be affected by environmental factors. Inhibitory molecules are produced by hepatic stellate cells, Kupffer cells, T-regulatory cells and myeloid-derived suppressor cells. Through a contact-dependent manner, NK cells can kill HBV-specific CD8$^+$ T-cells. Moreover, HBV-specific CD8$^+$ T-cells can be suppressed by inhibitory ligands such as programmed death-ligand 1 (Figure 1)[6,42]. However, considering HBV has adaptive and active strategies to evade innate immune responses and negative feedback exists in all immune responses, immune regulator therapy targeting only a single pathway is unlikely to be effective in treating HBV infection.

Host genetic variations associated with HBV infection

Researchers have made great efforts to confirm the associations between HBV infection and host immunogenetics. Host genetic variants, including mutations in TLRs, HLAs, vitamin D-related genes, cytokine and chemokine genes, microRNAs, and HBV receptor sodium taurocholate co-transporting polypeptide, have been observed to impact the outcomes of HBV infection (Table 2)[43-46]. The HLA genes are divided into two classes: HLA-class I (HLA-A, B, C, E, F and G) and HLA-class II (HLA-DP, DQ, DR, DM and DO). Polymorphisms in HLA genes were shown to be significantly associated with the

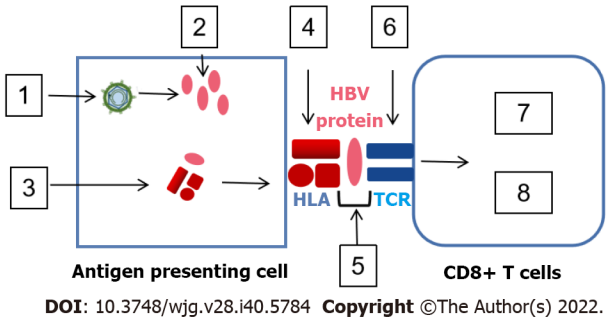
Table 2 Host genetic variants associated with hepatitis B virus infection[43-46]

Gene ontology	Gene	Genetic determinants (SNP/Hap/CNVs)
HLA	*HLA-A*	*33:03:01
	HLA-B	*13:01:01
	HLA-B	*07, *58
	HLA-C	Leu-15, rs2853953, rs3130542
	HLA-DOA	rs378352
	HLA-DP	rs9366816
	HLA-DPA1	rs3077, rs2301220, rs2395309, rs9277341
	HLA-DPB1	G-A-G-A-T-T[1], G-G-G-G-T-C[2], rs2281388, rs9277535, rs9277542, rs9277534, *0201, *0401, *0901, positions 84–87, *0402, *0501, *0201-*0401, *0201-*0402, *0201-*0501, *0401-*0402, *0401-*0501, *0402-*0402, *0402-*0501, *0501-*0501, *0501- *0901, *0501*others, rs9277378, rs10484569, rs3117222, rs9380343, rs3135021
	HLA-DQ	rs9275319, rs9275572, A1*0101-B1*0501, A1*0102-B1*0303, A1*0102-B1*0604, A1*0301-B1*0601, A1*0102-B1*0602, A1*0102-B1*0602, A1*0301-B1*0302, A1*0301-B1*0303, A1*0301-B1*0401, A1*0501-B1*0301
	HLA-DPA1/ DPB1	A-A[3], A-A[4], T-A-T[5],C-A-T[6], A-A-C-T[7], A-A-C-C//A-G-T-G-C-C[8], A-A-C-T//A-G-T-G-C-C[9], G-G-T-C//A-G-T-G-C-C[10], A1*0103-B1*0401, A1*0103-B1*0402, A1*0202-B1*0301, A1*0202-B1*0501
	HLA-DQA2	rs9276370
	HLA-DQB1	*0201, *0301, *0303, *0502, *0604, rs2856718, *0401-*0501, *0402-*0402, *0402-*0501, *0501-*0501
	HLA-DQB2	rs7453920, rs7756516
	HLA-DRB1	*13
	HLA-DP/DQ	T-T-G-A-T[11], T-T-G-G-T[12], carrying 4–6 variant alleles, G-A[13], A-G[14], A-A[15]
	HLA-J	rs400488
Cytokines	*IL-10*	−592
	IL-10RB	rs2834167
	IL-12B	rs3212227
	IL-16	rs11556218
	IL-21	rs2221903
	IL-12B	rs3212227
	IL-18	−137
	IFN-γ	+874
	IFN-α2	p.Ala120Thr
	IFN-αR2	rs1051393, rs12233338
	IFNLR1	rs4649203, rs7525481
	IFN-γR1	rs3799488
	IFN-γR2	rs1059293
	TNF-α	T-C-C-G-G-G[16], C-A-C-G-G-G[17] ,−238, −308, −857, −863
	TGF-α	+106151, +103461, A-T-G-T-T-T-T-C-T[18]
Chemokines	*CCR5*	Δ32
TLRs	*TLR-3*	rs3775291, rs1879026
	TLR-9	rs352140
MicroRNAs	*miR-30a*	rs1358379
	miR-101-2	T-C[19], rs12375841
	miR-106b-25	rs999885

	miR-122	rs3783553, rs4309483
	miR-196a-2	rs11614913
	miR-let-7c	rs6147150
	miR-219-1	rs107822, rs213210, rs421446, C-A-C[20], T-G-T[21]
	miR-323b	rs56103835
	miR-423	rs6505162
	miR-492	rs2289030
Others	*C2*	p.Glu318Asp, rs7746553, rs9267673, rs9267665, rs9267677, rs9279450, rs10947223
	CD40	rs1883832
	CFB	rs12614
	CTLA-4	C-A-C-C-G[22], T/C-A-C-C-G[23], T-A-C-C-A[24], rs231775,rs3087243, rs5742909
	EHMT2	rs7887, rs652888, rs35875104, rs41267090
	ESR1	+29
	IFN4/HLA-DQ	rs12971396-rs9275319, rs12971396-rs12979860-rs9275319
	INST10	rs7000921
	KIF1B	A-T-A[25]
	MCP1	−2518, −2518/−2076(−/ht2), −2518/−2076(ht2/ht2)
	MIF	rs755622
	MxA	−123
	MX1	rs467960
	NF-κB	rs2233406, rs3138053
	NLRX1	p.Arg707Cys
	NOTCH4	rs422951
	NTCP	rs2296651, rs943277, rs4646285
	OCT4	rs13409, rs885952, rs879882, rs1265163, rs2394882, rs3094193, rs3130501, rs3130503, rs3130931, rs3132526, rs3757349, rs9263800, rs117265349
	PAPL	rs423058
	SOCS3	C-C[26], T-T-C-T-A[27], rs111033850, rs12953258,
	SPP1	−1800
	STAT4	C-T-C-T-T[28], rs7574865,rs8179673, rs10168266, rs11889341,
	TCF19	rs1419881
	TMEM2	p.Ser1254Asn
	TMEM2/IFNA2/ NLRX1/C2	p.Ser1254-Asn/p.Ala120Thr/p.Arg707Cys/p.Glu318Asp
	UBE2L3	rs2266959, rs4821116
	VARS2	rs1043483, rs1264295, rs2249464, rs2517459, rs2532932, rs9394021,
	VDR	FokI
	ZNRD1	G-G-A[29], rs3757328

Haplotypes:
[1]G-A-G-A-T-T, rs9277535-rs10484569-rs3128917-rs2281388-rs3117222-rs9380343.
[2]G-G-G-G-T-C, rs9277535-rs10484569-rs3128917-rs2281388-rs3117222-rs9380343.
[3]A-A, rs3077-rs9277535.
[4]A-A, rs2395309-rs9277535.
[5]T-A-T, rs3077-rs9277378-rs3128917.
[6]C-A-T, rs3077-rs9277378-rs3128917.
[7]A-A-C-T, rs2395309-rs3077- rs2301220-rs9277341.

[8]A-A-C-C//A-G-T-G-C-C, rs2395309-rs3077-rs2301220-rs9277341//rs9277535-rs10484569-rs3128917 -rs2281388-rs3117222-rs9380343.
[9]A-A-C-T//A-G-T-G-C-C, rs2395309-rs3077-rs2301220-rs9277341//rs9277535-rs10484569-rs3128917 -rs2281388-rs3117222-rs9380343.
[10]G-G-T-C//A-G-T-G-C-C, rs2395309-rs3077-rs2301220-rs9277341//rs9277535-rs10484569-rs3128917 -rs2281388-rs3117222-rs9380343;
[11]T-T-G-A-T, rs9276370-rs7756516-rs7453920- rs9277535-rs9366816.
[12]T-T-G-G-T, rs9276370-rs7756516-rs7453920-rs9277535-rs9366816.
[13]G-A, rs2856718- rs9275572.
[14]A-G, rs2856718- rs9275572.
[15]A-A, rs2856718- rs9275572.
[16]T-C-C-G-G-G, -1031/-863/-857/-308/-238/-163.
[17]C-A-C-G-G-G, -1031/-863/-857/-308/-238/-163.
[18]A-T-G-T-T-T-T-C-T, +88344/+102906/+103432/+103437/+103461/+104261/+104802/+106151/+106318.
[19]T-C, rs12375841-rs17803780.
[20]C-A-C, rs421446-rs107822-rs213210.
[21]T-G-T, rs421446-rs107822-rs213210.
[22]C-A-C-C-G, -1722/-1661/-658/-319/+49.
[23]T/C-A-C-C-G, -1722/-1661/-658/-319/+49.
[24]T-A-C-C-A, -1722/-1661/-658/-319/+49.
[25]A-T-A, rs17401966-rs12734551-rs3748578.
[26]C-C, rs111033850-rs12953258.
[27]T-T-C-T-A, -1800/-1627/+4645/+5806/+6139.
[28]C-T-C-T-T, rs8179673-rs7574865-rs4274624-rs11889341-rs10168266.
[29]G-G-A, rs3757328-rs6940552-rs9261204.
SNPs/Hap/CNVs: Single nucleotide polymorphisms/Haplotype/Copy number variations; HLA: Human leukocyte antigen; TLR: Toll-like receptors.



DOI: 10.3748/wjg.v28.i40.5784 Copyright ©The Author(s) 2022.

Figure 2 Mechanism of immune escape in antigen-presenting cell/hepatitis B virus special T-cell. Hepatitis B virus (HBV)-infected hepatocytes produce various HBV antigens that are swallowed and digested by antigen-presenting cells (APCs), producing HBV peptide/human leukocyte antigen (HLA) complexes. Antigen processing escape mutants, down-regulating HLA expression and mutation of HLA binding residues may appear in APCs. The HBV peptide/HLA complexes are transferred to the surface of APC and make contact with T-cell receptor (TCR) on the surface of $CD8^+$ T-cells. Masking HLA/TCT binding residues with N-linked glycosylation and mutation of TCR binding residues influences TCR affinity/avidity, leading to $CD8^+$ T-cell stimulation or inhibition. The square icon displays: (1) Increase in viral antigen; (2) Antigen processing escape mutants; (3) Down-regulation of HLA expression; (4) Mutation of HLA binding residues; (5) Masking of HLA/TCT binging residues with N-linked glycosylation; (6) Mutation of TCR binding residues; (7) Stimulation induced by cytokine production and cytolytic activity; and (8) Inhibition caused by exhaustion, anergy and tolerance. HBV: Hepatitis B virus; TCR: T-cell receptor; HLA: Human leukocyte antigen.

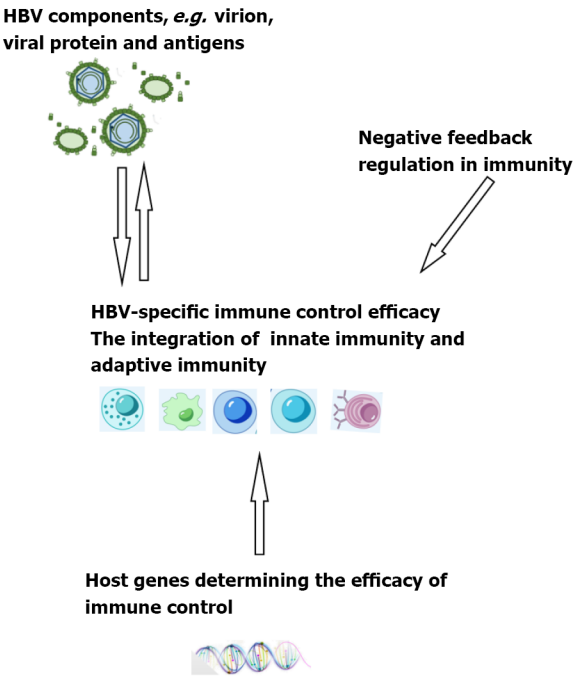
pathogenesis of HBV infection[47,48]. Studies have also reported that the genes encoding cytokines such as interleukins, TNF-α, IFNs and TGF-β, can influence the immune state of CHB patients[49-53]. In a study by Nitschke *et al*[54], the authors confirmed that specific HLA class I alleles restricted the efficacy of HBV-specific $CD8^+$ T-cells[54], indicating that the host's immune-related genes can affect the outcome of hepatitis B infection.

Researchers have observed significant differences in HBV infection rates between Western and East/Southeast Asian populations. Prior to HBV vaccination programs, the prevalence of HBsAg was less than 1% in the Caucasian population but higher than 10% in the Chinese population[43]. This difference was investigated in several studies, which showed that HLA molecules in European, Caucasian, Middle East, African-American and Asian populations affected the rate of HBV infection[43,55,56]. In addition, discordances in HBV-specific $CD8^+$ T-cell repertoires observed in different races, i.e., between Chinese and Caucasian populations, could be related to race-dependent HLA gene variants, leading to the different T-cell responses observed between different populations and ethnicities[57].

Thus, these findings underline the complexity of HBV-specific immune control efficacy, which is influenced by HBV components, negative feedback regulation in immunity and host genetic variants (Figure 3).

Heterogeneity of immune control in HBV infection

Heim *et al*[6] reviewed the heterogeneity of HBV-specific $CD8^+$ T-cells and described the functional



DOI: 10.3748/wjg.v28.i40.5784 **Copyright** ©The Author(s) 2022.

Figure 3 Interplay between hepatitis B virus-specific immune control, hepatitis B virus components, and negative feedback regulation in immunity and host genes. HBV: Hepatitis B virus.

deficiencies and distinct phenotypical characteristics associated with HBV-specific $CD8^+$ T-cells exhaustion. T-cell impairment demonstrates hierarchical and progressive loss in antiviral functions, from functional suppression to physical deletion in T-cells, which depend on the quantity of HBV antigens and the duration of T cell exposure to these antigens[31,58]. Moreover, exhausted $CD8^+$ T-cells do not represent a homogeneous T-cell population but are rather heterogeneous in function and phenotype. Kuipery *et al*[5] proposed concepts related to the heterogeneity of immune responses in CHB patients[5]. Based on reports from literature, we summarized the following concepts to improve our understanding on the heterogeneity of immune control.

Figure 1 illustrates the activation and inhibition of immune signaling pathways that overlap in HBV infection, multiple immune cell populations and integrated signals pathways that simultaneously respond to the stimulation of HBV components, and the ability of HBV-specific immune control depends on the overall immune responses of an individual rather than the capability of single immune cells or a single immune pathway.

Based on the immune escape mechanisms of APCs/$CD8^+$T-cells presented in Figure 2, the heterogeneous immune responses of T-cells are related to very fine mechanisms of immune regulation that influence the immune control of HBV-specific T-cells, or T-cells sensitivity/inhibition.

Figure 3 outlines the reasons for heterogeneous immune control. The overall immune control against HBV in an individual is influenced by HBV, negative feedback regulation in the immune signaling network and host genetic variants. Therefore, any changes in these three countenances could lead to fluctuations affecting the effectiveness of immune control. Thus, CHB infection is divided into four clinical phases: Immune tolerant with HBeAg-positive, HBeAg-positive immune-activation, inactive carrier with HBeAg-negative, and HBeAg-negative immune-activation. Further, heterogeneous immune controls can lead to different clinic phases and disease outcomes such as acute hepatitis, chronic hepatitis, cirrhosis, hepatocellular carcinoma and hepatic failure[43].

Reports have shown that host genetic polymorphisms are crucial determinants influencing HBV infectious rate and disease outcomes in Caucasian, Saudi Arabian, African-American, European, and Asian populations[56,59,60]. In addition, the host genetic variants of individuals from the same race can influence disease outcomes and the efficacies of antiviral therapy.

Researcher and immunologists who often overlook immune compartmentalization should be cautious when interpreting findings from the peripheral blood of patients.

IFN-α TREATMENT FOR CHB

Definition of partial cure and functional cure

A complete cure from HBV infection is currently hypothesized to be possible if the cccDNA and integrated HBV DNA are eliminated from hepatocytes. However, this is challenging as cccDNA can still persist in patients despite spontaneous recovery from an acute HBV infection. Since 2017, some advances in CHB therapeutics have been achieved[61], and researchers have proposed new definitions of cure. For instance, a partial cure has been defined as persistently undetectable HBV DNA and HBeAg in patients' serum after the completion of a limited course of antiviral therapy. Functional cure has been defined as sustained and undetectable HBV DNA and HBsAg in patients' serum, with or without seroconversion to hepatitis B surface antibody (anti-HBs), after a limited course of therapy. Complete sterilizing cure has been defined by the absence of HBsAg and eradication of HBV DNA, including HBV virion, integrated HBV DNA and cccDNA in the liver and serum of patients. However, because current treatments cannot deliver complete sterilizing cure, functional cure is the selected goal of therapy.

NAs and immunotherapy

Therapeutic strategies for CHB can be classified into two categories: NAs targeting HBV replication and immune modulators targeting immune control. NAs can cause rapid decay of HBV DNA in the peripheral blood but cannot completely eradicate HBsAg from patients' serum and cccDNA in hepatocytes[62,63]. Even though the virus might be undetectable in the serum after long-term treatment with NAs, low-level viral replication still persists due to the conservation of cccDNA in the nucleus of hepatocytes. Thus, prolonged NAs treatments are rarely associated with CHB cure and inevitably result in either NAs resistance or viral relapse[62-66].

In contrast, immunotherapy can target the innate and adaptive immunity to reinvigorate the host immune response to long-term inhibition of viral replication. Therapeutic strategies involving innate immunity include activating pattern recognition receptors (*i.e.*, TLRs and RIG-I), enhancing cytokine secretion, and improving the efficacy of NK cells. For adaptive immunity, therapies are directed at restoring the effects of HBV-specific T-cells and B-cells. Clinically, although immunotherapy can lead to sustained HBsAg loss, it cannot eradicate cccDNA from hepatocytes. Thus, being the more promising treatment compared to NAs, the ultimate goal of immunotherapy is currently targeted at achieving functional cure, enabling spontaneous control of HBV replication and maintaining disease remission without antiviral therapy[3]. Hoogeveen and Boonstra[32] reported that immunomodulators regulating a single immune pathway might not restore antiviral immunity as multiple immune pathways in the host enhance specific HBV immune responses[32].

Mechanism and clinical application of IFN-α therapy

IFNs are produced and released by immune cells in response to HBV components[67,68]. Of the known IFNs, IFN-α has broad-spectrum effects on viruses and tumors, and contributes to immune regulation by suppressing viral replication and cell growth. The antiviral function of IFN-α is cascaded by binding to IFN receptors on immune cells, activating signal transcription pathways, and inducing ISGs expression and related product secretion. Various ISGs products were found to inhibit different stages of the viral life cycle[69]. Further, epigenetics was shown to play a critical role in regulating cccDNA transcription[70-73]. IFN-α can regulate the epigenetic repression of cccDNA transcription by inducing cccDNA-bound histone hypo-acetylation and increasing the recruitment of transcription co-repressor on cccDNA[63,65,73]. In addition, IFN-α can upregulate HLAs expression to activate innate and adaptive immune responses. Many researchers have investigated the host genes associated with IFN-α treatment outcomes and observed its genetic polymorphisms[43,44,74-78] (Table 3).

As described earlier, due to negative feedback mechanisms, immune modulators targeting a single signal pathway might not improve the overall and long-term immune responses[61]. In this regard, the advantages of IFN-α treatment are that IFN-α can simultaneously affect multiple immune pathways and various immune cell populations in the host and integrate signals to improve the efficacy of immune control[10,11,15,36]. Currently, only IFN-α treatment was found to improve the efficacy of immune control[64,65].

IFN-α has been approved for the treatment of hepatitis B for over 20 years[36,61,65]. Compared with NAs, IFN-α has shown better efficacy in HBeAg seroconversion and HBsAg loss, with no risk of drug resistance[79]. For groups of patients with good prognoses, such as Caucasians, young age, low viral load, and females, IFN-α treatment has been more effective[80,81]. One study reported functional cure in 10%–20% of Caucasians who underwent IFN-α treatment, while it was < 5% in Asian patients[82]. However, most of the underlying mechanisms of IFN-α therapy are still unclear. More research is needed to investigate these significant differences in IFN-α efficacy between different groups of patients.

Table 3 Host genetic variants associated with interferon-α therapy[43,44,74-78,91]

Gene ontology	Gene	Genetic determinants (SNP/Hap/CNVs)
HLA	*HLA-DP*	rs3077, rs9277535
	HLA-DQA1-DQB1-DRB1	*0302-*0303-*09
	HLA-DQB1	*0303
	HLA-DRB1	*08
	HLA-A, B, C	*1101-*4601-*0102
Cytokines	*IL-28B*	A-C[1],rs8099917, rs12979860, rs12980275
Others	*CYP24A1*	rs2248359
	CYP27B1	rs10877012, rs4646536
	G3BP2	rs3821977
	OAS	G-T-G-A[2], C-C-T-A[3], C-C-C-A[4], A-C-T-A[5]
	OAS3	rs2072136
	PRELID2	rs371991
	STAT4	rs7574865
	TRAPPC9	rs78900671
	VDBP	rs7041
	VDR	rs1544410, rs731236, rs11568820, rs10735810

Haplotypes:
[1]A-C, rs12980275-rs12979860.
[2]G-T-G-A, rs3177979-rs1293747-rs4767043-rs10849829.
[3]C-C-T-A, rs2285934-rs2072138-rs2072136-rs10849829.
[4]C-C-C-A, rs2285934- rs2072138-rs2072136-rs10849829.
[5]A-C-T-A, rs2285934-rs2072138-rs2072136-rs10849829.
SNPs/Hap/CNVs: Single nucleotide polymorphisms/Haplotype/Copy number variations; HLA: Human leukocyte antigen.

IMPROVEMENT OF HBV-SPECIFIC IMMUNE CONTROL BY IFN-α RETREATMENT

IFN-α retreatment

In 1996, although IFN-α was already being used to treat CHB patients, only 20%-30% of the patients achieved viral suppression or partial cure with single IFN-α treatment. Then, it was found that IFN-α retreatment in these remaining patients could enhance treatment outcomes. Thus, multiple courses of IFN-α were implemented to treat these patients and researchers observed that three courses of IFN-α treatment were effective in treating HBeAg positive or negative patients. With multiple frequencies of IFN-α treatment, partial or functional cure rates gradually increased to approximately 25%-40% but were mostly observed in patients of white race[10-14] (Table 4).

By 2008, failures from combination therapy with nucleoside and nucleotide were reported, and multi-drug resistance with NAs treatment started to increase in China. Comparatively, IFN-α retreatment was associated with safe stopping of NAs administration and induced better-sustained responses to IFN-α [15]. Thus, when researchers started to investigate the effects of increasing the frequency and extending the total course of IFN-α treatment and found that these could significantly improve the rate of functional cure in Asian and Caucasian patients[73-75,80-83]. IFN-α retreatment was recommended by the Asian-Pacific clinical practice guidelines[16-18] and by Yin *et al*[64] (Table 4). Based on these promising findings and recommendations, we estimate that more CHB patients in Asia would receive IFN-α retreatment and experience better antiviral efficacy.

Interplay between IFN-α retreatment and the HBV-specific immune control

Recently, more and more HBV-specific immune mechanisms have been discovered, inspiring clinicians and immunologists to collaborate to study the interplay between immune mechanisms and clinical events in hepatitis B. Chang *et al*[84] summarized the relationship between hepatitis flare and immune responses in CHB patients to explore the underlying immune mechanism of hepatitis flares[84]. The observations made from the strategy of Chang's *et al*[84] were used below to discuss the immune control involved in IFN-α retreatment.

Table 4 Summary and timeline of interferon-α retreatment for chronic hepatitis B virus infection

Ref.	Year	The regimens of INF-α retreatment
van Zonneveld *et al*[10]	2004	One hundred and sixty-five patients received their first IFN-α treatment. Of them, 48 non-responders received 2-3 courses of IFN-α
Manesis and Hadziyannis[11]	2001	Two hundred and sixteen patients received IFN-α therapy, of whom 51 received a second IFN-α treatment and 9 were treated with three courses of IFN-α
Niederau *et al* [12]	1996	One hundred and three cases were treated IFN-α. Of them, 29 received a second course of therapy, and 17 received a third course of IFN-α
Carreño *et al*[13]	1999	Fifty-seven patients underwent a course of IFN-α therapy. Of them, 27 received a second course of IFN-α; and 30 others who did not receive IFN-α retreatment served as controls. IFN-α retreatment was found to enhance the antiviral effects against HBV
Ballauff *et al*[14]	1998	After all the children received the first course of IFN-α treatment, 15 were given the second course of IFN-α (study group), while the other 19 did not receive the second course of IFN-α, serving as the control group. HBV DNA clearance and anti-HBe seroconversion occurred in 5 of 15 children (33%) in the study group and 5 of 19 children (26%) in the control group
Yin and Zhong [15]	2016	Inappropriate therapies induced HBV resistance, multi-drug resistance and failure of combination therapy with nucleoside plus nucleotide in China. An IFN-α regimen, *i.e.* (1) Switch from nucleoside plus nucleotide to IFN-α therapy; and (2) subsequent IFN-α retreatment, was used to treat these patients. IFN-α switching therapy leaded to safe cessation of nucleoside plus nucleotide combination therapy, and IFN-α retreatment induced sustained response of IFN-α
Sarin *et al*[16]	2016	Asian-Pacific clinical practice guidelines 2015 recommended IFN-α retreatment to treat chronic HBV infection
Liaw *et al*[17]	2012	Asian-Pacific clinical practice guidelines 2012 recommended IFN-α retreatment to treat chronic HBV infection
Liaw *et al*[18]	2008	Asian-Pacific clinical practice guidelines 2008 recommended IFN-α retreatment to treat chronic HBV infection
Yin *et al*[64]	2021	IFN-α retreatment was recommended for patients on entecavir or tenofovir monotherapy with persistent low-level viremia

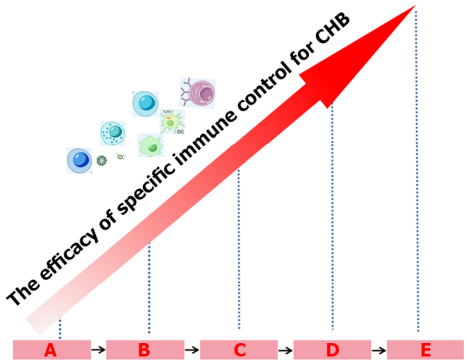
IFN-α: Interferon-α; HBV: Hepatitis B virus.

Asymptomatic persistence of cccDNA in the liver of patients who had acute hepatitis B or self-limiting HBV infection, despite the resolution of HBV infection[3], indicates that the host's immune system can fully inhibit HBV replication and that the specific HBV immune control in these individuals had an overwhelming advantage over HBV replication. In addition, investigations on the heterogeneous immune control of HBV infection have shown that the heterogeneity depends on the interplay between the host, virus and therapy, including host genes and immunity state, HBV load, duration of HBV infection, and IFN-α treatment and course of treatment[5,6,31,58]. However, the exact mechanism *via* which IFN-α retreatment exerts its benefits is yet to be fully elucidated.

Apart from HBV load, HBsAg and HBeAg, markers associated with the immune control of IFN-α treatment are lacking. In a study by Konerman and Lok[79], the authors proposed a scoring system that could help assess the efficacy of immune control[79]. The type of immune control could be estimated from a patient's HBV DNA, HBeAg seroconversion, HBsAg loss and times of IFN-α treatment, based on the following criteria: (1) Patients with acute hepatitis B or self-limiting HBV infection could achieve automatic cure without IFN-α treatment; (2) Patients with acute hepatitis B could achieve functional cure with one time IFN-α treatment; (3) CHB patients with one time IFN-α treatment could achieve functional cure; (4) CHB patients with one time IFN-α treatment could achieve partial cure; (5) CHB patients with multiple times of IFN-α treatment could achieve functional cure; and (6) CHB patients with multiple times of IFN-α treatment could achieve partial cure. These criteria suggest a step-like decline in immune control with increasing infection severity.

Clinical studies have confirmed that IFN-α retreatment could gradually increase the rate of partial and functional cure (Table 4)[10,11,13,15,36] and that CHB patients often have diverse HBV-specific immune control. Since 2016, researchers in China have reported numerous findings from clinical trials in which patients with inactive HBsAg carriers or low-level viremia were selectively enrolled and treated with IFN-α to evaluate their functional cure rate[85-88]. However, it should be noted that these were performed under trial settings because clinical guidelines do not recommend IFN-α therapy for the treatment of CHB in these patients[16,89,90]. A high rate of functional cure, 44.7%-84.2% of HBsAg loss and 20.2%-68.2% of HBsAg seroconversion were reported, in which a distinctive pattern of immune control whereby a close correlation between lower HBsAg at baseline and higher rates of HBsAg loss or HBsAg seroconversion was observed[85-88]. This pattern also appeared in the final course of IFN-α retreatment in previous studies[10,11,13,15,36], indicating that reducing HBsAg could be a prerequisite for achieving functional cure during IFN-α retreatment.

Taken together, current literature indicates that IFN-α retreatment could gradually enhance the overall immune control and improve the antiviral efficacy of IFN-α in CHB patients (Figure 4).



DOI: 10.3748/wjg.v28.i40.5784 **Copyright** ©The Author(s) 2022.

Figure 4 Interferon-α retreatment improves the efficacy of hepatitis B virus-specific immune control. Interferon-α (IFN-α) retreatment can lead to various treatment outcomes, namely no response, hepatitis B virus (HBV) decline, partial cure and functional cure. Multiple frequencies of IFN-α treatment can potentially restore specific immune control to HBV infection and simultaneously increase the rate of partial cure and functional cure. A: Exhausted immune control to HBV before IFN-α therapy (Baseline); B: Without HBV decline following IFN-α therapy; C: HBV decline; D: Partial cure; E: Functional cure. CHB: Chronic hepatitis B.

CONCLUSION

The interactions between immune cells and cytokines form a complex immune response network that exerts immune control over HBV infection. The efficacy of HBV-specific immune control is affected by HBV components, negative feedback regulation in the immune system, host genetic variants, and heterogeneity in the function and phenotype of immune control to HBV. Treatment with IFN-α can simultaneously affect multiple immune pathways and various immune cell populations in the host and integrate signals to improve the efficacy of immune control. Clinically, increasing the frequency and extending the total course of IFN-α retreatment have improved functional cure rates, indicating that IFN-α retreatment could gradually enhance the overall immune control. Further research on IFN-α retreatment could help promote this strategy in CHB patients with.

Altogether, this article outlined immune control without detailed discussions on immunity-related markers during immune transformation. In future studies, the discovery of detailed markers associated with immune transformation could provide important clues in understanding the underlying mechanism of immune control to improve the treatment of HBV infection.

ACKNOWLEDGEMENTS

We are very grateful to Prof. Gao-Jun Teng in Zhong-Da Hospital, Southeast University and Prof. Bei Zhong in the sixth Affiliated Hospital of Guangzhou medical University/Qingyuan People's Hospital for the comprehensive evaluation of the manuscript and valuable advices. Authors acknowledge Dr. Cun Shan in the Department of infectious disease, Nanjing Zhong-Da Hospital for data collection.

FOOTNOTES

Author contributions: All authors contributed to the study conception and design; The first draft of the manuscript was written by Yin GQ; All authors commented on previous versions of the manuscript, they all read and approved the final manuscript.

Conflict-of-interest statement: All the authors report no relevant conflicts of interest for this article.

Open-Access: This article is an open-access article that was selected by an in-house editor and fully peer-reviewed by external reviewers. It is distributed in accordance with the Creative Commons Attribution NonCommercial (CC BY-NC 4.0) license, which permits others to distribute, remix, adapt, build upon this work non-commercially, and license their derivative works on different terms, provided the original work is properly cited and the use is non-commercial. See: https://creativecommons.org/Licenses/by-nc/4.0/

Country/Territory of origin: China

ORCID number: Guo-Qing Yin 0000-0002-8972-3752; Ke-Ping Chen 0000-0002-8601-7481; Xiao-Chun Gu 0000-0002-7289-8054.

S-Editor: Fan JR

L-Editor: A
P-Editor: Fan JR

REFERENCES

1 **Revill PA**, Chisari FV, Block JM, Dandri M, Gehring AJ, Guo H, Hu J, Kramvis A, Lampertico P, Janssen HLA, Levrero M, Li W, Liang TJ, Lim SG, Lu F, Penicaud MC, Tavis JE, Thimme R; Members of the ICE-HBV Working Groups; ICE-HBV Stakeholders Group Chairs; ICE-HBV Senior Advisors, Zoulim F. A global scientific strategy to cure hepatitis B. *Lancet Gastroenterol Hepatol* 2019; **4**: 545-558 [PMID: 30981686 DOI: 10.1016/S2468-1253(19)30119-0]
2 **Rehermann B**, Thimme R. Insights From Antiviral Therapy Into Immune Responses to Hepatitis B and C Virus Infection. *Gastroenterology* 2019; **156**: 369-383 [PMID: 30267712 DOI: 10.1053/j.gastro.2018.08.061]
3 **Gehring AJ**, Protzer U. Targeting Innate and Adaptive Immune Responses to Cure Chronic HBV Infection. *Gastroenterology* 2019; **156**: 325-337 [PMID: 30367834 DOI: 10.1053/j.gastro.2018.10.032]
4 **Lang J**, Neumann-Haefelin C, Thimme R. Immunological cure of HBV infection. *Hepatol Int* 2019; **13**: 113-124 [PMID: 30600480 DOI: 10.1007/s12072-018-9912-8]
5 **Kuipery A**, Gehring AJ, Isogawa M. Mechanisms of HBV immune evasion. *Antiviral Res* 2020; **179**: 104816 [PMID: 32387476 DOI: 10.1016/j.antiviral.2020.104816]
6 **Heim K**, Neumann-Haefelin C, Thimme R, Hofmann M. Heterogeneity of HBV-Specific CD8$^+$ T-Cell Failure: Implications for Immunotherapy. *Front Immunol* 2019; **10**: 2240 [PMID: 31620140 DOI: 10.3389/fimmu.2019.02240]
7 **Ma Z**, Cao Q, Xiong Y, Zhang E, Lu M. Interaction between Hepatitis B Virus and Toll-Like Receptors: Current Status and Potential Therapeutic Use for Chronic Hepatitis B. *Vaccines (Basel)* 2018; **6** [PMID: 29337856 DOI: 10.3390/vaccines6010006]
8 **Burton AR**, Pallett LJ, McCoy LE, Suveizdyte K, Amin OE, Swadling L, Alberts E, Davidson BR, Kennedy PT, Gill US, Mauri C, Blair PA, Pelletier N, Maini MK. Circulating and intrahepatic antiviral B cells are defective in hepatitis B. *J Clin Invest* 2018; **128**: 4588-4603 [PMID: 30091725 DOI: 10.1172/JCI121960]
9 **Salimzadeh L**, Le Bert N, Dutertre CA, Gill US, Newell EW, Frey C, Hung M, Novikov N, Fletcher S, Kennedy PT, Bertoletti A. PD-1 blockade partially recovers dysfunctional virus-specific B cells in chronic hepatitis B infection. *J Clin Invest* 2018; **128**: 4573-4587 [PMID: 30084841 DOI: 10.1172/JCI121957]
10 **van Zonneveld M**, Honkoop P, Hansen BE, Niesters HG, Darwish Murad S, de Man RA, Schalm SW, Janssen HL. Long-term follow-up of alpha-interferon treatment of patients with chronic hepatitis B. *Hepatology* 2004; **39**: 804-810 [PMID: 14999700 DOI: 10.1002/hep.20128]
11 **Manesis EK**, Hadziyannis SJ. Interferon alpha treatment and retreatment of hepatitis B e antigen-negative chronic hepatitis B. *Gastroenterology* 2001; **121**: 101-109 [PMID: 11438498 DOI: 10.1053/gast.2001.25524]
12 **Niederau C**, Heintges T, Lange S, Goldmann G, Niederau CM, Mohr L, Häussinger D. Long-term follow-up of HBeAg-positive patients treated with interferon alfa for chronic hepatitis B. *N Engl J Med* 1996; **334**: 1422-1427 [PMID: 8618580 DOI: 10.1056/NEJM199605303342202]
13 **Carreño V**, Marcellin P, Hadziyannis S, Salmerón J, Diago M, Kitis GE, Vafiadis I, Schalm SW, Zahm F, Manzarbeitia F, Jiménez FJ, Quiroga JA. Retreatment of chronic hepatitis B e antigen-positive patients with recombinant interferon alfa-2a. The European Concerted Action on Viral Hepatitis (EUROHEP). *Hepatology* 1999; **30**: 277-282 [PMID: 10385667 DOI: 10.1002/hep.510300117]
14 **Ballauff A**, Schneider T, Gerner P, Habermehl P, Behrens R, Wirth S. Safety and efficacy of interferon retreatment in children with chronic hepatitis B. *Eur J Pediatr* 1998; **157**: 382-385 [PMID: 9625334 DOI: 10.1007/s004310050834]
15 **Yin GQ**, Zhong B. Efficacy of interferon for chronic hepatitis B in patients with nucleoside and nucleotide combination therapy failure. *J Gastroenterol Hepatol* 2016; **31**: 248-255 [PMID: 26456953 DOI: 10.1111/jgh.13191]
16 **Sarin SK**, Kumar M, Lau GK, Abbas Z, Chan HL, Chen CJ, Chen DS, Chen HL, Chen PJ, Chien RN, Dokmeci AK, Gane E, Hou JL, Jafri W, Jia J, Kim JH, Lai CL, Lee HC, Lim SG, Liu CJ, Locarnini S, Al Mahtab M, Mohamed R, Omata M, Park J, Piratvisuth T, Sharma BC, Sollano J, Wang FS, Wei L, Yuen MF, Zheng SS, Kao JH. Asian-Pacific clinical practice guidelines on the management of hepatitis B: a 2015 update. *Hepatol Int* 2016; **10**: 1-98 [PMID: 26563120 DOI: 10.1007/s12072-015-9675-4]
17 **Liaw YF**, Kao JH, Piratvisuth T, Chan HL, Chien RN, Liu CJ, Gane E, Locarnini S, Lim SG, Han KH, Amarapurkar D, Cooksley G, Jafri W, Mohamed R, Hou JL, Chuang WL, Lesmana LA, Sollano JD, Suh DJ, Omata M. Asian-Pacific consensus statement on the management of chronic hepatitis B: a 2012 update. *Hepatol Int* 2012; **6**: 531-561 [PMID: 26201469 DOI: 10.1007/s12072-012-9365-4]
18 **Liaw YF**, Leung N, Kao JH, Piratvisuth T, Gane E, Han KH, Guan R, Lau GK, Locarnini S; Chronic Hepatitis B Guideline Working Party of the Asian-Pacific Association for the Study of the Liver. Asian-Pacific consensus statement on the management of chronic hepatitis B: a 2008 update. *Hepatol Int* 2008; **2**: 263-283 [PMID: 19669255 DOI: 10.1007/s12072-008-9080-3]
19 **Megahed FAK**, Zhou X, Sun P. The Interactions between HBV and the Innate Immunity of Hepatocytes. *Viruses* 2020; **12** [PMID: 32151000 DOI: 10.3390/v12030285]
20 **Han JW**, Shin EC. Liver-Resident Memory CD8$^+$ T Cells: Possible Roles in Chronic HBV Infection. *Int J Mol Sci* 2020; **22** [PMID: 33396596 DOI: 10.3390/ijms22010283]
21 **Faure-Dupuy S**, Lucifora J, Durantel D. Interplay between the Hepatitis B Virus and Innate Immunity: From an Understanding to the Development of Therapeutic Concepts. *Viruses* 2017; **9** [PMID: 28452930 DOI: 10.3390/v9050095]
22 **Bertoletti A**, Ferrari C. Adaptive immunity in HBV infection. *J Hepatol* 2016; **64**: S71-S83 [PMID: 27084039 DOI: 10.1016/j.jhep.2016.01.026]
23 **Zhong B**, Huang MP, Yin GQ, Gao X. Effects of costimulation on intrahepatic immunopathogenesis in patients with

chronic HBV infection. *Inflamm Res* 2014; **63**: 217-229 [PMID: 24337678 DOI: 10.1007/s00011-013-0691-3]
24 **Yin JW**, Ping Huang M, Zhong B. Intrahepatic Toll-Like Receptor 3 in Chronic HBV Infection Subjects: Asymptomatic Carriers, Active Chronic Hepatitis, Cirrhosis, and Hepatocellular Carcinoma. *Hepat Mon* 2016; **16**: e34432 [PMID: 27630720 DOI: 10.5812/hepatmon.34432]
25 **Stoop JN**, Claassen MA, Woltman AM, Binda RS, Kuipers EJ, Janssen HL, van der Molen RG, Boonstra A. Intrahepatic regulatory T cells are phenotypically distinct from their peripheral counterparts in chronic HBV patients. *Clin Immunol* 2008; **129**: 419-427 [PMID: 18823821 DOI: 10.1016/j.clim.2008.07.029]
26 **Peppa D**, Micco L, Javaid A, Kennedy PT, Schurich A, Dunn C, Pallant C, Ellis G, Khanna P, Dusheiko G, Gilson RJ, Maini MK. Blockade of immunosuppressive cytokines restores NK cell antiviral function in chronic hepatitis B virus infection. *PLoS Pathog* 2010; **6**: e1001227 [PMID: 21187913 DOI: 10.1371/journal.ppat.1001227]
27 **Pandey S**, Kawai T, Akira S. Microbial sensing by Toll-like receptors and intracellular nucleic acid sensors. *Cold Spring Harb Perspect Biol* 2014; **7**: a016246 [PMID: 25301932 DOI: 10.1101/cshperspect.a016246]
28 **Protzer U**, Maini MK, Knolle PA. Living in the liver: hepatic infections. *Nat Rev Immunol* 2012; **12**: 201-213 [PMID: 22362353 DOI: 10.1038/nri3169]
29 **Wu J**, Meng Z, Jiang M, Pei R, Trippler M, Broering R, Bucchi A, Sowa JP, Dittmer U, Yang D, Roggendorf M, Gerken G, Lu M, Schlaak JF. Hepatitis B virus suppresses toll-like receptor-mediated innate immune responses in murine parenchymal and nonparenchymal liver cells. *Hepatology* 2009; **49**: 1132-1140 [PMID: 19140219 DOI: 10.1002/hep.22751]
30 **Lumley SF**, McNaughton AL, Klenerman P, Lythgoe KA, Matthews PC. Hepatitis B Virus Adaptation to the CD8+ T Cell Response: Consequences for Host and Pathogen. *Front Immunol* 2018; **9**: 1561 [PMID: 30061882 DOI: 10.3389/fimmu.2018.01561]
31 **Boni C**, Barili V, Acerbi G, Rossi M, Vecchi A, Laccabue D, Penna A, Missale G, Ferrari C, Fisicaro P. HBV Immune-Therapy: From Molecular Mechanisms to Clinical Applications. *Int J Mol Sci* 2019; **20** [PMID: 31195619 DOI: 10.3390/ijms20112754]
32 **Hoogeveen RC**, Boonstra A. Checkpoint Inhibitors and Therapeutic Vaccines for the Treatment of Chronic HBV Infection. *Front Immunol* 2020; **11**: 401 [PMID: 32194573 DOI: 10.3389/fimmu.2020.00401]
33 **Murphy CM**, Xu Y, Li F, Nio K, Reszka-Blanco N, Li X, Wu Y, Yu Y, Xiong Y, Su L. Hepatitis B Virus X Protein Promotes Degradation of SMC5/6 to Enhance HBV Replication. *Cell Rep* 2016; **16**: 2846-2854 [PMID: 27626656 DOI: 10.1016/j.celrep.2016.08.026]
34 **Livingston CM**, Ramakrishnan D, Strubin M, Fletcher SP, Beran RK. Identifying and Characterizing Interplay between Hepatitis B Virus X Protein and Smc5/6. *Viruses* 2017; **9** [PMID: 28368357 DOI: 10.3390/v9040069]
35 **Tsunematsu S**, Suda G, Yamasaki K, Kimura M, Izumi T, Umemura M, Ito J, Sato F, Nakai M, Sho T, Morikawa K, Ogawa K, Tanaka Y, Watashi K, Wakita T, Sakamoto N. Hepatitis B virus X protein impairs α-interferon signaling *via* up-regulation of suppressor of cytokine signaling 3 and protein phosphatase 2A. *J Med Virol* 2017; **89**: 267-275 [PMID: 27459003 DOI: 10.1002/jmv.24643]
36 **Tan G**, Song H, Xu F, Cheng G. When Hepatitis B Virus Meets Interferons. *Front Microbiol* 2018; **9**: 1611 [PMID: 30072974 DOI: 10.3389/fmicb.2018.01611]
37 **Matthews PC**, Carlson JM, Beloukas A, Malik A, Jooste P, Ogwu A, Shapiro R, Riddell L, Chen F, Luzzi G, Jesuthasan G, Jeffery K, Jojic N, Ndung'u T, Carrington M, Goulder PJ, Geretti AM, Klenerman P. HLA-A is a Predictor of Hepatitis B e Antigen Status in HIV-Positive African Adults. *J Infect Dis* 2016; **213**: 1248-1252 [PMID: 26655301 DOI: 10.1093/infdis/jiv592]
38 **Mohamadkhani A**, Sotoudeh M, Bowden S, Poustchi H, Jazii FR, Sayehmiri K, Malekzadeh R. Downregulation of HLA class II molecules by G1896A pre-core mutation in chronic hepatitis B virus infection. *Viral Immunol* 2009; **22**: 295-300 [PMID: 19811086 DOI: 10.1089/vim.2009.0031]
39 **Hakim MS**, Rahmadika N, Jariah ROA. Expressions of inhibitory checkpoint molecules in acute and chronic HBV and HCV infections: Implications for therapeutic monitoring and personalized therapy. *Rev Med Virol* 2020; **30**: e2094 [PMID: 31825155 DOI: 10.1002/rmv.2094]
40 **Beyer M**, Abdullah Z, Chemnitz JM, Maisel D, Sander J, Lehmann C, Thabet Y, Shinde PV, Schmidleithner L, Köhne M, Trebicka J, Schierwagen R, Hofmann A, Popov A, Lang KS, Oxenius A, Buch T, Kurts C, Heikenwalder M, Fätkenheuer G, Lang PA, Hartmann P, Knolle PA, Schultze JL. Tumor-necrosis factor impairs CD4(+) T cell-mediated immunological control in chronic viral infection. *Nat Immunol* 2016; **17**: 593-603 [PMID: 26950238 DOI: 10.1038/ni.3399]
41 **Wilson EB**, Yamada DH, Elsaesser H, Herskovitz J, Deng J, Cheng G, Aronow BJ, Karp CL, Brooks DG. Blockade of chronic type I interferon signaling to control persistent LCMV infection. *Science* 2013; **340**: 202-207 [PMID: 23580528 DOI: 10.1126/science.1235208]
42 **Boni C**, Fisicaro P, Valdatta C, Amadei B, Di Vincenzo P, Giuberti T, Laccabue D, Zerbini A, Cavalli A, Missale G, Bertoletti A, Ferrari C. Characterization of hepatitis B virus (HBV)-specific T-cell dysfunction in chronic HBV infection. *J Virol* 2007; **81**: 4215-4225 [PMID: 17287266 DOI: 10.1128/JVI.02844-06]
43 **Zhang Z**, Wang C, Liu Z, Zou G, Li J, Lu M. Host Genetic Determinants of Hepatitis B Virus Infection. *Front Genet* 2019; **10**: 696 [PMID: 31475028 DOI: 10.3389/fgene.2019.00696]
44 **O'Brien TR**, Yang HI, Groover S, Jeng WJ. Genetic Factors That Affect Spontaneous Clearance of Hepatitis C or B Virus, Response to Treatment, and Disease Progression. *Gastroenterology* 2019; **156**: 400-417 [PMID: 30287169 DOI: 10.1053/j.gastro.2018.09.052]
45 **Akcay IM**, Katrinli S, Ozdil K, Doganay GD, Doganay L. Host genetic factors affecting hepatitis B infection outcomes: Insights from genome-wide association studies. *World J Gastroenterol* 2018; **24**: 3347-3360 [PMID: 30122875 DOI: 10.3748/wjg.v24.i30.3347]
46 **Wang L**, Zou ZQ, Wang K. Clinical Relevance of HLA Gene Variants in HBV Infection. *J Immunol Res* 2016; **2016**: 9069375 [PMID: 27243039 DOI: 10.1155/2016/9069375]
47 **He D**, Tao S, Guo S, Li M, Wu J, Huang H, Guo X, Yan G, Zhu P, Wang Y. Interaction of TLR-IFN and HLA polymorphisms on susceptibility of chronic HBV infection in Southwest Han Chinese. *Liver Int* 2015; **35**: 1941-1949

[PMID: 25469587 DOI: 10.1111/liv.12756]
48 **Wasityastuti W**, Yano Y, Ratnasari N, Triyono T, Triwikatmani C, Indrarti F, Heriyanto DS, Yamani LN, Liang Y, Utsumi T, Hayashi Y. Protective effects of HLA-DPA1/DPB1 variants against Hepatitis B virus infection in an Indonesian population. *Infect Genet Evol* 2016; **41**: 177-184 [PMID: 27051043 DOI: 10.1016/j.meegid.2016.03.034]
49 **Eskandari E**, Metanat M, Pahlevani E, Nakhzari-Khodakheir T. Association between TGFβ1 polymorphisms and chronic hepatitis B infection in an Iranian population. *Rev Soc Bras Med Trop* 2017; **50**: 301-308 [PMID: 28700046 DOI: 10.1590/0037-8682-0266-2016]
50 **Karra VK**, Gumma PK, Chowdhury SJ, Ruttala R, Polipalli SK, Chakravarti A, Kar P. IL-18 polymorphisms in hepatitis B virus related liver disease. *Cytokine* 2015; **73**: 277-282 [PMID: 25802197 DOI: 10.1016/j.cyto.2015.02.015]
51 **Karataylı SC**, Bozdayı M, Karataylı E, Öztürk T, Husseini AA, Albayrak R, Özkan M, Kalaylıoğlu Z, Yalçın K, Çınar K, İdilman R, Yurdaydın C. Interleukin-28 gene polymorphisms may contribute to HBsAg persistence and the development of HBeAg-negative chronic hepatitis B. *Liver Int* 2015; **35**: 846-853 [PMID: 24840315 DOI: 10.1111/liv.12595]
52 **Talaat RM**, Dondeti MF, El-Shenawy SZ, Khamiss OA. Association between IL-10 gene promoter polymorphism and hepatitis B viral infection in an Egyptian population. *Biochem Genet* 2014; **52**: 387-402 [PMID: 24838671 DOI: 10.1007/s10528-014-9655-8]
53 **Saxena R**, Chawla YK, Verma I, Kaur J. Effect of IL-12B, IL-2, TGF-β1, and IL-4 polymorphism and expression on hepatitis B progression. *J Interferon Cytokine Res* 2014; **34**: 117-128 [PMID: 24161121 DOI: 10.1089/jir.2013.0043]
54 **Nitschke K**, Luxenburger H, Kiraithe MM, Thimme R, Neumann-Haefelin C. CD8+ T-Cell Responses in Hepatitis B and C: The (HLA-) A, B, and C of Hepatitis B and C. *Dig Dis* 2016; **34**: 396-409 [PMID: 27170395 DOI: 10.1159/000444555]
55 **Matsuura K**, Isogawa M, Tanaka Y. Host genetic variants influencing the clinical course of hepatitis B virus infection. *J Med Virol* 2016; **88**: 371-379 [PMID: 26255971 DOI: 10.1002/jmv.24350]
56 **Trinks J**, Nishida N, Hulaniuk ML, Caputo M, Tsuchiura T, Marciano S, Haddad L, Blejer J, Bartoli S, Ameigeiras B, Frías SE, Vistarini C, Heinrich F, Remondegui C, Ceballos S, Echenique G, Charre Samman M, D'Amico C, Rojas A, Martínez A, Ridruejo E, Fernández RJ, Burgos Pratx L, Salamone H, Nuñez F, Galdame O, Gadano A, Corach D, Sugiyama M, Flichman D, Tokunaga K, Mizokami M. Role of HLA-DP and HLA-DQ on the clearance of hepatitis B virus and the risk of chronic infection in a multiethnic population. *Liver Int* 2017; **37**: 1476-1487 [PMID: 28267888 DOI: 10.1111/liv.13405]
57 **Tan AT**, Loggi E, Boni C, Chia A, Gehring AJ, Sastry KS, Goh V, Fisicaro P, Andreone P, Brander C, Lim SG, Ferrari C, Bihl F, Bertoletti A. Host ethnicity and virus genotype shape the hepatitis B virus-specific T-cell repertoire. *J Virol* 2008; **82**: 10986-10997 [PMID: 18799575 DOI: 10.1128/JVI.01124-08]
58 **McLane LM**, Abdel-Hakeem MS, Wherry EJ. CD8 T Cell Exhaustion During Chronic Viral Infection and Cancer. *Annu Rev Immunol* 2019; **37**: 457-495 [PMID: 30676822 DOI: 10.1146/annurev-immunol-041015-055318]
59 **Thomas R**, Thio CL, Apps R, Qi Y, Gao X, Marti D, Stein JL, Soderberg KA, Moody MA, Goedert JJ, Kirk GD, Hoots WK, Wolinsky S, Carrington M. A novel variant marking HLA-DP expression levels predicts recovery from hepatitis B virus infection. *J Virol* 2012; **86**: 6979-6985 [PMID: 22496224 DOI: 10.1128/JVI.00406-12]
60 **Al-Qahtani AA**, Al-Anazi MR, Abdo AA, Sanai FM, Al-Hamoudi W, Alswat KA, Al-Ashgar HI, Khalaf NZ, Eldali AM, Viswan NA, Al-Ahdal MN. Association between HLA variations and chronic hepatitis B virus infection in Saudi Arabian patients. *PLoS One* 2014; **9**: e80445 [PMID: 24465366 DOI: 10.1371/journal.pone.0080445]
61 **Lok AS**, Zoulim F, Dusheiko G, Ghany MG. Hepatitis B cure: From discovery to regulatory approval. *J Hepatol* 2017; **67**: 847-861 [PMID: 28778687 DOI: 10.1016/j.jhep.2017.05.008]
62 **Boyd A**, Lacombe K, Lavocat F, Maylin S, Miailhes P, Lascoux-Combe C, Delaugerre C, Girard PM, Zoulim F. Decay of ccc-DNA marks persistence of intrahepatic viral DNA synthesis under tenofovir in HIV-HBV co-infected patients. *J Hepatol* 2016; **65**: 683-691 [PMID: 27210429 DOI: 10.1016/j.jhep.2016.05.014]
63 **Martinez MG**, Testoni B, Zoulim F. Biological basis for functional cure of chronic hepatitis B. *J Viral Hepat* 2019; **26**: 786-794 [PMID: 30803126 DOI: 10.1111/jvh.13090]
64 **Yin GQ**, Li J, Zhong B, Yang YF, Wang MR. New therapeutic options for persistent low-level viremia in patients with chronic hepatitis B virus infection: Increase of entecavir dosage. *World J Gastroenterol* 2021; **27**: 666-676 [PMID: 33716446 DOI: 10.3748/wjg.v27.i8.666]
65 **Goh ZY**, Ren EC, Ko HL. Intracellular interferon signalling pathways as potential regulators of covalently closed circular DNA in the treatment of chronic hepatitis B. *World J Gastroenterol* 2021; **27**: 1369-1391 [PMID: 33911462 DOI: 10.3748/wjg.v27.i14.1369]
66 **Liang TJ**, Block TM, McMahon BJ, Ghany MG, Urban S, Guo JT, Locarnini S, Zoulim F, Chang KM, Lok AS. Present and future therapies of hepatitis B: From discovery to cure. *Hepatology* 2015; **62**: 1893-1908 [PMID: 26239691 DOI: 10.1002/hep.28025]
67 **Meng Z**, Chen Y, Lu M. Advances in Targeting the Innate and Adaptive Immune Systems to Cure Chronic Hepatitis B Virus Infection. *Front Immunol* 2019; **10**: 3127 [PMID: 32117201 DOI: 10.3389/fimmu.2019.03127]
68 **Lee S**, Baldridge MT. Interferon-Lambda: A Potent Regulator of Intestinal Viral Infections. *Front Immunol* 2017; **8**: 749 [PMID: 28713375 DOI: 10.3389/fimmu.2017.00749]
69 **Liu SY**, Aliyari R, Chikere K, Li G, Marsden MD, Smith JK, Pernet O, Guo H, Nusbaum R, Zack JA, Freiberg AN, Su L, Lee B, Cheng G. Interferon-inducible cholesterol-25-hydroxylase broadly inhibits viral entry by production of 25-hydroxycholesterol. *Immunity* 2013; **38**: 92-105 [PMID: 23273844 DOI: 10.1016/j.immuni.2012.11.005]
70 **Ji M**, Hu K. Recent advances in the study of hepatitis B virus covalently closed circular DNA. *Virol Sin* 2017; **32**: 454-464 [PMID: 29280054 DOI: 10.1007/s12250-017-4009-4]
71 **Kim W**, Lee S, Son Y, Ko C, Ryu WS. DDB1 Stimulates Viral Transcription of Hepatitis B Virus *via* HBx-Independent Mechanisms. *J Virol* 2016; **90**: 9644-9653 [PMID: 27535046 DOI: 10.1128/JVI.00977-16]
72 **Tropberger P**, Mercier A, Robinson M, Zhong W, Ganem DE, Holdorf M. Mapping of histone modifications in episomal HBV cccDNA uncovers an unusual chromatin organization amenable to epigenetic manipulation. *Proc Natl Acad Sci U S A* 2015; **112**: E5715-E5724 [PMID: 26438841 DOI: 10.1073/pnas.1518090112]
73 **Dandri M**. Epigenetic modulation in chronic hepatitis B virus infection. *Semin Immunopathol* 2020; **42**: 173-185 [PMID:

32185454 DOI: 10.1007/s00281-020-00780-6]

74 **Brouwer WP**, Chan HLY, Lampertico P, Hou J, Tangkijvanich P, Reesink HW, Zhang W, Mangia A, Tanwandee T, Montalto G, Simon K, Ormeci N, Chen L, Tabak F, Gunsar F, Flisiak R, Ferenci P, Akdogan M, Akyuz F, Hirankarn N, Jansen L, Wong VW, Soffredini R, Liang X, Chen S, Groothuismink ZMA, Santoro R, Jaroszewicz J, Ozaras R, Kozbial K, Brahmania M, Xie Q, Chotiyaputta W, Xun Q, Pazgan-Simon M, Oztas E, Verhey E, Montanari NR, Sun J, Hansen BE, Boonstra A, Janssen HLA; GIANT-B Global Consortium. Genome-wide Association Study Identifies Genetic Variants Associated With Early and Sustained Response to (Pegylated) Interferon in Chronic Hepatitis B Patients: The GIANT-B Study. *Clin Infect Dis* 2019; **69**: 1969-1979 [PMID: 30715261 DOI: 10.1093/cid/ciz084]

75 **Thanapirom K**, Suksawatamnuay S, Sukeepaisarnjareon W, Tanwandee T, Charatcharoenwitthaya P, Thongsawat S, Leerapun A, Piratvisuth T, Boonsirichan R, Bunchorntavakul C, Pattanasirigool C, Pornthisarn B, Tantipanichtheerakul S, Sripariwuth E, Jeamsripong W, Sanpajit T, Poovorawan Y, Komolmit P. Genetic variation in the vitamin D pathway CYP2R1 gene predicts sustained HBeAg seroconversion in chronic hepatitis B patients treated with pegylated interferon: A multicenter study. *PLoS One* 2017; **12**: e0173263 [PMID: 28296915 DOI: 10.1371/journal.pone.0173263]

76 **Jiang DK**, Wu X, Qian J, Ma XP, Yang J, Li Z, Wang R, Sun L, Liu F, Zhang P, Zhu X, Wu J, Chen K, Conran C, Zheng SL, Lu D, Yu L, Liu Y, Xu J. Genetic variation in STAT4 predicts response to interferon-α therapy for hepatitis B e antigen-positive chronic hepatitis B. *Hepatology* 2016; **63**: 1102-1111 [PMID: 26704347 DOI: 10.1002/hep.28423]

77 **Tseng TC**, Yu ML, Liu CJ, Lin CL, Huang YW, Hsu CS, Liu CH, Kuo SF, Pan CJ, Yang SS, Su CW, Chen PJ, Chen DS, Kao JH. Effect of host and viral factors on hepatitis B e antigen-positive chronic hepatitis B patients receiving pegylated interferon-α-2a therapy. *Antivir Ther* 2011; **16**: 629-637 [PMID: 21817184 DOI: 10.3851/IMP1841]

78 **Wu X**, Shi W, Wu J, Zhu X, Chen K, Zheng S, Li Z, Duan Z, Li H, Liu Y. A functional polymorphism in ADAR1 gene affects HBsAg seroclearance both spontaneously and interferon induced. *Liver Int* 2014; **34**: 1560-1565 [PMID: 24351124 DOI: 10.1111/liv.12444]

79 **Konerman MA**, Lok AS. Interferon Treatment for Hepatitis B. *Clin Liver Dis* 2016; **20**: 645-665 [PMID: 27742005 DOI: 10.1016/j.cld.2016.06.002]

80 **Sokal EM**, Conjeevaram HS, Roberts EA, Alvarez F, Bern EM, Goyens P, Rosenthal P, Lachaux A, Shelton M, Sarles J, Hoofnagle J. Interferon alfa therapy for chronic hepatitis B in children: a multinational randomized controlled trial. *Gastroenterology* 1998; **114**: 988-995 [PMID: 9558288 DOI: 10.1016/s0016-5085(98)70318-x]

81 **Roberts EA**. Why treat chronic hepatitis B in childhood with interferon alpha? *Gut* 2000; **46**: 591-593 [PMID: 10764697 DOI: 10.1136/gut.46.5.591a]

82 **Chu CM**, Liaw YF. Hepatitis B surface antigen seroclearance during chronic HBV infection. *Antivir Ther* 2010; **15**: 133-143 [PMID: 20386068 DOI: 10.3851/IMP1497]

83 **Wu H**, Zhao G, Qian F, Liu K, Xie J, Zhou H, Xu J, Xu Y, Han Y, Xie Q, Wang H. Association of IL28B polymorphisms with peginterferon treatment response in Chinese Han patients with HBeAg-positive chronic hepatitis B. *Liver Int* 2015; **35**: 473-481 [PMID: 24517415 DOI: 10.1111/liv.12491]

84 **Chang ML**, Liaw YF. Hepatitis B Flare in Hepatitis B e Antigen-Negative Patients: A Complicated Cascade of Innate and Adaptive Immune Responses. *Int J Mol Sci* 2022; **23** [PMID: 35163476 DOI: 10.3390/ijms23031552]

85 **Cao Z**, Liu Y, Ma L, Lu J, Jin Y, Ren S, He Z, Shen C, Chen X. A potent hepatitis B surface antigen response in subjects with inactive hepatitis B surface antigen carrier treated with pegylated-interferon alpha. *Hepatology* 2017; **66**: 1058-1066 [PMID: 28407271 DOI: 10.1002/hep.29213]

86 **Wu F**, Lu R, Liu Y, Wang Y, Tian Y, Li Y, Li M, Wang W, Zhang X, Jia X, Dang S. Efficacy and safety of peginterferon alpha monotherapy in Chinese inactive chronic hepatitis B virus carriers. *Liver Int* 2021; **41**: 2032-2045 [PMID: 33896094 DOI: 10.1111/liv.14897]

87 **Huang Y**, Qi M, Liao C, Xun J, Zou J, Huang H, Long LY, Chen J, Fan X, Chen R. Analysis of the Efficacy and Safety of PEGylated Interferon-α2b Treatment in Inactive Hepatitis B Surface Antigen Carriers. *Infect Dis Ther* 2021; **10**: 2323-2331 [PMID: 34350562 DOI: 10.1007/s40121-021-00511-w]

88 **Li MH**, Xie Y, Zhang L, Lu Y, Shen G, Wu SL, Chang M, Mu CQ, Hu LP, Hua WH, Song SJ, Zhang SF, Cheng J, Xu DZ. Hepatitis B surface antigen clearance in inactive hepatitis B surface antigen carriers treated with peginterferon alfa-2a. *World J Hepatol* 2016; **8**: 637-643 [PMID: 27239256 DOI: 10.4254/wjh.v8.i15.637]

89 **Terrault NA**, Lok ASF, McMahon BJ, Chang KM, Hwang JP, Jonas MM, Brown RS Jr, Bzowej NH, Wong JB. Update on Prevention, Diagnosis, and Treatment of Chronic Hepatitis B: AASLD 2018 Hepatitis B Guidance. *Clin Liver Dis (Hoboken)* 2018; **12**: 33-34 [PMID: 30988907 DOI: 10.1002/cld.728]

90 **European Association for the Study of the Liver**. EASL 2017 Clinical Practice Guidelines on the management of hepatitis B virus infection. *J Hepatol* 2017; **67**: 370-398 [PMID: 28427875 DOI: 10.1016/j.jhep.2017.03.021]

91 **Cusato J**, Boglione L, De Nicolò A, Imbornone R, Cardellino CS, Ghisetti V, Carcieri C, Cariti G, Di Perri G, D'Avolio A. Association of vitamin D pathway SNPs and clinical response to interferon in a cohort of HBeAg-negative patients. *Pharmacogenomics* 2017; **18**: 651-661 [PMID: 28453395 DOI: 10.2217/pgs-2016-0041]

World Journal of Gastroenterology

Submit a Manuscript: https://www.f6publishing.com

World J Gastroenterol 2022 October 28; 28(40): 5801-5806

DOI: 10.3748/wjg.v28.i40.5801

ISSN 1007-9327 (print) ISSN 2219-2840 (online)

MINIREVIEWS

Interaction between gut microbiota and COVID-19 and its vaccines

John S M Leung

Specialty type: Gastroenterology and hepatology

Provenance and peer review: Invited article; Externally peer reviewed.

Peer-review model: Single blind

Peer-review report's scientific quality classification

Grade A (Excellent): 0
Grade B (Very good): 0
Grade C (Good): C, C
Grade D (Fair): D
Grade E (Poor): 0

P-Reviewer: Almeida C, Portugal; Amedei A, Italy

Received: June 30, 2022
Peer-review started: June 30, 2022
First decision: August 1, 2022
Revised: September 7, 2022
Accepted: October 14, 2022
Article in press: October 14, 2022
Published online: October 28, 2022

John S M Leung, Cardiothoracic Unit, St. Paul's Hospital, Hong Kong, China

Corresponding author: John S M Leung, FRCS (Ed), MBBS, Doctor, Cardiothoracic Unit, St. Paul's Hospital, 2 Eastern Hospital Road, Hong Kong, China. leungsiumanjohn@yahoo.com.hk

Abstract

The whole world has been continuously afflicted by the coronavirus disease 2019 (COVID-19) pandemic for the past 3 years. Many countries have tried many methods to control this virus infection with varying successes and failures. The gut microbiota is a biosystem spanning the entire length of the digestive tract and playing important roles in health and disease. It is much affected by COVID-19. In return it also substantially impacts infection. In particular, the gut microbiota has established a bidirectional interaction with the COVID-19 vaccines, enhancing or reducing vaccine efficacy by virtue of its varying components. Conversely, COVID-19 vaccines also make a substantial impact on the gut microbiota, reducing its overall population and biodiversity. It is hoped that by exploring and harnessing this bidirectional interaction we may break new ground and develop new methods to prevent and treat this formidable virus infection.

Key Words: Gut microbiota; COVID-19 vaccines; Vaccine interactions; Gut microbiota alterations

©The Author(s) 2022. Published by Baishideng Publishing Group Inc. All rights reserved.

Core Tip: The gut microbiota is a biosystem spanning the entire length of the digestive tract and playing important roles in health and disease. It is much affected by coronavirus disease 2019 (COVID-19). In return it has impacts on the infection and a bidirectional interaction with the COVID-19 vaccines has been established, which enhances or reduces vaccine efficacy. Conversely, COVID-19 vaccines also make a substantial impact on the gut microbiota, reducing its overall population and biodiversity. By exploring and harnessing this bidirectional interaction we may hopefully break new ground and develop new methods to fight this formidable pandemic.

Citation: Leung JSM. Interaction between gut microbiota and COVID-19 and its vaccines. *World J Gastroenterol* 2022; 28(40): 5801-5806
URL: https://www.wjgnet.com/1007-9327/full/v28/i40/5801.htm
DOI: https://dx.doi.org/10.3748/wjg.v28.i40.5801

INTRODUCTION

The gut microbiota is a highly important and intriguing biosystem extending throughout the alimentary tract, covering an area of 400 square meters and with a biodiversity spanning over 2000 species, including protozoa, fungi, bacteria and viruses[1]. These organisms could be intraluminal or attached to the linings of the gut. Some even occupy an intracellular or subepithelial intercellular residence, while others enter the tissue fluid, the lymphatics and even the blood stream[1].

With such a background, the gut microbiota is constantly engaged in interactions with the various systems of the host and plays an important part both in health and in disease. In health, it is an integral part of digestion, absorption and nutrition. The contribution of gut microbiota in the production of vitamins of the B family and vitamin K has become common knowledge. More recently, it has been shown that gut microbiota, with their rich endowment of enzymes, could digest far more varieties of carbohydrates than their host could do alone[2]. Gut microbiota could also synthesize essential amino acids from inorganic nitrogen so that the host could survive even on a protein-free diet.

In fat metabolism, some bacteria are able to synthesize long chain fatty acids, contributing to the host energy supply as well as obesity, while many others, typically the strict anaerobes, ferment carbohydrates into short chain fatty acids (SCFAs). SCFAs inhibit histone deacetylase and activate G-protein coupled receptors with benefits in antioxidant, anti-inflammatory, antitumorigenic and antide-generative functions[3]. Indeed, research has shown the potential of fecal SCFA content as a marker of intestinal health, being at a lower level in colon cancer *vs* healthy controls[4]. Further studies of serum free fatty acid profiles especially the SCFA profiles show distinct patterns for healthy colon, colonic adenomatous polyps, colon cancer and coeliac disease reflecting the differences of gut microbiota among these conditions[5].

It is beyond the scope of this review to cover all aspects of the gut microbiota in health and disease but rather to focus on the intriguing interaction between the gut microbiota and coronavirus disease 2019 (COVID-19). The COVID-19 pandemic has been continuously ravaging the whole world for the past 2.5 years. Up to August 22, 2022, the World Health Organization's statistics showed the cumulative number of infected cases exceeded 211 million and was still increasing at 4.5 million *per* week, while the cumulative number of deaths had exceeded 4.4 million and was still increasing at around 68000 *per* week[6]. Various well-established methods of infection control have been tried, mostly with only partial success, and complete control remained elusive. Meanwhile, the phenomenon of "pandemic fatigue" has set in, and people become less inclined to adhere to control measures instead of tightening infection control measures[7]. In this review, aspects of gut microbiota that are relevant to the pandemic and its potential contribution to pandemic control was the focus.

GUT MANIFESTATION IN COVID-19 AND MICROBIOTA ALTERATIONS

The earliest report of COVID-19 in The Lancet on January 24, 2020 on the first 41 cases in Wuhan stated that diarrhea was the presenting symptom in only 1 case[8]. Three months later, when a New York center reported its first 393 cases of COVID-19[9], diarrhea was the presenting symptom in 23.7%. The incidence of diarrhea in the two districts remained almost unchanged over the next year with China at 3.80% diarrhea among 1141 cases[10] and New York at 20.14% diarrhea among 278 cases[11]. The difference is obvious and significant. Conceivably the diet in the Wuhan population is quite different from that in New York. It is probable that the gut microbiota in these two localities would also have a considerable difference, offering a plausible explanation of the increased diarrhea among the New York patients. In addition a Western diet, rich in processed meat but deficient in microbiota accessible carbohydrates, would have lower biodiversity[12] and less favorable to health. Unfortunately for the research investigator, most of these early studies did not report details of gut microbiota status, and the opportunity to study the influence of the gut microbiota on the early phase of the pandemic was lost.

GUT MICROBIOTA ALTERATIONS AND COVID-19 SEVERITY

By 2021, it became obvious that gut involvement and diarrhea were associated with greater severity of COVID-19[13]. An investigation in Hong Kong further demonstrated that certain components of the gut microbiota with immune-modulatory potential were depleted in severe and long-lasting COVID-19, notably *Faecalibacterium prausnitzii*, *Eubacterium rectale* and bifidobacterial species[14]. The investigators proposed that depletion of these bacteria could be taken as biomarkers predictive of severe and prolonged COVID-19. It is tempting to suggest that further studies might even explore the therapeutic value of replenishing these organisms to mitigate the disease.

GUT MICROBIOTA AND THE IMMUNE SYSTEM AND IMMUNE THERAPY

The interaction between the gut microbiota and the immune system goes far beyond the three groups of bacteria mentioned in the last section. In fact, beginning with the first colonization of the gut at birth or even before birth, the gut microbiota continuously evolve and influence the development of the host immune system, fostering reactivity against pathogenic invaders and tolerance towards harmless colonizers or beneficial symbionts[15]. Such actions are mediated by both regulatory cytokines (like interleukin-10 and interferon-beta) and T regulatory cells. This not only promotes diversity and increases beneficial microbes but actually helps to reduce host autoimmune disorders.

On the other hand, antibiotics have been shown to reduce the gut microbiota in both quantity and diversity, with reduced efficacy of immune checkpoint inhibitors in immunotherapy of cancer, and fecal transplantation has been shown to successfully restore the immune therapeutic response in such patients[16].

GUT MICROBIOTA'S IMPACT ON COVID-19 VACCINES: EFFICACY AND SIDE EFFECTS

With the foregoing background we now come to the important consideration of controlling the ongoing COVID-19 pandemic. It is common knowledge that pandemic control rests on five pathways: (1) Isolation of patients at the infectious stage by quarantines and social distancing; (2) Blocking the routes of infection by masking, air filtering/exchanging and sanitation; (3) Building up resistance among the population with vaccination; (4) Development of effective medicines to cure the infected patients and eliminate the carrier status; and (5) Letting the pandemic run its natural course, eliminating all susceptible components of the population and leaving those with inborn or naturally acquired immunity to survive.

The first four measures at present run into many obstacles, including social, economic, political, even personal egocentric considerations and biased sentiments. What is left is the fifth choice, otherwise called "herd immunity," a rather primitive, counter-intuitive and inhuman approach. Fortunately, amidst these dark looming clouds appears a silver lining. The gut microbiota might not only modify the COVID-19 disease but actually improve the efficacy and reduce the side effects of its vaccines, winning more skeptics to accept this highly important preventive measure.

This seminal work, a combined effort of the two universities in Hong Kong, was reported by Ng *et al*[17] and published on February 9, 2022[17]. It showed that for vaccine recipients of the inactivated virus, CoronaVac, the relatively low induction of neutralizing antibodies could be increased with a higher level of *Bifidobacterium adolescentis* (*B. adolescentis*) in the gut microbiota, while *Bacteroides vulgaris*, *Bacteroides thetaiotaomicron* and *Ruminococcus gnavus* were enriched in low responders. Another vaccine, the viral spike protein-encoded messenger RNA, BNT-162b, under the brand name Comirnaty, although capable of eliciting high antibody levels, could be further improved by the abundance of flagellate and fimbriate bacteria like *Roseburia faecis*. In addition, for both vaccines, enrichment of *Prevotella copri* and two *Megamonas* species led to fewer side effects, likely due to the anti-inflammatory influence of these organisms.

Interestingly, the role of *B. adolescentis* in CoronaVac seems very specific. So far, according to these researchers, any other species of the same *Bifidobacterium* genus tested would not work. As the species *B. adolescentis* is not present in commonly available health food or probiotic preparations, there seems no way to simply make an off-the-counter purchase of "health foods" to obtain such benefit. By contrast, the requirements of BNT-162b for *Roseburia faecis* seem less fastidious, and various bacteria with flagella and fimbriae might also impart benefit. Even *Bacteroides thetaiotaomicron*, known to be associated with low antibody production in CoronaVac, joins the company of antibody-enhancers for BNT-162b. This list may also include a minimal existence of *B. adolescentis* because the only BNT-162b recipient who failed to develop adequate antibody level was entirely devoid of *B. adolescentis*.

IMPACT OF COVID-19 VACCINES ON GUT MICROBIOTA: A BIDIRECTIONAL INTERACTION

Ng *et al*[17] not only showed the impact of gut microbiota on vaccine efficacy but also showed the impact of vaccination on gut microbiota 1 mo after delivering two doses[17]. For CoronaVac, only *Bacteroides caccae* was increased. For BNT-162b2, both *B. caccae* and *Alistipes shahii* increased. Common to both vaccines, a large number of species were diminished including *Adlercreutzia equolifaciens*, *Asaccharobacter celatus*, *Blautia obeum*, *Blautia wexlerae*, *Dorea formicigenerans*, *Dorea longicatena*, *Coprococcus comes*, *Streptococcus vestibularis*, *Collinsella aerofaciens* and *Ruminococcus obeum*[17]. There seemed to be a substantial loss of biodiversity, but no further elaboration on the clinical and pathological significance was mentioned. With such substantial changes in the gut microbiota one would expect some alterations in bowel habits after vaccination. On a theoretical basis, vaccine-induced loss of diversity would

Table 1 Diarrhea in persons aged 19-55 years after Pfizer-BioNTech coronavirus disease 2019 vaccination based on The Centers for Disease Control online published table[23] under the title "Vaccines and Immunizations"

Subjects	First injection number		Second injection number	
	Vaccine 2291	Placebo 2298	Vaccine 2098	Placebo 2103
Symptoms				
Any diarrhea	255 (11.10%)	270 (11.70%)	219 (10.40%)	177 (8.40%)
Severe diarrhea	3 (0.13%)	1 (0.04%)	4 (0.19%)	1 (0.05%)

increase the opportunity of pathogens to thrive in the intestine. There would be less competition for nutrition and for the niche of bacteria habitat, with less antagonistic factors produced by healthy bacteria such as bacteriocin and SCFAs to discourage the growth of pathogenic organisms[18]. With the proliferation of pathogenic organisms, the chance of diarrhea would be increased. Minor changes in bowel habits, however, tend to be under-reported, and severe diarrhea would tend to be so uncommon that it is often underpowered to establish a statistically significant conclusion. Table 1 was constructed from data published online by the Centers for Disease Control and Prevention (United States).

While there is no significant difference in mild diarrhea between recipients of vaccine and placebo, a signal of increased severe diarrhea among vaccine recipients seems to show up in the bottom row for both first and second injections, possibly reflecting the increase in severe diarrhea by 3.2 times (for first injection) to 3.8 times (for second injection) as a result of diminished diversity of gut microbiota. This table has two limitations. First, the actual number of severe diarrhea cases are too small for statistically significant computation. Second, no information is given for the composition of the microbiota of these patients, and it is not possible to relate the diarrhea to any particular organism or to the vaccine itself.

BIDIRECTIONAL INTERACTION BETWEEN GUT MICROBIOTA AND IMMUNE ACTIVITIES BEYOND COVID-19

Therapeutic agents, including vaccines, may have therapeutic value well beyond their originally intended effects. One of the best-known examples is the anti-tuberculosis BCG vaccine, whose role in protection against leprosy is well studied and documented[19]. For over 40 years it has also played a role in the treatment of non-muscle-invasive bladder cancer[20]. Indeed, many vaccines have been actively studied as a platform for anticancer treatment[21]. In certain areas, like hepatocellular carcinoma and carcinoma of the cervix, anti-viral vaccines have successfully prevented the cancer by preventing infection of the respective oncogenic virus. In other cancers, the mRNA technology has played a pivotal role in stimulating the patient's immune system to recognize and react against tumor-associated neo-antigens[22].

For three decades scientists have been struggling to iron out technical obstacles and the overall reluctance of recruiting the body's immune cells to produce an antigen and provoke an immune reaction, which is like retracing the steps of autoimmune disorders (the same sentiment still prevails among COVID-19 vaccine doubters today). Consequently, the predominant form of cancer immunotherapy at present is immune checkpoint inhibition, which involves abolishing major mechanisms of evasion of cancer from the host immunity *via* immune checkpoints. Even in this context, certain components of the gut microbiota, notably *Bifididobacterium longum* and *Akkermansia muciniphila* are found to be associated with good response to checkpoint inhibitors in melanoma and lung cancer, respectively, while lowered diversity and population of the gut microbiota under antibiotic treatment would have the opposite effect[16]. When the COVID-19 pandemic broke out, the mRNA-based vaccines, backed by years of research in previous anticancer immunotherapy, had a chance to be tested extensively and speedily with resounding success.

CONCLUSION

As mentioned earlier in the study of Ng *et al*[17], certain gut microbes could enhance vaccine efficacy in antibody stimulation while other microbes have the opposite effect[17]. Conversely, COVID-19 vaccines could impact the gut microbiota, enhancing the growth of some microbes but suppressing the growth of many others[17]. This bidirectional interaction between gut microbiota and COVID-19 vaccine is highly reminiscent of that between gut microbiota and anticancer immunotherapy. Conceivably, modifying the gut microbiota might enhance the vaccine-induced therapeutic value for both infection and cancer. It will take further study to understand and possibly harness such interactions and convert their potential therapeutic value into reality.

FOOTNOTES

Author contributions: Leung JSM is the sole author and contributed to the entire article.

Conflict-of-interest statement: JSM Leung has received no fees for serving as a speaker, holds no paid position for any organization, received no funding from any source. Nor is he an employee of any company or establishment. He owns no stocks or shares in any commercial company, nor any patency in any form or context.

Open-Access: This article is an open-access article that was selected by an in-house editor and fully peer-reviewed by external reviewers. It is distributed in accordance with the Creative Commons Attribution NonCommercial (CC BY-NC 4.0) license, which permits others to distribute, remix, adapt, build upon this work non-commercially, and license their derivative works on different terms, provided the original work is properly cited and the use is non-commercial. See: https://creativecommons.org/Licenses/by-nc/4.0/

Country/Territory of origin: China

ORCID number: John S M Leung 0000-0001-9283-2733.

S-Editor: Fan JR
L-Editor: Filipodia
P-Editor: Fan JR

REFERENCES

1 **Lazar V**, Ditu LM, Pircalabioru GG, Gheorghe I, Curutiu C, Holban AM, Picu A, Petcu L, Chifiriuc MC. Aspects of Gut Microbiota and Immune System Interactions in Infectious Diseases, Immunopathology, and Cancer. *Front Immunol* 2018; **9**: 1830 [PMID: 30158926 DOI: 10.3389/fimmu.2018.01830]
2 **Morowitz MJ**, Carlisle EM, Alverdy JC. Contributions of intestinal bacteria to nutrition and metabolism in the critically ill. *Surg Clin North Am* 2011; **91**: 771-785, viii [PMID: 21787967 DOI: 10.1016/j.suc.2011.05.001]
3 **Tan J**, McKenzie C, Potamitis M, Thorburn AN, Mackay CR, Macia L. The role of short-chain fatty acids in health and disease. *Adv Immunol* 2014; **121**: 91-119 [PMID: 24388214 DOI: 10.1016/B978-0-12-800100-4.00003-9]
4 **Niccolai E**, Baldi S, Ricci F, Russo E, Nannini G, Menicatti M, Poli G, Taddei A, Bartolucci G, Calabrò AS, Stingo FC, Amedei A. Evaluation and comparison of short chain fatty acids composition in gut diseases. *World J Gastroenterol* 2019; **25**: 5543-5558 [PMID: 31576099 DOI: 10.3748/wjg.v25.i36.5543]
5 **Baldi S**, Menicatti M, Nannini G, Niccolai E, Russo E, Ricci F, Pallecchi M, Romano F, Pedone M, Poli G, Renzi D, Taddei A, Calabrò AS, Stingo FC, Bartolucci G, Amedei A. Free Fatty Acids Signature in Human Intestinal Disorders: Significant Association between Butyric Acid and Celiac Disease. *Nutrients* 2021; **13** [PMID: 33652681 DOI: 10.3390/nu13030742]
6 **WHO Team**. Weekly epidemiological update on COVID-19. Edition 54. [cited 24 August 2021]. Available from: https://www.who.int/
7 **Chan EYY**, Kim JH, Kwok KO, Huang Z, Hung KKC, Wong ELY, Lee EKP, Wong SYS. Population Adherence to Infection Control Behaviors during Hong Kong's First and Third COVID-19 Waves: A Serial Cross-Sectional Study. *Int J Environ Res Public Health* 2021; **18** [PMID: 34769694 DOI: 10.3390/ijerph182111176]
8 **Huang C**, Wang Y, Li X, Ren L, Zhao J, Hu Y, Zhang L, Fan G, Xu J, Gu X, Cheng Z, Yu T, Xia J, Wei Y, Wu W, Xie X, Yin W, Li H, Liu M, Xiao Y, Gao H, Guo L, Xie J, Wang G, Jiang R, Gao Z, Jin Q, Wang J, Cao B. Clinical features of patients infected with 2019 novel coronavirus in Wuhan, China. *Lancet* 2020; **395**: 497-506 [PMID: 31986264 DOI: 10.1016/S0140-6736(20)30183-5]
9 **Goyal P**, Choi JJ, Pinheiro LC, Schenck EJ, Chen R, Jabri A, Satlin MJ, Campion TR Jr, Nahid M, Ringel JB, Hoffman KL, Alshak MN, Li HA, Wehmeyer GT, Rajan M, Reshetnyak E, Hupert N, Horn EM, Martinez FJ, Gulick RM, Safford MM. Clinical Characteristics of Covid-19 in New York City. *N Engl J Med* 2020; **382**: 2372-2374 [PMID: 32302078 DOI: 10.1056/NEJMc2010419]
10 **Luo S**, Zhang X, Xu H. Don't Overlook Digestive Symptoms in Patients With 2019 Novel Coronavirus Disease (COVID-19). *Clin Gastroenterol Hepatol* 2020; **18**: 1636-1637 [PMID: 32205220 DOI: 10.1016/j.cgh.2020.03.043]
11 **Nobel YR**, Phipps M, Zucker J, Lebwohl B, Wang TC, Sobieszczyk ME, Freedberg DE. Gastrointestinal Symptoms and Coronavirus Disease 2019: A Case-Control Study From the United States. *Gastroenterology* 2020; **159**: 373-375.e2 [PMID: 32294477 DOI: 10.1053/j.gastro.2020.04.017]
12 **Turnbaugh PJ**, Ridaura VK, Faith JJ, Rey FE, Knight R, Gordon JI. The effect of diet on the human gut microbiome: a metagenomic analysis in humanized gnotobiotic mice. *Sci Transl Med* 2009; **1**: 6ra14 [PMID: 20368178 DOI: 10.1126/scitranslmed.3000322]
13 **Baradaran A**, Malek A, Moazzen N, Abbasi Shaye Z. COVID-19 Associated Multisystem Inflammatory Syndrome: A Systematic Review and Meta-analysis. *Iran J Allergy Asthma Immunol* 2020; **19**: 570-588 [PMID: 33463127 DOI: 10.18502/ijaai.v19i6.4927]
14 **Yeoh YK**, Zuo T, Lui GC, Zhang F, Liu Q, Li AY, Chung AC, Cheung CP, Tso EY, Fung KS, Chan V, Ling L, Joynt G, Hui DS, Chow KM, Ng SSS, Li TC, Ng RW, Yip TC, Wong GL, Chan FK, Wong CK, Chan PK, Ng SC. Gut microbiota composition reflects disease severity and dysfunctional immune responses in patients with COVID-19. *Gut* 2021; **70**: 698-706 [PMID: 33431578 DOI: 10.1136/gutjnl-2020-323020]

15 **Kabat AM**, Srinivasan N, Maloy KJ. Modulation of immune development and function by intestinal microbiota. *Trends Immunol* 2014; **35**: 507-517 [PMID: 25172617 DOI: 10.1016/j.it.2014.07.010]
16 **Pierrard J**, Seront E. Impact of the gut microbiome on immune checkpoint inhibitor efficacy-a systematic review. *Curr Oncol* 2019; **26**: 395-403 [PMID: 31896938 DOI: 10.3747/co.26.5177]
17 **Ng SC**, Peng Y, Zhang L, Mok CK, Zhao S, Li A, Ching JY, Liu Y, Yan S, Chan DLS, Zhu J, Chen C, Fung AC, Wong KK, Hui DS, Chan FK, Tun HM. Gut microbiota composition is associated with SARS-CoV-2 vaccine immunogenicity and adverse events. *Gut* 2022; **71**: 1106-1116 [PMID: 35140064 DOI: 10.1136/gutjnl-2021-326563]
18 **Li Y**, Xia S, Jiang X, Feng C, Gong S, Ma J, Fang Z, Yin J, Yin Y. Gut Microbiota and Diarrhea: An Updated Review. *Front Cell Infect Microbiol* 2021; **11**: 625210 [PMID: 33937093 DOI: 10.3389/fcimb.2021.625210]
19 **Merle CS**, Cunha SS, Rodrigues LC. BCG vaccination and leprosy protection: review of current evidence and status of BCG in leprosy control. *Expert Rev Vaccines* 2010; **9**: 209-222 [PMID: 20109030 DOI: 10.1586/erv.09.161]
20 **Redelman-Sidi G**, Glickman MS, Bochner BH. The mechanism of action of BCG therapy for bladder cancer--a current perspective. *Nat Rev Urol* 2014; **11**: 153-162 [PMID: 24492433 DOI: 10.1038/nrurol.2014.15]
21 **Liu J**, Fu M, Wang M, Wan D, Wei Y, Wei X. Cancer vaccines as promising immuno-therapeutics: platforms and current progress. *J Hematol Oncol* 2022; **15**: 28 [PMID: 35303904 DOI: 10.1186/s13045-022-01247-x]
22 **Miao L**, Zhang Y, Huang L. mRNA vaccine for cancer immunotherapy. *Mol Cancer* 2021; **20**: 41 [PMID: 33632261 DOI: 10.1186/s12943-021-01335-5]
23 **CDC Website COVID-19 Vaccination>Product Info by U.S. Vaccine>Pfizer-BioNTech Vaccines**. Pfizer-BioNTech COVID-19 vaccine reactions & adverse events. [cited 10 July 2022]. Available from: https://www.cdc.gov/coronavirus/2019-ncov/

World Journal of Gastroenterology

Submit a Manuscript: https://www.f6publishing.com

World J Gastroenterol 2022 October 28; 28(40): 5807-5817

DOI: 10.3748/wjg.v28.i40.5807

ISSN 1007-9327 (print) ISSN 2219-2840 (online)

MINIREVIEWS

Improving the prognosis before and after liver transplantation: Is muscle a game changer?

Alexis Goffaux, Alicia Delorme, Géraldine Dahlqvist, Nicolas Lanthier

Specialty type: Gastroenterology and hepatology

Provenance and peer review: Invited article; Externally peer reviewed.

Peer-review model: Single blind

Peer-review report's scientific quality classification

Grade A (Excellent): 0
Grade B (Very good): B
Grade C (Good): C
Grade D (Fair): 0
Grade E (Poor): 0

P-Reviewer: Srpcic M, Slovenia; Tsoulfas G, Greece

Received: July 8, 2022
Peer-review started: July 8, 2022
First decision: August 19, 2022
Revised: August 30, 2022
Accepted: October 11, 2022
Article in press: October 11, 2022
Published online: October 28, 2022

Alexis Goffaux, Nicolas Lanthier, Laboratory of Hepato-Gastroenterology, Institut de Recherche Expérimentale et Clinique, Université catholique de Louvain, Brussels 1200, Belgium

Alexis Goffaux, Alicia Delorme, Géraldine Dahlqvist, Nicolas Lanthier, Service d'Hépato-Gastroentérologie, Cliniques universitaires Saint-Luc, Université catholique de Louvain, Brussels 1200, Belgium

Corresponding author: Nicolas Lanthier, MD, PhD, Doctor, Professor, Laboratory of Hepato-Gastroenterology, Institut de Recherche Expérimentale et Clinique, Université catholique de Louvain, Avenue Mounier, 52, Brussels 1200, Belgium. nicolas.lanthier@saintluc.uclouvain.be

Abstract

Liver transplantation (LT) is currently the only curative treatment option for selected patients with end stage liver disease or hepatocellular carcinoma. Improving waiting list-mortality, post-transplant morbidity and mortality and refining the selection of the patients remain our current central objectives. In this field, different concepts dealing with nutrition and the muscle such as sarcopenia, malnutrition, frailty or myosteatosis have emerged as possible game changers. For more than a decade, many prospective studies have demonstrated that sarcopenia and frailty are major predictive factors of mortality in the waiting list but also after LT. Malnutrition is also a well-known risk factor for morbidity and mortality. Muscle composition is a newer concept giving insight on muscle quality which has also been shown to be linked to poorer outcomes. Each of these terms has a precise definition as well as pathophysiological mechanisms. The bi-directional liver-muscle axis makes sense in this situation. Defining the best, easy to use in clinical practice tools to assess muscle quality, quantity, and function in this specific population and developing quality prospective studies to identify interventional strategies that could improve these parameters as well as evaluate the effect on mortality are among the important challenges of today.

Key Words: Muscle; Liver; Transplantation; Sarcopenia; Myosteatosis; Frailty

©The Author(s) 2022. Published by Baishideng Publishing Group Inc. All rights reserved.

Core Tip: Patients suffering from end stage liver disease currently have liver transplantation as the only curative treatment. In order to improve the pre and post transplantation management of patients, muscle related concepts such as sarcopenia, myosteatosis, frailty and malnutrition could be important potential game changers. Considering a bidirectional axis between the muscle and the liver, it is therefore justified to characterize the condition of the muscles adequately and to identify interventional strategies that could improve both muscle parameters and patient survival.

Citation: Goffaux A, Delorme A, Dahlqvist G, Lanthier N. Improving the prognosis before and after liver transplantation: Is muscle a game changer? *World J Gastroenterol* 2022; 28(40): 5807-5817
URL: https://www.wjgnet.com/1007-9327/full/v28/i40/5807.htm
DOI: https://dx.doi.org/10.3748/wjg.v28.i40.5807

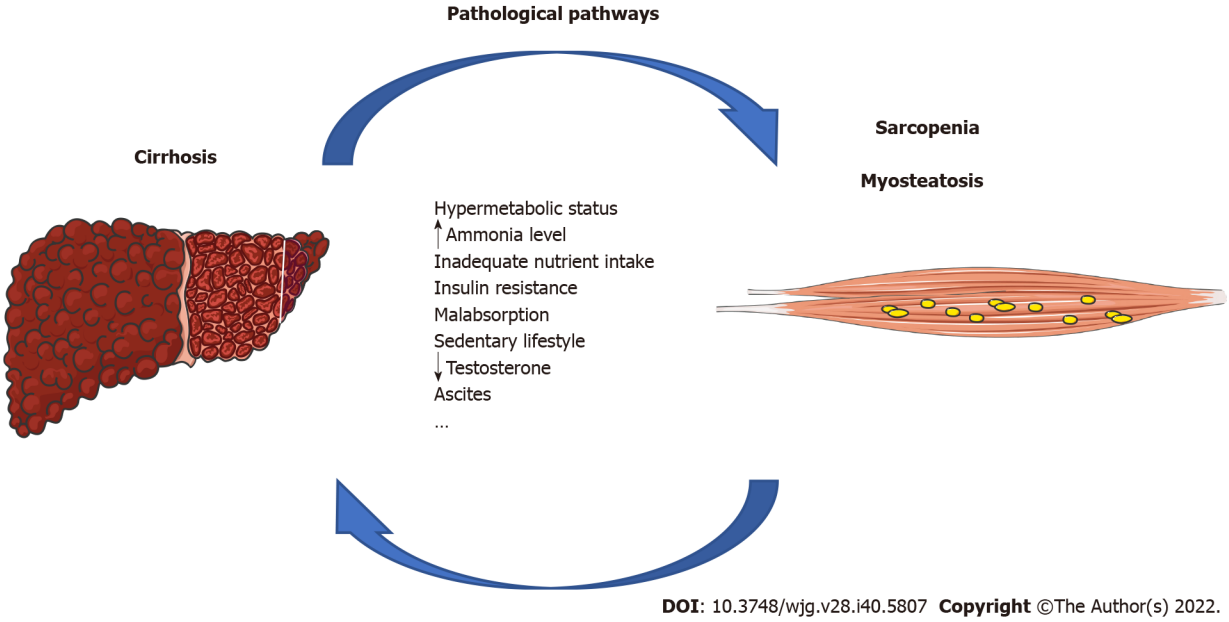
INTRODUCTION

To date, despite medical developments in knowledge and drug treatments, liver transplantation (LT) remains the only curative treatment option for selected patients with acute liver failure, end-stage liver disease (ESLD), liver cancer and acquired or genetic metabolic liver disease[1]. ESLD is the most frequent indication for LT with alcohol-related liver disease as the main etiology[2]. Other common etiologies are metabolic dysfunction-associated fatty liver disease (MAFLD) and viral hepatitis[3,4]. Autoimmune related liver diseases and cholestatic diseases are rarer indications in Western countries. The epidemiology of LT has changed over the last 20 years since the selection of patients suffering from hepatocellular carcinoma (HCC) with the Milan criteria and the progressive eradication of hepatitis C virus since the universal use of direct-acting antivirals[5]. MAFLD is probably becoming one of the main indications for LT in parallel with the epidemic of obesity in Western countries. This disease can coexist with other causes and act as an important co-factor. This specific population represents a series of challenges in the pre-, peri- and post-transplant settings due to the presence of medical comorbidities that include obesity, type 2 diabetes and cardiovascular risk factors[6,7].

For years, graft allocation has been based on the model for end-stage liver disease (MELD) score that has been used to predict 3-mo mortality on the waiting list. The use of the MELD score has led to a better selection of patients requiring LT but also to a reduction in waiting time and a reduction in mortality on the waiting list[8]. However, the score suffers from several limitations: Patients with cholestatic liver diseases, severe portal hypertension as well as those with hepatic encephalopathy are disadvantaged due to a preserved synthesis function which does not reflect the severity of the disease and the related morbimortality. Another major limitation is the absence of assessment of malnutrition and more specifically of sarcopenia[8-10]. Abnormalities of body composition are frequently found in patients with chronic diseases such as cirrhosis. Interestingly, there is a close relationship between the skeletal muscle compartment and liver function (Figure 1)[11].

In the field of chronic liver disease (CLD) and particularly ESLD and LT, different concepts have emerged and are commonly used, such as sarcopenia, malnutrition, frailty or myosteatosis[12]. They affect between 40%-70% of cirrhotic patients with important clinical outcomes. They have been evaluated independently in different studies and it is confirmed that they are robust predictors of poor outcomes[13]. This fragile population is at increased risk of hepatic decompensation, reduced quality of life, increased risk of infection, and prolonged hospitalization. It leads to a higher morbidity and mortality[14,15]. Adding the concept of frailty on the waiting list prioritization, specifically helps a population that is listed with low priority based on a low MELD score (< 15). While adding muscle surface to the MELD score had limited added value for organ allocation in a global cirrhotic population, this measurement is highly correlated with waiting list mortality in patients with low MELD score (< 15) [16]. It is therefore important to define the best tools to evaluate these functional concepts in the field of liver diseases and LT[13].

Understanding these different concepts and their implications in our clinical practice is of major interest to improve the management of our patients. There is clearly a certain overlap in these definitions, but it is important to understand them separately to develop tailored behavioral interventions and targeted pharmacotherapies for these conditions[17]. It is necessary to clearly define the gold standard of sarcopenia management with standardized cut-offs for this specific cirrhotic population. These clear definitions will allow us to evaluate the impact of interventions on patients' outcome[13]. We then review the pathophysiology of cirrhosis-related sarcopenia and myosteatosis, provide a narrative review of the major studies on the subject and discuss the tools available for muscle assessment and treatment.



DOI: 10.3748/wjg.v28.i40.5807 **Copyright** ©The Author(s) 2022.

Figure 1 Summary of pathways linking sarcopenia and myosteatosis to cirrhosis: A bi-directional communication. This figure was partly created using Servier Medical Art templates (https://smart.servier.com).

DEFINITIONS OF COMMONLY USED YET DISTINCT CONCEPTS

As explained above, various terms are now frequently used in the field of CLD, sometimes incorrectly or inappropriately. However, they each have a precise definition.

Malnutrition

Malnutrition can be defined as a state resulting from an insufficient intake of nutrients or an imbalance in essential nutrients and/or in their utilization. This imbalance will have a deleterious impact on the body composition and body cell mass that could lead to diminished physical and mental function, as well as impaired clinical outcomes from disease. Malnutrition has multiple causes combined or take alone, which are starvation and diseases such as CLD and aging[18]. It is also important to note that malnutrition can affect the entire body mass index (BMI) spectrum from obese to anorexic[17]. Different clinical scores exist to estimate the presence of malnutrition such as the nutritional risk score or the Global Leadership Initiative on Malnutrition criteria. Malnutrition is associated with increased mortality in cirrhotic patients[19].

Sarcopenia

The term sarcopenia comes from Greek origin and literally means the "loss of flesh". Sarcopenia is characterized by 3 components: Decreased muscle mass, decreased muscle strength as well as decreased physical performance[20]. Initially, sarcopenia was described as associated with aging. The term is now also used in association with chronic diseases such as cirrhosis[12]. Nevertheless, even today, the criteria to be included as well as the cut-off values are still discussed. The diagnosis of sarcopenia is still complicated today as the criteria can be so variable, especially in obese people[21]. Cutoffs for muscle mass depletion exist but are still currently under debate. Nevertheless, the use of muscle area measurement at the level of the third lumbar vertebra on a computed tomography (CT) slice is recognized as acceptable by relating the muscle area to the patient's height squared [skeletal muscle index (SMI)]. By extension, the term sarcopenia is often used based on the sole criterion of low muscle area. Sarcopenia is then defined when SMI is < 41 cm^2/m^2 for a woman and < 53 cm^2/m^2 for a man in the field of obesity[22] or < 39 cm^2/m^2 for a woman and < 50 cm^2/m^2 for a man in the field of ESLD[23]. In the field of liver diseases, this measure is particularly interesting because it is minimally affected by hydro-sodium retention. Measurement of the brachial circumference (BC) or mid-arm muscle circumference and arm strength using the hand dynamometer are other frequently used techniques.

Myosteatosis

Myosteatosis can be defined as the ectopic accumulation of fat in the muscle. This increased accumulation around and within the myocyte can lead to an impairment of normal physiological function. We will therefore speak of intra and extra cellular fat. It can be estimated on the basis of the decrease in muscle density on an ultrasound image or a CT scan section for example[24,25]. A skeletal muscle radiation attenuation below 41 Hounsfield units (HU) in normal weight patients (BMI up to 24.9 kg/m^2)

and 33 HU in overweight patients (BMI ≥ 25 kg/m²) could be used[24]. Muscle density can also be related to the muscle surface to give an idea of the absolute amount of intramuscular fat[26]. This leads to the following parameters: The skeletal muscle density index (SMDI)[27] and the skeletal muscle fat index (SMFI) described in patients with MAFLD without ESLD[26,28]. Different groups of patients are compared in clinical studies, but pathological cut-offs for SMDI or SMFI are not yet defined[26-28]. Finally, imaging allows us to assess the homogeneous or heterogeneous distribution of fat in the muscle. This parameter can be associated with certain pathological conditions[29].

Frailty

Defined in the field of geriatrics, frailty is considered a metabolic syndrome associated with a decrease in physiological reserves and an increase in vulnerability to stress factors. In the case of cirrhosis, the stressors are variable, ranging from a dysfunction in protein synthesis to muscle toxicity. A reproducible and objective assessment of patients with liver disease is offered by several simple, non-invasive tests. For example, based on the results of handgrip, sit to stand and balance tests, the liver frailty index (LFI) can be calculated. A patient is considered frail if the score is between 4.5 and 6[15].

Physical exercise

Physical exercise is defined as activity requiring physical effort, performed specifically to maintain or improve health and fitness. The term is therefore relevant to physical activity interventions offered to patients with CLD to improve their condition. The data available so far concerns patients with compensated liver disease with no separate results for patients with ESLD[30]. An increase in functional capacity, strength and muscle mass is noted in the patients with compensated cirrhosis who are subjected to physical exercise for 12 wk and then compared to a group of patients with relaxation activity[31]. In patients awaiting LT, specific protocols are being evaluated (NCT04604860, NCT05061576, NCT05237583, *etc*). The type (endurance and/or resistance), duration and frequency should be determined, bearing in mind that these programs must be adapted to the patients' situation (safety, absence of contraindications).

PATHOPHYSIOLOGICAL BASIS OF SARCOPENIA AND MYOSTEATOSIS IN END STAGE LIVER DISEASE

Several mechanisms exist that link sarcopenia to CLD and ESLD. Nevertheless, these exact mechanisms are particularly not well known. Sarcopenia is often a feature of malnutrition. The reasons for this malnutrition, in the case of cirrhosis, are multiple and often result from the combination of several factors (Figure 1)[32]. The first factor in the context of CLD and cirrhosis is the presence of a hypermetabolic status resulting from chronic inflammation and altered gut barrier function[33]. Low liver glycogen content induces muscle protein catabolism for blood glucose maintenance[34]. In addition, ascites present in cirrhotic patients may be responsible for an increase of energy expenditure and therefore increase the catabolism of protein[35]. Partly due to the pro-inflammatory environment, patients with cirrhosis and HCC showed accelerated sarcopenia[36]. Second, the hyperammonemia level is also increased due to its poor elimination because of a pathological architecture of the liver. The consequence of this increase will be the activation of myostatin and consequently the inactivation of protein synthesis which will lead to sarcopenia. Third, inadequate intake of micro and macronutrients can be due in cirrhotic patients to loss of appetite (dysgeusia, cytokines), prolonged gastric emptying or a restrictive diet (sodium and protein) for example. The sedentary lifestyle is probably the most obvious factor in sarcopenia. Indeed, a study showed that one of the causes of sarcopenia in the elderly was partly due to lack of physical exercise[20]. It is therefore easy to think that decompensated cirrhotic patients with high frailty and malnutrition may also suffer from a lack of physical activity aggravating their sarcopenia even more. Fourth, cirrhosis is associated with some degree of cholestasis. An increase in bile acids related to deregulation of the enterohepatic cycle (also due to the dysbiosis associated with cirrhosis) is observed. These have a potentially toxic effect, particularly on the muscle that expresses some bile acid receptors, inducing muscle atrophy[37]. Malabsorption in the context of cirrhosis also plays an important role. A decrease in bile excretion will result in a decrease in the reabsorption of lipids and certain lipo-soluble vitamins. Altered intestinal motility as well as changes in the composition of the gut microbiota will also affect nutrient absorption and utilization[33]. Finally, in cirrhotic patients, a decrease of testosterone levels has been associated with a decrease of muscle mass that could favor sarcopenia[34].

The mechanism through which myosteatosis occurs is still not well understood. Myosteatosis is a well-known characteristic of patients with CLD due to MAFLD[27]. Cirrhotic patients are also characterized by muscle insulin resistance, regardless of the cause of the cirrhosis[34]. This insulin resistance status may also be responsible for myosteatosis[34]. Other proposed mechanisms include hyperammonemia (inducing impaired mitochondrial oxidative phosphorylation and decreased lipid oxidation in muscle), decreased lipid storage capacity within the subcutaneous adipose tissue and age-related differ-

entiation of muscle stem cells into adipocytes[38].

WHY IS IT IMPORTANT TO CONSIDER THE MUSCLE IN A LIVER TRANSPLANT SETTING?

Screening and preventing sarcopenia and frailty is of major interest to patients with CLD. The challenge is big because muscle composition and muscle function have a direct impact on the prognosis of the cirrhotic patient. Sarcopenia and frailty will condition the prognosis of the cirrhotic patients awaiting LT, independently of the severity of the liver disease (MELD score)[39]. Table 1 summarizes the main studies investigating the deleterious role of sarcopenia, frailty and myosteatosis in the context of LT.

For more than a decade, many prospective studies have demonstrated that low muscle mass is a major predictive factor of mortality in the waiting list but also after LT. In a study involving more than 200 patients on the waiting list, both low muscle quantity and quality were independent risk factors for mortality in patients with ESLD[40]. Low muscle mass is more frequent in patients with hepatic encephalopathy and associates with poor survival[41]. Two meta-analyses confirm these results, the first one includes more than 19 studies with 3800 patients awaiting LT. Sarcopenia was assessed by a wide range of CT-assessed skeletal muscle mass cut-points. Despite these limitations, the study described an independent association between low muscle mass and the post-LT and the waiting list mortality[42]. The second meta-analysis, although it has multiple biases, shows an association between sarcopenia in the pre-LT period and greater post-operative mortality, higher infection risk and post-operative complications, longer intensive care unit stay and ventilator dependency[43].

In patients with cirrhosis (decompensated or not), frailty, easily measured by the LFI, is an independent predictor of death, cirrhosis progression and unplanned hospitalizations (mainly due to infections)[44]. Frail cirrhotic patients also have an increased risk of acute kidney injury[45] and hepatorenal syndrome[46]. In cirrhotic patients awaiting LT, frailty is associated with a 2-fold increased risk of mortality, regardless of the presence of ascites or hepatic encephalopathy[15]. Frail cirrhotic LT recipients have increased postoperative morbidity with prolonged hospital stays[47] and an increased risk of acute rejection[48].

While the link between sarcopenia and mortality is well established, the long-term prognostic value of skeletal muscle quality is less clear. However, several studies tend to demonstrate that pre-transplant myosteatosis is an important prognostic marker for LT recipients in the post-operative period. The prognosis value of myosteatosis seems to be particularly important in the early post-operative phase with higher rates of deaths due to respiratory and septic complications[48]. Unfortunately, most studies are retrospective and the clinical impact of myosteatosis on the transplant waiting list still needs to be demonstrated with prospective studies.

In view of these results, the American Association for the Study of Liver Diseases guidance document suggests that all cirrhotic patients should be assessed for sarcopenia and frailty with standardized tools both at baseline and longitudinally[17]. These recommendations are consistent with the implementation of specific protocols such as "enhanced recovery after surgery" protocols to improve recovery after surgery, especially for LT candidates[49].

HOW TO EVALUATE THE MUSCLE IN ROUTINE PRACTICE?

To assess physical activity, muscle function, composition and mass, several tools exist. It is important to note that many tests, questionnaires and radiological methods are possible. A non-exhaustive list of these tools is presented in Table 2 with their advantages and disadvantages. Some of them have been included in a recent review manuscript[50]. It is interesting to note that patients' baseline physical activity can be assessed by questionnaire or objective measurement (Table 2). Easy tests are possible in consultation or at the patient's bedside, such as measuring BC or handgrip strength. Tests that are more complex to implement in routine practice are also available, such as the 6 min walk test, which correlates well with survival in patients awaiting LT[51], or isokinetic testing, the detailed results of which have given interesting information in other diseases such as type 2 diabetes[29]. Finally, among imaging techniques, the same dilemma exists between easier and less expensive techniques (such as ultrasound)[52,53] and time-consuming but probably more objective and reproducible techniques (such as CT or magnetic resonance imaging)[54] (Table 2).

HOW TO IMPROVE THE MUSCLE IN CLINICAL PRACTICE?

It is well defined that malnutrition plays a major role in the prognosis of the cirrhotic patient and that the resulting loss of muscle mass is a real complication of cirrhotic disease with a significant impact on the morbidity and mortality of these patients. All patients with CLD should be evaluated for nutrition

Table 1 Main studies investigating the deleterious role of frailty, low muscle mass, sarcopenia and myosteatosis in patients undergoing pre-transplant assessment

Ref.	Patient selection	Patients, *n*	Sarcopenia, myosteatosis	Frailty parameters	Outcome	Results
Lai *et al* [15], 2019	Ambulatory cirrhotic patients awaiting LT	1014	Non applicable	LFI	Waiting list mortality	Frailty: 25%. HR = 1.82; 95%CI: 1.31-2.52; P < 0.001
Fozouni *et al*[48], 2020	LT recipients	241	Non applicable	LFI	Acute cellular rejection within 3 mo post-LT	Frailty: 19%. OR = 3.3; 95%CI: 1.2-9.3; P = 0.02
Lai *et al* [47], 2022	LT recipients	1166	Non applicable	LFI	LT LOS. ICU stay. Inpatient days within 3 mo post-LT. Overall survival (1-3 and 5-yr mortality)	Frailty: 21%. Prolonged LT LOS: OR = 2.00; 95%CI: 1.47-2.73. ICU stay: OR = 1.56; 95%CI: 1.12-2.14. Inpatient days within 3 mo. post-LT: OR = 1.72; 95%CI: 1.25-2.37. Overall survival: P = 0.02
Bhanji *et al*[41], 2018	Cirrhotic patients assessed for LT	675	L3-MA (HU). L3-SMI	Non applicable	HE. Mortality	Sarcopenia: 36%. HE: OR = 2.42; 95%CI: 1.43-4.10; P = 0.001. Mortality: Univariate HR = 2.02; 95%CI: 1.57-2.58; P < 0.001. Multivariate: HR = 2.15; 95%CI: 1.52-3.05; P < 0.001. Myosteatosis: 52%. HE: OR = 2.25; 95%CI: 1.32-3.85; P = 0.003. Mortality: Univariate: HR = 1.45; P = 0.004; 95%CI: 1.16-2.91. Multivariate: P = 0.69
Van Vugt *et al*[42], 2016	LT candidates/recipients	3804. Meta-analysis	SMI. Total psoas area	Non applicable	Waiting list mortality. Post-LT mortality	Waiting list mortality: HR = 1.72; 95%CI: 0.99-3.00; P = 0.02. Post-LT mortality: HR = 1.84; 95%CI: 1.11-3.05; P = 0.05
Bot *et al* [40], 2021	ESLD patients awaiting LT	262	L3-SMI (cm^2/m^2). L3-MA (HU)	Non applicable	Waiting list mortality	Low SMI: HR = 2.580; 95%CI: 1.055-6.308. MA: HR = 9.124; 95%CI: 2.871-28.970
Czigany *et al*[24], 2020	LT recipients	225	L3-SMI. L3-MA (HU)	Non applicable	Major morbidity. ICU stay. LT LOS	Sarcopenia: 37%. Myosteatosis: 44%. Major morbidity: OR = 2.772; 95%CI: 1.516-5.066; P = 0.001. ICU stay: 18 ± 25 *vs* 11 ± 21 d, P < 0.001. LT LOS: 56 ± 55 *vs* 33 ± 24 d, P < 0.001

LFI: Liver frailty index; HR: Hazard ratio; CI: Confidence interval; LT: Liver transplantation; OR: Odds ratio; LT LOS: Liver transplantation length of stay; ICU: Intensive care unit; L3-MA: Lumbar 3-muscle attenuation; HU: Hounsfield unit; L3-SMI: Lumbar 3-skeletal muscle index; HE: Hepatic encephalopathy; SMI: Skeletal muscle index; ESLD: End stage liver disease.

and sarcopenia at the time of diagnosis and then regularly at least annually for compensated cirrhosis and every 8-12 wk for decompensated cirrhosis[17]. The ultimate goal of the medical practitioner is the prevention of the occurrence of complications that may result from sarcopenia and undernutrition. Nevertheless, although there is no clear evidence for an appropriate guideline for patients at present, the current management in transplant centers is that patients with cirrhosis who are placed on the list benefit from efforts by the multidisciplinary team to try to preserve muscle mass and function, through the interventions of dieticians (screening for undernutrition, implementation of standard nutritional measures, early oral intake) and physical therapists (mobilization)[54]. However, it is not yet proven that we are able to slow down the progression of complications or reverse advanced situations *via* muscle targeted interventions[13]. There are two main options, non-exclusive: Dietary interventions and physical activity. Additional specific pharmacological measures are under investigation.

The current nutrition guidelines for patients with CLD recommend a weight-based daily caloric intake of at least 35 kcal/kg/d with a protein intake of 1.2-1.5 g/kg/d[18]. These recommendations are derived from data assessing energy expenditure (indirect calorimetry). They are difficult to achieve in routine practice. Protein intake is easily found in staple foods such as meat and vegetables. Several studies have analyzed the benefit of branched-chain amino acid (BCAA) supplementation but the results of these data are contradictory. While some authors suggest that BCAA improve hepatic encephalopathy and muscle mass[55], a meta-analysis shows that there is no effect on mortality and nutritional parameters[56]. Because of these contradictions and the limitations of clinical studies, BCAA supplementation is not currently recommended. Prolonged periods of fasting should be avoided in cirrhosis and it is important to favor split meals associated with a late evening snack or an early morning breakfast[17]. Oral nutritional supplements given before bedtime showed a muscle benefit in Child A patients but not Child B or C[57]. If not achieved *via* oral route, energy intake *via* enteral nutritional supplementation may be considered to achieve targets.

Besides these nutritional recommendations, physical activity improvement is also important. The latest recommendations propose to assess frailty and/or sarcopenia with standardized tools in order to define a personalized approach for the sarcopenic patient. This personalized activity prescription is

Table 2 Set of techniques to evaluate the physical activity as well as the quantity and quality of muscle

Technique	Goal	Advantages	Disadvantages
Physical activity assessment			
IPAQ	Reflects physical activity over the last 7 d	Easier to implement. Understandable for the patient. Representative over 7 d	Subjective. Poor estimation by the patient
Pedometer	Measures walking activity	Inexpensive and easy to set up. Represents the physical activity of walking	Reliability decreases with walking speed. Could induce changes in patient's habits. Does not measure other physical activities
Accelerometer	Measures walking activity	Takes slope and weight carried in consideration	Long to wear for good representation. Not sensitive to the inclination of the walk or the load worn during the walk. Could induce changes in patient's habits
Anthropometric measurement			
BC	Gives information on arm circumference and stage of muscle mass depletion	Very easy to perform (requires only a tape measure)	User dependent
MAMC (BC-TSF)	Gives information on arm muscle volume	Well described and easy to perform. Assesses muscle volume better than BC alone	User dependent. Requires a caliper
BIA	Allows to assess the body composition	Simple. Non-invasive. Reproductible	Requires specific equipment. Varies with fluid retention (common in cirrhosis)
Function tests			
Handgrip	Allows to measure the strength of the forearm and wrist muscles	Low cost. Easy to perform. Gold standard	Not representative of total body strength
6MWT	Measures distance walked for 6 min	Easy to perform. Reflects endurance and general fitness	Caution in patients with cardiac and respiratory problems
LFI	Measures frailty of patients calculated with a score	Easy to perform. Little training	Not assessable in severe encephalopathy
Isokinetic	Measures the function and strength of a of group muscles	Gold standard. Reproducible	Cost. Requires training and collaboration. Caution in patients with cardiac and respiratory problems
Leg press	Measures the strength of the lower limbs	Simple device	Requires collaboration. Rougher assessment. Not well evaluated/used
Imaging techniques			
US	Allows to measure the echogenicity of the muscle	Non-invasive. Not expensive	User dependent. Variability with fat thickness, position of the probe. Requires training
CT-scan	Allows to measure the surface of the muscle (easily) as well as its density	Clear image. Reproduceable	Radiation exposition
MRI	Can be used to evaluate the muscle surface. Measures the amount of fat within the muscle (PDFF)	Clear image. Reproduceable	Cost. Time consuming. Contra-indications (claustrophobia, pacemaker, *etc*)
DXA	Allows to measure the body composition (muscle, fat, water, *etc*)	Clear image. Reproduceable	Radiation exposition. Varies with fluid retention (common in cirrhosis)

IPAQ: International physical activity questionnaire; BMI: Body mass index; BC: Brachial circumference; TSF: Tricipital skin fold; MAMC: Mid-arm muscle circumference; BIA: Bio-impedance analysis; 6MWT: 6 min walk test; LFI: Liver frailty index; US: Ultrasound; CT-Scan: Computed tomography scan; MRI: Magnetic resonance imaging; PDFF: Proton density fat fraction; DXA: Dual x-ray absorptiometry.

guided by the principles of frequency-intensity-time-type: A combination of aerobic exercise that improves cardiorespiratory endurance and resistance exercise that improves strength and skeletal muscle mass[17]. Personalized physical activity allows patients to improve their cardiopulmonary capacity and quality of life. Unfortunately, current randomized controlled data are limited by small samples of well-compensated cirrhosis patients (mean MELD = 10)[31,58]. Despite these promising results, there are no randomized controlled studies with patients with ESLD or a waiting list for LT. It is therefore not currently possible to conclude whether a personalized physical activity program would improve the outcomes in the waiting list and post-LT surgery.

Several randomized controlled trials evaluating the benefit of nutritional and/or physical exercise on muscle mass (SMI) and frailty (LFI) pre- and post-LT would help to answer these uncertainties. Finally, pharmacological treatments are being studied to treat sarcopenia (hormone replacement therapy such as testosterone or growth hormone, ammonia reduction and myostatin inhibition)[59].

CONCLUSION

Malnutrition, sarcopenia and frailty are very common in patients with cirrhosis, especially in cases of disease requiring organ transplantation. Bi-directional pathophysiological links exist between muscle and liver that underlie this association. This highlights the interest of prospective studies comparing the different tools at our disposal to evaluate the cirrhotic patient as well as translational studies to understand these mechanisms and find a possible therapeutic or diagnostic target. Through a better understanding of mechanistic links, the muscle can become a game changer. A better understanding of the situation will also allow us to prioritize fragile patients who need a faster LT or to identify negative factors in certain recipients in whom the situation would be irreversible post-LT and deleterious to the graft. Interventional strategies (nutritional, physical exercise and pharmacological treatments) are also being evaluated. The rationale for their efficacy is clear, even if at this ESLD, evidence of their impact on reducing pre-LT and post-LT mortality is lacking, as well as a precise characterization of the protocols to be implemented. Again, quality prospective studies will be able to answer this question.

FOOTNOTES

Author contributions: Goffaux A, Delorme A, Dahlqvist G and Lanthier N participated in the writing of this manuscript (literature review, first versions and corrections); and all authors have read and approve the final manuscript.

Conflict-of-interest statement: All the authors report no relevant conflicts of interest for this article.

Open-Access: This article is an open-access article that was selected by an in-house editor and fully peer-reviewed by external reviewers. It is distributed in accordance with the Creative Commons Attribution NonCommercial (CC BY-NC 4.0) license, which permits others to distribute, remix, adapt, build upon this work non-commercially, and license their derivative works on different terms, provided the original work is properly cited and the use is non-commercial. See: https://creativecommons.org/Licenses/by-nc/4.0/

Country/Territory of origin: Belgium

ORCID number: Alexis Goffaux 0000-0002-0126-699X; Géraldine Dahlqvist 0000-0002-4661-7650; Nicolas Lanthier 0000-0002-7651-9314.

S-Editor: Wang JJ
L-Editor: Filipodia
P-Editor: Wang JJ

REFERENCES

1 **Mahmud N**. Selection for Liver Transplantation: Indications and Evaluation. *Curr Hepatol Rep* 2020; **19**: 203-212 [PMID: 32837824 DOI: 10.1007/s11901-020-00527-9]
2 **Singal AK**, Kwo P, Kwong A, Liangpunsakul S, Louvet A, Mandrekar P, McClain C, Mellinger J, Szabo G, Terrault N, Thursz M, Winder GS, Kim WR, Shah VH. Research methodologies to address clinical unmet needs and challenges in alcohol-associated liver disease. *Hepatology* 2022; **75**: 1026-1037 [PMID: 34496071 DOI: 10.1002/hep.32143]
3 **Lanthier N**, Vanuytsel T. Metabolic dysfunction-associated fatty liver disease: a new clearer nomenclature with positive diagnostic criteria. *Acta Gastroenterol Belg* 2020; **83**: 513-515 [PMID: 33321005]
4 **Hamoir C**, Horsmans Y, Stärkel P, Dahlqvist G, Negrin Dastis S, Lanthier N. Risk of hepatocellular carcinoma and fibrosis evolution in hepatitis C patients with severe fibrosis or cirrhosis treated with direct acting antiviral agents. *Acta Gastroenterol Belg* 2021; **84**: 25-32 [PMID: 33639690 DOI: 10.51821/84.1.420]
5 **Dahlqvist G**, Moreno C, Starkel P, Detry O, Coubeau L, Jochmans I. Innovations in liver transplantation in 2020, position of the Belgian Liver Intestine Advisory Committee (BeLIAC). *Acta Gastroenterol Belg* 2021; **84**: 347-359 [PMID: 34217187 DOI: 10.51821/84.2.347]
6 **Gill MG**, Majumdar A. Metabolic associated fatty liver disease: Addressing a new era in liver transplantation. *World J Hepatol* 2020; **12**: 1168-1181 [PMID: 33442446 DOI: 10.4254/wjh.v12.i12.1168]
7 **Lanthier N**. Les nouveaux traitements de la stéatohépatite non-alcooliqueNew therapies in non-alcoholic steatohepatitis. *Nutr Clin Metab* 2020; **34**: 216-222 [DOI: 10.1016/j.nupar.2020.04.003]

8 **Durand F**, Buyse S, Francoz C, Laouénan C, Bruno O, Belghiti J, Moreau R, Vilgrain V, Valla D. Prognostic value of muscle atrophy in cirrhosis using psoas muscle thickness on computed tomography. *J Hepatol* 2014; **60**: 1151-1157 [PMID: 24607622 DOI: 10.1016/j.jhep.2014.02.026]

9 **Ebadi M**, Montano-Loza AJ. Sarcopenia and Frailty in the Prognosis of Patients on the Liver Transplant Waiting List. *Liver Transpl* 2019; **25**: 7-9 [PMID: 30472786 DOI: 10.1002/lt.25386]

10 **Artru F**, le Goffic C, Pageaux GP, Saliba F, Louvet A. Sarcopenia should be evaluated in patients with acute-on-chronic liver failure and candidates for liver transplantation. *J Hepatol* 2022; **76**: 983-985 [PMID: 34536432 DOI: 10.1016/j.jhep.2021.09.004]

11 **Sinclair M**, Gow PJ, Grossmann M, Angus PW. Review article: sarcopenia in cirrhosis--aetiology, implications and potential therapeutic interventions. *Aliment Pharmacol Ther* 2016; **43**: 765-777 [PMID: 26847265 DOI: 10.1111/apt.13549]

12 **Lanthier N**, Stärkel P, Dahlqvist G. Muscle mass depletion in chronic liver diseases: An accelerated model of aging or a distinct entity? *Clin Res Hepatol Gastroenterol* 2021; **45**: 101721 [PMID: 34087426 DOI: 10.1016/j.clinre.2021.101721]

13 **Lanthier N**, Stärkel P, Dahlqvist G. Frailty, sarcopenia and mortality in cirrhosis: what is the best assessment, how to interpret the data correctly and what interventions are possible? *Clin Res Hepatol Gastroenterol* 2021; **45**: 101661 [PMID: 33667732 DOI: 10.1016/j.clinre.2021.101661]

14 **Mazumder N**, Rinella M. Editorial: sarcopenia in liver transplantation-our weakest patients may need the strongest push. *Aliment Pharmacol Ther* 2019; **49**: 1100-1101 [PMID: 30920044 DOI: 10.1111/apt.15204]

15 **Lai JC**, Rahimi RS, Verna EC, Kappus MR, Dunn MA, McAdams-DeMarco M, Haugen CE, Volk ML, Duarte-Rojo A, Ganger DR, O'Leary JG, Dodge JL, Ladner D, Segev DL. Frailty Associated With Waitlist Mortality Independent of Ascites and Hepatic Encephalopathy in a Multicenter Study. *Gastroenterology* 2019; **156**: 1675-1682 [PMID: 30668935 DOI: 10.1053/j.gastro.2019.01.028]

16 **van Vugt JLA**, Alferink LJM, Buettner S, Gaspersz MP, Bot D, Darwish Murad S, Feshtali S, van Ooijen PMA, Polak WG, Porte RJ, van Hoek B, van den Berg AP, Metselaar HJ, IJzermans JNM. A model including sarcopenia surpasses the MELD score in predicting waiting list mortality in cirrhotic liver transplant candidates: A competing risk analysis in a national cohort. *J Hepatol* 2018; **68**: 707-714 [PMID: 29221886 DOI: 10.1016/j.jhep.2017.11.030]

17 **Lai JC**, Tandon P, Bernal W, Tapper EB, Ekong U, Dasarathy S, Carey EJ. Malnutrition, Frailty, and Sarcopenia in Patients With Cirrhosis: 2021 Practice Guidance by the American Association for the Study of Liver Diseases. *Hepatology* 2021; **74**: 1611-1644 [PMID: 34233031 DOI: 10.1002/hep.32049]

18 **European Association for the Study of the Liver**. EASL Clinical Practice Guidelines on nutrition in chronic liver disease. *J Hepatol* 2019; **70**: 172-193 [PMID: 30144956 DOI: 10.1016/j.jhep.2018.06.024]

19 **Dumont C**, Wuestenberghs F, Lanthier N, Piessevaux H, Dahlqvist G. Malnutrition is highly prevalent in hospitalized cirrhotic patients and associates with a poor outcome. *Acta Gastroenterol Belg* 2022; **85**: 311-319 [PMID: 35709775 DOI: 10.51821/85.2.9016]

20 **Dhillon RJ**, Hasni S. Pathogenesis and Management of Sarcopenia. *Clin Geriatr Med* 2017; **33**: 17-26 [PMID: 27886695 DOI: 10.1016/j.cger.2016.08.002]

21 **Cruz-Jentoft AJ**, Sayer AA. Sarcopenia. *Lancet* 2019; **393**: 2636-2646 [PMID: 31171417 DOI: 10.1016/S0140-6736(19)31138-9]

22 **Martin L**, Birdsell L, Macdonald N, Reiman T, Clandinin MT, McCargar LJ, Murphy R, Ghosh S, Sawyer MB, Baracos VE. Cancer cachexia in the age of obesity: skeletal muscle depletion is a powerful prognostic factor, independent of body mass index. *J Clin Oncol* 2013; **31**: 1539-1547 [PMID: 23530101 DOI: 10.1200/JCO.2012.45.2722]

23 **Carey EJ**, Lai JC, Wang CW, Dasarathy S, Lobach I, Montano-Loza AJ, Dunn MA; Fitness, Life Enhancement, and Exercise in Liver Transplantation Consortium. A multicenter study to define sarcopenia in patients with end-stage liver disease. *Liver Transpl* 2017; **23**: 625-633 [PMID: 28240805 DOI: 10.1002/lt.24750]

24 **Czigany Z**, Kramp W, Bednarsch J, van der Kroft G, Boecker J, Strnad P, Zimmermann M, Koek G, Neumann UP, Lurje G. Myosteatosis to predict inferior perioperative outcome in patients undergoing orthotopic liver transplantation. *Am J Transplant* 2020; **20**: 493-503 [PMID: 31448486 DOI: 10.1111/ajt.15577]

25 **Czigany Z**, Kramp W, Lurje I, Miller H, Bednarsch J, Lang SA, Ulmer TF, Bruners P, Strnad P, Trautwein C, von Websky MW, Tacke F, Neumann UP, Lurje G. The role of recipient myosteatosis in graft and patient survival after deceased donor liver transplantation. *J Cachexia Sarcopenia Muscle* 2021; **12**: 358-367 [PMID: 33525056 DOI: 10.1002/jcsm.12669]

26 **Nachit M**, Lanthier N, Rodriguez J, Neyrinck AM, Cani PD, Bindels LB, Hiel S, Pachikian BD, Trefois P, Thissen JP, Delzenne NM. A dynamic association between myosteatosis and liver stiffness: Results from a prospective interventional study in obese patients. *JHEP Rep* 2021; **3**: 100323 [PMID: 34355155 DOI: 10.1016/j.jhepr.2021.100323]

27 **Lanthier N**, Rodriguez J, Nachit M, Hiel S, Trefois P, Neyrinck AM, Cani PD, Bindels LB, Thissen JP, Delzenne NM. Microbiota analysis and transient elastography reveal new extra-hepatic components of liver steatosis and fibrosis in obese patients. *Sci Rep* 2021; **11**: 659 [PMID: 33436764 DOI: 10.1038/s41598-020-79718-9]

28 **Nachit M**, Kwanten WJ, Thissen JP, Op De Beeck B, Van Gaal L, Vonghia L, Verrijken A, Driessen A, Horsmans Y, Francque S, Leclercq IA. Muscle fat content is strongly associated with NASH: A longitudinal study in patients with morbid obesity. *J Hepatol* 2021; **75**: 292-301 [PMID: 33865909 DOI: 10.1016/j.jhep.2021.02.037]

29 **Bell KE**, Paris MT, Avrutin E, Mourtzakis M. Altered features of body composition in older adults with type 2 diabetes and prediabetes compared with matched controls. *J Cachexia Sarcopenia Muscle* 2022; **13**: 1087-1099 [PMID: 35174664 DOI: 10.1002/jcsm.12957]

30 **Tandon P**, Montano-Loza AJ, Lai JC, Dasarathy S, Merli M. Sarcopenia and frailty in decompensated cirrhosis. *J Hepatol* 2021; **75** Suppl 1: S147-S162 [PMID: 34039486 DOI: 10.1016/j.jhep.2021.01.025]

31 **Román E**, García-Galcerán C, Torrades T, Herrera S, Marín A, Doñate M, Alvarado-Tapias E, Malouf J, Nácher L, Serra-Grima R, Guarner C, Cordoba J, Soriano G. Effects of an Exercise Programme on Functional Capacity, Body Composition and Risk of Falls in Patients with Cirrhosis: A Randomized Clinical Trial. *PLoS One* 2016; **11**: e0151652 [PMID: 27011355 DOI: 10.1371/journal.pone.0151652]

32 **Mazurak VC**, Tandon P, Montano-Loza AJ. Nutrition and the transplant candidate. *Liver Transpl* 2017; **23**: 1451-1464

[PMID: 29072825 DOI: 10.1002/lt.24848]
33 **Quigley EM**, Stanton C, Murphy EF. The gut microbiota and the liver. Pathophysiological and clinical implications. *J Hepatol* 2013; **58**: 1020-1027 [PMID: 23183530 DOI: 10.1016/j.jhep.2012.11.023]
34 **Clarembeau F**, Bale G, Lanthier N. Cirrhosis and insulin resistance: current knowledge, pathophysiological mechanisms, complications and potential treatments. *Clin Sci (Lond)* 2020; **134**: 2117-2135 [PMID: 32820802 DOI: 10.1042/CS20200022]
35 **Dolz C**, Raurich JM, Ibáñez J, Obrador A, Marsé P, Gayá J. Ascites increases the resting energy expenditure in liver cirrhosis. *Gastroenterology* 1991; **100**: 738-744 [PMID: 1993495 DOI: 10.1016/0016-5085(91)80019-6]
36 **Perisetti A**, Goyal H, Yendala R, Chandan S, Tharian B, Thandassery RB. Sarcopenia in hepatocellular carcinoma: Current knowledge and future directions. *World J Gastroenterol* 2022; **28**: 432-448 [PMID: 35125828 DOI: 10.3748/wjg.v28.i4.432]
37 **Abrigo J**, Gonzalez F, Aguirre F, Tacchi F, Gonzalez A, Meza MP, Simon F, Cabrera D, Arrese M, Karpen S, Cabello-Verrugio C. Cholic acid and deoxycholic acid induce skeletal muscle atrophy through a mechanism dependent on TGR5 receptor. *J Cell Physiol* 2021; **236**: 260-272 [PMID: 32506638 DOI: 10.1002/jcp.29839]
38 **Ebadi M**, Tsien C, Bhanji RA, Dunichand-Hoedl AR, Rider E, Motamedrad M, Mazurak VC, Baracos V, Montano-Loza AJ. Myosteatosis in Cirrhosis: A Review of Diagnosis, Pathophysiological Mechanisms and Potential Interventions. *Cells* 2022; **11** [PMID: 35406780 DOI: 10.3390/cells11071216]
39 **Lai JC**, Feng S, Terrault NA, Lizaola B, Hayssen H, Covinsky K. Frailty predicts waitlist mortality in liver transplant candidates. *Am J Transplant* 2014; **14**: 1870-1879 [PMID: 24935609 DOI: 10.1111/ajt.12762]
40 **Bot D**, Droop A, Lucassen CJ, van Veen ME, van Vugt JLA, Shahbazi Feshtali S, Leistra E, Tushuizen ME, van Hoek B. Both muscle quantity and quality are predictors of waiting list mortality in patients with end-stage liver disease. *Clin Nutr ESPEN* 2021; **42**: 272-279 [PMID: 33745592 DOI: 10.1016/j.clnesp.2021.01.022]
41 **Bhanji RA**, Moctezuma-Velazquez C, Duarte-Rojo A, Ebadi M, Ghosh S, Rose C, Montano-Loza AJ. Myosteatosis and sarcopenia are associated with hepatic encephalopathy in patients with cirrhosis. *Hepatol Int* 2018; **12**: 377-386 [PMID: 29881992 DOI: 10.1007/s12072-018-9875-9]
42 **van Vugt JL**, Levolger S, de Bruin RW, van Rosmalen J, Metselaar HJ, IJzermans JN. Systematic Review and Meta-Analysis of the Impact of Computed Tomography-Assessed Skeletal Muscle Mass on Outcome in Patients Awaiting or Undergoing Liver Transplantation. *Am J Transplant* 2016; **16**: 2277-2292 [PMID: 26813115 DOI: 10.1111/ajt.13732]
43 **Ooi PH**, Hager A, Mazurak VC, Dajani K, Bhargava R, Gilmour SM, Mager DR. Sarcopenia in Chronic Liver Disease: Impact on Outcomes. *Liver Transpl* 2019; **25**: 1422-1438 [PMID: 31242345 DOI: 10.1002/lt.25591]
44 **Wang S**, Whitlock R, Xu C, Taneja S, Singh S, Abraldes JG, Burak KW, Bailey RJ, Lai JC, Tandon P. Frailty is associated with increased risk of cirrhosis disease progression and death. *Hepatology* 2022; **75**: 600-609 [PMID: 34528267 DOI: 10.1002/hep.32157]
45 **Cullaro G**, Verna EC, Duarte-Rojo A, Kappus MR, Ganger DR, Rahimi RS, Boyarsky B, Segev DL, McAdams-DeMarco M, Ladner DP, Volk ML, Hsu CY, Lai JC. Frailty and the Risk of Acute Kidney Injury Among Patients With Cirrhosis. *Hepatol Commun* 2022; **6**: 910-919 [PMID: 34676697 DOI: 10.1002/hep4.1840]
46 **Schleicher EM**, Kremer WM, Kalampoka V, Gairing SJ, Kaps L, Schattenberg JM, Galle PR, Wörns MA, Nagel M, Weinmann-Menke J, Labenz C. Frailty as Tested by the Clinical Frailty Scale Is a Risk Factor for Hepatorenal Syndrome in Patients With Liver Cirrhosis. *Clin Transl Gastroenterol* 2022; **13**: e00512 [PMID: 35905416 DOI: 10.14309/ctg.0000000000000512]
47 **Lai JC**, Shui AM, Duarte-Rojo A, Ganger DR, Rahimi RS, Huang CY, Yao F, Kappus M, Boyarsky B, McAdams-Demarco M, Volk ML, Dunn MA, Ladner DP, Segev DL, Verna EC, Feng S; from the Multi-Center Functional Assessment in Liver Transplantation (FrAILT) Study. Frailty, mortality, and health care utilization after liver transplantation: From the Multicenter Functional Assessment in Liver Transplantation (FrAILT) Study. *Hepatology* 2022; **75**: 1471-1479 [PMID: 34862808 DOI: 10.1002/hep.32268]
48 **Fozouni L**, Mohamad Y, Lebsack A, Freise C, Stock P, Lai JC. Frailty Is Associated With Increased Rates of Acute Cellular Rejection Within 3 Months After Liver Transplantation. *Liver Transpl* 2020; **26**: 390-396 [PMID: 31655014 DOI: 10.1002/lt.25669]
49 **Crespo G**, Hessheimer AJ, Armstrong MJ, Berzigotti A, Monbaliu D, Spiro M, Rapti DA, Lai JC. Which preoperative assessment modalities best identify patients who are suitable for enhanced recovery after liver transplantation? *Clin Transplant* 2022; e14644 [PMID: 35293025 DOI: 10.1111/ctr.14644]
50 **Hari A**. Muscular abnormalities in liver cirrhosis. *World J Gastroenterol* 2021; **27**: 4862-4878 [PMID: 34447231 DOI: 10.3748/wjg.v27.i29.4862]
51 **Carey EJ**, Steidley DE, Aqel BA, Byrne TJ, Mekeel KL, Rakela J, Vargas HE, Douglas DD. Six-minute walk distance predicts mortality in liver transplant candidates. *Liver Transpl* 2010; **16**: 1373-1378 [PMID: 21117246 DOI: 10.1002/lt.22167]
52 **Kara M**, Kaymak B, Ata AM, Özkal Ö, Kara Ö, Baki A, Şengül Ayçiçek G, Topuz S, Karahan S, Soylu AR, Çakır B, Halil M, Özçakar L. STAR-Sonographic Thigh Adjustment Ratio: A Golden Formula for the Diagnosis of Sarcopenia. *Am J Phys Med Rehabil* 2020; **99**: 902-908 [PMID: 32941253 DOI: 10.1097/PHM.0000000000001439]
53 **Razaq S**, Kara M, Özçakar L. Measure grip strength, gait speed and quadriceps muscle in cirrhosis. Comment to "Frailty, sarcopenia and mortality in cirrhosis: What is the best assessment, how to interpret the data correctly and what interventions are possible? *Clin Res Hepatol Gastroenterol* 2021; **45**: 101727 [PMID: 34087427 DOI: 10.1016/j.clinre.2021.101727]
54 **Brustia R**, Monsel A, Skurzak S, Schiffer E, Carrier FM, Patrono D, Kaba A, Detry O, Malbouisson L, Andraus W, Vandenbroucke-Menu F, Biancofiore G, Kaido T, Compagnon P, Uemoto S, Rodriguez Laiz G, De Boer M, Orloff S, Melgar P, Buis C, Zeillemaker-Hoekstra M, Usher H, Reyntjens K, Baird E, Demartines N, Wigmore S, Scatton O. Guidelines for Perioperative Care for Liver Transplantation: Enhanced Recovery After Surgery (ERAS) Recommendations. *Transplantation* 2022; **106**: 552-561 [PMID: 33966024 DOI: 10.1097/TP.0000000000003808]
55 **Hernández-Conde M**, Llop E, Gómez-Pimpollo L, Fernández Carrillo C, Rodríguez L, Van Den Brule E, Perelló C, López-Gómez M, Abad J, Martínez-Porras JL, Fernández-Puga N, Ferre C, Trapero M, Fraga E, Calleja JL. Adding

Branched-Chain Amino Acids to an Enhanced Standard-of-Care Treatment Improves Muscle Mass of Cirrhotic Patients With Sarcopenia: A Placebo-Controlled Trial. *Am J Gastroenterol* 2021; **116**: 2241-2249 [PMID: 34074812 DOI: 10.14309/ajg.0000000000001301]

56 **Gluud LL**, Dam G, Les I, Marchesini G, Borre M, Aagaard NK, Vilstrup H. Branched-chain amino acids for people with hepatic encephalopathy. *Cochrane Database Syst Rev* 2017; **5**: CD001939 [PMID: 28518283 DOI: 10.1002/14651858.CD001939.pub4]

57 **Plank LD**, Gane EJ, Peng S, Muthu C, Mathur S, Gillanders L, McIlroy K, Donaghy AJ, McCall JL. Nocturnal nutritional supplementation improves total body protein status of patients with liver cirrhosis: a randomized 12-month trial. *Hepatology* 2008; **48**: 557-566 [PMID: 18627001 DOI: 10.1002/hep.22367]

58 **Aamann L**, Dam G, Borre M, Drljevic-Nielsen A, Overgaard K, Andersen H, Vilstrup H, Aagaard NK. Resistance Training Increases Muscle Strength and Muscle Size in Patients With Liver Cirrhosis. *Clin Gastroenterol Hepatol* 2020; **18**: 1179-1187.e6 [PMID: 31394282 DOI: 10.1016/j.cgh.2019.07.058]

59 **Allen SL**, Quinlan JI, Dhaliwal A, Armstrong MJ, Elsharkawy AM, Greig CA, Lord JM, Lavery GG, Breen L. Sarcopenia in chronic liver disease: mechanisms and countermeasures. *Am J Physiol Gastrointest Liver Physiol* 2021; **320**: G241-G257 [PMID: 33236953 DOI: 10.1152/ajpgi.00373.2020]

World Journal of Gastroenterology

Submit a Manuscript: https://www.f6publishing.com

World J Gastroenterol 2022 October 28; 28(40): 5818-5826

DOI: 10.3748/wjg.v28.i40.5818

ISSN 1007-9327 (print) ISSN 2219-2840 (online)

MINIREVIEWS

Management of liver diseases: Current perspectives

Gautam Ray

Specialty type: Gastroenterology and hepatology

Provenance and peer review: Invited article; Externally peer reviewed.

Peer-review model: Single blind

Peer-review report's scientific quality classification

Grade A (Excellent): A
Grade B (Very good): B
Grade C (Good): 0
Grade D (Fair): 0
Grade E (Poor): 0

P-Reviewer: Ji G, China; Rodrigues AT, Brazil

Received: July 10, 2022
Peer-review started: July 10, 2022
First decision: July 31, 2022
Revised: August 4, 2022
Accepted: September 21, 2022
Article in press: September 21, 2022
Published online: October 28, 2022

Gautam Ray, Gastroenterology Unit, Department of Medicine, B.R.Singh (Railway) Hospital, Kolkata 700014, West Bengal, India

Corresponding author: Gautam Ray, DNB, MD, Academic Research, Chief Doctor, Doctor, Teacher, Gastroenterology Unit, Department of Medicine, B.R.Singh (Railway) Hospital, Parikshit Roy Lane, Near Sealdah Bus Stop, Beliaghata, Kolkata 700014, West Bengal, India. gautam1910@yahoo.com

Abstract

There is increasing incidence and prevalence of acute and chronic liver diseases (CLDs) all over the world which influence the quality of life and can give rise to life threatening complications. The burden of advanced liver disease due to hepatitis B has been controlled by antivirals but its eradication is difficult soon. Highly effective directly acting antiviral therapy has reduced the burden of hepatitis C but is partially offset by increasing IV drug abuse. Non-alcoholic fatty liver disease pandemic is on and there is recent alarming increase in alcohol related liver disease, both of which have no drug cure apart from control of the risk factors. Genetic factors have been identified in progression of all forms of CLD. Due to better management of complications of CLD, the life span of patients have increased spiking the number of hepatocellular carcinoma (HCC) and patients needing liver transplantation (LT). The present severe acute respiratory syndrome coronavirus pandemic has affected the outcome CLD including LT in addition to causing acute hepatitis. Better diagnostics and therapeutics are available for liver fibrosis, portal hypertension, HCC and post LT management and many drugs are under trial. The present review summarises the current scenario of the epidemiology and the advances in diagnosis and treatment of liver diseases including their complications like portal hypertension, HCC and LT.

Key Words: Chronic liver disease; Genes; Biomarkers; Therapy; Hepatocellular carcinoma; Liver transplantation; Recent advances

©The Author(s) 2022. Published by Baishideng Publishing Group Inc. All rights reserved.

Core Tip: The incidence and prevalence of liver disease is rising all over the world. Hepatitis B is difficult to eradicate and the benefit of directly acting antiviral therapy for hepatitis C is partially offset by increasing IV drug abuse. Non-alcoholic fatty liver disease pandemic is on and alcohol related liver disease is rising alarmingly, both having no drug cure. Due to better management of complications, patients of chronic liver disease are living longer spiking the number of hepatocellular carcinoma (HCC) and patients needing liver transplantation (LT). Better diagnostics and therapeutics are available for fibrosis, portal hypertension, HCC and post LT management which are discussed.

Citation: Ray G. Management of liver diseases: Current perspectives. *World J Gastroenterol* 2022; 28(40): 5818-5826
URL: https://www.wjgnet.com/1007-9327/full/v28/i40/5818.htm
DOI: https://dx.doi.org/10.3748/wjg.v28.i40.5818

INTRODUCTION

Chronic liver disease (CLD) and cirrhosis pose substantial health burden worldwide. In the period 2007-2017, the age standardised prevalence increased 10.4% with 1.5 billion cases in 2017[1]. Of the four chief etiology, hepatitis B virus (HBV) and hepatitis C virus (HCV) burden still remains high [though decreased due to availability of vaccination for HBV and directly acting antiviral therapy (DAA) for HCV] although with the non-alcoholic fatty liver disease (NAFLD) pandemic and increasing global alcohol consumption, they are fast catching up. NAFLD is the leading cause in developed nations, it is also gradually becoming important in newly developed nations like India, China[2,3]. The age standardised prevalence of HBV/HCV related CLD rose by 9%/10.2% in the last decade whereas for NAFLD it was 23.5%[1]. The high HBV and HCV burden is mostly due to poor diagnostic coverage and linkage to treatment and care of the susceptible population.

HBV

The HBV pool is chiefly contributed to by the Western Pacific and Subsaharan Africa region (mostly tribals) and some southeast Asian countries (China, Vietnam, Thailand, Laos) where the load remains high despite the success of HBV vaccination programme at birth. It is the leading cause of hepatocellular carcinoma (HCC) in these countries[4]. Among some developed and newly developing nations where prevalence is intermediate to low, its burden is contributed by the indigenous tribal population like India, Australia[5,6] maintained through intracaste marriages, close living, tribal customs, illiteracy and poor access to health care resources. With the present attrition rate (present burden of 296 million from 350 million 3 decades back and present annual mortality of 8 lakh and addition of 1.5 million cases in 2019[7]), it is still a long way for natural elimination of the pool. In future some redistribution is also likely due to population migration from high to low endemicity regions. World Health Organization (WHO)'s ambitious programme for eradication of HBV by 2030 therefore incorporate the best preventive measures *i.e.*, increase vaccination at birth, prevent vertical and horizontal transmission among toddlers by treating at risk mothers, and scale up screening, care and treatment services. Curative treatment is difficult and < 20% who receive the currently approved drugs [interferon, nucleos(t)ide analog (NA) or combination as sequential/add on/switch therapy] achieve loss of HBsAg (functional cure). Combination strategies are less cost effective than first line NA monotherapy although this may lead to more HBsAg loss in some subgroup of HBV patients[8]. Even with long term NA monotherapy (Tenofovir disoproxil for 5 years) half fail to achieve fibrosis regression[9] and there is high relapse rate in e negative patients (RETRACT B study showing relapse rate of 47.8% at 6 mo, 68.9% at 12 mo, 83.4% at 48 mo)[10]. The other problem is the risk of relapse in previously exposed person or inactive HBsAg carriers (who constitute a sizable majority of the present pool not requiring drug therapy) needing immunosuppression (IS) or cancer chemotherapy. Fortunately, highly active antivirals are capable of controlling the virus and reducing the burden of advanced liver disease from HBV. The chief impediments to HBV functional cure are intrahepatic viral reservoir cccDNA with integrated sequencing, high HBsAg levels, and defective host innate and adaptive immune responses. Newer strategies target these *e.g.*, targeting HBV life cycle without damaging hepatocyte by inhibiting ccc DNA replenishment pathways or degrading them by entry inhibitors like Bulevirtide [used for HBV/HDV coinfection including post liver transplantation (LT)], nucleic acid polymer assembly inhibitors (Lonafarnib), CRISPR/Cas9 protein base editors (DNA endonucleases), siRNAs, core protein modulators (Morphothiadin,Vebicorvir, Bersacapavir) and antisense oligonucleotide (Bepirovirsen)[2], immunomodulation to safely eliminate infected cells. Potential targets in innate immune response pathway include pathogen recognition receptors [Toll-like receptors 7/8, retinoic acid-inducible gene

(RIG)-1-like receptors and nucleotide-binding oligomerization domain (NOD)-like receptors], natural killer cells and antigen presenting cells (dendritic cells and Kupffer cells) whereas in adaptive immune response pathway, it includes modulation of HBV-specific CD4+ and CD8+ T cell (especially the relative functional and numerical deficiency of CD8+ T-cells by PD-1 checkpoint inhibitors), regulatory T cell, HBV-specific T and B cell (autologous, engineered or by vaccine).

HCV

Gratifying results have been obtained with the introduction of affordable short term (3-6 mo) DAA therapy for HCV (with sustained viral response rates of > 95%, decreased fibrosis and HCC) with increasing treatment coverage in newly developed and developing nations which have decreased the HCV burden to 58 million as of 2019[7]. HCV still remains the leading cause of HCC in the developed world (Western countries, Japan) though alcohol related liver disease (ALD)/NAFLD are fast taking the lead due to treatment with DAA. But challenges still remain like limited drug availability, interaction with other drugs used to treat comorbidities (HIV, coronary artery disease and hyperlipidemia), inability to afford even the low drug cost by patients who pay from their own pocket and increasingly recognized metabolic dysfunctions associated with hepatitis C. Even in Denmark, 50% HCV patients are yet to attend specialist care especially IV drug users[11]. HIV coinfection is also a deterrent for good treatment outcome for both HBV and HCV. In future the HCV pool is likely to be maintained by intravenous drug users and the increasing population with drug/alcohol abuse and other psychiatric disorders, those needing repeated blood transfusion (for haematological disorders, hemodialysis) and reinfection in those who continue to have risk factors even after cure by DAA. WHO recommends increased access to treatment by onsite diagnosis by dried blood spot and initiating treatment at point of care and by trained non specialist doctors and nurses at harm reduction centres.

NAFLD

NAFLD is the most common liver disease worldwide affecting about a quarter population with regional differences[12]. It is fast becoming the leading cause of cirrhosis in developed nations. Genetic inheritance (25%-34%), ancestry (HispanicAmerican/Asian/Indian > European > African American), advancing age and male sex are non modifiable whereas obesity (especially central), diabetes mellitus, hyperlipidemia and insulin resistance are modifiable risk factors. There is currently no approved pharmacological therapy for NAFLD apart from those treating the risk factors. Weight loss through dietary alteration, physical exercises and bariatric surgery leads to improved liver histology but only small percentage of patients can achieve and maintain the degree of weight loss needed for sustaining the benefit and 50% fail to improve histology[13]. Ursodeoxycholic acid (UDCA)/obeticholic acid (OCA), Vitamin E have no proven benefit. Therefore it is the hottest area of newer drug research which modulate key metabolic, inflammatory, and fibrogenic pathway. Pan PPAR agonists (Lanifibranor), GLP 1 agonists (Semaglutide), CCR 5 inhibitors (Leronlimab), thyroid hormone receptor agonist (Resmetirom) and hepatic SCD1 inhibitor (Aramchol) are in phase 2 and 3 clinical trial (Table 1). Other antifibrotic and disease modifying agents as well as genetic factors are discussed below. But considering the multiple risk factors and complex pathophysiology, it is unlikely that a panacea will be discovered soon.

ALCOHOL

Approximately 2 billion people worldwide consume alcohol of whom 283 million suffer from AUD[14]. ALD is most prevalent in the western world and in some affluent Asian countries (South Korea, Japan) though there is increasing global trend especially in newly industrialised southeast Asian nations (China, India, Vietnam, Thailand) where it was low due to traditional"dry" culture. ALD has become the leading cause of CLD/cirrhosis in India[5]. The recent coronavirus disease 2019 (COVID-19) pandemic has significantly increased the incidence of ALD in young adults. DALYs per 1000 people due to ALD was highest in India (2356.4), followed by the United States (467.9), China (466.3), Nigeria (424.5) and Indonesia (365.1). For alcohol related liver cancer, DALYs were highest for China followed by Vietnam, Russia, Thailand, India[15]. Consumption depends on age, sex, religion, culture, health status and national income distribution. Globally it is a tussle between national income from alcohol retail *vs* health expenditure for AUD, the latter being dismal even in developed nations. Being a fully preventable disease, WHO's "best buys" are the most cost effective ways for prevention, *i.e.*, increasing taxation on alcoholic beverages, enforcing bans or comprehensive restrictions on exposure to alcohol advertising and restricting physical availability of retailed alcohol. A recent global study shows no safe dose for alcohol[16]. Abstinence can reverse fatty liver and halt the progression of CLD. It is responsible

Table 1 Interrim results of selective drug trials for non-alcoholic fatty liver disease and liver fibrosis

Agent	Mechanism	Phase	ClinicalTrials.gov number	Results
Simtuzumab	Lysyl oxidase-like 2 monoclonal antibody	IIb	NCT01672879	Ineffective in decreasing hepatic venous pressure gradient
Selonsertib	Selective inhibitor of apoptosis signal-regulating kinase 1	III	NCT03053063	Ineffective in improving fibrosis without worsening NASH
Emricasan	Pan-caspase inhibitor	II	NCT03205345	No reduction in composite outcome of mortality and decompensation
Pegbelfermin	PEGylated fibroblast growth factor 21 analogue	IIa	NCT03486912	Ineffective in improving fibrosis without worsening NASH
Lanifibranor	Pan peroxisome proliferator-activated receptor agonists	III	NCT04849728	Decrease of ≥ 2 points in the Steatosis Activity Fibrosis score without worsening of fibrosis in phase 2b trial
Resmetirom	Thyroid hormone receptor agonist	III	NCT03900429	Significant reductions in liver fat content and serum atherogenic lipids in phase 2 trial
Aramchol	Hepatic stearoyl-CoA desaturase1 inhibitor	IIb	NCT02279524	Insignificant decrease in liver triglycerides but significant improvement in liver inflammation and improvement of fibrosis ≥ 1 stage and serum ALT level
Leronlimab	Chemokine receptor 5 monoclonal antibody	II	NCT04521114	Significant drops in liver fat, inflammation and fibrosis values as also in liver enzymes and multiple inflammation markers at week 14 compared to placebo

NASH: Non-alcoholic steatohepatitis; ALT: Alanine transaminase.

for 50% of deaths due to CLD because no specific drug therapy is available apart from some short term benefit of steroids in pure acute hepatitis. Tumour necrosis factor alpha, growth hormone, pentoxyfylline and antioxidants at best show mixed results from highly variable to weak, efficacy depending on the stage of disease. The unclear molecular mechanism of disease deter identifying treatment target and disincetivize drug development. Naltrexone, disulfiram and acamprosate helps to decrease addiction. Obesity and cigarette smoking are known risk factors so weight control and quitting smoking are routinely encouraged. A poor overall nutritional status (protein calorie malnutrition, micronutrient deficiencies) often accompanies ALD and correlates positively with the development of serious complications hence a well-conceived nutrition support by oral, enteral, and parenteral routes is an essential part of standard care. Recent evidence also strongly implicates intestinal dysbiosis in ALD progression. These targets are being addressed by trials of probiotics, fecal microbiota transplantation, growth factors (granulocyte colony stimulating factor, bovine colostrum), antioxidants (ω5 and synthetic fatty acids, S-adenosyl methionine + choline, N-Acetyl cysteine, vitamin C), in addition to liver regenerative biologics and device assisted behavioural alteration[17]. The other hindrances are disease stratification for early identification when it is most reversible, monitoring abstinence (as recidivism is high) and identifying risky drinking behaviour like binges. Various biomarkers under study for this purpose include circulating small noncoding RNAs, long noncoding RNAs, selective cytokines profiles, phosphatidyl ethanol and urine ethyl glucuronide and ethyl sulphate[18-21].

AUTOIMMUNE LIVER DISEASE

Autoimmune hepatitis appears to be increasing in incidence as a part of the general increase in immune mediated and allergic diseases resulting from decreasing infectious disease with mounting antibiotics use globally. Some antibiotics like nitrofuranotin, minocycline and coamoxyclav can induce autoimmune hepatitis by themselves and some antibiotic associated drug induced liver disease (DILI) may resemble autoimmune hepatitis. The standard treatment of autoimmune hepatitis is with steroids with/without azathioprine. Mycophenolate mofetil is a second line drug. Substantial advances in treatment of autoimmune cholangiopathies has been achieved with PPAR α agonist bezafibrate, FXR agonist OCA and recombinant FGF 19 (which alter bile acid synthesis along with antifibrogenic effect [22], see below) and drugs inhibiting intestinal apical sodium-dependent bile acid transporter (linerixibat, maralixibat, odevixibat)[23]. in addition to bile acid resins and UDCA. Combinations of such enterohepatic with cholehepatic and/or anti-fibrotic drugs could result in synergistic/additive effects in decreasing the fibrosis along with the pruritus.

ADVANCES IN DIAGNOSIS

Non invasive biomarkers of CLD (patented ones like fibrotest, fibrometer, Hepascore, ELF model and non patented ones like FIB 4 index, APRI, BARD, NFS) and elastography (fibroscan, MRE, point SWE, 2D-SWE, 3D Velacur™) or their combination (MEFIB, MAST, FAST) have been investigated across the whole spectrum of NAFLD to delineate the stage as well as correlating genes with liver fat, enzymes and fibrosis[24]. Novel ones like computerised tomography (CT) scan with objective measures of liver nodularity and shunts, multiparametric magnetic resonance imaging (MRI) (iron corrected T1, cT1), extracellular vesicles, microbiome (stool microbial profiles), biomarker for extracellular matrix remodelling (TGF-β, MMP, TIMP)[25-27] are being investigated. Graph convolution networks (a deep learning technique) is being tested for quantitative assessment of fibrosis[28].

GENETIC FACTORS IN CLD

Genetic factors are important in progression of all forms of CLD (ALD, NAFLD, metabolic associated fatty liver disease, chronic hepatitis) including HCC with interplay of genes involved in glucose, lipid and iron metabolism, insulin signalling, oxidative stress, inflammatory pathways and fibrogenesis. Most reliable fatty liver genes include PNPLA3, TM6SF2, HSD17B13, GCKR and MBOAT7 (associated with increased liver fat, NASH, cirrhosis, HCC). The evidence for others like MARC1, GPAM, APOE, ALDH1B, PCKS7, SERPINA1, HNF1A etc are less robust. Rare variants like APOB and MTTP are associated with an increased risk of fat accumulation leading to HCC while protecting at the same time against dyslipidemia and cardiovascular risk[24]. Polygenetic risk score [with/without clinical risk markers] are being investigated to stratify disease risk *e.g.*, PNPLA3 and TM6SF2 can become a reason for HCC surveillance whilst giving protection from cardiovascular complications[29] It can also help in proper drug selection. Genetic therapies in CLD include gene silencing approaches (PNPLA3, HSD17B13), CRISPR/Cas9-based approaches[30] (which alter responsible genes) and modulating genes involved in liver regeneration.

ACUTE HEPATITIS

The etiology of acute liver failure (in those with normal liver) varies in different countries at different times. Most commonly these include viruses (hepatitis A, B and E), DILI (CAM, anti tuberculous drugs, paracetamol, anticonvulsants, antibiotics), toxins (herbs, alcohol) and autoimmune flares; else these may precipitate acute liver failure in those with CLD (acute-on-chronic liver failure, ACLF). Hepatitis E virus may be associated with fulminant course in pregnancy. In tropical areas, malaria, dengue, enteric fever, leptospirosis and scrub typhus may also cause acute hepatitis. Traditionally Wilson disease and autoimmune hepatitis has been considered to cause acute liver failure but in adults majority of such acute flares occur on background CLD. Most acute hepatitis of viral etiology recover by themselves and of drug/toxin on their discontinuation, some DILI may need corticosteroid (especially those resembling autoimmune hepatitis). Bacterial infections respond to antibiotics. But the course of ACLF depends on the stage of the background CLD and the precipitating cause, alcohol having the worst outcome[31,32]. Undefined number of acute hepatitis are occurring recently due to COVID-19 infection, recreational drugs and alcohol.

PORTAL HYPERTENSION AND LIVER FIBROSIS

With the increasing prevalence of CLD, portal hypertension and its complications are also increasing. Refractory ascites/hepatorenal syndrome/hydrothorax are now being better managed with terlipressin, noradrenaline, midodrine, octreotide and long-term albumin supplementation (with its newly discovered wider pleiotropic non-oncotic properties positively impacting decompensated CLD). Sodium-dependent glucose cotransporter 2 inhibitors and Alfa pump are under trial. Endohepatology (the application of endoscopic ultrasound in liver disease treatment)[33] has brought about dramatic improvement in the treatment of variceal bleed by better delineation of collaterals and guided treatment (coiling, balloon retrograde transvenous occlusion of collaterals, glue injection in gastric varix), directed liver biopsy, portal pressure gradient measurement and deployment of dedicated esophageal stents. Pre emptive transjugular intrahepatic portasystemic shunt has been used for uncontrollable ascites or variceal bleed.

Fibrosis in the liver is caused by activated HSC whose biology connects damage, regeneration and cancer. Severe hepatic fibrosis represses regeneration and accumulation of senescent HSCs creates a pro-inflammatory, pro-fibrotic environment. Fibrogenesis inhibitor drugs resolve inflammation, cause loss of activated myofibroblasts, and ECM degradation Those under investigation (Table 1) include [FXR

agonist OCA/cilofexor, acetyl-coenzyme A carboxylase inhibitor Firsocostat, ASK-1 inhibitor Selonsertib, CCR 2/5 inhibitor Cenicriviroc, FGF 19 analog Aldafermin/21 analogue Pegbelfermin, PPAR α/δ agonist Elafibranor, PPARγ agonist pioglitazone, PPAR α/γ agonist Saroglitazar, galectin 3 inhibitor Belapectin, CB1 antagonist Rimonabant, ECM production inhibitors like TIMP and MMP, lysyl oxidase 2 inhibitor Simtuzumab, HSP 47 inhibitor Pirfenidone, pan caspase inhibitor Emricasan and anti inflammatory lipids derivatives of PUFA (lipoxins, resolvins, protectins, and maresins)][34-36]. Statins have been found to have beneficial effect in halting the progress of CLD[37].

HCC

The chief cause of HCC in the West is hepatitis C followed by NAFLD and alcohol whereas it is hepatitis B in Asia and Africa. Eighty percent occur in low and middle resource countries. Screening programme for HCC in cirrhotics is cost effective and better cancer surveillance can be achieved by the recently developed GALAD (incorporating AFP, AFP-L3, PIVKA, age and sex) screening tool[38] along with radiologic strategies (contrast enhanced ultrasonogram using Li-RADS, multiphasic CT/aMRI scan) every 6 mo in high risk patients. Ninety percent HCC occur on background CLD which pose additional health risk to HCC itself. Liver biopsy carries risk hence liquid biopsy using detection of circulating tumor cells specific to HCC, mutation or methylation of circulating tumor DNA, and transcriptomic profiling of extracellular vesicles are promising. The widely followed BCLC staging system have been upgraded (to be more inclusive for surgery with/without downgrading of tumor) and provide better platform for optimal use of different treatment modalities like ablation, resection, LT, stereotactic body radiation, locoregional and systemic therapy. LT has been extended outside Milan criteria to include more patients by various expanded selection criteria with reduced but excellent long term results[39]. Cancer in non cirrhotic liver is treated by LT with better understanding of transplant oncology. Newer drugs like multikinase inhibitors (Lenvatinib, Regorafinib, Cabozantinib, Ramucirumab), checkpoint inhibitors (atezolizumab, bevacizumab, durvalumab, pembrolizumab, nivolumab, ipilimumab and tremelimumab) are now available over sorafenib for systemic therapy with better outcome[40]. Limitations are their unclear safety profile in Child Pugh stage B, best response not more than 50%, unclear treatment sequence and use in early stage of tumor.

LT

ALD is now the predominant cause for LT followed by HCV and NAFLD in the West[41] whereas it is still HBV/HCV in the East with ALD at its heels[42]. With good patient selection, the present 1 year survival is 90% and 5 year of 70%. Good outcome has been substantially influenced by betterment of surgical techniques, perioperative management, organ preservation (normothermic machine perfusion), recipient selection (through organ sharing network), post transplant immunosuppressive management and of viral etiology (DAA for HCV. Bulevirtide/NA for HBV/HDV). The challenge of limited organ availability has been addressed by accepting marginal and extended criteria donors (donors of cardiac death, 30%-60% steatotic liver explant without inflammation, HBsAg and HCV positive donors), split liver grafts and live donor transplant especially in Asia[41]. Liver regeneration based approaches like stem cell therapy and organ bioengineering can also help. Most post transplant morbidity arise from prolonged use of immunosuppressive with resultant infections, hypertension, dyslipidemia, cardiovascular events, renal failure, malignancy and chronic organ rejection. Long term outcome can be improved by minimising/late introduction of standard IS or withdrawing it completely (20% become operationally tolerant) and using less toxic IS drugs (mToR inhibitors, interleukin 2 receptor blockers). With increased understanding of transplant immunology, research is on whether IS can be completely withdrawn after finite treatment by modulating recipient immunity (by CD4 Treg cells, regulatory dendritic cells or hematopoietic stem cell transplantation)[43]. The problem of HCV relapse leading to cirrhosis in 30% has been addressed by DAA. Present challenges for liver transplant are: (1) High alcohol recidivism; (2) ACLF grade 3 and severe acute alcohol related hepatitis; (3) NAFLD/non-alcoholic steatohepatitis with high comorbities; (4) Frailty in advance CLD; (5) Recipient and caregiver challenges; (6) Genetic variants; and (7) COVID-19. Severe acute respiratory syndrome coronavirus vaccine fails to decrease mortality as the patient's immunity is already weakened.

Artificial intelligence and digital transformation of various diagnostic modalities, decision making tool and management will further advance the treatment of liver diseases.

CONCLUSION

The current scenario of the epidemiology and the advances in diagnosis and treatment of liver diseases including their complications are summarised in this review.

FOOTNOTES

Author contributions: Ray G conceptualized the topic, collected data, drafted, edited and approved the final manuscript.

Conflict-of-interest statement: The author reports no relevant conflicts of interest for this article.

Open-Access: This article is an open-access article that was selected by an in-house editor and fully peer-reviewed by external reviewers. It is distributed in accordance with the Creative Commons Attribution NonCommercial (CC BY-NC 4.0) license, which permits others to distribute, remix, adapt, build upon this work non-commercially, and license their derivative works on different terms, provided the original work is properly cited and the use is non-commercial. See: https://creativecommons.org/Licenses/by-nc/4.0/

Country/Territory of origin: India

ORCID number: Gautam Ray 0000-0003-4859-8729.

S-Editor: Gao CC
L-Editor: A
P-Editor: Gao CC

REFERENCES

1 **GBD 2017 Disease and Injury Incidence and Prevalence Collaborators**. Global, regional, and national incidence, prevalence, and years lived with disability for 354 diseases and injuries for 195 countries and territories, 1990-2017: a systematic analysis for the Global Burden of Disease Study 2017. *Lancet* 2018; **392**: 1789-1858 [PMID: 30496104 DOI: 10.1016/S0140-6736(18)32279-7]
2 **De A**, Duseja A. Nonalcoholic Fatty Liver Disease: Indian Perspective. *Clin Liver Dis (Hoboken)* 2021; **18**: 158-163 [PMID: 34691404 DOI: 10.1002/cld.1141]
3 **Xiao J**, Wang F, Wong NK, He J, Zhang R, Sun R, Xu Y, Liu Y, Li W, Koike K, He W, You H, Miao Y, Liu X, Meng M, Gao B, Wang H, Li C. Global liver disease burdens and research trends: Analysis from a Chinese perspective. *J Hepatol* 2019; **71**: 212-221 [PMID: 30871980 DOI: 10.1016/j.jhep.2019.03.004]
4 **World Health Organization**. WHO Global Hepatitis Report 2017. [cited 30 June 2022]. In: World Health Organization [Internet]. Available from: www.who.int/hepatitis/publications/global-hepatitis-report2017/en/
5 **Ray G**. Current Scenario of Hepatitis B and Its Treatment in India. *J Clin Transl Hepatol* 2017; **5**: 277-296 [PMID: 28936409 DOI: 10.14218/JCTH.2017.00024]
6 **Hanson J**, Fox M, Anderson A, Fox P, Webster K, Williams C, Nield B, Bagshaw R, Hempenstall A, Smith S, Solomon N, Boyd P. Chronic hepatitis B in remote, tropical Australia; successes and challenges. *PLoS One* 2020; **15**: e0238719 [PMID: 32881958 DOI: 10.1371/journal.pone.0238719]
7 **World Health Organization**. Hepatitis B and Hepatitis C. WHO bulletin 24 June 2022. [cited 30 June 2022]. In: World Health Organization [Internet]. Available from: www.who.in/Factsheets/Detail/Hepatitis
8 **Yin XR**, Liu ZH, Liu J, Liu YY, Xie L, Tao LB, Jia JD, Cui FQ, Zhuang GH, Hou JL. First line nucleos(t)ide analog monotherapy is more cost-effective than combination strategies in hepatitis B e antigen-positive chronic hepatitis B patients in China. *Chin Med J (Engl)* 2019; **132**: 2315-2324 [PMID: 31567376 DOI: 10.1097/CM9.0000000000000445]
9 **Marcellin P**, Gane E, Buti M, Afdhal N, Sievert W, Jacobson IM, Washington MK, Germanidis G, Flaherty JF, Aguilar Schall R, Bornstein JD, Kitrinos KM, Subramanian GM, McHutchison JG, Heathcote EJ. Regression of cirrhosis during treatment with tenofovir disoproxil fumarate for chronic hepatitis B: a 5-year open-label follow-up study. *Lancet* 2013; **381**: 468-475 [PMID: 23234725 DOI: 10.1016/S0140-6736(12)61425-1]
10 **Hirode G**, Choi HSJ, Chen CH, Su TH, Seto WK, Van Hees S, Papatheodoridi M, Lens S, Wong G, Brakenhoff SM, Chien RN, Feld J, Sonneveld MJ, Chan HLY, Forns X, Papatheodoridis GV, Vanwolleghem T, Yuen MF, Hsu YC, Kao JH, Cornberg M, Hansen BE, Jeng WJ, Janssen HLA; RETRACT-B Study Group. Off-Therapy Response After Nucleos(t)ide Analogue Withdrawal in Patients With Chronic Hepatitis B: An International, Multicenter, Multiethnic Cohort (RETRACT-B Study). *Gastroenterology* 2022; **162**: 757-771.e4 [PMID: 34762906 DOI: 10.1053/j.gastro.2021.11.002]
11 **Nielsen S**, Hansen JF, Hay G, Cowan S, Jepsen P, Omland LH, Krarup HB, Søholm J, Lazarus JV, Weis N, Øvrehus A, Christensen PB. Hepatitis C prevalence in Denmark in 2016-An updated estimate using multiple national registers. *PLoS One* 2020; **15**: e0238203 [PMID: 32881877 DOI: 10.1371/journal.pone.0238203]
12 **Cotter TG**, Rinella M. Nonalcoholic Fatty Liver Disease 2020: The State of the Disease. *Gastroenterology* 2020; **158**: 1851-1864 [PMID: 32061595 DOI: 10.1053/j.gastro.2020.01.052]
13 **Vilar-Gomez E**, Martinez-Perez Y, Calzadilla-Bertot L, Torres-Gonzalez A, Gra-Oramas B, Gonzalez-Fabian L, Friedman SL, Diago M, Romero-Gomez M. Weight Loss Through Lifestyle Modification Significantly Reduces Features of Nonalcoholic Steatohepatitis. *Gastroenterology* 2015; **149**: 367-78.e5; quiz e14 [PMID: 25865049 DOI: 10.1053/j.gastro.2015.04.005]
14 **World Health Organization**. Global status report on alcohol and health 2018. [cited 30 June 2022]. In: World Health Organization [Internet]. Available from: www.who.int/publications/overview/Global_status_report_on_alcohol_and_health_2018
15 **World Health Organization**. Global health estimates 2016: Disease burden by cause, age,sex, by country and by region,

2000–2016. Global status report on alcohol and health 2018. [cited 30 June 2022]. In: World Health Organization [Internet]. Available from: www.who.int/data/Global_Health_Estimate

16 **Wood AM**, Kaptoge S, Butterworth AS, Willeit P, Warnakula S, Bolton T, Paige E, Paul DS, Sweeting M, Burgess S, Bell S, Astle W, Stevens D, Koulman A, Selmer RM, Verschuren WMM, Sato S, Njølstad I, Woodward M, Salomaa V, Nordestgaard BG, Yeap BB, Fletcher A, Melander O, Kuller LH, Balkau B, Marmot M, Koenig W, Casiglia E, Cooper C, Arndt V, Franco OH, Wennberg P, Gallacher J, de la Cámara AG, Völzke H, Dahm CC, Dale CE, Bergmann MM, Crespo CJ, van der Schouw YT, Kaaks R, Simons LA, Lagiou P, Schoufour JD, Boer JMA, Key TJ, Rodriguez B, Moreno-Iribas C, Davidson KW, Taylor JO, Sacerdote C, Wallace RB, Quiros JR, Tumino R, Blazer DG 2nd, Linneberg A, Daimon M, Panico S, Howard B, Skeie G, Strandberg T, Weiderpass E, Nietert PJ, Psaty BM, Kromhout D, Salamanca-Fernandez E, Kiechl S, Krumholz HM, Grioni S, Palli D, Huerta JM, Price J, Sundström J, Arriola L, Arima H, Travis RC, Panagiotakos DB, Karakatsani A, Trichopoulou A, Kühn T, Grobbee DE, Barrett-Connor E, van Schoor N, Boeing H, Overvad K, Kauhanen J, Wareham N, Langenberg C, Forouhi N, Wennberg M, Després JP, Cushman M, Cooper JA, Rodriguez CJ, Sakurai M, Shaw JE, Knuiman M, Voortman T, Meisinger C, Tjønneland A, Brenner H, Palmieri L, Dallongeville J, Brunner EJ, Assmann G, Trevisan M, Gillum RF, Ford I, Sattar N, Lazo M, Thompson SG, Ferrari P, Leon DA, Smith GD, Peto R, Jackson R, Banks E, Di Angelantonio E, Danesh J; Emerging Risk Factors Collaboration/EPIC-CVD/UK Biobank Alcohol Study Group. Risk thresholds for alcohol consumption: combined analysis of individual-participant data for 599 912 current drinkers in 83 prospective studies. *Lancet* 2018; **391**: 1513-1523 [PMID: 29676281 DOI: 10.1016/S0140-6736(18)30134-X]

17 **Xiao J**, Wang F, Wong NK, Lv Y, Liu Y, Zhong J, Chen S, Li W, Koike K, Liu X, Wang H. Epidemiological Realities of Alcoholic Liver Disease: Global Burden, Research Trends, and Therapeutic Promise. *Gene Expr* 2020; **20**: 105-118 [PMID: 32690129 DOI: 10.3727/105221620X15952664091823]

18 **Choudhuri S**. Small noncoding RNAs: biogenesis, function, and emerging significance in toxicology. *J Biochem Mol Toxicol* 2010; **24**: 195-216 [PMID: 20143452 DOI: 10.1002/jbt.20325]

19 **Han S**, Zhang T, Kusumanchi P, Huda N, Jiang Y, Yang Z, Liangpunsakul S. Long non-coding RNAs in liver diseases: Focusing on nonalcoholic fatty liver disease, alcohol-related liver disease, and cholestatic liver disease. *Clin Mol Hepatol* 2020; **26**: 705-714 [PMID: 33053941 DOI: 10.3350/cmh.2020.0166]

20 **Walsham NE**, Sherwood RA. Ethyl glucuronide and ethyl sulfate. *Adv Clin Chem* 2014; **67**: 47-71 [PMID: 25735859 DOI: 10.1016/bs.acc.2014.09.006]

21 **Gerbase FE**, Tegner M, Krutzmann ME, Muller VV, Alff JA, da Silva VB, Sagrilo OP, Linden R, Antunes MV. Blood phosphatidyl ethanol levels as a tool to detect alcohol misuse in trauma patients. *Clin Toxicol (Phila)* 2021; **59**: 418-425 [PMID: 33021410 DOI: 10.1080/15563650.2020.1822531]

22 **Gerussi A**, Lucà M, Cristoferi L, Ronca V, Mancuso C, Milani C, D'Amato D, O'Donnell SE, Carbone M, Invernizzi P. New Therapeutic Targets in Autoimmune Cholangiopathies. *Front Med (Lausanne)* 2020; **7**: 117 [PMID: 32318580 DOI: 10.3389/fmed.2020.00117]

23 **Al-Dury S**, Marschall HU. Ileal Bile Acid Transporter Inhibition for the Treatment of Chronic Constipation, Cholestatic Pruritus, and NASH. *Front Pharmacol* 2018; **9**: 931 [PMID: 30186169 DOI: 10.3389/fphar.2018.00931]

24 **Du X**, DeForest N, Majithia AR. Human Genetics to Identify Therapeutic Targets for NAFLD: Challenges and Opportunities. *Front Endocrinol (Lausanne)* 2021; **12**: 777075 [PMID: 34950105 DOI: 10.3389/fendo.2021.777075]

25 **Nakao Y**, Amrollahi P, Parthasarathy G, Mauer AS, Sehrawat TS, Vanderboom P, Nair KS, Nakao K, Allen AM, Hu TY, Malhi H. Circulating extracellular vesicles are a biomarker for NAFLD resolution and response to weight loss surgery. *Nanomedicine* 2021; **36**: 102430 [PMID: 34174416 DOI: 10.1016/j.nano.2021.102430]

26 **Oh TG**, Kim SM, Caussy C, Fu T, Guo J, Bassirian S, Singh S, Madamba EV, Bettencourt R, Richards L, Yu RT, Atkins AR, Huan T, Brenner DA, Sirlin CB, Downes M, Evans RM, Loomba R. A Universal Gut-Microbiome-Derived Signature Predicts Cirrhosis. *Cell Metab* 2020; **32**: 878-888.e6 [PMID: 32610095 DOI: 10.1016/j.cmet.2020.06.005]

27 **Yilmaz Y**, Eren F. Serum biomarkers of fibrosis and extracellular matrix remodeling in patients with nonalcoholic fatty liver disease: association with liver histology. *Eur J Gastroenterol Hepatol* 2019; **31**: 43-46 [PMID: 30134384 DOI: 10.1097/MEG.0000000000001240]

28 **Wojciechowska M**, Malacrino S, Martin NG, Fehri H, Rittscher J. Early detection of liver fibrosis using graph convolutional networks. Medical image computing and computer assisted intervention – MICCAI 2021: 24th International Conference, Strasbourg, France, September 27 – October 1, 2021, Proceedings, Part VIII, 2021: 217-226

29 **Jonas W**, Schürmann A. Genetic and epigenetic factors determining NAFLD risk. *Mol Metab* 2021; **50**: 101111 [PMID: 33160101 DOI: 10.1016/j.molmet.2020.101111]

30 **Alves-Bezerra M**, Furey N, Johnson CG, Bissig KD. Using CRISPR/Cas9 to model human liver disease. *JHEP Rep* 2019; **1**: 392-402 [PMID: 32039390 DOI: 10.1016/j.jhepr.2019.09.002]

31 **Gawande A**, Gupta GK, Gupta A, Wanjari SJ, Goel V, Rathore V, Bhardwaj H, Nijhawan S. Acute-on-Chronic Liver Failure: Etiology of Chronic and Acute Precipitating Factors and Their Effect on Mortality. *J Clin Exp Hepatol* 2019; **9**: 699-703 [PMID: 31889750 DOI: 10.1016/j.jceh.2019.04.050]

32 **Ray G**, Manjubhargav P. Clinical Presentation and Mortality Determinants of Alcohol-Related Liver Disease: A Single-Center Experience of the Rising Menace from Eastern India. *Inflamm Intest Dis* 2019; **4**: 104-114 [PMID: 31559262 DOI: 10.1159/000501274]

33 **Rudnick SR**, Conway JD, Russo MW. Current state of endohepatology: Diagnosis and treatment of portal hypertension and its complications with endoscopic ultrasound. *World J Hepatol* 2021; **13**: 887-895 [PMID: 34552695 DOI: 10.4254/wjh.v13.i8.887]

34 **Zhang J**, Liu Q, He J, Li Y. Novel Therapeutic Targets in Liver Fibrosis. *Front Mol Biosci* 2021; **8**: 766855 [PMID: 34805276 DOI: 10.3389/fmolb.2021.766855]

35 **Tan Z**, Sun H, Xue T, Gan C, Liu H, Xie Y, Yao Y, Ye T. Liver Fibrosis: Therapeutic Targets and Advances in Drug Therapy. *Front Cell Dev Biol* 2021; **9**: 730176 [PMID: 34621747 DOI: 10.3389/fcell.2021.730176]

36 **Maciejewska-Markiewicz D**, Stachowska E, Hawryłkowicz V, Stachowska L, Prowans P. The Role of Resolvins, Protectins and Marensins in Non-Alcoholic Fatty Liver Disease (NAFLD). *Biomolecules* 2021; **11** [PMID: 34202667 DOI:

10.3390/biom11070937]
37 **Bosch J**, Gracia-Sancho J, Abraldes JG. Cirrhosis as new indication for statins. *Gut* 2020; **69**: 953-962 [PMID: 32139553 DOI: 10.1136/gutjnl-2019-318237]
38 **Johnson PJ**, Pirrie SJ, Cox TF, Berhane S, Teng M, Palmer D, Morse J, Hull D, Patman G, Kagebayashi C, Hussain S, Graham J, Reeves H, Satomura S. The detection of hepatocellular carcinoma using a prospectively developed and validated model based on serological biomarkers. *Cancer Epidemiol Biomarkers Prev* 2014; **23**: 144-153 [PMID: 24220911 DOI: 10.1158/1055-9965.EPI-13-0870]
39 **Yang JD**, Heimbach JK. New advances in the diagnosis and management of hepatocellular carcinoma. *BMJ* 2020; **371**: m3544 [PMID: 33106289 DOI: 10.1136/bmj.m3544]
40 **Zhang H**, Zhang W, Jiang L, Chen Y. Recent advances in systemic therapy for hepatocellular carcinoma. *Biomark Res* 2022; **10**: 3 [PMID: 35000616 DOI: 10.1186/s40364-021-00350-4]
41 **Burke NT**, Maurice JB, Nasralla D, Potts J, Westbrook R. Recent advances in liver transplantation. *Frontline Gastroenterol* 2022; **13**: 57-63 [PMID: 34970429 DOI: 10.1136/flgastro-2020-101425]
42 **Choudhary NS**, Bhangui P, Soin AS. Liver Transplant Outcomes in India. *Clin Liver Dis (Hoboken)* 2022; **19**: 32-35 [PMID: 35106148 DOI: 10.1002/cld.1166]
43 **Jadlowiec CC**, Taner T. Liver transplantation: Current status and challenges. *World J Gastroenterol* 2016; **22**: 4438-4445 [PMID: 27182155 DOI: 10.3748/wjg.v22.i18.4438]

World Journal of Gastroenterology

Submit a Manuscript: https://www.f6publishing.com

World J Gastroenterol 2022 October 28; 28(40): 5827-5844

DOI: 10.3748/wjg.v28.i40.5827

ISSN 1007-9327 (print) ISSN 2219-2840 (online)

MINIREVIEWS

Pancreatic acinar cell carcinoma: A comprehensive review

Luis Fernando Calimano-Ramirez, Taher Daoud, Dheeraj Reddy Gopireddy, Ajaykumar C Morani, Rebecca Waters, Kazim Gumus, Albert Russell Klekers, Priya R Bhosale, Mayur K Virarkar

Specialty type: Gastroenterology and hepatology

Provenance and peer review: Invited article; Externally peer reviewed.

Peer-review model: Single blind

Peer-review report's scientific quality classification

Grade A (Excellent): 0
Grade B (Very good): B, B
Grade C (Good): C
Grade D (Fair): 0
Grade E (Poor): 0

P-Reviewer: Hiyoshi M, Japan; Nithiyaraj E, India; Rama N, Portugal

Received: August 25, 2022
Peer-review started: August 25, 2022
First decision: September 8, 2022
Revised: September 14, 2022
Accepted: October 14, 2022
Article in press: October 14, 2022
Published online: October 28, 2022

Luis Fernando Calimano-Ramirez, Department of Radiology, University of Florida College of Medicine Jacksonville, Jacksonville, FL 32209, United States

Taher Daoud, Ajaykumar C Morani, Albert Russell Klekers, Priya R Bhosale, Department of Diagnostic Radiology, The University of Texas MD Anderson Cancer Center, Houston, TX 77030, United States

Dheeraj Reddy Gopireddy, Mayur K Virarkar, Department of Diagnostic Radiology, University of Florida College of Medicine Jacksonville, Jacksonville, FL 32209, United States

Rebecca Waters, Department of Pathology and Lab Medicine, The University of Texas MD Anderson Cancer Center, Houston, TX 77030, United States

Kazim Gumus, Department of Research and Diagnostic Radiology, University of Florida College of Medicine Jacksonville, Jacksonville, FL 32209, United States

Corresponding author: Luis Fernando Calimano-Ramirez, MD, Research Assistant, Department of Radiology, University of Florida College of Medicine Jacksonville, 655 8th St. W 2nd Floor, Jacksonville, FL 32209, United States. luis.calimanoramirez@jax.ufl.edu

Abstract

Acinar cell carcinoma (ACC) is a rare pancreatic malignancy with distinctive clinical, molecular, and morphological features. The long-term survival of ACC patients is substantially superior to that of pancreatic adenocarcinoma patients. As there are no significant patient series about ACCs, our understanding of this illness is mainly based on case reports and limited patient series. Surgical resection is the treatment of choice for patients with the disease restricted to one organ; however, with recent breakthroughs in precision medicine, medicines targeting the one-of-a-kind molecular profile of ACC are on the horizon. There are no standard treatment protocols available for people in which a total surgical resection to cure the condition is not possible. As a result of shared genetic alterations, ACCs are chemosensitive to agents with activity against pancreatic adenocarcinomas and colorectal carcinomas. The role of neoadjuvant or adjuvant chemoradiotherapy has not been established. This article aims to do a comprehensive literature study and present the most recent information on acinar cell cancer.

Key Words: Acinar cell carcinoma; Pancreas; Imaging; Immunohistochemical stains; Molecular features; Surgery; Chemotherapy

©The Author(s) 2022. Published by Baishideng Publishing Group Inc. All rights reserved.

Core Tip: Acinar cell carcinoma (ACC) of the pancreas is a rare, malignant neoplasm that accounts for a small percentage of all pancreatic neoplasms. Our understanding of this disease remains unclear as there are no large series of patients with ACC. This review article aims to conduct a comprehensive literature review and present current knowledge about ACC.

Citation: Calimano-Ramirez LF, Daoud T, Gopireddy DR, Morani AC, Waters R, Gumus K, Klekers AR, Bhosale PR, Virarkar MK. Pancreatic acinar cell carcinoma: A comprehensive review. *World J Gastroenterol* 2022; 28(40): 5827-5844
URL: https://www.wjgnet.com/1007-9327/full/v28/i40/5827.htm
DOI: https://dx.doi.org/10.3748/wjg.v28.i40.5827

INTRODUCTION

The rising prevalence of abdominal imaging has resulted in an uptick in historically rare pancreatic cancer cases. The exocrine pancreas primarily comprises acinar and ductal cells[1]. Although acinar tissue accounts for most of the pancreatic organ, pancreatic neoplasms that mainly exhibit acinar differentiation are rare. The expression of various pancreatic enzymes, such as chymotrypsin, trypsin, and lipase, leads to acinar differentiation in the exocrine pancreas[1]. Most acinar neoplasms are solid, malignant, and not well-recognized[2]. Acinar cell cystadenoma is the sole benign acinar neoplasm documented; uncommon benign cystic, malignant cystic, and mixed carcinomas also exist.

Acinar cell carcinoma (ACC) of the pancreas is a rare, malignant tumor composed of cells with morphological resemblance to acinar cells and with evidence of exocrine enzyme synthesis by the neoplastic cells, accounting for 1%-2% of all pancreatic neoplasms[2-4]. ACC of the pancreas is a high-grade malignancy with no apparent site preference; it can occur in any section of the pancreas, but the head is the most common location.

Currently, there is no definitive course of treatment for ACC; however, vigorous surgical resection with negative margins has been linked to improved long-term survival[5]. Particularly with the use of computerized tomography (CT) and magnetic resonance imaging (MRI), as well as with the confirmation of fine needle aspiration (FNA) biopsies, early recognition and diagnosis are of particular relevance. Knowledge of these lesions' morphologic and immunohistochemical characteristics is also essential for a precise clinical diagnosis. In addition, extensive molecular analyses of acinar neoplasms have identified genomic alterations that may be amenable to specific therapies, thereby increasing the likelihood of widespread clinical molecular testing of these tumors.

This article aims to do a comprehensive literature study and present the most recent information on acinar cell cancer.

EPIDEMIOLOGY

ACC of the pancreas accounts for 1%-2% of all adult exocrine pancreatic neoplasms and 15% of pediatric neoplasms. ACC occurs most frequently in white males and is usually bimodal in age, with peaks in childhood at 8-15 years of age and adulthood with a peak incidence at 60 and is rare between the ages of 20 and 40. ACC has a 3.6 male-to-female ratio. No known racial relationships exist[1,6,7].

CLINICAL FEATURES

Most ACC s exhibit vague symptoms, which include weight loss (45%), abdominal pain (60%), back pain (50%), nausea and vomiting (20%), melena (12%), weakness, anorexia, and diarrhea (8%) are typical non-specific symptoms of ACC[8,9]. In distinction to ductal adenocarcinoma, ACC infrequently obstructs the bile duct and causes jaundice only in 12% of patients. ACC causes a mass effect and displaces those organs but does not infiltrate[10].

Some patients experience paraneoplastic disease known as "Schmid's Triad" or lipase hypersecretion syndrome due to increased lipase levels reaching over 10000 U/dL[11,12]. Elevated lipase may be the first sign of ACC. Patients may present with multiple nodular foci of subcutaneous fat necrosis, polyarthralgia may occur due to fat necrosis in the cancellous bone, and may have peripheral blood eosinophilia[13,14]. On imaging, fat necrosis within the bone can appear as a focal area of sclerosis.

Paraneoplastic syndrome may occur following tumor recurrence. Most patients have hepatic metastases at presentation; however, some may present with only a bulky pancreatic mass. The serum lipase levels may normalize after surgical resection of the tumor, and patients may have symptomatic relief. Lipase may be used as a tumor marker in these patients. Alpha-fetoprotein (AFP) blood levels can be elevated in young patients[15].

MACROSCOPY (GROSS FEATURES)

On FNA, an abundance of cells with fluctuating degrees of acinar differentiation but no endocrine or ductal cells are seen. The aspirates consist primarily of cohesive fragments creating acini, cellular cords, or solid nests of neoplastic epithelium, composed of clusters of uniform cells with smoothly contoured, eccentric nuclei containing one or two prominent nuclei nucleoli[16,17].

ACCs can occur in any region of the pancreas and, on average, are 10 to 11 cm in size at the time of diagnosis[18-20]. The tumors are well circumscribed and have a soft, fleshy, tan to red appearance[2]. They occasionally exhibit lobulated appearances, necrosis, and cystic degeneration[20]. On occasion, the neoplasm is found attached to the surface of the pancreas. Involvement of the duct system by ACCs can sometimes be observed grossly as polypoid or fingerlike projections extending from the primary tumor mass toward the duct[21].

PATHOLOGY

ACCs are cellular neoplasms with minimal stroma on microscopic examination. Multiple architectural patterns, including acinar (Figure 1A), solid (Figure 1B), glandular (Figure 1C), and trabecular (Figure 1D), can be observed. Solid and acinar patterns are the most prevalent. The acinar pattern is characterized by structures resembling normal acini, with small lumina and cells arranged in a monolayer with basally located nuclei. Large sheets of cells depict the solid pattern without lumina. Acinar structures with the dilated lumen characterize the less common granular pattern. The trabecular pattern, which resembles the architecture of well-differentiated neuroendocrine tumors, consists of more pronounced palisading with thinner, interlacing ribbons of cells. Multiple architectural patterns are visible within a single tumor.

IMMUNOHISTOCHEMISTRY

The immunohistochemical labeling of enzyme production from pancreatic cells aids in confirming the diagnosis of ACC (Table 1). There are commercially available antibodies for chymotrypsin, trypsin, lipase, and amylase, with the first three being the most frequently used in clinical settings (Figure 1E). These enzymes exhibit varying degrees of specificity and sensitivity. In approximately 95% of cases, trypsin and chymotrypsin reactivity can be demonstrated, and this combination is reportedly the most sensitive for diagnosing ACC[10,22].

ACC is also positive for CK8 and CK18, and as a result, they will label for AE1/AE3 and CAM5.2. CK7 (Figure 1F) and CK19, which are usually expressed in ductal adenocarcinomas, are generally missing in ACC but may be expressed in a subgroup of ACCs[15,23]. Focal labeling for chromogranin and synaptophysin is observed in a substantial proportion of ACCs, displaying the need to assess with further clear-cut acinar markers, especially in small samples, to avoid misidentifying an ACC as a neuroendocrine tumor or mixed acinar-neuroendocrine differentiation[10,24,25]. Recent research on histological and cytological samples has proven that the monoclonal antibody directed against the COOH-terminal region of the BCL10 protein, which identifies the COOH-terminal portion of CEL, is a highly specific and sensitive approach for detecting ACCs[26,27].

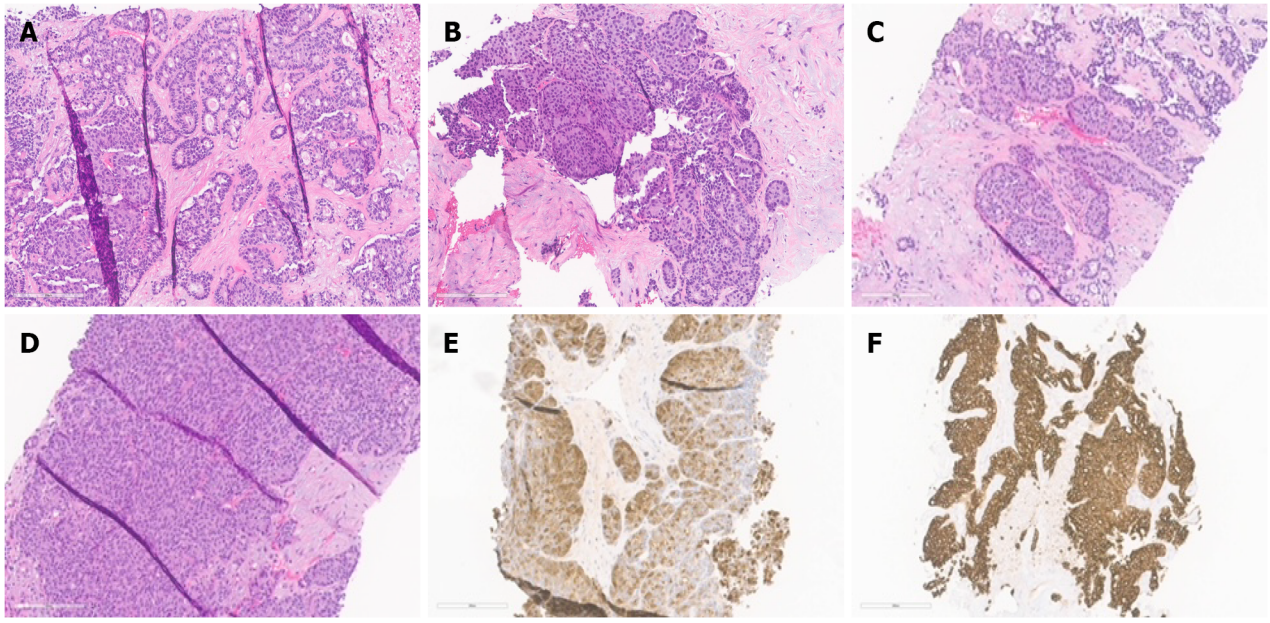
MOLECULAR FEATURES

The genetic alterations driving ACC have been thoroughly characterized and sequenced. The outcomes of these studies have emphasized the diversity of modified genes and pathways among various tumors, as well as the marked genomic instability in a subset of instances, including at the base pairs and chromosomes level. Several studies analyzed ACC for mutations in gene changed in pancreatic ductal adenocarcinoma (PDAC), the most prevalent subtype of pancreatic cancer, before the wide availability of whole genome and exome. Several of these studies reported uncommon mutations in *TP53*, *KRAS*, and *SMAD4*, in addition to the unusual loss of SMAD4 expression in acinar neoplasms, while others reported no modifications in these genes[28-33]. In these studies, the most prevalent ACC mutations

Table 1 Immunohistochemical profile from the differential diagnosis

Tumor type	PCK	Trypsin/chymotrypsin/BCL-10	BCL-10	B-Catenin	Synaptophysin	Chromogranin	Others
ACC	+	+	+	+/-	-/+	-/+	Amylase. Lipase. PAS
PDAC	+	-	-	-	-	-	P53, DPC4 loss
SPN	-/+	-	-	+[1]	-	-	PR, CD56, Alpha 1-antitrypsin
PanNET	+	-	-	-	+	+	CD56, PAX8[3], ISL1[3]
PBL	+	+	-	+[2]	-	-	Alpha fetoprotein, CEA

[1]Nuclear.
[2]Nuclear/Cytoplasmic and positive in squamous morules.
[3]PAX8 and ISL1 are specific markers for PanNETs.
ACC: Acinar cell carcinoma; PCK: Pancytokeratin; PanNET: Pancreatic neuroendocrine tumors; PBL: Pancreatoblastoma; SPN: Solid pseudopapillary neoplasm; PDAC: Pancreatic ductal carcinoma; PAS: Periodic acid-Schiff; ISL 1: Islet 1; CEA: Carcinoembryonic antigen.



DOI: 10.3748/wjg.v28.i40.5827 **Copyright** ©The Author(s) 2022.

Figure 1 Histopathological patterns. A: Acinar cell carcinoma with the predominant acinar pattern. The acinar pattern is characterized by structures resembling normal acini, with small lumina and cells arranged in a monolayer with basally located nuclei; B: Acinar cell carcinoma with the predominant glandular pattern. Acinar structures with dilated lumina characterize the glandular pattern; C: Acinar cell carcinoma with the predominant trabecular pattern. The trabecular pattern is characterized by ribbons of cells resembling those of pancreatic neuroendocrine tumors; D: Acinar cell carcinoma with a predominant solid pattern. Large sheets of cells characterize the solid pattern without lumina; E: Acinar cell carcinoma, immunohistochemical staining for trypsin; F: Acinar cell carcinoma, immunohistochemical staining for cytokeratin 7.

affected WNT signalings, such as mutations in APC that rendered inactive and mutations in CTNNB1 that rendered it active; these alterations were found in roughly 20% of ACCs[30]. Recent sequencing studies of the entire exome have highlighted the diversity of mutated genes in the ACC[34,35]. Several other studies have shown substantial chromosomal gains and losses in ACCs and altered regions in various carcinomas; nevertheless, the target genes (if any) in these regions have not been detected[29,30,36,37].

Multiple potentially targetable genetic alterations in pancreatic ACC have been identified. A subset of cases exhibits genomic instability due to mutations in genes involved in DNA repairs, such as *ATM*, *BRCA1*, *BRCA2*, *PALB2*, and *MSH2*[34,35]. According to various studies, microsatellite instability has been documented in fluctuating proportions of ACC, ranging from 7% to 14%[30,35,38]. Also, platinum agents and PARP inhibitors treat tumors with mutations in BRCA pathway genes[39,40]. Even though it has not yet been proven in major clinical trials, preliminary findings indicate that tumors with BRAF fusions react to MEK inhibitors, providing ACC with targeted therapy[41-43]. In a subgroup of ACCs,

Table 2 Summary of pertinent differential diagnostic features

Differential diagnoses	Age/sex	Imaging/gross findings	Histology	Prognosis
ACC	Predominant in males; mean age of 62 yr	Solid, well-circumscribed, bulky tumors; hemorrhage and necrosis are also frequent	Predominant acinar or solid architecture; uniform cells; basally located nuclei; eosinophilic granular cytoplasm; prominent single nucleoli. minimal stroma	Overall aggressive, with high rates of recurrence and metastasis
PDAC	Slightly higher in males; 6th-8th decade of life	Solid, poorly defined mass	Large, medium, or small malignant ducts with a tubular pattern; desmoplastic stroma. Processes of mitosis and necrosis	Poor survival rates
PanNET	Even distribution between the genders; more prevalent in adults; mean age of 40	Solid, well-circumscribed. 5% are cystic	Variable architectural patterns; uniform cells; oval or spherical nuclei; granular cytoplasm; undetected nucleoli; minimal stroma	Relatively languid, but with variable results
SPN	Almost exclusively female; average age of 28	Well-defined and encased with cystic degeneration	Pseudopapillae; cells with hyaline/myxoid stroma surrounding vessels; large cytoplasmic hyaline globules; nuclear groove	Overall low malignant potential: The majority are successfully treated surgically
PBL	First decade of life, mean age of 4; adults can be affected	Partially encapsulated, frequently lobulated, and substantial	Solid and acinar structure; cellular stroma; keratinization of squamoid nests; heterologous mesenchymal elements	Aggressive; better outcomes for children

ACC: Acinar cell carcinoma; PanNET: Pancreatic neuroendocrine tumors; PBL: Pancreatoblastoma; SPN: Solid pseudopapillary neoplasm; PDAC: Pancreatic ductal carcinoma

MYC abnormalities, including chromosome 8 polysomy and gene amplification, have been identified recently[44].

DIAGNOSIS

Laboratory analysis

Besides an increase in serum lipase levels associated with the syndrome of lipase hypersecretion, serum tumor markers are not consistently elevated in ACC. Even in the absence of lipase hypersecretion syndrome, lipase might be high. There have been numerous AFP increases, especially in younger patients[2]. Typically, Serum tumor markers such as carbohydrate antigen 19-9, alpha-fetoprotein, and carcinoembryonic antigen are expressed.

Radiological features (imaging)

In recent years, the incidence of uncommon pancreatic cancers has grown, likely due to the increased use of cross-sectional imaging[45]. In most instances, pancreatic cancers are incidentally found by CT. MRI is often used as a secondary test for further characterization. ACC of the pancreas is a well-defined, primarily oval or round exophytic mass in cross-sectional imaging[46,47]. Rarely have cystic variations been described. Typically, it manifests as a dense, largely solid tumor devoid of noticeable cystic alterations[46,48]. One-third of patients may exhibit calcifications, and the majority of the tumor increases constantly, but less so than the adjacent pancreatic parenchyma[49]. The tumor displays heterogeneous enhancement after intravenous infusion of contrast material[46]. Other studies also concluded that when confronted with a large mass with an ovoid shape, exophytic, well-circumscribed arising from the pancreas, with slight and persistent enhancement after contrast administration, and without appreciable biliary or pancreatic dilation, the diagnosis of ACC should be considered[18,47,50]. Another study stated that MRI is better than CT for identifying tumor margination, intratumoral bleeding, tissue invasion, and ductal dilation[51]. On the other hand, CT is more sensitive to detecting central calcification and is commonly utilized due to its accessibility and quickness[50,51]. CT and MRI accurately depict most ACC imaging characteristics, and the two modalities correlate well[51].

Differential diagnosis

Pancreatic endocrine neoplasms that are well-differentiated, solid pseudopapillary neoplasms (SPNs), mixed acinar neoplasms, pancreatoblastoma (PBL), and PDACs should be included in the differential diagnosis (Table 2). Well-differentiated endocrine neoplasm, also commonly known as pancreatic neuroendocrine tumors (PanNET), is the entity most widely confused and misdiagnosed[2]. Both neoplasms typically contain a high number of cells and little amount of stroma, are capable of forming cell sheets and can consist of medium-sized, spherical, monomorphic cells with a microglandular or

solid pattern of growth[2]. In addition, the red cytoplasmic zymogen and neurosecretory granules from ACC and PanNETs, respectively, are similar with appropriate differentiation. PanNETs are associated with a more favorable prognosis, making differentiation crucial. ACCs are distinguished from PanNETs by their primary acinar development, cytoplasmic granulation, basally oriented nuclei, and individual conspicuous nucleoli. However, hyalinized stroma, plasmacytoid cell appearance, and a "salt and pepper" chromatin pattern are indicative of PanNET[6]. Immunohistochemistry is advantageous, but it must be utilized with care. Using general neuroendocrine markers such as synaptophysin and chromogranin A alone may be unsafe because several ACCs contain neuroendocrine cells, which are particularly abundant in 30% of cases, as stated before[10,24]. Therefore, the demonstration of acinar cell products is mandatory if an ACC is suspected.

SPNs present as massive, dense pancreatic masses that are clinically identical to ACC; however, SPNs virtually entirely affect women of young age[52]. Cytological smears are characterized by delicately branched vasculature with lightly adherent cells generating pseudopapillary structures, a homogenous population of microscopic cells with cuboidal formation, and a unique hyaline myxoid matrix[52]. Additionally, cytoplasmic hyaline globules are occasionally visible. Moreover, the SPNs nuclei are often normochromic, with numerous indentations, and lack the conspicuous nucleoli found in acinar cells [53]. Typically, SPNs exhibit nuclear immunoreactivity for β-catenin and high expression of CD10, which are also detectable in roughly 10% and 60% of ACCs, respectively. As a result, these two markers must be utilized in conjunction with markers specific to acinar cells, such as trypsin and BCL10[53-55].

PBL is another entity with stroma-poor acinar differentiation that must be evaluated in the differential diagnosis. Similar to ACCs, upon the appearance, PBLs are typically large, with an average size of 10 cm ranging from 1.5 to 20 cm[56]. This uncommon tumor shares nearly all of the cytologic and clinical characteristics of ACC, notably in the population of younger age, where it is frequently observed [2,57]. Cytologically, the neoplasms may be indistinguishable because they both display a predominant acinar-cell differentiation[2]. Heterologous components and squamous nests, such as osseous and cartilage development, characterize PBL[2]. In addition to immunochemistry and clinicopathologic data, the heterogeneous cytologic elements of the types of the tumor-cell present, including a combination of squamoid, mesenchymal, and glandular cells, are a general clue to diagnosing PBL[58]. Histologically, the presence of squamoid nests in PBL is the distinguishing characteristic of the two entities.

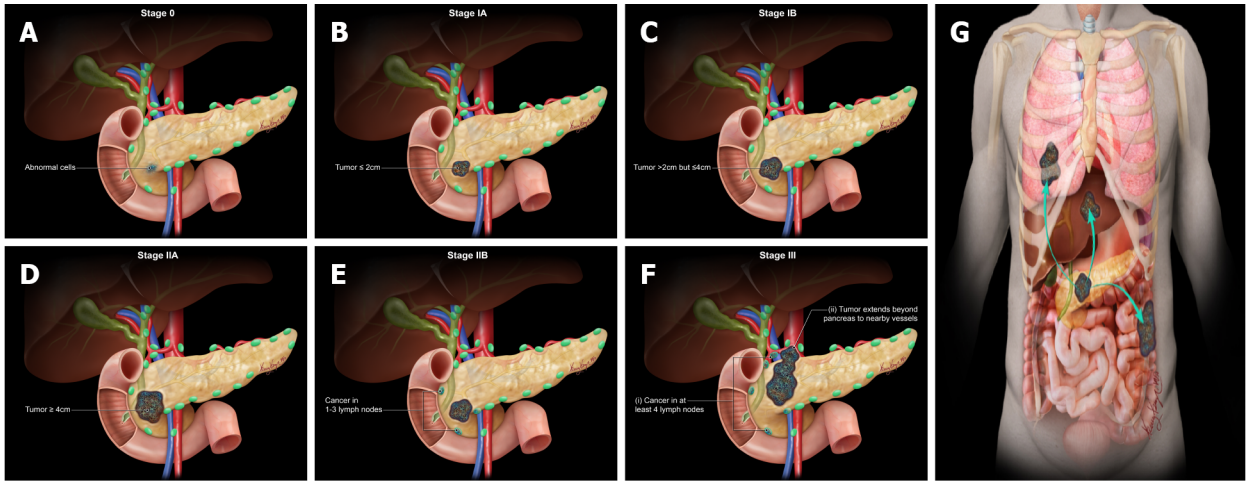
ACCs typically lack the characteristic cytomorphologic features of PDACs, allowing these two tumors to be distinguished easily. PDACs typically exhibit "drunk honeycomb" and "tombstone cells" arrangements alongside nuclear heterogeneity and nuclear silhouette abnormalities[59]. This is in contrast to the relatively homogeneous polygonal cells of ACCs, which are arranged in three-dimensional arrays and tissue fragments[1]. ACCs lack the large desmoplastic stroma that describes PDACs and display an overall solid and acinar architecture, whereas PDACs feature a prominent desmoplastic stroma[10,59,60].

STAGING FOR ACINAR PANCREATIC CARCINOMA

The staging system for acinar pancreatic cancer is undergoing continuous development. Clinical staging is determined by resectability, which is heavily impacted by surgical expertise. The agreed guidelines for the resectability of surgical procedures continue to be refined (*e.g.*, National Comprehensive Cancer Network, MD Anderson Cancer Center, American Hepato-Pancreato-Biliary Association, and International Hepato-Pancreato-Biliary Association). Traditionally, they are categorized as resectable, borderline resectable, locally progressed, and metastatic. To begin with, resectable tumors lack vascular involvement. Next, the borderline resectable tumors involve vascular, local structures, or other signs indicating a high risk of R1 resection. Local invasions (particularly vascular involvement) prevent surgical intervention for locally progressed malignancies. Lastly, metastatic cancer has spread to other organs beyond the main pancreatic tumor. The American Joint Committee on Cancer (AJCC) has classified staging by TNM (tumor, node, metastasis) classification using the consensus guidelines for resectability (Table 3 and Figure 2)[61]. Imaging cases with different AJCC TNM staging were added in chronological order (Figures 3 - 7) to appreciate the differences in changes.

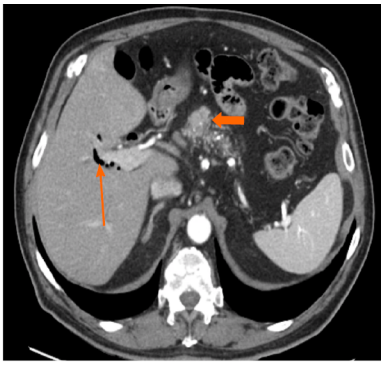
PROGNOSIS, FACTORS OF PREDICTION, SPREAD, AND METASTASES

ACCs are exceptionally malignant neoplasms; relatively 50% of patients have metastasis during diagnosis[62]. Initial studies indicate that the prognosis for ACCs is better than that for ductal carcinomas but worse than that for PanNETs[5,63,64]. Previous research using population-based cancer databases and epidemiological methods indicated that individuals diagnosed with ACCs have a median overall survival time of roughly 47 mo for patients with localized disease and 14 mo for patients with metastatic disease, with a 5-year survival rate ranging from 36.2% to 72.8% for resected cancers[5,64,65]. A recent study shows that ACC has a better prognosis than adenocarcinoma. They found that the prognosis was deteriorating with a decrease of 25% in a 5-year survival rate to previously reported rates



DOI: 10.3748/wjg.v28.i40.5827 **Copyright** ©The Author(s) 2022.

Figure 2 American Joint Committee on Cancer 8th Edition cancer staging for exocrine pancreatic tumor such as pancreatic acinar cell carcinoma. A: Stage 0 (TNM: Tis, N0, M0). Tis = Carcinoma in situ. N0 = No regional lymph node metastases. M0 = No distant metastasis; B: Stage IA (TNM: T1, N0, M0). T1 = Tumor ≤ 2 cm in greatest dimension. N0 = No regional lymph node metastases. M0 = No distant metastasis; C: Stage IB (TNM: T2, N0, M0). T2 = Tumor > 2 cm and ≤ 4 cm in greatest dimension. N0 = No regional lymph node metastases. M0 = No distant metastasis; D: Stage IIA (TNM: T3, N0, M0). T3 = Tumor > 4 cm in greatest dimension. N0 = No regional lymph node metastases. M0 = No distant metastasis; E: Stage IIB (TNM: T 1/2/3, N1, M0). T 1/2/3 = Tumor ≤ 2 cm > 4 cm in greatest dimension. N1 = Metastasis in one to three regional lymph nodes. M0 = No distant metastasis; F: Stage III (TNM: T 1/2/3, N2, M0 or T4, Any N, M0). T 1/2/3 = Tumor ≤ 2 cm > 4 cm in greatest dimension. N2 = Metastasis in four or more regional lymph nodes. T4 = Tumor involves celiac axis, superior mesenteric artery, and common hepatic artery, regardless of size; G: Stage IV (TNM: Any T, Any N, M1). M1 = Distant metastasis. T = Primary tumor; N = Regional lymph node; M = Distant metastasis.



DOI: 10.3748/wjg.v28.i40.5827 **Copyright** ©The Author(s) 2022.

Figure 3 Stage IA (T1, N0, M0). A 77-year-old male patient with acinar cell carcinoma. Axial post-contrast portal-venous phase computed tomography image shows a solid mass (short arrows) measuring 1.8 cm × 1.6 cm and involving the region of the pancreatic head/body. Incidental findings are calcifications seen throughout the pancreas (likely related to changes in chronic pancreatitis) and mild dilatation of the biliary tree with pneumobilia (long arrow).

[66]. However, data from a few studies published and anecdotal reports hint that some patients with ACCs have a greater survival rate than expected; unfortunately, no parameters are available to identify this group of patients[67,68].

Rarely do patients with ACC are diagnose with lung, cervical lymph nodes, and ovary metastases. Metastatic illness is typically detected in regional lymph nodes and the liver[69]. Patients presenting as their first disease symptom with distant metastases are infrequent. It has been proposed that ACCs in patients younger than 20 may be less aggressive than in adults[10]. The most significant prognostic indicator is the tumor stage, with patients without lymph nodes or distant metastases having a better prognosis[5,70]. In addition, a poor prognosis is also associated with being male, being over 60, and having a tumor larger than 10 cm[5].

TREATMENT

Current, surgical, radiotherapeutic, and chemotherapeutic treatments used for PDAC are typically used to treat ACC (Table 4). Surgery is regarded as the optimal treatment modality for ACCs that are

Table 3 American Joint Committee on Cancer 8th Edition cancer staging for exocrine pancreatic tumor such as pancreatic acinar cell carcinoma

Stage	TNM	Description
0	Tis	Carcinoma in situ[1]
	N0	No regional lymph node metastases
	M0	No distant metastasis
IA	T1	T1 = Tumor is ≤ 2 cm in any direction
		T1a = Tumor is ≤ 0.5 cm in any direction
		T1b = Tumor is > 0.5 cm and < 1 cm in any direction
		T1c = Tumor is 1–2 cm in any direction
	N0	No regional lymph node metastases
	M0	No distant metastasis
IB	T2	Tumor is > 2 cm and ≤ 4 cm in any direction
	N0	No regional lymph node metastases
	M0	No distant metastasis
IIA	T3	Tumor is > 4 cm in any direction
	N0	No regional lymph node metastases
	M0	No distant metastasis
IIB	T1	T1 = Tumor is ≤ 2 cm in any direction
		T1a = Tumor is ≤ 0.5 cm in any direction
		T1b = Tumor is > 0.5 cm and < 1 cm in any direction
		T1c = Tumor is 1–2 cm in any direction
	N1	Metastasis in one to three regional lymph nodes
	M0	No distant metastasis
	T2	Tumor is > 2 cm and ≤ 4 cm in any direction
	N1	Metastasis in one to three regional lymph nodes
	M0	No distant metastasis
	T3	Tumor is > 4 cm in any direction
	N1	Metastasis in one to three regional lymph nodes
	M0	No distant metastasis
III	T1	T1 = Tumor is ≤ 2 cm in any direction
		T1a = Tumor is ≤ 0.5 cm in any direction
		T1b = Tumor is > 0.5 cm and < 1 cm in any direction
		T1c = Tumor is 1–2 cm in any direction
	N2	Metastasis in four or more regional lymph nodes
	M0	No distant metastasis
	T2	Tumor is > 2 cm and ≤ 4 cm in any direction
	N2	Metastasis in four or more regional lymph nodes
	M0	No distant metastasis
	T3	Tumor is > 4 cm in any direction
	N2	Metastasis in four or more regional lymph nodes
	M0	No distant metastasis
	T4	Regardless of tumor size, the cancer has grown outside the pancreas, into the nearby

		large blood vessels[2]
	Any N	NX = Regional lymph nodes cannot be assessed
		N0 = No regional lymph node metastases
		N1 = Metastasis in one to three regional lymph nodes
		N2 = Metastasis in four or more regional lymph nodes
	M0	No distant metastasis
IV	Any T	TX = Primary tumor cannot be assessed
		T0 = No evidence of primary tumor
		Tis = Carcinoma in situ[1]
		T1 = Tumor is ≤ 2 cm in any direction
		T1a = Tumor is ≤ 0.5 cm in any direction
		T1b = Tumor is > 0.5 cm and < 1 cm in any direction
		T1c = Tumor is 1–2 cm in any direction
		T2 = Tumor is > 2 cm and ≤ 4 cm in any direction
		T3 = Tumor is > 4 cm in any direction
		T4 = Regardless of tumor size, the cancer has grown outside the pancreas, into the nearby large blood vessels[2]
	Any N	NX = Regional lymph nodes cannot be assessed
		N0 = No regional lymph node metastases
		N1 = Metastasis in one to three regional lymph nodes
		N2 = Metastasis in four or more regional lymph nodes
	M1	Distant metastasis

[1]Included in this category are high-grade pancreatic intraepithelial neoplasia, intraductal papillary mucinous neoplasm with high-grade dysplasia, intraductal tubulopapillary neoplasm with high-grade dysplasia, and mucinous cystic neoplasm with high-grade dysplasia.
[2]Celiac axis, superior mesenteric artery, and/or common hepatic artery are involved.
T: Primary tumor; N: Regional lymph node; M: Distant metastasis.

Table 4 Acinar cell carcinoma treatment options

Clinical stage	Treatment options
Resectable or borderline resectable	Neoadjuvant therapy[1]
	Surgery
	Postoperative chemotherapy
	Postoperative chemoradiation therapy
Locally advance	Chemotherapy[2]
	Chemoradiation therapy
	Surgery
	Palliative surgery
Recurrent or metastatic	Chemotherapy[2]

[1]Chemotherapy with or without chemoradiation therapy given before surgery.
[2]With or without target therapy.

regionally circumscribed and resectable. Holen *et al*[8] found that median survival for surgically resected cases was 36 mo, compared to 14 mo for those without surgical resection[8]. Another systematic research by Glazer *et al*[71] indicated that the total median survival rate for patients with ACC who had resection was approximately 47 mo[71]. More aggressive therapeutic regimens must be



DOI: 10.3748/wjg.v28.i40.5827 **Copyright** ©The Author(s) 2022.

Figure 4 Stage IB (T2, N0, M0). An 89-year-old male patient with acinar cell carcinoma. Axial post-contrast computed tomography arterial phase image shows a large mass in the body of the pancreas (arrow) measuring 3.3 cm × 3 cm. No regional adenopathy is identified.



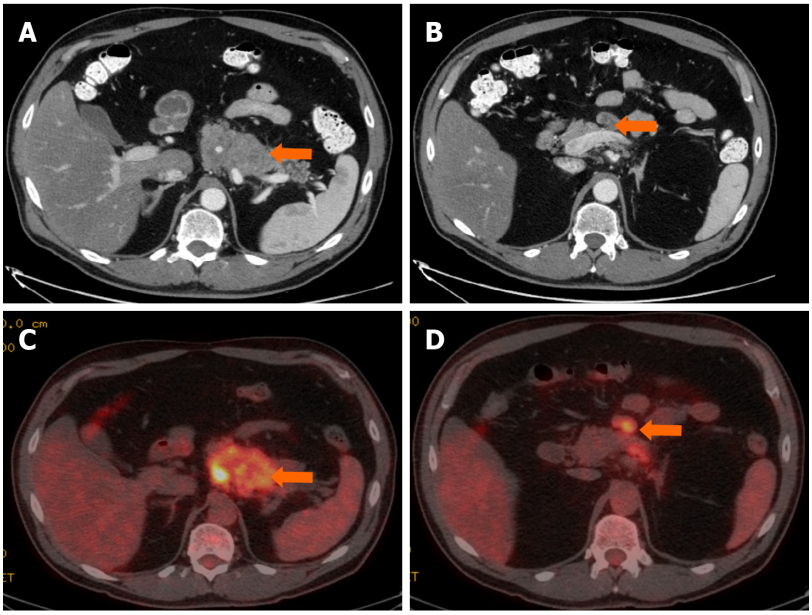
DOI: 10.3748/wjg.v28.i40.5827 **Copyright** ©The Author(s) 2022.

Figure 5 Stage IIA (T3, N0, M0). A 66-year-old patient with acinar cell carcinoma. Axial post-contrast computed tomography image in the arterial phase shows a solid lobulated mass measuring 6.5 cm × 5.4 cm arising from the tail of the pancreas (arrow). The mass is heterogeneous in density with areas of low-density and solid-enhancing areas. No regional or distant lymphadenopathy was detected.

sought when surgery is unavailable for locally advanced and metastatic diseases.

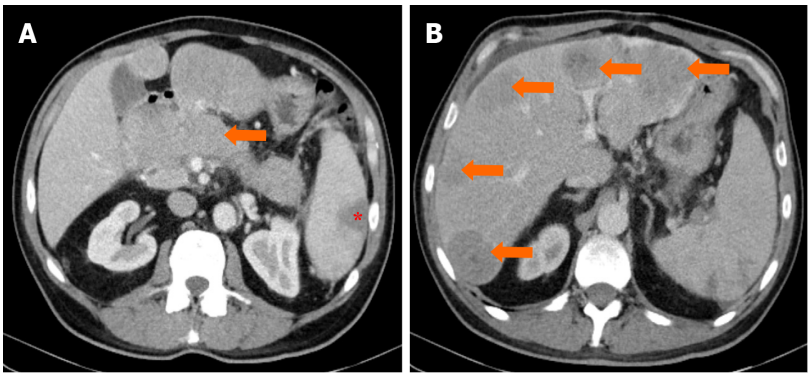
Due to the rareness of ACC and the absence of sufficient randomized trials comparing different treatment approaches, the role of adjuvant therapy remains debatable. Table 5 enlists characteristics of studies on various regimes used for treating ACC. In a study at Memorial Sloan-Kettering Cancer Center, systemic chemotherapy for ACC was determined to be ineffective[8]. Following surgical resection, there are no clear treatment guidelines, and most adjuvant therapies are individualized with variable response rates. Lack of prospective data to create therapy guidelines and genetic variation in the *APC* gene/β-catenin pathway observed in pancreatic acinar cells, ACC patients are frequently treated with chemotherapeutic agents known to be active against PDAC or colorectal cancer[72]. Most study participants received combination chemotherapy protocols based on gemcitabine or fluoropyrimidine[11,73]. If the ACC cannot be resected, the patient should undergo neoadjuvant or palliative 5-FU chemotherapy[70,74]. Combination fluoropyrimidine-based chemotherapies have increased disease control rates[8,11,73,75-77]. Glazer *et al*[71] systematic review showed that patients with a high-performance status typically receive folinic acid/fluorouracil/oxaliplatin or folinic acid/fluorouracil/irinotecan. In contrast, patients with a lower performance status typically receive gemcitabine/protein-bound paclitaxel[71].

Conventional fractionation and hypofractionated stereotactic body radiotherapy are used to "down-stage" or convert a borderline resectable tumor to one that is resectable[73]. Patients who could potentially benefit from resection can be identified through the absence of ACC development following neoadjuvant radiotherapy. Several studies reported a "major response" rate from 25% to 35% of these individuals[8,11].



DOI: 10.3748/wjg.v28.i40.5827 **Copyright** ©The Author(s) 2022.

Figure 6 Stage IIB (T3, N1, M0). A 61-year-old patient with acinar cell carcinoma. A: Axial post-contrast computed tomography (CT) image in the portovenous phase shows an infiltrative mass arising from the pancreatic body and tail (arrow); B: axial post-contrast CT images in the portovenous phase shows an enlarged mesenteric lymph node (arrow) measuring 2.6 cm × 1.2 cm; C: Axial positron emission tomography/CT image in the portovenous phase shows hypermetabolic pancreatic body and tail mass (arrow); D: Axial post-contrast CT images in the portovenous phase shows hypermetabolic enlarged mesenteric lymph node (arrow). Pathology of the mass revealed Acinar cell carcinoma with a metastatic mesenteric lymph node.



DOI: 10.3748/wjg.v28.i40.5827 **Copyright** ©The Author(s) 2022.

Figure 7 Stage IV. A 64-year-old patient with acinar cell carcinoma. A: Axial post-contrast image port venous phase shows a pancreatic head mass measuring about 3.2 cm × 2.8 cm (arrow); B: Axial post-contrast image port venous phase shows multiple bilobar variable-sized hepatic metastatic lesions (arrows). An incidental finding is an area of splenic infarction (asterisk in image A).

CONCLUSION

Pancreatic acinar neoplasms are a molecularly and morphologically heterogeneous group of diseases far less prevalent than ductal neoplasms. Due to its low surgical resectability, high rate of recurrence, and high frequency of metastases at diagnosis, pancreatic ACC has been regarded as cancer with a poor prognosis. At least a subset of the neoplastic cells exhibits acinar differentiation, as defined morphologically (granular cytoplasm, single prominent nucleoli) or immunohistochemically. The molecular system underlying the advancement of ACCs has been elucidated, revealing potentially targetable mutations that offer optimism for developing additional curative options. ACC usually appears as a bulky mass that does not obstruct the pancreatic or bile duct and does not cause jaundice. Elevated lipase levels, subcutaneous nodules, and the presence of bone infarct should help clinch a diagnosis of ACC. Also, these tumors have large lymph nodes at presentation. In the future, molecular diagnostics to detect lesions susceptible to targeted therapy will likely play an important role in patient care.

Table 5 Characteristics of studies on various acinar cell carcinoma treatment regimes

Ref.	Year of publication	ACC sample size	Type of treatment	No. of patients	Conclusion
Holen *et al* [8]	2002	39	Resection	9	A high recurrence rate following complete surgical resection suggests that micrometastases are present even in localized disease, and that adjuvant therapies may be indicated. Chemotherapy and radiation are ineffective, however, and novel treatments are required
			RT alone	22	
			Fluoropyrimidine-based chemotherapy and RT	1	
			Fluoropyrimidine-based chemotherapy	7	
Kitagami *et al*[65]	2007	115	Resection	88	To improve prognosis, surgical resection should be pursued if possible. If ACC cannot be resected or recurs, chemotherapy is likely to be beneficial. A multidisciplinary treatment centered on the role of surgery must be developed
			Palliative operation	12	
			Exploratory laparotomy	4	
			Other treatment[1]	11	
Seth *et al* [11]	2008	14	Resection	10	When feasible, surgical resection is the optimal first-line treatment for resectable ACC due to its superior survival, which can be further improved by the addition of a planned neoadjuvant and/or adjuvant chemoradiation regimen
			Resection, mixed chemotherapy[2] and RT	4	
Wisnoski *et al*[64]	2008	672	Resection	266	ACC surgical resection appears to improve survival, and the findings support an aggressive strategy for resectable disease. In order to define the role of chemoradiation in the palliative, adjuvant, and neoadjuvant settings, additional research is required
			Other treatment[1]	406	
Schmidt *et al*[5]	2008	865	Resection	190	In these favorable pancreatic cancers, aggressive surgical resection with negative margins is associated with long-term survival. Second, cancer registries lack certain information, such as the specific type of chemotherapy administered and radiation therapy details. Consequently, institutional and multi-institutional reports of ACC continue to be essential for performing a more comprehensive analysis of the presentation, pathology, natural history, and treatment-related outcomes of ACC
			Resection and chemotherapy	33	
			Resection and RT	10	
			Resection and chemoradiation	100	
			Other treatment[1]	532	
Matos *et al* [75]	2009	17	Resection	12	ACC requires aggressive surgical resection. Importantly, some patients with locally advanced ACC have responded to a neoadjuvant approach allowing resection of a downstaged tumor; therefore, a combined modality approach should be considered for these patients
			Mixed chemotherapy[2]	3	
			Mixed chemotherapy[2] and RT	2	
Seki *et al* [76]	2009	4	Gemcitabine-based chemotherapy	1	A partial response suggested that fluoropyrimidine-based chemotherapy may have some activity against this tumor. To confirm the efficacy of fluoropyrimidine in treating pancreatic ACC, prospective clinical trials are required
			Fluoropyrimidine-/gemcitabine-based chemotherapy	3	
Lee *et al* [78]	2010	29	Resection	12	In Korea, the clinical characteristics of ACC include a young age, a large size, a location in the tail, and nonspecific tumour markers. ACC should always be actively treated with surgery, regardless of its size
			Resection, mixed chemotherapy[2] and RT	10	
			Mixed chemotherapy[2] and RT	1	
			Other treatment[1]	6	
Butturini *et al*[73]	2011	9	Resection	2	Using multiple chemotherapy regimens and regional treatments sequentially for recurrent disease allowed for 45-, 85-, and 52-mo post-primary survival. Long-term survival and clinical benefit may be possible with repeated surgery, neoadjuvant and adjuvant chemoradiation therapies, and locoregional therapy
			Resection and gemcitabine-based chemotherapy	7	
Hartwig *et al*[79]	2011	17	Resection	13	ACC of the pancreas is a relatively uncommon tumor entity for which resection may lead to long-term survival, even in the presence of limited metastatic disease. Optimized adjuvant treatment protocols are required to improve the long-term survival of ACC patients
			Resection and gemcitabine-based chemotherapy	4	

Lowery *et al*[77]	2011	20	Gemcitabine-based chemotherapy	20	Observed efficacy of combination chemotherapy in metastatic patients. ACC supports the use of combination therapies based on gemcitabine or 5-fluorouracil and incorporating irinotecan, a platinum analog, or docetaxel in patients with advanced disease. A potential association between germline mutations in DNA mismatch repair genes and ACC warrants further evaluation
Zheng *et al*[80]	2015	15	Resection	12	Clinicians generally regard pancreatic acinar cell carcinoma as a low-grade malignancy due to its unique clinical features. Positive sentiments towards ACC should be held
			Resection and gemcitabine-based chemotherapy	3	
Kruger *et al*[81]	2016	15	Resection	3	In contrast to PDAC, gemcitabine alone does not appear to have significant activity in ACC. Based on the findings, advanced ACC should be treated with chemotherapy regimens containing 5-FU and/or a platinum compound (such as oxaliplatin). Undetermined is whether this observation also applies to adjuvant chemotherapy administered after surgical resection of ACC
			Resection and gemcitabine-based chemotherapy	8	
			Chemoradiation	1	
			Mixed chemotherapy[2]	3	
Seo *et al* [82]	2017	20	Resection	9	Compared to PDAC, patients with resectable pancreatic ACC had a favorable prognosis after curative resection. Although adjuvant chemotherapy was not associated with improved survival in this study, it is unknown whether this was due to a selection bias or the ineffectiveness of 5-FU monotherapy in pancreatic ACC. On the basis of molecular analysis utilizing innovative genetic analytic tools, additional research on effective adjuvant chemotherapy is required
			Resection and 5-fluorouracil-based chemotherapy	9	
			Resection and gemcitabine-based chemotherapy	1	
			Resection and etoposide plus cisplatin-based chemotherapy	1	
Pishvaian *et al*[83]	2020	12	Mixed chemotherapy[2]	12	Molecularly guided treatments targeting oncogenic drivers and the DNA damage response and repair pathway require further prospective evaluation, based on these real-world findings
Zong *et al* [84]	2020	11	Resection	4	For pancreatic acinar cell carcinoma, surgery is a potentially curative treatment contributing to long-term survival. It has been confirmed that adjuvant systemic therapy, including chemotherapy and chemoradio-therapy, significantly improves survival compared to surgery alone for resectable ACC. To investigate the role and protocol of perioperative and palliative treatments, additional research with a large sample size is required
			Resection and gemcitabine-based chemotherapy	4	
			Resection and capecitabine	1	
			Resection and mixed chemotherapy[2]	2	
Xu *et al* [85]	2022	22	Resection	6	Although the value of adjuvant chemotherapy remains obscure, fluoropyrimidine-based chemotherapy merits consideration. Fluorouracil-based chemotherapy, such as FOLFIRINOX, may be the preferred treatment for patients with metastasis, but additional research is required due to the small sample size in this study
			Resection and S1-based chemotherapy	3	
			Resection and SOX-based chemotherapy	2	
			Resection and fluoropyrimidine-based chemotherapy	3	
			Resection and AG-based chemotherapy	1	
			Resection and gemcitabine-based chemotherapy	7	
Chen *et al* [86]	2022	26	Resection	11	After radical resection, patients with ACC had a longer overall survival than those with PDAC. ACC is also an aggressive tumor with a similar recurrence-free survival trend to PDAC, necessitating multidisciplinary treatment for resectable ACC disease
			Resection and adjuvant chemotherapy	15	

[1]Not specified in manuscript.

[2]Treatment using more than one anticancer drug including FOLFIRNOX (5-FU + oxaliplatin + leucovorin + irinotecan), CAPOX (oxaliplatin + capecitabine), and S1 (tegafur/gimeracil/potassium).

ACC: Acinar cell carcinoma; PDAC: Pancreatic ductal adenocarcinoma; RT: Radiotherapy; 5-FU: 5-fluorouracil; SOX: S1 + Oxaliplatin; AG: Albumin-bound paclitaxel + gemcitabine; FOLFIRNOX: 5-FU + oxaliplatin + leucovorin + irinotecan.

ACKNOWLEDGEMENTS

We thank Kelly Kage for the beautiful illustrations.

FOOTNOTES

Author contributions: All authors equally contributed to this paper with the conception and design of the study, literature review and analysis, drafting, critical revision, editing, and approval of the final version.

Conflict-of-interest statement: All the authors report no relevant conflicts of interest for this article.

Open-Access: This article is an open-access article that was selected by an in-house editor and fully peer-reviewed by external reviewers. It is distributed in accordance with the Creative Commons Attribution NonCommercial (CC BY-NC 4.0) license, which permits others to distribute, remix, adapt, build upon this work non-commercially, and license their derivative works on different terms, provided the original work is properly cited and the use is non-commercial. See: https://creativecommons.org/Licenses/by-nc/4.0/

Country/Territory of origin: United States

ORCID number: Luis Fernando Calimano-Ramirez 0000-0003-2599-3179; Taher Daoud 0000-0001-9161-1314; Dheeraj Reddy Gopireddy 0000-0001-8441-7804; Ajaykumar C Morani 0000-0002-2936-0291; Rebecca Waters 0000-0002-8163-7497; Kazim Gumus 0000-0002-1450-6868; Albert Russell Klekers 0000-0003-1202-7369; Priya R Bhosale 0000-0003-4014-4941; Mayur K Virarkar 0000-0002-5825-3102.

S-Editor: Fan JR
L-Editor: A
P-Editor: Fan JR

REFERENCES

1 **Toll AD**, Hruban RH, Ali SZ. Acinar cell carcinoma of the pancreas: clinical and cytomorphologic characteristics. *Korean J Pathol* 2013; **47**: 93-99 [PMID: 23667367 DOI: 10.4132/KoreanJPathol.2013.47.2.93]
2 **Klimstra DS**. Nonductal neoplasms of the pancreas. *Mod Pathol* 2007; **20** Suppl 1: S94-112 [PMID: 17486055 DOI: 10.1038/modpathol.3800686]
3 **Béchade D**, Desjardin M, Salmon E, Désolneux G, Bécouarn Y, Evrard S, Fonck M. Pancreatic Acinar Cell Carcinoma. *Case Rep Gastroenterol* 2016; **10**: 174-180 [PMID: 27403122 DOI: 10.1159/000445867]
4 **Fontenot J**, Spieler B, Hudson C, Boulmay B. Pancreatic acinar cell carcinoma--literature review and case report of a 56-year-old man presenting with abdominal pain. *Radiol Case Rep* 2020; **15**: 39-43 [PMID: 31737144 DOI: 10.1016/j.radcr.2019.10.009]
5 **Schmidt CM**, Matos JM, Bentrem DJ, Talamonti MS, Lillemoe KD, Bilimoria KY. Acinar cell carcinoma of the pancreas in the United States: prognostic factors and comparison to ductal adenocarcinoma. *J Gastrointest Surg* 2008; **12**: 2078-2086 [PMID: 18836784 DOI: 10.1007/s11605-008-0705-6]
6 **Chaudhary P**. Acinar Cell Carcinoma of the Pancreas: A Literature Review and Update. *Indian J Surg* 2015; **77**: 226-231 [PMID: 26246707 DOI: 10.1007/s12262-014-1049-y]
7 **Lack EE**, Cassady JR, Levey R, Vawter GF. Tumors of the exocrine pancreas in children and adolescents. A clinical and pathologic study of eight cases. *Am J Surg Pathol* 1983; **7**: 319-327 [PMID: 6307069 DOI: 10.1097/00000478-198306000-00003]
8 **Holen KD**, Klimstra DS, Hummer A, Gonen M, Conlon K, Brennan M, Saltz LB. Clinical characteristics and outcomes from an institutional series of acinar cell carcinoma of the pancreas and related tumors. *J Clin Oncol* 2002; **20**: 4673-4678 [PMID: 12488412 DOI: 10.1200/JCO.2002.02.005]
9 **Sridharan V**, Mino-Kenudson M, Cleary JM, Rahma OE, Perez K, Clark JW, Clancy TE, Rubinson DA, Goyal L, Bazerbachi F, Visrodia KH, Qadan M, Parikh A, Ferrone CR, Casey BW, Fernandez-Del Castillo C, Ryan DP, Lillemoe KD, Warshaw AL, Krishnan K, Hernandez-Barco YG. Pancreatic acinar cell carcinoma: A multi-center series on clinical characteristics and treatment outcomes. *Pancreatology* 2021 [PMID: 34023183 DOI: 10.1016/j.pan.2021.05.011]
10 **Klimstra DS**, Heffess CS, Oertel JE, Rosai J. Acinar cell carcinoma of the pancreas. A clinicopathologic study of 28 cases. *Am J Surg Pathol* 1992; **16**: 815-837 [PMID: 1384374 DOI: 10.1097/00000478-199209000-00001]
11 **Seth AK**, Argani P, Campbell KA, Cameron JL, Pawlik TM, Schulick RD, Choti MA, Wolfgang CL. Acinar cell carcinoma of the pancreas: an institutional series of resected patients and review of the current literature. *J Gastrointest Surg* 2008; **12**: 1061-1067 [PMID: 17957440 DOI: 10.1007/s11605-007-0338-1]

12 **Burns WA**, Matthews MJ, Hamosh M, Weide GV, Blum R, Johnson FB. Lipase-secreting acinar cell carcinoma of the pancreas with polyarthropathy. A light and electron microscopic, histochemical, and biochemical study. *Cancer* 1974; **33**: 1002-1009 [PMID: 4819206 DOI: 10.1002/1097-0142(197404)33:4<1002::aid-cncr2820330415>3.0.co;2-r]

13 **Borowicz J**, Morrison M, Hogan D, Miller R. Subcutaneous fat necrosis/panniculitis and polyarthritis associated with acinar cell carcinoma of the pancreas: a rare presentation of pancreatitis, panniculitis and polyarthritis syndrome. *J Drugs Dermatol* 2010; **9**: 1145-1150 [PMID: 20865849]

14 **Radin DR**, Colletti PM, Forrester DM, Tang WW. Pancreatic acinar cell carcinoma with subcutaneous and intraosseous fat necrosis. *Radiology* 1986; **158**: 67-68 [PMID: 3940400 DOI: 10.1148/radiology.158.1.3940400]

15 **La Rosa S**, Sessa F, Capella C. Acinar Cell Carcinoma of the Pancreas: Overview of Clinicopathologic Features and Insights into the Molecular Pathology. *Front Med (Lausanne)* 2015; **2**: 41 [PMID: 26137463 DOI: 10.3389/fmed.2015.00041]

16 **Samuel LH**, Frierson HF Jr. Fine needle aspiration cytology of acinar cell carcinoma of the pancreas: a report of two cases. *Acta Cytol* 1996; **40**: 585-591 [PMID: 8669201 DOI: 10.1159/000333921]

17 **Ishihara A**, Sanda T, Takanari H, Yatani R, Liu PI. Elastase-1-secreting acinar cell carcinoma of the pancreas. A cytologic, electron microscopic and histochemical study. *Acta Cytol* 1989; **33**: 157-163 [PMID: 2467480]

18 **Raman SP**, Hruban RH, Cameron JL, Wolfgang CL, Kawamoto S, Fishman EK. Acinar cell carcinoma of the pancreas: computed tomography features--a study of 15 patients. *Abdom Imaging* 2013; **38**: 137-143 [PMID: 22349806 DOI: 10.1007/s00261-012-9868-4]

19 **Chiou YY**, Chiang JH, Hwang JI, Yen CH, Tsay SH, Chang CY. Acinar cell carcinoma of the pancreas: clinical and computed tomography manifestations. *J Comput Assist Tomogr* 2004; **28**: 180-186 [PMID: 15091120 DOI: 10.1097/00004728-200403000-00005]

20 **Thompson ED**, Wood LD. Pancreatic Neoplasms With Acinar Differentiation: A Review of Pathologic and Molecular Features. *Arch Pathol Lab Med* 2020; **144**: 808-815 [PMID: 31869246 DOI: 10.5858/arpa.2019-0472-RA]

21 **Fabre A**, Sauvanet A, Flejou JF, Belghiti J, Palazzo L, Ruszniewski P, Degott C, Terris B. Intraductal acinar cell carcinoma of the pancreas. *Virchows Arch* 2001; **438**: 312-315 [PMID: 11315630 DOI: 10.1007/s004280000342]

22 **Ordóñez NG**, Mackay B. Acinar cell carcinoma of the pancreas. *Ultrastruct Pathol* 2000; **24**: 227-241 [PMID: 11013963 DOI: 10.1080/01913120050176680]

23 **Mustafa S**, Hruban RH, Ali SZ. Acinar cell carcinoma of the pancreas: a clinicopathologic and cytomorphologic review. *J Am Soc Cytopathol* 2020; **9**: 586-595 [PMID: 32461075 DOI: 10.1016/j.jasc.2020.04.005]

24 **Yantiss RK**, Chang HK, Farraye FA, Compton CC, Odze RD. Prevalence and prognostic significance of acinar cell differentiation in pancreatic endocrine tumors. *Am J Surg Pathol* 2002; **26**: 893-901 [PMID: 12131156 DOI: 10.1097/00000478-200207000-00007]

25 **Kim JY**, Brosnan-Cashman JA, Kim J, An S, Lee KB, Kim H, Park DY, Jang KT, Oh YH, Hruban RH, Heaphy CM, Hong SM. Pancreatic acinar cell carcinomas and mixed acinar-neuroendocrine carcinomas are more clinically aggressive than grade 1 pancreatic neuroendocrine tumours. *Pathology* 2020; **52**: 336-347 [PMID: 32111396 DOI: 10.1016/j.pathol.2020.01.437]

26 **La Rosa S**, Franzi F, Marchet S, Finzi G, Clerici M, Vigetti D, Chiaravalli AM, Sessa F, Capella C. The monoclonal anti-BCL10 antibody (clone 331.1) is a sensitive and specific marker of pancreatic acinar cell carcinoma and pancreatic metaplasia. *Virchows Arch* 2009; **454**: 133-142 [PMID: 19066953 DOI: 10.1007/s00428-008-0710-x]

27 **Hosoda W**, Sasaki E, Murakami Y, Yamao K, Shimizu Y, Yatabe Y. BCL10 as a useful marker for pancreatic acinar cell carcinoma, especially using endoscopic ultrasound cytology specimens. *Pathol Int* 2013; **63**: 176-182 [PMID: 23530562 DOI: 10.1111/pin.12045]

28 **Hoorens A**, Lemoine NR, McLellan E, Morohoshi T, Kamisawa T, Heitz PU, Stamm B, Rüschoff J, Wiedenmann B, Klöppel G. Pancreatic acinar cell carcinoma. An analysis of cell lineage markers, p53 expression, and Ki-ras mutation. *Am J Pathol* 1993; **143**: 685-698 [PMID: 8362971]

29 **de Wilde RF**, Ottenhof NA, Jansen M, Morsink FH, de Leng WW, Offerhaus GJ, Brosens LA. Analysis of LKB1 mutations and other molecular alterations in pancreatic acinar cell carcinoma. *Mod Pathol* 2011; **24**: 1229-1236 [PMID: 21572398 DOI: 10.1038/modpathol.2011.83]

30 **Abraham SC**, Wu TT, Hruban RH, Lee JH, Yeo CJ, Conlon K, Brennan M, Cameron JL, Klimstra DS. Genetic and immunohistochemical analysis of pancreatic acinar cell carcinoma: frequent allelic loss on chromosome 11p and alterations in the APC/beta-catenin pathway. *Am J Pathol* 2002; **160**: 953-962 [PMID: 11891193 DOI: 10.1016/s0002-9440(10)64917-6]

31 **Moore PS**, Orlandini S, Zamboni G, Capelli P, Rigaud G, Falconi M, Bassi C, Lemoine NR, Scarpa A. Pancreatic tumours: molecular pathways implicated in ductal cancer are involved in ampullary but not in exocrine nonductal or endocrine tumorigenesis. *Br J Cancer* 2001; **84**: 253-262 [PMID: 11161385 DOI: 10.1054/bjoc.2000.1567]

32 **Terhune PG**, Memoli VA, Longnecker DS. Evaluation of p53 mutation in pancreatic acinar cell carcinomas of humans and transgenic mice. *Pancreas* 1998; **16**: 6-12 [PMID: 9436856 DOI: 10.1097/00006676-199801000-00002]

33 **Rigaud G**, Moore PS, Zamboni G, Orlandini S, Taruscio D, Paradisi S, Lemoine NR, Klöppel G, Scarpa A. Allelotype of pancreatic acinar cell carcinoma. *Int J Cancer* 2000; **88**: 772-777 [PMID: 11072247 DOI: 10.1002/1097-0215(20001201)88:5<772::aid-ijc14>3.0.co;2-w]

34 **Furukawa T**, Sakamoto H, Takeuchi S, Ameri M, Kuboki Y, Yamamoto T, Hatori T, Yamamoto M, Sugiyama M, Ohike N, Yamaguchi H, Shimizu M, Shibata N, Shimizu K, Shiratori K. Whole exome sequencing reveals recurrent mutations in BRCA2 and FAT genes in acinar cell carcinomas of the pancreas. *Sci Rep* 2015; **5**: 8829 [PMID: 25743105 DOI: 10.1038/srep08829]

35 **Jiao Y**, Yonescu R, Offerhaus GJ, Klimstra DS, Maitra A, Eshleman JR, Herman JG, Poh W, Pelosof L, Wolfgang CL, Vogelstein B, Kinzler KW, Hruban RH, Papadopoulos N, Wood LD. Whole-exome sequencing of pancreatic neoplasms with acinar differentiation. *J Pathol* 2014; **232**: 428-435 [PMID: 24293293 DOI: 10.1002/path.4310]

36 **Taruscio D**, Paradisi S, Zamboni G, Rigaud G, Falconi M, Scarpa A. Pancreatic acinar carcinoma shows a distinct pattern of chromosomal imbalances by comparative genomic hybridization. *Genes Chromosomes Cancer* 2000; **28**: 294-299

[PMID: 10862035 DOI: 10.1002/1098-2264(200007)28:3<294::aid-gcc7>3.0.co;2-n]

37 **Dewald GW**, Smyrk TC, Thorland EC, McWilliams RR, Van Dyke DL, Keefe JG, Belongie KJ, Smoley SA, Knutson DL, Fink SR, Wiktor AE, Petersen GM. Fluorescence in situ hybridization to visualize genetic abnormalities in interphase cells of acinar cell carcinoma, ductal adenocarcinoma, and islet cell carcinoma of the pancreas. *Mayo Clin Proc* 2009; **84**: 801-810 [PMID: 19720778 DOI: 10.1016/S0025-6196(11)60490-4]

38 **Liu K**, Peng W, Zhou Z. The CT findings of pancreatic acinar cell carcinoma in five cases. *Clin Imaging* 2013; **37**: 302-307 [PMID: 23465983 DOI: 10.1016/j.clinimag.2012.06.003]

39 **Golan T**, Hammel P, Reni M, Van Cutsem E, Macarulla T, Hall MJ, Park JO, Hochhauser D, Arnold D, Oh DY, Reinacher-Schick A, Tortora G, Algül H, O'Reilly EM, McGuinness D, Cui KY, Schlienger K, Locker GY, Kindler HL. Maintenance Olaparib for Germline *BRCA*-Mutated Metastatic Pancreatic Cancer. *N Engl J Med* 2019; **381**: 317-327 [PMID: 31157963 DOI: 10.1056/NEJMoa1903387]

40 **Le DT**, Durham JN, Smith KN, Wang H, Bartlett BR, Aulakh LK, Lu S, Kemberling H, Wilt C, Luber BS, Wong F, Azad NS, Rucki AA, Laheru D, Donehower R, Zaheer A, Fisher GA, Crocenzi TS, Lee JJ, Greten TF, Duffy AG, Ciombor KK, Eyring AD, Lam BH, Joe A, Kang SP, Holdhoff M, Danilova L, Cope L, Meyer C, Zhou S, Goldberg RM, Armstrong DK, Bever KM, Fader AN, Taube J, Housseau F, Spetzler D, Xiao N, Pardoll DM, Papadopoulos N, Kinzler KW, Eshleman JR, Vogelstein B, Anders RA, Diaz LA Jr. Mismatch repair deficiency predicts response of solid tumors to PD-1 blockade. *Science* 2017; **357**: 409-413 [PMID: 28596308 DOI: 10.1126/science.aan6733]

41 **Chmielecki J**, Hutchinson KE, Frampton GM, Chalmers ZR, Johnson A, Shi C, Elvin J, Ali SM, Ross JS, Basturk O, Balasubramanian S, Lipson D, Yelensky R, Pao W, Miller VA, Klimstra DS, Stephens PJ. Comprehensive genomic profiling of pancreatic acinar cell carcinomas identifies recurrent RAF fusions and frequent inactivation of DNA repair genes. *Cancer Discov* 2014; **4**: 1398-1405 [PMID: 25266736 DOI: 10.1158/2159-8290.CD-14-0617]

42 **Ross JS**, Wang K, Chmielecki J, Gay L, Johnson A, Chudnovsky J, Yelensky R, Lipson D, Ali SM, Elvin JA, Vergilio JA, Roels S, Miller VA, Nakamura BN, Gray A, Wong MK, Stephens PJ. The distribution of BRAF gene fusions in solid tumors and response to targeted therapy. *Int J Cancer* 2016; **138**: 881-890 [PMID: 26314551 DOI: 10.1002/ijc.29825]

43 **Lee NV**, Lira ME, Pavlicek A, Ye J, Buckman D, Bagrodia S, Srinivasa SP, Zhao Y, Aparicio S, Rejto PA, Christensen JG, Ching KA. A novel SND1-BRAF fusion confers resistance to c-Met inhibitor PF-04217903 in GTL16 cells through [corrected] MAPK activation. *PLoS One* 2012; **7**: e39653 [PMID: 22745804 DOI: 10.1371/journal.pone.0039653]

44 **La Rosa S**, Bernasconi B, Vanoli A, Sciarra A, Notohara K, Albarello L, Casnedi S, Billo P, Zhang L, Tibiletti MG, Sessa F. c-MYC amplification and c-myc protein expression in pancreatic acinar cell carcinomas. New insights into the molecular signature of these rare cancers. *Virchows Arch* 2018; **473**: 435-441 [PMID: 29721608 DOI: 10.1007/s00428-018-2366-5]

45 **Fitzgerald TL**, Hickner ZJ, Schmitz M, Kort EJ. Changing incidence of pancreatic neoplasms: a 16-year review of statewide tumor registry. *Pancreas* 2008; **37**: 134-138 [PMID: 18665072 DOI: 10.1097/MPA.0b013e318163a329]

46 **Tatli S**, Mortele KJ, Levy AD, Glickman JN, Ros PR, Banks PA, Silverman SG. CT and MRI features of pure acinar cell carcinoma of the pancreas in adults. *AJR Am J Roentgenol* 2005; **184**: 511-519 [PMID: 15671372 DOI: 10.2214/ajr.184.2.01840511]

47 **Bhosale P**, Balachandran A, Wang H, Wei W, Hwang RF, Fleming JB, Varadhachary G, Charnsangavej C, Tamm E. CT imaging features of acinar cell carcinoma and its hepatic metastases. *Abdom Imaging* 2013; **38**: 1383-1390 [PMID: 23232580 DOI: 10.1007/s00261-012-9970-7]

48 **Lalwani N**, Mannelli L, Ganeshan DM, Shanbhogue AK, Dighe MK, Tiwari HA, Maximin S, Monti S, Ragucci M, Prasad SR. Uncommon pancreatic tumors and pseudotumors. *Abdom Imaging* 2015; **40**: 167-180 [PMID: 25063236 DOI: 10.1007/s00261-014-0189-7]

49 **Hu S**, Hu S, Wang M, Wu Z, Miao F. Clinical and CT imaging features of pancreatic acinar cell carcinoma. *Radiol Med* 2013; **118**: 723-731 [PMID: 23358813 DOI: 10.1007/s11547-012-0908-5]

50 **Tian L**, Lv XF, Dong J, Zhou J, Zhang Y, Xi SY, Zhang R, Xie CM. Clinical features and CT/MRI findings of pancreatic acinar cell carcinoma. *Int J Clin Exp Med* 2015; **8**: 14846-14854 [PMID: 26628966]

51 **Hsu MY**, Pan KT, Chu SY, Hung CF, Wu RC, Tseng JH. CT and MRI features of acinar cell carcinoma of the pancreas with pathological correlations. *Clin Radiol* 2010; **65**: 223-229 [PMID: 20152279 DOI: 10.1016/j.crad.2009.11.010]

52 **Klöppel G**, Kosmahl M. Cystic lesions and neoplasms of the pancreas. The features are becoming clearer. *Pancreatology* 2001; **1**: 648-655 [PMID: 12120249 DOI: 10.1159/000055876]

53 **Abraham SC**, Klimstra DS, Wilentz RE, Yeo CJ, Conlon K, Brennan M, Cameron JL, Wu TT, Hruban RH. Solid-pseudopapillary tumors of the pancreas are genetically distinct from pancreatic ductal adenocarcinomas and almost always harbor beta-catenin mutations. *Am J Pathol* 2002; **160**: 1361-1369 [PMID: 11943721 DOI: 10.1016/s0002-9440(10)62563-1]

54 **La Rosa S**, Adsay V, Albarello L, Asioli S, Casnedi S, Franzi F, Marando A, Notohara K, Sessa F, Vanoli A, Zhang L, Capella C. Clinicopathologic study of 62 acinar cell carcinomas of the pancreas: insights into the morphology and immunophenotype and search for prognostic markers. *Am J Surg Pathol* 2012; **36**: 1782-1795 [PMID: 23026929 DOI: 10.1097/PAS.0b013e318263209d]

55 **Notohara K**, Hamazaki S, Tsukayama C, Nakamoto S, Kawabata K, Mizobuchi K, Sakamoto K, Okada S. Solid-pseudopapillary tumor of the pancreas: immunohistochemical localization of neuroendocrine markers and CD10. *Am J Surg Pathol* 2000; **24**: 1361-1371 [PMID: 11023097 DOI: 10.1097/00000478-200010000-00005]

56 **Ohike N**, Morohoshi T. Exocrine Pancreatic Neoplasms of Nonductal Origin: Acinar Cell Carcinoma, Pancreatoblastoma, and Solid-Pseudopapillary Neoplasm. *Surg Pathol Clin* 2011; **4**: 579-588 [PMID: 26837489 DOI: 10.1016/j.path.2011.03.001]

57 **Klimstra DS**, Wenig BM, Adair CF, Heffess CS. Pancreatoblastoma. A clinicopathologic study and review of the literature. *Am J Surg Pathol* 1995; **19**: 1371-1389 [PMID: 7503360 DOI: 10.1097/00000478-199512000-00005]

58 **Reid MD**, Bhattarai S, Graham RP, Pehlivanoglu B, Sigel CS, Shi J, Saqi A, Shirazi M, Xue Y, Basturk O, Adsay V. Pancreatoblastoma: Cytologic and histologic analysis of 12 adult cases reveals helpful criteria in their diagnosis and distinction from common mimics. *Cancer Cytopathol* 2019; **127**: 708-719 [PMID: 31581358 DOI: 10.1002/cncy.22187]

59 **Conrad R**, Castelino-Prabhu S, Cobb C, Raza A. Cytopathology of the pancreatobiliary tract-the agony, and sometimes,

the ease of it. *J Gastrointest Oncol* 2013; **4**: 210-219 [PMID: 23730518 DOI: 10.3978/j.issn.2078-6891.2012.022]
60 **Sigel CS**, Klimstra DS. Cytomorphologic and immunophenotypical features of acinar cell neoplasms of the pancreas. *Cancer Cytopathol* 2013; **121**: 459-470 [PMID: 23408736 DOI: 10.1002/cncy.21279]
61 **Board PATE**. Pancreatic Cancer Treatment (Adult) (PDQ®). 2022 [DOI: 10.1097/01893697-199109010-00011]
62 **Kryklyva V**, Haj Mohammad N, Morsink FHM, Ligtenberg MJL, Offerhaus GJA, Nagtegaal ID, de Leng WWJ, Brosens LAA. Pancreatic acinar cell carcinoma is associated with *BRCA2* germline mutations: a case report and literature review. *Cancer Biol Ther* 2019; **20**: 949-955 [PMID: 31002019 DOI: 10.1080/15384047.2019.1595274]
63 **La Rosa S**, Klersy C, Uccella S, Dainese L, Albarello L, Sonzogni A, Doglioni C, Capella C, Solcia E. Improved histologic and clinicopathologic criteria for prognostic evaluation of pancreatic endocrine tumors. *Hum Pathol* 2009; **40**: 30-40 [PMID: 18715612 DOI: 10.1016/j.humpath.2008.06.005]
64 **Wisnoski NC**, Townsend CM Jr, Nealon WH, Freeman JL, Riall TS. 672 patients with acinar cell carcinoma of the pancreas: a population-based comparison to pancreatic adenocarcinoma. *Surgery* 2008; **144**: 141-148 [PMID: 18656619 DOI: 10.1016/j.surg.2008.03.006]
65 **Kitagami H**, Kondo S, Hirano S, Kawakami H, Egawa S, Tanaka M. Acinar cell carcinoma of the pancreas: clinical analysis of 115 patients from Pancreatic Cancer Registry of Japan Pancreas Society. *Pancreas* 2007; **35**: 42-46 [PMID: 17575544 DOI: 10.1097/mpa.0b013e31804bfbd3]
66 **Duorui N**, Shi B, Zhang T, Chen C, Fang C, Yue Z, Wu P, Wu Z, Huang X, Li M. The contemporary trend in worsening prognosis of pancreatic acinar cell carcinoma: A population-based study. *PLoS One* 2020; **15**: e0243164 [PMID: 33332471 DOI: 10.1371/journal.pone.0243164]
67 **Armstrong MD**, Von Hoff D, Barber B, Marlow LA, von Roemeling C, Cooper SJ, Travis P, Campbell E, Paz-Fumagalli R, Copland JA, Colon-Otero G. An effective personalized approach to a rare tumor: prolonged survival in metastatic pancreatic acinar cell carcinoma based on genetic analysis and cell line development. *J Cancer* 2011; **2**: 142-152 [PMID: 21475719 DOI: 10.7150/jca.2.142]
68 **Suzuki A**, Sakaguchi T, Morita Y, Oishi K, Fukumoto K, Inaba K, Takehara Y, Baba S, Suzuki S, Konno H. Long-term survival after a repetitive surgical approach in a patient with acinar cell carcinoma of the pancreas and recurrent liver metastases: report of a case. *Surg Today* 2010; **40**: 679-683 [PMID: 20582524 DOI: 10.1007/s00595-009-4128-0]
69 **Nasser F**, Motta Leal Filho JM, Affonso BB, Galastri FL, Cavalcante RN, Martins DLN, Segatelli V, Yamaga LYI, Gansl RC, Tranchesi Junior B, Macedo ALV. Liver Metastases in Pancreatic Acinar Cell Carcinoma Treated with Selective Internal Radiation Therapy with Y-90 Resin Microspheres. *Case Reports Hepatol* 2017; **2017**: 1847428 [PMID: 29158927 DOI: 10.1155/2017/1847428]
70 **Distler M**, Rückert F, Dittert DD, Stroszczynski C, Dobrowolski F, Kersting S, Grützmann R. Curative resection of a primarily unresectable acinar cell carcinoma of the pancreas after chemotherapy. *World J Surg Oncol* 2009; **7**: 22 [PMID: 19239719 DOI: 10.1186/1477-7819-7-22]
71 **Glazer ES**, Neill KG, Frakes JM, Coppola D, Hodul PJ, Hoffe SE, Pimiento JM, Springett GM, Malafa MP. Systematic Review and Case Series Report of Acinar Cell Carcinoma of the Pancreas. *Cancer Control* 2016; **23**: 446-454 [PMID: 27842335 DOI: 10.1177/107327481602300417]
72 **Ordóñez NG**. Pancreatic acinar cell carcinoma. *Adv Anat Pathol* 2001; **8**: 144-159 [PMID: 11345238 DOI: 10.1097/00125480-200105000-00003]
73 **Butturini G**, Pisano M, Scarpa A, D'Onofrio M, Auriemma A, Bassi C. Aggressive approach to acinar cell carcinoma of the pancreas: a single-institution experience and a literature review. *Langenbecks Arch Surg* 2011; **396**: 363-369 [PMID: 20803029 DOI: 10.1007/s00423-010-0706-2]
74 **Antoine M**, Khitrik-Palchuk M, Saif MW. Long-term survival in a patient with acinar cell carcinoma of pancreas. A case report and review of literature. *JOP* 2007; **8**: 783-789 [PMID: 17993731]
75 **Matos JM**, Schmidt CM, Turrini O, Agaram NP, Niedergethmann M, Saeger HD, Merchant N, Johnson CS, Lillemoe KD, Grützmann R. Pancreatic acinar cell carcinoma: a multi-institutional study. *J Gastrointest Surg* 2009; **13**: 1495-1502 [PMID: 19495891 DOI: 10.1007/s11605-009-0938-z]
76 **Seki Y**, Okusaka T, Ikeda M, Morizane C, Ueno H. Four cases of pancreatic acinar cell carcinoma treated with gemcitabine or S-1 as a single agent. *Jpn J Clin Oncol* 2009; **39**: 751-755 [PMID: 19666905 DOI: 10.1093/jjco/hyp085]
77 **Lowery MA**, Klimstra DS, Shia J, Yu KH, Allen PJ, Brennan MF, O'Reilly EM. Acinar cell carcinoma of the pancreas: new genetic and treatment insights into a rare malignancy. *Oncologist* 2011; **16**: 1714-1720 [PMID: 22042785 DOI: 10.1634/theoncologist.2011-0231]
78 **Lee JH**, Lee KG, Park HK, Lee KS. [Acinar cell carcinoma of the pancreas in Korea--clinicopathologic analysis of 27 patients from korean literature and 2 cases from our hospital--]. *Korean J Gastroenterol* 2010; **55**: 245-251 [PMID: 20389178 DOI: 10.4166/kjg.2010.55.4.245]
79 **Hartwig W**, Denneberg M, Bergmann F, Hackert T, Hinz U, Strobel O, Büchler MW, Werner J. Acinar cell carcinoma of the pancreas: is resection justified even in limited metastatic disease? *Am J Surg* 2011; **202**: 23-27 [PMID: 21440887 DOI: 10.1016/j.amjsurg.2010.06.004]
80 **Zheng C**, Lang M, Xu C, Li N, Ren H, Hao J. Diagnosis and treatment analysis of 15 pancreatic acinar cell carcinoma patients. *Chin J Clin Oncol* 2015; **42**: 287-291 [DOI: 10.1007/s11805-008-0235-8]
81 **Kruger S**, Haas M, Burger PJ, Ormanns S, Modest DP, Westphalen CB, Kleespies A, Angele MK, Hartwig W, Bruns CJ, Kirchner T, Werner J, Heinemann V, Boeck S. Acinar cell carcinoma of the pancreas: a rare disease with different diagnostic and therapeutic implications than ductal adenocarcinoma. *J Cancer Res Clin Oncol* 2016; **142**: 2585-2591 [PMID: 27629876 DOI: 10.1007/s00432-016-2264-7]
82 **Seo S**, Yoo C, Kim KP, Ryoo BY, Chang HM, Hong SM, Lee JH, Song KB, Hwang DW, Kim KH, Hwang S, Kim SC. Clinical outcomes of patients with resectable pancreatic acinar cell carcinoma. *J Dig Dis* 2017; **18**: 480-486 [PMID: 28671770 DOI: 10.1111/1751-2980.12505]
83 **Pishvaian MJ**, Blais EM, Brody JR, Lyons E, DeArbeloa P, Hendifar A, Mikhail S, Chung V, Sahai V, Sohal DPS, Bellakbira S, Thach D, Rahib L, Madhavan S, Matrisian LM, Petricoin EF 3rd. Overall survival in patients with pancreatic cancer receiving matched therapies following molecular profiling: a retrospective analysis of the Know Your Tumor

registry trial. *Lancet Oncol* 2020; **21**: 508-518 [PMID: 32135080 DOI: 10.1016/S1470-2045(20)30074-7]

84 **Zong Y**, Qi C, Peng Z, Shen L, Zhou J. Patients With Acinar Cell Carcinoma of the Pancreas After 2005: A Large Population Study. *Pancreas* 2020; **49**: 781-787 [PMID: 32541633 DOI: 10.1097/MPA.0000000000001573]

85 **Xu JY**, Guan WL, Lu SX, Wei XL, Shi WJ, Ren C, Li YH, Li SP, Qiu MZ, Wang FH. Optimizing Chemotherapy of Pancreatic Acinar Cell Carcinoma: Our Experiences and Pooled Analysis of Literature. *Clin Med Insights Oncol* 2022; **16**: 11795549221090186 [PMID: 35509769 DOI: 10.1177/11795549221090186]

86 **Chen H**, Xu Z, Shen Z, Weng Y, Wang W, Ying X, Wang X, Deng X, Shen B. Clinical characteristics and surgical outcomes of resectable acinar cell carcinoma of the pancreas-propensity score matching analysis with pancreatic ductal adenocarcinoma. *Eur J Surg Oncol* 2022; **48**: 1062-1067 [PMID: 34887166 DOI: 10.1016/j.ejso.2021.11.135]

World Journal of Gastroenterology

Submit a Manuscript: https://www.f6publishing.com

World J Gastroenterol 2022 October 28; 28(40): 5845-5864

DOI: 10.3748/wjg.v28.i40.5845

ISSN 1007-9327 (print) ISSN 2219-2840 (online)

ORIGINAL ARTICLE

Basic Study

Expression of the methylcytosine dioxygenase ten-eleven translocation-2 and connexin 43 in inflammatory bowel disease and colorectal cancer

Mohammad El-Harakeh, Jessica Saliba, Kawthar Sharaf Aldeen, May Haidar, Layal El Hajjar, Mireille Kallassy Awad, Jana G Hashash, Margret Shirinian, Marwan El-Sabban

Specialty type: Gastroenterology and hepatology

Provenance and peer review: Unsolicited article; Externally peer reviewed.

Peer-review model: Single blind

Peer-review report's scientific quality classification

Grade A (Excellent): 0
Grade B (Very good): B
Grade C (Good): C
Grade D (Fair): 0
Grade E (Poor): E

P-Reviewer: Feng Y, China; Ruan X, China; Wan XH, China
A-Editor: Nakaji K, Japan

Received: February 6, 2022
Peer-review started: February 6, 2022
First decision: April 10, 2022
Revised: May 6, 2022
Accepted: June 13, 2022
Article in press: June 13, 2022
Published online: October 28, 2022

Mohammad El-Harakeh, Kawthar Sharaf Aldeen, May Haidar, Layal El Hajjar, Marwan El-Sabban, Department of Anatomy, Cell Biology and Physiological Sciences, Faculty of Medicine, American University of Beirut, Beirut 1107, Lebanon

Mohammad El-Harakeh, Mireille Kallassy Awad, UR GPF Laboratory of Biodiversity and Functional Genomics, Faculty of Science, Université Saint-Joseph de Beyrouth, Beirut 1107, Lebanon

Jessica Saliba, Department of Biology, Faculty of Sciences, Lebanese University, Beirut 1533, Lebanon

Jessica Saliba, Department of Public Health, Faculty of Health Sciences, University of Balamand, Dekwaneh, Sin el Fil 1552, Lebanon

Jana G Hashash, Department of Internal Medicine, Division of Gastroenterology and Hepatology, Faculty of Medicine, American University of Beirut, Beirut 1107, Lebanon

Margret Shirinian, Department of Experimental Pathology, Immunology and Microbiology, Faculty of Medicine, American University of Beirut, Beirut 1107, Lebanon

Corresponding author: Marwan El-Sabban, PhD, Professor, Department of Anatomy, Cell Biology and Physiological Sciences, Faculty of Medicine, American University of Beirut, Bliss Street, Beirut 1107, Lebanon. me00@aub.edu.lb

Abstract

BACKGROUND

Inflammatory bowel disease (IBD) constitutes a substantial risk factor for colorectal cancer. Connexin 43 (Cx43) is a protein that forms gap junction (GJ) complexes involved in intercellular communication, and its expression is altered under pathological conditions, such as IBD and cancer. Recent studies have implicated epigenetic processes modulating DNA methylation in the pathogenesis of diverse inflammatory and malignant diseases. The ten-eleven translocation-2 (TET-2) enzyme catalyzes the demethylation, hence, regulating the activity of various cancer-promoting and tumor-suppressor genes.

AIM
To investigate Cx43 and TET-2 expression levels and presence of 5-hydroxymethylcytosine (5-hmC) marks under inflammatory conditions both *in vitro* and *in vivo*.

METHODS
TET-2 expression was evaluated in parental HT-29 cells and in HT-29 cells expressing low or high levels of Cx43, a putative tumor-suppressor gene whose expression varies in IBD and colorectal cancer, and which has been implicated in the inflammatory process and in tumor onset. The dextran sulfate sodium-induced colitis model was reproduced in BALB/c mice to evaluate the expression of TET-2 and Cx43 under inflammatory conditions *in vivo*. In addition, archived colon tissue sections from normal, IBD (ulcerative colitis), and sporadic colon adenocarcinoma patients were obtained and evaluated for the expression of TET-2 and Cx43. Expression levels were reported at the transcriptional level by quantitative real-time polymerase chain reaction, and at the translational level by Western blotting and immunofluorescence.

RESULTS
Under inflammatory conditions, Cx43 and TET-2 expression levels increased compared to non-inflammatory conditions. TET-2 upregulation was more pronounced in Cx43-deficient cells. Moreover, colon tissue sections from normal, ulcerative colitis, and sporadic colon adenocarcinoma patients corroborated that Cx43 expression increased in IBD and decreased in adenocarcinoma, compared to tissues from non-IBD subjects. However, TET-2 expression and 5-hmC mark levels decreased in samples from patients with ulcerative colitis or cancer. Cx43 and TET-2 expression levels were also investigated in an experimental colitis mouse model. Interestingly, mice exposed to carbenoxolone (CBX), a GJ inhibitor, had upregulated TET-2 levels. Collectively, these results show that TET-2 levels and activity increased under inflammatory conditions, in cells downregulating gap junctional protein Cx43, and in colon tissues from mice exposed to CBX.

CONCLUSION
These results suggest that TET-2 expression levels, as well as Cx43 expression levels, are modulated in models of intestinal inflammation. We hypothesize that TET-2 may demethylate genes involved in inflammation and tumorigenesis, such as Cx43, potentially contributing to intestinal inflammation and associated carcinogenesis.

Key Words: Demethylation; Inflammation-induced carcinogenesis; Ulcerative colitis; Colorectal cancer; Connexins

©The Author(s) 2022. Published by Baishideng Publishing Group Inc. All rights reserved.

Core Tip: Chronic inflammation of the colon is a risk factor for colorectal cancer. Intestinal inflammation has been associated with reduced gap junction-mediated intercellular communication and downregulation connexins [mainly connexin 43 (Cx43)]. The involvement of the demethylating enzyme ten-eleven translocation-2 (TET-2) (methylcytosine dioxygenase) in the inflammatory process has motivated the investigation of Cx43 and TET-2 expression in colitis and colorectal carcinoma. *In vitro* and *in vivo* data report on the upregulation of Cx43 in inflammatory states and a downregulation of TET-2. In human samples of colon adenocarcinoma, both TET-2 and Cx43 were downregulated, potentially implicating them in the malignant transformation of inflamed intestinal tissues.

Citation: El-Harakeh M, Saliba J, Sharaf Aldeen K, Haidar M, El Hajjar L, Awad MK, Hashash JG, Shirinian M, El-Sabban M. Expression of the methylcytosine dioxygenase ten-eleven translocation-2 and connexin 43 in inflammatory bowel disease and colorectal cancer. *World J Gastroenterol* 2022; 28(40): 5845-5864
URL: https://www.wjgnet.com/1007-9327/full/v28/i40/5845.htm
DOI: https://dx.doi.org/10.3748/wjg.v28.i40.5845

INTRODUCTION

The gastrointestinal tract is constantly exposed to environmental insults that may potentially lead to pathologies. Inflammatory bowel disease (IBD) is a relapsing and remitting inflammatory disorder affecting distinct parts of the gastrointestinal tract. It comprises two primarily encountered disorders: Crohn's disease and ulcerative colitis, which can be distinguished by their localization in the different

parts of the gut and the endoscopic appearance of the inflamed segment[1-3]. IBD increases the risk of developing colon adenocarcinoma[4], and colitis-associated colon adenocarcinoma remains a fundamental consequence of sustained IBD, possibly because both IBD and colon adenocarcinoma share etiological factors implicated in their development[5].

Gap junctions (GJs), components of junctional complexes, have a potential role in regulating epithelial integrity and function. GJs are formed by the docking of two hemichannels (connexin hexamers) contributed from two adjacent cells, allowing the direct exchange of ions and small signaling molecules (< 2 kDa)[6]. Connexins play a pivotal role in cellular proliferation, differentiation, and function and are recognized as putative tumor-suppressor genes[7-9]. The library of connexin-related diseases has been emerging for many years, and includes various types of syndromes and disorders, such as inflammatory diseases and cancer. Several studies have revealed that the inflammatory response relies in part on connexins and GJ-mediated intercellular communication (GJIC)[10]. More specifically, alteration in the expression of connexin 43 (Cx43) in the gastrointestinal tract is associated with IBD, gastrointestinal infections, and impaired motility[11,12]. We have previously shown an alteration of Cx43 expression and localization, as well as a direct heterocellular communication between intestinal epithelial cells (IECs) and macrophages, which may contribute to IBD pathogenesis[12].

In complex diseases, such as IBD and colon adenocarcinoma, in addition to the heritable component, environmental and epigenetic (DNA methylation and demethylation, histone marks, higher order chromatin structure, *etc.*) factors are likely to influence onset[13]. DNA methylation state is controlled by the interplay between DNA methyltransferases and demethylating enzymes, such as ten-eleven translocation (TET) proteins. Methylation occurs at normally demethylated CpG-rich regions named "CpG islands", of which 70% overlap with human gene promoters, and results in gene silencing[14]. DNA methylation profiles from IBD patients are considerably altered compared to healthy counterparts[15]. Moreover, in IBD-associated colon adenocarcinoma, DNA methylation status was distinct from sporadic colon adenocarcinoma, with different gene expression profiles[16]. DNA methylation is counteracted by demethylation mechanisms, catalyzed by TET enzymes (TET-1, TET-2, TET-3), thus activating gene transcription[17]. Following a series of oxidation reactions by TET enzymes, previously methylated 5-methylcytosine is converted to 5-hydroxymethylcytosine (5-hmC) and further oxidized products that will be recognized and excised by thymine-DNA glycosylase/base enzyme repair pathway to result in an unmethylated cytosine residue[18]. TET genes are mutated in a variety of diseases and cancers. In inflammatory diseases, TET-2 is crucial for the repression of the pro-inflammatory cytokine, interleukin (IL)-6[19], while in several cancers, TET-2 expression is downregulated[20]. In particular, tumors of the digestive tract express different levels of TET enzymes, which are explored as potential factors informing prognosis[21]. Downregulation of TET-1, TET-2, and TET-3 have been reported in gastric cancers with concomitant loss of 5-hmC marks[22] and in colorectal carcinoma[23], with TET-2 transcriptional levels potentially serving as indicators for treatment outcome and disease recurrence [23]. In addition, a recent study reported that the human gene coding for TET-2 contains three promoter elements which are differently regulated in different tissues and developmental stages[24] and may play a role in cancer development.

While many studies have reported the Cx43 promoter to be hypermethylated during the transition from inflammation to cancer[25-27], the expression statuses of Cx43 and TET-2 in IBD and colorectal cancer have not been simultaneously described. This study investigated the effect of inflammation and Cx43 expression levels on the intestinal cell membrane integrity and described TET-2 expression and 5-hmC marks under inflammatory states *in vitro, in vivo*, and in human samples of ulcerative colitis and sporadic colon carcinoma.

MATERIALS AND METHODS

Cell lines and culture conditions

The HT-29 and Caco-2 cell lines derived from colorectal adenocarcinoma tissues were used as models for human IECs. When grown in monolayer, these cells become more differentiated and IEC-like[12,28,29] and are widely used as a model of intestinal transport and pathology, including inflammation. Human embryonic kidney cells (packaging HEK 293T cells) were used for production of viral supernatant for transduction purposes.

In addition, the human monocytic cell line (THP-1) was used as an *in vitro* model for activated macrophages[12,30,31] for the production of conditioned inflammatory medium. After exposure to phorbol myristate acetate (PMA) and lipopolysaccharide (LPS), THP-1 cells become activated; they adhere to the cell culture vessel and show increased transcriptional levels of connexins, Toll-Like Receptor (TLR)-2, TLR-4, NF-κB p65, COX-2, inflammatory cytokines tumor necrosis factor-α (TNF-α), and IL-1β[12]. In this study, suspension THP-1 cells were activated with 50 ng/mL PMA (Sigma-Aldrich, St Louis, MO, United States) for 24 h, followed with 1 μg/mL of LPS (Sigma-Aldrich) for 4 additional hours. When activated THP-1 cells adhered to the cell culture plate, they were washed with PMA- and LPS-free media and left to grow for 72 h. Conditioned media was then collected, filtered, and applied *in vitro* onto colon cell lines to create an inflammatory milieu.

Cells were maintained in complete RPMI-1640 (Sigma-Aldrich) for HT-29 and THP-1 cells or Dulbecco's Modified Eagle's medium (DMEM AQ; Sigma-Aldrich) for HEK 293T cells supplemented with 10% FBS (Sigma-Aldrich), 100 U/mL penicillin G, and 100 µg/mL streptomycin (Sigma-Aldrich). Cells were grown at 37 °C in a humidified incubator with 5% CO_2 atmosphere.

Generation of HT-29 cells upregulating Cx43 gene

The Cx43-pDendra2N construct (Evrogen, Moscow, Russia) was previously cloned into pCSCW lentiviral vectors[12]. The plasmid was then used to transform DH5α competent *Escherichia coli* bacteria, which were then left to proliferate. Plasmid was then isolated and purified using the EndoFree Maxi plasmid purification kit (Qiagen, Hilden, Germany) to be used for transfection along with other plasmids (gag/pol/env) into HEK 293T cells for production of viral supernatant, which carries the Cx43-pDendra2 chimeric proteins. The viral supernatant was used to transduce HT-29 cells. Following the transduction, HT-29 cells were cultured, expanded, and highly positive cells (referred to as HT-29 Cx43D cells thereafter) were sorted using the BD FACSAria™ III sorter (BD Biosciences, Franklin Lakes, NJ, United States). Viral supernatants were obtained from HEK 293T cells and used to transduce HT-29 cells. These cells, named HT-29 Cx43D, were then isolated using a BD Fluorescence-Activated Cell Sorting Aria SORP cell sorter in the single-cell mode. Green fluorescence in HT-29 Cx43D cells attests to the successful upregulation of exogenous Cx43 in these cells.

Generation of HT-29 cells downregulating Cx43 gene using CRISPR/Cas9 system

HT-29 cells knocking down Cx43, referred to as HT-29 Cx43$^-$ cells, were generated using the CRISPR/Cas9 gene-editing system. After cloning the Cx43 target sequence (20 bp) into the guide RNA scaffold of the pX330-CRISPR plasmid, the bacterial transformation was performed as above and 10-15 colonies were picked to check for the correct insertion of the guide RNA by sequencing. Transfection of HT-29 cells with positive clones was performed, and cells were selected with puromycin (1 µg/mL) until isolated colonies were obtained. Several positive clones were validated for Cx43 knockdown at the RNA and protein levels. One specific clone resulted in more than 90% down-regulation of Cx43 mRNA, generating the experimental HT-29 Cx43$^-$ cells. This downregulation was confirmed by western blot and immunofluorescence assays.

Cell growth assay

Parental HT-29, HT-29 Cx43D, and HT-29 Cx43$^-$ cells were seeded in 24-well plates at a density of 25000 cells/cm^2. At 24 h, 48 h, and 72 h, cells were washed with PBS and trypsinized. Viable cells were counted using the trypan blue exclusion dye.

Evaluation of barrier integrity

Trans-epithelial electrical resistance: This method evaluates barrier integrity of epithelial cells grown in monolayer; by describing the impedance of barrier-forming cell cultures. Briefly, electrodes are placed on both sides of the cellular barrier and an electric current is applied. The resulting current established in the circuit is measured and trans-epithelial electrical resistance (TEER) is calculated. The higher the TEER, the better the membrane integrity[32]. In this study, HT-29, HT-29 Cx43D, and HT-29 Cx43$^-$ cells were cultured on Transwell® inserts with 0.4 µm-pore size filters (Corning, Corning, NY, United States). TEER was measured on confluent cells in the presence or absence of 2% dextran sulfate sodium (DSS) using an EVOM voltmeter with an ENDOHM-12 (World Precision Instruments, Sarasota, FL, United States). Electrical resistance was expressed as Ω × cm^2. DSS was applied onto the cells to reproduce *in vitro* the membrane breach it is known to induce *in vivo* and characterize the loss of membrane integrity. TEER was calculated by subtracting the resistance of blank filters from that of filters covered with a monolayer of parental HT-29, HT-29 Cx43D, or HT-29 Cx43$^-$ cells.

Evans blue assay

Epithelial cells form tight junctions that prevent paracellular transit. Evans blue is a dye that strongly binds to serum albumin *in vivo* and *in vitro*, becoming a protein tracer[33]. When Evans Blue is added on the apical aspect of cells in culture, it is retained in this compartment due to the established epithelial barrier. Any perturbation of barrier integrity will result in seeping of Evans Blue to the basolateral aspect of the cells. HT-29, HT-29 Cx43D, and HT-29 Cx43$^-$ cells were grown on transparent PET membrane cell culture inserts with 0.4 µm-pore size (Corning) until confluent (monolayer). Evans Blue solution (Sigma-Aldrich) was prepared in a 1% bovine serum albumin (cell culture grade; GIBCO®, Paisley, Scotland) at a concentration of 170 µg/mL and then filtered through 0.22 µm-filters (Corning®, Wiesbaden, Germany). At confluence, cells were exposed to 2% DSS for 24 h. Cells were then washed twice with PBS and 400 µL of Evans Blue solution were added on top of the cells (seeded in inserts). Plate wells were rinsed and 1 mL of PBS was added into each well. Cells were then incubated at 37 °C. Every 30 min, 200 µL of solution from the well were collected and replaced with fresh 200 µL PBS, for a total of 2 h. The optic density of collected solution was recorded at 630 nm and concentrations of Evans Blue were calculated.

DSS-induced colitis mouse model

This study was approved by the Institutional Animal Care and Utilization Committee of the American University of Beirut (IACUCC# 18-03-476). The acute DSS-induced colitis mouse model was performed as previously reported[34]. The DSS colitis model in mice is a well-established model for IBD. Using this mouse model, studies have shown disruption of the epithelial barrier function with the infiltration of immune cells, as well as an uncommon production of cytokines[35,36]. In addition, DSS has been previously used *in vitro* to induce a cell membrane breach in a monolayer of colon cells, mimicking the intestinal mucosal barrier. DSS exposure resulted in impairment of protein trafficking and alterations in membrane composition in the intestinal Caco-2 cell line[37,38], resembling the intestinal mucosa integrity breach that occurs in IBD.

In this study, carbenoxolone (CBX) was used as a non-specific GJ inhibitor, injected intraperitoneally at the dose of 30 mg/kg every other day. Briefly, adult BALB/c male mice were distributed into the following experimental groups, each comprised of five mice: (1) Control group that received normal drinking water with no CBX injections; (2) CBX group that received normal drinking water with CBX injections starting on day 11; (3) DSS group where mice were exposed to 2.5% DSS in their drinking water for 10 d, followed by normal drinking water as of day 11; and (4) DSS + CBX group that received DSS-containing drinking water for 10 d followed by CBX injections. All four groups were given normal drinking water from day 11 to day 21 (end of experimental duration) and body weights were measured daily. All mice were given standard chow *ad libitum* and were housed in a temperature-controlled environment on a 12-h automated light/dark cycle. On day 21, mice were anesthetized with isoflurane and then euthanized by cervical dislocation. Colon lengths were measured using a ruler and colon tissues were collected for histological and molecular examinations to assess tissue integrity and expression of inflammatory markers, Cx43, and TET-2.

RNA isolation

Cells in culture: Cells were washed with PBS and total RNA was extracted using the RNeasy® Plus mini kit (Qiagen) as *per* manufacturers' instructions.

Cryopreserved tissues: Colon tissues from experimental mice were collected and snap-frozen in liquid nitrogen. RNA was then isolated using TRI reagent (Sigma), as *per* manufacturers' protocol. Since DSS treatment inhibits mRNA amplification from tissues by quantitative polymerase chain reaction (qPCR) by inhibiting the activities of both polymerase and reverse transcriptase, RNA purification for all samples in all conditions was done by the lithium chloride method according to Viennois *et al*[38].

qPCR

One μg of total RNA was reverse-transcribed to cDNA using the iScriptTM cDNA synthesis kit (Bio-Rad, Hercules, CA, United States). qPCR was conducted using a homemade SYBR green mix in a CFX96 system (Bio-Rad). Products were amplified using primers that recognize Cx43, TET-2, IL-1β, TNF-α, and glyceraldehyde 3-phosphate dehydrogenase (GAPDH) (Table 1). PCR settings were as follows: A pre-cycle at 95 °C for 5 min followed by 40 cycles consisting of 95 °C for 10 s, 52-62 °C for 30 s, and 72 °C for 30 s with a final extra-elongation at 72 °C for 5 min. The fluorescence threshold cycle value (Ct) was obtained for each gene and normalized to the corresponding GAPDH Ct value. All experiments were carried out in technical duplicates and independently performed at least three times.

Protein extraction and Western blot

Cells in culture: Cells were washed with ice-cold PBS, and scraped on ice in lysis buffer (0.5 M Tris-HCl buffer, pH 6.8; 2% SDS, and 20% glycerol) containing protease and phosphatase inhibitors (Roche, Basel, Switzerland).

Cryopreserved tissues: Snap-frozen mouse colon tissues were homogenized on ice in ice-cold RIPA buffer containing 10% of a 0.5 M Tris-HCl buffer, pH 7.5, 3% of 5 M NaCl, 1% NP-40, 10% sodium deoxycholate, and 1% SDS as well as phosphatase and protease inhibitors.

The lysate was then sonicated. Proteins were quantified, loaded onto 10% SDS-polyacrylamide gels, and subjected to electrophoresis. Migrated proteins were transferred to polyvinylidene fluoride membranes (Bio-Rad) and membranes were blocked with 5% fat-free milk in PBS. Membranes were then incubated with either human or mouse primary antibodies for 3 h at room temperature or overnight at 4 °C. Primary antibodies were hybridized with horseradish peroxidase-conjugated secondary antibodies (anti-rabbit: SC-2357 and anti-mouse SC-2005; Santa Cruz Biotechnology, Dallas, TX, United States) and blots were visualized using an enhanced chemiluminescence detection kit. GAPDH (MAB5476; Abnova, Taipei, Taiwan) and β-actin (A2228; Sigma-Aldrich) were used as loading controls. The quantification of bands was performed using the ImageJ software (United States National Institutes of Health, Bethesda, MD, United States). Immunoreactivity of proteins under study was reported as a ratio of protein-of-interest expression to the housekeeping gene used as loading control.

Table 1 Quantitative polymerase chain reaction human and mouse primer sequences

Gene	Primer sequences, 5' to 3'	Annealing temperature, °C
hCx43	F: CTTCACTACTTTTAAGCAAAAGAG	52
	R: TCCCTCCAGCAGTTGAG	
hTET-1	F: TTCGTCACTGCCAACCTTAG	60
	R: ATGCCTCTTTCACTGGGTG	
hTET-2	F: CACTGCATGTTTGGACTTCTG	60
	R: TGCTCATCCTCAGGTTTTCC	
hTET-3	F: GCCCACAAGGACCAGCATAA	60
	R: CGCAGCGATTGTCTTCCTTG	
hGAPDH	F: TGGTGCTCAGTGTAGCCCAG	52-62
	R: GGACCTGACCTGCCGTCTAG	
mCx43	F: ACAGCGGTTGAGTCAGCTTG	60
	R: GAGAGATGGGGAAGGACTTGT	
mTET-2	F: CAAGGTGTGCTTGGCAATTTT	60
	R: CATCACTGTGCGTCAATCAAGA	
mIl-1β	F: CTCCACCTCAATGGACAGAA	57
	R: GCCGTCTTTCATTACACAGG	
mTNF-α	F: AATGGCCTCCCTCTCATCAGT	57
	R: CCACTTGGTGGTTTGCTACGA	
mGAPDH	F: CATGGCCTTCCGTGTTCCTA	58
	R: CCTGCTTCACCACCTTCTTGAT	

Cx43: Connexin 43; F: Forward; GAPDH: Glyceraldehyde 3-phosphate dehydrogenase; h: Human; Il-1β: Interleukin-1β; m: Mouse; R: Reverse; TET: Ten-eleven translocation; TNF-α: Tumor necrosis factor-α.

Specimens from human patients

Archived formaldehyde-fixed paraffin-embedded (FFPE) colon blocks (ulcerative colitis, sporadic colon adenocarcinoma and normal) were obtained from the American University of Beirut Medical Center. All patients' identifiers were kept confidential from the study team.

Histological evaluation

Sections obtained from animals and human samples were stained with hematoxylin and eosin (H&E) for observation under the light microscope (CX41; Olympus, Tokyo, Japan).

Immunofluorescence microscopy

Cells in culture: Cells were grown on coverslips and then fixed either with 4% paraformaldehyde and permeabilized with 0.05% Triton X-100 for 20 min for Cx43 probing (SAB4501175; Sigma-Aldrich) or with ice-cold methanol at -20 °C for TET-2 (ab94580; Abcam, Cambridge, United Kingdom) and 5-hmC (ab214728; Abcam) probing before blocking of non-specific binding.

FFPE tissues: Human and murine 5-μm-thick tissue sections were immune-stained using antibodies against Cx43, TET-2, 5-hmC, and CD68 (ab201340, Abcam, United States). Briefly, paraffin blocks were sectioned using a microtome and sections were mounted onto glass slides. Specimens were deparaffinized in xylene and rehydrated using a gradient series of alcohol to water. Antigen retrieval was performed by incubating sections in sodium citrate buffer (pH 6.0) in a steamer for 30 min. Sections were allowed to cool, then washed twice with deionized water before blocking of non-specific binding.

Non-specific binding was blocked with 5% normal goat serum (Chemicon, Burlington, MA, United States) in PBS for 1 h in a humidified chamber and incubated with the primary antibody against Cx43, TET-2, and 5-hmC overnight at 4 °C. Cells were then washed and incubated with IgG-conjugated secondary antibody: Either Texas Red (T862; Life Technologies, Carlsbad, CA, United States) or Alexa Fluor 488 (A11070; Life Technologies) at 1 μg/mL for 1 h at room temperature. Nuclei were counter-stained with 4',6-diamidino-2-phenylindole at 1 μg/mL for 10 min. Coverslips were then mounted onto

the glass slides using Prolong Anti-fade kit (Life Technologies).

Slides were examined under a fluorescence microscope and images were acquired using a 63×/1.46 Oil Plan-Apochromatic objective (on the laser scanning confocal microscope LSM 710, operated by the Zeiss LSM 710 software; Carl Zeiss, Oberkochen, Germany).

Statistical analyses

Numerical values were expressed as mean ± SEM or mean ± SD. The *P* value was determined and considered significant for $P < 0.05$. Differences between experimental groups were assessed using Student *t*-test, one-way analysis of variance (ANOVA) or by two-way ANOVA followed by Tukey's multiple comparisons test.

RESULTS

Characterization of the HT-29 cell model used in this study

In an attempt to investigate TET-2 modulation in the context of different Cx43 expression levels in HT-29 cells, Cx43 was upregulated (HT-29 Cx43D cells) or downregulated (HT-29 Cx43$^-$ cells). Increases and decreases in Cx43 levels were reflected at the translational level: Western blot analysis (Figure 1A) shows upregulation of exogenous Cx43 protein levels in HT-29 Cx43D and loss of endogenous Cx43 protein expression in HT-29 Cx43$^-$ cells compared to parental HT-29 cells ($P < 0.001$). Figure 1B also shows increased expression of Cx43 in HT-29 Cx43D cells and their localization at the cell periphery, where they form GJ plaques, and a decrease in Cx43 levels in HT-29 Cx43$^-$ cells.

Cells manipulated for *Cx43* gene showed differential proliferation rates 48 h and 72 h post-seeding. As depicted in Figure 1C, Cx43 upregulation (HT-29 Cx43D cells) significantly decreased the number of viable cells compared to parental HT-29 cells ($P < 0.05$ at 48 h and $P < 0.001$ at 72 h). However, cells devoid of Cx43 (HT-29 Cx43$^-$ cells) demonstrated a significantly greater proliferation rate compared to parental HT-29 cells at 48 h and 72 h post-seeding ($P < 0.001$). The increased proliferation rate of HT-29 Cx43$^-$ cells was also accompanied by increased migratory potential, as suggested by the wound healing and the invasion assays (Supplementary Figure 1). Compared to parental cells, HT-29 Cx43$^-$ cells seemed more efficient at closing the artificially created gap ($P < 0.05$).

These observations are in accordance with the tumor suppressor role of Cx43, greatly inhibiting the proliferation of HT-29 cells.

Modulation of TET expression in HT-29 cellular subsets

Transcriptional levels of TET-1, TET-2, and TET-3 were evaluated in HT29 cells, manipulated for Cx43 expression. TET-2 specifically demonstrated the highest transcriptional levels between all three TET genes (Figure 1D). TET-2 protein expression was verified by immunofluorescence in parental HT-29 cells (Figure 1D). While TET-1 and TET-3 levels were not significantly different in HT-29 cells expressing lower or higher levels of Cx43, TET-2 levels significantly increased in HT-29 Cx43$^-$ cells compared to parental HT-29 ($P < 0.05$) and to HT-29 Cx43D ($P < 0.001$) cells.

For the remainder of this study, TET-2 expression levels and 5-hmC mark were evaluated given the greater expression of TET-2 in HT-29 cells and the prevalence of loss-of-function mutations of TET-2 in cancer[21,39-41].

Inflammation induces increase in Cx43 and TET-2 expression levels in HT-29 cells

In order to explore a potential pattern of expression for TET-2 and Cx43 in inflammation, parental HT-29, HT-29 Cx43D, and HT-29 Cx43$^-$ cells were screened for TET-2 mRNA and protein expressions, as well as 5-hmC marks by immunofluorescence using an antibody against 5-hmC, a product of the reaction catalyzed by TET-2. In Cx43-expressing cells, the addition of inflammatory media (supernatant from activated THP-1 cells) resulted in upregulation of Cx43 (Figure 2A). Similarly, under inflammatory conditions, all three cellular subsets upregulated their TET-2 expression ($P < 0.05$) at the transcriptional and translational levels (Figure 2B). Interestingly, HT-29 cells down-regulating Cx43 showed higher expression of TET-2 compared to parental cells or cells overexpressing Cx43 (Figure 2B). The 5-hmC marks also increased with increased TET-2 levels in HT-29 Cx43$^-$ cells. Levels of TET-2 and 5-hmC both increased in cells exposed to inflammation, as shown by quantified immunofluorescence micrographs (Figure 2C). Changes in TET-2 expression were less pronounced in HT-29 Cx43D cells than in HT-29 Cx43$^-$ cells. This trend was also evident with the 5-hmC marks (Figure 2C) where increased expression of TET-2 correlated with increased amounts of 5-hmC.

In order to strengthen these findings, experiments were performed on Caco-2 cells. Levels of Cx43 and TET-2 were also upregulated in Caco-2 cells exposed to inflammatory medium (Figure 2D), with a five-fold increase in Cx43 levels ($P < 0.001$) and two-fold increase in TET-2 levels ($P < 0.01$).

Downregulating Cx43 contributes to the disruption of epithelial membrane integrity

Parental HT-29, HT-29 Cx43D, and HT-29 Cx43$^-$ cells were grown as monolayers and exposed to 2% DSS

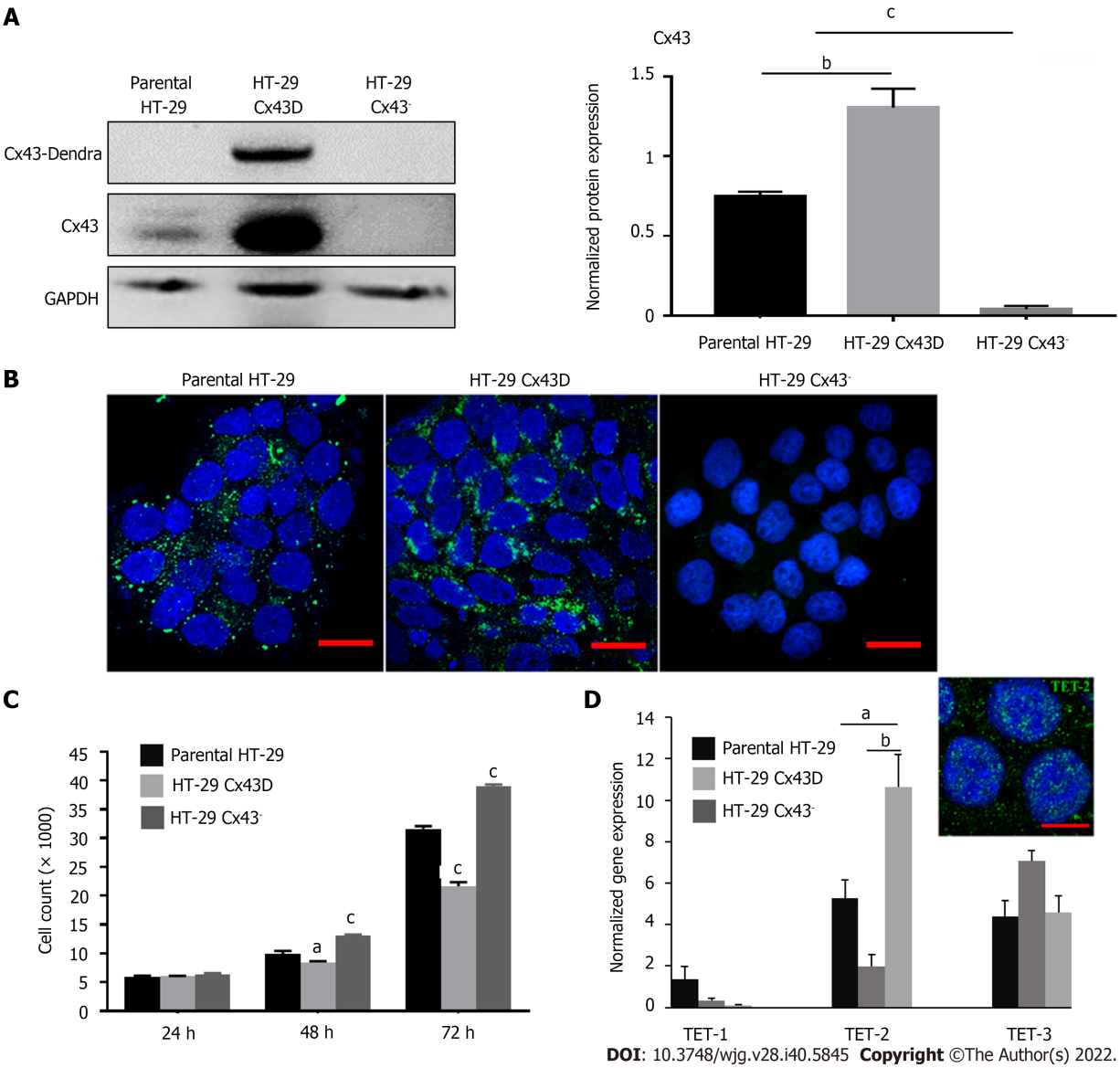
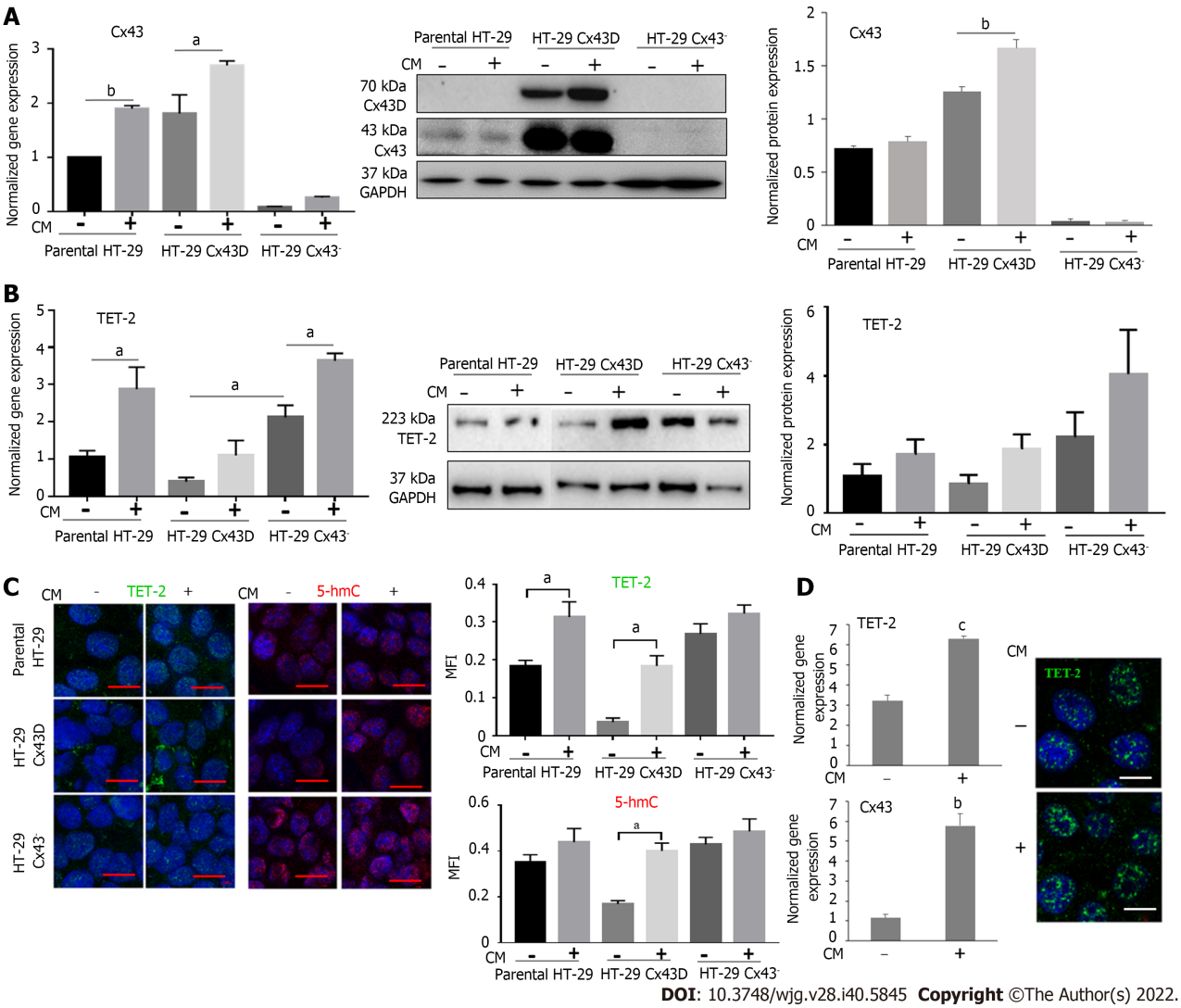


Figure 1 Characterization of the *in vitro* HT-29 cell model. A: Western blot of connexin 43 (Cx43) protein expression in parental HT-29, HT-29 Cx43-Dendra (Cx43D), and in HT-29 Cx43- cells. Bar graphs display mean densitometric analysis (of three independent experiments) after normalizing protein expression to glyceraldehyde 3-phosphate dehydrogenase (GAPDH); B: Immunofluorescence micrographs of parental HT-29 and HT-29 Cx43- cells, as well as a fluorescent micrograph of HT-29 cells transduced with the GFP-Cx43 construct. Highly GFP positive cells were sorted using BD-Fluorescence-Activated Cell Sorting cell sorter, generating the HT-29 Cx43D. Scale bar 10 μm; C: Cells were counted at three different time points (24, 48 and 72 h), using the trypan blue dye exclusion assay. Compared to parental HT-29 cells, HT-29 Cx43D cells had a slower proliferation rate and HT-29 Cx43- cells a faster proliferation rate at 48 and 72 h; D: Histograms show normalized gene expression of ten-eleven translocation (TETs) in parental HT-29, HT-29 Cx43D and HT-29 Cx43- cells, as detected by quantitative polymerase chain reaction (qPCR). TET-2 was the highest expressed TET in HT-29 cells, and cells with differential Cx43 expression also had significantly different TET-2 expression levels. The inset is an immunomicrograph of TET-2 in HT-29 C43D cells. Scale bar 5 μm. Results are presented as means ± SEM of three independent qPCR runs in duplicates. One-way ANOVA, [a]$P < 0.05$; [b]$P < 0.001$; [c]$P < 0.0005$. Cx43: Connexin 43; GAPDH: Glyceraldehyde 3-phosphate dehydrogenase.

for 24 h to evaluate if differential Cx43 levels would have any bearing on DSS-induced membrane integrity breach. DSS was previously shown to impair IEC membrane integrity *in vitro*[42] and it was used in our study to induce membrane injury similar to that observed upon chronic inflammation. Figure 3A shows that DSS resulted in decreased cell contacts and increased spaces between cells (red arrows), indicating loss of membrane integrity. The TEER assay was performed to assess how Cx43 modulation affects membrane integrity in the presence of DSS. Figure 3B shows that, in the absence of DSS, differentially expressed Cx43 had no major impact on epithelial barrier integrity, with an average TEER of 20 Ω × cm^2 in parental and in HT-29 Cx43- cells and 23 Ω × cm^2 in HT-29 Cx43D cells. However, the addition of DSS resulted in a significant decrease in TEER values by approximately 37% in parental cells and 50% in HT-29 Cx43- cells ($P < 0001$). Therefore, overexpression of Cx43 in HT-29 Cx43D cells seemed to be protective against DSS-induced loss of membrane integrity (Figure 3B).

The Evans Blue permeability assay was then performed to evaluate the monolayer integrity under DSS exposure and in cells with different Cx43 expression status. The level of cell permeability or "leakage" was correlated to the concentration of Evans Blue measured at the bottom of the well. As



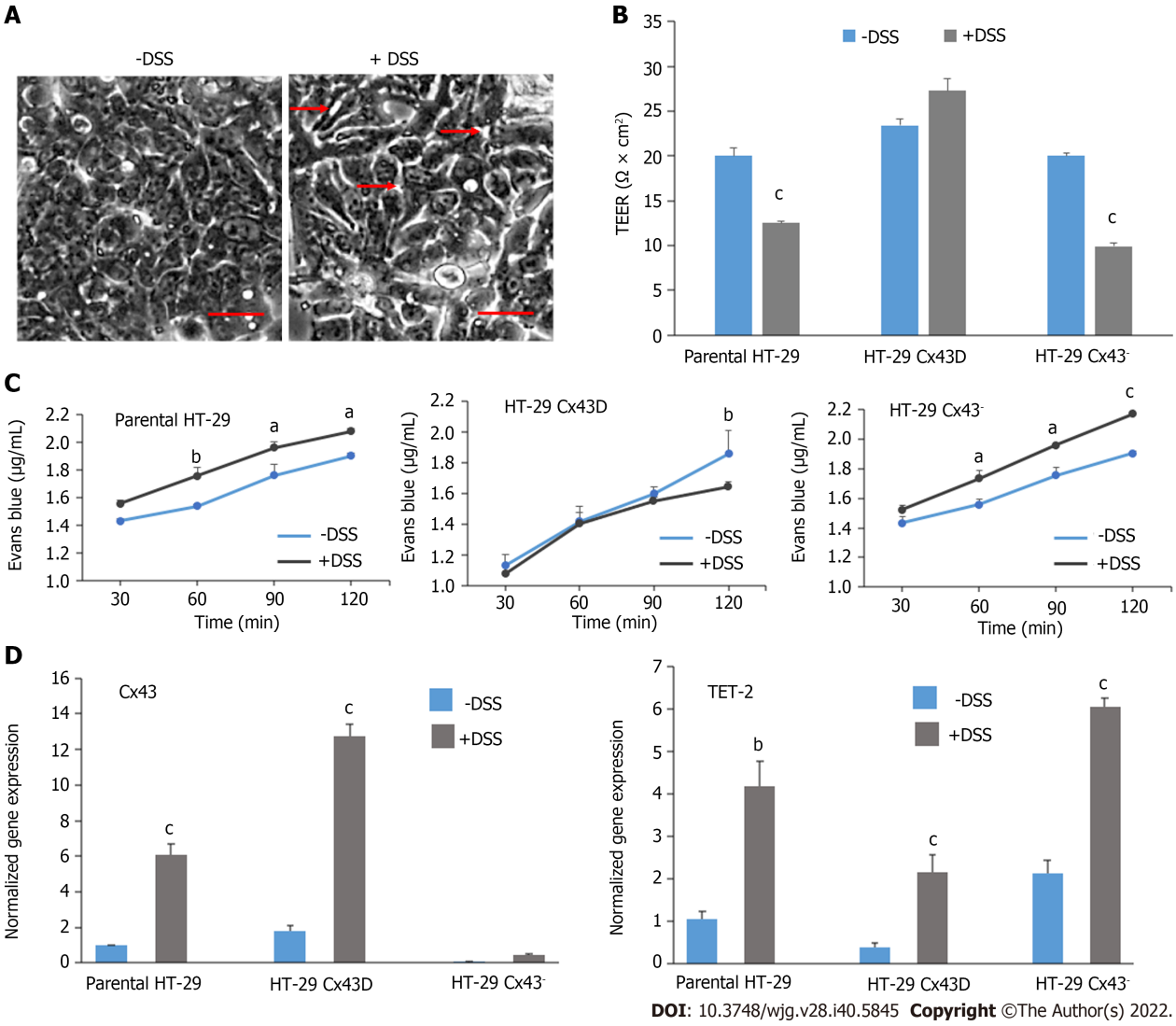
DOI: 10.3748/wjg.v28.i40.5845 **Copyright** ©The Author(s) 2022.

Figure 2 Connexin 43 and ten-eleven translocation-2 expression increases in cells exposed to inflammation. Parental HT-29, HT-29 connexin 43-Dendra (Cx43D), and HT-29 Cx43$^-$ cells were exposed to inflammatory conditioned media (CM) obtained from activated THP-1 cells for 24 h. A: Histograms show the normalized gene expression of Cx43, as detected by quantitative polymerase chain reaction. Cx43 mRNA levels increase in parental HT-29 and HT-29 Cx43D, in the presence of inflammatory media. Western blot of endogenous Cx43 and exogenous Cx43D protein expression in parental HT-29, HT-29 Cx43D, and in HT-29 Cx43$^-$ cells. Densitometric analysis (ratio of protein-of-interest to loading control band intensity) shows a slight increase in Cx43 levels upon exposure to inflammation; B: Bar graphs show ten-eleven translocation-2 (TET-2) transcriptional levels increase in all three HT-29 cellular subsets when exposed to CM. Western blots of TET-2 and densitometric analysis shows increased protein levels of TET-2 in CM-treated cells; C: Immunofluorescence images showing TET-2 expression and 5-hmC marks in parental HT-29, HT-29 Cx43D, and HT-29 Cx43$^-$ cells. Bar graphs in the right panel reflect mean fluorescence intensity of at least five different fields acquired from three different experiments. Levels and activity of TET-2 increase in all CM-exposed cells. Scale bar 5 μm; D: Bar graphs display levels of Cx43 and TET-2 in Caco-2 cells exposed to CM. Fluorescent micrographs show increased levels of TET-2 in the nucleus upon exposure to CM. Scale bar 5 μm. Experiments were repeated at least three different times. One-way ANOVA, $^aP < 0.05$; $^bP < 0.001$; $^cP < 0.0005$. TET-2: Translocation-2; Cx43: Connexin 43; GAPDH: Glyceraldehyde 3-phosphate dehydrogenase; MFI: Mean fluorescence intensity.

shown in Figure 3C, after 60 min of incubation with Evans Blue, the concentration of the dye significantly and rapidly increased in DSS-treated parental HT-29 ($P < 0.05$) and HT-29 Cx43$^-$ cells ($P < 0.0001$). However, within the two-hour timeframe, cells overexpressing Cx43 (HT-29 Cx43D cells) had not leaked substantial levels of Evans Blue dye.

DSS was subsequently used to reproduce the murine colitis model to evaluate modulation of Cx43 and TET-2 levels in the inflamed colons of mice. Figure 3D shows that upon exposure of HT-29 cells to DSS *in vitro*, levels of Cx43 and TET-2 vary. Specifically, in Cx43-expressing cells, DSS exposure results in upregulation of Cx43 ($P < 0.001$). Levels of TET-2 also significantly increase in all HT-29 cellular subsets ($P < 0.01$).

In summary, *in vitro* results suggest that inflammation leads to upregulation of Cx43 and of TET-2 in HT-29 cells. TET-2 upregulation was more pronounced in HT-29 cells devoid of Cx43. Moreover, Cx43 knockdown rendered HT-29 cells more sensitive to DSS-induced membrane integrity breach, in favor of a role of Cx43 protein in the maintenance of epithelial barrier integrity. Modulation of Cx43 and TET-2 *in vitro* displayed similar trends whether cells were exposed to conditioned inflammatory media



DOI: 10.3748/wjg.v28.i40.5845 **Copyright** ©The Author(s) 2022.

Figure 3 Dextran sulfate sodium treatment disrupts the integrity and permeability of intestinal epithelial barrier, notably in HT-29 connexin 43- cells. A: Light microscopy images of HT-29 cells in the presence or absence of 2% dextran sulfate sodium (DSS). Scale bar 50 μm; B: The membrane integrity of parental HT-29, HT-29 connexin 43-Dendra (Cx43D), and HT-29 Cx43- cells in the presence or absence of 2% DSS was measured by trans-epithelial electrical resistance (TEER). Bar graphs indicate average TEER measurements; C: Membrane permeability was evaluated by Evans Blue permeability assay in all three cell subsets. Levels of Evans Blue that crossed are measured by spectrophotometry and are plotted as means over time; D: Quantitative polymerase chain reaction data show that transcriptional levels of Cx43 and ten-eleven translocation-2 (TET-2) significantly increase in DSS-treated cells. All experiments have been repeated at least three times. Two-way ANOVA, $^{a}P < 0.05$; $^{b}P < 0.001$; $^{c}P < 0.0005$. Cx43: Connexin 43; DSS: Dextran sulfate sodium; TEER: Trans-epithelial electrical resistance.

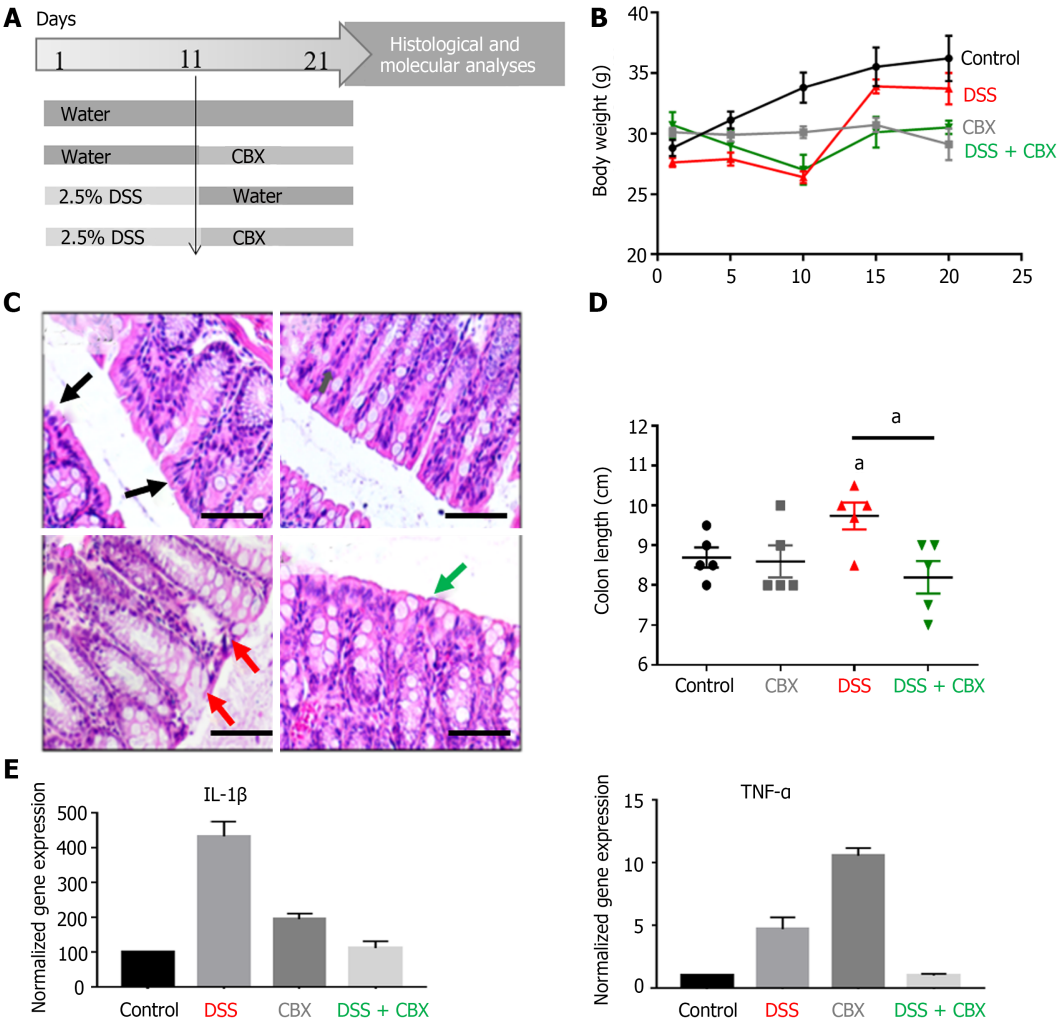
(obtained from activated THP-1 cells) or to DSS (subsequently used in the colitis mouse model).

An established and widely used DSS-induced colitis mouse model was reproduced[34] to evaluate Cx43 and TET-2 expression. A subset of mice was also administered CBX, a GJ inhibitor, to examine TET-2 expression modulation in varying functional states of GJs.

DSS-induced colitis in mice is attenuated by CBX-induced GJ blockade

The experimental design was as described in Figure 4A, where each group comprised five mice. Body weight was recorded daily, throughout the 21-d experimental duration. Figure 4B reflects weight changes; while mice in the control group (Group 1) consistently gained weight over the 21-d experiment, mice exposed to CBX alone (Group 2) maintained their baseline weight throughout the experiment. On the other hand, DSS-exposed mice lost a moderate amount of weight until day 10, after which they were switched to normal drinking water (Group 3) and their average weight picked up to almost control group levels. Mice in the DSS group who were injected with CBX starting day 11 recovered some of the weight lost until day 10, but did not reach the normal weight recorded in the control group.

At the end of the experimental duration, mice were euthanized and their colons examined and collected for measurement purposes and a biopsy was used for histological and molecular analyses.



DOI: 10.3748/wjg.v28.i40.5845 **Copyright** ©The Author(s) 2022.

Figure 4 Dextran sulfate sodium induces inflammation in mice and carbenoxolone restores the normal phenotype. A: A flowchart schematizing the *in vivo* experimental design. BALB/c male mice were distributed into four experimental groups, each comprised of five mice: (1) Control group that received normal drinking water with no carbenoxolone (CBX) injections; (2) CBX group that received normal drinking water with CBX injections starting day 11; (3) Dextran sulfate sodium (DSS) group where mice were administered with 2.5% DSS in their drinking water for 10 d but not subjected to any CBX injections; and (4) DSS + CBX group that received DSS-containing drinking water as well as CBX injections. Mice were given 30 mg/kg CBX *via* intraperitoneal injections from day 11 every other day to the end of the experiment; B: Variation of animal body weight over 21 d. DSS-exposed mice lost weight. Significance in body weight change was detected between days 4 and 12 in DSS-treated mice, and days 11 and 21 in CBX-injected mice only; C: Hematoxylin and eosin images showing the architecture of mice colon tissues from all experimental groups. Arrows indicate representative sites in each experimental condition. Scale bar 50 μm; D: Colon length was measured at the end of the experiment. DSS-treated mice showed significantly longer colons compared to the control group; E: Bar graphs showing the normalized gene expression of interleukin-1β and tumor necrosis factor-α in mouse colon tissues, as detected by quantitative polymerase chain reaction. Experiments were repeated five times and results are displayed as means ± SEM. One-way ANOVA, $^{a}P < 0.05$. IL: Interleukin; CBX: Carbenoxolone; DSS: Dextran sulfate sodium; TNF-α: Tumor necrosis factor-α.

Histological examination of H&E stained sections of colons showed a disruption of epithelial barrier as well as an increase in infiltrating cells in crypts of colons from DSS-treated mice compared to control. CBX-treated animals seem to have retained (albeit not fully) some normalcy (Figure 4C). DSS-treated mice showed significantly longer colons compared to the control group ($P < 0.05$). CBX significantly reduced the length of DSS-treated colons to approximately normal levels ($P < 0.05$) (Figure 4D).

Levels of inflammatory cytokines, IL-1β and TNF-α, previously shown to be modulated in IBD models[12,38,43], were evaluated by qPCR. In accordance with weight changes and colon length indicative of intestinal damage, DSS-treated mice of Group 3 had increased expression of both IL-1β and TNF-α, compared to control Group 1 ($P < 0.05$) (Figure 4E).

These data propose that CBX alleviates DSS-induced inflammation in mice, as demonstrated by normalized colon length and histology, as well as decreased levels of inflammatory mediator transcripts in colon tissues.

DSS-induced inflammation increases Cx43 and TET-2 expression in vivo

Colon tissues obtained from mice on day 21 (end of experimental duration) were processed for total

RNA and protein extraction. Cx43 expression was significantly higher in tissues from mice exposed to DSS both at the transcriptional (Figure 5A, $P < 0.0001$) and translational levels (Figure 5A, middle and right panels). However, CBX injections restored Cx43 mRNA and protein levels back to control levels. Not only did GJ inhibition attenuate the inflammatory state in the colon, it also led to downregulated Cx43 expression.

Levels of TET-2 were also evaluated in the colon tissues obtained from mice in all four experimental groups. Gene expression analysis pointed to an increase of TET-2 mRNA levels in the CBX-treated group (Group 2, Figure 5B, $P < 0.001$). In the tissues of mice from Group 4 (DSS + CBX), TET-2 levels were similar to those in the DSS group (slightly, but not significantly, higher than control levels). The same pattern was observed at the protein level (Figure 5B, middle and right panels). Changes in TET-2 levels were accompanied by changes in Cx43 levels, which increased in DSS-treated (inflamed) colons and decreased upon addition of CBX (Figure 5C). Inflammation was further underscored by immunostaining using CD68 antibody. As shown in Figure 5D, levels of infiltrated $CD68^+$ cells (macrophages) increased significantly by six-fold in colons of DSS-treated mice as opposed to those of control or CBX-treated mice alone ($P < 0.0001$). In accordance with CBX effects on inflammatory mediators and histological aspects, CBX injections following DSS exposure resulted in a decreased amount of macrophages. Sections from colons of mice in the DSS group also showed considerable levels of TET-2 protein in epithelial cells with neighboring macrophages, both indicative of an active inflammatory process. TET-2 levels increased further in colons of CBX-treated mice. In addition, and consistent with transcriptional and translational data, CBX-treated mice had upregulated TET-2 protein levels in their colons (Figure 5D). Immunofluorescent micrographs reflect TET-2 level increase in mucosal cells, though not to the same extent as qPCR data; due to the contribution of TET-2 mRNA from $CD68^+$ macrophages in the vicinity of IECs.

These data indicate that inhibiting GJs in inflamed tissues mitigates DSS-induced inflammation. In addition, the increase in Cx43 expression upon exposure to DSS is accompanied by an increase in TET-2 protein expression levels, and disabling GJs by CBX is paralleled by a significant increase in TET-2 levels. Data therefore suggest that, under inflammatory conditions (DSS), GJ inhibition by CBX restores Cx43 levels down to control. In accordance with *in vitro* data where HT-29 $Cx43^-$ cells had upregulated TET-2 levels, chemical inhibition of Cx43 *in vivo* also was accompanied by increased TET-2 levels.

Collectively, *in vitro* and *in vivo* data indicate that under inflammatory conditions, levels of both TET-2 and Cx43 increase.

Cx43 levels increase and TET-2 levels decrease in colons of patients with ulcerative colitis

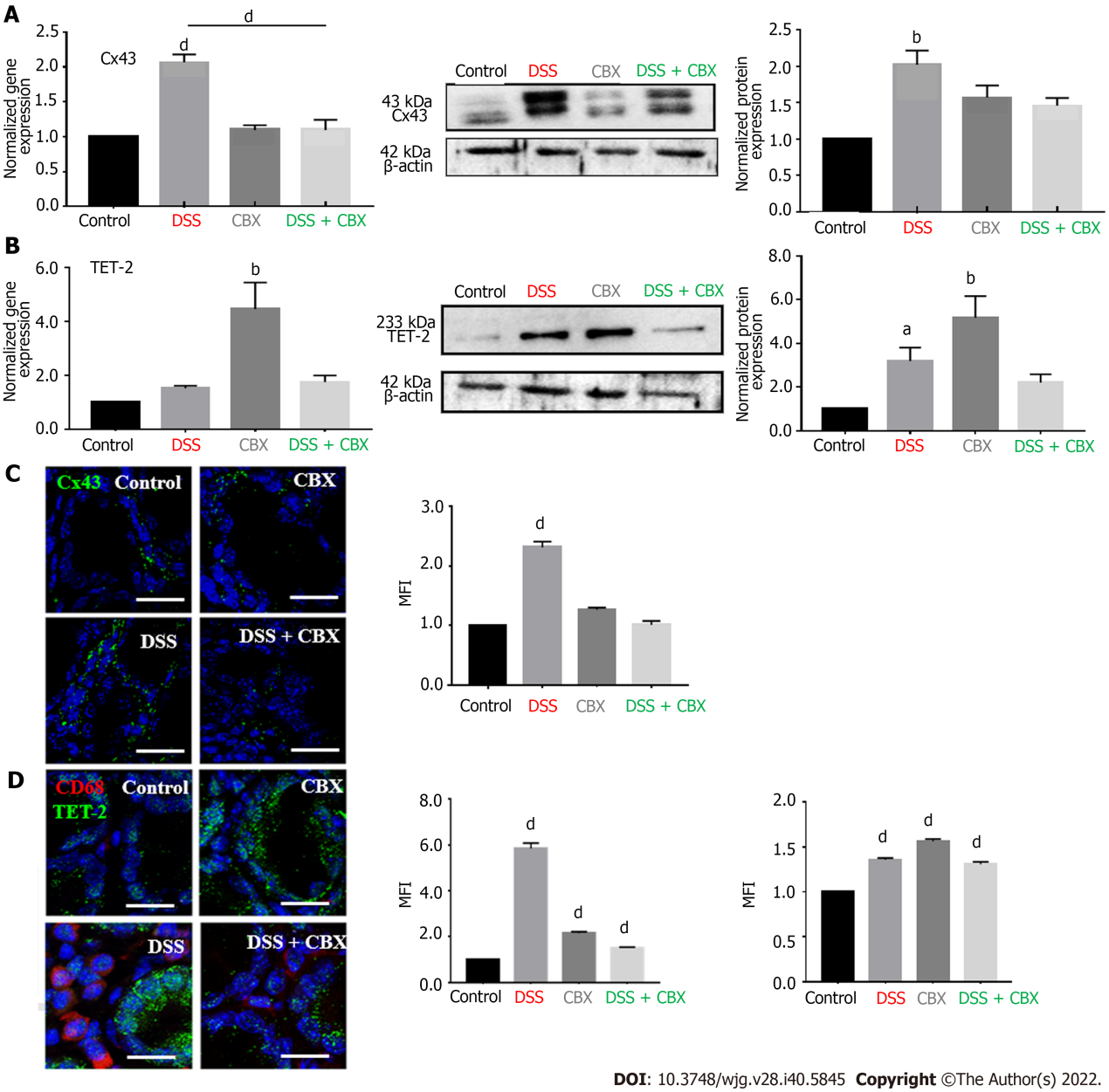
In an attempt to correlate *in vitro* and *in vivo* findings with clinical data, FFPE colon biopsies from normal non-dysplastic non-inflamed colons ($n = 7$), ulcerative colitis ($n = 5$), and colon adenocarcinoma ($n = 7$) patients were obtained anonymously. Sections were stained with H&E for light microscopy, as well as with antibodies against CD68 (macrophage marker), Cx43, and TET-2 for immunofluorescence analyses.

Histological staining exposed a clearly disorganized intestinal mucosal layer in ulcerative colitis and sporadic colon adenocarcinoma tissues as compared to normal tissues (Figure 6A). The disrupted architecture was due to extensive immune activity in the tissues underlying the mucosa. Figure 6B shows $CD68^+$ macrophages infiltrating tissues from ulcerative colitis patients ($P < 0.0001$), underscoring the inflammatory profile. Tissues obtained from patients with sporadic adenocarcinoma of the colon also displayed macrophage foci, but to a much lesser extent than ulcerative colitis tissues ($P < 0.001$). Although comparable to control in terms of fluorescence intensity, $CD68^+$ cells in the adenocarcinoma specimen were not uniformly distributed in the tissue.

Moreover, Cx43 and TET-2 expression and localization were evaluated by immunofluorescence (Figure 6C and D). Consistent with data obtained *in vitro* (Figures 2 and 3) and *in vivo* (Figure 5), Cx43 protein levels were significantly increased in ulcerative colitis (*i.e.* inflamed) tissues ($P < 0.005$) and sharply decreased in adenocarcinoma. Unlike *in vitro* and *in vivo* data that reflect parallel patterns of Cx43 and TET-2 expression in inflammatory conditions, Cx43 level increase in ulcerative colitis was accompanied by a decrease in TET-2 expression ($P < 0.001$). This observation, however, resembles the *in vitro* scenario illustrated in Figure 2. In fact, while TET-2 expression had increased upon exposure of cells to an inflammatory milieu, Cx43 upregulation in HT-29 Cx43D cells was associated with lower overall TET-2 expression compared to parental cells, and Cx43 knockdown resulted in elevated TET-2 levels.

DISCUSSION

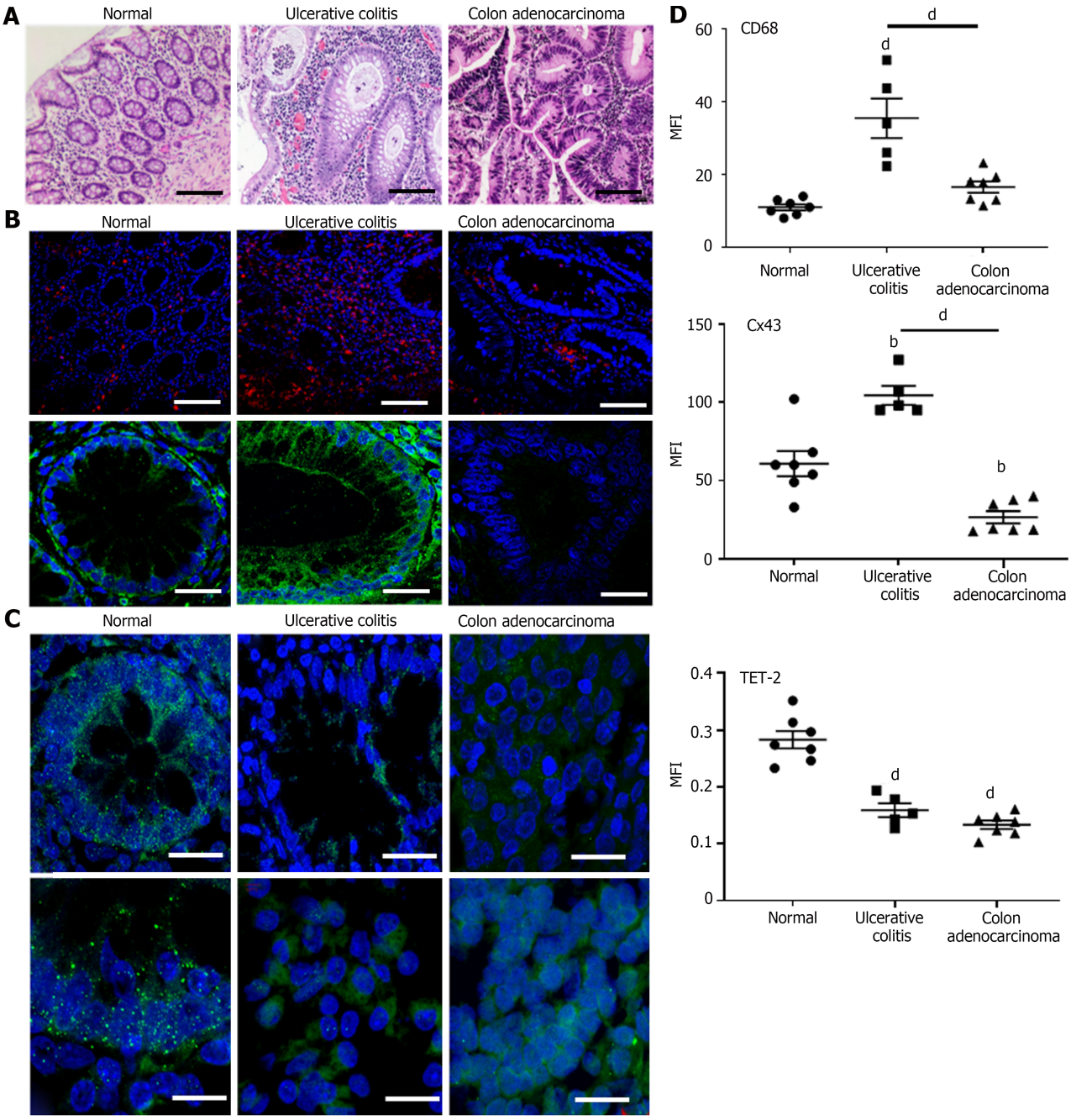
In various pathologies, including inflammation and cancer, the alteration of the expression, regulation, and association of junctional complexes with other proteins have been reported. Epigenetic methylation and demethylation processes are also major players in a cell's malignant transformation. Specifically, GJ-forming Cx43 and demethylating enzyme TET-2 have both been documented to be impaired in inflammation and cancer[10-12,19,20].



DOI: 10.3748/wjg.v28.i40.5845 **Copyright** ©The Author(s) 2022.

Figure 5 Dextran sulfate sodium increases connexin 43 and ten-eleven translocation-2 expressions *in vivo*. A: Left panel: Histograms show the normalized gene expression of connexin 43 (Cx43) in mice colon tissues, as detected by quantitative polymerase chain reaction (qPCR). Middle panel: Western blot of Cx43 protein in mouse colon tissues. Right panel: Densitometric analysis of protein expression after normalization to β-actin. Dextran sulfate sodium (DSS)-treated mice had the highest expression of Cx43 in their colons; B: Left panel: Histograms display the normalized gene expression of ten-eleven translocation-2 (TET-2) in mouse colon tissues, as detected by qPCR. Middle panel: Western blot of TET-2 protein expression in mouse colon tissues. Right panel: Densitometric analysis of protein expression after normalization to β-actin. DSS exposure resulted in enhanced TET-2 transcription and carbenoxolone inhibition of gap junctions significantly increased TET-2 expression; C: Immunofluorescence images of colon tissues stained for Cx43 with the mean fluorescence intensity (MFI) analysis. Scale bar 20 μm; D: Immunofluorescence images of mouse colon tissues stained for CD68 and TET-2. Histograms reflect the MFI analysis. High levels of CD68$^+$ cells correlated with greater expression of Cx43 and TET-2 in DSS-exposed mice. Scale bar 10 μm. Experiments were repeated five times. One-way ANOVA, $^aP < 0.05$; $^bP < 0.005$; $^dP < 0.0001$. MFI: Mean fluorescence intensity; CBX: Carbenoxolone; DSS: Dextran sulfate sodium.

Studies have shown that the inflammatory response relies in part on intercellular communication mediated by channel-forming connexins. The role of GJ-mediated signaling in the initiation of inflammation is mainly through the transfer of ATP between neighboring cells. ATP molecules are then released in the extracellular environment where they act as signaling molecules that activate purinergic receptors, amplifying the inflammatory response[10]. Wong *et al*[11] partly elucidated the role of Cx43 in intestinal epithelial barrier injury. TLR activation in the disrupted intestinal epithelium translates intracellularly into Cx43 transcription, translation, post-translational modification, and assembly into connexons. GJIC regulates intestinal epithelial function during both acute and chronic inflammation [11]. Furthermore, Al-Ghadban *et al*[12] demonstrated a role of GJs in the pathogenesis of IBD by a direct communication between IECs and macrophages enhanced by basement membrane degradation [12]. Long-term IBD associates with amplified risk of colon carcinogenesis, and the deregulation of



DOI: 10.3748/wjg.v28.i40.5845 **Copyright** ©The Author(s) 2022.

Figure 6 Modulation of connexin 43 and ten-eleven translocation-2 expression in human colon tissues under pathological conditions. A: Hematoxylin and eosin images of human colon tissues. Compared to normal (histopathologically unchanged) samples, tissues from inflamed (ulcerative colitis) and sporadic malignant colons show disorganization of colon crypts and infiltration of immune cells within the lamina propria. Scale bar 50 μm; B: Immunofluorescence images of $CD68^+$ cells (macrophages) and connexin 43 (Cx43) show that Cx43 expression increases in inflamed tissues. Scale bar 10 μm; C: Immunofluorescence images of ten-eleven translocation-2 (TET-2) in human colon tissues (upper panel: Low magnification; lower panel: Higher magnification). TET-2 protein was minimally detected in ulcerative colitis and colon adenocarcinoma tissues. Scale bar 10 μm; D: Mean fluorescence intensity (MFI) analyses reflecting the expression of CD68, Cx43, and TET-2. One-way ANOVA, $^bP < 0.005$; $^dP < 0.0001$. MFI: Mean fluorescence intensity; TET: Ten-eleven translocation.

connexin expression is regarded as one of the hallmarks of different cancers. Shilova *et al*[44] reviewed *in vitro* and *in vivo* studies that point at a correlation between the loss of connexin expression and cancer onset. In fact, downregulation of Cx26, Cx32, and Cx43 accompanies the development of human bladder cancer, hepatocarcinoma, and breast cancer, respectively[44]. A recent study on breast cancer proposed that Cx43 upregulation in a triple negative breast cancer cell line led to a reversal of its mesenchymal phenotype *in vitro* and to a decreased metastatic potential *in vivo*[7]. While connexin downregulation is observed in many cancers, elevated Cx43 levels have also been associated with increased malignancy. In a hepatocellular carcinoma cell line, Cx43 was shown to enhance malignancy by inhibiting Cx32-mediated GJIC[45], and, in prostate cancer, Cx43 promoted invasion and metastasis[46]. Variability of data on connexin involvement in cancer onset and progression warrants more research to identify the

underlying factors that dictate a tumor-suppressing or tumor-enhancing activity of connexins. Epigenetic regulation of various genes could explain the differential expression of tumor-suppressor and tumor-enhancer genes in inflammation and cancer onset and progression.

The role of demethylating enzyme TET-2 in IBD and colorectal adenocarcinoma has not been fully described. In fact, TET proteins have mostly been studied in hematological malignancies. TET-1 was characterized as a partner gene to the *Mixed-Lineage Leukemia* gene in acute myeloid leukemia (AML), and the *TET-2* gene was described in a study on the myelodysplastic syndrome[47]. Recent investigations report that frequent point mutations in the *TET-2* gene can lead to the truncation of the resulting protein and loss of enzymatic activity, reflected by reduced global levels of the 5-hmC marks in AML patients[41,48]. However, although mutations in the *TET-1* and *TET-3* genes are rare in hematological malignancies compared to *TET-2*, both still exhibit a tumor-suppressor role: TET-1 in B-cell lymphomas [41] and TET-3, together with TET-2, in murine aggressive myeloid cancer[49]. Mutations and reduced expression of TET proteins were also observed in solid tumors, and decreased translational levels of TETs seem like an important hallmark of different cancers, including cancers of the digestive system[50-52].

In addition to carcinogenesis, a study by Zhang *et al*[19] shows an anti-inflammatory role for TET-2, which, under inflammatory conditions, repressed IL-6 transcription in dendritic cells and macrophages [19]. Moreover, TET-2-deficient bone marrow-derived dendritic cells and macrophages had high transcriptional levels of IL-6 upon LPS challenge. Another study also reported an increase of TET-2 transcriptional levels in colon tissues from patients with IBD[53].The present study examined the expression of Cx43 and TET-2 in an *in vitro* model of colon epithelium, where HT-29 cells were used in their parental state or with upregulated or knocked-out Cx43 in the presence or absence of inflammation (induced by DSS or by the addition of an inflammatory medium). A DSS-induced colitis murine model was used to describe how inflammation modulates the expression of Cx43 and TET-2. Data were then compared to Cx43 and TET-2 expression levels in tissues obtained from patients with ulcerative colitis or sporadic colorectal cancer.

Results from this study indicate that knockout of Cx43 in the HT-29 intestinal cell line leads to disruption of membrane integrity exacerbated by the DSS chemical insult. In Cx43-deficient cells and in mice that were subjected to chemical inhibition of GJs by CBX, loss of GJs was paralleled with increased TET-2 expression, further intensified in the presence of inflammation. In fact, inflammation triggered an upregulation of Cx43 and TET-2 expression in all cell subsets, which is in accordance with the literature [19,47]. An exploratory analysis of human colon samples obtained from ulcerative colitis patients revealed an increase in Cx43 and a decrease in TET-2 protein levels accompanied by the disruption of colon architecture. Though these findings are not aligned with the overall trend implicating TET-2 in intestinal inflammatory conditions, little is known about characteristics of patients whose colon biopsies were examined, including potential pharmacological agents that could lead to TET-2 degradation *via* one of the four pathways reviewed by Cong *et al*[54] in October 2020: A caspase-dependent pathway, calpain1-promoted degradation of TET-2, proteasome-dependent degradation, and p53-facilitated autophagy of TET-2 proteins[54]. Moreover, TET-2 seems to be implicated in both initiation of the inflammatory process by activating innate pro-inflammatory signaling pathways and its resolution by inducing the repression of pro-inflammatory mediators[55]. Therefore, the exact status of TET-2 in the colon of IBD patients remains to be elucidated, in light of multiple factors governing post-transcriptional and post-translational TET-2 regulation. In specimens from sporadic colon adenocarcinoma, both TET-2 and Cx43 proteins were considerably downregulated, underscoring the tumor-suppressor role of Cx43.

In the context of IBD (specifically ulcerative colitis) and colon cancer, we propose that Cx43 upregulation in inflamed colons could attenuate or slow down the onset of malignancy. Therefore, loss of Cx43 in tissues from colon cancer could be attributed to a malignant switch, turning off tumor-suppressor genes and activating tumor-promoting genes. The presence of $CD68^+$ cells (macrophages) was concomitant with loss of TET-2 expression in the colon adenocarcinoma samples. This could be explained by an immune-active phenotype in tumors, with tumor-associated macrophages having little to no TET-2 expression[55]. A 2018 study reported increased levels of TET-2 in T lymphocytes from colorectal tumor tissues, leading to demethylation and activation of FOXP3 and regulation of regulatory T cell (Treg) function[56], further implicating TET-2 in immune-related processes. In particular, TET-2 has been reported to regulate the innate immune response[57,58]. While it serves to activate the inflammatory response, TET-2 has also been implicated in inflammation resolution, where in response to IL-1/RMyD88 signaling, TET-2 downregulates the expression of inflammatory cytokines, such as IL-6 in innate myeloid cells and IL-1β in macrophages by recruiting HDACs for histone deacetylation[19,57]. This property might explain low levels of TET-2 in human ulcerative colitis samples where unresolved inflammation can be attributed to persistent inflammatory cytokines.

TET-2 status and role in digestive cancers remain unclear and variable, depending on the cancer site and grade, but also on possible mutations that could lead to cancer progression and resistance to chemotherapy, as recently reviewed[21].

CONCLUSION

Data presented in this manuscript show that exposure of intestinal cells to inflammation is associated with Cx43 and TET-2 upregulation *in vitro* and *in vivo*. We propose that, as part of its potential anti-inflammatory role and through its demethylating activity, TET-2 might be responsible for promoting the expression of anti-inflammatory genes and for indirectly repressing the expression of pro-inflammatory genes under inflammatory conditions. Similarly, we hypothesize that the demethylating TET-2 enzyme might promote the expression of tumor-suppressor genes (among others, Cx43) in the inflamed colon. Extrapolating from observations made on human colon samples, a malignant switch could happen in chronically inflamed colons. This malignant switch could be associated with downregulation of TET-2 (and potentially other TET enzymes[20,23]) in ulcerative colitis, possibly resulting in the hypermethylation of genes that are relevant in the context of carcinogenesis, such as Cx43. Although we present evidence on the modulation of TET-2 expression and we reiterate the role of Cx43 in intestinal inflammation, further investigation is under way to more solidly explore the mechanism of action behind a potential interplay between Cx43 and TET-2 that might, at least partly and indirectly, bridge chronic inflammation (such as in IBD) and IBD-induced carcinogenesis in the colon.

ARTICLE HIGHLIGHTS

Research background

Patients with inflammatory bowel disease (IBD) have a higher propensity to acquire colorectal cancer. The link between inflammation and cancer has long been established; however, the molecular players in the switch to cancer are still poorly defined.

Research motivation

In previous work, we have demonstrated a potential role for connexin 43 (Cx43) in inflamed intestinal cells. Recognizing the tumor-suppressor role of Cx43 in several cancers, we set out to explore whether the loss of Cx43 is associated with the switch to carcinogenesis. One potential mechanism for downregulating Cx43 expression is through methylation. We hypothesized that ten-eleven translocation-2 (TET-2), a demethylating enzyme, previously described to have a role in inflammation, may be involved in this process.

Research objectives

Using cell culture, a colitis animal model, and archived human tissues, we assessed the expression of both Cx43 and TET-2 in intestinal inflammation. Specific objectives include: (1) Assessment of the expression levels of Cx43 and TET-2 under inflammatory conditions; (2) Assessment of the expression and activity of TET-2 in HT-29 cell lines with up- or down-regulated for Cx43 expression; (3) Reproduction of a colitis mouse model and assessment of Cx43 and TET-2 levels in colons of mice; and (4) Explore Cx43 and TET-2 expression levels in archived biopsies obtained from patients with ulcerative colitis and colon adenocarcinoma.

Research methods

This study employed several modalities to verify the hypothesis, which include intestinal epithelial cell (IEC) line modified for Cx43 expression grown under inflammatory conditions. A dextran sulfate sodium-induced colitis mouse model was reproduced and tissues from different experimental conditions were analyzed. Gene expression profile, protein expression levels, morphology and cellular localization were described. In addition, archived formalin-fixed paraffin-embedded tissues were sectioned and evaluated for Cx43 and TET-2 expression.

Research results

In vitro, TET-2 expression was elevated under inflammatory conditions and even more so in HT-29 cells devoid of Cx43. The barrier function of IECs was breached when Cx43 levels were down-regulated. These results were corroborated in the murine colitis model. In archived biopsies from ulcerative colitis patients, Cx43 expression was upregulated compared to non-inflamed counterparts. In sporadic colon adenocarcinoma sections, both TET-2 and Cx43 expression levels were decreased.

Research conclusions

Under inflammatory conditions, levels of Cx43 and of the demethylating enzyme TET-2 are upregulated. Through demethylation, TET-2 would turn on the expression of several factors involved in inflammation (presumably Cx43 included). When TET-2 levels were diminished in sporadic colon adenocarcinoma, we also observed that Cx43 was downregulated, which may indicate a role of TET-2 in shutting down Cx43 and its tumor-suppressing potential.

Research perspectives

In vitro, manipulation of TET-2 levels in intestinal cells may yield further insight into the mechanism of action. Methylation studies will also be undertaken. The animal model will be expanded to allow for the development of colon carcinoma, and timed evaluation of molecular players will be performed. More stringent criteria will be implemented for prospective tissue collection from non-inflamed subjects, patients with IBD, and with IBD-associated colorectal cancer.

FOOTNOTES

Author contributions: El-Harakeh M, Saliba J, Haidar M, and Sharaf Aldeen K equally contributed to the study; El-Sabban M conceived and designed the study; Hashash JG, Awad MK, Shirinian M, and El-Sabban M provided the material and resources for the experiments; El-Harakeh M, Haidar M, Sharaf Aldeen K, and El Hajjar L performed the experiments; Saliba J and El-Harakeh M analyzed the data and wrote the manuscript; Shirinian M and Hashash JG critically reviewed the manuscript; Saliba J and El-Sabban M revised the manuscript; All authors read and approved the final version of the manuscript.

Institutional review board statement: Archived formaldehyde-fixed paraffin-embedded (FFPE) colon blocks (ulcerative colitis, sporadic colon adenocarcinoma and normal) were obtained from the American University of Beirut Medical Center (AUBMC). All patients' identifiers were kept confidential and all samples were anonymous, hence exempted from ethics committee approval.

Institutional animal care and use committee statement: All procedures involving animals were reviewed and approved by the Institutional Animal Care and Use Committee of the American University of Beirut, No. 18-03-476.

Conflict-of-interest statement: All the authors report no relevant conflicts of interest for this article.

Data sharing statement: Raw data are available upon reasonable request.

ARRIVE guidelines statement: The authors have read the ARRIVE guidelines, and the manuscript was prepared and revised according to the ARRIVE guidelines.

Open-Access: This article is an open-access article that was selected by an in-house editor and fully peer-reviewed by external reviewers. It is distributed in accordance with the Creative Commons Attribution NonCommercial (CC BY-NC 4.0) license, which permits others to distribute, remix, adapt, build upon this work non-commercially, and license their derivative works on different terms, provided the original work is properly cited and the use is non-commercial. See: https://creativecommons.org/Licenses/by-nc/4.0/

Country/Territory of origin: Lebanon

ORCID number: Mohammad El-Harakeh 0000-0003-3014-3937; Jessica Saliba 0000-0002-9117-8773; Kawthar Sharaf Aldeen 0000-0002-9546-104X; May Haidar 0000-0002-4345-0621; Layal El Hajjar 0000-0003-3123-5577; Mireille Kallassy Awad 0000-0003-1489-8686; Jana G Hashash 0000-0001-8305-9742; Margret Shirinian 0000-0003-4666-2758; Marwan El-Sabban 0000-0001-5084-7654.

S-Editor: Fan JR
L-Editor: Filipodia
P-Editor: Cai YX

REFERENCES

1 **Khor B**, Gardet A, Xavier RJ. Genetics and pathogenesis of inflammatory bowel disease. *Nature* 2011; **474**: 307-317 [PMID: 21677747 DOI: 10.1038/nature10209]
2 **Gajendran M**, Loganathan P, Catinella AP, Hashash JG. A comprehensive review and update on Crohn's disease. *Dis Mon* 2018; **64**: 20-57 [PMID: 28826742 DOI: 10.1016/j.disamonth.2017.07.001]
3 **Gajendran M**, Loganathan P, Jimenez G, Catinella AP, Ng N, Umapathy C, Ziade N, Hashash JG. A comprehensive review and update on ulcerative colitis. *Dis Mon* 2019; **65**: 100851 [PMID: 30837080 DOI: 10.1016/j.disamonth.2019.02.004]
4 **Fleming M**, Ravula S, Tatishchev SF, Wang HL. Colorectal carcinoma: Pathologic aspects. *J Gastrointest Oncol* 2012; **3**: 153-173 [PMID: 22943008 DOI: 10.3978/j.issn.2078-6891.2012.030]
5 **Du L**, Kim JJ, Shen J, Chen B, Dai N. KRAS and TP53 mutations in inflammatory bowel disease-associated colorectal cancer: a meta-analysis. *Oncotarget* 2017; **8**: 22175-22186 [PMID: 28077799 DOI: 10.18632/oncotarget.14549]
6 **Beyer EC**, Berthoud VM. Gap junction gene and protein families: Connexins, innexins, and pannexins. *Biochim Biophys Acta Biomembr* 2018; **1860**: 5-8 [PMID: 28559187 DOI: 10.1016/j.bbamem.2017.05.016]
7 **Kazan JM**, El-Saghir J, Saliba J, Shaito A, Jalaleddine N, El-Hajjar L, Al-Ghadban S, Yehia L, Zibara K, El-Sabban M.

Cx43 Expression Correlates with Breast Cancer Metastasis in MDA-MB-231 Cells In Vitro, In a Mouse Xenograft Model and in Human Breast Cancer Tissues. *Cancers (Basel)* 2019; **11** [PMID: 30939738 DOI: 10.3390/cancers11040460]

8 **Kou Y**, Ji L, Wang H, Wang W, Zheng H, Zou J, Liu L, Qi X, Liu Z, Du B, Lu L. Connexin 43 upregulation by dioscin inhibits melanoma progression *via* suppressing malignancy and inducing M1 polarization. *Int J Cancer* 2017; **141**: 1690-1703 [PMID: 28677156 DOI: 10.1002/ijc.30872]

9 **Zhou JZ**, Riquelme MA, Gu S, Kar R, Gao X, Sun L, Jiang JX. Osteocytic connexin hemichannels suppress breast cancer growth and bone metastasis. *Oncogene* 2016; **35**: 5597-5607 [PMID: 27041582 DOI: 10.1038/onc.2016.101]

10 **Willebrords J**, Crespo Yanguas S, Maes M, Decrock E, Wang N, Leybaert L, Kwak BR, Green CR, Cogliati B, Vinken M. Connexins and their channels in inflammation. *Crit Rev Biochem Mol Biol* 2016; **51**: 413-439 [PMID: 27387655 DOI: 10.1080/10409238.2016.1204980]

11 **Wong J**, Chopra J, Chiang LLW, Liu T, Ho J, Wu WKK, Tse G, Wong SH. The Role of Connexins in Gastrointestinal Diseases. *J Mol Biol* 2019; **431**: 643-652 [PMID: 30639409 DOI: 10.1016/j.jmb.2019.01.007]

12 **Al-Ghadban S**, Kaissi S, Homaidan FR, Naim HY, El-Sabban ME. Cross-talk between intestinal epithelial cells and immune cells in inflammatory bowel disease. *Sci Rep* 2016; **6**: 29783 [PMID: 27417573 DOI: 10.1038/srep29783]

13 **Amatullah H**, Jeffrey KL. Epigenome-metabolome-microbiome axis in health and IBD. *Curr Opin Microbiol* 2020; **56**: 97-108 [PMID: 32920333 DOI: 10.1016/j.mib.2020.08.005]

14 **Grosser C**, Wagner N, Grothaus K, Horsthemke B. Altering TET dioxygenase levels within physiological range affects DNA methylation dynamics of HEK293 cells. *Epigenetics* 2015; **10**: 819-833 [PMID: 26186463 DOI: 10.1080/15592294.2015.1073879]

15 **Ryan FJ**, Ahern AM, Fitzgerald RS, Laserna-Mendieta EJ, Power EM, Clooney AG, O'Donoghue KW, McMurdie PJ, Iwai S, Crits-Christoph A, Sheehan D, Moran C, Flemer B, Zomer AL, Fanning A, O'Callaghan J, Walton J, Temko A, Stack W, Jackson L, Joyce SA, Melgar S, DeSantis TZ, Bell JT, Shanahan F, Claesson MJ. Colonic microbiota is associated with inflammation and host epigenomic alterations in inflammatory bowel disease. *Nat Commun* 2020; **11**: 1512 [PMID: 32251296 DOI: 10.1038/s41467-020-15342-5]

16 **Pekow J**, Hernandez K, Meckel K, Deng Z, Haider HI, Khalil A, Zhang C, Talisila N, Siva S, Jasmine F, Li YC, Rubin DT, Hyman N, Bissonnette M, Weber C, Kibriya MG. IBD-associated Colon Cancers Differ in DNA Methylation and Gene Expression Profiles Compared With Sporadic Colon Cancers. *J Crohns Colitis* 2019; **13**: 884-893 [PMID: 30753380 DOI: 10.1093/ecco-jcc/jjz014]

17 **Liu XS**, Wu H, Ji X, Stelzer Y, Wu X, Czauderna S, Shu J, Dadon D, Young RA, Jaenisch R. Editing DNA Methylation in the Mammalian Genome. *Cell* 2016; **167**: 233-247.e17 [PMID: 27662091 DOI: 10.1016/j.cell.2016.08.056]

18 **Wawrzyniak M**, Scharl M. Genetics and epigenetics of inflammatory bowel disease. *Swiss Med Wkly* 2018; **148**: w14671 [PMID: 30378641 DOI: 10.4414/smw.2018.14671]

19 **Zhang Q**, Zhao K, Shen Q, Han Y, Gu Y, Li X, Zhao D, Liu Y, Wang C, Zhang X, Su X, Liu J, Ge W, Levine RL, Li N, Cao X. Tet2 is required to resolve inflammation by recruiting Hdac2 to specifically repress IL-6. *Nature* 2015; **525**: 389-393 [PMID: 26287468 DOI: 10.1038/nature15252]

20 **Rasmussen KD**, Helin K. Role of TET enzymes in DNA methylation, development, and cancer. *Genes Dev* 2016; **30**: 733-750 [PMID: 27036965 DOI: 10.1101/gad.276568.115]

21 **Wang F**, Zhang J, Qi J. Ten-eleven translocation-2 affects the fate of cells and has therapeutic potential in digestive tumors. *Chronic Dis Transl Med* 2019; **5**: 267-272 [PMID: 32055786 DOI: 10.1016/j.cdtm.2019.12.001]

22 **Du C**, Kurabe N, Matsushima Y, Suzuki M, Kahyo T, Ohnishi I, Tanioka F, Tajima S, Goto M, Yamada H, Tao H, Shinmura K, Konno H, Sugimura H. Robust quantitative assessments of cytosine modifications and changes in the expressions of related enzymes in gastric cancer. *Gastric Cancer* 2015; **18**: 516-525 [PMID: 25098926 DOI: 10.1007/s10120-014-0409-4]

23 **Rawluszko-Wieczorek AA**, Siera A, Horbacka K, Horst N, Krokowicz P, Jagodziński PP. Clinical significance of DNA methylation mRNA levels of TET family members in colorectal cancer. *J Cancer Res Clin Oncol* 2015; **141**: 1379-1392 [PMID: 25557833 DOI: 10.1007/s00432-014-1901-2]

24 **Lou H**, Li H, Ho KJ, Cai LL, Huang AS, Shank TR, Verneris MR, Nickerson ML, Dean M, Anderson SK. The Human *TET2* Gene Contains Three Distinct Promoter Regions With Differing Tissue and Developmental Specificities. *Front Cell Dev Biol* 2019; **7**: 99 [PMID: 31231651 DOI: 10.3389/fcell.2019.00099]

25 **Aasen T**, Leithe E, Graham SV, Kameritsch P, Mayán MD, Mesnil M, Pogoda K, Tabernero A. Connexins in cancer: bridging the gap to the clinic. *Oncogene* 2019; **38**: 4429-4451 [PMID: 30814684 DOI: 10.1038/s41388-019-0741-6]

26 **Wang Y**, Huang LH, Xu CX, Xiao J, Zhou L, Cao D, Liu XM, Qi Y. Connexin 32 and 43 promoter methylation in Helicobacter pylori-associated gastric tumorigenesis. *World J Gastroenterol* 2014; **20**: 11770-11779 [PMID: 25206281 DOI: 10.3748/wjg.v20.i33.11770]

27 **Yi ZC**, Wang H, Zhang GY, Xia B. Downregulation of connexin 43 in nasopharyngeal carcinoma cells is related to promoter methylation. *Oral Oncol* 2007; **43**: 898-904 [PMID: 17306607 DOI: 10.1016/j.oraloncology.2006.11.004]

28 **Ferraretto A**, Bottani M, De Luca P, Cornaghi L, Arnaboldi F, Maggioni M, Fiorilli A, Donetti E. Morphofunctional properties of a differentiated Caco2/HT-29 co-culture as an *in vitro* model of human intestinal epithelium. *Biosci Rep* 2018; **38** [PMID: 29540534 DOI: 10.1042/BSR20171497]

29 **Lea T**, Verhoeckx K, Cotter P, López-Expósito I, Kleiveland C, Lea T, Mackie A, Requena T, Swiatecka D, Wichers H. Caco-2 Cell Line. In: The Impact of Food Bioactives on Health: in vitro and ex vivo models [Internet]. Cham (CH): Springer; 2015. Chapter 10 [PMID: 29787057]

30 **Hyun J**, Romero L, Riveron R, Flores C, Kanagavelu S, Chung KD, Alonso A, Sotolongo J, Ruiz J, Manukyan A, Chun S, Singh G, Salas P, Targan SR, Fukata M. Human intestinal epithelial cells express interleukin-10 through Toll-like receptor 4-mediated epithelial-macrophage crosstalk. *J Innate Immun* 2015; **7**: 87-101 [PMID: 25171731 DOI: 10.1159/000365417]

31 **Sáez PJ**, Shoji KF, Aguirre A, Sáez JC. Regulation of hemichannels and gap junction channels by cytokines in antigen-presenting cells. *Mediators Inflamm* 2014; **2014**: 742734 [PMID: 25301274 DOI: 10.1155/2014/742734]

32 **Poenar DP**, Yang G, Wan WK, Feng S. Low-Cost Method and Biochip for Measuring the Trans-Epithelial Electrical Resistance (TEER) of Esophageal Epithelium. *Materials (Basel)* 2020; **13** [PMID: 32443854 DOI: 10.3390/ma13102354]

33 **Yao L**, Xue X, Yu P, Ni Y, Chen F. Evans Blue Dye: A Revisit of Its Applications in Biomedicine. *Contrast Media Mol Imaging* 2018; **2018**: 7628037 [PMID: 29849513 DOI: 10.1155/2018/7628037]

34 **Mizoguchi A**. Animal models of inflammatory bowel disease. *Prog Mol Biol Transl Sci* 2012; **105**: 263-320 [PMID: 22137435 DOI: 10.1016/B978-0-12-394596-9.00009-3]

35 **Dieleman LA**, Ridwan BU, Tennyson GS, Beagley KW, Bucy RP, Elson CO. Dextran sulfate sodium-induced colitis occurs in severe combined immunodeficient mice. *Gastroenterology* 1994; **107**: 1643-1652 [PMID: 7958674 DOI: 10.1016/0016-5085(94)90803-6]

36 **Kitajima S**, Takuma S, Morimoto M. Tissue distribution of dextran sulfate sodium (DSS) in the acute phase of murine DSS-induced colitis. *J Vet Med Sci* 1999; **61**: 67-70 [PMID: 10027168 DOI: 10.1292/jvms.61.67]

37 **Toutounji M**, Wanes D, El-Harakeh M, El-Sabban M, Rizk S, Naim HY. Dextran Sodium Sulfate-Induced Impairment of Protein Trafficking and Alterations in Membrane Composition in Intestinal Caco-2 Cell Line. *Int J Mol Sci* 2020; **21** [PMID: 32326391 DOI: 10.3390/ijms21082726]

38 **Viennois E**, Chen F, Laroui H, Baker MT, Merlin D. Dextran sodium sulfate inhibits the activities of both polymerase and reverse transcriptase: lithium chloride purification, a rapid and efficient technique to purify RNA. *BMC Res Notes* 2013; **6**: 360 [PMID: 24010775 DOI: 10.1186/1756-0500-6-360]

39 **Feng Y**, Li X, Cassady K, Zou Z, Zhang X. TET2 Function in Hematopoietic Malignancies, Immune Regulation, and DNA Repair. *Front Oncol* 2019; **9**: 210 [PMID: 31001476 DOI: 10.3389/fonc.2019.00210]

40 **Ko M**, Huang Y, Jankowska AM, Pape UJ, Tahiliani M, Bandukwala HS, An J, Lamperti ED, Koh KP, Ganetzky R, Liu XS, Aravind L, Agarwal S, Maciejewski JP, Rao A. Impaired hydroxylation of 5-methylcytosine in myeloid cancers with mutant TET2. *Nature* 2010; **468**: 839-843 [PMID: 21057493 DOI: 10.1038/nature09586]

41 **Weissmann S**, Alpermann T, Grossmann V, Kowarsch A, Nadarajah N, Eder C, Dicker F, Fasan A, Haferlach C, Haferlach T, Kern W, Schnittger S, Kohlmann A. Landscape of TET2 mutations in acute myeloid leukemia. *Leukemia* 2012; **26**: 934-942 [PMID: 22116554 DOI: 10.1038/leu.2011.326]

42 **Homaidan FR**, Chakroun, Dbaibo GS, El-Assaad W, El-Sabban ME. IL-1 activates two phospholipid signaling pathways in intestinal epithelial cells. *Inflamm Res* 2001; **50**: 375-381 [PMID: 11506393 DOI: 10.1007/PL00000259]

43 **Homaidan FR**, El-Sabban ME, Chakroun I, El-Sibai M, Dbaibo GS. IL-1 stimulates ceramide accumulation without inducing apoptosis in intestinal epithelial cells. *Mediators Inflamm* 2002; **11**: 39-45 [PMID: 11926594 DOI: 10.1080/09629350210313]

44 **Shilova ON**, Shilov ES, Lieber A, Deyev SM. Disassembling a cancer puzzle: Cell junctions and plasma membrane as targets for anticancer therapy. *J Control Release* 2018; **286**: 125-136 [PMID: 30030181 DOI: 10.1016/j.jconrel.2018.07.030]

45 **Zhang D**, Kaneda M, Nakahama K, Arii S, Morita I. Connexin 43 expression promotes malignancy of HuH7 hepatocellular carcinoma cells *via* the inhibition of cell-cell communication. *Cancer Lett* 2007; **252**: 208-215 [PMID: 17275998 DOI: 10.1016/j.canlet.2006.12.024]

46 **Zhang A**, Hitomi M, Bar-Shain N, Dalimov Z, Ellis L, Velpula KK, Fraizer GC, Gourdie RG, Lathia JD. Connexin 43 expression is associated with increased malignancy in prostate cancer cell lines and functions to promote migration. *Oncotarget* 2015; **6**: 11640-11651 [PMID: 25960544 DOI: 10.18632/oncotarget.3449]

47 **Langemeijer SM**, Kuiper RP, Berends M, Knops R, Aslanyan MG, Massop M, Stevens-Linders E, van Hoogen P, van Kessel AG, Raymakers RA, Kamping EJ, Verhoef GE, Verburgh E, Hagemeijer A, Vandenberghe P, de Witte T, van der Reijden BA, Jansen JH. Acquired mutations in TET2 are common in myelodysplastic syndromes. *Nat Genet* 2009; **41**: 838-842 [PMID: 19483684 DOI: 10.1038/ng.391]

48 **Zhao Z**, Chen L, Dawlaty MM, Pan F, Weeks O, Zhou Y, Cao Z, Shi H, Wang J, Lin L, Chen S, Yuan W, Qin Z, Ni H, Nimer SD, Yang FC, Jaenisch R, Jin P, Xu M. Combined Loss of Tet1 and Tet2 Promotes B Cell, but Not Myeloid Malignancies, in Mice. *Cell Rep* 2015; **13**: 1692-1704 [PMID: 26586431 DOI: 10.1016/j.celrep.2015.10.037]

49 **Zibara K**, Awada Z, Dib L, El-Saghir J, Al-Ghadban S, Ibrik A, El-Zein N, El-Sabban M. Anti-angiogenesis therapy and gap junction inhibition reduce MDA-MB-231 breast cancer cell invasion and metastasis *in vitro* and in vivo. *Sci Rep* 2015; **5**: 12598 [PMID: 26218768 DOI: 10.1038/srep12598]

50 **Yang H**, Liu Y, Bai F, Zhang JY, Ma SH, Liu J, Xu ZD, Zhu HG, Ling ZQ, Ye D, Guan KL, Xiong Y. Tumor development is associated with decrease of TET gene expression and 5-methylcytosine hydroxylation. *Oncogene* 2013; **32**: 663-669 [PMID: 22391558 DOI: 10.1038/onc.2012.67]

51 **Lian CG**, Xu Y, Ceol C, Wu F, Larson A, Dresser K, Xu W, Tan L, Hu Y, Zhan Q, Lee CW, Hu D, Lian BQ, Kleffel S, Yang Y, Neiswender J, Khorasani AJ, Fang R, Lezcano C, Duncan LM, Scolyer RA, Thompson JF, Kakavand H, Houvras Y, Zon LI, Mihm MC Jr, Kaiser UB, Schatton T, Woda BA, Murphy GF, Shi YG. Loss of 5-hydroxymethylcytosine is an epigenetic hallmark of melanoma. *Cell* 2012; **150**: 1135-1146 [PMID: 22980977 DOI: 10.1016/j.cell.2012.07.033]

52 **Liu C**, Liu L, Chen X, Shen J, Shan J, Xu Y, Yang Z, Wu L, Xia F, Bie P, Cui Y, Bian XW, Qian C. Decrease of 5-hydroxymethylcytosine is associated with progression of hepatocellular carcinoma through downregulation of TET1. *PLoS One* 2013; **8**: e62828 [PMID: 23671639 DOI: 10.1371/journal.pone.0062828]

53 **Cong B**, Zhang Q, Cao X. The function and regulation of TET2 in innate immunity and inflammation. *Protein Cell* 2021; **12**: 165-173 [PMID: 33085059 DOI: 10.1007/s13238-020-00796-6]

54 **Dziaman T**, Gackowski D, Guz J, Linowiecka K, Bodnar M, Starczak M, Zarakowska E, Modrzejewska M, Szpila A, Szpotan J, Gawronski M, Labejszo A, Liebert A, Banaszkiewicz Z, Klopocka M, Foksinski M, Marszalek A, Olinski R. Characteristic profiles of DNA epigenetic modifications in colon cancer and its predisposing conditions-benign adenomas and inflammatory bowel disease. *Clin Epigenetics* 2018; **10**: 72 [PMID: 29875879 DOI: 10.1186/s13148-018-0505-0]

55 **Pan W**, Zhu S, Qu K, Meeth K, Cheng J, He K, Ma H, Liao Y, Wen X, Roden C, Tobiasova Z, Wei Z, Zhao J, Liu J, Zheng J, Guo B, Khan SA, Bosenberg M, Flavell RA, Lu J. The DNA Methylcytosine Dioxygenase Tet2 Sustains Immunosuppressive Function of Tumor-Infiltrating Myeloid Cells to Promote Melanoma Progression. *Immunity* 2017; **47**: 284-297.e5 [PMID: 28813659 DOI: 10.1016/j.immuni.2017.07.020]

56 **Ma H**, Gao W, Sun X, Wang W. $STAT_5$ and TET_2 Cooperate to Regulate $FOXP_3$-TSDR Demethylation in CD_4^+ T Cells of Patients with Colorectal Cancer. *J Immunol Res* 2018; **2018**: 6985031 [PMID: 30013992 DOI: 10.1155/2018/6985031]

57 **Cull AH**, Snetsinger B, Buckstein R, Wells RA, Rauh MJ. Tet2 restrains inflammatory gene expression in macrophages. *Exp Hematol* 2017; **55**: 56-70.e13 [PMID: 28826859 DOI: 10.1016/j.exphem.2017.08.001]

58 **Montagner S**, Leoni C, Emming S, Della Chiara G, Balestrieri C, Barozzi I, Piccolo V, Togher S, Ko M, Rao A, Natoli G, Monticelli S. TET2 Regulates Mast Cell Differentiation and Proliferation through Catalytic and Non-catalytic Activities. *Cell Rep* 2016; **15**: 1566-1579 [PMID: 27160912 DOI: 10.1016/j.celrep.2016.04.044]

World Journal of Gastroenterology

Submit a Manuscript: https://www.f6publishing.com

World J Gastroenterol 2022 October 28; 28(40): 5865-5880

DOI: 10.3748/wjg.v28.i40.5865

ISSN 1007-9327 (print) ISSN 2219-2840 (online)

ORIGINAL ARTICLE

Basic Study

Curcumin alleviates experimental colitis *via* a potential mechanism involving memory B cells and Bcl-6-Syk-BLNK signaling

Si-Yi Wei, Tian-Tian Wu, Jia-Qi Huang, Zeng-Ping Kang, Meng-Xue Wang, You-Bao Zhong, Wei Ge, Bu-Gao Zhou, Hai-Mei Zhao, Hai-Yan Wang, Duan-Yong Liu

Specialty type: Pharmacology and pharmacy

Provenance and peer review: Unsolicited article; Externally peer reviewed.

Peer-review model: Single blind

Peer-review report's scientific quality classification

Grade A (Excellent): 0
Grade B (Very good): B, B, B
Grade C (Good): 0
Grade D (Fair): 0
Grade E (Poor): 0

P-Reviewer: Di Leo A, Italy; Losurdo G, Italy; Zhao G, China

Received: July 25, 2022
Peer-review started: July 25, 2022
First decision: August 19, 2022
Revised: August 20, 2022
Accepted: October 13, 2022
Article in press: October 13, 2022
Published online: October 28, 2022

Si-Yi Wei, Tian-Tian Wu, Jia-Qi Huang, Zeng-Ping Kang, Meng-Xue Wang, Department of Postgraduate, Jiangxi University of Chinese Medicine, Nanchang 330004, Jiangxi Province, China

You-Bao Zhong, Laboratory Animal Research Center for Science and Technology, Jiangxi University of Chinese Medicine, Nanchang 330004, Jiangxi Province, China

Wei Ge, Affiliated Hospital, Jiangxi University of Chinese Medicine, Nanchang 330004, Jiangxi Province, China

Bu-Gao Zhou, Hai-Mei Zhao, Hai-Yan Wang, Duan-Yong Liu, Formula-Pattern Research Center, Jiangxi University of Chinese Medicine, Nanchang 330004, Jiangxi Province, China

Corresponding author: Duan-Yong Liu, PhD, Director, Full Professor, Professor, Formula-Pattern Research Center, Jiangxi University of Chinese Medicine, No. 1688 Meiling Road, Nanchang 330004, Jiangxi Province, China. liuduanyong@163.com

Abstract

BACKGROUND

Immune dysfunction is the crucial cause in the pathogenesis of inflammatory bowel disease (IBD), which is mainly related to lymphocytes (T or B cells, including memory B cells), mast cells, activated neutrophils, and macrophages. As the precursor of B cells, the activation of memory B cells can trigger and differentiate B cells to produce a giant variety of inducible B cells and tolerant B cells, whose dysfunction can easily lead to autoimmune diseases, including IBD.

AIM

To investigate whether or not curcumin (Cur) can alleviate experimental colitis by regulating memory B cells and Bcl-6-Syk-BLNK signaling.

METHODS

Colitis was induced in mice with a dextran sulphate sodium (DSS) solution in drinking water. Colitis mice were given Cur (100 mg/kg/d) orally for 14 consecutive days. The colonic weight, colonic length, intestinal weight index, occult blood scores, and histological scores of mice were examined to evaluate the curative effect. The levels of memory B cells in peripheral blood of mice were measured by flow cytometry, and IL-1β, IL-6, IL-10, IL-7A, and TNF-α expression

in colonic tissue homogenates were analyzed by enzyme-linked immunosorbent assay. Western blot was used to measure the expression of Bcl-6, BLNK, Syk, and other signaling pathway related proteins.

RESULTS

After Cur treatment for 14 d, the body weight, colonic weight, colonic length, colonic weight index, and colonic pathological injury of mice with colitis were ameliorated. The secretion of IL-1β, IL-6, TNF-α, and IL-7A was statistically decreased, while the IL-35 and IL-10 levels were considerably increased. Activation of memory B cell subsets in colitis mice was confirmed by a remarkable reduction in the expression of IgM, IgG, IgA, FCRL5, CD103, FasL, PD-1, CD38, and CXCR3 on the surface of $CD19^+CD27^+$ B cells, while the number of $CD19^+CD27^+$ IL-10^+ and $CD19^+CD27^+$ Tim-3^+ B cells increased significantly. In addition, Cur significantly inhibited the protein levels of Syk, p-Syk, Bcl-6, and CIN85, and increased BLNK and p-BLNK expression in colitis mice.

CONCLUSION

Cur could effectively alleviate DSS-induced colitis in mice by regulating memory B cells and the Bcl-6-Syk-BLNK signaling pathway.

Key Words: Curcumin; Experimental colitis; Memory B cell; Bcl-6; BLNK

©The Author(s) 2022. Published by Baishideng Publishing Group Inc. All rights reserved.

Core Tip: As the precursor of B cells, the activation of memory B cells can trigger the activation of B cells, thus producing numerous inducible B cells and tolerant B cells, whose dysfunction can easily result in inflammatory bowel disease (IBD). Also, the disorder of humoral immune function mediated by memory B cells has a critical position in the pathogenesis of IBD. As an immune suppressant, curcumin (Cur) has a therapeutic role in treating many immune diseases, such as IBD and rheumatoid arthritis. Meanwhile, it has proven efficacy in experimental colitis mice and patients with ulcerative colitis (UC), while the disturbances in memory B cells have been observed in IBD. However, few studies have explored whether Cur treatment of colitis is closely related to memory B cells. In the present research, our results indicated that Cur effectively alleviated DSS-induced UC in mice *via* a potential mechanism involving memory B cells and the Bcl-6-Syk-BLNK signaling pathway.

Citation: Wei SY, Wu TT, Huang JQ, Kang ZP, Wang MX, Zhong YB, Ge W, Zhou BG, Zhao HM, Wang HY, Liu DY. Curcumin alleviates experimental colitis *via* a potential mechanism involving memory B cells and Bcl-6-Syk-BLNK signaling. *World J Gastroenterol* 2022; 28(40): 5865-5880
URL: https://www.wjgnet.com/1007-9327/full/v28/i40/5865.htm
DOI: https://dx.doi.org/10.3748/wjg.v28.i40.5865

INTRODUCTION

Curcuma longa L, also named turmeric, is a perennial herb pertaining to the genus Curcuma in the *Zingiberaceae* of the *Scitamineae,* native to China, Indonesia, and India. According to the existing literature, *Curcuma longa L* can promote Qi, break blood stasis, facilitate menstruation, and relieve pain [1]. The bioactive natural polyphenols extracted from the rhizome of *Zingiberaceae* are called curcumin (Cur) [1,7-bis(4-hydroxy-3-methoxyphenyl)- 1,6-heptadiene-3,5-dione]. They are also known as diferuloylmethane, and their molecular formula $C_{21}H_{20}O_6$ accounts for 75% to 80% of curcumin compounds[2] (a structure is shown in Figure 1A)[3]. According to recent carefully designed clinical studies, with an excellent safety profile, Cur has the potential effect of prevention and/or management of various diseases including inflammatory bowel disease, dysentery, chronic enteritis, gastrointestinal syndrome, and so on, due to its anti-oxidant, anti-apoptotic, and anti-inflammatory properties[4]. In addition, many preclinical studies have indicated that Cur has perfect anti-cancer properties to inhibit carcinogenesis and the proliferation of various cancer cells[5], including prostate, oral epithelial leukemia, hepatic, breast, and colon cancers in human and animals, and the probable mechanisms are closely related to modulating the activation of a variety of cellular signals as apoptosis and angiogenesis [6].

As a chronic nonspecific inflammatory disorder, inflammatory bowel disease (IBD), classified into ulcerative colitis (UC) and Crohn's disease (CD), is characterized by recurrent abdominal pain, diarrhea, anemia, bleeding, and weight loss. However, the pathogenesis of IBD is still unclear, and is closely

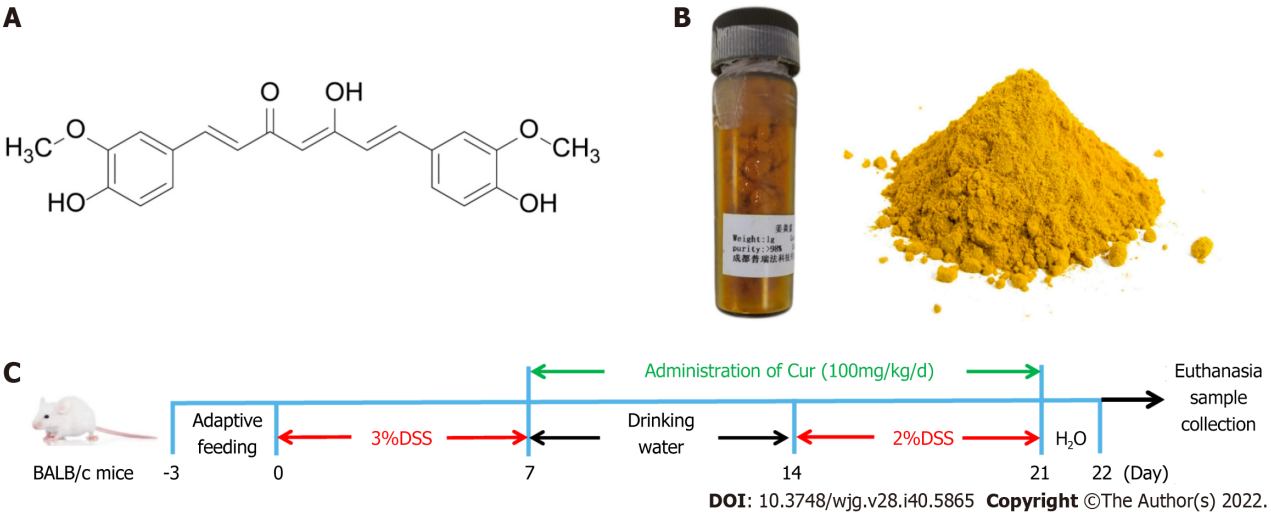


Figure 1 Drugs and protocols used in the study. A: Molecular structural formula of curcumin (Cur); B: Cur used in the experiment; C: Colitis induction and Cur administration. The experiment lasted for 22 d, including 3 d of adaptive feeding, 0-7 d of treatment with 3% DSS treatment with drinking water, and 7 d of free drinking water. Animals were divided into four groups: Control (n = 10), DSS (n = 10), DSS + Cur (100 mg/kg/d, n = 10), and Ctrl + Cur (100 mg/kg/d, n = 10) groups.

associated with heredity, environment, infection, immunity, and so on[7]. Among these, immune system dysfunction has been regard as the main cause of IBD, which is mainly involving abnormal lymphocytes (including T and B cells, including memory B cells), macrophages, mast cells, and activated neutrophils[8]. As a precursor to B cells, the activation of memory B cells can trigger the activation of B cells, thus producing numerous inducible B cells and tolerant B cells, whose dysfunction predisposes to autoimmune diseases, including IBD[9]. Pararasa *et al*[10] reported a decrease in $CD27^+IgD^-$ memory B cells in the blood of patients with IBD, but a concomitant increase in $CD27^-IgD^-$ memory B cells in gut-associated lymphoid tissue, which suggests that the disorder of humoral immune function mediated by memory B cells has a very important role in the pathogenesis of IBD.

Many previous studies have demonstrated that Cur can be used to effectively treat UC patients and animals. An endoscopic study revealed that NCB-02 enema (containing 140 mg Cur) used once per day for 8 wk could ameliorate the disease symptoms in patients with UC[11]. In an animal study, Cur administration effectively alleviated the colonic mucosal inflammation, restored colonic length, and reduced colonic weight and colonic damage[10]. Potential mechanisms of Cur for treating UC are diverse, including regulating immune function (such as regulating the function and level of T cells, regulatory T cells, memory T cells, macrophages, and dendritic cells), inhibiting the secretion of IL-2, IL-6, IL-12, IL-17, and TNF-α[12], downregulating the expression of costimulatory molecules[13], inhibiting the chemotaxis of chemokines and neutrophils, and inducing antioxidant effect[14]. Cur may induce apoptosis in colorectal cancer as it induces reactive oxygen species production, suppressing NF-κB signaling activation and cyclooxygenase-2 expression, activating caspase 3 and c-Jun N-terminal kinases (JNK), and inducing the release of cytochrome C. It is known that Cur can promote the activation of caspase 3, caspase 8, caspase 9, Bax, and poly (ADP-ribose) polymerase (PARP) to induce apoptosis in HCT-116 colon cancer cells[15]. Furthermore, it also exerts its effect on other autoimmune diseases by effectively regulating memory B cells. Elham and colleagues[16] found that Cur achieved effective results for autoimmune diseases such as RA and systemic lupus erythematosus (SLE) by targeting B lymphocyte stimulating factor (BLYS), which is an important cytokine for memory B cell proliferation. However, it is unclear whether Cur exerts a therapeutic effect on IBD by regulating the subsets or function of memory B cells. Therefore, in this study, DSS-induced colitis model, a classic animal model replicating human UC, was used to evaluate and explore the mechanism and therapeutic effect of Cur on IBD. Flow cytometry and other experiments were performed to explore the possible mechanisms and the changes in memory B cell subsets after Cur treatment.

MATERIALS AND METHODS

Mice

BALB/c male mice, aged 8-9 wk and weighing 20-22 g, were purchased from the Hunan Silaike Jingda Experimental Animal Co. Ltd. (Changsha, China; Animal Certificate No. SCXK 2016-0002). Mice were provided with standard food and water *ad libitum*, and lived under specific pathogen-free (SPF) conditions at the temperature of 23 °C ± 2 °C and relative humidity of 55% ± 10% with alternating light/darkness for 12 h. They were acclimatized for 3 d prior to the start of the experiment. All animal

experiments were conducted and performed in line with the regulations and guidelines of the Jiangxi University of Chinese Medicine Animal Care and Use Committee and the AAALAC and the IACUC (Permit No. JZLLSC2021-196).

All experimental mice were randomly divided into the following four groups: Control group, in which mice were fed normal food without DSS or drug treatment; Control + Cur group, in which normal mice were given Cur treatment; DSS group, in which mice with DSS-induced colitis were administrated with Cur; DSS + Cur group, in which mice with DSS-induced colitis were treated with Cur.

DSS-induced experimental colitis

As previously described, mice with colitis were freely given a 3% (w/v) solution of DSS (Batch No. 160110) in drinking water for 7 d (Figure 1C), then with sterile drinking water for 7 d, and finally with 2% (w/v) DSS for 7 d. Meanwhile, mice in the control group were given tap water. Cur was provided by Chengdu Purifa Technology Development Co., LTD (Chengdu, China; Batch No. PRF10052344, purity > 98%), as shown in Figure 1B. In order to better dissolve the drug, Cur was dissolved in 1.5% sodium carboxymethylcellulose. According to our previous study[17], mice in the DSS + Cur group and Control + Cur group were administrated with Cur (100 mg/kg/d) by gavage for 14 consecutive days, while mice in the Control and DSS groups were administrated with an equal volume of saline starting from day 8. The mice were weighed daily to evaluate body weight changes, and their fecal character, stool bleeding, and live state were monitored[18].

Histological evaluation

After the last administration, the mice were fasted for 12 h. All mice were weighed before anesthesia with sodium pentobarbital (20 mg/kg *i.p.*). After euthanasia, the whole colons were rapidly separated on the ice box, and their length and weight were measured to calculate the colon weight index (CWI) as [colon weight/body weight] × 100%, and the colon length index (CLI) as (colon weight/colon length) × 100%. The distal colon tissue was fixed in 4% paraformaldehyde for 72 h. After embedding in paraffin to cut 4 μm thick sections, the sections were dehydrated in an ethanol gradient series and stained with hematoxylin-eosin for histopathological analysis. Finally, the slices were sealed with neutral gum. And then the colonic pathological changes were observed and double-blindly scored by two pathologists under a microscope (Leica, Wetzlar, Germany, Product model: DM2500). According to the previous standards, a composite score was computed and totalized with inflammatory cell infiltration (scores 0-3), mucosal damage (scores 0-3), crypt damage (scores 0-4), and regeneration (scores 0-4)[19].

Flow cytometry

In order to isolate peripheral lymphocytes, 500 μL of peripheral blood from each mouse was collected and treated with 1 mL of lysing buffer (BD Biosciences, Franklin Lakes, NJ, United States) and incubated for 15 min in the darkness to remove red blood cells. The cell suspension was combined with an Fcγ receptor-blocking mAb (CD16/32; BioLegend, San Diego, CA, United States) for 15 min at 4 °C. Later on, the cells were detected for surface antigens by labelling with BV510 rat anti-mouse CD19 (Lot No. BD562956), AF488 rat anti-mouse CD27 (Lot No. BD124222), PE-A rat anti-mouse IgM (Lot No. BD553409), BV421 rat anti-mouse IgG (Lot No. BD742475), APC rat anti-mouse IL-10 (Lot No. BD505010), BV421 rat anti-mouse IgA (Lot No. BD743293), APC rat anti-mouse FCRL5 (Lot No. BD340305), PE-A rat anti-mouse CD103 (Lot No. BD562772), BV421 rat anti-mouse FasL (Lot No. BD740054), APC rat anti-mouse PD-1 (Lot No. BD562671), BV421 rat anti-mouse CXCR3 (Lot No. BD126529), and PE-A rat anti-mouse Tim-3 (Lot No. BD119704), which were purchased from BD Bioscience (San Jose, CA, United States). Finally, the single-cell suspensions were analyzed with a FACS Canto II flow cytometer (BD Biosciences, Franklin Lakes, NJ, United States). Gates were set for the quadrant markers based on negative populations and isotype controls. FlowJo VX software (TreeStar, San Carlos, CA, United States) was used to analyze all data to differentiate the memory B cell subgroups.

Enzyme-linked immunosorbent assay (ELISA)

One hundred micrograms of mouse colon tissue was homogenized by adding 1000 μL of RIPA lysis buffer (Cell Signaling Technology, Danvers, MA, United States). The samples were incubated at 4 °C for 1 h, ultrasonically homogenized, and centrifuged at 13000 rpm for 10 min, and the supernatant was taken to obtain colonic tissue homogenate. The total protein in colonic tissue homogenate was quantified with a total protein detection kit (Aidlab Biotechnologies Co., Ltd., Beijing, China; Lot No. PP0102). According to the manufacturer's instructions, commercial ELISA kits (Thermo Fisher Scientific, Waltham, MA, United States) were used to detect the secretion of IL-1β (Lot No. BMS6002TEN), IL-6 (Lot No. BMS603-2), IL-10 (Lot No. 88-7105-88), IL-35 (Lot No. BMS616), IL-17A (Lot No. BMS6001), and TNF-α (Lot No. BMS607-3).

Western blot analysis

Colon tissue homogenate was prepared and protein concentration determination was performed

according to the above methods. First, equal amounts of colonic mucosa protein were resolved by polyacrylamid gel electrophoresis and transferred onto PVDF membranes, which were then blocked with 3% bovine serum albumin (BSA) solution for 1 h at room temperature and then incubated with the following primary antibodies overnight at 4 °C: BLNK (Abcam, ab32418, 1:500), p-BLNK (Abcam, ab174837, 1:1000), Syk (Abcam, ab40781, 1:1000), p-Syk (Abcam, ab300410, 1:1000), CIN85 (1:1000), Bcl-6 (Abcam, ab19011, 1:1000), and anti-GAPDH (Abcam, ab181602, 1:1000) antibodies. Next, the corresponding HRP-coupled secondary antibody (Abcam, ab205718, 1:5000) was added and incubated for 2 h at room temperature, and the ECL hypersensitive solution (Thermo, Rockford, IL, United States) was used to visualize the protein blotting. Photographs were taken by using the Highly Sensitive Chemiluminescence Imaging system (UVP ChemStudio 515; Analytik Jena, Jena, Germany). Image-Pro Plus 6.0 software (Media Cybernetic, Bethesda, MD, United States) was used to quantify the images, and the gray value of the band and the ratio to that of the internal reference GAPDH was used for statistical analysis.

Statistical analysis

GraphPad Prism 7.0 software (San Diego, CA, United States) was used to analyze the difference between groups by performing independent samples *t*-test, one-way analysis of variance, least-significant difference test, and Turkey test for multiple comparisons. All data are presented as the mean ± SE. $P < 0.05$ was considered statistically significant.

RESULTS

Cur alleviates DSS-induced colitis

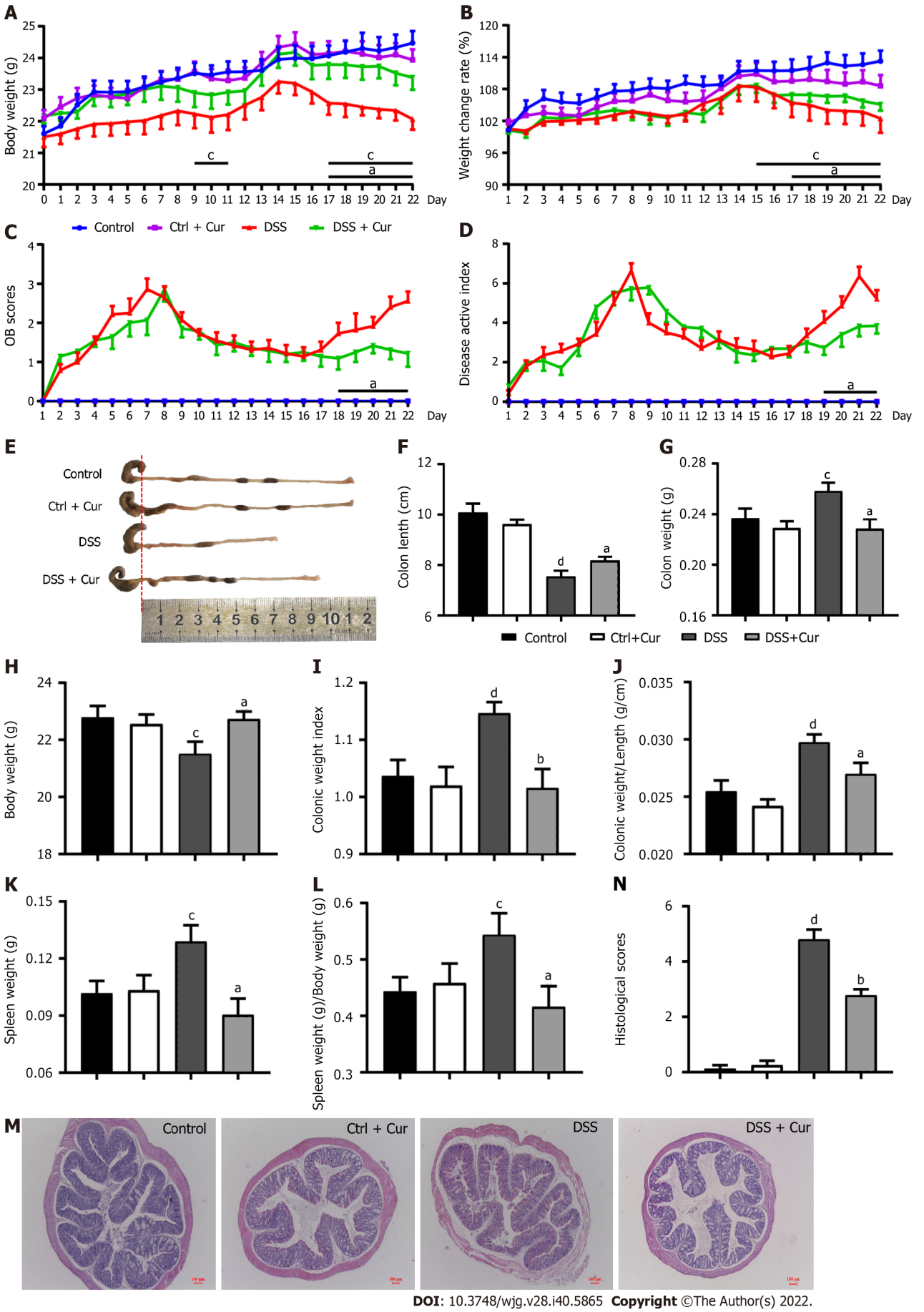
Many studies have shown that mice with DSS-induced colitis may present diarrhea, abdominal pain, bloody stool, weight loss, shortened colon length, increased colon weight, and other symptoms[20]. Under the microscope, altered colonic gland structure, a decrease in the number of goblet cells, massive infiltration of inflammatory cells in the mucosa and submucosa, and obvious erosive ulcer in DSS-induced colitis can be observed[21]. In our pilot study, DSS-induced colitis mice exhibited significant weight loss from day 4 to day 21 of the experiment (Figure 2A), and the changes in body weight (Figure 2B) were significantly lower in contrast with those of the Control group. From days 1 to 22, the occult blood (OB) test score (Figure 2C) gradually started to be different from that of the Control group, while disease activity index (DAI) scores (Figure 2D), which were significantly higher than those of the Control group, exhibited a similar trend to OB scores. In addition, the colonic weight (Figure 2G), index of colon length (Figure 2I), index of colonic weight (Figure 2J), spleen weight (Figure 2K), and the spleen weight index (Figure 2L) of mice in the DSS group statistically increased, whereas the body weight in the last day (Figure 2H) and colonic length (Figure 2E and F) decreased significantly. Meanwhile, the histopathological analysis (Figure 2M) showed that the colonic mucosa of mice was intact in the control group, with no obvious ulceration or inflammatory cell infiltration, neat arrangement of cup-shaped cells, and no congestion or edema, while the colitis mice showed exudation of the colonic mucosal epithelium, changes in crypt structure, disordered arrangement, local ulcer formation, hyperemia and edema in the colon mucosa, and infiltration of inflammatory cells in the lamina propria and submucosa, and the pathological injury scores were significantly increased (Figure 2N), which was consistent with our previous study. The above findings indicated that the chronic colitis model has been successfully constructed.

After Cur gavage administration, significant changes in body weight (Figure 2A), weight change rate (Figure 2B), OB scores (Figure 2C), and DAI scores (Figure 2D) were effectively reversed in colitis mice. Also, colon weight (Figure 2G), colon mass per unit length (Figure 2J), index of colonic weight (Figure 2I), spleen weight (Figure 2K), and spleen weight index (Figure 2L) were significantly decreased when compared with those in the DSS group, while the body weight in the last day (Figure 2H) and colonic length (Figure 2E and F) were obviously higher in the DSS + Cur group than in the DSS group. Meanwhile, ulceration and inflammatory infiltration in the colitis mice treated with Cur were distinctly improved (Figure 2M), and the pathological injury scores (Figure 2N) were observably decreased compared to those of colitis mice without treatment. Moreover, the above data were not evidently different between the Control and Control + Cur groups. Therefore, these data suggest that Cur can effectively alleviate DSS-induced colonic injury.

Cur regulates inflammatory cytokine expression

UC is a form of IBD characterized by rising levels of pro-inflammatory factors and declining levels of anti-inflammatory factors[22]. Disruption of the balance between pro-inflammatory and anti-inflammatory factors is one of the important characteristics of IBD[23].

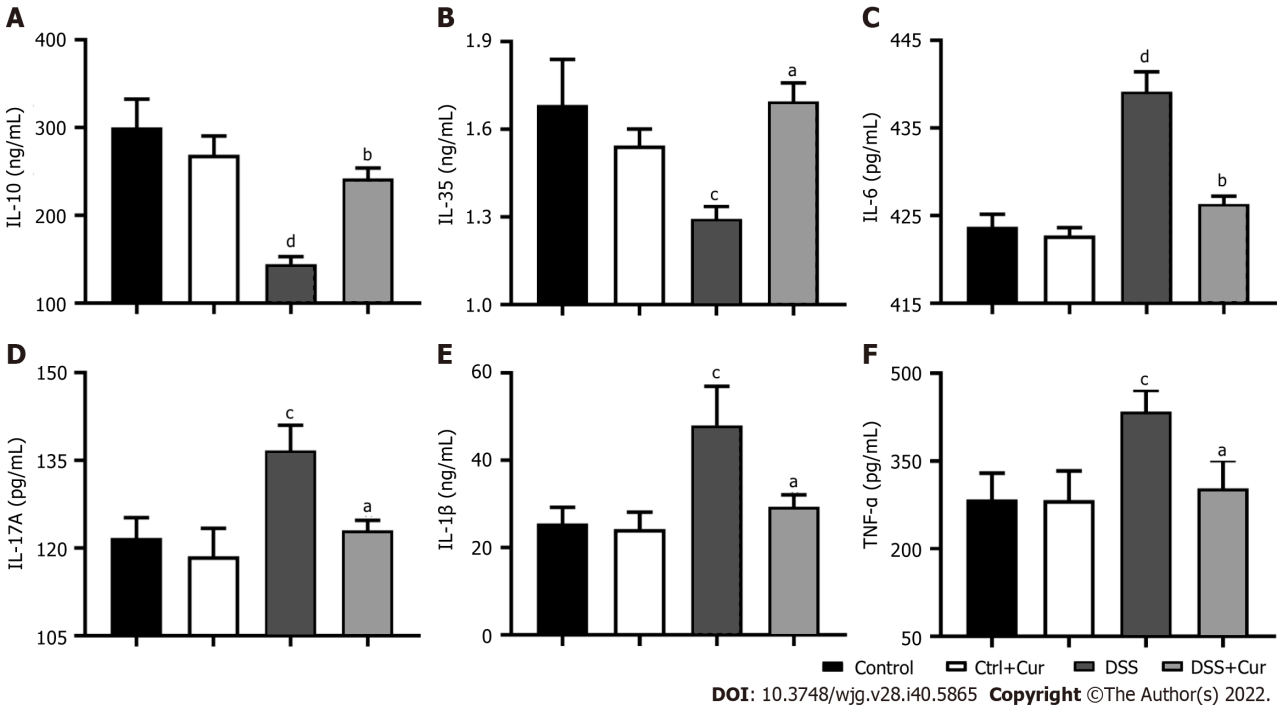
In our experiment, we found that the levels of IL-6 (Figure 3C), IL-17A (Figure 3D), IL-1β (Figure 3E), and TNF-α (Figure 3F) were remarkably increased in the DSS group compared to the Control group, while the IL-10 (Figure 3A) and IL-35 levels (Figure 3B) in the DSS group were dramatically decreased, suggesting that the imbalance of pro-inflammatory and anti-inflammatory factors was one of the



DOI: 10.3748/wjg.v28.i40.5865 **Copyright** ©The Author(s) 2022.

Figure 2 Therapeutic evaluation of curcumin on DSS-induced experimental colitis. A: Body weight of mice from days 0-22; B: Weight change of rate

in mice from days 1-22; C: OB scores of mice in the four groups from days 1-22; D: DAI scores of mice in the four groups from days 1-22; E: Gross changes in colonic length; F: Colonic length of mice on day 22 in the four groups; G: Colonic weight; H: Body weight; I: Colonic weight index; J: Colonic weight/colonic length; K: Spleen weight; L: Spleen weight/body weight; M: Histological appearance of colons from individual groups of mice (hematoxylin and eosin staining, magnification 50 ×, scale bar = 100 μm); N: Pathological injury score. Data are presented as the mean ± SE (n = 8-10). $^{a}P < 0.05$, $^{b}P < 0.01$ *vs* Control group; $^{c}P < 0.05$, $^{d}P < 0.01$ *vs* DSS group.



DOI: 10.3748/wjg.v28.i40.5865 **Copyright** ©The Author(s) 2022.

Figure 3 Curcumin effectively regulates inflammatory cytokine expression. A: Concentration of IL-10 in colonic tissue; B: Concentration of IL-35 in colonic tissue; C: Concentration of IL-6 in colonic tissue; D: Concentration of IL-17A in colonic tissue; E: Concentration of IL-1β in colonic tissue; F: Concentration of TNF-α in colonic tissue. Data are presented as the mean ± SE (n = 8-10). $^{a}P < 0.05$, $^{b}P < 0.01$ *vs* Control group; $^{c}P < 0.05$, $^{d}P < 0.01$ *vs* DSS group.

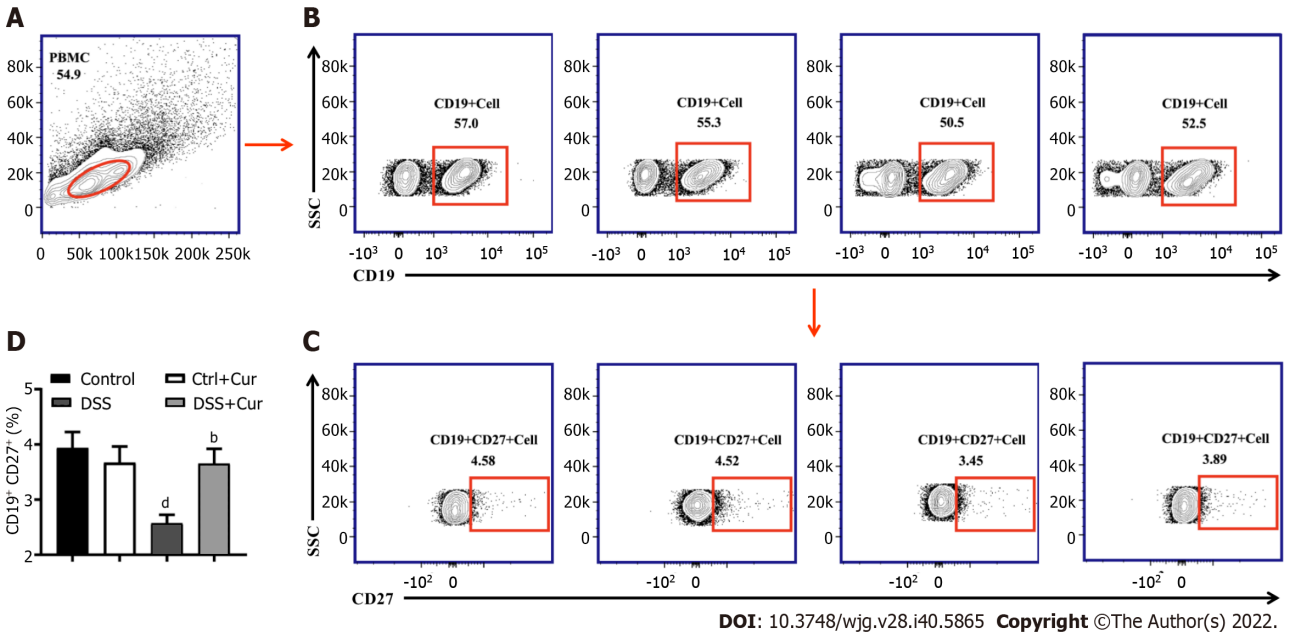
important characters in DSS-induced colitis. More importantly, the IL-6 (Figure 3C), IL-17A (Figure 3D), IL-1β (Figure 3E), and TNF-α (Figure 3F) expression was significantly downregulated, while IL-10 (Figure 3A) and IL-35 (Figure 3B) expression was observably upregulated in colitis mice after Cur treatment. Altogether, Cur could effectively decrease IL-1β, IL-6, IL-17A and TNF-α production and increase IL-10 level, thus reestablishing the equilibrium between anti-inflammatory and pro-inflammatory factors in colitis.

Cur regulates memory B cell subsets

In the humoral immune response, there are two layers of memory cells, namely, long-lived B memory cells and B effector cells (plasma cells). The production of long-lived cells depends on the antigenic activation of B cells in the presence of T helper cells to induce germinal centers[24]. When the body comes in second contact with an antigen, memory B cells are quickly activated, differentiate into new tolerant or inducible plasma cells, secrete high-quality antibodies, and produce more efficient, faster, and more specific humoral immunity[9]. The tolerant type generally expresses factors such as IL-10 and TIM-3, while the induced type usually expresses molecules such as IgG, IgM, IgA, PD-1, CD38, CXCR3, FCRL5, CD103, and FasL, thus having opposite roles in the process of disease development[25]. Their balance determines the development, genesis, and development of memory B cells, while their dysfunction is one of the pathogenesis of IBD.

Recent studies have revealed that CD27 is expressed at higher levels in memory B cells than in plasma blasts and can be used as a biological biomarker of memory B cells. The CD19-positive cells were selected as the gate of B cells. Memory B cells ($CD19^+CD27^+$) could be marked and separated according to the expression of CD27 and CD19, which could then be divided into many subgroups in accordance with the expression of different cytokines on the surface of memory B cells[26,27].

In this study, compared with mice in the Control group, the level of $CD19^+CD27^+$ memory B cells in peripheral blood of colitis mice was significantly decreased (Figure 4A-D), the percentages of $CD19^+CD27^+IgM^+$ (Figure 5A and B), $CD19^+CD27^+IgG^+$ (Figure 5C and D), and CD19 + $CD27^+IgA^+$ (Figure 5E and F) cells were obviously increased, and the percentages of $CD19^+CD27^+FCRL5^+$ (Figure 6A and B),



DOI: 10.3748/wjg.v28.i40.5865 **Copyright** ©The Author(s) 2022.

Figure 4 Curcumin regulates differentiation of memory B cells in DSS-induced ulcerative colitis mice. A: Representative flow cytometry profile of peripheral blood mononuclear cells (PBMC); B: Representative flow cytometry profile of CD19$^+$ cells in peripheral blood; C: Representative flow cytometry profile of CD19$^+$ CD27$^+$ cells in peripheral blood; D: Bar chart of CD19$^+$ CD2$^+$ memory B cells. Data are presented as the mean ± SE (n = 8-10). $^aP < 0.05$, $^bP < 0.01$ *vs* Control group; $^cP < 0.05$, $^dP < 0.01$ *vs* DSS group.

CD19$^+$ CD27$^+$ CD103$^+$ (Figure 6C and D), CD19$^+$ CD27$^+$ FasL$^+$ (Figure 6G and H), CD19$^+$ CD27$^+$ PD-1$^+$ (Figure 7A and B), CD19$^+$ CD27$^+$ CD38$^+$ (Figure 7C and D), and CD19$^+$ CD27$^+$ CXCR3$^+$ (Figure 7E and F) cells were significantly increased. These percentages were significantly decreased after DSS-induced colitis mice were treated with Cur for 14 d. Meanwhile, the percentages of CD19$^+$ CD27$^+$ IL-10$^+$ (Figure 6E and F) and CD19$^+$ CD27$^+$ Tim-3$^+$ (Figure 7G and H) cells were remarkably decreased in mice of the DSS group, whereas the percentages of CD19$^+$ CD27$^+$ Tim-3$^+$ and CD19$^+$ CD27$^+$ IL-10$^+$ cells were markedly increased after experimental colitis mice were treated with Cur. These results suggested that Cur could effectively regulate memory B cell subsets in mice with colitis.

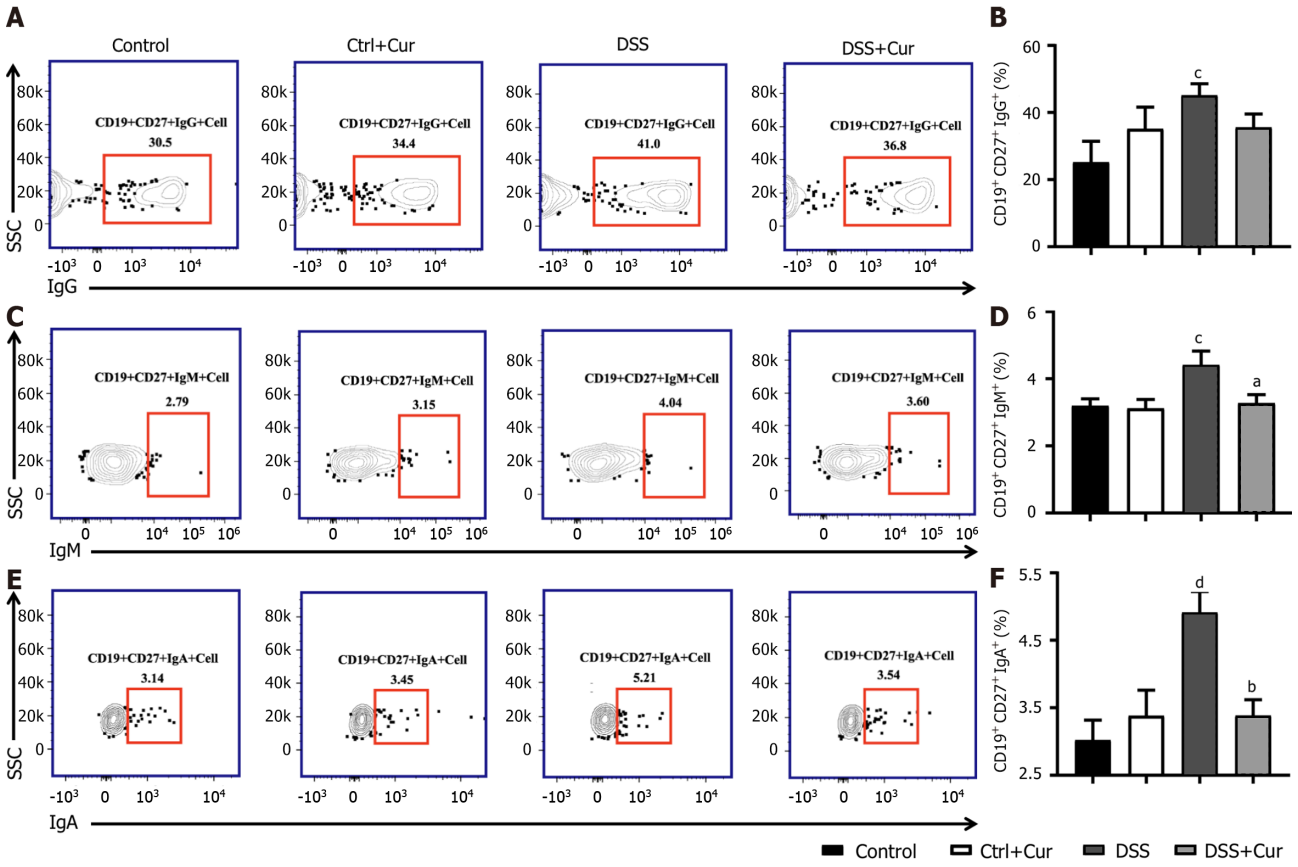
Cur regulates the activation of the Bcl-6-Syk-BLNK signaling pathway

Next, we used Western blot analysis to explore the effect of Cur on the regulation of memory B-cell-related signaling pathways in mice with colitis. The Bcl-6-Syk-BLNK signaling pathway is a crucial signaling pathway involved in the activation, differentiation, proliferation, and functional display of immune cells, including B cells and memory B cells. In our experiments, the expression levels of Bcl-6 (Figure 8A and B), CIN85 (Figure 8A and E), Syk (Figure 8A and F), and p-Syk (Figure 8A and G) were higher in the DSS group than in the Control group. After 14 d of Cur treatment, Bcl-6, CIN85, Syk, and p-Syk expression in the colonic tissues of colitis mice was significantly inhibited. In addition, the expression levels of BLNK (Figure 8A and C) and p-BLNK (Figure 8A and D) were obviously lower in the DSS group than in the Control group, and the expression levels of BLNK and p-BLNK in the treatment group were evidently increased compared with the DSS group. Thus, these results suggested that Cur effectively regulates the activation of the Bcl-6-Syk-BLNK signaling pathway in colitic mice.

DISCUSSION

The incidence of UC has been gradually increasing worldwide, especially in adults between 30 and 40 years old. Patients with UC have mucosal inflammation, which starts in the rectum but continues into the proximal colon, usually presenting with bloody stool. Its pathogenesis is multifactorial, involving destroyed epithelial barrier, dysregulated immune responses, genetic predisposition, and imbalance of the gut microbiota. The dysfunction of immune cells and the destruction of immune homeostasis are deemed as the direct causes of UC[28,29].

B cells have an important role in adaptive immunity, and can differentiate into plasma cells and participate in inflammatory responses by producing a large number of antibodies and suppressing immune responses by releasing anti-inflammatory cytokines[30]. Previous studies on the role of B cells in immune diseases have indicated that the disruption of B cell subsets was a common characteristic in various autoimmune diseases. The variations in B cell frequency, abnormal molecular expression, key



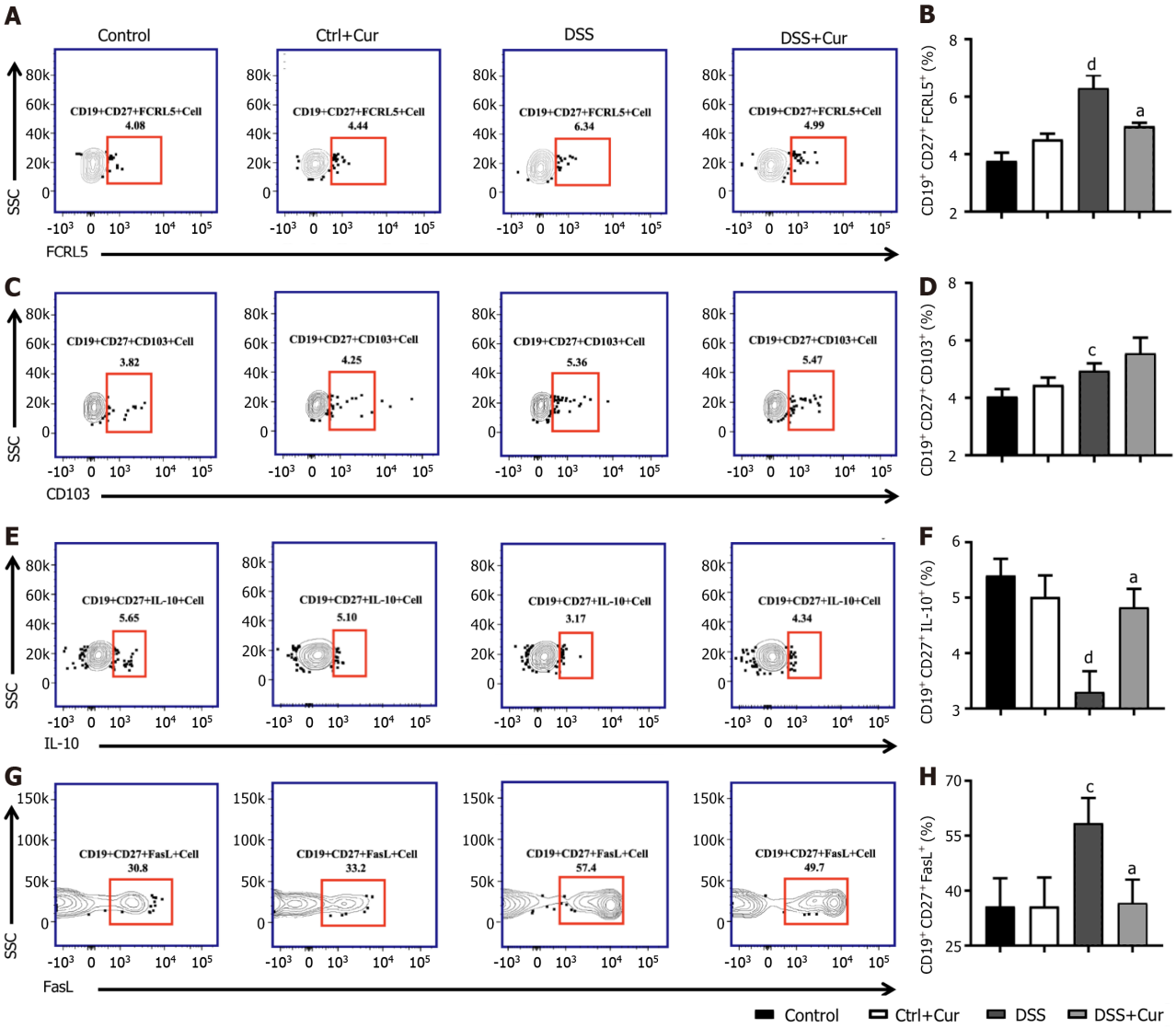
DOI: 10.3748/wjg.v28.i40.5865 **Copyright** ©The Author(s) 2022.

Figure 5 Curcumin regulates differentiation of memory B cells in DSS-induced ulcerative colitis mice. A: Representative flow cytometry profile of $CD19^+$ $CD27^+$ IgG^+ cells in peripheral blood; B: Bar chart of $CD19^+$ $CD27^+$ IgG^+ cells; C: Representative flow cytometry profile of $CD19^+$ $CD27^+$ IgM^+ cells in peripheral blood; D: Bar chart of $CD19^+$ $CD27^+$ IgM^+ cells; E: Representative flow cytometry profile of $CD19^+$ $CD27^+$ IgA^+ cells in peripheral blood; F: Bar chart of $CD19^+$ $CD27^+$ IgA^+ cells. Data are presented as the mean ± SE (n = 8-10). $^aP < 0.05$, $^bP < 0.01$ *vs* Control group; $^cP < 0.05$, $^dP < 0.01$ *vs* DSS group.

pathways, and the imbalance in subgroup distribution are closely related to the immunological pathogenesis of many diseases. Different B cell subsets can promote and inhibit inflammation. Overactivation of B cell responses, abnormal expression of signaling factors and cytokines, and imbalance in subpopulations, including memory B cells, are involved in the pathogenesis of many immune diseases. Meanwhile, memory B cells were considered as the source of several pro-inflammatory cytokines, which are involved in the pathogenesis of many autoimmune diseases[31]. In recent years, domestic and foreign scholars have extensively focused on this special class of B cells and their relationship with autoimmune diseases, such as myasthenia grais, Gillan barre syndrome, and other immune system diseases[32]. Dysregulation of memory B cells was found in several autoimmune diseases. Previous studies[17] have found that the B cell immune response, namely, the antibody response, is abnormally activated, and the memory B cells are significantly reduced in UC patients.

It is known that the body's immune system generates memory during the body's first antigen-antagonism and antibody response to specific antigens. The initial B cells can transform into memory B cells to complete the rapid category conversion in the next immunization[33]. These plasma cells migrate to bone marrow and lymphoid tissue, secrete specific antibodies such as immunoglobulins, inflammatory cytokines, and chemokines, mediate rapid and effective secondary immune response, and have an important role in humoral immunity[34].

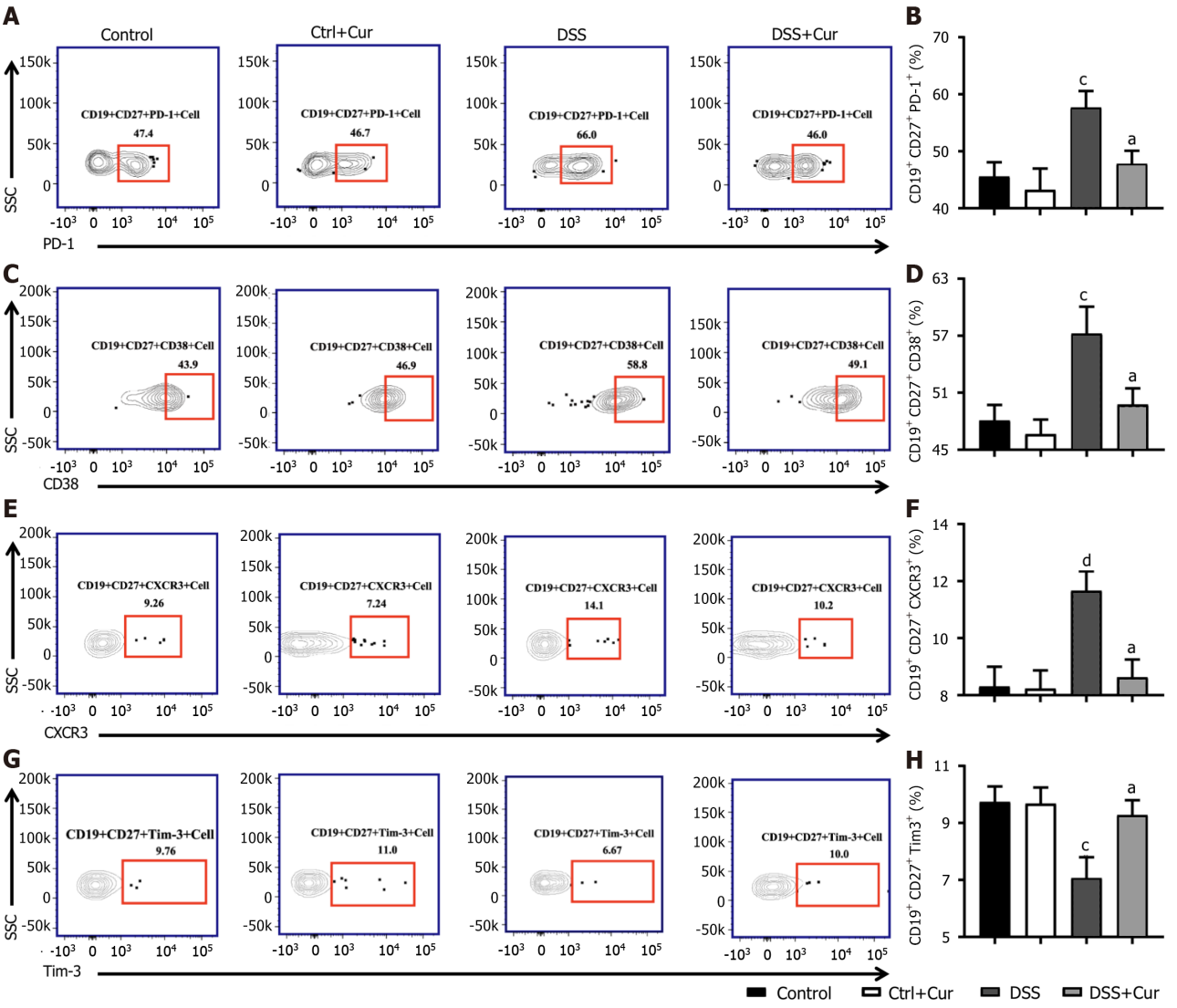
When memory B cells are stimulated again by the same antigen, they are rapidly activated to produce IgG, IgM, IgA, FCRL5, CD103, IL-10, FasL, PD-1, CD38, CXCR3, Tim3, and so on. It is known that the destruction of the intestinal mucosal barrier during the onset of IBD causes abnormal expression of immunoglobulins, which are a major participant in humoral immunity, including IgG, IgA, IgM, *etc* [35]. IgG has the function of opsonizing phagocytes and neutralizing toxins, IgA has an antibacterial and antiviral function, while IgM has the function of lysing pathogens and binding antigens. Previous studies have shown that the increased number of endoplasmic cells in the intestinal mucosa of IBD patients leads to an increase in the secretion of IgG, IgA, IgM, and other immunoglobulins, which further participate in the formation of local immune complexes in the intestinal mucosa and trigger intestinal inflammation[36]. "FCR-like" (FCRL) is an evolutionarily conserved gene family associated with IgG and IgE Fc receptors (FCRS). FCRL5 is preferentially expressed in B cells and encodes



DOI: 10.3748/wjg.v28.i40.5865 **Copyright** ©The Author(s) 2022.

Figure 6 Curcumin regulates differentiation of memory B cells in DSS-induced ulcerative colitis mice. A: Representative flow cytometry profile of $CD19^+CD27^+FCRL5^+$ cells in peripheral blood; B: Bar chart of $CD19^+CD27^+FCRL5^+$ cells; C: Representative flow cytometry profile of $CD19^+CD27^+CD103^+$ cells in peripheral blood; D: Bar chart of $CD19^+CD27^+CD103^+$ cell; E: Representative flow cytometry profile of $CD19^+CD27^+IL\text{-}10^+$ cells in peripheral blood; F: Bar chart of $CD19^+CD27^+IL\text{-}10^+$ cells; G: Representative flow cytometry profile of $CD19^+CD27^+FasL^+$ cells in peripheral blood; H: Bar chart of $CD19^+CD27^+FasL^+$ cells. Data are presented as the mean ± SE (n = 8-10). $^aP < 0.05$, $^bP < 0.01$ *vs* Control group; $^cP < 0.05$, $^dP < 0.01$ *vs* DSS group.

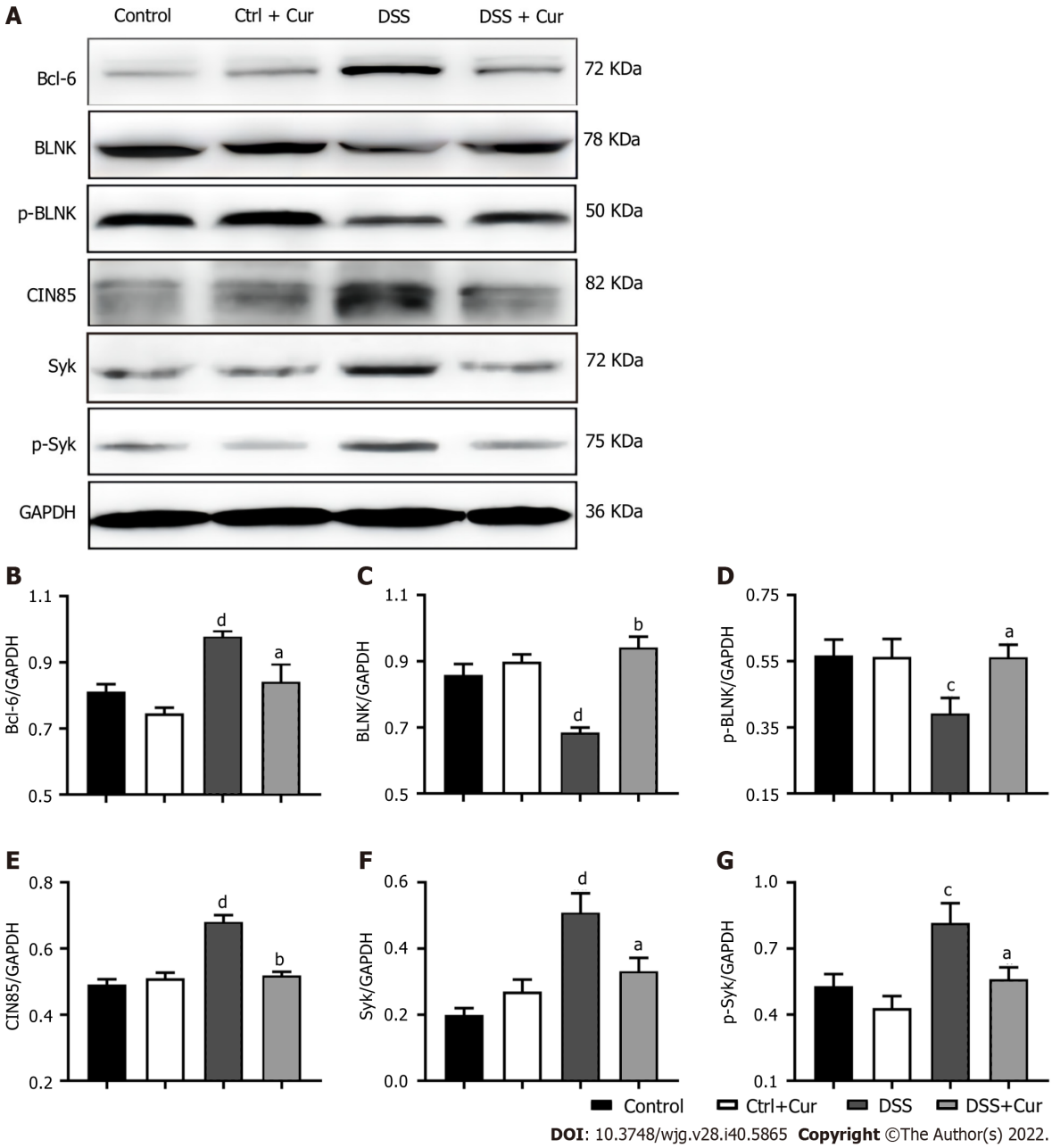
transmembrane proteins with tyrosine-based immunoregulatory motifs[37]. CD103 (human mucosal lymphocyte antigen-1) is highly expressed at mucosal sites, and CD103-positive lymphocytes have a remarkable ability to move directly toward the intestinal epithelial cell model and immobilize mucosal lymphocytes with E-cadherin at the basolateral side of the intestinal epithelium[38]. IL-10 has anti-inflammatory effects by inhibiting inflammation and cellular immune response, improving B cell survival rate, B cell proliferation, MHC II antigen expression, and immunoglobulin secretion, and inhibiting the production of NK cytokines, monocytes, and macrophage pro-inflammatory factors[39]. In the gastrointestinal tract, IL-10 is secreted by T cells, B cells, macrophages, neutrophils, and natural killer cells, and maintains mucosal homeostasis and immune tolerance during inflammation[40]. FasL is a membrane receptor protein that belongs to the superfamily of nerve growth factor receptors. It has a signal transduction role in cell apoptosis, and can induce colon epithelial cells and protect Th2 cells from apoptosis or even directly kill Th2 cells. In colonic epithelial cells, FasL can mediate the apoptosis of colonic epithelial cells through caspase-mediated apoptosis, which ultimately leads to the destruction of the colonic mucosal barrier and the formation of ulcers[41]. Indeed, expressed of Fas L in B cells is upregulated by IL-10 in some autoimmune diseases and GVHD models. CD5 is expressed in both $FasL^+$ B cells and IL-10-producing B10 cells, suggesting the possibility of a feedforward cycle in which B cells can express IL-10 to enhance their other immunomodulatory mechanisms[42]. Programmed death receptor 1 (PD-1) is a coinhibitory receptor expressed on T cells, B cells, natural killer cells, and monocytes. It has been confirmed that PD-1 is highly expressed in intestinal mucosal cells. Its ligand



DOI: 10.3748/wjg.v28.i40.5865 **Copyright** ©The Author(s) 2022.

Figure 7 Curcumin regulates differentiation of memory B cells in DSS-induced ulcerative colitis mice. A: Representative flow cytometry profile of $CD19^+CD27^+$ $PD\text{-}1^+$ cells in peripheral blood; B: Bar chart of $CD19^+CD27^+$ $PD\text{-}1^+$ cells; C: Representative flow cytometry profile of $CD19^+CD27^+$ $CD38^+$ cells in peripheral blood; D: Bar chart of $CD19^+CD27^+CD38^+$ cells; E: Representative flow cytometry profile of $CD19^+CD27^+CXCR3^+$ cells in peripheral blood; F: Bar chart of $CD19^+CD27^+CXCR3^+$ cells; G: Representative flow cytometry profile of $CD19^+CD27^+$ $Tim\text{-}3^+$ cells in peripheral blood; H: Bar chart of $CD19^+CD27^+$ $Tim\text{-}3^+$ cells. Data are presented as the mean ± SE (n = 8-10). $^aP < 0.05$, $^bP < 0.01$ *vs* Control group; $^cP < 0.05$, $^dP < 0.01$ *vs* DSS group.

binding can participate in the occurrence of intestinal mucositis by activating initial T lymphocytes, inhibiting activated effector T lymphocytes, and regulating the secretion of cytokines[43]. Studies have shown that in patients with UC, the expression level of PD-1 in inflammatory sites is significantly increased, while intestinal mucositis is alleviated when the PD-1 pathway is blocked[44]. CD38 is expressed on intestinal inflammatory cells, which has been reported to promote intestinal inflammation. Therefore, CD38 indirectly promotes intestinal inflammation[45]. CXCR3 is a chemokine receptor of the CXC family, expressed in epithelial and endothelial cells, as well as various lymphocytes such as NK cells, B cells, memory T cells, monocytes, and neutrophils. In IBD patients, CXCR3 and its corresponding ligands are strongly expressed in the intestinal mucosa. They can also recruit pro-inflammatory cells into the colon during colitis, leading to IBD[46]. As an important immune checkpoint molecule, Tim-3 regulates immune response. According to previous studies, Tim-3 is also expressed on the surface of B cells, while B cell activation affects the expression of Tim-3. After knocking out Tim-3, its protective effect disappeared, and the protective effect of B cells depended on Tim-3. Wang *et al*[47] found that during the development of acute enteritis, the expression of Tim-3 on the surface of infiltrated immune cells, especially B cells in the lamina propria of the colon, significantly decreased. After knocking out Tim-3, enteritis was significantly aggravated, and the protective effect of B cells on enteritis potentially depended on Tim-3. When the humoral immune balance related to memory B cells is disrupted, the expression of proinflammatory factors is induced, and the expression of anti-inflammatory factors is inhibited, leading to a variety of autoimmune diseases, including IBD[48].



DOI: 10.3748/wjg.v28.i40.5865 **Copyright** ©The Author(s) 2022.

Figure 8 Curcumin regulates expression of memory B cell-related proteins in DSS-induced ulcerative colitis mice. A: Expression of Bcl-6, BLNK, p-BLNK, CIN85, Syk, and p-Syk in colon tissues as revealed by Western blot analysis. GAPDH served as the internal reference; B-G: Quantitative evaluation of (B) Bcl-6, (C) BLNK, (D) p-BLNK, (E) CIN85, (F) Syk, and (G) p-Syk. Data are presented as the mean ± SE (n = 8-10). $^{a}P < 0.05$, $^{b}P < 0.01$ *vs* Control group; $^{c}P < 0.05$, $^{d}P < 0.01$ *vs* DSS group.

Our experimental results revealed that the level of memory B cells in the peripheral blood of DSS-induced colitis mice was obviously abnormal, which was consistent with other literature reports. In our experiment, induced memory B cells (IgG^+, IgM^+, IgA^+, $FCRL5^+$, $CD103^+$, $FasL^+$, $PD\text{-}1^+$, $CD38^+$, and $CXCR3^+$ memory B cells) were over-expressed and tolerant memory B cells ($IL\text{-}10^+$ and $Tim\text{-}3^+$ memory B cell) were under-expressed. After Cur administration, the levels of induced memory B cells with pro-inflammatory factor expression were significantly inhibited, while the levels of tolerant memory B cells and anti-inflammatory factors were increased. These phenomena were accompanied by Cur's effective inhibition of pathological damage in colitis mice, which indicated that Cur could effectively regulate the balance of memory B cells in colitis mice, so as to restore the balance of pro-inflammatory factors and anti-inflammatory factors and alleviate the symptoms of DSS-induced colitis. These findings suggest that the therapeutic effect of Cur on UC in mice might be closely related to the balance regulation of memory B cells.

In order to explore the mechanisms by which Cur regulates the balance of memory B cells, we examined the activation of the Bcl-6-Syk-BLNK signaling pathway in colon tissue. Bcl-6 protein is highly expressed in germinal B cells, and the germinal response is the maturation of antigen-specific B cells

into memory B cells, which constitute the cellular components of immune memory of the B cell lines [49]. Previous studies have suggested that Bcl-6 expression is necessary to enable germinal center B cells to differentiate into memory B cells. Bcl-6 expression was also found to enhance B cell survival and thereby regulate self-renewal of memory B cell. High expression of Bcl-6 sustains a germinal center B cell phenotype and inhibits the differentiation of memory B cells *in vitro*. Furthermore, it has been established that Syk/p-Syk is a key signal pathway, which is required to couple the BCR to all downstream signaling pathways in mature B cells. Also, the B cells with Syk deficiency could not differentiate into the germinal center or plasma cells, suggesting that Syk is required for the survival of memory B cells[50,51]. When BLNK/p-BLNK is deficient, the transformation of primordial B cells into memory B cells is disrupted, and the level of memory B cells is significantly reduced[52]. CIN85 is widely involved in various physiological activities in the body, especially vesicle transport, membrane transport, and invasion and migration of various cancer cells. It also participates in cell differentiation, cell cycle, and apoptosis[53,54]. According to the above analysis, the Bcl-6-Syk-BLNK signaling pathway plays a crucial role in the development, activation, and differentiation of B cells and memory B cells.

In our experiment, after Cur administration, the levels of other proteins were increased, but BLNK and p-BLNK protein expression was decreased. This result indicated that Cur could significantly inhibit the activation of the Bcl-6-Syk-BLNK signaling pathway, which is consistent with its regulatory effect on memory B-cell balance.

As a new member of regulatory immunity, the biological characteristics and functions of memory B cells have been studied extensively, providing a new perspective for studying immune regulation mode and a new method for treating IBD. It has been proven that Cur is effective against DSS-induced micron colitis. In this experiment, we found that Cur could effectively improve the mucosal damage of DSS-induced colitis mice and significantly regulate the balance of induced type and tolerance memory B cells in colitis mice. As a result, the Bcl-6-Syk-BLNK signaling pathway was significantly inhibited. The effectiveness of Cur for murine UC was closely related to the regulation of memory B cell balance. Cur regulated the balance of memory B cell subgroups in mice with colitis, which was realized by activating the Bcl-6-Syk-BLNK signaling pathway. These results suggest that through the activation of the Bcl-6-Syk-BLNK signaling pathway, Cur harmonizes the differentiation and activation of inducible and inhibitory memory B cells, promotes the balance between them, reduces the expression of chemokines related to the inhibition of inducible memory B cells, and prevents excessive accumulation of inflammatory cells. It can also prevent overproduction of pro-inflammatory factors, increase the expression of tolerant memory B cells and anti-inflammatory factors to alleviate the immune damage by correcting memory B cell disorder, and maintain the humoral immune homeostasis mediated by memory B cells.

CONCLUSION

Cur could effectively alleviate DSS-induced colitis in mice by regulating memory B cells and the Bcl-6-Syk-BLNK signaling pathway.

ARTICLE HIGHLIGHTS

Research background

Curcumin (Cur) has shown promising efficacy in experimental colitis mice and ulcerative colitis patients. Disturbance in memory B cells has been observed in various autoimmune diseases, including inflammatory bowel disease. However, few studies have explored whether Cur treatment of colitis is associated with memory B cells.

Research motivation

To the best of our knowledge, this is the first study to explore the mechanisms by which Cur regulates memory B cells in the treatment of experimental colitis.

Research objectives

To investigate whether Cur can alleviate experimental colitis induced by DSS through regulating memory B cells and Bcl-6-Syk-BLNK signaling.

Research methods

Cur (100 mg/kg/d) was intragastrically administered in mice with colitis induced by DSS for 14 consecutive days. The effect of Cur was evaluated by macroscopic and histological observation. The levels of memory B cell subgroups in mouse peripheral blood were detected by flow cytometry, and the levels of cytokines in colonic tissue homogenates were measured by using ELISA. The expression of Bcl-6, BLNK, and Syk was measured by Western blot analysis.

Research results

After mice were treated with Cur for 14 d, the body weight, colonic weight and length, colonic weight index, and histopathological injury were ameliorated. In colitis mice, the concentrations of IL-1β, IL-6, TNF-α, and IL-7A were significantly decreased, while the concentrations of anti-inflammatory cytokines IL-35 and IL-10 were obviously increased. Activation of memory B cell subsets in colitis mice was confirmed by a remarkable reduction in the expression of IgM^+, IgG^+, IgA^+, $FCRL5^+$, $CD103^+$, $FasL^+$, $PD\text{-}1^+$, $CD38^+$, and $CXCR3^+$ on the surface of $CD19^+CD27^+$B cells, while the number of $CD19^+$ $CD27^+$ $IL\text{-}10^+$ and $CD19^+CD27^+$ $Tim\text{-}3^+$ B cells increased significantly. In addition, Cur observably decreased the protein levels of Syk, p-Syk, Bcl-6, and CIN85, and increased BLNK and p-BLNK expression in colitis mice.

Research conclusions

Cur could effectively alleviate DSS-induced colitis in mice, which is realized *via* a potential mechanism involving memory B cells and the Bcl-6-Syk-BLNK signaling pathway.

Research perspectives

In the present study, Cur effectively ameliorated the pathological colonic injury induced by DSS, which was achieved through a potential mechanism involving regulating the balance of memory B cells and activating the Bcl-6-Syk-BLNK signaling pathway.

FOOTNOTES

Author contributions: Wei SY and Wu TT contributed equally to this work and should be regarded as co-first authors; Huang JQ, Zhong YB, Kang ZP, Wang MX, Zhou BG, Zhao HM, and Ge W performed the experiments; Liu DY and Wang HY contributed reagents/materials/analytical tools; Liu DY and Zhong YB analyzed the data; Wei SY, Wu TT, and Liu DY wrote the paper; Liu DY and Wang HY conceived and designed the experiments.

Supported by the National Natural Science Foundation of China, No. 81760808; and Jiangxi University of Chinese Medicine Science and Technology Innovation Team Development Program, No. CXTD22008.

Institutional animal care and use committee statement: The study was reviewed and approved by the Jiangxi University of Chinese Medicine Animal Care and Use Committee and were performed in accordance with its prescribed guidelines (Approval No. JZLLSC2021-196).

Conflict-of-interest statement: There are no conflicts of interest to report.

Data sharing statement: No additional data are available.

ARRIVE guidelines statement: The authors have read the ARRIVE Guidelines, and the manuscript was prepared and revised according to the ARRIVE Guidelines.

Open-Access: This article is an open-access article that was selected by an in-house editor and fully peer-reviewed by external reviewers. It is distributed in accordance with the Creative Commons Attribution NonCommercial (CC BY-NC 4.0) license, which permits others to distribute, remix, adapt, build upon this work non-commercially, and license their derivative works on different terms, provided the original work is properly cited and the use is non-commercial. See: https://creativecommons.org/Licenses/by-nc/4.0/

Country/Territory of origin: China

ORCID number: Duan-Yong Liu 0000-0003-2855-2811.

S-Editor: Chen YL
L-Editor: Wang TQ
P-Editor: Chen YX

REFERENCES

1 **Perrone D**, Ardito F, Giannatempo G, Dioguardi M, Troiano G, Lo Russo L, DE Lillo A, Laino L, Lo Muzio L. Biological and therapeutic activities, and anticancer properties of curcumin. *Exp Ther Med* 2015; **10**: 1615-1623 [PMID: 26640527 DOI: 10.3892/etm.2015.2749]
2 **Pulido-Moran M**, Moreno-Fernandez J, Ramirez-Tortosa C, Ramirez-Tortosa M. Curcumin and Health. *Molecules* 2016; **21**: 264 [PMID: 26927041 DOI: 10.3390/molecules21030264]
3 **Rao EV**, Sudheer P. Revisiting curcumin chemistry part I: a new strategy for the synthesis of curcuminoids. *Indian J*

Pharm Sci 2011; **73**: 262-270 [PMID: 22457548 DOI: 10.4103/0250-474X.93508]
4 **Mantzorou M**, Pavlidou E, Vasios G, Tsagalioti E, Giaginis C. Effects of curcumin consumption on human chronic diseases: A narrative review of the most recent clinical data. *Phytother Res* 2018; **32**: 957-975 [PMID: 29468820 DOI: 10.1002/ptr.6037]
5 **Kotecha R**, Takami A, Espinoza JL. Dietary phytochemicals and cancer chemoprevention: a review of the clinical evidence. *Oncotarget* 2016; **7**: 52517-52529 [PMID: 27232756 DOI: 10.18632/oncotarget.9593]
6 **Aggarwal BB**, Kumar A, Bharti AC. Anticancer potential of curcumin: preclinical and clinical studies. *Anticancer Res* 2003; **23**: 363-398 [PMID: 12680238]
7 **Neurath MF**. Targeting immune cell circuits and trafficking in inflammatory bowel disease. *Nat Immunol* 2019; **20**: 970-979 [PMID: 31235952 DOI: 10.1038/s41590-019-0415-0]
8 **Yu Y**, Sitaraman S, Gewirtz AT. Intestinal epithelial cell regulation of mucosal inflammation. *Immunol Res* 2004; **29**: 55-68 [PMID: 15181270 DOI: 10.1385/IR:29:1-3:055]
9 **Cancro MP**, Tomayko MM. Memory B cells and plasma cells: The differentiative continuum of humoral immunity. *Immunol Rev* 2021; **303**: 72-82 [PMID: 34396546 DOI: 10.1111/imr.13016]
10 **Pararasa C**, Zhang N, Tull TJ, Chong MHA, Siu JHY, Guesdon W, Chavele KM, Sanderson JD, Langmead L, Kok K, Spencer J, Vossenkamper A. Reduced CD27^{-}IgD^{-} B Cells in Blood and Raised CD27^{-}IgD^{-} B Cells in Gut-Associated Lymphoid Tissue in Inflammatory Bowel Disease. *Front Immunol* 2019; **10**: 361 [PMID: 30891036 DOI: 10.3389/fimmu.2019.00361]
11 **Singla V**, Pratap Mouli V, Garg SK, Rai T, Choudhury BN, Verma P, Deb R, Tiwari V, Rohatgi S, Dhingra R, Kedia S, Sharma PK, Makharia G, Ahuja V. Induction with NCB-02 (curcumin) enema for mild-to-moderate distal ulcerative colitis-a randomized, placebo-controlled, pilot study. *J Crohns Colitis* 2014; **8**: 208-214 [PMID: 24011514 DOI: 10.1016/j.crohns.2013.08.006]
12 **Patel SS**, Acharya A, Ray RS, Agrawal R, Raghuwanshi R, Jain P. Cellular and molecular mechanisms of curcumin in prevention and treatment of disease. *Crit Rev Food Sci Nutr* 2020; **60**: 887-939 [PMID: 30632782 DOI: 10.1080/10408398.2018.1552244]
13 **Zhao G**, Han X, Zheng S, Li Z, Sha Y, Ni J, Sun Z, Qiao S, Song Z. Curcumin induces autophagy, inhibits proliferation and invasion by downregulating AKT/mTOR signaling pathway in human melanoma cells. *Oncol Rep* 2016; **35**: 1065-1074 [PMID: 26573768 DOI: 10.3892/or.2015.4413]
14 **Wan P**, Chen H, Guo Y, Bai AP. Advances in treatment of ulcerative colitis with herbs: from bench to bedside. *World J Gastroenterol* 2014; **20**: 14099-14104 [PMID: 25339799 DOI: 10.3748/wjg.v20.i39.14099]
15 **Ismail NI**, Othman I, Abas F, H Lajis N, Naidu R. Mechanism of Apoptosis Induced by Curcumin in Colorectal Cancer. *Int J Mol Sci* 2019; **20** [PMID: 31108984 DOI: 10.3390/ijms20102454]
16 **Abdollahi E**, Momtazi AA, Johnston TP, Sahebkar A. Therapeutic effects of curcumin in inflammatory and immune-mediated diseases: A nature-made jack-of-all-trades? *J Cell Physiol* 2018; **233**: 830-848 [PMID: 28059453 DOI: 10.1002/jcp.25778]
17 **Zhong YB**, Kang ZP, Zhou BG, Wang HY, Long J, Zhou W, Zhao HM, Liu DY. Curcumin Regulated the Homeostasis of Memory T Cell and Ameliorated Dextran Sulfate Sodium-Induced Experimental Colitis. *Front Pharmacol* 2020; **11**: 630244 [PMID: 33597887 DOI: 10.3389/fphar.2020.630244]
18 **Sann H**, Erichsen Jv, Hessmann M, Pahl A, Hoffmeyer A. Efficacy of drugs used in the treatment of IBD and combinations thereof in acute DSS-induced colitis in mice. *Life Sci* 2013; **92**: 708-718 [PMID: 23399699 DOI: 10.1016/j.lfs.2013.01.028]
19 **Chassaing B**, Aitken JD, Malleshappa M, Vijay-Kumar M. Dextran sulfate sodium (DSS)-induced colitis in mice. *Curr Protoc Immunol* 2014; **104**: 15.25.1-15.25.14 [PMID: 24510619 DOI: 10.1002/0471142735.im1525s104]
20 **Rogler G**, Singh A, Kavanaugh A, Rubin DT. Extraintestinal Manifestations of Inflammatory Bowel Disease: Current Concepts, Treatment, and Implications for Disease Management. *Gastroenterology* 2021; **161**: 1118-1132 [PMID: 34358489 DOI: 10.1053/j.gastro.2021.07.042]
21 **Das S**, Batra SK, Rachagani S. Mouse Model of Dextran Sodium Sulfate (DSS)-induced Colitis. *Bio Protoc* 2017; **7**: e2515 [PMID: 34541176 DOI: 10.21769/BioProtoc.2515]
22 **Sarlos P**, Kovesdi E, Magyari L, Banfai Z, Szabo A, Javorhazy A, Melegh B. Genetic update on inflammatory factors in ulcerative colitis: Review of the current literature. *World J Gastrointest Pathophysiol* 2014; **5**: 304-321 [PMID: 25133031 DOI: 10.4291/wjgp.v5.i3.304]
23 **Kiernan MG**, Coffey JC, Sahebally SM, Tibbitts P, Lyons EM, O'leary E, Owolabi F, Dunne CP. Systemic Molecular Mediators of Inflammation Differentiate Between Crohn's Disease and Ulcerative Colitis, Implicating Threshold Levels of IL-10 and Relative Ratios of Pro-inflammatory Cytokines in Therapy. *J Crohns Colitis* 2020; **14**: 118-129 [PMID: 31241755 DOI: 10.1093/ecco-jcc/jjz117]
24 **Sabatino JJ Jr**, Pröbstel AK, Zamvil SS. B cells in autoimmune and neurodegenerative central nervous system diseases. *Nat Rev Neurosci* 2019; **20**: 728-745 [PMID: 31712781 DOI: 10.1038/s41583-019-0233-2]
25 **Good-Jacobson KL**. Strength in diversity: Phenotypic, functional, and molecular heterogeneity within the memory B cell repertoire. *Immunol Rev* 2018; **284**: 67-78 [PMID: 29944763 DOI: 10.1111/imr.12663]
26 **Potter KN**, Mockridge CI, Rahman A, Buchan S, Hamblin T, Davidson B, Isenberg DA, Stevenson FK. Disturbances in peripheral blood B cell subpopulations in autoimmune patients. *Lupus* 2002; **11**: 872-877 [PMID: 12529053 DOI: 10.1191/0961203302lu309oa]
27 **Sato S**, Fujimoto M, Hasegawa M, Takehara K. Altered blood B lymphocyte homeostasis in systemic sclerosis: expanded naive B cells and diminished but activated memory B cells. *Arthritis Rheum* 2004; **50**: 1918-1927 [PMID: 15188368 DOI: 10.1002/art.20274]
28 **Ungaro R**, Mehandru S, Allen PB, Peyrin-Biroulet L, Colombel JF. Ulcerative colitis. *Lancet* 2017; **389**: 1756-1770 [PMID: 27914657 DOI: 10.1016/S0140-6736(16)32126-2]
29 **Kobayashi T**, Siegmund B, Le Berre C, Wei SC, Ferrante M, Shen B, Bernstein CN, Danese S, Peyrin-Biroulet L, Hibi T. Ulcerative colitis. *Nat Rev Dis Primers* 2020; **6**: 74 [PMID: 32913180 DOI: 10.1038/s41572-020-0205-x]
30 **Klinker MW**, Lundy SK. Multiple mechanisms of immune suppression by B lymphocytes. *Mol Med* 2012; **18**: 123-137

[PMID: 22033729 DOI: 10.2119/molmed.2011.00333]
31 **Duddy M**, Niino M, Adatia F, Hebert S, Freedman M, Atkins H, Kim HJ, Bar-Or A. Distinct effector cytokine profiles of memory and naive human B cell subsets and implication in multiple sclerosis. *J Immunol* 2007; **178**: 6092-6099 [PMID: 17475834 DOI: 10.4049/jimmunol.178.10.6092]
32 **Dizon BLP**, Pierce SK. The tangled web of autoreactive B cells in malaria immunity and autoimmune disease. *Trends Parasitol* 2022; **38**: 379-389 [PMID: 35120815 DOI: 10.1016/j.pt.2022.01.005]
33 **Pape KA**, Taylor JJ, Maul RW, Gearhart PJ, Jenkins MK. Different B cell populations mediate early and late memory during an endogenous immune response. *Science* 2011; **331**: 1203-1207 [PMID: 21310965 DOI: 10.1126/science.1201730]
34 **Jin W**, Luo Z, Yang H. Peripheral B Cell Subsets in Autoimmune Diseases: Clinical Implications and Effects of B Cell-Targeted Therapies. *J Immunol Res* 2020; **2020**: 9518137 [PMID: 32280720 DOI: 10.1155/2020/9518137]
35 **Rai T**, Wu X, Shen B. Frequency and risk factors of low immunoglobulin levels in patients with inflammatory bowel disease. *Gastroenterol Rep (Oxf)* 2015; **3**: 115-121 [PMID: 25638221 DOI: 10.1093/gastro/gou082]
36 **Gouni-Berthold I**, Baumeister B, Berthold HK, Schmidt C. Immunoglobulins and IgG subclasses in patients with inflammatory bowel disease. *Hepatogastroenterology* 1999; **46**: 1720-1723 [PMID: 10430330]
37 **Zhu Z**, Li R, Li H, Zhou T, Davis RS. FCRL5 exerts binary and compartment-specific influence on innate-like B-cell receptor signaling. *Proc Natl Acad Sci U S A* 2013; **110**: E1282-E1290 [PMID: 23509253 DOI: 10.1073/pnas.1215156110]
38 **Oshitani N**, Watanabe K, Maeda K, Fujiwara Y, Higuchi K, Matsumoto T, Arakawa T. Differential expression of homing receptor CD103 on lamina propria lymphocytes and association of CD103 with epithelial adhesion molecules in inflammatory bowel disease. *Int J Mol Med* 2003; **12**: 715-719 [PMID: 14532999]
39 **Shouval DS**, Biswas A, Goettel JA, McCann K, Conaway E, Redhu NS, Mascanfroni ID, Al Adham Z, Lavoie S, Ibourk M, Nguyen DD, Samsom JN, Escher JC, Somech R, Weiss B, Beier R, Conklin LS, Ebens CL, Santos FG, Ferreira AR, Sherlock M, Bhan AK, Müller W, Mora JR, Quintana FJ, Klein C, Muise AM, Horwitz BH, Snapper SB. Interleukin-10 receptor signaling in innate immune cells regulates mucosal immune tolerance and anti-inflammatory macrophage function. *Immunity* 2014; **40**: 706-719 [PMID: 24792912 DOI: 10.1016/j.immuni.2014.03.011]
40 **Morhardt TL**, Hayashi A, Ochi T, Quirós M, Kitamoto S, Nagao-Kitamoto H, Kuffa P, Atarashi K, Honda K, Kao JY, Nusrat A, Kamada N. IL-10 produced by macrophages regulates epithelial integrity in the small intestine. *Sci Rep* 2019; **9**: 1223 [PMID: 30718924 DOI: 10.1038/s41598-018-38125-x]
41 **Liu D**, Huang X, Cheng S, Tong W, Wan P, Guan Y, Zhao H. [Regulation of sishen wan on Bax/Bcl-2 mRNA, Fas/FasL in colonic tissue from rats with colitis]. *Zhongguo Zhong Yao Za Zhi* 2011; **36**: 3484-3488 [PMID: 22368862]
42 **Ray A**, Wang L, Dittel BN. IL-10-independent regulatory B-cell subsets and mechanisms of action. *Int Immunol* 2015; **27**: 531-536 [PMID: 25999596 DOI: 10.1093/intimm/dxv033]
43 **Collins M**, Michot JM, Danlos FX, Mussini C, Soularue E, Mateus C, Loirat D, Buisson A, Rosa I, Lambotte O, Laghouati S, Chaput N, Coutzac C, Voisin AL, Soria JC, Marabelle A, Champiat S, Robert C, Carbonnel F. Inflammatory gastrointestinal diseases associated with PD-1 blockade antibodies. *Ann Oncol* 2017; **28**: 2860-2865 [PMID: 29045560 DOI: 10.1093/annonc/mdx403]
44 **Roosenboom B**, Horjus Talabur Horje CS, Smids C, Leeuwis JW, van Koolwijk E, Groenen MJM, Wahab PJ, van Lochem EG. Distribution of mucosal PD-1 expressing T cells in patients with colitis of different etiologies. *Scand J Gastroenterol* 2021; **56**: 671-679 [PMID: 33779456 DOI: 10.1080/00365521.2021.1906316]
45 **Ning L**, Shan G, Sun Z, Zhang F, Xu C, Lou X, Li S, Du H, Chen H, Xu G. Quantitative Proteomic Analysis Reveals the Deregulation of Nicotinamide Adenine Dinucleotide Metabolism and CD38 in Inflammatory Bowel Disease. *Biomed Res Int* 2019; **2019**: 3950628 [PMID: 31179321 DOI: 10.1155/2019/3950628]
46 **Yuan YH**, ten Hove T, The FO, Slors JF, van Deventer SJ, te Velde AA. Chemokine receptor CXCR3 expression in inflammatory bowel disease. *Inflamm Bowel Dis* 2001; **7**: 281-286 [PMID: 11720316 DOI: 10.1097/00054725-200111000-00001]
47 **Wang S**, Liu Y, Yuan X, Yao L, Yang S, Ma R. Fecal bacteria from ulcerative colitis patients downregulate Tim-3-mediated inhibitory effects on monocytes *in vitro*. *Microb Pathog* 2019; **128**: 147-152 [PMID: 30594639 DOI: 10.1016/j.micpath.2018.12.043]
48 **Klein U**, Rajewsky K, Küppers R. Human immunoglobulin (Ig)M+IgD+ peripheral blood B cells expressing the CD27 cell surface antigen carry somatically mutated variable region genes: CD27 as a general marker for somatically mutated (memory) B cells. *J Exp Med* 1998; **188**: 1679-1689 [PMID: 9802980 DOI: 10.1084/jem.188.9.1679]
49 **Crotty S**, Johnston RJ, Schoenberger SP. Effectors and memories: Bcl-6 and Blimp-1 in T and B lymphocyte differentiation. *Nat Immunol* 2010; **11**: 114-120 [PMID: 20084069 DOI: 10.1038/ni.1837]
50 **Ackermann JA**, Nys J, Schweighoffer E, McCleary S, Smithers N, Tybulewicz VL. Syk tyrosine kinase is critical for B cell antibody responses and memory B cell survival. *J Immunol* 2015; **194**: 4650-4656 [PMID: 25862820 DOI: 10.4049/jimmunol.1500461]
51 **Iwata S**, Tanaka Y. B-cell subsets, signaling and their roles in secretion of autoantibodies. *Lupus* 2016; **25**: 850-856 [PMID: 27252261 DOI: 10.1177/0961203316643172]
52 **Li N**, Wu J, Wu Y, Xu Y, Yao R, Li G, Zhang J, Zhou Y, Yin L, Yin Y, Yu T, Wang J. Further delineation of primary B cell immunodeficiency caused by novel variants of the BLNK gene in two Chinese patients. *Clin Immunol* 2020; **214**: 108387 [PMID: 32194234 DOI: 10.1016/j.clim.2020.108387]
53 **Kometani K**, Yamada T, Sasaki Y, Yokosuka T, Saito T, Rajewsky K, Ishiai M, Hikida M, Kurosaki T. CIN85 drives B cell responses by linking BCR signals to the canonical NF-kappaB pathway. *J Exp Med* 2011; **208**: 1447-1457 [PMID: 21708930 DOI: 10.1084/jem.20102665]
54 **Anderson SM**, Tomayko MM, Ahuja A, Haberman AM, Shlomchik MJ. New markers for murine memory B cells that define mutated and unmutated subsets. *J Exp Med* 2007; **204**: 2103-2114 [PMID: 17698588 DOI: 10.1084/jem.20062571]

World Journal of Gastroenterology

Submit a Manuscript: https://www.f6publishing.com

World J Gastroenterol 2022 October 28; 28(40): 5881-5892

DOI: 10.3748/wjg.v28.i40.5881

ISSN 1007-9327 (print) ISSN 2219-2840 (online)

ORIGINAL ARTICLE

Observational Study

Liver transplantation is beneficial regardless of cirrhosis stage or acute-on-chronic liver failure grade: A single-center experience

Eduardo Cervantes-Alvarez, Mario Vilatoba, Nathaly Limon-de la Rosa, Osvely Mendez-Guerrero, David Kershenobich, Aldo Torre, Nalu Navarro-Alvarez

Specialty type: Transplantation

Provenance and peer review: Invited article; Externally peer reviewed.

Peer-review model: Single blind

Peer-review report's scientific quality classification

Grade A (Excellent): A
Grade B (Very good): B
Grade C (Good): C
Grade D (Fair): 0
Grade E (Poor): 0

P-Reviewer: Cassese G, Italy; Mogahed EA, Egypt; Sahin TT, Turkey

Received: April 25, 2022
Peer-review started: April 25, 2022
First decision: May 30, 2022
Revised: June 21, 2022
Accepted: September 21, 2022
Article in press: September 21, 2022
Published online: October 28, 2022

Eduardo Cervantes-Alvarez, PECEM, Facultad de Medicina, Universidad Nacional Autónoma de México, Mexico City 14080, Mexico

Eduardo Cervantes-Alvarez, Nathaly Limon-de la Rosa, Osvely Mendez-Guerrero, David Kershenobich, Aldo Torre, Nalu Navarro-Alvarez, Department of Gastroenterology, Instituto Nacional de Ciencias Médicas y Nutrición Salvador Zubirán, Mexico City 14080, Mexico

Mario Vilatoba, Department of Trasplant, Instituto Nacional de Ciencias Médicas y Nutrición Salvador Zubirán, Mexico City 14080, Mexico

Nalu Navarro-Alvarez, Department of Molecular Biology, Universidad Panamericana School of Medicine, Mexico City 03920, Mexico

Nalu Navarro-Alvarez, Department of Surgery, University of Colorado Anschutz Medical Campus, Denver, CO 80045, United States

Corresponding author: Nalu Navarro-Alvarez, MD, PhD, Assistant Professor, Department of Gastroenterology, Instituto Nacional de Ciencias Médicas y Nutrición Salvador Zubirán, Vasco de Quiroga #15, Mexico City 14080, Mexico. nalu.navarroa@incmnsz.mx

Abstract

BACKGROUND

Liver transplantation for the most critically ill remains controversial; however, it is currently the only curative treatment option.

AIM

To assess immediate posttransplant outcomes and compare the short (1 year) and long-term (6 years) posttransplant survival among cirrhotic patients stratified by disease severity.

METHODS

We included cirrhotic patients undergoing liver transplantation between 2015 and 2019 and categorized them into compensated cirrhosis (CC), decompensated cirrhosis (DC), and acute-on-chronic liver failure (ACLF). ACLF was further divided into severity grades. Our primary outcomes of interest were total days of intensive care unit (ICU) and hospital stay, development of complications and posttransplant survival at 1 and 6 years.

RESULTS

235 patients underwent liver transplantation (CC = 11, DC = 129 and ACLF = 95). Patients with ACLF had a significantly longer hospital stay [8.0 (6.0-13.0) *vs* CC, 6.0 (3.0-7.0), and DC 7.0 (4.5-10.0); $P = 0.01$] and developed more infection-related complications [47 (49.5%), *vs* CC, 1 (9.1%) and DC, 38 (29.5%); $P < 0.01$]. Posttransplant survival at 1- and 6-years was similar among groups ($P = 0.60$ and $P = 0.90$, respectively). ACLF patients stratified according to ACLF grade [ACLF-1 $n = 40$ (42.1%), ACLF-2 $n = 33$ (34.7%) and ACLF-3 $n = 22$ (23.2%)], had similar ICU and hospital stay length ($P = 0.68$, $P = 0.54$), as well as comparable frequencies of overall and infectious post-transplant complications ($P = 0.58$, $P = 0.80$). There was no survival difference between ACLF grades at 1 year and 6 years ($P = 0.40$ and $P = 0.15$).

CONCLUSION

Patients may benefit from liver transplantation regardless of the cirrhosis stage. ACLF patients have a longer hospital stay and frequency of infectious complications; however, excellent, and comparable 1 and 6-year survival rates support their enlisting and transplantation including those with ACLF-3.

Key Words: Liver transplantation; Acute-on-chronic liver failure; Prognosis; Survival analysis; Critical care

©The Author(s) 2022. Published by Baishideng Publishing Group Inc. All rights reserved.

Core Tip: Cirrhotic patients classified into compensated or decompensated cirrhosis and acute-on-chronic liver failure (ACLF) underwent liver transplantation. Patients with ACLF have a longer hospital stay and a higher frequency of infectious complications, but despite that, have similar posttransplant survival at one year and up to 6 years of follow-up.

Citation: Cervantes-Alvarez E, Vilatoba M, Limon-de la Rosa N, Mendez-Guerrero O, Kershenobich D, Torre A, Navarro-Alvarez N. Liver transplantation is beneficial regardless of cirrhosis stage or acute-on-chronic liver failure grade: A single-center experience. *World J Gastroenterol* 2022; 28(40): 5881-5892
URL: https://www.wjgnet.com/1007-9327/full/v28/i40/5881.htm
DOI: https://dx.doi.org/10.3748/wjg.v28.i40.5881

INTRODUCTION

Cirrhosis is the consequence of chronic liver disease originated by a variety of etiological factors, characterized by the disruption of the normal hepatic architecture due to fibrosis with consequent hemodynamic repercussions. Unless the hepatic insult is removed, patients with this condition will suffer progression and transition from a stage of compensated cirrhosis (CC) to a stage of decompensated cirrhosis (DC) with the occurrence of portal hypertension-related symptoms[1]. An entity of recent definition known as acute-on-chronic liver failure (ACLF) is now recognized[2,3], which imposes the highest mortality risk given by a state of profound cirrhosis-associated immune dysfunction and the development of organ failures additional to that of the liver[4,5].

Currently, liver transplantation (LT) is the only definitive therapeutic measure for any of these patients, albeit with the implied risks including posttransplant complications and the long-term use of immunosuppressive drugs. However, patients benefit in general from excellent posttransplant survival.

There is controversial literature, and uncertainty prevails concerning the possible futility of assigning a liver to a patient with advanced cirrhosis and systemic alterations such as in those with ACLF. Some studies have demonstrated the presence of ACLF at the time of LT as a risk factor for mortality and graft loss, and that these patients may have lower short and long-term survival after transplant[6-8]. However, others have shown non-significant survival differences between ACLF and non-ACLF patients including a marked improvement in the prognosis of those with the highest severity (ACLF-3) [9-12]. The development of early allograft dysfunction and renal dysfunction is also comparable between these groups, as well as long-term liver and kidney function[12,13]. However, unfavorable outcomes can be expected and a higher frequency of perioperative and postoperative complications has been reported[8,9]. Differences may be found when ACLF patients are subdivided by ACLF grade, however, survival disparities are still controversial[7,9].

We here report our transplant center's experience in an effort to further contribute to the evidence on the benefit of LT in ACLF. The aim was to assess immediate posttransplant outcomes and to compare the short (1 year) and long-term (6 years) posttransplant survival among cirrhotic patients stratified by

disease severity. Unlike other studies so far, this study specifically compares survival and outcomes between compensated, decompensated cirrhosis and ACLF, thus distinctly contrasting the extremes of disease severity. Additional analyses were performed to determine possible differences between ACLF grades. These results should encourage further transplantation in those with this severe form of cirrhosis and even in patients with ACLF grade 3.

MATERIALS AND METHODS

Patients and operational definitions

This study included all patients undergoing LT between January 1st 2015 and December 31st 2019. Patients with a previous transplant, malignancies other than hepatocellular carcinoma, fulminant hepatic failure, and amyloidosis were excluded. Patients were classified into compensated cirrhosis (CC), decompensated cirrhosis (DC), and ACLF, and the latter were further subdivided into ACLF grades 1, 2 and 3 (Figure 1). Diagnoses of CC and DC were based on the absence or presence of symptoms related to portal hypertension, including ascites, encephalopathy, or variceal bleeding, respectively, as previously described[14]. All CC patients received liver transplant because of hepatocarcinoma mainly due to hepatitis C virus (HCV) infection.

ACLF was diagnosed in a patient that fulfilled ACLF criteria any time during their clinical course while waiting to receive a LT according to the EASL-CLIF consortium criteria[2] which state the following organ failure (OF) definitions: liver (total bilirubin ≥ 12 mg/dL); kidney (creatinine ≥ 2 mg/dL); brain (encephalopathy grade 3 or 4 according to West-Haven criteria); coagulation (INR ≥ 2.5); circulation (vasopressor use due to circulatory failure); and lung ($PaO_2/FiO_2 \leq 200$ or $SpO_2/FiO_2 \leq 214$ or mechanical ventilation due to lung failure). ACLF grading was performed as follows: ACLF-1, patients with single kidney OF or non-renal OF plus kidney dysfunction (creatinine between 1.5-1.9 mg/dL) and/or brain dysfunction (encephalopathy grade 1 or 2 according to West-Haven criteria); ACLF-2, patients with two OFs; and ACLF-3, patients with three or more OFs.

Patients at our center are considered for LT based on cirrhosis disease severity according to an unrestricted evaluation of the Model for End-Stage Liver Disease (MELD), MELD-Na and CLIF-C scores and are ultimately listed according to an interdisciplinary consensus reached by the gastroenterology, cardiology, pneumology, infectology, otorhinolaryngology, psychiatry, surgery, anesthesiology, and stomatology specialties. Liver transplants were carried out in their majority with classic technique. Briefly, recipient hepatectomy involved a bilateral subcostal incision with or without midline extension. Then dissection and clamping of the portal vein, hepatic artery, bile duct, and superior and inferior vena cava were done. Implantation of the donor's liver was attained by anastomosing first the superior vena cava from the donor with that of the recipient, followed by the inferior vena cava, and portal vein, after which reperfusion of the donor liver was begun. Total reperfusion was then obtained by anastomosing the hepatic artery of the graft with the junction of the gastroduodenal artery and the common hepatic artery of the recipient. The procedure was completed after performing cholecystectomy and duct to-duct anastomosis.

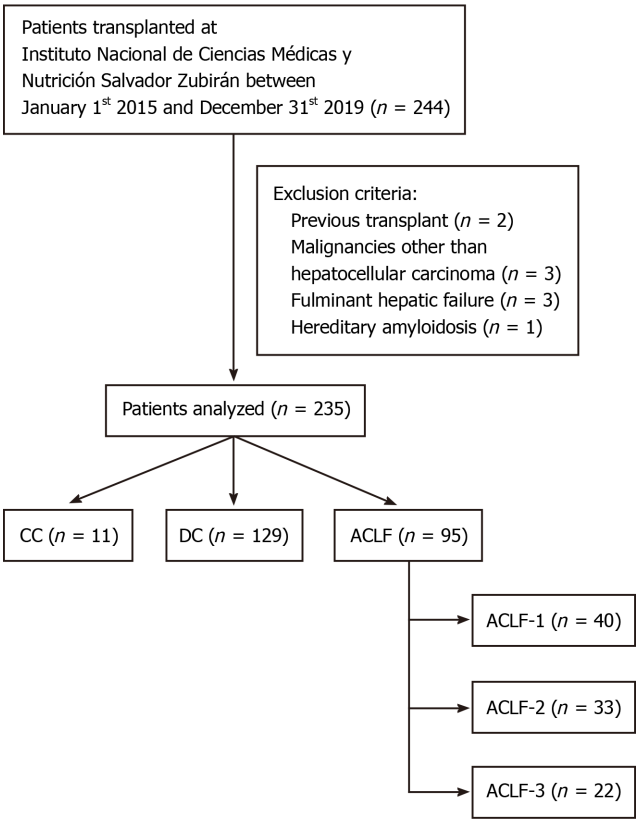
The immunosuppressive regimen in all patients following the procedure consisted of all or a combination of the following drugs: a calcineurin inhibitor (tacrolimus or cyclosporine), corticosteroids, mycophenolate mofetil and the interleukin-2 (IL-2) receptor antagonist basiliximab. In the event of renal disease in the post-orthotopic liver transplant period, modifications to the immunosuppression regimen including CNI dose reduction with the addition of MMF, were performed.

No donor organs were obtained from executed prisoners or other institutionalized people.

This study was approved by the ethics committee of our institution (GAS-2368-17-20) and conforms to the provisions of the Declaration of Helsinki. Requirement of informed consent was waived due to its observational nature.

Data collection and primary outcomes

Medical records of all patients were examined to extract the following demographic and clinical variables [gender, age, cirrhosis etiology, presence of ascites and encephalopathy, vasopressor use, PaO_2/FiO_2 or SpO_2/FiO_2 relation, requirement of mechanical ventilation and precipitant event (bacterial infection, gastrointestinal hemorrhage, active alcoholism, other or unknown)]. Laboratory data measured at the time of LT necessary to determine disease severity and for the computation of the MELD-Na score was further registered: total bilirrubin (mg/dL), creatinine (mg/dL), INR, and leukocyte count ($\times 10^9$/L). Our primary outcomes of interest were: the development of immediate posttransplant infectious complications, defined as any type of nosocomial-acquired, donor-derived or surgery-related infection presented during the immediate hospital stay following LT until the patients' discharge; the development of any type of immediate postoperative complication according to Clavien-Dindo classification[15]; and post-LT survival at 1 year and 6 years. Similarities in donor liver graft quality were assessed by evaluation of the donor risk index (DRI[16]) which considers the donor's age, height, race and cause of death, donation after cardiac death, split/partial graft, organ allocation and cold ischemia time.



DOI: 10.3748/wjg.v28.i40.5881 **Copyright** ©The Author(s) 2022.

Figure 1 Flowchart of the patients analyzed in this study. CC: Compensated cirrhosis; DC: Decompensated cirrhosis; ACLF: Acute-on-chronic liver failure.

Statistical analyses

Results of categorical variables are presented as frequencies and percentages, and as means and standard deviations or medians with interquartile range (IQR) for normally or not normally distributed continuous variables, respectively. Univariate statistical comparisons between categorical variables were performed with Pearson's Chi-squared test or Fisher's exact test and between continuous variables with the analysis of variance test or the Kruskal-Wallis test according to the normal distribution. Paired *t*-tests were carried out between disease severity scores among ACLF groups. Posttransplant survival was analyzed with the Kaplan-Meier method and survival curves were compared with the log-rank test. Statistical analyses were done with SPSS version 28.0 for Windows, IBM Corp., Armonk, NY, United States and survival curves were plotted using R version 4.1.0 (R Foundation for Statistical Computing, Vienna, Austria; www.r-project.org) with the survminer package. Statistical significance was considered at a P value less than 0.05.

RESULTS

Non-ACLF and ACLF patient characteristics

A total of 235 patients that underwent LT from 2015 to 2019 were included in this study, of which 95 (38.9%) fulfilled ACLF criteria, 129 (52.9%) were classified as DC, and 11 (4.5%) as CC (Table 1). When compared to the CANONIC study, we identified an overall younger population with ACLF patients being even younger than those with DC and CC [50.0 years (IQR 37.0-59.0) *vs* 52.0 years (IQR 43.0-61.0) and 57.0 years (IQR 53.0-59.0), respectively; $P = 0.02$]. Autoimmune etiologies (autoimmune hepatitis, primary biliary cholangitis, primary sclerosing cholangitis and overlapping syndromes) were the most frequent in ACLF patients (44.2% *vs* 27.9% DC, and 9.1% CC; $P < 0.01$), whereas the leading cause in DC and CC patients was HCV infection (72.7% CC, 32.6% DC, and 13.7% ACLF; $P < 0.0001$). With regard to comorbidities, no statistical differences were observed between cirrhosis groups for frequencies of either type 2 diabetes mellitus or primary hypertension ($P = 0.44$ and $P = 0.06$, respectively). ACLF patients had the highest MELD-Na score (25 ± 6 *vs* 19 ± 4 and 11 ± 3, DC and CC respectively), and accordingly the highest bilirubin and creatinine values. The presence of clinical ascites and encephalopathy (including West-Haven grade 3-4 encephalopathy) was also significantly higher in ACLF patients (Table 1).

Table 1 Patient characteristics (*n* = 235)

	CC, *n* = 11 (4.5%)	DC, *n*= 129 (52.9%)	ACLF, *n* = 95 (38.9%)	*P* value
Male gender, *n* (%)	6 (54.5)	64 (49.6)	47 (49.5)	0.95
Age, yr	57.0 (53.0-59.0)[a]	52.0 (43.0-61.0)[c]	50.0 (37.0-59.0)[a,c]	0.02
Liver cirrhosis etiology, *n* (%)				
Autoimmune	1 (9.1)[a]	36 (27.9)[c]	42 (44.2)[a,c]	< 0.01
HCV	8 (72.7)[a,b]	42 (32.6)[b,c]	13 (13.7)[a,c]	< 0.0001
Alcoholic liver disease	1 (9.1)	11 (8.5)	9 (9.5)	0.93
NASH	0 (0.0)	7 (5.4)	6 (6.3)	0.88
Cryptogenic	1 (9.1)	22 (17.1)	18 (18.9)	0.76
Other[1]	0 (0.0)	11 (8.5)	7 (7.4)	0.84
Comorbidities, *n* (%)				
Type 2 diabetes mellitus	3 (27.3)	22 (17.1)	13 (13.7)	0.44
Primary hypertension	2 (18.2)	20 (15.5)	6 (6.3)	0.06
Pre-transplant clinical data				
MELD-Na	11 ± 3[a,b]	19 ± 4[b,c]	25 ± 6[a,c]	< 0.0001
Total bilirubin (mg/dL)	1.18 (1.03-1.45)[a,b]	3.39 (2.3-5.46)[b,c]	7.70 (4.14-16.63)[a,c]	< 0.0001
INR	1.1 (1.1-1.2)[a,b]	1.5 (1.3-1.7)[b]	1.5 (1.3-2.0)[a]	< 0.0001
Serum creatinine (mg/dL)	0.67 (0.57-0.71)[a]	0.73 (0.61-0.88)[c]	0.97 (0.75-1.35)[a,c]	< 0.0001
Leukocyte count (× 10^9/L)	2.9 (2.4-3)[a]	4 (3.1-5)[c]	5.4 (3.8-6.8)[a,c]	< 0.0001
Disease manifestations[2], *n* (%)				
Clinical ascites	0 (0.0)[a,b]	88 (68.2)[b,c]	88 (92.6)[a,c]	< 0.0001
Encephalopathy	0 (0.0)[a,b]	69 (53.5)[b,c]	80 (84.2)[a,c]	< 0.0001
Grade 3-4 encephalopathy (West- Haven)	0 (0.0)[a,b]	7 (5.4)[b,c]	37 (38.9)[a,c]	< 0.0001

[1]Includes secondary biliary cirrhosis, drug-induced liver injury, and congenital liver diseases.
[2]Disease manifestations during the whole clinical course until liver transplantation.
Comparisons between groups are shown with superscript letters.
[a]Significant difference between CC and ACLF.
[b]Significant difference between CC and DC.
[c]Significant difference between DC and ACLF.
ACLF: Acute-on-chronic liver failure; CC: Compensated cirrhosis; DC: Decompensated cirrhosis; HCV: Hepatitis C virus; INR: International normalized ratio; MELD Na: Model for End-Stage Liver Disease-Sodium; NASH: Non-alcoholic steatohepatitis.

When assessing the last ACLF event of these patients before undergoing LT, the majority were classified as ACLF grade 1 [*n* = 40 (42.1%)] followed by ACLF-2 [*n* = 33 (34.7%)] and ACLF-3 [*n* = 22 (23.2%)] (Table 2). Overall median time to LT since their ACLF event was 31 d (IQR 11.0-88.0). However, those with ACLF-1 had a significantly longer time to LT compared to ACLF-2 and ACLF-3 [54.0 (IQR 21.3-122.8) *vs* 31.0 (IQR 7.0-59.5) and 22.0 (IQR 9.5-46.8), respectively; *P* = 0.03]. Demographic data and etiologies were similar within these three groups, with autoimmune etiologies being the most frequent among all ACLF grades (*P* = 0.30). The most common ACLF precipitant overall were bacterial infections and the absence of an identifiable factor (unknown). Other precipitants including pharmacological and procedure-related complications, were more frequent in ACLF-1 patients (*P* = 0.01). Kidney OF was the only one that did not differ significantly between ACLF groups [18 (45.0%) ACLF-1, 11 (33.3%) ACLF-2, and 14 (63.6%) ACLF-3; *P* = 0.09], whereas liver, brain, coagulation, circulation and lung failure were significantly higher in patients with ACLF-3 (Table 2).

Parameters reflecting disease severity including MELD-Na, CLIF-C OF and CLIF-C ACLF scores, total bilirubin, INR and leukocyte count were higher in ACLF-3 and lower in ACLF-1. We observed a generalized improvement of clinical parameters in ACLF patients at the time of LT, with a concomitant reduction of the disease severity scores evaluated. For instance, MELD-Na decreased significantly among all three ACLF grades (*P* < 0.01), and an improvement in the CLIF-C OF score was also observed. Interestingly, the CLIF-C ACLF score became similar within ACLF-1, 2 and 3 patients with no significant difference among them (*P* = 0.18), as well as INR and leukocyte count (*P* = 0.05 and *P* = 0.92,

Table 2 Acute-on-chronic liver failure patients characteristics (*n* = 95)

	ACLF-1, *n* = 40 (42.1%)	ACLF-2, *n* = 33 (34.7%)	ACLF-3, *n* = 22 (23.2%)	*P* value
Male gender, *n* (%)	21 (52.5)	17 (51.5)	11 (50.0)	0.98
Age, yr	55.0 (39.8-60.0)	44.0 (36.5-53.0)	49.0 (37.5-59.3)	0.14
Time to LT since ACLF event	54.0 (21.3-122.8)[a,b]	31.0 (7.0-59.5)[b]	22.0 (9.5-46.8)[a]	0.03
Liver cirrhosis etiology, *n* (%)				
Autoimmune	14 (35.0)	17 (51.5)	11 (50.0)	0.30
HCV	9 (22.5)	2 (6.1)	2 (9.1)	0.14
Alcoholic liver disease	2 (5.0)	4 (12.1)	3 (13.6)	0.44
NASH	3 (7.5)	2 (6.1)	1 (4.5)	0.99
Cryptogenic	10 (25.0)	5 (15.2)	3 (13.6)	0.50
Other[1]	2 (5.0)	3 (9.1)	2 (9.1)	0.69
ACLF precipitant, *n* (%)				
Bacterial infection	14 (35.0)	16 (48.5)	11 (50.0)	0.39
Gastrointestinal hemorrhage	1 (2.5)	3 (9.1)	1 (4.5)	0.44
Active alcoholism	0 (0.0)	0 (0.0)	0 (0.0)	0.99
Other	10 (25.0)[a]	2 (6.1)	0 (0.0)[a]	0.01
Unknown	15 (37.5)	12 (36.4)	10 (45.5)	0.77
Organ failures, *n* (%)				
Liver	14 (35.0)[a,b]	22 (66.7)[b]	16 (72.7)[a]	< 0.01
Kidney	18 (45.0)	11 (33.3)	14 (63.6)	0.09
Brain	5 (12.5)[a]	10 (30.3)	11 (50.0)[a]	< 0.01
Coagulation	3 (7.5)[a,b]	12 (36.4)[b]	11 (50.0)[a]	< 0.001
Circulation	0 (0.0)[a,b]	8 (24.2)[b,c]	14 (63.6)[a,c]	< 0.0001
Lung	1 (2.5)[a]	3 (9.1)	7 (31.8)[a]	< 0.01
ACLF event clinical data				
MELD-Na	27 ± 4[a,b]	29 ± 5[b,c]	35 ± 4[a,c]	< 0.0001
CLIF-C OF	9 ± 1[a,b]	10 ± 1[b,c]	12 ± 2[a,c]	< 0.0001
CLIF-C ACLF	39 ± 8[a]	43 ± 6[c]	52 ± 6[a,c]	< 0.0001
Total bilirubin (mg/dL)	6.31 (2.99-12.91)[a,b]	13.07 (6.39-22.31)[b]	23.08 (10.56-27.76)[a]	< 0.001
INR	1.5 (1.2-1.9)[a,b]	1.9 (1.4-2.5)[b]	2.2 (1.7-2.8)[a]	< 0.001
Serum creatinine (mg/dL)	1.86 (1.18-2.27)[b]	0.93 (0.71-1.99)[b,c]	2.25 (1.42-2.87)[c]	< 0.01
Leukocyte count (× 10^9/L)	6.55 (4.73-9.43)[a]	6.60 (4.55-8.25)[c]	8.75 (6.88-13.05)[a,c]	< 0.01
Pre-transplant clinical data				
MELD-Na	23 ± 4[a]	25 ± 5[c]	29 ± 8[a,c]	< 0.0001
CLIF-C OF	8 ± 2[a]	9 ± 2	10 ± 2[a]	0.01
CLIF-C ACLF	37 ± 9	37 ± 8	41 ± 12	0.18
Total bilirubin (mg/dL)	4.58 (2.94-8.60)[a]	9.75 (5.40-16.62)	19.59 (5.48-34.11)[a]	< 0.01
INR	1.4 (1.3-1.7)	1.6 (1.3-2.2)	1.9 (1.4-2.6)	0.05
Serum creatinine (mg/dL)	0.96 (0.75-1.29)[a]	0.88 (0.72-1.17)[c]	1.23 (0.94-1.95)[a,c]	< 0.01
Leukocyte count (× 10^9/L)	4.40 (3.23-6.70)	4.80 (2.90-6.30)	4.75 (2.48-10.45)	0.92

[1]Includes secondary biliary cirrhosis, drug-induced liver injury, and congenital liver diseases.

Comparisons between groups are shown with superscript letters.
[a]Significant difference between CC and ACLF.
[b]Significant difference between CC and DC.
[c]Significant difference between DC and ACLF.
ACLF: Acute-on-chronic liver failure; CLIF-C OF: Chronic Liver Failure Consortium: Organ Failure score; CLIF-C ACLF: Chronic Liver Failure Consortium: acute-on-chronic liver failure score; HCV: Hepatitis C virus; INR: International normalized ratio; MELD Na: Model for End-Stage Liver Disease-Sodium; NASH: Non-alcoholic steatohepatitis.

respectively) (Table 2).

ACLF patients have a more complicated posttransplant stay, but comparable short and long-term survival

Although severity of cirrhosis clearly differed between CC, DC and ACLF patients, posttransplant outcomes were mostly similar. While total days at the intensive care unit (ICU) were comparable and non-significant among these groups, patients with ACLF had a significantly longer hospital stay [8.0 d (IQR 6.0-13.0) *vs* 6.0 d (IQR 3.0-7.0) and 7.0 d (IQR 4.5-10.0), CC and DC, respectively; $P = 0.01$]. The frequency of patients who developed any type of complication (Clavien-Dindo I-V complications[15]) during their immediate hospital stay following LT was also similar, however those with ACLF more commonly presented an infectious complication ($P < 0.01$) (Table 3). When comparing days of hospital stay and posttransplant outcomes between ACLF-grades no significant differences were observed, thus the clinical course after LT of ACLF-3 patients was similar to that of those with ACLF-1 and 2 (Table 4).

Assessment of posttransplant mortality revealed that ACLF, DC and CC patients have a comparable survival at 1 and 6 years after LT [87 (91.6%), 114 (88.4%), 11 (100%) at 1 year, respectively; $P = 0.60$. 80 (84.2%), 112 (86.8%), and 10 (90.9%) at 6 years, respectively; $P = 0.90$]. Early transplant mortality at the critical periods of 30 d and 3 mo was also non-significant ($P = 0.38$ and $P = 0.30$, respectively).

All groups received the same quality grafts as there were no significant differences between groups in the DRI ($P = 0.13$) (Table 5). Survival as assessed by Kaplan-Meier analysis showed no significant differences among groups ($P = 0.79$; Figure 2A). These analyses were additionally performed in the ACLF population by subdividing them into their severity grades and no significant differences were observed at 30-d and 3-mo mortality ($P = 0.17$ and $P = 0.65$, respectively), 1-year and overall survival ($P = 0.40$ and $P = 0.15$, respectively). Likewise, no differences were observed in the DRI index ($P = 0.08$) (Table 5). This was reflected in a non-significant Kaplan-Meier analysis ($P = 0.17$; Figure 2B), which confirms similar posttransplant outcomes even among ACLF-3 patients.

DISCUSSION

Despite controversies, LT has been increasingly encouraged in patients with ACLF, including those with the highest severity grade. Hemodynamic derangements and systemic inflammation may restrain clinicians from considering an ACLF patient as a candidate for this procedure; however, the decision is so urgent that mortality on the waiting list may be even higher than that of status-1a patients[17]. In support of LT benefit for critically ill patients, this study demonstrates that according to our single-center experience, posttransplant outcomes in ACLF are favorable and in fact comparable with those of CC and DC patients. Moreover, even when comparing between ACLF grades a worse prognosis was not observed in those with ACLF-3.

In contrast to the CANONIC study[2], our patient population was in general younger, and interestingly ACLF patients were also the youngest even though no differences were found by ACLF grade. However, the main etiology in this group was of autoimmune nature. Although autoimmune diseases in cirrhosis follow a progressive and complicated clinical course, autoimmune ACLF patients in our center showed non-significant posttransplant survival differences in comparison with non-ACLF patients regardless of ACLF grade, which goes accordingly to the reported excellent survival observed in ACLF patients with autoimmune etiology[18]. A clear clinical difference between ACLF, CC and DC patients was evident by a significantly higher MELD-Na score and leukocyte count at the time of the ACLF event. These two parameters along with the CLIF-C and CLIF C-ACLF decrease at the time of LT, indicating improvement of the ACLF syndrome and hence a more favorable profile that allowed eventual transplantation. Indeed, Kim *et al*[19] has previously reported that both lower MELD scores and no ACLF progression are considered independent factors associated with a high survival rate after LT. Moreover, we also observed that the CLIF-C ACLF score at the time of LT was now similar between ACLF grades, which may further explain improvement and thus equally excellent posttransplant outcomes within these subgroups.

Compared to other studies[9,20-22], ACLF-3 patients in our center benefited from an even greater 1-year survival rate (90.9%) which remained higher even after our 6 year follow-up (77.3%). There are several risk factors associated with worse 1-year posttransplant mortality in ACLF-3 patients, such as

Table 3 Posttransplant outcomes (*n* = 235)

	CC, *n* = 11 (4.5%)	DC, *n* = 129 (52.9%)	ACLF, *n* = 95 (38.9%)	*P* value
ICU stay (d)	2.0 (1.0-4.0)	2.0 (1.5-4.0)	3.0 (2.0-5.0)	0.05
Hospital stay (d)	6.0 (3.0-7.0)[a]	7.0 (4.5-10.0)	8.0 (6.0-13.0)[a]	0.01
Any type of complication, *n* (%)	7 (63.6)	105 (81.4)	85 (89.5)	0.05
Infectious complications, *n* (%)	1 (9.1)[a]	38 (29.5)[b]	47 (49.5)[a,b]	< 0.01
Complications (Clavien-Dindo), *n* (%)				
I	4 (36.4)	17 (13.2)	19 (20.0)	0.08
II	2 (18.2)	51 (39.5)	32 (33.7)	0.31
III	1 (9.1)	14 (10.9)	17 (17.9)	0.27
IV	0 (0.0)	9 (7.0)	12 (12.6)	0.23
V	0 (0.0)	14 (10.9)	5 (5.3)	0.24

Comparisons between groups are shown with superscript letters.
[a]Significant difference between CC and ACLF.
[b]Significant difference between CC and DC.
[c]Significant difference between DC and ACLF.
ACLF: Acute-on-chronic liver failure; CC: Compensated cirrhosis; DC: Decompensated cirrhosis; ICU: Intensive care unit.

Table 4 Acute-on-chronic liver failure posttransplant outcomes (*n* = 95)

	ACLF-1, *n* = 40 (42.1%)	ACLF-2, *n* = 33 (34.7%)	ACLF-3, *n* = 22 (23.2%)	*P* value
ICU stay (d)	3.0 (2.0-4.0)	3.0 (2.0-6.0)	3.0 (2.0-6.0)	0.68
Hospital stay (d)	8.0 (5.0-11.8)	8.0 (6.0-15.5)	6.0 (5.8-14.3)	0.54
Any type of complication, *n* (%)	35 (87.5)	31 (93.9)	19 (86.4)	0.58
Infectious complications, *n* (%)	20 (50.0)	15 (45.5)	12 (54.5)	0.80
Complications (Clavien-Dindo), *n* (%)				
I	7 (17.5)	6 (18.2)	6 (27.3)	0.62
II	17 (42.5)	11 (33.3)	4 (18.2)	0.15
III	5 (12.5)	7 (21.2)	5 (22.7)	0.50
IV	4 (10.0)	6 (18.2)	2 (9.1)	0.49
V	2 (5.0)	1 (3.0)	2 (9.1)	0.61

ACLF: Acute-on-chronic liver failure; ICU: Intensive care unit.

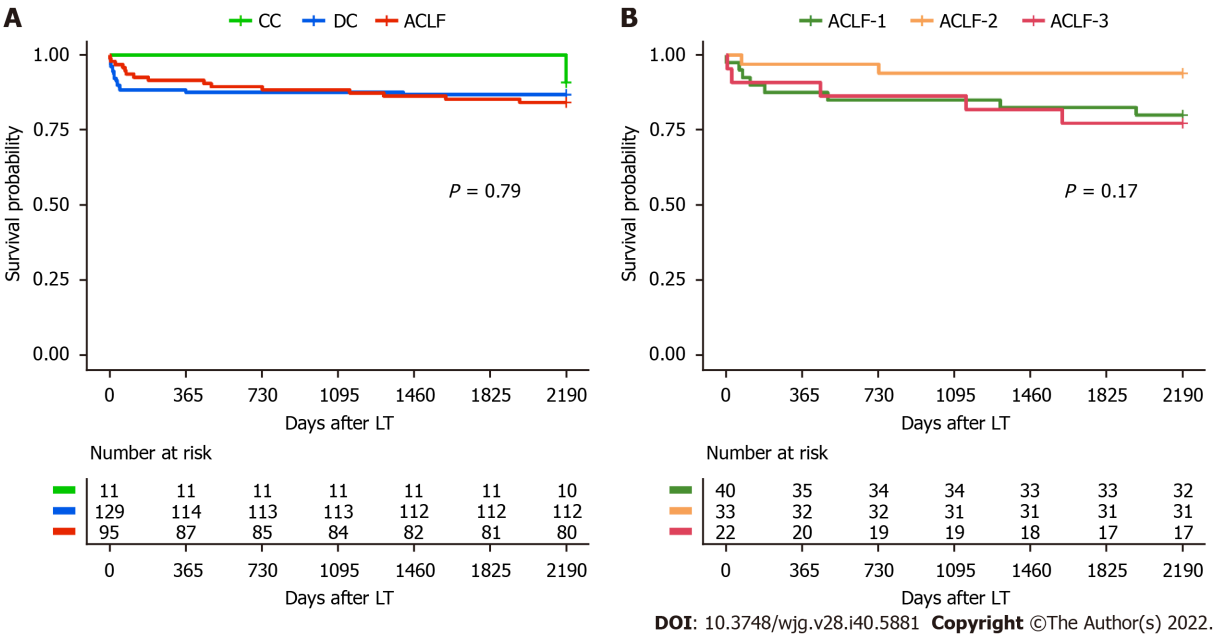
older age (≥ 53 years), high pretransplant arterial lactate levels, mechanical ventilation and high leukocyte count (≤ 10 g/L)[23]. Contributing to the favorable outcome observed in our ACLF population, including those with ACLF-3, several of the above mentioned reported risk factors for worse posttransplant mortality were not present in our patients. First, a younger age characterized our ACLF population and clinical parameters were mostly stable across all severity grades at the time of LT. Leukocyte counts were higher than in DC and CC patients, but generally always lower than 10×10^9/L either during the ACLF event or at LT. While bacterial infections were the main ACLF precipitant followed by unknown factors, important differences regarding other cohorts can be found with the frequency of certain OFs. Respiratory failure which is a risk factor for lower posttransplant survival[11,20,23] was uncommon as lung OF seldom occurred. Instead, liver OF prevailed in those with severe ACLF although closely followed by extrahepatic OFs including kidney OF, which was the most frequent in those with ACLF-1.

Inevitably, ACLF patients will have a longer and more complicated hospital stay after LT as has been reported thus far[9,22]. This was true in our center, where the latter required more days of ICU and hospital stay. Posttransplant complications by the Clavien-Dindo classification[15], were not different between ACLF and non-ACLF patients (CC and DC) in accordance with a systematic review[22]. Despite this encouraging finding, infectious complications were specifically more common in the

Table 5 Posttransplant survival overall and by acute-on-chronic liver failure grade, *n* (%)

	CC, *n* = 11 (4.5%)	DC, *n* = 129 (52.9%)	ACLF, *n* = 95 (38.9%)	*P* value	ACLF-1, *n* = 40 (42.1%)	ACLF-2, *n* = 33 (34.7%)	ACLF-3, *n* = 22 (23.2%)	*P* value
DRI	1.41 (1.36-2.26)	1.38 (1.21-1.53)	1.32 (1.19-1.54)	0.13	1.43 (1.24-1.62)	1.27 (1.20-1.43)	1.38 (1.20-1.69)	0.08
30-d mortality	0 (0.0)	10 (7.8)	3 (3.2)	0.38	1 (2.5)	0 (0.0)	2 (9.1)	0.17
3-mo mortality	0 (0.0)	15 (11.6)	6 (6.3)	0.30	3 (7.5)	1 (3.0)	2 (9.1)	0.65
1-yr survival	11 (100)	114 (88.4)	87 (91.6)	0.60	35 (87.5)	32 (97.0)	20 (90.9)	0.40
Overall survival[1]	10 (90.9)	112 (86.8)	80 (84.2)	0.90	32 (80.0)	31 (93.9)	17 (77.3)	0.15

[1]Survival was analyzed until 6 years of follow-up, when the study was ended.
ACLF: Acute-on-chronic liver failure; CC: Compensated cirrhosis; DC: Decompensated cirrhosis.



DOI: 10.3748/wjg.v28.i40.5881 **Copyright** ©The Author(s) 2022.

Figure 2 Kaplan-Meier analyses for survival after liver transplant between compensated cirrhosis, decompensated cirrhosis, and acute-on-chronic liver failure (A), and between acute-on-chronic liver failure grades (B). LT: Liver transplant; CC: Compensated cirrhosis; DC: Decompensated cirrhosis; ACLF: Acute-on-chronic liver failure.

former, occurring in over half of them, which is also in agreement with the study of Artru *et al*[9]. This may warrant a more directed antibiotic regimen in ACLF patients and physicians should be aware of this frequent outcome to promote a longer posttransplant survival. Interestingly, infections were equally prevalent in ACLF-3 patients according to our experience, which may be due to the similar pretransplant profile identified among severity grades including non-significant CLIF-C ACLF score differences. A good donor liver graft quality which was comparable between CC, DC and ACLF patients is another factor that may have contributed to an overall excellent outcome; however, optimal graft quality must not impede the decision for LT given its lesser impact compared to early transplantation, as has been recently reported[24]. Overall, our results encourage further transplantation in those with ACLF, considering that this procedure is the only effective treatment option and that survival was not significantly different compared to patients with less advanced cirrhosis, despite a more complicated posttransplant clinical course.

This study is limited by its retrospective nature and its single-center design; hence, findings must be compared to those of other authors. We report here the experience of one of the largest transplant centers in Mexico; however, demographics in this center will certainly vary with those seen in the rest of the country. This may explain the high proportion of autoimmune patients compared to HCV or alcoholic hepatitis. Regardless, during the five-year study period we have found a comparable proportion of ACLF patients who undergo LT, whose disease severity is markedly different from CC and DC patients. In spite of these differences, we observed a clear LT benefit as has been supported by

previous studies.

CONCLUSION

In conclusion, out of 235 liver transplantation procedures that were carried out between 2015 and 2019 in our center, 38.9% corresponded to ACLF patients. Although important clinical differences were found with non-ACLF patients (CC and DC) and among each other when divided by severity grade, posttransplant survival was uniformly excellent. A longer hospital stay and frequency of infectious complications is to be expected, however, this should not restrain the decision to transplant those with ACLF. Furthermore, our observations support benefit even in the most critically ill patients (ACLF-3), given comparable 1-year and 6-year survival rates.

ARTICLE HIGHLIGHTS

Research background

Currently, liver transplantation (LT) is the only definitive therapeutic measure for patients with cirrhosis, albeit with the implied risks including posttransplant complications and the long-term use of immunosuppressive drugs. However, these patients benefit in general from excellent posttransplant survival. The benefit and survival of this procedure for patients with more advanced cirrhosis such as those with acute-on-chronic liver failure (ACLF), still remains controversial, with some reports showing a clear benefit, while others reporting lower short and long-term survival after transplant.

Research motivation

In order to contribute to the current literature regarding the benefit of LT even in those with more severe diseases, we evaluate the immediate posttransplant outcomes and compared the posttransplant survival in patients stratified by disease severity.

Research objectives

To assess immediate posttransplant outcomes and compare the short (1 year) and long-term (6 years) posttransplant survival among cirrhotic patients stratified by disease severity.

Research methods

We included cirrhotic patients undergoing liver transplantation between 2015 and 2019 and categorized them into compensated cirrhosis (CC), decompensated cirrhosis (DC), and ACLF. ACLF was further divided into severity grades. Medical records of all patients were examined to extract demographic and clinical variables as well as laboratory data measured at the time of LT and in the posttransplant period. Our primary outcomes of interest were: the development of immediate posttransplant infectious complications, defined as any type of nosocomial-acquired, donor-derived or surgery-related infection presented during the immediate hospital stay following LT until the patients' discharge; the development of any type of immediate postoperative complication according to Clavien-Dindo classification; and post-LT survival at 1 year and 6 years. Posttransplant survival was analyzed with the Kaplan-Meier method and survival curves were compared with the log-rank test.

Research results

A total of 235 patients underwent liver transplantation (CC = 11, DC = 129 and ACLF = 95). Patients with ACLF had a significantly longer hospital stay and developed more infection-related complications. Posttransplant survival at 1- and 6-years was similar among groups. When ACLF patients were stratified according to ACLF grade, similar intensive care unit and hospital stay lengths were found, as well as comparable frequencies of overall and infectious posttransplant complications. Despite that, there was no survival difference between ACLF grades at 1 year and 6 years.

Research conclusions

Patients may benefit from liver transplantation regardless of the cirrhosis stage. Despite having a longer hospital stay and a higher frequency of infectious complications, ACLF patients have excellent and comparable 1 and 6-year survival rates.

Research perspectives

A multicenter study would be required to determine the value of LT in advanced disease patients such as those with ACLF according to disease etiology.

ACKNOWLEDGEMENTS

We would like to thank Elizabeth Costello for her important contribution in editing the English language text of this manuscript.

FOOTNOTES

Author contributions: Cervantes-Alvarez E and Navarro-Alvarez N envisioned the study and wrote the manuscript; Cervantes-Alvarez E, Limon-de la Rosa N and Mendez-Guerrero O supported the data collection and made the formal analysis; Navarro-Alvarez N, Kershenobich D, Vilatoba M, Torre A, Limon-de la Rosa N, Mendez-Guerrero O and Cervantes-Alvarez E reviewed and edited the manuscript; all authors read and approved the final manuscript.

Institutional review board statement: This study was reviewed and approved by the Research Ethics Committee of Instituto Nacional de Ciencias Médicas y Nutrición Salvador Zubirán (GAS-2368-17-20).

Informed consent statement: Requirement of informed consent was waived due to the observational nature of this study.

Conflict-of-interest statement: All the authors report no relevant conflicts of interest for this article.

Data sharing statement: The data that support the findings of this study are available from the corresponding author upon reasonable request.

STROBE statement: The authors have read the STROBE Statement—checklist of items, and the manuscript was prepared and revised according to the STROBE Statement—checklist of items.

Open-Access: This article is an open-access article that was selected by an in-house editor and fully peer-reviewed by external reviewers. It is distributed in accordance with the Creative Commons Attribution NonCommercial (CC BY-NC 4.0) license, which permits others to distribute, remix, adapt, build upon this work non-commercially, and license their derivative works on different terms, provided the original work is properly cited and the use is non-commercial. See: https://creativecommons.org/Licenses/by-nc/4.0/

Country/Territory of origin: Mexico

ORCID number: Eduardo Cervantes-Alvarez 0000-0002-7791-0489; Mario Vilatoba 0000-0002-7141-4337; Nathaly Limon-de la Rosa 0000-0002-1175-3126; Osvely Mendez-Guerrero 0000-0002-9308-9352; David Kershenobich 0000-0001-6178-9170; Aldo Torre 0000-0002-9299-3075; Nalu Navarro-Alvarez 0000-0003-0118-4676.

Corresponding Author's Membership in Professional Societies: American Association for the Study of Liver Diseases, No. 135418.

S-Editor: Gong ZM
L-Editor: A
P-Editor: Gong ZM

REFERENCES

1 **Garcia-Tsao G**, Friedman S, Iredale J, Pinzani M. Now there are many (stages) where before there was one: In search of a pathophysiological classification of cirrhosis. *Hepatology* 2010; **51**: 1445-1449 [PMID: 20077563 DOI: 10.1002/hep.23478]

2 **Moreau R**, Jalan R, Gines P, Pavesi M, Angeli P, Cordoba J, Durand F, Gustot T, Saliba F, Domenicali M, Gerbes A, Wendon J, Alessandria C, Laleman W, Zeuzem S, Trebicka J, Bernardi M, Arroyo V; CANONIC Study Investigators of the EASL–CLIF Consortium. Acute-on-chronic liver failure is a distinct syndrome that develops in patients with acute decompensation of cirrhosis. *Gastroenterology* 2013; **144**: 1426-1437, 1437.e1 [PMID: 23474284 DOI: 10.1053/j.gastro.2013.02.042]

3 **Jalan R**, Yurdaydin C, Bajaj JS, Acharya SK, Arroyo V, Lin HC, Gines P, Kim WR, Kamath PS; World Gastroenterology Organization Working Party. Toward an improved definition of acute-on-chronic liver failure. *Gastroenterology* 2014; **147**: 4-10 [PMID: 24853409 DOI: 10.1053/j.gastro.2014.05.005]

4 **Albillos A**, Lario M, Álvarez-Mon M. Cirrhosis-associated immune dysfunction: distinctive features and clinical relevance. *J Hepatol* 2014; **61**: 1385-1396 [PMID: 25135860 DOI: 10.1016/j.jhep.2014.08.010]

5 **Laleman W**, Claria J, Van der Merwe S, Moreau R, Trebicka J. Systemic Inflammation and Acute-on-Chronic Liver Failure: Too Much, Not Enough. *Can J Gastroenterol Hepatol* 2018; **2018**: 1027152 [PMID: 30155448 DOI: 10.1155/2018/1027152]

6 **Levesque E**, Winter A, Noorah Z, Daurès JP, Landais P, Feray C, Azoulay D. Impact of acute-on-chronic liver failure on 90-day mortality following a first liver transplantation. *Liver Int* 2017; **37**: 684-693 [PMID: 28052486 DOI:

10.1111/liv.13355]

7 **Agbim U**, Sharma A, Maliakkal B, Karri S, Yazawa M, Goldkamp W, Podila PSB, Vanatta JM, Gonzalez H, Molnar MZ, Nair SP, Eason JD, Satapathy SK. Outcomes of Liver Transplant Recipients With Acute-on-Chronic Liver Failure Based on EASL-CLIF Consortium Definition: A Single-center Study. *Transplant Direct* 2020; **6**: e544 [PMID: 32309630 DOI: 10.1097/TXD.0000000000000984]

8 **Huebener P**, Sterneck MR, Bangert K, Drolz A, Lohse AW, Kluge S, Fischer L, Fuhrmann V. Stabilisation of acute-on-chronic liver failure patients before liver transplantation predicts post-transplant survival. *Aliment Pharmacol Ther* 2018; **47**: 1502-1510 [PMID: 29611203 DOI: 10.1111/apt.14627]

9 **Artru F**, Louvet A, Ruiz I, Levesque E, Labreuche J, Ursic-Bedoya J, Lassailly G, Dharancy S, Boleslawski E, Lebuffe G, Kipnis E, Ichai P, Coilly A, De Martin E, Antonini TM, Vibert E, Jaber S, Herrerro A, Samuel D, Duhamel A, Pageaux GP, Mathurin P, Saliba F. Liver transplantation in the most severely ill cirrhotic patients: A multicenter study in acute-on-chronic liver failure grade 3. *J Hepatol* 2017; **67**: 708-715 [PMID: 28645736 DOI: 10.1016/j.jhep.2017.06.009]

10 **Belli LS**, Duvoux C, Artzner T, Bernal W, Conti S, Cortesi PA, Sacleux SC, Pageaux GP, Radenne S, Trebicka J, Fernandez J, Perricone G, Piano S, Nadalin S, Morelli MC, Martini S, Polak WG, Zieniewicz K, Toso C, Berenguer M, Iegri C, Invernizzi F, Volpes R, Karam V, Adam R, Faitot F, Rabinovich L, Saliba F, Meunier L, Lesurtel M, Uschner FE, Fondevila C, Michard B, Coilly A, Meszaros M, Poinsot D, Schnitzbauer A, De Carlis LG, Fumagalli R, Angeli P, Arroyo V, Jalan R; ELITA/EF-CLIF working group. Liver transplantation for patients with acute-on-chronic liver failure (ACLF) in Europe: Results of the ELITA/EF-CLIF collaborative study (ECLIS). *J Hepatol* 2021; **75**: 610-622 [PMID: 33951535 DOI: 10.1016/j.jhep.2021.03.030]

11 **Finkenstedt A**, Nachbaur K, Zoller H, Joannidis M, Pratschke J, Graziadei IW, Vogel W. Acute-on-chronic liver failure: excellent outcomes after liver transplantation but high mortality on the wait list. *Liver Transpl* 2013; **19**: 879-886 [PMID: 23696006 DOI: 10.1002/lt.23678]

12 **O'Leary JG**, Bajaj JS, Tandon P, Biggins SW, Wong F, Kamath PS, Garcia-Tsao G, Maliakkal B, Lai J, Fallon M, Vargas HE, Thuluvath P, Subramanian R, Thacker LR, Reddy KR. Outcomes After Listing for Liver Transplant in Patients With Acute-on-Chronic Liver Failure: The Multicenter North American Consortium for the Study of End-Stage Liver Disease Experience. *Liver Transpl* 2019; **25**: 571-579 [PMID: 30724010 DOI: 10.1002/lt.25426]

13 **Marciano S**, Mauro E, Giunta D, Torres MC, Diaz JM, Bermudez C, Gutierrez-Acevedo MN, Narvaez A, Ortíz J, Dirchwolf M, Pollarsky F, Rojas-Saunero LP, Gadano A. Impact of acute-on-chronic liver failure on post-transplant survival and on kidney outcomes. *Eur J Gastroenterol Hepatol* 2019; **31**: 1157-1164 [PMID: 31385871 DOI: 10.1097/MEG.0000000000001467]

14 **Cervantes-Alvarez E**, Limon-de la Rosa N, Vilatoba M, Pérez-Monter C, Hurtado-Gomez S, Martinez-Cabrera C, Argemi J, Alatorre-Arenas E, Yarza-Regalado S, Tejeda-Dominguez F, Lizardo-Thiebaud MJ, Mendez-Guerrero O, Gamboa-Dominguez A, Aguilar-Salinas CA, Huang CA, Kershenobich D, Bataller R, Torre A, Navarro-Alvarez N. Galectin-3 is overexpressed in advanced cirrhosis and predicts post-liver transplant infectious complications. *Liver Int* 2022; Online ahead of print [PMID: 35635536 DOI: 10.1111/liv.15326]

15 **Dindo D**, Demartines N, Clavien PA. Classification of surgical complications: a new proposal with evaluation in a cohort of 6336 patients and results of a survey. *Ann Surg* 2004; **240**: 205-213 [PMID: 15273542 DOI: 10.1097/01.sla.0000133083.54934.ae]

16 **Feng S**, Goodrich NP, Bragg-Gresham JL, Dykstra DM, Punch JD, DebRoy MA, Greenstein SM, Merion RM. Characteristics associated with liver graft failure: the concept of a donor risk index. *Am J Transplant* 2006; **6**: 783-790 [PMID: 16539636 DOI: 10.1111/j.1600-6143.2006.01242.x]

17 **Sundaram V**, Shah P, Wong RJ, Karvellas CJ, Fortune BE, Mahmud N, Kuo A, Jalan R. Patients With Acute on Chronic Liver Failure Grade 3 Have Greater 14-Day Waitlist Mortality Than Status-1a Patients. *Hepatology* 2019; **70**: 334-345 [PMID: 30908660 DOI: 10.1002/hep.30624]

18 **Singal AK**, Wong RJ, Jalan R, Asrani S, Kuo YF. Primary biliary cholangitis has the highest waitlist mortality in patients with cirrhosis and acute on chronic liver failure awaiting liver transplant. *Clin Transplant* 2021; **35**: e14479 [PMID: 34510550 DOI: 10.1111/ctr.14479]

19 **Kim JE**, Sinn DH, Choi GS, Kim JM, Joh JW, Kang W, Gwak GY, Paik YH, Choi MS, Lee JH, Koh KC, Paik SW. Predictors and outcome of emergent Liver transplantation for patients with acute-on-chronic liver failure. *Dig Liver Dis* 2021; **53**: 1004-1010 [PMID: 33931340 DOI: 10.1016/j.dld.2021.03.030]

20 **Sundaram V**, Patel S, Shetty K, Lindenmeyer CC, Rahimi RS, Flocco G, Al-Attar A, Karvellas CJ, Challa S, Maddur H, Jou JH, Kriss M, Stein LL, Xiao AH, Vyhmeister RH, Green EW, Campbell B, Cranford W, Mahmud N, Fortune BE; Multi-Organ Dysfunction and Evaluation for Liver Transplantation (MODEL) Consortium. Risk Factors for Posttransplantation Mortality in Recipients With Grade 3 Acute-on-Chronic Liver Failure: Analysis of a North American Consortium. *Liver Transpl* 2022; **28**: 1078-1089 [PMID: 35020260 DOI: 10.1002/lt.26408]

21 **Sundaram V**, Mahmud N, Perricone G, Katarey D, Wong RJ, Karvellas CJ, Fortune BE, Rahimi RS, Maddur H, Jou JH, Kriss M, Stein LL, Lee M, Jalan R; Multi-Organ Dysfunction, Evaluation for Liver Transplantation (MODEL) Consortium. Longterm Outcomes of Patients Undergoing Liver Transplantation for Acute-on-Chronic Liver Failure. *Liver Transpl* 2020; **26**: 1594-1602 [PMID: 32574423 DOI: 10.1002/lt.25831]

22 **Abdallah MA**, Waleed M, Bell MG, Nelson M, Wong R, Sundaram V, Singal AK. Systematic review with meta-analysis: liver transplant provides survival benefit in patients with acute on chronic liver failure. *Aliment Pharmacol Ther* 2020; **52**: 222-232 [PMID: 32490550 DOI: 10.1111/apt.15793]

23 **Artzner T**, Michard B, Weiss E, Barbier L, Noorah Z, Merle JC, Paugam-Burtz C, Francoz C, Durand F, Soubrane O, Pirani T, Theocharidou E, O'Grady J, Bernal W, Heaton N, Salamé E, Bucur P, Barraud H, Lefebvre F, Serfaty L, Besch C, Bachellier P, Schneider F, Levesque E, Faitot F. Liver transplantation for critically ill cirrhotic patients: Stratifying utility based on pretransplant factors. *Am J Transplant* 2020; **20**: 2437-2448 [PMID: 32185866 DOI: 10.1111/ajt.15852]

24 **Zhang S**, Suen SC, Gong CL, Pham J, Trebicka J, Duvoux C, Klein AS, Wu T, Jalan R, Sundaram V. Early transplantation maximizes survival in severe acute-on-chronic liver failure: Results of a Markov decision process model. *JHEP Rep* 2021; **3**: 100367 [PMID: 34825154 DOI: 10.1016/j.jhepr.2021.100367]



Published by **Baishideng Publishing Group Inc**
7041 Koll Center Parkway, Suite 160, Pleasanton, CA 94566, USA
Telephone: +1-925-3991568
E-mail: bpgoffice@wjgnet.com
Help Desk: https://www.f6publishing.com/helpdesk
https://www.wjgnet.com



© 2022 Baishideng Publishing Group Inc. All rights reserved.